Virchows Arch (2009) 455:1–13
DOI 10.1007/s00428-009-0783-1

REVIEW AND PERSPECTIVE

Stem cells and solid cancers

Stuart A. C. McDonald · Trevor A. Graham · Stefanie Schier · Nicholas A. Wright · Malcolm R. Alison

Received: 9 March 2009 / Revised: 22 April 2009 / Accepted: 28 April 2009 / Published online: 5 June 2009

Abstract Recently, there have been significant advances in our knowledge of stem cells found in tissues that can develop solid tumours. In particular, novel stem cell markers have been identified for the first time identifying multipotential cells: a required characteristic of a stem cell. The scarcity of cancer stem cells has been questioned. Current dogma states that they are rare, but novel research has suggested that this may not be the case. Here, we review the latest literature on stem cells, particularly cancer stem cells within solid tumours. We discuss current thinking on how stem cells develop into cancer stem cells and how they protect themselves from doing so and do they express unique markers that can be used to detect stem cells. We attempt to put into perspective these latest advances in stem cell biology and their potential for cancer therapy.

Keywords Stem cell · Cancer stem cell · Intestine · Liver · Lung

Stuart A. C. McDonald, Trevor A. Graham and Stefanie Schier contributed equally to this work.

S. A. C. McDonald (✉)
Centre for Gastroenterology, Institute of Cell and Molecular Science, Barts and the London School of Medicine and Dentistry, Blizard Building, 4 Newark Street, Whitechapel, London E1 2AT, UK
e-mail: stuart.mcdonald@cancer.org.uk

S. A. C. McDonald · T. A. Graham · S. Schier · N. A. Wright · M. R. Alison
Histopathology Unit, Cancer Research UK, London Research Institute, London, UK

M. R. Alison
Centre for Diabetes, Institute of Cell and Molecular Science, Barts and the London School of Medicine and Dentistry, London, UK

N. A. Wright
Institute of Cell and Molecular Science, Barts and the London School of Medicine and Dentistry, London, UK

Introduction

Cancer is most likely a disease of stem cells. This appears to be a rather didactic statement and can be argued for and against; however, the hypothesis that stem cells are at the root of a hierarchical cellular organization of the majority of cancers seems intuitive. The fact that stem cells appear to be the only cell type that can self-renew heavily implicates them in cancer development that can also be seen as a disease with dysregulated self-renewal [1]. They are also one of the limited number of cell types that survive long enough to accrue sufficient numbers of mutations needed to develop into a tumour: the mutation and selection theory of cancer development [2]. Furthermore, there can be multiple differentiated cell types within tumours, which can be readily explained if there is a multipotent stem cell at its source [3].

The cancer stem cell theory was first proposed by Hamburger and Salmon [4] who demonstrated that only a small percentage of tumour cells were able to form colonies in soft agar. This raises the possibility that only a minority of self-renewing cells within a tumour are capable of sustaining it, and therefore, therapies need only target the cancer stem cell (CSC). The identification of this population of CSCs has been at the forefront of tumour biology.

Here, we review the current literature describing how a normal tissue stem cell develops into a cancer stem cell, potential markers of such cells, the mechanisms behind the

mutation and selection theory and finally how such mutations spread through rapidly renewing tissues such as the gastrointestinal tract. We discuss recent developments, which have questioned the role of stem cells in cancer development, their numbers in individual tumours and molecular signatures.

Cells with stem cell-like characteristics were first described in the bone marrow in 1961 by Till and McCulloch [5] as cells that gave rise to multilineage haematopoietic colonies in the spleen. Stem cells can be defined by two essential features: first they have the ability of indefinite self-renewal, so-called longevity. Second, they are multipotent, meaning they can differentiate into various cell lineages within their tissue of origin. Adult stem cells are immature, undifferentiated cells, which are thought to exist in small numbers in nearly all post-embryonic tissue [6]. These key properties of adult stem cells enable them to replenish terminally differentiated cell populations and facilitate tissue repair within their tissue of origin [7–10]. The differences in developmental potential between stem cells and progenitor cells form a hierarchical structure with stem cells residing at the base and their progeny above, becoming more differentiated with each division [11].

Tissues such as blood, skin or the gut perpetually renew their cell populations; however, a large number of tissues in adult mammalians exhibit very low cellular turnover under normal circumstances. Some of these even respond poorly to tissue damage such as the heart, whilst others, like the liver, respond well. Although adult stem cells have been widely studied in the haematopoietic system, candidates for tissue stem cells have been described in the nervous system [12], the myocardium[13], skeletal muscle [14], epidermis [15], intestinal track [16–20], liver [21] and pancreas [22].

The stem cell niche

Adult stem cells are thought to reside in a *stem cell niche* [23]. The niche is a specialised microenvironment that contains the signalling molecules required to maintain stem cell identity. Within the niche, a cell that has intrinsic stem cell potential will have a stem cell phenotype. Upon leaving the niche, such a cell will lose its stemness. A number of stem cell niches have been characterised. In the intestinal crypt for example, stem cells are thought to reside towards the crypt base (see Fig. 1a). Surrounding stromal cells, the *pericryptal myofibroblasts* secrete messenger proteins, including members of the Wnt and BMP families, which contribute to cell fate determination and regulate proliferation in the stem cell compartment (reviewed in [24]). The colonic crypt illustrates the

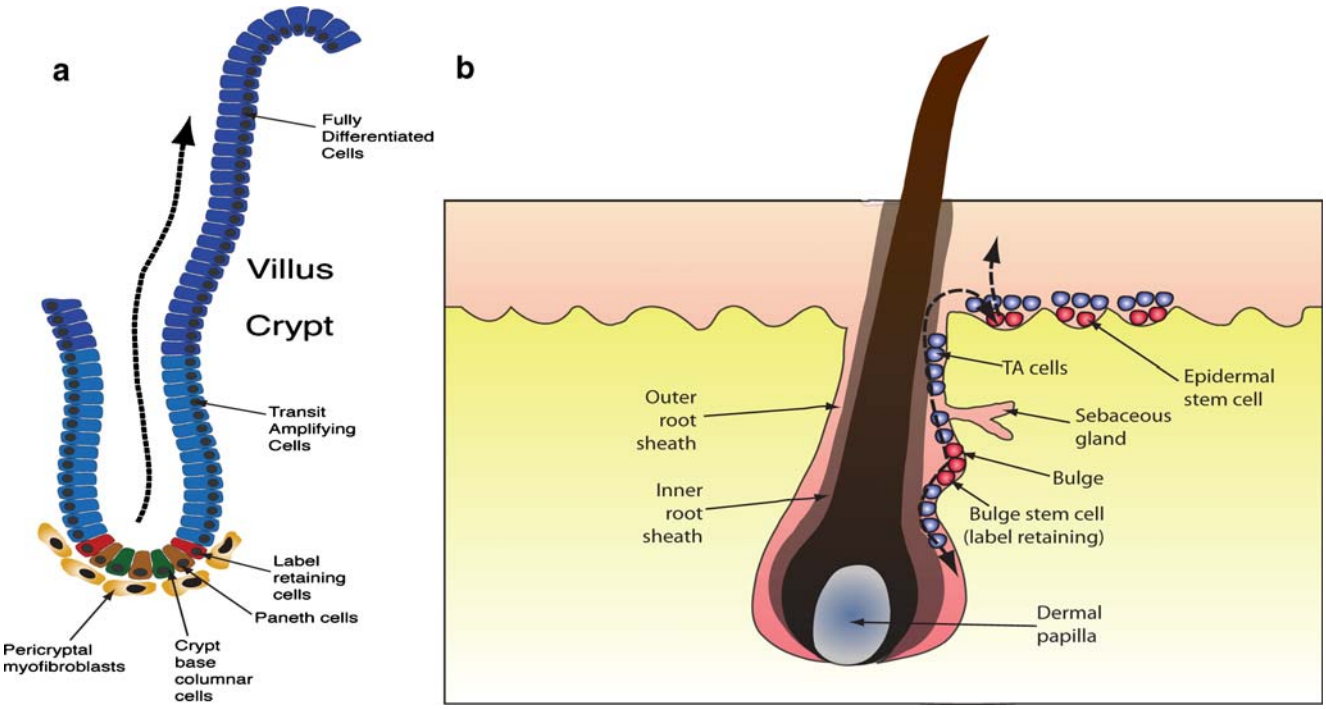

Fig. 1 The stem cell niche. **a** The small intestinal crypt. The stem cell zone is believed to be superior to the Paneth cell zone, but recent evidence suggests that Lgr5-expressing cells are located within the Paneth cell zone. These are entirely distinct from Paneth cells and have been called crypt base columnar cells (CBCs). The crypt is surrounded by a pericryptal myofibroblast sheath and this defines the crypt niche. Cross-talk between the stem cell and the myofibroblast is thought to maintain 'stemness'. **b** Epidermis. Here there are two populations of stem cells, one in the basal layer of the epidermis and one in the bulge region below the sebaceous gland. The progeny of the latter are thought differentiate into the follicle itself

reciprocal relationship in maintaining stemness that is shared between cells and their niche. In the crypt, epithelial cells themselves also express signalling molecules: for example, expression of the Hedgehog (Hh) ligands *Indian* and *Sonic Hedgehog* is restricted to the epithelial cells away from the crypt base [25, 26]. Hedgehog signalling antagonises proliferative Wnt signals, inhibiting proliferation in Hh^{+} cells and so restricting cell division to the stem cell compartment. In the fly testis, germline stem cells are clustered around a hub of non-dividing cells, which express the niche-ligand *Unpaired* (*Upd*). Upd stimulates the JAK–STAT pathway, which maintains stem cell identity [27, 28]. Spradling et al. have argued that a stem cell niche should persist on the removal of the stem cells [29]. Indeed, transplantation of germline stem cells from donor mice into the testes of sterile mice restored spermatogenesis [30]. Correspondingly, in the murine intestinal crypt, the stem cell compliment is readily restored following depletion by radiation or mutagen.

Given the remarkable proliferative potential of stem cells, tight regulation of stem cell division is required to prevent aberrant growth. Proliferation of stem cells must balance the need for self-renewal of the stem cell population with the constant requirement for new short-lived tissue-specific differentiated cells. One mechanism to balance this trade-off between renewal and proliferation is *asymmetric* stem cell division. Asymmetric division results in a stem cell producing one differentiated daughter cell and one daughter stem cell. In this manner, the normal stem cell compliment is maintained. The immediate differentiating cell progeny of the stem cells are thought to be *transit amplifying cells* (TA cells). TA cells have limited replicative potential and divide only a relatively small number of times to produce the bulk of the specialised, terminally differentiated (TD) cells in the tissue. Ohlstein and Spradling show clear evidence of this hierarchical tissue structure in the fly mid-gut [31]. Crypt-like structures in the fly are maintained by a single proliferative stem cell, which divides asymmetrically to produce differentiated enterocyte and enteroendocrine progeny. Hierarchical tissue structure has also been demonstrated in the mammalian intestine [32, 33]. Hierarchical tissue structures may have evolved to restrict the accumulation of mutations and so could be an anti-cancer mechanism. This idea is discussed in the next section.

Are all stem cell divisions asymmetric? The answer to this question is almost certainly no. Mutant stem cells can repopulate an entire niche [34–36], and further, analysis of the diversity of heritable methylation patterns in colon crypts is incompatible with a model where all stem cell lineages are immortal [37]. Thus, some stem cell divisions must be *symmetric*, producing either two stem cell progeny or two differentiated cell progeny. In order maintain a constant number of stem cells in the niche, the symmetric divisions resulting in two daughter stem cells (growth of a stem cell clone) must occur at the same frequency as symmetric divisions resulting in two differentiating daughter cells (death of a stem cell clone). Disruption to this balance can lead to aberrant growth and the formation of a tumour.

In the small intestinal crypt, cells migrate from the base of the crypt, along the vertical crypt axis and onto the villus (Fig. 1a). Thus, the crypt stem cells, the source of the differentiated cells, are very likely to be located at the base. Indeed, localisation of the putative stem cell marker Lgr5 (described later) to the cells at positions 1–3, suggests the intestinal stem cells reside between the Paneth cells at the crypt base [38]. Contrastingly, label retaining cells are located at positions 4–5 [39], where the putative stem cell marker Bmi1 [40] is also localised (described later). Proliferation in the crypt tends to be restricted to the bottom two-thirds [41]. Stem cells produce transit amplifying cells whose progeny constitute the bulk of the crypt cell population [33]. Regulation of cell division and differentiation of stem cell progeny into either Goblet or enteroendocrine cells or enterocytes are provided by a range of signalling pathways including Wnt, Notch and BMP pathways (reviewed in [42]).

Stem cell niches are thought to be present in all proliferative tissues. The structure of the epidermal stem cell niche has also been extensively investigated. Figure 1b schematically describes the structure of the follicle and surrounding epidermis. Briefly, there are two putative stem cell zones within the epidermis: the basal layer of the epidermal proliferative unit (EPU) of epidermis and the bulge region of the hair follicle. Each stem cell zone has its own independent niche. It should be noted that only thin, relatively unexposed skin exhibits EPUs: thicker, more exposed skin does not and is heavily keratinised. However, within an EPU, the basal layer is the most proliferative and high expression of adhesion markers such as β1 intergrins have been proposed as a stem cell marker in the basal layer [23] particularly in conjunction with a physical connection to the basement membrane. Stem cells in the bulge region primarily appear to be responsible for hair growth and maintenance of the sebaceous gland. Bulge cells have been characterised by their ability to retain DNA label and express the α4 integrin, transplanting these cells led to patches of hair-producing epidermis [43].

Self-defence in stem cell populations

Since DNA replication is not perfect, mutations occur each time a cell divides. In renewing tissues, such as the gastrointestinal epithelium, many millions of cell divisions

occur each day. When viewed in this light, the eventual acquisition of a tumorigenic mutation by a stem cell clone seems inevitable. Yet, cancers are relatively rare. Why is this? One persuasive answer is that the mechanisms that regulate stem cell divisions have evolved to limit somatic evolution in the stem cell population. Mathematical modelling shows that *hierarchical tissue structures*, whereby a few infrequently dividing stem cells produce short-lived transit amplifying cells that generate the bulk of the tissue mass, restrict the likelihood of oncogenic transformation of stem cells in a niche [44].

In 1975, John Cairns introduced his 'immortal strand hypothesis' (Fig. 2a) as a mechanisms by which adult stem cells protect themselves from accumulation mutations and hence minimising the risk of developing cancer [45]. The basic assumption is that the template DNA is selectively retained in asymmetrical division whilst the newly synthesised strand is passed on to the daughter cell, the transit-amplifying cell. Thus, any errors in replication will be transferred to progenitor cells and lost from the population [45]. Experimentally proving the hypothesis has been challenging; however, the presence of cells that apparently are able to segregate their template DNA strand has been observed in a limited number of tissues including small intestinal [46] and breast [47] epithelial cells and muscle satellite cells [48].

The hypothesis has been challenged, however, and no molecular mechanism for the selective retention of template DNA has been proposed. Furthermore, the immortal strand hypothesis requires that such label-retaining cells undergo

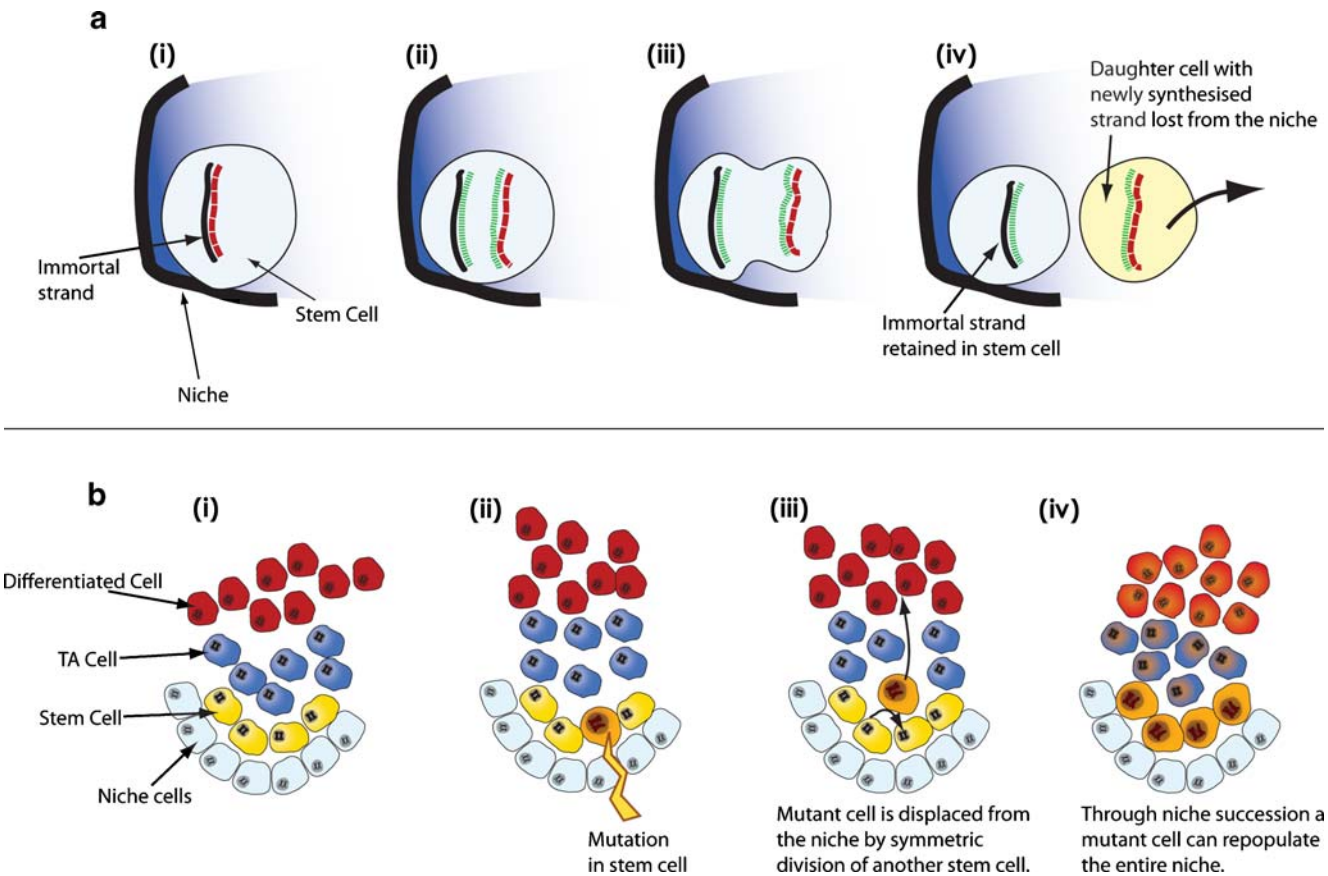

Fig. 2 Niche defence mechanisms. **a** The immortal strand hypothesis. Stem cells may selectively segregate newly formed, and hence error-prone, DNA strands to their short-lived progeny, and retain the original, error-free, template strand. *i* A stem cell in its niche with an immortal DNA strand (*black*), and the complementary new strand (*red*). *ii* DNA replication, with newly synthesised strands (*dashed green*). *iii* Mitosis. Chromatids are aligned in preparation for selective chromatid segregation. *iv* The stem cell retains the immortal strand, whilst the daughter cell inherits the newly synthesised DNA. **b** Hierarchical tissue structures restrict the accumulation of mutations. *i* The stem cell niche is maintained by a small number of stem cells (*yellow*), which produce transit amplifying progeny (*blue*) that divide frequently to produce the bulk of the differentiated cell population (*red*). *ii* A stem cell in the niche acquires a mutation (*orange*). Mutations could result from exposure to a mutagen or simply through random DNA replication errors. *iii* A symmetric division of an adjacent stem cell displaces the mutant cell from the niche. The mutant cell will be subsequently lost from the niche, and the niche reverts to being entirely wild-type. *iv* Alternatively, through niche succession, the mutant cell can repopulate the entire niche. The niche is now described as mono-clonally converted. Some stem cell mutations will provide a selective advantage for the mutant cell compared to the other stem cells in the niche, increasingly the likelihood the mutation is retained in the niche

further division but retain the template strand: this has yet to be shown experimentally. Lansdorp [49] recently proposed the 'silent sister' hypothesis, suggesting that cell fate in asymmetric division is co-directed by epigenetic differences between sister chromatids, inducing a non-random segregation of sister chromatids during mitosis. The daughter cell remaining as a stem cell selectively retains chromatids with active stem cell genes, with the loss of stem cell properties in the cell that inherits the opposite 'silent' sister chromatids [49]. Not all studies agree with the hypothesis. Haematopoietic stem cells (HSCs) with long-term repopulating activity have been shown not to segregate their template DNA strand nor do they retain label [50].

Occasional *symmetric divisions* of stem cells, which result in a stem cell producing two daughter stem cells, or two daughter differentiated cells, also restrict the rate at which mutations can accumulate in the stem cells in a niche [51]. This is because symmetric divisions eventually result in the loss of a stem cell clone: in order to keep the number of stem cells in a niche roughly constant, symmetric division of stem cells, producing two daughter stem cells, must be balanced by a second symmetric stem cell division which results in two differentiated cells and the eventual loss of the stem cell clone. Correspondingly, if a niche contains N stem cells, these random losses and expansions of stem cell lineages mean that the probability that a neutral mutation will become *fixed* in the niche is $1/N$, so that most neutral mutations are shed from the niche. This could therefore act as a defence mechanism whereby a neutral mutation, if it was allowed to continue to survive within the niche, may propagate a field of genetic instability encouraging further, possibly tumorigenic, mutations. This is illustrated in Fig. 2b.

Stem cells are also thought to have developed strategies in order to protect them from toxic environment agents. This seems to confer them with a resistance to xenobiotics, including many drugs used to treat cancer. A well-described defence mechanism involves the expression of members of the ATP-binding cassette (ABC) superfamily of membrane transporters. These proteins have the ability to hydrolyse ATP to support substrate efflux against steep concentrations, usually from the intra- to the extracellular space. Goodell et al. first reported the isolation of HSCs on the basis of their ability to efflux a fluorescent dye, Hoechst 33342 [52]. Cells that actively efflux the Hoechst dye appear as a distinct population of cells called the 'side population' (SP). Many studies suggest that the ABCG2 transporter, a member of the ABC superfamily [52], also known as the breast cancer resistance protein, determines the SP phenotype. The SP fraction often equates to the stem cell population in normal tissues as well as tumours [53, 54]; however, not all SP cells are stem cells [55]. The expression of such ABC transporters in cancer stem cells could enable them to efflux drugs and hence contribute to relapses and drug resistance in cancer.

There are other mechanisms known to protect stem cells in healthy tissue and possibly lead to resistance in cancer stem cells. HSCs for example have high levels of aldehyde dehydrogenase (ALDH), a detoxifying enzyme that confers resistance to alkylating reagents such as cyclophosphamide [56]. Indeed, a subpopulation of cells with high levels of ALDH has been found to define a poor prognosis group in acute myeloid leukemia (AML) [57]. In the bronchiolar epithelium, stem cells appear to be rare pollutant-resistant cells linked to a deficiency in phase 1 drug metabolising enzyme CYP450 [58]. In the liver, progenitor cells have been shown to expand despite exposure to pyrrolizidine alkaloids due to a similar deficiency in cytochrome P450 [59].

Markers of adult stem cells

It is not possible to morphologically distinguish a tissue stem cell from its 'non-stem' cell neighbour. As such, there has been a rush to find a stem cell marker that not only is specific for a stem cell area but can also demonstrate the multipotential properties of such cells. Recently, there have been significant advances in the identification of adult stem cell markers; no longer do we rely on markers that tag the supposed stem cell zone but instead use techniques that actually demonstrate multipotentiality, a crucial property of stem cells.

There is no doubt that the Wnt (reviewed elsewhere [60]) signalling pathway is inextricably linked to stem cell renewal and maintenance of the niche. Nuclear β-catenin has been shown to be present in normal basal intestinal crypt cells [61], and these could be stem cells; however, Paneth cells can also express nuclear β-catenin during their maturation [62], so this is probably not a reliable marker of stem cells. Barker et al. [38] have demonstrated a Wnt target gene, leucine-rich-repeat-containing-G protein-coupled receptor 5 (*Lgr5*) as a potential stem cell marker within the gastrointestinal tract of mice. After crossing *Lgr5-Cre-lox* transgenic mice with ROSA26-*LacZ* mice [38], this group was able to trace the development of Lgr5+ve cells within crypts via the expression of LacZ. Initially, cells appeared in crypt base columnar (CBC) cells in the small intestine and at the base of the colon. Over time, LacZ expression spread throughout the crypt telling us that Lgr5 expression was induced in a stem cell and the progeny eventually formed all the differentiated epithelial phenotypes within the crypt, therefore demonstrating multipotentiality. Furthermore, a recent paper by the same group has elegantly shown that isolation and culture of *lgr5*+ve cells results in the in vitro

formation of rudimentary crypts and villi in an organoid fashion [63]. What is so interesting about this paper is that crypts and villi appear to form in the absence of an obvious niche. If this can be repeated in other systems, we may have to rethink the dogma that a stem cell only remains a stem cell whilst is in a niche.

Subsequent to this, another marker of murine intestinal stem cells was proposed using a similar approach. Bmi1, a member of the Polycomb group gene family, was first described as an oncogene that induces leukaemias [64] and appears to play a role in stem cell self-renewal [65]. Bmi1 has been shown to be over-expressed in intestinal cancers [66, 67]. By using a transgenic mouse model that expressed *Cre* under the *Bmi1* locus crossed with a *Cre*-inducing *LacZ* (Rosa26) mouse, Sangiorgi and Capecchi [40] demonstrated that 20 h post-tamoxifen injection, Bmi1+ve cells (by β-gal expression) appeared at cell position 4, the originally proposed stem cell position [68]. Over time, these cells expanded eventually taking over the entire crypt, in a similar fashion to that shown by Barker et al., with Lgr5. Interestingly, the Lgr5 transgenic mice showed little in the way of intestinal epithelial abnormalities; however, when the Bmi1 transgenic mice were crossed with a mouse expressing the diphtheria toxin, tamoxifen injections resulted in a loss of crypt number over time, indicating that there has been a loss of the stem cell compartment and that Bmi1 has an important function in the maintenance of tissue stem cells. Thus, maybe a two-tier system operates in the small intestine, with rapidly cycling CBC stem cells supported by slowly cycling, so-called label retaining stem cells at cell positions 4–5.

There have been a number of other markers that have been suggested, the most notable being Musashi-1 (Msi1). Msi1 is an RNA-binding protein that blocks the translation of *m-Numb* RNA and so has a positive regulating effect on Notch signalling [69]. Msi1 is expressed at the base of the colonic crypt and at cell positions 3–4 in the small intestinal crypt [70]. It is also expressed in the so-called CBC cells (small, slender cells that sit in amongst the Paneth cells) within the small intestine, which are also positive for Lgr5 [67]. It has been shown to suppress the differentiation of Paneth cells and may have a role in maintaining 'stemness' [71]. Before Msi1 can be considered a true marker of intestinal stem cells, it must be shown to be expressed on cells that demonstrate multipotentiality. Other markers of intestinal stem cells have been proposed including DCAMKL-1 [72], EphB receptors [73] and label-retaining cells [46], all of which have been shown to be expressed in the stem cell zone but have not yet been shown to have any robust stem cell properties.

Unlike the intestine, the liver does not have a well-defined niche; indeed, the liver is normally proliferatively quiescent. This has led to the belief that there may not be a stem cell population within the liver, but rather a slow but continuous turnover of cells such as hepatocytes. However, upon partial hepatectomy, a fast regenerative response occurs which involves all hepatic cell types, restoring the liver to its original state [74], suggesting that there may be progenitor/stem cell-like populations in the liver. Recently, our group has shown that mitochondrial DNA mutations can be used as a marker of clonal expansion of a stem cell clone from the portal area in vivo [34]. Markers of hepatic stem cells have been proposed (label-retaining cells [75], STAT3 and Oct4 [76]), and indeed these cells are located proximal to the portal area, but none have adequately been demonstrated as stem cells.

Cancer stem cells

For many years, it has been apparent that stem cells feature in processes as diverse as wound healing, metaplasia and cancer. Two-stage models of skin cancer in rodents carried out in the 1950s strongly suggested that cancers had their origins in long-lived epidermal stem cells, but the idea that cancers themselves might have malignant CSCs is only just gaining widespread acceptance, despite the fact that Hamburger and Salmon in 1977 [4] using colony formation in soft agar as a surrogate stem cell assay found that for many human tumours, only one in 1,000 to one in 5,000 cells was able to form a macroscopic colony.

Cancer could arise from the dedifferentiation of mature cells that have retained the ability to divide, or it could result from the 'maturation arrest' of immature stem cells [77]. The idea of 'blocked ontogeny' has gained wide acceptance, and we now believe that the arrested differentiation of tissue-based stem cells or their immediate progenitors is closely linked to the development of not only tetratocarcinomas and haematological malignancies, but also carcinomas. Some of the most frequent cancers occur in tissues with a high cell turnover such as the skin and the epithelial lining of the gastrointestinal tract. It is argued, not unreasonably in our view, that in these tissues the stem cells are the only cells with sufficient life span to acquire the requisite number of genetic abnormalities for malignant transformation. Additionally, with a self-renewal mechanism already in place, seemingly fewer alterations are required to change normal stem cells into CSCs. In the now classical two-stage model of mouse skin carcinogenesis, severely delaying the interval between 7,12-dimethylbenz(*a*)anthracene initiation and the application of the phorbol ester promoter had no bearing on subsequent tumour yield—strongly suggestive of an origin in a long-lived cell, an epidermal stem cell [78].

Direct genetic labelling of adult stem cells in the mouse small intestine has revealed that tumours, in this case, adenomas, arise directly from adult stem cells [79,

80]. Notwithstanding the current debate about whether cancer stem cells, or more correctly tumour-initiating cells (TICs), are rare or quite common, it is quite clear that more than one marker has been used to enrich for TICs from a given tumour type. For example, both CD133 and CD44 have been employed for enrichment of TICs in both colorectal [81, 82] and pancreatic cancer [83, 84]. Indeed, there may well be phenotypic diversity amongst the CSC population within a single tumour population as suggested for gliobastoma multiforme [85]. In fact, the CSC population may be a moving target as cells lose or acquire properties of 'stemness', as seen when Twist or Snail is up-regulated in breast cancer epithelial cells resulting in epithelial–mesenchymal transition (EMT)—remarkably these mesenchymal-like cells also acquired the widely perceived breast CSC phenotype, $CD44^{+}CD24^{low}$ [86]. The development of metastasis might well involve the dissemination of CSCs, particularly involving those cells at the tumour margins that have undergone EMT—the so-called migrating cancer stem cells [43]. This process may be aided by the expression of chemokine receptors on CSCs as observed in pancreatic cancer [83]. These concepts are depicted in Fig. 3.

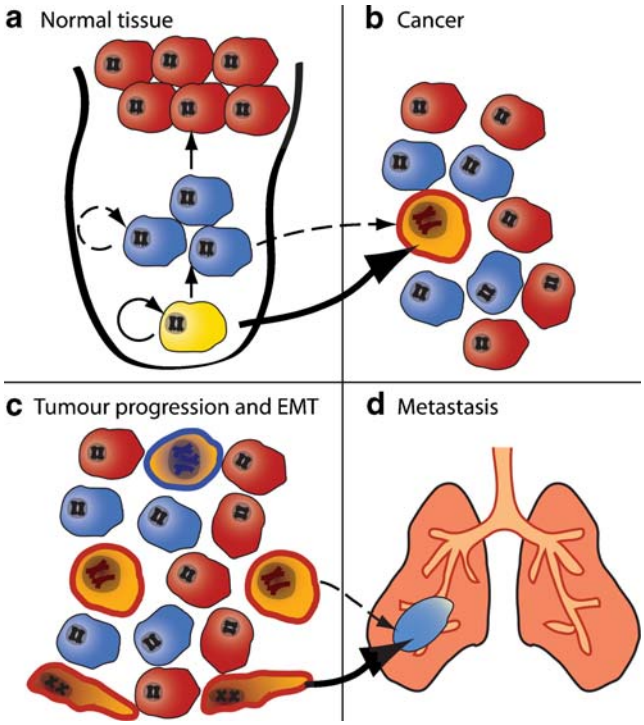

Fig. 3 Current concepts regarding stem cells and tumour evolution in tissues with ordered structure such as epithelia. **a** In normal tissues, adult stem cells (ASC, *yellow*) self-renew and give rise to transit amplifying cells (TAC, *blue*) that divide several times before undergoing terminal differentiation (TD, *red*). Many lines of evidence, including direct lineage tracing from genetically marked ASC indicate that tumours arise from ASCs, though an origin from TACs is also possible. **b** Tumours also have a hierarchical structure, albeit a relatively disorganised one, the cancer stem cells (CSC, *yellow*, altered chromosomes) may have a single phenotype (X surface colour denotes a specific surface phenotype, e.g., $CD44^{+}CD24^{low/-}$ in breast cancer) and be rare or relatively common. **c** Genetic or epigenetic events may result in new clones driven by phenotypically diverse populations of CSCs (*yellow cells* with Y surface colour). Further genetic or epigenetic changes may result in some cells undergoing epithelial–mesenchymal transition (EMT, *yellow* fibroblast-like cell) equipping them with CSC properties, and **d** metastasis may be caused by migrating CSCs detaching from the tumour mass, in particular these may be the CSCs formed through EMT that may respond to chemotactic gradients by virtue of expression of chemokine receptors such as CXCR4

Markers of CSCs

Considerable effort is being expended in the search for 'markers' of stem cells, with every expectation that many of the molecules expressed by normal stem cells will also be found in their malignant counterparts. Collectively, these molecules appear to be involved in maintaining 'stemness' (transcription factors such as Oct-4 and Nanog), ensuring adhesion to the niche and be involved in cytoprotection [87]. Many putative stem cells have acquired the ability to withstand cytotoxic insults through either efficient enzyme-based detoxification systems or by the ability to rapidly export potentially harmful xenobiotics. This would include high expression of ABC transporters, responsible for the SP and ALDH gene superfamily encoding detoxifying enzymes for many pharmaceuticals and environmental pollutants [88]. As expected, high expression of ALDH can be detrimental to tumour eradication; cyclophosphamide treatment of human colonic xenografts enriches for CD44+ALDH+ cells, and these double positive cells were more tumorigenic than cells selected by solely CD44 positivity [89].

As discussed earlier, another proposed stem cell marker is Bmi1, required, for example, for the self-renewal of HSCs. Loss of Bmi1 leads to a depletion of neural stem cells, associated with upregulation of $p16^{Ink4a}$ [90]. The premature senescence of murine neural stem cells is prevented by Bmi1, suppressing transcription at the *Ink4a/Arf* locus that encodes $p16^{Ink4a}$ and $p19^{Arf}$ [90].

Perhaps, the most 'popular' marker of putative stem cells is Prominin-1 (CD133), the first identified member of the rapidly growing prominin family of pentaspan membrane proteins [91, 92]. The specific functions and ligands of the prominins are still relatively unclear, but they are distinct in their restricted expression within plasma membrane protrusions, such as epithelial microvilli [93]. Two antibodies, CD133/1 (aka AC133) and CD133/2 (aka AC141) recognise different glycosylated epitopes, and most studies use CD133/1. In combination with other markers, CD133 has been used to isolate HSCs and endothelial progenitor cells (EPCs), but its greatest utility has been in the enrichment of cells with tumour-initiating ability (so-called cancer stem

cells) in immune-deficient mice from a variety of human solid tumours, including brain, prostate, liver and colon [94]. However, a recent study has found that most normal and malignant colonic epithelial cells express CD133, and moreover, CD133-negative cells isolated from colorectal liver metastases were at least as tumorigenic as their CD133-positive counterparts [95].

Cancer stem cells in solid tumours

Colorectal cancer is one of the most common forms of solid tumour in the western world and accounts for approximately 10% of cancer-related deaths in Europe [96]. There is therefore a distinct need to develop markers to develop our understanding of the origins of colorectal cancer at a cellular level and evaluate the contribution of stem cells in this disease.

CD133 (Prominin-1) has received the most attention as such a colorectal cancer stem cell marker. Initial publications by O'Brien et al. and Ricci-Vitiani et al. demonstrated that when CD133-positive cells were purified from clinical colorectal tumours they were capable of initiating tumours in immunodeficient mice. Indeed, tumours were established by transplanting as few as 3,000 CD133-positive cells and grew faster than when 10^6 whole tumour cell populations were injected; when CD133-negative cells were injected, no tumours arose. This was potentially a very significant observation, showing for the first time a specific population of cancer cells that expressed a marker that was easily identified and was able to initiate tumour growth although the true function of CD133 in such cells has not been identified. As with nearly every other potential marker of cancer stem cells, it was not long before CD133 as a cancer stem cell marker in the intestine was called into question. Shmelkov et al. created a knock-in *LacZ* reporter mouse whose LacZ expression was driven by the CD133 promoter. They showed that CD133 expression was not restricted to the stem cell zone of the crypt, but expressed all over the intestinal epithelium. When they crossed $CD133^{LacZ/+}$ mice with IL-$10^{-/-}$ mice (who develop spontaneous colonic inflammation progressing to adenocarcinoma [95]), the entire tumour expressed CD133. Furthermore, they also demonstrated that both CD133-positive and CD133-negative metastatic colon cancer cells, derived from clinical material, were able to initiate tumours. This does not hold true for all cancer stem cell systems. In cells isolated from brain cancer, clonogenicity and self-renewal seem to be exclusive to a subpopulation of cells expressing CD133 and nestin, regardless of the tumour phenotype [97].

The observation that SP cells, characterised by their ability to efflux Hoechst 33342 dye, represents a stem cell or even cancer stem cell population has been proposed [98], but does not apply to all tissues. In the mouse hair follicle for example, the SP cells are found beneath the label-retaining bulge and thus correspond to TACs [99]. Likewise, in human epidermis and the murine haematopoietic system, the SP phenotype does not appear to be specific for stem cells [99]. Haraguchi et al. [100] demonstrated that human colorectal cancers do contain a SP and that these cells expressed ABCG2. However, recent evidence from our group has suggested that SP cells are not enriched for cancer stem cells [101] and SP-enriched or SP-negative cells are both equally able to induce tumours in immunodeficient mice.

Despite the vast amount of research into putative cancer stem cell markers in colorectal tumours, only Lgr5 has been shown to be a marker of normal crypt stem cells, and it also has been used to demonstrate that crypt stem cells can be the TIC population that gives rise to colorectal cancer. Barker et al. [102] elegantly demonstrated that deletion of *Apc* in a *Lgr5* knock-in transgenic mouse quickly lead to transformation (dysplastic cells expressing β-catenin) within a few days. Over time, this spreads in a bottom-up fashion [103] leading to the development of monocryptal adenoma-like crypts and eventually to large adenomas (Fig. 4). Along with evidence that the expression of Lgr5 is greatly increased in advanced colorectal cancers [104], this has the potential to be an extremely promising marker for targeted therapy.

Evidence for the existence of CSCs in the lung was first described more than 25 years ago in a study by Carney et al. [105]. In this study, a small population of cells (<1.5%) isolated from the tumours of both adenocarcinoma of the lung and small cell lung cancer (SCLC) patients were able to form colonies in a soft agar cloning assay. As with other solid tumours, CD133 expression features predominantly in the search for CSCs in the lung. In non-small cell lung cancer (NSCLC), 1,000 $CD133^+$ cells could form tumours in SCID mice, but 10^4 CD133-negative cells never did [106]. The CD133-positive cells showed enhanced expression of Oct-4 and ABCG2; siRNA knockdown of Oct-4 blocked clonogenicity and enhanced chemosensitivity. In both SCLC and NSCLC a small (<1%) population of CD133-posiive cells has been found, with 10^4 of these cells capable of forming tumours in SCID mice with features of the parent tumours [107]. These in vitro sphere-forming cells often expressed Oct-4 and Nanog along with CCSP and SP-C. Exploiting the perceived chemoresistance of CSCs, CSCs have been enriched in a NSCLC cell line by treating with the likes of cisplatin and doxorubicin [108]; 5×10^3 drug selected cells regularly formed tumours in SCID mice. These cells expressed CD133 and CD117 and the embryonic stem cell markers SSEA-3, TRA1-81 and Oct-4 and had nuclear β-catenin. In the cell line, the SP fraction was 5.2%, but

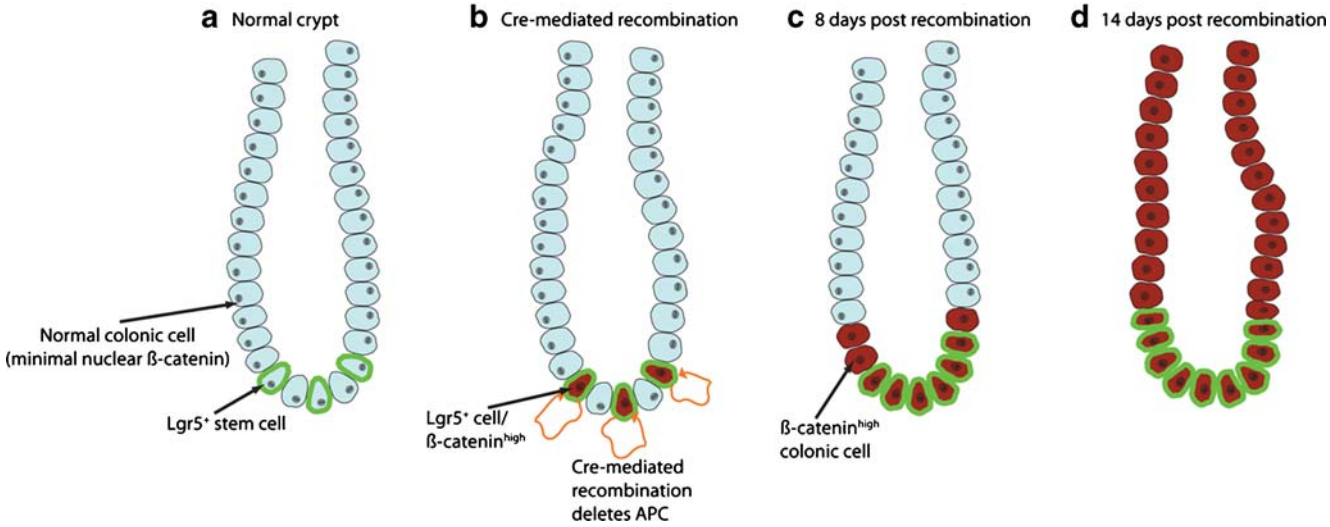

Fig. 4 To demonstrate the process by which a stem cell at the base of a crypt can transform the crypt to an adenoma, we illustrate the work done by Barker et al. [102]. **a** A normal colon crypt contains between 4 and 6 Lgr5+ stem cells (*green border*) located at the crypt base, between the Paneth cells. In Lgr5-EGFP-IRES-creER mice, Lgr5-expressing cells are transiently labelled with GFP and also express creER. **b** Following tamoxifen injection, the creER, which is expressed only in Lgr5+ cells, is activated and the resulting cre-mediated recombination removes the floxed APC gene in these cells. The transformed cells rapidly become strongly positive for β-catenin (*brown cells*), a marker of adenomatous growth. **c** At 8 days post-recombination, the β-catenin high cells were still restricted to the base of the crypts. **d** At 2 weeks post-recombination, crypts entirely composed of β-catenin high cells were observed—therefore niche succession and monoclonal conversion has occurred. In these adenomatous crypts, Lgr5 expression was still localised to the putative stem cell zone at the crypt base (*brown cells*, *green border*). At 36 days post-recombination, multiple β-catenin high adenomas were observed throughout the intestine

after drug treatment this was increased to 35%. Clearly, drug resistance and lung CSCs are heavily entwined. In the A549 NSCLC cell line, a large (24%) SP has been found, with enhanced resistance to doxorubicin and methotrexate related to ABCG2 activity [109].

Using the CD133/1 antibody, a number of studies have suggested that the CD133-positive fraction enriches for hepatocellular carcinoma (HCC) CSCs [110, 111]. As might be expected of CSCs, they appear as a minority (<2%) population in primary tumours, though continued passaging has resulted in considerable enrichment of $CD133^+$ cells in some HCC cell lines, up to 90% [110]. HCCs with higher than the median number (1.32%) of CD133-positive cells are correlated with shorter survival, higher recurrence rates and higher tumour grade [112], and $CD133^+$ cells appear highly resistant to conventional therapeutic drugs such as 5-FU and doxorubicin [113].

Are cancer stem cells rare?

CSCs are believed to have stem cell characteristics, particularly the ability to self-renew and to give rise to a hierarchy of progenitor and differentiated cells, albeit in a disorganised manner that gives rise to more CSCs. Operationally at present, CSCs are regarded as prospectively purified cells that are more tumorigenic than the bulk or the marker-negative tumour population in a suitable tumour development assay, e.g., after transplantation to NOD/SCID mice. More stringently, a CSC should be a cell that can reconstitute, in a recipient animal, a tumour identical to the original tumour in the patient, which can then be serially xenotransplanted indefinitely. At present, most putative CSCs are identified by their tumour-initiating ability and are thus referred to as TICs. The conventional wisdom is that CSCs are rare based upon having to xenotransplant large numbers of human tumour cells into immunodeficient mice to further propagate the tumours; however, this might have more to do with a hostile murine microenvironment. For example, a few as ten mouse lymphoma or AML cells can regularly propagate the tumours when transplanted into histocompatible mice, so are all cells in these tumours possible TICs? [114]. Using standard immunodeficient mice, the frequency of TICs in human melanoma has been reported to be in the order of one in 10^6 [115], but even single human melanoma cells can form tumours in more highly immunocompromised NOD/SCID/IL2Rγ null mice [116]. The rarity of cancer stem cells has also been questioned in lung cancer; using up to a dozen murine lung cancer cell lines, cell colonies could be regularly generated from randomly selected cells, and when 2×10^5 cells from these clonally derived colonies were allografted into histocompatible mice, tumours were consistently produced, suggesting that perhaps that the

TICs do not have a unique surface marker signature [117]. Thus, perhaps we need to modify the CSC hypothesis accordingly:

1. CSCs are cells that can be prospectively isolated and initiate malignant growth in vivo.
2. CSCs are not necessarily rare, but they must be effectively targeted for definitive cures since they can often be especially radioresistant and chemoresistant.

Implications for treatment

For tomorrow's oncologist, a variety of druggable targets and strategies related to CSCs present themselves and include:

- Wnt signalling
- Hedgehog signalling
- Notch/Delta signalling
- mTOR
- ABC transporters
- Targeting the stem cell niche
- Small molecule cancer therapeutics (miRNAs, tyrosine kinase inhibitors)
- Gene therapy

Proliferation of CSCs is likely to involve dysregulation of the pathways present in normal stem cell self-renewal such as the Wnt-/β-catenin, PTEN, Notch and Hedgehog pathways, as well as the products of the *Bmi1* and other polycomb genes. In many tissues, key regulators of stem cell renewal appear to be members of the Polycomb group protein family of transcriptional repressors (Bmi1, Rae28, Mel-18). Bmi1 targets genes such as $p16^{INK4A}$ and $p14^{ARF}$ preventing stem cell senescence by respectively maintaining cyclinD/Cdk4 signalling and Mdm2 destruction of p53. Bmi1 is in fact a downstream target of the morphogen Sonic hedgehog (Shh) through the latter's activation of the Gli family of latent transcription factors. Shh acts on the receptor complex of Patched (PTCH) and Smoothened (SMO), blocking the restraining influence of PTCH on SMO, resulting in SMO signalling activating the Gli family of transcription factors and so activating target genes like *Bmi1*. Inhibiting the action of SMO with the antagonist cyclopamine is a highly effective strategy against some cancers. It has been claimed that almost all SCLCs ubiquitously express Bmi1 [117], and antisense *Bmi1* RNA therapy reduces proliferation of A549 cells [118]. The Notch family of receptors is also critical for stem cell self-renewal. Engagement of ligands of the Delta and Jagged families causes cleavage, mediated by the γ-secretase protease complex, of the intracellular portion of Notch and its translocation to the nucleus where it binds to the transcription factor CSL, changing it from a transcriptional repressor to an activator. The use of γ-secretase inhibitors may have utility in cancers where Notch signalling is inappropriately activated [119].

Apart from the renewal and proliferation pathways, there are many other potential molecular targets relating to CSCs. As many tumours have SP fractions, almost certainly enriched for CSCs, targeting ABC transporter activity will be an obvious strategy for overcoming chemoresistance as well as directly eradicating stem cells, drug resistance being particularly problematic in SCLCs [120].

Antibody-based targeting of CSCs exploiting the over-expression of the likes of CD133 is another possible approach, while CSCs may reside in areas rich in blood vessels, so-called vascular niches. So while anti-angiogenic therapy is not new, used to debulk tumours through disruption of their blood supply, the destruction of the CSC niche adds a new twist to the story. Small molecule therapeutics that target growth factors, growth factor receptors and their kinases, and more specifically tyrosine kinase inhibitors such as imatinib that target c-Kit-positive cells are also gaining widespread usage.

Conclusions

Novel markers of tissue stem cells have recently been proposed that are able to identify cells that are multipotential in nature. These include Lgr5 and Bmi1. Although further research is required to demonstrate these molecules as definitive stem cell markers within human tissues, work done in transgenic mice has opened up their potential. Whether or not such markers identify tumour-initiating cells in cancer patients is unclear. It is likely that tumour-initiating cells are indeed stem cells and that tumours themselves are maintained by a population of cancer stem cells—these may not be the same cell. Cancer stem cells are thought to be rare; however, recent studies have shown that these may be far more common within the tumour than was initially thought.

Acknowledgement SACM is funded by CORE (Formerly Digestive Disorders Foundation).

Conflict of interest statement We declare that we have no conflict of interest.

References

1. Radtke F, Clevers H (2005) Self-renewal and cancer of the gut: two sides of a coin. Science 307:1904–1909
2. Tomlinson I, Bodmer W (1999) Selection, the mutation rate and cancer: ensuring that the tail does not wag the dog. Nat Med 5:11–12
3. Pierce GB, Nakane PK, Martinez-Hernandez A et al (1977) Ultrastructural comparison of differentiation of stem cells of

murine adenocarcinomas of colon and breast with their normal counterparts. J Natl Cancer Inst 58:1329–1345
4. Hamburger AW, Salmon SE (1977) Primary bioassay of human tumor stem cells. Science 197:461–463
5. Till JE, Mc CE (1961) A direct measurement of the radiation sensitivity of normal mouse bone marrow cells. Radiat Res 14:213–222
6. Mayhall EA, Paffett-Lugassy N, Zon LI (2004) The clinical potential of stem cells. Curr Opin Cell Biol 16:713–720
7. Cheng H, Leblond CP (1974) Origin, differentiation and renewal of the four main epithelial cell types in the mouse small intestine. V. Unitarian Theory of the origin of the four epithelial cell types. Am J Anat 141:537–561
8. Cheng H, Leblond CP (1974) Origin, differentiation and renewal of the four main epithelial cell types in the mouse small intestine. I. Columnar cell. Am J Anat 141:461–479
9. Cheng H, Leblond CP (1974) Origin, differentiation and renewal of the four main epithelial cell types in the mouse small intestine. III. Entero-endocrine cells. Am J Anat 141:503–519
10. Niemann C, Watt FM (2002) Designer skin: lineage commitment in postnatal epidermis. Trends Cell Biol 12:185–192
11. Rossi DJ, Jamieson CH, Weissman IL (2008) Stems cells and the pathways to aging and cancer. Cell 132:681–696
12. Stemple DL, Anderson DJ (1993) Lineage diversification of the neural crest: in vitro investigations. Dev Biol 159:12–23
13. Beltrami AP, Barlucchi L, Torella D et al (2003) Adult cardiac stem cells are multipotent and support myocardial regeneration. Cell 114:763–776
14. Mauro A (1961) Satellite cell of skeletal muscle fibers. J Biophys Biochem Cytol 9:493–495
15. Alonso L, Fuchs E (2003) Stem cells of the skin epithelium. Proc Natl Acad Sci U S A 100(Suppl 1):11830–11835
16. Bjerknes M, Cheng H (1981) The stem-cell zone of the small intestinal epithelium. IV. Effects of resecting 30% of the small intestine. Am J Anat 160:93–103
17. Bjerknes M, Cheng H (1981) The stem-cell zone of the small intestinal epithelium. III. Evidence from columnar, enteroendocrine, and mucous cells in the adult mouse. Am J Anat 160:77–91
18. Bjerknes M, Cheng H (1981) The stem-cell zone of the small intestinal epithelium. II. Evidence from paneth cells in the newborn mouse. Am J Anat 160:65–75
19. Bjerknes M, Cheng H (1981) The stem-cell zone of the small intestinal epithelium. I. Evidence from Paneth cells in the adult mouse. Am J Anat 160:51–63
20. Bjerknes M, Cheng H (1981) The stem-cell zone of the small intestinal epithelium. V. Evidence for controls over orientation of boundaries between the stem-cell zone, proliferative zone, and the maturation zone. Am J Anat 160:105–112
21. Forbes S, Vig P, Poulsom R et al (2002) Hepatic stem cells. J Pathol 197:510–518
22. Bonner-Weir S, Sharma A (2002) Pancreatic stem cells. J Pathol 197:519–526
23. Watt FM, Hogan BL (2000) Out of Eden: stem cells and their niches. Science 287:1427–1430
24. Crosnier C, Stamataki D, Lewis J (2006) Organizing cell renewal in the intestine: stem cells, signals and combinatorial control. Nat Rev Genet 7:349–359
25. Madison BB, Braunstein K, Kuizon E et al (2005) Epithelial hedgehog signals pattern the intestinal crypt–villus axis. Development 132:279–289
26. van den Brink GR, Bleuming SA, Hardwick JC et al (2004) Indian Hedgehog is an antagonist of Wnt signaling in colonic epithelial cell differentiation. Nat Genet 36:277–282
27. Kiger AA, Jones DL, Schulz C et al (2001) Stem cell self-renewal specified by JAK–STAT activation in response to a support cell cue. Science 294:2542–2545
28. Tulina N, Matunis E (2001) Control of stem cell self-renewal in Drosophila spermatogenesis by JAK–STAT signaling. Science 294:2546–2549
29. Spradling A, Drummond-Barbosa D, Kai T (2001) Stem cells find their niche. Nature 414:98–104
30. Brinster RL, Zimmermann JW (1994) Spermatogenesis following male germ-cell transplantation. Proc Natl Acad Sci U S A 91:11298–11302
31. Ohlstein B, Spradling A (2006) The adult Drosophila posterior midgut is maintained by pluripotent stem cells. Nature 439:470–474
32. Barker N, Clevers H (2007) Tracking down the stem cells of the intestine: strategies to identify adult stem cells. Gastroenterology 133:1755–1760
33. Bjerknes M, Cheng H (1999) Clonal analysis of mouse intestinal epithelial progenitors. Gastroenterology 116:7–14
34. Greaves LC, Preston SL, Tadrous PJ et al (2006) Mitochondrial DNA mutations are established in human colonic stem cells, and mutated clones expand by crypt fission. Proc Natl Acad Sci U S A 103:714–719
35. Gutierrez-Gonzalez L, Deheragoda M, Elia G et al (2009) Analysis of the clonal architecture of the human small intestine establishes a common stem cell for all lineages and reveals a mechanism for the fixation and spread of mutations. J Pathol 217:489–496. doi:10.1002/path.2502
36. McDonald SA, Greaves LC, Gutierrez-Gonzalez L et al (2008) Mechanisms of field cancerization in the human stomach: the expansion and spread of mutated gastric stem cells. Gastroenterology 134:500–510
37. Yatabe Y, Tavare S, Shibata D (2001) Investigating stem cells in human colon by using methylation patterns. Proc Natl Acad Sci U S A 98:10839–10844
38. Barker N, van Es JH, Kuipers J et al (2007) Identification of stem cells in small intestine and colon by marker gene Lgr5. Nature 449:1003–1007
39. Cai WB, Roberts SA, Potten CS et al (1997) The number of clonogenic cells in crypts in three regions of murine large intestine. Int J Radiat Biol 71:573–579
40. Sangiorgi E, Capecchi MR (2008) Bmi1 is expressed in vivo in intestinal stem cells. Nat Genet 40:915–920
41. Wright NA, Alison MR (1984) The biology of epithelial cell populations. Oxford University Press, Oxford
42. Brabletz S, Schmalhofer O, Brabletz T (2009) Gastrointestinal stem cells in development and cancer. J Pathol 217:307–317
43. Jensen UB, Lowell S, Watt FM (1999) The spatial relationship between stem cells and their progeny in the basal layer of human epidermis: a new view based on whole-mount labelling and lineage analysis. Development 126:2409–2418
44. Pepper JW, Sprouffske K, Maley CC (2007) Animal cell differentiation patterns suppress somatic evolution. PLoS Comput Biol 3:e250
45. Cairns J (1975) Mutation selection and the natural history of cancer. Nature 255:197–200
46. Potten CS, Owen G, Booth D (2002) Intestinal stem cells protect their genome by selective segregation of template DNA strands. J Cell Sci 115:2381–2388
47. Smith GH (2005) Label-retaining epithelial cells in mouse mammary gland divide asymmetrically and retain their template DNA strands. Development 132:681–687
48. Shinin V, Gayraud-Morel B, Gomes D et al (2006) Asymmetric division and cosegregation of template DNA strands in adult muscle satellite cells. Nat Cell Biol 8:677–687
49. Lansdorp PM (2007) Immortal strands? Give me a break. Cell 129:1244–1247
50. Kiel MJ, He S, Ashkenazi R et al (2007) Haematopoietic stem cells do not asymmetrically segregate chromosomes or retain BrdU. Nature 449:238–242

51. van Leeuwen IM, Byrne HM, Jensen OE et al (2006) Crypt dynamics and colorectal cancer: advances in mathematical modelling. Cell Prolif 39:157–181
52. Goodell MA, Brose K, Paradis G et al (1996) Isolation and functional properties of murine hematopoietic stem cells that are replicating in vivo. J Exp Med 183:1797–1806
53. Alison MR, Poulsom R, Otto WR et al (2003) Plastic adult stem cells: will they graduate from the school of hard knocks? J Cell Sci 116:599–603
54. Hirschmann-Jax C, Foster AE, Wulf GG et al (2005) A distinct "side population" of cells in human tumor cells: implications for tumor biology and therapy. Cell Cycle 4:203–205
55. Morita Y, Ema H, Yamazaki S et al (2006) Non-side-population hematopoietic stem cells in mouse bone marrow. Blood 108:2850–2856
56. Storms RW, Trujillo AP, Springer JB et al (1999) Isolation of primitive human hematopoietic progenitors on the basis of aldehyde dehydrogenase activity. Proc Natl Acad Sci U S A 96:9118–9123
57. Cheung AM, Wan TS, Leung JC et al (2007) Aldehyde dehydrogenase activity in leukemic blasts defines a subgroup of acute myeloid leukemia with adverse prognosis and superior NOD/SCID engrafting potential. Leukemia 21: 1423–1430
58. Giangreco A, Shen H, Reynolds SD et al (2004) Molecular phenotype of airway side population cells. Am J Physiol Lung Cell Mol Physiol 286:L624–630
59. Vig P, Russo FP, Edwards RJ et al (2006) The sources of parenchymal regeneration after chronic hepatocellular liver injury in mice. Hepatology 43:316–324
60. Barker N (2008) The canonical Wnt/beta-catenin signalling pathway. Methods Mol Biol 468:5–15
61. van de Wetering M, Sancho E, Verweij C et al (2002) The beta-catenin/TCF-4 complex imposes a crypt progenitor phenotype on colorectal cancer cells. Cell 111:241–250
62. van Es JH, Jay P, Gregorieff A et al (2005) Wnt signalling induces maturation of Paneth cells in intestinal crypts. Nat Cell Biol 7:381–386
63. Sato T, Vries RG, Snippert HJ, et al (2009) Single Lgr5 stem cells build crypt-villus structures in vitro without a mesenchymal niche. Nature. doi:10.1038/nature07935
64. Bea S, Tort F, Pinyol M et al (2001) BMI-1 gene amplification and overexpression in hematological malignancies occur mainly in mantle cell lymphomas. Cancer Res 61:2409–2412
65. Baylin SB, Herman JG, Graff JR et al (1998) Alterations in DNA methylation: a fundamental aspect of neoplasia. Adv Cancer Res 72:141–196
66. Kim HK, Song KS, Kim HO et al (2003) Circulating numbers of endothelial progenitor cells in patients with gastric and breast cancer. Cancer Lett 198:83–88
67. Reinisch C, Kandutsch S, Uthman A et al (2006) BMI-1: a protein expressed in stem cells, specialized cells and tumors of the gastrointestinal tract. Histol Histopathol 21:1143–1149
68. Potten CS, Booth C, Pritchard DM (1997) The intestinal epithelial stem cell: the mucosal governor. Int J Exp Pathol 78:219–243
69. Nakamura M, Okano H, Blendy JA et al (1994) Musashi, a neural RNA-binding protein required for Drosophila adult external sensory organ development. Neuron 13:67–81
70. Potten CS, Booth C, Tudor GL et al (2003) Identification of a putative intestinal stem cell and early lineage marker; musashi-1. Differentiation 71:28–41
71. Murayama M, Okamoto R, Tsuchiya K et al (2009) Musashi-1 suppresses expression of Paneth cell-specific genes in human intestinal epithelial cells. J Gastroenterol 44:173–182
72. May R, Riehl TE, Hunt C et al (2008) Identification of a novel putative gastrointestinal stem cell and adenoma stem cell marker, doublecortin and CaM kinase-like-1, following radiation injury and in adenomatous polyposis coli/multiple intestinal neoplasia mice. Stem Cells 26:630–637
73. Horwitz E, Prockop D, Fitzpatrick L et al (1999) Transplantability and therapeutic effects of bone marrow-derived mesenchymal cells in children with osteogenesis imperfecta. Nat Med 5:309–313
74. Alison M, Islam S, Lim S (2009) Stem cells in liver regeneration, fibrosis and cancer: the good, the bad and the ugly. J Pathol 217:282–298
75. Kuwahara R, Kofman AV, Landis CS et al (2008) The hepatic stem cell niche: identification by label-retaining cell assay. Hepatology 47:1994–2002
76. Tang Y, Kitisin K, Jogunoori W et al (2008) Progenitor/stem cells give rise to liver cancer due to aberrant TGF-beta and IL-6 signaling. Proc Natl Acad Sci U S A 105:2445–2450
77. Sell S, Pierce GB (1994) Maturation arrest of stem cell differentiation is a common pathway for the cellular origin of teratocarcinomas and epithelial cancers. Lab Invest 70:6–22
78. Berenblum I (1949) The carcinogenic action of 9, 10-dimethyl-1, 2-benzanthracene on the skin and subcutaneous tissues of the mouse, rabbit, rat and guinea pig. J Natl Cancer Inst 10:167–174
79. Barker N, Ridgway RA, van Es JH et al (2009) Crypt stem cells as the cells-of-origin of intestinal cancer. Nature 457:608–611
80. Zhu L, Gibson P, Currle DS et al (2009) Prominin 1 marks intestinal stem cells that are susceptible to neoplastic transformation. Nature 457:603–607
81. Dalerba P, Dylla SJ, Park IK et al (2007) Phenotypic characterization of human colorectal cancer stem cells. Proc Natl Acad Sci U S A 104:10158–10163
82. Ricci-Vitiani L, Lombardi DG, Pilozzi E et al (2007) Identification and expansion of human colon-cancer-initiating cells. Nature 445:111–115
83. Hermann PC, Huber SL, Herrler T et al (2007) Distinct populations of cancer stem cells determine tumor growth and metastatic activity in human pancreatic cancer. Cell Stem Cell 1:313–323
84. Li C, Heidt DG, Dalerba P et al (2007) Identification of pancreatic cancer stem cells. Cancer Res 67:1030–1037
85. Borovski T, Vermeulen L, Sprick MR et al (2009) One renegade cancer stem cell? Cell Cycle 8(6):803–808
86. Mani SA, Guo W, Liao MJ et al (2008) The epithelial–mesenchymal transition generates cells with properties of stem cells. Cell 133:704–715
87. Alison MR, Islam S (2009) Attributes of adult stem cells. J Pathol 217:144–160
88. Vasiliou V, Nebert DW (2005) Analysis and update of the human aldehyde dehydrogenase (ALDH) gene family. Hum Genomics 2:138–143
89. Dylla SJ, Beviglia L, Park IK et al (2008) Colorectal cancer stem cells are enriched in xenogeneic tumors following chemotherapy. PLoS ONE 3:e2428
90. Molofsky AV, He S, Bydon M et al (2005) Bmi-1 promotes neural stem cell self-renewal and neural development but not mouse growth and survival by repressing the p16Ink4a and p19Arf senescence pathways. Genes Dev 19:1432–1437
91. Alison MR, Murphy G, Leedham S (2008) Stem cells and cancer: a deadly mix. Cell Tissue Res 331:109–124
92. Mizrak D, Brittan M, Alison MR (2008) CD133: molecule of the moment. J Pathol 214:3–9
93. Bauer N, Fonseca AV, Florek M et al (2008) New insights into the cell biology of hematopoietic progenitors by studying prominin-1 (CD133). Cells Tissues Organs 188:127–138
94. Burkert J, Wright NA, Alison MR (2006) Stem cells and cancer: an intimate relationship. J Pathol 209:287–297
95. Shmelkov SV, Butler JM, Hooper AT et al (2008) CD133 expression is not restricted to stem cells, and both CD133+ and

CD133− metastatic colon cancer cells initiate tumors. J Clin Invest 118:2111–2120
96. Ferlay J, Autier P, Boniol M et al (2007) Estimates of the cancer incidence and mortality in Europe in 2006. Ann Oncol 18:581–592
97. Singh SK, Clarke ID, Terasaki M et al (2003) Identification of a cancer stem cell in human brain tumors. Cancer Res 63:5821–5828
98. Goodell MA (2002) Multipotential stem cells and 'side population' cells. Cytotherapy 4:507–508
99. Triel C, Vestergaard ME, Bolund L et al (2004) Side population cells in human and mouse epidermis lack stem cell characteristics. Exp Cell Res 295:79–90
100. Haraguchi N, Utsunomiya T, Inoue H et al (2006) Characterization of a side population of cancer cells from human gastrointestinal system. Stem Cells 24:506–513
101. Alison MR, Poulsom R, Brittan M et al (2006) Isolation of gut SP cells does not automatically enrich for stem cells. Gastroenterology 130:1012–1013 author reply 1013–1014
102. Barker N, Ridgway RA, van Es JH et al (2008) Crypt stem cells as the cells-of-origin of intestinal cancer. Nature
103. Preston SL, Wong WM, Chan AO et al (2003) Bottom-up histogenesis of colorectal adenomas: origin in the monocryptal adenoma and initial expansion by crypt fission. Cancer Res 63:3819–3825
104. McClanahan T, Koseoglu S, Smith K et al (2006) Identification of overexpression of orphan G protein-coupled receptor GPR49 in human colon and ovarian primary tumors. Cancer Biol Ther 5:419–426
105. Carney DN, Gazdar AF, Bunn PA Jr et al (1982) Demonstration of the stem cell nature of clonogenic tumor cells from lung cancer patients. Stem Cells 1:149–164
106. Chen YC, Hsu HS, Chen YW et al (2008) Oct-4 expression maintained cancer stem-like properties in lung cancer-derived CD133-positive cells. PLoS ONE 3:e2637
107. Eramo A, Lotti F, Sette G et al (2008) Identification and expansion of the tumorigenic lung cancer stem cell population. Cell Death Differ 15:504–514
108. Levina V, Marrangoni AM, DeMarco R et al (2008) Drug-selected human lung cancer stem cells: cytokine network, tumorigenic and metastatic properties. PLoS ONE 3:e3077
109. Sung JM, Cho HJ, Yi H et al (2008) Characterization of a stem cell population in lung cancer A549 cells. Biochem Biophys Res Commun 371:163–167
110. Ma S, Chan KW, Hu L et al (2007) Identification and characterization of tumorigenic liver cancer stem/progenitor cells. Gastroenterology 132:2542–2556
111. Ma S, Chan KW, Lee TK et al (2008) Aldehyde dehydrogenase discriminates the CD133 liver cancer stem cell populations. Mol Cancer Res 6:1146–1153
112. Song W, Li H, Tao K et al (2008) Expression and clinical significance of the stem cell marker CD133 in hepatocellular carcinoma. Int J Clin Pract 62:1212–1218
113. Ma S, Lee TK, Zheng BJ et al (2008) CD133+ HCC cancer stem cells confer chemoresistance by preferential expression of the Akt/PKB survival pathway. Oncogene 27:1749–1758
114. Kelly PN, Dakic A, Adams JM et al (2007) Tumor growth need not be driven by rare cancer stem cells. Science 317:337
115. Schatton T, Murphy GF, Frank NY et al (2008) Identification of cells initiating human melanomas. Nature 451:345–349
116. Quintana E, Shackleton M, Sabel MS et al (2008) Efficient tumour formation by single human melanoma cells. Nature 456:593–598
117. Yoo MH, Hatfield DL (2008) The cancer stem cell theory: is it correct? Mol Cells 26:514–516
118. Yu Q, Su B, Liu D et al (2007) Antisense RNA-mediated suppression of Bmi-1 gene expression inhibits the proliferation of lung cancer cell line A549. Oligonucleotides 17:327–335
119. Grosveld GC (2009) Gamma-secretase inhibitors: Notch so bad. Nat Med 15:20–21
120. Subramanian J, Govindan R (2008) Small cell, big problem! Stem cells, root cause? Clin Lung Cancer 9:252–253

Virchows Arch (2009) 455:15–19
DOI 10.1007/s00428-009-0794-y

ORIGINAL ARTICLE

Art and the teaching of pathological anatomy at the University of Florence since the nineteenth century

Gabriella Nesi · Raffaella Santi · Gian Luigi Taddei

Received: 14 January 2009 / Revised: 12 May 2009 / Accepted: 17 May 2009 / Published online: 9 June 2009

Abstract In 1840, the University of Florence was the first university in Italy to confer a Professorship in Pathological Anatomy. The origin of this teaching post is linked to the history of the Pathology Museum founded in 1824 by the Florentine *Accademia Medico-Fisica*. The Museum houses anatomical specimens and waxworks depicting pathological conditions in the nineteenth century. Both the need to instruct medical students in pathology without resorting to corpse dissection and the difficulty of the lengthy preservation of anatomical preparations made it necessary to produce life-sized wax duplicates of diseased parts of the body. Through the history of the Pathology Museum of Florence, we describe how pathology developed and, in particular, how pathologists from a literary circle laid the foundations of modern surgical pathology in Italy. Museum visits for the medical students guided by lecturers are still today a component of the course of Pathological Anatomy.

Keywords Historical materials · Didactic materials · Museum specimens · Anatomy · Wax models · Pathology

The foundation of the Pathology Museum of the University of Florence

The Pathology Museum of the University of Florence houses a vast collection of anatomical casts and more than a hundred waxworks that document the most common diseases in the nineteenth century, when the collection was set up [1].

It was created by the Florentine *Accademia Medico-Fisica*, which stemmed from the prestigious association of "men of letters", which was the *Gabinetto Vieusseux*, founded in 1819 by Giovan Pietro Vieusseux (1779–1863) [2]. Originally a reading room that provided leading European periodicals for Florentines and visitors from abroad, the *Gabinetto* soon became a reference point in the panorama of Italian nineteenth century culture. In 1820, Vieusseux inaugurated the *Antologia*, a periodical of intellectual and political commitment. Substantially dedicated to the natural sciences, geography, and travel, it also published medical articles and the minutes of the meetings of the Florentine *Accademia Medico-Fisica* [3].

Among the better-known members were Pietro Betti (1784–1863) and Filippo Pacini (1812–1883). In 1835, the latter delivered a report illustrating sensorial corpuscles, which were subsequently given the denomination "Pacini's corpuscles". Of particular interest was the lively discussion on the nature of cholera, which led to the rules of hygiene and potability of water [2].

It was during the first assembly of the *Accademia* on 4 February 1824 that the proposal by Pietro Betti to allow each member to contribute anatomical specimens was accepted, and after a few months, it was decided to institute a pathology museum, following the wishes of Angiolo Nespoli (1786–1839), then President of the *Accademia* [4].

Pietro Betti, rightfully considered the mastermind of the Museum, was appointed custodian of pathological casts and dedicated himself to looking after the Museum and increasing its value both in quantity and quality [5]. On 5 May 1824, he suggested ways for recording pathological casts, thus preluding the Catalogue, which, as well as chemical analyses, provided case histories and illustrations [1].

G. Nesi (✉) · R. Santi · G. L. Taddei
Department of Human Pathology and Oncology,
University of Florence,
Viale G.B. Morgagni 85,
50134 Florence, Italy
e-mail: gabriella.nesi@unifi.it

In a short time, the museum treasures had outgrown the assembly hall of the *Gabinetto Vieusseux* and non-medical members aspired to more pleasurable surroundings for their meetings. Such a situation drove Museum supporters in January 1825 to seek temporary accommodation in private premises at No. 3 *Via delle Belle Donne* [4]. The *Accademia Medico-Fisica* was then moved to the *Imperiale e Reale Arcispedale di Santa Maria Nuova* in March 1838, and the Pathology Museum was incorporated into the one already existing in that hospital.

In 1959, the Institute of Pathological Anatomy and the Museum were transferred to Careggi General Hospital, the foremost medical institution in Florence. The Museum is currently housed in the Department of Human Pathology and Oncology of the University of Florence (Fig. 1).

Visits to the Pathology Museum guided by the lecturers are nowadays a standard component of the course of Pathological Anatomy at the Faculty of Medicine, while students of the Fine Arts periodically visit the collection to sketch the wax models and anatomical casts.

The rise of pathological anatomy in Italy

In 1839, the *Ordinamento delle Autopsie nell'Arcispedale* was approved, where it was specified that every autopsy was to be presided over by the director of the Pathology Museum and that the medical history of every deceased patient was to be archived. Clinical diagnoses were to be compared with the autopsy findings, and the diseased parts of the body which had been surgically removed handed over to the Museum. Finally, if the patient was instead cured, the doctor was required to send the Museum a report on the therapy employed [6]. This handling of matters suggested an approach to modern clinico-pathological correlation in Italy, and a network was created among clinicians, surgeons, and pathologists.

Fig. 1 Overall view of the pathology museum at the Department of Human Pathology and Oncology of the University of Florence

A *Registro delle Autopsie* was set up in 1839; the practice of recording autopsies having never been suspended since. Included in the volumes are the 1,469 clinical histories of autopsy cases performed between 1839 and 1881 [1]. In actual fact, the protocol for carrying out and registering the autopsies was considered so effective that it constituted a model for the first legislation on the subject after the establishment of the Kingdom of Italy.

These were fertile years for pathology. As Superintendent of the *Imperiale e Reale Arcispedale di Santa Maria Nuova*, Betti proposed to institute a Professorship of Pathological Anatomy in Florence in his *Progetto di coordinamento degli Studi medico-chirurgici in S. M. Nuova coll'insegnamento già sanzionato per l'Università di Pisa* [5]. In this document, he also stated that the main responsibility of the Assistant to the Professor of Pathological Anatomy was the management of the Museum. In 1840, the first Chair of Pathological Anatomy in Italy was set up and entrusted to the surgeon Carlo Burci (1815–1875), previously curator of the Museum and translator of the treatise *De abditis nonnullis ac mirandis morborum et sanationum causis* by Antonio Benivieni (1443–1502).

The foundation of the Pathology Museum went hand in hand with the Pathological Anatomy Professorship, as did the nominations of the Professor and the curator of the pathological casts. Giuseppe Ricci was appointed Assistant to the Professor of Pathological Anatomy. Formerly Anatomy Dissector, he moulded most of the waxworks (about 60) seen today in the Museum [1].

Succeeding Burci as Professor of Pathological Anatomy was the Director of the Museum, Ferdinando Zannetti (1801–1881), well known for having removed a bullet from the hip of General Garibaldi at the battle of Aspromonte in 1862, thus avoiding amputation of the leg [7].

Ceroplastics and waxes as didactic tools in medicine

The decision to set up wax duplicates of diseased parts of the body was prompted by difficulties in conserving pathological material and by the need to instruct young doctors without resorting to corpse dissection. All the same, the artistic value of these works should not be underestimated (Fig. 2). They are an admirable example of symbiosis between Art and Science, in the wake of the Bolognese school of wax modelling acclaimed in the eighteenth century, with the works of Ercole Lelli (1702–1766), Giovanni Manzolini (1700–1755) and his wife, Anna Morandi (1716–1774) [8, 9].

Building on the anatomical discoveries made in the age of scientific enlightenment, wax models gave medical

Fig. 2 Wax model showing warty skin bumps of Darier disease, also known as "keratosis follicularis". Artist anonymous

students hands-on experience of both normal and aberrant processes not provided by fixed organs and tissues, considering that, in addition to tri-dimensionality, they offered the "dimension" of colour, an essential element for a correct gross diagnosis [10].

Since antiquity, wax votive figures had been offered to the divinities in propitiation, in requesting divine intervention in an ailment or as token of gratitude for grace received. Often, such works were made in the form of the body part, which needed the healing favour. For a long time after 1400, the Florentine church of the Annunziata housed the most splendid series of this type of figure (*boti* in the Florentine dialect). There were carpenter and wax workshops in the precincts of the church. One of these belonged to the Benintendi family, of whom the artist Orsino was a member, mentioned by Vasari as a pupil of Verrocchio [8, 11].

The use of wax was well known to artists and particularly to sculptors, both because they moulded wax models (whether the finished or the preparatory versions) and because of the increasing application of the so-called *cire perdue* or "lost wax" technique, in use since 2000 BC [12, 13].

It was from the fifteenth to the eighteenth centuries that the art of ceroplastics enjoyed its climax. With the contributions of Leonardo da Vinci and the impulse imparted by Paolo Mascagni (1755–1815), these specimens, especially dedicated to the study of lymph vessels, came closer to technical perfection [11].

In 1775, the *Imperiale e Regio Museo di Fisica e Storia Naturale* was established under the patronage of the first Hapsburg duke of Tuscany, Pietro Leopoldo, a remarkably enlightened and progressive leader. Attached was a wax studio, called *La Specola* after an astronomical and meteorological observation tower housed in the same building (Fig. 3). This laboratory produced a truly conspicuous number of waxworks of normal anatomy under the supervision first of Felice Fontana (1730–1805), a professor of Logic from Pisa, followed by a string of skilful dissectors and modellers, among whom were Clemente Susini (1754–1814), Luigi Calamai (1796–1851), Francesco Calenzuoli (1796–1829), Filippo Uccelli (1770–1832) and Egisto Tortori (1829–1893) [8, 13–15].

Produced on commission of Emperor Joseph II were the anatomical casts from the *Josephinum* collection at the Viennese Institute of the History of Medicine. These waxes, totalling 1,190 pieces, were at that time paid 30,000 gold coins. Other waxworks were sent to Perugia, Genoa and Cagliari and attracted a cultured, elitist class of tourists not often acquainted with medicine [16].

Moulage production in Berlin began immediately after the International Congress in Paris in 1889, thanks to Oskar Lassar (1849–1907), founder of the Dermatological Society in Berlin [17]. Lassar was of the opinion that the diagnostic ability of specialists in dermatology would be improved if they themselves were able to create moulages. One of the courses was held by Lassar himself and his mouleur Heinrich Kasten. For a specialist in dermatology, this 1-month course would have been enough to expand basic knowledge in moulaging. However, if there were no knowledge of skin diseases, the learning process would have taken much longer. These courses were, therefore, restricted to doctors trained in dermatology, who, apart from the technique of moulaging, could then instruct their

Fig. 3 Life-sized model of a skinned male figure, showing superficial veins and lymph vessels, by C. Susini, housed at *La Specola* (courtesy of Saulo Bambi)

Fig. 4 Wax model by L. Calamai displaying conjunctival ulcer of the left eye associated with ectropion. The three wax casts mounted on a wooden board show the patient's face before and after blepharoplasty

own mouleurs in the morphology of normal and diseased skin. Lassar and Kasten kept an approachable stance towards education in the art of moulaging, in contrast to other places in Europe where the few respected mouleurs were reluctant to give any details about the preparation of the plaster and wax mixtures, colouring methods, refinement and mounting [17].

At the beginning of the nineteenth century, a second revolution in biological investigations was started, with the physiological and histological sciences taking root. Although major anatomical institutes remain important components of medical education, they became largely inactive regarding research. The poor techniques of cadaver fixation limited the study of anatomical specimens. For this reason, dissections were best carried out in winter within 4 days. The introduction of more advanced fixation techniques allowed dissections to continue over the course of many days or weeks. Dissected specimens could also be preserved for long periods, which allowed for a more detailed study.

Fig. 5 Wax model by E. Tortori of a monoventricular heart in a newborn infant

Fig. 6 One of the four volumes of the Museum Catalogue detailing case histories and pathological specimens

Although the Florentine production of anatomical waxes ceased on Tortori's death in 1893, modelling in a more modest form has been carried on to the present day. Such models, produced by firms like Auzoux and Somso, represent valid tools in modern medical education [13].

The Pathology Museum of Florence: collection of anatomical casts and wax models

The Pathology Museum of the University of Florence, lodged on the top floor of the Department of Human Pathology and Oncology at Careggi Hospital, covers an area of 200 m^2. The collection includes wax reproductions and pathological specimens, both dried and fixed in formalin, displayed in elegant wooden cabinets. All in all,

Fig. 7 Detail of the so-called "Leper", a full-scale reproduction by L. Calamai of a man affected by Norwegian scabies

there are 116 waxes, mostly the work of Giuseppe Ricci, with the contribution of two talented artists from *La Specola* workshop, Luigi Calamai and his pupil Egisto Tortori (Figs. 4 and 5).

The general condition of the waxworks is variable with occasional fissures, crevices, small wax defects and yellowish discolouration. The wax models are often mounted on white canvas and fixed to black wooden boards, with the diagnosis written on card labels. Details of the patients and their case histories are described in the original four-volume Catalogue (Fig. 6).

The waxwork considered to be the jewel in the crown of the Museum is the so-called "Leper" by Luigi Calamai (Fig. 7). This is a life-sized model, realistically reproducing the body of a man affected with an acute form of Norwegian scabies. Cast in 1851, it may have caused the celebrated wax master's death from his prolonged exposure to the mercury solution used for the preservation of the corpse during the moulding of the statue [15].

The Museum also houses a large collection of anatomical specimens, perfectly preserved and amenable to investigation by means of modern biomolecular techniques, for the study of the aetiology and pathomorphosis of diseases in relation to the profound modifications in the composition and socio-economic conditions of the resident Florentine population over the nineteenth and twentieth centuries. These specimens are a macroscopic demonstration of rare disease entities. In the realm of teratology, the collection comprises general malformations, including veritable monstruosities (e.g., the "two-sided Janus", the "Siren" and the "Cyclops"). Most of the anatomical casts are kept in antique glass jars, filled with buffered formalin solution, hermetically sealed with wax between the lid and the lip of the jar. The specimens are labelled in obsolete terms, often at odds with present-day medical terminology, thus making histology mandatory in order to establish the correct diagnosis. As an example, one cast labelled *mollusco con morbo follicolare di Rayer*, on histological examination, proved to be neurofibromatosis type I.

Conclusions

Since the beginning, the Pathology Museum of the University of Florence has contributed to the teaching of Pathological Anatomy to medical students, for whom it constitutes a unique, three-dimensional teaching tool. At the same time, it is a culturally formative experience bringing to their attention the history of Florence, particularly that of public hygiene and of figurative art. Radiological and molecular biology investigation of the pathological specimens could provide an aetiological background relevant to present-day knowledge. An additional project which could be undertaken is the digitalization of specimens (ideally in 3-D) in order to make them informatically available to pathologists, anatomists, artists and historians all over the world.

Acknowledgements Thanks are due to the Ente Cassa di Risparmio di Firenze for their support of the Pathology Museum of the University of Florence. The authors wish to express their gratitude to Dr. Marta Poggesi and the staff of *La Specola* for the invaluable cooperation.

Conflict of interest statement We declare that we have no conflict of interest.

References

1. Costa A, Weber G, Zampi G, Dini S (1963) La prima Cattedra Italiana di Anatomia Patologica (Firenze 1840) e le sue premesse nelle istituzioni culturali e scientifiche del primo '800 fiorentino ed europeo. Arch de Vecchi 34:939–993
2. Funghi MS (1983) Accademia Medico-Fisica Fiorentina. In: Adorno F (ed) Accademie e Istituzioni culturali a Firenze. Olschki, Firenze
3. Sestan E (1986) La Firenze di Vieusseux e di Capponi. Olschki, Firenze
4. Corsini A (1924) Le origini dell'Accademia Medico-Fisica Fiorentina. Lo Sperimentale, a. 78:181–200
5. Morelli C (1865) Cenni storici della vita scientifica del Prof. Pietro Betti. Tipografia M. Cellini e C., Firenze
6. Filippi A (1875) Alla memoria di Carlo Burci. Lettura all'Accademia Medico-Fisica Fiorentina 13 giugno 1875. Tipografia Cenniniana, Firenze-Roma
7. Paolini G (ed) (2004) La ferita di Garibaldi ad Aspromonte. Documenti e lettere inedite di Ferdinando Zannetti. Polistampa, Firenze
8. Lanza B, Azzaroli Puccetti ML, Poggesi M, Martelli A (1979) Le cere anatomiche della Specola. Arnaud, Firenze
9. Accademia delle scienze dell'Istituto di Bologna (1981) Le cere anatomiche bolognesi del Settecento: Università degli Studi di Bologna, Accademia delle scienze, settembre-novembre 1981. CLUEB, Bologna
10. Gonzalez-Crussi F (1995) Suspended animation: six essays on the preservation of bodily parts. Harcourt Brace, New York
11. Terribile Wiel Marin V (1988) Il Museo dell'Istituto di Anatomia Patologica dell'Università degli Studi di Padova. Museol Sci IV:193–219
12. Dacome L (2006) Waxworks and the performance of anatomy in mid-18th-century Italy. Endeavour 30:29–35
13. Chen JCT, Amar AP, Levy ML, Apuzzo ML (1999) The development of anatomic art and sciences: the "ceroplastica" anatomic models of La Specola. Neurosurgery 45:883–891
14. During MV, Poggesi M, Didi-Huberman G, Bambi S (1999) Encyclopaedia Anatomica. Taschen, Cologne
15. Negri L, Weber G (1954) La "scabbia norvegese" in una cera del 1851 appartenente alla raccolta dell'Istituto di Patologia di Firenze. Studio sul cosiddetto "Lebbroso" di Luigi Calamai. Arch de Vecchi 20:893–911
16. Maraldi NM, Mazzotti G, Cocco L, Manzoli FA (2000) Anatomical waxwork modeling: the history of the Bologna anatomy museum. Anat Rec 261:5–10
17. Worm AM, Hadjivassiliou KA (2007) The Greek moulages: a picture of skin diseases in former times. J Eur Acad Dermatol Venereol 21:515–519

Virchows Arch (2009) 455:21–33
DOI 10.1007/s00428-009-0798-7

ORIGINAL ARTICLE

Thyroid tumours of uncertain malignant potential: frequency and diagnostic reproducibility

Véronique Hofman · Sandra Lassalle · Christelle Bonnetaud · Catherine Butori · Céline Loubatier · Marius Ilie · Olivier Bordone · Patrick Brest · Nicolas Guevara · José Santini · Brigitte Franc · Paul Hofman

Received: 14 April 2009 / Revised: 19 May 2009 / Accepted: 3 June 2009 / Published online: 20 June 2009

Abstract The term thyroid tumours of uncertain malignant potential (TT-UMP) has been proposed for a subgroup of follicular-patterned thyroid tumours for which benignancy or malignancy cannot be assessed with certainty. The frequency, diagnostic reproducibility, immunohistochemistry and molecular genetic profiling of such tumours have been poorly explored. We, therefore, investigated (1) the frequency of TT-UMP diagnosed in a single institution (Nice, France: 2004–2008), (2) the observer variation among four pathologists, (3) whether immunohistochemical and molecular genetic profiling of TT-UMP provide additional information concerning such lesions. A series of 31 diagnosed TT-UMP (2.9%) out of 1,078 consecutive thyroidectomies were analysed. It comprised 15 follicular thyroid tumours of UMP (FT-UMP) and 16 well-differentiated tumours of UMP (WDT-UMP). Observer concordance was 70% for all TT-UMP. More than 50% of FT-UMP expressed galectin-3 and CK19, whereas more than 50% of WDT-UMP expressed HBME-1. Five cases of TT-UMP showed N-RAS mutations, while one showed H-RAS mutation and another PAX8/PPARγ rearrangement. In conclusion, the frequency of TT-UMP is low in our institution. Diagnostic reproducibility is within the same range as other published data on follicular-patterned thyroid tumours. The ancillary methods have a low impact on aiding diagnosis of such lesions.

V. Hofman · S. Lassalle · C. Butori · P. Brest · P. Hofman
Inserm ERI-21, Faculty of Medicine,
University of Nice Sophia Antipolis,
avenue de Valombrose,
06107 Nice, France

V. Hofman · S. Lassalle · C. Butori · P. Brest · P. Hofman
EA 4319, Faculty of Medicine,
University of Nice Sophia Antipolis,
avenue de Valombrose,
06107 Nice, France

V. Hofman · S. Lassalle · C. Butori · M. Ilie · P. Hofman (✉)
Laboratory of Clinical and Experimental Pathology,
Louis Pasteur Hospital,
30 avenue de la voie Romaine,
06002 Nice Cedex 01, France
e-mail: hofman@unice.fr

V. Hofman · S. Lassalle · C. Bonnetaud · C. Butori · C. Loubatier · O. Bordone · P. Hofman
Human Biobank CHU-CAL-UNSA/CRB INSERM,
Louis Pasteur Hospital,
30 avenue de la voie Romaine,
06002 Nice, France

N. Guevara · J. Santini
Department of Otorhinolaryngology,
Louis Pasteur Hospital,
30 avenue de la voie Romaine,
06002 Nice, France

B. Franc
Laboratory of Pathology,
Ambroise Paré Hospital (Assistance Publique-Hôpitaux de Paris),
Boulogne 92104, France

B. Franc
Faculty of Medicine Paris Ile de France Ouest,
University of Versaille Saint Quentin en Yvelines,
Versailles cedex, France

Keywords Thyroid · Follicular lesion · Uncertain malignant potential tumour · Observer variation · Molecular biology · Immunochemistry

Introduction

For decades, conventional histology has failed to classify some encapsulated follicular thyroid tumours as benign or malignant because these lesions share overlapping histological features [1–9]. This difficulty is underscored by recently reported substantial inter-observer variability, either in the pathological assessment of thyroid nodules or in the identification of underlying diagnostic criteria, such as papillary nuclear features, vascular and/or capsular invasion [10–12]. These difficulties are especially relevant in some encapsulated follicular-patterned thyroid tumours in determining whether they belong to strict adenomas or to differentiated thyroid carcinomas. To point out to the physicians such difficulties, several terminologies have been given to avoid performing either unnecessary aggressive surgery or missing out on using necessary aggressive surgical therapy and the general term of "thyroid tumours of uncertain malignant potential" (TT-UMP) has been recently proposed [5, 13, 14]. For tumours showing questionable capsular and/or vascular invasion, it is recommended to call them "follicular tumour of uncertain malignant potential" (FT-UMP) if papillary carcinoma-type nuclear changes are absent and "well-differentiated tumour of uncertain malignant potential" (WDT-UMP) if these nuclear changes are imprecise [13].

In these lesions, immunohistochemistry and the detection of somatic mutations via genotyping have not been extensively adopted in the routine practice of surgical pathology [15–19]. The use of this terminology has been actively discussed by pathologists since it is controversial, particularly for surgeons when considering the therapeutic strategy point of view and because observer variation among pathologists may be high [4, 20].

The frequency of TT-UMP is difficult to determine since this condition has only been defined recently and since it is not an international classification and not adopted by all pathologists. Thus, as formulated in the last edition of the WHO publication concerning the term TT-UMP, "the use of this nomenclature has not been generally accepted" [13].The observer variation among pathologists of different institutions for the diagnosis of FT-UMP and WDT-UMP has not yet been evaluated. Finally, the usefulness of a combined morphological, immunohistochemical and molecular biological approach in optimising the diagnosis and the prognosis of such borderline follicular lesions has been poorly studied to date.

The purpose of this work was to evaluate the incidence of TT-UMP diagnosed in a single institution (Pasteur Hospital, Nice, France) by using the criteria defined in the last edition of the WHO publication [13] in a prospective study performed between 2004 and 2008. We analysed the observer variation among four surgical pathologists from two different institutions. In parallel, we examined the clinicopathological characteristics of such diagnosed cases. In addition, the impact on diagnosis of ancillary methods, such as immunohistochemistry and molecular genetic profiling of a series of diagnosed TT-UMP was determined.

Materials and methods

Cases

The cases were selected from the records of the Laboratory of Clinical and Experimental Pathology (Pasteur Hospital, Nice France) from January 2004 to January 2008. Thirty-one TT-UMP were initially diagnosed by one or more of the three pathologists of the same institution (pathologists B, C or D). However, the diagnosis of TT-UMP was finally made in 31 tumours after a second evaluation. These 31 TT-UMP (15 FT-UMP and 16 WDT-UMP) were diagnosed according to the WHO 2004 diagnostic criteria [13]. The clinical (age, sex, previous medical history and ultrasound analysis) and pathological (fine-needle aspiration (FNA), frozen section, tumour size and location and diagnosis) data were recorded. Each case was processed as follows: complete analysis of the interface of the tumour capsule was performed. For this purpose, specimens of 3-mm thickness of the interface were obtained, fixed in 10% formaldehyde and 10 serial sections of each embedded specimen were stained with haematoxylin–eosin safran (HES). Different features were noted in the initial report that was made by one of the pathologists (pathologist A). The capsule was described as thick, thin or incomplete or poorly formed. Absence of capsular invasion or incomplete protrusion of the capsule (only the inner half of the capsule) with single or multiple foci was noted. The cellularity was divided into three groups: low, with abundant colloid simulating an adenomatoid nodule, moderate and high with compact cell growth. Nuclear-papillary thyroid carcinoma (PTC) changes were classified as questionable and corresponded to diffuse or focal not well-developed nuclear features or focal obvious nuclear changes. Absence or questionable vascular invasion was noted. Finally, the presence of associated lesions in the adjacent thyroid parenchyma was noted: nodular hyperplasia, lymphocytic thyroiditis, PTC, papillary microcarcinoma and C cell hyperplasia.

Observer variation analysis

A set of 10% formaldehyde fixed, paraffin-embedded tissue sections, stained with HES comprising 10 slides per case

was sent to the four panellists. Each case among the 31 diagnosed TT-UMP was previously randomly anonymised without knowledge of the initial diagnosis. Each panellist reviewed the cases independently. A file per case and per panellist was filled. Three pathologists belonged to the same institution (CB: B, VH: C, SL: D) and one to a different institution (BF: A).

Immunohistochemistry

Immunostaining for HBME-1, galectine-3 and CK19 were performed on paraffin-embedded sections using the Ventana Benchmark automated system (entire procedure, from pretreatment to counterstaining; Ventana Benchmark, Ventana, Tucson AZ). Deparaffinized sections were incubated with the following monoclonal antibodies for 30 min: HBME-1 (Dako, Coppenhagen, Denmark; dilution 1/200), galectin-3 (Novocastra, Newcastle, UK; dilution, 1/100) and CK19 (Dako, dilution 1/30). Paraffin sections from a PTC positive for these antibodies were used as a positive control. The immunoreactivity was scored as negative (−), focally positive (±: less than 10% positive cells), positive (+: 10% to 50% positive cells) and strongly positive (++: more than 50% positive cells). Signals showed a membranous and apical staining for HBME-1, a cytoplasmic and/or membranous staining for galectin-3 (predominantly cytoplasmic) and CK19. Combined expression of two or three proteins was analysed.

Molecular biology

B-RAF, N-RAS, K-RAS and H-RAS mutations Genomic DNA from frozen tissue samples was extracted using the MagNA Pure Compact Nucleic Acid Isolation Kit Large Volume (Roche) according to the manufacturer′s instructions. After initial denaturation at 95 C for 5 min, gDNA (50 ng) for B-RAF, K-RAS and N-RAS analysis was subjected to 35 cycles of polymerase chain reaction (PCR; 95 C for 30 s, 57 C for 30 s and 72 C for 30 s) using Taq platinum (Invitrogen, San Diego, CA) followed by final extension at 72 C for 7 min. The primer pairs used for amplification are given in Table 1. Negative controls were included in each set of amplification. After amplification, post-PCR purification was performed using the Qiaquick Purification PCR kit (Qiagen, Basle, Switzerland) in accordance with the manufacturer′s recommendations. All samples were bidirectionally sequenced on an ABI 310 sequencer using the Big Dye Terminator kit (Applied Biosystems, Inc., Foster City, CA). B-RAF (Exon 15: Codon 600/T1799A and 601/A1801G) and RAS (Exon 1: Codons 12 and 13 for K-RAS and H-RAS, Exon 2: Codon 61 for N-RAS and H-RAS) genes found mutated in patients were reanalyzed by a second amplification and sequencing. Genomic DNA extracted from A375 cells (harbouring a B-RAF mutation), T84 and A549 cells (K-RAS mutations), THP1 and HL60 cells (N-RAS mutations) were used as positive controls.

RET/PTC1, RET/PTC3 and PAX8/PPARγ rearrangements Total RNA was extracted from frozen samples with Trizol solution (Invitrogen, San Diego, CA), and the integrity of the RNA was assessed using an Agilent BioAnalyser 2100 (Palo Alto, CA). Synthesis of cDNA was performed with 2 μg of total RNA at 37 C for 90 min, using random hexamer primers and reverse transcriptase Superscript III in

Table 1 Primer pairs used for mutation and rearrangement analysis

Gene name	Exons	Sequences
BRAF	Forward exon 15	TgCTTgCTCTgATAggAAAATg
	Reverse exon 15	AgCATCTCAgggCCAAAAAT
KRAS	Forward exon 1	gACTgAATATAAACTTgTgg
	Reverse exon 1	CTgTATCAAAgAATggTCCT
NRAS	Forward exon 2	ggTgAAACCTgTTTgTTggA
	Reverse exon 2	ggTTAATATCCgCAAATgACTTgC
HRAS	Forward exon 1	CAggCCCCTgAggAgCgATg
	Reverse exon 1	TTCgTCCACAAAATggTTCT
HRAS	Forward exon 2	TCCTgCAggATTCCTACCgg
	Reverse exon 2	ggTTCACCTgTACTggTggA
PAX8/PPARγ	Forward PAX8 exon 7	gCATTgACTCACAgAgCAgCA
	Forward PAX8 exon 8	gCTCAACAgCACCCTggA
	Reverse PPAR exon 2	CATTACggAgAgATCCACgg
RET/PTC1	Forward H4 exon 1	ATTgTCATCTCgCCgTTC
	Reverse RET exon 13	TgCTTCAggACgTTgAAC
RET/PTC3	Forward RFG exon 6	TggAgAAgAgAggCTgTATC
	Reverse RET exon 13	TgCTTCAggACgTTgAAC

accordance with the manufacturer′s recommendations (Invitrogen). The thermoprofile for cDNA generation was 25 C for 10 min, 42 C for 50 min, 70 C for 15 min and 4 C for 5 min. RT-PCR with primers specific for the human GAPDH gene was performed for the mRNA control. After initial denaturation at 95 C for 5 min, cDNA was subjected to 40 cycles of PCR (95 C for 30 s, 55 C for 2 min and 72 C for 2 min) for RET/PTC1 and 3 and 40 cycles of PCR (95 C for 1 min, 61 C for 1 min and 72 C for 1 min) for PAX8/PPARγ, using Taq platinium (Invitrogen), followed by final extension at 72 C for 10 min. The primer pairs used for amplification are given in Table 1. Negative controls were included in each set of amplification. Total RNA extracted from TPC1 cells (kind gift of Pr Santoro, Napoli, Italy) was used as a positive control for RET/PTC1 PCR. For the PAX8/PPARγ PCR, cDNA (kind gift of Dr. V Leite, Lisbon, Portugal) isolated from RNA extracted from previously characterised thyroid samples was used as a positive control. After positive amplification, post-PCR purification was performed using the Qiaquick Purification PCR kit (Qiagen) in accordance with the manufacturer′s recommendations. Patients′ samples positive for a rearrangement were bidirectionally sequenced on an ABI 310 sequencer using the Big Dye Terminator kit (Applied Biosystems, Inc., Foster City, CA).

Statistical analysis

The cumulative agreement (and percent) between the pathologists for WDT-UMP, FT-UMP and TT-UMP diagnosis was calculated for the 31 TT-UMP diagnosed cases by one or more of the four pathologists. The concordant rate was examined for the three pathologists of the same institution and for the four pathologists. A study of sample parameters allowing differentiation of FT-UMP and WDT-UMP was done. The statistical significant of the studied parameters was examined using the χ^2. A p value of 0.05 or less was considered to be significant.

Results

The TT-UMP frequency in a prospective series of thyroidectomy from a single institution (Nice Hospital, France)

A total of 1,078 thyroidectomies were performed from January 2004 to January 2008 in our hospital (Department of ORL, Pasteur Hospital, Nice, France). Among these specimens, 166 were malignant tumours and 31 TT-UMP. Among the TT-UMP, there were 15 FT-UMP and 16 WDT-UMP, representing 2.9% of total thyroidectomy specimens.

Observer variation

Observer variation was studied taking into consideration the initial diagnosis of 31 TT-UMP made by at least one of the four pathologists. The diagnostic concordance was 70% (22/31) for the four pathologists. Diagnostic concordances were 87% (14/16) and 53% (8/15), for the diagnosis of WDT-UMP and FT-UMP, respectively (Table 2). The diagnosis made by each pathologist is shown in Table 3.

Clinicopathological characteristics

Among the 31 TT-UMP, the patient age ranged from 16 to 78 years (mean, 54.1 years) for FT-UMP and from 26 to 78 years (mean, 52.1 years) for WDT-UMP. Females predominated with a female to male ratio of 2/1 (10 females and five males) for FT-UMP and 3/1 (12 females

Table 2 Agreement between pathologists for the diagnosis of TT-UMP, WDT-UMP, and FT-UMP

	All pathologists (A/B/C/D)			Pathologists from the same institution (B/C/D)	
Agreement/Pathologists	4/4	3/4	2/4	3/3	2/3
TT-UMP					
Cumulative agreement/cases	22/31	30/31	31/31	25/31	31/31
(%)	(70)	(97)	(100)	(80)	(100)
WDT-UMP					
Cumulative agreement/cases	14/16	16/16	16/16	15/16	16/16
(%)	(87)	(100)	(100)	(94)	(100)
FT-UMP					
Cumulative agreement/cases	8/15	14/15	15/15	10/15	15/15
(%)	(53)	(93)	(100)	(66)	(100)

TT-UMP thyroid tumour of uncertain malignant potential; *WDT-UMP* well-differentiated tumour of uncertain malignant potential; *FT-UMP* follicular tumour of uncertain malignant potential

Table 3 Distribution of the diagnosis of WDT-UMP and FT-UMP by the four pathologists

Case N°	Pathologists			
	A	B	C	D
1	WDT-UMP	WDT-UMP	WDT-UMP	WDT-UMP
2	WDT-UMP	WDT-UMP	WDT-UMP	WDT-UMP
3	WDT-UMP	WDT-UMP	WDT-UMP	WDT-UMP
4	WDT-UMP	WDT-UMP	WDT-UMP	WDT-UMP
5	WDT-UMP	WDT-UMP	WDT-UMP	WDT-UMP
6	WDT-UMP	WDT-UMP	WDT-UMP	WDT-UMP
7	WDT-UMP	WDT-UMP	WDT-UMP	WDT-UMP
8	WDT-UMP	FA	WDT-UMP	WDT-UMP
9	WDT-UMP	WDT-UMP	WDT-UMP	WDT-UMP
10	WDT-UMP	WDT-UMP	WDT-UMP	WDT-UMP
11	WDT-UMP	WDT-UMP	WDT-UMP	WDT-UMP
12	WDT-UMP	WDT-UMP	WDT-UMP	WDT-UMP
13	WDT-UMP	WDT-UMP	WDT-UMP	WDT-UMP
14	WDT-UMP	WDT-UMP	WDT-UMP	WDT-UMP
15	WDT-UMP	WDT-UMP	WDT-UMP	WDT-UMP
16	FV-PTC	WDT-UMP	WDT-UMP	WDT-UMP
17	FT-UMP	FT-UMP	FT-UMP	FT-UMP
18	FT-UMP	FT-UMP	FT-UMP	FT-UMP
19	FT-UMP	FT-UMP	FA	FT-UMP
20	FT-UMP	FA	FT-UMP	FT-UMP
21	FT-UMP	FT-UMP	FT-UMP	FT-UMP
22	FT-UMP	FC	FT-UMP	FT-UMP
23	FT-UMP	FT-UMP	FT-UMP	FT-UMP
24	FT-UMP	FT-UMP	FT-UMP	FT-UMP
25	FT-UMP	FT-UMP	FT-UMP	FA
26	FT-UMP	FT-UMP	FT-UMP	FT-UMP
27	FT-UMP	FT-UMP	FT-UMP	FT-UMP
28	FT-UMP	FT-UMP	FT-UMP	FT-UMP
29	FA	FT-UMP	FT-UMP	FT-UMP
30	FA	FA	FT-UMP	FT-UMP
31	FA	FT-UMP	FT-UMP	FT-UMP

WDT-UMP well-differentiated tumour of uncertain malignant potential; *FT-UMP* follicular tumour of uncertain malignant potential; *FA* follicular adenoma; *FC* follicular carcinoma; *FV-PTC* follicular variant of papillary carcinoma

and four males) for WDT-UMP. No statistical difference for age or sex was noted for WDT-UMP and FT-UMP. FNA performed on 10 patients with FT-UMP was interpreted as non-diagnostic (one case) and an uncertain malignancy (nine cases: follicular neoplasm (seven cases) and Hurthle cell neoplasm (two cases)). FNA performed on 10 patients with WDT-UMP was interpreted as nondiagnostic (two cases), benign lesion (two cases) and uncertain malignancy (two cases: follicular neoplasm (three cases) and cellular, suspicious for malignancy (three cases)). It was noteworthy that nuclear abnormalities typical of papillary carcinoma were not observed in this latter group of tumours. The mean size of tumours was 3 cm (range from 0.8 to 7.0 cm) for FT-UMP and 3.2 cm (range from 1.0 to 8.0 cm) for WDT-UMP. No preferential localization on the thyroid gland was noted for these two groups of tumours. The diagnosis made from frozen sections was "epithelial tumours without uncertain signs of malignancy" in 26/31 TT-UMP. Diagnosis of a strict benign tumour was not immediately made from frozen sections since the capsule was thick, not well-defined and with possible invasion by follicles. Diagnosis of "follicular adenoma" was made in 5/31 TT-UMP (all WDT-UMP). Data concerning these different cases are shown in Table 4. The majority of TT-UMP were moderately or highly cellular, with a vesicular or, less frequently, with a trabecular architecture. Two cases of WDT-UMP were poorly cellular, with macrovesicular architecture. All FT-UMP showed a capsule, generally thick, or thin, in a few cases. This capsule was thin, not well-defined, not complete or complete in WDT-UMP. Capsular invasion (not complete, isolated or multiple) was present in all FT-UMP (Fig. 1a, b) and in two WDT-UMP. Questionable vascular invasion was noted in one FT-UMP and in one WDT-UMP. Nuclear abnormalities looking like those observed in PTC were observed in WDT-UMP (Fig. 1c–f). These abnormalities were not complete, isolated or diffuse (Fig. 1c, d) or characteristics of PTC (Fig. 1e, f) and isolated. Thyroid tissue adjacent to tumours was normal in 31% of WDT-UMP and 40% of FT-UMP. Other TT-UMP showed at their periphery, nodular hyperplasia and thyroiditis, and interestingly, four WDT-UMP were associated with PTC. Table 5 summarises the main histological criteria observed in our series. For 22/31 (71%) patients, a thyroid nodule that was surgically removed was clinically present between 24 and 37 months (mean=30 months) before surgery. For all cases, no additional therapy was given and non-recommended by the clinician. However, medical supervision was enhanced and consisted in a medical examination with ultrasound examination of the thyroid every 6 months. Finally, for all cases, no tumour recurrence has been noted to date after surgery (follow-up range from 12 to 48 months, mean=31 months).

Immunohistochemical results

The tumours of the WDT-UMP group showed HBME-1, galectin-3 and CK19 expression (more than 10% positive cells) in 9/16 (56%), 9/16 (56%) and 10/16 (62%) tumours, respectively. HBME-1 was expressed in more than 50% of the cells in 7/16 (44%) cases (Fig. 2a) and sometimes showed a more intense signal in regions where nuclear anomalies were obvious (Fig. 2b), whereas galectin-3 and CK19 were expressed in 4/16 (25%) and 3/16 (19%) cases, respectively (Fig. 2c, d). Immunostaining with two or three of these antibodies was found in 56% of the cases. The

Table 4 Main clinicopathological characteristics of WDT-UMP and FT-UMP

Case no.	Diagnosis	Sex	Age (year)	FNA	Frozen section	Tumour size/cm	Lobe location (Left/Right)
1	WDT-UMP	F	29	Follicular	Benign	3.0	L
2	WDT-UMP	F	76	Not done	Undeterminated	2.8	R
3	WDT-UMP	F	62	Not done	Benign	8.0	L
4	WDT-UMP	F	34	Follicular	Benign	2.5	L
5	WDT-UMP	M	66	Cellular	Undeterminated	2.5	R
6	WDT-UMP	M	78	Not done	Undeterminated	2.5	L
7	WDT-UMP	F	57	Not done	Undeterminated	6.0	R
8	WDT-UMP	F	77	Cellular	Undeterminated	5.0	R
9	WDT-UMP	F	20	Not done	Undeterminated	3.5	R
10	WDT-UMP	F	47	Non diagnostic	Benign	1.5	R
11	WDT-UMP	M	26	Non diagnostic	Undeterminated	3.0	L
12	WDT-UMP	F	58	Not done	Benign	1.0	L
13	WDT-UMP	F	63	Benign	Undeterminated	2.0	R
14	WDT-UMP	F	52	Follicular	Undeterminated	2.5	R
15	WDT-UMP	M	40	Benign	Undeterminated	1.5	L
16	WDT-UMP	F	49	Cellular	Undeterminated	4.5	R
17	FT-UMP	F	78	Follicular	Undeterminated	6.0	R
18	FT-UMP	F	61	Not done	Undeterminated	1.3	R
19	FT-UMP	F	35	Follicular	Undeterminated	0.8	L
20	FT-UMP	F	66	Non diagnostic	Undeterminated	2.5	L
21	FT-UMP	M	45	Follicular	Undeterminated	3.0	R
22	FT-UMP	F	77	Not done	Undeterminated	7.0	L
23	FT-UMP	F	60	Oncocytic	Undeterminated	1.2	L
24	FT-UMP	F	55	Follicular	Undeterminated	3.5	L
25	FT-UMP	F	43	Oncocytic	Undeterminated	3.0	R
26	FT-UMP	M	46	Follicular	Undeterminated	1.8	R
27	FT-UMP	F	16	Follicular	Undeterminated	1.2	R
28	FT-UMP	M	75	Cellular	Undeterminated	2.0	L
29	FT-UMP	M	60	Not done	Undeterminated	6.5	L
30	FT-UMP	M	59	Not done	Undeterminated	3.0	L
31	FT-UMP	F	36	Not done	Undeterminated	3.0	R

WDT-UMP well-differentiated tumour of uncertain malignant potential; *FT-UMP* follicular tumour of uncertain malignant potential; *FNA* fine needle aspiration; *F* female; *M* male

tumours of the FT-UMP group showed galectin-3 and CK19 immunoreactivity (more than 10% positive cells) in 6/15 (40%) and 8/15 (53%) cases, respectively, and most often in more than 50% of the cells (Fig. 2e, f). HBME-1 was expressed in 3/15 (20%) cases and on more than 50% of cells; 6/15 (40%) cases showed co-expression of two or three antigens. Finally, none of these three proteins were significantly expressed in either of the two subgroups of TT-UMP. The details of the immunohistochemical results are summarised in Table 6.

Molecular biology

The results of the molecular biological analyses are summarised in Table 7. None of the 31 TT-UMP showed B-RAF mutations and RET-PTC1 or RET-PTC3 rearrangements. Two FT-UMP and three WDT-UMP showed a N-RAS mutation and one FT-UMP showed H-RAS mutation. One FT-UMP showed a PAX8-PPARγ rearrangement. The cases of mutated N-RAS WDT-UMP corresponded to highly cellular tumours with microvesicular and trabecular patterns and diffuse questionable nuclear abnormalities (one associated with capsular invasion). Two of these latter cases were associated with a micropapillary carcinoma. No statistical differences were noted for the group of TT-UMP showing N-RAS mutation for the following criteria: age, sex, tumour size, cellularity, capsular invasion, HBME-1, galectin-3 and CK19 staining. Finally, FT-UMP with H-RAS mutation and PAX8-PPARγ rearrangement were histologically similar to other FT-UMP studied in this series.

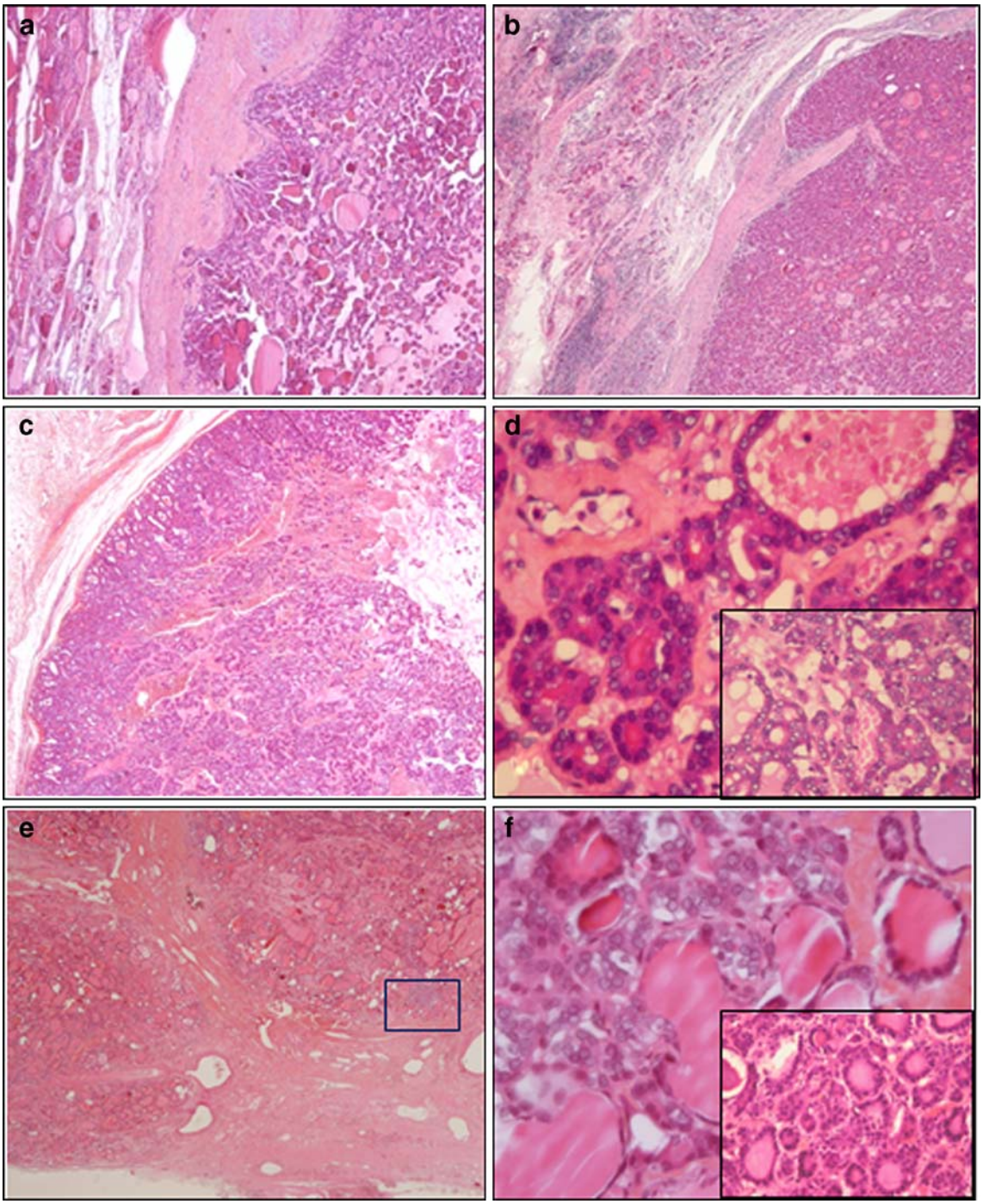

Fig. 1 FT-UMP: **a** Multiple questionable capsular invasion (case no. 26). **b** Isolated capsular invasion (case no. 24; **a**, **b**, HES, original magnification ×40). WDT-UMP: **c**, **d** Microfollicular lesion with diffuse questionable PTC-nuclear changes (case no. 8). *Inset* in **d** shows very small area of nuclei looking like PTC-nuclear changes (**c** HES, original magnification, ×40; **d** HES, original magnification ×400; *inset*, HES, original magnification ×400); **e**, **f** heterofollicular lesion with small foci of obvious PTC-nuclear changes (case no. 9). *Inset* in **f** shows large area of nuclei without PTC-nuclear changes (**c**, **e**, HES, original magnification ×40; **d**, **f**, HES, original magnification ×400, **f** *inset*, HES, original magnification ×400)

Discussion

Our study should be considered as a complement to the previous studies published, in the last decade, into observer variation in the diagnosis of encapsulated follicular lesions of the thyroid [10–12]. Moreover, none of these studies specifically focused on the generally not accepted nomenclature of TT-UMP. It remains to be determined whether or

Table 5 Histological features of FT-UMP and WDT-UMP

Histological criteria	Total FT-UMP (n=15)	Total WDT-UMP (n=16)
Cellularity		
Low	0	2
Moderate	6	8
High	9	6
Capsule		
Thick	10	2
Thin	5	7
Incomplete	0	7
Capsular invasion		
Absence	0	14
Questionable	15	2
Single foci	6	1
Multiple foci	9	1
Vascular invasion		
Absence	14	15
Questionable	1	1
PTC-nuclear changes		
Absence	11	0
Questionable	4	12
Small foci	4	4
Diffuse	0	8
Obvious	0	4
Small foci	0	4
Peritumoural parenchyma		
No disease	6	5
Nodular hyperplasia	4	9
Lymphocytic thyroiditis	3	1
PTC	0	2
Micro-PTC	2	2
C cell hyperplasia	1	1

not this category of disease, initially defined by Williams et al. [14] and then classified in the last edition of the WHO publication [13] should or should not still be defined separately. Our inter-observer variation lies within the value already reported in other studies but with a higher level of agreement in the WDT-UMP group [10–12]. Even if we consider a "centre effect" (three of the observers belonging to the same institution) the level of agreement between the four pathologists was 87% for the WDT-UMP cases and 53% for the FT-UMP cases. In addition, we note that most of the discord concerned diagnosis of a follicular adenoma instead of a TT-UMP either in 1/16 (6%) WDT-UMP and in 6/15 (40%) FT-UMP. A pending diagnosis of malignancy was made in 1/16 (6%) WDT-UMP and in 1/15 (7%) FT-UMP. Therefore, the reticence expressed in the most recent publication of the WHO [13] is fully justified, and our study highlights the fact that the TT-UMP diagnosis tips more toward diagnosis of a follicular adenoma diagnosis than of a malignancy.

Numerous previous studies have demonstrated that the use of ancillary techniques such as immunohistochemistry can significantly improve diagnosis in thyroid pathologies [21–28]. However, a single marker is usually suboptimal in terms of sensitivity and specificity. Panels of two or more antibodies are usually more effective and can improve diagnostic accuracy when based on paraffin-embedded tissue. Our immunohistochemical data (HBME-1, galectin-3, CK19) still demonstrate that the "TT-UMP lesions" had an immunohistological profile that was not typical of a follicular adenoma, which has already been suggested by others for WDT-UMP [29–34]. The immunohistochemical profile has been less studied in the FT-UMP group, a pathology that is not as well-known in North America as in Europe, where it is a matter of concern [31, 32]. Moreover, most of the published studies used only HBME-1 [33] or galectin-3 [29, 30], HBME-1 and galectin-3 [32] or HBME-1, galectin-3 and CK19 [31, 34]. Previous reports showed that WDT-UMP, also called "encapsulated

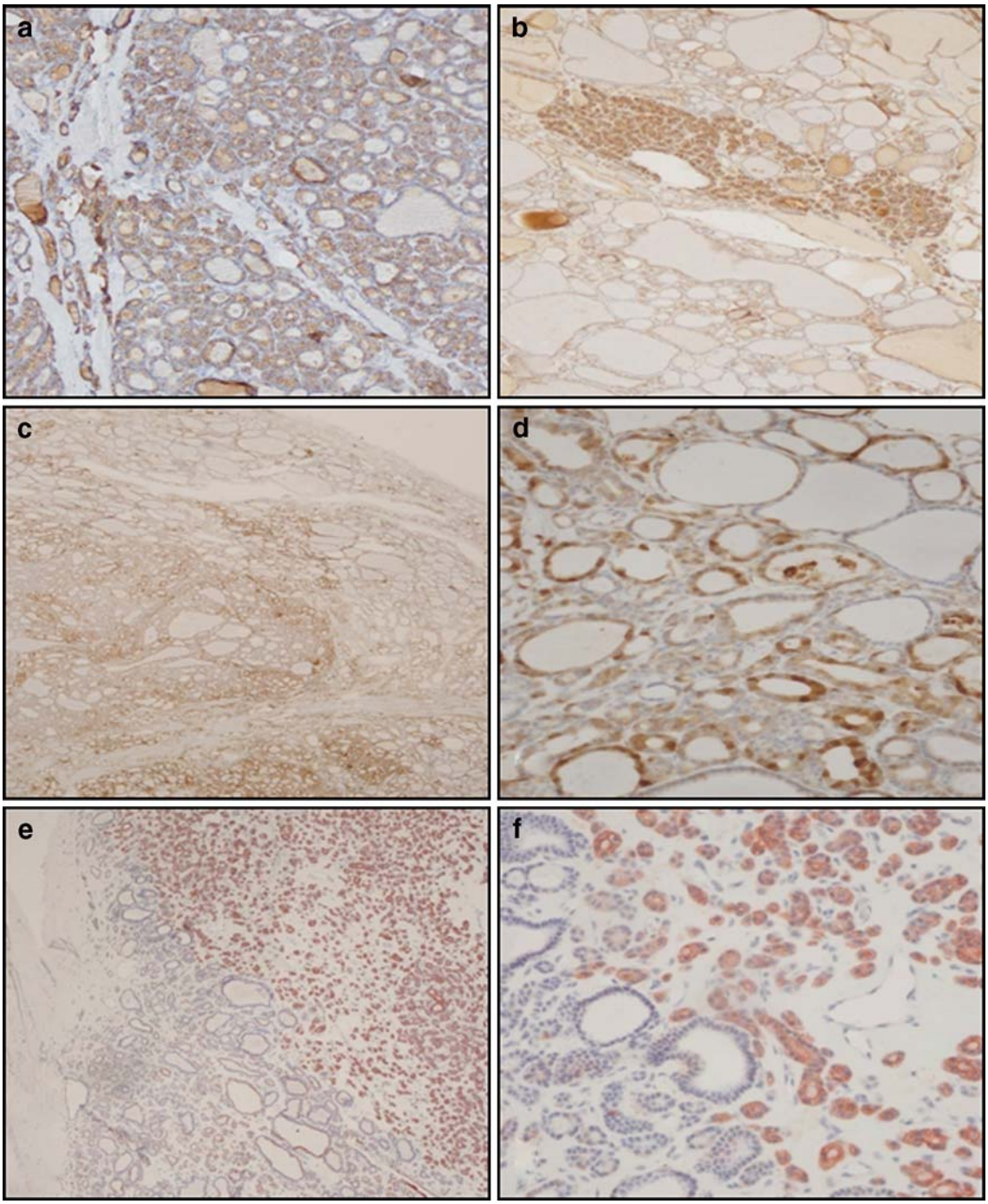

Fig. 2 WDT-UMP: **a** Diffuse questionable PTC-nuclear changes with >50% positive cells (case no. 3; HBME-1, original magnification ×40). **b** Small foci of obvious PTC-nuclear changes (case no. 16; HBME-1, immunoperoxidase, original magnification ×200). **c**, **d** Diffuse questionable PTC-nuclear changes with 10% to 50% positive cells (case no. 4; Galectin-3, immunoperoxidase, original magnification, ×40 (**c**) and ×400 (**d**)). FT-UMP: up to 50% positive cells (case no. 28; CK19, immunoperoxidase, original magnification; ×40 (**e**) and ×400 (**f**))

lesions with questionable features of PTC" by Sconamiglio et al. [34], expressed HBME-1 in around 60% to 70% cases, and galectin-3 in around 60% to 80% cases [32, 34]. In one series, WDT-UMP expressed CK19 in 63% tumours [34]. In our series, the results were quite similar since WDT-UMP expressed HBME-1, galectin-3 and CK19 in respectively, 56%, 56% and 62% cases. In the study of Papotti et al., FT-UMP expressed HBME-1 and galectin-3 in 62% and 37% of tumours [32], whereas in our series, HBME-1 and galectin-3 were expressed in 25% and 50% of tumours, respectively. Previous studies using the terminology of atypical adenoma or follicular neoplasm of

Table 6 Immunohistochemical analysis of WDT-UMP and FT-UMP

Case no.	Diagnosis	HBME-1	galectin-3	CK19
1	WDT-UMP	++	+	+
2	WDT-UMP	−	−	+
3	WDT-UMP	++	++	++
4	WDT-UMP	−	+	−
5	WDT-UMP	++	+	+
6	WDT-UMP	−	−	−
7	WDT-UMP	+	+	++
8	WDT-UMP	−	++	+
9	WDT-UMP	++	+	+
10	WDT-UMP	−	++	+
11	WDT-UMP	++	−	+
12	WDT-UMP	−	−	−
13	WDT-UMP	−	+	−
14	WDT-UMP	++	+	+
15	WDT-UMP	+	+	+
16	WDT-UMP	++	++	++
17	FT-UMP	−	−	+
18	FT-UMP	−	−	+
19	FT-UMP	−	−	+
20	FT-UMP	−	−	−
21	FT-UMP	−	+	+
22	FT-UMP	−	−	++
23	FT-UMP	−	++	++
24	FT-UMP	++	++	++
25	FT-UMP	++	++	++
26	FT-UMP	−	++	−
27	FT-UMP	++	−	+
28	FT-UMP	−	++	++
29	FT-UMP	−	−	−
30	FT-UMP	−	−	−
31	FT-UMP	+	−	+

(−) negative; (±) <10% positive cells; (+) 10% to 50% positive cells; (++) >50% positive cells

undefined malignant behaviour showed HBME-1 expression in 45–60% tumours, galectin-3 expression in 70–85% tumours and CK19 expression in 20% tumours [29, 31, 33]. Interestingly, in the present study, HBME-1 was more often expressed in WDT-UMP, whereas galectin-3 and CK19 were similarly expressed in FT-UMP and WDT-UMP. As in our series, previous reports showed that around half of the WDT-UMP expressed both HBME-1 and galectin-3 [22, 32]. Coli et al. have suggested that tumours demonstrating "cytological atypia suggestive but not diagnostic of PTC" may have started to change phenotype towards a PTC [22]. Interestingly, in the present study, HBME-1 was more often expressed in WDT-UMP, whereas galectin-3 and CK19 were similarly expressed in FT-UMP and WDT-UMP. However, when associated, the three antibodies did not discriminate between FT-UMP and WDT-UMP. In addition, we demonstrate that the immunohistological profiles of TT-UMP are not tumour-size-dependant.

TT-UMP represent a true "grey zone" of lesions that need to be further characterised in order to determine whether or not they represent a borderline category requiring specific curative procedures and postoperative follow-up. The "exponential increase in papers" on this topic [4, 13, 14, 20, 35, 36] has permitted more precise definition of the underlying criteria necessary, as highlighted by our good inter-observer agreement in WDT-UMP. However, it is less obvious in FT-UMP which is less frequent, and for which "questionable invasive criteria" are still poor and less convincing. As the nomenclature for TT-UMP is recent and since not all pathologists recognise the controversial entity, the current incidence of TT-UMP is difficult to appreciate. In our institution, TT-UMP represented 2.9% of thyroid surgical pathologies. However, it is necessary to point out that such problematic histological cases in the field of thyroid pathology make up only a very small fraction of thyroid cases but when seen by experienced surgical pathologists in thyroid pathology. Moreover, in a routine diagnostic setting, the current histological criteria for classification tumours, especially follicular-patterned thyroid tumours, is hampered by considerable variability depending on experience. In this regard, the terms TT-UMP, FT-UMP and WDT-UMP have not been introduced as an easy option for the surgical pathologists when dealing with the evaluation of difficult cases or as a way of avoiding the commitment required in making a clear diagnosis of malignancy or benignity.

Recently, major advances in the molecular characterisation of the well-differentiated carcinoma of the thyroid have been made [37–48]. We report here one of the first analyses of mutations and chromosomic rearrangements in a large series of TT-UMP. None of the WDT-UMP had mutations for B-RAF V600. RAS mutations were noted in a few tumours belonging to the two subgroups of TT-UMP. Among the latter tumours, a poorly differentiated carcinoma was ruled out in particular in the three cases of WDT-UMP corresponding to highly cellular tumours with microvesicular and trabecular patterns. Interestingly, one FT-UMP showed a PAX8/PPAR γ rearrangement. Secondary histological analysis in this latter case did not modify the diagnosis of minimally invasive FC. No RET mutation was observed in cases of TT-UMP, which contrasts with results obtained by Fontaine et al. who found three RET/PTC1 rearrangements and did not detect any N-RAS mutations in exon 2 [31]. However, other larger studies are lacking in this field. Moreover, it may be useful to increase the sensitivity of these molecular biology methods by using laser capture microdissection followed by RT-PCR amplification in archival samples [49, 50]. This approach will procure pure-

Table 7 Mutations and rearrangements in WDT-UMP and FT-UMP

Case no.	Diagnosis	BRAF	HRAS	KRAS	NRAS	RET/PTC-1	RET/PTC-3	PAX8/PPAR©
1	WDT-UMP	-	-	-	-	-	-	-
2	WDT-UMP	-	-	-	-	-	-	-
3	WDT-UMP	-	-	-	+ exon 2	-	-	-
4	WDT-UMP	-	-	-	-	-	-	-
5	WDT-UMP	-	-	-	+ exon 2	-	-	-
6	WDT-UMP	-	-	-	-	-	-	-
7	WDT-UMP	-	-	-	-	-	-	-
8	WDT-UMP	-	-	-	-	-	-	-
9	WDT-UMP	-	-	-	-	-	-	-
10	WDT-UMP	-	-	-	-	-	-	-
11	WDT-UMP	-	-	-	-	-	-	-
12	WDT-UMP	-	-	-	-	-	-	-
13	WDT-UMP	-	-	-	+ exon 2	-	-	-
14	WDT-UMP	-	-	-	-	-	-	-
15	WDT-UMP	-	-	-	-	-	-	-
16	WDT-UMP	-	-	-	-	-	-	-
17	FT-UMP	-	-	-	-	-	-	-
18	FT-UMP	-	+ exon 1	-	-	-	-	-
19	FT-UMP	-	-	-	-	-	-	-
20	FT-UMP	-	-	-	-	-	-	-
21	FT-UMP	-	-	-	-	-	-	+ PAX8/PPAR©
22	FT-UMP	-	-	-	-	-	-	-
23	FT-UMP	-	-	-	+ exon 2	-	-	-
24	FT-UMP	-	-	-	-	-	-	-
25	FT-UMP	-	-	-	-	-	-	-
26	FT-UMP	-	-	-	-	-	-	-
27	FT-UMP	-	-	-	-	-	-	-
28	FT-UMP	-	-	-	-	-	-	-
29	FT-UMP	-	-	-	-	-	-	-
30	FT-UMP	-	-	-	-	-	-	-
31	FT-UMP	-	-	-	+ exon 2	-	-	-

WDT-UMP well-differentiated tumour of uncertain malignant potential; *FT-UMP* follicular tumour of uncertain malignant potential

cell populations showing questionable PTC-nuclear changes when looking for rearrangements and mutations of interest.

Taken together, these data confirm that the ancillary methods are not prognostic in TT-UMP. This is not surprising, since these methods are of low significance in evaluating the potential aggressiveness of most epithelial thyroid tumours. The discovery of new biomarkers, particularly to evaluate the potential onset of metastasis or recurrence of TT-UMP will be useful. In this regard, some studies have shown the potential interest of using microarray technology in thyroid pathology [51–54]. Based on a recent study, it is promising to note that a DNA microarray gene expression approach was able to define a gene expression signature which can clearly distinguish the different TT-UMP from other epithelial thyroid tumours [31].

In conclusion, the clinical course of TT-UMP is currently unknown since their incidence is certainly underestimated, and because, if any, their recurrence and metastatic onset can occur several years after the initial surgical resection. After making the diagnosis, treatment of TT-UMP is most of the time the same as for benign epithelial thyroid tumours. We strongly believe that the terminology of TT-UMP should be quickly tested in different referent centres. Moreover, some ancillary methods, particularly for the PAX8/PPARγ rearrangement in FT-UMP should be examined in a larger series. In the present study, immunohistochemistry and molecular genetic profiling were not useful in detecting a low- and high-risk population of patients among the different TT-UMP subgroups. Standardisation of the different procedures, particularly for sampling thyroid

tumours is critical in improving our knowledge of these controversial issues. In this regard, we are still waiting for a biomarker to appreciate the real aggressiveness of such lesions. Only long-term survival data of the follow-up of patients over at least 20 years will prove whether TT-UMP are able to metastasize or whether surgical pathologists are just over-cautious in front of such features suggesting they are actually dealing with benign tumours mimicking features of WDT carcinoma.

Acknowledgements This work was supported by the Institut National du Cancer (VH, PB, CL, PH), the Canceropole PACA (CB) and the CHUN-CNRS (SL) [VH: RA N°1233; PB: RA No. 1233; CL and PH: RA1235 No.; PH: RA No. 1287; SL: Grant CHUN-CNRS 2007; CB: Procan 2008-2011]. We acknowledge the excellent support of the LPCE Platform of the Marseille-Nice Canceropole PACA where the immunohistochemistry and molecular biological analyses were carried out.

Conflict of interest statement We declare that we have no conflict of interest.

References

1. Baloch ZW, Livolsi VA (2002) Follicular-patterned lesions of the thyroid: the bane of the pathologist. Am J Clin Pathol 117:143–150
2. Evans HL (1984) Follicular neoplasms of the thyroid. A study of 44 cases followed for a minimum of 10 years, with emphasis on differential diagnosis. Cancer 54:535–540
3. Fonseca E, Soares P, Cardoso-Oliveira M et al (2006) Diagnostic criteria in well-differentiated thyroid carcinomas. Endocr Pathol 17:109–117
4. Livolsi VA, Baloch ZW (2004) Follicular neoplasms of the thyroid: view, biases, and experiences. Adv Anat Pathol 11:279–287
5. Rosai J (2005) Handling of thyroid follicular patterned lesions. Endocr Pathol 16:279–283
6. Rosai J, Kuhn E, Cargangiu ML (2006) Pitfalls in thyroid tumour pathology. Histopathology 49:107–120
7. Sobrinho-Simões M, Magalhaes J, Foncesa E et al (2005) Diagnostic pitfalls of thyroid pathology. Curr Diag Pathol 11:52–59
8. Suster S (2006) Thyroid tumours with a follicular growth pattern: problems in differential diagnosis. Arch Pathol Lab Med 130:984–988
9. Vasko VV, Gaudart J, Allasia C et al (2004) Thyroid follicular adenomas may display features of follicular carcinoma and follicular variant of papillary carcinoma. Eur J Endocrinol 151:779–786
10. Franc B, de la Salmonière P, Lange F et al (2003) Interobserver and intraobserver reproductibility in the histopathology of follicular thyroid carcinoma. Hum Pathol 34:1092–1100
11. Hirokawa M, Carney JA, Goellner JR et al (2002) Observer variation of encapsulated follicular lesions of the thyroid gland. Am J Surg Pathol 26:1508–1514
12. Lloyd RV, Erickson LA, Casey MB et al (2004) Observer variation in the diagnosis of follicular variant of papillary thyroid carcinoma. Am J Surg Pathol 28:1336–1340
13. De Lellis RA, Lloyd RV, Heitz PU (2004) Pathology and genetics: tumours and endocrine organs, 3rd edn. WHO, Geneva
14. Williams ED (2000) Guest editorial: two proposals regarding the terminology of thyroid tumours. Int J Surg Pathol 8:181–183
15. Cheung CC, Ezzat S, Freeman JL (2001) Immunohistochemical diagnosis of papillary thyroid carcinoma. Mod Pathol 14:338–342
16. Fischer S, Asa S (2008) Application of immunochemistry to thyroid neoplasm. Arch Pathol Lab Med 132:359–372
17. Mehrotra P, Okpokam A, Bouhaidar R et al (2004) Galectin-3 does not reliably distinguish benign from malignant thyroid neoplasm. Histopathology 45:493–500
18. Nakamura N, Erickson LA, Jin L et al (2006) Immunohistochemical separation of follicular variant of papillary thyroid carcinoma from follicular adenoma. Endocr Pathol 17:213–223
19. Sobrino-Simoes M, Preto A, Rocha AS et al (2005) Molecular pathology of well-differentiated thyroid carcinomas. Virchows Arch 447:787–793
20. Baloch ZW, LiVolsi VA (2007) Our approach to follicular-patterned lesions of thyroid. J Clin Pathol 60:244–250
21. Barroeta JE, Baloch ZW, Lal P et al (2006) Diagnostic value of differential expression of CK19, Galectin-3, HBME-1, ERK, RET, and p16 in benign and malignant follicular-derived lesions of the thyroid: an immunohistochemical tissue microarray analysis. Endocr Pathol 17:225–234
22. Coli A, Bigotti G, Parente P et al (2007) Atypical thyroid nodules express both HBME-1 and Galectin-3, two phenotypic markers of papillary thyroid carcinoma. J Exp Clin Cancer Res 26:221–227
23. Ito Y, Yoshida H, Tomoda C et al (2005) HBME-1 expression in follicular tumour of the thyroid: an investigation of whether it can be used as a marker to diagnose follicular carcinoma. Anticancer Res 25:179–182
24. Mase T, Funahashi H, Koshikawa T et al (2003) HBME-1 immunostaining in thyroid tumours especially in follicular neoplasm. Endocrinol J 50:173–177
25. Miettinen M, Karkkainen P (1996) Differential reactivity of HBME-1 and CD15 antibodies in benign and malignant thyroid tumours. Preferential reactivity with malignant tumours. Virchows Arch 429:213–219
26. Prasad ML, Pellegata NS, Huang Y et al (2005) Galectin 3, fibronectin-1, CITED-1, HBME-1 and cytokeratin 19 immunochemistry is useful for the differential diagnosis of thyroid tumours. Mod Pathol 18:48–57
27. Sahoo S, Hoda S, Rosai J et al (2001) Cytokeratin 19 immunoreactivity in the diagnosis of papillary thyroid carcinoma: a note of caution. Am J Clin Pathol 116:696–702
28. Torregrossa L, Faviana P, Camacci T et al (2007) Galectin-3 is highly expressed in nonencapsulated papillary thyroid carcinoma but weakly expressed in encapsulated type; comparison with Hector Battifora mesothelial cell 1 immunoreactivity. Hum Pathol 38:1482–1488
29. Bartolazzi A, Gasbarri A, Papotti M et al (2001) Thyroid Cancer Study Group. Application of an immunodiagnostic method for improving preoperative diagnosis of nodular thyroid lesions. Lancet 357:1644–1650
30. Bartolazzi A, Orlandi F, Saggiorato E et al (2008) Galectin-3 expression analysis in the surgical selection of follicular thyroid nodules with indeterminate fine-needle aspiration cytology: a prospective multicentre study. Lancet Oncol 9:543–549
31. Fontaine JF, Mirebeau-Prunier D, Franc B et al (2007) Microarray analysis refines classification of non-medullary thyroid tumours of uncertain malignancy. Oncogene 29:1–9
32. Papotti M, Rodriguez J, De Pompa R et al (2005) Galectin-3 and HBME-1 expression in well-differentiated thyroid tumours with follicular architecture of uncertain malignant potential. Mod Pathol 18:541–546
33. Rigau V, Martel B, Evrard C et al (2001) HBME-1 immunostaining in thyroid pathology. Ann Pathol 21:15–20

34. Scognamiglio T, Hyjek E, Kao J et al (2006) Diagnostic usefulness of HBME1, galectin-3, CK19, and CITED1 and evaluation of their expression in encapsulated lesions with questionable features of papillary thyroid carcinoma. Am J Clin Pathol 126: 700–708
35. Chan JK (2002) Strict criteria should be applied in the diagnosis of encapsulated follicular variant of papillary thyroid carcinoma. Am J Clin Pathol 117:16–18
36. Renshaw AA, Gould EW (2002) Why there is the tendency to "overdiagnose" the follicular variant of papillary thyroid carcinoma. Am J Clin Pathol 117:19–21
37. Castro P, Rebocho AP, Soares RJ et al (2006) PAX8-PPARgamma rearrangement is frequently detected in the follicular variant of papillary thyroid carcinoma. J Clin Endocrinol Metab 91:213–220
38. Di Cristofaro J, Marcy M, Vasko V et al (2006) Molecular genetic study comparing follicular variant versus classic papillary thyroid carcinomas: association of N-ras mutation in codon 61 with follicular variant. Hum Pathol 37:824–830
39. Elisei R, Romei C, Vorontsova T et al (2001) RET/PTC rearrangements in thyroid nodules: studies in irradiated and not irradiated, malignant and benign thyroid lesions in children and adults. J Clin Endocrinol Metab 81:3211–3216
40. Fusco A, Chiappetta G, Hui P et al (2002) Assessment of RET/PTC oncogene activation and clonality in thyroid nodules with incomplete morphological evidence of papillary carcinoma: a search for the early precursors of papillary cancer. Am J Pathol 160:2157–2167
41. Kroll TG, Sarraf P, Pecciarini L et al (2000) PAX8-PPARgamma1 fusion oncogene in human thyroid carcinoma [corrected]. Science 289:1357–1360
42. Lupi C, Giannini R, Ugolini C et al (2007) Association of B-RAF V600E mutation with poor clinicopathological outcomes in 500 consecutive cases of papillary thyroid carcinoma. J Clin Endocrinol Metab 92:4085–4090
43. Marques AR, Espadinha C, Catarino AL et al (2002) Expression of PAX8-PPAR gamma 1 rearrangements in both follicular thyroid carcinomas and adenomas. J Clin Endocrinol Metab 87:3947–3952
44. Nikiforov YE (2002) RET-PTC rearrangement in thyroid tumours. Endocr Pathol 13:3–16
45. Soares P, Trovisco V, Rocha AS et al (2003) B-RAF mutations and RET/PTC rearrangements are alternative events in the etiopathogenesis of PTC. Oncogene 22:4578–4580
46. Trovisco V, Soares P, Preto A et al (2005) Type and prevalence of B-RAF mutations are closely associated with papillary thyroid carcinoma histotype and patients' age but not with tumour aggressiveness. Virchows Arch 446:589–595
47. Vasko V, Ferrand M, Di Cristofaro J et al (2003) Specific pattern of RAS oncogene mutations in follicular thyroid tumours. J Clin Endocrinol Metab 88:2745–2752
48. Zhu Z, Gandhi M, Nikiforova MN et al (2003) Molecular profile and clinical-pathologic features of the follicular variant of papillary thyroid carcinoma. An unusually high prevalence of ras mutations. Am J Clin Pathol 120:71–77
49. Denning KM, Smyth PC, Cahill SF et al (2007) A molecular expression signature distinguishing follicular lesions in thyroid carcinoma using preamplification RT-PCR in archival samples. Mod Pathol 20:1095–1102
50. Tallini G, Brandao G (2005) Assessment of RET/PTC oncogene activation in thyroid nodules utilizing laser capture microdissection followed by nested RT-PCR. Methods Mol Biol 293:103–111
51. Barden CB, Shister KW, Zhu B et al (2003) 3rd. Classification of follicular thyroid tumours by molecular signature: results of gene profiling. Clin Cancer Res 9:1792–1800
52. Chevillard S, Ugolin N, Viehl P et al (2004) Gene expression profiling of differentiated thyroid neoplasms: diagnostic and clinical implications. Clin Cancer Res 10:6586–6597
53. Finley DJ, Zhu B, Barden CB et al (2004) Discrimination of benign and malignant thyroid nodules by molecular profiling. Ann Surg 240:436–437
54. Finn SP, Smyth P, Cahill S et al (2007) Expression microarray analysis of papillary thyroid carcinoma and benign thyroid tissue: emphasis on the follicular variant and potential markers of malignancy. Virchows Arch 450:249–260

Virchows Arch (2009) 455:35–41
DOI 10.1007/s00428-009-0789-8

ORIGINAL ARTICLE

RET/PTC rearrangements arising from a small population of papillary thyroid carcinoma cells, possible candidate for passenger mutation

Tadao Nakazawa · Shin-ichi Murata · Tetsuo Kondo · Dongfeng Niu · Kunio Mochizuki · Tomonori Kawasaki · Tetsu Yamane · Nobuki Nakamura · Ryohei Katoh

Received: 2 March 2009 / Revised: 6 May 2009 / Accepted: 9 May 2009 / Published online: 3 June 2009

Abstract *RET* rearrangements (*RET*/PTC) is a major genetic alteration in papillary thyroid carcinomas. However, the prevalence of *RET*/PTC differs considerably among investigators, and its impact on cancer progression has been controversial. In the current study, we applied interphase fluorescence in situ hybridization (FISH) to touch imprint cytology of 14 papillary thyroid carcinomas along with reverse-transcription polymerase chain reaction (RT-PCR) analysis. FISH DNA probes included *RET* locus, and PCR primers were designed targeting *RET*/PTC1 or *RET*/PTC3. Split FISH signals of *RET* was observed in 78.6% (11/14) of tumors. Proportions of tumor cells having split *RET* signals ranged from 1.8% to 19.6% (mean 9.7%) in those 11 tumors. In RT-PCR analysis, *RET*/PTC was found in 28.6% (4/14) of tumors. Among tumors with split *RET* signals, 36.4% (4/11) of tumors exhibited detectable messenger RNA of *RET*/PTC1 or *RET*/PTC3. The remaining seven tumors with split *RET* signals had no *RET*/PTCs amplicon. In conclusion, the current study disclosed that *RET*/PTCs occur in a small population of tumor cells in papillary thyroid carcinomas. Even though *RET*/PTC is a specific genetic event in the carcinomas, our results suggested the possibility of *RET*/PTC as "passenger" abnormalities rather than "driver" oncogenic mutation during thyroid cancer progression, warranting further studies on mechanisms and implication of *RET* gene instability.

Keywords Papillary thyroid carcinoma · *RET* rearrangements · Interphase FISH · RT-PCR · TTF-1

T. Nakazawa (✉) · T. Kondo · D. Niu · K. Mochizuki · T. Kawasaki · T. Yamane · N. Nakamura · R. Katoh
Department of Pathology, University of Yamanashi Interdisciplinary Graduate School of Medicine and Engineering, 1110 Shimokato,
Chuo, Yamanashi 409-3898, Japan
e-mail: tadaon@yamanashi.ac.jp

S.-i. Murata
Department of Pathology, Saitama Medical University, International Medical Center,
Saitama, Japan

Introduction

Papillary carcinoma is the most common thyroid malignancy and shows a favor prognosis even when the patient has metastasis in the regional lymph nodes. Molecular studies in papillary thyroid carcinomas have provided several genetic alterations, such as point mutations in the *BRAF* and *RAS* genes and rearrangements of *RET* gene (*RET*/PTC) [1–3]. The *RET* proto-oncogene, which is located in the long arm of chromosome 10 at band q11.2, encodes a receptor tyrosine kinase for the glial cell-line-derived neurotrophic factor [4]. The somatic rearrangements of *RET* proto-oncogene always involve intron 11 of *RET* and lead to the juxtaposition of its intracellular tyrosine kinase domain to the 5′ portion of different donor genes [5, 6]. *RET*/PTC generates a novel amino-terminal portion and consecutively ligand-independent *RET* tyrosine kinase activation [7, 8]. The fusion protein of *RET*/PTC permits the binding of SHC and activation of RAS-RAF-MAPK cascade [9]. Although a number of *RET*/PTC subtypes have been reported so far, the main forms of *RET*/PTC are *RET*/PTC1 and *RET*/PTC3, resulting from paracentric inversion on chromosome 10q. The tyrosine kinase domains of *RET* fuses with *H4* (*RET*/PTC1) and *RFG/ELE1* (*RET*/PTC3) [6, 10, 11].

Table 1 Summary of clinicopathological features of 14 patients with papillary thyroid carcinoma

Case	Age/sex	Tumor size (mm)	LN METS	Subtype
1	53/F	18	+	Classical
2	64/F	17	−	Classical
3	49/F	11	+	Classical
4	43/F	12	+	Classical
5	62/M	20	+	Classical
6	34/F	32	+	Classical
7	46/M	15	−	Classical
8	36/F	25	+	Classical
9	52/M	31	na	Classical
10	46/F	10	+	Classical
11	56/F	10	+	Classical
12	51/F	50	+	Classical
13	53/F	13	−	Classical
14	61/F	11	na	Classical

na not available

Interpretation of *RET* rearrangements in thyroid cancers is still controversial. The high frequency of *RET* rearrangements in subclinical papillary microcarcinomas is consistent with these changes representing early events in the neoplastic process [12]. Meanwhile, heterogeneity of *RET* rearrangements in a single large tumor has been interpreted as indicating a relatively late event [13]. The low prevalence of expression of *RET*/PTCs in poorly differentiated and undifferentiated thyroid carcinoma might indicate a minor role in tumor progression [14, 15]. Furthermore, the prevalence rates of *RET* rearrangements in papillary thyroid carcinomas are considerably wide among investigators, raising a possibility of methodological differences [16].

In the current study, we applied interphase fluorescence in situ hybridization (FISH) analysis on touch cytology specimens to investigate the distribution of *RET* rearrangements in papillary carcinoma cells and also performed conventional reverse-transcription polymerase chain reaction (RT-PCR) analysis for both *RET*/PCT1 and *RET*/PTC3 using same tissue samples. We compared the different methodologies for detecting *RET* rearrangements and discussed heterogeneity in the prevalence of *RET*/PTCs in papillary thyroid carcinomas.

Materials and methods

Patients

We studied 14 surgical specimens from thyroid papillary carcinomas collected from the Yamanashi University Hospital. A thorough review of clinical data revealed nothing to suggest radiation exposure of the neck in any patients. Informed consent was obtained before resection in all patients. The pathological diagnoses were made on the basis of the second edition of *Histological Typing of Thyroid Tumours* (World Health Organization) [17]. Histologically, all thyroid papillary carcinomas studied for this report were the classical type of papillary carcinoma without foci of poorly differentiated and/or anaplastic components and more than 9 mm in size. Summary of clinicopathological features was shown in Table 1. Numbers of case listed in Table 1 are in accordance with those in Table 2.

Cell and tissue preparation

For FISH analysis and immunofluorescence, touch imprint cytology specimens were prepared from fresh tissue taken from the pure tumorous lesions and the normal tissues. Normal thyroid tissue samples are obtained from six patients who underwent subtotal or total thyroidectomy for papillary carcinomas (case nos. 1, 3, 4, 10, 11, and 13). They were fixed for 30 min with 95% ethanol and stored at −80°C. The formalin-fixed paraffin-embedded tissue was routinely processed for pathological diagnosis and RT-PCR analysis.

Microdissection and RNA extraction from paraffin-embedded tissue

Four serial sections, 10 μm thick, were cut from routinely processed, formalin-fixed, and paraffin-embedded tissue blocks. These sections were stained with hematoxylin after deparaffinization. Microscopically comparing the sections for orientation, each tumor tissue was microdissected with a

Table 2 Population of tumor cells with *RET*/PTC and *RET*/PTC by RT-PCR in 14 papillary thyroid carcinomas

Cases	FISH Rearranged cell population (%)	RT-PCR
1	6.0	+ (PTC1)
2	18.8	+ (PTC1)
3	19.6	+ (PTC1)
4	11.9	+ (PTC1)
5	9.4	−
6	6.5	−
7	2.9	−
8	12.2	−
9	1.8	−
10	9.9	−
11	7.8	−
12	0	−
13	0	−
14	0	−

disposable syringe needle under a stereomicroscope, as previously described [1]. Total RNA was extracted using the acid guanidinium–phenol–chloroform system (ISOGEN PB Kit, NipponGene, Toyama, Japan) according to the manufacturer's instructions.

Reverse-transcription polymerase chain reaction analysis

One microgram of total RNA was reverse-transcribed (RT) using Moloney murine leukemia virus reverse transcriptase (Wako, Osaka, Japan) primed with random hexamers (Roche, Tokyo, Japan). All RT reactions were performed at 25°C for 10 min, 42°C for 45 min, and 95°C for 5 min. After RT reactions, amplification of complementary DNA corresponding to *RET*/PTC1 and *RET*/PTC3 was performed by PCR using a thermal cycler. The primary and nested amplifications were performed as previously described [1].

The human thyroid cancer cell line, TPC-1, kindly provided by Dr. Noboru Takamura, Nagasaki University, served as positive control for *RET*/PTC1 [18]. Amplification of glyceraldehyde-3-phosphate dehydrogenase was used as quality control for RNA integrity.

Immunofluorescence

Monoclonal mouse antithyroid transcription factor (TTF) 1 antibody (ZYMED Laboratories, CA, USA) was used as a primary antibody. After a 60-min incubation with the primary antibody, the sections were incubated with a 1:100 dilution of rhodamine-labeled goat antimouse F $(ab)'_2$ fragment (DAKO, Hamburg, Germany) in 1% phosphate saline buffer containing bovine serum albumin. After a 30-min incubation, images were obtained with a fluorescence microscope IX71 (Olympus, Tokyo, Japan) and a scientific-grade, cooled, charge-coupled device camera, Sensys (Photometric, Tucson, AZ, USA), connected to a personal computer.

Multicolor fluorescence in situ hybridization

Figure 1 shows the color scheme for the multicolor FISH strategy using *RET*-, *H4*-, and chromosome-10-specific DNA probes to detect *RET* rearrangements. After microscopic observation for fluorescence of TTF-1, the preparations were refixed with 95% ethanol overnight. FISH was performed on the same preparations using bacterial artificial chromosome clones: RP11-351D16 (Advanced Geno Tech Co.), spanning the entire region of *RET* proto-oncogene, and RP11-368L1 (Advanced Geno Tech Co. Japan) containing the telomeric region of *H4*. DNA was extracted and labeled with digoxigenin-11-dUTP (RP11-351D16) and biotin-16-dUTP (RP11-368L1) by nick translation (Vysis Inc; Downers Grove, IL, USA). Whole chromosome 10 probe labeled with Cy3 (Cambio Ltd., Cambridge, UK) was used to confirm the locations of these genes. The preparations were then pretreated and subjected to hybridization with the DNA probes and detected with antibodies labeled with fluorescein isothiocyanate (FITC; RP11-351D16) and Alexa 647 (RP11-368L1). Nuclei were counterstained with 4′,6-diamiono-2-phenylindole (DAPI). We used normal (46, XY) Metaphase CGH Target Slides (Vysis Inc.; Downers Grove, IL, USA) as control to verify the specificity of above-mentioned DNA probes. Two and four FISH signals were observed in the nuclei in interphase and metaphase cells, respectively.

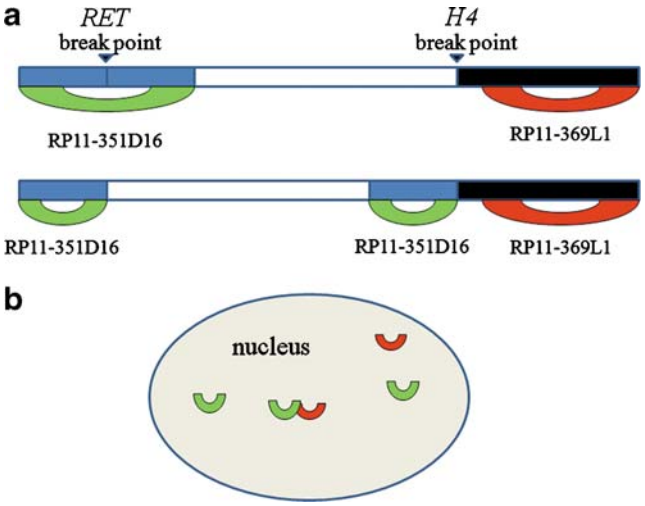

Fig. 1 Scheme of the multicolor FISH strategy to detect *RET*/PTC1. **a** Paracentric inversion on chromosome 10q (inv(10)(q11.2 q21)) suggests *RET*/PTC1 (break point, *arrow head*). *RET* (*blue*)—specific DNA probe covers the entire region of *RET* (RP11-351D16, *green*). *H4* (*black*)—specific DNA probe covers the telomeric region of H4 (RP11-369L1, *red*). **b** The nucleus having *RET* rearrangements is designed to demonstrate attachment of one split signal suggesting *RET* (*green*) and one signal suggesting H4 (*red*)

After staining by the immunofluorescence method for TTF-1 and prior to interphase FISH, we took pictures at low and high magnifications. During fluorescence microscopy of FISH, we searched the same areas at low magnification and identified the same nuclei comparing the immunofluorescence images. We estimated FISH signals only in isolated tumor cells because of the difficulty in estimating these signals in clustered or overlapping tumor cells. We counted 217–267 cells (average 225.6) per tumor and 211–253 cells (average 227.3) per normal thyroid tissue.

Statistic analysis

Statistic analysis was carried out using Fisher's exact test, comparing prevalence rates of the *RET* rearrangements as determined by FISH and RT-PCR. To compare the pairs of means of tumor cells with *RET* rearrangements, Student *t* test was used with a significance level of 5%.

Results

Prevalence rate of *RET* rearrangements

It is difficult to discriminate tumor cell nuclei from nontumor cells such as stromal fibroblasts, vascular endothelium, and inflammatory cells on interphase FISH examination using touch imprint cytology. Therefore, we performed immunofluorescent staining for TTF-1, a marker of thyroid follicular cells, on the same preparation prior to interphase FISH analysis to evaluate the cancer cell population with *RET* rearrangements. TTF-1 was diffusely positive in the large and irregular-shaped nuclei, suggesting papillary thyroid carcinoma cells (Fig. 2b, d).

Interphase FISH analyses with the *RET*-specific DNA probe were performed in 12 papillary carcinomas. By using this method, *RET* gene rearrangements were seen as three signals (Figs. 2a and 3a) and lack of *RET* gene rearrangements as two signals (Figs. 2b and 3a) in the nuclei of tumor cells.

On interphase FISH analysis, the tumor cells with split signals, suggesting *RET* rearrangements, were demonstrated in 11 of 14 papillary thyroid carcinomas (78.6%). We observed split signals in none of the nuclei of the non-tumorous follicular cells from the six normal thyroid tissues.

In contrast, RT-PCR analyses with specific primers for *RET*/PTC1 and *RET*/PTC3 revealed that *RET*/PTC1 was detected in four (28.6%) tumors and *RET*/PTC3 in no tumors (Table 2, Fig. 4). The prevalence rate of *RET* rearrangements (78.6%) as determined by interphase FISH was significantly higher than that (28.6%) by RT-PCR ($p < 0.05$). All four papillary thyroid carcinomas that were positive for *RET*/PTC1 by RT-PCR were also positive by interphase FISH. However, RT-PCR analysis did not detect *RET*/PTCs in seven papillary carcinomas which were positive by interphase FISH (Table 2).

Tumor cell population having *RET* rearrangements

Interphase FISH analysis suggested that tumor cells with and without *RET* rearrangements coexisted in the same tumor (Fig. 3a). Therefore, we assessed the percentage of rearranged cells in 11 papillary thyroid carcinomas having *RET* rearrangements. The percentage of rearranged tumor cells were ranged from 1.8% to 19.6% (average 9.7%), indicating that majority of tumor cell were nonrearranged cells in all 11 tumors (Table 2).

In four papillary carcinomas with *RET* rearrangements detected by both RT-PCR and interphase FISH, the population of rearranged tumor cells ranged from 6.0% to 19.6% (average 14.1%). In contrast, in the seven papillary thyroid carcinomas with *RET* rearrangements demonstrated by interphase FISH alone, the population of rearranged

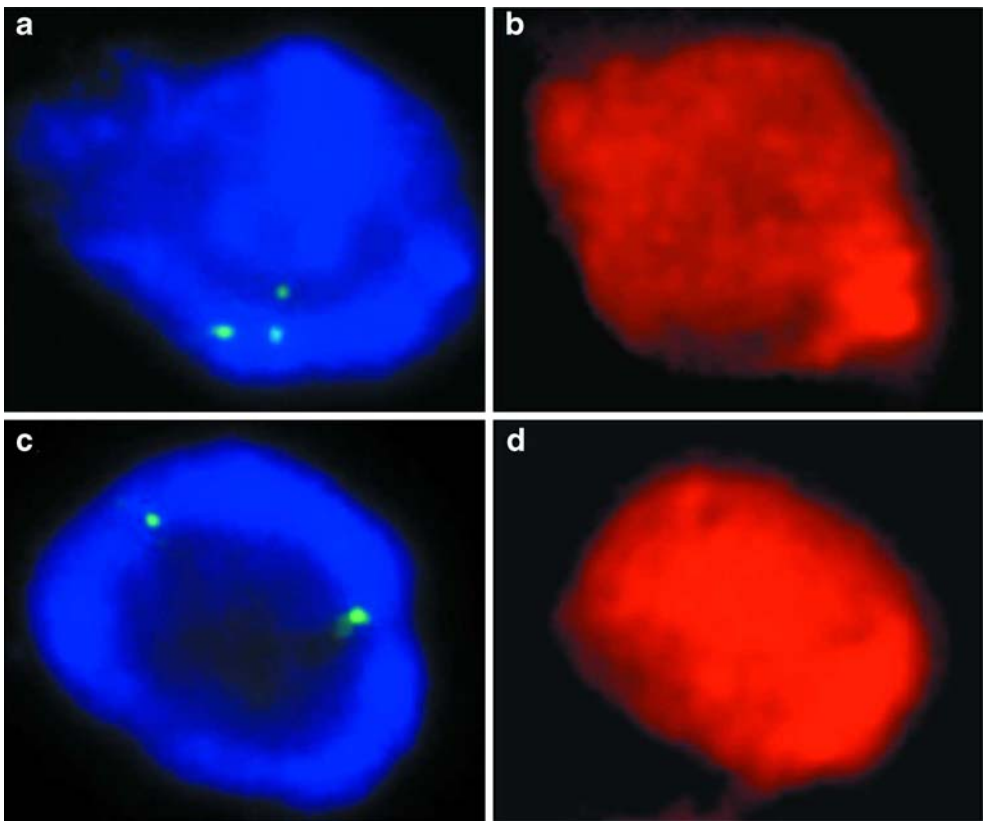

Fig. 2 Immunofluorescence microscopic findings of interphase FISH analysis with the *RET*-specific DNA probe and immunofluorescence for TTF-1 performed in the same nuclei of the papillary thyroid carcinoma cells. **a** A nucleus stained with DAPI (*blue*) having three FISH signals (FITC, *green*) suggests *RET* rearrangement. **b** Same nuclei showing immunopositivity for TTF-1 (rhodamine, *red*). **c** A nucleus stained with DAPI (*blue*) having two FISH signals (FITC, *green*) suggests lack of *RET* rearrangement. **d** Same nuclei showing immunopositivity for TTF-1 (rhodamine, *red*) TTF-1, thyroid transcription factor-1; *DAPI*, 4′,6-diamiono-2-phenylindole; *FITC*, fluorescein isothiocyanate

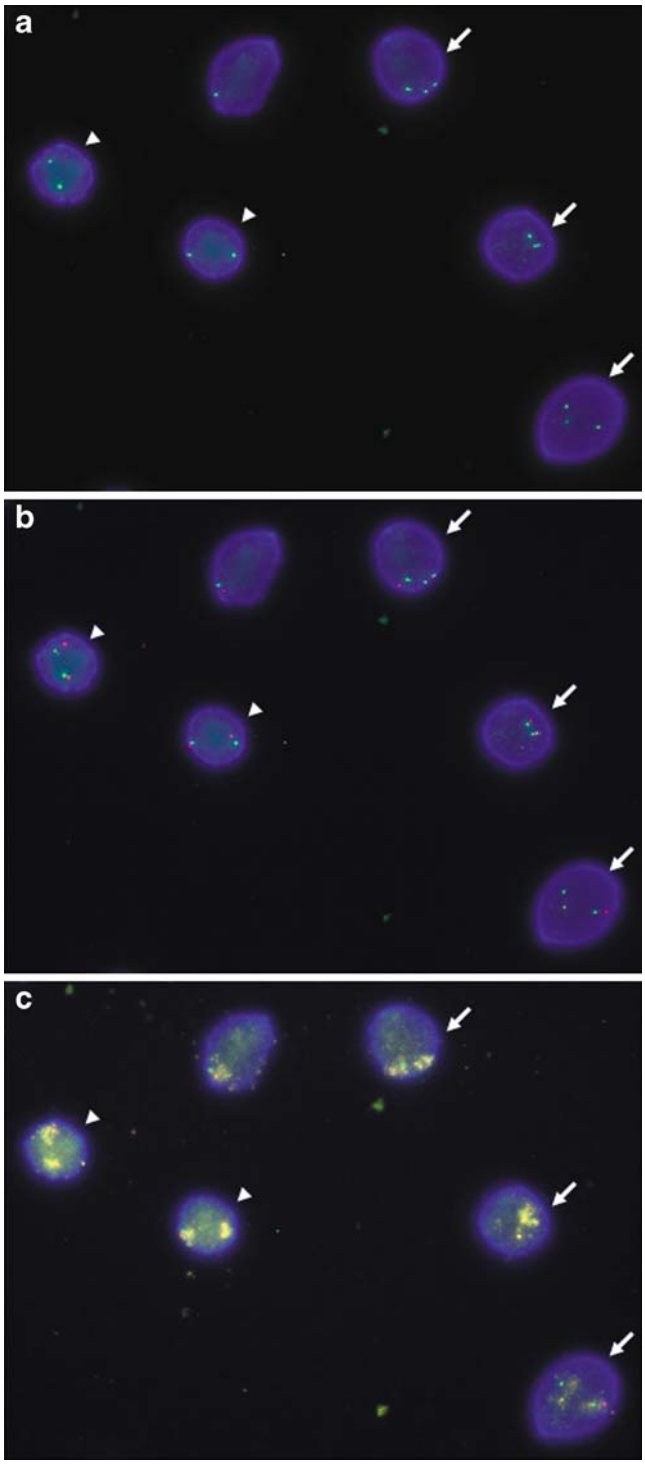

Fig. 3 Multicolor FISH analysis using *RET*- and *H4*-specific DNA probes and whole chromosome-10-specific probe in the same nuclei of a papillary thyroid carcinoma. **a** Tumor cell nuclei with three RET gene signals suggesting *RET* rearrangement (*arrows*) and with two *RET* gene signals suggesting lack of *RET* rearrangement (*arrow head*) are intermingled. **b** One *H4* gene signal (*red*) is attached to a *RET* gene signal (*green*), suggesting *RET*/PTC1 in the rearranged tumor cell nuclei (*arrow*). **c** All signals of *RET* and *H4* genes are located in chromosome 10. *RET* gene signal: FITC, *green*; *H4* gene signal: Alexa 647, *red*; chromosome 10 signal: Cy3, *yellow*

tumor cells ranged from 1.8% to 12.2% (average 7.2%). Although the population of tumor cells with *RET* rearrangements was greater in the former group (detected by both RT-PCR and interphase FISH) than in the latter group (detected by interphase FISH alone), it was not a statistically significant difference in the rearranged tumor cell population between these two groups.

Interphase FISH analysis for *RET*, *H4*, and chromosome 10

We also performed multicolor FISH analyses using *RET*-, *H4*-, and chromosome-10-specfic DNA probes in the cases positive for *RET*/PTC1 by RT-PCR. Multicolor imaging for FISH signals in rearranged tumor cells revealed that one of three *RET* signals attached to one signal of *H4*, and all these signals were located in chromosome 10, suggesting *RET*/PTC1 (Fig. 3b, c).

Discussion

RET rearrangements (*RET*/PTC) in papillary thyroid carcinomas have been studied by RT-PCR using formalin-fixed and paraffin-embedded tissues [1, 16]. The reported prevalence rates of *RET*/PTC in papillary thyroid carcinomas extensively varied from 0% to 85% between studies [19, 20]. It is conceivable that this wide range of prevalence in RT-PCR analysis is due, in part, to technical or methodological factors. For example, degradation of RNA during processing tissues through formalin fixation and paraffin embedment or the difficulties in discriminating tumor cells and interstitial cells largely affect the results.

Touch imprint cytology specimens fixed with ethanol have some advantages for evaluating exact prevalence rates of *RET* rearrangement. On FISH analysis, cytology specimens allow us to observe the exact number of FISH signals in the whole cell nucleus. In addition, it is important that nucleic acids are well preserved in cells with ethanol fixation. Therefore, we employed interphase FISH analysis on touch cytology specimens from 14 papillary thyroid carcinomas to detect *RET* rearrangements.

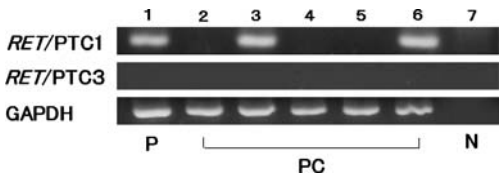

Fig. 4 Representative results of *RET*/PTC1 and *RET*/PTC3 detected by RT-PCR analysis in papillary thyroid carcinomas (PC; *lanes 2–6*). Positive bands for *RET*/PTC1 are shown in *lanes 3* and *6*. No bands for *RET*/PTC3 were demonstrated. *Lane 1* (*P*) is positive control for *RET*/PTC1 (TPC-1 cell line) and *lane 7* (*N*) is negative control (no template)

In the current study, interphase FISH analysis revealed a high prevalence rate (78.6%, 11/14) of *RET* rearrangements. To date, as shown in Table 3, there has been five papers on *RET* rearrangements in papillary thyroid carcinomas using interphase FISH analysis [13, 21–24]. The prevalence rates of *RET* rearrangements in these studies varied from 33.3% to 92.3%. Therefore, our data were not too high compared to other previous reports. We also performed RT-PCR analyses with the specific primers for *RET*/PTC1 and *RET*/PTC3 and found that *RET*/PTC1 was detected in 28.6% of papillary thyroid carcinomas. The prevalence rate of *RET*/PTC as determined by RT-PCR was apparently lower than that by interphase FISH.

Several explanations are raised to explain the discrepant prevalence between FISH and RT-PCR in papillary thyroid carcinomas. In this study, RT-PCR analysis was performed with primers targeting *RET*/PTC1 and *RET*/PTC3, while interphase FISH, with the probe covering the whole region of *RET*, might pick up the other types of *RET*/PTC rearrangements. The other possible reason is that interphase FISH can detect small number of cells with DNA rearrangement, while the messenger RNA transcript of the gene rearrangements would be undetectable by RT-PCR when the population of rearranged cell is small. Therefore, it is not surprising that interphase FISH is more sensitive than RT-PCR in detecting *RET* rearrangements.

In the previous studies using the FISH procedures, they used the cutoff levels (less than 10%) in the estimation of *RET*/PTC for tumor tissues because *RET*/PTC was observed in a small number of the nuclei of the nontumorous thyroid tissues. In this FISH study, we did not recognize *RET*/PTC in the nuclei of the nontumorous follicular cells despite of careful microscopic observations and, therefore, no cutoff level was set to elucidate *RET*/PTC in tumor tissues. It has been reported that variable stimuli, such as Hashimoto's thyroiditis and irradiation, induce genetic instability (*RET*/PTC) in nonneoplastic follicular cells [22, 25]. We have reassessed the histological and clinical findings of normal control and found Hashimoto's thyroiditis in none of the patients for normal control. We have also verified that none of the patients had neck irradiation.

The mean tumor cell populations containing *RET*/PTC has been reported to range from 9.8% to 54%. In the current study, the percentage of tumor cells with *RET*/PTC was rather low in papillary thyroid carcinomas, ranging from 1.8% to 19.6% (mean 9.7%). These data suggested that most papillary thyroid carcinomas with *RET* rearrangements are comprised of nonrearranged tumor cell. Unger et al. [13] described that this genetic heterogeneity of *RET*/PTC can be interpreted in two different ways: *RET*/PTC is the first event with new clones emerging later or *RET*/PTC is, at least in some carcinomas, a late event in thyroid carcinogenesis. Of these two hypotheses, the latter hypothesis could be more likely because the population of *RET* rearranged cells is small in all papillary thyroid carcinomas examined.

Recently, "driver and passenger" theory is discussed in cancer genomics [26, 27]. Cancer cells carry the DNA abnormalities that initiate malignant proliferation and induce additional genetic events. Some of these secondary mutations will be accelerating pathogenic factors during the cancer progression (driver mutation), while others may be incidental abnormalities as nononcogenic or less oncogenic (passenger mutation), resulting from mutational exposures, genome instability, or simply the large number of cell doublings. Flavin et al. found the presence of *RET* rearrangements in a small population of primary peritoneal carcinomas by FISH analysis. They presumed that *RET* rearrangements in peritoneal carcinomas represent as "passenger mutation" reflecting *RET* instability in subclone rather than oncogenic mutation [28]. These observations lead us to conjecture that some of *RET* rearrangements reflect passenger mutation in thyroid cancers, congruent with low prevalence of *RET* rearrangements in poorly and undifferentiated thyroid carcinomas. However, our previous study confirmed restrictive detection of *RET*/PTCs in papillary carcinoma among thyroid neoplasms. Furthermore, thyroid-targeted expression of *RET*/PTC1or *RET*/PTC3 induces thyroid neoplasms in transgenic mice. These

Table 3 Reported prevalence rates and cell populations of *RET*/PTC in papillary thyroid carcinomas examined by interphase FISH analysis

Authors (years)	No. of case	% of positive cases (cutoff %)	Mean cell population (%) in positive cases	Radiation	Specimen
Cinti et al. (2000) [21]	69	18.8 (10)/33.3 (5)	NA	−	Cytology
Zhu et al. (2006) [24]	26	53.8 (9)	54.1	−	Cytology
Rhoden et al. (2006) [22]	26	92.3 (3.5)	9.8	−	Histology
Unger et al. (2004) [13]	30	71.9 (7.1)	14.3	+	Histology
Unger et al. (2006) [23]	44	81.8 (7.1)	17.2	+	Histology
Current study	14	78.6 (0)	9.7	−	Cytology

NA not available

findings implies oncogenic roles *RET* rearrangements in thyroid carcinomas, conflicting with the idea of passenger mutation.

In conclusion, we disclosed that *RET* rearrangements occur in a small population of tumor cells in papillary thyroid carcinomas using interphase FISH analysis on touch imprint cytology. Even though *RET*/PTCs is a specific genetic event in papillary thyroid carcinomas, heterogeneity of *RET* rearrangements, shown in the present study, implies *RET* rearrangements is subclonal event. Our results raised the possibility of *RET* rearrangements as "passenger" abnormalities rather than "driver" oncogenic mutation on thyroid carcinogenesis, warranting further studies on mechanisms and implication of *RET* gene instability.

Acknowledgements The authors thank Ms. Miyuki Ito, Ms. Mikiko Yoda, and Mr. Yoshihito Koshimizu for their excellent technical assistance and Ms. Kayoko Kono for executive assistance. This work was supported by the Ministry of Education, Culture, Sports, Science, and Technology, Japan: Grant in-Aid for Young Scientists (17790232) for Tadao Nakazawa.

Conflict of interest statement We declare that we have no conflict of interest.

References

1. Nakazawa T, Kondo T, Kobayashi Y et al (2005) RET gene rearrangements (RET/PTC1 and RET/PTC3) in papillary thyroid carcinomas from iodine-rich country (Japan). Cancer 104:943–953
2. Kondo T, Ezzat S, Asa SL (2006) Pathogenic mechanisms in thyroid-follicular cell neoplasia. Nat Rev Cancer 6:292–306
3. Nikiforov YE (2008) Thyroid carcinoma: molecular and therapeutic targets. Mod Pathol 21:S37–S43
4. Airaksinen MS, Titievsky A, Saarma M (1999) GDNF family neurotrophic factor signaling: four masters, one servant? Mol Cell Neurosci 13:313–325
5. Takahasi M, Ritz J, Cooper GM (1985) Activation of a novel transforming gene, ret, by DNA rearrangements. Cell 42:581–588
6. Grieco M, Santoro M, Berlingieri MT et al (1990) PTC is a novel rearrangement form of the *ret* proto-oncogene and is frequently detected in vivo in human thyroid papillary carcinomas. Cell 60:557–563
7. Tong Q, Xing S, Jhiang SM (1997) Leucine zipper-mediated dimerization is essential for the PTC1 oncogenic activity. J Biol Chem 272:9043–9047
8. Jhiang SM (2000) The RET proto-oncogene in human cancers. Oncogene 19:5590–5597
9. Knauf JA, Kuroda H, Basu S et al (2003) RET/PTC-induced dedifferentiation of thyroid cells is mediated through Y1062 signaling through SHC-RAS-MAP kinase. Oncogene 22:4406–4412
10. Santoro M, Dathan NA, Berlingieri MT et al (1994) Molecular characterization of RET/PTC3: a novel rearranged version of the RET proto-oncogene in a human thyroid papillary carcinoma. Oncogene 9:509–516
11. Bongarzone I, Butti MG, Coronelli S et al (1994) Frequent activation of ret proto-oncogene by fusion with a new activating gene in papillary thyroid carcinomas. Cancer Res 54:2979–2985
12. Viglietto G, Chiappetta G, Martinez-Tello FJ et al (1995) RET/PTC oncogene activation is an early event in thyroid carcinogenesis. Oncogene 21:1207–1210
13. Unger K, Zitzelsberger H, Salvatore G et al (2004) Heterogeneity in the distribution of RET/PTC rearrangements within individual post-Chernobyl papillary thyroid carcinomas. J Clin Endocrinol Metab 89:4272–4279
14. Santro M, Papotti M, Chiapetta M et al (2002) RET activation and clinicopathologic features in poorly differentiated thyroid tumors. J Clin Endocrinol Metab 87:370–379
15. Tallini G, Santoro M, Helie M et al (1998) RET/PTC oncogene activation defines a subset of papillary thyroid carcinomas lacking evidence of progression to poorly or undifferentiated tumor phenotypes. Clin Cancer Res 4:287–294
16. Nikiforov YE (2002) RET/PTC rearrangement in thyroid tumors. Endocr Pathol 13:3–16
17. Hedinger H, Williams ED, Sobin LH (1988) Histological classification of thyroid tumors. In: Hedinger C, Williams ED, Sobin LH (eds) Histological typing of thyroid tumors. World Health Organization international histological classification of tumours, 2nd edn. Springer, Paris, pp 3–18
18. Ishizuka Y, Ushijima T, Sugimura T, Nagao M (1990) cDNA cloning and characterization of ret activated in a human papillary thyroid carcinoma cell line. Biochem Biophys Res Commun 168:402–408
19. Namba H, Yamashita S, Pei HC et al (1991) Lack of PTC gene (*ret* proto-oncogene) in human thyroid tumors. Endocrinol Jpn 38:627–632
20. Chua EL, Wu WM, Tran KT et al (2000) Prevalence and distribution of *ret*/ptc 1, 2, and 3 in papillary thyroid carcinoma in New Caledonia and Australia. J Clin Endocrinol Metab 85:2733–2739
21. Cinti R, Yin L, Ilic K et al (2000) RET rearrangements in papillary thyroid carcinomas and adenomas detected by interphase FISH. Cytogenet Cell Genet 88:56–61
22. Rhoden KJ, Unger K, Salvatore G et al (2006) RET/papillary thyroid cancer rearrangement in nonneoplastic thyrocytes: follicular cells of Hashimoto's thyroiditis share low-level recombination events with a subset of papillary carcinomas. J Clin Endocrinol Metab 91:2040–2042
23. Unger K, Zurnadzhy L, Walch A et al (2006) RET rearrangements in post-Chernobyl papillary thyroid carcinomas with a short latency analyzed by interphase FISH. Br J Cancer 94:1472–1477
24. Zhu Z, Ciampi R, Nikiforova MN, Gandhi M, Nikiforov YE (2006) Prevalence of RET/PTC rearrangements in thyroid papillary carcinomas: effects of the detection methods and genetic heterogeneity. J Clin Endocrinol Metab 91:3603–3610
25. Caudill CM, Zhu Z, Ciampi R, Stringer JR, Nikiforov YE (2005) Dose-dependent generation of RET/PTC in human thyroid cells after in vitro exposure to gamma-radiation: a model of carcinogenic chromosomal rearrangement induced by ionizing radiation. J Clin Endocrinol Metab 90:2364–2369
26. Lui ET (2008) Functional genomics of cancer. Curr Opin Genet Dev 18:251–256
27. Haber DA, Settleman J (2007) Cancer: drivers and passengers. Nature 446:145–146
28. Flavin R, Jackl G, Finn S et al (2009) RET/PTC rearrangements occurring in primary peritoneal carcinoma. Int J Surg Pathol 17:187–197

Virchows Arch (2009) 455:43–48
DOI 10.1007/s00428-009-0786-y

ORIGINAL ARTICLE

Tenascin C in medullary thyroid microcarcinoma and C-cell hyperplasia

Oskar Koperek · Astrid Prinz · Christian Scheuba · Bruno Niederle · Klaus Kaserer

Received: 5 March 2009 / Revised: 24 April 2009 / Accepted: 27 April 2009 / Published online: 30 May 2009

Abstract Tenascin C (Tn-C) is an extracellular matrix glycoprotein that is expressed early in carcinogenesis including intraepithelial neoplastic lesions of different organs. In this study, we analyze whether stroma reaction seen by Tn-C expression is detected early in tumorigenesis of medullary thyroid carcinoma (MTC) including medullary microcarcinoma and C-cell hyperplasia (CCH), which is accepted to be a precursor lesion of MTC in the setting of RET oncogene germ-line mutation. Tn-C was expressed in the stroma of all medullary microcarcinoma and in the stroma next to CCH. Stromal Tn-C expression was significantly more often seen in CCH with concomitant MTC than in isolated CCH of hereditary as well as nonhereditary cases (p=0.001 and p=0.016, respectively). We conclude that Tn-C expression and thus early stroma remodeling is seen in medullary microcarcinoma and CCH. Stromal Tn-C expression seems to be an indicator of a further step in carcinogenesis of MTC irrespective of a RET oncogene germ-line mutation.

Keywords Medullary thyroid carcinoma · C-cell hyperplasia · Tenascin C

Introduction

Molecular genetic studies, calcitonin screening, and the resulting prophylactic thyroidectomies allowed studying early C-cell lesions including medullary thyroid microcarcinoma and C-cell hyperplasia (CCH) in familial but also sporadic cases [1–5].

In the setting of RET oncogene germ-line mutation, CCH is accepted to be a precancerous lesion. Results of several studies indicate an age-related progression of C-cell lesions from CCH towards medullary thyroid carcinoma (MTC) in patients with germ-line mutations of the RET oncogene [6–8]. In nonhereditary (sporadic) cases, the role of CCH in carcinogenesis is discussed controversially [5, 9–11]. Perry et al. suggested that only CCH of hereditary cases show morphologic atypia, and nonhereditary, so-called reactive CCH do not [9]. However, other authors did not find morphologic differences between CCH of hereditary and nonhereditary cases, indicating that CCH might be a precursor of MTC in a sporadic setting as well [5, 12, 13].

In MTC, we could show that only tumors with a desmoplastic stroma reaction may show lymph node metastasis and hence concluded that stroma remodeling might play an important role in the progression of MTC [14–16]. However, its role in the early tumorigenesis in MTC is not analyzed.

An extracellular matrix glycoprotein expressed in the stroma of malignant tumors including MTC is tenascin C (Tn-C) [15, 17, 18]. It promotes cell migration, inhibits cell adhesion to fibronectin, and induces tumor proliferation and metastasis in model systems [19–22]. Tenascin C is expressed early in carcinogenesis including intraepithelial neoplastic lesions of various organs such as breast (DCIS), prostate (PIN), vulva (VIN), and cervix (CIN) [23–26]. Hence, it is considered an indicator of early stroma remodeling in carcinogenesis.

The aim of this study was to investigate Tn-C expression systematically in medullary thyroid microcarcinoma as well as in concomitant and isolated CCH in sporadic and hereditary cases.

O. Koperek · A. Prinz · K. Kaserer (✉)
Department of Clinical Pathology, Medical University of Vienna, Währinger Gürtel 18-20, 1090 Vienna, Austria
e-mail: klaus.kaserer@meduniwien.ac.at

C. Scheuba · B. Niederle
Section of Endocrine Surgery, Division of General Surgery, Department of Surgery, Medical University of Vienna, Vienna, Austria

Materials and methods

Case selection

Seventy-seven cases of isolated C-cell hyperplasia and 70 cases of medullary thyroid microcarcinoma were obtained from the Department of Clinical Pathology of the Medical University of Vienna. Clinicopathologic data including gender, age, and lymph node status were available. Additionally, all cases were examined for germ-line mutations in exons 8, 10, 11, 13, 14, 15, and 16 of the RET proto-oncogene as described by Fink et al. [27].

One hundred thirty-three of 147 cases were retrieved from a consecutive series where basal calcitonin levels were routinely measured in patients with thyroid and parathyroid disorders who were referred to the Department of Surgery at the University of Vienna. An elevated basal calcitonin level and an abnormal pentagastrin-stimulated calcitonin level indicated surgical removal. For calcitonin measurements, either a modified two-site radioimmunometric assay (CIS-Biointernational, Gif-sur-Yvette, France) or a chemiluminescence immunoassay (Nichols Institute Diagnostics, San Clemente, CA, USA) was used as described [4, 28, 29]. In three nonfamilial cases (one case of MTC and two cases of CCH), normal basal calcitonin level was detected, but suspect nodular lesion of the thyroid led to the surgical procedure. In 11 cases (seven cases of MTC and four cases of CCH), prophylactic total thyroidectomy was performed based on the known germ-line mutation of the RET proto-oncogene. In the other hereditary cases including six cases with isolated CCH, elevated basal calcitonin level and an abnormal pentagastrin-stimulated calcitonin level indicated surgical removal.

Total thyroidectomy was done in each case. The thyroid gland was cut in 2–3 mm sections, fixed in 4% formaldehyde, and embedded in paraffin. Serial 3 μm sections were cut and used for histopathological and immunohistochemical evaluation. One section of each block was stained with hematoxylin–eosin. In addition, we performed immunohistochemical staining with antibodies against calcitonin (monoclonal mc, Chemicon, Temecula, California, USA, 1:600) for all blocks and additionally Tn-C (TN2, mc, DAKO, Golstrup, Denmark, 1:200) in representative blocks of the medullary microcarcinoma and of the CCH. In four cases, Tn-C expression could not be investigated in MTCs as the small tumors were not seen on the consecutive sections. The lymph node metastasis were not investigated by Tn-C immunohistochemistry.

Antigen retrieval for Tn-C was performed by incubating 10 min in protease X. Slides were incubated at room temperature for 1 h with the primary antibodies followed by incubation with biotinylated secondary antibodies and the avidin–biotin peroxidase complex (ABC) using the Vectastin ABC kit (Vector Laboratories, Burlingame, CA, USA). The final reaction was visualized with 3,3′ diaminobenzidine. Sections were counterstained with Harris' hematoxylin. Negative controls included omission or substitution of primary antibodies by nonspecific, isotype-matched antibodies.

Histomorphology

C-cell hyperplasia is defined by more than 50 C cells in a low-power field (magnification, ×100) in both thyroid lobes [5]. For the C-cell count, the calcitonin immunostained sections were scanned at low magnification (×40), and the area with the highest density (hot spot) of C cells was selected. The C-cell count was determined by counting all C cells per low-power field (×100 magnifications, area of 3.33 mm^2).

Medullary thyroid microcarcinoma was defined as an MTC according to the WHO criteria [30] and a tumor diameter of 1 cm or less.

Statistical evaluation

For statistical analysis, the SPSS program (SPSS, Chicago, IL, USA) was used. Tn-C expression was correlated with gender, age, calcitonin level, and number of C cells in isolated and concomitant CCH. Tenascin C expression was considered as positive whenever an expression is seen in the extracellular matrix surrounding C cells in at least one focus of C cells (stromal Tn-C expression) or when it was seen within C cells (intracellular Tn-C expression). Both expression patterns were calculated separately. Familial (hereditary) and nonfamilial (sporadic) cases were analyzed separately. For statistical analysis, qui-quadrate calculations and Student's t test were applied whenever appropriate. A two-tailed p value of <0.05 was considered as significant.

Results

Patients data

Hereditary cases

Ten of 77 cases of isolated CCH and 30/70 cases of MTC showed germ-line mutations in the RET proto-oncogene. Different mutations in the exons 10, 11, 13, 14, and 15 were detected (see Table 1).

The ten cases of isolated CCH consisted of seven male and three female patients with a mean age of 39±22 years, ranging from 6 to 69 years. The 30 cases of medullary thyroid microcarcinoma consisted of 14 male and 16 female patients with a mean age of 45±22 years, ranging from 5 to 80 years.

Table 1 Stromal tenascin C expression next to CCH in hereditary cases

RET-oncogene germ-line mutation (exon/codon mutation)	Isolated CCH	Concomitant CCH	Patients age in years (isolated and concomitant CCH)
10/611 TGC-TAC		1/2	42, 56
10/611 TGC-TGG	0/3	1/1	23, 34, 36, and 80
10/620 TGC-CGC	1/2	2/2	6, 7 and 36, 38
10/620 TGC-TAC		1/1	19
11/634 TGC-AGC		1/1	8
11/634 TGC-CGC		4/4	5, 11, 34, 39
13/791 TAT-TTT	1/4	0/1	48, 55, 66, 69, and 69
14/804 GTG-ATG		8/8	26, 28, 55, 58, 58, 69, 71, 76
15/891 TCG-GCG	1/1	4/5	43 and 11, 50, 52, 72
15/907 AAG-ATG		2/2	24, 29

CCH C-cell hyperplasia

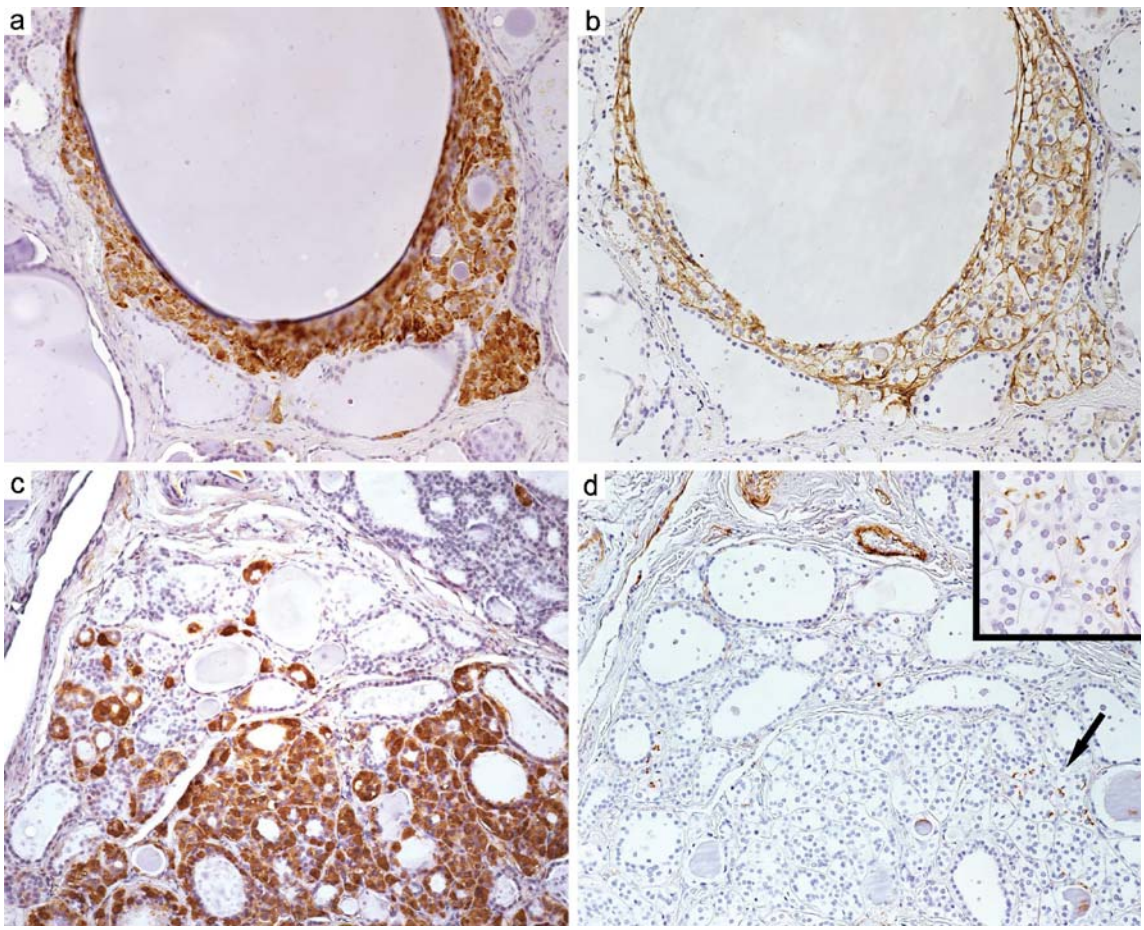

Fig. 1 Tenascin C immunoreactivity in C-cell hyperplasia. **a** Calcitonin immunoreactivity in C cells of an isolated C-cell hyperplasia in a patient without RET oncogene germ-line mutation (magnification, ×40). **b** Prominent stromal tenascin C expression in an adjacent section of the C-cell hyperplasia (magnification, ×40). **c** Calcitonin immunoreactivity in C cells of an isolated C-cell hyperplasia in a patient without RET oncogene germ-line mutation (magnification, ×40). **d** Intracellular tenascin C expression in C cells (enlarged in the *upper right corner*) but lack of stromal tenascin C expression in an adjacent section of the C-cell hyperplasia (magnification, ×40; enlargement in the *upper right corner*, ×400)

Sporadic cases

The 67 cases of isolated CCH consisted of 55 male and 12 female patients with a mean age of 55±11 years, ranging from 23 to 75 years. The 40 cases of medullary thyroid microcarcinoma consisted of 25 male and 15 female patients with a mean age of 61±12 years, ranging from 26 to 82 years.

Histomorphology

Hereditary cases

In the 30 cases of micro-MTC, the mean tumor diameter was 4.4±2.7 mm, ranging from 1 to 10 mm. Six of 30 (20%) MTCs had metastasized to the regional lymph nodes. Concomitant CCH was seen in 27/30 (90%) cases. In all cases, the concomitant CCH was seen in close proximity to an MTC. The mean number of C cells was 337±169 ranging from 97 to 751. Tenascin C expression was seen in the stroma of all investigated MTCs and in the stroma of the concomitant CCH in 89% (24/27). In MTC, the stromal tenascin expression was often accentuated at the peritumoral invasion front. Tenascin expression in CCH was seen in the stroma surrounding non-invasive C-cell clusters.

In the ten patients with isolated CCH, the mean number of C cells was 497±271 ranging from 195 to 1,025. Stromal Tn-C expression next to isolated CCH was observed in 30% (3/10) of the cases (Table 1). The expression pattern of stromal tenascin C did not differ from the pattern seen in concomitant CCH.

The difference in the frequency of stromal Tn-C expression comparing isolated and concomitant CCH was significant (p= 0.001). Stromal Tn-C expression was not correlated with gender, age, calcitonin level, and number of C cells.

Intracellular Tn-C immunoreactivity of C cells was detected in 2/27 (5%) concomitant and in 1/10 (10%) isolated CCH and additionally in invasive C cells of 2/28 (7%) MTC. No correlation was seen between intracellular Tn-C expression with any of the investigated clinicopathologic parameters and stromal tenascin expression.

Seventeen of forty specimens showed nodular goiter. Inflammatory thyroid disease was seen in 5/40 cases, and nonmedullary neoplastic diseases was observed in three cases (one follicular adenoma, two papillary thyroid carcinomas—both microcarcinomas).

Sporadic cases

Concerning the 40 cases of medullary thyroid microcarcinoma, the mean tumor diameter was 4±2.9 mm, ranging from 0.5 to 10 mm. Five of the 40 (13%) MTCs had metastasized to the regional lymph nodes. Concomitant CCH was seen in 32/40 (80%) cases. In all cases, concomitant CCH was seen in the vicinity of the MTC. The mean number of C cells was 445±299 ranging from 61 to 1,259.

Tn-C expression was seen in the stroma of all investigated MTCs and in the stroma next to concomitant CCH in 78% (25/32) of the cases. The staining pattern of stromal tenascin C in MTC and CCH was similar to the pattern seen in the hereditary cases. In the 67 cases with isolated CCH, the mean number of C cells was 490±278 ranging from 111 to 1,231. Half of the cases (52%, n=35) with isolated CCH showed Tn-C expression (see Fig. 1). The difference in the frequency of stromal Tn-C expression comparing isolated and concomitant CCH was significant (p=0.016). Stromal Tn-C expression was not correlated with gender, age, calcitonin level, and number of C cells.

Intracellular immunoreactivity of C cells was detected in 6/32 (19%) concomitant and in 16/67 (24%) isolated CCH and additionally in invasive C cells of 10/38 (26%) MTC (see Fig. 1). Six cases of CCH without stromal Tn-C deposition showed intracellular Tn-C expression. No correlation was seen between intracellular Tn-C expression with any of the investigated clinicopathologic parameters and stromal tenascin expression.

Concerning the MTC cases, nodular thyroid disease was observed in 25/40 specimens, inflammatory thyroid disease in 9/40 cases, and nonmedullary neoplastic diseases in 15/

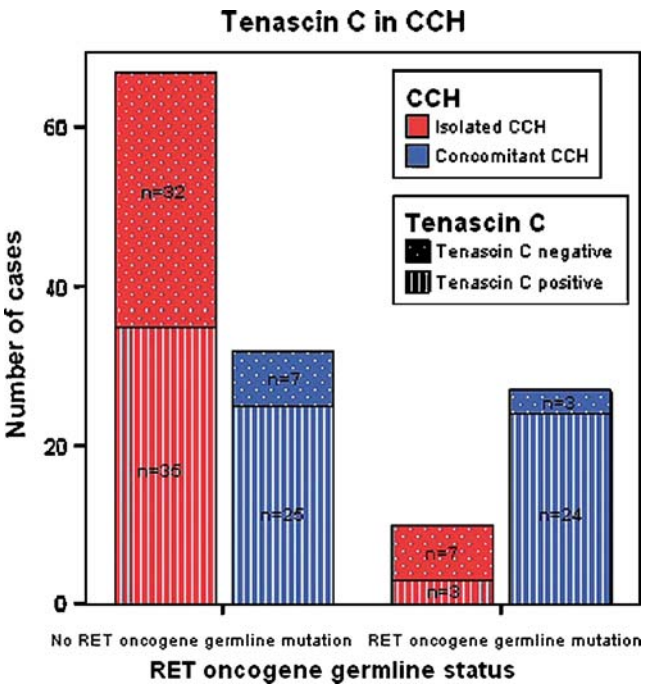

Fig. 2 Tenascin C in isolated and concomitant CCH of familial and sporadic cases. In patients with and without RET oncogene germ-line mutation, stromal tenascin C expression is more often seen in concomitant CCH (24/27 and 32/40, respectively) than in isolated CCH (3/10 and 35/67, respectively)

40 cases (11 papillary thyroid carcinomas—all microcarcinomas—and four follicular thyroid adenomas).

Fifty-one of 67 patients with isolated CCH showed nodular thyroid disease. Inflammatory disease was seen in 11/67 cases. Concomitant neoplastic diseases include 18 cases of papillary thyroid carcinomas—including 17 microcarcinomas—and four cases of follicular adenomas.

Discussion

Tenascin C is an extracellular matrix glycoprotein that contributes to pattern formation during development. Connective tissue of adult organs such as thyroid shows no tenascin expression under physiologic conditions [31] but under various pathologic conditions, e.g., wound healing, inflammation, and tumorigenesis [32]. It is expressed early in carcinogenesis including intraepithelial neoplastic lesions of different organs like breast, prostate, vulva, and cervix [23–26].

C-cell hyperplasia in the setting of germ-line RET oncogene mutation is accepted as precancerous lesion [6, 33], however, its role in nonhereditary cases is discussed controversially [5, 9–11]. Hence, our aim was to analyze whether Tn-C expression is seen in the context of carcinogenesis of MTC.

We observed stromal Tn-C expression in all medullary thyroid microcarcinomas and additionally in most concomitant as well as in a fraction of isolated CCHs irrespective of the RET oncogene germ-line status (Fig. 2). Thus, Tn-C expression in CCH parallels early stromal remodeling described next to intraepithelial neoplasia of diverse organs [23–26].

A recent study indicated a distinct age-related progression of hereditary medullary thyroid carcinoma in carriers of the different RET oncogene germ-line mutations. Depending on the RET oncogene mutation CCH, MTC and its lymph node metastasis developed on different consecutive time points [33].

Regarding the hereditary cases, we found stromal Tn-C expression in 24 of 27 CCHs concomitant to MTC, whereas only three of ten isolated CCHs expressed stromal Tn-C. Hence, the Tn-C expression could indicate a step in the progression from CCH to MTC. However, due to the low number of hereditary cases and the high variability of RET germ-line mutations, no reliable genotype/phenotype/age correlation can be made.

In our study, the nonhereditary cases parallel the findings of the hereditary cases. Tenascin-C expression was more frequent in concomitant CCH (25/32) than in isolated CCH (35/67). These observations together with the findings that the stromal deposition of Tn-C is seen in the development of other preneoplastic conditions such as CIN, PIN, etc. strongly suggest that many CCHs of sporadic cases might represent a preneoplastic lesion with the same stepwise progression to MTC as seen in the hereditary cases.

Additionally to the stromal expression, Tn-C was also seen in the cytoplasm of the tumor cells. Expression of tenascin in tumor cells was seen in other carcinomas and correlated with prognosis in breast carcinoma [34, 35]. We found intracytoplasmatic Tn-C immunoreactivity not only in C cells of MTC but also in some isolated and concomitant CCH. No correlation was seen between intracellular Tn-C expression with any of the investigated clinicopathologic parameters and stromal Tn-C expression. Due to the expression of tenascin in neural crest cells, the expression in C cells may be an incidental phenomenon due to its neurocrest origin [36–39].

We conclude that the Tn-C expression and consequently the stromal remodeling seem to indicate a further step in the carcinogenesis of MTC. We cannot exclude that the Tn-C expression is only a side effect rather than it plays a pivotal role in tumorigenesis. For this question, further experimental studies are necessary. As the stromal activation in sporadic cases was similar to that seen in hereditary forms, a progression of CCH to MTC as seen in hereditary cases seems likely.

Conflict of interest statement We declare that we have no conflict of interest.

References

1. Lips CJ, Landsvater RM, Hoppener JW et al (1994) Clinical screening as compared with DNA analysis in families with multiple endocrine neoplasia type 2A. N Engl J Med 331:828–835
2. Barbot N, Calmettes C, Schuffenecker I et al (1994) Pentagastrin stimulation test and early diagnosis of medullary thyroid carcinoma using an immunoradiometric assay of calcitonin: comparison with genetic screening in hereditary medullary thyroid carcinoma. J Clin Endocrinol Metab 78:114–120
3. Pacini F, Fontanelli M, Fugazzola L et al (1994) Routine measurement of serum calcitonin in nodular thyroid diseases allows the preoperative diagnosis of unsuspected sporadic medullary thyroid carcinoma. J Clin Endocrinol Metab 78:826–829
4. Vierhapper H, Raber W, Bieglmayer C et al (1997) Routine measurement of plasma calcitonin in nodular thyroid diseases. J Clin Endocrinol Metab 82:1589–1593
5. Kaserer K, Scheuba C, Neuhold N et al (1998) C-cell hyperplasia and medullary thyroid carcinoma in patients routinely screened for serum calcitonin. Am J Surg Pathol 22:722–728
6. Krueger JE, Maitra A, Albores-Saavedra J (2000) Inherited medullary microcarcinoma of the thyroid: a study of 11 cases. Am J Surg Pathol 24:853–858
7. Diaz-Cano SJ, de Miguel M, Blanes A et al (2001) Germline RET 634 mutation positive MEN 2A-related C-cell hyperplasias have genetic features consistent with intraepithelial neoplasia. J Clin Endocrinol Metab 86:3948–3957
8. Machens A, Niccoli-Sire P, Hoegel J et al (2003) Early malignant progression of hereditary medullary thyroid cancer. N Engl J Med 349:1517–1525

9. Perry A, Molberg K, Albores-Saavedra J (1996) Physiologic versus neoplastic C-cell hyperplasia of the thyroid: separation of distinct histologic and biologic entities. Cancer 77:750–756
10. Kaserer K, Scheuba C, Neuhold N et al (2001) Sporadic versus familial medullary thyroid microcarcinoma: a histopathologic study of 50 consecutive patients. Am J Surg Pathol 25:1245–1251
11. Saggiorato E, Rapa I, Garino F et al (2007) Absence of RET gene point mutations in sporadic thyroid C-cell hyperplasia. J Mol Diagn 9:214–219
12. Verga U, Ferrero S, Vicentini L et al (2007) Histopathological and molecular studies in patients with goiter and hypercalcitoninemia: reactive or neoplastic C-cell hyperplasia? Endocr Relat Cancer 14:393–403
13. Guyetant S, Josselin N, Savagner F et al (2003) C-cell hyperplasia and medullary thyroid carcinoma: clinicopathological and genetic correlations in 66 consecutive patients. Mod Pathol 16:756–763
14. Koperek O, Scheuba C, Cherenko M et al (2008) Desmoplasia in medullary thyroid carcinoma: a reliable indicator of metastatic potential. Histopathology 52:623–630
15. Koperek O, Scheuba C, Puri C et al (2007) Molecular characterization of the desmoplastic tumor stroma in medullary thyroid carcinoma. Int J Oncol 31:59–67
16. Scheuba C, Kaserer K, Kaczirek K et al (2006) Desmoplastic stromal reaction in medullary thyroid cancer—an intraoperative "marker" for lymph node metastases. World J Surg 30:853–859
17. Jones PL (2001) Extracellular matrix and tenascin-C in pathogenesis of breast cancer. Lancet 357:1992–1994
18. Hauptmann S, Zardi L, Siri A et al (1995) Extracellular matrix proteins in colorectal carcinomas. Expression of tenascin and fibronectin isoforms. Lab Invest 73:172–182
19. Hauptmann S, Budianto D, Denkert C et al (2003) Adhesion and migration of HRT-18 colorectal carcinoma cells on extracellular matrix components typical for the desmoplastic stroma of colorectal adenocarcinomas. Oncology 65:174–181
20. Chiquet-Ehrismann R, Tucker RP (2004) Connective tissues: signalling by tenascins. Int J Biochem Cell Biol 36:1085–1089
21. Sethi T, Rintoul RC, Moore SM et al (1999) Extracellular matrix proteins protect small cell lung cancer cells against apoptosis: a mechanism for small cell lung cancer growth and drug resistance in vivo. Nat Med 5:662–668
22. Maschler S, Grunert S, Danielopol A et al (2004) Enhanced tenascin-C expression and matrix deposition during Ras/TGF-beta-induced progression of mammary tumor cells. Oncogene 23:3622–3633
23. Tuxhorn JA, Ayala GE, Smith MJ et al (2002) Reactive stroma in human prostate cancer: induction of myofibroblast phenotype and extracellular matrix remodeling. Clin Cancer Res 8:2912–2923
24. Iskaros BF, Koss LG (2000) Tenascin expression in intraepithelial neoplasia and invasive carcinoma of the uterine cervix. Arch Pathol Lab Med 124:1282–1286
25. Goepel C, Stoerer S, Koelbl H (2003) Tenascin in preinvasive lesions of the vulva and vulvar cancer. Anticancer Res 23:4587–4591
26. Howeedy AA, Virtanen I, Laitinen L et al (1990) Differential distribution of tenascin in the normal, hyperplastic, and neoplastic breast. Lab Invest 63:798–806
27. Fink M, Weinhusel A, Niederle B et al (1996) Distinction between sporadic and hereditary medullary thyroid carcinoma (MTC) by mutation analysis of the RET proto-oncogene. "Study Group Multiple Endocrine Neoplasia Austria (SMENA)". Int J Cancer 69:312–316
28. Scheuba C, Kaserer K, Moritz A et al (2009) Sporadic hypercalcitoninemia: clinical and therapeutic consequences. Endocr Relat Cancer 16(1):243–253
29. Bieglmayer C, Scheuba C, Niederle B et al (2002) Screening for medullary thyroid carcinoma: experience with different immunoassays for human calcitonin. Wien Klin Wochenschr 114:267–273
30. DeLellis R (2004) Pathology and Genetics of Tumors of the Endocrine Organs. IARC, Lyon
31. Mackie EJ (1994) Tenascin in connective tissue development and pathogenesis. Perspect Dev Neurobiol 2:125–132
32. Mackie EJ (1997) Molecules in focus: tenascin-C. Int J Biochem Cell Biol 29:1133–1137
33. Machens A, Holzhausen HJ, Thanh PN et al (2003) Malignant progression from C-cell hyperplasia to medullary thyroid carcinoma in 167 carriers of RET germline mutations. Surgery 134:425–431
34. Brunner A, Mayerl C, Tzankov A et al (2004) Prognostic significance of tenascin-C expression in superficial and invasive bladder cancer. J Clin Pathol 57:927–931
35. Ishihara A, Yoshida T, Tamaki H et al (1995) Tenascin expression in cancer cells and stroma of human breast cancer and its prognostic significance. Clin Cancer Res 1:1035–1041
36. Tucker RP, McKay SE (1991) The expression of tenascin by neural crest cells and glia. Development 112:1031–1039
37. Martinez L, Ceano-Vivas MD, Gonzalez-Reyes S et al (2005) Decrease of parafollicular thyroid C-cells in experimental esophageal atresia: further evidence of a neural crest pathogenic pathway. Pediatr Surg Int 21:175–179
38. Russo AF, Clark MS, Durham PL (1996) Thyroid parafollicular cells. An accessible model for the study of serotonergic neurons. Mol Neurobiol 13:257–276
39. Kameda Y (1995) Evidence to support the distal vagal ganglion as the origin of C cells of the ultimobranchial gland in the chick. J Comp Neurol 359:1–14

Virchows Arch (2009) 455:49–54
DOI 10.1007/s00428-009-0804-0

ORIGINAL ARTICLE

Differential expression of microRNA 181b and microRNA 21 in hyperplastic polyps and sessile serrated adenomas of the colon

Klaus Juergen Schmitz · Sascha Hey · Anja Schinwald · Jeremias Wohlschlaeger · Hideo Andreas Baba · Karl Worm · Kurt Werner Schmid

Received: 17 April 2009 / Revised: 8 June 2009 / Accepted: 8 June 2009 / Published online: 23 June 2009

Abstract This study was designed to analyse the potential diagnostic value of miR-181b and miR-21 for discriminating hyperplastic polyps (HP) from sessile serrated adenomas (SSA) without cytologic dysplasia. Using real-time polymerase chain reaction expression levels of miR-181b and miR-21 in 18 HPs, 19 SSAs without cytologic dysplasia and 20 normal colonic mucosal specimens were examined. In addition, 20 colorectal cancers specimen were analysed for miR-181b expression. Data were normalised to RNU48 as an internal control. A differential expression of miR-181b and miR-21 was found in HPs, SSAs, and normal colonic mucosa with highest expression levels in SSAs. Levels of miR-181b but not miR-21 differed in HPs and normal mucosa. SSAs exhibited both significantly higher miR-181b levels (up to 2.01-fold; $P<0.001$) and miR-21 levels (up to 1.82-fold; $P=0.011$) than HPs. In contrast to HPs, SSAs are characterised by high levels of miR-181b and miR-21 expression. However, due to the overlap of values, miR-181b and miR-21 evaluation did not allow discrimination of the two lesions in every case.

Keywords MicroRNA · Hyperplastic polyp · Sessile serrated adenoma · Polymerase chain reaction

K. J. Schmitz (✉) · S. Hey · A. Schinwald · J. Wohlschlaeger · H. A. Baba · K. Worm · K. W. Schmid
Institute of Pathology and Neuropathology,
University Hospital Essen, University of Duisburg-Essen,
Hufelandstr. 55,
45122 Essen, Germany
e-mail: klausjschmitz@versanet.de

H. A. Baba · K. W. Schmid
West German Cancer Center,
Essen, Germany

Introduction

Hyperplastic polyps (HP) are common lesions in the large bowel, especially in the distant bowel [1]. Typical HPs are small, usually <5 mm in diameter, symmetrical, and uniform. While adenomatous polyps have been documented to progress into colorectal carcinoma [2], such evidence has not been documented for HPs. Thus, the non-neoplastic nature of HPs has developed into an unchallenged dogma for several decades. Most HPs are typically located in the recto-sigmoid and are still considered as lesions lacking a malignant potential [3, 4]. The recognition of a morphologically different variant of HP, which is mainly located in the proximal colon, has led to the identification of a lesion we now call sessile serrated adenoma (SSA). The SSA is part of a novel pathway called the serrated pathway [5]. Various lesions may show serrated epithelial infolding and are united into the term "serrated polyp". This has led to a currently proposed classification [6] that includes four morphological categories (HPs, SSA, admixed polyps, and traditional serrated adenomas). Although HPs and SSAs share some morphological features, several distinct characteristics have been recognised [5, 7] that help to differentiate between these two type of lesions. Nevertheless, histopathological diagnosis of SSA still remains difficult.

MicroRNAs (miRNAs) are a class of recently discovered small RNA molecules that regulate the expression of genes at the translational level [8, 9]. Our understanding of these recently discovered tiny RNA molecules is still in its infancy, but studies indicate that microRNA-mediated gene regulation is likely to play key roles in human development, cellular differentiation, and oncogenesis. MicroRNA are endogenously expressed short noncoding RNAs, which are 18–25 nucleotides in length and that are capable of

repressing protein translation through binding to target messenger RNA (mRNA). The single-stranded miRNAs, derived from miRNA duplex complexes, can associate with the RNA-induced silencing complex (RISC) [10]. The miRNA-RISC has been shown to bind to specific mRNA targets and cause the translational repression or cleavage of these mRNA sequences.

For pathologists, the measurement of microRNA levels might offer a new set of diagnostic tools that may also be used to improve our understanding of cancer. This study focuses on potential diagnostic value of several microRNAs (miR-181b, miR-21, miR-133, and miR-let 7c) that have been found to be differentially expressed in colorectal tumour tissue [11].

Materials and methods

Patient material

The study comprised SSAs, HPs, colorectal cancers, and specimens with normal colonic mucosa. Table 1 depicts the exact numbers of specimens used for microRNA analysis. Diagnosis of SSA was performed according to diagnostic criteria published by Torlakovic et al. [6]. Figure 1 represents a typical SSA with its peculiar morphological features. Patients with SSAs and HPs had a mean age of 60.1 and 62.5 years, respectively. Tissue was retrieved from paraffin-embedded material using a punching tool of 0.6 mm diameter. At least three cores were taken from each specimen and the whole cores were used for RNA extraction. Standard H&E staining was performed on each cored specimen in order to ensure that removed tissue samples were representative for the lesion (Fig. 2). The normal colon mucosa was retrieved from resections margins of diverticulosis specimens lacking any inflammatory activity. Colorectal cancer specimens were collected from diagnostic tumour biopsies. Patients were not subject to any neoadjuvant or adjuvant therapies.

RNA isolation and reverse transcription

Total RNA isolation was performed using the Rneasy FFPE isolation kit (Qiagen, Hilden, Germany) according to the manufacturer's instructions. miR-181b, miR-21, miR-133, and miR-let 7c were analysed by the real-time reverse transcription (RT)-polymerase chain reaction (PCR) scheme for miRNA quantification according to the protocol of Applied Biosystems (P/N: 4364031). The RNA concentration and purity (A260:A280>2.0; A260:A230>1.8) were measured using NanoDrop™ 1000 spectrophotometer (Thermo Scientific, Wilmington, DE, USA). The reverse transcriptase reaction was carried out in a 15-µl reaction mixture containing gene-specific stem-loop primers according to the TaqMan MicroRNA Assay protocol (Applied Biosystems, Darmstadt, Germany), 5× RT buffer, 10 mM deoxynucleotide triphosphate (dNTPs) (ROTH, Ultrapure dNTP-Set), 200 U/µl RT (Fermentas, RevertAid M-MuLV Reverse Transcriptase, Vilnius, Lithuania), 40 U/µl Ribo-Lock RNase Inhibitor (Fermentas), and 20 ng/µl RNA. The reaction was performed in a peqlab cycler (primus 25 advanced, MWG Biotech, Ebersberg, Germany) for 30 min at 16°C, 30 min at 42°C, and 5 min at 85°C, and the reaction mixture containing the resulting complementary DNA (cDNA) was stored at 4°C.

Real- time PCR

The 12-µl real-time PCR mixture contained 5.25 µl cDNA (diluted 1:25), TaqMan Universal PCR master mix (No AmpErase UNG), and 1 µl of TaqMan MicroRNA assay hsa-181b/hsa-21/hsa-133/hsa-let7c and RNU48 (Applied Biosystems). The reaction was initiated at 95°C for 10 min, followed by 40 cycles of 95°C for 15 s, and 60°C for 1 min. The reaction was carried out using an Applied Biosystems 7500 fast real-time PCR system (Applied Biosystems Inc., Foster City, CA, USA).

Statistical analysis

Default threshold settings were used to determine the threshold cycle data. The relative amount of each miRNA was calculated using the comparative threshold (Ct) method with $\Delta Ct = Ct\,(miRNA) - Ct\,(RNU48)$. Relative quantification of miRNA expression was calculated with the $2^{-\Delta\Delta Ct}$ method (Applied Biosystems User Bulletin No. 2 [P/N: 4303859]). This method is called the comparative C_T method, which is widely used to present relative gene

Table 1 Cases analysed for miR-181b, miR-21, miR-133, and miR-let 7c expression

	miR-181b	miR-21	miR-133	miR-let 7c
Normal mucosa	20	20	8	4
Hyperplastic polyp	19	19	4	4
Sessile serrated adenoma	18	18	5	5
Colorectal cancer	20	0	24	4

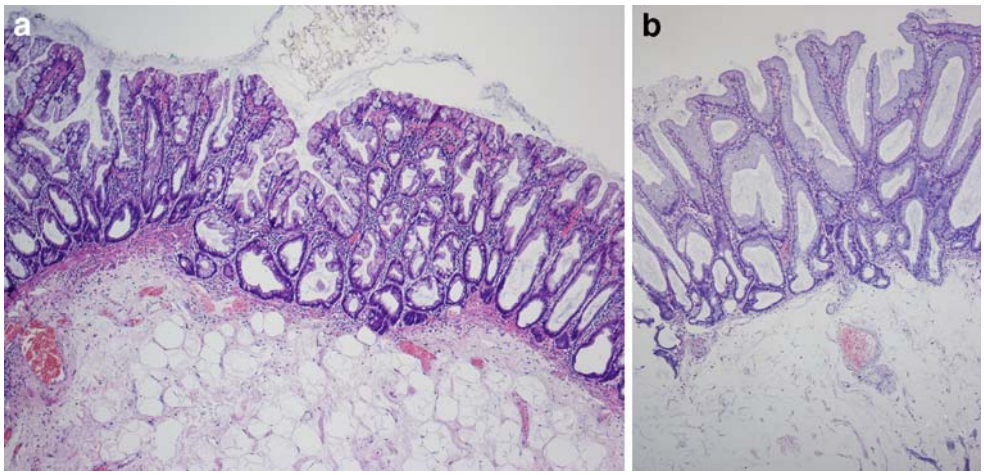

Fig. 1 Sessile serrated adenoma without cytological dysplasia. The lesion shows characteristic architectural features such as branching of crypts, dilatation of the base of the crypts, and a specific growth pattern in which crypts seem to grow parallel to the muscularis mucosae (**a**). Note the peculiar feature of so-called microherniation with herniation of crypts through the muscularis mucosae (**b**)

expression [12]. Normalisation is an essential step for the accurate quantification levels. In our study, three different approaches were used for data normalisation. MicroRNA expression data were normalised to levels of RNU48, RNU6b, and let-7a-1. Out of these three internal standards, RNU48 was proven to have the lowest variability, and the values were therefore calculated by normalisation with RNU48.

Statistical differences between localization and lesion type were performed using chi-square analysis. Differences between microRNA expression levels among the two groups were evaluated using nonparametric Mann–Whitney *U* test and the Kruskal–Wallis test for three or more groups. *P* values <0.05 were considered significant. Statistics were performed with Statistical Package for the Social Sciences version 17 (SPSS Inc., Chicago, IL, USA).

Results

Anatomical localization of HPs and SSAs

Out of 18 HPs, three (16.7%) were located in the proximal colon, four (22.2%) in the transversal or distal colon, and

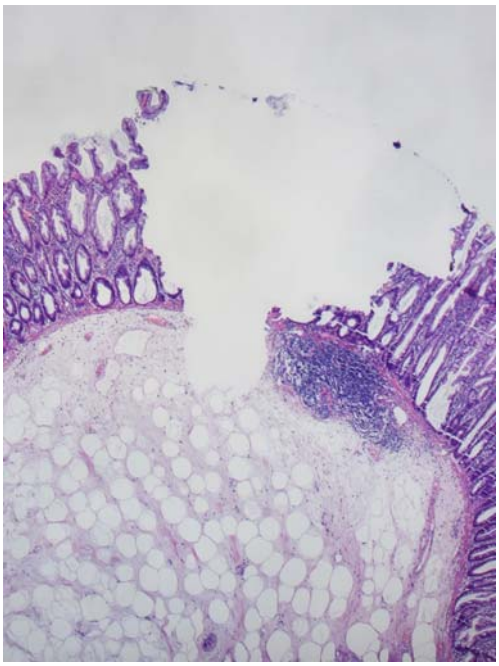

Fig. 2 Micrograph showing a control staining demonstrating the area of which the cores were taken for microRNA analysis. At least three cores of 0.6 mm diameter were taken from each specimen

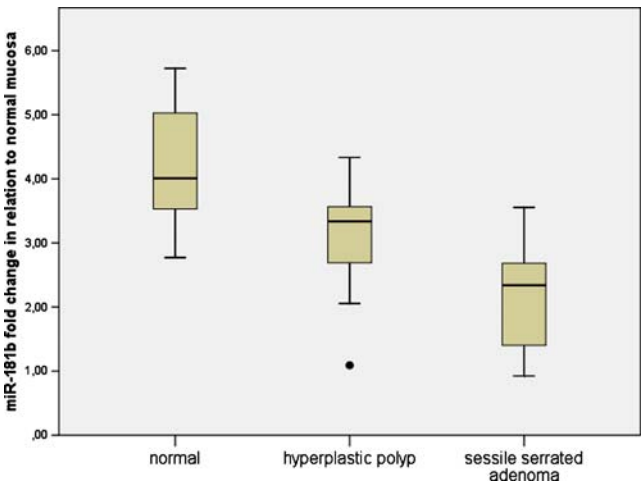

Fig. 3 Boxplot showing the different levels of miR-181b expression (data presented in ΔCT of relative threshold cycles indicating fold changes over normal mucosa; low values indicate high levels of miRNA). miR-181b is expressed at higher levels in sessile serrated adenomas compared to normal colonic mucosa and hyperplastic polyps ($P<0.001$; Kruskal–Wallis test). *Circles* indicate outliers. *Inside the boxes* lies a *central line* demonstrating the median value

Table 2 MicroRNA expression in sessile serrated adenomas in relation to hyperplastic polyps

	Sessile serrated adenoma	
	Fold change	*P* value
miR-181b	2.01 ↑	<0.001
miR-21	1.82 ↑	0.011

Fold change normalised to hyperplastic polyp

11 (61.1%) in the rectum. In contrast, out of 19 SSAs, 11 (57.9%) were located in the proximal colon, six (31.6%) in the transversal or distal colon; whereas, only two (5.4%) were located in the rectum. Thus, there was a specific distribution pattern with SSAs being located more frequently in the proximal colon and HP in the rectum (chi-square analysis, $P=0.006$).

Expression levels of microRNA

High values of relative threshold cycles indicate low microRNA quantity, and data were normalised to RNU48 expression.

Expression levels of miR-181b

The highest level of miR-181b was found in the group of SSAs (2.14, SD 0.78), followed by colorectal cancer (2.21, SD 1.36), HPs (3.14, SD 0.82), and normal colonic mucosa (4.19, SD 0.92). When comparing all groups, miR-181b expression levels showed a differential expression among normal mucosa, HPs, SSAs, and colorectal cancers ($P=0.001$; Fig. 3).

In the subgroup of HPs and SSAs, miR-181b expression of HPs was distinctly different from that of SSAs with an upregulation of miR-181b in SSAs of up to 2.01-fold. Compared to normal colon mucosa, we found elevated miR-181b expression levels in SSAs up to 4.16-fold. In addition, normal colon mucosa and HPs exhibited significant differences with miR-181b being upregulated in HPs up to 2.06-fold. Tables 2 and 3 depict data on miR-181b expression levels.

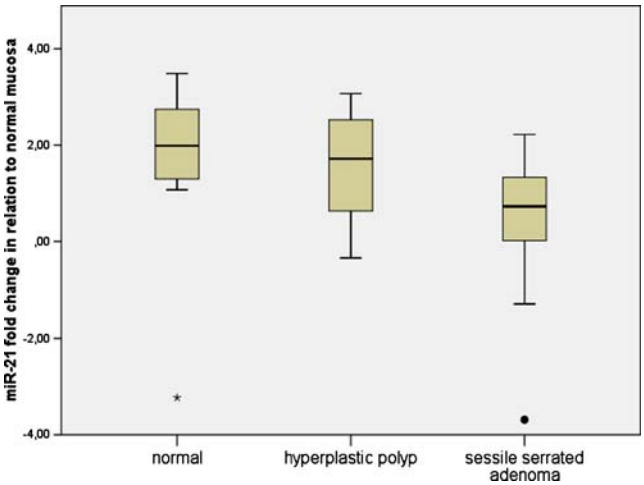

Fig. 4 Boxplot showing the different levels of miR-21 expression (data presented in ΔCT of relative threshold cycles indicating fold changes over normal mucosa; low values indicate high levels of miRNA). miR-21 is expressed at higher levels in sessile serrated adenomas compared to normal colonic mucosa and hyperplastic polyps ($P=0.003$; Kruskal–Wallis test). *Circles* indicate outliers. *Stars* indicate extreme values. *Inside the boxes* lies a *central line* demonstrating the median value

Expression levels of miR-21

Data from miR-21 expression in colorectal cancer was not available. The highest level of miR-21 was found in the group of SSAs (0.48, SD 1.33), followed by HPs (1.69, SD 1.09), and normal colonic mucosa (1.82, SD 1.39). When comparing all groups, MiR-21 expression levels showed a differential expression among normal mucosa, HPs, and SSAs ($P=0.003$; Fig. 4).

In the subgroup of HP and SSA, miR-21 expression of HPs was distinctly different from that of SSA with an upregulation of miR-21 in SSA of up to 1.82-fold. Compared to normal colon mucosa, we found elevated miR-21 expression levels in SSA; whereas, normal colon mucosa and HPs exhibited no differences. Tables 2 and 3 depict data on miR-21 expression levels.

Expression levels of miR-133

The highest level of miR-133 was found in the group of normal colonic mucosa (5.43, SD 2.44). Levels decreased

Table 3 MicroRNA expression in hyperplastic polyps, sessile serrated adenomas, and colorectal cancers in relation to normal mucosa

[a] Fold change normalised to normal colonic mucosa

Variants	Hyperplastic polyp		Sessile serrated adenoma		Colorectal cancer	
	Fold change[a]	*P* value	Fold change	*P* value	Fold change	*P* value
miR-181b	2.06	0.004	4.16	<0.001	3.94	<0.001
miR-21	1.17	NS	2.13	<0.001	–	–

to 5.77 (SD 0.98) in SSAs and 6.86 (SD 1.01) in HPs. Lowest expression values were found in colorectal cancers (7.91, SD 1.99). When comparing all groups, MiR-133 expression levels showed no differential expression among normal mucosa, HPs, and SSAs; whereas, colorectal cancers exhibited significant lower expression levels of miR-133 compared to normal colonic mucosa (P=0.025). In the subgroup of HPs and SSAs, miR-133 expression did not differ significantly.

Expression levels of miR-let 7c

The highest level of miR-let 7c was found in colorectal cancer (4.09, SD 1.05), followed by SSAs (4.78, SD 0.75), normal colonic mucosa (5.28, SD 0.28), and HPs (5.82, SD 0.95). When comparing all groups, due to overlapping values, miR-let 7c expression levels showed no differential expression among normal mucosa, HPs, SSAs, and colorectal carcinomas. In the subgroup of HPs and SSAs, miR-let 7c expression did not differ significantly.

Discussion

Altered microRNA expression has been identified in many human cancers. Comparison between human cancers and their normal counterparts has revealed that microRNA exhibit differential expression profiles in normal versus cancer tissues [13, 14]. Thus, unique microRNA expression signatures or even expression levels of certain microRNAs might be used to differentiate tumours or precursor lesions. This study focused on miR-181b and miR-21, since both these microRNA were shown to be upregulated in colorectal cancer tissue [11]. The study is based on paraffin-embedded tissue, which recently has been shown to be suitable for microRNA expression studies [15]. Initially, we started with two additional microRNAs (miR-133a and miR-let7c) that have been described to be upregulated in colorectal cancer [11]. However, our investigation of a small primary series revealed no differential expression of these microRNAs in HPs versus SSAs. Thus, we proceeded with miR-181b and miR-21 in serrated lesions.

Our data shows that these two lesions with close morphological resemblance, namely, HP and SSA, without cytologic dysplasia, exhibit significantly different miR-181b and miR-21 expression levels. miR-21 is one of the most prominent microRNAs implicated in the genesis and progression of human cancer. Recently, it was shown for the first time that a tumour suppressor (Pdcd4) was negatively regulated by miR-21 in colorectal cancer [16]. This study demonstrated miR-21 association with invasion, intravasation, and metastasis in colorectal cancer cells. Little is known about the target genes of miR-181b. It is possible to utilise TargetScan (http://www.targetscan.org) to identify putative target genes regulated by this microRNA. However, such data remains speculative only, thus, we have refrained from discussing possible target mRNAs. Future investigations are necessary to link the miR-181b and miR-21 expression levels with genetic and epigenetic alterations of SSA.

The presented study has focused on the differential expression of miRNA in serrated lesions. Moreover, we have compared miR-181b expression levels in SSA and colorectal cancer specimens. We are aware that the present series of 20 colorectal cancers is likely to represent mostly sporadic colorectal cancers and not adenocarcinomas evolved through the so-called serrated pathway. Reproducible histopathological criteria for serrated adenocarcinoma have recently been established and have been qualified by DNA expression analysis for 7,928 genes. Tuppurainen et al. were able to identify serrated adenocarcinomas as a molecular entity distinct from conventional adenocarcinoma [17]. We did not perform additional methods to characterise the genetic background of the present series of colorectal cancers. It would be desirable in the future to examine miRNA profiles in an established series of colorectal cancer with a “serrated” morphology and distinct genetic profile.

In conclusion, assessment of miR-181b and miR-21 expression in serrated polyps might help separating SSAs without cytologic dysplasia from ordinary HPs. Unfortunately, due to overlap of values of miR-181b and miR-21 expression observed in the groups of SSAs and HPs studied, measurement of these parameters is not likely to allow a clear separation of these lesions at individual patient level. Nevertheless, our results point towards a potential biological relevance of these microRNAs in the serrated polyp development.

Conflict of interest We declare that we have no conflict of interest.

References

1. Estrada RG, Spjut HJ (1980) Hyperplastic polyps of the large bowel. Am J Surg Pathol 4:127–133
2. Kinzler KW, Vogelstein B (1996) Lessons from hereditary colorectal cancer. Cell 87:159–170
3. Higuchi T, Sugihara K, Jass JR (2005) Demographic and pathological characteristics of serrated polyps of colorectum. Histopathology 47:32–40
4. Torlakovic E, Snover DC (1996) Serrated adenomatous polyposis in humans. Gastroenterology 110:748–755
5. Makinen MJ (2007) Colorectal serrated adenocarcinoma. Histopathology 50:131–150
6. Torlakovic E, Skovlund E, Snover DC et al (2003) Morphologic reappraisal of serrated colorectal polyps. Am J Surg Pathol 27:65–81

7. Goldstein NS, Bhanot P, Odish E et al (2003) Hyperplastic-like colon polyps that preceded microsatellite-unstable adenocarcinomas. Am J Clin Pathol 119:778–796
8. Wightman B, Ha I, Ruvkun G (1993) Posttranscriptional regulation of the heterochronic gene lin-14 by lin-4 mediates temporal pattern formation in *C. elegans*. Cell 75:855–862
9. Lee RC, Feinbaum RL, Ambros V (1993) The *C. elegans* heterochronic gene lin-4 encodes small RNAs with antisense complementarity to lin-14. Cell 75:843–854
10. Bartel DP (2004) MicroRNAs: genomics, biogenesis, mechanism, and function. Cell 116:281–297
11. Schetter AJ, Leung SY, Sohn JJ et al (2008) MicroRNA expression profiles associated with prognosis and therapeutic outcome in colon adenocarcinoma. JAMA 299:425–436
12. Schmittgen TD, Livak KJ (2008) Analyzing real-time PCR data by the comparative C(T) method. Nat Protoc 3:1101–1108
13. Volinia S, Calin GA, Liu CG et al (2006) A microRNA expression signature of human solid tumors defines cancer gene targets. Proc Natl Acad Sci U S A 103:2257–2261
14. Yanaihara N, Caplen N, Bowman E et al (2006) Unique microRNA molecular profiles in lung cancer diagnosis and prognosis. Cancer Cell 9:189–198
15. Siebolts U, Varnholt H, Drebber U et al (2009) Tissues from routine pathology archives are suitable for microRNA analyses by quantitative PCR. J Clin Pathol 62:84–88
16. Asangani IA, Rasheed SA, Nikolova DA et al (2008) MicroRNA-21 (miR-21) post-transcriptionally downregulates tumor suppressor Pdcd4 and stimulates invasion, intravasation and metastasis in colorectal cancer. Oncogene 27:2128–2136
17. Tuppurainen K, Makinen JM, Junttila O et al (2005) Morphology and microsatellite instability in sporadic serrated and non-serrated colorectal cancer. J Pathol 207:285–294

Virchows Arch (2009) 455:55–65
DOI 10.1007/s00428-009-0795-x

ORIGINAL ARTICLE

Structural changes in the epithelium of the small intestine and immune cell infiltration of enteric ganglia following acute mucosal damage and local inflammation

Louise Pontell · Patricia Castelucci · Mária Bagyánszki · Tanja Jovic · Michelle Thacker · Kulmira Nurgali · Romke Bron · John B. Furness

Received: 16 April 2009 / Revised: 24 May 2009 / Accepted: 25 May 2009 / Published online: 11 June 2009

Abstract An acute enteritis is commonly followed by intestinal neuromuscular dysfunction, including prolonged hyperexcitability of enteric neurons. Such motility disorders are associated with maintained increases in immune cells adjacent to enteric ganglia and in the mucosa. However, whether the commonly used animal model, trinitrobenzene sulphonate (TNBS)-induced enteritis, causes histological and immune cell changes similar to human enteric neuropathies is not clear. We have made a detailed study of the mucosal damage and repair and immune cell invasion following intralumenal administration of TNBS. Intestines from untreated, sham-operated and TNBS-treated animals were examined at 3 h to 56 days. At 3 h, the mucosal surface was completely ablated, by 6 h an epithelial covering was substantially restored and by 1 day there was full re-epithelialisation. The lumenal epithelium developed from a squamous cell covering to a fully differentiated columnar epithelium with mature villi at about 7 days. Prominent phagocytic activity of enterocytes occurred at 1–7 days. A surge of eosinophils and T lymphocytes associated with the enteric nerve ganglia occurred at 3 h to 3 days. However, elevated immune cell numbers occurred in the lamina propria of the mucosa until 56 days, when eosinophils were still three times normal. We conclude that the disruption of the mucosal surface that causes TNBS-induced ileitis is brief, a little more than 6 h, and causes a transient immune cell surge adjacent to enteric ganglia. This is much briefer than the enteric neuropathy that ensues. Ongoing mucosal inflammatory reaction may contribute to the persistence of enteric neuropathy.

Keywords Enteritis · Mucosal inflammation · Enteric neuropathy · Small intestine · Irritable bowel syndrome · Epithelial repair · Immune cells

L. Pontell · P. Castelucci · M. Bagyánszki · T. Jovic · M. Thacker · R. Bron · J. B. Furness (✉)
Department of Anatomy and Cell Biology,
University of Melbourne,
Parkville,
Melbourne, Victoria 3010, Australia
e-mail: j.furness@unimelb.edu.au

P. Castelucci
Department of Anatomy, University of São Paulo,
São Paulo, Brazil

M. Bagyánszki
Department of Physiology, Anatomy and Neuroscience,
University of Szeged,
Szeged 6726, Hungary

K. Nurgali
Department of Physiology, University of Melbourne,
Parkville,
Melbourne, Victoria 3010, Australia

Introduction

A considerable body of evidence links intestinal inflammation and intestinal neuromuscular disorders, both in the clinical literature and in animal models [1–6]. Even though the period of inflammation may be brief, and the region of overt inflammatory damage is circumscribed, the effects on enteric neurons are long-lasting [7, 8] and significant changes in organ function are observed in regions that are remote from the inflammation [9–12].

In experimental animals, inflammation causes substantial increases in the excitability of enteric neurons [13–16]. These studies investigated the enteric nervous system 3–

10 days after the induction of inflammation, a time when the inflammatory response, in terms of tissue damage and immune cell activation, is still apparent. Two animal studies have extended the investigation of neuronal changes to 8 weeks [8, 17]. In both cases, the structural effects of inflammation were resolved before 8 weeks, as judged by histological examination and assay of myeloperoxidase activity in tissue extracts, but the changes in the physiological properties of myenteric neurons [17] and submucosal neurons [8] persisted. This implies that the inflammation may cause a prolonged change in the intrinsic properties of the neurons. On the other hand, histopathological studies in human indicate that an on-going inflammation of enteric ganglia (ganglionitis), including infiltration of the ganglionated plexuses by lymphocytes, can occur in intestinal neuromuscular disorders [3, 18]. Inflammatory changes in the mucosa have also been associated with persistent changes in motility and pain perception, for example in irritable bowel syndrome patients [19] and changes in the mucosa persist for 6 months or more following an acute episode of clinical enteritis [20]. However, there is not a detailed study of the time course of immune cell infiltration of enteric ganglia and inflammatory cell presence in the mucosa in the animal models which have been used for functional studies of enteric neurons. Thus, we have investigated the process of mucosal repair and inflammatory cell attraction to enteric ganglia in an animal model previously used to investigate the changes in enteric neuron function that follow inflammation.

Materials and methods

Experiments were performed on guinea pigs (150–275 g) of either sex from the inbred Hartley strain colony of the Department of Anatomy and Cell Biology at the University of Melbourne. All procedures were conducted according to the Code of Practice of the National Health and Medical Research Council of Australia and were approved by the University of Melbourne Animal Experimentation Ethics Committee.

Inflammation was induced in the guinea pig ileum as previously described [16]. 2,4,6-Trinitrobenzene sulphonic acid (TNBS, Wako Industries, Nagoya, Japan) was given in an amount of 30 mg/kg in 1 mL of 30% ethanol into the distal ileum. Animals were taken at intervals from 3 h to 56 days after TNBS injection. Sham animals were treated identically, except that phosphate buffered saline (PBS, 0.15 M NaCl in 0.01 M sodium phosphate buffer, pH 7.2) was injected into the lumen. At the time of taking tissue, animals were stunned by a blow to the head and killed by cutting the carotid arteries and severing the spinal cord.

Histology

Samples for histology were taken from the site of application of TNBS or sham and placed into PBS containing 1 μm nicardipine, pinned on balsa board mucosa up and fixed in fixative (2% formaldehyde plus 0.2% picric acid in 0.1 M sodium phosphate buffer, pH 7.2) at 4°C overnight. Tissue was also taken from untreated guinea pigs and from 10 and 20 cm proximal to the region of inflammation. Tissue was placed into histology cassettes and dehydrated through graded ethanol to histolene and embedded in paraffin. Sections were cut transversely at 5 μm thickness and processed for standard haematoxylin and eosin (H&E) and the periodic acid-Schiff reaction (PAS). Following staining, the tissue was mounted using permanent mounting medium.

Immunohistochemistry

T cells were localised in whole mounts of the myenteric and submucosal plexuses that were double stained with anti-calbindin to reveal the ganglia. Preparations were incubated in 10% normal horse serum to block non-specific binding of labelled immunoglobulins. They were then incubated in a mixture of mouse anti-guinea pig T-cell antibody (Fitzgerald Laboratories, Niagara Falls, NY, USA; 1:1,000) and rabbit anti-calbindin (Swant, Bellinzona, Switzerland; 1:2,500), overnight at 4°C. After washing in PBS, the preparations were incubated for 1 h in a mixture of horse anti-mouse gamma globulin coupled to biotin (1:100, Vector Laboratories, Burlingame, CA, USA) and donkey anti-rabbit gamma globulin coupled to Alexa488 1:1,000 (Molecular Probes, Eugene, OR, USA), followed by streptavidin coupled to Texas Red 1:400 (Amersham, Melbourne, Australia), also for 1 h.

Results

Macroscopic and histological observations

Macroscopically, at 3 h after TNBS injection into the lumen of the ileum, there was obvious bleeding within the wall of the ileum, over a distance of about 5–8 cm oral to the site of injection. The extent of haemorrhage was variable in this region. Histological examination at 3 h showed an almost complete loss of the mucosal epithelium facing the lumen, and parts of the mucosal surface that had separated were found in the lumen (Fig. 1). The villi were completely ablated, but the bases of the glands remained and the crypts had normal appearance (Fig. 1b). At 6 h, the macroscopic appearance was similar, but the histology showed a substantial restoration of the mucosal epithelium (Fig. 1c),

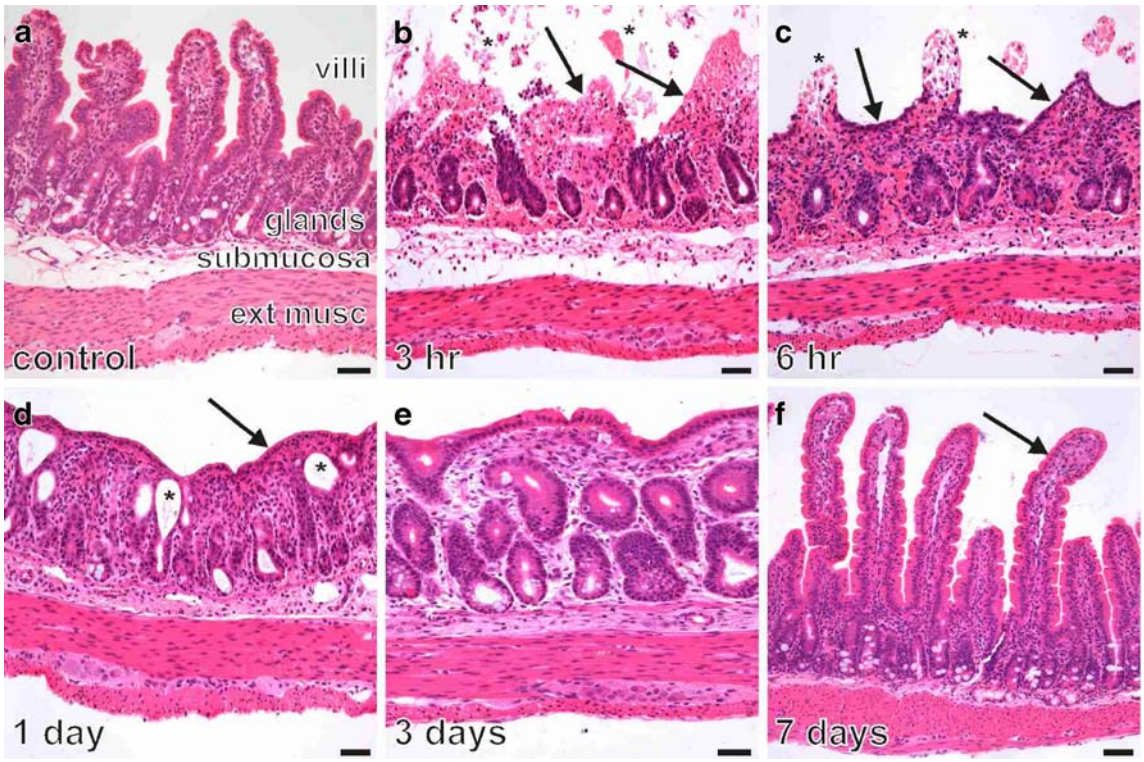

Fig. 1 Time course of histological change in the ileum after intralumenal application of TNBS. Sections are stained with haematoxylin and eosin. **a** Control ileum, with principal components of the organ labelled: external muscle layers (*ext musc*), submucosa, mucosal glands and villi. **b** The appearance 3 h after TNBS. The surface epithelium has been completely stripped from the villi (*arrows*), and the villi have broken up and formed debris in the lumen (*asterisks*). However, crypts and crypt epithelium are normal. **c** At 6 h, a partial covering of squamous epithelium (*arrows*) has formed over a flattened mucosal surface. Numerous haemorrhagic foci (*asterisks*) were seen at this stage. **d** At 1 day, a complete covering of squamous or low cuboidal epithelium has formed (*arrow*), which separates the lamina propria from the lumen. Some cysts have been included beneath the reformed epithelium (*asterisks*). **e** At 3 days, the mucosa has thickened and the surface epithelium has matured, but villi have not yet formed. **f** At 7 days, the structure of the mucosa appears similar to that of control ileum. Villi (*arrow*) have normal height and morphology. *Scale bars* 50 μm

which at this stage had a squamous or low cuboidal profile (Fig. 2a). The restored epithelium was breached at intervals, which provided microscopic haemorrhagic foci, from which there was bleeding into the lumen (Fig. 1c).

At 12 h and 1 day, the mucosal epithelium facing the lumen was continuous and haemorrhages into the lumen were not found (Fig. 1d). The epithelium was now composed of cuboidal cells (Fig. 2b). At 3 and 7 days

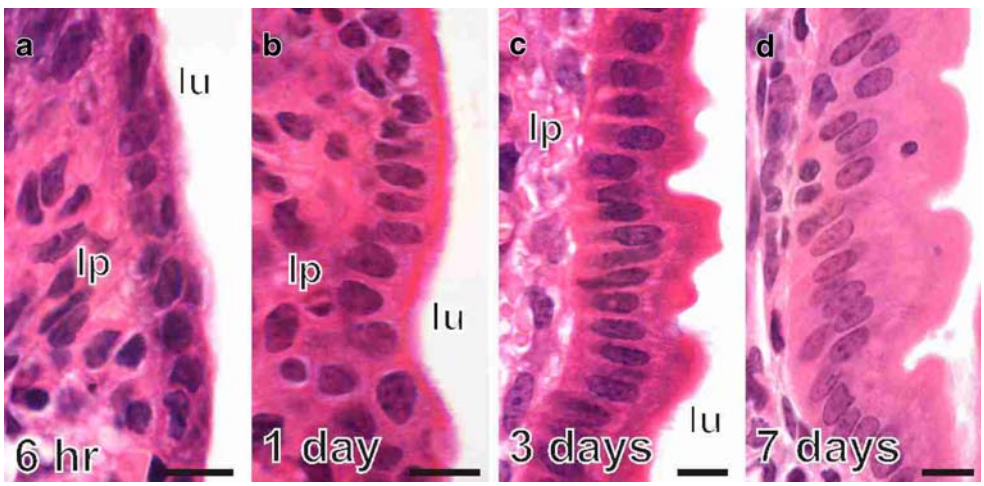

Fig. 2 Re-differentiation of enterocytes following TNBS-mediated disruption of the mucosal surface. **a** At 6 h after TNBS, the epithelium has formed as a continuous layer of squamous epithelial cells over most of the surface. *lp* lamina propria, *lu* lumen. **b** At 1 day, the epithelium is formed by a regular layer of cuboidal cells. **c** At 3 days, the epithelial cells have elongated and are similar to those in the normal ileum. **d** By 7 days, the epithelium has its normal appearance. *Scale bars* 10 μm

(Fig. 1e, f), the epithelium was intact. Villi began to be recognisable at 3 days, although there were still flattened regions. They were normal at 7 days. From 1 to 7 days, numerous small enclosed haemorrhages (petechiae) were observed in the wall, and the muscle layers were usually thickened. Sub-epithelial cysts were observed at 1 and 3 days (Fig. 1d), but these had resolved by 7 days. There was slight crypt dilatation at 1 and 3 days (Fig. 1d, e). At 7, 28 and 56 days, the intestine appeared macroscopically and histologically normal, except for increased numbers of eosinophils in the lamina propria, which is described below. The change in epithelial cell morphology from squamous to columnar between 6 h and 7 days (Fig. 2) was accompanied by the re-appearance of goblet cells (Fig. 3). In the first stages of re-epithelialisation, at 6 h, the proportion of goblet cells in the epithelium was lower than normal and there was no continuous brush border revealed by PAS staining (Fig. 3b). At 1 day, although goblet cell numbers had barely increased, the brush border and glycocalyx had returned. Goblet cell numbers continued to increase and had returned to normal proportions between 7 and 28 days (Fig. 3).

At 1, 3 and 7 days, numerous surface epithelial cells contained lysosome-like inclusions (Fig. 4). Many of the inclusions were strongly basophilic. Occasional intra-epithelial lymphocytes and eosinophils were found. Basophilic inclusions that were observed at 7 days were almost exclusive in epithelial cells at the tips of villi (Fig. 4d). In some cases, the engulfed material had the appearance of eosinophil or neutrophil cell residues (Fig. 4c), similar to the phagocytosed plasma cells that have been described in

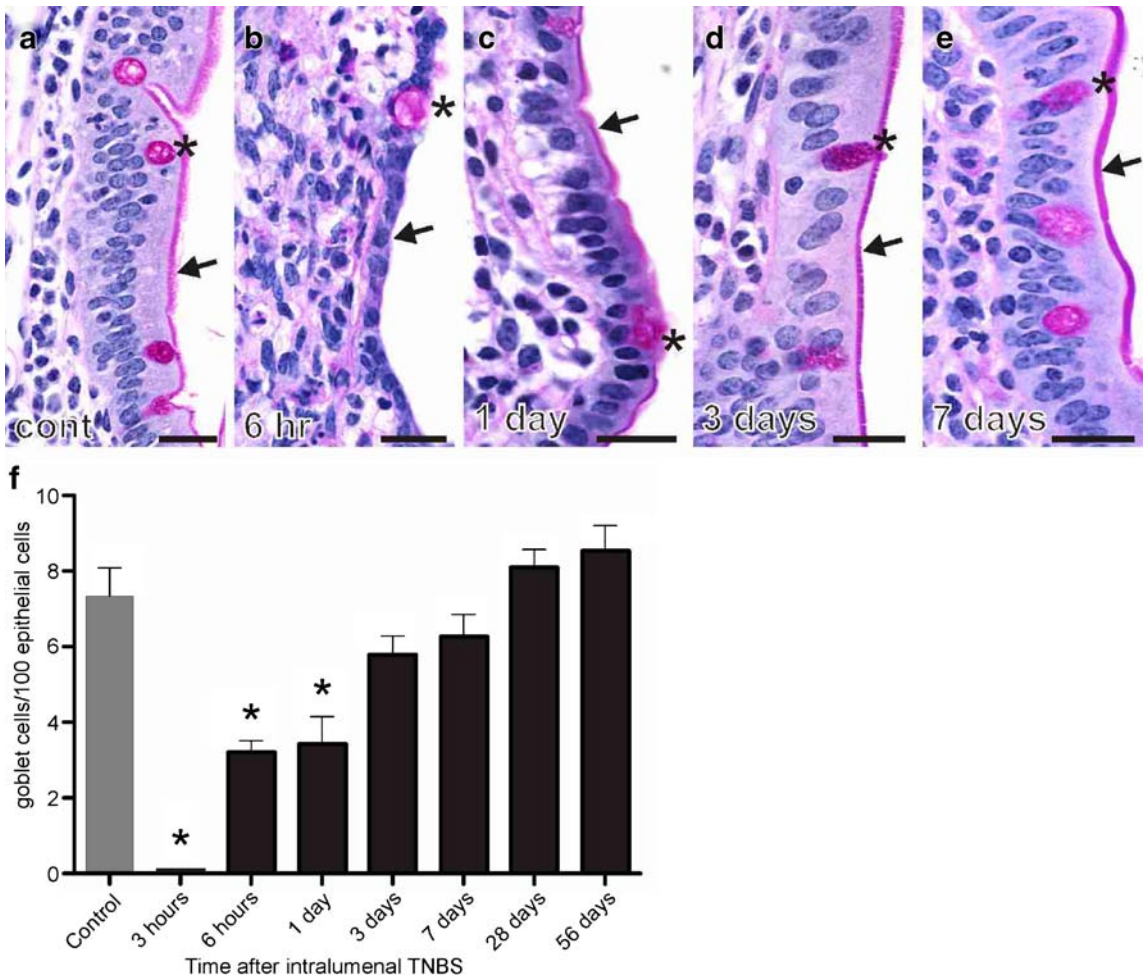

Fig. 3 Changes in goblet cells and surface mucus following inflammation with TNBS. **a** In the control, the goblet cells (*asterisk*) appear regularly in the epithelium, and a coating of mucus covers the lumenal surface (*arrow*). **b** At 6 h, goblet cells (*asterisk*) are rare at the surface, and a brush border and glycocalyx has not formed (*arrow*). **c** At 1 day, although goblet cells in the epithelium are still rare, the surface mucus layer is present (*arrow*). **d** At 3 days, the goblet cells (*asterisk*) appear mature, and there is a well-formed brush border. **e** The goblet cells and brush border appear to be normal at 7 days. **f** Goblet cell numbers at different times after infusion of TNBS into the lumen (mean ± SEM, $n=3$ animals for each time). TNBS treatment has a significant effect on goblet cell numbers (one-way ANOVA, $P<0.0001$). Numbers of goblet cells at 3 and 6 h and 1 day are significantly different to control (Dunnett's multiple comparison test, $P<0.05$, *asterisks*). *Scale bars* 20 μm

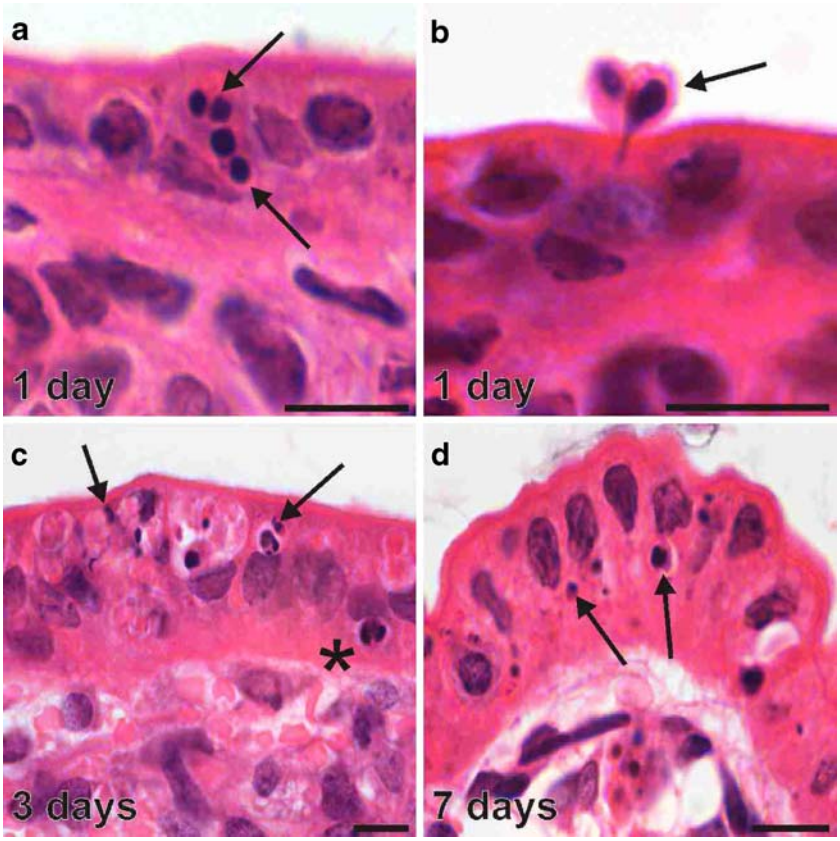

Fig. 4 Intra-epithelial inclusions, many probably being apoptotic bodies, indicative of the assumption of a phagocytic role by enterocytes. No inclusions were found in the normal intestine or in intestine from sham operations. **a** One day after TNBS, dark inclusion bodies are seen in healthy-looking enterocytes (*arrows*). **b** Small cytoplasmic extrusions into the lumen (*arrow*) that contain dense inclusions. These may indicate that debris is removed from the lamina propria and expelled into the lumen by phagocytic enterocytes. **c** Intra-epithelial inclusions 3 days after TNBS (*arrows*). An inclusion with the appearance of a neutrophil is indicated by the *asterisk*. **d** Inclusions at 7 days. Most of the enterocytes that have inclusions are at the tips of villi at this time. *Scale bars* 10 μm

the lung [21]. Some of the basophilic inclusions, surrounded by small amounts of cytoplasm, could be seen in the apparent process of extrusion at the luminal surface (Fig. 4b). No histological changes were observed in the intestine from sham-operated animals.

Immune cells

Eosinophils

Eosinophils were readily recognised in the haematoxylin and eosin-stained sections (Fig. 5). In the external layers, they were found close to myenteric ganglia, but they were not seen within the ganglia (Fig. 5a, d). The close eosinophils often appeared to be adhering to the surfaces of the ganglia (Fig. 5a, d). No eosinophils were found adjacent to myenteric ganglia in tissue from untreated guinea pigs, or from sham-operated guinea pigs, or in intestinal samples taken 10–20 cm proximal to the region affected by TNBS. In contrast to the infiltration of the spaces around the myenteric ganglia, eosinophils did not invade the circular or longitudinal muscle layers (Figs. 5a and 6). Eosinophil numbers also increased in the lamina propria and submucosa (Fig. 5b, c). The increase in eosinophil numbers peaked at about 6 h in each of the lamina propria, submucosa and myenteric plexus (Fig. 6). An increase was already apparent at 3 h in the lamina propria and submucosa, but not adjacent to myenteric ganglia. Eosinophil numbers declined and were no different to those of untreated guinea pigs by 3 days after TNBS in the submucosa and myenteric plexus (Fig. 6). However, the numbers remained elevated until 56 days in the lamina propria of the mucosa. In the tissue from sham animals, there was a slight increase in cell numbers at 6 h in the lamina propria and submucosa, but there was no increase in the region adjacent to the myenteric ganglia. There were no significant differences of shams from untreated animals at other time points.

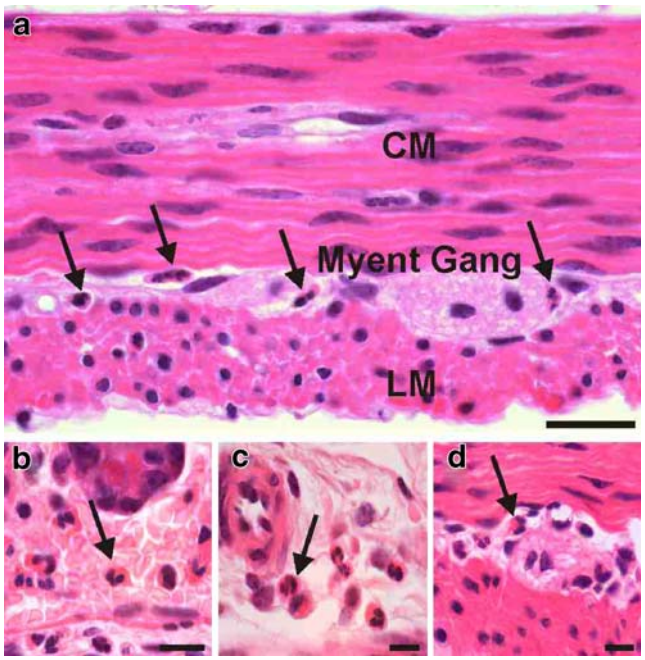

Fig. 5 The localisation of eosinophils in the wall of the ileum following inflammation. **a** Eosinophils located close to myenteric ganglia in the inflamed region, 1 day after the injection of TNBS into the lumen. Eosinophils are commonly found close to the ganglia (*arrows*), but were rare in the circular muscle (*CM*) and longitudinal muscle (*LM*). **b** Eosinophils in the lamina propria, 6 h after TNBS. At this stage, eosinophil numbers were already significantly elevated; six cells can be seen in this small field, one of which is indicated by the *arrow*. **c** Eosinophils in the submucosa, 1 day after TNBS (example at *arrow*). **d** An eosinophil close to a myenteric ganglion at 6 h. *Scale bars* 20 μm (**a**), 10 μm (**b**–**d**)

T lymphocytes

Very few T lymphocytes occurred adjacent to the myenteric ganglia of the control ileum, greater numbers were found in the submucosa and lymphocytes in the mucosa were numerous. TNBS injection into the lumen caused a substantial increase in submucosal lymphocyte numbers, 8-fold over the control at 6 h and 1 day (Fig. 7). Lymphocyte numbers declined to about half of the 1 day peak at 3 days, but were still above control at 7 and 28 days. They had returned to control at 56 days. In non-inflamed regions oral to the inflammation, there was a transient increase at 6 h, but the numbers were not different to control at 3, 7, 28 and 56 days.

TNBS injection into the lumen caused a greater than 50-fold increase in T-lymphocyte numbers in the myenteric plexus at 1 day at the site of mucosal exposure to TNBS (Fig. 8). The numbers of lymphocytes had dropped to a tenth of the 1-day value by 7 days and were back to control numbers at 28 and 56 days. In non-inflamed regions, there was a much smaller increase in T-cell number, less than 10% of the response in the area of TNBS injection.

Discussion

This study has defined the sequence of histological changes that occur following acute damage to the small intestinal lining by the hapten, TNBS, which is one of the agents commonly used to induce inflammation in animal models of acute human inflammatory bowel conditions, primarily because the immune reaction to TNBS resembles that observed in human mucosal inflammation [22].

Time course of mucosal repair

We observed that the mucosal surface is almost completely ablated at 3 h after TNBS, and that re-epithelialisation is extremely rapid, with the surface being almost fully covered, except for small foci of haemorrhage, by 6 h. It is notable that the crypts and crypt epithelium remained intact. By 12 and 24 h, surface re-epithelialisation is complete, but the epithelium has not differentiated. At this time, there are very few goblet cells; these did not return to normal numbers until after 7 days. Prior to 1 day, the lack of goblet cells was associated with a lack of brush border and associated glycocalyx at the epithelial surface, suggesting that the mucosa would be susceptible to further damage at this stage. A transient loss of goblet cells has also been reported following dextran sodium sulphate-induced colitis in the rat [23]. Inclusion cysts occurred in the early period after the restitution of the epithelium, as is also apparent in the paper of Gaudio [23]. A rapid return of epithelium is also observed after other destructive treatments [24, 25]. Experiments similar to ours, but on mouse colon, have shown re-epithelialisation at 1 day after dinitrobenzene sulphonate (DNBS; 300 mg/kg in 0.1 mL) and a similar early loss of mucin [26]. Epithelial repair was still incomplete in the rat colon 7 days after TNBS (150 mg/kg in 0.25 mL) in another study [27]. This compares with our use of 30 mg/kg in 1 mL. Slower repair is associated with deep erosion of the intestinal wall [25].

In the present study, the primary trigger for the inflammatory events, the disruption of the mucosal surface, allowing the entry of TNBS and gut flora, was largely over by 6 h, and there was an apparently complete sealing of the mucosal epithelium by 12 h. Experimentally, this provides a well-defined time of initiation of the events which follow, including the changes in enteric neuron properties, that are observed from 7 days to at least 56 days after TNBS [8, 14, 16, 17].

Mucosal phagocytic activity

A prominent feature of the epithelial changes was the appearance of dense lysosome-like intracellular inclusions at 1, 3 and 7 days. Thus, the epithelial cells assume a

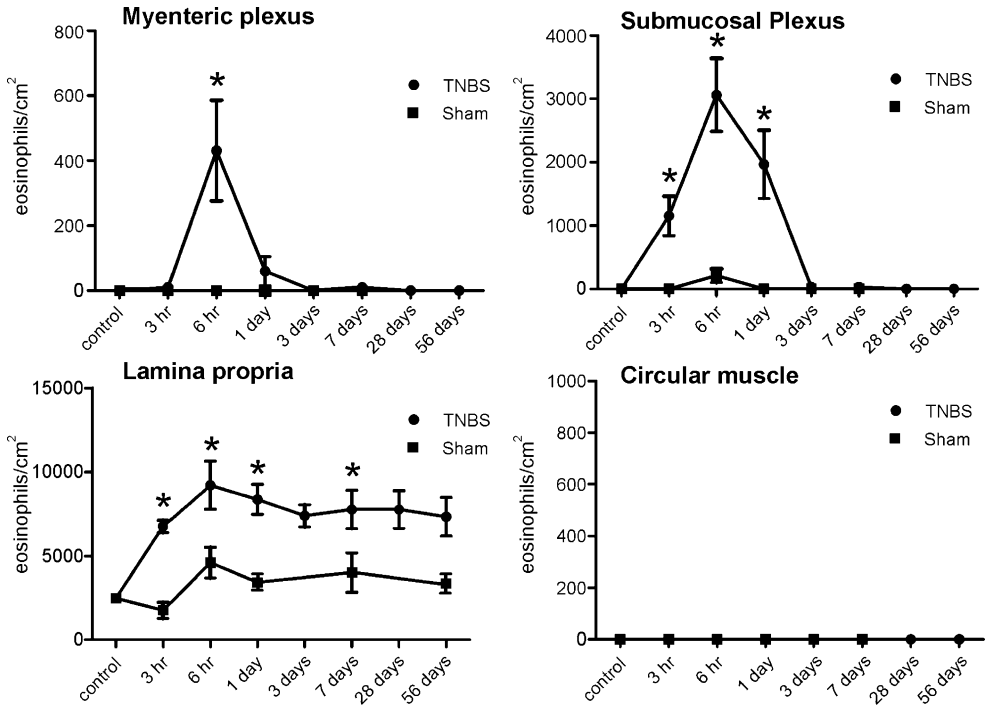

Fig. 6 The time course of changes in eosinophil numbers adjacent to ganglia of the myenteric plexus, submucosal plexus, lamina propria and circular muscle following the injection of TNBS into the lumen of the distal ileum. *Filled squares*, data from sham operations; *filled circles*, data from TNBS-treated guinea pigs. Myenteric plexus: eosinophils are normally absent from the myenteric plexus; numbers peaked at 6 h after TNBS and then subsided quickly; sham operation had no effect. Submucosal plexus: numbers rose very quickly, even at 3 h, peaked at 6 h and declined quickly; only a slight transient elevation in numbers occurred in the shams. Lamina propria: Cell numbers rose quickly and remained at an elevated level for at least 56 days; numbers after sham operation rose slightly. Circular muscle: Eosinophils did not occur in the circular muscle after TNBS or in the shams. Numbers of eosinophils are significantly changed by TNBS treatment in the myenteric plexus, submucosal plexus and lamina propria (two-way ANOVA, $P<0.001$). Differences are significant at 6 (myenteric plexus), 3 and 6 h and 1 day (submucosal plexus) and at all time points in the lamina propria (Bonferroni's test, post hoc, $P<0.05$, *asterisks*). Data are mean ± SEM, $n=3$ animals for each time

phagocytic phenotype, similar to that observed in other damaged surface epithelia [21, 28, 29]. This phagocytic activity of epithelia is thought to be important in clearing tissues of apoptotic cells, especially dying immune cells and cell debris [28]. We have observed the apparent extrusion of phagocytosed material into the lumen, suggesting that this process is important to remove debris from the lamina propria of the intestinal mucosa. Phagocytic activity continued for at least a week in our study, that is, it continues for 6 days after the epithelium has sealed and points to a very active role of the epithelium in dealing with the early stages of mucosal damage. Phagocytic inclusions in gastrointestinal epithelial cells have also been reported after aspirin damage to the gastric lining [30] and acid damage to the duodenal mucosa [31], but not previously after hapten-induced enteritis, as far as we have been able to determine.

Immune cells in the lamina propria

Increased numbers of immune cells in the lamina propria after inflammation have been seen in animal models [32] and in human post-infectious irritable bowel syndrome [19, 20, 33]. In humans, increased immune cell numbers in the rectal mucosa have been documented for at least a year after an acute *Campylobacter* enteritis [20]. Increased mucosal immune cell numbers are also seen in patients with long-standing intestinal neuromuscular dysfunction [6, 19]. In a previous investigation of the mucosa after intralumenal TNBS, increased mucosal lymphocyte numbers were observed at 10–14 days, but compared to the present study, this was a much more severe challenge that caused transmucosal necrosis [32]. In the present work, after TNBS causing only superficial mucosal damage, we found that eosinophil numbers peaked at 6 h and then remained elevated to about the same extent up to 56 days, in the mucosa of the guinea pig ileum. Our data suggest that in both experimental animals and in human, an acute injurious insult to the mucosa causes a long-term inflammatory reaction.

Immune cells and enteric ganglia

In a previous study, neutrophils were detected close to the myenteric ganglia 6 h following injection of DNBS into the colon lumen of rats, their numbers peaking at about 2 days

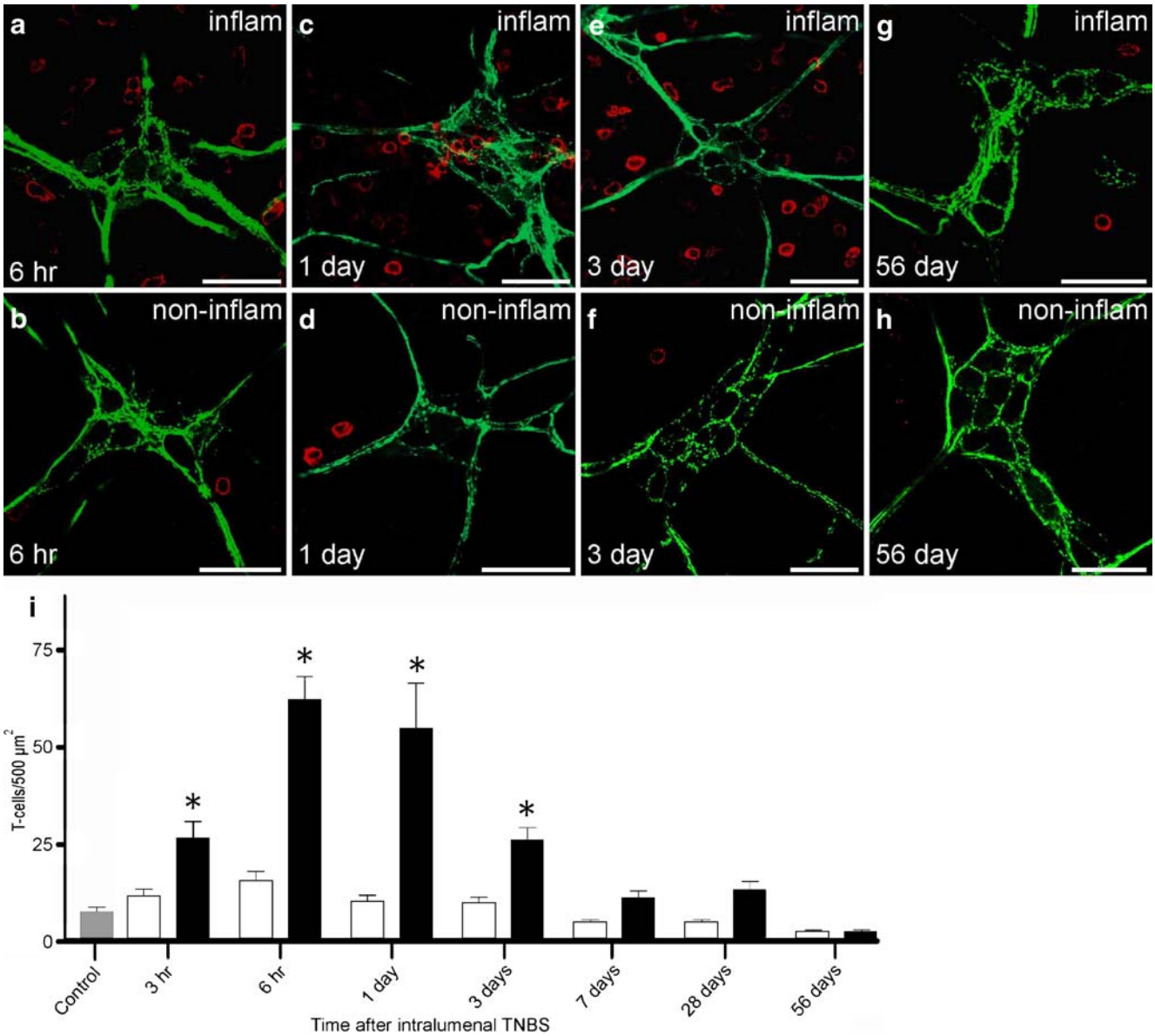

Fig. 7 T lymphocytes adjacent to submucosal ganglia of inflamed and non-inflamed regions of guinea pig small intestine at 3 h to 56 days after the injection of TNBS into the lumen. Tissue was taken from the region of inflammation and from intestine that was 10–20 cm proximal to the inflammation. T cells are *red* and the myenteric ganglia are revealed by immunoreactivity for calbindin (*green*). **a**, **b** At 6 h after injection of TNBS, T cells were observed adjacent to the ganglia from the inflamed region in increased numbers. **c**, **d** At 1 day, there were substantial numbers of T cells adjacent to the ganglia. Cell numbers were still elevated at 3 days (**e**, **f**), but had subsided by 56 days, when very few cells were observed close to ganglia (**g**, **h**). **i** Quantitation of T-cell numbers at different times after the inflammatory stimulus (mean ± SEM, n=3 animals for each time). Data are from inflamed (*black bars*) and non-inflamed (*open bars*) regions of the small intestine of the same guinea pigs at 3 h to 56 days after the application of TNBS. Numbers of T cells are significantly changed by TNBS treatment in the submucosal plexus (two-way ANOVA, $P<0.001$). Differences are significant at 3 and 6 h and 1 and 3 days (Bonferroni's test, post hoc, $P<0.05$, *asterisks*). Control: *grey bar*. *Scale bars* 50 µm

[34]. Similar observations were made in the guinea pig colon; neutrophils, eosinophils and lymphocytes, identified by their morphology, increased in numbers close to myenteric ganglia at 2 to 24 h after TNBS [35]. The next time point examined was 6 days, at which time the numbers of immune cells had declined to be close to control. Our data are consistent with these observations: we observed a rapid and transient appearance of eosinophils and T cells immediately adjacent to myenteric ganglia, whereas no eosinophils and few T cells were close to the ganglia in normal intestine. In addition, we investigated the submucosa where there was also a rapid early increase in immune cell numbers. TNBS increased the immune cell numbers in the submucosa at 3 h to 3 days. The increase in eosinophil

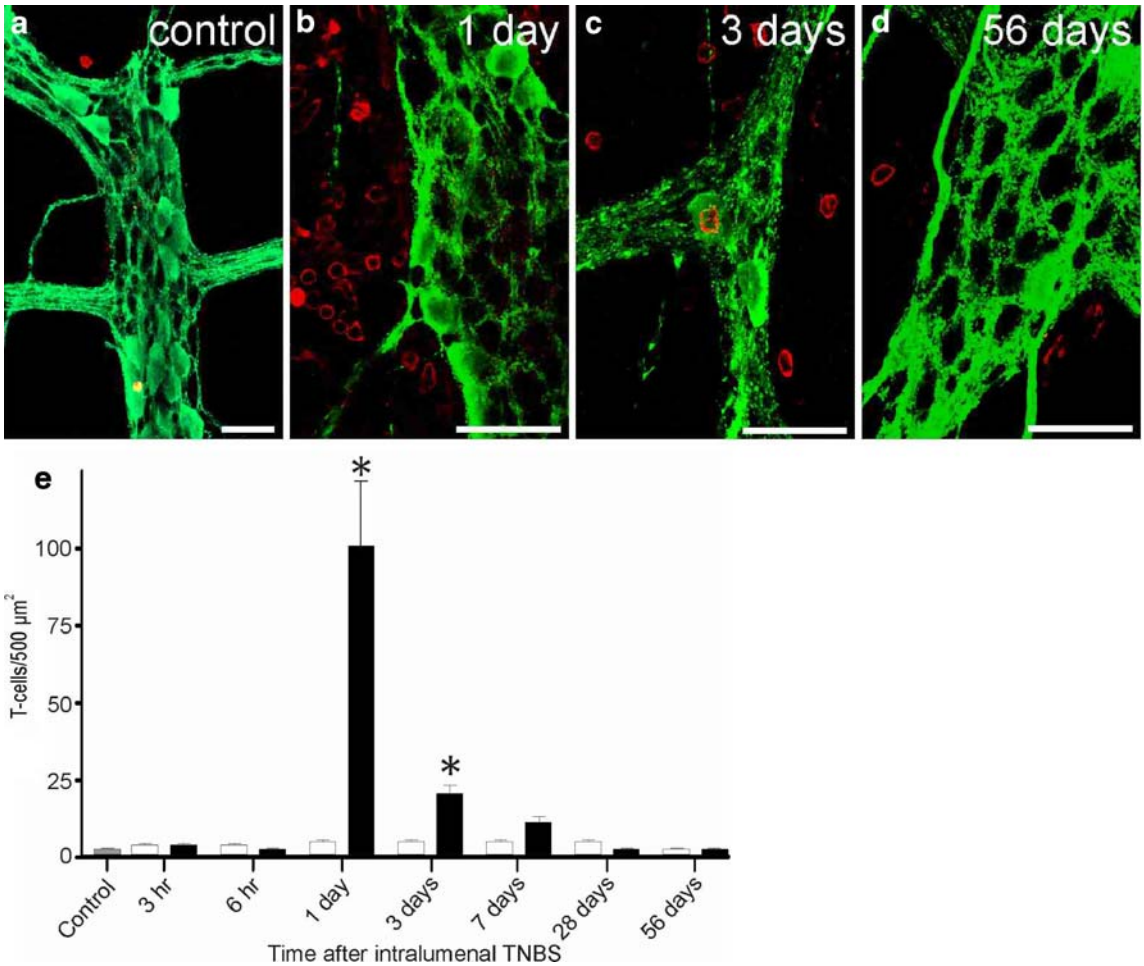

Fig. 8 The time course of changes in T-cell numbers at the level of the myenteric plexus. **a** Control preparation, in which T cells are *red* and the myenteric ganglia are revealed by immunoreactivity for calbindin (*green*). Few lymphocytes were found. **b** Numerous lymphocytes were adjacent to myenteric ganglia 1 day after TNBS treatment. **c** At 3 days after TNBS, numbers of lymphocytes were elevated, but were many fewer than at 1 day. **d** T-lymphocyte numbers were similar to control at 28 and 56 days. **e** Quantitation of T-cell numbers at different times after the inflammatory stimulus (mean ± SEM, $n=3$ animals for each time). Data are from inflamed (*black bars*) and non-inflamed (*open bars*) regions of guinea pig small intestine at 3 h to 56 days after the application of TNBS. Control: *grey bar*. Numbers of T cells are significantly changed by TNBS treatment in the myenteric plexus (two-way ANOVA, $P<0.001$). Differences are significant at 1 and 3 days (Bonferroni's test, post hoc, $P<0.05$, *asterisks*). *Scale bars* 50 µm

and T-cell numbers in the vicinity of submucosal ganglia was apparent at 3 h, whereas the rise in the myenteric plexus occurred slightly later. Eosinophils were first observed adjacent to myenteric ganglia at 6 h, and T cells were observed at 1 day. The time differences may reflect the fact that resident immune cells are common in the submucosa and can increase by local proliferation, whereas cells probably need to extravasate to colonise the myenteric ganglia. Following TNBS, eosinophils and T cells were common adjacent to myenteric ganglia but were rare in the muscle layers, indicating a specific targeting to enteric ganglia. Such selective targeting of immune cells to the ganglia, rather than the muscle, is also observed in human myenteric ganglia following inflammation [18, 36].

Implications

In normal intestine, there are no eosinophils associated with myenteric ganglia, and T cells are found in their vicinity only rarely. Thus, their presence in elevated numbers is an indication of ganglionitis and suggestive of neuropathology [6]. In this experimental model, the presence of immune cells adjacent to myenteric ganglia and the increased numbers close to submucosal ganglia were transient (peaks at about 6 h to 1 day which subsided by about 7 days), whereas the hyperexcitability of myenteric and submucosal neurons remains prominent for at least 56 days [8, 17]. This suggests that there is an enteric neuronal memory of previous insult. However, persistent mucosal inflammation

(indicated by increased eosinophil numbers) is still observed at 56 days, when the numbers of these cells are only slightly fewer than the peak at 6 h and about three times the numbers found in control. Thus, the immune state of the mucosa is re-set by a severe insult that ablates the mucosal surface. The major neuron type in myenteric ganglia whose properties are changed by a brief severe inflammation are the intrinsic primary afferent neurons (IPANs) [14, 16]. These neurons have processes in the mucosa that are stimulated by local mediators, for example short-chain fatty acids, adenosine triphosphate, 5-hydroxytryptamine and dietary amino acids [37–39]. Thus, the exposure of their nerve terminal in the mucosa to the products of immune cells may contribute to the maintenance of increased excitability of IPANs.

Conclusions

The immediate damage to the mucosa caused by TNBS is rapidly reversed (<1 day), and the increases in immune cell numbers close to enteric ganglia peak at 6 h to 1 day and have subsided by 3 days. However, the re-constituted epithelium is actively involved in clearing debris from the sub-epithelial connective tissue for at least a week and increased immune cell numbers in the mucosa and elevated enteric neuron excitability persist for at least 8 weeks. Thus, the ongoing hyperexcitability of enteric neurons is not due to a persistent ganglionitis, but ongoing mucosal inflammation may be a contributing factor.

Acknowledgements This work was supported by the National Health and Medical Research Council of Australia (NHMRC) grant 400020, a University of Melbourne visiting scholar award and a Fellowship of the Fundação de Amparo à Pesquisa do Estado de São Paulo, number 2008/05718-9 (to PC) and G8 Fellowship to MB. We thank Dr. Trung Nguyen for statistical analysis. Histology facilities were provided by the Australian Phenomics Network Histopathology and Organ Pathology Node.

Conflict of interest The authors declare that they have no conflict of interest.

References

1. Collins SM (1996) The immunomodulation of enteric neuromuscular function: implications for motility and inflammatory disorders. Gastroenterology 111:1683–1699
2. Sharkey KA, Kroese ABA (2001) Consequences of intestinal inflammation of the enteric nervous system: neuronal activation induced by inflammatory mediators. Anat Rec 262:79–90
3. De Giorgio R, Guerrini S, Barbara G et al (2004) Inflammatory neuropathies of the enteric nervous system. Gastroenterology 126:1872–1883
4. Khan WI, Collins SM (2005) Gut motor function: immunological control in enteric infection and inflammation. Clin Exp Immunol 143:389–397
5. Lomax AE, Linden DR, Mawe GM et al (2006) Effects of gastrointestinal inflammation on enteroendocrine cells and enteric neural reflex circuits. Auton Neurosci 126:250–257
6. Knowles CH, De Giorgio R, Kapur RP et al (2009) Gastrointestinal neuromuscular pathology: guidelines for histological techniques and reporting on behalf of the Gastro 2009 International Working Group. Acta Neuropathol (in press)
7. Barbara G, Vallance BA, Collins SM (1997) Persistent intestinal neuromuscular dysfunction after acute nematode infection in mice. Gastroenterology 113:1224–1232
8. Lomax AE, O'Hara JR, Hyland NP et al (2007) Persistent alterations to enteric neural signaling in the guinea pig colon following the resolution of colitis. Am J Physiol 292:482–491
9. Jacobson K, McHugh K, Collins SM (1995) Experimental colitis alters myenteric nerve function at inflamed and noninflamed sites in the rat. Gastroenterology 109:718–722
10. Pérez-Navarro R, Martínez-Augustin O, Ballester I et al (2005) Experimental inflammation of the rat distal colon inhibits ion secretion in the proximal colon by affecting the enteric nervous system. Naunyn Schmiedebergs Arch Pharmacol 371:114–121
11. De Schepper HU, De Man JG, Van Nassauw L et al (2007) Acute distal colitis impairs gastric emptying in rats via an extrinsic neuronal reflex pathway involving the pelvic nerve. Gut 56:195–202
12. X-x D, Thacker M, Pontell L et al (2008) Effects of intestinal inflammation on specific subgroups of guinea-pig celiac ganglion neurons. Neurosci Lett 444:231–235
13. Palmer JM, Wong Riley M, Sharkey KA (1998) Functional alterations in jejunal myenteric neurons during inflammation in nematode-infected guinea pigs. Am J Physiol 275:G922–G935
14. Linden DR, Sharkey KA, Mawe GM (2003) Enhanced excitability of myenteric AH neurones in the inflamed guinea-pig distal colon. J Physiol (Lond) 547:589–601
15. Lomax AE, Mawe GM, Sharkey KA (2005) Synaptic facilitation and enhanced neuronal excitability in the submucosal plexus during experimental colitis in guinea-pig. J Physiol (Lond) 564:863–875
16. Nurgali K, Nguyen TV, Matsuyama H et al (2007) Phenotypic changes of morphologically identified guinea-pig myenteric neurons following intestinal inflammation. J Physiol (Lond) 583:593–609
17. Krauter EM, Strong DS, Brooks EM et al (2007) Changes in colonic motility and the electrophysiological properties of myenteric neurons persist following recovery from trinitrobenzene sulfonic acid colitis in the guinea pig. Neurogastroenterol Motil 19:990–1000
18. Törnblom H, Lindberg G, Nyberg B et al (2002) Full-thickness biopsy of the jejunum reveals inflammation and enteric neuropathy in irritable bowel syndrome. Gastroenterology 123:1972–1979
19. Chadwick VS, Chen W, Shu D et al (2002) Activation of the mucosal immune system in irritable bowel syndrome. Gastroenterology 122:1778–1783
20. Spiller RC, Jenkins D, Thornley JP et al (2000) Increased rectal mucosal enteroendocrine cells, T lymphocytes, and increased gut permeability following acute *Campylobacter* enteritis and in post-dysenteric irritable bowel syndrome. Gut 47:804–811
21. Sexton DW, Blaylock MG, Walsh GM (2001) Human alveolar epithelial cells engulf apoptotic eosinophils by means of integrin- and phosphatidylserine receptor-dependent mechanisms: a process upregulated by dexamethasone. J Allergy Clin Immunol 108:962–969

22. Elson CO, Sartor RB, Tennyson GS et al (1995) Experimental models of inflammatory bowel disease. Gastroenterology 109:1344–1367
23. Gaudio E, Taddei G, Vetuschi A et al (1999) Dextran sulfate sodium (DSS) colitis in rats. Dig Dis Sci 44:1458–1475
24. Argenzio RA, Henrikson CK, Liacos JA (1988) Restitution of barrier and transport function of porcine colon after acute mucosal injury. Am J Physiol 255:G62–G71
25. Dignass AU (2001) Mechanisms and modulation of intestinal epithelial repair. Inflamm Bowl Dis 7:68–77
26. Boyer L, Ghoreishi M, Templeman V et al (2005) Myenteric plexus injury and apoptosis in experimental colitis. Auton Neurosci 117:41–53
27. Poli E, Lazzaretti M, Grandi D et al (2001) Morphological and functional alterations of the myenteric plexus in rats with TNBS-induced colitis. Neurochem Res 26:1085–1093
28. Monks J, Rosner D, Geske FJ et al (2005) Epithelial cells as phagocytes: apoptotic epithelial cells are engulfed by mammary alveolar epithelial cells and repress inflammatory mediator release. Cell Death Differ 12:107–114
29. Ichimura T, EJPv A, Humphreys BD et al (2008) Kidney injury molecule-1 is a phosphatidylserine receptor that confers a phagocytic phenotype on epithelial cells. J Clin Invest 118:1657–1668
30. Morris GP, Harding RK (1979) Phagocytosis of cells in the gastric surface epithelium of the rat. Cell Tissue Res 196:449–454
31. Feil W, Wenzl E, Vattay P et al (1987) Repair of rabbit duodenal mucosa after acid injury in vivo and in vitro. Gastroenterology 92:1973–1986
32. Elson CO, Beagley KW, Sharmanov AT et al (1996) Hapten-induced model of murine inflammatory bowel disease. J Immunol 157:2174–2185
33. Barbara G, De Giorgio R, Stanghellini V et al (2002) A role for inflammation in irritable bowel syndrome. Gut 51:i41–i44
34. Sanovic S, Lamb DP, Blennerhassett MG (1999) Damage to the enteric nervous system in experimental colitis. Am J Pathol 155:1051–1057
35. Linden DR, Couvrette JM, Ciolino A et al (2005) Indiscriminate loss of myenteric neurones in the TNBS-inflamed guinea-pig distal colon. Neurogastroenterol Motil 17:751–760
36. De Giorgio R, Camilleri M (2004) Human enteric neuropathies: morphology and molecular pathology. Neurogastroenterol Motil 16:515–531
37. Bertrand PP, Kunze WAA, Bornstein JC et al (1997) Analysis of the responses of myenteric neurons in the small intestine to chemical stimulation of the mucosa. Am J Physiol 273:G422–G435
38. Furness JB, Jones C, Nurgali K et al (2004) Intrinsic primary afferent neurons and nerve circuits within the intestine. Prog Neurobiol 72:143–164
39. Gwynne RM, Bornstein JC (2007) Local inhibitory reflexes excited by mucosal application of nutrient amino acids in guinea pig jejunum. Am J Physiol 292:G1660–G1670

Virchows Arch (2009) 455:67–75
DOI 10.1007/s00428-009-0793-z

ORIGINAL ARTICLE

Expression of Wnt gene family and frizzled receptors in head and neck squamous cell carcinomas

Silvia Maria Díaz Prado · Vanessa Medina Villaamil · Guadalupe Aparicio Gallego · Moisés Blanco Calvo · José Luis López Cedrún · Sheila Sironvalle Soliva · Manuel Valladares Ayerbes · Rosario García Campelo · Luis M. Antón Aparicio

Received: 21 October 2008 / Revised: 9 April 2009 / Accepted: 17 May 2009 / Published online: 19 June 2009

Abstract Genes of the Wnt and Frizzled class, expressed in HNSCC tissue and cell lines, have an established role in cell morphogenesis and differentiation, and also they have oncogenic properties. We studied Wnt and Fz genes as potential tumor-associated markers in HNSCC by qPCR. Expression levels of Wnt and Fz genes in 22 unique frozen samples from HNSCC were measured. We also assessed possible correlation between the expression levels obtained in cancer samples in relation to clinicopathologic outcome. Wnt-1 was not expressed in the majority of the HNSCC studied, whereas Wnt-5A was the most strongly expressed by the malignant tumors. Wnt-10B expression levels were related with higher grade of undifferentiation. Related to Fz genes, Fz-5 showed more expression levels in no-affectation of regional lymph nodes. Kaplan–Meier survival analyses suggest a reduced time of survival for low and high expression of Wnt-7A and Fz-5 mRNA, respectively. qPCR demonstrated that HNSCC express Wnt and Fz members, and suggested that Wnt and Fz signaling is activated in HNSCC cells.

Keywords Wnt · Frizzled · Head and neck squamous cell carcinoma · Quantitative real-time PCR · Molecular marker

S. M. Díaz Prado · L. M. Antón Aparicio
Medicine Department, University of La Coruña,
La Coruña, Spain

S. M. Díaz Prado · V. Medina Villaamil · G. Aparicio Gallego · M. Blanco Calvo · M. Valladares Ayerbes
Research Unit, Biomedical Research Institute (INIBIC),
Complexo Hospitalario Universitario A Coruña,
La Coruña, Spain

J. L. López Cedrún · S. Sironvalle Soliva
Maxillofacial Surgery Service,
Complexo Hospitalario Universitario A Coruña,
La Coruña, Spain

M. Valladares Ayerbes · R. García Campelo · L. M. Antón Aparicio (✉)
Medical Oncology Service,
Complexo Hospitalario Universitario A Coruña,
As Xubias S/N. 15.006,
La Coruña, Spain
e-mail: luis.miguel.anton.aparicio@sergas.es

Introduction

Squamous cell carcinoma (SCC) is the most frequent malignant tumor of the head and neck area. In the last years, there has been great progress in identifying molecular changes that occur during the malignant transformation of cells.

Although many molecular markers have been evaluated, the role of Wnt and Fz in carcinogenesis of HNSCC remains poorly understood. The diverse receptor–ligand pairs of the Wnt and Frizzled families play essential roles in the regulation of the cell growth, motility, and differentiation during embryonic development [1, 2]. Genes of the wingless (Wnt) and frizzled (Fz) class have an established role in cell morphogenesis and cellular differentiation [3–5].

Wnt genes encode a large family of secreted glycoproteins expressed in species ranging from *Drosophila* to human. The Wnt family constitutes 19 members in the human genome. The Wnt glycoproteins are ligands for the Fz receptors, which exert their effects through activation of distinct intracellular signaling pathways. The intracellular Wnt signaling have been recognized in four

distinct branches: the canonical β-catenin pathway, which activates the target genes in the nucleus; the planar cell polarity pathway, which involves JNK (Jun N-terminal kinase) and cytoskeletal rearrangements; the Wnt/Ca^{2+} pathway, which involves activation of PLC (phospholipase C) and PKC (protein kinase); and a pathway that regulates spindle orientation and asymmetric cell division [6–10].

Aberrant activation of the Wnt signaling pathway has been reported during neoplastic progression, and became evident in cancer with the discovery that a number of Wnt genes have now been associated with the development of various human cancers [11–17].

To date, different roles for Wnt have been recognized in squamous cell carcinomas of the oral cavity [18, 19]. Also, it is known that Wnt and Fz proteins are expressed in HNSCC cell lines, suggesting that they play a role in cell growth and survival. However, no examination has been made on Wnt and Fz expression in human oral carcinomas specimens by qPCR.

In the present study, we have studied expression levels of Wnt and Fz family members. The hypothesis that prompted this study was that human HNSCC might show different Wnt and Fz expression patterns than to those shown in tumor cell lines. We examined frozen human samples of HNSCC for the expression of five Wnt and two Fz genes.

Materials and methods

Processing of clinical tissue specimens

Fresh primary tumor samples of head and neck squamous cell carcinomas (HNSCC) from 22 patients, who underwent surgical removal of their tumors, were obtained from the Maxillofacial Surgery Service, A Coruña University Hospital. Among the total specimens, 22 samples comprised central tumor tissue and 16 comprised peritumoral tissue; both tissues were obtained from the same HNSCC patient (Table 1). As control, a pool of healthy human oral mucosa (n=19) was used. The study was approved by the Institutional Review Board of the Ethic Committee of Clinical Investigation of Galicia (Spain). All tumor samples were confirmed by histopathological analysis. Tissue samples were dissected under stringent sterile conditions to prevent RNA contamination and immediately were frozen in liquid nitrogen and stored at −80°C until RNA extraction.

RNA extraction

Isolation of total RNA from frozen healthy and malignant specimens was performed, following manufacturer's protocols, using Tripure Isolation Reagent (Roche, Mannheim, Germany).

Table 1 Clinicopathologic data from tumors analyzed

N	Localization	Type	G	Stage	TNM	Gender	Age (years)
1	Tongue	SCC	4	IV	T4N1M1	F	60
2	Tongue	SCC	1	IV	T3N0M0	M	80
3	Floor of mouth	SCC	3	IV	T4N2M0	M	47
4	Oropharynx	SCC	1	II	T2N0M0	M	71
5	Tongue	SCC	2	III	T2N1M0	M	65
6	Retromolar trigone	SCC	3	III	T3N0M0	M	73
7	Floor of mouth	SCC	3	III	T2N1M0	M	54
8	Floor of mouth	SCC	3	IV	T1N2M0	M	44
9	Cheek	SCC	1	IV	T4N0M0	M	80
10	Oropharynx	SCC	2	IV	T3N2M0	M	55
11	Tongue	SCC	2	IV	T4N1M1	F	39
12	Tongue	SCC	1	II	T2N1M0	M	52
13	Palate	SCC	2	IV	T1N2M0	M	49
14	Tongue	SCC	3	IV	T3N0M0	M	64
15	Floor of mouth	SCC	2	IV	T4N0M0	M	55
16	Tongue	SCC	2	IV	T2N2M0	M	75
17	Retromolar trigone	SCC	2	IV	T4N0M0	M	73
18	Maxilla	SCC	2	IV	T4N0M0	M	61
19	Oropharynx	SCC	2	II	T2N0M0	F	53
20	Tongue	SCC	1	II	T2N0M0	M	56
21	Retromolar trigone	SCC	1	I	T1N0M0	M	65
22	Maxilla	SCC	3	IV	T4N0M0	M	69

Characteristics of the head and neck tumors analyzed

SCC squamous cell carcinoma, *TNM* TNM status, *F* female, *M* male

For the isolation of each tissue sample, 50 to 100 mg was processed. Total RNA were treated with DNase I.

RNA integrity was confirmed by 2% agarose gel electrophoresis stained with ethidium bromide. RNA was also assessed for quantity at 260 nm using a GENIOUS UV spectrophotometer. A260/A280 relation was calculated for quality, quantity, and purity.

cDNA synthesis

Reverse-transcription PCR (RT-PCR) was performed using Super-Script™ First-Strand Synthesis System for RT-PCR (Invitrogen, Spain) up to a total volume of 20 µl. One microgram of total RNA, 2.5 nM random hexamers, 0.5 mM dNTP mix, and 3 µl of DEPC-treated water were denatured at 65°C for 5 min and chilled on ice for at least 1 min. On the other hand, 2 µl of 10× RT buffer, 5 mM $MgCl_2$, 0.01 M DTT, and 40 U of RNase-OUT™ Recombinant Ribonuclease Inhibitor were mixed, collected by centrifugation, and incubated at 25°C for 2 min. After incubation, 50 U of Super-Script™ II RT was added and incubated at 25°C for 10 min, 42°C for 50 min, and 70°C for 15 min in a Thermocycler (Gene AMP PCR System 9700, Applied Biosystems, Spain). Finally, samples were chilled on ice and incubated with 2 U of RNAse H for 20 min at 37°C before proceeding to the amplification of the target cDNA. Positive and negative controls were included in each experiment.

RNA extraction, reverse-transcription PCR assay setup, and post reverse-transcription PCR product analysis were carried out in separate designated rooms to prevent cross-contamination. cDNA was quantified and assessed for purity using a Genious UV spectrophotometer. cDNA concentration was measured at 260 nm. Also, A_{260}/A_{280} relation was calculated in order to know cDNA quality, quantity, and purity.

Quantitative real-time PCR (qPCR)

Quantitative real-time PCR analysis was performed, using LightCycler® 480 SYBR Green I Master Kit (Roche), on a LightCycler® 480 Real Time PCR System (Roche). PCR reaction consisted of 10 µl of Master Mix 2× conc., 0.35 µM of each forward and reverse primer, template cDNA, and PCR-grade water up to a final volume of 20 µl in the LightCycler 480 Multiwell Plate 96. Multiwell plate was centrifuged at 3,000 rpm for 2 min and was loaded in the LightCycler 480 Instrument until the PCR program started. An initial activation at 95°C for 5 min followed by an amplification target sequence 50 cycles of 95°C for 10 s, 59–60°C (depending on the primers pair used) for 10 s, and 72°C 9–20 s (depending on the amplicon size amplified) was used. For melting curve analysis, one cycle of 95°C for 5 s, 70°C for 15 s, and 95°C for 1 s was used. Finally, a cooling step was used at 40°C for 10 s. PCR primers for the amplification of the different Wnt and Fz genes were carefully designated using the web-based ProbeFinder software (Universal ProbeLibrary Design Center) accessible at [43] or via Roche Applied Science home page [44]. PCR primers were positioned to span exon–intron boundaries in order to reduce the risk of detecting genomic DNA. Primers were purchased from Roche Mannheim (Germany). The following list summarizes the primer pairs used: Wnt-1: 5′ TCT TCG GCA AGA TCG TCA A 3′ (forward); 5′ ACA CGT GCA GGA TTC GAT G 3′ (reverse). Wnt-5A: 5′ TGG TGC CTG ATA TCT CAA AGT C 3′ (forward); 5′ GAG AAA TAA CCC CAG AGT AAA CTG TAA 3′ (reverse). Wnt-7A: 5′ GGG AAG GAG CTC AAA GTG G 3′ (forward); 5′ CTG GCC TTG CYY CYC TTT GT 3′ (reverse). Wnt-10B: 5′ AAT GCG AAT CCA CAA CAA CA 3′ (forward); 5′ TCC AGC ATG TCT TGA ACT GG 3′ (reverse). Wnt-13: 5′ AAG ATG GTG CCA ACT TCA CCG 3′ (forward); 5′ CTG CCT TCT TGG GGG CTT TGC 3′ (reverse). Fz-2: 5′ CAT CGA GGC CAA CTC TCA GT 3′ (forward); 5′ AGG CCT ACG AAG CAC ACG 3′ (reverse). Fz-5: 5′ TAC CCA GCC TGT CGC TAA AC 3′ (forward); 5′ GGA TTC CAG GGA AAG GAC TCT 3′ (reverse). HPRT: 5′ TGA CCT TGA TTT ATT TTG CAT ACC (forward); 5′ CGA GCA AGA CGT TCA GTC CT 3′ (reverse). Suitable selection of housekeeping gene was performed using Human Endogenous Control Gene Panel (TATAA Biocenter, Sweden). The Excel macro named GeNorm VBA applet for Microsoft Excel was used to determine the gene with the most correlated expression in the set of samples. HPRT (hypoxanthine-guanine phosphoribosyltransferase) was used as internal control. Also, housekeeping gene was used to verify integrity of RNA and efficacy of reverse transcription. Any specimen with inadequate housekeeping mRNA level was excluded from the study.

We verified that amplifications and the expected size of each qPCR product were specific. Agarose gel electrophoresis (1.8%) of all PCR products revealed a single band that corresponded to the single-amplified products as predicted by the melting curve analysis of the PCR. The amplification efficiency was determined for both target and housekeeping genes and was equal (99–100%).

Data analysis was performed with LightCycler® 480 Relative Quantification software (Roche). Relative expression levels (R.E.L) were calculated by the $2^{-\Delta\Delta Ct}$ method [20]. Each assay was done at least in triplicate and it included marker-positive and marker-negative controls and reagent with no template controls.

DNA sequencing

Al least one qPCR product coming from each quantitative real-time PCR experiment was used as template

DNA in order to verify the specificity of the amplified amplicon. Products were purified by enzymatic method (ExoSAP-IT, Amersham USB). DNA sequencing was performed on an ABI 3700 system (Applied Biosystems) using Big Dye terminators. Forward and reverse primers used in sequencing reactions were the same as for the real-time PCR.

Statistical analysis

Statistical analysis of the results was performed with SPSS program (version 12.0 for Windows). The relationship between Wnt and Fz expression values and clinicopathological data was studied by non-parametric statistic, Kruskal–Wallis, and Mann–Whitney *U* tests. The relationship among the different markers tested with patient's survival was performed by Cox regression and Kaplan–Meier curves analyses. Statistical significance of differences was evaluated at the 95% confidence level; p values <0.05 were considered to be significant.

Other procedures

Standard procedures for manipulation of nucleic acids were essentially those previously reported [21].

Results

Expression of Wnt genes in head and neck squamous cell carcinoma and healthy human oral mucosa of head and neck

To assay Wnt gene expression as potential tumor-associated markers in HNSCC, we analyzed various tumors by qPCR. With the exception of Wnt-1, all the genes tested showed expression in peritumoral and central tumor tissues of oral mucosa. Of the Wnt genes, Wnt-1 was not expressed in the majority of the HNSCC studied; only three cases showed expression. Wnt-5A was the most strongly expressed by the central zones of the malignant tumors, followed by Wnt-13, Wnt-10B, and Wnt-7A. Regarding peritumoral tissues, Wnt-5A was also the most strongly expressed, followed by Wnt-10B, Wnt-13, and Wnt-7A. Wnt-5A, Wnt-7A, and Wnt-13 showed higher mRNA expression levels in central tumor tissues than in the peritumoral zones (Fig. 1a). When we compared Wnt mRNA expression levels in human central tumor tissues against healthy human oral mucosa, we observed that the higher levels were obtained in central tumor zones (Fig. 1b). When we compared Wnt mRNA expression levels in human peritumoral tissues against healthy human oral mucosa, we observed that the higher levels were obtained in peritumoral zones (Fig. 1c).

Expression of Fz genes in head and neck squamous cell carcinoma and healthy human oral mucosa of head and neck

To assay Fz gene expression as potential tumor-associated markers in HNSCC, we analyzed various tumors by qPCR. Both genes tested showed expression in peritumoral and central tumor tissues of oral mucosa. Of the Fz genes, Fz-2 was the most strongly expressed by the central tumor zones of the malignant tumors, followed by Fz-5. Regarding peritumoral tissues, Fz-2 was the most strongly expressed, followed by Fz-5 (Fig. 1a). When we compared Fz mRNA expression levels in human central tumor tissues against healthy human oral mucosa, we observed that the higher levels were obtained in central tumor zones (Fig. 1b). When we compared Fz mRNA expression levels in human peritumoral tissues against healthy human oral mucosa, we observed that the higher levels were obtained in peritumoral zones (Fig. 1c).

Correlation of Wnt and Fz gene expression with clinicopathological parameters and patient's survival

mRNA expression levels of the different Wnt genes tested in central tumor zones were correlated, by means of non-parametric statistics, with different clinicopathological parameters that included TNM status, stage, tumor localization, degree of differentiation, sex, and age (Table 2). Among all Wnt genes, WNT10B expression levels were correlated with higher grade of undifferentiation (Mann–Whitney *U* test, $p=0.013$). Related to Fz genes, Fz-5 showed higher expression in no-affectation of regional lymph nodes (Mann–Whitney *U* test, $p=0.009$). Fz-5 was not correlated with TNM status (Kruskal–Wallis test, $p>0.05$), although it could seem to exist a direct relation between them. More tumor specimens of HNSCC should be screened to validate these findings.

In order to know if there is any relationship among the different markers tested and patient's survival, we performed Cox regression and Kaplan–Meier curves analyses. Cox regression analyses showed that there is no statistically significant relationship among the different markers studied with patient's survival. However, when we performed Kaplan–Meier curves analyses, using the median of the R.E.L for each marker tested as cut-off value, we could appreciate that for Wnt-7A and Fz-5 we obtained values with statistical significance. Regarding Wnt-7A marker, we suggest that patients with R.E.L above the median (median=1.056) have higher survival than those with R.E.L. below the median ($p=0.024$). Also, for Fz-5 marker, we suggest that patients with R.E.L. above the median (median=5.859) have lower survival than those with R.E.L. below the median ($p=0.011$). In this way, Kaplan–Meier survival analyses

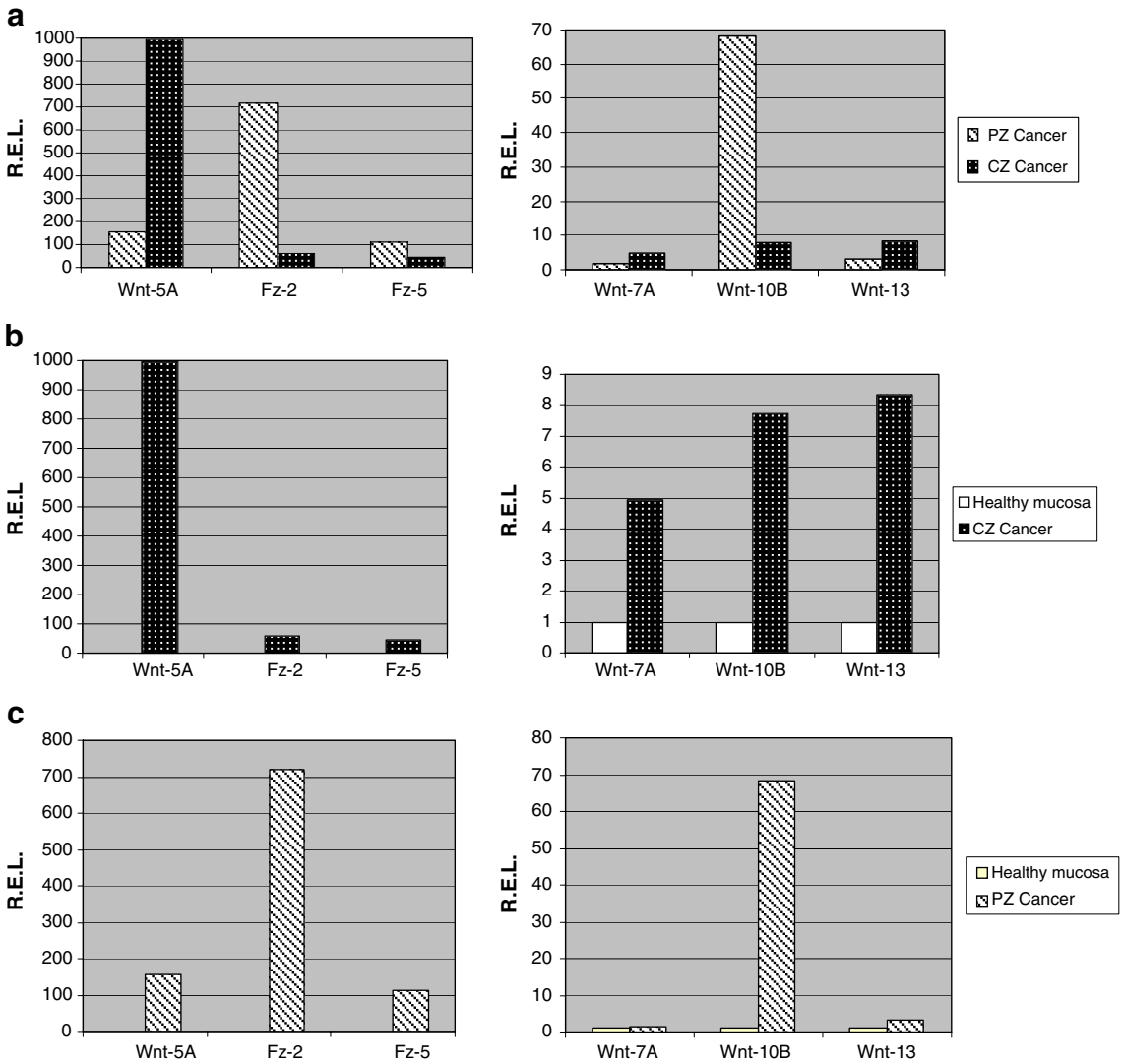

Fig. 1 Wnt and Fz mRNA expression levels in different human HNSCC, peritumoral zone (*PZ Cancer*, $n=16$) versus central tumor zone of the tumor (*CZ Cancer*, $n=22$) (**a**). Wnt and Fz mRNA expression levels in a pool of healthy human oral mucosa ($n=19$) versus central tumor tissue (*CZ Cancer*, $n=22$) (**b**). Wnt and Fz mRNA expression levels in a pool of healthy human oral mucosa ($n=19$) versus peritumoral tissue (*PZ Cancer*, $n=16$) (**c**). *Y* axis represents Wnt and Fz mRNA relative expression levels (*R.E.L.*) and *X* axis represents the different human Wnt and Fz genes tested. mRNA levels were measured by quantitative real-time PCR as described in Materials and methods. Quantitative real-time PCR results are the mean of at least three independent measurements. Data were normalized versus the values obtained in healthy human oral mucosa which were considered equal to 1

suggest a reduced time of survival for low R.E.L. of Wnt-7A mRNA and for high R.E.L. of Fz-5 mRNA (Fig. 2).

Discussion

To evaluate Wnt and Fz gene expression as potential tumor-associated markers in HNSCC, we screened various tumors by qPCR. The results revealed that Wnt-5A was the most strongly expressed by the central tumor tissues, but Wnt-1 was not expressed in the majority of the HNSCC studied (only three cases expressed Wnt-1). On the contrary, Rhee et al. [14] observed that Wnt-1 was one of the most expressed in HNSCC cell lines besides Wnt-10B and Wnt-5A. Also, they observed no differences in Fz-5 expression in HNSCC cell lines against normal human broncho-epithelial and oral squamous epithelial cell lines, whereas in HNSCC tissues we obtained an increased expression of Fz-5 with regard to healthy human oral mucosa. Among all Wnt genes, expression levels of Wnt-10B in central tumor zone were related with higher grade of undifferentiation. The present study demonstrates that HNSCC express Wnt and Fz members and that all Wnt and Fz genes tested were overexpressed not only in peritumoral zone but also in central tumor tissues of human HNSCC specimens.

Table 2 Correlation among different expression levels and clinicopathologic data

Variable	%	Wnt-1	Wnt-5A	Wnt-7A	Wnt-10B	Wnt-13	Fz-2	Fz-5
Sex								
Male	86.4	$p>0.05$a	$p>0.05$a	$p>0.05$a	$p>0.05$a	$p>0.05$a	$p>0.05$a	$p>0.05$a
Female	13.6							
Stage								
I	4.5							
II	18.2	$p>0.05$b	$p>0.05$b	$p>0.05$b	$p>0.05$b	$p>0.05$b	$p>0.05$b	$p>0.05$b
III	13.7							
IV	63.6							
T								
T1	13.6							
T2	31.8	$p>0.05$b	$p>0.05$b	$p>0.05$b	$p>0.05$b	$p>0.05$b	$p>0.05$b	$p>0.05$b
T3	18.2							
T4	36.4							
N								
N0	54.6	$p>0.05$a	$p>0.05$a	$p>0.05$a	$p>0.05$a	$p>0.05$a	$p>0.05$a	$p=0.009$a
N1, N2	45.4							
M								
M0	90.9	$p>0.05$a	$p>0.05$a	$p>0.05$a	$p>0.05$a	$p>0.05$a	$p>0.05$a	$p>0.05$a
M1	9.1							
G								
G1	27.3	$p>0.05$a	$p>0.05$a	$p>0.05$a	$p=0.013$a	$p>0.05$a	$p>0.05$a	$p>0.05$a
G2, G3, G4	72.7							
Localization								
Tongue	36.4							
Mouth floor	18.2							
Alveolar ridge	4.5							
Retromolar trigone	9.1	$p>0.05$b	$p>0.05$b	$p>0.05$b	$p>0.05$b	$p>0.05$b	$p>0.05$b	$p>0.05$b
Oropharyx	13.7							
Cheek	4.5							
Palate	4.5							
Maxilla	9.1							

Correlation between Wnt and Fz expression status and various clinicopathologic variables

a Mann–Whitney *U* test, *b* Kruskal–Wallis test

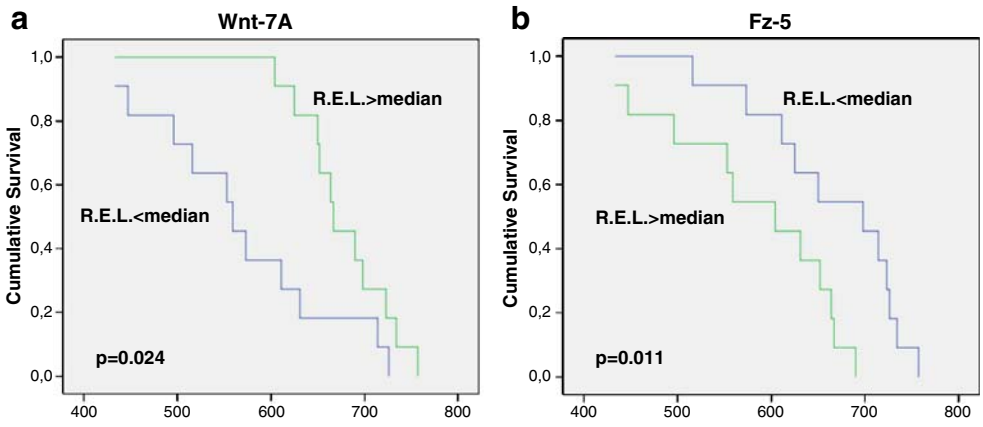

Fig. 2 Kaplan–Meier graphs for time of survival according to R. E.L. of Wnt-7A (**a**) and Fz-5 (**b**) mRNA in central tumor tissue of HNSCC; *p* values are given for log rank tests

Aberrant activation of the Wnt and Fz signaling pathway has been reported in HNSCC lines [14]. These investigators found that Wnt-1, Wnt-10B, Wnt-13, and Fz-2 were overexpressed in ten HNSCC lines in comparison to normal human bronchial epithelium, suggesting that the growth and survival of a subset of this tumor may depend on the Wnt/Fz pathway. Other studies focusing on the involvement of Wnt family expression in oral squamous cell carcinomas (OSCC) tissue samples and cell lines showed that carcinoma cells express many Wnt family members [18, 19].

Our finding of a weak expression of Wnt-1 and a high Wnt-10B expression not only in central tumor zone but also in peritumoral tissue is compatible with the idea that Wnt-1 and Wnt-10B have a redundant function [22]. If this is true, it may be speculated that, in differentiated HNSCC, Wnt-1 plays a role in the control of differentiation, proliferation, and invasiveness of cells. This cellular defense mechanism may subsequently be lost in undifferentiated steps and while the Wnt-1 expression is silenced the expression of Wnt-10B is emerging in undifferentiated carcinomas. Wnt-1 is part of a Wnt cluster conserved in all vertebrates comprising Wnt-1 and Wnt-10B. The function of Wnt-10B during oncogenesis has not been explored yet. In zebrafish, Wnt-10B is expressed in a pattern overlapping extensively with that of Wnt-1; Wnt-1 and Wnt-10B provide partially redundant functions [22].

Interestingly, in human genome, Wnt-1 maps to linkage group (LG) 23 in close proximity to another Wnt paralog, Wnt-10B [23, 24]. The linkage of Wnt-1 and Wnt-10B paralogs has been conserved in the vertebrate linkage, and this relationship may reflect the existence of three ancient Wnt paralogs present before the divergence of protostomes and deuterostomes, Wnt-1, Wnt-6, and Wnt-10 [25]. The conservation of the spatial arrangement of Wnt-1 and Wnt-10B raises the possibility that their expression may be regulated in a coordinated and sequential fashion [26, 27]. In support of this assertion, a fragment of Wnt-10B gene showed an expression pattern that may be similar to that shown by Wnt-1 [28].

Our study demonstrates an increased expression of Wnt-10B mRNA in HNSCC, whereas Wnt-1 expression was low or undetectable. This pattern does not fit to observations in oral squamous cell carcinoma lines where Wnt-1 mRNA was overexpressed [14]. This Wnt-1 strong expression in carcinoma cell lines but a complete loss in human head and neck squamous cell carcinomas could indicate a post-translational deregulation. Discrepancy between transcriptional and translational control fits to observations in other tumor types as aggressive invasive breast ductal cancers where, in the undifferentiated state, a selective loss of protein expression was found in parallel to an aggressive state of the tumor [29].

Although many Wnt genes have been evaluated in HNSCC, the role of Wnt-5A remains poorly understood. In the study of Rhee et al. [14] and in the study of Uraguchi et al. [18], Wnt-5A was expressed in 4/10 and 5/14 carcinoma HNSCC cells lines, respectively. In contrast, we found a strong expression of WNT-5A not only in peritumoral zone but also in central tumor tissue of HNSCC specimens. The importance of Wnt-5A signaling and their function in HNSCC are currently incompletely understood. It is known that in other human tumorsWnt-5A serves as an antagonist to the canonical Wnt signaling pathway with tumor suppressor activity in differentiated carcinomas. Also, Wnt-5A expression is compatible with the idea that Wnt-5A has a tumor activity; Wnt-5A plays a role in the control of tumor differentiation, proliferation, and invasiveness of cells [30–33].

While some Wnt genes, expressed in normal tissues during embryonic or post-natal period, induce cell morphological changes and cellular differentiation, the same Wnt genes can be expressed in both normal adult and tumoral tissues. These disappointing behaviors suggest that members of the Wnt family implicated in normal physiologic tissue development or repair are not expressed when the tissue has ceased proliferating and exhibit overexpression in hyperplastic or oncogenic transformation. Wnt proteins have a different function in carcinogenesis, and based on their ability to transform mouse mammary epithelial cells, they can be divided into three different classes: Wnt-1, Wnt-3A, and Wnt-7A have the greatest transforming capacity; Wnt-2, Wnt-5B, and Wnt-7B have an intermediate transforming capacity; and Wnt-4, Wnt-5A, and Wnt-6 are non-transforming [34]. Although detailed mechanisms are not well understood why Wnts are overexpressed in one tumor and downregulated in another, the pleiotropism of Wnt signaling is evident [35]. Previous results confirmed that some components of the Wnt family have aberrant expression that affects the tumor proliferation in non-small cell lung carcinomas (NSCLCs) [36–38].

The present study demonstrated that HNSCC of the oral cavity express a set of Wnt and Fz genes, and suggests as in other published works that this signaling pathway is activated in carcinoma cells. The implication of both Wnt and Fz signaling pathways in the pathogenesis of human cancer is becoming more clearly understood [39–41]. A recent work demonstrated a relationship among Wnt signaling pathway and expression values of COX-2 and Ku [42]. If more Wnt gene expression in HNSCC are studied in the future, the role of the Wnt pathway during oral squamous cell carcinoma induction and its significance in HNSCC will be well understood. Development of targeted therapies and novel drugs, perhaps based on Wnt-7A, Wnt-10B, and Fz-5, could represent an attractive field for suppression of tumor progression.

Acknowledgements The authors thank Mrs. M. Haz Conde and I. Santamarina Caínzos for technical support and S. Pértega Díaz for statistical assistance. S.M. Díaz Prado is supported by an Isidro Parga Pondal research contract by Xunta de Galicia (A Coruña, Galicia, Spain). Cancer research in our laboratory is supported by "Fundación Juan Canalejo-Marítimo de Oza".

Authors' disclosures of potential conflicts of interest The authors declare that they have no competing interests.

Authors' contributions Conception and design: S.M. Díaz Prado, L.M. Antón Aparicio.
Provision of study materials and patients: J.L. López Cedrún, S. Sironvalle Soliva.
Collection and assembly of data: S.M. Díaz Prado, G. Aparicio Gallego, V. Medina Villaamil.
Data analysis and interpretation: S.M. Díaz Prado, L.M. Antón Aparicio, M. Blanco Calvo.
Manuscript writing: S.M. Díaz Prado, L.M. Antón Aparicio, R. García Campelo, M Valladares Ayerbes.
Final approval of manuscript: S.M. Díaz Prado, V. Medina Villaamil, G. Aparicio Gallego, M. Blanco Calvo, J.L. López Cedrún, S. Sironvalle Soliva, M. Valladares Ayerbes, R. García Campelo, L.M. Antón Aparicio.

References

1. Hunter T (1997) Oncoprotein networks. Cell 88:333–346
2. Ramsdell AF, Yost HJ (1998) Molecular mechanisms of vertebrate left-right development. Trends Genet 14:459–465
3. Parr BA, Shea MJ, Vassileva G et al (1993) Mouse Wnt genes exhibit discrete domains of expression in the early embryonic CNS and limb buds. Development 119:247–261
4. Riddle RD, Ensini M, Nelson C et al (1995) Induction of the LIM homeobox gene Lmx1 by WNT7a establishes dorsoventral pattern in the vertebrate limb. Cell 83:631–640
5. Vogel A, Rodriguez C, Warnken W et al (1995) Dorsal cell fate specified by chick Lmxl during vertebrate limb development. Nature 378:716–720
6. Dale TC (1998) Signal transduction by the Wnt family ligands. Biochem J 329:209–223
7. Thorpe CJ, Schlesinger A, Bowerman B (2000) Wnt signaling in *Caenorhabditis elegans:* regulating repressors and polarizing the cytoskeleton. Trends Cell Biol 10:10–17
8. Kuhl M, Sheldahl LC, Park M et al (2000) The Wnt/Ca^{2+} pathway: a new vertebrate Wnt signaling pathway takes shape. Trends Genet 16:279–283
9. Krasnow RE, Wong LL, Adler PN (1995) Dishevelled is a component of the frizzled signaling pathway in *Drosophila*. Development 121:4095–4102
10. Bienz M (2001) Spindles cotton on to junctions, APC and EB1. Nat Cell Biol 3:E67–E68
11. Bui TD, Zhang L, Rees MC et al (1997) Expression and hormone regulation of Wnt2, 3, 4, 5a, 7a, 7b and 10b in normal human endometrium and endometrial carcinoma. Br J Cancer 75:1131–1136
12. Holcombe RF, Marsh JL, Waterman ML et al (2002) Expression of Wnt ligands and Frizzled receptors in colonic mucosa and in colon carcinoma. Mol Pathol 55:220–226
13. Howng SL, Wu CH, Cheng TS et al (2002) Differential expression of Wnt genes, beta-catenin and E-cadherin in human brain tumors. Cancer Lett 183:95–101
14. Rhee CS, Sen M, Lu D et al (2002) Wnt and frizzled receptors as potential targets for immunotherapy in head and neck squamous cell carcinomas. Oncogene 21:6598–6605
15. Ricken A, Lochhead P, Kontogiannea M et al (2002) Wnt signaling in the ovary: identification and compartmentalized expression of wnt-2, wnt-2b, and frizzled-4 mRNAs. Endocrinology 143:2741–2749
16. Saitoh T, Mine T, Katoh M (2002) Frequent up-regulation of WNT5A mRNA in primary gastric cancer. Int J Mol Med 9:515–519
17. Pham K, Milovanovic T, Barr RJ et al (2003) Wnt ligand expression in malignant melanoma: pilot study indicating correlation with histopathological features. Mol Pathol 56:280–285
18. Uraguchi M, Morikawa M, Shirakava M et al (2004) Activation of Wnt family expression and signaling in squamous cell carcinomas of the oral cavity. J Dent Res 83:327–332
19. Zhang W-M, Lo Muzio L, Rubini C et al (2005) Effect of Wnt-1 on β-catenin expression and its relation to Ki-67 and tumor differentiation in oral squamous cell carcinoma. Oncol Rep 13:1095–1099
20. Livak KJ, Schmittgen TD (2001) Analysis of relative gene expression data using real-time quantitative PCR and the $2^{-\Delta\Delta Ct}$ method. Methods 25:402–408
21. Sambrook J, Maniatis T, Fritsch EF (1989) Molecular cloning: a laboratory manual. Cold Spring Harbor Laboratory Press, New York
22. Lekven AC, Buckler GR, Kostakis N et al (2003) Wnt1 and Wnt10B function redundantly at the zebrafish midbrain–hindbrain boundary. Dev Biol 254:172–187
23. Postletwait JH, Yan YL, Gates MA et al (1998) Vertebrate genome evolution and the zebrafish gene map. Nat Genet 18:345–349
24. Gellner K, Brenner S (1999) Analysis of 148 kb of genomic DNA around the Wnt 1 locus of *Fungu rubripes*. Genome Res 9:251–258
25. Nusse R (2001) An ancient cluster of Wnt paralogues. Trends Genet 17:443
26. Rastegar S, Fridle H, Frommer F et al (1999) Transcriptional regulation of Xvent homeobox genes. Mech Dev 1:139–149
27. Melby AE, Beach C, Mullius M et al (2002) Patterning the early zebrafish by the opposing actions of *bozozok* and *vox/vent*. Development 129:2987–2089
28. Kraus S, Kork V, Fjose A et al (1992) Expression of four zebrafish Wnt-related genes during embryogenesis. Development 116:249–259
29. Jonsson M, Dejmek J, Bendahl PO et al (2002) Loss of Wnt-5a protein is associated with early relapse in invasive ductal breast carcinomas. Cancer Res 62:409–416
30. Olson DJ, Papkoff J (1994) Regulated expression of Wnt family members during proliferation of C57mg mammary cells. Cell Growth Differ 5:197–206
31. Olson DJ, Gibo DM, Saggers G et al (1997) Reversion of uroepithelial cell tumorigenesis by the ectopic expression of human wnt-5a. Cell Growth Differ 8:417–423
32. Olson DJ, Oshimura M, Otte AP et al (1998) Ectopic expression of wnt-5a in human renal cell carcinoma cells suppresses in vitro growth and telomerase activity. Tumour Biol 19:244–252
33. Kremenevskaja N, von Wasielewski R, Rao AS et al (2005) Wnt-5a has tumor suppressor activity in thyroid carcinoma. Oncogene 24:2144–2154
34. Dejmek J, Leandersson K, Manjer J et al (2005) Expression and signaling activity of Wnt-5a/Discoidin domain receptor-1 and Syk plays distinct but decisive roles in breast cancer patient survival. Clin Cancer Res 11:520–528
35. Paul S, Dey A (2008) Wnt signaling and cancer development: therapeutic implication. Neoplasma 55:165–176

36. He B, Jablons DM (2006) Wnt signaling in stem cells and lung cancer. Ernst Schering Found Symp Proc 5:27–58
37. Tennis M, Van Scoyk M, Winn RA (2007) Role of the Wnt signaling pathway and lung cancer. J Thorac Oncol 2:889–892
38. Nakashima T, Liu D, Nakano J et al (2008) Oncol Rep 19:203–209
39. Lo Muzio L (2001) A possible role for the Wnt-1 pathway in oral carcinogenesis. Crit Rev Oral Biol Med 12:152–165
40. Lo Muzio L, Pannone G, Staibano S et al (2002) WNT-1 expression in basal cell carcinoma of head and neck. An immunohistochemical and confocal study with regard to the intracellular distribution of beta-catenin. Anticancer Res 22:565–576
41. Yeh KT, Chang JG, Lin TH et al (2003) Correlation between protein expression and epigenetic and mutation changes of Wnt pathway-related genes in oral cancer. Int J Oncol 23:1001–1007
42. Chang HW, Roh JL, Jeong EJ et al (2008) Wnt signaling controls radiosensitivity via cyclooxygenase-2-mediated Ku expression in head and neck cancer. Int J Cancer 122:100–107
43. Roche Applied Science [database on the Internet] [cited December 20, 2005]. Assay Design Center/ProbeFinder. *Homo sapiens* (Human). Available from http://www.universalprobelibrary.com
44. Roche Applied Science [database on the Internet] [cited December 20, 2005]. Universal ProbeLibrary. Universal ProbeLibrary interest site. Assay Design Center/ProbeFinder. Homo sapiens (Human). Available from http://www.roche-applied-science.com

Virchows Arch (2009) 455:77–85
DOI 10.1007/s00428-009-0790-2

ORIGINAL ARTICLE

Topographical distribution of bronchial eosinophilia: significance for biopsy diagnosis

Russell P. Sherwin · Valda Richters

Received: 29 January 2009 / Revised: 8 April 2009 / Accepted: 8 May 2009 / Published online: 3 June 2009

Abstract Field-by-field (0.324 × 0.09 μM) counts of eosinophils were applied to the lamina propria of cartilaginous bronchi from 47 Los Angeles and 22 Miami residents 11 to 30 years of age who died suddenly from violence. A highly variable topographical distribution was found that appeared to be due mainly to variations in confluent eosinophil-positive fields and "hot spots" (≥3 eosinophils per field). Since biopsy is the gold standard for the diagnosis of bronchial eosinophilia, there is a need to resolve the problem of non-uniformity. New measurements applicable to biopsy diagnosis are presented having potential usefulness for providing insight into the severity and topographical distribution of eosinophilia within bronchi that are the sites of biopsy. The additional finding of a 30.4% incidence of moderate to marked eosinophilia (>1.5 eosinophils/mm reticular basement membrane) suggests a high level of asthma or asthmatic-like disease in the young subjects of this study.

Keywords Eosinophilia · Main stem bronchus · Topographic quantitation

Introduction

Recent reports [1–4] have challenged a long-standing belief that bronchial eosinophilia in the asthmatic is uniformly distributed when measurements are adequately controlled [5–9]. Should bronchial eosinophilia not be uniform, it could substantially undermine the reliability of biopsy in view of the exceedingly small amount of the bronchial tree that is sampled. What is needed to help answer the question of uniformity is information on the topographical distribution of eosinophils within cartilaginous bronchi, but to date, there are no reports affording that information. An opportunity to obtain quantitative data on topographical distributions of bronchial eosinophilia was provided by an independent and ongoing medical examiner autopsy study of young Los Angeles (LAC) and Dade-Miami County (DMC) residents who died suddenly from violence [10]. Feasibility was supported by an earlier subjective study [11] of a similar group of individuals where a 10% incidence of bronchial eosinophilia was found in association with an apparent highly variable topographical distribution of eosinophils. The specific aim was to establish topographical distributions through field-by-field counts of eosinophils within the lamina propria of cartilaginous bronchi and to derive quantitative measurements for biopsy use that could provide insight into the level and extent of eosinophilia within the bronchial tree. An additional goal was to determine the prevalence of eosinophilic airway inflammation (EAI) in young victims of sudden and violent death, with special attention given to the question of what is an abnormal level of eosinophilia for an individual bronchus since there are no uniformly defined or uniformly applied criteria.

Materials and methods

As described previously [10], main stem bronchi were obtained from autopsies of LAC and MDC residents who died suddenly from homicide, vehicular accident, or

R. P. Sherwin · V. Richters
Department of Pathology, Keck School of Medicine,
University of Southern California,
2011 Zonal Avenue,
Los Angeles, CA 90089, USA

R. P. Sherwin (✉)
2011 Zonal Avenue HMR 209,
Los Angeles, CA 90089-9092, USA
e-mail: russell.sherwin@keck.usc.edu

other violence. Criteria for acceptance into the study were sudden death from violence, five or more years of LAC or MDC residency, ages 11 to 30, no history of drug use, no history or gross autopsy evidence of disease, and a postmortem time no more than 3 days. A left or right lung was perfusion-fixed with 10% buffered formalin at 25 cm water pressure for at least 24 h using an apparatus of identical construction at each site. A transverse section of main stem bronchus was excised at a level ~2 mm proximal to the carina. Gross and microscopic examinations were carried out by the principal investigator (RPS).

Quantitative measurements

Paraffin sections (4 μM) of main stem bronchi were stained with hematoxylin and eosin (H&E). Eosinophil counts were limited to the lamina propria, defined as the connective tissue layer between the reticular basement membrane (RBM) of the mucosal lining and the adluminal margins of smooth muscle, cartilaginous plates, submucosal fibrocollagenous tissue, and submucosal glands. Autolyzed or otherwise technically unsatisfactory segments of bronchi were excluded from counting. Areas of suboptimal preservation of one or more continuous fields within the lamina propria were included in the counting when there was good preservation of at least a part of the overlying epithelial lining, leucocytes in general, and/or submucosal glands. Each 500× high power field (HPF), measuring 0.324 μM in length and 0.09 μM in depth, of lamina propria was examined using a 10× Zeiss ocular, 1.25× Zeiss Optovar, 40× objective, and a calibrating eyepiece reticule having a 1.0-mm scale divided into 0.10-mm increments. Eosinophils were identified as monolobed or bilobed cells containing coarse eosinophilic granules. Eosinophils were counted with the assistance of a Veeder-Root hand counter, with overlap of contiguous fields controlled by tissue landmarks. Intraepithelial eosinophils were excluded from the counting. Measurements included eosinophils/HPF, HPFs/bronchus, eosinophil-positive HPFs/bronchus, and eosinophils/mm RBM. Additional measurements were derived from an observation identified as a confluent eosinophil-positive field (CEF) and defined as aggregates or clusters of two or more abutting eosinophil-positive HPFs. Two quantitative derivatives relating to CEFs were obtained, CEF density (eosinophils/CEF) and CEF length (HPFs/CEF). The integrity of the epithelial lining was graded on a scale of 0–10, with 10 being fully intact. A micrometer was used to obtain from one to several measurements of RBM thickness, excluding poorly preserved tissue and tangentially sectioned areas. Data were analyzed by *t* tests, with significance based on critical two-tail values ($p<0.05$).

Demographic study

For all MDC cases, autopsy permission was obtained and interviews with next-of-kin successfully carried out prior to lung accessioning. The LAC autopsies were authorized under a legislative mandate. Contact of next-of-kin for interview followed lung accessioning over varying periods of time, with about half of the interviews successful. Medical examiner investigational reports (LAC) provided additional data. Accessioned lungs that were not suitable for processing or histopathological examination were excluded from the study. The respective transplantation services carried out all next-of-kin interviews in accord with a protocol modified from the independent investigation noted earlier [10]. Demographic data were not made available to the principal investigator until the pathological studies had been completed.

Results

Main stem bronchi from 69 subjects were suitable for study, 47 LAC (26 with and 21without next-of-kin interviews) and 22 MDC. Approximately half of the bronchi had been obtained from subjects of the prior independent study [10]. Mean ages were 21.0 [11–29] and 21.5 [13–30], LAC and MDC, respectively (NS). Levels of EAI were defined as follows: marked (≥5 eosinophils/mm), moderate EAI (>1.5–<5 eosinophils/mm), slight (0.15–<1.5 eosinophils/mm), and totally absent, with frequencies of 15.9%, 14.5%, 44.9%, and 8.7%, respectively. The frequency of marked eosinophilia was not significantly different between the LAC and DMC groups, 14.9% vs. 18.2%, respectively. The highest mean EAI level for a single bronchus was 17.8 eosinophils/mm per RBM. Comparisons between LAC and MDC groups showed a consistent but not significant trend towards higher mean EAI levels (eosinophils/mm) for the DMC group (Table 1). There was a trend toward longer CEHs for the DMC group in that mean HPFs/CEF (CEF lengths in mm/RBM) were higher for the MDC group (4.0 ± 5.2 and 5.7 ± 6.9, respectively), but with significance only for individual bronchi ($p=0.02$) and not by group analysis. No differences in measurements were found between the interviewed and non-interviewed LAC groups.

Four main topographical distributions of eosinophilia were observed in the transverse bronchial sections: widespread, multifocal, skewed or polarized, and scattered isolates or clusters. A *widespread* distribution (Fig. 1a), defined as ≥75% eosinophil-positive HPFs, was observed in 8.7% (6/69), and all had mean EAI levels greater than 5 eosinophils/mm in association with numerous CEFs. The predominant presentation of EAI (62.3% of bronchi) was multifocal eosinophilia with 9.9% to 68.1% of the lamina

Table 1 Quantitative data

Los Angeles—not interviewed						Los Angeles—interviewed						MIAMI—interviewed					
Age/ Sex	EB/ SK	Eosinophils/ mm	Eosinophils/ HPF	HPFs	BM mean (μm)	Age/ Sex	EB/ SK	Eosinophils/ mm	Eosinophils/ HPF	HPFs	BM mean (μm)	Age/ Sex	EB/ SK	Eosinophils/ mm	Eosinophils/ HPF	HPFs	BM mean (μm)
23/M	H[a]	13.46	767	176	16.7	17/M	H+	17.75	374	65	14.7	25/M	B−	15.06	835	171	5.5[b]
24/M	H[a]	8.3	207	77	8.3	21/M	H−	8.77	310	109	td	26/M	B−	11.14	831	230	td
20/M	H[a]	7.35	336	141	9.2[b]	11/M	H?	5.96	288	149	td	17/M	C−	10.49	687	202	17.5
19/M	H[a]	5.99	219	113	11.1[b]	11/M	H−	2.13	100	146	4.6	15/M	H−	5.56	312	173	td
24/M	H[a]	3.83	138	111	13.8	26/M	B−	1.98	61	95	8.3[b]	30/M	C+	2,69	163	188	16.6[b]
23/M	H[a]	1.98	74	115	12	26/M	B+	1.67	88	158	7.4[b]	19/F	C−	2.56	137	165	9.2[b]
18/M	H[a]	1.91	90	145	7.4[b]	21/M	H+	1.7	55	101	6.5	21/F	B−	2.47	123	155	7.4[a]
24/M	H[a]	1.3	58	138	9.4[b]	19/M	C−	1.39	37	82	3.7[b]	22/M	B−	0.83	31	113	7.4[b]
21/M	H[a]	1.3	52	125	9.4[b]	21/M	B+	1.33	26	61	7.4[b]	13/F	C−	0.65	21	100	14.7[b]
25/M	H[a]	0.77	30	121	4.6	21/M	H+	1.14	51	139	td	21/M	B−	0.59	29	153	4.6
21/M	H[a]	0.74	33	136	td	19/M	B+	1.02	43	129	10.2	19/M	C+	0.46	12	79	4.6[a]
20/M	H[a]	0.43	17	124	9.2[b]	16/M	H−	0.9	38	133	5.5[b]	17/M	H−	0.34	8	72	td
26/F	H[a]	0.4	14	108	8.3	17/M	B−	0.46	18	119	6.5[b]	25/F	B−	0.31	18	177	9.2[b]
15/F	H[a]	0.37	13	110	7.4[b]	15/F	C+	0.46	18	121	5.5[b]	25/M	B−	0.28	14	150	td
20/M	H[a]	0.31	13	127	9.2	20/M	C/A −	0.37	12	103	6.5	16/F	C−	0.22	6	90	9.4[b]
19/M	H[a]	0.31	9	93	td	22/M	H−	0.34	8	76	5.5[b]	26/M	C−	0.15	7	128	7.4[b]
27/M	H[a]	0.28	8	94	4.6	23/F	C+	0.25	10	132	7.4[b]	21/F	C−	0.12	5	147	td
26/M	H[a]	0.25	10	130	td	16/M	H+	0.22	8	115	8.3	28/M	C+	0.03	1	73	9.2[b]
20/M	H[a]	0.15	5	107	7.4[b]	19/M	B+	0.22	6	93	4.6	26/M	C+	0	0	121	td
20/M	H[a]	0.09	4	115	td	16/M	H−	0.12	4	92	3.7[b]	22/M	C−	0	0	103	6.5
16/M	H[a]	0.03	1	116	7.4[b]	25/M	C[a]	0.09	3	114	3.7[b]	17/M	H[a]	0	0	91	6.5
						16/M	C[a]	0.06	2	103	11.1[b]	24/M	H−	0	0	73	4.5
						29/M	C−	0.03	1	111	7.4[b]						
						18/M	H[a]	0	0	109	5.5[b]						
						23/M	C[a]	0	0	75	6.5						
Total		–	2,098	2,522	–	Total		–	1,562	2,828	–	Total		–	3,240	2,954	–
Mean		2.4	99.9	120.1	9.1	Mean		1.9	60.1	108.8	6.8	Mean		2.35	147.3	134.3	8.8

EB ethnic background, *B* Afro-American, *C* Caucasian, *H* Hispanic, *C/A* Caucasian–Asian, *SK* smoking history, *td* technical difficulty

[a] SK not known

[b] One reading

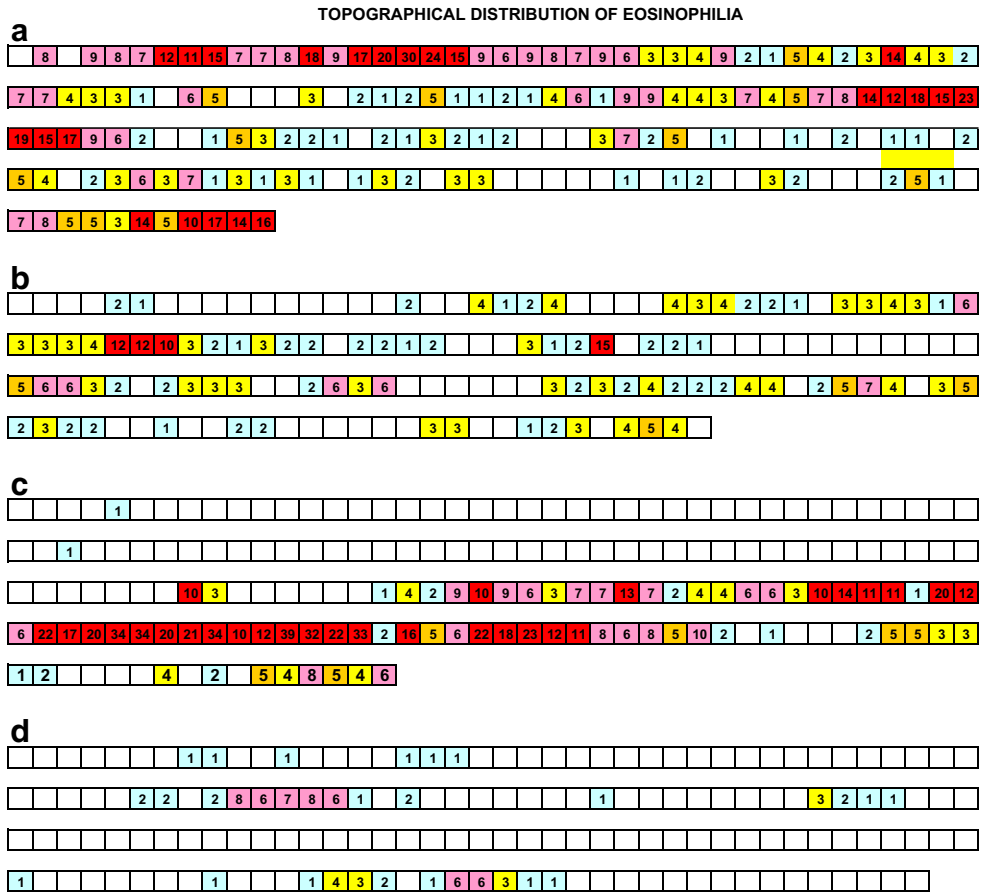

Fig. 1 **a** Widespread EAI (26 B/M). Of 171 HPFs, 80.1% contain one or more eosinophils. "Hot spots" ≥10 eosinophils/HPF appear as apparent epicenters within abutting eosinophil-positive HPFs (CEHs). **b** Marked multifocal EAI (11 H/M with "slight asthma"). Of 149 HPFs, 58.4% are eosinophil-positive. The presence of 17 CEHs contrasts with only two isolated eosinophil-positive HPFs. A hypothetical biopsy sampling a CEH of three HPFs (each with 12, 12, and 10 eosinophils) would yield a mean of 35 eosinophils/mm vs. 6.0 eosinophils/mm for the bronchus. **c** Polarized or skewed EAI (24 H/M). Half of the lamina comprised mostly eosinophil-positive HPFs, with a 17.8-mm-long CEH (55 HPFs) occupying 31% of the bronchial circumference. The other half is largely eosinophil-negative. The entire lamina exhibits a moderate to marked round cell infiltrate that is mainly lymphocytic, with eosinophils most prominent in densely packed nodular aggregates of lymphocytes. Chains of eosinophil-positive HPFs (CEHs) separated by a few eosinophil-negative HPFs may be part of a longer chain separated by artifact or postmortem loss of eosinophils. **d** Moderate multifocal EAI (19 B/M). Only 21% of 158 HPFs are eosinophil-positive, but a single hypothetical biopsy 0.972 mm in diameter could yield a level as high as 22 eosinophils/mm and three biopsies might result in a mean EAI as high as 15.1 eosinophils/mm vs. the bronchial mean of 1.7 eosinophils/mm

propria occupied by eosinophil-positive HPFs and ranging from slight (Fig. 2b) to marked (Fig. 2d). *Skewed* or *polarized* localizations were observed in 5.8% (4/69), with from 9.9% (Fig. 2a) to 46.6% (Fig. 1c) eosinophil-positive HPFs and with mean EAI levels ranging from 1.7 to 13.5 eosinophils/mm, respectively. Eosinophils most frequently presented as scattered isolates or clusters of eosinophil-positive HPFs. In the latter respect, bronchial involvement ranged from 0.09% to 4.3%, with mean EAI levels <0.15 eosinophils/mm and with CEFs usually absent or, when present, being very short (aggregates of two or three eosinophil-positive HPFs). Long CEFs tended to have frequent "hot spots" (≥3 eosinophils/HPF) and were usually associated with high mean bronchial EAI levels, e.g., a CEF 17.8 mm in length (Fig. 1c) in a bronchus having a mean EAI of 13.5 eosinophils/mm. A caveat is that just a few "hot spots" in an otherwise eosinophil-negative bronchus can result in an abnormal EIA level, e.g., two CEFs occupying only 9.9% of the lamina (Fig. 2a) but with a bronchial mean EAI of 1.7 eosinophils/mm. "Hot spots" ≥10 eosinophils/HPF were almost invariably associated with marked (≥5 eosinophils/mm) bronchial mean EAI levels (Figs. 1a–c and 2d), with one exception of a bronchus with moderate EAI (3.8 eosinophils/mm) despite a content of four HPFs, each containing ≥10 eosinophils (Fig. 2c).

An abnormal level of EAI (>1.5 eosinophils/mm) was found in 30.4% (21/69), with no significant differences between groups, i.e., 33%, 27%, and 32% for LAC non-interviewed, LAC interviewed, and MDC groups, respectively (Table 1). Of four subjects with a history of asthma, EAI was identified in

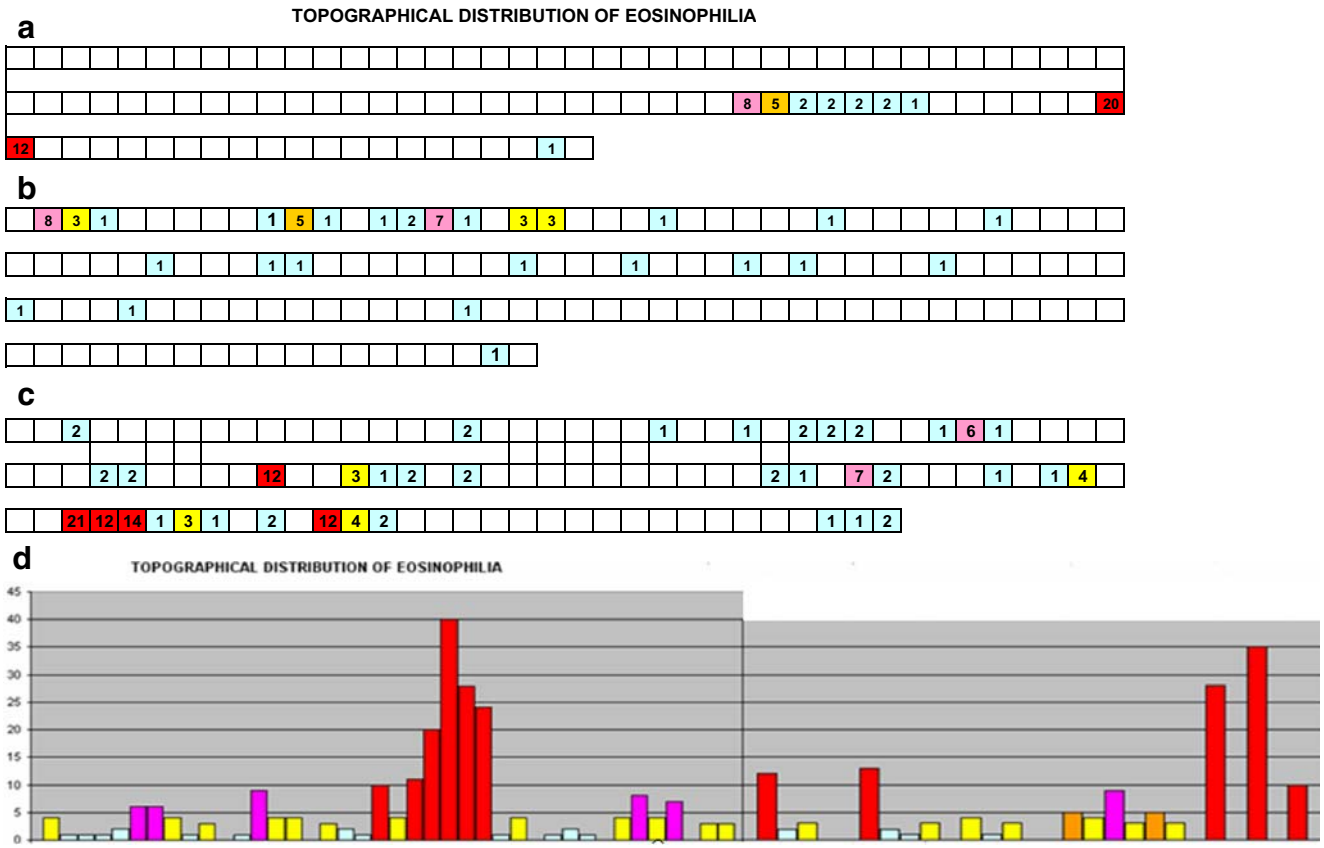

Fig. 2 **a** Polarized or skewed distribution of eosinophil-positive HPFs (20 H/M). A hypothetical 0.972-mm biopsy that sampled the 0.972 mm CEH comprising 20, 12, and 0 eosinophils would yield an EAI as high as 32.9 eosinophils/mm vs. as high as 15 eosinophils/mm for the second CEH (eight, five, and two eosinophils) vs. the bronchial mean of 1.7 eosinophils/mm. Of course, biopsy sampling that is entirely negative is more likely. **b** Multifocal slight and polarized EAI (19 C/M). At one pole of the lamina, there are four closely associated CEHs containing "hot spots" ranging from three to eight eosinophils/HPF. HPFs containing a single eosinophil are scattered elsewhere. A hypothetical 0.972-mm biopsy might result in an EAI level as high as 12.4 eosinophils/mm vs. the bronchial mean of 1.1 eosinophils/mm vs. a most likely very low or totally negative result. **c** Multifocal moderate EAI (18 H/M). Hypothetically, a 0.972-mm biopsy might yield a level as high as 47 eosinophils/mm for a single CEH vs. the bronchial mean of 3.8 eosinophils/mm. One CEH containing exceptionally dense "hot spots," beginning with 21, 12, and 14 eosinophils/HPF, would probably have encompassed at least 12 eosinophil-positive HPFs, but fell short by two interspersed eosinophil-negative HPPs that are probably falsely negative due to degranulation or poor postmortem preservation. **d** Profile of topographical distribution of eosinophilia (17 H/M who worked with metals and wood dust). The "hot spots" appear as multiple epicenters in a widespread eosinophilia that involves 83.1% of the bronchial circumference. A hypothetical single 0.972-mm biopsy might vary from a high of 94.7 eosinophils/mm to a low of 3.0 eosinophils/mm vs. the bronchial mean of 17.8 eosinophils/mm

two (Table 2), one with marked and one with moderate EAI, 6 eosinophils/mm (Fig. 1b) and 2.1 eosinophils/mm, respectively. A pathologic diagnosis of asthma was not sustainable in any of the 69 subjects. With respect to seven subjects where mention was made of environmental exposure, marked eosinophilia was observed in three (42.9%; Table 2).

Discussion

Historical background

Earlier reports considered the distribution of eosinophilia to be uniform throughout the bronchial tree, as for example statements that a tissue sample 1.0 × 0.1 mm along the basement membrane is sufficient to obtain constant cell numbers [8]; cell counts can be restricted to "one airway level only" [5], and small samples of either large or small airways are "likely to be representative when comparing cases," the latter with the reservation that an "up to fivefold variation" was occasionally seen between proximal and distal airways in fatal cases of asthma [7]. However, recent studies have found substantial intrasubject variation with respect to upper vs. lower lobes [1], proximal vs. distal airway generations [2, 4], between as well as within biopsy sections [3, 12], and between sections of a single biopsy [13]. Moreover, a "mapping" of eosinophilia from nasal mucosa to lung parenchyma found "great variability of

Table 2 Demographic data

City	Age	Sex	Ethnicity	SK	Historical Information	Eosinophils/mm
LAC	17	M	H	+	Wood work; metal dusts (student)	17.75
LAC	21	M	H	+	Cotton cloth dust (machine operator)	8.77
LAC	26	M	B	+	Road fumes (truck driver)	1.39
LAC	21	M	B	+	Wood work; construction/roofing; metal dusts	1.33
MDC	25	M	B	−	Solid wast (truck driver)	5.56
MDC	25	M	B	−	Wood work	0.15
MDC	28	M	C	+	Welding fumes; metals (electrician)	0.03
LAC	11	M	H	?	Mild asthma; recent history of insect bites	5.96
LAC	21	M	H	+	10 years	2.13
LAC	26	M	B	−	Slightly asthmatic since birth	0.9
LAC	20	M	C/A	−	Athletic asthma	0.48

− Non-smoker, + Cigarettes

B Afro-American, *C* Caucasian, *H* Hispanic, *C/A* Caucasian-Asian, *SK* Smoking history

eosinophil content within different regions in the same patient" [14]. The uncertainty raised is a serious challenge to the reliability of biopsy measurements of bronchial eosinophilia, bearing in mind that biopsy "still remains the gold standard" for assessing airway inflammation in asthma [15] and "will continue to have a major role in asthma research" [1]. Further, recent validation of bronchial biopsy as a safe procedure [16] is likely to increase utilization, and this adds to a well-recognized need to "optimize quantification of the cellular infiltrate" [3]. In the latter respect, Richmond et al. [1] recommended "power calculations" applied to data from groups of ~15 subjects to control wide intrasubject variability between anatomic site, which compares to other reports recommending groups of five to 15 [7] and eight to 25 [3] subjects. With respect to bronchial biopsy of an individual, little information is available on measures to control quantitation other than the recommendation by Sont et al. [3] for "counting the largest possible area within a biopsy and/or averaging data obtained from multiple sections and/or biopsies." The special need is for insight on biopsy examination into the severity and extent of eosinophilia within the bronchial tree. A first step towards gaining that insight is the acquisition of data on topographical distributions of eosinophilia within large bronchi.

Baselines of eosinophilia

There is no prior report on the topographical distribution of bronchial eosinophilia. Two studies providing measurements of eosinophilia within transverse sections of bronchi have been found which shared basic materials and methods in common, i.e., medical examiner cases of sudden death, cell counts based on H&E-stained transverse tissue sections of cartilaginous bronchi, and measurements according to numbers of eosinophils/mm per RBM [17, 18]. The two reports primarily presented data on EAI levels for groups of subjects, with measurements for individual bronchi limited for the most part to graphic displays, e.g., maxima of 3.8 eosinophils/mm [17] and ~10 eosinophils/mm [18]. In the absence of baselines on eosinophilia for individual bronchi, we defined a normal EAI level as ≤1.5 eosinophils/mm by arbitrarily selecting the higher of the two reported group control means, namely, 1.5 eosinophils/mm [17] vs. 1.0 eosinophils/mm [18], and also with guidance from a ranking of our data (Table 1). We assumed that EAI levels >1.5 eosinophils/mm reported in both control groups [17, 18] represented cases of either clinically covert asthma or non-asthmatic eosinophilic bronchitis. An EAI level >0.15 and ≤1.5 eosinophils/mm was defined as a *slight* but clinically normal eosinophilia, and isolated eosinophil-positive HPFs were considered to be incidental infiltrates. With the foregoing reported results in mind and with reference to a ranking of our data, we defined an abnormal level of EAI for an individual bronchus as greater than 1.5 eosinophils/mm. We noted that the reported group means for non-fatal asthmatics [17] and subjects with cystic fibrosis cases [18] were very low and virtually identical (1.8 eosinophils/mm) vs. the 11.0 [17] and 62.7 [18] eosinophils/mm reported for fatal asthmatics. We defined marked EAI as ≥5 eosinophils/mm based largely on observations by Carroll et al. [17] showing that 100% of fatal cases of asthma had group means of ≥5 eosinophils/mm vs. 20% for non-fatal cases of asthma.

Interpretation of biopsy data

With respect to insight on biopsy into the probable level of eosinophilia within the bronchial tree, we believe that measurements of numbers and magnitude of "hotspots" (≥3 eosinophils/HPF) offer the most potential for reliability.

Even a single HPF containing three eosinophils within biopsy tissue will in itself more likely than not reflect an abnormal level of eosinophilia for a hypothetical transverse bronchial section, i.e., 51.2% (20/41) of main stem bronchi having three eosinophils in at least one HPF had a mean EAI level >1.5 eosinophils/mm. As might be expected, a "hot spot" of ≥5 eosinophils/HPF tended to be associated with more frequent and higher levels of eosinophilia. Of 26 bronchi with one or more HPFs containing ≥5 eosinophils/HPF, a marked mean EAI level (≥5.0 eosinophils/mm) was found in 44% and some level of abnormality (>1.5 eosinophils/mm) in 84%. The finding that mean EAI was normal for the remaining 16% despite the presence of ≥5 eosinophils in one or more HPFs raises the question of underdiagnosis from inadequate sampling or poor tissue preservation. Figure 2a is an example of a bronchus with 91% of the lamina propria comprising eosinophil-negative HPFs and a slightly elevated mean EAI (1.7 eosinophils/mm), but "hot spots" present raise the question of underdiagnosis. Specifically, biopsy sampling of two ~1 mm in length sites (three HPFs each 0.324 mm long) would yield mean EAI levels of 33 and 15.4 eosinophils/mm if the two "hot spots" present are selected, i.e., 20,12, and 0 eosinophils per 0.972 mm and 8, 5, and 2 eosinophils per 0.972 mm, respectively. Moreover, a highly elevated mean bronchial EAI may understate localized EAI, e.g., the mean EAI of 17.2 eosinophils/mm of the bronchus shown in Fig. 2d is the highest we recorded, but sampling limited to "hot spots" could hypothetically result in a single EAI level as high as 94.7 eosinophils/mm or a mean EAI of 65.5 eosinophils/mm. Conversely, mean EAI of that same bronchus (Fig. 2d) could be greatly understated since one fifth (19.4%) of the HPFs is entirely eosinophil-negative and nearly half of the eosinophil-positive HPFs (43.6%) contains less than three eosinophils.

Localized aggregation of eosinophils in the assessment of eosinophilic airway inflammation

Clustering has been reported to have special meaning in eosinophilic airway inflammation. Sont et al. [3] stated that "clustering might provide specific information about the inflammatory process," and Sullivan et al. [13] suggested that clustering of eosinophils within airway tissue is a "likely explanation" for the variability of eosinophilia. Of related pertinence, a report on tumor-infiltrating eosinophils [19] pointed out that eosinophils "invariably" presented as clusters, making counts of the highest density of eosinophils within tumor tissue more in accord with functional status than classical counts of eosinophils. Our introduction of the term CEF expands the concept of clustering to allow for new quantitative measurements on frequency, density, and extent of clustering, specifically: numbers of CEFs/biopsy tissue (frequency), eosinophils/CEF (density), and eosinophil-positive HPFs/CEF (extent). Measurements of numbers and severity of "hot spots" (≥3 eosinophils/HPF) within CEFs have been given special attention since they commonly present as apparent epicenters of CEFs (Figs. 1c, b and 2d), which suggests that they play a central role in the development and progression of eosinophilia. With the latter in mind, we attempted to relate "hot spots" to focal epithelial sloughing, but the results were inconclusive due mainly to unsatisfactory postmortem tissue preservation. While sloughing has been dismissed as artifact [9, 20], a strong rebuttal argument has been made [21] and a number of studies report a relationship of eosinophilia to increased epithelial cell loss [22–24]. Additional encouragement for exploring a relationship of "hot spots" to injury are reports of localized eosinophil infiltrates adversely affecting tissues other than the epithelial lining, notably neural injury [25–27] and the "clustering of eosinophils around airway nerves" [28]. Long CEFs (Fig. 1c) seem especially likely to be a reflection of injury, in particular patchy infiltrates which are by definition ≥10 mm in diameter. The latter were seemingly anticipated by Sont et al. [3] who called attention to "a patchy focal phenomenon sometimes in clusters of indefinable numbers." Patchy CEFs will ordinarily not be demonstrable in biopsy tissue, but four or more tissue samples at 2 mm [29] or 2.6 mm [30] in diameter may afford observations of ~24 HPFs, i.e., 8 mm of total tissue with three HPFs/0.972 mm. Thus, patchy or widespread eosinophilia may be suspected when long CEFs predominate in multiple tissue specimens. Assessment of eosinophilia in general may benefit from a scoring methodology that gives weight to frequency, density, and extent of CEFs and "hot spots."

Eosinophilia in asthma and asthma-like diseases

Our recording of a 30.4% frequency of moderate to marked EAI (>1.5 eosinophils/mm) appears to be reasonably acceptable as a reflection of asthma and asthma-like diseases, the latter including possible environmental exposures. Pertinently, four LAC subjects had historical information suggestive of environmental exposures at work or in the classroom, and two of the four had eosinophilia, a frequency 7.7% for the group (2/26; Table 2). Of related pertinence, a Minnesota report found 37.3% of children having one or more recorded diagnoses of asthma and asthma-like diseases, the latter without a diagnosis of asthma and represented by reactive airway disease, exercise-induced bronchospasm, or recurrent wheezing or bronchospasm [31]. Further, a cross-sectional survey of 5- to 18-year-old New Orleans schoolchildren found lifetime prevalences of wheezing and asthma to be 39.4% and 24.4%, respectively [32]. The demographic data of the

present study are too limited for conclusions, but it is of interest that 15.4% (4/26) of the LAC youths with next-of-kin interviews had a history of asthma and two of the four had abnormal EAI levels (>1.5 eosinophils/mm). In comparison, California data show a 23% frequency of asthma and asthma-like breathing problems, with asthma alone having an incidence of 13% [33]. It should be noted that none of the 69 subjects had pathological findings in support of a diagnosis of asthma. Mention should also be made that neither the presence of eosinophilia or thickening of the RBM necessarily supports a diagnosis of asthma. While eosinophilia is well recognized as a characteristic of both childhood and adult asthma [24], the finding has been said to be "untenable" as a "hallmark feature of asthma," and that is also the case with RBM thickening [34]. Moreover, there are studies showing that EAI may not be accompanied by airway hyperresponsiveness and RBM thickening can be found in non-eosinophilic asthma [35–37].

Covert chronic lung inflammation and eosinophilia

A final consideration is the significance of bronchial eosinophilia in the absence of known clinical manifestations. Our earlier subjective measurements of chronic inflammation of airways [11, 38] and airspaces [10] of comparable groups found eosinophilia in 10% and chronic lung inflammation in approximately one of four. In some of those subjects, lung remodeling was observed that included peribronchiolar fibrosis, alveolar airspace derangement, and/or parenchymal scarring [10]. Moreover, we noted that four LAC subjects included in the present study had earlier been shown to have chronic lung inflammation, eosinophilia, and remodeling [10], the latter including one individual with peribronchiolar fibrosis and, as shown in the present study, an EAI level of 2.0 eosinophils/mm. Two other subjects had airspace derangement but normal EAI levels (≤1.5 eosinophils/mm). The foregoing findings suggest that bronchial eosinophilia in some young residents of metropolitan cities with or without clinically manifested asthmatic disease is likely to be associated with chronic lung inflammation and remodeling, which tends to support the suggestion by Pohunek et al. [39] that early remodeling in children may occur with developing asthma "before a reliable diagnosis of asthma could be made based on clinical features." Of potentially equal if not greater significance is that those living cohorts of the present study who share in common marked EAI and chronic lung inflammation may be experiencing an inordinate rate of depletion of functional and structural lung reserves sufficient to place them at risk as an especially susceptible subpopulation. Of special interest in the latter respect is a report on sudden unexpected deaths in soldiers which attributed death of 10 of the 151 soldiers (6.7%) to asthma. Further, three of the ten soldiers who died from asthma had no prior history of asthma, with the reservation that historical information may have been withheld due to an eagerness to serve [40].

Acknowledgments This study was supported by a Cooperative Agreement (CR 8215756) between the National Health and Environmental Effects Research Laboratory (NHEERL), US Environmental Protection Agency, and the University of Southern California. The authors wish to acknowledge the assistance of R. B. Everson, PhD, formerly of the Human Studies Division (MD-58C) of the National Health and Environmental Effects Research Laboratory, US Environmental Protection Agency, Research Triangle Park, Raleigh, NC 27711. The autopsy cases were provided by the Los Angeles County Department of Coroner and the Dade County Medical Examiner's Office. We are indebted to Dr. Lakshmanan Sathyavagiswaran, Chief Medical Examiner of the Los Angeles County Department of Coroner, and to Drs. Joseph H. Davis and Roger E. Mittleman of the Dade County Medical Examiner's Office. Assistance has also been provided by Scott Hanks, Ann C. Hughes, Jeffrey A. Thomas, and Margaret Acosta. We thank Dr. Arnis Richters for technical assistance. The project was approved by the Institutional Review Board of the Los Angeles County-University of Southern California Medical Center and the Research Committee of the Department of Coroner of Los Angeles County.

Disclaimer Although the research described in this article has been supported by the United States Environmental Protection Agency through Cooperative Agreement CR 821576-01-0 with the University of Southern California, it has not been subjected to Agency review and therefore does not necessarily reflect the views of the Agency, and no official endorsement should be inferred. Mention of trade names or commercial products does not constitute endorsement or recommendation for use.

The authors declare that they have no conflict of interest.

References

1. Richmond I, Booth H, Ward C et al (1996) Intrasubject variability in airway inflammation in biopsies in mild to moderate stable asthma. Am J Respir Crit Care Med 153:899–903
2. Faul JL, Tormey VJ, Leonard C et al (1997) Lung immunopathology in cases of sudden asthma death. Eur Respir J 10:301–307
3. Sont JK, Willems LN, Evertse CE et al (1997) Repeatability of measures of inflammatory cell number in bronchial biopsies in atopic asthma. Eur Respir J 10:2602–2608
4. Haley KJ, Sunday ME, Wiggs BR et al (1998) Inflammatory cell distribution within and along asthmatic airways. Am J Respir Crit Care Med 158:565–572
5. Bradley BL, Azzawi M, Jacobson M et al (1991) Eosinophils, T-lymphocytes, mast cells, neutrophils, and macrophages in bronchial biopsy specimens from atopic subjects with asthma: comparison with biopsy specimens from atopic subjects without asthma and normal control subjects and relationship to bronchial hyperresponsiveness. J Allergy Clin Immunol 88:661–674
6. Haahtela T, Laitinen A, Laitinen LA (1993) Using biopsies in the monitoring of inflammation in asthmatic patients. Allergy 48(17 Suppl):65–69
7. Carroll N, Lehmann E, Barret J et al (1996) Variability of airway structure and inflammation in normal subjects and in cases of nonfatal and fatal asthma. Pathol Res Pract 192:238–248

8. Ten Hacken NH, Aleva RM, Oosterhoff Y et al (1998) Submucosa 1.0 x 0.1 mm in size is sufficient to count inflammatory cell numbers in human airway biopsy specimens. Mod Pathol 11:292–294
9. Turcotte H, Laviolette M, Boutet M et al (2003) Variability of inflammatory cell counts on bronchial biopsies of normal subjects. Lung 181:9–21
10. Sherwin RP, Richters V, Kraft P et al (2000) Centriacinar region inflammatory disease in young individuals: a comparative study of Miami and Los Angeles residents. Virchow Arch 437:422–428
11. Sherwin RP, Richters V (1992) Inflammation of the bronchial lamina propria in young adults. Tropospheric Ozone and Environment TR-20, pp 11–23
12. Letter to the Editor: Stone BD, Elias-Todd T, Parrino J (2001) EG-1 positive eosinophils in asthma. Response from the Authors: Faul, JL, Burke, CM, Poulter, LW. Am J Respir Crit Care Med 164:171–172
13. Sullivan P, Stephens D, Ansari T et al (1998) Variation in the measurements of basement membrane hickness and inflammatory cell number in bronchial biopsies. Eur Respir J 12:811–815
14. de Magalhães Simões S, dos Santos MA, da Silva Oliveira M et al (2005) Inflammatory cell mapping of the respiratory tract in fatal asthma. Clin Exp Allergy 35:602–611
15. Jeffery PK (1996) Bronchial biopsies and airway inflammation. Eur Respir J 9:1583–1587
16. Elston WJ, Whittaker AJ, Khan LN, Flood-Page P, Ramsay C, Jeffery PK, Barnes NC (2004) Safety of research bronchoscopy, biopsy and bronchoalveolar lavage in asthma. Eur Respir J 24:375–377
17. Carroll N, Cooke C, James A (1997) The distribution of eosinophils and lymphocytes in the large and small airways of asthmatics. Eur Respir J 10:292–300
18. Azzawi M, Johnston PW, Majumdar S et al (1992) T lymphocytes and activated eosinophils in airway mucosa in fatal asthma and cystic fibrosis. Am Rev Respir Dis 145:1477–1482
19. Alkhabuli JO, High AS (2006) Significance of eosinophil counting in tumor associated tissue eosinophilia (TATE). Oral Oncol 42:849–850
20. Ordonez CL, Fahy JV (2000) Epithelial desquamation in asthma. Am J Respir Crit Care Med 162:2324–2329
21. Holgate ST, Davies DE (2001) Epithelial desquamation in asthma. Am J Respir Crit Care Med 164:1997–1998
22. Amin K, Lúdvíksdóttir D, Janson C et al (2000) Inflammation and structural changes in the airways of patients with atopic and nonatopic asthma. BHR Group. Am J Respir Crit Care Med 162:2295–2301
23. Shahana S, Björnsson E, Lúdvíksdóttir D et al (2005) Ultrastructure of bronchial biopsies from patients with allergic and non-allergic asthma. Respir Med 99:429–443
24. Barbato A, Turato G, Baraldo S et al (2006) Epithelial damage and angiogenesis in the airways of children with asthma. Am J Respir Crit Care Med 174:975–981
25. Dakhama A, Kanehiro A, Makela MJ et al (2002) Regulation of airway hyperresponsiveness by calcitonin gene-related peptide in allergen sensitized and challenged mice. Am J Respir Crit Care Med 165:1137–1144
26. Durcan N, Costello RW, McLean WG et al (2006) Eosinophil-mediated cholinergic nerve remodeling. Am J Respir Cell Mol Biol 34:775–786
27. Nie Z, Nelson CS, Jacoby DB et al (2007) Expression and regulation of intercellular adhesion molecule-1 on airway parasympathetic nerves. J Allergy Clin Immunol 119:1415–1422
28. Jacoby DB, Costello RM, Fryer AD (2001) Eosinophil recruitment to the airway nerves. J Allergy Clin Immunol 107:211–218
29. Jeffery P, Holgate S, Wenzel S (2003) Endobronchial Biopsy Workshop. Methods for the assessment of endobronchial biopsies in clinical research: application to studies of pathogenesis and the effects of treatment. Am J Respir Crit Care Med 168:S1–S17
30. Aleva RM, Kraan J, Smith M et al (1998) Techniques in human airway inflammation: quantity and morphology of bronchial biopsy specimens taken by forceps of three sizes. Chest 113:182–185
31. Yawn BP, Wollan P, Kurland M et al (2002) A longitudinal study of the prevalence of asthma in a community population of school-age children. J Pediatr 140:576–581
32. Mvula M, Larzelere M, Kraus M et al (2005) Prevalence of asthma and asthma-like symptoms in inner-city schoolchildren. J Asthma 42:9–16
33. Babey SH, Meng YY, Brown ER et al (2006) Nearly six million Californians suffer from asthma symptoms or asthma-like breathing problems. Policy Brief UCLA Cent Health Policy Res (PB2006-5), pp 1–7
34. Gibson PG (2007) What do non-eosinophilic asthma and airway remodelling tell us about persistent asthma? Thorax 62:1034–1036
35. Wenzel SE, Schwartz LB, Lankmack EL et al (1999) Evidence that severe asthma can be divided pathologically into two inflammatory subtypes with distinct physiologic and clinical characteristics. Am J Respir Crit Care Med 160:1001–1008
36. Douwes J, Gibson P, Pekkanen J et al (2002) Non-eosinophilic asthma: importance and possible mechanisms. Thorax 57:643–648
37. Berry M, Morgan A, Shaw DE, Parker D et al (2007) Pathological features and inhaled corticosteroid response of eosinophilic and non-eosinophilic asthma. Thorax 62:1043–1049
38. Sherwin RP, Richters V, Everson RB et al (1998) Chronic glandular bronchitis in young individuals residing in a metropolitan area. Virchow Arch 433:341–348
39. Pohunek P, Warner JO, Turzíková J, Kudrmann J, Roche WR (2005) Markers of eosinophilic inflammation and tissue remodelling in children before clinically diagnosed bronchial asthma. Pediatr Allergy Immunol 16:43–51
40. Amital H, Glikson M, Burstein M, Afek A, Sinnreich R, Weiss Y, Israeli V (2004) Clinical characteristics of unexpected death among young enlisted military personnel: results of a three-decade retrospective surveillance. Chest 126:528–533

Virchows Arch (2009) 455:87–92
DOI 10.1007/s00428-009-0781-3

ORIGINAL ARTICLE

Immune cell subsets in necrotizing fasciitis: an immunohistochemical analysis

A. J. Saenz · A. F. Koreishi · A. E. Rosenberg · R. L. Kradin

Received: 16 December 2008 / Revised: 9 April 2009 / Accepted: 17 April 2009 / Published online: 16 June 2009

Abstract Current concepts of the pathophysiology of necrotizing fasciitis (NF), a life-threatening infection of soft tissues associated with a toxic shock syndrome, emphasizes the role of bacterial superantigens as mediators of cytokine release by immune lymphocytes. In order to assess the cellular basis of immune activation, immunohistochemistry was applied to the analysis of inflammatory cell subsets in situ in 13 patients with NF. The percentage of inflammatory cells in skin and soft tissue was scored from 0 to 3+ (>50%). Substantial numbers of CD15+ polymorphonuclear leukocytes were present in 12 of 13 patients. CD3+ T-lymphocytes accounted for >10%, CD68+ macrophages for >50%, and Factor XIIIa+ mononuclear cells for >10% of the mononuclear cell infiltrates, respectively, in 10 of 13 patients, whereas CD1a+ cells were present in only 3 of 13 cases and accounted for <10% of mononuclear inflammatory cells. We conclude that immune lymphocytes and accessory immune cells are represented in substantial numbers in the early lesions of NF, and their presence supports current concepts with respect to the pathophysiology of this disorder.

A. J. Saenz · A. F. Koreishi · A. E. Rosenberg · R. L. Kradin (✉)
Department of Pathology,
Massachusetts General Hospital and Harvard Medical School,
Boston, MA 02114, USA
e-mail: rlkradin@partners.org

A. J. Saenz · A. F. Koreishi · A. E. Rosenberg · R. L. Kradin
James Homer Wright Pathology Laboratories,
Massachusetts General Hospital and Harvard Medical School,
Boston, MA 02114, USA

R. L. Kradin
Department of Medicine,
Massachusetts General Hospital and Harvard Medical School,
Boston, MA 02114, USA

Keywords Skin · Immunohistochemistry · Toxic shock · Streptococci

Introduction

Necrotizing fasciitis (NF) is an uncommon life-threatening infection of subcutaneous tissues. The disease is attributable to bacterial infection that spreads along fascial planes, producing extensive liquefactive necrosis that largely spares the superficial skin and skeletal muscle associated with a syndrome of toxic shock. The treatment of NF generally requires a combination of antibiotics, surgical debridement, and hemodynamic support. Clinically, NF has been subclassified into three types [1]. Type I occurs most commonly following surgery in diabetic patients and in those with peripheral vascular disease and is caused by a mixed aerobic and anaerobic infection [1]; type II is caused predominantly by group A beta hemolytic streptococci, but community-acquired methicillin resistant *Staphylococcus aureus* (MRSA) infection has also been reported [2]; type II infection occurs in all age groups; predisposing factors include drug injection, local trauma, and burns. Type III is caused by *Vibrio vulnificus* introduced into tissues via puncture wounds or the ingestion of shellfish in patients with hepatic compromise [1, 3].

The diagnosis of NF by the surgical pathologist often requires intraoperative examination of frozen sections. Stamenkovic and Lew [4] have suggested that the key criterion for the diagnosis of NF is the presence of neutrophils in fascial tissues, associated with liquefactive necrosis of fascia, fat necrosis, thrombosis of blood vessels, vasculitis, and abundant microorganisms [4, 5].

Although tissue neutrophils have been regarded as the sine qua non of the inflammatory response in NF

[4], current concepts of pathogenesis favor a primary role for bacterial toxin mediated cytokine release by T-lymphocytes rather than the pyogenic response that often accompanies bacterial infection. But diagnostic pathologists have paid little attention to the presence of T-lymphocytes and accessory cells, including dendritic cells, monocytes, and Langerhans cells, in NF. In the present study, we investigated the representation of immune cell subsets in NF by in situ immunohistochemical staining.

Materials and methods

Cases

The computerized electronic medical records of the Department of Pathology at the Massachusetts General Hospital from 2004 to 2007 were searched for the diagnosis "necrotizing fasciitis". Thirteen patients were identified with both clinical and histological evidence of necrotizing fasciitis. Rapid frozen sections were examined in five cases (38%). In these cases, the diagnosis was suggested by rapid frozen section examination and subsequently confirmed on examination of the permanent sections. A diagnosis compatible with necrotizing fasciitis on the rapid frozen section resulted in a larger surgical procedure in all cases, including either debridement and/or amputation.

Histopathology

The specimens were derived from the definitive surgical procedures. Full thickness specimens of skin that included the deep fascia and microscopic fragments of skeletal muscle were examined in all cases. Sections were fixed in 10% buffered formalin, routinely processed, sectioned at 5 μM, and stained with hematoxylin and eosin.

Immunohistochemistry

Serial 5-μm tissue sections were mounted on Superfrost slides. Immunohistochemical staining was performed with monoclonal antibodies (all Ventana Medical Systems) directed at CD3 (predilute), CD15 (predilute), CD1a (predilute), CD68 (predilute), and Factor XIIIa (1:1,400). All staining was performed on an automated Ventana Benchmark Autostainer (Ventana Medical Systems, Tucson, AZ, USA) with the Ultra View Detection Kit incubated for 32 min. Sections were deparaffinized, and antigen retrieval was performed by heating sections in CC1 (Ventana Medical Systems) EDTA at a pH of 8 for 30 min.

Data analysis

The hematoxylin-and-eosin-stained slides and immunohistochemical results were reviewed and scored by consensus of two pathologists (AS, RLK). Inflammatory cells were enumerated in five randomly selected high-power fields, including the dermis and fascia. Immunostaining was scored as a percentage of the total mononuclear cell infiltrate in each field and an average score ranging from negative, 1+ (<10%), 2+ (10–50%), to 3+ (>50%) was calculated.

Results

The pertinent clinical information is summarized in Table 1. There were six men and seven women, with ages ranging from 48 to 90 (mean=63) years. All patients were treated with antibiotics, surgical debridement, and/or amputation. The underlying disorders in these patients are listed in Table 1. Diabetes mellitus was the most common associated medical disorder (6 of 13). A history of either major or minor trauma was elicited in 2 of 13. Chronic obstructive pulmonary disease (3 of 13), cancer (2 of 13), cirrhosis (1 of 13), ethanolism (1 of 13), and peripheral vascular disease were other concomitant disorders. All of the patients survived their acute infection to leave the hospital; however, three died subsequently from complications of their underlying disease.

Gram-positive bacteria were identified in situ by tissue gram or GMS stains (gram-positive cocci) in 11 of 13. Gram-negative bacteria were not identified by tissue gram stain and were isolated in the microbiology laboratory. Bacteria were isolated from tissues in all cases. Three patients showed laboratory evidence of polymicrobial infection. These included group A beta hemolytic *Streptococcus* (3 of 13), *Enterococcus* (2 of 13), alpha hemolytic *Streptococcus* (1 of 13), non-hemolytic *Streptococcus* (1 of 13), *Staphylococcus* spp. (4 of 13), *Escherichia coli* (2 of 13), and *Proteus mirabilis* (1 of 13).

The key histopathologic findings of NF in the present series are listed in Table 2. All cases were diagnosed within 48 h of developing clinical symptoms and were judged to be in the acute phase of the disease. Dermal and fascial inflammation with neutrophils and mononuclear inflammatory cells was present in all cases (13 of 13; Fig. 1), necrosis of dermis and fascia (13 of 13; Fig. 2), vascular thrombi (7 of 13; Fig. 3), and microorganisms within necrotic dermis and fascia (11 of 13; Fig. 4).

The immunohistochemical findings are summarized in Table 3. CD15+ polymorphonuclear leukocytes were present in all cases and accounted for >10% of all inflammatory cells in 12 of 13 patients. CD3+ T-

Table 1 Pertinent clinical information

Patient	Age	Sex	Clinical status	Anatomic site (frozen section)	Microbiology	Clinical outcome
1	69	F	Peripheral vascular disease, hypertension	Left forearm (NF)	Beta hemolytic *Streptococcus* group A (very rare)	Surgical debridement; healed skin graft; alive at 2 years
2	52	M	Hepatitis B cirrhosis	Right leg (F)	Beta hemolytic *Streptococcus* group A (moderate)	Surgical debridement; healed skin graft; alive at 2 years
3	52	F	Diabetes mellitus	Left thigh (NF)	Non-hemolytic *Streptococcus* (abundant); coagulase negative *Staphylococcus* (moderate)	Surgical debridement and skin grafts; healed skin graft; alive at 2 years
4	84	M	Congestive heart failure, chronic obstructive pulmonary disease, S/P radiation prostatic carcinoma	Right leg fascia (F)	Beta hemolytic *Streptococcus* group A (abundant)	Below the knee amputation; dead
5	63	F	Ovarian carcinoma, chemotherapy	Right thigh (NF)	Septicum (very rare); *Staphylococcus aureus* (abundant); *Enterococcus* (abundant); *Corynebacterium* species (moderate)	Surgical debridement; skin grafting; healed graft; dead
6	90	M	Diabetes mellitus, chronic obstructive pulmonary disease	Left hand and forearm (NF)	*Staphylococcus aureus*	Surgical debridement; dead
7	64	F	Diabetes mellitus, hypertension	Left foot (F)	*Escherichia coli*	Surgical debridement; alive at 5 years
8	48	F	Diabetes mellitus, chronic obstructive pulmonary disease	Right abdomen/ right lower extremity (NF)	*Enterococcus*	Surgical debridement and split-thickness skin graft; alive at 4 years
9	71	F	Diverticulitis, peripheral vascular disease	Buttocks (NF)	*Proteus mirabilis*	Advancement flap and full thickness skin graft closure of large sacral wound; healed skin graft; alive at 3 years
10	56	M	Ethanol abuse, wasp sting	Right leg (NF)	*Escherichia coli* (few)	Surgical debridement of left buttock with left hip disarticulation and amputation of the left lower extremity; alive at 5 years
11	51	M	Diabetes mellitus, opioid abuse, trauma	Perineum, scrotum, and gluteus (F)	Alpha hemolytic *Streptococcus* (abundant)	S/P diverting sigmoid colostomy for Fournier's gangrene, post-op course complicated by wound infection that resolved; alive at 2 years
12	49	M	Psoriasis	Buttock (NF)	Coagulase negative *Staphylococcus*	Surgical debridement; alive at 2 years
13	72	F	Diabetes mellitus, urinary tract infection	Abdomen, perianal region (NF)	Coagulase negative *Staphylococcus* (few); *Staphylococcus aureus* (very rare); *Enterococcus* (very rare); *Proteus mirabilis* (very rare)	Surgical debridement; alive at 2 years

F frozen section examination conducted, *NF* no frozen section determination conducted

Table 2 Histopathologic findings in necrotizing fasciitis

Variegate appearance at low power
Dermal edema and necrosis
Fascial necrosis with interstitial fibrin deposition
Lobular panniculitis
Relative sparing of deep striated muscle
Neutrophils
Macrophages and lymphocytes
Vascular thrombi

lymphocytes were also present in all cases, as were CD68+ macrophages and Factor XIIIa+ mononuclear cells. CD1a+ dendritic cells were identified in 3 of 13 cases. Representative immunohistochemical staining results are shown in Fig. 4.

Discussion

Previous studies have addressed the histopathology of NF [4, 5]. Stamenkovic and Lew identified necrosis, neutrophilic infiltration, microorganisms, vasculitis, and thrombosis in the superficial fascia, deep dermis, and proximal adipose tissue in NF [4]. In this disorder, low-power screening invariably reveals a sparsely inflamed and edematous superficial dermis, whereas the deep dermis has a "dirty" appearance due to liquefactive necrosis of fascia and fat of the subcutis.

In the present study, mononuclear cell inflammation was demonstrated to be a common feature of NF, and CD68+ macrophages and Factor XIIIa+ mononuclear cells accounted for the majority of macrophages leukocytes.

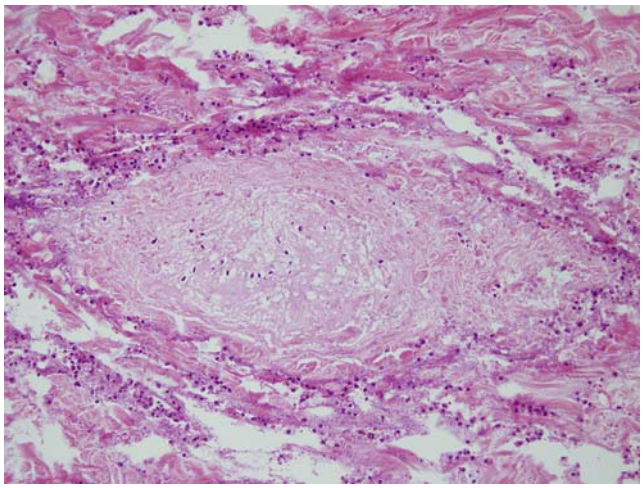

Fig. 2 Skin biopsy demonstrates subtle liquefactive necrosis of the fascia with microorganisms and acute inflammation. H&E, magnification ×200

Factor XIIIa+ dendritic macrophages and Langerhans' cells are effective class II MHC-restricted antigen presenting cells, and together with activated subsets of CD68+ macrophages, they provide accessory activities for the local proliferation of immune T-lymphocytes and for cytokine release. The presence of substantial numbers of CD3+ lymphocytes and putative accessory cells in the early lesions of NF support current concepts with respect to its pathogenesis.

Necrotizing fasciitis is a potentially fatal deep infection of skin with risk factors that include immunosuppressed states, minor cuts, burns, surgical procedures, chronic skin disease, insect bites, and blunt trauma [6]. The early clinical findings include edema of the involved area followed by bulla formation and erythema. The latter typically extends rapidly and progress to gangrene, with

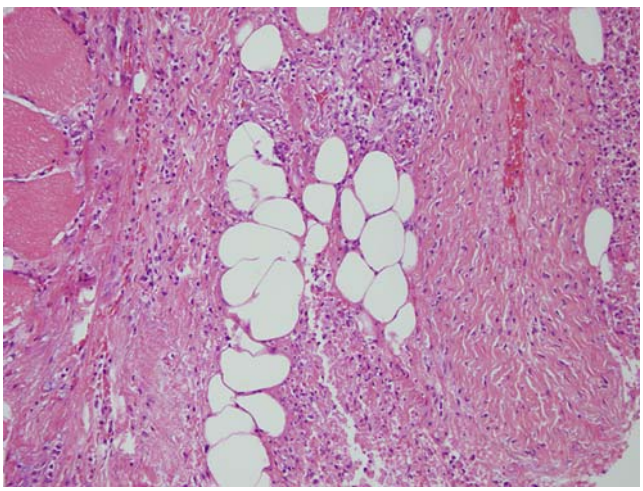

Fig. 1 Subcutaneous adipose tissue and fascia showing acute inflammation and mononuclear cell infiltrate with sparing of contiguous skeletal muscle. H&E, magnification ×200

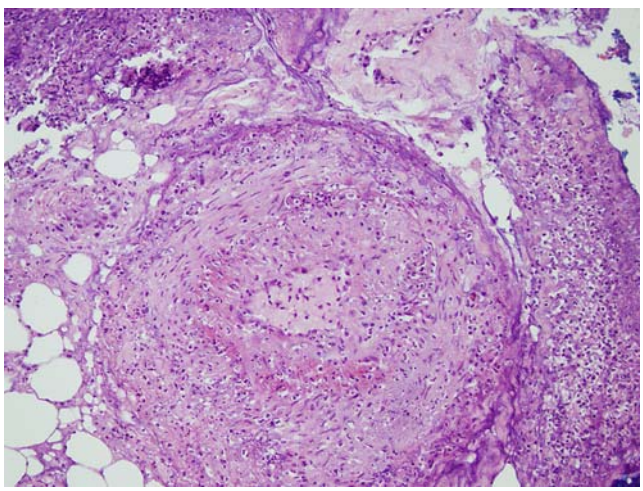

Fig. 3 Skin biopsy demonstrates vasculitis with surrounding necrosis, acute inflammation, and mononuclear cell infiltrate. H&E, magnification ×200

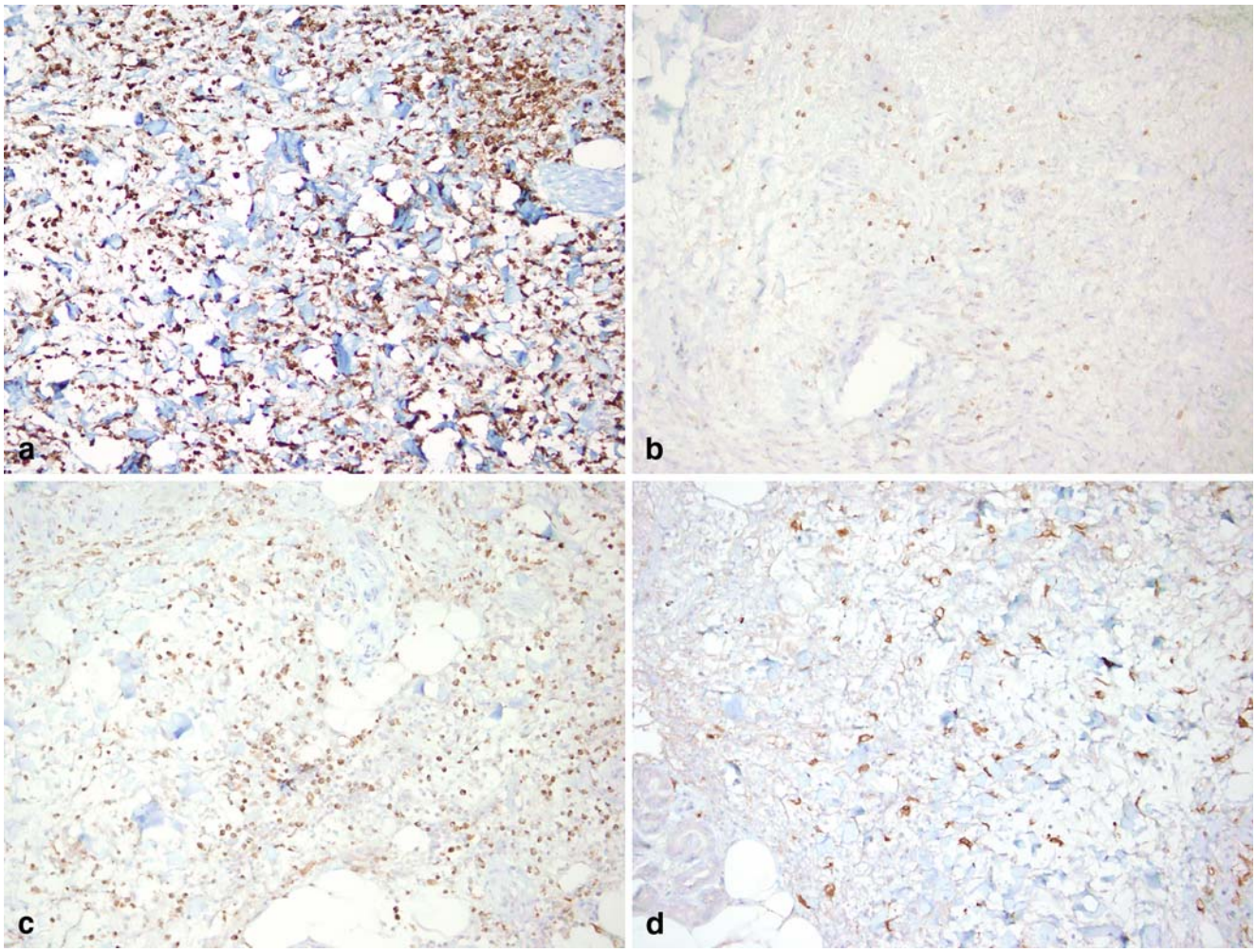

Fig. 4 The cellular infiltrate in NF showing **a** CD15+, **b** CD3+, **c** CD68+, and **d** Factor XIIIa+ mononuclear cells. Peroxidase, magnification ×200

systemic symptoms, shock, and multiorgan failure [7, 8]. The clinical findings mimic those of the toxic shock syndrome caused by staphylococcal and streptococcal infections [7–9].

Associations exist between group A streptococcal (GAS) strains, especially those of M-protein types of 1, 3, 12, and 28, and the toxic shock syndrome [7, 10]. Like the streptococcal disease scarlet fever, pyrogenic exotoxins

Table 3 Immunohistochemical staining results in necrotizing fasciitis

Patient no.	CD3+	CD68+	CD1a+	CD15+	Factor XIIIa+
1	1+	3+	Negative	3+	1+
2	1+	2+	1+	3+	3+
3	1+	2+	Negative	3+	1+
4	1+	3+	Negative	3+	3+
5	1+	2+	Negative	2+	1+
6	2+	3+	Negative	3+	3+
7	1+	3+	Negative	3+	2+
8	2+	3+	1+	3+	3+
9	2+	3+	Negative	3+	3+
10	1+	3+	1+	3+	2+
11	2+	3+	1+	3+	3+
12	3+	3+	Negative	3+	2+
13	1+	3+	Negative	3+	2+

produced by GAS appear to be responsible for the systemic effects that accompany localized infections [7, 10–12]. Streptococcal exotoxins A and B can mediate both local tissue damage and systemic toxicities [13]. Furthermore, GAS M-proteins can serve as superantigens that bind to major histocompatibility complex class II antigens on professional antigen presenting cells, linking them to specific variable beta regions of the T-cell receptor [6, 14] and leading to the release of potent cytokines, including tumor necrosis factor alpha and beta, interleukin-1 beta, interleukin-6, interleukin-2, and interferon gamma [15, 16]. Other streptococcal toxins that can function as superantigens include streptolysin O, streptococcal superantigen, and mitogenic factor [17, 18]. *Streptococcus* spp. are often a component of polymicrobial infections [4, 19].

Mononuclear cell inflammation is a constant and likely significant feature of the histopathology of NF. With respect to the three clinical subtypes of NF, only patients with type I (diabetes with polymicrobial disease) and II (group A streptococci) were examined in this study. There was no discernible difference in the histopathology or representation of mononuclear subsets between these groups. Immune lymphocytes and mononuclear accessory cells appear to play a critical role in mediating the local and systemic effects of this disease. Whereas the presence of fascial and dermal neutrophils is consistent with the histopathological diagnosis of NF, it is not specific and can be seen, e.g., in cellulitis. For this reason, the surgical pathologist should query the surgeon as to the presence of the characteristic "dish water" exudate, particularly at the time of frozen section, and the concomitant presence of mononuclear cell inflammation should be sought, as it may lend further support to the correct diagnosis.

References

1. Salcido R (2007) Necrotizing fasciitis: reviewing the causes and treatment strategies. Adv Skin Wound Care 20:288–293
2. Miller LG, Perdreau Remington F, Rieg G et al (2005) Necrotizing fasciitis caused by community-acquired methicillin resistant Staphylococcus aureus in Los Angeles. N Engl J Med 352:1445–1451
3. Roldan CJ (2007) Necrotizing fasciitis. J Emerg Med 16:1–2
4. Stamenkovic I, Lew PD (1984) Early recognition of potentially fatal necrotizing fasciitis. The use of frozen-section biopsy. N Engl J Med 310:1689–1693
5. Wong C, Wang Y (2005) The diagnosis of necrotizing fasciitis. Curr Open Infect Dis 18:101–106
6. Bisno AL, Stevens DL (1996) Streptococcal infections of skin and soft tissues. N Engl J Med 334:240–245
7. Stevens DL (1992) Invasive group A streptococcus infections. Clin Infect Dis 14:2–11
8. Wang YS, Wong CH, Tay YK (2007) Staging of necrotizing fasciitis based on the evolving cutaneous features. Int J Dermatol 46:1036–1041
9. Dahl PR, Perniciaro C, Holmkvist KA, O'Connor MI, Gibson LE (2002) Fulminant group A streptococcal necrotizing fasciitis: clinical and pathologic findings in 7 patients. J Am Acad Dermatol 47:489–492
10. Stevens DL, Tanner MH, Winship J (1989) Severe group A streptococcal infections associated with a toxic shock-like syndrome and scarlet fever toxin A. N Eng J Med 321:1–7
11. Hauser AR, Stevens DL, Kaplan EL, Schlievert PM (1991) Molecular analysis of pyrogenic exotoxins from Streptococcus pyogenes isolates associated with toxic shock-like syndrome. J Clin Microbiol 29:1562–1567
12. Marrack P, Kapler JW (1990) The staphylococcal enterotoxins and their relatives. Science 248:705–711
13. Green RJ, Dafoe DC, Raffin TA (1996) Necrotizing fasciitis. Chest 110:219–229
14. Mollick JA, Rich RR (1991) Characterization of a superantigen from a pathogenic strain of Streptococcus pyogenes. Clin Res 39:213A
15. Hackett SP, Stevens DL (1992) Streptococcal toxic shock syndrome: synthesis of tumor necrosis factor and interleukin-1 by monocytes stimulated with pyrogenic exotoxin A and streptolysin O. J Infect Dis 165:879–885
16. Fast DJ, Schlievert PM, Nelson RD (1989) Toxic shock syndrome-associated staphylococcal and streptococcal pyrogenic toxins are potent inducers of tumor necrosis factor production. Infec Immun 57:291–294
17. Norrby-Teglund A, Newton D, Kotb M (1994) Superantigenic properties of the group A streptococcal exotoxin SpeF (MF). Infec Immun 62:5227–5233
18. Mollick JA, Miller GG, Musser JM (1993) A novel superantigen isolated from pathogenic strains of Streptococcus pyogenes with aminoterminal homology to staphylococcal enterotoxins B and C. J Clin Invest 92:710–719
19. Hasham S, Matteucci P, Stanley PRW, Hart NB (2005) Necrotizing fasciitis. BMJ 330:830–833

Virchows Arch (2009) 455:93–94
DOI 10.1007/s00428-009-0758-2

LETTER TO THE EDITOR

Cytokeratin RNA amplification as a molecular method for the detection of lymph node metastases in breast cancer patients

Hans Kreipe

Received: 25 February 2009 / Accepted: 4 March 2009 / Published online: 24 March 2009

Keywords Sentinel lymph node · Breast cancer · Cytokeratin · RNA expression

Dear Sir:
In their recently published study, Schem and coworkers state that analysis of sentinel lymph node specimens in breast cancer patients by polymerase chain reaction (PCR) for expression of cytokeratin genes yields a reliable and standardized instrument with benefit for patients equalling histological analysis [1].

The data presented, however, could be read in a different way resulting in an opposing interpretation. A major shortcoming of the study is that no sensitivity tests have been performed: how many single cytokeratin-positive cells can be detected among how many lymphocytes? This could have been evaluated by simple mixing experiments with cell lines and lymphocytes isolated from the blood or from tissue samples. No quantitative analysis at all appears to be possible from what has been described in the paper because no calibration experiments have been performed.

Furthermore, the study suffers from a lack of gold standard to evaluate the sensitivity and specificity of the new technique to detect tumor cells in extracts of lymph node tissues. Histological proof of tumor cells could have been the gold standard as it provides the method currently used in practice. If this gold standard had been accepted, then an intolerable rate of discordance would have been the result. Rate of falsely positive samples would have amounted to 25 out of 343 equalling 7.3% and falsely negative samples to four out of 343 equalling 1.2%. A total discordance rate of 8.5% would have been the consequence.

Results become even worse when macrometastases, which might have been noticed by macroscopic evaluation alone and not requiring elaborate PCR methodology, are omitted: out of nine micrometastatic cases, two were falsely negative in the PCR assay (22.2%) and out of three samples with isolated tumor cells, two were negative in PCR. Hence, in samples with macroscopically nonvisible metastasis, four out of 12 samples were discordant (25%). The authors decided to compromise histology as a gold standard because of potential sampling bias. A second principle of verification was introduced consisting of additional evidence of the presence of epithelial cells by Western blot and three additional PCR reactions for putatively cancer-specific transcripts (CK19, SPDEF, and FOXA1). This principle, however, was not applied to every sample in the study, which could have meant a gold standard, but only to a selected subgroup of discordant cases. Sampling bias was assumed when at least one of the additional tests for epithelial gene expression was positive. Again, no experiments with controlled conditions, e.g., by mixing experiments, have been performed to evaluate how frequently only one of the additional markers turned positive and what, for example, the significance might be if CK19 PCR and Western blot are negative, whereas FOXA1 is the only further marker in support of the one-step nucleic acid amplification (OSNA) result (e.g., sample 11). What is the justification for assuming that one additional positive marker is sufficient to prove sampling bias, whereas three

H. Kreipe (✉)
Institute of Pathology, Medizinische Hochschule Hannover,
Carl Neuberg Strasse 1,
30625 Hannover, Germany
e-mail: Kreipe.Hans@mh-hannover.de

negative markers do not argue in favor of a discordant result?

The approach of the study to prove sampling bias as a major source of discordant results could be further questioned if those four cases are considered from which different samples with discordant results between positive OSNA and negative histology were derived. Three of these four cases yielded mixed results, with one sample being in favor of sampling bias and the others demonstrating discordance. The only case out of the four with a uniform result in all samples (7 and 13) homogeneously showed discordance. The other cases were constantly negative in histology (except one ITC) but yielded varying results with regard to RNA or protein detection of tumor cells in lymph node lysates, shedding light on the limited reproducibility of these evaluation methods (1 and 15; 22, 23, and 24; 18 and 20).

No information about the reproducibility of OSNA can be extracted from the description of the experiments. Were they done in duplicate or triplicate and what was the concordance between repeated tests?

Besides the methodological concerns, the conclusion of the authors that the adoption of the method as a clinical approach could lead to a benefit for the patients appears hard to follow when further consequences of the technique are considered. Material which has been used for PCR analysis is lost for histological evaluation. Consequently, a prognostically relevant discrimination between micrometastasis and isolated tumor cell involvement is no longer possible if the sample was the only part of the lymph node involved. As stated by the authors, the PCR reaction in terms of copy number did not correlate with the amount of tumor cells in the sample.

The most effective way to study the value of the new OSNA technique would have been to perform a randomized study comparing the ability of histology versus PCR-based techniques to predict from the analysis of the sentinel node further axillary lymph node involvement by breast cancer. Until that has been done, histology of the sentinel lymph node will remain the ultimate gold standard.

The intention of Schem and coworkers to test potential alternatives to intraoperative frozen section investigation of sentinel lymph nodes, which is not available everywhere in the world, is appreciated and there is no doubt that alternative techniques have to be evaluated. However, being confronted, as many of my colleagues in Germany have been in recent months, with an aggressive marketing strategy of companies trying to force the corresponding devices onto the market, I felt inclined to give a critical reappraisal of the currently available evidence for improved sentinel lymph node diagnostics by molecular means.

Conflicts of interest I declare that I do not have any conflicts of interest in this matter.

Reference

1. Schem C, Maass N, Bauerschlag DO, Carstensen MH, Löning T, Roder C, Batic O, Jonat W, Tiemann K (2009) One-step nucleic acid amplification—a molecular method for the detection of lymph node metastases in breast cancer patients; results of the German study group. Virchows Arch 454:203–210

Virchows Arch (2009) 455:95–96
DOI 10.1007/s00428-009-0797-8

LETTER TO THE EDITOR

One-step nucleic acid amplification—a molecular method for the detection of lymph node metastases in breast cancer patients; results of the German study group

Christian Schem

Received: 27 May 2009 / Accepted: 30 May 2009 / Published online: 23 June 2009

Abstract On behalf of all co-authors, I appreciate Prof. Kreipe's thoughts concerning our presented study results very much. In order to sustain this fruitful discussion about new developments and techniques in pathological diagnostics, we would like to comment on the questions raised in the Letter to the editor.

Keywords Breast · Metastasis · Lymph nodes

This published study describes the use of a commercially available molecular system, designed for the detection of lymph node metastases in breast cancer patients, in comparison with intensive histology.

Any experiments related to basic research of the IVD-CE marked product, such as the establishment of sensitivity and reproducibility of the one-step nucleic acid amplification (OSNA) assay, were not part of this study but reported elsewhere [1] and declared in the product information provided by the manufacturer (Sysmex, Kobe, Japan). Amplification of CK19 mRNA as part of OSNA is not based on PCR, as mentioned by H. Kreipe, but on reverse-transcription loop-mediated isothermal amplification (RT-LAMP) which includes six primers and is carried out at an isothermal temperature. The use of six primers ensures a high degree of specificity.

The OSNA system can detect macrometastases and micrometastases but not isolated tumor cells [1, 2] which are, according to the TNM classification of the UICC 6th edition [3], designated as pN0(i+) and therefore were recorded as histology negative in this study. In contrast to what Prof. Kreipe stated in his letter, OSNA detected all macrometastases (97/97) and seven out of nine micrometastases indicated by histological analysis in this study. Homogenates of the two discordant samples showed negative results upon further investigation with quantitative reverse-transcription PCR (QRT-PCR) and Western blotting.

In a recent publication, Daniele et al. [4] pointed out that, for studies in which alternating sections of the same sentinel lymph node are used for a comparison of molecular and histological methods, tissue allocation bias is the main source of discordant results. We therefore performed further analysis with molecular methods of the homogenates (discordant case investigation=DCI) in order to confirm this concept for our study.

DCI was established with a cohort of lymph nodes from histologically negative and positive lymph nodes (LN) from breast cancer patients according to the criteria described in Tsujimoto et al. [1] and Visser et al. [2]. A panel of three markers was used for QRT-PCR in order to supplement for potential downregulation of any of those markers in the tumor deposits. All markers can distinguish well between histologically positive and negative cases [1]; however, FOXA1 mRNA and SPDEF mRNA are less strongly expressed in histologically positive lymph nodes [1] than CK19 mRNA. On the other hand, rare cases with low CK19 expression can occur. Because of this, different results among the three markers for one sample can be observed. Since CK19 protein expression is partially regulated on a post-transcriptional level [5], even a positive result in QRT-PCR and a negative result in Western blotting for CK19 can be obtained.

In another study using a different molecular system for SLN analysis, DCI with a multi-marker panel was

C. Schem (✉)
Department of Obstetrics and Gynecology,
University Clinic of Schleswig-Holstein, Campus Kiel,
Michaelisstr. 16,
24105 Kiel, Germany
e-mail: Christian.Schem@uk-sh.de

performed in a similar fashion, and likewise a subgroup of assay positive/histology negative as well as assay positive/histology positive cases could not be confirmed by additional molecular testing [6].

As for the importance of OSNA as an intra-operative diagnostic tool for the detection of SLN metastasis, large multi-centric studies were recently performed in the UK and France with manuscripts in preparation. Up-to-date several institutes in five European countries are using OSNA as an intra-operative diagnostic tool for the assessment of the SLN status, with some users analyzing the whole SLN with OSNA and others leaving a 1 mm middle slice of the SLN for histological analysis. Ultimately, more published data and randomized studies will have to shed more light on the value of this innovative technique in the future.

Conflict of interest statement We declare that we have no conflict of interest.

References

1. Tsujimoto M, Nakabayashi K, Yoshidome K et al (2007) One-step nucleic acid amplification (OSNA) for intraoperative detection of lymph node metastasis in breast cancer patients. Clin Can Res 13:4807–4816
2. Visser M, Jiwa M, Horstman A et al (2008) Intra-operative rapid diagnostic method based on CK19 mRNA expression for the detection of lymph node metastases in breast cancer. Int J Cancer 122:2562–2567
3. Sobin LH, Wittekind C et al (2002) UICC TNM classification of malignant tumours, 6th edn. Wiley, New York
4. Daniele L, Annaratone L, Allia E et al (2008) Technical limits of comparison of step-sectioning, immunohistochemistry and RT-PCR on breast cancer sentinel nodes: a study on methacarn fixed tissue. J Cell Mol Med Jul 30 epub
5. Su L, Morgan PR, Lane EB (1996) Expression of cytokeratin messenger RNA versus protein in the normal mammary gland and in breast cancer. Hum Pathol 8:800–806
6. Julian TB, Blumencranz P, Deck K et al (2008) Novel intraoperative molecular test for sentinel lymph node metastases in patients with early-stage breast cancer. J Clin Oncol 26:3338–45

Virchows Arch (2009) 455:97–98
DOI 10.1007/s00428-009-0792-0

LETTER TO THE EDITOR

Primary thyroid-like renal tumor or renal metastasis from the thyroid?

William Sterlacci · Gregor Mikuz

Received: 4 May 2009 / Accepted: 17 May 2009 / Published online: 18 June 2009

Dear Editor,

With great interest, we read the comment by Insabato et al. [1] and the original report by Amin et al. [2], underlining the importance of distinguishing metastatic thyroid carcinoma to the kidney from a primary thyroid-like renal neoplasm. The authors accurately describe six cases of this extremely rare renal epithelial tumor, providing a comprehensive and noteworthy discussion. Our comment is as follows.

The renal tumor we described, resembling a follicular thyroid carcinoma and lacking immunohistochemical expression of thyreoglobulin as well as thyroid transcription factor-1 (TTF-1) [3], was not accepted as such by Amin et al. [2], due to a subsequent pulmonary nodule demonstrating immunoreactivity with TTF-1. The antibody panel, consisting of CK-7, CK-20, CAM5.2, vimentin, CD-10, CD-117, TTF-1, and thyreoglobulin, was examined in both tumors. We reported all staining results concerning the renal neoplasm and the differing results for the lung focus. Accordingly, the pulmonary tumor did not express thyreoglobulin. As previously discussed [4], TTF-1 positivity alone does not prove this pulmonary neoplasm originating from the thyroid. Possible explanations include non-neoplastic lung tissue entrapped within metastatic renal thyroid-like follicular cancer, TTF-1 immunoreactive tumor cells reflecting microenvironmental influences by lung tissue, or a separate primary lung carcinoma showing thyroid-like follicular carcinoma morphology. Amin et al. point out that metastatic carcinoma from the thyroid is usually widespread by the time of renal involvement, which is associated with poor survival, especially for follicular thyroid carcinoma. The patient we reported on is disease-free to date, amounting to a follow-up period of 7 years.

An extremely small thyroid carcinoma remaining undetected is possible though unlikely. At our institute, all thyroids excised due to malignancy are completely embedded in paraffin in maximally 3-mm-thick sections. Therefore a tumor must be smaller than 3 mm to escape histological diagnosis. The described renal tumor predominantly demonstrated typical follicular architecture, which would most likely be associated with a large primary and an advanced tumor stage in the case of a primary thyroid carcinoma. Follicular carcinoma of the thyroid disseminates hematogenously and predominantly metastasizes to bone, lungs, brain, and liver, whereas renal metastasis is a very rare occurrence. The vast majority of incidental carcinomas present with papillary histology. In addition, it is known that the normalization of iodine supply in an endemic goiter region, which is our situation, results in an increase of papillary carcinomas and a reduction of follicular carcinomas, as well as a shift towards earlier tumor stages at diagnosis. Also arguing against an overlooked occult primary of the thyroid is the fact that, after a thorough workup, all clinical examinations including ultrasound, laboratory parameters, 99-technetium scintigraphy, 18-fluordeoxyglucose positron emission tomography, and 131-iodine whole-body scans were without pathological findings.

Tumors resembling thyroid carcinoma have also been reported in other organs [5]. In conclusion, a crucial aspect when differentiating between a primary thyroid-like tumor and a metastasis from the thyroid is exact clinicopathologic correlation. Especially in cases that are not straight forward, this gains immense importance.

W. Sterlacci (✉) · G. Mikuz
Department of Pathology, Medical University of Innsbruck,
Muellerstrasse 44,
6020 Innsbruck, Austria
e-mail: William.sterlacci@i-med.ac.at

Conflict of interest The authors declare that they have no conflict of interest.

References

1. Insabato L, Ben-Dor D, Galliani CA et al (2009) Primary thyroid and thyroid-like follicular carcinoma of the kidney versus solitary metastatic carcinoma of the thyroid: a vexing issue. Virchows Arch 454:717–718
2. Amin MB, Gupta R, Ondrej H et al (2009) Primary thyroid-like follicular carcinoma of the kidney: report of 6 cases of a histologically distinctive adult renal epithelial neoplasm. Am J Surg Pathol 33:393–400
3. Sterlacci W, Verdorfer I, Gabriel M et al (2008) Thyroid follicular carcinoma-like renal tumor: a case report with morphologic, immunophenotypic, cytogenetic, and scintigraphic studies. Virchows Arch 452:91–95 Erratum in: Virchows Arch 452:471 William, Sterlacci [corrected to Sterlacci, William]; Irmgard, Verdorfer [corrected to Verdorfer, Irmgard]; Michael, Gabriel [corrected to Gabriel, Michael]; Gregor, Mikuz [corrected to Mikuz, Gregor]
4. Bisceglia M, Ragazzi M, Galliani CA et al (2009) TTF-1 expression in nephroblastoma. Am J Surg Pathol 33:454–461
5. Eusebi V, Damiani S, Ellis IO et al (2003) Breast tumor resembling the tall cell variant of papillary thyroid carcinoma: report of 5 cases. Am J Surg Pathol 27:1114–1118

Virchows Arch (2009) 455:99–100
DOI 10.1007/s00428-009-0796-9

LETTER TO THE EDITOR

Anti-MTOC-MT antibody is commonly detected by AIT test in colorectal cancer patients

Jung-UK Sir · Think-You Kim

Received: 25 May 2009 / Accepted: 27 May 2009 / Published online: 10 June 2009

Keywords Anti-MTOC-MT · Colorectal cancer · AIT test · Macrophage · IT-1 cell line

Abbreviations

AIT	Autoimmune target
MTOC	Microtubule organizing center
MT	Microtubule

To the Editor:

After reading the article, "β_{III}-tubulin at the invasive margin of colorectal cancer: possible link to invasion", by Portyanko et al. [1], we would like to express our experiences and opinions on host immune reaction in cancer patients.

In the article, the expression of β_{III}-tubulin, which is an isotype of tubulin, a major component of microtubule (MT) found in the budding margin of colorectal cancer tissue, was confirmed by immunohistochemical staining using anti-β_{III}-tubulin, and this phenomenon was considered to have deep relations with invading activity of cancer cell.

J.-U. Sir
Institute of Rheumatism, The Hospital for Rheumatic Diseases,
Hanyang University Medical Center,
Seoul, South Korea

T.-Y. Kim (✉)
Department of Early Arthritis/Laboratory Medicine, The Hospital for Rheumatic Diseases, Hanyang University Medical Center,
17 Haengdang-Dong Sungdong-Gu,
Seoul 133-792, South Korea
e-mail: tykim@hanyang.ac.kr

Up until current times, there had been several reports that confirmed the existence of various autoantibodies in cancer patients, and that these antibodies do affect the process of cancer growth [2].

We had discovered the existence of autoantibody against microtubule organizing center with microtubule (MTOC-MT) in the serum of cancer patients for a long time, and many extensive studies in various cancers are currently in progress [3]. The anti-MTOC-MT positive rates were 15.2% in our colorectal cancer cases and 10.8% (20/186) in gastrointestinal cancer cases (Table 1). Anti-MTOC-MT was measured by AIT (autoimmune target) test that uses indirect immunofluorescence method. Instead of using HEp-2 cell as in the conventional test, AIT test uses the human macrophage cell (IT-1) as a substrate that plays a pivotal role in the autoimmune and tumor immune pathways, and this test can detect various spectrums of autoantibody that were not possible to be seen by conventional antinuclear antibody test. Due to the unique nature of high intracellular and intercellular activity of macrophage, the size of MTOC-MT is especially large and is easy to observe [4, 5].

In terms of host immunity, our results provide evidence that can support and reinterpret the results of the above article. In other words, MT is playing an important role in the metastatic invasion of cancer cell, and can create anti-MTOC-MT by 'spitting out' a MT-related soluble form of autoantigen into host immune network. Looking at the fluorescence pattern of anti-MTOC-MT by AIT test, involved autoantigen can be related to various types of MT-associated components including β_{III}-tubulin. Also, anti-MTOC-MT formed by such process could be understood as playing a role of host defense mechanism against cancer cell invasion. As a conclusion, we think that, when

Table 1 Prevalence of anti-MTOC-MT pattern of AIT test in gastrointestinal cancer patients (n=186)

Type of malignancy	Anti-MTOC-MT positive cases	Total cases	Percent
Esophagus	2	22	9.1
Stomach	11	118	9.3
Colorectal	7	46	15.2
Total cases	20	186	10.8

MTOC-MT microtubule organizing center with microtubule, *AIT* autoimmune target

β_{III}-tubulin could be a marker in estimating the invading activity of cancer cell, anti-MTOC-MT could be considered as a new cancer marker that can represent the host immune reaction against cancer cell.

Conflict of interest statement T.Y. Kim holds patent relating to the IT-1 cell line.

References

1. Portyanko A, Kovalev P, Gorgun J et al (2009) β_{III}-tubulin at the invasive margin of colorectal cancer: possible link to invasion. Virchows Arch 454:541–548
2. Bei R, Masuelli L, Palumbo C et al (2008) A common repertoire of autoantibodies is shared by cancer and autoimmune disease patients: inflammation in their induction and impact on tumor growth. Cancer Lett . doi:10.1016/j.canlet.2008.11.009
3. Mihn DC, Kim TY (2009) Various autoantibodies are found in small-cell lung cancer. Lung Cancer 64:250
4. Le Goff P, Saraux A, Youinou P (1997) New autoantibodies in rheumatoid arthritis. Rev Rhum Engl Ed 64:638–644
5. Kim TY, Chang SY (1999) Anti-MTOC, the new marker antibody for rheumatoid arthritis, is different from centrosome autoantibodies. Korean J Lab Med 19(Suppl):S280

Virchows Arch (2009) 455:101–108
DOI 10.1007/s00428-009-0803-1

ORIGINAL ARTICLE

Multiple sporadic gastrointestinal stromal tumours arising at different gastrointestinal sites: pattern of involvement of the muscularis propria as a clue to independent primary GISTs

Abbas Agaimy · Bruno Märkl · Hans Arnholdt · Peter H. Wünsch · Luigi M. Terracciano · Stephan Dirnhofer · Arndt Hartmann · Luigi Tornillo · Michel P. Bihl

Received: 20 April 2009 / Revised: 7 June 2009 / Accepted: 8 June 2009 / Published online: 2 July 2009

Abstract Multifocal sporadic gastrointestinal stromal tumours (GISTs) may be misinterpreted as recurrent or metastatic disease, leading to inappropriate treatment. As molecular analysis is generally not available in routine practise, histological criteria that would facilitate diagnosis of multiple primary GISTs in routine slides are needed. We studied 14 GISTs (mean size, 2.7 cm) from six men and one woman (mean age, 70 years) applying morphological features and direct sequencing of *KIT*, *PDGFRA*, *BRAF*, and *KRAS*. Diagnosis was synchronous in five and metachronous in two patients. Paired tumours originated in stomach/small bowel (n=5), duodenum/jejunum (n=1), and stomach/oesophagus (n=1) and revealed spindle (n=10) and mixed spindle and epithelioid (n=4) phenotype. Tumours were well circumscribed and have involved the muscularis propria in a pattern typical of primary GISTs. Different somatic *KIT* mutations were found in tumours from four patients. One patient had a *KIT*-mutated and a *BRAF*-mutated (V600E) tumour. Two patients had wild-type tumours. No *PDGFRA* or *KRAS* mutations were detected. Our results underscore the molecular heterogeneity of sporadic multifocal GISTs. The characteristic involvement of the muscularis propria and the site-typical morphology and immunophenotype facilitated the diagnosis of primary GISTs in all cases and correlated with molecular findings, emphasising the value of conventional histology in recognising independent primary GISTs.

Keywords Multiple GIST · KIT · BRAF · KRAS

A. Agaimy · A. Hartmann
Institute of Pathology, University Hospital,
Erlangen, Germany

B. Märkl · H. Arnholdt
Institute of Pathology, Klinikum Augsburg,
Augsburg, Germany

P. H. Wünsch
Institute of Pathology, Klinikum Nürnberg,
Nürnberg, Germany

L. M. Terracciano · S. Dirnhofer · L. Tornillo · M. P. Bihl
Institute of Pathology, University of Basel,
Basel, Switzerland

A. Agaimy (✉)
Pathologisches Institut, Universitätsklinikum Erlangen,
Krankenhausstraße 12,
91054 Erlangen, Germany
e-mail: abbas.agaimy@uk-erlangen.de

Introduction

A majority of gastrointestinal stromal tumours (GISTs) occur as sporadic solitary neoplasms in adults with a mean age of 65 years [1]. Somatic *KIT* (80%) and *PDGFRA* (10%) mutations represent mutually exclusive gatekeeper molecular events in GISTs [2, 3]. A subset of GISTs (approximately 10%), in particular, paediatric GISTs [4] and GISTs in patients with neurofibromatosis 1 (NF1) [5], and the Carney triad [6] lack mutations in *KIT* and *PDGFRA* (wild-type GISTs). Of the latter, approximately 4% were found to harbour the *V600E BRAF* mutation as alternative molecular oncogenic events in two recent studies [7, 8]. Paediatric and Carney triad-associated GISTs

arise commonly as multifocal or multinodular gastric tumours [4, 9]. On the other hand, patients with NF1 [5] and those with germline mutations in *KIT* [10] and *PDGFRA* [11] are characterised by the development of numerous GISTs in one or different parts of the GI tract, usually in a background of diffuse interstitial cell of Cajal (ICC) hyperplasia. The small intestine (duodenum, jejunum, and ileum) represents predilection sites for NF1-associated GISTs, but other sites may be involved as well [5]. On the other hand, patients with *KIT* or *PDGFRA* germline mutations develop GISTs at different sites including stomach, small bowel, and other rare locations [10, 11].

Recent studies revealed a predilection for multiple sporadic GISTs to develop in the proximal gastric body as a result of distinct *KIT* and *PDGFRA* mutations, suggesting a possible "field effect" [12, 13]. However, GISTs originating multifocally in different GI sites in patients lacking familial GIST syndromes and NF1 are probably under-recognised; many such GISTs might have been interpreted as recurrent or metastatic disease. Accordingly, their molecular pathogenesis is not sufficiently studied. To date, less than ten such cases have been analysed in three previous studies [14–16], but molecular findings have been inconsistent in some of the cases analysed.

Although the growth pattern and relationship of a neoplasm to surrounding tissue/mucosa has been long applied to resolve the dilemma of *primary* versus *metastatic tumour* in surgical pathology practise, to our knowledge, this aspect has not been addressed in GISTs to date. Accordingly, there exist no criteria that permit a diagnosis of primary versus recurrent tumour in patients with a history of GIST and those presenting initially with multifocal disease. Previous reports have focused mainly on the mutational status as the only hint to their multifocal primary nature, but no detailed description of gross and microscopic features was given. Thus, it is not surprising that tumours completely localised in the peritoneum, a common site for metastatic spread in GIST, were included in previous studies and turned out to be metastatic disease [16]. Furthermore, a proportion of previously studied cases revealed identical mutations [14], findings that in conjunction with peritoneal location and high-risk histology would favour metastatic spread.

In this study, we analysed 14 GISTs from seven patients for their gross and histopathological features, with emphasis on the pattern of involvement of the muscularis propria as a clue for distinct primaries. In addition to *KIT* and *PDGFRA*, we investigated for the first time the presence of *BRAF* and *KRAS* mutations in multiple sporadic GISTs. The results indicate the value of histological features in initial recognition of primary GISTs, supplemented by molecular analysis in equivocal cases.

Materials and methods

Cases were retrieved from the surgical pathology files of our institutions. Only cases in which GISTs were diagnosed at distinct GI sites (e.g., stomach and any other part of the GI tract) or originated in different parts of the small bowel (duodenum, jejunum, or ileum) were considered. Tumours that were closely associated in the proximal stomach have been published previously and are not included here [13]. The BRAF-mutated tumour from one patient has been included in a recent study [8]. No patient had a known history of NF1, familial GIST syndrome, or features of the Carney triad, and none had received imatinib therapy prior to surgery. All gross descriptions and available gross photographs as well as conventional slides from all tumours have been evaluated by an experienced pathologist (A. A.) without knowledge of the molecular findings. No cases with apparently advanced metastatic tumours involving the peritoneum have been included. A minimum of five blocks were submitted from tumours ≥5 cm. Tumours were carefully analysed, both grossly and microscopically, for any association with the muscularis propria as was described previously in so-called extra-gastrointestinal GIST [17]. In particular, the following was noted as suggestive of primary GIST: (1) at least partial intramural localization with or without dissection of the muscularis propria along the plane of the Auerbach plexus, (2) attachment of a predominantly extramural lesion to the outermost gut wall by a narrow pedicle partially obliterating the external muscle layer, and (3) evidence of remnant muscle fibres at the tumour periphery/capsule. If applicable, tumours have been classified into one of the eight histological subtypes described by Miettinen et al. for gastric GISTs [18] in order to correlate their morphologies with anatomic sites. Risk assessment was based on the National Institutes of Health consensus criteria [19]. Immunohistochemistry was performed using the methods and primary antibodies described previously [20].

Molecular analysis for *KIT*, *PDGFRA*, *BRAF*, and *KRAS* mutations

Extraction of tumour DNA from formalin-fixed paraffin embedded material, polymerase chain reaction (PCR) amplification, direct sequencing of *KIT* exons 2, 9, 11, 13, and 17 and *PDGFRA* exons 12, 14, and 18, and verification PCR were performed using the methods previously described [20]. For *BRAF* and *KRAS* mutation

analysis, the sequences of primers used for the PCR were as follows:

BRAF exon 15 forward	5′ CTTCATGAAGACCTCACAGTAAAAATAGG 3′
BRAF exon 15 reverse	5′ TAGCCTCAATTCTTACCATCCACAAA 3′
KRAS exon2 forward	5′ TTTTTATTATAAGGCCTGCTGAAAATG 3′
KRAS exon2 forward nested	5′ TATTATAAGGCCTGCTGAAAATGACTG 3′
KRAS exon2 reverse	5′ AATGGTCCTGCACCAGTAATATGCATAT 3′
KRAS exon2 reverse nested	5′ GTCCACAAAATGATTCTGAATTAGCTGTA 3′

BRAF and *KRAS* amplification required one step and two steps of amplification, respectively. For the first and the nested PCR, a 50-cycles amplification step was performed using an AmpliTaq Gold (Applied Biosystem) under the following conditions: 20 s at 95°C for the denaturation, 10 s at 55°C for the annealing, and 40 s at 72°C for the elongation.

Results

General incidence and localization of multiple primary GISTs

Initially, a total of ten patients (with two distinct GISTs each) fulfilled the above criteria for independent primary GISTs. Two patients with small bowel GISTs had a known NF1 and were excluded from further analysis. A third patient had two simultaneous duodenal and jejunal GISTs expressing S100 protein. NF1 was suspected, but our initial enquiries were inconclusive for NF1. However, upon a thorough review of old pathology request forms, it turned out that this patient had clinical signs of NF1. Thus, this patient was also excluded from further analysis. The remaining seven patients represented 1.6% of 419 consecutive GISTs at our departments and are the subject of this study. Paired tumours originated from the stomach body/fundus and small bowel (n=5), stomach body and oesophagus (n=1), and duodenum and jejunum (n=1).

Clinical features and patients characteristics

The clinicopathological features of all patients are summarised in Table 1. There were six men and one woman. Patient ages at diagnosis of the first tumour ranged from 39 to 84 years (mean age, 70 years). Presenting symptoms were upper GI bleeding (n=2), extensive peritoneal sarcomatosis from ileal GIST (n=1), intermittent abdominal pain with palpitation (n=1), and non-specific abdominal symptoms (n=2). Four small tumours were incidental findings during abdominal surgery for malignant (n=2) and benign (n=2) diseases. Two tumours were incidental to surgery for symptomatic GIST. The duodenal GIST in patient 5 was thought to represent a pancreatic head tumour on computed tomography scan. A second jejunal GIST was detected in this patient intra-operatively. In one patient, both tumours were incidental finding at autopsy. Diagnosis of both tumours was synchronous in five patients and metachronous in two. The interval between first and second tumour in the patients with metachronous presentation was 5 and 6 years, respectively.

Pathological findings

Gross features

Tumours ranged from 0.1 to 7.5 cm in size (mean, 2.7 cm). Gross features were similar to those previously reported for GIST in general, the majority being tan to grey-whitish with variable areas of cystic degeneration and haemorrhage. All tumours were well circumscribed grossly (Fig. 1a, b). Larger symptomatic tumours were commonly transmural with both peritoneal and luminal growths (Fig. 1c). Almost all incidentally detected second tumours (n=8) were predominantly extramural or partially subserosal nodules attached to the outer layer of the gut wall by a narrow pedicle. The tumour pedicle obliterated the muscularis propria, indicating intramural origin of the tumour with subsequent extramural growth (Fig. 1d).

Microscopic and immunohistochemical features

All tumours revealed a variable degree of involvement of the muscularis propria in a pattern typical of primary GISTs, and none was completely intra-peritoneal/extra-gastrointestinal or confined to the subserosa, contrasting with metastatic deposits (Table 1). Dissecting growth along the plane of the myenteric plexus was a common feature, at least focally (Fig. 2a, b). Of interest, it was remarkable that tumour tissue in the vicinity of the muscularis propria was generally hypocellular and spindled with bland histology, even in tumours with otherwise high cellularity and epithelioid morphology (Fig. 2c). Residual muscle fibres were consistently seen at tumour periphery (Fig. 2d). Intimate association with the myenteric plexus and the Cajal cells was well recognisable in most cases (Fig. 2e, f). Gastric tumours revealed sclerosing spindle (n=4), cellular spindle (n=1), and mixed spindle and epithelioid (n=1) morphology according to Miettinen et al. [18]. The duodenal tumour from patient 4 and the gastric tumour from patient 5 displayed distinct lobules of cellular

Table 1 Clinicopathologic and molecular features of sporadic multifocal GISTs from the current study (n=7)

No.	Age/ gender	Tumours	Site	Chronology	Clinical features	Histotype/mitotic count per 50 HPFs	Size (cm), risk	CD34	SMA	Follow-up	KIT exons 9, 11, 13, and 17	PDGFRA exons 12, 14, and 18	BRAF exon 15	KRAS exon 2	Normal tissue
1A	79, M	first GIST	Stomach fundus		Incidental finding	Sclerosing spindle; focal calcification 0/50	0.4, VLR	+++	−		*KIT* exon 11 Del W557-K558, W557F	WT	WT	WT	WT
1B		second GIST	Ileum	Meta 5 years	GI bleeding and peritoneal MTS	Sarcomatous spindle; 15/50	7.5, HR	++	+	AWD under Glivec at 8 months	*KIT* exon 9 Dupl: A502-Y503	WT	WT	WT	WT
2A	61, M	first GIST	Stomach body		Incidental to Barrett adenocarcinoma	Sclerosing spindle; focal calcification 0/50	0.5, VLR	+++	−		WT	WT	WT	WT	WT
2B		second GIST	Oesophagus	Syn	Incidental microscopic finding	Sclerosing spindle 0/50	0.1, VLR	+++	−	NA	*KIT* exon 11 V560D	WT	WT	WT	WT
3A	81, M	first GIST	Stomach fundus		Both incidental to gastric cancer	Sclerosing spindle 0/50	0.5, VLR	+++	−		*KIT* exon 11 V559D	WT	WT	WT	WT
3B		second GIST	Jejunum	Syn		Cellular spindle, SF 0/50	0.4, VLR	++	+	Recent case	WT	WT	V600E	WT	WT
4A	39, M	first GIST	Stomach body		Non-specific symptoms	Cellular spindle, 3/50	6, IR	+++	−		*KIT* exon 11 Del A555-Q556	WT	WT	WT	WT
4B		second GIST	Duodenum	Meta 6 years		Sclerosing epithelioid, sclerosing/cellular spindle, 4/50	3.5, LR	++	−	ANED 119 months from 1st GIST, 47 months from 2nd GIST	*KIT* exon 11 W557G	WT	WT	WT	WT
5A	82, M	first GIST	Stomach body		Upper GI bleeding	cellular epithelioid +sclerosing spindle 10/50	4.5, IR	++	−		*KIT* exon 11 Del M552-Y553	WT	WT	WT	WT
5B		second GIST	Small bowel	Syn	Found during surgery for GIST	Cellular spindle, SF 0/50	0.5, VLR	+	+++	ANED at 13 months	*KIT* exon 11 Del M552-Y553+ V560D+ E554E	WT	WT	WT	WT
6A	69, F	first GIST	Duodenum		Abdominal pain, palpitation	Cellular spindle+ cellular epithelioid, SF; 1/50	7, IR	+++	+		WT	WT	WT	WT	WT
6B		second GIST	Jejunum	Syn	Incidental finding on resection of GIST	Sclerosing/cellular spindle+cellular epithelioid, SF; 1/50	5.8, IR	+	++	ANED at 44 months	WT	WT	WT	WT	WT
7A	84, M	first GIST	Stomach fundus		Died of CVD, both autopsy findings	Sclerosing spindle +calcification; 0/50	0.4, VLR	+++	−		WT	WT	WT	WT	WT
7B		second GIST	Small bowel	Syn		Cellular spindle, SF 0/50	0.5, VLR	−	+++	Both GISTs autopsy findings	WT (L472L)	WT	WT	WT	WT

SF skeinoid fibres, *HPF* high power field, *VLR* very low risk, *LR* low risk, *IR* intermediate risk, *HR* high risk, *MTS* metastasis, *NA* not available, *ANED* alive with no evidence of disease, *AWD* alive with disease, *Syn* synchronous, *Meta* metachronous, *CVD* cardiovascular disease, *WT* wild-type

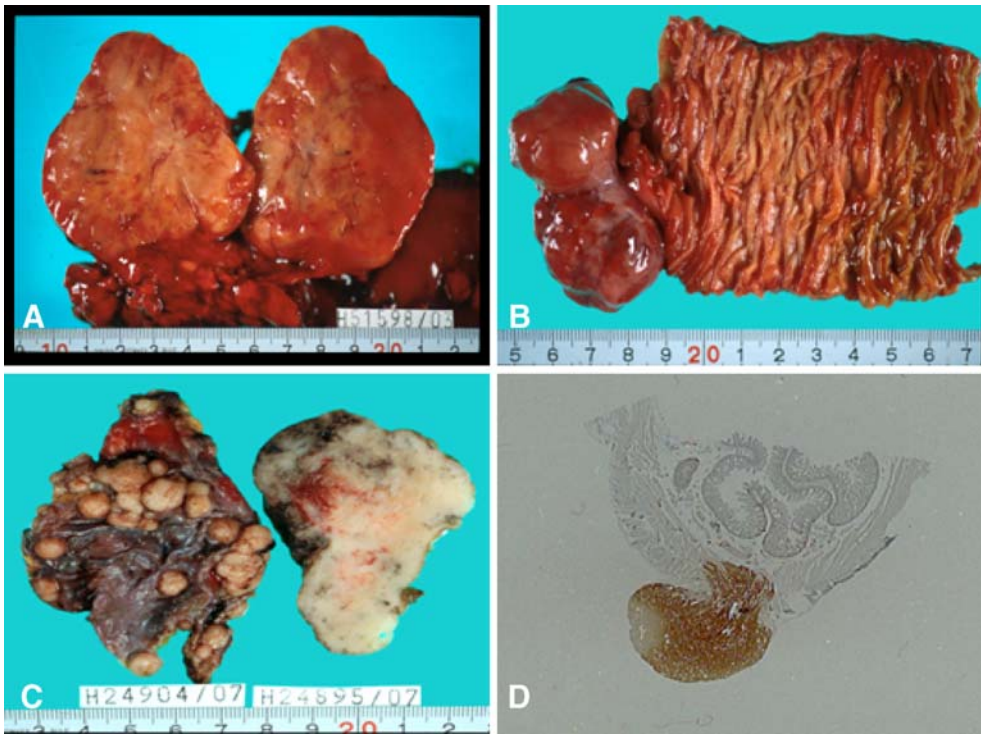

Fig. 1 Gross features of multiple primary and metastatic GISTs. **a** Large duodenal extramural GIST on cross section (case 6). **b** Second tumour from the same patient found intra-operatively attached to the jejunum by a thin pedicle. **c** Large malignant transmural ileal GIST (*right*) presenting initially with multiple confluent peritoneal metastases (*left*) in case 1. **d** Overview of the small bowel GIST found intra-operatively in case 5. Note tumour pedicle obliterating the external muscle coat (CD117)

epithelioid and sclerosing/cellular spindle morphology separated by residual muscle fibres with focally recognisable transitional areas (Fig. 2g, h). Small bowel tumours revealed high to moderate cellularity with numerous skeinoid fibres seen in most of them (Fig 2i). No precursor lesions (ICC hyperplasia) were seen in the surrounding muscularis propria in any of the cases.

Immunohistochemically, all tumours were strongly KIT positive (Fig. 1f). However, expression of CD34 and smooth muscle actin (SMA) was site-dependant. In particular, gastric tumours were uniformly CD34 positive and SMA negative. On the other hand, small bowel tumours were more commonly CD34 negative or only focally positive, and diffusely SMA positive. None of the tumours expressed S100 protein or desmin.

Molecular findings

In nine of 14 tumours (64%) corresponding to five of seven patients (71%), a mutation was detected in *KIT* (n=8) and *BRAF* (n=1; Table 1). No mutations were detected in *PDGFRA* or *KRAS*. *KIT* mutations involved exon 11 in seven tumours (five-point mutations and four deletions) and exon 9 in one tumour. Two tumours had both deletions and point mutations. The mutational status for paired tumours was as follows: *KIT* exon 11/*KIT* exon 11 (three patients), *KIT* exon 11/*KIT* exon 9 (one patient), *KIT* exon 11/*BRAF* (one patient), and wild-type/wild-type (two patients). Patient 3 had a gastric GIST with V559D and a small bowel GIST harbouring the V600E *BRAF* mutation (Fig. 3). Different mutations were detected in four of the five mutation-positive cases. Patient 5 had the same *KIT* exon 11 deletion in both tumours, in addition to a point mutation and a silent mutation detected only in his small bowel GIST. However, tumours from this patient showed a strikingly distinct morphology (Fig. 2g–i). Of note, no multiple mutations involving more than one gene or different exons of the same gene were detected in the same tumour in any of the cases. Analysis of normal tissue revealed wild-type sequences in all cases, thus ruling out germline mutations.

Discussion

This is the first study to analyse the gross and histological pattern of involvement of the muscularis propria as a potentially reliable clue to the primary nature of GISTs. We applied the same method we used previously to critically assess the origin of so-called extra-gastrointestinal GISTs (EGIST) [17]. Typical patterns of involvement of the muscularis propria seen in the current cases included (1) splitting of the muscularis propria at a level corresponding to the intermuscular plane of the Auerbach plexus; (2) non-destructive dissecting infiltration of the muscle coat by bland-looking less cellular spindled tumour tissue with occasional sclerosis, even in otherwise hypercellular and epithelioid neoplasms; (3) presence of compressed capsule-like smooth muscle fibres at the tumour periphery in extramural tumours; (4) small myenteric nerves or residual ganglionic elements within the tumour; (5) presence of a

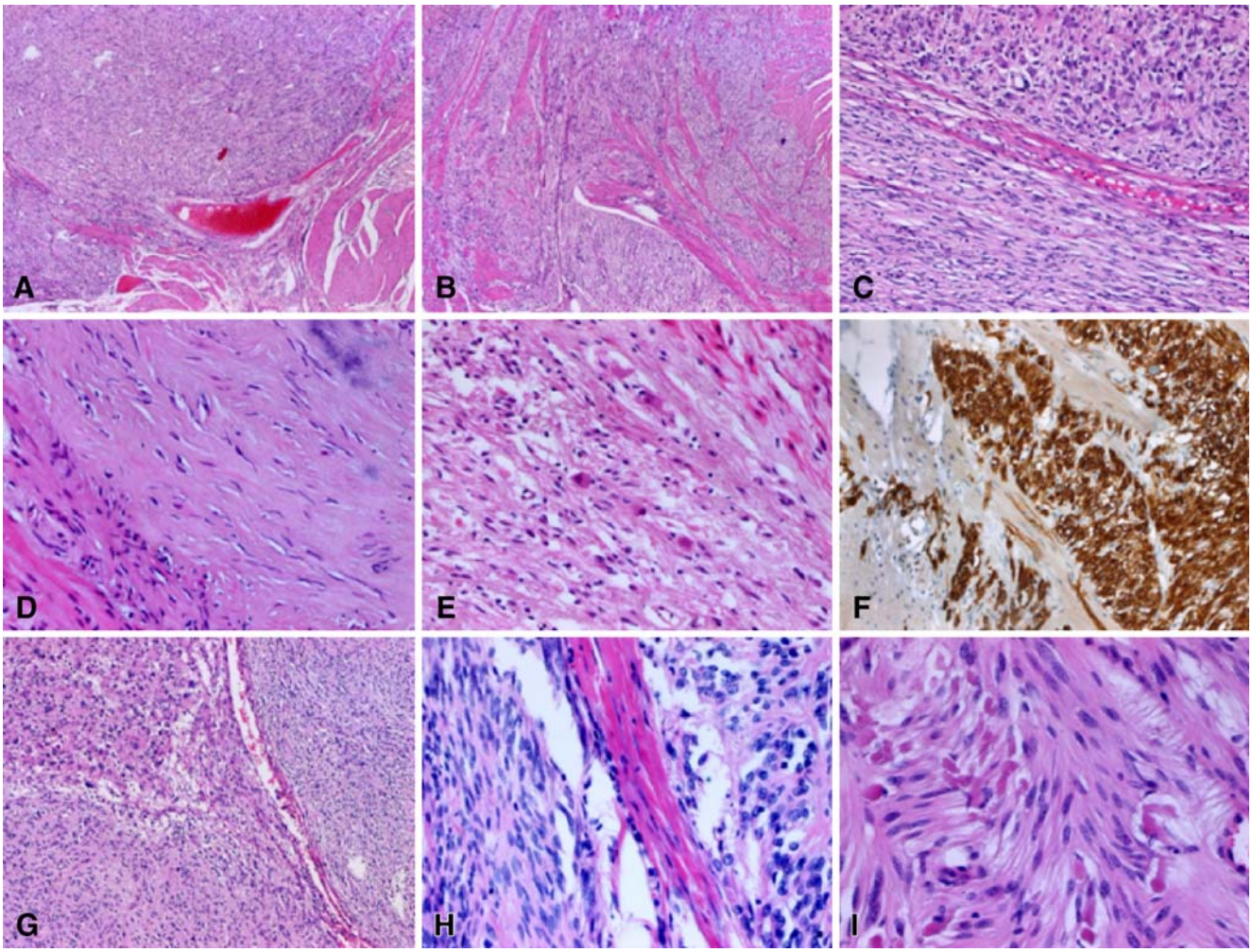

Fig. 2 **a** Typical splitting of the muscularis propria along the plane of the myenteric plexus. **b** Sheets of tumour cells diffusely dissecting the muscle coat. **c** Cellular epithelioid gastric GIST (*upper field*) with a bland-looking spindle cell focus at the border to the muscularis propria. **d** Sclerosing spindle cell gastric GIST showing residual muscle tissue at the tumour periphery. **e** Residual myenteric nerve and ganglion cells at the border to the muscle coat in a small bowel GIST. **f** CD117 highlighting close association of GIST (*upper right*) with ICCs (*lower left*). **g** Typical multinodular spindle and epithelioid pattern in gastric GIST (patient 5) with intervening fibromuscular septum deriving from the muscularis propria in **h**. **i** Second tumour from the same patient found intra-operatively showing small bowel-typical histology with skeinoid fibres

tumour pedicle obliterating the external muscle coat and abutting the myenteric plexus; and (6) presence of thin fibromuscular septa arising from the muscularis propria and traversing tumour nodules, particularly in epithelioid and mixed neoplasms. These observations were consistent with the notion that GISTs, as tumours of ICCs, do arise invariably within the muscularis propria but may adopt varied growth patterns in the later course of the disease [17]. Although infiltration of the muscularis propria may occur in metastatic GIST, in our experience, this is uncommon and if occurred, such metastatic tumours generally have high-grade features, are less well circumscribed, and have irregular infiltrative borders with entrapment of fat and other tissue derivatives besides the muscularis propria. Furthermore, the above-listed features typical of primary GISTs are unusual in metastatic GISTs infiltrating the GI musculature.

The site-typical morphology and immunophenotype represent further criteria that may be of great value in identifying primary GISTs. Gastric GISTs reveal a strikingly varied but characteristic morphology with eight reproducible histological types [18] that generally differ from small bowel GISTs [21]. In our study, paired tumours originating in the stomach and small bowel in the same patient displayed discordant, site-typical morphology, respectively. In particular, gastric tumours showed sclerosing spindle, cellular spindle, or mixed morphology with a common expression of CD34, but not SMA in most of the cases. On the other hand, small bowel tumours were typically moderately cellular with numerous skeinoid fibres and commonly

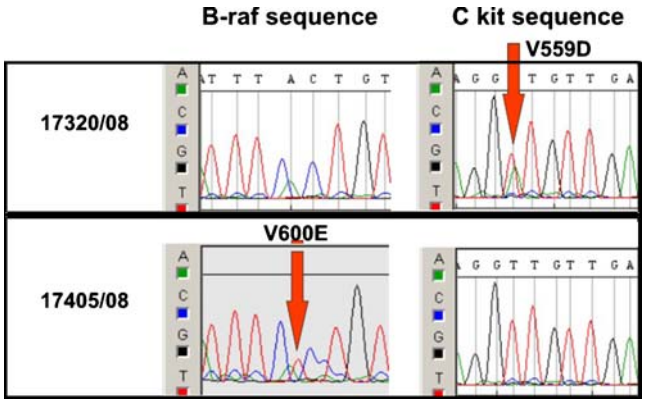

Fig. 3 Chromatograms of the complementary reverse sequence of *BRAF* exon 15 and the forward sequence of *KIT* exon 11 from the gastric GIST (*above*) and small bowel GIST (*below*) in patient 3. The two mutually exclusive mutations detected in his two tumours are indicated by the *red arrow*

CD34+/SMA−. Furthermore, the generally bland histology seen in many tumours and the low mitotic activity should also suggest independent neoplasms. A careful analysis of these distinct morphological features in different tumours from the same patient allowed appropriate interpretation and were also in line with their distinct molecular pathogenesis demonstrated by mutational analysis.

Recognising multiple primary GISTs developing synchronously in a patient with a history of GIST is mandatory to avoid misinterpretation as metastasis with the hazard of unnecessary over-treatment. Our two cases with metachronous presentation of primary GISTs in patients without a syndrome represent a hitherto unreported observation and should be distinguished from tumour recurrence. Mutational analysis plays an important role in equivocal cases. While detection of distinct mutations in imatinib-naïve multiple GISTs clearly indicates independent primary tumours, the occurrence of the same mutation in two tumours fulfilling histological criteria for independent GISTs should warrant analysis of the normal tissue to confirm or rule out a germline mutation. Rarely, independent GISTs may arise from ICCs harbouring the same somatic mutation [13]. On the other hand, patients with a germline *KIT* mutation may present with metachronous-isolated disease mimicking recurrent solitary sporadic GIST [22]. The latter case points to the potential pitfalls related to dependence on molecular analysis alone in confirming recurrent GISTs. While the presence of numerous variably sized and confluent nodules localised mainly to the peritoneum and showing high-grade histological features are typical of metastatic disease, rare extramural gastric GISTs may present as multiple omental EGIST, thus mimicking metastatic disease [23, 24]. Combined careful analysis of morphological and molecular features will facilitate correct diagnosis in equivocal cases (Fig. 4).

A novel finding in this study is the detection of the V600E *BRAF* mutation in the small bowel GIST of one patient who had a *KIT*-mutated gastric tumour. Both mutations were mutually exclusive. *BRAF V600E* mutation has been detected in 4% and 7% of *KIT/PDGFRA* wild-type GISTs in two recent studies [7, 8]. This case demonstrates that multiple GISTs in the same patient can be initiated by mutations involving different genes, as reported by Haller et al. and Miselli et al. [12, 15]. The wild-type in the tumours from case 7 could be the result of poor DNA preservation and contamination by abundant hyaline fibrous tissue. However, the pathogenesis of the wild-type intestinal GISTs in patient 6, who displayed no clinical features of NF1, remains unclear. This patient might have either an undiagnosed NF1 or have tumours initiated by other rare types of mutations.

In summary, we described further seven patients with sporadic GISTs arising multifocally at different GI sites, demonstrating a great heterogeneity in their molecular profiles and emphasising the value of histological features in their appropriate initial interpretation as independent

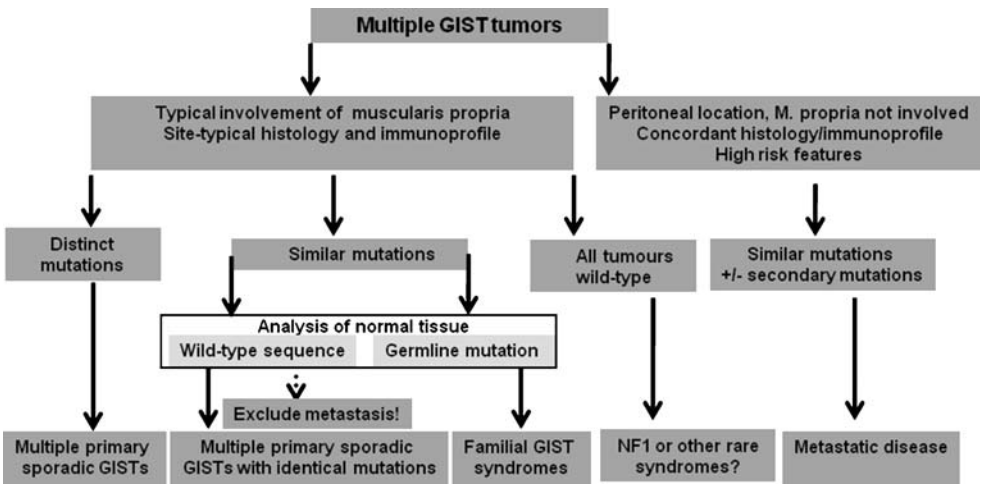

Fig. 4 An algorithm for evaluating multiple GIST nodules of unknown pathogenesis

primary neoplasms. It is mandatory to exclude multiple independent tumours, particularly in patients with an apparent recurrence or metastasis from a previously treated low risk GISTs.

Conflict of interest statement We declare that we have no conflict of interest.

References

1. Miettinen M, Lasota J (2006) Gastrointestinal stromal tumors: pathology and prognosis at different sites. Semin Diagn Pathol 23:70–83
2. Lasota J, Miettinen M (2006) KIT and PDGFRA mutations in gastrointestinal stromal tumors (GISTs). Semin Diagn Pathol 23:91–102
3. Wardelmann E, Hrychyk A, Merkelbach-Bruse S et al (2004) Association of platelet-derived growth factor receptor alpha mutations with gastric primary site and epithelioid or mixed cell morphology in gastrointestinal stromal tumors. J Mol Diagn 6:197–204
4. Miettinen M, Lasota J, Sobin LH (2005) Gastrointestinal stromal tumors of the stomach in children and young adults. A clinicopathologic, immunohistochemical, and molecular genetic study of 44 cases with long-term follow-up and review of the literature. Am J Surg Pathol 29:1373–1381
5. Miettinen M, Fetsch JF, Sobin LH et al (2006) Gastrointestinal stromal tumors in patients with neurofibromatosis 1: a clinicopathologic and molecular genetic study of 45 cases. Am J Surg Pathol 30:90–96
6. Matyakhina L, Bei TA, McWhinney SR et al (2007) Genetics of carney triad: recurrent losses at chromosome 1 but lack of germline mutations in genes associated with paragangliomas and gastrointestinal stromal tumors. J Clin Endocrinol Metab 92:2938–2943
7. Agaram NP, Wong GC, Guo T et al (2008) Novel V600E BRAF mutations in imatinib-naive and imatinib-resistant gastrointestinal stromal tumors. Genes Chromosomes Cancer 47:853–859
8. Agaimy A, Terracciano LM, Dirnhofer S et al (2009) V600E BRAF mutations are alternative early molecular events in a subset of KIT/PDGFRA wild-type gastrointestinal stromal tumors (GISTs). J Clin Pathol 62:613–616
9. Carney JA (1999) Gastric stromal sarcoma, pulmonary chondroma and extra-adrenal paraganglioma (Carney triad): natural history, adrenocortical component and possible familial occurrence. Mayo Clin Proc 74:543–552
10. Chen H, Hirota S, Isozaki K et al (2002) Polyclonal nature of diffuse proliferation of interstitial cells of Cajal in patients with familial and multiple gastrointestinal stromal tumours. Gut 51:793–796
11. Chompret A, Kannengiesser C, Barrois M et al (2004) PDGFRA germline mutation in a family with multiple cases of gastrointestinal stromal tumor. Gastroenterology 126:318–321
12. Haller F, Schulten HJ, Armbrust T et al (2007) Multicentric sporadic gastrointestinal stromal tumors (GISTs) of the stomach with distinct clonal origin: differential diagnosis to familial and syndromal GIST variants and peritoneal metastasis. Am J Surg Pathol 31:933–937
13. Agaimy A, Dirnhofer S, Wünsch PH et al (2008) Multiple sporadic gastrointestinal stromal tumors (GISTs) of the proximal stomach are caused by different somatic *KIT* mutations suggesting a field effect. Am J Surg Pathol 32:1553–1559
14. Kang DY, Park CK, Choi JS et al (2007) Multiple gastrointestinal stromal tumors: clinicopathologic and genetic analysis of 12 cases. Am J Surg Pathol 31:224–232
15. Miselli F, Conca E, Casieri P et al (2008) Sporadic multiple GIST with unusual pathologic, molecular, and genetic features. Am J Surg Pathol 32:340–341
16. Gasparotto D, Rossi S, Bearzi I et al (2008) Multiple primary sporadic gastrointestinal stromal tumors in the adult: an underestimated entity. Clin Cancer Res 14:5715–5721
17. Agaimy A, Wünsch PH (2006) Gastrointestinal stromal tumours: a regular origin in the muscularis propria, but an extremely diverse gross presentation. A review of 200 cases to critically re-evaluate the concept of so-called extra-gastrointestinal stromal tumours. Langenbecks Arch Surg 391:322–329
18. Miettinen M, Sobin LH, Lasota J (2005) Gastrointestinal stromal tumors of the stomach: a clinicopathologic, immunohistochemical, and molecular genetic study of 1765 cases with long-term follow-up. Am J Surg Pathol 29:52–68
19. Fletcher CD, Berman JJ, Corless C et al (2002) Diagnosis of gastrointestinal stromal tumors: a consensus approach. Hum Pathol 33:459–465
20. Agaimy A, Wünsch PH, Dirnhofer S et al (2008) Microscopic gastrointestinal stromal tumors in esophageal and intestinal surgical resection specimens. A clinicopathologic, immunohistochemical, and molecular study of 19 lesions. Am J Surg Pathol 32:867–873
21. Miettinen M, Makhlouf H, Sobin LH et al (2006) Gastrointestinal stromal tumors of the jejunum and ileum: a clinicopathologic, immunohistochemical, and molecular genetic study of 906 cases before imatinib with long-term follow-up. Am J Surg Pathol 30:477–489
22. Woźniak A, Rutkowski P, Sciot R et al (2008) Rectal gastrointestinal stromal tumors associated with a novel germline KIT mutation. Int J Cancer 122:2160–2164
23. Kim JH, Boo YJ, Jung CW et al (2007) Multiple malignant extragastrointestinal stromal tumors of the greater omentum and results of immunohistochemistry and mutation analysis: a case report. World J Gastroenterol 13:3392–3395
24. Terada T (2008) Primary multiple extragastrointestinal stromal tumors of the omentum with different mutations of c-kit gene. World J Gastroenterol 14:7256–7259

Virchows Arch (2009) 455:109–115
DOI 10.1007/s00428-009-0808-9

ORIGINAL ARTICLE

The distribution of lesions in 1–14-mm invasive breast carcinomas and its relation to metastatic potential

Tibor Tot · Gyula Pekár · Syster Hofmeyer · Thomas Sollie · Mária Gere · Miklós Tarján

Received: 9 April 2009 / Revised: 19 June 2009 / Accepted: 24 June 2009 / Published online: 21 July 2009

Abstract We analyzed 301 consecutive cases of 1–14-mm invasive breast carcinomas documented in large-format histological sections to determine the distribution of invasive and in situ foci. We also aimed to determine whether this distribution was related to the frequency of demonstrable vascular invasion and lymph node metastases. One third of the carcinomas (31.9%, 96 cases) had a multifocal invasive component and a more than doubled relative risk of vascular invasion (RR=2.3642, 95% confidence interval (CI)= 1.5077–3.7073) and lymph node metastasis (RR=2.7760, 95% CI=1.6337–4.7171) compared to unifocal invasive carcinomas. Invasive carcinomas with diffuse in situ component had an elevated relative risk for vascular invasion (RR=2.2201, 95% CI=1.4049–3.5083) and lymph node metastasis (RR=1.9201, 95% CI=1.1278–3.2691) compared to those with unifocal or multifocal in situ lesions. However, multifocality of the invasive component was associated with a substantially elevated risk of vascular invasion and lymph node metastasis, even in cases with diffuse in situ component. Similar observations were made in the 1–9- and 10–14-mm invasive carcinoma subgroups. These findings indicate that lesion distribution has prognostic relevance for 1–14-mm invasive breast carcinomas and underline the importance of using special techniques in breast pathology for proper assessment of this parameter.

T. Tot (✉) · G. Pekár · S. Hofmeyer · M. Gere · M. Tarján
Department of Pathology and Clinical Cytology,
Central Hospital Falun,
Falun, Sweden
e-mail: tibor.tot@ltdalarna.se

T. Sollie
Department of Laboratory Medicine, Örebro University Hospital,
Örebro, Sweden

Keywords Breast cancer · Multifocality · In situ component · Vascular invasion · Lymph node metastasis · Sick lobe theory

Introduction

Breast carcinoma is the most common malignancy among women in the Western world and is the leading cause of premature death in younger women [1]. The prognosis depends largely on tumor stage at the time of detection. While advanced carcinomas, which are larger and may have metastasized, often have an unfavorable outcome, the vast majority of patients with small tumors without metastatic spread have excellent disease-free survival and overall survival prognosis [2]. Population-based mammography screening has substantially increased detection of small, early-stage, nonmetastatic carcinomas with favorable prognosis; this has contributed to lower mortality from breast cancer during the last few decades [3, 4]. However, some patients with early-stage breast cancer still have an unfavorable outcome indicating that additional prognostic parameters are needed in order to identify and properly treat higher-risk patients even in this category of the tumors.

Many studies have addressed the value of various prognostic parameters in predicting the outcome of early breast carcinomas, sometimes generating conflicting results [5]. Regarding lymph node metastasis (LNM) in T1 tumors, increasing tumor size, poor histological grade, the presence of lymph vessel invasion (LVI), and younger age are the most important predictive variables [6–11]. We recently reported that multifocality of the invasive component of breast carcinomas is associated with increased frequency of vascular invasion and lymph node metastasis and that this seems to be unrelated to tumor size [12, 13]. In the present study, we focused on 1–14-mm carcinomas with invasive

foci, assessed the distribution of the tumor foci using large-format histological sections, and tested whether this distribution was related to the metastatic capacity of the tumors.

Materials and methods

A consecutive series of breast carcinoma cases with 1–14-mm invasive tumors was selected from the files of the Department of Pathology and Clinical Cytology at the Central Hospital in Falun, Sweden, from January 2005 to December 2008. All cases were documented in large-format standard histological sections (maximum size, 10×8 cm). The technical protocol has been described previously in detail [14–16]. The large sections represented coronal cross sections of entire sector resection specimens and sagittal cross sections from mastectomies. Cross sections that were larger than the maximal dimension of the standard object glass were bisected and embedded in two or three adjoining blocks. One to eight blocks were prepared for each case and were sectioned at two to 14 levels. Large thick sections, also called three-dimensional histology slides [16], were prepared for selected cases.

A dedicated team of experts analyzed all cases in diagnostic routine. Detailed preoperative and postoperative radiological/pathological correlation of the mammogram, ultrasonogram, and magnetic resonance image findings to the large-format histological sections findings were used by the pathologist to assess the distribution of the lesions and the extent of the disease. The clinical, radiological, and pathological data were registered in a database. One of the authors (TT) reviewed all the large sections in this series for the purposes of the present study.

We analyzed the distribution of the in situ and the invasive components of the tumors separately using our previously published criteria [12, 13]. In brief, we defined multifocality of the invasive component as the presence of two or more well-defined invasive tumor foci separated from each other by tissue that did not contain invasive tumor structures. A unifocal tumor was characterized by a solitary invasive focus. A diffuse invasive component was defined as a tumor growing without forming a well-defined tumor body, much like a spider's web. The in situ component was also assessed and categorized as unifocal, multifocal, or diffuse. Unifocal in situ tumors were defined as a well-delineated cluster of tumor-filled dilated acini corresponding to a distended lobule or to several neighboring distended lobules without uninvolved breast tissue in between them. Multifocal in situ component was characterized by distended lobules containing in situ carcinomas separated from each other by uninvolved breast tissue; larger ducts were generally tumor free in these cases. Diffuse in situ carcinomas involved mainly the larger ducts and were difficult to delineate. Tumor size was measured at the largest diameter of the largest invasive focus. Figures 1 and 2 show typical examples of tumors with unifocal and multifocal invasive components; Fig. 3 shows a typical example of an invasive tumor with a diffuse in situ component.

To assess the metastatic capacity of the tumors, we correlated the distribution of the in situ and the invasive components with the presence or absence of vascular invasion and lymph node metastasis. Vascular invasion was defined as tumor cells or tumor cell groups surrounded by endothelial cell-lined spaces and was assessed in routinely stained large histological sections and in peritumoral regions. D2-40 antibody staining (Dako Glostrup, Denmark) helped identify LVI in tumors diagnosed in 2007–2008. Lymph node metastases data, comprising the summarized results of the sentinel lymph node procedure and/or axillary clearance, were obtained from our database. Only macrometastases with a diameter greater than 2 mm were included in the statistical analysis. Relative risk was calculated using a commercially available statistical program (MedCalc Statistics for Biomedical Research; MedCalc Software, Belgium).

Results

During the study period, 815 breast carcinomas were diagnosed in our department. Of these, 119 (14.6%) were purely in situ and 696 had an invasive component. Of the invasive tumors, 301 (43.2%) were 1–14 mm in size. All

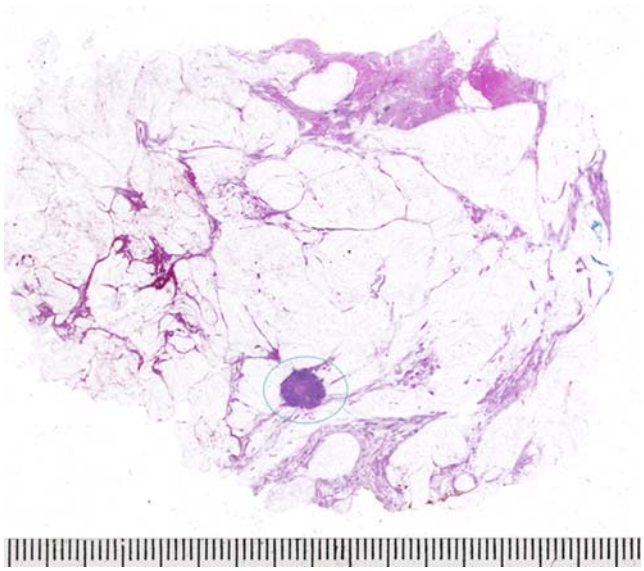

Fig. 1 Large-format histology image of a 6-mm unifocal invasive breast carcinoma (*encircled*) with no multifocal or diffuse in situ components

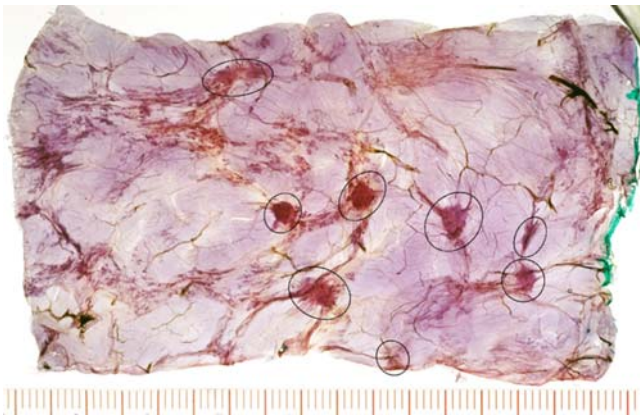

Fig. 2 Large-format thick-section histology image of a multifocal invasive breast carcinoma with eight individual tumor foci (*encircled*) that are less than 10 mm

but 26 of the 301 invasive tumors contained an in situ component. The distribution data for the lesions in relation to LVI and LNM in 1–14-mm carcinomas are summarized in Table 1.

In this series of 301 1–14-mm invasive carcinomas, 205 (68.1%) had unifocal and 96 (31.9%) had multifocal invasive components. None had a diffuse invasive growth pattern. LVI was observed in 19.6% (59/301) of the tumors: in 32.3% (31/96) of the multifocal tumors and in 13.7% (28/205) of the unifocal tumors. The relative risk of having LVI in multifocal versus unifocal carcinomas was 2.3642 (95% CI=1.5077–3.7073). Macrometastasis in the axillary lymph node(s) was present in 15.3% (46/301) of the cases: in 27.1% (26/96) of the multifocal cases and in 9.8% (20/205) of the unifocal cases, giving a relative risk of 2.7760 (95% CI=1.6337–4.7171).

An in situ component was found in large sections from 275 of the 301 invasive carcinomas. The in situ component was unifocal in 108 (39.3%), multifocal in 91 (33.1%), and diffuse in 76 (27.6%) cases. Invasive carcinomas with a diffuse in situ component had an elevated risk of LVI (RR=2.2201, 95% CI=1.4049–3.5083) and LNM (RR=1.9201, 95% CI=1.1278–3.2691) compared to those with unifocal or multifocal in situ components.

The carcinomas were divided into two subcategories by size. There were 137 (45.5%) 1–9-mm and 164 (54.5%) 10–14-mm invasive carcinomas. The invasive component was unifocal in 97 (70.8%) of the 1–9-mm carcinomas and multifocal in 40 (29.2%) cases. The multifocal tumors exhibited an elevated relative risk for LVI (RR=3.8144, 95%CI=1.7960–8.0870) and for LNM (RR=2.4250, 95% CI=0.7424–7.9266) compared to their unifocal counterparts. The presence of a diffuse in situ component carried a substantially elevated risk for LNM (RR=4.667, 95% CI=1.2724–17.1154). For 10–14-mm invasive carcinomas, multifocality of the invasive component also conferred an elevated risk for LVI (RR=1.7256, 95% CI=0.9766–3.0488) and for LNM (RR=2.7000, 95% CI=1.5127–4.8159), as did the presence of a diffuse in situ component. These results are summarized in Tables 2 and 3.

We also asked whether the distribution of the invasive component influenced the frequency of LVI and LNM in the group of invasive 1–14-mm carcinomas having a diffuse in situ component. Multifocality of the invasive component was associated with a substantially elevated risk of LVI (7.4286, 95% CI=1.8196–30.3273) and LNM (3.4286, 95% CI=0.7174–16.3847) in 1–9-mm tumors having a diffuse in situ component. Risk of LNM was elevated in 10–14-mm such tumors (2.000, 95% CI=0.6360–6.2891). Regarding multifocal 1–14-mm invasive carcinomas having diffuse in situ component versus unifocal tumors, the relative risk of LVI was 2.1438 (95% CI=1.0878–4.2249) and the relative risk of LNM 2.8941 (95% CI1.1316–7.4017).

Discussion

The definition of “early breast carcinoma” is still ambiguous. Historically, tumors up to 5 cm in diameter and involving up to three metastatic axillary lymph nodes have been called “early” in some studies, as reviewed by Tot [5]. Other studies use the term “minimal breast carcinoma” and define it as in situ carcinoma and/or invasive carcinoma up to 5 mm [17] or 10 mm [18]. The common characteristic of these tumors is ≥90% long-term survival of the patient. As we demonstrated previously, mammography screening and improved therapy modalities have resulted in excellent long-term survival prognosis for patients with invasive carcinomas up to 14 mm [19]. This motivated us to focus

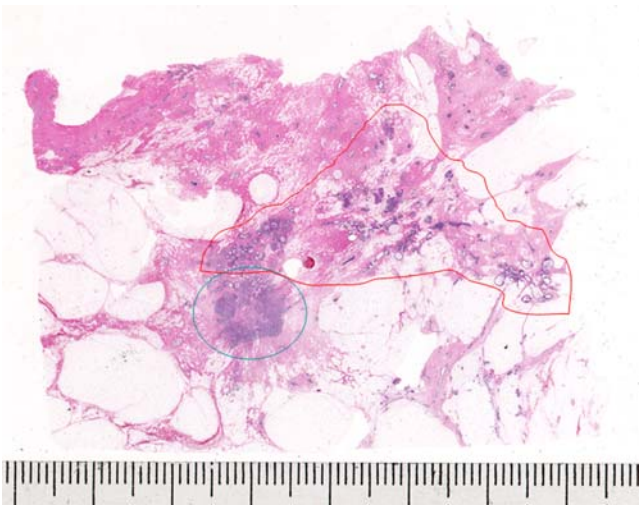

Fig. 3 Large-format histology image of a 9-mm invasive carcinoma (*blue circle*) with extensive diffuse in situ component (*red area*)

Table 1 Distribution of lesions in 301 invasive 1–14-mm breast carcinomas in relation to lymphovascular invasion (LVI) and axillary lymph node metastasis (LNM)

		Unifocal	Multifocal	Diffuse	Sum	Relative risk
In situ component	LVI	15.7% (17/108)	17.6% (16/91)	31.6% (24/76)	20.7% (57/275)	2.2201[a]
						95% CI=1.4049–3.5083
	LNM	10.2% (11/108)	18.7% (17/91)	23.7% (18/76)	16.7% (46/275)	1.9201[a]
						95% CI=1.1278–3.2691
Invasive component	LVI	13.7% (28/205)	32.3% (31/96)	–	19.6% (59/301)	2.3642
						95% CI=1.5077–3.7073
	LNM	9.8% (20/205)	27.1% (26/96)	–	15.3% (46/301)	2.7760
						95% CI=1.6337–4.7171

[a] Relative risk of LVI and LNM in tumors with diffuse in situ component compared to that in tumors with unifocal or multifocal in situ components

on this category of invasive carcinomas in the present study.

Defining and measuring the diameter of an invasive breast carcinoma is not always easy. The most widely accepted way to define the size of a unifocal tumor is to measure the largest dimension of the largest invasive focus. In multifocal tumors, however, using the combined diameter of the invasive foci has been proposed as being more accurate than using the largest dimension of the largest invasive focus [20, 21]. Recent studies have not confirmed the value of using a combined diameter to define these tumors [22, 23]; thus, in the present study, we used the standard definition, i.e., the largest dimension of the largest invasive focus, to define tumor size.

Similarly, the definition of tumor multifocality is still being debated. On one hand, the current TNM classification states "…tumors are defined as arising independently only if they occur in different quadrants of the breast…" [24]. On the other hand, some studies count and measure every individual tumor focus [25], while others call the tumor multifocal if there is 1, 2, or 4 cm between individual foci [26, 27]. In this study, we considered well-defined invasive foci to be individual foci when they were delineated from each other by tissue that did not contain invasive structures, irrespective of the distance between the foci or the quadrant localization of the foci. Our criteria for defining the distribution of in situ structures have been published previously (i.e., unifocal localized in one lobule or in neighboring lobules, multifocal localized in lobules distant to each other, diffuse involving larger ducts) [28, 29]. In this study, we did not use the combined distribution of in situ and invasive components as this may give a large number of combinations and complicate the analysis [12]. Instead, we assessed the distribution of the in situ and the invasive components of the same tumor separately and also tested their individual influence on metastatic potential separately.

A limitation of our study is that follow-up results were not included. This is primarily because the follow-up period is still very short. However, testing the metastatic capacity of tumors by assessing LVI and LNM is reliable: LVI is a strong prognostic factor for operable patients with breast carcinoma as a predictor of poor prognosis in both lymph-node-negative and lymph-node-positive cases [30, 31]. LVI

Table 2 Distribution of lesions in 137 invasive 1–9-mm breast carcinomas in relation to lymphovascular invasion (LVI) and axillary lymph node metastasis (LNM)

		Unifocal	Multifocal	Diffuse	Sum	Relative risk
In situ component	LVI	15.6% (7/45)	16.2% (6/37)	24.4% (10/41)	18.7% (23/123)	1.5385[a]
						95% CI=0.7383–3.2060
	LNM	0.0% (0/45)	8.1% (3/37)	17.1% (7/41)	8.1% (10/123)	4.6667[a]
						95% CI=1.2724–17.1154
Invasive component	LVI	9.3% (9/97)	35.0% (14/40)	–	16.8% (23/137)	3.8144
						95% CI=1.7960–8.0870
	LNM	5.2% (5/97)	12.5% (5/40)	–	7.3% (10/137)	2.4250
						95% CI=0.7424–7.9266

[a] Relative risk of LVI and LNM in tumors with diffuse in situ component compared to that in tumors with unifocal or multifocal in situ components

Table 3 Distribution of lesions in 164 invasive 10–14-mm breast carcinomas in relation to lymphovascular invasion (LVI) and axillary lymph node metastasis (LNM)

		Unifocal	Multifocal	Diffuse	Sum	Relative risk
In situ component	LVI	15.9% (10/63)	18.5% (10/54)	40.0% (14/35)	22.4% (34/152)	2.3400[a]
						95% CI=1.3245–4.1341
	LNM	17.5% (11/63)	25.9% (14/54)	31.4% (11/35)	23.7% (36/152)	1.4709[a]
						95% CI=0.8075–2.6808
Invasive component	LVI	17.6% (19/108)	30.4% (17/56)	–	22.0% (36/164)	1.7256
						95% CI=0.9766–3.0488
	LNM	13.9% (15/108)	37.5% (21/56)	–	22.0% (36/164)	2.7000
						95% CI=1.5127–4.8159

[a] Relative risk of LVI and LNM in tumors with diffuse in situ component compared to that in tumors with unifocal or multifocal in situ components

correlates significantly with LNM [30], and LNM is a well-established morphological prognostic parameter. We included only cases with macrometastasis because the prognostic significance of micrometastases and isolated cancer cells in lymph nodes is still unclear [32].

The proportion of "multifocal" invasive cases varies in different series of breast carcinomas and depends on the histological method, the diagnostic criteria, and the case selection. Values as low as 11% [33] and as high as 75% have been reported [34]. Use of the large-section technique clearly facilitates identification of multiple foci in breast tissue [35]. Gallager and Martin [34], using a technique that was very similar to that used in the present study, reported "extensive neoplastic transformation of the ductal epithelium and multiplicity of the invasive sites" in three quarters of the 38 mastectomy specimens studied; most of these cases were large advanced tumors. Holland et al. [36] reported that 63% of the Tis and T1-2 breast carcinomas had tumor foci around the "referent mass," 20% within 2 cm, and 43% that were even more distant (27% being in situ foci). Using whole-organ sectioning, Luttges [37] reported 46% (76/166) multifocal and 22% (36/166) multicentric cases. Large-section technique has been used routinely in our laboratory for every operated breast cancer specimen for more than 20 years. Our dedicated and experienced technicians produce large-format histological slides of the same high quality as those obtained with conventional small-block technique. In our experience, large-format histology together with detailed preoperative and postoperative radiological–pathological correlation represent the best currently available tool for assessing tumor size and extent and distribution of the lesions. Using this approach in the present study, we found that 31.9% of carcinomas had multifocal invasive components; 31.1% had multifocal in situ and 27.6% had diffuse in situ components. These results are comparable to the results of the cited studies and are in agreement with our previous series [13]. This also indicates that the distribution of in situ and invasive tumor foci of 1–14-mm invasive carcinomas is similar to the distribution of lesions in larger tumors.

The prognostic parameters cited most often for 1–14-mm invasive carcinomas are tumor grade [38], tumor size [5], extent of the in situ component [39], casting-type microcalcifications associated with invasive carcinoma as detected by mammography [19], and lymph node status. The most important predictors of LNM in 1–14-mm invasive breast carcinomas are increasing tumor size, poor histological grade, presence of LVI, and younger patient age [6–11]. Based on the results of the present study, multifocality of the invasive component and diffuse pattern of the in situ component are additional predictors of increased risk for LNM in this tumor category.

The prognostic significance of multifocality is seldom addressed in the literature, and typically only the invasive component is considered. Methodological differences and differing definitions of multifocality make it difficult to compare study results. Worse overall survival rates were reported for patients with multifocal carcinomas versus single-site tumors by Egan [40], but more recent studies have not confirmed these results [41, 42]. Regarding disease-free survival, some studies have found higher local recurrence rates for multifocal tumors compared to unifocal tumors [41, 42]. In a recent study, multifocality was the only parameter significantly associated with residual disease in reexcision specimens for close margins for patients with invasive carcinoma [43].

Tumor size correlates with lymph node positivity [7, 12, 13] as well as with LVI [8, 13, 31]. Thus, the percentage of cases with LVI and LNM in the present series of 1–14-mm carcinomas was expected to be relatively low. In the study by Maibenco et al., LNM was found in 9.6% of T1a tumors and in 14.2% of T1b cases [7]. Yip et al. found LNM in 7.7% of T1a, 12.3% of T1b, 29.2% of T1c, and 48.2% of T2 tumors [11]. Chadha et al. reported LNM in 27% of T1

cases [6]. Gajdos et al. found LVI in 35% of tumors larger than 1 cm and in 13% of smaller carcinomas [8]; Gurleyik et al. reported LVI in 29% of T1, in 54% of T2, and in 100% of T3 tumors [31]. Thus, our results, i.e., 15.3% LNM and 19.6% LVI for the entire study group of 1–14-mm invasive breast carcinomas, were comparable to the results reported in these studies. In addition, we found LNM in 7.3% and LVI in 16.3% of 1–9-mm tumors and in 22% (both parameters) of 10–14-mm tumors. Our results in this series thus confirmed the positive correlation between tumor size and metastatic potential.

The elevated risk of LVI and LNM in multifocal carcinomas compared to their unifocal counterparts has been previously reported regarding breast carcinomas not categorized by size [20, 33, 41] and also in the 1–14-mm size category [13]; those studies reported results similar to the findings in the present study. Others found no significant difference in the risk of LNM between unifocal and multifocal tumors [22]. Comparing the results of the present study with our previous findings [12, 13], a doubled risk of LVI and LNM in multifocal versus unifocal invasive breast carcinomas seems to be the general rule, regardless of tumor size. Theoretically, two types of invasive tumor multifocality are observed in breast cancers: separate foci that develop independently from each other from in situ carcinomas and foci that are the result of intramammary tumor spread. In the first type, the multifocal tumor is really an early carcinoma, and, in the second type, this is less clear. Intramammary spread of the tumor may be the initial step in generating LNM and is probably associated with involvement of the prelymphatic system [44] and/or with LVI [45]. Involvement of the prelymphatic system was previously demonstrated in invasive lobular carcinomas using large-format histology sections [46].

The elevated risk of LVI and LNM in cases with a diffuse in situ component versus those with unifocal and multifocal in situ components in this series may be interpreted as an unexpected finding. However, diffuse distribution of the in situ lesions (involvement of the larger ducts) is associated with high nuclear grade, comedo necrosis, and casting-type microcalcifications in the majority of cases [29]. LNM has been reported not only in invasive breast carcinoma but also in rare cases of ductal carcinoma in situ without demonstrable invasive component; these cases were mostly high-grade comedo lesions [47, 48]. Casting-type calcifications on the mammogram are also associated with higher rate of LNM than the cases without such calcifications [49]. These findings indicate a possible association between diffuse distribution of the in situ component, its grade, and the risk of LNM and may explain the findings of the present study. Our findings are concordant with the experience of some leading experts who, although advocating restrictive approach in offering sentinel lymph node biopsy in cases of in situ carcinomas, recommend such procedure in cases with "diffuse or pluricentric microcalcifications" [48].

In the present study, we also demonstrated that multifocal distribution of the invasive component had prognostic significance in cases with a diffuse in situ component. According to the sick lobe theory [28, 50], malignant transformation in the breast is initially restricted to a single lobe that had abnormal embryonic development. This transformation may involve the lobules and/or the larger ducts within the sick lobe. In contrast to lobular localization, involvement of the larger ducts of the sick lobe seems to confer an unfavorable prognosis associated with an elevated risk of LVI and LNM as demonstrated in the present study and is also associated with higher mortality [19] observed in patients with 1–14-mm invasive breast carcinomas.

In conclusion, multifocality of the invasive component and diffuse distribution of the in situ component are associated with elevated risk of LVI and LNM in 1–14-mm invasive breast carcinomas. Thorough histological assessment of these parameters is essential in modern breast pathology.

Conflict of interest statement We declare that we have no conflict of interest.

References

1. Boyle P, Ferlay J (2005) Cancer incidence and mortality in Europe 2004. Ann Oncol 16:481–188
2. Tavassoli FA, Devilee P (eds) (2003) World Health Organization Classification of tumours, pathology & genetics. Tumors of the breast and female genital organs. IARC, Lyon, pp 56–59
3. Smith RA, Duffy SW, Gabe R et al (2004) The randomized trials of breast cancer screening: what have we learned? Radiol Clin North Am 42:793–806
4. The Swedish Organized Service Screening Evaluation Group (2006) Reduction in breast cancer mortality from organized service screening with mammography: 1. Further confirmation with expanded data. Cancer Epidemiol Biomarkers Prev 15:45–51
5. Tot T (2006) The limited prognostic value of measuring and grading small breast carcinomas: the whole sick lobe versus the details within it. Med Sci Monit 12RA:170–175
6. Chadha M, Chabon AB, Friedmann P et al (1994) Predictors of axillary lymph node metastases in patients with T1 breast cancer. A multivariate analysis. Cancer 73:350–353
7. Maibenco DC, Weiss LK, Pawlish KS et al (1999) Axillary lymph node metastases associated with small invasive breast carcinomas. Cancer 85:1530–1536
8. Gajdos CS, Tartter PI, Bleiweiss IJ (1999) Lymphatic invasion, tumor size, and age are independent predictors of axillary lymph node metastases in women with T1 breast cancers. Ann Surg 230:692–696
9. Shoup M, Malinzak L, Weisenberger J et al (1999) Predictors of axillary lymph node metastasis in T1 breast carcinoma. Am Surg 65:748–752

10. Rivadeneira DE, Simmons RM, Christos PJ et al (2000) Predictive factors associated with axillary lymph node metastasis in Ta1 and Tb1 breast carcinomas: analysis in more than 900 patients. J Am Coll Surg 191:1–6
11. Yip CH, Taib NA, Tan GH et al (2009) Predictors of axillary lymph node metastases in breast cancer: is there a role for minimal axillary surgery? World J Surg 33:54–57
12. Tot T (2007) The clinical relevance of the distribution of the lesions in 500 consecutive breast cancer cases documented in large-format histological sections. Cancer 110:2551–2560
13. Tot T (2009) The metastastic capacity of multifocal breast carcinomas: extensive tumors versus tumors of limited extent. Hum Pathol 40:199–205
14. Tot T, Tabár L, Dean PB (2002) Practical breast pathology. Thieme, Stuttgart, pp 116–123
15. Tot T (2005) Colorectal cancer: Atlas of large section histopathology. Thieme, Stuttgart, pp 130–144
16. Tabár L, Tot T, Dean PB (2005) Breast cancer: the art and science of early detection with mammography: perception, interpretation, histopathologic correlation. Thieme, Stuttgart, pp 405–438
17. Gallager HS (1976) Treatment selection in primary breast cancer. Pathologic considerations. Am J Roentgenol 126:135–138
18. Hartmann WH (1984) Minimal breast cancer. An update. Cancer 53(3 suppl):681–684
19. Tabar L, Tony Chen HH, Amy Yen MF et al (2004) Mammographic tumor features can predict long-term outcomes reliably in women with 1–14-mm invasive breast carcinoma. Cancer 101:1745–1759
20. Andea AA, Bouwman D, Wallis T et al (2004) Correlation of tumor volume and surface area with lymph node status in patients with multifocal/multicentric breast carcinoma. Cancer 100:20–27
21. Andea AA, Wallis T, Newman LA et al (2002) Pathologic analysis of tumor size and lymph node status in multifocal/multicentric breast carcinoma. Cancer 94:1383–1390
22. Tresserra F, Rodriguez I, Garcia-Yuste M et al (2007) Tumor size and lymph node status in multifocal breast cancer. Breast J 13:68–71
23. O'Daly BJ, Sweeney KJ, Ridgway PF et al (2007) The accuracy of combined versus largest diameter in staging multifocal breast cancer. J Am Coll Surg 204:282–285
24. Greene FL et al (eds) (2002) AJCC cancer staging handbook. TNM classification of malignant tumors, 6th edn. Springer, New York, pp 255–281
25. Lagios MD, Westdahl PR, Rose MR (1981) The concept and implications of multicentricity in breast carcinoma. Pathol Annu 16:1123–1130
26. Silverstein MJ, Cohlan BF, Gierson ED et al (1992) Duct carcinoma in situ: 227 cases without microinvasion. Eur J Cancer 28:630–634
27. Faverly DRG, Burgers L, Bult P et al (1994) Three-dimensional imaging of mammary ductal carcinoma in situ: clinical implications. Sem Diagn Pathol 11:193–198
28. Tot T (2005) DCIS, cytokeratins and the theory of the sick lobe. Virchows Arch 447:1–829
29. Tot T, Tabár L (2006) Radiologic-pathologic correlation of ductal carcinoma in situ of the breast using two- and three-dimensional large histologic sections. Semin Breast Dis 8:144–151
30. Lauria R, Perrone F, Carlomagno C et al (1995) The prognostic value of lymphatic and blood vessel invasion in operable breast cancer. Cancer 76:1772–1778
31. Gurleyik G, Gurleyik E, Aker F et al (2007) Lymphovascular invasion, as a prognostic marker in patients with invasive breast cancer. Acta Chir Belg 107:284–287
32. Cserni G, Bianchi S, Vezzosi V et al (2008) Variations in sentinel node isolated tumour cells/micrometastasis and non-sentinel node involvement rates according to different interpretations of the TNM definitions. Eur J Cancer 44:2185–2191
33. Coombs NJ, Boyages J (2005) Multifocal and multicentric breast cancer: does each focus matter? J Clin Oncol 23:7497–7502
34. Gallager HS, Martin JE (1969) The study of mammary carcinoma by mammography and whole organ sectioning. Cancer 23:855–873
35. Jackson PA, Merchant W, McCormick CJ et al (1994) A comparison of large block macrosectioning and conventional techniques in breast pathology. Virchows Arch 425:243–248
36. Holland R, Veling SH, Mravunac M et al (1985) Histologic multifocality of Tis, T1–2 breast carcinomas. Implications for clinical trials of breast-conserving surgery. Cancer 56:979–990
37. Luttges J, Kalbfleisch H, Prinz P (1987) Nipple involvement and multicentricity in breast cancer. A study of whole organ sections. J Cancer Res Clin Oncol 113:481–487
38. Rakha EA, El-Sayed ME, Lee AH et al (2008) Prognostic significance of Nottingham histologic grade in invasive breast carcinoma. J Clin Oncol 26:3153–3158
39. Zafrani B, Vielh P, Fourquet A et al (1989) Conservative treatment of early breast cancer: prognostic value of the ductal in situ component and other pathological variables on local control and survival. Long-term results. Eur J Cancer Clin Oncol 25:1645–1650
40. Egan RI (1982) Multicentric breast carcinomas: clinical–radiographic pathologic whole organ studies and 10-year survival. Cancer 49:1123–1130
41. Pedersen L, Gunnarsdottir KA, Rassmussen BB et al (2004) The prognostic influence of multifocality in breast cancer patients. Breast 13:188–193
42. Joergensen LE, Gunnarsdottir KA, Lanng C et al (2008) Multifocality as a prognostic factor in breast cancer patients registered in Danish Breast Cancer Cooperative Group (DBCG) 1996–2001. Breast 17:587–591
43. Sabel MS, Rogers K, Griffith K et al (2009) Residual disease after re-excision lumpectomy for close margins. J Surg Oncol 99:99–103
44. Asioli S, Eusebi V, Gaetano L et al (2008) The pre-lymphatic pathway, the rooths of the lymphatic system in breast tissue: a 3D study. Virchows Arch 453:401–406
45. Cserni G (2008) Editorial: commentary on in-transit lymph node metastases in breast cancer: a possible source of local recurrence after sentinel node procedure. J Clin Pathol 61:1233–1235
46. Foschini MP, Righi A, Cucchi MC et al (2006) The impact of large section and 3D technique on the study of lobular in situ and invasive carcinoma of the breast. Virchows Arch 448:256–261
47. Pendas S, Dauway E, Giuliano R et al (2000) Sentinel node biopsy in ductal carcinoma in situ patients. Ann Surg Oncol 7:15–20
48. Veronesi P, Intra M, Vento AR et al (2005) Sentinel lymph node biopsy for localized ductal carcinoma in situ? Breast 14:520–522
49. Tabár L, Tot T, Dean PB (2007) Breast cancer: early detection with mammography. Casting type calcifications: signs of subtype with deceptive features. Thieme, Stuttgart, pp 214–215
50. Tot T (2007) The theory of the sick lobe and the possible consequences. Int J Surg Pathol 15:369–375

Virchows Arch (2009) 455:117–123
DOI 10.1007/s00428-009-0809-8

ORIGINAL ARTICLE

Overexpression of PTK6 (breast tumor kinase) protein—a prognostic factor for long-term breast cancer survival—is not due to gene amplification

Michaela Aubele · Sanja Vidojkovic · Herbert Braselmann · Dominique Ritterswürden · Gert Auer · Mike J. Atkinson · Soile Tapio · Heinz Höfler · Sandra Rauser · John M. S. Bartlett

Received: 8 April 2009 / Revised: 10 June 2009 / Accepted: 6 July 2009 / Published online: 21 July 2009

Abstract In a previous retrospective study, we demonstrated the prognostic value of protein tyrosine kinase 6 (PTK6) protein expression in breast carcinomas. Here, we analyzed PTK6 gene amplification using fluorescence in situ hybridization technique in a cohort of 426 invasive breast carcinomas and compared it with PTK6 expression level as well as with the clinical outcome of patients. Forty-five percent of tumors show increased PTK6 gene copy numbers when compared to normal tissue. Most of these, however, were related to chromosome 20 polysomy (30%), while gene amplification accounted for only 15%. Only "low level" amplification of the PTK6 gene, with up to eight signals per nucleus, was found. The PTK6 cytogenetic status (normal, gene amplification, polysomy 20) was not associated with histopathological parameters or with the protein expression of HER receptors. No statistical association was identified between PTK6 gene status and expression level. Further, the PTK6 gene status does not influence the disease-free survival of patients at ≥240 months. Based on these results, we state that the PTK6 overexpression is not essentially attributed to gene amplification, and the PTK6 protein expression—but not gene status—is of prognostic value in breast carcinomas. PTK6 protein overexpression may result from polysomy 20 in a minority of the tumors. In a marked proportion of tumors, however, the overexpression is likely to be caused by posttranscriptional regulation mechanisms.

Keywords PTK6 (BRK) · Gene amplification · FISH · Overexpression · Breast cancer · Prognosis

M. Aubele (✉) · S. Vidojkovic · D. Ritterswürden · H. Höfler · S. Rauser
Institute of Pathology, Helmholtz Zentrum München,
German Research Center for Environmental Health,
85764 Neuherberg, Germany
e-mail: aubele@helmholtz-muenchen.de

H. Braselmann
Institute of Molecular Radiation Biology,
Helmholtz Zentrum München,
German Research Center for Environmental Health,
85764 Neuherberg, Germany

G. Auer
Department of Oncology and Pathology,
Karolinska Institute and Hospital,
17176 Stockholm, Sweden

M. J. Atkinson · S. Tapio
Institute of Radiation Biology, Helmholtz Zentrum München,
German Research Center for Environmental Health,
85764 Neuherberg, Germany

M. J. Atkinson
Klinik für Strahlentherapie, Technische Universität München,
Ismaningerstr. 22,
81675 Munich, Germany

H. Höfler
Institute of Pathology, Technische Universität München,
Trogerstr. 18,
81675 Munich, Germany

J. M. S. Bartlett
Endocrine Cancer Group, Cancer Research Centre,
Western General Hospital,
Crewe Road South,
Edinburgh EH4 2XR, UK

Introduction

Gene amplification represents a key mechanism leading to gene activation and overexpression [1]. Amplification is widely observed in human tumors where it represents an oncogene-activating genetic mechanism [2] that may indicate an aggressive behavior of the tumor and a poor prognosis [3]. Among the various proto-oncogenes amplified in primary breast cancer, HER2/neu, located on chromosome 17q11–12, is the best studied [4]. Approximately 20–25% of primary breast cancers show amplification of the Her2/neu proto-oncogene with amplification values in many cases up to 20 gene copies [4]. Her2/neu overexpression/amplification is associated with worse prognosis [5, 6]. Anti-HER2/neu receptor antibody therapy with Trastuzumab induces tumor regression in approximately 30–35% of patients with HER2-amplified metastatic breast cancer [7]. This response rate indicates that additional signaling molecules may influence the biological response to Trastuzumab.

Signal transduction of the HER receptor family (EGFR/HER1, HER2/neu, HER3, and HER4) is thought to be transmitted through the action of nonreceptor protein tyrosine kinases (TK) in the cytoplasm. These TK proteins frequently show alterations in their activities in human tumorigenesis [8], and selective inhibitors of TKs are being investigated for the treatment of cancers [9]. One of these TKs is protein tyrosine kinase 6 (PTK6, BRK), a cytoplasmic tyrosine kinase, which is not only overexpressed in two thirds of breast carcinomas [10–15] but is also overexpressed in colon and prostate tumors and several cancer cell lines [11, 12, 16–18]. In vitro studies to define the physiological role and to identify the PTK6 interaction partners confirmed that PTK6 functions downstream of the HER receptors [18, 19]. This makes PTK6 an interesting tumor marker and a potential new therapy target.

Knowledge of PTK6 expression in tumor tissues is limited, although PTK6 overexpression is established in breast carcinogenesis [15, 19, 20]. High levels of PTK6 are also observed in differentiating noncancerous epithelial tissues such as the gastrointestinal tract, skin [12, 21], and prostate [17]. The extent of PTK6 expression may be influenced by the level of differentiation of breast tissue with evidence for an association with estrogen receptor expression [22] and with the expression of HER receptors [13, 15]. More significantly, the expression of PTK6 has been shown to be a prognostic indicator of outcome in invasive breast carcinomas [15].

The mechanisms behind increases in PTK6 protein overexpression as well as its role in tumorigenesis and prognosis are not understood. We are not aware of studies of PTK6 protein expression or gene status in relation to clinical outcome in invasive breast carcinomas. We conducted a study to compare the prognostic impact of PTK6 gene copy number and protein expression. We performed fluorescence in situ hybridization (FISH) for PTK6 and for the chromosome 20 alpha satellite and studied associations between the FISH signal counts and histopathological and immunohistochemical parameters as well as with the clinical course of disease. We demonstrate that increased PTK6 gene copy number is mainly attributed to polysomy of chromosome 20, not to gene amplification, and that there is no statistical association between PTK6 gene status and PTK6 protein levels. Furthermore, unlike PTK6 protein levels, gene status is not a significant predictor of disease-free survival.

Material and methods

Tumor samples and patient data

Formalin-fixed and paraffin-embedded archival material was obtained from 426 patients with invasive breast carcinomas, as recently described [23]. This cohort contains 244 lymph node negative and 182 node positive tumors, and a total of 234 tumors were less than 2 cm in size. The median follow-up of patients was 80 months (mean 94, maximum 264 months) with 121 (28%) of the patients showing disease recurrence by distant metastases and/or local recurrence. In addition to the standard histopathological parameters (lymph node status, tumor size, and histological grade and type), immunohistochemical data were available for HER2, HER3, HER4, PTK6, estrogen receptor (ER), and progesterone receptor (PrR).

Tissue microarrays (TMAs) were produced as described [15] using a tissue-arraying instrument (Beecher Instruments Inc., Silver Spring, MD, USA). Five-micrometer sections were cut and transferred to adhesive slides using the "paraffin-tape-transfer system" (Instrumedics, Hackensack, NJ, USA). Hematoxylin- and eosin-stained sections from the TMAs, as well as from the original paraffin block, were reexamined to validate representative sampling.

FISH

FISH was performed on 5-μm thick TMA sections. Pretreatment of the sections was done by heating the slides for 12 min in a microwave oven (750 W), digestion with Pronase E (0.05%) for 6 min, and denaturation at 75°C for 15 min, as described elsewhere [24].

The DNA hybridization probes were obtained from Chrombios (Molecular Cytogenetics Chrombios, Raubling, Germany). The PTK6 probe was labeled with Cy3 (red fluorescence), and the centromere 20 probe (20q11.21, CEP20) was labeled with FITC (green fluorescence).

Counterstaining of the sections was done using 4',6-diamidino-2-phenylindole (DAPI). The probes were applied sequentially; after the first hybridization using the PTK6 probe, slides were washed as described [24] and the hybridization procedure repeated using the centromeric probe.

Image acquisition and evaluation of FISH signals

The hybridized slides were viewed under a confocal laser scanning microscope (LSM 510, Zeiss, Jena, Germany) equipped with the Apotome Extension (Zeiss Vision) and appropriate filters [24]. Images were captured using a C-Apochromat ×63/1.2 W objective, and 3-dimensional image projections (AxioVision software) were used for PTK6 signal counting. Multiple tumor areas were scored from each case, and FISH signals were evaluated by counting at least 50 non-overlapping tumor nuclei. Signals were also counted in normal tissues involved in the TMAs, with a mean signal count of 1.54 (± 0.15 SD). Consequently, the presence of ≤2 PTK6 signals per nucleus (corresponding to mean + 3 times SD) were considered normal.

The signals for centromere 20 were counted directly under the microscope and registered as normal (≤2 signals per nucleus) or as increased (>2 signals per nucleus).

The ratio PTK6/CEP20 was interpreted as normal (PTK6 and CEP20≤2 signals), as polysomy of chromosome 20 (>2 signals for PTK6 and for CEP20) or as gene amplification (>2 PTK6 signals and ≤2 CEP20 signals).

Quantitative mRNA analysis

From 90 randomly selected cases, total RNA was isolated and purified from paraffin sections as described elsewhere [13], and RNA was reverse-transcribed using Superscript II Reverse Transcriptase (Invitrogen) according to manufacturer's directions. Intron-spanning primers and probes (FAM™ dye-labeled) were obtained from Applied Biosystems (Assay-on-Demand™, PE Applied Biosystems, PTK6: HS00178742). For the TBP reference gene (*T*ATA-*B*ox binding protein), intron-spanning primers and oligonucleotide probes with 5' fluorescent reporter dye (FAM) and a 3' quencher dye (TAMRA) were designed (Primer-Express software, PE Applied Biosystems, Weiterstadt, Germany) [13]. Polymerase chain reaction (PCR) amplifications were performed as described elsewhere [13], following established criteria. Relative expression levels for the target gene were determined by the standard curve method using a reference RNA (MCF7 breast cancer cell line) [13], and the target amount was divided by the endogenous reference amount to obtain a normalized target value. Final results are expressed as *N*-fold differences in expression relative to the TBP gene. In normal tissues, the mean PTK6 mRNA expression was 0.55 (± 0.8). Therefore, values ≥10-fold (corresponding to mean +2-fold logarithmic SD) were considered as increased mRNA expression.

Statistics

The Spearman rank correlation test was used to examine the relationship between two markers and between markers and clinical parameters. Statistical significance was considered at the $p \leq 0.05$ level.

Survival analysis was performed using disease-free survival, which was defined as the interval from the date of surgery to the first loco-regional recurrence and/or distant metastases.

For univariate survival analysis, Kaplan–Meier curves were calculated, and differences between strata were tested with the log-rank Chi-Square value. Multivariate analyses were performed using Cox proportional hazards regression and a combined stepwise selection algorithm (SAS Inst., Cary, NC, USA). All parameters reaching a significance level of $p \leq 0.15$ in univariate analysis were offered to multivariate analysis. In all other tests, statistical significance was considered proven if $p \leq 0.05$.

Results

PTK6 gene amplification and polysomy 20 in invasive breast cancer

PTK6 FISH signals were detectable in 389 of the tumors examined. A normal PTK6 gene copy number (signal frequency ≤2 signals/nucleus) was found in 55% (n=213) of the invasive breast carcinomas (Table 1). An increased PTK6 gene copy number (>2 signals, as defined in normal tissue) was present in 45% (n=171) of the tumors. In most of these cases, overrepresentation of the gene copy number was caused by polysomy of chromosome 20 (30%); gene amplification was seen in only 15% (Table 1). In Fig. 1, examples for polysomy 20 (a) and for PTK6 amplification (b) are shown. The highest PTK6 gene copy number in our tumors was eight signals/nucleus (corresponding to a 4-fold

Table 1 Frequency of PTK6 gene copy number in comparison with the cytogenetic status

PTK6 signal frequency	Percent of cases	Cytogenetic status*	Percent of cases
≤2.0	55% (n=213)	n	55%
>2.0	45% (n=171)	Polysomy	30% (n=115)
		Amplification	15% (n=56)

Cytogenetic status = ratio of PTK6/CEP20 signals

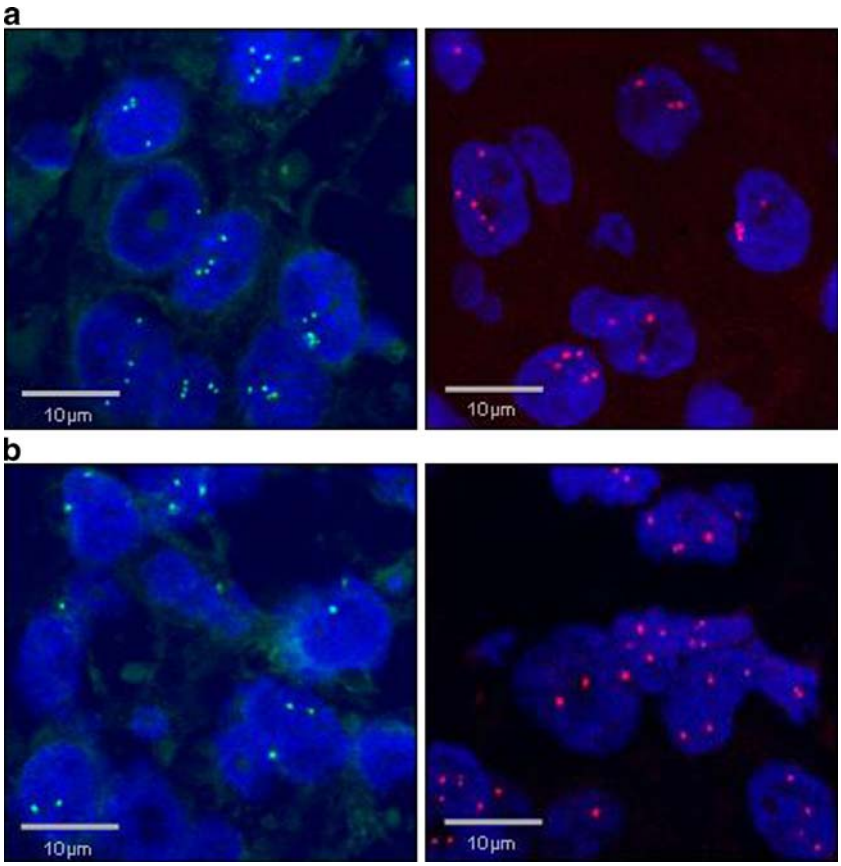

Fig. 1 Examples for an increased PTK6 signal count in breast cancer, caused by polysomy 20 (**a**) or by PTK6 gene amplification (**b**). PTK6 signals = red fluorescence; CEP20 signals = green fluorescence; counterstaining: DAPI

gene dosis); no higher levels of amplification were found. The majority of tumors with an increased signal count showed between two and four signals (n=150); only a minority of cases showed >4 signals (n=18). Therefore, in comparison to other gene amplifications like the HER2 receptor in breast cancer, the PTK6 gene is amplified only on low level.

Correlations between FISH signal counts and other parameters

As shown in Table 2, the PTK6 signal count was significantly associated ($p \leq 0.05$) with ER status, histological grade, and tumor size. The number of tumors with normal and increased signal counts in the three different histological grades is given in Table 3. Most of the cases with normal PTK6 signal counts are classified as grade 1 or 2 (n=152 vs. n=37), whereas the majority of cases with increased signals are grade 2 or 3 (n=142 vs. n=35). The number of centromeric CEP20 signals correlated with tumor size and histological grade. The cytogenetic status (ratio PTK6/CEP20) does not show association with any of the histopathological parameters (Table 2).

The number of PTK6 gene copies was significantly correlated with the immunohistochemical staining intensities of HER3 and HER4 (Table 4), and CEP20 signals revealed significant correlation with HER2, HER3, and HER4 receptor staining. The ratio of PTK6/CEP20 signals does not show any significant correlation with the immunohistochemical parameters (Table 4). Remarkably, there was neither any statistical association between PTK6 IHC and PTK6 FISH gene copy numbers (p=0.5).

To compare gene copy number with mRNA expression and with protein expression, we performed quantitative RT-

Table 2 Associations between FISH signals (PTK6, CEP20, ratio PTK6/CEP20), the PTK6 mRNA, and the histopathological parameters

	Lymph node status	Histological grade	Tumor size	ER	PrR
PTK6 FISH	0.2	**0.0015** 0.17	**0.02** 0.12	**0.003** 0.15	0.15
FISH CEP20	0.6	**0.023** 0.13	**0.036** 0.12	0.06	0.8
ratio PTK6/CEP20	0.2	0.6	0.9	0.4	0.4
PTK6 mRNA	0.3	0.2	0.99	**0.009** 0.27	**0.011** 0.27

Significant correlations are highlighted in bold, and in addition, the Spearman correlation coefficients are given

Table 3 Number of tumors with normal and increased PTK6 signal counts in the three different histological grades

Grade	≤2 signals/nucleus (n=189)	>2 signals/nucleus (n=177)
1	50 (26.4%)	35 (19.8%)
2	102 (54.0%)	82 (46.3%)
3	37 (19.6%)	60 (33.9%)

Spearman rank correlation test p=0.02

PCR for PTK6 in 90 of our tumors. An increased expression (≥10-fold) was found in 71% of cases. PTK6 mRNA expression showed significant association with the expression of ER and PrR ($p \leq 0.01$; Table 2), and at least a trend (p=0.08) was indicated between PTK6 mRNA and PTK6 IHC (Table 4). No significant association was found between mRNA expression and the FISH results (PTK6 signals, p=0.95; CEP20 signals, p=0.6; ratio PTK6/CEP20, p=0.85).

Correlations with the disease-free survival of patients

As recently published by us, the PTK6 protein expression showed significant correlation with the disease-free survival of patients in multivariate analysis, together with the lymph node status and the tumor size [23]. In the study presented here, which was performed on the same tumor cohort, no statistical significant association was present for normal (≤2) or increased (>2) PTK6 signal counts and the clinical course (p=0.36). Further, neither CEP20 signals nor the ratio PTK6/CEP20 shows association with the clinical course of patients in univariate analysis. Parameters, positively correlated with a disease-free survival of patients in univariate analysis, were lymph node status and tumor size ($p \leq 0.0001$) and histological grade (p=0.002), and an inverse association was found for PTK6 IHC ($p \leq 0.0001$), progesterone receptor status (p=0.02), and HER4 staining intensity (p=0.03), as published else [23].

In multivariate analysis for a disease-free survival of patients, all parameters reaching a significance level of ≤0.15 in univariate analysis were offered. We found an independent prognostic value for lymph node status (p=0.0003, relative risk 2.13), protein expression of PTK6 (p=0.0007, 0.62), and tumor size (p=0.003, 1.55) [23]. The FISH values (PTK6, CEP20, PTK6/CEP20) as well as the mRNA expression values do not influence this result due to insufficient significance.

Discussion

PTK6 is overexpressed in about two thirds of breast carcinomas [10–15], but the mechanisms behind this overexpression are still unknown, and the physiological role of PTK6 in overexpressing cells is not defined. In this study, we show that most tumors with increased PTK6 gene copies are attributed to polysomy of chromosome 20, not to gene amplification, and that there is no statistical association between PTK6 gene status and protein or mRNA expression. Hence, besides an increased dose caused by polysomy 20, there may be additional mechanisms contributing to overexpression as, for example, posttranscriptional regulation mechanisms.

Gene amplification is one major mechanism to increase gene dosage and has importance for both prognosis and targeted therapy. For example, amplification of HER2, MYC, and CCND1 have been reported to be significantly associated with high grade in breast cancer, and a decrease of survival was observed with increasing number of co-amplifications [25]. Amplification is also one of the underlying causes of resistance to therapy [4] as, for example, BCR-ABL gene amplification in patients with chronic myeloid leukemia [26] or clinical resistance to 5-fluorouracil in liver metastases [26].

Although enhanced expression is often the consequence of gene amplification, there are alternative pathways to increase protein expression such as activating regulatory mutations or posttranscriptional and posttranslational mechanisms [4] and, especially in the case of PTK6, via activation by other kinases. Protein overexpression without gene amplification was also described for HER2 protein in some urothelial carcinomas [27] and for hypoxia inducible factor-1alpha in human breast cancer [28].

About half of the tumors analyzed in our study showed increased PTK6 signals; however, most of them had 2–4 signals and only a minority had >4 PTK6 signals. This and, in particular, that most tumors with increased PTK6 signals are caused by polysomy let as state that PTK6 amplification in breast cancers is present only on low level and that it cannot account for the protein overexpression found in two thirds of the tumors. There are also indications that

Table 4 Associations between FISH signals (PTK6, CEP20, ratio PTK6/CEP20), the PTK6 mRNA expression, and the immunohistochemically determined expression of HER2, HER3, HER4, PTK6, and the hormone receptors

	HER2	HER3	HER4	PTK6 IHC
PTK6 FISH	0.2	**0.01** −0.15	**0.01** −0.13	0.5
FISH CEP20	**0.04** −0.11	**<.0001** −0.46	**<.0001** −0.29	0.7
ratio PTK6/ Cep20	0.7	0.5	0.6	0.4
PTK6 mRNA	0.8	0.1	0.4	0.08

Significant correlations are highlighted in bold, and in addition, the Spearman correlation coefficients are given

chromosomal polysomy may, to a certain degree, cause protein overexpression, as has been reported for chromosome 17 polysomy and HER2 in breast carcinomas [29, 30] and in esophageal and gastric carcinomas [31]. In the current study, the majority of tumors with increased PTK6 signals exhibited polysomy 20.

We found no association between the signal ratio PTK6/CEP20 and tumor size or histological grade, whereas both PTK6 and CEP20 signals showed a significant correlation with these histopathological parameters. This indicates that increased signal counts are predominantly found in high histological grades and in tumors larger in size. The cytogenetic status, as described by the ratio PTK6/CEP20, is indicative for gene amplification and does not show significant correlation. Consequently, these associations with histopathological parameters are based upon polysomy of chromosome 20, not on gene amplification. Likewise, the PTK6/CEP20 ratio was not associated with the HER2, HER3, or HER4 protein expression, whereas PTK6 signals as well as CEP20 signals showed significant inverse correlations with HER receptor expressions, indicating that polysomy 20 is associated with normal or low HER receptor expression. There is growing evidence in the literature that HER3 overexpression is associated with worse, HER4 with good prognosis [32, 33]. Some other studies, however, have indicated that HER3 overexpression may be a good prognostic factor [34]. In our tumor cohort, both markers showed a similar (inverse) tendency in univariate survival analysis, although HER3 did not reach significance. This explains the inverse correlation of CEP20 and PTK6 signals with HER3 and HER4. It is remarkable that there was no statistical association between PTK6 IHC or mRNA and the PTK6 gene status. This further emphasizes that overrepresentation of PTK6 appears at the messenger RNA or protein level. Consequently, the altered synthesis and degradation rates of the gene products seem to play a crucial role.

We further show that PTK6 protein expression—but not PTK6 gene status or mRNA expression—is significantly associated with the clinical course of patients. So far, no other study described PTK6 FISH analysis on breast carcinomas with correlation with the clinical outcome. Only one study [9] reported that six of seven high-grade ovarian carcinomas showed PTK6 amplification with an up to 3-fold increase of the PTK6 gene. The authors concluded that gene amplification may be responsible for the observed protein overexpression in ovarian tumors. However, such a small cohort may not allow to draw the conclusion that increased gene dosage may be the reason for protein overexpression. Further, in comparison to our results here with a maximum of eight PTK6 gene signals (corresponding to a 4-fold gene dosage), the level of gene dosage in ovarian carcinomas was up to 3-fold [9]. Compared to other oncogene amplifications in breast cancer, e.g., HER2/neu with >20 gene copies, we would classify those PTK6 gene increases from both studies only as "low level" amplifications. After all, such low-level amplifications in only part of our tumors (15%) cannot account for PTK6 protein overexpression in two thirds of breast carcinomas.

PTK6 has been linked to proliferation of carcinoma cells [35] and represents a potential target for the development of novel cancer therapies based on interfering with its functions [35]. Therefore, it is important to understand how it contributes to the phenotypic effect. Here, we showed that gene amplification cannot account for the protein overexpression in two thirds of breast cancers. Further studies, however, are necessary to define protein–protein interactions and to further uncover therapeutic opportunities.

Acknowledgements This project was supported by the Deutsche Krebshilfe, contract 107379, and partly by the European Commisson, "TRANSBIG" Project, no. LSHC-CT-2004-503426. We gratefully acknowledge the excellent technical assistance of Uli Reich and Ilse DiGrazia.

Disclosure of Conflict of Interest We, the authors, declare that we have no conflict of interest.

References

1. Savelyeva L, Schwab M (2001) Amplification of oncogenes revisited: from expression profiling to clinical application. Cancer Lett 167:115–123
2. Imoto I, Yang ZQ, Pimkhaokham A et al (2001) Identification of cIAP1 as a candidate target gene within an amplicon at 11q22 in esophageal squamous cell carcinomas. Cancer Res 61:6629–6634
3. Ohta JI, Miyoshi Y, Uemura H et al (2001) Fluorescence in situ hybridization evaluation of c-erbB-2 gene amplification and chromosomal anomalies in bladder cancer. Clin Cancer Res 7:2463–2467
4. Schwab M (1998) Amplification of oncogenes in human cancer cells. Bioessays 20:473–479
5. Slamon DJ (1990) Studies of the HER-2/neu proto-oncogene in human breast cancer. Cancer Invest 8:253
6. Jukkola A, Bloigu R, Soini Y et al (2001) c-erbB-2 positivity is a factor for poor prognosis in breast cancer and poor response to hormonal or chemotherapy treatment in advanced disease. Eur J Cancer 37:347–354
7. Hsieh AC, Moasser MM (2007) Targeting HER proteins in cancer therapy and the role of the non-target HER3. Br J Cancer 97:453–457
8. Hahn WC, Weinberg RA (2002) Rules for making human tumor cells. N Engl J Med 347:1593–1603
9. Schmandt RE, Bennett M, Clifford S et al (2006) The BRK tyrosine kinase is expressed in high-grade serous carcinoma of the ovary. Cancer Biol Ther 5:1136–1141
10. Mitchell PJ, Barker KT, Martindale JE et al (1994) Cloning and characterisation of cDNAs encoding a novel non-receptor tyrosine kinase, brk, expressed in human breast tumours. Oncogene 9:2383–2390

11. Barker KT, Jackson LE, Crompton MR (1997) BRK tyrosine kinase expression in a high proportion of human breast carcinomas. Oncogene 15:799–805
12. Llor X, Serfas MS, Bie W et al (1999) BRK/Sik expression in the gastrointestinal tract and in colon tumors. Clin Cancer Res 5:1767–1777
13. Born M, Quintanilla-Fend L, Braselmann H et al (2005) Simultaneous over-expression of the Her2/neu and PTK6 tyrosine kinases in archival invasive ductal breast carcinomas. J Pathol 205:592–596
14. Ostrander JH, Daniel AR, Lofgren K et al (2007) Breast tumor kinase (protein tyrosine kinase 6) regulates heregulin-induced activation of ERK5 and p38 MAP kinases in breast cancer cells. Cancer Res 67:4199–4209
15. Aubele M, Auer G, Walch AK et al (2007) PTK (protein tyrosine kinase)-6 and HER2 and 4, but not HER1 and 3 predict long-term survival in breast carcinomas. Br J Cancer 96:801–807
16. Meric F, Lee WP, Sahin A et al (2002) Expression profile of tyrosine kinases in breast cancer. Clin Cancer Res 8:361–367
17. Derry JJ, Prins GS, Ray V et al (2003) Altered localization and activity of the intracellular tyrosine kinase BRK/Sik in prostate tumor cells. Oncogene 22:4212–4220
18. Kamalati T, Jolin HE, Fry MJ et al (2000) Expression of the BRK tyrosine kinase in mammary epithelial cells enhances the coupling of EGF signalling to PI 3-kinase and Akt, via erbB3 phosphorylation. Oncogene 19:5471–5476
19. Zhang P, Ostrander JH, Faivre EJ et al (2005) Regulated association of protein kinase B/Akt with breast tumor kinase. J Biol Chem 280:1982–1991
20. Petro BJ, Tan RC, Tyner AL et al (2004) Differential expression of the non-receptor tyrosine kinase BRK in oral squamous cell carcinoma and normal oral epithelium. Oral Oncol 40:1040–1047
21. Haegebarth A, Heap D, Bie W et al (2004) The nuclear tyrosine kinase BRK/Sik phosphorylates and inhibits the RNA-binding activities of the Sam68-like mammalian proteins SLM-1 and SLM-2. J Biol Chem 279:54398–54404
22. Zhao C, Yasui K, Lee CJ et al (2003) Elevated expression levels of NCOA3, TOP1, and TFAP2C in breast tumors as predictors of poor prognosis. Cancer 98:18–23
23. Aubele M, Walch AK, Ludyga N et al (2008) Prognostic value of protein tyrosine kinase 6 (PTK6) for long-term survival of breast cancer patients. Br J Cancer 99:1089–1095
24. Walch A, Bink K, Hutzler P et al (2001) Sequential multilocus fluorescence in situ hybridization can detect complex patterns of increased gene dosage at the single cell level in tissue sections. Lab Invest 81:1457–1459
25. Al-Kuraya K, Schraml P, Torhorst J et al (2004) Prognostic relevance of gene amplifications and coamplifications in breast cancer. Cancer Res 64:8534–8540
26. Gorre ME, Mohammed M, Ellwood K et al (2001) Clinical resistance to STI-571 cancer therapy caused by BCR-ABL gene mutation or amplification. Science 293:876–880
27. Caner V, Turk NS, Duzcan F et al (2008) No strong association between HER-2/neu protein overexpression and gene amplification in high-grade invasive urothelial carcinomas. Pathol Oncol Res 14(3):261–266
28. Vleugel MM, Bos R, Buerger H et al (2004) No amplifications of hypoxia-inducible factor-1alpha gene in invasive breast cancer: a tissue microarray study. Cell Oncol 26:347–351
29. Hyun CL, Lee HE, Kim KS et al (2008) The effect of chromosome 17 polysomy on HER-2/neu status in breast cancer. J Clin Pathol 61:317–321
30. Lal P, Salazar PA, Ladanyi M et al (2003) Impact of polysomy 17 on HER-2/neu immunohistochemistry in breast carcinomas without HER-2/neu gene amplification. J Mol Diagn 5:155–159
31. Bizari L, Borim AA, Leite KR et al (2006) Alterations of the CCND1 and HER-2/neu (ERBB2) proteins in esophageal and gastric cancers. Cancer Genet Cytogenet 165:41–50
32. Tovey S, Dunne B, Witton CJ et al (2005) Can molecular markers predict when to implement treatment with aromatase inhibitors in invasive breast cancer? Clin Cancer Res 11:4835–4842
33. Koutras AK, Fountzilas G, Kalogeras KT et al (2009) The upgraded role of HER3 and HER4 receptors in breast cancer. Crit Rev Oncol Hematol, in press
34. Pawlowski V, Revillion F, Hebbar M et al (2000) Prognostic value of the type I growth factor receptors in a large series of human primary breast cancers quantified with a real-time reverse transcription-polymerase chain reaction assay. Clin Cancer Res 6:4217–4225
35. Harvey AJ, Crompton MR (2003) Use of RNA interference to validate Brk as a novel therapeutic target in breast cancer: Brk promotes breast carcinoma cell proliferation. Oncogene 22:5006–5010

Statement

Ethical approval for this study was obtained from the Ethics Committee of the Medical Faculty of the Technische Universität München, Germany.

Virchows Arch (2009) 455:125–132
DOI 10.1007/s00428-009-0812-0

ORIGINAL ARTICLE

Clinical relevance of neuroendocrine differentiation in non-small cell lung cancer assessed by immunohistochemistry: a retrospective study on 405 surgically resected cases

William Sterlacci · Michael Fiegl · Wolfgang Hilbe · Jutta Auberger · Gregor Mikuz · Alexandar Tzankov

Received: 27 May 2009 / Revised: 16 July 2009 / Accepted: 17 July 2009 / Published online: 4 August 2009

Abstract Neuroendocrine differentiation in non-small cell lung cancer is a common feature, which has caused contradictory conclusions concerning survival estimates and responsiveness to therapy. Aiming to clarify this conflict, we analyzed neuroendocrine differentiation by immunohistochemistry in 405 surgically resected non-small cell lung carcinomas using standardized tissue microarray platform and the currently recommended antibody panel consisting of chromogranin-A, synaptophysin, and neural-cell adhesion molecule. Diagnostic criteria provided by the World Health Organization were applied. Histological subtypes were primarily reclassified according to current guidelines, assisted by auxiliary immunohistochemistry. Extensive clinical data was acquired, enabling detailed clinicopathological correlation. Importantly, neuroendocrine differentiation assessed by immunohistochemistry showed no significant relation to overall survival estimates, which remained unaffected by histological subtype, neuroendocrine marker type, adjuvant therapy, and recurring disease. The only exception was a small group consisting of three large cell carcinomas, each expressing all three neuroendocrine markers and demonstrating decreased survival. In conclusion, additional immunohistochemical detection of neuroendocrine differentiation in non-small cell lung cancer is presently not of prognostic importance and does not justify a distinct consideration.

Keywords Non-small cell lung cancer · Neuroendocrine differentiation · Immunohistochemistry · Survival

W. Sterlacci (✉) · G. Mikuz
Institute for Pathology, Medical University Innsbruck,
Muellerstrasse 44,
6020 Innsbruck, Austria
e-mail: william.sterlacci@i-med.ac.at

M. Fiegl · W. Hilbe · J. Auberger
Division of Haematology and Oncology,
Department of Internal Medicine, Medical University Innsbruck,
Anichstrasse 35,
6020 Innsbruck, Austria

A. Tzankov
Institute for Pathology, University Hospital Basel,
Schoenbeinstrasse 40,
4031 Basel, Switzerland

Introduction

Lung cancer is the most common cancer in the world and the leading cause of cancer-related mortality [1]. Nearly all lung cancers are carcinomas and about 80% thereof are non-small cell carcinomas (NSCLC) [2]. Exact histological classification is required for proper therapy and prognostic estimates. Neuroendocrine differentiation may occur in any entity, although the relevance of this feature has not yet been entirely clarified. The four major categories of morphologically distinguishable neuroendocrine lung tumors recognized at present are small cell carcinoma, typical carcinoid, atypical carcinoid, and large cell neuroendocrine carcinoma (LCC-NE), which all show varying degrees of neuroendocrine features by light microscopy [3]. LCC-NE requires additional confirmation of neuroendocrine differentiation by immunohistochemistry [3]. Some pulmonary carcinomas without neuroendocrine morphology by light microscopy demonstrate immunohistochemical expression of neuroendocrine markers and are termed non-small cell carcinoma with neuroendocrine differentiation (NSCLC-ND) [3]. This entity has generated controversial conclusions concerning survival time and responsiveness to chemotherapy resulting in the current

recommendation to note neuroendocrine differentiation in NSCLC without an according separate category. This implies immunohistochemistry or electron microscopy of all NSCLC to determine neuroendocrine expression. Studies report improved [4], decreased [5], and unaffected survival [6] as well as better [4] and worse [7] responses to chemotherapy in NSCLC-ND. Reports also show discrepancies concerning the definition of neuroendocrine differentiation [8], the panel of antibodies used [9], and the interpretation of immunohistochemical results [10], providing possible explanations for such conflicting data. Thus, it still remains to be determined what prognostic significance, if any, is associated with immunohistochemical neuroendocrine differentiation in NSCLC. Furthermore, uniform standards should be followed in order to compare results.

This study analyzes the prognostic significance of neuroendocrine differentiation in 405 surgically resected NSCLC using a standardized tissue microarray (TMA) platform and the currently recommended antibody panel [3, 11]. Diagnostic criteria comply with the current guidelines by the World Health Organization (WHO) [3]. Extensive clinical data for each case enabled detailed evaluation.

Patients, materials, and methods

Cases

NSCLC cases diagnosed at the Institute for Pathology, Medical University of Innsbruck, between 1992 and 2004 were selected from the pathology archives. Cases were selected only based on tissue preservation. Hematoxylin and eosin (H&E) stains from all available slides (whole tumor sample) of all cases were reclassified by two pathologists (W.S. and A.T.) without knowledge of patient information, according to the current WHO classification of tumors of the lung [3]. Categories included squamous cell carcinoma (SCC), adenocarcinoma (ACA), large cell carcinoma (LCC), adenosquamous carcinoma (ASC), pleomorphic carcinoma (PLM), and mucoepidermoid carcinoma (MEC). ACA included growth type (bronchioloalveolar, papillary, acinar, solid, and mixed) as well as mucin status as assessed on alcyan–PAS-stained slides. In morphologically equivocal cases, expression of thyroid transcription factor-1 (TTF-1) and cytokeratin 7 (CK 7) in favor of ACA as well as p63, cytokeratin 34βE12 (CK 34βE12), and cytokeratin 5/6 (CK 5/6) in favor of SCC were also considered for proper tumor classification. LCCs were diagnosed on light microscopy by lack of cytological and architectural features described for small cell, glandular, or squamous differentiation [3] and categorized as LCC "classical" type (LCC-CL) or LCC with neuroendocrine features (LCC-ND). Features suggestive of neuroendocrine differentiation by light microscopy (LCC-ND) consisted of trabecular growth, rosettes, or perilobular palisading patterns [3]. Organoid nesting in LCC-ND was not taken into account because nesting is also a feature described for LCC-CL, and the distinction between organoid nesting and nesting is not clearly defined. LCC-ND with additional immunohistochemical expression of at least one neuroendocrine marker is currently defined as large cell neuroendocrine carcinoma (LCC-NE) [3]. Accordingly, a group of LCC-CL with neuroendocrine differentiation arises (LCC-CLNE). Around 50% of LCC-NE is known to express TTF-1, whereas expression of CK 34βE12 is uncommon [3]. Currently, no specific immunohistochemical profile for LCC-CL is recognized. Extensive necrosis was noted independently of tumor category. Tumors were also regraded according to well, moderate, or poor differentiation. Typical and atypical carcinoids were not included. The clinical information was documented within the TYROL survey (Twelve Years Retrospective of Lung Cancer), a project aiming at analyzing various features of a large number of lung cancer patients. These patients mainly originated from the Austrian county of Tyrol and were all diagnosed and treated at the Medical University Hospital of Innsbruck and associated hospitals (Table 1). Approval for data acquisition and analysis was obtained from the Medical University of Innsbruck Ethics Committee (the local Institutional Review Board). In this project, the basic patients' characteristics including symptoms at presentation, smoking habits, comorbidities, and laboratory parameters, as well as the complete course of treatment modalities, including surgery, all lines of chemo-, and radiotherapy, were documented. Regarding therapy modalities, the patients were routinely discussed at the Medical University of Innsbruck Tumor Board, and a state of the art recommendation of therapy adapted to the condition of the patient was given. Accordingly, there was a continuous shift of therapy modalities routinely applied in this comparably large interval of patients recruited into the survey. Efficacy of the different therapy lines in routine patients can therefore be evaluated in detail [12, 13].

Tissue microarray construction

Tumor material consisted of paraffin embedded tissue after fixation in 10% neutral buffered formalin. Representative tumor areas were marked on H&E stained slides, and four cylindrical 0.6-mm tissue cores each were arrayed from the corresponding paraffin blocks into a recipient block using an arraying machine from Breecher Instruments. The core coordinates were recorded for exact location using Microsoft Excel, and printouts assisted the subsequent immunohistochemical evaluation. Four micrometer-thick paraffin sections were cut from a total of three resulting

Table 1 Patient characteristics

	Total	Male	Female	pUICC stage					Mean age (range), in years	Mean survival (±SD), in years	Median survival (years)	Relative 5-year survival rate (%)	Adjuvant therapy
				I	II	IIIA	IIIB	IV					
SCC	126	107	19	65	27	15	4	2	63.5 (38–83)	6.3±0.6	4.9	49	22
ACA	207	125	82	92	26	32	14	9	62 (23–82)	5.7±0.3	5.2	50.5	36[a]
LCC	58	46	12	30	8	5	0	2	63 (43–82)	4.8±0.7	3.5	45.9	11
ASC	9	8	1	6	0	1	1	0	62.2 (49–77)	3.1±0.7	1.9	0	1
PLM	4	3	1	2	0	1	0	1	55.2 (35–75)	0.9±0.4	0.8	0	1
MEC	1	1	0	1	0	0	0	0	40.9				0

pUICC pathological Union Internationale Contre le Cancer, *SD* standard deviation, *SCC* squamous cell carcinoma, *ACA* adenocarcinoma, *LCC* large cell carcinoma, *ASC* adenosquamous carcinoma, *PLM* pleomorphic carcinoma, *MEC* mucoepidermoid carcinoma

[a] One case neoadjuvant

array blocks. The first sections were stained with H&E to confirm validity, the following used for alcyan staining and immunohistochemistry (Fig. 1). Adhesive transfer tape was not used.

Immunohistochemistry

Immunohistochemistry was performed using the automated staining system Ventana Benchmark XT by Ventana Medical Systems Inc. The primary antibodies used and their dilutions are listed in Table 2.

Evaluation

Only spots containing at least twenty vital tumor cells were evaluated. If all four spots of a case did not meet this criterion for any marker diagnostic of neuroendocrine differentiation, it was excluded from further analysis. Tumor cells were counted independently by two pathologists (W.S. and A.T.), and the percentage of positive cells were noted for each spot, followed by the calculation of the arithmetic mean value. Staining was considered positive for chromogranin-A (CHA), synaptophysin (SYN), protein gene product 9.5 (PGP9.5), and neuron-specific enolase (NSE) when located within the cytoplasm, usually demonstrating a finely granular pattern. Neural-cell adhesion molecule (N-CAM, CD56) was regarded positive when a membranous pattern was observed. Neuroendocrine differentiation was diagnosed when one marker was positive, excluding PGP9.5 and NSE. Staining for cytokeratins (CK 7, CK 5/6, and CK 34βE12) was considered positive when located within the cytoplasm; positive staining for TTF-1 and p63 was diagnosed when a nuclear pattern was observed. These five auxiliary markers were classified as negative or positive, as with the daily routine practice in Innsbruck and Basel. Actually, there were no cases expressing the respective markers in less than one third of the tumor cells. Staining intensity for neuroendocrine markers was noted as weak, moderate, or strong but not taken into account. Intensity for all other markers was not assessed.

The prognostic relevance of respective markers was assessed by means of receiver operating characteristic-analysis, selecting death as the state variable. Optimal cutoff values were calculated using the Youden index (*J*) [14].

Statistical analysis

Association between variables was analyzed using the Spearman test. Kaplan–Meier curves were calculated for survival estimates and a log-rank statistic used to determine differences between groups. P values <0.05 were considered significant. Statistical calculations were performed using SPSS 15.0 software (SPSS, Chicago, IL).

Results

Reclassification of histology on surgical tumor samples

After revision of all 405 cases using all available tumor material, 207 were diagnosed ACA, 126 SCC, 58 LCC (44 LCC-CL and 14 LCC-ND), 9 ASC, 4 PLM, and 1 MEC. Histological subtypes were altered in 108 cases; the largest group consisting of 31 LCC reverted to ACA, followed by 17 ACA reclassified as LCC. For equivocal cases, auxiliary immunohistochemistry was taken into account (Table 3). The alteration of histological subtype in part of the cases, resulting in modified overall survival estimates, was mainly due to the revised diagnostic guidelines published by the WHO in 2004 as well as extensive immunophenotypic workup of equivocal cases [3].

When comparing cumulative overall survival estimates between original and reclassified histology, a significant

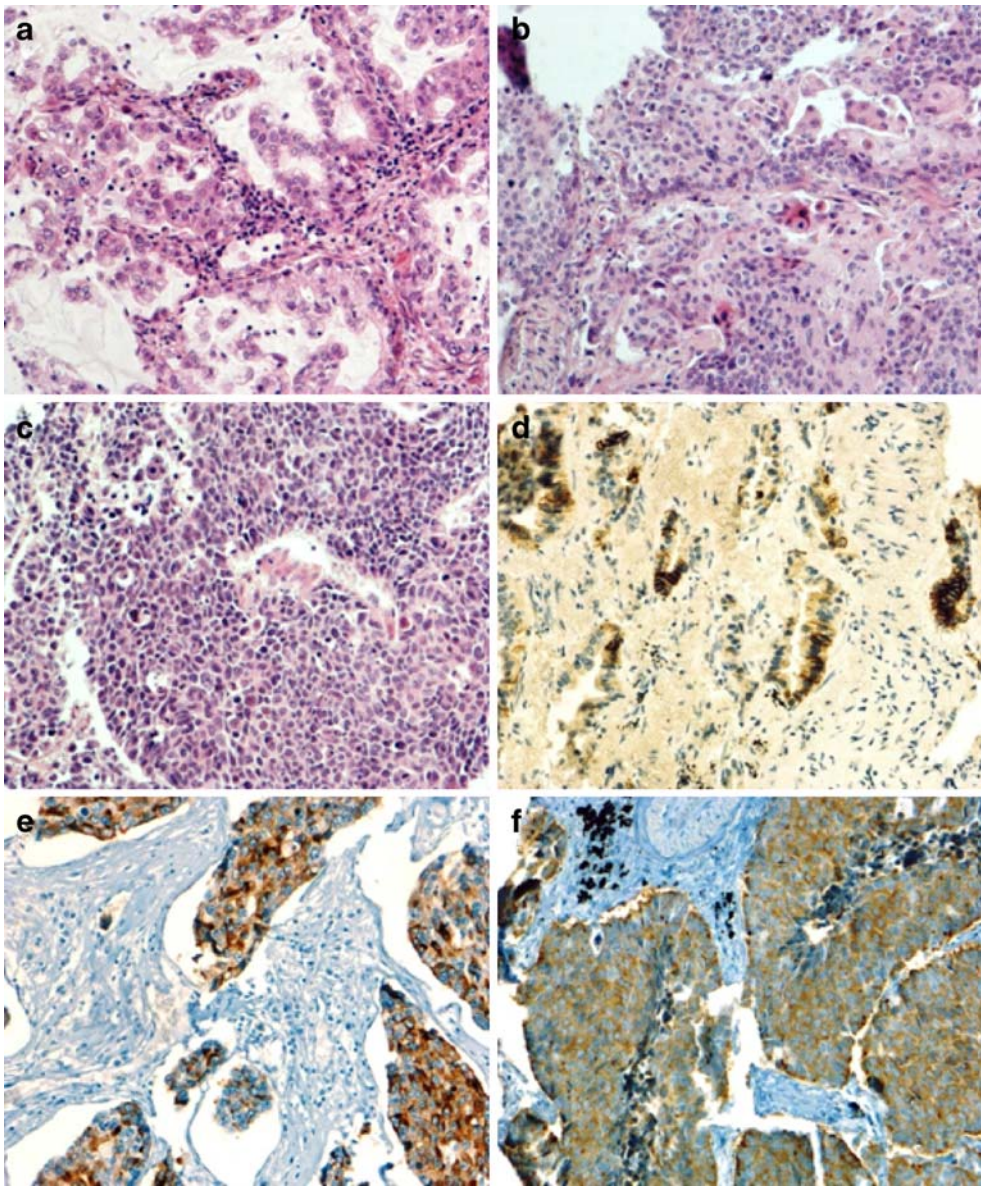

Fig. 1 Hematoxylin and eosin stains of NSCLC-ND: ACA (**a**), squamous cell carcinoma (**b**), and LCC, triple positive, (**c**). Positive immunohistochemical staining results of ACA for neural-cell adhesion molecule (**d**), squamous cell carcinoma for SYN (**e**), and LCC for chromogranin (**f**). Original magnification ×20

Table 2 Applied antibody panel

Antibody	Source	Dilution	Retrieval
Chromogranin-A	Neomarkers, MS-382-P	1:400	MW 98°/30′, citrate buffer pH 6
Neural-cell adhesion molecule	Ventana	Ready-to-use kit	
Synaptophysin	Novocastra, NCL-SYNAP-299	1:100	MW 98°/30′, citrate buffer pH 6
Neuron-specific enolase	Ventana	Ready-to-use kit	
Protein gene product 9.5	Novocastra, NCL-9.5	1:20	MW 98°/60′, citrate buffer pH 6
Cytokeratin 7	Progen, 61025	1:50	Pronase 1, 8′
Cytokeratin 5/6	Ventana	Ready-to-use kit	
Thyroid transcription factor-1	Neomarkers, MS-699-P	1:25	MW 98°/30′, citrate buffer pH 6
Cytokeratin 34βE12	Ventana	Ready-to-use kit	

MW microwave

Table 3 Distribution (%) of diagnostically auxiliary markers among non-small cell lung cancer subtypes

	CK 5/6	CK 34βE12	p63	CK 7	TTF-1
SCC	115/119 (96.6)	118/121 (97.5)	116/122 (95.1)	33/116 (28.4)	18/118 (15.3)
ACA	27/203 (13.3)	18/193 (9.3)	10/204 (4.9)	197/203 (97)	161/197 (81.7)
LCC	28/56 (50)	27/55 (49.1)	23/57 (40.4)	38/55 (69.1)	21/56 (37.5)
ASC	6/9 (66.7)	5/9 (55.6)	5/9 (55.6)	7/9 (77.8)	4/9 (44.4)
PLM	0/4 (0)	2/3 (66.7)	0/4 (0)	4/4 (100)	3/4 (75)
MEC	1/1 (100)	1/1 (100)	1/1 (100)	1/1 (100)	0/1 (0)

CK cytokeratin, *TTF-1* thyroid transcription factor-1, *SCC* squamous cell carcinoma, *ACA* adenocarcinoma, *LCC* large cell carcinoma, *ASC* adenosquamous carcinoma, *PLM* pleomorphic carcinoma, *MEC* mucoepidermoid carcinoma

difference of overall survival between the reclassified histologies was noted due to the group of PLM showing extraordinary dismal outcome (Fig. 2a, b). When solely comparing ACA, SCC, and LCC (excluding ASC and PLM), these types did not show any difference in overall survival for the reclassified cases ($p=0.17$). Distribution of pathological tumor stage by Union Internationale Contre le Cancer (UICC) revealed 196 (57%) stage I, 61 (18%) stage II, 54 (16%) stage IIIA, 19 (5%) stage IIIB, and 14 (4%) stage IV. The patient population comprised 290 men and 115 women with an average age of 62 years (range 23 to 83 years).

Tissue microarray evaluation: immunohistochemistry

Three hundred eighty-five cases were valid for evaluation of immunohistochemical expression of CHA, SYN, and N-CAM, revealing 62 (16.1%) NSCLC-ND (Table 4). Calculated potentially prognostically relevant cutoff values were 2% for CHA and 5% each for SYN, N-CAM, PGP9.5, and NSE. Staining was usually focal and weak, except for N-CAM, which mostly demonstrated a moderate intensity. Strong staining was only noted for CHA in one ACA, for N-CAM in one LCC, and for SYN in three LCC. LCC and ACA demonstrated neuroendocrine expression more

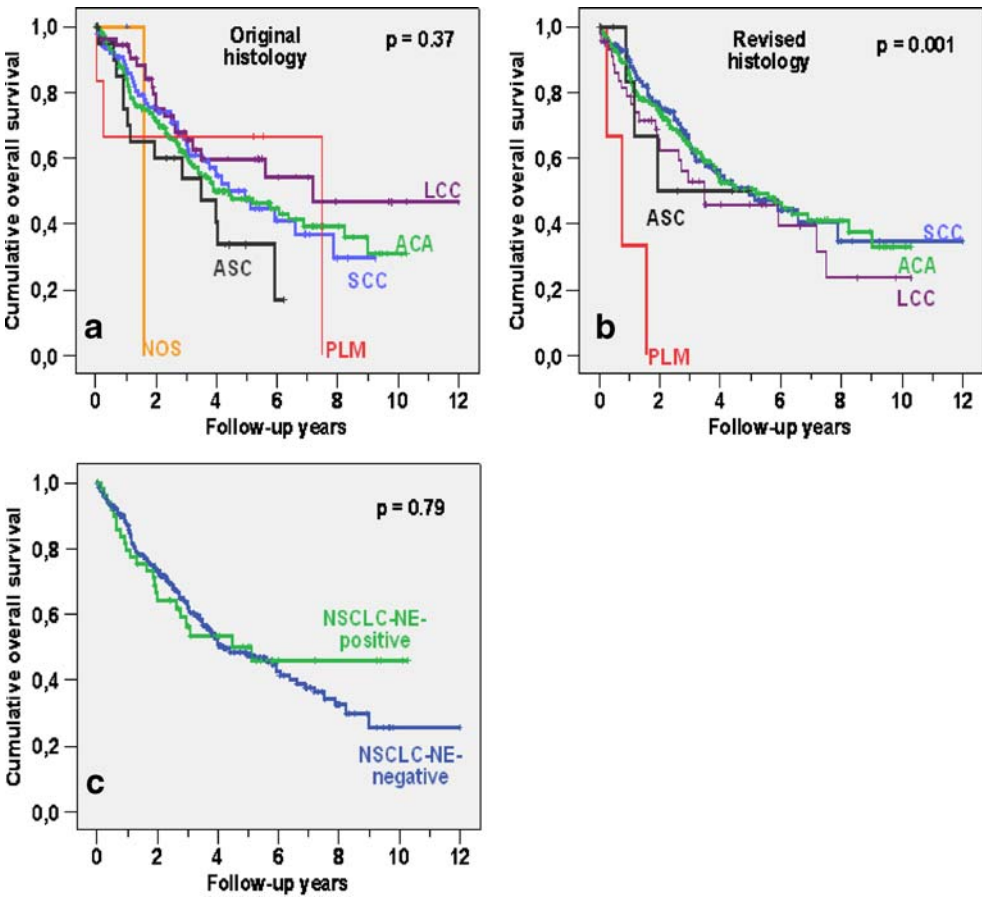

Fig. 2 Kaplan–Meier survival estimate graphs for the original histology (**a**), revised histology (**b**), and non-small cell lung cancer with and without neuroendocrine differentiation (**c**). *ACA* adenocarcinoma, *ASC* adenosquamous carcinoma, *LCC* large cell carcinoma, *MEC* mucoepidermoid carcinoma, *NOS* non-small cell lung cancer not otherwise specified, *NSCLC-NE* non-small cell lung cancer neuroendocrine, *PLM* pleomorphic carcinoma, *SCC* squamous cell carcinoma

Table 4 Neuroendocrine differentiation (%) of non-small cell lung cancer subtypes and distribution (%) of neuroendocrine markers

	NSCLC-ND	CHA	N-CAM	SYN	PGP9.5	NSE
ACA	38/197 (19)	2/197 (1)	10/196 (5)	28/197 (16)	91/195 (46)	16/197 (8)
SCC	7/119 (6)	0/119 (0)	3/119 (3)	4/119 (3)	79/119 (66)	12/119 (10)
LCC	16/56 (29)	6/56 (11)	12/56 (21)	7/56 (14)	48/55 (87)	7/56 (12)
ASC	1/9 (11)	0/9 (0)	1/9 (11)	1/9 (12)	3/9 (33)	1/9 (11)
PLM	0/3 (0)	0/3 (0)	0/3 (0)	0/3 (0)	2/3 (67)	0/3 (0)
MEC	0/1 (0)	0/1 (0)	0/1 (0)	0/1 (0)	0/1 (0)	0/1 (0)
Total	62/385 (16)	8/385 (2)	26/384 (7)	40/385 (10)	223/382 (58)	36/385 (9)

NSCLC-ND non-small cell lung cancer with neuroendocrine differentiation, *CHA* chromogranin-A, *N-CAM* neural-cell adhesion molecule, *SYN* synaptophysin, *PGP9.5* protein gene product 9.5, *NSE* neuron-specific enolase, *SCC* squamous cell carcinoma, *ACA* adenocarcinoma, *LCC* large cell carcinoma, *ASC* adenosquamous carcinoma, *PLM* pleomorphic carcinoma, *MEC* mucoepidermoid carcinoma

frequently than SCC ($p<0.001$ and $p=0.001$). Six tumors were positive for two neuroendocrine markers. Coexpression of SYN and CHA was found in two ACA as well as in two LCC. Coexpression of SYN and N-CAM was detected in one case each of LCC and ASC. A positive combination of CHA and N-CAM was not present. Only three cases were positive for all three markers, and restricted to LCC-CL. Altogether, LCC-CL revealed 11/42 (26%) and LCC-ND 5/14 (36%) cases with neuroendocrine marker expression.

Tissue microarray evaluation: survival analysis

There was no significant difference in overall survival time when comparing NSCLC without neuroendocrine differentiation to NSCLC-ND (Fig. 2c). This remained unaffected by histological subtype, neuroendocrine marker type, adjuvant therapy, and recurring disease. A further clinical substratification for overall survival analysis was not feasible due to the many various settings of therapies (e.g., neoadjuvant, adjuvant, palliative; chemotherapy, radiotherapy, combination of both). Concerning the amount of positive markers, a significantly reduced survival time ($p=0.044$) was determined only for triple positive NSCLC-ND when compared with all other NSCLC. The former group consisted of only three cases, exclusively LCC-CLNE, two in pathological UICC (pUICC) stage IIIA and one in stage II. Analyzed only within the LCC group, this statistical significance was not apparent.

Discussion

The present study demonstrated that neuroendrocine differentiation is a common phenomenon in NSCLC, being present in 16% of cases overall, which is consistent with the commonly reported 10–20% [3]. This confirms the applied antibody panel as well as staining interpretation, calculated cutoff values, and the representativeness of the study material.

In accordance with previous reports, neuroendocrine differentiation was not associated with a significant difference in overall survival [10, 15]. Others, however, have reported contradictory results demonstrating decreased [16] as well as increased [17] survival times, particularly when smaller cohorts were analyzed, or the chosen antibodies did not meet current recommendations for diagnosis of neuroendocrine differentiation. To strengthen validity, the present study evaluated a large number of patients as recommended by Howe et al. and applied a standardized TMA platform [10]. TMA technique offers an ideal method to evaluate a large number of cases. Compared with standard viewing of slides, this approach reduces staining variations and minimizes observer differences since (1) all samples are processed and evaluated in one day, which minimizes biases due to staining variability and daily variations in the gaging of the observer, and (2) interpretation of immunostains is based on the findings within a well-defined small area of well-preserved tissue (and not immunohistochemical "hot spots") in which absolute cell counts can be easily assessed to determine the percentage of positively stained cells [18]. Quadruplicate cores, as analyzed here, improve accuracy compared with the usual duplicate core method and reduce microheterogeneity biases to a neglectable minimum [19].

Concerning prognostic relevance, the present data showed no correlation between histological subtype, neuroendocrine marker expression, and overall survival. Others, however, have linked ACA to a worse prognosis when neuroendocrine expression was present [16, 20]. LCC showed the highest rate of neuroendocrine differentiation, with three cases positive for all three neuroendocrine markers diagnostic of NSCLC-ND. All three patients had a short survival, which, primarily, may be attributed to their locally advanced stages at initial diagnosis. When examining neuro-

endocrine differentiation within the histological subtypes, LCC and ACA were those with the largest proportion of neuroendocrine differentiation which is in accordance with previous reports focusing on ACA [15, 21]. Other groups failed to define a correlation between neuroendocrine differentiation and histological NSCLC subtype [5, 10].

In our study, we had four groups of LCC, which resulted from a simple algorithm: either LCC-CL or LCC-ND by light microscopy, followed by the possible presence of neuroendocrine differentiation by immunohistochemistry, resulting in the additional groups LCC-CLNE and LCC-NE, respectively. Only LCC with immunohistochemical confirmation of neuroendocrine differentiation (LCC-CLNE and LCC-NE) were included in the group of NSCLC-ND. It has been stated that LCC-ND consistently demonstrates immunoreactivity for neuroendocrine markers [16], which was not the case here. Indeed, 5/14 (36%) of LCC with definite neuroendocrine features by light microscopy showed expression of neuroendocrine markers, thus representing the group with the highest proportion of cases with neuroendocrine phenotype, but, importantly, 9/14 (64%) of those tumors with definite neuroendocrine features by light microscopy (trabecular growth, rosettes, perilobular palisading patterns) were negative for all markers. This emphasizes the necessity of additional confirmation of neuroendocrine differentiation by immunohistochemistry using the immunhistochemical markers CHA, SYN, and N-CAM for the diagnosis LCC-NE, independent of neuroendocrine morphology by light microscopy, as required by the WHO [3]. We applied this approach to NSCLC subtypes other than LCC-ND for defining neuroendocrine differentiation since no separate guidelines are provided. LCCs with neuroendocrine differentiation are known to have a worse overall survival rate than stage-comparable NSCLCs without neuroendocrine differentiation and should benefit from a systemic adjuvant standard small cell lung cancer (SCLC)-based chemotherapy [22, 23]. Marchevsky et al. even claimed that LCC-NE and SCLC should be merged as a single group of high-grade neuroendocrine carcinomas [24]. A resulting debate, which occurred, was whether to exclude LCC with neuroendocrine differentiation from survival analysis. This is not a straightforward matter since two morphologically different groups were present within LCC demonstrating neuroendocrine differentiation (LCC-CLNE and LCC-NE). Complicating matters further is the group of LCC with light microscopical features of neuroendocrine differentiation though lacking immunohistochemical confirmation (LCC-ND). Which entity or entities deserve exclusion? Does a logical or validated approach exist? The present study aims at analyzing neuroendocrine differentiation in NSCLC since this entity is still controversial. Unfeasible comparison between studies is often due to differences regarding inclusion criteria, interpretation of results, and lack of generally accepted definitions. With this in mind, we used the current diagnostic criteria by the WHO to design our study [3]. We acknowledge that this is not optimal, considering the behavior of LCC with neuroendocrine differentiation. On the other hand, accurately following current recommendations has the advantage of reproducibility, comparability, and less bias, which is what we opted for here. From the clinical point of view, it would be worth studying a large collective of LCC-CLNE and LCC-NE, whether the response rates to chemotherapy and survival rates are similar. In our small series of 5 LCC-NE and 11 LCC-CLNE cases, we found no survival differences (data not shown).

Some of the previously mentioned differences between studies concerning prognostic value of phenotypic neuroendocrine differentiation in NSCLC may be due to inconsistencies of the panels of antibodies used. Another source of discrepancy is the determination of cutoff values for positive staining results and incorporation of staining intensity into “scores” [10]. Evidence suggests that staining intensity is particularly prone to variation between cases, runs, and batches due to different tissue preservation, applied batches, detection/amplification systems, and even to minimal changes in chromogen incubation duration [25]. Interestingly, by incorporating staining intensity to determine neuroendocrine differentiation, only two more cases would have been positive, raising the incidence by a mere 0.5%. This suggests that staining intensity may be disregarded when assessing neuroendocrine differentiation. Studies using the same antibodies have reported relative proportions of N-CAM> SYN>CHA [10]. In our series, however, SYN was the most frequently positive marker, followed by N-CAM and CHA. NSE revealed positive staining results comparable to SYN, which does not entirely reflect its reported low specificity [10]. PGP9.5, on the other hand, was positive in 58% of the specimens and should not be considered as part of a diagnostic panel when examining neuroendocrine expression due to obviously lacking specificity.

Why at all is it a matter of interest to discriminate NSCLC into two subentities characterized by neuroendocrine differentiation? Indeed, the entity NSCLC-ND has generated many controversial conclusions concerning survival time and responsiveness to therapy. We conclude that, in addition to classical light microscopy analysis, neuroendocrine immunohistochemical subdifferentiation of NSCLC is not of high importance in terms of clinical consequences at present, except for LCC-NE, in which cases with phenotypic expression of multiple neuroendocrine markers might be accompanied by a worse outcome. With the development of new targeted therapies, this insignificance may change, and more differentiated, tailored treatment modalities may aim at phenotypic profiles studied here.

Conflict of interest statement The authors declare that they have no conflict of interest.

References

1. Kamangar F, Dores GM, Anderson WF (2006) Patterns of cancer incidence, mortality, and prevalence across five continents: defining priorities to reduce cancer disparities in different geographic regions of the world. J Clin Oncol 24:2137–2150
2. Parkin DM, Whelan SL, Ferlay J et al (2002) Cancer incidence in five continents, vol VIII. IARC, Lyon
3. Travis W, Brambilla E, Müller-Hermelink H et al (2004) Pathology and genetics of tumours of the lung, pleura, thymus and heart. IARC, Lyon
4. Carles J, Rosell R, Ariza A et al (1993) Neuroendocrine differentiation as a prognostic factor in non-small cell lung cancer. Lung Cancer 10:209–219
5. Schleusener JT, Tazelaar HD, Jung SH et al (1996) Neuroendocrine differentiation is an independent prognostic factor in chemotherapy-treated nonsmall cell lung carcinoma. Cancer 77:1284–1291
6. Gajra A, Tatum AH, Newman N et al (2002) The predictive value of neuroendocrine markers and p53 for response to chemotherapy and survival in patients with advanced non-small cell lung cancer. Lung Cancer 36:159–165
7. Graziano SL, Mazid R, Newman N et al (1989) The use of neuroendocrine immunoperoxidase markers to predict chemotherapy response in patients with non-small-cell lung cancer. J Clin Oncol 7:1398–1406
8. Carnaghi C, Rimassa L, Garassino I et al (2001) Clinical significance of neuroendocrine phenotype in non-small-cell lung cancer. Ann Oncol 2:S119–S123
9. Segawa Y, Takata S, Fujii M et al (2009) Immunohistochemical detection of neuroendocrine differentiation in non-small-cell lung cancer and its clinical implications. J Cancer Res Clin Oncol 135:1055–1059
10. Howe MC, Chapman A, Kerr K et al (2005) Neuroendocrine differentiation in non- small cell lung cancer and its relation to prognosis and therapy. Histopathology 46:195–201
11. Attanoos RL (2000) Management of small biopsies in pulmonary disease. CPD Bull, Cell Pathol 2:138–141
12. Fiegl M, Hilbe W, Auberger J, Schmid T et al (2008) Twelve-year retrospective analysis of lung cancer—the TYROL study: daily routine in 1,424 patients (1995–2006). J Clin Oncol 26, abstract 19063
13. Hilbe W, Aigner K, Dittrich C et al (2007) Expert recommendations 2006 on the rationale for second-line therapy for non-small cell bronchial neoplasms. Wien Klin Wochenschr 119:259–266
14. Perkins NJ, Schisterman EF (2006) The inconsistency of "optimal" cutpoints obtained using two criteria based on the receiver operating characteristic curve. Am J Epidemiol 163:670–675
15. Ionescu DN, Treaba D, Gilks CB et al (2007) Nonsmall cell lung carcinoma with neuroendocrine differentiation—an entity of no clinical or prognostic significance. Am J Surg Pathol 31:26–32
16. Pelosi G, Pasini F, Sonzogni A et al (2003) Prognostic implications of neuroendocrine differentiation and hormone production in patients with stage I nonsmall cell lung carcinoma. Cancer 97:2487–2497
17. Petrovic M, Tomic I, Plavec G et al (2008) Neuron specific enolase tissue expression as a prognostic factor in advanced non small cell lung cancer. J BUON 13:93–96
18. Tzankov A, Went P, Zimpfer A et al (2005) Tissue microarray technology: principles, pitfalls and perspectives—lessons learned from hematological malignancies. Exp Gerontol 40:737–744
19. Camp RL, Charette LA, Rimm DL (2000) Validation of tissue microarray technology in breast carcinoma. Lab Invest 80:1943–1949
20. Hiroshima K, Iyoda A, Shibuya K et al (2002) Prognostic significance of neuroendocrine differentiation in adenocarcinoma of the lung. Ann Thorac Surg 73:1732–1735
21. Baldi A, Groger AM, Esposito V et al (2000) Neuroendocrine differentiation in non-small cell lung carcinomas. In Vivo 14:109–114
22. Rossi G, Cavazza A, Marchioni A et al (2005) Role of chemotherapy and the receptor tyrosine kinases KIT, PDGFRalpha, PDGFRbeta, and Met in large-cell neuroendocrine carcinoma of the lung. J Clin Oncol 23:8774–8785
23. Takei H, Asamura H, Maeshima A et al (2002) Large cell neuroendocrine carcinoma of the lung: a clinicopathologic study of eighty-seven cases. J Thorac Cardiovasc Surg 124:285–292
24. Marchevsky AM, Gal AA, Shah S et al (2001) Morphometry confirms the presence of considerable nuclear size overlap between "small cells" and "large cells" in high-grade pulmonary neuroendocrine neoplasms. Am J Clin Pathol 116:466–472
25. Atkins D, Reiffen KA, Tegtmeier CL et al (2004) Immunohistochemical detection of EGFR in paraffin-embedded tumor tissues: variation in staining intensity due to choice of fixative and storage time of tissue sections. J Histochem Cytochem 52:893–901

Virchows Arch (2009) 455:133–142
DOI 10.1007/s00428-009-0807-x

ORIGINAL ARTICLE

Differences in the expression of histamine-related genes and proteins in normal human adrenal cortex and adrenocortical tumors

Peter M. Szabó · Zoltán Wiener · Zsófia Tömböl · Attila Kovács · Péter Pócza · János Horányi · Janina Kulka · Peter Riesz · Miklós Tóth · Attila Patócs · Rolf C. Gaillard · András Falus · Károly Rácz · Peter Igaz

Received: 6 April 2009 / Revised: 28 May 2009 / Accepted: 18 June 2009 / Published online: 1 July 2009

Abstract Histamine is involved in the pathogenesis of several tumors; however, there are no data on its possible involvement in human adrenocortical tumorigenesis. The expression of genes and proteins involved in the biosynthesis (histidine decarboxylase, HDC), action (histamine receptors: HRH1–HRH4), and metabolism of histamine is largely unknown both in the normal human adrenal cortex and in adrenocortical tumors. In this study, we examined the expression of histamine-related genes and proteins and histamine content in normal adrenal cortex, benign adrenocortical adenomas, and malignant adrenocortical cancer (ACC). Fifteen normal adrenals and 43 tumors were studied. mRNA expression was examined by real time RT-PCR. Western-blotting and immunohistochemistry were used for the study of proteins. Tissue histamine content was determined by enzyme-linked immunosorbent assay. We found that all proteins involved in histamine biosynthesis and action are present both in the normal adrenal cortex and in the tumors studied. HDC expression and histamine content was highest in the normal tissues and lower in benign tumors, whereas it was significantly less in ACCs. HRH3 expression was significantly higher in ACC samples than in the other groups. Adrenocortical tumorigenesis might, thus, be characterized by reduced histamine biosyn-

P. M. Szabó · Z. Tömböl · M. Tóth · K. Rácz · P. Igaz (✉)
2nd Department of Medicine, Faculty of Medicine,
Semmelweis University,
1088 Budapest, Szentkirályi str. 46,
Hungary
e-mail: igapet@bel2.sote.hu

Z. Wiener · P. Pócza · A. Falus
Department of Genetics,
Cell and Immunobiology Faculty of Medicine,
Semmelweis University,
1089 Budapest, Nagyvárad square 4,
Hungary

A. Kovács · J. Kulka
2nd Department of Pathology Faculty of Medicine,
Semmelweis University,
1091 Budapest, Üllői str. 93,
Hungary

J. Horányi
1st Department of Surgery, Faculty of Medicine,
Semmelweis University,
Üllői str. 78,
1083 Budapest, Hungary

P. Riesz
Department of Urology, Faculty of Medicine,
Semmelweis University,
1082 Budapest, Üllői str. 78/B,
Hungary

A. Patócs
Molecular Medicine Research Group,
Hungarian Academy of Sciences and Semmelweis University,
1088 Budapest, Szentkirályi str. 46,
Hungary

R. C. Gaillard
Service d'Endocrinologie, Diabétologie et Métabolisme,
Centre Hospitalier Universitaire Vaudois,
1011 Lausanne, Rue de Bugnon 46,
Switzerland

A. Falus
Inflammation Biology and Immune Genomics Research Group,
Hungarian Academy of Sciences and Semmelweis University,
1089 Budapest, Nagyvárad square 4,
Hungary

thesis; furthermore, different adrenocortical tumor subtypes may show unique histamine receptor expression profiles.

Keywords Adrenal cortex · Adrenocortical tumor · Histamine · mRNA · Protein · Receptor

Abbreviations

ACC	Adrenocortical carcinoma
ACTH	Adrenocorticotropin
APA	Aldosterone producing adenoma
cAMP	Cyclic AMP
CPA	Cortisol-producing adenoma
DAO	Diamino-oxydase
DHEA	Dehydroepiandrosterone
DHEAS	Dehydroepiandrosterone sulfate
GAPDH	Glyceraldehyde-3-phosphate dehydrogenase
HDC	Histidine decarboxylase
HNMT	Histamine-*N*-methyltransferase
HRH1	Histamine receptor H1
HRH2	Histamine receptor H2
HRH3	Histamine receptor H3
HRH4	Histamine receptor H4
IA	Hormonally inactive adenoma
IFN-γ	Interferon-γ
IL-10	Interleukin-10
IL-12	Interleukin-12
PKA	cAMP-dependent protein kinase
PRKAR1A	Protein kinase A regulatory-subunit type-I alpha
QRT-PCR	Quantitative real-time RT-PCR

Introduction

The biogenic amine histamine is involved in the regulation of numerous physiological and pathological processes. Histamine has been implicated in the pathogenesis of several human tumors, e.g., malignant melanoma [1], breast [2], colon cancer [3–5], and pancreatic endocrine tumors [6]. In malignant melanoma and breast cancer tissues, histamine may act as an autocrine growth factor being secreted by the tumor cells themselves [1, 2]. Although there are some reports on the action of histamine on adrenal functioning, the relevance of histamine in normal adrenal gland physiology is not clear, and there are no data on its possible involvement in adrenal tumorigenesis.

Adrenal tumors are common; their prevalence reaches up to 5–9% in pathological series [7]. More than 80% of adrenal tumors are of adrenocortical origin. The majority of these tumors are hormonally inactive benign adenomas, but cortisol- or aldosterone-producing adenomas are also found. If left untreated, hormonally active benign tumors are associated with significant morbidity and mortality [8]. Adrenocortical carcinoma (ACC) is rare, and its prognosis is poor with an overall 5-year survival below 30% [9–11]. The pathogenesis of sporadic adrenocortical tumors is poorly elucidated. In this study, we attempted to characterize the expression of histamine-related genes and proteins both in normal and neoplastic adrenocortical tissues.

Histamine is synthesized from the amino acid L-histidine by the single enzyme histidine decarboxylase (HDC). Its action is realized via four receptors: histamine receptor 1 (HRH1) is a major regulator of allergic responses, histamine receptor 2 (HRH2) is involved in the regulation of gastric acid secretion, and both of them are involved in many immune processes and tumorigenesis, as well. Histamine receptor 3 (HRH3) is primarily localized on the presynaptic membranes of central nervous system neurons. The recently discovered histamine receptor 4 (HRH4) is mostly involved in immune cell migration and inflammatory mediator release [12]. Two enzymes, the diamino-oxydase (DAO) and histamine-*N*-methyltransferase (HNMT), are involved in histamine degradation [13, 14].

Most available data on the relevance of adrenal histamine involve adrenomedullary actions. The first described action of histamine on adrenal functioning was the stimulation of catecholamine secretion that did not depend on splanchnic nerve innervation [15]. Histamine was found to be present in the adrenal gland: immunhistochemical studies of adult rat adrenal glands localized histamine to clusters of noradrenergic chromaffin cells in the medulla but failed to detect it in nerve fibers, adrenaline-containing chromaffin, and cortical cells [16]. HDC immunoreactivity has been documented both in normal human adrenomedullary chromaffin cells, as well as in human adrenomedullary tumors (phaeochromocytomas) [17]. Histamine evoked catecholamine secretion from bovine chromaffin cells via HRH1 [18]. HRH2 mRNA expression was detected in guinea pig adrenal medulla [19], but there is no evidence for expression of functional HRH3 and HRH4 receptors in chromaffin cells [20].

The expression pattern of histamine-related genes and proteins in the normal human adrenal cortex and adrenocortical tumors is unknown.

Materials and methods

Tissue samples

The study, approved by the Ethical Committee of the Hungarian Health Council, involved 58 tissue samples: 18 hormonally inactive adenomas (all from females, mean

age=49.4, range=30.8–61.8 years), eight cortisol-producing adenomas (CPA; seven females and one male, mean age=38.3, range=24–46.8 years), nine aldosterone-producing adenomas (APA; six females and three males, mean age=45.9, range=20.7–69.1 years), eight ACC (six females and two males, mean age=55.9, range=26.1–70.4 years), and 15 normal adrenal tissues (11 females and four males, mean age=49.7, range=19.3–67.9 years). All patients were of Caucasian descent. All malignant adrenocortical tumors were cortisol-secreting. Only tumor samples where clinical, laboratory, and histological data were all available and clear-cut were included in our study. Normal adrenocortical tissues were obtained from adrenal glands removed during operations for kidney tumors.

Immunohistochemistry

Formalin-fixed and paraffin-embedded tissues were cut and mounted onto SuperFrost slides. Specimens were deparaffinized, then two slides were stained with hematoxylin–eosin and toluidine blue [21]. Immunohistochemistry was carried out on a Ventana ES automated staining system (Ventana Medical Systems, INC, Tucson, AZ, USA) according to the instructions of the manufacturer. Rabbit polyclonal anti-human HRH1 (H1R12-A), HRH2 (H2R21-A), HRH3 (H3R32-A), HRH4 (H4R41-A; Alpha Diagnostic International, San Antonio, TX), HDC (ab37291), HNMT (ab63147; Abcam plc, Cambridge, UK), and DAO (WH0001610M1; Sigma–Aldrich Corp., MO, USA) antibodies at a dilution of 1:100 and iWIEW DAB Detection Kit (Ventana Medical Systems, INC, Tucson, AZ, USA) for automatization were used. Cleaned coverslips were mounted on the slides using Tissue Tek GLC Class Coversiper with GLC Mounting Medium (Sakura Finetek Europe B.V., Zoeterwoude, The Netherlands). Immunostainings were examined by a Nikon Eclipse i80 microscope (Nikon Spot Advanced Program, Nikon, Tokyo, Japan). Normal human colon and antral stomach tissues were used as positive controls. All negative controls, performed by omitting the primary antibodies, demonstrated negligible background.

RNA isolation, reverse transcription, and QRT-PCR

Samples were snap frozen in liquid nitrogen immediately after adrenalectomy. Total RNA was isolated using RNeasy Lipid tissue Mini Kit (Qiagen GmbH, Hilden, Germany). RNA quality was verified by an Agilent 2100 bioanalyzer (Agilent Tech. Inc., Santa Clara, CA, USA). Samples with RNA integrity number above 7.0 were used. One microgram RNA was transcribed to cDNA using high capacity cDNA Reverse Transcription Kit (Applied Biosystems, Foster City, CA, USA). QRT-PCR was performed by TaqMan Fast Universal Master Mix on a 7500 Fast Real-Time PCR system according to the manufacturer's instructions. TaqMan assays were used as follows: HDC (Hs00157914_m1), human HRH1 (Hs00911670_s1), HRH2 (Hs00254569_s1), HRH3 (Hs00200610_m1), HRH4 (Hs0222094_m1), histamine-*N*-methytransferase (HNMT, Hs00199373_m1), DAO (Hs00266481_m1), and glyceraldehyde-3-phosphate dehydrogenase (GAPDH, Hs02758991_g1) as internal housekeeping gene (all materials from Applied Biosystems, Foster City, CA, USA). All samples were run in triplicate. Normalized signal levels were calculated using the comparative CT ($\Delta\Delta$CT) [22] method relative to GAPDH according to the manufacturer's instructions (SDS program, Applied Biosystems, Foster City, CA, USA).

Western-blotting

Tissue samples were lysed in lysis buffer (10 nM Tris-HCL (pH 8.0), 10 mg/ml leupeptin, 0.5 mM EGTA, 25 mM PMSF, 2% NaF, 1% Triton X-100, 2% Na-orthovanadate). Fifteen-microgram heat-denaturized and β-mercaptoethanol-treated protein samples were loaded on 10% Ready Gel Tris-HCl gels (Bio-rad Lab., Hercules, CA, USA) and blotted to PVDF-membranes (Bio-rad Lab., Hercules, CA, USA). Membranes were probed with rabbit anti-human polyclonal HRH1 (H1R12-A), HRH2 (H2R21-A), HRH3 (H3R32-A), HRH4 (H4R41-A; all from Alpha Diagnostics Int., San Antonio, TX, USA), HDC (ab37291), and HNMT (ab63147; Abcam plc, Cambridge, UK) antibodies at concentrations of 1 μg/ml. Secondary peroxidase-conjugated goat polyclonal anti-rabbit IgG (Sigma–Aldrich Corp., MO, USA) antibodies were used at a concentration of 0.1 μg/ml. As loading control, rabbit anti-β-actin antibody (A5060; Sigma–Aldrich Corp., MO, USA) was applied (concentration=1 μg/ml). Specificity of primary antibodies has been previously checked with blocking peptides [3]. Relative protein expression levels were calculated from X-ray film densitometry data normalized to the respective β-actin bands. Image analysis was done using Fluorchem 8000 image analysis platform and the Chemilmager 5500 image analysis software package (Alpha Innotech Corp., San Leandro, CA, USA).

ELISA

Histamine was extracted from 100 mg of homogenized sample by 0.2 M perchloric acid and 1 M potassium borate. All measurements of histamine concentration were performed using EIA Histamine Kit (Beckman Coulter, Inc., Fullerton, CA, USA) according to the manufacturers' instructions. Absorbance was measured at 405 nm on a microplate reader (Multiskan MS, Labsystems, Finland).

Detection of mast cells

The presence of mast cells was examined by toluidine blue staining [21] and CD117 (c-kit receptor) immunohistochemistry [23, 24] in normal adrenal tissue samples. Immunohistochemistry was performed as above.

Statistical analysis

Results were analyzed by one-way ANOVA with Scheffé post hoc test using the STATISTICA 7 and Microsoft EXCEL softwares (Microsoft Inc., Redmond, WA, USA).

Results

Immunohistochemistry of histamine-related proteins in normal adrenocortical tissues

HDC was detected in all three layers of the adrenal cortex (zona glomerulosa, fasculata, and reticularis; Fig. 1a).

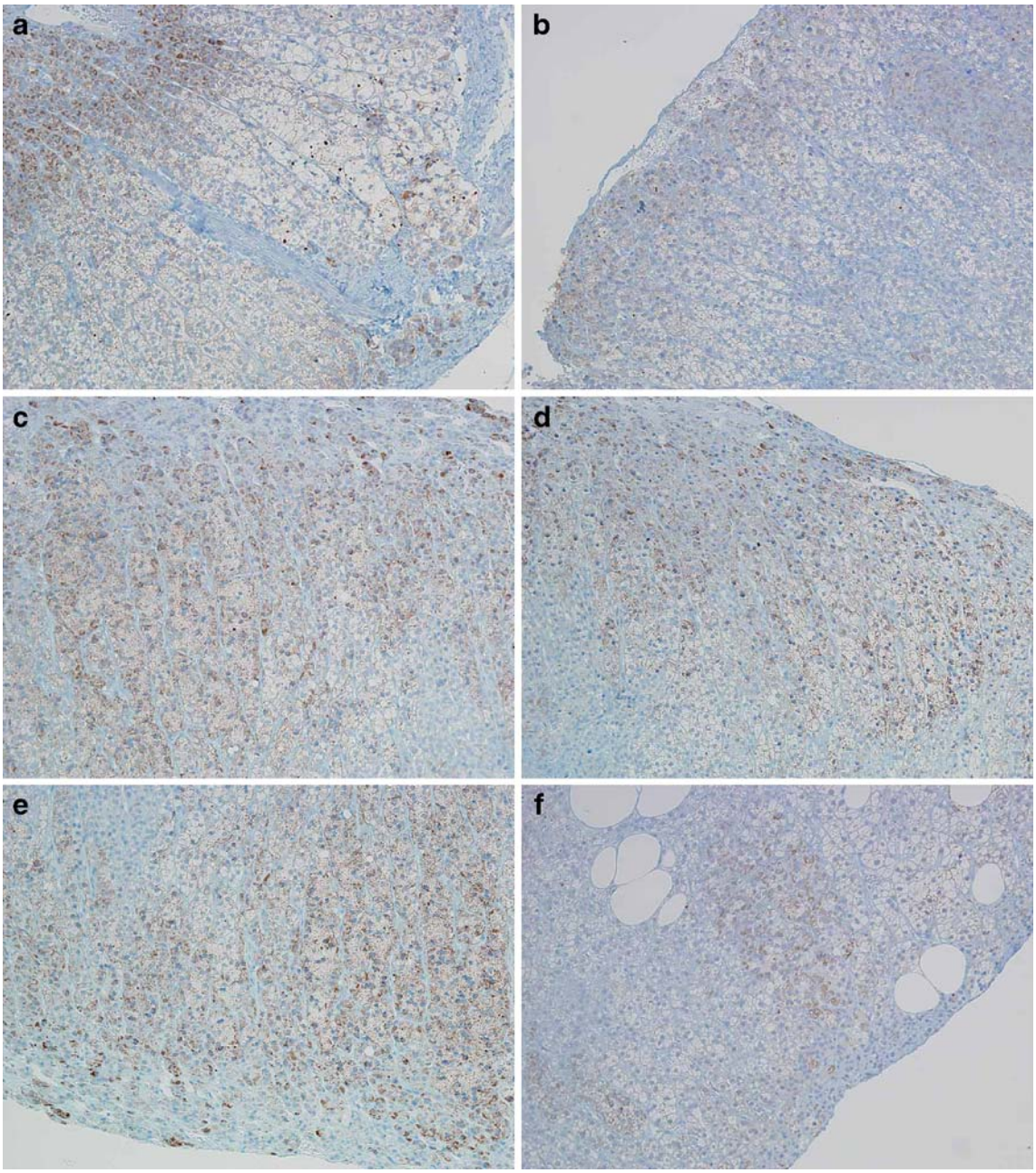

Fig. 1 Immunohistochemistry of histamine-related proteins in the normal adrenal cortex (representative images). **a** HDC, **b** HRH1, **c** HRH2, **d** HRH3, **e** HRH4, **f** HNMT (magnification ×20)

HRH1 immunohistochemistry showed focal staining in all adrenocortical layers (Fig. 1b). HRH2 and HRH3 were positive in the fasciculata and reticularis layers, but they were absent from the zona glomerulosa (Fig. 1c, d). HRH4 showed focal staining in the zona fasciculata (Fig. 1e). HNMT was colocalized with HDC in all three layers (Fig. 1f). DAO was undetectable (data not shown).

The pattern of HDC and HNMT immunohistochemistry was dot-like cytoplasmic. HRH1 and HRH2 immunohistochemistry revealed diffuse cytoplasmic staining, whereas HRH3 and HRH4 expression was dot-like. Available literature data on HRH1 and HRH2 expression in epithelial and mesenchymal cells show similar staining patterns (e.g., basolateral cytoplasmic in gastric epithelial cells and dot-like cytoplasmic in chondrocytes) [25, 26].

Having confirmed the presence of all proteins involved in histamine physiology in the normal adrenal cortex at the protein level, we next examined their mRNA and protein expression in adrenocortical tumors.

Expression of HDC and histamine content in adrenocortical tumors

HDC expression was detected in all examined tumors both at the mRNA and protein levels. Both quantitative real-time PCR and Western-blotting showed that the expression of HDC mRNA and protein was the highest in the normal adrenal cortex and benign hormonally inactive adenomas, somewhat lower in hormone-producing adenomas, whereas significantly lower expression was found in the ACC group (Fig. 2a–c). Immunohistochemical analysis revealed the presence of HDC in both benign and malignant tumor cells (Fig. 2e, f). Having proven the presence and different expression of the histamine biosynthetic enzyme HDC in adrenocortical samples, we next examined whether histamine content (by ELISA) of normal and neoplastic adrenocortical tissues was different. Parallel to the results of HDC mRNA and protein expression, histamine content was significantly lower in all tumor samples compared to normal adrenocortical tissues (Fig. 2d).

Histamine receptors in adrenocortical tumors

Quantitative RT-PCR and Western-blotting studies failed to demonstrate any significant differences in the expression of HRH1 (Fig. 3a, b). Expression of HRH2 was significantly lower in CPA and APA (Fig. 3c, d) and HRH4 showed significantly lower expression in CPA compared to normal adrenocortical tissues and other tumors (Fig. 3g, h). HRH3 expression was significantly higher both at the mRNA and protein levels in malignant tumors than in both normal tissues and benign tumors (Fig. 3e, f and 4). All types of histamine receptors were detected in adrenocortical tumor cells by immunohistochemistry (data not shown).

Histamine metabolizing enzymes

HNMT was detected both by Western-blotting and immunohistochemistry; however, no differences in expression were found either at the mRNA or protein levels (Fig. 3i, j). DAO was undetectable both at the mRNA level and by immunohistochemistry (data not shown).

Detection of mast cells

We have not detected metachromatic cells characteristic for mast cells by toluidine blue staining and only very few c-kit-positive cells were found by immunohistochemistry (data not shown).

Discussion

The present study provides novel data on the expression of histamine-related genes and proteins, and histamine content in the normal human adrenal cortex and adrenocortical tumors. We demonstrated the expression of HDC, HNMT, and all histamine receptors both at the mRNA and protein levels in the normal adrenal cortex and compared these data to those observed in various benign and malignant adrenocortical tumor subtypes. We found significant differences in HDC expression, histamine content, and receptor expression profiles.

Only few studies on the adrenocortical actions of histamine have been reported to date, and these presented contradictory results [27–30] that may be in part due to species differences. Yoshida et al. failed to detect any effect of histamine on basal cortisol secretion of isolated bovine adrenocortical cells; however, if co-cultured with bovine adrenomedullary cells, histamine dose-dependently induced cortisol secretion acting indirectly via the stimulation of adrenomedullary catecholamine secretion [27]. In another study, however, performed on isolated human adrenocortical cell cultures without adrenomedullary cells, histamine decreased aldosterone and cortisol and increased dehydroepiandrosterone sulfate (DHEAS) production [28]. When histamine was administered together with adrenocorticotropin (ACTH), it increased ACTH-stimulated DHEA production, decreased ACTH-stimulated cortisol and aldosterone production, and did not affect ACTH-stimulated DHEA levels [29]. The molecular mechanism of these actions was unclear, but a direct action of histamine on adrenocortical cells may be supposed. There have been no available data on the expression of histamine receptors in the normal human adrenal cortex.

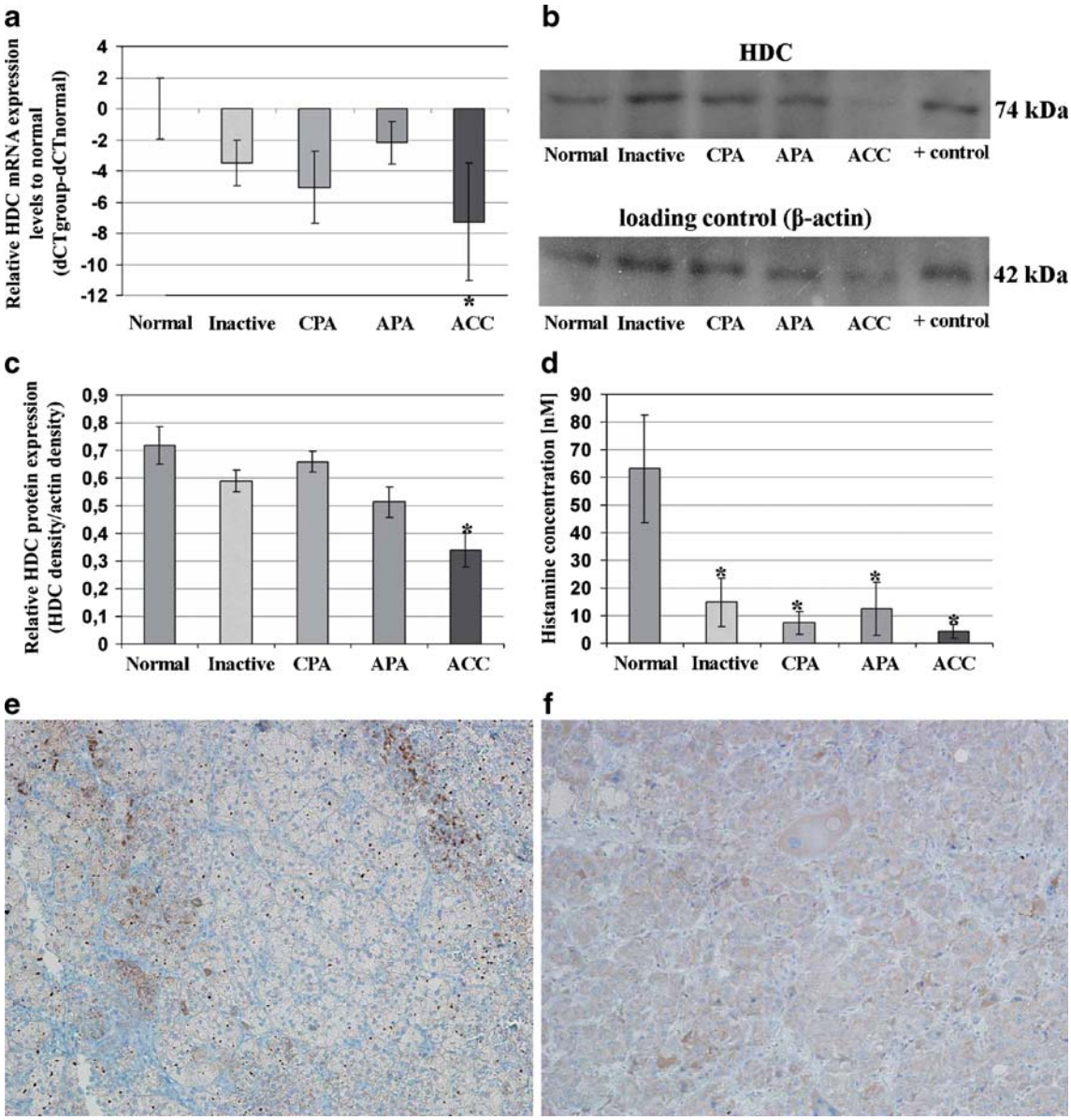

Fig. 2 Expression of HDC (**a** quantitative RT-PCR results expressed as ΔΔCT values relative to normal samples, **b** results of a representative Western-blotting experiment, **c** densitometric analysis of Western-blotting results using β-actin as loading control) and histamine content (**d**) in adrenocortical tumors. Representative images of HDC immunohistochemistry in a cortisol-producing benign (**e**) and malignant (**f**) tumor (magnification ×20). Mean±SE. *$p<0.05$,+*control* positive control (mRNA from antral stomach mucosa)

Our study may present a possible basis for these phenomena, as all histamine receptors were detected in adrenocortical cells. It seems, therefore, likely that histamine may directly influence the functioning of the human adrenal cortex without the intervention of adrenomedullary cells. Previous reports indicated that HRH1 may be implicated in the regulation of steroid hormone production in normal adrenocortical cells [28, 29]. We identified HRH1 on both normal and neoplastic adrenocortical cells; however, no difference was noted in HRH1 expression in the tissues studied.

HDC immunoreactivity has been described both in rat and human adrenomedullary chromaffin cells [16, 17]. Our results show that all three layers of the adrenal cortex harbor HDC-positive adrenocortical cells, as well. In addition, the quantity of HDC-positive cells in our samples was invariably much higher in the cortex than in the medulla (data not shown).

Mast cells are considered to be the major cellular source of histamine in most tissues [31]. In the rat adrenal gland, mast cells have been detected in the adrenal capsule. ACTH appears to increase adrenal blood flow via the induction of

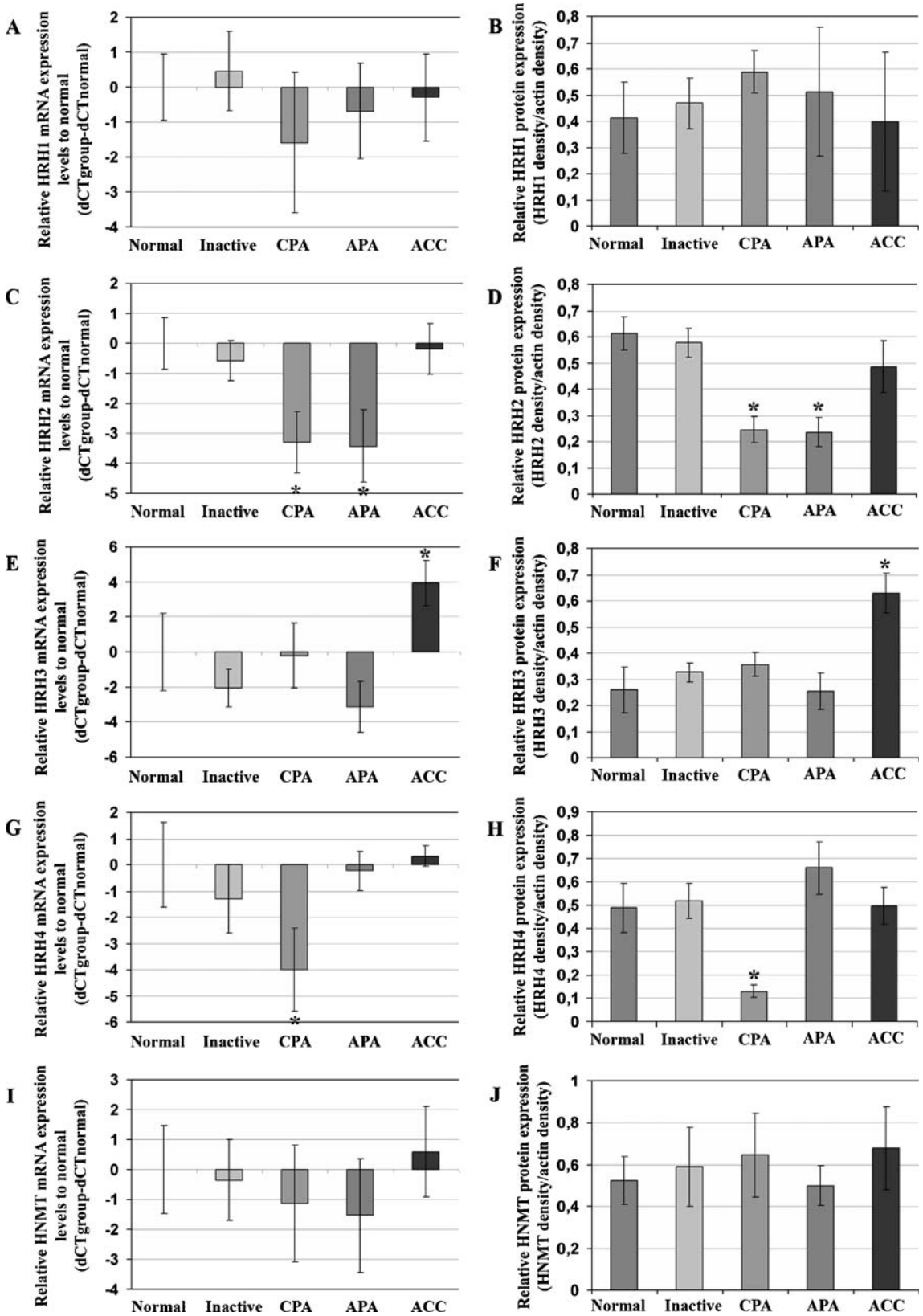

Fig. 3 Expression of histamine receptors and HNMT in adrenocortical tumors. Results of quantitative RT-PCR expressed as ΔΔCT values relative to normal samples (**a** HRH1, **c** HRH2, **e** HRH3, **g** HRH4, **i** HNMT). Densitometric analysis of Western blots using β-actin as loading control (**b** HRH1, **d** HRH2, **f** HRH3, **h** HRH4, **j** HNMT). Mean±SE. *$p<0.05$

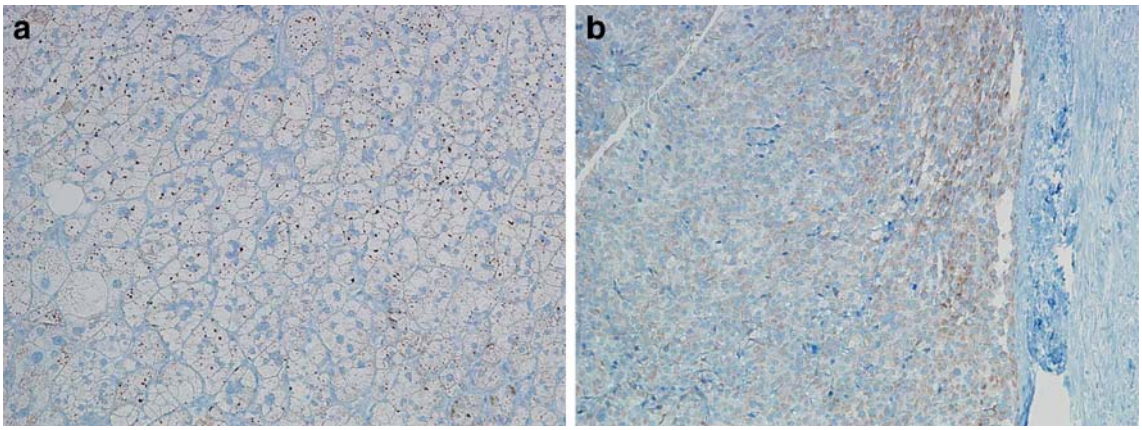

Fig. 4 Immunohistochemistry for HRH3 in a representative benign CPA (**a**) and an ACC (**b**) (magnification ×20)

mast cell degranulation. Both mast cell-derived histamine and serotonin may be implicated in this phenomenon [32]. Lefebvre et al. detected isolated, perivascular mast-like cells in the human adrenal cortex [33]. Serotonin secreted by these cells stimulated adrenocortical cortisol secretion and may, thus, be implicated in the paracrine regulation of cortisol release [33].

In the study by Aiba et al., abundant mast cells were found in a rare 11-deoxycorticosterone-producing adrenocortical tumor but were absent from CPAs. Few mast cells were identified in some normal adrenocortical tissues and several in APA samples [34]. Serotonin released by mast-like cells in APAs may exert a tonic stimulatory effect on aldosterone secretion and may, thus, be implicated in the pathophysiology of these tumors [35].

In contrast with serotonin that seems to be exclusively produced by intraadrenal mast-like cells in the normal adrenal cortex [33], our studies show that the histamine biosynthetic enzyme HDC is mostly expressed by the adrenocortical cells. The regulation of secretion of these two major biogenic amines, thus, seems to be different in the adrenal cortex.

We revisited the question of mast cell presence in the normal adrenal cortex both by toluidine blue staining [21] as well as c-kit (CD117) immunohistochemistry that is regarded as a specific detection method for mast cells [23, 24]. Only few c-kit-positive cells were found in our samples. Zhang et al. failed to detect c-kit-positive cells in the normal adrenal cortex [36]. Moreover, histamine content in APA samples (that were previously shown to harbor several mast cells [34]) has been significantly inferior to that in normal adrenocortical samples. This may support our hypothesis that mast cells do not represent a major source of histamine either in the normal cortex or in adrenocortical tumors. It can, therefore, be concluded that adrenocortical cells may be an important source of adrenal histamine in humans.

Histamine is involved in the pathogenesis of several tumors. These effects are realized via both direct histamine–tumor interactions and indirect tumor–stroma interactions [2]. In human melanoma cell lines, histamine may act as an autocrine growth factor inducing tumor progression via HRH1 and HRH2 [37]. In transgenic BF16-F10 melanoma cells, higher HDC expression induced tumor progression in vivo [38]. Furthermore, histamine may also influence tumor progression via modulation of antitumor immunity. Histamine may dysregulate the local balance between Th1, Th2, and Treg lymphocytes in neoplastic tissues [39]. Systematic histamine treatment decreased Th1-promoting IL-12 and IFN-γ expression and increased Th2-facilitating IL-10 expression in murine colorectal tumor implants [40].

HDC immunoreactivity was detected in all adrenocortical tumors studied, and malignant adrenocortical cancer tissues were characterized by significantly decreased HDC expression. Histamine content was significantly lower in both benign and malignant tumors. Reduced expression of some other genes and proteins has already been described in ACC (e.g., aldo-keto reductase family 1, member B1 (*AKR1B1*) and *novH*) that, together with the loss of HDC expression, may be interpreted as signs of loss of differentiation [41].

Remarkable differences in histamine receptor expression were also noted. Benign hormone-secreting adenomas (CPA and APA) displayed significantly lower HRH2 expression, and HRH4 was significantly lower in CPA than in hormonally inactive benign tumors or ACC. The marked overexpression of HRH3 (10-fold relative to normal) in ACC that is a non-neuronal tumor is noteworthy.

Signaling of histamine receptors involves mainly G-protein-mediated pathways. HRH2 is primarily associated with cyclic AMP (cAMP) accumulation, whereas HRH3 and HRH4 activation mostly inhibits adenylate cyclase activity [42, 43]. Alterations of the ACTH-cAMP-PKA pathway may be involved in adrenocortical tumorigenesis, but several contradictory findings have been reported to

date [44]. Germline mutations of the *PRKAR1A* gene were identified in Carney complex involving primary pigmented nodular adrenocortical disease [45].

If the relative underexpression of HRH2 in CPA and APA, together with the overexpression of HRH3 in cortisol-secreting ACCs, were considered, one might have the impression that histamine might be associated with reduced cAMP signaling in hormone-secreting tumors. It should also be taken into consideration, however, that the histamine content in all tumors was significantly lower than in normal tissues, and no studies on histamine receptor signaling in adrenocortical tissues have been performed to date.

In contrast with other neoplasms, where histamine seems to act in a tumor-promoting manner (malignant melanoma, gastric, and colorectal cancer), we found decreased histamine content and HDC expression in malignant tumors. It is, therefore, likely that the action of histamine is different in tumors of various organs. The significant differences among histamine receptor expression patterns may also have pathogenetic relevance; however, it is very difficult to interpret these findings without the mastery of histamine effects on adrenal functioning and gene expression in normal and neoplastic adrenocortical cells. Further, in vitro studies on adrenocortical cell cultures and cell lines are necessary to elucidate the physiological and pathophysiological relevance of histamine.

In conclusion, these findings raise the possibility that histamine might be involved in the pathogenesis of adrenocortical tumors. Expression of histamine-related genes and proteins was detected in both normal and neoplastic adrenocortical tissues; thus, the whole histaminergic machinery including biosynthetic and degrading enzymes as well as histamine receptors were found to be present. Since histamine mainly acts in a paracrine fashion, its secretion by adrenocortical cells might influence steroid biosynthesis, adrenocortical blood flow [30, 32], immune response, etc. Further, experimental studies (e.g., actions of histamine receptor agonists and antagonists on adrenocortical cancer cell lines) are needed to clarify the relevance of histamine in the normal adrenal cortex and to examine the consequences of decreased histamine biosynthesis and altered receptor repertoire in adrenocortical tumor development.

Acknowledgements Hungarian Ministry of Health 089/2006, Semmelweis University Research Grant, Hungarian Scientific Research Fund (OTKA) PD72306, Swiss National Fund (FNRS) 3200BO-105657/1) and Fondation pour la Recherche en Endocrinologie, Diabétologie et Métabolisme. Attila Patócs MD PhD is a recipient of a János Bolyai Research Grant. The authors would also like to thank Dr. Gábor L. Kovács (National Health Center, Budapest, Hungary) for supplying some tissue samples.

Conflict of interest The authors have no conflict of interest to report.

References

1. Tomita K, Nakamura E, Okabe S (2005) Histamine regulates growth of malignant melanoma implants via H2R receptors in mice. Inflammopharmacol 13:281–289
2. Medina V, Croci M, Crescenti E et al (2007) The role of histamine in human mammary carcinogenesis: H3R and H4R receptors as potential therapeutic targets for breast cancer treatment. Cancer Biol Ther 7:28–35
3. Boer K, Helinger E, Helinger A et al (2008) Decreased expression of histamine H1R and H4R receptors suggests disturbance of local regulation in human colorectal tumors by histamine. Eur J Cell Biol 87:227–236
4. Tomita K, Izumi K, Okabe S (2003) Roxatidine- and cimetidine-induced angiogenesis inhibition suppresses growth of colon cancer implants in syngeneic mice. J Pharmacol Sci 93:321–330
5. Morris DL, Adams WJ (1995) Cimetidine and colorectal cancer–old drug, new use? Nat Med 1:1243–1244
6. Tanimoto A, Matsuki Y, Tomita T et al (2004) Histidine decarboxylase expression in pancreatic endocrine cells and related tumors. Pathol Int 54:408–412
7. Koch CA, Pacak K, Chrousos GP (2002) The molecular pathogenesis of hereditary and sporadic adrenocortical and adrenomedullary tumors. J Clin Endocrinol Metab 87:5367–5384
8. Terzolo M, Bovio S, Pia A et al (2005) Midnight serum cortisol as a marker of increased cardiovascular risk in patients with a clinically inapparent adrenal adenoma. Eur J Endocrinol 153:307–315
9. Assié G, Antoni G, Tissier F et al (2007) Prognostic parameters of metastatic adrenocortical carcinoma. J Clin Endocrinol Metab 92:148–154
10. Libé R, Fratticci A, Bertherat J (2007) Adrenocortical cancer: pathophysiology and clinical management. Endcrine-Related Cancer 14:13–28
11. Patalano A, Brancato V, Mantero F (2009) Adrenocortical cancer treatment. Horm Res 71:99–104
12. Huang JF, Thurmond RL (2008) The new biology of histamine receptors. Curr Allergy Asthma Rep 8:21–27
13. Chanda R, Ganguly AK (1995) Diamine-oxidase activity and tissue di- and poly-amine contents of human ovarian, cervical and endometrial carcinoma. Cancer Lett 89:23–28
14. Pacifici GM, Donatelli P, Giuliani L (1992) Histamine N-methyl transferase: inhibition by drugs. Br J Clin Pharmacol 34:322–327
15. Kellaway CH, Cowell SJ (1922) On the concentration of the blood and the effects of histamine in adrenal insufficiency. J Physiol 57:82–99
16. Häppölä O, Soinila S, Päivärinta H et al (1985) Histamine-immunoreactive endocrine cells in the adrenal medulla of the rat. Brain Res 339:393–396
17. Matsuki Y, Tanimoto A, Hamada T et al (2003) Histidine decarboxylase expression as a new sensitive and specific marker for small cell lung carcinoma. Mod Pathol 16:72–78
18. Marley PD, Thomson KA, Jachno K et al (1991) Histamine-induced increases in cyclic AMP levels in bovine adrenal medullary cells. Br J Pharmacol 104:839–846
19. Traiffort E, Vizuete ML, Tardivel-Lacombe J et al (1995) The guinea pig histamine H2 receptor: gene cloning, tissue expression and chromosomal localization of its human counterpart. Biochem Biophys Res Commun 211:570–577
20. Marley PD (2003) Mechanisms in histamine-mediated secretion from adrenal chromaffin cells. Pharmacol Ther 98:1–34
21. Horny HP, Ruck P, Kröber S et al (1997) Systemic mast cell disease (mastocytosis). General aspects and histopathological diagnosis. Histol Histopathol 12:1081–1089

22. Livak KJ, Schmittgen TD (2001) Analysis of relative gene expression data using real-time quantitative PCR and the 2(-Delta Delta C(T)) Method. Methods 25:402–408
23. Galli SJ, Tsai M, Wershil BK (1993) The c-kit receptor, stem cell factor and mast cells. What each teaching us about the others. Am J Pathol 142:965–974
24. Shukla SA, Veerappan R, Whittimore JS et al (2006) Mast cell ultrastructure and saining in tissue. Methods Mol Biol 315:63–76
25. Fukushima Y, Ohmachi Y, Asano T et al (1999) Localization of the histamine H2 receptor, a target for antiulcer drugs, in gastric parietal cells. Digestion 60:522–527
26. Tetlow LC, Wooley DE (2005) Histamine, histamine receptors (H1 and H2) and histidine decarboxylase expression by chondrocytes of osteoarthritic cartilage: an immunohistochemical study. Rheumatol Int 26:173–178
27. Yoshida T, Mio M, Tasaka K et al (1997) Histamine-induced cortisol secretion from bovine adrenocortical cells: co-cultured with bovine adrenomedullary cells. Jpn J Pharmacol 75:115–121
28. Orsó E, Szalay KS, Tóth IE et al (1995) Effect of histamine on corticosteroid secretion of isolated human and rat adrenocortical cells. Inflamm Res 44:S48–S49
29. Orsó E, Szalay KS, Fehér T (1997) Interaction of histamine with adrenocorticotropic hormone: a local modulatory role for adrenocortical androgen synthesis? Inflamm Res 46:S57–S58
30. Zhang DX, Gauthier KM, Campbell WB (2005) Mechanisms of histamine-induced relaxation in bovine small adrenal cortical arteries. Am J Physiol Endocrinol Metab 289:E1058–E1063
31. Krishnaswamy G, Ajitawi O, Chi DS (2006) The human mast cell: an overview. Methods Mol Biol 315:13–34
32. Hinson JP, Vinson GP, Kapas S et al (1991) The relationship between adrenal vascular events and steroid secretion: the role of mast cells and endothelin. J Steroid Biochem Mol Biol 40:381–389
33. Lefebvre H, Contesse V, Delarue C et al (1992) Serotonin-induced stimulation of cortisol secretion from human adrenocortical tissue is mediated through activation of a serotonin4 receptor subtype. Neuroscience 47:999–1007
34. Aiba M, Iri H, Suzuki H et al (1985) Numerous mast cells in an 11-deoxycorticosterone-producing adrenocortical tumor. Arch Pathol Lab Med 109:357–360
35. Lefebvre H, Cartier D, Duparc C et al (2002) Characterization of serotonin4 receptors in adrenocortical aldosterone-producing adenomas: in vivo and in vitro studies. J Clin Endocrinol Metab 87:1211–1216
36. Zhang PJ, Genega EM, Tomaszewsky JE et al (2003) The role of calretinin, inhibin, melan-A, BCL-2, and c-kit in differentiating adrenal cortical and medullary tumors: an immunohistochemical study. Mod Pathol 16:591–597
37. Falus A, Hegyesi H, Lázár-Molnár E et al (2001) Paracrine and autocrine interactions in melanoma: histamine is a relevant player in local regulation. Trends Immunol 22:648–652
38. Pós Z, Wiener Z, Pócza P et al (2008) Histamine suppresses fibulin-5 and insulin-like growth factor-II receptor expression in melanoma. Cancer Res 68:1997–2005
39. Jelinek I, László V, Buzás E et al (2007) Increased antigen presentation and T(h)1 polarization in genetically histamine-free mice. Int Immunol 19:51–58
40. Tomita K, Okabe S (2005) Exogenous histamine stimulates colorectal cancer implant growth via immunosuppression in mice. J Pharmacol Sci 97:116–123
41. Igaz P, Wiener Z, Szabó P et al (2006) Functional genomics approaches for the study of sporadic adrenal tumor pathogenesis. Clinical implications. J Steriod Biochem Mol Biol 101:87–96
42. de Esch IJ, Thurmond RL, Jongejan A et al (2005) The histamine H4 receptor as a new therapeutic target for inflammation. Trends Pharmacol Sci 26:462–469
43. Akdis CA, Simons FE (2006) Histamine receptors are hot in immunopharmacology. Eur J Pharmachol 533:69–76
44. Soon PS, McDonald KL, Robinson BG et al (2008) Molecular markers and the pathogenesis of adrenocortical cancer. Oncologist 13:548–561
45. Groussin L, Horvath A, Jullian E et al (2006) A PRKAR1A mutation associated with primary pigmented nodular adrenocortical disease in 12 kindreds. J Clin Endocrinol Metab 91:1943–1949

Virchows Arch (2009) 455:143–148
DOI 10.1007/s00428-009-0806-y

ORIGINAL ARTICLE

Lymphangiomatoid pattern in diffuse malignant mesothelioma of the pleura: a report of six cases

Ruchira Ruangchira-urai · Eugene J. Mark

Received: 30 March 2009 / Revised: 3 June 2009 / Accepted: 17 June 2009 / Published online: 18 July 2009

Abstract The multiplicity of epithelioid and mesenchymal forms of diffuse malignant mesothelioma includes patterns that may mimic another process. Identification of the multiplicity of patterns may help in the diagnosis of diffuse malignant mesothelioma. One pattern that has not been described is lymphangiomatoid. We observed six cases with ovoid or elongated or irregular anastomosing vascular-like spaces lined by flattened cells simulating lymphangioma. The luminal spaces could contain proteinaceous material simulating lymph but not erythrocytes. The cells lining the spaces were mesothelial by immunohistochemical staining. The lymphangiomatoid areas never constituted more than 40% of the area of the tumor on the slides. When seen in more solid areas of tumor, the lymphangiomatoid structures generally did not produce diagnostic difficulty. However, when seen at the edge of solid tumor or forming an irregular nodule or invading into adjacent adipose tissue, these lymphangiomatoid structures could be confusing. All six patients had been exposed to asbestos either by occupation or by spousal exposure. Three patients received chemotherapy. One patient died of diffuse malignant mesothelioma of the pleura.

Keywords Lymphangiomatoid · Diffuse malignant mesothelioma

R. Ruangchira-urai · E. J. Mark (✉)
Department of Pathology, Harvard Medical School,
Massachusetts General Hospital,
55 Fruit Street,
Boston, MA, USA 02114
e-mail: emark@partners.org

R. Ruangchira-urai
Department of Pathology, Siriraj Hospital, Mahidol University,
Bangkok, Thailand

Introduction

Diffuse malignant mesothelioma (DMM) can have epithelioid or mesenchymal attributes, and a combination of the two together is useful in the diagnosis. The epithelioid and mesenchymal aspects reflect the histogenesis of the mesothelial cell as it arises from the schizocoelom, whereby mesenchymal tissue separates to form a cavity and the resulting surface cells acquire both mesenchymal and epithelioid attributes.

The epithelioid forms include solid epithelioid areas, squamoid solid areas, stranding, complex lace-like network, papillae, cotyledonous structures, deciduoid cells, glomeruloid features, insular features, macrocysts, microcysts, jelly roll-like structures, lymphohistiocytoid forms, tubuloglandular structures, small cells, clear cells, foam cells, and rhabdoid cells [1-16]. Transitions between these epithelioid forms generally occur.

In the course of reviewing several hundred cases of malignant mesothelioma, we observed seven cases where a large portion of the tumor resembled lymphangioma to a degree that the pattern could lead to an erroneous consideration of a lymphatic proliferation including either lymphatic dilatation due to obstruction or lymphangiomatosis or lymphangioma.

A pattern resembling lymphangioma in DMM has not been described to our knowledge and constitutes this report.

Materials and methods

Four hundred and seventy-two cases of DMM reviewed in consultation form the basis for the data in this report. These cases were tabulated with an emphasis on distinctive

Table 1 Clinical features of six DMMs with lymphangiomatoid pattern

Case	Age/sex	Signs and symptoms	Radiological findings	Operative findings	Treatment	Exposure to asbestos
1	69/M	SOB	Rt pleural effusion and a pleural mass	Rt lung encased with thick and dense fibrous peel	Partial decortication; chemotherapy	Laborer and maintenance helper
2	55/M	SOB and nonproductive cough	Lt pleural effusion, pleural thickening and calcification	NA	Talc pleurodesis; radical extrapleural pneumonectomy; intraoperative heated chemotherapy	Household exposure through his father, who worked as a laborer Father's uncle with DMM Great uncle and aunt with asbestosis
3	74/M	SOB	Rt pleural effusion, circumferential nodular pleural thickening and bilat pleural plaques	Extensive pleural based nodules	NA	Laborer, seaman, carpenter, drywaller and tile installer
4	67/M	Dyspnea, weight loss, and recurrent pleural effusion	Pleural effusion	White deposits in pleura	Talc pleurodesis; chemotherapy	Laborer and paper machine worker
5	82/F	SOB	Rt pleural effusion and loss of volume at the lung base	Marked thickening pleura	NA (Died 4 months after Dx)	Exposed through her husband, who worked as a millwright and mechanic
6	72/M	SOB	Lt pleural effusion with pleural based masses and bilat plaques	NA	NA	Worked around boilers

Bilat bilateral, *DMMs* diffuse malignant mesotheliomas; *Dx* diagnosis; *F* female; *Lt* left; *M* male; *NA* not available; *Rt* right; *SOB* shortness of breath

patterns of growth of both epithelioid and mesenchymal forms of DMM. Six cases of DMM of the pleura showed lymphangioma-like areas and constitute the body of this report. A seventh case of a malignant mesothelioma of the peritoneum with such a pattern was also encountered. All seven cases were medical-legal in origin. As the slides could not be retained, we recorded detailed histologic description and digital photomicrographic images in addition to clinical history and treatment record and exposure to asbestos.

Immunohistochemical staining had been done at the original laboratory in all cases. Because of the multiple laboratories involved, a variety of markers were performed,

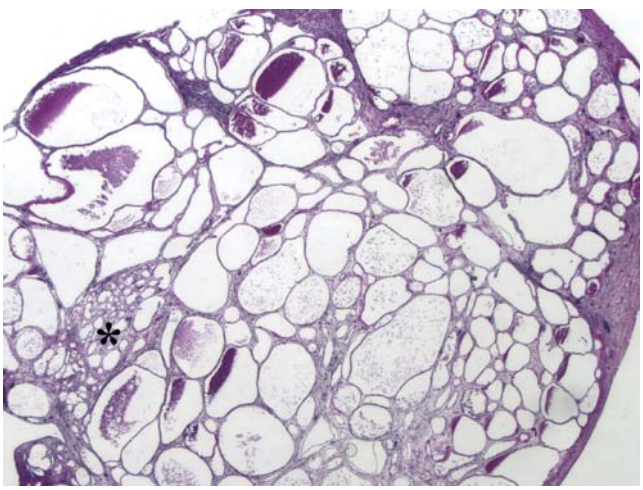

Fig. 1 Ovoid spaces lined by flattened cells and containing pink proteinaceous material mimicking lymphatic spaces. A small adenomatoid component (*asterisk*) is present

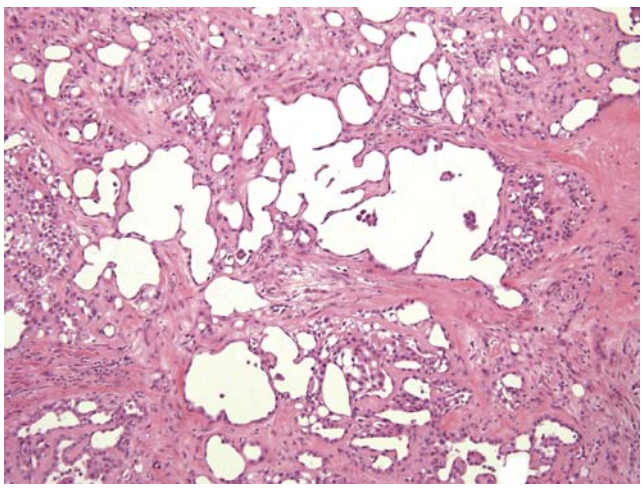

Fig. 2 Irregularly contoured and branching and serpentine structures lined by flattened cells

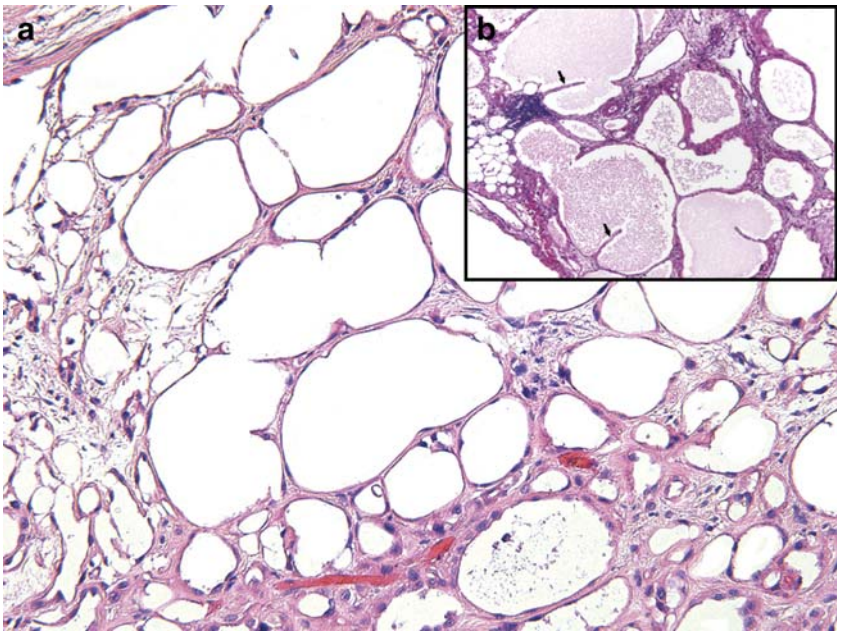

Fig. 3 Thin membranous structures forming vascular-like spaces, and filled with proteinaceous material (*inset*) and with valve-like structures (*arrows*)

including AE1/AE3, calretinin, CK5/6, CK7, CK20, WT-1, vimentin, MOC-31, D2-40, CEA, HBME-1, TTF-1, B72-3, BerEp4, CDX2, CD15, desmin, prostate-specific antigen, and prostate-specific acid phosphatase. Stains for keratins and calretinin were performed in all cases. Among other markers, staining for D2-40 was performed in two cases. The immunohistochemical stains were performed at multiple laboratories. Because these were cases referred for medical legal reasons, blocks were not available to perform additional staining, and this would include endothelial markers other than WT-1 and D2-40.

Results

Patient demographics and clinical findings

The summary of the patients' clinical features including occupational exposure to asbestos are given in Table 1. Five of the patients were males, and one was female. The age range was 55 to 82 years with a mean of 69.8 years. All patients presented with shortness of breath. Three patients were treated with chemotherapy, one with pleural decortication, and one with radical extrapleural pneumonectomy.

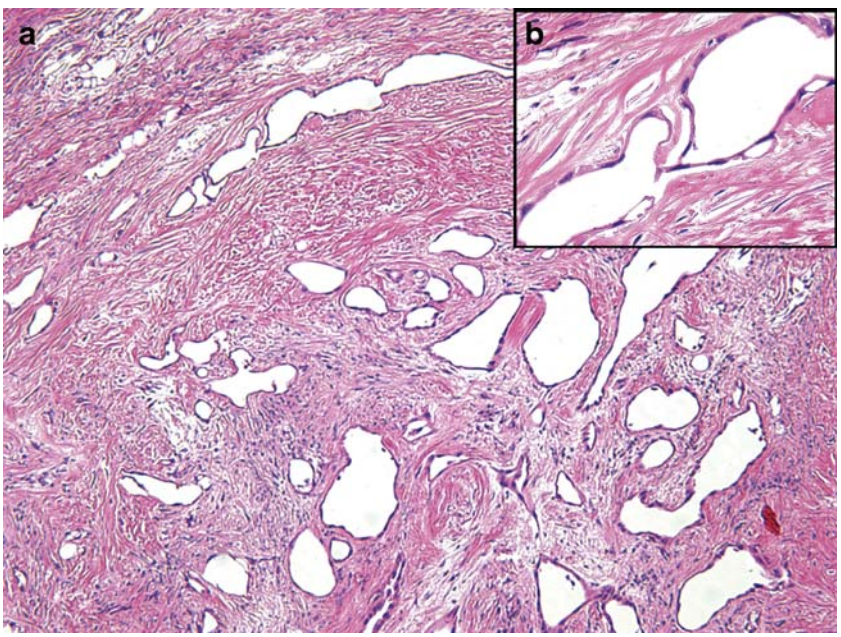

Fig. 4 Lymphangiomatoid structures within dense collagen and aligned along the axis of bundles of the collagen (*inset*), and lined by thin attenuated mesothelial cells

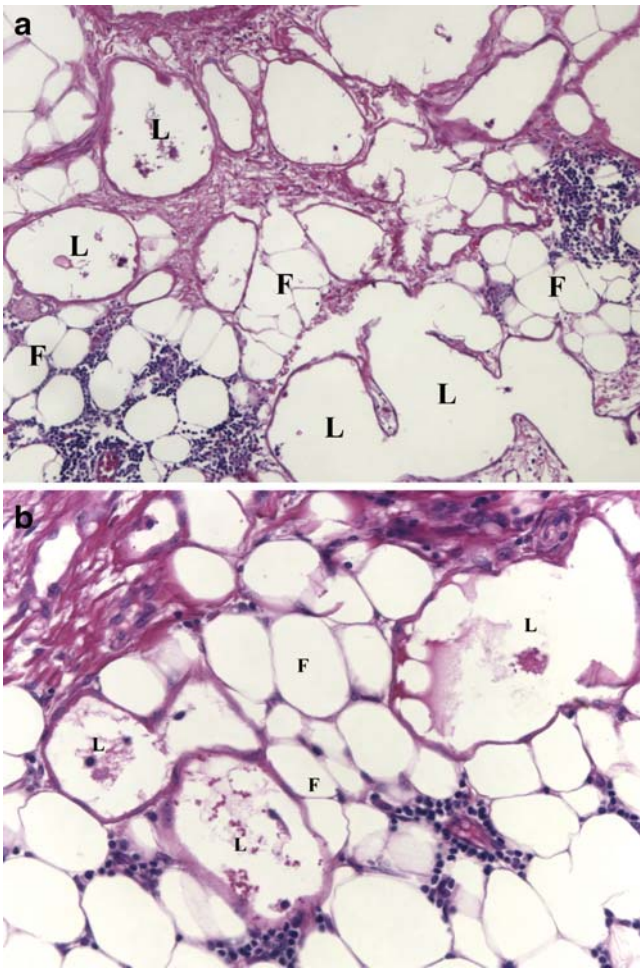

Fig. 5 Irregular but smoothly contoured structures resembling lymphangioma (**a**) invading into fat and causing fat necrosis with focal lymphocytic inflammation (**b**). *L* lymphangioma-like structures; *F* fat

All patients had pleural effusions on initial radiographic studies of the chest. Four of the patients had either a pleural mass or pleural thickening. Initial pathological diagnosis was made on specimens obtained by thoracoscopic biopsy in three patients, wedge biopsy of pleura and lung in one, pleural decortication in one, and radical extrapleural pneumonectomy in one. Follow-up is short. Six patients were alive 6 months or less after the diagnosis of DMM. One patient has died of DMM.

Two of the cases had pleural hyaline plaques noted on X-ray bilaterally, and three other cases had pleural hyaline plaques found pathologically in the operative specimen. All patients were exposed to asbestos.

Histopathological findings

Four of the cases were entirely epithelioid, and two were biphasic.

Ovoid (Fig. 1) or serpentine (Fig. 2) structures bounded by flattened cells comprise the commonality in all cases. The lymphangiomatoid structures constituted from 10% to 40% of the overall area examined histologically in the slides available for review. The lymphangiomatoid areas were found in more solid epithelioid areas in all cases. Leaflet- or valve-like membranous structures extended into the vascular-like spaces (Fig. 3 inset) in two cases. The lymphangiomatoid structures could be found in dense pleural fibrous tissue (Fig. 4 inset). The lymphangiomatoid structures could extend beyond the main tumor and into adipose tissue and cause fat necrosis (Fig. 5a, b).

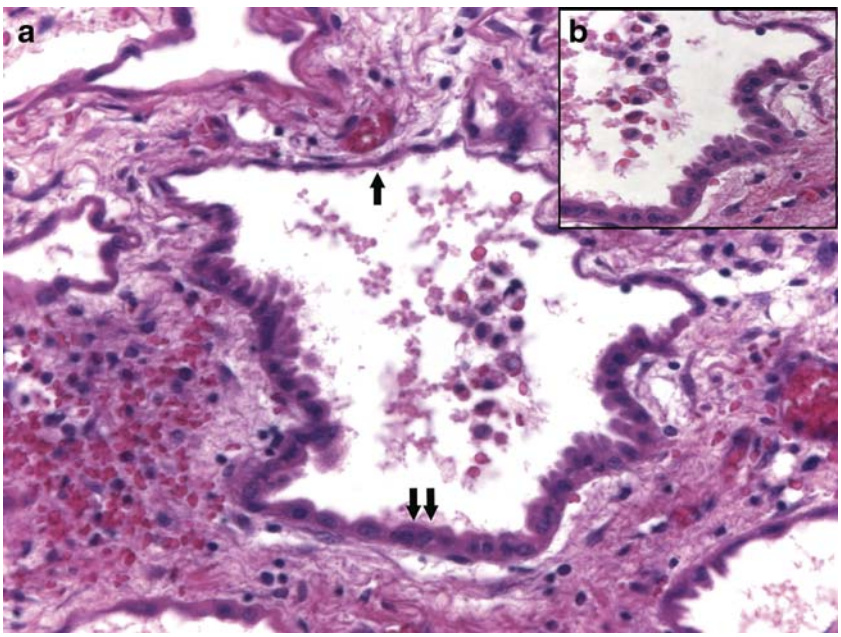

Fig. 6 Irregular space lined by flattened mesothelial cells (*single arrow*) to cuboidal cell (*double arrow*) and a gradual transition between the two. Cuboidal cells have more epithelioid aspects and a hobnail appearance (*inset*)

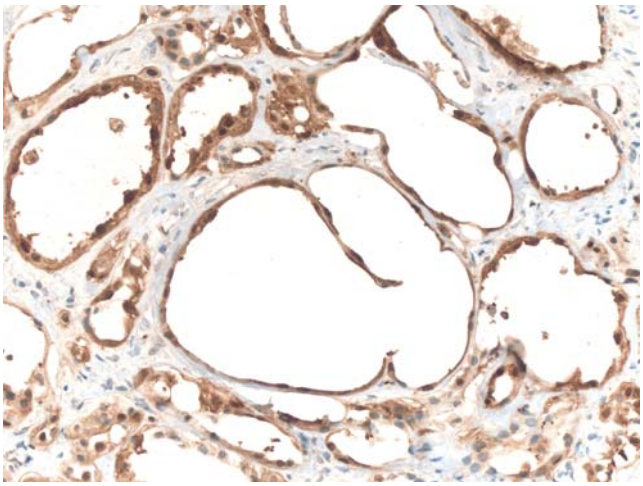

Fig. 7 Immunostain for calretinin highlighted the cells lining lymphangiomatoid spaces

The attenuated cells generally could be traced to cells with more copious cytoplasm and bland regular nuclei typical of DMM in early phase (Fig. 6 inset).

Lymphangiomatoid pattern was particularly evident in those cases which also had coexistent adenomatoid patterns. The lymphangiomatoid pattern was not seen in mesenchymal components of DMM in the two cases with a mesenchymal component.

Immunohistochemically, cells lining the lymphangiomatoid spaces stained for calretinin in all cases (Fig. 7), for cytokeratin 5/6 in five cases, for cytokeratin 7 in two cases, and for Wilms tumor-1 in five cases. In none of the cases did the cells not stain for these three agents. Staining for D2-40, a marker for both mesothelial cells and for endothelial cells, was positive in the two cases in which it was performed. Expected negative expression in DMM are documented in all cases. Five cases were negative for TTF-1 and CEA, three cases for CK20 and MOC-31, two cases for B72.3 and prostate specific antigen, and one case for prostate-specific acid phosphatase and CD15. One case weakly positive for MOC-31. Results of immunohistochemical staining are included in Table 2.

Discussion

Historically, DMM was not identified as a distinct entity until the late 1940s. In a 30-volume encyclopedia of pathology edited by Henke and Lubarsch in the interval of 1928–1931, the statement was made that if malignant mesothelioma existed, it was so rare that pathologists were not sure of its existence [13-15]. Of note for our paper is that among the various descriptions and terminology used for controversial cases of pleural tumors at that time was endothelioma of the pleura. One author of a treatise on pathology of tumors in 1960 stated that all tumors called pleural mesotheliomas were, in fact, metastases from an undiscovered primary carcinoma [16].

The differential diagnosis of pleural-based tumors includes epithelioid hemangioendothelioma. This malignant tumor of endothelial origin generally has epithelioid features, moderate to marked nuclear pleomorphism, and intracytoplasmic lacunes thought to represent incipient vascular lumina. Such cases are not similar to what we are describing.

Lymphangiomatoid pattern could be an accentuation of the more frequent adenomatoid pattern. However, the distinctive distended lymphatic-like spaces in lymphangiomatoid pattern differ from slit-like or pseudotubular spaces in adenomatoid pattern.

Lymphangiomatosis can involve the mediastinum or lung, particularly in children [17]. The lymphangiomatosis may permeate through the lung following lymphatic pathway and, thus, proliferate in the pleura. Pleural lymphangiomatosis typically causes a chylous pleural effusion. A differential diagnosis between lymphangiomatosis and the lymphangiomatoid pattern in DMM is unlikely to arise because no solid mass is present in lymphangiomatosis, the condition is seen mainly in younger patients, and the entire lesion consists of vascular spaces lined by the attenuated endothelial cells. In our cases, the lymphangiomatoid pattern could be traced into more solid areas of epithelioid DMM, and in these areas, the true nature of the tumor was apparent.

However, a diagnostic difficulty may arise when the lymphangiomatoid pattern is seen apart from the more solid

Table 2 Immunohistochemical results

Case	Stains							
	Calretinin	AE/AE3	WT-1	CK5/6	CK7	HBME-1	D2-40	Vimentin
1	+	NA	+[a]	+	NA	NA	NA	+
2	+	+	+	+	+	NA	NA	NA
3	+	+	+	NA	+	NA	+	NA
4	+	+	NA	+	NA	+	+	NA
5	+	NA	+	+	NA	NA	NA	NA
6	+	NA	+	+	NA	NA	NA	NA

[a] Weakly positive

areas of tumor. Particularly when the lymphangiomatoid pattern is seen in adipose tissue of chest wall apart from solid tumor, the impression may be that these are dilated lymphatics rather than invasive tumor. If there is a doubt as to whether these spaces are lymphatic or DMM, immunohistochemical staining for mesothelial markers and lymphatic endothelial markers, respectively, should provide the solution. However, we call attention to lymphangiomatoid DMM because there may be cases where the biopsy specimen samples principally lymphangiomatoid histology and leads to a problem in correct interpretation.

Conclusion

Lymphangiomatoid pattern occurs rarely in DMM. When invasive into fibroadipose tissue, it should be recognized as such rather than as lymphatic dilatation due to obstruction or lymphangioma. Recognition of a lymphangiomatoid pattern facilitates the diagnosis of DMM based on slides stained with hematoxylin and eosin alone because it adds to one of the distinctive patterns of DMM, but immunohistochemical studies can be performed in confusing cases to make the distinction of endothelial cells from mesothelial cells.

Conflict of interest statement Dr. Mark has served as an expert in legal cases where the patient believed his or her disease was related to asbestos.

References

1. Allen TC (2005) Recognition of histopathologic patterns of diffuse malignant mesothelioma in differential diagnosis of pleural biopsies. Arch Pathol Lab Med 129:1415–1420
2. Attanoos RL, Gibbs AR (1997) Pathology of malignant mesothelioma. Histopathology 30:413–418
3. Baker PM, Clement PB, Young RH (2005) Malignant peritoneal mesothelioma in women: a study of 75 cases with emphasis on their morphologic spectrum and differential diagnosis. Am J Clin Pathol 123:724–737
4. Galateau-Sallé F, Attanoos R, Gibbs AR et al (2007) Lymphohistiocytoid variant of malignant mesothelioma of the pleura: a series of 22 cases. Am J Surg Pathol 31:711–716
5. Galateau-Sallé F (2006) Pathology of malignant mesothelioma. Springer, London
6. Nascimento GA, Keeney GL, Fletcher CD (1994) Deciduoid peritoneal mesothelioma: an unusual phenotype affecting young females. Am J Surg Pathol 18:439–445
7. Shanks JH, Harris M, Banerjee SS et al (2000) Mesotheliomas with deciduoid morphology: a morphologic spectrum and a variant not confined to young females. Am J Surg Pathol 24:285–294
8. Shia J, Erlandson RA, Klimstra DS (2002) Deciduoid mesothelioma: a report of 5 cases and literature review. Utrastruct Pathol 26:355–363
9. Mayall FG, Gibbs AR (1992) The histology and immunohistochemistry of small cell mesothelioma. Histopathology 20:47–51
10. Ordóñez NG (2006) Mesothelioma with rhabdoid features: an ultrastructural and immunohistochemical study of 10 cases. Mod Pathol 19:373–383
11. Ordóñez NG (2005) Mesothelioma with clear cell features: an ultrastructural and immunohistochemical study of 20 cases. Hum Pathol 36:465–473
12. Cavazza A, Pasquinelli G, Agostini L et al (2002) Foamy cell mesothelioma. Histopathology 41:369–371
13. Henke, F. & O. Lubarsch, Eds. (1928) Handbuch der speziellen pathologischen Anatomie und Histologie, vol. III/I. Springer Verlag, Berlin
14. Henke F, Lubarsch O (eds) (1930) Handbuch der speziellen pathologischen Anatomie und Histologie, vol. III/2. Springer, Berlin
15. Henke F, Lubarsch O (eds) (1931) Handbuch der speziellen pathologischen Anatomie und Histologie, vol. III/3. Springer, Berlin
16. Willis RA (1960) Pathology of tumors, 3rd edn. Butterworths, London, p 186
17. Tazelaar HD, Kerr D, Yousem SA et al (1993) Diffuse pulmonary lymphangiomatosis. Hum Pathol 24:1313–1322

Virchows Arch (2009) 455:149–157
DOI 10.1007/s00428-009-0802-2

ORIGINAL ARTICLE

Involvement of centrosomes in nuclear irregularity of thyroid carcinoma cells

Dongfeng Niu · Shin-ichi Murata · Tetsuo Kondo · Tadao Nakazawa · Tomonori Kawasaki · Defu Ma · Tetsu Yamane · Nobuki Nakamura · Ryohei Katoh

Received: 4 February 2009 / Revised: 27 May 2009 / Accepted: 6 June 2009 / Published online: 9 July 2009

Abstract Nuclear irregularities including nuclear pseudoinclusions and nuclear grooves are characteristic of papillary thyroid carcinoma cells and are regarded as important diagnostic clues in histopathology. We observed nuclear features of thyroid carcinoma cell lines (KTC-1 and TPC-1) in various culture conditions and performed immunocytochemical examinations for cytoskeleton molecules to clarify the morphogenesis of thyroid carcinoma nuclei. We found that nuclear irregularities presenting as bean-like nuclei (BLNs) and donut-like nuclei (DLNs) appeared in cells from confluent cultures, but not in cells from sparse cultures. On immunocytofluorescence analyses, clusters of γ-tubulin, representing a centrosome, frequently localized at the indentation of BLNs or in the hole of DLNs of thyroid carcinoma cells. In conclusion, we suggest that cell-to-cell contact may affect nuclear changes such as BLNs and DLNs in cancer cell lines and that centrosomes may be involved in the morphogenetic process of these nuclear changes.

Keywords Thyroid gland · Papillary carcinoma · Immunofluorescence · Nuclear inclusion · Centrosome

D. Niu · T. Kondo · T. Nakazawa · T. Kawasaki · D. Ma · T. Yamane · N. Nakamura · R. Katoh (✉)
Department of Human Pathology, Interdisciplinary Graduate School of Medicine and Engineering, University of Yamanashi, Yamanashi 409-3898, Japan
e-mail: rkatoh@yamanashi.ac.jp

S.-i. Murata
Department of Pathology, Saitama Medical University International Medical Center,
Saitama, Japan

Introduction

Normal cells have round or oval nuclei with a smooth nuclear contour. In contrast, carcinoma cells generally display nuclear atypia, being irregular in size and shape [1, 2]. In particular, papillary thyroid carcinoma (PTC), the most common subtype of thyroid malignancies, has characteristic nuclear figures, including nuclear grooves and nuclear pseudoinclusions. Nuclear grooves are notches in the nuclear contours usually evident parallel to the long axis of the nucleus, and nuclear pseudoinclusions are invaginations of nuclear contours with cytoplasm appearing as circumscribed punched-out holes [3, 4]. These nuclear shapes are important clues for the diagnosis of PTC in fine-needle aspirates as well as histological sections [5, 6]; however, little is known about the morphogenetic mechanism of these nuclear features of PTC cells.

Past reports suggest that these nuclear features form cooperatively between the nuclear envelope and cytoskeletons [7-12]. The cytoskeleton is a dynamic network which plays an important structural role in such things as orientation of organelles, cell division, cellular organization, and maintenance of cell shape [9, 10]. Cytoskeletons are classified into three groups which include microtubules, intermediate filaments, and microfilaments, and all three groups have a connection with nuclear membrane proteins [8, 11]. Microtubules are composed of α- and β-tubulin heterodimers, along with γ-tubulin, the functional unit of the centrosome which stabilizes and anchors the minus end of the microtubule [13, 14]. The intermediate filament group includes many kinds of proteins such as cytokeratin, vimentin, and desmin.

Nuclear irregularities are common in PTCs. These features may be associated with vimentin and desmin [15]; however, it was reported that distribution and

expression of the major structural proteins of the nuclear envelope, including lamin A, lamin B1, and lamin C, were not altered relative to the nuclear irregularities of PTCs [16]. Thus, we hypothesize that aberrant cytoskeleton molecules may contribute to the abnormal nuclear shapes in PTCs.

In the current study, we cultured papillary thyroid carcinoma-derived cell lines which contained donut-like nuclei (DLNs) and bean-like nuclei (BLNs) within a confluent cell density to clarify the morphogenesis of nuclear irregularities. We studied the relationship between nuclear morphology and various cytoskeleton molecules using immunocytofluorescence.

Materials and methods

Cell lines and cell culture

We selected KTC-1 cells (papillary carcinoma) [17], TPC-1 cells (papillary carcinoma) [18], WRO cells (follicular carcinoma), and 8505C (undifferentiated carcinomas) to represent various histological types of human thyroid carcinomas [19]. Cells were maintained in RPMI 1640 (Gibco, Grand Island, NY, USA) supplemented with 10% fetal bovine serum, streptomycin sulfate (100 mg/L), and penicillin G sodium (100 mg/L). Cells were cultured in a standard humidified incubator at 37°C in a 5% CO_2 atmosphere.

Thyroid carcinoma cells were plated in 3.5-cm glass-bottom dishes with different numbers of cells (1×10^4, 1×10^5, or 1×10^6 cells) and then microscopically examined for nuclear morphology on the first, third, and seventh days of incubation.

Preparation for imprint cytology

Touch imprint cytology was prepared from fresh PTC tissues taken from patients undergoing lobectomy or total thyroidectomy at the University of Yamanashi Hospital. Touch imprint specimens were washed three times with phosphate-buffered saline (PBS) and then fixed with 3.7% formaldehyde in PBS at room temperature for 30 min. Hematoxylin–eosin stain at room temperature and nuclear DNA stain by 0.8 mM Hoechst 33258 (Molecular Probes, OR, USA) or propidium iodide (PI) were performed at 4°C for 30 min. PI staining required pretreatment for RNA digestion using 0.01% Raze at 37°C for 30 min. The institutional ethics board of the University of Yamanashi approved all protocols.

Immunocytofluorescence

We stained culture cells and touch imprint specimens for indirect immunofluorescence using primary antibodies: anti-α-tubulin, anti-β-tubulin, anti-γ-tubulin, anti-cytokeratin-19, anti-vimentin, anti-lamin B, and anti-emerin. Detailed information of the primary antibodies, their resources, dilutions, and pretreatment are presented in Table 1. For antigen retrieval, slides were treated by autoclave at 120°C for 5 min in the 0.01 M citrate buffer, pH 6.0. Then, the samples were incubated first with primary antibody at room temperature for 1 h, then with fluorescent dye-conjugated second antibody at room temperature for 1 h. Biotin-conjugated secondary antibody was visualized using streptavidin Alexa Fluor 647 (1:50; Molecular Probes) at room temperature for 1 h. For double immunofluorescence stains, appropriate secondary antibodies were selected based on the primary antibody host. After the nuclear counter stain, the samples were mounted by ProLong Gold antifade reagent (Molecular Probes).

Phalloidin (Alexa Fluor 546, Molecular Probes) was used to visualize actin filament in the cytoplasm. After pretreatment with acetone at −20°C, the cells were treated with phalloidin for 20 min at room temperature.

The fluorescence images were acquired through an epi-illuminant fluorescence microscope, BX50, equipped with a scientific grade, cooled CCD camera (DP30BW, Olympus, Tokyo, Japan) connected to a personal computer. Confocal images were obtained using laser scanning confocal microscopy (FV1000, Olympus).

Table 1 Lists of primary antibodies used for immunofluorescence staining

Antibody	Host	Dilution	Antigen retrieval	Resource
α-Tubulin	Mouse	1:100	Citrate buffer, pH 6.0, autoclave, 5 min	Molecular Probes (Eugene, OR, USA)
β-Tubulin	Rabbit	1:100	Citrate buffer, pH 6.0, autoclave, 5 min	Lab Vision (CA, USA)
γ-Tubulin	Rabbit	1:100	Citrate buffer, pH 6.0, autoclave, 5 min	Sigma-Aldrich (St. Louis, MO, USA)
Cytokeratin 19	Mouse	1:100	Citrate buffer, pH 6.0, autoclave, 5 min	Dako (Glostrup, Denmark)
Vimentin	Mouse	1:100	Citrate buffer, pH 6.0, autoclave, 5 min	Dako (Glostrup, Denmark)
Lamin B	Goat	1:100	Citrate buffer, pH 6.0, autoclave, 5 min	Santa Cruz Biotecnology (Santa Cruz, CA, USA)
Emerin	Mouse	1:20	Citrate buffer, pH 6.0, autoclave, 5 min	Novocastra Lab (Newcastle, UK)

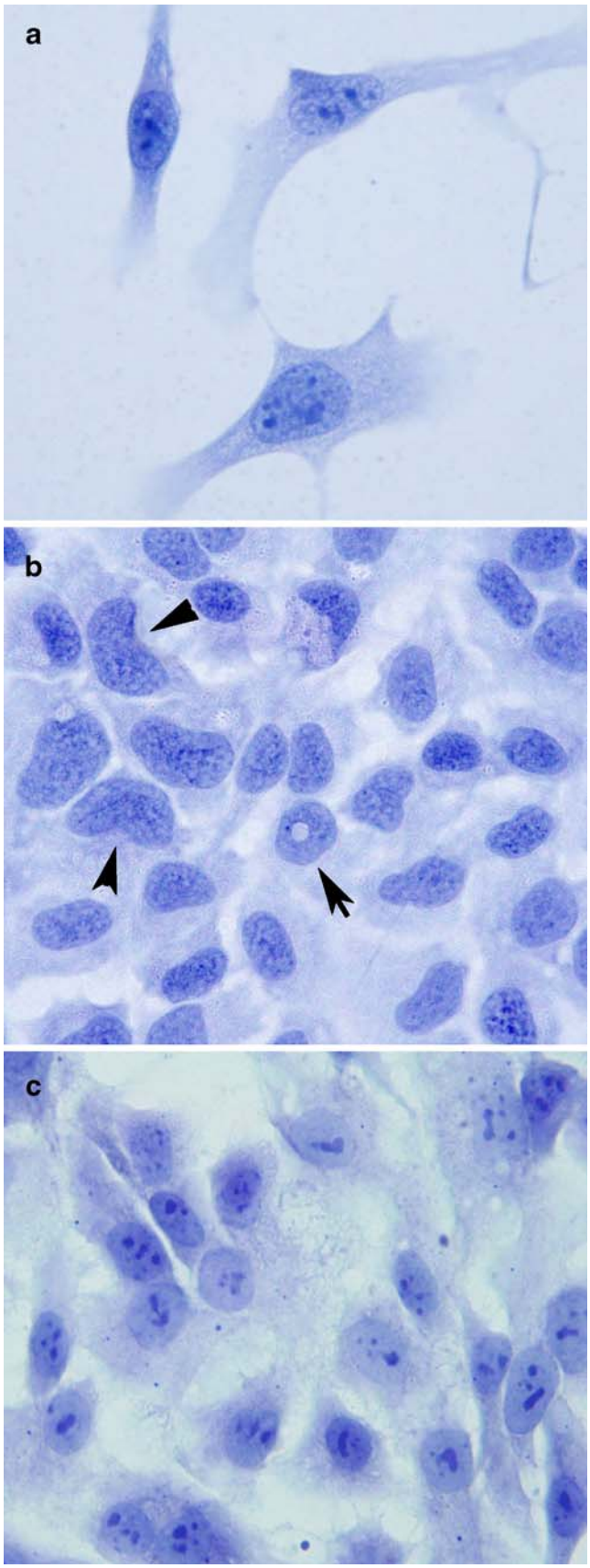

◀ **Fig. 1** The morphology of KTC-1 cells relative to cell density in the dishes. **a** Early during culturing, the nuclei of cells were round with smooth a contour. **b** Cells from a confluent cell density had nuclei with irregular nuclear contours; BLN (*arrowhead*) and sporadically DLN (*arrow*). **c** The nuclei of 8505C cells show neither BLNs nor DLNs within the confluent cultures

Results

Nuclear morphology of thyroid carcinoma cell lines

The nuclei of the KTC-1 and TPC-1 cells from the sparsely populated cultures had round, smooth contours during early culturing (Fig. 1a). However, we found the characteristic nuclear features such as BLNs and DLNs within the confluent cultures. BLNs had a dent in their nuclear contour, creating a bean or horseshoe shape, and DLNs looked as though they had a punched-out hole (Fig. 1b). We did not observe these unique nuclear figures in non-papillary thyroid carcinoma cell lines (WRO and 8505C cells) from the sparsely populated or confluent cultures (Fig. 1c).

Frequencies of BLNs and DLNs

The frequencies of BLNs and DLNs in KTC-1 cells and TPC-1 cells are shown in Table 2. BLNs were seen on the third and seventh days in the dishes containing 1×10^5 and 1×10^6 plated cells from both cell lines. Frequency of BLNs tended to be higher in the TPC-1 cell line (3.6% to 6.4%) than in the KTC-1 cell line (1.2% to 3.9%). DLNs were identified only on day 7 in dishes containing 1×10^5 and 1×10^6 plated cells in the KTC-1 cell line and on days 3 and 7 in the dishes containing 1×10^6 plated cells from the TPC-1 cell line. Neither BLNs nor DLNs were identified at any time in the dishes of the 1×10^4 plated cells.

Table 2 Frequency of bean-like nuclei and donut-like nuclei in thyroid carcinoma cells

Cell lines	No. of plated cell/dish	Frequency of BLNs (%)			Frequency of DLNs (%)		
		Day 1	Day 3	Day 7	Day 1	Day 3	Day 7
KTC-1	1×10^4	0	0	0	0	0	0
	1×10^5	0	1.2	2.4	0	0	3.1
	1×10^6	0	2.6	3.9	0	0	2.6
TPC-1	1×10^4	0	0	0	0	0	0
	1×10^5	0	3.9	5.1	0	0	2.6
	1×10^6	0	3.6	6.4	0	2.3	1.9

BLNs bean-like nuclei, *DLNs* donut-like nuclei

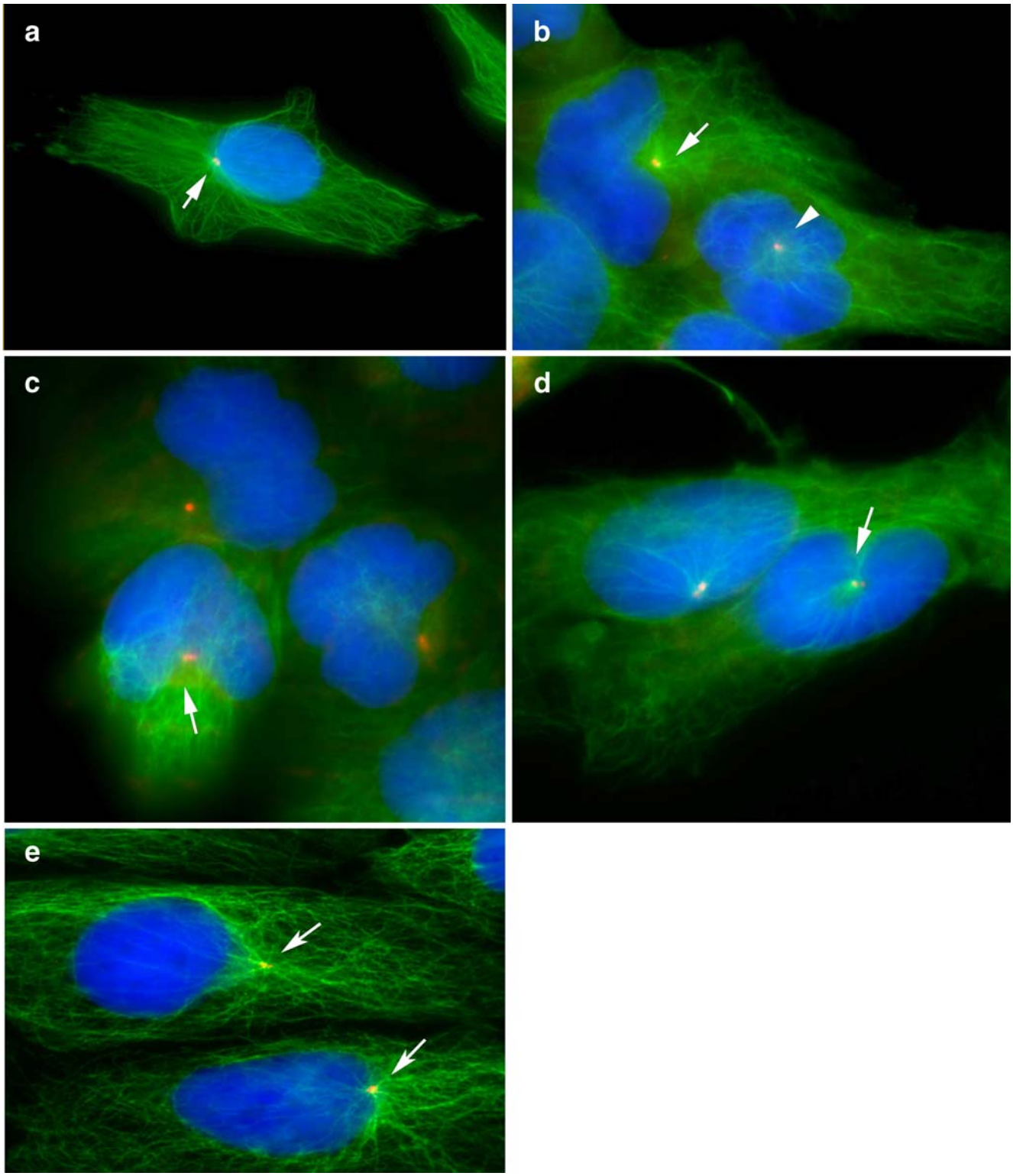

Fig. 2 Double immunofluorescence staining of alpha-tubulin (FITC: *green*) and gamma-tubulin (TRCR: *red*) in culture cells. Nuclei were stained by Hoechst (*blue*). The red color is seen as yellow due to an overlap with green color. **a** A KTC-1 cell with round nucleus from a sparsely populated cell culture. An accumulated cluster of gamma-tubulin (centrosome: *arrow*) near the nucleus and linear filaments of alpha-tubulin (microtubules) are growing out from a cluster of gamma-tubulin. **b** KTC-1 cells with irregular nuclear contours from a confluent cell population. Clusters of gamma-tubulin are located near a BLN (*arrow*) and in a DLN (*arrowhead*). **c** TPC-1 cells with irregular nuclear contours from a confluent cell population. A cluster of gamma-tubulin is located in a BLN (*arrows*). **d** TPC-1 cells with irregular nuclear contours from a confluent cell density. A cluster of gamma-tubulin located in a DLN (*arrows*). **e** In 8505C cells, cluster of γ-tubulin localize near the nuclei

Table 3 Ratios of centrosomes in the hole of DLNs

Cell lines	DLNs	Centrosome within DLNs (%)
KTC-1	48	64.6
TPC-1	63	55.6

DLNs donut-like nuclei

Immunocytochemistry

We carried out our immunofluorescence study for microtubules using antibodies against α-tubulin, β-tubulin, γ-tubulin, cytokeratin-19, vimentin, lamin B, and emerin. Double immunofluorescence techniques for α- and γ-tubulins on papillary thyroid carcinoma-derived cells (KTC-1 and TPC-1 cells) from sparsely plated cultures revealed γ-tubulin in a cluster and localized near the nuclei representing a centrosome, while α-tubulin was immunoreactive in fibers, or microtubules, growing from the centrosome to the cell membrane (Fig. 2a). Within the confluent culture, we found that a γ-tubulin centrosome was occasionally localized at the dent of a BLN and in the hole of a DLN, while microtubules positive for α-tubulin were most consistently found within the sparsely cultured cells (Fig. 2b–d). After carefully examining all DLNs, we estimated the frequency of those having a cluster of γ-tubulin in their hole to be 64.6% (31 of 48 DLNs) from the KTC-1 cell line and 55.6% (35 of 63 DLNs) from the TPC-1 cell line (Table 3). In non-papillary thyroid carcinoma cell lines (WRO and 8505C cells), cluster of γ-tubulin localized near the nuclei representing a centrosome with the same pattern as papillary thyroid carcinoma-derived cells from sparsely plated cultures (Fig. 2e)

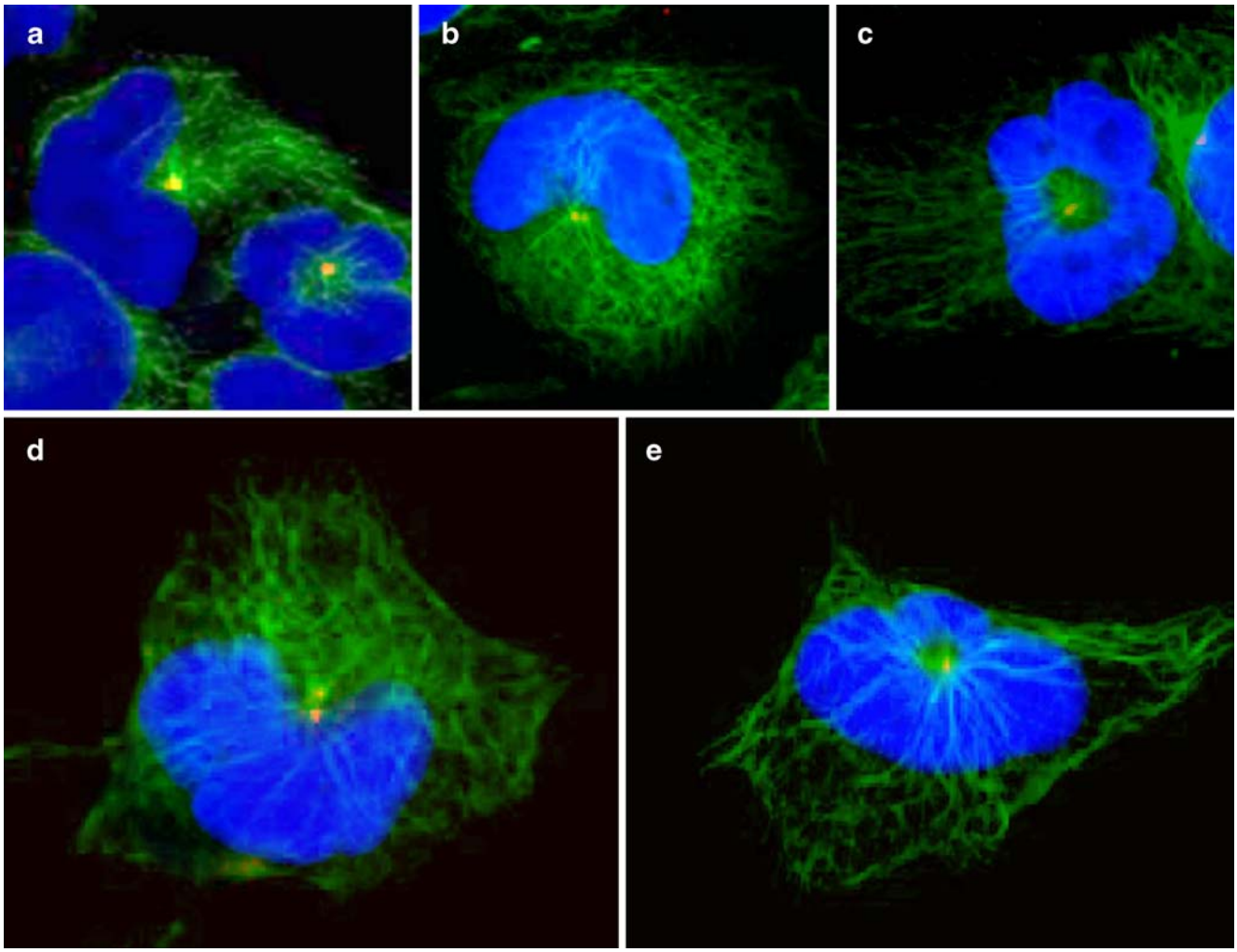

Fig. 3 Confocal images of double immunofluorescence staining of tubulins in culture cells. Alpha-tubulin and gamma-tubulin are visualized by FITC (*green*) and TRCR (*red*), respectively. Red color is seen as yellow due to an overlap with green color. Nuclei are stained by Ho (*blue*). Confocal images of alpha-tubulin and gamma-tubulin of KTC-1 (**a**–**c**) and TPC–1 (**d**–**e**) cell lines, respectively. Alpha-tubulin filaments are radiating from a gamma-tubulin centrosome. **a** Confocal image of the same cells shown in Fig. 2b. **b**, **d** The gamma-tubulin is positioned close to the BLN. **c**, **e** The positioning of gamma-tubulin centralized within the DLN is confirmed by confocal laser scanning microscopy

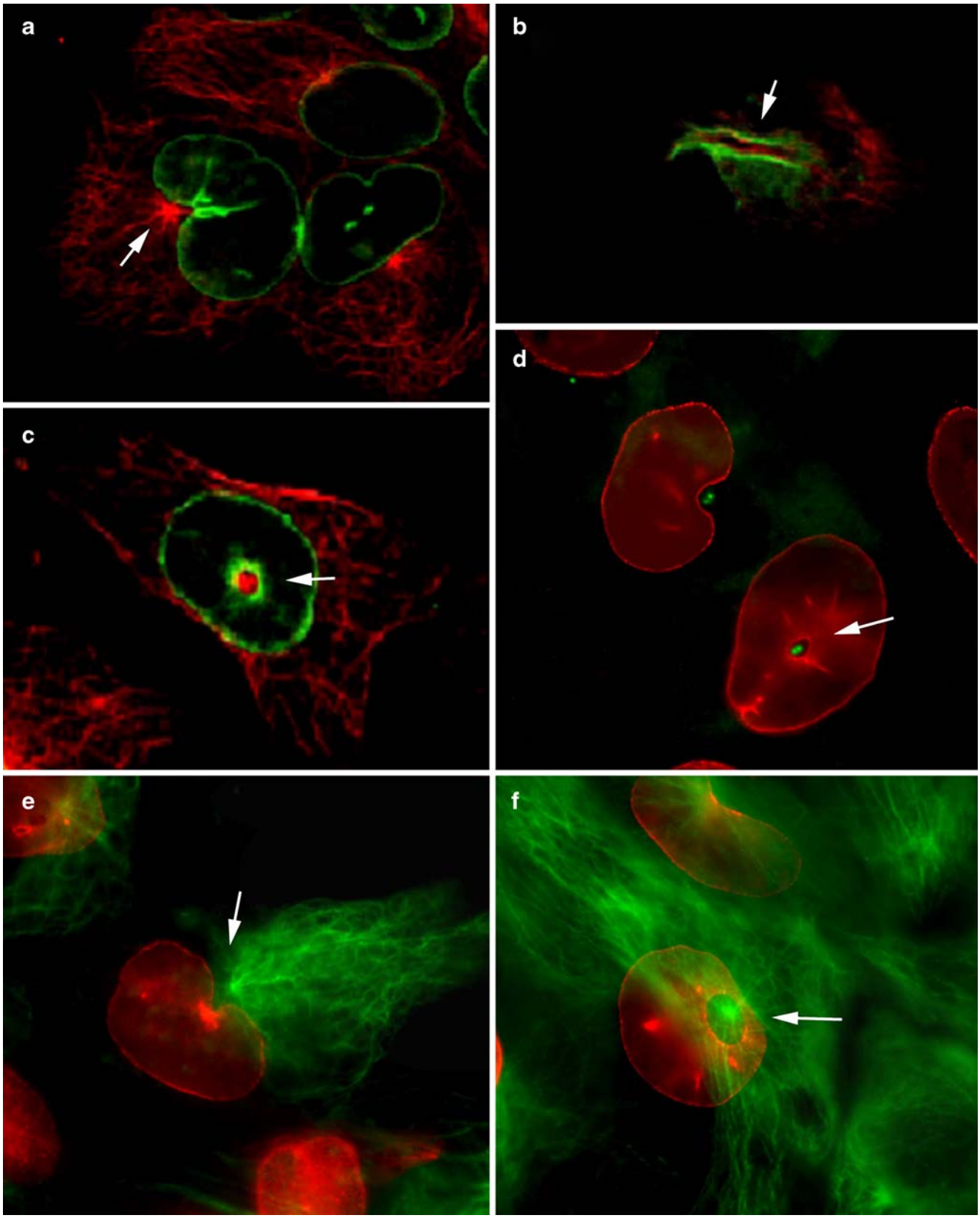
a
b
c
d
e
f

Immunohistochemistry using confocal laser scanning microscopy confirmed that γ-tubulin centrosomes localized at dents of BLNs and in the holes of DLNs (Fig. 3). In addition, our double immunofluorescence study for nuclear membrane proteins (lamin B and emerin) and γ- or β-tubulin also supported the close relationship between DLNs/BLNs, centrosomes, and microtubules (Fig. 4). Although we also stained for F-actin and intermediate filaments including cytokeratin-19 and vimentin, we did not find any distributional association with the nuclear figs of BLNs and DLNs (Fig. 5).

Human papillary thyroid carcinoma

We examined touch-imprinted cells from human papillary thyroid carcinoma tissues in the same manner as our plated cells. Immunofluorescent examination revealed γ-tubulin centrosomes in nuclear pseudoinclusions or near nuclear grooves in the human papillary carcinoma cells (Fig. 6).

Discussion

In our current study, we examined nuclear irregularities of thyroid carcinoma cells, focusing on cytoskeletal molecules using light and confocal microscopy. We found unique morphological figures such as BLNs and DLNs in papillary thyroid carcinoma cell lines (KTC-1 and TPC-1). The BLNs and DLNs appearing in these cell lines were morphologically similar to nuclear grooves and nuclear pseudoinclusions in papillary thyroid carcinoma cells. Similar nuclear findings in a papillary carcinoma cell line (NPA cell line) have been described by Papotti et al. [4] in 2004. Using confocal microscopic analysis and tridimensional reconstruction, they demonstrated that the nuclear holes and grooves seen during light microscopy correspond to invaginations and tunnels. From a morphological point of view, the BLNs and DLNs in KTC-1 and TPC-1 cell lines can be related to invaginations and tunnels of cancer cell nuclei.

Overlapping nuclei representing high cell density is a characteristic of papillary thyroid carcinomas [5, 20, 21]. Interestingly, the frequency of BLNs and DLNs corre-

◀ **Fig. 4** Images of both KTC-1 cells with double immunofluorescence staining of beta-tubulin and lamin B (**a**–**c**) and TPC-1 cells with double immunofluorescence staining of beta-tubulin and emerin and gamma-tubulin and emerin (**d**–**f**). Beta- and gamma-tubulins are visualized with FITC (*green*); lamin B and emerin are visualized with TRCR (*red*). **a**, **e** Beta-tubulin filaments accumulated in the cytoplasm near and extending to the nuclear envelope (lamin B, emerin) at the side of the BLN (*arrow*). **b** Confocal image of the top plane of cells is shown. Beta-tubulin is expressed parallel to the long axis of the BLN (*arrow*). **c**, **f** Condensation of beta-tubulin is seen in a DLN (*arrow*). **d** A gamma-tubulin centrosome in the central cytoplasm within a DLN (arrow)

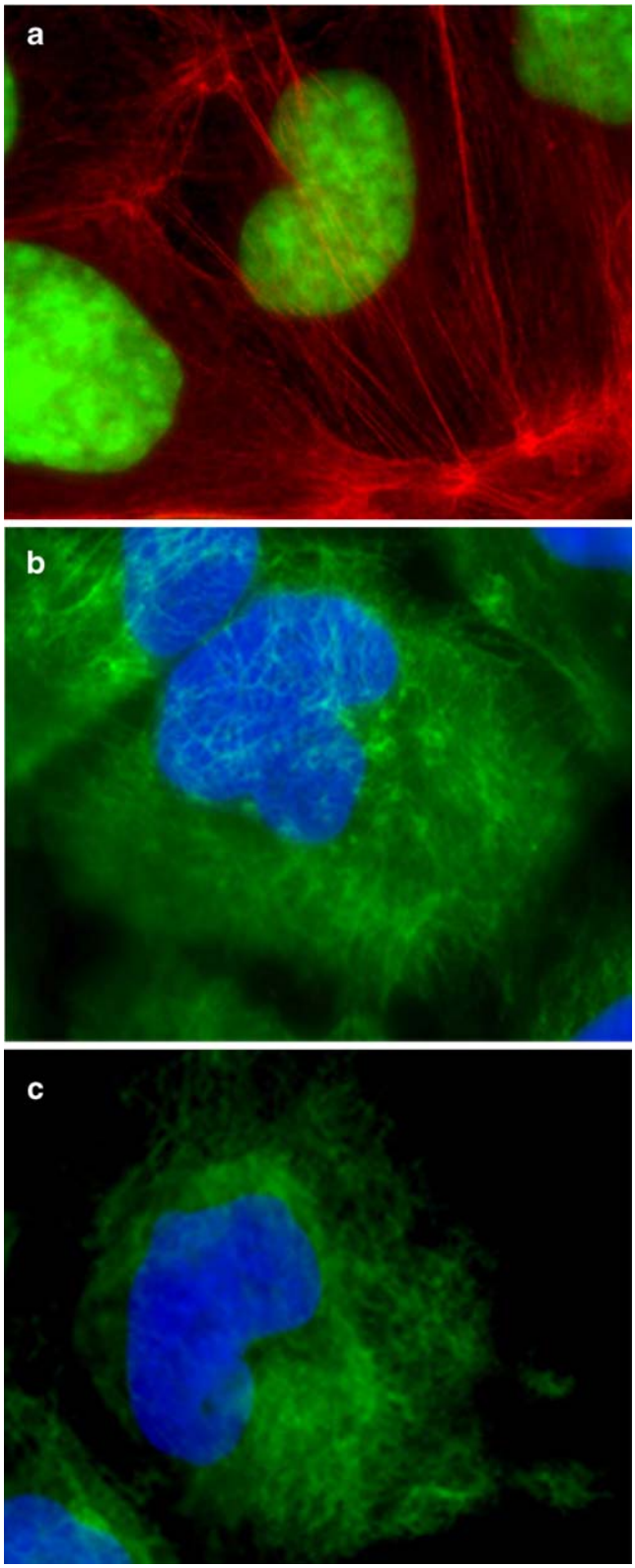

Fig. 5 Expression of F-actin filaments and intermediate filaments in KTC-1 cells. **a** F-actin filaments are expressed almost parallel in the cytoplasm along the long axis of the cell and no association with nuclear contour was found. **b** Filaments of cytokeratin-19 are evenly distributed around the nucleus with no association to nuclear contour. **c** Filaments of vimentin were also evenly distributed around the nucleus, similar to the cytokeratin-19 expression

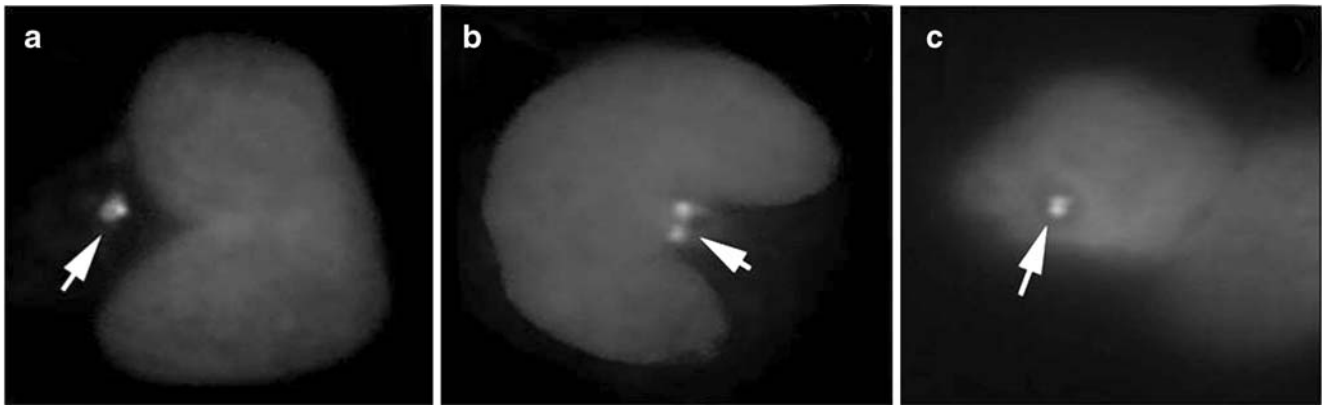

Fig. 6 Gamma-tubulin in touch imprint specimens of papillary thyroid carcinoma. *Arrows* indicate gamma-tubulin centrosomes in the cytoplasm near the nuclear groove (**a**, **b**) and in the nuclear pseudoinclusion (**c**)

sponded with the number of plated cells and days of incubation: BLNs and DLNs were found more frequently in cultures that were initially plated with a higher number of cells and/or at later days of incubation. These findings suggest that cell-to-cell contact and/or cell density may be related to the morphogenesis of nuclear irregularities.

The nuclear envelope is firmly fastened to the cytoskeleton [22], and the cellular scaffold that comprises the nuclear matrix and cytoskeleton provides mechanical support for the cell and may play some role in nuclear structure. Therefore, we performed an immunofluorescence study for several cytoskeleton molecules and nuclear membrane proteins such as α-tubulin, β-tubulin, γ-tubulin, cytokeratin-19, vimentin, lamin B, and emerin in the cultured cells with and without BLNs and DLNs. We found that a cluster of γ-tubulin, a centrosome, was positioned in the hole of a DLN or near a BLN, whereas α- and β-tubulin heterodimers accumulated more within the BLNs and DLNs. In addition, we had similar findings in the touch imprint specimens of PTCs. Therefore, it is conceivable that centrosomes and microtubules may be involved with the nuclear irregularities of PTC cells.

It has been reported that a significant fraction of emerin is located at the outer nuclear membrane and linked directly with the centrosome [23]. Also, we know that numerical and structural aberrations of centrosomes play an initial role in the carcinogenic process [24, 25]. These data support our hypothesis that centrosomes may be related to the nuclear morphogenesis of PTCs.

In conclusion, we suggest that cell-to-cell contact may affect nuclear changes such as BLNs and DLNs in cancer cell lines and that centrosomes may be involved in the morphogenetic process of these nuclear changes. Our findings contribute to the understanding of characteristic nuclear features in papillary thyroid carcinomas.

Acknowledgments The authors thank Ms. Miyuki Ito, Ms. Mikiko Yoda, and Mr. Yoshihito Koshimizu for technical support and Ms. Kayoko Kono for executive assistance.

Conflict of interest We declare that we have no conflict of interest.

References

1. Murata S-I, Mochizuki K, Nakazawa T et al (2002) Detection of underlying characteristics of nuclear chromatin patterns of thyroid tumor cells using texture and factor analyses. Cytometry 49:91–95
2. Murata S-I, Mochizuki K, Nakazawa T et al (2003) Morphological abstraction of thyroid tumor cell nuclei using morphometry with factor analysis. Microsc Res Tech 61:457–462
3. Das DK, Sharma PN (2005) Intranuclear cytoplasmic inclusions and nuclear grooves in fine needle aspiration smears of papillary thyroid carcinoma and its variants: advantage of the count under an oil-immersion objective over a high-power objective. Anal Quant Cytol Histol 27:83–94
4. Papotti M, Manazza AD, Chiarle R et al (2004) Confocal microscope analysis and tridimensional reconstruction of papillary thyroid carcinoma nuclei. Virchows Arch 444:350–355
5. Chan JK, Saw D (1986) The grooved nucleus. A useful diagnostic criterion of papillary carcinoma of the thyroid. Am J Surg Pathol 10:672–679
6. Das DK (2005) Intranuclear cytoplasmic inclusions in fine-needle aspiration smears of papillary thyroid carcinoma: a study of its morphological forms, association with nuclear grooves, and mode of formation. Diagn Cytopathol 32:264–268
7. D'Assoro AB, Lingle WL, Salisbury JL (2002) Centrosome amplification and the development of cancer. Oncogene 21:6146–6153
8. Djabali K (1999) Cytoskeletal proteins connecting intermediate filaments to cytoplasmic and nuclear periphery. Histol Histopathol 14:501–509
9. Helfand BT, Chang L, Goldman RD (2004) Intermediate filaments are dynamic and motile elements of cellular architecture. J Cell Sci 117:133–141
10. Malek AM, Izumo S (1996) Mechanism of endothelial cell shape change and cytoskeletal remodeling in response to fluid shear stress. J Cell Sci 109(Pt 4):713–726

11. Starr DA (2007) Communication between the cytoskeleton and the nuclear envelope to position the nucleus. Mol Biosyst 3:583–589
12. Wilhelmsen K, Litjens SHM, Kuikman I et al (2005) Nesprin-3, a novel outer nuclear membrane protein, associates with the cytoskeletal linker protein plectin. J Cell Biol 171:799–810
13. Desai A, Mitchison TJ (1997) Microtubule polymerization dynamics. Annu Rev Cell Dev Biol 13:83–117
14. Urbani L, Stearns T (1999) The centrosome. Curr Biol 9:R315–R317
15. Echeverria OM, Hernandez-Pando R, Vazquez-Nin GH (1998) Ultrastructural, cytochemical, and immunocytochemical study of nuclei and cytoskeleton of thyroid papillary carcinoma cells. Ultrastruct Pathol 22:185–197
16. Fischer AH, Taysavang P, Weber CJ et al (2001) Nuclear envelope organization in papillary thyroid carcinoma. Histol Histopathol 16:1–14
17. Kurebayashi J, Tanaka K, Otsuki T et al (2000) *All-trans*-retinoic acid modulates expression levels of thyroglobulin and cytokines in a new human poorly differentiated papillary thyroid carcinoma cell line, KTC-1. J Clin Endocrinol Metab 85:2889–2896
18. Namba H, Yamashita S, Pei HC et al (1991) Lack of PTC gene (ret proto-oncogene rearrangement) in human thyroid tumors. Endocrinol Jpn 38:627–632
19. Kondo T, Nakazawa T, Murata S et al (2007) Enhanced B-Raf protein expression is independent of V600E mutant status in thyroid carcinomas. Hum Pathol 38(12):1810–1018
20. Hapke MR, Dehner LP (1979) The optically clear nucleus. A reliable sign of papillary carcinoma of the thyroid? Am J Surg Pathol 3:31–38
21. Deligeorgi-Politi H (1987) Nuclear crease as a cytodiagnostic feature of papillary thyroid carcinoma in fine-needle aspiration biopsies. Diagn Cytopathol 3:307–310
22. Schatten H, Hedrick J, Chakrabarti A (1998) The cytoskeleton of *Drosophila*-derived Schneider line-1 and Kc23 cells undergoes significant changes during long-term culture. Cell Tissue Res 294:525–535
23. Salpingidou G, Smertenko A, Hausmanowa-Petrucewicz I et al (2007) A novel role for the nuclear membrane protein emerin in association of the centrosome to the outer nuclear membrane. J Cell Biol 178:897–904
24. D'Angelo MA, Hetzer MW (2006) The role of the nuclear envelope in cellular organization. Cell Mol Life Sci 63:316–332
25. Kayser G, Gerlach U, Walch A et al (2005) Numerical and structural centrosome aberrations are an early and stable event in the adenoma–carcinoma sequence of colorectal carcinomas. Virchows Arch 447:61–65

Virchows Arch (2009) 455:159–170
DOI 10.1007/s00428-009-0791-1

ORIGINAL ARTICLE

LANA-1, Bcl-2, Mcl-1 and HIF-1α protein expression in HIV-associated Kaposi sarcoma

E Long · M Ilie · V Hofman · K Havet · E Selva · C Butori · J P Lacour · A M Nelson · G Cathomas · P Hofman

Received: 5 March 2009 / Revised: 2 May 2009 / Accepted: 10 May 2009 / Published online: 30 May 2009

Abstract Human herpesvirus 8 (HHV8) is necessary for Kaposi sarcoma (KS) to develop, but whether the tissue viral load is a marker of KS progression is still unclear. Little is known about the level of expression of apoptosis-regulating proteins and of hypoxia-inducible factors (HIFs) in KS tumour cells relative to HHV8 expression. We therefore investigated the expression of the latency-associated nuclear antigen (LANA-1) of HHV8, Bcl-2, Mcl-1, Bax, Bcl-xL, caspase 3 and HIF-1αin KS tissue specimens at different stages of the disease. The expression of these proteins was evaluated immunohistochemically using tissue microarrays (TMAs) in tissue specimens from 245 HIV-positive patients at different stages of the disease. Both LANA-1 and HIF-1α were expressed in KS biopsies taken at different stages, but their level increased throughout tumour progression. Additionally, the levels of Bcl-2 and Mcl-1 were higher in visceral KS lesions compared to levels observed in cutaneous and mucosal KS. This study demonstrates that late tumour stages of KS in tissues from HIV-positive patients are associated with high levels of LANA-1, HIF-1α and of the anti-apoptotic proteins, Bcl-2 and Mcl-1. Finally, the expression of these proteins can be potentially used as a tissue biomarker in defining patients with a higher risk of disease progression.

Keywords HIV · Kaposi sarcoma · LANA-1 · Apoptosis · Hypoxia · Tumour progression

E. Long · M. Ilie · V. Hofman · K. Havet · C. Butori · P. Hofman (✉)
Laboratory of Clinical and Experimental Pathology,
Louis Pasteur Hospital,
30 avenue de la voie romaine,
Nice 06002, France
e-mail: hofman@unice.fr

V. Hofman · C. Butori · P. Hofman
INSERM ERI-21/EA 4319,
Nice, France

V. Hofman · E. Selva · C. Butori · P. Hofman
Human Tissue Biobank Unit/CRB INSERM,
Nice, France

J. P. Lacour
Department of Dermatology, University of Nice Sophia Antipolis,
Nice 06002, France

A. M. Nelson
Armed Forces Institute of Pathology,
Washington, DC 20306-6000, USA

G. Cathomas
Institute for Infectious Pathology,
Liestal, Switzerland

Introduction

By 1989, 15% of all reported acquired immunodeficiency syndrome (AIDS) cases in the USA had Kaposi sarcoma (KS) as the primary AIDS-defining illness [1]. KS is still the most common tumour in HIV-infected individuals, but in different parts of the world the epidemiological trend is changing. In the era of highly active anti-retroviral therapy (HAART), the incidence of AIDS-KS has declined considerably [2, 3]. In contrast, the prevalence of KS remains high in untreated HIV patients, in particular amongst Africans [4]. Finally, the increase in KS after initiation of HAART may be a manifestation of the immune reconstitution inflammatory syndrome [5, 6].

A better understanding of the pathogenesis of KS came with the identification of the human herpesvirus 8 (HHV8) in all forms of KS [7–9]. Viral oncogenesis and cytokine-induced growth, as well as some immunocompromised

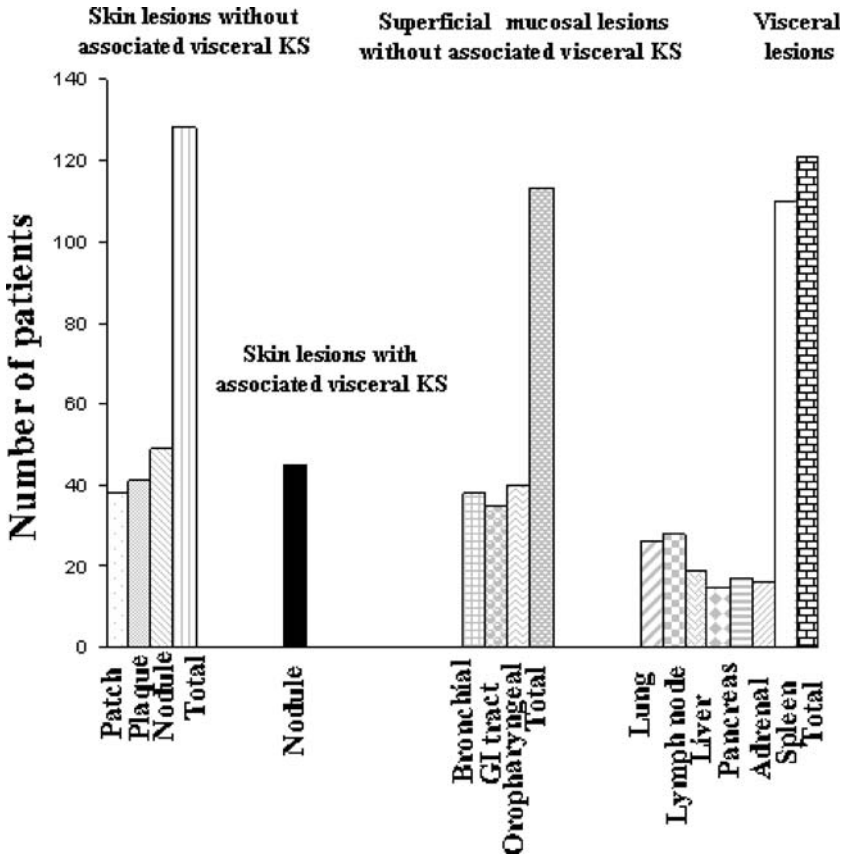

Fig. 1 Summary of the tissue lesions included for tissue microarray construction

states, contribute to its development. Clinically, AIDS-KS commonly presents with cutaneous lesions beginning as macules and papules, which frequently evolves into plaque-like and then into nodular tumours [10]. Histologically, patch-stage KS is the earliest pattern, followed by the plaque stage and nodular stage [11]. Similar lesions are observed at mucosal surfaces, mostly in the conjunctiva and in the oropharyngeal, gastrointestinal (GI) and bronchial tracts. These lesions can be unique or multiple, with or without associated visceral involvement [10, 11]. Finally, progression of AIDS-KS causes significant mortality with different organ manifestations and post-mortem studies suggest that more than 25% of patients with cutaneous AIDS-KS also have visceral lesions [12–14]. KS most commonly involves the lung, spleen, liver, lymph nodes, stomach, rectum/anus and liver, but any organ can be involved [13, 14].

Several HHV8 genes that are expressed during latency or during the lytic life cycle can affect binding, cell growth, proliferation, inflammation and angiogenesis [15]. HHV8 has developed alternative means of expressing proteins that overcome the usual responses to viral infection by helping to oppose cell cycle arrest, apoptosis and activation of cellular immunity. Amongst the different molecules acting during KS development and progression, the latency-associated nuclear antigen (LANA) of HHV8 (encoded by ORF 73) may act as a transcriptional regulator and modify gene expression of viral and cellular genes [16]. HHV8 seems to have pirated some relevant cellular genes linked to apoptosis and angiogenesis that leads to dysregulation of these processes [17]. In this regard, it has been suggested that the pathogenesis of KS in the HIV-infected population may be related to escape from apoptosis rather than to an increase in proliferation [18, 19]. However, it is still not clear whether the development and progression of KS in HIV-positive individuals infected by HHV8 are related to increased cell growth and/or to decreased cell death. Recent research has demonstrated that the hypoxia-inducible factor-1α (HIF-1α), a key player in angiogenesis, is highly expressed in KS lesions [20, 21]. Finally, it is not clear if the level of viral antigens, such as LANA-1, is linked to stages of the disease and whether it is correlated with the level of apoptosis-related and/or the HIF-1α protein.

The aim of this study was to investigate and to quantify the expression of LANA-1, anti-apoptotic (Bcl-2, Mcl-1)

Fig. 2 **a** Clinical appearance of cutaneous patch (*a1*), plaque (*b1*), ▶ nodule (*c1*) and mucosal (tongue; *d1*) KS lesions. Tissue microarrays of cutaneous patches (*a2*, *a3*, *a4*), plaques (*b2*, *b3*, *b4*), nodules (*c2*, *c3*, *c4*) and mucosal (tongue; *d2*, *d3*, *d4*) KS lesions (*a2–d2*: haematoxylin eosin, ×150; anti-LANA-1 immunostaining: *a3–d3*, ×100; *a4–d4*, ×400). **b** Number of cell nuclei expressing LANA-1 in patch, plaque and nodular isolated KS cutaneous lesions and in isolated mucosal lesions. *$p<0.05$

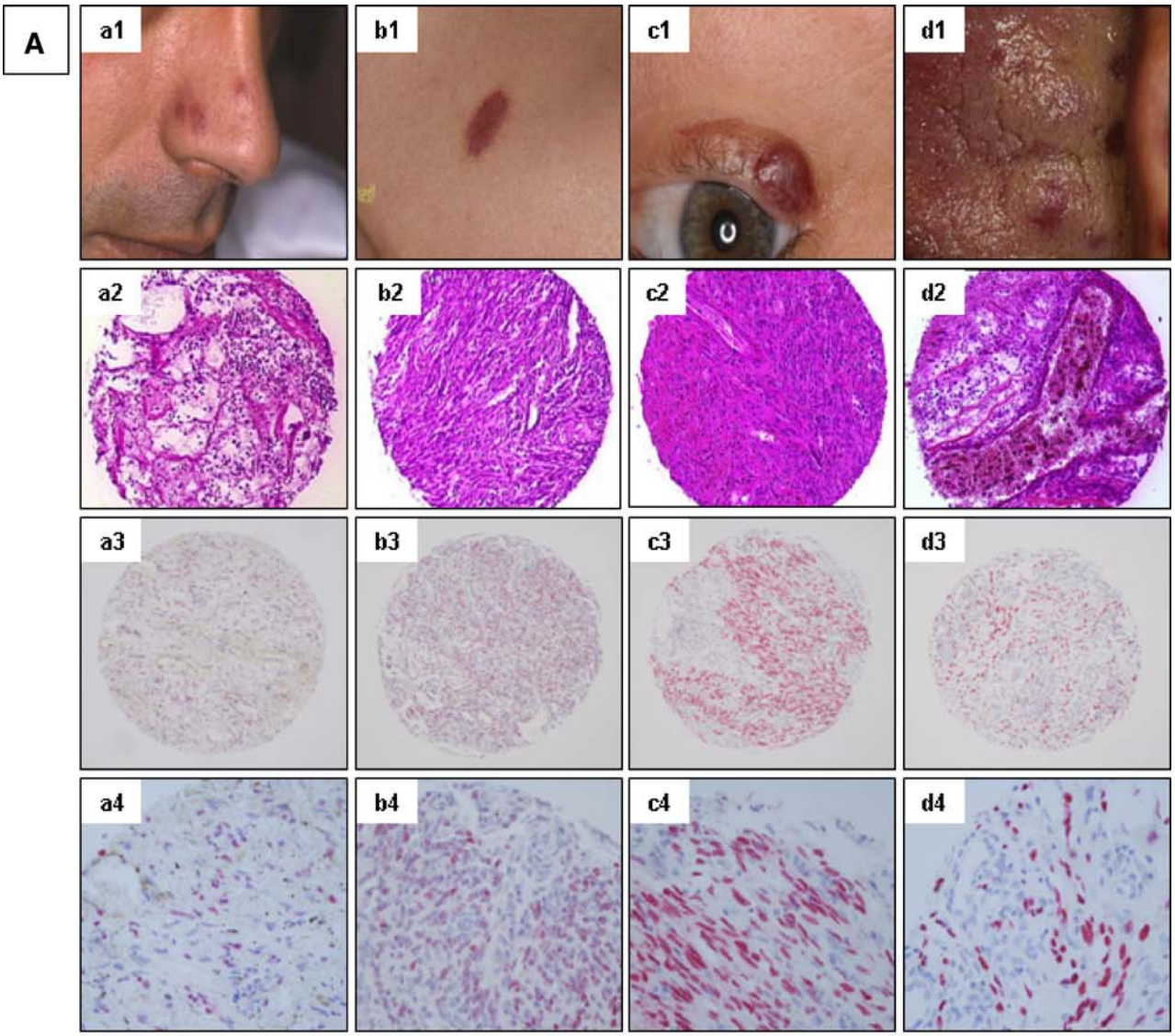
A
a1
b1
c1
d1
a2
b2
c2
d2
a3
b3
c3
d3
a4
b4
c4
d4

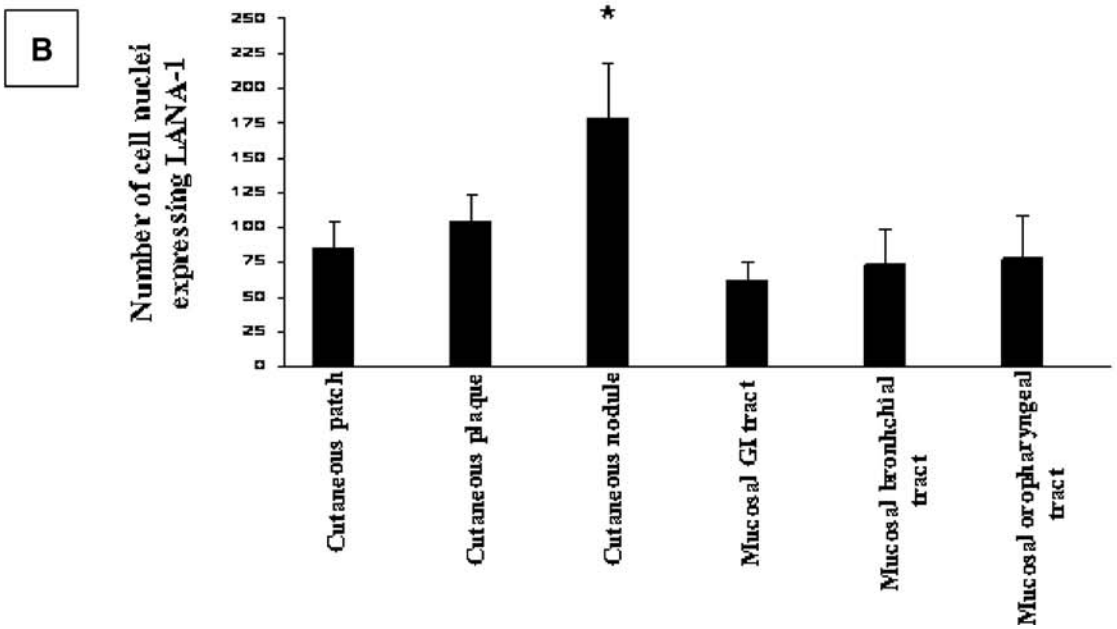
B
Number of cell nuclei expressing LANA-1
250
225
200
175
150
125
100
75
50
25
0
*
Cutaneous patch
Cutaneous plaque
Cutaneous nodule
Mucosal GI tract
Mucosal bronhchial tract
Mucosal oropharyngeal tract

pro-apoptotic (caspase 3, Bcl-xl, Bax) and HIF-1α proteins, at different stages of KS disease progression. These proteins were identified immunohistochemically using TMA technology, from tissue specimens of 245 HIV-infected individuals and their level compared to KS clinico-pathological features. LANA-1 protein expression was compared to Bcl-2, Mcl-1 and HIF-1α protein expression.

Materials and methods

Patients and samples

The medical records of the Department of Pathology of Pasteur Hospital (Nice, France) were searched from 1983 to 2004 for cases of KS in HIV-positive patients not treated with HAART. Tissue specimens of 245 patients were included in this study. These patients ranged in age from 28 to 74 years, with a mean of 37 years. All except 18 were men and all were Caucasian living in the Nice area. Risk factor(s) for HIV infection were noted in all patients; 28 men were intravenous drug users; 199 men were homosexuals or bisexuals. Women were heterosexuals without known risk. CD4+ T cell counts ranged from 8 to 122 per cubic millimetre, with a mean of 49 per cubic millimetre. For patients with cutaneous KS, clinical data were obtained from the Department of Dermatology of the Archet Hospital (Nice, France). Seventy-nine patients presented with KS lesions of different stages (patch 25 cases, plaque 27 cases, nodule 27 cases) isolated from the skin (Figs. 1 and 2a). Sixty-three patients presented with KS mucosal lesions of different sites (bronchial tract 18 cases, GI tract 24 cases, oropharynx 21 cases). Finally, 118 patients presented with a visceral KS lesion of different organs (liver 19 cases, lymph node 21 cases, pancreas 13 cases, lung 23 cases, adrenal 21 cases, spleen 21 cases; Fig. 1**).**

Tissue microarray and immunohistochemistry

Representative KS lesions obtained for each patient for building TMAs were selected from haematoxylin and eosin (HE)-stained sections. TMA construction and high-throughput analysis of tissue samples were performed in accordance with institutional guidelines. HE sections of KS lesions were reviewed by five pathologists (EL, IL, VH, CB and PH), and areas of tumours were marked on the slides. Areas of necrosis, large haemorrhage and normal tissue were avoided. TMAs were set up as previously described [22, 23]. Briefly, three tissue cores (600 μm in diameter) corresponding to three representative central areas of the lesion were selected. The tissue cores were arrayed into a recipient paraffin block as previously described [24]. TMAs with KS specimens contained normal skin tissue (6 tissue cores), which served both as a control and as a regulating mark spacing of 1 mm between core centres. A 4-μm HE-stained section was reviewed to confirm the presence of morphologically representative areas of the original lesions.

Immunohistochemical methods were performed using the automated immunostainer Bond-X system (Medite, Nunningen, Switzerland) on serial 2-μm deparaffinized TMA sections. Briefly, these sections were incubated with 0.1% trypsin (Sigma Chemical Co, St. Louis, MO, USA) in phosphate-buffered saline (PBS, pH7.5) for 10 min at 37°C. After washing with distilled water, sections were incubated with 0.03% hydrogen peroxide containing 0.2% sodium azide for 20 min (for blocking intrinsic peroxydase), then washed with PBS. In studies into Bcl-2, Bcl-X and caspase 3, antigen retrieval was carried out as reported previously in ethylenediaminetetraacetic acid (EDTA) buffer pH8.6 by heating in a microwave oven for 5 min and repeated three times. Citrate buffer (0.01 mol/l, pH6.0) microwave antigen retrieval was used in place of the EDTA buffer in studies into Mcl-1. The monoclonal mouse anti-LANA-1 (Novocastra, Newcastle, UK; clone 13B10) antibody was added at a dilution of 1:25 in Tris buffer for 1 h. Immunostaining was performed following heat-induced epitope retrieval with retrieval ER 2 solution (Novocastra) at 95°C for 20 min. The anti-human Bcl-2 mouse antibody (monoclonal immunoglobulin G (IgG), DAKO, Carpinteria, CA, USA, clone 124; diluted 1: 50), mouse anti-human Bcl-xL antibody (monoclonal IgG, Santa Cruz, San Diego, CA, USA; clone H-5, diluted 1:400), rabbit anti-human antibody Mcl-1 (polyclonal IgG, Lot 057; diluted 1:30), mouse anti-human Bax (A3533; diluted 1:100) and anti-caspase 3 (A3537; diluted 1:50) antibodies were all from DAKO, and the mouse anti-HIF-1α monoclonal antibody (BD Biosciences Pharmingen; San Diego, CA, USA; clone 54; diluted 1:500) was incubated on sections at room temperature for 1 h. After rinsing with PBS, sections were incubated with peroxidase-labelled anti-mouse Igs or peroxidase-labelled anti-rabbit Igs (DAKO) for 45 min. Negative controls were performed by omission of the primary antibody and by using normal mouse IgG_1 (DAKO) in each experiment. Sections were then washed with PBS, coloured with 3-amino-9-ethylcarbazole in acetate buffer containing hydrogen peroxide, counterstained with haematoxylin and mounted with aqueous mounting medium. After staining, slides were analysed with an image analysis workstation (Spot Browser version 7, Alphelys,

Fig. 3 Comparison of the number of cell nuclei expressing LANA-1 ▶ in visceral KS lesions, in isolated cutaneous KS and in cutaneous KS associated with secondary visceral KS lesions. **a** Tissue microarrays of lung (*a1*, *a2*), liver (*b1*, *b2*) and spleen (*c1*, *c2*) KS (anti-LANA-1 immunostaining; *a1–c1*, ×100; *a2–c2*, ×400). **b** Number of cell nuclei expressing LANA-1

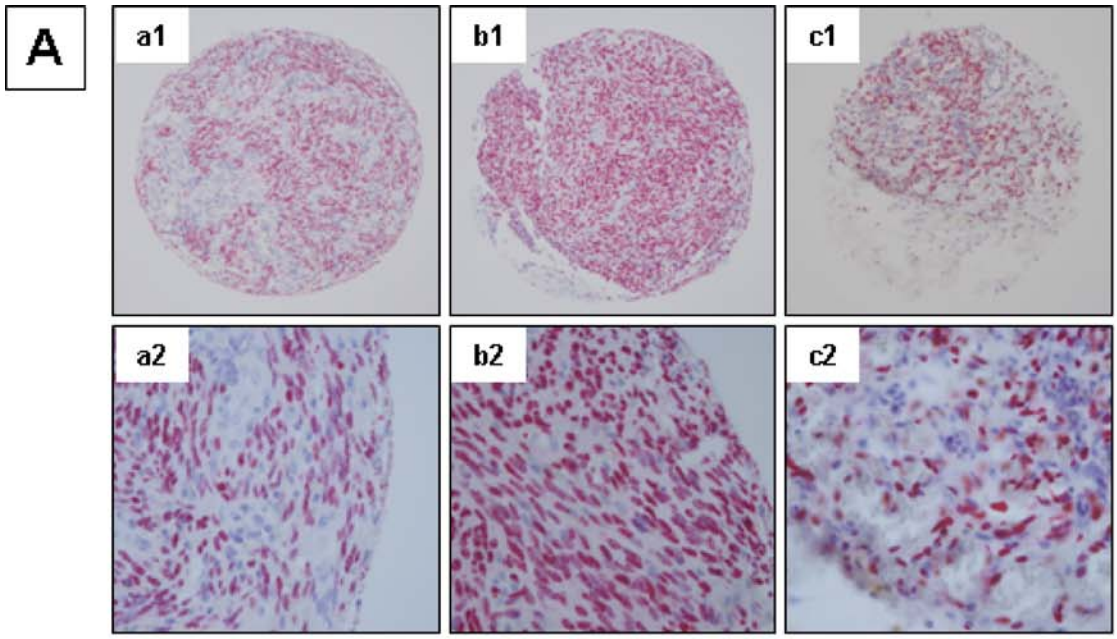
A
a1
b1
c1
a2
b2
c2

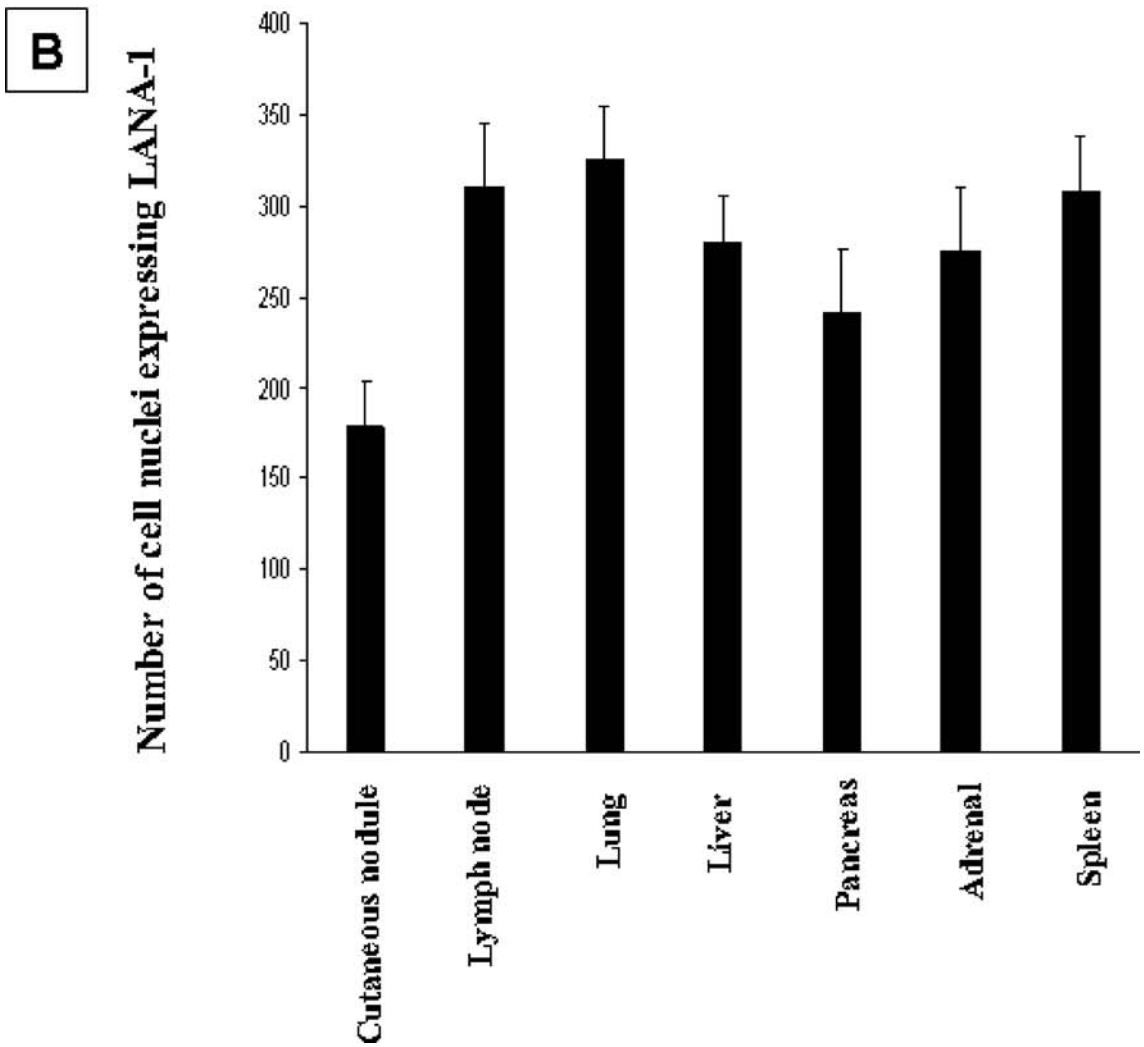
B
Number of cell nuclei expressing LANA-1
400
350
300
250
200
150
100
50
0
Cutaneous nodule
Lymph node
Lung
Liver
Pancreas
Adrenal
Spleen

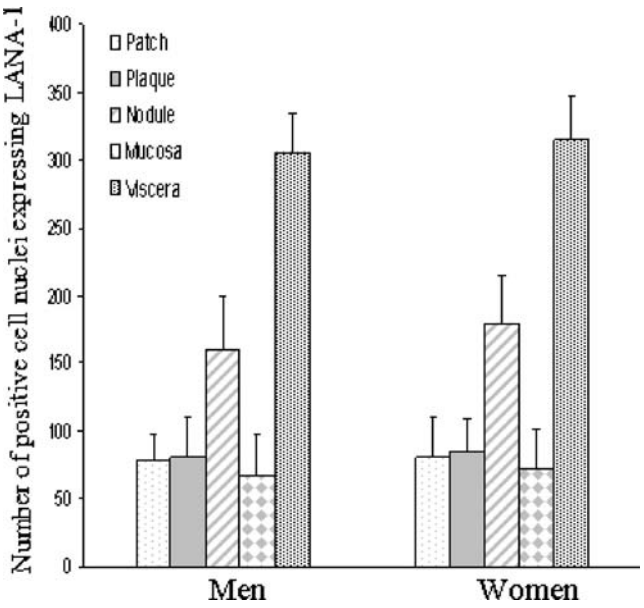

Fig. 4 Comparison of the number of cell nuclei expressing LANA-1 in KS lesions in females and males

Paris, France) as previously described [24, 25]. Briefly, the signal intensity and number of positive nuclei of digitised images were determined using Spot Browser software. For each patient, the mean of the score of a minimum of two core biopsies was calculated. Discrepancies were resolved by five pathologists (EL, MI, VH, CB and PH) under a multiheaded microscope. Correlation of staining for LANA-1 and HIF-1α, Bcl-2 or Mcl-1 was done by comparing the percentage of positive cells obtained for HIF-1α, Bcl-2, Mcl-1 and the number of LANA-1-positive cell nuclei in different KS lesions. They were classified into different groups (from 1 to 9, according to the number of LANA-1-positive detected cells): group 1 five to ten positive nuclei cells, group 2 ten to 50 positive nuclei; group 3 50–100 positive nuclei; group 4 100–150 positive nuclei cells; group 5 150–200 positive nuclei cells; group 6 200–250 positive nuclei cells; group 7 250–300 positive nuclei cells; group 8 300–350 positive nuclei cells; group 9 350–400 positive nuclei cells. Moreover, whole-tissue sections from tumour blocks of a subset of 20 cutaneous nodular KS were stained and compared by visual inspection with the corresponding TMA discs. For figures, polychromatic high-resolution spot images (1,392×1,040 pixels) were obtained using a Leica DMR optic microscope (Leica Microsystems, Rueil-Malmaison, France).

Statistical analysis

Histospots containing less than 10% of a lesion were excluded from additional analyses. Nonparametric correlation (Spearman's *P* coefficient; SPSS release 12.01) was used to compare data from whole-tissue sections and discs as previously described [24]. The number of positive nuclei was compared between the groups of studied lesions using the Mann–Whitney test. Correlation between the number of positive nuclei for LANA-1 staining, the number of positive nuclei for cells protected against apoptosis and/or the positive nuclei for HIF-1α staining was evaluated with the Spearman's rank correlation test. Values were expressed as a mean (±SEM). A $p<0.05$ was considered statistically significant.

Results

LANA-1 expression in nodular, patch and plaque cutaneous KS lesions and in mucosal KS lesions

Immunohistochemistry with an anti-LANA-1 antibody was performed on biopsies taken from cutaneous patch, plaque and nodule lesions and from mucosal lesions without associated visceral or disseminated disease (Fig. 2a, a1–d1). Evaluation of the density of nuclei expressing LANA-1 was performed only on representative spots (Fig. 2a, a2–d2). Positive nuclei were observed mainly in endothelial cells lining vessels and in a few other spindle cells (Fig. 2a). In patients with cutaneous patch (Fig. 2a, a3–a4) and plaque lesions (Fig. 2a, b3–b4), positive nuclei were 77±22 and 104±21 cells per square millimetre, respectively (Fig. 2b). The density of nuclei expressing LANA-1 increased strongly in patients with cutaneous nodules (178±45 per square millimetre; $p<0.05$; Figs. 2a, c3–c4, and 2b). Nuclei positive for LANA-1 staining were similarly found in patients with isolated mucosal lesions from the GI, bronchial and oropharyngeal tract (Fig. 2a, d3–d4, and 2b). Positive nuclei were observed both in endothelial lining vessels and in other spindle cells.

LANA-1 expression in visceral KS lesions and in nodular KS lesions with or without associated visceral KS lesions

The number of positive nuclei detected by immunostaining with an anti-LANA-1 antibody was strongly increased in

Fig. 5 Expression of apoptotic proteins in different lesions of KS. **a** ▶ Number of anti-apoptotic and pro-apoptotic molecules in patch, plaque and nodular isolated cutaneous lesions and in mucosal lesions (*a1*). Correlation of cells with positive nuclei for Bcl-2 (*a2*) and Mcl-1 (*a3*) and LANA-1 staining in patch, plaque and nodular isolated cutaneous lesions and in mucosal lesions. **b** Number of anti-apoptotic and pro-apoptotic molecules in cutaneous KS associated with secondary visceral KS lesions and in visceral KS lesions (*b1*). Correlation of cells with positive nuclei for Bcl-2 (*b2*) and Mcl-1 (*b3*) and LANA-1 for staining in cutaneous KS associated with secondary visceral KS lesions and in visceral KS lesions. The number of LANA-1-positive cell nuclei in different KS lesions was classified into nine different groups according to the number of positive cells, as described in the "Materials and methods" section

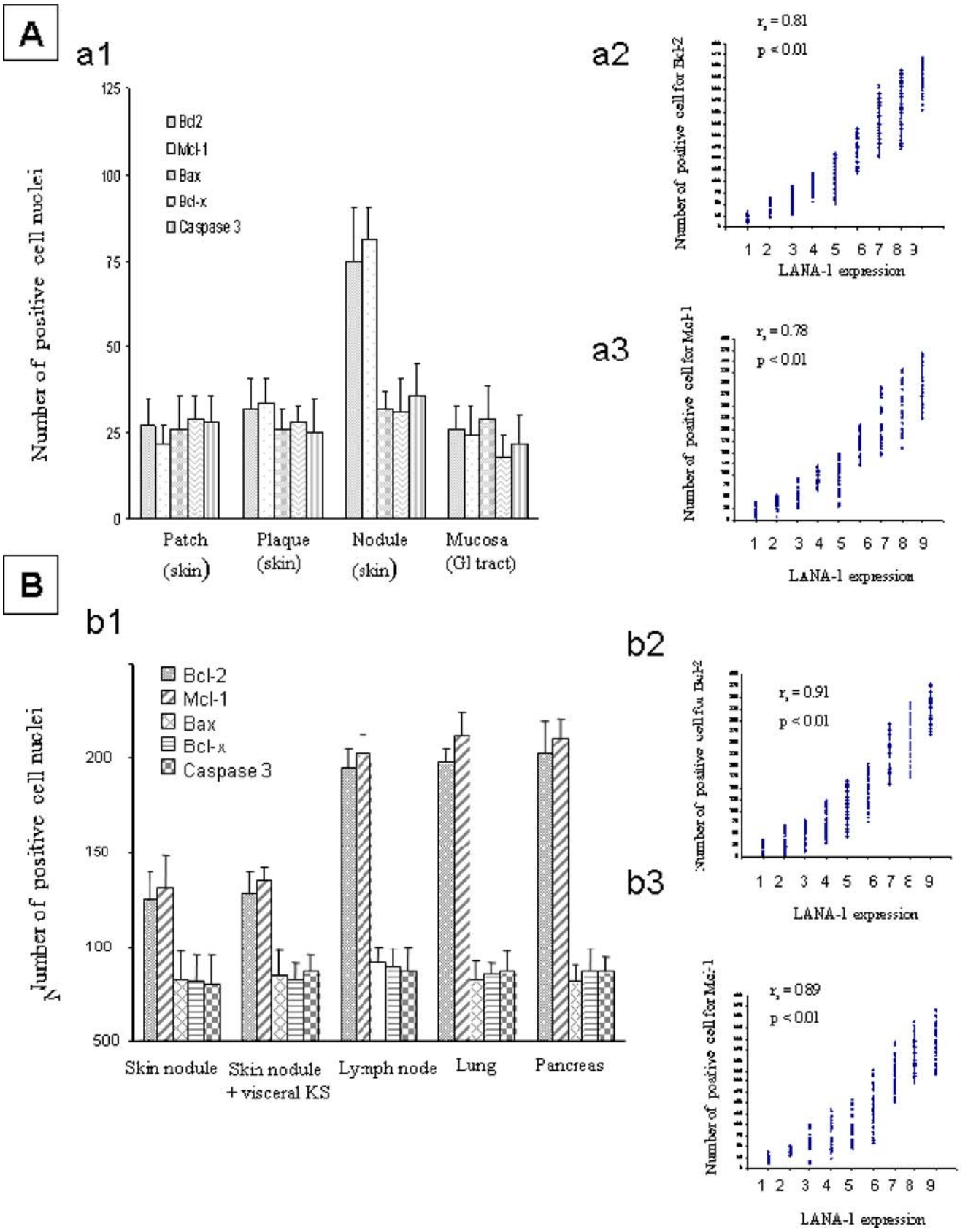
A
a1
Number of positive cell nuclei
125
100
75
50
25
0
Bcl2
Mcl-1
Bax
Bcl-x
Caspase 3
Patch (skin)
Plaque (skin)
Nodule (skin)
Mucosa (GI tract)
a2
$r_s = 0.81$
$p < 0.01$
Number of positive cell for Bcl-2
1 2 3 4 5 6 7 8 9
LANA-1 expression
a3
$r_s = 0.78$
$p < 0.01$
Number of positive cell for Mcl-1
1 2 3 4 5 6 7 8 9
LANA-1 expression
B
b1
Number of positive cell nuclei
200
150
100
500
Bcl-2
Mcl-1
Bax
Bcl-x
Caspase 3
Skin nodule
Skin nodule + visceral KS
Lymph node
Lung
Pancreas
b2
$r_s = 0.91$
$p < 0.01$
Number of positive cell for Bcl-2
1 2 3 4 5 6 7 8 9
LANA-1 expression
b3
$r_s = 0.89$
$p < 0.01$
Number of positive cell for Mcl-1
1 2 3 4 5 6 7 8 9
LANA-1 expression

visceral KS lesions in comparison with nodular cutaneous KS lesions with or without associated visceral and disseminated KS disease (Fig. 3a, b). Nuclei positive for LANA-1 staining in visceral KS lesions were observed in endothelial cells lining vessels and in other spindle cells (Fig. 3a).

LANA-1 expression in female and male KS lesions

The number of positive nuclei for LANA-1 staining was evaluated by immunohistochemistry in the cutaneous (patch, plaque, nodule), mucosal and visceral KS lesions according to gender (Fig. 4). No significant differences were found in the number of positive cell nuclei expressing LANA-1 in the different tissue specimens obtained from women and men (Fig. 4).

Expression of apoptosis-related proteins in KS lesions and correlation with LANA-1 staining

Cell apoptosis in different KS lesions was evaluated by immunohistochemical staining for Bcl-2, Mcl-1, Bax, Bcl-xL and caspase 3. Interestingly, the number of cells expressing the anti-apoptotic (Bcl-2, Mcl-1) proteins was increased in nodular cutaneous KS lesions when compared to patch and plaque cutaneous and mucosal KS lesions (Fig. 5a, a1). Moreover, the number of cells expressing Bcl-2 and Mcl-1 correlated with the density of cell nuclei positive for LANA-1 staining (Fig. 5a, a2 and a3). The number of cells expressing Bax, Bcl-xL and caspase 3 was similar in patch, plaque and nodular cutaneous and mucosal KS lesions (not shown). The nine different groups were classified arbitrarily according to the number of LANA-1-positive cell nuclei. Groups 1–3 corresponded to patch KS specimens, groups 4 and 5 to plaque and mucosal KS specimens and groups 6–9 to nodular and visceral KS specimens. Additionally, the number of apoptotic cells was lower in visceral KS lesions in comparison with those observed in cutaneous KS lesions associated with visceral KS dissemination (Fig. 5b, b1). In all these lesions, the number of Bcl-2- and Mcl-1-expressing cells correlated with the density of positive cell nuclei for LANA-1 staining (Fig. 5b, b2 and b3).

HIF-1α expression in KS lesions and correlation with LANA-1 expression

Immunohistochemistry with an anti-HIF-1α antibody was performed on biopsies taken from cutaneous patch, plaque and nodule lesions and mucosal KS lesions without associated visceral or disseminated disease and from different visceral KS lesions (Fig. 6a, b, b1). In patients with cutaneous patch and plaque lesions, positive nuclei were 50±18 and 54±22 cells per square millimetre, respectively (Fig. 6b, b1). Positive nuclei were observed mainly in endothelial cells lining vessels. The density of nuclei expressing HIF-1α was strongly increased in patients with cutaneous nodules (250±15 cells per square millimetre, $p<0.05$; Fig. 6a, b, b1). Most positive nuclei were noted in spindle cells. Nuclei positive for HIF-1α staining were also found in patients with isolated mucosal lesions from GI, bronchial and oropharyngeal tracts (Fig. 6b, b1). Positive nuclei were observed both in endothelial lining vessels and in other spindle cells. The number of positive nuclei after immunostaining with HIF-1α antibody was strongly increased in all visceral KS lesions in comparison to nodular cutaneous KS lesions associated with visceral and disseminated KS disease (Fig. 6a, b, b1). Nuclei positive for HIF-1α staining were mostly observed in all spindle cells. Interestingly, the number of cells expressing LANA-1 staining correlated with the density of positive cells for HIF-1α (Fig. 6b, b2). The nine different groups classified arbitrarily according to the number of LANA-1-positive cell nuclei revealed that groups 1–3 corresponded to patch, plaque skin KS and GI tract, bronchial and oropharyngeal mucosal KS specimens, groups 4–6 to nodular cutaneous KS and groups 7–9 to visceral KS lesions.

Discussion

The natural history and pathogenesis of HHV8 infections in immunosuppressed patients has been extensively studied by different groups [21, 26–30]. The identification of KS patients with poor survival is essential in determining the treatment strategy. However, discrepant results have been reported with reference to the HHV8 viral load in patients' sera in early and late stages of HIV-associated KS. Some studies reported an increase in the KSH/HHV8 DNA load of patients with clinical KS [21, 28, 29]. In contrast, other studies showed a decrease in the HHV8 viral load in sera from patients with late stages of KS, indicating the probability of suppression of HHV8 release and/or immunosegregation of virus during these later stages [26, 30–32]. Another study showed that measurement of the HHV8 load

Fig. 6 Detection of the HIF-1α protein in different KS lesions **a** Tissue microarrays of cutaneous patch (*a*), plaque (*b*), nodule (*c*), bronchial (*d*), digestive (*e*) and oral (*f*) mucosa and lung (*g*), liver (*h*) and pancreatic (*i*) KS lesions (anti-HIF-1α immunostaining; *a1–a6*, ×400). **b** (*b1*) Quantification of the number of cell nuclei positive for the HIF-1α protein. (*b2*) Correlation of the number of positive nuclei for HIF-1α staining and the number of nuclei positive for LANA-1 staining in the different KS specimens evaluated in this series. The number of LANA-1 positive cell nuclei in different KS lesions was classified into nine different groups according to the number of positive detected cells, as described in the "Materials and methods" section

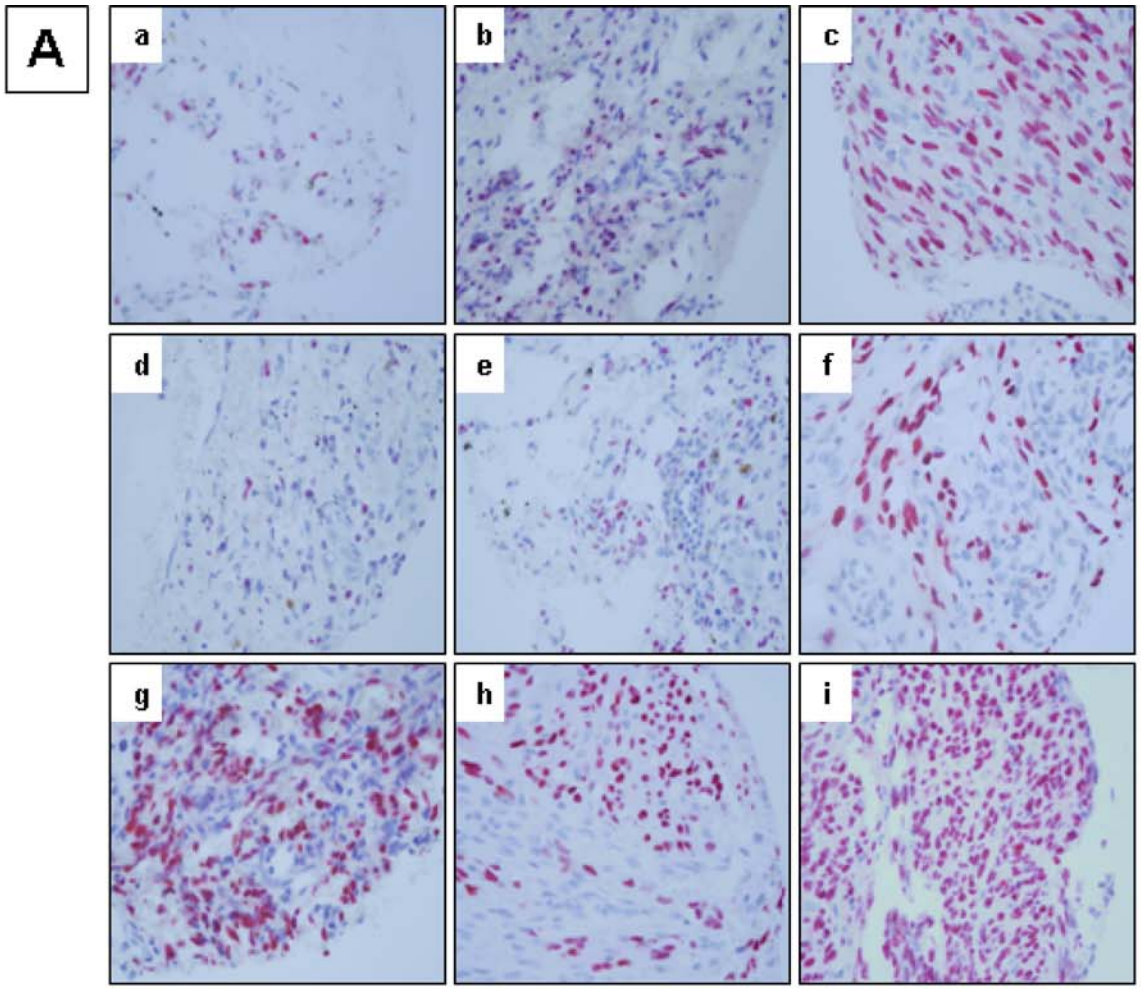
A
a
b
c
d
e
f
g
h
i

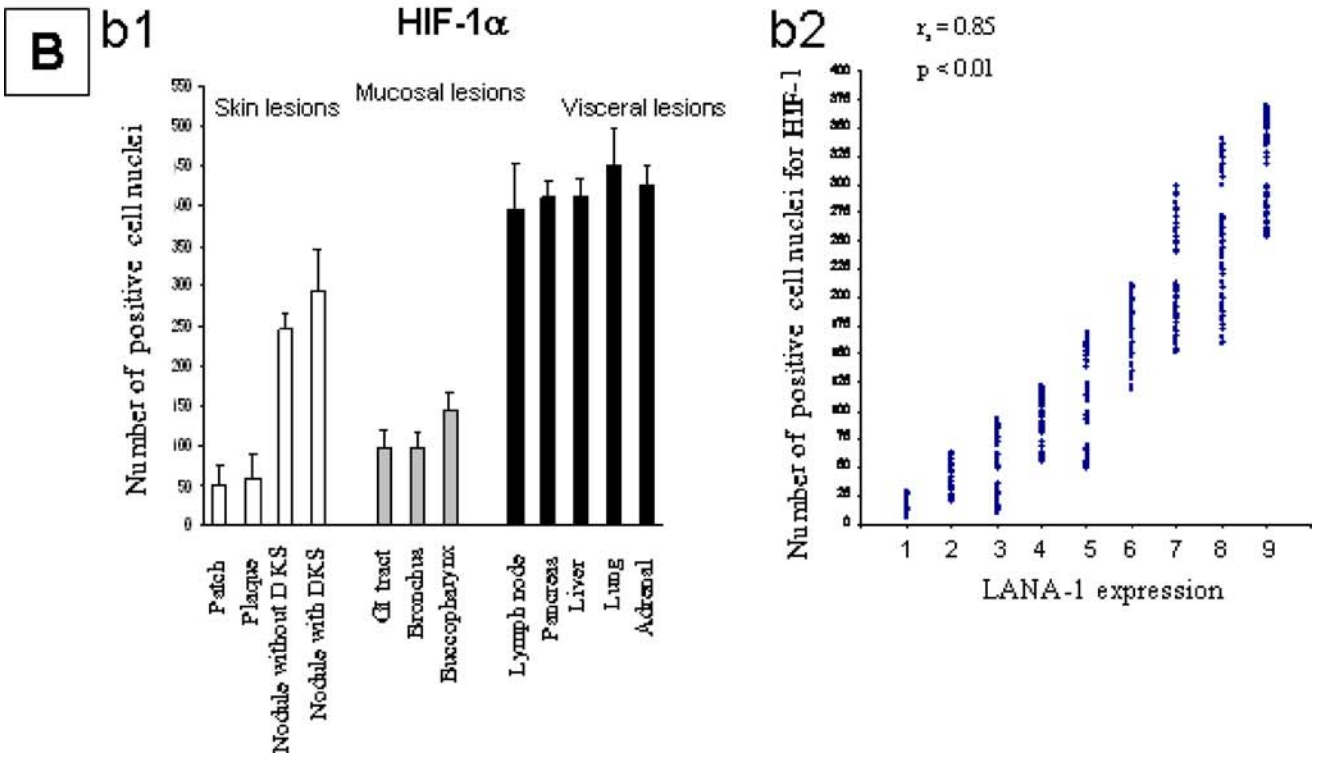
B
b1
HIF-1α
Skin lesions
Mucosal lesions
Visceral lesions
Number of positive cell nuclei
Patch
Plaque
Nodule without D KS
Nodule with DKS
GI tract
Bronchus
Bronchopharynx
Lymph node
Pancreas
Liver
Lung
Adrenal
b2
r_s = 0.85
p < 0.01
Number of positive cell nuclei for HIF-1
LANA-1 expression

in peripheral blood mononuclear cells provided a limited correlation with the clinical stage of KS [33]. A recent study performed in AIDS-related KS from Uganda demonstrated that the HHV8 load in peripheral blood was positively and significantly associated with the rate of KS progression but not with the KS burden [34]. Finally, a clinical scoring system to predict survival in HIV-associated KS, which includes the CD4 count, age, association with another AIDS-associated illness, has been established previously in cases with KS as the AIDS-defining illness [35]. Although HIV infection is neither necessary nor sufficient for KS development, it is associated with an increased incidence and a more aggressive course of KS. Moreover, decreased CD4 and/or CD8 lymphocyte counts have been associated with KS progression in HIV-positive patients.

Discrepancies exist between tissue biomarkers and their potential usefulness in various clinico-pathological stages of KS. In this regard, our study was conducted so as to determine the level of expression of LANA-1 in tissues taken from cutaneous, mucosal and visceral HIV-associated KS. LANA encoded by ORF73 is one of the few HHV8-encoded proteins that is highly expressed in all latently infected tumour cells, which strongly suggests that LANA-1 plays a critical role in the maintenance of a latent HHV8 infection. A previous study showed that the highly concentrated expression of LANA-1, anchored to the host genome in the nuclear foci of latently infected cells and replicated through each cell generation, may function as an epigenetic modifier [36]. In our study, we demonstrate that LANA-1 expression is increased in later stages of KS in HIV-positive patients. In cutaneous KS, immunostaining showed a significantly ($p<0.005$) higher rate of positive nuclear nodules than in patch and plaque lesions. Moreover, the level of LANA-1-positive nuclei was dramatically increased in all visceral KS compared to superficial mucosal KS ($p<0.001$) and to nodular cutaneous KS ($p<0.005$). Thus, our observations indicate a strong correlation between the presence of HHV8 in tissue specimens and the KS clinico-pathological features. These results indicate that the viral infection is not aborted during KS progression and that the higher clinical aggressiveness of visceral KS could be linked to a higher HHV8 load in tissues. This is in accordance with a previous study that showed by polymerase chain reaction an increase in the HHV8/KSHV load in cutaneous lesions of AIDS-KS during progression from early (patch/plaque) to late (nodular) stages [37].

In Western countries, AIDS-KS has a clear male predominance [1]. The paucity of KS in women was initially attributed to lower androgenic hormones. However, KS occurs infrequently in women in the Western world since they are only rarely infected with HHV8. In our study, we demonstrate that the level of LANA-1 positive nuclei was similar in tissue specimens from HIV-positive men and women and correlated similarly to the clinico-pathological stages of the disease.

Most people infected with HHV8 do not develop KS, suggesting that HHV8 is a necessary but not sufficient factor for the development and probably the progression of the disease. Thus, in addition to the expression of LANA-1, different molecules involved in cell growth and cell death have been studied in KS biopsy specimens, but data on the development and progression of KS related expression of these molecules are controversial [38–45]. Studies have implicated some genes of HHV8 in the reduction of apoptosis in KS lesions. HHV8 encodes homologues of proteins that are involved in the control of apoptosis (i.e., v-Bcl-2, v-IL6, v-FLIP) or in the control of cellular proliferation and/or differentiation (i.e., v-cyclins, v-G protein-coupled receptors)[17, 18]. Stürzl et al. have shown in a small series of biopsies that sequences encoding the anti-apoptotic protein viral-FLIP are expressed at very low levels in early KS lesions, but expression increases dramatically in late-stage lesions [44]. Other studies suggested several mechanisms to explain the high apoptotic rate in early stage KS. For example, high concentrations of inflammatory cytokines, such as TNF-α and interferon-γ may induce endothelial cell apoptosis [45]. Alternatively, apoptosis in early lesions could be due to activated T cells expressing the pro-apoptotic Fas ligand [19]. However, it is still not clear whether the development and progression of KS are related to increased cell growth or to decreased cell death or both mechanisms. The rather low number of mitoses seen in most KS lesions, together with the absence of a correlation between the histological progression of KS and its proliferation fraction, suggests that the pathogenesis of KS may be related to escape from apoptosis rather than to increased proliferation. In our study, Bcl-2 and Mcl-1 were found to be highly expressed in tumour cells of late-stage KS lesions. Moreover, the level of both these anti-apoptotic proteins strongly correlated with the level of LANA-1 during the different pathological KS stages These findings obtained in a large series of patients strongly support the premise that anti-apoptotic mechanisms have to be operative to allow growth of KS lesions.

In this study, we were interested in looking at the potential role of HIFs in KS progression. It is well known that tumour hypoxia and the critical molecular mediators of hypoxia, HIFs, regulate multiple steps of tumourigenesis including tumour formation, progression and response to therapy [46–48]. HIF-1α is commonly increased in a variety of human tumours [49]. A study demonstrated that hypoxia has a protective effect on apoptotic cell death [50]. Moreover, angiogenesis is critical for tumour progression and HIF can directly activate the expression of a number of pro-angiogenic factors, including VEGF and VEGF recep-

tors [46]. In this regard, recent work has demonstrated that LANA-1 can function as an inhibitor of HIF-1α suppressor proteins, but can also induce nuclear accumulation of HIF-1α during latent infection [20]. Moreover, it has been shown in vitro, that HHV8 infection of primary cultures leads to increased expression of HIF-1α and the activation of HIF may play a role in KS formation, localization and tumour progression [51]. Our present work clearly demonstrates that the levels of HIF-1α and LANA-1 are significantly correlated.

Although the mechanism(s) by which HHV8 is involved in the progression of KS lesions cannot be elucidated from the mostly descriptive data presented here, we can put forward different hypotheses. Our finding that LANA-1 expression increases from early patch to late nodular cutaneous and visceral KS lesions are consistent with several previous reports of increased cell survival caused by the inhibition of apoptosis by viral gene [31, 42, 44]. In this regard, a bimodal model of KS tumour development from an early (cutaneous patch) reactive lesion to late (cutaneous nodule and visceral involvement) progressively clonal tumour cell proliferation can be proposed. In addition, a significant difference in proliferation between LANA-1 positive and negative spindle cells was found previously and suggests that LANA-1 positive spindle cells may have a proliferative advantage [37]. However, the reason why the HHV8 load increases during tumour progression is still unclear and further studies are needed to determine if viral permissiveness is increased in the different subpopulations of cells present in KS lesions during tumour progression. A potential mechanism to explain how HHV8 stimulates tumour progression could implicate the action of virally encoded G-protein-coupled receptor (vGPCR), an HHV8 lytic gene product that has been functionally linked to HHV8-mediated tumourigenesis [52]. By activating the Ras, Raf and Rac intracellular signalling pathways, vGPCR could induce the expression and secretion of vascular endothelial growth factor in an autocrine and paracrine manner [53]. Moreover, this process might also involve the direct phosphorylation of HIF-1α [54].

Finally, we demonstrated, in a large series of AIDS patients with KS, a stage-related increase in LANA-1, Bcl-2, Mcl-1 and HIF-1 α protein levels that is strongly associated with a strong correlation of these molecules in KS progression. In future, the data may be useful in distinguishing between patients with a low- and high-risk of disease progression and in predicting their survival.

Acknowledgements The authors thank Christiane Brahimi-Horn for editing the manuscript. This work is supported by the Canceropôle PACA (LPCE Platform).

Conflict of interest statement No conflict of interest

References

1. Beral V, Peterman TA, Berkelman RL et al (1990) Kaposi's sarcoma among persons with AIDS: a sexually transmitted infection ? Lancet 335:123–128
2. Cattelan AM, Calabro ML, De Rossi A et al (2005) Long-term clinical outcome of AIDS-related Kaposi's sarcoma during highly active antiretroviral therapy. Int J Oncol 27:779–785
3. Jones JL, Hanson DL, Dworkin MS et al (1999) Effects of antiretroviral therapy on recent trends in selected cancers among HIV-infected persons. J Acquir Immune Defic Syndr 21:S11–S17
4. Parkin DM, Wabinga H, Nambooze S et al (1999) AIDS-related cancers in Africa: maturation of the epidemic in Uganda. AIDS 13:2563–2570
5. Bower M, Nelson M, Young AM et al (2005) Immune reconstitution inflammatory syndrome associated with Kaposi's sarcoma. J Clin Oncol 23:5224–5228
6. Hofman P, Nelson AM (2006) The pathology induced by highly active antiretroviral therapy against human immunodeficiency virus: an update. Curr Med Chem 13:3121–3132
7. Chang Y, Cesarman E, Pessin MS et al (1994) Identification of herpesvirus-like DNA sequences in AIDS-associated Kaposi's sarcoma. Science 266:1865–1869
8. Hiatt KM, Nelson AM, Lichy JH et al (2008) Classic Kaposi Sarcoma in the United States over the last two decades: a clinicopathologic and molecular study of 438 non-HIV-related Kaposi Sarcoma patients with comparison to HIV-related Kaposi sarcoma. Mod Pathol 21:572–582
9. Schalling M, Ekman M, Kaaya EE et al (1995) A role for a new herpes virus (KSHV) in different forms of Kaposi's sarcoma. Nat Med 1:707–708
10. Hengge UR, Ruzicka T, Tyring ST et al (2002) Update on Kaposi's sarcoma and other HHV8 associated diseases. Part 1: epidemiology, environmental predispositions, clinical manifestations, and therapy. Lancet Infect Dis 2:281–292
11. Weiss SW, Goldblum JR (2001) Enzinger and Weiss's soft tissue tumors, 4th edn. Mosby, St. Louis, pp 917–954
12. Afessa B, Green W, Chiao J et al (1998) Pulmonary complications of HIV infection: autopsy findings. Chest 113:1225–1229
13. Hofman P, Saint-Paul MC, Battaglione V et al (1999) Autopsy findings in the acquired immunodeficiency syndrome (AIDS). A report of 395 cases from the south of France. Pathol Res Pract 195:209–217
14. Klatt EC, Nichols L, Nogushi TT (1994) Evolving trends revealed by autopsies of patients with the acquired immunodeficiency syndrome. 565 autopsies in adults with the acquired immunodeficiency syndrome, Los Angeles, Calif, 1982–1993. Arch Pathol Lab Med 118:884–890
15. Hengge UR, Ruzicka T, Tyring SK et al (2002) Update on Kaposi's sarcoma and other HHV8 associated diseases. Part 2: pathogenesis, Castleman's disease, and pleural effusion lymphoma. Lancet Infect Dis 2:344–352
16. Renne R, Barry C, Dittmer D et al (2001) Modulation of cellular and viral gene expression by the latency-associated nuclear antigen of Kaposi sarcoma-associated herpesvirus. J Virol 75:458–468
17. Bais C, Santomasso B, Coso O et al (1998) G-protein-coupled receptor of Kaposi sarcoma-associated herpesvirus is a viral oncogene and angiogenesis activator. Nature 391:86–89
18. Cheng EH, Nicholas J, Bellows DS et al (1997) A Bcl-2 homolog encoded by Kaposi sarcoma-associated virus, human herpesvirus 8, inhibits apoptosis but does not heterodimerize with Bax or Bak. Proc Natl Acad Sci U S A 94:690–694
19. Kirchoff S, Sebens T, Baumann S et al (2002) Viral IFN-regulatory factors inhibit activation-induced cell death via two

positive regulator factor 1-dependent domains in the CD95 ligand promoter. J Immunol 168:1226–1234
20. Cai Q, Murakami M, Si H et al (2007) A potential a-helix motif in the amino terminus of LANA encoded by Kaposi sarcoma-associated Herpesvirus is critical for nuclear accumulation of HIF-1α in normoxia. J Virol 81:10413–10423
21. Campbell TB, Borok M, Gwanzura L (2000) Relationship of human herpesvirus 8 peripheral blood virus load and Kaposi sarcoma clinical stage. AIDS 14:2109–2116
22. Giltane JM, Rimm DL (2004) Technology insight: identification of biomarkers with tissue microarray technology. Nat Clin Pract 1:104–111
23. Hoos A, Cordon-Cardo C (2001) Tissue microarray profiling of cancer specimens and cell lines opportunities and limitations. Lab Invest 81:1331–1338
24. Hofman P, Butori C, Havet K et al (2008) Prognostic significance of cortactin levels in head and neck squamous cell carcinoma: comparison with epidermal growth factor receptor status. Br J Cancer 98:956–964
25. Hofman V, Lassalle S, Selva E et al (2007) Involvement of mast cells in gastritis caused by *Helicobacter pylori*: a potential role in epithelial cell apoptosis. J Clin Pathol 60:600–607
26. Cannon MJ, Dollard SC, Black JB (2003) Risk factors for Kaposi sarcoma in men seropositive for both human herpesvirus 8 and human immunodeficiency virus. AIDS 17:215–222
27. Laney AS, Dollard SC, Jaffe HW et al (2004) Repeated measures study of human herpesvirus 8 (HHV8) DNA and antibodies in men seropositive for both HHV8 and HIV. AIDS 18:1819–1826
28. Laney AS, Cannon MJ, Jaffe HW et al (2007) Human herpesvirus 8 presence and viral load are associated with the progression of AIDS-associated Kaposi sarcoma. AIDS 21:1541–1545
29. Marcelin AG, Gorin I, Morand P et al (2004) Quantification of Kaposi sarcoma-associated herpesvirus in blood, oral mucosa, and saliva in patients with Kaposi sarcoma. AIDS Res Hum Retroviruses 20:704–708
30. Pak F, Mwakigonja AR, Kokhaei P et al (2007) Kaposi sarcoma herpes virus load in biopsies of cutaneous and oral Kaposi sarcoma lesions. Eur J Cancer 43:1877–1882
31. Hayward GS (1999) Human herpesvirus 8 latent-state gene expression and apoptosis in Kaposi sarcoma lesions. J Natl Cancer Inst 9:1705–1707
32. Massambu C, Pyakurel P, Kaaya E et al (2003) Serum HHV8 DNA and Tat antibodies in Kaposi sarcoma patients with and without HIV-1 infection. Anticancer Res 23:2389–2395
33. Guttman-Yassky E, Abada R, Kra-Oz Z (2007) Relationship between human herpesvirus 8 loads and disease stage in classic Kaposi sarcoma patients. Diagn Microbiol Infect Dis 57:387–392
34. Nsubuga MM, Biggar RJ, Combs S et al (2008) Human herpesvirus 8 load and progression of AIDS-related Kaposi sarcoma lesions. Cancer Lett 263:182–188
35. Stebbing J, Sanitt A, Nelson M et al (2006) A prognostic index for AIDS-associated Kaposi ‘s sarcoma in the era of highly active antiretroviral therapy. Lancet 367:1495–1502
36. Stuber G, Mattsson K, Flaberg E et al (2007) HHV8 encoded LANA-1 alters the higher organization of the cell nucleus. Mol Cancer 6:28
37. Pyakurel P, Massambu C, Castaños-Vélez E et al (2004) Human herpesvirus 8/Kaposi sarcoma herpesvirus cell association during evolution of Kaposi sarcoma. J Acquir Immune Defic Syndr 36:678–683
38. Dada MA, Chetty R, Biddolph SC et al (1996) The immunoexpression of bcl-2 and p53 in Kaposi’s sarcoma. Histopathology 29:159
39. Foreman KE, Wrone-Smith T, Boise LH et al (1996) Kaposi’s sarcoma tumor cells preferentially express Bcl-xL. Am J Pathol 149:795–803
40. Hodak E, Hammel I, Feinmesser M et al (1999) Differential expression of p53 and Ki-67 proteins in classic and iatrogenic Kaposi’s sarcoma. Am J Dermatopathol 21:138–145
41. Ramos da Silva S, Bacchi MM, Bacchi CE et al (2007) Human bcl-2 expression, cleaved caspase-3, and KSHV LANA-1 in Kaposi sarcoma lesions. Am J Clin Pathol 128:794–802
42. Simonart T, Degraef C, Noel JC et al (1998) Overexpression of Bcl-2 in Kaposi’s sarcoma-derived cells. J Invest Dermatol 111:349–353
43. Widmer I, Wernli M, Bachmann F et al (2002) Differential expression of viral Bcl-2 encoded by Kaposi’s sarcoma-associated herpesvirus and human Bcl-2 in primary effusion lymphoma cells and Kaposi’s sarcoma lesions. J Virol 76:2551–2556
44. Stürzl M, Hohenadl C, Zietz C et al (1999) Expression of K13/v-FLIP gene of human herpesvirus 8 and apoptosis in Kaposi’s sarcoma spindle cells. J Natl Cancer Inst 91:1725–1733
45. Rezaee SA, Cunningham C, Davison AJ et al (2006) Kaposi’s sarcoma-associated herpesvirus immune modulation: an overview. J Gen Virol 87:1781–1804
46. Brahimi-Horn MC, Chiche J, Pouysségur J (2007) Hypoxia and cancer. J Mol Med 85:1301–1317
47. Harris AL (2002) Hypoxia-a key regulatory factor in tumour growth. Nat Rev Cancer 2:38–47
48. Hickey MM, Simon MC (2006) Regulation of angiogenesis by hypoxia and hypoxia-inducible factors. Curr Top Dev Biol 76:217–257
49. Talks KL, Turley H, Gatter KC et al (2000) The expression and distribution of the hypoxia-inducible factors HIF-1alpha and HIF-2 alpha in normal tissues, cancers, and tumor-associated macrophages. Am J Pathol 157:411–421
50. Sermeus A, Cosse JP, Crespin M et al (2008) Hypoxia induces protection against etoposide-induced apoptosis: molecular profiling of changes in gene expression and transcription factor activity. Mol Cancer 7:27
51. Carroll PA, Kenerson HL, Yeung RS et al (2006) Latent Kaposi’s sarcoma-associated herpesvirus infection of endothelial cells activates hypoxia-induced factors. J Virol 80:10802–10812
52. Thirunarayanan N, Cifire F, Fichtner I et al (2007) Enhanced tumorigenicity of fibroblasts transformed with human herpesvirus 8 chemokine receptor vGPCR by successive passage in nude and immunocompetent mice. Oncogene 26:5702–5712
53. Glaunsinger B, Ganem D (2004) Highly selective escape from KSHV-mediated host mRNA shutoff and its implications for viral pathogenesis. J Exp Med 200:391–398
54. Montaner S, Sodhi A, Servitja JM et al (2004) The small GTPase Rac1 links the Kaposi sarcoma-associated herpesvirus vGPCR to cytokine secretion and paracrine neoplasia. Blood 104:2903–2911

Virchows Arch (2009) 455:171–185
DOI 10.1007/s00428-009-0800-4

ORIGINAL ARTICLE

Differentiation patterning of vascular smooth muscle cells (VSMC) in atherosclerosis

Sebastian Stintzing · Matthias Ocker · Andrea Hartner · Kerstin Amann · Letterio Barbera · Daniel Neureiter

Received: 9 March 2009 / Revised: 11 May 2009 / Accepted: 6 June 2009 / Published online: 26 June 2009

Abstract To investigate the involvement of transdifferentiation and dedifferentiation phenomena inside atherosclerotic plaques, we analyzed the differentiation status of vascular smooth muscle cells (VSMC) in vitro and in vivo. Forty normal autoptic and 20 atherosclerotic carotid endarterectomy specimens as well as 20 specimens of infrarenal and suprarenal aortae were analyzed for the expression of cytokeratins 7 and 18 and β-catenin as markers (epithelial transdifferentiation) as well as CD31 and CD34 (embryonic dedifferentiation) by conventional and double fluorescence immunohistochemistry and reverse transcription polymerase chain reaction. Looking at these markers, additional cell culture experiments with human aortic (HA)-VSMC were done under stimulation with IL-1β, IL-6, and TNF-α. Cytokeratins and β-catenin were expressed significantly higher in atherosclerotic than in normal carotids primarily localized in VSMC of the shoulder/cap region of atherosclerotic lesions. Additionally, heterogeneous cellular coexpression of CD31 and/or CD34 was observed in subregions of progressive atherosclerotic lesions by VSMC. The expression of those differentiation markers by stimulated HA-VSMC showed a time and cytokine dependency in vitro. Our findings show that (1) VSMC of progressive atheromas have the ability of differentiation, (2) that transdifferentiation and dedifferentiation phenomena are topographically diverse localized in the subregions of advanced atherosclerotic lesions, and (3) are influenced by inflammatory cytokines like IL-1β, IL-6, and TNF-α.

Keywords Atherosclerosis · Smooth muscle cells · Differentiation · Dedifferentiation · Transdifferentiation

Sebastian Stintzing and Matthias Ocker contributed equally to this work.

S. Stintzing (✉)
Department of Medicine III, University Hospital Großhadern,
LMU Munich,
Marchioninistrasse 15,
81377 Munich, Germany
e-mail: sebastian.stintzing@med.uni-muenchen.de

S. Stintzing · M. Ocker
Department of Medicine 1, University Hospital Erlangen,
Erlangen, Germany

A. Hartner
Hospital for Children and Adolescents,
University Hospital Erlangen,
Erlangen, Germany

K. Amann · D. Neureiter
Institute of Pathology, University Hospital Erlangen,
Erlangen, Germany

L. Barbera
Department of Vascular Surgery, University of Bremen,
Bremen, Germany

D. Neureiter
Institute of Pathology, Landeskliniken Salzburg,
Paracelsus Medical University,
Salzburg, Austria

Introduction

The process of atherosclerosis is described as a chronic and complex immune-mediated inflammatory disease [1]. This model is supported by the detection of an enlarged inflammatory cell infiltrate in atherosclerotic plaques, possibly caused by infectious agents (like viruses [cytomegalovirus or herpes virus] or bacteria [*Chlamydia pneumoniae* or *Helicobacter pylori*]) [2]. Additionally, the response-to-injury hypothesis of atherosclerosis focuses on the central role of activated and proliferating vascular

smooth muscle cells (VSMC) that are histologically observed in the early and late stages of atherosclerosis, thus being a key event in atherosclerosis [3–5].

It is now accepted that VSMC can display at least two different phenotypes in the pathogenesis of atherosclerotic lesions: (1) highly differentiated, contractile cells of the media and (2) synthetically active and proliferating cells invading the intima [6]. Inside normal arteries, VSMC are highly differentiated cells being responsible for the regulation of blood pressure and vascular tension. In atherosclerotic plaques, VSMC can display a more active cell type, i.e., proliferating, migrating, and secreting different proteins leading to intimal thickening and fibrosis of the vascular wall [7]. Intimal thickening seems to be the first sign of atherosclerosis, but until today, it is not known what kind of injury leads to the response of initiating atherosclerosis.

The gene expression pattern of end-differentiated VSMC is well characterized (e.g., α- and β-smooth muscle actin, smooth muscle 22α, calponin, smoothelin, and smooth muscle myosin heavy chain) [6]. Many studies dealing with proliferating VSMC show evidence that VSMC of artery walls have a multilineage potential [8] and express many different cell line antigens. Until now, a specific marker of the synthetic state of VSMC has not been established [6, 9]. The phenomena of transdifferentiation and dedifferentiation are highly conserved processes of organism development as well as of organ regeneration and reparation [10]. Recent hypotheses raised the question whether unregulated processes of the transition state could essentially be involved in chronic degenerative and inflammatory diseases like atherosclerosis as has been shown for tumorigenesis [11–13]. Therefore, understanding these processes could help to develop new therapeutic targets. Relevant and systematically evaluated data of transdifferentiation and dedifferentiation phenomena analyzing the phenotypic states of typical cellular components of normal arterial walls and of progressive atherosclerotic lesions in vitro and in vivo are still sparse or missing [14].

Therefore, in our studies, we aimed to investigate the capacity of VSMC to transdifferentiate and dedifferentiate by investigating the expression of (1) cytokeratin 7 (CK7)/cytokeratin 18 (CK18) and β-catenin (transdifferentiation) and of (2) CD31/CD34 (dedifferentiation) in vivo (normal vessels vs. early and advanced atherosclerotic lesions) as well as in vitro.

Materials and methods

Tissue preparation

In our study, 20 carotid arteries of patients (mean age 69± 11.4 years [median, 67 years; range, 55–81 years]; 58% male) who underwent carotid endarterectomy at the Department of Vascular Surgery, University Hospital Bochum and University of Bremen after ischemic stroke were analyzed by histology and immunohistochemistry. All of them showed at least type VI atherosclerotic lesions according to the American Heart Association (AHA) classification of human atherosclerotic lesions [15]. Stroke was diagnosed according to the World Health Organization criteria [16]. Patients with evidence of any cerebral disease proven by brain autopsy were excluded from the control group. Forty unaltered carotids from autopsy cases which were morphologically free of atherosclerosis and showed at most early lesions corresponding to type I/II of the AHA classification at light microscopy served as controls.

To evaluate atherosclerotic lesions in other localizations and of different plaque category, 20 aorta specimens from routine autopsy cases were acquired and classified histologically into three groups: normal arteries, early lesions, and advanced atherosclerotic lesions (mean age 63± 12.4 years [median, 62 years; range, 51–82 years]; 54.2% male) representing types I to VII grade atherosclerotic lesions according to the AHA classification.

All specimens were divided in halves. One part was frozen immediately and stored at −80°C; the other half was routinely fixed with buffered formalin (5% [*v*/*v*]), decalcified in 0.4 M ethylenediaminetetraacetic acid, dehydrated, and embedded in paraffin. Five-micrometer-thick paraffin sections were cut and stored at room temperature until use.

Histochemical methods

Routine hematoxylin and eosin staining was used to classify the extent of atherosclerosis according to the AHA classification [15].

Immunohistochemical analysis

For the purpose of detecting CK7 and CK18, β-catenin (monoclonal and polyclonal), CD31, and CD34 immunohistochemical (IHC) staining was performed. In short, mouse antibodies (IgG1) against CK7, CK18, β-catenin, as well as CD31/34 were applied (Table 1), followed by a biotinylated rabbit antimouse (goat antirabbit in the case of the CD154 and the polyclonal β-catenin antibody; both from Dako, Denmark) secondary antibody. Immunoreactivity was detected by peroxidase staining using the streptavidin–biotin–peroxidase method (Dako, Denmark), based on alkaline phosphatase and 3-hydroxy-2-naphtylacid 2,4-dimethylanilid (Fast Red, Sigma-Aldrich, Germany) as chromogen following Dako's recommendations. Nuclei were counterstained with hematoxylin.

To compare the expression levels of CK7, CK18, β-catenin, as well as of CD31 and CD34, all cells (stained

Table 1 Primary antibodies and antigen retrieval methods used for IHC and immunofluorescence analysis

Antigen specificity	Type	Dilution	Antigen retrieval	Vendor	Cat. no.
CK7	Mouse monoclonal	1:100	P	Biogenex, Germany	ab. no. 255M
CK18	Mouse monoclonal	1:50	P	Sigma, Germany	C8541
β-Catenin	Mouse monoclonal	1:50	none	Transduction Laboratories, USA	C 19220
β-Catenin	Rabbit polyclonal	1:750	TRS	Sigma Germany	C 2206
CD31	Mouse monoclonal	1:20	Citrate	Dako, Denmark	M 0823
CD34	Mouse monoclonal	1:50	Citrate	Dianova-Immunotech, Germany	0786
CD40	Mouse monoclonal	1:250	Trypsin 0.1%	Abcam, UK	ab19684
CD68	Mouse monoclonal	1:200	Citrate	Dako, Denmark	M 0814
CD154	Rabbit polyclonal	1:250	none	Santa Cruz Biotechnology CA, USA	sc-978
Smooth muscle actin	Mouse monoclonal	1:300	Citrate	Dako, Denmark	M 0851
Secondary antibodies					
Mouse IgG	Rabbit antimouse	1:500	na	Dako, Denmark	E 0354
Rabbit IgG	Goat antirabbit	1:500	na	Dako, Denmark	E 0432
Fluorescence antibodies					
Mouse IgG	Goat antimouse Alexa Fluor 488 green	1:250	na	Life Technologies, USA	A 11001
Mouse IgG	Goat antimouse Alexa Fluor 568 red	1:250 1:50	na	Life Technologies, USA	A 11004
Rabbit IgG	Goat antirabbit Alexa Fluor 488 green	1:250	na	Life Technologies, USA	A 11008
DAPI	FluoroPure	na		Life Technologies, USA	D 21490
IgG, F(ab)2-fragment	Goat antimouse	1:10	na	Dianova, Germany	005-000-006

P pronase (2 mg/mL, PBS, pH7.4, 10 min at 37°C; Sigma, Germany), *Pt* protease XXIV (0.05 mg/mL, PBS, pH7.2, 10 min at 37°C; Sigma, Germany), *MW* microwave (10 mmol/L citrate buffer, pH6.0; 10 min at 800 W and 10 min at 560 W), *TRS* target retrieval solution (pH6.0; DakoCytomation, Denmark) used instead of citrate buffer, *na* not applicable

positive and negative) were counted in ten randomly selected high-power fields by two independent observers, and the number of immunohistochemically positive cells are given as the percentage of all cells in the investigated areas. Furthermore, immunohistochemistry for CD68, smooth muscle actin, and CD40/CD40L (CD154) was performed on consecutive slides in order to characterize the cells expressing these markers. CD40/CD40L staining was done as described above but with 3,3′-diaminobenzidine instead of Fast Red as peroxidase substrate.

Double immunofluorescence staining was done as follows. In formalin-fixed, paraffin-embedded tissue sections, antigen retrieval was done using Dako TRS® (target retrieval solution, Dako Denmark code S1700). In short, after rehydration and washing with 10% Tris-buffered saline (TBS), every slide was coated with Dako TRS® for 30 min at room temperature. In chamber slide probes, the fixation was done with ice-cold methanol (−20°C); so after rehydration, no antigen retrieval had to be done. Primary antibodies were applied after washing with 10% TBS in the same dilutions as done with conventional immunohistochemistry (see Table 1), but secondary antibodies were replaced by goat antimouse antibodies labeled with Alexa Fluor® (Molecular Probes, Invitrogen, Germany; dilution 1:250) dye with a maximum excitation at 488 nm (green) or 568 nm (red). Using the polyclonal rabbit anti-β-catenin primary antibody, a goat antirabbit antibody labeled with Alexa Flour® 488 (Molecular Probes, Invitrogen, Germany) was applied as secondary antibody. In all stainings, Alexa Fluor® 568 (red) was applied to mark smooth muscle cell actin whereas green (Alexa Fluor® 488) labeled the second epitope. Nuclear staining was done using 4′,6-diamidino-2-phenylindole (DAPI, dihydrochloride; FluoroPure®, Invitrogen, Germany). For the use of two different secondary antibodies from the same species, the technique of Negeoscu et al. [17] was used. In short, the first secondary antibody was used at five times higher concentration (dilution 1:50) than in normal immunohistochemistry (1:250) and incubated for 4 h at room temperature. After washing, the sections were incubated overnight with goat antimouse IgG, F(ab)2-fragment (1:10, Danova, Germany) in order to saturate all antimouse binding sites. Then the second primary antibody was applied and further staining was done as in conventional immunohistochemistry. The staining was evaluated using a Leica microscope (Leica DM6000B, Germany) with ImagicAccess Enterprise 5® software (Imagic AG, Switzerland) to

Table 2 Sequences of human primers used for real-time PCR experiments

Human primers used for real-time PCR		
CD31	Forward	5′-GAAGCTAACAGTCATTACGGTCACAA-3′
	Reverse	3′-CCACGGCATCAGGGGACA-5′
	Amplicon	202 bp
CD34	Forward	5′-TCCTAAGTGACATCAAGGCAGAAA-3′
	Reverse	3′-TTAAACTCCGCACAGCTGGA-5′
	Amplicon	109 bp
CK18	Forward	5′-GAGACGTACAGTCCAGTCCTTGG-3′
	Reverse	3′-CCACCTCCCTCAGGCTGTT-5′
	Amplicon	86 bp
CK7	Forward	5′-TGAATGATGAGATCAACTTCCTCAG-3′
	Reverse	3′-TGTCGGAGATCTGGGACTGC-5′
	Amplicon	75 bp
β-Catenin	Forward	3′-CACCAGAGTGAAAAGAACGATAGCTA-5′
	Reverse	5′-CTTGGAATGAGACTGATGATCTTG-3′
	Amplicon	102 bp
GAPDH	Forward	5′-GAAGGTGAAGGTCGGAGTC-3′
	Reverse	3′-GAAGATGGTGATGGGATTTC-5′
	Amplicon	226 bp
18S rRNA	Forward	5′-TTGATTAAGTCCCTGCCCTTTGT-3′
	Reverse	5′-CGATCCGAGGGCCTCACTA-3′
	Amplicon	77 bp

Primers were designed by use of the Primer Express software (version 2.0.0; Perkin-Elmer Applied Biosystems, Foster City, CA, USA)

assemble the images. The quantification of the fluorescence immunohistochemistry was performed using the image-processing software Photoshop® from Adobe with the background corrected fluorescence methods as described before by Kirkeby et al. [18].

Human gastric and colorectal carcinoma specimens served as positive controls for CK7 and CK18 as well as β-catenin. Placental specimens served as positive controls for CD31 and CD34. In control experiments, PBS replaced primary or secondary antibodies and the samples were

Table 3 Expression of CK7, CK18, and β-catenin as well as of CD31 and CD34 inside normal controls and atherosclerotic carotids overall and the plaque subregions

	Mean of all cells [%] (± standard deviation)	Controls	Cases				
			Overall[a]	Distributed to each plaque area			
		Overall		Cap	Shoulder	Core	Basis	Boundary
Transdifferentiation	CK7	0.6±0.8[b,*]	7.7±1.2*,**	9.5±2.3	12.0±2.0	6.0±1.0	3.5±1.0	1.5±0.7
	CK18	0.8±0.9[b],*	4.8±1.1*,**	5.4±1.5	7.1±1.5	4.3±1.1	2.3±0.8	1.2±0.7
Activation	β-Cat m	2.8±1.7[c],*	5.5±0.8*,***	5.5±1.1	6.8±1.2	4.7±1.4	5.1±0.8	2.1±0.7
	β-Cat p	3.4±1.8[c,*]	9.6±1.2*,***	10.9±2.2	12.5±2.3	8.2±1.2	6.9±1.4	3.2±1.4
Dedifferentiation	CD31	0.3±0.4*	2.0±0.3*,****	1.9±0.6	2.2±0.6	1.9±0.7	2.0±0.3	0.5±0.5
	CD34	1.7±0.9*	2.8±0.5*,****	2.7±0.7	3.6±0.7	2.4±0.6	2.5±0.6	1.8±0.5

m monoclonal, *p* polyclonal

*$p<0.05$, significant differences between controls and cases; **, ***, ****$p<0.05$, significant differences of cases (overall) for different markers

[a] Mean of cap, shoulder, core, and basis regions

[b] Mainly sparsely expressed in the intima and focally by endothelial cells

[c] Mainly expressed in the media

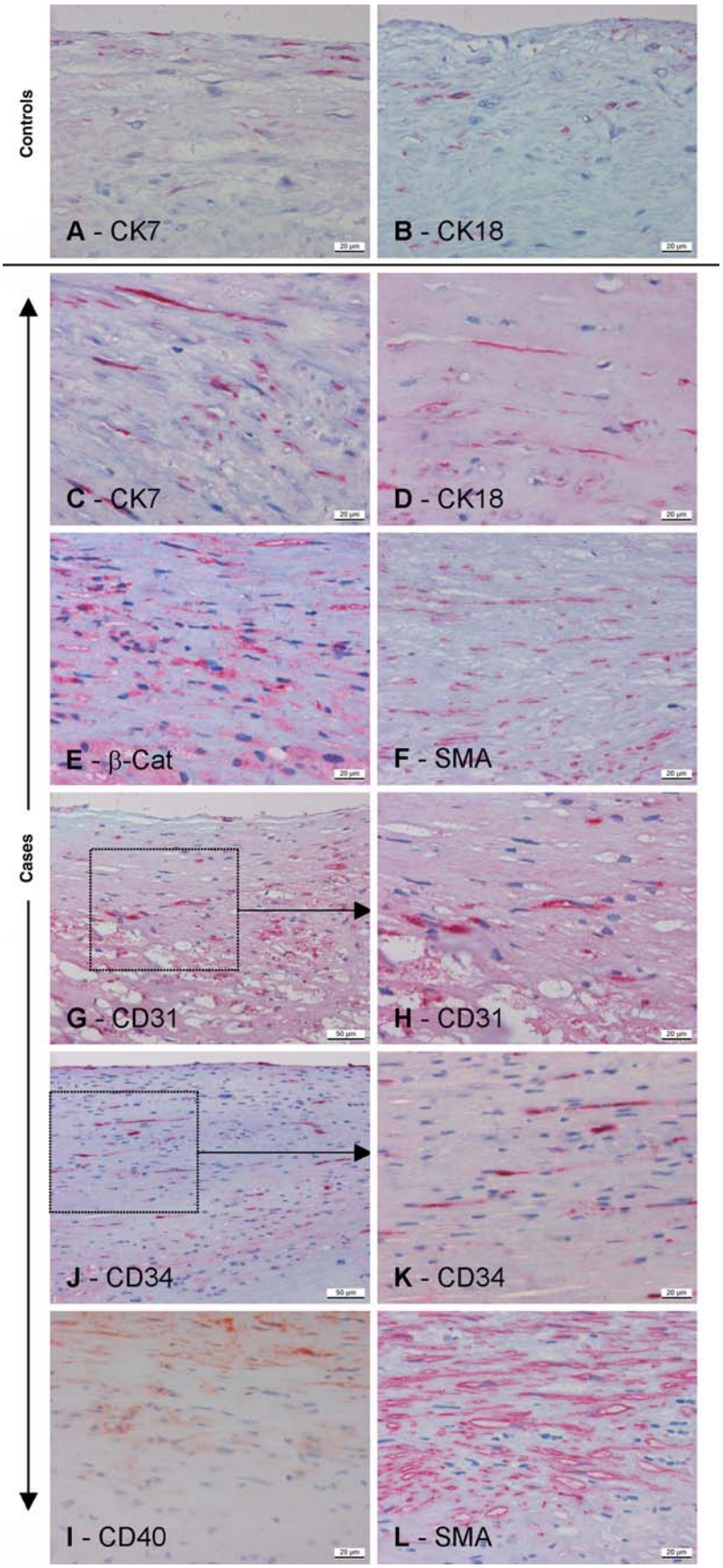

Fig. 1 Typical IHC distribution of CK7, CK18, β-catenin, CD31, and CD34 in normal controls (**a**, **b**) and in atherosclerotic lesions (**c**–**l**). In short, expression of CK7 (**a**; control PASN04) and CK18 (**b**; control PASN12) was very focally in controls, whereas higher frequency of CK7-positive (**c**; case GCH_B12) and CK18-positive (**d**; case GCH_B12) cells could be observed in cases. In comparison to CK7 and CK18, β-catenin (**e**; case GCH_B12), CD31 (**g** and, in detail, **h**; case GCH_B28), and CD34 (**j** and, in detail, **k**; case GCH_B28) as well as CD40 (**i**; case GCHB_28) were expressed sparse to low in cells of atherosclerotic plaques in cases in comparison with the expression of smooth muscle actin on consecutives slides (**f**; case GCH_B12 and **l**; case GCH_B28). Magnifications ×400 (**a**–**f**, **h**, **l**, **k**, and **i**) and ×200 (**g** and **j**)

processed as described above. All control samples were negative (not shown).

To estimate the extent of CD31-positive and CD34-positive signals derived from macrophages, all immunofluorescence stainings were repeated with an anti-CD68 antibody (to mark macrophages) replacing the anti-SMA antibody.

To investigate the reliability of the categories for evaluating the expression of CK7, CK18, β-catenin, as well as CD31 and CD34, the analyses were repeated in all specimens by an independent observer. The agreement of the classification was good ($\kappa \geq 0.70$).

RNA isolation and reverse transcription

For RNA analysis, approximately 10 mg of frozen tissue or the content of one cell culture well of a six-well plate was homogenized for 30 s in 1 mL (700 µL for cell culture) RNAPure™ (PeqLab Biotechnology, Erlangen, Germany). Further RNA isolation was done by peqGOLD RNAPure™ according to the manufacturer's recommendations. Total RNA concentration was evaluated photometrically and RNA integrity was confirmed on an agarose gel. RNAs were frozen instantly and stored at −80°C until further processing. For reverse transcription, we used 1 µg of the isolated RNA, 100 pmol oligo-dT, 50 pmol random primer, and 100 U Superscript II (Invitrogen) following the recommendations of the supplier. The cDNA was stored at −20°C until use.

Quantitative real-time PCR

Real-time reverse transcription polymerase chain reaction (RT-PCR) was performed as recently described [19]. In short, the LightCycler FastStart DNA Master SYBR Green I Kit (Roche, Mannheim, Germany) was used according to the manufacturer's instructions. The 20-µL probe contained 5 mM $MgCl_2$, 0.4 µM of each primer, 2 µL of the DNA template, and 2 µL of the Master Mix (including polymerase, dNTP). The PCR was performed as follows: (1) initial denaturation at 95°C for 10 min; (2) 40 cycles of denaturation at 95°C for 10 s, annealing at 60°C for 5 s, and elongation at 72°C for 10 s; and (3) a melting curve was arranged at 95°C, 60°C, and 95°C following the manufacturer's recommendations. Measurements were done in triplicate and standardized to GAPDH. To exclude variations in the expression of GAPDH [20, 21], 18S rRNA of the human specimen was measured as a second reference to substantiate our results. The expression of 18S rRNA and GAPDH showed a positive significant correlation ($p<0.001$, Pearson's $r=0.964$). The quantitative real-time PCR analyses were performed on a LightCycler real-time PCR machine (Roche).

The sequences of primers are listed in Table 2 and were synthesized at MWG Biotech AG (Ebersberg, Germany).

Fig. 2 Double immunofluorescence staining for CK7, CK18, β-catenin, as well as for CD31 and CD34 using Alexa Fluor® 488 (*green*) in combination with staining for smooth muscle cells with Alexa Fluor® 568 (*red*). Nuclear staining was done with DAPI. Overall, colocalization of fluorescence signals in the cytoplasm (in descending order of intensity) of CK7, CK18, β-catenin, CD31, and CD34 with SMA could be observed, whereas the expression of CD31 and CD34 (see *arrows*) was very low by SMA-positive VSMC showing no lumen. Magnifications ×630 (CK7, CK18, and β-catenin) and ×1,000 (CD31 and CD34)

Each PCR assay was repeated three times for each cDNA sample. To monitor the amplification of possible contaminating DNA, distilled water served as a negative control.

Cell culture experiments

In order to reflect inflammatory conditions in atherosclerosis, we carried out stimulation experiments of VSMC with the major proinflammatory and proatherosclerotic cytokines IL-1β, IL-6, and TNF-α [22, 23].

Human aorta VSMC (T/G HA-VSMC, Promochem, London, UK) were cultivated on six-well tissue plates (Becton Dickinson, Mannheim, Germany) in Dulbecco's modified Eagle's medium high-glucose medium with L-glutamine (PAA Laboratories, Pasching, Austria) containing 10% fetal bovine serum (Biochrom) at 37°C and 5% CO_2. According to the manufacturer (ATCC), the HA-VSMC smooth muscle cell line was derived from the normal aorta of an 11-month-old female, blood type O rhesus positive. The cell line has been reported to undergo a total of 30 to 35 passages before the onset of senescence. Cells were grown to 75% confluence before stimulation with TNF-α (25 ng/mL), IL-1β (10 ng/mL), and IL-6 (10 ng/mL; Strathmann Biotech, Hannover, Germany). Cells were harvested after 6, 12, and 24 h of stimulation. RNA isolation with RNAPure was carried out immediately as described. For statistical reasons, all stimulation experiments were repeated thrice. Data shown on Fig. 5 are based on three independent experiments. For immunohistochemistry, cells were grown in chamber slides (NUNC®, Germany) and fixed after stimulation in ice-cold methanol (−20°C) for 20 min before immunohistochemistry was carried out as described above.

Ethics

The study was approved by the local ethics committee (# 1041/1998) and the Data Protection Committee of the University of Erlangen–Nuremberg. Informed consent was obtained from all case and control subjects. The participants who were not able to consent for themselves had given consent through their next of kin or guardian.

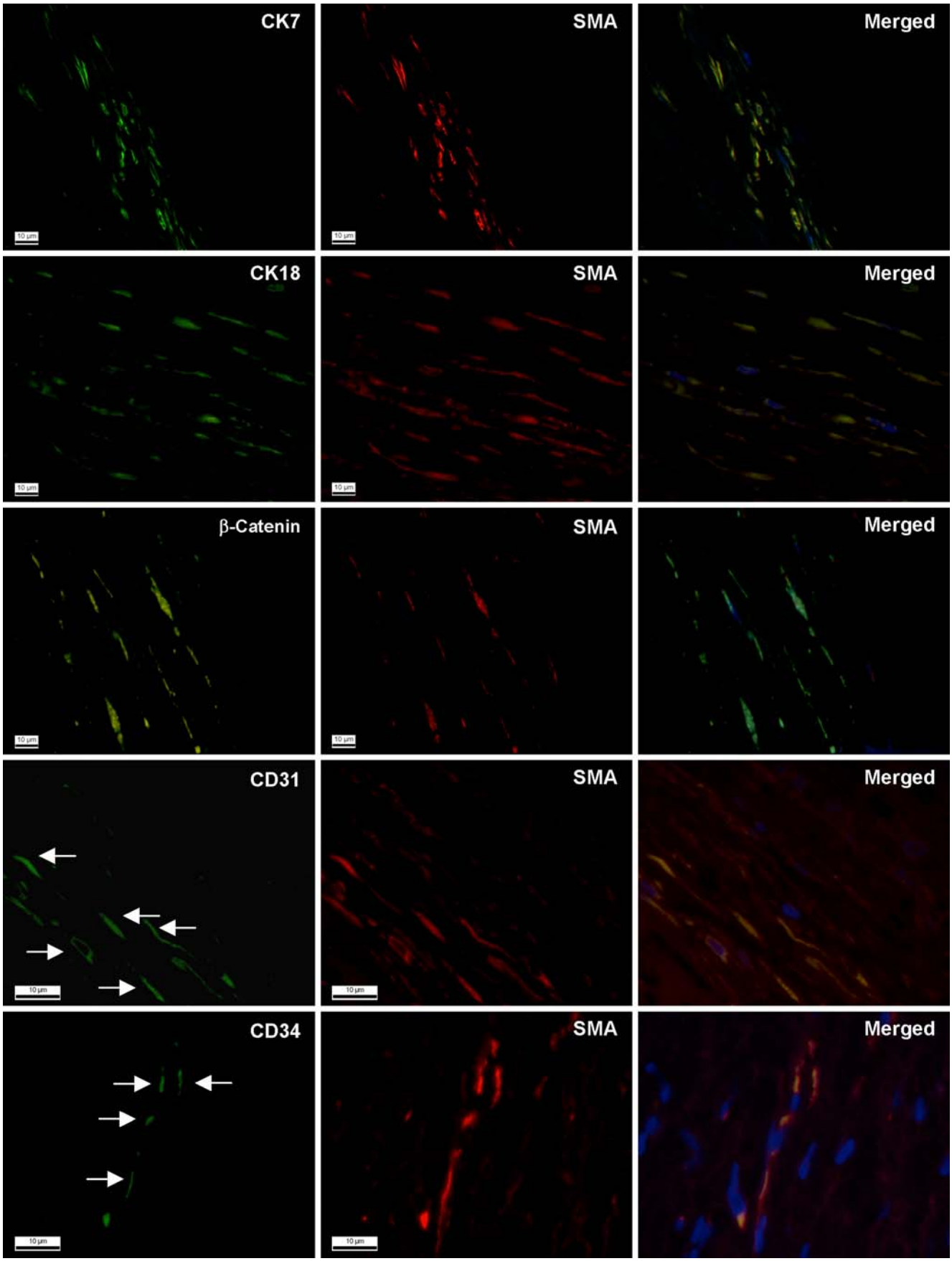
CK7
SMA
Merged
CK18
SMA
Merged
β-Catenin
SMA
Merged
CD31
SMA
Merged
CD34
SMA
Merged

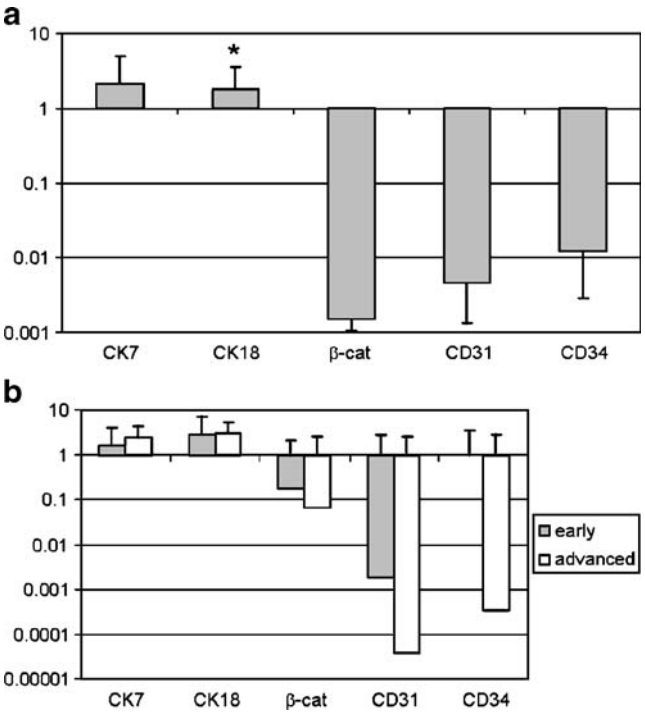

Fig. 3 Quantitative RT-PCR. Relative mRNA content of atherosclerotic lesions of arteries of elastic type [carotid artery (**a**) and abdominal aorta (**b**)]. mRNA content was normalized to GAPDH and is expressed in relation to normal vessels (set at 1.0) for each gene of interest. Mean values (with standard deviation) of three independent PCR analyses are shown. *$p<0.05$, significant changes (Student's *t* test)

Statistics

Statistical analysis was done using the SPSS 15 software package (SPSS, USA). The Student's *t* test and Mann–Whitney *U* test were used to proof differences in interval and ordinal variables. For testing the reliability of the quantification of CK7, CK18, β-catenin, as well as CD31 and CD34 expression between the investigators, kappa statistic was used. All tests were two-tailed, and statistical significance was determined at an alpha level of 0.05.

Results

Immunohistochemistry of carotids

Expression of CK7 and CK18 as well as β-catenin as markers for epithelial transdifferentiation was significantly ($p<0.05$) higher in symptomatic than in normal carotids. The percentage of positively stained cells decreased from β-catenin, CK7, and CK18 in cases and from β-catenin, CK18, and CK7 in controls (see Table 3). Although it is assumed that IHC staining with polyclonal antibodies against β-catenin is better for detecting nuclear β-catenin expression, we did not find a difference in the cellular distribution but in the amount of β-catenin between monoclonal or polyclonal antibodies (see Table 3).

Looking closer at the subregions of the plaques, the expression of cytokeratins and β-catenin was, besides the core region, maximal in the shoulder and/or cap region of atherosclerotic lesions (see Table 3). Additionally, expression levels of monoclonal β-catenin were similar in the cap and basis plaque subregions. On the cellular level (VSMC, fibroblasts, macrophages, and endothelial cells), positive staining of CK7 and CK18 as well as β-catenin was higher in VSMC and macrophages, whereas in endothelial cells, their expression was only a rare event interpreting immunohistochemistry of consecutive slides with smooth muscle actin and CD68 (Fig. 1). β-Catenin staining showed increased cytoplasmatic positivity of VSMC inside atherosclerotic lesions while staining of the nuclei could rarely be observed. Coexpression of β-catenin and CD40 could be observed on serial sections (Fig. 1).

Although the rate of CD31-positive and CD34-positive cells with VSMC morphology indicating embryonic dedifferentiation was low in controls and cases, the amount of CD31-positive or CD34-positive cells was significantly higher in atherosclerotic plaques of cases than in normal arteries of controls ($p<0.05$; see Table 3). Overall, the expression of CD34 was significantly higher than of CD31 ($p<0.05$). Inside the plaques, CD31 and CD34 were, besides the endothelium, mainly expressed in the shoulder region of the plaques (see Table 3 and Fig. 1), whereas the expression levels inside the cap and basis regions were comparable in contrast to CK7 and CK18.

No association between expression of cytokeratins, β-catenin, CD31, and CD34 was found looking at the whole plaque or plaque subregions expression using correlation analysis.

Double immunofluorescence of carotid specimen

Double immunofluorescence stainings of selected carotid samples confirmed the results of the conventional immunohistochemistry: inside the shoulder and core regions, SMA-positive VSMC had a strong coexpression of CK7 and CK18 with a sizeable overlapping of fluorescence

Fig. 4 **a** Typical IHC expression of CK7, CK18, β-catenin, CD31, and CD34 of smooth muscle cell lines after treatment with IL-1β (10 ng/mL), IL-6 (10 ng/mL), or TNF-α (25 ng/mL) compared to untreated controls (magnification ×400). **b** Double immunofluorescence staining for β-catenin using Alexa Fluor® 488 (*green*) in combination with staining for smooth muscle cells with Alexa Fluor® 568 (*red*) after treatment with TNF-α (25 ng/mL) compared to untreated controls. Nuclear staining was done with DAPI. Overall, β-catenin expression changed from diffuse cytoplasmatic distribution in controls to a predominant perinuclear pattern during stimulation (magnification ×400) ▶

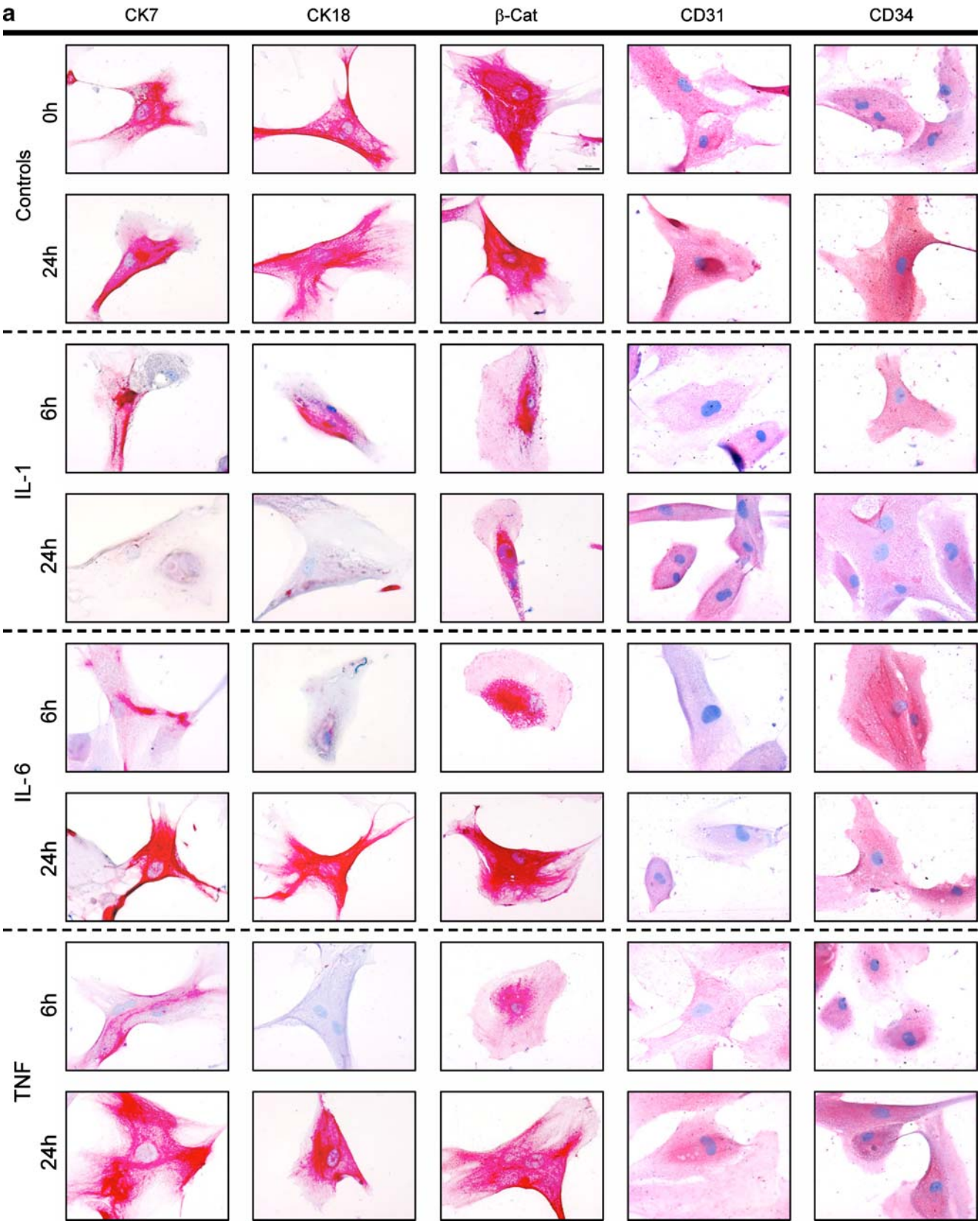
a
CK7
CK18
β-Cat
CD31
CD34
Controls
0h
24h
IL-1
6h
24h
IL-6
6h
24h
TNF
6h
24h

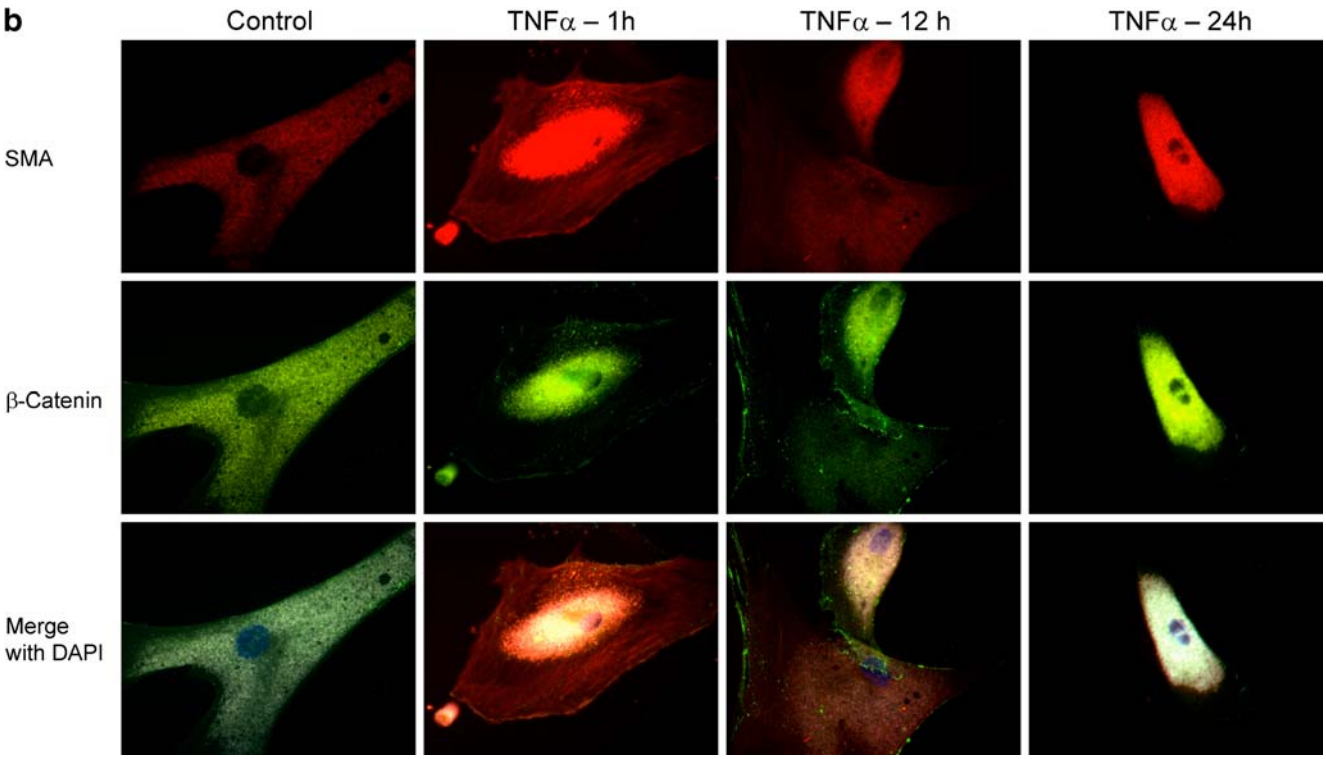

Fig. 4 (Continued)

signals in the cytoplasm (Fig. 2). A nuclear expression of CK7 or CK18 was not detected. The level of expression of β-catenin was lower than with CK7 and CK18 but with a similar cytoplasmatic overlap as seen in CK7 and CK18. Partially, β-catenin could be localized predominantly cytoplasmatic near the nucleus using DAPI nucleus staining (Fig. 2). Finally, CD31 and CD34 were focally coexpressed by SMA-positive VSMC showing no lumen (see arrows Fig. 2).

The double immunofluorescence staining of CD68 (for macrophages) and CK7, CK18, β-catenin, as well as CD31 and CD34 showed that coexpression of these markers (especially CK7 and CK18) is a very sparse event, indicating that, inside atherosclerotic lesions, the process of transdifferentiation and dedifferentiation is mainly associated with VSMCs (data not shown).

RNA analysis of carotids and infrarenal aorta specimen

The normalized expression levels of CK7, CK18, β-catenin, CD31, and CD34 were comparable in carotid and aortal specimens. Corroborating the IHC results, mRNA levels of CK7 and CK18 were significantly higher inside the plaques (Fig. 3a, b) and especially the CK7 levels increased with progression of the atherosclerotic lesion (Fig. 3b). Unlike the IHC results, β-catenin, CD31, and CD34 expressions were lower with a trend towards significance in atherosclerotic plaques. The levels declined in dependence of the atherosclerotic lesion (see Fig. 3b).

Cell culture experiments of human aorta vascular smooth muscle cells

Immunohistochemical results of stimulated HA-VSMC

The modification of markers for transdifferentiation and dedifferentiation during stimulation inside chamber slides with IL-1β, IL-6, and TNF-α is shown in Fig. 4a: In summary, the basal expression levels of all investigated markers were low (CD31 and CD34) to moderate (CK7, CK18, and β-catenin) within the time range investigated. IL-1β-stimulated HA-VSMC showed a lower intensity of all investigated markers in comparison to untreated controls independent of time. HA-VSMC treated with TNF-α or IL-6 also express lower levels of all markers analyzed for the first 12 h. After 24 h of stimulation with TNF-α or IL-6, staining for CK7, CK18, and β-catenin was more intense in comparison to the untreated controls, whereas CD31 and CD34 displayed negative or low positive pattern during the entire experiment. Noteworthy, β-catenin stained cytoplasm of controls but was located in a perinuclear pattern during stimulation with IL-1β, IL-6, and TNF-α being exemplarily highlighted using double immunofluorescence stainings after treatment with TNF-α (see Fig. 4b).

mRNA analysis of stimulated HA-VSMC

The results of RT-PCR analysis of HA-VSMC stimulated in six-well plates with the same cytokines as described above are shown in Fig. 5 and are corroborative with the immunohistological findings. In short, IL-1β reduced the expression of all investigated markers over the whole observation period. Particularly, CD31, CD34, CK7, and CK18 expressions were suppressed, whereas β-catenin remained unaffected. The reduction of the mRNA expression of CK7 and CK18 was time-dependent.

Stimulation with IL-6 lowered the expression levels of CD31 and CD34 throughout the period of surveillance. In contrast to that, the expression of CK7, CK18, and β-catenin was diminished during the first 12 h. After 24 h of stimulation with IL-6, the expression of CK7, CK18, and β-catenin was higher than in the controls.

Under the influence of TNF-α, all investigated cytokeratins showed a decreased expression for the first 12 h. After that, parallel to the effect seen under IL-6 stimulation, CK7, CK18, and β-catenin exceeded the levels seen in the controls. CD31 and CD34 expression after 24 h of stimulation with TNF-α was higher than in the controls.

Discussion

The process of atherosclerosis is in the beginning characterized by intimal thickening caused by hyperplasia of VSMC. Different models of how migrating, secreting, and proliferating VSMC appear inside the arterial wall are currently discussed: One possibility is that circulating smooth muscle precursor cells of myeloid or hematopoietic lineage relocate from the blood into atherosclerotic lesions [24] and start to proliferate. Another possibility is that local VSMC of the contractile phenotype reobtain the embryonic potential of proliferation and migration [25–32] via transdifferentiation and dedifferentiation processes as a response to injury. Additionally, the reactivation of localized predisposed smooth muscle cells are regarded as being essentially involved in these of process intimal thickening using embryonic pathways, too [33].

In our study, we were able to show that, inside atherosclerotic specimens, (1) VSMC of progressive atheromas have the ability of differentiation, (2) transdifferentiation and dedifferentiation phenomena are topographically dependent on subregions of advanced atherosclerotic lesions, and (3) this phenotype plasticity is influenced by inflammatory stimuli and associated with plaque progression and possibly also plaque rupture. These findings corroborate that VSMC could exhibit high plasticity which is associated with and is possibly involved in advanced atherosclerosis.

Whereas the gene expression pattern of differentiated VSMC is well characterized [6], many in vivo and in vitro studies dealing with proliferating VSMC showed heterogeneous cell marker expressions of multilineage differentiation [8, 9]. Very well known is the capacity of VSMC for phenotypic changes in cell culture stimulation experiments emphasizing the differentiation potency of VSMC [34]. One possible way to characterize the multilineage potential of VSMC is to analyze gene expression indicating differential gene regulation being associated with extracellular matrix remodeling as well as with cell motility in general [35]. Another way to approach understanding the morphological and molecular phenotype switching of VSMC is to look at vascular development. Interestingly, similar to atherosclerosis, processes of multilineage differentiation with transition states could be observed during vascular development [9, 34, 36, 37]. Embryonic VSMC derive from different cells of origin via transdifferentiation, e.g., coronary VSMC from epicardial lining, aortic VSMC from local mesenchyme (for details, see [38]).

Interestingly, VSMC can express cytokeratins during development and in atherosclerotic lesions, indicating a highly conserved phenomenon of transdifferentiation, too [11, 25–32]. Overall, the expression of cytokeratin by VSMC is linked to a proliferative state of VSMC (see also review [39]). We were able to confirm these findings of high expression of cytokeratins inside progressive atherosclerotic lesions on mRNA and protein level. Our results are, therefore, in line with previous reports of a distinct CK18 expression in either proliferating fetal smooth muscle cells, in dedifferentiated cultured smooth muscle cells, or in atherosclerotic lesions [29, 32, 39]. Additionally, using immunohistochemistry, we were able to localize cytokeratins and β-catenin in subregions of progressive plaques, emphasizing the importance to discriminate different plaque regions. In detail, markers of transdifferentiation such as CK7 and CK18 were predominantly found in areas being relevant for plaque instability, whereas markers of activation such as β-catenin were detected all over the plaque indicating an enhanced level of whole plaque remodeling. Another marker of activation, CD40, which plays a key role in the inflammatory scenario of atherosclerosis [40], is coexpressed in β-catenin-positive cells. Interestingly, different expression levels of cytokeratins were found in atherosclerotic arteries of muscular type (data not shown). Our cell culture experiments confirmed these findings and highlight the importance of VSMC in the progression of atherosclerosis. Obviously, cytokeratin expression of smooth muscle cells is influenced by inflammatory cytokines such as IL-1β, IL-6, and TNF-α. These findings are in line with cDNA array data showing that reduced expression of cytoskeleton proteins (such as cytokeratins) is linked with an invasive phenotype [35].

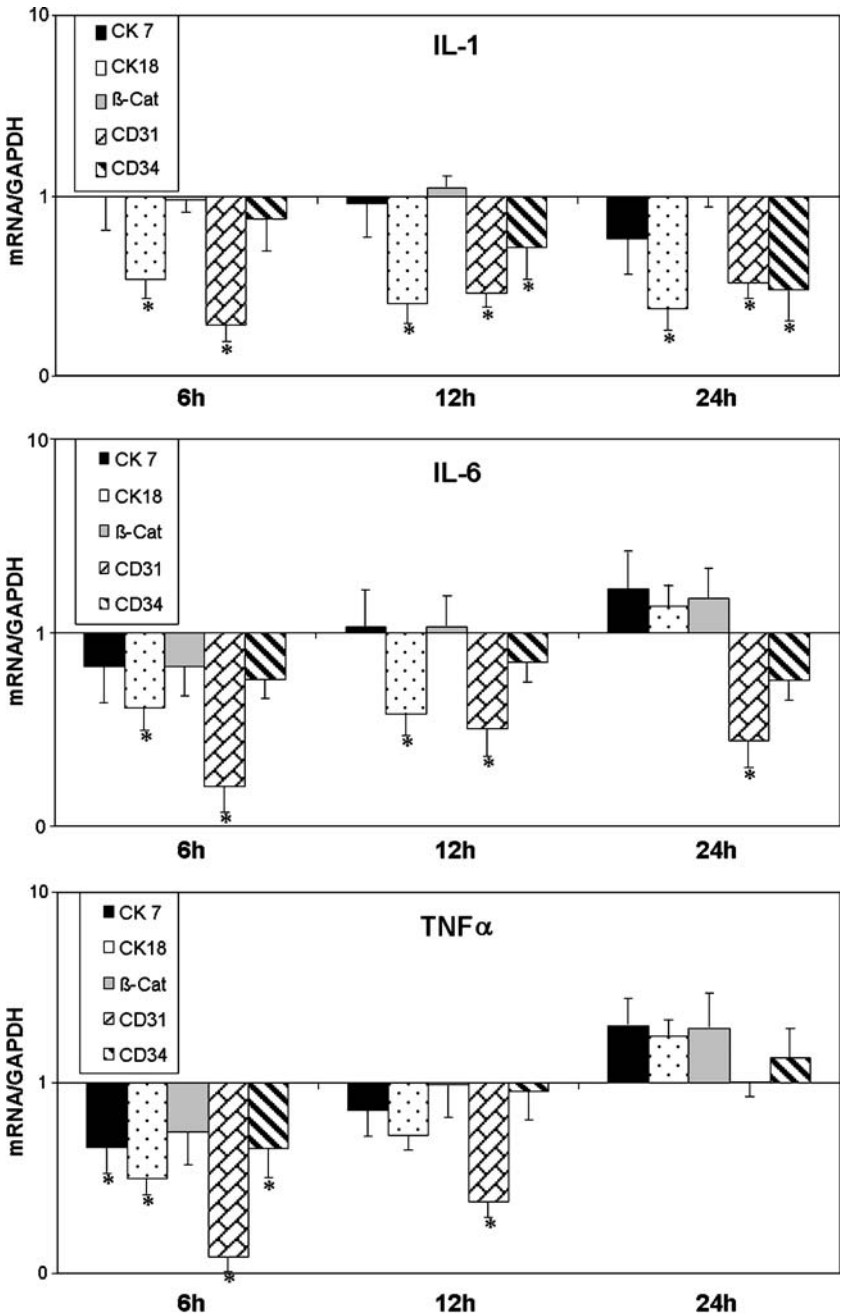

Fig. 5 Quantitative RT-PCR. Relative mRNA content of smooth muscle cell lines after treatment with IL-1β (concentration 10 ng/mL), IL-6 (10 ng/mL), or TNF-α (25 ng/mL); mRNA content was normalized to GAPDH and is expressed in relation to untreated controls (set at 1.0) for each gene of interest. Mean values (with standard deviation) of three independent PCR analyses are shown. *$p<0.05$, significant changes (Student's *t* test)

Another possible link to the process of embryonic dedifferentiation of VSMC is the finding that multipotent CD34-positive stem cells could display a VSMC-like phenotype [14, 34, 41–46]. The term of dedifferentiation describes an embryonic-like status with temporary multilineage potency [10]. Looking at atherosclerosis and VSMC, there is a lot of evidence that VSMC progenitor cells are essentially involved in the progression of atherosclerosis [47]. The origin of such VSMC progenitor cells is under debate, i.e., whether these cells derive from bone marrow or dedifferentiated intimal cells. This indicates, however, that there may be many possible origins of VSMC [47–49]. It has been recently shown that vascular progenitor cells exist inside normal vessel walls and the number is increased in atherosclerotic lesions [50]. Serial sections of carotid specimens showed a heterogeneous expression of CD31 and CD34 of cells displaying typical smooth muscle cell morphology, being in line with the hypothesis that, not only bone marrow, but also local vascular-derived stem cells could be detected in atherosclerotic lesions [50]. Overall, the analysis of expression levels of these markers of dedifferentiation indicates that processes of dedifferentiation are low but increase in progressive atherosclerotic lesions in all areas. Our cell culture experiments illustrated

a heterogeneous response to stimulation with proinflammatory cytokines, indicating an influence of those cytokines on the differentiation status of VSMC. Overall, the prolonged suppression of the CD34 and CD31 expression over the observation period suggested that dedifferentiation is not an early event under inflammatory influence in vitro.

Additionally, the β-catenin/Wnt signaling pathway could modulate the proliferation, activation, and differentiation state of VSMC [14, 51–55] similar to what is known and well established for different cancer types. In our cell culture experiments, after a downregulation over the first 12 h, we could observe a β-catenin upregulation after 24 h of stimulation being in line with the observations of an upregulation of β-catenin after experimental balloon injury of rat vessels [53]. It is noteworthy that we found a discrepancy between β-catenin mRNA levels as determined by RT-PCR and IHC staining results which indicate a phenotypic stabilization of the protein with transcriptional suppression of the cognate mRNA. Interestingly, low-density lipoprotein receptor protein is associated with VSMC proliferation and survival via β-catenin linking the β-catenin signaling cascade not only with mechanic (such as balloon injury) but also with lipid status and biochemical pathways [56]. Furthermore, differentiation phenomena in epithelial cell types, e.g., colorectal or pancreatic cancer, have also been shown to involve Notch or β-catenin signaling as has also been demonstrated for VSMC during atherosclerosis [13, 39]. Other growth factors like platelet-derived growth factor (PDGF) have been linked to vascular homeostasis and atherogenesis, predominantly after mechanical or rheological stress and release from macrophages in vivo [57, 58]. The role of PDGF in vitro, in contrast, is still controversial with studies reporting proatherogenic and proproliferative effects on smooth muscle cells [59] or induction of apoptosis in fibroblasts [60]. We, therefore, investigated the effect of classical inflammatory cytokines in our setting, although we acknowledge that PDGF, fibroblast growth factor, or vascular endothelial growth factor may also play a role in the complex pathogenesis of atherosclerosis in vivo.

Taken together, our in vitro experiments show that markers of transdifferentiation are re-expressed sooner than those of dedifferentiation in vitro. Possibly, the earliest main effect of the VSMC is cell cycle arrest and, after that, starting differentiation pathways. Although early molecular events should be observed, our in vitro time period of 24 h after stimulation could not exclude that differentiation markers raised dramatically. Another possible explanation is that, in our in vitro experiments, only a selection of inflammatory cytokines was used. In vivo, there are not only additional influences by extracellular matrix molecules, but there is also a combination of different cytokines affecting VSMC differentiation.

Unregulated processes of a transition state could essentially be involved in tumor genesis as well as in chronic degenerative and inflammatory diseases like atherosclerosis [11–13]. Our study shows that the observed activation of differentiation pathways is essentially associated with progressive atherosclerosis-like inflammation and matrix remodeling (see review [4, 12]).

In summary, our experiments give evidence that transdifferentiation and dedifferentiation processes of VSMC are present in atherosclerosis and that expression of several differentiation markers can be influenced by proinflammatory cytokines known to be relevant in atherosclerosis.

Acknowledgements This work was supported by a Research Grant from the University of Erlangen–Nuremberg (ELAN-Fond 98.08.14.1) and in part by the IZKF Erlangen (A11). The expert technical assistance of S. Söllner, Gudrun Hülsmann-Volkert, and W. Wurm is gratefully acknowledged.

Conflicts of interest statement We declare that we have no conflicts of interest.

References

1. Ross R (1999) Atherosclerosis—an inflammatory disease. N Engl J Med 340:115–126
2. Neureiter D, Heuschmann P, Stintzing S et al (2003) Detection of *Chlamydia pneumoniae* but not of *Helicobacter pylori* in symptomatic atherosclerotic carotids associated with enhanced serum antibodies, inflammation and apoptosis rate. Atherosclerosis 168:153–162
3. Ross R, Glomset JA (1973) Atherosclerosis and the arterial smooth muscle cell: proliferation of smooth muscle is a key event in the genesis of the lesions of atherosclerosis. Science 180:1332–1339
4. Dzau VJ, Braun-Dullaeus RC, Sedding DG (2002) Vascular proliferation and atherosclerosis: new perspectives and therapeutic strategies. Nat Med 8:1249–1256
5. Owens GK (1998) Molecular control of vascular smooth muscle cell differentiation. Acta Physiol Scand 164:623–635
6. Shanahan CM, Weissberg PL (1999) Smooth muscle cell phenotypes in atherosclerotic lesions. Curr Opin Lipidol 10:507–513
7. Shanahan CM, Weissberg PL (1998) Smooth muscle cell heterogeneity: patterns of gene expression in vascular smooth muscle cells in vitro and in vivo. Arterioscler Thromb Vasc Biol 18:333–338
8. Tintut Y, Alfonso Z, Saini T et al (2003) Multilineage potential of cells from the artery wall. Circulation 108:2505–2510
9. Owens GK (1995) Regulation of differentiation of vascular smooth muscle cells. Physiol Rev 75:487–517
10. Neureiter D, Herold C, Ocker M (2006) Gastrointestinal cancer—only a deregulation of stem cell differentiation? Int J Mol Med 17:483–489 Review
11. Neureiter D, Zopf S, Dimmler A et al (2005) Different capabilities of morphological pattern formation and its association with the expression of differentiation markers in a xenograft model of human pancreatic cancer cell lines. Pancreatology 5:387–397
12. Brabletz T, Jung A, Spaderna S et al (2005) Opinion: migrating cancer stem cells—an integrated concept of malignant tumour progression. Nat Rev Cancer 5:744–749

13. Iyemere VP, Proudfoot D, Weissberg PL et al (2006) Vascular smooth muscle cell phenotypic plasticity and the regulation of vascular calcification. J Intern Med 260:192–210
14. Moiseeva EP (2001) Adhesion receptors of vascular smooth muscle cells and their functions. Cardiovasc Res 52:372–386
15. Stary HC, Chandler AB, Dinsmore RE et al (1995) A definition of advanced types of atherosclerotic lesions and a histological classification of atherosclerosis. Circulation 92:1355–1374
16. Hatano S (1976) Experience from a multicentre stroke register: a preliminary report. Bull World Health Organ 54:541–553
17. Negoescu A, Labat-Moleur F, Lorimier P et al (1994) F(ab) secondary antibodies: a general method for double immunolabeling with primary antisera from the same species. Efficiency control by chemiluminescence. J Histochem Cytochem 42:433–437
18. Kirkeby S, Thomsen CE (2005) Quantitative immunohistochemistry of fluorescence labelled probes using low-cost software. J Immunol Methods 301:102–113
19. Neureiter D, Zopf S, Leu T et al (2007) Apoptosis, proliferation and differentiation patterns are influenced by Zebularine and SAHA in pancreatic cancer models. Scand J Gastroenterol 42:103–116
20. Barber RD, Harmer DW, Coleman RA et al (2005) GAPDH as a housekeeping gene: analysis of GAPDH mRNA expression in a panel of 72 human tissues. Physiol Genomics 21:389–395
21. Bayliss J, Maguire JA, Bailey M et al (2008) Increased vascular endothelial growth factor mRNA in endomyocardial biopsies from allografts demonstrating severe acute rejection: a longitudinal study. Transpl Immunol 18:264–274
22. Hansson GK, Libby P, Schonbeck U et al (2002) Innate and adaptive immunity in the pathogenesis of atherosclerosis. Circ Res 91:281–291
23. Libby P (2002) Inflammation in atherosclerosis. Nature 420:868–874
24. Metharom P, Liu C, Wang S et al (2008) Myeloid lineage of high proliferative potential human smooth muscle outgrowth cells circulating in blood and vasculogenic smooth muscle-like cells in vivo. Atherosclerosis 198:29–38
25. Bader BL, Jahn L, Franke WW (1988) Low level expression of cytokeratins 8, 18 and 19 in vascular smooth muscle cells of human umbilical cord and in cultured cells derived therefrom, with an analysis of the chromosomal locus containing the cytokeratin 19 gene. Eur J Cell Biol 47:300–319
26. Bar H, Bea F, Blessing E et al (2001) Phosphorylation of cytokeratin 8 and 18 in human vascular smooth muscle cells of atherosclerotic lesions and umbilical cord vessels. Basic Res Cardiol 96:50–58
27. Bar H, Wende P, Watson L et al (2002) Smoothelin is an indicator of reversible phenotype modulation of smooth muscle cells in balloon-injured rat carotid arteries. Basic Res Cardiol 97:9–16
28. Bauriedel G, Schewe K, Windstetter U et al (1991) Differential cytokeratin expression in cultivated smooth muscle cells of primary and re-stenosed plaque tissue? Vasa Suppl 32:216–219
29. Denger S, Jahn L, Wende P et al (1999) Expression of monocyte chemoattractant protein-1 cDNA in vascular smooth muscle cells: induction of the synthetic phenotype: a possible clue to SMC differentiation in the process of atherogenesis. Atherosclerosis 144:15–23
30. Glukhova MA, Shekhonin BV, Kruth H et al (1991) Expression of cytokeratin 8 in human aortic smooth muscle cells. Am J Physiol 261:72–77
31. Jahn L, Franke WW (1989) High frequency of cytokeratin-producing smooth muscle cells in human atherosclerotic plaques. Differentiation 40:55–62
32. Jahn L, Kreuzer J, von Hodenberg E et al (1993) Cytokeratins 8 and 18 in smooth muscle cells. Detection in human coronary artery, peripheral vascular, and vein graft disease and in transplantation-associated arteriosclerosis. Arterioscler Thromb 13:1631–1639
33. Garcia-Ramirez M, Martinez-Gonzalez J, Juan-Babot JO et al (2005) Transcription factor SOX18 is expressed in human coronary atherosclerotic lesions and regulates DNA synthesis and vascular cell growth. Arterioscler Thromb Vasc Biol 25:2398–2403
34. Chamley-Campbell JH, Campbell GR, Ross R (1981) Phenotype-dependent response of cultured aortic smooth muscle to serum mitogens. J Cell Biol 89:379–383
35. Blindt R, Vogt F, Lamby D et al (2002) Characterization of differential gene expression in quiescent and invasive human arterial smooth muscle cells. J Vasc Res 39:340–352
36. Slomp J, Gittenberger-de Groot AC, Glukhova MA et al (1997) Differentiation, dedifferentiation, and apoptosis of smooth muscle cells during the development of the human ductus arteriosus. Arterioscler Thromb Vasc Biol 17:1003–1009
37. Glukhova MA, Frid MG, Koteliansky VE (1990) Developmental changes in expression of contractile and cytoskeletal proteins in human aortic smooth muscle. J Biol Chem 265:13042–13046
38. Liu C, Nath KA, Katusic ZS et al (2004) Smooth muscle progenitor cells in vascular disease. Trends Cardiovasc Med 14:288–293
39. Johansson B, Eriksson A, Virtanen I et al (1997) Intermediate filament proteins in adult human arteries. Anat Rec 247:439–448
40. Campean V, Neureiter D, Nonnast-Daniel B et al (2007) CD40-CD154 expression in calcified and non-calcified coronary lesions of patients with chronic renal failure. Atherosclerosis 190:156–166
41. Matsumura G, Miyagawa-Tomita S, Shin'oka T et al (2003) First evidence that bone marrow cells contribute to the construction of tissue-engineered vascular autografts in vivo. Circulation 108:1729–1734
42. Simper D, Stalboerger PG, Panetta CJ et al (2002) Smooth muscle progenitor cells in human blood. Circulation 106:1199–1204
43. Yeh ET, Zhang S, Wu HD et al (2003) Transdifferentiation of human peripheral blood CD34+-enriched cell population into cardiomyocytes, endothelial cells, and smooth muscle cells in vivo. Circulation 108:2070–2073
44. Bea F, Bar H, Watson L et al (2000) Cardiac alpha-actin in smooth muscle cells: detection in umbilical cord vessels and in atherosclerotic lesions. Basic Res Cardiol 95:106–113
45. Amore B, Chiavegato A, Paulon T et al (1996) Atherosclerosis resistance in rats correlates with lack of expansion of an immature smooth muscle cell population. J Vasc Res 33:442–453
46. Trosheva M, Dikranian K, Nikolov S (1996) Expression of cytoskeletal proteins and ATPase activity in bovine femoral artery and vein intima. Histol Histopathol 11:335–342
47. Roberts N, Jahangiri M, Xu Q (2005) Progenitor cells in vascular disease. J Cell Mol Med 9:583–591
48. Majesky MW (2007) Developmental basis of vascular smooth muscle diversity. Arterioscler Thromb Vasc Biol 27:1248–1258
49. Medbury HJ, Tarran SL, Guiffre AK et al (2008) Monocytes contribute to the atherosclerotic cap by transformation into fibrocytes. Int Angiol 27:114–123
50. Torsney E, Mandal K, Halliday A et al (2007) Characterisation of progenitor cells in human atherosclerotic vessels. Atherosclerosis 191:259–264

51. Bobryshev YV, Lord RS, Watanabe T et al (1998) The cell adhesion molecule E-cadherin is widely expressed in human atherosclerotic lesions. Cardiovasc Res 40:191–205
52. Uglow EB, Slater S, Sala-Newby GB et al (2003) Dismantling of cadherin-mediated cell–cell contacts modulates smooth muscle cell proliferation. Circ Res 92:1314–1321
53. Wang X, Xiao Y, Mou Y et al (2002) A role for the beta-catenin/T-cell factor signaling cascade in vascular remodeling. Circ Res 90:340–347
54. George SJ, Beeching CA (2006) Cadherin:catenin complex: a novel regulator of vascular smooth muscle cell behaviour. Atherosclerosis 188:1–11
55. George SJ, Dwivedi A (2004) MMPs, cadherins, and cell proliferation. Trends Cardiovasc Med 14:100–105
56. Wang X, Adhikari N, Li Q et al (2004) LDL receptor-related protein LRP6 regulates proliferation and survival through the Wnt cascade in vascular smooth muscle cells. Am J Physiol Heart Circ Physiol 287:H2376–H2383
57. Heldin CH, Westermark B (1999) Mechanism of action and in vivo role of platelet-derived growth factor. Physiol Rev 79:1283–1316
58. Andrae J, Gallini R, Betsholtz C (2008) Role of platelet-derived growth factors in physiology and medicine. Genes Dev 22:1276–1312
59. Ross R, Glomset J, Kariya B et al (1974) A platelet-dependent serum factor that stimulates the proliferation of arterial smooth muscle cells in vitro. Proc Natl Acad Sci U S A 71:1207–1210
60. Kim HR, Upadhyay S, Li G et al (1995) Platelet-derived growth factor induces apoptosis in growth-arrested murine fibroblasts. Proc Natl Acad Sci U S A 92:9500–9504

Virchows Arch (2009) 455:187–190
DOI 10.1007/s00428-009-0801-3

CASE REPORT

Pulmonary histiocytic sarcoma mimicking pulmonary Langerhans cell histiocytosis in a young adult presenting with spontaneous pneumothorax: a potential diagnostic pitfall

Elvira Stacher · Christine Beham-Schmid · Hans-Joachim Terpe · Nektaria Simiantonaki · Helmut Hans Popper

Received: 23 February 2009 / Revised: 1 June 2009 / Accepted: 6 June 2009 / Published online: 27 June 2009

Abstract We present a case of a histiocytic sarcoma incidentally detected in peripheral lung tissue resected for a spontaneous pneumothorax. Furthermore, we discuss the practical approach to pulmonary Langerhans cell histiocytosis, the main differential diagnosis of this lesion in the lung, based on morphological and immunohistochemical features. A 23-year-old male patient presented with recurrent pneumothoraces. The pulmonary tissue showed a single round granuloma-like lesion measuring 4 mm in diameter in close neighbourhood to a bronchial wall. The granuloma consisted of histiocytic cells with enlarged pale nuclei, plasma cells, lymphocytes and scanty eosinophilic granulocytes giving the impression of a granuloma of pulmonary Langerhans cell histiocytosis on haematoxylin and eosin (H&E) stains. Immunohistochemically, the histiocytic cells were negative for CD1a and S-100. They were positive for CD68, HLA-DR, CD14, CD4, CD11c, CD45LCA and lysozyme. MIB1 (Ki67) showed a nuclear staining of approximately 10% of the histiocytic cells. In summary, these findings were in keeping with a histiocytic sarcoma, a rare haematopoetic neoplasm. By demonstrating this particular case, we emphasise the importance of proving the diagnosis of pulmonary Langerhans cell histiocytosis by means of immunohistochemistry. In case of a negative CD1a reaction in a histiocytic lesion, further immunohistochemical studies have to be performed in order not to misdiagnose a malignant haematopoetic lesion.

Keywords Histiocytic sarcoma · Lung · Immunohistochemistry · Pulmonary Langerhans cell histiocytosis · Pneumothorax

E. Stacher (✉) · C. Beham-Schmid · H. H. Popper
Department of Pathology, Medical University of Graz,
Auenbruggerplatz 25,
8036 Graz, Austria
e-mail: elvira.stacher@medunigraz.at

H.-J. Terpe · N. Simiantonaki
Department of Pathology, Klinikum Leverkusen,
Am Gesundheitspark 11,
51375 Leverkusen, Germany

Introduction

A variety of underlying or concomitant conditions and diseases in the occurrence of spontaneous pneumothoraces is known. Apart from the frequently seen different emphysematous changes including juvenile, bullous or scarring emphysema, smoking-related diseases like respiratory bronchiolitis (RB) and respiratory bronchiolitis–interstitial lung disease (RB-ILD) as well as pulmonary Langerhans cell histiocytosis (PLCH) have recently been reported more often in the context with spontaneous pneumothoraces [1, 2]. In contrast, malignant lesions in this setting are encountered to a far lesser extent.

In this article, we present a case of a histiocytic sarcoma incidentally detected in a peripheral lung specimen resected for a spontaneous pneumothorax. Furthermore, we discuss the practical approach to the differential diagnosis of PLCH based on morphological and immunohistochemical features.

Clinical history

In February 2008, a 23-year-old male patient, a never-smoker without any relevant past medical history, presented with his second spontaneous pneumothorax of his right lung. On conventional X-ray and on computed tomography (CT) scans,

the lung parenchyma was unremarkable except for focal emphysematous changes and the pneumothorax itself.

Video-assisted thoracoscopic surgery for a bullae resection and pleurodesis was performed. On macroscopic examination, a firm greyish nodule with a diameter of 4 mm was found and embedded completely. The surrounding peripheral lung tissue was unremarkable except for minor emphysematous changes.

Materials and methods

The lung tissue was fixed in 4% buffered formalin and processed routinely according to standard protocols. H&E-stained sections of 4-µm thickness were obtained. Immunohistochemistry using commercially available antibodies was performed according to the manufacturers' recommendations. The list of antibodies used and the results are displayed in Table 1.

Results

Histologically, the bronchi and bronchioles were essentially unremarkable. The peripheral lung tissue showed mild emphysematous changes according to the macroscopic impression. In close neighbourhood of a bronchial wall, the tissue displayed a single, round tumour-like or granulomatous lesion measuring 4 mm in diameter. It was sharply demarcated, but not encapsulated and showed no foci of necrosis. The lesion consisted of cells with a histiocytic appearance with moderately polymorphic enlarged pale nuclei and fine but unevenly distributed chromatin. Nuclear folding was frequently observed. In most histiocytic-like cells, one or two nucleoli were visible, some of them quite prominent. Mitotic figures were not encountered. Within the lesion, inflammatory infiltrates consisting of plasma cells and lymphocytes were present and scanty eosinophilic granulocytes were scattered within the granulomatous lesion. Based on H&E sections, the tentative diagnosis of PLCH was rendered.

Table 1 Panel of antibodies used

Antibody	Clone	Company	Dilution	Results
CD1a	O10	Immunotech	r.t.u.	0
CD1a	O10	Dako	1:50	0
S-100		Dako	1:2,000	0
CD68	KP1	Dako	1:300	3+
HLA-DR	CR3/43	Dako	1:200	3+
CD45LCA	2811+DD7/26	Dako	1:50	3+
Lysozyme	EC3.2.1.17	Dako	1:300	2+
CD4	BC/1F6	Biocare	1:50	2+
CD11c	B-6	Santa Cruz	1:25	3+
CD14	7	Novocastra	1:50	3+
MIB-1	Ki-67	Ventana	r.t.u.	10–15%
CD3	T3	Dako	1:200	0
CD10	56C6	Novocastra	1:10	0
CD21	1F8	Dako	1:200	0
CD35	BerNACDRC	Dako	1:10	0
PLAP	SP15	NeoMarkers	1:50	0

Immunohistochemical staining refers to tumour cells

0: negativity; 2+: moderate positive; 3+: strong positivity

r.t.u. ready to use

Using immunohistochemistry, the histiocytic-like cells were negative for CD1a. This staining was repeated with a different antibody to CD1a provided by another company giving a negative result again. Also, the staining with an antibody to S-100-protein revealed a negative result. In contrast, the cells strongly expressed CD68. In additionally performed stains with antibodies to HLA-DR, CD45LCA and lysozyme positive results in the vast majority of tumour cells were observed. Most tumour cells expressed CD4 and all tumour cells expressed CD11c and CD14, proving the histiocytic origin. With an antibody to CD3, the intermingled T lymphocytes cells were stained positively. A few interspersed follicular dendritic cells were stained positively using antibodies to CD21 and CD35, whereas the tumour cells themselves did not express these markers. Furthermore, the tumour cells did express neither CD10 nor PLAP. MIB1 (Ki67) demonstrated a nuclear staining of approximately 10–15% of the histiocytic tumour cells. In summary, these findings were in keeping with a histiocytic sarcoma.

Photographs of the lesion (H&E stains, immunohistochemical stains) are displayed in Fig. 1a–h.

Discussion

Histiocytic sarcoma (HS), previously named "true histiocytic lymphoma", is a rare haematological neoplasm usually affecting the lymph nodes, the skin and the gastrointestinal tract. In case of a multiple involvement of different sites, this systemic presentation is referred to as "malignant histiocytosis" [3]. HS arising in the lung has rarely been reported; indeed, only few well-documented reports of cases in humans exist [4, 5]. According to the WHO, HS should be regarded as an aggressive haematopoetic neoplasm with a poor response to therapy being reflected by the study of Vos et al. [6] who reported five cases of HS. Four patients died within 2 to 15 months of their disease. In another patient group, two patients out of 14 died 4 and 5 months, respectively, following initial diagnosis [5].

In our case, the very small tumour was discovered incidentally and completely excised. The patient has been

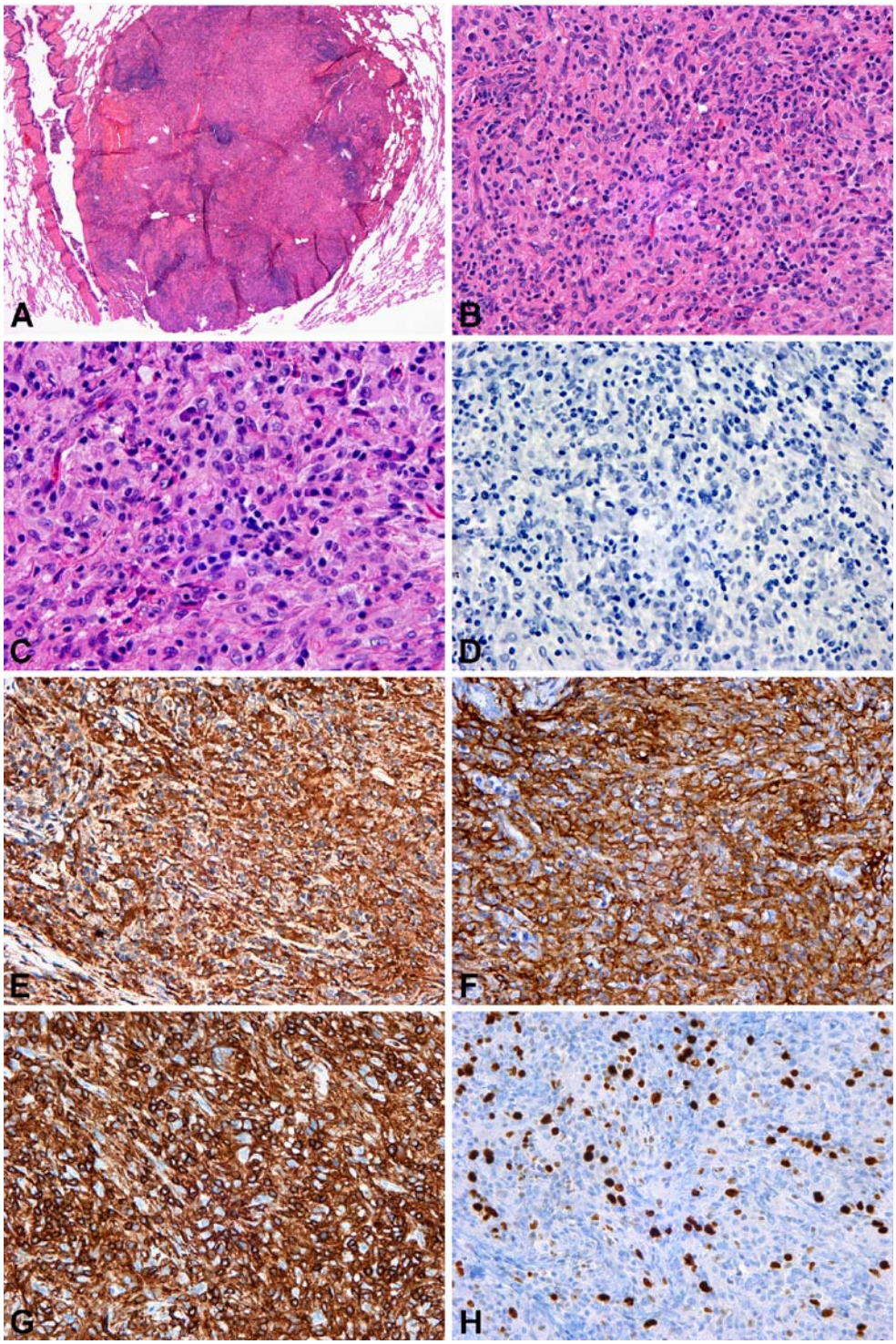

Fig. 1 **a** Well-circumscribed unencapsulated lesion closely attached to a bronchiolar wall. **b**, **c** Cells with a histiocytic appearance with moderately polymorphic enlarged pale nuclei and fine chromatin surrounded by inflammatory infiltrates consisting of plasma cells and lymphocytes. Few eosinophilic granulocytes. **d** CD1a. **e** CD68. **f** CD11c. **g** CD45LCA. **h** MIB-1

followed up on a three-monthly basis including clinical examinations, CT scans and a bone marrow biopsy. Neither a recurrence nor an involvement of other organs has been found. Until today, he has not received any chemotherapy. Meanwhile, the unfortunate patient suffered a third spontaneous pneumothorax 3 months after the initial diagnosis of the HS which was treated by a resection of the right upper lobe. On histological examination of the lung tissue, no residual tumour was found.

It is very unlikely that the tumour itself led to the spontaneous pneumothorax, as we think that it just happened to be an incidental finding. Interestingly, it has been questioned whether the routine histological examination of lung tissue excised in case of a pneumothorax is justified at all,

as it hardly ever changes the treatment of the patient [7]. We think that this particular case once more demonstrates that the histological examination can indeed be pivotal in order not to miss an underlying malignancy.

Focusing on pulmonary diseases, a differential diagnosis of this entity one has to consider is PLCH. In its active phase, it shows airway-centred interstitial infiltrates consisting of a special type of histiocytes, the so-called Langerhans cell histiocyte. This cell is regularly CD-1a as well as S-100-positive, but does not express CD68. Eosinophilic granulocytes in variable amount most often accompany these histiocytes, which reflects the historical term "eosinophilic granuloma". The surrounding peripheral lung parenchyma usually is either unremarkable or may display foci of RB [8, 9]. As PLCH progresses, its diagnostic hallmark is the airway-centred stellate scar. The cellular infiltrates decrease in number with the age of the granulomas; finally, the Langerhans cell histiocytes as well as the eosinophilic granulocytes may even be absent.

By demonstrating this case, we emphasise the importance of proving the diagnosis of PLCH by means of immunohistochemistry. We recommend the use of an antibody to CD1a preferably to antibodies to S-100-protein since an S-100 positivity has been reported in a certain percentage of cases of HS [5, 10, 11], which, taken by itself, may in fact not help to distinguish between these two entities. Recently, the use of antibodies to Langerin, a lectin associated with the formation of Birbeck granules, was reported to be a highly sensitive marker for Langerhans cells. However, it has to be borne in mind that also in a minority of cases tumour cells of a HS might be Langerin-positive [12].

The newly characterised CD163, a haemoglobin scavenger receptor, is a promising marker in the diagnosis of true histiocytic malignancies [6, 13, 14]. Its expression in cells of Langerhans cell histiocytosis has not been extensively studied; however, in one report dealing with this objective, a positive expression in three of five cases has been observed [15].

Given the fact that PLCH is a well-known cause for spontaneous pneumothoraces, we feel that it might be a diagnostic pitfall to rely on H&E sections alone when a histiocytic lesion in this setting is encountered. We strongly recommend immunohistochemical stainings, and in the case of a presumed PLCH with a negative CD1a reaction, further immunohistochemical studies have to be performed in order not to misdiagnose a malignant haematopoetic lesion.

Acknowledgement We are grateful to the expert haematopathologist Prof. Annette Schmitt-Gräff (Medical University of Freiburg, Germany) who reviewed this case and confirmed the diagnosis of a histiocytic sarcoma.

Conflict of interest We declare that we have no conflict of interest.

References

1. Mendez JL, Nadrous HF, Vassallo R et al (2004) Pneumothorax in pulmonary Langerhans cell histiocytosis. Chest 125(3):1028–1032
2. Cottin V, Streichenberger N, Gamondes JP et al (1998) Respiratory bronchiolitis in smokers with spontaneous pneumothorax. Eur Respir J 12(3):702–704
3. Jaffe ES, Harris NL, Stein H et al (2001) World health organization classification of tumours. Pathology and genetics of tumours of haematopoetic and lymphoid tissues. IARC, Lyon
4. Buonocore S, Valente AL, Nightingale D et al (2005) Histiocytic sarcoma in a 3-year-old male: a case report. Pediatrics 116(2): e322–e325
5. Hornick JL, Jaffe ES, Fletcher CD (2004) Extranodal histiocytic sarcoma: clinicopathologic analysis of 14 cases of a rare epithelioid malignancy. Am J Surg Pathol 28(9):1133–1144
6. Vos JA, Abbondanzo SL, Barekman CL et al (2005) Histiocytic sarcoma: a study of five cases including the histiocyte marker CD163. Mod Pathol 18(5):693–704
7. Khan OA, Tsang GM, Barlow CW et al (2006) Routine histological analysis of resected lung tissue in primary spontaneous pneumothorax—is it justified? Heart Lung Circ 15(2):137–138
8. Katzenstein A (2006) Surgical pathology of non-neoplastic lung disease. Saunders, Philadelphia
9. Cagle PT, Allen TC, Barrios R et al (2005) Color atlas and text of pulmonary pathology. Lippincott Williams & Wilkins, Philadelphia
10. Copie-Bergman C, Wotherspoon AC, Norton AJ et al (1998) True histiocytic lymphoma: a morphologic, immunohistochemical, and molecular genetic study of 13 cases. Am J Surg Pathol 22 (11):1386–1392
11. Pileri SA, Grogan TM, Harris NL et al (2002) Tumours of histiocytes and accessory dendritic cells: an immunohistochemical approach to classification from the International Lymphoma Study Group based on 61 cases. Histopathology 41(1):1–29
12. Lau SK, Chu PG, Weiss LM (2008) Immunohistochemical expression of Langerin in Langerhans cell histiocytosis and non-Langerhans cell histiocytic disorders. Am J Surg Pathol 32 (4):615–619
13. Kristiansen M, Graversen JH, Jacobsen C et al (2001) Identification of the haemoglobin scavenger receptor. Nature 409(6817):198–201
14. Walter RB, Bachli EB, Schaer DJ et al (2003) Expression of the hemoglobin scavenger receptor (CD163/HbSR) as immunophenotypic marker of monocytic lineage in acute myeloid leukemia. Blood 101(9):3755–3756
15. Nguyen TT, Schwartz EJ, West RB et al (2005) Expression of CD163 (hemoglobin scavenger receptor) in normal tissues, lymphomas, carcinomas, and sarcomas is largely restricted to the monocyte/macrophage lineage. Am J Surg Pathol 29(5):617–624

Virchows Arch (2009) 455:191–192
DOI 10.1007/s00428-009-0799-6

MEETING REPORT

Protein analysis of tissues—current views and clinical perspectives

Karl-Friedrich Becker · Axel Walch · Marius Ueffing

Received: 2 June 2009 / Accepted: 3 June 2009 / Published online: 26 June 2009

Abstract Proteomics raises high expectations in finding novel and reliable biomarkers for diagnosis, prognosis and therapy prediction. The goal of the 2-day workshop "Protein analysis of tissues—current views and clinical perspectives" was to bring together scientists from multiple areas of protein research interested in tissue analysis.

Keywords Proteomics · Molecular pathology · Meeting report

Much progress in tissue proteomics has been made for applications in basic sciences; translation of these methods for treatment of patients, however, is slow because the realities in the clinic are rarely taken into account and proteomic changes in cultured cell lines might not fully reflect human diseases due to the lack of the tissue (micro) environment. The goal of the 2-day workshop "Protein analysis of tissues" was to bring together scientists from multiple areas of protein research. The workshop was conceived by molecular and cell biologists, pathologists and protein scientists, supported by industry, the German Society of Protein Research and a Coordination Action funded by the European Union. A key strength of the meeting was that it combined lectures and practical aspects (wet lab courses).

Researchers from 12 European countries participated in the meeting. The fact that about 80% of the participants described themselves as primarily involved in protein analysis and only 20% were involved in histology indicated that pathologists may not be aware that there has been recent progress in protein studies—other than immunohistochemistry—in human tissues, including the use of samples stored for decades in huge archives in pathology departments.

Proteomics raises high expectations in finding novel and reliable biomarkers for diagnosis, prognosis and therapy prediction. H. Meyer (Bochum, Germany) presented data for the identification of biomarkers for liver cirrhosis using tissue microdissection, differential gel electrophoresis (DIGE) technology and mass spectrometry. Applications of laser microdissection, 2D-DIGE and matrix-assisted laser desorption/ionisation (MALDI) time-of-flight from heterogenous prostate carcinoma tissues in biomarker discovery were presented by S. Skvortsov (Innsbruck, Austria). F. Lottspeich (Martinried, Germany) presented results for the comparison of 2D-DIGE, Sypro-2D, and isotope-coded protein labelling for quantitative proteome analysis of brain tissues. H. Langen (Basel, Switzerland) explained in his talk why biomarker tests should be developed as "companion diagnostics" and escort the drug development at all stages (pharmacodiagnostic tests). This is crucial for the effective development and successful commercialisation of medicines and innovative drugs.

G. Schmidt (München, Germany) introduced an image analysis software platform for robust and fully automated means to extract quantitative information from tissues slide scans.

A joint workshop between Helmholtzzentrum München and Technische Universität München, München, 6–7 March 2009.

K.-F. Becker (✉)
Institut für Pathologie, Technische Universität München,
Trogerstrasse 18,
München 81675, Germany
e-mail: kf.becker@lrz.tum.de

A. Walch
Institut für Pathologie, Helmholtzzentrum München,
München, Germany

M. Ueffing
Abteilung Proteinanalytik, Helmholtzzentrum München,
München, Germany

Clinical tissues are typically formalin-fixed and paraffin-embedded (FFPE) for histopathological diagnosis. In order to shift diagnosis to prediction, novel tools are needed for precise protein measurements of FFPE tissues. The alternatives include the use of frozen tissues and the development of novel tissue fixatives. It is estimated that more than one billion FFPE tissue blocks exist worldwide. Many of those samples are connected to clinical data. Some lively debate at the conference focused on the use of FFPE tissues for protein analysis. KF Becker (Munich, Germany) and T. Geoui (Hilden, Germany) gave overviews about recently established methodologies for the suitability of FFPE tissue samples for protein studies. They focused on the extraction of full-length proteins from FFPE samples and the quantitative analysis of the extracted proteins using protein microarray technology. Other applications for FFPE tissues include mass spectrometry and 2D polyacrylamide gel electrophoresis.

T. Joos (Reutlingen, Germany) described applications and future challenges for protein microarrays. This technology is likely to evolve into a key technology for the characterisation of complex samples.

The almost complete absence of protein synthesis of platelets makes them ideal systems for protein studies. A. Sickmann (Dortmund, Germany) presented data on the identification of more than 2,500 proteins, more than 1,000 phosphorylation sites and more than 350 glycosylation sites. Using these data, the knowledge about platelet function will certainly benefit.

MALDI mass spectrometry has become a powerful tool in biological research, especially in proteomics. Recently, MALDI techniques were developed for direct tissue analysis and molecular imaging, allowing the detection and localisation of a large number of compounds directly from tissue sections in one acquisition. Unlike other visualisation techniques such as immunohistochemistry or fluorescence microscopy, so-called MALDI-IMAGING does not require a target-specific reagent (e.g. antibody) and, therefore, is a valuable discovery tool, since it can survey a broad range of proteins simultaneously. The advantage of maintaining the spatial location of proteins is critical in achieving a comprehensive analysis of heterogeneous tissue samples, such as cancers. S.O. Deininger (Bremen, Germany) and A. Walch (München, Germany) presented exciting novel data about the use of MALDI-IMAGING for tumour proteomics.

M. Ueffing presented data for the interactome of lebercilin, which is genetically linked to a severe form of blindness, Leber congenital amaulrosis. The interactome links this protein to the transport of vesicular cargo to the outer segment along ciliar structures.

One of the major health challenges of the twenty-first century is type 2 diabetes. H. Sarioglu (München, Germany) used liquid chromatography tandem mass spectrometry to identify 4,000 quantitative profiles of protein markers in a type 2 diabetes mouse model.

The second day of the workshop focussed on practical aspects of protein analysis from tissues. Protocols were provided and explained in detail for protein extraction from FFPE tissue samples and subsequent protein microarray analysis, MALDI-IMAGING, quantitative immunohistochemistry and quantitative approaches for mass spectrometry-based and gel-based proteomics. After a short theoretical introduction to each of the topics, participants were allowed to try some of the assays by themselves.

Because of the great success of the workshop, the organisers plan to repeat the meeting in 2011, hoping to attract more histology-oriented researchers.

Virchows Arch (2009) 455:193–196
DOI 10.1007/s00428-009-0810-2

MEETING REPORT

From virtual microscopy to systems pathology

A meting report of the 1st European workshop on tissue imaging and analysis, Heidelberg, Germany, 13–14 February 2009

Niels Grabe · Peter Schirmacher

Received: 9 July 2009 / Accepted: 10 July 2009 / Published online: 4 August 2009

Introduction

Virtual microscopy encompasses the high-resolution scanning of tissue slides and cell preparation and derived technologies including automatic digitalization and computational processing of whole microscopic slides, cytological preparations and tissue arrays, and web-based easy accessibility and analyses. For the first time, it enables high-throughput imaging and quantitative measurements of tissue structures. By integrating mass tissue data and derived analyses, virtual microscopy creates novel synergies between technological disciplines such as pathology/histology, bioinformatics, medical informatics, image analysis, as well as cell and molecular biology. These technical synergies may pave the way for new structures in research, clinical diagnostics, education, and training and fundamentally support newly arising disciplines like medical systems biology. The 1st European Workshop on Tissue Imaging and Analysis, held in Heidelberg on 13th and 14th February 2009 intended to provide a discussion forum for multiple disciplines related to virtual microscopy, like pathology, systems biology and pathology, computer-assisted high-throughput diagnostics, cell-based cancer diagnostics, bioinformatics and image processing, and the scientific exchange of key players in the field. Over 140 participants from 10 European countries as well as USA and Japan took part in the meeting.

N. Grabe (✉) · P. Schirmacher
Hamamatsu Tissue Imaging and Analysis (TIGA) Center,
BIOQUANT, INF 267, University of Heidelberg,
Heidelberg, Germany
e-mail: niels.grabe@bioquant.uni-heidelberg.de

N. Grabe
Institute of Medical Biometry and Informatics,
University Hospital Heidelberg,
Heidelberg, Germany

P. Schirmacher
Institute of Pathology, University Hospital Heidelberg,
Heidelberg, Germany

Sessions

Research applications

Several speakers covered topics from tissue banking over the systematic evaluation of tissue morphology using image processing up to systems biological modeling of tissues. *Niels Grabe* (*University Heidelberg*, *Germany*) introduced virtual microscopy as a tool and its increasing role in Medical Systems Biology as it generates the necessary data of tissue morphology in which molecular computational models of diseases will be embedded. This has motivated the foundation of the first interdisciplinary institutions linking Pathology, Systems Biology, and Medical Informatics, such as the Tissue Imaging and Analyses Center at the University of Heidelberg [1]. *Ulf-Dietrich Braumann* (*University Leipzig*, *Germany*) presented how microscopy is presently undergoing a transformation due to the increasing availability of digital image acquisition devices. He demonstrated how growth of carcinoma of the cervix, prostate, and skin as well as regeneration processes and tissue formation, for example of nerves and joint cartilage, can be quantified using image data obtained by virtual microscopy [2]. *Nobert Wey* (*University Zurich*, *Switzerland*) showed what is needed to quantify Alzheimer plaque on virtual slides. His work provided an excellent example for the necessity of having an efficient work flow allowing

the automated analysis of high volume imaging data. *Pascal Tomakidi* (*University Freiburg*, *Germany*) provided data on the use of virtual microscopy in epithelial tissue cultures, especially how quantitative spatial profiles of markers of epithelial homeostasis were generated. These analyses may form the basis for prospective simulation attempts of epithelia formation and regeneration [3]. *Andreas Heffel* (*University Leipzig*, *Germany*) reported how automated image segmentation and classification provide an indispensable requirement for a large-scale analysis of in situ hybridization gene expression patterns (GEP). He presented an automated process flow for segmentation, classification, and clustering in large-scale sets of Drosophila melanogaster GEP that is capable of dealing with most of the technical problems implicated in these images. *Peter Schirmacher* (*University Heidelberg*, *Germany*) described tissue banks as essential platforms for modern biomedical and translational research. Besides tissue storage, distribution, project management, and support in morphology-based techniques, tissue banks offer an optimal platform for decentralized tissue-based research projects, including centralized scanning of decentrally obtained stains, especially multi-tissue arrays, data storage, and data analysis as well as decentralized access to data, their analyses as well as reference slides. These tools can be extended through further integration of additional tissue technologies (e.g., fluorescence techniques) and bioinformatics.

Industrial applications

Technical capabilities and the application potential of currently available virtual microscopy technologies as a key technology in industrial research were discussed by several speakers. *Maria Athelogou* (*Definiens*, *Germany*) described how "Intelligent Image Analysis" plays an important role and moves into the heart of R&DS and Diagnostics. She stressed that accurate information from image processing is critical for pathologists and oncologists as it determines the predictive and prognostic outcome of morphological studies. *Niels Foged* (*Visiopharm*, *Denmark*) demonstrated that the quantitative analysis of the HER-2 immunostaining in breast cancer tissue sections represents an important challenge for digital pathology. He introduced a novel, highly discriminative algorithm for scoring HER-2 and thereby also presented the widely applicable principles of image sampling, data management, and quantification in whole slide images. *Heinrich Bürgers* (*TissueGnostics*, *Austria*) sketched a novel approach to imaging, analysis, diagnosis, and documentation of histological slides by the use of FACS equivalents for cells in tissue slides and smears. *Catherine Conway* and *Lynn Dobson* (*Slidepath*, *Ireland*) showed quantitative data resulting from a study using the application of image analysis as adjunct to manual evaluation of HER-2 status. They described the development of a HER-2 image analysis algorithm that classified cases based on both the intensity and continuity of membrane staining. The performance of the algorithm was validated across a large cohort of clinical cases and achieved a 91% concordance with manual review by a pathologist. Agreement with gene amplification status as the gold standard was also found to be higher for the automated review, suggesting a potential of this technology as a support to increase the diagnostic standardization of HER-2 evaluation [4]. *Lars Schmidt* (*Agfa*, *Germany*) described the technical requirements for the embedding of virtual microscopy in a hospital setting as an example for an administrative–medical workflow in the field of digital pathology. *Masafumi Oshiro* (*Hamamatsu Photonics*, *Japan*) elaborated on the basic concepts of virtual microscopy already introduced in 1997, since then becoming rapidly an indispensable tool to support digital pathology applications. Thereby, the technical implications of slide scanning determine the potential of virtual microscopy. Furthermore, new features, such as virtual fluorescence slides and Z-stack for focusing, were presented, which may enable the introduction of novel clinical applications.

Education and training

Research and training represent the areas where virtual microscopy has first entered practical application, and in this field, the most advanced experiences exist. *Jim Diamond and Peter Hamilton* (*Queens University Belfast*, *Ireland*) noted that we currently experience a tipping point in tissue-based research and education [5]. The importance of pathology diagnostics as a central discipline for translational research and biomarker discovery was stressed, and the technical challenges including storage, remote slide viewing, and high-performance image processing were sketched. From this, novel opportunities for application in education, quality management, tissue archiving, and research were elaborated. *Peter Riegman* (*Erasmus Medical Center*, *Rotterdam*, *The Netherlands*) showed how virtual microscopy is increasingly replacing conventional microscopy in students training at Rotterdam Medical School. He reported VM to enable teachers to spend more time on teaching and collaboratively discussing histology and pathology topics. He also showed that students appreciated virtual microscopy far more than conventional microscopy. *Alberto Pérez-Bouza* (*RWTH Aachen*, *Germany*) demonstrated his innovative approaches and experiences when implementing virtual microscopy in histology courses since June 2006. He analyzed the acceptance of the web-based digital microscopy by questionnaires filled out by students and also by an analysis of

the number of visits on the web server. He found that students not only appreciated the possibility of learning microscopy through the Web but also used the system intensively for training purposes and self-assessment prior to examinations. Moreover, the integration of the virtual histology into a video podcast containing macroscopic images, drawings, etc. has improved the acceptance of clinical pathology as an attractive and modern subject. *Katharina Glatz* (*University of Basel*, *Switzerland*) presented Pathorama as a publicly accessible modular e-learning platform used at all levels of pathology education, including a searchable atlas containing more than 600 virtual slides. Various contributors have fed categorized metadata including the slide URL into the central slide database while the slides are stored on servers at the contributing institutes [6]. *Marco Novelli* (*University College London*, *Great Britain*) reported positives experiences of applying the virtual microscopy technology, including fast remote virtual slide access; reported improvements were benefits in the quantitative measurements of virtual slides (Breslow's thickness measurement, proliferation index), remote reporting, and greatly improved e-learning. He also elaborated on difficulties like hospital firewalls, the need of technical education, as well as relatively high costs for image processing, storage, and scanning.

Clinical applications

Peter Hufnagl, *Karsten Schlüns*, and *Norman Zerbe* (*University Berlin-Charité*) discussed the basic requirements for the use of virtual microscopy in routine pathology. Despite being widely accepted in Pathology for educational purposes and teleconsultation, they stated that the broad routine use of VM in surgical pathology is currently not in sight due to the technical requirements and some further limitations. Instead, they identified application potential in the fields of education, second opinion, and interdisciplinary tumor centers, routine marker quantification for small departments as well as large university institutes [7]. Furthermore, the rise of tumor centers is expected to promote the routine use of VM. In conclusion, similarities to digital radiology were identified although the introduction was estimated to take some years. *Peter Sinn* (*University Heidelberg*, *Germany*) reported recent experiences in the application of virtual microscopy in reference pathology and external clinical services. Telepathology and teleconsultation were presented as important application fields. He showed results from a diagnostic trial in cryosection evaluation. He concluded that telepathology is almost equivalent to conventional microscopy in the evaluation of frozen sections if no evaluation of the macroscopic aspects of the specimen is required, e.g., in the frozen section diagnoses of sentinel lymph node biopsies [8]. *Thomas Fuchs* (*ETH-Zürich*, *Switzerland*) presented a framework for biomarker quantification using tissue microarrays based on experiences with clear cell renal cancer by computational pathology including correlation with survival analysis [9]. Quantified histological assessment of human tissues was identified as the key point for the automation and objective assessment in predictive pathology. *Manfred Schmitt and Lina Seiz* (*Technical University München*, *Germany*) reported on the assessment of Urokinase plasminogen activator (uPA) and its inhibitor (PAI-1) which are accepted predictive markers in breast cancer by virtual microscopy. Automated scanning, followed by computer-assisted quantitative scoring of uPA and PAI-1 immunohistochemistry, may represent a potential alternative to the established ELISA measurements, recently recommended for clinical application in the ASCO guidelines 2007. *Niels Halama* (*National Center for Tumor Diseases*, *University Heidelberg*, *Germany*) presented a quantitative analysis of immune infiltrates in primary colorectal cancers and their liver metastases. Quantitative cell counts based on immune cell surface molecules (CD3, CD8, Granzyme B, and CD45RO) were independent predictors of patient outcome. Using virtual microscopy, the intratumoral heterogeneity of the investigated immune cells was assessed. Computational simulation of tissue microarrays from the virtual slides showed that intratumoral heterogeneity of all measured surface molecules was so high that a reliable measurement of the surface molecules for an individual patient was only achieved by analysis of full-size tissue sections. He suggested studies for the definition of potential biomarker cutoffs. Potential diagnostic tests should include quantitative assessments of intratumoral heterogeneity. This could be reliably achieved by measurements in full-size tissue slides using virtual microscopy [10]. *Thomas Schrader* (*University of Applied Sciences*, *Brandenburg*, *Germany*) elaborated on the need for standardization when embedding virtual microscopy in the Integrated Healthcare Enterprise [11]. A communication concept was presented connecting virtual slide scanners and pathology laboratory information systems. *Nicolas Wentzensen* (*National Cancer Institute*, *Bethesda*, *MD*, *USA*) presented the innovative application scenario of virtual microscopy in cervical cancer screening cytology. Virtual microscopy has the potential to improve this process at several levels. Novel biomarkers allow the automated detection of abnormal cells with increasing sensitivity and a reduced evaluation time. Web-based evaluation allows cytologists to analyze specimens without the need for circulating glass slides. Archiving of digital microscopy images preserves slides under optimal conditions and saves storage space.

Conclusions

The workshop provided a comprehensive overview over novel technologies and applications of virtual microscopy and a forum for stimulating interdisciplinary discussions, representing diverse fields such as pathology, computer sciences, systems biology, biomedical informatics, biotechnology, epidemiology as well as basic biomedical research. It is intended to be pursued in a regular, most likely annual format.

References

1. Grabe N (2008) Virtual microscopy in systems pathology. Pathologe 29(Suppl 2):259–263
2. Braumann UD, Scherf N, Einenkel J et al (2007) Large histological serial sections for computational tissue volume reconstruction. Methods Inf Med 46(5):614–622
3. Grabe N, Pommerencke T, Steinberg T et al (2007) Reconstructing protein networks of epithelial differentiation from histological sections. Bioinformatics 23(23):3200–3208
4. Conway C, Dobson L, O'Grady A et al (2008) Virtual microscopy as an enabler of automated/quantitative assessment of protein expression in TMAs. Histochem Cell Biol 130(3):447–463
5. Hamilton PW, van Diest PJ, Williams R et al (2009) Do we see what we think we see? The complexities of morphological assessment. J Pathol 218(3):285–291
6. Glatz K, Bubendorf L, Glatz D (2007) Cytology in the internet. Pathologe 28(5):318–324
7. Hufnagl P, Schluns K (2008) Virtual microscopy and routine diagnostics. A discussion paper. Pathologe 29(Suppl 2):250–254
8. Sinn HP, Andrulis M, Mogler C et al (2008) Virtual microscopy in pathology teaching and postgraduate training (continuing education). Pathologe 29(Suppl 2):255–258
9. Fuchs E (2008) Skin stem cells: rising to the surface. J Cell Biol 180(2):273–284
10. Halama N, Michel S, Kloor M et al (2009) The localization and density of immune cells in primary tumors of human metastatic colorectal cancer shows an association with response to chemotherapy. Cancer Immun 9:1
11. Wienert S, Beil M, Saeger K et al (2009) Integration and acceleration of virtual microscopy as the key to successful implementation into the routine diagnostic process. Diagn Pathol 4:3

The given references do not reflect the contents of the individual talks but provide further information concerning that matter.

Virchows Arch (2009) 455:197–211
DOI 10.1007/s00428-009-0813-z

ORIGINAL ARTICLE

A combined histologic and molecular approach identifies three groups of gastric cancer with different prognosis

Enrico Solcia · Catherine Klersy · Luca Mastracci · Paola Alberizzi · Maria Elena Candusso · Marta Diegoli · Francesca Tava · Roberta Riboni · Rachele Manca · Ombretta Luinetti

Received: 27 May 2009 / Revised: 6 July 2009 / Accepted: 15 July 2009 / Published online: 12 August 2009

Abstract The limited prognostic value of currently used histologic classifications of gastric cancer and their failure to account for the complexity of the disease as revealed by more recent investigations prompted a combined reinvestigation of histologic, molecular, and clinicopathologic patterns in 294 extensively sampled, invasive gastric cancers representing all main histotypes and stages of the disease and followed for a median of 150 months. Among histologic parameters tested, only cellular atypia, angio-lympho- or neuroinvasion, Ki67 proliferation index, expansile/infiltrative type growth, and T8 cell-rich high lymphoid intra-/peritumor response (HLR) proved to be stage-independent predictors of patient survival. Among molecular tests, p53 gene exon 7 (loop 3) and 8 (loop-sheet-helix motif and S-10 band), but not p53 protein overexpression, TP53 LOH or 18qLOH, were found to worsen prognosis. Microsatellite DNA instability was a favorable prognostic factor when coupled with HLR. Patient survival analysis of the main histotypes and their subtypes confirmed the favorable prognosis of HLR, well-differentiated tubular, muconodular, and low grade diffuse desmoplastic cancers, and highlighted the worse prognosis of anaplastic and infiltrative-lymphoinvasive mucinous cancers compared to ordinary cohesive and diffuse cancers. Distinct roles of individual morphologic and molecular factors in tumor progression of the different histotypes have been recognized. The combination of survival-predictive histotypes and individual histologic or molecular parameters allowed us to develop a classification of all gastric cancers into three grades of increasing malignancy which proved to be of high prognostic value.

Keywords Gastric cancer · Prognostic factors · Lymphoid cell response · P53 gene mutations · Histotype grading

E. Solcia · P. Alberizzi · M. E. Candusso · F. Tava · R. Riboni · R. Manca · O. Luinetti
Anatomic Pathology Service,
IRCCS Policlinico S. Matteo Foundation,
Pavia, Italy

E. Solcia · M. Diegoli
Department of Pathology and Genetics, University of Pavia,
Pavia, Italy

C. Klersy
Statistics Unit, Scientific Direction,
IRCCS Policlinico S. Matteo Foundation,
Pavia, Italy

L. Mastracci
Department of Anatomic Pathology, University of Genova,
Genova, Italy

M. Diegoli
Inherited Cardiovascular Diseases Center,
IRCCS Policlinico S. Matteo Foundation,
Pavia, Italy

E. Solcia (✉)
Istituto Anatomia Patologica,
via Forlanini 16,
27100 Pavia, Italy
e-mail: solciae@smatteo.pv.it

Introduction

Currently used histologic classifications are of limited value in the prognostic evaluation of gastric cancer [1–3]. Separation of gland-forming 'intestinal' from scattered-cell 'diffuse' tumors according to Lauren [4] is known to predict the natural history of gastric cancer, including its association with intestinal metaplasia and blood-borne liver metastases or with direct serosal invasion and peritoneal carcinosis, respectively [5]. Different molecular changes

have also been detected in the two tumor types: p53 gene mutation, p53 protein accumulation, microsatellite DNA instability, 18qLOH, or c-erbB-2 expression are preferentially associated with the intestinal type and cadherin E mutation or loss of membrane expression with the diffuse type [6–12]. However, despite early suggestions that diffuse tumors had a poorer prognosis [13], Lauren's classification failed to predict patient survival independently from tumor stage [1, 3]. Attempts to improve prediction power by considering the type of local tumor growth (expansile vs. infiltrative) [14], by introducing different degrees of glandular differentiation (well vs. moderate vs. poor) [15, 16], by combining glandular differentiation with mucin production [17–19], or by separating solid and mixed from glandular and diffuse cancers [2, 3] had limited success and failed to impact significantly on clinical practice.

However, a few histologic features have consistently been found to predict tumor behavior such as vascular invasion [2, 3, 20] and intratumor lymphoid cell infiltration [21–24]. In addition, some molecular findings have also been reported to be prognostically informative, i.e., high level instability of microsatellite DNA (MSI-H) [10, 11], Epstein–Barr virus (EBV) infection [25], p53 gene mutation [8, 26], 18qLOH [27], SMAD4 or 7 gene expression [28, 29], c-erbB2 expression [30], E cadherin gene mutation [7], and gene loss or gain by comparative genomic hybridization [31]. Unfortunately, so far, none of these molecular findings have proven to be contributive and cost effective enough to enter routine diagnostic practice.

Nevertheless, some of the histologic, phenotypic, or molecular patterns were helpful in identifying tumor subsets predictive of patient survival. Those showing better survival included very well-differentiated tubular cancers with intestinal phenotype [32, 33], the muconodular-expansile subtype of mucinous cancer [33], and the low grade, tumor cell-embedding variant of diffuse desmoplastic cancer [34], in addition to MSI-H [10, 11] and lymphocyte-rich cancers [21–24]. On the contrary, various kinds of anaplastic cancers with poor outcome have been identified, with or without neuroendocrine features, from small to intermediate or large cell [35–37], diffuse to solid in structure, sometimes with signs of hepatoid, choriocarcinomatous, or squamoid differentiation [3, 34, 38, 39].

Thus, in order to develop a more informative and practical classification system, a systematic reinvestigation of potentially predictive histological and molecular parameters seems to be required on a sufficiently large series of invasive gastric cancers covering all the main stages and histotypes and with long-term follow-up (fundamental in identifying long survivors with low grade tumors). The aim of this study was to: (a) further check the prognostic power of individual parameters; comparatively and simultaneously in the same patient series; (b) search for possible histotype restriction of their distribution and diagnostic or prognostic power; (c) test the prognostic value of resulting tumor types and subtypes; (d) develop a simple grading system based on predictive histologic factors or histotypes, into which contributive molecular findings could be easily incorporated.

Materials and methods

Tumor selection Invasive (T1b to T4) gastric cancers were selected from cases undergoing surgery with curative intent at the San Matteo General Hospital in Pavia from 1984 to 2000 or at San Martino General Hospital in Genova in 1998–1999. The study considered only cases with extensive sampling of the tumor (two to 12 blocks, depending on size) and surrounding non-tumor tissue and carefully assessed perioperative TNM stage [40]. Special attention was paid to tumors whose invasion was limited to the deep submucosa (penetrating T1b, 44 cases) or muscularis propria (T2a, 55 cases) or whose histologic patterns suggested low or high malignancy or showed a structure differing from that of ordinary glandular and diffuse cancers. In all, 294 cases were collected. Corresponding patients by the end of January 2009 had either died of the disease or other causes or were still alive and had been followed for at least 7 years, with a median follow-up of 150 months (25th–75th=90–186).

Histologic and histochemical stains Paraffin sections were stained with hematoxylin–eosin, Alcian blue–PAS, Giemsa, or immunoperoxidase using specific antibodies for MUC1, MUC2, MUC5AC, and MUC6 mucins [33, 34]; cytokeratins 7, 19, 20, and AE1/AE3 (Dako, Denmark); CD8 antigen (C8/144B clone, Dako); Ki67 protein (MIB1 clone, Dako); p53 protein (D07 clone, Dako); and h-MLH1 (G-168.15 clone, Pharmingen, San Diego, CA, USA) or h-MSH2 (Fe11 clone, Oncogene, Cambridge, MA, USA) mismatch repair proteins. In situ hybridization for the EBER-1 gene [3] or for EBER-1 and EBER-2 genes (probe Y5200, Dako) was used to detect Epstein–Barr virus (EBV) infection.

For molecular investigation, tumor tissue was carefully dissected under microscopic control to enrich the tumor cell component to more than 60%. A PCR-based denaturing gradient gel electrophoresis (DGGE) method, followed by DNA sequencing with a 3100 Applied Biosystems equipment, was used to detect p53 gene mutations at exons 5 to 8 [8]. For microsatellite instability analysis, Bat 25 and Bat 26 loci were first investigated; tumors showing concordant stability or instability at both loci were classified as either stable (MSS) or highly unstable (MSI-H), respectively. Those showing discordant findings were further tested at Bat 40, D5S346, and D2S123 loci. Only tumors with

instability involving at least two of the five loci were classified as MSI-H; the others were classified as low instability (MSI-L) and included in the MSI-negative tumor group together with MSS cases [10, 11, 41]. In most MSI-H cases, loss of MLH1 nuclear stain was observed immunohistochemically while only two cases lacked MSH2 reactivity.

Loss of heterozygosity (LOH) at chromosome 18 was examined as previously described [12] in paired tumor and non-tumor DNAs using 12 highly polymorphic microsatellite markers (D18S56, D18S67, D18S34, D18S460, D18D450, D18S474, D18S484, DCC-vNTR, D18S69, D18S55, D18S58, and D18S70) spanning most of the long arm of the chromosome, from band 18q11.2 up to q23 near the q-ter. For TP53 LOH at 17p13.1, a CCA117-732 probe was used in accordance with Vogelstein et al. [42].

Histologic evaluation Glandular differentiation was scored 0 (predominantly diffuse or solid structure), 1 (mixed diffuse/solid and glandular structure, at least 40% each of the two components), 2 (>60% glandular structure), or 3 (well-differentiated, purely glandular structure). Assessment of tumor cell anaplasia was mainly, but not exclusively, based on nuclear features [43]. Score 1 tumors were characterized by monomorphous, small- to medium-sized nuclei of regular shape, fairly uniform chromatin distribution, and small to inapparent nucleoli inside cells with fairly abundant cytoplasm. They often presented signs of functional differentiation (including mucin secretion), with or without cell polarization and well-developed intercellular junctions or glandular structure. In contrast, score 3 tumors showed larger, polymorphic nuclei, ranging from vesicular with prominent nucleoli to dense, hyperchromatic with relatively small nucleoli, inside poorly cohesive, non-polarized cells with scarce (small cells) to abundant (large cells) cytoplasm, usually mucin free, albeit sometimes with signs of abortive endocrine (poorly differentiated neuroendocrine cancers), hepatoid, chorionepitheliomatous, or squamoid differentiation, often with multifocal necrosis [3, 34, 36, 37, 39]. Tumors showing moderate to considerable nuclear pleomorphism in cells of various size, shape, and aggregation status, with intermediate patterns between those of score 1 and 3, were classified as score 2.

Mitotic figures were counted in ten high power fields (HPF, ×400) while the percent of Ki67 positive nuclei was assessed at ×250 magnification by counting at least 1,000 cells in areas showing the highest proliferation [34]. Routine hematoxylin–eosin preparations were adequate in most cases to assess lymphatic and blood vessel invasion. When tumor cells were found in vessel-like spaces of doubtful interpretation, the CD31 endothelial cell marker (M823 antibody, Dako) was applied. Lymphoinvasion and neuroinvasion were graded 0 (absent), 1 (sporadic, i.e., no more than one invaded vessel or nerve in a tumor section), or 2 (multifocal); only score 2 invasion proved to be unquestionably predictive of survival in this study. A single finding of unequivocal blood vessel invasion was sufficient to classify the tumor as angioinvasive, while the presence of either score 2 lymphoinvasion and/or angioinvasion indicated vascular invasion. Both endoneural and closely adherent perineural invasion were considered [34]. Only those cases which showed a well-demarcated regular boundary between a "pushing" tumor growth and surrounding non-tumor tissues were classified as expansile; all the remaining cases were considered as infiltrative.

Tumor types Of the 294 tumors, careful investigation of hematoxylin–eosin, Alcian blue–PAS, and Giemsa-stained sections identified 74 cases with diffusely infiltrating, poorly cohesive cells dispersed in the stroma as single elements or in small aggregates with little or no gland formation (diffuse cancers) [34], 42 cases with prominent extracellular mucin (mucinous cancers) [33], and 21 cases formed predominantly or exclusively by anaplastic, highly proliferative (≥20 mitoses/10 high power fields) small to large cells with scarce stroma and frequent necrosis, regardless of their diffuse or cohesive structure and usually poor expression of endocrine or exocrine markers (anaplastic cancers) [3, 34, 36].

Among the remaining 157 tumors, 56 cases showed increased intra-peritumor lymphoid cell infiltration (lymphocyte-rich or LR cancers) [21, 24], of which 47 "high lymphoid response" (HLR) cancers showed either (a) lymphoepithelioid (LEP; 17 cases, 12 of which are EBV positive) pattern with intimate admixture of abundant lymphoid cells and epithelial tumor cells, often dissociated from each other by the infiltrate, or (b) ≥300 CD8+ cells/10 HPF inside the tumor growth, coupled with a prominent band of lymphoid cells, rich in CD8+ cells, surrounding the expansile edge of the tumor or its nodules. The remaining 110 non-HLR tumors formed the cohesive cancers group, with more or less prominent glandular (tubular, papillary, or cystopapillary) differentiation or even with solid histology.

In addition, three low grade subtypes were identified according to previously published criteria, i.e., muconodular cancer, characterized by prominent mucin lakes with expansile growth and moderately numerous tumor cells freely floating in them [33], separated from the remaining mucinous cancers showing an infiltrative pattern, low grade diffuse desmoplastic cancer with prominent desmoplasia entrapping tumor cells with a limited or no invasive pattern, to be separated from ordinary diffuse cancer [34], and very well-differentiated tubular cancer with monostratified, low grade epithelium and a limited or no invasive pattern [32, 33], somewhat reminiscent of tubular breast cancer [44], to be separated from ordinary cohesive cancers.

Statistical analysis Data distribution was expressed as counts and percents for categorical variables and was compared by means of the Fisher exact test. The Spearman R correlation coefficient was used to measure the association of variables on a continuous scale.

The follow-up extended from the date of surgery to the date of death from gastric cancer or to the last available assessment. Patients dying from other causes were censored at the date of their death. Median follow-up and its interquartile range (25th–75th) was computed by means of the inverse Kaplan–Meier method. Cox regression was used to assess the prognostic role of cytologic atypia and of a series of other potential risk factors. Uni- and multivariable models were fitted. Clinically relevant variables were included in the multivariable model in addition to stage, provided they were not collinear. Hazard ratios (HR) and their 95% confidence intervals (95% CI) were computed. The proportional hazard assumption was tested based on Schoenfeld residuals. Death rates per 100 persons per year (95% CI) were also computed as summary measures. To assess model performance, we also calculated the Royston explained variation, Harrell's *C* statistic for discrimination, and the Le Cessie–van Houwellingen shrinkage coefficient (and noise in model=1—shrinkage) for calibration. A two-sided p value <0.05 was considered statistically significant. Stata 10.1 (StataCorp, College Station, TX, USA) was used for computation.

Results

In the 294 tumors under investigation, a series of potentially prognostic, histologic, or molecular parameters were analyzed for patient survival (Table 1). Several histologic features (Figs. 1, 2, and 3) proved to be predictive at univariable as well as at stage-inclusive bivariable analysis, among which grade 2 and 3 anaplasia, expansile vs. infiltrative growth, vascular (either score 2 lymph or any blood vessel) invasion, and high lymphoid intra-/peritumor response. The outcome predictive value of lymphoinvasion and angioinvasion was also supported by their strong association with local T invasion level, lymph node metastases, and distant metastases (Fisher exact test, $p<0.001$ for all associations).

Glandular differentiation showed significant prognostic influence at univariable analysis, which, however, largely vanished at stage-inclusive analysis; a trend toward improved survival was retained only by high tubular differentiation. Neuroinvasion (score 2), though significantly predictive of worse survival regardless of stage, was often difficult to ascertain, especially in T1b or T2a tumors sparing deep muscularis propria, where larger nerves and ganglia are likely to be found. It was assessed only in 244 of the 294 cases investigated. Both mitotic and Ki67 proliferative indices predicted worse survival independently of stage when cases above/below the median were compared. When comparing tertiles of their distribution, Ki67 proved to be superior (log rank test for Ki67 $p=0.002$, for mitoses $p=0.023$), especially in discriminating the lower (death rate=6.21, 4.50–8.56) from the intermediate tertile (death rate=12.45, 9.84–15.77); however, both Ki67 ($p=0.071$) and mitoses ($p=0.297$) failed to survive stage-inclusive Cox bivariable analysis. Mucin production, either intracellular or extracellular, failed *per se* to predict survival, while showing an inverse relationship with intra- and peritumor lymphoid cell response and a trend towards lower tumor cell proliferation.

Among molecular tests (Figs. 4 and 5), only exon 7 and 8 p53 gene mutations (of which 33/37, 89%, were in the L3 loop, 12 cases, S-10 strand, two cases, or the loop-sheet-helix motif, 19 cases, three regions crucial for target DNA interaction) proved to be stage-independent predictors of worse survival; p53 exon 5 to 8 mutations, p53 gene locus LOH, or p53 protein nuclear accumulation, though significantly predictive on univariable analysis, showed only borderline trends when stage was included. Exon 5 and 6 mutations lacked any prognostic value. High level microsatellite instability and 18qLOH revealed non-significant trends for improved or worse survival, respectively.

Of the 56 lymphoid cell-rich (LR) tumors, lymphoid infiltrates were distributed unequally in nine cases leaving significant lymphocyte poor tumor areas or lacked a T_8 cell-rich peritumor band, thus failing to fulfill all criteria for HLR cases. The remaining 47 tumors formed the HLR group, which showed highly improved survival (HR 0.26, 0.15–0.47, $p<0.001$) compared to the 247 non-HLR cases. The interplay between HLR, EBV, MSI-H, and p53 status in terms of prognosis is analyzed in Table 2, where it appears that the HLR pattern *per se* represents the most powerful prognostic factor and that the favorable effect of MSI-H may act mostly through HLR, as suggested by its inefficacy among HLR-negative cases. In addition, Table 2 shows that, besides EBV and MSI-H positive tumors, a third group of 12 tumors developed HLR, possibly through expression of increased, highly antigenic, and mutated proteins like p53. Indeed, eight such tumors (67%) showed either p53 gene mutation (seven cases, six of which in exons 5 or 6) and/or p53 protein overexpression (seven cases), in contrast to the reduced trend for both changes among EBV+ or MSI-H tumors.

Among the 80 tumors (including all 56 LR and 47 HLR cases) tested for EBV infection by in situ hybridization, 16 cases, all from the HLR group, proved to be EBV positive and showed worse survival compared to the remaining 31 HLR tumors at univariable analysis. This, however, was not confirmed by stage-inclusive bivariable analysis (Table 2).

Table 1 Patient survival analysis as a function of tumor histologic or molecular findings

	N (%)	Death rate	95% CI	HR	95% CI	*p* value	
						Univariable	With stage[a]
Glandular diff.	294					<0.001	0.127
Grade 0	127 (43)	13.95	11.21–17.37	1			
Grade 1	70 (24)	10.04	7.34–13.74	0.79	0.54–1.15	0.216	0.773
Grade 2	76 (26)	11.07	8.26–14.82	0.77	0.53–1.10	0.154	0.176
Grade 3	21 (7)	2.23	0.93–5.36	0.20	0.09–0.50	0.001	0.035
Anaplasia	294					<0.001	<0.001
Grade 1	141 (48)	4.62	3.52–6.07	1			
Grade 2	132 (45)	21.58	17.69–26.33	3.53	2.39–4.71	<0.001	<0.001
Grade 3	21 (7)	109.07	70.37–169.07	10.65	6.18–18.34	<0.001	<0.001
LR							
Yes	56 (19)	4.17	2.63–6.63	0.35	0.21–0.57	<0.001	0.022
No	238 (81)	13.31	11.33–15.62	1			
Exp. growth							
Yes	66 (22)	2.65	1.76–4.54	0.21	0.13–0.36	<0.001	<0.001
No	228 (78)	15.49	13.22–18.15	1			
Vascular invasion							
No	139 (47)	3.50	2.59–4.73	1			
Yes	155 (53)	32.41	27.24–38.57	6.66	4.65–9.53	<0.001	<0.001
Neuroinvasion							
No	174 (71)	7.57	6.11–9.38	1			
Yes	70 (29)	43.34	33.65–55.82	4.17	2.96–5.88	<0.001	<0.001
Mitoses							
0–18	151 (52)	7.63	6.10–9.56	1			
19–110	137 (48)	16.44	13.38–20.18	1.65	1.22–2.25	0.001	0.002
Ki67							
<40%	135 (46)	7.33	5.75–9.35				
≥40%	159 (54)	14.73	12.16–17.86	1.74	1.27–2.37	<0.001	0.001
P53 protein							
No	177 (60)	8.59	7.01–10.54	1			
Yes	117 (40)	14.75	11.80–18.44	1.48	1.09–2.00	0.011	0.078
p53 Gene:	292					<0.001[b]	<0.001[b]
Wild type	226 (77)	9.40	7.87–11.24	1			
Mutated							
Exons 5–8	66 (23)	16.25	12.21–21.63	1.49	1.06–2.09	0.021	0.084
Exons 5, 6	29 (10)	8.46	5.19–13.82	0.91	0.54–1.52	0.708	0.379
Exons 7, 8	37 (13)	30.93	21.75–43.28	2.25	1.51–3.35	<0.001	<0.001
TP53							
Heter	150 (66)	9.09	7.30–11.32	1			
LOH	79 (34)	16.61	12.75–21.63	1.61	1.14–2.27	0.007	0.360
MSS+L	253 (86)	11.23	9.57–13.17	1			
MSI-H	41 (14)	7.27	4.58–11.54	0.65	0.39–1.06	0.081	0.246
18q							
Heter	144 (66)	10.11	8.12–12.59	1			
LOH	75 (34)	14.65	11.08–19.39	1.38	0.97–1.97	0.076	0.618

LR lymphocyte-rich

[a] Bivariable Cox analysis inclusive of stage; stage I vs. II vs. III+IV, TNM system

[b] Model: wild type vs. mutated exon 5, 6 vs. mutated exon 7, 8

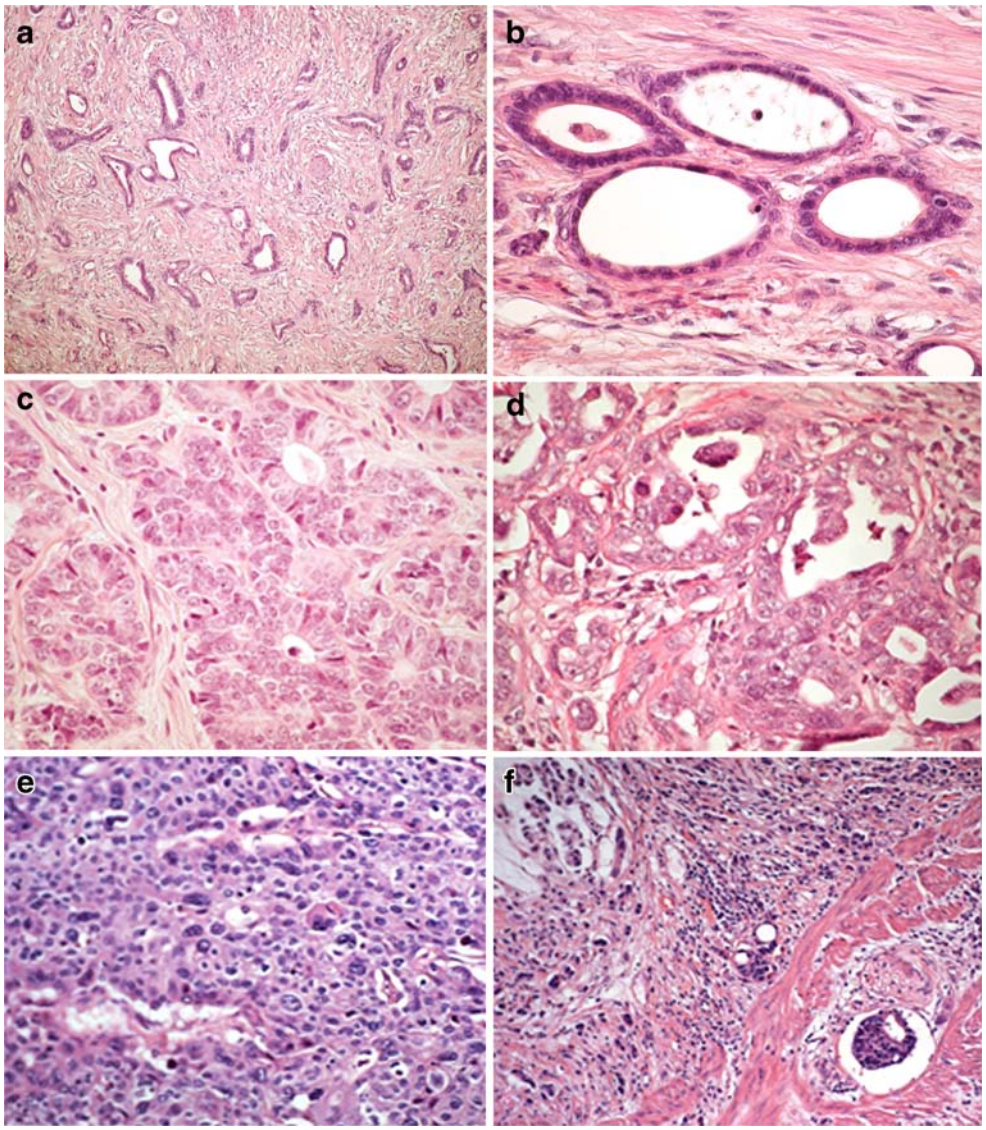

Fig. 1 **a**, **b** Well-differentiated (glandular score 3), low grade tubular cancer with moderately atypical (score 1 anaplasia), polarized cells arranged in a monostratified epithelium. **c** Ordinary cohesive (tubulo-trabecular), intermediate grade cancer formed by moderately atypical (score 1 anaplasia) cells with relatively regular nuclei. **d** Ordinary cohesive (tubulopapillary) cancer with frankly atypical (score 2 anaplasia) cells of pleomorphic nuclei and an exon 8 p53 gene mutation. Intermediate (Table 6A) to high (Table 6B) grade. **e** Anaplastic, high grade cancer formed by highly atypical, disorganized cells (score 3 anaplasia). **f** Diffusely infiltrative component of an high grade mucinous cancer with lymphoinvasion (*bottom right*)

Compared with the 247 non-HLR tumors, EBV+ cases showed only a slight, non-significant trend toward improved survival.

In Table 3, a Cox multivariable analysis confirms that, in addition to tumor diameter and stage, anaplasia, vascular invasion, expansile growth, Ki67 index, and p53 exons 7 or 8 mutations are independent survival predictors. HLR, which showed high collinearity (0.64) with expansile growth, also proved to be predictive (HR 0.36, 0.20–0.68, p=0.002) when substituted for expansile growth in the same model. Mitoses, when substituted for Ki67 index, failed to show significant predictive power.

We then analyzed the histotype distribution of parameters proven (see Tables 1, 2, and 3) to be of prognostic value in our gastric cancer population taken as a whole. We first considered five histotypes: cohesive (i.e., glandular+solid), diffuse, mucinous, anaplastic, and HLR cancers. Table 4 illustrates that the 21 anaplastic cases showed an obvious concentration of worsening factors like higher T (T_3–T_4), N (N_2–N_3), stage (III–IV), distant metastases, larger diameter, blood and/or lymph vessel invasion, neuroinvasion, proliferative indices (including a median of 45 mitoses/10 HPFs for the 21 cases, well above the median of 18 to 19 in the whole series), and p53 exon 7 or

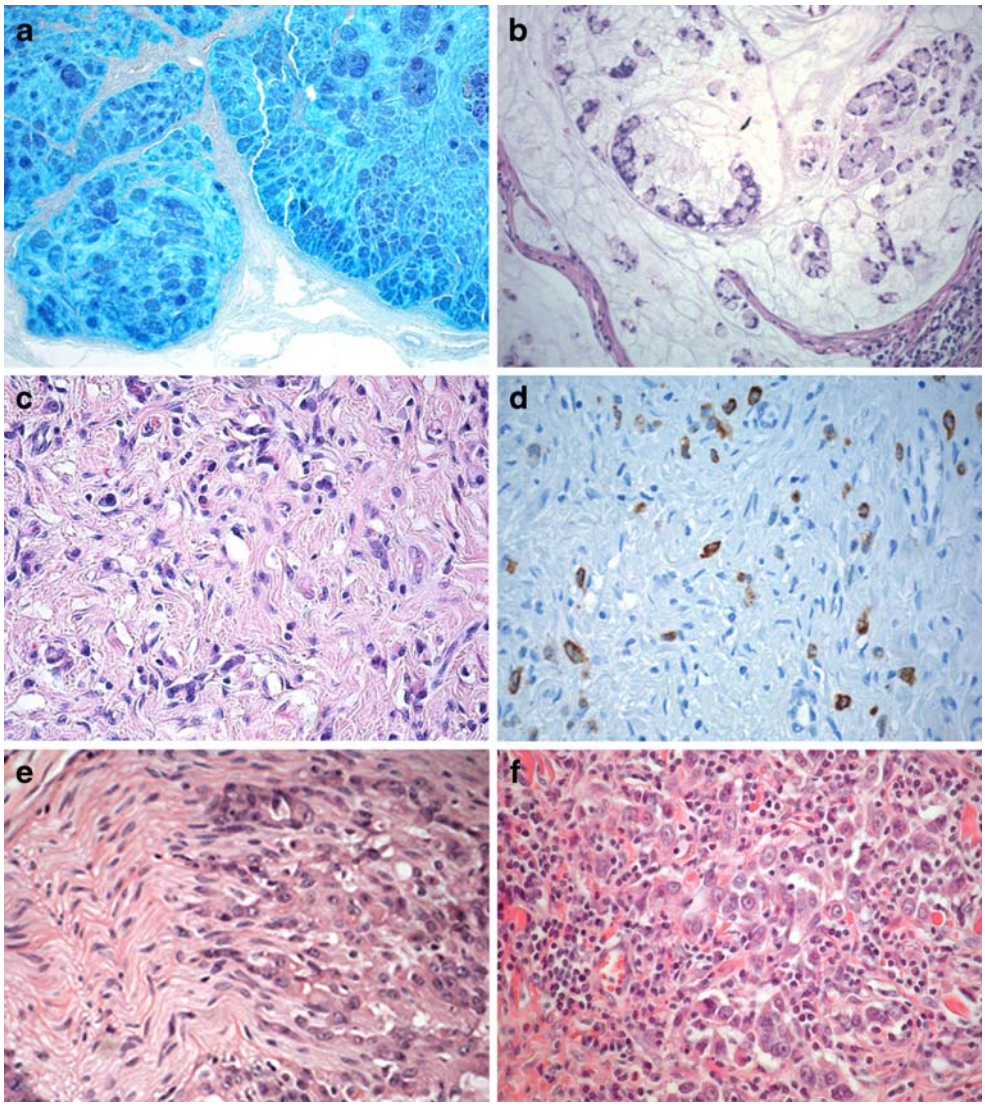

Fig. 2 **a** Alcian blue/PAS reactive mucin lakes with expansile borders in a low grade muconodular cancer. **b** Predominance of unstained extracellular mucin over tumor cells, either signet ring or forming small cords, inside a muconodule of a low grade case. **c** Epithelial tumor cells , cytokeratin reactive in (**d**) are scattered inside an overwhelming, fibroblast-rich stroma of a low grade desmoplastic cancer. **e** Gastric wall nerve invaded by neoplastic cells from an intermediate grade, ordinary diffuse cancer. **f** Low grade HLR cancer showing a lymphoepithelioid pattern resulting from heavy intratumor lymphoid cell infiltration dissociating cancerous cells of apparently prominent nuclear atypia (score 2 anaplasia)

8 mutations, in addition to score 3 anaplasia, their main diagnostic feature. Among cohesive, diffuse, and mucinous tumors, no major T, N, or M stage difference was found; however, we found a trend towards higher blood vessel invasion, proliferative rates, p53 protein expression, and exon 7+8 mutations in cohesive compared to diffuse and mucinous as well as towards neuroinvasion in diffuse compared to cohesive cancers. Unexpectedly, a significantly higher rate of 18qLOH, mainly involving from q21.1 up to q-ter loci, was found among mucinous compared to all other cancers as a whole (Fisher test, $p<0.001$) or taken individually ($p<0.001$ vs. diffuse and HLR; $p=0.007$ vs. cohesive; $p=0.021$ vs. anaplastic).

Given their frequently borderline structure between cohesive (solid-medullary or glandular) and diffuse (lymphoepithelioid) histology as well as their distinctive, mostly favorable prognosis, we considered the 47 HLR tumors separately. They turned out to show lower T, N, M stage, lymph or blood vessel invasion, neuroinvasion, p53 protein expression, and 18qLOH, in addition to more expansile growth and higher MSI-H rate, all features predicting favorable survival. The only exceptions were mitotic and Ki67 proliferative rates, which were increased ($p<0.001$ for both) compared to the remaining tumors, excepting anaplastic cancers.

We also tested parameter distribution among three histologic subtypes recently proposed to imply a favorable

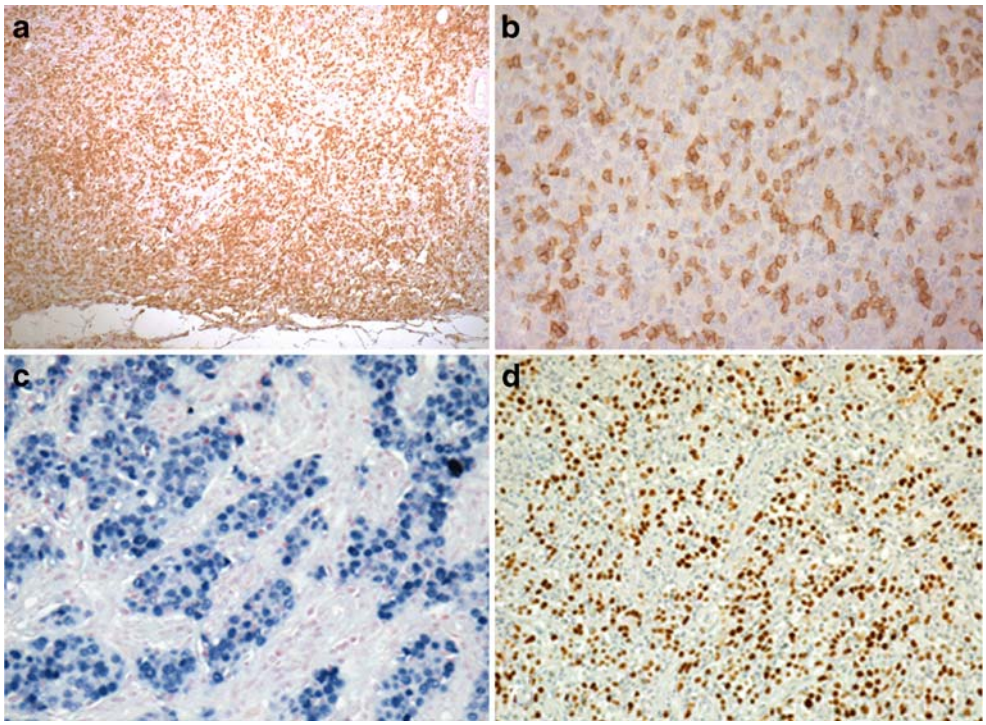

Fig. 3 **a** Low grade HLR cancer with heavy intratumor infiltration of CD8 positive T cells enveloping unreactive epithelial cells; note a regular, expansile border (*bottom*) mostly formed by CD8 reactive lymphocytes. **b** MLH1 unreactive neoplastic epithelial cells inside a low grade, MSI-H and HLR cancer with medullary structure; note MLH1 reactivity of intratumor lymphoid cells. **c** Positive EBV in situ hybridization of cancer cells forming islets and trabeculae separated by unreactive, abundant lymphoid cells (low grade HLR case). **d** Nuclear p53 protein immunoreactivity in a low grade, lymphoepithelioid type HLR tumor negative for both EBV and microsatellite DNA instability, while showing an exon 5 p53 gene mutation

prognosis, i.e., low grade mucinous (muconodular) cancer [33], low grade desmoplastic cancer [34], and very well-differentiated tubular cancer [32]. In all three subtypes, a clear-cut concentration of prognostically favorable parameters was observed, compared to remaining non-low grade cohesive (100 cases), diffuse (59), and mucinous (23) cancers (Table 4). It should be added that the 99 tumors showing invasion confined within the muscularis propria included 22 (47%) HLR, six (60%) well-differentiated tubular, nine (60%) low grade diffuse desmoplastic, and 15 (75%) muconodular cases. Collectively, the four low grade histotypes accounted for 52/99 (53%) T1b+T2a

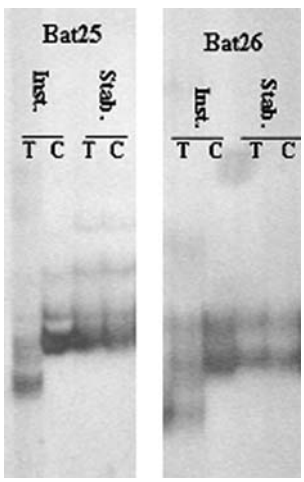

Fig. 4 Microsatellite DNA instability (*Inst.*) at Bat 25 and 26 loci of the same MSI-H (and HLR) tumor to be compared with a stable case (*Stab.*). *T* tumor, *C* non-tumor control tissue. DGGE

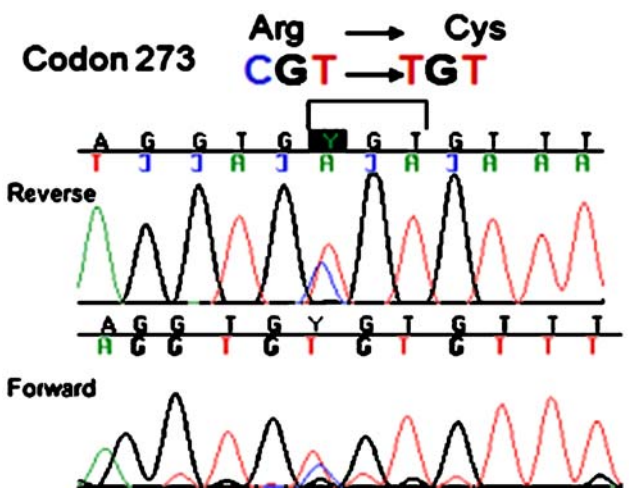

Fig. 5 Exon 8 (codon 273) p53 gene mutation of a high grade cancer. DGGE followed by sequence electropherogram

Table 2 Interplay of tumor HLR, EBV, MSI, and p53 changes with patient survival

	N	p53		Death rate	95% CI	*p* value		Vs.
		Mutation	Protein expr.			Univariable	With stage	
HLR								
All	47	11 (24)[a]	11 (23)	3.14	1.79–5.54	<0.001	0.006	No HLH, all
EBV+	16	2 (12.5)	0	6.71	3.20–14.08	0.014	0.162	MSI-H+other
MSI-H	19	2 (11)	4 (21)	1.81	0.58–5.62	0.031	0.196	EBV+
Other	12	7 (58)	7 (58)[b]	1.79	0.45–7.14	0.087	0.292	EBV+
No HLR								
All	247	55 (22)[c]	106 (43)	12.97	11.09–15.16	0.122	0.081	EBV+
MSI-H	22	4 (18)	4 (18)	18.26	11.00–30.29	<0.001	0.005	HLR–MSI-H
Fisher exact test:								
HLR all, vs. no HLR all, *p*:		0.848	0.014					
HLR, other vs. EBV+, *p*:		0.017	0.001					
HLR other vs. MSI-H, *p*:		0.013	0.056					
HLR other vs. no HLR, *p*:		0.009	0.375					
No HLR, MSI-H vs. no MSI-H, *p*:		0.791	0.014					

[a] Only 46 cases successfully tested due to lack of amplification of an MSI-H case

[b] Eight cases showed either mutation or protein expression

[c] Only 246 cases successfully tested due to lack of amplification of a non MSI-H case

cases, as against only 2/68 (3%) T3+4 cases ($p<0.001$ vs. non-low grade tumors). On the other hand, the 23 infiltrative mucinous cancers turned out to show an increased diameter (median 8 cm, 5–12, vs. 5.3–6; $p<0.001$, Kruskal–Wallis test), invasion level ($p=0.042$), lymph node metastases ($p=0.059$), stage ($p=0.038$), and lymphoinvasion ($p=0.062$) compared to ordinary cohesive and diffuse cancers.

Table 3 Cox multivariable analysis of 292 gastric tumors[a]

Parameter	HR	95% CI	*p* value
Age[b]	1.01	0.99–1.02	0.200
Sex (male)	1.35	0.97–1.89	0.078
Expansile growth[c]	0.25	0.14–0.44	<0.001
Vascular invasion	2.51	1.65–3.83	0.001
Anaplasia, scores 2+3	1.53	1.05–2.24	0.027
Ki67, >40%	1.54	1.08–2.19	0.017
P53 mut, ex. 7,8	1.66	1.09–2.52	0.019
Diameter[b]	1.14	1.08–1.20	<0.001
Stage			<0.001
Stage II	2.22	1.29–3.80	0.004
Stage III+IV	4.11	2.38–7.09	<0.001

Harrell's C: 0.84; Royston explained variation=0.70; noise in model=0.037. When mitoses (>18/10 HPF) were substituted for Ki67: HR 1.26 (0.89–1.78), $p=0.192$

[a] Two cases missing due to lack of p53 mutation data for technical reasons

[b] On continuous scale

[c] When replaced with HLR: HR 0.36 (0.20–0.68), $p=0.001$

Table 5 analyzes patient survival of the five main histologic types as well as of the three additional low grade subtypes and corresponding non-low grade cohesive, diffuse, or mucinous cancers. The results outline a favorable prognosis in HLR and low grade tubular, desmoplastic diffuse, or muconodular tumors and a worse prognosis in both anaplastic and infiltrative mucinous cancers, compared to ordinary cohesive and diffuse cases. No significant survival difference was observed between cohesive and diffuse or between anaplastic and infiltrative mucinous tumors or even among the three low grade subtypes and HLR cases. Therefore, all histologic types/subtypes were grouped into three categories of increasing malignant potential: (1) low grade histotypes (91 cases) encompassing 47 HLR, 10 well-differentiated tubular, 15 diffuse with embedding desmoplasia, and 19 muconodular tumors; (2) intermediate grade histotypes (159 cases) with ordinary cohesive and diffuse cancers; and (3) high grade histotypes (44 cases) corresponding to infiltrative mucinous and anaplastic cancers (Table 6A). The three groups showed clear-cut survival differences.

Based on the histologic parameters proven to predict survival in Tables 1, 2, and 3, another, more refined and flexible, though more complex, approach to a three-level grading system of gastric cancers was also developed. Thus, 47 tumors with HLR and score 1 or 2 anaplasia

Table 4 Distribution of prognostic parameters among histologic types and subtypes

		Main histologic groups								
		1	2		3		4		5	
Histotype	All	HLR	Cohesive (110 cases)		Diffuse (74 cases)		Mucinous (42 cases)		Anaplastic	*p* value (8 subtypes)
Subtype			W.d. tubular (a subtype)	Ordinary (b subtype)	Lg desm (a subtype)	Ordinary (b subtype)	Muconodular (a subtype)	Infiltrative (b subtype)		
N (%)	294 (100)	47 (16)	10 (3)	100 (34)	15 (5)	59 (20)	19 (6)	23 (8)	21 (7)	Pearson's
Diameter, mean (SD)[a]	54 (35)	48 (28)	37 (17)	50 (28)	29 (13)	56 (42)	45 (29)	82 (40)	83 (40)	<0.001[b]
T1b	44 (15)	6 (13)	2 (20)	13 (13)	6 (40)	10 (17)	7 (37)	0	0	<0.001
T2	182 (62)	41 (87)	8 (80)	63 (63)	9 (60)	29 (49)	10 (53)	12 (52)	10 (48)	
T3–T4	68 (23)	0	0	24 (24)	0	20 (34)	2 (10)	11 (48)	11 (52)	
N0	96 (33)	28 (60)	5 (50)	24 (24)	10 (67)	14 (24)	11 (58)	1 (4)	3 (14)	<0.001
N1	102 (35)	17 (36)	5 (50)	40 (40)	4 (26)	18 (32)	4 (21)	9 (39)	5 (24)	
N2+3	94 (32)	2 (4)	0	36 (36)	1 (7)	25 (44)	4 (21)	13 (57)	13 (62)	
M+	28 (9.5)	0	0	1 (11)	0	5 (8.5)	0	4 (17)	8 (38)	<0.001
Stage										
I	104 (35)	29 (62)	5 (50)	28 (28)	11 (73)	15 (25)	13 (68)	1 (4)	2 (10)	<0.001
II	73 (25)	15 (32)	5 (50)	22 (22)	3 (20)	16 (27)	2 (11)	6 (26)	4 (19)	
III+IV	117 (40)	3 (6)	0	50 (50)	1 (7)	28 (48)	4 (21)	16 (70)	15 (71)	
Lymphoinvasion	145 (49)	10 (21)	0	67 (67)	0	31 (53)	0	19 (83)	18 (86)	<0.001
Angioinvasion	48 (16)	1 (2)	0	29 (29)	0	4 (7)	0	2 (9)	12 (57)	<0.001
Neuroinvasion	69 (28)	1 (3)	0	22 (29)	0	27 (48)	1 (8)	9 (39)	9 (53)	<0.001
Exp. growth	66 (22.5)	39 (83)	1 (10)	5 (5)	1 (7)	0	17 (89)	0	3 (14)	<0.001
Anaplasia										
1	141 (48)	28 (60)	10 (100)	30 (30)	15 (100)	29 (49)	19 (100)	9 (39)	0	<0.001
2	132 (45)	19 (40)	0	70 (70)	0	30 (51)	0	14 (61)	0	
3	21 (7)	0	0	0	0	0	0	0	21 (100)	
Ki67										
<30%	82 (29)	2 (4)	5 (50)	20 (20)	12 (86)	25 (45)	10 (59)	8 (35)	0	<0.001
30–49%	113 (39)	22 (47)	2 (20)	47 (47)	2 (14)	23 (41)	7 (41)	7 (30)	3 (16)	
≥50%	91 (32)	23 (49)	3 (30)	33 (33)	0	8 (14)	0	8 (35)	16 (84)	
MSI-H	41 (14)	19 (40)	1 (10)	7 (7)	2 (13)	2 (3)	3 (15)	5 (23)	2 (10)	<0.001
p53 Protein	117 (40)	11 (23)	3 (30)	59 (59)	2 (13)	18 (30.5)	5 (26)	7 (30)	12 (57)	<0.001
p53 Mut (5–8)	66 (23)	11 (24)	0	31 (31)	1 (7)	8 (14)	2 (11)	5 (22)	8 (38)	0.018
p53 Mut (7+8)	37 (13)	4 (9)	0	19 (19)	0	4 (7)	0	2 (9)	8 (38)	<0.001
18qLOH	75 (34)	6 (16)	2 (29)	29 (38)	1 (11)	9 (24)	9 (60)	13 (72)	6 (32)	<0.001

[a] Millimeters

[b] Kruskal–Wallis test

Table 5 Prognostic profile of gastric cancer histotypes and their subtypes

Type	*N* (%)	Death rate	95% CI	HR	95% CI	*p* value		HR	95% CI	*p* value	
						Univariable	With stage			Univariable	With stage
1. HLR	47 (16)	3.14	1.78–5.54	1				0.21	0.11–0.39	<0.001	0.005
2. Cohesive	110 (37)	13.79	10.93–17.40	3.84	2.08–7.10	<0.001	0.020				
(a) W.d. tubular	10 (3)	0.88	0.12–6.21	0.33	0.04–2.56	0.331	0.336	0.07	0.01–0.51	0.009	0.058
(b) Ordinary	100 (34)	17.47	13.82–22.08	4.71	2.55–8.71	<0.001	0.005	1			
3. Diffuse	74 (25)	10.37	7.72–13.93	3.28	1.73–6.22	<0.001	0.005				
(a) Desm., low gr.	15 (5)	1.92	0.62–5.96	0.67	0.19–2.38	0.634	0.508	0.14	0.04–0.46	0.001	0.023
(b) Ordinary	59 (20)	15.28	11.25–20.76	4.73	2.48–9.01	<0.001	<0.001	1.00	0.68–1.48	0.985	0.100
4. Mucinous	42 (14)	8.69	5.79–13.20	2.99	1.48–6.04	0.002	0.094				
(a) Muconodular	19 (6)	1.38	0.44–4.26	0.55	0.16–1.96	0.689	0.151	0.12	0.04–0.37	<0.001	0.002
(b) Infiltrative	23 (8)	54.23	34.59–85.03	10.46	5.02–21.78	<0.001	<0.001	2.22	1.33–3.71	0.002*	0.005**
5. Anaplastic	21 (7)	109.07	70.37–169.07	17.88	8.54–37.43	<0.001	<0.001	3.79	2.27–6.35	<0.001	<0.001

*p=0.005 vs. diffuse ordinary, p=0.002 vs. ordinary diffuse+cohesive, and p=0.096 vs. anaplastic; **p=0.144 vs. diffuse ordinary, p=0.015 vs. ordinary diffuse+cohesive, and p=0.138 vs. anaplastic

(regardless of their angio-, lympho-, or neuroinvasive pattern) and 62 non-HLR tumors with score 1 anaplasia in the absence of angiolymphoinvasion or neuroinvasion formed the 109 cases in the grade 1 group. Grade 3 tumors included, in addition to 21, score 3 anaplasia cases and 19 infiltrative mucinous cancers also showing lymphoinvasion, a further 16 cases showing exon 7 or 8 p53 gene mutations coupled with score 2 anaplasia and angio-lympho or neuroinvasion. The remaining 129 cohesive (78 cases), diffuse (47), or mucinous (four) tumors formed the grade 2 group. Table 6B shows clear-cut survival differences among the three groups at both univariable and stage-inclusive bivariable analysis. Kaplan–Meier curves of patient groups in Table 6A and B are reported in Fig. 6.

Discussion

A number of histologic features have been found to be prognostically informative by univariable survival analysis in a large series of invasive (T1b to T4) gastric cancers. On stage-inclusive bivariable and multivariable analysis, only high intra- and peritumor lymphoid cell response (HLR) and expansile type local growth, largely correlated to each other, were confirmed to predict improved prognosis, while tumor lymph or blood vessel invasion, cellular anaplasia, and a high (≥40%) Ki67 index proved to worsen prognosis. Another stage-independent predictor of worse survival, neuroinvasion, proved difficult to assess in a substantial proportion (26%) of tumors, while mitotic counts above the median (>18/10 HPF) failed to survive multivariable analysis.

Out of several molecular changes tested, including p53 gene mutation or protein expression, TP53 LOH, microsatellite DNA instability, and 18q11.2–23 LOH, only exon 7 and 8 p53 gene mutations had a clear-cut negative influence on patient survival. This finding on gastric cancer p53 gene mutations fits in with previous results on lung [45, 46], head and neck [47], and colorectal cancers [48]; it is likely to be related to the high concentration of DNA contact and gain of function mutations in exons 7 and 8, with special reference to L3 loop, S-10 band, and loop-sheet-helix (LSH) mutations [49]. Indeed, 89% of exon 7 or 8 mutations that we found in our gastric cancers were of this type, with hot spots at codons 248 (exon 7, L3) and 273 (exon 8, LSH). It should be added that the lack of prognostic influence of exon 5 and 6 mutations is likely to account for the reduced predictive power of p53 mutations as a whole and, possibly, also of related parameters like p53 protein expression and TP53 LOH.

In our series, high level microsatellite DNA instability failed *per se* to predict a favorable outcome unless coupled with a high intra- and peritumor, T_8-rich lymphoid cell response. The higher proportion of mucinous, high grade,

Table 6 Survival analysis of three tumor grade groups

Grade	*N* (%)	Death rate	95% CI	HR	95% CI	*p* value	
						Univariable	With stage
A. Histotype based (see types in Table 5):							
Low: HLR (1)+w.d. tubular (2a)+diff. lg desm (3a) +muconodular (4a)	91 (31)	2.18	1.39–3.42	1			
Intermediate: ordinary cohesive (2b)+ordinary diffuse (3b)	159(54)	16.59	13.78–19.98	6.15	3.77–10.04	<0.001	<0.001
High: mucinous infiltrative (4b)+anaplastic (5)	44 (15)	73.08	53.39–100.02	17.19	9.74–30.36	<0.001*	<0.001*
B. Based on histotypes and prognostic parameters:							
Low: as in A, +18 cases with score 1 anaplasia and no invasive pattern	109 (37)	2.18	1.45–3.27	1			
Intermediate: 78 ordinary cohesive+47 ordinary diffuse+4 non-lymphoinvasive mucinous	129 (44)	19.42	15.85–23.80	7.20	4.53–11.43	<0.001	<0.001
High: 19 lymphoinvasive mucinous+21 anaplastic+ 16 exon 7,8 p53 mutated	56 (19)	94.14	71.92–123.23	23.99	14.09–40.85	<0.001*	<0.001*

Model A, with stage: Harrell's C=0.81 (univariable=0.72); Royston explained variation=0.61; noise=0.009. Model B, with stage: Harrell's C= 0.82 (univariable=0.76); Royston explained variation=0.65; noise=0.008

*p<0.001 vs. the intermediate group

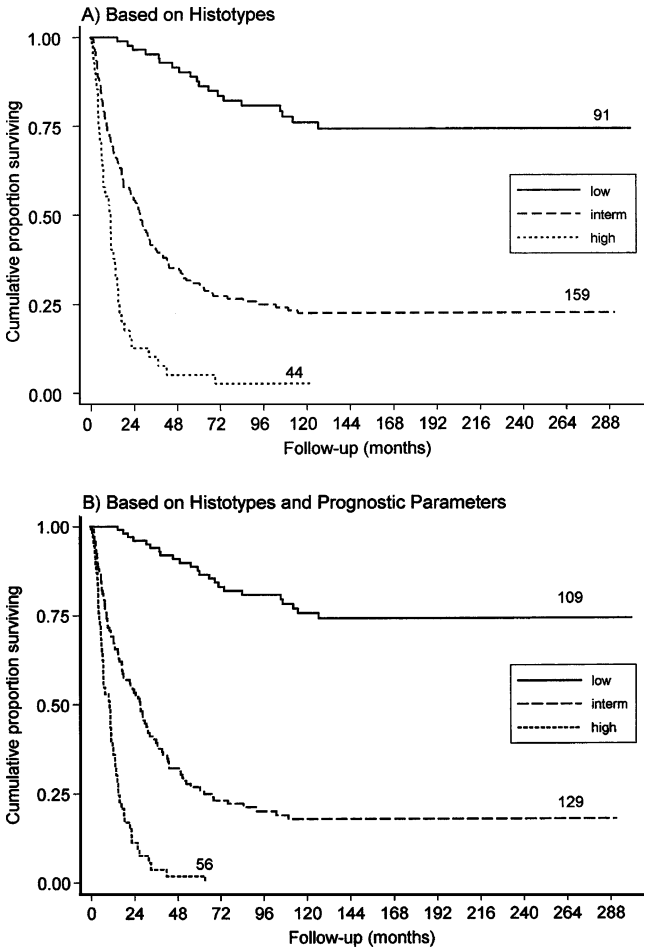

Fig. 6 Kaplan–Meier curves of patient groups from Table 6A and B

and advanced stage cases we found among MSI-H tumors lacking HLR, compared to their HLR positive counterpart, is likely to account for the present failure to confirm the prognostic value of MSI-H *per se* reported in other series [10, 11]. Our results confirm previous findings on colon and gastric cancer [23, 50] in showing the prognostic dominance of HLR. In addition, we have seen that HLR, invariably present in all our EBV positive tumors, was also found in a third small subset of tumors negative for both microsatellite instability and EBV infection.

Expression of a wide range of mutated proteins coded by unstable microsatellite DNA genes [51], as yet undefined EBV virus proteins [52, 53] and other highly antigenic and/or mutated proteins like p53 [54, 55], may explain the high lymphoid cell response. Interestingly, both MSI-H/HLR positive and the third group of HLR tumors showed a preference for the distal stomach (antrum) with an obviously favorable prognosis. On the contrary, tumors in the EBV+ group, as already observed [25], were concentrated significantly in the proximal stomach and showed a trend towards an intermediate prognosis between that of the above two groups and of the HLR-negative tumors as a whole. The oncogenic potential of the EBV virus itself might work as a progression factor in EBV tumors, thus partly counteracting their strong T cell antitumor response, as well as favoring immune escape phenomena [52, 56].

In addition to individual histologic or molecular parameters, some tumor histologic types have also been suggested to predict patient survival, among which lymphoid cell-rich [21–24], very well-differentiated tubular [32], muconodular

[33], and a low grade subset of diffuse desmoplastic cancers [34] were all associated with a more favorable outcome, whereas various kinds of anaplastic cancers, with or without poor neuroendocrine, gut exocrine, hepatoid, choriocarcinomatous, or epidermoid differentiation, were associated with worse outcome. Therefore, the predictive power for the outcome of individual histologic types and subtypes was extensively reinvestigated in the whole series. The results, besides confirming previous suggestions [21–24, 32–34], allowed us to recognize infiltrative mucinous cancer, especially when associated with lymphoinvasion, as a highly malignant cancer with a significantly worse prognosis than ordinary cohesive or diffuse cancers and no substantial difference from anaplastic cancer. It should be recalled that mucinous cancers as a whole have been repeatedly shown to have a higher incidence of lymph node metastases, lymph vessel invasion, deep gastric wall invasion, large size and advanced stage, as well as worse overall survival which, however, was essentially accounted for by their more advanced stage [57, 58]. We confirm that no significant survival difference was found when the whole population of mucinous, cohesive, and diffuse cancers were compared to each other; however, when their respective low grade subtypes were taken out, infiltrative mucinous cancers showed a poorer stage-independent survival rate than that of ordinary cohesive and diffuse cancers comparable to that of anaplastic cancers.

These findings suggest that infiltrative mucinous cancers should be added to anaplastic cancers in a high grade tumor group having a significantly worse prognosis than ordinary cohesive or diffuse cancers. Thus, gastric cancer has been categorized into three malignancy grades, where HLR, very well-differentiated tubular, embedding desmoplasia diffuse and muconodular tumors make up the low grade, anaplastic and infiltrative mucinous cancers the high grade, and the remaining cohesive or diffuse cancers the intermediate grade group.

A systematic investigation of the distribution of survival-predictive histologic, molecular, or stage-linked parameters among main histologic types and subtypes disclosed a considerable histotype dependence of many such factors. For instance, expansile growth, long known to predict more favorable outcome [14], was a prominent and informative finding only among HLR and muconodular tumors, both showing better survival. In addition, 18qLOH was highly concentrated among mucinous tumors and, albeit less evidently, among cohesive tumors, with no significant prognostic value despite its known association with advanced stage [12, 27]. Of interest were also the increased proliferative rates found among favorable outcome HLR tumors as well as the lower rates found among worse outcome diffuse cancers. These findings, contrasting with the otherwise general parallelism between proliferative rates and survival, may weaken the prognostic value of both mitotic counts and the Ki67 index. They might also explain in part the failure of the predictive power of mitotic counts (which may be affected by the amount of stroma, abundant in many diffuse cancers) to survive multivariable analysis. Apparently, only vascular invasion and cellular anaplasia were distributed fairly equally among histotypes, essentially according to their malignancy grade.

Clarification of the selective role played by some of the histologic or molecular factors in the behavior of individual histotypes may open the possibility of a more fruitful reconstruction of their distinctive natural history, including pathogenetic and therapeutic aspects. It should be outlined that most parameters predicting worse survival were highly represented among anaplastic cancers and that many of them, especially histologic lymphoinvasion, lymph node metastases, T level invasion, and high maximum diameter, were also prominent among infiltrative mucinous cancers. In general, the differential distribution of many parameters among histotypes supported their characterization as individual neoplastic growths with distinctive morphology, molecular background, and, to some extent, natural history. For instance, the high 18qLOH shown by mucinous cancers compared with its low prevalence among diffuse cancers, with special reference to its signet-ring cell subtype, outlines the substantial difference between the two neoplastic diseases, despite their common excessive production of mucins, either extracellular (mucinous cancer) or intracellular (signet-ring cancer). The precise molecular link between 18qLOH and mucin dislocation, whose impact on tumor natural history has already been outlined [17–19, 59], remains to be investigated, with special reference to a possible relationship between DCC and SMAD genes (at 18q21 band) activity and tumor cell functional polarization and stroma interaction [12, 33].

The unequal distribution of predictive parameters among different histotypes and their complex reciprocal interplay has discouraged any attempt to develop a global scoring system for gastric cancer similar to that used, for instance, for ductal breast cancer [43]. However, the spectrum of survival-predictive histologic and molecular patterns obtained was taken as a base to further develop a three-grade classification of high prognostic value. Thus HLR tumors and, in addition, non-HLR tumors with score 1 cellular anaplasia and without angio-lympho- or neuro-invasion made up the grade 1 group (109 cases, 37%); tumors with score 3 anaplasia, invasive mucinous cancers as well as score 2 anaplasia tumors showing an exon 7 or 8 p53 gene mutation coupled with angio-, lympho-, or neuroinvasion formed the grade 3 group (56 cases, 19%); while the remaining 129 cases (44%) formed the grade 2 group. Further investigations on continuous, non-selected series are warranted in order to assess reliable figures of

tumor distribution among the three different grades. Despite this limit, the classification system appears to contribute substantially to the prognostic evaluation of gastric cancer as a whole.

It should be outlined that the two grading systems developed gave largely similar and partly overlapping findings. The histotype-based system has the advantage of allowing an easier identification and clinicopathologic characterization of distinctive tumor entities from well-recognizable structural patterns. On the other hand, the more complex system, integrating histotypes with individual parameters, provides a more balanced tumor distribution among the three grades while retaining stage-independent predictive power.

In conclusion, extensive investigation of histologic and molecular parameters, as well as histotypes of potential prognostic value in a large series of invasive gastric cancers, identified a limited number of independent, survival-predictive factors which were used to classify each tumor according to a three-grade highly discriminative scale of increasing malignancy. While the present investigation adds feasibility and scientific background to our approach, its effectiveness in routine diagnostic practice should be checked further on independent, continuous tumor series extensively sampled so as to ensure an appropriate grading, especially when identifying low grade histotypes.

Acknowledgements This investigation was supported by grants from the Italian Ministry of Health (RF-PSM-2006-401346) and the Fondazione IRCCS Policlinico San Matteo to ES.

We declare that we have no conflict of interest.

References

1. Ribeiro MM, Seixas M, Sobrinho-Simoes M (1988) Prognosis in gastric carcinoma. The preeminence of staging and futility of histological classification. Dig Dis Pathol 1:51–68
2. Carneiro F, Seixas M, Sobrinho-Simoes M (1995) New elements for an updated classification of the carcinomas of the stomach. Pathol Res Pract 191:571–584
3. Chiaravalli AM, Cornaggia M, Furlan D et al (2001) The role of histological investigation in prognostic evaluation of advanced gastric cancer. Analysis of histological structure and molecular changes compared with invasive pattern and stage. Virchows Arch 439:158–169
4. Lauren P (1965) The two histological main types of gastric carcinoma: diffuse and so-called intestinal-type carcinoma. An attempt at a histo-clinical classification. Acta Pathol Microbiol Scand 64:31–49
5. Esaki Y, Hirayama R, Hirokawa K (1990) A comparison of patterns of metastasis in gastric cancer by histologic type and age. Cancer 65:2086–2090
6. Uchino S, Noguchi M, Ochiai A, Saito T, Kobayashi M, Hirohashi S (1993) P53 Mutation in gastric cancer: a genetic model for carcinogenesis is common to gastric and colorectal cancer. Int J Cancer 54:759–764
7. Becker KF, Atkinson MJ, Reich U, Becker I, Nekarda H, Siewert JR, Hofler H (1994) E-cadherin gene mutations provide clues to diffuse type gastric carcinomas. Cancer Res 54:3845–3852
8. Ranzani GN, Luinetti O, Padovan LS et al (1995) p53 gene mutations and protein nuclear accumulation are early events in intestinal type gastric cancer but late events in diffuse type. Cancer Epidemiol Biomarkers Prev 4:223–231
9. Solcia E, Fiocca R, Luinetti O et al (1996) Intestinal and diffuse gastric cancers arise in a different background of *Helicobacter pylori* gastritis through different gene involvement. Am J Surg Pathol 20(Suppl 1):S8–S22
10. Oliveira C, Seruca R, Seixas M, Sobrinho-Simoes M (1998) The clinicopathological features of gastric carcinomas with microsatellite instability may be mediated by mutations of different "target genes": a study of the TGFbeta RII, IGFII R, and BAX genes. Am J Pathol 153:1211–1219
11. Yamamoto H, Perez-Piteira J, Yoshida T et al (1999) Gastric cancers of the microsatellite mutator phenotype display characteristic genetic and clinical features. Gastroenterology 116:1348–1357
12. Candusso ME, Luinetti O, Villani L et al (2002) Loss of heterozygosity at 18q21 region in gastric cancer involves a number of cancer-related genes and correlates with stage and histology, but lacks independent prognostic value. J Pathol 197:44–50
13. Stemmermann GN, Brown C (1974) A survival study of intestinal and diffuse types of gastric carcinoma. Cancer 33:1190–1195
14. Ming SC (1977) Gastric carcinoma. A pathobiological classification. Cancer 39:2475–2485
15. Kubo T (1971) Histologic appearance of gastric carcinoma in high and low mortality countries: comparison between Kyushu, Japan and Minnesota, USA. Cancer 28:726–734
16. Watanabe H, Jass JR and Sobin LH in collaboration with pathologists in eight countries (1990) Histological typing of oesophageal and gastric tumors, 2nd ed. Edited by the World Health Organization (WHO). Springer, Berlin, pp. 20–26
17. Goseki N, Takizawa T, Koike M (1992) Differences in the mode of the extension of gastric cancer classified by histological type: new histological classification of gastric carcinoma. Gut 33:606–612
18. Martin IG, Dixon MF, Sue-Ling H, Axon AT, Johnston D (1994) Goseki histological grading of gastric cancer is an important predictor of outcome. Gut 35:758–763
19. Songun I, van de Velde CJ, Arends JW et al (1999) Classification of gastric carcinoma using the Goseki system provides prognostic information additional to TNM staging. Cancer 85:2114–2118
20. Gabbert HE, Meier S, Gerharz CD, Hommel G (1991) Incidence and prognostic significance of vascular invasion in 529 gastric-cancer patients. Int J Cancer 49:203–207
21. Watanabe H, Enjoji M, Imai T (1976) Gastric carcinoma with lymphoid stroma. Its morphologic characteristics and prognostic correlations. Cancer 38:232–243
22. Minamoto T, Mai M, Watanabe K et al (1990) Medullary carcinoma with lymphocytic infiltration of the stomach. Clinicopathologic study of 27 cases and immunohistochemical analysis of the subpopulations of infiltrating lymphocytes in the tumor. Cancer 66:945–952
23. Grogg KL, Lohse CM, Pankratz VS, Halling KC, Smyrk TC (2003) Lymphocyte-rich gastric cancer: associations with Epstein–Barr virus, microsatellite instability, histology, and survival. Mod Pathol 16:641–651
24. Chiaravalli AM, Feltri M, Bertolini V et al (2006) Intratumour T cells, their activation status and survival in gastric carcinomas characterised for microsatellite instability and Epstein–Barr virus infection. Virchows Arch 448:344–353
25. Nakamura S, Ueki T, Yao T, Ueyama T, Tsuneyoshi M (1994) Epstein–Barr virus in gastric carcinoma with lymphoid stroma. Special reference to its detection by the polymerase chain reaction

and in situ hybridization in 99 tumors, including a morphologic analysis. Cancer 73:2239–2249
26. Shiao YH, Palli D, Caporaso NE et al (2000) Genetic and immunohistochemical analyses of p53 independently predict regional metastasis of gastric cancers. Cancer Epidemiol Biomarkers Prev 9:631–633
27. Inoue H, Matsuyama A, Mimori K, Ueo H, Mori M (2002) Prognostic score of gastric cancer determined by cDNA microarray. Clin Cancer Res 8:3475–3479
28. Xiangming C, Natsugoe S, Takao S et al (2001) Preserved Smad4 expression in the transforming growth factor beta signaling pathway is a favorable prognostic factor in patients with advanced gastric cancer. Clin Cancer Res 7:277–282
29. Kim YH, Lee HS, Lee HJ et al (2004) Prognostic significance of the expression of Smad4 and Smad7 in human gastric carcinomas. Ann Oncol 15:574–580
30. Yonemura Y, Ninomiya I, Ohoyama S et al (1991) Expression of c-erbB-2 oncoprotein in gastric carcinoma. Immunoreactivity for c-erbB-2 protein is an independent indicator of poor short-term prognosis in patients with gastric carcinoma. Cancer 67:2914–2918
31. Weiss MM, Kuipers EJ, Postma C et al (2004) Genomic alterations in primary gastric adenocarcinomas correlate with clinicopathological characteristics and survival. Cell Oncol 26:307–317
32. Endoh Y, Tamura G, Motoyama T, Ajioka Y, Watanabe H (1999) Well-differentiated adenocarcinoma mimicking complete-type intestinal metaplasia in the stomach. Hum Pathol 30:826–832
33. Solcia E, Luinetti O, Tava F et al (2004) Identification of a lower grade muconodular subtype of gastric mucinous cancer. Virchows Arch 445:572–579
34. Chiaravalli AM, Klersy C, Tava F et al (2009) Lower and higher grade subtypes of diffuse gastric cancer. Human Pathol (in press). doi:10.1016/j.humpath.2009.04.004
35. Matsui K, Kitagawa M, Miwa A, Kuroda Y, Tsuji M (1991) Small cell carcinoma of the stomach: a clinicopathologic study of 17 cases. Am J Gastroenterol 86:1167–1175
36. Rindi G, Azzoni C, La Rosa S et al (1999) ECL cell tumor and poorly differentiated endocrine carcinoma of the stomach: prognostic evaluation by pathological analysis. Gastroenterology 116:532–542
37. Jiang SX, Mikami T, Umezawa A, Saegusa M, Kameya T, Okayasu I (2006) Gastric large cell neuroendocrine carcinomas: a distinct clinicopathologic entity. Am J Surg Pathol 30:945–953
38. Krulewski T, Cohen LB (1988) Choriocarcinoma of the stomach: pathogenesis and clinical characteristics. Am J Gastroenterol 83:1172–1175
39. Nagai E, Ueyama T, Yao T, Tsuneyoshi M (1993) Hepatoid adenocarcinoma of the stomach. A clinicopathologic and immunohistochemical analysis. Cancer 72:1827–1835
40. Sobin LH, Wittekind C (1997) TNM classification of malignant tumors, 5th edn. Wiley-Liss, New York, pp 59–62
41. Boland CR, Thibodeau SN, Hamilton SR et al (1998) A national cancer institute workshop on microsatellite instability for cancer detection and familial predisposition: development of international criteria for the determination of microsatellite instability in colorectal cancer. Cancer Res 58:5248–5257
42. Vogelstein B, Fearon ER, Hamilton SR et al (1988) Genetic alterations during colorectal tumor development. N Engl J Med 319:525–532
43. Elston CW, Ellis IO (1991) Pathological prognostic factors in breast cancer. I. The value of histological grade in breast cancer: experience from a large study with long-term follow-up. Histopathology 19:403–410
44. Stalsberg H, Hartmann WH (2000) The delimitation of tubular carcinoma of the breast. Hum Pathol 31:601–607
45. Huang C, Taki T, Adachi M, Konishi T, Higashiyama M, Miyake M (1998) Mutations in exon 7 and 8 of p53 as poor prognostic factors in patients with non-small cell lung cancer. Oncogene 16:2469–2477
46. Skaug V, Ryberg D, Kure EH et al (2000) P53 Mutations in defined structural and functional domains are related to poor clinical outcome in non-small cell lung cancer patients. Clin Cancer Res 6:1031–1037
47. Erber R, Conradt C, Homann N et al (1998) TP53 DNA contact mutations are selectively associated with allelic loss and have a strong clinical impact in head and neck cancer. Oncogene 16:1671–1679
48. Borresen-Dale AL, Lothe RA, Meling GI, Hainaut P, Rognum TO, Skovlund E (1998) TP53 and long-term prognosis in colorectal cancer: mutations in the L3 zinc-binding domain predict poor survival. Clin Cancer Res 4:203–210
49. Cho Y, Gorina S, Jeffrey PD, Pavletich NP (1994) Crystal structure of a p53 tumor suppressor–DNA complex: understanding tumorigenic mutations. Science 265:346–355
50. Guidoboni M, Gafa R, Viel A et al (2001) Microsatellite instability and high content of activated cytotoxic lymphocytes identify colon cancer patients with a favorable prognosis. Am J Pathol 159:297–304
51. dos Santos NR, Seruca R, Constancia M, Seixas M, Sobrinho-Simoes M (1996) Microsatellite instability at multiple loci in gastric carcinoma: clinicopathologic implications and prognosis. Gastroenterology 110:38–44
52. Saiki Y, Ohtani H, Naito Y, Miyazawa M, Nagura H (1996) Immunophenotypic characterization of Epstein–Barr virus-associated gastric carcinoma: massive infiltration by proliferating CD8+ T-lymphocytes. Lab Invest 75:67–76
53. van Beek J, zur Hausen A, Snel SN et al (2006) Morphological evidence of an activated cytotoxic T-cell infiltrate in EBV-positive gastric carcinoma preventing lymph node metastases. Am J Surg Pathol 30:59–65
54. Ciernik IF, Berzofsky JA, Carbone DP (1996) Human lung cancer cells endogenously expressing mutant p53 process and present the mutant epitope and are lysed by mutant-specific cytotoxic T lymphocytes. Clin Cancer Res 2:877–882
55. Vierboom MP, Nijman HW, Offringa R et al (1997) Tumor eradication by wild-type p53-specific cytotoxic T lymphocytes. J Exp Med 186:695–704
56. Koriyama C, Akiba S, Itoh T et al (2002) Prognostic significance of Epstein–Barr virus involvement in gastric carcinoma in Japan. Int J Mol Med 10:635–639
57. Adachi Y, Mori M, Kido A, Shimono R, Maehara Y, Sugimachi K (1992) A clinicopathologic study of mucinous gastric carcinoma. Cancer 69:866–871
58. Wu CY, Yeh HZ, Shih RT, Chen GH (1998) A clinicopathologic study of mucinous gastric carcinoma including multivariate analysis. Cancer 83:1312–1318
59. Park JM, Jang YJ, Kim JH et al (2008) Gastric cancer histology: clinicopathologic characteristics and prognostic value. J Surg Oncol 98:520–525

Virchows Arch (2009) 455:213–223
DOI 10.1007/s00428-009-0814-y

ORIGINAL ARTICLE

High resolution analysis of DNA copy-number aberrations of chromosomes 8, 13, and 20 in gastric cancers

Tineke E. Buffart · Nicole C. T. van Grieken · Marianne Tijssen · Jordy Coffa · Bauke Ylstra · Heike I. Grabsch · Cornelis J. H. van de Velde · Beatriz Carvalho · Gerrit A. Meijer

Received: 21 June 2009 / Revised: 12 July 2009 / Accepted: 16 July 2009 / Published online: 21 August 2009

Abstract DNA copy-number gains of chromosomes 8q, 13q, and 20q are frequently observed in gastric cancers. Moreover gain of chromosome 20q has been associated with lymph node metastasis. The aim of this study was to correlate DNA copy-number changes of individual genes on chromosomes 8q, 13q, and 20q in gastric adenocarcinomas to clinicopathological data. DNA isolated from 63 formalin-fixed and paraffin-embedded gastric adenocarcinoma tissue samples was analyzed by whole-genome microarray comparative genomic hybridization and by multiplex ligation-dependent probe amplification (MLPA), targeting 58 individual genes on chromosomes 8, 13, and 20. Using array comparative genomic hybridization, gains on 8q, 13q, and 20q were observed in 49 (77.8%), 25 (39.7%), and 49 (77.8%) gastric adenocarcinomas, respectively. Gain of chromosome 20q was significantly correlated with lymph node metastases (p=0.05) and histological type (p=0.02). MLPA revealed several genes to be frequently gained in DNA copy number. The oncogene c-*myc* on 8q was gained in 73% of the cancers, while *FOXO1A* and *ATP7B* on 13q were both gained in 28.6% of the cases. Multiple genes on chromosome 20q showed gains in more than 60% of the cancers. DNA copy-number gains of *TNFRSF6B* (20q13.3) and *ZNF217* (20q13.2) were significantly associated with lymph node metastasis (p=0.02) and histological type (p=0.02), respectively. In summary, gains of chromosomes 8q, 13q, and 20q in gastric adenocarcinomas harbor DNA copy-number gains of known and putative oncogenes. *ZNF217* and *TNFRSF6B* are associated with important clinicopathological variables, including lymph node status.

Keywords DNA copy-number · Gastric cancer · Lymph node status · MLPA

T. E. Buffart · N. C. T. van Grieken · M. Tijssen · J. Coffa · B. Ylstra · B. Carvalho · G. A. Meijer (✉)
Department of Pathology, VU University Medical Center, PO Box 7057, 1007 Amsterdam, The Netherlands
e-mail: ga.meijer@vumc.nl

J. Coffa
MRC-Holland, Amsterdam, The Netherlands

H. I. Grabsch
Pathology and Tumour Biology, Leeds Institute of Molecular Medicine, University of Leeds, Leeds, UK

C. J. H. van de Velde
Department of Surgery, Leiden University Medical Center, Leiden, The Netherlands

Introduction

Gastric cancer is a major health problem and ranks second as a cause of cancer death worldwide [1]. The only possible curative treatment is complete surgical resection. One of the hallmarks of solid cancers, including gastric cancer, is chromosomal instability leading to gains and losses of parts of, or even whole chromosomes [2]. The mechanisms underlying this instability phenotype in gastric cancers are still poorly understood. Patterns of DNA copy-number aberrations can be analyzed at high resolution by array comparative genomic hybridization (CGH). Gains of chromosomes 3q, 7p, 7q, 8q, 13q, 17q, and 20q and losses of chromosomes 4q, 5q, 6q, 9p, 17p, and 18q have been consistently described in gastric cancer studies using CGH or array CGH analysis [3–11]. In addition, gains of chromosomes 7q, 8q, 9q, 11q, 13q, and 20q and losses of chromosomes 4p, 5q, 6, 9p, 17p, and 18q can already be

detected in gastric cancer precursor lesions with direct malignant potential, indicating these as early events in the pathogenesis of gastric cancer [12–16]. Results from array CGH studies have shown that patterns of chromosomal aberrations can be correlated with clinicopathological variables. In previous studies, we have shown different patterns of chromosomal instability to correlate with lymph node status and with age of onset of the disease [17, 18].

DNA copy-number gains of chromosomes 8, 13, and 20 have been described to play an important role in colorectal adenoma to carcinoma progression [19, 20]. Also in gastric adenomas and adenocarcinomas, gains of these chromosomes have frequently been detected, indicating the importance of genetic events on these chromosomes for gastric cancer pathogenesis. Moreover, gain of chromosome 20q has been described to correlate with lymph node metastasis in gastric cancer and poor clinical outcome in colorectal cancer [3, 21, 22]. The most widely used array CGH platforms, so far, use spotted bacterial artificial chromosomes (BACs), which means that the probe sequences on the arrays cover up to 1 kb of DNA. This approach is very suitable for detecting patterns of DNA copy-number changes but has limitations in pinpointing individual genes whose normal function is disrupted due to these chromosomal aberrations. Multiplex ligation-dependent probe amplification (MLPA) [23] allows to determine in a single experiment DNA copy-number ratios of up to 40 individual genes and can be used to zoom in on chromosomal areas that show aberrations with array CGH [24, 25]. The aim of the present study is a detailed analysis of DNA copy-number changes of individual genes within gained areas on chromosomes 8, 13, and 20 in gastric adenocarcinomas and to correlate gene specific alterations to clinicopathological data.

Materials and methods

Materials and DNA isolation

DNA of 63 formalin-fixed and paraffin-embedded (FFPE) gastric adenocarcinomas of which 53 were obtained from Leeds (Leeds University Hospital, UK) and 10 were obtained from the Dutch D1/D2 trial [26], was isolated as previously described [17] using a commercial available DNA isolation kit (QIAmp DNA microkit, Qiagen, Hilden, Germany). Briefly, areas of at least 70% tumor cells were demarcated on a 4-μm haematoxylin- and eosin-stained tissue section. Adjacent serial sections of 10 μm were cut, and after deparaffination, the tumor tissue was macrodissected using a needle. After an overnight incubation with sodium thiocyanate (1 M) at 37°C, followed by proteinase K treatment, DNA was extracted. DNA concentrations were measured on a Nanodrop ND-1000 spectrophotometer (Isogen, IJsselstein, The Netherlands), and DNA quality was assessed by isothermal amplification as previously described [27]. Only DNA of excellent, good, and intermediate quality was used for further analysis.

Table 1 An overview of DNA copy number gains of chromosomes 8q, 13q and 20q detected by array CGH in 63 gastric adenocarcinomas, and the correlation to lymph node status and histological type of the tumor

Chromosome	Status	All cases	Lymph node status		*P* value	Histological type			*P* value
			LN0	LN1		Intestinal	Diffuse	Mixed	
		n=63	*n*=22	*n*=41		*n*=38	*n*=17	*n*=8	
8q	Gain	49 (77.8%)	18 (81.8%)	31 (75.6%)	0.57	29 (76.3%)	13 (76.5%)	7 (87.5%)	0.78
	No gain	14 (22.2%)	4 (18.2%)	10 (24.4%)		9 (23.7%)	4 (23.5%)	1 (12.5%)	
13q	Gain	25 (39.7%)	10 (45.5%)	15 (36.6%)	0.49	19 (50.0%)	4 (23.5%)	2 (25.0%)	0.12
	No gain	38 (60.3%)	12 (54.5%)	26 (63.4%)		19 (50.0%)	13 (76.5%)	6 (75.0%)	
20q	Gain	49 (77.8%)	14 (63.6%)	35 (85.4%)	**0.048**	33 (86.8%)	9 (52.9%)	7 (87.5%)	**0.016**
	No gain	14 (22.2%)	8 (36.4%)	6 (14.6%)		5 (13.2%)	8 (47.1%)	1 (12.5%)	
8q+13q+20q	Gain	17 (27.0%)	6 (27.2%)	11 (26.8%)	0.97	13 (34.2%)	2 (11.8%)	2 (25.0%)	0.22
	No gain	46 (73.0%)	16 (72.7%)	30 (73.2)		25 (65.8%)	15 (88.2%)	6 (75.0%)	
8q+13q	Gain	4 (6.3%)	3 (13.6%)	1 (2.4%)	0.082	2 (5.3%)	2 (11.8%)	0 (0.0%)	0.48
	No gain	59 (93.7%)	19 (86.4%)	40 (97.6%)		36 (94.7%)	15 (88.2%)	8 (100.0%)	
8q+20q	Gain	24 (38.1%)	8 (36.4%)	16 (39.0%)	0.84	14 (36.8%)	6 (35.3%)	4 (50.0%)	0.76
	No gain	39 (61.9%)	14 (63.6%)	25 (61.0%)		24 (63.2%)	11 (64.7%)	4 (50.0%)	
13q+20q	Gain	3 (4.8%)	0 (0.0%)	3 (7.3%)	0.19	3 (7.9%)	0 (0.0%)	0 (0.0%)	0.36
	No gain	60 (95.2%)	22 (100.0%)	38 (92.7%)		35 (92.1%)	17 (100.0%)	8 (100.0%)	

Gain of 20q is significantly correlated to lymph node status and histological tumor type (in *bold*)

LN0 lymph node-negative, *LN1* lymph node-positive

DNA labeling and array CGH)

DNA labeling and array CGH were essentially performed as previously described [17, 28]. In short, tumor and normal DNA were differentially labeled using random priming (Bioprime DNA Labeling System; Invitrogen, Breda, The Netherlands) and hybridized on a BAC array containing approximately 5,000 clones printed in triplicate, consisting of the Sanger BAC clone set with an average resolution along the whole genome of 1.0 Mb (http://www.ensembl.org/Homo_sapiens/cytoview), the OncoBac set (http://informa.bio.caltech.edu/Bac_onc.html), containing approximately 600 clones corresponding to 200 cancer-related genes, and selected clones of interest obtained from the Children's Hospital Oakland Research Institute (CHORI) to fill any gaps larger than 1 Mb on chromosome 6 and to have full-coverage contigs of regions on chromosomes 8, 11, 13, and 20. All clones were printed on Codelink™ slides (Amersham BioSciences, Roosendaal, The Netherlands) at a concentration of 1 μg/μl in 150-mM sodium phosphate, pH 8.5, using an OmniGrid 100 microarrayer (Genomic Solutions, Ann Arbor, MI, USA) equipped with SMP3 pins (TeleChem International, Sunnyvale, CA, USA), and processed according to the manufacturer's protocol.

After hybridization, images of the arrays were acquired by scanning (Microarray scanner G2505B; Agilent technologies, Palo Alto, USA), and spot analysis and quality control were automatically performed using BlueFuse 3.4 software (BlueGnome, Cambridge, UK). When the Blue-

Table 2 Overview of patient and tumor characteristics of the 63 gastric adenocarcinomas analyzed in the study

Tumor ID	Gender	Age	Histological type	T status	N status	Tumor ID	Gender	Age	Histological type	T status	N status
1	Female	78	Intestinal	T3	N1	33	Male	75	Intestinal	T2	N3
2	Female	81	Diffuse	T3	N1	34	Male	61	Intestinal	T3	N3
3	Female	54	Intestinal	T2	N0	35	Female	82	Diffuse	T3	N1
4	Male	73	Intestinal	T3	N1	36	Male	74	Mixed	T2	N1
5	Male	81	Mixed	T2	N2	37	Female	87	Diffuse	T3	N2
6	Male	58	Intestinal	T2	N1	38	Female	78	Intestinal	T1	N0
7	Female	72	Intestinal	T2	N0	39	Male	78	Diffuse	T2	N0
8	Male	86	Intestinal	T2	N2	40	Female	84	Intestinal	T2	N0
9	male	71	Intestinal	T3	N0	41	Male	85	Diffuse	T3	N2
10	Female	75	Intestinal	T4	N1	42	Male	62	Diffuse	T3	N3
11	Female	75	Intestinal	T3	N2	43	Male	68	Intestinal	T3	N1
12	Male	64	Mixed	T3	N1	44	Male	58	Intestinal	T4	N1
13	Male	81	Intestinal	T2	N2	45	Male	61	Diffuse	T3	N1
14	Male	63	Intestinal	T2	N0	46	Female	58	Intestinal	T3	N1
15	Male	63	Intestinal	T3	N1	47	Male	81	Intestinal	T3	N1
16	Male	68	Mixed	T2	N0	48	Female	65	Intestinal	T2	N1
17	Female	72	Intestinal	T2	N1	49	Female	65	Intestinal	T2	N1
18	Male	73	Intestinal	T2	N2	50	Male	82	Intestinal	T1	N0
19	Male	71	Intestinal	T3	N2	51	Female	74	Mixed	T1	N0
20	Female	67	Intestinal	T2	N0	52	Male	72	Diffuse	T3	N2
21	Male	67	Diffuse	T3	N1	53	Female	60	Diffuse	T3	N0
22	Female	64	Intestinal	T3	N2	54	Male	47	Diffuse	T2	N0
23	Female	72	Diffuse	T3	N2	55	Female	74	Diffuse	T2	N0
24	Male	74	Intestinal	T2	N1	56	Male	65	Mixed	T2	N2
25	Male	58	Intestinal	T3	N3	57	Female	49	Intestinal	T1	N0
26	Male	71	Intestinal	T1	N0	58	Male	74	Intestinal	T1	N0
27	Female	68	Mixed	T3	N1	59	Male	58	Intestinal	T1	N0
28	Male	74	Intestinal	T2	N0	60	Male	53	Diffuse	T2	N0
29	Male	57	Mixed	T3	N1	61	Male	61	Diffuse	T2	N1
30	Male	69	Diffuse	T3	N1	62	Male	69	Diffuse	T2	N1
31	Male	67	Intestinal	T2	N0	63	Male	56	Intestinal	T2	N0
32	Female	71	Intestinal	T2	N1						

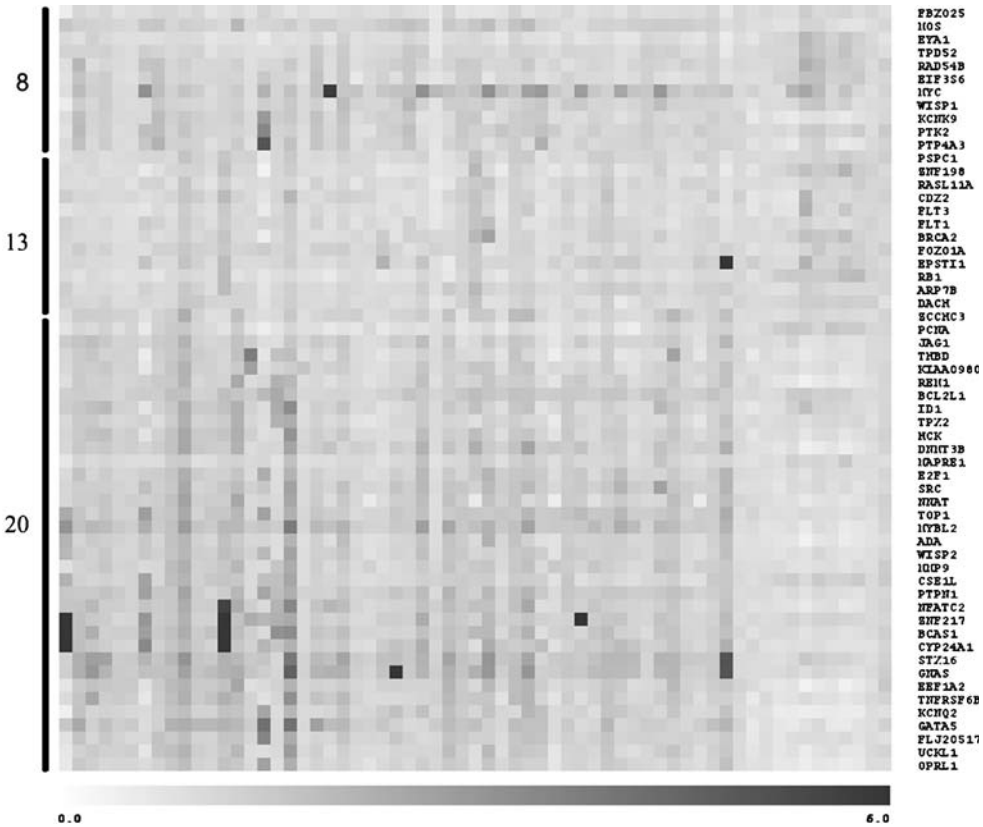

Fig. 1 Heatmap of DNA copy number ratios of 11 genes on chromosome 8, 12 genes on chromosome 13, and 35 genes on chromosome 20. The *columns* represent different gastric adenocarcinomas, and the *rows* represent the different genes. *Darker squares* indicate higher DNA copy number ratios

Fuse quality flag was below one or the confidence value was below 0.1, spots were excluded from further analysis. The $\log_2$ tumor to normal fluorescence ratio was calculated for each spot and normalized against the mode of the ratios of all autosomes. The package CGH call was used for data segmentation and defining copy-number gains and losses of each clone in the array CGH profile [29].

Multiplex ligation-dependent probe amplification

MLPA was performed, as previously described, [24] using two different probe mixes. One probemix contained 38 probes representing 31 different genes on chromosome 20 and 10 control probes located on chromosomes 2, 3, 4, 5, 12, and 16. The second probemix contained 11 probes on chromosome 8, 12 probes on chromosome 13, 16 probes on chromosome 20 representing 14 different genes, and 8 control probes located on chromosomes 2, 4, 12, and 16. Some genes on chromosome 20 are present in both probe mixes, leaving 35 different genes on chromosome 20 by combining these two probe mixes. DNA of the cell line HT29, showing a gain on chromosomes 8, 13, and 20, was used as positive control. A human pool of DNA isolated from blood of 36 healthy individuals and a pool of DNA isolated of 30 normal gastric and colon mucosa, spleen, liver, and kidney tissue samples (FFPE), were used as normal controls.

Of each sample, approximately 100 ng of DNA in a volume of 5 µl was denaturated at 98°C for 5 min. A mixture of 1.5-µl salsa probes (1–4 fmol of each short synthetic probe oligonucleotide and each phage M13-derived long probe oligonucleotide in TE (10 mM Tris-HCl, pH 8.2, 1 mM ethylenediamine tetraacetic acid (EDTA))) and 1.5 µl of MLPA buffer (1.5 M KCl, 300 mM Tris-HCl, pH 8.5, 1 mM EDTA) was added. The mixture was heated for 1 min at 95°C followed by 16 h of incubation at 60°C to allow the MLPA hemipobes to hybridize. Next, 32 µl of ligase-65 mixture (dilution buffer containing 2.6 mM $MgCl_2$, 5 mM Tris-HCl, pH 8.5, 0.013% non-ionic detergents, 0.2 mM of nicotinamide adenine dinucleotide (NAD), and 1 U of ligase-65 enzyme) was added to each sample for ligation of hybridized hemiprobes during a 10–15 min of incubation at 54°C, followed by a 5 min of incubation at 98°C to inactivate the ligase.

Polymerase chain reaction (PCR) was performed with 10 µl of polymerase mixture containing the PCR primers (10 pmol), dNTPs (2.5 nmol), and 2.5 U *Taq* polymerase (promega), 4 µl of PCR buffer (2.6 mM $MgCl_2$, 5 mM Tris-HCl, pH 8.5, 0.013% non-ionic detergents, 0.2 mM NAD), 26 µl of water and 10 µl of MLPA ligation reaction.

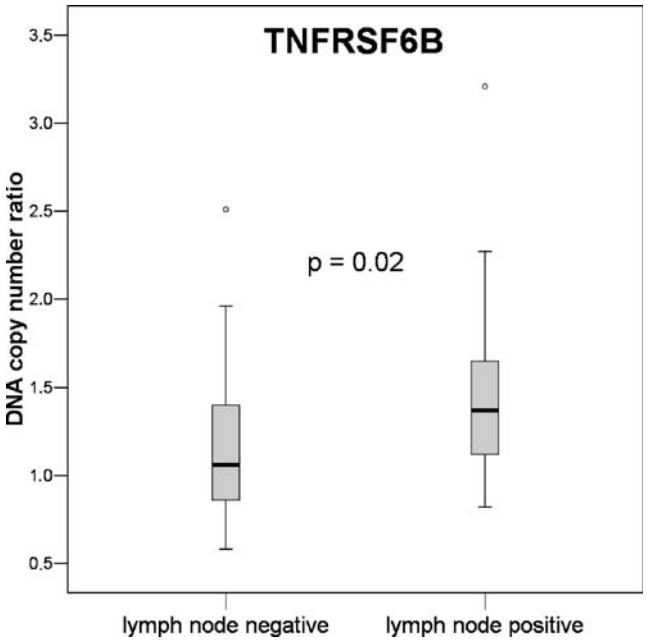

Fig. 2 Box plot of DNA copy number ratios of the gene *TNFRFS6B* between lymph node-negative and lymph node-positive gastric adenocarcinomas. Lymph node-positive gastric adenocarcinomas have significantly higher DNA copy number ratios of *TNFRFS6B* compared with lymph node-negative gastric adenocarcinomas (p=0.02). The *central box* covers the middle 50% of the data values between the upper and lower quartiles. The *line* across the box indicates the median. The *whiskers* extend from the box to the minimum and maximum values with the exception of outliers, which are marked by *circles*

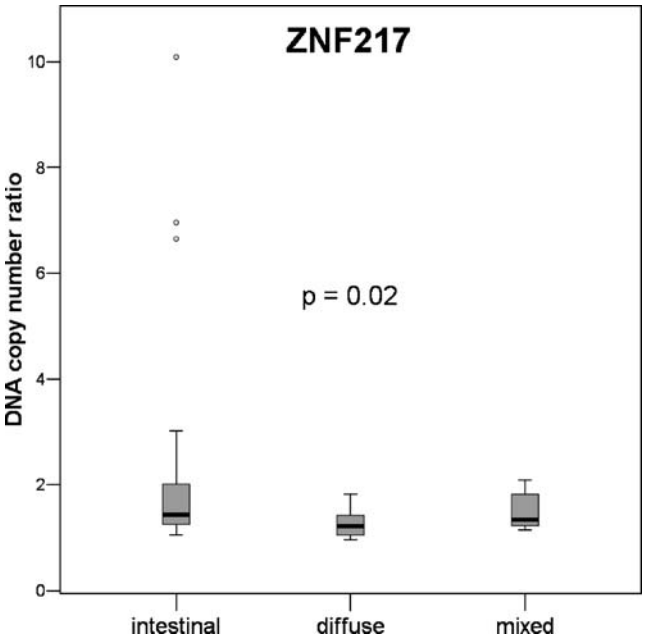

Fig. 3 Box plot of DNA copy number ratios of the gene *ZNF217* between intestinal-, diffuse-, and mixed-type gastric adenocarcinomas. DNA copy number ratios of *ZNF217* are significantly different between gastric adenocarcinomas of different histological types (p=0.02)

Multiplex ligation-dependent probe amplification data analysis

Analysis of the MLPA PCR products for each gene was performed on an ABI 3100 capillary sequencer (Applied Biosystems, Warrington, UK) in a mixture of 8.5 µl of deionized formamide (Applied Biosystems, Warrington, UK), 1 µl of PCR product and 0.5 µl marker including a ROX-labeled internal size standard (ROX-500 Genescan; Applied Biosystems, Warrington, UK). Data analysis was performed using the MLPAnalyzer version 8.0 (http://www.mlpa.com/coffalyser/) [30]. For each tumor, peak heights for every probe were derived from the ABI output and median peak heights of at least two different ligation reactions and three different PCR reactions were calculated. For each sample, tumor to normal DNA copy-number ratios was calculated per probe by dividing the median peak heights in the tumor tissue by the median peak heights in the reference DNA. All ratios were normalized by setting the median of the tumor to reference DNA copy-number ratios of the control genes in the probe mixture to 1.0. When multiple probes were present for one gene, the mean value of the probes was calculated and used for further analysis. Tumor to normal ratios below 0.7 and above 1.3 was considered as a loss or gain, respectively. TMEV software 3.1 (http://www.tigr.org/) was used to present descriptive data.

Statistical analysis

Box and scatter plots were used to present descriptive statistics. Chi-square test was used to evaluate associations of DNA copy-number gain of chromosomes 8q, 13q, and 20q with clinicopathological variables. t Test was used to evaluate differences in DNA copy-number aberrations and age of the patients. Mann-Whitney U test and Kruskal-Wallis H test were used to evaluate differences in DNA copy-number changes of each gene between lymph node status and histological tumor type according to the Laurén classification [31], respectively. Correlation coefficients between the $\log_2$ ratios for the array CGH and MLPA analysis were obtained by Spearman correlation (SPSS 12.0.1 for Windows; SPSS Inc. Chicago, IL, USA). A threshold of 0.05 for significance was used.

Results

Array CGH analysis and correlation with lymph node status and histological type

Of the 63 gastric adenocarcinomas analyzed by array CGH, 49 (77.8%) showed gains on chromosome 8, 25 (39.7%)

Table 3 A detailed overview of the frequencies of DNA copy number gains per gene, determined by MLPA analysis and mean DNA copy number ratio and range, per tumor group, i.e., lymph node-positive versus lymph node-negative gastric adenocarcinomas and intestinal- versus diffuse- versus mixed-type gastric carcinomas

Gene	Location	Gains	LN-negative	LN-positive	*p* value	Intestinal	Diffuse	Mixed	*p* value
FBXO25	8p23.3	1.6%	1.04 (0.68–1.46)	0.97 (0.48–1.26)	NS	0.98 (0.48–1.46)	1.08 (0.81–1.26)	0.87 (0.63–1.29)	0.01
MOS	8q11	39.7%	1.20 (0.78–2.02)	1.31 (0.73–1.96)	NS	1.34 (0.92–2.02)	1.15 (0.77–1.71)	1.23 (0.73–1.96)	NS
EYA1	8q13.3	9.5%	1.08 (0.55–2.07)	0.96 (0.65–1.35)	NS	1.01 (0.66–2.07)	1.05 (0.75–1.64)	0.86 (0.55–1.25)	NS
TPD52	8q21	25.4%	1.26 (0.67–1.98)	1.15 (0.68–1.59)	NS	1.20 (0.90–1.98)	1.22 (0.96–1.74)	1.04 (0.67–1.59)	NS
RAD54B	8q21.3	34.9%	1.33 (0.88–2.29)	1.22 (0.90–2.06)	NS	1.30 (0.90–2.29)	1.20 (0.88–2.06)	1.19 (0.90–1.59)	NS
EIF3S6	8q22	28.6%	1.27 (0.85–1.82)	1.12 (0.64–1.74)	0.04	1.19 (0.74–2.82)	1.13 (0.64–1.70)	1.18 (0.76–1.59)	NS
MYC	8q24.12	73.0%	1.75 (0.95–3.22)	1.76 (0.90–5.81)	NS	1.74 (0.94–3.22)	1.74 (0.90–5.81)	1.84 (1.03–2.74)	NS
WISP1	8q24	36.5%	1.26 (0.79–1.68)	1.26 (0.51–2.08)	NS	1.28 (0.51–1.88)	1.20 (0.79–1.64)	1.27 (0.79–2.08)	NS
KCNK9	8q24.3	34.9%	1.16 (0.59–2.92)	1.24 (0.58–1.90)	NS	1.22 (0.77–1.90	1.11 (0.59–1.87)	1.37 (0.58–2.92)	NS
PTK2	8q24	47.6%	1.40 (0.96–3.47)	1.29 (0.83–1.97)	NS	1.33 (0.83–1.86)	1.25 (0.91–1.97)	1.51 (0.63–5.02)	NS
PTP4A3	8q24.3	33.3%	1.37 (0.62–5.02)	1.23 (0.63–2.24)	NS	1.27 (0.86–2.20)	1.18 (0.62–2.24)	1.55 (0.63–5.02)	NS
PSPC1	13q11	22.2%	1.12 (0.65–1.48)	1.18 (0.71–1.75)	NS	1.20 (0.89–1.75)	1.15 (0.82–1.48)	1.01 (0.65–1.51)	NS
ZNF198	13q11	20.6%	1.05 (0.38–2.17)	1.08 (0.55–2.04)	NS	1.08 (0.55–2.04)	1.15 (0.74–2.17)	0.88 (0.38–1.41)	NS
RASL11A	13q12.2	11.1%	1.09 (0.87–1.35)	1.10 (0.61–1.66)	NS	1.15 (0.84–1.66)	1.08 (0.75–1.52)	0.93 (0.61–1.15)	0.03
CDX2	13q12	22.2%	1.09 (0.70–2.11)	1.19 (0.67–2.09)	NS	1.21 (0.76–2.11)	1.14 (0.70–1.73)	0.91 (0.67–1.30)	0.03
FLT3	13q12	12.7%	1.04 (0.56–2.23)	1.05 (0.65–1.70)	NS	1.08 (0.69–2.23)	1.05 (0.71–1.55)	0.87 (0.56–1.51)	NS
FLT1	13q12.2	20.6%	1.10 (0.85–1.42)	1.13 (0.67–1.85)	NS	1.17 (0.77–1.85)	1.09 (0.82–1.48)	0.98 (0.67–1.34)	NS
BRCA2	13q12.3	22.2%	1.15 (0.53–1.85)	1.22 (0.91–2.62)	NS	1.23 (0.83–2.62)	1.17 (0.93–1.85)	1.08 (0.53–1.31)	NS
FOXO1A	13q14.1	28.6%	1.18 (0.80–1.58)	1.19 (0.79–1.59)	NS	1.20 (0.79–1.59)	1.15 (0.80–1.45)	1.18 (0.89–1.46)	NS
EPSTI1	13q14.11	17.5%	1.51 (1.02–6.32)	1.21 (0.62–2.20)	NS	1.30 (0.94–2.20)	1.17 (0.62–1.68)	1.70 (0.90–6.32)	NS
RB1	13q14.2	14.3%	1.12 (0.72–1.87)	1.04 (0.60–1.97)	NS	1.06 (0.69–1.89)	1.13 (0.60–1.97	1.01 (0.72–1.55)	NS
ATP7B	13q14.2	28.6%	1.15 (0.77–1.45)	1.21 (0.90–1.99)	NS	1.24 (0.91–1.99)	1.14 (0.86–1.53)	1.05 (0.77–1.42)	NS
DACH	13q21.32	20.6%	1.13 (0.82–1.42)	1.13 (0.62–1.72)	NS	1.15 (0.62–1.72)	1.15 (0.88–1.42)	1.05 (0.71–1.36)	NS
ZCCHC3	20p13–p12.2	38.1%	1.19 (0.81–1.82)	1.28 (0.94–2.29)	NS	1.26 (0.81–2.29)	1.21 (0.91–1.92)	1.27 (0.94–1.96)	NS
PCNA	20pter–p12	17.5%	1.09 (0.48–1.65)	1.01 (0.45–1.61)	NS	1.02 (0.45–1.65)	1.06 (0.64–1.50)	1.06 (0.48–1.61)	NS
JAG1	20p12.1–p11.23	42.9%	1.24 (0.69–2.05)	1.29 (0.85–2.13)	NS	1.31 (0.69–2.13)	1.17 (0.85–1.68)	1.31 (0.97–2.05)	NS
THBD	20p12–cen	31.7%	1.04 (0.48–1.79)	1.26 (0.71–3.81)	NS	1.25 (0.48–3.81)	1.07 (0.60–1.66)	1.10 (0.74–1.34)	NS
KIAA0980	20p11.22–p11.1	42.9%	1.17 (0.70–1.76)	1.31 (0.84–2.73)	NS	1.32 (0.70–2.73)	1.12 (0.77–1.55)	1.29 (0.92–1.76)	NS
REM1	20q11.21	34.9%	1.19 (0.42–2.43)	1.24 (0.75–2.21)	NS	1.29 (0.42–2.43)	1.08 (0.60–1.51)	1.24 (0.75–1.79)	NS
BCL2L1	20q11.21	73.0%	1.44 (0.97–1.98)	1.45 (1.04–2.44)	NS	1.50 (1.10–2.44)	1.31 (0.97–1.76)	1.51 (1.19–1.98)	NS
ID1	20q11	29.2%	1.29 (0.66–2.25)	1.41 (0.80–3.33)	NS	1.48 (0.77–3.33)	1.15 (0.66–1.62)	1.32 (1.00–1.73)	NS
TPX2	20q11.2	27.0%	1.26 (0.58–2.22)	1.21 (0.71–2.35)	NS	1.28 (0.58–2.35)	1.13 (0.80–1.57)	1.21 (0.97–1.75)	NS
HCK	20q11–q12	46.0%	1.23 (0.71–2.27)	1.37 (0.90–3.12)	NS	1.40 (0.71–3.12)	1.16 (0.73–1.58)	1.28 (0.93–1.69)	NS
DNMT3B	20q11.2	54.0%	1.29 (0.43–2.26)	1.42 (0.72–2.60)	NS	1.42 (0.43–2.55)	1.20 (0.54–1.74)	1.51 (0.94–2.60)	NS
MAPRE1	20q11.21	20.6%	1.16 (0.84–1.78)	1.14 (0.70–1.78)	NS	1.15 (0.70–1.78)	1.12 (0.84–1.53)	1.17 (0.83–1.54)	NS

E2F1	20q11.2	44.4%	1.35 (0.80–2.31)	1.33 (0.93–2.26)	NS	1.37 (0.82–2.26)	1.21 (0.80–1.72)	1.47 (0.95–2.31)	NS
SRC	20q12–q13	57.1%	1.38 (0.71–2.12)	1.45 (0.77–2.70)	NS	1.51 (0.88–2.70)	1.22 (0.71–1.67)	1.48 (1.02–2.12)	NS
NNAT	20q11.2–q12	52.4%	1.30 (0.47–2.50)	1.30 (0.55–2.65)	NS	1.36 (0.47–2.65)	1.16 (0.69–1.78)	1.27 (0.91–1.91)	NS
TOP1	20q12–q13.1	63.5%	1.57 (0.85–2.78)	1.47 (0.88–2.40)	NS	1.57 (1.00–2.78)	1.29 (0.85–1.72)	1.67 (0.94–2.69)	NS
MYBL2	20q13.1	73.0%	1.49 (0.58–2.79)	1.73 (0.70–3.83)	NS	1.79 (0.58–3.83)	1.34 (0.58–2.51)	1.62 (0.95–2.65)	NS
ADA	20q12–q13.11	41.3%	1.17 (0.42–1.80)	1.28 (0.67–2.24)	NS	1.32 (0.42–2.24)	1.08 (0.53–1.74)	1.22 (0.74–1.80)	NS
WISP2	20q12–q13.1	52.4%	1.31 (0.78–2.03)	1.33 (0.78–2.62)	NS	1.37 (0.82–2.62)	1.18 (0.78–1.69)	1.40 (0.95–2.03)	NS
MMP9	20q11.2–q13.1	47.6%	1.26 (0.76–2.06)	1.33 (0.87–2.37)	NS	1.38 (0.81–2.37)	1.18 (0.76–1.72)	1.27 (0.87–1.81)	NS
CSE1L	20q13	49.2%	1.40 (0.85–2.65)	1.31 (0.88–2.54)	NS	1.37 (0.85–2.65)	1.25 (0.94–1.60)	1.43 (1.11–1.82)	NS
PTPN1	20q13.1–q13.2	65.1%	1.46 (0.85–2.76)	1.51 (0.87–2.62)	NS	1.55 (0.85–2.76)	1.32 (0.96–1.82)	1.57 (1.04–2.54)	NS
NFATC2	20q13.2–q13.3	55.6%	1.31 (0.63–2.34)	1.60 (0.77–5.60)	NS	1.61 (0.63–5.60)	1.27 (0.65–2.09)	1.45 (0.83–2.50)	NS
ZNF217	20q13.2	57.1%	1.74 (0.99–6.65)	1.79 (0.96–10.09)	NS	2.06 (1.05–10.09)	1.27 (0.96–1.82)	1.50 (1.15–2.09)	0.02
BCAS1	20q13.2–q13.3	58.7%	1.42 (0.80–2.77)	1.94 (0.95–12.17)	NS	2.03 (0.80–12.17)	1.29 (0.85–1.88)	1.47 (1.05–2.19)	NS
CYP24A1	20q13	60.3%	1.47 (0.85–3.43)	1.81 (0.80–9.16)	NS	1.92 (0.85–9.16)	1.26 (0.80–1.91)	1.52 (0.96–2.27)	NS
STX16	20q13.32	77.8%	1.78 (0.91–5.05)	1.81 (0.95–3.95)	NS	1.90 (1.11–3.95)	1.47 (0.91–2.62)	2.03 (1.09–5.05)	0.03
GNAS	20q13.3	76.2%	2.00 (0.94–7.97)	1.82 (0.87–4.68)	NS	2.02 (0.94–7.97)	1.48 (0.87–2.26)	2.12 (1.16–4.99)	NS
EEF1A2	20q13.3	47.6%	1.20 (0.41–2.52)	1.41 (0.63–2.20)	NS	1.39 (0.41–2.52)	1.21 (0.42–2.18)	1.40 (0.83–2.09)	NS
TNFRSF6B	20q13.3	49.2%	1.20 (0.58–2.51)	1.45 (0.82–3.21)	0.02	1.41 (0.67–3.21)	1.25 (0.58–2.01)	1.36 (0.82–2.13)	NS
KCNQ2	20q13.3	38.1%	1.18 (0.49–2.59)	1.30 (0.43–2.08)	NS	1.27 (0.43–2.08)	1.13 (0.52–1.85)	1.48 (0.55–2.59)	NS
GATA5	20q13.33	60.3%	1.44 (0.60–4.15)	1.58 (0.62–4.12)	NS	1.54 (0.63–4.12)	1.38 (0.60–2.46)	1.82 (0.62–4.15)	NS
FLJ20517	20q13.33	41.3%	1.28 (0.65–3.54)	1.34 (0.80–2.38)	NS	1.30 (0.80–2.38)	1.24 (0.65–1.74)	1.60 (0.95–3.54)	NS
UCKL1	20q13.33	39.7%	1.13 (0.56–2.03)	1.30 (0.67–2.86)	NS	1.29 (0.56–2.86)	1.13 (0.67–1.87)	1.24 (0.85–1.65)	NS
OPRL1	20q13.33	28.6%	1.15 (0.49–2.70)	1.19 (0.62–2.28)	NS	1.18 (0.49–2.28)	1.08 (0.51–1.57)	1.38 (0.67–2.70)	NS

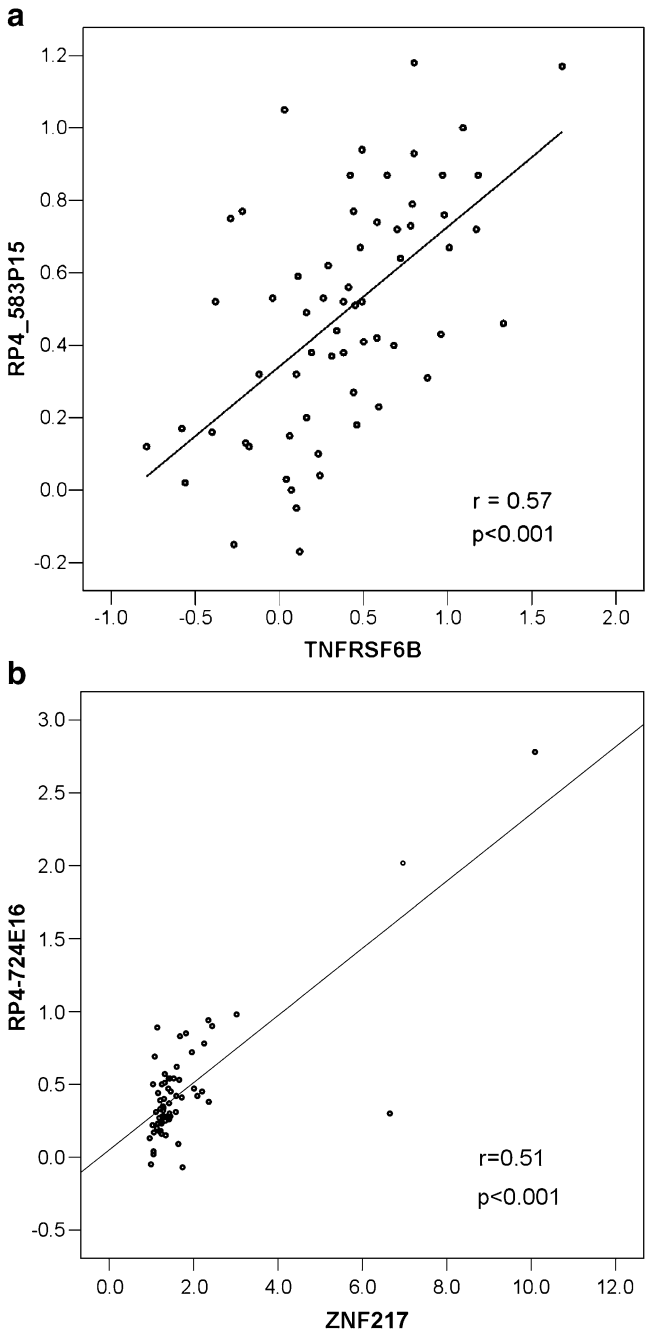

Fig. 4 Scatter plots of the $\log_2$ ratios of the BAC clone and MLPA probe of the *TNFRFS6B* (**a**) and *ZNF217* (**b**) genes. A significant correlation was detected for both genes ($p<0.001$, $r=0.57$ and $r=0.51$, respectively)

showed gains on chromosome 13, and 49 (77.8%) showed gains on chromosome 20. Concurrent gains of chromosomes 8 and 13, 8 and 20, and 13 and 20 were observed in four (6.3%), 24 (38.1%), and three (4.8%) of the gastric adenocarinomas, respectively. Concurrent gains of chromosomes 8, 13, and 20 were observed in 17 (27%) gastric adenocarcinomas. Gain of chromosome 20q was significantly correlated with lymph node status ($p=0.05$) and histological type of the tumor ($p=0.02$), being more common in lymph node-positive gastric cancers (85%) than in lymph node-negative gastric cancers (64%) and more common in intestinal-type (87%) and mixed-type (88%) gastric cancers than in diffuse-type (53%) gastric cancers. No significant (NS) correlation was found between 20q gain and age and gender of the patients and tumor size. No correlation of 8q gain or 13q gain with clinicopathological variables was found. An overview of the frequencies of copy-number gains on chromosomes 8q, 13q, and 20q detected by array CGH analysis is given in Table 1. An overview of patient and tumor characteristics is given in Table 2.

Multiplex ligation-dependent probe amplification analysis of DNA copy-number aberrations and correlation with lymph node status and histological type

All 63 gastric adenocarcinomas analyzed by array CGH were analyzed by MLPA. An overview of the DNA copy-number ratios of all individual genes on chromosomes 8, 13, and 20 in all tumor samples is presented as a heatmap in Fig. 1.

Gains of genes on chromosome 8q were observed in 9.5%–73.0% of the gastric adenocarcinomas, with the highest frequencies of gains observed in c-*myc* (73.0%). Gains of genes on chromosome 13q were detected in 11.1%–28.6%, with the highest frequencies of gains observed in *FOXO1A* and *ATP7B* (both 28.6%). Frequent DNA copy-number gains of multiple genes on chromosome 20q were observed. Gain of *TOP1*, *PTPN1*, *CYP24A1*, and *GATA5* was observed in more than 60% of the gastric adenocarcinomas, and gain of *BCL2L1*, *MYBL2*, *STX16*, and *GNAS* was observed in more than 70% of the gastric adenocarcinomas. When correlating gene-specific copy-number status to lymph node status, *EIF3S6* ($p=0.04$), located on chromosome 8q22 and *TNFRSF6B* ($p=0.02$), located on chromosome 20q13.3, were significantly different between lymph node-positive and lymph node-negative gastric adenocarcinomas. Although Mann-Whitney *U* test yielded a significant difference in copy-number of the gene *EIF3S6* between lymph node-positive and lymph node-negative gastric adenocarcinomas, mean copy-number ratio of both carcinoma groups were within the normal copy-number range (DNA copy-number ratio between 0.7 and 1.3). Lymph node-positive gastric adenocarcinomas showed gain (DNA copy-number ratio >1.3) of *TNFRSF6B* while lymph node negative gastric adenocarcinomas showed normal copy-number ratios of this gene (Fig. 2). When correlating gene-specific copy-number ratio to histological tumor type, Kruskall-Wallis *H* test yielded five significant genes. Mean copy-number ratios of *FBXO25* ($p=0.01$), located on 8p23.3, *RASL11A* ($p=0.03$), located on 13q12.2 and *CDX2* ($p=0.03$), located on 13q12, were within the normal copy-number range for all three tumor types. Mean

copy-number ratio of *ZNF217* (p=0.02), located on 20q13.2, showed gain in intestinal and mixed histological gastric cancer types versus normal in the diffuse histological types (Fig. 3). *STX16* (p=0.03), located on 20q13.32, showed mean copy-number gain in all three tumor types, but higher mean copy-number ratios in the intestinal and mixed types of gastric carcinomas compared with diffuse-type gastric carcinomas (1.90, 2.03, and 1.47, respectively). A detailed overview of the frequencies of gains per gene and mean copy-number ratio per tumor group, i.e., lymph node-positive versus lymph node-negative gastric adenocarcinomas and intestinal- versus diffuse- versus mixed-type gastric carcinomas are given in Table 3.

Correlation of copy-number status of MLPA and array CGH

The BAC clones RP4-583P15 and RP4-724E16 comprised the location of the *TNFRSF6B* and *ZNF217* genes, respectively. To evaluate the correlation between the array CGH and MLPA data, the MLPA DNA copy-number ratios were transformed to a $\log_2$ scale. Spearman correlation yielded a significant correlation between array CGH and MLPA data for both *TNFRSF6B* (r=0.57, p<0.001; Fig. 4a) and *ZNF217* (r=0.51, p<0.001; Fig. 4b).

Discussion

Gastric cancer is a common disease with a poor prognosis [1]. Chromosomal instability is a major mechanism of genetic instability in gastric cancers which has been widely studied by array CGH analysis [2, 32]. Frequent copy-number gains of chromosomes 8q, 13q, and 20q have been detected in gastric adenocarcinomas by this technique [3–10]. In this study, we report a detailed analysis of DNA copy-number changes of genes located on chromosomes 8, 13, and 20 in gastric adenocarcinomas aiming to correlate gene-specific alterations to clinicopathological data.

In the present study of 63 gastric adenocarcinomas studied by array CGH, nearly 80% of the cancers showed gain of chromosomes 8q and 20q. These frequencies of gains are consistent with previous studies where gains of chromosomes 8q and 20q were reported in 40–80% and 50–80% of gastric cancers, respectively [4, 10, 13, 14, 17, 33]. Both gains and losses of chromosome 13q have been detected in gastric cancers. Losses of chromosome 13q have been described in up to 30% of gastric cancers and gains of 13q have been described in up to 40% of gastric cancers [4, 10, 13–15, 17, 33], which is consistent with the findings of the present study.

When analyzing DNA copy-number gain at the gene level, mean copy-number ratio of two genes, *EIF3S6*E (8q22) and *TNFRSF6B* (20q12.3), correlated significantly with lymph node status. Mean copy-number ratios of *EIF3S6E* were within the normal range for both lymph node-positive and lymph node-negative gastric cancers, corresponding to the array CGH results in this study. Mean copy-number ratio of *TNFRSF6B* was significantly higher in lymph node-positive compared with lymph node-negative gastric cancers and was within the range of DNA copy-number gain and normal, respectively. Although 20q gain CGH data correlated with lymph node metastasis, of the 20q genes tested, only DNA copy-number gain of *TNFRSF6B* was significantly correlated with lymph node metastasis. *TNFRSF6B* is a member of the tumor necrosis factor receptor superfamily and is also known as decoy receptor 3 (DrR3). *TNFRSF6B* binds to FasL and inhibits FasL-induced apoptosis [34]. Overexpression of this gene has been observed in multiple cancer types, including cancers of the gastrointestinal tract. Interestingly, gastric cancers with pN2 and pN3 diseases have been shown to have significantly higher *TNFRSF6B* expression compared with gastric cancers with pN0 and pN1 diseases. Serum levels of *TNFRSF6B* were correlated with TNM stage in gastric cancers [35, 36]. We found *TNFRSF6B* DNA copy-number ratios on average to be gained in gastric cancers metastasized to the lymph nodes (pN1–3) compared with on average normal DNA copy-number ratios of *TNFRSF6B* in non-metastasized gastric cancers (pN0). Although previous studies have reported overexpression of *TNFRSF6B* without gene amplification [37], results of the present study indicate that DNA copy-number status of *TNFRSF6B* could be a valuable marker for identifying lymph node-positive gastric cancers.

DNA copy-number status of five genes, *FBXO25* (8p23.3), *RASL11A* (13q12.2), *CDX2* (13q12), *ZNF217* (20q13.2), and *STX16* (20q13.32), correlated significantly with histological tumor type, i.e., intestinal-, diffuse-, or mixed-type gastric cancer. Mean DNA copy-number ratios of *FBXO25*, *RASL11A*, and *CDX2*, however, were within the normal copy-number range for all three histological types, in consistence with the array CGH data of this study. The biological meaning of this difference, therefore, is not immediately clear, but could, e.g., relate to only a subpopulation of tumor cells being affected.

STX16 showed significantly higher mean copy-number ratios in intestinal- and mixed-type compared with diffuse-type gastric cancers; however, DNA copy-number gain was observed in all three tumor groups. *STX16* encodes a syntaxin protein which plays a role in intracellular trafficking [38], but its role in cancer still has to be elucidated.

ZNF217 encodes a transcription factor which was shown to be involved in immortalization of breast cancer cells when overexpressed [39]. High-level amplifications of *ZNF217* have been previously described in approximately 10% of gastric cancers [9, 10, 40]. In the study of Weiss et

al. on three tumors, all of the intestinal-type, out of 27 gastric adenocarcinomas, showed an amplification on 20q13. Fluorescence in situ hybridization (FISH) analysis was performed on these three tumors, confirming the copy-number increase at this locus [9]. Results from the present study suggest that DNA copy-number gain of *ZNF217* plays a more important role in intestinal- and mixed-type compared with diffuse-type gastric cancers, since gains of mean copy-number ratios are observed in intestinal- and mixed-type gastric cancers and normal mean copy-number ratio in diffuse-type gastric cancers.

In summary, we present a detailed DNA copy-number analysis of a panel of genes located on chromosomes 8, 13, and 20 in gastric adenocarcinomas. We found that DNA copy-number gain of *ZNF217* plays a role mainly in intestinal- and mixed-type but not in diffuse-type gastric adenocarcinomas. In addition, we showed that DNA copy-number gain of *TNFRSF6B* is significantly correlated to gastric cancers with lymph node metastasis, indicating a potential role for this gene as a biomarker for identifying patients at high risk of lymph node metastasis, who might, therefore, benefit from extended lymph node resection or neoadjuvant chemotherapy to improve gastric cancer outcome.

Acknowledgements This study was financially supported by the Dutch Cancer Society, grant KWF2004-3051.

Conflict of interest statement We declare that we have no conflict of interest.

References

1. Parkin DM, Bray F, Ferlay J et al (2005) Global cancer statistics, 2002. CA Cancer J Clin 55:74–108
2. Lengauer C, Kinzler KW, Vogelstein B (1998) Genetic instabilities in human cancers. Nature 396:643–649
3. Hidaka S, Yasutake T, Kondo M et al (2003) Frequent gains of 20q and losses of 18q are associated with lymph node metastasis in intestinal-type gastric cancer. Anticancer Res 23:3353–3357
4. Kimura Y, Noguchi T, Kawahara K et al (2004) Genetic alterations in 102 primary gastric cancers by comparative genomic hybridization: gain of 20q and loss of 18q are associated with tumor progression. Mod Pathol 17:1328–1337
5. Koo SH, Kwon KC, Shin SY et al (2000) Genetic alterations of gastric cancer: comparative genomic hybridization and fluorescence In situ hybridization studies. Cancer Genet Cytogenet 117:97–103
6. Sakakura C, Mori T, Sakabe T et al (1999) Gains, losses, and amplifications of genomic materials in primary gastric cancers analyzed by comparative genomic hybridization. Genes Chromosomes Cancer 24:299–305
7. Takada H, Imoto I, Tsuda H et al (2005) Screening of DNA copy-number aberrations in gastric cancer cell lines by array-based comparative genomic hybridization. Cancer Sci 96:100–110
8. van Grieken NC, Weiss MM, Meijer GA et al (2000) *Helicobacter pylori*-related and -non-related gastric cancers do not differ with respect to chromosomal aberrations. J Pathol 192:301–306
9. Weiss MM, Snijders AM, Kuipers EJ et al (2003) Determination of amplicon boundaries at 20q13.2 in tissue samples of human gastric adenocarcinomas by high-resolution microarray comparative genomic hybridization. J Pathol 200:320–326
10. Weiss MM, Kuipers EJ, Postma C et al (2004) Genomic alterations in primary gastric adenocarcinomas correlate with clinicopathological characteristics and survival. Cell Oncol 26:307–317
11. Wu MS, Shun CT, Wang HP et al (1997) Genetic alterations in gastric cancer: relation to histological subtypes, tumor stage, and *Helicobacter pylori* infection. Gastroenterology 112:1457–1465
12. Buffart TE, Carvalho B, Mons T et al (2007) DNA copy-number profiles of gastric cancer precursor lesions. BMC Genomics 8:345
13. Kim YH, Kim NG, Lim JG et al (2001) Chromosomal alterations in paired gastric adenomas and carcinomas. Am J Pathol 158:655–662
14. Kokkola A, Monni O, Puolakkainen P et al (1998) Presence of high-level DNA copy-number gains in gastric carcinoma and severely dysplastic adenomas but not in moderately dysplastic adenomas. Cancer Genet Cytogenet 107:32–36
15. van Dekken H, Alers JC, Riegman PH et al (2001) Molecular cytogenetic evaluation of gastric cardia adenocarcinoma and precursor lesions. Am J Pathol 158:1961–1967
16. Weiss MM, Kuipers EJ, Postma C et al (2003) Genome wide array comparative genomic hybridisation analysis of premalignant lesions of the stomach. Mol Pathol 56:293–298
17. Buffart T, Carvalho B, Hopmans E et al (2007) Gastric cancers in young and elderly patients show different genomic profiles. J Pathol 211:45–51
18. Weiss MM, Kuipers EJ, Postma C et al (2003) Genomic profiling of gastric cancer predicts lymph node status and survival. Oncogene 22:1872–1879
19. Carvalho B, Postma C, Mongera S et al (2008) Integration of DNA and expression microarray data unravels seven putative oncogenes on 20Q amplicon involved in colorectal adenoma to carcinoma progression. Cell Oncol 30:145–146
20. Hermsen M, Postma C, Baak J et al (2002) Colorectal adenoma to carcinoma progression follows multiple pathways of chromosomal instability. Gastroenterology 123:1109–1119
21. Aust DE, Muders M, Kohler A et al (2004) Prognostic relevance of 20q13 gains in sporadic colorectal cancers: a FISH analysis. Scand J Gastroenterol 39:766–772
22. Postma C, Terwischa S, Hermsen MA et al (2007) Gain of chromosome 20q is an indicator of poor prognosis in colorectal cancer. Cell Oncol 29:73–75
23. Schouten JP, McElgunn CJ, Waaijer R et al (2002) Relative quantification of 40 nucleic acid sequences by multiplex ligation-dependent probe amplification. Nucleic Acids Res 30:e57
24. Buffart TE, Coffa J, Hermsen MA et al (2005) DNA copy-number changes at 8q11–24 in metastasized colorectal cancer. Cell Oncol 27:57–65
25. Postma C, Hermsen MA, Coffa J et al (2005) Chromosomal instability in flat adenomas and carcinomas of the colon. J Pathol 205:514–521
26. Bonenkamp JJ, Hermans J, Sasako M et al (1999) Extended lymph-node dissection for gastric cancer. Dutch Gastric Cancer Group. N Engl J Med 340:908–914
27. Buffart TE, Tijssen M, Krugers T et al (2007) DNA quality assessment for array CGH by isothermal whole genome amplification. Cell Oncol 29:351–359

28. Snijders AM, Nowak N, Segraves R et al (2001) Assembly of microarrays for genome-wide measurement of DNA copy-number. Nat Genet 29:263–264
29. van de Wiel MA, Kim KI, Vosse SJ et al (2007) CGHcall: calling aberrations for array CGH tumor profiles. Bioinformatics 23:892–894
30. Coffa J, van de Wiel MA, Diosdado B et al (2008) MLPAnalyzer: data analysis tool for reliable automated normalization of MLPA fragment data. Cell Oncol 30:323–335
31. Laurén P (1965) The two histological main types of gastric carcinoma: diffuse and so-called intestinal-type carcinoma. An attemt at a histo-clinical classification. Acta Pathol Microbiol Scand 64:31–49
32. Pinkel D, Albertson DG (2005) Array comparative genomic hybridization and its applications in cancer. Nat Genet 37(Suppl): S11–S17
33. Carvalho B, Buffart TE, Reis RM et al (2006) Mixed gastric carcinomas show similar chromosomal aberrations in both their diffuse and glandular components. Cell Oncol 28:283–294
34. Pitti RM, Marsters SA, Lawrence DA et al (1998) Genomic amplification of a decoy receptor for Fas ligand in lung and colon cancer. Nature 396:699–703
35. Wu Y, Han B, Sheng H et al (2003) Clinical significance of detecting elevated serum DcR3/TR6/M68 in malignant tumor patients. Int J Cancer 105:724–732
36. Wu Y, Guo E, Yu J et al (2008) High DcR3 expression predicts stage pN2–3 in gastric cancer. Am J Clin Oncol 31:79–83
37. Bai C, Connolly B, Metzker ML et al (2000) Overexpression of M68/DcR3 in human gastrointestinal tract tumors independent of gene amplification and its location in a four-gene cluster. Proc Natl Acad Sci U S A 97:1230–1235
38. Simonsen A, Bremnes B, Ronning E et al (1998) Syntaxin-16, a putative Golgi t-SNARE. Eur J Cell Biol 75:223–231
39. Nonet GH, Stampfer MR, Chin K et al (2001) The ZNF217 gene amplified in breast cancers promotes immortalization of human mammary epithelial cells. Cancer Res 61:1250–1254
40. Yang SH, Seo MY, Jeong HJ et al (2005) Gene copy-number change events at chromosome 20 and their association with recurrence in gastric cancer patients. Clin Cancer Res 11:612–620

Virchows Arch (2009) 455:225–233
DOI 10.1007/s00428-009-0825-8

ORIGINAL ARTICLE

Neutrophil gelatinase-associated lipocalin (NGAL/Lcn2) is upregulated in gastric mucosa infected with *Helicobacter pylori*

Warner Alpízar-Alpízar · Ole Didrik Laerum · Martin Illemann · José A. Ramírez · Adriana Arias · Wendy Malespín-Bendaña · Vanessa Ramírez · Leif R. Lund · Niels Borregaard · Boye Schnack Nielsen

Received: 22 June 2009 / Revised: 13 August 2009 / Accepted: 14 August 2009 / Published online: 1 September 2009

Abstract *Helicobacter pylori* infection is one of the most significant risk factors for gastric cancer. The infection is established early in life and persists lifelong leading to a sustained chronic inflammation. Iron is essential for most living organisms. Bacteria use several mechanisms to acquire iron from their hosts, including the synthesis of the potent iron chelators known as siderophores. Hosts cells may express the siderophore-binding protein neutrophil gelatinase-associated lipocalin (NGAL/lipocalin-2 (Lcn2)) in response to infection, thus preventing bacterial iron uptake. We have characterized here the pattern of expression of NGAL/Lcn2 in gastric mucosa (45 non-neoplastic and 38 neoplastic tissue samples) and explored the connection between NGAL/Lcn2 expression and *H. pylori* infection. Immunohistochemical analysis showed high NGAL/Lcn2 expression in normal and gastritis-affected mucosa compared to low expression in intestinal metaplasia, dysplasia, and gastric cancer. In normal and gastritis-affected mucosa (n=36 tissue samples), NGAL/Lcn2 was more frequently seen in epithelial cells located at the neck and base of the glands in *H. pylori*-positive cases than in similar epithelial cells of noninfected cases (Fisher's exact test, p=0.04). In conclusion, the high expression of NGAL/Lcn2 in normal and gastritis-affected mucosa infected with *H. pylori* suggests that NGAL/Lcn2 is upregulated locally in response to this bacterial infection. It is discussed whether this may have a causal relation to the development of gastric cancer.

W. Alpízar-Alpízar · O. D. Laerum
The Gade Institute,
University of Bergen and Department of Pathology,
Haukeland University Hospital,
Bergen, Norway

W. Alpízar-Alpízar · W. Malespín-Bendaña · V. Ramírez
Cancer Research Program, Health Research Institute (INISA),
University of Costa Rica,
San José, Costa Rica

W. Alpízar-Alpízar · M. Illemann · B. S. Nielsen
The Finsen Laboratory,
Rigshospitalet,
Copenhagen, Denmark

J. A. Ramírez · A. Arias
Department of Pathology,
Dr. Rafael A. Calderón Guardia Hospital,
San José, Costa Rica

L. R. Lund
Department of Biology, Section for Cell
and Developmental Biology, University of Copenhagen,
Copenhagen, Denmark

N. Borregaard
The Granulocyte Research Laboratory,
Department of Haematology, University of Copenhagen,
Rigshospitalet,
Copenhagen, Denmark

W. Alpízar-Alpízar (✉)
The Gade Institute, Department of Pathology,
Haukeland University Hospital,
5021 Bergen, Norway
e-mail: awarnercr@yahoo.com
e-mail: Warner.Alpizar@student.uib.no

Present Address:
B. S. Nielsen
Exiqon A/S, Diagnostic Product Development,
Vedbæk, Denmark

Keywords NGAL/Lcn2 · *Helicobacter pylori* · Inflammation · Gastritis · Intestinal metaplasia · Gastric cancer

Abbreviations

IM	Intestinal metaplasia
mAb	Monoclonal antibody
pAbs	Polyclonal antibodies
TNP	Trinitrophenyl hapten
NGAL	Neutrophil gelatinase-associated lipocalin
Lcn2	Lipocalin-2

Introduction

Gastric cancer is the second most common cause of cancer deaths worldwide [1]. It is the final result of a multistep process initiated by environmental factors, including diet and *Helicobacter pylori* infection [2, 3]. *H. pylori* infection is one of the most important risk factors for this malignancy [4, 5]. The infection is usually established early in life and persists lifelong in the absence of treatment [6]. The infection leads to a sustained chronic inflammation characterized by infiltration of a number of inflammatory cells in the gastric mucosa and expression of inflammatory mediators by immune and epithelial cells [7]. It is the combination of bacterial factors, host immune response, and environmental insults that drives the stepwise transformation starting with mucosal atrophy through metaplasia and dysplasia to overt gastric cancer [8, 9].

Iron is an essential element for a number of metabolic processes in almost all living organisms. During infection, bacteria utilize several mechanisms to obtain iron from their hosts, including synthesis of so-called siderophores, which chelate Fe^{3+} with high affinity and facilitate its transport into the pathogen [10–12]. An important host defense mechanism, which interferes with bacterial uptake of iron has been unraveled by the discovery of neutrophil gelatinase-associated lipocalin (NGAL or lipocalin-2 (Lcn2)) [13, 14] or NGAL-homologous proteins (24p3 in mouse and NRL in rats) [15] as siderophore-binding proteins [16]. NGAL/Lcn2 binds some bacterial siderophores and prevents their uptake into bacteria [17]. NGAL/Lcn2 expression has been shown to be upregulated in response to inflammation in epithelial cells of several mucosal surfaces including the gastrointestinal tract and the lower respiratory tract [18–20]. Elevated expression of the NGAL-homologous proteins has also been found in animal models (mice and rats) in response to bacterial infections [21, 22]. The significance of this was demonstrated in a mouse model, where NGAL-deficient mice challenged with a clinical strain of *Escherichia coli* (H9049 strain) had a substantial increase in bacteremia and bacterial burden in some organs, including liver and spleen and a strikingly decreased survival compared to the wild-type mice [23], and also in response to pulmonary *Klebsiella pneumoniae* infection [22].

Iron is fundamental for the pathogenesis of *H. pylori.* The ability of *H. pylori* to acquire iron is considered important for colonization, persistence, and virulence of this microorganism in the gastric mucosa [24–27]. Expression of NGAL/Lcn2 in the stomach has been reported both at the protein and mRNA level [14, 28]. In a mouse model, immunoreactivity for the NGAL-homologous protein, 24p3, was observed in epithelial, endothelial, and infiltrating inflammatory cells in the stomach in response to various forms of gastrointestinal injury [29]. Recently, increased expression of NGAL/Lcn2 was reported in rhesus macaques challenged with *H. pylori* [30]. These observations suggest that NGAL/Lcn2 is expressed in gastric mucosa in response to inflammation/infection. Here, we study the expression of NGAL/Lcn2 in human gastric mucosa and show for the first time that NGAL/Lcn2 is upregulated in response to *H. pylori* infection and inflammation.

Material and methods

Tissue samples

Formalin-fixed and paraffin-embedded tissue samples were obtained from patients undergoing surgery for gastric cancer in two hospitals in Costa Rica (Max Peralta Hospital and Rafael Angel Calderón Guardia Hospital) and one in Bergen, Norway (Haukeland University Hospital). The samples encompassed non-neoplastic mucosa adjacent to the malignant tissue (n=45; 37 from Costa Rica and eight from Norway) and neoplastic lesions (n=38; 32 from Costa Rica and six from Norway). Three to four micrometer thick paraffin-embedded tissue sections were cut from the non-neoplastic material, stained with H&E, and evaluated by a pathologist (ODL). Among the 45 non-neoplastic sections, there were foci characterized as normal mucosa (with some degree of inflammation; n=6), gastritis (n=30), intestinal metaplasia (IM; n=17), and dysplasia (n=11). Information regarding the histopathological subtype of gastric cancer was collected for all 38 neoplastic lesions. The histopathological classification was according to Laurén's classification system (Norwegian cases) and Japanese classification system (Costa Rican cases). For the purposes of this study, Costa Rican cases were reclassified according to Laurén's classification system following established criteria given by the Japanese Gastric Cancer Association [31]. Of the 38 cases, 20 were classified as intestinal subtype and 18 as diffuse subtype, and they were all non-cardia cancers (from corpus and antrum regions of the stomach). The study was

approved by the ethics committees and institutional review boards of each institution (Costa Rica: VI 742-94-571, VI 742-99-340; Norway: REK 053228) and performed in accordance with the World Medical Association Declaration of Helsinki, 1996.

Antibodies

Affinity purified mouse monoclonal antibody (mAb) against human NGAL/Lcn2 (clone 211.1) has been described previously [32]. Rat mAb against human NGAL/Lcn2 was purchased from R&D systems (Minneapolis, USA). mAbs against cytokeratins (CKs, clones AE1/AE3), neutrophil elastase (clone NP57), and rabbit polyclonal antibodies (pAbs) against *H. pylori* (code no. B0471), fluorescein isothiocyanate (FITC)-conjugated goat anti-mouse IgG and nonimmune rabbit IgG were purchased from Dako (Glostrup, Denmark). Cy3-conjugated goat anti-rabbit was obtained from Jackson Immunoresearch (West Grove, PA, USA). Monoclonal antibody directed against trinitrophenyl hapten (TNP, IgG1) was previously described [33].

Immunoperoxidase staining

Three micrometer thick paraffin-embedded tissue sections were deparaffinized with xylene and hydrated in gradual series of ethanol–water dilutions. For NGAL immunohistochemistry with mouse and rat mAbs, sections were heat-treated in a T/T micromed microwave processor (Milestone, Sorisol, Italy) at 98°C for 30 min in target retrieval solution pH 6,0 (code no. S1699, Dako). For immunohistochemistry with antibodies against neutrophil elastase, CKs, *H. pylori*, and TNP, sections were pretreated with proteinase K (10 μg/mL) for 20–25 min at 37°C. Endogenous peroxidase activity was blocked by incubation in 1% hydrogen peroxide solution for 15 min and washed briefly in Tris Buffered Saline (TBS; 50 mM Tris, 150 mM NaCl, pH 7.6) containing 0.5% triton X-100. The primary antibodies were diluted in antibody diluent (Dako) and incubated for 2 h in Shandon racks (Thermo Shandon, Pittsburg, PA, USA) at the following dilutions: NGAL mouse mAb 1:200 (5.0 μg/mL), NGAL rat mAb 1:350 (1.4 μg/mL), Neutrophil Elastase 1:200, CKs 1:300, and anti-*H. pylori* 1:150. Subsequently, the primary antibodies were detected with EnVision reagent using either anti-mouse IgG or anti-rabbit IgG horseradish peroxidase-conjugated polymers (Dako) and polyclonal rabbit anti-rat immunoglobulins/HRP (code no. P0450, Dako). The reactions were visualized by incubating the sections with NovaRED (Vector Laboratories, Burlingame CA, USA) or DAB chromogen (Dako; for *H. pylori* pAbs) according to manufacturer's instructions and counterstained with Mayer´s haematoxylin.

Negative controls

The sections were pretreated in the same way as described above for the NGAL antibody. The mouse NGAL monoclonal antibody was substituted with anti-TNP mAb incubated at the same concentrations as that for NGAL.

Double immunofluorescence staining

The sections were processed as described above for the NGAL mouse mAb using heat-induced retrieval in target retrieval solution pH 6.0 (code no. S1699, Dako). The anti-NGAL mouse mAb (1:150, 6.7 μg/mL) was diluted in antibody diluent (Dako) together with anti-*H. Pylori* pAbs (1:150) and incubated in the tissue sections for 2 h at room temperature. The antibodies were subsequently detected with FITC-conjugated goat-anti-mouse IgG, 1:200, and Cy3-conjugated goat anti-rabbit IgG, 1:200, respectively. After brief rinses with TBS, the sections were mounted with ProLong Gold antifade (Molecular Probes, Eugene, Oregon).

Confocal microscopy

The double stained sections were analyzed using a confocal laser-scanning microscope, LSM 510 META (Carl Zeiss, Jena, Germany), equipped with a 488 nm argon laser and a 543 nm HeNe1 laser, as previously described [34].

Scoring for the immunoperoxidase stainings

The tissue sections stained with NGAL mouse mAb from both non-neoplastic gastric mucosa adjacent to cancer tissue and from gastric cancer lesions were evaluated by two independent investigators (WAA and ODL). Neutrophils present in the microvasculature and within the tissue served as internal positive control for NGAL/Lcn2 expression. NGAL/Lcn2 immunoreactivity was scored, according to the estimated percentage of crypts showing NGAL/Lcn2-positive epithelial cells, in the following four types of non-neoplastic gastric mucosa: normal mucosa, gastritis, IM, and dysplasia. The scoring was as follows: 0, less than 10% positive crypts; 1+, between 10% and 30% positive crypts; 2+, between 30% and 60% positive crypts; and 3+, more than 60% positive crypts. In gastric cancer lesions, NGAL/Lcn2 immunoreactivity was scored based on the estimated percentage of positive cancer cells seen in the whole section. Thus, the percentages of positive cancer cells were grouped into the following categories: 0, less than 5% NGAL/Lcn2-positive cancer cells detected; 1, between 5% and 30% positively stained cells; 2, between 30% and 60% positive tumor cells; and 3, when more than 60% of cancer cells were positive.

H. pylori positivity was scored based on the density of bacteria and the number of crypts containing bacteria into the following categories: −, no evidence of *H. pylori* on the section; +, less than three crypts with small clusters of bacteria; ++, either less than three crypts with dense clusters of bacteria or more than three crypts with small clusters; and +++, three or more crypts with dense clusters of bacteria.

Statistical analysis

χ^2 analysis was performed to evaluate the differences regarding the frequency of cases having NGAL/Lcn2-positive cancer cells in intestinal versus diffuse subtypes of gastric cancer. χ^2 analysis and Fisher's exact test were used to assess the correlation between NGAL/Lcn2 expression in gastric epithelial cells and *H. pylori* infection in normal-like and gastritis-affected mucosa. $p \leq 0.05$ was considered statistically significant in all cases.

Results

NGAL/Lcn2 expression in non-neoplastic and neoplastic gastric mucosa

Immunoperoxidase staining for NGAL/Lcn2 in non-neoplastic and neoplastic tissue sections demonstrated NGAL/Lcn2 staining in all the specimens studied. We separately characterized the pattern of expression of NGAL/Lcn2 for each of the different states of the gastric mucosa: normal mucosa, gastritis, IM, dysplasia, and cancer. In general, the NGAL/Lcn2-positive cells observed in the non-neoplastic and neoplastic tissue samples included neutrophils, epithelial cells, and cancer cells. The NGAL/Lcn2 immunoreactivity of the normal mucosa (with some degree of inflammation) and gastritis-affected mucosa was intense (high frequency of sections scored as 3+), while that of IM, dysplasia, and cancer was low (high frequency of the sections scored as 0–1+; Table 1). This suggests that the expression of NGAL/Lcn2 is upregulated locally in the early steps of the gastric carcinogenesis that are characterized by chronic inflammation of the gastric mucosa.

The pattern of expression of NGAL/Lcn2 varied substantially according to the level of affection of the gastric mucosa. In normal and gastritis affected mucosa, NGAL/Lcn2 immunoreactivity was mainly seen in epithelial cells (Fig. 1a–d). NGAL/Lcn2 was, however, differentially expressed depending on the location of the epithelial cells in the crypts, with the most intense signal being observed in epithelial cells located at the neck and base of the crypts and weak or negative immunoreactivity at the surface epithelial cells (Fig. 1d). The expression of NGAL/Lcn2 was absent at foci with IM, where scattered NGAL/Lcn2-positive neutrophils were seen in the lamina propria (Fig. 1c–e). In dysplastic mucosa, NGAL/Lcn2 immunoreactivity was seen in epithelial cells of the glands located deeper into the gastric mucosa (Fig. 1f). In gastric cancer lesions, NGAL/Lcn2 staining was seen in 53% (20 out of 38) of the cases in cancer cells widespread within the malignant growth, with similar frequency in intestinal (Fig. 1g) and diffuse (Fig. 1h) histological subtypes (Table 1; $p=0.84$; $\chi^2=0.04$). NGAL/Lcn2 immunoreactivity in neoplasia was heterogeneous, being intense in some areas of the tumor growth and weak and/or negative in other areas (not shown).

Table 1 NGAL/Lcn2 immunoreactivity in non-neoplastic and neoplastic tissue sections according to the different states of the gastric mucosa and histological subtypes of gastric cancer

Lesion	*n*	NGAL/Lcn2 scoring[a]			
		0	1+	2+	3+
Normal-appearing[b]	6	2	0	0	4
Gastritis[b]	30	3	1	1	25
IM[c]	17	15	2	0	0
Dysplasia	11	4	5	1	1
Cancer[d]	38	18	11	5	4
Intestinal	20	10	5	2	3
Diffuse	18	8	6	3	1

NGAL neutrophil gelatinase-associated lipocalin, *Lcn2* lipocalin-2, *IM* intestinal metaplasia

[a] Scoring method is described in Material and methods section

[b] Scoring according to *Helicobacter pylori* status is shown in Table 2

[c] χ^2 analysis for normal and gastritis vs intestinal metaplasia and dysplasia, $p<0.0001$

[d] χ^2 analysis for intestinal versus diffuse, $p=0.84$

The specificity of NGAL/Lcn2 immunoreactivity was verified by analysis of a series of positive and negative controls. Similar NGAL/Lcn2 staining was obtained with mouse and rat mAbs against NGAL/Lcn2 in both non-neoplastic (Fig. 1i, j) and neoplastic tissue (not shown) in all of 15 cases tested. As negative control, we substituted the NGAL mouse mAb with a mAb against TNP. No specific staining was obtained with this antibody when incubated at similar immunoglobulin concentration as the respective anti-NGAL antibody preparation (Fig. 1k, l).

H. pylori infection associates with the induction of NGAL/Lcn2 in gastric mucosa

We observed, as described above, a clear and consistent NGAL/Lcn2 immunoreactivity in epithelial cells of normal mucosa and from gastritis (Table 1, Fig. 2b). Since it is known that *H. pylori* infection induces a chronic inflammatory

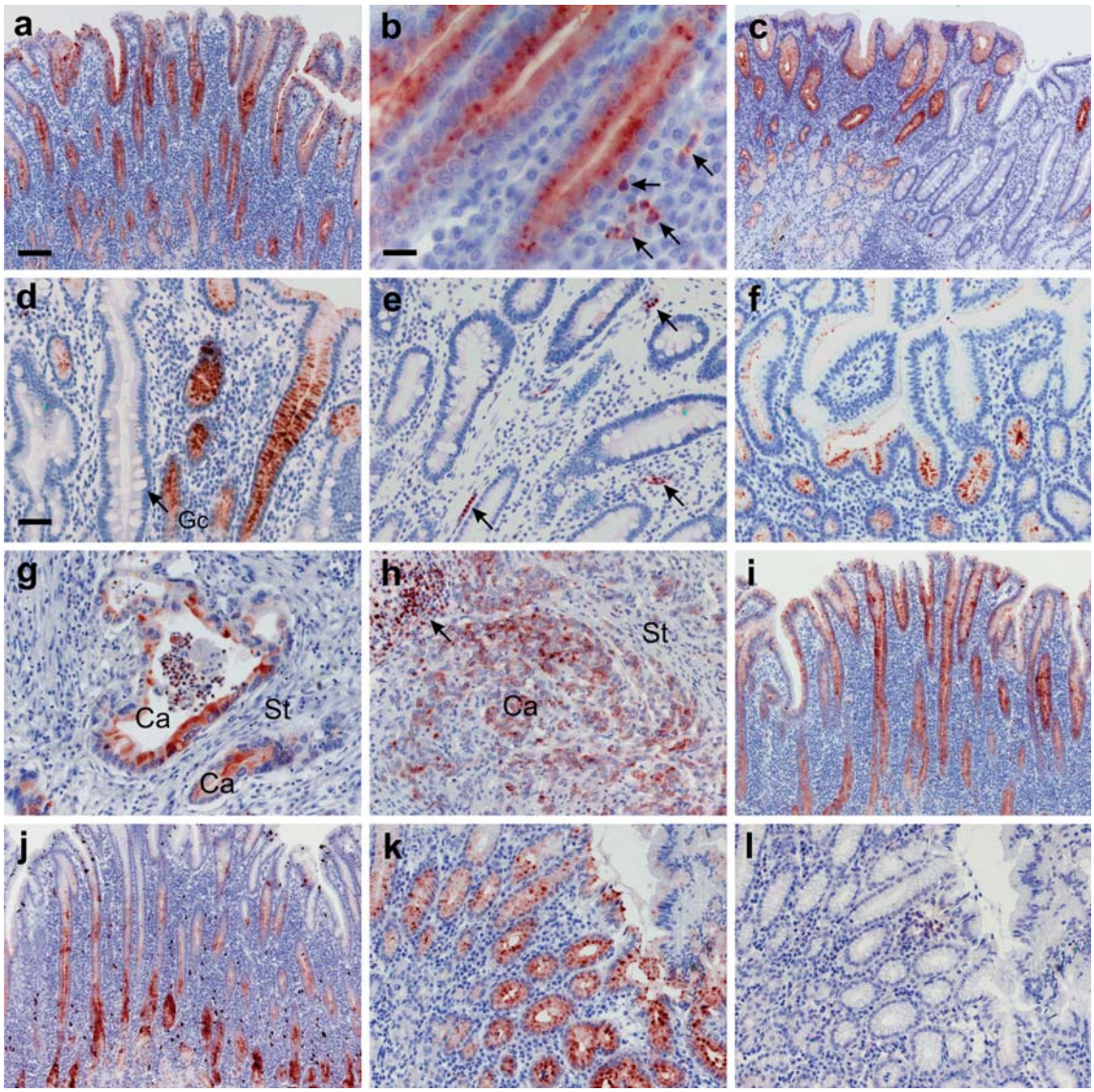

Fig. 1 Immunoperoxidase staining for NGAL/Lcn2 in non-neoplastic and neoplastic gastric tissue. Paraffin sections from non-neoplastic (**a**–**f**, **i**–**l**) and neoplastic (**g**–**h**) gastric mucosa were incubated with mouse mAb against NGAL/Lcn2 (**a**–**i**, **k**), rat mAb against NGAL/Lcn2 (**j**), and a mAb against TNP (**l**). Panels **i**–**j** and **k**–**l** represent adjacent sections. In gastritis-affected mucosa (**a**–**d**), NGAL/lcn2 is expressed by epithelial cells of gastric mucosa and scattered neutrophils in the lamina propia (**b**; neutrophils (*arrows*)). NGAL/Lcn2 is seen in epithelial cells located at the neck and base of the crypts more evidently than in surface epithelial cells (**d**). NGAL/Lcn2 expression is absent in intestinal metaplasia (**c**–**e**), next to gastritis foci showing intense immunoreactivity (**c** and **d**; goblet cells (*Gc*)), where only scattered NGAL/Lcn2-positive neutrophils are observed in the lamina propia (**e**; *arrows*). In dysplasia (**f**), NGAL/Lcn2 is observed in epithelial cells of glands located deep into the mucosa. In the gastric cancer lesions, NGAL/Lcn2 immunoreactivity is observed in cancer cells that are widespread within the tumor growth in both intestinal (**g**; stroma (*St*), cancer (*Ca*)) and diffuse subtype (**h**). A similar staining pattern is seen with mouse mAb (**i**) and rat mAb (**j**). As negative control, the mAb against NGAL/Lcn2 (**k**) was substituted with a mAb against TNP (**i**), and no specific staining is seen. Sections were counterstained with hematoxylin. *Scale bars*: ~100 μm (**a**, **c**, **i**, **j**), ~50 μm (**d**–**h**, **k**, **l**), ~25 μm (**b**)

response in gastric mucosa [35] and that NGAL/Lcn2 expression is upregulated in response to bacterial infection and inflammation [36], we explored the possibility that the expression of NGAL/Lcn2 in epithelial cells of the gastric mucosa is associated with *H. pylori* infection. Tissue samples from non-neoplastic mucosa, with foci of normal and gastritis affected mucosa, were selected and stained for *H. pylori*. Immunoperoxidase staining showed *H. pylori* in 72% (26 out of 36) of the cases. *H. pylori* clusters were observed at the luminal edge of the crypts, in deeper areas of the crypts, and inside some of the mucosal glands, with the highest density of bacteria in gastritis-affected mucosa (Fig. 2c). We next scored the NGAL/Lcn2 immunoreactivity in epithelial cells of the normal and gastritis-affected mucosa from adjacent

tissue sections, as described in Material and methods, and noticed that the majority of the *H. pylori*-positive cases had an elevated expression of NGAL/Lcn2 (scores 2–3+) as compared to *H. pylori*-negative cases (Table 2). It has been shown that NGAL/Lcn2 is expressed at a basal low level in a number of human epithelial tissues such as the respiratory tract, the gastrointestinal and urinary tracts that are exposed to the external environment and thereby prone to infections [14, 18, 28], indicating that a low expression level is to be expected in mucosal surfaces. We, therefore, dichotomized the expression of NGAL/Lcn2 into NGAL/Lcn2 low immunoreactivity (scores 0, 1+) and NGAL/Lcn2 high immunoreactivity (scores 2+, 3+; Table 2) for a statistical analysis. Using this classification, we found a significant association between the expression of NGAL/Lcn2 in epithelial cells and *H. pylori* infection ($p=0.02$; $\chi^2=5.43$; df=1; Fisher exact test $p=0.04$). Double immunofluorescence analysis for NGAL/Lcn2 combined with *H. pylori* in non-neoplastic normal and gastritis-affected mucosa from 24 of the gastric cancer patients (18 *H. pylori*-positive and 6 *H. pylori*-negative), indeed showed intense and consistent NGAL/Lcn2 immunoreactivity in crypts where epithelial cells were in direct contact with *H. pylori* bacteria in the *H. pylori*-positive cases (Fig. 2d, f). In contrast, in *H. pylori*-negative cases, the NGAL/Lcn2 signal was weak in epithelial cells at similar locations (not shown).

Discussion

We have investigated the expression of NGAL/Lcn2 in each of the pre-neoplastic stages leading to gastric cancer, focusing on the potential induction of this protein in response to *H. pylori* infection. By performing immunohistochemistry and immunofluorescence analysis, we show that NGAL/Lcn2 is upregulated in epithelial cells of normal and gastritis-affected mucosa infected with *H. pylori.* These are typical sites of robust inflammatory activity [7]. Interestingly, we also observed that the expression of NGAL/Lcn2 is absent at foci with IM adjacent to areas of gastritis. At IM, *H. pylori* infection is spontaneously eradicated and inflammation is partially resolved [2, 37]. Our results, therefore, support the role of NGAL/Lcn2 as a component of the innate immunity and suggest that *H. pylori* infection is causatively associated with upregulation of this molecule in gastric mucosa.

In the present study, we found a significant higher NGAL/Lcn2 immunoreactivity in gastric epithelial cells of *H. pylori*-infected individuals than in those non-infected, which was substantiated by observing *H. pylori* clusters in close proximity to NGAL/Lcn2-positive epithelial cells in our double immunofluorescence analysis. NGAL/Lcn2 has been shown to be constitutively expressed in epithelial cells of a number of tissues that are often challenged by microorganisms such as the respiratory tract and the urinary and gastrointestinal tracts [14, 28]. NGAL/Lcn2 mRNA and protein levels are greatly increased in response to pneumococcal and mycobacterial infections in the respiratory tract and urinary tract infections, in both animal models and humans [22, 36, 38, 39]. Taking together these observations and our results, we suggest that the constitutive basal expression of NGAL/Lcn2 that is observed in the gastric epithelium ([14, 28] and this paper) is substantially upregulated upon *H. pylori* infection. A recent study in rhesus macaques, showing that NGAL/Lcn2 is induced in gastric mucosa of monkeys challenged with certain *H. pylori* strains [30], is in agreement with our observations and suggests that the upregulation of NGAL/Lcn2 by *H. pylori* may be related to specific bacterial virulence factors.

A particularly interesting finding of this study was the abrupt down-regulation of NGAL/Lcn2 expression observed at IM foci located next to normal and gastritis *H. pylori*-infected mucosa showing intense NGAL/Lcn2 immunoreactivity. A number of histological and physiological changes occur in the gastric epithelium during the pre-neoplastic stages leading to gastric cancer, including a focal loss of glands and specialized cells (atrophic gastritis), followed by the transformation of the stomach mucosa into an intestinal-like epithelium (IM) [8, 40]. These changes are not well tolerated by *H. pylori* and results in its spontaneous disappearance from the transformed epithelium [37, 41]. Accordingly, we did not observe *H. pylori* bacteria at intestinal metaplastic glands. It is, therefore, tempting to suggest that the abolition of NGAL/Lcn2 expression on IM is a consequence of the natural eradication of *H. pylori* occurring at these foci. Thus, our findings in IM argue in favor of the potential link between *H. pylori* infection and the upregulation of NGAL/Lcn2 in the gastric epithelium.

Iron is an essential element for the growth and virulence of *H. pylori*, and the general consensus is that *H. pylori* obtains this element from human molecules, mainly lactoferrin and heme [27, 42–44]. Despite one study suggesting the production of siderophores by *H. pylori* [45], most investigations have been unable to reproduce that finding or to demonstrate the use of exogenous siderophores as a source of iron by this bacterium [44, 46]. Nevertheless, the induction of NGAL/Lcn2 is not restricted to microorganisms that produce or uptake siderophores.

The induction of NGAL/Lcn2 has been consistently linked to inflammation. High NGAL/Lcn2 mRNA and protein levels have been found in epithelial cells in inflammatory colorectal diseases such as inflammatory bowel disease, appendicitis [18], as well as in other processes associated with intense inflammatory activity [20, 47]. As part of the inflammatory response against *H. pylori* infection, a complex set of inflammatory mediators are released by

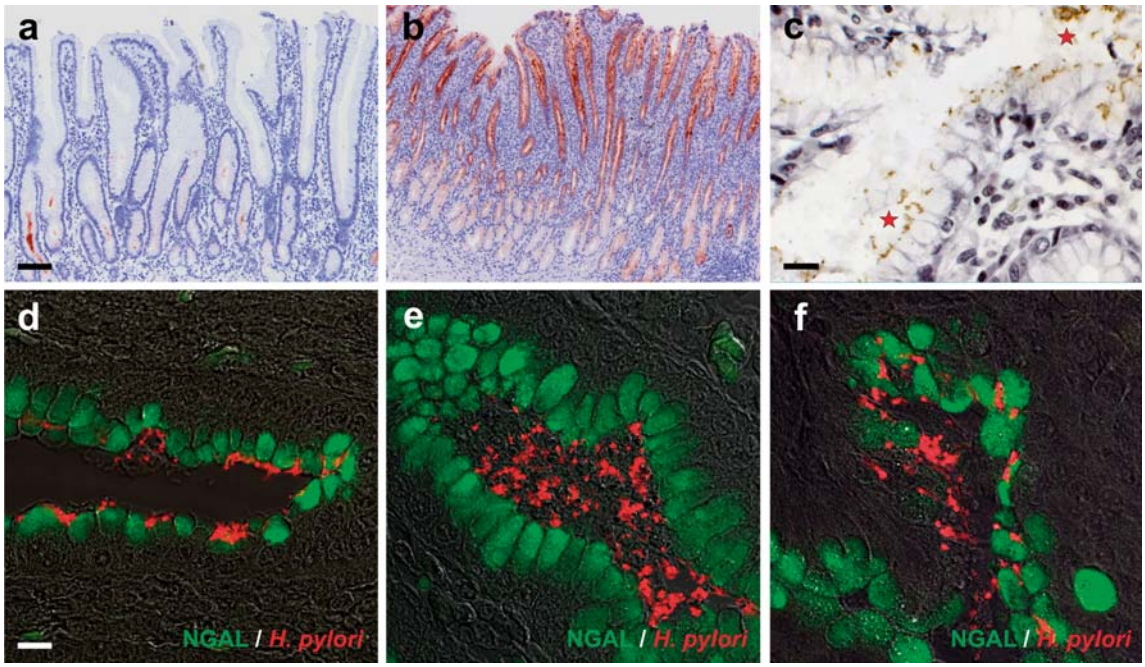

Fig. 2 Immunohistochemical analyses of NGAL/Lcn2 and *H. pylori* in non-neoplastic gastric mucosa. Sections from samples with gastric mucosa adjacent to the neoplastic lesion were processed for immunoperoxidase staining for NGAL/Lcn2 (**a**, **b**), *H. pylori* (**c**), or for immunofluorescence analysis (**d–f**) using mAb against NGAL/Lcn2, pAbs against *H. pylori*, and NGAL mAb together with *H. pylori* pAbs, respectively. NGAL/Lcn2 immunoreactivity is weak, if observed, in *H. pylori*-negative mucosa (**a**). In *H. pylori*-infected mucosa, NGAL/Lcn2 is strongly expressed on epithelial cells (**b**). *H. pylori* clusters (*red stars*) can be observed at the luminal side in some of the crypts along the gastric epithelium with the highest density in gastritis-affected mucosa (**c**). In the double immunofluorescence analysis, mAb against NGAL/Lcn2 together with pAbs against *H. pylori* (double staining in **d–f**) were detected with FITC-conjugated goat antimouse (green fluorescence) and Cy3-conjugated goat antirabbit (red fluorescence), respectively. Intense NGAL/Lcn2 immunoreactivity is seen in epithelial cells that are in direct contact with *H. pylori* bacteria (**d-f**). Nomarsky DIC imaging technique was used in **d–f**. *Scale bars*: ~100 μm (**a**, **b**), ~12 μm (**c**), ~20 μm (**d–f**)

epithelial and infiltrating inflammatory cells into the gastric mucosa, including IL-1β and NF-κβ [48]. Certain *H. pylori* virulence factors have been shown to potentiate this inflammatory response [49]. It has been demonstrated that IL-1β and NF-κβ (stabilized by its cofactor IκB-ζ) play a central role in the induction of NGAL/Lcn2 in epithelial cells [19, 50]. Thus, it is likely that the upregulation of NGAL/Lcn2 by *H. pylori* in gastric epithelial cells is driven by mediators of inflammation being released into the gastric epithelium in response to the bacterial infection.

Table 2 NGAL/Lcn2 immunoreactivity in epithelial cells in relation to the *Helicobacter pylori* status in non-neoplastic tissue sections diagnosed as normal-appearing and gastritis-affected mucosa

	n	NGAL/Lcn2 scoring			
		0	1+	2+	3+
H. pylori negative[a]	10	3	1	1	5
H. pylori positive[a]	26	2	0	0	24
Total	36	5	1	1	29

NGAL neutrophil gelatinase-associated lipocalin, *Lcn2* lipocalin-2

[a] Fisher's exact test for *H. pylori*-positive versus *H. pylori*-negative, $p=0.04$

It was recently demonstrated in animal models (rhesus macaques and mice) that pathogenic strains of *Salmonella enterica* induce NGAL/Lcn2 in colonic mucosa, which confers a competitive advantage to the bacterium for colonizing and growing in the inflamed intestine [51]. In agreement to this view, Hornsby et al. [30] hypothesized that the induction of a set of antimicrobial molecules, including NGAL/Lcn2, in rhesus monkeys infected with *H. pylori* may indeed serve to increase the competitive advantage of this bacterium. We, therefore, do not exclude the possibility that high expression of NGAL/Lcn2 in gastric mucosa may facilitate *H. pylori* infection.

Other functions have been suggested for NGAL/Lcn2 in addition to its antimicrobial role [52]. NGAL/Lcn2 has been shown to be expressed on neoplastic cells in several types of adenocarcinomas including breast, pancreas, colon, and ovarian cancer [28, 53–56], and elevated protein levels have been correlated with poor prognosis in some of these malignancies [56, 57]. In the current study, we observed

NGAL/Lcn2 immunoreactivity in gastric cancer cells in one half of the studied cases, with similar frequency in both intestinal and diffuse gastric cancer histological subtypes. A recent study found that NGAL/Lcn2 levels in tissue and urine from breast cancer patients are associated with invasion and metastasis and demonstrated, in cell lines transfected with NGAL/Lcn2, that this molecule promotes breast cancer progression by inducing epithelial to mesenchymal transition [58]. The molecular mechanisms explaining the role of NGAL/Lcn2 in carcinogenesis remain entirely unknown, but it has been speculated that expression of NGAL/Lcn2 provides the carcinoma cells the ability to acquire iron and thus, supporting their growth [52, 59]. Therefore, the expression of NGAL/Lcn2 in gastric cancer in connection to progression and prognosis of the disease should be further investigated.

Acknowledgements We thank Ms. Öznur Turan and Ms. Agnieszka Ingvorsen for their excellent technical assistance and Mr. John Post for his photographic assistance. This study was supported by the Danish Cancer Society, the Lundbeck Foundation, Haukeland University Hospital (Helse-Vest), and Vicerrectoría de Investigación of the University of Costa Rica.

Conflict of interest statement We declare that we have no conflict of interest.

References

1. Parkin DM, Bray FI, Devesa SS (2001) Cancer burden in the year 2000. The global picture. Eur J Cancer 37(Suppl 8):S4–S66
2. Stemmermann GN, Fenoglio-Preiser C (2002) Gastric carcinoma distal to the cardia: a review of the epidemiological pathology of the precusors to a preventable cancer. Pathology 34:494–503
3. Correa P (1992) Human gastric carcinogenesis: a multistep and multifactorial process—First American Cancer Society Award Lecture on cancer epidemiology and prevention. Cancer Res 52:6735–6740
4. Uemura N, Okamoto S, Yamamoto S, Matsumura N, Yamaguchi S et al (2001) Helicobacter pylori infection and the development of gastric cancer. N Engl J Med 345:784–789
5. Huang JQ, Zheng GF, Sumanac K, Irvine EJ, Hunt RH (2003) Meta-analysis of the relationship between cagA seropositivity and gastric cancer. Gastroenterology 125:1636–1644
6. Wilson KT, Crabtree JE (2007) Immunology of Helicobacter pylori: insights into the failure of the immune response and perspectives on vaccine studies. Gastroenterology 133:288–308
7. Robinson K, Argent RH, Atherton JC (2007) The inflammatory and immune response to Helicobacter pylori infection. Best Pract Res Clin Gastroenterol 21:237–259
8. Correa P, Houghton J (2007) Carcinogenesis of Helicobacter pylori. Gastroenterology 133:659–672
9. Fox JG, Wang TC (2007) Inflammation, atrophy, and gastric cancer. J Clin Invest 117:60–69
10. Neilands JB (1995) Siderophores: structure and function of microbial iron transport compounds. J Biol Chem 270:26723–26726
11. Braun V, Braun M (2002) Active transport of iron and siderophore antibiotics. Curr Opin Microbiol 5:194–201
12. Krewulak KD, Vogel HJ (2008) Structural biology of bacterial iron uptake. Biochim Biophys Acta 1778:1781–1804
13. Kjeldsen L, Johnsen AH, Sengelov H, Borregaard N (1993) Isolation and primary structure of NGAL, a novel protein associated with human neutrophil gelatinase. J Biol Chem 268:10425–10432
14. Cowland JB, Borregaard N (1997) Molecular characterization and pattern of tissue expression of the gene for neutrophil gelatinase-associated lipocalin from humans. Genomics 45:17–23
15. Kjeldsen L, Cowland JB, Borregaard N (2000) Human neutrophil gelatinase-associated lipocalin and homologous proteins in rat and mouse. Biochim Biophys Acta 1482:272–283
16. Goetz DH, Holmes MA, Borregaard N, Bluhm ME, Raymond KN et al (2002) The neutrophil lipocalin NGAL is a bacteriostatic agent that interferes with siderophore-mediated iron acquisition. Mol Cell 10:1033–1043
17. Holmes MA, Paulsene W, Jide X, Ratledge C, Strong RK (2005) Siderocalin (Lcn 2) also binds carboxymycobactins, potentially defending against mycobacterial infections through iron sequestration. Structure 13:29–41
18. Nielsen BS, Borregaard N, Bundgaard JR, Timshel S, Sehested M et al (1996) Induction of NGAL synthesis in epithelial cells of human colorectal neoplasia and inflammatory bowel diseases. Gut 38:414–420
19. Cowland JB, Sorensen OE, Sehested M, Borregaard N (2003) Neutrophil gelatinase-associated lipocalin is up-regulated in human epithelial cells by IL-1 beta, but not by TNF-alpha. J Immunol 171:6630–6639
20. Sorensen OE, Cowland JB, Theilgaard-Monch K, Liu L, Ganz T et al (2003) Wound healing and expression of antimicrobial peptides/polypeptides in human keratinocytes, a consequence of common growth factors. J Immunol 170:5583–5589
21. Berger T, Togawa A, Duncan GS, Elia AJ, You-Ten A et al (2006) Lipocalin 2-deficient mice exhibit increased sensitivity to Escherichia coli infection but not to ischemia-reperfusion injury. Proc Natl Acad Sci U S A 103:1834–1839
22. Chan YR, Liu JS, Pociask DA, Zheng M, Mietzner TA et al (2009) Lipocalin 2 is required for pulmonary host defense against Klebsiella infection. J Immunol 182:4947–4956
23. Flo TH, Smith KD, Sato S, Rodriguez DJ, Holmes MA et al (2004) Lipocalin 2 mediates an innate immune response to bacterial infection by sequestrating iron. Nature 432:917–921
24. van Amsterdam K, van Vliet AH, Kusters JG, van der Ende A (2006) Of microbe and man: determinants of Helicobacter pylori-related diseases. FEMS Microbiol Rev 30:131–156
25. Velayudhan J, Hughes NJ, McColm AA, Bagshaw J, Clayton CL et al (2000) Iron acquisition and virulence in Helicobacter pylori: a major role for FeoB, a high-affinity ferrous iron transporter. Mol Microbiol 37:274–286
26. Waidner B, Greiner S, Odenbreit S, Kavermann H, Velayudhan J et al (2002) Essential role of ferritin Pfr in Helicobacter pylori iron metabolism and gastric colonization. Infect Immun 70:3923–3929
27. Perez-Perez GI, Israel DA (2000) Role of iron in Helicobacter pylori: its influence in outer membrane protein expression and in pathogenicity. Eur J Gastroenterol Hepatol 12:1263–1265
28. Friedl A, Stoesz SP, Buckley P, Gould MN (1999) Neutrophil gelatinase-associated lipocalin in normal and neoplastic human tissues. Cell type-specific pattern of expression. Histochem J 31:433–441
29. Playford RJ, Belo A, Poulsom R, Fitzgerald AJ, Harris K et al (2006) Effects of mouse and human lipocalin homologues 24p3/lcn2 and neutrophil gelatinase-associated lipocalin on gastrointestinal mucosal integrity and repair. Gastroenterology 131:809–817
30. Hornsby MJ, Huff JL, Kays RJ, Canfield DR, Bevins CL et al (2008) Helicobacter pylori induces an antimicrobial response in

rhesus macaques in a cag pathogenicity island-dependent manner. Gastroenterology 134:1049–1057
31. Japanese Gastric Cancer A (1998) Japanese classification of gastric carcinoma - 2nd english edition. Gastric Cancer 1:10–24
32. Kjeldsen L, Koch C, Arnljots K, Borregaard N (1996) Characterization of two ELISAs for NGAL, a newly described lipocalin in human neutrophils. J Immunol Methods 198:155–164
33. Boulianne GL, Hozumi N, Shulman MJ (1984) Production of functional chimaeric mouse/human antibody. Nature 312:643–646
34. Nielsen BS, Rank F, Illemann M, Lund LR, Dano K (2007) Stromal cells associated with early invasive foci in human mammary ductal carcinoma in situ coexpress urokinase and urokinase receptor. Int J Cancer 120:2086–2095
35. Atherton JC (2006) The pathogenesis of Helicobacter pylori-induced gastro-duodenal diseases. Annu Rev Pathol 1:63–96
36. Xu S, Venge P (2000) Lipocalins as biochemical markers of disease. Biochim Biophys Acta 1482:298–307
37. Valle J, Kekki M, Sipponen P, Ihamaki T, Siurala M (1996) Long-term course and consequences of Helicobacter pylori gastritis. Results of a 32-year follow-up study. Scand J Gastroenterol 31: 546–550
38. Nelson AL, Barasch JM, Bunte RM, Weiser JN (2005) Bacterial colonization of nasal mucosa induces expression of siderocalin, an iron-sequestering component of innate immunity. Cell Microbiol 7:1404–1417
39. Saiga H, Nishimura J, Kuwata H, Okuyama M, Matsumoto S et al (2008) Lipocalin 2-dependent inhibition of mycobacterial growth in alveolar epithelium. J Immunol 181:8521–8527
40. Gutierrez-Gonzalez L, Wright NA (2008) Biology of intestinal metaplasia in 2008: more than a simple phenotypic alteration. Dig Liver Dis 40:510–522
41. Kokkola A, Kosunen TU, Puolakkainen P, Sipponen P, Harkonen M et al (2003) Spontaneous disappearance of Helicobacter pylori antibodies in patients with advanced atrophic corpus gastritis. APMIS 111:619–624
42. Dhaenens L, Szczebara F, Husson MO (1997) Identification, characterization, and immunogenicity of the lactoferrin-binding protein from Helicobacter pylori. Infect Immun 65:514–518
43. Worst DJ, Otto BR, de Graaff J (1995) Iron-repressible outer membrane proteins of Helicobacter pylori involved in heme uptake. Infect Immun 63:4161–4165
44. Husson MO, Legrand D, Spik G, Leclerc H (1993) Iron acquisition by Helicobacter pylori: importance of human lactoferrin. Infect Immun 61:2694–2697
45. Illingworth DS, Walter KS, Griffiths PL, Barclay R (1993) Siderophore production and iron-regulated envelope proteins of Helicobacter pylori. Zentralbl Bakteriol 280:113–119
46. Dhaenens L, Szczebara F, Van Nieuwenhuyse S, Husson MO (1999) Comparison of iron uptake in different Helicobacter species. Res Microbiol 150:475–481
47. Sorensen OE, Thapa DR, Roupe KM, Valore EV, Sjobring U et al (2006) Injury-induced innate immune response in human skin mediated by transactivation of the epidermal growth factor receptor. J Clin Invest 116:1878–1885
48. Algood HM, Cover TL (2006) Helicobacter pylori persistence: an overview of interactions between H. pylori and host immune defenses. Clin Microbiol Rev 19:597–613
49. Brandt S, Kwok T, Hartig R, Konig W, Backert S (2005) NF-kappaB activation and potentiation of proinflammatory responses by the Helicobacter pylori CagA protein. Proc Natl Acad Sci U S A 102:9300–9305
50. Cowland JB, Muta T, Borregaard N (2006) IL-1beta-specific up-regulation of neutrophil gelatinase-associated lipocalin is controlled by IkappaB-zeta. J Immunol 176:5559–5566
51. Raffatellu M, George MD, Akiyama Y, Hornsby MJ, Nuccio SP et al (2009) Lipocalin-2 resistance confers an advantage to *Salmonella enterica* serotype Typhimurium for growth and survival in the inflamed intestine. Cell Host Microbe 5:476–486
52. Clifton MC, Corrent C, Strong RK (2009) Siderocalins: siderophore-binding proteins of the innate immune system. Biometals 22:557–564
53. Stoesz SP, Friedl A, Haag JD, Lindstrom MJ, Clark GM et al (1998) Heterogeneous expression of the lipocalin NGAL in primary breast cancers. Int J Cancer 79:565–572
54. Furutani M, Arii S, Mizumoto M, Kato M, Imamura M (1998) Identification of a neutrophil gelatinase-associated lipocalin mRNA in human pancreatic cancers using a modified signal sequence trap method. Cancer Lett 122:209–214
55. Lim R, Ahmed N, Borregaard N, Riley C, Wafai R et al (2007) Neutrophil gelatinase-associated lipocalin (NGAL) an early-screening biomarker for ovarian cancer: NGAL is associated with epidermal growth factor-induced epithelio-mesenchymal transition. Int J Cancer 120:2426–2434
56. Bauer M, Eickhoff JC, Gould MN, Mundhenke C, Maass N et al (2008) Neutrophil gelatinase-associated lipocalin (NGAL) is a predictor of poor prognosis in human primary breast cancer. Breast Cancer Res Treat 108:389–397
57. Devarajan P (2007) Neutrophil gelatinase-associated lipocalin: new paths for an old shuttle. Cancer Ther 5:463–470
58. Yang J, Bielenberg DR, Rodig SJ, Doiron R, Clifton MC et al (2009) Lipocalin 2 promotes breast cancer progression. Proc Natl Acad Sci U S A 106:3913–3918
59. Devireddy LR, Gazin C, Zhu X, Green MR (2005) A cell-surface receptor for lipocalin 24p3 selectively mediates apoptosis and iron uptake. Cell 123:1293–1305

Virchows Arch (2009) 455:235–243
DOI 10.1007/s00428-009-0818-7

ORIGINAL ARTICLE

Immunohistochemical expression of ubiquitin and telomerase in cervical cancer

Toro de Méndez Morelva · Llombart Bosch Antonio

Received: 23 February 2009 / Revised: 7 July 2009 / Accepted: 27 July 2009 / Published online: 14 August 2009

Abstract Ubiquitin and telomerase immunohistochemical expression patterns in cervical cancer were compared with normal cervical tissue samples. Eighty-one cervical cancer cases and 22 normal exo–endocervical tissue were examined with polyclonal antibody for ubiquitin and 44G12 clone for telomerase using tissue microarrays. The results were interpreted using a semiquantitative scale The average age of patients was 50.67 years. The most frequent histological types were moderately differentiated epidermoid carcinoma (43.5%), according to the degree of differentiation, and endocervical adenocarcinoma (42.1%). Immunohistochemical findings were as follows: 98.7% of cervical cancers showed immunoexpression for ubiquitin and 52.6% for telomerase. Statistically significant differences were found in tumor immunoreactivity when compared with control tissue ($p<0.0007$) for both biomarkers. There was no significant difference in biomarker expression at different histological types of tumors, although telomerase was less expressed in endocervical adenocarcinoma. Our findings confirm that abnormal immunoexpression pattern of ubiquitin and telomerase is common in HPV-positive cervical cancer, indicating the existence of an intense degradation of proteins, subsequent cellular immortalization and maintenance of the malignant phenotype.

Keywords Cervical cancer · Immunohistochemical expression · Telomerase · Ubiquitin

This study was carried out with support from the AECC (Junta Provincial) and Fundación Instituto Valenciano de Oncología (FIVO), Valencia, Spain.

T. de Méndez Morelva
Exfoliative Cytology,
Faculty of Pharmaceutics and Analytical Biosciences,
University of Los Andes,
Mérida, Venezuela

L. B. Antonio
Departament of Pathology, School of Medicine,
University of Valencia,
Valencia, Spain

T. de Méndez Morelva (✉)
Facultad de Farmacia y Bioanálisis, Universidad de Los Andes,
Sector Campo de Oro,
5101 Mérida, Venezuela
e-mail: tmorelva@ula.ve

L. B. Antonio (✉)
Facultad de Medicina y Odontología, Universidad de Valencia,
Av. Blasco Ibáñez, 17,
46010 Valencia, España
e-mail: antonio.llombart@uv.es

Introduction

Cervical cancer and precursor lesions are induced by persistent infection with certain types of high-risk human papillomavirus (HR-HPV) [1, 2]. These viruses are able to activate different molecular mechanisms by inducing the development of a cellular clone with malignant phenotype [3, 4]. Such mechanisms are mediated by proteins used as molecular markers and alteration indicators in cellular control mechanisms. Thus, the study of these complex molecular pathways using different diagnostic techniques such as immunohistochemistry can be conducted. The continual expression of the E6 and E7 HR-HPV oncogenes in high-grade squamous intraepithelial lesions (HSIL) as well as in invasive cancer alter the functionality of a great variety of regulating cellular proteins [5–8]. HPV infection alone is thought to be insufficient for the development of invasive carcinoma.

Telomere length stability is required for the survival of germline human cells and differentiating cells and also for the immortalization of the cellular phenotype derived from

cancer. This characteristic is achieved through telomerase, a ribonucleoprotein enzyme capable of extending chromosome ends with specific telomeric DNA sequences. This enzyme compensates for the end replication problem and allows cells to proliferate indefinitely [9, 10].

Multiple studies have been carried out to evaluate telomerase as a possible HSIL and invasive cervical cancer marker, considering that detection of telomerase activity is useful for cytological screening of cervical lesions using cellular and tissue samples of uterine cervix [6, 11–14]. The HR-HPV E6 oncoprotein activates the oncogenic hTERT enzyme, mainly by stimulating the transcription of *hTERT* gene [15–17], and by immortalizing transformed cervical cells [6, 17]. Studies have shown that the activity of this enzyme is increased in comparison to normal cervical tissue in cervical cancer and in HSIL HPV 16- and 18-positive samples [17–21].

The rapid removal of enzymes and proteins is essential for the control of cellular growth and metabolism. A rapid intracellular protein degradation pathway is created with the addition of multiple ubiquitin monomers, followed by the recognition and degradation of specific substrate-protein by the 26S proteasome [22]. The ubiquitin-proteasome degrades a variety of cellular proteins, which generally have a short half life and include cyclines (D1 and E), cycline-dependent kinase inhibitors (specifically the p27KIP1), tumor-suppressor gene products (p53 and Retinoblastoma protein), transcription factors (E2F), and membrane receptors, among others. Furthermore, those mutated proteins that might also affect cellular homeostasis may be degraded by this pathway [5, 23].

Apart from protein degradation, ubiquitin is involved in physiological and pathological cell signaling processes such as gene transcription, DNA repair, and intracellular traffic. This signaling mechanism functions similarly to protein phosphorylation [24]. Substrate proteins that should be degraded are polyubiquitinized during an adenosine triphosphate (ATP)-dependent reaction. Several ubiquitin molecules are added in chains to these proteins. This polyubiquitinized substrate is recognized by the 26S proteasome and catalyzes the rupture of the substrate protein until it obtains small peptides of six to 12 amino-acids [25, 26].

In many human tumors, the ubiquitin-proteasome protein degradation pathway remains active, with the subsequent rapid degradation of many proteins conveying the lack of control known in cellular proliferation of neoplasias [22]. In the process of cervical carcinogenesis, the integration of HR-HPV in the cellular genome accepts the continuous uncontrolled expression of the HPV E6 and E7 oncogens; both E6/E7 are required for efficient immortalization of their natural host cells. Covalent union of HPV oncoproteins with ubiquitin and other related proteins modifies and induces cellular protein degradation. The E6/E7 oncoproteins are a target of the ubiquitin-proteasome system, and the resultant complex attracts target cellular proteins for their degradation. The ability of E6 and E7 to deactivate the normal function of the main tumor suppressors contributes to their oncogenic potential [3, 7].

The HR-HPV 16 and 18 use the cellular proteolytic ubiquitin-proteasome system to target p53 and pRb by eliciting rapid degradation of these regulating proteins through the continuous expression of E6 and E7 oncogenes. To facilitate HR-HPV replication and persistence, the infected cells must be irreversibly directed towards the synthesis phase of the cell cycle; as a result, the HR-HPV E7/pRb complex releases the E2F transcription factor. This interaction leads toward the ubiquitin-proteosome-mediated degradation of pRb [27, 28]. The HR-HPV E7 recruits the E3 ubiquitin-ligase enzyme to target the pRb and cause later degradation. It is also possible that the HR-HPV E7 serves as a direct link between pRb and the 26S proteasome, so that the pRb may degrade rapidly without previous ubiquitinization [7, 29]. Thus, the pRb may be deactivated and rapidly degraded in those cervical epithelial cells infected by HR-HPV.

The specific action of the HR-HPV E6 on p53 is functionally equivalent to p53 inactivation through mutation, which indicates that the HR-HPV E6/p53 complex represents one of the most important events in cervical carcinogenesis, given the interruption of the control points and apoptosis inhibition. The HR-HPV E6 protein binds to E6-AP, a cellular E3 ubiquitin-ligase, to form a dimer that binds p53. The complex results in E6AP-mediated ubiquitine and degradation p53 degradation. As a consequence, the immunohistochemical expression of p53 in neoplastic cervical cells could be negative. This effect could also be affected by the MDM2 protein that induces the ubiquitination and proteasomal degradation of p53 [7]. Degradation of p53 induced by E6-AP is a significant achievement of the HR-HPV, and results in malignant transformation of cervical epithelial cells together with the inactivation and degradation of pRb [5].

In this study, ubiquitin and telomerase immunohistochemical expression patterns were evaluated in cervical cancer in comparison with normal cervical tissue samples.

Materials and methods

Materials

Normal tissue samples (22 cases) and cancer from the uterine cervix were collected from archives of the Pathology Department of the University Hospital of Valencia, Spain. Two groups of cervical cancer samples were

included; the first with 66 cases diagnosed from 2000 to 2005 and the second with 15 cases of cervical cancer diagnosed between 1969 and 1998. The original hematoxylins of well-preserved cervical cancer cases were reevaluated [21]. Also, 22 cases of normal exocervical and endocervical tissues were included as a control group.

Immunohistochemical study

The tissue microarrays were constructed with distinct tumor areas of squamous cell cervical carcinoma and cervical adenocarcinoma. Tissue microarrays of normal exocervical (n=22) and normal endocervical (n=22) were also prepared taking the exocervical and endocervical sections from each block. Immunohistochemical staining was then carried out. In summary, deparaffinization in xylene and hydration in decreasing alcohol series was performed. Antigen retrieval with citrate buffer pH 6.0 was cooled in the same buffer; subsequently, endogenous peroxidase with 3% hydrogen peroxide at room temperature for 30 min was blocked. Similarly, tissue collagen was blocked to avoid nonspecific unions with a 20% horse serum solution at room temperature for 20 min.

The tissue microarrays were then incubated with primary antibodies for ubiquitin: a polyclonal antibody (DAKO Cytomation, Denmark) diluted at 1:500 and telomerase: 44F12 clone (Novocastra, UK) for 1 h at room temperature. The tissue microarrays were then incubated with biotin-labeled secondary antibody contained in the LSAB+ System-horseradish peroxidase (HRP) kit (DAKO Cytomation, Denmark), and liquid diaminobenzidin (DAB)+ Substrate Chromogen System (DAKO Cytomation, Denmark) was used to develop the reaction. All rinses were carried out with phosphate buffered saline (PBS; pH 6) and finally, the tissue microarrays were counterstained with Harris's hematoxylin before mounting. In the specific case of telomerase, the EnVision™ detection kit, the HRP (DAKO Cytomation, Denmark), and later the chromogene (EnVision™) substrate-DAB solution were used. Immunostaining against the telomerase antigen (diluted at 1:50) was carried out following conventional procedures and contrasting it with Harris's hematoxylin. However, since no satisfactory results were obtained in the case of cervical neoplasia, despite the positive control (lymphoma) showing intense reactivity (+++) for telomerase, a second immunostaining was carried out with diluted antibody 1:20, again using (EnVision™) and counterstaining with hematoxylin again. Finally, a third immunostaining was carried out, but contrasting with 0.5% methylium green. Thus, cases with no reactivity (true negatives) were confirmed while those with doubtful reactivity (false negatives) were reclassified.

All rinses were carried out with PBS (pH 6). Negative control included the substitution of a subclass-matched monoclonal antibody that was generated against an irrelevant antigen. Positive controls were made up of neoplastic tissue with known reactivity against the biomarkers under study, from a vesicular tumor, a breast tumor and a lymphoma. These controls were included in each one of the tissue microarrays. Cell counting was carried out including the entire diameter of the tumor disc as the total (100%). The positive reaction was represented by the presence of brown precipitation at the membrane, cytoplasm or in both cellular compartments. The percentage of neoplastic or normal cells with reactivity was estimated considering a minimum of 100 cells per tissue. The distribution of the immunoreactive cells was classified according to the following scale: negative=<5%; positive= >5% to <25%; ++=between 25% and 50%; +++=>50%. In the case of telomerase, any nuclear staining was interpreted as positive and considered overexpression or abnormal expression. In the case of ubiquitin, cytoplasmic and nuclear immunostaining were considered overexpression or abnormal expression. Moreover, we estimated staining intensity and scored as follows: low, moderate, or high. All tissue microarrays were evaluated first by an observer and later by an experienced pathologist without knowledge of clinical data.

Detection and genotypification of HPV DNA

Only tumor samples were submitted to HPV evaluation. A paraffin block with no embedded tissue (empty block) was prepared previously. The following recommendations were followed: gloves were used and changed regularly; the microtome was cleaned first with disinfectant, then with xylene, and finally with ethanol; a new knife was used to cut each block and its corresponding empty paraffin block. Five 5 μm thick cuts were made and placed in 1.5 ml Eppendorf tubes. We removed the block, cleaned as indicated previously, changed the knife, and cut the corresponding empty paraffin block. The same procedure was used for the subsequent tumor blocks. For isolation of cell DNA, five cuts were submitted for deparaffinization with xylene and washed with absolute ethanol. The pellet was resuspended in 500 μl of lysis solution (SDS, 0.5%; Tris-HCl, 10 mM; pH 8; NaCl, 0.15 M; EDTA, 5 mM). 25 μl of proteinase K (0.5 mg/ml) were added to each tube and incubated overnight at 55°C. DNA was extracted using phenol-chloroform-isoamilic alcohol, and then precipitated by adding one tenth volume of sodium acetate and 2.5 volumes of ethanol. A polymerase chain reaction (PCR) test was carried out before estimating the quality of DNA extracted through amplification of the interferon gene INF primers INF150DR: CTGGGATGCTCTTCGACCTC and INT150DF: TCTTTTCTTTCCCGATAGGT. Samples with a clear band of electrophoresis for INF150 were submitted

Table 1 Ubiquitin and telomerase expression in case controls and cervical cancer cases

	Controls (*n* (%))		Cases (*n* (%))		*p* value
	Positive	Negative	Positive	Negative	
Ubiquitin	34 (76.8)	10 (23.2)	79 (98.7)	1 (1.3)	0.0007
Telomerase	10 (22.7)	34 (77.3)	41 (52.6)	37 (47.4)	0.0007

for amplification of the 65 pb segment of the L1 region of HPV DNA using the set of SPF10 primers (INNO-LiPA; Innogenetics Inc., Belgium). The reaction was carried out at a final volume of 50 μl containing 2 mM of $MgCl_2$, Triton X-100 at 0.1%, 200 μM for each dNTPs, 10 μl of the mixture of SPF10-biotinylated primers, 1.5 UI of AmpliTaq Gold DNA polymerase (Perkin-Elmer), and 10 μl of isolated DNA. The PCR conditions were as follows: initial denaturalization and activation of the polymerase for 9 min at 94°C was followed by 40 cycles of 30 s at 94°C, 45 s at 52°C, and 45 s at 72°C, and a final extension for 5 min at 72°C. Positive and negative HPV 6 (Innogenetics, Belgium) controls containing only master mix reaction were included. PCR products were analyzed by electrophoresis in 2% agarose gel stained with ethidium bromide. The samples resulting from positive HPV DNA for SPF10 PCR were submitted for genotypification of HPV using the reverse hybridization band probe assay method (INNO-LiPA; Innogenetics Inc., Belgium). The SPF10 PCR products were mixed with a denaturing and hybridized solution with specific probes to identify 24 different HPV types (namely, HPV 6, 11, 16, 18, 31, 33, 35, 39, 40, 42, 43, 44, 45, 51, 52, 53, 54, 56, 58, 59, 66, 68, 70 and 74).

Statistical analysis

Association between different variables was determined using the Chi-square (X^2) test with the Yates and the Fisher's Exact Probability Test. The SPSS® statistical package was used for the statistical analysis and statistical significance was set at $p<0.05$.

Results

For this study, the age for each cervical cancer case was obtained from the clinical information originally found at the hospital service (range, 28–79 years; mean, 50.67 years). For the control group the age range was 36–75 years, with a mean age of 51.82 years. A total of 81 cases of cervical cancer were studied: 62 (76.5%) squamous cell cervical carcinomas (SCC) and 19 (23.5%) cervical adenocarcinomas. In SCC, the moderately differentiated (MD) group tumors (43.5%) predominated, followed by well-differentiated (WD) tumors (21%). The group of carcinomas with less differentiation was made up of 22.6% poorly-differentiated (PD) and 12.9% undifferentiated (UD). The greater portion of adenocarcinomas belonged to the endocervical type (42.1%), followed by the endometrioid type (26.3%); the villoglandular and papillary types reached 15.8% and 10.5%, respectively; the remaining 5.3% represented a mucinous type. Forty-four normal cervical tissues (control group: 22 exocervical/22 endocervical) were also included.

Of the 81 cervical tumors, three (3.7%) were excluded due to inadequate DNA; the remaining 78 cases (96.3%) were all HPV positive, of these, 67 (85.9%) cases showed a single HPV infection and 11 (14.1%) multiple HPV type infections. The most frequent specific viral type was HPV 16 in 46 (58.97%) cases, followed by HPV 18 in 12 (15.38%), HPV 45 in three (3.84%), HPV 58 in two (2.56%), and viral types HPV 31, HPV 66, HPV 68, and HPV X in equal numbers, one of each (1.28%). The squamous cell carcinomas as well as the adenocarcinomas showed predominantly one type of viral sequence 83.1% and 94.7%, although they did not reach statistical significance ($p=0.208$). HPV 16 was the most frequent viral type in SCC 35 (71.4%) as well as in cervical adenocarcinomas ten (55.6%), with equal *p* value 0.248; the HPV 18 was detected in 44.4% of the cervical adenocarcinomas and in 10.2% of SCC, which were statistically significant ($p<0.001$). These results are not shown.

Immunoexpression of biomarkers in tumors and controls

Ubiquitin A 98.7% of cervical cancers showed ubiquitin overexpression; only one case was negative (1.3%). With respect to case controls, 23.2% were negative for ubiquitin. We found highly significant differences ($p<0.0007$) when comparing ubiquitin expression in tumors and case controls; protein degradation was more intense in tumors than in case controls (See Table 1 and Fig. 1).

Fig. 1 Telomerase immunoexpression showing as tiny dots (**a** and **b** normal cervical tissue; **c** and **d** cervical cancer) within the nuclei and nucleoli (**c** poorly differentiated carcinoma). The normal exocervical tissue shows telomerase staining at the level of isolated nuclei in the deep strata, while being negative in the endocervix. Ubiquitin (**e** and **f** normal cervical tissue; **g** and **h** cervical cancer) showed marked expression, both nuclear and cytoplasmic. The normal endocervical epithelium also expresses a low positivity at nuclear and cytoplasmic level. Immunohystochemistry, original magnification: **a**, **e** ×100 and **b**, **c**, **d**, **f**, **g**, **h** ×400

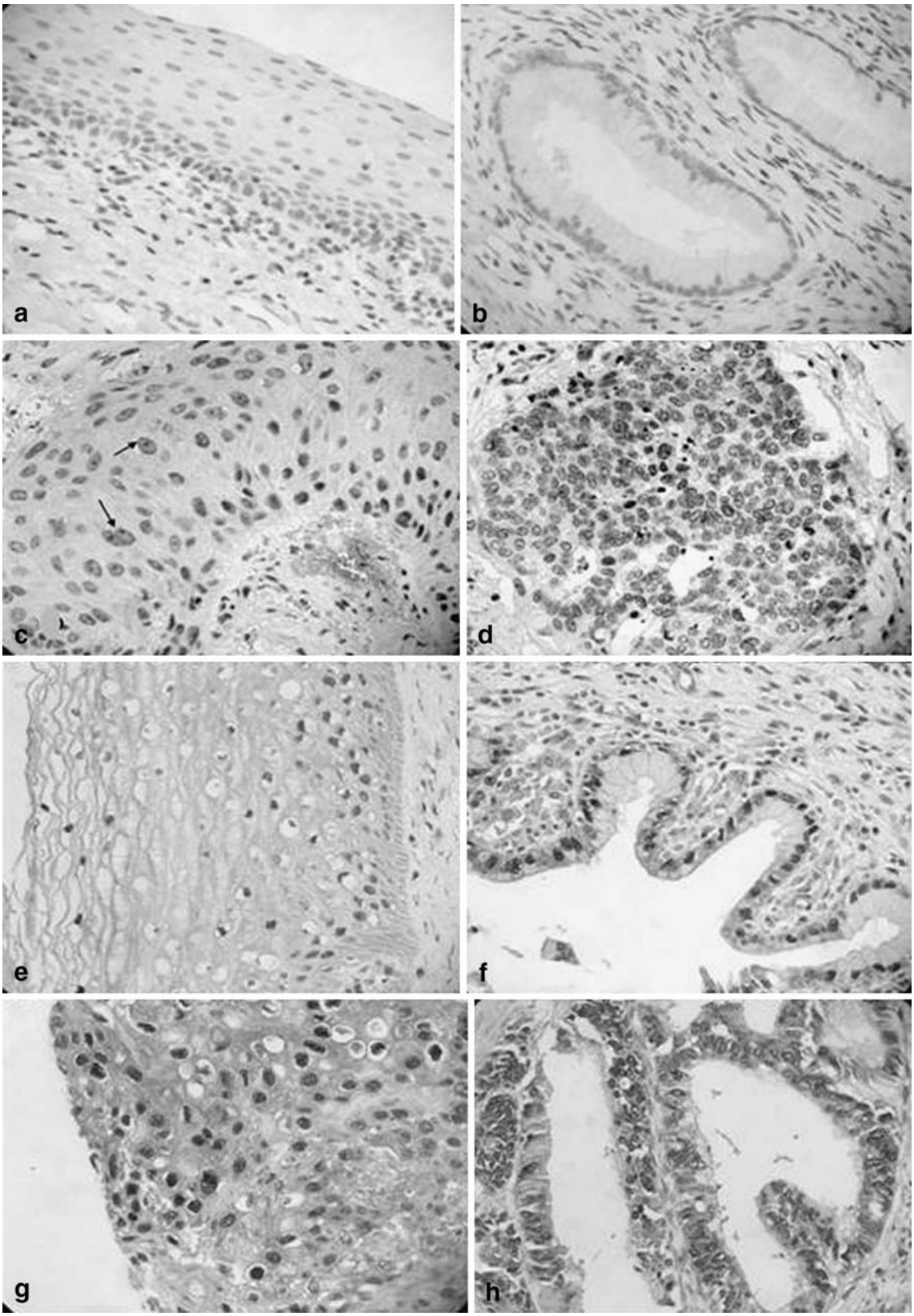
a
b
c
d
e
f
g
h

Table 2 Ubiquitin and telomerase expression in histological types of cervical cancer

	Squamous cells carcinoma (*n* (%))		Adenocarcinoma (*n* (%))		*p* value
	Positive	Negative	Positive	Negative	
Ubiquitin	60(98.4)	1(1.6)	19(100)	–	0.620
Telomerase	32(52.5)	29(47.5)	9(52.9)	8(47.1)	0.595

Telomerase Nuclear staining in the lymphocytes was used as a positive internal control in addition to the external positive control that corresponded to a lymphoma. The counterstaining with cytoplasmic 0.5% methylium green confirmed the negative cases and permitted reclassification with doubtful reactivity. Both internal and external, positive and negative controls showed the expected reactivity. From the cervical cancers, 41 (52.6%) were positive for telomerase, while 37 (47.4%) did not show reactivity. Case controls were evaluated completely: ten (22.7%) positive and 34 (77.3%) negative. No cytoplasmic staining was observed in any case or in case controls. Telomerase immunoexpression from both tumors and case controls also showed highly significant differences ($p<0.0007$) given that this enzyme expression was greater in tumors (Table 1).

Immunoexpression of the biomarkers in histological types of cervical tumors

Ubiquitin A 98.4% of SCCs and 100% of the adenocarcinomas were positive for ubiquitin, without showing significant differences ($p=0.620$) (Table 2). Cervical carcinomas showed immunoreactivity for ubiquitin in the nucleus as well as in the cytoplasm. In many cases, nuclear staining was more evident than cytoplasmic, which indicates that protein degradation is constant and occurs in both cellular compartments. Staining intensity was moderate and/or marked. In the stroma, reactivity was also positive (Fig. 1b, d). Ubiquitin was expressed in 100% of the WD, MD, and UD carcinomas, and 92.9% of PD ($p=0.879$). It was also expressed in 100% of the histological subtypes of the cervical adenocarcinoma without significant differences ($p=0.329$). The greatest case proportion 14/19 (73.7%) was expressed in more than 50% of malignant cells. These results are summarized in Table 3.

Telomerase Regarding the distribution of cervical carcinomas with or without telomerase expression, we observed that both types of tumors were positive, showing similar percentages (52.5% for SCCs and 52.9% for adenocarcinomas) and with no statistically significant differences ($p=0.595$) (Table 2). The immunoreactivity was only nuclear and nucleolar. The staining pattern was characterized by a very fine granular homogenous appearance and a pale sharp-edge aspect. The nucleus of both malignant cells and stromal lymphocytes showed reactivity, this being more intense. The nucleoli turned greyish-brown and became highly noticeable within the nucleus. In general, staining was less intense. In Table 3, telomerase immunoexpression in the histological types of cervical cancer is shown in detail. Reactivity resulted in similar percentages between the various degrees of SCCs differentiation, being higher at UD (62.5%), followed by the MD (55%), and the same proportion in the WD and PD (46.2%), with no significant differences ($p=0.667$). Cervical adenocarcinoma showed telomerase expression with statistically significant differences between the different histological types ($p<0.028$): in 100% of the villoglandular type and in the unique mucinous case, followed by the endometrioid and papillary histological subtypes in equal proportions (50%). The endocervical adenocarcinoma showed a small proportion of reactive cells (28.6%). No correlation between HPV presence, and ubiquitin ($p=0.305$) and telomerase ($p=0.656$) immunoexpression was observed.

Immunoexpression of biomarkers in normal cervical tissues

Ubiquitin The nucleus at the deep layer of exocervical tissue together with some intermediate cells were stained moderately-to-slightly. Pale cytoplasmic staining was also observed. Stroma staining was more evident in the vascular endothelium (Fig. 1a). In normal endocervical epithelium, staining was nuclear, intense, and focally cytoplasmic. Stroma cells nuclei and cytoplasms were stained (Fig. 1c). We included a special positive case control to compare ubiquitin immunostaining which corresponded to a non-gestational endometrial tissue. This resulted in mainly cytoplasmic staining and some highly intense nuclei.

Telomerase Occasional staining in cellular nuclei was observed (less than 10% of cells) in deep layer exocervical tissue. There was no nuclear staining in intermediate and superficial layers. Stroma staining was sporadic. Some endocervical cells and stromal nuclei were stained.

Discussion

In this study, highly significant differences in ubiquitin detection between study cases and case controls have been observed. In cervical lesions associated with HR-HPV,

Table 3 Immunoreactivity of malignant cells in the squamous cell carcinomas according to degree of differentiation and in the histological subtypes of cervical adenocarcinoma

Cervical cancer		Scale	Ubiquitin	*p* value	Scale	Telomerase	*p* value
Squamous cell carcinoma	Grade of differentiation			0.879			0.667
	WD	<5%	–		<5% (−)	53.8	
		5–50%	23.1		>5% (+)	46.2	
		>50%	76.9				
	MD	<5%	–		<5% (−)	44.4	
		5–50%	38.5		>5% (+)	55.6	
		>50%	61.5				
	PD	<5%	7.1		<5% (−)	53.8	
		5–50%	28.6		>5% (+)	46.2	
		>50%	64.3				
	UD	<5%	–		<5% (−)	37.5	
		5–50%	12.5		>5% (+)	62.5	
		>50%	87.5				
Cervical adenocarcinoma	Histological subtypes			0.329			0.028
	Endocervical	25–50%	25		<5% (−)	71.4	
		>50%	75		>5% (+)	28.6	
	Mucinous	25–50%	–		<5% (−)	–	
		>50%	100		>5% (+)	100	
	Endometrioid	25–50%	20		<5% (−)	50	
		>50%	80		>5% (+)	50	
	Papillary	25–50%	–		<5% (−)	50	
		>50%	100		>5% (+)	50	
	Villoglandular	25–50%	66.7		<5% (−)	–	
		>50%	33.7		>5% (+)	100	

WD well differentiated, *MD* moderately differentiated, *PD* poorly differentiated, *UD* undifferentiated

these viruses are considered a vital mechanism for the degradation of the main regulating cell proteins, through the elimination of the check points that protect the cell from alterations of its internal homeostasis, such as the tumor suppressing protein p53 [7, 30, 31] and the Retinoblastoma protein [7, 28]. Similarly, HR-HPV oncoproteins use the ubiquitin-proteosome system to target many other cell regulatory proteins for degradation [8]. In consequence, not only cell proteins are functionally inactive, but their expression levels tend to be lower due to intense degradation [7]. In this study, we have found a high expression of ubiquitin in cervical carcinoma, which indicates an intense protein degradation, regardless of the degree of differentiation in squamous cell carcinoma, although more intense in the poorly differentiated cases, and quite similar in the various subtypes of adenocarcinomas.

Immortalization of telomerase enzyme activation has been detected in malignant neoplasias, considering its expression as an essential step towards malignant transformation of human tissue [6, 32, 33]. This capacity allows unlimited multiplication of malignant cells. Multiple studies have been carried out to evaluate telomerase as a possible marker of HSIL and cancer and have found it useful as a complement to cytological diagnosis, especially in patients with cytological abnormalities associated with HR-HPV [6, 11–14]. These studies used the Telomeric Repeat Amplification Protocol TRAP method, which permitted the determination of enzymatic activity by amplifying PCR, in which up to 100% of this enzyme expression has been reported [19, 21, 33, 34]. In the present study, 52.6% of cervical cancer cases showed telomerase immune expression. These differences are possibly due to a higher sensitivity of the method used for capturing and amplifying the reduced quantity of telomerase synthesized in malignant and premalignant cervical cells and to the criteria used for evaluating enzymatic expression. Despite the advantages offered by molecular techniques, it is also possible to estimate telomerase expression in human cervical samples through immunohistochemistry. This technique has the advantage of allowing accurate observation of localized protein expression in premalignant and malignant cells in cervical tissue samples [35].

Efficiency of telomerase immunodetection depends on the conditions related to an adequate dilution of primary antibodies and on the use of highly sensitive antigen-antibody reaction detection systems. In addition, for doubtful cases, due to the observation of a fine and homogeneous sharp-edged immunoreactive pattern, it is necessary to use a cytoplasmic counterstaining that permits better nuclear observation and differentiation staining. It is possible that, the percentage of this enzyme expression may be higher in our tumor series because it may influence a dilution of inappropriate anti-hTERT antibodies. This could be proved in future research studies, where other forms of antigenic recovery [35, 36] might be considered.

In this study, 53.8% of the WD carcinomas were negative for telomerase, while UD showed positively in 62.5% of the cases. It is possible that tumor heterogeneity may influence the enzymatic analysis. As Jorboe et al. [6] explained, the telomerase activity could be related to the degree of tumor differentiation. In fact, well-differentiated tumors have less enzymatic expression, as shown in our results.

With respect to the endocervical adenocarcinomas, 71.4% were negative telomerase (<5% of reactive cells). These tumor cells may be found in apoptosis [35], telomerase inhibiting factors may exist when blocking their activation, and the enzyme may present qualitative modifications (hypophosphorylation) [36, 37]. In addition, hTERT variants not transported to the cytoplasm nucleus could be detected for their activation [35]. Finally, perhaps the cell may synthesize at minimum or nondetectable enzymatic levels, together with the development of other mechanisms that may keep the malignant phenotype, among other causes [38]. Future research could give answers to these hypotheses.

Normal cervical epithelium showed less immunoreactivity against the studied biomarkers when compared with the neoplastic tissue, which revealed abnormal expression in tumors with statistically significant differences. The biomarker immunoexpression in neoplastic tissue compared with the normal cervical tissue confirmed that in malignant cervical neoplasia, a diversity of interactions and altered molecular mechanisms induce cycle deregulation and uncontrolled cell proliferation. These alterations are apparently produced by HR-HPV E6/E7 oncoproteins associated with telomerase activation in cells with genomic instability and activated *myc* gene. The formation of E6-*myc* complex stimulates the expression of the *hTERT* gene by activating the promoter of this gene [39, 40]. HR-HPV E6 expression is relevant for the process of cell immortalization and suggests that other cell genes (*myc*) could be regulated by this viral protein in favor of cellular progression and immortalization [41].

The present findings confirm that an abnormal immunoexpression pattern of ubiquitin and telomerase, determined by immunodetection, is common in HPV-positive cervical cancer in comparison with normal cervix. This may be related to the existence of an intense protein degradation, with a consequent cellular immortalization which leads to the maintenance of a malignant phenotype.

Acknowledgments The authors thank Alejo Sempere and Laura Martínez from the Department of Pathology, School of Medicine, University of Valencia, for their invaluable support and training immunohistochemical technicians.

Conflict of interest statement We declare that we have no conflict of interest.

References

1. Muñoz N, Bosch FX, de Sanjosé S et al (2003) Epidemiologic classification of human papillomavirus types associated with cervical cancer. N Engl J Med 348:518–527
2. Moscicki A-B, Schiffman M, Kjaer S et al (2006) Updating the natural history of HPV and anogenital cancer. Vaccine 24S3:S3/42–S3/51
3. zur Hausen H (2000) Papillomaviruses causing cancer: evasion from host-cell control in early events in carcinogenesis. J Natl Cancer Inst 92:690–698
4. von Knebel-Doeberitz M (2001) Aspects of molecular pathogenesis of cervical cancer in establishing new tumor markers for early detection and diagnosis. Zentralbl Gynakol 123:186–191
5. Scheffner M (1998) Ubicuitin, E6-AP, and their role in p53 inactivation. Pharmacol Ther 78:129–139
6. Jarboe EA, Liaw K-L, Thompson LC et al (2002) Analysis of telomerase as a diagnostic biomarker of cervical dysplasia and carcinoma. Oncogene 21:664–673
7. Scheffner M, Whitaker NJ (2003) Human papillomavirus-induced carcinogenesis and the ubicutin-proteosome system. Sem Cancer Biol 13:59–67
8. Kim YT, Zhao M (2005) Aberrant cell cycle regulation in cervical cancer. Yonsei Medical J 46:597–613
9. Hanahan D, Weinberg R (2000) The hallmark of cancer. Cell 100:57–70
10. Hiyama E, Hiyama K (2007) Telomere and telomerase in stem cell. British J Cancer 96:1020–1024
11. Reesink-Peters N, Helder MN, Wisman GBA et al (2003) Detection of telomerase, its components, and human papillomavirus in cervical scrapings as a tool for triage in women with cervical dysplasia. J Clin Pathol 56:31–35
12. Braviccini S, Sanchini MA, Amadori A et al (2005) Potencial of telomerase expresión and activity in cervical specimens as a diagnostic tool. J Clin Pathol 58:911–914
13. Jarboe EA, Thompson LC, Heinz D et al (2004) Telomerase and human papillomavirus as diagnosis adjuncts for cervical dysplasia and carcinoma. Hum Pathol 35:396–402
14. Pinto-Tang CT, Premoli G (2005) Detection of telomerase activity in cervical lesions by non-radioactive telomeric repeat amplification protocol (TRAP). Invest Clin 46:255–263
15. Gewin L, Galloway DA (2001) E box-dependent activation of telomerase by human papillomavirus type 16 E6 does not require induction of c-*myc*. J Virol 75:7198–7201

16. Oh ST, Kyo S, Laimins LA (2001) Telomerase activation by human papillomavirus type 16 E6 protein: induction of human telomerase reverse transcrptase expression through *Myc* and GC-rich Sp1 binding sites. J Virol 75:5559–5566
17. Branca M, Giorgi C, Ciotto M et al (2006) Upregulation of telomerase (hTERT) is related to the grade of cervical intra-epithelial neoplasia, but is not an independent predictor of high-risk human papilomavirus, virus persistence, or disease outcome in cervical cancer. Diagn Cytopathol 34:739–748
18. Takakura M, Saturo K, Taro K et al (1998) Expression of human telomerase subunits and correlation with telomerase activity in cervical cancer. Cancer Res 58:1558–1561
19. Wang S-Z, Sun J-H, Zhang W et al (2004) Telomerase activity in cervical intraepithelial neoplasia. Chinese Med J 117:202–206
20. Anderson S, Shera K, Ihle J et al (1997) Telomerase activation in cervical cancer. Am J Pathol 151:25–31
21. Yashima K, Ashfaq R, Nowak J et al (1998) Telomerase activity and expression of its RNA component in cervical lesions. Cancer 82:1319–1327
22. Pagano M (1997) Cell cycle regulation by the ubicutin pathway. FASEB J 11:1067–1075
23. Rolfe M, Chiu I, Pagano M (1997) The ubicutin-mediated proteolytic pathway as a therapeutic area. J Mol Med 75:5–17
24. Haglund K, Dikic I (2005) Ubicuitylation and cell signaling. EMBO J 24:3353–3359
25. Huibregtse JM, Scheffner M, Beaudenon S et al (1995) A family of proteins structurally and functionally related to the E6-AP ubiquitin-protein ligase. Proc Natl Acad Sci USA 92:2563–2567
26. Mitch WE, Goldberg AL (1996) Mechanisms of muscle wasting-the role of the ubiquitin-proteosome pathway. New Engl J Med 335:1897–1905
27. Boyer SN, Wazer DE, Band V (1996) E7 protein of human papilloma virus-16 induces degradation of retinoblastoma protein through the ubicutin-proteosome pathway. Cancer Res 56:4620–4624
28. González SL, Stremlau M, He X et al (2001) Degradation of the retinoblastoma tumor suppressor by the human papillomavirus type 16 E7 oncoprotein is important for functional inactivation and is separable from proteosomal degradation of E7. J Virol 75:7583–7591
29. Berezutskaya E, Bagchi S (1997) The human papillomavirus E7 oncoprotein functionally interacts with the S4 subunit of the 26S proteosome. J Biol Chem 272:30135–30140
30. Kao WH, Beaudenon SL, Talis AL et al (2000) Human papillomavirus type 16 E6 induces self-ubicuitination of the E6AP ubiquitin-protein ligase. J Virol 74:6408–6417
31. Hengstermann A, Linares LK, Ciechanover A et al (2001) Complete switch from Mdm2 to human papillomavirus E6-mediated degradation of p53 in cervical cancer cells. Proc Natl Acad Sci USA 98:1218–1223
32. Shay JW, Bacchetti S (1997) A survey of telomerase activity in human cancer. Eur J Cancer 33:787–791
33. Yokoyama Y, Takahashi Y, Shinohara A et al (1998) Telomerase activity in the female reproductive tract and neoplasms. Gynecol Oncol 68:145–149
34. Shroyer KR, Thompson LC, Enomoto T et al (1998) Telomerase expression in normal epithelium, reactive atypia, squamous dysplasia, and squamous cell carcinoma of the uterine cervix. Am J Clin Pathol 109:153–162
35. Yan P, Benhattar J, Seelentag W et al (2004) Immunohistochemical localization of hTERT protein in human tissues. Histochem Cell Biol 121:391–397
36. Kyo S, Masutomi K, Maida Y et al (2003) Significance of immunological detection of human telomerase reverse transcriptase. Re-evaluation of expression and localization of human telomerase reverse transcriptase. Am J Pathol 163:859–867
37. Liu K, Hodes RJ, Weng NP (2001) Cutting edge: telomerase activation in human T lymphocytes does not require increase in telomerase reverse transcriptase (hTERT) protein but is associated with hTERT phosphorylation and nuclear translocation. J Immunol 166:4826–4830
38. Kakihana M, Yahata N, Hirano T et al (2002) Telomerase activity during carcinogenesis in the bronchus. Oncol Rep 9:43–49
39. Veldman T, Horikawa I, Barrett JC et al (2001) Transcriptional activation of the telomerase *hTERT* gene by human papillomavirus type 16 E6 oncoprotein. J Virol 75:4467–4472
40. Fehrmann F, Laimins LA (2003) Human papillomaviruses: targeting differentiation epithelial cells malignant transformation. Oncogene 22:5201–5207
41. Veldman T, Liu X, Yuan H et al (2003) Human papillomavirus E6 and *Myc* proteins associate in vivo and bind to and cooperatively activate the telomerase reverse transcriptase promoter. PNAS 100:8211–8216

Virchows Arch (2009) 455:245–251
DOI 10.1007/s00428-009-0811-1

ORIGINAL ARTICLE

Adhesion molecules and p16 expression in endocervical adenocarcinoma

Elisabetta Carico · Franco Fulciniti · Maria Rosaria Giovagnoli · Nunzia Simona Losito · Gerardo Botti · Giulio Benincasa · Maria Giuseppina Farnetano · Aldo Vecchione

Received: 15 April 2009 / Revised: 1 July 2009 / Accepted: 13 July 2009 / Published online: 13 August 2009

Abstract An immunohistochemical (IHC) study has been conducted on 34 cases of untreated endocervical adenocarcinomas collected among three institutions (Ospedale S. Andrea, Rome; Istituto Nazionale Tumori "Fondazione G. Pascale", Naples; and Clinica Malzoni, Avellino). The E-cadherin and α- and β-catenin complex status has been investigated along with p16INK4a in all studied cases with the aim to study whether the pattern of expression of the cadherin–catenin complex could be causally related to the expression of P16INK4a protein. Results were evaluated for statistical significance by a non-parametric test (Kruskal–Wallis). Endocervical adenocarcinomas as a group were uniformly expressing p16INK4a except for two cases, and all lesions displayed downregulation of the cadherin–catenin complex, without demonstrating statistically significant differences among the different histotypes. The lack of nuclear accumulation of β-catenin found in this group of lesions probably implies that no alteration of the β-catenin/Wnt metabolic pathway is present in endocervical adenocarcinoma, as opposed to what is found in the literature for squamous carcinoma of the cervix. The diffuse expression of p16INK4a protein in this group of neoplasms stresses the important role of high-risk human papillomavirus infection in neoplastic causation possibly via the viral E7-mediated inactivation of pRB tumor-suppressor protein and also underlines the useful role of p16INK4a immunostaining in the diagnostic algorithm of endocervical adenocarcinomas. In consideration of these findings, investigation of downstream β-catenin genes c-myc and cyclin D1 is sought as possibly contributive in the molecular pathogenesis of endocervical adenocarcinoma.

Keywords p16INK4a · Cadherin–catenin complex · Endocervical adenocarcinoma

E. Carico · M. R. Giovagnoli
U.O. Citopatologia, IIa Facoltà Medicina e Chirurgia La Sapienza, Rome, Italy

F. Fulciniti · N. S. Losito · G. Botti
A.F. Anatomia Patologica e Citopatologia, Istituto Tumori "Fondazione G. Pascale, Napoli", Naples, Italy

G. Benincasa · M. G. Farnetano
Divisione di Anatomia Patologica e di Ginecologia Oncologica, Clinica Malzoni, Avellino, Italy

F. Fulciniti (✉)
S.S.D. di Citopatologia, A.F. di Anatomia Patologica, Istituto Nazionale Tumori "Fondazione G. Pascale", Via Mariano Semmola, 80131 Naples, Italy
e-mail: franco.fulciniti@gmail.com

A. Vecchione
Istituto Tumori "Fondazione G. Pascale, Napoli", Naples, Italy

Introduction

The rising incidence of endocervical adenocarcinoma in relation to squamous cell carcinoma of the uterine cervix, as well as the increasing rate of adenocarcinoma per population at risk, have raised the attention of researchers to primary glandular neoplasms of the uterine cervix [1]. Endocervical adenocarcinoma is a heterogeneous group of neoplasms with a wide variability of histological patterns but generally showing an aggressive biological behavior. Furthermore, its early detection in a screened population is often negatively affected by sampling and/or diagnostic pitfalls [2].

E-Cadherin and its cytoplasmic-associated cell adhesion molecules such as catenins have been recognized to be important biomarkers of tumor differentiation [3, 4]. E-Cadherin, which is an epithelial cell adhesion molecule, is a transmembrane protein with a cytoplasmic domain that connects to the actin cytoskeleton through a complex with its associated cytoplasmic proteins, α-, β-, and γ-catenins [5, 6]. Calcium is required for E-cadherin to mediate its adhesive function, and the extracellular portion of E-cadherin contains several calcium-binding sites. E-Cadherin molecules form homodimers on the cell surface and carry out their adhesive function by binding to E-cadherin molecules on adjacent cells (homotypic adhesion), being also able to form extensive multidimers of E-cadherin [7]. Loss of E-cadherin expression has been correlated with the in vitro invasive phenotype of cancer cell lines [8, 9]. Furthermore, previous studies reported the reduced or aberrant expression of E-cadherin and/or catenins in different human cancers: in neoplastic thyroid tissue [10], in esophageal cancer [11], in breast cancer [12, 13], in gastric [14] and pancreatic carcinoma [15], in bladder [16] and prostatic cancer [17], and in melanoma [18] and meningioma [19]. Defects in the E-cadherin/catenin adhesion complex have also been described in several gynecologic cancers, mainly in cervical [20, 21], endometrial [22–24], and ovarian tumors [25].

Fewer studies have recently focused also on the E-cadherin–catenin complex expression in endocervical adenocarcinomas [26–28], and all have showed decreased expression of the E-cadherin–catenin complex with atypical patterns of α- and β-catenin expression.

P16INK4a is known to play a critical role as a negative regulator of cell cycle progression and differentiation by controlling the activity of the tumor-suppressor protein pRb. Increased levels of p16 appear to be indirectly related to high-risk human papillomavirus (HR-HPV), possibly via the production of the viral oncoprotein E7, which binds and inactivates the host cellular tumor-suppressor proteins pRB [29]. In this respect, the cyto-histological study of p16 expression has overcome many of the conceptual and practical problems associated with the detection of HR-HPV types as an adjunctive test and, as a matter of fact, it is now widely used as a surrogate test to diagnose HR-HPV infection, often with superior sensitivity to DNA-hybridization [30].

Notwithstanding the important role of HR-HPV infection in the initiation and progression of cervical cancer, it has also been demonstrated that HPV is a necessary but not sufficient cause to develop invasive carcinoma and, at least in the pathogenesis of squamous cell carcinoma, a "second hit" or metabolical disturbance is required to develop cervical cancer. Pérez-Plasencia et al. [31, 32] used wide genome analysis to identify altered metabolic pathways in cervical squamous cell carcinomas carrying HPV 16 infection; in their study, they found an alteration of the β-catenin/Wnt pathway. In particular, the so-called canonical activation pathway of Wnt gene transcripts impedes phosphorylation of β-catenin, causing its stabilization with nuclear accumulation and abnormal cytoplasmic expression. This, in turn, leads to the activation of target genes involved in cell proliferation and cell cycle progression, like c-myc and cyclin D1.

In this paper, we evaluated the tissue distribution of adhesion molecules such as E-cadherin and α- and β-catenin in endocervical adenocarcinoma by IHC techniques with the aim to investigate whether differences in the expression of these molecules exist in the different histotypes of endocervical adenocarcinoma and their possible biological significance. In this study, parallel staining for p16INK4a was also performed to investigate the role of HR-HPV infection as indirectly shown by p16INK4a expression in endocervical carcinogenesis.

Materials and methods

Thirty-four tissue specimens (14 biopsies from curettings and 20 surgical samples) previously diagnosed as endocervical adenocarcinoma were collected among three institutions (Ospedale S. Andrea, Rome; Istituto Nazionale Tumori "Fondazione G. Pascale", Naples; and Clinica Malzoni, Avellino). The original diagnoses concerned patients who had not received preoperative therapy at the time of diagnosis and were reviewed by three of us (E.C., F.F., and N.S.L.) by using newly cut 5 μm histopathological sections stained with hematoxylin and eosin, alcian, and alcian-periodic acid Schiff; tumor grading and histological reclassification of the neoplasms were performed according to current criteria by World Health Organization System. The age of the patients varied between 36 and 74 years, with a median age of 52. Pathological staging information was available only in 20 cases: among these, there were two cases (10%) of in situ adenocarcinoma, five cases (25%) were classified as pT1a, 11 cases (55%) as pT2, two cases (10%) were classified as pT4.

To be enrolled in this study, all cases had already undergone preliminary IHC staining for vimentin, monoclonal carcinoembryonic antigen (mCEA), and estrogen and progesterone receptors (ER and PR) using commercially available antibodies and performed in the participating institutions. This material had been made available to us and, when unavailable, preliminary immunocytochemical staining for the above stated markers had been repeated by us on new sections taken from the available tissue blocks. Only cases showing cytoplasmic positivity for mCEA and negativity for ER, PR, and vimentin were considered for

Table 1 Scores for immunohistochemical protein expression of p16, E-cadherin, α-catenin, and β-catenin in the different diagnostic categories

Diagnostic category	Grading	p16	E-Cad	α-Cat	β-Cat
Mucinous ca. (n=20)					
Median	2	105	0	85	15
Min	1	0	0	0	0
Max	3	300	160	200	80
Adenosquamous ca. (n=3)					
Median	3	130	5	60	0
Min	3	160	0	30	0
Max	3	205	20	100	0
Endometrioid ca. (n=6)					
Median	2	240	10	90	30
Min	1	100	0	80	0
Max	3	290	80	160	140
Serous ca. (n=3)					
Median	3	120	0	100	5
Min	3	90	0	30	0
Max	3	170	10	180	80
Inter-group differences					
Kruskal–Wallis test (p)	0.005		NS	NS	NS
Clear cell ca. (n=1)	3	150	10	80	80
Signet ring mucinous cell ca. (n=1)	2	80	20	70	200

E-cad E-cadherin, *α-cat* α-catenin, *β-cat* β-catenin (see also text for explanation)

further study. All tissue samples had been fixed in 10% buffered formalin. Table 1 synthetically shows the histological diagnoses, tumor grade, and data from IHC score of all the studied specimens. To assess reactivity for adhesion molecules, immunohistochemistry was performed according to a standard streptavidin-biotin peroxidase complex method (Zymed, San Francisco, CA, USA). E-Cadherin, α-catenin, and β-catenin expression were assessed by using commercial specific mouse monoclonal antibodies (Zymed, San Francisco, CA, USA): HECD-1 specific for human E-cadherin, α-CAT-7A4 raised against a synthetic peptide corresponding to the C-terminus of mouse α-catenin (dilution 1:100), and CAT-5H10 raised against a recombinant protein corresponding to the C-terminus of chicken β-catenin (dilution 1:100). Four-micrometer sections were deparaffinized in xylene, rehydrated in graded ethanols, and washed with phosphate-buffered saline, then treated in a microwave oven for 15 min in 0.01 M citrate buffer (pH 6.0) and cooled down at room temperature for 20 min. Endogenous peroxidases were quenched by incubation in 0.3% hydrogen peroxide, and sections were then incubated in serum-blocking solution to reduce non-specific labeling. No further inhibition of endogenous biotin was performed as this was already contained in the developing kit. Anti-E-cadherin primary antibody, anti-α-catenin, and anti-β-catenin primary antisera were added, and sections were then incubated for 1 h at room temperature. Positive controls were known E-cadherin and α- and β-catenin expressing epithelial tissues; negative controls were carried out by using unrelated isotype matching antibody. The secondary biotinylated antibody was incubated as previously described. The reaction was developed by adding diaminobenzidine-tetrahydrochloride (DAB) chromogen mixture (Zymed, San Francisco, CA, USA). After hematoxylin counterstaining, slides were permanently mounted and analyzed for the presence and distribution of the immunostaining. Staining was scored by two of us (E.C. and F.F.) based on semiquantitative assessment of the distribution pattern of staining (nucleus, plasma membrane, and/or cytoplasm) and number of immunoreactive epithelial cells. In order to obtain data in the proper format for statistical evaluation, the following scoring system was employed: the number of immunoreactive nuclei/cytoplasms/cell membranes and total of immunoreactive cells (independently of the subcellular distribution of IHC signal) were expressed on a percent basis and were added sequentially, so as to generate an absolute numerical value (range 0–400), where numbers between 0 and 100 indicated low levels of IHC reactivity, numbers between 101 and 200 indicated moderate immunoreactivity, and numbers >200 indicated strong immunoreactivity for a given IHC marker.

For p16INK4a IHC analysis, a commercially available monoclonal antibody (clone E6H4, CINtec $p16^{INK4a}$, MTM Laboratories, Heidelberg) was used. Briefly, after antigen unmasking in epitope retrieval solution in heated water bath for 10 min at 95–99°C and endogenous peroxidase block, slides were stained with the primary antibody for 30′ at room temperature and subsequently with visualization

reagent solution. After developing with substrate-chromogen solution (DAB), slides were counterstained with hematoxylin and evaluated for both nuclear and cytoplasmic staining. A reaction in <1% of cells was considered negative, according to a previous study [26].

Statistical analysis

Statistical differences with relation to histological grading and to the expression of p16INK4a, E-cadherin, and α- and β-catenin in the different diagnostic categories were analyzed by using the non-parametric Kruskal–Wallis test. A p value <0.05 was considered statistically significant.

Statistical correlation with pathological tumor stage was not performed, as this data was not complete and limited only to 20 cases with surgical samples.

Results

The histopathological reclassification of 34 endocervical adenocarcinomas and their histological grading are shown in Table 1 along with their immune reactivity scores for P16INK4a, E-cadherin, and α- and β-Catenin.

Table 2 illustrates the IHC score distribution for each antiserum tested.

p16INK4a reactivity

Two of 34 (5.9%) of the tested cases, both mucinous adenocarcinomas, showed no reactivity for p16INK4a, even after repetition of the IHC staining and tissue pre-treatment with trypsin. Twelve cases (35.3%) showed low-level reactivity, ten cases (29.4%) moderate, and ten cases (29.4%) high level of immunoreactivity.

Nuclei of the neoplastic cells were most commonly stained (Fig. 1); cytoplasms and cell membranes were progressively decorated with increasing IHC scores. The diagnostic categories with the higher median IHC scores for p16 were represented by adenosquamous (with more marked expression in the squamoid areas) and endometrioid adenocarcinomas (Fig. 2; respectively, 130 and 240); serous and mucinous adenocarcinomas showed decreasing median IHC scores (Tables 1 and 2).

Table 2 Immunocytochemical score distribution for each tested antiserum in 34 cases of endocervical adenocarcinoma

IC score	0	≤100	101–200	201–300	301–400
P16INK4a	2	9	12	10	0
E-Cad	17	12	1	4	0
α-Cat	1	24	9	0	0
β-Cat	13	19	2	0	0

E-cad E-cadherin, *α-cat* α-catenin, *β-cat* β-catenin (see also text for explanation)

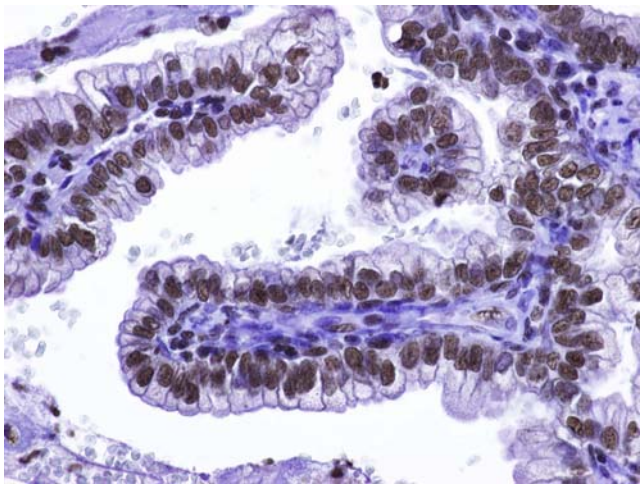

Fig. 1 Exclusive nuclear expression of p16INK4a protein in moderately differentiated mucinous-type endocervical adenocarcinoma (immunoperoxidase, ×400). E-Cadherin and α- and β-catenin staining were completely negative in this case

E-cadherin staining

A typical membranous expression of E-cadherin with strong decoration of the lateral (and often also apical) cytoplasmic cell borders was found in 6/34 cases only (17.6%; Fig. 3). In the other three cases (8.8%), a combined membranous and cytoplasmic expression was found, while in eight cases (23.5%), pure cytoplasmic staining without lateral membranous staining was obtained. Seventeen of 34 cases (50%) resulted negative. The highest IHC score for E-cadherin were found in the mucinous adenocarcinoma

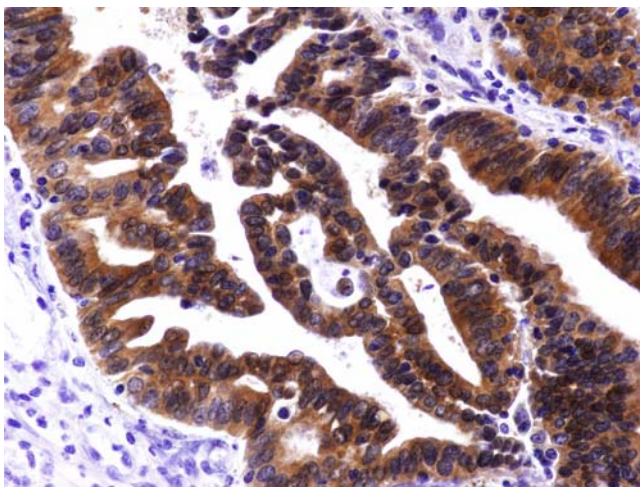

Fig. 2 Nucleocytoplasmic expression of p16INK4a protein in endometrioid adenocarcinoma (immunoperoxidase, ×400, original magnification)

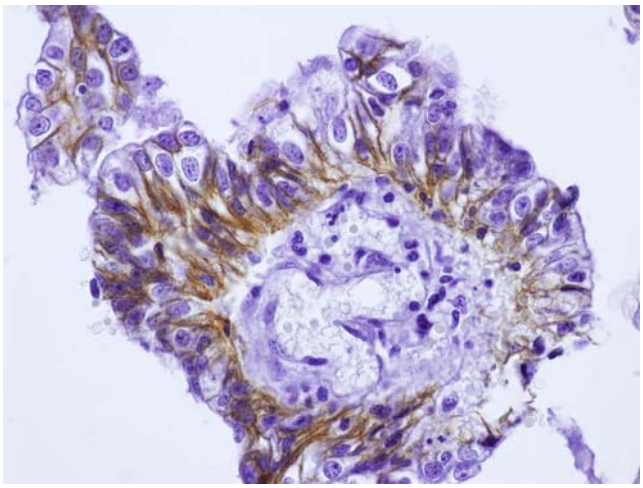

Fig. 3 E-Cadherin staining in mucinous adenocarcinoma of the cervix. Besides the lateral cell borders, there seems to be a tendency for circumferential cytoplasmic staining (immunoperoxidase, ×400, original magnification)

category (max score: 160; Tables 1 and 2). In our series, we could verify the findings by Heathley [26] on the circumferential rather than lateral membranous expression of E-cadherin in endocervical adenocarcinoma in cases with strong expression of the molecule. No statistical correlation was found, however, between histological grading of the neoplasms and E-cadherin IHC staining score.

α- and β-catenin expression

α-Catenin expression was slightly more conserved than that of E-cadherin, with median scores in the low range of expression (between 30 and 90; Table 1).

In particular, 1/34 (2.9%) cases scored 0, 24/34 cases (70%) showed low-range expression, and 9/34 (26.4%) showed moderate expression. No cases were found in the strong to very strong range of expression (Table 2).

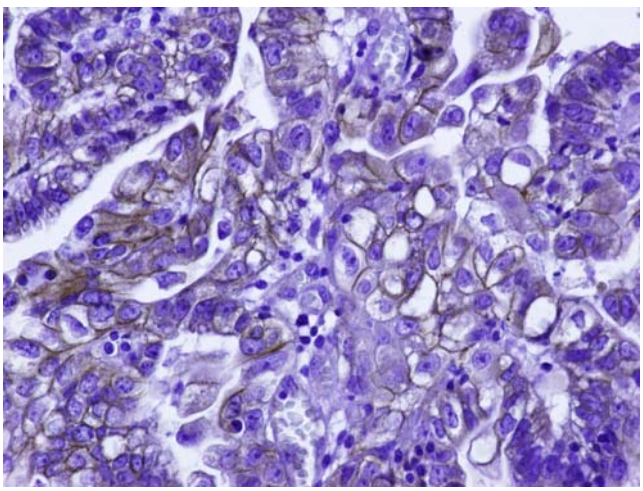

Fig. 4 α-Catenin staining in clear adenocarcinoma of endocervix. Pure membranous pattern of slight to moderate intensity can be observed (immunoperoxidase, ×600, original magnification)

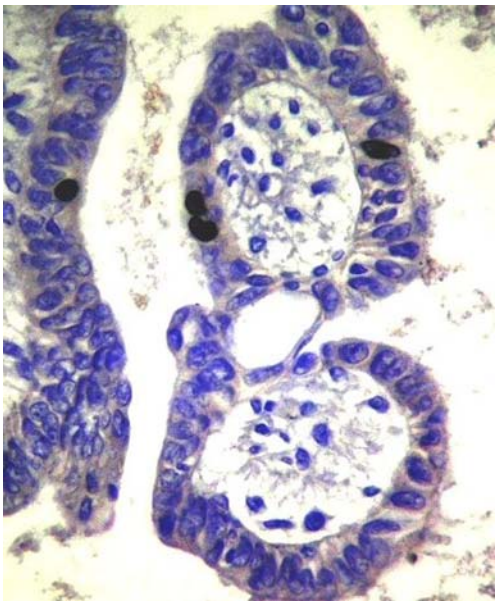

Fig. 5 α-Catenin staining in adenocarcinoma of the cervix. Notice focal nuclear staining in rare neoplastic cells (immunoperoxidase, ×400, original magnification)

The IHC distribution of the staining was membranous in 20/34 cases (59%; Fig. 4), membranous and cytoplasmic in 11/34 cases (32.3%), and cytoplasmic in two cases (5.8%). One case was totally negative. In one case of endometrioid adenocarcinoma, pure nuclear staining was found in rare nuclei only, coupled to focal cytoplasmic staining (Fig. 5).

β-Catenin was the least expressed adhesion molecule (median scores between 0 and 30), and its expression was

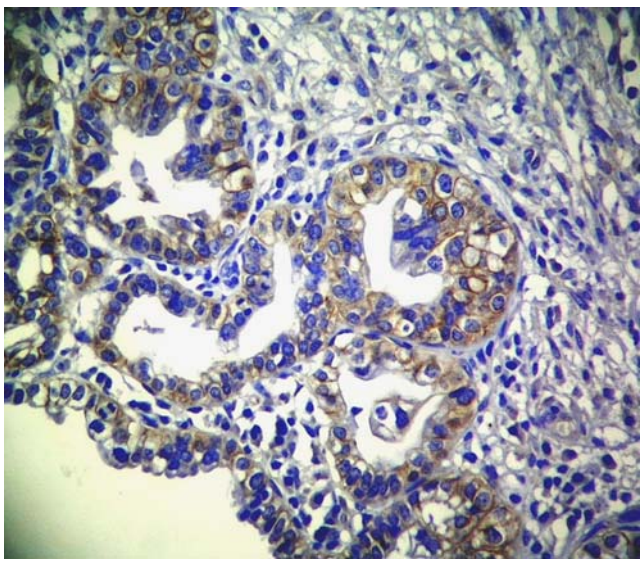

Fig. 6 β-Catenin staining in mucinous adenocarcinoma with clear cell differentiation. Notice moderate membranous positivity (immunoperoxidase, ×400, original magnification)

totally lost in the adenosquamous adenocarcinoma category (Table 1). In particular, 13/34 (38.2%) cases scored 0, 19/34 (55.8%) were in the low reactivity range, and only 2/34 cases (5.8%) were in the moderate reactivity range (Fig. 6; Table 2).

Statistical evaluation

Statistical evaluation of IHC scores by using a non-parametric (Kruskal–Wallis) test did not show significant differences among the various histopathological categories, while showing significant variation in the homogeneity of the histological grading scores, with $p=0.005$.

Discussion

In this paper, the authors have examined a relatively large series of endocervical adenocarcinomas collected among four different institutions.

The histopathological reclassification of the neoplasms has lead to the identification of four main histotypes (mucinous, adenosquamous, endometrioid, and serous adenocarcinomas, with one case of clear cell carcinoma and one case of signet ring mucinous carcinoma). The numerical consistence of the histological categories reflects their relative frequencies in the literature [1, 2].

IHC study of this group of lesions has shown that p16INK4a is consistently expressed at a variable intensity in cervical adenocarcinomas, with the only exception, in this series of 2/34 cases (5.9%). The diffuse expression of p16INK4a in this group of lesions most probably links endocervical adenocarcinoma to HR-HPV infection, possibly through inactivation of the pRB protein by E7 HPV protein [26, 27].

The study of E-cadherin and α- and β-catenin expression in our series has fully confirmed previously published reports dealing with reduced expression of the E-cadherin–catenin complex in many human epithelial neoplasms [9–18, 20–25].

With reference to β-catenin pattern of expression, our results, while confirming its diffuse downregulation in endocervical adenocarcinomas, do not fully support in this group of lesions the findings of Pérez-Plasencia et al. [28, 29] in squamous carcinoma. These authors found, besides to diffuse downregulation of the cadherin–catenin complex, also frequent nuclear accumulation of β-catenin. This led to the pathogenetical hypothesis of a possible "second hit" mutation causing a disturbance of the β-catenin-Wnt metabolic pathway in squamous carcinoma of the cervix. In our series, as a matter of fact, we were not able to demonstrate any nuclear accumulation of β-catenin, notwithstanding the frequent finding of its pure cytoplasmic expression, that is suggestive of an altered functional activity of this protein.

In this, endocervical adenocarcinoma, though sharing with squamous carcinoma of the cervix, the strong association with p16INK4a expression (and hence HR-HPV infection) may show a different pathogenetic mechanism implying a more direct interaction between the accumulation of p16INK4a protein and derangement of pRB protein.

Anyhow, further studies are needed in our opinion to definitively exclude alterations of the β-catenin/Wnt pathway in order to determine the status of downstream oncogenes, like C-myc and cyclin D1.

The high frequency of p16INK4a expression in our series of endocervical adenocarcinomas (32/34 cases; 94.11%) confirms what was already found by Negri et al. [29] on the usefulness of this immunocytochemical staining in the diagnostic algorithm of endocervical adenocarcinoma.

Acknowledgments The authors gratefully thank Dr. Emiliano Palmieri, M.D., for performing statistical evaluation of data, and the Lega Ialiana per la Lotta ai Tumori (LILT, Sezione di Napoli) for the generous contribution to this study. The authors would like to thank Dr. Alessandra Trocino for her excellent bibliographic services.

Conflict of interest statement We declare that we have no conflict of interest.

References

1. Smith HO, Tiffany MF, Qualls CR et al (2000) The rising incidence of adenocarcinoma relative to squamous cell carcinoma of the uterine cervix in the United States. A 24-year population-based study. Gynecol Oncol 78:97–105
2. Schoolland M, Allpress S, Sterret GF (2002) Adenocarcinoma of the cervix. Cancer 96:5–13
3. Takeichi M (1993) Cadherins in cancer: implication for invasion and metastasis. Curr Opin Cell Biol 5:806–811
4. Shiozaki H, Oka H, Inoue M et al (1996) E-cadherin mediated adhesion system in cancer cells. Cancer 77:1605–1613
5. Piepenhagen PA, Nelson WJ (1993) Defining E-cadherin associated protein complexes in epithelial cells: plakoglobin, β-catenin and γ-catenin are distinct components. J Cell Sci 104:751–762
6. Hinck L, Nathke IS, Papkoff J et al (1994) Dynamics of cadherin/catenin complex formation: novel protein interactions and pathways of complex assembly. J Cell Biol 125:1327–1340
7. Boggon TJ, Murray J, Chappuis-Flament S et al (2002) C-cadherin ectodomain structure and implications for cell adhesion mechanisms. Science 296:1308–1313
8. Frixen UH, Beherens J, Sachs M et al (1991) E-cadherin mediated cell-cell adhesion prevents invasiveness of human carcinoma cells. J Cell Biol 113:173–185
9. Van Aken E, De Wever O, Correia da Rocha AS et al (2001) Defective E-cadherin/catenin complexes in human cancer. Virchows Arch 439:725–751
10. Cerrato A, Fulciniti F, Avallone A et al (1998) Beta- and gamma-catenin expression in thyroid carcinomas. J Pathol 185(3):267–272

11. Buongiorno PF, al-Kasspooles M, Lee SW et al (1995) E-cadherin expression in primary and metastatic thoracic neoplasms and in Barrett's oesophagus. Br J Cancer 71:166–172
12. Siitonen SM, Kononen JTT, Helin HJ et al (1996) Reduced E-cadherin expression is associated with invasiveness and unfavorable prognosis in breast cancer. Am J Clin Pathol 105:394–402
13. Sung-Chul L, Mi-Sook L (2002) Significance of E-cadherin/β-catenin complex and Cyclin D1 in breast cancer. Oncol Rep 9:915–928
14. Oka H, Shiozaki H, Kobayashi K et al (1992) Immunohistochemical evaluation of E-cadherin adhesion molecule expression in human gastric cancer. Virchows Arch A Pathol Anat Histopathol 421:149–156
15. Weinel RJ, Neumann K, Kisker O et al (1996) Expression and potential role of E-cadherin in pancreatic carcinoma. Int J Pancreatol 19:25–30
16. Wakatsuki S, Watanabe R, Saito K et al (1996) Loss of human E-cadherin (ECD) correlated with invasiveness of transitional cell cancer in the renal pelvis, ureter and urinary bladder. Cancer Lett 103:11–17
17. Cheng L, Nagabhushan M, Pretlow TP et al (1996) Expression of E-cadherin in primary and metastatic prostate cancer. Am J Pathol 148:1375–1380
18. Danen EH, de Vries TJ, Morandini R et al (1996) E-cadherin expression in human melanoma. Melanoma Res 6:127–131
19. Tohma Y, Yamashima T, Yamashita J (1992) Immunohistochemical localization of cell adhesion molecule epithelial cadherin in human arachnoid villi and meningiomas. Cancer Res 52:1981–1987
20. Vessey CJ, Wilding J, Folarin N et al (1995) Altered expression and function of E-cadherin in cervical intraepithelial neoplasia and invasive squamous cell carcinoma. J Pathol 176:151–159
21. Carico E, Atlante M, Bucci B et al (2001) E-Cadherin and α-catenin expression during tumor progression of cervical epithelium. Gynecol Oncol 80:156–161
22. Hideyuki N, Tsuyoshi S, Hiroshi Y et al (1999) Nuclear localization of β-catenin in normal and carcinogenic endometrium. Mol Carcinog 25:207–218
23. Moreno-Bueno G, Hardisson D, Sarrio D et al (2003) Abnormalities of E- and P-cadherin and catenin (beta-, gamma catenin, and p120ctn) expression in endometrial cancer and endometrial atypical hyperplasia. J Pathol 199:471–478
24. Shih HC, Shiozawa T, Miyamoto T et al (2004) Immunohistochemical expression of E-cadherin and beta-catenin in the normal and malignant human endometrium: an inverse correlation between E-cadherin and nuclear beta-catenin expression. Anticancer Res 24:3843–3850
25. Veatch AL, Carson LF, Ramakrishnan S (1994) Differential expression of the cell-cell adhesion molecule E-cadherin in ascites and solid human ovarian tumor cells. Int J Cancer 58:393–399
26. Heathley MK (2004) E-cadherin and catenin expression in normal and neoplastic endocervical epithelium. Histopathology 45:200–202
27. Imura J, Ichikawa K, Takeda J et al (2001) Beta catenin expression as a prognostic indicator in cervical adenocarcinoma. Int J Mol Med 8:353–358
28. Fadare O, Reddy H, Wang J et al (2005) E- cadherin and β-catenin expression in early stage cervical carcinoma: a tissue microarray study of 147 cases. World J Surg Oncol 3:38
29. Negri G, Egarter-Vigl E, Kasal A et al (2003) p16INK4a is a useful marker for the diagnosis of adenocarcinoma of the cervix uteri and its precursors: an immunohistochemical study with immunocytochemical correlations. Am J Surg Pathol 2:187–193
30. Carozzi F, Confortini M, Dalla Palma P, New Technologies for Cervical Cancer Screening (NTCC) Working Group et al (2008) Use of p16-INK4A overexpression to increase the specificity of human papillomavirus testing: a nested substudy of the NTCC randomised controlled trial. Lancet Oncol 10:937–945
31. Pérez-Plasencia C, Vázquez-Ortiz G, López-Romero R et al (2007) Genome wide expression analysis in HPV 16 Cervical cancer: identification of altered metabolic pathways. Infect Agents Cancer 2:16
32. Pérez-Plasencia C, Duenas-Gonzalez A, Alatorre-Tavera B (2008) Second hit in cervical carcinogenesis process: involvement of Wnt/beta catenin pathway. Int Arch Med 1(1):10

Virchows Arch (2009) 455:253–259
DOI 10.1007/s00428-009-0823-x

ORIGINAL ARTICLE

Prevalence, viral load, and physical status of HPV 16 and 18 in cervical adenosquamous carcinoma

Tomomi Yoshida · Takaaki Sano · Tetsunari Oyama · Tatsuya Kanuma · Toshio Fukuda

Received: 3 June 2009 / Revised: 24 July 2009 / Accepted: 12 August 2009 / Published online: 29 August 2009

Abstract Adenosquamous carcinoma of the uterine cervix is a rare mixture of malignant squamous and glandular epithelial elements and accounts for approximately 10% of cervical carcinomas. The aims of the present study were to evaluate the prevalence, physical status, and viral load of HPV 16 and 18 in adenosquamous carcinoma. Formalin-fixed paraffin-embedded tissue samples from 20 cases of histologically diagnosed adenosquamous carcinoma were examined. The squamous and glandular components were separately microdissected and analyzed for their HPV DNA subtype, viral load, and physical status using real-time polymerase chain reaction (PCR). The percentages of HPV 16- and 18-positive cases among all the HPV-positive cases were 36.8% (7/19) and 57.9% (11/19) in the squamous epithelial elements and 33.3% (6/18) and 61.1% (11/18) in the glandular elements, respectively. PCR analysis with E2 primers revealed that seven of eleven (63.6%) HPV 18-positive cases had the pure integrated form in both elements. The mean HPV 16 DNA copy numbers/cell was 7.22 in the squamous elements and 1.33 in the glandular elements ($p=0.04$) while the corresponding mean HPV 18 DNA copy numbers/cell was 1.50 and 0.89, respectively. The prevalence of HPV 18 in adenosquamous carcinoma was high and many HPV 18-positive cases were the pure integrated form resulting in very low copy numbers/cell. It is possible that more aggressive transformation with early integration of HPV 18 results in cases with greater chromosomal instabilities, higher growth rates, and rapid progression.

Keywords Adenosquamous carcinoma · Uterine cervix · Human papillomavirus (HPV) · Viral load · Physical status

T. Yoshida (✉) · T. Fukuda
School of Health Sciences, Faculty of Medicine,
Gunma University,
3-39-15 Showa-machi,
Maebashi, Gunma 371-8511, Japan
e-mail: toyosida@health.gunma-u.ac.jp

T. Sano · T. Oyama
Department of Diagnostic Pathology, Faculty of Medicine,
Gunma University Graduate School of Medicine,
3-39-15 Showa-machi,
Maebashi, Gunma 371-8511, Japan

T. Kanuma
Department of Gynecology and Reproductive Medicine,
Faculty of Medicine,
Gunma University Graduate School of Medicine,
3-39-15 Showa-machi,
Maebashi, Gunma 371-8511, Japan

Introduction

Up to 80% of uterine cervical carcinomas are squamous cell carcinoma while the majority of the remainder is adenocarcinoma and adenosquamous carcinoma. Adenosquamous carcinoma of the uterine cervix is a rare mixture of malignant squamous and glandular epithelial elements. Adenosquamous carcinoma of the cervix is less common than adenocarcinoma. Recent studies have reported that the incidence of adenosquamous carcinoma is increasing especially among young women even though the overall incidence of cervical carcinoma has declined [1, 2].

It has been clearly established that the strong association of human papillomavirus (HPV) infection with the development of cervical squamous lesions and the risk of cervical squamous cell carcinoma is related to high-risk HPV subtypes, viral physical status, and viral load. However, the relationship between HPV and adenosquamous carcinoma remains unclear owing to the limited data

available. Previous studies reported that the prevalence of HPV DNA in adenocarcinoma varies significantly (32–100%) and that the high-risk HPV type 18 is more frequently detected in adenocarcinoma and adenosquamous carcinoma than HPV 16 [3–9]. A few studies have reported differing rates of HPV DNA detection in adenosquamous carcinoma (30–100%) [10–13], and the pathogenic role of HPV in the development of adenosquamous carcinoma remains uncertain.

Several pathways for the histogenesis of adenosquamous carcinoma have been proposed, namely that (1) neoplastic columnar cells may turn into squamous metaplasia in a subset of adenocarcinomas, (2) reserve cells may become neoplastic and differentiate into both glandular and squamous lineages, or (3) pure adenocarcinoma and pure squamous cell carcinoma may collide with each other [14, 15]. However, the detailed mechanism remains unclear. Although a few studies on HPV 18 DNA integration in squamous cell carcinoma have been reported, the importance and necessity of viral DNA integration in the pathogenesis of adenosquamous carcinoma are not well established [16]. The aims of the present study were to evaluate the prevalence, physical status, and viral load of HPV 16 and 18 in adenosquamous carcinoma.

Materials and methods

Case selection and subclassification

Formalin-fixed paraffin-embedded tissue samples from 20 cases of histologically diagnosed adenosquamous carcinoma were chosen from the pathology files of routine surgical specimens of the Gunma University Hospitals. The specimens were removed by cone biopsies or hysterectomies between 1998 and 2008. The subjects ranged in age from 27–62 years (mean, 39 years). Three cervical cancer cell lines (SiHa, CaSki, and HeLa) and HPV 18 in a plasmid vector were used as controls.

All cases were reconfirmed by pathologists according to the World Health Organization (WHO) criteria [17] and subclassified into histological subtypes A–C according to the features of the malignant glandular and squamous components. Each case was subclassified as follows: type A, both the squamous and glandular elements are well-differentiated and well-bordered with foci of clear keratinizing and glandular components; type B, ill-defined mixture of poorly differentiated carcinoma components, with partial squamous and glandular differentiation; type C, predominance of solid or sheet-like cancer cells consisting of squamous differentiation within foci of goblet cells, but glandular formation is not seen. Type C may correspond to mucoepidermoid carcinoma in previous criteria [17].

Microdissection and HPV DNA detection and typing

The squamous and glandular components were separately microdissected from paraffin sections using a microtome blade. DNA was isolated from each microdissected sample by digestion with proteinase K in 10 mM Tris-HCl buffer (pH 8.0) containing 1 mM EDTA and 1% Tween-20. HPV DNA was amplified by polymerase chain reaction (PCR) using consensus primers (L1C1/L1C2) for the L1 open reading frame (ORF). The primers for the L1 region allowed the identification of at least seven types of genital HPV DNA (16, 18, 31, 33, 35, 52, and 58) on the basis of restriction fragment length polymorphisms with three restriction enzymes and direct sequencing. The PCR conditions were described previously [18]. HPV 16- and 18-positive cases were further analyzed by quantitative real-time PCR with HPV 16- and 18-specific primers for the E2 and E6 regions [19].

Quantitative real-time PCR for HPV 16 and 18 DNA

All HPV 16- and 18-positive cases were further examined for quantification of the viral load and analysis of the physical status of their HPV DNA. Two sets of primers for the E6 and E2 segments were used for HPV 16 or 18 genome amplification [19, 20]. For HPV DNA quantification by real-time PCR, primers for the HMBS gene were used as internal controls to quantify the cell DNA [21]. This gene was chosen as a control because no differences were detected between its levels of expression in normal and cancerous cervical tissues.

An aliquot (1 μl) of template DNA was added to a final reaction volume of 50 μl containing 25 μl of Platinum SYBR Green qPCR SuperMix-UDG (Invitrogen Corporation, Carlsbad, CA), 0.2 μM of each primer (forward and reverse) in 5 μl and 14 μl of H_2O. PCR amplification was performed using an Mx3000P™ Multiplex Quantitative PCR System (Stratagene Japan, Tokyo, Japan). The PCR amplification was initiated at 95°C for 10 min and completed by 45 amplification cycles (denaturation at 95°C for 10 s and annealing and extension at 60°C for 25 s). During the thermal cycling, the emission from each sample was recorded, and the fluorescence data were processed by the Mx3000 software (Stratagene Japan) to produce a threshold cycle (Ct) value for each sample. SiHa and CaSki cell DNA (HPV 16-positive) as well as HeLa DNA and HPV 18 in a plasmid vector (HPV 18-positive) samples were used as positive controls. The viral load was expressed as the HPV copy number/cell in each sample according to a previously reported formula [22]. The copy number/cell of each sample was measured in a relative manner by setting the SiHa cell line at 1 copy/cell.

Physical status of the HPV 16 and 18 genomes by real-time PCR

The primer sequences were located in the E2 and E6 segments of HPV types 16 and 18. The E2 region is usually deleted upon viral DNA integration into the host genome, and preferential disruption of E2 causes absence of the E2 product in PCR amplification. We defined an HPV as the pure integrated form if the E2 product was not detected but the E6 product was amplified.

Statistical analysis

The data were analyzed statistically using Student's *t* test. Values of $p<0.05$ were considered to indicate statistical significance.

Results

Subclassification of histological patterns

The 20 cases were histologically subdivided into type A (9/20, 45%), type B (6/20, 30%), and type C (5/20, 25%; Fig. 1a–c). The mean ages of the patients with the three subtypes were 41, 35, and 41 years, respectively. No relationships were detected between the histological subtypes and the patient ages.

Detection and typing of HPV DNA by consensus primer PCR

Using consensus primer PCR, HPV DNA infection was detected in 95% (19/20) of the squamous epithelial elements and 90% (18/20) of the glandular or goblet cell elements in adenosquamous carcinoma. The percentages of HPV 16- and 18-positive cases among all the HPV-positive cases was 36.8% (7/19) and 57.9% (11/19) in the squamous epithelial elements and 33.3% (6/18) and 61.1% (11/18) in the glandular elements, respectively (Table 1). These data revealed that >50% of the cases was HPV 18-positive in both elements of the adenosquamous carcinomas. The remaining one case was HPV 31-positive in both elements. The mean ages of the HPV 16- and 18-positive cases was 38.6 and 37.2 years, respectively. The relationships between HPV 16- and 18-positivities and the histological patterns were 3/7 (42.9%) and 4/7 (57.1%) for type A, 1/6 (16.7%) and 5/6 (83.3%) for type B, and 2/4 (50%) and 2/4 (50%) for type C, respectively. These data showed that HPV 18 was detected more frequently in type B cases, but the differences were not significant. Interestingly, the detected HPV subtypes were identical in the glandular

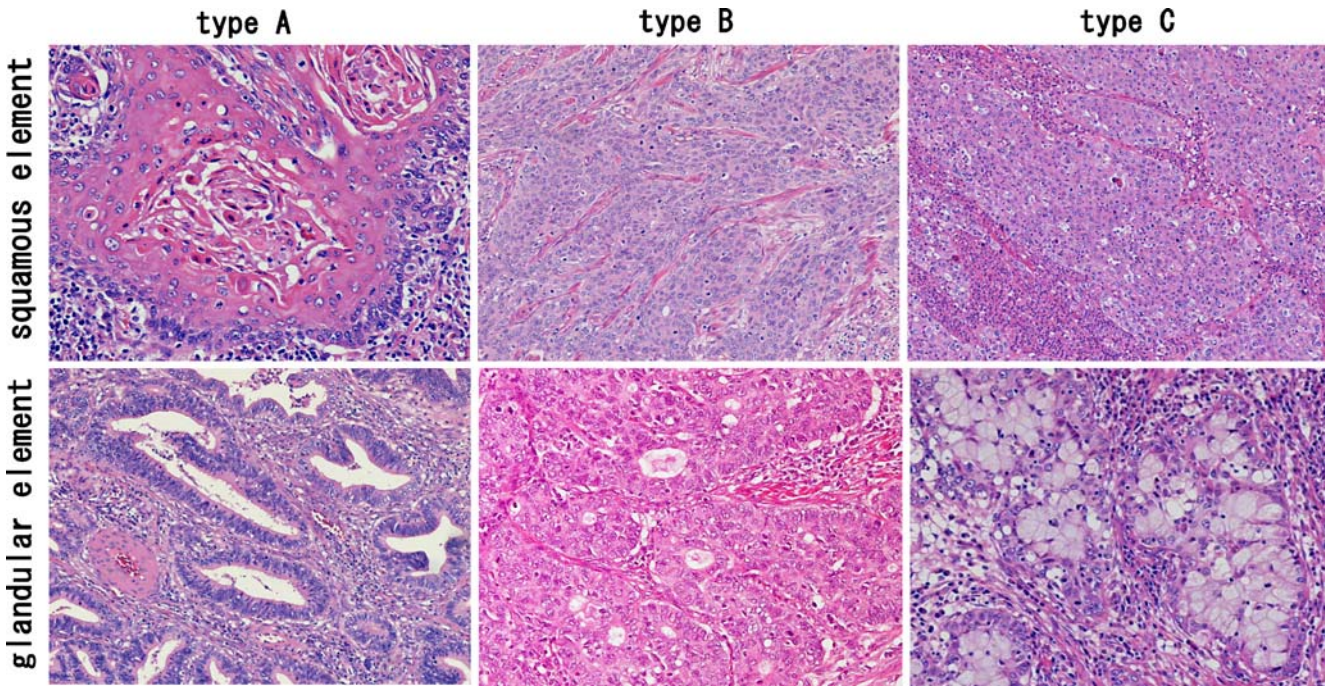

Fig. 1 Histological subtypes of adenosquamous carcinoma. *Type A*: Both squamous and glandular elements are well differentiated and well bordered, with foci of clear keratinizing and clear glandular components. Type B: Ill-defined mixture of poorly differentiated components, with partial squamous and glandular differentiation. Type C: Predominance of solid or sheet-like cancer cells showing squamous differentiation with foci of goblet cells, but glandular formation is absent

Table 1 Rates of HPV infection and integration in each element of adenosquamous carcinoma

	Squamous element	Glandular element
All HPV-positive	19/20[a] (95%)	18/20[b] (90%)
HPV 16	7/19 (36.8%)	6/18 (33.3%)
Integrated	1/7 (14.3%)	1/6 (16.7%)
HPV 18	11/19 (57.9%)	11/18 (61.1%)
Integrated	7/11 (63.3%)	7/11 (63.6%)

[a] One case was HPV 31-positive

[b] One case was HPV 31-positive and one case was HPV-negative

and squamous elements in all cases with the exception of one case in which the squamous element was HPV 16-positive, but the adenocarcinoma component was HPV-negative.

Physical statuses

PCR analysis with the E2 primers revealed that seven of 11 (63.6%) HPV 18-positive cases had the pure integrated form in both the squamous and glandular elements. Meanwhile, one of seven (14.3%) and one of six (16.7%) HPV 16-positive cases had the pure integrated form in the squamous and glandular elements, respectively, and each integrated form in the squamous and glandular elements was identical. It is very interesting that most of the HPV 18-positive cases contained the integrated form while only a few HPV 16-positive cases contained the integrated form among adenosquamous carcinomas as one histological subtype of cervical cancer (Table 1).

Assessment of the HPV 16 and 18 DNA copy numbers by real-time PCR

The mean HPV DNA copy numbers/cell in the three histological categories of adenosquamous carcinoma was 4.36 for type A, 1.04 for type B, and 0.48 for type C. The mean HPV DNA copy number/cell for type A cases with a well-differentiated squamous cell carcinoma component was higher, and significant differences were observed between type A and types B and C (Fig. 2).

The mean HPV DNA copy numbers/cell was 3.52 for the squamous epithelial elements and 1.05 for the glandular elements (p=0.04; Fig. 3). Among the HPV subtypes, the mean HPV DNA copy numbers/cell was 4.27 for the HPV 16-positive cases and 1.20 for the HPV 18-positive cases (Fig. 4). The mean copy number/cell was higher for cases infected with HPV 16 and significantly lower for cases infected with HPV 18 (p=0.02). Furthermore, the mean HPV 16 DNA copy numbers/cell was 7.22 in the squamous epithelial elements and 1.33 in the glandular elements (p=0.04) while the corresponding mean HPV 18 DNA copy numbers/cell was 1.50 and 0.89, respectively. The mean copy numbers/cell in both the HPV 16- and 18-infected cases tended to be higher in the squamous epithelial elements without any significant difference for the HPV 18-positive cases.

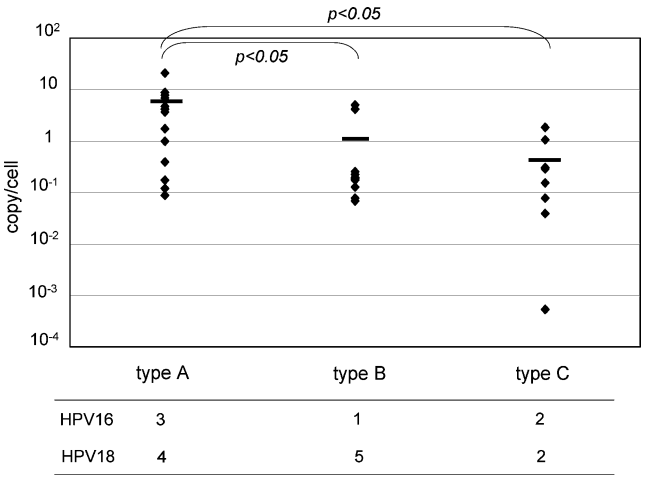

Fig. 2 HPV subtypes and viral loads in the histological subtypes. Significant differences are observed between type A and types B and C

The mean HPV DNA copy number/cell was significantly lower in the pure integrated cases, in which PCR products for the E2 region were absent, than in the nonintegrated cases (0.43 vs. 6.13, p=0.02; Fig. 5). The mean copy number/cell of the pure integrated cases, especially the HPV 18-positive cases, was much lower than that in the nonintegrated cases (0.28 vs. 2.81, p=0.009). Furthermore, the mean copy number/cell in the HPV 18-positive pure integrated cases was significantly lower than that in the HPV 16-positive pure integrated cases (0.28 vs. 1.51, p=0.001). The physical statuses were not related to the histological types or patient ages.

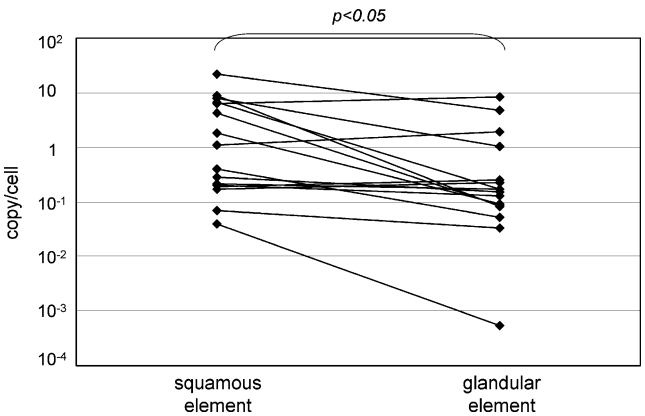

Fig. 3 Viral loads in the histological elements. The HPV copy numbers/cell are higher in the squamous component and lower in the glandular component in all cases

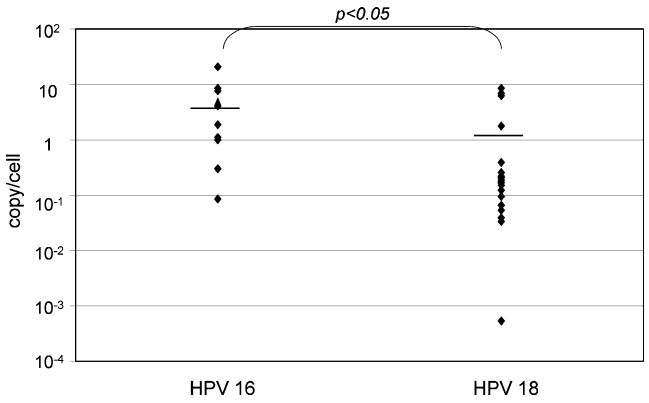

Fig. 4 Viral loads in the HPV subtypes. The mean copy numbers/cell are higher in cases infected with HPV 16 and significantly lower in cases infected with HPV 18

Discussion

Many reports have suggested that the incidence of cervical cancer in young women is continuing to increase steadily [23–25]. The majority of invasive cancers are squamous cell carcinomas, although greater prevalence of adenocarcinoma and adenosquamous carcinoma in young women have been reported [25–28]. In the present study, the mean age of the subjects was 39 years (range, 27–62 years), which is younger than the squamous cell carcinoma cases examined in our previous study in Japan [29]. Liu et al. [30] also showed that obvious increases in the overall incidence rates of adenocarcinoma and adenosquamous carcinoma were mainly observed in women aged 20–49 years.

The age-related high-risk HPV prevalence rates among women with normal cytology in Japan are 23.1% in women aged 20–29 years and 7.9% in women aged 30–49 years [31]. In Japan, a study on the prevalence of HPV 18 reported rates of 0% for women with normal cytology and low-grade squamous intraepithelial lesions, 4.7% for high-grade squamous intraepithelial lesions, and 11.1% for

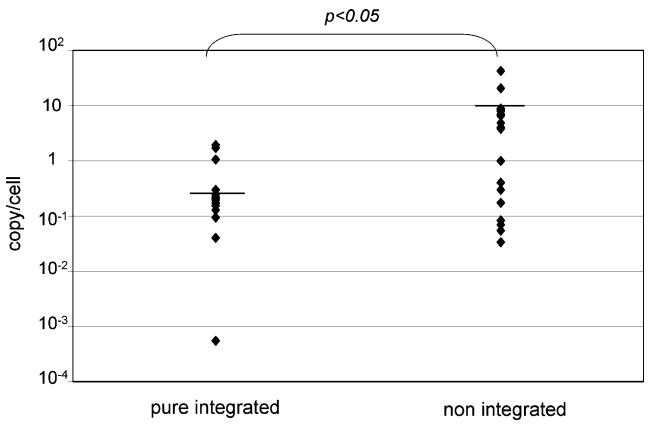

Fig. 5 Viral loads in different physical statuses. The mean copy numbers/cell is significantly lower in the pure integrated cases

cervical cancer [32]. In the present study, HPV DNA was detected in 95% of squamous lesions and 90% of glandular lesions. HPV 16 DNA was detected in 36.8% of squamous lesions and 33.3% of glandular lesions while HPV 18 DNA was detected in 57.9% of squamous lesions and 61.1% of glandular lesions. The reported HPV DNA detection rates in adenosquamous carcinoma vary among previous studies ranging from 30–100% [10–13]. Our present data revealed a high prevalence of HPV 18 DNA in adenosquamous carcinoma compared with HPV 16 DNA, but no difference was observed between the components. The frequencies of HPV 18 in adenocarcinoma and adenosquamous carcinoma are known to be much higher than those of HPV 16, although HPV 16 is the most common viral type identified in cervical cancers.

In the present study, we subclassified all the adenosquamous carcinoma cases into three subtypes, type A, B, and C. Examination of the relationships between the HPV subtypes and the histological types showed that HPV 18 was most frequently observed in type B cases (5/6, 83.3%). This finding is probably caused by the fact that most of the type B cases were poorly differentiated carcinomas, suggesting that type B cases may be classified as poorly differentiated adenocarcinomas. No relationships between the three histological types and the patient ages were observed.

Integration of high-risk HPV types into the host genome is considered to be an important step in malignant transformation. It is well established that HPV integration indicates an advanced stage of cervical lesions [33, 34]. The integration usually occurs within the E1 or E2 ORF in a manner that results in loss of its expression. The E1 or E2 ORF is an important viral regulator encoding transcriptional modulators, and disruption of E2-dependent negative feedback controlling E6 and E7 transcription is considered to be a selective event in tumor development and progression [35–37]. In the present study, the rates of integration were 63.6% in HPV 18-positive cases for both the squamous and glandular components compared with only 14.3% and 16.7% in the HPV 16-positive cases, respectively. Badaracco et al. [38] showed that HPV 18 integration occurred with significantly higher frequency than HPV 16 integration and was even detected in preneoplastic lesions. These findings are consistent with our data showing the predominant presence of HPV 18 pure integrated cases. Similar findings were reported by Cullen et al. [39], who detected a significant difference in viral integration between HPV 16 and 18, and indicated that many cases of HPV 16-positive cervical cancers only contain episomal forms of the virus. Our results showed that adenosquamous carcinoma tends to occur in a younger age group (mean age, 39 years) than squamous cell carcinoma, and this may be associated with early integration of HPV 18 [40] and its clinically higher aggressiveness

than HPV 16 [39, 41], although no significant difference in clinical tumor stages between HPV16 and HPV 18 positive cases was observed in this study. This difference may be derived from the different biological behaviors of the individual viral subtypes.

During integration, disruption of the E2 gene has been proposed as a mechanism of tumor progression, since it allows expression of the E6/E7 viral oncogenes. Meanwhile, Casas et al. [42] reported that Asian-American E2 variants of HPV 16 with retention of E1/E2 were present in some clinical samples and showed high levels of viral amplification with episomal multimeric or tandem integration. These findings suggest that disruption of the E2 gene, especially that of HPV 16, is not necessary for deregulation of the expression of the E6/E7 viral oncogenes and that the E2 variants may be an alternative mechanism for deregulating the expression of viral oncogenes. If this mechanism is operative, these data suggest that the Asian-American E2 variants of HPV 16 with retention of E1/E2 may also be present in the nonintegrated form in the categories defined in the present study.

Berumen et al. [43] suggested that integration and inactivation of E2 are not always essential for the development of HPV 16-positive carcinomas, which differ from HPV 18-positive cancers in this respect, and reported that the mean copy number/cell for HPV 18-positive tumors was significantly lower than that for HPV 16-positive tumors. Our data provide evidence that E2 integrity is essential for viral replication in invasive carcinoma and that its disruption impairs the ability of the viral genome to replicate. Badaracco [38] suggested that viral genome deletions may affect the production of infection particles, thereby limiting diffusion of the virus. Therefore, it is conceivable that the variable integration levels between HPV 16 and 18 are responsible for different viral diffusions and consequently different viral prevalence.

Our data revealed significant relationships between the viral copy numbers and the squamous and glandular components. The copy numbers/cell was 3.52 for squamous epithelial elements and 1.05 for glandular elements ($p<0.05$) and 4.36 for type A, 1.04 for type B, and 0.48 for type C ($p<0.05$). A previous study showed that high viral copy numbers/cell were always associated with E1/E2 amplification in keratinizing invasive tumors compared with nonkeratinizing tumors [43] and obtained similar data to our data showing that the copy number/cell was highest in type A tumors, which include a squamous keratinizing component. However, few reports have independently detected HPV DNAs in squamous and glandular lesions. A previous study using in situ hybridization showed that the HPV DNA localization in each component in adenosquamous carcinoma gradually increased from the pure adenocarcinoma component (28.6%) through the mixed component (54.5%) to the pure squamous cell carcinoma component (83.3%) [44]. These results can be explained by the sensitivity of the in situ hybridization method judging from our finding that the HPV copy number was higher in the squamous component and lower in the glandular component.

Various pathways for the histogenesis of adenosquamous carcinoma have been proposed in the past; however, the detailed mechanism remains unclear. Ueda et al. [45] suggested that adenosquamous carcinoma is derived from single stem cells, which have pluripotency to differentiate into both squamous and glandular cells. Interestingly, we observed that the same subtype of HPV was detected, and the physical status was the same in both the glandular and squamous elements in all of the HPV-positive cases. Therefore, our results agree with the above proposal that the main pathway for the histogenesis of adenosquamous carcinoma is from primitive reserve cells that become neoplastic and differentiate into two different cell types while collision of pure adenocarcinoma and pure squamous cell carcinoma with each other is a rare pathway for the histogenesis of adenosquamous carcinoma.

In the present study, we investigated 20 adenosquamous carcinomas for HPV infection, physical status, and viral load. In particular, the prevalence rate of HPV 18 was high, and many cases of HPV 18-positive cancer were the pure integrated form resulting in very low copy numbers/cell. It is possible that more aggressive transformation with early integration of HPV 18 results in cases with greater chromosomal instabilities, higher growth rates, and rapid progression.

Conflict of interest statement The authors declare that there are no conflicts of interest.

References

1. Parazzini F, La Vecchia C (1999) Epidemiology of adenocarcinoma of the cervix. Gynecol Oncol 39:40–46
2. Warton V (1995) Neoplasms of the cervix. In: Holland JF, Frei E III, Bast RC Jr et al (eds) Cancer medicine, Vol. II, 4th edn. Williams & Wilkins, Toronto, pp 2227–2261
3. Ferguson AW, Svobada-Newman SM, Frank TS (1998) Analysis of human papillomavirus infection and molecular alterations in adenocarcinoma of the cervix. Mod Pathol 11:11–18
4. Lombard I, Vincent-Salman A, Validire P et al (1998) Human papillomavirus genotype as a major determinant of the course of cervical cancer. J Clin Oncol 16:2613–2619
5. Anciaux D, Lawrence WD, Gregoire L (1997) Glandular lesions of the uterine cervix: prognostic implications of human papillomavirus status. Int J Gynecol Obstet 16:103–110
6. Parker MF, Arroyo GF, Geradts J et al (1997) Molecular characterization of adenocarcinoma of the cervix. Gynecol Path 64:242–251

7. Uchiyama M, Iwasaki T, Matsuo N et al (1997) Correlation between human papillomavirus positivity and *p53* gene overexpression in adenocarcinoma of the uterine cervix. Gynecol Oncol 65:23–29
8. Duggan MA, McGregor SE, Benoit JL et al (1995) The human papillomavirus status of invasive cervical adenocarcinoma: a clinicopathological and outcome analysis. Hum Pathol 26:319–325
9. Tenti P, Romagnoli S, Silini E et al (1996) Human papillomavirus types 16 and 18 infection in infiltrating adenocarcinoma of the cervix: PCR analysis of 138 cases and correlation with histologic type and grade. Am J Clin Pathol 106:52–56
10. Gordon AN, Bornstein J, Kaufman RH et al (1989) Human papillomavirus associated with adenocarcinoma and adenosquamous carcinoma of the cervix: analysis by in situ hybridization. Gynecol Oncol 35:345–348
11. Yamakawa Y, Forslund O, Teshima H et al (1994) Human papillomavirus DNA in adenocarcinoma and adenosquamous carcinoma of the uterine cervix detected by polymerase chain reaction (PCR). Gynecol Oncol 53:190–195
12. Tase T, Okagaki T, Clark BA et al (1988) Human papillomavirus types and localization in adenocarcinoma and adenosquamous carcinoma of the uterine cervix: a study by in situ DNA hybridization. Cancer Res 48:993–998
13. Teshima H, Beaudenon S, Koi K et al (1997) Human papillomavirus type 18 DNA sequences in adenocarcinoma and adenosquamous carcinoma of the uterine cervix. Arch Gynecol Obstet 259:169–177
14. Adcock LL, Julian TM, Okazaki T et al (1982) Carcinoma of the uterine cervix FIGO Stage I-B. Gynecol Oncol 14:199–208
15. Yajima A, Fukuda M, Noda K (1984) Histopathological findings concerning the morphogenesis of mixed carcinoma of the uterine cervix. Gynecol Oncol 18:157–164
16. Corden SA, Sant-Cassia LJ, Easton AJ et al (1999) The integration of HPV-18 DNA in cervical carcinoma. J Clin Pathol: Mol Pathol 52:275–282
17. Wells M, Nesland JM, Ostor AG et al (2003) Epithelial tumors. In: Tavassoli FA, Devilee P (eds) World Health Organization classification of tumors. Pathology and genetics of tumors of the breast and female genital organs. IARC Press, Lyon, pp 262–279
18. Fujinaga Y, Shimada M, Okazawa K et al (1991) Simultaneous detection and typing of genital human papillomavirus DNA using the polymerase chain reaction. J Gen Virol 72:1039–1044
19. Fujii T, Masumoto N, Saito M et al (2005) Comparison between in situ hybridization and real-time PCR technique as a means of detecting the integrated form of human papillomavirus 16 in cervical neoplasia. Diagn Mol Pathol 14(2):103–108
20. Ho CM, Chien TY, Huang SH et al (2006) Integrated human papillomavirus types 52 and 58 are infrequently found in cervical cancer, and high viral loads predict risk of cervical cancer. Gynecol Oncol 102:54–60
21. Moberg M, Gustavsson I, Gyllensten U (2003) Real-time PCR-based system for simultaneous quantification of human papillomavirus types associated with high risk of cervical cancer. J Clin Microbiol 41:3221–3228
22. Yoshida T, Sano T, Kanuma T et al (2008) Quantitative real-time polymerase chain reaction analysis of the type distribution, viral load, and physical status of human papillomavirus in liquid-based cytology samples from cervical lesions. Int J Gynecol Cancer 18:121–127
23. Ito T, Ishizuka T, Suzuki K et al (2000) Cervical cancer in young Japanese women. Arch Gynecol Obstet 264:68–70
24. Clark MA, Naahas W, Marker RJ et al (1991) Cervical cancer: women aged 35 and younger compared with women aged 36 and older. Am J Clin Oncol 14:352–356
25. Elliot PM, Tattersall MHN, Coppleson M et al (1989) Changing character of cervical cancer in young women. BMJ 298:288–290
26. Schwartz W, Weiss B (1986) Increased incidence of adenocarcinoma of the cervix in young women in the United States. Am J Epidemiol 124:1045
27. Zheng T, Holford TR, Ma Z et al (1996) The continuing increase in adenocarcinoma of the uterine cervix: a birth cohort phenomenon. Int J Epidemiol 25:252–258
28. Kjaer SK, Brinton LA (1993) Adenocarcinomas of the uterine cervix: the epidemiology of an increasing problem. Epidemiol Rev 15:486–498
29. Yoshida T, Fukuda T, Sano T et al (2004) Usefulness of liquid-based cytology specimens for immunocytochemical study of p16 expression and human papillomavirus testing. Cancer Cytopathol 102:100–1008
30. Liu S, Semenciw R, Mao Y (2001) Cervical cancer: the increasing incidence of adenocarcinoma and adenosquamous carcinoma in younger women. CMAJ 164(8):1151–1152
31. Inoue M, Sakaguchi J, Sasagawa T et al (2006) The evaluation of human papillomavirus DNA testing in primary screening for cervical lesions in a large Japanese population. Int J Gynecol Cancer 16:1007–1013
32. Konno R, Shin HR, Kim YT et al (2008) Human papillomavirus infection and cervical cancer prevention in Japan and Korea. Vaccine 26S:30–42
33. Schneider-Maunoury S, Croissant O, Orth G (1987) Integration of human papillomavirus type 16 DNA sequences: a possible early event in the progression of genital tumors. J Virol 61:3295–3298
34. Schwarz E, Fresse UK, Gissmann L et al (1985) Structure and transcription of human papillomavirus sequences in cervical carcinoma cells. Nature 314:111–114
35. Ham J, Dostatni N, Gauthier J et al (1991) The papillomavirus E2 protein: a factor with many talents. TIBS 16:440–444
36. Choo KB, Pan CC, Han SH (1987) Integration of human papillomavirus type 16 into cellular DNA of cervical carcinoma: preferential deletion of the E2 gene and invariable retention of the long control region and the E6/E7 open reading frames. Virology 161:259–261
37. Wilczynski SP, Pearlman L, Walker J (1988) Identification of HPV 16 early genes retained in cervical carcinomas. Virology 166:624–627
38. Badaracco G, Venuti A, Sedati A et al (2002) HPV16 and HPV18 in genital tumors: significantly different levels of viral integration and correlation to tumor invasiveness. J Med Virol 67:574–582
39. Cullen AP, Reid R, Campion M et al (1991) Analysis of the physical state of different human papillomavirus DNAs in intraepithelial and invasive cervical neoplasm. J Virol 65:606–612
40. Cheung JLK, Cheung TH, Ng CWY et al (2008) Analysis of HPV 18 viral load and integration status from low-grade cervical lesion to invasive cervical cancer. J Clin Microbiol 47(2):287–293
41. Park JS, Hwang ES, Park SN et al (1997) Physical status and expression of HPV genes in cervical cancers. Gynecol Oncol 65:121–129
42. Casas L, Galvan SC, Ordonez RM et al (1999) Asian-American variants of human papillomavirus type 16 have extensive mutations in the *E2* gene and are highly amplified in cervical carcinomas. Int J Cancer 83:449–455
43. Berman J, Casas L, Segura E et al (1994) Genome amplification of human papillomavirus types 16 and 18 in cervical carcinomas is related to the retention of *E1*/*E2* genes. Int J Cancer 56:640–645
44. Ogura K, Ishi K, Masumoto T et al (2006) Human papillomavirus localization in cervical adenocarcinoma and adenosquamous carcinoma using in situ polymerase chain reaction: review of the literature of human papillomavirus detection in these carcinomas. Pathol Int 56:301–308
45. Ueda Y, Miyatake T, Okazawa M et al (2008) Clonality and HPV infection analysis of concurrent glandular and squamous lesions and adenosquamous carcinomas of the uterine cervix. Am J Clin Pathol 130:389–400

Virchows Arch (2009) 455:261–270
DOI 10.1007/s00428-009-0816-9

ORIGINAL ARTICLE

An allelotype analysis indicating the presence of two distinct ovarian clear-cell carcinogenic pathways: endometriosis-associated pathway vs. clear-cell adenofibroma-associated pathway

Sohei Yamamoto · Hitoshi Tsuda · Kozue Suzuki · Masashi Takano · Seiichi Tamai · Osamu Matsubara

Received: 4 June 2009 / Revised: 21 July 2009 / Accepted: 21 July 2009 / Published online: 5 August 2009

Abstract Patterns of allele loss (loss of heterozygosity (LOH)) were studied to identify the genetic backgrounds underlying the two putative carcinogenic pathways of ovarian clear-cell adenocarcinoma: carcinomas thought to arise in endometriosis (endometriosis-associated carcinomas, 20 cases) and carcinomas thought to be derived from clear-cell adenofibroma ((CCAF)-associated carcinomas, 14 cases). Each tumor was assessed for LOH at 24 polymorphic loci located on 12 chromosomal arms: 1p, 3p, 5q, 8p, 9p, 10q, 11q, 13q, 17p, 17q, 19p, and 22q. For all informative loci, the frequency of LOH was not statistically different between the two carcinoma groups: 38% (66/172 loci) in the endometriosis-associated carcinomas and 35% (40/113 loci) in the CCAF-associated carcinomas. In the endometriosis-associated carcinomas, LOH was detected at high frequencies (>50%) at 3p, 5q, and 11q and at low frequencies (<20%) at 8p, 13q, and 17p. In the CCAF-associated carcinomas, LOH was detected at high frequencies at 1p, 10q, and 13q and at low frequencies at 3p, 9p, 11q, and 17q. The frequencies of LOH at chromosomes 3p, 5q, and 11q were significantly higher in the endometriosis-associated carcinomas than in the CCAF-associated carcinomas (P=0.026, 0.007, and 0.011, respectively). Immunohistochemical analysis demonstrated a close association between the allelic status of the 3p25–26 locus and levels of von Hippel–Lindau (VHL) protein expression (P=0.0026). These data further support the presence of two distinct carcinogenic pathways to ovarian clear-cell adenocarcinoma; the allelic status of the 3p, 5q, and 11q loci may provide a means to identify the precursor lesions of these carcinomas.

Keywords Ovarian clear-cell adenocarcinoma · Loss of heterozygosity · Endometriosis · Clear-cell adenofibroma · Carcinogenesis

S. Yamamoto · H. Tsuda (✉) · K. Suzuki · O. Matsubara
Department of Basic Pathology, National Defense Medical College,
3-2 Namiki, Tokorozawa,
Saitama 359-8513, Japan
e-mail: dr21001@ndmc.ac.jp

M. Takano
Department of Obstetrics and Gynecology,
National Defense Medical College,
3-2 Namiki, Tokorozawa,
Saitama 359-8513, Japan

S. Tamai
Department of Laboratory Medicine,
National Defense Medical College,
3-2 Namiki, Tokorozawa,
Saitama 359-8513, Japan

H. Tsuda
Pathology Section, Clinical Laboratory Division,
National Cancer Center Hospital,
Tokyo 104-0045, Japan

Introduction

Clear-cell adenocarcinomas comprise 5% to 10% of epithelial ovarian cancer in Western countries and, for unknown reasons, 15% to 20% of such tumors in Japan [1–6]. Ovarian clear-cell adenocarcinoma is characterized by its distinctive histology and highly chemoresistant nature, resulting in an extremely poor prognosis when surgical cytoreduction is insufficient [1–4]. Although the etiology of ovarian clear-cell adenocarcinoma has not been fully elucidated, two distinct precursor lesions have been suggested, namely, endometriosis and clear-cell adenofibroma (CCAF).

Histological and epidemiological observations have consistently demonstrated a close association between endometriosis and ovarian clear-cell adenocarcinoma [7–13], and the molecular basis of the transformative pathway from endometriosis to clear-cell adenocarcinoma has been described, i.e., genetic instability or DNA aneuploidy in the endometriotic lesions, with loss of heterozygosity (LOH) or mutation of the tumor-suppressor gene *PTEN* detected in both endometriosis and co-existing clear-cell adenocarcinomas [14–17].

On the other hand, CCAF, a major form of benign or borderline ovarian clear-cell tumor, may also be a precursor of clear-cell adenocarcinoma [1, 4, 18–22]. Benign or borderline CCAF is a rare form of neoplasm, accounting for less than 5% of all ovarian clear-cell tumors [1, 4, 18, 19]. However, a study from our institution demonstrated that CCAF components co-existed in 21% of surgically resected clear-cell adenocarcinomas [20]. The CCAF components co-existing with clear-cell adenocarcinoma often contain both benign CCAF and borderline CCAF [18–20]. Recently, we analyzed LOH using 17 polymorphic markers to examine the genetic linkage between CCAF and co-existing clear-cell adenocarcinoma of the ovary and suggested that CCAF can be a clonal precursor for clear-cell adenocarcinoma in certain cases [21]. In that study, allelic losses were observed to accumulate from benign CCAF through borderline CCAF to co-existing clear-cell adenocarcinoma, and several specific chromosomal regions appeared to undergo genetic changes earlier (i.e., 5q, 10q, and 22q) or later (i.e., 1p and 13q) in the CCAF-associated clear-cell carcinogenic pathway [21].

These observations suggest, but do not yet establish, that clear-cell adenocarcinoma associated with CCAF components is a distinct clinicopathological entity in ovarian clear-cell adenocarcinoma [20, 23]. A study from our institution showed that, in comparison with clear-cell adenocarcinoma without CCAF components, clear-cell adenocarcinoma with CCAF components shows several distinct clinicopathological characteristics, such as a lower frequency of co-existing endometriosis, a higher frequency of histologically low-grade tumor with tubulocystic proliferative architecture, a lower cancer cell proliferative activity, and better patient prognosis [20]. In that study, carcinomas without CCAF components frequently harbored endometriosis in the ipsilateral adnexa to the carcinoma, and therefore, these two distinct carcinogenic pathways might contribute to the distinct clinicopathological features of the tumors [20]. However, the molecular genetic evidence underlying the differences between these putative pathways has not been elucidated.

Because the development of many cancers is believed to be the result of a multistep process involving a series of genetic events and the subsequent clonal evolution of cells with accumulated genetic errors, the chromosomal loci most frequently showing LOH would be expected to differ between tumors arising via distinct developmental pathways. Therefore, to clarify whether differences in genetic background underline the two possible carcinogenic pathways to ovarian clear-cell adenocarcinoma (endometriosis-associated pathway vs. CCAF-associated pathway), we performed polymerase chain reaction (PCR)-based LOH analyses using 24 polymorphic markers located on 12 chromosomal arms where relatively frequent LOH has been reported in ovarian epithelial tumors, including clear-cell adenocarcinoma or endometriosis [15–17, 24–31]. We then compared the allelic patterns of carcinomas with putative distinct precursors, since demonstrating the presence or absence of divergent carcinogenic pathways in ovarian clear-cell adenocarcinoma will provide insight into the genetic origin of this tumor.

Materials and methods

Cases analyzed

According to the histopathological criteria described previously [20–22], a total of 20 clear-cell adenocarcinomas with synchronous endometriosis (endometriosis-associated carcinomas) and a total of 14 clear-cell adenocarcinomas with adjacent CCAF component (CCAF-associated carcinomas) were identified from the files of the Department of Laboratory Medicine, National Defense Medical College Hospital, Japan (Fig. 1). All of the 34 patients underwent surgical resection between 1988 and 2006, and none had undergone chemotherapy or radiation therapy prior to surgery. All specimens were formalin-fixed and paraffin-embedded. The presence of cytological or structural atypia in the putative precursor lesions was not considered in this study. Although histologic examination revealed endometriotic lesions in two of the 14 cases with CCAF-associated carcinomas, these endometriotic lesions were present in the adnexa contralateral to the carcinomas and none of these 20 cases with endometriosis-associated carcinoma and 14 cases with CCAF-associated carcinoma overlapped. Clinical staging of disease was done according to the International Federation of Gynecology and Obstetrics system. Of the 20 cases with endometriosis-associated carcinoma, 14 (70%) were stage I, one (5%) was stage II, four (20%) were stage III, and one (5%) was stage IV. Of the 14 cases with CCAF-associated carcinoma, ten (71%) were stage I, one (7%) was stage II, two (14%) were stage III, and one (7%) was stage IV. The research protocol was approved by the ethics committee of the National Defense Medical College, Tokorozawa, Japan.

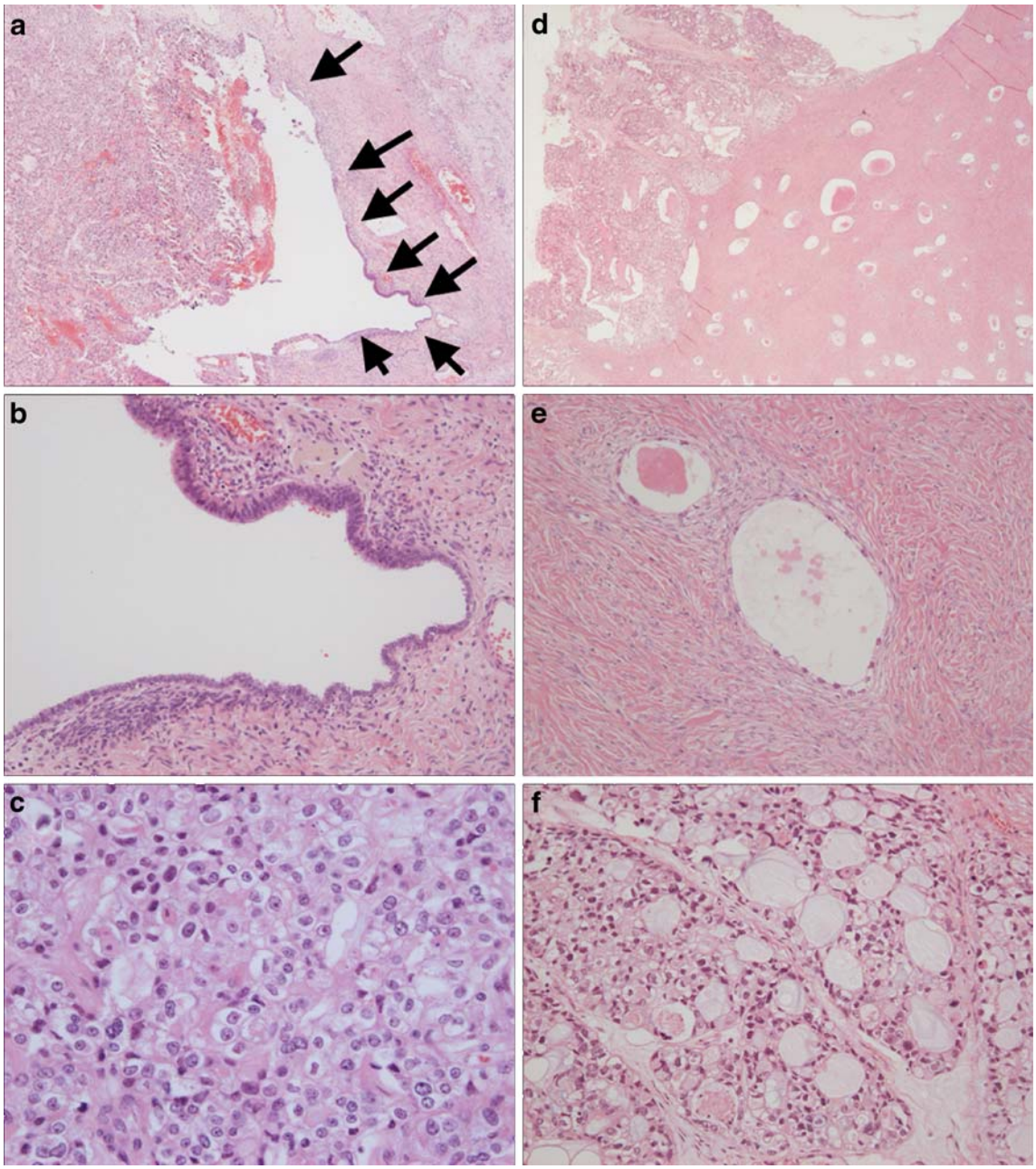

Fig. 1 Representative histological features of ovarian clear-cell adenocarcinoma with synchronous endometriosis (**a**, **b**, and **c**) and ovarian clear-cell adenocarcinoma with adjacent CCAF component (**d**, **e**, and **f**). **a** Clear-cell adenocarcinoma (middle to left side) arising within endometriotic cyst. *Arrows* indicate endometriotic epithelium. **b** High magnification of the endometriosis shown in (**a**). **c** High magnification of the clear-cell adenocarcinoma component shown in (**a**). **d** Clear-cell adenocarcinoma (left side) with adjacent CCAF component (middle to right side). **e** High magnification of the CCAF shown in (**d**). Glands are delineated with monolayers of cuboidal glandular cells with clear cytoplasm. Cytological atypia is not evident in this case. **f** High magnification of the clear-cell adenocarcinoma component shown in (**d**). HE stain, original magnification ×20 for (**d**); ×40 for (**a**); ×200 for (**b**), (**e**), and (**f**); ×400 for (**c**)

Tissue microdissection and DNA extraction

DNA was extracted from selected regions of carcinomas in which tumor histology was highly representative for a diagnosis for clear-cell adenocarcinoma and apart from tissue degeneration or inflammation, and normal areas by laser microdissection using a Leica LMD 6000 (Leica; Narishige Micromanipulator, Wetzlar, Germany) as described previously [21]. We performed constitutional microdissection from at least five serial 8-μm-thick tissue sections of the 10×10 mm or larger representative cancer tissues. DNA extraction was performed using the same

methods as described previously [21], and the concentration of DNA from each sample was adjusted to 0.05 μg/μl. Extracted DNA samples were stored at 4°C until use.

Selection of polymorphic markers

Twenty-four polymorphic markers, located on 12 chromosomal arms, were selected on the basis of the following criteria: (1) the markers were localized on regions in which frequent LOH events have been reported in primary ovarian carcinomas and/or endometriosis [15–17, 24–31], (2) the sizes of the amplified fragments were expected to be smaller than 200 bp for reliable amplification of template DNA from formalin-fixed tissue.

Two paired polymorphic markers were used for each chromosomal locus examined, and pairs of forward and reverse primers of 24 oligonucleotide polymorphic markers corresponding to the sequences retrieved from the Genome Database (http://gdbwww.gdb.org/gdb/) were synthesized commercially and purchased from Perkin Elmer (Applied Biosystems, Foster City, CA). Chromosomal regions and paired markers used were as follows: 1p36.12–36.32 (*D1S199, D1S2663*), 3p25–26 (*D3S1110, D3S1038*), 5q13.3–23 (*D5S424, D5S346*), 8p21.3–22 (*D8S261, D8S254*), 9p21 (*D9S161, D9S1748*); 10q23.2–23.3 (*D10S608, D10S574*), 11q23–24 (*D11S1336, D11S1356*), 13q12.3–13 (*D13S263, D13S267*), 17p13.1 (*D17S786, D17S1289*), 17q21 (*D17S579, D17S1322*), 19p13.3 (*D19S413, D19S894*), 22q13 (*D22S284, D22S304*). The 5' ends of the forward primers were labeled with 6-carboxyfluorescein.

Polymerase chain reaction and analysis of allelic pattern

PCR amplification of genomic DNA was performed in a total volume of 25 μl of reaction mixture containing 2 μl of DNA solution corresponding to 100 ng of genomic DNA, 0.4 pmol/μl of each primer, and 1× TaqMan Universal PCR Master Mix (Applied Biosystems) using a GeneAmp® PCR system 9600 (Applied Biosystems). Details of PCR-cycling conditions have been described previously [21].

Aliquots of the PCR products were then mixed with size standards and formamide, denatured, and run on an ABI 3130 automated capillary electrophoresis DNA sequencer (Applied Biosystems). The allelic products were assessed for peak height and peak area with GeneMapper software version 3.7 (Applied Biosystems).

Non-cancerous DNA samples with two different amplified bands were defined as informative cases for LOH analysis. LOH was considered to exist if the relative ratio of peak heights calculated by the following formula was lower than 0.5 or greater than 1.5: [Peak height of the affected allele (allele A) of the tumor × peak height of the unaffected allele (allele B) of normal cells] / [peak height of allele A of normal cells × peak height of allele B of tumor cells]. When tumor DNA samples showed a significant reduction in the relative ratio of peak height in the initial PCR, the cases were reexamined at least twice to confirm that the LOH data were reproducible. Results were considered non-informative when the normal tissue was homozygous, when the tissue lysate failed to be amplified, or when the results could not be interpreted unambiguously. A case was considered to be positive for LOH when at least one of the two paired markers on each chromosomal region showed a pattern of allelic loss.

Immunohistochemistry

Sections of 4-μm-thick tissue were deparaffinized in xylene and rehydrated through a series of alcohols. Antigen retrieval was achieved by microwave heating (97°C for 30 min) in 0.01 mol/l citrate buffer (pH 6.0), followed by cooling at room temperature. Endogenous peroxidase was blocked using 5% hydrogen peroxide, and non-specific binding of secondary antibody was blocked by incubation with normal swine serum. Individual sections were incubated at 4°C overnight with primary antibodies against VHL (ab11191, mouse monoclonal, dilution 1/100; Abcam, Cambridge, UK). The slides were then reacted with a dextran polymer reagent combined with secondary antibodies and peroxidase (DAKO, Glostrup, Denmark) for 1 h at room temperature. Specific antigen–antibody reactions were visualized with 0.2% diaminobenzidine tetrahydrochloride and hydrogen peroxide, and counterstaining was performed using Mayer's hematoxylin. Non-neoplastic kidney tissue was used as a positive control, and sections without the primary antibody were used as negative controls.

We evaluated cell membranous and cytoplasmic immunoreaction and did not separate these because distinction between cytoplasmic and membranous expression was often difficult in the tumor cells with scant cytoplasm or rich in cytoplasmic glycogen. Cases were considered as positive for VHL protein expression if more than 10% of the tumor cells examined showed membranous/cytoplasmic immunoreactivity with intensity equal to or more than that in the positive control; otherwise, cases were considered as representing downregulation of VHL protein expression.

Statistical analyses

Statistical analyses were performed using StatMate III software (ATMS, Tokyo, Japan). To compare the frequencies of LOH occurrence or the immunohistochemical results, the chi-squared test or Fisher's exact test was used as appropriate. Differences at $P<0.05$ were considered to be statistically significant.

Results

Allelotype analysis

A representative case showing LOH at the *D3S1038* locus is presented in Fig. 2. LOH data derived from the allelotype analysis are summarized in Tables 1 and 2. When all the chromosomal regions studied and all the informative cases were combined, the total frequency of LOH events was 37% (106 of 285 informative loci), and there was no statistically significant difference in the frequency of LOH between the endometriosis-associated carcinomas (38%, 66 of 172 informative loci) and the CCAF-associated carcinomas (35%, 40 of 113 informative loci). In all the 34 cases examined, LOH events were detected at high frequencies (>50%) at chromosomes 5q (72%, 18 of 25 informative cases), 1p (54%, 14 of 26), and 10q (50%, 7 of 14), followed by 11q (42%, 13 of 31), 3p (39%, 13 of 33), 19p (35%, 9 of 26), 22q (33%, 10 of 30), 13q (33%, 3 of 9), 8p (27%, 9 of 33), 17q (20%, 4 of 20), and detected at low frequencies (<20%) at chromosomes 9p (19%, 5 of 27) and 17p (8%, 1 of 12). In the 20 endometriosis-associated carcinomas, LOH events were detected at high frequencies (>50%) at chromosomes 5q (93%, 14 of 15 informative

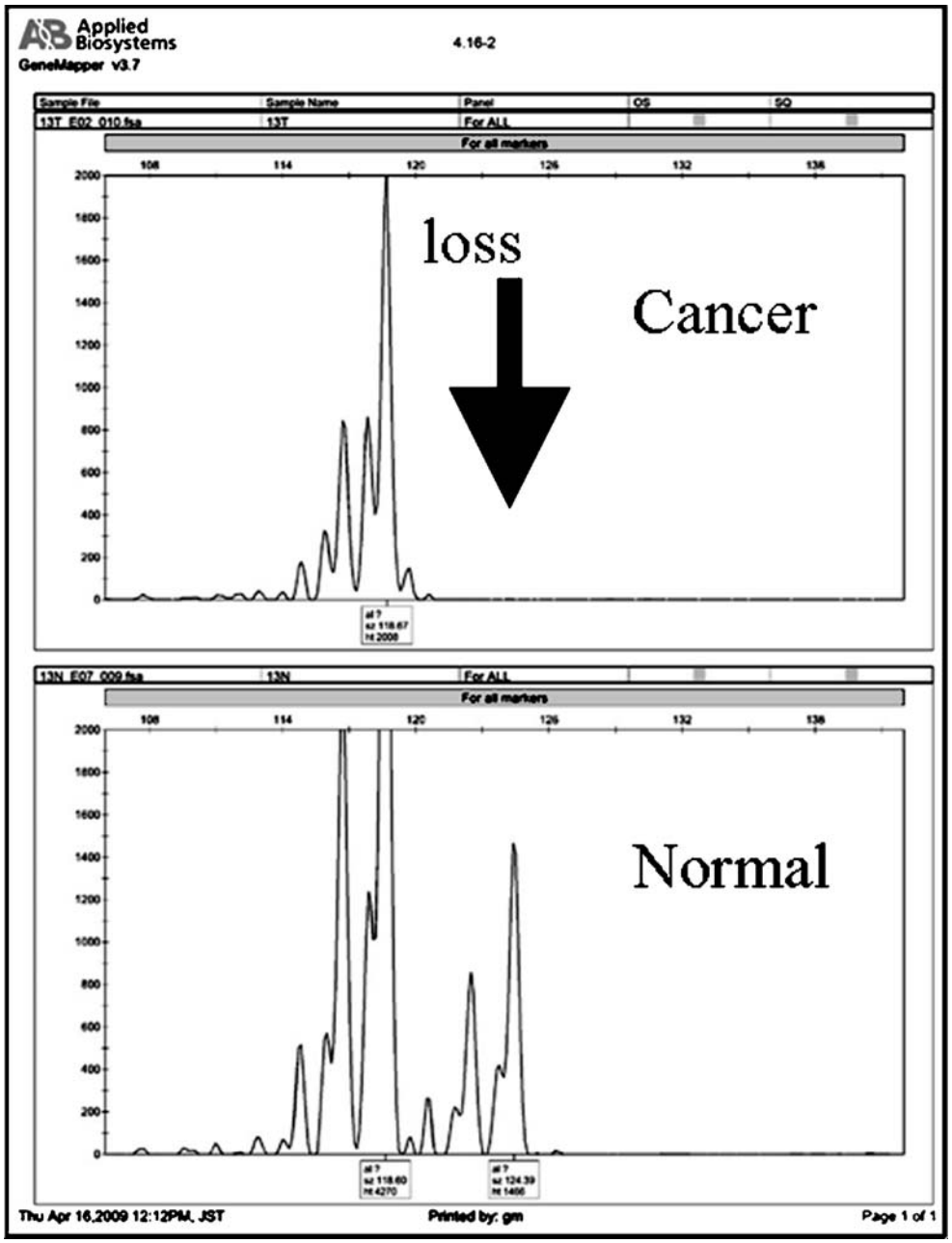

Fig. 2 An electrophoretogram showing allelic loss at the *D3S1038* locus on chromosome 3p25–26 in a case of ovarian clear-cell adenocarcinoma. Loss of heterozygosity is identified as a reduction of the relative intensity of one of the two alleles in the cancer DNA to less than 50% of that in the corresponding normal DNA. The longer allele is deleted (*arrow*). According to the definition given in the text, the case was judged to carry LOH

Table 1 Frequency of LOH at 24 polymorphic chromosomal loci in endometriosis-associated carcinomas and CCAF-associated carcinomas

Marker	Chromosome location	No. of cases with LOH/ no. of informative cases (%)		
		Total cases	Endometriosis-associated	CCAF-associated
D1S199	1p36.12–36.21	14/26 (54)	6/15 (40)	8/11 (73)
D1S2663	1p36.31–36.32	2/5 (40)	1/2 (50)	1/3 (33)
D3S1110	3p25–26	8/32 (25)	7/19 (37)	1/13 (8)
D3S1038	3p25–26	7/23 (30)	5/14 (36)	2/9 (22)
D5S424	5q13.3	13/24 (54)	10/15 (67)	3/9 (33)
D5S346	5q22–23	10/19 (53)	8/11 (73)	2/8 (25)
D8S261	8p21.3–22	0/2 (0)	0/0 (0)	0/2 (0)
D8S254	8p22	9/33 (27)	3/19 (16)	6/14 (43)
D9S161	9p21	1/14 (7)	1/10 (10)	0/4 (0)
D9S1748	9p21	4/26 (15)	3/16 (19)	1/10 (10)
D10S608	10q23.2	6/13 (46)	3/6 (50)	3/7 (43)
D10S574	10q23.3	2/10 (20)	1/5 (20)	1/5 (20)
D11S1336	11q23	10/28 (36)	9/17 (53)	1/11 (9)
D11S1356	11q23–24	4/21 (19)	3/14 (21)	1/7 (14)
D13S267	13q12.3–13	2/7 (29)	0/4 (0)	2/3 (67)
D13S263	13q12.3–13	1/6 (17)	1/4 (25)	0/2 (0)
D17S1289	17p13.1	0/0 (0)	0/0 (0)	0/0 (0)
D17S786	17p13.1	1/12 (8)	0/7 (0)	1/5 (20)
D17S1322	17q21	3/20 (15)	2/13 (15)	1/7 (14)
D17S579	17q21	1/16 (6)	1/10 (10)	0/6 (0)
D19S413	19p13.3	8/26 (31)	5/17 (29)	3/9 (33)
D19S894	19p13.3	1/1 (100)	0/0 (0)	1/1 (100)
D22S304	22q13	5/18 (28)	2/11 (18)	3/7 (43)
D22S284	22q13	7/29 (24)	4/19 (21)	3/10 (30)

CCAF clear-cell adenofibroma, *LOH* loss of heterozygosity

cases), 11q (61%, 11 of 18), and 3p (55%, 11 of 20), followed by 10q (43%, 3 of 7), 1p (40%, 6 of 15), 19p (29%, 5 of 17), 22q (26%, 5 of 19), 9p (25%, 4 of 16), 17q (23%, 3 of 13), and detected at low frequencies (<20%) at chromosomes 13q (17%, 1 of 6) and 8p (16%, 3 of 19; Table 2). At chromosome 17p, LOH was not observed in the endometriosis-associated carcinomas (0 of seven informative cases). In the 14 CCAF-associated carcinomas, LOH events were detected at high frequencies (>50%) at chromosomes 1p (73%, 8 of 11 informative cases), 13q

Table 2 Compared frequencies of LOH on chromosomal regions analyzed in this study

Chromosome location	No. of cases with LOH/ no. of informative cases (%)			
	Total	Endometriosis-associated	CCAF-associated	*P* value
1p36.12–36.32	14/26 (54)	6/15 (40)	8/11 (73)	0.104
3p25–26	13/33 (39)	11/20 (55)	2/13 (15)	**0.026**
5q13.3–23	18/25 (72)	14/15 (93)	4/10 (40)	**0.0068**
8p21.3–22	9/33 (27)	3/19 (16)	6/14 (43)	0.092
9p21	5/27 (19)	4/16 (25)	1/11 (9)	0.302
10q23.2–23.3	7/14 (50)	3/7 (43)	4/7 (57)	0.500
11q23–24	13/31 (42)	11/18 (61)	2/13 (15)	**0.011**
13q12.3–13	3/9 (33)	1/6 (17)	2/3 (67)	0.226
17p13.1	1/12 (8)	0/7 (0)	1/5 (20)	0.364
17q21	4/20 (20)	3/13 (23)	1/7 (14)	0.561
19p13.3	9/26 (35)	5/17 (29)	4/9 (44)	0.884
22q13	10/30 (33)	5/19 (26)	5/11 (45)	0.284

Bold figures indicate statistical significance

LOH loss of heterozygosity, *CCAF* clear-cell adenofibroma

Table 3 Results of immunohistochemistry for VHL protein expression

	No. of cases (%)			*P* value
	Total	Positive	Downregulated	
I. Comparison of cases classified by the putative precursor lesions				
Endometriosis-associated	20 (100)	14 (60)	6 (30)	0.261
CCAF-associated	14 (100)	12 (86)	2 (14)	
II. Comparison of cases subdivided by allelic status on chromosome 3p25–26				
LOH-positive	13 (100)	6 (46)	7 (54)	0.0026
LOH-negative	20 (100)	19 (95)	1 (5)	

CCAF clear-cell adenofibroma, *LOH* loss of heterozygosity

(67%, 2 of 3), and 10q (57%, 4 of 7), followed by 22q (45%, 5 of 11), 19p (44%, 4 of 9), 8p (43%, 6 of 14), 5q (40%, 4 of 10), and 17p (20%, 1 of 5), and detected at low frequencies (<20%) at chromosomes 3p (15%, 2 of 13), 11q (15%, 2 of 13), 17q (14%, 1 of 7), and 9p (9%, 1 of 11; (Table 2). In comparison with the CCAF-associated carcinomas, the incidences of LOH on chromosomes 3p, 5q, and 11q were statistically significantly higher in the endometriosis-associated carcinomas (P=0.026, 0.0068, and 0.011, respectively; Table 2). On chromosomes 1p, 8p, and 13q, the incidences of LOH were substantially higher in the CCAF-associated carcinomas than in the endometriosis-associated carcinomas (1p, 73% in the former and 40% in the latter; 8p, 43% in the former and 16% in the latter; and 13q, 67% in the former and 17% in the latter), but these differences were not statistically significant (P=0.104, 0.092, and 0.226, respectively; Table 2).

Immunohistochemical analysis for VHL protein expression

The results of immunohistochemical detection of VHL protein are summarized in Table 3. A case showing positive immunoreactivity for VHL protein and another case showing downregulated expression of VHL protein are presented in Fig. 3. Of the 34 clear-cell adenocarcinomas, 26 (76%) and eight (24%) were considered as positive and downregulated for VHL protein, respectively. There was no statistically significant difference in the score of VHL immunoreactivity between endometriosis-associated carcinomas and CCAF-associated carcinomas (Table 3). However, of the 33 cases in which information on LOH on chromosome 3p25–26 was available, the score of VHL immunoreactivity was strongly and significantly associated with allelic status on chromosome region 3p25–26: seven (54%) of 13 LOH-positive tumors and only one (5%) of 20 tumors with constitutional heterozygosity were scored as downregulated expression of VHL protein, respectively (P=0.0026).

Discussion

It is generally accepted that genetic instability and alterations play an important role in human carcinogenesis, and the development of many cancers is believed to be the

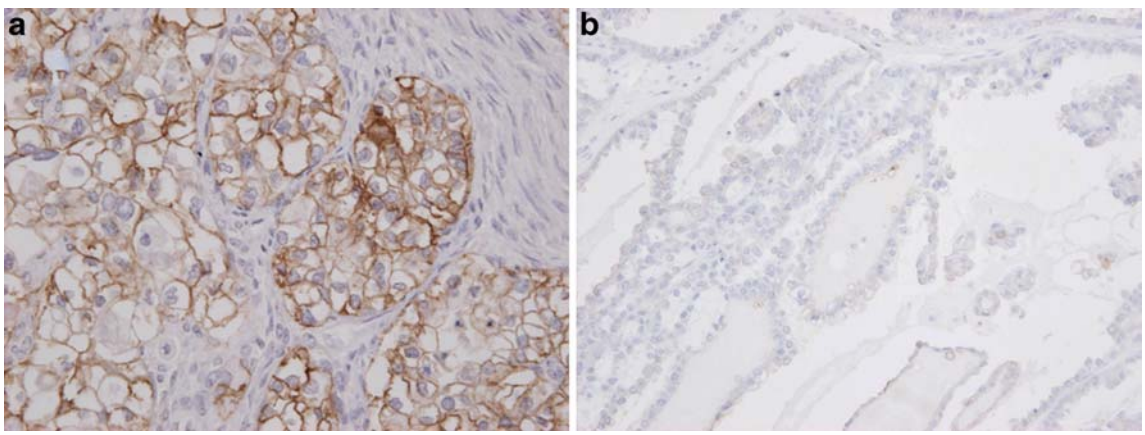

Fig. 3 Immunohistochemistry for VHL protein in ovarian clear-cell adenocarcinoma. **a** A case of clear-cell adenocarcinoma showing diffuse membranous/cytoplasmic immunoreactivity for VHL protein. **b** A case of clear-cell adenocarcinoma assessed as showing reduced expression of VHL protein. Immunoperoxidase stain, original magnification ×400 for (**a**) and ×200 for (**b**)

result of a multistep process involving a series of genetic events and the subsequent clonal evolution of cells with accumulated genetic errors. Consequently, if different chromosomal alterations play particular roles in tumors with distinct clinicopathological features, the chromosomal loci most frequently showing LOH would differ among these tumors, and divergent genetic backgrounds would underlie the development of each tumor type.

In the present study, we have demonstrated that the total frequency of LOH on all informative chromosomal loci in the endometriosis-associated carcinomas and the CCAF-associated carcinomas was 38% and 35%, respectively, suggesting that the overall extent of genetic alterations was not different between the two carcinoma groups. However, analysis with respect to specific chromosomal loci did reveal differences between the two carcinoma groups. These loci were chromosomes 3p25–26, 5q13.3–23, and 11q23–24, where the endometriosis-associated carcinomas exhibited LOH with frequencies of 55%, 93%, and 61%, respectively, compared with 15%, 40%, and 15% in the CCAF-associated carcinomas. These data suggest that these less frequently altered regions in CCAF-associated carcinomas may harbor genes responsible for the clinicopathological characteristics of the type, namely, a higher frequency of histologically low-grade tumors with tubulocystic proliferative architecture as well as lower cancer cell proliferative activity [20].

As our previous study suggested a relatively better prognosis for patients with CCAF-associated carcinomas [20], a point of interest is whether allelic losses on chromosomes 3p25–26, 5q13.3–23, or 11q23–24 are associated with tumor aggressiveness, i.e., ability to metastasize or resistance to chemotherapy. Therefore, tumor suppressor genes (TSGs) mapping to these chromosomal regions, such as *VHL* on 3p, *adenomatous polyposis coli* (*APC*) on 5q, and *ataxia telangiectasia mutated* (*ATM*) on 11q, or products of these genes, are of interest [32–34]. Although there have been conflicting reports on the association of LOH at 3p with histological grade or clinical stage of ovarian cancers [25, 35, 36], Zheng et al. [35] have shown that 3p deletions are associated with high-grade ovarian carcinomas. Allan et al. [37] demonstrated LOH on 5q in 50% of sporadic ovarian carcinomas, but the *APC* TSG was not mutated in these tumors, suggesting that this gene is not responsible for ovarian tumorigenesis. A study by Gabra et al. [38] reported that LOH on chromosome 11q23–24 was significantly associated with advanced stage and poor prognosis in patients with ovarian or breast cancer, and suggested that a late-acting progression-suppressor may be located within this region.

We have demonstrated that immunohistochemical expression of VHL protein was significantly correlated with the allelic status of the clear-cell adenocarcinomas studied. The *VHL* gene is located at 3p25–26, and alterations on chromosome 3q or the *VHL* locus have been described to occur in a variable proportion of ovarian carcinomas [25, 28, 35, 36, 39]. However, in some series, a significant number of tumors, including those with allelic deletion at the *VHL* locus, showed a normal VHL protein-staining pattern [39]. However, our observation that seven (54%) of 13 LOH-positive tumors and only one (5%) of 20 LOH-negative tumor showed reduced expression of VHL protein indicates that, at least in our series, LOH at the *VHL* locus is associated with decreased *VHL* gene function, suggesting a tumor suppressor role of VHL in a proportion of ovarian clear-cell adenocarcinomas.

The best understood function of VHL relates to its ability to target hypoxia-inducible factor (HIF) for poly-ubiquitination, and hence destruction [40]. HIF is a heterodimer composed of DNA-binding alpha/beta complexes and directs various transcriptional responses involving the induction of genes responsible for tumor growth and angiogenesis [41]. The HIF-1alpha subunit interacts with VHL protein and is degraded by ubiquitin-mediated proteolysis in the presence of oxygen. An increased level of HIF-1alpha has been reported in various human malignancies, including ovarian clear-cell adenocarcinoma [39, 41–43]. Osada et al. [39] reported that patients with ovarian carcinomas showing nuclear HIF-1alpha expression had poor prognosis, and that the topological distributions of HIF-1alpha and VHL protein were inversely correlated in the ovarian clear-cell adenocarcinoma specimens. Therefore, it is possible that the decreased levels of VHL protein have an accelerating role in ovarian clear-cell carcinogenesis via upregulation of HIF1-alpha, and this merits future study.

Overall, however, there appears to be some overlap of the patterns of allelic loss between the two groups of ovarian clear-cell carcinomas, for example, involvement of 1p36 and 10q23.3, and these points of overlap may represent common areas where genetic alterations play fundamental roles in the carcinogenesis of this tumor. Mutational analysis of the remaining alleles may yield additional information concerning the significance of LOH at these loci in ovarian clear-cell carcinogenesis.

In summary, we have assessed patterns of allelic loss in two groups of ovarian clear-cell adenocarcinomas with possible distinct precursor lesions. We found significant differences in the frequencies of LOH at chromosomal regions 3p25–26, 5q13.3–23, and 11q23–24. These data further support the presence of two distinct carcinogenic pathways to ovarian clear-cell adenocarcinoma; the allelic status of the 3p, 5q, and 11q loci may be useful in differentiating the distinct precursor lesions of these carcinomas.

Acknowledgments This work was supported in part by a grant-in-aid for promotion of defense medicine from the Ministry of Defense, Japan (S.Y., H.T., and O.M.), and by a grant-in-aid for cancer research from the Ministry of Health, Labour, and Welfare, Japan (H.T.).

Conflict of interest statement The authors declare no actual or potential conflicts of interest in this study.

References

1. Seidman JD, Russell P, Kurman RJ (2001) Surface epithelial tumors of the ovary. In: Kurman RJ (ed) Blaustein's pathology of the female genital tract, 5th edn. Springer, New York, pp 791–904
2. Sugiyama T, Kamura T, Kigawa J et al (2000) Clinical characteristics of clear cell carcinoma of the ovary: a distinct histologic type with poor prognosis and resistance to platinum-based chemotherapy. Cancer 88:2584–2589
3. Ikeda K, Sakai K, Yamamoto R et al (2003) Multivariate analysis for prognostic significance of histologic subtype, GST-pi, MDR-1, and p53 in stages II–IV ovarian cancer. Int J Gynecol Cancer 13:776–784
4. Tavassoli FA, Devilee P (eds) (2003) World Health Organization classification of tumours. Pathology and genetics of tumours of the breast and female genital organs. IARC Press, Lyon
5. Kaku T, Ogawa S, Kawano Y et al (2003) Histological classification of ovarian cancer. Med Electron Microsc 36:9–17
6. Gynecologic Cancer Comittee, Japan Society of Obstetrics and Gynecology (2008) Annual report of gynecological cancer patients in Japan 2006. Acta Obstet Gynaecol Jpn 60:1001–1085 (in Japanese)
7. Sampson JA (1925) Endometrial carcinoma of the ovary arising in endometrial tissue in that organ. Arch Surg 10:1–72
8. Vercellini P, Parazzini F, Bolis G et al (1993) Endometriosis and ovarian cancer. Am J Obstet Gynecol 169:181–182
9. Fukunaga M, Nomura K, Ishikawa E et al (1997) Ovarian atypical endometriosis: its close association with malignant epithelial tumours. Histopathology 30:249–255
10. Ogawa S, Kaku T, Amada S et al (2000) Ovarian endometriosis associated with ovarian carcinoma: a clinicopathological and immunohistochemical study. Gynecol Oncol 77:298–304
11. LaGrenade A, Silverberg SG (1988) Ovarian tumors associated with atypical endometriosis. Hum Pathol 19:1080–1084
12. Mostoufizadeh M, Scully RE (1980) Malignant tumors arising in endometriosis. Clin Obstet Gynecol 23:951–963
13. Seidman JD (1996) Prognostic importance of hyperplasia and atypia in endometriosis. Int J Gynecol Pathol 15:1–9
14. Varma R, Rollason T, Gupta JK et al (2004) Endometriosis and the neoplastic process. Reproduction 127:293–304
15. Jiang X, Hitchcock A, Bryan EJ et al (1996) Microsatellite analysis of endometriosis reveals loss of heterozygosity at candidate ovarian tumor suppressor gene loci. Cancer Res 56:3534–3539
16. Jiang X, Morland SJ, Hitchcock A et al (1998) Allelotyping of endometriosis with adjacent ovarian carcinoma reveals evidence of a common lineage. Cancer Res 58:1707–1712
17. Sato N, Tsunoda H, Nishida M et al (2000) Loss of heterozygosity on 10q23.3 and mutation of the tumor suppressor gene PTEN in benign endometrial cyst of the ovary: possible sequence progression from benign endometrial cyst to endometrioid carcinoma and clear cell carcinoma of the ovary. Cancer Res 60:7052–7056
18. Bell DA, Scully RE (1985) Benign and borderline clear cell adenofibromas of the ovary. Cancer 56:2922–2931
19. Roth LM, Langley FA, Fox H et al (1984) Ovarian clear cell adenofibromatous tumors. Benign, of low malignant potential, and associated with invasive clear cell carcinoma. Cancer 53:1156–1163
20. Yamamoto S, Tsuda H, Yoshikawa T et al (2007) Clear cell adenocarcinoma associated with clear cell adenofibromatous components: a subgroup of ovarian clear cell adenocarcinoma with distinct clinicopathologic characteristics. Am J Surg Pathol 31:999–1006
21. Yamamoto S, Tsuda H, Takano M et al (2008) Clear-cell adenofibroma can be a clonal precursor for clear-cell adenocarcinoma of the ovary: a possible alternative ovarian clear-cell carcinogenic pathway. J Pathol 216:103–110
22. Yamamoto S, Tsuda H, Takano M et al (2008) Expression of platelet-derived growth factors and their receptors in ovarian clear-cell carcinoma and its putative precursors. Mod Pathol 21:115–124
23. Veras E, Mao TL, Ayse A et al (2009) Cystic and adenofibromatous clear cell carcinomas of the ovary: distinctive tumors that differ in their pathogenesis and behavior: a clinicopathologic analysis of 122 cases. Am J Surg Pathol 33:844–853
24. Cliby W, Ritland S, Hartmann L et al (1993) Human epithelial ovarian cancer allelotype. Cancer Res 53:2393–2398
25. Dodson MK, Hartmann LC, Cliby WA et al (1993) Comparison of loss of heterozygosity patterns in invasive low-grade and high-grade epithelial ovarian carcinomas. Cancer Res 53:4456–4460
26. Sato T, Saito H, Morita R et al (1991) Allelotype of human ovarian cancer. Cancer Res 51:5118–5122
27. Osborne RJ, Leech V (1994) Polymerase chain reaction allelotyping of human ovarian cancer. Br J Cancer 69:429–438
28. Simsir A, Palacios D, Linehan WM et al (2001) Detection of loss of heterozygosity at chromosome 3p25–26 in primary and metastatic ovarian clear-cell carcinoma: utilization of microdissection and polymerase chain reaction in archival tissues. Diagn Cytopathol 24:328–332
29. Okada S, Tsuda H, Takarabe T et al (2002) Allelotype analysis of common epithelial ovarian cancers with special reference to comparison between clear cell adenocarcinoma with other histological types. Jpn J Cancer Res 93:798–806
30. Dent J, Hall GD, Wilkinson N et al (2003) Cytogenetic alterations in ovarian clear cell carcinoma detected by comparative genomic hybridisation. Br J Cancer 88:1578–1583
31. Suehiro Y, Sakamoto M, Umayahara K et al (2000) Genetic aberrations detected by comparative genomic hybridization in ovarian clear cell adenocarcinomas. Oncology 59:50–56
32. Shuin T, Yamasaki I, Tamura K et al (2006) Von Hippel–Lindau disease: molecular pathological basis, clinical criteria, genetic testing, clinical features of tumors and treatment. Jpn J Clin Oncol 36:337–343
33. Kinzler KW, Nilbert MC, Su LK et al (1991) Identification of FAP locus genes from chromosome 5q21. Science 253:661–665
34. Savitsky K, Bar-Shira A, Gilad S et al (1995) A single ataxia telangiectasia gene with a product similar to PI-3 kinase. Science 268:1749–1753
35. Zheng JP, Robinson WR, Ehlen T et al (1991) Distinction of low grade from high grade human ovarian carcinomas on the basis of losses of heterozygosity on chromosomes 3, 6, and 11 and HER-2/neu gene amplification. Cancer Res 51:4045–4051
36. Lounis H, Mes-Masson AM, Dion F et al (1998) Mapping of chromosome 3p deletions in human epithelial ovarian tumors. Oncogene 17:2359–2365
37. Allan GJ, Cottrell S, Trowsdale J et al (1994) Loss of heterozygosity on chromosome 5 in sporadic ovarian carcinoma is a late event and is not associated with mutations in APC at 5q21–22. Hum Mutat 3:283–291

38. Gabra H, Watson JE, Taylor KJ et al (1996) Definition and refinement of a region of loss of heterozygosity at 11q23.3–q24.3 in epithelial ovarian cancer associated with poor prognosis. Cancer Res 56:950–954
39. Osada R, Horiuchi A, Kikuchi N et al (2007) Expression of hypoxia-inducible factor 1alpha, hypoxia-inducible factor 2alpha, and von Hippel–Lindau protein in epithelial ovarian neoplasms and allelic loss of von Hippel–Lindau gene: nuclear expression of hypoxia-inducible factor 1alpha is an independent prognostic factor in ovarian carcinoma. Hum Pathol 38:1310–1320
40. Kaelin WG Jr (2002) Molecular basis of the VHL hereditary cancer syndrome. Nat Rev Cancer 2:673–682
41. Semenza GL (2003) Targeting HIF-1 for cancer therapy. Nat Rev Cancer 3:721–732
42. Lee S, Garner EI, Welch WR et al (2007) Over-expression of hypoxia-inducible factor 1 alpha in ovarian clear cell carcinoma. Gynecol Oncol 106:311–317
43. Yasuda M, Miyazawa M, Fujita M et al (2008) Expression of hypoxia inducible factor-1alpha (HIF-1alpha) and glucose transporter-1 (GLUT-1) in ovarian adenocarcinomas: difference in hypoxic status depending on histological character. Oncol Rep 19:111–116

Virchows Arch (2009) 455:271–275
DOI 10.1007/s00428-009-0817-8

CASE REPORT

Fibroadenoma and intraduct papilloma—a common pathogenesis?

Margaret C. Cummings · Leonard da Silva · David J. Papadimos · Sunil R. Lakhani

Received: 5 July 2009 / Accepted: 27 July 2009 / Published online: 11 August 2009

Abstract This report describes two cases, each showing fibroepithelial proliferation, admixed with intraduct papillomas. Case 1 was from a 13-year-old female who presented with a breast mass, while case 2 was from a 60-year-old female who also had a breast lump. Case 1 showed proliferative breast disease with multiple small papillomas, some with leaf-like contours. Broad-based parenchymal proliferations protruding into ducts were also seen, and there were overlap features between the two ends of this spectrum. Case 2, similarly, demonstrated a mixed intraductal proliferation, with papillomas on narrow stalks together with low-grade phyllode areas extending into ducts from a wider base. That fibroadenoma and intraduct papilloma may have a common pathogenesis is discussed.

M. C. Cummings (✉) · L. da Silva · S. R. Lakhani
Molecular and Cellular Pathology, Centre for Clinical Research,
University of Queensland,
Brisbane, Queensland, Australia
e-mail: m.cummings@uq.edu.au

M. C. Cummings · S. R. Lakhani
Royal Brisbane and Women's Hospital,
Herston,
Brisbane, Queensland 4029, Australia

S. R. Lakhani
The School of Medicine, University of Queensland,
Brisbane, Queensland, Australia

D. J. Papadimos
Sullivan Nicolaides Pathology,
Brisbane, Queensland, Australia

Keywords Fibroadenoma · Intraduct papilloma · Pathogenesis

Introduction

Fibroadenomas are benign tumours of the breast with both epithelial and fibrous connective tissue elements. They are round or ovoid, and, while not encapsulated, are well demarcated and are easily separated from the surrounding breast tissue. Phyllode lesions also have stromal and epithelial elements but have a more leaf-like architecture and a relatively greater stromal component. Intraduct papillomas have a branching connective tissue core invested by a layer of epithelial and myoepithelial cells and are connected to the wall of their surrounding duct by a narrow stalk.

We present two cases, each showing a predominantly intraductal architecture, with varying proportions of fibroepithelial and papilloma components together with elements showing overlap features.

Clinical history

Case 1

The patient was a 13-year-old female, who presented with a large right-sided breast mass, which, clinically, was thought to be a papilloma. A wide local excision was performed, with two pieces of tissue removed.

Case 2

The patient was a 60-year-old female who presented with a lesion superior and lateral to the right nipple. A wide local excision was undertaken.

Materials and methods

The surgical specimens were fixed in 10% buffered neutral formalin and embedded in paraffin. All sections were stained with haematoxylin and eosin. On selected paraffin sections for case 1, immunohistochemical examination was performed for oestrogen receptor protein (ER; Clone 6F11/2, 1:100, Leica Microsystems), progesterone receptor protein (PR; Clone 16, 1:500, Leica Microsystems), Ki67 (Clone MIB-1, 1:50, Dako) and HER2 (Dako Herceptest Kit, K5207). Staining for ER, PR and Ki67 was performed automatically using the Leica Bond Max immunostainer with Bond Polymer Refine Detection Kits (Leica, DS9800) and heat-induced epitope retrieval pH 9.0 (Leica, ER2, AR9640) for 40 min, 30 min and 20 min, respectively. Staining for HER2 was performed using the Dako Herceptest Kit (K207) according to the kit insert.

ER, PR and Ki67 were considered positive when there was nuclear staining, and HER2 was assessed using the HERCEPT test guidelines.

Results

Pathology

Macroscopic findings

Case 1 The specimen comprised two irregular pieces of breast tissue, the smaller measuring 30 x 15 x 10 mm and the larger measuring 50 x 40 x 35 mm. On more than one surface, papillary tissue was seen, and, on sectioning, there were large and small spaces filled with papillary material seen throughout the specimen. A small amount of adjacent white breast tissue was also present.

Case 2 The specimen was a piece of breast parenchyma measuring 55 x 40 x 20 mm, within which was a firm nodule measuring 23 x 20 x 14 mm.

Microscopic findings

Case 1 Histological examination of the breast tissue showed a range of appearances with widespread proliferative breast disease (Fig. 1a). There were many greatly dilated ducts in which multiple, crowded, small papillomas were seen, many with rounded contours and prominent sclerosis (Fig. 1b). Some of the papillomas had more convoluted, somewhat leaf-like contours, reminiscent of a phyllode pattern. Compared with these intraduct papillomas, with their characteristically narrow stalks, other areas showed breast parenchyma protruding into ducts from a far broader base. This varied from only slightly encroaching on the involved duct to projecting into and filling the lumen and even apparently compressing and distending the opposite wall of the duct, giving an appearance of early, small fibroadenomas (Fig. 1c). In some ducts, there was a mixture of broad-based papillary protrusions extending into them together with some connected to the duct walls by only very narrow stalks (Fig. 1d). Much of the covering surface epithelium showed a relatively flattened layer of cuboidal epithelial cells; although, in areas, there were more pronounced hyperplastic features. Overall, the main features were of small fibroadenomas, admixed with intraduct papillomas and areas resembling phyllode tumour.

Immunostaining for the proliferation marker Ki67 showed 1–2% of cell staining, and these were mostly epithelial cells rather than stromal. There were relatively more positively staining glandular epithelial cells in the broad-based projections compared with the epithelium seen in the opposite indented side of the ducts (Fig. 2a, b).

There was strong staining for both ER and PR in approximately 95% of the epithelial cells (Fig. 2c, d). Staining for HER2 was negative (0).

Case 2 Histological examination showed breast parenchyma with a fibroepithelial proliferation extending into and distorting and surrounding some ducts. Distension of the ducts with compression of the overlying ductal epithelium was seen. In areas, there was a relatively prominent stroma. A leaf-like contour was focally present. Some of the intraduct proliferations were more broadly based while in others there was a narrow stalk with the characteristic appearance of benign intraduct papillomas. The overall diagnosis was of a composite lesion with fibroadenoma, intraduct papilloma and low-grade phyllode features (Fig. 1e).

Discussion

There have been many studies concerning the pathogenesis of fibroadenomas, but there is little information available concerning the pathogenesis of intraduct papillomas. We show two cases here whose features suggest that these two entities may share a common pathogenesis. Both cases include foci comprising typical intraduct papillomas; both also show fibroepithelial type proliferation, in the first, giving fibroadenoma areas and, in the second, giving a low-grade phyllode appearance. Both also show features which are intermediate or transitional between the two entities, suggesting that both entities develop along similar pathways, sharing a common evolution.

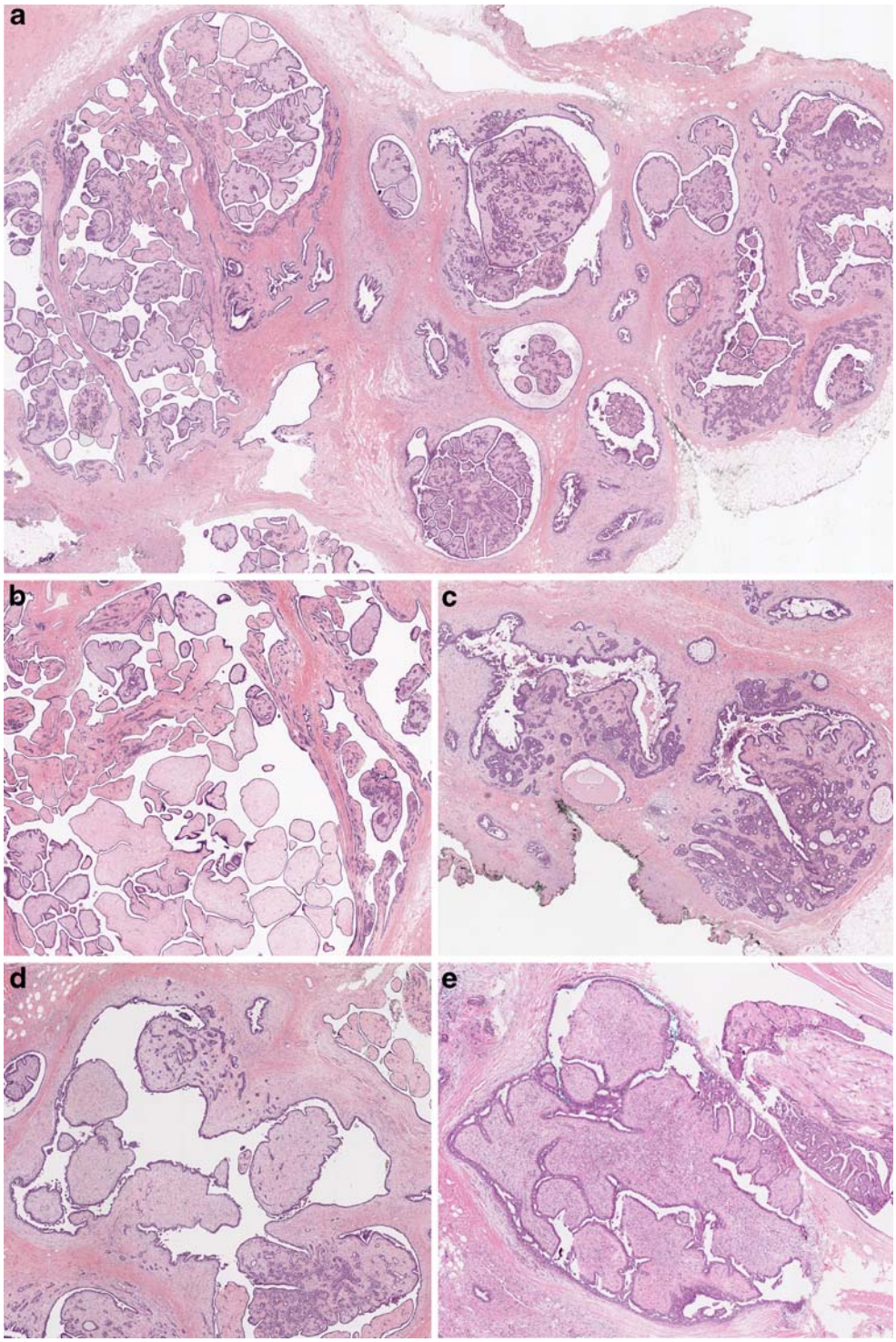

Fig. 1 **a** Low-power view showing the range of intermingled intraductal proliferations. **b** Multiple papillomas of varying shapes. **c** Fibroepithelial protrusion into ducts on broad fronts. **d** Narrow stalks and wide bases within a single duct. **e** Phyllode-like proliferation in one duct with adjacent duct containing an intraduct papilloma

Several old and very elegant studies have been performed concerning the origin and nature of fibroadenomas. Delbet, in 1898, held that epithelial proliferation and the formation of cysts was the initial step in their development and that subsequent connective tissue overgrowth and the invagination of cysts later produced the characteristic architecture [1]. Cheatle, on the other hand, felt that fibroadenomas arose predominantly because of stromal proliferation, both around terminal ducts and within lobules [2]. In a particularly thorough study, Demetrakopoulos made a three-dimensional reconstruction of a small fibroadenoma using composite drawings of serial histological sections [3]. He also felt that the key component of a fibroadenoma was the connective tissue proliferation and that that accounted for its architectural features. He observed that the connective tissue often invaginated the

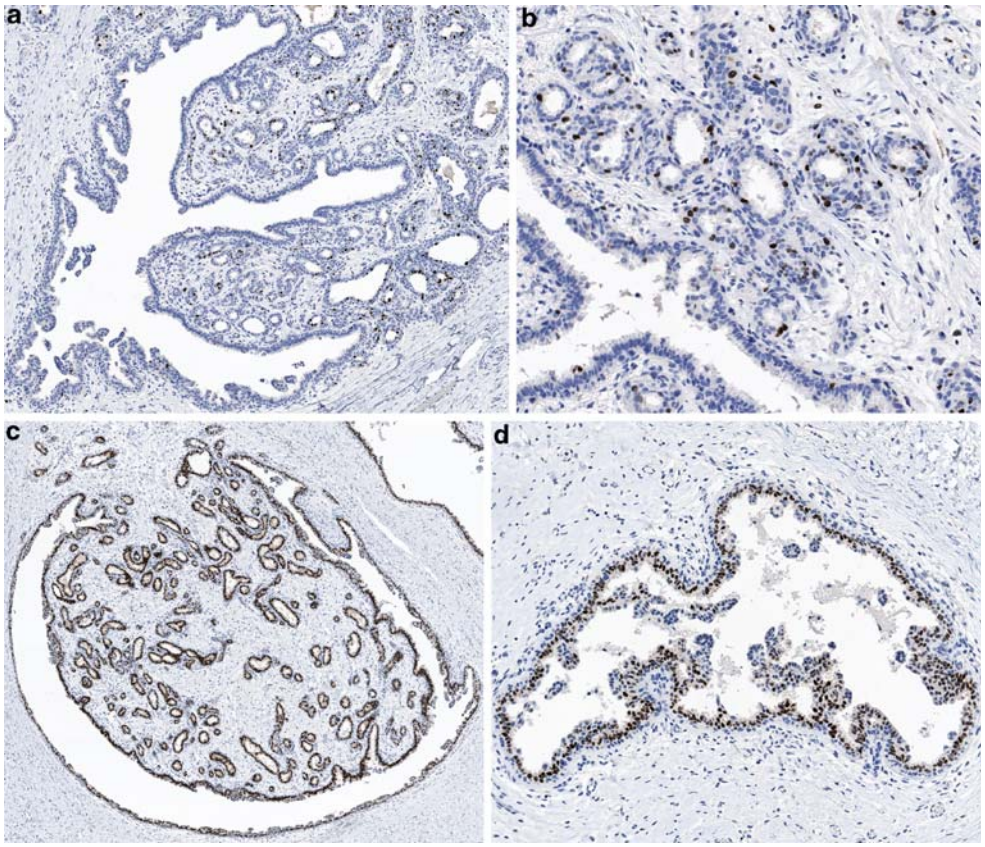

Fig. 2 **a** Greater staining with Ki67 in glands protruding into ducts compared with the opposite duct wall. **b** Ki67 staining of luminal cells and occasional myoepithelial cells and fibroblasts. **c** Widespread ER staining. **d** ER-positive duct cells with more central ER negative ones

walls of ducts, and, similar to what the current cases show, the intraluminal connective tissue was sometimes so prominent that it pushed one wall of the involved duct against the opposite wall, partly occluding the lumen. He also noticed that in other instances, the connective tissue projected in a tongue-like fashion in either direction within the lumen of the duct, similar to the intraduct papilloma components of the current cases.

In their comprehensive study on the origins of fibroadenomas, Koerner and O'Connell concluded that the stromal cells of fibroadenomas arose from the loose, specialised connective tissue seen around ducts and lobules and that the glandular epithelial component was merely caught up within the growing stroma [4]. They felt that, while the epithelial elements of a fibroadenoma are thought to derive largely from a single ductal system, as the process evolves, more ducts and lobules may gradually become included within the growing mass.

That fibroadenomas are hyperplastic rather than neoplastic was supported by the work of Noguchi et al. who showed that both the epithelial and stromal components were polyclonal [5]. The diffuse and strong staining for both oestrogen and progesterone receptor proteins seen in case 1 is consistent with a hyperplastic process; this is compared with the usual staining pattern for the hormone receptor proteins where only occasional cells are stained. While mitoses were not seen and Ki67 showed infrequent positivity, there did appear to be relatively more proliferative activity in the glandular epithelium of the parenchymal component that was protruding into the duct lumen, indicating that it may be the glandular proliferation in particular that promotes the development of fibroadenomas rather than that of the accompanying dependent stroma.

Compared with fibroadenomas, there appears to have been relatively little interest in how intraduct papillomas develop and evolve. An intraduct papilloma has a fibrovascular stromal core, sometimes with branching fronds and it is covered by a layer of epithelial and myoepithelial cells. The stromal connective tissue core, generally, has only a narrow stalk linking it to the duct wall. The so-called solid intraduct papilloma is thought to arise when there are multiple papillary projections within a duct that somehow merge together. Showing some aspects that are similar to the present cases, Chung et al. described a case of intraductal fibroadenomatosis with overlap features of papillomas, intraductal adenomas, fibroadenomas and benign phyllode tumours [6].

When fibroadenomas or intraduct papillomas are seen by one histologically, these have usually been there for quite some time and, so, are well advanced in terms of their own natural history. Earlier on, they would generally not cause symptoms. Case 1 described here is very unusual in that it shows features of both fibroade-

noma and intraduct papilloma, both in their initial developing stages. Case 2 shows an admixed fibroepithelial proliferation with intraduct papillomas. The early evolution of both components occurring together in case 1, sometimes within the one duct, suggests that the two entities, fibroadenoma and intraduct papilloma, could share a common pathogenesis. If breast parenchyma projects into a cavity on a narrow stalk or base, an intraduct papilloma occurs. Conversely, if there is a wider or a more broad base to the projection, then the opposite duct wall becomes compressed over it, eventually attenuates, and a fibroadenoma occurs. Why one develops and not the other, and generally not both together, is unclear.

References

1. Delbet P (1898) Fibroadenoma of the breast. Duplat-Reclus, Traite de Chir. 7:157–165
2. Cheatle GL (1923) Hyperplasia of epithelial and connective tissues in the breast: its relation to fibro-adenoma and other pathological conditions. Br J Surg 10:436–455
3. Demetrakopoulos NJ (1958) Three-dimensional reconstruction of a human mammary fibroadenoma. Q Bull Northwest Univ Med Sch 32:221–228
4. Koerner FC, O'Connell JX (1994) Fibroadenoma: morphological observations and a theory of pathogenesis. Pathol Annu 29:1–19
5. Noguchi N, Motomura K, Inaji H, Imaoka S, Kiyama H (1993) Clonal analysis of fibroadenoma and phyllodes tumour of the breast. Cancer Res 53:4071–4074
6. Chung A, Scharre K, Wilson M (2008) Intraductal fibroadenomatosis: an unusual variant of fibroadenoma. Breast J 14:193–195

Virchows Arch (2009) 455:277–284
DOI 10.1007/s00428-009-0821-z

ORIGINAL ARTICLE

Loss of RKIP expression is associated with poor survival in GISTs

Olga Martinho · António Gouveia · Paula Silva · Amadeu Pimenta · Rui Manuel Reis · José Manuel Lopes

Received: 8 June 2009 / Revised: 17 July 2009 / Accepted: 30 July 2009 / Published online: 25 August 2009

Abstract Gastrointestinal stromal tumours (GISTs) are rare mesenchymal tumours of the digestive tract and are commonly driven by oncogenic mutations in *KIT* and *PDGFRA* genes. Tumour size, location, mitotic index and *KIT/PDGFRA* mutations are the most important prognostic parameters in GISTs. However, additional studies screening for new molecular prognostic markers in GISTs are missing. Raf kinase inhibitor protein (RKIP) has been considered as a suppressor of metastasis and a prognostic marker in several neoplasms. In the present study we aimed to examine whether RKIP expression is associated with GIST clinical–pathological features. Using immunohistochemistry, we determined RKIP expression levels in a well-characterised series of 70 GISTs. We found that RKIP is expressed in the great majority of cases, and absent in approximately 9% of GISTs. Additionally, we found that loss of RKIP expression was not due to the promoter methylation as assessed by methylation-specific PCR. Loss of RKIP expression was associated with poor disease-specific survival and with tumour necrosis in GISTs. Furthermore, a statistical tendency was observed between the positive RKIP expression and absence of metastasis. So far, this is the first study assessing RKIP expression levels in GISTs. We conclude that loss of RKIP expression could have an important role as prognostic marker in GISTs.

Keywords RKIP · Expression · Survival · GISTs

Olga Martinho and António Gouveia contributed equally to the study.

O. Martinho · R. M. Reis
Life and Health Sciences Research Institute (ICVS),
School of Health Sciences, University of Minho,
Braga, Portugal

A. Gouveia · P. Silva · A. Pimenta · J. M. Lopes (✉)
IPATIMUP, Institute of Molecular Pathology
and Immunology of the University of Porto,
Rua Dr. Roberto Frias, s/n,
4200-465 Porto, Portugal
e-mail: jmlopes@ipatimup.pt

A. Gouveia · A. Pimenta
Department of Surgery,
Porto, Portugal

J. M. Lopes
Department of Pathology, H.S. João,
Porto, Portugal

A. Gouveia · P. Silva · A. Pimenta · J. M. Lopes
Medical Faculty of Porto University,
Porto, Portugal

Introduction

Gastrointestinal stromal tumours (GISTs) are rare mesenchymal tumours of the digestive tract [1, 2]. Gain-of-function mutations in *KIT* and *PDGFRA* oncogenes have been identified in a great majority of GISTs and are considered to be one of the first molecular events in their pathogenesis [3, 4]. The tyrosine kinase inhibitor imatinib mesylate is the gold standard in the treatment of metastatic GISTs, leading up to 75% response rates [5]. Several studies have shown the importance of *KIT* and *PDGFRA* molecular status in imatinib response [6, 7].

Tumour size, location and mitotic index are the most important prognostic parameters of GISTs [8, 9]. Several authors have proven the usefulness of these and other classification parameters in GISTs clinical follow-up [10, 11]. Moreover, other studies have shown that molecular

genetic markers, such as the type of *KIT* and *PDGFRA* mutations, might also have prognostic value [12, 13]. However, a part of GISTs behave unpredictably leading to the need of screening new molecular prognostic markers.

The MAP kinase (RAS/RAF/MEK/ERK) pathway, one of the KIT downstream cascades, is highly preserved and implicated in cell growth, differentiation, migration and survival [14]. Activated RTK phosphorylates RAS, which binds RAF-1 kinase that phosphorylates MEK1/2, leading to ERK1/2 activation. Phosphorylated ERKs translocates into nucleus and regulates gene expression through several transcription factors like c-Myc, CREB and AP-1, ultimately leading to changes in gene expression [14]. Recently, we and others observed activation of this pathway in GISTs by presence of *BRAF* activating mutations [15, 16]. In addition, we described the absence of *RAS* mutations, and suggest that MAP kinase could also be activated through SCF/KIT autocrine/paracrine mechanisms in a subset of *KIT/PDGFRA* wild-type GISTs [16].

Raf kinase inhibitory protein (RKIP; also known as PEBP, for phosphatidylethanolamine-binding protein) was originally identified as an endogenous inhibitor of the RAS/RAF/MEK/ERK pathway by interfering with the phosphorylation and activation of MEK by Raf-1 [17, 18]. Subsequently, RKIP was shown also to suppress the activation of the nuclear factor Kappa B (NFkB) cell survival pathway by blocking the inactivation of the inhibitor of NFkB, namely IkB [19]. In mammals, RKIP is also a negative regulator of G-protein coupled receptors [GPCRs] by inhibiting GRK-2 [20], and may be involved in regulating the partitioning of chromosomes and mitosis progression through RKIP binding to centrosomal and kinetochore regions of metaphase chromosomes [21]. The collective evidence indicates that RKIP regulates the activity and mediates the crosstalk between several important cellular signalling pathways including cell differentiation, cell cycle, apoptosis and cell migration. Attenuation of RKIP function is implicated in several human diseases, such as neurologic diseases and metastases in cancer [22, 23].

RKIP is a widely expressed and highly conserved protein [24–26], which is downregulated in several tumours, including highly metastatic prostate carcinoma, breast, colon and gastric carcinoma, hepatocellular carcinoma, melanoma, insulinoma and ovarian carcinoma [27–36]. Furthermore, RKIP is also a prognostic marker in prostate, colorectal and gastric carcinomas [34, 36–38]. The molecular mechanisms underlying RKIP downregulation in cancer is not yet fully understood. Some authors suggested *RKIP* promoter methylation as a potential RKIP silencing event [21, 39].

In the present study we aimed to clarify the role of RKIP in the prognosis of GISTs.

Materials and methods

Tissue samples

Seventy formalin-fixed paraffin-embedded primary sporadic GISTs, classified according to WHO criteria and risk group [40], previously characterised immunohistochemically for CD117, actin, S100, desmin and CD34, and molecularly for *KIT* and *PDGFRA* mutations, were retrieved from the Pathology Department of S. João Hospital files (1989–2005), Porto, Portugal [10, 41]. All patients were Caucasian and of Portuguese origin, with a mean age of 62.1 years (range 20–88). Thirty-six (51.4%) patients were female and 34 (48.6%) were male. Most frequent tumour location was gastric (n=40) and small intestine (n=23); other location were: colon (n=2), rectum (n=1), oesophagus (n=1) and omentum/mesentery (n=3). Three GIST patients with surgically resected tumours were treated with imatinib (400 mg daily, with escalation to 600 mg daily whenever indicated), because of tumour recurrence. Of these patients, two are alive with stable disease and one died due to the disease. Follow-up data was available in all patients, as at December 2007, and collected through direct interview with patients or their relatives, and by review of in-hospital patient files. The median follow-up time of patients was 54.1 months (range, 1–206). The diagnosis of metastases, including the two cases with very limited biopsy material, was based on definitive imagiological evidence obtained during the follow-up of the patients.

Immunohistochemistry analysis for RKIP

Representative 3-μm thick sections were subjected to immunohistochemical analysis according to the streptavidin–biotin peroxidase complex system (UltraVision Large Volume Detection System Anti-Polyvalent, HRP; Lab Vision Corporation). Briefly, deparaffinised and rehydrated slides were submitted to heat-induced antigen retrieval for 20 min at 98°C with 10 mM citrate buffer (pH6.0). After incubation with the primary antibodies raised against RKIP (dilution 1:600; incubation 2 h at RT; Upstate Biotechnology, Lake Placid, NY), the secondary biotinylated goat anti-polyvalent antibody was applied for 10 min followed by incubation with the streptavidin–peroxidase complex. The immune reaction was visualised by 3,3′-diamonobenzidine as a chromogen. All sections were counterstained with Gill-2 haematoxylin. For negative controls, primary antibody was replaced by a universal negative control antibody (CEA, rabbit anti-human, DAKO Corporation, Carpinteria, CA). A prostate carcinoma was used as positive control.

Tumour samples were evaluated for both extension and intensity of the immunoreactions. The score used was the

sum of the percentage of positive cells (0, negative; 1, less than 25% positive cells; 2, 26% to 50% positive cells and 3, more than 50% positive cells) and the staining intensity (0, negative; 1, weak; 2, moderate and 3, strong). Scores between 0 and 2 were classified as negative, 3 and 4 as moderate positive and 5 and 6 as strongly positive.

DNA isolation

Selected areas contained at least 85% of tumour tissue were macrodissected into a microfuge tube using a sterile needle (Neolus, 25G-0.5 mm) and DNA isolation was performed using Qiagen's QIAamp® DNA Micro Kit, as previously described [42].

Methylation analysis of *RKIP* promoter

DNA methylation pattern in the promoter region of the *RKIP* gene was determined by methylation-specific PCR (MSP), as previously described [39] with some modifications. Briefly, bisulphite treatment of 200 ng DNA was done using EZ DNA Methylation Golf Kit (Zymo Research Corporation, USA) according to the manufactures instructions. The PCR was carried out in a total volume of 15 µl, consisting of 1 µl of bisulphite modified DNA, 0.2 µM of both sense and anti-sense primers (MWG-Biotech, Ebersberg, Germany), 200 µM of dNTPs (Fermentas, USA), 1,5 mM of MgCl2 (Bioron, Germany), 1× Taq Buffer incomplete (Bioron, Germany) and 1 U of Taq Superhot DNA Polymerase (Bioron, Germany). The reaction consisted of an initial denaturation at 95°C for 10 min, followed by 40 cycles with denaturation at 95°C for 30 s, annealing at 52–58°C for 30 s and extension at 72°C for 30 s, followed by a final extension for 10 min at 72°C, in a Thermocycler (BioRad). To MSP reaction, were used specific primers to distinguish methylated DNA (204 bp PCR product) from unmethylated DNA (205 bp PCR product), as described [39]. CpGenome Universal Methylated DNA (Chemicon International, USA) was used as methylated control. Blood DNA of a young healthy individual was used as unmethylated control.

Statistical analysis

The available clinical–pathological and immunohistochemistry data were analysed with SPSS software for Windows,

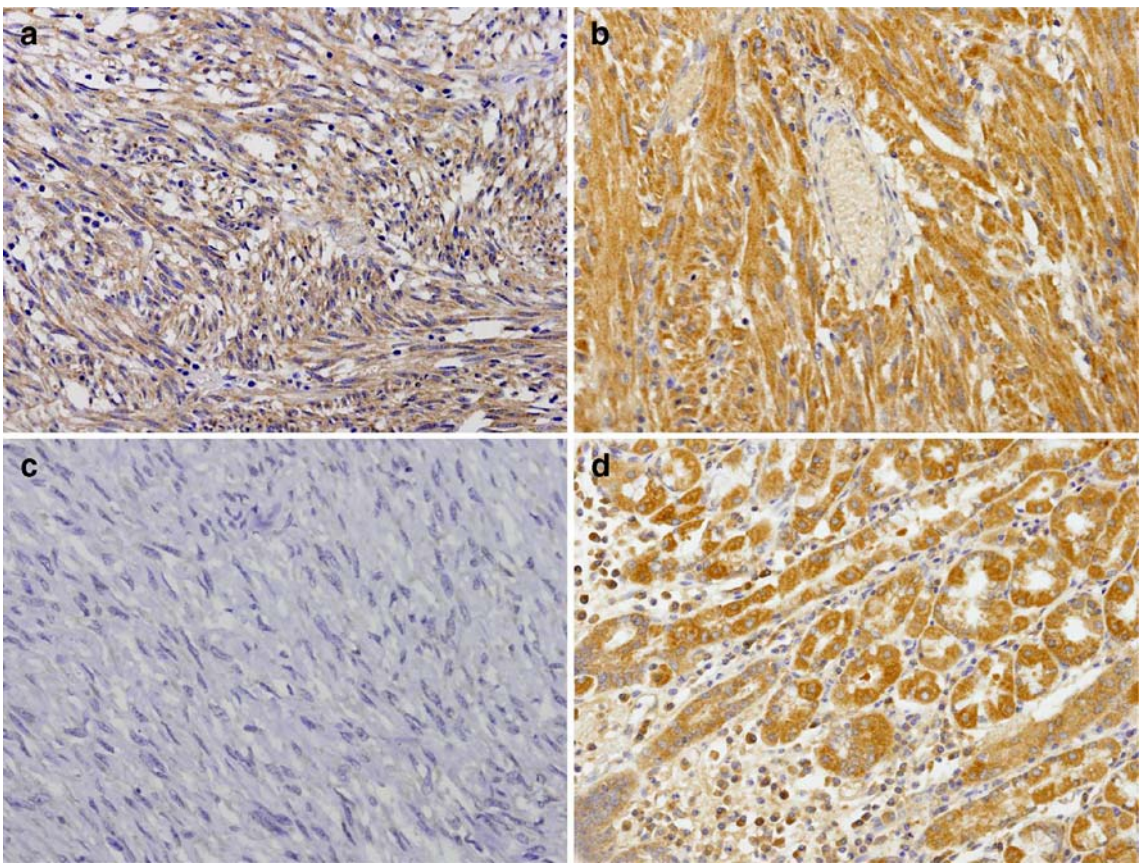

Fig. 1 Immunohistochemistry analysis of RKIP in GISTs. **a** Weak expression (×200), **b** strong expression (×200), **c** negative expression (×200), **d** positive expression of RKIP in normal adjacent tissue (×200)

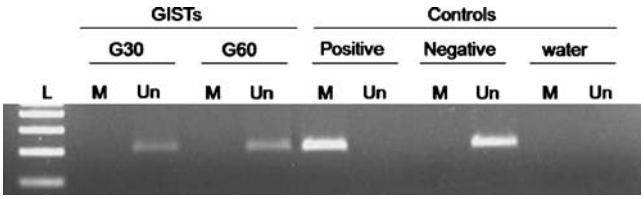

Fig. 2 Agarose gel (2%) showing MSP result for methylation analysis of *RKIP* gene in the two cases with RKIP loss of expression (G30 and G60). *Un* unmethylated, *M* methylated, *L* 100 bp ladder

version 15.0. Correlations between categorical variables were performed using Fischer's exact test. Disease-specific survival (DSS) was calculated from the time of diagnosis until death related with the disease, or censored at the time of latest follow-up, as described [10]. Cumulative survival probabilities were calculated using the Kaplan–Meier method. Differences between survival rates were tested with the log-rank test. p value inferior to 0.05 was considered significant.

Table 1 Association between RKIP expression and clinical–pathological parameters in GISTs (n=70)

Parameter	RKIP expression			
	N	Negative (%)	Positive (%)	p[a]
CD117 expression				
Negative	6	2 (33.3)	4 (66.7)	0.079
Positive	64	4 (6.3)	60 (93.7)	
KIT/PDGFRA mutations				
Mutant	44	4 (9.1)	40 (90.9)	1.000
Wild-type	26	2 (7.7)	24 (92.3)	
Age (years)				
≤60	30	2 (6.7)	28 (93.3)	0.694
>60	40	4 (10)	36 (90)	
Gender				
Male	34	3 (8.8)	31 (91.2)	1.000
Female	36	3 (8.3)	33 (91.7)	
Tumour local				
Small intestine	23	0 (0)	23 (100)	0.051
Gastric	40	4 (10)	36 (90)	
Other	7	2 (28.6)	5 (71.4)	
Risk grade				
Very low/low/intermediate	41	2[b] (4.9)	39 (95.1)	0.224
High	29	4 (13.8)	25 (86.2)	
Cellular morphology				
Spindle	45	4 (8.9)	41 (91.1)	0.842
Epithelioid	8	0 (0)	8 (100)	
Mixed	17	2 (11.8)	15 (88.2)	
Tumour size (cm)				
≤5	29	1 (3.4)	28 (96.6)	0.268
>5 to ≤10	23	2 (8.7)	21 (91.3)	
>10	18	3 (16.7)	15 (83.3)	
Mitotic index (50/HPF)				
≤5	50	3 (6)	47 (94)	0.343
>5	20	3 (15)	17 (85)	
Necrosis				
Absent	29	0 (0)	29 (100)	0.038*
Present	41	6 (14.6)	35 (85.4)	
Metastasis				
Absent	58	3 (5.2)	55 (94.8)	0.058
Present	12	3 (25)	9 (75)	
Mean survival time (months ± SD)	70	60.60±20.07	167.87±10.35	0.023*[c]

N number of cases, *HPF* high power field (×400)

*p<0.05, statistically significant values

[a] Fischer´s exact test

[b] One case low and one case intermediate risk

[c] Log-rank test

Results

RKIP expression

In the present study, we used a series of 70 GISTs which comprises 91.4% of CD117 positive cases and 63% of *KIT/PDGFRA* mutated GISTs, as previously characterised [41]. Immunohistochemical approach was done to detect RKIP protein expression and distribution in GIST cases. We observed cytoplasmatic expression of RKIP in 64 (91.5%) of the 70 GISTs studied: 30 cases showed moderate and 34 strong positivity (Fig. 1a and b). The remaining 8.5% (6/70) of cases were considered as negative for RKIP expression (Fig. 1c). In a subset of cases, it was possible to analyse the normal adjacent tissue that showed to be strongly positive for RKIP expression (Fig. 1d).

RKIP methylation

To determine whether absence of RKIP expression was due to gene promoter hypermethylation, we performed methylation-specifc PCR in all six cases without RKIP expression. None of the cases exhibited *RKIP* promoter hypermethylation (Fig. 2).

Clinical–pathological features and statistical analysis

After univariate statistical analysis we observed that there is no correlation between RKIP expression and CD117 staining and *KIT/PDGFRA* mutations status (Table 1). Concerning clinical–pathological data, no significant correlations ($p>0.05$) were found between RKIP expression and age, gender, risk grade, cellular morphology, tumour size and mitotic index (Table 1). RKIP negativity was correlated with presence of necrosis ($p=0.038$). There was a tendency ($p=0.051$) for absence of RKIP expression in gastric GISTs and a tendency ($p=0.058$) for the development of metastasis in RKIP negative cases (Table 1).

Regarding clinical–pathological parameters and disease-specific survival (univariate analysis), we found that a shorter DSS was significantly associated with male gender ($p=0.014$), high-risk GISTs ($p<0.001$), tumour size >10 cm ($p=0.001$), mitotic index >5 ($p=0.009$) and development of metastasis ($p<0.001$). Loss of RKIP expression was significantly ($p=0.023$) associated with poor DSS (Table 1 and Fig. 3). Only three cases were treated with imatinib-based therapy, hampering any statistical analysis. The low number of cases precluded multivariate analysis of the studied parameters.

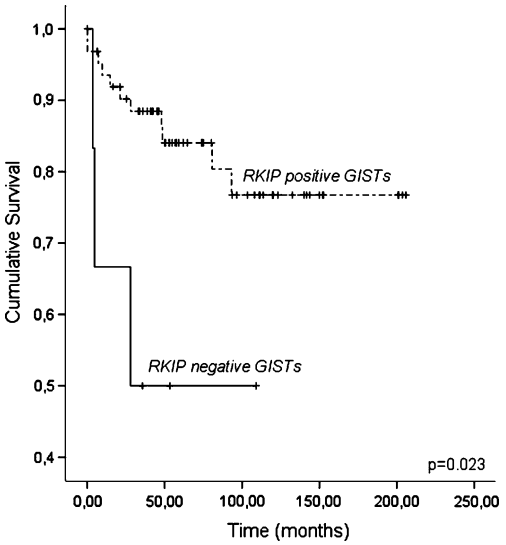

Fig. 3 Disease-specific survival (DSS) according to RKIP expression in GISTs ($n=70$). Cumulative survival is significantly lower in cases with RKIP loss of expression ($p=0.023$)

Discussion

Unresectable or metastatic GIST is a fatal disease resistant to conventional cytotoxic chemo and radiotherapy. The median survival time for patients with metastatic GIST is approximately 20 months, and 9–12 months for patients with local recurrences [43]. Treatment with imatinib mesylate is the first option for metastatic disease [44]. However, further molecular characterization is warranted for the treatment of primary and secondary imatinib-resistant GISTs. Furthermore, excepting *KIT* and *PDGFRA* mutations, no other molecular alterations have been consistently associated with prognosis of GISTs [12, 13].

RKIP is considered to be a signal transduction modulator and a metastasis suppressor [45]. The first evidence came from cell lines derived from metastatic prostate carcinomas, which display decreased levels of RKIP as compared with primary tumour cell lines [27]. In human breast carcinoma [32] and metastatic colorectal carcinoma [34, 46], RKIP expression is consistently lost in lymph node metastases but not in primary tumours, supporting the suggestion that RKIP is downregulated in metastatic development. Moreover, overexpression of RKIP in vitro and in vivo prostate and melanoma tumour models suggest that RKIP represent an important suppressor of metastasis by decreasing vascular invasion [27, 29]. Consistent with the role of RKIP as a potent suppressor of metastatic development, several studies described that highly metastatic prostate carcinoma [27], malignant melanoma [29], breast cancer lymph node metastases [32], insulinoma [31], colorectal carcinoma [46], hepatocarcinoma [33], ovarian carcinoma [35], Merckel cell carcinoma [47] and thyroid carcinoma [48] display frequently a marked decrease in RKIP expression.

Work by Eves et al. [49] also indicates that the absence of RKIP may increase the genetic instability of the cell

while work with hepatoma cells suggests that the absence of RKIP may increase the rate of cell division [33].

Furthermore, loss of cytoplasmatic RKIP has also been associated with colorectal carcinoma recurrence [34] and with poor prognosis in prostate, colorectal and gastric adenocarcinomas [34, 36–38]. Recently, it was proposed that the level of RKIP in the blood can be used as a prognostic marker for prostate cancer patients [38]. Thus, loss of RKIP expression may be considered as a marker of tumour progression.

In our series, well-established prognostic markers (male gender, high risk, tumour size >10 cm, mitotic index >5 and development of metastasis) were significantly associated with DSS [10]. Regarding RKIP expression, our results in GISTs has shown that a negative cytoplasmatic expression, found in approximately 9% of the cases, is significantly correlated with the presence of necrosis and with DSS of GIST patients. Furthermore, a tendency was observed between the presence of RKIP expression and absence of metastasis. So far, there are no reported studies of RKIP expression in GISTs. We recently demonstrated that MAPK pathway alterations occur at low frequency in *KIT* and *PDGFRA* wild-type GISTs, corroborating the low percentage of RKIP absence of expression in the present study [16]. Further studies with a largest series are needed to validate RKIP expression as a prognostic marker in GISTs. Furthermore, it will be also interesting in the future to assess the expression levels of RKIP in the metastatic biopsies of GISTs.

Despite the increasing evidence that RKIP is lost during tumour progression, especially in metastasis, the mechanisms of RKIP down-regulation remains to be unraveled [21]. To further elucidate the genetic event that underlies RKIP down-regulation in GISTs, we analysed the methylation status of the CpG islands of RKIP promoter in RKIP negative GISTs. All six GISTs without RKIP expression were found unmethylated for RKIP promoter. Former studies concerning RKIP methylation are discrepant. RKIP methylation was described in a cohort of 12 patients with hyperplastic polyposis coli [39]. Noteworthy, the same authors, using 28 colorectal carcinomas, reported that methylation of the RKIP promoter was not responsible for loss of RKIP expression [46]. Recently, Al-Mulla et al. [21] reported that 72.5% of 40 RKIP negative colorectal carcinomas were methylated at the RKIP promoter, and suggested it as the major mechanism by which RKIP is silenced [21].

The role of RKIP in tumour progression and in metastases development raises hope for tailored therapeutic approaches, using drug-induced modulation of RKIP expression, to control tumour aggressiveness. Locostatin has already been shown to abrogate the ability of RKIP to inhibit Raf-1 [50]. In some prostate and breast carcinoma cell lines, increasing levels of RKIP expression re-sensitise cells to drug-induced apoptosis. In drug-sensitive cell lines, down-regulation of RKIP led to the resistance to DNA-damaging drugs [9-nitrocamptothecin, taxol and cisplatin] [28]. Rituximab up-regulates RKIP, which has been shown to sensitise non-Hodgkin's lymphoma cell lines to chemotherapeutic-induced apoptosis [51]. Both inhibition of the MEK–ERK pathway and inhibition of the NFkB pathway were suggested as possible mechanisms for these drug-sensitising effects [51]. Recently, RKIP expression levels in pituitary adenomas were found to correlate with both acute and long-term clinical response to octreotide [52]. Furthermore, Bonavida et al. demonstrated that nitric oxide mediated chemo/immunosensitization via inhibition of NFkB may also involve the induction of RKIP. Induction of RKIP inhibits anti-apoptotic pathways that regulate tumour cell sensitivity to apoptotic stimuli [53].

In the present study we describe for the first time that GIST RKIP expression levels correlate with clinical–pathological parameters in univariate analysis. We found that the loss of RKIP expression was independent of promoter methylation in a subset of GISTs. Most important, loss of RKIP was associated with tumour necrosis and with a poor survival, i.e., a potential prognostic marker for GIST patients. Further studies with larger series and with in vivo/in vitro tumour models are warranted to evaluate the role of RKIP in metastatic development and survival of GIST patients.

Acknowledgements OM is recipient of a PhD fellowship (SFRH/BD/36463/2007) from FCT, Portugal. This study was partially supported by NOVARTIS Oncology, Portugal.

Conflicts of interest statement We declare that we have no conflict of interest.

References

1. Tryggvason G, Gislason HG, Magnusson MK et al (2005) Gastrointestinal stromal tumors in Iceland, 1990–2003: the icelandic GIST study, a population-based incidence and pathologic risk stratification study. Int J Cancer 117:289–293
2. Nilsson B, Bumming P, Meis-Kindblom JM et al (2005) Gastrointestinal stromal tumors: the incidence, prevalence, clinical course, and prognostication in the preimatinib mesylate era—a population-based study in western Sweden. Cancer 103:821–829
3. Hirota S, Isozaki K, Moriyama Y et al (1998) Gain-of-function mutations of c-kit in human gastrointestinal stromal tumors. Science 279:577–580
4. Heinrich MC, Corless CL, Duensing A et al (2003) PDGFRA activating mutations in gastrointestinal stromal tumors. Science 299:708–710
5. Heinrich MC, Blanke CD, Druker BJ et al (2002) Inhibition of KIT tyrosine kinase activity: a novel molecular approach to the treatment of KIT-positive malignancies. J Clin Oncol 20:1692–1703

6. Heinrich MC, Corless CL, Demetri GD et al (2003) Kinase mutations and imatinib response in patients with metastatic gastrointestinal stromal tumor. J Clin Oncol 21:4342–4349
7. Tornillo L, Terracciano LM (2006) An update on molecular genetics of gastrointestinal stromal tumours. J Clin Pathol 59:557–563
8. Miettinen M, Lasota J (2006) Gastrointestinal stromal tumors: review on morphology, molecular pathology, prognosis, and differential diagnosis. Arch Pathol Lab Med 130:1466–1478
9. Corless CL, Heinrich MC (2008) Molecular pathobiology of gastrointestinal stromal sarcomas. Annu Rev Pathol 3:557–86
10. Gouveia AM, Pimenta AP, Capelinha AF et al (2008) Surgical margin status and prognosis of gastrointestinal stromal tumor. World J Surg 32(11):2375–82
11. Takahashi T, Nakajima K, Nishitani A et al (2007) An enhanced risk-group stratification system for more practical prognostication of clinically malignant gastrointestinal stromal tumors. Int J Clin Oncol 12:369–374
12. Wardelmann E, Buttner R, Merkelbach-Bruse S et al (2007) Mutation analysis of gastrointestinal stromal tumors: increasing significance for risk assessment and effective targeted therapy. Virchows Arch 451:743–749
13. Wardelmann E, Losen I, Hans V et al (2003) Deletion of Trp-557 and Lys-558 in the juxtamembrane domain of the c-kit proto-oncogene is associated with metastatic behavior of gastrointestinal stromal tumors. Int J Cancer 106:887–895
14. Dhillon AS, Hagan S, Rath O et al (2007) MAP kinase signalling pathways in cancer. Oncogene 26:3279–3290
15. Agaram NP, Wong GC, Guo T et al (2008) Novel V600E BRAF mutations in imatinib-naive and imatinib-resistant gastrointestinal stromal tumors. Genes Chromosomes Cancer 47:853–859
16. Martinho O, Gouveia A, Viana-Pereira M et al (2009) Low frequency of MAP kinase signalling pathway alterations in KIT & PDGFRA wild-type GISTs. Histopathology 55:53–62
17. Yeung K, Seitz T, Li S et al (1999) Suppression of Raf-1 kinase activity and MAP kinase signalling by RKIP. Nature 401:173–177
18. Yeung K, Janosch P, McFerran B et al (2000) Mechanism of suppression of the Raf/MEK/extracellular signal-regulated kinase pathway by the raf kinase inhibitor protein. Mol Cell Biol 20:3079–3085
19. Yeung KC, Rose DW, Dhillon AS et al (2001) Raf kinase inhibitor protein interacts with NF-kappaB-inducing kinase and TAK1 and inhibits NF-kappaB activation. Mol Cell Biol 21:7207–7217
20. Lorenz K, Lohse MJ, Quitterer U (2003) Protein kinase C switches the Raf kinase inhibitor from Raf-1 to GRK-2. Nature 426:574–579
21. Al-Mulla F, Hagan S, Al-Ali W et al (2008) Raf kinase inhibitor protein: mechanism of loss of expression and association with genomic instability. J Clin Pathol 61:524–529
22. Keller ET, Fu Z, Brennan M (2004) The role of Raf kinase inhibitor protein (RKIP) in health and disease. Biochem Pharmacol 68:1049–1053
23. Klysik J, Theroux SJ, Sedivy JM et al (2008) Signaling crossroads: the function of Raf kinase inhibitory protein in cancer, the central nervous system and reproduction. Cell Signal 20:1–9
24. Bernier I, Jolles P (1984) Purification and characterization of a basic 23 kDa cytosolic protein from bovine brain. Biochim Biophys Acta 790:174–181
25. Hori N, Chae KS, Murakawa K et al (1994) A human cDNA sequence homologue of bovine phosphatidylethanolamine-binding protein. Gene 140:293–294
26. Seddiqi N, Bollengier F, Alliel PM et al (1994) Amino acid sequence of the Homo sapiens brain 21–23-kDa protein (neuropolypeptide h3), comparison with its counterparts from Rattus norvegicus and Bos taurus species, and expression of its mRNA in different tissues. J Mol Evol 39:655–660
27. Fu Z, Smith PC, Zhang L et al (2003) Effects of raf kinase inhibitor protein expression on suppression of prostate cancer metastasis. J Natl Cancer Inst 95:878–889
28. Chatterjee D, Bai Y, Wang Z et al (2004) RKIP sensitizes prostate and breast cancer cells to drug-induced apoptosis. J Biol Chem 279:17515–17523
29. Schuierer MM, Bataille F, Hagan S et al (2004) Reduction in Raf kinase inhibitor protein expression is associated with increased Ras-extracellular signal-regulated kinase signaling in melanoma cell lines. Cancer Res 64:5186–5192
30. Schuierer MM, Bataille F, Weiss TS et al (2006) Raf kinase inhibitor protein is downregulated in hepatocellular carcinoma. Oncol Rep 16:451–456
31. Zhang L, Fu Z, Binkley C et al (2004) Raf kinase inhibitory protein inhibits beta-cell proliferation. Surgery 136:708–715
32. Hagan S, Al-Mulla F, Mallon E et al (2005) Reduction of Raf-1 kinase inhibitor protein expression correlates with breast cancer metastasis. Clin Cancer Res 11:7392–7397
33. Lee HC, Tian B, Sedivy JM et al (2006) Loss of Raf kinase inhibitor protein promotes cell proliferation and migration of human hepatoma cells. Gastroenterology 131:1208–1217
34. Al-Mulla F, Hagan S, Behbehani AI et al (2006) Raf kinase inhibitor protein expression in a survival analysis of colorectal cancer patients 1. J Clin Oncol 24:5672–5679
35. Li HZ, Wang Y, Gao Y et al (2008) Effects of raf kinase inhibitor protein expression on metastasis and progression of human epithelial ovarian cancer. Mol Cancer Res 6:917–928
36. Chatterjee D, Sabo E, Tavares R et al (2008) Inverse association between Raf Kinase Inhibitory Protein and signal transducers and activators of transcription 3 expression in gastric adenocarcinoma patients: implications for clinical outcome. Clin Cancer Res 14:2994–3001
37. Zlobec I, Baker K, Minoo P et al (2008) Node-negative colorectal cancer at high risk of distant metastasis identified by combined analysis of lymph node status, vascular invasion, and raf-1 kinase inhibitor protein expression. Clin Cancer Res 14:143–148
38. Fu Z, Kitagawa Y, Shen R et al (2006) Metastasis suppressor gene Raf kinase inhibitor protein (RKIP) is a novel prognostic marker in prostate cancer. Prostate 66:248–256
39. Minoo P, Baker K, Goswami R et al (2006) Extensive DNA methylation in normal colorectal mucosa in hyperplastic polyposis. Gut 55(10):1467–1474
40. Fletcher CD, Berman JJ, Corless C et al (2002) Diagnosis of gastrointestinal stromal tumors: a consensus approach. Int J Surg Pathol 10:81–89
41. Gomes AL, Gouveia A, Capelinha AF et al (2008) Molecular alterations of KIT and PDGFRA in GISTs: evaluation of a Portuguese series. J Clin Pathol 61:203–208
42. Basto D, Trovisco V, Lopes JM et al (2005) Mutation analysis of B-RAF gene in human gliomas. Acta Neuropathol (Berl) 109:207–210
43. Dematteo RP, Lewis JJ, Leung D et al (2000) Two hundred gastrointestinal stromal tumors: recurrence patterns and prognostic factors for survival. Ann Surg 231:51–58
44. Demetri GD, von Mehren M, Blanke CD et al (2002) Efficacy and safety of imatinib mesylate in advanced gastrointestinal stromal tumors. N Engl J Med 347:472–480
45. Granovsky AE, Rosner MR (2008) Raf kinase inhibitory protein: a signal transduction modulator and metastasis suppressor. Cell Res 18:452–457
46. Minoo P, Zlobec I, Baker K et al (2007) Loss of Raf-1 kinase inhibitor protein expression is associated with tumor progression and metastasis in colorectal cancer. Am J Clin Pathol 127:820–827

47. Houben R, Michel B, Vetter-Kauczok CS et al (2006) Absence of classical MAP kinase pathway signalling in Merkel cell carcinoma. J Invest Dermatol 126:1135–1142
48. Akaishi J, Onda M, Asaka S et al (2006) Growth-suppressive function of phosphatidylethanolamine-binding protein in anaplastic thyroid cancer. Anticancer Res 26:4437–4442
49. Eves EM, Shapiro P, Naik K et al (2006) Raf kinase inhibitory protein regulates aurora B kinase and the spindle checkpoint. Mol Cell 23:561–574
50. Zhu S, Mc Henry KT, Lane WS et al (2005) A chemical inhibitor reveals the role of Raf kinase inhibitor protein in cell migration. Chem Biol 12:981–991
51. Jazirehi AR, Vega MI, Chatterjee D et al (2004) Inhibition of the Raf-MEK1/2-ERK1/2 signaling pathway, Bcl-xL down-regulation, and chemosensitization of non-Hodgkin's lymphoma B cells by Rituximab. Cancer Res 64:7117–7126
52. Fougner SL, Bollerslev J, Latif F et al (2008) Low levels of raf kinase inhibitory protein in growth hormone-secreting pituitary adenomas correlate with poor response to octreotide treatment. J Clin Endocrinol Metab 93:1211–1216
53. Bonavida B, Baritaki S, Huerta-Yepez S et al (2008) Novel therapeutic applications of nitric oxide donors in cancer: roles in chemo- and immunosensitization to apoptosis and inhibition of metastases. Nitric Oxide 19:152–157

Virchows Arch (2009) 455:285–293
DOI 10.1007/s00428-009-0827-6

ORIGINAL ARTICLE

Diffuse large B-cell lymphoma with a high number of epithelioid histiocytes (lymphoepithelioid B-cell lymphoma): a study of Osaka Lymphoma Study Group

Naoki Wada · Junichiro Ikeda · Masaharu Kohara · Hiroyasu Ogawa · Masayuki Hino · Shirou Fukuhara · Akihisa Kanamaru · Haruo Sugiyama · Yuzuru Kanakura · Eiichi Morii · Katsuyuki Aozasa

Received: 29 April 2009 / Revised: 22 July 2009 / Accepted: 18 August 2009 / Published online: 1 September 2009

Abstract The aim of this study was to clarify whether diffuse large B-cell lymphoma (DLBCL) with a high number of epithelioid histiocytes (DLBCL-EH) could have distinctive clinicopathological characteristics. Clinicopathological findings in 22 cases with DLBCL-EH and, as a control, 96 cases with ordinary type of DLBCL were analyzed. There were ten men and 12 women with ages ranging from 38 to 91 (median, 64) years. The primary site was lymph node in 16 cases, extranodal organs in three, and unknown in three. Stage of disease was I in five cases, II in three, III in nine, and IV in five. Histologically, there was a diffuse proliferation of large lymphoid cells admixed with numerous clusters of epithelioid histiocytes sprinkling throughout the lesions. Immunohistochemically, the large lymphoid cells were $CD20^{+}$, $CD15^{-}$, and $CD3^{-}$ and positive for CD10, bcl-6, and MUM1 in nine (41%), eight (36%), and 12 (55%) of 22 cases, respectively. Epstein–Barr virus positive rate was higher in DLBCL-EH (23.8%) than that in ordinary DLBCL (4.5%; $P<0.05$). Clonality analysis revealed monoclonal bands in all of the examined 20 cases with DLBCL-EH. Multivariate analysis revealed the prominent epithelioid reaction to be an independent factor for favorable prognosis. These findings suggest that DLBCL-EH could be a specific morphological variant of DLBCL associated with a better prognosis.

Keywords B-cell lymphoma · Epithelioid cells · Epstein–Barr virus · Prognosis

Introduction

In the World Health Organization (WHO) classification for lymphoid neoplasias, malignant lymphomas are largely divided into B-cell neoplasia, T/NK-cell neoplasia, and Hodgkin's lymphoma (HL). Diffuse large B-cell lymphoma (DLBCL), the most common category constituting about 30% of all lymphomas in the world, is defined as a diffuse proliferation of large neoplastic lymphoid B cells [1, 2]. Based on this criteria, it is

N. Wada · J. Ikeda · M. Kohara · E. Morii · K. Aozasa (✉)
Department of Pathology,
Graduate School of Medicine,
Osaka University,
2-2 Yamadaoka, Suita,
Osaka 565-0871, Japan
e-mail: aozasa@molpath.med.osaka-u.ac.jp

H. Ogawa
Department of Internal Medicine,
Hyogo College of Medicine,
Nishinomiya, Hyogo, Japan

M. Hino
Department of Clinical Haematology and Diagnostics,
Graduate School of Medicine,
Osaka City University, Osaka, Japan

S. Fukuhara
First Department of Internal Medicine,
Kansai Medical University, Moriguchi, Osaka, Japan

A. Kanamaru
Department of Hematology, School of Medicine,
Kinki University, Sayama, Osaka, Japan

H. Sugiyama
Department of Functional Diagnostic Science,
Graduate School of Medicine, Osaka University,
Suita, Osaka, Japan

Y. Kanakura
Department of Hematology and Oncology,
Graduate School of Medicine, Osaka University,
Suita, Osaka, Japan

postulated that DLBCL comprises morphologically, immunohistochemically, and clinically heterogeneous tumors with each unique clinical and pathologic features. Therefore, attempts have been undertaken to classify the DLBCL into biologically and clinically relevant subgroups. On the basis of the gene expression profile, DLBCL could be categorized into the germinal center B-cell type (GCB) and activated B-cell type (ABC) [3, 4]. Approximately 50% of adult DLBCLs are reported to be GCB subgroup [3].

DLBCL is categorized as one of the aggressive non-Hodgkin's lymphomas (NHL). At present, the International Prognostic Index (IPI) is widely adopted for the prediction of outcome in patients with aggressive NHL [5]. It incorporates patient age, performance status, serum lactate dehydrogenase (LDH), clinical stage, and number of extranodal lesions.

Through a review of cases registered with Osaka Lymphoma Study Group (OLSG), we found 22 cases of DLBCL with a high number of epithelioid histiocytes (DLBCL-EH). Follow-up study revealed that patients with DLBCL-EH showed a much more favorable course than ordinary DLBCL.

Patients and methods

Patients

From November 1999 to December 2007, a total of 3,468 cases were registered with OLSG, Japan. Histologic specimens obtained by biopsy were fixed in 10% formalin and routinely processed for paraffin embedding. Histologic sections, cut at 4 μm, were stained with hematoxylin and eosin and immunoperoxidase procedure (ABC method). All of the histologic sections were reviewed by one of the authors (KA) and classified according to the WHO classification. A diagnosis of malignant lymphoma was confirmed in 2,808 of 3,468 cases (81.0%). Of these 2,808 cases, 2,541 (90.5%) were NHL and 267 (9.5%) HL. The number of DLBCL cases was 1,220, which constituted 48.0% of all NHL. In 22 cases (1.8%) of DLBCL, there was a diffuse proliferation of large B-lymphoid cells admixed with numerous clusters of epithelioid histiocytes sprinkling throughout the lesions mimicking "Lennert lymphoma": They were selected for the present study. Ninety-six cases of DLBCL registered during August 2000–May 2005 were used as the control group (DLBCL-CG) because adequate clinical data and unstained sections for additional immunohistochemical analyses and in situ hybridization were available. Clinicopathological findings of DLBCL-EH and DLBCL-CG are summarized in Table 1.

Adequate clinical information was available in all patients. There were ten men and 12 women with ages ranging from 38 to 91 (median, 64) years. Primary site was lymph node in 16 cases and extranodal organs (spleen, orbit, and spinal epidural region) in three. Primary site could not be defined in three cases due to advanced disease involving both lymph nodes and extranodal organs. On the basis of the records of physical examinations, surgical notes, and pathologic examinations of the specimens, the Ann Arbor staging system was applied. Stage of disease was I in five cases, II in three, III in nine, and IV in five. The IPI score was calculated with five adverse factors (age>60 years, Ann Arbor stages III and IV, Eastern

Table 1 Brief clinicopathological findings

Characteristic	DLBCL-EH	DLBCL-CG	*P* value
Age (years): range (mean/median)	38–91 (65.2/64)[a]	24–86 (62.8/64)[b]	NS
Age>60 years, *n* (%)	17/22 (77.3%)	58/96 (60.4%)	NS
Sex, male/female	10:12	56:40	NS
Primary site, nodal/extranodal	16:3	39:35	0.013
Serum LDH level>normal, *n* (%)	11/22 (50%)	48/96 (50%)	NS
Performance status 2–4, *n* (%)	4/22 (18.2%)	26/96 (27.1%)	NS
Stage 3/4, *n* (%)	14/22 (63.6%)	43/96 (44.8%)	NS
Involved extranodal organ>1, *n* (%)	6/22 (27.3%)	22/96 (22.9%)	NS
IPI, HI/H, *n* (%)	9/22 (40.9%)	39/96 (40.6%)	NS
Response, SD/PD, *n* (%)	3/22 (13.6%)	15/96 (15.6%)	NS
Proliferation pattern			
Monomorphous, *n* (%)	0 (0%)	79 (82.3%)	<0.001
Polymorphous, *n* (%)	22 (100%)	17 (17.7%)	
Fibrosis, present/absent	17:5	47:49	0.016
Mitotic count (/high-power field)			
mean (range)	2.7 (0–8)[a]	3.0 (0–10)[b]	NS
MIB-1,%, mean (range)	57.1 (20–90)[c]	60 (20–90)[d]	NS
GCB/non-GCB	10:12	42:49	NS
EBV positive, *n* (%)	5/21 (23.8%)	2/44 (4.5%)	0.031

DLBCL-EH diffuse large B-cell lymphoma (DLBCL) with a high number of epithelioid histiocytes, *DLBCL-CG* DLBCL-control group, *IPI* International prognostic index, *HI/H* high-intermediate/high, *SD* stable disease, *PD* progressive disease, *GCB* germinal center B-cell type, *NS* not significant

[a] *n*=22

[b] *n*=96

[c] *n*=21

[d] *n*=35

Cooperative Oncology Group performance scores 2–4, elevation of serum LDH, and two or more extranodal lesions) present at the time of diagnosis [5]. For cases under 60 years, an age-adjusted IPI score was applied, in which advanced stage, low performance score, and elevation of LDH were considered as adverse factors [5]. In one patient (67-year-old man) with stage II disease at presentation, lymphadenopathy disappeared without any adjuvant therapy and the complete remission continued for more than 4 years. Chromosomal analysis in this case revealed t(8;14)(q24.1;q32). All of the remaining patients with DLBCL-EH received the combination chemotherapy, cyclophosphamide, doxorubicin, vincristine, and prednisolone (CHOP) in 15 cases, pirarubicin, cyclophosphamide, vincristine, and prednisolone (THP-COP) in three, and etoposide, mitoxantrone, cyclophosphamide, vincristine, prednisolone, and bleomycin (VNCOP-B) in two. One patient underwent combined chemotherapy and radiotherapy. In the latter half of 2003, rituximab was included in the regimen for most patients. Rituximab (R) was used in 14 (63.6%) of 22 DLBCL-EH patients: ten received R-CHOP, two R-THP-COP, one R-VNCOP-B, and one R only. Rituximab was used in 51 (53.1%) of 96 DLBCL-CG patients. There was not a statistically significant difference in frequency of patients receiving rituximab between DLBCL-EH and DLBCL-CG. Clinical outcome was evaluated according to the guidelines of the International Workshop to standardize response criteria for NHL [6]. Recurrence of disease after the chemotherapy was found in three patients with DLBCL-EH: All these patients underwent biopsy.

Immunohistochemistry

Monoclonal antibodies used for immunophenotyping were CD20, CD3, CD8, Bcl-6, MUM1, CD68, MIB-1, CD15, CD30 (Dakocytomation, Glostrup, Denmark, dilution at 1:400, 1:50, 1:100, 1:50, 1:100, 1:100, 1:1, 1:25, 1:50, respectively), CD4 (Novocastra Laboratories, Newcastle, UK, 1:40), CD10, CD23 (Nichirei Biosciences, Tokyo, Japan, used as prediluted antibodies), and programmed cell death 1 (PD-1; abcam, Tokyo, Japan, 1:50). Tonsils with reactive lymphoid hyperplasia served as external control tissues. In MIB-1 staining, the number of positive cells among 300–1,000 large lymphoid cells was counted: MIB-1 index was calculated as positive cells/100 cells.

In situ hybridization

RNA in situ hybridization using the Epstein–Barr encoded RNAs (EBER-1) probe was performed to examine the presence of Epstein–Barr virus (EBV) genome on the formalin-fixed paraffin-embedded sections according to the method previously described with some modifications [7]. Briefly, a 30-base oligonucleotide probe, 5′-AGACACCGTCCTCACCACC CGGGACTTGTA-3′, which was the sense and antisense for a portion of the EBER-1 gene, a region of the EBV genome that is actively transcribed in latently infected cells, was synthesized using a DNA synthesizer. As a positive control, the Raji cell line was used. As negative controls, the hybridizing mixture containing sense or antisense probe after RNase treatment was used. The presence of EBV genomes was evaluated in 21 cases of DLBCL-EH and 44 cases of DLBCL-CG. When the in situ hybridization yielded positive signals in the nuclei of more than 1% of the proliferating cells, such cases were defined as EBV positive.

Clonality analysis with the use of Ig and BCL2-IgH gene rearrangement

One to five sections with 4–10 μm thickness were cut from the paraffin-embedded samples, deparaffinized with xylene, washed with absolute and 70% ethanol, and subsequently digested in lysis buffer (50 mM Tris–HCl, 10 mM EDTA, 150 mM NaCl, 0.5% sodium dodecyl sulfate, and 0.4 mg/l proteinase K) at 55°C for overnight. DNA was extracted with phenol-chloroform extraction-based protocol, followed by ethanol precipitation and re-dissolved in TE buffer. Immunoglobulin (Ig) gene rearrangement was assessed by eight PCRs with 41 primers according to BIOMED-2 protocols [four multiplex PCRs and one single PCR with 28 primers for Ig heavy chain (IgH) gene; two multiplex PCRs with ten primers for Ig kappa light chain (Igκ) gene; one multiplex PCR with three primers for Ig lambda light chain (Igλ) gene] [8]. When the PCR amplification was not sufficient because of small amount of extracted DNA or fragmentation of DNA, we modified PCR condition of BIOMED-2 protocols as described in Table 2. The amplified PCR products were electrophoresed in 5.0% or 6.6% polyacrylamide gel based on fragment

Table 2 Summary of the PCR protocols for the original and modified BIOMED-2 PCR reactions

	Original BIOMED-2	Modified BIOMED-2
PCR reaction mix		
Template DNA	40 ng/50 μL	20 ng/50 μL
dNTP	200 μM	No change
Buffer ($MgCl_2$)	1.5 mM	No change
Primer	0.2 μM	0.5 μM
AmpliTaq Gold	1 U/50 μL	2.5 U/50 μL
PCR run parameters		
Denature	30 s	No change
Annealing	30 s	No change
Extention	30 s	No change
Cycles	35	40

sizes. For detection of BCL2-IgH chimera gene generated by t(14;18)(q32;q21), BIOMED-2 PCR protocol for MBR, 3′MBR, and mcr was applied as described previously [8]. Genotypic study could not be performed in two DLBCL-EH cases because enough amounts of paraffin-embedded materials for DNA extraction were not available.

Follow-up

The DLBCL-EH patients were followed until June 2008; the follow-up periods for survivors ranged from 2.8 to 98.8 (average, 35.1) months. Nineteen of 22 patients were alive at the end of the observation period. The Kaplan–Meier estimated survival rate for the DLBCL-EH at 5 years was 85.9%. As for the control group, the follow-up periods for survivors ranged from 11 to 99 (average, 45) months. Forty-nine of 96 patients were alive at the end of the observation period: 5-year survival rate was 50%.

Statistical analysis

Differences in frequencies of various clinical and pathologic factors between cases with DLBCL-EH and DLBCL-CG were compared with the chi-square test or the Fisher's exact probability test. Differences of means were compared with the *t* test or the Mann–Whitney test. Survival curves and overall survival rates were calculated with the Kaplan–Meyer method and were compared by the log-rank test. Multivariate analysis was performed with the Cox proportional hazard regression model.

Results

Histologic and immunohistochemical findings

Outstanding feature of DLBCL-EH is the presence of numerous clusters of epithelioid histiocytes sprinkled throughout the lesion with appearance of Langhans type or foreign body-type giant cells in two cases; among them, large lymphoid cells were discernible with occasional formation of large areas of the proliferating cells. This histologic appearance could be called lymphoepithelioid lymphoma (Fig. 1). Varying amount of small lymphocytes were present in the lesions but never predominated over the epithelioid histiocytes even when they were numerous. They were predominantly CD8 positive in 13 of 21 cases examined and rather equal in number of CD4- and CD8-positive lymphocytes in the remaining eight cases. Immunohistochemistry of CD4 and CD8 was not available in one DLBCL-EH case. More than 10% of small T lymphocytes were PD-1 positive in three of 21 DLBCL-EH cases. Staining with CD23 revealed the absence of follicular dendritic cells in 18 cases and faintly stained meshwork in two. Plasma cells and eosinophils were frequent in two cases. As a result, all of DLBCL-EH showed a polymorphous pattern of proliferation. Necrotic foci were occasional in three cases. Appearance of fine fibrous tissues in the background of the lesions was more frequent in the DLBCL-EH (17 of 22 cases) compared to that in DLBCL-CG (47 of 96 cases; $P<0.05$; Table 1).

Morphologic appearances of the large lymphoid cells were identical to centroblasts in 13 cases, centroblasts and immunoblasts in five, and unclassifiable because of tissue artifacts in four. Immunohistochemically, the large lymphoid cells were $CD20^+$ (Fig. 1), $CD3^-$, and positive for CD10, bcl-6, and MUM1 in nine (41%), 8 (36%) and 12 (55%) of 22 cases, respectively. DLBCL-EH could be categorized into GCB with $CD10^+$ or $CD10^-$/$bcl\text{-}6^+$/$MUM1^-$ and non-GCB with $CD10^-$/$bcl\text{-}6^-$ or $CD10^-$/$bcl\text{-}6^+$/$MUM1^+$ [9]. Ratio of GCB to non-GCB between DLBCL-EH and DLBCL-CG was similar in the present series. Large lymphoid cells were CD15 negative in all cases (0/21) and CD30 positive in three of 20 cases. Mean mitotic count per high-power field and MIB-1 labeling index among large lymphoid cells were 2.7 and 57.1, respectively.

Recurrence of disease was found in three patients: They were biopsied. The histology of two cases was also DLBCL-EH with appearance of Reed–Sternberg (R–S)-like cells and increased number of eosinophils in one. R–S-like cells were never found in the initial biopsy of any cases. In one case, precise evaluation was not possible because of tissue artifacts.

In situ hybridization

In situ hybridization with EBER-1 probe yielded positive signals in the nucleus of large lymphoid cells in five (23.8%) of 21 cases with DLBCL-EH (Fig. 1). Percentage of EBV-positive cells among large lymphoid cells was 3% in one case, 20% in two, 30% in one, and 70% in one. The EBV positive rate in DLBCL-EH was higher than that in two (4.5%) of 44 cases with DLBCL-CG ($P<0.05$). DLBCL-EH in one patient, who showed the spontaneous regression of lymphadenopathy without adjuvant therapy, was EBV positive.

Molecular genetic study

Genotypic study was performed in 20 cases with DLBCL-EH. All cases showed the monoclonal rearrangement of Ig genes with at least one primer. Monoclonal bands for both IgH and Ig light chain (IgL) genes were found in 17 cases, only for IgH gene in one, and only for IgL gene in two (Fig. 2). The BCL2-IgH gene rearrangement was detected in two (10%) of 20 cases examined. Tumor cells in these two cases showed the positive immunoreactivity for CD10.

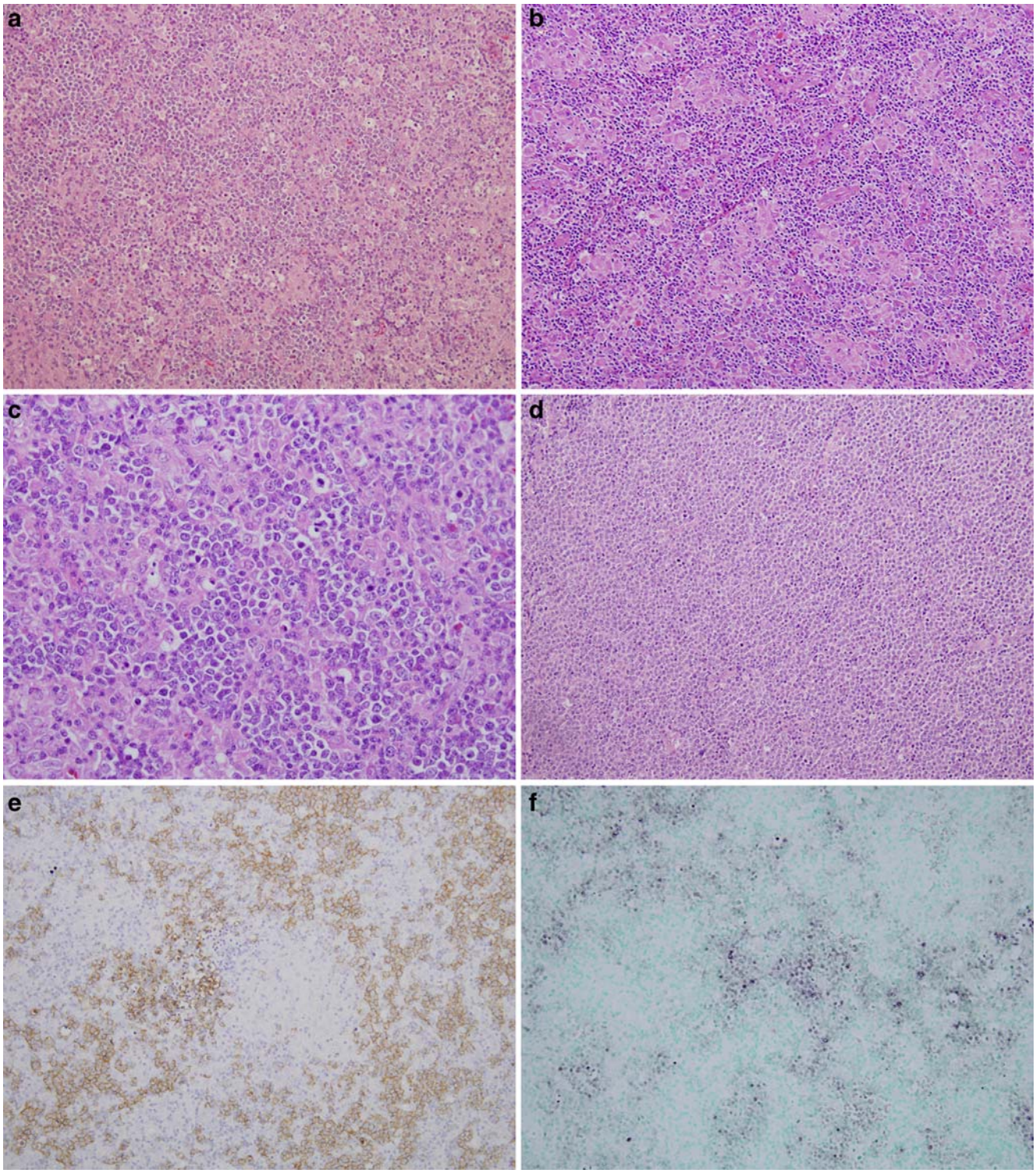

Fig. 1 **a** Diffuse large B-cell lymphoma (DLBCL) with a high number of epithelioid histiocytes (DLBCL-EH). There was a diffuse proliferation of large lymphoid cells admixed with numerous clusters of epithelioid histiocytes sprinkling throughout the lesions. A few small lymphoid cells were found, H&E ×200. **b** Many reactive lymphoid cells were found among clusters of epithelioid histiocytes together with diffuse proliferation of large lymphoid cells in some cases with DLBCL-EH, H&E ×200. **c** Higher magnification illustrating the immunoblast- and centroblast-like proliferating cells in DLBCL-EH, H&E ×400. **d** DLBCL with the ordinary histology showing almost monomorphous proliferation of large lymphoid cells, H&E ×200. **e** Immunohistochemically, the large lymphoid cells in DLBCL-EH were $CD20^{+}$, ×200. **f** In situ hybridization with EBER-1 probe revealed positive signals in the nucleus of large lymphoid cells in DLBCL-EH, x200

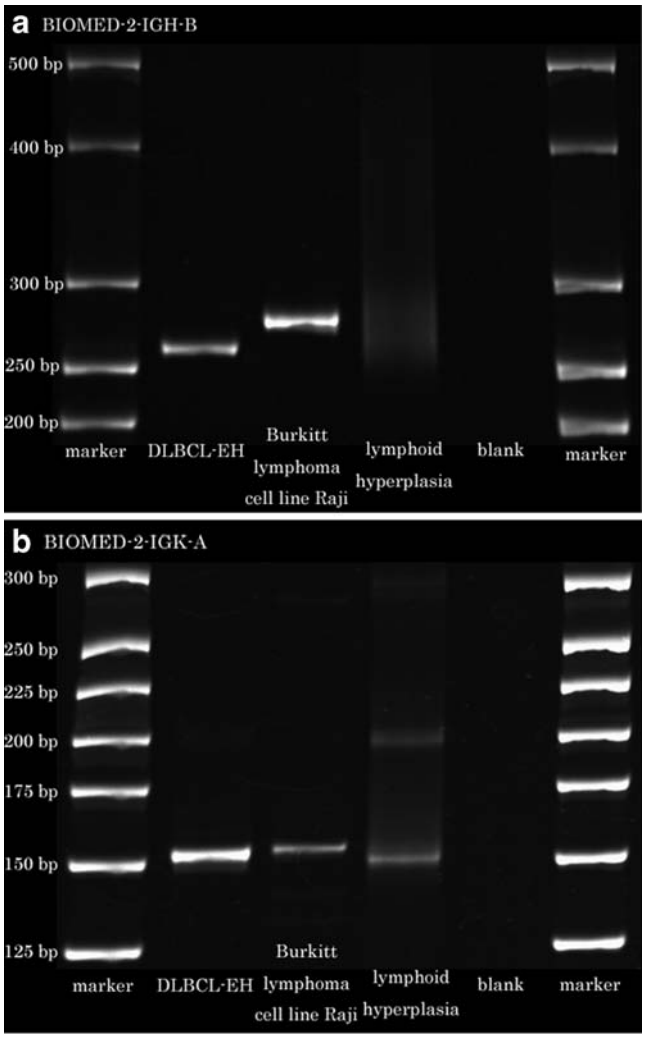

Fig. 2 Clonality analysis with use of immunoglobulin (Ig) heavy chain (IgH) gene (**a**) and Ig kappa light chain (Igκ) gene (**b**). Monoclonal bands were found in lanes of diffuse large B-cell lymphoma with a high number of epithelioid histiocytes (DLBCL-EH) and Burkitt lymphoma cell line Raji

Clinical findings

Brief clinical and pathological findings are summarized in Table 1. There were no findings suggestive of the presence of immunodeficient conditions. Two patients had a past history of autoimmune diseases, one each of idiopathic thrombocytopenic purpura and rheumatoid arthritis. One patient had a past history of chronic hepatitis caused by hepatitis B virus. One patient suffered from chronic hepatitis caused by hepatitis C virus and prostatic cancer. Agents supposed to cause immunosuppression such as methotrexate, steroid, or chemotherapeutic drugs for cancer were never used in these patients. No significant differences were found in age, serum LDH level, performance status, number of involved extranodal organ, IPI, response for chemotherapy, and the ratio of GCB to non-GCB subgroup between cases with DLBCL-EH and DLBCL-CG. Female preponderance and the higher frequency of advanced disease (stage III+IV) were found in DLBCL-EH, but the differences of these factors between DLBCL-EH and DLBCL-CG were not significant. Significant difference was found in the primary site (nodal vs extranodal) between DLBCL-EH (16:3) and DLBCL-CG (39:35; $P<0.05$).

Prognostic factors

The estimated survival rate at 5 years for the DLBCL-EH (85.9%) was significantly higher than that for DLBCL-CG (50%; log-rank, $P<0.05$) (Fig. 3). Results of the univariate analysis are shown in Table 3. Elevated serum LDH level, low PS, advanced stage, involved extranodal organ>1, and high IPI score were unfavorable factors for prognosis. The presence of prominent epithelioid cell response and GCB subgroup were favorable factors for prognosis. Multivariate analysis revealed that low PS was an independent factor for poor prognosis, and prominent epithelioid cell response was a favorable prognostic factor (Table 4). GCB subgroup showed a marginal significance for favorable prognosis ($P=0.062$).

Discussion

In the WHO classification (2008), several variants of DLBCL, not otherwise specified, are listed such as T cell/histiocyte-rich large B-cell lymphoma (THRLBCL), primary DLBCL of the central nervous system, primary cutaneous DLBCL, leg type, and EBV-positive DLBCL of the elderly [1]. At first, a difference of DLBCL-EH from THRLBCL should be commented. The new classification provides a description that "THRLBCL is characterized by a limited number of scattered, large, atypical B-cells embedded in a background of abundant T cells and frequent histiocytes" [10]. In the DLBCL-EH, large B cells are numerous and form sheets of

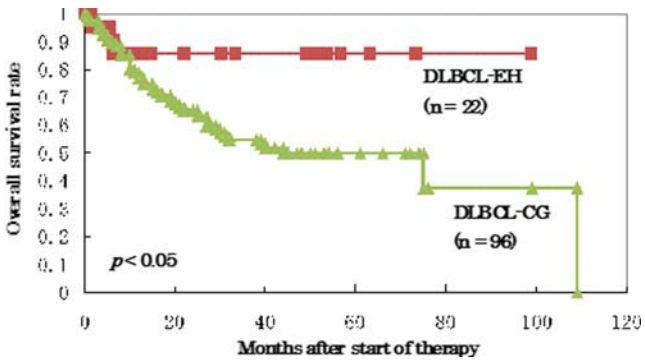

Fig. 3 Overall survival curve for patients with diffuse large B-cell lymphoma (DLBCL) with a high number of epithelioid histiocytes (DLBCL-EH) and DLBCL-control group (DLBCL-CG; Kaplan–Meier method). The estimated survival rate in patients with DLBCL-EH at 5 years (85.9%) was significantly favorable than that in DLBCL-CG (50.0%) (log-rank, $P=0.045$)

Table 3 Univariate analysis for overall survival of patients with DLBCL-EH and DLBCL-CG

Characteristic	No. of patients	Five-year OS (%)	*P* value
Age, years			
Age≦60	43	60.2	NS
Age > 60	75	51.1	
Sex			
Male	66	52.4	NS
Female	52	57.8	
Primary site			
Nodal	55	55.2	NS
Extranodal	38	67.7	
Serum LDH level			
Normal or lower	59	72.4	0.0014
Higher than normal	59	38.3	
Performance status			
ambulatory (0–1)	88	67.0	<0.001
not ambulatory (2–4)	30	13.7	
Ann Arbor stage			
Stage 1/2	61	72.8	<0.001
Stage 3/4	57	34.1	
Extranodal involvement			
0–1 site	90	63.6	<0.001
> 1 sites	28	25.0	
International Prognostic Index			
L/LI	70	75.9	<0.001
HI/H	48	23.2	
GCB/non-GCB			
GCB	52	65.7	0.017
Non-GCB	61	45.6	
Prominent epithelioid cell response			
Present	22	85.9	0.045
Absent	96	50.0	

DLBCL-EH diffuse large B-cell lymphoma (DLBCL) with a high number of epithelioid histiocytes; *DLBCL-CG* DLBCL-control group, *OS* overall survival, *L/LI* low/low-intermediate, *HI/H*, high-intermediate/high, *GCB* germinal center B-cell type, *NS* not significant

cells as shown in Fig. 1a and e. Marked appearance of cluster of epithelioid histiocytes, as shown in this study (Fig. 1), is not described and illustrated. Lymphoepithelioid B-cell lymphoma was differentiated from THRLBCL by predominance of histiocytes to small lymphocytes and their epithelioid morphologies, not by percentages of histiocytes and lymphocytes in the present study as also in the study by Achten et al. [11]. Achten et al. described that histiocytes in their cases with histiocyte-rich, T-cell-rich B-cell lymphoma, which corresponds to the THRLBCL, were not epithelioid in appearances. Chetaille et al. [12] reported that the T cells in all of THRLBCL cases expressed PD-1 antigen. This showed a clear contrast to the present cases, in which only three of 21 cases were PD-1 positive.

Table 4 Multivariate analysis of clinicopathological factors for overall survival of patients with DLBCL-EH and DLBCL–CG

Characteristic	Relative risk	95% CI	*P* value
Serum LDH level>normal	1.43	0.65–3.15	NS
Performance status 2–4	2.95	1.52–5.72	0.0014
Stage 3/4	1.88	0.61–5.85	NS
Involved extranodal organ>1	1.77	0.88–3.56	NS
IPI, HI/H	1.34	0.34–5.32	NS
Germinal center B-cell type	0.53	0.28–1.03	0.062
Prominent epithelioid cell response	0.26	0.077–0.86	0.028

DLBCL-EH diffuse large B-cell lymphoma (DLBCL) with a high number of epithelioid histiocytes, *DLBCL-CG* DLBCL control group, *CI* confidence interval, *IPI* International prognostic index, *HI/H* high-intermediate/high, *NS* not significant

Some of the similar cases to the present series were included in the previous reports under the headings of TCR-, T/HR- or TC/HR-(L)BCL [13–15], but prognosis of this special type of THRLBCL was not commented in comparison with representative cases of THRLBCL without prominent epithelioid reaction. Large B-cell lymphomas generally fail to provoke a substantial immune reaction; therefore, prominent epithelioid cell reaction is exceptional: Frequency of DLBCL-EH among all DLBCL cases registered with the OLSG is only 1.8%.

Patients with DLBCL-EH showed the significantly favorable prognosis than those with DLBCL-CG, i.e., ordinary type of DLBCL. This finding contrasts to the disease diagnosed as THRLBCL by the WHO criteria, which shows similar prognosis to stage- and IPI-matched ordinary DLBCL [15–18]. The present multivariate analysis revealed that the prominent epithelioid cell response was an independent factor for favorable prognosis. The present clonality analysis based on the Ig gene rearrangement confirmed the clonal nature of B-cell proliferation in the DLBCL-EH. Proliferative activity, as revealed by MIB-1 labeling index, was rather similar between DLBCL-EH and DLBCL-CG. It has been reported that DLBCL of non-GCB subgroup showed a more unfavorable prognosis than that of GCB subgroup [4, 9, 19]. Frequency of GCB and non-GCB cases in the present series was rather similar, which is identical to the previous reports on DLBCL [3].

DLBCL is divided into the two types based on the gene expression profiles of the proliferating cells, i.e., GCB type and ABC with more favorable prognosis of the former than the latter type [3, 4]. Recently, Lenz et al. [20] reported that DLBCL could be categorized based on the gene expression signatures of stromal cells surrounding the neoplastic large B-lymphoid cells. The stromal cell gene signature found in cases showing histiocyte-rich host reaction to the lymphoma cells was correlated with favorable prognosis of the patients. This finding is concordant with the present finding that DLBCL-EH shows a favorable prognosis.

DLBCL-EH is characterized by a predominantly nodal presentation and higher EBV positive rate compared to DLBCL-CG. EBV positive rate in the ordinary type of DLBCL is reported to be less than 10% worldwide. Therefore, the higher EBV-positive rate in the DLBCL-EH is unique. One of the present patients with EBV-positive DLBCL-EH showed the spontaneous regression without adjuvant therapy. Spontaneous regressions of EBV-positive DLBCL were reported previously [21, 22], but their histologies were not epithelioid rich.

Present findings suggest that DLBCL-EH could be a morphological variant of DLBCL that has an apparent better clinical outcome than conventional DLBCL. The peculiar morphological aspect of the tumor raises several important differential diagnoses. Then, differential points of this lymphoma from other types of diseases are discussed below. Firstly, distinction of DLBCL-EH from the lymphoepithelioid cell variant of peripheral T-cell lymphoma, not otherwise specified (PTCL-NOS) is necessary. Indeed, the authors, as the pathology board members of the OLSG, initially interpreted the histologic pictures of DLBCL-EH as the lymphoepithelioid cell variant of PTCL-NOS on the purely morphological grounds. However, the immunohistochemistry revealed the B-cell nature of the proliferating large lymphoid cells. In addition, genotypic study confirmed the clonal proliferation of B cells. The presence of fine fibrous tissues and necrotic foci might be frequent to occasional in DLBCL-EH but uncommon in the lymphoepithelioid cell variant of PTCL-NOS.

Classical HL of mixed cellularity type (CHL-MC) occasionally show the histology containing a high content of epithelioid histiocytes, with rather favorable clinical course than ordinary CHL-MC [23]. Thus, distinction of DLBCL-EH from CHL-MC may be needed in some cases. Indeed, Reed–Sternberg cell-like cells appeared in the recurrent lesion of one of the present cases. However, diagnostic Reed–Sternberg cells were absent even in this lesion. Such kind of cells was never found in the initial biopsy of any cases. Complete absence of CD15-positive cells and presence of CD30-positive cells in a quite limited number of the present DLBCL-EH cases indicated that a diagnosis of CHL-MC was unlikely. CD30 immunoreactivity seems not to be a distinguishing feature of CHL, as it may be observed in the THRLBCL as well [11]. In addition, clonal B-cell proliferation was confirmed in all of the DLBCL-EH cases examined. Although mononuclear Hodgkin and multinucleated Reed–Sternberg (HRS) cells contain monoclonal Ig gene in greater than 98% of cases and monoclonal T-cell receptor gene in rare cases in the DNA isolated from the single HRS cells, the monoclonal rearrangements are usually not detectable in the whole tissue DNA [24]. With combination of histologic, immunohistologic findings and genotypic study, distinction of DLBCL-EH from CHL-MC with a high content of epithelioid histiocytes is possible.

In conclusion, the DLBCL-EH is distinct from ordinary DLBCL in its higher EBV-positive rate, predominant nodal presentation, and favorable prognosis. Because the follow-up period in the present series was rather short, further study on the DLBCL-EH with more high number of cases and adequately long follow-up period would provide a robust conclusion.

Acknowledgements The authors thank Ms. T. Sawamura, M. Sugano, K. Fujikawa, and E. Maeno for their technical assistance and Mr. Toshimitsu Hamasaki, Department of Biomedical Statistics, Osaka University, for advice on the statistical analyses. This study is supported in part by a Grant from the Ministry of Education, Culture, Sports, and Science (20014012), Japan

Conflict of interest statement We declare that we have no conflict of interest.

References

1. Stein H, Warnke RA, Chan WC et al (2008) Diffuse large B-cell lymphoma, not otherwise specified. In: Swerdlow SH et al (eds) WHO classification of tumours of haematopoietic and lymphoid tissues. World health organization classification of tumours, 4th edn. IARC, Lyon, pp 233–237
2. The Non-Hodgkin's Lymphoma Classification Project (1997) A clinical evaluation of the International Lymphoma Study Group classification of non-Hodgkin's lymphoma. Blood 89:3909–3918
3. Rosenwald A, Wright G, Chan WC et al (2002) The use of molecular profiling to predict survival after chemotherapy for diffuse large-B-cell lymphoma. N Engl J Med 346:1937–1947
4. Alizadeh AA, Eisen MB, Davis RE et al (2000) Distinct types of diffuse large B-cell lymphoma identified by gene expression profiling. Nature 403:503–511
5. The International Non-Hodgkin's Lymphoma Prognostic Factors Project (1993) A predictive model for aggressive non-Hodgkin's lymphoma. N Engl J Med 329:987–994
6. Cheson BD, Horning SJ, Coiffier B et al (1999) Report of an international workshop to standardize response criteria for non-Hodgkin's lymphomas. NCI Sponsored International Working Group. J Clin Oncol 17:1244–1253
7. Weiss LM, Jaffe ES, Liu XF, Chen YY, Shibata D, Medeiros LJ (1992) Detection and localization of Epstein–Barr viral genomes in angioimmunoblastic lymphadenopathy and angioimmunoblastic lymphadenopathy-like lymphoma. Blood 79:1789–1795
8. Van Dongen JJ, Langerak AW, Brüggemann M et al (2003) Design and standardization of PCR primers and protocols for detection of clonal immunoglobulin and T-cell receptor gene recombinations in suspect lymphoproliferations: report of the BIOMED-2 Concerted Action BMH4-CT98–3936. Leukemia 17:2257–2317
9. Hans CP, Weisenburger DD, Greiner TC et al (2004) Confirmation of the molecular classification of diffuse large B-cell lymphoma by immunohistochemistry using a tissue microarray. Blood 103:275–282
10. De Wolf-Peeters C, Delabie J, Campo E et al (2008) T cell/histiocyte-rich large B-cell lymphoma. In: Swerdlow SH et al (eds) WHO classification of tumours of haematopoietic and lymphoid tissues. World health organization classification of tumours, 4th edn. IARC, Lyon, pp 238–239
11. Achten R, Verhoef G, Vanuytsel L, De Wolf-Peeters C (2002) Histiocyte-rich, T-cell-rich B-cell lymphoma: a distinct diffuse large B-cell lymphoma subtype showing characteristic morphologic and immunophenotypic features. Histopathology 40:31–45
12. Chetaille B, Bertucci F, Finetti P et al (2009) Molecular profiling of classical Hodgkin lymphoma tissues uncovers variations in the tumor microenvironment and correlations with EBV infection and outcome. Blood 113:2765–2775
13. Macon WR, Williams ME, Greer JP, Stein RS, Collins RD, Cousar JB (1992) T-cell-rich B-cell lymphomas. A clinicopathologic study of 19 cases. Am J Surg Pathol 16:351–363
14. Baddoura FK, Chan WC, Masih AS, Mitchell D, Sun NC, Weisenburger DD (1995) T-cell-rich B-cell lymphoma. A clinicopathologic study of eight cases. Am J Clin Pathol 103:65–75
15. Abramson JS (2006) T-cell/histiocyte-rich B-cell lymphoma: biology, diagnosis, and management. Oncologist 11:384–392
16. Bouabdallah R, Mounier N, Guettier C et al (2003) T-cell/histiocyte-rich large B-cell lymphomas and classical diffuse large B-cell lymphomas have similar outcome after chemotherapy: a matched-control analysis. J Clin Oncol 21:1271–1277
17. Aki H, Tuzuner N, Ongoren S et al (2004) T-cell-rich B-cell lymphoma: a clinicopathologic study of 21 cases and comparison with 43 cases of diffuse large B-cell lymphoma. Leuk Res 28:229–236
18. El Weshi A, Akhtar S, Mourad WA et al (2007) T-cell/histiocyte-rich B-cell lymphoma: clinical presentation, management and prognostic factors: report on 61 patients and review of literature. Leuk Lymphoma 48:1764–1773
19. Sjö LD, Poulsen CB, Hansen M, Møller MB, Ralfkiaer E (2007) Profiling of diffuse large B-cell lymphoma by immunohistochemistry: identification of prognostic subgroups. Eur J Haematol 79:501–507
20. Lenz G, Wright G, Dave SS et al., Lymphoma/Leukemia Molecular Profiling Project (2008) Stromal gene signatures in large-B-cell lymphomas. N Engl J Med 359:2313–2323
21. Abe R, Ogawa K, Maruyama Y, Nakamura N, Abe M (2007) Spontaneous regression of diffuse large B-cell lymphoma harbouring Epstein–Barr virus: a case report and review of the literature. J Clin Exp Hematopathol 47:23–26
22. McCabe MG, Hook CE, Burke GA (2008) Spontaneous regression of an EBV-associated monoclonal large B cell proliferation in the mastoid of a young child following surgical biopsy. Pediatr Blood Cancer 51:557–559
23. Sacks EL, Donaldson SS, Gordon J, Dorfman RF (1978) Epithelioid granulomas associated with Hodgkin's disease: clinical correlations in 55 previously untreated patients. Cancer 41:562–567
24. Stein H, Delsol G, Pileri SA et al (2008) Classical Hodgkin lymphoma, introduction. In: Swerdlow SH et al (eds) WHO classification of tumours of haematopoietic and lymphoid tissues. World health organization classification of tumours, 4th edn. IARC, Lyon, pp 326–329

Virchows Arch (2009) 455:295–299
DOI 10.1007/s00428-009-0819-6

ORIGINAL ARTICLE

DLK is a novel immunohistochemical marker for adrenal gland tumors

Eszter Turányi · Katalin Dezső · Sándor Paku · Peter Nagy

Received: 13 March 2009 / Revised: 19 June 2009 / Accepted: 30 July 2009 / Published online: 14 August 2009

Abstract Delta-like protein (DLK) is expressed in fetal and adult adrenal glands. We have investigated if this expression is maintained in adrenal gland-derived tumors. All the studied 37 cortical tumors, including five carcinomas, stained positively as well as the 13 examined pheochromocytomas. Thus, DLK is a very sensitive marker for adrenal tumors of cortical and medullary origin. Renal cell carcinomas, presenting the major differential diagnostic problem for cortical tumors, were all negative, as well as melanomas, which are similar to high portion of adrenocortical tumors that react with melan-A. However, all paragangliomas, some carcinoids, and thyroid medullary carcinomas were also positive for DLK. Therefore, this novel immunohistochemical marker seems useful for the identification of adrenocortical tumors while it has limited value for the distinction of pheochromocytomas from diagnostically related neuroendocrine tumors.

Keywords Immunohistochemistry · Adrenocortical tumor · DLK

Abbreviations

DLK	delta-like protein
EGF	epidermal growth factor
PEC	perivascular epithelioid cell

This study is supported by the OTKA K67697.

E. Turányi · K. Dezső · S. Paku · P. Nagy (✉)
First Department of Pathology and Experimental Cancer Research, Semmelweis University,
Üllői út 26,
Budapest 1085, Hungary
e-mail: nagy@korb1.sote.hu

Introduction

Delta-like protein (DLK), an epidermal growth factor like multidomain glycoprotein, is expressed in several fetal tissues, e.g., in immature liver and in adult adrenal glands [1]. We have recently described [2] that DLK expression is maintained in the hepatoblasts upon malignant transformation, and it can be applied as a diagnostic immunohistochemical marker for hepatoblastomas. DLK expression has been reported in normal adrenal cortex [3], in ganglioneuroblastomas, in pheochromocytomas, and in other endocrine tumors [4–6], but no comprehensive immunohistochemical analysis has been performed on adrenocortical tumors. In this present work, we have collected adrenal gland-derived and differential diagnostically related tumors from our archives and investigated their DLK expression by standard immunohistochemistry. All the investigated adrenal gland-derived tumors are positive for DLK, and this immunophenotype, especially in cortical tumors, can be useful to resolve certain aspects of diagnostic challenges.

Materials and methods

Formalin-fixed, paraffin-embedded tissue was used for immunohistochemical staining. The most important parameters of the investigated tumors are listed in Tables 1 and 2. No peculiar variants of cortical adenomas (black, oncocytic, etc.) occurred among the investigated tumors.

Traditional, avidin biotin-based immunohistochemistry was performed. In brief, after blocking the endogenous peroxidase activity in methanol and hydrogen peroxide, the antigens were retrieved by heating in 10 mmol citrate buffer (pH 7.0) in a microwave oven for 10 min. The sections were then blocked with normal horse serum (blocking

Table 1 Clinical characteristics of investigated tumors

	Gender (M/F)	Mean age (years)	Number
Adrenocortical carcinoma	1/4	60.2	5
Adrenocortical adenoma	6/26	50.6	32
Pheochromocytoma	8/5	40.4	13
Paraganglioma	0/4	40.2	4
Angiomyolipoma	1/8	49.6	9
Renal cell carcinoma	18/13	57.8	31
Melanoma	3/8	62.6	11
Carcinoid	7/15	52.2	22
Thyroid medullary carcinoma	2/9	46.7	11

M male, *F* female

serum from the kit) diluted in phosphate-buffered saline before overnight incubation with the primary antibodies (DLK: R&D Systems, Minneapolis, MN, USA, Catalog number: AF1144; goat polyclonal antibody, dilution 1:100) at 4°C. The VECTASTAIN Elite ABC Kit (goat; Vector Laboratories, Burlingame, CA, USA, Catalog number: PK-6105) was used for developing the reactions with diaminobenzidine as chromogen. The negative control slides were covered by normal goat serum (Vector Laboratories, Catalog number: S-1000) instead of the primary antibody. No staining was observed on the negative controls (data not shown). Hepatoblastomas were used as positive controls.

Results

DLK expression in normal adrenal gland

In our immunohistochemical staining in the peritumoral, normal adrenal gland confirms earlier observations [1, 3]. DLK is present in both substances of the glands, contrary to their different embryological origin. The staining pattern is usually not even; the reaction is stronger in the cells of the zona glomerulosa and decreases in central direction (data not shown).

Table 2 DLK immunostaining of the investigated tumors

	+	++	+++	Negative	All
Adrenocortical carcinoma	0	0	5	0	5
Adrenocortical adenoma	0	13	19	0	32
Pheochromocytoma	0	1	12	0	13
Paraganglioma	0	0	4	0	4
Angiomyolipoma	0	0	0	9	9
Renal cell carcinoma	0	0	0	31	31
Melanoma	0	0	0	11	11
Carcinoid	1	0	2	19	22
Thyroid medullary carcinoma	3	2	0	6	11

+ positive reaction in less than 5%, ++ positive reaction between 5% and 50%,+++ positive reaction over 50% of the tumor area

DLK expression in adrenal gland tumors

Each of the examined 37 adrenocortical tumors stained positively for DLK (Fig. 1a, b). The reaction was usually diffuse; it always covered at least 20% of the tumorous areas. The staining pattern on cellular level was variable. In most cases, in addition to the diffuse cytoplasmic staining, strong paranuclear dots were observed, and membranous reaction was present occasionally (Fig. 1b). The different staining patterns were mixed sometimes in the same tumor, but usually, there was a dominant type of distribution. We could not observe any correlation among the reaction patterns and/or the clinical, morphological characteristics, and the endocrine activity of the tumors (data not shown). The situation was similar to hepatoblastomas [2], when no connection was recognized between the distribution of the DLK immunostaining and other features of the tumors.

Metastasis formation proved the malignant nature of five of the investigated cortical tumors. Neither the intensity nor the distribution of the reaction was different in the carcinomas and adenomas. The pulmonary metastasis of one carcinoma was available, and it was positive for DLK.

Similar to the cortical tumors, each investigated pheochromocytomas proved to be DLK positive (Fig. 1c). The dominant but not exclusive reaction was the dot formation in paranuclear position. The immunostaining was confined to the tumor cells, and no reliable reaction was present on the endothelial cells.

DLK expression in differential diagnostically related tumors

We stained several kidney tumors consisting of clear cells: 31 renal cell carcinomas (29 clear cell, 1 papillary, and 1 chromophobe carcinomas) and 9 angiomyolipomas for DLK, but no positive reaction was observed (Fig. 2a).

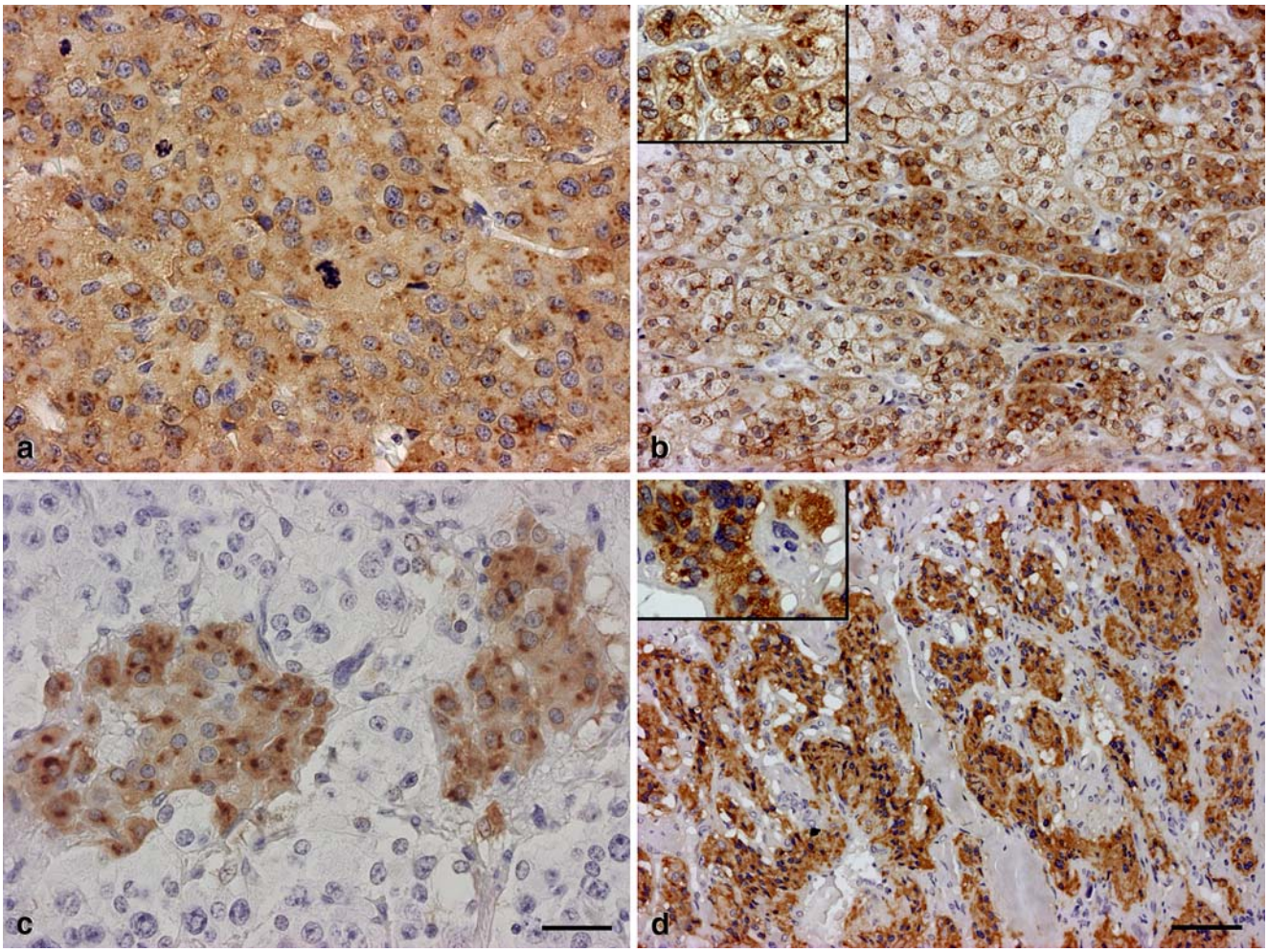

Fig. 1 DLK immunostaining in adrenocortical carcinoma (**a**), adrenocortical adenoma (**b**), pheochromocytoma (**c**), and paraganglioma (**d**). Note the membranous staining and paranuclear dots on the high magnification *inserts*. *Scale bars* for **a**, **c**: 50 μm; **b**, **d**: 100 μm

In the histogenesis of extra-adrenal pheochromocytomas, paragangliomas is basically identical with those of the adrenal tumors. So, it was not surprising that these tumors could not be distinguished from adrenal pheochromocytomas by DLK stainings (Fig. 1d). The majority of the other investigated neuroendocrine tumors: carcinoids (14 stomachs, 4 appendices, 1 ileum, 1 colon, 1 pancreas, and 1 lung) and thyroid medullary carcinomas were DLK negative, but positively stained tumors also occurred (Fig. 2b, c). There was diffuse reaction in one lung and one stomach tumors. Furthermore, in one additional stomach carcinoid, the DLK positivity was focal. Five of the 11 studied medullary carcinomas also reacted with the DLK antibody. The staining pattern was focal in three and intermediate in two samples. Neither of the melanomas were decorated by DLK (Fig. 2d). Finally, the negative control sections of all the investigated specimens remained unstained. The results of DLK immunostainings are summarized in Table 2.

Discussion

We have investigated the expression of DLK by immunohistochemistry in adrenal gland neoplasms and differential diagnostically related tumors. Each of the studied adrenocortical tumors and pheochromocytomas proved to be positive, but occasional reaction occurred in the other tumors as well. Thus, the sensitivity of DLK for adult adrenal tumors was 100% while the specificity on our samples was 87%. No neuroblastomas were included in this work, because DLK expression in this group of tumors has been thoroughly analyzed [4]. Neuroblastomas were reported negative while the differentiating cells of ganglioneuromas became positive. We observed similar staining on a few investigated tumors [2]. The presence of DLK messenger RNA (mRNA) in a human neuroblastoma cell line [5] also has been described.

The occurrence of DLK mRNA and protein has been documented in the normal adrenal gland several times [1,

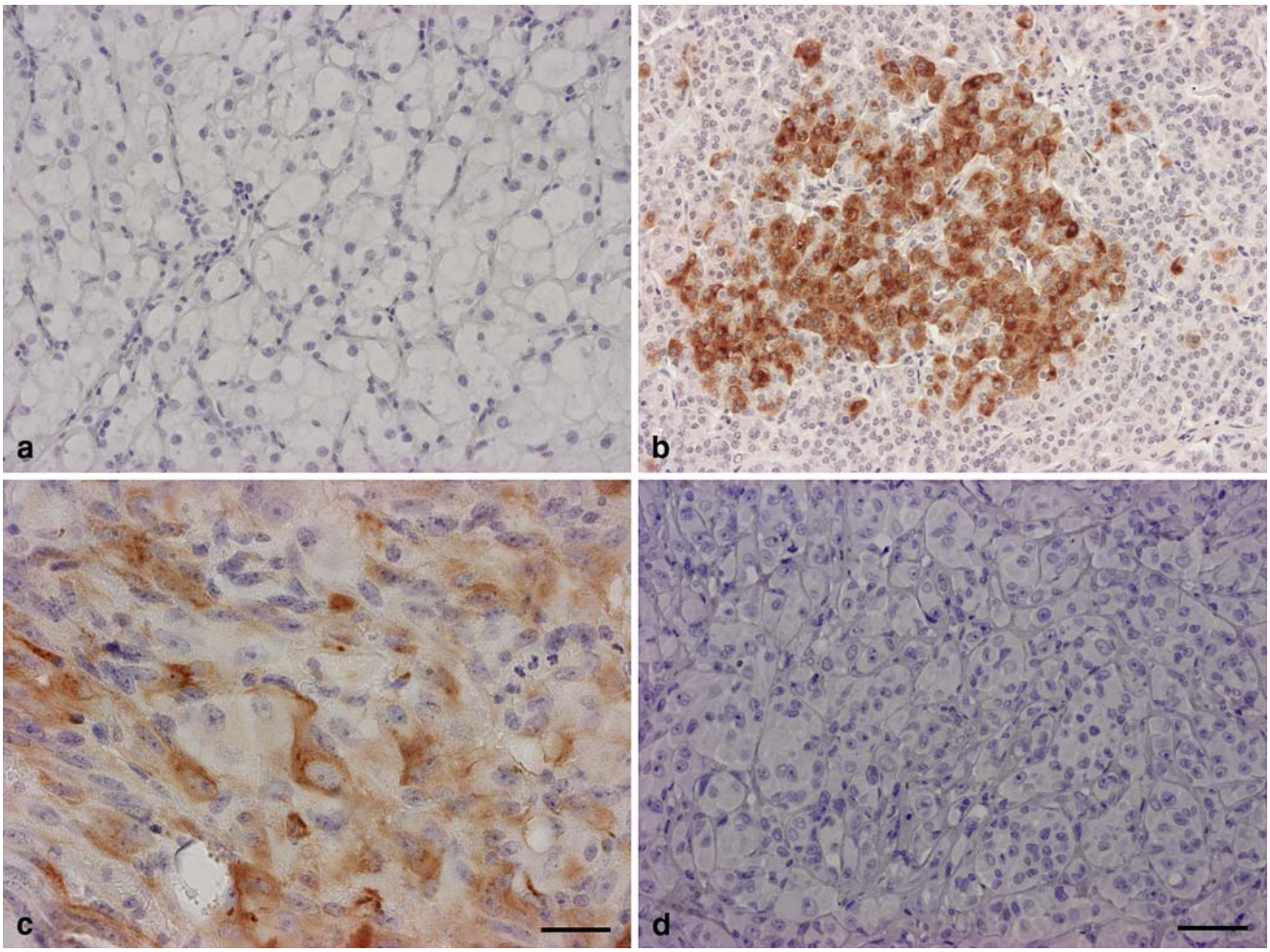

Fig. 2 DLK immunostaining in renal cell carcinoma (**a**), stomach carcinoid (**b**), thyroid medullary carcinoma (**c**), and melanoma (**d**). *Scale bars* for **a**, **b**, and **d** 100 μm; **c** 50 μm

7–9]. In fact, one of the alternative names for DLK is human adrenal-specific complementary DNA [8]. The presence of this antigen is well-documented in different neuroendocrine tumors. DLK is an established marker of small cell lung carcinoma and pulmonary carcinoids [5, 9]. It is present in certain endocrine tumors of the pancreas [6]. The tumor cells of pheochromocytomas were reported negative for DLK while it could be detected in the tumor vasculature [4]. Others reported the presence of DLK mRNA in a pheochromocytoma cell line [5].

As far as we know, nobody analyzed the DLK expression in adrenocortical tumors so far. All the studied adrenal cortex-derived tumors were positive in our present experiment. Although DLK is a new player among the routinely used immunohistochemical markers, its expression in adrenocortical tumors is not a unique feature. However, in certain context, our observation could be utilized in diagnostic algorithms. If we are challenged by a clear cell tumor from the adrenal region, the three major differential diagnostic problems are: (1) distinction between adrenal tumors and renal cell carcinomas, (2) distinction between adrenal cortical and medullar tumors, and (3) distinction between cortical adenomas and carcinomas. DLK, based on our results, cannot contribute to answer the latter two questions, but may be the key issue regarding the first problem. There are several overlaps between the immunophenotypes of renal cell carcinomas and adrenocortical tumors (vimentin positivity and uncertain keratin staining) [10, 11], and the clear cells of perivascular epithelioid cell component in angiomyolipomas may be also similar to adrenal tumors. Each investigated renal cell carcinomas and kidney angiomyolipomas were clearly negative, so the DLK staining would strongly support the diagnosis of adrenal tumors in such cases.

The value of the exact histopathological diagnosis from metastatic tumors will increase in the upcoming age of molecular targeted therapy. So far, no specific immunohistochemical marker for adrenocortical tumors has been established. There are a few new candidates (Ad4BP/SF-1, DAX-1) with very little available data [12]. Zhang et al.

[13] recommended the combination of melan-A, calretinin, and inhibin alpha for the differential diagnosis of adrenocortical tumors from other clear cell neoplasms. All of these antibodies recognize other tumors as well. Depending on the special differential diagnostic problem (e.g., distinction from melanomas), DLK may be an equally useful member of this battery.

DLK seems equally sensitive to recognize pheochromocytomas and paragangliomas. However, since other diagnostically related neuroendocrine tumors may be also positive, the diagnostic value of DLK among neuroendocrine tumors is not clear yet.

The function of DLK is largely unknown [14], but considering that it is a transmembrane protein with a quite restricted distribution in healthy adults [5], it may be a readily accessible target for antibody imaging or therapy.

Conflict of interest statement We declare that we have no conflict of interest.

References

1. Jensen CH, Teisner B, Hojrup P et al (1993) Studies on the isolation, structural analysis and tissue localization of fetal antigen 1 and its relation to a human adrenal-specific cDNA, pG2. Hum Reprod 8:635–641
2. Dezső K, Halász J, Bisgaard HC et al (2008) Delta-like protein (DLK) is a novel immunohistochemical marker for human hepatoblastoma. Virchows Arch 452:443–448
3. Floridon C, Jensen CH, Thorsen P et al (2002) Does fetal antigen 1 (FA1) identify cells with regenerative, endocrine and neurogenic potentials? A study of FA1 in embryonic, fetal, and placental tissue and in maternal circulation. Differentiation 66:49–59
4. Hsiao CC, Huang CC, Sheen JM et al (2005) Differential expression of delta-like gene and protein in neuroblastoma, ganglioneuroblastoma and ganglioneuroma. Mod Pathol 18:665–662
5. Laborda J, Sausville EA, Hoffman T et al (1992) Dlk, a putative mammalian homeostatic gene differentially expressed in small cell lung carcinoma and neuroendocrine tumor cell line. J Biol Chem 268:3817–3820
6. Tornehave D, Jensen CH, Teisner B et al (1996) FA1 immunoreactivity in endocrine tumours and during development of the human fetal pancreas, negative correlation with glucagon expression. Histochem Cell Biol 106:535–542
7. Halder SK, Takemori H, Hatano O et al (1998) Cloning of a membrane-spanning protein with epidermal growth factor-like repeat motifs from adrenal glomerulosa cells. Endocrinology 139:3316–3328
8. Helman LJ, Sack N, Plon SE et al (1990) The sequence of an adrenal specific human cDNA, pG2. Nucleic Acid Res 18:685
9. Jensen CH, Krogh TN, Hojrup P et al (1994) Protein structure of fetal antigen 1 (FA1). Eur J Biochem 225:83–92
10. Pan CC, Chen PC, Tsay SH et al (2005) Differential immunoprofiles of hepatocellular carcinoma, renal cell carcinoma, and adrenocortical carcinoma: a systemic immunohistochemical survey using tissue array technique. Appl Immunohistochem Mol Morphol 13:347–352
11. Skinnider BF, Amin MB (2005) An immunohistochemical approach to the differential diagnosis of renal tumors. Semin Diagn Pathol 22:51–68
12. Kaneko T, Kojima Y, Umemoto Y et al (2008) Usefulness of transcription factor Ad4BP/SF-1 and DAX-1 as immunohistologic markers for diagnosis of advanced adrenocortical carcinoma. Horm Res 70:294–299
13. Zhang H, Bu H, Hen H et al (2008) Comparison of immunohistochemical markers in the differential diagnosis of adrenocortical tumors: immunohistochemical analysis of adrenocortical tumors. Appl Immunohistochem Mol Morphol 16:32–39
14. Laborda J (2000) The role of the epidermal growth factor-like protein dlk in cell differentiation. Histol Histopathol 15:131–142

Virchows Arch (2009) 455:301–305
DOI 10.1007/s00428-009-0820-0

EDITORIAL

Hermann Lebert (1813–1878): a pioneer of diagnostic pathology

Hellmuth Pickel · Olaf Reich · Raimund Winter · Robert H. Young

Received: 17 July 2009 / Accepted: 31 July 2009 / Published online: 18 August 2009

Abstract Hermann Lebert (1813–1879) was a pioneer of diagnostic pathology and medical iconography. He was born in Breslau, then Prussia, and died in Nice (France). He lived in Switzerland as a general physician, in France as a pathologist, and eventually became the chairman for internal medicine in Zurich and Breslau, respectively. The significance of Hermann Lebert for medical posterity has three aspects: firstly, scientific linking of the French (Parisian) school and its distinctive clinical/practical orientation to the later clinical/pathological German school of Johann Lukas Schönlein, Johannes Müller, and Rudolf Virchow; secondly, his pioneering of the diagnostic use of the microscope in pathological anatomy; and finally, his remarkable book, *Traité d'anatomie pathologique générale et spéciale*, which has almost fallen into oblivion, being unknown to most contemporary workers.

Keywords Pathologist · Microscopy · Cytology · Pathologic atlas

Most who read these words use a microscope as part of their routine work as a diagnostic pathologist without giving any thought, quite reasonably, to when this modality first became used in medical care. If they do, they may think it has been since not long after the time of Van Leeuwenhoek. However, at least one authority on the history of pathology has noted the rather surprising delay in the utilization of the microscope in the practice of pathology [1], and indeed, if one views our discipline from the broad perspective of human history, light microscopic analysis of tumors and other lesions is still relatively "new." In this essay, we consider one of the pioneers of microscopy in pathology, Hermann Lebert, and discuss his books, one of which is surely one of the most magnificent in the rich tradition of diagnostic pathology.

It is a sad reality that, with the passage of time, remarkable contributions of prior investigators and even the investigators themselves often become progressively overlooked and, in some cases, end up completely unknown by current workers. This includes some whose innovation can be considered fundamental to the development of our field. We recently came across the stunning book *Traité d'anatomie pathologique générale et spéciale* [2] by the French/German physician–pathologist Hermann Lebert. It stimulated us to investigate his life and other contributions [3, 4], which, although noted in standard books on the history of pathology [1, 5, 6], we suspect, are either not known or are little known by most readers. Our researches clearly indicated a person of great substance whose contributions merited exposition for the current generation.

Paris was the center of the medical world in the early years of the nineteenth century when a transition from speculative medicine to medicine based on rational observation was taking place. The new "philosophy of observation" had its breakthrough due to the Enlightenment and the French Revolution of 1789. In 1794, the teaching of medicine and the organization of the hospitals in France underwent a radical reform. It was mostly clinicians, and primarily surgeons, who benefited from this. Thanks to the

H. Pickel (✉) · O. Reich · R. Winter
Department of Gynecology, Medical University of Graz,
Auenbruggerplatz 14,
A-8036 Graz, Austria
e-mail: ulli.pickel@aon.at

R. H. Young
James Homer Wright Pathology Laboratories,
Department of Pathology, Massachusetts General Hospital,
Harvard Medical School,
Boston, USA

vast number of patients in the large Parisian hospitals; they had ample opportunity to practice bedside observation. Aside from focusing on observation and care of patients, they also emphasized pathological anatomy, largely autopsy based. In France and Great Britain, clinicians were regularly in charge of postmortem examination at the large hospitals up to the twentieth century. The first half of the nineteenth century saw the creation of textbooks and manuals of pathological anatomy, mainly in France, which remained standard works for a long time. They were profusely illustrated masterpieces of macroscopic iconography, with little to no consideration of the microscopic dimension, which was yet to be fully developed [7].

Hermann Lebert was born in Breslau (then in the kingdom of Prussia, now Wroclaw in Silesia/Poland) on June 9, 1813, the son of a Prussian merchant Isidore Jakob Lebert and his wife Johanna, nee Fanty [8]. His parents lived primarily in Berlin (then the capital of the Kingdom of Prussia) but fled to Breslau for a brief period of time to escape the conditions caused by one of the Napoleonic wars (1813–1814).

Lebert studied medicine and the natural sciences in Berlin and then in Zurich under Johann Lukas Schönlein (1793–1864). Before and after receiving his medical doctorate at the University of Zurich in 1834, Lebert traveled with his close friend Jean de Charpentier (1786–1855) throughout Switzerland and studied botany. After receiving a doctorate with a thesis on botany, he focused on theoretical and practical medicine for the next 1 1/2 years. In Paris, he attended postgraduate courses, particularly under two famous figures in the history of medicine, the surgeon Guillaume Dupuytren (1777–1835) and the physician–pathologist Pierre Charles Alexandre Louis (1787–1872), the father of medical statistics. In 1838, Lebert began to work as a country doctor in Bex, a mountainous village in the Rhone Valley in the Swiss Canton of Vaud. During the summer months, he practiced medicine in Bex, but he spent the winter months of 1842–1845 in Paris, occupied with both clinical and microscopic studies in the great Paris hospitals. He attended the microscopic courses of the prominent French clinician and microscopist Alfred Francois Donné (1801–1878) (chef de clinique at the Hopital de la Charite in Paris, the discoverer of thrombocytes, trichomonades, and *Candida albicans* and the inventor of microphotography) [9]. In Paris, he became friends with his later pupils, the pathologist/clinician Charles Robin (1821–1885) and Paul Broca (1824–1880). In 1844, he witnessed the short but bloody civil war in the Swiss canton of Valais, where he served as an army doctor. During a stay in Berlin in the winter of 1845–1846, he made the acquaintance of two promising German pathologists (later to become legendary figures), Johannes Müller (1801–1858) and Rudolf Virchow (1821–1902), who both became his friends.

Fig. 1 **a** Portrait of Professor Hermann Lebert. **b** Frontispiece of the main work of Lebert. **c** Diseases of the liver (*above* abscess of the liver, *below* cirrhosis hepatis). On the *right side* of the picture under *figure 4*, cytologic native preparations of degenerated liver cells. **d** Native cytologic preparations of diverse tumors, epidermoid cancer cells with psammoma bodies (*figures 1 and 2*), isolated cells with multiple nuclei (*figure 4*). **e** Kidneys with hydronephrotic alterations (*figure 1*, *upper left* and *right*) and polycystic alterations in the *middle bottom* (*figure 4*). Between the figures, native preparations of sedimentary crystals. **f** Gynecological cancers: cancer of the cervix (*upper left* and *right*, *figures 1 and 4*), Cervical cancers with perforation into the bladder (*figures 2* and *6*). On the *bottom right* (*figure 7*, endometritis after artificial abortus with perforation. In the *middle on the right side* (*figure 3*), native cytologic preparations of squamous cancer cells. In *figure 5* (*middle bottom*) native cancer tissue with blood vessels

In 1846, Lebert finally moved to Paris, devoting his efforts to his extensive private practice in the morning and to his scientific work in the afternoon and evening. These years saw the beginning of his work on his monumental iconography of pathological anatomy (see later). The previous year, 1845, saw the publication of his first book, considered by us later. In 1848, he experienced the February revolution in Paris, and in 1849, he witnessed the outbreak of cholera, in the same city, which resulted in 10,000 deaths. For his work combating that epidemic, he received the cross of the Legion d'honneur from the French president Louis Napoleon Bonaparte (later Emperor Napoleon III, 1808–1873). He left Paris and went to Zurich in 1852; there, he was appointed professor of clinical medicine at the university. He resigned from this position in 1859 when he was offered a similar position at the University of Breslau. In the same year, 1853, he married Isaline Fayod with whom he had five children. He witnessed the Austro-Prussian war in Breslau in 1866 and served again as a high-ranking military officer in the Prussian army. In 1869, he took part in the fight in Silesia against another epidemic, typhoid fever, as the medical adviser for the city of Breslau. He resigned from his position in Breslau in 1874 and divided his time in the last 4 years of his life between Nice, France and Vevey and Bex in Switzerland. He died in Bex on August 1, 1878, from rupture of an aortic aneurysm. He is buried in Nice [8].

Hermann Lebert was a very prolific author and added greatly to the knowledge of biology, pathology, and clinical medicine of his time [10, 11]. In his autobiography, published in 1869, he listed 101 major contributions [12]. However, Reichert, in a subsequent biography, listed 124 publications [8]. The most prominent among them is the colossal *Traité d'anatomie pathologique générale et spéciale* published in four volumes (two volumes text and two volumes atlas) edited by Baillière in Paris in 1857 and 1861 [2]. Lebert subtitled his work *Description et iconographie pathologique*. This is one of the most comprehensive and important work of the pre-photographic era of medical


a
Hermann LEBERT (1813 - 1878)

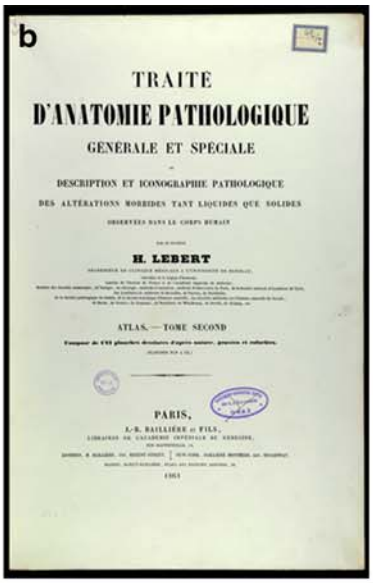
b
TRAITE
D'ANATOMIE PATHOLOGIQUE
GENERALE ET SPECIALE
DESCRIPTION ET ICONOGRAPHIE PATHOLOGIQUE
H. LEBERT
ATLAS. — TOME SECOND
PARIS,

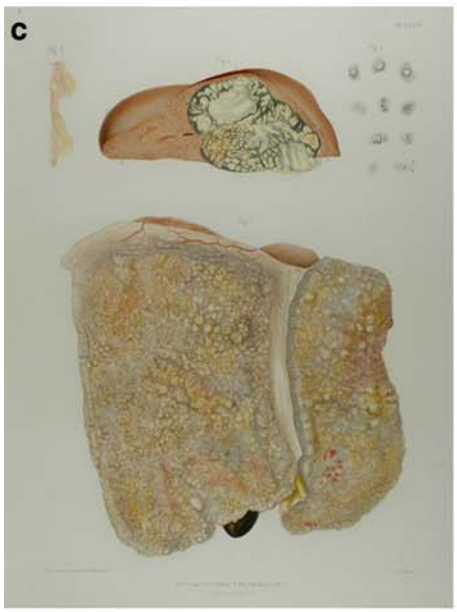
c

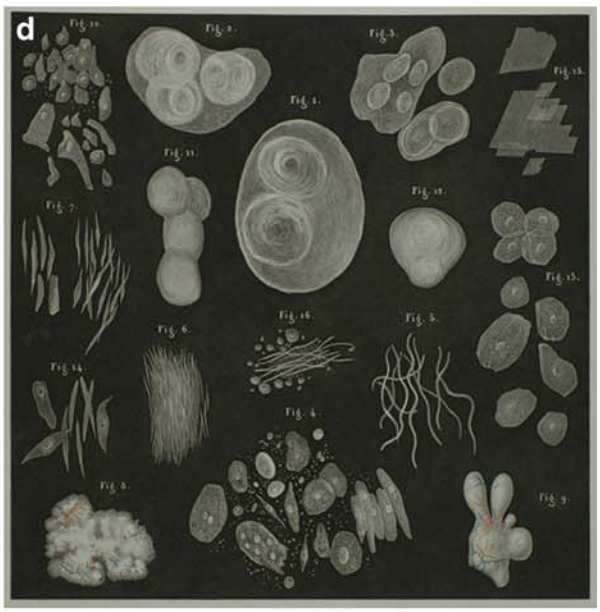
d


e

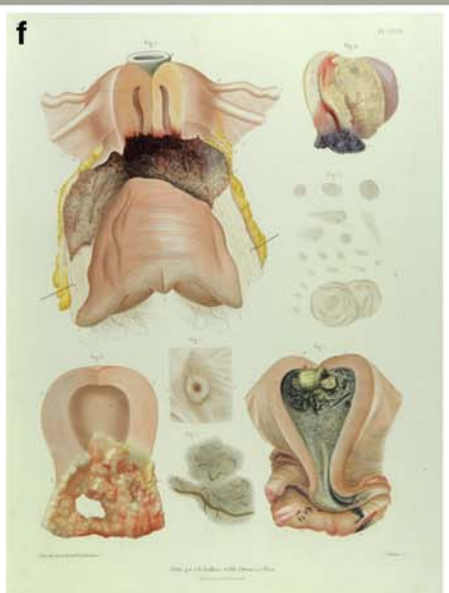
f

illustration (Fig. 1). Contributors to the enormous pathological and clinical material contained within it were physicians from Paris, most notably the surgeons Alfred-Armand Velpeau (1795–1867) and Charles Marie Edouard Chassaignac (1805–1879) as well as the syphilidologist Philippe Ricord (1799–1889).

The quality of Lebert's work has only been equaled in our times by means of color photography. Apparently, the illustrations were steel-faced copper engravings using multiple plates printing ("Planches dessinées d'aprés nature, gravées et coloriées"), and their technical quality is superb [7]. This was aided by having it printed by the most renowned publishing house of that time, J.-B. Baillière et fils in Paris, which had also published and printed Cruveilhier's magnum opus. The composition of Lebert's atlas resembles the work of his great predecessor Cruveilhier, but it is much larger and has a richer layout. In contrast to Cruveilhier's work, Lebert combines his text in two complete and well-arranged volumes and provides detailed and clear explanations in the two atlases [1] Lebert surpasses the work of Cruveilhier by not only describing microscopic findings but also by documenting them in detail in his illustrations as well.

The work consists of four volumes in large folio size (12 1/4 in. wide×18 3/4 in. tall): two text volumes (766 and 733 pages) as well as two atlas volumes (the first volume featuring 94 tables ("planches") including several illustrations and 46 pages of explanations, and the second volume 106 tables with several pictures and 44 pages of explanations). This work was sold to more than 300 subscribers throughout the world. Most of the subscribers were large university libraries both in Europe and the Americas, primarily the USA. However, bookstores and individuals also appear as subscribers. In 1863, Lebert's work received an award from the Imperial French Medical Academy. These words do not do justice to Lebert's work, which proverbially "needs to be seen to be believed."

The first volume contains a historical overview of pathological–anatomical iconography followed by a comprehensive essay on general pathology with relevant clinical case histories. The second volume is entirely dedicated to special pathology and also includes case histories and, among them, cases of tumor pathology. The scope of the two atlases is remarkable with the 200 large and mainly colored plates of the highest quality designed by outstanding artists such as the draftsman Lackerbauer and the engravers Oudet and Visto. The complete work was produced by the fine-art printers L. Martinet in Paris. To further emphasize the magnificence of the work, we note that each plate contains a minimum of ten and usually many more individual illustrations.

Lebert's most historically significant other publication was his two-volume *Physiologie pathologique* published in 1845 [3]. In it, he combines clinical observation, animal experiments, and microscopic observations as well as biochemistry. The first volume deals with inflammatory disorders. The second volume deals exclusively with tumors. Lebert expresses his theory of the characteristics of malignant cells for the first time in this work; this would become very controversial later. By means of uncolored cytological preparations, he described the morphological features of neoplastic cells, which are still valid today, such as those pertaining to the nucleolus.

The importance of the aforementioned work was brought home to us while we were preparing this essay, devised initially mainly to draw attention to the remarkable two volume text and atlas already considered. As part of the associated reading of various texts, we consulted the small but wonderfully detailed and strongly recommended book on the history of pathology by Dr. E. B. Krumbhaar published in 1937 [1]. In his chapter on "cellular pathology," which considers primarily Virchow, Krumbhaar reflects on the relatively late application of the microscope in the study of morbid anatomy we noted earlier. The first work Krumbhaar credits for applying microscopy to pathologic anatomy is the 1843 book of Julius Vogel *Icones Histologicae Pathologicae*. He then notes the 1845 work of Lebert, making it, obviously, one of the earliest works in which microscopy was used in the pathology literature. Similar significance is given to Lebert's 1845 book in Long's consideration of the *History of Pathology* [5], and these observations are reinforced by Dr. Steven Hajdu [13], in a much more recent contribution, and in the outstanding recent book on the *History of Histopathology* by Professor Georg Dhom [9].

Lebert figures in a significant way in the second chapter of the latter work when Dhom discusses the Paris school. Indeed, Lebert gets more coverage in that chapter than any other individual, and Dhom illustrates the frontispiece of two of his books as well as a number of other illustrations from his texts. The mention Lebert has received in these contributions only heightened our feeling that his role in the development of diagnostic pathology merited further highlighting. However, despite the attention he received in the works just noted, we feel that, overall, he is not as well-known as he should be to most current workers. Lebert wrote a third book published in 1851 [4]. Like all his works, the work is an impressive one, albeit not as monumental as the Atlas we have focused on. The 1851 book runs to 885 pages and is divided into two parts. The first has four chapters concerning the microscopic characteristics of neoplasia and the second part ten chapters considering separate organs and systems of the body in turn. Among those he dedicates the work, three are giants, such as Cruveilhier, Louis, and Müller.

Very early in his career, Lebert advocated the diagnostic use of the microscope in the assessment of biopsy material [14] following the pioneering work of Alfred Donné. There

was no practical technique for dying tissue at the time, and observers had to rely on the assessment of individual cells or, at best cell clusters, from cytological preparations [9]. Thus, Lebert propagated the "Stückchen-diagnose" (small piece diagnosis of malignant tumors) decades before Ruge [15] and Veit [16] did. In his role as director of the Medical Clinic in Breslau/Wroclaw, Lebert emphasized: "Uterine cancer must be diagnosed directly in life by means of a microscope in that one can examine larger pieces of tissue" [17].

Lebert's other important publications (for a complete list, see references) focused on botany and zoology (entomology) as well as medical/historical topics. Publications from his early years were in French, but the majority of those dating from the beginning of his academic career and his call to Zurich in 1853 was written in German.

The significance of Hermann Lebert for medical posterity has three aspects: firstly, scientific linking of the French (Parisian) school and its distinctive clinical/practical orientation to the later clinical/pathological German school of Johann Lukas Schönlein, Johannes Müller and Rudolf Virchow; secondly, his pioneering of the diagnostic use of the microscope in pathological anatomy; and finally, his remarkable book, *Traité d'anatomie pathologique générale et spéciale*, which has almost fallen into oblivion, being unknown to most contemporary workers.

Acknowledgements Mr. Jack Eckert, Senior Librarian at the Center for the History of Medicine at the Francis A. Countway Library of Medicine at Harvard Medical School, was most helpful in enabling review by one of the authors (RHY) of the three books of Lebert noted herein. His assistance is much appreciated. Dr. Gregory Y. Lauwers, Director of Surgical Pathology at the Massachusetts General Hospital kindly translated selected portions of Lebert's atlas for RHY.

References

1. Krumbhaar EB (1937) Pathology. In: Hoeber PB (ed) Clio Medica: a series of primers on the history of medicine, vol 19. Hoeber, New York, pp 96–106
2. Lebert H (1857) Traité d'anatomie pathologique générale et speciale. Description et iconographie pathologique des altérations morbides tant liquides que solides. J.-B. Baillière et fils, Paris (2 volumes en grand in-folio et 2 volumes du même format de 200 planches gravées en acier et coloriées)
3. Lebert H (1845) Physiologie pathologieque ou reserches cliniqiues, experimentales et microscopiques. Sur l'inflammation, la tuberculisation, les tumeur la formation du cal. Chez J-B Baillière, Paris
4. Lebert H (1851) Traité pratique des maladies cancéreuses et des affections curables confondues avec le cancer. Chez J-B Baillière, Paris
5. Long ER (1965) A history of pathology. Dover, New York
6. Malkin H (1993) Out of the mist. The foundations of modern pathology and medicine during the nineteenth century. Vesalius, Berkeley
7. Goldschmid E (1925) Entwicklung und Bibliographie der pathologisch anatomischen Abbildung (Development and bibliography of the pathological–anatomical illustration). Hiersemann, Leipzig
8. Reichert B (1973) La vie et les oevres de Hermann Lebert. Thèse pour le doctorat en médecine, Académie de Paris, Université René Descartes, Faculté de médecine Necker-Enfants-Malades, Paris
9. Dhom G (2001) Geschichte der Histopathologie (History of histopathology). Springer, Berlin
10. Kaufmann G (1911) Festschrift zur Feier des hundertjährigen Bestehens der Universität Breslau (Publication celebrating the 100th anniversary of the university of Breslau). Hirt, Breslau
11. Nachruf auf H. Lebert (Obituary on H. Lebert) (1878) Berliner Klin Wochenschr 15:589
12. Lebert H (1869) Biographische Skizzen und Überblick der von mir bekannt gemachten Werke und kleineren Arbeiten (Biographical sketches and overview of my works and smaller treatises). Korn, Breslau
13. Hajdu SI (2004) A note from history: the first cellular pathologists. Annals of Clinical & Laboratory Science 34:481–483
14. Lebert H (1848) Einige Bemerkungen über die Erkenntnis des Krebses vor der Operation und am Lebenden überhaupt (Some remarks on the knowledge of the cancer before the operation and on the living also). Roses und Wunderlichs Archiv für physiologische Heilkunde 7:441–445
15. Dallenbach-Hellweg G, Schmidt D (2003) History of gynecological pathology. XV. Dr. Carl Arnold Ruge. Int J Gynecol Pathol 23:83–90
16. Pickel H, Winter R, Young RH (2009) History of gynecological pathology. XXII. Johann Veit. Int J Gynecol Pathol 28:103–106
17. Lebert H (1860) Handbuch der praktischen Medizin (Handbook of the practical medicine), 2nd edition, 2nd volume. Laupp'sche Buchhandlung, Tübingen

Virchows Arch (2009) 455:307–313
DOI 10.1007/s00428-009-0836-5

ORIGINAL ARTICLE

The importance of precise pT diagnosis for prognostic prediction of uterine cervical cancer—a single institutional report at a Japanese comprehensive cancer hospital

Norihiro Teramoto · Rieko Nishimura · Koichi Mandai · Takashi Matsumoto · Takamitsu Nogawa · Masamichi Hiura

Received: 23 April 2009 / Revised: 9 August 2009 / Accepted: 7 September 2009 / Published online: 24 September 2009

Abstract We previously reported that the majority of Japanese pathologists misunderstand the International Union against Cancer-pT2 criteria for uterine cervical cancer (UCC). We compared the prognosis of originally diagnosed pT2 (ori-pT) UCC cases at our hospital with reclassified pT2 (re-pT) cases to assess the importance of making a correct pT diagnosis. There were 43 International Federation of Gynecology and Obstetrics (FIGO) II (i.e., cT2) and/or ori-pT2 UCC cases who received surgery without neoadjuvant chemotherapy at Shikoku Cancer Center from 1991 to 2003. The cases (seven ori-pT1 and 36 ori-pT2; 43 cN0 with six pN1) were reclassified as 22 re-pT1 and 21 re-pT2. Fifteen of the 23 ori-pT2a cases (65%) were re-pT1 because their vaginal extension had only been intraepithelial. The difference in the 5-year survival rate (5Y-SR) was not significant between the ori-pT1 and ori-pT2 cases using Fisher's exact test (F test): $P=0.236>0.05$, whereas 5Y-SR of re-pT1 cases was significantly higher than re-pT2, including pN1 cases and excluding them (F test: $P=0.00164<0.01$ and $P=0.0108<0.05$, respectively). The 5Y-SR of ori-pT2-re-pT1 (overdiagnosed pT2) was significantly higher that of ori-pT2-re-pT2 (true pT2) including pN1 cases and excluding them (F test: $P=0.00694<0.01$ and $P=0.0305<0.05$, respectively). These results indicated that pT2 of UCC could be frequently misdiagnosed at an institutional level, and that misdiagnosed pT2 might impair the evidence-based medicine of UCC. Multi-institutional assessment of the accuracy of pTNM is recommended, because it is not likely that this is an endemic problem to our hospital.

Keywords UICC · FIGO · Uterine cervical cancer · Quality assurance · pTNM · Staging

Abbreviations

UICC	International Union against Cancer
FIGO	the International Federation of Gynecology and Obstetrics
UCC	Uterine cervical cancer

Introduction

To establish evidence-based cancer therapy, cancer stages must be evaluated uniformly among institutions with as little error as possible. For cancers at most sites, the cancer stage provides corroborating evidence for estimating the risk to the patient's life [1, 2]. Therefore, the cancer stage is an extremely important indicator for the selection of the treatment method and for grouping patients for various kinds of investigations.

This work was partly supported by a grant-in-aid for cancer research from the Ministry of Education, Science, Sports, Culture and Technology of Japan.

N. Teramoto (✉) · R. Nishimura
Department of Pathology, Shikoku Cancer Center,
Minami-Umenomoto Kou 160,
Matsuyama City, Ehime 791-0288, Japan
e-mail: teramoto@shikoku.cc

K. Mandai
Department of Pathology and Laboratory,
Higashihiroshima Medical Center,
Higashihiroshima City, Japan

T. Matsumoto · T. Nogawa · M. Hiura
Department of Gynecology, Shikoku Cancer Center,
Matsuyama City, Japan

In most cancers, the cancer stage is defined by the combination of TNM, which stands for the local extent of primary tumor (T), regional lymph node metastasis (N), and distant metastasis (M) [1, 2]. Grouping of the combinations of TNM according to the risk to life indicates the stage. International Union against Cancer (UICC)-TNM classification consists of the clinical TNM classification before treatment (cTNM) and the pathological TNM after tumor resection (pTNM). In uterine cervical cancers, the International Federation of Gynecology and Obstetrics (FIGO) stage is widely accepted among gynecologists [3]. The FIGO stage classification is similar to the UICC stage, except for the stipulations that the FIGO stage of uterine cervical cancer (UCC) be determined only by clinical data collected before therapy, not by postsurgical information, and that lymph node metastasis is not included in the FIGO stage. Therefore, FIGO II UCC is cT2N0M0 or cT2N1M0, while FIGO II UCC is not always pT2N0M0 or pT2N1M0.

Despite its importance, little attention has been paid to the accuracy of pTNM classifications for UCC as well as cancers of other sites. Recently, we reported the result of a questionnaire survey of pathologists working in the *Gan-shinryo-renkei-kyoten Byoin* (Local Core Cancer Hospitals) on pTNM classification [4]. The results suggested that Japanese pathologists have insufficient knowledge about the UICC-TNM, which might lead to inaccurate TNM classification. The percentage of correct answers to questions concerning the following important criteria was only about 60%, despite the fact that the questions were yes–no ones: "When it is difficult to judge TNM, the lesion is classified into the lower category", and "Direct invasion of the lymph node is a N component" [4]. In the survey, more than half of Japanese pathologists regarded a UCC as T2a if the carcinoma in situ accompanying UCC extended to the vagina, [4] although an intraepithelial component does not raise the UICC-T stage [5]. The results clearly indicated that pT2 of UCC was misdiagnosed in many institutions. Recently, we also reported that the pTNM staging of lung cancer was frequently done incorrectly when a clear description of the UICC-TNM was not provided to pathologists, including a clear description of the distinction between intrapulmonary metastasis vs synchronous tumor. Thus, the inaccurate use of pTNM might lead to the misperception of its prognostic significance [6].

The Shikoku Cancer Center is a comprehensive cancer hospital in the Chugoku and Shikoku districts of Japan. It handles the largest number of patients with gynecological tumors in these districts. The Gynecology Department of our hospital is a member of the Gynecology Oncology Group and the Japanese Gynecology Oncology Group. Our hospital's former chief pathologist was a pathology committee member of the group that produced the *General Rules for the Clinical and Pathological Study of Uterine Cervical Cancer in Japan* (GR-UCC) [7] and was responsible for the diagnosis of a small proportion of the cases assessed in the present study.

In this study, we assessed the accuracy of pT diagnosis of UCCs, with a focus on T2 lesions that were diagnosed as locally advanced and were surgically treated at our hospital, the Shikoku Cancer Center. We compared the prognosis of patients with correctly diagnosed T2 lesions to that of patients whose T2 lesions were misdiagnosed to assess the importance of making an accurate pT diagnosis.

Materials and methods

Case selection and rules for reclassification

The list of UCC cases treated between 1991 and 2003 that belonged to either FIGO II or pT2 was obtained from the files of the pathology department of the Shikoku Cancer Center. The cases were reexamined microscopically with reference to pathological reports and macroscopic photos of the excised specimens by N.T. and R.N. to reclassify the pT according to the UICC-TNM, 6th edition [2]. The definitions of T1 and T2 did not change from 1991 to 2003 [2]. The reasons why pathologists deviated from making an accurate diagnosis of pT are shown in Tables 1 and 2. The original pT recorded in the pathological report is hereinafter referred to as ori-pT, and the reclassified pT as re-pT. ori-pTX reclassified as re-pTX is referred to as ori-pTX-re-pTX, ex ori-pT2-re-pT1. In this study, we considered the re-pT to be the true pT. As in the UICC supplement book, only the extension of an invasive component of a carcinoma raises T [5], and a cancer component in the lymphovascular space of the parametrial tissue does not assure pT2b [8]. The subdivision of pT1a1 vs. pT1a2 and pT1b1 vs. pT1b2 was not conducted because this study was focused on T2 lesions. Information about the prognosis was obtained from the hospital-based cancer registry. Prognosis was analyzed by overall survival. Follow-up data longer than 5 years were available for 40 patients. Eight patients died within 5 years, and two others died within 5 to 10 years.

Table 1 Pitfalls of the TNM classification of uterine cervical cancer (only vaginal involvement by the invasive component deserves classification into T2a)

T2a	ori-pT2a	ori-pT2a-re-pT2a	Concordance rate
No. of cases	23	8	35%

Vaginal extension of the intraepithelial component is not considered to be T2a

ori-pT original-pT, *re-pT* reclassified-pT, *ori-pT2a-re-pT2a* ori-pT2a cases reclassified as re-pT2a

Table 2 Pitfalls of the TNM classification of uterine cervical cancer (only grossly or histologically evident continuous invasion beyond the myometrium is classified as T2b)

T2b	ori-pT2b	ori-pT2b-re-pT2b	Concordance rate
No. of cases	13	12	93%

Questionable invasion is not T2b. Intravascular or lymphaticular extension to the parametrium is not considered to be T2b

ori-pT original-pT, *re-pT* reclassified-pT, *ori-pT2b* cases reclassified as re-pT2b.

Statistical analysis

Using Fisher's exact test (F test), we examined the 5-year survival rate after surgery with StatMate (ATMS, Tokyo, Japan). The survival function of ori-pT1-re-pT2 and that of ori-pT2-re-pT2 were compared using the Kaplan–Meier estimator. Differences were considered significant at $P<0.05$.

Results

Results of reclassification

At Shikoku Cancer Center, there were 537 hysterectomy cases between 1991 and 2003. Of 537 cases, 126 cases were diagnosed as either FIGO II (i.e., cT2) or ori-pT2. Forty-three of the cases had not received preoperative chemotherapy or radiotherapy. The 43 cases consisted of 17 FIGO I (FIGO IA: three, FIGO IB: 14) and 26 FIGO II (FIGO IIA: 20, FIGO IIB: six). The ori-pT of the 43 cases were seven ori-pT1 (ori-pT1a: one, ori-pT1b: six) and 36 ori-pT2 (ori-pT2a: 23, ori-pT2b: 13). These 43 cases comprised all the cT2 and/or ori-pT2 cases at the Shikoku Cancer Center during this period. All 43 cases were cN0M0, and six of them were proven to be pN1 at the pathology examination. They were reexamined with regard to their pTNM. According to the UICC-TNM, 6th edition, the 43 cases were reclassified into re-pT1 in 22 cases (re-pT1a: three, re-pT1b: 19) and re-pT2 in 21 patients (re-pT2a: eight, re-pT2b: 13). None of the pN and M had to be revised. These results are summarized in Tables 3 and 4.

None of the cases with re-pT2 lesions were ori-pT1, suggesting that in our hospital, there was a tendency to overdiagnose the stage in the ori-pT evaluation (Table 3). Fourteen of the 23 ori-pT2a cases (61%) were re-pT1 and one was ori-pT2b (Table 3). The overestimation of stage was due to the intravaginal extension of intraepithelial neoplasia (Fig. 1). An ori-pT2b case was downgraded to re-pT1 because cancer tissue in the parametrial lymphovascular space had been regarded as evidence of pT2b. Seventeen of the 43 cases were FIGO I-ori-pT2, and ten were re-pT2 (Table 4). The number of FIGO I cases without preoperative chemotherapy between 1991 and 2003 was 248. Therefore, the rate of underdiagnosis of FIGO I to re-pT2 was about 4% (10/248). Conversely, 15 of the 26 FIGO II cases were re-pT1 lesions. The rate of misdiagnosis of FIGO II to re-pT1 was 58% (15/26). Details of the patients are shown in Table 5.

Table 3 The correlation between reclassified pT versus original pT

		ori-pT				
		T1a	T1b	T2a	T2b	Total
re-pT	T1a	0	0	3	0	3
	T1b	1	6	11	1	19
	T2a	0	0	8	0	8
	T2b	0	0	1	12	13
	Total	1	6	23	13	43

Note that no case was in the squares consisting of re-pT2a-2b and ori-T1a-1b, but that 15 cases belonged to the squares consisting of re-pT1a-1b and ori-T2a-2b

Relationship between the reclassified pT lesions and the prognoses

The prognosis could be followed up for more than 5 years after the surgery in 40 of the 43 patients. Eight of them died within 5 years after the operation, and two others died in the next 5 years. None of the patients with ori-pT1 or re-pT1 lesions died within 5 years.

The 5-year survival rates were compared by the F test between the patients with FIGO I and FIGO II lesions ($P>0.05$), between ori-pT1 and ori-pT2 lesions ($P>0.05$), and between re-pT1 and re-pT2 lesions ($P<0.01$). Only re-pT was correlated with the 5-year survival rate (Table 6). Even if pN1 cases were excluded, the difference of the 5-year survival rate was still significant between the re-pT1 and re-

Table 4 The correlation between reclassified pT versus FIGO stage

		FIGO				
		IA	IB	IIA	IIB	Total
re-pT	T1a	3	0	0	0	3
	T1b	0	4	13	2	19
	T2a	0	3	4	1	8
	T2b	0	7	3	3	13
	Total	3	14	20	6	43

Note that only 11 of 26 FIGO II cases were in the squares consisting of re-pT2a-2b

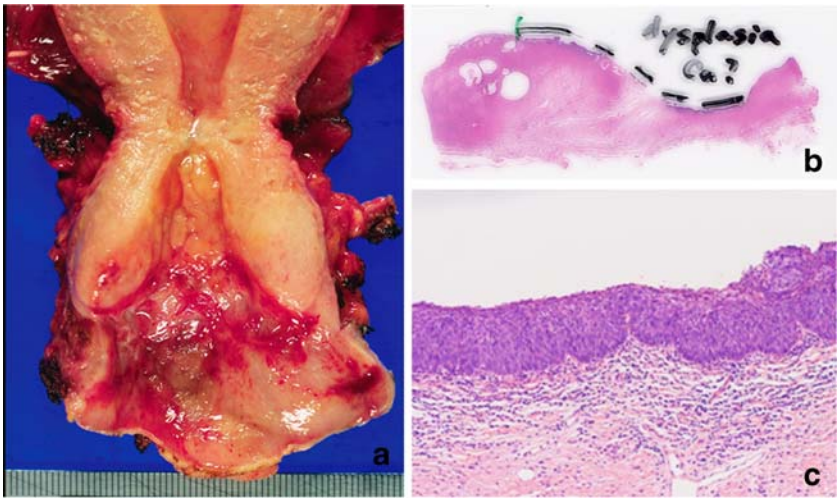

Fig. 1 Intravaginal growth of UCC. **a**–**c** Uterine cervical cancer diagnosed as FIGO IIA, ori-pT2a but re-pT1b. **a** A macroscopic image. **b** A panoramic image. Note that the person making the original diagnosis wrote "dysplasia-Ca(ncer)?" on the glass. **c** Only CIN3 was observed in the vagina

pT2 lesions ($P<0.05$) but not between the ori-pT1 and ori-pT2 lesions ($P>0.05$; Table 6).

Eight of the 20 patients with ori-pT2-re-pT2 lesions/true pT2 (40%) died within 5 years after surgery, while none of the ori-pT2-re-pT1 patients/overdiagnosed pT2 (0/14) died within 5 years of the operation. The 5-year survival rate was significantly lower in true pT2 than in overdiagnosed pT2 (F test: $P<0.01$). Since two patients, including one ori-pT2-re-pT1 case, died between the sixth and tenth year, the survival risk for 10 years of ori-pT2-re-pT2 and that of ori-pT1-re-pT2 were compared using the Kaplan–Meier estimator. The prognosis of the former was significantly worse than that of the latter, either including pN1 cases (Logrank, $P<0.01$) or excluding them (Logrank, $P<0.05$; Fig. 2).

Among the nine FIGO I-re-pT2 patients (pT2 cases underdiagnosed as FIGO I), four (44%) died within 5 years after surgery, while none of the 13 patients with FIGO II-re-pT1 lesions (pT1 cases overdiagnosed as FIGO II) died within 5 years of the operation. The prognosis was significantly worse in the former than in the latter cases ($P<0.05$). This showed again that the pathologic stage correlates better with prognosis than the clinical stage correlates with prognosis [1, 2]. These findings are summarized in Table 6.

Discussion

As shown in our past report, the majority of Japanese pathologists do not seem to know the precise TNM rules of UCC [4]. Therefore, it is not likely that stage classification of UCC at our hospital is particularly less accurate among Japanese hospitals. Brierley et al. reported that the accuracy of pTNM classification for all gynecological cancers in Princess Margaret Hospital in Canada was 81% [9]. We have not found any reports on interinstitutional or international pTNM accuracy. Thus far, not much attention has been paid to the pitfalls of pTNM classification in certain conditions.

GR-UCC is the textbook for cervical cancer diagnosis in Japan, published collectively by the Japan Society of Obstetrics and Gynecology, the Japanese Society of Pathology, and the Japan Radiation Society [7]. The statements of the rules of the UICC-TNM as well as the GR-UCC are not detailed enough to allow users to make a precise TNM classification [2, 7]. The UICC-TNM rules state that a carcinomatous component in the parametrial lymphovascular space is not a T2b component, but the GR-UCC rules do not have this stipulation in the text [2, 7]. It is not clearly stated in either the GR-UCC or the UICC-TNM, 6th edition, that vaginal involvement by a noninvasive component of UCC is not a T2a component [2, 7]. With regard to pT2 lesions of UCC, the rules established by the UICC provide the following broad descriptions: "pT2: beyond uterus but not pelvic wall or lower third vagina. T2a: no parametrium, T2b: parametrium" [2, 8]. Obviously, more detailed descriptions are needed. Another reason for inaccurate pTNM staging in Japan is that the pTNM staging is not considered the main responsibility of pathologists and is thus mainly conducted by clinical physicians at many institutions who do not actually check the pathology specimens.

There was a significant difference in prognosis between re-pT1 and re-pT2, but not between ori-pT1 and ori-pT2 (Table 6). The difference in the mortality between the ori-pT2-re-pT2 cases and ori-pT2-re-pT1 cases accentuates the importance of an accurate pT diagnosis on the prediction of prognosis of locally advanced UCC patients.

Table 5 Patients' data of the cases examined

Original pT		Revised pT	FIGO	pN	Outcome	Follow-up (months)	5-year survival
2b	>	1b	IIA		Alive	42	Lost
2b	=	2b	IIB		Died	10	No
2b	=	2b	IIB	pN1	Alive	60	Yes
2b	=	2b	IIB	pN1	Died	19	No
2b	=	2b	IIA		Died	17	No
2b	=	2b	IIA	pN1	Died	16	No
2b	=	2b	IB		Died	40	No
2b	=	2b	IB		Alive	72	Yes
2b	=	2b	IB		Died	109	Yes
2b	=	2b	IB		Alive	121	Yes
2b	=	2b	IB		Alive	121	Yes
2b	=	2b	IB		Alive	100	Yes
2b	=	2b	IB		Died	28	No
2a	>	1b	IIA		Alive	69	Yes
2a	>	1b	IIA		Alive	121	Yes
2a	>	1b	IIA		Alive	121	Yes
2a	>	1b	IIA		Alive	72	Yes
2a	>	1b	IIA		Died	74	Yes
2a	>	1b	IIA		Alive	121	Yes
2a	>	1b	IIA		Alive	121	Yes
2a	>	1b	IB		Alive	78	Yes
2a	>	1b	IB		Alive	121	Yes
2a	>	1b	IB		Alive	121	Yes
2a	>	1b	IB		Alive	115	Yes
2a	>	1a	IA		Alive	81	Yes
2a	>	1a	IA		Alive	108	Yes
2a	>	1a	IA		Alive	60	Yes
2a	=	2a	IIB		Alive	73	Yes
2a	=	2a	IIA		Alive	71	Yes
2a	=	2a	IIA		Alive	65	Yes
2a	=	2a	IIA		Alive	68	Yes
2a	=	2a	IIA		Alive	101	Yes
2a	=	2b	IIA	pN1	Alive	121	Yes
2a	=	2a	IB	pN1	Died	25	No
2a	=	2a	IB		Died	24	No
2a	=	2a	IB		Alive	22	Lost
1b	=	1b	IIB		Alive	8	Lost
1b	=	1b	IIB		Alive	121	Yes
1b	=	1b	IIA	pN1	Alive	121	Yes
1b	=	1b	IIA		Alive	72	Yes
1b	=	1b	IIA		Alive	121	Yes
1b	=	1b	IIA		Alive	99	Yes
1a	=	1b	IIA		Alive	82	Yes

Follow up longer than 10 years was indicated as 121 months. 5-year survival; "Yes", "No" and "Lost" mean "alive more than 59 months after surgery", "dead within 59 months of surgery", and "lost in follow-up within 59 months", respectively.

pN only pN1 cases are indicated, *pN0* cases are left blank

We analyzed only FIGO II and/or ori-pT2 cases in this study. Before conducting this study, however, we already had data showing that these cases are a frequently misdiagnosed group in UCC-TNM diagnosis (data not shown). Ori-pT1 and ori-pT2 did not show a significant difference of vital risk in this study (Table 6), because ori-pT2 was contaminated with ori-pT2-re-pT1. However, because the number of ori-pT1-FIGO I cases at our hospital, which were not analyzed in this study, is several-fold greater than the number of ori-pT1-FIGO II cases

Table 6 5-year survival of FIGO, original pT and re-classified pT

	Total cases	Died	Alive	Fisher's exact test
FIGO I	16	4	12	P=0.853>0.05
FIGO II	24	4	20	
ori-pT1	6	0	6	P=0.236>0.05
ori-pT2	34	8	26	
ori-pT1 w/o N1	5	0	5	P=0.427>0.05
ori-pT2 w/o N1	29	5	24	
re-pT1	20	0	20	P=0.00164<0.01
re-pT2	20	8	12	
re-pT1 w/o N1	19	0	19	P=0.0108<0.05
re-pT2 w/o N1	15	5	10	
ori-pT2-re-pT2	20	8	12	P=0.00694<0.01
ori-pT2-re-pT1	14	0	14	
ori-pT2-re-pT2 w/o N1	15	5	10	P=0.0305<0.05
ori-pT2-re-pT1 w/o N1	13	0	13	
FIGO I-re-pT2	9	4	5	P=0.0172<0.05
FIGO II-re-pT1	13	0	13	

ori-pT original-pT, *re-pT* reclassified-pT, *w/o N1* without pN1 cases, *ori-pT2-re-pT2* ori-pT2 cases reclassified as pT2 (i.e., true pT2), *ori-pT1-re-pT2* ori-pT2 cases reclassified as pT1 (i.e., overdiagnosed pT2), *FIOGI-re-pT2* FIGO I cases classified as re-pT2 (underdiagnosed FIGO I/cT1), *FIOGII-re-pT1* FIGO II cases classified as re-pT1 (overdiagnosed FIGO II/cT2).

analyzed in this study, there would be a significant difference in the prognosis between ori-pT1 and ori-pT2 cases if ori-pT1-FIGO I cases were included. However, this might have hitherto concealed the problem of UCC-pT2 diagnosis.

In operated cases, the prognosis can be predicted more reliably by the pTNM classification than by the FIGO stage, which is a pure clinical staging without lymph node evaluation. An accurate pT diagnosis in operated cases is important for the accurate FIGO stage classification system itself, because a misdiagnosed pT could lead clinicians to incorrectly judge the FIGO stage for the next UCC case at the institution.

It is important to assess the accuracy of the pTNM classification of UCC [1, 2]. For example, the evaluation of pT in stage I and II UCC cases is extremely important for researching the efficacy of postoperative chemotherapy as well as for assessing the risk of recurrence in specific histological subtypes and gene types. Without appropriate pT evaluation, it is virtually impossible to compare patients whose prognostic risks are homogeneous. The desired level of accuracy of TNM is not defined in the UICC-TNM. In clinical cancer research studies, the pathology exclusion rate should not be higher than 10% of the cases [10, 11], and for the therapeutic purpose of a patient, it should be far less than 10%.

Our past report suggested that the pTNM may be misdiagnosed in many institutes due to insufficient knowledge about TNM [4]. We also showed that pTNM diagnoses were not actually accurate, especially in certain situations where the description of TNM was unclear [6]. Although the present study was a single-institutional study, it suggested the possibility that misdiagnosed pT might threaten the evidence-based medicine of locally advanced cancer. Misdiagnoses of UCC-pT2 were frequent, and would impair both the prognostic predictability of pTNM

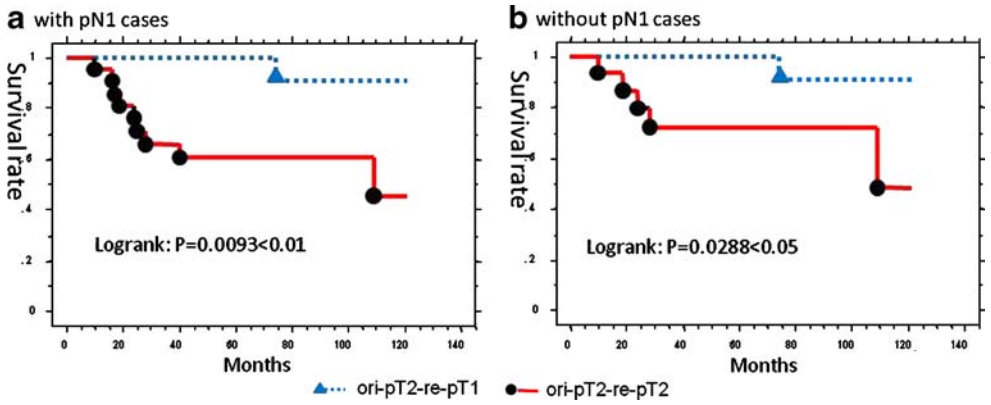

Fig. 2 Survival function of pT2 uterine cervical cancers. Prognosis of ori-pT2-re-pT1 (cases originally diagnosed as pT2 and reclassified as pT1, i.e., overdiagnosed uterine cervical cancers) is significantly better than that of ori-pT2-re-pT2 (cases originally diagnosed as pT2 and reclassified as pT2, i.e., true pT2 uterine cervical cancer). **a** Logrank: P=0.0093<0.01, including pN1 cases. **b** Logrank: P=0.0288<0.05, excluding pN1 cases

on a patient basis and the quality of the clinical research of locally advanced UCC. Here, we have only described the results of assessment at a single institution. Multi-institutional assessment of the accuracy of pT in Japan is needed because we believe that this problem is not endemic to our hospital. The misdiagnosis of pT2 may also occur in other countries. In addition, we are certain that this problem is not specific to UCC, but occurs with other cancers[6].

Acknowledgments We would like to thank Dr. Shosuke Moriwaki, the former director of the Shikoku Cancer Center, for collecting and storing detailed data. Thanks also go to the past and present laboratory technicians of the pathology department of our hospital for their enthusiastic preparation and management of the specimens, and to the staff of the intrahospital cancer registration of our hospital.

Conflict of interest statement We declare that we have no conflict of interest. All the authors are employees of the National Hospital Organization of Japan. This work was partly supported by a grant-in-aid for cancer research from the Ministry of Education, Science, Sports, Culture and Technology of Japan.

References

1. American Joint Committee on Cancer (2002) AJCC cancer staging manual. Springer, New York
2. Sobin LH, Wittekind CH (2002) TNM classification of malignant tumours. Wiley-Liss, New York
3. Pecorelli S, Benedet JL, Creasman WT et al (1999) FIGO staging of gynecologic cancer. 1994–1997 FIGO Committee on Gynecologic Oncology. International Federation of Gynecology and Obstetrics. Int J Gynaecol Obstet 64:5–10
4. Teramoto N, Tanimizu M, Nishimura R (2009) The present situation of pTNM classification in Japan: a questionnaire survey of the pathologists of Gan-shinryo-renkei-kyoten Byoin (Local Core Cancer Hospitals) on pTNM classification. Pathol Int 59:167–174
5. Wittekind CH, Greene FL, Henson DE (2003) Explanatory notes—general. TNM supplement—a commentary on use. Wiley, New York, pp 1–24
6. Teramoto N, Nishimura R, Takahata T et al (2009) Self-assessment of pTNM classification for lung cancer — a single institutional report at a Japanese comprehensive cancer hospital. Pathol Int 59:376–381
7. Japan Society of Obstetrics and Gynecology, The Japanese Society of Pathology, Japan Radiation Society (1999) General rules for clinical and pathological study of uterine cervical cancer in Japan. Kanehara, Tokyo
8. Wittekind CH, Greene FL, Henson DE (2003) Explanatory notes—specific anatomic sites (Uterine cervix). TNM supplement—a commentary on use. Wiley, New York, pp 58–59
9. Brierley JD, Catton PA, O'Sullivan B et al (2002) Accuracy of recorded tumor, node, and metastasis stage in a comprehensive cancer center. J Clin Oncol 20:413–419
10. Gilchrist KW, Harrington DP, Wolf BC et al (1988) Statistical and empirical evaluation of histopathologic reviews for quality assurance in the Eastern Cooperative Oncology Group. Cancer 62:861–868
11. Kempson RL (1985) Pathology quality control in the cooperative clinical cancer trial programs. Cancer Treat Rep 69:1207–1210

Virchows Arch (2009) 455:315–322
DOI 10.1007/s00428-009-0841-8

ORIGINAL ARTICLE

Acute and chronic placental membrane hypoxic lesions

Jerzy Stanek

Received: 17 April 2009 / Revised: 8 September 2009 / Accepted: 18 September 2009 / Published online: 15 October 2009

Abstract Laminar necrosis (LN) and microscopic chorionic pseudocysts (MCP) are the two histological placental membrane lesions. This study retrospectively compares the clinical and placental associations of LN and MCP on a large placental material. Four hundred seventy-nine placentae featuring membrane LN (group 1), 220 placentae with MCP (group 2), and 50 placentae with both LN and MCP were identified in the database of consecutively signed by the author 4,853 placentae from 18 to 42 weeks pregnancies in years 1994–2007. Frequencies or averages of several clinical conditions and gross and microscopic placental features were compared among the groups (Yates chi-square or analysis of variance, where appropriate). Statistically significant differences were observed for preeclampsia, diabetes mellitus, stillbirths, cesarean section deliveries, placental weight, gross chorionic cysts, maternal chorioamnionitis, fetal chorioamnionitis, marginate placentae, and excessive amount of extravillous trophoblasts, respectively. Based on the above results, LN, a membrane infarction, appears to be an acute membrane hypoxic lesion, while MCP is a chronic lesion related to a more widespread extravillous trophoblasts accumulation in the placental disk. There was a substantial overlap of other clinical and placental conditions among the groups, paralleling not uncommon coexistence of acute and chronic placental hypoxia, therefore, LN and MCP, in same placentae.

Presented at the Paediatric Pathology Society 54th Annual Meeting, 4–6 September, 2008, Helsinki, Finland.

J. Stanek (✉)
Division of Pathology and Laboratory Medicine,
Cincinnati Children's Hospital Medical Center,
3333 Burnet Avenue,
Cincinnati, OH 45229-3039, USA
e-mail: jerzy.stanek@cchmc.org

Keywords Placental membranes · Laminar necrosis · Microscopic chorionic pseudocysts · Extravillous trophoblasts · Preeclampsia · Hypoxia · Placenta · Surgical path · Obstetrics · Chorionic pseudocyst

Introduction

Several hypoxic–ischemic placental lesions can be identified by pathology consultation [1–5]. The real diagnostic significance of many of them has not been firmly established. The time honored villous placental lesions are placental infarction (a focal lesion) and global (diffuse) hypoxic pattern of placental injury. Both are evaluated in the chorionic disk. Recently, two placental membrane lesions have been added to the pathologist's armamentarium and separately correlated with pregnancy outcome, fetal condition, and other placental features. These are laminar necrosis (LN), a band of coagulative necrosis (infarction) present at the choriodecidual interface of the placental membranes [6, 7] (Fig. 1), and microscopic chorionic pseudocysts (MCP), which are lakes of fibrinoid material, surrounded by migratory extravillous trophoblast of the chorionic layer of placental membranes [8] (Fig. 2a, b). LN was observed in 27% placentas from mothers with hypertensive disorders (preeclampsia or chronic hypertension) and was linked to other maternal, fetal, neonatal, and placental conditions known to be associated with perinatal hypoxia, with hypoxia-inducible factor, apoptosis, and oxidative stress playing role in the pathomechanisms [7, 9, 10]. Recently, a leukocytoclastic necrosis of the decidua basalis, a lesion histologically very similar to LN and similarly to LN associated with preeclampsia, preterm birth, and decreased fetal growth, but involving the maternal floor, was described [11]. MCP are even more strongly

associated with preeclampsia and diabetes mellitus, with their incidence almost mirroring the incidence of preeclampsia throughout gestation, peaking in early third trimester [8]. MCP are also statistically associated with placental hypoxic lesions, such as placental infarction, global hypoxic pattern of placental injury, and LN [8].

As LN and MCP have never been mutually compared, this analysis is intended to retrospectively compare the frequency of selected clinical and placental factors associated with LN and MCP on a large placental material.

Material and methods

All consecutive placentas from ≥20-week pregnancies with histological diagnosis of LN and MCP were extracted from the database of 4,853 placentas signed by the author at three institutions (University of Cincinnati Hospital Medical Center, Cincinnati, Ohio, U.S.A; Sheffield Children's NHS Trust, Sheffield, United Kingdom; and Canterbury Health Laboratories, Christchurch, New Zealand) in years 1994–2007. Four hundred seventy-nine placentas featuring membrane LN constituted group 1, 220 placentas with MCP constituted group 2, and 50 placentas with both LN and MCP constituted group 3. Frequencies or averages of several clinical conditions and gross and microscopic placental features were compared among the three groups (Yates chi-square at two degrees of freedom, or analysis of variance (ANOVA), where appropriate).

The placentas were submitted for examination at discretion of obstetricians because of high risk nature of the pregnancies, fetal distress, poor condition of the neonate, operative delivery, or grossly abnormal placenta. Placental examination was performed according to generally accepted criteria; specifically, two sections of placental membrane rolls and at least two paracentral full thickness

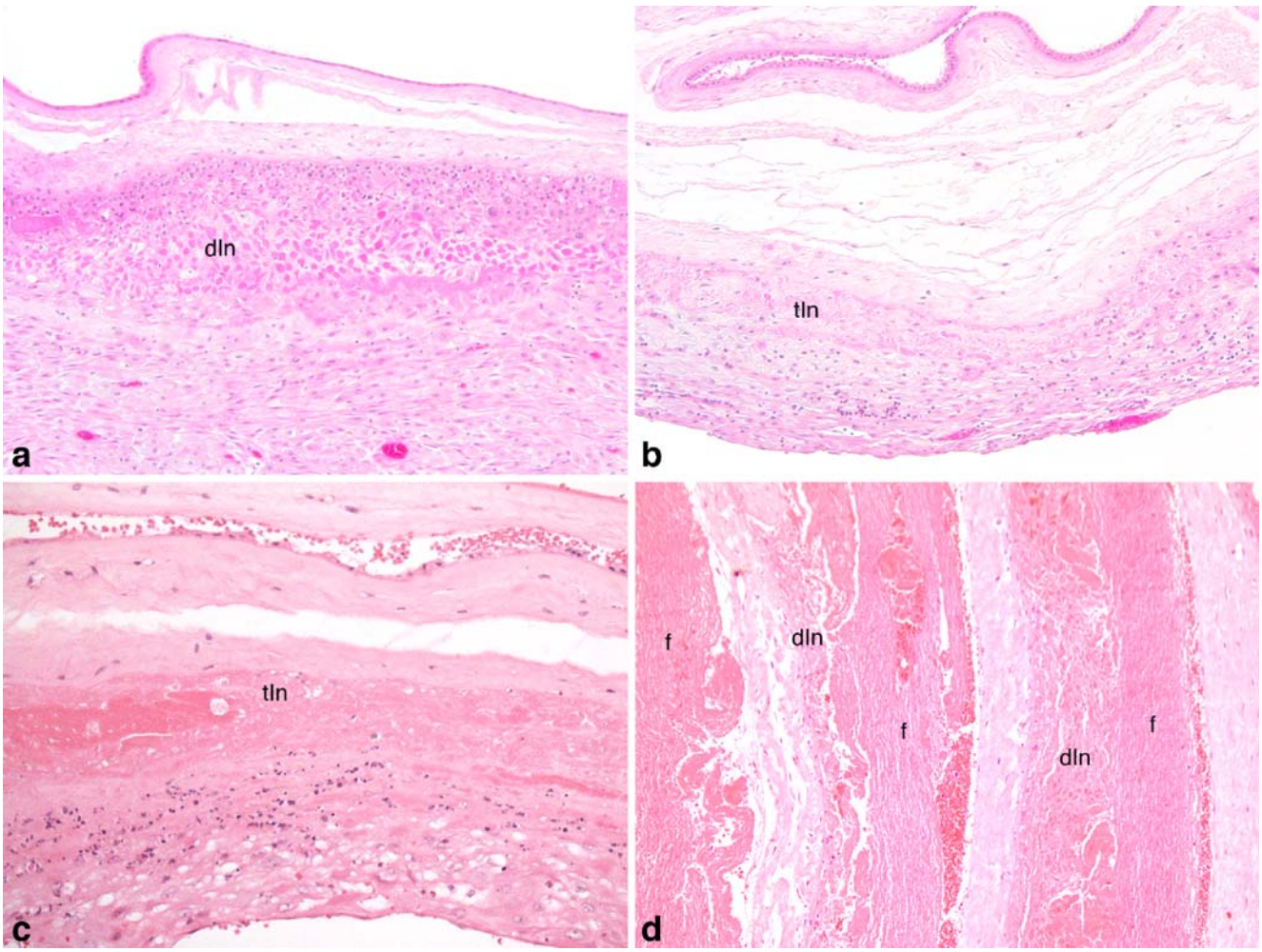

Fig. 1 Laminar necrosis. **a** Decidual laminar necrosis (*dln*) of placental membranes. **b** Trophoblastic laminar necrosis (*tln*) of placental membranes. **c** Leukocytoclastic trophoblastic laminar necrosis (*tln*) of placental membranes. Leukocytes and nuclear "dust" is seen on the decidual side of the band of necrosis of extravillous trophoblast. **d** Decidual laminar necrosis (*dln*) associated with extracellular fibrin (*f*) deposition in placental membranes

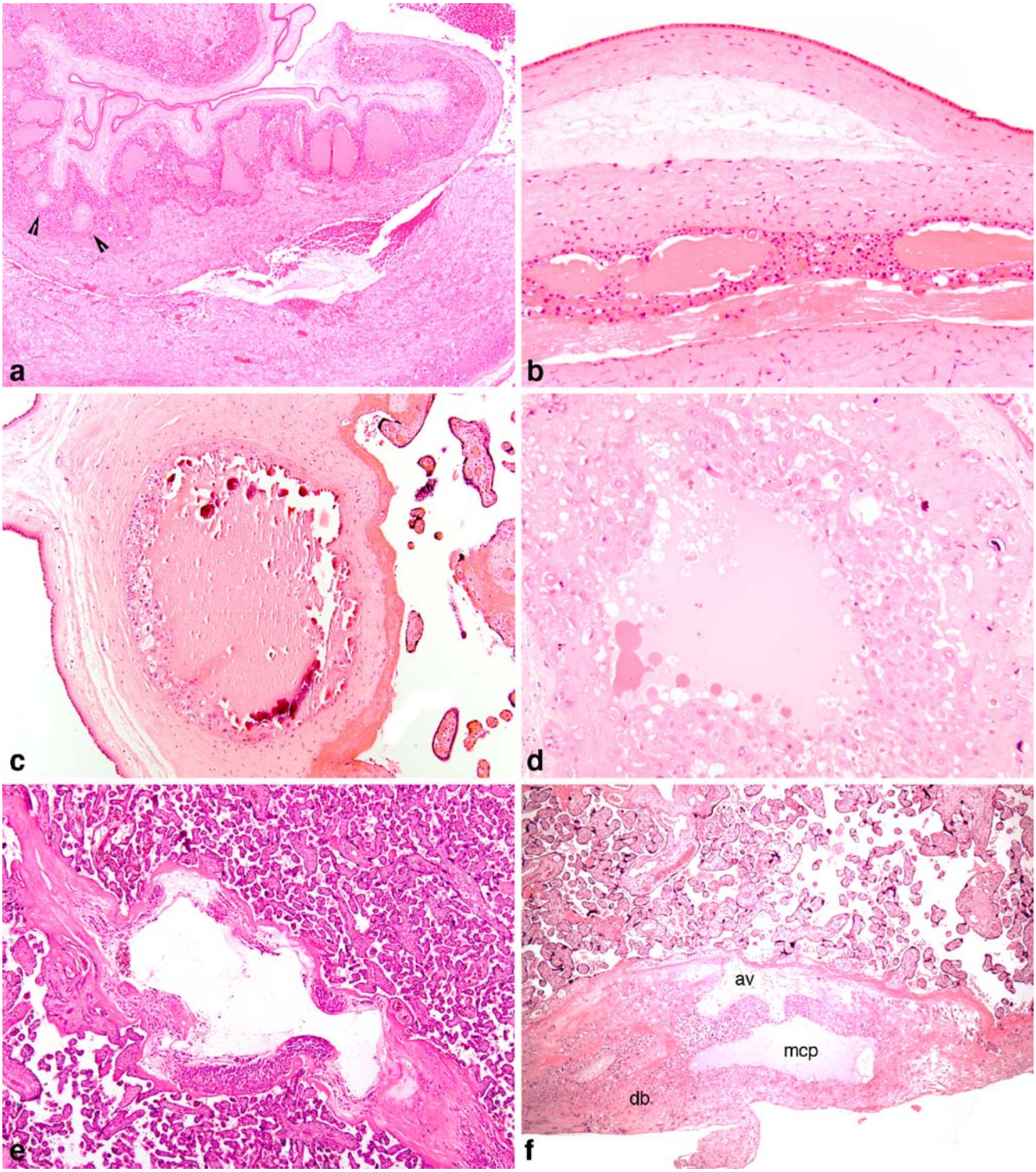

Fig. 2 Microscopic chorionic pseudocysts. **a** Microscopic chorionic pseudocysts (MCP) and two atrophic chorionic villi of chorion laeve (*arrowheads*) in placental membranes. **b** Microscopic chorionic pseudocysts in dividing membranes of dichorionic twin placenta. **c** Focally calcified microscopic chorionic pseudocyst of the chorionic plate. **d** Microscopic cell island pseudocyst, probably of secretory origin. **e** Microscopic septal pseudocyst, probably of degenerative origin. **f** Microscopic chorionic pseudocyst (*mcp*) of basal plate, anchoring villus (*av*), and decidua basalis (*db*)

Table 1 Pregnancy factors

	Group 1		Group 2		Group 3		Statistical significance	
	LN		MCP		Both LN and MCP		χ^2 or F, p	
Number	479		220		50			
Gestational age (weeks, M±SD)	34.0±5.5		34.8±4.0		35.5±3.8			
Multiple pregnancy	27	5.6%	20	9.1%	4	8%		
Pregnancy-induced hypertension	9	0.4%	2	0.9%	2	4%		
Preeclampsia	85	17.7%	57	25.9%	5	10.0%	6.63	$p<0.05$
Mild	30	6.3%	20	9.1%	0			
Severe	40	8.3	28	12.7%	4			
HELLP	11	2.3	8	3.6%	1			
Eclampsia	4	0.8%	1	0.4%	0			
Chronic hypertension	11	2.3%	10	4.5%	2	4%		
Diabetes mellitus	17	3.5%	23	10.4%	0		14.9	$p<0.001$
Substance abuse	24	5.0%	6	2.7%	1	2%		
Oligohydramnios or polyhydramnios	30	6.3%	14	6.4%	3	6%		
Absent/reversed diastolic blood flow by dopplers	9	1.9%	6	2.7%	0			
Induction of labor	40	8.3%	23	10.4%	7	14%		
Abnormal fetal heart rate tracing	64	13.4%	36	16.4%	9	18%		
Antepartum hemorrhage	60	12.5%	23	10.4%	8	16%		
Premature rupture of labor	39	8.1%	14	6.4%	0	0%		
Meconium-stained amniotic fluid	30	6.3%	10	4.5%	2	4%		
Umbilical cord compromise (encirclement, true knot, prolapse)	16	3.3%	8	3.6%	0	0%		
Cesarean section	154	32.1%	104	47.3%	22	44%	14.8	$p<0.001$
Complications of third stage of labor	10	2.1%	2	0.9%	2	4%		

LN laminar necrosis, *MCP* microscopic chorionic pseudocysts, *M* mean, *SD* standard deviation, χ^2 Yates chi-square, *F* statistics of ANOVA, *HELLP* hemolysis, elevated liver enzymes, and low platelets syndrome

chorionic disk sections were routinely taken as a part of the placental examination if no gross lesions were identified. All grossly seen lesions were additionally sampled. The samples were fixed in buffered formalin, followed by routine paraffin embedding, cutting, and staining with hematoxylin and eosin [1–3, 12]. Only cases with at least three microscopic chorionic lakes in membranes were reported as MCP in the placental diagnosis and as LN only

Table 2 Fetal/neonatal factors

	Group 1		Group 2		Group 3		Statistical significance	
	LN		MCP		Both LN and MCP		χ^2 or F, p	
Birth weight (grams, M±SD)	2,078±1,004		2,303±951		2,671±1,016			
Apgar score 1 min (M±SD)	6.4±2.7		7.1±2.2		7.6±2.0			
Apgar score 5 min (M±SD)	7.8±2.0		8.2±1.7		8.6±1.2			
Perinatal mortality	65	13.6%	8	3.6%	1	2%	20.4	$p<0.001$
Neonatal deaths	8	1.7%	2	0.9%	0	0%		
Nonmacerated stillbirths	27	5.6%	3	1.4%	1	2%	6.1	$p<0.05$
Macerated stillbirths	30	6.3%	3	1.4%	0	0%	9.0	$p<0.05$
Intrauterine growth restriction	62	12.9%	30	13.6%	8	16%		
Congenital malformations	36	7.5%	8	3.6%	0		5.8	$p=0.05$

LN laminar necrosis, *MCP* microscopic chorionic pseudocysts, *M* mean, *SD* standard deviation, χ^2 Yates chi-square, *F* statistics of ANOVA

Table 3 Placental factors

	Group 1		Group 2		Group 3		Statistical significance
	LN		MCP		Both LN and MCP		χ^2 or F, p
Placental weight (gm, M±SD)	364.8±165.1		423.1±170.8		445.5±144.2		F=12.6 p<0.001
Two-vessel umbilical cord	8	1.7%	4	1.8%	1	2%	
Hypocoiled or hypercoiled umbilical cord	32	6.7%	11	5.0%	3	6%	
Other umbilical cord pathology	33	6.9%	11	5.0%	1	2%	
Acute chorioamnionitis	120	25.0%	38	17.3%	9	18%	
Maternal	106	22.1%	19	8.6%	8	16%	χ^2=17.9 p<0.001
Fetal	14	2.9%	19	8.6%	1	2%	χ^2=10.4 p<0.05
Chronic villitis of unknown etiology	54	11.3%	20	9.1%	5	10%	
Plasma cell deciduitis	14	2.9%	4	1.8%	3	6%	
Hypertrophic decidual arteriolopathy	109	22.8%	60	27.3%	13	26%	
Atherosis of spiral arterioles	35	7.3%	21	9.5%	5	10%	
Infarction[a]	65	13.6%	35	15.9%	2	4%	
Perivillous fibrin deposition/maternal floor infarction	34	7.1%	22	10.0%	4	8%	
Meconium macrophages	183	38.2%	68	30.9%	15	30%	
Amnion	101	21.1%	52	23.6	8		
Chorion	19	4.0%	6	2.7%	2		
Decidua	63	13.1%	10	4.5%	5		
Global placental hypoxia[b]	82	17.1%	45	20.4%	5	10%	
Preuterine	25	5.2%	12	5.4%	1		
Uterine	37	7.7%	20	9.1%	4		
Postuterine	20	4.2%	13	5.9%	0		
Microscopic cell island chorionic pseudocysts	23	4.8%	18	8.2%	2	4%	
Microscopic chorionic plate pseudocysts	6	1.2%	6	2.7%	1	2%	
Excessive amount of extravillous trophoblasts[c]	20	4.2%	29	13.2%	2	4%	χ^2=18.2 p<0.001
Chorangiosis	94	19.6%	37	16.8%	12	24%	
Erythroblastosis of fetal blood	26	5.4%	14	6.4%	3	6%	
Obliterative endarteritis of stem vessels	25	5.2%	17	7.7%	3	6%	
Increased placental site giant cells	68	14.2%	34	15.4%	7	14%	
Placenta accreta (clinical or occult)	16	3.3%	14	6.4%	0	0%	
Chorangioma	5	1.0%	2	0.9%	0	0%	
Amnion nodosum	18	3.8%	4	1.8%	1	2%	
Battledore placenta	50	10.4%	18	8.2%	6	12%	
Velamentous insertion of umbilical cord	5	1.0%	1	0.4%	1	2%	
Retroplacental hematoma	2	0.4%	5	2.3%	2	4%	
Decidual hemosiderosis	26	5.4%	9	4.1%	4	8%	
Marginate/vallate placenta	57	11.9%	13	5.9%	9	18%	χ^2=7.5 p<0.05
Thrombi in fetal circulation	12	2.5%	12	5.4%	0		
Clusters of avascular chorionic villi	18	3.8%	10	4.5%	2	4%	
Hemorrhagic endovasculitis	13	2.7%	5	2.3%	1	2%	
Intimal cushions of fetal veins	21	4.4%	10	4.5%	2	4%	
Luminal abnormalities of chorionic vessels	42	8.8%	12	5.4%	2	4%	
Diffuse fibrosis of chorionic villi	31	6.5%	6	2.7%	3	6%	

Table 3 (continued)

	Group 1		Group 2		Group 3		Statistical significance
	LN		MCP		Both LN and MCP		χ^2 or F, p
Edema of chorionic villi	9	1.9%	4	1.8%	0	0%	
Intervillous thrombi	57	11.9%	20	9.1%	5	10%	
Intravillous hemorrhage	8	1.7%	1	0.4%	0	0%	
Macroscopic chorionic cysts	10	2.1%	12	5.4%	4	8%	χ^2=6.2 p<0.05
Ferrugination of basement membranes of chorionic villi	8	1.7%	1	0.4%	1	4%	
Succenturiate lobe	8	1.7%	9	1.9%	1	4%	

[a] Only central/paracentral placental infarctions involving at least 5% of placental parenchyma were included

[b] Global (diffuse) placental hypoxia (preuterine, uterine, or postuterine) was histologically diagnosed based on the type of placental maturation (heterogenous or homogenous), excessive syncytial knotting (granular or smudgy chromatin), amount of extracellular matrix of chorionic villi (increased or decreased), density of villous cytotrophoblastic cells (increased or decreased), density of Hofbauer cells (increased or decreased), and villous vascularity (increased or decreased branching of capillaries) [17–19]

[c] More than five cell islands/placental septa per slide

cases in which this lesion involved at least 10% of membrane rolls [7, 8].

Results

LN was found in 9.9% of placentas and MCP in 4.5% placentas, thus LN was twice more common than MCP in this high-risk pregnancy population. There were no statistically significant differences in gestational age between the groups studied. One ninth of LN placentas showed also MCP, and one fourth of MCP placentas also showed LN. Of pregnancy risk factors (Table 1), MCP were statistically significantly associated more frequently than LN with preeclampsia (25.9% vs 17.7%) and diabetes mellitus (10.4% vs 3.5%) but not pregnancy-induced hypertension (0.9% vs 0.4%) or chronic hypertension (4.5% vs 2.3%, respectively). Cesarean deliveries were also more common in groups 2 and 3 than group 1 (47% vs 32%, respectively). Of fetal factors (Table 2), total perinatal mortality was four times more prevalent in group 1 than in groups 2 and 3, this being true both for macerated and nonmacerated stillbirths but not neonatal deaths. Congenital malformations were also more common in group 1. Of placental factors (Table 3), higher placental weight, fetal chorioamnionitis, marginate or vallate placentas, excessive amount of extravillous trophoblasts, and macroscopic chorionic cysts were seen more frequently with MCP than LN. Only maternal chorioamnionitis was seen more commonly with LN than MCP. Fetal–placental weight ratio was lower with MCP (5.4) than with LN (5.7). Although proportions of such clinical conditions as abnormal fetal heart tracings (Table 1), intrauterine growth restriction (Table 2), or other placental hypoxic lesions such as global placental hypoxia or infarction (Table 3) were higher in each group than in this high-risk placental population (not shown), they did not differ statistically significantly between groups 1, 2 and 3 (p>0.05).

Discussion

In this analysis, we intentionally did not analyze separately a specific clinical diagnosis (e.g., preeclampsia) but rather a pair of placental membrane morphologic features (LN and MCP) in a population of high-risk pregnancy. The two discussed membrane lesions are easy to appreciate during placental examination. The LN is easily recognizable despite concerns expressed by some authors [9] who doubt whether this lesion can be reliably distinguished from membrane fibrin deposition. Paying attention to the presence of trophoblastic and/or decidual ghost cells, one can easily distinguish between the two (Fig. 1d). Also, inflammatory necrosis is usually of the liquefactive type, with obliteration of cellular details and stratification of membranes. Leukocytoclastic LN must be distinguished from acute chorioamnionitis. In the former, leukocytes and leukocyte-derived nuclear fragments are adjacent to the decidual aspect of a band of LN (Fig. 1c) and are absent elsewhere in the membranes where necrosis is absent. The mechanism of the leukocyte accumulation is most likely same as in other infarction-associated inflammation, as for example in myocardial infarction. By contrast, chorioamnionitis-associated leukocytes are usually observed at the maternofetal interface of the membranes, frequently without necrosis (except in the most severe acute chorioamnionitis where diagnosis of LN cannot be rendered). MCP are also easily recognizable as they clearly stand out on microscopic

examination even on low power magnification. The only differential diagnosis is fibrosed/hyalinized/atrophic chorionic villi [8], which do not pose a significant diagnostic differential problem (Fig. 2a).

Based on analysis of the presented clinical material, LN, a membrane infarction, appears to be an acute membrane hypoxic lesion, statistically associated with intrauterine fetal death, while MCP are related to a more widespread extravillous trophoblasts accumulation, both in membranes [13] and in chorionic disk (Table 3). This excessive accumulation of extravillous trophoblasts in the chorionic disk may be associated with an increased number of chorionic plate (Fig. 2c), cell island (Fig. 2d), placental septa (Fig. 2d, e), and maternal floor (Fig. 2f) microscopic chorionic pseudocysts as well as macroscopically seen gross chorionic cysts (Table 3). The increased accumulation of extravillous trophoblast (EVT) cells may predispose to secondary pseudocyst formation as the aggregates are avascular [2, 3]. It is reasonable to conclude that such accumulation needs time to develop; MCP is, therefore, a chronic placental lesion. This observation corresponds to the findings of Redline et al. that showed an increased amount of proliferating (by proliferating cell nuclear antigen) and immature (by decreased amount human placental lactogen) trophoblasts in the maternal floor in preeclamptic placentas [14]. It is interesting that the frequency of massive perivillous fibrin deposition which is even larger EVT and fibrinoid deposition was not different among the studied groups, meaning that it is a qualitatively distinct lesion and not a part of the spectrum of increased number of placental septa/placental cell islands. Association of MCP with chronic complications of pregnancy such as preeclampsia and maternal diabetes mellitus and frequent deliveries by cesarean section but less with perinatal mortality could indicate that more generous cesarean section deliveries might have prevented fetal deaths in many cases of groups 2 and 3. Likewise, the greater amount of congenital malformations in group 1 might have accounted for the differences. While the differences in frequency of chorioamnionitis were not statistically significant, maternal chorioamnionitis (acute inflammation of the membranous chorion and amnion and/or acute subchorial intervillositis) was significantly more common in LN, while fetal chorioamnionitis (umbilical cord vasculitis, chorionic vasculitis) in MCP. The cause of this remains unclear. The substantial overlap of high-risk clinical conditions and complications and placental features between groups 1 and 2 may be explained by the tendency of the acute in utero hypoxia to occur more frequently in conditions complicated by chronic uteroplacental insufficiency (the "acute-on-chronic hypoxia"). That is probably why LN occurs more frequently in smaller placentas and why both lesions may be seen together (group 3).

While the pathomechanism of LN is clearly the placental hypoxia and oxidative stress [8] with contribution of the hypoxia-inducible factor2α [10], two pathomechanisms may be operative in formation of MCP [8]: (1) The MCP formation may be a result of increased secretory activity of extravillous trophoblasts. The microscopic appearance of most MCP indicates their secretory nature since the cysts have smooth walls with their content usually uninterrupted, intensely eosinophilic and granular, with occasional scalloping at the cell/matrix border, similar to that seen in thyrotoxic goiter (Fig. 1a, d, f) [4]; (2) The pseudocysts may also form secondary to degeneration of exuberant extravillous trophoblasts and its subsequent liquefaction. In that case, MCP feature their ragged walls with frequent absence of content (Fig. 1e); (3) Both mechanisms may be operative and be hypoxia driven, as some MCP morphologically show mixed features (Fig. 1c).

In summary, because of insufficient sensitivity and specificity of the known and time-honored placental hypoxic lesions, any additional one that can improve the accuracy of placental consultation should be considered for implementation. Placental lesion multiplicity rather than a single lesion poses a risk for fetal growth restriction and neurological impairment [15, 16]. The current analysis proved the relevance and usefulness in retrospective analysis of pregnancy outcome of MPC and LN, the yet relatively unknown placental membrane lesions to general pathologists.

Conflict of interest statement I declare that I have no conflict of interest.

References

1. Kraus FT, Redline RW, Gersell DJ et al (2004) Placental pathology. American Registry of Pathology, Washington, DC
2. Baergen RN (2005) Manual of Benirschke and Kaufmann's pathology of the human placenta. Springer, New York
3. Benirschke K, Kaufmann P, Baergen RN (2006) Pathology of the human placenta. Springer, New York
4. Faye-Petersen OM, Heller DS, Joshi VV (2006) Handbook of placental pathology. Taylor, London
5. Fox H, Sebire NJ (2007) Pathology of the placenta. Saunders, London
6. Salafia CM, Pezzullo JC, López-Zeno JA et al (1995) Placental pathologic features of preterm preeclampsia. Am J Obstet Gynecol 173:1097–1105
7. Stanek J, Al-Ahmadie H (2005) Laminar necrosis of placental membranes: a histologic sign of uteroplacental hypoxia. Pediatr Dev Pathol 8:34–42
8. Stanek J, Weng E (2007) Microscopic chorionic pseudocysts in placental membranes: a histologic lesion of in utero hypoxia. Pediatr Dev Pathol 10:192–198

9. McDonald B, Moore L (2006) IUGR and laminar necrosis of the placental membranes. Pediatr Dev Pathol 9:170
10. Stanek J, Heil J (2006) Direct evidence of hypoxia by immunohistochemistry in placental membranes with laminar necrosis from patients with severe preeclampsia. Pediatr Dev Pathol 9:406
11. Goldenberg RL, Faye-Petersen O, Andrews WW et al (2007) The Alabama preterm birth study: diffuse leukocytoclastic necrosis of the decidua basalis, a placental lesion associated with preeclampsia, indicated preterm birth and decreased fetal growth. J Matern Fetal Neonat Med 20:391–395
12. Langston C, Kaplan C, Macpherson T et al (1997) Practice guideline for examination of the placenta. Arch Pathol Lab Med 121:449–476
13. Stanek J (2008) Increased number of migratory trophoblastic cells in placental membranes with microscopic chorionic pseudocysts (abstract). Mod Path 21:210–211
14. Redline RW, Patterson P (1995) Pre-eclampsia is associated with an excess of proliferative immature intermediate trophoblast. Hum Pathol 26:594–600
15. Viscardi RM, Sun CC (2001) Placental lesion multiplicity: risk factor for IUGR and neonatal cranial ultrasound abnormalities. Early Hum Dev 62:1–10
16. Kraus FT (2007) Clinical syndromes with variable pathologic features. Semin Diagn Pathol 24:43–47
17. Kingdom JC, Kaufmann P (1997) Oxygen and placental villous development: origins of fetal hypoxia. Placenta 18:613–621
18. Chen CP, Aplin JD (2003) Placental extracellular matrix: gene expression, deposition by placental fibroblasts and the effect of oxygen. Placenta 24:316–325
19. Stanek J, Eis ALW, Myatt L (2001) Nitrotyrosine immunostaining correlates with increased extracellular matrix: evidence of postplacental hypoxia. Placenta 22:S56–S62

Virchows Arch (2009) 455:323–336
DOI 10.1007/s00428-009-0837-4

ORIGINAL ARTICLE

Nodular pattern of bone marrow infiltration: frequent finding in immunosuppression-related EBV-associated large B-cell lymphomas

Deborah W. Sevilla · Erin M. Weeden · Suzy Alexander · Vundavalli V. Murty · Bachir Alobeid · Govind Bhagat

Received: 30 June 2009 / Revised: 29 August 2009 / Accepted: 14 September 2009 / Published online: 6 October 2009

Abstract Different patterns of bone marrow (BM) infiltration by diffuse large B cell lymphomas (DLBCL) have been described. A pure nodular pattern is uncommon, and the pathologic features, as well as the clinical correlates of DLBCL manifesting this pattern in the BM have not been well characterized. We evaluated BM biopsies involved by large B cell lymphomas diagnosed at our institute over an 11-year period to assess the morphology, phenotype, cytogenetic abnormalities, and clinical features of cases associated with a nodular pattern. A distinct nodular pattern of BM involvement was noted in 14 out of 55 (25%) cases. Although both EBV+ and EBV− DLBCL with this pattern were identified, a pure nodular pattern was significantly more common in EBV+ DLBCL compared to EBV− DLBCL (8/9, 89% versus 6/46, 13%; P=0.00002). The majority of EBV+ DLBCL associated with a nodular pattern had distinctive morphologic features (polymorphic cellular infiltrate and pleomorphic cytology), and CD30 expression was more commonly observed in this group (P=0.0163). All EBV+ DLBCL and two out of six (33%) EBV− DLBCL had nongerminal center phenotypes. No recurrent cytogenetic abnormalities were detected in either group. Importantly, all EBV+ DLBCL occurred in individuals with immune dysfunction (organ transplant recipients, HIV infection) or in those >50 years of age. Our study indicates a much higher predilection for EBV+ DLBCL to involve the marrow in a nodular pattern compared to EBV− cases and highlights similarities in the morphologic pattern of BM involvement by previously recognized subsets of immunodeficiency-related EBV+lymphomas and the newer entity of "EBV+ DLBCL of the elderly."

Keywords Diffuse large B cell lymphoma · Epstein–Barr virus · Bone marrow · Nodular pattern

D. W. Sevilla · E. M. Weeden · S. Alexander · V. V. Murty · B. Alobeid · G. Bhagat
Department of Pathology, Columbia University Medical Center, New York Presbyterian Hospital, 630 W. 168th Street, 14th Floor, New York, New York 10032, USA

G. Bhagat (✉)
Department of Pathology, College of Physicians and Surgeons, Columbia University, 630 West 168th Street, Vanderbilt Clinic Room 14-228, New York, New York 10032, USA
e-mail: gb96@columbia.edu

Introduction

Bone marrow (BM) examination is an integral part of the Ann Arbor staging system for B cell non-Hodgkin lymphomas (B-NHL). Bone marrow involvement indicates stage IV disease, which is an adverse prognostic factor in the International Prognostic Index (IPI), but it is also independently associated with a worse prognosis [1]. The frequency of BM involvement by B-NHL varies according to disease subtype. Marrow infiltration is more commonly observed in patients with low grade B-NHL, ranging from 30% for marginal zone lymphomas to virtually 100% for chronic lymphocytic leukemias [2–7], compared to diffuse large B cell lymphomas (DLBCL; 8–35%) [2, 3, 8–13]. Differences in the frequency of BM involvement by DLBCL, with regard to their phenotype or association with Epstein–Barr virus (EBV) infection, are currently unclear. Characteristic patterns of BM infiltration by different subtypes of B-NHL have also been reported, with the paratrabecular pattern more commonly seen in follicular lymphoma, the interstitial

diffuse and/or nodular pattern frequently observed in chronic lymphocytic leukemia/small lymphocytic lymphoma and lymphoplasmacytic lymphoma, and the sinusoidal pattern most often associated with splenic marginal zone lymphoma [2, 14, 15]. Only a few studies have described different patterns of BM involvement by DLBCL [2, 6, 16]. These include diffuse, interstitial, paratrabecular, nodular, and mixed patterns. A pure nodular pattern appears to be one of the least common, observed in 0–23% of cases [2, 4–6, 16], and DLBCL manifesting this pattern of BM infiltration have not been well-characterized. Thus, we undertook this study to assess the morphology, phenotype, associated cytogenetic abnormalities, and clinical features of DLBCL with a distinct nodular pattern of BM involvement. We observed nodular BM infiltrates in both EBV− and EBV+ DLBCL; however, this pattern was significantly more common in EBV+ DLBCL. All of the EBV+ DLBCL in our series occurred in immunosuppressed patients and included cases representing the recently described entity of EBV+ DLBCL of the elderly.

Methods

Case selection and clinical characteristics

A search of our departmental database was performed to identify BM biopsies, which had infiltrates of DLBCL over a period of 11 years (January 1997–December 2007). Morphologic features were assessed using H&E stained sections of Bouin's fixed paraffin-embedded BM biopsies. The pattern of BM involvement was analyzed to identify cases with pure nodular infiltrates of DLBCL. A distinct or pure nodular pattern was defined as the presence of well-delineated or circumscribed aggregates of large neoplastic lymphocytes with <10% of the neoplastic cells demonstrating a different pattern of infiltration (i.e., single scattered cells) [2]. The corresponding formalin-fixed paraffin-embedded lymph node (LN) or soft tissue biopsies of the DLBCL, where available, were also evaluated to characterize architectural and cytologic features.

Data regarding patient demographics, EBV viral load and/or serology, immune status, immunosuppressive regimen, chemotherapy and/or radiation therapy, and clinical outcomes were obtained from our laboratory information system. Epstein–Barr virus reactivation was defined as detection of >100 copies per milliliter of EBV antigen by polymerase chain reaction (PCR) analysis.

Immunohistochemistry and in situ hybridization

Immunohistochemical stains were performed on the BM biopsies and LN or soft tissue biopsies, using the primary antibodies listed in Table 1, after heat-induced antigen retrieval, and were visualized with Envision plus (DAKO, Carpinteria, California, USA) and DAB. Cases were scored as positive for the antigen of interest if >30% of the neoplastic cells expressed it. Based on the expression of CD10, BCL6, and IRF4, the DLBCL were classified as either germinal center (GC) type (CD10+ or CD10−/BCL6+/IRF4−) or non-GC type (CD10−/BCL6+/ IRF4+ or CD10−/BCL6−/IRF4+) [17]. Semiquantitative assessment of the reactive T cells within the nodules of DLBCL was performed on CD3-stained sections (<10%=mild, >10–50%=moderate, >50%=marked).

In situ hybridization for EBV-encoded small RNAs (EBER) was performed using the supplied protocol (INFORM EBER, Ventana, Tuscon, Arizona, USA). Cases were considered EBV+ when the vast majority (>90%) of neoplastic cells expressing one or more of the B cell antigens (CD20/PAX5/OCT2) demonstrated a positive signal by EBER.

Cytogenetic analysis

Giemsa banding was performed on metaphase preparations obtained after short term (12 h) unstimulated cultures of the BM aspirate, LN, or soft tissue biopsies using standard methods. Karyotypes were described according to the International System for Human Cytogenetic Nomenclature [18]. Fluorescence in situ hybridization (FISH) was performed on methanol/acetic acid fixed cells using immunoglobulin heavy chain gene (*IGH*), *BCL6*(3q27), and *c-MYC*(8q24) dual color break-apart probes (VYSIS, Downers Grove, Illinois, USA) or locus specific probes for *TP53/ATM* (VYSIS) and *BLIMP1*(*PRDM1*)(6q21) [19], as indicated, according to standard protocols. Fluorescence signals were captured after analyzing 200–300 cells and counterstaining with DAPI using the Cytovision Imaging system attached to a Nikon Eclipse 600 microscope (Applied Imaging, Santa Clara, California, USA).

Immunoglobulin heavy chain gene rearrangement

Polymerase chain reaction analysis to detect *IGH* variable region gene rearrangement was performed on bone marrow aspirates and LN or soft tissue biopsies, using the Biomed-2 primers (IVS Gene Clonality Assay Kit, InVivo Scribe Technologies, San Diego, CA, USA).

Statistical analysis

The observed data were tested for normalcy using a Kolmogorov–Smirnov test. Statistical significance of differences between groups was calculated using the one-tailed Student's *t* test with a significance threshold of $P<0.001$ or

Table 1 Immunohistochemical staining profile of DLBCL with a nodular pattern of bone marrow infiltration

Antibody, clone, company	EBV+ (n=8)						EBV− (n=6)							
Case number	1	2	3	4	5	6	7	8	9	10	11	12	13	14
CD45, 2B11+PD7/26, DAKO, Carpinteria, California, USA	+	+	+	+	+	+	+	+	+	+	+	+	+	+
CD20, L26, DAKO	−	+	+	+	+	+	+	+	+	+	+	+	+	+
PAX5, 24, Cell Marque, Rocklin, California, USA	−	+	+	+	+	+	+	+	+	+	+	+	+	+
CD79a, JCB117, DAKO	+	+	+	+	+	+	+	+	+	+	+	+	+	+
Pu-1, G148-74, BDPharm, Franklin Lakes, New Jersey	+	+	+	−	−	+	+	−	+	+	+	+	+	+
OCT2, N/A, Santa Cruz	+	+	+	+	+	+	+	+	+	+	+	+	+	+
CD10, Calla (56C6), Novacastra, Newcastle upon Tyne, UK	−	−	−	−	−	−	−	−	+	−	−	−	+	−
BCL6, PG-B6P, DAKO	−	+	−	−	+	+	−	−	+	+	−	+	+	+
IRF4, MUM1p, DAKO	+	+	+	+	+	+	+	+	−	−	+	−	−	+
CD138, M115, DAKO														
CD30, Ber-H2, DAKO	+	−	+	+	+	+	+	+	−	−	−	−	−	+
BCL2, 124, DAKO	+	−	−	+	+	+	+	+	+	+	+	+	+	+
CD15, LEUM1, DAKO	−	−	−	−	−	−	−	−	−	−	−	−	−	−
CD5, CD5/54/P6, DAKO	−	−	−	−	−	−	−	−	−	−	−	−	−	−
Fascin, 55 K2, DAKO	−	−	+	−	−	−	−	−	−	−	−	−	−	−
p53[a], BP53-12-1, BIOGENEX, San Ramon, California, USA	+	−	−	−	−	−	−	−	−	+	−	−	−	+
Ki-67[b], MIB1, DAKO	90	80	80	50	80	60	90	70	30	90	50	60	70	80
HHV8 (LANA), 13B10, Cell Marque	−	−	−	−	−	−	−	−	−	−	−	−	−	−
EBNA2, PE2, DAKO	−	+	−	−	−	+	−	−	−	−	−	−	−	−
LMP1, CSI-4DAKO	+	+	+	+	+	+	+	+	−	−	−	−	−	−
EBER, in situ hybridization; Ventana, Tucson, Arizona, USA	+	+	+	+	+	+	+	+	−	−	−	−	−	−
CD3[c], F7.2.38, DAKO	1	1	2	1	2	1	3	3	1	1	2	1	3	1
CD4:CD8[d]CD4, SP35, Cell Marque CD8, C8/144B, DAKO	1:10	1:2	1:2	1:7	1:2	1:3	1:1	1:2	1:2	1:2	1:1	1:2	1:2	1:1

[a] p53 considered positive if >30% of the neoplastic cells demonstrated nuclear expression

[b] Ki-67 expressed as percentage of neoplastic cells

[c] CD3 staining profile refers to nonneoplastic T cells within the nodules, 1=mild, 2=moderate, and 3=marked

[d] CD4:CD8 ratio refers to relative proportions of reactive T cells within the nodules

Fisher's exact probability test, and a P value of <0.05 was considered significant.

Results

Case and patient characteristics

Fifty-five cases of DLBCL involving the BM were diagnosed at our institute during the study period, and the most common primary pattern of BM involvement was diffuse (23/55, 42%), followed by nodular (18/55, 32%), interstitial single-cell (12/55, 22%), and paratrabecular (2/55, 4%). Of the 18 cases with a nodular component, four were eliminated since they exhibited a mixed pattern and did not fulfill our definitional criteria (three had a component of diffuse infiltrate and one had numerous single scattered cells). Thus, 14 of 55 (25%) BM biopsies exhibited a pure nodular pattern. In all, except one case, besides the nodular aggregates, the minor component of single scattered or small clusters of neoplastic cells, represented <5% of the DLBCL infiltrate; one case had an additional component of scattered neoplastic cells approaching 10% of the total DLBCL infiltrate. EBV− DLBCL with a nodular pattern accounted for six of 46 of all EBV− cases (13%), whereas EBV+ DLBCL with a nodular pattern represented eight of nine (89%) of all EBV+ cases involving the BM (P=0.00001967868), only one EBV+ DLBCL with a non-nodular pattern (single cell interstitial infiltrate) was seen in our series.

Clinical characteristics of the patients are described in Table 2. All patients presented with de novo DLBCL, except one patient with an EBV+ DLBCL who had a history of B-NHL, not otherwise specified, 14 years prior to the current BM biopsy. The morphology was identical in the previous BM biopsy; however, no material was available to perform in situ hybridization for EBER in the prior biopsy. A male predominance was observed for EBV+ DLBCL (M:F=5:3), while patients with EBV− DLBCL had an equal gender distribution (M:F=3:3). There was no significant difference in the median age of patients that had EBV+ or EBV− DLBCL (66 years versus 59 years, range 3–83 years and 34–84 years, respectively; P=0.4192). Additionally, no difference in the mean age of patients with EBV− nodular DLBCL, and those that had EBV− DLBCL with other patterns of BM involvement was noted. No significant difference in lactate dehydrogenase (LDH) levels, IPI, Eastern Cooperative Oncology Group (ECOG) performance status, or response rates was seen between the two groups. EBV+ DLBCL with a nodular pattern were seen exclusively in immunocompromised patients: HIV+ (n=2), solid organ transplant (n=3), and old age (>50 years, n=3); two of the recipients of solid organ transplants were >50 years of age, while five of six (83%) individuals with EBV− nodular DLBCL were >50 years of age, but none of the latter had any apparent immune dysfunction. None of the patients had a concurrent (or prior) T cell lymphoma or an autoimmune or collagen vascular disease, and with the exception of PTLD patients, none received immunosuppressive medication (e.g. methotrexate).

At diagnosis, PCR-based EBV viral load assessment was performed in five of eight patients with EBV+ DLBCL and in two of six patients with EBV− DLBCL. An elevated serum EBV viral load was noted at the time of diagnosis in all five EBV+ DLBCL (range 411,000–1,352,000 copies per milliliter; mean 852,000). Epstein–Barr virus was undetectable on follow-up evaluation in two of the five cases, both PTLD patients (1 month and 1 year after diagnosis). None of the tested EBV− cases had measurable viral loads at the time of diagnosis.

Morphology and phenotype

The nodules in all eight EBV+ DLBCL were discrete and had rounded contours, with numerous admixed histiocytes, small lymphocytes, occasional plasma cells, and variable numbers of neoplastic cells (Fig. 1). Histiocyte-rich nodules (highlighted with a stain for PGM-1), with histiocytes comprising >50% of the nodule cellularity, were seen in five of eight (62%) cases. The nodules varied in size, both within the same biopsy and between different biopsies, ranging from small (nodules occupying ≤1/2 of a high power field, 400×) to large and expansile (nodules occupying at least one high power field; Table 3). BM biopsies in three of eight cases (38%) showed only interstitial nodules, and only paratrabecular nodules were seen in three cases (38%); two (25%) had both paratrabecular and interstitial nodules (Table 3). A single case showed one nodule in which the neoplastic cells displayed an angiocentric pattern with accompanying coagulative necrosis (Fig. 2f); while in three cases, the nodules had single-scattered apoptotic cells. Neoplastic cells were quantified based on CD20, PAX5 and/or OCT2 staining as assessment of H&E stained slides always underestimated the number of neoplastic cells. In the majority of biopsies (5/8, 62%), large neoplastic cells comprised a minority of the cellular elements (20–30%) that were either seen as scattered cells at the periphery (targetoid pattern) or randomly distributed throughout the nodules (Fig. 3). In the remaining cases (3/8, 38%), neoplastic cells comprised >30% of the nodular cellular infiltrate (Fig. 2h). The neoplastic cells had centroblastic morphology (large lymphocytes with scant to moderate amphophilic cytoplasm, round to ovoid nuclear contours, fine chromatin, and multiple small nucleoli) in only two of eight (25%) cases (Fig. 2h), with the majority (6/8, 75%) displaying pleomorphic cytologic features (large lymphocytes with angulated or irregular nuclear contours) and bizarre or Reed–Sternberg (RS)-like cells were identified in four (66%) of the latter biopsies (Fig. 2d).

Table 2 Clinical characteristics of patients with nodular infiltration of bone marrow by DLBCL

Variables	EBV+ cases (n=8)	EBV− cases (n=6)
Sex (male/female)	5/3	3/3
Age, median (range; years)	66 (3–83)	59 (34–84)
Older than 60	6 (75%)[a]	3 (50%)[a]
ECOG PS 2–4	3 (38%)[a]	1 (17%)[a]
Bsymptoms, presence	6 (75%)[a]	3 (50%)[a]
LDH elevated	8 (100%)[a]	6 (100%)[a]
Ann Arbor stage III/IV	8 (100%)[a]	6 (100%)[a]
Extranodal involvement (>1 site)	4 (50%)[a]	2 (33%)[a]
IPI,high intermediate/high	6 (75%)[a]	4 (66%)[a]

ECOG Eastern Cooperative Oncology Group, *PS* performance status, *LDH* lactate dehydrogenase, *IPI* International Prognostic Index

[a] Number of cases (%)

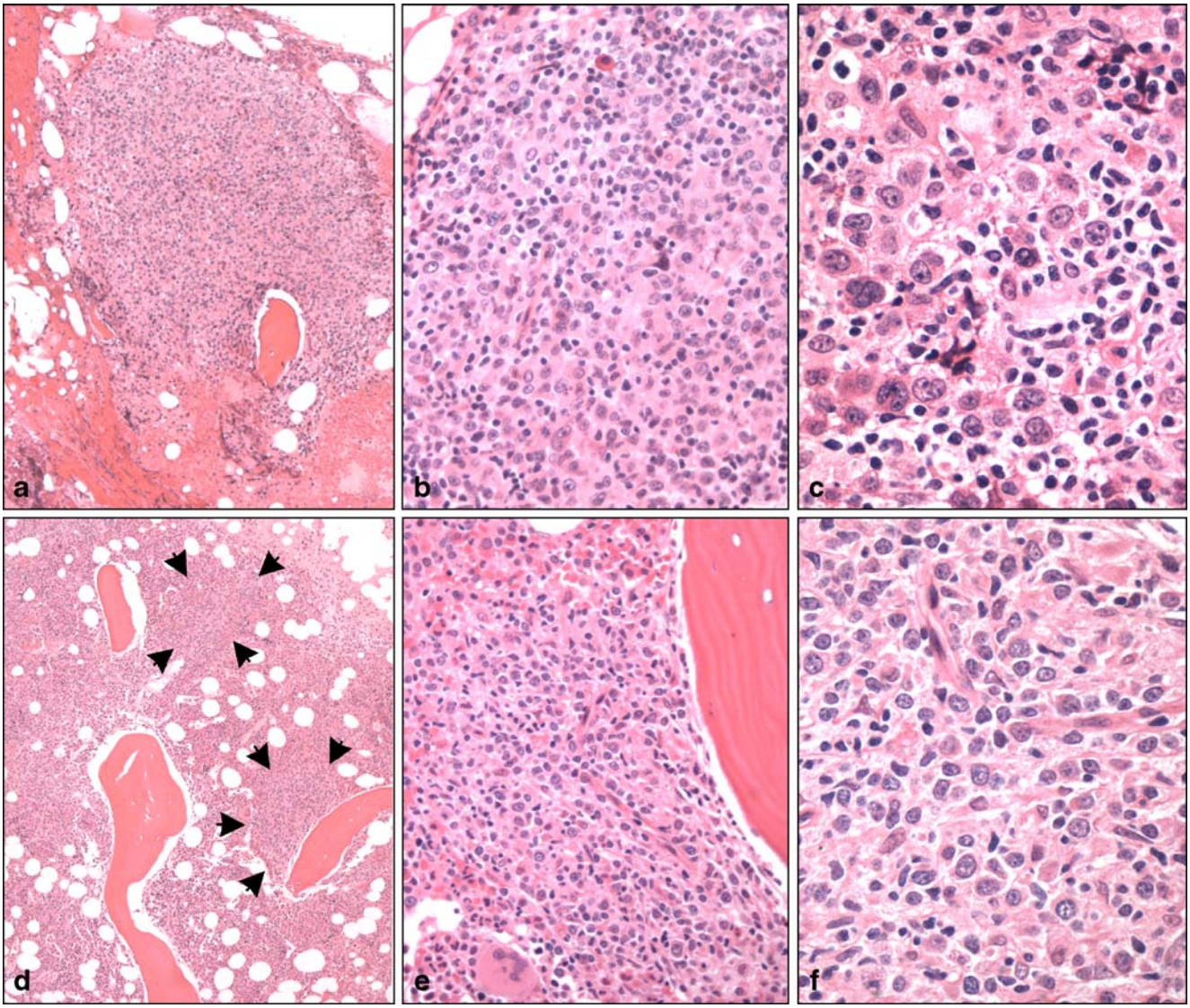

Fig. 1 EBV+ DLBCL of the elderly involving the BM in a nodular pattern (case number 7). **a** BM shows a well-defined paratrabecular nodular infiltrate, clearly visible at low magnification (H&E, 40×). **b** The polymorphic cell population including histiocytes, small lymphocytes, and intermixed neoplastic cells is demonstrated at intermediate magnification (H&E, 200×), while **c** high magnification highlights pleomorphic cytology and occasional RS-like cells (H&E, 400×). EBV− DLBCL with a nodular pattern (case number 12). **d** BM biopsy shows less conspicuous nodules delineated by *arrowheads* (H&E, 40×). **e** Intermediate (H&E, 200×) and **f** high magnification (H&E, 400×) images show a high proportion of centroblast-like cells within the nodules

In contrast, nodules of the six EBV− DLBCL had irregular contours in the majority of cases (4/6, 66%; Fig. 1). Only a few admixed histiocytes were noted (10–30% of all cellular elements within the nodules) that were present in similar numbers as the adjacent uninvolved marrow, and two cases had fewer histiocytes within the nodules compared to the uninvolved marrow, imparting a "negative image" (Fig. 4f). The nodules also had a higher number and density of neoplastic cells compared to most of the EBV+ cases (Fig. 1; Table 3). In all EBV− DLBCL, the neoplastic cells comprised at least 50% of the cellular elements, and in the majority (4/6, 66%), large cells comprised >80% of the nodular cellular infiltrate (Fig. 4e). Half of the biopsies (n= 3) showed only interstitial nodules, while the remaining half showed both interstitial and paratrabecular nodules. The neoplastic cells in the majority of cases (5/6, 83%) demonstrated centroblastic morphology; only one (17%) DLBCL had pleomorphic cytology. The numbers of admixed T cells were variable in EBV+, as well as EBV– DLBCL, and most cases showed a predominance of CD8+ T cells. The inverted CD4:CD8 ratio was especially marked in the 2 EBV+ HIV-associated DLBCL (Table 1). None of the nodules showed evidence of follicular dendritic cell meshworks as assessed by immunohistochemical stains for CD21 and CD23.

Table 3 Diffuse large B cell lymphoma involving the bone marrow in a nodular pattern: patient demographics, morphologic features, phenotype, molecular and cytogenetic characteristics, treatment, and outcome

Case no./ sex/age (year)	Etiology (if applicable)	Morphologic features of nodules				Phenotype	EBER	Karyotype	FISH	Clonality (PCR)	Treatment	Outcome
		Size[a]	Location	Neoplastic cell %	Unique features							
1/F/41	HIV+	S	P	20	RS-like cells	Non-GC	+	89–91<4N>,XXXX, 1, der(3)t(1;3)(q21;p13)×2,+ sder(3)t(3;?)(q11;?),−4,+7×2, t(8;14)(q24;q32)×2,−10,+ del(11)(p11),−12,+i(12)(p10), −13,−16,−17,−18,−21×2,+ mar1−4[cp10]/46,XX[7]	ND	C	None	DOD
2/M/63	Post-tx and elderly	L	I	20		Non-GC	+	46,XY[20]	ND	ND	A-based ChemoRx	DOD
3/M/72	Elderly	S	I	20	RS-like cells	Non-GC	+	46,XY,del(3)(q22q24),der (7)add(7)(p22)add(7) (q36)[14]/46,XY[6]	ND	ND	None	DOD
4/M/57	HIV+and elderly	L	P	60	RS-like cells few apoptotic cells	Non-GC	+	46,XY[20]	ND	ND	A-based ChemoRx	DOD
5/F/70	Post-tx and elderly	S & L	P	60	Few apoptotic cells	Non-GC	+	45−46,X,−X,dup(1)(q41q42; q41q42),+6,+add(7)(q36), ins(11;?)(q22.2;?),dup(12) (q15q24.3),−14, add(14) (p11.2)(q32),del(15) (q22q23),+1−2mar[cp17]/ 46,XX[3]	IgH T BCL6 NT MYC NT Tp53 del	C	A-based ChemoRx	PR, 9 months
6/M/3	Post-tx	S	I	80		Non-GC	+	46,XY[20]	IgH NT	C	A-based ChemoRx	CR, 13 months
7/M/68	Elderly	S & L	I & P	30	RS-like cellsangiocentric with coagulative necrosis	Non-GC	+	46,XY[20]	IgH NT BCL2 NT BCL6 NT c-MYC NT	Poly	Non-A ChemoRx	DOD
8/F/83	Elderly	S & L	I & P	20		Non-GC	+	45,X,−X,t(14;19)(q32;q13) [15]/46,XX[1]	IgH T	C	Non-A ChemoRx	Unknown
9/M/68		S & L	I	80	Nodules devoid of histiocytes	GC	−	ND	ND	ND	A-based ChemoRx	DOD
10/M/51		S & L	I & P	80		GC	−	46, XY[20]	ND	ND	A-based ChemoRx	DOD
11/M/51		S & L	I	80	Nodules devoid of histiocytes	Non-GC	−	51–52,XY,+add(X)(q22),+ add(1))p13,+der(1)t(1;?) (p12;?),+3,+7,t(8;14)(q24; q32), del(15)(q11q21),+ 18,+21[cp20]	ND	ND	A-based ChemoRx	CR, 43 months
13/F/34		S	I & P	50		GC	−	97–101,<4N>,XX,−X,−X,t (3;14)(q27;q32)×2,+t(3;14) (q27;q32),add(6)(q13)×2, del(7)(p14)×2,+hsr(7)(q22)×2,+ i(7)(q10)hsr(7)(q22),−8,add(9)	IgH T BCL6 T BLIMP1 del	C	A-based ChemoRx	CR, 21 mo

14/F/84	S & L	I & P	80	RS-like cells	Non-GC	–	49–51,XX,−2,−5,+1–7mar [cp3]/46,XX[18]	IgH NT BCL6 NT	C	Non-A ChemoRx	DOD
							(p21)×2,+10,−11,−12×2,-15,-17× 2,+18×4, add(19)(q13)×2,+20, + del(20)(q11.2)×2,+1–7mar,+ r(?)×4[cp8]/46,XX[12]				

[a] Please refer to the results section for the parameters used to determine size of nodules

F female, *M* male, *HIV* human immunodeficiency virus, *Post-tx* post solid organ transplant, *S* small, *L* large, *I* interstitial, *P* paratrabecular, *RS* Reed-Sternberg, *GC* germinal center, *Poly* polyclonal, *C* clonal, *T* translocation present, *NT* no translocation detected, *ND* not done, *A-based ChemoRx* anthracycline-based chemotherapy, *non-A ChemoRx* chemotherapy without anthracycline, *CR* complete response, *PR* partial response, *DOD* died of disease

In 11 of 14 (79%) cases, corresponding LN or tissue biopsies were available. Of the seven cases of EBV+ DLBCL available for review, four occurred at extranodal sites (two gastrointestinal tract, one liver, and one kidney), while three were LN-based (one axillary, one mediastinal, and one cervical). Four cases showed variable areas of a polymorphic infiltrate, comprising histiocytes, plasma cells, and small-sized reactive lymphocytes with scattered neoplastic cells being the minority component (Fig. 2a). The two PTLD cases were of the monomorphic type, and the LNs showed near total effacement by sheets of large neoplastic lymphocytes, one had pleomorphic neoplastic cells (Fig. 2i), while the other displayed plasmacytoid features. Overall, pleomorphic neoplastic cells were seen in five cases, and numerous anaplastic or RS-like cells were seen in the majority (4/7, 57%) of cases, similar to findings in the BM biopsies (Fig. 2c). Four of the six EBV− DLBCL, with tissue biopsies available for review, were equally distributed between those occurring at extranodal sites (one testes and one retroperitoneal mass) and LNs (one axillary and one cervical). All these cases displayed centroblastic morphology. As in the corresponding BM biopsies, only a minimal infiltrate of admixed histiocytes was observed. One of the two EBV− nodular BM DLBCL, without available tissue biopsies, demonstrated pleomorphic morphology.

All DLBCL expressed one or more B lineage antigens (CD20, PAX5, OCT2) (Table 1). All EBV+ DLBCL (n=8) were EBER+ by in situ hybridization and had non-GC phenotypes, while two of six (33%) and four of six (66%) EBV– DLBCL had non-GC and GC phenotypes, respectively (Table 3). The neoplastic cells of EBV+ DLBCL more commonly expressed CD30 compared to EBV– DLBCL (7/8, 88% versus 1/6, 17%; P=0.016317; Fig. 4d). All EBV– DLBCL were fascin-negative, while only one of eight (12%) EBV+ DLBCL showed weak fascin staining. Six of eight (75%) EBV+ DLBCL had a type II viral latency pattern (LMP1+ and EBNA2−), and two cases (25%) displayed type III latency (LMP1+ and EBNA2+), both of the latter were PTLDs. In the latter, the number of EBER+ cells was greater than the EBNA2+ and LMP1+ cells combined, and nonoverlapping EBNA2+, and LMP1+ subsets were also seen, consistent with the presence of cell populations with different, as well as transitional, EBV latency types. None of the cases showed any staining for LANA.

Cytogenetic analysis

In 12 of 14 (86%) cases, either BM aspirates or LN/soft tissue biopsies were submitted for cytogenetic analysis. Of these, seven cases had abnormal karyotypes, and all but one exhibited a complex karyotype (Table 3). The most

common cytogenetic aberrations were rearrangements of *IGH* (14q32) detected in five cases (71%). Two cases (one EBV+ and one EBV−), both with non-GC phenotypes, showed t(8;14)(q24;q32) indicative of balanced reciprocal translocations involving *IGH* and *c-MYC*. One EBV+ DLBCL showed t(14;19)(q32;q13) involving *IGH*, and the region encoding *BCL3* and one EBV− DLBCL demonstrated t(3;14)(q27;q32) confirmed to represent a translocation involving *IGH* and *BCL6*. An EBV− DLBCL showed rearrangement of *IGH* only detected by FISH; however, due to the complexity of the karyotype, the partner could not be determined (FISH excluded *BCL6* and *c-MYC*).

Immunoglobulin heavy chain gene rearrangement

In seven of 14 (50%) cases, PCR analysis for *IGH* variable region gene rearrangement was performed, and clonal products were detected in six of seven (86%) cases (Table 3).

Discussion

Bone marrow involvement by DLBCL is less common than low grade B-NHL and occurs in 8–35% of cases [2, 3, 8–13]. However, EBV-associated DLBCL, which represent a small subset of DLBCL (8–12%) [10, 20–24] were shown to have a slightly greater proclivity for the BM (39%) in a recent study [10], compared to EBV − DLBCL. Similar to low grade B-NHLs, different morphologic patterns of BM involvement by DLBCL have been described, which include a predominant or near exclusive presence of diffuse (15–50%), paratrabecular (0–53%), nodular (0–23%), or single cell (17–24%) infiltrates of neoplastic cells [2, 4–6, 13, 16]. Similar patterns and frequencies of marrow involvement by DLBCL were also observed in our series. We decided to focus on DLBCL with a pure nodular pattern in this study since little is known about the phenotypic and clinical spectrum of such cases. A nodular pattern of BM infiltration was noted in 25% of all our cases with BM involvement by DLBCL, and although both EBV− and EBV+ cases were observed, the latter predominated. Of interest, among all cases of EBV+ DLBCL with BM involvement, the vast majority (89%) exhibited a nodular pattern, and EBV+ nodular DLBCL were exclusively seen in patients with documented (organ transplantion, HIV infection) or presumed (old age) immune dysfunction. Differences in the morphologic, phenotypic, and clinical characteristics of EBV+ and EBV– DLBCL with a nodular pattern of BM infiltration were also noted.

EBV+ nodular DLBCL had distinctive morphologic features. The nodules were well circumscribed, and the neoplastic cells usually represented a minor component scattered within a heterogenous population of nonneoplastic inflammatory cells, including histiocytes in most cases. Pleomorphic cytology was quite common, and RS-like cells were observed in 50% of cases. In contrast, the nodules of EBV− DLBCL had more irregular contours, and centroblast-like neoplastic cells comprised the major cellular component in the majority of cases. Lymph node and soft tissue biopsies of the EBV+ DLBCL displayed features similar to those observed in the BM with at least some areas demonstrating neoplastic cells scattered within a polymorphic nonneoplastic background, while all LN biopsies of EBV− DLBCL evaluated showed diffuse infiltrates of centroblast-like cells, similar to what is seen in routine cases of DLBCL.

All EBV+ and one third of the EBV− DLBCL had non-GC phenotypes, and a significant number of EBV+ DLBCL showed CD30 expression by at least a proportion of neoplastic cells compared to EBV − DLBCL, in agreement with prior studies [22, 25]. Staining for fascin, a protein involved in the formation of dendritic processes that is expressed by RS cells in virtually all cases of classical Hodgkin lymphoma (CHL) [26], and approximately 50% of anaplastic large cell lymphomas [27], was seen in the BM and corresponding LN biopsy in only one (13%) of our EBV+ DLBCL, similar to the frequency reported previously [27]. Previous studies of EBV+ DLBCL in PTLD patients have shown high frequencies (36–64%) of type III latency profiles [28, 29]. Lower frequencies of this latency type have been reported in HIV patients (41–50%) [30, 31]. All, except two of the EBV+ cases in our series, displayed type II latency. Both PTLDs, which were of the monomorphic subtype (DLBCL), exhibited type III latency profiles, but populations of cells with different latency types were seen in these cases, similar to previous observations [28, 29]. Our three cases of EBV+ DLBCL of the elderly (see below) showed type II latency, which is the more common latency profile described in these lymphomas [23, 25]. Type III

Fig. 2 EBV+ DLBCL of the elderly (case number 8). An area showing neoplastic lymphocytes scattered in a polymorphic nonneoplastic background in the **a** LN (H&E, 200×) with a similar pattern in the **b** corresponding bone marrow biopsy (H&E, 400×). EBV+ DLBCL of the elderly (case number 3). Markedly pleomorphic neoplastic and RS-like cells in the **c** LN (H&E, 200×) and **d** corresponding bone marrow biopsy (H&E, 400×). EBV+ DLBCL of the elderly (case number 7). A diffuse infiltrate of large neoplastic cells is evident in the **e** LN (H&E, 200×) while the **f** corresponding BM biopsy exhibits angiocentricity with cellular debris and coagulative necrosis (H&E, 400×). EBV+ DLBCL in an HIV patient (case number 4). A high proportion of neoplastic cells are present in the **g** LN (H&E, 200×) and **h** corresponding bone marrow biopsy (H&E, 400×). EBV+ DLBCL in a PTLD patient (case number 2). Sheets of neoplastic cells consistent with monomorphic type of PTLD (DLBCL) are seen in the **i** LN (H&E, 200×), the **j** corresponding BM biopsy shows a moderate infiltrate of nonneoplastic cellular elements (H&E, 400×) ▶

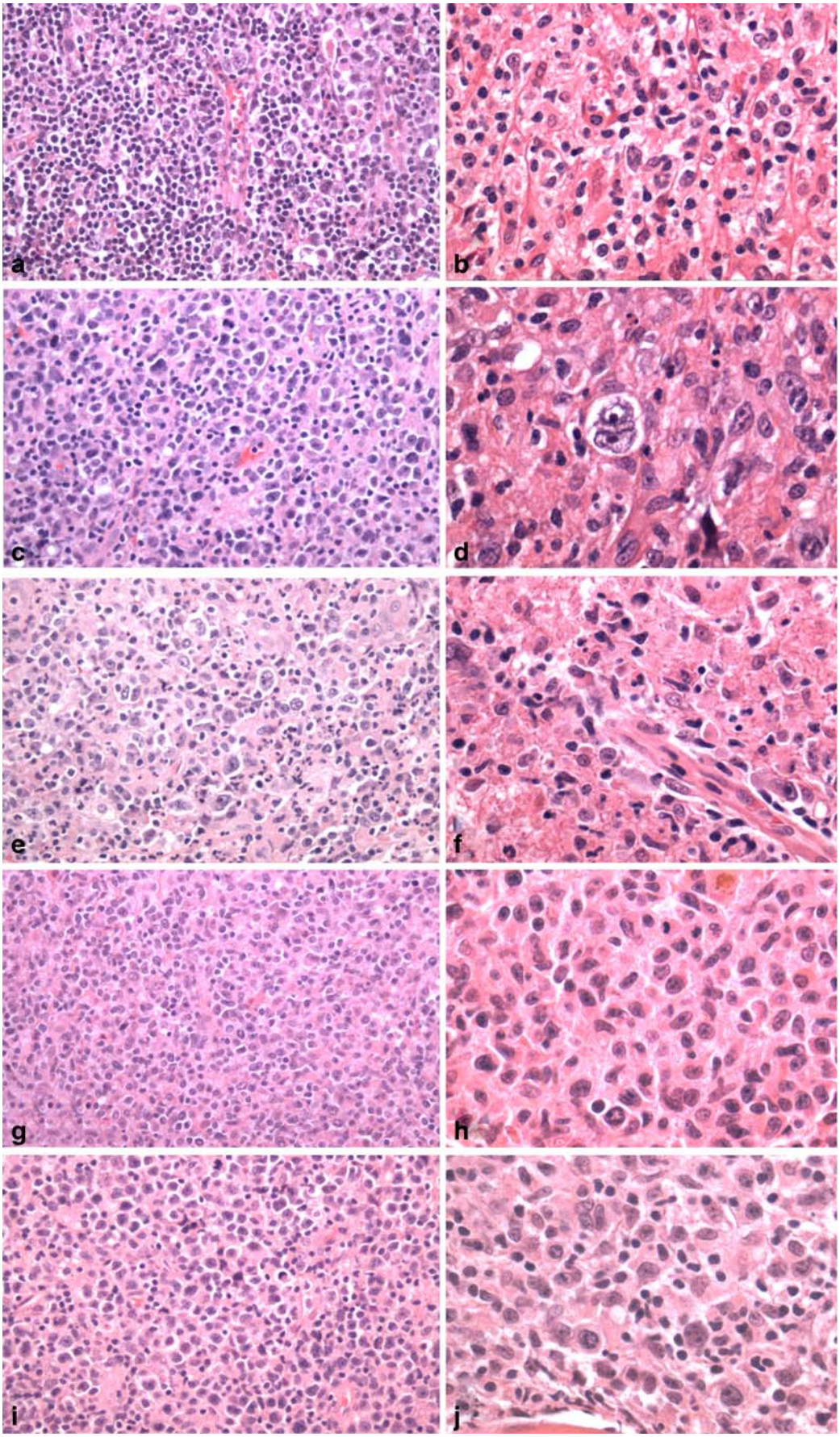
a
b
c
d
e
f
g
h
i
j

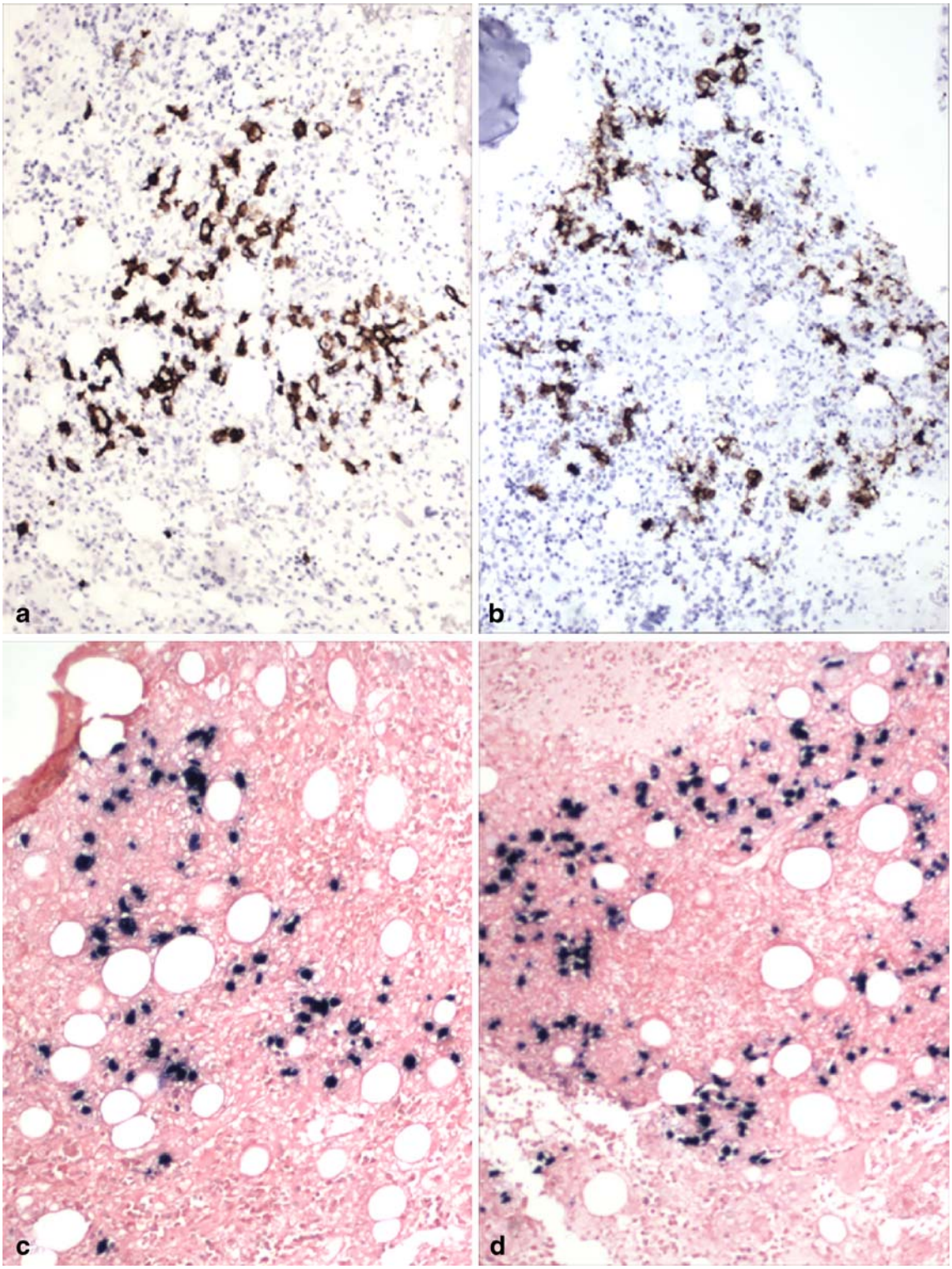

Fig. 3 Distribution patterns of CD20+ and EBER+ neoplastic cells within nodules in the bone marrow biopsies in cases of EBV+ DLBCL (100×). Neoplastic cells are scattered throughout the nodules (**a**, **c**) or seen in a targetoid pattern at the periphery of the nodule (**b**, **d**)

latency has, however, been described in a small proportion of such cases (14–36%) [12, 20, 22, 23, 25, 32].

An interesting finding in our study relates to the presence of EBV+ DLBCL that fulfill the criteria of the recently recognized entity termed EBV+ DLBCL of the elderly [15, 23, 32, 33]. The current World Health Organization classification defines these lymphomas as those occurring in patients >50 years old without any known predisposing

immunodeficiency [15, 23, 32, 33]. A recent survey of EBV-associated lymphomas by Cho et al. described 29 patients with EBV+ DLBCL, 24 of whom were elderly or had a prior history of hepatitis B or C virus infection, tuberculosis, or CHL, suggesting decreased immunity associated with old age and/or environmental cofactors as contributors to lymphomagenesis [20]. It is thought that age associated immune dysfunction, a phenomenon described as "immune senescence," predisposes older individuals to EBV+ lymphomas [34]. Similarities of EBV+ DLBCL of the elderly to B-NHL arising in immunodeficient or immunocompromised patients have been previously described, including a propensity for extranodal disease and the morphologic spectrum of lymphoproliferations, ranging from polymorphic lymphomas resembling polymorphic PTLDs to large cell monomorphic lymphomas indistinguishable from conventional DLBCL [12, 15, 20, 23, 25, 32, 33, 35, 36]. Although, BM involvement has been documented in EBV+ DLBCL of the elderly, to the best of our knowledge, the patterns of BM involvement have not been described. It remains to be seen whether a nodular pattern is the most prevalent pattern of BM involvement in this entity, as seen in our study. Virtually, all prior studies of EBV+ DLBCL have been reported from Asia, whereas, all our three patients were Caucasian and of European descent. Moreover, in contrast to the Asian experience, our cases did not show extranodal involvement.

The morphologic and phenotypic features of our nodular DLBCL also showed an overlap with other types of B cell malignancies, which include T cell/histiocyte-rich large B cell lymphoma (THRLBCL), especially the micronodular variant [37], lymphomatoid granulomatosis (LG), and CHL. Bone marrow involvement, although rare in some of these entities, has been described [38, 39]. The paucity of neoplastic cells and the presence of a polymorphic background, often rich in histiocytes and small reactive T cells, in all these entities, can pose a diagnostic challenge, especially, when reviewing BM biopsies. T cell/histiocyte-rich large B cell lymphomas are usually EBV−; however, rare cases of EBV+ THRLBCL with CD30+ neoplastic cells showing RS-like morphology have been described [40]. However, by definition, the diagnosis of THRLBCL requires the presence of at least a 90% component of nonneoplastic cells, without any aggregates or sheets of large neoplastic cells [15]. All our DLBCL, though rich in nonneoplastic cells, had clusters and/or sheets of neoplastic cells that comprised at least 20% of all cellular elements of the nodules of EBV+ DLBCL and >50% of the EBV− DLBCL. Lymphomatoid granulomatosis also has a polymorphic infiltrate with variable numbers of large EBV+ lymphocytes that may also express CD30. However, these lymphoproliferations show angiocentricity and/or angiodestruction and although occasional bizarre lymphocytes may be seen, classic RS-like cells are infrequent [15]. Angiocentricity and angiodestruction with associated coagulative necrosis was observed focally in only one BM biopsy of our EBV+ DLBCL, within a nodular aggregate that had a large proportion of neoplastic cells. Nodal involvement, which is rare in LG, is usually characterized by a predominance of small-sized T cells in the background, while the LN biopsy of the aforementioned case showed a diffuse infiltrate of predominantly large neoplastic cells, and there was no evidence of extranodal disease arguing against the possibility of LG [41]. Classical Hodgkin lymphoma often presents as nodular polymorphic lymphohistiocytic infiltrates with infrequent CD30+ RS-like cells in the BM [42]. RS cells in CHL coexpress CD30 and CD15 in the majority of cases (80%), are uniformly positive for fascin, and although a minority can express bright CD20 (30%), they usually do not express OCT2 or PU-1 [15, 26]. The CD30+ RS-like cells in our EBV+ DLBCL were uniformly negative for CD15, expressed CD20 in the majority of cases (88%), expressed PU-1 in 50%, and fascin was only expressed in one case. Moreover, all except one case tested, showed clonal immunoglobulin gene rearrangements, which are less commonly detected in CHL by the current assays. The morphologic and phenotypic features of one of our EBV+ cases was similar to the so-called mediastinal gray zone lymphomas, although there was no evidence of mediastinal disease and the latter tend to be EBV− [43]. Methotrexate-related lymphoproliferative disorders can also display similar features, but none of our patients received methotrexate therapy [44]. Although, even nonneoplastic disorders (especially infectious mononucleosis) could morphologically mimic the findings we describe, involvement of the bone marrow is exceptionally rare in these situations. Our study highlights the utility of an extensive immunophenotypic panel, examination of tissue from other sites, and correlation with the clinical features in order to distinguish between these different diagnostic considerations when a nodular pattern of DLBCL is encountered in BM biopsies.

Cytogenetic analysis demonstrated complex cytogenetic aberrations in approximately 50% of our EBV+ and EBV− DLBCL evaluated, but recurrent cytogenetic abnormalities were not observed. Translocations involving *IGH* (14q32) were the most frequently encountered abnormality, detected in almost half of the cases with cytogenetic abnormalities; however, the partners varied. Translocations of *IGH* and *c-MYC* were detected in one case each of EBV+ and EBV− DLBCL. Both had complex karyotypes and non-GC phenotypes, effectively ruling out a diagnosis of Burkitt lymphoma. Intriguingly, an EBV+ DLBCL showed a t(14;19)(q32;q13) on karyotypic analysis, potentially involving the *BCL3* locus, which has been previously reported in a variety of B-NHLs [45]; however, FISH was not performed to confirm involvement of *BCL3* in this case.

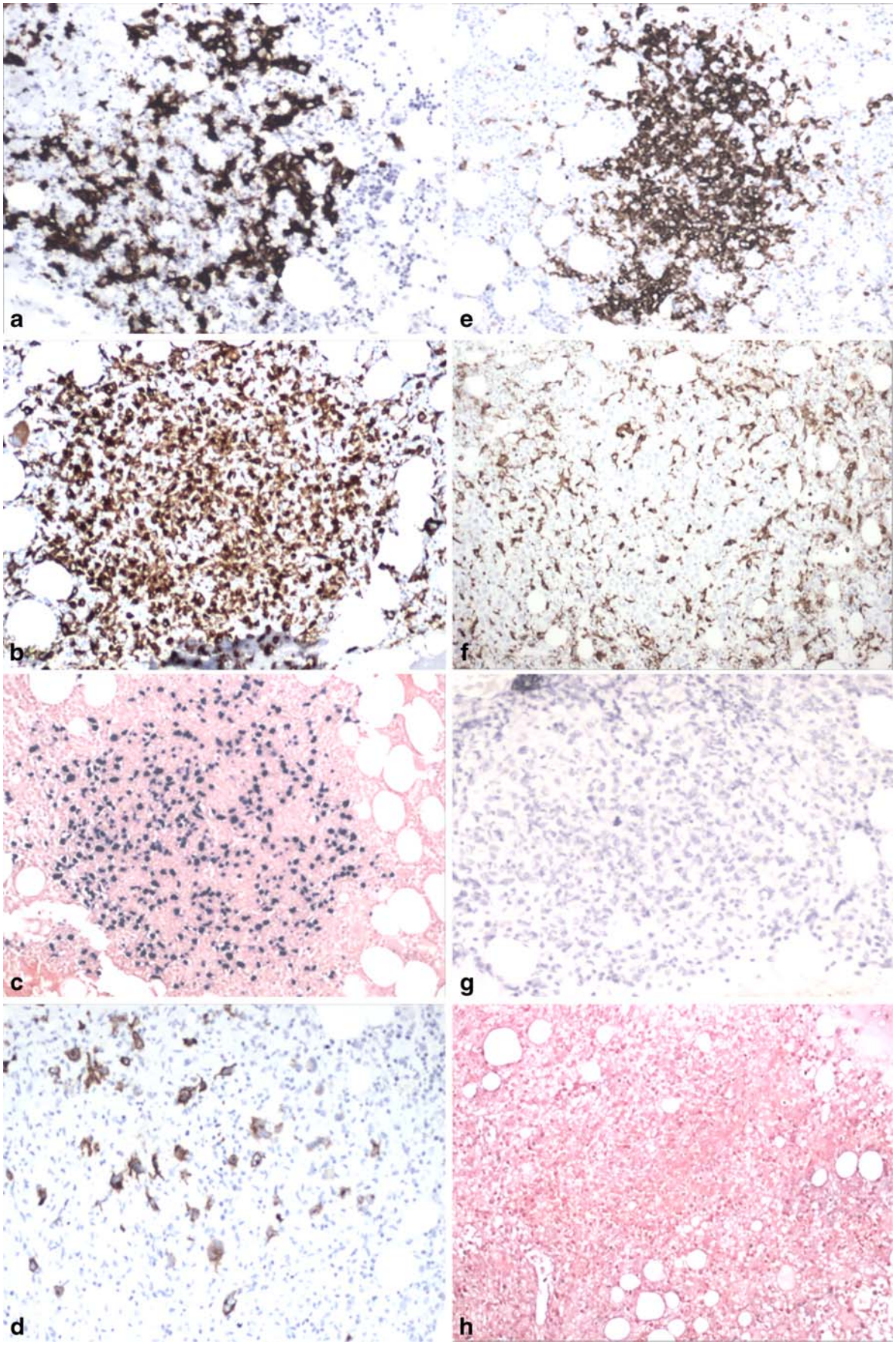
a
e
b
f
c
g
d
h

Cytogenetic findings have not been previously described in surveys of EBV+ DLBCL of the elderly. Our results suggest that the spectrum of cytogenetic aberrations in these cases might be similar to conventional DLBCL [46]. All, but one of our cases, showed clonal IgH gene rearrangement products by PCR analysis. Addition of PCR assays for Ig light chains might have increased the yield of our clonal cases, since cases have been described that show clonality only on using light chain (IgK) primers [47].

Lastly, but importantly, our study suggests investigation of the patient's immune status and evaluation for EBV infection if one observes a nodular pattern of BM involvement by DLBCL with the described features. Determination of EBV status is clinically relevant as multiple studies have demonstrated that EBV+ DLBCL patients have significantly lower overall survival rates, compared to individuals with EBV– DLBCL [10, 22, 24, 33]. We did not see any significant difference in ECOG status, LDH levels, IPI, or clinical outcomes between EBV+ and EBV– DLBCL patients, which might be attributable to our small sample size and/or selection of patients with advanced stage disease (BM involvement). High mortality was seen in both groups, and the small number of patients precludes any assessment of the type of therapy. Since immunosuppressed patients with T cell dysfunction are at risk for "reactivation" of EBV and subsequent development of EBV-associated lymphoproliferative disorders, viral load monitoring in patients with EBV+ PTLDs is performed to detect early disease recurrence and response to treatment [48, 49]. EBV viral load assessment performed in five of our patients at diagnosis of EBV+ B-NHL, which included individuals with PTLD, HIV associated DLBCL, and EBV– DLBCL of the elderly, showed evidence of viral reactivation. Future studies need to investigate the utility of serial serologic or EBV viral load monitoring, as performed in PTLD patients, in detecting early disease recurrence in EBV+ DLBCL of the elderly. Clinical trials using targeted therapies that induce the lytic form of infection in EBV+ lymphoid malignancies in conjunction with gancyclovir treatment have shown promising results [50]. This strategy might also be useful in treating EBV+ DLBCL of the elderly. Since altered lymphocyte development and function contribute to immunosenescence in the elderly, recently proposed treatment approaches aimed at rejuvenating the immune system and augmenting innate immunity in the elderly might be alternative therapeutic options [51].

◀ **Fig. 4** Immunohistochemical studies of the bone marrow (100×). Case number 7 (EBV+ DLBCL), **a** Scattered CD20+ neoplastic B cells representing less than 50% of all cells within the nodule. **b** The nodule is rich in histiocytes (PGM1); **c** neoplastic cells express EBER; and **d** many are CD30+. In contrast, case number 12 (EBV− DLBCL), **e** has numerous CD20+ neoplastic cells within the nodules and **f** fewer histiocytes (PGM1); **g** EBER is negative; and **h** the neoplastic cells do not express CD30

Conflict of interest statement We declare that we have no conflict of interest.

References

1. Wilder RB, Rodriguez MA, Medeiros LJ et al (2002) International prognostic index-based outcomes for diffuse large B-cell lymphomas. Cancer 94:3083–3088
2. Arber DA, George TI (2005) Bone marrow biopsy involvement by non-Hodgkin's lymphoma: frequency of lymphoma types, patterns, blood involvement, and discordance with other sites in 450 specimens. Am J Surg Pathol 29:1549–1557
3. Conlan MG, Bast M, Armitage JO et al (1990) Bone marrow involvement by non-Hodgkin's lymphoma: the clinical significance of morphologic discordance between the lymph node and bone marrow. Nebraska Lymphoma Study Group. J Clin Oncol 8:1163–1172
4. Bartl R, Hansmann ML, Frisch B et al (1988) Comparative histology of malignant lymphomas in lymph node and bone marrow. Br J Haematol 69:229–237
5. McKenna RW, Hernandez JA (1988) Bone marrow in malignant lymphoma. Hematol Oncol Clin North Am 2:617–635
6. Schmid C, Isaacson PG (1992) Bone marrow trephine biopsy in lymphoproliferative disease. J Clin Pathol 45:745–750
7. Kremer M, Quintanilla-Martinez L, Nahrig J et al (2005) Immunohistochemistry in bone marrow pathology: a useful adjunct for morphologic diagnosis. Virchows Arch 447:920–937
8. Campbell J, Seymour JF, Matthews J et al (2006) The prognostic impact of bone marrow involvement in patients with diffuse large cell lymphoma varies according to the degree of infiltration and presence of discordant marrow involvement. Eur J Haematol 76:473–480
9. Hodges GF, Lenhardt TM, Cotelingam JD (1994) Bone marrow involvement in large-cell lymphoma. Prognostic implications of discordant disease. Am J Clin Pathol 101:305–311
10. Park S, Lee J, Ko YH et al (2007) The impact of Epstein–Barr virus status on clinical outcome in diffuse large B-cell lymphoma. Blood 110:972–978
11. Yamauchi A, Fujita S, Ikeda J et al (2007) Diffuse large B-cell lymphoma in the young in Japan: a study by the Osaka Lymphoma Study Group. Am J Hematol 82:893–897
12. Ohshima K, Suzumiya J, Tasiro K et al (1996) Epstein–Barr virus infection and associated products (LMP, EBNA2, vIL-10) in nodal non-Hodgkin's lymphoma of human immunodeficiency virus-negative Japanese. Am J Hematol 52:21–28
13. Foucar K (2001) Bone marrow pathology. ASCP, Chicago
14. Foucar K, McKenna RW, Frizzera G et al (1982) Bone marrow and blood involvement by lymphoma in relationship to the Lukes–Collins classification. Cancer 49:888–897
15. Swerdlow SH, Campo E, Harris NL et al (eds) (2008) WHO classification of tumours of haematopoietic and lymphoid tissues. IARC, Lyon
16. Jeong SY, Chang YH, Lee JK et al (2007) Incidence and histologic patterns of bone marrow involvement of malignant lymphoma based on the World Health Organization classification: a single institution study. Korean J Lab Med 27:383–387
17. Hans CP, Weisenburger DD, Greiner TC et al (2004) Confirmation of the molecular classification of diffuse large B-cell

lymphoma by immunohistochemistry using a tissue microarray. Blood 103:275–282
18. Shaffer LG (2005) An international system for human cytogenetic nomenclature. Karger, Basel
19. Pasqualucci L, Compagno M, Houldsworth J et al (2006) Inactivation of the PRDM1/BLIMP1 gene in diffuse large B cell lymphoma. J Exp Med 203:311–317
20. Cho EY, Kim KH, Kim WS et al (2008) The spectrum of Epstein–Barr virus-associated lymphoproliferative disease in Korea: incidence of disease entities by age groups. J Korean Med Sci 23:185–192
21. Hummel M, Anagnostopoulos I, Korbjuhn P et al (1995) Epstein–Barr virus in B-cell non-Hodgkin's lymphomas: unexpected infection patterns and different infection incidence in low- and high-grade types. J Pathol 175:263–271
22. Kuze T, Nakamura N, Hashimoto Y et al (2000) The characteristics of Epstein–Barr virus (EBV)-positive diffuse large B-cell lymphoma: comparison between EBV(+) and EBV(−) cases in Japanese population. Jpn J Cancer Res 91:1233–1240
23. Oyama T, Yamamoto K, Asano N et al (2007) Age-related EBV-associated B-cell lymphoproliferative disorders constitute a distinct clinicopathologic group: a study of 96 patients. Clin Cancer Res 13:5124–5132
24. Yoshino T, Nakamura S, Matsuno Y et al (2006) Epstein–Barr virus involvement is a predictive factor for the resistance to chemoradiotherapy of gastric diffuse large B-cell lymphoma. Cancer Sci 97:163–166
25. Shimoyama Y, Yamamoto K, Asano N et al (2008) Age-related Epstein–Barr virus-associated B-cell lymphoproliferative disorders: special references to lymphomas surrounding this newly recognized clinicopathologic disease. Cancer Sci 99:1085–1091
26. Pinkus GS, Pinkus JL, Langhoff E et al (1997) Fascin, a sensitive new marker for Reed-Sternberg cells of hodgkin's disease. Evidence for a dendritic or B cell derivation? Am J Pathol 150:543–562
27. Bakshi NA, Finn WG, Schnitzer B et al (2007) Fascin expression in diffuse large B-cell lymphoma, anaplastic large cell lymphoma, and classical Hodgkin lymphoma. Arch Pathol Lab Med 131:742–747
28. Shaknovich R, Basso K, Bhagat G et al (2006) Identification of rare Epstein–Barr virus infected memory B cells and plasma cells in non-monomorphic post-transplant lymphoproliferative disorders and the signature of viral signaling. Haematologica 91:1313–1320
29. Vakiani E, Basso K, Klein U et al (2008) Genetic and phenotypic analysis of B-cell post-transplant lymphoproliferative disorders provides insights into disease biology. Hematol Oncol 26:199–211
30. Delecluse HJ, Hummel M, Marafioti T et al (1999) Common and HIV-related diffuse large B-cell lymphomas differ in their immunoglobulin gene mutation pattern. J Pathol 188:133–138
31. Hamilton-Dutoit SJ, Rea D, Raphael M et al (1993) Epstein–Barr virus-latent gene expression and tumor cell phenotype in acquired immunodeficiency syndrome-related non-Hodgkin's lymphoma. Correlation of lymphoma phenotype with three distinct patterns of viral latency. Am J Pathol 143:1072–1085
32. Oyama T, Ichimura K, Suzuki R et al (2003) Senile EBV+B-cell lymphoproliferative disorders: a clinicopathologic study of 22 patients. Am J Surg Pathol 27:16–26
33. Shimoyama Y, Oyama T, Asano N et al (2006) Senile Epstein–Barr virus-associated B-cell lymphoproliferative disorders: a mini review. J Clin Exp Hematop 46:1–4
34. Ouyang Q, Wagner WM, Walter S et al (2003) An age-related increase in the number of CD8+ T cells carrying receptors for an immunodominant Epstein–Barr virus (EBV) epitope is counteracted by a decreased frequency of their antigen-specific responsiveness. Mech Ageing Dev 124:477–485
35. Tao J, Wasik MA (2001) Epstein–Barr virus associated polymorphic lymphoproliferative disorders occurring in nontransplant settings. Lab Invest 81:429–437
36. Nador RG, Chadburn A, Gundappa G et al (2003) Human immunodeficiency virus (HIV)-associated polymorphic lymphoproliferative disorders. Am J Surg Pathol 27:293–302
37. Dogan A, Burke JS, Goteri G et al (2003) Micronodular T-cell/histiocyte-rich large B-cell lymphoma of the spleen: histology, immunophenotype, and differential diagnosis. Am J Surg Pathol 27:903–911
38. Robak T, Kordek R, Urbanska-Rys H et al (2006) High activity of rituximab combined with cladribine and cyclophosphamide in a patient with pulmonary lymphomatoid granulomatosis and bone marrow involvement. Leuk Lymphoma 47:1667–1669
39. Skinnider BF, Connors JM, Gascoyne RD (1997) Bone marrow involvement in T-cell-rich B-cell lymphoma. Am J Clin Pathol 108:570–578
40. Lim MS, Beaty M, Sorbara L et al (2002) T-cell/histiocyte-rich large B-cell lymphoma: a heterogeneous entity with derivation from germinal center B cells. Am J Surg Pathol 26:1458–1466
41. Takiyama A, Nishihara H, Tateishi U et al (2008) CNS lymphomatoid granulomatosis with lymph node and bone marrow involvements. Neuropathology 28:640–644
42. Franco V, Tripodo C, Rizzo A et al (2004) Bone marrow biopsy in Hodgkin's lymphoma. Eur J Haematol 73:149–155
43. Traverse-Glehen A, Pittaluga S, Gaulard P et al (2005) Mediastinal gray zone lymphoma: the missing link between classic Hodgkin's lymphoma and mediastinal large B-cell lymphoma. Am J Surg Pathol 29:1411–1421
44. Kamel OW, Weiss LM, van de Rijn M et al (1996) Hodgkin's disease and lymphoproliferations resembling Hodgkin's disease in patients receiving long-term low-dose methotrexate therapy. Am J Surg Pathol 20:1279–1287
45. Martin-Subero JI, Ibbotson R, Klapper W et al (2007) A comprehensive genetic and histopathologic analysis identifies two subgroups of B-cell malignancies carrying a t(14;19)(q32;q13) or variant BCL3-translocation. Leukemia 21:1532–1544
46. Dave BJ, Nelson M, Pickering DL et al (2002) Cytogenetic characterization of diffuse large cell lymphoma using multi-color fluorescence in situ hybridization. Cancer Genet Cytogenet 132:125–132
47. van Dongen JJ, Langerak AW, Bruggemann M et al (2003) Design and standardization of PCR primers and protocols for detection of clonal immunoglobulin and T-cell receptor gene recombinations in suspect lymphoproliferations: report of the BIOMED-2 Concerted Action BMH4-CT98–3936. Leukemia 17:2257–2317
48. Cohen JI (2000) Epstein–Barr virus infection. N Engl J Med 343:481–492
49. Tsai DE, Douglas L, Andreadis C et al (2008) EBV PCR in the diagnosis and monitoring of posttransplant lymphoproliferative disorder: results of a two-arm prospective trial. Am J Transplant 8:1016–1024
50. Perrine SP, Hermine O, Small T et al (2007) A phase 1/2 trial of arginine butyrate and ganciclovir in patients with Epstein–Barr virus-associated lymphoid malignancies. Blood 109:2571–2578
51. Dorshkind K, Montecino-Rodriguez E, Signer RA (2009) The ageing immune system: is it ever too old to become young again? Nat Rev Immunol 9:57–62

Virchows Arch (2009) 455:337–341
DOI 10.1007/s00428-009-0830-y

ORIGINAL ARTICLE

Splenic micronodular T-cell/histiocyte-rich large B-cell lymphoma: effect of prior corticosteroid therapy

Elena Kan · Itai Levy · Daniel Benharroch

Received: 20 April 2009 / Revised: 16 August 2009 / Accepted: 24 August 2009 / Published online: 9 September 2009

Abstract We report on three patients who were treated with corticosteroids only prior to the diagnosis of splenic lymphoma. Corticosteroids were administered for different conditions, at different doses, and for various periods of time. The primary diagnosis was splenic micronodular T-cell/histiocyte-rich large B-cell lymphoma in the three cases, and it was reached with variable difficulty. We suggest that the corticosteroid treatment was one of the causes for the complications in reaching a diagnosis. The morphologic appearance of the microscopic splenic nodules was the most variable feature and may possibly reflect the dose and duration of the corticosteroid therapy. However, the histopathologic changes are probably not related with Epstein-Barr virus-induced immunosuppression.

Keywords Splenic micronodular lymphoma · T-cell/histiocyte-rich large B-cell lymphoma · Corticosteroids

Introduction

Splenic micronodular T-cell/histiocyte-rich large B-cell lymphoma (SMTHLBCL) is a rare lymphoma variant related to T-cell/histiocyte-rich large B-cell lymphoma (THLBCL), which occurs at other body sites as well as in the spleen. First described as SMTHLBCL by Dogan et al. in 2003, it presents with systemic symptoms, anemia, and splenomegaly, with minimal to usually absent lymphadenopathy [1]. In this condition, the spleen shows multiple micronodules and a mixed population of small T cells and plasma cells. The tumoral cells dispersed among the previously mentioned population are large lymphoid cells that are $CD20^+$, $Bcl\text{-}6^+$, and to a variable extent EMA^+, $CD30^+$, and $Bcl\text{-}2^+$. The features of this variant lymphoma are similar to those of THLBCL [2]. Most of the 17 patients described by Dogan et al. died within 2 years of diagnosis [1].

A search into the older literature disclosed three cases of lymphoma described by Braylan et al. These patients presented with splenomegaly but no lymphadenopathy. In these spleens, multiple epithelioid granulomas masked the neoplasm and delayed diagnosis. It is possible that these authors had described prematurely the same lymphoma variant [3].

Sarcoid-like granulomas, as seen in Hodgkin as well as in non-Hodgkin lymphomas, often obscure the neoplasm. Moreover, sarcoidosis by itself may be related to non-Hodgkin lymphoma. These two conditions may be extremely difficult to distinguish, especially when no clinical evidence of sarcoidosis is present [4, 5].

Patients with suspected malignant hematolymphoid disease have at times been subjected to exclusive corticosteroid therapy prior to a primary biopsy [6]. Indications for the steroid therapy have varied from hemolytic anemia, dermatologic disorders, asthma, and auto-immune diseases, to life-threatening conditions such as superior vena cava syndrome and respiratory insufficiency [7–9]. Except for the rare tumor lysis syndrome, complications of corticosteroid administration prior to a biopsy have rarely been reported [9]. In an ongoing study on this subject (manuscript in preparation), we found that a complication in the primary diagnosis was the most frequent consequence of this preliminary corticosteroid therapy. Among the patients

E. Kan · D. Benharroch (✉)
Department of Pathology, Soroka University Medical Center and Faculty of Health Sciences, Ben-Gurion University of the Negev, P.O. Box 151, Beer-Sheva 84101, Israel
e-mail: benaroch@bgu.ac.il

I. Levy
Department of Hematology, Soroka University Medical Center, Beer-Sheva, Israel

with lymphomas examined in the previously mentioned study, there were three who received corticosteroids before bone marrow biopsy, liver biopsy, and splenectomy were performed. These three patients, diagnosed with variable difficulty as suffering from SMTHLBCL, are the subject of this report. No additional SMTHLBCL case was found in our Registry that was not related with prior corticosteroid treatment.

Case histories

Case 1. C.R., a 70-year-old woman with asthma, presented because of weight loss. She was found to have splenomegaly and hemolytic anemia for which she was given 60 mg prednisone a day for 6 months. As lymphoma was suspected, in the absence of lymphadenopathy, splenectomy was carried out. The patient was given six courses of rituximab, cytoxan, adriamycin, vincristine, and Prednisone (R-CHOP), and 1 year after the first marrow biopsy, she showed evidence of complete remission. At that time, a bone marrow biopsy showed no evidence of malignancy.

Case 2. B.E., a 59-year-old man, was admitted because of fever of 3 months' duration, weight loss of 15 kg, night sweats, splenomegaly, and anemia of 12.8 g%. He was obese, a heavy smoker, and suffered from diabetes. He was given 60 mg prednisone because of fever of unknown origin in the absence of peripheral lymphadenopathy or a clear-cut malignant tumor. A diagnostic splenectomy was performed. The patient was treated with six courses of R-CHOP and was in remission 15 months after diagnosis.

Seven years after presentation, the patient was admitted because of a right orbital tumor. It was located in the lacrimal gland and its histology was that of a low-grade marginal zone B-cell lymphoma. The patient refused treatment and is well, 26 months following complete resection of the lacrimal gland.

Case 3. S.M., a 63-year-old woman, complained of fever, weight loss, fatigue, and pruritus, and was found to have splenomegaly. Anemia and hypogammaglobulinemia were evident. The patient received prednisone 40 mg a day for 3 months for dermatitis followed by tapering off the dose. A laparoscopic splenectomy was performed. No additional abdominal organ seemed to be involved in the process. The patient was treated with six cycles of R-CHOP. She suffered neutropenic fever on several occasions. The patient is now in complete remission, 36 months after presentation.

Materials and methods

The three patients reported herein are part of a larger cohort retrospectively investigated as they were treated with corticosteroids only prior to a primary lymphoma biopsy. They presented with isolated involvement with what seemed to be a splenic lymphoma.

The history of the patients and splenic, marrow, and liver biopsies, when available, were reviewed. The possible effect of prior corticosteroid therapy was studied. Notably, we scrutinized the size and composition of the microscopic nodules. We evaluated the degree to which the diagnoses of Hodgkin lymphoma, peripheral T-cell lymphoma, and benign granulomatous lesions were tenable.

These patients are reported since we reached a diagnosis of SMTHLBCL in the three cases. Clinical features were retrieved from the patients' files (Table 1). To evaluate a possible link between this outstanding occurrence and EBV-induced immune suppression, we carried out Epstein-Barr virus small RNA (EBER) in situ hybridization (ISH), using the kit from Biogenex, (San Ramon, CA, USA).

Results

The bone marrow biopsies showed predominant groups of epithelioid histiocytes, numerous $CD3^+$ or $CD5^+$ T cells, and a small number of large $CD20^+$ B cells. In two of the three cases, the infiltrates were paratrabecular (Fig. 1a).

In case 2, a first liver biopsy showed several epithelioid aggregates (Fig. 1b), numerous small T cells, and a few large lymphoid cells that were $CD20^+$, $CD30^+$, $CD15^-$. In a second liver biopsy, the microscopic nodules were fibrotic (Fig. 1c), at least in part, and lacked epithelioid histiocytes and most of the small T lymphocytes.

The spleens weighed 744, 850, and 540 g. The cut section was uniformly dark red. On histology, multiple microscopic nodules included epithelioid cell aggregates at their centers (Fig. 1d). They also included isolated large B cells (Fig. 1e) and some $CD30^+$ (Fig. 1f), focally positive for EMA, Bcl-6, and BCl-2. Immunostains for CD10, CD15, CD23, and LMP-1 were all negative. EBER ISH was negative in all three cases. A few small B cells were also found. A reticulin stain highlighted the fine nodularity of the spleens. The red pulp was often spared. The microscopic nodules varied in size and composition from case to case. In some of these, as in case 1, all the components were well represented. In the other cases, epithelioid and small T cells were few. In case 2, some micronodules were fibrotic.

The following diseases were initially considered as a probable diagnosis: granulomatous inflammation (cases 1

Table 1 Splenic micronodular T-cell/histiocyte-rich large B-cell lymphoma—clinical features

Patient	1 CR	2 BE	3 SM
Age	70	59	61
Gender	F	M	F
Symptoms	Weight loss	Fever, weight loss, night sweats	Fever, weight loss pruritus
Signs	Splenomegaly	Splenomegaly	Splenomegaly
Laboratory	Pancytopenia, hemolytic anemia	Anemia	Anemia, hypoglobulinemia
Prior therapy	Prednisone	Prednisone	Prednisone
Dosage	60 mg/day	60 mg/day	40 mg/day
Duration	6 months	Several months	3 months
Indication	Hemolytic anemia	F.U.O.	Dermatitis
Medical history	Asthma	Obesity, diabetes, heavy smoker	Obesity, diabetes, hepatitis B
Preliminary diagnosis	Splenic micronodular lymphoma	T-cell-rich large B-cell lymphoma	Lymphoma
Treatment	R-CHOP X 6	R-CHOP X 6	R-CHOP X 6
Follow-up	Complete remission	MZBCL of right lacrimal gland	Complete remission

and 2), Hodgkin lymphoma, peripheral T-cell lymphoma (case 3), granulomas reactive to and masking a malignant lymphoma (case 1), and nodular lymphocyte-predominant Hodgkin lymphoma (case 2). However, in establishing the diagnosis of splenic micronodular T-cell/histiocyte-rich large B-cell lymphoma, we were influenced by the similarity of the microscopic nodules to T-cell/histiocyte-rich large B-cell lymphoma as it presents in lymph nodes. We may have been biased by the SMTHLBCL case that we reported several months ago.

Patient 2 developed marginal B-cell lymphoma of the right lacrimal gland 7 years after the splenic lymphoma. The three patients are in complete remission from 12 to 36 months following last evidence of lymphoma.

Discussion

Splenic micronodular T-cell/histiocyte rich large B-cell lymphoma has rarely been described. In fact, the diagnosis is a very difficult one to make and several conditions have to be excluded first. Follicular lymphoma has rarely involved the spleen in the absence of nodal disease. Moreover, bone marrow involvement by SMTHLBCL has been diagnosed before as follicular lymphoma [10].

Granulomatous inflammation of the spleen should also be considered and is difficult to rule out. The microscopic nodules, in contrast to granulomas, show a morphologic and immunophenotypic composition similar to that of T-cell/histiocyte-rich large B-cell lymphomas. The presence of large CD30-positive lymphoid cells, small T cells, and eosinophils should suggest the diagnosis of Hodgkin lymphoma, but a micronodular pattern with uniformly large CD20-positive B cells, even though few in number, should exclude this lymphoma. Involvement of the spleen by a T-cell lymphoma is usually marked by extensive necrosis and an admixture of lymphoid cells of all sizes. Nodular lymphocyte predominant Hodgkin lymphoma rarely presents with isolated involvement of the spleen [1, 10].

Difficult as it may be to diagnose, it seems that prior treatment with corticosteroids renders the diagnosis of SMTHLBCL even more remote. Such preliminary therapy is given to patients with conditions such as hemolytic anemia, idiopathic thrombocytopenic purpura, dermatoses, and autoimmune diseases [6, 7].

It is of note that although few patients with SMTHLBCL have been described to date, none are reported to have received pretreatment with corticosteroids. Variation in the appearance of the microscopic nodules is marked in our patients, from well-developed microgranuloma-like nodules to more cellular nodules with predominant small T cells and at times fibrosed nodules. These changes may reflect the dose and duration of the prior corticosteroid therapy.

It is possible that in several of the 40 or so cases of SMTHLBCL that have been identified to date, prior corticosteroid treatment was administered but unreported [10]. This may have contributed to the complexity of the diagnostic approach. Is it possible that the SMTHLBCL variant itself is the consequence of corticosteroid treatment in patients with an unrelated lymphoma entity or a benign lesion?

Glucocorticoids are known for their marked effect on a variety of mammalian cells. These hormones modify both cellular metabolism and gene expression and show a cytotoxic effect on some cell types, most markedly on lymphocytes [11]. Corticosteroids have been shown to cause apoptosis in most nucleated cells of the hemolymphatic system: thymocytes [12], T lymphocytes [13], B lymphocytes [14], monocytes, and macrophages [15].

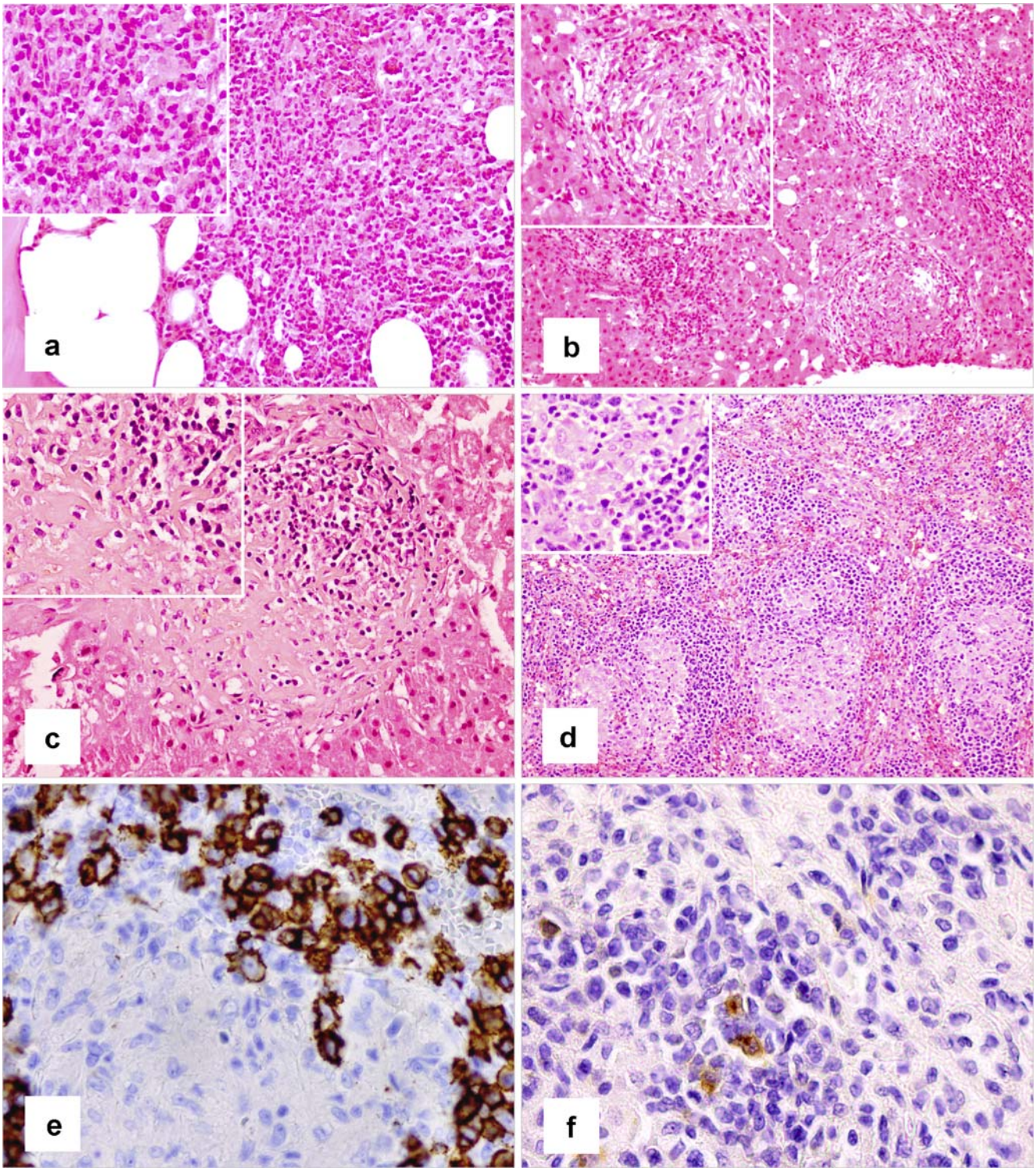

Fig. 1 **a** Micronodular involvement of bone marrow by tumor (H & E, ×240). The presence of a mixed population, including small and larger lymphoid cells is seen (*inset*). **b** Three microscopic tumor nodules in liver biopsy of case2 (H & E, ×240). The *inset* shows the margin of a tumor nodule. **c** Predominantly fibrosed nodule in second liver biopsy of case2 (H & E, ×310). The fibrosis is emphasized (*inset*). **d** Case1, section of spleen—several micronodules with predominant epithelioid cells (H & E, ×240). In addition, large lymphoid cells (see *inset*). **e** Large CD20-positive cells in splenic nodule (Immunoperoxidase with Diaminobezidine substrate, ×360). **f** Large CD30-positive cells in splenic microscopic nodule (Immunoperoxidase with Diaminobenzidine substrate, ×360)

When, however, T lymphocytes over-expressed the Bcl-2 oncogene, the glucocorticoids inhibit apoptosis [16]. As a consequence of this therapy, the lesions are expected to present reduced numbers of these cells.

In this context, one should note the association between immune suppression and the subsequent development of lymphomas. Corticosteroids are notable for their immune suppressive effect. The negative results both with LMP1 immunostains and with EBER RNA ISH do not support such an occurrence in our cases, as such lymphomas are most often EBV-associated. Knowledge of the effect of corticosteroids on the lymphoreticular system, as a most important component of the immune system, and its neoplasms, is at best incomplete [17]. Corticosteroids are an integral part of the CHOP regimen; however, remission may be obtained with corticosteroids alone, and may even be sustained.

It seems that malignant lymphomas of the central nervous system are more prone than other lymphomas to the masking effect of prior corticosteroids [18, 19]. An extensive search of the effect of prior corticosteroid therapy in lymphomas in general did not disclose further data.

The present cases were selected from a larger cohort of lymphomas that were diagnosed following steroid therapy. This expanded study is pending and is the subject of a future publication.

The splenic pathology that may precede the corticosteroid effect would therefore be richer in T and B cells and in histiocytes, and may well be of the common brand of THRLBCL. The unknown component, though critical, is the micronodular pattern and should not be a priori consequence of corticosteroids. Thus, although it is tempting to relate the occurrence of SMTHLBCL to this iatrogenic effect, this is not probable.

We eventually reached the diagnosis of SMTHLBCL because we had been made aware of this lymphoma variant following our publication of a single case report of patient 3 (S.M.). In this report, we had missed the significance of the prebiopsy corticosteroid treatment [10].

Although the primary diagnosis of SMTHLBCL is extremely difficult by itself, the use of corticosteroids in the reported cases may have postponed establishment of the diagnosis by supporting alternative diagnoses. Moreover, it would have complicated the diagnosis by modifying the size and composition of the microscopic nodules.

In conclusion, we have described three patients who received a preliminary treatment with corticosteroids for different conditions and who eventually, with differing difficulties, were diagnosed as having splenic micronodular T-cell/histiocyte-rich large B-cell lymphoma. We have been unable to identify a case of SMTHLBCL in our registry that was not related with corticosteroid treatment.

Conflict of interest statement We declare that we have no conflict of interest.

References

1. Dogan A, Burke JS, Goteri G, Stitson RNM, Wotherspoon AC, Isaacson PG (2003) Micronodular T-cell/histiocyte-rich large B-cell lymphoma of the spleen. Histology, immunophenotype and differential diagnosis. Am J Surg Pathol 27:903–911
2. Mollejo M, Algara P, Mateo MS, Menargez J, Pascual E, Fresno MF, Camacho FI, Piris MA (2003) Large B-cell lymphoma presenting in the spleen. Identification of different clinicopathological conditions. Am J Surg Pathol 27:895–902
3. Braylan RC, Long JC, Jaffe ES, Greco FA, Orr SL, Berard CW (1977) Malignant lymphoma obscured by concomitant extensive epithelioid granulomas: report of three cases with similar clinicopathologic features. Cancer 39:1146–1155
4. Dunphy CH, Panella MJ, Grosso LE (2000) Low grade B-cell lymphoma and concomitant extensive sarcoid-like granulomas: a case report and review of the literature. Arch Pathol Lab Med 124:152–156
5. Li S, Mann KP, Holden JT (2004) T-cell-rich B-cell lymphoma presenting in the spleen: a clinicopathologic analysis of three cases. Int J Surg Pathol 12:31–37
6. Borenstein SH, Gerstle T, Thorner P, Filler RM (2000) The effect of pre-biopsy corticosteroid treatment on the diagnosis of mediastinal lymphoma. J Pediatr Surg 35:973–976
7. Magrath IT (1989) Malignant non-Hodgkin's lymphoma. In: Pizzo PA, Poplack DG (eds) Principles and practice of pediatric oncology. Lippincott, Philadelphia, pp 442–443
8. Lowenthal R, Jestrimsk R (1986) Corticosteroid drugs: their role in oncological practice. Med J Aust 144:81–84
9. Duzova A, Cetin M, Gumruk F, Yetgin S (2001) Acute tumour lysis syndrome following a single dose corticosteroid in children with acute lymphoblastic leukaemia. Eur J Haematol 66:404–407
10. Kan E, Levy I, Benharroch D (2008) Splenic micronodular T-cell/histiocyte-rich large B-cell lymphoma. Ann Diagn Pathol 12:290–292
11. Wood AC, Elvin P, Hickman JA (1995) Induction of apoptosis by anti-cancer drugs with disparate modes of action: kinetics of cell death and changes in *c-myc* expression. Br J Cancer 71:937–941
12. Pruschy M, Shi YQ, Crompton NE, Steinbach J, Aquzzi A, Glanzmann C (1997) The proto-oncogene c-fos mediates apoptosis in murine T-lymphocytes induced by ionizing radiation and dexamethasone. Biochem Biophys Res Commun 241:519–524
13. Herold MJ, McPherson KG, Reichardt HM (2006) Glucocorticoids in T-cell apoptosis and function. Cell Mol Life Sci 63:60–72
14. Andreau K, Lemaire C, Souvannavong V, Adam A (1998) Induction of apoptosis by dexamethasone in the B-cell lineage. Immunopharmacology 40:67–76
15. Shmidt M, Pauels HG, Lugering N, Lugering A, Domschke W, Kwcharzik T (1999) Glucocorticoids induce apoptosis in human monocytes: potential role of IL-1 beta. J Immunol 163:3484–3490
16. Huang ST, Cidlowski JA (1999) Glucocorticoids inhibit serum depletion-induced apoptosis in T-lymphocytes expressing Bcl-2. FASEB J 13:467–476
17. Lennert K (1975) Letter: corticosteroid effect in lymphogranulomatosis. Dtsch Med Wochenschr 100:2183
18. Choi YL, Suh YL, Kim D, Ko YH, Co S, Lee JI (2006) Malignant lymphoma of the central nervous system: difficult histologic diagnosis after glucocorticoid therapy prior to biopsy. Clin Neuropathol 25:29–36
19. Geppert M, Ostertag CB, Seitz G, Kiessling M (1990) Glucocorticoid therapy obscures the diagnosis of cerebral lymphoma. Acta Neuropathol 80:629–634

Virchows Arch (2009) 455:343–351
DOI 10.1007/s00428-009-0829-4

ORIGINAL ARTICLE

CpG island hypermethylation and repetitive DNA hypomethylation in premalignant lesion of extrahepatic cholangiocarcinoma

Baek-hui Kim · Nam-Yun Cho · So Hyun Shin · Hyeong-Ju Kwon · Ja June Jang · Gyeong Hoon Kang

Received: 16 April 2009 / Revised: 5 August 2009 / Accepted: 24 August 2009 / Published online: 10 September 2009

Abstract Biliary intraepithelial neoplasia (BilIN) is the premalignant lesion of extrahepatic cholangiocarcinoma (EHC), and there are no published data regarding epigenetic changes throughout disease progression from normal biliary epithelia to BilIN to EHC. The objective of this study was to identify the occurrence of CpG island hypermethylation and repetitive DNA hypomethylation in BilIN. A total of 50 EHCs, 31 BilINs, and 31 normal cystic duct samples were analyzed for their methylation status in seven genes and two repetitive DNA elements. The number of methylated genes increased with disease progression (normal bile duct, 0.6; BilIN, 2.0; EHC, 3.6; $P<0.001$). The methylation level of examined genes was significantly higher in BilIN than in normal samples (*TMEFF2*, *HOXA1*, *NEUROG1*, and *RUNX3*, $P<0.05$) and in EHC than in BilIN samples (*TMEFF2*, *HOXA1*, *NEUROG1*, *RUNX3*, *RASSF1A*, and *APC*, $P<0.05$). Long interspersed nucleotide element-1 (*LINE-1*) and juxtacentromeric satellite 2 (*SAT2*) methylation levels were markedly lower in EHC than in normal duct and BilIN samples, and BilIN samples showed a decrease of *SAT2* methylation levels but no decrease of *LINE-1* methylation levels compared to normal samples. These findings suggest that most of cancer-specific CpG island hypermethylation occur in the stage of BilIN and that CpG island hypermethylation seems to occur earlier than repetitive DNA element hypomethylation.

Keywords Biliary intraepithelial neoplasia · Cholangiocarcinoma · CpG island · DNA hypermethylation · DNA hypomethylation

Electronic supplementary material Supplementary material is available in the online version of this article at http://dx.doi.org/10.1007/s00428-009-0829-4 and is accessible to authorized users.

B.-h. Kim
Department of Pathology, Korea University Medical School, Seoul, South Korea

N.-Y. Cho · S. H. Shin · G. H. Kang
Laboratory of Epigenetics, Cancer Research Institute and BK21 2nd Stage, College of Medicine, Seoul National University, Seoul, South Korea

H.-J. Kwon · J. J. Jang · G. H. Kang (✉)
Department of Pathology, College of Medicine, Seoul National University, 28 Yongon-dong, Jongno-gu, Seoul 110-744, South Korea
e-mail: ghkang@snu.ac.kr

Introduction

Extrahepatic cholangiocarcinoma (EHC) is an uncommon malignant neoplasm that arises from the extrahepatic bile ducts. The pathogenesis of EHC is not fully understood, but it has been proposed that EHC develops through a multistep carcinogenesis process and that EHC is preceded by a precursor lesion, biliary intraepithelial neoplasia (BilIN) [1]. BilINs are found adjacent to carcinoma lesions in 20–80% of EHCs, supporting the hypothesis that BilIN is a premalignant lesion of invasive carcinoma [2–4]. The lack of standard classification, relatively low incidence, difficulty in approach to the anatomic location, and the small tissue sample size of BilIN make it hard to investigate the BilIN–EHC sequence [5]. For this reason, few studies concerning BilIN have been reported, even though certain molecular alterations, including *KRAS* and *p53* mutations, have been revealed in EHC [6, 7]. However, there have been some studies regarding morphologic and molecular features of premalignant lesions arising from intrahepatic bile ducts [8–11]. Results of these studies support that BilIN of large intrahepatic bile duct is also a precursor lesion of intrahepatic cholangiocarcinoma.

In the traditional concept of molecular carcinogenesis, genetic alterations play a pivotal role in cancer progression. Recent advancements in epigenetic studies have changed this concept, however, and much data support the contribution of epigenetics to tumorigenesis [12]. Aberrant DNA hypermethylation and hypomethylation are the most consistently observed and widely studied epigenetic events in human cancers. Hypermethylation of promoter CpG islands is closely related to silencing of tumor suppressor genes, which is a common finding in human cancers regardless of tissue types [13]. However, various tissue types of human cancers show distinct methylation profiles that differ from those of normal tissues [13]. On the other hand, genome-wide DNA hypomethylation causes chromosomal instability and is believed to play an important role in cancer progression [14, 15]. Measurements of methylation of repetitive DNA sequences, including long interspersed nucleotide element-1 (*LINE-1*) and juxtacentromeric satellite 2 (*SAT2*), are reproducible and correlate well with genome-wide methylation levels [16]. In the multistep carcinogenesis model, genetic changes as well as epigenetic changes accumulate with tumor progression [12, 17–20]. In this regard, a stepwise increase in promoter CpG island methylation and a stepwise decrease in genome-wide methylation levels are expected in the normal bile duct–BilIN–EHC sequence. Little is known, however, about DNA methylation changes in BilIN of the extrahepatic bile duct.

We previously determined methylation profiles for 24 CpG island loci in EHCs using methylation-specific polymerase chain reaction (PCR; MSP) and found that methylation frequencies of seven individual CpG island loci (*HOXA1*, *TMEFF2*, *NEUROG1*, *CDH1*, *RUNX3*, *RASSF1A*, and *APC*) were >23% in EHC [21]. Their methylation frequencies were significantly higher in EHCs than in normal bile ducts, indicative of cancer-related hypermethylation. In the present study, we analyzed BilIN and EHC samples for their methylation status in the seven CpG island loci using real-time PCR-based quantitative methylation analysis (MethyLight technology) to determine whether promoter CpG island hypermethylation is an early event in multistep carcinogenesis of EHC. In addition, we examined whether repetitive DNA hypomethylation occurs in EHC and BilIN.

Materials and methods

Patients and tissue samples

A total of 112 formalin-fixed, paraffin-embedded archival tissue samples (50 EHC, 31 BilIN, and 31 cholecystitis) were previously obtained from 84 patients (53 EHC and 31 cholecystitis) who underwent surgical resection for EHC or chronic cholecystitis at the Seoul National University Hospital, Seoul, South Korea between January 2001 and December 2004. From the surgical specimens of EHC patients (n=53), we obtained 31 BilIN samples, 28 of which were matched samples of EHC and BilIN. The remaining three BilIN samples were obtained from three EHC cases in which archival tissue blocks of invasive cancers were not available for the present study. All samples of EHC and BilIN were obtained from extrahepatic biliary tree (distal and proximal common bile ducts, common hepatic duct, confluence of hepatic duct, and cystic duct), and gallbladder lesions were not included in this study (Table 1 and Supplemental Table 1). We classified BilIN into two grades (low and high) instead of three grades (BilIN-1, BilIN-2, and BilIN-3), and low-grade BilIN corresponds to BilIN-1, and high-grade BilIN corresponds to BilIN-2 and BilIN-3 of the consensus proposal [5]. We selected high-grade BilIN more than 1 cm away from invasive carcinoma to eliminate potential contamination of carcinoma cells. Loss of cellular polarity, nuclear pseudostratification reaching upper third of cytoplasm, and nuclear changes including enlargement, hyperchromasia, and irregular nuclear membrane were used as diagnostic criteria for high-grade BilIN. Dysplastic lesions showing abrupt severe nuclear atypia or nuclear atypia equivalent to invasive carcinoma were excluded to eliminate the possibility of sampling cells from intraepithelial or lateral spreading of adenocarcinoma. We also excluded low-grade BilIN from the study because of the ambiguity of diagnostic criteria for hyperplastic or reactive epithelial lesions and low-grade BilINs. We considered dysplastic lesions with basally located nuclei, mild nuclear atypia, and relatively uniform nuclei as low-grade BilIN [5]. EHC samples were obtained from invasive tumor portions of surgical specimens. Cystic duct portions from cholecystectomy specimens were used as surrogates for normal bile duct samples, which are usually denuded of their epithelium in the surgical specimens submitted for histologic examination. Two pathologists reviewed all slides of surgical specimens and pathologic stages, and tumor grade was determined using the latest criteria of the cancer staging manual of the American Joint Committee on Cancer and World Health Organization classification system [22, 23]. This study was approved by the Institutional Review Board of Seoul National University Hospital.

DNA extraction and bisulfite modification

Five serial sections (8 μm thick) from each paraffin block sample were stained with hematoxylin and eosin and were examined microscopically. Regions consisting of more than 70% neoplastic cells were marked and manually dissected

Table 1 Locations and histologic features of extrahepatic cholangiocarcinoma and biliary intraepithelial neoplasia

	EHC	BilIN
Total number	50	31
Location		
Distal CBD	26	7
Proximal CBD	12	10
CHD	3	10
Hepatic duct confluence	9	3
Cystic duct	0	1
Differentiation of invasive tumor		
Well differentiated	16	
Moderately differentiated	28	
Poorly differentiated	6	
Pattern of BilIN		
Adenoma like with glandular extension		16
Tufting		9
Micropapillary		6
Background biliary lesions		
Gallbladder stone	2[a]	2[a]
Choledocal cyst	1[a]	1[a]
No identified background lesions	47	28

EHC extrahepatic cholangiocarcinoma, *BilIN* biliary intraepithelial neoplasia, *CBD* common bile duct, *CHD* common hepatic duct

[a] These patients are both included in extrahepatic cholangiocarcinoma and biliary intraepithelial neoplasia groups

and placed in microtubes. The collected tissue samples were digested in lysis buffer containing proteinase K. Bisulfite modification of the digested tissue samples (18 μl) was performed using the EZ DNA methylation kit (Zymo Research Co., Orange, CA, USA) according to the manufacturer's protocol.

DNA hypermethylation assay

We quantified hypermethylation using MethyLight technology. Based on a previous study, we selected seven promoter CpG island loci that were methylated in EHC at frequencies significantly higher than those in normal bile ducts [21]. Primer and probe sequences are listed in Table 2. PCR was performed in 30 μl containing 0.2 mM deoxyribonucleotide triphosphates, 0.3 μM forward and reverse primers, 0.05 μM probe, 3.5 mM $MgCl_2$, 0.05% gelatin, 0.01% Tween-20, 1× PCR buffer, and 0.5 U of AmpliTaq Gold polymerase. The amplification conditions for all primers consisted of 95°C for 10 min, followed by 50 cycles of 95°C for 20 s and 59°C for 40 s. *ALU* repeats were used as an internal reference to normalize input DNA and to generate a standard curve. Bisulfite-modified placental genomic DNA treated with M.*Sss*I was used as a control reaction for the *ALU* repeat and selected promoter CpG loci. The percentage of methylated reference (PMR) of each genetic locus was calculated as 100 times the *GENE*/*ALU* methylation ratio of each sample divided by the *GENE*/*ALU* methylation ratio of reference DNA treated with M.*Sss*I. The methylation status of each sample was determined as positive when PMR >4, which cutoff value was based on validated data [24].

DNA hypomethylation assay

Methylation levels of repetitive DNA elements, including *LINE-1* and *SAT2*, correlate with global DNA methylation levels [25, 26]. *LINE-1* methylation level was measured using the combined bisulfite restriction analysis (COBRA) technique as described [20]. *LINE-1* sequences in bisulfite-modified DNA were amplified, and the PCR products were digested with *Tas*I and *Taq*I to digest unmethylated and methylated *LINE-1* alleles, respectively. Then, the digested DNA fragments were separated using polyacrylamide gel electrophoresis. The methylation level of *LINE-1* was calculated as the intensity of *Taq*I-digested band divided by the sum of intensities of *Taq*I- and *Tas*I-digested bands. Measurement of band intensity was performed with ImageJ software (http://rsb.info.nih.gov/ij). We measured methylation of *SAT2* using MethyLight technology as described [16]. Primers and probe for *SAT2* are shown in Table 2.

Statistical analysis

The two-tailed Student's *t* test and one-way analysis of variance (ANOVA) test were used to evaluate the significance of the differences observed between two means and among three or more means, respectively. All statistical analyses were performed using SPSS software (SPSS version 12.0, Chicago, IL, USA). *P* values less than 0.05 were considered statistically significant.

Results

Histologic features of EHCs and BilINs

We analyzed histologic features of EHCs and BilINs. Gross morphology and histologic differentiation of invasive adenocarcinoma were determined according to World Health Organization classification system. Among 53 EHC patients, background biliary disease was noted in three patients (two gallbladder stone and one choledochal cyst), and *Clonorchis sinensis* infection was not identified in serologic, histologic, and cytopathologic examination. Data are shown in Table 1 and Supplemental Table 1.

Table 2 MethyLight primers and probes

Gene	Primer and probe sequences	AT (°C)	Size (bp)
APC	F: GAACCAAAACGCTCCCCAT R: TTATATGTCGGTTACGTGCGTTTATAT	59	74
	Pr: 6FAM-CCCGTCGAAAACCCGCCGATTA-TAMRA		
CDH1	F: AGGGTTATCGCGTTTATGCG R: TTCACCTACCGACCACAACCA	59	96
	Pr: 6FAM-ACTAACGACCCGCCCACCCGA-TAMRA		
HOXA1	F: TTGTTTATTAGGAAGCGGTCGTC R: TCGAACCATAAAATTACAACTTTCCA	59	83
	Pr: 6FAM-TCGTACGCGATCAACGCCAACAATTA-TAMRA		
HPP1/TMEFF2	F: CGACGAGGAGGTGTAAGGATG R: CAACGCCTAACGAACGAACC	59	73
	Pr: 6FAM-TATAACTTCCGCGACCGCCTCCTCCT-TAMRA		
NEUROG1	F: CGTGTAGCGTTCGGGTATTTGTA R: CGATAATTACGAACACACTCCGAAT	59	88
	Pr: 6FAM-CGATAACGACCTCCCGCGAACATAAA-TAMRA		
RASSF1A	F: ATTGAGTTGCGGGAGTTGGT R: ACACGCTCCAACCGAATACG	59	65
	Pr: 6FAM-CCCTTCCCAACGCGCCCA-TAMRA		
RUNX3	F: CGTTCGATGGTGGACGTGT R: GACGAACAACGTCTTATTACAACGC	59	117
	Pr: 6FAM-CGCACGAACTCGCCTACGTAATCCG-TAMRA		
SAT2	F: TGGAATGGAATTAATATTTAACGGAAAA R: CCATTCGAATCCATTCGATAATTCT	59	79
	Pr: 6FAM-CGATTCCATTCGATAATTCCGTTT-TAMRA		

AT annealing temperature, *F* forward primer, *R* reverse primer, *Pr* probe

Histologic patterns of BilINs are divided into three groups (adenoma like with glandular extension, tufting, and micropapillary pattern; Fig. 1). Multiple patterns were noted when remaining epithelium of BilINs was sufficiently large. When multiple patterns are present in BilIN, most prominent pattern was recorded (Table 1 and Supplemental Table 1).

Methylation profiles of seven CpG island loci in normal, BilIN, and EHC tissue samples

We performed MethyLight analysis of seven CpG island loci on 112 DNA samples from normal cystic duct (n=31), BilIN (n=31), and EHC (n=50) tissue samples. PMR values for each sample and each locus were calculated using MethyLight reaction data (Fig. 2). The DNA methylation frequencies (PMR≥4) for each gene were calculated in normal cystic duct, BilIN, and EHC tissue samples. The number of methylated CpG island loci was 0.6, 2.0, and 3.6 in normal cystic duct, BilIN, and EHC tissue samples, respectively (P<0.001, ANOVA test; Fig. 3a). When methylation levels of individual CpG island loci were compared among normal cystic duct, BilIN, and EHC samples (Fig. 4a), *TMEFF2*, *HOXA1*, *NEUROG1*, and *RUNX3* were methylated in BilIN samples at levels significantly higher than those in normal cystic duct samples (P<0.05, Student's t test). The methylation levels of six CpG island loci (*CDH1* was the exception) were significantly higher in EHC samples than in BilIN samples (P<0.05, Student's t test).

The above-mentioned six CpG island loci showed methylation frequencies >20% in EHC tissue samples with *HOXA1* and *TMEFF2* methylation frequencies >90%. Five genes were not methylated or rarely methylated (methylation frequency <4%) in normal bile duct samples except for *TMEFF2*, for which the methylation frequency was >50% in normal bile duct samples. Four genes exhibited >14% methylation frequencies in BilIN samples. Based on methylation frequencies of these six genes in three tissue types, three different groups of genes were recognizable according to their methylation behaviors during multistep carcinogenesis (Fig. 4b): (1) genes methylated in a non-neoplastic stage, including *TMEFF2*; (2) genes methylated in an early neoplastic stage, including *HOXA1*, *NEUROG1*, and *RUNX3*; and (3) genes methylated in a late neoplastic stage, including *RASSF1A* and *APC*.

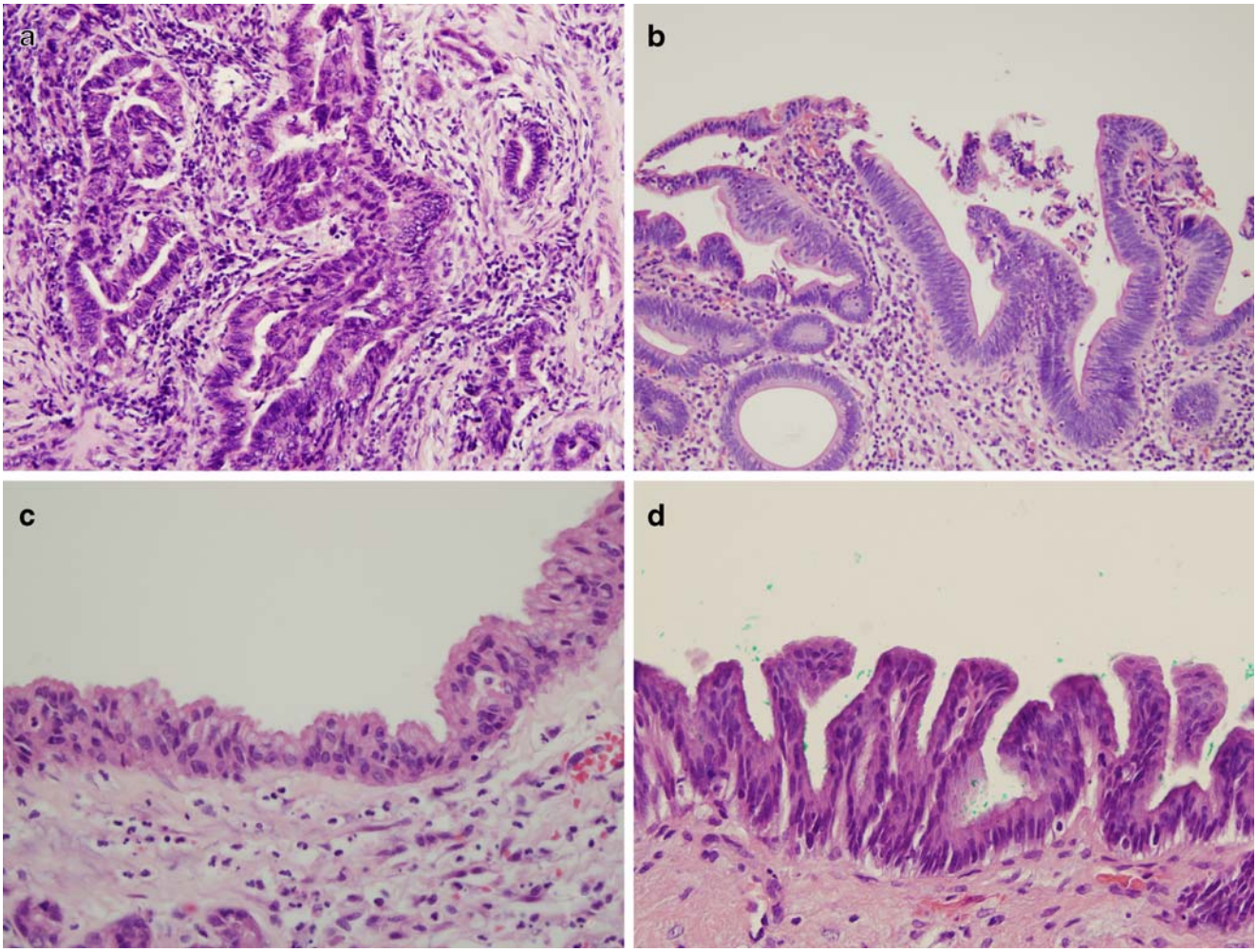

Fig. 1 Histologic pictures of extrahepatic cholangiocarcinoma and biliary intraepithelial neoplasia. **a** Invasive portion of EHC. **b**–**d** BilINs with adenoma like with glandular extension, tufting, and micropapillary pattern, respectively (hematoxylin and eosin; **a**, **b** ×200; **c**, **d** ×400)

Hypomethylation of repetitive DNA elements in biliary intraepithelial neoplasia and EHC tissue samples

We performed the COBRA assay to determine *LINE-1* methylation levels and the MethyLight assay to determine *SAT2* methylation levels using 112 DNA samples from normal cystic duct (n=31), BilIN (n=31), and EHC (n=50) tissue samples. When compared with methylation levels of *LINE-1* and *SAT2* in normal cystic duct samples (Fig. 3b, c), the methylation levels of *LINE-1* did not change in BilIN but sharply declined in EHC samples, whereas methylation levels of *SAT2* decreased in BilIN and further decreased in EHC samples.

Discussion

Aberrant DNA methylation in human cancer cells is characterized by both focal hypermethylation of gene-associated CpG islands and generalized genome-wide reduction in 5-methylcytosine, which are found in virtually all tissue types of human cancers [27–29]. Subsets of CpG island loci which are hypermethylated in a cancer-specific manner have been demonstrated to be hypermethylated in premalignant or in situ neoplastic lesions, including colon adenomas [30], gastric adenomas [31], pancreatic intraepithelial neoplasia [32], and prostatic intraepithelial neoplasia [33], although the methylation frequencies or methylation levels at each locus are generally lower in premalignant lesions than in their malignant counterparts. Of the six CpG island loci showing cancer-specific methylation in EHC samples, four loci, *TMEFF2*, *HOXA1*, *NEUROG1*, and *RUNX3*, were found to be methylated in BilIN samples at levels significantly higher than those of normal bile duct samples. These findings suggest that promoter CpG island hypermethylation occurs at an early stage of multistep choledochal carcinogenesis and likely contributes to the development of BilIN or the progression of BilIN to EHC.

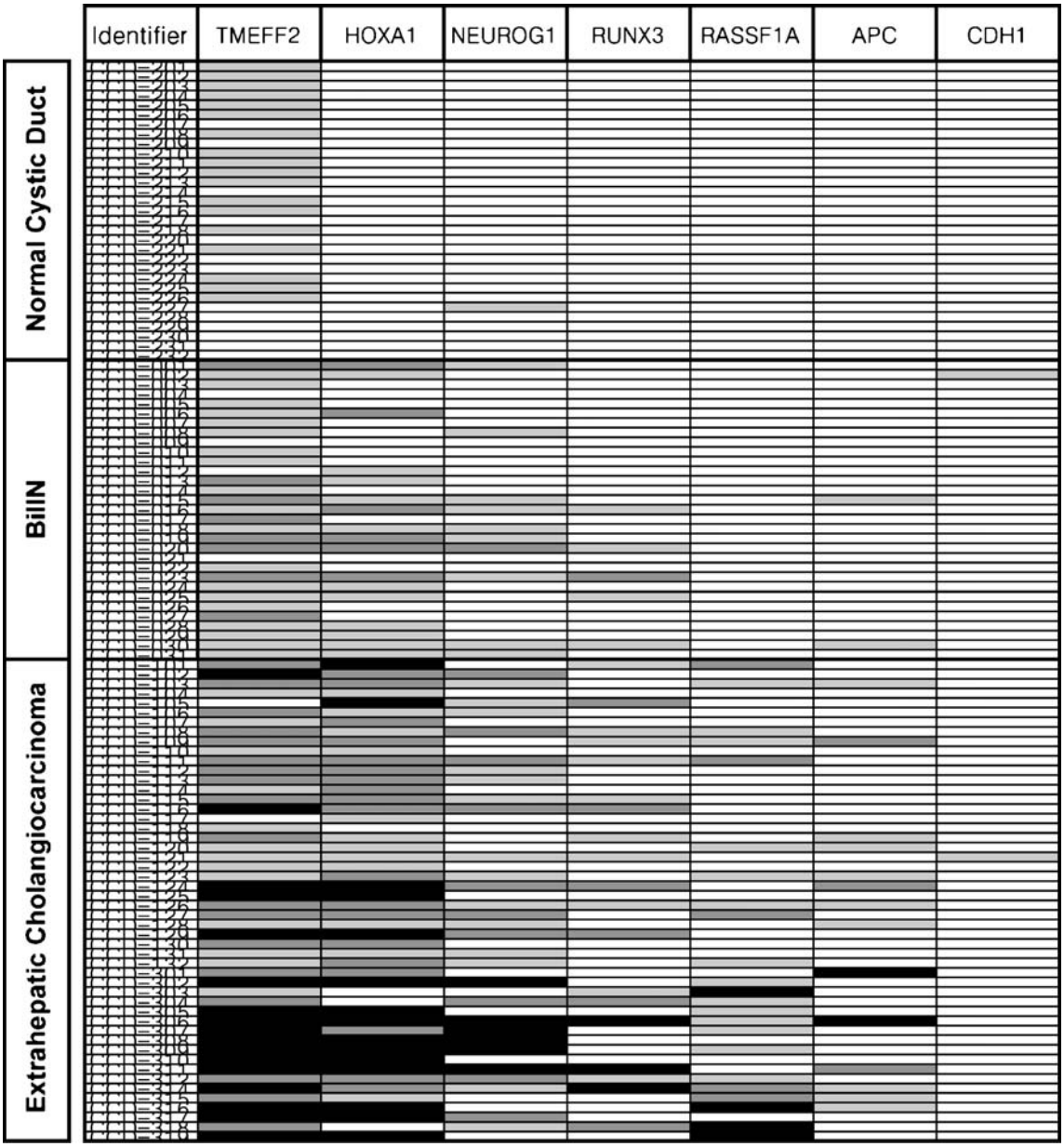

Fig. 2 Map of gene methylation in extrahepatic cholangiocarcinoma, biliary intraepithelial neoplasia, and normal cystic duct tissue samples. *Box color* represents the degree of allele methylation [PMR≥50 (*black*), 20≤PMR<50 (*dark gray*), 4≤PMR<20 (*light gray*)], and *open boxes* represent PMR<4

Repetitive DNA elements, comprising 45% of the genomic DNA, consist of tandem repeats, such as *SAT2*, and interspersed repeats, such as *LINE-1*. The methylation levels of the repetitive DNA elements are closely correlated with 5-methylcytosine content of the genome [16]. In the present study, EHC samples demonstrated hypomethylation of *LINE-1* and *SAT2* compared with normal cystic duct samples, whereas BilIN samples showed decreased methylation levels of *SAT2* but similar methylation levels of *LINE-1* compared with the respective ones of normal cystic duct samples. From our findings, it can be speculated that genomic hypomethylation begins with pericentromeric satellite DNA in the early stages and then involves *LINE-1* on chromosomal arms in a later stage along the multistep process of carcinogenesis. Differential hypomethylation of repetitive DNA elements also has been found in cancers of other tissue types, including stomach and liver, during disease progression [34].

When comparing the methylation frequencies of the seven CpG island loci between our previous study [34] and the present study, the methylation frequencies of six loci (*TMEFF2*, *HOXA1*, *NEUROG1*, *RUNX3*, *RASSF1A*, and

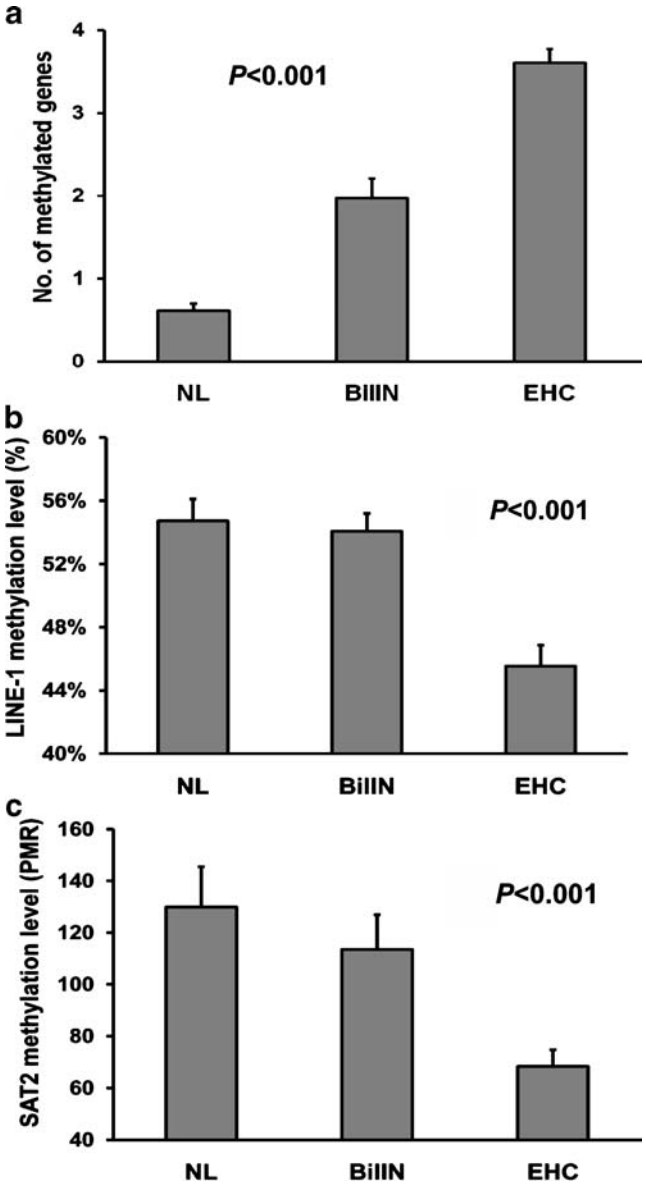

Fig. 3 Number of methylated genes of the seven loci tested (**a**) and *LINE-1* (**b**) and *SAT2* (**c**) methylation levels in extrahepatic cholangiocarcinoma (*EHC*), biliary intraepithelial neoplasia (*BilIN*), and normal cystic duct (*NL*) tissue samples. Data represent means± standard error of the mean (*error bars*). The significance (*P*) after ANOVA analysis is shown

APC) were similar, but the methylation frequency of *CDH1* was markedly lower in the present study. This discrepancy of *CDH1* methylation frequency might be attributable to the inadequacy of the oligonucleotide primers used in our previous *CDH1* MSP assay. The oligonucleotide primers contain three CpG sites (two forward primers and one reverse primer) that do not fulfill the minimal requirements for designing MSP primers recommended by the Herman group [35, 36]. Thus, *CDH1* MSP might give rise to false positives. Alternatively, the heterogeneity of methylated DNA alleles with respect to the methylation status of each CpG site within a given segment may differ. Notably, bisulfite genomic sequencing has shown that different alleles of *CDH1* are differentially methylated at individual CpG sites [37]. Thus, *CDH1* MSP may detect DNA alleles having differentially methylated CpG sites within the segment between the forward and reverse primer sequences. In contrast, *CDH1* MethyLight detected near-perfect methylated DNA alleles because the primers and probe for *CDH1* MethyLight targeted seven CpG sites within a 96-bp DNA sequence. Thus, traditional MSP can detect both partially methylated alleles as well as the highly methylated alleles detected by MethyLight technology, which might explain the discrepancy in *CDH1* methylation frequencies produced by MSP and the MethyLight assay.

EHCs generally have a low rate of preoperative histologic or cytologic diagnosis [38], and the poor prognosis of EHC patients is related to the delayed diagnosis of the disease. Because of technical difficulties in EHC tissue biopsy via choledochoscopy, several inves-

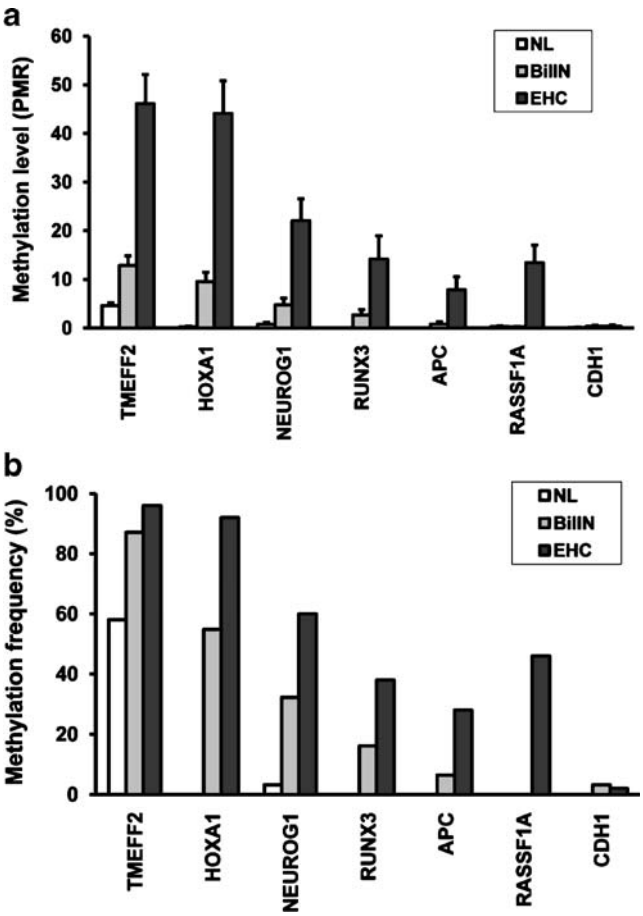

Fig. 4 Comparison of the methylation levels of seven CpG island loci among extrahepatic cholangiocarcinoma (*EHC*), biliary intraepithelial neoplasia (*BilIN*), and normal cystic duct (*NL*) tissue samples (**a**). The means and the standard errors (*error bars*) are shown. **b** Comparison of the methylation frequency of the individual CpG island loci among EHC, BilIN, and NL tissue samples

tigators have attempted to develop molecular markers to detect EHC in bile juice. To date, however, no sensitive/specific molecular markers for EHC have been identified [39]. Still, promising markers include DNA methylation marks, which are chemically stable and relatively easy to detect. In our present and previous studies, *HOXA1* was hypermethylated in more than 95% of EHC tissue samples but never hypermethylated in normal bile duct samples. Thus, *HOXA1* methylation looks promising as a tumor biomarker in bile juice for the detection of biliary epithelial tumors.

In conclusion, using quantitative methylation analysis technologies, we have demonstrated that promoter CpG island hypermethylation occurs not only in malignant tumors of biliary epithelia but also in premalignant lesions. Promoter CpG island hypermethylation appears to precede repetitive DNA hypomethylation. Lastly, *HOXA1* hypermethylation may constitute a highly sensitive and specific marker for biliary epithelial neoplasms.

Acknowledgments This study was supported by a grant from the Cancer Research Institute Research Fund, a grant from the Seoul National University Hospital Research Fund (03-2008-020-0), and the Korea Research Foundation Grant (MOEHRD; KRF-2008-041-E00099).

Conflict of interest The authors declare that they have no conflict of interest.

References

1. Fleming KA, Boberg KM, Glaumann H et al (2001) Biliary dysplasia as a marker of cholangiocarcinoma in primary sclerosing cholangitis. J Hepatol 34:360–365
2. Laitio M (1983) Carcinoma of extrahepatic bile ducts. A histopathologic study. Pathol Res Pract 178:67–72
3. Kim JPY, Kim H (1998) Immunohistochemical characteristics of biliary tract carcinoma and its precancerous lesions. Korean J Pathol 32:985–992
4. Suzuki M, Takahashi T, Ouchi K et al (1989) The development and extension of hepatohilar bile duct carcinoma. A three-dimensional tumor mapping in the intrahepatic biliary tree visualized with the aid of a graphics computer system. Cancer 64:658–666
5. Zen Y, Adsay NV, Bardadin K et al (2007) Biliary intraepithelial neoplasia: an international interobserver agreement study and proposal for diagnostic criteria. Mod Pathol 20:701–709
6. Scarpa A, Zamboni G, Achille A et al (1994) ras-family gene mutations in neoplasia of the ampulla of Vater. Int J Cancer 59:39–42
7. Suto T, Habano W, Sugai T et al (2000) Aberrations of the K-ras, p53, and APC genes in extrahepatic bile duct cancer. J Surg Oncol 73:158–163
8. Nakanishi Y, Zen Y, Kondo S et al (2008) Expression of cell cycle-related molecules in biliary premalignant lesions: biliary intraepithelial neoplasia and biliary intraductal papillary neoplasm. Hum Pathol 39:1153–1161
9. Sasaki M, Yamaguchi J, Itatsu K et al (2008) Over-expression of polycomb group protein EZH2 relates to decreased expression of p16 INK4a in cholangiocarcinogenesis in hepatolithiasis. J Pathol 215:175–183
10. Zen Y, Aishima S, Ajioka Y et al (2005) Proposal of histological criteria for intraepithelial atypical/proliferative biliary epithelial lesions of the bile duct in hepatolithiasis with respect to cholangiocarcinoma: preliminary report based on interobserver agreement. Pathol Int 55:180–188
11. Tsuneyama K, Sasaki M, Shimonishi T et al (2004) Expression of MAGE-A3 in intrahepatic cholangiocarcinoma and its precursor lesions. Pathol Int 54:181–186
12. Baylin SB, Herman JG (2000) DNA hypermethylation in tumorigenesis: epigenetics joins genetics. Trends Genet 16:168–174
13. Esteller M, Corn PG, Baylin SB et al (2001) A gene hypermethylation profile of human cancer. Cancer Res 61:3225–3229
14. Gaudet F, Hodgson JG, Eden A et al (2003) Induction of tumors in mice by genomic hypomethylation. Science 300:489–492
15. Ogino S, Kawasaki T, Nosho K et al (2008) LINE-1 hypomethylation is inversely associated with microsatellite instability and CpG island methylator phenotype in colorectal cancer. Int J Cancer 122:2767–2773
16. Weisenberger DJ, Campan M, Long TI et al (2005) Analysis of repetitive element DNA methylation by MethyLight. Nucleic Acids Res 33:6823–6836
17. Isaacs WB, Bova GS, Morton RA et al (1994) Molecular biology of prostate cancer. Semin Oncol 21:514–521
18. Hake SB, Xiao A, Allis CD (2004) Linking the epigenetic 'language' of covalent histone modifications to cancer. Br J Cancer 90:761–769
19. Lee S, Lee HJ, Kim JH et al (2003) Aberrant CpG island hypermethylation along multistep hepatocarcinogenesis. Am J Pathol 163:1371–1378
20. Cho NY, Kim JH, Moon KC et al (2009) Genomic hypomethylation and CpG island hypermethylation in prostatic intraepithelial neoplasm. Virchows Arch 454:17–23
21. Kim BH, Cho NY, Choi M et al (2007) Methylation profiles of multiple CpG island loci in extrahepatic cholangiocarcinoma versus those of intrahepatic cholangiocarcinomas. Arch Pathol Lab Med 131:923–930
22. Greene FL, American Joint Committee on Cancer, American Cancer Society (2002) AJCC cancer staging manual, 6th edn. Springer, New York
23. Aaltonen LA, Hamilton SR, World Health Organization, International Agency for Research on Cancer (2000) Pathology and genetics of tumours of the digestive system. IARC, Lyon
24. Ogino S, Kawasaki T, Brahmandam M et al (2006) Precision and performance characteristics of bisulfite conversion and real-time PCR (MethyLight) for quantitative DNA methylation analysis. J Mol Diagn 8:209–217
25. Chalitchagorn K, Shuangshoti S, Hourpai N et al (2004) Distinctive pattern of LINE-1 methylation level in normal tissues and the association with carcinogenesis. Oncogene 23:8841–8846
26. Eads CA, Danenberg KD, Kawakami K et al (2000) MethyLight: a high-throughput assay to measure DNA methylation. Nucleic Acids Res 28:E32
27. Jones PA, Baylin SB (2002) The fundamental role of epigenetic events in cancer. Nat Rev Genet 3:415–428
28. Feinberg AP, Vogelstein B (1983) Hypomethylation distinguishes genes of some human cancers from their normal counterparts. Nature 301:89–92
29. Gama-Sosa MA, Slagel VA, Trewyn RW et al (1983) The 5-methylcytosine content of DNA from human tumors. Nucleic Acids Res 11:6883–6894
30. Lee S, Hwang KS, Lee HJ et al (2004) Aberrant CpG island hypermethylation of multiple genes in colorectal neoplasia. Lab Invest 84:884–893

31. Kang GH, Lee S, Kim JS et al (2003) Profile of aberrant CpG island methylation along the multistep pathway of gastric carcinogenesis. Lab Invest 83:635–641
32. Sato N, Fukushima N, Hruban RH et al (2008) CpG island methylation profile of pancreatic intraepithelial neoplasia. Mod Pathol 21:238–244
33. Yamanaka M, Watanabe M, Yamada Y et al (2003) Altered methylation of multiple genes in carcinogenesis of the prostate. Int J Cancer 106:382–387
34. Lee HS, Kim BH, Cho NY et al (2009) Prognostic implications of and relationship between CpG island hypermethylation and repetitive DNA hypomethylation in hepatocellular carcinoma. Clin Cancer Res 15:812–820
35. Herman JG, Graff JR, Myohanen S et al (1996) Methylation-specific PCR: a novel PCR assay for methylation status of CpG islands. Proc Natl Acad Sci U S A 93:9821–9826
36. Brandes JC, Carraway H, Herman JG (2007) Optimal primer design using the novel primer design program: MSPprimer provides accurate methylation analysis of the ATM promoter. Oncogene 26:6229–6237
37. Graff JR, Herman JG, Myohanen S et al (1997) Mapping patterns of CpG island methylation in normal and neoplastic cells implicates both upstream and downstream regions in de novo methylation. J Biol Chem 272:22322–22329
38. Ponchon T, Gagnon P, Berger F et al (1995) Value of endobiliary brush cytology and biopsies for the diagnosis of malignant bile duct stenosis: results of a prospective study. Gastrointest Endosc 42:565–572
39. Tada M, Yokosuka O, Omata M et al (1990) Analysis of ras gene mutations in biliary and pancreatic tumors by polymerase chain reaction and direct sequencing. Cancer 66: 930–935

Virchows Arch (2009) 455:353–361
DOI 10.1007/s00428-009-0826-7

ORIGINAL ARTICLE

$p16^{INK4}$ and CEA can be mutually exchanged with confidence between both relevant three-marker panels (ER/Vim/CEA and ER/Vim/$p16^{INK4}$) in distinguishing primary endometrial adenocarcinomas from endocervical adenocarcinomas in a tissue microarray study

Chih-Ping Han · Ming-Yung Lee · Yeu-Sheng Tyan · Lai-Fong Kok · Chung-Chin Yao · Po-Hui Wang · Jeng-Dong Hsu · Szu-Wen Tseng

Received: 31 May 2009 / Revised: 2 August 2009 / Accepted: 16 August 2009 / Published online: 9 September 2009

Abstract The accurate distinction between primary endocervical adenocarcinomas (ECA) and endometrial adenocarcinomas (EMA) may require the use of multiple ancillary monoclonal antibodies in panels of immunohistochemistry stains. In addition to reappraising the expressions of four commonly used individual monoclonal antibodies [estrogen receptor (ER), Vimentin (Vim), carcinoembryonic antigen (CEA), and $p16^{INK4}$], this study was designed to investigate whether CEA and $p16^{INK4}$ can be effectively exchanged between two relevant three-marker panels (ER/

C.-P. Han, M.-Y. Lee, and Y.-S. Tyan have equally contributed to this article.

C.-P. Han · P.-H. Wang
Department of Obstetrics and Gynecology,
Chung-Shan Medical University Hospital,
Taichung, Taiwan

C.-P. Han
Institute of Medicine, Chung-Shan Medical University,
Taichung, Taiwan

C.-P. Han (✉)
Clinical Trial Center, Chung-Shan Medical University Hospital,
Taichung, Taiwan
e-mail: hanhaly@gmail.com

M.-Y. Lee
Department of Statistics and Informatics Science,
Providence University,
Taichung, Taiwan

Y.-S. Tyan
Department of Medical Imaging,
Chung-Shan Medical University Hospital,
Taichung, Taiwan

Y.-S. Tyan
Department of Medical Imaging and Radiological Science,
Chung-Shan Medical University,
Taichung, Taiwan

L.-F. Kok
Department of Pathology, China Medical University Hospital,
Taichung, Taiwan

C.-C. Yao
Department of Surgery, Chung-Shan Medical University Hospital,
Taichung, Taiwan

J.-D. Hsu
Department of Pathology, Chung Shan Medical University Hospital,
Taichung, Taiwan

J.-D. Hsu (✉)
Department of Pathology, School of Medicine,
Chung Shan Medical University,
Taichung, Taiwan
e-mail: dongdong@csmu.edu.tw

S.-W. Tseng
Department of Internal Medicine, Division of Medical Oncology,
Chung Shan Medical University Hospital,
Taichung, Taiwan

S.-W. Tseng (✉)
Department of Internal Medicine, School of Medicine,
Chung Shan Medical University,
Taichung, Taiwan
e-mail: doc1592@yahoo.com.tw

Vim/CEA vs. ER/Vim/p16^{INK4}) in distinguishing ECA from EMA. A tissue microarray was constructed using paraffin-embedded, formalin-fixed tissues from 35 hysterectomy specimens, including 14 ECA and 21 EMA. Utilizing the avidin–biotin technique, tissue array sections were immunostained with the four aforementioned individual markers (ER, Vim, CEA, and p16^{INK4}). In addition to the four individual monoclonal antibodies, both their respective three-marker panels, proposed here, showed statistically significant ($p<0.05$) frequency differences between these two gynecologic tumors (ECA vs. EMA). The panel performance and test effectiveness revealed that both three-marker panels are promising and very helpful. According to our data, when histomorphological and clinical doubt exists as to the primary site of origin, we recommend using either of these two conventional three-marker panels, which consist of ER/Vim/CEA and ER/Vim/p16^{INK4}. CEA and p16^{INK4} can be interchanged with confidence without significantly influencing the panel presentations and efficiencies in distinguishing between adenocarcinomas of endocervical and endometrial origin.

Keywords Endocervical adenocarcinomas (ECA) · Endometrial adenocarcinomas (EMA) · Endocervical (EC) · Endometrial (EM) · Tissue microarray (TMA) · Immunohistochemistry (IHC) · Estrogen receptor (ER) · Vimentin (Vim) · Carcinoembryonic antigen (CEA) · p16^{INK4} (p16)

Background

Although careful morphological examination usually allows a confident diagnosis, the distinction between a primary endometrial (EMA) and endocervical adenocarcinoma (ECA) may be difficult with small biopsies or curetted tissue specimens. In some cases, tumors may be present in both endometrial and endocervical sites, and preoperative imaging does not help to establish the site of origin. Difficulties may also occur in the pathologic examination of large surgically resected specimens when the tumor involves both the lower uterine segment and upper endocervix. Since the initial choice of therapy may differ substantially, it is important to ascertain the cancer site of origin. For EMA, staging is surgical; while for ECA, staging is clinical. Treatment plans and adjuvant therapies are totally different between these two gynecologic malignancies (ECA vs. EMA) [1, 2].

McCluggage et al. [3] have already proposed that a conventional three-marker [estrogen receptor (ER)/Vimentin (Vim)/carcinoembryonic antigen (CEA)] panel generally allows a confident preoperative distinction between primary ECA and EMA. Recent studies have also demonstrated that p16^{INK4} immunohistochemistry (IHC) is of diagnostic value in distinguishing primary ECA from EMA [4–7]. In this study, we plan to reappraise the expression status of four individual monoclonal antibodies (ER, Vim, CEA, and p16^{INK4}) and investigate whether CEA and p16^{INK4} can be effectively interchanged between their relevant traditional three-marker panels (ER/Vim/CEA vs. ER/Vim/p16^{INK4}) without influencing the panel performance in distinguishing ECA from EMA.

Methods

Study materials

The study materials consisted of slides and selected formalin-fixed, paraffin-embedded tissue blocks from 35 hysterectomy specimens retrieved from the archives of the Tissue Bank of the Clinical Trial Center at Chung-Shan Medical University Hospital. These endocervical (endocervical-type ECA, $n=14$) and endometrial (endometroid-type EMA, $n=21$) specimens were acquired between 2004 and 2008. Two board-certified pathologists (CP Han and LF Kok) reviewed all the hematoxylin–eosin (H&E)-stained slides for these cases. A slide with representative tumor tissue was selected from each case, and the tumor area of interest was circled. The area corresponding to the selected area on the slide was also circled on the block with an oil marker. All donor tissue blocks were sent to the Bio-Chiefdom International Co. Ltd, Taiwan for tissue microarray (TMA) slide construction. They were cored with a 1.5-mm diameter needle and transferred to a recipient paraffin block. The recipient block was sectioned at 5 μm and transferred to silanized glass slides.

Immunohistochemical staining

Using the avidin–biotin complex technique, slides were stained with monoclonal antibodies whose main characteristics are summarized in Table 1. Formalin-fixed, paraffin-embedded tissue array specimens with 1.5-mm, 5-μm individual cores were deparaffinized in xylene, rehydrated through serial dilutions of alcohol, and washed in phosphate-buffered saline (PBS; pH 7.2). The pH 7.2 PBS buffer was used for all subsequent washes. Slides were stained with the following monoclonal antibodies: ER (NCL-L-ER-6F11, Leica Microsystems), 1:100 dilution; Vim (NCL-L-VIM-V9, Leica Microsystems), 1:400 dilution; CEA (NCL-L-CEA-2, Leica Microsystems), 1:100 dilution; and p16^{INK4a} (F12, sc-1661, Santa Cruz), 1:200 dilution (Table 1). Negative controls were obtained by excluding the primary antibody. Appropriate positive controls were applied. The slides were mounted for examination, and images were captured

Table 1 Antibodies used in this study

Antigen	Clone	Product code	Antibody class	Supplier	Dilution	Antigen retrieval
ER	Mouse Monoclonal, 6F11	NCL-L-ER-6F11	IgG1	Leica Microsystems	1:100	Citrate
Vim	Mouse monoclonal, V9	NCL-L-VIM-V9	IgG1	Leica Microsystems	1:400	Citrate
CEA	Mouse monoclonal, 12-140-10	NCL-L-CEA-2	IgG1	Leica Microsystems	1:100	Trypsin
$p16^{INK4a}$	Mouse monoclonal, F12	sc-1661	IgG2a	Santa Cruz	1:200	Citrate

by the Olympus BX51 microscopic DP71 Digital Camera System for study comparison.

Scoring of immunostaining

In this study, the TMA slides were simultaneously reviewed and scored by the two aforementioned pathologists, using a two-headed microscope. Since both nucleic and cytoplasmic IHC scoring algorithms have not been optimized and standardized, all CEA, ER, Vim, and $p16^{INK4a}$ expressions were interpreted using the German semi-quantitative scoring system in considering the intensity and extent of staining. The intensity of marker expression was quantified using the following scores: 0=negative, 1=weakly positive, 2=moderately positive, and 3=strongly positive. The extent of marker expression was quantified by evaluating the percentage of the positive staining areas in relation to the whole cancer area in the core. A score of 0 points was given for 0% reactivity, 1 point was assigned for 1–10% reactivity, 2 points were assigned for 11–50% reactivity, 3 points were assigned for 51–80% reactivity, and 4 points were assigned for 81–100% reactivity.

Although the term "semiquantitative" lacks clear definition, it implies having both features of "quantitative" and "qualitative." In fact, the "semiquantitative" scoring mechanism has generally been defined as the calculation of the expression index, which associates the "quantitative" area fraction of labeled tumor cells with their "qualitative" immunostaining intensity. The final immunoreactive score was determined by multiplying the positive intensity and the extent of positive area scores, yielding a range from 0 to 12 [8–12]. The threshold for differentiating between final positive and negative immunostaining was set at 4 for interpretation. This optimal cutoff value for this study was determined using receiver operating characteristic curve analysis [13–15]. The results are expressed by dividing cases into scores of 0–3 (essentially negative) and 4–12 (at least moderately positive in at least 11–50% of cells). This method of assessment has been widely accepted and used in previous studies [15–23].

Statistical analysis

A chi-square test or Fisher's exact test was performed to test the frequency difference of immunostaining (positive vs. negative) between each IHC biomarker and the two adenocarcinomas. The results are expressed by dividing cases into scores of 0–3 (negative) and 4–12 (positive; at least moderately positive in at least 11–50% of cells). The Mann–Whitney *U* test was used to analyze the immunostaining raw scores between the two adenocarcinomas, given the lack of normally distributed IHC scores. To distinguish between primary ECA and EMA, the sensitivity and specificity of EC- and EM-type immunoprofiles were compared. Sensitivity was defined as a ratio of accurate expression of a typical immunoprofile type among the primary adenocarcinoma of origin. Specificity was defined as the number of tissues that lacked a typical immunoprofile type of expression over the number of tissues that were not actually the primary adenocarcinoma of origin [24]. Analyses were performed using SPSS statistical software (SPSS, Inc., Chicago, IL). All tests were two-sided, and a $p<0.05$ was considered significant.

Results

In this study, we reappraised the expressional status of four individual monoclonal antibodies (ER, Vim, CEA, and $p16^{INK4}$). H&E and immunoreactivities for ER, Vim, CEA, and $p16^{INK4a}$ can be seen in two cases representative of primary ECA (tissue code 18) and EMA (tissue code 40; Fig. 1). The IHC findings of all four immunomarkers are summarized in Table 2. Using a score of ≧4 points as a cutoff, the immunomarkers (ER, Vim, CEA, and $p16^{INK4a}$) showed significant frequency differences in ECA and EMA tissue immunostainings. The ER marker stained positive in two of 14 (14.3%) ECA tumors with a median staining score of 0.50 and a range of 0–6. The ER marker stained positive in 15 of 21 (71.4%) EMA tumors ($p<0.001$), with a median staining score of 6.00 and a range of 0–12 ($p<0.001$). The Vim marker stained positive in one of 14 (7.1%) ECA tumors with a median staining score of 0.00 and a range of 0–6. The Vim marker stained positive in 15 of 21 (71.4%) EMA tumors ($p<0.001$) with a median staining score of 6.00 and a range of 0–12 ($p<0.001$). The CEA marker stained positive in ten of 14 (71.4%) ECA tumors with a median staining score of 5.00 and a range of 1–12. The CEA marker stained positive in

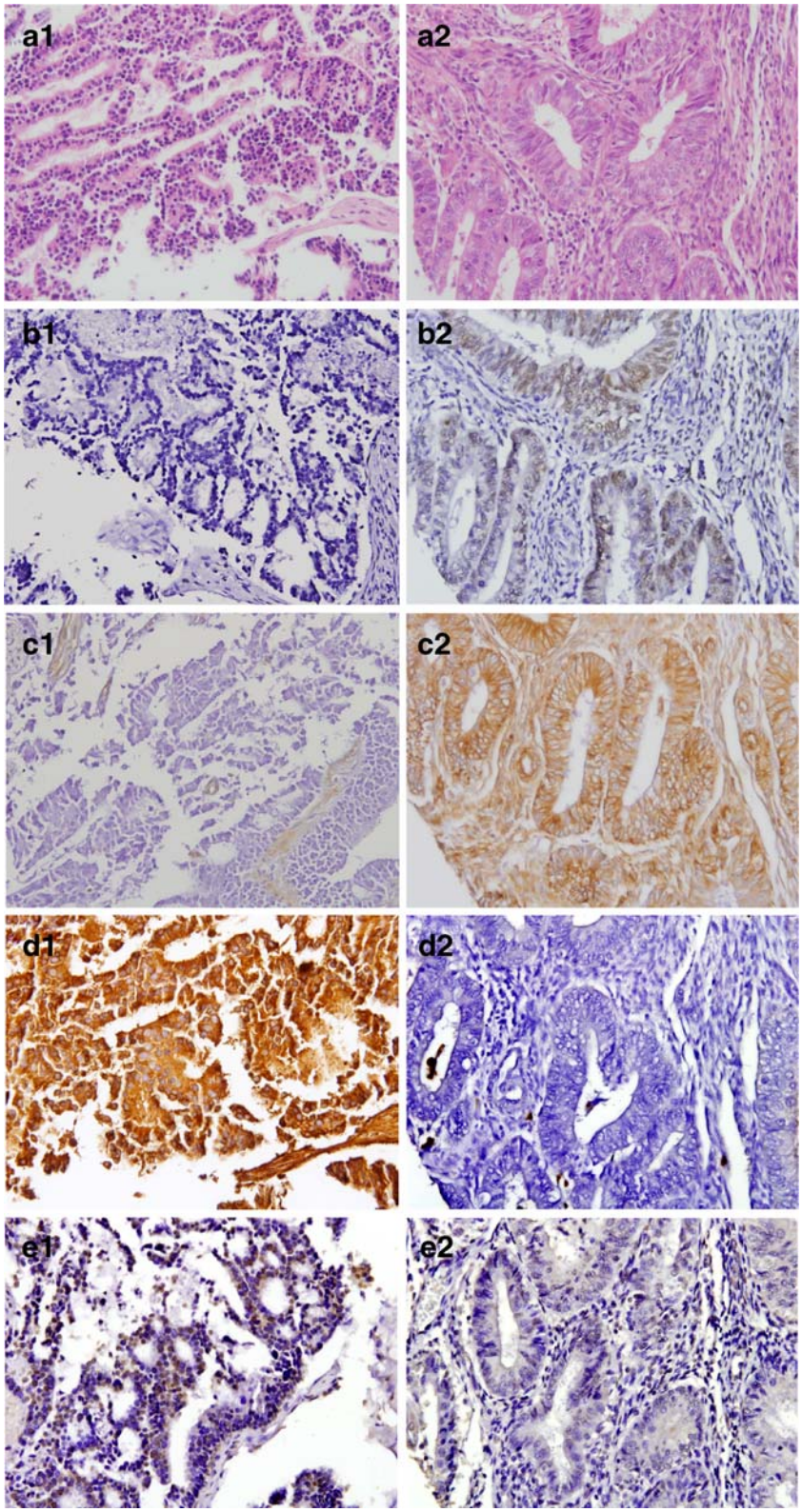

Fig. 1 H&E and immunohistochemical stains for ER, Vim, CEA, and p16^{INK4a} identified in endocervical adenocarcinomas (ECA) versus endometrial adenocarcinomas (EMA). Photographs *a1*, *b1*, *c1*, *d1*, and *e1* are from an ECA case (code no. 18), while photographs *a2*, *b2*, *c2*, *d2*, and *e2* are from an EMA case (code no. 40). *a1* H&E stain of endocervical type endocervical adenocarcinoma. *a2* H&E stain of endometroid type endometrial adenocarcinoma. *b1* Negative estrogen receptor (ER) IHC stain of ECA tumor cells, score: 0 points. *b2* Positive estrogen receptor (ER) IHC stain of EMA tumor cells, score: 9 points. *c1* Negative Vimentin IHC stain of ECA tumor cells, score: 0 points (**c2**) positive Vimentin IHC stain of EMA tumor cells, score: 9 points. Internal controls of stromal tissues were also positive in both *c1* and *c2*. *d1* Positive carcinoembryonic antigen (CEA) IHC stain of ECA tumor cells, score: 12 points. *d2* Negative carcinoembryonic antigen (CEA) IHC stain of EMA tumor cells, score: 0 points. *e1* Positive p16^{INK4a} (p16) IHC stain of ECA tumor cells, score: 6 points. Only nucleic p16^{INK4a} (p16) labeling in tumor cells was considered positive, regardless of the unexpected cytoplasmic reactivity. *e2* Negative p16^{INK4a} (p16) IHC stain of EMA tumor cells, score: 2 points (all images are ×400 magnification)

four of 21 (19.0%) EMA tumors (p=0.004) with a median staining score of 2.00 and a range of 0–9 (p=0.001). The p16^{INK4a} marker stained positive in 11 of 14 (78.6%) ECA tumors with a median staining score of 5.00 and a range of 2–12. The p16^{INK4a} marker stained positive in seven of 21 (33.3%) EMA tumors (p=0.009) with a median staining score of 2.00 and a range of 0–9 (p=0.001). The marker frequency differences in Taiwanese women

Table 2 Immunohistochemical staining results

		ECA (n=14)	EMA (n=21)	p value
ER	Score 0–3	12 (85.7%)	6 (28.6%)	0.002[a]
	Score 4–12	2 (14.3%)	15 (71.4%)	
	Median (range)	0.50 (0–6)	6.00 (0–12)	<0.001[b]
Vim	Score 0–3	13 (92.9%)	6 (28.6%)	<0.001[a]
	Score 4–12	1 (7.1%)	15 (71.4%)	
	Median (range)	.00 (0–6)	6.00 (0–12)	<0.001[b]
CEA	Score 0–3	4 (28.6%)	17 (81.0%)	0.004[a]
	Score 4–12	10 (71.4%)	4 (19.0%)	
	Median (range)	5.00 (1–12)	2.00 (0–9)	0.001[b]
$p16^{INK4a}$	Score 0–3	3 (21.4%)	14 (66.7%)	0.009[a]
	Score 4–12	11 (78.6%)	7 (33.3%)	
	Median (range)	5 (2–12)	2.00 (0–9)	0.001[b]

Using a score of ≧ 4 points as a cutoff, the immunostainings are defined as "negative" for scores from 0 to 3 and "positive" for scores from 4 to 12 points.

[a] Chi-square test with continuity correction or Fisher's exact test

[b] Mann–Whitney U test using exact significance

correspond with previous reports on Caucasian women [9–11, 14].

In addition, we also compared the performances between two three-marker panels (ER/Vim/CEA vs. ER/Vim/$p16^{INK4}$). A typical EC-type immunoprofile is defined as ER-/Vim-/CEA+ or ER-/Vim-/$p16^{INK4a}$+, whereas a typical EM-type immunoprofile is defined as ER+/Vim+/CEA or ER+/Vim+/$p16^{INK4a}$. A non-typical immunoprofile is defined as the three-marker expressions other than typical EC- and typical EM-type expression patterns [3, 5–7, 15–23] (Tables 3, 4, and 5).

Despite the typical expression patterns of the ECA and EMA immunoprofiles, there were several other non-typical expression patterns for both three-marker panels. Table 3 represents the panel expression patterns in primary ECA. Of the 14 ECA cases, there were (1) eight cases with a typical EC-type immunoprofile and six cases with a non-typical immunoprofile in the three-marker (ER/Vim/CEA) panel containing CEA, as well as (2) eight cases with a typical EC-type immunoprofile and six cases with a non-typical immunoprofile in the three-marker panel (ER/Vim/$p16^{INK4}$) containing $p16^{INK4a}$. Table 4 exhibits the panel expression patterns in primary EMA. Of the 21 EMA cases, there were (1) ten cases with a typical EM-type immunoprofile and 11 cases with a non-typical immunoprofile in the three-marker (ER/Vim/CEA) panel containing CEA, as well as (2) seven cases with a typical EM-type immunoprofile and 14 cases with a non-typical type immunoprofile in the three-marker (ER/Vim/$p16^{INK4}$) panel containing $p16^{INK4a}$.

As seen in Table 5, in the three-marker (ER/Vim/CEA) panel containing CEA, the typical EC-type immunoprofile was present in eight of 14 (57.1%) ECA tumors as well as in one of 21 (4.76%) EMA tumors (p=0.001). The typical EM-type immunoprofile was present in none of 14 (0%) ECA tumors as well as in ten of 21 (47.62%) EMA tumors (p=0.002). The non-typical immunoprofile was present in six of 14 (42.86%) ECA tumors, as well as in ten out of 21 (47.62%) EMA tumors. In the three-marker (ER/Vim/$p16^{INK4a}$) panel containing $p16^{INK4a}$, the typical EC-type immunoprofile was present in eight of 14 (57.14%) ECA tumors as well as none of 21 (0.0%) EMA tumors (p<0.001). The typical EM-type immunoprofile panel was present in none out of 14 (0%) ECA tumors as well as in seven of 21

Table 3 Immunoprofiles for three-marker panels for primary ECA (sample size 14)

ER>3	Vim>3	CEA>3	$p16^{INK4a}$>3	Number	Percent with this panel
Three-marker panel (ER/Vim/CEA)					
−	−	−		3	21.43
−	−	+		***8***	***57.14***
−	+	+		1	7.14
+	−	+		1	7.14
+	−	−		1	7.14
Three-marker panel (ER/Vim/$p16^{INK4a}$)					
−	−		−	3	21.43
−	−		+	***8***	***57.14***
−	+		+	1	7.14
+	−		+	2	14.29

The row in italic bolds is defined as typical EC-type immunoprofile. Other rows are defined as non-typical immunoprofile

(−) score negative, (+) score positive

Table 4 Immunoprofiles for three-marker panels for primary EMA (sample size 21)

ER>3	Vim>3	CEA>3	p16INK4a>3	Number	Percent with this panel
Three-marker panel (ER/Vim/CEA)					
−	−	−		2	9.52
−	−	+		1	4.76
−	+	−		3	14.29
+	−	−		1	4.76
+	−	+		2	9.52
+	+	−		***10***	***47.62***
+	+	+		2	9.52
Three-marker panel (ER/Vim/p16INK4a)					
−	−		−	3	14.29
−	+		−	2	9.52
−	+		+	1	4.76
+	−		−	3	14.29
+	+		−	***7***	***33.33***
+	+		+	5	23.81

The row in italic bolds is defined as typical EM-type immunoprofile. Other rows are defined as non-typical immunoprofile

(−) score negative, (+) score positive

(33.33%) EMA tumors (p=0.027). The non-typical type immunoprofile panel was present in six of 14 (42.86%) ECA tumors as well as in 14 of 21 (66.67%) EMA tumors.

Table 6 presents the comparisons of the test effectiveness and performance between the two three-marker panels with typical EC-type or typical EM-type in diagnostically distinguishing between 14 ECA and 21 EMA. Of the expressions of typical immunoprofiles in the first conventional three-marker (ER/Vim/CEA) panel, the sensitivity and negative predictive value (NPV) were 57.1% and 76.9% in ECA as well as 47.6% and 56.0% in EMA. On the other hand, the specificity and positive predictive value (PPV) were 95.2% and 88.9% in ECA as well as 100% and 100% in EMA. The accuracy rate was 80.0% in ECA and 68.6% in EMA. Of the expressions of typical immunoprofiles in the second three-marker (ER/Vim/p16^{INK4a}) panel, the sensitivity and NPV were 57.1% and 87.8% in ECA as well as 33.3% and 50.0% in EMA. On the other hand, the specificity and PPV were 100% and 100% in ECA as well as 100% and 100% in EMA. The accuracy rate was 82.9% in ECA and 60.0% in EMA.

Discussion

Distinguishing between primary ECA and EMA before planning the patient treatment is clinically important. The primary EMAs of the endometroid type usually have distinctly different histological appearances from ECAs of the endocervical type; therefore, careful gross and histomorphological examinations often allow a confident distinction. Generally speaking, the former is usually composed of tubular glands with a complex tubulopapillary and cribriform architecture that are mostly dilated and lined by stratified or pseudostratified columnar cells that may have cilia. However, the glands of the latter are frequently smaller and obscurely mucinous. Their lining cells tend to have more intense amphophilic to eosinophilic cytoplasm,

Table 5 The typical and non-typical IHC performances of the three-marker panels (ER/Vim/CEA vs.ER/Vim/p16^{INK4a}) between primary ECA and EMA

		ECA	EMA	p value
Three-marker panel (ER/Vim/CEA)	Typical EC-type	8/14 (57.14%)	1/21 (4.76%)	0.001
	Typical EM-type	0/14 (0.0%)	10/21 (47.62%)	0.002
	Non-typical	6/14 (42.86%)	10/21 (47.62%)	
Three-marker panel (ER/Vim/p16^{INK4a})	Typical EC-type	8/14 (57.14%)	0/21 (0.0%)	<0.001
	Typical EM-type	0/14 (0.0%)	7/21 (33.33%)	0.027
	Non-typical	6/14 (42.86%)	14/21 (66.67%)	

Three-marker panel (ER/Vim/CEA) with typical EC-type immunoprofile: ER-/Vim-/CEA+. Three-marker panel (ER/Vim/CEA) with typical EM-type immunoprofile: ER+/Vim+/CEA−. Three-marker panel (ER/Vim/p16^{INK4a}) with typical EC-type immunoprofile: ER-/Vim-/p16^{INK4a}+. Three-marker panel (ER/Vim/p16^{INK4a}) with typical EM-type immunoprofile: ER+/Vim+/p16^{INK4a}−. Non-typical types: immunoprofile other than the typical types in all the above mentioned

Table 6 Comparisons of the test effectiveness and performance between the three-marker panels with typical EC-type or typical EM-type in distinguishing between ECA and EMA

	Panel expression typical EC-type in ECA (N=14)		Panel expression typical EM-type in EMA (N=21)	
	ER/Vim/CEA	ER/Vim/p16^{INK4a}	ER/Vim/CEA	ER/Vim/p16^{INK4a}
Sensitivity (95% CI)	0.571 (0.407, 0.735)	0.571 (0.407, 0.735)	0.476 (0.311, 0.642)	0.333 (0.177,0.490)
Specificity (95% CI)	0.952 (0.882, 1.000)	1.000 (1.000,1.000)	1.000 (1.000, 1.000)	1.000 (1.000,1.000)
Positive predictive value (95% CI)	0.889 (0.785, 0.993)	1.000 (1.000,1.000)	1.000 (1.000, 1.000)	1.000 (1.000,1.000)
Negative predictive value (95% CI)	0.769 (0.630, 0.909)	0.778 (0.640,0.916)	0.560 (0.396, 0.724)	0.5 (0.334,0.666)
Accuracy (95% CI)	0.800 (0.667,0.933)	0.829 (0.704,0.953)	0.686 (0.532,0.840)	0.600 (0.438,0.762)

Three-marker panel (ER/Vim/CEA) with typical EC-type immunoprofile: ER-/Vim-/CEA+. Three-marker panel (ER/Vim/CEA) with typical EM-type immunoprofile: ER+/Vim+/CEA−. Three-marker panel (ER/Vim/p16^{INK4a}) with typical EC-type immunoprofile: ER-/Vim-/p16^{INK4a}+. Three-marker panel (ER/Vim/p16^{INK4a}) with typical EM-type immunoprofile: ER+/Vim+/p16^{INK4a}−. Non-typical types: immunoprofile other than the typical types in all the above mentioned

are more mitotically active, and show more apoptosis, etc. Despite these morphological differences in the majority of cases, there are other cases in which morphological overlap is such that other findings may aid in this distinction [25, 26]. When there is still doubt and indistinguishable primaries, IHC may assist. McCluggage et al. [3] has reported that the conventional three-marker (ER/Vim/CEA) panel generally allows distinction between a primary endometrial and ECA. We also know that the p16^{INK4a} marker is currently the most important focus of attention and carries more diagnostic weight than the others. However, no single antibody is totally specific or any one neoplasm [4–7, 15–22]. Herein, we have re-evaluated these two commonly used three-marker (ER/Vim/CEA and ER/Vim/p16^{INK4a}) panels to see whether they both show similar promising performance and effectiveness in distinguishing between primary ECA and EMA.

ECA tends to be ER-/Vim-/CEA+ and EMA tends to be ER+/Vim+/CEA− in the first traditional three-marker (ER/Vim/CEA) panel, whereas ECA tends to be ER-/Vim-/p16^{INK4a}+ and EMA tends to be ER+/Vim+/p16^{INK4a}− in the second three-marker (ER/Vim/p16^{INK4a}) panel [3–7, 15–23]. In this study, we reappraised the expressional status of four individual markers (ER, Vim, CEA, and p16^{INK4a}) and investigated whether p16^{INK4a} and CEA are mutually interchangeable between both their relevant three-marker (ER/Vim/CEA and ER/Vim/p16^{INK4a}) panels in distinguishing ECA from EMA. We demonstrated that all these four individual monoclonal antibodies and their two commonly applied three-marker panels revealed significant frequency differences (p<0.05) between these two gynecologic tumors (ECA vs. EMA). Our data will help in the referral and management of ECA and EMA cases worldwide. On the other hand, immunohistochemical overlap may exist, and the immunoprofiles are not always definitive in some cases. Unexpected "aberrant" expressions can occur with any of the markers from the two panels discussed. This diagnostic dilemma still remains unresolved, as there are many kinds of non-typical immunoprofiles.

Regarding the typical EC- or EM-type immunoprofile, the sensitivity and NPV were 57.1% and 76.9% in ECA as well as 47.6% and 56.0% in EMA in the first three-marker (ER/Vim/CEA) panel and 57.1% and 77.8% in ECA as well as 33.3% and 50.0% in EMA in the second three-marker (ER/Vim/p16^{INK4}) panel. All of these results indicate a high false-negative rate. If the staining results are not in agreement with the typical EC- or EM-type immunoprofile, despite the panel used, there is a high probability that the corresponding ECA or EMA tumor diagnosis would be doubtful and inconclusive. The low sensitivity and NPV are the limiting factors for applying either three-marker panel as the screening tool for ECA and EMA. On the other hand, the specificity and PPV were 95.8% and 88.9% in ECA as well as 100% and 100% in EMA in the first conventional three-marker (ER/Vim/CEA) panel and 100% and 100% in ECA as well as 100% and 100% in EMA in the second three-marker (ER/Vim/p16^{INK4}) panel. Both indicated a low false-positive rate. If the staining result matches up with the typical EC- or EM-type immunoprofile, despite the panel used, there is a high probability that the corresponding ECA or EMA tumor diagnosis will be accurate and conclusive. The high specificity and PPV of both panels are the favorable factors for applying either three-marker panel as a confirmatory tool for ECA and EMA.

Above all, accuracy means the degree of veracity. When using both three-marker panels with typical EC-type (ER-/Vim-/CEA+ and ER-/Vim-/p16^{INK4}+) immunoprofiles in definitively diagnosing primary ECA, the ER/Vim/p16^{INK4} panel has a more favorable accuracy rate than the ER/Vim/CEA panel (82.9% vs. 80.0%). When using both three-marker panels with typical EM-type (ER+/Vim+/CEA− and ER+/Vim+/p16^{INK4}−) immunoprofiles in definitively diagnosing primary EMA, the ER/Vim/CEA panel has a more favorable accuracy rate than the ER/Vim/p16^{INK4} panel

(68.6% vs. 60.0%). All these similar promising values and possible trade-offs in statistical characteristics provide evidence-based information that $p16^{INK4}$ and CEA can be mutually interchanged with confidence between both relevant three-marker panels (ER/Vim/CEA and ER/Vim/$p16^{INK4}$) in distinguishing primary EMAs from ECAs in this tissue microarray study.

In summary, no single antibody is totally specific for any one neoplasm. It should be stressed that IHC results should always be interpreted in the context of morphology, and, in general, panels of antibodies should be used rather than relying on a single antibody. It is known that each of the four monoclonal antibodies directed against ER, Vim, CEA, and $p16^{INK4a}$, as well as their two respective panels comprised of three-markers each (ER/Vim/CEA and ER/Vim/$p16^{INK4a}$), could help in distinguishing between adenocarcinomas of endocervical and endometrial origin. After assessing the parameters of panel performance and test effectiveness, such as sensitivity, specificity, NPV, PPV, and accuracy rate of the two three-marker panels, this study has demonstrated that both three-marker panels are similarly promising and helpful. CEA and $p16^{INK4}$ can be interchanged with confidence. Despite the limited number of cases, these data provide significant and valuable references for further investigations of other useful markers or panels, which will definitively distinguish between primary ECA and EMA.

Conclusions

Distinguishing between primary ECA and EMA can often be accomplished by routine gross and histological examination, but some cases reveal tumors with undetermined origins or overlapping histomorphological features. Accurate diagnosis may require the use of ancillary IHC stains. The results from this TMA study provide valuable references of consistency between Taiwanese and Caucasian women. We found that both three-marker panels (ER/Vim/CEA and ER/Vim/$p16^{INK4a}$) can sufficiently provide an advantageous, cost-effective, and easier means of appropriately distinguishing between ECA and EMA. Based on our data, we scientifically demonstrated that CEA and $p16^{INK4a}$ are of similar importance and are mutually interchangeable between both of their relevant panels (ER/Vim/CEA and ER/Vim/$p16^{INK4a}$) in distinguishing primary ECA from EMA.

Acknowledgments This work was supported in part by grants from Department of Health (DOH98-PAB-1001-E and DOH98-PAB-1009-I), Chung-Shan Medical University Hospital (CSH-97-A-09 and CSH-2009-B-007), Taiwan, ROC.

Conflict of interest statement The authors declare that there are no conflicts of interest.

References

1. Lurain JR, Bidus MA, Elkas JC (2007) Uterine cancer, cervical and vaginal cancer. In: Berek RS (ed) Novak's gynecology, 14th edn. Lippincott Williams & Wilkins (LWW), Philadelphia, pp 1343–1402
2. Schorge JO, Knowles LM, Lea JS (2004) Adenocarcinoma of the cervix. Curr Treat Options Oncol 5:119–127
3. McCluggage WG, Sumathi VP, McBride HA et al (2002) A panel of immunohistochemical stains, including carcinoembryonic antigen, vimentin, and estrogen receptor, aids the distinction between primary endometrial and endocervical adenocarcinomas. Int J Gynecol Pathol 21:11–15
4. Yao CC, Kok LF, Lee MY et al (2009) Ancillary p16(INK4a) adds no meaningful value to the performance of ER/PR/Vim/CEA panel in distinguishing between primary endocervical and endometrial adenocarcinomas in a tissue microarray study. Arch Gynecol Obstet 280:405–413
5. Han CP, Lee MY, Kok LF et al (2009) Adding the p16INK4a-marker to the traditional 3-marker (ER/Vim/CEA) panel engenders no supplemental benefit in distinguishing between primary endocervical and endometrial adenocarcinomas in a tissue microarray study. Int J Gynecol Pathol 28:489–496
6. McCluggage WG, Jenkins D (2003) p16 immunoreactivity may assist in the distinction between endometrial and endocervical adenocarcinoma. Int J Gynecol Pathol 22:231–235
7. Mittal K, Soslow R, McCluggage WG (2008) Application of immunohistochemistry to gynecologic pathology. Arch Pathol Lab Medicine 132:402–423
8. Walker RA (2006) Quantification of immunohistochemistry—issues concerning methods, utility and semiquantitative assessment I. Histopathology 49:406–410
9. Taylor CR, Levenson RM (2006) Quantification of immunohistochemistry—issues concerning methods, utility and semiquantitative assessment II. Histopathology 49:411–424
10. Remmele W, Schicketanz K-H (1993) Immunohistochemical determination of estrogen and progesterone receptor content in human breast cancer. Computer-assisted image analysis (QIC score) vs. subjective grading (IRS). Pathol Res Pract 189:862–866
11. Klein M, Vignaud JM, Hennequin V et al (2001) Increased expression of the vascular endothelial growth factor is a pejorative prognosis marker in papillary thyroid carcinoma. J Clin Endocrinol Metab 86:656–658
12. Kamoi S, AlJuboury MI, Akin MR et al (2002) Immunohistochemical staining in the distinction between primary endometrial and endocervical adenocarcinomas: another viewpoint. Int J Gynecol Pathol 21:217–223
13. Matos LL, Stabenow E, Tavares MR et al (2006) Immunohistochemistry quantification by a digital computer-assisted method compared to semiquantitative analysis. Clinics 61:417–424
14. Zweig MH, Campbell G (1993) Receiver-operating characteristic (ROC) plots: a fundamental evaluation tool in clinical medicine. Clin Chem 39:561–577
15. Metz CE (1978) Basic principles of ROC analysis. Semin Nucl Med 8:283–98
16. Kamoi S, AlJuboury MI, Akin MR et al (2002) Immunohistochemical staining in the distinction between primary endometrial and endocervical adenocarcinomas: another viewpoint. Int J Gynecol Pathol 21:217–223
17. Khoury T, Tan D, Wang J et al (2006) Inclusion of MUC1 (Ma695) in a panel of immunohistochemical markers is useful for distinguishing between endocervical and endometrial mucinous adenocarcinoma. BMC Clin Pathol 6:1
18. Reid-Nicholson M, Iyengar P, Hummer AJ et al (2006) Immunophenotypic diversity of endometrial adenocarcinomas: implications for differential diagnosis. Mod Pathol 19:1091–1100

19. Dabbs DJ, Sturtz K, Zaino RJ (1996) Distinguishing endometrial from endocervical adenocarcinoma. Hum Pathol 27:172–177
20. Castrillon DH, Lee KR, Nucci MR (2002) Distinction between endometrial and endocervical adenocarcinoma: an immunohistochemical study. Int J Gynecol Pathol 21:4–10
21. Alkushi A, Irving J, Hsu F et al (2003) Immunoprofile of cervical and endometrial adenocarcinomas using a tissue microarray. Virchows Arch 442:271–277
22. Han CP, Lee MY, Tzeng SL (2008) Nuclear receptor interaction protein (NRIP) expression assay using human tissue microarray and immunohistochemistry technology confirming nuclear localization. J Exp Clin Cancer Res 27:25
23. Han CP, Kok LF, Wang PW et al (2009) Scoring p16INK4a immunohistochemistry based on independent nucleic staining alone can sufficiently distinguish between endocervical and endometrial adenocarcinomas in a tissue microarray study. Mod Path 22:797–806
24. Bodner G, Schocke MF, Rachbauer F et al (2002) Differentiation of malignant and benign musculoskeletal tumors: combined color and power Doppler US and spectral wave analysis. Radiology 223:410–416
25. Young RH, Clement PB (2004) Pathology of endometrial carcinoma. In: Fuller AF, Seiden MV, Young RH, American Cancer Society (eds) Uterine cancer, 1st edn. PMPH, USA, pp 52–77
26. Young RH, Clement PB (2002) Endocervical adenocarcinoma and its variants: their morphology and differential diagnosis. Histopathology 41:185–207

Virchows Arch (2009) 455:363–373
DOI 10.1007/s00428-009-0832-9

ORIGINAL ARTICLE

Tissue transglutaminase expression in celiac mucosa: an immunohistochemical study

Julia Gorgun · Anna Portyanko · Yuri Marakhouski · Eugeni Cherstvoy

Received: 2 June 2009 / Revised: 23 August 2009 / Accepted: 25 August 2009 / Published online: 12 September 2009

Abstract Tissue transglutaminase (tTG) constitutes the main autoantigen in celiac disease (CD). The aim of the study was to clarify weather celiac disease is associated with changes in tTG expression in duodenal mucosa. Tissue transglutaminase was assessed immunohistochemically (clone CUB 7402) in duodenal biopsy specimens from 22 untreated CD patients, ten normal controls (NC) with unremarkable duodenal mucosa, and nine disease nonceliac controls (DC). In 15 CD patients duodenal biopsy specimens were repeatedly assessed after these patients had been prescribed gluten-free diet. Positive pixel count algorithm of ImageScope was used for quantitative evaluation of immunohistochemistry. Tissue transglutaminase expression in superficial epithelium differed significantly between the three groups ($p<0.001$). It was increased in DC in relation to NC ($p<0.001$) and in CD—in relation to NC ($p<0.001$) and DC ($p=0.003$). In CD and DC, cryptal epithelium was stained more intensively than in NC ($p<0.001$), but there was no difference between CD and DC ($p=0.507$). The same pattern was seen in lamina propria. A significant decrease in tTG expression in all the compartments was seen in repeatedly assessed samples. Untreated CD is associated with tTG overexpression, which is reversible. Tissue transglutaminase up-regulation does not seem to be specific for CD and can appear in other pathological conditions.

J. Gorgun (✉) · Y. Marakhouski
Department of Gastroenterology and Nutrition,
Belarusian Medical Academy of Postgraduate Education,
P Brovky st 3-3,
Minsk 220013, Belarus
e-mail: julia.gorgun@mail.ru

A. Portyanko · E. Cherstvoy
Department of Pathology, Belarusian State Medical University,
Dzerzhynsky Avenue 83,
220116 Minsk, Belarus

Keywords Celiac disease · Transglutaminase 2 · Duodenal mucosa · Immunohistochemistry · Inflammation

Introduction

Transglutaminase (TG) family includes enzymes which cross-link proteins through an acyl transfer reaction between the γ-carboxamide group of glutamine in glutamine-donor proteins and the ε-amino group of lysine in glutamine acceptor proteins, which results in the formation of the irreversible ε-(γ-glutamyl)-lysine (isopeptidyl) bond [1]. One of the members of this family, type II TG or tissue TG (tTG), is an ubiquitous multifunctional protein, which is involved in cell death and differentiation, matrix stabilization, and cell adhesion [2]. Today, type II TG rate is a key player in a number of human pathological states [1]. Celiac disease (CD) is a gluten-triggered autoimmune enteropathy in which tTG constitutes a main autoantigen [3]. The exact pathogenesis of CD is not yet fully understood, but there is convincing evidence of the important role of tTG in the disease development. According to present-day knowledge, tTG deamidates glutamine residues of the glutamine-rich gliadins, which results in the increased affinity for HLA-DQ2/DQ8 molecules on antigen presenting cells and consequent T cell stimulation [4–7].

Apart from this, tTG could be implicated in CD pathogenesis by some other mechanisms:

– tTG catalyzed cross-linking of gliadin peptides with extracellular matrix molecules; it creates long-term reservoirs of antigenically potentiated gluten components and forms immunogenic neoepitopes, which may play a role in secondary autoimmune diseases associated with CD [8];

- tTG itself cross-links with gliadin and might act as a hapten for the formation of antibodies; the presentation of gliadin-tTG complexes results in the formation of antibodies against gliadin, tTG, and the cross-linked proteins [9];
- tTG autoantibodies may be involved in the activation of the epithelial cell proliferation by interacting with the extracellular membrane-bound tTG [10];
- expression of tTG in celiac mucosa seems to be subjected to up-regulation effect of gliadin peptides as opposed to nonceliac mucosa [11].

Considering a special role of tTG in CD, it seems logical to suppose that celiac mucosa might have some specific characteristics of tTG expression or activity. If it is really so, it could be useful in CD diagnostic and helpful in understanding of CD pathogenesis more exactly. At present, there is evidence of tTG overexpression in jejunal mucosa of CD patients [12–14], but the mechanism causing increased tTG activity is not yet understood. The data about tTG distribution pattern in celiac mucosa are controversial, and the source of its increased activity remains unclear [15]. It remains also unclear whether tTG up-regulation in intestinal mucosa is specific for CD or constitutes a universal reaction to tissue damage. Thus, our aim was to assess tTG expression and its distribution pattern in intestinal mucosa of CD patients.

Materials and methods

Patients

Four groups of patients have been studied (Table 1).

The first group (normal duodenal controls—NC) included ten controls with unremarkable duodenal mucosa who were negative for anti-tTG-IgA and did not have Ig-A deficiency.

The second group (untreated CD patients—CD) consisted of 22 untreated patients with celiac disease (Table 2). Celiac disease was diagnosed on the basis of commonly accepted histological and serological criteria. All CD patients were positive for at least one of the following serological markers: anti-tTG-IgA, antigliadin-IgA (AGA-IgA), antigliadin-IgG (AGA-IgG). All of them, but two, had HLA DQ2 or DQ8. DQ2/DQ8-negative cases, malabsorbtion, showed typical celiac serology and histology, and dramatically improved on gluten-free diet (GFD), so there was not any doubt in diagnosis.

The third group (treated CD patients) included 15 patients from group CD who were repeatedly assessed after the prescription of GFD.

The fourth group (disease controls—DC) consisted of nine anti-tTG-IgA and AGA-negative patients with the following duodenal changes: 5—acid-related duodenitis with atrophy in duodenal bulb, 1—Waldenstrom macroglobulinemia with prominent lymphangiectasia, 1—focal atrophic active duodenitis in Crohn's disease, 1—abetalipoproteinemia, 1—diffuse atrophic enteritis associated with *Campylobacter jejuni* infection.

The study was approved by the local ethics committee, and each patient gave an informed consent before the endoscopy.

Biopsy/histology

In all the patients, the upper endoscopy was performed and multiple biopsy samples were obtained in the patients with acid-related duodenitis from duodenal bulb and in the other patients from the distal duodenum. All biopsy samples were placed on filter paper luminal side upward just after they had been obtained and then fixated in 40 g/L formaldehyde. After dehydration, the biopsy specimens were embedded in paraffin, cut in 4 μm thick sections, and stained with hematoxylin/eosin. A routine histology assessment was performed, and the changes in CD samples were classified according to Marsh criteria.

Immunohistochemistry

The immunohistochemical staining was performed on formalin-fixed, paraffin-embedded 4 μm sections. The slides were deparaffinized, rehydrated, and the endogenous peroxidase activity was blocked for 20 min by 30 g/L hydrogen peroxide. After that, the slides were subjected to antigen retrieval by boiling (16 min) in 10 mM citrate buffer, pH 6 and then incubated with 10 g/L bovine serum albumin in tris-buffered saline (TBS) for 30 min to block nonspecific binding. Next, the slides were incubated overnight (4°C) with anti-tTG antibody (clone CUB 7402, LabVision, UK), diluted 1:100 in blocking solution. Subsequently, they were extensively washed with TBS and incubated with a secondary reagent (Envision kit) according to the manufacturer's (Dako, Denmark) instructions. Following additional washes, color

Table 1 Demographic data of investigated patients

Group of patients	NC	CD	Treated CD	DC
Total number of patients	10	22	15	9
M:F ratio	4:6	5:17	4:11	4:5
Age, mean (min ÷ max)	34.5 (17÷58)	37.1 (15÷72)	40.8 (17÷72)	32.3 (16÷62)

Table 2 Serological and histological data of CD patients

Serology	*n*
Isolated AGA-IgA positivity	2
Isolated AGA-IgG positivity	1
AGA - IgA + AGA - IgG positivity	2
Anti - tTG - IgA + AGA - IgA positivity	1
Anti - tTG - IgA + AGA - IgG positivity	1
Anti - tTG - IgA + AGA - IgA + AGA - IgG positivity	15
Histological grade	
Marsh IIIA	5
Marsh IIIB	1
Marsh IIIC	16

was developed with DAB (Dako, Denmark), the sections were counterstained with hematoxylin and mounted. For a negative control, the primary antibody was replaced with an isotype control antibody (Zymed, Invitrogen Corp.).

Evaluation of immunohistochemical staining

All the specimens were evaluated using a Leica DM5000B microscope with HC PL FLUOTAR objectives. For each patient, the best oriented section was chosen, and images were obtained at ×100 using a DFC420C Leica digital camera (1798×1438 pixels). The images were analyzed by the image analysis software, ImageScope version 9.0.19.1516 (Aperio Technologies, Inc.). Bamboo pen tablet (Wacom Co. Ltd.) was used for drawing out different image compartments. Villus or superficial epithelium, cryptal epithelium, and lamina propria compartments were outlined using pen tool of ImageScope and thus, selected for subsequent analysis. Artifacts were excluded from analyses with negative pen tool. Each compartment was divided into separate regions according to the opportunity to draw a non-breaking curve.

Positive pixel count algorithm version 9 was used for quantitative evaluation of immunohistochemical staining. From the automatically calculated parameters the following were selected for our study:

- Total number of pixels: TN = number positive + number negative,
- Positivity = number positive/TN, and
- Average intensity of all pixels: Iavg = (Iweak positive+ Ipositive + Istrong positive) / (Nweak positive + Npositive+Nstrong positive). According to the manufacturer instructions, intensity is the measure of brightness of the pixel, which ranges from zero (black) to 255 (bright white), so that a large intensity value means that

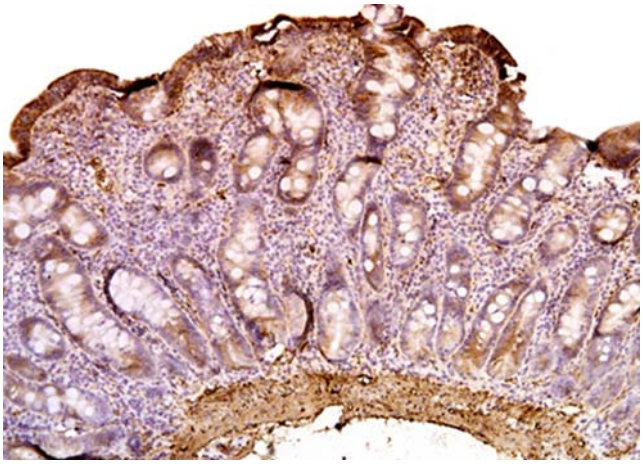

Fig. 2 Duodenal mucosa from a newly diagnosed CD patient (Marsh IIIC) × 100. There is strong staining of superficial epithelium, tTG expression in cryptal epithelium, and lamina propria is also seen

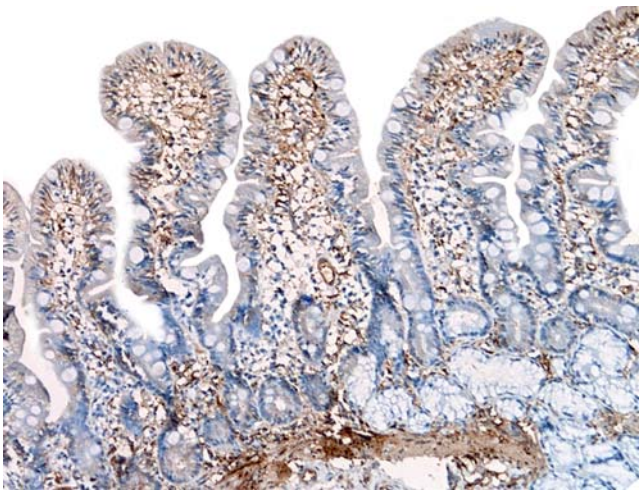

Fig. 1 Normal duodenal mucosa stained with anti-tTG antibodies × 100. Only weak epithelial TTG expression on the top of villi is seen, but it is strong in muscularis mucosae and lamina propria

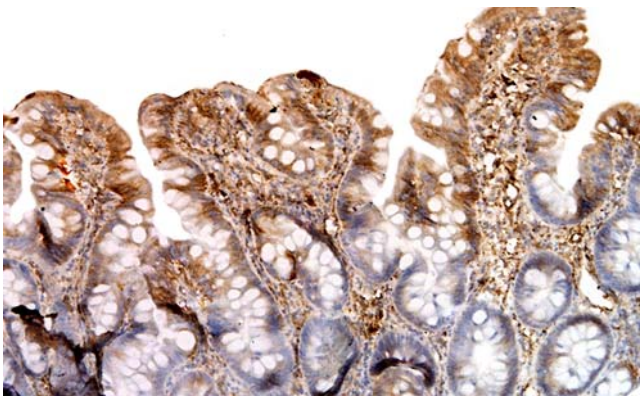

Fig. 3 Duodenal mucosa from patient with atrophic enteritis associated with *Campylobacter jejuni* infection × 200. Strong staining of villus epithelium and lamina propria

the pixel is brighter. To avoid confusion due to change of parameters in opposite directions, we have introduced one more parameter, which is index of intensity= 255−Iavg, and used it as a measure of staining intensity.

All the parameters were separately calculated for every epithelial region and were used for group comparison. For pair comparison of the same patient's data during follow up, the mean parameters, calculated together automatically for all the regions of each patient, were used.

Statistics

Mann–Whitney's U test, Wilcoxon matched pairs test, and Kruskal–Wallis' test were used to analyze the data. For multiple (three) pair comparisons, we used Bonferroni correction and considered p value <0.017 to indicate statistical significance. In the rest of cases, the differences were considered to be significant at $p<0.05$.

Results

Comparison of normal controls, celiac disease patients, and disease controls

In negative control slides, no staining was observed. In control group, tTG expression in epithelium was mostly absent or quite weak (Fig. 1). The ascending gradient along the crypt-villus axis was noticeable, and some foci of strong staining were seen on the top of villus in two controls. Tissue transglutaminase expression was also found in both villus and intercryptal lamina propria. All CD patients were remarkable by significant staining of superficial epithelium

Table 3 Quantitative evaluation of tTG expression in normal controls, celiac disease patients, and disease controls

	Normal controls (NC)	Celiac disease (CD)	Disease controls (DC)	p for multiple comparison[b]	p for pair comparison[c]: CD vs NC DC vs NC CD vs DC
Villus/superficial epithelium					
Number of regions	225	138	106		
Positivity (%)[a]	12.9 (4.2–31.8)	78.1 (38.3–99.1)	59.7 (18.6–90.1)	=0.000[d]	<0.000[d] <0.000[d] =0.003[d]
Intensity index[a]	96.3 (85.6–111.0)	113.3 (91.2–140.9)	108.8 (85.3–127.9)	<0.000[d]	<0.000[d] <0.007[d] <0.037
Cryptal epithelium					
Number of regions	210	667	165		
Positivity (%)	1.1 (0.3–3.7)	17.5 (1.3–77.1)	20.3 (6.3–42.8)	=0.000[d]	<0.000[d] <0.000[d] =0.507
Intensity index	96.7 (83.7–109.3)	84.4 (75.1–102.7)	79.5 (66.6–97.2)	<0.000[d]	<0.000[d] <0.000[d] <0.000[d]
Lamina propria					
Number of regions	238	478	165		
Positivity (%)	23.5 (13.0–41.5)	45.7 (21.2–75.1)	37.2 (20.4–75.3)	<0.000[d]	<0.000[d] <0.000[d] =0.171
Intensity index	99.7 (88.3–111.2)	97.2 (82.7–110.4)	99.9 (85.6–114.0)	=0.066	

[a] Median (lower and upper quartiles)

[b] Kruskal–Wallis ANOVA

[c] Mann–Whitney's U test

[d] Difference considered to be significant

(Fig. 2). Cryptal tTG distribution was absent in some cases, but in most patients, weak or focal staining was evident. Tissue transglutaminase was also present in lamina propria and seemed to be more concentrated in its upper part beneath superficial epithelium or around crypts. In disease controls, the staining of epithelium varied from full absence (one case of acid-associated duodenitis) to being rather strong (Crohn's duodenitis and atrophic enteritis associated with *C. jejuni* infection; Fig. 3). The last case also showed increased tTG expression in lamina propria while the other pathological controls did not demonstrate any evident peculiarities of the staining in lamina propria.

The results of quantitative evaluation of tTG expression are shown in Table 3. The positivity of superficial/villus epithelium differed significantly between the three groups. It was increased in both CD and DC, and CD patients showed more conspicuous increase. In relation to NC, both these groups also demonstrated stronger tTG expression, which was proved by higher index of intensity, although, the difference between CD and DC was not significant. Cryptal epithelium in CD group had a higher level of positivity than NC, but low index of intensity showed that this extensive positive area was stained rather weak. The same pattern was seen in DC which showed even a lower intensity level than CD patients. In lamina propria, we also found an increase in positivity in CD and DC while the intensity was similar in all the three groups.

Comparing the average index of intensity in different compartments of each group, we also revealed a difference in tTG distribution in duodenal mucosa. In NC, the index of intensity was similar in villus epithelium, cryptal epithelium, and lamina propria ($p=0.407$, Kruskal–Wallis ANOVA). In contrast, the index of intensity was different among these three compartments in CD ($p<0.0001$) and DC ($p<0.0001$). In both groups, the level of intensity in superficial epithelium was higher than in cryptal epithelium ($p<0.0001$), and in CD, it was even higher than in lamina propria ($p<0.0001$).

Table 4 Individual histological and serological data before and after a follow-up period

Number of case	Marsh grade, initial assessment	Increased serological markers, initial assessment	Follow-up period (month)	Marsh grade, repeated assessment	Increased serological markers, repeated assessment	Comments
1	IIIC	anti-tTG-IgA, AGA-IgA	5	IIIB	↓anti-tTG-IgA, ↓AGA-IgA	strict GFD
2	IIIC	AGA-IgA	6	0	None	strict GFD, NSAID
3	IIIC	AGA-IgG	10	0	↓AGA-IgG	strict GFD
4	IIIC	anti-tTG-IgA, AGA-IgA, AGA-IgG	14	0	None	strict GFD
5	IIIC	anti-tTG-IgA, AGA-IgA, AGA-IgG	18	I	None	strict GFD
6	IIIC	AGA-IgA, AGA-IgG	19	0	↓AGA-IgG	strict GFD, prednisolone
7	IIIC	anti-tTG-IgA, AGA-IgA, AGA-IgG	20	I	None	strict GFD
8	IIIC	anti-tTG-IgA, AGA-IgA, AGA-IgG	15	IIIC	anti-tTG-IgA, AGA-IgA, AGA-IgG	GFD for 6 months followed by HGD
9	IIIA	AGA-IgA	24	0	AGA-IgA	GFD for 6 months followed by HGD
10	IIIC	anti-tTG-IgA, AGA-IgA, AGA-IgG	7	IIIC	anti-tTG-IgA, AGA-IgA, AGA-IgG	HGD
11	IIIB	AGA-IgA, AGA-IgG	13	IIIA	AGA-IgA, AGA-IgG	HGD, prednisolone
12	IIIC	anti-tTG-IgA, AGA-IgA, AGA-IgG	15	IIIC	anti-tTG-IgA, AGA-IgA, AGA-IgG	HGD
13	IIIC	anti-tTG-IgA, AGA-IgA, AGA-IgG	21	IIIC	anti-tTG-IgA, AGA-IgA, AGA-IgG	HGD
14	IIIC	anti-tTG-IgA, AGA-IgA, AGA-IgG	25	IIIC	anti-tTG-IgA, AGA-IgA, AGA-IgG	HGD
15	IIIC	anti-tTG-IgA, AGA-IgA, AGA-IgG	60	IIIB	None	strict GFD, collagenous sprue, resistant to GFD, prednisolone, and azathioprine

The *downward arrow* indicates a marker showing a significant decrease in relation to the initial level, but is still above the normal limit

GF gluten-free diet, *HGD* hypogluten diet

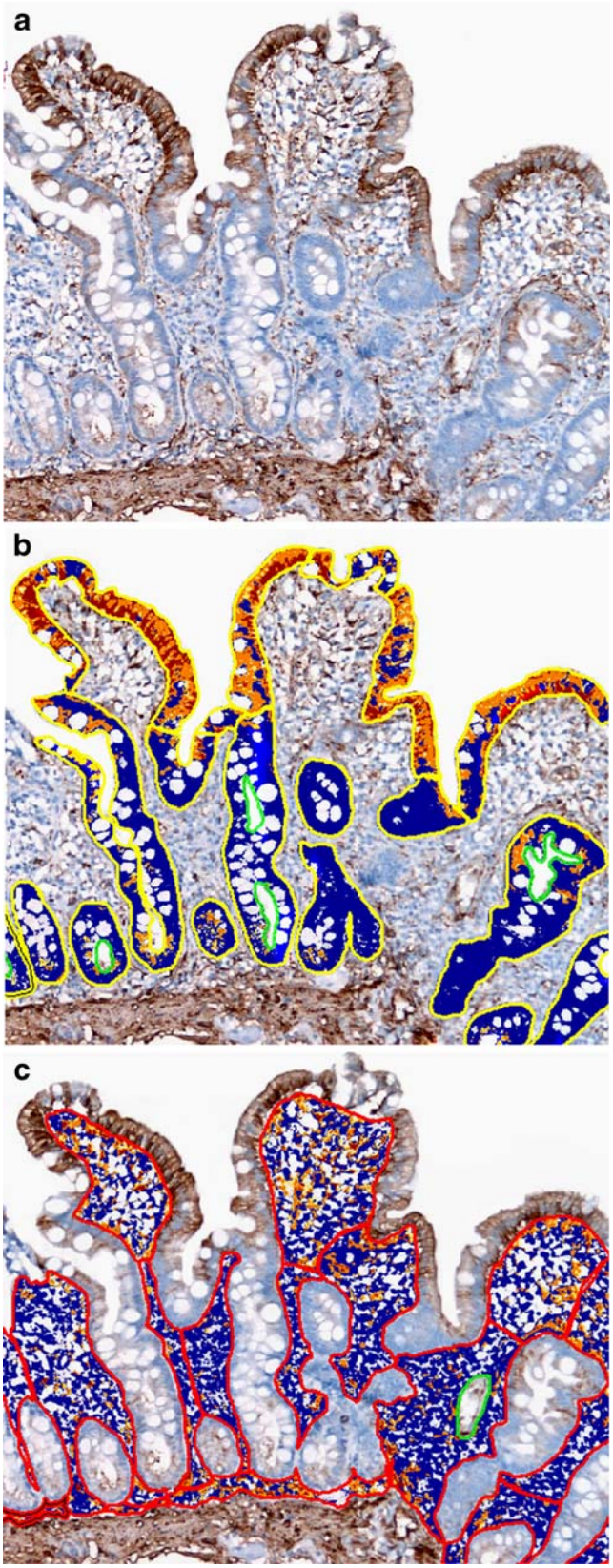

Fig. 4 Duodenal mucosa from a patient with untreated CD (Marsh IIIB) × 100. **a** Native immunohistochemical image. **b** Markup image after evaluation of the epithelial staining by positive pixel count algorithm. **c** Markup image after evaluation of the lamina propria. Color meanings on the markup images are as follows: *blue*—negative pixels, *yellow*—weak positive pixels, *orange*—positive pixels, and *red*—strong positive pixels

Follow-up of celiac disease patients

After CD diagnosis, all the patients were recommended to keep on GFD, and in 15 of them, tTG expression was assessed repeatedly (Table 4). All these patients reported a decrease in gluten intake and had clinical improvement. Eight out of 15 complied with the GFD and significantly decreased or normalized their serological markers during the follow-up period (strict GFD); the others did not fully comply as reported by the patients themselves and supported by a persistently elevated level of serological markers (hypogluten diet). There was one case of CD complicated with collagenous sprue in this group. This patient followed strict GFD and normalized her serological markers, but mucosal atrophy and significant clinical symptoms persisted that is why GFD was supplemented with permanent taking of prednisolone or azathioprine. In two more cases, prednisolone was given initially due to severe condition and then stopped.

Pair analyses of the each patient's results showed a significant decrease in positivity and/or index of intensity in superficial epithelium for 12 patients (Fig. 4, 5, 6a). In most cases, a decrease in positivity of cryptal epithelium and lamina propria was also seen, but the intensity in these compartments seemed to be quite variable (Fig. 6b-c). Three of 15 patients had opposite changes in all the compartments and were remarkable by the following peculiarities: patient 2—persistently taking nonsteroidal anti-inflammatory drugs (NSAID) due to rheumatoid arthritis; patient 10—not fully compliant with GFD; patient 15—suffering from collagenous sprue with persisting atrophy despite GFD. Excluding this last case, we also performed a pair group comparison (14 pairs) using Wilcoxon matched pair test and found that the positivity of superficial epithelium, cryptal epithelium, and lamina propria significantly decreased in the follow-up group (Fig. 7), while there were no significant changes in intensity.

Fig. 5 Duodenal mucosa from the same patient as in Fig. 4 after GFD (Marsh IIIA) × 100. **a** Native immunohistochemical image. **b** Markup image after evaluation of the epithelial staining by positive pixel count algorithm. **c** Markup image after evaluation of the lamina propria. In comparison with Fig. 4, decrease in tTG expression is evident. Color meanings on the markup images are as follows: *blue*—negative pixels, *yellow*—weak positive pixels, *orange*—positive pixels, and *red*—strong positive pixels

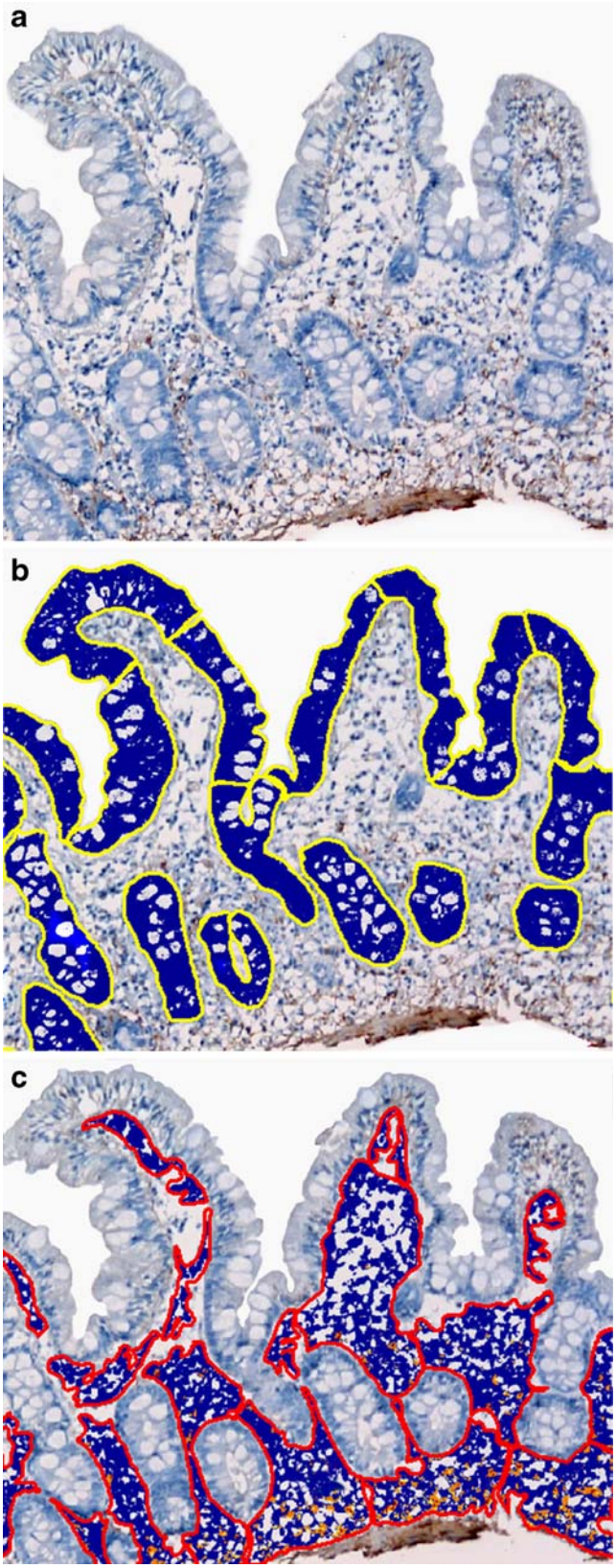

Discussion

The previous studies have shown that tTG appears in normal intestinal mucosa. It does not raise doubts that it can be found just beneath the epithelium, in lamina propria, and in the muscularis mucosae [16–19], but the data about its epithelial localization is conflicting. Some investigators have revealed epithelial tTG expression in normal duodenal mucosa [20], but the others have not [16, 17, 21]. We also have not found any significant epithelial tTG expression in most patients with normal duodenal mucosa except two cases with small focal areas of staining and believe that epithelial tTG expression is not usual for the normal duodenum. There is evidence from many studies conducted in the last 20 years that tTG is up-regulated in celiac mucosa [12–14], but till now, there exists some controversy concerning tTG distribution pattern in celiac mucosa and the source of its increased activity [11, 17, 19, 20, 22].

Our study has shown that celiac duodenal mucosa differs from normal controls by a significant increase in tTG expression in lamina propria, which agrees with the data of the other authors [17]. This tTG overexpression can be explained by externalization of tTG by lamina propria cells [23], namely, macrophages, which are present in increased numbers in celiac mucosa [20] or production of tTG by endothelial cells [22].

Our study has also demonstrated that the epithelial tTG expression is a characteristic for CD. We have revealed the significant increase in tTG expression in cryptal and, especially, in superficial epithelium in patients with untreated CD. Earlier, the presence of tTG in intestinal epithelium in CD was found by some investigators [17, 21, 24], but the number of examined patients with untreated CD in those studies was rather small (5–10). So, we have confirmed these results on a larger group of CD patients. Apart from that, following up the patients who were recommended to stop gluten intake, we have demonstrated a decrease in tTG expression in epithelium and lamina propria in a repeatedly taken mucosa samples. It testifies that a high tTG expression in CD patients is not constitutive and might be affected by some factors. Due to a relatively small number of pairs, we did not further stratify these patients, although, the analysis of individual cases showed that the data of some individuals were inconsistent with the group data. It can be supposed that such factors as mucosal atrophy, inflammation, gluten intake, and medication like prednisolone, azathioprine, or NSAID could influence the tTG expression. Biagi F. et al., being based on their own study, concluded that epithelial distribution of tTG was gluten dependent [21]. Our results, based on the follow-up of the same patients before and after GFD, do not fully allow in agreeing with that statement as we did not find any decrease in tTG expression in some patients keeping to

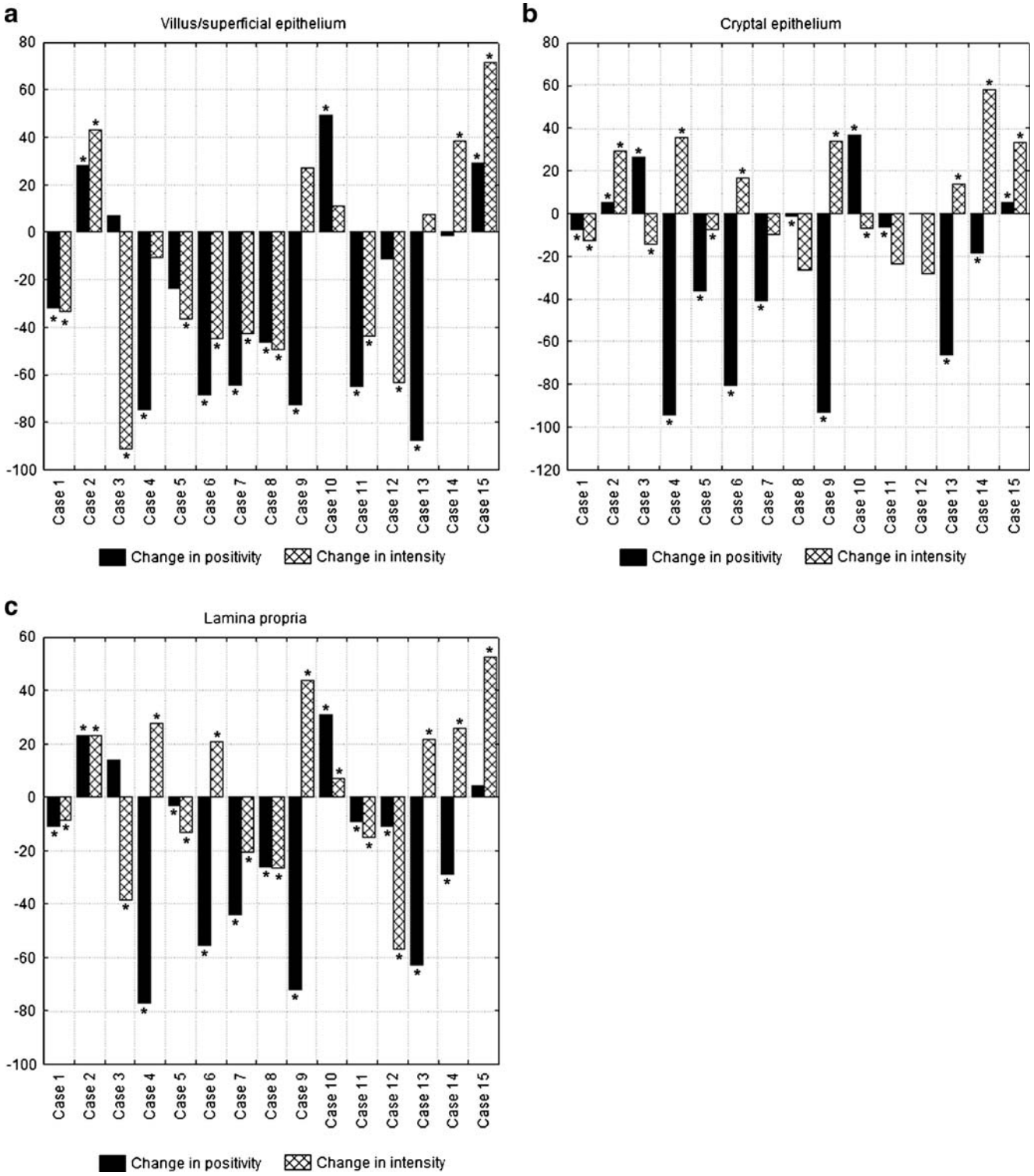

Fig. 6 Individual changes in positivity and index of intensity after prescription of GFD. **a** Superficial/villus epithelium. **b** Cryptal epithelium. **c** Lamina propria. Positive values mean an increase in parameters while negative ones—a decrease. The *asterisk* indicates that the difference is significant; $p<0.05$; Mann–Whitney's U test

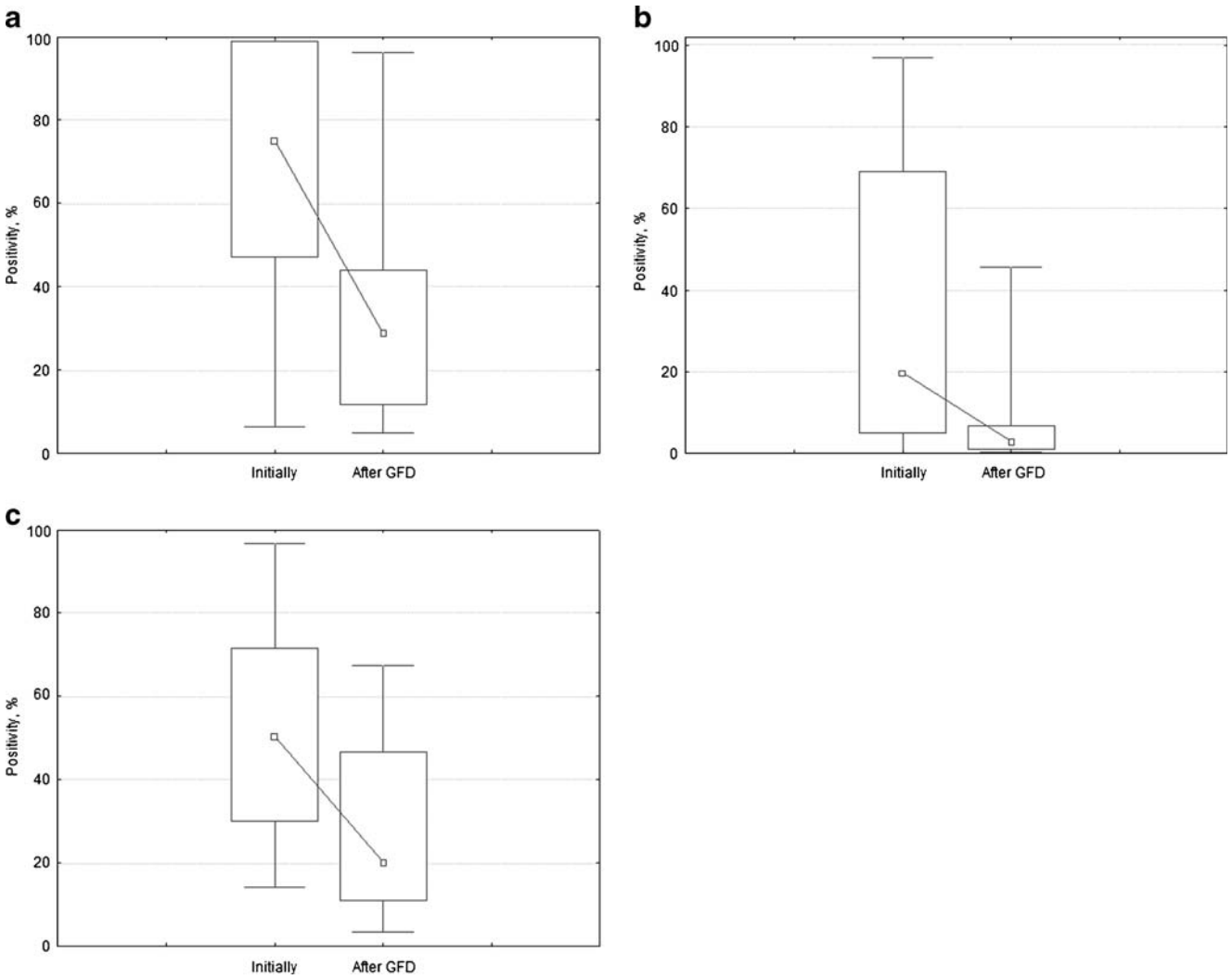

Fig. 7 TTG positivity in CD patients before and after prescription of GFD. **a** Superficial/villus epithelium, $p=0.019$. **b** Cryptal epithelium, $p=0.041$. **c** Lamina propria, $p=0.041$. Median values are shown by an *empty square*; the *box* represents values between the 25th and the 75th percentiles; the *lower* and *upper bars* indicate minimal and maximal values

strict GFD. On the other hand, as the sensitivity of AGA and anti-tTG in assessment of adherence to gluten-free diet is not the same, the possibility of misinterpretation of compliance to GFD cannot be fully excluded.

Contrary to the above-mentioned studies, W. Sakly et al. found that in CD group there were significantly less patients displaying tTG expressing enterocytes than in the control group [20]. Maiuri L. et al. did not manage to discover epithelial tTG expression in both treated and untreated celiac mucosa using anti-tTG CUB 7402 [11]. There are also some studies which failed to reveal any difference in tTG expression pattern between CD patients and normal controls [5, 6, 17]. Such controversy regarding tTG expression in celiac mucosa could be possibly explained by heterogeneity of CD, but can also be due to methodological differences. In contrast with other authors who assessed immunohistochemical or immunofluorescent staining qualitatively or semi-quantitatively, we used special image analysis software to analyze our samples. Although such approach needs much more time for all samples to be analyzed, it allows subjectivity to minimize and to prove significant differences even in relatively small group of samples. Thus, based on our own data and similar results of other investigators, we believe that CD, at least in part of patients, is associated with changes in tTG distribution in intestinal mucosa.

At present, there is no one opinion concerning the specificity of epithelial tTG expression in CD [17, 21]. That is why our study has been also designed to assess if the tTG distribution pattern found in CD is disease specific. Investigating our pathological controls, we revealed that the changes in tTG distribution are similar to those ones in CD group, namely, increase in tTG expression in epithelium and lamina propria. So, we believe that these changes of

the tTG expression are not specific for CD and could represent a universal mucosa reaction to inflammation or atrophy. Contrary to us, Biagi F. et al. had found epithelial tTG expression to be specific for CD, but only one non-CD condition, such as autoimmune enteropathy, served as pathological control in that study [21]. Thus, it could be also supposed that absence of tTG expression in enterocytes might be specific for autoimmune enteropathy. Our conclusion concerning nonspecificity of tTG overexpression is supported by the results of other authors. The increase in tTG expression in small bowel Crohn's disease has already been shown in the study of D'Argenio G. et al. [25] and was also noticeable in our pathological control with duodenal Crohn's disease. Just recently, Villanacci V. et al. have found that mucosal tTG distribution in duodenitis is the same as in CD, and the positivity in this study was similar in frozen and fixed material [22]. It is also known that tTG overexpression can be found in inflammatory conditions affecting other organs, e. g., idiopathic inflammatory myopathies [26] or anterior polar cataracts [27]. The inflammatory cytokines (IFN-gamma and TGF-beta) seem to be responsible for the tTG up-regulation, at least partly [28, 29]. In its turn, the increased tTG activity triggers NF-kappaB activation inducing the polymerization of NF-kappaB inhibitory protein I-kappaB-alpha and participating in that way in the regulation of inflammation [30, 31].

In conclusion, finding tTG overexpression in lamina propria and intestinal epithelium is a characteristic but not specific for celiac mucosa, which seems to agree with the recent data about involving tTG in the inflammation process. Further investigations are needed to clear up how far an altered expression and distribution of tTG contributes to CD pathogenesis.

Acknowledgments We express our gratitude to Dr. O. Karatysh, Dr. I. Dergacheva, Dr. H. Usau, and Dr. S. Kondrashov for their collaboration and help with the clinical part of the study. The excellent technical assistance of Mrs. S. Klimovich and Mrs. M. Pavlova is also gratefully acknowledged.

Conflict of interest statement We declare that we have no conflict of interest.

Funding This work was supported by the Belarusian Republican Foundation for Basic Research (number 20052078).

References

1. Griffin M, Casadio R, Bergamini CM (2002) Transglutaminases: nature's biological glues. Biochem J 368(Pt 2):377–396
2. Wodzinska JM (2005) Transglutaminases as targets for pharmacological inhibition. Mini Rev Med Chem 5:279–292
3. Reif S, Lerner A (2004) Tissue transglutaminase—the key player in celiac disease: a review. Autoimmun Rev 3:40–45
4. van de Wal Y, Kooy Y, van Veelen P et al (1998) Selective deamidation by tissue transglutaminase strongly enhances gliadin-specific T cell reactivity. J Immunol 161:1585–1588
5. Arentz-Hansen H, Körner R, Molberg O et al (2000) The intestinal T cell response to alpha-gliadin in adult celiac disease is focused on a single deamidated glutamine targeted by tissue transglutaminase. J Exp Med 191:603–612
6. Facchiano F, Facchiano A, Facchiano AM (2006) The role of transglutaminase-2 and its substrates in human diseases. Front Biosci 11:1758–1773
7. Piper JL, Gray GM, Khosla C (2002) High selectivity of human tissue transglutaminase for immunoactive gliadin peptides: implications for celiac sprue. Biochemistry 41:386–393
8. Dieterich W, Esslinger B, Trapp D et al (2006) Cross-linking to tissue transglutaminase and collagen favours gliadin toxicity in coeliac disease. Gut 55:478–484
9. Sollid LM, Molberg O, McAdam S et al (1997) Autoantibodies in coeliac disease: tissue transglutaminase—guilt by association? Gut 41:851–852
10. Barone MV, Caputo I, Ribecco MT et al (2007) Humoral immune response to tissue transglutaminase is related to epithelial cell proliferation in celiac disease. Gastroenterology 132:1245–1253
11. Maiuri L, Ciacci C, Ricciardelli I et al (2005) Unexpected role of surface transglutaminase type II in celiac disease. Gastroenterology 129:1400–1413
12. Bruce SE, Bjarnason I, Peters TJ (1986) Human jejunal transglutaminase: demonstration of activity, enzyme kinetics, and substrate specificity with special relation to gliadin and coeliac disease. Clin Sci (Lond) 68:573–579
13. D'Argenio G, Sorrentini I, Ciacci C et al (1989) Human serum transglutaminase and coeliac disease: correlation between serum and mucosal activity in an experimental model of rat small bowel enteropathy. Gut 30:950–954
14. Skovbjerg H, Hansen GH, Niels-Christiansen LL et al (2004) Intestinal tissue transglutaminase in coeliac disease of children and adults: ultrastructural localization and variation in expression. Scand J Gastroenterol 39:1219–1227
15. Kim SY, Jeitner TM, Steinert PM (2002) Transglutaminases in disease. Neurochem Int 40:85–103
16. Ciccocioppo R, Di Sabatino A, Biagi F et al (2003) Gliadin and tissue transglutaminase complexes in normal and coeliac duodenal mucosa. Clin Exp Immunol 134:516–524
17. Esposito C, Paparo F, Caputo I et al (2003) Expression and enzymatic activity of small intestinal tissue transglutaminase in celiac disease. Am J Gastroenterol 98:1813–1820
18. Molberg O, Mcadam SN, Körner R et al (1998) Tissue transglutaminase selectively modifies gliadin peptides that are recognized by gut-derived T cells in celiac disease. Nat Med 4:713–717
19. Brusco G, Muzi P, Ciccocioppo R et al (1999) Transglutaminase and coeliac disease: endomysial reactivity and small bowel expression. Clin Exp Immunol 118:371–375
20. Sakly W, Sriha B, Ghedira I et al (2005) Localization of tissue transglutaminase and N (epsilon)-(gamma) -glutamyl lysine in duodenal mucosa during the development of mucosal atrophy in coeliac disease. Virchows Arch 446:613–618
21. Biagi F, Campanella J, Laforenza U et al (2006) Transglutaminase 2 in the enterocytes is coeliac specific and gluten dependent. Dig Liver Dis 38:652–658
22. Villanacci V, Not T, Sblattero D et al (2009) Mucosal tissue transglutaminase expression in celiac disease. J Cell Mol Med 13:334–340
23. Aeschlimann D, Thomazy V (2000) Protein cross-linking in assembly and remodelling of extracellular matrices: the role of transglutaminases. Connect Tissue Res 41:1–27
24. Hansson T, Ulfgren AK, Lindroos E et al (2002) Transforming growth factor-beta (TGF-beta) and tissue transglutaminase ex-

pression in the small intestine in children with coeliac disease. Scand J Immunol 56:530–537
25. D'Argenio G, Biancone L, Cosenza V et al (1995) Transglutaminases in Crohn's disease. Gut 37:690–695
26. Choi YC, Kim TS, Kim SY (2004) Increase in transglutaminase 2 in idiopathic inflammatory myopathies. Eur Neurol 51: 10–14
27. Wan XH, Lee EH, Koh HJ et al (2002) Enhanced expression of transglutaminase 2 in anterior polar cataracts and its induction by TGF-beta in vitro. Br J Ophthalmol 86:1293–1298
28. Ientile R, Caccamo D, Griffin M (2007) Tissue transglutaminase and the stress response. Amino Acids 33:385–394
29. Kim SY, Jeong EJ, Steinert PM (2002) IFN-gamma induces transglutaminase 2 expression in rat small intestinal cells. J Interferon Cytokine Res 22:677–682
30. Kim SY (2006) Transglutaminase 2 in inflammation. Front Biosci 11:3026–3035
31. Lee J, Kim YS, Choi DH et al (2004) Transglutaminase 2 induces nuclear factor-kappaB activation via a novel pathway in BV-2 microglia. J Biol Chem 279:53725–53735

Virchows Arch (2009) 455:375–381
DOI 10.1007/s00428-009-0833-8

ORIGINAL ARTICLE

Intra- and interobserver reproducibility of interpretation of immunohistochemical stains of prostate cancer

Sara Jonmarker Jaraj · Philippe Camparo · Helen Boyle · François Germain · Bo Nilsson · Fredrik Petersson · Lars Egevad

Received: 22 July 2009 / Revised: 27 August 2009 / Accepted: 1 September 2009 / Published online: 18 September 2009

Abstract The evaluation of immunohistochemistry (IHC) is usually semiquantitative, and thus subject to observer variability. We analyzed the reproducibility of different IHC measures. Fifty TMA cores of prostate cancer were stained for PDX-1, a transcription factor overexpressed in the cytoplasm of prostate cancer cells. The strongest intensity was scored 0–3 and 1–3 was used for extent (1–33%, 34–66%, and 67–100%). The stains were evaluated twice by four observers: two genitourinary pathologists, and two medical doctors with no formal pathology training. Staining intensity was also measured with automated image analysis. The pathologists read the slides faster than nonpathologists (total time 88 and 178 min, respectively, $p=0.03$). Mean weighted kappa for intraobserver agreement was 0.85 (range 0.81–0.89) for intensity and 0.43 (range 0.38–0.51) for extent with similar results among pathologists and nonpathologists. Mean weighted kappa for interobserver agreement was 0.80 (range 0.77–0.84) for intensity and 0.21 (range 0.11–0.26) for extent. The subjective estimations of intensity correlated with results of image analysis ($r=0.61$–0.66, $p<0.001$), but the correlation between observers was stronger ($r=0.75$–0.81) and correlated better with Gleason grade. Thus, subjective assessment of intensity can be done with a high level of reproducibility while estimation of staining extent is less reliable. Although educated pathologists were faster, the level of pathology training is not crucial for obtaining reproducible results in the analysis of TMA-based studies.

Keywords Adenocarcinoma of the prostate · Immunohistochemistry · Reproducibility · Image analysis · Tissue microarray

S. Jonmarker Jaraj · B. Nilsson · F. Petersson · L. Egevad (✉)
Department of Oncology-Pathology, Karolinska Institutet,
Karolinska University Hospital Solna,
171 76 Stockholm, Sweden
e-mail: lars.egevad@ki.se

P. Camparo
Service d'Anatomie et Cytologie Pathologiques, Hopital Foch,
Paris, France

H. Boyle
Department of Oncology, Centre Leon Berard,
Lyon, France

F. Germain
Noesis,
Gif sur Yvette, France

L. Egevad
International Agency for Research on Cancer,
Lyon, France

Introduction

Immunohistochemistry (IHC) has been widely used for protein detection in tissue sections for more than 30 years. Although many other methods have appeared recently, IHC is still extensively used in both diagnostic pathology and research. It is therefore essential that the procedures of immunostaining and evaluation are uniform and that human errors are minimized, thus providing reliable results.

Methodological issues of IHC laboratory techniques have been extensively addressed [1–4] but the assessment of staining is also of great importance [5, 6]. The evaluation of IHC is often semiquantitative, and thus subject to observer variability. The reproducibility of this evaluation is seldom considered. There is no consensus on the preferred evaluation method. The intensity and extent of staining are often assessed [7–14]; but the scales and calculation methods vary. In our group, the strongest

intensity and the extent of this intensity are graded and multiplied to obtain a product from 0–9 [7, 11, 13, 14]. Some groups multiply several intensity levels in the same specimen by their extents and then add them [8, 15]. Depending on the scales for intensity and extent, this scoring system is sometimes referred to as the Histon score [16, 17]. In the Allred score, the proportion of positive cells is added to the average intensity [18]. The quickScore has a similar scoring system but with other scales [19, 20]. Volante et al. used a system where subcellular localization and extent of staining is scored simultaneously on a four-tier scale that includes both intensity and subcellular location [21]. Other scoring systems such as percentage of positive stained cells, without regard to the intensity, exist as well [22].

Often, more than one observer is used for validation [9, 18]. The slides may be read by several observers in an open discussion at a multiheaded microscope [17] or the observers may do individual and independent observations, followed either by calculation of an average score [7, 11, 13, 14] or by an open discussion about the cases that obtain conflicting results [21, 23].

Tissue microarrays (TMA) were first described in 1998 [24] and have since then become a common method for evaluation of large series of tissue samples, both using IHC and other methods such as fluorescent in situ hybridization. Compared to full mount tissue samples, TMA is a high-throughput method. Thus, less antibody is needed, staining time is shorter, evaluation is quicker and simpler, and less space is needed for storage. It may be argued that only small parts of samples are studied, but this is the case also in full mounts since only thin sections are stained.

Rubin et al. showed that three cores per tumor were required for correct assessment of prostate cancer IHC [25]. Singh et al. reported that a minimum of five cores per tumor was necessary in order to take tissue heterogeneity into account [26]. Number of cores that are required most likely depends on the investigated marker. In studies of prostate cancer, one [12, 27], two [23, 28] or three cores [7, 11, 13, 14, 29, 30] of tumor tissue per case are commonly used but sometimes even more than that [15]. TMA requires a careful selection of material for core harvesting. This is particularly true for prostate cancer since this is a very heterogeneous tumor type.

Our aim was to analyze inter- and intraobserver reproducibility of scoring of a cytoplasmic staining. Pancreatic duodenal homeobox-1 (PDX-1) was used as test staining. PDX-1 is a Hox-type transcription factor expressed during early embryonic stages of pancreatic development. The main function involves regulation of glucose-dependent insulin gene transcription. PDX-1 expression and overexpression has been seen in several forms of human carcinomas [31–33]. Our group has recently demonstrated a cytoplasmic overexpression of PDX-1 in prostate cancer [11]. In the current study, we also attempted to evaluate subjective scoring against results of image analysis, i.e., presumably objective methods.

Materials and methods

Tissue collection and preparation

The cores selected for this study were part of a larger tissue microarray series consisting of 289 formalin-fixed, paraffin-embedded radical prostatectomy specimens collected from 1998 to 2002 at Karolinska Hospital, Solna, Sweden. None of the patients had received hormonal therapy or radiotherapy prior to surgery. TMAs were constructed using a Beecher Manual Arrayer I (Beecher Instruments Inc, Sun Prairie, WI, USA). Three tumor cores with a diameter of 1 mm were collected from each specimen.

Immunohistochemistry

After rehydration, endogenous peroxidase was inactivated for 30 min in 0.3% H_2O_2 in methanol. Slides were boiled in a microwave oven for 15 min in Vector H 3300 antigen unmasking solution (Vector Laboratories, Burlingame, CA, USA). Nonspecific binding sites were blocked with 5% skimmed milk in PBS with 0.1% BSA. The slides were incubated with a primary rabbit polyclonal antibody against PDX-1 (Abcam, Cambridge, MA, USA) at 1:4,000 dilutions at 4°C overnight. The secondary antibody (Elite kit Vector 5 ml/ml in PBS with 0.1% BSA) was applied for 30 min at room temperature. The signal was increased with the ABC kit (20 ml A+20 ml B/ml PBS-0.1% BSA) at 37°C for 45 min and detected with DAB (Vector kit SK 4100). The slides were counterstained with hematoxylin. Human breast cancer was used as positive and negative control according to the manufacturer's instructions.

Core selection

After immunostaining, 50 cores from the first three blocks were selected. The selection was done in consecutive order, with one core from each case. Only cores containing a large amount of cancer were selected. This was done to simplify the evaluation and minimize error due to difficulty in distinguishing prostate cancer from benign or premalignant changes. Therefore, cores containing prostatic intraepithelial neoplasia (PIN) or a large percentage of benign glands were not chosen. As we included observers with little pathological training this selection was considered necessary to ensure that the correct glands were graded. Reference cores for standardization of intensity levels were selected from the same three blocks and were not included in the reproducibility study dataset.

Evaluation of TMA

Subjective

Intensity and extent of immunoreactivity (IR) and their product (IRP) were evaluated in each core by four independent observers (HB, LE, SJ, FP), including two senior pathologists specialized in urogenital pathology (LE, FP), and two medical doctors with no formal training in pathology (an oncology resident with no training in evaluation of IHC and a PhD student with experience of reading IHC slides). The material was evaluated at two occasions with a two-week interval. The intensity was scored from 0 (no staining) to 3 (most intense staining) based on the strongest staining of the core. The extent of positive intracytoplasmic staining was evaluated in a semiquantitative manner. Scoring was based on percentage of stained epithelial cells and graded from 1 to 3, signifying 1–33%, 34–66%, and >66%, respectively.

Digital image analysis

Color intensity (brown) was measured by digital image analysis (Noesis, Paris, France). No selection was made of areas involved by color intensity measurement, i.e., false positive areas in stroma were not excluded. Regression analysis was calculated between the results of the automated measurement and against the subjective assessments. A second measurement with digital image analysis was performed on the same TMA spots 6 months later and compared with the first measurement by regression analysis.

Statistical analysis

Weighted kappa statistics were used for assessment of inter- and intraobserver variability of immunoreactivity scores. Kappa statistics measures the agreement between observers. A kappa value of 1 indicates perfect concordance, 0 means agreement at the level of chance, and negative values agreement worse than chance agreement. A weighted kappa also takes the magnitude of the disagreement into account so that for example 1 vs. 3 on a three-tier scale is worse than 2 vs. 3. A kappa value of 0 to 0.2, 0.21 to 0.4, 0.41 to 0.6, 0.61 to 0.8, and 0.81 to 1 was considered as slight, fair, moderate, substantial, and almost perfect agreement, respectively. Spearman rank regression analysis was used for comparison of the results of image analysis and subjective assessments. Paired and unpaired Student's t test was used when appropriate for comparisons of time spent on the analyses. A p value of <0.05 was considered significant.

Ethics committee decision

The study was approved by the ethics committees at the Karolinska University Hospital, Stockholm (2006/4:10) and at IARC, Lyon (06–08).

Results

The pathologists needed less than half the time of that required by the nonpathologists to perform the first evaluation ($p=0.001$; Table 1). In the second evaluation, the nonpathologists improved their speed considerably and there was no longer a significant difference in time needed for evaluation compared to the pathologists ($p=0.32$). The total time taken to read the slide twice was less for the pathologists ($p=0.025$).

Mean weighted kappa for intraobserver agreement of intensity, extent, and IRP were 0.85 (range 0.81=0.89), 0.43 (range 0.38–0.51), and 0.83 (range 0.73–0.89), respectively (Table 2). Pathologists and nonpathologists had similar intraobserver agreement evaluation 2 for intensity (mean 0.84 and 0.86), extent (mean 0.41 and 0.45), and IRP (mean 0.81 and 0.85). Mean weighted kappa for interobserver agreement of intensity, extent and IRP were 0.80 (range 0.77–0.84), 0.21 (range 0.11–0.26), and 0.79 (range 0.67–0.88), respectively (Table 3). Pathologists and nonpathologists had similar interobserver

Table 1 Time (min) spent on the evaluations

Observer	Training	Evaluation 1 (min)	Evaluation 2 (min)	Total (min)	Evaluation 1 vs. 2 p value
1	P	50	45	95	
2	P	45	35	80	
	Mean	95	80	175	0.20
3	NP	120	70	190	
4	NP	120	45	165	
	Mean	240	115	355	0.13
Average		83.8	48.8	132.5	0.13
P vs. NP p value		0.001	0.32	0.025	

P pathologists, *NP* nonpathologists

Table 2 Intraobserver agreement (weighted kappa) of the four observers

Observer	Training	Intensity	Extent	IRP
1	P	0.874	0.437	0.889
2	P	0.810	0.383	0.730
3	NP	0.828	0.506	0.872
4	NP	0.891	0.396	0.829
Average		0.851	0.431	0.830

P pathologists, *NP* nonpathologists, *IRP* immunoreactivity product (the product of intensity and extent)

Table 4 Correlation coefficient between the four observers (evaluation 1)

Observer	Intensity	Extent	IRP
1 vs. 2	0.805	0.169	0.734
1 vs. 3	0.802	0.169	0.783
1 vs. 4	0.799	0.332	0.815
2 vs. 3	0.754	0.415	0.721
2 vs. 4	0.804	0.453	0.758
3 vs. 4	0.750	0.475	0.787

IRP immunoreactivity product (the product of intensity and extent)

agreement for intensity (0.81 and 0.79), extent (0.24 and 0.25), and IRP (0.79 and 0.82).

The correlation coefficients between observers for intensity, extent and IRP were 0.75–0.81, 0.17–0.48, and 0.72–0.82, respectively, in evaluation 1 (Table 4), and 0.77–0.86, 0.30–0.43, and 0.72–0.86, respectively, in evaluation 2 (Table 5). The subjective estimation of intensity by each observer correlated with results of automated image analysis (r=0.61–0.66, p<0.001). The results of the two automated measurements were not identical, but correlated strongly with each other (r=1.0, p<0.001). The mean difference in measured intensity was only 0.012% (0–0.24%).

The subjective estimation of the staining intensity correlated with the Gleason pattern of the core in three observers (r=0.31–0.39, p=0.015–0.028), but not in one of the nonpathologists (r=0.19, p=0.19). The automated analysis showed no correlation with Gleason pattern (r=−0.001, p=0.99).

Discussion

IHC is a standard method for protein detection and quantitation in research and clinical work, but has many potential sources of error. Technical and methodological aspects of the staining have been thoroughly investigated, while the evaluation of slides has received less attention. Microscopic evaluation of IHC is subjective and based on different scoring systems and scales with poor standardization. In research, this leads to a lack of reproducibility, while in clinical applications it is even more problematic, since IHC results may alter treatment with great effect for the individual patients. There is no gold standard for IHC annotation, and perhaps there never will be, as each antibody must be considered individually. Some proteins are easily classified as cytoplasmic, membranous or nuclear, while others are expressed in several cell compartments, e.g., both in the cytoplasm and nucleus. Blotchy, heterogeneous staining is also common and may benefit from a different evaluation scale. It is conceivable that the clinical implication of staining varies between different proteins and tissues. Whereas, the mere existence of hormone receptors may be an indication for hormone therapy in breast cancer, the varying levels of other proteins in cancer tissue may be important.

In this study, evaluation of staining intensity reached a surprisingly strong intraobserver agreement that was almost perfect as measured by kappa statistics. Interobserver agreement was likewise high, ranging from substantial to almost perfect. This indicates that subjective estimation of the staining intensity may be sufficient for reliable and

Table 3 Interobserver agreement (weighted kappa) between the four observers

Observer	Intensity	Extent	IRP
1 vs. 2	0.807	0.245	0.794
1 vs. 3	0.799	0.255	0.882
1 vs. 4	0.842	0.206	0.802
2 vs. 3	0.771	0.216	0.770
2 vs. 4	0.817	0.109	0.671
3 vs. 4	0.786	0.250	0.817
Average	0.804	0.214	0.789

IRP immunoreactivity product (the product of intensity and extent)

Table 5 Correlation coefficient between the four observers (evaluation 2)

Observer	Intensity	Extent	IRP
1 vs. 2	0.848	0.402	0.859
1 vs. 3	0.815	0.419	0.864
1 vs. 4	0.848	0.401	0.834
2 vs. 3	0.770	0.426	0.776
2 vs. 4	0.857	0.300	0.715
3 vs. 4	0.814	0.413	0.819

IRP immunoreactivity product (the product of intensity and extent)

robust measurement of IHC in TMA. The use of internal reference cores representing each intensity grade may have contributed to the high intra- and interobserver agreement (Fig. 1). It has been suggested that an internal control should be used to overcome batch variations [6].

By contrast, extent of staining showed a poor intra- and interobserver agreement. In previous studies, we have found that extent generally correlate less well with outcome measures than intensity [11]. We have also routinely calculated the product of intensity and extent, although this measure has provided no or marginal improvement over intensity alone for e.g., prediction of prognosis. These earlier results indicate that extent of staining may be of less importance than previously assumed. The present study raises serious concern about extent as a reproducible measure in TMA assessment. Standard cores for extent were not used, but whether this would be useful is questionable. Interestingly, the weighted kappa values of IRP were almost as good as those of intensity. This indicates that the poor reproducibility of extent may be balanced by the intensity. If an observer hesitates between an intensity of 2 with extent 3 and an intensity of 3 with extent 1, the relative discrepancy of extent exceeds that of the product of intensity and extent.

There was no difference in the reproducibility achieved by trained pathologists and nonpathologists, which indicates that IHC assessments can be performed with a high accuracy early in pathology training. In the current study, cores were selected to contain sufficient amount of invasive carcinoma because our aim was to measure the ability to evaluate IHC itself and not the ability to accurately diagnose prostate cancer. If the series would have been unselected and included pitfalls such as PIN, benign proliferations or unusual cancer types, the results may have been different. However, we nevertheless believe that it is possible to train devoted junior colleagues to do IHC assessment in research.

The evaluation of the slides was more time-consuming for nonpathologists than for pathologists in the first evaluation, while the difference decreased in the second evaluation. Thus, junior observers seem to have compensated lack of experience with more careful observation. Both groups of participants increased their speed in the second evaluation, probably because the observers had already seen the slides once and established their internal references.

To obtain a more objective and reproducible evaluation of IHC, it has been suggested that subjective assessment should be replaced by automated image analysis [34, 35]. The correlation between Noesis, the automatic image analysis system used in this study, and subjective analyses was significant but weaker than the correlation between the human observers. For image analysis, a representative area was chosen manually. To obtain adequate results, it is critical that the appropriate tissue compartment is measured, in this case cancerous epithelium, while benign epithelium, premalignant lesions, and stroma need to be avoided. The lower correlation between Noesis and manual analyses compared to the correlation between human observers may be explained by the difficulty involved in segmentation of microscopic images. As shown in this study, objective assessment by image analysis is not necessarily better than subjective estimation and a standardization of this system is necessary to stabilize the analysis in the future. Interestingly, the subjective assessments correlated better with tumor grade than automated analysis. There are two possible explanations of this finding. Subjective assessment may better reflect the biology of the tumor as the observer can make sure artifacts is excluded and that the appropriate invasive cancer

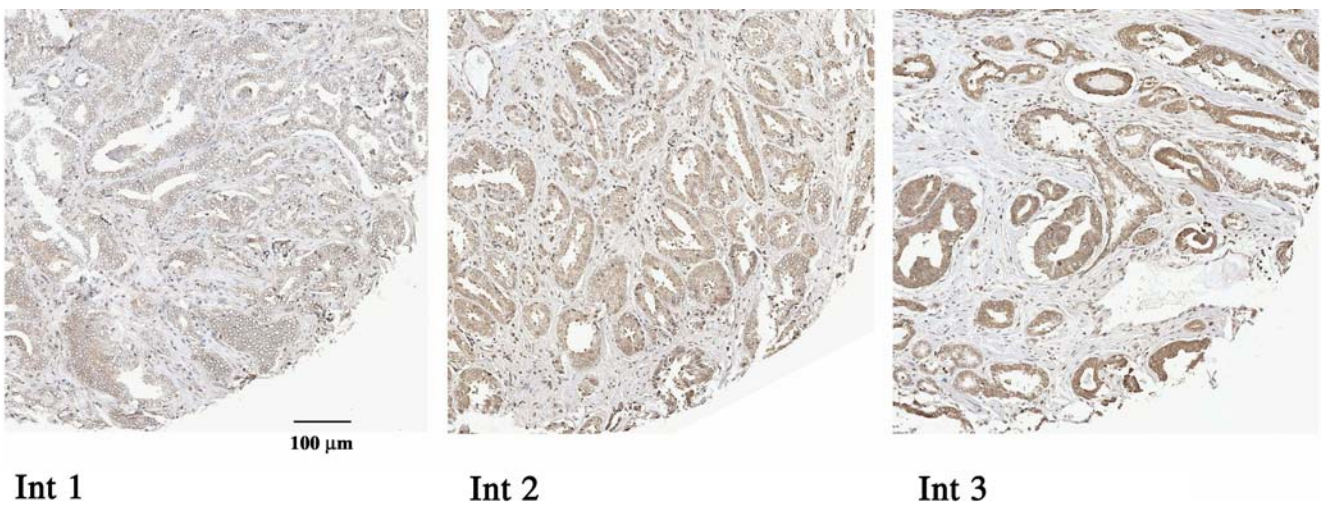

Fig. 1 TMA cores used for standardization of staining intensity grading. Reference cores for intensities 1, 2, and 3. Immunohistochemical staining against PDX-1

component is measured. On the other hand, subjective observers may be biased by their knowledge of tumor grade (as it is not possible to be entirely blinded for when reading slides) and staining intensity. It may be no coincidence that the only subjective observer that did not reach a significant correlation with tumor grade was a nonpathologist who had not received any systematic training in prostate cancer grading. Whether subjective or automated measurements are the best predictors of patient outcome is not possible to evaluate based on the current series of 50 patients. It should also be emphasized that the current study for practical reasons was performed on one single antibody and results may theoretically differ between different biomarkers.

We have compared intra- and inter reproducibility of IHC evaluation in prostatic TMA both using subjective and digital analysis. We have shown that subjective assessment of IHC staining intensity is highly reproducible, regardless of previous training of the observer. Although one single scale of evaluation may not be desirable, we want to emphasize the importance of standardized scoring systems, in order to improve reproducibility within and between research groups.

Conflict of interest statement We declare that we have no conflict of interest. The Noesis company has let us use the Noesis digital analysis system free of charge, however, it has not been possible for the company to influence the results of this study

References

1. Chan JK (1998) Advances in immunohistochemical techniques: toward making things simpler, cheaper, more sensitive, and more reproducible. Adv Anat Pathol 5:314–325
2. Pileri SA, Roncador G, Ceccarelli C et al (1997) Antigen retrieval techniques in immunohistochemistry: comparison of different methods. J Pathol 183:116–123
3. Werner M, Chott A, Fabiano A et al (2000) Effect of formalin tissue fixation and processing on immunohistochemistry. Am J Surg Pathol 24:1016–1019
4. Leong AS, Leong TY (2006) Newer developments in immunohistology. J Clin Pathol 59:1117–1126
5. Seidal T, Balaton AJ, Battifora H (2001) Interpretation and quantification of immunostains. Am J Surg Pathol 25:1204–1207
6. Walker RA (2006) Quantification of immunohistochemistry—issues concerning methods, utility and semiquantitative assessment I. Histopathology 49:406–410
7. Valdman A, Häggarth L, Cheng L, Lopez-Beltran A, Montironi R, Ekman P, Egevad L: Expression of redox pathway enzymes in human prostatic tissue (Anal Quant Cytol Histol, in press)
8. Rimm DL, Camp RL, Charette LA et al (2001) Amplification of tissue by construction of tissue microarrays. Exp Mol Pathol 70:255–264
9. Witton CJ, Hawe SJ, Cooke TG et al (2004) Cyclooxygenase 2 (COX2) expression is associated with poor outcome in ER-negative, but not ER-positive, breast cancer. Histopathology 45:47–54
10. Davol PA, Bagdasaryan R, Elfenbein GJ et al (2003) Shc proteins are strong, independent prognostic markers for both node-negative and node-positive primary breast cancer. Cancer Res 63:6772–6783
11. Jonmarker S, Glaessgen A, Culp WD et al (2008) Expression of PDX-1 in prostate cancer, prostatic intraepithelial neoplasia and benign prostatic tissue. Apmis 116:491–498
12. Kollermann J, Schlomm T, Bang H et al (2008) Expression and prognostic relevance of annexin a3 in prostate cancer. Eur Urol 54:1314–1323
13. Rosenblatt R, Valdman A, Cheng L, Lopez-Beltran A, Montironi R, Ekman P, Egevad L: Endothelin-1 expression in prostate cancer and high-grade PIN (Anal Quant Cytol Histol. 2009 Jun;31(3):137–42
14. Glaessgen A, Jonmarker S, Lindberg A, Nilsson B, Lewensohn R, Ekman P, Valdman A, Egevad L (2008) Heat shock proteins 27, 60 and 70 as prognostic markers of prostate cancer. Acta Pathol Microbiol Immunol Scand B 116(10):888–895
15. Chung S, Hammarsten P, Josefsson A, Stattin P, Granfors T, Egevad L, Mancini G, Lutz B, Bergh A, Fowler C et al (2009) A high cannabinoid CB1 receptor immunoreactivity is associated with disease severity and outcome in prostate cancer. Eur J Cancer 45:172–182
16. McCarty KS Jr, Miller LS, Cox EB et al (1985) Estrogen receptor analyses. Correlation of biochemical and immunohistochemical methods using monoclonal antireceptor antibodies. Arch Pathol Lab Med 109:716–721
17. Gee JM, Barroso AF, Ellis IO et al (2000) Biological and clinical associations of c-jun activation in human breast cancer. Int J Cancer 89:177–186
18. Harvey JM, Clark GM, Osborne CK et al (1999) Estrogen receptor status by immunohistochemistry is superior to the ligand-binding assay for predicting response to adjuvant endocrine therapy in breast cancer. J Clin Oncol 17:1474–1481
19. Reiner A, Neumeister B, Spona J et al (1990) Immunocytochemical localization of estrogen and progesterone receptor and prognosis in human primary breast cancer. Cancer Res 50:7057–7061
20. Detre S, Saclani Jotti G, Dowsett M (1995) A "quickscore" method for immunohistochemical semiquantitation: validation for oestrogen receptor in breast carcinomas. J Clin Pathol 48:876–878
21. Volante M, Brizzi MP, Faggiano A et al (2007) Somatostatin receptor type 2A immunohistochemistry in neuroendocrine tumors: a proposal of scoring system correlated with somatostatin receptor scintigraphy. Mod Pathol 20:1172–1182
22. Montironi R, Mazzucchelli R, Barbisan F et al (2007) Immunohistochemical expression of endothelin-1 and endothelin-A and endothelin-B receptors in high-grade prostatic intraepithelial neoplasia and prostate cancer. Eur Urol 52:1682–1689
23. Paju A, Hotakainen K, Cao Y et al (2007) Increased expression of tumor-associated trypsin inhibitor, TATI, in prostate cancer and in androgen-independent 22Rv1 cells. Eur Urol 52:1670–1679
24. Kononen J, Bubendorf L, Kallioniemi A et al (1998) Tissue microarrays for high-throughput molecular profiling of tumor specimens. Nat Med 4:844–847
25. Rubin MA, Dunn R, Strawderman M et al (2002) Tissue microarray sampling strategy for prostate cancer biomarker analysis. Am J Surg Pathol 26:312–319
26. Singh SS, Qaqish B, Johnson JL et al (2004) Sampling strategy for prostate tissue microarrays for Ki-67 and androgen receptor biomarkers. Anal Quant Cytol Histol 26:194–200
27. Schlomm T, Kirstein P, Iwers L et al (2007) Clinical significance of epidermal growth factor receptor protein overexpression and gene copy number gains in prostate cancer. Clin Cancer Res 13:6579–6584
28. Wegiel B, Bjartell A, Ekberg J et al (2005) A role for cyclin A1 in mediating the autocrine expression of vascular endothelial growth factor in prostate cancer. Oncogene 24:6385–6393

29. Kwabi-Addo B, Wang J, Erdem H et al (2004) The expression of Sprouty1, an inhibitor of fibroblast growth factor signal transduction, is decreased in human prostate cancer. Cancer Res 64:4728–4735
30. Feng S, Agoulnik IU, Bogatcheva NV et al (2007) Relaxin promotes prostate cancer progression. Clin Cancer Res 13:1695–1702
31. Leys CM, Nomura S, Rudzinski E et al (2006) Expression of Pdx-1 in human gastric metaplasia and gastric adenocarcinoma. Hum Pathol 37:1162–1168
32. Koizumi M, Doi R, Toyoda E et al (2003) Increased PDX-1 expression is associated with outcome in patients with pancreatic cancer. Surgery 134:260–266
33. Sakai H, Eishi Y, Li XL et al (2004) PDX1 homeobox protein expression in pseudopyloric glands and gastric carcinomas. Gut 53:323–330
34. Press MF, Pike MC, Chazin VR et al (1993) Her-2/neu expression in node-negative breast cancer: direct tissue quantitation by computerized image analysis and association of overexpression with increased risk of recurrent disease. Cancer Res 53:4960–4970
35. Diaz LK, Sneige N (2005) Estrogen receptor analysis for breast cancer: current issues and keys to increasing testing accuracy. Adv Anat Pathol 12:10–19

Virchows Arch (2009) 455:383–388
DOI 10.1007/s00428-009-0835-6

ORIGINAL ARTICLE

Atypical lipomatous tumors of the tongue: report of six cases

Jan Laco · Thomas Mentzel · Helena Hornychova · Ales Kohout · Zdenek Jirousek · Ales Ryska

Received: 27 July 2009 / Revised: 1 September 2009 / Accepted: 3 September 2009 / Published online: 9 October 2009

Abstract The occurrence of liposarcoma in the tongue is rare with only 34 cases published so far. We report six new cases of atypical lipomatous tumor (ALT) of the tongue, and detection of mdm-2 and CDK4 expression by immunohistochemistry and fluorescence in situ hybridization (FISH), respectively, was performed. The series comprised three males and three females, aged 11–78 years. The tumors arose at the lateral side of the tongue, and in one case, multiple tumor nodules were noted. Follow-up information in five cases (range from 4 to 159 months) revealed one local recurrence at 6 months. Microscopically, four cases had features of lipoma-like ALT, whereas two cases displayed patterns of sclerosing ALT. Immunohistochemically, tumor cells revealed expression of vimentin (five of five), S100 (five of five), mdm-2 (three of five), and CDK4 (four of five). Two cases were also examined by FISH; amplification of mdm-2 gene was found in both cases, whereas amplification of CDK4 gene was present in one case only. To the best of our knowledge, this is the third largest series reporting occurrence of ALT in the tongue and the first one where analysis of mdm-2 and CDK4 proteins/genes expression/amplification was performed. Both these markers may be of help in the differential diagnosis of ALT versus lipoma. Although most ALTs of the tongue behave in the nonaggressive fashion, they may recur locally. Based on current data, the term ALT is strongly recommended for tumors occurring in the tongue to prevent inadequate treatment.

Keywords Atypical lipomatous tumor · Well differentiated liposarcoma · Tongue · Oral cavity · Head and neck

Introduction

Liposarcoma (LS) is the most common soft tissue sarcoma in adulthood. According to current WHO classification of soft tissue tumors [1], LSs are categorized into five subtypes: atypical lipomatous tumor (ALT)/well-differentiated LS (WDLS), dedifferentiated LS, myxoid/round cell LS, pleomorphic LS, and mixed-type LS. Since it has become apparent that WDLS and ALT are identical tumors which show no metastatic potential unless they undergo dedifferentiation, the term ALT has been proposed for surgically amenable WDLSs, which are curatively treated by wide excision with free margins [1].

ALT accounts for about 40–45% of all LSs occurring as extremity or retroperitoneal tumor in late adult life, mainly between the fifth and the seventh decades. ALT is further subclassified into the lipoma-like, sclerosing, inflammatory, and spindle cell subtypes [1].

J. Laco · H. Hornychova · A. Kohout · A. Ryska
The Fingerland Department of Pathology, Charles University Medical Faculty and Faculty Hospital in Hradec Kralove, Hradec Kralove, Czech Republic

T. Mentzel
Dermatopathology Bodensee, Friedrichshafen, Germany

Z. Jirousek
Department of Dentistry, Charles University Medical Faculty and Faculty Hospital in Hradec Kralove, Hradec Kralove, Czech Republic

J. Laco (✉)
The Fingerland Department of Pathology, Faculty Hospital, Sokolska 581,
500 05 Hradec Kralove, Czech Republic
e-mail: lacoj@lfhk.cuni.cz

The occurrence of LS in the tongue is extremely rare, with only 34 cases reported in the English-written literature so far, as reviewed by Allon et al. [2] in 2005 with two subsequent cases reported by DeWitt et al. [3] in 2008. Among the histological subtypes, ALT is by far the most common in this particular location [2]. It has very good prognosis with a tendency for local recurrences, namely if incompletely excised, but with virtually no metastatic potential.

We report herein six new cases of ALT of the tongue, where detection of mdm-2 (murine double minutes) and CDK4 (cyclin-dependent kinase 4) by both immunohistochemistry and fluorescence in situ hybridization (FISH) was used in the diagnostics. The clinical course, diagnostic criteria as well as differential diagnosis are discussed.

Materials and methods

Six cases of ALT of the tongue examined during the years 1996–2009 were retrieved from the archive and consultation files of the authors. The paraffin blocks for additional immunohistochemical and FISH analysis were available all but one case (no. 4). The specimens were immediately fixed in formalin, embedded in paraffin, and routinely processed.

Indirect immunohistochemistry using monoclonal/polyclonal antibodies against vimentin (clone V9, dilution 1:50, Dako (Glostrup, Denmark)), S100 protein (S100; polyclonal, 1:6,000, Dako), mdm-2 (IF2, 1:200, Invitrogen (Carlsbad, CA, USA)), CDK4 (DC9-31, 1:400, Biosource (Nivelles, Belgium)), and Ki-67 (MIB-1, 1:50, Dako) was performed. For antigen retrieval of vimentin, the tissue was processed in the microwave vacuum histoprocessor RHS 1 (Milestone) at pH 6.0 at 120°C for 4 min. For detection of other antigens, the retrieval was performed in a water bath for 40 min at 97°C in the target retrieval buffers at different pH values—at pH 6.0 for S100 and at pH 9.0 for Ki-67—and in a water bath for 30 min at 95°C at pH 9.0 for mdm-2 and CDK4, respectively.

Endogenous peroxidase activity was inhibited by immersing the sections in 3% hydrogene peroxide. Finally, for vimentin, S100, and Ki-67, the sections were incubated with EnVision+ Dual Link System-HRP (Dako) and for mdm-2 and CDK4 with LSAB™ Kit (Dako), respectively. The reactions were visualized using diaminobenzidine.

The FISH was performed on 3-μm sections of formalin fixed, paraffin-embedded tissue after baking at 65°C for 16 h, deparaffinization with xylene, and dehydration with ethanol. All tissue sections were pretreated with a 30% solution of pretreatment solution and digested with proteinase K following the instructions of the suppliers (Q-Biogene, Heidelberg, Germany). Digestion times were optimized on a case-by-case basis. Amplification of the mdm-2 and CDK4 genes was detected by hybridization of digoxigenin-labeled bacterial artificial chromosomes followed by binding to fluorescein isothiocyanate antidigoxigenin. After a second hydration step, the probes were applied to the sections, and the cover slides were sealed with a rubber cement, heat-denaturated, and hybridized at 37°C for 16 h. After stringent washing with 50% formamide in 2× standard sodium citrate, the sections were counterstained with 4′,6-diamidino-2-phenylindole II in mounting medium (125 ng/ml, Vysis, Bergisch Gladbach, Germany) and visualized under a Zeiss Axioplan 2 microscope using a HBO103 lamp and the appropriate filters for three fluorescence dyes.

Results

The clinicopathological features of the patients are summarized in Table 1. There were three males and three females, aged 11–78 years (mean 51±11 years; median 58 years). In all cases, the tumors arose at the lateral side of the tongue. In one case (no. 3), there were multiple tumor nodules, localized at both sides of the tongue (Fig. 1). All lesions were treated by local excision. Follow-up information in five cases (range from 4 to 159 months; mean 69± 25 months; median 59 months) revealed one local recurrence in case no. 3 6 months after initial surgical treatment, and the patient died 8 months later on complications of ischemic heart disease. Autopsy was not performed.

Grossly, the tumors had the appearance of lipoma, i.e., they were yellow-tan, lobulated, and covered by intact mucosa. Microscopically, all lesions were partly circumscribed, but not encapsulated; focally, the neoplasms infiltrated into the surrounding striated muscle and fibrous tissue (Fig. 2). The tumors were of lobular arrangement, composed of adipocytes with striking variations in size and shape having hyperchromatic nuclei. Scattered lipoblasts, both univacuolar and multivacuolar, were present in four cases. Four cases had the features of lipoma-like ALT (Fig. 3), whereas in two cases, prominent interstitial fibrillary sclerosis (Fig. 4) was in keeping the diagnosis of sclerosing ALT. Additionally, in two cases only, isolated spindle-shaped primitive looking stromal cells were found, presumably of a precursor nature. Mitotic activity was very low; only few typical mitoses were found in all the slides examined. Foci of dedifferentiation were not present (not even in the recurrent case (no. 3)).

Immunohistochemically, the tumor cells revealed expression of vimentin (five of five), of S100 (five of five), of mdm-2 (three of five; Fig. 5), and of CDK4 (four of five; Fig. 6). Proliferative antigen Ki-67 was positive in less than 0.5% of tumor cells. Two cases (nos. 1 and 3) were examined also by FISH. Amplification of mdm-2 gene was

Table 1 Clinicopathological data of patients

Case no.	Sex	Age (years)	Tumor size (mm)	Type of ALT	Follow-up (months)	Follow-up result
1	F	78	11	LL	63	NED
2	F	27	7	LL	58	NED
3	M	65	20	LL	59	Local recurrence
4	M	11	8	S	NA	NA
5	M	75	10	S	159	NED
6	F	50	12	LL	4	NED

M male, *F* female, *ALT* atypical lipomatous tumor, *LL* lipoma-like type, *S* sclerosing type, *NED* no evidence of disease, *NA* not available

found in both cases (Fig. 5, inset), whereas amplification of CDK4 gene was present in one case (no. 1) only. The results of immunohistochemical and FISH analysis of expression and amplification of mdm-2 and CDK4 proteins/genes are summarized in Table 2.

Discussion

Liposarcoma, first described by Virchow in 1857 (as cited by DeWitt et al. [3]), is the most common mesenchymal malignancy of adulthood, arising in deep soft tissues of the extremities and in the retroperitoneum and in the abdominal cavity. However, its occurrence in the head and neck region, particularly within the oral cavity, is rare. In the largest review of 23 cases of LS of the oral cavity [4], the tongue was the preferred site in 52% (12 of 23) cases, whereas in the second largest series of 18 cases of LS of the oral cavity and salivary glands [5], LS occurred most frequently in the buccal mucosa in 39% (seven of 18) of cases, respectively. Other anatomic locations included lip, floor of mouth, gingiva and alveolar mucosa, soft palate, and parotid and submandibular gland [4, 5].

Since the comprehensive review of LS of the tongue from 2005 [2], analyzing a total of 32 cases included in two large series [4, 5] and in several case reports [6–18], only one paper reporting two additional cases has been published [3]. Thus, together with our cases, there are only 40 cases of LS of the tongue reported so far.

Compared to LS of other parts of the body, LS of the tongue occurs in older patients with the mean age of about 60 years [2]. However, it may affect younger persons as well, since two of our patients were aged 11 and 27 years, respectively; the former appears to be the youngest patient reported so far. According to gender distribution, LS of the tongue shows a male-to-female ratio of about 2.5:1 [2] which is higher than that for LS in other locations [19].

Two gross patterns of LS of the tongue have been recognized—solitary or multiple nodules, the former being by far the commonest. Typically, the tumor presents as a submucosal mass covered by intact mucosa, occurring on lateral and/or dorsolateral aspects of the tongue. The clinical diagnosis usually includes benign tumors, e.g., fibroma, lipoma, and neurogenic and salivary gland tumors [2]. Some rare neoplasms which show predilection for tongue involvement, e.g., low-grade myofibroblastic sarco-

Fig. 1 Multinodular atypical lipomatous tumor at the lateral margin of the tongue (case no. 3)

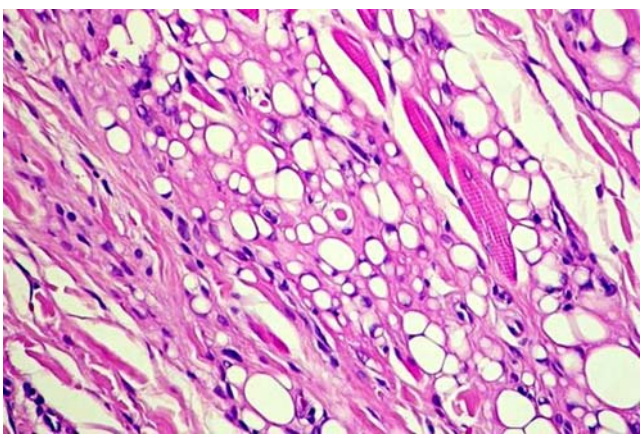

Fig. 2 Focal infiltration of tumor cells among bundles of skeletal muscle (HE, original magnification ×200)

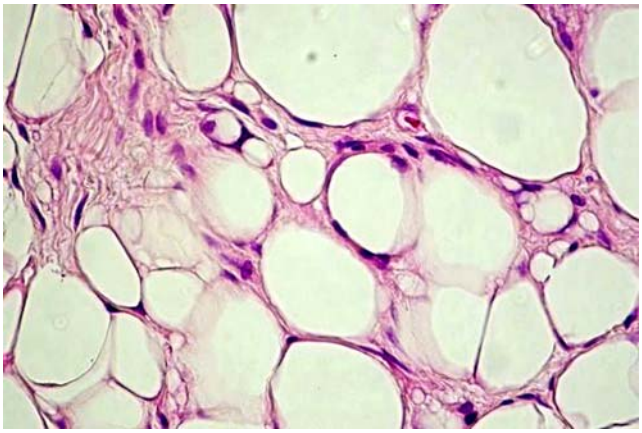

Fig. 3 Isolated lipoblasts interspersed among mature adipocytes (HE, original magnification ×400)

ma [20, 21] and ectomesenchymal chondromyxoid tumor [22], may enter the differential diagnosis as well.

Regarding the LS variants, the most LSs of the tongue are of ALT subtype, comprising about 75% of cases, followed by myxoid/round cell and dedifferentiated variants [2]. This distribution differs from LSs of retroperitoneal and of head and neck origin, which are dominated by myxoid/round cell variant in 50% and in 40% of cases, respectively [19, 23]. The majority of cases of ALTs of the tongue show features of the lipoma-like subtype, while only several cases display, usually focally, the sclerosing subtype pattern [2].

The differential diagnosis of ALT of the tongue includes particularly a lipoma with regressive changes and an intramuscular lipoma. Traumatization of lipoma due to repeated biting may lead to degenerative changes—edema, fibrosis, and entrapment of adipocytes within the scar tissue—thus mimicking appearance of the sclerosing variant of ALT. However, the typical hallmark of ALT—hyperchromatic nuclei—is typically absent. The vacuolated histiocytes present in areas of fat necrosis may simulate lipoblasts; however, their origin may be demonstrated using immunohistochemical detection of lysosome-associated antigens, e.g., CD68 or lysozyme. Presence of a central intranuclear vacuole, so-called *Lochkern*, which is considered either an intranuclear cytoplasmic lipid invagination or a cutting artifact and may mimic a lipoblast, may eventually disappear on thinner sections. Despite its infiltrative growth pattern, intramuscular lipoma is composed of more uniform adipocytes and lipoblasts are absent. Since ALT may, although rarely, occur in younger patients as shown above, a lipoblastoma enters the differential diagnosis. However, lipoblastoma is most commonly found within the first 3 years of life, and it frequently displays myxoid stroma with plexiform vascular pattern on microscopy, both these characteristics being not the features of ALT. In addition, the cytogenetic hallmark of lipoblastoma, i.e., rearrangement of chromosome 8q11–13 [1], is absent in ALT whereas an amplification of mdm-2 and CDK4 genes is seen in the latter [24]. Being the second most common type of lipoma in the oral and maxillofacial region, spindle cell/pleomorphic lipoma (SC/PL) should be included in the differential diagnosis as well [25]. Contrary to ALT, SC/PL shows no striking variation of size and shape of the adipocytic cells, atypical and/or hyperchromatic nuclei are absent, frequently displays thick rope-like collagen bundles—the latter being extremely useful diagnostic feature—and shows mdm-2- and CDK4-negative immunohistochemical profile. Furthermore, SC/PL is characterized by monosomy or partial loss of chromosomes 13 and/or 16; these cytogenetic findings are absent in ALT [1].

Immunohistochemically, the ALT shows consistent expression of vimentin and of S100, although the spindle cell component may feature variable results of the latter [2]. In addition, expression of three novel antigens was detected in ALTs [24]. These include mdm-2, a nuclear phosphoprotein able to inhibit the p53 transactivating domain [26], CDK4 with catalytic kinase function, and HMGI-C, a transcription factor [27]. The genes coding all these proteins are located in the chromosomal region 12q13–15. These DNA sequences are the major constituents of the supernumerary ring and giant rod chromosomes, the cytogenetic hallmarks of ALTs being present in about 93% of the cases [28–31]. In one series [24], the expression of mdm-2, CDK4, and HMGI-C was found in 50%, in 100%, and in 83% cases of ALTs, respectively, whereas all lipomas were mdm-2 negative and CDK4 and HMGI-C expression was detected in only 11% and 44% cases of lipomas, respectively. In our study, which is the first series of ALT of the tongue where immunohistochemical expression of both mdm-2 and CDK4 was performed, we have obtained similar results. Thus, immunohistochemical detection of both mdm-2 and CDK4 may be

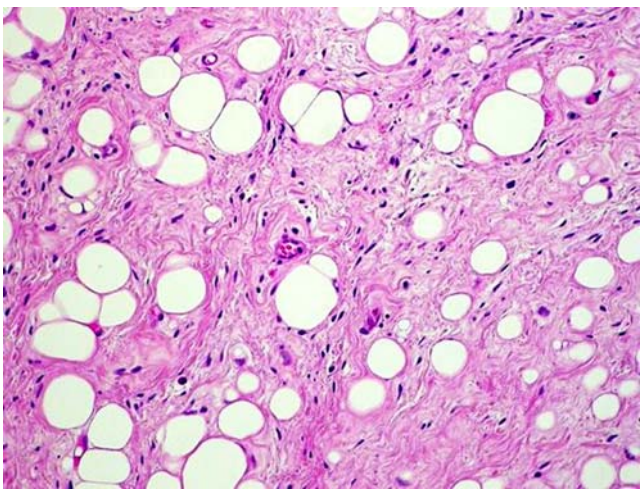

Fig. 4 Prominent interstitial sclerosis (HE, original magnification ×200)

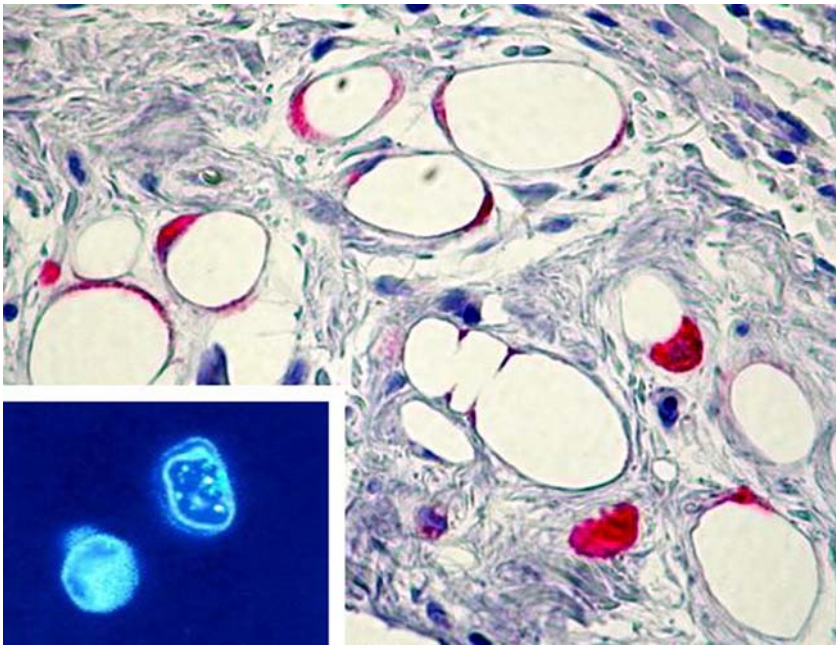

Fig. 5 Nuclear expression of mdm-2 in the majority of tumor cells (original magnification ×400). *Inset*: Amplification of mdm-2 gene as multiple green signals in the nucleus of a tumor cell (original magnification ×1,000)

useful in differential diagnosis of lipoma versus ALT. On the other hand, the above stated data have led some investigators to a hypothesis that lipomas and ALTs may be two extremes of the molecular, genetic, and morphological continuum [24, 32].

The optimal treatment for ALT of the tongue is wide surgical excision with free margins. Among the reported cases of ALT of the tongue, including our cases, 15% (six of 40) of tumors had recurred and 7.5% (three of 40) lesions demonstrated multiple recurrences (up to five times) during a follow-up period ranging from 4 months to 37 years (mean 6±9 years; median 2 years). Although 5% (two of 40) of the published cases displayed foci of dedifferentiation [4, 5], no metastases from lingual ALT have been reported so far.

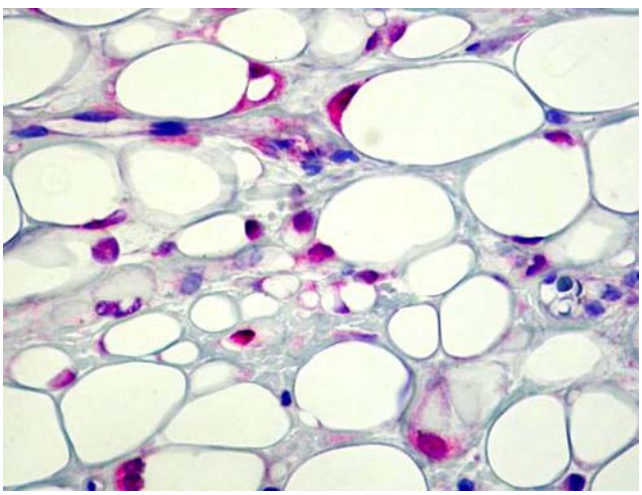

Fig. 6 Nuclear expression of CDK4 in the majority of tumor cells (original magnification ×400)

In summary, we report six new cases of ALT of the tongue—a rare neoplastic entity which should be always considered in the differential diagnosis when dealing with adipocytic lesion in this particular location. To the best of our knowledge, this is the third largest series reporting occurrence of ALT in this anatomic area and the first one where both immunohistochemical analysis of mdm-2 and CDK4 proteins expression and FISH analysis of genes amplification were used in the diagnostics. Although the diagnosis of ALT can be made on hematoxylin–eosin, our results and data of other investigators indicate that both these markers may be of help in the differential diagnosis of ALT versus lipoma. Based on current data, the use of term ALT over the designation WDLS is strongly recommended for tumors occurring in the tongue to prevent inadequate

Table 2 Results of immunohistochemical and FISH analysis of expression and amplification of mdm-2 and CDK4 proteins/genes

Case no.	Immunohistochemistry		FISH	
	mdm-2	CDK4	mdm-2	CDK4
1	−	−	+	+
2	−	+	NP	NP
3	+	+	+	−
4	NP	NP	NP	NP
5	+	+	NP	NP
6	+	+	NP	NP

FISH fluorescence in situ hybridization, *NP* not performed

treatment. Most ALTs of the tongue behave in a nonaggressive fashion; however, they may recur locally if incompletely excised. Thus, long-term follow-up of the patients is mandatory.

Acknowledgments The work was supported by Research Project of the Ministry of Health of the Czech Republic No. 00179906. The study complies with the current laws of the Czech Republic and of Germany.

Conflict of interest statement The authors declare that they have no conflict of interest.

References

1. Fletcher ChDM, Unni KK, Mertens F (2002) Adipocytic tumours. In: Fletcher ChDM, Unni KK, Mertens F (eds) WHO classification of tumours. Pathology and genetics of tumours of soft tissue and bone, 1st edn. IARC, Lyon, pp 19–46
2. Allon I, Vered M, Dayan D (2005) Liposarcoma of the tongue: clinico-pathologic correlations of a possible underdiagnosed entity. Oral Oncol 41:657–665
3. DeWitt J, Heidelman J, Summerlin DJ et al (2008) Atypical lipomatous tumors of the oral cavity: a report of 2 cases. J Oral Maxillofac Surg 66:366–369
4. Nascimento AF, McMenamin ME, Fletcher ChDM (2002) Liposarcomas/atypical lipomatous tumors of the oral cavity: a clinicopathologic study of 23 cases. Ann Diagn Pathol 6:83–93
5. Fanburg-Smith JC, Furlong MA, Childers ELB (2002) Liposarcoma of the oral and salivary gland region: a clinicopathologic study of 18 cases with emphasis on specific sites, morphologic subtypes, and clinical outcome. Mod Pathol 15:1020–1031
6. Larson DL, Cohn AM, Estrada RG (1976) Liposarcoma of the tongue. J Otolaryngol 5:410–414
7. Wescott WB, Correll RW (1984) Multiple recurrences of a lesion at the base of the tongue. J Am Dent Assoc 108:231–233
8. Guest PG (1992) Liposarcoma of the tongue: a case report and review of the literature. Br J Oral Maxillofac Surg 30:268–269
9. Minic AJ (1995) Liposarcomas of the oral tissues: a clinicopathologic study of four tumors. J Oral Pathol Med 24:180–184
10. Saddik M, Oldring DJ, Mourad WA (1996) Liposarcoma of the base of tongue and tonsillar fossa: a possibly underdiagnosed neoplasm. Arch Pathol Lab Med 120:292–295
11. Kacker A, Taskin M (1996) Atypical intramuscular lipoma of the tongue. J Laryngol Otol 110:189–191
12. Nelson W (1998) Enlarging tongue mass. J Oral Maxillofac Surg 56:224–227
13. Kasper HU, Freigang B, Buhtz P et al (2000) Lipoma-like liposarcoma of the tongue. Laryngorhinootologie 79:50–52
14. Orita Y, Nishizaki K, Yorizane S et al (2000) Liposarcoma of the tongue: case report and literature update. Ann Otol Rhinol Laryngol 109:683–686
15. Moore PL, Goede A, Phillips DE et al (2001) Atypical lipoma of the tongue. J Laryngol Otol 115:859–861
16. Nunes FD, Loducca SV, de Oliveira EM et al (2002) Well-differentiated liposarcoma of the tongue. Oral Oncol 38:117–119
17. Bengezi OA, Kearns R, Shuhaibar H et al (2002) Myxoid liposarcoma of the tongue. J Otolaryngol 31:327–328
18. Capodiferro S, Scully C, Maiorano E et al (2004) Liposarcoma circumscriptum (lipoma-like) of the tongue: report of a case. Oral Dis 10:398–400
19. Enzinger FM, Weiss SW (2001) Liposarcoma. In: Weiss SW, Goldblum JR (eds) Soft tissue tumors, 4th edn. Mosby, St. Louis, pp 641–690
20. Mentzel T, Dry S, Katenkamp D et al (1998) Low-grade myofibroblastic sarcoma: analysis of 18 cases in the spectrum of myofibroblastic tumors. Am J Surg Pathol 22:1228–1238
21. Laco J, Simakova E, Slezak R et al (2006) Low grade myofibroblastic sarcoma of the tongue: a case report. Cesk Patol 42:150–153
22. Allen CM (2008) The ectomesenchymal chondromyxoid tumor: a review. Oral Dis 14:390–395
23. Golledge J, Fisher C, Rhys-Evans PH (1995) Head and neck liposarcoma. Cancer 76:1051–1058
24. Dei Tos AP, Doglioni C, Piccinin S et al (2000) Coordinated expression and amplification of the MDM2, CDK4, and HMGI-C genes in atypical lipomatous tumours. J Pathol 190:531–536
25. Furlong MA, Fanburg-Smith JC, Childers ELB (2004) Lipoma of the oral and maxillofacial region: site and subclassification of 125 cases. Oral Surg Oral Med Oral Pathol Oral Radiol Endod 98:441–450
26. Xiao ZX, Chen J, Levine AJ et al (1995) Interaction between the retinoblastoma protein and the oncoprotein MDM2. Nature 375:694–697
27. Rogalla P, Drechsler K, Frey G et al (1996) HMGI-C expression patterns in human tissues. Implication for the genesis of frequent mesenchymal tumors. Am J Pathol 149:775–779
28. Dal Cin P, Kools P, Sciot R et al (1993) Cytogenetic and fluorescence in situ hybridization investigation of ring chromosomes characterizing a specific pathologic subgroup of adipose tissue tumors. Cancer Genet Cytogenet 68:85–90
29. Fletcher CD, Akerman M, Dal Cin P et al (1996) Correlation between clinicopathological features and karyotype in lipomatous tumors. A report of 178 cases from the Chromosomes and Morphology (CHAMP) Collaborative Study Group. Am J Pathol 148:623–630
30. Rosai J, Akerman M, Dal Cin P et al (1996) Combined morphologic and karyotypic study of 59 atypical lipomatous tumors. Evaluation of their relationship and differential diagnosis with other adipose tissue tumors (a report of the CHAMP Study Group). Am J Surg Pathol 20:1182–1189
31. Pedeutour F, Forus A, Coindre JM et al (1999) Structure of the supernumerary ring and giant rod chromosomes in adipose tissue tumors. Genes, Chromosomes Cancer 24:30–41
32. Mentzel T (2000) Biological continuum of benign, atypical, and malignant mesenchymal neoplasms—does it exist? J Pathol 190:523–525

Virchows Arch (2009) 455:389–394
DOI 10.1007/s00428-009-0831-x

CASE REPORT

Intestinal type of mucinous borderline tumor arising from mixed epithelial and stromal tumor of kidney

Peiguo G. Chu · Sean K. Lau · Lawrence M. Weiss · Zhong Jiang

Received: 13 May 2009 / Revised: 22 July 2009 / Accepted: 24 August 2009 / Published online: 15 September 2009

Abstract We report a mucinous borderline tumor arising from a mixed epithelial and stromal tumor of left kidney (MESTK). The patient was an 82-year-old woman who presented with gross hematuria and recurrent urinary tract infection for years. The patient had a cytoscopy with a retrograde pyelogram, which indicated a dilated left kidney with a central mass lesion. Subsequently, she underwent a radical left nephrectomy. Cross-sections of left kidney showed a 4.5×3.5×1.5 cm ill-defined cystic lesion with mucinous and solid areas. Histologic sections of the lesion showed numerous variable-sized dilated cysts with fibrous, fatty, vascular, and smooth muscle stroma. The cysts were lined by a various types of epithelium, including single layer of flat, cuboidal and mucinous epithelium, urothelium, intestinal epithelium, and endocervical epithelium. In areas, the mucinous epithelium showed complex proliferation with stratification, papillae formation, and nuclear atypia, resembling that of an ovarian mucinous borderline tumor, a colorectal tubular adenoma, or a low-grade appendiceal mucinous carcinoma. Immunohistochemically, the mucinous borderline tumor showed a colorectal phenotype, being strongly positive for CK20, CDX-2, and MUC2. There was no invasive mucinous tumor identified. We believe that this case represents the first reported example of mucinous borderline tumor arising from a MESTK.

Keywords Mucinous borderline tumor · Mixed epithelial and stromal tumor · Adult cystic nephroma · Kidney

P. G. Chu (✉) · S. K. Lau · L. M. Weiss
Department of Pathology, City of Hope National Medical Center,
1500 East Duarte Road,
Duarte, CA 91010, USA
e-mail: PChu@coh.org

Z. Jiang
Department of Pathology, School of Medicine,
University of Massachusetts,
Worcester, MA, USA

Introduction

Mixed epithelial and stromal tumor of the kidney (MESTK) is a rare renal tumor, which is composed of a mixture of stromal and epithelial elements [1–3]. The tumor is usually composed of many large and small cysts lined by different types of epithelium. The most common epithelial elements are single layer of flattened or cuboidal cells [4, 5], followed by urothelium [4]. The stroma is usually composed of fibroblasts and smooth muscle cells. While MESTK has a strong association with the female sex and hormonal milieu, adult cystic nephroma (ACN; more common than MESTK) can affect both sexes and, on occasion, may have a hormonal association [6]. Despite the facts that there is considerable overlap between both tumors morphologically and both tumors have a similar molecular profile [6, 7], the relationship between CAN and MESTK is still highly controversial. Some authors believe that MESTK often display features of Müllerian differentiation [8].

The vast majority of cases of MESTK follow a benign clinical course. Nephrectomy is the treatment of choice [3, 6]. However, rare cases with heterologous epithelial or malignant stromal components have been reported. Yang et al. [9] described a case of MESTK with cervical and intestinal differentiation, which contained Paneth and goblet cells. Beiko et al. [10] reported a case of MESTK

with estrogen receptor expressing müllerian type epithelium. Cases of malignant MESTK have been reported [11–15]. All three cases had a sarcomatoid stromal component, while the epithelial components were benign. To our knowledge, borderline or malignant epithelial tumors in a MESTK have not been described in literature.

Here, we report the first case of mucinous borderline tumor arising from a MESTK-exhibiting mucinous, intestinal, and endocervical epithelium.

Case report

The patient was an 82-year-old woman with a clinical history of stage I breast cancer diagnosed 8 years prior to presentation. She presented to her urologist with a history of gross hematuria and recurrent urinary tract infections. She had no clinical and radiologic evidence of gastrointestinal or ovarian malignancy. The patient first had a cystoscopy with a retrograde pyelogram, which indicated a dilated left kidney with hydronephrosis. She then underwent left ureteroscopy and a ureteral stent replacement. At the time, she was noted to have a 1.5-cm renal mass in the left upper calyx. The patient then underwent a left radical nephrectomy. The patient is alive and well without recurrent disease 2 months after surgery.

The left kidney weighed 361 g. The cut surface of the left kidney showed dilated calyces ranging from 1.5 to 2.0 cm in diameter (Fig. 1). In the center of the kidney, there was a 4.5×3.5×1.5 cm ill-defined cystic mass with solid areas and a mucinous appearance. The dilated calyces grossly communicated with the mass.

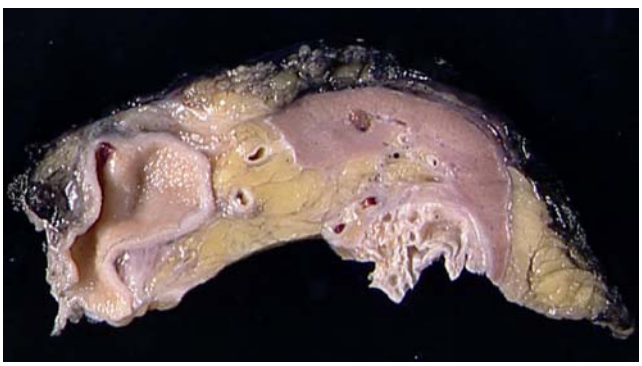

Fig. 1 Gross appearance (part of tumor) of formalin-fixed mixed epithelial and stromal tumor of the kidney. Residual normal kidney is present in the *right upper field*. The cystic tumor with solid and mucinous areas is present in the *right lower field*. The dilated calyx is present in the *left field*. Entrapped fatty and vascular tissue are present between the tumor and the dilated calyx

Materials and methods

The specimen was formalin-fixed and routinely processed for light microscopy. Fifteen tissue blocks were submitted for histologic examination. Immunohistochemistry was performed in a Dako Autostainer (Dako, Carpinteria, CA) using the dual Link Envision+ Detection System with antibodies directed against keratin 7 (clone OV-TL 12/30, dilution 1:2,000, Dako), keratin 20 (clone IT-KS.20.8, dilution 1:8, APR, Belmont, MA), CDX-2 (clone CDX2-88, dilution 1:50, Biogenex Laboratories, San Ramon, CA), MUC2 (clone Ccp58, dilution 1:100, Novocastra Laboratories, Newcastle, UK), PAX-2 (polyclonal, dilution 1:60, Zymed, Carlsbad, CA), WT-1 (clone 6F-H2, dilution 1:50, Dako), CD56 (clone NK-1, dilution 1:50, Novocastra Laboratories), HMB-45 (clone HMB-45, dilution 1:400, Dako), and ER-α (clone 1D5, dilution 1:600, Immunotech, Marceille, France), and PR (clone PR88, dilution 1:100, Biogenex Laboratories).

Microsatellite instability/mismatch repair (MSI/MMR) protein expression was performed by immunohistochemical staining with antibodies against MLH-1 (clone G168-15, dilution 1:5, BD Biosciences, San Jose, CA), MSH-2 (clone FE11, dilution 1:100, Calbiochem, Gibbstown, NJ), MSH-6 (clone 11/MSH6, dilution 1:50, BD Biosciences), and PMS-2 (clone A16-4, dilution 1:25, BD Biosciences).

Results

Pathology

The tumor was characterized by macrocysts, microcysts, and clusters of tubules (Fig. 2a). The cysts were lined by single layer of flattened, cuboidal epithelium (Fig. 2b), and urothelium (Fig. 2c). In areas, mucinous epithelium (Fig. 3) and intestinal-type mucosa was present with prominent Paneth and goblet cells (Fig. 2d). In other areas, endocervical mucosa was present (Fig. 2e). The stroma between cysts was composed of predominantly fibroblasts and smooth muscle cells with marked chronic inflammatory cell infiltration. In addition, there were large-caliber blood vessels and fatty tissue (Fig. 1, middle). Adjacent to benign mucinous epithelium, there were multiple foci of borderline mucinous tumor (Fig. 3a). The tumor was composed of intracystic complex mucinous epithelial proliferation with stratification and filiform papillae formation. Occasional Paneth cells were present at the base. The nuclei were hyperchromatic and slightly enlarged with occasional mitotic figures present. The overall histologic features resembled mucinous borderline tumor of the ovary or pancreas, a low-grade mucinous tumor of the appendix, or

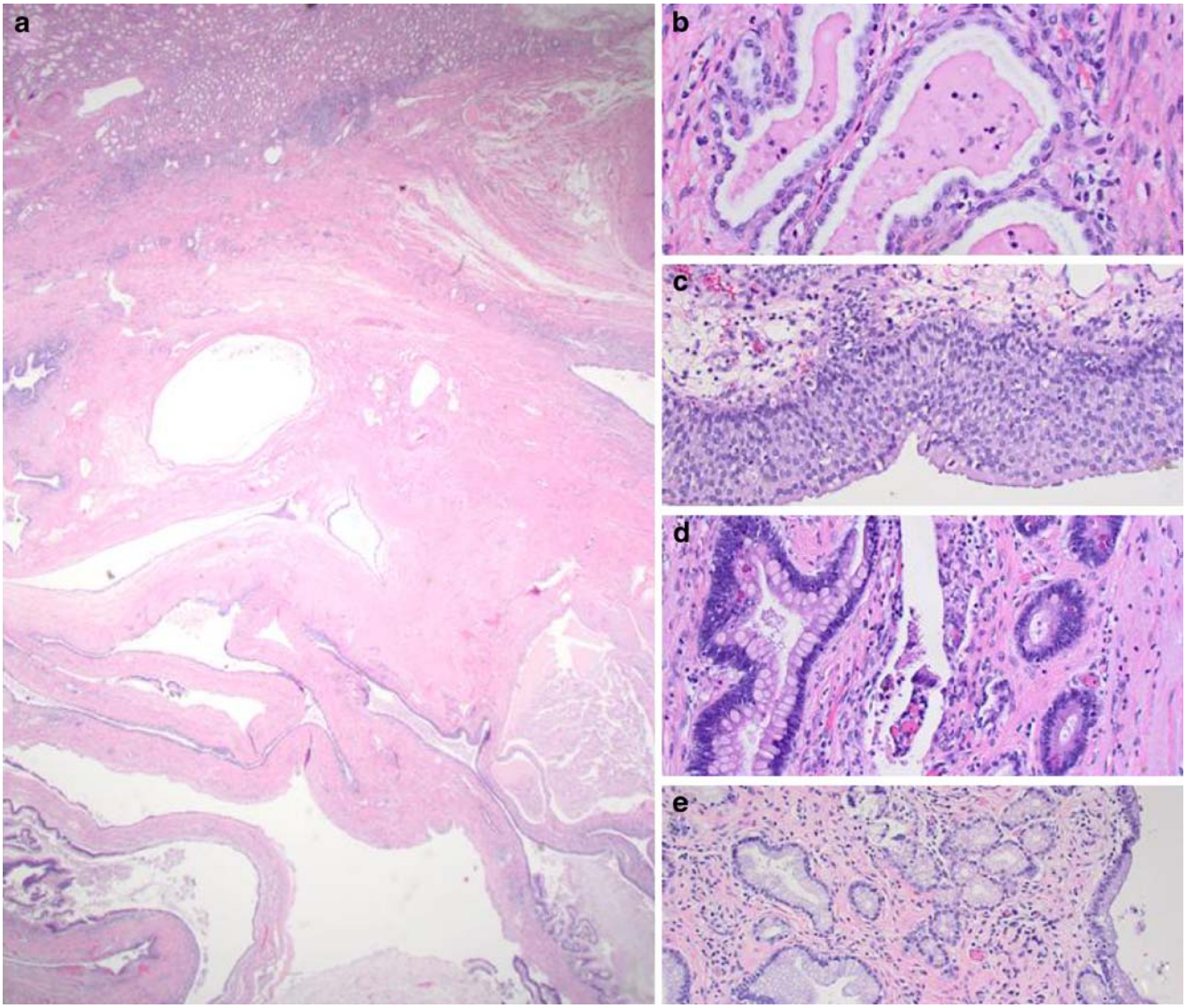

Fig. 2 In low power magnification (×20; **a**), the mixed epithelial and stromal tumor of the kidney adjacent to normal renal tissue is seen (*top*) and shows numerous variable-sized cysts with abundant stroma. Two foci of mucinous borderline tumor are seen in the *left lower* and *right lower* corners. On high power magnification, different cystic lining epithelia are seen, including simple cuboidal epithelium (**b**, ×200), urothelium (**c**, ×200), intestinal mucosa with Paneth and goblet cells (**d**, ×200), and endocervical mucosa (**e**, ×200)

colorectal tubular adenoma. No invasive mucinous tumor was identified.

Immunohistochemistry

Immunohistochemically, the flattened and cuboidal epithelial cells were positive for CK7 (Fig. 3b) and PAX-2 (Fig. 3c) and negative for CK20, CDX-2, and MUC2, suggesting renal tubular differentiation. In contrast, the benign mucinous epithelium next to the mucinous borderline tumor (Fig. 3a, insert) was strongly positive for CK7 and CK20 and negative for CDX-2, an immunophenotype similar to that of an ovarian mucinous tumor. The borderline mucinous tumor was strongly positive for CK20 (Fig. 3d), CDX-2 (Fig. 3e), and MUC2 (Fig. 3f), and was negative for CK7, suggesting a colorectal immunophenotype. The stromal cells were focally positive for ER and PR, with the strongest nuclear staining in stromal cells surrounding the mucinous borderline tumor. The stromal cells were negative for WT1 and CD56.

MSI/MMR protein immunohistochemistry

The mucinous borderline tumor cells were positive for MLH-1, MSH-2, MSH-6, and PMS-2, providing no evidence for microsatellite instability, mismatch repair.

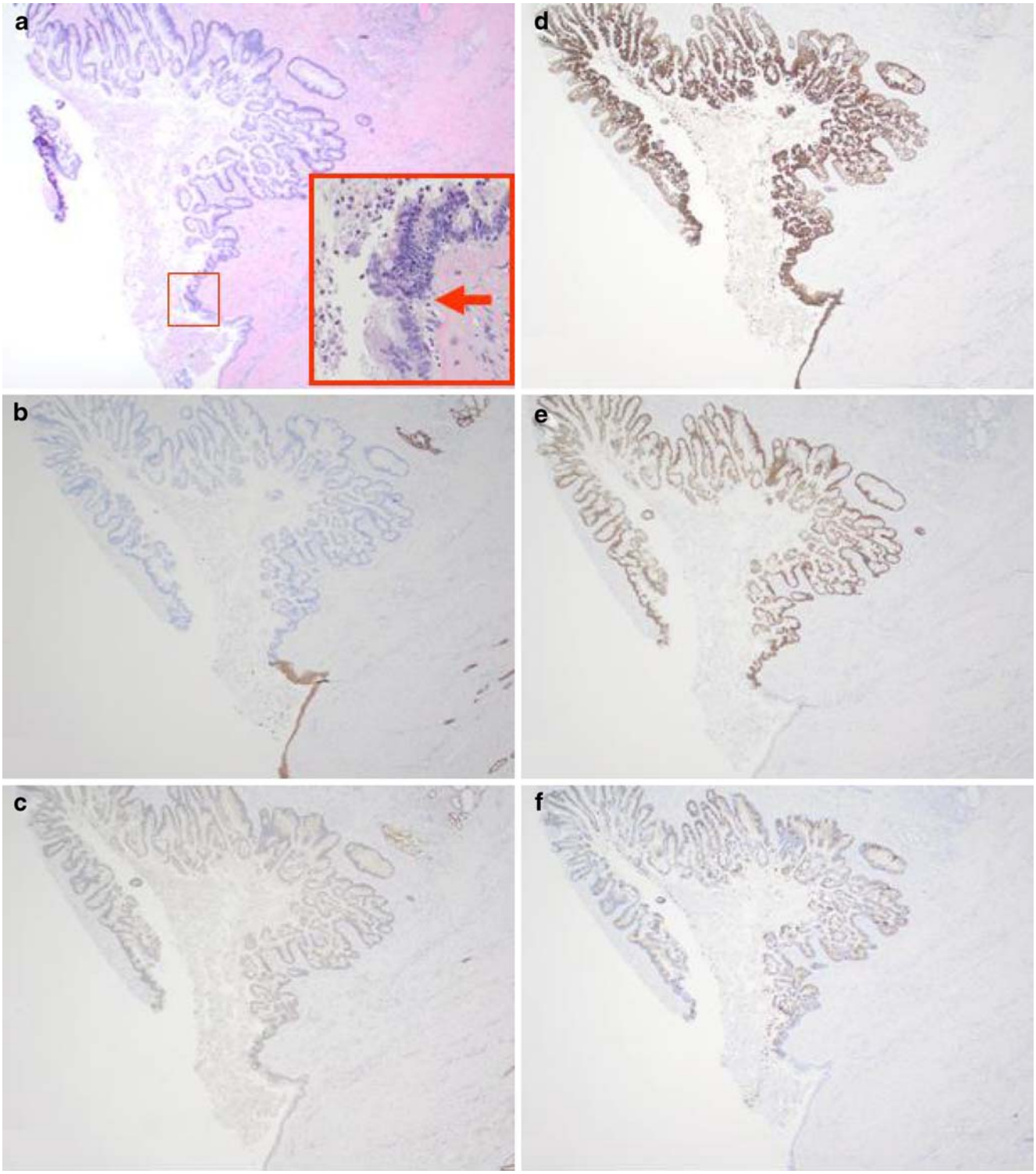

Fig. 3 A mucinous borderline tumor (**a**, ×40) is seen adjacent to benign mucinous epithelium (**a**, *insert*, ×400). The *arrow* marks the transition point between benign mucinous epithelium (*lower portion*) and the mucinous borderline tumor (*upper portion*). The benign mucinous epithelium is positive for CK7 (**b**, ×40) and CK20 (**d**, ×40) and negative for PAX-2 (**c**, ×40), CDX-2 (**e**, ×40), and MUC2 (**f**, ×40), whereas the mucinous borderline tumor is positive for CK20, CDX-2, and MUC2 and negative for CK7 and PAX-2. The small tubules and cysts lined with single layer of flattened or cuboidal epithelia (*right upper* and *right lower fields*) are positive for CK7 and PAX-2 and negative for CK20, CDX-2, and MUC2

Discussion

The patient described in the present study had characteristic clinical and histological features of MESTK, including repeated urinary tract infection, ureteral dilation, and a multicystic renal lesion with abundant stroma. Although MESTK is a rare benign renal tumor, several large case studies have described this lesion [4, 5, 7], and MESTK is recognized in the recent WHO classification of tumors of the urinary system as a distinct entity [2]. MESTK has very similar clinical, histological, and molecular features to that of ACN [6, 7, 9].

Two unusual histologic features make the present case different from previously reported MESTKs. First, unlike most described cases, the current case has unique epithelial components: columnar mucinous epithelium, intestinal mucosa, and endocervical mucosa. The columnar mucinous epithelium showed benign histology and was associated with marked chronic inflammation, suggesting a metaplastic process. Immunohistochemically, the benign mucinous epithelium was strongly positive for CK7 and CK20, which is an immunophenotype similar to that seen in ovarian mucinous tumor [16] and appendiceal low-grade mucinous carcinoma [17]. One case of MESTK associated with intestinal and endocervical mucosa was reported in the literature [9]. In both the current and reported cases, the intestinal epithelium contained Paneth and goblet cells, while the endocervical mucosa was composed of mucinous glands. Both epithelial components showed no cytological atypia.

Second, a mucinous borderline was present adjacent to the mucinous epithelium. Borderline mucinous tumors or other malignant epithelial components have not been reported in MESTK. However, seven MESKT cases with malignant stromal components have been reported. Five of these cases showed a fibrosarcoma-like component with a positive immunohistochemical staining of vimentin, smooth muscle actin, and muscle-specific actin. Two of these patients died of disease [15], and other three patients lived well at the time of description [11, 12]. One case showed stromal cells with rhabdoid features and positive immunohistochemical staining for WT1, CD99, and CD56. This patient was alive 17 months after nephrectomy [14]. One case had carcinosarcoma component with malignant epithelial component resembling endometrioid adenocarcinoma [13]. It is important to rule out a metastatic low-grade mucinous tumor from the ovary, appendix, or other gastrointestinal locations. The mucinous borderline tumor in the current case appeared to arise de novo in the MESTK because (1) there was no clinical and radiological evidence of ovarian or gastrointestinal tumor, (2) histologically, the mucinous borderline tumor merged with the adjacent mucinous columnar epithelium (Fig. 3a, insert), and (3) immunohistochemically, the mucinous tumor cells were strongly positive for CK20 and CDX-2 and negative for CK7, WT1, and ER. The latter three markers are usually expressed in ovarian mucinous tumors.

Immunohistochemical studies for MSI/MMR protein defects showed the borderline mucinous tumor to be strongly positive for MLH-1, MSH-2, MSH-6, and PMS-2. Thus, the defects in MSI/MMR proteins are unlikely to be involved in the neoplastic transformation of the mucinous borderline tumor.

The stromal component in the current case contained fibroblasts, smooth muscle cells, large-size vessels, and fat. Despite its morphological similarity to renal angiomyolipoma, the smooth muscle cells, perivascular cells, and fat were negative for HMB-45 and melan-A by immunohistochemistry, suggesting that they represented entrapped benign fatty and muscular and vascular tissue rather than a neoplastic process. Ovarian like stoma has been reported in mucinous tumors of other locations, such as the pancreas. Ovarian-like stroma is also typically identified in MESTK and CAN, owing its positivity for ER and PR. Similar to previously reported cases, the stromal cells in the current case were also positive for ER-α and PR but negative for WT1 for CD56. In contrast, true ovarian stromal cells are typically negative for ER-α and positive for WT1 and CD56 [18]. Therefore, the ER-α positive stromal cells in MESTK have a different immunophenotype from that of ovarian stroma, and therefore, they should not be regarded as true ovarian stroma.

In summary, we report what we believe to be the first case of a mucinous borderline tumor arising from a MESTK. Immunohistochemically, the borderline mucinous tumor had an identical immunophenotype to that of colorectal adenoma and carcinoma but different from that of an ovarian mucinous tumor. Caution should be taken in surgical resection of the lesion because, as with mucinous neoplasms of other organs, its rupture could potentially lead to pseudomyxoma peritonei.

Conflict of interest statement We declare that we have no conflict of interest.

References

1. Michal M, Syrucek M (1998) Benign mixed epithelial and stromal tumor of the kidney. Pathol Res Pract 194:445–448
2. Eble JN, Sauter G, Epstein JI et al (2004) Pathology and genetics of tumors of the urinary system and male genital organs. IARC, Lyon
3. Pawade J, Soosay GN, Delprado W et al (1993) Cystic hematoma of the renal pelvis. Am J Surg Pathol 17:1169–1175

4. Turbiner J, Amin MB, Humphrey PA et al (2007) Cystic nephroma and mixed epithelial and stromal tumor of kidney: a detailed clinicopathologic analysis of 34 cases and proposal for renal epithelial and stromal tumor (REST) as a unifying term. Am J Surg Pathol 31:489–500
5. Adsay NV, Eble JN, Srigley JR et al (2000) Mixed epithelial and stromal tumor of the kidney. Am J Surg Pathol 24:958–970
6. Antic T, Perry KT, Harrison K et al (2006) Mixed epithelial and stromal tumor of the kidney and cystic nephroma share overlapping features: reappraisal of 15 lesions. Arch Pathol Lab Med 130:80–85
7. Zhou M, Kort E, Hoekstra P et al (2009) Adult cystic nephroma and mixed epithelial and stromal tumor of the kidney are the same disease entity: molecular and histologic evidence. Am J Surg Pathol 33:72–80
8. Michal M, Hes O, Bisceglia M et al (2004) Mixed epithelial and stromal tumors of the kidney. A report of 22 cases. Virchows Arch 445:359–367
9. Yang Y, Ondrej H, Zhang L et al (2005) Mixed epithelial and stromal tumor of the kidney with cervical and intestinal differentiation. Virchows Arch 447:669–671
10. Beiko DT, Nickel JC, Boag AH et al (2001) Benign mixed epithelial stromal tumor of the kidney of possible mullerian origin. J Urol 166:1381–1382
11. Jung SJ, Shen SS, Tran T et al (2008) Mixed epithelial and stromal tumor of kidney with malignant transformation: report of two cases and review of literature. Hum Pathol 39:463–468
12. Svec A, Hes O, Michal M et al (2001) Malignant mixed epithelial and stromal tumor of the kidney. Virchows Arch 439:700–702
13. Kuroda N, Sakaida N, Kinoshita H et al (2008) Carcinosarcoma arising in mixed epithelial and stromal tumor of the kidney. APMIS 116:1013–1015
14. Sukov WR, Cheville JC, Lager DJ et al (2007) Malignant mixed epithelial and stromal tumor of the kidney with rhabdoid features: report of a case including immunohistochemical, molecular genetic studies and comparison to morphologically similar renal tumors. Hum Pathol 38:1432–1437
15. Nakagawa T, Kanai Y, Fujimoto H et al (2004) Malignant mixed epithelial and stromal tumours of the kidney: a report of the first two cases with a fatal clinical outcome. Histopathology 44:302–304
16. Ji H, Isacson C, Seidman JD et al (2002) Cytokeratins 7 and 20, Dpc4, and MUC5AC in the distinction of metastatic mucinous carcinomas in the ovary from primary ovarian mucinous tumors: Dpc4 assists in identifying metastatic pancreatic carcinomas. Int J Gynecol Pathol 21:391–400
17. Vang R, Gown AM, Barry TS et al (2006) Cytokeratins 7 and 20 in primary and secondary mucinous tumors of the ovary: analysis of coordinate immunohistochemical expression profiles and staining distribution in 179 cases. Am J Surg Pathol 30:1130–1139
18. He H, Luthringer DJ, Hui P et al (2008) Expression of CD56 and WT1 in ovarian stroma and ovarian stromal tumors. Am J Surg Pathol 32:884–890

Virchows Arch (2009) 455:395–396
DOI 10.1007/s00428-009-0839-2

LETTER TO THE EDITOR

The term *cor bovinum* in anatomical pathology

Georg Reith · Bernd Busch · Marcel A. Verhoff

Received: 31 July 2009 / Revised: 9 September 2009 / Accepted: 14 September 2009 / Published online: 13 October 2009

Keywords Cor bovinum · Historical definition · Diagnostic criteria · Minimum weight

Dear Sir:

The term *cor bovinum* or ox heart is found in pathology literature as a somewhat arbitrarily used analogy for an enlarged heart. Thus, the German benchmark textbook *Pathologie* from 1999, which was edited by Remmele, uses the term to describe hearts weighing more than 600 g but less than 1,000 g, while, interestingly, referring to weights exceeding 1,000 g as an *extreme enlargement*. We, therefore, thought that it would be interesting to shed light on the historical origin and use of this quaint term.

Our research revealed that two authors can claim credit for coining the term *cor bovinum*. Even if he did not yet use the exact term [1], William Cowper was the first to compare an extremely enlarged human heart to the heart of an ox in a case study on aorta valve stenosis. A second trail leads to Giovanni Battista Morgagni, who, in his 1761 opus, *De sedibus et causis morborum per anatomen indagatis*, says, "…the heart, however, was so large, that it was in size like that of an ox." Here, in the Latin original, the term *cor bovinum* is first used for an enlarged heart [2].

In deciding whether Cowper or Morgagni should receive credit for the term, one must take into account that the two were probably familiar with each other. Morgagni, at least, frequently referred to the English surgeon and anatomist in his text [2]. It is, therefore, quite possible that Morgagni adopted the analogy from Cowper.

In subsequent centuries, the term kept cropping up in pathology textbooks and manuals. In his 1887 *Pathology* manual, Mönkenberg explains [3] that older authors used the terms *cor bovinum* and *aneurysma totale cordis* to describe general hypertrophy and dilation of the heart. In 1852, Virchow used the expression, *ox heart*, to describe seriously dilated hearts [4]. *Cor bovinum* was used both by Cohnheim in 1877 and Brugsch in 1947. Interestingly, in a handbook published by Kaufmann in 1931, the term *cor bovinum* could still be found, but it no longer appeared in the 1955 edition. While the descriptions of *cor bovinum* are similar in these sources, neither a clear definition of the term nor a weight specification is included.

The term first appears in connection with a specific weight in Remmele's 1984 manual. The weight given here is 600 g. This weight is also quoted in Blümke's textbook *Pathologie* from 1995. A paper from 2001 even designates all hearts exceeding a weight of 500 g as being *cor bovinum* (Praxis 90: 1964–1972).

Weight specifications as diagnostic criteria, thus, appear to be of modern origin, and we conclude that the term *cor bovinum* was not historically associated with a specific weight. Although weights of over 1,300 g have been described for human hearts, in direct comparison, the hearts of Jersey cattle, which is the smallest known race, weigh at least 1,800 g [5].

Cor bovinum should, thus, primarily be understood as a descriptive rather than a diagnostic term.

G. Reith · B. Busch · M. A. Verhoff (✉)
Department of Legal Medicine, University of Gießen,
Frankfurter Straße 58,
35392 Gießen, Germany
e-mail: Marcel.A.Verhoff@forens.med.uni-giessen.de

References

1. Cowper W (1705) Of ossifications or petrifacations in the coats of arteries particularly in the valves of the great artery. Philos Trans 24:1970–1974
2. Morgagni JB (1761) De sedibus et causis morborum per anatomen indagatis. Typographia Remondiniana, Venice, Italy
3. Mönckeberg JG (1887) In: Henke, Lubarsch (ed) Handbuch der speziellen Pathologischen Anatomie und Histologie. Vol. 1, Springer, Berlin, p 375
4. Lichthardt R (2003) In: Virchow R. (ed) Specielle pathologische Anatomie, Mitschriften des Studenten Justus Rabus aus dem Jahre 1852/53 Inauguraldissertation Med. Fak. Würzburg, p 443
5. Nickel, Schummer, Seiferle (eds) (1996) Lehrbuch der Anatomie der Haustiere. Parey, Berlin

Virchows Arch (2009) 455:397–411
DOI 10.1007/s00428-009-0842-7

ORIGINAL ARTICLE

Histological heterogeneity of Ewing's sarcoma/PNET: an immunohistochemical analysis of 415 genetically confirmed cases with clinical support

Antonio Llombart-Bosch · Isidro Machado · Samuel Navarro · Franco Bertoni · Patrizia Bacchini · Marco Alberghini · Apollon Karzeladze · Nikita Savelov · Semyon Petrov · Isabel Alvarado-Cabrero · Doina Mihaila · Philippe Terrier · Jose Antonio Lopez-Guerrero · Piero Picci

Received: 21 April 2009 / Revised: 15 September 2009 / Accepted: 25 September 2009 / Published online: 17 October 2009

Abstract Ewing's sarcoma (ES)/peripheral neuroectodermal tumor (PNET) are malignant neoplasms affecting children and young adults. We performed a study to typify the histological diversity and evaluate antibodies that may offer diagnostic/prognostic support. In total, 415 cases of genetically confirmed paraffin-embedded ES/PNET were analyzed on whole sections and in tissue microarrays. This study confirms the structural heterogeneity of ES/PNET, distinguishing three major subtypes: conventional ES (280 cases); PNET (53 cases); and atypical ES/PNET (80), including large cells, vascular-like patterns, spindle pattern, and adamantinoma-like configuration. All cases presented positivity for at least three of the four tested antibodies (CD99, FLI1, HNK1, and CAV1). CAV1 appeared as a diagnostic immunomarker of ES/PNET being positive in CD99-negative cases. Hence, the immunohistochemical analysis confirmed the diagnostic value of all four antibodies, which together cover more than 99% of the tumors, independently of the histological variety. The univariate analysis for survival revealed atypical ES as the only histological parameter apparently associated with less favorable clinical outcome, particularly in the subgroup of patients treated with surgery. In conclusion, the diagnosis of atypical ES is a challenge for the pathologist and needs support from molecular techniques to perform an optimal differential diagnosis with other small round cell tumors.

Keywords ESFT · Histopathology · Immunohistochemistry

A. Llombart-Bosch (✉) · I. Machado · S. Navarro
Department of Pathology, University of Valencia,
Ave. Blasco Ibañez, 17,
46010 Valencia, Spain
e-mail: antonio.llombart@uv.es

F. Bertoni · P. Bacchini · M. Alberghini · P. Picci
Institut Orthopedic Rizzoli,
Bologna, Italy

A. Karzeladze · N. Savelov
N.N. Blokhin National Cancer Research Center,
Moscow, Russia

S. Petrov
Cancer Oncology Center,
Kazan, Russia

I. Alvarado-Cabrero
Hospital General de Mexico DF,
Mexico, Mexico

D. Mihaila
Children's Hospital,
Iasi, Romania

P. Terrier
Institute Goustave Roussy,
Villejuif, France

J. A. Lopez-Guerrero
Instituto Valenciano Oncología,
Valencia, Spain

Introduction

Ewing's sarcoma (ES) of the bone configures a family of highly malignant neoplasms in children and young adults; the histology is constituted by undifferentiated small round cells distributed in a homogeneous pattern

without any particular architectural definition [1–3]. Occasionally, Homer-Wright pseudorosettes can be detected, a fact that has given support for a neuroectodermal nature, thus being also named peripheral neuroectodermal tumor (PNET) [4–7]. Atypical variants of this tumor have been described [4–12] due mainly to a high degree of cell heterogeneity or to the presence of pseudovascular structures [13]. In addition, neoadjuvant chemotherapy or radiotherapy induces tumor cell changes producing major structural anaplasia [14]. Thus, the histological diagnosis of this tumor is difficult [13–15]. Moreover, a number of small round cell tumors (SRCT), mostly located outside the bone, show a histologically similar configuration making its diagnosis even more difficult. The differential diagnosis of ES/PNET, compared with other malignant SRCT, is occasionally extremely complex or almost impossible when using only histological methods [7, 13–17].

Immunohistochemistry (IHC) has been reported to provide crucial support to the identification of these neoplasms as well as to the differential diagnosis when compared to other SRCT. Among the most well-recognized antibodies regularly expressed in this tumor are MIC2 (CD99) [15, 18–20], HNK1 (Leu7, CD57) [21–24], Fli1 [15, 22, 25, 26], and more recently, caveolin-1 (CAV1) [27]. Therefore, the simultaneous use of several antibodies becomes mandatory to histologically confirm an ES/PNET. Nevertheless, the definitive value of these markers for diagnosis and prognosis remains a matter of debate.

ES/PNET are cytogenetically characterized by a specific reciprocal translocation between chromosomes 11 and 22 in over 90% of cases, as well as other less frequent chromosomal rearrangements [t(21;22), t(7;22), t(2,22); 28–32], promoting the rearrangement of the *EWS* gene with one of the members of the *ETS* family of genes, mainly with the *FLI1* gene [33–39]. In this regard, cytogenetics and molecular biology have provided new tools for diagnosis as well as for the characterization of this group of SRCT, becoming today a necessary requisite before any therapeutical approach can be clinically undertaken.

The pathologists of the Prognosis and Therapeutic Targets in the Ewing Family of Tumors Consortium (PROTHETS, a 6FP grant EC project) undertook an extensive study, collecting SRCT from several laboratories participating in the project in order to gain a better view of the histology of this neoplasm and its microscopical diversity, as well as to typify those antibodies that could offer a better diagnostic support as well as prognostic information. To this end, a large number of formalin-fixed paraffin-embedded SRCT were collected and, after an extensive review and genetic confirmation, 415 ES/PNET cases were retained for the present study.

Material and methods

Patients and samples

A total of 857 SRCT were collected and made available for study at the Department of Pathology, University of Valencia Estudi General (UVEG). In 34 cases, only slides were obtained as these cases had been submitted for second expert opinion and no paraffin blocks were available. The centers of origin of the remaining cases were as follows: 447 from Instituto Ortopedici Rizzoli (IOR), Bologna, Italy; 183 from UVEG, Valencia, Spain; 111 from Blokhin Russian Cancer Research Center, Moscow and the Clinical Oncological Center, Kazan, Russia; 54 from Orthopedic Institut of Kiev, Ukraine; 32 from Hospital General de Mexico DF, Mexico; 12 from Children's Hospital, Iasi, Romania; nine from Institute Gustave Roussy (IGR), Villejuif, France; and two from Instituto Nacional de Oncologia y Radioterapia (INOR), La Habana, Cuba. The tissues were fixed in buffered formalin and paraffin embedded at the local laboratories. Solutions of formic acid/formalin, hydrochloric acid, or ethylenediaminetetraacetic acid were used as standard decalcifier agents for each institution [40].

Approval for data acquisition and analysis was obtained from the ethics committee of all the institutions involved in the study. The clinical data were reviewed and stored within a specific database.

Out of these 823 SRCT, 166 cases were excluded from the study due to technical problems, insufficient material, poor preservation resulting from overdecalcification, or massive tissue necrosis. Another 242 cases were not considered because genetically they were either negative or not informative for *EWS* rearrangements, leaving a total of 415 ES/PNET for inclusion in the present study.

The source of the analyzed material was known for 324 cases, the distribution being as follows: 272 primary tumors (84%), 22 disseminated primary tumors (7%), nine recurrences (3%), and 21 metastases (6%). For statistical considerations, disseminated primary tumors, recurrences, and metastasis were grouped in the same category (disseminated disease).

Histology

Following previous publications [5, 13, 15, 17, 22, 41], several histological varieties of ES/PNET are considered: conventional or classical ES, large cell ES with epithelioid cells, clear cell with hypernephroid cells, ES with spindle cells, vascular-like with hemangioendothelial features, ES with neuroectodermal features (isolated pseudorosettes),

PNET showing numerous well-configured Homer-Wright rosettes, synovial sarcoma-like PNET, sclerosing PNET, adamantinoma-like ES. In addition to this morphological subtyping, other structural parameters were reviewed in order to obtain supplementary criteria for prognosis, as previously described by several authors in primary ES before treatment [42–45]. It should be noted that these criteria were verified on the complete histological slide. The following histological structures were analyzed:

Presence/absence of necrosis: negative, either no or minimal necrosis (<25%) and positive (>25%) of the whole slide.

Chessboard or filigree pattern: presence of string-like figures motivated by the infiltration of tumor cells within a stroma displaying high sclerosis and causing a dense collagen response.

Lobular pattern: distribution of thin reticular fibers, scalloping the tumor cells in nests or lobules.

Mitotic count: detection of at least five or more mitosis in ten consecutive, randomly selected high power fields at a ×40 magnification. When fewer mitotic figures were found, the count was considered as negative.

Immunohistochemistry

For practical reasons and due to the large number of cases in the study, we have limited the immunophenotyping of the ES/PNET to a panel of four antibodies (Table 1). The choice of these antibodies was decided after an analysis of the literature, taking into account their confirmed expression in this tumor type and, therefore, excluding other immunomarkers, such as epithelial or neuroectodermal, that have been tested without major diagnostic or prognostic relevance [5, 7, 10, 13, 15–17, 22, 25, 26, 45–59]. The histopathological analyses were performed on the whole tissue sections. In addition, 24 tissue microarrays (TMAs) were constructed. Each TMA included two representative cores for each case (1 mm of diameter). Sections, 4-µm-thick, were processed for IHC. Antigen retrieval was performed by pressure cooker boiling at 1.2 atm for 3 min in 10 mmol/L citrate buffer (pH 6.0). The labeled streptavidin–biotin (LSAB) method (Dako) was performed, followed by revelation with 3,3-diaminobenzidine as conventional protocols. All sections were evaluated independently by three pathologists (IM, SN, and ALLB).

In order to test for the most appropriate antibody for CD99, four different clones of commercially available monoclonal antibodies, namely, HBA71, 013, HO36-1.1, and MEM131 [19, 60–62], were evaluated in a set of 157 cases with the objective of determining their sensitivity and specificity [63]. CD99 positivity was considered as "+3" when the stain was present in all tumor cells mainly defining the membrane, while the cytoplasm was either negative or also positive. When a lower delimitation of the cell membrane with coloring of the cytoplasm occurred, these were deemed "+2" when all the cells were stained, while scanty cell membrane or cytoplasmic staining in isolated groups of cells was noted as "+1." Negative staining was considered for no or very weak staining. Antibody positivity was scored in both the complete histological slide as well as in the TMA (core diameter 1 mm, two cores of the most representative fields from each case).

Molecular biology and fluorescence in situ hybridization

RNA was extracted and tested in all tumors with reverse transcription polymerase chain reaction (RT-PCR) in order to detect any of the following translocations: *EWS/FLI1*, *EWS/ERG*, and *EWS/FEV* as previously described [30]. In addition, a fluorescent in situ hybridization (FISH) analysis was carried out with the *EWSR1* break-apart probe on the TMA. More details are described elsewhere [39].

Statistical analysis

A FileMaker database was constructed and implemented to collect the main clinical, histopathological, and genetic data of all patients included in the project.

For the statistical analysis, we used binary variables reflecting the positivity status of the measures (yes or no). Association with histopathological parameters, all categorical, was also assessed using a chi-square test to determine homogeneity or linear trend for ordinal

Table 1 Antibodies used for the immunohistochemical analysis

Antibodies	Source	Clone	System	Dilution	Pretreatment
CD99	Dako	Monoclonal mouse HBA-71	LSAB	1/50	Citrate buffer (pH 6.0) pressure cooker boiling
FLI-1	Santa Cruz	Rabbit polyclonal	LSAB	1/50	Citrate buffer (pH 6.0) pressure cooker boiling
HNK	Cell line ATCC, Valencia	–	LSAB	10 µ/ml	Citrate buffer (pH 6.0) pressure cooker boiling
CAV1	Santa Cruz	Rabbit polyclonal	LSAB	1/200	Citrate buffer (pH 6.0) pressure cooker boiling

variables. The significance level was set at 5%. To study the impact of the histological, immunohistochemical, and molecular factors on the progression-free survival (PFS) and overall survival (OS), the Kaplan–Meier proportional risk test (log rank) was used [64, 65]. PFS is considered as the proportion of patients with no evidence of local or distant recurrence during follow-up, whereas OS reflects the proportion of patients alive (with or without disease) at the time of the last clinical review. Only cancer-specific deaths were considered for the statistical analysis of the OS. Evidence of the relative risk for each patient was also provided by means of a Cox proportional hazards model using stepwise selection to identify the independent predictors of poor outcome [66]. All the statistical analyses were carried out using the SPSS (version 15.0.1, SPSS, Chicago, IL, USA).

For the prognostic evaluation, we analyzed 217 patients with localized genetically confirmed ES/PNET. Due to the retrospective nature of the series and the variety of institutions involved, it was not always possible to obtain complete clinical information for some cases, such as margins, type of surgery, or TNM stage. Hence, given the limited quality of the clinical information, the survival data herein presented should be considered with reserve. Therefore, the variables used in the prognostic evaluation included: clinical (age, sex, location of the tumor, and type of treatment), histological (histological varieties, necrosis, lobular pattern, filigree pattern, and mitosis), immunohistochemical (CD99, HNK1, Fli1, and CAV1), and molecular parameters (fusion gene type).

Results

The characteristics of the series included in the present study are listed in Table 2. For the prognostic evaluation, only patients from IOR (198 cases) and UVEG (19 cases) with localized primary tumors (nondisseminated primary tumors) were considered, making a total of 217 patients. The median age of the series was 17 years (range=1–99 years) and the male–female ratio was 1.6. Sixty percent of tumors were appendicular skeleton. Seventy-six patients (35%) were treated with surgery and chemotherapy, whereas the remaining cases were treated with radiotherapy, chemotherapy, and/or surgery. The median follow-up was 39 months (range=0.17–452 months) with an OS of 55%.

Histology

Among the 415 ES/PNET cases, the following histological varieties were found:

Conventional or classical ES (264 cases, 63%) is defined as a tumor constituted by a diffuse and monotonous proliferation of homogeneous small round blue cells (in hematoxylin and eosin [H/E] due to the dark staining of the small nuclei; Fig. 1a, b) and, in some cases, adopting a perivascular distribution with a variable amount of necrosis extending about 200–250 μ distant from the most proximal vessel. Cell pleomorphism and mitosis are scarce (about two to three per ×40 in ten consecutive fields).

PNET (53 cases, 13%) are mainly represented by the existence of typical Homer-Wright neural rosettes provided with a central core (Fig. 1b, c). In addition, fibrillar structures appear as cytoplasm projections, while the tumor is lobulated by reticular fibers (Fig. 2e). The number of rosettes varies from isolated to numerous in continuous transitions, appearing within monotonous fields of conventional ES. We considered all cases in which these structures were present as PNET, independently of the degree of differentiation and the number of rosettes seen.

Large cell ES (33 cases, 8%): this histological variant is consistent with a SRCT that possesses cell and nuclear pleomorphism with large abundant acidophilic cytoplasm. The nuclei are voluminous, round or oval, occasionally binucleated, and contain one or more prominent nucleoli (Fig. 1e). The reticular network is more prominent with a tendency to lobulation. The cells may contain a large amount of glycogen within the cytoplasm adopting a clear cell hypernephroid appearance (Fig. 2a). In addition, the cells occasionally adopt a more spindle-like configuration with fusiform nuclei, affecting more than 50% of the tumor fields (Fig. 1f). This histological particularity can appear in both conventional ES and in the large cell subtype.

ES/PNET with vascular-like, hemangioendothelial features (nine cases, 2%): the cells display a pseudoendothelial pattern conforming vascular-like spaces, lined by tumor cells that progressively elongate and cover lacunae filled with erythrocytes and plasma material (Fig. 2b). These cells, lining the surface of the vessel-like spaces, lack basal membrane and are in continuity with the more solid cellular areas that maintain a typical ES configuration.

Regarding the varieties of *synovial sarcoma-like ES*, *sclerosing ES*, and *adamantinoma-like ES* [15], none of these subtypes were considered as an independent entity in our material. The presence of sclerotic areas is quite frequent in ES/PNET and is associated with tumor extension into cortical bone or with areas of soft tissue invasion (Fig. 2c, f), as well as with secondary interstitial hyaline deposits. Also, no true *adamantinoma-like ES/PNET* were identified, but we did observe cases in which the cells focally adopt a palisading architecture being sustained by a collagen basal-like membrane that could mimic an adamantinoma ES (Fig. 2d). All these cases were

Table 2 Characteristics of the series

Parameter	Number	Percentage
Sex		
Male	228	62
Female	142	38
Age (median years)=17 years (1–99 years)		
≤17 years	191	54
≥17 years	166	36
Histological varieties		
Conventional ES	280	67
PNET	53	13
Atypical ES	82	20
Location		
Axial	140	40
Appendicular	211	60
Surgery[a]		
Not done	63	29
Done	154	71
Radiotherapy[a]		
Not done	76	35
Done	141	65
Event-free survival[a]		
No progression	118	55
Progression	98	45
Final outcome[a]		
Alive	119	55
Died	98	45

[a] Data available from 217 cases

included within the category of atypical ES. In order to homogenize these ES/PNET varieties in larger statistical groups, the 415 cases were regrouped into three larger categories according to their predominant morphological criteria: conventional–typical ES [280 cases (67%)], PNET with the presence of neuroectodermal traces [53 cases (13%)], and atypical ES comprising all varieties distinct from the two above-mentioned types [82 cases (20%)]. The main histological findings are summarized in Table 3.

Immunohistochemistry

All sections were evaluated independently and read blinded by all three pathologists (IM, SN, and ALLB) with a high concordance rate between all examiners. Full concordance existed between whole sections and TMA sections by IHC for each pair of cores.

CD99 expression

Of the 415 cases, 402 (97% of the total) were valid for CD99 immunostaining. All but four cases expressed CD99 from a low to a high intensity (99%; Table 4). The majority of cases (289) presented both a membranous and cytoplasmic staining (+3; Fig. 3a), while a diffuse dense cytoplasm coloring was seen in 81 cases (+2). Finally, in 28 cases, there was a light cytoplasmic or membranous staining (+1). There were no differences in CD99 expression with respect to the distinct histological varieties of ES/PNET.

Fli1 expression

This antibody stains the cell nuclei of the tumors but is also present in endothelial cells and in the lymphocytes of the stroma. Eighty-nine percent of cases (344 from a total of 388 informative cases) expressed Fli1 with high intensity (Fig. 3b), while 44 cases were negative (11%; Table 4). As seen with CD99, no relationships could be found between Fli1 expression and the histological subgroups of ES/PNET.

HNK1 staining

HNK1 expression was detected in 215 cases out of 404 informative cases (53%; Fig. 3c, Table 4). Interestingly, PNET (57% of cases) and especially atypical ES/PNET (64%) stained HNK1 in a higher proportion than conventional ES/PNET (49%; $p=0.045$).

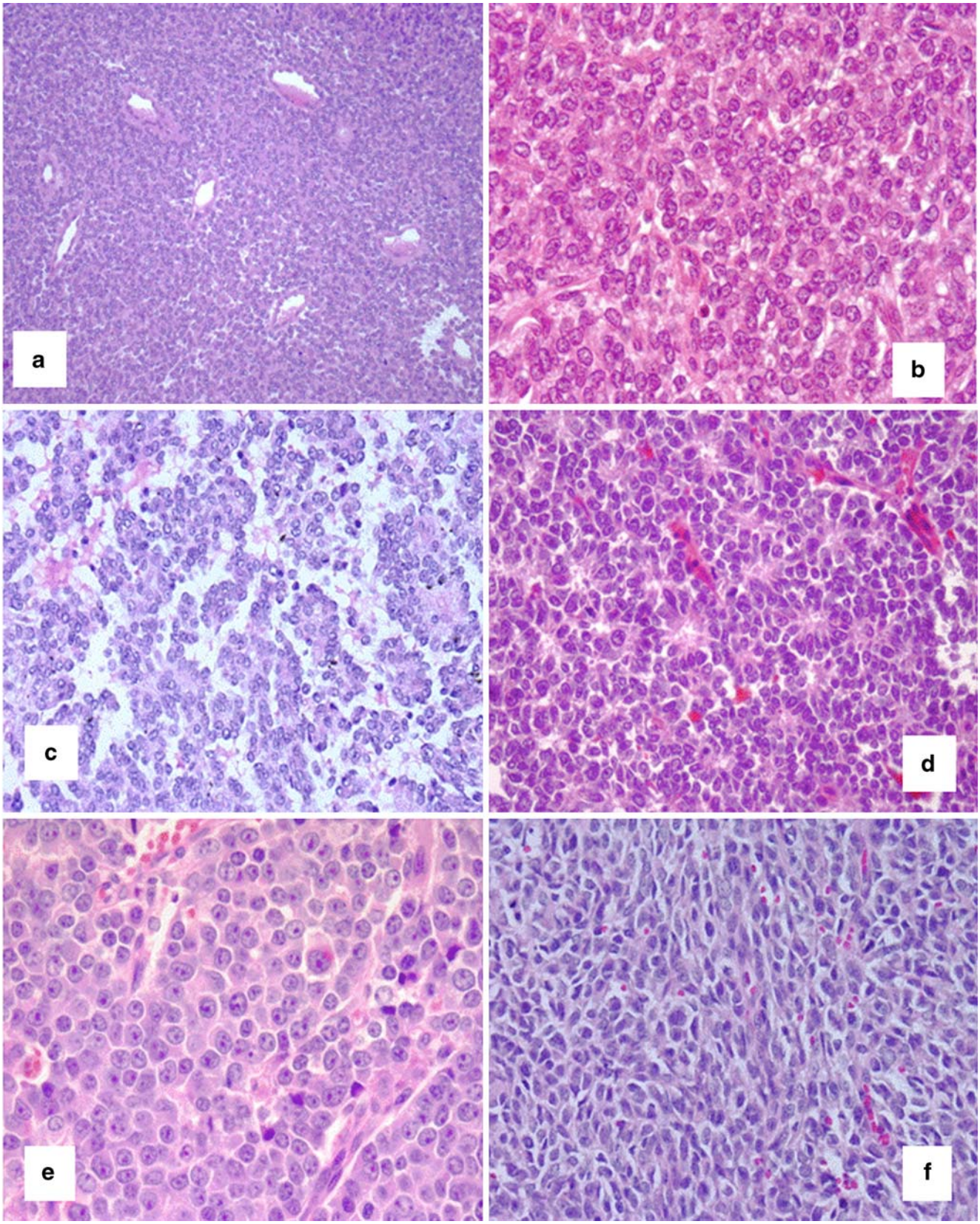

Fig. 1 **a** Classical ES with vascular formation (H/E, ×20), **b** classical ES (H/E, ×40), **c** and **d** PNET with abundant rosettes (H/E, ×40), **e** large cells ES (H/E, ×40), **f** atypical ES with spindle cell pattern (H/E, ×40)

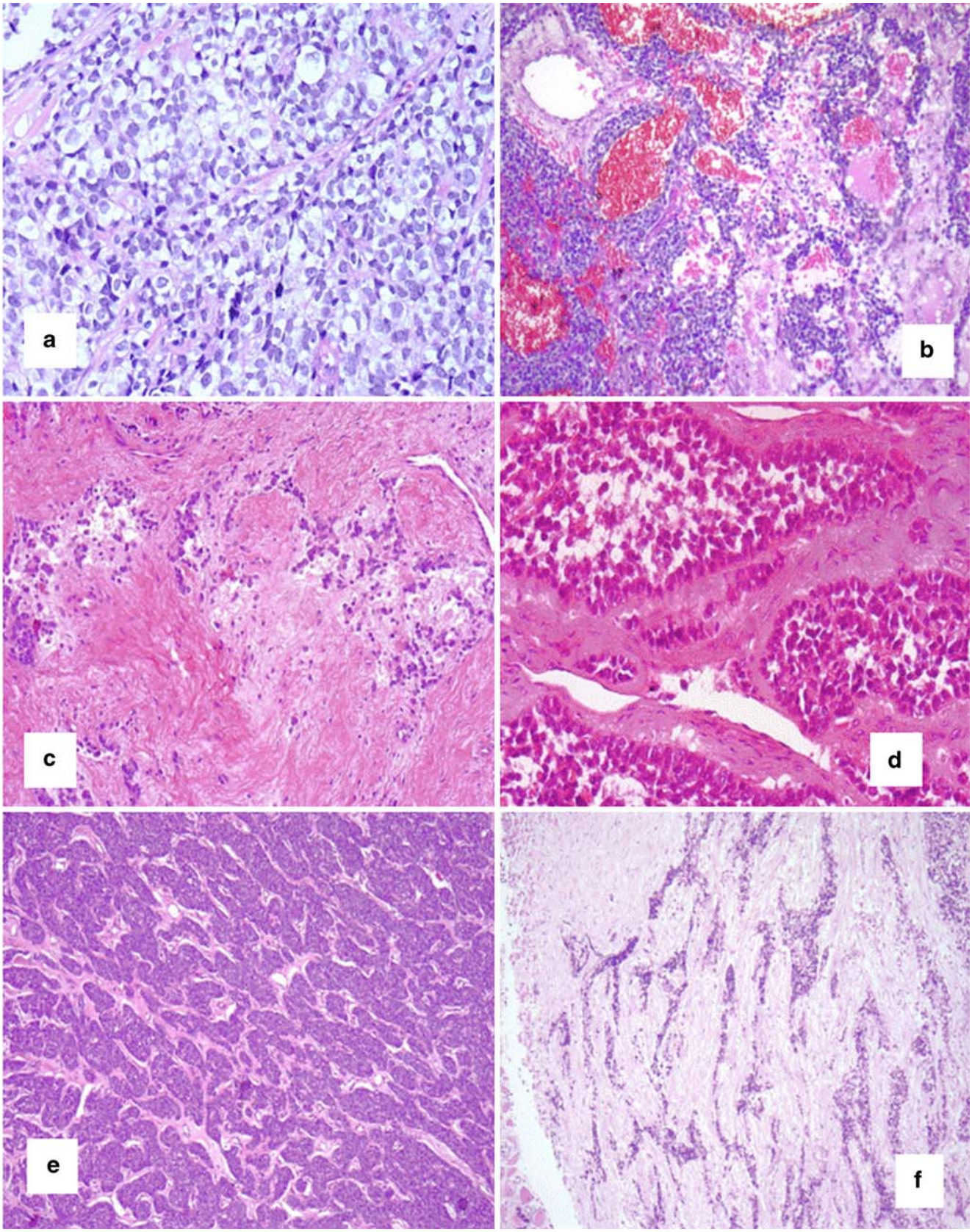

Fig. 2 **a** Clear cell ES (H/E, ×40), **b** hemangioendothelial ES (H/E, ×40), **c** sclerosing ES (H/E, ×20), **d** adamantinoma-like ES (H/E, ×40), **e** lobular pattern in PNET (H/E, ×20), **f** filigree pattern and sclerosis in ES (H/E, ×20)

Table 3 Frequencies of the histological parameters

Parameter	Number	Percentage
Histological varieties		
Conventional ES	280	67
PNET	53	13
Atypical ES	82	20
Necrosis		
No	208	52
Yes	193	48
Lobular pattern		
No	277	68
Yes	130	32
Filigree pattern		
No	261	64
Yes	147	36
Mitosis		
0–4	310	76
5–10	84	21
>10	12	3

Caveolin-1 expression

In our series, CAV1 was expressed in 96% of cases (368; Fig. 3d), while only 5% of tumors (17 cases) resulted negative (Table 4). No association with ES/PNET histological varieties or tumor progression was observed. However, CAV1 correlated highly with CD99 ($p<0.0001$) and, interestingly, the four CD99-negative cases expressed CAV1.

Association of the analyzed parameters with tumor progression

Taking into account the type of material analyzed, primary tumors vs. disseminated disease, we compared the difference in frequencies between these two groups for each of the different parameters analyzed in order to depict an association with tumor progression. The results are listed in Table 5. No association with progression was observed with the histological varieties of ES/PNET, although disseminated tumors were characterized by a high mitotic count. None of the immunohistochemical diagnostic markers, except Fli1, demonstrated association with tumor progression (Table 5).

Table 4 Immunohistochemical expression of the diagnostic markers

Immunohistochemical marker	Negative (%)	Positive (%)
CD99	4 (1)	398 (99)
HNK1	189 (47)	215 (53)
FLI1	44 (11)	344 (89)
CAV1	17 (4)	368 (96)

Molecular genetic studies

The diagnosis of Ewing's sarcoma family of tumors (ESFT) in all cases was genetically confirmed by FISH *EWSR1* break apart and/or RT-PCR positive results. These results are described in more detail elsewhere [39].

Progression-free and overall survival

Tables 6 and 7 show the results of the univariate and multivariate analysis for both PFS and OS. The multivariate analysis revealed that the lobular pattern ($p=0.044$) and the type of treatment ($p=0.00037$) constituted independent prognostic factors for PFS, probably due to the presence of inoperable cases ($n=63$) in the radiotherapy group. The same trend was observed for OS where the type of treatment remained as an independent prognostic factor ($p<0.0001$).

In order to avoid the influence of treatment type on prognostic behavior, two groups of patients were considered. The surgery group composed of 76 patients who received surgery with chemotherapy and the radiotherapy group composed of 141 patients in whom radiotherapy was included in their treatment regimen (78 patients with surgery and 63 patients without surgery). Tables 8 and 9 show the most relevant associations between the analyzed parameters and follow-up for the surgery group of patients. Interestingly, the histological variety of ES/PNET constitutes the unique independent prognostic factor for both PFS and OS (Tables 8 and 9). The atypical ES/PNET being the variety with the worst behavior (Fig. 4a, b). However, this association was not observed in the radiotherapy group in which only Fli1 expression provided favorable prognostic information in the univariate analysis for OS ($p=0.036$). No independent prognostic factor emerged from the multivariate analysis.

Discussion

Several unresolved problems remain regarding the histological diagnosis of ES/PNET due to the plurophenotypic histology and the diverse response to immunohistochemical staining. These facts have led to the need for molecular support in order to confirm the presence of any of the already-described genetic rearrangements, thus making morphology subsidiary to the molecular diagnosis. A major aim of the PROTHETS EC project (http://www.prothets.org) was to confirm the validity of histology and IHC as tools for diagnosis based on the experience obtained from the review of a large number of samples and adequate selection of immunostaining.

The present study, based upon a series of 415 genetically confirmed ES/PNET cases, substantiates the structural heterogeneity of this family of tumors in which three major

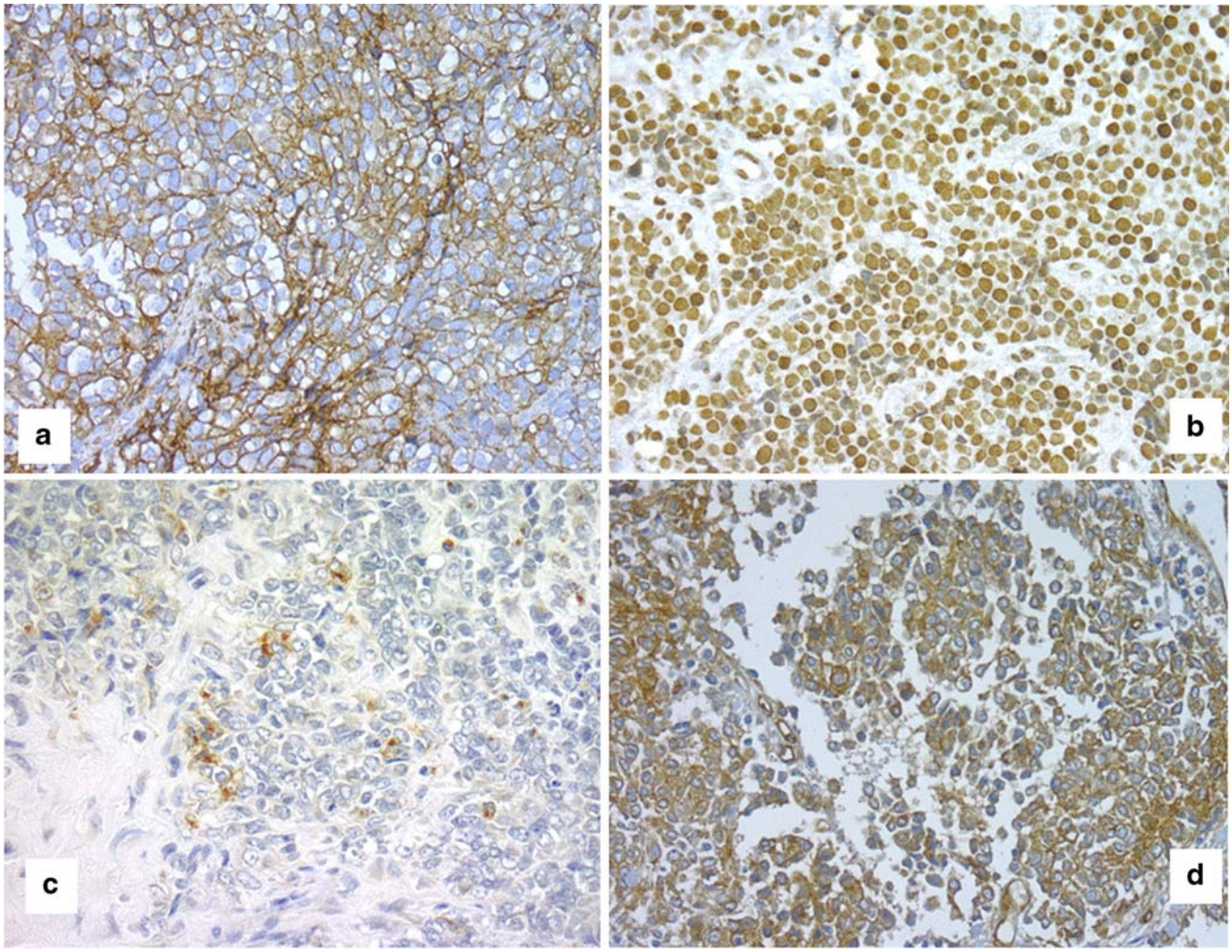

Fig. 3 **a** CD99 (HBA71) membranous staining (+++) in PNET (×40), **b** Fli1 nuclear staining (+++) in classic ES (×40), **c** HNK-1 cytoplasm staining (+) with focal dot-like pattern/Golgi staining (×40), **d** CAV1 cytoplasm and membrane staining (+++) in ES and endothelial cells as positive control (×40)

subtypes were distinguished: conventional or classical ES (67%), PNET with neuroectodermal phenotype (13%), and atypical ES/PNET (20%). The present results are similar to those described by other authors. Folpe et al. [15] observed 43 ES (73%) with typical features within a series of 66 ES cases; also in this publication, the PNET constituted 16%. In our series, a total of 82 cases were classified as atypical ES which displayed a heterogeneous histology when compared to conventional ES or PNET, comprising neoplasms composed of large cells with irregular nuclear contours (33 cases, 8%) or offering a vascular-like hemangiomatous appearance (eight cases, 2%). In addition, atypism of another 41 (10%) tumors was consistent when major structural variations that appeared within a conventional ES, including the presence of other microscopical components such as spindle cells, desmoplasia, sclerosis with a hyalinized matrix, focal adamantinoma-like, and chessboard or filigree configuration, together with a variable extent of necrosis and hemorrhages. These atypical ES have been described previously by our group and other authors [10, 13, 16, 17, 41], not only in bone, but also in soft tissues [12, 15, 67–69].

An additional point in the PROTHETS project was the search for histological patterns that could provide prognostic significance when evaluated on the H/E histological slide without any special immunostaining support. In previous publications, the extent of necrosis seen in the histological slide, together with presence of a "chessboard or filigree pattern" constituted by nests of tumor cells extending outside the bone invading soft tissue and clustered by dense hyalinized stroma, have been described as prognostic indicators of higher malignancy [16, 45, 70]. In the present study, none of these findings influence prognosis for the patients.

In a univariate analysis, the only histological pattern associated with poor clinical outcome was atypical ES

Table 5 Association of histological patterns with tumor progression

Parameter	Number	Primary tumor (%)	Disseminated (%)	*p* value
Histological diagnosis				
Conventional ES	216	188 (69)	28 (54)	0.101
PNET	40	31 (11)	9 (17)	
Atypical ES	68	53 (19)	15 (29)	
Histological parameters				
Filigree pattern	317	95 (36)	12 (24)	0.112
Lobular pattern	317	73 (27)	17 (33)	0.393
Mitosis	316	60 (23)	19 (37)	0.027
Necrosis	313	128 (49)	18 (36)	0.100
IHC				
CD99	315	259 (99)	52 (100)	0.371
HNK1	316	154 (58)	31 (60)	0.864
FLI1	305	213 (84)	49 (96)	0.022
CAV1	302	244 (96)	45 (96)	0.986

compared to conventional ES or PNET subtypes, especially in the subgroup of patients treated with surgery in which the histological subtype constituted an independent prognostic factor. These findings confirm the controversial issue [45, 71–74] on the significance of neuroectodermal differentiation associated to a different clinical outcome. In addition, no difference in disease-free survival, tumor progression, or presence/absence of metastasis was detected when analyzing the remaining histological parameters.

We also analyzed the value of several immunomarkers for diagnostic and prognostic purposes. Regarding the most commonly used marker, CD99 (p30/32mic2), we were able to confirm previous findings [15, 18, 19, 22, 25, 58] that have shown how CD99 expression constitutes a very reliable maker for the diagnosis of this family of tumors. This antigen is also expressed in a number of other SRCT (rhabdomyosarcoma, synovial sarcoma, and small cell anaplastic osteosarcoma) [17, 41, 56, 58, 75] but the staining reactions are generally weak and focal. These findings limit the specificity of this antibody to some extent and may cause difficulties for the diagnosis of ES/PNET when used alone as a single immunomarker.

The most significant observation was that all but four cases expressed CD99 with a high or moderate intensity (+++/+), either membranous or cytoplasmic, or both. The four negative cases for CD99 were histologically conventional ES and were tested with the other CD99 monoclonal antibodies (HO36-1, O13, and MEM131) [63] obtaining similar negative results. However, these cases were positive for the *EWS* rearrangements by FISH and RT-PCR, thus confirming the existence of CD99-negative ES/PNET, but in such a limited number of cases as to in fact make this result an exception.

Table 6 Log-rank and Cox regression tests for PFS

Parameters	Number	Events	%PFS	*p* univariate	HR [95%CI HR]	*p* multivariate
Clinical						
Treatment				<0.0001		0.00037
Surgery group	76	20	70		1	
Radiotherapy group	141	78	36		2.5 [1.5–4.05]	
Location				0.073		NS
Axial	72	35	39			
Appendicular	144	63	51			
Histological						
Lobular pattern				0.006		0.044
No	152	63	51		1	
Yes	59	35	33		1.5 [1.01–2.3]	
Histological subtype				0.379		
Conventional ES	148	65	49			
PNET	26	10	58			
Atypical ES	42	23	36			

NS not significant, *HR* hazard ratio

Table 7 Log-rank and Cox regression tests for OS

Parameters	Number	Events	%OS	*p* univariate	HR [95%CI HR]	*p* multivariate
Clinical						
Treatment				<0.0001		<0.0001
Surgery group	76	18	73		1	
Radiotherapy group	141	80	37		2.9 [2.1–5.03]	
Location				0.071		NS
Axial	73	36	40			
Appendicular	144	62	53			
Histological						
Lobular pattern				0.031		NS
No	153	65	51			
Yes	59	33	37			

NS not significant, *HR* hazard ratio

There were no statistical differences regarding intensity and distribution of CD99 expression patterns and the three major histological varieties of ES/PNET. Furthermore, no distinction was found between CD99 expression and tumor progression when analyzing the clinical situation of the patients (primary tumors, disseminated primary tumors, recurrences, and metastasis). In consequence, we confirm that CD99 expression is the most reliable immunohistochemical marker for ES/PNET, as has previously been observed in less numerous series of cases [15–17, 22, 41, 58, 76].

In many studies, Fli1 immunostaining [15, 22, 25, 26, 77, 78] as well as HNK1 (CD57) [23, 46, 53, 79–82] have been described as reliable markers for ES/PNET. Nevertheless, all authors agree that both markers lack specificity and their sensitivity is quite variable. In our material, 89% of tumors expressed Fli1 with high intensity, although as with CD99, no relationship was found between Fli1 expression and the histological subtypes. However, we report an association between Fli1 expression and a better OS in the group of patients treated with radiotherapy. In most of the human ES/PNET, Fli-1 is the target of a characteristic chromosomal-balanced translocation t (11;22) (q24:q12), which results in the production of the *EWS/FLI-1* fusion gene, and ES/PNET cases harboring the *EWS/FLI-1* transcript which seem to have a better prognosis than those containing other *EWS/ETS* transcripts have been described [83]. In our series, all studied cases carried a *EWS* rearrangement and the overexpression of Fli1 distinguished a group of patients with better outcome.

Unlike Fli1, only 53% of cases expressed HNK1. A relationship was found between HNK1 expression and the histological ES subtypes, the proportion of positive cases being higher in PNET and atypical ES. However, no relation with prognosis was seen.

CAV1 is a membrane protein that participates in the formation of caveolae [84]. The function of CAV1 is still under intensive investigation [85]. High expression of CAV1 leads to inhibition of cancer-related pathways, such as growth factor signaling pathways. However, certain

Table 8 Log-rank and Cox regression tests for PFS in the surgery group of patients

Parameters	Number	Events	%PFS	*p* univariate	HR [95%CI HR]	*p* multivariate
Clinical						
Sex				0.072		NS
Male	47	9	79			
Female	27	11	57			
Histological						
Mitosis (in 10 HPF)				0.076		NS
0–5	59	12	76			
6–10	13	6	51			
>10	3	2	33			
Histological subtype				0.027		0.045
Conventional ES	55	11	77		1	
PNET	7	2	71		3.3 [1.3–8.6]	
Atypical ES	14	7	37		2.5 [0.51–11.9]	
Fli1				0.091		NS
No expression	7	0	100			
Expression	66	20	65			

NS not significant, *HR* hazard ratio

Table 9 Log-rank and Cox regression tests for OS in the surgery group of patients

Parameters	Number	Events	%OS	*p* univariate	HR [95%CI HR]	*p* multivariate
Clinical						
Sex				0.070		NS
Male	47	8	79			
Female	27	10	62			
Histological						
Histological subtype						
Conventional ES	57	10	79	0.004	1	0.031
PNET	7	1	80		3.58 [1.4–9.3]	
Atypical ES	14	7	40		2.45 [0.5–11.9]	

NS not significant, *HR* hazard ratio

cancer cells that express CAV1 have been shown to be more aggressive and metastatic because of a potential for anchorage-independent growth [86]. Particularly in the case of ES, CAV1 has been described as a key determinant of tumorigenicity and could be considered as a potential target of new molecular therapeutic strategies. In these tumors, CAV1 is a direct target of the *EWS/FLI1* chimeric proteins, being overexpressed in a high proportion of cases [27], and has, therefore, been proposed as a potential diagnostic marker for ES/PNET [87]. The positivity of CAV1 antibody has been communicated in several carcinomas and sarcomas [27, 86, 88–98]. The experience of our group confirmed the high sensitivity of this antibody in ES/PNET when compared to other neuroectodermal and mesenchymal neoplasms such as neuroblastomas, undifferentiated synovial sarcomas, chondrosarcomas, and osteosarcomas (data not shown). In this study, CAV1 presented intense positivity in the cytoplasm of 96% of the ES/PNET, independently of the histological subtype or the clinical stage of the tumor. This is the first report to confirm the value of this antibody as a diagnostic marker. Nevertheless, as has also been indicated for CD99, this expression lacked prognostic significance.

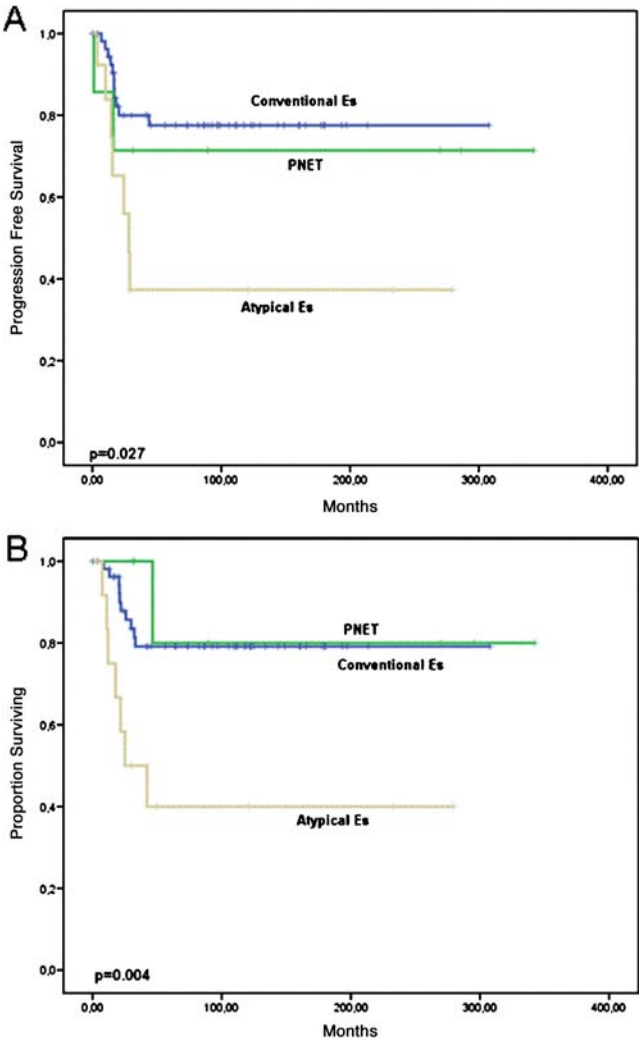

Fig. 4 Kaplan–Meier plots representing the effect of the three main histological varieties of ES/PNET on the PFS (**a**) and OS (**b**) in the group of patients treated with surgery and chemotherapy

In conclusion, the study of a large series of 415 ES/PNET, genetically confirmed by RT-PCR or FISH, corroborates the heterogeneity of the histology of the ESFT in which at least three clearly differentiated phenotypes exist: conventional ES, PNET, and atypical ES. Atypical ES, based upon the clinical data included in this study, seems to present a worse clinical outcome when compared to the two former subtypes. Moreover, the immunohistochemical analysis confirmed the diagnostic value of CD99 (HBA71), HNK1, Fli1, and CAV1, which together cover more than 99% of ES/PNET tumors, independently of the histological variety or clinical stage. All cases expressed at least three out of the four tested markers. Therefore, without questioning the additional value of molecular techniques such as FISH or RT-PCR, we confirm that adequate support can be provided for the diagnosis of ESFT based on the microscopical analysis by combining the immunostaining of these four antibodies. Particular attention has to be paid to the atypical ES in which histology might not be diagnostic and the clinical behavior more problematic. Here, the support of molecular techniques is mandatory in order to exclude an SRCT other than ES/PNET.

Acknowledgements This study was supported by and performed within the project Prognosis and Therapeutic Targets in the Ewing Family of Tumors (PROTHETS), European Community 6FP contract no. 503036.

Conflict of interest statement We declare that we have no conflict of interest.

References

1. Dahlin D (1978) Bone tumors: general aspects and data on 6,221 cases, 3rd edn. Thomas, Springfield, pp 274–287
2. Dorfman HD, Czerniak B (1998) Bone tumors. Mosby, St. Louis, pp 607–663
3. Ewing J (1921) Diffuse endothelioma of bone. Proc NY Soc Pathol 21:17–24
4. Dehner LP (1993) Primitive neuroectodermal tumor and Ewing's sarcoma. Am J Surg Pathol 17:1–13
5. Jaffe R, Santamaria M, Yunis EJ et al (1984) The neuroectodermal tumor of bone. Am J Surg Pathol 8:885–898
6. Verrill MW, Judson IR, Harmer CL et al (1997) Ewing's sarcoma and primitive neuroectodermal tumor in adults: are they different from Ewing's sarcoma and primitive neuroectodermal tumor in children? J Clin Oncol 15:2611–2621
7. Ushigome S, Machinami R, Sorensen PH (2002) Ewing sarcoma/primitive neuroectodermal tumour (PNET). In: Fletcher CDM, Mertens F (eds) Classification of tumours pathology and genetic of tumours of soft tissue and bone. World Health Organization, Geneva, pp 298–300
8. Askin FB, Rosai J, Sibley RK et al (1979) Malignant small cell tumor of the thoracopulmonary region in childhood: a distinctive clinicopathologic entity of uncertain histogenesis. Cancer 43:2438–2451
9. Fukunaga M, Ushigome S (1998) Periosteal Ewing-like adamantinoma. Virchows Arch 433:385–389
10. Llombart-Bosch A, Blache R, Peydro-Olaya A (1978) Ultrastructural study of 28 cases of Ewing's sarcoma: typical and atypical forms. Cancer 41:1362–1373
11. Meister P, Konrad E, Hubner G (1979) Malignant tumor of humerus with features of "adamantinoma" and Ewing's sarcoma. Pathol Res Pract 166:112–122
12. Nascimento AG, Unii KK, Pritchard DJ et al (1980) A clinicopathologic study of 20 cases of large-cell (atypical) Ewing's sarcoma of bone. Am J Surg Pathol 4:29–36
13. Navarro S, Noguera R, Pellin A et al (2002) Atypical pleomorphic extraosseous Ewing tumor/peripheral primitive neuroectodermal tumor with unusual phenotypic/genotypic profile. Diagn Mol Pathol 11:9–15
14. Maeda G, Masui F, Yokoyama R et al (1998) Ganglion cells in Ewing's sarcoma following chemotherapy: a case report. Pathol Int 48:475–480
15. Folpe AL, Goldblum JR, Rubin BP et al (2005) Morphologic and immunophenotypic diversity in Ewing family tumors: a study of 66 genetically confirmed cases. Am J Surg Pathol 29:1025–1033
16. Llombart-Bosch A, Contesso G, Henry-Amar M et al (1986) Histopathological predictive factors in Ewing's sarcoma of bone and clinicopathological correlations. A retrospective study of 261 cases. Virchows Arch A Pathol Anat Histopathol 409:627–640
17. Llombart-Bosch A, Contesso G, Peydro-Olaya A (1996) Histology, immunohistochemistry, and electron microscopy of small round cell tumors of bone. Semin Diagn Pathol 13:153–170
18. Fellinger EJ, Garin-Chesa P, Su SL et al (1991) Biochemical and genetic characterization of the HBA71 Ewing's sarcoma cell surface antigen. Cancer Res 51:336–340
19. Weidner N, Tjoe J (1994) Immunohistochemical profile of monoclonal antibody O13: antibody that recognizes glycoprotein p30/32MIC2 and is useful in diagnosing Ewing's sarcoma and peripheral neuroepithelioma. Am J Surg Pathol 18:486–494
20. CJ SA, Bertoni F et al (1994) CD99 (p30/32MIC2) neuroectodermal/Ewing's sarcoma antigen as an immunohistochemical marker: review of more than 600 tumors and the literature experience. Appl Immunohistochem Mol Morphol 2:231–240
21. Dierick AM, Roels H, Langlois M (1993) The immunophenotype of Ewing's sarcoma. An immunohistochemical analysis. Pathol Res Pract 189:26–32
22. Llombart-Bosch A, Navarro S (2001) Immunohistochemical detection of EWS and FLI-1 proteins in Ewing sarcoma and primitive neuroectodermal tumors: comparative analysis with CD99 (MIC-2) expression. Appl Immunohistochem Mol Morphol 9:255–260
23. Michels S, Swanson PE, Robb JA et al (1987) Leu-7 in small cell neoplasms. An immunohistochemical study with ultrastructural correlations. Cancer 60:2958–2964
24. Miettinen M, Chatten J, Paetau A et al (1998) Monoclonal antibody NB84 in the differential diagnosis of neuroblastoma and other small round cell tumors. Am J Surg Pathol 22:327–332
25. Folpe AL, Hill CE, Parham DM et al (2000) Immunohistochemical detection of FLI-1 protein expression: a study of 132 round cell tumors with emphasis on CD99-positive mimics of Ewing's sarcoma/primitive neuroectodermal tumor. Am J Surg Pathol 24:1657–1662
26. Mhawech-Fauceglia P, Herrmann F, Penetrante R et al (2006) Diagnostic utility of FLI-1 monoclonal antibody and dual-colour, break-apart probe fluorescence in situ (FISH) analysis in Ewing's sarcoma/primitive neuroectodermal tumour (EWS/PNET). A comparative study with CD99 and FLI-1 polyclonal antibodies. Histopathology 49:569–575
27. Tirado OM, Mateo-Lozano S, Villar J et al (2006) Caveolin-1 (CAV1) is a target of EWS/FLI-1 and a key determinant of the oncogenic phenotype and tumorigenicity of Ewing's sarcoma cells. Cancer Res 66:9937–9947
28. Bridge RS, Rajaram V, Dehner LP et al (2006) Molecular diagnosis of Ewing sarcoma/primitive neuroectodermal tumor in routinely processed tissue: a comparison of two FISH strategies and RT-PCR in malignant round cell tumors. Mod Pathol 19:1–8
29. Delattre O, Zucman J, Melot T et al (1994) The Ewing family of tumors—a subgroup of small-round-cell tumors defined by specific chimeric transcripts. N Engl J Med 331:294–299
30. Mangham DC, Williams A, McMullan DJ et al (2006) Ewing's sarcoma of bone: the detection of specific transcripts in a large, consecutive series of formalin-fixed, decalcified, paraffin-embedded tissue samples using the reverse transcriptase-polymerase chain reaction. Histopathology 48:363–376
31. Meier VS, Kuhne T, Jundt G et al (1998) Molecular diagnosis of Ewing tumors: improved detection of EWS-FLI-1 and EWS-ERG chimeric transcripts and rapid determination of exon combinations. Diagn Mol Pathol 7:29–35
32. Stegmaier S, Leuschner I, Aakcha-Rudel E et al (2004) Identification of various exon combinations of the ews/fli1 translocation: an optimized RT-PCR method for paraffin embedded tissue—a report by the CWS-study group. Klin Padiatr 216:315–322
33. Ahmed AA, Nava VE, Pham T et al (2006) Ewing sarcoma family of tumors in unusual sites: confirmation by rt-PCR. Pediatr Dev Pathol 9:488–495
34. Barr FG, Chatten J, D'Cruz CM et al (1995) Molecular assays for chromosomal translocations in the diagnosis of pediatric soft tissue sarcomas. JAMA 273:553–557
35. Dagher R, Pham TA, Sorbara L et al (2001) Molecular confirmation of Ewing sarcoma. J Pediatr Hematol Oncol 23:221–224
36. Dhulipal PD (1997) Ets oncogene family. Indian J Exp Biol 35:315–322
37. Downing JR, Head DR, Parham DM et al (1993) Detection of the (11;22)(q24;q12) translocation of Ewing's sarcoma and peripheral

neuroectodermal tumor by reverse transcription polymerase chain reaction. Am J Pathol 143:1294–1300
38. Lazar A, Abruzzo LV, Pollock RE et al (2006) Molecular diagnosis of sarcomas: chromosomal translocations in sarcomas. Arch Pathol Lab Med 130:1199–1207
39. Machado I, Noguera R, Pellin A, López-Guerrero JA, Piqueras M, Navarro S, Llombart-Bosch A (2009) Molecular diagnosis of Ewing sarcoma family of tumors. A comparative analysis of 560 cases with FISH and RT-PCR. Diagn Mol Pathol (in press)
40. Arka T, Anderson PJ (1963) Histochemistry: theory, practice and bibliography. Harper & Row, Hoeber Medical Division, New York
41. Llombart-Bosch A, Pellin A, Carda C et al (2000) Soft tissue Ewing sarcoma—peripheral primitive neuroectodermal tumor with atypical clear cell pattern shows a new type of EWS-FEV fusion transcript. Diagn Mol Pathol 9:137–144
42. Bernstein ML, Devidas M, Lafreniere D et al (2006) Intensive therapy with growth factor support for patients with Ewing tumor metastatic at diagnosis: pediatric oncology group/children's cancer group phase II study 9457—a report from the children's oncology group. J Clin Oncol 24:152–159
43. Parham DM, Hijazi Y, Steinberg SM et al (1999) Neuroectodermal differentiation in Ewing's sarcoma family of tumors does not predict tumor behavior. Hum Pathol 30:911–918
44. Paulussen M, Frohlich B, Jurgens H (2001) Ewing tumour: incidence, prognosis and treatment options. Paediatr Drugs 3:899–913
45. Terrier P, Henry-Amar M, Triche TJ et al (1995) Is neuroectodermal differentiation of Ewing's sarcoma of bone associated with an unfavourable prognosis? Eur J Cancer 31A:307–314
46. WL ADA (1995) CD57: a review. Appl Immunohistochem Mol Morphol 3:137–152
47. Bacci G, Ferrari S, Bertoni F et al (2000) Prognostic factors in nonmetastatic Ewing's sarcoma of bone treated with adjuvant chemotherapy: analysis of 359 patients at the Istituto Ortopedico Rizzoli. J Clin Oncol 18:4–11
48. Bridge JA, Fidler ME, Neff JR et al (1999) Adamantinoma-like Ewing's sarcoma: genomic confirmation, phenotypic drift. Am J Surg Pathol 23:159–165
49. Carter RL, al-Sams SZ, Corbett RP et al (1990) A comparative study of immunohistochemical staining for neuron-specific enolase, protein gene product 9.5 and S-100 protein in neuroblastoma, Ewing's sarcoma and other round cell tumours in children. Histopathology 16:461–467
50. Collini P, Sampietro G, Bertulli R et al (2001) Cytokeratin immunoreactivity in 41 cases of ES/PNET confirmed by molecular diagnostic studies. Am J Surg Pathol 25:273–274
51. Davicioni E, Wai DH, Anderson MJ (2008) Diagnostic and prognostic sarcoma signatures. Mol Diagn Ther 12:359–374
52. AF DPS, Miser J et al (1999) Pathology and prognosis in osseous Ewing's sarcoma-primitive neuroectodermal tumor (ES/PNET): preliminary data analysis from CCG 7881/POG 8850. Mod Pathol 12:2p
53. Gardner LJ, Polski JM, Fallon R et al (1998) Identification of CD56 and CD57 by flow cytometry in Ewing's sarcoma or primitive neuroectodermal tumor. Virchows Arch 433:35–40
54. Gu M, Antonescu CR, Guiter G et al (2000) Cytokeratin immunoreactivity in Ewing's sarcoma: prevalence in 50 cases confirmed by molecular diagnostic studies. Am J Surg Pathol 24:410–416
55. Jambhekar NA, Bagwan IN, Ghule P et al (2006) Comparative analysis of routine histology, immunohistochemistry, reverse transcriptase polymerase chain reaction, and fluorescence in situ hybridization in diagnosis of Ewing family of tumors. Arch Pathol Lab Med 130:1813–1818
56. Llombart-Bosch A (1996) Small round cell tumors of bone and soft tissue. Introduction. Semin Diagn Pathol 13:149–152
57. Llombart-Bosch A (1999) Ewing's sarcoma and peripheral primitive neuroectodermal tumor of bone and soft tissue. Int J Surg Pathol 7:185–192
58. Navarro S, Giraudo P, Karseladze AI et al (2007) Immunophenotypic profile of biomarkers related to anti-apoptotic and neural development pathways in the Ewing's family of tumors (EFT) and their therapeutic implications. Anticancer Res 27:2457–2463
59. Yamaguchi U, Hasegawa T, Morimoto Y et al (2005) A practical approach to the clinical diagnosis of Ewing's sarcoma/primitive neuroectodermal tumour and other small round cell tumours sharing EWS rearrangement using new fluorescence in situ hybridisation probes for EWSR1 on formalin fixed, paraffin wax embedded tissue. J Clin Pathol 58:1051–1056
60. Chan JK, Tsang WY, Seneviratne S et al (1995) The MIC2 antibody 013. Practical application for the study of thymic epithelial tumors. Am J Surg Pathol 19:1115–1123
61. Ramani P, Rampling D, Link M (1993) Immunocytochemical study of 12E7 in small round-cell tumours of childhood: an assessment of its sensitivity and specificity. Histopathology 23:557–561
62. Sandrin MS, Vaughan HA, Henning MM et al (1992) Expression cloning of cDNA clones encoding the human cell surface proteins HuLy-m6 and FMC29. Immunogenetics 35:283–285
63. Llombart Bosch ASM, Navarro S, Baccini P, Bertoni F, Savelov N, Lopez-Guerrero JA (2007) Evaluation of CD99 expression in a large series of Ewing's sarcomas. The experience of the PROTHETS Group. Lab Invest 87:18A
64. MP KE (1958) Nonparametric estimation from incomplete observations. J Am Stat Assoc 53:457–481
65. Peto R, Peto J (1987) Asymptomatically efficient rank invariant test procedures. J R Stat Soc 135:185–206
66. Cox D (1972) Regression models and life tables. J R Stat Soc 34:187–220
67. Contesso G, Llombart-Bosch A, Terrier P et al (1992) Does malignant small round cell tumor of the thoracopulmonary region (Askin tumor) constitute a clinicopathologic entity? An analysis of 30 cases with immunohistochemical and electron-microscopic support treated at the Institute Gustave Roussy. Cancer 69:1012–1020
68. Renshaw AA, Perez-Atayde AR, Fletcher JA et al (1996) Cytology of typical and atypical Ewing's sarcoma/PNET. Am J Clin Pathol 106:620–624
69. Terrier P, Llombart-Bosch A, Contesso G (1996) Small round blue cell tumors in bone: prognostic factors correlated to Ewing's sarcoma and neuroectodermal tumors. Semin Diagn Pathol 13:250–257
70. Hartman KR, Triche TJ, Kinsella TJ et al (1991) Prognostic value of histopathology in Ewing's sarcoma. Long-term follow-up of distal extremity primary tumors. Cancer 67:163–171
71. Bacci G, Ferrari S, Bertoni F et al (2000) Neoadjuvant chemotherapy for peripheral malignant neuroectodermal tumor of bone: recent experience at the Istituto Rizzoli. J Clin Oncol 18:885–892
72. Bacci G, Ferrari S, Comandone A et al (2000) Neoadjuvant chemotherapy for Ewing's sarcoma of bone in patients older than thirty-nine years. Acta Oncol 39:111–116
73. Luksch R, Sampietro G, Collini P et al (1999) Prognostic value of clinicopathologic characteristics including neuroectodermal differentiation in osseous Ewing's sarcoma family of tumors in children. Tumori 85:101–107
74. Wexler LH, Meyer WH, Parham DM et al (2000) Neural differentiation and prognosis in peripheral primitive neuroectodermal tumor. J Clin Oncol 18:2187–2188
75. Kang LC, Dunphy CH (2006) Immunoreactivity of MIC2 (CD99) and terminal deoxynucleotidyl transferase in bone marrow clot and core specimens of acute myeloid leukemias and myelodysplastic syndromes. Arch Pathol Lab Med 130:153–157

76. Scotlandi K, Serra M, Manara MC et al (1996) Immunostaining of the p30/32MIC2 antigen and molecular detection of EWS rearrangements for the diagnosis of Ewing's sarcoma and peripheral neuroectodermal tumor. Hum Pathol 27:408–416
77. Nilsson G, Wang M, Wejde J et al (1999) Detection of EWS/FLI-1 by immunostaining. An adjunctive tool in diagnosis of Ewing's sarcoma and primitive neuroectodermal tumour on cytological samples and paraffin-embedded archival material. Sarcoma 3:25–32
78. Rossi S, Orvieto E, Furlanetto A et al (2004) Utility of the immunohistochemical detection of FLI-1 expression in round cell and vascular neoplasm using a monoclonal antibody. Mod Pathol 17:547–552
79. Khoury JD (2008) Ewing sarcoma family of tumors: a model for the new era of integrated laboratory diagnostics. Expert Rev Mol Diagn 8:97–105
80. Olsen SH, Thomas DG, Lucas DR (2006) Cluster analysis of immunohistochemical profiles in synovial sarcoma, malignant peripheral nerve sheath tumor, and Ewing sarcoma. Mod Pathol 19:659–668
81. Makrigiannis AP, Parham P (2008) The evolution of NK cell diversity. Semin Immunol 20:309–310
82. Parham P (2008) The genetic and evolutionary balances in human NK cell receptor diversity. Semin Immunol 20:311–316
83. de Alava E, Kawai A, Healey JH et al (1998) EWS-FLI1 fusion transcript structure is an independent determinant of prognosis in Ewing's sarcoma. J Clin Oncol 16:1248–1255
84. Drab M, Verkade P, Elger M et al (2001) Loss of caveolae, vascular dysfunction, and pulmonary defects in caveolin-1 gene-disrupted mice. Science 293:2449–2452
85. Lu Z, Ghosh S, Wang Z et al (2003) Downregulation of caveolin-1 function by EGF leads to the loss of E-cadherin, increased transcriptional activity of beta-catenin, and enhanced tumor cell invasion. Cancer Cell 4:499–515
86. Williams TM, Lisanti MP (2005) Caveolin-1 in oncogenic transformation, cancer, and metastasis. Am J Physiol Cell Physiol 288:C494–C506
87. Baird K, Davis S, Antonescu CR et al (2005) Gene expression profiling of human sarcomas: insights into sarcoma biology. Cancer Res 65:9226–9235
88. Ando T, Ishiguro H, Kimura M et al (2007) The overexpression of caveolin-1 and caveolin-2 correlates with a poor prognosis and tumor progression in esophageal squamous cell carcinoma. Oncol Rep 18:601–609
89. Belanger MM, Roussel E, Couet J (2004) Caveolin-1 is down-regulated in human lung carcinoma and acts as a candidate tumor suppressor gene. Chest 125:106S
90. Bouras T, Lisanti MP, Pestell RG (2004) Caveolin-1 in breast cancer. Cancer Biol Ther 3:931–941
91. Campbell L, Jasani B, Edwards K et al (2008) Combined expression of caveolin-1 and an activated AKT/mTOR pathway predicts reduced disease-free survival in clinically confined renal cell carcinoma. Br J Cancer 98:931–940
92. Cantiani L, Manara MC, Zucchini C et al (2007) Caveolin-1 reduces osteosarcoma metastases by inhibiting c-Src activity and met signaling. Cancer Res 67:7675–7685
93. Davidson B, Goldberg I, Givant-Horwitz V et al (2002) Caveolin-1 expression in ovarian carcinoma is MDR1 independent. Am J Clin Pathol 117:225–234
94. Davidson B, Nesland JM, Goldberg I et al (2001) Caveolin-1 expression in advanced-stage ovarian carcinoma—a clinicopathologic study. Gynecol Oncol 81:166–171
95. Garcia E, Li M (2006) Caveolin-1 immunohistochemical analysis in differentiating chromophobe renal cell carcinoma from renal oncocytoma. Am J Clin Pathol 125:392–398
96. Ito Y, Yoshida H, Tomoda C et al (2005) Caveolin-1 and 14–3–3 sigma expression in follicular variant of thyroid papillary carcinoma. Pathol Res Pract 201:545–549
97. Mercier I, Bryant KG, Sotgia F et al (2009) Using caveolin-1 epithelial immunostaining patterns to stratify human breast cancer patients and predict the caveolin-1 (P132L) mutation. Cell Cycle 8:1396–1401
98. Racine C, Belanger M, Hirabayashi H et al (1999) Reduction of caveolin 1 gene expression in lung carcinoma cell lines. Biochem Biophys Res Commun 255:580–586

Virchows Arch (2009) 455:413–422
DOI 10.1007/s00428-009-0844-5

ORIGINAL ARTICLE

Aberrant expression of p27^{Kip1}-interacting cell-cycle regulatory proteins in ovarian clear cell carcinomas and their precursors with special consideration of two distinct multistage clear cell carcinogenetic pathways

Sohei Yamamoto · Hitoshi Tsuda · Kosuke Miyai · Masashi Takano · Seiichi Tamai · Osamu Matsubara

Received: 16 August 2009 / Revised: 27 September 2009 / Accepted: 29 September 2009 / Published online: 24 October 2009

Abstract We have previously reported that alterations of p27^{Kip1}-interacting cell-cycle proteins frequently occur during the development of endometriosis-associated ovarian clear cell adenocarcinoma (CCA; Yamamoto et al., Histopathology in press, 20). However, CCA also occurs in association with clear cell adenofibroma (CCAF). In this study, the expressions of p27^{Kip1}-interacting proteins, i.e., p27^{Kip1}, Skp2, Cks1, cyclin A, cyclin E, and the Ki-67 labeling index (LI), were analyzed in 25 CCAFs (11 benign and 14 borderline) and 15 CCAF-associated CCAs, and compared with the expression status of each protein in the 23 previously studied endometriosis-associated CCAs. Although aberrant expression of all p27^{Kip1}-interacting proteins was more frequent in the CCAF-associated CCAs than in the benign CCAFs, statistical significance was found only for Cks1 overexpression. The frequencies of p27^{Kip1} downregulation and overexpression of Skp2 and cyclin A were significantly lower in CCAF-associated than in endometriosis-associated CCAs ($P<0.05$, respectively). The frequencies of p27^{Kip1} downregulation and Skp2 over expression in borderline CCAFs were significantly lower than those in atypical endometriosis components in endometriosis-associated CCAs ($P<0.05$, respectively). Mean Ki-67 LI increased significantly through benign (4.9%) to borderline (11.1%) CCAF and to CCAF-associated CCA (30.6%), but the latter two values were significantly lower than those in atypical endometriosis (21.4%) and endometriosis-associated CCA (46.9%; $P<0.05$, respectively). These data suggest that accumulated alterations of p27^{Kip1}-interacting proteins may accelerate the development of CCAs regardless of their carcinogenetic pathways, but that tumor cells in the CCAF-associated pathway appear to show slower cell-cycle progression than those in the endometriosis-associated pathway, possibly accounting for the distinct clinicopathological features of the two CCA subtypes.

Keywords Ovarian clear cell adenocarcinoma · p27 · skp2 · cks1 · Cyclin · Clear cell adenofibroma · Endometriosis

S. Yamamoto · H. Tsuda (✉) · K. Miyai · O. Matsubara
Department of Basic Pathology,
National Defense Medical College,
3-2 Namiki,
Tokorozawa, Saitama 359-8513, Japan
e-mail: htsuda@ndmc.ac.jp

M. Takano
Department of Obstetrics and Gynecology,
National Defense Medical College,
3-2 Namiki,
Tokorozawa, Saitama 359-8513, Japan

S. Tamai
Department of Laboratory Medicine,
National Defense Medical College,
3-2 Namiki,
Tokorozawa, Saitama 359-8513, Japan

H. Tsuda
Pathology Section, Clinical Laboratory Division,
National Cancer Center Hospital,
5-1-1 Tsukiji,
Tokyo 104-0045, Japan

Introduction

Clear cell adenocarcinoma (CCA) accounts for 5–10% of all epithelial ovarian cancers in Western countries,

whereas for unknown reasons, it accounts for more than 20% in Japan [1–6]. CCA has a characteristic histology and is highly chemoresistant, resulting in an extremely poor prognosis when surgical cytoreduction is insufficient [1–4]. Although several chemotherapeutic regimens against CCA have been developed, including platinum analogues, taxanes, etoposide, and camptothecin, mortality has remained largely unchanged [7, 8]. Therefore, a better understanding of the pathways driving neoplastic transformation and tumor growth in CCA is needed to provide an insight into the disease and facilitate early identification and development of novel targeted therapeutic strategies.

Despite a lack of data on cause–effect relationships, evidence has emerged for a close association between endometriosis and ovarian CCA, and many investigators have suggested that ovarian endometriosis can give rise to CCA [9–15]. Additionally, atypical endometriosis, in which the endometrioid epithelium shows cytological and/or structural atypia, has been recognized as a precancerous lesion for some CCAs [11–13, 15]. Therefore, a transformative pathway from endometriosis to CCA may exist, and the molecular basis of this putative pathway has been described, i.e., genetic instability or DNA aneuploidy in endometriotic lesions and loss of heterozygosity or mutation of the tumor suppressor gene *PTEN* in both endometriosis and co-existing CCA [16–19].

Dysregulation of the normal cell-cycle machinery is integral to the process of neoplasia, and there is compelling evidence for loss of cell-cycle control in the development and progression of most human malignancies. Recently, we have reported that cumulative aberrations of $p27^{Kip1}$-related cell-cycle regulators are highly associated with the development of ovarian CCA presumably arising in endometriosis [20]. Our data suggested that downregulation of $p27^{Kip1}$ and overexpression of cyclin E and Cks1 may be associated with the early steps of endometriosis-associated clear cell carcinogenesis [20]. Moreover, overexpression of Skp2 and cyclin A may be late events and play a significantly important role in the atypical changes or malignant transformation of endometriosis [20].

Besides endometriosis, clear cell adenofibroma (CCAF), a major form of benign or borderline ovarian clear cell tumor, may also be able to give rise to CCA [1, 4, 21–25]. The CCAF components co-existing with CCA often contain both apparently benign clear cell adenofibroma (benign CCAF) and CCAF with cellular and structural atypia (borderline CCAF) [21–23]. Borderline CCAF is rare, accounting for 5–8% of all ovarian clear cell neoplasms, and benign CCAF is even rarer [21, 22]. However, another study at our institution demonstrated that CCAF components co-existed in 21% of surgically resected CCAs [23].

Moreover, in comparison with CCAs lacking CCAF components, CCAs with CCAF components show several distinct clinicopathologic characteristics, i.e., a lower frequency of co-existing endometriosis, a higher frequency of histologically low-grade tumor with tubulocystic proliferative architecture, and a correlation with better prognosis [23]. These data suggest that two possible distinct carcinogenic pathways contribute to the clinicopathological features of CCA. Up to now, however, little is known about molecular backgrounds to explain the differences between the two putative pathways of clear cell carcinogenesis.

In the present study, we histologically reviewed a number of surgically resected cases of ovarian CCA and selected cases with CCAF components. Using immunohistochemistry, we examined the altered expression of $p27^{Kip1}$ and $p27^{Kip1}$-interacting cell-cycle regulators, i.e., Skp2, Cks1, cyclin A, and cyclin E, and cell proliferation activity assessed in terms of the Ki-67 labeling index (LI) in the benign and borderline CCAF components and co-existing CCA components and compared them. Moreover, the results were also compared with those for the pathway of endometriosis-associated ovarian clear cell carcinogenesis reported previously [20]. It was anticipated that this information would provide not only a better understanding of the development of ovarian CCA but also suggest potentially promising treatment options for these carcinomas with distinct carcinogenetic pathways.

Materials and methods

Cases analyzed and histological features of CCAF

The research protocol was approved by the ethics committee of the National Defense Medical College, Tokorozawa, Japan. Seventy-nine cases of primary ovarian CCA were identified from the files of the Department of Laboratory Medicine, National Defense Medical College Hospital, Japan. These 79 cases of CCA had been surgically resected between 1988 and 2007, and the patients had not undergone chemotherapy or radiation therapy before surgery. All specimens were formalin-fixed and paraffin-embedded, and 4-μm-thick sections were prepared for hematoxylin and eosin staining. All pathology specimens were reviewed at our institution, and the tumors were classified according to the criteria of the World Health Organization [4].

The histological criteria for benign CCAF and borderline CCAF have been described previously [21–25]. In short, benign CCAF was a surface epithelial-stromal tumor containing tubulocystic epithelial components embedded in a fibromatous stroma (Fig. 1a). The epithelial cells were polygonal, flat, or hobnail in shape with clear, slightly granular, or eosinophilic cytoplasm, and nuclear atypia and

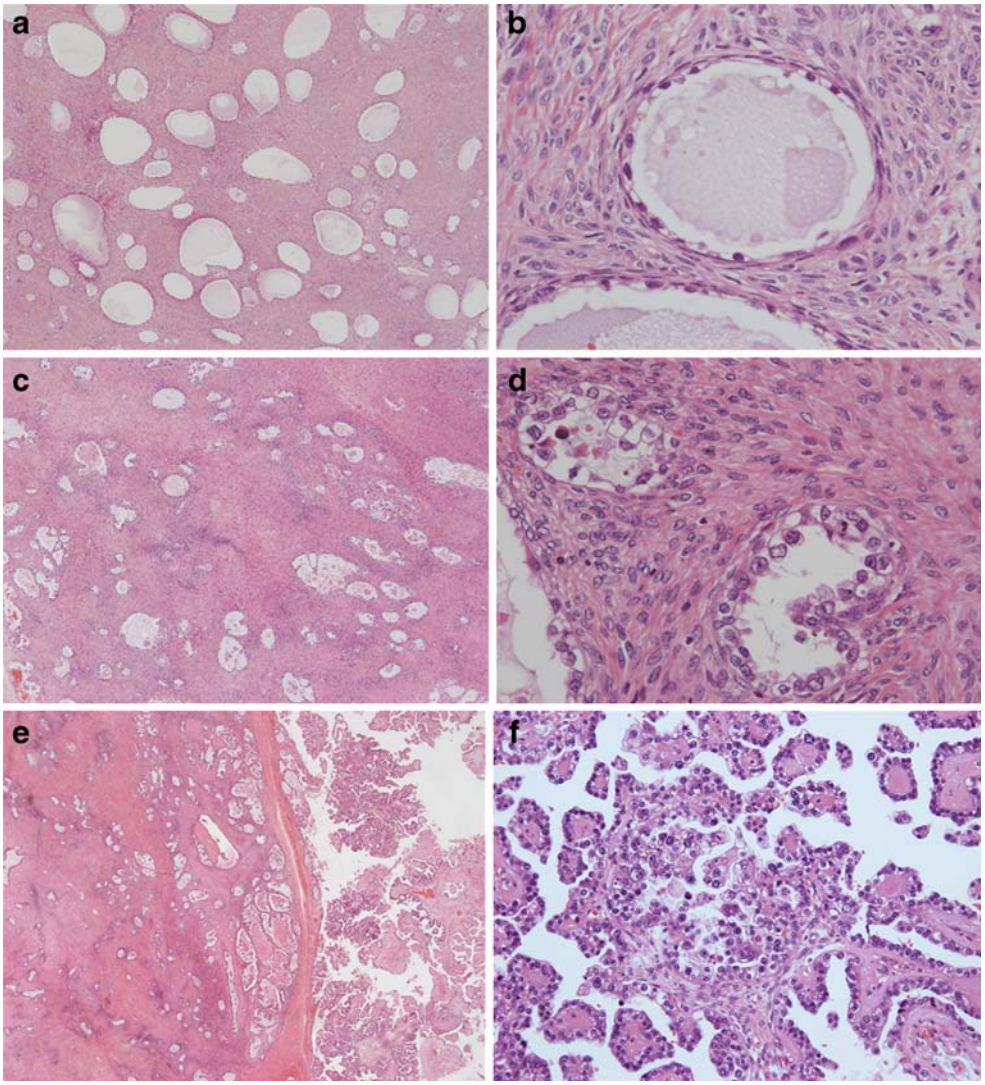

Fig. 1 Histological features of ovarian clear cell adenofibroma (CCAF) co-existing with clear cell adenocarcinoma. Benign CCAF: (**a**) a CCAF component shows simple cystic glands separated by wide fascicles of fibromatous stromal cells; (**b**) glands are delineated by monolayers of cuboidal or flattened glandular cells with clear cytoplasm and uniform nuclei. Borderline CCAF: (**c**) glands of various sizes and shapes are focally crowded; (**d**) glands are delineated by one to three layers of cells with clear cytoplasm and mildly pleomorphic and hyperchromatic nuclei. **e** Histological continuum between borderline CCAF (*left field*) and clear cell adenocarcinoma (*middle to right field*). **f** High-power view of clear cell adenocarcinoma component in **e**. HE stain, original magnification, ×20 for **e**; ×100 for **a** and **c**; ×200 for **f**; ×400 for **b** and **d**

epithelial stratification was minimal (Fig. 1b). In borderline CCAF, cellular (i.e., nuclear pleomorphism and stratification of the epithelium) and structural (i.e., size irregularity and crowding of the tubulocystic architecture) atypia were evident (Fig. 1c, d).

Consequently, 15 (19%) of the 79 CCA cases were found to have CCAF components. Of these 15 cases, ten (67%) had both benign CCAF and borderline CCAF components, four (27%) had borderline CCAF component only, and one (7%) had a benign CCAF component only. Therefore, 11 benign CCAF components, 14 borderline CCAF components, and 15 CCAs containing adjacent CCAF components were analyzed by immunohistochemistry.

Among the 15 cases enrolled, endometriotic lesions were found in three (20%): endometriosis in the uterine adnexa contralateral to the tumor in two cases and endometriosis in the adnexa ipsilateral to the tumor in one case. However, these endometriotic lesions were not regarded as synchronous with co-existing CCA because they were present at only a small focus located distantly from the main tumor. For this reason, they were not analyzed by immunohistochemistry.

Immunohistochemistry

All selected formalin-fixed, paraffin-embedded specimens were cut into 4-μm-thick serial sections and analyzed by immunohistochemistry. The primary antibodies used were those against $p27^{Kip1}$ (sc-528, rabbit polyclonal, dilution 1:100, Santa Cruz Biotechnology, Santa Cruz, CA, USA), Skp2 (2C8D9, mouse monoclonal, dilution 1:100, Zymed, San Francisco, CA, USA), Cks1 (4G12G7, mouse monoclonal, dilution 1:250, Zymed), cyclin A (sc-56299, mouse monoclonal, dilution 1:100, Santa Cruz Biotechnology), cyclin E (sc-481, rabbit polyclonal, dilution 1:100, Santa Cruz Biotechnology), and Ki-67 (MIB1, mouse monoclonal, dilution 1:100, DAKO, Glostrup, Demark), and the

immunohistochemistry protocols were the same as those described previously [20]. Non-neoplastic lymphoid tissue (tonsil) was used as a positive control for all the antibodies used. Sections without the primary antibody were used as negative controls.

Evaluation of immunohistochemical staining

Immunohistochemical staining was evaluated only in areas with well-preserved tissue morphology and located distant from necrosis or artifacts. Nuclear immunostaining for $p27^{Kip1}$, Skp2, Cks1, cyclin A, cyclin E, and Ki-67 was calculated as the percentage of positive epithelial cells among a total of 500 epithelial cells encountered in at least five to ten representative high-power fields. Although cells showed a range of staining intensities, moderately to strongly stained nuclei were considered to be positive. The results of immunohistochemistry were evaluated independently by two observers (S.Y. and K.M.), and any discrepancies between them were resolved by consensus using a multi-headed microscope. However, in all the cases examined, inter-observer discrepancy did not affect the expression status when the cut-off used for aberrant expression positivity described below was employed.

Except for Ki-67, the criteria used for assignment for aberrant expression of each protein was based on published criteria: $p27^{Kip1}$ was considered to be downregulated if <50% of nuclei were stained [26–28], Skp2 was considered to be overexpressed if >10% of nuclei were stained [28, 29], Cks1 was considered to be overexpressed if >40% of nuclei were stained [29], and cyclin A and cyclin E were considered to be overexpressed if >10% of nuclei were stained [28]. For Ki-67, the percentage of cells stained was taken as the LI.

Statistical analyses

Statistical analyses were performed using the StatMate III software package (ATMS, Tokyo, Japan). The frequency of overexpression or downregulation of each examined protein in the various components was compared using Fisher's exact test or chi-squared test. For a comparison of Ki-67 LI among the various histological components, the Kruskal–Wallis test was used, followed by the multiple comparison test. Differences at $P<0.05$ were considered to be statistically significant.

Results

Table 1 summarizes the results for all of the proteins examined.

Downregulation of $p27^{Kip1}$

Downregulation of $p27^{Kip1}$, as defined by <50% of the cells showing positive staining, was seen in the only one (9%) of 11 benign CCAFs (Fig. 2a, b), one (7%) of 14 borderline CCAFs, and two (13%) of 15 CCAs (Fig. 2c). No statistically significant differences in the frequency of

Table 1 Frequencies of aberrant expression of $p27^{Kip1}$-interacting cell-cycle regulators and Ki-67 labeling index (LI) in clear cell adenofibroma (CCAF) components and co-existing clear cell adenocarcinoma (CCA)

	No. of tumors (%)					
	$p27^{Kip1}$-downregulation	Skp2-overexpression	Cks1-overexpression	Cyclin A-overexpression	Cyclin E-overexpression	Ki-67 LI mean ± SE
Benign CCAF (n = 11)	1(9)	0(0)	4(36)	0(0)	6(55)	4.9±1.06
Borderline CCAF (n = 14)	1(7)	1(7)	9(60)	0(0)	11(79)	11.1±1.21
CCA (n = 15)	2(13)	3(20)	12(80)	1(7)	13(87)	30.6±3.03

LI labeling index, *SE* standard error

*Marginal significance (P=0.085)

**$P<0.05$

***$P<0.01$

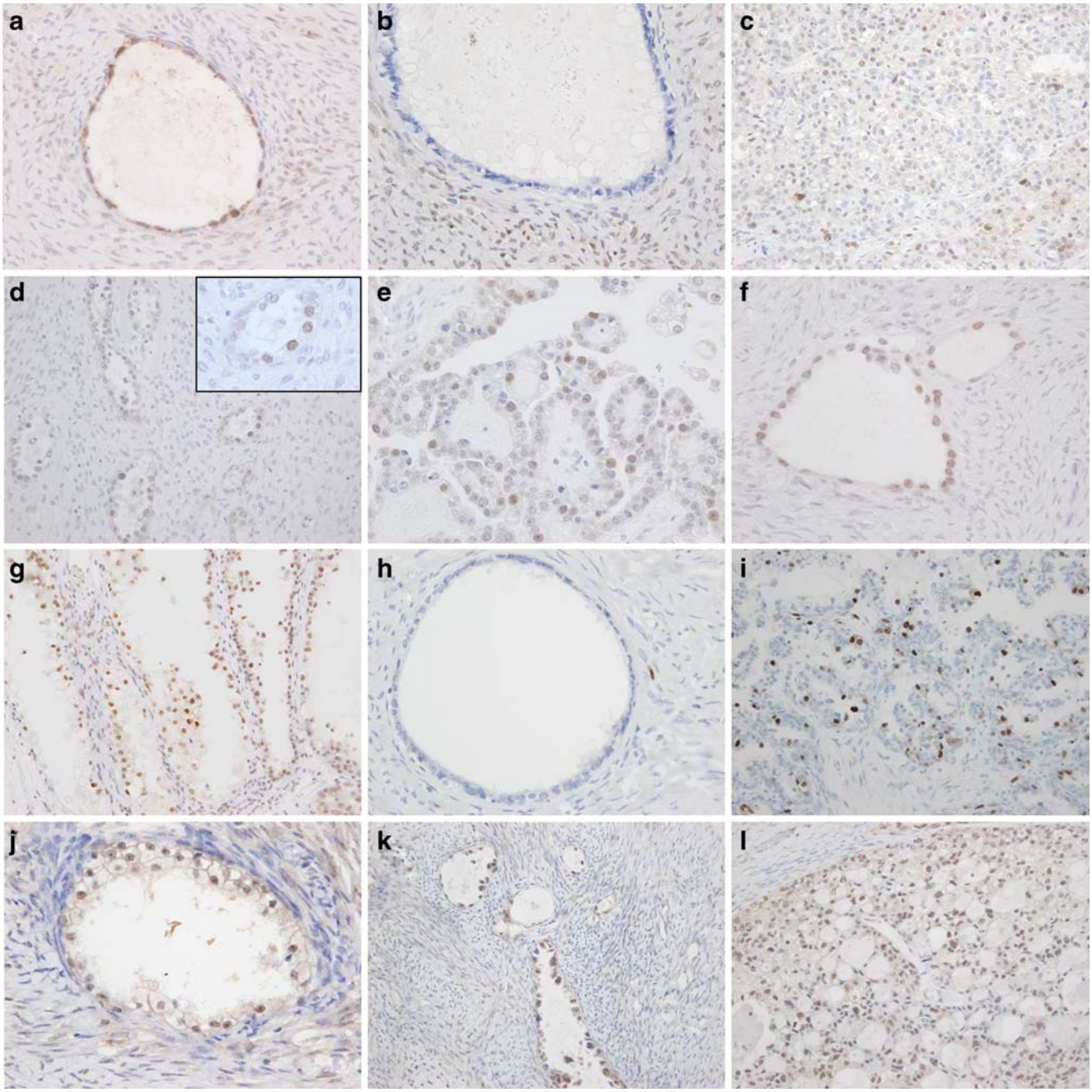

Fig. 2 Expression of $p27^{Kip1}$-interacting cell-cycle regulators in ovarian clear cell adenofibroma (CCAF) and co-existing clear cell adenocarcinoma. Immunohistochemistry for $p27^{Kip1}$ (**a**–**c**), Skp2 (**d**, **e**), Cks1 (**f**, **g**), cyclin A (**h**, **i**), and cyclin E (**j**–**l**) in the benign CCAF (**a**, **b**, **f**, **h**, **j**), the borderline CCAF (**d**, **k**), and clear cell adenocarcinoma (**c**, **e**, **g**, **i**, **l**). $p27^{Kip1}$ was positive in most of the benign CCAF (**a**). **b** and **c** show the $p27^{Kip1}$-downregulated benign CCAF (**b**) and clear cell adenocarcinoma (**c**) components in a CCAF-associated carcinoma. Note the stromal cells in **b** showing weak to moderate diffuse immunoreactivity for $p27^{Kip1}$. The borderline CCAF (**d**) and clear cell adenocarcinoma (**e**) components with Skp2 overexpression, showing immunoreactivity in more than 10% of the tumor cells. Benign CCAF (**f**) and clear cell adenocarcinoma (**g**) components with Cks1 overexpression, showing immunoreactivity in more than 40% of the tumor cells. Cyclin A is negative in the epithelial components of the benign CCAF but shows scattered positivity in a stromal cell (**h**). A clear cell adenocarcinoma showing immunoreactivity for cyclin A in more than 10% of the tumor cells (**i**). Benign CCAF (**j**), borderline CCAF (**k**), and clear cell adenocarcinoma (**l**) components with cyclin E overexpression, showing immunoreactivity in more than 10% of the tumor cells. Immunoperoxidase stain, original magnification ×200 for **c**, **d**, **g**, **i**, **k**, and **l**; ×400 for **a**, **b**, **d** inset, **e**, **f**, **h**, and **j**

$p27^{Kip1}$ downregulation were evident among the histological components. In one case that showed $p27^{Kip1}$ downregulation in the benign CCAF component, the co-existing borderline CCAF and CCA components also showed $p27^{Kip1}$ downregulation.

Overexpression of Skp2

Overexpression of Skp2 was not observed in the benign CCAF components. Only one (7%) of 14 borderline CCAF components and three (20%) of 15 CCAs demonstrated Skp2 overexpression (Fig. 2d, e). In this case, where borderline CCAF demonstrated Skp2 overexpression, the co-existing CCA component also retained Skp2 overexpression. No statistically significant differences in the frequency of Skp2 overexpression were evident among the histological components.

Overexpression of Cks1

Overexpression of Cks1, as defined by positivity in >40% of the cells, was seen in four (36%) of 11 benign CCAF components (Fig. 2f), nine (60%) of 15 borderline CCAF components, and 12 (80%) of 15 CCAs (Fig. 2g). There were statistically significant differences in the frequency of Cks1 overexpression between the benign CCAF and CCA components (P=0.032). In all cases that showed Cks1 overexpression in the benign CCAF component, the co-existing borderline CCAF or CCA components retained their Cks1 overexpression.

Overexpression of cyclin A

No overexpression of cyclin A was observed in benign or borderline CCAF components (Fig. 2h). As only one (7%) of 15 CCAF-associated CCAs demonstrated overexpression of cyclin A (Fig. 2i), the differences in frequency of overexpression did not reach a significant level. The case in which the CCA component showed cyclin A overexpression was different from that in which the CCA component showed Skp2 overexpression.

Overexpression of cyclin E

Overexpression of cyclin E was seen in six (55%) of 11 benign CCAFs (Fig. 2j), 11 (79%) of 14 borderline CCAFs (Fig. 2k), and 13 (87%) of 15 CCAs (Fig. 2l). Although the frequency of cyclin E overexpression in the CCA components tended to be higher than that in the benign CCAF components, the difference was only marginally significant (P=0.085). In all cases that showed cyclin E overexpression in the benign or borderline CCAF component, the co-existing CCA retained cyclin E overexpression.

Proliferative activity assessed by Ki-67 labeling index (LI)

The Ki-67 LIs (mean ± standard error (SE)) were 4.9±1.06 in the benign CCAF components, 11.1±1.21 in the borderline CCAF components, and 30.6±3.03 in the CCA components. Significant differences in the Ki-67 LIs were observed between borderline CCAF and CCA components (p<0.01; multiple comparison test followed by Kruskal–Wallis test).

We then looked for any correlation of Ki-67 LI with the expression of $p27^{Kip1}$-interacting cell-cycle regulators and also correlations of aberrant expression among the $p27^{Kip1}$-interacting cell-cycle regulators examined in benign CCAF, borderline CCAF, and CCAF-associated CCA components. However, no significant correlation was disclosed for any of the marker combinations.

Comparison of aberrant expression of $p27^{Kip1}$-interacting proteins and Ki-67 LI between the CCAF-associated and endometriosis-associated clear cell carcinogenetic pathways

Figure 3 graphically illustrates the cumulative aberrant expression of $p27^{Kip1}$-related cell-cycle regulators in the CCAF-associated ovarian clear cell carcinogenetic pathway, compared with the corresponding expressions in the endometriosis-associated clear cell carcinogenetic pathway described previously [20].

The frequency of $p27^{Kip1}$ downregulation in CCAF-associated carcinomas was significantly lower than that in endometriosis-associated carcinomas (13% vs 48%, P=0.030). Moreover, the frequency of $p27^{Kip1}$ downregulation in borderline CCAFs was significantly lower than that in the atypical endometrioses in endometriosis-associated carcinomas (7% vs 40%, P=0.049).

The frequency of Skp2 overexpression in the CCA components of CCAF-associated carcinomas was significantly lower than that in endometriosis-associated carcinomas (20% vs 91%, P<0.0001). Moreover, the frequency of Skp2 overexpression in the borderline CCAF components of CCAF-associated carcinomas was significantly lower than that in atypical endometriosis components of endometriosis-associated carcinomas (7% vs 48%, P=0.022).

The frequencies of Cks1 overexpression in the benign CCAF, borderline CCAF, and CCAF-associated carcinoma components were higher than those in non-atypical endometriosis (36% vs 19%), atypical endometriosis (64% vs 33%), and endometriosis-associated carcinomas (80% vs 65%), respectively, but the differences for each combination did not reach statistical significance.

The frequency of cyclin A overexpression in the CCAF-associated carcinomas was significantly lower than that in endometriosis-associated carcinomas (7% vs 87%, P<

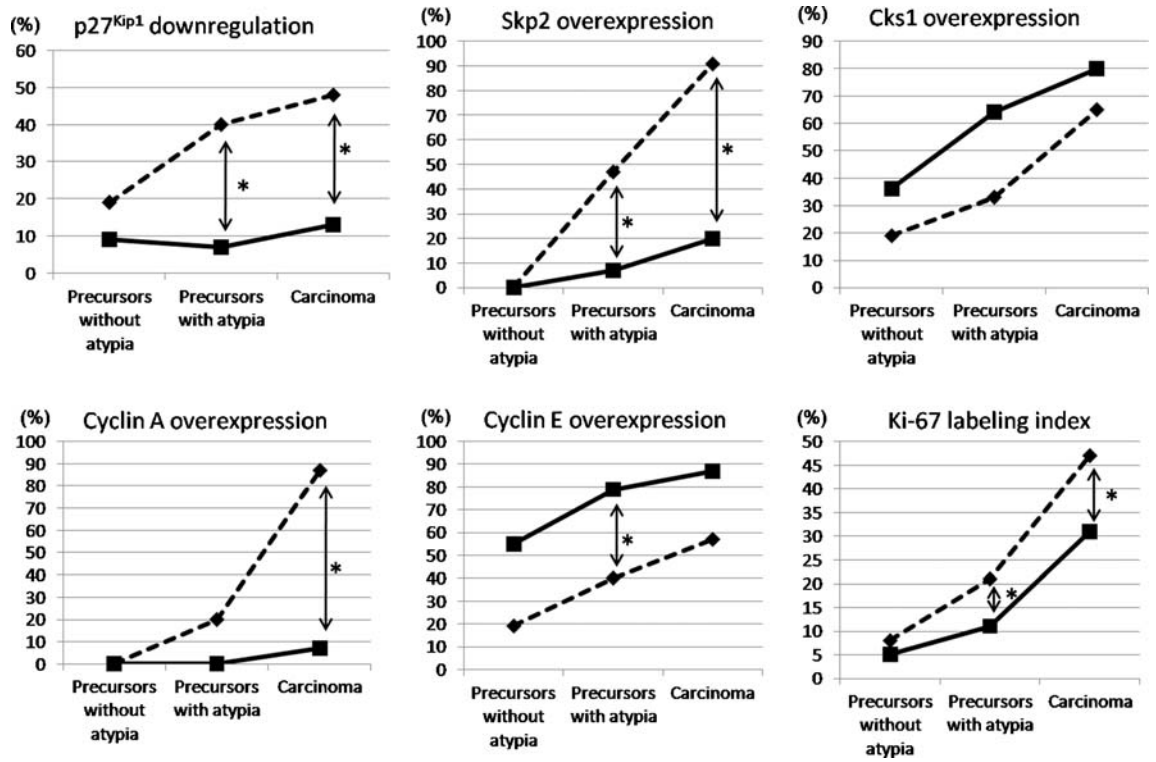

Fig. 3 Accumulated aberration of $p27^{Kip1}$-interacting cell-cycle regulatory proteins and the Ki-67 labeling index during the development of ovarian clear cell adenocarcinoma. Data are presented as the percentage of lesions positive for aberrant protein expression (downregulation of $p27^{Kip1}$, overexpression of Skp2, Cks1, cyclin A, and cyclin E) or as the Ki-67 labeling index. Precursors without atypia indicate the components of benign CCAF or non-atypical endometriosis. Precursors with atypia indicate the components of borderline CCAF or atypical endometriosis. The *solid lines* represent the data for the CCAF-associated pathway obtained in the present study; the *broken lines* represent the data for the endometriosis-associated pathway obtained from the previous study [20]. *Left–right arrow with asterisk* indicates statistically significant differences in the proportions of lesions demonstrating the stated aberration of the protein expression examined

0.0001). Cyclin A overexpression in borderline CCAF components of CCAF-associated carcinoma was less frequent than in atypical endometriosis components of endometriosis-associated carcinomas (0% vs 20%), but not to a statistically significant degree.

The frequencies of cyclin E overexpression in the benign CCAF, borderline CCAF, and CCAF-associated carcinoma components were significantly higher than those in the non-atypical endometriosis (55% vs 19%), atypical endometriosis (79% vs 40%), and endometriosis-associated carcinoma components (87% vs 57%), respectively. With regard to cyclin E overexpression, there was a statistically significant difference between the borderline CCAF and atypical endometriosis components (P=0.041), and marginally significant differences were found between the benign CCAF and non-atypical endometriosis components (P=0.050) and between CCAF-associated carcinomas and endometriosis-associated carcinomas (P=0.052).

The mean Ki-67 LI of CCAF-associated carcinomas was significantly lower than that of endometriosis-associated carcinomas (30.6 vs 46.9, P<0.01, by multiple comparison test followed by Kruskal–Wallis test). Moreover, the mean Ki-67 LI of borderline CCAF in CCAF-associated carcinomas was significantly lower than that of atypical endometriosis in endometriosis-associated carcinomas (11.1 vs 21.4, P<0.05, by multiple comparison test followed by Kruskal–Wallis test). The mean Ki-67 LI in benign CCAF of CCAF-associated carcinomas was lower than that in non-atypical endometriosis in endometriosis-associated carcinomas (4.9 vs 8.4), but the difference was not statistically significant.

Discussion

Our previous studies have demonstrated that a proportion of ovarian CCA can be derived from CCAF, and that CCA with CCAF components may constitute a distinct clinicopathological entity in ovarian CCAs [23–25]. One of our studies suggested that in comparison with CCAs lacking CCAF components, CCAs with CCAF components show several distinct clinicopathological features, e.g., infrequent coexistence of endometriosis, histologically lower tumor grade with tubulocystic architecture, and a better prognosis [23]. However, none of the findings were able to account

for the distinct clinicopathological characteristics of the CCAF-associated carcinomas.

In the present study, the frequencies of aberrant expression of all $p27^{Kip1}$-inetracting cell-cycle regulators examined in CCAF-associated CCAs were higher than those in the benign CCAF components, suggesting that accumulated aberration of these cell-cycle regulators is at least associated with the development of CCAF-associated CCA of the ovary. Moreover, overexpression of Cks1 and cyclin E was frequently observed in histologically benign CCAF lesions, and the frequency of this overexpression was increased in borderline CCAF and coexisting CCA components, suggesting that it might play a role in the malignant transformation of CCAF.

However, in contrast to the endometriosis-associated CCAs reported previously, Skp2, cyclin A, and $p27^{Kip1}$ were not altered so frequently in CCAF-associated carcinomas, suggesting that the magnitude of alterations of these proteins in the CCAF-associated pathway may not be so high in comparison with the endometriosis-associated carcinogenetic pathway [20].

Additionally, cell proliferative activity determined by Ki67 LI was significantly lower in CCAF-associated carcinomas than in endometriosis-associated carcinomas. Furthermore, Ki-67 LI was significantly lower in the borderline CCAF components of CCAF-associated carcinomas than in the atypical endometriosis components of endometriosis-associated carcinomas.

Skp2, an F-box protein necessary for DNA replication, was originally identified as a protein that interacts with the cyclin A–CDK2 complex [30]. It has been reported that increased Skp2 overexpression is associated with cyclin A overexpression and also with reduced $p27^{Kip}$ expression [31–33]. Skp2 protein is reportedly a negative prognostic factor in ovarian carcinomas [34, 35]. In our previous study, aberrant expression of $p27^{Kip1}$, cyclin A, and Skp2 was positively correlated with cell proliferative activity, as represented by Ki67 LI, in atypical endometriosis and invasive carcinoma components [20]. Moreover, Skp2 overexpression was highly correlated with $p27^{Kip1}$ downregulation in atypical endometriosis, suggesting that increased Skp2 overexpression may have a causative role in decreasing the expression of $p27^{Kip1}$ and the resulting overexpression of cyclin A, during endometriosis-associated ovarian clear cell carcinogenesis [20].

When taken together, the results of the previous and present studies may be able to explain the relatively better clinical outcome of CCAF-associated CCAs in terms of the relatively lower frequencies of overexpression of Skp2 and cyclin A and downregulation of $p27^{Kip1}$. Less frequent alterations of these cell-cycle regulators might account for the lower proliferative activity of cancer cells in comparison with endometriosis-associated carcinomas. Although follow-up data (i.e., patients' survival) on the cases presented were of interest, sample size was relatively small, and sufficient long-term follow-up data were not available for some of the cases, therefore, not mentioned in this study.

Itamochi et al. [36] suggested that the chemoresistant nature of ovarian CCA, which is the primary reason for its lethality, may result from the low proliferative activity of the tumor cells. In their study, CCAs with a high Ki-67 LI showed relatively better chemosensitivity and better prognosis when compared with CCAs showing a low Ki-67 LI [36]. However, the cases studied by Itamochi et al. [36] were limited to those at advanced stages (FIGO stages III or IV) with measurably residual tumors, and they did not subclass CCA from the viewpoint of co-existing precursor lesions. In contrast, our previous study demonstrating a better prognosis of CCAF-associated carcinomas included a larger number of early stage tumors (FIGO stage I or II; 72% of the cases) and cases that had been treated by optimal cytoreduction (79% of the cases) [23]. Therefore, the present data suggesting that low cell proliferative activity itself may account for the better prognosis of patients with CCA, especially those who have undergone optimal cytoreduction, may not necessarily be discordant with those of Itamochi et al. [36].

The study by Shimizu et al. [37] demonstrated that in comparison with other histologic subtypes (i.e., serous adenocarcinoma, mucinous adenocarcinoma, or endometrioid adenocarcinoma), ovarian CCA showed significantly high expression of $p21^{WAF1/CIP1}$ and cyclin E. However, in their study, cyclin E overexpression was not associated with tumor cell proliferative activity, as assessed by Ki-67 LI, a finding consistent with our present study. From the comparison study for aberrant expression of cyclin E between the CCAF-associated and endometriosis-associated clear cell carcinogenetic pathways, it could be speculated that cyclin E overexpression would have influence on CCAF-associated carcinogenesis equal to or greater than on endometriosis-associated carcinogenesis at the precursor stage, with and without atypia. The cyclin E-CDK2 complex is primarily regulated by the CDK inhibitors $p27^{Kip1}$ and $p21^{WAF1/CIP1}$ [38, 39]. Because, in this study, $p27^{Kip1}$ was not frequently downregulated in CCAF-associated carcinoma, alteration of $p21^{WAF1/CIP1}$ protein appears to be of interest, although downregulation of $p21^{WAF1/CIP1}$ is reportedly less frequent in CCAs than in non-clear cell carcinomas [37, 40].

In summary, we have demonstrated that cumulative alterations of cell-cycle regulators, especially $p27^{Kip1}$-interacting proteins, are associated with ovarian clear cell carcinogenesis but that the frequencies of some of these alterations, and the Ki67 LI, are significantly lower in CCAF-associated CCAs and their precursors than in

endometriosis-associated CCAs and their precursors. These results suggest that the former show slower cell-cycle progression and lower cell proliferative activity than the latter. Differences in the expression levels of these cell-cycle regulators appear to account for differences in the rates of tumor progression and metastatic potential, and consequently prognosis, between CCAF-associated and endometriosis-associated CCA of the ovary.

Acknowledgments This work was supported in part by a grant-in-aid for promotion of defense medicine from the Ministry of Defense, Japan (S.Y., H.T., and O.M.), and by a grant-in-aid for cancer research from the Ministry of Health, Labour, and Welfare, Japan (H.T.). The authors are thankful to Ms. Kozue Suzuki for technical assistance with immunohistochemistry.

Conflict of interest statement The authors declare no actual or potential conflicts of interest in this study.

References

1. Seidman JD, Russell P, Kurman RJ (2001) Surface epithelial tumors of the ovary. In: Kurman RJ (ed) Blaustein's pathology of the female genital tract, 5th edn. Springer-Verlag, New York, pp 791–904
2. Sugiyama T, Kamura T, Kigawa J et al (2000) Clinical characteristics of clear cell carcinoma of the ovary: a distinct histologic type with poor prognosis and resistance to platinum-based chemotherapy. Cancer 88:2584–2589
3. Ikeda K, Sakai K, Yamamoto R et al (2003) Multivariate analysis for prognostic significance of histologic subtype, GST-pi, MDR-1, and p53 in stages II-IV ovarian cancer. Int J Gynecol Cancer 13:776–784
4. Tavassoli FA, Devilee P (eds) (2003) World Health Organization classification of tumours. Pathology and genetics of tumours of the breast and female genital organs. IARC Press, Lyon
5. Kaku T, Ogawa S, Kawano Y et al (2003) Histological classification of ovarian cancer. Med Electron Microsc 36:9–17
6. Gynecologic cancer committee, Japan society of obstetrics and gynecology (2008) Annual report of gynecological cancer patients in Japan 2006. Acta Obstet Gynaecol Jpn 60:1001–1085 in Japanese
7. Takano M, Sugiyama T, Yaegashi N et al (2008) Low response rate of second-line chemotherapy for recurrent or refractory clear cell carcinoma of the ovary: a retrospective Japan Clear Cell Carcinoma Study. Int J Gynecol Cancer 18:937–942
8. Takano M, Kikuchi Y, Yaegashi N et al (2006) Clear cell carcinoma of the ovary: a retrospective multicentre experience of 254 patients with complete surgical staging. Br J Cancer 94:1369–1374
9. Sampson JA (1925) Endometrial carcinoma of the ovary arising in endometrial tissue in that organ. Arch Surg 10:1–72
10. Vercellini P, Parazzini F, Bolis G et al (1993) Endometriosis and ovarian cancer. Am J Obstet Gynecol 169:181–182
11. Fukunaga M, Nomura K, Ishikawa E et al (1997) Ovarian atypical endometriosis: its close association with malignant epithelial tumours. Histopathology 30:249–255
12. Ogawa S, Kaku T, Amada S et al (2000) Ovarian endometriosis associated with ovarian carcinoma: a clinicopathological and immunohistochemical study. Gynecol Oncol 77:298–304
13. LaGrenade A, Silverberg SG (1988) Ovarian tumors associated with atypical endometriosis. Hum Pathol 19:1080–1084
14. Mostoufizadeh M, Scully RE (1980) Malignant tumors arising in endometriosis. Clin Obstet Gynecol 23:951–963
15. Seidman JD (1996) Prognostic importance of hyperplasia and atypia in endometriosis. Int J Gynecol Pathol 15:1–9
16. Varma R, Rollason T, Gupta JK et al (2004) Endometriosis and the neoplastic process. Reproduction 127:293–304
17. Jiang X, Hitchcock A, Bryan EJ et al (1996) Microsatellite analysis of endometriosis reveals loss of heterozygosity at candidate ovarian tumor suppressor gene loci. Cancer Res 56: 3534–3539
18. Jiang X, Morland SJ, Hitchcock A et al (1998) Allelotyping of endometriosis with adjacent ovarian carcinoma reveals evidence of a common lineage. Cancer Res 58:1707–1712
19. Sato N, Tsunoda H, Nishida M et al (2000) Loss of heterozygosity on 10q23.3 and mutation of the tumor suppressor gene PTEN in benign endometrial cyst of the ovary: possible sequence progression from benign endometrial cyst to endometrioid carcinoma and clear cell carcinoma of the ovary. Cancer Res 60:7052–7056
20. Yamamoto S, Tsuda H, Miyai K, et al (2009) Cumulative alterations of $p27^{Kip1}$-related cell cycle regulators in the development of endometriosis-associated ovarian clear cell adenocarcinoma. Histopathology (in press)
21. Bell DA, Scully RE (1985) Benign and borderline clear cell adenofibromas of the ovary. Cancer 56:2922–2931
22. Roth LM, Langley FA, Fox H et al (1984) Ovarian clear cell adenofibromatous tumors. Benign, of low malignant potential, and associated with invasive clear cell carcinoma. Cancer 53:1156–1163
23. Yamamoto S, Tsuda H, Yoshikawa T et al (2007) Clear cell adenocarcinoma associated with clear cell adenofibromatous components: a subgroup of ovarian clear cell adenocarcinoma with distinct clinicopathologic characteristics. Am J Surg Pathol 31:999–1006
24. Yamamoto S, Tsuda H, Takano M et al (2008) Clear-cell adenofibroma can be a clonal precursor for clear-cell adenocarcinoma of the ovary: a possible alternative ovarian clear-cell carcinogenic pathway. J Pathol 216:103–110
25. Yamamoto S, Tsuda H, Takano M et al (2008) Expression of platelet-derived growth factors and their receptors in ovarian clear-cell carcinoma and its putative precursors. Mod Pathol 21:115–124
26. Filipits M, Puhalla H, Wrba F (2003) Low p27Kip1 expression is an independent prognostic factor in gallbladder carcinoma. Anticancer Res 23:675–679
27. Hui AM, Li X, Shi YZ, Torzilli G, Takayama T, Makuuchi M (2000) p27(Kip1) expression in normal epithelia, precancerous lesions, and carcinomas of the gallbladder: association with cancer progression and prognosis. Hepatology 31:1068–1072
28. Huang HY, Kang HY, Li CF et al (2006) Skp2 overexpression is highly representative of intrinsic biological aggressiveness and independently associated with poor prognosis in primary localized myxofibrosarcomas. Clin Cancer Res 12:487–498
29. Li SH, Li CF, Sung MT et al (2007) Skp2 is an independent prognosticator of gallbladder carcinoma among p27(Kip1)-interacting cell cycle regulators: an immunohistochemical study of 62 cases by tissue microarray. Mod Pathol 20:497–507
30. Zhang H, Kobayashi R, Galaktionov K, Beach D (1995) p19skp1 and p45skp2 are essential elements of the cyclin A-CDK2 S phase kinase. Cell 82:915–925
31. Gstaiger M, Jordan R, Lim M et al (2001) Skp2 is oncogenic and overexpressed in human cancers. Proc Natl Acad Sci USA 98:5043–5048
32. Chao Y, Shih Y-L, Chiu J-H et al (1998) Overexpression of cyclin A but not Skp2 correlated with the tumor relapse of human hepatocellular carcinoma. Cancer Res 58:985–990

33. Latres E, Chiarle R, Schulman BA et al (2001) Role of the F-box protein Skp2 in lymphomagenesis. Proc Natl Acad Sci USA 98:2515–2520
34. Shigemasa K, Gu L, O'Brien TJ, Ohama K (2003) Skp2 expression is a prognostic factor in patients with ovarian adenocarcinoma. Clin Cancer Res 9:1756–1763
35. Sui L, Dong Y, Watanabe Y et al (2006) Clinical significance of Skp2 expression, alone and combined with Jab1 and p27 in epithelial ovarian tumors. Oncol Rep 15:765–771
36. Itamochi H, Kigawa J, Sugiyama T et al (2002) Low proliferation activity may be associated with chemoresistance in clear cell carcinoma of the ovary. Obstet Gynecol 100:281–287
37. Shimizu M, Nikaido T, Toki T, Shiozawa T, Fujii S (1998) Clear cell carcinoma has an expression pattern of cell cycle regulatory molecules that is unique among ovarian adenocarcinomas. Cancer 85:669–677
38. Hwang HC, Clurman BE (2005) Cyclin E in normal and neoplastic cell cycles. Oncogene 24:2776–2786
39. Nakayama KI, Hatakeyama S, Nakayama K (2001) Regulation of the cell cycle at the G1-S transition by proteolysis of cyclin E and p27Kip1. Biochem Biophys Res Commun 282:853–860
40. Anttila MA, Kosma V-M, Hongxiu J et al (1999) p21/WAF1 expression as related to p53, cell proliferation and prognosis in epithelial ovarian cancer. Br J Cancer 79:1870–1878

Virchows Arch (2009) 455:423–429
DOI 10.1007/s00428-009-0843-6

ORIGINAL ARTICLE

Pathologic characteristics of resected squamous cell carcinoma of the trachea: prognostic factors based on an analysis of 59 cases

Jimmie Honings · Henning A. Gaissert · Ruchira Ruangchira-Urai · John C. Wain · Cameron D. Wright · Douglas J. Mathisen · Eugene J. Mark

Received: 14 August 2009 / Revised: 24 September 2009 / Accepted: 25 September 2009 / Published online: 17 October 2009

Abstract While squamous cell carcinoma (SCC) is the most common tracheal malignancy, few reports describe the pathologic considerations that may guide intraoperative decisions and prognostic assessment. We reviewed 59 tracheal SCC treated between 1985 and 2008 by segmental resection of the trachea, including resection of the carina in 24% and inferior larynx in 14%. We classified these tumors by grading histologic differentiation and microscopic features used in SCC of other sites. Of 59 tumors, 24% (14 of 59) were well differentiated, 49% (29 of 59) were moderately differentiated, and 27% (16 of 59) were poorly differentiated. Unfavorable prognostic factors were tumor extension into the thyroid gland (all of five so-afflicted patients died of tumor progression within 3 years) and lymphatic invasion (mean survival 4.6 versus 7.6 years). Keratinization, dyskeratosis, acantholysis, necrosis, and tumor thickness did not predict prognosis. As surgical resection is the only curative treatment; the surgeon should establish clean lines of resection using, as appropriate, intraoperative frozen section. The pathologist can provide additional important prognostic information, including tumor differentiation and extent, invasion of surgical margins, and extension into the thyroid.

J. Honings · H. A. Gaissert (✉) · J. C. Wain · C. D. Wright · D. J. Mathisen
Division of Thoracic Surgery,
Massachusetts General Hospital and Harvard Medical School,
32 Fruit Street, Blake 1570,
Boston, MA 02114, USA
e-mail: hgaissert@partners.org

R. Ruangchira-Urai · E. J. Mark
Department of Pathology,
Massachusetts General Hospital and Harvard Medical School,
Boston, MA, USA

Keywords Trachea · Squamous cell carcinoma · Airway resection · Pathologic staging · Histologic features of invasion

Introduction

Although squamous cell carcinoma (SCC) accounts for more than half of all tracheal tumors [1], the pathologic features in resection specimens and the impact of these features on survival have only been described in small series [2]. At least two staging systems have been proposed for tracheal malignancies; one, a cross-sectional analysis of a national cancer database by Bhattacharyya, is based on retrospective tumor–node–metastases (TNM) documentation correlated with survival statistics in 41 squamous cell carcinomas, 19 adenoid cystic carcinomas, and 32 tumors of other histology [3], although a TNM staging system validated by clinical and pathologic evidence for this disease does not exist. The other, by Macchiarini, is a nonvalidated TNM classification [4]. Both classifications are intended to be applied to all histologic types of tracheal cancer.

We describe specific pathologic features of primary tracheal SCC in a large series of surgical specimens from a single institution to identify prognostic predictors of survival.

Materials and methods

A retrospective analysis was conducted of consecutive patients who underwent resection for primary SCC of the trachea from 1985 to 2008 at Massachusetts General Hospital (MGH) and for whom pathology slides or blocks were available. All except four patients were included in a previous report describing the surgical results [5]. We

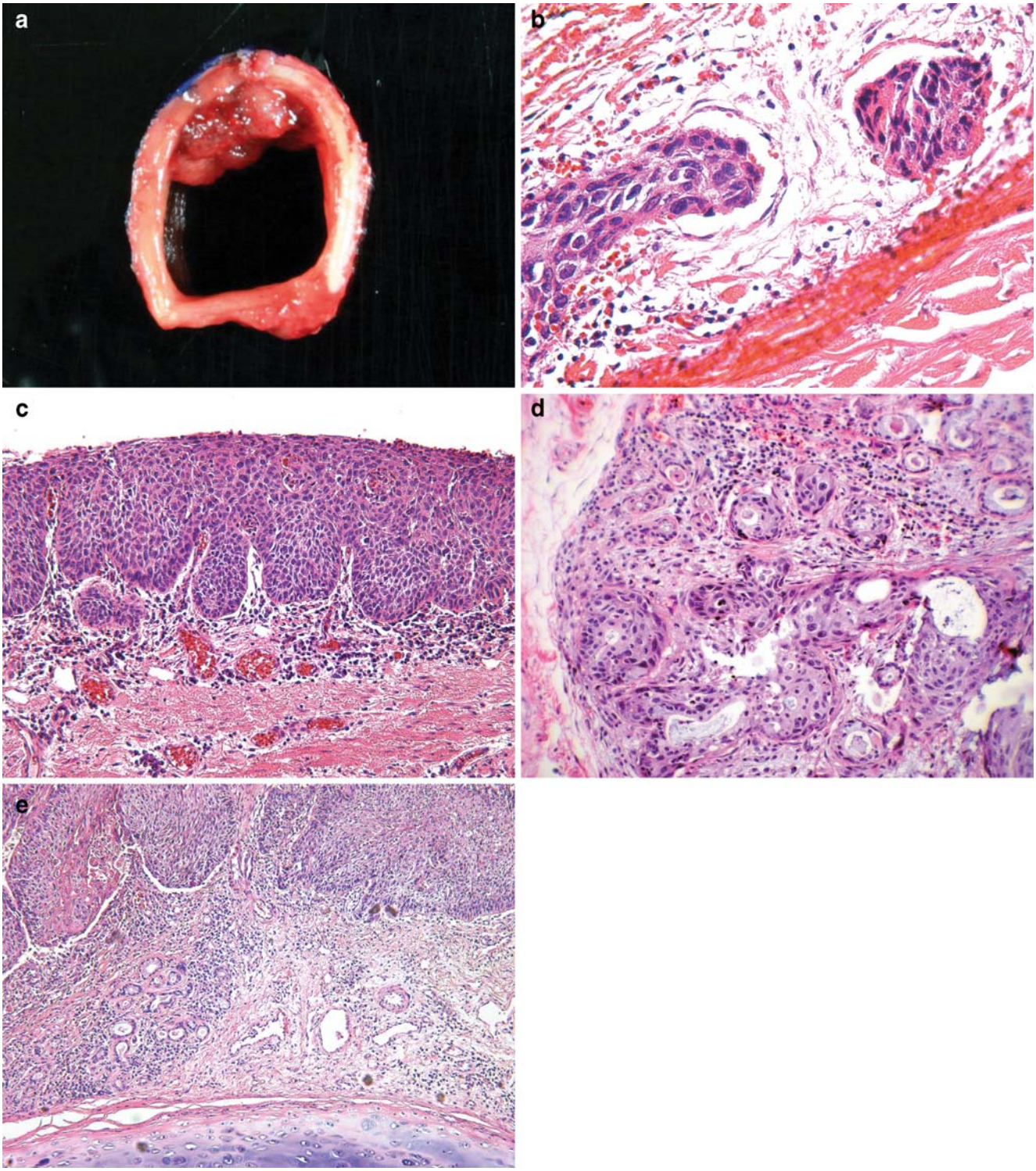

Fig. 1 **a** Cross section of trachea with exophitic tumor attached to anterior wall; **b** lymphatic invasion in peritracheal adventitia; **c** squamous cell carcinoma in situ, with full thickness replacement of epithelium by cells with hyperchromatic nuclei and lack of surface maturation; **d** cancerization of mucus ducts and glands by malignant squamous cells but no invasion beyond basement membrane; **e** squamous cell carcinoma invading from surface epithelium into lamina propria and eliciting inflammation and fibrosis but not as far as tracheal cartilage (bottom)

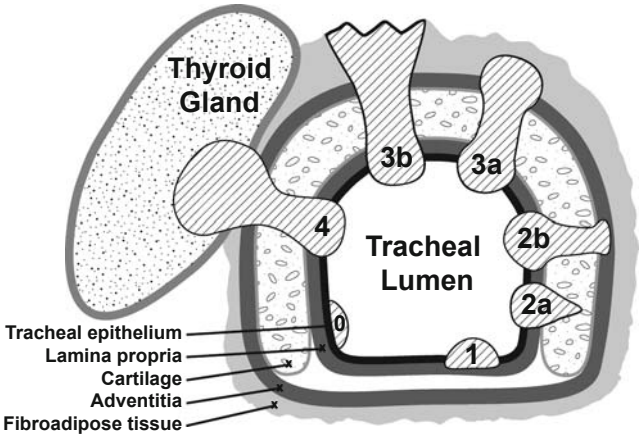

Fig. 2 Depth of invasion in tracheal squamous cell carcinoma ranked by levels. Tumor invaded between cartilage plates and not through the cartilage. Level definitions: *0* carcinoma in situ, *1* infiltrating lamina propria, *2a* abutting or extending between cartilage, *2b* invading beyond cartilage, *3a* invading peritracheal fibroadipose tissue, *3b* abutting soft tissue resection margin, *4* invading into thyroid gland

included one patient in whom a second resection at MGH completed tumor excision after a first resection elsewhere. One patient underwent three resections, but only the first, for tumor resection, was included in this study. Pathology reports, operative reports, and hospital charts were reviewed to exclude laryngeal cancer and tumors of the lung that extended to the carina. The MGH institutional review board approved the most recent protocol (no. 2008-P-000113) in January 2008.

Types of resection

The surgical technique has been detailed previously [6]. For standard tracheal resection, a sleeve of trachea was removed with end-to-end reconstruction, resulting in two airway margins and a radial soft tissue margin. When tracheal resection was combined with laryngectomy, cervical or mediastinal end-tracheostomy was required. For laryngotracheal resection, the tumor was removed with a portion of infraglottic larynx while preserving at least one recurrent laryngeal nerve not involved with tumor. Reconstruction was achieved by shaping the remaining trachea to conform to the laryngeal defect. Carinal resection was performed with or without concomitant lung resection resulting in either two or three airway margins, respectively. Systematic lymph node dissection is assumed to interfere with the tracheal blood supply and was therefore not performed. Regional lymph nodes were often not included in the specimen if not grossly enlarged. Absence of tumor at the airway margins was confirmed by frozen section, unless the limits of resection had been reached, and no additional trachea could be removed.

Pathologic review and tumor data

In all reviewed cases, photographs of the resected specimen (Fig. 1a) and slides stained with hematoxylin and eosin were retrieved. Slides were recut from stored blocks if necessary. Pathologic review of two or more slides per case was done in each case by a senior pulmonary pathologist (E.J.M.), on average four to six slides of the tumor itself and additional slides of resection margins and lymph nodes. The following histologic features were scored: degree of differentiation based on degree and extent of nuclear pleomorphism, using the criteria for well, moderately, or poorly differentiated subtypes in the Armed Forces Institute of Pathology *Atlas of Tumor Pathology* [7]; tumor thickness, defined as the distance from the luminal tumor surface to the farthest extent of invasion; keratinization; necrosis; dyskeratosis; acantholysis; and lymphatic invasion (Fig. 1b). Since no TNM-based staging system currently exists for tracheal carcinoma, depth of tumor invasion into the tracheal wall was scored according to a system devised for the study as shown in Fig. 2, with both squamous cell carcinoma in situ (Fig. 1c) and invasion of carcinoma into tracheal mucus glands and ducts (so-called cancerization, Fig. 1d) considered level 0 and superficially invasive (Fig. 1e) as grade 1.

Further, operative and pathology reports were reviewed for length of resection in the long axis of the airway and the presence of tumor metastasis in lymph nodes. Since lymph node excision in tracheal resection occurs merely sporadically, we combined cases with positive lymph node biopsy and cases with lymphatic invasion on histologic examination in order to provide a meaningful, albeit restricted, analysis.

Adjuvant radiotherapy

Postoperative radiotherapy was usually recommended at a dose of 54 Gy 6 to 8 weeks after resection and often administered outside Massachusetts General Hospital.

Follow-up

Patients and the MGH cancer registry were contacted for follow-up information. The Social Security Death Index was searched. Patients were determined to have died if name, date of birth, and social security number matched. The survival period began on the day of operation and was concluded by death.

Statistical analysis

Overall survival after airway resection was calculated using the Kaplan–Meier procedure with the log rank test

Table 1 Survival according to pathologic subgroups

Pathologic subgroup	Number	Percent	Mean survival (years)	*P* value	Survival (%)	
					5-year	10-year
Tumor differentiation						
Well differentiated	14	23.7	8.8	0.164	73	55
Moderately differentiated	29	49.2	6.3		44	25
Poorly differentiated	16	27.1	4.5		29	10
Keratinization						
Yes	39	66.1	6.5	0.719	50	28
No	20	33.9	6.6		39	26
Necrosis						
Extensive	12	20.3	7.2	0.726	46	27
Focal	28	47.5	6.1		45	26
No	19	32.2	6.2		47	30
Dyskeratosis						
Yes	35	59.3	6.7	0.942	51	34
No	24	40.7	6.3		39	20
Acantholysis						
Yes	16	27.1	5.6	0.307	47	31
No	43	72.9	6.9		46	26
Lymphatic invasion						
Yes	22	37.3	4.6	0.049	24	24
No	37	62.7	7.6		60	31
Depth of invasion						
Level 0	2	3.4	n.a.	0.001	100	100
Level 1	5	8.5	7.6		75	25
Level 2a	14	23.7	6.0		50	25
Level 2b	11	18.6	7.1		50	38
Level 3a	16	27.1	7.7		53	31
Level 3b	6	10.2	2.1			
Level 4	5	8.5	1.4		0	
Tumor thickness						
0.1–1.0 cm	29	49.2	6.8	0.650	48	32
1.1–2.0 cm	21	35.6	6.8		56	26
>2.0 cm	9	15.3	4.1		13	13
Overall	59	100.0	6.5		46	27

implemented in the SPSS 14.0 statistical software program (SPSS Inc, Chicago, IL), in contrast to the earlier report that used an actuarial method [5]. Categorical variables were compared with the chi-square test, and covariate analysis was done with Pearson's bivariate analysis.

Results

Since 1985, 75 patients have undergone surgical resection for tracheal SCC at Massachusetts General Hospital. There were no operative deaths. Slides or blocks were retrieved in 64 cases, of which five were excluded: there was no viable tumor after radiotherapy in three patients, a cutaneous SCC occurred at a tracheostomy site in one, and two separate SCC were present in one other patient, of which only one was resected. Thus, the study included 59 cases.

Overall characteristics

There were 44 men (75%) and 15 women (25%) with a mean age of 61.9 years (range 29 to 79 years). Prior locoregional or preoperative radiotherapy was administered in 24% (14 of 59). Resection involved trachea only in 63% (37 of 59), trachea and carina in 24% (14 of 59), and trachea and larynx in 14% (eight of 59) of cases. Mean length of resected airway was 3.2 cm (range 1 to 6 cm).

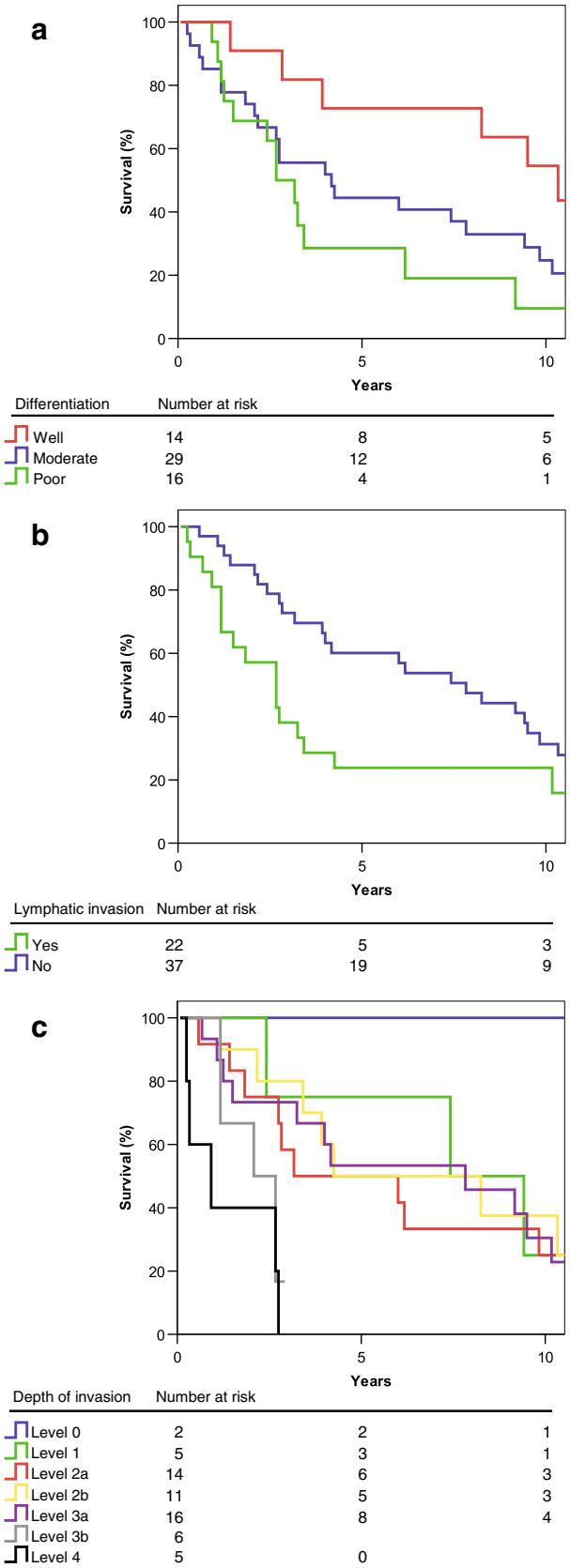

Fig. 3 **a**–**c** Overall survival according to: **a** tumor differentiation, **b** lymphatic invasion, **c** depth of tumor invasion

Pathologic characteristics are listed in Table 1. Postoperative radiation was documented in 42.4% of patients (25 of 59). We know of no patient who received postoperative chemotherapy.

Follow-up and overall survival

Mean follow-up in 59 cases was 5.5 years (range 1 month to 18.3 years). Survival information was complete in 90% of patients (53 of 59). Mean survival was 6.5 years, and the 5- and 10-year survivals were 46% and 27%, respectively. Table 1 shows the survival calculated for each subgroup.

Differentiation

A majority of tumors had moderate differentiation, while close to half were equally distributed between well and poorly differentiated. Survival was longer in well-differentiated tumors, though this difference was not significant (Fig. 3a). Survival in well-differentiated carcinomas was 8.8 years versus 5.8 years in the group of moderately and poorly differentiated carcinomas combined (P=0.117).

Keratinization, necrosis, dyskeratosis, and acantholysis

Two thirds of tumors (39 of 59) showed keratinization. Focal or extensive necrosis was present in 48% (28 of 59) and 20% (12 of 59), respectively. Necrosis was present significantly more frequently in moderately and poorly differentiated tumors (82%, 37 of 45) compared to well-differentiated tumors (21%, three of 14; P<0.001). Dyskeratosis was seen in 59% and acantholysis in 27%.

Survival was not significantly correlated with the presence or absence of keratinization, necrosis, dyskeratosis, or acantholysis.

Lymphatic invasion

In 22 cases (37%), there was tumor in peritracheal lymphatics on histologic examination (seven cases), a tumor-positive lymph node biopsy was present (nine), or both (six). In the other 36 cases (61%), neither lymphatic invasion nor lymph node metastasis was demonstrated. Lymphatic invasion was correlated with the degree of differentiation: histologic lymphatic invasion or tumor-positive lymph node biopsies were present in one of 14 well-differentiated (7%), 13 of 29 moderately differentiated (49%), and nine of 16 poorly differentiated (56%) tumors (P=0.015). Survival in patients without lymphatic invasion was higher than when lymphatic invasion was present (P=

Table 2 Pathologic characteristics according to depth of invasion

Depth of invasion	Number	Percent	Well differentiated		Lymphatic invasion		Tumor thickness >2cm	
			N	%	*N*	%	*N*	%
Level 0	2	3.4	2	100.0	0	0.0	0	0.0
Level 1	5	8.5	2	40.0	0	0.0	0	0.0
Level 2a	14	23.7	5	35.7	1	7.1	0	0.0
Level 2b	11	18.6	4	36.4	5	45.5	2	18.2
Level 3a	16	27.1	1	6.3	7	43.8	6	37.5
Level 3b	6	10.2	0	0.0	4	66.7	1	16.7
Level 4	5	8.5	0	0.0	5	100.0	0	0.0
Overall	59	100.0	14	23.7	22	37.3	9	15.3

0.049, Fig. 3b). There was no difference in survival between patients who had lymphatic invasion only versus patients with positive lymph nodes only, versus both (P=0.382).

Depth of invasion

Carcinomas in situ (level 0) were uncommon, while tumor invaded peritracheal fibroadipose tissue (level 3a) in 16 cases (27%), extended to the soft tissue resection margin (level 3b) in six cases (10%), and invaded the thyroid gland (level 4) in five cases (8%; Table 2). While both patients with carcinoma in situ were alive without disease 9.6 and 15 years after resection, there was no difference in survival between levels 1, 2 (a and b), and 3a (Table 1 and Fig. 3c). Incomplete resection and involvement of the thyroid gland were both negative prognostic markers: mean survival was 2.1 years in patients with tumor at the soft tissue resection margin (level 3b) and 1.4 years when tumor invaded the thyroid gland (level 4), both significantly lower than in other levels of invasion (P=0.025 and P<0.001, respectively). Lesser levels of invasion were associated with a higher incidence of well-differentiated histology (P=0.018) and a lower incidence of lymphatic invasion (P=0.002).

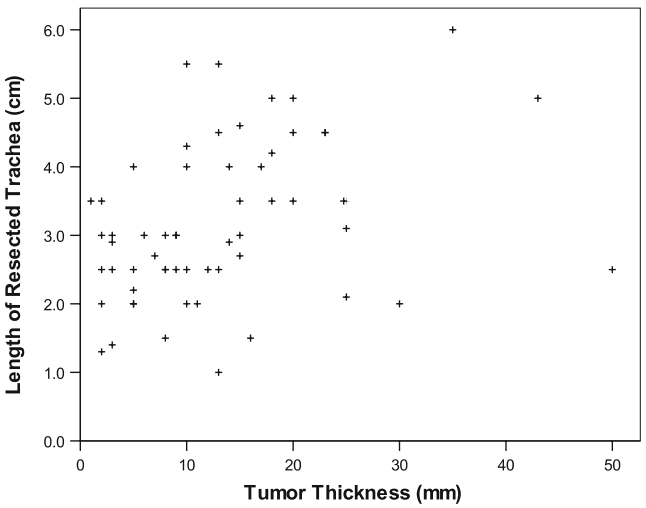

Fig. 4 Correlation between thickness and length of resected tracheal tumor. Each data point represents one tumor specimen

Tumor thickness

Mean tumor thickness was 1.3 cm (median 1.1 cm, range 0.1–5.5 cm). Tumors were 2 cm or smaller in 85%. Within this range, tumor thickness had no significant impact on survival (P=0.650). Tumors of greater thickness were associated with resections of greater (>3 cm) length (P= 0.008), although there were two resections of 2.0 and 2.5 cm in length of trachea with a tumor of 3 and 5 cm in thickness, respectively (Fig. 4, correlation coefficient 0.364). Tumors >2 cm in thickness had no different survival than tumors of 2 cm or less (P=0.353). Tumors >2 cm in thickness more frequently invaded peritracheal fibroadipose tissue (six of nine, 67%) than smaller tumors (ten of 50, 20%; P=0.004) but were not associated with levels 3b or 4 (Table 2).

Discussion

In this pathologic review of primary tracheal squamous cell carcinoma, the largest series to date, we show that completeness of resection, involvement of the thyroid gland, and lymphatic invasion are histopathologic features with important prognostic value. Increasing depth of invasion into the tracheal wall is associated with a loss of histologic differentiation and lymphatic invasion. Although survival in well-differentiated carcinomas is higher, this difference is not significant and may be attributed to the higher incidence of lymphatic invasion in moderately and poorly differentiated carcinomas. Further, we observed that

resected tracheal SCCs are mostly small tumors (median thickness 1.1 cm) and that tumor thickness within this range did not significantly affect prognosis. A possible explanation for this finding is that thickness may result from the exophitic portion of the tumor and thus is not conditioned on deeper invasion into the tracheal wall. A higher proportion of larger tumors, however, exhibit lymphatic invasion, a significant predictor of survival.

Surgical resection may lead to excellent survival even when the tumor violates the boundaries of the trachea and invades peritracheal fibroadipose tissue. To provide the best chances of survival, it is however important for the surgeon to achieve negative soft tissue resection margins. When faced with a tracheal SCC growing into the thyroid gland, our findings indicate that surgical resection should be applied to carefully selected patients, and palliative therapy may be considered when complete resection is otherwise compromised. Further, the pathologist reviewing SCC of the trachea should be aware of the importance of lymphatic invasion and specifically investigate the tumor for the presence of this feature.

There are some limitations to our study. We retrospectively analyzed large pathologic specimens of tracheal SCC, and only resected cases were included. Tumors growing into vital organs such as the heart or the great vessels and tumors involving long segments of airway judged unresectable were treated at the Massachusetts General Hospital but are not included in our study. We might have underestimated or misjudged the histologic characteristics, as only a limited number of representative slides for each case were available during histologic review; further, there were only five cases with invasion of the thyroid gland.

Tracheal SCC is a rare tumor, and few centers acquire proficiency in its surgical treatment. The dissemination of whatever prognostic information is available assumes therefore a greater importance. We confirm that lymphatic invasion predicts prognosis, while depth of invasion could not be correlated with survival, except for a marked decline when tumor was present at the resection margin or invaded the thyroid gland. We therefore conclude that even in cases where tumor invades peritracheal fibroadipose tissue, excellent survival can be achieved provided the patient undergoes surgical resection and the resection is complete. Positive resection margins in turn predict treatment failure. Our previous report showed that outcome in patients with unresected tumors is worse than in patients that underwent resection [5], a finding supported here by the poor prognosis in patients with incomplete resection. Thus, tumor resectability, usually dictated by tumor length in the long axis of the airway and invasion of vital organs, may possibly be the single most important prognostic factor in this very distinct type of cancer.

Conflicts of interest and funding None of the authors has had nor currently has any financial or personal relationships with other people or organizations that could inappropriately influence (bias) their work. There are no conflicts of interest. There were no sources of funding other than departmental funds.

References

1. Gelder CM, Hetzel MR (1993) Primary tracheal tumours: a national survey. Thorax 48:688–692
2. Sweeney EC, Hughes F (1977) Primary carcinoma of the trachea. Histopathology 1:289–299
3. Bhattacharyya N (2004) Contemporary staging and prognosis for primary tracheal malignancies: a population-based analysis. Otolaryngol Head Neck Surg 131:639–642
4. Macchiarini P (2006) Primary tracheal tumours. Lancet Oncol 7:83–91
5. Gaissert HA, Grillo HC, Shadmehr MB, Wright CD, Gokhale M, Wain JC, Mathisen DJ (2004) Long-term survival after resection of primary adenoid cystic and squamous cell carcinoma of the trachea and carina. Ann Thorac Surg 78:1889–1897
6. Grillo HC (2004) Surgical techniques. In: Grillo HC (ed) Surgery of the trachea and bronchi. BC Decker, Hamilton, pp 499–692
7. Colby TV, Koss MN, Travis WD (1994) Squamous cell carcinoma and variance. In: Colby TV, Koss MN, Travis WD (eds) Atlas of tumor pathology. Tumors of the lower respiratory tract. Armed Forces Institute of Pathology, Washington, DC, pp 157–167

Virchows Arch (2009) 455:431–440
DOI 10.1007/s00428-009-0838-3

ORIGINAL ARTICLE

Overexpression of Aurora B is associated with poor prognosis in epithelial ovarian cancer patients

Yi-Jen Chen · Chun-Ming Chen · Nae-Fang Twu · Ming-Shyen Yen · Chiung-Ru Lai · Hua-Hsi Wu · Peng-Hui Wang · Chiou-Chung Yuan

Received: 14 August 2009 / Revised: 13 September 2009 / Accepted: 14 September 2009 / Published online: 17 October 2009

Abstract Recent studies have indicated that Aurora B expression is related to cell proliferation and prognosis in many cancers, but its association with epithelial ovarian carcinoma is not fully understood. Therefore, we examined the Aurora B kinase expression in epithelial ovarian cancer patients. Using immunohistochemistry, the expression levels of Aurora B and phosphohistone H3 (Ser^{10}) (mitosis-specific marker) were measured in 156 patients with epithelial ovarian cancer. The expression levels of Aurora B at the protein and messenger RNA levels were examined using Western blotting and reverse transcriptase polymerase chain reaction. In total, 53 tumorous ovarian samples (34.0%) showed Aurora B overexpression, which was significantly higher than that found in the 15 normal ovarian tissue samples (0%, $p=0.006$). The overexpression of Aurora B was also significantly higher in cases showing phosphohistone H3 (Ser^{10}) overexpression (44.3% vs. 27.4%, $p=0.03$). In addition, the expression of Aurora B in poorly and moderately differentiated carcinomas of the ovary was significantly higher than in well-differentiated carcinomas (53.6% vs. 28.2% vs.10.0%, respectively, $p=0.02$). The overexpression of Aurora B was significantly higher in cases with lymph node metastasis ($p=0.01$) and a positive ascites cytology ($p=0.008$). Overall, the Aurora B overexpression group demonstrated a significantly shorter progression-free survival ($p=0.001$) and overall survival ($p=0.023$) than the Aurora B low expression group using univariate analysis (log-rank statistic). Aurora B is an effective predictor of aggressive epithelial ovarian carcinoma in terms of differentiation, metastasis, and prognosis.

Keywords Phosphohistone H3 · Aurora B · Epithelial ovarian cancer · Prognosis

C.-M. Chen and C.-C. Yuan contributed equally to this work.

Y.-J. Chen · N.-F. Twu · M.-S. Yen · H.-H. Wu · P.-H. Wang · C.-C. Yuan
Department of Obstetrics and Gynecology,
Taipei Veterans General Hospital,
Taipei, Taiwan

Y.-J. Chen · H.-H. Wu · P.-H. Wang · C.-C. Yuan
Institute of Clinical Medicine, National Yang-Ming University,
Taipei, Taiwan

C.-M. Chen · N.-F. Twu · M.-S. Yen
Department of Life Sciences and Institute of Genome Sciences,
National Yang-Ming University,
Taipei, Taiwan

C.-R. Lai
Department of Pathology, Taipei Veterans General Hospital,
Taipei, Taiwan

C.-C. Yuan (✉)
Department of Obstetrics and Gynecology,
Taipei Veterans General Hospital,
201, Section 2, Shih-Pai Road,
Taipei 112, Taiwan
e-mail: chenyj@vghpte.gov.tw

Introduction

Ovarian cancer is a common gynecological malignancy in Western countries and represents the fifth leading cause of death due to cancer among women [1]. More than 70% of presenting cases are already in an advanced stage of the disease at diagnosis. Despite advances in cytoreductive surgery and in chemotherapy regimens, therapeutic failure and disease progression are still quite frequent [1]. The prognosis of patients with ovarian carcinoma depends mainly on the stage of disease and, to a lesser extent, on the patient's age, the volume of residual disease following cytoreductive surgery, and the histological type and grade

of cancer [2]. The identification of additional prognostic parameters would be very helpful when developing a therapeutic strategy, particularly for patients with advanced disease.

Aurora B is a chromosomal passenger protein critical for accurate chromosome segregation, cytokinesis [3, 4], protein localization to the centromere and kinetochore, correct microtubule-kinetochore attachment, and regulation of the mitotic checkpoint. Aurora B is localized on the centromeres from prophase through to metaphase–anaphase transition [5–7]. A significant overexpression of Aurora B has been observed in thyroid, colorectal, and hepatocellular human cancer cell lines [8–10]. Furthermore, it has been observed that overexpression of Aurora B produces aneuploid cells with a malignant and aggressive phenotype, which suggests that the protein's aberrant expression is correlated with human tumorigenesis. Aurora B expression has been associated with cell proliferation and prognosis in thyroid cancer, lung cancer, hepatomas, prostate cancer, and endometrial cancer [11–15]. In a recent study, Kulkarni et al. [16] demonstrated that Aurora B is significantly associated with tumor grade and ploidy status in epithelial ovarian carcinoma. Therefore, it is reasonable to study whether Aurora B expression might have clinical significance in patients with ovarian cancer.

Histone H3 is a protein involved in chromosome condensation and mitotic entry and its phosphorylation at $Ser^0$is mediated by Aurora B [3–7]. The phosphorylation of histone H3 is a rare event in interphase cells and is a process that almost exclusively occurs during mitosis [17]; thus, phosphohistone H3 (PHH3) is a mitosis-specific marker [18]. However, the correlation between Aurora B protein and PHH3 in epithelial ovarian carcinoma is still unclear. To answer this question, we assessed the association of this mitosis-specific marker with Aurora B in ovarian cancer.

In this study, we used an immunohistochemical method to determine the expression of Aurora B and PHH3 (a mitosis marker) in surgical ovarian tumor specimens from ovarian cancer patients. The correlation between Aurora B, PHH3, and clinicopathological parameters was evaluated. The expression of Aurora B in ovarian cancer was also analyzed by reverse transcription–polymerase chain reaction (RT-PCR) and Western blotting. Finally, the prognostic significance of Aurora B expression was examined using the patient follow-up data.

Materials and methods

Study cohort

This study included 156 ovarian cancer patients who had been admitted, treated, and followed-up at the Division of Gynecologic Oncology, Department of Obstetrics and Gynecology, Taipei Veterans General Hospital, Taiwan, between January 1992 and December 2006. Written informed consent was obtained from all patients enrolled in this study. The study has been performed with the approval of Taipei Veterans General Hospital ethics committee (VGHIRB no. 97-08-19A). The patients were selected on the basis of available histological material. The histological specimens were reviewed by a gynecological pathologist (Dr. Lai). Pathological specimens were assessed using the WHO criteria for histological subtype and nuclear grade [19–21]. The median age of the patients was 53 years, and the mean age was 54.62±12.27 years (range, 26–87). Of these patients, 57 (40.1%) had stage I or II cancer, and 85 (59.9%) had stage III or IV cancer. Histologically, serous adenocarcinoma was the most frequent type of cancer presenting in this group (34.0%). The clinicopathological characteristics of the patients are shown in Table 1.

The following clinical information was obtained directly from patients' hospital notes: date of birth, date of diagnosis, operative findings, Federation of International Obstetricians and Gynecologists (FIGO) stage based on the findings at clinical examination, and surgical exploration together with cytology results, CA125 values at diagnosis and relapse, date of relapse, date of last follow-up, and date and cause of death [2].

The 156 cases had undergone primary staging or debulking surgery. Optimal debulking surgery (n=99) was defined as the presence of a residual tumor <1 cm after the procedure. In contrast, if the residual tumor was ≥1 cm, the surgery was then defined as suboptimal debulking (n=29). Seventy-two patients were treated with six cycles of cisplatin-based combination chemotherapy with a minimum total dose of 400 mg/m^2 of cisplatin 2–3 weeks after initial surgery. The cisplatin-based combination chemotherapy regimen consisted of either the cyclophosphamide plus cisplatin (CP) regimen or the cisplatin, adriamycin and cyclophosphamide (CAP) regimen. Seventy-eight patients were treated with six cycles of paclitaxel-based combination chemotherapy 2–3 weeks after initial surgery. This chemotherapy regimen consisted of paclitaxel plus cisplatin or paclitaxel plus carboplatin. Most patients were reviewed after completing treatment every 3–6 months for 5 years and annually thereafter.

Immunohistochemistry

Four-micron sections were cut from formalin-fixed ovarian tissue embedded in paraffin blocks and then mounted onto silane-coated slides. Sections were dewaxed in xylene and rehydrated in a graded alcohol series (100%, 95%, 75%, and 60%) and ddH_2O; antigens were retrieved by boiling in a citrate buffer (pH 6, target retrieval solution; Dako, Carpinteria, CA, USA) for 5 min. Endogenous peroxidase

Table 1 Patient characteristics

Characteristic	*n* (%)
Age	156
Mean	54.62±12.27 years
Range	26–87 years
FIGO stage	142
I+II	57 (40.1%)
III+IV	85 (59.9%)
Histotype	156
Serous	53 (34.0%)
Mucinous	19 (12.2%)
Endometrioid	49 (31.4%)
Clear cell	6 (3.8%)
Others	29 (18.6%)
Differentiation	77
Well	10 (13.0%)
Moderate	39 (50.6%)
Poor	28 (36.4%)
Cytoreduction	128
Optimal	99 (77.3%)
Sub-optimal	29 (22.7%)
Ascites cytology	108
Positive	63 (58.3%)
Negative	45 (41.7%)
CA-125	96
Positive	86 (89.6%)
Negative	10 (10.4%)
Lymph node metastasis	116
Positive	61 (52.6%)
Negative	55 (47.4%)

was inhibited by 3% H_2O_2 (R&D Systems, Minneapolis, MN, USA). Sections were incubated in primary antibody overnight at 4°C. Anti-Aurora B and PHH3 (Ser^{10}) polyclonal antibody (Abcam, Cambridge, UK) was diluted to 1:100 in antibody diluent (Dako) in the immunohistochemical staining procedures [16, 22]. Following overnight incubation, secondary biotinylated antibodies and streptavidin–horseradish peroxidise-conjugated reagent (R&D Systems) were applied to the sections. Immunoreactive complexes were detected using the peroxidase substrate 3-amino-9-ethyl-carbazole (R&D Systems). Slides then were counterstained with aqueous hematoxylin (Thermo Shandon, Waltham, MA, USA) and mounted on a crystal mount (Biomeda, Foster City, CA, USA).

Quantification of immunohistochemical staining

Two observers independently examined the immunohistochemistry slides. The specific staining by each antibody was identified in the nucleus. We utilized an immunohistochemical score (IHS) based on the German ImmunoReactive score; this method has been shown to provide approximate data based on an image analysis-based scoring system [23]. The IHS is calculated by combining an estimate of the percentage of immunoreactive cells (quantitative score) with an estimate of the staining intensity (staining intensity score): No staining is scored as 0, 1%–10% of cells stained scored as 1, 11%–50% as 2, 51%–80% as 3, and 81%–100% as 4. Staining intensity is rated on a scale of 0–3, with 0 being negative, 1 being weak, 2 being moderate, and 3 being strong. The raw data are converted to the IHS by multiplying the quantity and staining intensity scores. Theoretically, the scores could range from 0 to 12. An IHS score of 9–12 is considered strong immunoreactivity, 5–8 is considered moderate, 1–4 is considered weak, and 0 is scored as negative. Aurora B and PHH3 expressing at a moderate to strong level in the nucleus was considered to be overexpression; in contrast, Aurora B and PHH3 expressing at a negative to weak level was to be considered low expression. There were no major differences in overall interpretation of the IHC results between the two pathologists (Chiung-Ru Lai and Ching-Fen Yang).

Western blotting

To confirm the antigenic specificity of the antibodies used for immunostaining, Western blotting was performed as described previously [24]. In brief, seven fresh tissue specimens (two normal ovarian tissue samples, two samples of well-differentiated ovarian carcinomas, and three samples of poor-differentiated ovarian carcinomas) were homogenized and lysed in 0.5 mL NaCl, 0.5% NP-40 (Neu-Ulm, Germany), 1 mmol/L phenylmethylsulfonylfluoride (Sigma Chemical, St Louis, Mo, USA), 1 μg/mL aprotinin (Boehringer Mannheim, Indianapolis, Ind), 1 μg/mL leupeptin (Boehringer Mannheim), and 20 μg/mL tosyl phenylalanyl chloromethyl-ketone (Boehringer Mannheim). The lysates were centrifuged at 13,000×*g* for 20 min at 4°C, and the supernatants were then stored at −70°C until they were used. Extracts equivalent to 50 mg of total protein were separated on sodium dodecyl sulfate–polyacrylamide gels (10% acrylamide). The proteins were then transferred to a nitrocellulose membrane (Amersham, Buckinghamshire, UK) by applying 100 V for 60 min using a plate electrode apparatus (Semi Dry Blotter II; Ken En Tec, Copenhagen, Denmark). The filters were blocked for 1 h in Tris-buffered saline Tween-20 (TBST) consisting of 0.2 mol/L NaCl, 0.2% Tween-20, and 10 mmol/L Tris (pH 7.4), containing 5% nonfat dry milk and 0.02% NaN_3. Subsequently, the filters were incubated with antibodies against Aurora B (Abcam; diluted 1:1,000) and β-actin (Biomakor, Rehovot, Israel; diluted 1:5,000) in TBST containing 5% milk. Finally, they were incubated in

anti-mouse or anti-rabbit IgG (Amersham; diluted 1:5,000) in TBST containing 2% milk. The filters were washed several times with TBST after each step. The bound antibodies were detected using an enhanced chemiluminescence system (Amersham).

Semiquantitative RT-PCR

To assess the mechanism of the expression, the messenger RNA (mRNA) of Aurora B was investigated using RT-PCR. The primers for Aurora B were determined using the GenBank database (http://www.ncbi.nlm.nih.gov/blast) and are listed below. Total RNA was isolated from the same seven tissues used in the Western blotting. RNA extraction and gene amplification have been described previously [22, 25]. Briefly, total RNA was extracted from a frozen tissue sample using the Strata-Prep total RNA Miniprep kit (Stratagene, La Jolla, CA, USA), according to the manufacturer's instructions. First-strand complementary DNA (cDNA) was generated by reverse transcription from 1 μg total RNA using the SuperScript III first-strand synthesis system (Invitrogen, Carlsbad, CA, USA), according to the manufacturer's instructions. Approximately, 50–100 ng cDNA was used for amplifying the Aurora B gene (primers, 5′-CCTGAG CACCCTGCCCCAGCGAG-3′ and 5′-GCAGCTCCTTG TAGAGCTCC-3′) and the internal control, the GAPDH gene (primers, 5′-TGATGACATCAAGAAGGTGGTGAA-3′ and 5′-TCCTTGGAGGCCATGTGGGCCAT-3′). The PCR conditions were 4 min at 94°C, 35 cycles for 60 s at 94°C, 30 s at 52°C, 80 s at 72°C, and a final 7 min extension at 72°C. The amplified products were resolved on 1.5% agarose–ethidium bromide gel electrophoresis.

Statistical analysis

The relationship between Aurora B and PHH3 (Ser^{10}) overexpression and between Aurora B expression and the various clinicopathological parameters were analyzed by Fisher's exact test, the χ^2 test or linear by linear association. Progression-free survival (PFS) was calculated from the date of surgery to the date of relapse or the date last seen, whereas overall survival (OS) was calculated from the date of diagnosis to the date of death or the date last seen. Survival curves were plotted using the Kaplan–Meier method [26]. Statistical differences in survival between the different groups were compared by the log-rank test and univariable Cox regression model [27]. Multivariate analysis (Cox proportion hazard model) with forward stepwise progression was used to analyze the role of clinicopathological parameters and Aurora B staining as prognostic factors [28]. Statistical analysis was performed using SPSS statistical software (Chicago, IL, USA). Statistical significance was set at $p<0.05$.

Results

Aurora B and phosphohistone H3 (Ser^{10}) are overexpressed in human ovarian cancer

Immunohistochemistry was carried out on 156 paraffin-embedded samples obtained at the time of primary surgery and compared with 15 normal ovarian tissue samples. Normal ovary was obtained from 15 women (mean age, 54±3.55; range, 31–58) who received hysterectomy and oophorectomy for uterine prolapse ($n=15$). We cut the surface area of normal ovary for Western bolt. Aurora B and (Ser^{10}) were found to express in the nucleus (Fig. 1c, e, and f). Fifty-three tumor samples (53/156, 34%), including 21 serous adenocarcinomas, two mucinous adenocarcinomas, 15 endometrioid adenocarcinomas, three clear cell adenocarcinomas, and 12 unclassified ovarian cancers, were associated with Aurora B overexpression, which is significantly higher than the negligible expression (0/15, 0%) found for the control group of 15 normal ovarian tissues ($p=0.006$; Fig. 1a). Sixty-one tumor samples (61/156, 39.1%) were associated with PHH3 (Ser-10) overexpression, which was significantly higher than the low expression (1/15, 6.7%) found in the control group of 15 normal ovarian tissues ($p=0.011$; Fig. 1d).

Aurora B overexpression is associated with various clinicopathological parameters, including histotypes, cell differentiation, and lymph node metastasis

We found that overexpression of Aurora B in high-grade serous carcinoma of the ovary was significantly higher than that in endometrioid carcinomas (8/13, 61.5% vs. 33/106, 31.1%, $p=0.033$ one-sided Fisher's exact test) and significantly higher than that in non-high-grade serous carcinomas (8/13, 61.5% vs. 15/49, 30.6%, $p=0.043$ one-sided Fisher's exact test). It is noteworthy that the mucinous adenocarcinoma gave an overall lower frequency of Aurora B overexpression (10.5%). We found that overexpression of Aurora B in poor and moderately differentiated carcinomas of the ovary was significantly higher than that in well-differentiated carcinomas of the ovary (53.6% vs. 28.2% vs. 10.0%, respectively, $p=0.02$, linear by linear association). Overexpression of Aurora B was also significantly higher in cases with lymph node metastasis (50.8% vs. 27.3%, $p=0.01$) and positive ascites cytology (44.4% vs. 20.0%, $p=0.008$).

Expression of Aurora B in tumor cells by Western blotting and RT-PCR

Western blotting showed a specific band for Aurora B at 41 kD (Fig. 2). The expression of the Aurora B protein was

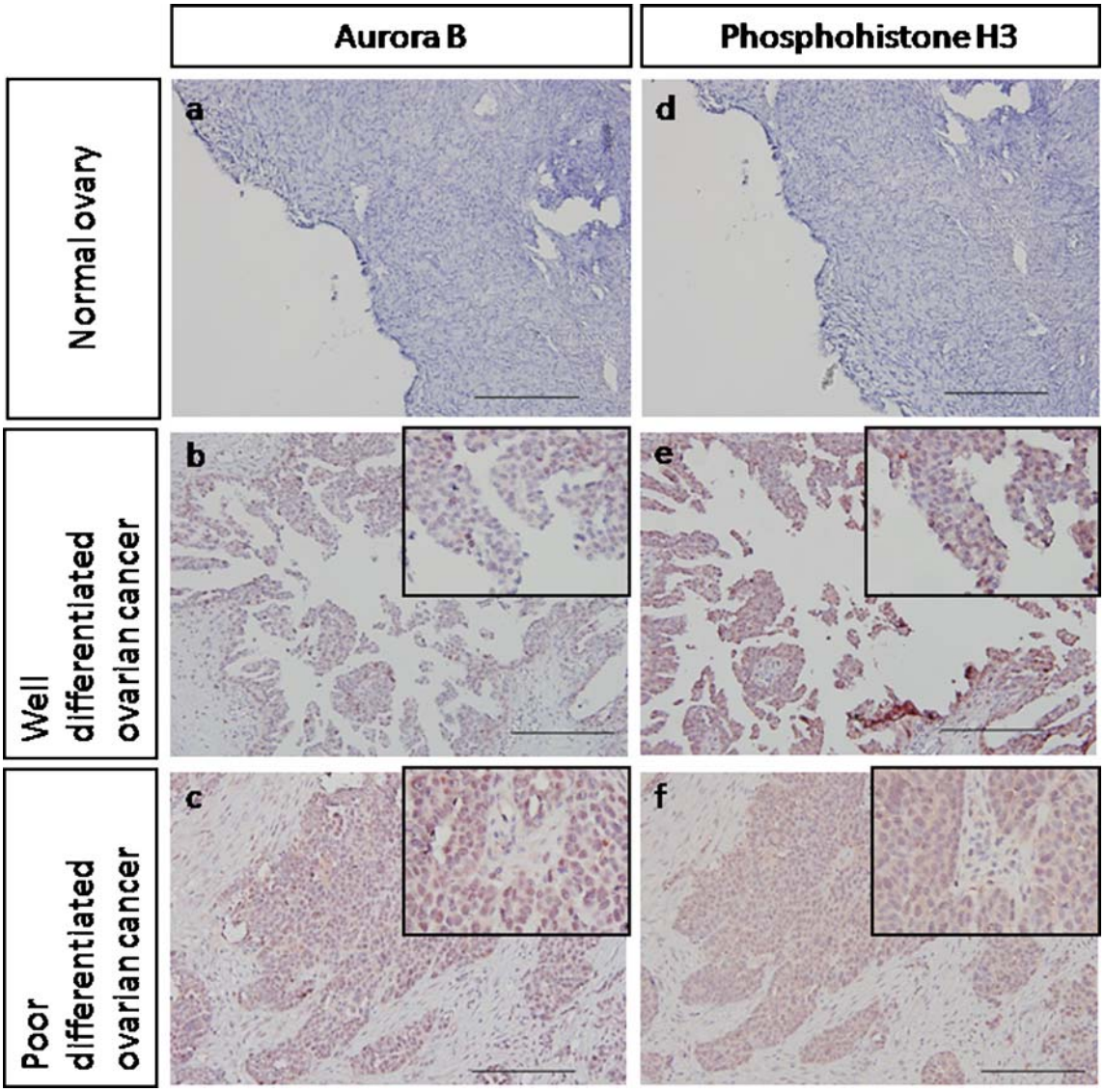

Fig. 1 Immunohistochemical staining for Aurora B and phosphohistone H3 (Ser[10]) in normal ovary and ovarian carcinoma. The normal ovarian epithelium exhibits negative staining of Aurora B (**a**). In the well-differentiated ovarian carcinomas, Aurora B-positive cells are sporadic in the tumor (**b**). In contrast, in poorly differentiated ovarian cancer, Aurora B-positive cells are present throughout the tumor (**c**). Expression patterns of Aurora B and phosphohistone H3 (Ser[10]) appear to be similar in serial sections of the same cases. **d**–**f** Original magnification, ×200; **b**, **c**, **e**, **f** higher magnification (×400) images are inserted. *Scare bars*, 100 μm

negative in all samples of normal ovarian tissue and was positive in all samples of the ovarian carcinoma tissue (case 3, endometrioid carcinoma; case 4, low grade serous carcinoma; case 5, endometrioid carcinoma; and cases 6 and 7, high grade serous carcinoma). The expression of the Aurora B protein was slightly increased in cases of well-differentiated carcinomas of the ovary and was markedly increased in all cases of poorly differentiated carcinomas of the ovary. These results are consistent with the immunohistochemical data on Aurora B for normal ovaries and for ovarian carcinoma.

The reverse transcriptase polymerase chain reaction studies showed a specific band of 209 bp for Aurora B (Fig. 2). The expression of Aurora B mRNA was increased in the carcinoma samples (n=5) compared to the normal ovary samples (n=2). In ovarian carcinoma, the mRNA expression of Aurora B was markedly increased in four cases but was very weak in the remaining case. Thus, Aurora B mRNA levels seem to be largely correlated with the protein expression levels.

Aurora B expression is associated with PHH3 (Ser[10]) expression

We next compared the expression of PHH3 (Ser[10]) with Aurora B expression in the ovarian cancer tissues. Expression patterns of PHH3 (Ser[10]) and Aurora B

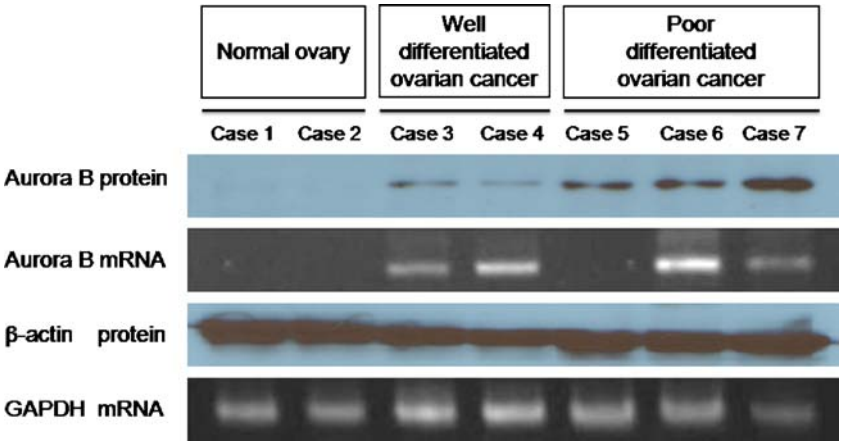

Fig. 2 Results of Western blotting and RT-PCR for Aurora B in normal ovary and epithelial ovarian cancer. Overexpression of Aurora B in epithelial ovarian cancer can be seen. Aurora B mRNA levels are largely correlated with protein levels (case 3, endometrioid carcinoma; case 4, low grade serous carcinoma; case 5, endometrioid carcinoma; cases 6 and 7, high grade serous carcinoma)

Table 2 Relationship of Aurora B expression and phosphohistone H3 and various clinicopathological factors in all patients with invasive ovarian carcinomas

	Aurora B positive cases	*p* value	Phosphohistone H3 (Ser-10) positive cases	*p* value
All case	53/156 (34.0%)		61/156 (39.1%)	
FIGO stage	142	0.169	142	0.130
I+II	17/57(29.8%)		17/57 (29.8%)	
III+IV	35/85(41.2%)		36/85 (42.4%)	
Histotype	156	0.130	156	0.164
Serous	21/53(39.6%)		20/53 (37.7%)	
Mucinous	2/19 (10.5%)		9/19 (47.4%)	
Endometrioid	15/49 (30.6%)		13/49 (26.5%)	
Clear	3/6 (50.0%)		3/6 (50%)	
Others	12/29 (41.3%)		16/29 (55.2%)	
Differentiation	77	0.02*	77	0.486
Well	1/10 (10.0%)		6/10 (60.0%)	
Moderate	11/39 (28.2%)		9/39 (23.1%)	
Poor	15/28 (53.6%)		15/28 (53.6%)	
Cytoreduction	128	0.799	128	0.554
Optimal	35/99 (35.4%)		35/99 (35.4%)	
Sub-optimal	11/29 (37.9%)		12/29 (41.4%)	
Ascites cytology	108	0.008*	108	0.247
Positive	28/63 (44.4%)		25/63 (39.7%)	
Negative	9/45 (20.0%)		13/45(28.9%)	
CA-125	96	0.306	96	0.006*
Positive	36/86 (41.9%)		37/86 (43.0%)	
Negative	2/10 (20%)		0/10 (0.0%)	
Lymph node Metastasis	116	0.01*	116	0.130
Positive	31/61 (50.8%)		26/61 (42.6%)	
Negative	15/55 (27.3%)		16/55 (29.1%)	
Phosphohistone H3 (Ser-10)	156	0.03*		
Positive	27/61 (44.3%)			
Negative	26/95 (27.4%)			

*$p<0.05$

appeared to be similar in serial sections of the same cases (Fig. 1). The overexpression of Aurora B was significantly higher in cases with PHH3 (Ser^{10}) overexpression (44.3% vs. 27.4%, $p=0.03$; Table 2).

Aurora B overexpression is associated with prognosis

OS follow-up data were available for 149 patients. There was no progression data for seven patients, so PFS data were available for 142 patients only. The median follow-up period was 1,073 days (range, 0–4,825 days). During this period, 77 (51.7%) patients died of the disease, and recurrence of the disease was observed in 77 (54%) cases.

Using univariate analysis, we found that the Aurora B overexpression group (median, 727 days, 95% confidence interval, 301–1,133) demonstrated a significantly shorter PFS than the Aurora B low expression group (median, 3,896 days) ($p=0.001$, log-rank statistic; Fig. 3a). The Aurora B overexpression group (median 1,418 days, 95% confidence interval, 836–2,000) also demonstrated a significantly shorter OS than the Aurora B low expression group (median, 2,482 days; 95% confidence interval, 1,233–3,731; $p=0.023$, log-rank statistic; Fig. 3b). Univariate Cox regression analysis for the variables of stage, high-grade serous carcinoma, optimal cytoreduction, and Aurora B was applied. Hazard ratios and p values are presented in Tables 3 and 4. Stage, high-grade serous carcinoma, suboptimal cytoreduction, and Aurora B were significantly correlated with poor PFS and OS. Finally, multivariate analysis using the Cox proportional hazards model was conducted, incorporating the variables of stage, high-grade serous carcinoma, optimal cytoreduction, and Aurora B. Both stage and suboptimal cytoreduction remained significant predictors of a poor PFS ($p<0.05$; Table 3). However, only the stage remained a significant predictor of OS in ovarian cancer (Table 4).

Using univariate analysis, high PHH3 (Ser^{10}) expression was not associated with poor PFS, with a median survival of 772 days vs. 1,353 days ($p=0.203$, log-rank statistic). Furthermore, high PHH3 (Ser^{10}) expression was not associated with poor OS, with a median survival of 1,492 vs. 1,780 days ($p=0.305$, log-rank statistic).

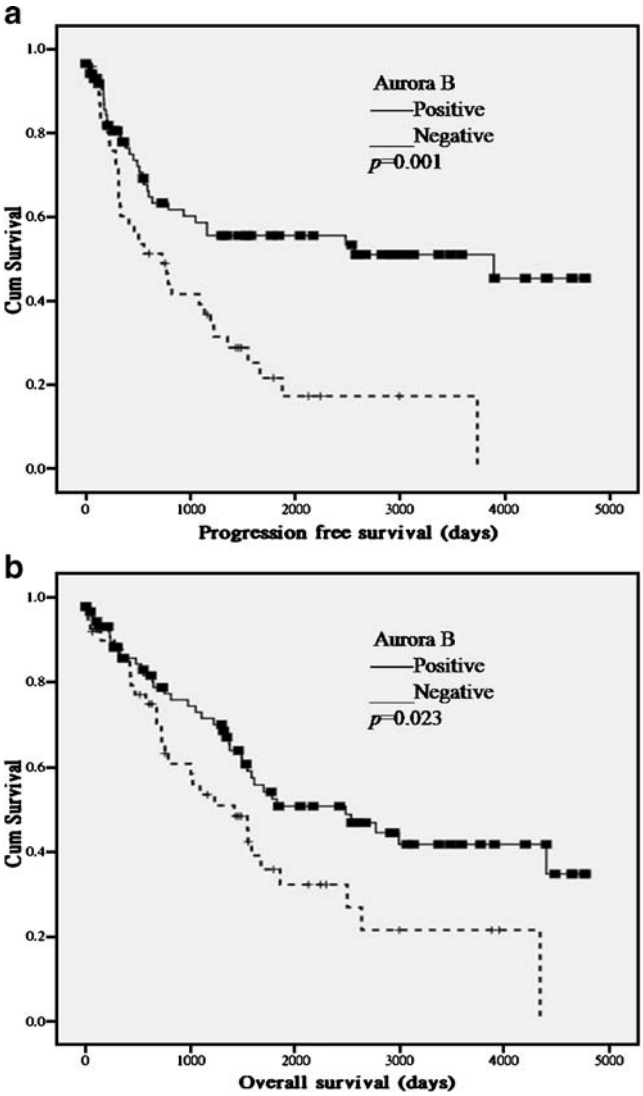

Fig. 3 Progression-free survival and overall survival curves for ovarian cancer according to Aurora B status. Survival curves were plotted using the Kaplan–Meier method. The Aurora B overexpression group (median, 727 days; 95% confidence interval, 301–1,133) demonstrated a shorter PFS than the Aurora B low expression group (median, 3,896 days; $p=0.001$, log-rank statistic; **a**). The Aurora B overexpression group (median, 1,418 days; 95% confidence interval, 836–2,000) also demonstrated a shorter overall survival than the Aurora B low expression group (median, 2,482 days; 95% confidence interval, 1,233–3,731; $p=0.023$, log-rank statistic; **b**)

Discussion

The key findings in this study are that Aurora B is much more frequently overexpressed in ovarian cancer than in normal ovaries and that the expression of Aurora B is related to epithelial ovarian cancer prognosis. Aurora B, a chromosome passenger protein that localizes to centromeres in early mitosis and then the spindle midzone in anaphase, is required for histone H3 phosphorylation, chromosome biorientation, the spindle assembly check point, and cytokinesis [29, 30]. Overexpression of Aurora B produces multinuclearity and increases ploidy; these are important factors during human cancer development [4, 6]. The serine 10 motif of histone H3, selectively phosphorylated in the G2/M phase of the cell cycle, is regulated by Aurora B kinase and is considered to have several important roles, including various ones in chromosome segregation [31–33]. However, the mechanism of histone H3 phosphorylation and the role of cell kinetics remain unclear. Since recent

Table 3 Univariate and multivariate Cox regression analysis of clinicopathological parameters and Aurora B status as predictors of progression-free survival in ovarian cancer patients

Variable	PFS			PFS		
	Univariate			Multivariate		
	HR	95% CI of HR	*p* value	HR	95% CI of HR	*p* value
Aurora B	2.195	1.365–3.531	0.001	1.160	0.600–2.244	0.695
Stage	2.767	2.011–3.806	<0.001	2.884	1.901–4.377	<0.001
High grade serous carcinoma	2.516	1.197–5.286	0.015	2.057	0.872–4.851	0.099
Optimal cytoreduction	0.327	0.189–0.266	<0.001	0.446	0.214–0.927	0.031

HR hazard ratio

studies have identified histone H3 protein as an important substrate of Aurora B kinase [34], nuclear localization of Aurora B is functionally important. Our immunostaining analysis showed a high PHH3 (Ser^{10}) index in ovarian cancers compared with non-cancerous tissue. This result suggests that the increased phosphorylation of histone H3 might have effects on the malignant transformation of ovarian epithelial cells and could act as a molecular marker reflecting carcinogenesis in ovarian cancer. Our study showed a correlation between PHH3 and Aurora B expression immunohistochemically Using immunohistochemical analysis of a large series of tumors, we showed frequent expression of Aurora B and PHH3 (Ser^{10}) in ovarian cancer samples, whereas normal ovarian tissue was negative for this phenomenon. Our study also showed a correlation between Aurora B and PHH3, a mitosis marker, immunohistochemically. This result is in agreement with those of other studies [35, 36]. Taken together, our findings also suggest a role for Aurora B and PHH3 (Ser^{10}) as tumor markers in ovarian cancer.

Our study also showed that Aurora B expression increases as tumor differentiation decreases. This observation is supported by previous findings where Aurora B expression inversely correlated with the degree of differentiation of other types of tumor, including colon cancer [19], hepatocellular carcinoma [10], prostate cancer [14], endometrial cancer [15], and thyroid carcinoma [8]. More recently, a well-designed study by Kulkarni and colleagues [16] showed that there was a significant correlation between Aurora B and tumor progression with epithelial ovarian cancer. We suggest that Aurora B may be involved in the development of malignant phenotypes, such as poor differentiation or multinuclear cells [6]. In this context, the mechanisms by which Aurora B has been proposed to promote tumor progression are loss of mitotic control and abnormal proliferation [6, 8, 15].

In the present study, we also found that Aurora B expression was strongly associated with lymph node metastasis in ovarian cancer. These observations are supported by previous findings that Aurora B expression is correlated with lymph node metastasis of other types of tumors, including oral cancer [37]. The detailed mechanism of metastasis caused by Aurora B overexpression is still unknown. In the future, we will examine the correlation between Aurora B overexpression and migration or invasion by ovarian cancer cells.

Overexpression of Aurora B has been related to a poor prognosis in recent reports of endometrial carcinoma and lung cancer [12, 15]. In our study, among the biomarkers tested, only Aurora B could predict the prognosis of the ovarian cancer patients. However, multivariate analysis failed to show that expression of Aurora B is an independent prognostic factor. This is due partly to the highly significant associations between the biomarkers and tumor grade and stage, making it difficult to separate its independent effects. Furthermore, Aurora B is an effective predictor of aggressive epithelial ovarian carcinoma in terms of differentiation and metastasis in our result. Thus, the immunohistochemistry of Aurora B provides significant information that cannot be obtained from staging alone.

The possible mechanism of an Aurora B-induced poor prognosis is probably through the phosphorylation of

Table 4 Univariate and multivariate cox regression analysis of clinicopathological parameters and Aurora B status as predictors of overall survival in ovarian cancer patients

Variable	OS			OS		
	Univariate			Multivariate		
	HR	95% CI of HR	*p* value	HR	95% CI of HR	*p* value
Aurora B	1.726	1.071–2.780	0.025	1.073	0.576–2.001	0.824
Stage	3.112	2.180–4.441	<0.001	3.800	2.375–6.080	<0.001
High grade serous	2.220	1.061–4.647	0.034	1.554	0.686–3.520	0.290
Optimal cytoreduction	0.368	0.217–0.625	<0.001	0.838	0.432–1.625	0.601

HR hazard ratio

histone H3, a direct impact on the process of ovarian carcinogenesis, or a high proliferation rate. Thus, the molecular effects of Aurora B on cancer prognosis are not completely clear. In future study, we will compare Aurora B and Ki67 staining to try to more clearly study this possibility. The limitation of our work was that we were using a non-quantitative methodology of RT-PCR to investigate the mRNA of Aurora B in only five carcinoma samples. Although this result needs further validation, our findings might be important for the clinical management of these patients.

Another limitation of our study is that we do not perform microdissection to collect the epithelial component of normal ovary. Even though we cut the surface area of normal ovary for Western bolt, but the ovary tissue still contain some stroma. It is possible to dilute the expression of Aurora B in the epithelium of normal ovary. However, these results for Western blot are consistent with the immunohistochemical data on Aurora B for normal ovaries.

In conclusion, Aurora B expression was well correlated with differentiation, metastasis, PFS, and OS in epithelial ovarian carcinoma. The study shows its value as a clinical relevant marker and as a potential therapeutic target for human ovarian cancer.

Authors' contributions Yi-Jen Chen carried out immunohistochemical staining, performed the statistical analysis, and drafted the manuscript. Chun-Ming Chen carried out the RT-PCR, Western blot and drafted the manuscript. Chiung-Ru Lai assessed the pathological specimens and evaluated the immunohistochemical score. Nae-Fang Twu, Ming-Shyen Yen, Hua-Hsi Wu, and Peng-Hui Wang participated in the design of the study and provided patients' data. Chiou-Chung Yuan conceived of the study and participated in its design and coordination. All authors read and approved the final manuscript.

Acknowledgments We thank Ching-Fen Yang for her evaluation of the immunohistochemical score. We appreciate Professor Ralphy Kirby's help in improving the style of written English. We thank Dr. Muh-Hwa Yang for his involvement in revising the manuscript. We are grateful for the assistance of Miss Tsui-Ying Huang in completing the RT-PCR and Western blots. This research was supported, in part, by grant 96-VGH-B1-010 from Veterans General Hospital and by a grant from the Ministry of Education "Aim for the Top University" Plan. This study was also supported by research grants from Yen-Tjing-Ling Medical Foundation (CI-97-6).

Conflict of interest statement We declare that we have no conflict of interest.

References

1. NCI Surveillance, E.a.E.R.S.P.a.t.N.C.f.H.S. National Cancer Institute—a snapshot of ovarian cancer: incidence and mortality rate trends 2006 Sep. http://planning.cancer.gov/disease/ovarian-snapshot.pdf
2. Hoskins WJ, Perez CA, Young RC (2000) Principles and practice of gynecologic oncology. Lippincott Williams and Wilkins, Philadelphia, pp 1005–1007
3. Adams RR, Carmena M, Earnshaw WC (2001) Chromosomal passengers and the (Aurora) ABCs of mitosis. Trends Cell Biol 11:49–54
4. Tatsuka M, Katayama H, Ota T et al (1998) Multinuclearity and increased ploidy caused by overexpression of the aurora- and Ipl1-like midbody-associated protein mitotic kinase in human cancer cells. Cancer Res 58:4811–4816
5. Kaitna S, Pasierbek P, Jantsch M et al (2002) The aurora B kinase AIR-2 regulates kinetochores during mitosis and is required for separation of homologous chromosomes during meiosis. Curr Biol 12:798–812
6. Ota T, Suto S, Katayama H et al (2002) Increased mitotic phosphorylation of histone H3 attributable to AIM-1/Aurora-B overexpression contributes to chromosome number instability. Cancer Res 62:5168–5177
7. Murata-Hori M, Wang YL (2002) Both midzone and astral microtubules are involved in the delivery of cytokinesis signals: insights from the mobility of aurora B. J Cell Biol 159:45–53
8. Sorrentino R, Libertini S, Pallante PL et al (2005) Aurora B overexpression associates with the thyroid carcinoma undifferentiated phenotype and is required for thyroid carcinoma cell proliferation. J Clin Endocrinol Metab 90:928–935
9. Katayama H, Ota T, Jisaki F et al (1999) Mitotic kinase expression and colorectal cancer progression. J Natl Cancer Inst 91:1160–1162
10. Sistayanarain A, Tsuneyama K, Zheng H et al (2006) Expression of Aurora-B kinase and phosphorylated histone H3 in hepatocellular carcinoma. Anticancer Res 26:3585–3593
11. Ulisse S, Delcros JG, Baldini E et al (2006) Expression of Aurora kinases in human thyroid carcinoma cell lines and tissues. Int J Cancer 119:275–282
12. Hayama S, Daigo Y, Yamabuki T et al (2007) Phosphorylation and activation of cell division cycle associated 8 by aurora kinase B plays a significant role in human lung carcinogenesis. Cancer Res 67:4113–4122
13. Remmele W, Schicketanz KH (1993) Immunohistochemical determination of estrogen and progesterone receptor content in human breast cancer. Computer-assisted image analysis (QIC score) vs subjective grading (IRS). Pathol Res Pract 8:227–245
14. Chieffi P, Cozzolino L, Kisslinger A et al (2006) Aurora B expression directly correlates with prostate cancer malignancy and influence prostate cell proliferation. Prostate 66:326–333
15. Kurai M, Shiozawa T, Shih HC et al (2005) Expression of Aurora kinases A and B in normal, hyperplastic and malignant human endometrium: Aurora B as a predictor for poor prognosis in endometrial carcinoma. Hum Pathol 36:1281–1288
16. Kulkarni AA, Loddo M, Leo E et al (2007) DNA replication licensing factors and aurora kinases are linked to aneuploidy and clinical outcome in epithelial ovarian carcinoma. Clin Cancer Res 13:6153–6161
17. Hendzel MJ, Wei Y, Mancini MA et al (1997) Mitosis-specific phosphorylation of histone H3 initiates primarily within pericentromeric heterochromatin during G2 and spreads in an ordered fashion coincident with mitotic chromosome condensation. Chromosoma 106:348–360
18. Kim YJ, Ketter R, Steudel WI et al (2007) Prognostic significance of the mitotic index using the mitosis marker anti-phosphohistone H3 in meningiomas. Am J Clin Pathol 128:118–125
19. Rosai J (2004) Ackerman's surgical pathology, 9th edn. Mosby, St. Louis
20. Köbel M, Kalloger SE, Boyd N et al (2008) Ovarian carcinoma subtypes are different diseases: implications for biomarker studies. PLoS Med 5:e232
21. Soslow RA (2008) Histologic subtypes of ovarian carcinoma: an overview. Int J Gynecol Pathol 27:161–174
22. Lee EC, Frolov A, Li R et al (2006) Targeting Aurora kinases for the treatment of prostate cancer. Cancer Res 66:4996–5002

23. Remmele W, Schicketanz KH (1993) Immunohistochemical determination of estrogen and progesterone receptor content in human breast cancer. Computer-assisted image analysis (QIC score) vs. subjective grading (IRS). Pathol Res Pract 189:862–866
24. Twu NF, Yuan CC, Yen MS et al (2009) Expression of aurora kinase A and B in normal and malignant cervical tissue: high Aurora A kinase expression in squamous cervical cancer. Eur J Obstet Gynecol Reprod Biol 142:57–63
25. Chen CM, Behringer RR (2004) Ovca1 regulates cell proliferation, embryonic development, and tumorigenesis. Genes Dev 18:320–332
26. Kaplan E, Meyer P (1958) Non parametric estimation from incomplete observations. J Am Stat Assoc 53:457–481
27. Altman DG, Lausen B, Sauerbrei W et al (1994) Dangers of using "Optimal" cut points in the evaluation of prognostic factors. J Natl Cancer Inst 86:829–835
28. Cox DR (1970) Analysis of binary data. Methuen, London
29. Andrews PD, Knatko E, Moore WJ et al (2003) Mitotic mechanics: the Auroras come into view. Curr Opin Cell Biol 15:672–683
30. Ruchaud S, Carmena M, Earnshaw WC (2007) The chromosomal passenger complex: one for all and all for one. Cell 131:230–231
31. Hsu JY, Sun ZW, Li X et al (2000) Mitotic phosphorylation of histone H3 is governed by Ipl1/aurora kinase and Glc7/PP1 phosphatase in budding yeast and nematodes. Cell 102:279–291
32. Hendzel MJ, Wei Y, Mancini MA et al (1997) Mitosis-specific phosphorylation of histone H3 initiates primarily within pericentromeric heterochromatin during G2 and spreads in an ordered fashion coincident with mitotic chromosome condensation. Chromosoma 106:348–360
33. Wei Y, Yu L, Bowen J et al (1999) Phosphorylation of histone H3 is required for proper chromosome condensation and segregation. Cell 97:99–109
34. Wheatley SP, Barrett RM, Andrews PD et al (2007) Phosphorylation by aurora-B negatively regulates survivin function during mitosis. Cell Cycle 6:1220–1230
35. Jacobberger JW, Frisa PS, Sramkoski RM et al (2008) A new biomarker for mitotic cells. Cytometry A 73:5–15
36. Kim YJ, Ketter R, Steudel WI et al (2007) Prognostic significance of the mitotic index using the mitosis marker anti-phosphohistone H3 in meningiomas. Am J Clin Pathol 128:118–125
37. Qi G, Ogawa I, Kudo Y et al (2007) Aurora-B expression and its correlation with cell proliferation and metastasis in oral cancer. Virchows Arch 450:297–302

Virchows Arch (2009) 455:441–448
DOI 10.1007/s00428-009-0846-3

ORIGINAL ARTICLE

Localization of indoleamine 2,3-dioxygenase in human esophageal squamous cell carcinomas

Jinzhong Liu · Gaofeng Lu · Fuai Tang · Yiqing Liu · Guanglin Cui

Received: 14 July 2009 / Revised: 8 September 2009 / Accepted: 5 October 2009 / Published online: 21 October 2009

Abstract Immunosuppressive factors derived from the tumor and nontumor cells present in the tumor microenvironment contribute to tumor escape from host immune attack. Recently, the tryptophan-catabolizing enzyme indoleamine 2,3-dioxygenase (IDO) derived from both the tumor cells and surrounding nontumor cells was found to function as a critical immunosuppressive factor. While the expression of IDO is intensively under investigation in many types of cancers, little information is available in esophageal squamous cell carcinomas (ESCC) thus far. In this study, we have therefore investigated the cellular localization of IDO in 45 ESSCs and ten morphologically normal esophageal tissues; the correlation of IDO with clinicopathological parameters was also analyzed. Immunohistochemistry (IHC) analysis revealed that the density of IDO-positive cells was increased in ESCCs relative to controls ($P<0.01$). These cells were distributed as clusters and formed a patchy pattern in both the cancerous epithelium and the surrounding noncancerous cells. Double IHC further confirmed that many IDO-positive cells in the tumor stroma were smooth-muscle-actin-alpha-positive myofibroblasts, CD68-positive macrophages, and S100-positive dendritic cells. Statistical analysis showed that the densities of IDO-positive cells were not significantly correlated with tumor clinical parameters (tumor invasion depth, node metastasis, and TNM stages) and lymphocytic infiltration. Our current findings suggested that the increased IDO expression in ESCCs is from a mixed cellular source (both cancer cells and noncancerous cells). Further studies on immune cell functional analysis are required in the future.

Keywords Immunosuppression · Carcinoma · Esophagus

Abbreviations

IDO	Indoleamine 2,3-dioxygenase
IHC	Immunohistochemistry
ESCC	Esophageal squamous cell carcinoma

Introduction

Esophageal cancer is a highly aggressive lethal malignancy worldwide with regional variations in incidence [1–3]. Asian countries have a high incidence, and the predominant histological type of esophageal cancers is esophageal squamous cell carcinoma (ESCC), which is in contrast with the reports from Western counties that a high incidence of esophageal adenocarcinoma was found. Our location (Henan Province, North China) has been reported to have the highest incidence of esophageal cancer in the world [2], and ESCC accounts for over 90% cases. In our

J. Liu
Department of Pathology,
The Fourth Affiliated Hospital of Zhengzhou University,
Zhengzhou, Henan, China

G. Lu · F. Tang · Y. Liu · G. Cui
Department of Medicine,
The Second Affiliated Hospital of Zhengzhou University,
Zhengzhou, Henan, China

G. Cui
Laboratory of Gastroenterology,
Institute of Clinical Medicine, University of Tromsø,
9037 Tromsø, Norway

G. Cui (✉)
Department of Gastroenterology,
The Second Affiliated Hospital of Zhengzhou University,
Zhengzhou 450014 Henan Province, China
e-mail: guanglin.cui@yahoo.com

Table 1 Basic clinicopathological information of ESCC patients

	Number	Tumor invasion			Lymph node involvement		Metastasis		TNM stages		
		T1	T2	T3	N0	N1	M0	M1	I	II	III
ESCC	45	1	9	35	35	10	45	0	1	34	10

province, over the past 40 years, there has been a strong attempt to make an early diagnosis for patients with ESCC, since an improved prognosis is heavily dependent on the disease stage. Unfortunately, the metastasis is often observed at the time of diagnosis, and curative surgery becomes impossible in many patients with ESCC. The prognosis is still very poor.

To seek potential therapeutic strategies for these ESCC patients with metastasis, a better understanding of the mechanisms of tumor cell growth control and progression is necessary. Several lines of evidence suggest that tumor cells can grow by escaping from the host immune system control and the malignant potential is significantly influenced by host immunity. One of the tumor's abilities to escape immune attack is to inhibit antitumor immunity by producing immunosuppressive factors [4, 5]. Indeed, a growing body of evidence has suggested that a variety of immunosuppressive factors derived from the tumor cells and surrounding cells contribute to the establishment of regional immunosuppressive networks in patients with ESCC [6–9]. Recently, indoleamine 2,3-dioxygenase (IDO), an intracellular enzyme that catalyzes the initial and rate-limiting steps in the metabolism of the essential amino acid tryptophan along the kynurenine pathway, is found to be increased and functions as a critical immunosuppressive factor in many types of human cancers [10–18]. However, little information is available concerning the expression of IDO in ESCC. The first study concerning IDO expression in patients with ESCC was reported by Sakurai et al. [19]. They showed that the mRNA level of IDO was remarkably increased in either the cancerous tissue or blood as compared with the controls. Furthermore, their statistical analysis suggested that the ESCC patients with higher levels of IDO expression had a worse survival rate than the IDO expression group with lower levels. It has been demonstrated that a variety of cells in the tumor microenvironment contribute to the IDO expression; IDO immunoreactivity is identified in both the cancer cells and the surrounding noncancerous cells (i.e., macrophages and dendritic cells) in many types of cancers [12, 20–22]. However, the phenotypic analysis of IDO expression in ESCCs is still lacking. In this study, we therefore investigated the cellular expression pattern of IDO in the tumor microenvironment and analyzed whether the IDO-positive cell density influenced the clinicopathological features in patients with ESCCs.

Materials and methods

Tissue specimens from ESCCS and controls

Forty-five surgical ESCC paraffin blocks tracked from the tissue bank in the Departments of Pathology, the Fourth Affiliated Hospital of Zhengzhou University, between August 2003 and November 2008 were included in the study according to the guidelines of the protocols approved by the institutional review board. There were 28 men and 17 women ranging in age from 32 to 76 years. The tumor location was in the upper third in seven patients, in the middle third in 25 patients, and in the lower third in 13 patients (for other information, see Table 1). None of the ESCC patients received immunomodulatory therapy, chemotherapy, or radiotherapy before surgery. Ten morphological normal esophageal mucosa without pathological evidence taken by endoscopy examinations served as controls (male/female 7/3; age 26–76 years; three were taken from upper third, four from middle third, and three from lower third esophagus).

Immunohistochemical examination of IDO and tumor-associated lymphocyte expression in the tumor microenvironment

Immunohistochemistry (IHC) was performed in 4-μm sections with Vectastatin Elite Universal ABC-HRP kits (Vector Lab., Burlingame, CA, USA) according to the manufacturer's instructions and our published methods [23, 24]. Antigen retrieval was achieved by incubating the

Fig. 1 Examination of the IDO expression patterns in the tissues of ESCCs by single IHC and DIHC. IDO-positive cells were only observed in low density in the control mucosa **a**), but they were present as cluster and formed a patchy distribution pattern with a high density in ESCC epithelium **b**) and surrounding noncancerous cells **c**). In tumor stroma, many of them had fibroblast morphological features (**d**), leukocytes (**e**), and microvessels (**f**). DIHC further confirmed that those IDO-positive surrounding noncancerous cells (*brown* in **g**, **h**, **i**) were myofibroblasts (*red color*, labeled by SMA-alpha in **g**), macrophages (*red color*, labeled by CD68 in **h**), and dendritic cells (*red color*, labeled by S100 in **i**). (**a**–**c**, single IHC, counterstained with hematoxylin, original magnification ×200; **d**–**f**, single IHC, counterstained with hematoxylin, original magnification ×400; **g**–**i**, DIHC, without nuclear counterstaining, original magnification ×400)

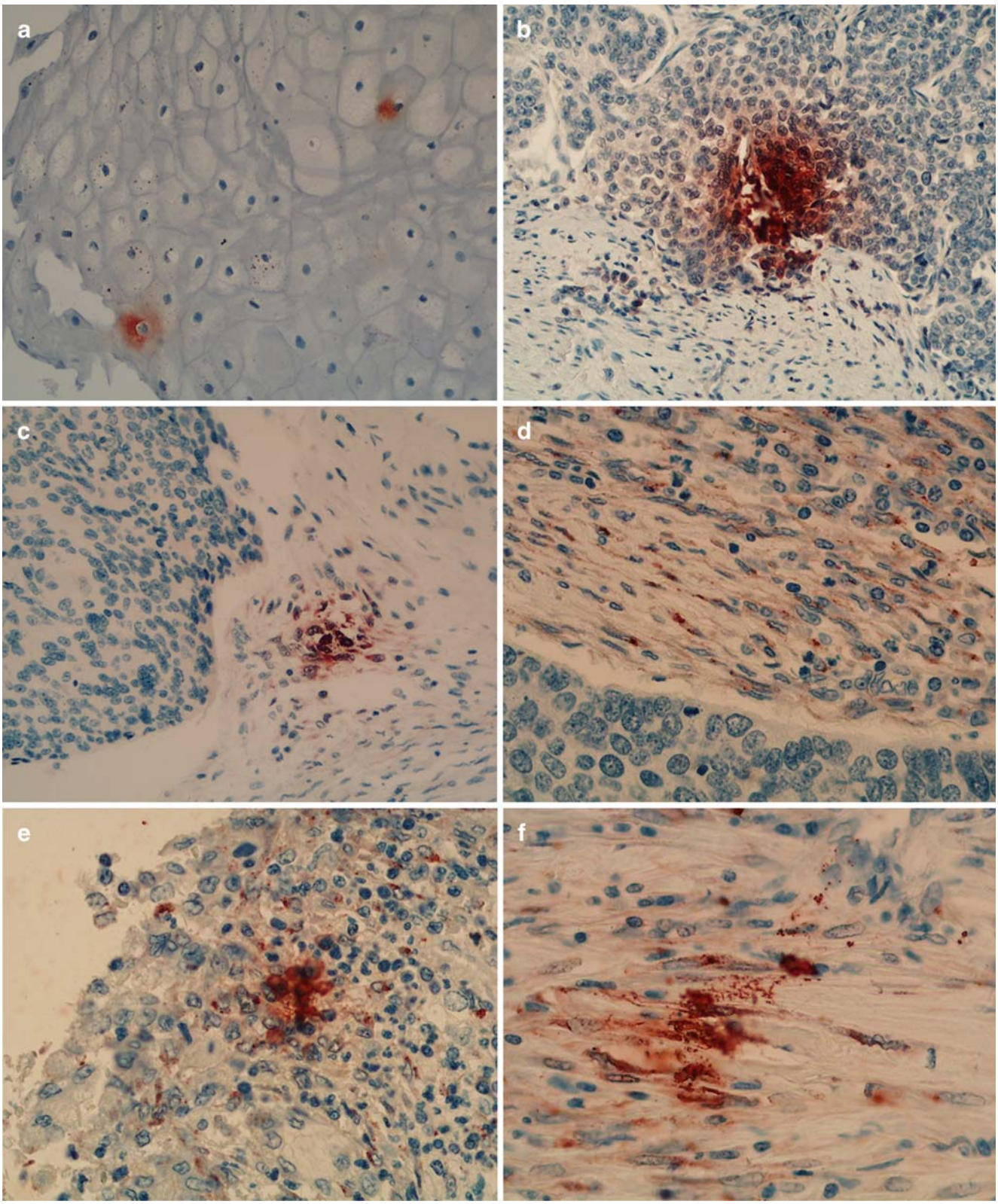

sections with ready-to-use Proteinase K solution (Dako, Carpinteria, CA, USA) for 10 min (for IDO IHC) or boiling sections in 0.01 M sodium citrate buffer (pH 6.0) through microwave processing for 15 min (for CD3 IHC), respectively. Then, the sections were incubated with the mouse anti-human IDO monoclonal antibody (working dilution 1:400, Oriental Yeast Co., Ltd., Tokyo, Japan) or anti-CD3 polyclonal antibody (1:50; Dako, Carpinteria, CA, USA)

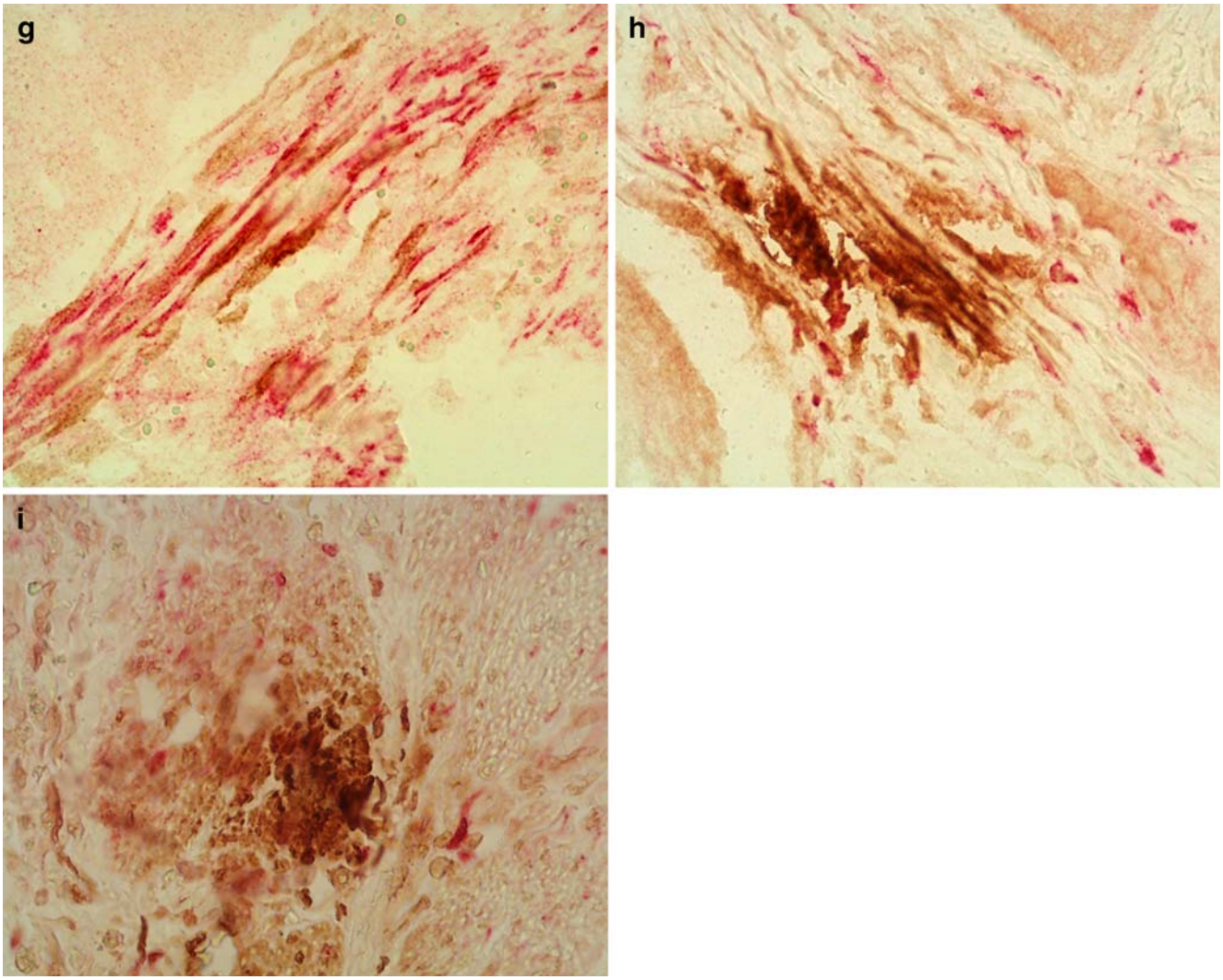

Fig. 1 (continued)

overnight at 4°C. 3-Amino-9-ethylcarbazole (Vector Laboratories, Burlingame, CA, USA) was used as chromogen and Mayer's hematoxylin as the counterstain. The negative control slides were performed routinely: (1) primary antibodies were substituted with the isotype-matched control antibodies; (2) secondary antibody was substituted with phosphate-buffered saline.

Double immunohistochemical identification of cellular phenotypes of IDO in the surrounding noncancerous cells

Since the expression of IDO in cancer cells was easily identified by the specific morphological features, here, we have only examined the cellular phenotypes of IDO in the tumor stromal cells. Double IHCs (DIHCs) were performed using EnVision G72 Doublestain System kit (Dako Demark, Glostrup, Denmark) with antibodies IDO/smooth muscle actin (SMA) alpha (to label myofibroblasts), IDO/CD68 (to label macrophages), and IDO/S100 (to label dendritic cells; monoclonal anti-SMA-alpha, anti-CD68, and anti-S100 antibodies were all purchased from Dako, Carpinteria, CA, USA) according to the manufacturer's instructions and the method described in our publications [25, 26]. In brief, the slides were incubated for 30 min with anti-IDO antibody after antigen retrieval and then incubated with labeled polymer–horseradish peroxidase–antimouse and antirabbit antibodies for 10 min at room temperature. Peroxidase activity was detected with the enzyme substrate 3,3′-diaminobenzidine tetrachloride. After quenching the enzyme reaction, the slides were incubated in Doublestain Block at room temperature for 4 min to block endogenous phosphates. The slides were then incubated with anti-S100, anti-CD68, and anti-SMA-alpha antibodies individually for 15 min at room temperature. After washing, the slides were incubated with rabbit/mouse link

for 10 min and then labeled with polymer–alkaline phosphates antimouse and antirabbit antibodies for 10 min. *Permanent Red* substrate solution was used for the visualization.

Morphometric evaluation

Since the numbers of IDO-positive cells in ESCCs were much lower than in other types of human cancers [10, 13, 15, 20, 27, 28], we used an absolute quantitative method for the IDO-positive density evaluation. The cells with IDO immunoreactivity were counted in malignant epithelium, intratumor stroma, and stroma in invading edges in at least five optical high-power magnification fields (×400) with abundant distribution from each slide. CD3-positive lymphocytes were scored according to the method described in our previous publication [29]. The average values per slide were used for statistical analysis.

Statistical analysis

Results were expressed as mean ± standard error of the mean unless otherwise stated. For statistical analysis of data, the Mann–Whitney tests were used. The level of significance was defined as $P<0.05$.

Results

The expression pattern of IDO in the tumor microenvironment of ESCC

In normal esophageal tissue sections, faint IDO immunoreactivity was occasionally observed in mucosal cells (Fig. 1a; normal controls taken by endoscopic forceps had little stroma; therefore, we could only describe the expression of IDO in mucosal cells). In contrast to the normal controls, the ESCC sections showed intense immunoreactivity for IDO in the cancer epithelium (Fig. 1b) and in the surrounding noncancerous stromal cells as well (Fig. 1c). Most IDO-positive cells were present as clusters and formed a patchy distribution pattern in the cancer epithelium and tumor stroma (Fig. 1b, c). IDO-positive cells in the tumor stroma had various morphological features; many of them were fibroblasts (Fig. 1d), and some were leukocytes (Fig. 1e) and microvessels (Fig. 1f). The intensity of IDO immunoreactivity in tumor cells (Fig. 1b), stromal immune cells (Fig. 1e), and microvessels (Fig. 1f) was stronger than that in fibroblasts (Fig. 1d). Increased IDO expression was confirmed by IDO-positive cell quantification, which showed a significant increase in IDO-positive cell density in the tumor microenvironment as compared with the normal mucosa (see Fig. 2). A particular high density of IDO-positive cells was demonstrated in the invading edges of ESCCs (see Fig. 2). In addition, the IDO-positive cell densities in the compartments of cancer epithelium and tumor stroma were significantly higher than that in the adjacent noncancerous epithelium and nontumor stroma (ESCC vs. adjacent mucosa 0.83±0.23 per field vs. 1.83±0.83 per field, $P\leq0.01$; ESCC tumor stroma vs. adjacent nontumor stroma 3.97±0.73 per field vs. 0.90±0.72 per field, $P\leq0.05$).

The influence of the total IDO-positive cell density on the clinicopathological features in patients with ESCCs was analyzed. The results showed that total IDO-positive cell densities were not significantly correlated with tumor invasion depth, node metastasis, and TNM stages (see Table 2). In addition, statistical analysis showed that the density of CD3-labeled lymphocytes in patients with high IDO cell density (≥10 per field) and with low IDO cell density (≤10 per field) was not different (low IDO cell group vs. high IDO cell group 2.33±0.16 per field vs. 2.59±0.17 per field, $P\geq0.05$).

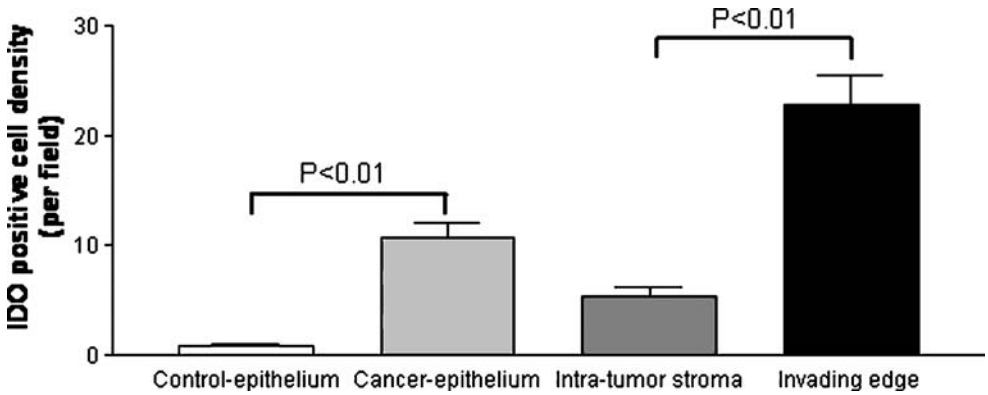

Fig. 2 Graphic analysis of IDO-positive cell densities in ESCCs. The IDO-positive cell density was significantly increased in the ESCC cancer epithelium (*light gray bar*) as compared with the controls (*white bar*); a particular high IDO-positive cell number was observed in the invading edges of ESCCs (*black bar*) as compared with the intratumoral stroma (*dark gray bar*). (The Mann–Whitney test was used for the statistical analysis)

Table 2 The correlation of the total IDO-positive cell density with clinicopathological factors

Factors	Total IDO cell density (field)	*P*
Tumor invasion depth		
T1/T2	12.92±3.66	>0.05
T3	15.25±1.97	
Lymph node involvement		
N0	14.91±1.87	>0.05
N1	18.83±5.37	
TNM stage		
I/II	14.50±1.88	>0.05
III	19.76±4.82	

Cellular phenotypes of IDO in the tumor stroma

The expression of IDO in cancer cells and microvessels can be easily identified by their specific morphological features. However, to identify IDO expression in immune cells (dendritic cells and macrophages) and myofibroblasts in the tumor stroma, DIHCs with specific antibodies (IDO/CD68, IDO/CD, and IDO/SMA alpha) need to be performed. The DIHC results revealed that IDO immunoreactivity could be frequently observed in SMA-alpha-positive myofibroblasts (Fig. 1g), CD68-positive macrophages (Fig. 1h), and S100-positive dendritic cells (Fig. 1i) in the tumor stroma.

Discussion

Immunosuppressive factors derived from the tumor microenvironment play a major role in extending immune escape and facilitating cancer progression. Since the study of Uyttenhove et al. showed that IDO expressed by the tumor cells have an immunoregulatory effect and reduce antitumor T cell attack in a marine tumor model [30], growing evidence from many studies carried out in different human cancers has demonstrated that IDO is expressed by both the tumor cells and nontumor cells in the tumor microenvironment [17]. In the present study, we revealed an increased IDO-positive cell density in the tumor microenvironment of ESCCs and identified that IDO is expressed by tumor cells and many types of cells in the tumor stroma.

IDO is an intracellular enzyme that catalyzes the initial and rate-limiting steps in the metabolism of the essential amino acid tryptophan along the kynurenine pathway [31]. Accumulated evidence has suggested that IDO could be a critical immunosuppressive factor and play an important role in inducing immune tolerance [32, 33]. Our present study has observed an increased number of IDO-positive cells in the microenvironment of ESCCs; these cells were both tumor cells and surrounding noncancerous stromal cells. Quantitative results showed that the IDO-positive cells were ~8 per field in the cancer epithelium and ~5 per field at the site of tumor stroma between cancer epithelium but significantly more common at the site of invading edges (~19 per field). As compared with the reported IDO densities in other types of human cancers [10, 13, 15, 20, 27, 28], IDO-positive cell density in the present study was lower. However, the IDO-positive cell densities were still significantly higher in ESCCs than in controls (see Fig. 2; $P \leq 0.01$). Sakurai et al. have reported that elevated IDO mRNA was found in ESCCs [19]. It is most likely that such increased IDO cell density may represent an increased IDO expression in the tumor microenvironment. In agreement with the findings of Sakurai et al., we also showed that the density of IDO-positive cells did not correlate to tumor invasion, lymph node metastasis, or TNM stage (all $P \geq 0.05$), although the IDO-positive cell densities are slightly increased, paralleling the degree of increase of these parameters. This may be because many factors released from the tumor cells and stroma cells participate in immunosuppression, and IDO only induces immunosuppression to a certain degree [34]. Since the ESCC samples in our study were procured very recently, survival follow-up analysis is not yet available. To further examine IDO-positive cell's prognostic significance, long-term follow-up and large sample studies will be required in the future.

Increased infiltration of immune cells and activated fibroblasts in the tumor stroma is one of the common histological features in ESCCs [35–38]. These cells in the tumor stroma may function as a double-edged sword because they play an important role in both the anticancer response [39, 40] and in favoring cancer progression in some certain conditions [26, 41, 42]. By both the quantitative and qualitative techniques, IDO has been found to be expressed by many types of cells in the tumor microenvironment including tumor cells, fibroblasts, endothelial cells (microvessels), dendritic cells, and macrophages in various cancers [12, 20, 43, 44]. In line with those studies, we were also able to observe IDO immunoreactivity in ESCCs in many types of stromal cells including microvessels, immune cells, and fibroblasts by single IHCs and DIHCs with specific antibodies (see Fig. 1). Those findings suggest that the IDO in ESCCs is most likely from a mixed cellular source, and tumor stroma is an active participant in local immunoregulation.

In addition, the suppressive effect of IDO on T cell function has been reported; we therefore examined the influence of IDO expression on infiltrating lymphocyte number in the tumor microenvironment; however, no statistically significant differences were noted between low and high IDO cell groups ($P > 0.05$). Possible explanations may be: first, T cell's function and number are

regulated by many factors [34]; secondly, T cell contains various subtype groups with different functions [39]; however, the influence of IDO on the different subtype T cells is still unclear; and finally the T cell function changes may be greater than the density changes. Thus, the functional analysis on certain subtype T cell is necessary for the comprehensive understanding of the IDO's effect on host immune functions in ESCCs.

In conclusion, our current findings suggest that increased expression of IDO in ESCCs is from a mixture cellular source in ESCCs and may potentially play an essential role in inducing immune tolerance. Since the use of IDO inhibitors as a possible cancer therapy has been intensively discussed in other types of cancers [45], its potential as a therapeutic application in ESCCs should be investigated in the future.

Acknowledgments We express our sincere gratitude to Ms. Dana Frederick, Department of Cell Biology, University of Massachusetts Medical School, for manuscript proofreading

Conflict of interest statement We declare that we have no conflict of interest.

References

1. Parkin DM, Bray FI, Devesa SS (2001) Cancer burden in the year 2000. The global picture. Eur J Cancer 37(Suppl 8):S4–S66
2. Li MX, Cheng SJ (1984) Carcinogenesis of esophageal cancer in Linxian, China. Chin Med J (Engl) 97:311–316
3. Wee JL, Christiansen D, Li YQ et al (2008) Suppression of cytotoxic and proliferative xenogeneic T-cell responses by transgenic expression of indoleamine 2,3-dioxygenase. Immunol Cell Biol 86:460–465
4. Hamilton DH, Bretscher PA (2008) Different immune correlates associated with tumor progression and regression: implications for prevention and treatment of cancer. Cancer Immunol Immunother 57:1125–1136
5. Croci DO, Zacarias Fluck MF, Rico MJ et al (2007) Dynamic cross-talk between tumor and immune cells in orchestrating the immunosuppressive network at the tumor microenvironment. Cancer Immunol Immunother 56:1687–1700
6. Westerterp M, Boermeester MA, Omloo JM et al (2008) Differential responses of cellular immunity in patients undergoing neoadjuvant therapy followed by surgery for carcinoma of the oesophagus. Cancer Immunol Immunother 57:1837–1847
7. Gholamin M, Moaven O, Memar B et al (2009) Overexpression and interactions of interleukin-10, transforming growth factor Beta, and vascular endothelial growth factor in esophageal squamous cell carcinoma. World J Surg 33:1439–1445
8. Shimada H, Nabeya Y, Okazumi S et al (2003) Prognostic value of preoperative serum immunosuppressive acidic protein in patients with esophageal squamous cell carcinoma. Dis Esophagus 16:102–106
9. O'Sullivan GC, Corbett AR, Shanahan F et al (1996) Regional immunosuppression in esophageal squamous cancer: Evidence from functional studies with matched lymph nodes. J Immunol 157:4717–4720
10. Brandacher G, Perathoner A, Ladurner R et al (2006) Prognostic value of indoleamine 2,3-dioxygenase expression in colorectal cancer: effect on tumor-infiltrating T cells. Clin Cancer Res 12:1144–1151
11. Curti A, Trabanelli S, Salvestrini V et al (2009) The role of indoleamine 2,3-dioxygenase in the induction of immune tolerance: focus on hematology. Blood 113:2394–2401
12. Feder-Mengus C, Wyler S, Hudolin T et al (2008) High expression of indoleamine 2,3-dioxygenase gene in prostate cancer. Eur J Cancer 44:2266–2275
13. Ino K, Yoshida N, Kajiyama H et al (2006) Indoleamine 2,3-dioxygenase is a novel prognostic indicator for endometrial cancer. Br J Cancer 95:1555–1561
14. Karanikas V, Zamanakou M, Kerenidi T et al (2007) Indoleamine 2,3-dioxygenase (IDO) expression in lung cancer. Cancer Biol Ther 6:1258–1262
15. Pan K, Wang H, Chen MS et al (2008) Expression and prognosis role of indoleamine 2,3-dioxygenase in hepatocellular carcinoma. J Cancer Res Clin Oncol 134:1247–1253
16. Prendergast GC (2008) Immune escape as a fundamental trait of cancer: focus on IDO. Oncogene 27:3889–3900
17. Zamanakou M, Germenis AE, Karanikas V (2007) Tumor immune escape mediated by indoleamine 2,3-dioxygenase. Immunol Lett 111:69–75
18. Lob S, Konigsrainer A, Zieker D et al (2009) IDO1 and IDO2 are expressed in human tumors: levo- but not dextro-1-methyl tryptophan inhibits tryptophan catabolism. Cancer Immunol Immunother 58:153–157
19. Sakurai K, Enomoto K, Amano S et al (2004) Study of indoleamine 2,3-dioxygenase expression in patients of esophageal squamous cell carcinoma. Gan To Kagaku Ryoho 31:1780–1782
20. Riesenberg R, Weiler C, Spring O et al (2007) Expression of indoleamine 2,3-dioxygenase in tumor endothelial cells correlates with long-term survival of patients with renal cell carcinoma. Clin Cancer Res 13:6993–7002
21. Sedlmayr P, Semlitsch M, Gebru G et al (2003) Expression of indoleamine 2,3-dioxygenase in carcinoma of human endometrium and uterine cervix. Adv Exp Med Biol 527:91–95
22. Ishio T, Goto S, Tahara K et al (2004) Immunoactivative role of indoleamine 2,3-dioxygenase in human hepatocellular carcinoma. J Gastroenterol Hepatol 19:319–326
23. Yuan A, Liu J, Liu Y et al (2008) Immunohistochemical examination of gastrin, gastrin precursors, and gastrin/CCK-2 receptor in human esophageal squamous cell carcinomas. Pathol Oncol Res 14:449–455
24. Yuan A, Liu J, Liu Y et al (2007) Chromogranin A-positive tumor cells in human esophageal squamous cell carcinomas. Pathol Oncol Res 13:321–325
25. Cui G, Yuan A, Goll R et al (2009) Dynamic changes of interleukin-8 network along the colorectal adenoma-carcinoma sequence. Cancer Immunol Immunother 58:1897–1905
26. Cui G, Yuan A, Vonen B et al (2009) Progressive cellular response in the lamina propria of the colorectal adenoma–carcinoma sequence. Histopathology 54:550–560
27. Muller AJ, Sharma MD, Chandler PR et al (2008) Chronic inflammation that facilitates tumor progression creates local immune suppression by inducing indoleamine 2,3 dioxygenase. Proc Natl Acad Sci USA 105:17073–17078
28. Witkiewicz A, Williams TK, Cozzitorto J et al (2008) Expression of indoleamine 2,3-dioxygenase in metastatic pancreatic ductal adenocarcinoma recruits regulatory T cells to avoid immune detection. J Am Coll Surg 206:849–854, discussion 854–846
29. Cui G, Goll R, Olsen T et al (2007) Reduced expression of microenvironmental Th1 cytokines accompanies adenomas–carcinomas sequence of colorectum. Cancer Immunol Immunother 56:985–995
30. Uyttenhove C, Pilotte L, Theate I et al (2003) Evidence for a tumoral immune resistance mechanism based on tryptophan degradation by indoleamine 2,3-dioxygenase. Nat Med 9:1269–1274

31. Takikawa O, Yoshida R, Kido R et al (1986) Tryptophan degradation in mice initiated by indoleamine 2,3-dioxygenase. J Biol Chem 261:3648–3653
32. Munn DH, Mellor AL (2007) Indoleamine 2,3-dioxygenase and tumor-induced tolerance. J Clin Invest 117:1147–1154
33. Muller AJ, Prendergast GC (2007) Indoleamine 2,3-dioxygenase in immune suppression and cancer. Curr Cancer Drug Targets 7:31–40
34. Kim R, Emi M, Tanabe K et al (2006) Tumor-driven evolution of immunosuppressive networks during malignant progression. Cancer Res 66:5527–5536
35. Guo SJ, Lin DM, Li J et al (2007) Tumor-associated macrophages and CD3-zeta expression of tumor-infiltrating lymphocytes in human esophageal squamous-cell carcinoma. Dis Esophagus 20:107–116
36. Sadanaga N, Kuwano H, Watanabe M et al (1994) Local immune response to tumor invasion in esophageal squamous cell carcinoma. The expression of human leukocyte antigen-DR and lymphocyte infiltration. Cancer 74:586–591
37. Zhang C, Fu L, Fu J et al (2009) Fibroblast growth factor receptor 2-positive fibroblasts provide a suitable microenvironment for tumor development and progression in esophageal carcinoma. Clin Cancer Res 15:4017–4027
38. Tsuzuki S, Ota H, Hayama M et al (2001) Proliferation of alpha-smooth muscle actin-containing stromal cells (myofibroblasts) in the lamina propria subjacent to intraepithelial carcinoma of the esophagus. Scand J Gastroenterol 36:86–91
39. Whiteside TL (2006) The role of immune cells in the tumor microenvironment. Cancer Treat Res 130:103–124
40. Brigati C, Noonan DM, Albini A et al (2002) Tumors and inflammatory infiltrates: friends or foes? Clin Exp Metastasis 19:247–258
41. Lewis CE, Pollard JW (2006) Distinct role of macrophages in different tumor microenvironments. Cancer Res 66:605–612
42. Lieubeau B, Heymann MF, Henry F et al (1999) Immunomodulatory effects of tumor-associated fibroblasts in colorectal-tumor development. Int J Cancer 81:629–636
43. Takikawa O (2005) Biochemical and medical aspects of the indoleamine 2,3-dioxygenase-initiated L-tryptophan metabolism. Biochem Biophys Res Commun 338:12–19
44. Popov A, Schultze JL (2008) IDO-expressing regulatory dendritic cells in cancer and chronic infection. J Mol Med 86:145–160
45. Lob S, Konigsrainer A, Rammensee HG et al (2009) Inhibitors of indoleamine-2,3-dioxygenase for cancer therapy: can we see the wood for the trees? Nat Rev Cancer 9:445–452

Virchows Arch (2009) 455:449–453
DOI 10.1007/s00428-009-0849-0

ORIGINAL ARTICLE

Full analysis of the prostatic urethra at the time of radical cystoprostatectomy for bladder cancer: impact on final disease stage

Justine Varinot · Philippe Camparo · Morgan Roupret · Marc Olivier Bitker · Fréderique Capron · Olivier Cussenot · J. Alfred Witjes · Eva Compérat

Received: 17 September 2009 / Revised: 6 October 2009 / Accepted: 8 October 2009 / Published online: 20 October 2009

Abstract Prostate involvement is a major prognostic element in urothelium carcinoma staging after radical cystoprostatectomy (RCP) for muscle invasive bladder cancer. While appropriate pTNM stage is necessary for adequate treatment, no standard procedure exists up to now for macroscopic sampling of the prostate in RCP in daily practice. We therefore propose a protocol where examination of the whole prostatic urethra (PU) is possible, without using whole mount sections. From 2008 to June 2009, RCP were sampled according to a macroscopic protocol permitting the whole length and the underlying stroma of PU to be visualized. Data were compared with our series or RCP from 2000–2007, when the PU was evaluated with a more simple protocol. One hundred and one specimens were examined between 2000–2007, 25 until June 2009. In the latter series, we found pT4 bladder cancer in 36% versus 21%, C*is* in the PU in 28% versus 14%, and additional prostate cancer was seen in 44% compared with 13% (p=0.0004) in the 2008–2009 group versus the 2000–2007 group, respectively. Our proposed protocol better detects prostate involvement by bladder cancer, therefore providing a better final stage of the patients. We propose a macroscopic protocol where the whole PU and the underlying stroma can be examined without the use of whole mount sections. Data are similar to those published in the recent literature, where whole mount sections were used. This protocol also permits better detection of concomitant prostate carcinomas.

Keywords Bladder cancer · Cystoprostatectomy · Urothelium · Stage · Prostate cancer

J. Varinot · F. Capron · E. Compérat
Department of Pathology, Pitie-Salpetriere Hospital, GHU Est, University PMC Paris VI,
Paris, France

P. Camparo · O. Cussenot · E. Compérat (✉)
Service d'Anatomie Pathologique, Hôpital La Pitié Salpêtrière, ER2, University PMC Paris VI, CeRePP,
83, Bd de l'Hopital,
75013 Paris, France
e-mail: eva.comperat@psl.aphp.fr

M. Roupret · M. O. Bitker
Department of Urology, Pitie-Salpetriere Hospital, GHU Est, University PMC Paris VI,
Paris, France

J. A. Witjes
Department of Urology, University Medical Center Nijmegen,
Nijmegen, The Netherlands

Introduction

In case of muscle invasive urothelial carcinoma (UC), radical cystoprostatectomy (RCP) is the gold standard of treatment [1]. Appropriate sampling of RCP specimen is necessary to obtain correct pTNM stage and treatment.

Staging UC in the prostatic urethra (PU) is controversial. The PU mucosa and large prostatic ducts that empty into the urethra are also lined by the same urothelium. In case of invasion of the PU, prostatic ducts or acini with UC without invasion of the prostatic stroma, the tumor has to be considered as pT*is*, making no difference whether it is a primary tumor or extension of an already existing UC of the bladder. In case of involvement of the underlying prostatic stroma, the UC becomes a pT4 tumor [2]. The proximity of prostatic urethra and bladder neck facilitate spreading of in situ carcinoma into prostatic urothelium. Many patients

with involvement of the bladder neck have spread of UC into the PU. To determine that the carcinoma does not invade the stroma of the underlying gland is a very important challenge in pathology. Up to now, no standard protocol for sampling the prostate in RCP specimens has been established. It is left to the pathologist to decide how many blocs should be taken. Montironi et al. suggest in a recent paper whole-mounted prostate sections with inclusion of the whole gland [3].

We propose a different protocol, permitting visualizing of the whole PU without the time-consuming technique of whole mount sections.

Materials and methods

We have collected 126 RCP specimens between January 2000 and June 2009. After taking material for snap frozen specimen if possible, the RCP was fixed in 10% neutral buffered formalin, 15 times the volume of the total specimen. Fixation lasted between 24 to 48 h according to the specimen's size. The following protocol was used for the samples from 2000–2007. After orientation and measuring and describing the RCP specimen, the apex, a slice in the middle of the prostate and a slice at the base of prostate were taken. Afterwards, the bladder was sampled according to necessity of macroscopic aspects.

From 2008 to 2009, the new standardized protocol was applied. After orientation, measuring, and describing the lesions and macroscopic findings, the RCP specimen was cut sagitally to separate the right and left half from anterior to posterior. Photos were taken systematically. Prostate tissue was inked to be able to mark resection margins precisely in case of concomitant prostate cancer as well as in case of invasion of the prostate by UC (Fig. 1). The most apical portion of the prostate was transected and submitted as for cone biopsies of cervix for evaluation of the apical margin, according to the Stanford protocol. Then the urethra was taken on both sides (right and left) in its total length to be able to study the whole PU (Fig. 2). The next step was sampling the bladder neck according to macroscopic findings including a sample of seminal vesicles and prostate tissue. Prostate samples were taken in the middle of the prostate (1 to 2 slices according to the size of the prostate). The procedure was similar on both sides (Fig. 3). Afterwards, the bladder was sampled according to the recommendations published by Lopez-Beltran et al. [4]. Tumors were classified according to the WHO classification 2004.

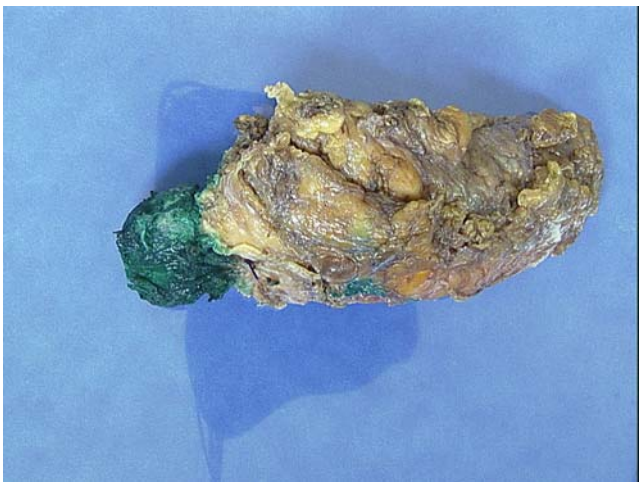

Fig. 1 The RCP specimen was oriented, prostate tissue was inked

Results

Between 2000 and June 2009 126 RCP were sent to our institution (Department of Pathology, Hôpital La Pitié-Salpetrière). All specimens examined before 2004 were reclassified according to the WHO classification 2004. Stages of the bladder tumor were distributed as follows (see Table 1). Between 2000 and 2007, we collected 101 RCP and 25 between 2008 and June 2009. Patients' age ranged from 39–85 years (mean, 70; median, 69; see Table 2).

Vascular invasion in perivesical fat was seen in 47 (37%) patients, 14 (11%) had C*is* in the bladder associated with invasive bladder tumor. Amongst the 30 pT4 patients, three

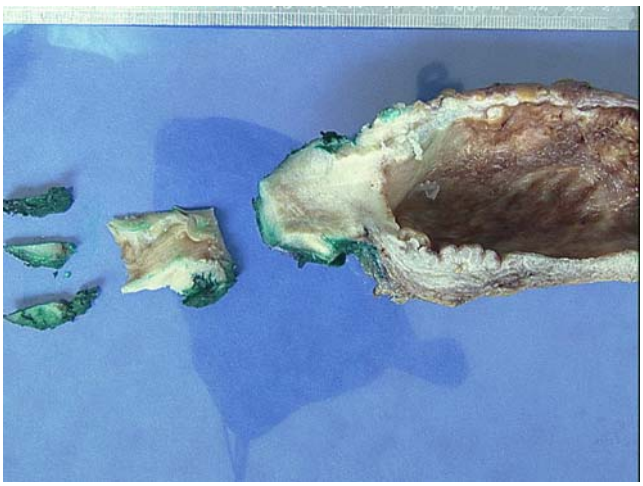

Fig. 2 Dissection of the most apical portion of the prostate, prepared as for cone biopsies of cervix for evaluation of the apical margin, the urethra was taken on both sides (right and left) in its total length to be able to study the whole PU (Fig. 2).Then we sampled the bladder neck according to macroscopic findings including a sample of seminal vesicles and prostate tissue. Prostate samples were taken in the middle of the prostate (1 to 2 slices according to the size of the prostate). The procedure was similar on both sides

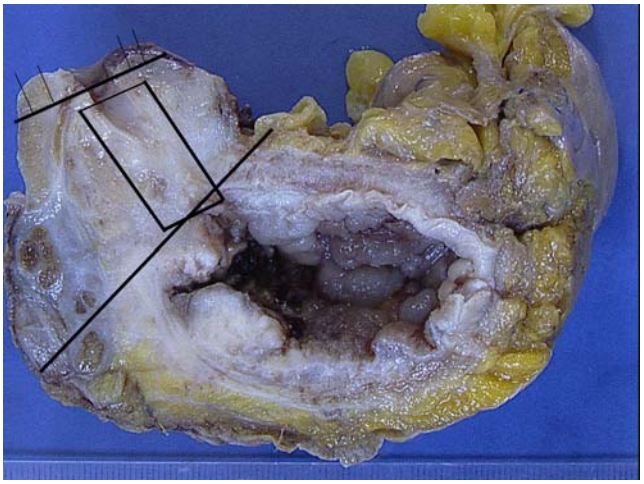

Fig. 3 Schema of sampling

were found to have urothelial carcinoma with an important squamous component, four had a micropapillary component in 20% to 80% of the tissue, all of these four cases displayed vascular invasion, and five had either particular bladder tumors or particular findings associated (one adenocarcinoma, one urothelial carcinoma with rhabdoid differentiation, one poorly differentiated carcinoma, one carcinoma had developed in a bladder substitution, and finally one patient had associated schistosomiasis, but no squamous component).

In our series, 24 patients (20%) were found to have concomitant adenocarcinoma of the prostate. Amongst them, five were considered as pT2a, three as pT2b, eleven as pT2c, one pT3a, 2 as pT3b, and two as pT4, both invading the bladder (immunohistologically confirmed). In the group 2000–2007, 13 cases (13%) of associated prostate cancer were described as compared with 11 cases (44%) in the recent group (p=0.0004).

When comparing cystoprostatectomies 2000–2007 data to 2008–2009, increasing numbers of PU invasion (plus 14%, nonsignificant), invasion of the prostatic stroma (18%, trend towards significance, p=0.08), and detection of concomittant prostate carcinoma (p=0.0004) could be observed with the new protocol (see Table 4). With this new protocol, six cases (24%) showed as well PU C*is* and invasion of the prostate (Fig. 4). One pT4 case with PU involvement displayed foci of C*is,* but without prostatic stroma invasion, the UC invaded the rectum. Increasing incidence of insignificant prostate carcinoma could also be observed.

A relationship between the presence of vascular invasion and micropapillary carcinoma (p=0.01), but also between vascular invasion and positive lymph nodes (p=0.0001) could be observed.

Table 1 Stages of RCP between January 2000 and June 2009

pT stage	Number of cases
pT0	0
pTa	1
pTis	3
pT1	10[a]
pT2	30
pT3a	11
pT3b	40
pT4	30

[a] Substaging (none according to the WHO classification 2004) was made for pT1 tumors, one case was pT1a; nine was pT1b

Table 2 Comparison of pT stages between 2000–2007 and 2008–2009

pT stage	Number of cases, 2000–2007 in %	Number of cases, 2008–2009 in %
pT1	9%	4%
pT2	25%	20%
pT3a	9%	8%
pT3b	32%	32%
pT4	21%	36%

Lymph nodes status were as follows (see Table 3)

Discussion

Sampling RCP specimens and correct staging are essential to decide on postsurgical treatment of urothelial carcinomas of the bladder [3, 5]. Up to now, no standard protocol has been established dealing with the method and extent of prostate sampling in RCP specimens.

We present a protocol where the PU of an RCP specimen can be examined as a whole without any lack of material. Using this new protocol, we could demonstrate that prostatic UC involvement is a common finding in more than a third of patients. Our results also showed that we were able to diagnose an increasing numbers of C*is* in the PU and increasing invasion of prostatic stroma (pT4). The

Table 3 Lymph node invasion of RCP between January 2000 and June 2009

pN stage	Number of cases, 2000–2007 in %	Number of cases, 2008–2009 in %
N0	72%	76%
N1	13%	8%
N2	12%	12%
Nx	4%	5%

Table 4 Comparison of prostate involvement by UC in our series

	2000–2007	2008–2009
invasion of PU	14 (14%)	7 (28%)
invasion of prostate stroma	18 (18%)	9 (36%)
prostate cancer	13 (13%)	11 (44%)
insignificant prostate cancer	2 (2%)	3 (12%)

current series come up with a 36% prostatic involvement, which is close to the results published by Shen et al., who included the prostate specimen in 5-mm intervals in the transverse plan from the apex to the base on whole mount sections [6]. Shen et al. found 32% of prostatic involvement in their series and specifically describe 21% of C*is* in the PU and prostatic ducts/acini, as compared with 24% of urothelial involvement in the prostate in our current series. These results are also close to those of Mazzucchelli et al., who worked one whole mount sections of 248 RCP and found 37.9% of UC involving the prostate [7].

Several disadvantages exist by using whole mount sections in prostate sampling. First of all, it is time-consuming and technically more demanding. Whole mount sections require well-trained technicians and new material for inclusion, cutting the blocs and different slides. In case of a need for immunohistochemistry, standard procedures cannot be deployed. Therefore, whole mount section technique is not commonly used.

Extension of UC in the PU is certainly underestimated [8], although it has significant prognostic importance. Direct extension of UC into the prostate has the worst prognosis as is reflected by the WHO 2004 classification, which stages these tumors as pT4. It has also a worse prognosis than nonstromal C*is* in the PU. Prostatic involvement has also been shown to be associated with a higher frequency of nodal metastasis and worse survival.

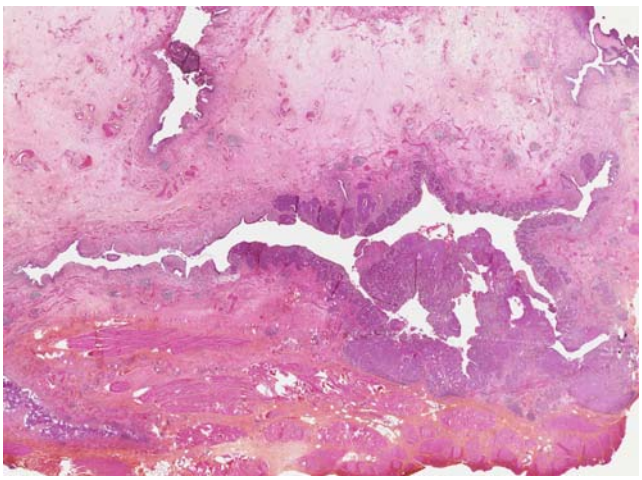

Fig. 4 Histological aspect of the whole urethra. Invasion of prostatic tissue and *Cis* of urothelium (HES, ×2.5)

Shen et al. demonstrated that UC involvement of the PU and lymph node metastasis were highly significant and independent prognostic factors for patients' survival [6].

On the other hand, Ayyathurai et al. found that involvement of PU did not alter the survival predicted by the primary bladder stage, but stromal involvement of the prostate always had poor prognosis, regardless of the mode of invasion [9].

Several studies have shown that there are different mechanisms of prostate invasion by UC. Development and pathogenesis of UC in the PU might be linked either to synchronous transformation of the prostatic and bladder urothelium or to pagetoid spread from an existing UC in the bladder into the PU. Another possibility is direct transmural invasion. In the last case, the stage immediately becomes pT4, either via posterior perivesical growth or directly through the bladder neck [10, 11]. The dominant mechanisms seem to be intraurethral spread with following transmural invasion. [6, 12]. Several studies suggested that transmural penetration has a worse prognosis than non-contiuous or intraurethral spread [12, 13]. Esrig et al. found that UC in the PU or ducts does not influence the prognosis as predicted by the primary bladder stage alone. But prostatic stromal invasion arising intraurethrally significantly decreased survival.

Since we have been able to show that in case of standardized sampling, an invasive component is found in the majority of cases, and all C*is* cases in the PU in the 2008–2009 group displayed stromal invasion, the method we describe might have significant clinical impact. Amongst the nine graded pT4 patients between 2008–2009, six received early additional chemotherapy, although the value of adjuvant systemic chemotherapy remains controversial, and follow-up in our series is not sufficient to prove real benefit. One patient died 4 days after surgery; two patients did not receive any therapy, one because of cardiac pathology, the other was affected by Alzheimer's disease. When comparing our two series, we can hypothesize that approximately 15% of patients were undergraded between 2000 and 2007 and did not receive additional treatment.

Additionally, we were able to demonstrate an increasing number of associated prostate cancers. With the new protocol, 44% adenocarcinomas of the prostate were found. These results are comparable to the series of Revelo et al., who found 41% of unexpected prostate cancers in RCP specimens [14]. These results are also in line with those of Montironi et al., who observed 49.6% of prostate cancers in RCP, of which he considered 18.7% insignificant [3]. In our study, five patients displayed nonsignificant prostate carcinoma, 2% in the group 2000–2007, 12% in the second group.

In conclusion, our study clearly demonstrates the importance of studying the whole PU. It prevents underestimation of its involvement and makes correct staging possible. For example, finding stromal invasion of the underlying prostate can be important for additional treatment decisions and prediction of patient's prognosis. Our protocol is a good alternative for sampling of the prostate of RCP specimens with similar results as published in the literature for whole mount sectioning. This proposed protocol better detects prostate involvement by bladder cancer, therefore providing a better final stage of the patients. A practical advantage, however, is that this technique permits to avoid whole mount sections, which is not available for everybody. This protocol is easy to use, and is not more time-consuming than other macroscopic protocols.

Acknowledgement We thank Annette Lesourd and Gilles Le Naour for perfect technical assistance.

Conflict of interest We declare that we have no conflict of interest.

References

1. Stenzl A, Cowan N, De Santis M et al (2009) The updated EAU guidelines on muscle-invasive and metastatic bladder cancer. Eur Urol 55:815–825
2. Eble JN, SG EJI, Sesterhenn IA (2004) WHO classification of tumors. Tumors of the genitourinary and male genital organs. IARC Press, Lyon
3. Montironi R, Cheng L, Mazzucchelli R et al (2009) Critical evaluation of the prostate from cystoprostatectomies for bladder cancer: insights from a complete sampling with the whole mount technique. Eur Urol 55:1305–1309
4. Lopez-Beltran A, Bassi P, Pavone-Macaluso M, Montironi R (2004) Handling and pathology reporting of specimens with carcinoma of the urinary bladder, ureter, and renal pelvis. Eur Urol 45:257–266
5. Wheeler TM (1989) Anatomic considerations in carcinoma of the prostate. Urol Clin North Am 16:623–634
6. Shen SS, Lerner SP, Muezzinoglu B et al (2006) Prostatic involvement by transitional cell carcinoma in patients with bladder cancer and its prognostic significance. Hum Pathol 37:726–734
7. Mazzucchelli R, Barbisan F, Santinelli A et al (2009) Prediction of prostatic involvement by urothelial carcinoma in radical cystoprostatectomy for bladder cancer. Urology 74:385–390
8. Liedberg F, Chebil G, Mansson W (2007) Urothelial carcinoma in the prostatic urethra and prostate: current controversies. Expert Rev Anticancer Ther 7:383–390
9. Ayyathurai R, Gomez P, Luongo T et al (2007) Prostatic involvement by urothelial carcinoma of the bladder: clinicopathological features and outcome after radical cystectomy. BJU Int 100:1021–1025
10. Donat SM, Genega EM, Herr HW, Reuter VE (2001) Mechanisms of prostatic stromal invasion in patients with bladder cancer: clinical significance. J Urol 165:1117–1120
11. Lerner SP, Shen S (2008) Pathologic assessment and clinical significance of prostatic involvement by transitional cell carcinoma and prostate cancer. Urol Oncol 26:481–485
12. Esrig D, Freeman JA, Elmajian DA et al (1996) Transitional cell carcinoma involving the prostate with a proposed staging classification for stromal invasion. J Urol 156:1071–1076
13. Herr HW, Donat SM (1999) Prostatic tumor relapse in patients with superficial bladder tumors: 15-year outcome. J Urol 161:185–187
14. Revelo MP, Cookson MS, Chang SS et al (2004) Incidence and location of prostate and urothelial carcinoma in prostates from cystoprostatectomies: implications for possible apical sparing surgery. J Urol 171:646–651

Virchows Arch (2009) 455:455–459
DOI 10.1007/s00428-009-0845-4

CASE REPORT

Metastatic potential of an aneurysmal bone cyst

Addy C. M. van de Luijtgaarden · Rene P. H. Veth · Piet J. Slootweg · Pauline M. Wijers-Koster · Leo J. Schultze Kool · Judith V. M. G. Bovee · Winette T. A. van der Graaf

Received: 29 July 2009 / Revised: 14 September 2009 / Accepted: 3 October 2009 / Published online: 17 October 2009

Abstract Aneurysmal bone cysts (ABCs) are benign bone tumors consisting of blood-filled cavities lined by connective tissue septa. Recently, the hypothesis that ABCs are lesions reactive to local hemodynamics has been challenged after the discovery of specific recurrent chromosomal abnormalities. Multiple cases of malignant transformation of ABC into (osteo)sarcoma have been described, as well as a number of cases of telangiectatic osteosarcoma which had been misdiagnosed as ABC. We herewith document a case of a pelvic ABC metastatic to the lung, liver, and kidneys. Diagnosis was confirmed by the presence of a break in the *USP6* gene, which is pathognomonic for ABC, in a pulmonary metastasis of our patient. Sarcomatous transformation as an explanation for this behavior was ruled out by demonstrating diploid DNA content in both the pulmonary lesion and the primary tumor.

A. C. M. van de Luijtgaarden (✉) · W. T. A. van der Graaf
Department of Medical Oncology (452),
Radboud University Nijmegen Medical Centre,
P.O. Box 9101, 6500 HB Nijmegen, The Netherlands
e-mail: a.luijtgaarden@onco.umcn.nl

R. P. H. Veth
Department of Orthopedic Surgery,
Radboud University Nijmegen Medical Centre,
Nijmegen, The Netherlands

P. J. Slootweg
Department of Pathology,
Radboud University Nijmegen Medical Centre,
Nijmegen, The Netherlands

P. M. Wijers-Koster · J. V. M. G. Bovee
Department of Pathology, Leiden University Medical Centre,
Leiden, The Netherlands

L. J. Schultze Kool
Department of Interventional Radiology,
Radboud University Nijmegen Medical Centre,
Nijmegen, The Netherlands

Keywords Bone cysts · Aneurysmal · Neoplasm metastasis · Image cytometry

Introduction

Primary aneurysmal bone cysts (ABC) account for 1–2% of all primary bone tumors and are usually present in the first two decades of life [1]. They are composed of blood-filled spaces separated by connective tissue septa that contain fibroblasts, osteoclast-type giant cells, and reactive woven bone [2]. The pathogenesis of primary ABC is still incompletely understood. In the past, ABCs were considered reactive lesions caused by altered local hemodynamics. More recently, it was shown that primary ABCs contain recurrent chromosomal abnormalities [3–13]. This suggests that primary ABCs are true neoplasms [1]. The differential diagnosis of primary ABC includes other giant cell-containing tumors of the bone, particularly giant cell tumor (GCT) [14]. ABC-like areas can also be seen in association with other tumors such as chondroblastoma (secondary ABC). Furthermore, cases of sarcomatous transformation of ABCs, often occurring after exposure to ionizing radiation, and of misdiagnosed telangiectatic osteosarcoma have been recognized. However, even without sarcomatous transformation, ABC may metastasize as is described in this report.

Clinical history

A 48-year-old woman was referred to our hospital for treatment of a giant ABC of the left ilium, measuring 27.6×22.4×15.9 cm (Fig. 1). Her medical history comprised of a hysterectomy for uterine cervical carcinoma in 1995, strumectomy for adenomatous thyroid hyperplasia in 1998,

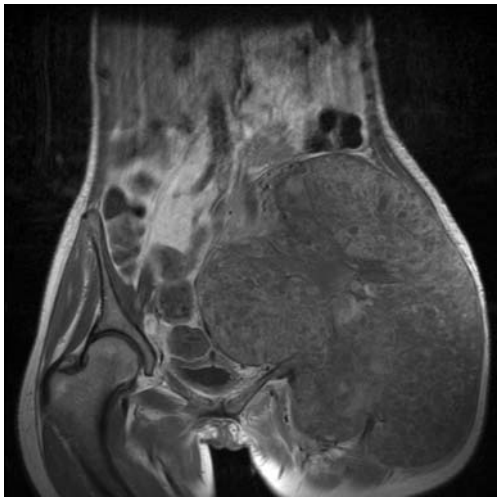

Fig. 1 Magnetic resonance image of the pelvis on admission showing a large ABC of the left ilium

and type II diabetes mellitus since 2004. For the ABC, she had been treated elsewhere with embolization (coiling and alcoholic zein injection; Ethibloc, Ethicon, Johnson & Johnson, New Brunswick, NJ, USA) and repeated surgery, all over a 1-year period. Wide local excision had not been achieved due to massive hemorrhage during surgical interventions. In our hospital, preoperative embolization and percutaneous intralesional alcohol injection were performed and staged resection of the alcohol-treated areas combined with cryosurgery was attempted. Furthermore, off-label systemic treatment with the monoclonal antivascular endothelial growth factor (VEGF) antibody bevacizumab (Avastin; Roche, Basel, Switzerland; Genentech, South San Francisco, California, USA) 10 mg/kg administered intravenously every other week was applied to reduce bleeding tendency. The latter was based on the reports by Kumta et al. and Shinde et al. showing VEGF positivity in 100% and 50% of primary ABCs, respectively [15, 16]. In our patient, plasma and cyst fluid VEGF levels were determined by enzyme-linked immunosorbent assay and found to be elevated (1.12 and 16.5 ng/ml, respectively; in-house control series of 23 healthy women: plasma average=0.166 ng/ml, range=0.028–0.966 ng/ml).

This strategy facilitated near-complete resection of the ABC by limiting intraoperative blood loss. However, clinical heart failure developed in our patient, prompting the discontinuation of bevacizumab. This was followed by a rapid regrowth of the pelvic lesion. After a total of seven surgical sessions, the patient's condition no longer allowed surgical interventions and it was decided to apply radiotherapy at a total dose of 39 Gy. Unexpectedly, at this time, radiographical treatment evaluation showed previously undiscovered lesions in both lungs and in the left kidney. Widespread metastatic behavior of this until then judged benign bone neoplasm was suspected, while differential diagnosis included secondary ABC in a yet unidentified primary bone malignancy, malignant transformation of ABC, misdiagnosed GCT, or telangiectatic osteosarcoma. The patient's condition no longer allowed any treatment and she died 2 years after ABC was first diagnosed. At autopsy, metastases were found in both lungs, both kidneys, and the liver.

Materials and methods

Pathology

Formalin-fixed paraffin-embedded specimens were available from all resections of the primary tumor. Sections from all samples were stained by the hematoxylin and

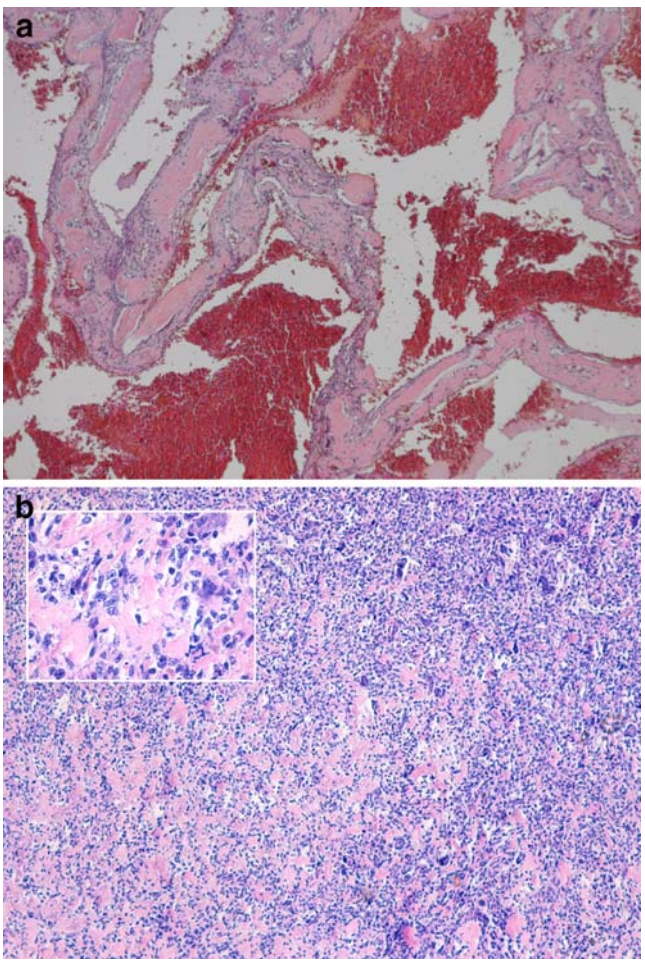

Fig. 2 **a** Photomicrograph of material from the first excision (hematoxylin and eosin, ×50) showing a blood-filled cavity and solid component containing strands of woven bone with interspersed fibroblasts. **b** Photomicrograph of the lung lesion removed at autopsy. A low-powered (hematoxylin and eosin, ×50) and high-powered (*inset*, hematoxylin and eosin, ×200) view show that no blood-filled cystic cavities were found at this site; the lesion only resembled the solid parts of the pelvic location

eosin method and re-examined for evidence of malignancy by multiple expert pathologists (PS, JB, and independent multidisciplinary revision by the Netherlands Committee on Bone Tumors).

Image cytometry

Three samples (two were obtained from the primary tumor at referral to our hospital and during the last resection, respectively, and the third was a pulmonary metastasis obtained during autopsy) were selected for DNA quantification by image cytometry. At least two 50-μm-thick sections were obtained of each sample followed by a 4-μm hematoxylin and eosin section to check for representativeness. An adaptation of the method described by Hedley [17] was used for cell nuclei extraction from the sections. The obtained suspensions were filtered with a Partec 50-μm CellTrics filter (Partec, Münster, Germany) and prepared into a monolayer by cytospin. Nuclei were stained with Feulgen's stain and periodic acid Schiff. The samples were evaluated using a cytometric image analysis system (QPATH, Leica Imaging Systems, Cambridge, UK) that consists of an automated microscope with a digital camera connected to a computer that runs DNA analysis software. Of each specimen, 5,000 nuclei were scanned and a minimum of 2,000 images of tumor cell nuclei were manually selected avoiding debris, necrotic or cut cells, and cell clusters. Lymphocytes were used as the standard internal controls. Histogram quality was evaluated by integrated optical density (IOD) values and its coefficient of variation (CV); $15 \leq IOD \leq 25$ and $CV \leq 5\%$ were considered acceptable. Criteria for ploidy classification were taken from the guidelines of the European Society for Analytical Cellular Pathology [18].

Fluorescence in situ hybridization

Fluorescence in situ hybridization (FISH) was performed on the lung metastasis using BAC probes flanking the *USP6* gene, largely as described [19].

Results

Histological examination of material obtained from the primary tumor in the pelvis during the first surgical procedure showed a multicystic lesion with blood-filled spaces (Fig. 2a). The septa consisted of fibroblasts which showed no cytological features of malignancy such as nuclear atypia or an increased number of mitoses. Interspersed were woven bone fragments. No evidence of an underlying primary lesion causing secondary ABC, neither of evident malignant transformation of ABC, GCT, nor telangiectatic osteosarcoma was found. The morphology of the primary lesion was thus consistent with a primary ABC. The other excision specimens subsequently obtained from this pelvic tumor showed similar histology. The lung lesion resembled the solid parts of the pelvic location; no blood-filled cystic spaces were found here (Fig. 2b). Again, no cytological features of malignancy were found. The three samples (two obtained from the primary tumor and one pulmonary lesion) that were evaluated for DNA content were diploid. FISH performed on the pulmonary lesion showed a break in the *USP6* gene in up to 43% of the nuclei: 24% of the nuclei showed segregation of the signal in addition to two normal (colocalization) chromosomes 17 (Fig. 3, left panel), 15% of the nuclei showed two normal chromosomes 17 and a single red signal (Fig. 3, middle panel), 4% showed one colocalization and one segregation of the signal (Fig. 3, right panel).

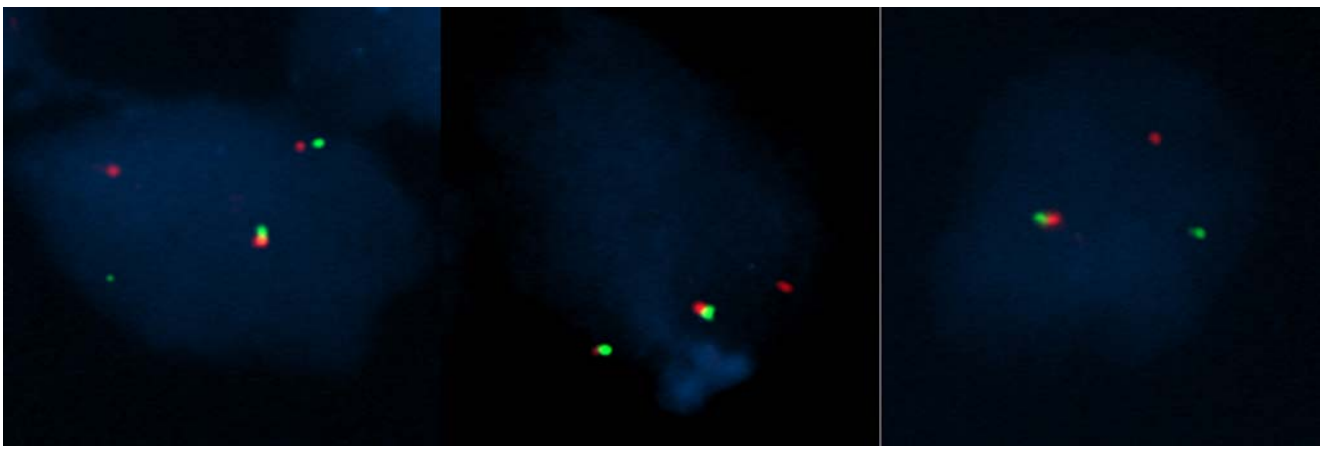

Fig. 3 FISH images of the lung lesion removed at autopsy using BAC probes flanking the *USP6* gene showing segregation of the signal and colocalization of two normal chromosomes 17 (*left panel*), two normal chromosomes 17 and a single red signal (*middle panel*), and one colocalization and one segregation of the signal (*right panel*)

Discussion

Since the discovery of recurrent chromosomal abnormalities, of which t(16;17)(q22;p13) is the most frequent [3–13], primary ABC is no longer considered a reactive lesion but rather a true benign neoplasm [1]. The t(16;17) translocation was later shown to relocate the promoter of CDH11, a gene that is strongly expressed in bone, in front of the *USP6* gene (TRE2, TRE17) [8]. Over the past few years, a series of different translocations has been described in ABC [8, 13], all resulting in oncogenic activation of the *USP6* gene on chromosome 17p13. Thus, the pathogenesis of most *primary* ABCs involves upregulation of USP6 transcription driven by other highly active promoters [20]. The mechanism by which USP6 upregulation causes ABC formation has not yet been elucidated. USP6 rearrangements were shown to be restricted to the spindle cells and were absent in the multinucleated giant cells, inflammatory cells, endothelial cells, and osteoblasts [8]. This suggests that the neoplastic spindle cells induce a vigorous, reactive host response mimicking young granulation tissue, explaining why for a long time the lesions were regarded reactive [8]. The majority of ABC patients are treated by local curettage combined with intraoperative adjuvant therapy (e.g., cryosurgery or phenol application) with local control rates as high as 70–90%. Almost all cases of recurrence can be treated by re-resection [1].

To our knowledge, there are no previous reports of metastatic behavior of primary ABC. Therefore, we considered the possibility of secondary ABC in a yet unidentified primary bone malignancy, malignant transformation of ABC, misdiagnosed GCT, or telangiectatic osteosarcoma. ABC-like areas can be seen in association with GCT, occasionally overgrowing the underlying primary tumor, and ABC can contain solid areas strongly resembling GCT [21]. In contrast with ABC, GCT may metastasize in 2–3% of cases, particularly to the lungs. The diploid DNA content we found cannot exclude GCT with metastatic potential [22, 23]. However, while chromosome 16 and 17 abnormalities have been found infrequently in GCT [24–26], the t(16;17)(q22;p13) translocation [8, 27] and USP6 upregulation [8] are absent in reported cases. We also tested three GCTs and could not detect a USP6 rearrangement (data not shown). Thus, it seems highly unlikely that our case represented metastasizing GCT of bone. Moreover, the USP6 rearrangement was demonstrated in the lung metastasis, indicating that, even if from the beginning it had been ABC secondary to and totally overgrowing an underlying primary bone lesion such as GCT, it is the ABC part that metastasized. Moreover, USP6 rearrangements have not been found in secondary ABC so far [19].

Telangiectatic osteosarcoma and ABC can be radiologically identical and histologically very difficult to distinguish [28–30]. Nuclear atypia and an increased number of mitoses favor telangiectatic osteosarcoma. As an additional diagnostic tool, several reports have suggested the use of DNA cytometry to distinguish these entities. Whereas ABCs are known for diploid DNA content, telangiectatic osteosarcomas show complex karyotypes and numerous gains and losses [31–33]. Moreover, in ABC, CDH11-USP6 fusions as well as USP6 upregulation are pathognomonic, while they are absent in osteosarcoma [8, 9]. So, the diploid nature of the lesion in our case, both in primary as well as metastatic deposits, adequately rules out telangiectatic osteosarcoma as an alternative diagnosis.

In summary, in our patient, all histological samples obtained over a 2-year period were consistent with ABC while lacking cytological features of malignancy. Absence of malignant transformation was supported by DNA content analysis: three selected samples including a pulmonary metastasis all had diploid DNA content. Finally, we found a rearrangement of the *USP6* gene by FISH in 43% of nuclei in the pulmonary lesion, which is within the highly variable range of positive cells (7–82%) reported for ABC [19].We ruled out sarcomatous transformation or GCT as cause of the metastatic behavior and confirmed the diagnosis of ABC by our FISH data.

It can be hypothesized that the numerous surgical and interventional radiological manipulations that were necessary in our patient have facilitated the hematogenous spread of ABC cell clusters. Furthermore, though bevacizumab proved successful in reducing bleeding tendency, recent reports about antiangiogenic therapy-induced malignant progression of tumors to increased invasion and accelerated metastasis raise concern about a similar effect in our patient.

Acknowledgements We thank Dr. K. Szuhai for the help with the FISH analysis and the Netherlands Committee on Bone Tumors for their critical reappraisal of all histological samples obtained from this patient.

Conflict of interest statement The authors declare that they have no conflict of interest.

References

1. Mendenhall WM, Zlotecki RA, Gibbs CP et al (2006) Aneurysmal bone cyst. Am J Clin Oncol 29(3):311–315
2. Rosenberg AE, Nielsen GP, Fletcher JA (2002) Aneurysmal bone cyst. In: Fletcher CDM, Unni KK, Mertens F (eds) World Health Organization classification of tumours: pathology and genetics of tumours of soft tissue and bone. International Agency for Research on Cancer, Lyon, pp 338–339
3. Althof PA, Ohmori K, Zhou M et al (2004) Cytogenetic and molecular cytogenetic findings in 43 aneurysmal bone cysts:

aberrations of 17p mapped to 17p13.2 by fluorescence in situ hybridization. Mod Pathol 17(5):518–525
4. Baruffi MR, Neto JB, Barbieri CH et al (2001) Aneurysmal bone cyst with chromosomal changes involving 7q and 16p. Cancer Genet Cytogenet 129(2):177–180
5. Dal CP, Kozakewich HP, Goumnerova L et al (2000) Variant translocations involving 16q22 and 17p13 in solid variant and extraosseous forms of aneurysmal bone cyst. Genes Chromosomes Cancer 28(2):233–234
6. Ellison DA, Sawyer JR, Parham DM et al (2007) Soft-tissue aneurysmal bone cyst: report of a case with t(5;17)(q33;p13). Pediatr Dev Pathol 10(1):46–49
7. Kenney B, Richkind KE, Zambrano E (2007) Solid variant of aneurysmal bone cyst with a novel (X;9) translocation. Cancer Genet Cytogenet 178(2):155–159
8. Oliveira AM, Hsi BL, Weremowicz S et al (2004) USP6 (Tre2) fusion oncogenes in aneurysmal bone cyst. Cancer Res 64 (6):1920–1923
9. Panoutsakopoulos G, Pandis N, Kyriazoglou I et al (1999) Recurrent t(16;17)(q22;p13) in aneurysmal bone cysts. Genes Chromosomes Cancer 26(3):265–266
10. Sciot R, Dorfman H, Brys P et al (2000) Cytogenetic–morphologic correlations in aneurysmal bone cyst, giant cell tumor of bone and combined lesions. A report from the CHAMP study group. Mod Pathol 13(11):1206–1210
11. Winnepenninckx V, biec-Rychter M, Jorissen M et al (2001) Aneurysmal bone cyst of the nose with 17p13 involvement. Virchows Arch 439(5):636–639
12. Wyatt-Ashmead J, Bao L, Eilert RE et al (2001) Primary aneurysmal bone cysts: 16q22 and/or 17p13 chromosome abnormalities. Pediatr Dev Pathol 4(4):418–419
13. Oliveira AM, Perez-Atayde AR, Dal CP et al (2005) Aneurysmal bone cyst variant translocations upregulate USP6 transcription by promoter swapping with the ZNF9, COL1A1, TRAP150, and OMD genes. Oncogene 24(21):3419–3426
14. Rosenberg AE, Nielsen GP (2001) Giant cell containing lesions of bone and their differential diagnosis. Curr Diagn Pathol 7(4):235–246
15. Kumta SM, Huang L, Cheng YY et al (2003) Expression of VEGF and MMP-9 in giant cell tumor of bone and other osteolytic lesions. Life Sci 73(11):1427–1436
16. Shinde A, Mehlman CT, Collins MH (2006) Aneurysmal bone cysts express vascular markers. Pediatr Dev Pathol 9(1):38–43
17. Hung IJ, Yang CP, Jaing TH (2003) Patterns of cancer distribution in a medical center among adolescents 14 to 17 years of age for the period 1995 to 2001. J Formos Med Assoc 102(9):631–636
18. Haroske G, Baak JP, Danielsen H et al (2001) Fourth updated ESACP consensus report on diagnostic DNA image cytometry. Anal Cell Pathol 23(2):89–95
19. Oliveira AM, Perez-Atayde AR, Inwards CY et al (2004) USP6 and CDH11 oncogenes identify the neoplastic cell in primary aneurysmal bone cysts and are absent in so-called secondary aneurysmal bone cysts. Am J Pathol 165(5):1773–1780
20. Oliveira AM, Chou MM, Perez-Atayde AR et al (2006) Aneurysmal bone cyst: a neoplasm driven by upregulation of the USP6 oncogene. J Clin Oncol 24(1):e1
21. Vergel De Dios AM, Bond JR, Shives TC et al (1992) Aneurysmal bone cyst. A clinicopathologic study of 238 cases. Cancer 69(12):2921–2931
22. Osaka S, Toriyama M, Taira K et al (1997) Analysis of giant cell tumor of bone with pulmonary metastases. Clin Orthop Relat Res 335:253–261
23. Takanami I, Imamura T, Morota N et al (1994) Recurrent pulmonary metastases from benign giant cell tumors of the bone: report of two cases and analysis of nuclear DNA content by flow cytometry. Surg Today 24(5):476–480
24. Bridge JA, Neff JR, Mouron BJ (1992) Giant cell tumor of bone. Chromosomal analysis of 48 specimens and review of the literature. Cancer Genet Cytogenet 58(1):2–13
25. Molenaar WM, van den Berg E, Dolfin AC et al (1995) Cytogenetics of fine needle aspiration biopsies of sarcomas. Cancer Genet Cytogenet 84(1):27–31
26. Gorunova L, von Vult SF, Storlazzi CT et al (2009) Cytogenetic analysis of 101 giant cell tumors of bone: nonrandom patterns of telomeric associations and other structural aberrations. Genes Chromosomes Cancer 48(7):583–602
27. Mitelman F, Johansson B, Mertens F (eds) (2008) Mitelman database of chromosome aberrations in cancer. Ref type: Data file. Available at http://cgap.nci.nih.gov/Chromosomes/Mitelman
28. Gomes H, Menanteau B, Gaillard D et al (1986) Telangiectatic osteosarcoma. Pediatr Radiol 16(2):140–143
29. Vanel D, Tcheng S, Contesso G et al (1987) The radiological appearances of telangiectatic osteosarcoma. A study of 14 cases. Skeletal Radiol 16(3):196–200
30. Vigliani F, Campailla E (1987) Mimickry in osteogenic sarcoma. Clinical considerations and report of 2 cases. Ital J Orthop Traumatol 13(4):425–436
31. el-Naggar AK, Hurr K, Tu ZN et al (1995) DNA and RNA content analysis by flow cytometry in the pathobiologic assessment of bone tumors. Cytometry 19(3):256–262
32. Werner M, Heintz A, Delling G (1996) DNA cytometry of solitary and aneurysmal bone cysts and low malignancy and high malignancy central osteosarcomas. Current significance within the scope of morphologic diagnosis of intraosseous cystic and osteoblastic lesions. Pathologe 17(1):44–49
33. Bauer HC, Kreicbergs A, Silfversward C et al (1988) DNA analysis in the differential diagnosis of osteosarcoma. Cancer 61(12):2532–2540

Virchows Arch (2009) 455:461–467
DOI 10.1007/s00428-009-0851-6

ORIGINAL ARTICLE

Vascular endothelial growth factor C mRNA expression is a prognostic factor in epithelial ovarian cancer as detected by kinetic RT-PCR in formalin-fixed paraffin-embedded tissue

Bruno V. Sinn · Silvia Darb-Esfahani · Ralph M. Wirtz · Areeg Faggad · Wilko Weichert · Ann-Christin Buckendahl · Aurelia Noske · Berit Maria Müller · Jan Budczies · Jalid Sehouli · Elena I. Braicu · Manfred Dietel · Carsten Denkert

Received: 31 July 2009 / Revised: 24 September 2009 / Accepted: 21 October 2009 / Published online: 13 November 2009

Abstract Vascular endothelial growth factor C (VEGF-C) is a well described chemotactic and growth factor for lymphatic endothelial cells. Its inhibition leads to suppression of lymphatic and distant metastases in mouse models. In ovarian cancer, the relationship between VEGF-C expression and tumor behavior has not yet been determined by a quantitative method *in vivo*. Therefore, we used a new technique of RNA extraction from formalin-fixed paraffin-embedded tissue samples and determined the expression levels of VEGF-C mRNA in a study group of 97 ovarian cancer patients. Expression levels were correlated with clinicopathological features and patient survival. High VEGF-C expression was associated with worse overall ($p=0.0393$) and progression-free ($p=0.0155$) patient survival. In the subgroups of serous tumors and high-grade tumors, VEGF-C mRNA was still a negative indicator for patient survival ($p=0.0190$ and 0.0311, respectively). A trend was observed among patients with high clinical stage ($p=0.0634$). In multivariate survival analysis VEGF-C mRNA retained its prognostic influence on progression-free survival ($p=0.006$, $HR=0.319$ with a 95% confidence interval of 0.142–0.720). High VEGF-C expression was further associated with an increased residual tumor mass after primary cytoreductive surgery. We found no correlation of VEGF-C expression with tumor grade, FIGO stage, lymph node, or distant metastases. Our study demonstrates that high VEGF-C expression is associated with aggressive tumor behavior in ovarian cancer. mRNA extracted from paraffin-embedded tumor samples is suitable for VEGF-C gene expression studies.

Keywords VEGF-C · FEPE tissue · Ovarian cancer · Lymphangiogenesis

Bruno V. Sinn and Silvia Darb-Esfahani contributed equally to the publication.

B. V. Sinn (✉) · S. Darb-Esfahani · A. Faggad · W. Weichert · A.-C. Buckendahl · A. Noske · B. M. Müller · J. Budczies · M. Dietel · C. Denkert
Institute of Pathology, Charité Universitätsmedizin Berlin, Campus Mitte,
Charitéplatz 1,
10117 Berlin, Germany
e-mail: bruno.sinn@charite.de

R. M. Wirtz
Siemens Healthcare Diagnostics,
Cologne, Germany

J. Sehouli · E. I. Braicu
Department of Gynaecology and Obstetrics,
Charité Universitätsmedizin Berlin,
Berlin, Germany

Introduction

Being the most common cause of death from malignancy of the female genital tract, ovarian cancer represents the 5th most common cause of cancer death in women [1]. Even though primary treatment with extensive surgery and adjuvant chemotherapy with paclitaxel/carboplatin is often successful in the first place, high relapse rates are observed. Overall 5-year-survival for patients with advanced ovarian cancer is only 25–45% [1, 2]. Therefore, an early detection of high-risk patients and new therapeutic strategies for advanced-stage patients are needed. Translational research on tumor tissue is very attractive to identify new prognostic markers and new targets for a tailored therapy. The tissue

archives of pathologic departments harbor large amounts of formalin-fixed paraffin-embedded (FFPE) tumor tissue samples, which together with data on clinicopathological features and follow-up are valuable sources for translational research projects in oncology. Until recently, RNA analysis from FFPE tissue was limited by low quality of the extracted RNA due to fragmentation of RNA and chemical modifications such as protein-RNA interactions [3, 4]. However, in the last few years, there have been some successful attempts proving that FFPE tissue is suitable for gene expression studies, especially by quantitative real-time polymerase chain reaction (PCR) [5–10]. In this study, we used a new RNA extraction technique to assess gene expression in archival FFPE tissue samples from ovarian carcinoma surgical specimens.

Vascular endothelial growth factor-C (VEGF-C) is a well-described chemotactic factor for lymphatic endothelial cells, and its overexpression leads to enhanced lymphangiogenesis and lymph node metastasis in animal cancer models [11–13]. It has also been shown to directly enhance the invasiveness of ovarian cancer cells in vitro [14].

VEGF-C belongs to the gene family of vascular endothelial growth factors and is secreted as a precursor molecule, which is processed by extracellular proteases. Overexpression of VEGF-C is a frequently seen feature of human cancer [15].

The affinity to its receptor vascular endothelial growth factor receptor 3 (VEGFR3), which is expressed on lymphatic endothelial cells in adult tissues, increases upon cleavage towards its major form. VEGFR3 is also expressed on a variety of cancer cells, among them ovarian cancer cells, where it mediates the action of VEGF-C in an autocrine manner [14]. Ovarian cancer spreads besides direct intraperitoneal and hematogenic routes also via lymph vessels. However, although the detection of the soluble tissue factor VEGF-C might be more suitable on the RNA than on the protein level, VEGF-C mRNA expression has not yet been determined in ovarian carcinoma. Therefore, we examined VEGF-C mRNA expression by kinetic reverse transcriptase-polymerase chain reaction (RT-PCR) in 97 epithelial ovarian cancer tissue samples that were formalin-fixed and paraffin-embedded for diagnostic purposes and examined a possible impact of VEGF-C mRNA expression levels on prognosis as well as a correlation with clinicopathological features.

Patients, materials, and methods

Study population and histopathological examination

The study group consisted of patients with primary epithelial ovarian cancer. All patients underwent radical surgery with the aim of maximal cytoreduction at the Department for Gynaecology and Obstetrics, Charité University Hospital (Berlin, Germany), between 1992 and 2005. Resection specimens were formalin-fixed and paraffin-embedded to render a diagnosis at the Institute of Pathology, Charité University Hospital, Berlin, Germany. Hematoxylin and eosin (H&E) stained sections were cut from paraffin-embedded blocks and used for histopathological evaluation. After histopathological diagnosis, the remaining tissue blocks were stored at room temperature. An experienced pathologist (C.D.) reevaluated tumor histopathology and grading. Grading of the tumors was assessed using the Silverberg grading system [16]. Patients were managed with extensive cytoreductive surgery followed by standard combination chemotherapy. Patients were selected by availability of both tissue material and follow-up data. The study was approved by the ethics committee of the Charité University Hospital.

RNA extraction from formalin-fixed paraffin-embedded tissue samples

RNA was extracted from formalin-fixed paraffin-embedded tissue samples of 126 patients by an automated method developed by Siemens Healthcare Diagnostics (Cologne, Germany). A 10-μm thick section was cut from each paraffin block and transferred to a 1.5-ml tube. All tumor samples included in the study contained at least 60% tumor tissue as evaluated by H&E staining. RNA was extracted using a technique based on magnetic beads. In brief, the FFPE section was deparaffinized in xylol and rehydrated in graded solutions of ethanol. The pellet was dried at room temperature for 10 min and subsequently lysed in lysis buffer and SDS for 5 min at 95ºC. Proteinase K was added and incubated for 2 h at 56ºC with shaking. A binding buffer and the magnetic beads were added for binding of the nucleic acids to the beads for 15 min at room temperature with shaking. On a magnetic rack, the supernatant was removed and the beads were washed several times with washing buffers. After addition of an elution buffer and incubation for 10 min at 70ºC with strong shaking, the supernatant was transferred to a new tube. This was followed by DNAse I treatment (NEB, Ipswich, MA, USA) according to the protocol provided by the manufacturer.

Kinetic RT-PCR

Intron-spanning primers and TaqMan fluorogenic probes for VEGF-C gene and the housekeeping gene *RPL37A* were provided by Siemens Healthcare Diagnostics (Cologne, Germany). All reactions were performed on an ABI Prism 7900 instrument (Applied Biosystems, Foster City, CA,

USA) using the Super Script III One-Step qRT-PCR Kit (Invitrogen, Karlsruhe, Germany) according to the manufacturer's instructions and a reaction volume of 10 μl on 384 well plates. PCR conditions were as follows: 30 min at 60°C for reverse transcription and 2 min at 95°C for Taq activation followed by 40 cycles of 95° for 30 s and 60°C for 60 s. All measurements were performed in triplicates. Cycle threshold (CT) values, which indicate the (interpolated) number of PCR cycles until the fluorescence reached its threshold, were determined. After initial measurement of RPL37A, its CT value was adjusted to 26 by dilution of each sample. Subsequently, the measurements for VEGF-C and RPL37A were performed in triplicate. Forty-ΔCT values were calculated as follows: $40-(CT_{VEGFC}–CT_{RPL37A})$. For quality control of raw data, the following preliminary conditions had to be fulfilled for each sample: CT value of the housekeeping gene was in a range between 22 and 28. At least two values were available for each sample and each gene whereas the single values differed by not more than 1 CT. CT values>40 were excluded. Ninety-seven samples met the quality criteria and were finally included in the statistical evaluation. Twenty-nine cases were excluded.

Statistical evaluation

Statistic analyses were computed using SPSS 15 (SPSS, Chicago, IL, USA), GraphPad Prism 4 statistical software (GraphPad Software, San Diego, CA, USA), and JMP 5.0.1.2 (SAS, Cary, NC, USA). The Mann–Whitney and Kruskal–Wallis tests were used for correlation with clinical and pathological features. For grouped data, Fisher's exact test was performed. Survival curves were compared by the Kaplan–Meier method and the log rank test. The Cox regression model was used for multivariate survival analysis. In general, p values<0.05 were considered as statistically significant. VEGF-C mRNA virtual copy numbers were divided in two groups. The cut-off point for survival analysis was chosen by application of a Chi-square based partitioning model of the JMP software.

Results

Study group of patients

The median age at diagnosis was 58 years with a range between 34 and 80 years. The medium follow-up time for event-free patients was 38 months (range, 2–83 months). In the follow-up period, 21 patients (21.6%) died. The median follow-up time for patients with non-progressive disease was 32 (0–67) months. Forty-six patients (47.4%) experienced disease relapse. Most patients had high-stage, high-grade serous adenocarcinomas in accordance with the general population of ovarian cancer patients. Data on adjuvant therapy were available for 92 patients; 89 (96.7%) received standard chemotherapy with a platinum compound and paclitaxel. Two FIGO stage I patients did not receive chemotherapy. The distribution of all clinicopathological factors is given in Table 1.

Expression of VEGF-C in ovarian cancer

RNA was isolated from archival tissue samples, and the expression of VEGF-C mRNA was determined by kinetic RT-PCR. The data distribution as illustrated in Fig. 1 shows

Table 1 Patient characteristics

Parameter	Cases (no)	Percent (%)
Age at surgery (years)		
≤60	55	56.7
>60	42	43.3
Histological type		
Serous	67	69.0
Mucinous	3	3.1
Endometroid	12	12.4
Clear cell	2	2.1
Transitional cell	5	5.2
Undifferentiated	8	8.2
FIGO stage		
I	18	18.6
II	7	7.2
III	66	68
IV	6	6.2
pT		
pT1	20	20.6
pT2	10	10.3
pT3	67	69.1
pN		
pN0	39	40.3
pN1	41	42.2
pNX	17	17.5
Silverberg grade		
G1	13	13.4
G2	43	44.3
G3	41	42.3
Postoperative residual tumor		
None	47	48.5
<2 cm	15	15.5
>2 cm	10	10.3
Missing	25	25.7
Chemotherapy (CTX)		
Platinum-based	89	91.8
Other CTX	1	1.0
No CTX	2	2.1
Missing	5	5.1

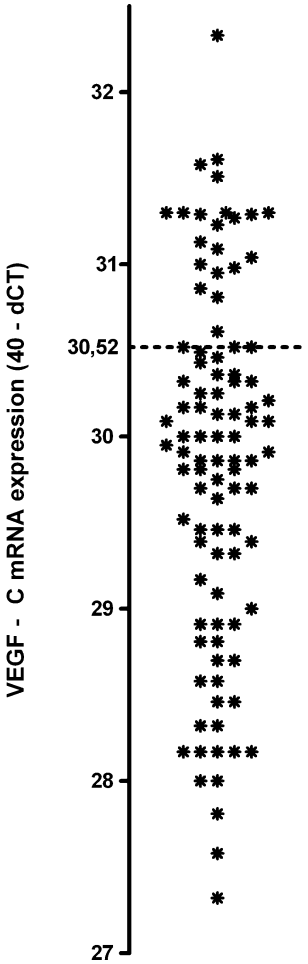

Fig. 1 Expression of VEGF-C in ovarian cancer: distribution of mRNA levels. *Dotted line*, cut-off for survival analysis

a separation of the study cohort in two groups of cases with low and high VEGF-C mRNA expression, respectively. The cutoff for statistical analyses was chosen as described above and defined as 30.52.

Correlation of VEGF-C expression with clinical and pathological features

We observed a correlation between higher VEGF-C expression and the residual tumor size after primary surgery (p=0.037, Fig. 2a). No significant correlation was found between VEGF-C expression and patient age (age≤60 vs. age>60 years; p=0.3495 years), histological type (serous and undifferentiated vs. other; p=0.9725), Silverberg grade (grade 1–2 vs. grade 3; p=0.0967), FIGO stage (FIGO I-II vs. III-IV; p=0.8078), pT stage (pT1–2 vs. pT 3; p=0.8331), or pN stage (pN1 vs. pN0, p=0.4812, Fig. 2b).

Impact of VEGF-C expression on patient survival

VEGF-C mRNA expression revealed its prognostic value in univariate survival analysis. Patients whose tumors expressed high levels of VEGF-C mRNA had a significantly shorter overall survival than patients with low VEGF-C expressing tumors (p=0.039). A favorable prognostic influence of low VEGF-C expression could also be observed for progression-free survival (p=0.016, Fig. 3). Other significant factors for overall and progression-free survival were tumor grade (p=0.011 and p=0.032, respectively), pN (p=0.006 and p<0.001), and residual tumor size <> 2 cm (p=0.001 and p=0.015).

In an exploratory multivariate survival analysis including VEGF-C expression as well as tumor grade, lymph node metastases, and residual tumor size, only a small residual tumor size after surgery was an independent predictor for favorable overall survival (p=0.008, hazard ratio (HR)= 0.176 with a 95% confidence interval (CI) of 0.048 to 0.642). However, in Cox regression analysis for progression-free survival, VEGF-C mRNA retained its prognostic influence (p=0.006, HR=0.319 with a 95% confidence interval of 0.142–0.720). Other significant factors were the postoperative residual tumor mass after surgery (p=0.024, HR=0.330 with a CI of 0.126–0.846) and lymph node metastasis (p=0.008, HR=0.362 with a CI of 0.170–0.770).

VEGF-C expression in ovarian cancer subgroups

We analyzed the influence of VEGF-C mRNA in the most important ovarian cancer subgroups. VEGF-C mRNA was still a negative predictor of overall and progression-free survival and in the subgroups of serous tumors (p=0.0190 and 0.0375, respectively), the group of high-grade (G2-3) tumors (p=0.0311 and 0.0010, respectively). In the group of patients with high clinical stage (FIGO III-IV), a trend could be observed (p=0.0634 and 0.0612, respectively; Fig. 4).

Discussion

Our study demonstrates that high VEGF-C mRNA expression in ovarian cancer is associated with poor patient

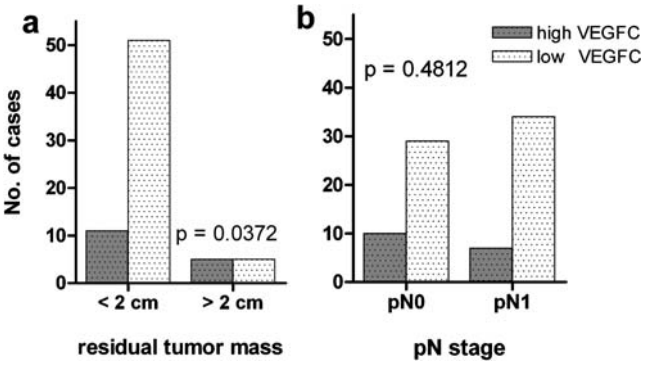

Fig. 2 **a** Correlation of VEGF-C expression with residual tumor mass after primary surgery. **b** Correlation with pN stage (Fisher's exact test, 2-tailed)

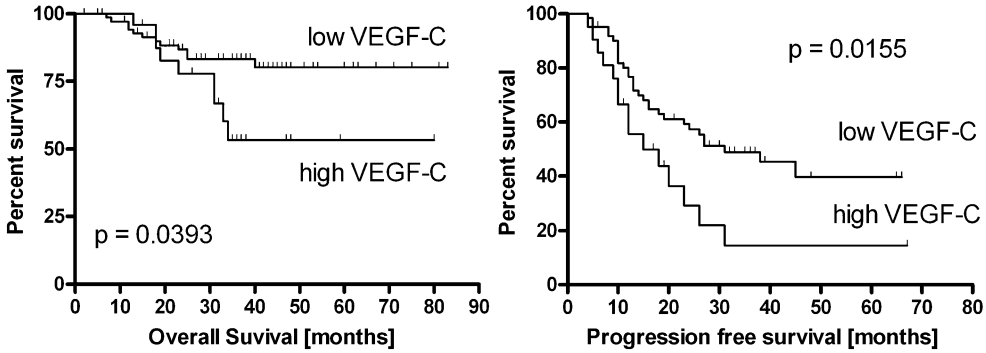

Fig. 3 Kaplan–Meier analysis. VEGF-C mRNA is a positive prognostic factor in ovarian cancer for overall (p=0.0393) and progression-free survival (p=0.0155, log rank test)

outcome and is an independent predictor of progression-free patient survival. Although we do not provide a direct comparison between VEGF-C mRNA determinations in fresh frozen and FFPE tissue, our study indicates that formalin-fixed paraffin-embedded tissue is suitable for the determination of VEGF-C gene expression using kinetic RT-PCR. The successful validation of markers identified in fresh frozen tissue after transfer into formalin fixed tissue analysis has recently been published for the prognostic role of estrogen receptor 1 mRNA expression in ovarian cancer [17, 18]. To our knowledge, this is the first study to determine VEGF-C expression in epithelial ovarian cancer using kinetic RT-PCR and the first to assess VEGF-C mRNA expression in formalin-fixed paraffin-embedded tissue samples. Although the determination of mRNA may not always directly reflect expression of the corresponding protein, in the case of a soluble tissue factor like VEGF-C, the analysis of mRNA levels seems more reasonable.

Our data characterize VEGF-C overexpression as a feature of aggressive ovarian carcinomas. The association with the strong prognostic factor residual tumor mass might explain the lack of independent prognostic value of VEGF-C expression on overall survival. We found a negative impact of high VEGF-C expression on patient outcome in the subgroups of serous tumors and high-grade tumors. A trend could be observed for patients with advanced clinical stage. However, the value of these data may be limited due to small patient subgroups.

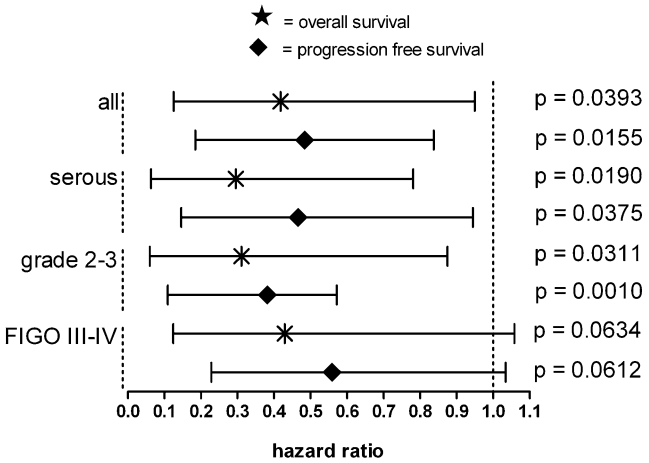

Fig. 4 Expression of VEGF-C mRNA in ovarian cancer subgroups: serous tumors, high grade tumors, and tumors with high clinical stage (log rank test, hazard ratio with 95% confidence interval)

In line with our findings, overexpression and association of VEGF-C with poor overall survival is described in a variety of human cancers [19, 20]. In ovarian cancer, a correlation of VEGF-C with lymph node metastases and worse overall survival is described by several studies using immunohistochemistry. In a study on 59 epithelial ovarian carcinomas, an increase of immunoreactivity was found from benign and borderline tumors towards invasive carcinomas. The expression correlated with lymph node metastases and peritoneal metastases outside the pelvic cavity. High levels of VEGF-C were also associated with worse patient survival [21]. Another study describes the correlation of VEGF-C with tumor grade, clinical stage, and lymph node metastases [22]. In a study on 80 specimens of ovarian cancer, patients with lower VEGF-C expression had a higher five-year survival rate than those with high expression. There was also a correlation between VEGF-C expression and peritoneal metastases outside the pelvic cavity and lymph node metastases [23]. In a study examining 73 ovarian carcinomas, a correlation is described between VEGF-C expression and clinical stage as well as lymph node metastases outside the pelvic cavity [14].

Contrary to the studies cited above, we did not detect an association between VEGF-C expression and nodal state, which indicates that VEGF-C mRNA expression in contrast to VEGF-C protein expression, might not be a predictive factor of lymph node metastasis but might rather reflect other mechanisms by which VEGF-C exerts an influence on tumor aggressiveness.

In vitro studies have elucidated the impact of VEGF-C expression on tumor progression. In cultured ovarian cancer cells, the influence of VEGF-C expression on tumor invasiveness was described as well as a correlation of VEGF-C expression with increased expression of matrix metalloproteinase 2 (MMP-2). An autocrine mechanism of

induction of invasiveness was proposed via VEGF-C-induced MMP-2 expression. This correlation could be confirmed in vivo [14]. VEGF-C exerts its effect on lymphatic endothelial cells through activation of tyrosine kinase receptors, manly VEGFR-3. In lymphatic endothelial cells, VEGFR-3 stimulation is followed by protein C-dependent activation of the p42/p44 mitogen-acivated proteine kinase (MAPK) pathway and induction of Akt phosphorylation [24, 25]. The VEGFR-3-mediated pathways are well described in lymphatic endothelial cells and VEGF-C levels have been shown to correlate with lymph node metastases in several human cancers [25]. However, VEGFR-3 is not solely expressed on lymphatic endothelial cells but also on a variety of different cancer cells, among them ovarian cancer [23], but also prostate cancer [26], leukemia [27], lung adenocarcinoma [28], colorectal carcinoma [29], head and neck cancer [30], and cervical cancer [31]. Thus, VEGF-C may affect cancer development or progression by direct effects on tumor cells. The VEGF-C/VEGFR-3 axis plays an important role in promoting invasion and metastasis of lung adenocarcinoma cells in vitro [28]. Transfection of cells with VEGF-C increased invasive abilities, and expression of both VEGFR-3 and VEGF-C led to an enhancement of invasion in an autocrine manner of stimulation. Blockade of the axis had inhibitory effects on cell invasiveness. Neural cell adhesion molecule CNTN-1 was described as downstream mediator of VEGF-C/VEGFR-3-induced invasion and metastasis through activation of Src/p38 MAPK-mediated C/EBP signaling. CNTN-1 regulates rearrangement of F-actin cytoskeleton and facilitated invasive behavior of carcinoma cells in vitro [28]. Inhibition of VEGF-C leads to inhibition of cellular motility in breast cancer cell lines demonstrating another mechanism of VEGF-C action in vitro [32]. Furthermore, VEGF-C also binds to other receptors like VEGFR-2, which main ligand is VEGF-A and neuropillin (NRP) pointing at another possible interaction with downstream effector cascades [33].

Our finding of an unfavorable prognosis of VEGF-C overexpression may reflect direct autocrine and paracrine effects of VEGF-C on cellular oncogenes. Further studies are needed to investigate the influence of VEGF-C expression on ovarian cancer cells for a better understanding of the VEGF-C action in this tumor.

In summary, VEGF-C expression as detected by quantitative RT-PCR (qRT-PCR) in RNA extracted from FFPE tissue provides additional information to detect high-risk tumors among patients with epithelial ovarian cancer. The validation of these data in future studies including larger numbers of patients seems promising.

Acknowledgements We would like to thank Mrs. Susanne Scharff for the excellent technical assistance.

Conflict of Interest Ralph M. Wirtz is an employee of Siemens Healthcare Diagnostics, Cologne, Germany. According to all other authors, there is no conflict of interest that could be perceived as prejudicing the impartiality of the research reported.

References

1. Jemal A, Siegel R, Ward E et al (2008) Cancer statistics. CA Cancer J Clin 58(2):71–96
2. Aletti GD, Gallenberg MM, Cliby WA et al (2007) Current management strategies for ovarian cancer. Mayo Clin Proc 82 (6):751–770
3. Srinivasan M, Sedmak D, Jewell S (2002) Effect of fixatives and tissue processing on the content and integrity of nucleic acids. Am J Pathol 161(6):1961–1971
4. Von Ahlfen S, Missel A, Bendrat K et al (2007) Determinants of RNA Quality from FFPE Samples. PLoS ONE 2(12):e1261
5. Lewis F, Maughan NJ, Smith V et al (2001) Unlocking the archive-gene expression in paraffin-embedded tissue. J Pathol 195(1):66–71
6. Abrahamsen HN, Steiniche T, Nexo E et al (2003) Towards quantitative mRNA analysis in paraffin-embedded tissues using real-time reverse transcriptase-polymerase chain reaction: a methodological study on lymph nodes from melanoma patients. J Mol Diagn 5(1):34–41
7. Penland SK, Keku TO, Torrice C et al (2007) RNA expression analysis of formalin-fixed paraffin-embedded tumors. Lab Invest 87(4):383–389
8. Cronin M, Pho M, Dutta D et al (2004) Measurement of gene expression in archival paraffin-embedded tissues: development and performance of a 92-gene reverse transcriptase-polymerase chain reaction assay. Am J Pathol 164(1):35–42
9. Godfrey TE, Kim SH, Chavira M et al (2000) Quantitative mRNA expression analysis from formalin-fixed, paraffin-embedded tissues using 5' nuclease quantitative reverse transcription-polymerase chain reaction. J Mol Diagn 2(2):84–91
10. Chang J, Makris A, Gutierrez M et al (2008) Gene expression patterns in formalin-fixed, paraffin-embedded core biopsies predict docetaxel chemosensitivity in breast cancer patients. Breast Cancer Res Treat 108(2):233–240
11. Jeltsch M (1997) Hyperplasia of lymphatic vessels in VEGF-C transgenic mice. Science 276(5317):1423–1425
12. Skobe M, Hawighorst T, Jackson DG et al (2001) Induction of tumor lymphangiogenesis by VEGF-C promotes breast cancer metastasis. Nat Med 7(2):192–198
13. Mandriota SJ, Jussila L, Jeltsch M et al (2001) Vascular endothelial growth factor-C-mediated lymphangiogenesis promotes tumour metastasis. EMBO J 20(4):672–682
14. Ueda M, Hung YC, Terai Y et al (2005) Vascular endothelial growth factor-C expression and invasive phenotype in ovarian carcinomas. Clin Cancer Res 11(9):3225–3232
15. Salven P, Lymboussaki A, Heikkila P et al (1998) Vascular endothelial growth factors VEGF-B and VEGF-C are expressed in human tumors. Am J Pathol 153:103–108
16. Silverberg SG (2000) Histopathologic grading of ovarian carcinoma: a review and proposal. Int J Gynecol Pathol 19(1):7–15
17. Zamagni C, Wirtz R, De Iaco P et al (2009) Oestrogen receptor 1 mRNA is a prognostic factor in ovarian cancer patients treated with neoadjuvant chemotherapy: determination by array and kinetic PCR in fresh frozen tissue biopsies. Endocr Relat Cancer [Epub ahead of print]
18. Darb-Esfahani, Wirtz R, Sinn B et al (2009) Estrogen receptor 1 mRNA is a prognostic factor in ovrian carcinoma: determination by kinetic PCR in formalin-fixed paraffin-embedded tissue. Enodcr Relat Cancer [Epub ahead of print]

19. Stacker S, Achen M, Jussila L et al (2002) Lymphangiogenesis and cancer metastasis. Nat Rev Cancer 2(8):573–583
20. Sugirua T, Inoue Y, Matsuki R et al (2009) VEGF-C and VEGF-D expression is correlated with lymphatic vessel density and lymph node metastasis in oral squamous cell carcinoma: Implications for use as a prognostic marker. Int J Oncol 34(3):673–680
21. Yokoyama Y, Charnock-Jones D, Licence D et al (2003) Vascular endothelial growth factor-D is an independent prognostic factor in epithelial ovarian carcinoma. Br J Cancer 88(2):237–24
22. Bolat F, Gumurdulu D, Erkanli S et al (2008) Maspin over-expression correlates with increased expression of vascular endothelial growth factors A, C, and D in human ovarian carcinoma. Pathol Res Pract 204(6):379–387
23. Nishida N, Yano H, Komai K et al (2004) Vascular endothelial growth factor C and vascular endothelial growth factor receptor 2 are related closely to the prognosis of patients with ovarian carcinoma. Cancer 101(6):1364–1374
24. Mäkinen T, Veikkola T, Mustjoki S et al (2001) Isolated lymphatic endothelial cells transduce growth, survival and migratory signals via the VEGF-C/D receptor VEGFR-3. EMBO J 20(17):4762–4773
25. Alitalo K, Carmeliet P (2002) Molecular mechanisms of lymphangiogenesis in health and disease. Cancer Cell 1(3):219–227
26. Kaushal V, Mukunyadzi P, Dennis RA et al (2005) Stage-specific characterization of the vascular endothelial growth factor axis in prostate cancer: expression of lymphangiogenic markers is associated with advanced-stage disease. Clin Cancer Res 11(2 Pt 1):584–593
27. Dias S, Choy M, Alitalo K et al (2002) Vascular endothelial growth factor (VEGF)-C signaling through FLT-4 (VEGFR-3) mediates leukemic cell proliferation, survival, and resistance to chemotherapy. Blood 99(6):2179–2184
28. Su J, Yang P, Shih J et al (2006) The VEGF-C/Flt-4 axis promotes invasion and metastasis of cancer cells. Cancer Cell 9(3):209–223
29. Witte D, Thomas A, Ali N et al (2002) Expression of the vascular endothelial growth factor receptor-3 (VEGFR-3) and its ligand VEGF-C in human colorectal adenocarcinoma. Anticancer Res 22 (3):1463–1466
30. Neuchrist C, Erovic BM, Handisurya A et al (2003) Vascular endothelial growth factor C and vascular endothelial growth factor receptor 3 expression in squamous cell carcinomas of the head and neck. Head Neck 25(6):464–474
31. Van Trappen PO, Steele D et al (2003) Expression of vascular endothelial growth factor (VEGF)-C and VEGF-D, and their receptor VEGFR-3, during different stages of cervical carcinogenesis. J Pathol 201(4):544–554
32. Timoshenko AV, Rastogi S, Lala PK (2007) Migration-promoting role of VEGF-C and VEGF-C binding receptors in human breast cancer cells. Br J Cancer 97(8):1090–1098
33. Favier B (2006) Neuropilin-2 interacts with VEGFR-2 and VEGFR-3 and promotes human endothelial cell survival and migration. Blood 108(4):1243–1250

Virchows Arch (2009) 455:469–475
DOI 10.1007/s00428-009-0858-z

ORIGINAL ARTICLE

Borderline and malignant phyllodes tumors display similar promoter methylation profiles

Jo-Heon Kim · Yoo Duk Choi · Ji Shin Lee · Jae Hyuk Lee · Jong Hee Nam · Chan Choi · Min Ho Park · Jung Han Yoon

Received: 5 October 2009 / Revised: 29 October 2009 / Accepted: 1 November 2009 / Published online: 19 November 2009

Abstract Mammary phyllodes tumors (PTs) are uncommon fibroepithelial neoplasms. On the basis of histologic criteria, PTs can be divided into benign, borderline, and malignant groups; however, the histologic distinction of PTs is often difficult and arbitrary. In breast cancer, promoter hypermethylation is a common phenomenon, but there are no data available concerning methylation status in PTs. The aim of this study was to assess whether the methylation profiles support the classification of PTs into three subgroups. A multiplex, nested, methylation-specific polymerase chain reaction approach was used to examine promoter methylation of five genes (GSTP1, HIN-1, RAR-β, RASSF1A, and Twist) in 87 PTs (54 benign, 23 borderline, and 10 malignant). Immunohistochemical staining for GSTP1 was performed using tissue microarray blocks to determine whether GSTP1 promoter hypermethylation correlated with loss of GSTP1 expression. There was a trend of increasing methylation frequency with increasing grade of PTs. The methylation frequency of all genes and the mean number of methylated genes in borderline and malignant PTs were higher than those in benign PTs; however, there were no statistically significant differences between borderline and malignant PTs. GSTP1 promoter hypermethylation was associated with loss of GSTP1 expression ($p<0.001$). These results suggest that PTs segregate into only two groups on the basis of their methylation profiles: the benign group and the combined borderline/malignant group.

Keywords Breast tumor · Phyllodes · Classification · Methylation

J.-H. Kim · Y. D. Choi · J. S. Lee · J. H. Lee · J. H. Nam · C. Choi
Department of Pathology, Chonnam National University Medical School and Research Institute of Medical Sciences, Gwangju, South Korea

M. H. Park · J. H. Yoon
Department of Surgery, Chonnam National University Medical School and Research Institute of Medical Sciences, Gwangju, South Korea

J. S. Lee (✉)
Department of Pathology,
Chonnam National University Hwasun Hospital,
160, IIsim-ri, Hwasun-eup,
Hwasun-gun, Jeollanam-do 519-809, Republic of Korea
e-mail: jshinlee@hanmail.net

Introduction

Phyllodes tumors (PTs) are rare tumors characterized by myoepitehlial and luminal epithelial component arranged in clefts surrounded by an overgrowing hypercellular mesenchymal component typically organized in leaf-like structure [1].

Several grading systems have been proposed consisting of either two or three subgroups [2–4]. Recently, the 2003 WHO classification of tumors proposed a classification of breast PTs in three categories (benign, borderline, and malignant). This grading system does have some correlation with the biological behavior of PTs [1]. It is important to distinguish benign from borderline and malignant PTs because the former do not metastasize [4]. Tumor grade has been correlated with expression of Ki-67, c-kit, vascular endothelial growth factor (VEGF), p53, CD10, and epidermal growth factor receptor (EGFR) [5–11]. Accurate classification of PTs continues to be challenging under many circumstances; therefore, additional biological markers based on molecular changes are needed.

There is mounting evidence that breast cancer develops by gradual accumulation of interacting epigenetic and genetic events over time [12]. Most recent studies of PTs have concentrated on the genetic changes detected in the tumors [13–15]. On the basis of patterns of chromosomal changes

by comparative genomic hybridization (CGH), Laé et al. classified PTs into two categories (benign and malignant) instead of three categories [13].

DNA methylation is an enzyme-induced chemical modification that usually occurs in cytosine–guanine dinucleotide rich regions (CpG islands) at the gene promoter sites. Aberrant promoter methylation of tumor suppressor genes has been established as an important epigenetic mechanism for gene silencing [16, 17]. Although inactivation of multiple tumor suppressor genes by aberrant promoter hypermethylation has been reported in breast cancer [12, 18, 19], methylation status in PTs has not been well documented in the literature with only one published report in a small series of eight PTs [14].

The purpose of this study was to assess whether the methylation profiles support the classification of PTs into three subgroups. A multiplex, nested, methylation-specific polymerase chain reaction (MSP) approach was used to examine promoter methylation of five genes [glutathione *S*-transferase pi gene (GSTP1), HIN-1, retinoic acid receptor-β (RAR-β), ras association domain family member 1 (RASSF1A), and Twist] in 87 PTs (54 benign, 23 borderline, and 10 malignant). These genes were selected because they are frequently methylated in breast cancer, but not in normal breast tissues [12, 18, 19]. We also studied the expression of GSTP1 protein by immunohistochemistry and compared its expression with GSTP1 methylation status.

Materials and method

Tumor samples

The histologic files of the four participating institutions (Chonnam National University Medical School Hospital, Chonnam National University Medical School Hwasun Hospital, Cell In All Private Clinics, and Foryou Private Clinics) between January 1999 and January 2009 were searched for PTs of the breast. Tumor tissue use was approved by the local ethical committee.

At least two pathologists reviewed and graded the cases as benign, borderline, or malignant PTs according to the WHO guidelines [1]. A total of 87 cases were reviewed, including 54 benign, 23 borderline, and 10 malignant PTs. These were obtained from 84 patients, with one tumor from each of 81 patients and two tumors (including the original and recurrent tumors) from each of three patients. One representative paraffin block from each case was subjected to methylation study and immunohistochemistry.

Sodium bisulfite treatment and MSP

For DNA extraction, one 5-μm tissue section was deparaffinized with xylene. On a mirror-imaged hematoxylyn–eosin-stained slide, the region of interest was manually scraped off to ensure a specific cell population of more than 80% in the preparation. The scraped tissue was extracted in 27 μL TNES (10 mM Tris, pH 8.0, 150 mM NaCl, 2 mM EDTA, 1% SDS) containing 3 μL proteinase K for 4 h at 52°C. The tissue extract was heat inactivated at 99°C for 10 min and separated by centrifugation at 13,000 rpm for 30 s. A 13.5 μL sample of the supernatant was used as a DNA source for sodium bisulfite treatment [20]. DNA was heated 10 min to 99°C, quick chilled, and incubated with 1.5 μL of 2 mol/L NaOH for 30 min at 42°C. Freshly prepared 3.6 mol/L sodium bisulfite containing 1 mmol/L hydroquinone was mixed with DNA, then overlaid with oil, and incubated at 55°C for 5 h in the dark. The sample was desalted using ion exchange columns (Amersham, Piscataway, NJ, USA). DNA was precipitated with 200 μL absolute alcohol, washed with 70% ethanol, air-dried, and resuspended in water (20 μL). Samples were stored at −80°C until use.

The methylation status of the five different genes was analyzed by MSP using a multiplex, nested PCR approach, as described previously [19]. Step 1 of the nested MSP was performed with primer sets (sense and antisense) for all five individual genes in each reaction. Step 1 primers contained no CpG dinucleotides and flanked the CpG-rich promoter regions of their respective targeted genes. Hence, these primers did not discriminate between methylated and unmethylated nucleotides after bisulfite treatment. A negative control for the assay (water only) and unmethylated (human sperm) and methylated (MDA-MB-231 breast cancer cells) DNA controls were included in each set of multiplex step 1 reactions. Depending upon the starting amount of DNA, PCR products from step 1 reactions were diluted (1:5 to 1:1,000) in water and subjected to the second step of the MSP reaction. This incorporated two sets of primers for each gene (labeled as unmethylated or methylated), which were designed to recognize differences arising from bisulfite-induced modifications of unmethylated cytosines. All of the primer sequences and PCR conditions for this nested MSP approach have been published previously [21–23]. The PCR products underwent electrophoresis on 2% agarose gel and were visualized under UV illumination using ethidium bromide staining. Any tumor sample that reliably yielded a PCR product in the methylated reaction was considered positive for promoter hypermethylation.

Tissue microarray construction

The arrays were constructed with a 2-mm punch on the Beecher arrayer. The array layout in grid format was designed using Microsoft Excel. Hematoxylin-and-eosin-

stained sections of PTs were reviewed, and the area of interest was marked on the slide. Using a marker pen, the corresponding region was circled on the archival "donor" paraffin block. The samples were then arrayed on to a "recipient" blank block. A total of 82 PTs were subjected to at least one punch per case; 78 cases had two microarray cores and four cases had one core.

Immunohistochemistry

Immunohistochemical analysis of GSTP1 protein expression was performed by the avidin–biotin–peroxidase complex method. Sections were deparaffinized and were placed in a microwave oven with a 2.1% citric acid buffer solution (pH 6.0) for 10 min to retrieve the antigens. After microwave processing, the sections were incubated overnight at 4°C with primary anti-GSTP1 antibody (1:100 dilution, clone GSTpi, Novocastra, Burlingame, CA, USA). The streptavidin–horseradish peroxidase (Research Genetics, Huntsville, AL, USA) detection system was applied, followed by 30 min of incubation at room temperature. After washing, the tissue sections were developed with a peroxidase substrate solution (3,3-diaminobenzidine tetrahydrochloride). The sections were counterstained with hematoxylin, dehydrated, and mounted. For negative controls, sections were treated similarly with the exception of the primary antibody. Because the epithelial component mostly displayed a reaction pattern as seen in the normal breast, GSTP1 immunohistochemical staining was only assessed in stromal components. GSTP1 expression was considered to be positive when >10% of stromal cells exhibited cytoplasmic or nuclear staining [24]. For cases with more than one TMA core, the decision of positivity was based on the average percentage of positive cells.

Statistical analysis

The linear by linear association for trend was used to assess the statistical significance in the proportion of samples in which methylation was detected with increasing grade of PTs. The trend of methylation increase with PTs grade was determined using the Spearman's rank correlation test. The χ^2 test was used to determine the difference in methylation frequencies between groups. One-way ANOVA was used to assess the differences of age and tumor size between the benign, borderline, and malignant PTs. When there was a statistically significant difference between three groups of PTs, the Bonferroni correlation was used to compare the difference. For all statistical analyses, the SPSS system for personal computer (version 13.5 for windows; SPSS INC., Chicago, IL, USA) was used, and $p<0.05$ was regarded as statistically significant.

Results

Clinicopathological characteristics

For the benign, borderline, and malignant PTs, the mean age was 40, 43, and 43 years, respectively, and the mean tumor size was 4.0, 5.4, and 5.5 cm, respectively. There was an increase in tumor size with increasing degree of malignancy, but the differences were not statistically significant. The median follow-up period was 30 months (range, 4–103 months). Nine patients experienced recurrent disease (seven benign and two borderline). Six of these had positive margins. The mean time to recurrence was 24 months, with a median of 22 months and range of 10–47 months. The original and recurrent tumors of three patients with benign PTs were included in this study. Histologically, two recurred as benign PTs and one recurred as a malignant PT.

Frequency of promoter hypermethylation

Representative examples of the MSP products obtained from step 2 of the nested MSP analysis for five genes are shown in Fig. 1. The frequency of methylation of each gene locus in benign, borderline, and malignant PTs is shown in Table 1. There was a trend of increasing methylation frequency with increasing grade of the PTs. Statistically significant differences among the three subgroups of PTs were found in all of the genes, except for GSTP1. Overall significant differences in methylation frequency were observed for HIN-1 ($p<0.005$), RAR-β ($p<0.001$), RASSF1A ($p<0.001$), and Twist ($p<0.001$; Table 1). In particular, RAR-β, RASSF1A, and Twist methylation frequency were significantly higher in borderline ($p<0.005$, $p<0.005$, and $p<0.001$, respectively) or malignant ($p<0.05$, $p<0.005$, and $p<0.01$, respectively) PTs compared to benign PTs; the methylation frequency was similar between borderline and malignant PTs. HIN-1 methylation frequency level was also higher in borderline

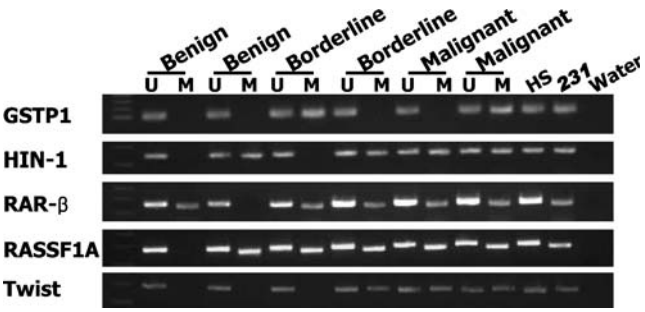

Fig. 1 Representative results of nested methylation-specific PCR analysis for HIN-1, GSTP1, RAR-β, RASSF1A, and Twist in phyllodes tumors of the breast. *Lanes U* and *M* correspond to unmethylated and methylated DNA, respectively. DNA from human sperm (*HS*) and MDA-MB-231 (*231*) breast cancer cell line served as positive controls for unmethylated and methylated genes, respectively. Water served as negative control

Table 1 Frequency of methylation in benign, borderline, and malignant phyllodes tumors

Gene	Frequency of methylation			*p* value			
	Benign (*n*=54)	Borderline (*n*=23)	Malignant (*n*=10)	Linear by linear	Be vs. Bo[a]	Be vs. Ma[a]	Bo vs. Ma[a]
GSTP1	6 (11.1%)	6 (26.1%)	3 (30.0%)	0.062	0.097	0.140	1.000
HIN-1	20 (37.0%)	14 (60.9%)	9 (90.0%)	0.001	0.054	0.004	0.123
RAR-β	31 (57.4%)	21 (91.3%)	10 (100%)	0.000	0.003	0.010	1.000
RASSF1A	26 (48.1%)	20 (87.0%)	10 (100%)	0.000	0.002	0.003	0.523
Twist	5 (9.3%)	11 (47.8%)	5 (50.0%)	0.000	0.000	0.006	1.000

Be benign, *Bo* borderline, *Ma* malignant, *NS* not significant

[a] Analyzed by χ^2 test

or malignant PTs compared to benign PTs; however, a statistically significant difference was only found between benign and malignant PTs ($p<0.01$). The methylation frequencies for HIN-1 did not differ significantly between borderline and malignant PTs.

The mean numbers of methylated genes were 1.63, 3.13, and 3.70 in benign, borderline, and malignant PTs, respectively. The differences between the benign and borderline and between the benign and malignant PTs were statistically significant ($p<0.001$ and $p=0.001$, respectively). A statistical difference was not detected between borderline and malignant PTs. There was a significant trend toward increased numbers of methylated genes with the increased grade of PTs (Spearman's $\rho=0.658$, $p<0.001$; Fig. 2). No differences were observed between the nonrecurrent and recurrent PTs for either the methylation frequency of all genes or the mean number of methylated genes (data not shown).

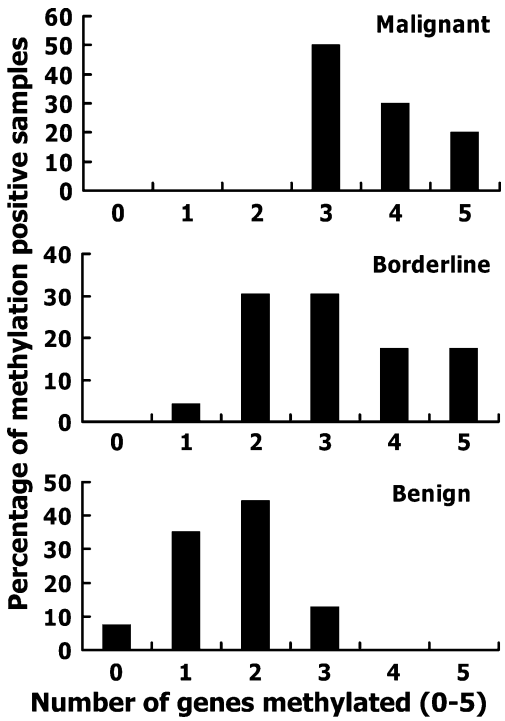

Fig. 2 Gene methylation increases with severity of phyllodes tumors. The trend was statistically significant ($p<0.001$)

Immunohistochemical analysis of GSTP1

Immunohistochemical staining using anti-GSTP1 antibody was performed to determine if GSTP1 promoter hypermethylation correlated with loss of GSTP1 expression. The epithelial and stromal cells of PTs showed both nuclear and cytoplasmic immunoreactivity for GSTP1 (Fig. 3). Loss of GSTP1 expression (negative) was observed in eight of 54 (14.8%) benign, four of 24 (17.4%) borderline, and three of 10 (30.0%) malignant PTs. Loss of GSTP1 expression was almost exclusively restricted to stromal cells. When the GSTP1 expression was compared against the methylation status of GSTP1, GSTP1 expression was more frequently lost in PTs with GSTP1 methylation than in PTs with unmethylated GSTP1 ($p < 0.001$; Table 2).

Discussion

This is the first large study comparing methylation profiles in the three subgroups of PTs. In this study, we have shown statistically significant differences in the methylation frequency and in the mean number of methylated genes between benign and borderline and between benign and malignant PTs. A statistical difference was not detected between the borderline and malignant PTs. On the basis of their methylation profiles, PTs can be segregated into two groups: the benign group and the combined borderline/malignant group.

Histologically, PTs are classified as benign, borderline, or malignant on the basis of stromal hypercellularity, cellular pleomorphism, mitotic rate, character of margins, stromal pattern, and existence of heterogeneous stromal elements [1]. Because only the borderline and malignant PTs metastasize, it is very important to distinguish benign from borderline and malignant PTs [4]. However, the

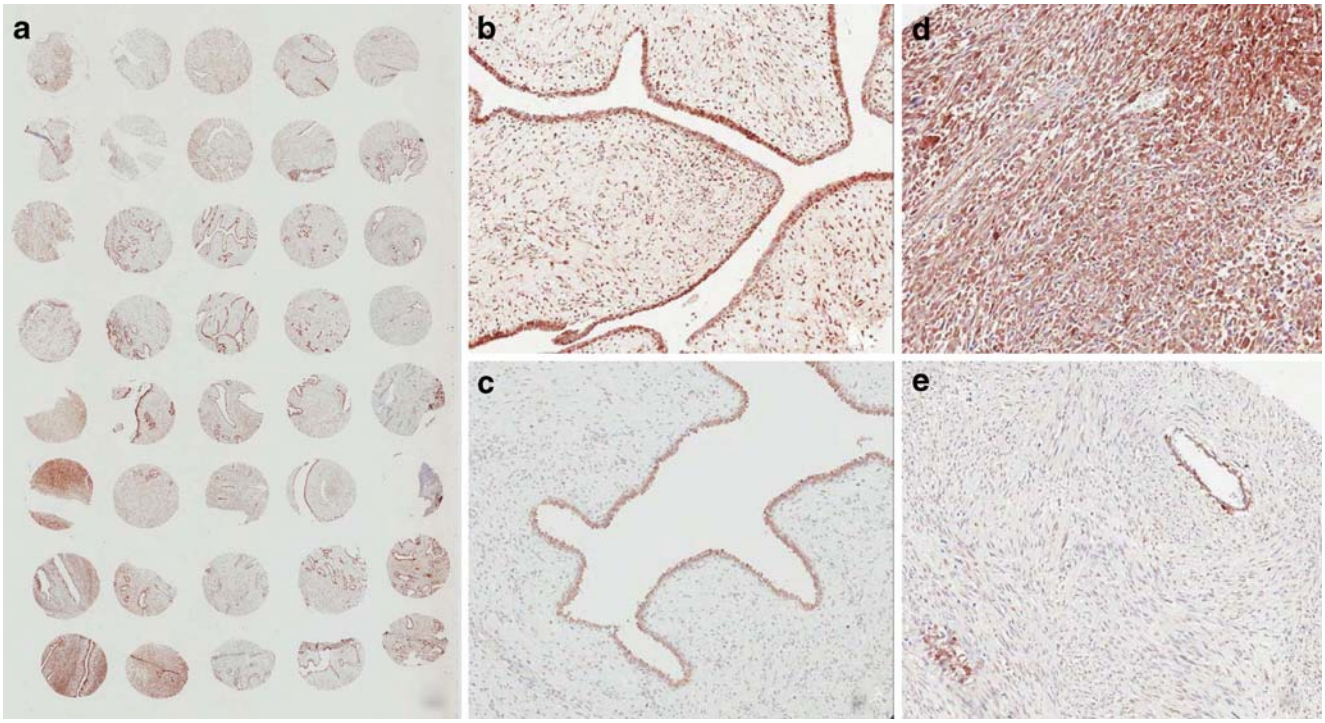

Fig. 3 Immunohistochemical staining of GSTP1 using tissue microarray blocks (**a**). Benign (**b**) and malignant (**d**) phyllodes tumor show diffuse nuclear and cytoplasmic staining representing a positive expression of GSTP1. Loss of GSTP1 expression is observed in benign (**c**) and malignant (**e**) PTs. Stromal cells were negative but epithelial cells were positive for GSTP1

distinction based on histological criteria between benign and borderline/malignant PTs can be difficult. Thus, many additional biological markers have been evaluated to distinguish benign from borderline/malignant PTs.

Many biological markers have been used in the evaluation of PTs. Stromal expression of Ki-67, p53, c-kit, VEGF, and EGFR was associated with grade of PTs [5–8, 11]. Benign, borderline, and malignant PTs differentially expressed CD10, p53, Ki-67, and c-kit [9, 10]. Expression of these markers significantly increased in borderline and malignant PTs vs. benign PTs, but there was no difference between borderline and malignant PTs.

Many genetic, epigenetic, and environmental factors contribute to the development of cancers. Most recent studies of PTs have concentrated on the genetic changes detected in the tumors. In a series of 30 PTs (nine benign, 12 borderline, and nine malignant), Laé et al. analyzed chromosomal changes detected by CGH in comparison with histological data [13]. Borderline and malignant PTs could not be differentiated on the basis of their genomic imbalances (e.g., presence and number of chromosomal changes and presence of 1q gain and/or 13q loss). Conversely, benign tumors could be significantly differentiated from the group composed of borderline and malignant tumors. This suggests that a classification of phyllodes tumors of the breast into two categories (benign and malignant) better reflects the genetic reality. Lv et al. also confirmed that molecular CGH features of borderline and malignant PTs were similar [15]. They used CGH to identify chromosomal aberrations in 36 cases of benign, borderline, or malignant PTs of the breast. That study demonstrated that in benign PTs, the number of gains and losses were in balance, while in the borderline and malignant groups, gains occurred more frequently than losses. A difference in chromosomal aberrations between borderline and malignant PTs was not evident. However, based on cluster analysis of array-CGH in 126 PTs (37 benign, 41 borderline, and 48 malignant), Jones et al. found more similarity between benign and borderline PTs compared to malignant tumors [14].

Table 2 GSTP1 expression in phyllodes tumor according to GSTP1 promoter methylation

	GSTP1 negative	GSTP1 positive	*p* value
GSTP1 unmethylated	7 (10.4%)	60 (89.6%)	<0.001
GSTP1 methylated	8 (53.3%)	7 (46.7%)	

Aberrant promoter methylation of tumor suppressor genes has been established as an important epigenetic mechanism for gene silencing [16, 17]. In this study, we have demonstrated a significant correlation between the promoter hypermethylation of GSTP1 and the data obtained

from immunohistochemical analyses. Promoter hypermethylation of GSTP1 resulted in the loss of GSTP1 protein expression in samples with methylation. These data provide evidence that GSTP1 promoter hypermethylation is a major mechanism involved in GSTP1 gene inactivation, resulting in impaired GSTP1 function during PTs development. However, PTs without GSTP1 hypermethylation were also negative for GSTP1 expression. These observations suggest that promoter hypermethylation is not the only mechanism of silencing the GSTP1 gene. Other mechanisms are implicated in the GSTP1 gene silencing in such tumors.

Although aberrant promoter hypermethylation has been well reported in breast cancer [12, 18, 19], there have not been many reports on the methylation status in PTs. There is only one study that has described the methylation of the p16 gene in eight borderline and malignant PTs [14]. They revealed p16 methylation in two of three malignant and five of five borderline PTs. In the present study, we graded PTs into benign, borderline, and malignant subgroups according to the guidelines of the WHO [1]. A panel of five gene promoters involved in breast carcinogenesis was assessed by nested MSP. Nested MSP is reported to be more sensitive than conventional MSP [25]. Methylation frequencies of HIN-1, RAR-β, RASSF1A, and Twist were significantly higher in borderline or malignant PTs than in benign PTs. However, no differences were observed between borderline and malignant PTs. The mean number of methylated genes was significantly different between benign and either borderline or malignant PTs, whereas the mean number of methylated genes was similar between borderline and malignant PTs. Promoter hypermethylation may aid in distinguishing benign from borderline or malignant PTs. This study provides evidence that borderline and malignant phyllodes tumors cannot be differentiated on the basis of promoter hypermethylation. Our study is limited by the small number of cases and by a relatively modest number of genes tested. Further studies with larger sample sizes and more genes are required to validate our results.

No association was identified between the methylation of each gene and the recurrence of PTs. Whether aberrant promoter methylation in PTs is associated with prognosis remains to be elucidated by long-term follow-up of our cohort.

In summary, we show for the first time that borderline and malignant PTs display similar promoter methylation profiles. These results suggest that PTs segregate by methylation profiles into only two groups: benign and borderline/malignant PTs.

Acknowledgments This work was supported by a grant (CRI08057-1) from the Chonnam National University Hospital Research Institute of Clinical Medicine and a Korea Research Foundation Grant funded by the Korean Government (MOEHRD, Basic Research Promotion Fund; KRF-2007-313-E00099) to Ji Shin Lee. We have no conflict of interests to declare.

References

1. Bellocq JP, Magro G (2003) Fibroepithelial tumors. In: Tavassoli FA, Devilee P (eds) World health organization classification of tumors: tumors of the breast and female genital organs. IARC, Lyon, pp 99–103
2. Layfield LJ, Hart J, Neuwirth H, Bohman R, Trumbull WE, Giuliano AE (1989) Relation between DNA ploidy and the clinical behavior of phyllodes tumors. Cancer 64:1486–1489
3. Parker SJ, Harries SA (2001) Phyllodes tumours. Postgrad Med J 77:428–435
4. Rosen PP (2001) Fibroepithelial neoplasms. In: Rosen PP (ed) Rosen's breast pathology, 2nd edn. Lippincott, Williams & Wilkins, Philadelphia, pp 163–200
5. Kleer CG, Giordano TJ, Braun T, Oberman HA (2001) Pathologic, immunohistochemical, and molecular features of benign and malignant phyllodes tumors of the breast. Mod Pathol 14:185–190
6. Sawyer EJ, Poulsom R, Hunt FT et al (2003) Malignant phyllodes tumours show stromal overexpression of c-myc and c-kit. J Pathol 200:59–64
7. Tse GM, Lui PC, Lee CS et al (2004) Stromal expression of vascular endothelial growth factor correlates with tumor grade and microvessel density in mammary phyllodes tumors: a multicenter study of 185 cases. Hum Pathol 35:1053–1057
8. Tan PH, Jayabaskar T, Yip G et al (2005) p53 and c-kit (CD117) protein expression as prognostic indicators in breast phyllodes tumors: a tissue microarray study. Mod Pathol 18:1527–1534
9. Tse GM, Tsang AK, Putti TC et al (2005) Stromal CD10 expression in mammary fibroadenomas and phyllodes tumours. J Clin Pathol 58:185–189
10. Esposito NN, Mohan D, Brufsky A, Lin Y, Kapali M, Dabbs DJ (2006) Phyllodes tumor: a clinicopathologic and immunohistochemical study of 30 cases. Arch Pathol Lab Med 130:1516–1521
11. Kersting C, Kuijper A, Schmidt H et al (2006) Amplifications of the epidermal growth factor receptor gene (egfr) are common in phyllodes tumors of the breast and are associated with tumor progression. Lab Invest 86:54–61
12. Widschwendter M, Jones PA (2002) DNA methylation and breast carcinogenesis. Oncogene 21:5462–5482
13. Laé M, Vincent-Salomon A, Savignoni A et al (2007) Phyllodes tumors of the breast segregate in two groups according to genetic criteria. Mod Pathol 20:435–444
14. Jones AM, Mitter R, Springall R, Graham T et al (2008) A comprehensive genetic profile of phyllodes tumours of the breast detects important mutations, intra-tumoral genetic heterogeneity and new genetic changes on recurrence. J Pathol 214:533–544
15. Lv S, Niu Y, Wei L, Liu Q, Wang X, Chen Y (2008) Chromosomal aberrations and genetic relations in benign, borderline and malignant phyllodes tumors of the breast: a comparative genomic hybridization study. Breast Cancer Res Treat 112:411–418
16. Wajed SA, Laird PW, DeMeester TR (2001) DNA methylation: an alternative pathway to cancer. Ann Surg 234:10–20
17. Momparler RL, Bovenzi V (2000) DNA methylation and cancer. J Cell Physiol 183:145–154
18. Lee JS, Lo PK, Fackler MJ et al (2007) A comparative study of Korean with Caucasian breast cancer reveals frequency of methylation in multiple genes correlates with breast cancer in young, ER, PR-negative breast cancer in Korean women. Cancer Biol Ther 6:1114–11120
19. Lee JS, Fackler MJ, Teo WW et al (2008) Quantitative promoter hypermethylation profiles of ductal carcinoma in situ in North

American and Korean women: potential applications for diagnosis. Cancer Biol Ther 7:1398–1406
20. Fackler MJ, Malone K, Zhang Z et al (2006) Quantitative multiplex methylation-specific PCR analysis doubles detection of tumor cells in breast ductal fluid. Clin Cancer Res 12:3306–3310
21. House MG, Herman JG, Guo MZ et al (2003) Aberrant hypermethylation of tumor suppressor genes in pancreatic endocrine neoplasms. Ann Surg 238:423–431
22. Fackler MJ, McVeigh M, Evron E et al (2003) DNA methylation of RASSF1A, HIN-1, RAR-beta, Cyclin D2 and Twist in in situ and invasive lobular breast carcinoma. Int J Cancer 107:970–975
23. Lee JS (2007) GSTP1 promoter hypermethylation is an early event in breast carcinogenesis. Virchows Arch 450:637–642
24. Huang J, Tan PH, Thiyagarajan J, Bay BH (2003) Prognostic significance of glutathione S-transferase-pi in invasive breast cancer. Mod Pathol 16:558–565
25. Palmisano WA, Divine KK, Saccomanno G et al (2000) Predicting lung cancer by detecting aberrant promoter methylation in sputum. Cancer Res 60:5954–5958

Virchows Arch (2009) 455:477–483
DOI 10.1007/s00428-009-0834-7

ORIGINAL ARTICLE

Encapsulated apocrine papillary carcinoma of the breast—a tumour of uncertain malignant potential: report of five cases

Melanie Seal · Christine Wilson · Gregory J. Naus · Stephen Chia · Terry C. Bainbridge · Malcolm M. Hayes

Received: 4 June 2009 / Revised: 24 August 2009 / Accepted: 1 September 2009 / Published online: 28 October 2009

Abstract Five cases of an unusual encapsulated apocrine papillary tumour are reported. All presented as cystic masses in the breast of women aged 44–84 years. Imaging studies showed a complex cyst often with one or more mural nodules. The key histological features are similar to those of classical encapsulated papillary carcinoma in that myoepithelial cells were absent within the papillary structures and at the periphery of the cyst. All were pure apocrine in type and showed variable degrees of cytological atypia and mitotic activity. All lacked evidence of malignancy in the breast tissue outside of the lesion. Sentinel lymph node biopsies performed in three of the cases were negative for metastases, and all have behaved in a benign fashion.

Keywords Breast neoplasms · Intracystic · Apocrine · Papillary carcinoma

M. Seal · S. Chia
The Department of Medical Oncology,
British Columbia Cancer Agency,
Vancouver, Canada

G. J. Naus · T. C. Bainbridge · M. M. Hayes (✉)
The Department of Pathology, British Columbia Cancer Agency,
Vancouver V5Z 4E6, Canada
e-mail: mhayes@bccancer.bc.ca

C. Wilson
The Department of Medical Imaging,
British Columbia Cancer Agency,
Vancouver, Canada

Introduction

Encapsulated papillary carcinoma (intracystic) of the breast (EPC) is a rare entity representing approximately 0.5–2.0% of all breast tumours [1]. Traditionally considered to be a variant of ductal carcinoma in situ (DCIS) characterised by papillary carcinoma within a cystically dilated duct, many authors now believe these tumours have malignant potential. This is based on evidence that they lack a myoepithelial cell layer at their periphery which pathologists consider a determinant for invasion. Furthermore, there have been case reports of intracystic papillary tumours metastatic to axillary lymph nodes and distant sites [1–3].

We present five cases of encapsulated apocrine papillary carcinoma of the breast and evaluate the clinical outcome of these patients. The objectives of this study are to describe the clinical, radiological, and pathological findings of these rare tumours and to discuss their malignant potential. Our goal is to aid clinicians and pathologists to make treatment decisions for patients who present with this diagnostic challenge.

Materials and methods

The clinical records, radiographical images, and pathology slides from five patients with suspected EPC of apocrine type seen during 1995–2009 at our centre were reviewed. Full ethics approval was obtained before commencing study.

Hematoxylin and Eosin (H&E) stained slides were available in all cases, and blocks were obtained for immunostaining of myoepithelial cells using a Ventana Benchmark XT autostainer. The antibodies used and staining protocols are summarised in Table 1.

Table 1 Antibodies and immunostaining protocols

Antibody	Clone	Dilution	Antigen retrieval	Indicator
P63	4A4 Dako	1:100	CCI-mild	VU-DAB
HCM	SMMS-1 Dako	1:50	CCI-standard	VU-DAB
CD10	56C6 Novo Castra	1:25	CCI-standard	VU-DAB
CK5/6	D5/16B4 Dako	1:50	CCI-standard	VU-DAB
CK14	LL002 Signet	1:50	CCI-mild	VU-DAB
MSA	HHF35 Dako	1:50	None	VU-DAB
ER	SP1 Ventana	Neat	CCI-mild	VU-DAB
PR	PGR636 Dako	1:100	CCI-standard	VU-DAB
HER2	4B5 Ventana	Neat	CCI-mild	VU-DAB
GCDFP-15	23A3 Dako	1:50	CCI-standard	VU-DAB

CCI Ventana proprietary buffer, *VU-DAB* Ventana UltraView diaminobenzidine kit, *HCM* smooth muscle heavy chain myosin, *MSA* muscle specific actin, *ER* oestrogen receptor, *PR* progesterone receptor, *HER2* Her2–neu, *CK* cytokeratin, *GCDFP-15* gross cystic disease fluid protein-15

Results

Clinical data

The clinical details are summarised in Table 2. All patients underwent partial mastectomy, and three had sentinel lymph node procedures. One patient received radiotherapy to the breast. None received systemic therapy. Although four patients had further biopsies, all were negative for malignancy, and no patient had recurrence. The length of follow-up in each case is given in Table 2.

Breast imaging

Mammograms were obtained in all cases. Four of the five patients showed soft tissue masses ranging in size from 3 to 12 cm (Fig. 1). Ultrasound examination showed a complex cyst with a mural nodule or intracystic papillary lesion in four patients. These nodules measured between 8 and 16 mm (Fig. 2). One case showed pleomorphic calcifications within the mass located in the cyst. One patient had multiple mural nodules with increased vascularity seen on Doppler ultrasound within them.

Table 2 Patient demographic information, treatment, and outcome

	Case 1	Case 2	Case 3	Case 4	Case 5
Age (years)	44	44	84	50	50
Clinical presentation	Patient palpated a new mass	Recurrent cyst requiring repeated drainage over several years. Mammogram showed area of concern	Bilateral recurrent cysts requiring drainage. New onset mastalgia in left breast	Bilateral recurrent cysts with pain (left>right)	Recurrent left breast cyst
Surgery	Left partial mastectomy	Left partial mastectomy and sentinel lymph node biopsy	Left partial mastectomy	Left partial mastectomy with reexcision and sentinel lymph node biopsy	Left partial mastectomy and sentinel lymph node biopsy
Radiation	No	42.5 Gy in 16 fractions	No	No	No
Systemic therapy	No	No	No	No	No
Follow-up (months)	36	17	41	7	3
Further procedures	Right breast biopsy for nodularity on clinical exam—negative for malignancy	Left breast pain with abnormal mammographic findings. Left breast biopsy—negative for malignancy	Left breast biopsies×2 due to new nodularity and pain at site of scar—negative for malignancy	MRI - bilateral cysts and enhancement at 6 o'clock right breast. US—hypoechoic nodular lesion. Biopsy—tubular adenoma	None
Postexcision recurrence	None	None	None	None	None
Status	Alive	Alive	Alive	Alive	Alive

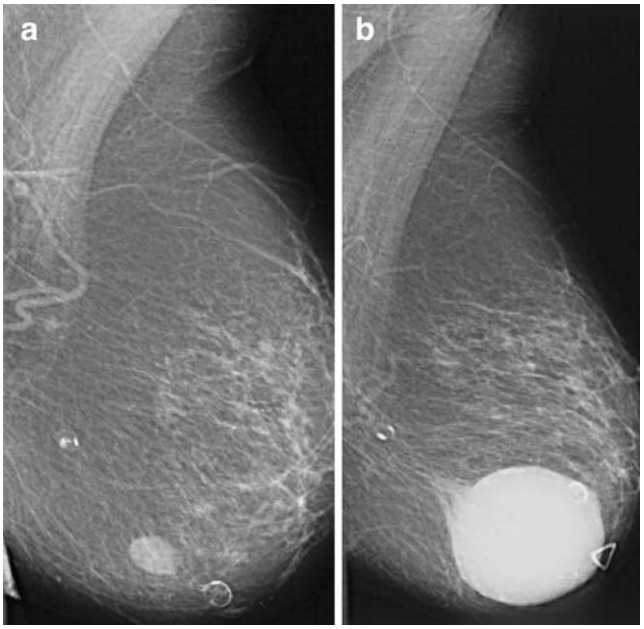

Fig. 1 Mammograms (left medial lateral oblique views) of case 3 **a** four years prior to diagnosis revealing small mass and **b** at diagnosis showing an increase in size of the mass

Pathological findings

Core biopsies were performed in four patients—two were interpreted as malignant (high-grade apocrine DCIS and low-grade apocrine papillary carcinoma), one as apocrine neoplasm of uncertain malignant potential, and one as fibrocystic change with apocrine metaplasia. These all went on to partial mastectomies with two requiring fine wire localisation prior to surgery. The cytology of the fine needle aspirates performed prior to excision in four of the cases showed apocrine cells and histiocytes that were interpreted as consistent with fibrocystic change.

Macroscopic findings

All cases showed a cystic mass that ranged in size from 1.2 to 4.5 cm. The cysts were received in a collapsed state which accounts for the discrepancy between the gross size and the size measured on imaging studies. The entire papillary component of the lesion was submitted for histological evaluation in all cases, and the encompassing cyst wall was sampled extensively. No other gross abnormalities were identified. The adjacent tissue was sampled in all cases. Fibrocystic changes were identified in the adjacent breast tissue.

Microscopic findings

All lesions were largely cystic with one or more papillary nodules attached to the wall of the cyst. A true papillary architecture characterised by cores of sclerotic fibrovascular stroma was observed within the tumours (Fig. 3). In all cases, the papillary structures were covered by a layer of proliferated apocrine cells (Fig. 4). The apocrine cell layer varied in complexity from a single cell layer through to multilayered epithelium forming a pseudopapillary and/or cribriform architecture. Apocrine cells also lined the cyst wall in all cases. There was no evidence of an infiltrative pattern outside the wall of the cyst. The apocrine cells showed a variable degree of cytological atypia but nuclear

Fig. 2 Left breast ultrasound from case 4 demonstrating a 10-cm cyst containing a 1.6-cm echogenic nodule

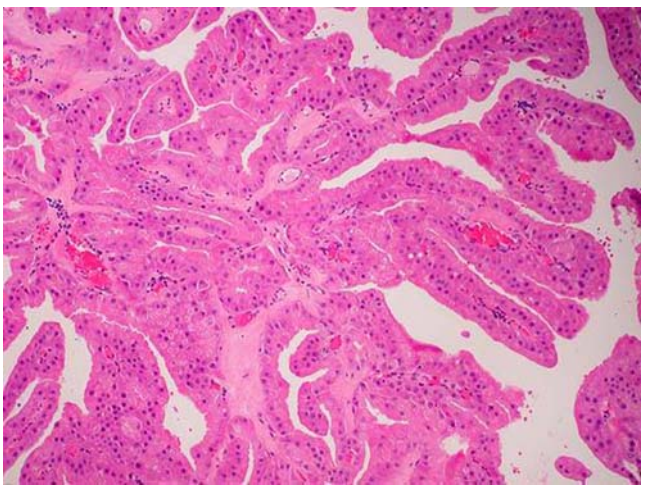

Fig. 3 Intracystic papillary tumour showing the prominent papillary architecture of the lesion (H&E×40)

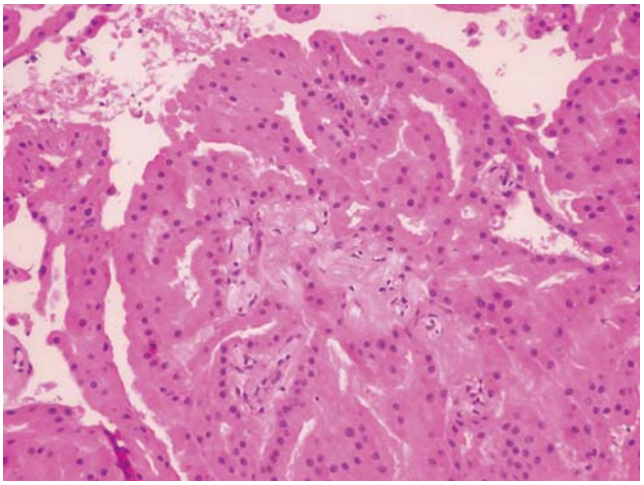

Fig. 4 Papillary structures covered by apocrine cells (H&E×100)

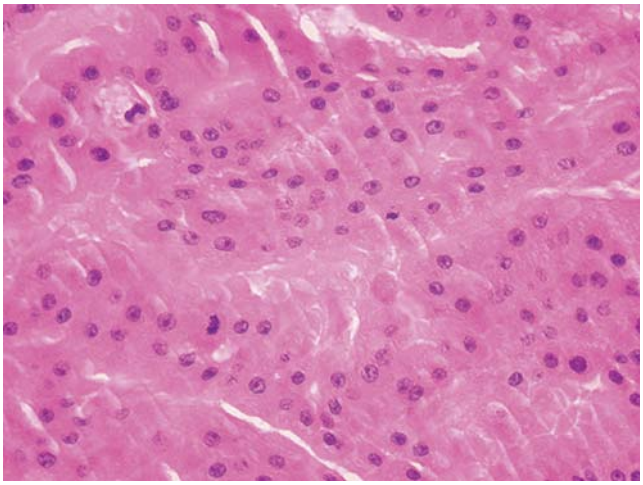

Fig. 6 Mitoses present within the apocrine cells of the papillary processes (H&E×200)

pleomorphism was mild in three cases. One case showed large nuclei with prominent nucleoli (Fig. 5). Mitoses were seen within the apocrine cells in four cases but no atypical mitoses were detected (Fig. 6). There was no zonal necrosis but individual cell necrosis was seen focally in all but one case, possibly attributable to ischaemia. Two cases contained calcifications. Lymphovascular invasion was absent. There was no evidence of in situ or invasive disease in the surrounding breast tissue but one case had a nearby focus of atypical ductal hyperplasia (ADH). Three patients underwent sentinel lymph node biopsies which were negative for metastases.

Immunohistochemical features

In all five cases, the presence of myoepithelial cells was investigated using a panel of immunostains (Table 1). No myoepithelial cells were detectable within the papillary structures or at the periphery of the cyst (Figs. 7 and 8). The normal adjacent breast tissue provided good internal control staining. Three of the five cases were tested for oestrogen receptor, progesterone receptor, and Her2–neu and were found to be negative. The apocrine nature of the lesions was confirmed by positive immunostaining for gross cystic disease fluid protein-15 (GCDFP-15; Fig. 9).

Discussion

Encapsulated (intracystic) papillary carcinomas often present as a palpable mass in the subareolar region most frequently in older women. They may be associated with nipple discharge which in some instances is blood-tinged. The associated cysts can vary in size from a few centimetres to 10 cm. [4]. Mammography of these

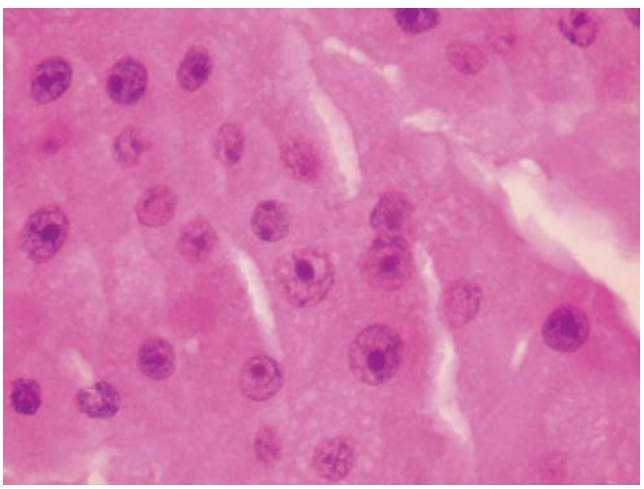

Fig. 5 Atypical apocrine cells lining the papillary processes in one case (H&E×400)

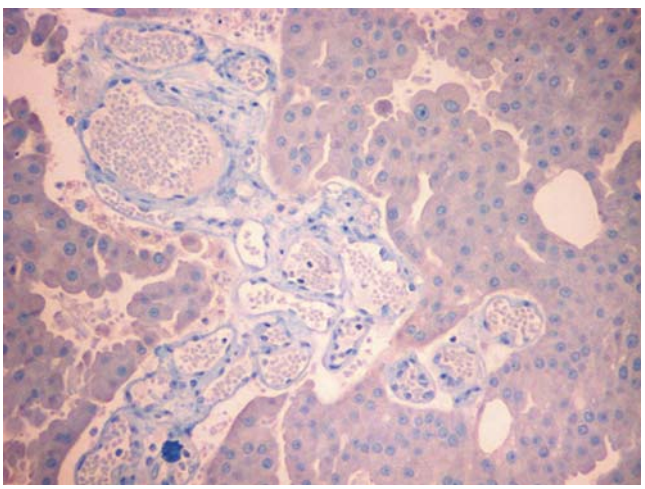

Fig. 7 Immunostain for p63/heavy-chain myosin exhibiting absence of myoepithelial cells within the papillary processes (×200)

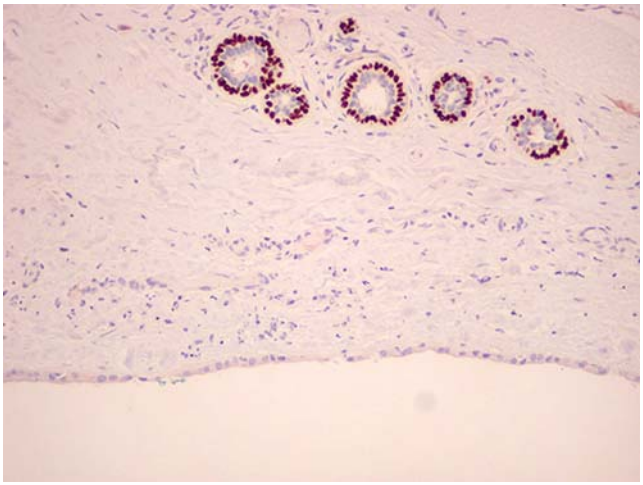

Fig. 8 Immunostain for p63 to show absence of myoepithelial cells at the periphery of the cyst and normal adjacent lobules (×200)

carcinomas reveals a well-circumscribed mass [5]. They are often single, ill-defined, and lobulated and occasionally show microcalcifications. Ultrasonographic findings include a hypoechoic lesion with posterior enhancement and a cystic portion that may show septation [6].

Originally thought to be a form of DCIS arising within a cyst, EPC is now thought to be a carcinoma with "expansile" or "pushing" invasion [2, 4, 7, 8] akin to the invasive pattern of nodular high-grade invasive ductal carcinomas. This conclusion is based on the absence of myoepithelial cells within the lesion and at its periphery, and because a few cases have been described to develop metastatic spread to the regional lymph nodes [3]. However, it has been shown that in some breast proliferations the myoepithelial cells show reduced staining or complete loss of expression of some myoepithelial markers [9, 10]. Alternatively, it has been argued that the myoepithelial cells could appear to be falsely absent due to attenuation secondary to distention of the cyst [11], and indeed, some cases otherwise acceptable as EPC show small foci of residual myoepithelial cells in the cyst wall that do not negate the diagnosis. Furthermore, given the observation that absence of myoepithelial cells is known to occur in some benign "infiltrative" lesions of the breast such as microglandular adenosis, this cannot be used as an absolute indicator of invasive malignancy. Other authors still consider EPC to be an in situ process because of the presence of basement membrane material at the periphery of the lesion [12]. However, one of the cases included in that report showed micrometastases to the axillary nodes which makes a purely in situ lesion improbable. Nevertheless, clinically malignant behaviour in EPC is distinctly unusual especially in lesions that measure less than 2 cm in diameter [13]. Moreover, most cases are treated effectively with complete surgical excision only. Currently, it is our practice pattern to recommend a sentinel lymph node biopsy at the time of wide excision but not an axillary lymph node dissection. Others recommend that EPC be treated the same as DCIS [13].

We report five patients with a pure apocrine papillary intracystic tumour very similar to classical EPC of the breast. These tumours are cystic and contain one or more mural nodules with a papillary architecture lined by apocrine epithelial cells that are apparently of one type. Furthermore, they lack identifiable myoepithelial cells both within the papillary component and at the periphery of the cyst. Care was taken in this series of cases to ensure that the myoepithelial layer was absent by performing multiple immunostains for these cells on many blocks from each case. Furthermore, the entire papillary component of the lesion was examined, and the cyst wall was sampled generously. Although several cytological and architectural patterns of EPC have been recognised [14, 15], to the best of our knowledge, a purely apocrine variant has not been described in the pathology literature. Certainly, there are no follow-up studies of lesions of this type upon which to base logical management decisions. There are two case reports of apocrine carcinomas that presented as cystic lesions [16, 17]. Both of these lesions showed focal infiltration beyond the wall of the cyst, and one case showed apocrine DCIS in adjacent ducts. In both cases, the apocrine cells showed cytological features of malignancy.

In most breast proliferations, particularly in papillary lesions, the presence of apocrine cells favours a benign process [13]. However, there is evidence that some apocrine lesions are clonal, are associated with ADH [18], and may progress to malignancy [19–23]. The absence of definite cytological features of malignancy including marked nuclear enlargement; marked variation in nuclear size, macronucleoli, irregular nucleoli, atypical mitotic figures,

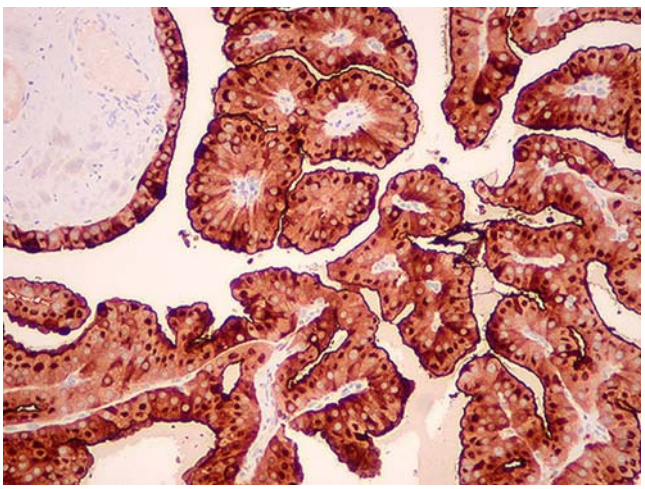

Fig. 9 Immunostain for GCDFP-15 confirming the apocrine nature of the lesion (×100)

and necrosis; and the absence of DCIS in the adjacent breast argue in favour of a benign lesion. Rigid cytological criteria for malignancy are a prerequisite for distinguishing between atypical apocrine adenosis and apocrine malignancy within the small tubular units of adenosis [20, 24], but low-grade apocrine DCIS involving large ducts outside of adenosis lesions may not show those overt cytological features of malignancy [25–28]. Benign apocrine cysts usually have a double layer of apocrine cells and myoepithelial cells while benign papillomas have myoepithelial cells within the papillary processes [29–31]. However, it has also been reported that benign apocrine lesions in the breast sometimes lack myoepithelial cells [32]. Therefore, this lesion could be interpreted as intracystic apocrine papillary hyperplasia or an intracystic apocrine papilloma.

In order to comply with the traditional terminology of World Health Organization classification of breast tumours, we have chosen to adopt the terminology of "encapsulated apocrine papillary carcinoma" for the lesion described herein. However, we stress that the malignant potential of this lesion has not yet been proven, and these lesions are probably best considered to be tumours of uncertain malignant potential for the purposes of clinical management. Furthermore, the term tumour is used in a broad way to indicate the uncertainty as to whether or not this lesion is a form of papillary hyperplasia or a true neoplasm. If neoplastic, distinction between papilloma and EPC remains an academic debate. Although the behaviour of the apocrine variant of EPC appears to be favourable based on this series of five cases, this study is limited by the small sample size and the short follow-up, particularly relevant to a low-grade malignancy. Since, in the available literature, there are no reports of such lesions behaving in a malignant fashion clinically, and since none of the cases has recurred or metastasized, we prefer to regard them as of uncertain malignant potential. This terminology is used to indicate to clinicians that this lesion should not be treated in the manner of typical invasive ductal carcinoma of the breast. In particular, the role of radiotherapy in the management of these lesions requires more evidence that these lesions are clinically malignant.

Conflict of interest statement We declare that we have no conflict of interest.

References

1. Fayanju OM, Ritter J, Gillanders WE et al (2007) Therapeutic management of intracystic papillary carcinoma of the breast: the roles of radiation and endocrine therapy. Am J Surg 194:497–500
2. Collins LC, Carlo VP, Hwang H et al (2006) Intracystic papillary carcinomas of the breast: a reevaluation using a panel of myoepithelial cell markers. Am J Surg Pathol 30:1002–1007
3. Mulligan AM, O'Malley FP (2007) Metastatic potential of encapsulated (intracystic) papillary carcinoma of the breast: a report of 2 cases with axillary lymph node micrometastases. Int J Surg Pathol 15:143–147
4. Mulligan AM, O'Malley FP (2007) Papillary lesions of the breast: a review. Adv Anat Pathol 14:108–119
5. Wagner AE, Middleton LP, Whitman GJ (2004) Intracystic papillary carcinoma of the breast with invasion. AJR Am J Roentgenol 183:1516
6. McCulloch GL, Evans AJ, Yeoman L et al (1997) Radiological features of papillary carcinoma of the breast. Clin Radiol 52:865–868
7. Leal C, Costa I, Fonseca D et al (1998) Intracystic (encysted) papillary carcinoma of the breast: a clinical, pathological, and immunohistochemical study. Hum Pathol 29:1097–1104
8. Lerwill MF (2004) Current practical applications of diagnostic immunohistochemistry in breast pathology. Am J Surg Pathol 28:1076–1091
9. Werling RW, Hwang H, Yaziji H et al (2003) Immunohistochemical distinction of invasive from noninvasive breast lesions: a comparative study of p63 versus calponin and smooth muscle myosin heavy chain. Am J Surg Pathol 27:82–90
10. Hilson JB, Schnitt SJ, Collins LC (2009) Phenotypic alterations in ductal carcinoma in situ-associated myoepithelial cells: biologic and diagnostic implications. Am J Surg Pathol 33:227–232
11. Bhargava R, Dabbs DJ (2007) Use of immunohistochemistry in diagnosis of breast epithelial lesions. Adv Anat Pathol 14:93–107
12. Esposito NN, Dabbs DJ, Bhargava R (2009) Are encapsulated papillary carcinomas of the breast in situ or invasive? A basement membrane study of 27 cases. Am J Clin Pathol 131:228–242
13. Collins LC, Schnitt SJ (2008) Papillary lesions of the breast: selected diagnostic and management issues. Histopathology 52:20–29
14. Carter D (1977) Intraductal papillary tumors of the breast: a study of 78 cases. Cancer 39:1689–1692
15. Lefkowitz M, Lefkowitz W, Wargotz ES (1994) Intraductal (intracystic) papillary carcinoma of the breast and its variants: a clinicopathological study of 77 cases. Hum Pathol 25:802–809
16. Mardi K, Sharma J, Sharma N (2004) Apocrine carcinoma of the breast presenting as a solitary cyst: cytological and histopathological study of a case. Indian J Pathol Microbiol 47:268–270
17. Angunawela P, de Silva MV, Yoheswaran K (1997) Apocrine carcinoma of the breast masquerading as a tension cyst. Ceylon Med J 42:104–105
18. Page DL, Dupont WD, Jensen RA (1996) Papillary apocrine change of the breast: associations with atypical hyperplasia and risk of breast cancer. Cancer Epidemiol Biomarkers Prev 5:29–32
19. Endoh Y, Tamura G, Kato N et al (2001) Apocrine adenosis of the breast: clonal evidence of neoplasia. Histopathology 38:221–224
20. Seidman JD, Ashton M, Lefkowitz M (1996) Atypical apocrine adenosis of the breast: a clinicopathologic study of 37 patients with 8.7-year follow-up. Cancer 77:2529–2537
21. Selim AA, El-Ayat G, Wells CA (2001) Immunohistochemical localization of gross cystic disease fluid protein-15, -24 and -44 in ductal carcinoma in situ of the breast: relationship to the degree of differentiation. Histopathology 39:198–202
22. Wells CA, El-Ayat GA (2007) Non-operative breast pathology: apocrine lesions. J Clin Pathol 60:1313–1320
23. Elayat G, Selim AG, Wells CA (2009) Cell cycle alterations and their relationship to proliferation in apocrine adenosis of the breast. Histopathology 54:348–354

24. Carter DJ, Rosen PP (1991) Atypical apocrine metaplasia in sclerosing lesions of the breast: a study of 51 patients. Mod Pathol 4:1–5
25. O'Malley FP, Bane AL (2004) The spectrum of apocrine lesions of the breast. Adv Anat Pathol 11:1–9
26. Leal C, Henrique R, Monteiro P et al (2001) Apocrine ductal carcinoma in situ of the breast: histologic classification and expression of biologic markers. Hum Pathol 32:487–493
27. Tavassoli FA, Norris HJ (1994) Intraductal apocrine carcinoma: a clinicopathologic study of 37 cases. Mod Pathol 7:813–818
28. O'Malley FP, Page DL, Nelson EH et al (1994) Ductal carcinoma in situ of the breast with apocrine cytology: definition of a borderline category. Hum Pathol 25:164–168
29. Papotti M, Eusebi V, Gugliotta P et al (1983) Immunohistochemical analysis of benign and malignant papillary lesions of the breast. Am J Surg Pathol 7:451–461
30. Hill CB, Yeh IT (2005) Myoepithelial cell staining patterns of papillary breast lesions: from intraductal papillomas to invasive papillary carcinomas. Am J Clin Pathol 123:36–44
31. Raju UB, Lee MW, Zarbo RJ et al (1989) Papillary neoplasia of the breast: immunohistochemically defined myoepithelial cells in the diagnosis of benign and malignant papillary breast neoplasms. Mod Pathol 2:569–576
32. Cserni G (2008) Lack of myoepithelium in apocrine glands of the breast does not necessarily imply malignancy. Histopathology 52:253–255

Virchows Arch (2009) 455:485–494
DOI 10.1007/s00428-009-0857-0

ORIGINAL ARTICLE

Prognostic implications of CpG island hypermethylator phenotype in colorectal cancers

Jung Ho Kim · So Hyun Shin · Hyeong Ju Kwon · Nam Yun Cho · Gyeong Hoon Kang

Received: 23 June 2009 / Revised: 22 October 2009 / Accepted: 27 October 2009 / Published online: 13 November 2009

Abstract CpG island methylator phenotype (CIMP) refers to a subset of colorectal cancers (CRCs) that are characterized by concordant hypermethylation of multiple CpG island loci. CIMP+ CRCs have peculiar clinicopathological features. However, controversy exists over prognostic implications of CIMP in CRCs. We analyzed 320 cases of CRCs for their CIMP status using the MethyLight assay and determined clinicopathological features and prognostic implications of CIMP alone or in combination with microsatellite instability (MSI). With methylation of five or more markers among eight markers examined, CIMP+ tumors were significantly associated with female gender, proximal tumor location, poor differentiation, nodal metastasis, more advanced cancer, *BRAF* mutations, MSI, and poor prognosis (all P values <0.05). Ogino's combined eight-marker panel outperformed the Ogino and the Laird five-marker panels in detecting these features. Of the four molecular subtypes generated by the combination of CIMP and MSI status, the CIMP+/MSI− subtype showed the worst clinical outcome (P=0.0003). However, poor prognosis of CIMP+/MSI− subtype was found to be attributed to *BRAF* mutation. In conclusion, the CIMP+/MSI− subtype tends to present with distinct clinicopathological and molecular features and shows the worst clinical outcome among the four molecular subtypes of CRCs.

Keywords Colon cancer · CpG island methylator phenotype · DNA methylation · Microsatellite instability

Electronic supplementary material The online version of this article (doi:10.1007/s00428-009-0857-0) contains supplementary material, which is available to authorized users.

J. H. Kim · H. J. Kwon · G. H. Kang (✉)
Department of Pathology,
Seoul National University College of Medicine,
28 Yongon-dong, Jongno-gu,
Seoul 110-744, South Korea
e-mail: ghkang@snu.ac.kr

S. H. Shin · N. Y. Cho · G. H. Kang
Laboratory of Epigenetics,
Cancer Research Institute and 2nd Stage Brain Korea,
Seoul National University College of Medicine,
Seoul, South Korea

Introduction

Epigenetics describes transmission through cell division of heritable changes in phenotype that do not involve DNA sequence changes. The underlying mechanisms for epigenetic transmission include DNA methylation, histone modification, and transmitted chromatin structure. Among these, the alteration of DNA methylation patterns is known to be a key component for altered gene expression associated with human cancers. Promoter CpG island hypermethylation is found in virtually all tissue types of human cancers and acts as an important mechanism for inactivation of tumor suppressor genes and tumor-related genes [1, 2]. Promoter CpG island hypermethylation and its associated histone modifications render the chromatin structure of a gene promoter into a closed compact structure inaccessible to transcription factors, which results in the inactivation of gene transcription [3]. Human cancer cells have both genetic changes and epigenetic changes in tumor-related genes. Recent studies have demonstrated that promoter CpG island hypermethylation is more frequent than genetic changes in human colorectal cancers [4, 5], which suggests that promoter CpG island hypermethylation is a potential mechanism of colorectal carcinogenesis.

In addition to two known molecular pathways in colorectal carcinogenesis, which involve chromosomal instability (CIN) and microsatellite instability (MSI), a third epigenetic instability pathway has been proposed by Dr. Issa's group [6]. The CpG island methylator phenotype (CIMP) refers to a subset of colorectal cancers (CRCs) that

occur through the epigenetic instability pathway. CIMP+ CRCs are characterized by widespread hypermethylation of promoter CpG island loci, which results in the inactivation of the involved genes. In the study of Weisenberger et al. [7], the presence of CIMP+ CRCs has been well documented; these tumors are distinct from CIMP− CRCs because of the higher methylation frequencies or higher methylation levels of the examined CpG island loci. A growing number of studies has consistently demonstrated close associations between CIMP+ CRCs and proximal colon location, MSI, and a high frequency of *BRAF* mutation, regardless of the methodology and CIMP marker panels used [7–11]. However, a marked controversy exists over the prognostic implications of CIMP: Some studies suggest an adverse effect of CIMP on survival of CRC patients [12–14], whereas other studies suggest little prognostic value of CIMP [15]. Furthermore, Ogino et al. [16] reported that CIMP was an independent predictor of good prognosis in colon cancers, which is contrary to previous findings. These differences may be related to differences in the methodology and CIMP marker panel used to determine CIMP status in these studies. The association of good prognosis with CIMP+ tumors was produced using MethyLight technology, whereas poor prognosis in CIMP+ tumors was seen using methylation-specific polymerase chain reaction (PCR) or combined bisulfite restriction analysis. Except for the study by Ogino et al. [16], no data are available regarding the prognostic implications of CIMP+ CRCs determined by MethyLight technology.

In the present study, we used MethyLight technology and analyzed 320 CRC cases for CIMP and MSI status and characterized the clinicopathological and molecular features of the CIMP+ CRCs. We then assessed the independent effect of CIMP and the combinatorial effect of CIMP and MSI on patient outcome.

Materials and methods

Tissue samples

Formalin-fixed, paraffin-embedded archival tissues from 320 CRC patients were retrieved from the Department of Pathology, Seoul National University Hospital (Seoul, Korea). These patients had undergone curative surgery at Seoul National University Hospital between 1999 and 2002. The selection was solely on the availability of archival tissue blocks for the study, and we did not exclude patients with a family history of CRCs. However, CRC patients treated with neoadjuvant therapy were excluded from the study. Clinicopathologic information including age, sex, histological differentiation, tumor location, tumor stage, and overall survival were obtained from these 320 patients. Tumor staging was based on the pTNM staging system of the American Joint Committee on Cancer (AJCC). The histological differentiation was determined using the World Health Organization criteria. This study was approved by the Institutional Review Board.

DNA extraction and bisulfite modification

Through light microscopic examination, we marked tumor areas where tumor cells occupied 50% or more of all cells and represented the main histology and differentiation of the tumor. Non-tumorous portions in matched CRC were obtained from normal colorectal mucosa and were confirmed by microscopy to be tumor free. Ten serial 10-μm-thick histologic slides of formalin-fixed tumor and normal tissue blocks were used for manual microdissection. Dissected tissue samples were subjected to tissue lysis using proteinase K lysis buffer. Sodium bisulfite conversion of genomic DNA was performed as described [17].

DNA methylation analysis

DNA methylation analyses were performed using MethyLight as previously described [18]. We quantified DNA methylation in eight CIMP markers—*CACNA1G*, *CDKN2A* (*p16*), *CRABP1*, *IGF2*, *MLH1*, *NEUROG1*, *RUNX3*, and *SOCS1*. The oligonucleotide sequences of the primers and probes used have been described [7]. The PCR conditions were as follows: initial denaturation at 95°C for 10 min followed by 50 cycles of 95°C for 15 s and 60°C for 1 min. *M.Sss*I-treated genomic DNA was used as a reference sample for complete methylation to determine the percentage of fully methylated alleles (percentage of methylated reference (PMR)) at a particular locus. The PMR value was calculated by dividing the *GENE*/*ALU* ratio of a sample by the *GENE*/*ALU* ratio of the *M.Sss*I-treated human genomic DNA sample and multiplying by 100 [19]. We considered a CpG island locus methylated if the PMR value was >4.

Optimal panel for CIMP determination

For the MethyLight-based determination of CIMP, three kinds of CIMP marker panels were available: Dr. Ogino's original five-marker panel (*CACNA1G*, *CRABP1*, *MLH1*, *NEUROG1*, and *p16*) [8], Dr. Laird's five-marker panel (*CACNA1G*, *IGF2*, *NEUROG1*, *RUNX3*, and *SOCS1*) [7], and Dr. Ogino's combined eight-marker panel (*CACNA1G*, *CRABP1*, *IGF2*, *MLH1*, *NEUROG1*, *p16*, *RUNX3*, and *SOCS1*) [21]. To determine which CIMP marker panel was optimal for CIMP diagnosis, the three CIMP marker panels were screened against 196 CRC cases. For the five-marker panels, CRC cases were considered CIMP+ if at least three of the markers were methylated; for the combined eight-

marker panel, cutoff values of five and six markers were each tested for CIMP determination. CIMP+ tumors defined by the three CIMP marker panels were compared regarding their associations with previously known clinicopathological features of CIMP+ CRCs, including poor prognosis, older age, female predominance, proximal colon location, poor differentiation, high frequency of *BRAF* mutations, and high frequency of MSI. Overall, the combined eight-marker panel with a cutoff value of five outperformed the five-marker panels and Dr. Ogino's combined eight-marker panel with a cutoff value of six in most comparisons based on the accuracy of association (Fig. 1 and Supplementary Table 1). Thus, we used the combined eight-marker panel with a cutoff value of five for subsequent determination of CIMP.

Mutation analysis of KRAS codons 12 and 13 and BRAF codon 600

KRAS codon 12 and 13 mutations were assayed by PCR–restriction fragment length polymorphism (RFLP) analysis, and suspected cases were confirmed by direct sequencing of the *KRAS* gene [20]. *BRAF* mutations were assayed using PCR–RFLP analysis and confirmatory sequencing as described [20].

Microsatellite analysis

The MSI status of each tumor was determined based on an examination of microsatellite markers (D2S123, D5S346, D17S250, BAT25, and BAT26). We classified MSI status

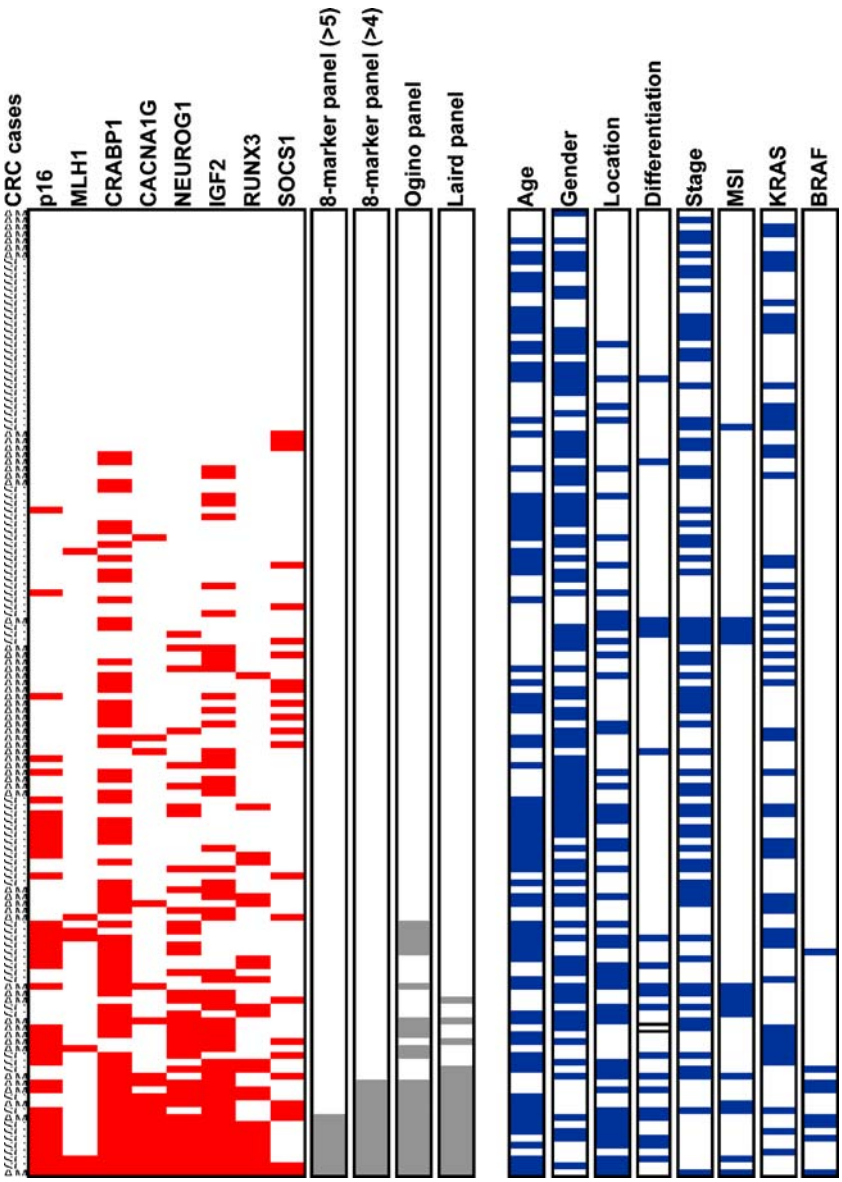

Fig. 1 Summary of comparative analysis among CIMP marker panels. *Red bars* indicate the presence of methylation in CIMP marker columns, and *gray bars* indicate CIMP+ status in four differently defined CIMP columns. *Blue bars* indicate older age (>61 years) in the *age column*, female in the *gender column*, proximal colon in the *location column*, poor differentiation in the *differentiation column*, higher stage (III, IV) in the *stage column*, MSI+ status in the *MSI column*, presence of mutant forms of *KRAS* in the *KRAS column*, and presence of mutant forms of *BRAF* in the *BRAF column*

Table 1 Clinicopathological or molecular features of four molecular subtypes generated by the combination of MSI and CIMP status

	CIMP−/MSI− 252 (78.8%)	CIMP−/MSI+ 31 (9.7%)	CIMP+/MSI− 25 (7.8%)	CIMP+/MSI+ 12 (3.8%)	*P* value
Age (years) (SD)	61.7 (12.0)	53.0 (12.4)	62.8 (13.2)	63.0 (16.3)	0.002
Female	99 (31.1%)	11 (35.5%)	15 (60.0%)	8 (66.7%)	0.055
Proximal location	64 (25.4%)	22 (71.0%)	19 (76.0%)	9 (75.0%)	<0.001
Differentiation (PD)	25 (10.0%)	8 (25.8%)	9 (36.0%)	6 50.0%	<0.001
Lymph node metastasis	137 (54.4%)	2 (6.4%)	22 (88.0%)	7 (58.3%)	<0.001
Higher stage					<0.001
Stage III	80 (31.7%)	1 (3.2%)	11 (44.0%)	7 (58.3%)	
Stage IV	69 (27.4%)	1 (3.2%)	11 (44.0%)	0	
BRAF mutation[a]	3/217 (1.4%)	0/25	7/21 (33.3%)	3/8 (37.5%)	<0.001
KRAS mutation[b]	90/226 (39.8%)	6/27 (22.2%)	3/22 (13.6%)	2/9 (22.2%)	0.027
5-year survival rate	64.4%	90.3%	44.0%	91.6%	0.003

[a] A total of 271 cases were analyzed for *BRAF* mutation

[b] A total of 284 cases were analyzed for *KRAS* mutation

as follows: MSI+ tumors had instability at two or more microsatellite markers, and MSI− tumors had instability at no more than one marker.

Statistical analysis

All statistical analyses were conducted using SPSS software version 12.0 (SPSS, Inc., Chicago, IL, USA). Pearson's chi-square test was used to test associations between clinicopathologic or molecular variables and CIMP+ tumors defined by different CIMP marker panels. Pearson's chi-square test was used to compare the frequency of each clinicopathological or genetic parameter in CRCs by four molecular subtypes. To compare the means of numeric variables among three or more groups, an analysis of variance test was used. Survival was measured from the date of resection of CRC to the date of death or the last clinical review before August 29, 2007. The average follow-up time (from surgery to death or the last follow-up) was 63.5 months (range, 1–99 months). Crude overall survival rates were assessed using the Kaplan–Meier log-rank test, and using Cox proportional-hazards regression models, multivariate analysis was performed in a backward manner to determine association between survival and CIMP, adjusting for variable suggested to be prognostic factors on univariate analysis. Hazard ratios and 95% confidence interval (95% CI) for death were computed using Cox survival modeling. All reported *P* values are two-sided, and *P* values of less than 0.05 were considered to indicate significance.

Results

Distinct clinicopathological features of the CIMP+/MSI− subtype

To study clinicopathological features of CIMP and MSI, we analyzed an additional 124 CRC cases, giving a total of 320 cases that were classified into four molecular subtypes (CIMP+/MSI+, CIMP+/MSI−, CIMP−/MSI+, and CIMP−/MSI−) using the eight-marker panel with a cutoff of five. The CIMP−/MSI− subtype was the most common, comprising 78.8% of CRCs, whereas the CIMP+/MSI+ subtype was the least common, comprising 3.8% of CRCs (Table 1). When these four molecular subtypes were compared regarding their associations with several clinicopathological features, the CIMP+/MSI− subtype (7.8%) showed close associations with proximal colon location, frequent poor differentiation, frequent nodal metastasis, frequent distant metastasis, high cancer stage, high frequency of *BRAF* mutation, and low frequency of *KRAS* mutation (Table 1). In survival analysis, the CIMP+/MSI− subtype showed the worst clinical outcome, whereas the CIMP−/MSI+ subtype showed the best clinical outcome (Fig. 2). These differences were statistically significant (Kaplan–Meier log-rank test,

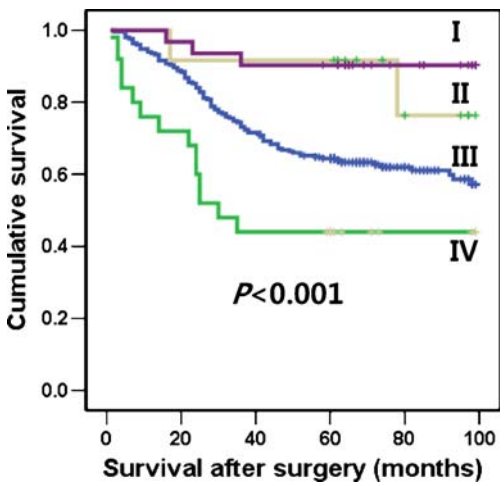

Fig. 2 Kaplan–Meier survival analysis in four molecular subtypes of colorectal cancers (n=318) according to status of CIMP and MSI. *I* CIMP−/MSI+ (n=31), *II* CIMP+/MSI+ (n=12), *III* CIMP−/MSI− (n=250), *IV* CIMP+/MSI− (n=25)

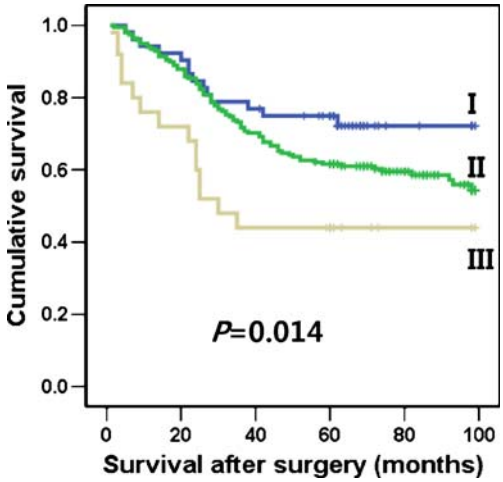

Fig. 3 Kaplan–Meier survival curves in MSI-negative colorectal cancers (n=275) according to CIMP status. *I* CIMP-0, *II* CIMP-low, *III* CIMP-high (or CIMP+). CIMP-low tumor was defined as a tumor with methylation at one to four DNA methylation markers

P<0.001). These results suggest that CIMP+/MSI− CRCs have distinct clinicopathological features.

The relationship between the degree of methylation and survival

A close association of CIMP+ with poor prognosis for MSI− CRC patients was still found after introduction, in the survival analysis, of CIMP-low group and resultant separation of CIMP− CRCs into CIMP-0 (lack of methylation in eight markers) and CIMP-low (with one to four methylated markers; Fig. 3). CIMP-low CRC patients showed clinical outcomes better than those of CIMP+ (or CIMP-high) CRC patients but worse than those of CIMP-0 CRC patients. When clinicopathological or molecular features were correlated with methylation status in MSI− CRCs, CIMP-low CRCs were similar to CIMP-0 CRCs in the examined features except for *KRAS* mutation (Table 2). *KRAS* mutation was more common in CIMP-low CRCs (45%) than in CIMP-0 (24%) or CIMP-high (14%) CRCs (P=0.001).

The effect of BRAF mutation on the prognostic effect of CIMP

In the present study, MSI− CRCs showed significantly different clinical outcomes depending on CIMP status, and particularly, the clinical outcomes of CIMP+/MSI− CRCs were worse than those of CIMP−/MSI− CRCs (P<0.001). In order to identify whether the prognostic effect of CIMP was related to the presence of *BRAF* mutation, we stratified MSI− CRCs into four subtypes according to CIMP and *BRAF* status: CIMP+/*BRAF*+, CIMP+/*BRAF*−, CIMP−/*BRAF*+, and CIMP−/*BRAF*−. CIMP+/*BRAF*+ CRCs showed worse clinical outcome than that of CIMP+/*BRAF*− CRCs, which was similar to that of CIMP−/*BRAF*− CRCs. This result clearly indicates that the worse clinical outcome of CIMP+/MSI− CRCs was clearly associated with the presence of *BRAF* mutation (Fig. 4).

Overall survival according to CIMP, MSI, and mutations of KRAS and BRAF

Survival was analyzed in 318 patients; two patients were excluded because of loss to follow-up. Univariate relationships between clinicopathogical or molecular factors and

Table 2 Relationship between clinicopathological or molecular parameters and methylation status in microsatellite instability-negative colorectal cancers

		MSI− CRCs			*P* value
		CIMP-0	CIMP-low	CIMP+	
Sex	Female	24 (46.2)	75 (37.5)	15 (60.0)	0.070
	Male	28 (53.8)	125 (62.5)	10 (40.0)	
Age	≤61 years	28 (53.8)	86 (43.0)	11 (44.0)	0.373
	>61 years	24 (46.2)	114 (57.0)	14 (56.0)	
Location	Proximal colon	12 (23.1)	52 (26.0)	19 (76.0)	<0.001
	Distal colon	19 (36.5)	69 (34.5)	2 (8.0)	
	Rectum	21 (40.4)	79 (39.5)	4 (16.0)	
Differentiation	WD or MD	44 (84.6)	182 (91.5)	16 (64.0)	<0.001
	PD	8 (15.4)	17 (8.5)	9 (36.0)	
Stage	I	4 (7.7)	13 (6.5)	1 (4.0)	0.062
	II	19 (36.5)	67 (33.5)	2 (8.0)	
	III	11 (21.2)	69 (34.5)	11 (44.0)	
	IV	18 (34.6)	51 (25.5)	11 (44.0)	
KRAS	Wild	39 (76.5)	97 (55.4)	19 (86.4)	0.001
	Mutant	12 (23.5)	78 (44.6)	3 (13.6)	
BRAF	Wild	51 (100)	163 (98.2)	14 (66.7)	<0.001
	Mutant	0	3 (1.8)	7 (33.3)	

Percentage is represented in parentheses

MSI microsatellite instability, *WD* well differentiated, *MD* moderately differentiated, *PD* poorly differentiated, *WT* wild type

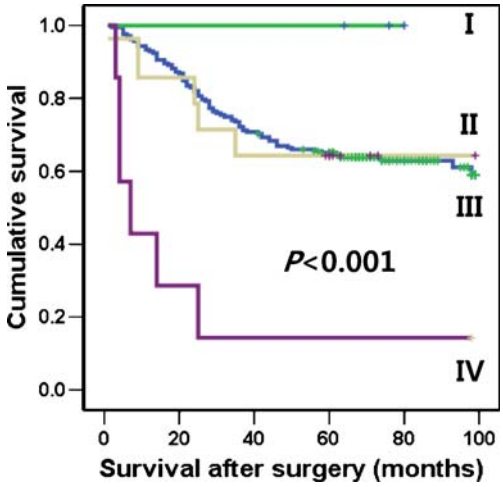

Fig. 4 Kaplan–Meier survival analysis in MSI-negative colorectal cancers (n=236) according to combined CIMP/*BRAF* status. *I* CIMP−/*BRAF*+ (n=3), *II* CIMP+/*BRAF*− (n=14), *III* CIMP−/*BRAF*− (n=212), *IV* CIMP+/*BRAF*+ (n=7)

the overall survival are summarized in Table 3. The factors showing significant associations with poor survival were poor differentiation, high cancer stage (AJCC), and older age (>61 years), whereas the factor significantly associated with good prognosis was MSI+ status. However, CIMP+ status was not a statistically significant factor. When we separated our study cases into colon cancer group and rectal cancer group (Table 4 and Supplementary Table 2), CIMP+ status was a significant factor in colon cancer group. For colon cancer group, besides CIMP+ status, older age, high cancer stage, MSI+ status, and *BRAF* mutation were significant factor associated with prognosis of colon cancer patients and differentiation was marginally significant. To determine association between CIMP and survival, multivariate analysis was performed with adjustment for above five variables, revealing that CIMP+ status was not an independent prognostic factor for colon cancers.

Table 3 Univariable analysis of clinicopathologic or molecular parameters with regard to survival in colorectal cancer patients

	No. of patients	No. of deaths	Overall survival (%)		Hazard ratio (95% confidence interval)	*P* value
			3years	5years		
Age (years)						0.020
≤61	153	47	80.4	72.5		
>61	165	69	68.5	60.6	1.523 (1.048–2.212)	
Differentiation						0.012
WD or MD	269	92	76.2	69.1		
PD	48	24	56.3	50.0	1.785 (1.138–2.801)	
Cancer stage						<0.001
I	22	1	93.3	93.3		
II	118	20	87.3	84.7	4.300 (0.577–32.053)	
III	98	30	81.6	72.5	8.236 (1.122–60.442)	
IV	80	64	37.5	22.4	39.305 (5.431–284.472)	
MSI						<0.001
Negative	275	111	70.6	62.5		
Positive	43	5	90.7	90.7	0.192 (0.071–0.522)	
KRAS						0.381
Wild	182	61	74.7	68.6		
Mutant	100	38	70.0	64.0	1.199 (0.799–1.800)	
BRAF						0.157
Wild	256	88	73.8	67.9		
Mutant	13	6	53.9	53.9	1.817 (0.794–4.158)	
CIMP (5/8)						0.243
CIMP-0	58	16	77.6	74.1		
CIMP-low	223	84	75.8	65.5	1.329 (0.778–2.270)	
CIMP-high	37	16	59.5	59.5	1.812 (0.906–3.625)	
CIMP (6/8)						0.047
CIMP-0	58	16	77.6	74.1		
CIMP-low	236	87	75.9	66.1	1.304 (0.764–2.224)	
CIMP-high	24	12	50.0	50.0	2.456 (1.161–5.193)	

WD well differentiated, *MD* moderately differentiated, *PD* poorly differentiated

Table 4 Univariate and multivariate prognostic analyses in 209 colon cancer patients

	No. of ases	Univariate analysis		Multivariate analysis	
		Mean survival (months) (95% CI)	*P* value[a]	HR (95% CI)	*P* value[b]
Age			0.033		0.056
≤61 years	104	81 (75–87)		Reference	
≥62 years	105	70 (63–77)		1.728 (0.986–3.030)	0.056
Stage			<0.001		<0.001
Stage I, II	100	91 (86–95)		Reference	
Stage III	61	82 (75–90)		3.248 (1.339–7.878)	0.009
Stage IV	48	35 (26–43)		21.731 (9.356–50.473)	<0.001
MSI			0.004		0.095
MSI−	172	72 (967–78)		Reference	
MSI+	37	91 (83–98)		0.351 (0.103–1.198)	
BRAF					<0.001
Wild	168	78 (73–83)	0.009	Reference	
Mutant	11	48 (23–74)		7.728 (2.999–19.916)	<0.001
CIMP			0.029	–	
CIMP-0	37	87 (78–96)			
CIMP-low	140	76 (70–82)			
CIMP-high	32	63 (48–77)			
Differentiation			0.094	–	
WD, MD	177	78 (73–83)			
PD	32	65 (52–79)			
KRAS				–	
Wild	133	77 (71–83)	0.661		
Mutant	54	74 (65–84)			

CI confidence interval, *HR* hazard ratio

[a] Log-rank test

[b] Cox proportional hazards regression model

Discussion

MSI and CIN are two important mechanisms of genetic instability in CRCs, but they cannot account for all CRCs because a proportion of CRCs have neither MSI nor CIN [22, 23]. A potential mechanism capable of filling the gap is CIMP, which is characterized by widespread hypermethylation of multiple promoter CpG island loci. CIMP has now been recognized as a potential alternative mechanism for genetic instability driving molecular diversity in CRCs. CIMP appears to overlap MSI, because a considerable proportion of sporadic MSI+ CRCs arise as a consequence of CIMP-related hypermethylation of *MLH1*. Recent studies suggested that CIMP and CIN are mutually exclusive pathways [24, 25].

Since the introduction of the CIMP concept to the molecular carcinogenesis of CRCs, many investigators have attempted to characterize the clinicopathologic and molecular features of CIMP+ CRCs using their own CIMP marker panels and cutoff values. Despite the lack of a reference marker panel, associations with proximal colon location, MSI, and a high frequency of *BRAF* mutation have been virtually consistent findings for CIMP+ CRCs. However, inconsistent findings among an accumulating series of studies include older age, female predominance, high frequency of *KRAS* mutation, poor differentiation, and poor clinical outcomes. Furthermore, the proportion of CIMP+ tumors in all CRCs varied from 48% and 12%. These inconsistencies are related to the fact that laboratories have developed their own tools to define CIMP, and the variety of approaches has made it difficult to compare results from different groups. It is necessary to define uniform criteria for CIMP. The technology for performing quantitative methylation analysis and producing high-throughput analysis, e.g., MethyLight or pyrosequencing, is likely to be adopted as the reference technology for CIMP diagnosis. For the MethyLight technology, the eight-marker panel appears to be superior to the five-marker panels based on the findings of the present study and that of Ogino et al. [21]. However, for the pyrosequencing methodology, CIMP marker panels have not been as thoroughly evaluated.

In contrast to the findings of Ogino et al. [26] that CIMP+ colon cancers had a better prognosis than CIMP− colon cancers and that CIMP was an independent prognostic factor, our study showed that CIMP was not an independent

prognostic factor for colon cancers. At present, we cannot explain why such a difference exists in the prognosis of CIMP+ tumors between the Ogino study and ours. In contrast to those studies reporting CIMP as an independent prognostic marker of poor prognosis in CRCs [12, 13], our study showed that CIMP was not a prognostic factor in CRCs and not an independent prognostic factor in colon cancers. The association of CIMP+ status with poor prognosis, which was statistically significant in colon cancer patients, remained no longer significant after adjusting for *BRAF* mutation. Previous studies reporting CIMP as an independent prognostic factor in CRCs did not analyze *BRAF* mutation in study samples and thus did not take the effect of *BRAF* mutation into consideration for the analysis of the association between CIMP+ status and prognosis of CRC patients [12, 13]. However, in the study of Barault et al. [14], CIMP+ status was closely associated with poor prognosis of MSI− colon cancers, and this association remained significant in multivariate analysis adjusted for age, stage, and *BRAF* and *KRAS* mutational status. The CIMP marker panel and methylation analysis technology used in the study of Barault et al. were classic five-marker panel (*MLH1*, *MINT1*, *MINT2*, *MINT31*, and *p16*) and methylation-specific PCR, respectively, and different from the panel and the analysis technology of the present study.

Compared with studies using Western patient populations, the present study showed discrepancies in the following respects: (1) the proportion of CIMP+ tumors in all CRCs, (2) the proportion of CIMP+ tumors in MSI+ CRCs, and (3) the rate of *BRAF* mutation in overall CRCs. In our study, 12% of CRCs were CIMP+, compared to 18% in the Ogino study [21]. Of MSI+ CRCs, 30% were CIMP+, compared to 71% in the Ogino study [21]. Studies having looked at specific causes of MSI+ CRCs not caused by germline mismatch repair gene mutation reported that majority (83–100%) of these cases have *MLH1* methylation [27–30]. Based on such a high frequency of *MLH1* methylation in MSI+ CRCs, Western researchers propose that virtually all sporadic MSI+ CRCs occur through the epigenetic instability pathway, with loss of *MLH1* gene expression through promoter CpG island hypermethylation. If this contention is true, the following interpretation can be deduced from our findings: either three quarters of MSI+ cases should be hereditary or our methylation assay had a lower sensitivity for detection of CIMP. The latter is unlikely because we tested and corroborated the precision of the MethyLight technology by comparing the results of the MethyLight analysis with those of bisulfite genomic sequencing in cancer cell lines (data not shown). The former possibility is also unlikely because we randomly selected study cases from the surgical files of our department without information about familial history. Our results suggest the possibility that sporadic MSI+ cases develop through mechanisms other than *MLH1* hypermethylation, including *MLH1* or *MSH2* gene mutation. Thus, it is plausible that there are ethnic differences in the causation of sporadic MSI+ CRCs, which explains the discrepancy in the percentage of CIMP positivity in MSI+ CRCs between Western data and the present study.

The rate of *BRAF* mutation (4.8%) in our CRC cases was similar to the rate (4.2%–9%) in other East Asian CRC studies [31–33], but lower than that in US, West Asian, and European CRC studies (9.5%–20.9%) [15, 34–36]. The rate of *BRAF* mutation was still low (6.1%, 11/181) when we excluded rectal cancers. However, the rate of *KRAS* mutation (101/285, 35.4%) was similar to that in other studies, regardless of geographic or ethnic differences (32%–34%) [9, 31, 37, 38]. The sensitivity of *BRAF* mutation detection could have been influenced by the mutation analysis methodology and use of the formalin-fixed paraffin-embedded tissues. But the former is unlikely because the enriched PCR–RFLP assay provides a highly sensitive means of detection and is capable of detecting one mutant allele in the presence of 1,000 normal alleles. In addition, we repeated *BRAF* mutation analysis at codon 600 (V600E) using real-time PCR-based allelic discrimination [36], giving the same result [20]. And it is also unlikely that use of the formalin-fixed tissue yielded lower detection of *BRAF* mutation because no difference was found in the mutation analysis of *BRAF* between the use of formalin-fixed tissues and the use of methanol-fixed tissues in a preliminary study (data not shown). At present, we cannot provide a satisfactory explanation for the discrepancy in *BRAF* mutation rates and the similarity of *KRAS* mutation rates between Western and East Asian CRC cases. Another point to address is the relationship between *BRAF* mutation and CIMP. One series of studies suggested that *BRAF* mutation is closely associated with sporadic MSI+ CRCs [39, 40], but this is disputed by recent studies indicating that *BRAF* mutation is closely associated with CIMP rather than MSI [16, 24]. Our study supports the close association of *BRAF* mutation with CIMP, because the *BRAF* mutation rate in CIMP+/MSI− CRCs was similar to that in CIMP+/MSI+ CRCs (33.3% and 37.5%, respectively).

In our study, CIMP+/MSI− CRCs exhibited the worst clinical outcomes among four molecular subtypes, which was attributed to *BRAF* mutation. However, *BRAF* mutation without CIMP was not associated with worse clinical outcome, which was consistent with our previous study [20]. Thus, CIMP+/MSI− CRCs with *BRAF* mutation pursued dismal clinical behavior, and the association of this molecular subtype with worse clinical outcome remained significant in multivariate analysis after adjusting for stage, differentiation, and age (data not shown). Because of the worse clinical outcome, molecular diagnostic tests to identify this subtype will be necessary in clinics, and targeted therapy against *BRAF* could be considered in the first-line adjuvant therapy.

Lastly, in our study, a close association of *KRAS* mutation with CIMP-low status was found for MSI− CRCs, which is consistent with the findings of the study of Ogino et al. [41] and furthermore in accordance with the study of Barault et al. using different CIMP marker panel and DNA methylation analysis technology [14]. Except for a strong association of *KRAS* mutation, CIMP-low tumors were similar to CIMP-0 tumors in several clinicopathological features, including *p53* mutation [41], suggesting that CIMP-low tumors might be derived from CIN pathway. Because tubulovillous adenoma or villous adenoma harbors higher frequencies of *KRAS* mutation and CpG island hypermethylation than those of tubular adenoma [42–44], tubulovillous or villous adenomas might be precursor lesions of CIMP-low CRCs. To support this speculation, a further study analyzing carcinoma–ex adenoma samples for their methylation status in each component will be necessary to identify whether CIMP-low CRCs tend to have tubulovillous or villous adenoma as their contiguous adenoma.

In conclusion, we analyzed 320 CRC cases for CIMP and MSI status and determined the prognostic implications of CIMP status in CRC patients. The CIMP+/MSI− subtype showed the worst clinical outcome among the four possible molecular subtypes of CRCs, and the worse clinical outcome of CIMP+/MSI− subtype was attributed to *BRAF* mutation.

Acknowledgments This study was supported by the 21C Frontier Functional Human Genome Project from the Ministry of Science & Technology in Korea (FG09-11-02) and by a grant from the National R&D Program for Cancer Control, Ministry of Health & Welfare, Republic of Korea (0720540).

Conflict of interest statement We declare that we have no conflict of interest.

References

1. Baylin SB, Herman JG, Graff JR, Vertino PM, Issa JP (1998) Alterations in DNA methylation: a fundamental aspect of neoplasia. Adv Cancer Res 72:141–196
2. Esteller M, Corn PG, Baylin SB, Herman JG (2001) A gene hypermethylation profile of human cancer. Cancer Res 61:3225–3229
3. Bird AP, Wolffe AP (1999) Methylation-induced repression—belts, braces, and chromatin. Cell 99:451–454
4. Wood LD, Parsons DW, Jones S et al (2007) The genomic landscapes of human breast and colorectal cancers. Science 318:1108–1113
5. Schuebel KE, Chen W, Cope L et al (2007) Comparing the DNA hypermethylome with gene mutations in human colorectal cancer. PLoS Genet 3:1709–1723
6. Toyota M, Ahuja N, Ohe-Toyota M et al (1999) CpG island methylator phenotype in colorectal cancer. Proc Natl Acad Sci USA 96:8681–8686
7. Weisenberger DJ, Siegmund KD, Campan M et al (2006) CpG island methylator phenotype underlies sporadic microsatellite instability and is tightly associated with BRAF mutation in colorectal cancer. Nat Genet 38:787–793
8. Ogino S, Cantor M, Kawasaki T et al (2006) CpG island methylator phenotype (CIMP) of colorectal cancer is best characterised by quantitative DNA methylation analysis and prospective cohort studies. Gut 55:1000–1006
9. Nagasaka T, Koi M, Kloor M et al (2008) Mutations in both KRAS and BRAF may contribute to the methylator phenotype in colon cancer. Gastroenterology 134:1950–1960.e1
10. Shen L, Toyota M, Kondo Y et al (2007) Integrated genetic and epigenetic analysis identifies three different subclasses of colon cancer. Proc Natl Acad Sci USA 104:18654–18659
11. Lee S, Cho NY, Yoo EJ, Kim JH, Kang GH (2008) CpG island methylator phenotype in colorectal cancers: comparison of the new and classic CpG island methylator phenotype marker panels. Arch Pathol Lab Med 132:1657–1665
12. Ward RL, Cheong K, Ku SL et al (2003) Adverse prognostic effect of methylation in colorectal cancer is reversed by microsatellite instability. J Clin Oncol 21:3729–3736
13. Shen L, Catalano PJ, Benson AB 3rd et al (2007) Association between DNA methylation and shortened survival in patients with advanced colorectal cancer treated with 5-fluorouracil based chemotherapy. Clin Cancer Res 13:6093–6098
14. Barault L, Charon-Barra C, Jooste V et al (2008) Hypermethylator phenotype in sporadic colon cancer: study on a population-based series of 582 cases. Cancer Res 68:8541–8546
15. Samowitz WS, Sweeney C, Herrick J et al (2005) Poor survival associated with the BRAF V600E mutation in microsatellite-stable colon cancers. Cancer Res 65:6063–6069
16. Ogino S, Goel A (2008) Molecular classification and correlates in colorectal cancer. J Mol Diagnostics 10:13–27
17. Yoo EJ, Park SY, Cho NY et al (2008) Helicobacter pylori-infection-associated CpG island hypermethylation in the stomach and its possible association with polycomb repressive marks. Virchows Arch 452:515–524
18. Kang GH, Lee S, Cho NY et al (2008) DNA methylation profiles of gastric carcinoma characterized by quantitative DNA methylation analysis. Lab Invest 88:161–170
19. Weisenberger DJ, Campan M, Long TI et al (2005) Analysis of repetitive element DNA methylation by MethyLight. Nucleic Acids Res 33:6823–6836
20. Lee S, Cho NY, Choi M et al (2008) Clinicopathological features of CpG island methylator phenotype-positive colorectal cancer and its adverse prognosis in relation to KRAS/BRAF mutation. Pathol Int 58:104–113
21. Ogino S, Kawasaki T, Kirkner GJ et al (2007) Evaluation of markers for CpG island methylator phenotype (CIMP) in colorectal cancer by a large population-based sample. J Mol Diagnostics 9:305–314
22. Georgiades IB, Curtis LJ, Morris RM, Bird CC, Wyllie AH (1999) Heterogeneity studies identify a subset of sporadic colorectal cancers without evidence for chromosomal or microsatellite instability. Oncogene 18:7933–7940
23. Goel A, Arnold CN, Niedzwiecki D et al (2003) Characterization of sporadic colon cancer by patterns of genomic instability. Cancer Res 63:1608–1614
24. Cheng YW, Pincas H, Bacolod MD et al (2008) CpG island methylator phenotype associates with low-degree chromosomal abnormalities in colorectal cancer. Clin Cancer Res 14:6005–6013
25. Goel A, Nagasaka T, Arnold CN et al (2007) The CpG island methylator phenotype and chromosomal instability are inversely correlated in sporadic colorectal cancer. Gastroenterology 132:127–138
26. Ogino S, Nosho K, Kirkner GJ et al (2009) CpG island methylator phenotype, microsatellite instability, BRAF mutation and clinical outcome in colon cancer. Gut 58:90–96

27. Herman JG, Umar A, Polyak K et al (1998) Incidence and functional consequences of hMLH1 promoter hypermethylation in colorectal carcinoma. Proc Natl Acad Sci USA 95:6870–6875
28. Kuismanen SA, Holmberg MT, Salovaara R, de la Chapelle A, Peltomaki P (2000) Genetic and epigenetic modification of MLH1 accounts for a major share of microsatellite-unstable colorectal cancers. Am J Pathol 156:1773–1779
29. Cunningham JM, Christensen ER, Tester DJ et al (1998) Hypermethylation of the hMLH1 promoter in colon cancer with microsatellite instability. Cancer Res 58:3455–3460
30. Cunningham JM, Kim CY, Christensen ER et al (2001) The frequency of hereditary defective mismatch repair in a prospective series of unselected colorectal carcinomas. Am J Hum Genet 69:780–790
31. Yuen ST, Davies H, Chan TL et al (2002) Similarity of the phenotypic patterns associated with BRAF and KRAS mutations in colorectal neoplasia. Cancer Res 62:6451–6455
32. Chang SC, Lin JK, Yang SH et al (2006) Relationship between genetic alterations and prognosis in sporadic colorectal cancer. Int J Cancer 118:1721–1727
33. Nagasaka T, Sasamoto H, Notohara K et al (2004) Colorectal cancer with mutation in BRAF, KRAS, and wild-type with respect to both oncogenes showing different patterns of DNA methylation. J Clin Oncol 22:4584–4594
34. Fransen K, Klintenas M, Osterstrom A et al (2004) Mutation analysis of the BRAF, ARAF and RAF-1 genes in human colorectal adenocarcinomas. Carcinogenesis 25:527–533
35. Vilkin A, Niv Y, Nagasaka T et al (2009) Microsatellite instability, MLH1 promoter methylation, and BRAF mutation analysis in sporadic colorectal cancers of different ethnic groups in Israel. Cancer 115:760–769
36. Young J, Barker MA, Simms LA et al (2005) Evidence for BRAF mutation and variable levels of microsatellite instability in a syndrome of familial colorectal cancer. Clin Gastroenterol Hepatol 3:254–263
37. Samowitz WS, Slattery ML, Sweeney C et al (2007) APC mutations and other genetic and epigenetic changes in colon cancer. Mol Cancer Res 5:165–170
38. Tanaka H, Deng G, Matsuzaki K et al (2006) BRAF mutation, CpG island methylator phenotype and microsatellite instability occur more frequently and concordantly in mucinous than non-mucinous colorectal cancer. Int J Cancer 118:2765–2771
39. Rajagopalan H, Bardelli A, Lengauer C et al (2002) Tumorigenesis: RAF/RAS oncogenes and mismatch-repair status. Nature 418:934
40. Oliveira C, Pinto M, Duval A et al (2003) BRAF mutations characterize colon but not gastric cancer with mismatch repair deficiency. Oncogene 22:9192–9196
41. Ogino S, Kawasaki T, Kirkner GJ, Loda M, Fuchs CS (2006) CpG island methylator phenotype-low (CIMP-low) in colorectal cancer: possible associations with male sex and KRAS mutations. J Mol Diagnostics 8:582–588
42. Rashid A, Shen L, Morris JS, Issa JP, Hamilton SR (2001) CpG island methylation in colorectal adenomas. Am J Pathol 159:1129–1135
43. Jass JR, Baker K, Zlobec I et al (2006) Advanced colorectal polyps with the molecular and morphological features of serrated polyps and adenomas: concept of a 'fusion' pathway to colorectal cancer. Histopathology 49:121–131
44. Kakar S, Deng G, Cun L, Sahai V, Kim YS (2008) CpG island methylation is frequently present in tubulovillous and villous adenomas and correlates with size, site, and villous component. Hum Pathol 39:30–36

Virchows Arch (2009) 455:495–503
DOI 10.1007/s00428-009-0856-1

ORIGINAL ARTICLE

Expression of MMP-10, MMP-21, MMP-26, and MMP-28 in Merkel cell carcinoma

Sari Suomela · Virve Koljonen · Tiina Skoog · Heli Kukko · Tom Böhling · Ulpu Saarialho-Kere

Received: 26 August 2009 / Revised: 14 October 2009 / Accepted: 23 October 2009 / Published online: 17 November 2009

Abstract Merkel cell carcinoma (MCC) is an aggressive cutaneous tumor with poor outcome and increasing incidence. We examined by immunohistochemistry the expression of three novel matrix metalloproteinases (MMPs)—MMP-21, MMP-26, and MMP-28—in 44 primary MCC tumors and six lymph node metastases while MMP-10 served as a positive control. Their mRNA expression was also studied in the UISO MCC cell line basally and after various stimulations using quantitative real-time PCR. MMP-28 was observed in tumor cells of 15/44 samples especially in tumors <2 cm in diameter (p=0.015) while 21/44 specimens showed MMP-28 in the tumor stroma. Expression of MMP-21 was demonstrated in tumor cells of 13/43 samples. MMP-26, instead, was positive in stromal cells (17/44) and its expression associated with tumors ≥2 cm in diameter (p= 0.006). Stromal expression of MMP-10 was the most frequent finding of the studied samples (31/44), but MMP-10 was detected also in tumor cells (17/44). Most of the metastatic lymph nodes expressed MMP-10 and MMP-26. MMP-10, MMP-21, and MMP-28 mRNAs were basally expressed by the UISO cells, and the corresponding proteins were detectable by immunostaining of cultured cells. IFN-α and TNF-α downregulated MMP-21 and MMP-28 expression. Our results suggest that novel MMPs may have a role in MCC pathogenesis: especially that MMP-26 expression in stroma is associated with larger tumors with poor prognosis. Expression of MMP-21 and MMP-28 seems to associate with the tumors of lesser malignant potential. We also confirm the previous finding on the role of MMP-10 in MCC pathogenesis.

Keywords Epilysin · Merkel cell carcinoma · Neuroendocrine carcinoma · MMP · Stromelysin-2

S. Suomela · U. Saarialho-Kere
Department of Dermatology,
University of Helsinki,
Meilahdentie 2, 00250, Helsinki, Finland

T. Böhling
Department of Pathology,
University of Helsinki and Helsinki University Central Hospital,
PO 400, 00290 HUS, Helsinki, Finland

V. Koljonen · H. Kukko
Department of Plastic Surgery,
Helsinki University Central Hospital,
PO 266, 00290 HUS, Helsinki, Finland

T. Skoog · U. Saarialho-Kere
Department of Clinical Science and Education and Section of Dermatology, Karolinska Institutet at Stockholm Söder Hospital,
Stockholm, Sweden

T. Skoog
Department of Biosciences and Nutrition,
Karolinska Institutet at Novum,
14157 Huddinge, Sweden

T. Böhling
HUSLAB, Helsinki University Central Hospital,
PO 720, 00290 HUS, Helsinki, Finland

S. Suomela (✉)
Department of Dermatology,
Helsinki University Central Hospital,
Meilahdentie 2, 00250 Helsinki, Finland
e-mail: sari.suomela@helsinki.fi

Introduction

Merkel cell carcinoma (MCC) is a rare primary neuroendocrine carcinoma of the skin, although the age-adjusted incidence of MCC has tripled between 1986 and 2001 in the USA [1]. It is a potentially fatal disease, and the

reported 5-year relative and disease-specific survival rates depend on the stage of the disease at presentation [2, 3]. The typical clinical course of the disease is rapid progression of the primary tumor with early and frequent metastasis to the regional lymph nodes. Several studies have established a close correlation between poor overall survival and large tumor size (≥2 cm) [4, 5]. MCC usually occurs in sun-damaged skin, the most common site being the head and neck region [6]. Ultraviolet irradiation and, very recently, the Merkel cell polyomavirus have been associated with the pathogenesis of MCC [7–9]. Interestingly, the incidence of MCC is abnormally high (8%) among immunosuppressed patients [10, 11], and HIV patients, with weakened immunity, have a 13.4-fold risk of acquiring MCC [12].

Matrix metalloproteinases (MMPs) are a group of 24 human enzymes that play a role at all stages of cancer progression from initiation to metastatic spread. Besides degrading various extracellular matrix and basement membrane proteins, they regulate growth factor activation, angiogenesis, inflammation, and apoptosis [13]. MMPs are regulated not only transcriptionally and translationally, but also by proenzyme activation and by specific inhibitors, tissue inhibitors of metalloproteinases (TIMPs) [14]. In a previous study on 33 MCCs, significant associations were found between metastatic tumor spread and high expression of MMP-7 and MMP-10 and their inhibitor TIMP-3, while the expression of MMP-1, MMP-2, MMP-3, MMP-13, and MMP-14 did not associate with prognosis [15]. In another study on 23 MCCs, high expression of MMP-1 and MMP-3 were significant negative prognostic factors [16] whereas no association was observed with the expression of MMPs-2, MMP-9, and MMP-14.

We have recently studied the role of several novel MMPs, such as MMP-21 [17], MMP-26 [18], and MMP-28 [19] in skin cancer. The aim of the present study was to elucidate the role of more novel MMPs in the biological behavior of MCC in vivo and in culture, correlating the findings with tumor size and presence of metastatic lymph nodes. MMP-10 was studied based on previous reports on its expression and prognostic significance in MCC. MMP-12 and MMP-8 were included since no previous data exist on them in MCC and since they have been suggested to have anti-tumor effects in certain cancer subtypes [13].

Materials and methods

Tissue samples

Individuals diagnosed with MCC in Finland within the time period of 1979 to 2004, were identified from the files of the Finnish Cancer Registry, which has coverage close to 100% of all malignancies diagnosed in Finland [20]. Clinical data were extracted from the hospital case records and records of the primary care centers. This study comprised 44 patients, 27 females (aged 59–95 years) and 17 males (aged 35–90 years), diagnosed with MCC (Table 1). Only two of the patients were immunosuppressed. Staging system from Memorial Sloan Kettering Cancer Center was used to stage the patients at the time of the MCC diagnosis [3]: briefly, stage I (T1N0M0, primary tumor <2 cm; no nodal involvement, no systemic metastasis), stage II (T2N0M0, primary tumor ≥2 cm; no nodal involvement, no systemic metastasis), stage III (any T, N1, M1; any tumor size, nodal involvement, no systemic metastasis), and stage IV (any T, any N, M1; any tumor size, nodal involvement, systemic metastasis). One primary tumor sample was collected from each patient. The diagnosis of MCC was then confirmed with immunohistochemical analysis: primary tumor samples were stained with hematoxylin and eosin, and immunohistochemistry using antibodies for cytokeratin-20 (CK-20, DakoCytomation, Glostrup, Denmark) and thyroid transcription factor-1 (TTF-1; Novocastra, Balliol Business Park West, Benton Lane, Newcastle Upon Tyne, UK) [21] was performed. The requirements for histological diagnosis of MCC were that tissue morphology was compatible with MCC by light microscopy and that the cancer cells stained positively for CK-20 and negatively for TTF-1. Although a few cases of MCC can be CK-20 negative, we used CK-20 positivity combined with TTF-1 negativity as inclusion criteria, to avoid the possibility that we studied tumors other than true MCCs. The longest diameter of the tumor was measured from hematoxylin and eosin stained slides, and in case of a large tumor, the diameter reported in the hospital case records was accepted. Tumor size (the greatest surface dimension) was measured from hematoxylin–eosin stained slides and documented as <2 cm or ≥2 cm. None of the patients received chemotherapy or radiation therapy preoperatively. In addition, six lymph node metastases were analyzed. The study was conducted in accordance to the Declaration of Helsinki principles and approved by the corresponding Ethical Review Board of the Helsinki University Central Hospital.

Immunohistochemistry

Immunohistochemistry was performed by the streptavidin–biotin–peroxidase complex technique (DakoCytomation, StreptABComplex/HRP Duet, Mouse/Rabbit, Glostrup, Denmark and Elite Goat (MMP-12) or Rabbit (MMP-21) IgG Vectastain ABC kit, Vector laboratories, Burlingame, CA, USA) or the antibody–polymer detection technique (PowerVision, Poly-HRP IHC Kit, ImmunoVision Technologies Co, Brisbane, CA, USA). Diaminobenzidine or 3-amino-9-ethylcarbazole was used as chromogenic substrate and Mayer's hematoxylin as counterstain. Monoclonal

Table 1 Clinical characteristics of MCC patients and MMP protein expression in MCC samples

Patient	Sex	Location	Size (mm)	Stage	Residive	Lymph node	Metastases	MMP-10		MMP-21		MMP-26		MMP-28	
								T	S	T	S	T	S	T	S
1	M	Scalp	3	1	0	1	0	0	1	0	0	0	0	0	1
2	M	Temple	4	1	0	0	0	0	1	0	0	0	0	0	0
3	M	Cheek	4	1	1	0	0	0	1	1	0	0	1	1	0
4	F	Nose	4	1	0	0	0	0	2	0	0	0	0	0	0
5	F	Nose	4	1	0	0	0	1	0	0	0	0	0	1	0
6	F	Nose	5	1	0	0	0	2	1	0	0	0	0	0	1
7	F	Buttock	5	1	0	1	0	0	1	0	0	1	0	1	0
8	F	Nose	6	1	0	0	0	1	2	1	0	0	0	1	1
9	M	Earlobe	6	1	0	0	0	1	1	0	1	0	0	0	1
10	F	Chin	7	1	1	1	0	1	0	1	0	0	0	0	0
11	F	Cheek	7	1	0	0	0	0	1	0	0	0	0	1	0
12	F	Cheek	8	1	1	0	0	0	1	1	1	0	1	0	0
13	M	Cheek	8	3	0	1	1	2	1	1	0	0	0	1	0
14	M	Cheek	8	1	0	1	0	1	2	0	0	0	0	0	1
15	M	Neck	9	1	0	0	0	0	0	0	0	0	0	0	0
16	F	Temple	9	1	0	1	0	2	1	2	0	0	1	1	2
17	M	Temple	9	1	1	1	0	0	0	0	0	0	0	0	1
18	M	Neck	10	1	0	1	0	0	0	0	0	0	1	0	1
19	M	Calf	10	1	0	0	0	0	1	1	0	0	0	0	0
20	M*	Hand	10	1	0	1	0	0	1	1	0	1	0	1	0
21	M	Brachium	11	1	0	0	0	1	2	0	0	0	1	1	1
22	F	Cheek	12	1	0	0	0	1	2	0	0	0	0	1	1
23	F	Thigh	12	1	0	0	0	0	1	1	0	0	1	0	0
24	F	Shin	13	1	0	1	1	0	0	0	0	0	0	1	0
25	F	Knee	14	3	0	0	1	1	0	1	1	1	0	0	1
26	F	Knee	14	1	0	0	0	0	0	0	0	0	0	0	1
27	F	Thigh	15	1	0	0	0	0	0	0	0	0	0	0	0
28	F	Brachium	16	1	0	0	0	0	0			1	1	1	1
29	M	Face	16	1	0	0	0	0	0	0	1	0	0	1	2
30	M*	Earlobe	16	3	0	1	1	1	1	0	0	1	0	1	0
31	F	Side	20	1	0	0	0	0	1	0	0	0	0	0	0
32	M	Scalp	22	2	0	1	0	1	0	0	0	0	1	1	1
33	F	Toe	22	1	1	0	0	0	1	0	1	0	2	0	2
34	F	Shin	24	1	0	0	0	2	2	0	0	1	1	0	2
35	F	Wrist	25	1	0	0	0	1	1	1	1	0	2	0	0
36	F	Cheek	25	1	0	0	0	0	1	1	0	0	0	0	0
37	M	Brachium	26	1	0	0	1	0	1	0	0	0	1	0	1
38	F	Shoulder	26	2	0	1	1	2	2	0	0	0	0	0	0
39	F	Cheek	27	1	0	0	0	1	1	1	1	0	1	0	0
40	F	Chin	30	1	0	0	0	0	2	0	2	2	1	0	1
41	F	Brachium	30	1	0	1	1	0	1	0	0	0	0	0	0
42	F	Thigh	30	1	1	0	0	0	1	0	0	0	2	0	0
43	F	Eye	40	1	0	1	1	0	0	0	0	0	1	0	1
44	M	Buttock	47	1	0	1	0	0	1	0	0	0	1	0	1

*Immunosuppressed; semiquantitative evaluation of immunosignal is described in Materials and methods

T Tumor cells, *S* surrounding stroma

antibodies were used to stain MMP-8 (10 ug/ml, 115-13D2, EMD Biosciences Inc., La Jolla, CA) and MMP-10 (1:300, 5E4, Novocastra Laboratories, New Castle upon Tyne, UK). Polyclonal antibodies raised by us against a synthetic peptide were used for MMP-21 [22], for MMP-26 (1:120, a gift from Prof. K. Isaka, Tokyo Medical University) [18], MMP-28 (1:100, M5066 Sigma-Aldrich, St. Louis, MO), and MMP-12 (1:80, SC-12361, Santa Cruz Biotechnology, Santa Cruz, California). MMP-10 and MMP-8 were pre-treated with 1% trypsin solution for 30 min at +37°C and MMP-26 and MMP-28 in a +95°C water bath for 25 min (Dako retrieval solution pH6; Dakocytomation). The incubation conditions for the antibodies were: +4°C overnight for MMP-28 and MMP-12, 2 h at RT for MMP-10, and 1 h at +37°C for MMP-26. For negative controls, parallel sections of the same samples were processed using preimmune sera or normal rabbit or mouse immunoglobulin. The positive controls used throughout the staining were formalin-fixed, paraffin-embedded sections of squamous cell cancers (MMP-10 and MMP-21), sarcoidosis (MMP-12), endometrium (MMP-26), and chronic wounds (MMP-8). Neutrophils, macrophages, and plasma cells were histologically identified from immunostained and corresponding hematoxylin–eosin stained sections by an experienced pathologist (T. B.).

Scoring

The intensity of MMP staining was scored independently in a blinded manner by two investigators (U. S-K. and T. B.). The investigators re-evaluated all specimens with discordant scores, and consensus score was used for further analyses. In MMP staining, the semiquantitative intensity of cytoplasmic expression was analyzed under a light-field microscope at ×100 magnification using a scale-marking staining intensity as follows: 0=less than 20 positive cells; 1=20–50 positive cells; 2=50–200 positive cells; 3=over 200 positive cells.

Cell cultures

The MCC cell line UISO, which has been established from a primary MCC tumor of a 46-year-old woman [23], was grown in RPMI 1640 supplemented with 10% fetal bovine serum, 100 U/ml penicillin, and 0.1 mg/ml streptomycin at 37°C in a humidified atmosphere of 5% CO2 and 95% air as previously described [24]. The medium was changed twice a week. UISO cells were also grown on Lab-Tek Chamber Slides and fixed with formalin for immunostaining 48 h after initiation of the culture [25]. To study the regulation of MMP-21, MMP-26, and MMP-28 expression, UISO cells were plated on tissue culture plates and allowed to reach 70–80% confluence. Then, the cells were depleted of serum overnight prior to stimulation with interferon (IFN)-α (10 and 50 U/ml), tumor necrosis factor (TNF)-α (10 and 50 ng/ml), or vascular endothelial growth factor (VEGF; 10 and 50 ng/ml; all from Sigma, St. Louis, MO). At 24 h and 48 h, the cells were lyzed, and total RNA was extracted using RNeasy Mini-Kit (Qiagen, Chatsworth, CA) as instructed by the manufacturer. Cells given fresh serum-free medium were used as controls. All treatments were carried out in triplicate, and the results were confirmed in at least three independent experiments.

Conventional and qRT-PCR

RNA was reverse transcribed to cDNA with SuperScript™ III First-Strand Synthesis System for RT-PCR (Invitrogen, Carlsbad, CA) with oligo dTs as primers and used as a template for conventional or for quantitative real-time polymerase chain reaction (qRT-PCR). Primers for MMP-10 were designed using the computer program Primer3 (http://frodo.wi.mit.edu/primer3/input.htm) and were 5′-GAC CTG GGC TTT ATG GAG ATA TT-3′ (forward) and 5′-GCT TCA GTG TTG GCT GAG TGA A-3′ (reverse). Primers and probes for MMP-21, MMP-26, and primers for MMP-28 were as described previously [17, 26, 27]. Human GAPDH (glyceraldehyde-3-phosphate dehydrogenase) labeled with VIC™ reporter dye (Pre-developed TaqMan™ assay reagents for endogenous control human GAPDH, Applied Biosystems, Warrington, UK) was used as an endogenous control in TaqMan™ (Applied Biosystems) qRT-PCR and GAPDH primers 5′-GGG AAG GTG AAG GTC GGR-3′ (forward) and 5′-GCA GCC CTG GTG ACC AG-3′ (reverse; Primer3) in conventional PCR and LightCycler® 480 SYBR Green (Roche Diagnostics, Mannheim, Germany) qRT-PCR. Placenta poly (A) RNA (Ambion, Austin, TX; MMP-10, MMP-21, and MMP-26) and total RNA prepared from A549 cells (overexpressing MMP-28) were used as positive controls. Conventional PCR assays were performed as described previously [25]. The reaction products were run on a 2.5% agarose gel, stained with 5 ng/ml ethidium bromide, and visualized under ultraviolet light. qRT-PCR reactions were performed with the the Applied Biosystems 7500 Fast Real-Time PCR System (MMP-21, MMP-26, and GAPDH) or the Roche Diagnostics LightCycler® 480 System (MMPs-10 and MMP-28 and GAPDH) with standard protocols. PCR amplifications were performed in 25-µl volumes in separate reactions. TaqMan™ qRT-PCR for MMP-21 and MMP-26, and GAPDH were run as described before [24]. MMP-10 and MMP-28 and GAPDH with LightCycler® 480 System were run in 15 µl SYBR Green mix containing 500 nM of forward and reverse primers, 5 µl of the undiluted cDNA, and 1× LightCycler 480 SYBR Green I Master mix (Roche Diagnostics). The PCR was started with 5 min pre-incubation at 95°C,

followed by a total of 45 cycles of 10 s denaturation at 95°C, 5 s annealing at 55°C and 8 s elongation at 72°C. The specificity of the SYBR Green primers was tested by running a melting curve after the qRT-PCR. The primers were ordered from Oligomer (Helsinki, Finland) or Sigma-Proligo (www.sigmaaldrich.com).

Statistical analysis

Statistical significance of the immunohistochemical scores were calculated using the Fisher's exact test. Statistical significance of the differences in mRNA expression levels in qRT-PCR analyses was calculated using the two-sample Student's *t* test. *P* value under 0.05 was considered as significant.

Results

Immunohistochemical detection of MMPs in primary MCC tumors

MMP-21 was expressed by MCC tumor cells in 13/43 cases and in eight samples by stromal neutrophils (Fig. 1a,

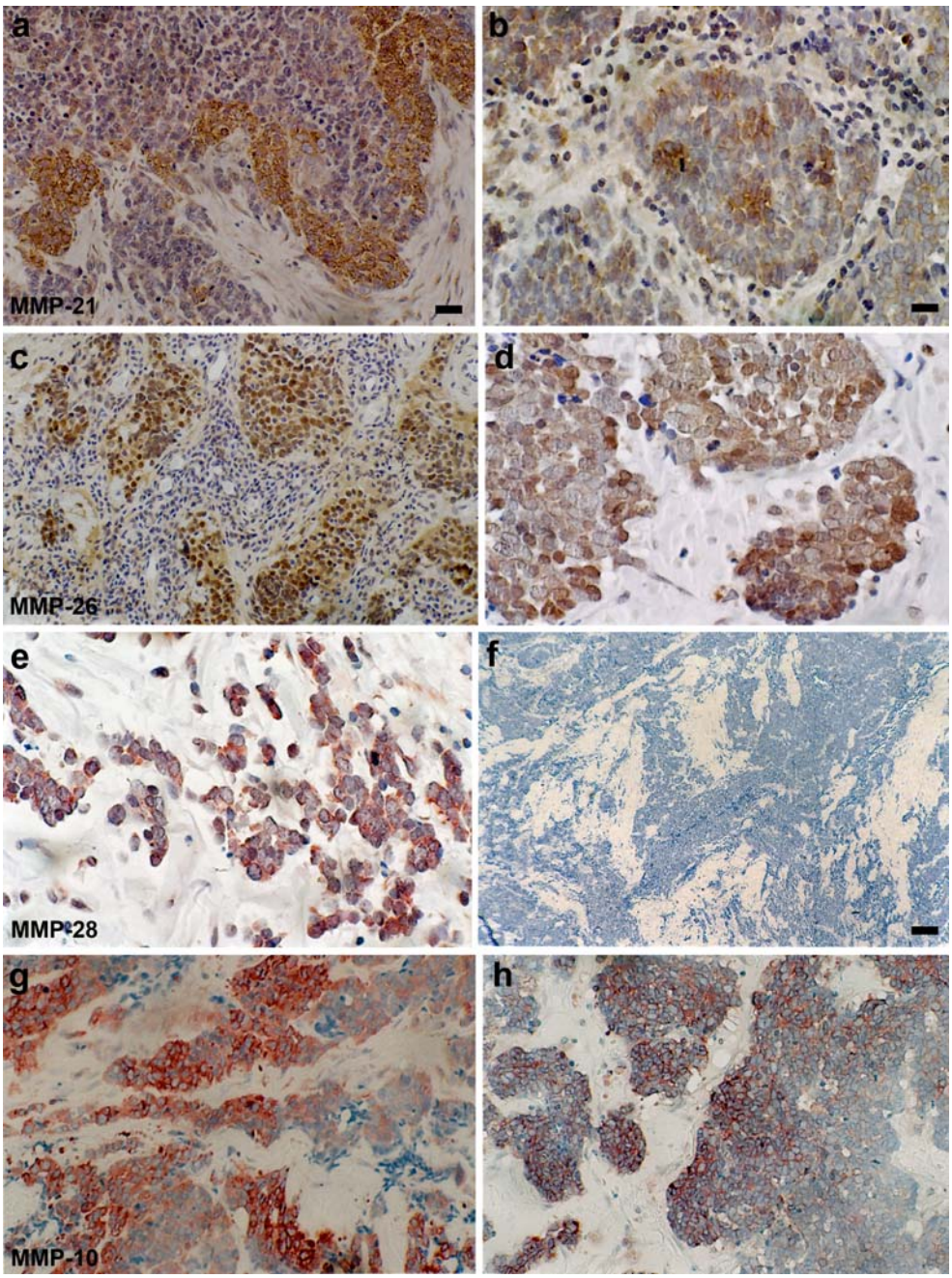

Fig. 1 Expression of MMP-21, MMP-26, MMP-28, and MMP-10 in MCC and its metastases. **a** Positive immunosignal for MMP-21 in tumor cells of a primary MCC and in a lymph node metastasis (**b**). **c** Staining for MMP-26 in a primary tumor and in metastasis of a lymph node (**d**). **e** Expression of MMP-28 in Merkel cells of a primary tumor. **f** Negative control for MMP-28. **g** Expression of MMP-10 in tumor cells and in a metastasis (**h**). Scale bars: 12 μm (**b**, **d**, **e**), 25 μm (**a**, **c**, **g**, **h**), 125 μm (**f**)

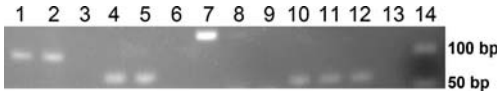

Fig. 2 MMP-10, MMP-21, and MMP-28 are expressed in UISO cells by conventional PCR. Specific primers for MMP-21 (lanes *1–3*), MMP-28 (*4–6*), MMP-10 (*7–9*), and GAPDH (*10–13*) were used. cDNA from UISO cells was used on lanes *2*, *5*, *8*, and *12*. Placenta (lanes *1*, *7*, and *10*) and A549 cells overexpressing MMP-28 (lanes *4* and *11*) were used as positive control and water (lanes *3*, *6*, *9*, and *13*) as negative control. Molecular weight ladder is on lane *14*

Table 1). None of the samples with MMP-21-expressing neutrophils had metastasized to the lymph nodes, while those tumors with lymph node metastasis (n=16) were all devoid of MMP-21 in the stroma (p=0.04).

MMP-26 (matrilysin-2) was expressed in only seven MCCs by tumor cells and by inflammatory cells, such as neutrophils, in 17/44 samples (Fig. 1c, Table 1). Stromal expression of MMP-26 was most intense in larger tumors (10/14 vs. 7/30, p=0.006). Invasion of tumor cells to dermal vessels was more common if MMP-26 expression was encountered in stromal cells, but this finding did not reach statistical significance (p=0.067).

MMP-28 (epilysin) was expressed in 15/44 MCCs in tumor cells (Fig. 1e, Table 1) and in 21/44 specimens by stromal cells, such as neutrophils and plasma cells. Tumors <2 cm in size were more likely to express MMP-28 in tumor cells than tumors with a diameter of ≥2 cm (14/30 vs. 1/14, respectively, p=0.015).

MMP-10, studied as a control [15], was observed in MCC tumor cells in 17/44 samples but in the stroma in 31 specimens in macrophages and lymphocytes (Fig. 1g, Table 1). In our samples, MMP-10 was most likely to be expressed by tumor cells in tumors of stages 2 or 3 (5/5 vs. 12/39, p=0.006).

Twenty-seven MCC samples were stained for MMP-12, and they were generally negative (data not shown). MMP-8 staining in 31 samples did not reveal positive tumor cells; only occasional neutrophils were positive in five samples (data not shown).

Immunohistochemical detection of MMPs in metastases of MCC

Sixteen of the 44 MCC patients had metastasis to the lymph nodes at the time of operation (Table 1). Eight patients

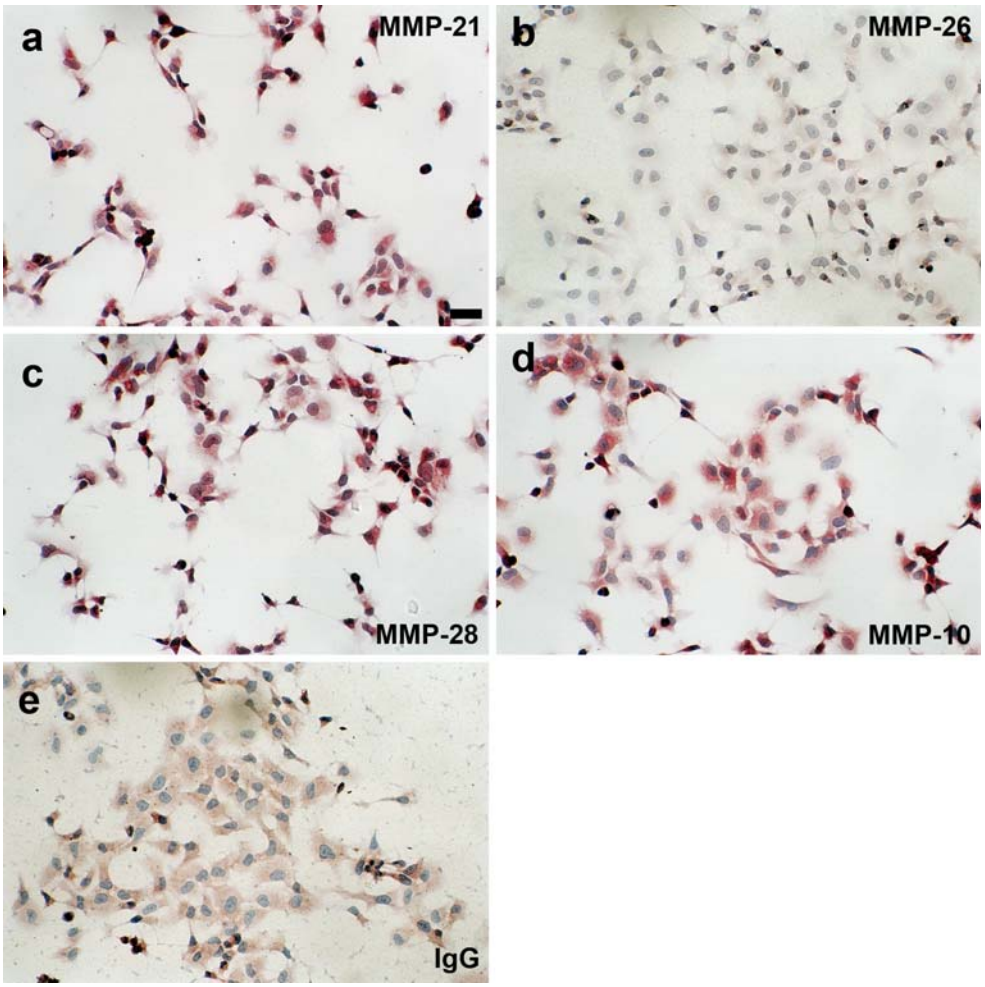

Fig. 3 Expression of MMP-21, MMP-26, MMP-28, and MMP-10 in UISO cells by immunohistochemistry. **a** MMP-21, MMP-28 (**c**), and MMP-10 (**d**) are expressed in the cytoplasm in the MCC cell line UISO. **b** MMP-26 was not expressed in UISO cells. **e** The corresponding negative mouse IgG control. Scale bar: 25 μm

developed systemic metastasis. We evaluated the MMP profile of six of the lymph node metastases by immunohistochemistry. MMP-21 expression was seen in cancer cells of one lymph node metastasis, and another lymph node metastasis had MMP-21 expression in inflammatory cells (Fig. 1b). MMP-26, however, was expressed in cancer cells of four metastatic lymph node samples and in the stroma of all metastases (Fig. 1d). None of the lymph node metastases expressed MMP-28 in tumor cells (data not shown). MMP-10 was expressed in macrophages or lymphocytes (6/6) and tumor cells (5/6) of the metastasis samples (Fig. 1h).

Expression and regulation of MMPs in UISO cells in vitro

To study whether UISO cells are able to express any of the MMPs found in tissue sections in culture, quantitative Taqman PCR was performed. In unstimulated cells, MMP-21 mRNA was expressed at low levels (at 33 cycles) whereas MMP-28 expression was more abundant (at 28 cycles). Very low expression of MMP-10 was detected (at 37 cycles) whereas no MMP-26 mRNA was found. This was confirmed by conventional PCR (Fig. 2). Analogously, when UISO cells cultured on Lab-Tek chamber slides were immunostained, expression of MMP-10, MMP-21, and MMP-28 proteins were detected, while staining for MMP-26 was negative (Fig. 3).

In order to understand the regulation of the studied MMPs in UISO cells, we cultured these cells in the presence of MCC-related cytokines or growth factors. Total RNA from these cells was analyzed using the TaqMan or SYBR Green quantitative real-time PCR [17, 27]. After 24 and 48 h of stimulation with IFN-α and TNF-α, a significant downregulation of MMP-21 and MMP-28 expression was observed (Fig. 4). VEGF did not affect the expression of any of the MMPs studied (data not shown). MMP-26 mRNA levels remained unaltered after various stimulations (data not shown).

Discussion

Due to the aggressiveness of MCC, novel targeted therapies are urgently needed for this rare neoplasm. To our knowledge, this is the first report on the expression of MMP-8, MMP-12, MMP-21, MMP-26, and MMP-28 in

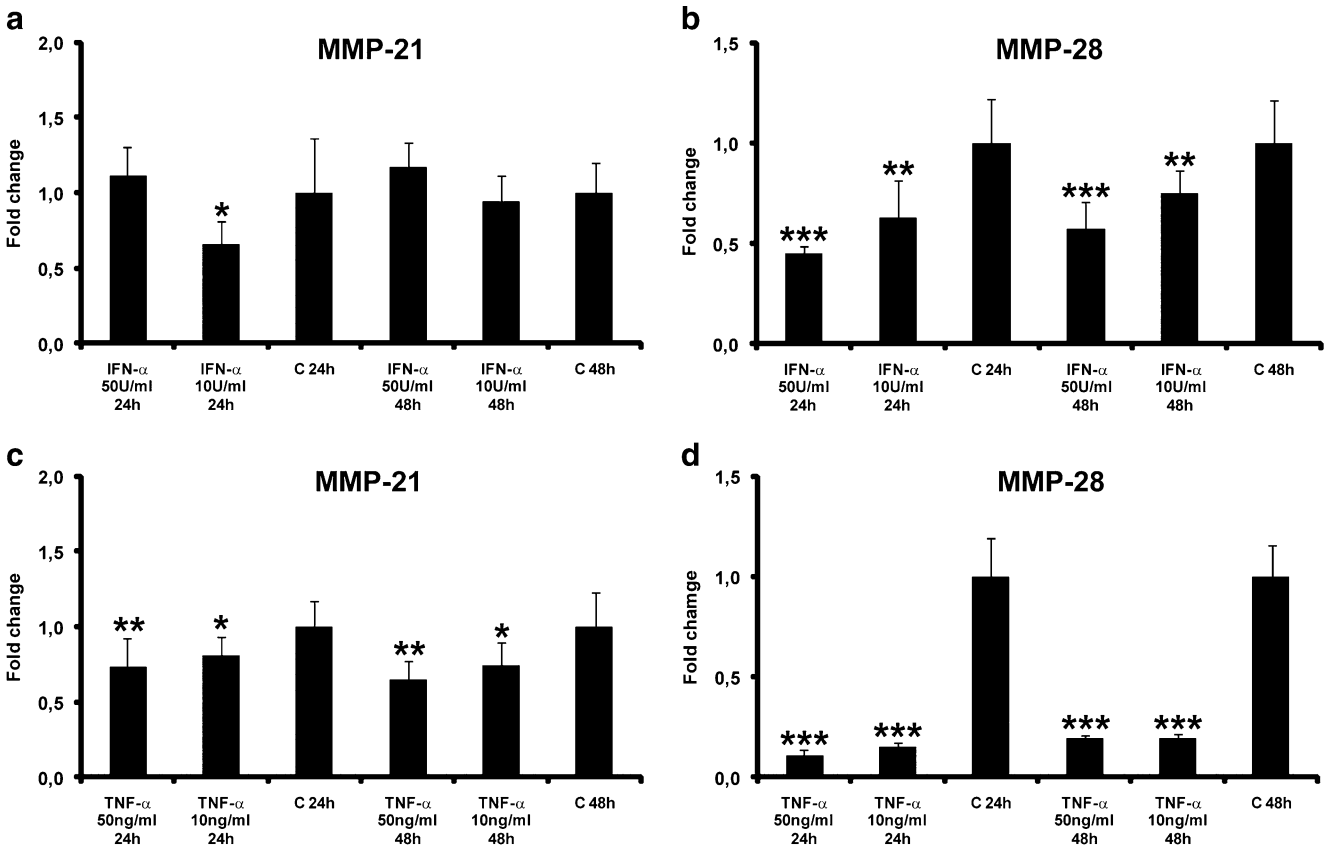

Fig. 4 Regulation of MMP-21 and MMP-28 expression in UISO MCC cell line as assessed by quantitative real-time PCR. MMP-21 and MMP-28 are significantly downregulated by IFN-α (a and b, respectively) and by TNF-α (c and d, respectively).The RT-PCR results are shown as mean fold changes relative to mRNA levels from corresponding control cells, assigned the value 1, +SEM (n=3) **p* value<0.05; ***p* value<0.01; ****p* value<0.001

MCC in vivo and in MCC cells in vitro. Furthermore, there is no data on the presence of MMPs in MCC lymph node metastases: here, we show that MMP-10 and MMP-26 may contribute to the rapid dissemination of MCC.

Tumors require angiogenesis to grow beyond a certain size. Positive regulators of angiogenesis include MMPs-1, MMP-2, MMP-9, MMP-10, and MT-MMPs [28]. Expression of MMP-7 and MMP-10 in MCC has been shown to correlate with VEGF expression levels [15]. We found MMP-10 capable of cleaving, e. g., pro MMP-1, MMP-2, and MMP-13, in most of our MCC samples confirming the importance of MMP-10 in MCC pathogenesis. Our results suggest that the more aggressive stage 2 and 3 tumors are associated with MMP-10 expression more often than stage 1 tumors. MMP-10 was also the most abundant MMP in metastasis samples.

MMP-26 is expressed in normal endometrial cells but in some carcinomas as well [29]. Our group has suggested MMP-26 not only to be associated with cancer but also with connective tissue remodeling during wound repair and pathobiology of various benign skin disorders [30]. MMP-26 has been linked to favorable prognosis in breast cancer patients, suggesting this protease to have anti-tumor properties [31]. Our present findings of stromal MMP-26 expression in especially larger tumors and in lymph node metastases suggest, however, that MMP-26 may, in some cancers, have a more notorious character. This agrees with our results on MMP-26 in esophageal [32] and pancreatic cancers [25].

In our MCC samples, MMP-21, cloned by our group [22], was the least expressed novel MMP in stroma and not associated with metastasis to the lymph nodes. It is also expressed in basal and squamous cell carcinomas [17] and may serve as a marker of malignant transformation of melanocytes in initial stages of tumorigenesis but not with micrometastases and poor outcome [19]. On the other hand, macrophages of granulomatous skin lesions and fibroblasts in dermatofibromas express MMP-21 [30]. MMP-21 has gelatinolytic activity, but its specific substrates are not known [33]. MMP-21 is upregulated by transforming growth factor-β1 in keratinocytes [17] and is a putative target of β-catenin transactivation in promoter analysis [34].

Here, we show that MMP-28, a proteinase thought to be involved in epithelial to mesenchymal transition [35], is expressed in primary MCC but not in lymph node metastases. Interestingly, tumors especially <2 cm in size expressed MMP-28 in tumor cells. MMP-28 is expressed in several normal tissues, suggesting a function in tissue homeostasis [36]. The role of MMP-28 seems to vary depending on tumor type as it is not overexpressed in melanoma [19] or colon cancer [37] but is upregulated in oral SCCs [38]. An interaction between TGF-β and MMP-28 has been suggested [36].

We also studied the regulation of MMP-21, MMP-26, and MMP-28 in UISO cells by VEGF, the expression of which correlates with aggressive behavior of MCC [15], but it did not alter the transcription of these MMPs. Instead IFN-α and TNF-α, used in the treatment of MCC [39–41], downregulated MMP-21 and MMP-28. Thus, some of the non-surgical therapeutic modalities for MCC may partly function through inhibition of proteolysis and angiogenesis via decreasing the levels of MMPs.

All the studied novel MMPs were expressed in less than half of the primary tumors either in tumor cells themselves or in stromal cells. Importantly, MMP expression is often associated with the supporting "host" cells rather than the tumor cells [28] emphasizing the importance of the microenvironment in tumorigenesis. The microenvironment contains several resident cell types (fibroblasts and vascular cells) and migratory cells derived from the bone marrow. Tumor-associated macrophages are able to produce several MMPs, and they may have both pro- and anti-tumor activities. Macrophage MMP-12 is required for the generation of angiostatin, an inhibitor of angiogenesis. Neutrophils produce MMP-8, which is supposed to have a protective role in cancer development [42]. Expression of MMP-8 or MMP-12 was not observed in MCC which may partly explain the aggressive behavior of these tumors.

In conclusion, our results show that several novel MMPs are upregulated in MCC tumors and cell lines and based on their expression in MCC metastasis, MMP-10 and MMP-26, in particular, may associate with aggressive disease.

Acknowledgments We thank Prof. Das Gupta and Dr. Roland Houben for UISO cells, Prof. Jorma Keski-Oja for MMP-28-overexpressing A549 cells, Ph. D. Jenita Pärssinen for contributions in the early phases of this study, and Ms. Alli Tallqvist and Ms. Jonna Jantunen for skillful technical assistance. This study was supported by the Academy of Finland, Finnish Cancer Foundation, Finska Läkaresällskapet, Helsinki University Central Hospital Research Fund (TYH2009233), Finland and Cancerfonden, the Swedish Research Council, and Edvard Welander–Finsen Foundation (TS), Sweden. Prof. Saarialho-Kere passed away during the processing of the manuscript. This article is dedicated to her memory.

Conflict of interest The authors declare that they have no conflict of interest.

References

1. Hodgson NC (2005) Merkel cell carcinoma: changing incidence trends. J Surg Oncol 89:1–4
2. Agelli M, Clegg LX (2003) Epidemiology of primary Merkel cell carcinoma in the United States. J Am Acad Dermatol 49:832–841
3. Allen PJ, Bowne WB, Jaques DP et al (2005) Merkel cell carcinoma: prognosis and treatment of patients from a single institution. J Clin Oncol 23:2300–2309
4. Tai PT, Yu E, Tonita J et al (2000) Merkel cell carcinoma of the skin. J Cutan Med Surg 4:186–195

5. Koljonen V, Bohling T, Granhroth G et al (2003) Merkel cell carcinoma: a clinicopathological study of 34 patients. Eur J Surg Oncol 29:607–610
6. Poulsen M (2005) Merkel cell carcinoma of skin: diagnosis and management strategies. Drugs Aging 22:219–229
7. Lawenda BD, Thiringer JK, Foss RD et al (2001) Merkel cell carcinoma arising in the head and neck: optimizing therapy. Am J Clin Oncol 24:35–42
8. Popp S, Waltering S, Herbst C et al (2002) UV-B-type mutations and chromosomal imbalances indicate common pathways for the development of Merkel and skin squamous cell carcinomas. Int J Cancer 99:352–360
9. Feng H, Shuda M, Chang Y et al (2008) Clonal integration of a polyomavirus in human Merkel cell carcinoma. Science 319: 1096–1100
10. Gooptu C, Woollons A, Ross J et al (1997) Merkel cell carcinoma arising after therapeutic immunosuppression. Brit J Dermatol 137:637–641
11. Buell JF, Trofe J, Hanaway MJ et al (2002) Immunosuppression and Merkel cell carcinoma. Transplant Proc 34:1780–1781
12. Engels EA, Frisch M, Goedert JJ et al (2002) Merkel cell carcinoma and HIV infection. Lancet 359:497–498
13. López-Otín C, Matrisian LM (2007) Emerging roles of proteases in tumour suppression. Nat Rev Cancer 7:800–808
14. Brew K, Dinakarpandian D, Nagase H (2000) Tissue inhibitors of metalloproteinases: evolution, structure and function. Biochim Biophys Acta 1477:267–283
15. Fernández-Figueras MT, Puig L, Musulén E et al (2007) Expression profiles associated with aggressive behaviour in Merkel cell carcinoma. Mod Pathol 20:90–101
16. Massi D, Franchi A, Ketabchi S et al (2003) Expression and prognostic significance of matrix metalloproteinases and their tissue inhibitors in primary neuroendocrine carcinoma of the skin. Hum Pathol 34:80–88
17. Ahokas K, Lohi J, Illman SA et al (2003) Matrix metalloproteinase-21 is expressed epithelially during development and in cancer and is up-regulated by transforming growth factor-beta1 in keratinocytes. Lab Invest 83:1887–1899
18. Kuivanen T, Jeskanen L, Kyllönen L et al (2009) Matrix metalloproteinase-26 is present more frequently in squamous cell carcinomas of immunosuppressed compared with immunocompetent patients. J Cutan Pathol 36:929–936
19. Kuivanen T, Ahokas K, Virolainen S et al (2005) MMP-21, unlike MMP-26 and -28, is induced at early stages of melanoma progression, but disappears with more aggressive phenotype. Virchows Arch 447:954–960
20. Teppo L, Pukkala E, Lehtonen M (1994) Data quality and quality control of a population-based cancer registry. Experience in Finland. Acta Oncol 33:365–369
21. Kaufmann O, Dietel M (2000) Expression of thyroid transcription factor-1 in pulmonary and extrapulmonary small cell carcinomas and other neuroendocrine carcinomas of various primary sites. Histopathology 36:415–420
22. Ahokas K, Lohi J, Lohi H et al (2002) Matrix metalloproteinase-21, the human orthologue for XMMP, is expressed during fetal development and in cancer. Gene 301:31–41
23. Ronan SG, Green AD, Shilkaitis A et al (1993) Merkel cell carcinoma: in vitro and in vivo characteristics of a new cell line. J Am Acad Dermatol 29:715–722
24. Houben R, Ortmann S, Schrama D (2007) Activation of the MAP kinase pathway induces apoptosis in the Merkel cell carcinoma cell line UISO. J Invest Dermatol 127:2100–2103
25. Bister V, Skoog T, Virolainen S et al (2007) Increased expression of matrix metalloproteinases-21 and -26 and TIMP-4 in pancreatic adenocarcinoma. Mod Pathol 20:1128–1140
26. Saarialho-Kere U, Kerkelä E, Jahkola T et al (2002) Epilysin (MMP-28) expression is associated with cell proliferation during epithelial repair. J Invest Dermatol 119:14–21
27. Ahokas K, Skoog T, Suomela S et al (2005) Matrilysin-2 (matrix metalloproteinase-26) is upregulated in keratinocytes during wound repair and early skin carcinogenesis. J Invest Dermatol 124:849–856
28. Noël A, Jost M, Maquoi E (2008) Matrix metalloproteinases at cancer tumor–host interface. Semin Cell Dev Biol 19:52–60
29. Marchenko ND, Marchenko GN, Weinreb RN (2004) Beta-catenin regulates the gene of MMP-26, a novel metalloproteinase expressed both in carcinomas and normal epithelial cells. Int J Biochem Cell Biol 36:942–956
30. Skoog T, Ahokas K, Orsmark C et al (2006) MMP-21 is expressed by macrophages and fibroblasts in vivo and in culture. Exp Dermatol 15:775–783
31. Strongin AY (2006) Mislocalization and unconventional functions of cellular MMPs in cancer. Cancer Metastasis Rev 25:87–98
32. Ahokas K, Karjalainen-Lindsberg ML, Sihvo E et al (2006) Matrix metalloproteinases 21 and 26 are differentially expressed in esophageal squamous cell cancer. Tumour Biol 27:133–141
33. Murphy G, Nagase H (2008) Progress in matrix metalloproteinase research. Mol Aspects Med 29:290–308
34. Marchenko GN, Marchenko ND, Strongin AY (2003) The structure and regulation of the human and mouse matrix metalloproteinase-21 gene and protein. Biochem J 372:503–515
35. Illman SA, Lehti K, Keski-Oja J et al (2006) Epilysin (MMP-28) induces TGF-beta mediated epithelial to mesenchymal transition in lung carcinoma cells. J Cell Sci 119:3856–3865
36. Illman SA, Lohi J, Keski-Oja J (2008) Epilysin (MMP-28)—structure, expression and potential functions. Exp Dermatol 17:897–907
37. Bister VO, Salmela MT, Karjalainen-Lindsberg ML et al (2004) Differential expression of three matrix metalloproteinases, MMP-19, MMP-26, and MMP-28, in normal and inflamed intestine and colon cancer. Dig Dis Sci 49:653–661
38. Lin MH, Liu SY, Su HJ et al (2006) Functional role of matrix metalloproteinase-28 in the oral squamous cell carcinoma. Oral Oncol 42:907–913
39. Bajetta E, Zilembo N, Di Bartolomeo M et al (1993) Treatment of metastatic carcinoids and other neuroendocrine tumors with recombinant interferon-alpha-2a. A study by the Italian trials in medical oncology group. Cancer 72:3099–3105
40. Hata Y, Matsuka K, Ito O et al (1997) Two cases of Merkel cell carcinoma cured by intratumor injection of natural human tumor necrosis factor. Plast Reconstr Surg 99:547–553
41. Krasagakis K, Krüger-Krasagakis S, Tzanakakis GN et al (2008) Interferon-alpha inhibits proliferation and induces apoptosis of Merkel cell carcinoma in vitro. Cancer Invest 26:562–568
42. Balbín M, Fueyo A, Tester AM et al (2003) Loss of collagenase-2 confers increased skin tumor susceptibility to male mice. Nat Genet 35:252–257

Virchows Arch (2009) 455:505–515
DOI 10.1007/s00428-009-0850-7

ORIGINAL ARTICLE

Immunosuppressive cytokine Interleukin-10 (IL-10) is up-regulated in high-grade CIN but not associated with high-risk human papillomavirus (HPV) at baseline, outcomes of HR-HPV infections or incident CIN in the LAMS cohort

Stina Syrjänen · Paulo Naud · Luis Sarian · Sophie Derchain · Cecilia Roteli-Martins · Adhemar Longatto-Filho · Silvio Tatti · Margherita Branca · Mojca Eržen · L. S. Hammes · S. Costa · Kari Syrjänen

Received: 14 July 2009 / Revised: 8 October 2009 / Accepted: 13 October 2009 / Published online: 12 November 2009

Abstract Bypassing the local immunological defense reactions in the cervix is one of the prerequisites for human papillomaviruses (HPV) infections to progress to intra-epithelial neoplasia (CIN). The role of potent immunosuppressive cytokines, e.g., interleukin-10 (IL-10), depressing these local virus-specific immunological responses is incompletely studied. To assess, whether IL-10 expression in cervical HPV lesions has any implications in the outcome of HPV infections or disease progression to CIN. Baseline cervical biopsies from 225 women of the LAMS study sub-cohort were analyzed for IL-10 expression using immunohistochemistry, to assess its associations with CIN grade, and high-risk HPV (HR-HPV) at baseline, as well as in predicting outcomes of HR-HPV infections, and development of incident CIN1+ and CIN2+ in this longitudinal setting. Expression of IL-10 in cervical lesions was up-

LAMS: Latin American Screening Study, funded by European Commission, INCO-DEV Contract # ICA4-CT-2001-10013.

S. Syrjänen
Department of Oral Pathology, Institute of Dentistry,
University of Turku,
Turku, Finland

P. Naud · L. S. Hammes
Hospital de Clinicas de Porto Alegre,
Porto Alegre, Brazil

L. Sarian · S. Derchain
Universidade Estadual de Campinas,
Campinas, Brazil

C. Roteli-Martins
Hospital Leonor M de Barros,
Sao Paulo, Brazil

A. Longatto-Filho
Instituto Adolfo Lutz, Sao Paulo, Brazil and University of Minho,
Braga, Portugal

S. Tatti
First Chair Gynecology Hospital de Clinicas,
Buenos Aires, Argentina

M. Branca
Unit of Cytopathology,
National Centre of Epidemiology,
Surveillance and Promotion of Health,
National Institute of Health (ISS),
Rome, Italy

M. Eržen
SIZE Diagnostic Center,
Ljubljana, Slovenia

S. Costa
Department of Obstetrics and Gynecology,
S.Orsola-Malpighi Hospital,
Bologna, Italy

K. Syrjänen (✉)
Department of Oncology and Radiotherapy,
Turku University Hospital,
Savitehtaankatu 1,
FIN-20521 Turku, Finland
e-mail: kari.syrjanen@tyks.fi

regulated most often in high-grade CIN, and IL-10 over-expression retained its value as independent predictor of CIN2+ (odds ratio (OR)=4.92) and CIN3+ (OR=7.51) also in multivariate model, including HR-HPV and several known covariates of IL-10 expression. Up-regulation was not related to HR-HPV detection, and showed no relationship to HR-HPV viral loads. Using longitudinal predictive indicators (SE, SP, PPV, NPV), IL-10 expression was of no value in predicting (1) the outcomes of HR-HPV infections, or (2) the surrogate endpoints (incident CIN1+, CIN2+) of progressive disease. IL-10 over-expression (along with HR-HPV) was one of the independent covariates of CIN2/3. This immunosuppressive cytokine might play an important role in creating a microenvironment that favors progressive cervical disease and immune evasion by HR-HPV.

Keywords High-risk HPV · Immunosuppressive cytokines · Interleukin-10 · Th cells · CIN · Viral outcomes · Disease progression · Longitudinal predictive values · Surrogate endpoints

Introduction

Practically all cervical carcinomas (CC) are caused by high-risk human papillomavirus (HR-HPV) infections, whereas the low-risk HPV (LR-HPV) types are rarely found in CC or its precursor (CIN) lesions [1–6]. This divergent oncogenic potential of LR-HPV and HR-HPV is mainly attributable to the differences of the two major viral oncoproteins (E6 and E7) to interact with the key regulatory cellular proteins, p53 and pRb [1, 4, 7–9]. While E6 of the HR-HPV (but not LR-HPV) initiates degradation of the p53 tumor suppressor protein, HPV E7 of HR-HPV (but not LR-HPV) binds to pRb resulting in G1/S transition of the cell cycle [1, 4, 7–11]. These two viral oncoproteins also play an important role in the processes, whereby HR-HPVs avoid recognition by the host immune surveillance mechanisms, leading to persistent HR-HPV infections, with increased risk of developing CIN and CC [1–4, 12, 13].

Both innate and adaptive immunity is needed to recognize and combat viral infections [1, 4, 12, 13], but HPV has developed several ingenious mechanisms on how to evade recognition by both of those. Of key importance in evading the innate immunity is the intraepithelial HPV life-cycle itself, which leaves little room for antigen presenting cells (APC) to recognize the virus [12, 13]. T lymphocytes are the key mediators of the adaptive immune system, consisting of two major subsets: CD4+ and CD8+ T cells [12, 13]. CD4+ T cells can be further subdivided into two subsets (Th1 and Th2) according to the profile of their cytokine expression. While Th1 cytokines (e.g. IFN-γ) enhance cell-mediated immunity (CMI), Th2 cytokines (interleukins (IL)) IL-4, IL-5, IL-6, IL-10, and IL-13 contribute to activation of humoral immune responses [12].

Of all these Th2 cytokines, IL-10 is of particular interest, because of its known anti-immune and anti-inflammatory properties [14, 15]. This cytokine is the first identified member [16] of a large family of ILs, with highly divergent biological functions [14, 15, 17]. Thus, IL-10 has (1) potent inhibitory effects on T-cell proliferation and inflammation, (2) it depresses the production of Th1 cytokines, and (3) in addition, IL-10 inhibits costimulatory activity of APCs, and (4) down-regulates MHC class II expression by monocytes [14, 15, 17, 18]. These properties make IL-10 the single most potent immunosuppressive cytokine and its increased expression could contribute to the development of cancer, because of suppressed Th1 cytokine production and concomitant absence of T-cell activation in tumor microenvironment [14, 15, 17, 18].

In the uterine cervix, such an immunosuppressive milieu would favor the development of immunological tolerance rather than immunological recognition of HPV antigens [12, 13]. Being produced by different type of cells, including keratinocytes [14, 15], IL-10 might potentially contribute to the development of such an immunosuppressive milieu in the uterine cervix. Until now, the specific role of IL-10 in cervical carcinogenesis has attracted little attention, despite some analysis on different cytokines in CIN and CC lesions [17, 19–22].

To further define the role of IL-10 in HR-HPV-associated cervical carcinogenesis, we analyzed a series of cervical biopsies derived from 225 women included in the Latin American Screening (LAMS) study cohort (n= 12,114) in Brazil and Argentina [23–26]. The study aimed to assess whether the expression of IL-10 is associated with (1) the grade of CIN, and (2) HR-HPV type at baseline, and whether it has any influence on (3) the outcome of these HR-HPV infections, or (4) development of incident CIN1+ and CIN2+ in this longitudinal setting.

Material and methods

General study design

The ongoing LAMS study is a multi-center screening trial targeting the female populations at different risk for CC in two Latin American countries, Brazil and Argentina [23]. At their baseline visit, a total of 12,114 consecutive women attending the four partner clinics: Campinas (CA), Sao Paulo (SP), Porto Alegre (PA), Buenos Aires (BA), were screened for HPV and CIN using eight different diagnostic tools, as detailed before [23–26]. Women that had a positive result with any of these diagnostic tests were examined by colposcopy (and biopsied) at their second visit. In addition,

a 5% random sample of PAP-negative women were recalled for a new PAP test at 12 months, as were 20% of those HCII negative, to assess the rates of incident PAP smear abnormalities and HPV infections, respectively [25, 26]. The women with biopsy-confirmed low-grade CIN comprise the prospective cohort (n=1,011), followed-up for a minimum of 24 months. All high-grade lesions were promptly treated and followed-up for the same period, using repeated PAP test, colposcopy, and HCII assay at 12-month intervals. For the present analysis of IL-10, baseline biopsies taken from 225 of these women were available.

Prospective follow-up

Using the above criteria, women were allocated in the prospective cohort, scheduled to be monitored in the clinic at 6-month intervals for a minimum of 24 months. A total of 1,011 women completed at least one FU visit including examination by PAP smear, visual inspection with acetic acid (VIA)/visual inspection with lugol's iodine, colposcopy, and biopsy, in case of abnormalities [24–26]. The mean FU time at this writing is 21.7 months (SD, 8.09 months; median, 24.2 months; range, 1–54 months).

Outcomes and endpoints of cervical lesions and HR-HPV infections

For the present analysis, the data of these 1,011 women were analyzed for the different surrogate endpoints of progressive disease: (1) progression to CIN1+, and (2) progression to CIN2+, as well as for different outcomes of their HR-HPV infections, including (1) incident infections, (2) virus persistence, and (3) HPV clearance. Progression to CIN1+ was based on detection (in baseline biopsy-negative woman) a biopsy-confirmed CIN1+ lesion in any of the consecutive FU visits. As a progression to CIN2+ was defined, any case where biopsy-confirmed progression from baseline negative, NCIN, or CIN1 biopsy was established in the subsequent FU-visits [27]. Times to progression into CIN1+ and CIN2+ were calculated from the baseline visit to the respective FU visit when the progression event was first detected. Progression rates were calculated dividing the numbers of progressed cases by women months at risk (WMR) and expressed per 1,000 WMR. Three outcomes of HR-HPV infections were recorded; incident, persistence, and clearance. As an incident HR-HPV infection, we recorded an appearance of positive hybrid capture 2 (HC2) test (at 1 pg/ml RLU/CO cut-off) among baseline HR-HPV-negative women at any of the FU visits. HR-HPV was considered cleared if the HC2 assay was negative at the last FU visit. Persistent HR-HPV infections were women in whom two or more subsequent HC2 assays were HR-HPV positive, and in whom the infection was not cleared at the last FU visit. Times to these three outcomes were also calculated and expressed as cases/1,000 WMR.

Methods

Because detailed in a series of recent reports [23–27], the methods used in the LAMS study are described here only as far as pertinent to elaborating the data necessary for the present analysis.

Epidemiological questionnaire

All women who gave their consent to participate (n= 12,114) filled in a detailed inquiry concerning the risk factors of HPV, CIN, and CC. This structured questionnaire contained questions exploring the reproductive history, sexual history, current sexual practices, sexual hygiene, medical history, smoking habits, and contraception [23].

Papanicolaou (Pap) smears

In the LAMS study, we compared the performance of three methods of cervical cytology: conventional PAP and two different LBC techniques (DNA-Citoliq®; Digene Brazil, Sao Paulo, and SurePath®; TriPath, Durham, NC, USA) [24]. In the present analysis, only the results of the conventional PAP test were used.

Directed punch biopsy

Directed punch biopsies (and cone biopsies) were fixed in formalin, embedded in paraffin, and processed into 5-µm-thick hematoxylin-eosin (HE) stained sections for light microscopy, following the routine procedures. All biopsies were examined among the daily routine in the Pathology Departments of the partner clinics in both studies, and diagnosed using the commonly agreed CIN nomenclature. The pathologists were also asked to notify the HPV-suggestive morphological changes in flat lesions with no CIN, i.e., HPV-NCIN (flat condyloma) [23, 24]. The slides from two of the centers (CA, SP) have been subjected to re-examination by two pathologists of the EC partners (ME, KS). The consensus diagnosis of the panel was considered as the final diagnosis.

Detection of HPV DNA by hybrid capture 2 assay

Primary HPV detection was done by HC2 assay, using cervical swabs (collected by a physician) and self-sampling devices (tampons), as described previously [23, 26]. HC2 assay (n=4,694 tests) was performed using the automated HC2 test system according to the manufacturer's protocol.

The samples were analyzed only for the presence of HR-HPV types 16, 18, 31, 33, 35, 39, 45, 51, 52, 56, 58, 59, and 68. The usual limit of 1 pg/ml of HPV 16 DNA was used as the positive control (CO), i.e., samples were classified as HR-HPV positive with the RLU/CO ≥1.0 pg/ml cut-off.

Immunohistochemical detection of IL-10

A total of 225 slides from the same number of women were available for immunohistochemical (IHC) analysis of IL-10. In brief, 4-μm-thick sections were cut on ChemMate Capillary Gap Microscope slides (Dako A/S, Glostrup, Denmark) and kept overnight at +55°C, deparaffinized in xylene, and rehydrated in graded alcohol. Before IHC, IL-10 antigen retrieval was done by heating the tissue sections in buffer of 10 mM Tris, 1 mM EDTA (pH 9.0) with a microwave oven for 10 min (600 W). The IHC staining for IL-10 was performed with the Dako TechMate™ 500 Plus Autostainer using monoclonal IL-10 antibody (MAB217; R & D Systems, Inc., Minneapolis, USA) diluted 1:50 and the reagents from Dako REAL-kit (Dako, Glostrup, Denmark). The sections were washed with distilled water and TBS-buffer. Then, the sections were stained with the primary antibody and the secondary biotinylated antibody (anti-mouse IgG) for 30 min. Endogenous peroxidase activity was blocked using 5% hydrogen peroxide for 3×2 min 30 s. This was followed by incubation with streptavidin peroxidase for 30 min. The counterstaining was performed with hematoxylin for 1 min, and the immunoperoxidase reaction was developed using 3, 3′-diaminobenzidine for 3×5 min. Finally, the sections were washed with distilled water and mounted with Aquamount (BDH Laboratory Supplies, Poole, England). Negative controls were similarly processed by omitting the primary antibody, and biopsies from tonsilla were used as positive controls.

Evaluation of the IHC staining for IL-10

In normal mature squamous epithelium, expression of IL-10 is invariably present, being cytoplasmic and confined to the cells in the basal cell layer of the epithelium (Fig. 1). In metaplastic squamous epithelium, IL-10 expression was often slightly increased in intensity, and also extended to the epithelial layers beyond the basal cells (Fig. 2). In CIN lesions, IL-10 expression was variable (normal or up-regulated), significant up-regulation being mostly confined to high-grade CIN (Figs. 3 and 4). In all biopsies, IL-10 expressing cells were also encountered among the inflammatory cell infiltrates in the connective tissue underlying the epithelial lesion (Figs. 1, 2, 3, and 4). In the original grading of the IL-10 staining, a semi-quantitative scoring into four categories was used, as follows: 0=no expression; 1=weak staining (equivalent to normal squamous epithelium); 2=

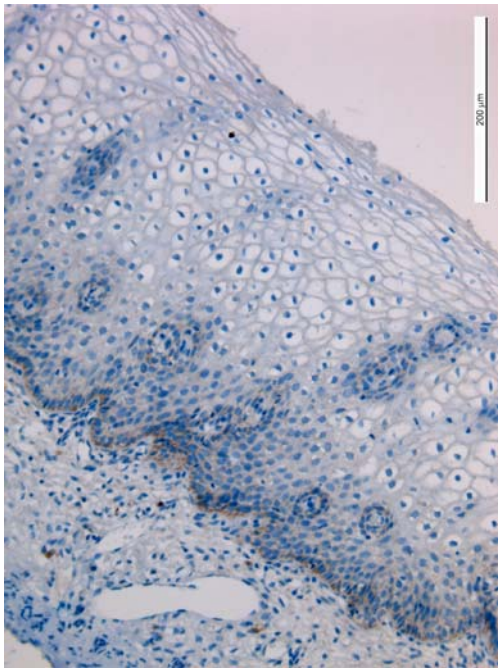

Fig. 1 Normal cervical epithelium with characteristic expression pattern of IL-10. IL-10 is regularly present, as cytoplasmic staining confined to the cells in the basal layer. In underlying connective tissue, scattered IL-10+ lymphocytes are also seen (IHC for IL-10, original magnification ×50)

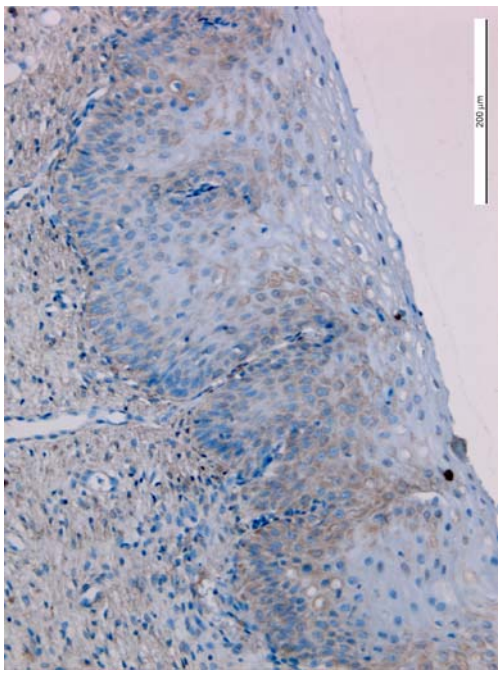

Fig. 2 Another site of squamous epithelium with characteristic features of metaplasia. As compared with the mature squamous epithelium in Fig. 1, cytoplasmic expression of IL-10 is extending to parabasal and lower intermediate layers. Staining is scattered in distribution, with some focal condensations. (IHC for IL-10, original magnification ×100)

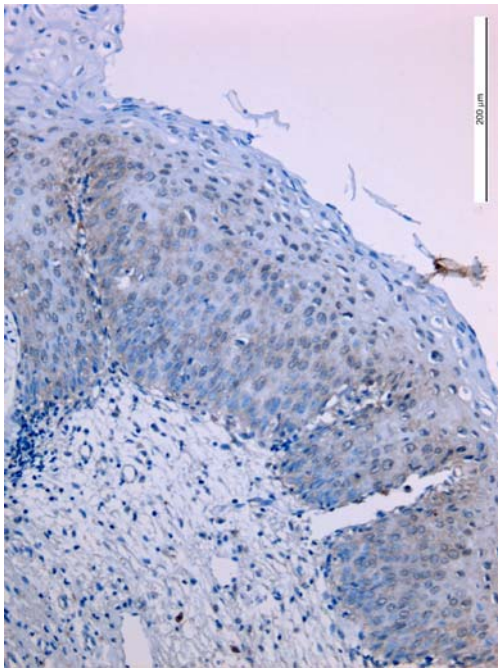

Fig. 3 A flat epithelial lesion with characteristic morphological features of HPV infection, associated with CIN2. IL-10 positive cells are confined to the dysplastic cells within the lowermost two thirds of epithelial thickness (CIN2 area), but also some koilocytes seem to be positive. A few IL-10+ lymphocytes appear in the underlying stroma (IHC for IL-10, original magnification ×100)

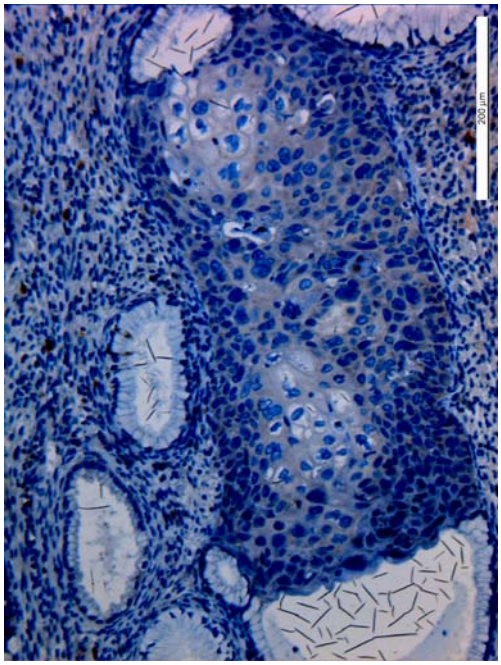

Fig. 4 A high-grade CIN3 lesion penetrating into an underlying glandular opening. IL-10 expression is found throughout the full thickness of the epithelium, indicating marked up-regulation. The staining is diffuse but its intensity shows some variability. In adjacent stroma, a few IL-10+ lymphocytes and macrophages are scattered among a loose inflammatory cell infiltrate (IHC for IL-10, original magnification ×250)

slightly to moderately increased staining (intermediate cells are stained); 3=strongly increased staining (all layers show positive IL-10 staining). In statistical analysis, the staining result was also treated as a dichotomous variable (normal vs. increased) to enable calculating the risk estimates (OR). In this analysis, no attempt was made to enumerate the cells expressing IL-10 among the inflammatory cell infiltrates.

Statistical methods

Statistical analyses were performed using the SPSS® and STATA software packages (SPSS for Windows, Version 16.0.2.1, and STATA/SE 10.1). In order to rule-out a selection bias caused by the non-systematic selection of the cases for IL-10 assessment, we compared the key clinical and epidemiological features of the 214 subjects who had material available for IL-10 assessment with those of the entire (1,011) LAMS cohort, forming three groups: women who had not undergone biopsy, women who underwent biopsy but the material was not available for IL-10 assessment and the study group (IL-10-available). Frequency tables for categorical variables were analyzed using the chi-square test. A multivariate linear model was fit to assess the distribution of these key epidemiological and clinical variables across the groups. In the subsequent analyses, using the IL-10 available subset, likelihood ratio (LR) or Fisher's exact test were used to assess the significance. Differences in the means of continuous variables were analyzed using non-parametric tests (Mann-Whitney) or analysis of variance (ANOVA). Performance indicators (sensitivity, specificity, PPV, NPV, and their 95% CI) for IL-10 as predictor of baseline CIN2/3 or HR-HPV, as well as the longitudinal predictive values for the three viral outcomes and incident CIN1+ and CIN2+, were all calculated using STATA/SE software and the algorithm of Seed et al. [28], which also calculates the area under ROC curve (AUC). In all tests, the values $p<0.05$ were regarded statistically significant.

Results

Table 1 depicts the key epidemiological and clinical features of the women that attended follow-up consultations during the prospective phase of the LAMS study, considering the availability of cervical biopsies and material for immunohistochemistry. Only women of the "IL-10 available" group were included in subsequent analyses. Most women (66.4%) were HPV-positive at baseline, on average they were 33 years of age at enrollment and most (70.3%) started sexual activity before 18 years of age. Approximately 40% of the sample consisted of current users of

Table 1 Comparison of the clinical and epidemiological baseline features of the LAMS cohort, considering the availability of samples for immunohistochemistry

Characteristic	No biopsy		IL-10 not available		IL-10 available		*p* value	
							Bivariate	Multivariate
Hr-HPV	No.	(%)	No.	(%)	No.	(%)		
Negative	142	(33.2)	55	(35.3)	37	(32.2)		
Positive	286	(66.8)	99	(64.7)	78	(67.8)	0.79	0.03
Not performed	133		82		99			
Age at enrollment								
<33 years	237	(42.4)	144	(61)	122	(57)		
≥33 years	322	(57.6)	92	(39)	92	(43)	<0.01	0.14
Ignored	2		0		0			
Pregnant								
Yes	534	(95.2)	228	(96.6)	212	(99.1)		
No	18	(4.8)	2	(3.4)	0	(0.9)	0.02	0.64
Ignored	9		6		2			
Onset of sexual activity								
<18 years	377	(67.2)	161	(68.2)	161	(75.6)		
≥18 years	184	(32.8)	75	(31.8)	52	(24.4)	0.07	0.11
Ignored	0		0		1			
Hormonal oral contraception								
Yes	222	(39.6)	98	(41.5)	101	(47.4)		
No	339	(60.4)	138	(58.5)	113	(52.6)	0.14	0.36
Smoking								
Yes (current or past)	219	(39.0)	85	(36.0)	98	(46.1)		
No	342	(61.0)	151	(64.0)	115	(53.9)	0.12	0.02
Ignored	0		0		1			
Lifetime sexual partners								
<4 partners	475	(84.7)	196	(83.4)	163	(76.5)		
≥4 partners	86	(15.3)	39	(16.6)	50	(23.5)	0.03	0.07
Ignored	0		1		1			
Years of formal education								
0 to 4	138	(24.6)	35	(14.8)	22	(10.3)		
5 to 10	183	(32.7)	86	(36.4)	58	(27.3)		
11 or more	239	(42.7)	115	(48.7)	133	(62.4)	<0.01	0.02
Ignored	1		0		1			

Table 2 Expression of IL-10 as related to lesion grade

Lesion grade	IL-10 expression						*p* value	
	Equivalent to normal expression		Slight to moderate up-regulation		Strong up-regulation			
Normal or HPV-NCIN	71	76.3%	14	15.1%	8	8.6%	$p=0.002$ (Fisher's exact test)	$p=0.008$ for linear trend
CIN1	51	79.7%	9	14.1%	4	6.2%		
CIN2	12	60.0%	8	40.0%	0	0.0%		
CIN3	16	44.4%	15	41.7%	5	13.9%		
SCC	1	100.0%	0	0.0%	0	0.0%		

HPV-NCIN flat HPV lesion with no CIN, *SCC* squamous cell carcinoma, *CIN* cervical intraepithelial neoplasia

Table 3 Expression of IL-10 as related to detection of HR-HPV and its viral load

HR-HPV Result	IL-10 expression						*p* value		Performance indicators of dichotomous (I/N) IL-10				
	Equivalent to normal expression		Slight to moderate up-regulation		Strong up-regulation				Sensitivity	Specificity	PPV	NPV	AUC
HC2 Assay									31.2% (95% CI 22.7–40.8)	78.0% (95% CI 65.3–87.7)	72.3% (95% CI 57.4–84.4)	38.0% (95% CI 29.3–47.3)	0.546 (95% CI 0.477–0.615)
HPV-positive	75	68.8%	28	25.7%	6	5.5%	p=0.313 (chi-square, LR)	p=0.417 for linear trend					
HPV-negative	46	78.0%	9	15.3%	4	6.8%							
Viral load (M±95% CI)[a]	2.19 (1.61–2.78) n=121		3.56 (2.46–4.67) n=37		2.34 (0.14–4.82) n=10		p=0.086 ANOVA	p=0.082 Kruskal–Wallis (M-C)					

M-C Monte-Carlo simulation with the 10,000 sample and 99% CI, *AUC* area under ROC curve, *I/N* increased vs. normal

[a] Semi-quantitative viral load determined by the RLU/CO ratio in hybrid capture 2 assay, log-transformed

hormonal contraception, and the same proportion of the women was of past or current smokers. Roughly 20% of the women had had four or more sexual partners during their lifetime. Multivariate analysis disclosed a slight, and clinically not significant, imbalance in HPV positivity rates between the groups formed considering the availability of material for histopathological analysis (p=0.03). These rates ranged from 64.7 in women that had a cervical biopsy, but whose material was not available for IHC, to 67.8% in women included in the present analysis (IL-10 assessment performed). No other imbalances in clinical and epidemiological features between groups were found.

The expression of IL-10 in cervical biopsies as related to the lesion grade is summarized in Table 2. There was a significant linear trend of increasing up-regulation of IL-10 (p=0.008) in parallel with increasing grade of CIN, with a major drop in normal expression upon transition from CIN2 to CIN3. When dichotomized (normal vs. increased), up-regulated IL-10 expression predicted CIN3+ with OR=3.66 (95% CI 1.76–7.6; p=0.001) and CIN2+ with OR=3.36 (95% CI 1.77–6.38; p=0.0001).

Table 3 depicts the association of IL-10 expression with the HR-HPV detection and semi-quantitative viral load measured by the HC2 assay. IL-10 expression pattern (3-tier grading) was clearly not related to detection of HR-HPV, showing similar distribution among HR-HPV+ and HR-HPV samples (p=0.313). Similarly, dichotomized expression was not associated with HR-HPV detection either: OR=1.60 (95% CI 0.76–3.35; p=0.201). The log-transformed semi-quantitative HR-HPV viral loads were not directly related to up-regulation of IL-10 (p=0.086). Not unexpectedly, when the performance indicators were calculated, IL-10 was not a useful marker of HR-HPV, with AUC=0.546 (95% CI 0.477–0.615).

Expression of IL-10 in the baseline biopsies was related to the outcomes of HR-HPV infections as presented in Table 4. IL-10 expression did not bear any relationship to the subsequent outcomes (incident infections, clearance, persistence) of HR-HPV infections during the follow-up, and no useful information was obtained calculating the longitudinal predictive values for the three outcomes. As to the time to clearance and time to incident HR-HPV (not calculable), there were no differences related to IL-10 expression.

Table 5 gives the data on IL-10 as predictor of the two surrogate endpoints of progressive disease (incident CIN1+, CIN2+). The 3-tier grading of IL-10 expression was practically identical in the baseline biopsies that subsequently progressed to incident CIN1+, with no significant difference. Longitudinal performance indicators did not provide any useful values, with AUC=0.472. The same is true with IL-10 as predictor of incident CIN2+ (AUC=0.506). However, NPV exceeds 90% implicating that

Table 4 Expression of IL-10as predictor of different outcomes of HR-HPV infection

Endpoint	IL-10 expression						*p* value		Longitudinal performance indicators of dichotomous (I/N) IL-10				
	Equivalent to normal expression		Slight to moderate up-regulation		Strong up-regulation		Fisher's exact	Linear trend	Sensitivity	Specificity	PPV	NPV	AUC
Incident HR-HPV									0.0% (95% CI 0.0–97.5)	85.5% (95% CI 73.3–93.5)	0.0 (95% CI 0.0–36.9)	97.9% (95% CI 88.9–99.9)	0.427 (95% CI 0.000–1.000)
Yes	1	100.0%	0	00.0%	0	00.0%	$p=1.000$	$p=0.703$					
No	47	85.5%	5	9.1%	3	5.5%							
HR-HPV cleared									7.1% (95% CI 0.2–33.9)	83.3% (95% CI 68.6–93.0)	12.5% (95% CI 0.3–52.7)	72.9% 95% CI 68.2–84.7)	0.452 (95% CI 0.362–0.543)
Yes	13	92.9%	0	00.0%	1	7.1%	$p=0.415$	$p=0.782$					
No	35	83.3%	5	11.9%	2	4.8%							
HR-HPV Persistence									0.0% (95% CI 0.0–28.5)	82.2% (95% CI 67.9–92.0)	0.0% (95% CI 0.0–36.9)	77.1% (95% CI 62.7–88.0)	0.411 (95% CI 0.355–0.468)
Yes	11	100.0%	0	00.0%	0	00.0%	$p=0.613$	$p=0.224$					
No	37	82.2%	5	11.1%	3	6.7%							

AUC area under ROC curve, *I/N* increased vs. normal

normal IL-10 expression precludes progression to CIN2+ with high accuracy (95% CI 82.4–96.3%). Times to progression to CIN1+ or CIN2+ were identical in different categories of IL-10 expression (data not shown in the Table).

Discussion

The first evidence on local immunological reactions as important mediators of host resistance against HPV infection [12, 13] was obtained in skin warts, where dense infiltrates of inflammatory cells were described in regressing lesions [13]. In the early 1980s, these studies were extended to cervical HPV lesions using newly introduced monoclonal antibodies to enumerate the cell subsets within these tissue-infiltrating lymphocytes (TIL) [29, 30]. Different subsets of lymphocytes (B cells, T helper cells; T suppressor cells) were present in abundance among these TILs, located subjacent to but also within the HPV lesions, CIN and CC [29, 30]. In addition, other types of immunocompetent cells, including Langerhans cells and natural killer cells were also detected among these infiltrates [31, 32]. Being hampered by the fact that serial samples were not available for analysis, these early studies failed to establish any meaningful correlations between the dynamic changes in TIL subsets (e.g., Th/Ts ratio) and the clinical outcome of HPV infections in a longitudinal setting [33, 34].

These enumeration studies have been subsequently complemented with the functional data on interleukins as key regulators of both humoral and CMI responses [12–15].

Table 5 Expression of IL-10 as predictor of the two surrogate endpoints of disease progression

Endpoint	IL-10 expression						*p* value		Longitudinal performance indicators of dichotomous (I/N) IL-10				
	Equivalent to normal expression		Slight to moderate up-regulation		Strong up-regulation		Fisher's exact	Linear trend	Sensitivity	Specificity	PPV	NPV	AUC
Incident CIN1+									16.7% (95% CI 3.6–41.4)	77.8% (95% CI 67.2–86.3)	14.3% (95% CI 3.–36.3)	80.6% (95% CI 70.3–88.8)	0.472 (95% CI 0.373–0.572)
Yes	15	83.3%	2	11.1%	1	5.6%	$p=1.000$	$p=0.687$					
No	63	77.8%	11	13.6%	7	8.6%							
Incident CIN2+									22.2% (95% CI 2.8–60.0)	78.9% (95% CI 69.0–86.8)	9.5% (95% CI 1.2–30.4)	91.0% (95% CI 82.4–96.3)	0.506 (95% CI 0.355–0.656)
Yes	7	77.8%	2	22.2%	0	00.0%	$p=0.668$	$p=0.798$					
No	71	78.9%	11	12.2%	8	8.9%							

AUC area under ROC curve, *I/N* increased vs. normal

Since its identification in 1989 [16], a huge amount of data have accumulated on IL-10 [14, 15]. It is now well established that IL-10 is produced by several different immune and non-immune cells, including T helper type 2 (Th2) cells, subsets of regulatory T cells designated as Tr1, Th1, and Th17 cells, CD8+ T cells, monocytes, and stimulated macrophages, some subsets of dendritic cells, B cells, as well as some granulocytes (eosinophils and mast cells) [14, 15]. Importantly, also some non-immune cells are rich sources of IL-10, most notably keratinocytes, epithelial cells, and even tumor cells [14, 35].

Including keratinocytes in this list of IL-10 secreting cells increases the interest in this cytokine as a potential modulator of cervical HPV infections, particularly through its known potent immunosuppressive effects [14, 15, 17, 18]. All these properties are potent enough to make IL-10 as an impending contributory factor in the development of cancer [14, 15]. Consistent with this, IL-10 expression has been shown to have increased in several different human malignancies (reviewed in [14]). Interpretation of these data is not straightforward, however, because elevated IL-10 expression can occur for multiple reasons with opposite implications, e.g., expressed by tumor cells themselves (suppressing antitumor responses), or produced by activated cells as a sign of a host antitumor reaction [14].

Taken the known complexity of the mechanisms whereby host immune responses attempt to control HPV infections on one hand and the cunning mechanisms developed by the virus to evade this control on the other hand [12, 13], there is little doubt that multiple potential sites of interaction between IL-10 and HR-HPV could exist in the microenvironment of CIN and/or CC. Under these circumstances, one could expect seeing some differences in IL-10 expression as related to (1) the grade of CIN, and (2) HR-HPV detection, as well as to (3) the outcome of these HR-HPV infections, and (4) development of incident CIN1+ and CIN2+, all having been examined in the present study. Instead of measuring cytokines in the serum [19] or in immune cells within TILs [20, 22], the present study analyzed the expression of IL-10 in the epithelial cells of CIN lesions, to assess whether the IL-10 expression patterns in cervical lesions have any associations with these four outcomes.

In the present study, IL-10 expression could be identified in practically all cervical biopsies, including normal epithelium and all grades of CIN (Table 1). IL-10 in normal squamous epithelium is confined to the basal cells, with rare extension to parabasal cells. IL-10 expression in normal cervical epithelium has been reported for the first time only recently, when Mindiola et al. [36], using a similar IHC approach, described increased IL-10 expression in normal epithelium adjacent to CIN or CC lesion. Using this IL-10 pattern in the normal squamous epithelium as a reference, we noticed that the expression of IL-10 seems to increase almost in parallel with the increasing grade of CIN. This is in full agreement with the observations reported in the recent studies using a similar approach [17, 36, 37]. In studies using different technique (e.g., RT-PCR for mRNA or cytokine tests in peripheral blood), IL-10 expression was shown to be decreased in HIV patients [22] as well as in CC as compared with CIN [20].

Interestingly, increased expression of IL-10 was shown to be associated with decreased risk of CIN2/3 lesions, when controlled for potential confounders using a multivariate model [38]. This is in sharp contrast to the present study, where up-regulated IL-10 expression predicted CIN3+ with OR=3.66 and CIN2+ with OR=3.36. When controlled for the most important confounder (HR-HPV), IL-10 up-regulation retained its significant association to both outcomes, with common OR=4.6 (95%CI 2.03–10.64) and OR=5.6 (95%CI 2.43–13.08) for CIN3+ and CIN2+, respectively (p=0.0001). However, it must be emphasized that these results were obtained with radically different methodologies. First, the IL-10 detection was performed using RT-PCR [38], contrasted to IHC in the present study. However, the most striking methodological dissimilarity is the fact that the quantification of IL-10 has been performed in cervical cytological specimens [38], collected with cytology brush, which may impart a wide variability of concentrations of the protein depending on how the collection has been done. Other analytical features of both studies, e.g., control variables used to balance for clinical factors contributing to CIN development, may also have partially contributed to these conflicting results.

In our series, up to 60% of CIN2 lesions still retained only weak expression of IL-10, equivalent to that found in the normal epithelium. In alignment with the recent reports [36, 37], IL-10 expression reached a peak in CIN3 lesions, of which only 44.4% retained the baseline profile, and almost 14% showed a significant over-expression (Table 1). It is tempting to speculate that this obvious up-regulation upon transition from CIN2 to CIN3 might bear some association with HR-HPV. In such a case, up-regulated IL-10 in these high-grade lesions could implicate a progressively increasing immunosuppression in a microenvironment favoring progressive cervical disease. This concept does not seem to hold true, however. Instead, the present data (Table 2) indicate that the expression profile of IL-10 is completely unrelated to the detection of HR-HPV in these lesions. Albeit previously described [17] (and confirmed by us) in typical HPV-harboring cells, IL-10 expression was shown to be completely unrelated to the detection of HPV also in another recent study [36]. In addition, we demonstrated no association between IL-10 expression and viral load of HR-HPV in the present series. As expected, then, IL-10 was not a useful marker of HR-HPV (AUC=0.546), unlike some other

markers ($p16^{INK4A}$, Survivin and hTERT) recently established as such [39].

Considering the potent immunosuppressive properties of IL-10 in the local microenvironment [14, 15, 17, 19–22], one would expect that its abundant expression should have some unfavorable impact on (1) the outcome of HR-HPV infections or (2) progression to CIN. This concept was challenged in the present study, however, when we failed to provide any confirmatory evidence to support the view that IL-10 expression could modify these viral and clinical outcomes. Thus, incident HR-HPV infections, virus clearance or HR-HPV persistence did not show any direct association with IL-10 expression (Table 3). Similarly, there was practically no difference in the baseline IL-10 expression patterns among progressive and non-progressive lesions (Table 4), and IL-10 was of no value in discriminating the incident CIN1+ and CIN2+ cases from those that did not progress.

Like studies enumerating immunocompetent cells among TILs in the baseline biopsies [29–34], also the present study suffers from the failure to provide any longitudinal data from the biopsies taken at FU visits [23, 27]. It is to be emphasized that like the traffic (recirculation) of immunocompetent cells in the cervix, also the production of immune regulatory cytokines (like IL-10) is a highly dynamic process [14, 15], being balanced and counterbalanced by a multitude of local and systemic stimuli that are impossible to record in single biopsies without a longitudinal setting. As recently discussed, several regulators of cytokine expression are currently known, including age, days since the last intercourse, current use of OC, current cigarette smoking, period of menstruation) [38], which are potential confounders of any analysis of IL-10 expression alone. To test the impact of these covariates, we constructed a multivariate model, including HR-HPV and the following potential confounders of IL-10 expression: age, time since last menstruation, current use of OC, and current smoking. Interestingly, the significant association of IL-10 with CIN2 and CIN3 was not confounded, but IL-10 retained its value as independent covariate of both CIN2 and CIN3 endpoints (together with HR-HPV, age and use of OC; data not shown).

In alignment with other recent reports [17, 36, 37], IL-10 up-regulation in the baseline biopsies was most consistently associated with high-grade CIN. The expression profile of this cytokine was unrelated to HR-HPV or its viral load, however, and was not a predictor of viral outcome and disease progression in a longitudinal setting. Together with HR-HPV, age and use of OC, IL-10 was an independent covariate of CIN2/3, suggesting that this immunosuppressive cytokine might play an important role in creating a milieu that favors progressive cervical disease. To better understand the role of IL-10 as a potential means contributing to the effective immune evasion by HR-HPV, several questions remain unanswered. Among these is the question whether HPV (like EBV, EHV2, Pox, CMV) [14, 15] does, indeed, have IL-10 gene homologs in their genome. Taken the close amino acid sequence homology between these known viral IL-10s and human IL-10 [14], one cannot exclude the possibility that IL-10 expression recently reported in koilocytes [17] and confirmed by observations in the present study might not be due to IL-10 of a viral (HPV) origin.

Acknowledgements This study has been supported by the European Commission, INCO-DEV Programme (Contract# ICA4-CT-2001-10013). The generous contribution of former DIGENE Inc. (USA) donating the HC2 tests at our disposal is gratefully acknowledged.

Conflict of interest statement We declare that we have no conflict of interest.

References

1. zur Hausen H (2009) Papillomaviruses in the causation of human cancers—a brief historical account. Virology 384:260–265
2. Syrjänen KJ (1987) Biology of human papillomavirus (HPV) infections and their role in squamous cell carcinogenesis. Med Biol 65:21–39
3. Syrjänen K, Syrjänen S (2000) Papillomavirus infections in human pathology. Wiley, New York, pp 1–615
4. Syrjänen S, Syrjänen K (2008) The history of papillomavirus research. Cent Eur J Public Health 16(Suppl):S7–13
5. Munoz N, Bosch FX, de Sanjose S et al (2003) Epidemiologic classification of human papillomavirus types associated with cervical cancer. N Engl J Med 348:518–527
6. Cliffort GM, Gallus S, Herrero R et al (2005) Worldwide distribution of human papillomavirus types in cytologically normal women in the International Agency for research on Cancer HPV prevalence surveys: pooled analysis. Lancet 366:991–998
7. Syrjänen SM, Syrjänen KJ (1999) New concepts on the role of human papillomavirus in cell cycle regulation. Ann Med 31:175–187
8. von Knebel Doeberitz M (2002) New markers for cervical dysplasia to visualise the genomic chaos created by aberrant oncogenic papillomavirus infections. Eur J Cancer 38:2229–2242
9. Munger K, Baldwin A, Edwards KM et al (2004) Mechanisms of human papillomavirus-induced oncogenesis. J Virol 78:11451–11460
10. Branca M, Ciotti M, Santini D et al (2004) $p16^{INK4A}$ expression is related to grade of CIN and high-risk human papillomavirus but does not predict virus clearance after conization or disease outcome. Int J Gynecol Pathol 23:354–365
11. Santopietro R, Shabalova IP, Petrovichev N et al (2006) Cell cycle regulators p105, p107, Rb2/p130, E2F4, $p21^{CIP1/WAF1}$, cyclin-A in predicting CIN, high-risk human papillomavirus infections and their outcome in women screened in three New Independent States of the Former Soviet Union. Cancer Epidemiol Biomark Prev 15:1250–1256
12. Stanley M (2006) Immune responses to human papillomavirus. Vaccine 24S:16–22
13. Syrjänen K (2000) Immunology of HPV infections and prospects for vaccination. Chapter 21. In: Syrjänen K, Syrjänen S (eds)

Papillomavirus infections in human pathology. Wiley, New York, pp 459–490
14. Moore KW, de Waal MR, Coffman RL et al (2001) Interleukin-10 and the interleukin-10 receptor. Annu Rev Immunol 19:683–765
15. Mosser DM, Zhang X (2008) Interleukin-10: new perspectives on an old cytokine. Immunol Rev 226:205–218
16. Fiorentino DF, Bond MW, Mosmann TR (1989) Two types of mouse T helper cell. IV. Th2 clones secrete a factor that inhibits cytokine production by Th1 clones. J Exp Med 170:2081–2095
17. Alcocer-Gonzalez JM, Berumen J, Tamez-Guerra R et al (2006) In vivo expression of immunosuppressive cytokines in human papillomavirus-transformed cervical cancer cells. Viral Immunol 19:481–491
18. de Waal Malefyt R, Haanen J, Spits HM et al (1991) Interleukin-10 (IL-10) and viral IL-10 strongly reduce antigen specific human T-cell proliferation by diminishing the antigen-presenting capacity of monocytes via down-regulation of class II major histocompatibility complex expression. J Exp Med 174:915–920
19. Clerici M, Merola M, Ferrario E et al (1997) Cytokine production patterns in cervical intraepithelial neoplasia: association with human papillomavirus infection. J Natl Cancer Inst 89:245–50
20. de Gruijl TD, Bontkes HJ, van den Muysenberg AJ et al (1999) Differences in cytokine mRNA profiles between premalignant and malignant lesions of the uterine cervix. Eur J Cancer 35:490–497
21. Santin AD, Hermonat PL, Ravaggi A et al (2000) Interleukin-10 increases Th1 cytokine production and cytotoxic potential in human papillomavirus-specific CD8(+) cytotoxic T lymphocytes. J Virol 74:4729–4737
22. Kobayashi A, Greenblatt RM, Anastos K et al (2004) Functional attributes of mucosal immunity in cervical intraepithelial neoplasia and effects of HIV infection. Cancer Res 64:6766–6774
23. Syrjänen K, Naud P, Derchain SM et al (2005) Comparing PAP smear cytology, aided visual inspection, screening colposcopy, cervicography and HPV testing as optional screening tools in Latin America. Study design and baseline data of the LAMS study. Anticancer Res 25:3469–3480
24. Longatto-Filho A, Maeda MYS, Eržen M et al (2005) Conventional PAP smear and liquid-based cytology as screening tools in low-resource settings of Latin America. Experience of the Latin American Screening Study. Acta Cytol 49:500–506
25. Sarian L, Derchain SM, Naud P et al (2005) Evaluation of visual inspection with acetic acid (VIA), Lugol's iodine (VILI) cervical cytology and HPV testing as cervical screening tools in Latin America. This report refers to partial results from the LAMS (Latin American Screening) study. J Med Screen 12:142–149
26. Longatto-Filho A, Eržen M, Branca M et al (2006) Human papillomavirus (HPV) testing as an optional screening tool in low-resource settings of Latin America. Experience from the LAMS study. Int J Gynecol Cancer 16:955–962
27. Syrjänen K, Shabalova I, Naud P et al (2009) Persistent high-risk human papillomavirus (HPV) infections and other endpoint markers of progressive cervical disease among women prospectively followed-up in the NIS and LAMS cohorts. Int J Gynecol Cancer 19:934–942
28. Seed PT, Tobias A (2001) Summary statistics for diagnostic tests. Stata Techn Bull 59:9–12
29. Syrjänen KJ (1983) Immunocompetent cells in uterine cervical lesions of human papillomavirus (HPV) origin. Gynecol Obstet Invest 16:327–340
30. Väyrynen M, Syrjänen K, Mäntyjärvi R et al (1985) Immunophenotypes of lymphocytes in prospectively followed up human papillomavirus lesions of the cervix. Genitourin Med 61:190–196
31. Väyrynen M, Syrjänen K, Mäntyjärvi R et al (1984) Langerhans cells in human papillomavirus (HPV) lesions of the uterine cervix identified by the monoclonal antibody OKT-6. Int J Gynaecol Obstet 22:375–383
32. Syrjänen K, Väyrynen M, Mäntyjärvi R et al (1986) Natural killer (NK) cells with HNK-1 phenotype in the cervical biopsies of women followed-up for human papillomavirus (HPV) lesions. Acta Obstet Gynecol Scand 65:139–145
33. Syrjänen K, Väyrynen M, Castren O et al (1984) The relation between the type of immunoreactive cells found in human papillomavirus (HPV) lesions of the uterine cervix and the subsequent behaviour of these lesions. Arch Gynecol 234:189–196
34. Syrjänen K, Väyrynen M, Hippeläinen M et al (1985) The in situ immunological reactivity and its significance in the clinical behaviour of the cervical human papillomavirus lesions. Neoplasma 32:181–190
35. Williams LM, Ricchetti G, Sarma U et al (2004) Interleukin-10 suppression of myeloid cell activation—a continuing puzzle. Immunology 113:281–292
36. Mindiola R, Caulejas D, Nunez-Troconis J et al (2008) Increased number of IL-2, IL-2 receptor and IL-10 positive cells in premalignant lesions of the cervix. Invest Clin 49:533–545
37. Giannini SL, Al-Saleh W, Piron H et al (1998) Cytokine expression in squamous intraepithelial lesions of the uterine cervix: implications for the generation of local immunosuppression. Clin Exp Immunol 113:183–189
38. Scott ME, Ma Y, Kuzmich L, Moscicki AB (2009) Diminished IFN-gamma and IL-10 and elevated Foxp3 mRNA expression in the cervix are associated with CIN 2 or 3. Int J Cancer 124:1379–1383
39. Branca M, Ciotti M, Giorgi C et al (2008) Predicting high-risk human papillomavirus (HPV) infection, progression of cervical intraepithelial neoplasia (CIN) and prognosis of cervical cancer with a panel of 13 biomarkers tested in multivariate modelling. Int J Gynecol Pathol 27:265–273

Virchows Arch (2009) 455:517–526
DOI 10.1007/s00428-009-0848-1

ORIGINAL ARTICLE

Establishment and characterization of a novel human malignant peripheral nerve sheath tumor cell line, FMS-1, that overexpresses epidermal growth factor receptor and cyclooxygenase-2

Michiyuki Hakozaki · Hiroshi Hojo · Michiko Sato · Takahiro Tajino · Hitoshi Yamada · Shinichi Kikuchi · Masafumi Abe

Received: 23 April 2009 / Revised: 10 August 2009 / Accepted: 9 October 2009 / Published online: 18 November 2009

Abstract Malignant peripheral nerve sheath tumor (MPNST) is a rare soft tissue sarcoma. We established a new human MPNST cell line (designated FMS-1) from MPNST of the right brachial plexus of a 69-year-old woman with NF1. The cell line has been maintained for >24 months with >100 passages. FMS-1 cells showed a fibrosarcoma-like or epithelioid pattern in the heterotransplanted tumor, compared with a fascicular growth pattern of short-spindle tumor cells in the primary tumor. Immunophenotypically, FMS-1 cells showed almost the same characteristics as the primary tumor. Cytogenetic and molecular analyses revealed a deletion in exons 5-8 of the p53 gene. Epidermal growth factor receptor (EGFR) and cyclooxygenase (COX)-2 were expressed in FMS-1 cells. To improve the highly aggressive course and poor prognosis and establish new therapeutic methods, molecular genetic and biological characterizations of MPNST are required. Thus, FMS-1 cells might be useful for investigating biological behaviors and developing new molecular-targeting antitumor drugs for MPNST expressing EGFR or COX-2.

M. Hakozaki (✉) · H. Hojo · M. Sato · M. Abe
First Department of Pathology,
Fukushima Medical University School of Medicine,
1 Hikarigaoka, Fukushima-shi,
Fukushima 960-1295, Japan
e-mail: paco@fmu.ac.jp

M. Hakozaki · T. Tajino · H. Yamada · S. Kikuchi
Department of Orthopaedic Surgery,
Fukushima Medical University School of Medicine,
Fukushima, Japan

Keywords Malignant peripheral nerve sheath tumor · FMS-1 cell line · Neurofibromatosis type 1 · Epidermal growth factor receptor · Cyclooxygenase-2

Introduction

Malignant peripheral nerve sheath tumor (MPNST), also called malignant schwannoma or neurofibrosarcoma, is a rare soft tissue sarcoma, accounting for approximately 5% of soft tissue sarcomas. Approximately half of MPNSTs manifest in patients with neurofibromatosis type 1 (NF1; von Recklinghausen disease) [1], and patients with NF1 have a 5–10% lifetime risk of MPNST [2, 3].

MPNST frequently shows highly aggressive behavior, resistance to multi-agent chemotherapy, and fatal metastasis. About 60% of patients with MPNST die of the disease and the overall 5- and 10-year survival rates are 34% and 23%, respectively [1]. Therefore, to improve the aggressive course or prognosis, new therapeutic developments including molecular-targeting drugs based on molecular genetic and biological characterizations of MPNST are required.

To the best of our knowledge, only nine human MPNST cell lines from eight patients with MPNST have been reported to date [4–9]. However, these cell lines have been adequately investigated from the perspectives of molecular genetics and biological behaviors. To clarify the biological behavior of MPNST, the present study established and characterized a new MPNST cell line, FMS-1, derived from a patient with NF1. Moreover, for the purpose of developing the potentialities for new therapeutic targets of MPNST, since there is no established remedy for MPNST other than surgical exclusion,

we also investigated whether epidermal growth factor receptor (EGFR) and cyclooxygenase (COX)-2 are over-expressed in FMS-1.

Materials and methods

Case report

A 69-year-old Japanese woman with a past medical history of NF1 on the basis of clinical findings (multiple cutaneous neurofibromas and café au lait spots) was admitted to our hospital with a 6-year history of palsy in the right arm. Physical examination showed a tumor in the right axilla, and her illness was clinically diagnosed as right brachial plexus palsy due to brachial plexus tumor. Magnetic resonance imaging revealed a tumor in the right brachial plexus involving the right subclavian/axillary artery and vein, measuring 173×93×77 mm in size. This lesion was hypointense on T1-weighted imaging and intermediate to hyperintense on T2-weighted imaging, showing diffuse enhancement on Gd-enhanced T1-weighted imaging. No distant metastases were found on radiological analysis. Light microscopy of incisional biopsy specimens from the right brachial plexus tumor showed diffuse proliferation of short spindle-shaped cells with focal arrangement in a fibrosarcoma-like pattern and occasional large pleomorphic cells (Fig. 1). Spindle-shaped and pleomorphic cells showed atypical nuclei, and mitotic figures were frequently seen. Immunohistochemically, tumor cells were positive for vimentin, S-100 protein, and nerve growth factor receptor (NGFR). Characteristics from light microscopy and immunohistochemistry led us to a diagnosis of MPNST. The criteria for diagnosis of MPNST have previously been outlined by Fletcher [10, 11]. The patient had not undergone any therapy such as palliative operation, chemotherapy, or radiotherapy, as the patient and her family were hoping to avoid therapy. The patient died of the disease 5 months after biopsy.

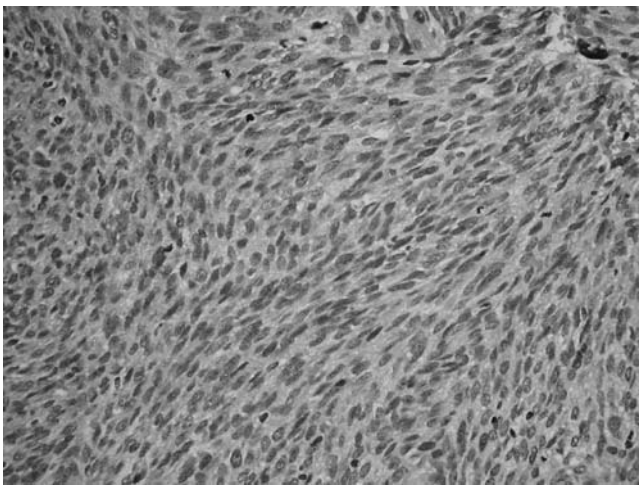

Fig. 1 Histology of the primary right brachial plexus tumor. Tumor cells show diffuse proliferation and are short spindle-shaped cells arranged in a fibrosarcoma-like pattern, accompanied by scattered pleomorphic cells (hematoxylin and eosin, ×200)

Establishment of cell line

Tumor cells were obtained from the biopsy specimen. The tumor tissue was cut into small pieces measuring about 0.5×0.5×0.5 mm with a scalpel, rinsed with phosphate-buffered saline twice. After the treatment with 0.25% trypsin-EDTA solution (Sigma, St. Louis, MO, USA), cells were cultured at an initial concentration of 1.0×10^6 viable cells/ml in RPMI-1640 medium (#R8758; Sigma) supplemented with 15% heat-inactivated fetal calf serum (FCS; JRH Biosciences, Lenexa, KS, USA), 50 units/ml penicillin G and 50 μg/ml streptomycin. Next, cells were inoculated into 100-mm plastic dishes (BD Falcon #353003; BD Biosciences, Franklin Lakes, NJ, USA) and incubated at 37°C in a humidified atmosphere with 5% CO_2. The culture medium was changed twice per week. To harvest and transfer the cell line, cells were treated with 0.25% trypsin-EDTA solution after reaching a sub-confluent state. The cell line has been maintained for >24 months under these culture conditions.

Morphological study

Growth and morphology of cultured cells in vitro were observed using an inverted microscope. Morphological characteristics were further determined by May-Giemsa staining on cytospin preparations and by hematoxylin–eosin staining on paraffin-embedded sections.

Immunohistochemistry

Immunohistochemical analysis was performed on the primary tumor, cultured cells at the 48th passage and heterotransplanted tumors using the streptavidin-biotin complex method. Antibodies used in this study are summarized in Table 1.

Cell population doubling time

To determine the doubling time, 3.5×10^5 cells at the 49th passage were seeded on 35-mm plastic dishes (BD Falcon #353046; BD Biosciences) with fresh culture medium containing 15% FCS. Dishes were harvested, and the number of viable cells in each dish was counted using the dye exclusion test (0.1% trypan blue in phosphate-buffered saline) every 24 h for 7 days.

Table 1 Antibodies used in the present study

Antibody	Clone	Dilution	Source
Vimentin	V9	1:1,000	Dako[a]
S-100 protein	Polyclonal	1:2,000	Dako[a]
NSE	Polyclonal	1:3	Nichirei[b]
Neurofilament	2F11	1:100	Dako[a]
Synaptophysin	SY38	1:20	Dako[a]
PGP9.5	10A1	1:40	Novocastra[c]
NGFR	NGFR 5	1:100	Dako[a]
CD34	NU-4A1	1:50	Nichirei[b]
CD56	123C3	1:300	Zymed Laboratories[d]
CD57 (Leu-7)	HNK-1	1:50	Becton Dickinson[e]
CD99 (MIC-2)	12E7	1:200	Dako[a]
Desmin	D33	1:20	Dako[a]
α-SMA	1A4	1:100	Dako[a]
AE1/AE3	AE1 and AE3	1:200	Dako[a]
Ki-67 (MIB-1)	MIB-1	1:300	Dako[a]
p53	DO-7	1:150	Dako[a]
EGFR	EGFR.25	1:100	Novocastra[c]
COX-2	4H12	1:100	Novocastra[c]

NSE neuron-specific enolase, *PGP9.5* protein gene product 9.5, *NGFR* nerve growth factor receptor, *α-SMA* α-smooth muscle actin, *EGFR* epidermal growth factor receptor, *COX-2* cyclooxygenase-2

[a] Glostrup, Denmark

[b] Tokyo, Japan

[c] Newcastle upon Tyne, UK

[d] San Francisco, CA, USA

[e] San Jose, CA, USA

Heterotransplantation

Severe combined immunodeficiency (SCID) mice (lcr/scid, female) and athymic nude mice (BALB/cA-nu/nu, female) were purchased at 6 weeks old from CLEA Japan (Tokyo, Japan) and kept under sterile conditions. All animal experiments were performed under the control of our committee in accordance with the Guidelines on Animal Experiments at Fukushima Medical University, the Japanese Government Animal Protection and Management Law (No. 105) and the Japanese Government Notification of Feeding and Safekeeping of Animals (No. 6). Mice were given a single subcutaneous injection of 1×10^7 cells at the 65th passage from cultured cells in the log phase of growth.

Cytogenetics

Karyotype analysis of FMS-1 cells at the 71st passage was performed commercially by SRL (Tokyo, Japan) using the trypsin G-banding technique.

Polymerase chain reaction-single strand conformational polymorphism (PCR-SSCP) and direct sequencing analysis for p53 gene

Genomic PCR-SSCP in p53 gene exons 5-8, which are considered the mutational hot spot for this gene, was performed on FMS-1 cells at the 78th passage (Mitsubishi Kagaku Bio-Clinical Laboratories, Tokyo, Japan). Moreover, oligonucleotide sequences in exons 5–9 of the p53 gene were analyzed by direct sequencing. DNA samples were extracted from FMS-1 cells at the 80th passage using Sepagene (Sanko-Junyaku, Tokyo, Japan), in accordance with to the protocol provided by the manufacturer. Using Takara Ex Taq HS polymerase (Takara Bio, Shiga, Japan), 0.5 μg of DNA was amplified in a total volume of 50 μl. The sequencing primers were as follows [12]: exons 5-6 (sense), 5′-TTCCTCTTCCTGCAGTACTC-3′; exons 5–6 (antisense), 5′-AGTTGCAAACCAGACCTCAG-3′; exon 7 (sense), 5′-GTGTTGCCTCCTAGGTTGGC-3′; exon 7 (antisense), 5′-CAAGTGGCTCCTGACCTGGA-3′; exons 8–9 (sense), 5′-CCTATCCTGAGTAGTGGTAA-3′; exons 8–9 (antisense), 5′-CCAAGACTTAGTACCTGAAG-3′. These primers were obtained from Sigma-Aldrich Japan (Hokkaido, Japan). PCR was performed as follows: denaturing at 94°C for 10 min followed by 30 cycles of amplification (94°C for 1 min, 60°C for 1 min, and 72°C for 1 min) and a 10-min extension at 72°C, in a thermal cycler (i-cycler, Bio-Rad Laboratories, Hercules, CA, USA). One microliter of the PCR product was applied for PCR under conditions consisting of 1 cycle of 95°C for 5 min and 25 cycles of 95°C for 30 s and 60°C for 30 s by the direct sequencing method (Thermo Sequenase core sequencing kit with 7-deaza-dGTP; Amersham, Cleveland, OH, USA). Subsequently, oligonucleotide sequences of exons 5–9 of the p53 gene were analyzed using a sequencer (SQ-5500, Hitachi, Tokyo, Japan) and compared with the germline sequences recorded in the GenBank database.

Western blotting analysis for EGFR and COX-2

Protein samples were separated from cell pellets of FMS-1 cells at the 66th passage. Methods for Western blotting analysis, reagents and antibodies (EGFR (1,005; sc-03, 1:1,000 dilution; Santa Cruz Biotechnology, Santa Cruz, CA, USA) and COX-2 (H-62; sc-7951, 1:200 dilution; Santa Cruz Biotechnology)) used in this study were the same as previously described [13]. The FPS-1 cell line, derived from human undifferentiated pleomorphic sarcoma and established in our laboratory [14], was used as a positive control for EGFR and COX-2 proteins.

RNA preparation and reverse transcription-PCR (RT-PCR) analysis for EGFR and COX-2 mRNA expression

Total RNA from FMS-1 cells at the 64th passage was isolated using ISOGEN reagent (Wako Pure Chemical Industries, Osaka, Japan) according to the manufacturer's protocol. Methods and sequencing primers were the same as previously described [13]. The FPS-1 cell line [14] was used as a positive control for EGFR and COX-2 mRNAs.

Results

Immunohistochemical analysis for p53, EGFR, and COX-2 on primary tumor cells

Primary tumor cells showed strong immunopositivity for EGFR and COX-2 (Table 2), but no immunoreactivity for p53.

Establishment of cell line

A new human MPNST cell line, designated FMS-1, was established from the right brachial plexus tumor of a patient with NF1. Doubling time of this cell line was approximately 38.5 h. The cell line has been stably maintained for >100 passages (a period of >24 months). Cultured cells comprised small, polygonal, or short-spindle-shaped cells with occasional large pleomorphic cells (Fig. 2). Loss of contact inhibition was observed. Immunohistochemically, cultured cells were positive for vimentin, S-100 protein (Fig. 3a), CD57, CD56, neurofilament, NGFR, CD99, protein gene product 9.5, AE1/AE3, Ki-67, EGFR (Fig. 3b), and COX-2 (Fig. 3c), but were negative for neuron-specific enolase, synaptophysin, CD34, desmin, α-smooth muscle actin, and p53 (Fig. 3d; Table 2).

Heterotransplantation

The FMS-1 cell line showed successful heterotransplantation into SCID mice and athymic nude mice. In two of two SCID mice and one of two nude mice given a single subcutaneous injection of FMS-1 cells, a tumor with a diameter of approximately 15 mm developed 9 weeks after inoculation (Fig. 4a). The cut surface of the xenografted tumor was solid and white. Under light microscopy, the tumor of SCID mouse showed various morphological patterns: spindle-shaped cells arranged in a fascicular and fibrosarcoma-like herringbone pattern (fascicular area, Fig. 4b) or focally in a nuclear palisading pattern (palisading area, Fig. 4c). An epithelioid-cellular area was also observed in the same tissue fragment (epithelioid area, Fig. 4d). Microscopically, tumor in nude mouse showed diffuse proliferation of epithelioid tumor cells with frequent mitotic figures (Fig. 4e). Focally, short-spindle-shaped tumor cells showed a structured fascicular pattern. A nuclear palisading pattern was not observed in tumor in nude mouse. No metastases were found at other sites, such as the brain, lungs or liver, in either SCID or nude mice. FMS-1 cells and heterotransplanted tumor cells showed almost the same immunophenotype as primary tumor cells. Primary tumor cells, FMS-1 cells, and heterotransplanted tumor cells all expressed EGFR and COX-2, but not p53 (Table 2).

Table 2 Immunohistochemical reactivity of primary tumor, FMS-1 cell line (in vitro), and heterotransplanted tumor (FMS-1 in nude mouse; in vivo) to various antibodies

Antibody	Primary tumor	FMS-1 (in vitro)	FMS-1 (in vivo)
Vimentin	4+	4+	4+
S-100 protein	1+	1+	+/–
NSE	–	–	3+
Neurofilament	–	2+	1+
Synaptophysin	–	–	–
PGP9.5	+/–	4+	3+
NGFR	2+	+/–	1+
CD34	–	–	–
CD56	1+	1+	2+
CD57 (Leu-7)	1+	1+	+/–
CD99 (MIC-2)	–	3+	+/–
Desmin	–	–	–
α-SMA	–	–	–
AE1/AE3	+/–	2+	2+
Ki-67 (MIB-1)	2+	3+	3+
p53	–	–	–
EGFR	3+	4+	4+
COX-2	3+	4+	4+

– negative, +/– rare cell positive (<1% positive cells), *1+* <10% positive cells, *2+* 10–50% positive cells, *3+* >50–90% positive cells, *4+* >90% positive cells

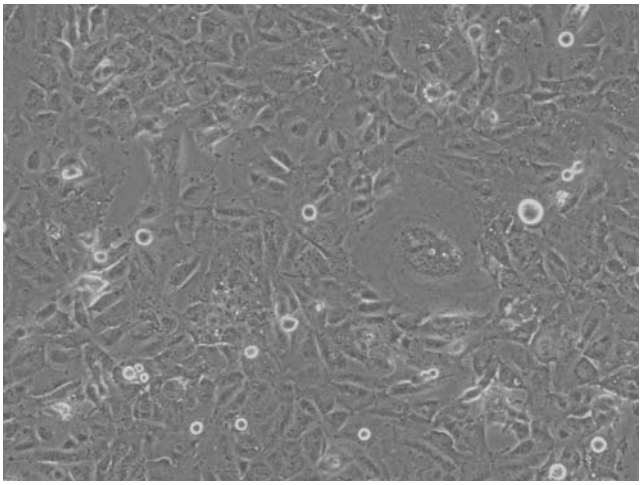

Fig. 2 Inverted microscopy of FMS-1 cells in vitro. Adherent cultured cells are atypical, small, polygonal, or short-spindle-shaped without contact inhibition. Large pleomorphic cells are also observed

Cytogenetics

Karyotype analysis of G-banded chromosomes for FMS-1 cells revealed the following composite karyotype: 79–84<4n>(modal number: 83), XX, −X[10], −X[10], der(1)add(1)(p36)add(1)(q21)[4], add(2)(p23)×2[10], add(4)(p16)[10], der(4)add(4)(p16)add(4)(q35)[6], der(4)add(4)(p16)del(4)(q?)[3], der(4)add(4)(p15)?t(4;11)(q35;q23)×2[9], +add(6)(p11)[10], add(6)(p11)×2[10], add(6)(q11)[6], der(6;15)(p10;q10)[10], der(6;15)[4], +7[2], +add(7)(p22)[10], add(7)[9], del(7)(q11)[6], del(7)(q32)[3], +add(8)(q21)[4], add(8)[10], add(8)[7], add(8)[2], add(8)(p11)[5], add(8)(p11)[4], add(8)[3], add(8)(p11)[3], −9[10], add(9)(q21)[4], add(9)(q32)[9], add(9)(q32)[3], der(9)t(8;9)(q11;p13)[9], −10[10], −10[10], del(11)(p13)[2], del(11)(p15)[10], del(11)[8], der(11)add(11)(p15)del(11)(q23)[10], der(11;13)(13qter→13p11::?::11p15→11q23:)[9],+del(12)(q13)×2[10], del(12)(q24q24)×2[10], del(12)[2], −13[8], der(13)t(13;13)(p11;q12)ins(13;?)(p11;?)[10], −14[10], −14[10], add(14)(p13)[5], −15[7], add(15)(p13)

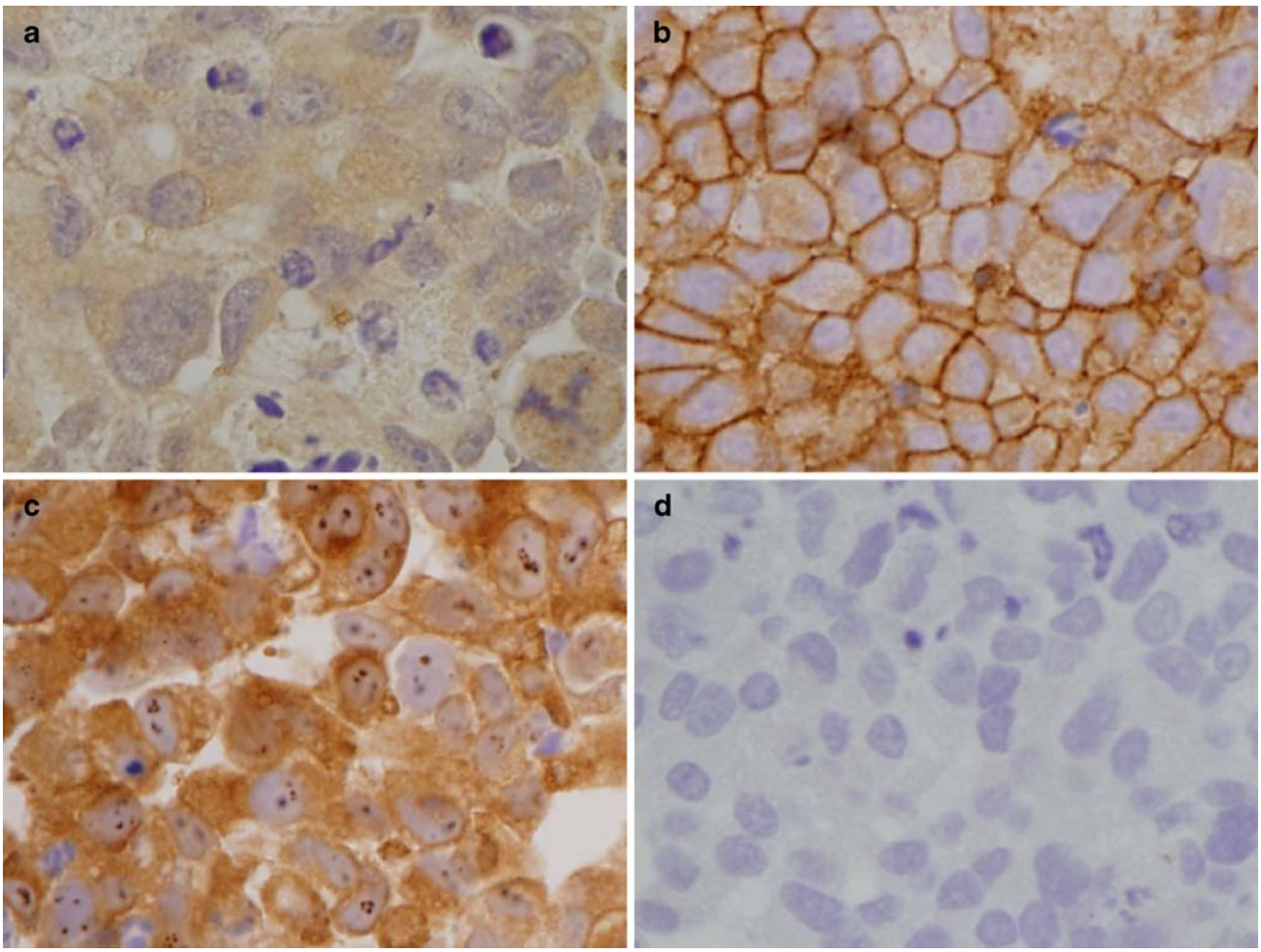

Fig. 3 FMS-1 cells immunohistochemically display positive immunoreactivity for S-100 protein (**a**), EGFR (**b**), and COX-2 (**c**), but not for p53 (**d**) (immunoperoxidase stain, ×400)

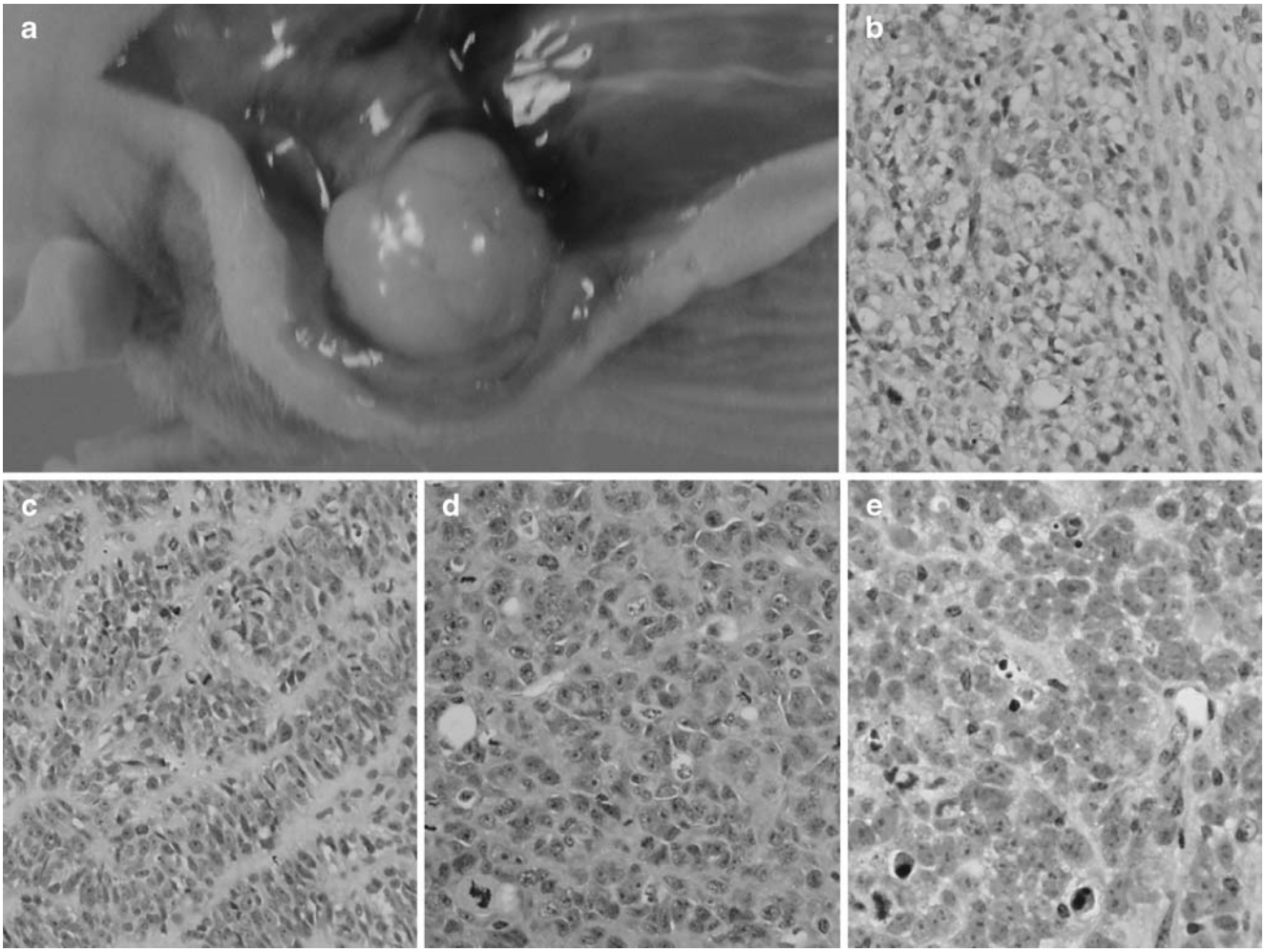

Fig. 4 Gross findings of heterotransplanted tumor in the nude mouse (**a**) and microscopic findings of heterotransplanted tumor in the SCID mouse (**b**–**d**), or athymic nude mouse (**e**) (hematoxylin and eosin, ×400). Tumor from SCID mouse shows a fascicular, fibrosarcoma-like herringbone pattern (**b**), a nuclear palisading pattern (**c**), or an epithelioid pattern (**d**). Tumor from nude mouse shows diffuse growth of epithelioid tumor cells with frequent mitotic figures (**e**)

[10], add(15)[8], −16[10], −17[10], −17[10], −17[6], add(17)(q25)[10], add(17)[2], +18[3], −19[8], add(19)(p13)[4], −20[10], −20[8], −21[3], −22[10], −22[10], add(22)(q13)[10], add(22)[8], +der(?)t(?;8)(?;q13)[6], +mar1×2[5], +mar2[9], +mar3[4], +1–4mar; cp10 (Fig. 5).

PCR-SSCP and direct sequencing analysis for p53 gene

In the FMS-1 cell line, PCR transcripts of the exons 5–9 or 5–8 of the p53 gene were not amplified both by PCR or PCR-SSCP. Direct sequencing was unable to show meaningful results (data not shown).

Western blotting for EGFR and COX-2 proteins

Western blot analysis demonstrated that FMS-1 and FPS-1 cells as a positive control expressed both EGFR and COX-2 proteins (Fig. 6).

RT-PCR analysis for EGFR and COX-2 mRNA

RT-PCR analysis showed both EGFR and COX-2 mRNA in FMS-1 cells, and also in FPS-1 cells as a positive control (Fig. 7).

Discussion

We established the FMS-1 cell line from human MPNST in a patient with NF1. FMS-1 cells showed various morphological characteristics in heterotransplanted tumor, with short-spindle-shaped tumor cells structured in a fascicular pattern, or polygonal cells with atypical nuclei arranged in an epithelioid pattern with scattered uninucleated anaplastic cells. An epithelioid component was observed in the heterotransplanted tumor, but not in the primary tumor. FMS-1 cells in vitro and in vivo showed almost the same

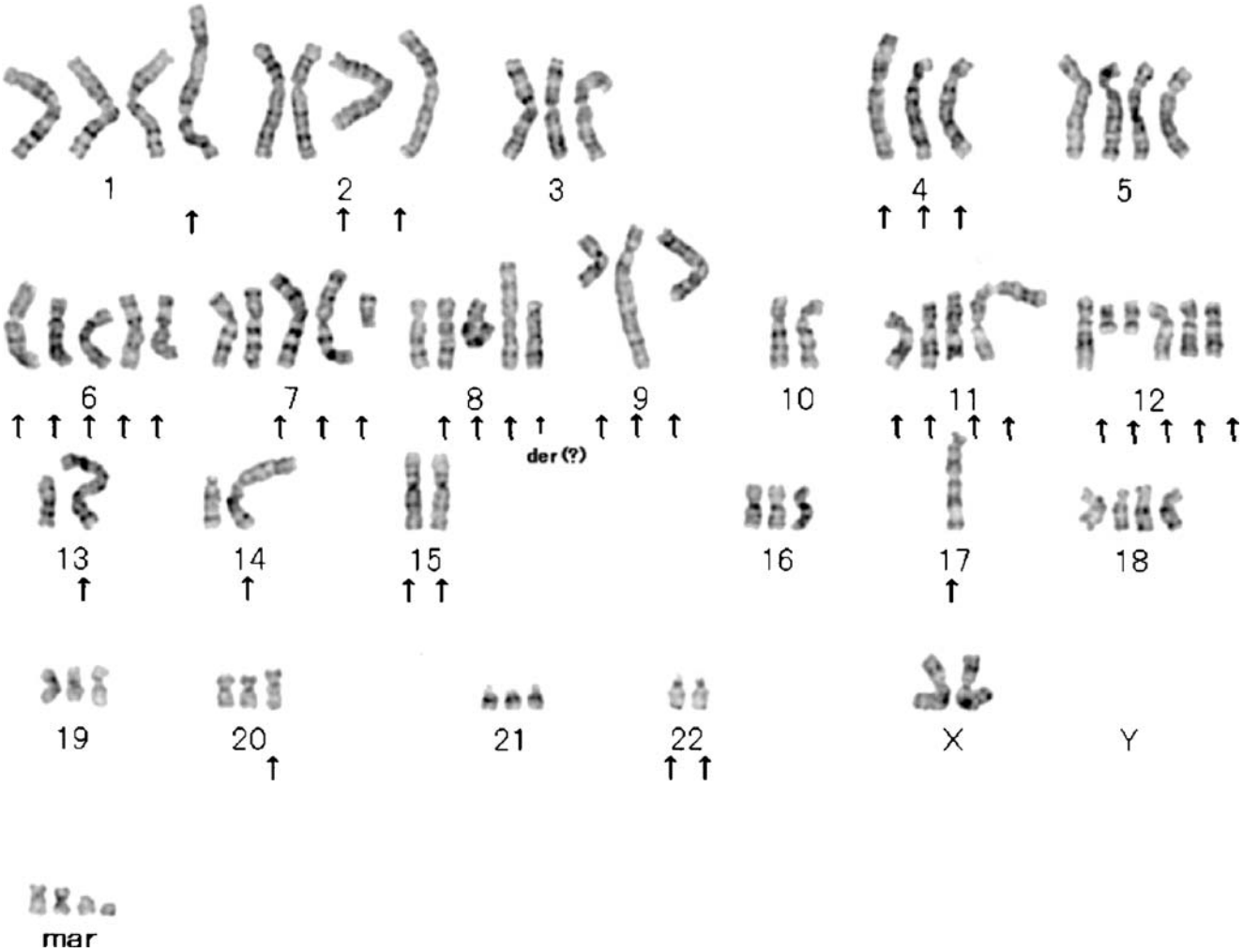

Fig. 5 Representative G-banded karyotype of the FMS-1 cell line at passage 71, exhibiting the following abnormal complement: 79, XX, −X, −X, der(1)add(1)(p36)add(1)(q21), add(2)(p23)×2, −3, −4, add(4)(p16), der(4)add(4)(p15)?t(4;11)(q35;q23)×2, +6, +add(6)(p11)×3, der(6;15)(p10;q10)×2, +7, +add(7)(p22)×2, del(7)(q11), +8, +add(8)(q21)×2, add(8)(p11), +der(?)t(?;8)(?;q13), −9, add(9)(q21), add(9)(q32), der(9)t(8;9)(q11;p13), −10, −10, del(11)(p15)×2, der(11)add(11)(p15)del(11)(q23), der(11;13)(13qter→13p11::?::11p15→11q23:), +12, +12, +del(12)(q13)x2, del(12)(q24q24)x3, −13, −13, der(13)t(13;13)(p11;q12)ins(13;?)(p11;?), −14, −14, add(14)(p13), −15, −15, add(15)(p13)×2, −16, −17, −17, −17, add(17)(q25), −19, −20, −21, −22, −22, add(22)(q13)×2, +mar1×2, +mar2, +mar3, +1–4mar. *Arrows* indicate the abnormal chromosomes

immunophenotype as primary tumor cells, suggesting MPNST, and FMS-1 was thus thought to be derived from the primary MPNST. Only immunoexpression of the neurofilament and CD99 shows difference between in the primary tumor and in the FMS-1 (in vitro and in vivo). Previously, there are no reports concerning with the expression of neurofilament or CD99 in MPNST. We speculate that difference of the circumstance of tumor cells lead to different immunoreactivity in tumor cells.

Mutations of two tumor suppressor genes, NF1 gene and p53 gene, reportedly participate in malignant tumorigenesis for patients with NF1 (2-stage carcinogenesis) [15]. Especially, alterations of NF1 gene is highly observed in NF1-associated MPNST [16]. Chromosome 17 loss parallels molecular evidence of allelic loss at the NF1 locus (17q11.2) in sporadic and NF1-associated MPNSTs, in addition to functional inactivation of the p53 tumor suppressor gene localized to 17p13.1 [17–20]. Bridge et al. reported that loss of chromosome 17 (chromosome 17 monosomy) is found in 43% of MPNST cases [21]. Cytogenetic analysis of FMS-1 confirmed chromosome 17 monosomy. Although mutation analysis of NF1 gene was not performed and PCR transcripts of p53 gene were not amplified by PCR or PCR-SSCP, loss of chromosome 17 seems to be related to the process of carcinogenesis in FMS-1 cells. Previous studies of the p53 gene in MPNST identified deletions and other mutations in approximately 29–75% of this tumor [18, 19, 22]. Previous immunohistochemical analysis showed overexpression of p53 gene product protein without clarified p53 gene mutation in

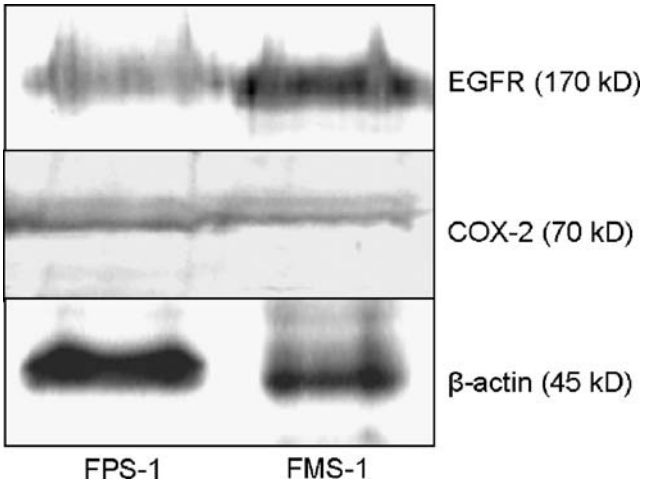

Fig. 6 Western blot analyses of EGFR (170 kD), COX-2 (70 kD), and β-actin (45 kD; loading control) proteins from FMS-1 and FPS-1 (positive control) cell lines. Bands of membranous protein EGFR and cytoplasmic protein COX-2 are detected

MPNST cases [23]. On the other hand, several cases or cell lines of other malignancies with a nonsense mutation have shown undetectable or low levels of p53 gene product protein [24–26]. We speculate that complete immunonegativity for the p53 gene product protein of primary tumor and FMS-1 cells both in vitro and in vivo (heterotransplanted tumor) were attributable to the clone harboring a serious mutation, particularly deletion of the p53 gene.

EGFR is a receptor tyrosine kinase and is widely expressed in a variety of epithelial malignancies [27]. EGFR activation promotes tumor growth by increasing cell proliferation, motility or angiogenesis, and by blocking apoptosis [28]. Recently, some EGFR tyrosine kinase inhibitor has seen clinical use against carcinomas, and antitumor effects on several types of malignancies including sarcomas have been investigated. Expression of EGFR and its ligands in sarcomas including MPNST has been reported [29–33]. Particularly, Holtkamp et al. had reported the effectiveness of erlotinib (EGFR tyrosine kinase inhibitor) and transzumab (humanized antibody targeting the extracellular domain of erbB2) against MPNST cells in vitro [34]. Our data also indicate that EGFR is a potential target in the treatment of MPNST patients and FMS-1 is useful for such investigations.

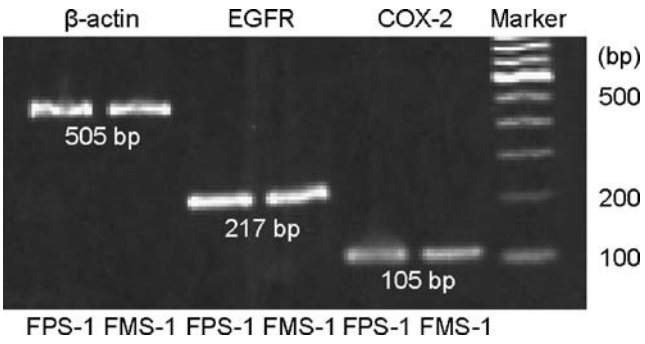

Fig. 7 RT-PCR analysis of EGFR and COX-2 mRNA in FMS-1 and FPS-1 (positive control) cell lines. *Lane 1*, marker, 100-bp DNA ladder; *Lanes 2* and *3*, β-actin (505 bp); *Lanes 4* and *5*, EGFR (217 bp); *Lanes 6* and *7*, COX-2 (105 bp). EGFR and COX-2 mRNA are detected

COX, also known as prostaglandin H2 synthase or prostaglandin endoperoxide synthase, is the key enzyme in the conversion of arachidonic acid to prostanoids [35]. Two COX genes have been cloned. COX-1 is a constitutive enzyme produced constantly in most tissue types, and is probably responsible for the production of prostanoids under physiological conditions. COX-2 is undetectable in most normal tissues, but can be induced in various cell types by pro-inflammatory agents, growth factors and carcinogens [36]. Overexpression of COX-2 is found in a variety of malignancies, including carcinomas, lymphomas and some sarcomas. In addition, COX-2 activation promotes tumor growth through the production of prostaglandin E2, which may block apoptosis or activate vascular endothelial growth factor and angiogenesis [37]. Recent studies have shown antitumor effects of some selective COX-2 inhibitors for sarcomas, particularly for osteosarcomas [38–43], as well as for carcinomas. No reports appear to have described COX-2 expression in MPNST, but COX-2 might offer a novel target for therapy against MPNST or to prevent malignancy in NF1 patients.

FMS-1 cells expressed both EGFR and COX-2. Crosstalk between EGFR and COX-2 has recently been found [44, 45], and cooperative cell-growth inhibition by combined treatment using an EGFR tyrosine kinase inhibitor and a selective COX-2 inhibitor in some carcinomas has been reported [46–49]. However, combined antitumor effect of an EGFR tyrosine kinase inhibitor and a selective COX-2 inhibitor in sarcoma has yet to be described. The FMS-1 cell line may thus be useful for investigating the antitumor effects of EGFR tyrosine kinase inhibitors combined with selective COX-2 inhibitors.

Conclusions

We have established a new human MPNST cell line, FMS-1, derived from a patient with NF1. FMS-1 cells show almost the same morphological characteristics and immunophenotype as the primary tumor cells that are characteristic of MPNST, and displayed a loss of chromosome 17 and lack of the p53 gene product protein as well as expression of EGFR and COX-2. The FMS-1 cell line will prove useful for investigating biological behaviors and developing therapies against MPNST.

Acknowledgments The authors would like to thank Mrs. Hiromi Kaneko and Miss Satomi Hikichi for their skillful technical assistance.

Conflict of interest statement We declare that we have no conflict of interest.

References

1. Woodruff JM, Kourea HP, Louis DN et al (2000) Malignant peripheral nerve sheath tumour (MPNST). In: Kleihues P, Cavenee WK (eds) World Health Organization classification of tumours. Tumours of the nervous system. IARC Press, Lyon, pp 172–174
2. Weiss SW, Goldblum JR (2007) Malignant tumors of the peripheral nerves. In: Weiss SW, Goldblum JR (eds) Enzinger and Weiss's soft tissue tumors, 5th edn. Mosby/Elsevier, Philadelphia, pp 903–917
3. Grobmyer SR, Reith JD, Shahlaee A et al (2008) Malignant peripheral nerve sheath tumor: molecular pathogenesis and current management considerations. J Surg Oncol 97:340–349
4. Ono I, Ishiwata I, Nakaguchi T et al (1989) Establishment and characterization of a human malignant schwannoma cell line (HKMS). Hum Cell 2:272–277 (in Japanese with English abstract)
5. Nagashima Y, Ohaki Y, Tanaka Y et al (1990) Establishment of an epithelioid malignant schwannoma cell line (YST-1). Virchows Arch [B] 59:321–327
6. Reynolds JE, Fletcher JA, Lytle CH et al (1992) Molecular characterization of a 17q11.2 translocation in a malignant schwannoma cell line. Hum Genet 90:450–456
7. Imaizumi S, Motoyama T, Ogose A et al (1998) Characterization and chemosensitivity of two human malignant peripheral nerve sheath tumour cell lines derived from a patient with neurofibromatosis type 1. Virchows Arch 433:435–441
8. Sonobe H, Takeuchi T, Furihata M et al (2000) A new human malignant peripheral nerve sheath tumour-cell line, HS-sch-2, harbouring p53 point mutation. Int J Oncol 17:347–352
9. Aoki M, Nabeshima K, Nishio J et al (2006) Establishment of three malignant peripheral nerve sheath tumor cell lines, FU-SFT8611, 8710 and 9817: conventional and molecular cytogenetic characterization. Int J Oncol 29:1421–1428
10. Fletcher CDM, Dal Cin P, de Wever I et al (1999) Correlation between clinicopathological features and karyotype in spindle cell sarcomas. A report of 130 cases from the CHAMP study group. Am J Pathol 154:1841–1847
11. Fletcher CDM (2000) Peripheral neuroectodermal tumors. In: Fletcher CDM (ed) Diagnostic histopathology of tumors, 2nd edn. Churchill Livingstone, London, pp 1695–1698
12. Murakami Y, Hayashi K, Sekiya T (1991) Detection of aberrations the p53 alleles and the gene transcript in human tumor cell lines by single-strand conformation polymorphism analysis. Cancer Res 51:3356–3361
13. Hakozaki M, Hojo H, Sato M et al (2006) Establishment and characterization of a new cell line, FRTK-1, derived from human malignant rhabdoid tumor of the kidney, with overexpression of epidermal growth factor receptor and cyclooxygenase-2. Oncol Rep 16:265–271
14. Hakozaki M, Hojo H, Sato M et al (2006) Establishment and characterization of a new cell line, FPS-1, derived from human undifferentiated pleomorphic sarcoma, overexpressing epidermal growth factor receptor and cyclooxygenase-2. Anticancer Res 26:3393–3401
15. Carroll SL, Stonecypher MS (2004) Tumor suppressor mutations and growth factor signaling in the pathogenesis of NF1-associated peripheral nerve sheath tumors. I. The role of tumor suppressor mutations. J Neuropathol Exp Neurol 63:1115–1123
16. Bottillo I, Ahlquist T, Brekke H et al (2009) Germline and somatic NF1 mutations in sporadic and NF1-associated malignant peripheral nerve sheath tumours. J Pathol 217:693–701
17. Legius E, Marchuk DA, Collins FS et al (1993) Somatic deletion of the neurofibromatosis type 1 gene in a neurofibrosarcoma supports a tumour suppressor gene hypothesis. Nat Genet 3:122–126
18. Menon AG, Anderson KM, Riccardi VM et al (1990) Chromosome 17p deletions and p53 gene mutations associated with the formation of malignant neurofibrosarcomas in von Recklinghausen neurofibromatosis. Proc Natl Acad Sci USA 87:5435–5439
19. Legius E, Dierick H, Wu R et al (1994) TP53 mutations are frequent in malignant NF1 tumors. Genes Chromosomes Cancer 10:250–255
20. Lothe RA, Slettan A, Saeter G et al (1995) Alterations at chromosome 17 loci in peripheral nerve sheath tumors. J Neuropathol Exp Neurol 54:65–73
21. Bridge RS Jr, Bridge JA, Neff JR et al (2004) Recurrent chromosomal imbalances and structurally abnormal breakpoints within complex karyotypes of malignant peripheral nerve sheath tumour and malignant triton tumour: a cytogenetic and molecular cytogenetic study. J Clin Pathol 57:1172–1178
22. Birindelli S, Perrone F, Oggionni M et al (2001) Rb and TP53 pathway alterations in sporadic and NF1-related malignant peripheral nerve sheath tumors. Lab Invest 81:833–844
23. Mawrin C, Kirches E, Boltze C et al (2002) Immunohistochemical and molecular analysis of p53, RB, and PTEN in malignant peripheral nerve sheath tumors. Virchows Arch 440:610–615
24. Davidoff AM, Pence JC, Shorter NA et al (1992) Expression of p53 in human neuroblastoma- and neuroepithelioma-derived cell lines. Oncogene 7:127–133
25. Villuendas R, Piris MA, Algara P et al (1993) The expression of p53 protein in non-Hodgkin's lymphomas is not always dependent on p53 gene mutations. Blood 82:3151–3156
26. Lepelley P, Preudhomme C, Vanrumbeke M et al (1994) Detection of p53 mutations in hematological malignancies: comparison between immunocytochemistry and DNA analysis. Leukemia 8:1342–1349
27. Nicholson RI, Gee JM, Harper ME (2001) EGFR and cancer prognosis. Eur J Cancer 37:S9–S15
28. Holbro T, Civenni G, Hynes N (2003) The ErbB receptors and their role in cancer progression. Exp Cell Res 284:99–110
29. Dobashi Y, Takei N, Suzuki S et al (2004) Aberration of epidermal growth factor receptor expression in bone and soft-tissue tumors: protein overexpression, gene amplification and activation of downstream molecules. Mod Pathol 17:1497–1505
30. Yamamoto T, Fujita I, Akisue T et al (2004) Amphiregulin and epidermal growth factor receptor expression in human malignant fibrous histiocytoma of soft tissues. Anticancer Res 24:1307–1310
31. Beech D, Pollock RE, Tsan R et al (1998) Epidermal growth factor receptor and insulin-like growth factor-I receptor expression and function in human soft-tissue sarcoma cells. Int J Oncol 12:329–336
32. Abdiu A, Walz TM, Nishikawa BK et al (1998) Human malignant fibrous histiocytomas in vitro: growth characteristics and their association with expression of mRNA for platelet-derived growth factor, transforming growth factor-alpha and their receptors. Eur J Cancer 34:2094–2100
33. Tawbi H, Thomas D, Lucas DR et al (2008) Epidermal growth factor receptor expression and mutational analysis in synovial sarcomas and malignant peripheral nerve sheath tumors. Oncologist 13:459–466

34. Holtkamp N, Malzer E, Zietsch J et al (2008) EGFR and erbB2 in malignant peripheral nerve sheath tumors and implications for targeted therapy. Neuro Oncol 10:946–957
35. Vane JR, Bakhle YS, Botting RM (1998) Cyclooxygenases 1 and 2. Annu Rev Pharmacol Toxicol 38:97–120
36. Dubois RN, Abramson SB, Crofford L et al (1998) Cyclooxygenase in biology and disease. FASEB J 12:1063–1073
37. Gately S, Li WW (2004) Multiple roles of COX-2 in tumor angiogenesis: a target for antiangiogenic therapy. Semin Oncol 31:2–11
38. Yamashita H, Osaki M, Honjo S et al (2003) A selective cyclooxygenase-2 inhibitor, NS-398, inhibits cell growth by cell cycle arrest in a human malignant fibrous histiocytoma cell line. Anticancer Res 23:4671–4676
39. Naruse T, Nishida Y, Hosono K et al (2006) Meloxicam inhibits osteosarcoma growth, invasiveness and metastasis by COX-2-dependent and independent routes. Carcinogenesis 27:584–592
40. Hakozaki M, Hojo H, Kikuchi S et al (2007) Etodolac, a selective cyclooxygenase-2 inhibitor, induces apoptosis by activating caspases in human malignant rhabdoid tumor cells (FRTK-1). Oncol Rep 17:169–173
41. Naruse T, Nishida Y, Ishiguro N (2007) Synergistic effects of meloxicam and conventional cytotoxic drugs in human MG-63 osteosarcoma cells. Biomed Pharmacother 61:338–346
42. Lee EJ, Choi EM, Kim SR et al (2007) Cyclooxygenase-2 promotes cell proliferation, migration and invasion in U2OS human osteosarcoma cells. Exp Mol Med 39:469–476
43. Liu B, Shi ZL, Feng J et al (2008) Celecoxib, a cyclooxygenase-2 inhibitor, induces apoptosis in human osteosarcoma cell line MG-63 via down-regulation of PI3K/Akt. Cell Biol Int 32:494–501
44. Dannenberg AJ, Lippman SM, Mann JR et al (2005) Cyclooxygenase-2 and epidermal growth factor receptor: pharmacologic targets for chemoprevention. J Clin Oncol 23:254–266
45. Lippman SM, Gibson N, Subbaramaiah K et al (2005) Combined targeting of the epidermal growth factor receptor and cyclooxygenase-2 pathways. Clin Cancer Res 11:6097–6099
46. Tortora G, Caputo R, Damiano V et al (2003) Combination of a selective cyclooxygenase-2 inhibitor with epidermal growth factor receptor tyrosine kinase inhibitor ZD1839 and protein kinase A antisense causes cooperative antitumor and antiangiogenic effect. Clin Cancer Res 9:1566–1572
47. Chen Z, Zhang X, Li M et al (2004) Simultaneously targeting epidermal growth factor receptor tyrosine kinase and cyclooxygenase-2, an efficient approach to inhibition of squamous cell carcinoma of the head and neck. Clin Cancer Res 10:5930–5939
48. Zhang X, Chen ZG, Choe MS et al (2005) Tumor growth inhibition by simultaneously blocking epidermal growth factor receptor and cyclooxygenase-2 in a xenograft model. Clin Cancer Res 11:6261–6269
49. Melisi D, Caputo R, Damiano V et al (2005) Zoledronic acid cooperates with a cyclooxygenase-2 inhibitor and gefitinib in inhibiting breast and prostate cancer. Endocr Relat Cancer 12:1051–1058

Virchows Arch (2009) 455:527–531
DOI 10.1007/s00428-009-0852-5

CASE REPORT

Colonic carcinoma with a pancreatic acinar cell differentiation. A case report

Anna Maria Chiaravalli · Giovanna Finzi · Valentina Bertolini · Stefano La Rosa · Carlo Capella

Received: 18 July 2009 / Revised: 23 September 2009 / Accepted: 16 October 2009 / Published online: 12 November 2009

Abstract A case of a colonic carcinoma showing a pancreatic acinar cell differentiation is described for the first time. A 65-year-old woman underwent surgical resection for an ulcerated protruding tumour of 4×2.5 cm in size on the anterior wall of the sigmoid colon. Histologically, tumour cells were organized in acinar structures resembling pancreatic acini and in solid nests and ribbons or diffusely infiltrated as poorly cohesive cells. Lymph nodes and femur metastases displayed the same histological features. The ultrastructural analysis of the primary tumour indicated the presence of zymogen-like granules in the cytoplasm of tumour cells. Immunohistochemically, both acinar and diffuse patterns of growth showed an intense staining for trypsin, chymotrypsin and BCL10 and a weaker immunoreactivity for lipase and carboxyl ester hydrolase. Most tumour cells were cytokeratin 20, CDX2 and p53 positive; whereas, mucin (MUC)2 immunoreactivity was observed only in the signet ring cells present in the diffuse pattern and chromogranin A in rare isolated tumour cells. No immunoreactivity was observed for cytokeratin 7, MUC1, MUC5AC, pancreatic amylase or PDX1. There was no evidence of a pancreatic acinar cell carcinoma or of heterotopic pancreatic tissue. A colonic origin ought to be suspected when a metastatic carcinoma of unknown primary shows an acinar differentiation.

A. M. Chiaravalli (✉) · G. Finzi · S. La Rosa
Department of Pathology, Ospedale di Circolo,
viale Borri 57,
21100 Varese, Italy
e-mail: annamaria.chiaravalli@tin.it

V. Bertolini · C. Capella
Department of Human Morphology, Anatomic Pathology Unit,
University of Insubria,
Varese, Italy

Keywords Acinar cell carcinoma · Colon cancer · Immunohistochemistry

Introduction

Acinar cell carcinoma of the pancreas is a rare malignant epithelial tumour representing 1–2% of all exocrine pancreatic neoplasms. It is composed of relatively uniform tumour cells arranged in acinar and solid structures. The diagnosis of acinar cell carcinoma requires immunohistochemical demonstration of the production of pancreatic enzymes, such as trypsin, lipase and chymotrypsin by tumour cells or ultrastructural demonstration of zymogen granules [1, 2]. In the gastrointestinal tract, other than in the pancreas, tumours with acinar cell differentiation have been described in the stomach [3–5] and jejunum [6] but, to our knowledge, no colonic localization has been reported in the literature.

Here, we report the first case of colon cancer with acinar cell differentiation.

Clinical history

A 65-year-old woman was hospitalized for intestinal occlusion. The colonic endoscopy showed a circumferential constriction just before the sigmoid-rectal junction. The patient underwent surgical resection, and a colonic segment of 15.5 cm was removed. Macroscopically, an ulcerated lesion of 4×2.5 cm in size was present on the anterior wall of the colon. Metastases were observed in eight of 17 regional lymph nodes.

Eighteen months later, a right femur metastasis appeared and the patient died with diffuse metastases to dorsal vertebrae and ribs 24 months after surgery.

Materials and methods

Immunohistochemical studies were performed on formalin-fixed paraffin-embedded sections using a peroxidase polymeric detection system (Ultravision, LabVision, Fremont CA) and 3-3′ diaminobenzidine as a chromogen. The primary antibodies used for staining are listed in Table 1.

For the ultrastructural study, samples of the tumour were retrieved from the paraffin block. After paraffin removal by chloroform the samples were fixed for 2 h at 4°C in a mixture of 2% paraformaldehyde and 2% glutaraldehyde in 0.05 M pH 7.3 cacodylate buffer and embedded in epoxy resins. Thin sections were counterstained with uranyl acetate and lead citrate and examined with a Philips (Morgagni 268 D) electron microscope.

Results

Histological findings The tumour extended from the mucosa, throughout the muscularis propria, into the adipose tissue under the serosa. It was characterized by two main intermingled growth patterns: acinar-solid and diffuse (Fig. 1a). In mucosa and submucosa, the acinar-solid pattern was prevalent: tumour cells were organized in acinar structures resembling normal pancreatic acini (Fig. 1b) and in solid nests and ribbons.

Foci with acinar architecture were also present in the muscularis propria and in the adipose tissue and were accompanied by a diffuse growth of single tumour cells that infiltrated separately.

The acinar and solid areas consisted of clusters of cuboidal to pyramidal cells separated by fine fibrous strands. The nuclei were round to oval, with single nucleoli. Nuclear atypia was moderate. Cytoplasms were moderately abundant, prevalently eosinophilic, with PAS positive fine granules. In acinar structures, tumour cells had basally located nuclei and surrounded small undefined lumina.

By contrast, the diffuse growth pattern was characterized by poorly cohesive, diffusely infiltrating, pleomorphic tumour cells with irregular-shaped nuclei and various degrees of atypia. The cytoplasms, more or less abundant, were clear or eosinophilic. Signet ring cells with cytoplasmic accumulation of Alcian Blue positive mucus were also present.

The adjacent non neoplastic colonic mucosa showed a normal appearance. Lymph nodes and femur metastases displayed all the histological features described in the primary tumour: acini, ribbons, solid nests and isolated cells were present.

Immunohistochemical findings Both acinar and diffuse patterns showed an intense immunostaining for trypsin (Fig. 1c), BCL10 (Fig. 1e) and chymotrypsin (Fig. 1f) and a

Table 1 List of primary antibodies

Antibodies/Antisera anti-	P/M (clone)	Dilution	Treatment	
Trypsin	P rabbit	1:400	PT 1	Biodesign International, Saco, ME, USA
Trypsin	M (MAB1482)	1:100	PT1	Millipore, Temecula, CA, USA
Chymotrypsin	P rabbit	1:100	HIER	AbD Serotec, Oxford UK
Pancreatic type amylase	M (6103)	1:200	PT 2	Biogenex Laboratories, San Ramon, CA, USA
Lipase	M	1:1,000	HIER	Chemicon Int. Inc, Temecula,CA, USA
BCL10 (C-terminal)	M (331.3)	1:200	HIER	Santa Cruz Biotech. Inc, Santa Cruz CA, USA
CEH (CEL[a], D-20)	P goat	1:50	HIER	Santa Cruz Biotechnology Inc
MUC 1	M (Ma695)	1:100	HIER	Novocastra, New Castle, UK
MUC 5AC	M (CLH2)	1:100	HIER	Novocastra
MUC 6	M (CLH5)	1:100	HIER	Novocastra
MUC 2	M (Ccp58)	1:200	HIER	Novocastra
Chromogranin A	M (LK2H10)	Undiluted	HIER	Ventana Medical System, Cedex, F
P53	M (DO-7)	Undiluted	HIER	Ventana
CDX 2	M (CDX2-88)	1:100	HIER	Biogenex Laboratories
CK 20	M (Ks20.8)	1:100	HIER	Dako, Glustrup, Denmark
CK7	M (OV-TL 12/30)	Undiluted	HIER	Cell Marque, Hot Spring, AR, USA
PDX1	P goat	1:200	HIER	Santa Cruz Biotechnology Inc

[a] In the Santa Cruz catalogue, the protein is named with the synonym carboxyl ester lipase

M monoclonal, *P* polyclonal, *PT 1* proteolytic treatment with 0.05 trypsin (Sigma), *PT 2* proteolytic treatment with 0.004 protease XXIV (Sigma), *HIER* heat-induced epitope retrieval with Tris-EDTA buffer

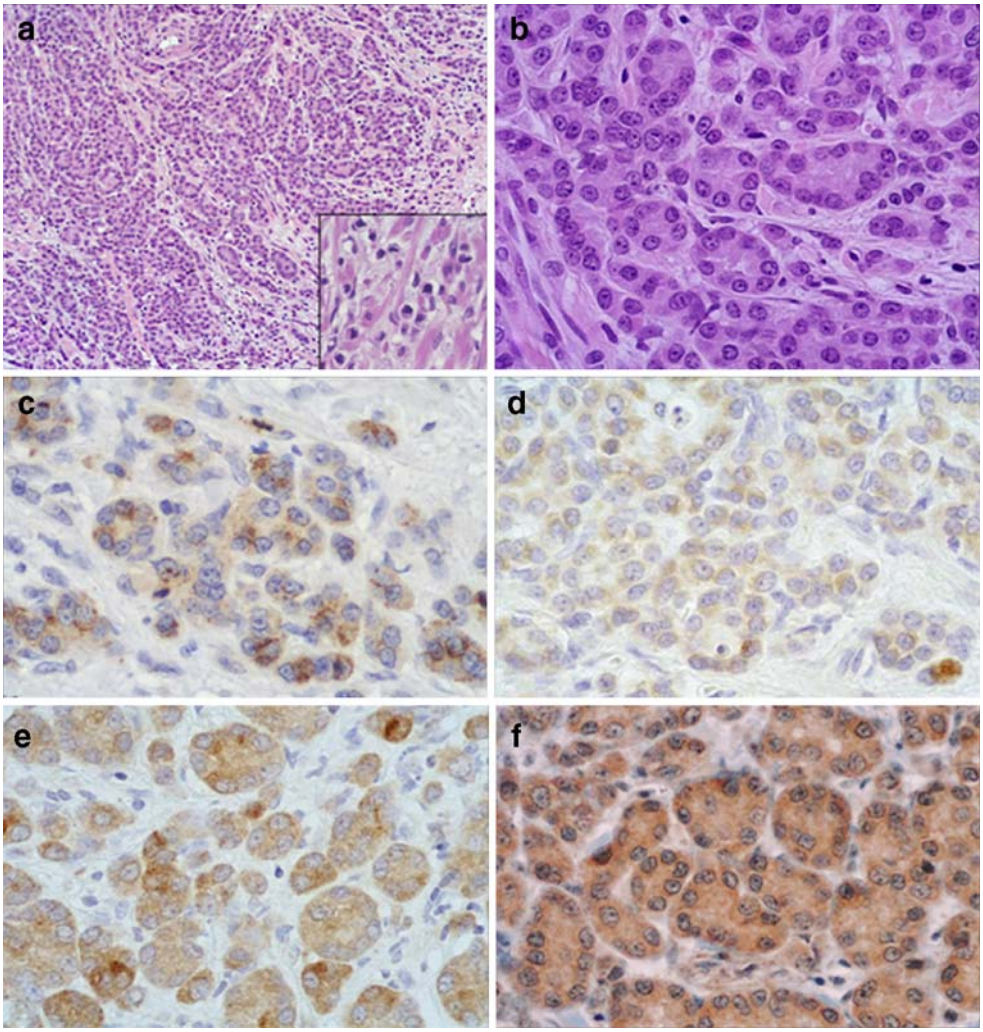

Fig. 1 Colonic carcinoma showing acinar-solid and diffuse (*inset*) growth pattern (**a**). Acinar arrangement: tumour cells have basally located nuclei and surround small undefined lumina (**b**). Intense immunoreactivity for trypsin (**c**), BCL10 (**e**) and chymotrypsin (**f**) and weak immunostaining for lipase (**d**). **a** and **b** haematoxylin–eosin; **c** to **f** immunoperoxidase, DAB–haematoxylin; **a** ×100; *inset*, **b** to **f** ×400)

weaker immunoreactivity for lipase (Fig. 1d) and carboxyl ester hydrolase. No pancreatic amylase immunoreactivity was observed in tumour cells. MUC2 immunoreactivity was present in the cytoplasm of most of the signet ring cells. Rare superficial tumour cells showed weak MUC6 immunoreactivity; whereas, no positivity was observed using MUC1 and MUC5AC antibodies. Most tumour cells were CK20, CDX2 and p53 immunoreactive, while no nuclear staining for PDX1 or cytoplasm immunoreactivity for CK7 was present.

Scattered isolated chromogranin-positive endocrine cells were also present among exocrine tumour cells.

Both lymph nodes and bone metastases displayed BCL10 and CEH immunoreactivity, the former displayed intensely and the latter more weakly. A light trypsin and lipase immunoreactivity was observed only in the lymph node metastases.

Ultrastructural findings Observed with the electron microscope, the neoplastic cells forming the acini showed some secretory granules, accumulated in the apical cytoplasm. The granules measured approximately 210 nm in diameter and showed a dense homogenous matrix, suggesting a zymogen-like aspect (Fig. 2). Among them, sparse cells had irregularly shaped endocrine-type secretory granules, accumulated in the basal cytoplasm, similar to those of intestinal enterochromaffin cells [7]

Discussion

The histological aspect of the present case of carcinoma suggested a pancreatic acinar carcinoma, but it occurred in the colon and the patient did not have a primary pancreatic neoplasm. The results of immunohistochemical and ultrastructural studies confirmed the acinar cell differentiation hypothesised on the basis of the histological features. In particular, electron dense zymogen-like granules were ultrastructurally documented in the cytoplasm of tumour cells. As far as enzymatic production was concerned, in addition to trypsin, the expression of which has already been documented

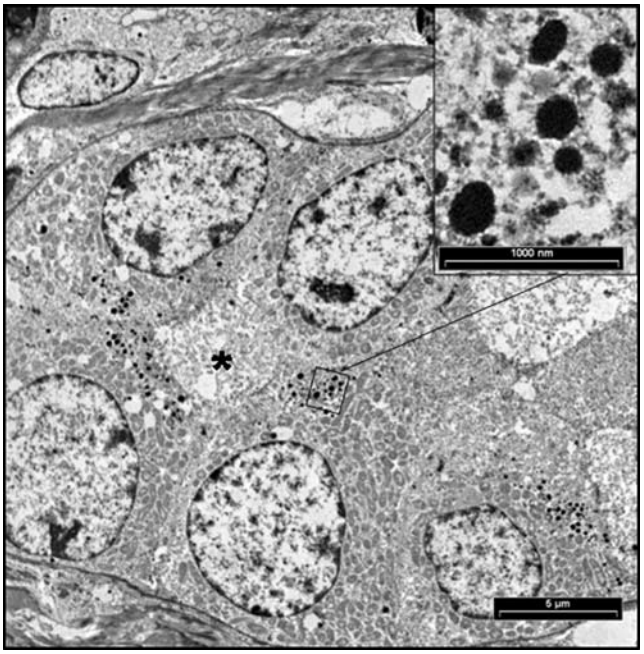

Fig. 2 Ultrastructural picture of an acinar structure. The acinar cells show dense homogeneous secretory granules (*inset*) accumulated in the apical cytoplasm. The acinar lumen is indicated by *asterisk*

in ordinary type colorectal carcinomas [8, 9], tumour cells showed immunoreactivity for other pancreatic enzymes such as lipase, chymotrypsin and carboxyl ester hydrolase (CEH). CEH is a glycoprotein secreted by pancreatic acinar cells [10] and lactating mammary gland [11] involved in cholesterol and lipid-soluble vitamin ester hydrolysis and absorption. It has been previously observed in pancreatic acinar cell carcinomas [12, 13] but not in pancreatic ductal adenocarcinomas. As recently demonstrated by La Rosa et al. [14], its presence in tumour cells may be proved immunohistochemically using a specific anti-CEH antibody as well as an anti-C-terminal BCL10 monoclonal antibody, because the C-terminal extremities of both CEH and BCL10 protein share the same amino acidic sequence. Tumour cells showed a weak immunoreactivity for CEH and a stronger positivity for BCL10. In addition, lymph nodes and above all bone metastases, which suffered from the hard decalcification treatment, were more intensely stained by anti-BCL10 than by anti-CEH antibody, confirming the major sensitivity of the anti-C-terminal BCL10 antibody in detecting carboxyl ester hydrolase.

In the literature, a few carcinomas with acinar cell differentiation have been described in the stomach [3–5] and in the jejunum [6]. For some of them, an origin from heterotopic pancreatic tissue has been suspected [6]. Pancreatic rests have been documented both in the stomach and in the small intestine [6, 15] but not in the large bowel. No evidence of heterotopic pancreatic tissue was observed in our case and all the clinical investigations excluded the possibility that the tumour could be a metastasis of a pancreatic acinar carcinoma. The most likely hypothesis about the histogenesis of the tumour is that it could have developed from a colonic stem cell with the potential for pancreatic differentiation. Indeed, most tumour cells expressed CK20 and CDX2, a transcription factor indispensable for intestine development [16] and a specific marker of adenocarcinomas of intestinal origin [17, 18], and displayed p53 nuclear accumulation which is a frequent genetic alteration in colorectal tumours but is not involved in the pathogenesis of pancreatic acinar cell carcinomas [19]. On the contrary, no tumour nuclei were immunoreactive for pancreatic and duodenal homeobox-1 (PDX-1), a transcriptional activator of several genes essential for the early development of pancreatic exocrine, endocrine and duct cells, duodenum and antrum [20–22].

A few cases of gastric carcinomas with acinar cell differentiation occur as mixed exocrine-endocrine tumours [4, 5]. Although endocrine cells were present in our case, they were so scattered that we cannot consider our case a composite glandular-endocrine tumour.

The fast negative evolution of the disease was unusual, more similar to pancreatic acinar than colonic carcinomas. In colonic adenocarcinomas, the spreading is preferentially via lymphatic or blood vessels to regional lymph nodes and the liver, whereas our patient developed bone metastases and died within 2 years. Enzyme production by tumour cells could explain, at least in part, the aggressive behaviour and the poor prognosis observed in this particular case. In fact, trypsin seems to promote, both directly and indirectly through the activation of other proteinase cascades, proliferation, invasion and metastases [9]. Yamamoto et al. [9] observed that, in colorectal carcinomas, trypsin expression at the invasive front correlated significantly with depth of invasion, lymphatic and venous invasion, lymph node and distant metastasis as well as recurrence.

To our knowledge this is the first reported case of colonic carcinoma showing a pancreatic acinar differentiation. Taking into account that lymph node and bone metastases of our case displayed acinar features, a colonic origin ought to be suspected when a metastatic carcinoma of unknown primary shows an acinar differentiation.

Conflict of interests statement We declare that we have no conflict of interest.

References

1. Klimstra DS, Longnecker D (2000) Acinar cell carcinoma. In: Hamilton SR, Aaltonen LA (eds) World Health Organization classification of tumours. Pathology and genetics of tumors of the digestive system. IARC Press, Lyon, pp 241–243

2. Hruban RH, Pitman MB, Klimstra DS (2007) Acinar neoplasms. In: Silverberg SG, Sobin LH (eds) Atlas of tumor pathology. Tumors of the pancreas. ARP and AFIP, Washington DC, pp 191–218
3. Fukunaga M (2002) Gastric carcinoma resembling pancreatic mixed acinar-endocrine carcinoma. Hum Pathol 33:569–573
4. Jain D, Eslami-Varzaneh F, Takano AM et al (2005) Composite glandular and endocrine tumors of the stomach with pancreatic acinar differentiation. Am J Surg Pathol 29:1524–1529
5. Sun Y, Wasserman PG (2004) Acinar cell carcinoma arising in the stomach: a case report with literature review. Hum Pathol 35:263–265
6. Maklouf HR, Almeida JL, Sobin LH (1999) Carcinoma in Jejunal Pancreatic Heterotopia. Arch Pathol Lab Med 123:707–711
7. Solcia E, Capella C, Buffa R et al (1979) Endocrine cell of the gastrointestinal tract and related tumors. Pathobiol Annual 9:163–203
8. Yamamoto H, Iku S, Adachi Y et al (2003) Association of trypsin expression with tumour progression and matrilysin expression in human colorectal cancer. J Pathol 199(2):176–184
9. Soreide K, Janssen EA, Komer H et al (2006) Trypsin in colorectal cancer: molecular biological mechanisms of proliferation, invasion and metastasis. J Pathol 209:147–156
10. Carrère J, Figarella-Branger D, Senegas-Balas F et al (1992) Immunohistochemical study of secretory proteins in the developing human exocrine pancreas. Differentiation 51:55–60
11. Nilsson J, Blackberg L, Crlsson P et al (1990) cDNA cloning of human-milk bile-salt-stimulated lipase and evidence for its identity to pancreatic carboxylic ester hydrolase. Eur J Biochem 192:543–550
12. Kuopio T, Ekfors TO, Nikkanen TJ et al (1995) Acinar cell carcinoma of the pancreas. Report of three cases. APMIS 103:69–78
13. Reuss R, Aberle S, Klingel K et al (2006) The expression of carboxyl ester lipase gene in pancreas and pancreatic adenocarcinomas. Int J Oncol 29:649–654
14. La Rosa S, Franzi F, Marchet S et al (2009) The monoclonal anti BCL-10 antibody (clone 331.1) is a sensitive and specific marker of pancreatic acinar cell carcinoma and pancreatic metaplasia. Virchows Arch 454:133–142
15. Ashida K, Egashira Y, Tutumi A et al (1997) Endocrine neoplasm arising from duodenal heterotopic pancreas: a case report. Gastrointest Endosc 46:172–176
16. Suh ER, Traber PG (1996) An intestine specific homeobox gene regulates proliferation and differentiation. Mol Cell Biol 16:619–625
17. Barbareschi M, Murer B, Colby TV et al (2003) CDX-2 homeobox gene expression is a reliable marker of colorectal adenocarcinoma metastases to the lungs. Am J Surg Pathol 27:141–149
18. Werling RW, Yaziji H, Bacchi CE et al (2003) CDX2, a high sensitive and specific marker of adenocarcinomas of intestinal origin. An immunohistochemical survey of 476 primary and metastatic carcinomas. Am J Surg Pathol 27:303–310
19. Abraham SC, Wu TT, Hruban RH et al (2002) Genetic and immunohistochemical analysis of pancreatic acinar cell carcinoma: frequent allelic loss on chromosome 11p and alterations in the APC/beta-catenin pathway. Am J Pathol 160(3):953–962
20. Offield MF, Jettan TL, Laboscky PA et al (1996) PDX-1 is required for pancreatic outgrowth and differentiation of the rostral duodenum. Development 122:983–995
21. Sakai H, Eishi Y, Li X et al (2004) PDX1 homeobox protein expression in pseudopyloric glands and gastric carcinomas. Gut 53:323–330
22. Shiraki N, Yoshida T, Araki K et al (2008) Guided differentiation of embryonic stem cells into Pdx1-expressing regional-specific definitive endoderm. Stem Cell 26:874–885

Virchows Arch (2009) 455 (Suppl 1):S1–S482
DOI 10.1007/s00428-009-0805-z

Oral presentations 1

Electron microscopy — Neuropathology — Miscellaneous

OP1.1

Immunohistochemical and electron-microscopic study in Henoch-Schoenlein nephritis

Wozniak A.; Pluta K.; Zurawski J.; Janicka M.; Kaczmarek E.; Zachwieja J.; Piechocka I.; Bulak J.
Department of Clinical Pathology, Karol Marcinkowski University of Medical Sciences, Poznan, Poland

Background Henoch-Schoenlein purpura is a form of systemic vasculitis with deposits of IgA, involving small vessels in skin, gut and glomeruli. Henoch-Schoenlein nephritis (HSN) is the most common secondary childhood nephropathy and leads to ESRD in up to 20% of pediatric patients after 20 years of follow-up.
Methods 44 cases of HSN: 32 children and 12 adults. EM was performed in 6 cases and IH in all. We evaluated mesangial proliferation (Ki-67, PCNA), mesangial expression of α-SMA and podocytes expression of p27.
Results LM study revealed the following grades: II (18), III (15), IV (3) and VI (8) (differences in prognosis between grades were not found). The initial symptoms and outcome were less severe in patients with grade II or III. Presence of glomerular sclerosis was important prognostic marker. EM study was was useful in recognition of early glomerular sclerosis. No significant correlations were found between mesangial cells Ki-67 and PCNA positivity and clinical presentation. Important finding was progressive decrease in p27 positive podocytes with more severe HSN grades. Significant correlations regarding the area of mesangial expression of α-SMA were observed. That expression was stronger in patients, who had foci of infection (independently of HSN grade).
Conclusion(s) The area of α-SMA expression have proved to be a useful marker of mesangial cells activation. The decreased expression of p27 in podocytes of HSN patients suggests their role in disease process. Our study did not demonstrated the prognostic usefulness of proliferation markers (Ki-67, PCNA).

OP1.2

Remodeling of adipose tissue from lipodystrophic patients with LMNA mutations

Cervera P.; Béréziat V.; Verpont M.; Le Dour C.; Antuna-Puente B.; Dumont S.; Somja-Azzi M.; Vantyghem M.; Capeau J.; Flejou J.; Vigouroux C.
Hôpital Saint Antoine, Paris, France

Background A-type lamins, encoded by the LMNA gene, are ubiquitous nuclear intermediate filament proteins that are required for the structural and functional integrity of the nucleus. Inherited laminopathies, due to LMNA mutations, represent a wide spectrum of diseases, including lipodystrophies, with peripheral subcutaneous fat loss, increase visceral fat and metabolic alterations; among them, the Dunningan-type familial partial lipodystrophy (FPLD2; OMIM 151660). The morphological alterations of adipose tissue in laminopathies have not been reported so far. In the present work, we have studied the pathological and ultrastructural alterations of adipose tissue from LMNA-mutated patients, together with the expression of specific adipocytes markers and mitochondrial proteins.
Methods Cervical fat was obtained from three patients with LMNA mutation, from one patient with mtDNA tRNA lys A8344G mutation, from three treated lipodystrophic HIV-infected men and three controls. Light microscopy, immunohistochemical and ultrastructural studies were performed on the fat samples and compared with mRNA assay, performed with the light cycler software (Roche diagnostics) and Western blot analysis.
Results Adipose tissue from LMNA-mutated patients shows a heterogeneous structure with decreased adipose size, altered extra-cellular matrix : thick fibrils invade the intercellular area without macrophages or inflammation, increased fibrosis, mitochondria disturbances, accumulation of prelamin A and altered expression of adipogenic transcription factors.
Conclusion(s) This study show here severe remodeling of adipose tissue from patients with FPLD and metabolic laminopathies. The accumulation of prelamin A could impair SREBP1 function and adipocyte differentiation but also induce oxidative stress leading to fibrosis.

OP1.3
Ultrastructural remodeling of cardiomyocytes during isolated atrial amyloidosis

Mandache E.; Gherghiceanu M.; Macarie C.; Popescu Mircea L.
"V. Babes" National Institute of Pathology, Bucharest, Sector 5, Romania

Background The heart is commonly affected by a localized organ-limited amyloidosis called isolated atrial amyloidosis (IAA). The IAA incidence increases with age, up to over 90%. The fibril protein deposited in this condition is the atrial natriuretic peptide, a hormone synthesized and secreted mainly by atrial cardiomyocytes.
Methods Thirty-six atrial biopsies from the surgery unit have been processed for electron microscopy. The investigation was intended to emphasise the features of cardiac remodelling during atrial arrhythmias (mostly atrial fibrillation).
Results One-third of the biopsies proved to contain small deposits of fibrilar material in the interstitial area, around the cardiomyocytes and/or small vessels with characteristic feature (randomly arranged, nonbranching filaments of about 10 nm in diameter). The ultrastructural features of these minute fibrilar deposits are presented. The close contacts of amyloid fibrils with the peripheral lamina of atrial myocytes are emphasized. They occurred only in the extracellular space. We have noticed the presence of sarcolemal small niches where the fibrils are concentrated. When these niches were deeper, they could be transversely sectioned, giving the false impression of intracellular inclusions. These sites seemed to be placed near the intercellular junctions. On the interstitial side, the peri-myocyte fibrilar deposits had a particular attraction for some particular, slender, interstitial Cajal-like cells, which have the tendency to wrap the fibrils.
Conclusion(s) In LM the atrial myocytes profiles were smaller, having more irregular contours, and appeared dispersed. The myofibrils were centrally gathered, and the mitochondria and glycogen peripherally placed.

OP1.4
A new variant of oralfacialdigital syndrome

Stenram U.; Cramnert C.; Axfors-Olsson H.
Department of Pathology, Lund, Sweden

Background The columnar epithelial cells of the respiratory tract have several cilia. Most other cells of the body have one immotile cilium, called monocilium or primary cillium. Mutations in their genes give strange malformation syndromes, ciliopathies. Respiratory tract symptoms are seldom reported. In these entities nasal/tracheal cilia have only been examined in single cases of Usher syndrome and the polysplenia syndrome.
Methods Case report. A girl presented with polydactyly, high arched palate, tongue lipoma and dysmorphic face. She had respiratory tract problems from birth, atelectasis, pneumonia and later bronchiectasis, and viscous secretions in the middle ears. The fourth ventricle is slightly enlarged. From 4½ years she shows growth retardation. At 5 years she uses a walker outdoors and speaks only short sentences. Electron microscopy of nasal brush biopsies at four occasions revealed almost total ciliary aplasia, but long, sometimes branched microvilli. There were a few cilia in the cytoplasm and also lumens. The basal bodies/centrioles were found deep in the cytoplasm. Some procentrioles were seen.
Results The cases has resemblances with the oralfacialdigital syndrome (OFDS) but in addition respiratory tract problems from birth. This and four other syndromes are due to mutations affecting the basal bodies, which in this case were displaced.
Conclusion(s) Such a cases has not previously been described. It was approved by POSSUM dysmorphology database and London Dysmorphology & Neurogenetics Databases as OFDS, Stenram type.

OP1.5
Ultrastructural characteristics of systemic and localized AL-lambda amyloid deposits

Bély M.; Apáthy A.; Kapp P.
Department of Pathology, Policlinic of the Order of the Brothers of Saint John of God in Budapest, Budapest, Hungary

Background The aim of this study was to define the ultrastructural characteristics of systemic and localized AL deposits.
Methods Amyloidosis was studied in a selected autopsy population of 5 in-patients with B-cell lymphoma and compared with 5 biopsies of extranodal plasmacytoma of epipharynx (nasopharynx) or vocal cord with localized AL deposits. Systemic immunoglobulin light-chain AL.
Results Electron microscopically the filaments or fibrils in systemic or localized AL amyloidosis revealed no morphologic difference, and the pattern of deposition was in both "lake"-like. However, there was a difference (1) in relation to the blood vessels, (2) in the arrangement of filaments, or fibrils within the amyloid deposits. The systemic AL amyloid deposits were always present within the vessel walls, or around the capillaries (with, or without deposits between the collagen fibrils). The localized AL amyloid deposits were never observed within the vessel walls, or between pericytes (excentric deposits may be present near vessels). In case of localized AL amyloidosis electron dense territories of clusters composed of regularly (parallel)

arranged, closely packed filaments and fibrils were present. In some cases this was bordered by circularly arranged, condensed fibrils at the periphery. This type of arrangement corresponded to the "crystalloid like" birefringence of the localized AL amyloid deposits.
Conclusion(s) The free vessels and the "crystalloid like" deposition of amyloid filaments are characteristics of localized AL amyloidosis electron microscopically. The "crystalloid like" arrangement represent the stage dependent maturation (or fragmentation) of deposited amyloid protein filaments, indicative of an advanced stage of deposition.

OP1.6
P53 as a prognostic marker for astrocytic gliomas: a meta-analysis and review

Levidou G.; El-Habr E.; Korkolopoulou P.; Saetta A.A.; Katsougiannis K.; Patsouris E.
National and Kapodistrian University of Athens, Department of Pathology, Athens, Greece

Background For decades researchers have been looking for parameters with an impact on the prognosis of patients with astrocytic tumours. p53 is one of the most widely investigated molecules in human gliomas. We aimed to review comprehensively the evidence for use of changes in p53 immunohistochemical expression in paraffin-embedded tissue specimens to predict astrocytomas mortality.
Methods We conducted a systematic review through December 2007 to identify cohort studies that evaluated p53 immunohistochemical expression as a prognostic marker for astrocytomas. Estimates of significance were extracted from association tests and hazard ratios (HR) with 95% CI. A meta-analysis was performed on the studies that applied Cox models adjusted with tumour grade and patients' age.
Results We reviewed 44 (n=3627) publications, 13 of which included the estimates (HR and 95% CI) derived from Cox regression. The descriptive analysis showed that most of the published articles did not contain information on important variables such as sex and age (27% and 31% of studies), previous treatment, tissue-retrieval and follow-up period (56%). The quantitative synthesis showed that p53 expression in not a significant prognostic factor (combined HR= 1.034, p=0.531). There was no significant between-study heterogeneity and publication bias. Meta-regression analysis selected tumour histologic grade and the publication of patients' treatment details as important factors.
Conclusion(s) After 18 years of research, evidence is not sufficient to conclude whether changes in p53 immunohistochemical expression act as a marker of outcome in patients with astrocytic neoplasms.

OP1.7
Chromosome 1p36 loss and Cox-2 overexpression are independent predictors of recurrence in completely removed meningiomas Grade I and II. Analysis of their association with clinicopathological and immunohistochemical variables

Sanz J.; Ruiz J.; Martinez A.; Hernandez S.; Asenjo J.; Zimman H.
Hospital Clinico San Carlos, Madrid, Spain

Background The WHO grading system is used to clasify meningiomas as grade I (benign), II (atypical) and III (anaplastic). 15–20% of benign and atypical meningiomas will recurr despite agressive surgery with complete removal.
Methods 247 meningiomas grade I and II with a mean follow-up perios of 7.6 years were analyzed with 30 IHC biomarkers and chromosomal loss of 1p36 was analyzed by FISH. Univariate and multivariate analysis for recurrence-free survival of the completely removed meningiomas.
Results Two molecular pathways characterized by the loss of 1p36 and Cox2 overexpression were associated with recurrent meningiomas. The loss of chromosome 1p36 was also associated with necrosis, nuclear atypia and alterations in the AKT/MAPK patway(AKTp, PDGF, CyclinE, p21). The overexpression of COX2 characterized meningiomas with increased celullar stress and overexpression of Growth Factors. (VEGF, PDGF, Her2, MDMD2). The prognostic significance of both pathways has an antagonic effect. MIB1 overexpression was also an important predictor of recurrence.
Conclusion(s) There is a need of new predictors of tumour recurrence for meningiomas grade I and II. We describe two molecular biomarkers: loss of 1p36 and COX-2 overexpression. Thay are associated with molecular pathways consistent with the more aggresive behaviour. Chemopreventive treatment can be used for the subgroup of meningiomas with Cox-2 overexpression.

OP1.8
Mitotic count and brain invasion are independent predictors of recurrence free survival in primary atypical and malignant meningiomas. A study of 86 patients

Pizem J.; Vranic A.; Popovic M.; Coer A.; Prestor B.
Institute of Pathology, Medical Faculty, Ljubljana, Slovenia

Background There is only sparse information about possible prognostic factors in the group of atypical and malignant meningiomas (AMM). Our aim was to evaluate the prognostic significance of various histological and clinical parameters, with an emphasis on mitotic count, brain invasion and Ki67 labelling index, in a series of primary AMM.

Methods We analysed 86 primary AMM, 76 of which were atypical and 10 malignant, diagnosed according to 2000 WHO. Multivariate recurrence free and overall survival analyses were performed.
Results High mitotic count (as a continuous variable), brain invasion and the parasagital-falcine location of the tumour were associated with decreased recurrence free survival in multivariate analysis. Brain invasion was present in 25 of 37 cases in which brain tissue was identified in the tumour specimens. When brain invasion was not included in the analysis due to the limited number of cases in which it could be assessed, high mitotic count, Ki67 index ≥4%, the presence of macronucleoli and parasagital-falcine location were significant predictors of shorter recurrence free survival.
Conclusion(s) Brain invasion and mitotic count as a continuous variable are the two most important parameters associated with survival of patients with AMM. AMM are biologically heterogeneous and recurrence free survival can be further stratified by histological parameters, especially mitotic count, brain invasion and Ki67 labelling index.

OP1.9

Dendritic cells from human peripheral lymphoid tissues express AIRE (autoimmune regulator)

Poliani L.P.; Kisand K.; Marrella V.; Ravanini M.; Notarangelo D.L.; Villa A.; Peterson P.; Facchetti F.
Department of Pathology, University of Brescia, Brescia, Italy

Background Self-reactive T-cells are eliminated in the thymus by central tolerance (CT), a process predominantly mediated by AIRE, a transcription factor driving the expression of tissue-restricted antigens (TRAs). Although remarkably efficient, potentially autoreactive T-cells escape CT selection and reach the periphery, where peripheral tolerance (PT) induction is required to prevent autoimmunity. AIRE-expressing cells (AEC) involved in PT induction have been recently identified in murine lymph-nodes (LN) although their phenotype and evidence in humans have yet to be defined.
Methods We investigated at mRNA and protein level AIRE expression in a large number of human lymphoid and non-lymphoid tissues and characterized AEC phenotype by double-immunohistochemistry and FACS analysis.
Results AEC were exclusively identified in LN, tonsils and mucosal-associated lymphoid tissues. AEC consistently co-expressed HLA-DR, fascin and most of them S100, CD11c and activated dendritic cell (DC) markers (DC-LAMP/CD208, CD40, CD83), suggesting a DC phenotype. Other antigens specific for lymphoid/myeloid, stromal/endothelial and epithelial cell lineages were negative. Cell sorting confirmed the presence in LNs of rare CD45lo/HLA-DRhi +/AIRE + cells with a DC phenotype and expressing TRAs (insulin and CYP17A1). Interestingly, LNs biopsies from different primary immunodeficiencies, particularly when associated with autoimmunity, and lymphadenitis from HIV patients, showed dramatic depletion of AECs, suggesting that normal T-cell homeostasis is crucial to maintain AIRE expression.
Conclusion(s) These data show that human lymphoid tissues contain a rare subset of DCs (most of which with an activated phenotype) expressing AIRE and TRAs and possibly involved in PT.

OP1.10

Isolation of cancer stem cells from dog glioblastoma multiforme

Stoica G.; Lungu G.; Martini-Stoica H.
Texas A&M University, College Station, TX, USA

Background Cancer stem cell migration in gliomas is a multifactorial event regulated by the interactions among a minority of tumor cells with stem cell-like properties and the host microenvironment. Necrosis and angiogenesis in gliomas occurs in a hypoxic environment. A working hypothesis that links tumor hypoxia, necrosis and angiogenesis appears to emerge in dog glioblastoma.
Methods The isolated gliomas cells were cultured in DMEM media and neurobasal media supplemented with growth factors. In vitro flow cytometry determined the phenotype of cancer stem cells isolated from dogs: a grade IV D-GBM and grade I pilocytic astrocytoma (PA). Tumor cells migration assayed using the Matrigel invasion assay. An intracranial orthotopic model using nude mice was utilized for in vivo evaluation of D-GBM tumorigenicity. Immunohistochemistry demonstrated glial and neuronal differentiation.
Results In the present study we demonstrate that glioblastoma multiforme isolated from a Boxer dog (D-GBM) has cells with phenotypical characteristics of CSCs. As a proof of concept, we characterized this cell line's morphophenotype and its specific stem cell markers such as nestin and CD133. CSCs demonstrated glial and neuronal differentiation when exposed to differentiation growth factors in vitro.
Conclusion(s) This is the first report demonstrating the presence of CSCs in dog GBM. Our data also demonstrate the similarity between human and dog GBM and emphasize the importance of studying dog spontaneous brain tumors in order to elucidate the mechanism(s) of tumor dispersal, post surgical reoccurrence, and resistance to therapy.

OP1.11

Silver enhanced in situ hybridisation detects of BK virus DNA in renal biopsies from renal transplant patients

Fritzsche R.F.; Gaspert A.; Pianca S.; Wang L.; Farrell M.; Chen X.; Fehr T.; Tubbs R.; Moch H.
University Hospital Zurich, Zurich, Zurich, Switzerland

Background SV40, BK and JC viruses are members of the polyomavirus family. The BK virus rarely causes disease, but BK virus nephropathy (BKN) is a well known complication of renal transplantations associated with high rates of graft loss. The diagnosis of BKN has to be made histologically by detection of the typical intranuclear viral inclusion bodies. Although the BKN morphology is relatively specific, other viruses have to be ruled out. The detection of BK-virus DNA by PCR can serve as a surrogate marker, but diagnostic confirmation of the infected tubular epithelial cells can be achieved by immunohistochemistry with antibodies directed against SV40.
Methods We have developed a new silver-enhanced in situ hybridisation (SISH) technique for the detection of BK virus in renal transplant kidney specimen. From archival cases, we selected 26 immunohistochemically (SV40 antibody) confirmed polyomavirus infections. We applied the SISH analysis on a Ventana Benchmark platform to detect BK virus infections.
Results The BK virus SISH positivity was highly concordant with the immunohistochemical results using a SV40 antibody. The SISH signal showed a distinct nuclear signal. Interestingly, in most cases less cells and tubules were positive with the SISH signal in comparison to the SV40 staining.
Conclusion(s) BK SISH is a sensitive and specific tool for the detection of BK virus infections in renal transplant patients.

OP1.12

Malaria and malignant non-burkitt-lymphomas. A review of studies from Uganda

Schmauz R.; Wright H.D.
Institute of Pathology, Papenburg, Superfluous, Germany

Background While well recognized for Burkitt-lymphoma, such an association with the remainder of these tumours is not taken into consideration in many and particularly recent studies. Six epidemiological studies from Uganda are therefore reviewed which use geographical comparisons to underline the possibility that malaria plays a major role in lymphomagenesis.
Methods The material is provided by the Kampala Cancer Registry which in the sixties and seventies of the last century covered the whole of Uganda. Information about malarial endemicity was available from a survey conducted during the years 1963–1966.
Results In a meta-analysis two early studies published in 1965 and 1973 show similar geographical distributions for Hodgkin's disease, reticulum cell sarcoma, lymphosarcoma and BL. Two further studies (1970 and 1974) confirm that certain NBL are more common in northern Uganda where BL is of the highest incidence. Finally, aggressive or high-grade HL and NHNBL (1) vary in a similar way in incidence with BL and (2) as the BL are rare or common in areas of low or high malarial endemicity, respectively, with gradients in incidence which are less marked than in BL. This is in contrast to low grade NBL which showed no such regional incidence patterns (1989 and 1990).
Conclusion(s) In studies related to the aetiology of malignant lymphomas in tropical Africa malaria as a causal factor deserves more attention.

Oral presentations 2

Cytopathology

OP2.1

Activity criteria of demyelinization process

Filipovich Nicolaevich A.
Research Institute of Medical Assessment and Rehabilitation, Minsk, Belarus, Minsk, Belarus

Background A latent phase (the first group, 79 patients, 19.9%) is characterized by slight increase in MTA of blood serum (7.6±1.2 units; control group - 3.9±0.82 units; $p<0.001$), decrease of CD4+ in blood (34.8±1.64%) and CIC levels (92.56±3.1).
Methods Clinical methods, immunoassays, myelinotoxic activity (MTA), CT and MRI of cerebrum and spinal cord, myelinotoxic activity (MTA).
Results A slow progradient phase of MS (second group, 156 patients, 39.4%) is distinguished by moderate evident(apparent) increase in MTA of blood serum (22.3; $p<0.01$ in comparison with 1st group), significant decrease of T-lymphocyte in blood serum by 32.4%, CD22+ by 71.1%, CD4+ by 33.9%, CIC levels by 12.4%, along increase in CD8+ by 1.3 times, weak induction of TNF-α at 84.3%; IL-8 at 4.8% patients. An acute phase (third group, 144 patients, 36.3%) coupled with significant increase in MTA of blood serum (40.4± 1.22 units) in comparison with 1st and 2nd groups. Acute condition of MS distinguished by significant increase in blood CD8+, IL-2P+, Ig G,A,M, CIC level along decrease

of T-lymphocyte (51.7%±1.56%) and CD22+ levels. Increase in IL-2P+ at 64.1% patients coupled with significant increased TNF-α и IL-8. In the fourth group (17 patients, 4.4%) fast progress of MS distinguished by high MTA level of blood serum (78.2±4.4 units), persistent immunological changes: increase in CD4+, CD8+, IL-2P+, IgG, IgM, IgA, CIC.

Conclusion(s) Measurement of blood serum MTA and immune reactivity in combination with clinical and MRI findings helps to correctly estimate the rate of demyelinization in multiple sclerosis patients.

OP2.2

KRAS mutation testing on matched cytological and histological specimens of metastatic colo-rectal cancer

Malapelle U.; Russo M.; Salatiello M.; Campione S.; Cozzolino I.; Zeppa P.; Palombini L.; D'Armiento F.; Troncone G.
Università degli studi Federico II, Naples, Italy

Background Metastatic colo-rectal carcinomas harboring a mutation in the KRAS gene do not derive benefit from EGFR targeted therapy. Cytological samples performed on metastasis may represent the only type of specimen available for KRAS mutation testing. To date, studies directly comparing mutation detection rates in cytological and paraffin embedded samples have not been performed yet.

Methods We carried out a retrospective search for cytological cases positive for adenocarcinoma and in which there was an unquestionable evidence of a colorectal cancer origin. Particular care was taken to process also the matched histological samples when available for review. Eighteen cytological cases represented this study series. Eleven fine needle aspiration (FNA) samples (lung $n=7$; liver $n=3$; soft tissue $n=1$) and seven peritoneal washings were assessed for codon 12 and 13 KRAS by direct gene sequencing. Histological samples were available in 13 cases. The same procedure was carried out on the matched cyto-histological samples.

Results Nearly in all instances (17/18; 94%) the cytological specimens were suitable for the molecular analysis. The data from FNA and surgical samples were matched. In this undergoing study, a high rate of concordance between the two samples types is being found.

Conclusion(s) We demonstrated that KRAS mutation can be performed from genomic DNA extracted from metastatic colorectal FNAs and peritoneal washings. This can be of pivotal relevance in patients with advanced colo-rectal cancer whose histological specimens are not available for KRAS testing

OP2.3

Pitfalls in FNA of lipomatous tumours

Pohar Marinsek Z.
Institute of Oncology, Ljubljana, Slovenia

Background At the Institute of Oncology in Ljubljana many soft tissue tumours are operated on the basis of cytology. A correct differentiation between benign and malignant is therefore imperative and specific diagnosis desirable. The objective of our study: morphological analysis of various lipomatous tumours in order to recognize pitfalls which can lead to false cytological diagnosis.

Methods We reviewed FNA samples of 120 histologicaly verified lipomatous tumours, 72 benign and 48 malignant. Characteristics noted: cellularity, cell shape, degree of atypia, presence of capillaries, mixoid background.

Results Pitfalls in benign lipomatous tumours which can lead to incorrect diagnosis of a malignant tumour: 1. Atypia in pleomorphic lipomas; 2. Degenerative changes in lipoma NOS with macrophages simulating lipoblasts; 3. Abundant myxoid material and capillaries simulating myxoid liposarcoma; 4. High cellularity, myxoid material and lipoblasts in lipoblastomas. Pitfalls in liposarcomas which can lead to a false benign diagnosis: 1. Lack of atypia in some well differentiated and myxoid liposarcomas; 2. Presence of spindle cells in dedifferentiated liposarcomas. Pitfalls in recognizing the lipomatous lineage: 1. Round cells in liposarcoma simulating lymphoma and other small round cell neoplasms: 2. Pleomorphic cells in liposarcoma, morphologically indistinguishable from other pleomorphic sarcomas and from pleomorphic metastatic carcinomas.

Conclusion(s) Since there is lack of obvious malignancy features in some liposarcomas and pronounced atypia in certain benign lipomatous tumours, cytopathologists should be cautious in rendering a definitive diagnosis. Myxoid background is very common in lipomatous tumours and represents an important pitfall.

OP2.4

Review of negative or low grade smears in women with invasive cervical cancer in Slovenia

Repse Fokter A.; Strojan Flezar M.; Pogacnik A.; Snoj V.; Primic Zakelj M.
Departrment of Pathology and Cytology, Celje Teaching Hospital, Slovenia, Celje, Slovenia

Background The purpose of this study was to review the smears which were taken from 0 to 3 years prior to the diagnosis of invasive cervical cancer in 2006 and were originally classified as low grade findings or normal.

Methods 59 smears from 37 women obtained between 2003 and 2006 were included in the study. In order to provide more objective assessment, two controls were added to each smear in question. Altogether, 177 smears were reexamined at the laboratory where original diagnosis was performed and then independently by a group of four experienced cytopathologists, members of the advisory board of the national screening programme. To avoid focused reviewing of any slide, the time for screening was limited to that in routine daily work.
Results Of the 37 cases of invasive cervical carcinoma, 19 were squamous cell carcinomas, 15 adenocarcinomas and 3 adenosquamous carcinomas. On reexamination at the laboratory where original diagnosis was made, 19 out of 59 smears were upgraded. After the review by the expert group, 22 smears were upgraded to the diagnosis requiring a biopsy, among them only 4 in patients with adenocarcinoma.
Conclusion(s) A subgroup of smears can be diagnosed as low grade or even negative despite the presence of high-grade findings that are detectable on reexamination, which is in concordance with some previous studies. Nevertheless, true negative smears occured more likely in patients with adenocarcinoma.

OP2.5

Thin layer cytology and immunocytochemistry in pleural fluids and ascites: quick and accurate

Kornegoor R.; Tiemessen N.; Van Benthem J.; Schaap W.; Bülbül M.; Peters M.H.
Gelre Ziekenhuizen Apeldoorn, Apeldoorn, Gelderland, Netherlands

Background Thin layer technique (ThinPrep) is applied successfully on a routinely basis in cervical and pulmonary cytology in our department. Therefore we decided to use this technique in pleural fluids and ascites and test the applicability and usefulness of immunocytochemistry.
Methods In 18 months 237 pleural fluid and 171 ascites (n=408) samples were evaluated. Several immunocytochemistry panels were performed in a 3-hour procedure. Diagnostic procedure and patient outcome was analysed and compared with patients medical history. Cases of malignancy were divided into “known primary”, “unknown primary” and “discordant known primary”.
Results Cellular preservation and nuclear morphology was improved in the majority of cases compared to conventional cytology. 295 body fluids were diagnosed benign, 14 showed atypia and 92 were malignant. There was an unknown primary in 39% (n =36), known primary in 54% (n=50) and discordant known primary in 7% (n=6) of all malignant cases. In 21% immunocytochemistry was performed to distinguish reactive mesothelial cells from carcinoma and to evaluate primary source in case of metastatic tumour. In the discordant known primary’s there were 5 pleural samples of patients, respectively known with breast cancer (n=3), transitional cell cancer and colon cancer. All turned out to have lung cancer. 1 ascites sample showed ovarian metastasis while the patient was known to have breast cancer.
Conclusion(s) Thin layer technique can be used successfully in pleural fluids and ascites diagnostics. Additional immunocytochemistry improves diagnostic accuracy, reduces time required for final diagnosis and can guide clinical approach.

OP2.6

Fractal characteristics of nuclear chromatin in routinely stained cytology are independent prognostic factors in patients with multiple myeloma

Metze K.; Ferro Peixoto D.; Falconi Almeida M.; Adam L.R.; Ortega M.; Lima Passos C.; De Souza A.C.; Lorand-Metze G.I.
University of Campinas, Campinas, SP, Brazil

Background Nuclear texture features examined by computerized analysis can provide important prognostic information. Recently, the fractality of the chromatin structure has shown to be an independent prognostic factor in acute leukemia. In this study we investigated the influence of the fractal dimension (FD) of chromatin on global survival of patients with multiple myeloma.
Methods We studied 78 newly diagnosed patients from our Institution. They were treated according to the Brazilian Multicentric Protocol. Diagnostic work-up consisted of peripheral blood counts, bone marrow cytology, bone radiograms, biochemistry and cytogenetics. The international Prognostic Index (ISS) was used for staging. In every patient gray scale transformed pseudo-3D images of 100 nuclei in May-Grünwald-Giemsa stained bone marrow smears were analyzed. FD was determined by the Minkowski-Bouligand method extended to three dimensions. Goodness-of-fit of FD was estimated by the R2 values in the log-log plots. Uni-and multivariate Cox-regressions were calculated.
Results When stratifying for the ISS stage, both FD and its goodness-of-fit were significant prognostic factors in the univariate analyses. Patients with higher FD dimension or lower goodness-of-fit (equivalent to accentuated “coarseness” of the chromatin pattern) indicated a poor prognosis. In the multivariate Cox-regression, FD, R2, and ISS stage entered the final model, which showed to be stable in bootstrap resampling study.
Conclusion(s) In conclusion, fractal characteristics of the chromatin in routine cytology reveal relevant prognostic information in patients with multiple myeloma.

OP2.7
Rapid pre-screening as a quality assurance measure in cervical cytology

Repse Fokter A.; Sramek Zatler S.; Caks Golec T.
Celje Teaching Hospital, Celje, Slovenia

Background Efficient cytologic interpretation of Pap smears is a crucial factor that contributes to the success of cervical cancer screening. The aim of current study was to assess the diagnostic validity of rapid prescreening as a quality control method in our laboratory.
Methods All consecutive routine conventional Pap smears (n=521) underwent RPS before full screening. 30 to 60 seconds were allowed to prescreen each slide. The threshold for pathologic smear was ASCUS or more. Smear adequacy, infections and presence of endometrial cells, if observed, were not noted on the worksheet. All smears subsequently underwent routine full screening. Results of RPS and full screening were compared.
Results Of a total of 2521 smears, 294 were diagnosed as abnormal (ASCUS and more) after final diagnosis. Of those, 158 were also detected on rapid prescreening. The average sensitivity of RPS was 62.2%. 25 cases were detected on RPS only, among them 15 ASCUS, 8 low-grade squamous intraepithelial lesions and 2 high-grade squamous intraepithelial lesions.
Conclusion(s) RPS is an efficient quality control method. It reduces false- negative rate, but it impacts on the work flow and in case of its implementation to the routine praxis the daily workload of 50 smears per day should be lowered.

OP2.8
Performance appraisail for cytologists: an experience from the United States

Sugrue C.
Long Island Jewish Medical Center, Garden City, New York, USA

Background This presentation intends to discuss the application of objective methods for the performance appraisal of cytologists in an era of great changes in European Cytopathology Laboratories by sharing United States experience.
Methods 1. Identify the role and modalities of a well conducted Performance in the evolving healthcare industry. 2. Demonstrate the United States experience of quality control and quality assurance. 3. Examples of metrix will be demonstrate and discussed
Results This presentation will demonstrate how effectively integrate regulation requirements by creating objective measures for evaluation. Implementatioon of ideas for remediation will also be discussed.
Conclusion(s) Performance Appraisal is an essential tool to monitor and empower staff members in any business and currently is being adopt in the fast evolving healthcare setting.

OP2.9
Preliminary investigation of the clinical relevance of detecting circulating tumor cells by isolation by size of epithelial tumor cells (ISET) technique from cutaneous melanoma patients

Panelos I.; De Giorgi V.; Pinzani P.; Salvianti F.; Paglierani M.; Janoska A.; Grazzini M.; Orlando C.; Santucci M.; Lotti T.; Pazzagli M.; Massi D.
Department of Pathology, University of Ioannina Medical School, Ioannina, Greece
Departments of Clinical Physiopathology, Dematological Sciences and Human Pathology and Oncology, University of Florence, Italy

Background The isolation by size of epithelial tumor cells (ISET) is a direct method for identification of circulating tumor cells (CTC) in the peripheral blood due to their large size. So far, ISET has been applied only to CTC detection from epithelial cancer patients, and has never been validated in cutaneous melanoma patients.
Methods We investigated the presence of CTC by ISET from the peripheral blood of patients with cutaneous melanomas (n=72), melanocytic nevi (n=11), non-melanoma skin tumors (n=4) and healthy volunteers (n=18).
Results CTC were detected neither in the control groups nor in the blood from patients with melanocytic nevi. Conversely, the detection of CTC paralleled tumor progression rising from 7.1% in the in situ melanomas to 32.6% in the primary invasive melanoma category to 66.6% among metastatic melanoma patients (p=0.006). CTC detection was significantly associated with mRNA tyrosinase levels by real-time RT-PCR in blood samples (p = 0.002). No significant correlation was demonstrated between CTC detection and clinico-pathological parameters.
Conclusion(s) We demonstrated that ISET-isolated CTC can be identified in the bloodstream of primary and metastatic melanoma patients. The clinical relevance of this finding is still under scrutiny and the biology of circulating melanoma cells must be carefully investigated.

Oral presentations 3

Dermatopathology

OP3.1
Cell adhesion molecules cadherins E, N, P and Catenins in nevi and melanomas

Stoemmer Erasmus P.; Torres-Galea P.
Forschungslabor Prof Dr. Stoemmer, Augsburg, Bavaria, Germany

Background In vitro experiments on melanoma cells show an important role of cell-adhesion molecules in melanomas. The subtypes of classical cadherins, E-, N-, P-cadherin, are expressed in a cell-, tissue-, and development-specific manner Especially N-cadherin is involved in the tumor-progression in melanomas;
Methods The immunohistochemical expression of E-cadherin, N-cadherin, P-cadherin, Catenins alpha and ß and of CAM CD44v was examined using 60 FFPE various benign and malignant melanocytic tumors (malignant melonomas (SSM, NMM), junctional, compound and dermal nevi, and blue nevi. Provider: E-Cadherin (Biologo, Dr.Schultheiss, Kronshagen, Klon 5H9, IgG1, IHC), N-Cadherin (Biozol, Eching GeneTex.Inc; IgG, polyclonal, IHC); ß-catenin Fisher Scientific Fremont CA USA), H-HAM CD44 Novocastra laboratories LM
Results E-Cadherin: Good membranous and intracytoplasmic expression is found in junctional nevi.. Dermal and especially regressive nevuscells show loss of E-Cadherin.In NMM there is a high expression, whereas SSM and LMM are completely negative. N-Cadherin: Nearly no N-cadherin is found in NMM; in contrast, high cytoplasmic and membranous expression in superficial cells of SSM is seen; in the deeper, seconddary nodular parts of these tumors, no N-cadherin is found. P-Cadherin: is seen in junctional nevus/melanoma cells: in junctional-N, upper parts of compound-N and superficial parts of NMM an SSM; deeper parts are completely negative. ß-Catenin: All junctional nevus/melanoma cells as well as those in deeper parts show a membranous expression H-CAM (CD44v): is positive in all nevus and melanoma cells
Conclusion(s) N-, E and P-Cadherin are involved inmelanocytic tumorprogression and invasivity. Mechanisms are und discussion.

OP3.2

Patterns of MCV in Merkel cell carcinoma (MCC) analyzed by fluorescence in situ hybridization (FISH)

Schmidt A.; Speel E.; Willi N.; Zsikla V.; Baumann M.; Haesevoets A.; Diebold J.; Hofman P.; Kurrer M.; Offner F.; Sauter G.; Cathomas G.
Liestal, Switzerland

Background MCC has recently been associated with a polyomavirus named Merkell cell polyomavirus (MCV). Aim of the study was the evaluation of viral DNA in MCC.
Methods The presence of MCV was analyzed by PCR and visualized by FISH, using a 5 kb biotinylated viral DNA probe.
Results Using PCR, MCV DNA was detected in 51 (74.5%) of 68 tumors; 51 were available for FISH, including 13 (25.5%) PCR negative cases. MCV was detected by FISH in 32 (84.2%) of PCR positive, but in none of PCR negative samples. FISH positive tumors showed 3 distinctive fluorescence patterns: i) a single signal per tumor cells, indicating chromosomal integration (in 25%), ii) a granular fluorescence pattern without a dominant signal spot, indicating episomal viral DNA/RNA expression (in 50%) and iii) a combination of the two patterns described (in 25%).
Conclusion(s) Combining PCR and FISH, 5 groups of MCC can be distinguished: 1) Chromosomal integration of MCV, 2) viral episomal or RNA expression without evidence of chromosomal integration 3) a combined pattern with evidence of integration and episomal/RNA expression, 4) MCV PCR positive tumors lacking any FISH signals and 5) MCC without evidence of MCV infection. Further studies have to elucidate whether these patterns represent different stages of MCC development or distinctive tumor groups.

OP3.3

Analysis of tumor suppressor gene TP53 mutations in atypical vascular lesions of the breast skin following radiotherapy

Santi R.; Cetica V.; Franchi A.; Delfino C.; Cesinaro A.; Miracco C.; Bianchi S.; Santucci M.; Sardi I.; Massi D.
University of Florence, Florence, Florence, Italy

Background Atypical vascular lesions (AVL) arise in the setting of breast-conserving surgical treatment with adjuvant radiation therapy. Clinical and histopathological findings suggest that AVL represent a reactive phenomenon secondary to radiotherapy although it has been suggested that in some cases AVL represent precursors of angiosarcoma. A better understanding of the biology of AVL is essential to establish appropriate patients' management. The aim of the present study was to investigate alterations of tumor suppressor gene TP53 in radiation-induced AVL.
Methods A series of 12 AVL (patients' age range 47–70 years, mean 59 years) developed in the irradiation field of a primary breast carcinoma following radiotherapy was analyzed. Immunohistochemical stainings for CD31, CD34, D2–40, and p53 protein were performed. Exons 4–9 of TP53 gene were analyzed by direct sequencing.
Results Atypical endothelial cells decorating anastomosing vascular channels were constantly CD31 positive whereas stainings for CD34, D2–40 and p53 were weakly and focally positive in the majority of cases. Sequencing analysis of TP53 gene showed the presence of at least one variation in 10 of 12 samples (83%). The most common alteration was P72R, found in 6 samples.
Conclusion(s) The presence of p53 alterations suggests that its mutational inactivation may be implicated in the

pathogenesis of AVL. It is conceivable that the expression of p53 mutant proteins may stimulate vessels' sprouting through ROS up-regulation causing activation of HIF1/VEGF-A pathway. However, further molecular investigations are needed to support this hypothesis.

OP3.4

Cell cycle regulator p16ink4a in cutaneous cylindromas and spiradenomas and its role as a morphogenetic factor

Stoemmer Erasmus P.; Torres-Galea P.
Forschungslabor Prof Dr.Stoemmer, Augsburg, Bavaria, Germany

Background Cutaneous cylindromas and spiradenomas are rare tumors mostly in young female patients. They exist in two different clinical manifestations: spontaneous solitary type in face and sclap and as a multiple variety as Turban tumor (Spiegler- Ancell) and together with trichoepitheliomas, spiradenomas or basal cell carcinomas. Their peculiar architecture is only incompletely undersatood.
Methods Ten spiradenomas and five cylindromas (FFPE) were processed according to conventional histologic and immunohistochemical methods for p16Ink4a, p63 protein S100, smooth muscle actin and proliferationmarker Ki-67 (MIB-1).
Results Defective laminin 5- processing induces characteristical broad PAS-positive hyaline sheath at the periphery of the tumorcomplexes and perhaps their peculiar jig-saw-puzzle pattern. The tumorcomplexes consist out of two different cell types: larger central cells and cuboidal cells at the periphery. Immunohistochemical results: basal cell marker p63 is highly expressed in the nuclei of the peripheral cells of these tumors, whereas p16INK4a is highly expressed in the cvytpolasm and the nuclei central cells in these tumors.
Conclusion(s) P16Ink4a is expressed in cytolasm and nuclei of multiple tumors; but only in cutaneous cylindromas and spiradenom, there is a strict separation between its expression in different compartiments of the tumors. The different expression in these cells may give an explanation for the characteristic two-cell-type architecture of these tumors.

OP3.5

Expression of neural crest stem cells markers in cutaneous amelanotic melanomas

Massi D.; De Giorgi V.; Pizzichetta M.A.; Maio V.; Santucci M.; Canzonieri V.
Dept of Human Pathology and Oncology, University of Florence, Florence, Italy

Background Amelanotic melanoma (AM) shows little or no pigment at visual inspection, thus featuring a diagnostic challenge. Despite recently gained insights on the dermoscopical features and unfavourable outcome of AM, its phenotypic profile has been poorly investigated. Sox proteins are transcription factors that belong to the HMG box superfamily of DNA-binding proteins and play a key role in regulating pigmentation. SOX10 modulates the expression of microphthalmia-associated transcription factor (MITF), which in turn controls genes critical for pigment cell development and pigmentation, including tyrosinase. Members of the SOX family and MITF were found expressed at higher levels in pigmented in comparison with non pigmented melanoma cell lines but there are no data on their expression in relation to melanoma pigmentation status in tissue specimens.
Methods The study included 27 AM (15F/12 M, 47–88 yrs.), retrieved from the authors' archives. Immunohistochemical analyses were performed with anti-SOX10 and anti-MITF antibodies.
Results Moderate to strong SOX10 expression was found in 27/27 cases, irrespective from thickness. MITF nuclear expression was detected in all AM.
Conclusion(s) SOX10 and MITF expression in AM suggests that downstream MITF factors, such as tyrosinase degradation, down-regulate pigmentation in amelanotic cells. Mechanistic studies are needed to prove SOX10 functionality, since MITF induces tyrosinase expression only in presence of functional SOX10. The preservation of transcription factors in AM is also consistent with the possibility that they could play a role in melanoma cell survival and proliferation, possibly affecting the activation of the stem cell marker nestin.

OP3.6

Gene signature of the metastatic potential of cutaneous melanoma: a meta-analysis

Jozsef T.; Balazs G.; Erzsebet R.
2nd Department of Pathology, Budapest, Hungary

Background Despite the stunning success of genomics in defining markers or gene signatures for breast cancer prognosis and predicting therapies, there is virtually no progression in malignant melanoma.
Methods We have evaluated gene signature studies published and collected their publicly available data-bases.
Results Four studies attempted to define the prognostic signature of skin melanoma but only one based the study on the primary tumor resulting in heterogenous signatures with a minimal overlap (MCM3 and NFKBIZ). Four study attempted to define the invasiveness-signature in the primary tumor based on thickness or growth pattern

discrimination identifying a 9-gene overlap which proved to be different from the prognostic signatures. On the other hand, seven studies analyzed various types of metastatic tissues (rarely visceral-, mostly cutaneous or lymphatic metastases) to define the metastasis-signatures, again with minimal overlap (AQP3, LGALS7 and SFN). Using seven GEO-based melanoma datasets we have performed a meta-analysis of the metastasis-gene signatures using normalization protocols. This analysis identified a 350-gene signature, the core of which was a 17-gene signature characterizing locoregional metastases where the individual components occuring in 3 studies: several members of this signature were extensively studied before in context of melanoma metastasis including WNT5A, EGFR, BCL2A1 and OPN.

Conclusion(s) These data suggest that only efficient inter-disciplinary collaboration throughout genomic analysis of human skin melanoma could lead to major advances in defining relevant gene-sets appropriate for clinical prognostication or revealing basic molecular pathways of melanoma progression.

OP3.7

Histopathology of cutaneous GvHD in the era of reduced-intensity conditioning

Fondi C.; Nozzoli C.; Arbarello L.; Avellini C.; Bonoldi E.; Cesinaro A.; Colombetti V.; Fortunato M.; Fratoni S.; Negri G.; Ponzoni M.; Rafaniello P.; Salomone E.; Villari L.; Santucci M.; Bosi A.; Massi D.
University of Florence, Pistoia, Italy

Background In recipients of allogenic transplants with reduced intensity conditioning (RIC) regimens the separation of acute from chronic GvHD before or after day 100 is no longer tenable and there is limited information on the histopathological features observed in GvHD skin biopsies in this context.

Methods Sixty skin biopsies from 55 patients (37 M and 18F) undergoing non myeloablative conditioning regimens were evaluated. 39 received transplants from related donors, 16 from unrelated ones. Stem cell source was bone marrow (n=8), peripheral blood (n=46) and cord blood (n=8). Thirty-two patients developed classical aGvHD, 2 patients late-onset aGvHD, 19 patients classic cGvHD and 7 patients overlap syndrome. GvHD-related deaths were 14/32, 1/2, 3/19 and 2/7, respectively.

Results Histopathological diagnostic categories were no GvHD (n=20), possible GvHD (n=16), consistent with GvHD (n=21) and definite GvHD (n=3). Histopathology in classical aGvHD and cGvHD was similar to that observed in conventional myeloablative transplantation. Biopsies from patients with overlap syndrome showed composite histological features: i) aGvHD with concomitant features of lichenoid cGvHD, ii) sclerodermiform cGvHD associated with basal vacuolar change, as observed in aGvHD.

Conclusion(s) Skin biopsy in GVHD is a snapshot in time and can give false negative results since tissue changes reflect duration of activity and degree of immunosuppressive treatment. Clinical pictures of aGvHD several months post-transplant or cGvHD features within 50–60 days post-HCT can be observed. Biopsies from patients with overlap syndrome may disclose peculiar composite features of acute and chronic GvHD.

OP3.8

Malignant melanomas can be differentiated from atypical nevi by Collagen XVII expression, which can be a target of immunotherapy

Krenacst T.; Kiszner G.; Stelkovics E.; Korom I.; Varga E.; Plotar V.; Orosz Z.; Timar J.; Raso E.
1st Deapartment of Pathology and Experimental Cancer Resrearch, Semmelweis University, Budapest, Hungary

Background Collagen XVII, a transmembrane receptor of laminin-5 is lost in mature keratinocytes but expressed early in squamous cell carcinomas. We detected it in activated melanocytes and melanocytic neoplasias.

Methods Using a mouse monoclonal antibody for the aa507–529 sequence, collagen XVII expression was tested in samples of 9 normal skin, 22 dysplastic- and 20 Spitz nevi, 83 primary and 18 metastatic melanomas, melanoma xenografts and cell lines, which were also treated with collagen XVII antibody. Immunostains were digitalized (Mirax Scan) and analyzed (HistoQuant, 3DHISTECH, Budapest).

Results Malignant melanomas showed moderate-to-strong collagen XVII immunostaining while nevi were negative. In melanomas collagen XVII expression paralleled with atypia, showed positive correlation with vertical growth and elevated expression on the tumor fronts, and it was seen in some HMB-45 or Melan A negative melanomas. Sensitivity and selectivity of melanoma markes were: Collagen XVII 85% in melanomas, 6% in nevi; Melan A 87/92%; S-100 94/90% and HMB-45 72/38%. Constitutive Collagen XVII mRNA and protein expression was detected in melanoma cell lines, primary metastatic and circulating HT199 cells of mouse xenografts and in re-cultured tumors. Collagen XVII antibody reduced cell proliferation, and elevated cell adhesion and apoptosis in a concentration dependent manner in HT199 cells.

Conclusion(s) Collagen XVII, a melanogenesis independent protein is an efficient marker of malignant melanomas differentiating malignant and benign lesions and it can be a target of melanoma immunotherapy. Supported by OTKA_K 62758.

OP3.9

Morphological and immunohistochemical features of atypical fibroxanthoma - potential diagnostic pitfalls

Luzar B.; Calonje Jaime E.
Medical Faculty University of Ljubljana, Institute of Pathology, Ljubljana, Slovenia

Background Genuine focal positivity for CD31 was occasionally observed among referral cases of atypical fibroxanthomas (AFX), leading to erroneous diagnosis of angiosarcoma. The present study gives emphasis on recognizing morphological variants of AFX, on validation of immunohistochemical markers, and on discussing potential diagnostic pitfalls.
Methods Histological features analysed were: ulceration, morphological variants, growth pattern, location in the skin, and vascular/perineural invasion. The antibodies used were CK-MNF116, CK-AE1/AE3, S100, smooth muscle actin, desmin, CD31, and EMA.
Results We analysed 66 AFXs (59 males, 7 females, age 55–95 yrs, mean 77 yrs). All developed on sun damaged skin. Morphological patterns were: pleomorphic spindle and epithelioid cells (60%), predominantly spindle cells (21%), predominantly epithelioid cells (6%), and purely spindle-cell non-pleomorphic variant (12%). Most were localized in the dermis (56%). An expansile (21%) rather than infiltrative (6%) growth into superficial subcutis was noted. No vascular/perineural invasion was seen. Additional changes were haemorrhagic and pseudoangiomatous areas (24%), granular cell change (23%), keloid-like change (9%) regression (9%), myxoid change (8%), osteoclast-like giant cells (4%), clear cell change (2%), and minute foci of necrosis (2%). AFX were consistently negative for S100, CK-MNF116, CK-AE1/AE3 and desmin. Focal positivity for SMA (44%), EMA (24%), and CD 31 (10%) was seen.
Conclusion(s) While SMA and EMA positivity are well recognized in AFXs, genuine focal CD31 positivity is a unique observation. Together with pseudoangiomatous/haemorrhagic areas, CD31 positivity in AFXs represents a potential diagnostic pitfall. This study further expands spectrum of non-vascular CD31 positive lesions.

Oral Presentation 4

Gynecopathology

OP4.1

Diagnostic and histogenetic significance of PAX8 expression in papillary serous carcinoma of the peritoneum

Tong G.; Hemale-Bena D.
Columbia University Medical Center, New York, NY, USA

Background Papillary serous carcinoma (PSC) of the peritoneum (PSCP) is a rare malignant tumor. Itoccurs almost exclusively in women and should be differentiated with peritoneal malignant mesothelioma (PMM), metastatic carcinoma of the peritoneum, peritoneal spread of ovarian epithelial carcinoma (OEC) and breast carcinoma (BC). Although similar to PSC of the ovary (PSCO), Müllerian origin of PSCP has not been confirmed. We investigated expression of PAX8, a new Müllerian marker, in PSCP utilizing immunohistochemistry (IHC).
Methods PAX8 IHC was performed on 7 PSCP (4 with positive ascites and 1 with axillary lymph node metastasis) and TMAs containing 10 PMM of female patients, 33 BC, 28 OEC, and 10 cases of reactive mesothelial cells (RMC) as control tissues, using the avidin-biotin peroxidase method following antigen retrieval.
Results All PSCP were consistently positive for BerEP4, CK7, negative for calretinin and CK20. Staining of ER, PR, WT-1 and CA125 was variable and 5, 3, 5, and 5 of 7 cases were positive, respectively. PAX8 was detected in all primary tumors, ascites, and lymph node metastasis of PSCP. No PAX8 staining was detected in BC, PMM, or RMC. PAX8 was detected in 23 of 28 OEC as previously reported.
Conclusion(s) Expression of PAX8 in PSCP supports its Müllerian origin arising probably from the fimbriae of the fallopian tube as shown for PSCO recently or Müllerian remnants in coelomic epithelium. PAX8 IHC is a useful differential tool in the diagnosis of PSCP in female patients.

OP4.2

A multiinstitutional consensus study on the pathologic diagnosis of ovarian mucinous borderline tumors and adenocarcinomas

Chun Y.; Chang E.; Kim M.; Kwon S.; Park M.; Suh K.; Yoon H.; Hwang T.; An H.; Park J.; Hong S.; Jun S.; Kim I.
Cheil General Hospital, Kwandong University College of Medicine, Seoul, Republic of Korea

Background This study was designed to assess the reproducibility of both the diagnosis and subtypes of ovarian mucinous borderline tumors (MBT) and the mucinous adenocarcinomas(MC).
Methods We collected 218 cases of MBT or MC from 11 hospitals in Korea and reviewed independently by 11 pathologists of the Gynecologic Pathology Study Group using a checklist. The checklist consisted of 4 major histologic categories–benign, MBT, MC and others including metastatic tumor-and 6 subclassification categories-endocervical-like type, intestinal type, microinvasion and intraepithelial carcinoma for MBT, and expansile type and infiltrative type for MC.

Results We excluded 7 cases showing mixed or other cell types and 9 cases having the likelihood of metastatic tumor. Of the remaining 202 cases, the original diagnoses were 37 (18%) MC and 165 (82%) MBT. After consensus study, 163 (80.7%) cases were reclassified as MBT (13 endocervical-like and 150 intestinal). 24 (11.9%) were MC and 9 (4.4%) were benign. Six cases (3.0%) could not get a consensus on diagnosis. The original diagnosis of MC showed low reproducibility and only 11 cases (30%) reached the agreement among more then two thirds of reviewers. But MBT showed a higher concordance rate. The differential diagnosis of MBT with intraepithelial carcinoma and expansile MC was problematic. Confusion with microinvasion and mucin granuloma was noted.
Conclusion(s) We need the more strict diagnostic criteria for the diagnosis of MBT with intraepithelial carcinoma and expansile type of invasion. The concept of MBT with microinvasion should need more qualification and quantification.

OP4.3
HER2 and ovarian cancer

Sarancone S.; Acosta Haab G.; Nocito A.; Frahm I.; Lupo E.; Cáceres V.
Rosario, Santa Fe, Argentina

Background Variable rates of HER2 over-expression/amplification have been reported in advanced ovarian cancers (AOC) with widely discordant results, ranging from 11 to 32%. There is growing interest in its role in prognosis, pathogenesis and treatment implications for AOC patients, due to the future introduction of trastuzumab and pertuzumab therapy. The aim of the study was to examine HER2 over-expression in AOC and to correlate with classic histological features.
Methods 155 H&E-stained, formalin fixed paraffin embedded AOC tissue samples with required criteria were collected HER-2 analysis was performed using policlonal antibody anti Her 2 (DAKO), microwave antigenic recovery, detection system EnVision (Dako) and developed with diaminobenzidine. Results were interpreted as hercepTest® guideline's. 40 cases were also screened by fluorescence in situ hybridization (FISH).
Results HER2 was over-expressed in 16 patients (10,3%), and all were also FISH +, and remaining 139 (89,7%) were score 0. Among, HER2 + patients: 6 were serous, 3 mucinous, 3 endometroid and 4 undifferentiated tumors.
Conclusion(s) HER2+ prevalence in our sample (10.3%) is in line with previously published onesThere was 100% correlation between ICH and FISH. No significant relationship was found among HER2 score and main pathological features. Identifying HER2 + patients enables specific therapy leading to a significant change in treatment and prognosis. Technique standardization is a key to success in identifying HER 2 over-expression in an accurate, precise and truthful way, although patterns may differ from breast cancer.

OP4.4
The prevalence of mix HRHPV infection among women of reproductive age in Tuzla Canton, Bosnia and Herzegovina

Iljazovic E.; Mehinovic N.; Ljuca D.; Avdic S.; Karasalihovic Z.
University Clinical Center Tuzla, Tuzla, Bosnia and Herzegovina

Background The prevalence of high risk Human papilloma virus infection (HRHPV) in woman of reproductive age in Tuzla Canton is around 45%. Mostly, HRHPV infection was identified in women with normal and mildly abnormal PAP smear. We aimed to set out the presence of mix HPV infection (HPV 16, 18, and 45) as one of the most common mix types.
Methods HRHPV DNA was detected by Hybride Capture HRHPV DNA II. In order to identify the presence of mix infection in HRHPV positive women was used the new Digene HPV 16/18/45 Probe Set (for research use only).
Results Most of the tested women had mix HPV infection
Conclusion(s) In one of our previous study HPV 16 was the most common type (> 46%), while HPV 18 and 45 were detected in 1,8% only. Detection of the mix infection of those HRHPV types in women with normal and mild cellular abnormality is important for the follow up intervals and prognosis.

OP4.5
Value of p16INK4a as a marker of progression/regression in cervical intraepithelial neoplasia Grade 1

Castillo P.; Del Pino M.; Garcia S.; Fusté V.; Alonso I.; Torné A.; Ordi J.
Department of Pathology, Hospital Clinic, IDIBAPS, Universidad de Barcelona, Barcelona, Catalunya, Spain

Background Low-grade squamous intraepithelial lesions (LSIL) and their histological counterpart CIN1, frequently regress spontaneously in 1–2 years. Nevertheless, 10–15% of LSIL/CIN1 lesions progress to CIN2/3. p16INK4a has recently been proposed as a biomarker for cervical lesions. In contrast with the consistent positive staining of CIN2–3 lesions, CIN1 show a marked variability in staining, with some lesions being positive and others showing a negative reaction. The objective of this study was to evaluate whether this immunohistochemical variability in p16INK4a

staining could provide information on the evolution of LSIL/CIN1 lesions.
Methods Patients with a histological diagnosis of CIN1 were prospectively recruited (n=138). Simultaneous detection of HR-HPV, and p16INK4a evaluation in the biopsy were performed. Follow-up was conducted every 6 months by cytology and colposcopy, and annually by HR-HPV testing, for at least 12 months (mean 29.0).
Results Progression was observed in 14 women (10.1%); 66 (47.6%) regressed, and 58 (42.0%) had a persistent disease. p16INK4a was positive in 77 (55.8%) initial biopsies. Progression to CIN2–3 was identified in 14/77 (18.2%) women with positive and 0/61 (0.0%) with negative p16INK4a immunostaining (p<0.001).
Conclusion(s) CIN1 lesions positive for p16INK4a have a significantly higher tendency to progress to CIN2–3. Patients with CIN1 lesions negative for p16INK4a rarely progress and may benefit from a less intensive clinical follow-up.

OP4.6
Adhesion molecules and p16 expression in endocervical adenocarcinoma

Fulciniti F.; Carico E.; Giovagnoli R.M.; Losito S.N.; Botti G.; Benincasa G.; Farnetano G.; Vecchione A.
Istituto Nazionale Tumori "Fondazione G. Pascale", Naples, Italy

Background Defects in the E-Cadherin/Catenin adhesion complex have been described in several gynecologic cancers, mainly in cervical, endometrial and ovarian tumors. Fewer studies have recently focused also on the the E-cadherin-catenin complex expression in endocervical adenocarcinomas.
Methods An immunohistochemical study has been conducted on 34 cases of untreated endocervical adenocarcinomas. The E-cadherin and α- and β-catenin complex status has been investigated along with p16INK4a in all studied cases with the aim to study whether the pattern of expression of the Cadherin-Catenin complex could be causally related to the expression of P16INK4a protein. Results were evaluated for statistical significance by a non parametric test (Kruskall Wallis).
Results Endocervical adenocarcinomas were uniformly expressing p16INK 4a except for two cases and all lesions displayed down regulation of the Cadherin-catenin complex, without demonstrating statistically significant differences among the different histotypes. The lack of nuclear accumulation of β-catenin found in this group of lesions probably implies that no alteration of the β-catenin/ wnt metabolic pathway is present in endocervical adenocarcinoma, as opposed to what found in the literature for squamous carcinoma of the cervix. The diffuse expression of p16INK4a protein in this group of neoplasms stresses the important role of high risk HPV infection in neoplastic causation possibly via the viral E7 mediated inactivation of pRB tumor suppressor protein.
Conclusion(s) In consideration of these findings, investigation of downstream β-catenin genes c-myc and Cyclin D1 is sought as possibly contributive in the molecular pathogenesis of endocervical adenocarcinoma.

OP4.7
Investigation of GLUT-1 and galectin-3 in endometrioid and serous carcinomas of the endometrium

Ege Cigdem B.; Akbulut M.; Zekioglu O.; Ozdemir N.
Pamukkale University, School of Medicine, Denizli, Turkey

Background GLUT-1 and galectin-3 have been shown to function in tumor progression and metastatic spread. The aim of this study was to investigate the relationship between GLUT-1 and galectin-3 expression and well-known prognostic factors. 64 endometrial carcinomas, which includes 24 serous type were obtained from previously untreated patients.
Methods Immunohistochemical analysis of 64 carcinomas, 20 endometrial hyperplasia (ten simple hyperplasia and ten complex atypic hyperplasia) and 20 normal endometria (ten proliferative and ten secretory) was performed.
Results The percentage of GLUT-1 expression was found to be significantly higher in serous carcinomas when compared to endometrioid adenocarcinomas. The percentage of GLUT-1 expression was significantly correlated with lymph node metastasis, adnexial metastasis, positive periton cytology and classified stage. GLUT-1 expression was also significantly higher in hyperplasias than normal endometrium. Epitelial and stromal galectin-3 expression was significantly decreased in both endometrioid and serous carcinomas compared to the control group. Stromal galectin-3 expression was also correlated with lymph node metastasis.
Conclusion(s) This study shows that GLUT-1 expression increases from secretory endometrium to hyperplastic endometrium and the two types of carcinoma of the endometrium and provides further evidence of a relationship between atypical hyperplasia and endometrioid carcinoma. GLUT-1 can serve as an indicator of the aggresive potential of endometrial cancers. This investigation suggests decreased expression of galectin-3 to be involved in the pathogenesis of endometrial carcinomas from normal endometrium to carcinoma. Down-regulated stromal expression of galectin-3 in endometrial carcinoma may be involved in lymph node metastasis.

OP4.8

Molecular basis of stromal-parenchymal interactions in foci of active and non-active adenomyosis

Kogan E.; Demura T.; Grechukhina O.; Unanyan A.; Sidorova I.
Scientific centre of obtetrics and gynecology, Moscow, Russian Federation

Background The aim of our study was to investigate molecular aspects of stromal-parenchymal interactions in active and non-active foci of adenomyosis.
Methods The study was performed on serial sections of uteri taken from 94 patients of reproductive age with diffuse adenomyosis (12 non-active and 82 active). Immunohistochemical detection of MMP-1,2,7,9, TIMP-1,4, E-cadherin, COX2, SOD (Lab Vision), PCNA, CD34 (DAKO), Apo, EGF, EGFR (Novocastra) was used. Results were evaluated with the help of quantitative and semi quantitative methods and statistic analysis.
Results Active foci with cytogenic stroma demonstrated relatively low apoptosis, high levels of PCNA and MMPs both in epithelial, stromal and endothelial cells, while non-active had higher levels of TIMPs and increased apoptosis. MMP1, MMP7 were detected predominantly in epithelium of active foci, while MMP2 and 9 were mostly expressed in stroma and endothelium of active adenomyosis. Non-active foci had high levels of TIMPs in epithelium. CD34 was much higher in active foci compared to non-active. Both types of foci revealed similar levels of E-cadherin expression.
Conclusion(s) Adenomyosis is a condition with the disturbances in stromal-parenchimal interactions including misbalance between processes of apoptosis and proliferation, MMPs and TIMPs and high level of neoangiogenesis. Increased stromal expression of MMP2 and 9 which are known to degrade extracellular matrix and trigger neoangiogenesis in active adenomyosis may indicate the aggressiveness of stroma.

OP4.9

Morphogenetic relationships between foci of adenomyosis and basalis of eutopic endometrium

Grechukhina O.; Kogan E.; Demura T.; Unanjan A.; Sidorova I.
Sechenov Moscow Medical Academy, Moscow, Russian Federation

Background Adenomyosis is a very common gynecological disorder. Despite high incidence of the disease precise developmental events leading to the condition remain unknown. The aim of our study was to investigate and compare the expression of markers of proliferation, apoptosis, invasion and neoangiogenesis in foci of adenomyosis and in eutopic endometrium and to assess their potential role in the pathogenesis of the disease.
Methods The study was performed on biopsy samples of uterus taken from 94 women with adenomyosis. Immunohistochemical staining of tissues was performed with antibodies to MMP1,2,7,9, TIMP1,4, E-cadherin, PCNA, Apo, EGF, EGFR.
Results The basal layer of eutopic endometrium and foci of adenomyosis were found to express similar levels of PCNA and Apo, markers of invasion and growth factors with their receptors in epithelium. The functionalis had different molecular features. E-cadherin was highly expressed in epithelium of eutopic and ectopic endometrium. Stroma in foci of adenomyosis showed higher levels of MMP2,9, whilst epithelium was more active in expressing MMP1,7, TIMP1,4, E-cadherin, EGF and EGFR.
Conclusion(s) The obtained data suggests that morphogenesis of adenomyosis is based on the disturbances in stromal-parenchimal interactions in the basal layer of endometrium. Alterations on molecular levels may result in the invasion of the basalis into the myomertium which occurs mostly due to the hyperactivity stromal elements, while epithelial cells reveal prominent cell-to-cell adhesion.

Oral presentations 5

Haematopathology

OP5.1

Diffuse large b-cell lymphoma-clear cell variant. Case report

Manxhuka-Kerliu S.; Petruseska G.; Kryeziu E.; Loxha S.; Kerliu A.; Baruti A.; Shahini L.; Gashi G.
University of Prishtina, Faculty of Medicine, Institute of Pathology, Prishtina, Kosovo, Serbia and Montenegro

Background Diffuse large B-cell lymphoma (DLBCL) is a diffuse proliferation of large neoplastic B lymphoid cells.
Methods. The aim of this study was to report a case of DLBCL-clear cell variant involving the lymph node in the neck, which was clinically suspected for metastatic carcinoma. A 39 years old man presented with rapidly enlarged lymph node in the neck, disclosing B symptoms and fatigue. FNAB disclosed pleomorphic feature. Large excision was performed for histopathology and IH examination.
Results The lymph node biopsy showed a partially nodular growth pattern with 2 distinct components with respect to morphological, phenotypic and genetic features: 1. large nodules / diffuse areas, composed of large cells with slightly irregular nuclei clear cytoplasm, admixed with a

few immunoblasts. Some pseudoadenoid structures were found. In these areas, there was a high mitotic activity, and numerous macrophages with tangible bodies responsible for some starry sky pattern. Stainings for cytokeratins and Mean A were negative. There was strong positivity to vimentin as well. These areas disclosed the following phenotype: CD20+, CD5-, CD10+, bcl-2+, bcl-6+ and exhibited a high proliferative rate (MIB1/Ki67 80%). 2. The areas with folliclura structures were composed of centrocytes and rare centroblasts with a CD20+, CD5, CD10+ (strong), bcl-2+, bcl-6+ phenotype, and a relatively low proliferative index (MIB1/Ki67 20%).
Conclusion(s) A number of high grade B-cell lymphomas, correspond to « de novo » transformation of low grade lymphoma, mainly FL and B-CLL.

OP5.2

Intact B cell follicles identify mixed cellularity (MC) Hodgkin lymphomas (HL) with clinical and prognostic features of lymphocyte rich classical hl (cHL)

Kurrer M.; Giger S.; Korol D.; Renner C.; Moch H.; Probst Hensch N.
Pathologisches Institut, Kantonsspital Aarau, Aarau, Switzerland

Background The WHO distinguishes nodular lymphocyte predominant (LP) HL from cHL. cHL is divided into nodular sclerosis (NS), MC and lymphocyte rich cHL (LR). The WHO separated MC from LR by the presence of eosinophils. Follicular and interfollicular cHL have been described to complement the WHO scheme. We hypothesized that preservation of follicular architecture would reclassify MC as cHL related to LR (LRcHL).
Methods Slides and files were reviewed from 131 patients diagnosed from 1991 to 2007. B cell follicles and absence of sclerosis was used to separate MC and NS from LRcHL. EBER, CD20, CD30 and CD15 was used to separate LP from LRcHL.
Results Review resulted in 65 NS, 19 MC, 32 LRcHL and 15 NP cases. B-symptoms were frequent in MC (11/15) compared to LRcHL (6/28) and LP (1/6). Advanced stage III/IV was seen in 10/52 NS, 12/15 MC, 1/26 LRcHL and 0/5 LP patients. Patients died in 8/65 NS, 6/17 MC, 1/27 LRcHL and 3/14 LP. Male to female ratio was for NS 33:32 (1:1), MC 13:6 (2:1), LR 23:9 (2.6:1) and LP 14:1. MC patients were older, higher stage and B-symptoms were more frequent than in NS and LRcHL. Recurrence was similar in all HL.
Conclusion(s) Follicles imparting a follicular or interfollicular pattern to HL identify a subgroup of MC with clinical features of LR. Other MC patients are older, have B-symptoms, advanced stage and bad outcome.

OP5.3

Aberrant hypermethylation of DAP-kinase cpg island in immune suppression associated B-cell lymphoproliferative disorders/lymphomas and immune competent diffuse large B-cell lymphoma – correlation with EBV-association

Ibrahim Ahmed Hamed H.; Menasce P.L.; Bower M.; Pomplun S.; Naresh N.K.
Imperial College London, London, United Kingdom

Background Post-transplant lymphoproliferative disorders (PTLDs) and HIV-related B-cell lymphomas (BCL) are well known examples of Immunodeficiency lymphoproliferative disorders (IDLDs). Aberrant hypermethylation (AH) of DAP-kinase, a proapoptotic gene, is involved in the pathogenesis of IDLDs. Epstein Barr virus (EBV) has been shown to play a major role in the pathogenesis of IDLDs in the majority of cases. We have investigated whether B-PTLDs and HIV-associated BCL significantly differ from immunocompetent (IC) diffuse large B-cell lymphomas (DLBCL) with regard to AH of DAP- kinase gene. We further correlated AH with EBV association.
Methods DNA was extracted from paraffin sections of 28, 19 and 18 samples of B-PTLD, HIV-related BCL, and IC-DLBCL respectively. In addition, DNA from 8 samples of peripheral blood lymphocytes was used as a control. Methylation specific PCR was carried out for AH detection. EBV association was assessed by In-Situ Hybridisation for EBER RNA on tissue Microarrays.
Results 23/28 of B-PTLD, 16/19 of HIV-lymphomas, and 14/18 IC-DLBCL showed AH of DAP-kinase while normal blood samples were negative. Overall, AH of the DAP-kinase gene was noted in 81% of the Lymphoproliferative disorders/lymphomas and EBV association was noted in 58% cases. While 83% of the cases that lacked DAP-kinase AH were EBV-associated, only 52% of the cases with DAP-kinase AH showed EBV-association ($p=0.045$).
Conclusion(s) 83% of IDLD and 78% of IC-DLBCL showed aberrant DAP-kinase hypermethylation. Hypermethylation status and EBV-association showed an inverse correlation.

OP5.4

Accelerated CLL is a morphological variant involving lymphoid tissues with high proliferation and prognostic implications

Martinez D.; Gine E.; Villamor N.; López-Guillermo A.; Bosch F.; Emili M.; Campo E.; Martinez A.
Hospital Clínic, Barcelona, Spain

Background CLL/SLL has a small lymphocytic component and a proliferative compartment, the proliferative

growth centers (PC). PC's are in similar composition to lymphoid follicles but lack a support of FDC meshwork. Increase of cell size and proliferative activity as well as enlarged and confluent PC may be seen in CLL although the clinical meaning is controversial.

Methods 145CLL/SLL patients diagnosed between the period from 1990–2008 from which a biopsy was obtained were stained with p27, p53 and ki67. The pattern of involvement, presence and size of proliferative growth centers and proliferation were assessed. The clinical and biological data were collected and analyzed.

Results Involvement by CLL/SLL was identified in 103 cases. Enlarged and confluent PC broader than ≥2,5 mm^2, ≥2.4 mitosis and/or ≥30% ki-67 in the PC identified cases with poor survival. A score based on these features classify CLL/SLL patients: patternA (≤ 1 parameter), 84 (82%) and patternB (≥ 2 parameters), 19 (18%) with worse survival from biopsy (34 months vs 80 months; $p=0.0014$). Transformation to DLBCL occurred in 23 cases, median survival of 4 months. Only one pattern B patient transformed to DLBCL. Unfavorable biological risk factors were evenly distributed among all subsets. Pattern B patients presented with high ZAP-70 expression and short lymphocyte doubling time.

Conclusion(s) Expanded PC and high proliferation identifies a group of CLL/SLL patients with poor survival. These patients do not transform to DLBCL and present an intermediate outcome. The term accelerated CLL/SLL is proposed.

OP5.5

Epstein Barr virus genotypes in immunodeficiency lymphoproliferative disorders/lymphomas

Ibrahim Ahmed Hamed H.; Menasce P.L.; Bower M.; Pomplun S.; Naresh N.K.
Imperial College London, London, United Kingdom

Background Immunodeficiency lymphoproliferative disorders (IDLDs) are a group of diseases that range from polyclonal to monoclonal lymphoid proliferations. Post-transplant lymphoproliferative disorders (PTLDs) and HIV-related B-cell lymphomas (BCL) are well known examples of these disorders. They usually develop as a result of some genetic and epigenetic alterations. Epstein Barr virus (EBV) has been shown to play a major role in the pathogenesis of IDLDs in the majority of cases. We have investigated the prevalence of different EBV genotypes among IDLD samples.

Methods We screened IDLDs and immune competent diffuse large B-cell lymphomas (IC-DLBCL) for EBV association by performing In-Situ Hybridization for EBER on tissue microarrays. We preformed PCR analysis with primers directed at EBNA3C to distinguish the two EBV genotypes.

Results We selected 26 B-PTLDs, 12 HIV-BCLs and 2 IC-DLBCL for EBV genotyping. Among B-PTLDs, 24 were of type A (92%) and 2 were of type B. Among HIV-BCLs, 6 were of type A (50%) and 6 were of type B. Differences in the EBV genotype between B-PTLD and HIV-BCL were statistically significant ($p=0.003$). Both cases of IC-DLBCL were of type A. None of the cases examined were positive for both types of EBV.

Conclusion(s) PTLD samples are more frequently associated with EBV type A as compared to HIV-BCLs.

OP5.6

Prognostic markers and angiogenesis in diffuse large B-cell lymphoma and follicular lymphoma

Mezei T.; Gurzu S.; Raica M.; Cîmpean A.; Szentirmay J.; Jung J.
University of Medicine and Pharmacy, Targu Mures, Romania

Background In later years great efforts have been done to elucidate different characteristics of immunohistochemical prognostic markers and tumour angiogenesis. This is especially valid for various solid tumours. There are however only a few papers that discuss microvascular characteristics of malignant B-cell lymphomas. The purpose of this study was to correlate some well known immunohistochemical prognostic markers with microvascular characteristics of two types of malignant B-cell lymphoma: Diffuse Large B-cell Lymphoma (DLBCL) and Follicular Lymphoma (FL).

Methods Randomly chosen 29 cases of DLBCL and 20 cases of FL were used. Conventional immunohistochemical methods were used for both the prognostic markers (Bcl-2, Bcl-6, CD10, MUM1) and to mark microvessels using the CD34 antibody. We measured the endothelial area fraction (EAF), defined by the CD34 positive area and total tissue area fraction, using digital morphometric analysis. DLBCL was divided into GC (germinal center) and nGC (non-germinal center) subtypes, FL into group A and B according to previously published protocolls.

Results We found a strong correlation between the adverse prognostic markers and high EAF values wich were the following (represented in percentages): DLBCL GC: 1,1±0,617; nGC 3,3±0,886; FL group A 1:0,9± 1,07; FL group B: 2,7±0,536.

Conclusion(s) Our findings indicate that low microvascular density might represent a better prognosis whilst high microvascular density is more likely to be linked with a negative outcome, in our cases these latter groups

were the in the case of DLBCL the nGC subgroup, in the FL the B subgroup.

Oral presentations 6

Pediatric and fetal pathology – Molecular pathology

OP6.1

Calretinin immunohistochemistry: a simple and efficient tool to diagnose Hirschsprung's disease

Berrebi D.; Guinard-Samuel V.; De Lagausie P.; Bonnard A.; Philippe-Chomette P.; Peuchmaur M.
Robert Debré, Paris, France

Background Diagnosis of Hirschsprung disease (HD) is quite entirely based on the histology on rectal biopsy inadequately helped by AChE staining. The aim of this study was to assess the diagnostic value of Calretinin immunochemistry to diagnose HD.
Methods 131 initial rectal biopsies performed for suspicion of HD in children were retrieved and Calretinin immunohistochemistry was performed on paraffin-embedded biopsies. Diagnosis of HD was made when no staining was observed. The results were statistically analyzed in comparison with our standard method (histology and AChE staining).
Results 130 biopsies were accurately diagnosed based on positivity or negativity of the Calretinin staining. The senior pathologists diagnosed all cases of HD with no false positive. 12 additional cases initially considered as doubtful for HD with the standard method was accurately diagnosed by Calretinin immunohistochemistry. The false negative was a case of HD with a Calretinin positive biopsy. We also demonstrate the easiness of Calretinin interpretation compared to AChE for the junior pathologist.
Conclusion(s) Calretinin histochemistry overcomes most of difficulties encountered using the combination of histology and AChE and detect almost all cases of HD with confident, with no false positive. Thus, we demonstrate that Calretinin is superior to AChE to complete histology and could advantageously substituted to AChE.

OP6.2

Fetal brain tumours

Fallet-Bianco C.; Joubert M.; Jossic F.; Blesson S.; Loget P.; Yacoubi T.; Mehaut S.; Bessieres B.; Miquel C.; Villa C.; Andreiuolo F.; Daumas-Duport C.
Sainte-Anne Hospital, Paris, France

Background Fetal brain tumours are rare and have a poor evolution. The aim of this study was to report on a large series of 31 fetal brain tumours diagnosed at our institution.
Methods All cases were examined post mortem. 27/31 were fetuses examined after a prenatal diagnosis between 26 and 36 weeks of gestation and a medical termination of pregnancy in accordance with French laws. Two neonates born at term had a normal prenatal ultrasonographic examination at 32 weeks of gestattion: they died shortly after birth, because of a massive hemorrhage (1) and rapid growth of the tumour (1). The karyotype was normal when sudied. The sex ratio was 13 females: 18 males.
Results Our series included two main categories, namely subependymel giant cell astrocytomas (SEGA) associated with tuberous sclerosis (n=16) and mixed tumours (n = 15). SEGA were associated, in all cases, with numerous cortical tubers and large subcortical lesions. There was a familial history of tuberous sclerosis only in 1 case. Other tumours included teratomas (n=5), choroid plexus papillomas (n= 3), glial and glioneuronal tumours (n=6) and atypical teratoid/rhabdoid tumour (1). Most of these tumours, mainly diagnosed in the 3rd trimester, exhibited a detectable intracranial mass with macrocephaly and rapid growth on imaging. They were sporadic, except in 1 case.
Conclusion(s) Our study confirms that fetal brain tumours are uncommon entities with a particular clinical, imaging and histopathological features. In most cases, the prognosis is severe either as a consequence of major hydrocephaly, a particularly rapid tumoral growth or hemorrrhagic complications.

OP6.3

FISH on extracted nuclei from formalin fixed and paraffin embedded tissues for the diagnosis of chromosomal aneuploidies in malformed fetuses

Yacoubi Tahar M.; Mougou S.; Letaief A.; Lahmar A.; Trabelsi A.; Hmissa S.; Gazal H.; Saad A.
Departement of Pathology, F. Hached Hospital, Sousse, Tunisia

Background The most frequent chromosomal anomalies in human pathology are aneuploidies especially the trisomy 13, 18 and 21 and the monosomy X since they are compatible with a postnatal life. Theses anomalies generally produce severe malformations that could terminate the pregnancy without any prenatal karyotype. The use of fluorescent in situ hybridization (FISH) to detect and characterize theses chromosomal anomalies is largely applied in lymphocytes and amniocytes but its use on formalin- fixed and paraffin-embedded tissues is not routinely made. The aim of this study is to detect above mentioned anomalies using FISH technique.

Methods 20 fetuses have been screened for the specific malformations of these chromosomal aneuploidies. Nuclei have been extracted from kidney and liver formalin- fixed and paraffin embedded tissues. FISH then was tested on the extracted nuclei by a combination of a contig of probes from chromosome 21, 13 on one hand and centromeric probes of chromosomes X and 18 on the other hand.
Results Trisomy 21 was detected in one case, trisomy 18 was confirmed in 4 cases, trisomy13 in 4 cases and monosomy X in 2 cases.
Conclusion(s) The application of FISH on fetal tissues is very useful in detecting chromosomal anomalies in embryofetopathology. FISH can so, straighten the diagnosis what constitutes a help to the genetic counseling for the related couples or in the cases where a differential diagnosis exists.

OP6.4

Placental hemosiderosis: relation to adverse obstetric events and neonatal outcome

Khong Y.; Toering T.; Erwich J.
SA Pathology, North Adelaide, South Australia, Australia

Background Placental hemosiderosis has been reported to be associated with chronic abruption oligohydramnios syndrome, prematurity and pulmonary hypertension of the newborn and chronic lung disease. The aim was to ascertain the incidence and to review the obstetric and neonatal correlates of placental hemosiderosis.
Methods A retrospective case-review of 100 consecutive singleton placentas with an indication for pathologic examination and 113 consecutive singleton placentas from uncomplicated pregnancies without an indication for pathologic examination. Sections were stained for iron to uncover hemosiderosis in membranes, chorionic plate and/or basal plate of the placenta. The obstetric and neonatal data were analysed.
Results Hemosiderosis was observed in 51.6% (110/213). Only two features were significantly related to hemosiderosis in the placenta: early decelerations during fetal heart rate monitoring ($p=0.0498$) and, negatively, maternal thrombophilia ($p=0.0496$). Preterm delivery, chronic separation of the placenta or procedures performed during pregnancy or delivery were significantly related to hemosiderosis. Different patterns of iron staining were observed but these were not correlated with any maternal or neonatal factors.
Conclusion(s) The incidence of hemosiderosis is considerably higher than previously reported. Placental hemosiderosis is not significantly correlated with adverse obstetric events and in particular, contrary to published data, is not a useful indicator for chronic placental abruption. Adverse neonatal outcome is not significantly correlated with placental hemosiderosis. Hemosiderosis in the amniochorial membranes is likely to be physiological in most cases. Which placentas displaying hemosiderosis have pathological causes remains to be determined.

OP6.5

Potential prognostic importance of MCM2 protein in chosen solid tumor in children. A preliminary study

Kobos J.; Taran K.; Sitkiewicz A.; Andrzejewska E.
Department of Pathology of the Age of Development, Medical University of Lodz, Lodz, Poland

Background Recent studies have shown that minichromosome maintenance 2 (MCM2) protein may be promising proliferation marker in some neoplasms and may be applied as biomarker for prognostication. The aim of this study was to evaluate the expression of MCM2 in chosen group of solid children tumors.
Methods Tissues from 32 pediatric solid tumors were used in our study. There were 8 cases of Rhabdomyosarcoma, 12 cases of neuroblastic tumors, 3 PNETs, 2 cases of fibromatosis and 7 cases of other sarcomas. For our research we used MCM2 (Clone CRCT2.1) antibody produced by Thermo Scientific Comp. Labelling index (LI) of the protein positive cells was scored in 10 HPF in every case.
Results MCM2 expression was very intense in RMSs. The higher score was observed in alveolar type in comparison to embryonal type, especially in the solid areas of Arms. Among neuroblastic tumors the highest LI was noted in undifferentiated tumors. In PNETs the highest score was related to unfavourable course. The lower LI of MCM2 was seen in fibromatosis as well as in alveolar soft part sarcoma and malignant fibrous histiocytoma (inflammatory type).
Conclusion(s) Our results suggest that MCM2 may be a useful marker in prognostication of solid tumors in children. Further studies are necessary in order to assess the clinical value of MCM2 protein in this group of tumors. Supported by: Medical University in Lodz Grant (502-11-752).

OP6.6

Challenges in the diagnosis of malignant primitive tumors of pediatric nasal cavity and sinuses (MPTPNCS). A review of 3 cases

Ngan B.; Taylor P.G.; Phillips Melville J.; Zielenska M.; Shago M.; Chan H.; James H.A.; Forte V.
Div. of Pathology, Hospital for Sick Children, University of Toronto, Toronto, Ontario, Canada

Background A majority of the primitive pediatric malignancies have defined histological, immunohistological and/

or molecular genetic abnormalities. We encountered 3 cases of highly aggressive MPTPNCS presented as huge masses with extension either to the skull base, anterior cranial fossa, orbit or the nasopharynx. The diagnostic results were extremely challenging to interpret. None of the characteristic diagnostic immunohistological or molecular abnormalities was present.

Methods Combined H&E, histochemistry, electron microscopy (EM), immunohistochemistry, cytogenetic and molecular analyses were used. A comprehensive panel of antibodies and PCR procedures for the detection of molecularly defined tumors such as the t(X;18),t(11;22),t(12;22), t(1;13),t(2;13),t(12;15),t(2;5) & t(15;19,NUT/BRD4) by PCR, and appropriate FISH analyses were performed.

Results One case was a EWS/PNET without EWS rearrangement. The patient had a complete remission from the VADRIAC-POG9354 chemotherapy protocol. The only helpful features were rare neurosecretory granules and cell processes. The second case was a high grade pleomorphic sarcoma with myofibroblastic sarcoma features by EM. The only useful diagnostic feature was the presence of fibronexus junctions. The third case was a poorly differentiated carcinoma (?NUT carcinoma variant). RT-PCR for NUT/BRD4 showed a broad range of amplified products and NUT/BRD4-FISH-ve. The most useful features by EM were long intercellular junctions and annulate lamellae.

Conclusion(s) Our experience with the diagnosis of MPTPNCS was challenging. Despite the availability of comprehensive immunohistological and molecular markers, analysis by EM offered crucial information about their histological origins.

OP6.7

Chronic lower respiratory disorders in children: high frequency of viral genomes in nasal-wash and bronchoalveolar lavage

Lunardi F.; Bertuola F.; Barbato A.; Valente M.; Alessandrini L.; Calabrese F.
University of Padua, Padua, Italy

Background Paediatric chronic lower respiratory disorders (CLRDs) include different pathological processes often difficult to recognize and problematic to treat. The role of viruses, well known in acute respiratory diseases is not clearly determined in CLRDs. The purpose of the study was to evaluate the frequency of viruses in CLRDs and nasal-wash specimens (NW).

Methods Polymerase chain reaction (PCR) was used to detect principal respiratory viruses such as Rhinovirus (RV), Cytomegalovirus (CMV), Adenovirus (AV), Influenzavirus A and B, Parainfluenzavirus 1 and 3, Metapneumovirus (MPV), Herpesvirus 6 (HHV6), Epstein-Barr Virus (EBV) and Parvovirus B19 (PV). NW were obtained from 45 children (mean age: 81 months) with CLRDs. Bronchoalveolar lavages (BAL) and NW performed at the same time were analysed by PCR. Other conventional microbiological tools were also used (culture, serology and antigen detection methods).

Results Viral genomes were detected in 32 samples (71%) with 16/32 samples positive for multiple viral genomes (50%). Amplified viral sequences included RV (23/32), HHV6 (12/32), EBV (10/32), CMV (2/32), PV (5/32), AV (4/32) RSV (1/32) and MPV (1/32). In 27/32 (84%) cases the same viral genome, mainly represented by RV, was amplified from NW and BAL.

Conclusion(s) The study shows that high frequency of viral genomes, mainly represented by RV, is present in CLRDs. NW, a less invasive tool, appears to be excellent for viral analysis.

OP6.8

Right-sided diaphragmatic eventration: a rare cause of non-immune hydrops fetalis.

Zankl A.; Osterheld M.; Vial Y.; Beurret N.; Meuli R.; Meagher-Villemure K.; Roth-Kleiner M.
Lausanne, Vaud, Switzerland

Background Congenital diaphragmatic eventration (CDE) is defined as an abnormal displacement of the whole or a portion of an attenuated but otherwise intact diaphragm into the thoracic cavity. Clinically it mimics the features of congenital diaphragmatic hernia (CDH) with displacement of abdominal organs into the thorax.

Methods We report 2 cases of non-immune hydrops fetalis (NIHF) in which autopsy findings revealed an association with right-sided CDE. Both patients born at 30 weeks of gestation presented skin oedema, pleural effusions and ascitis. They died shortly after birth of cardiorespiratory insufficiency with lung hypoplasia and low output failure.

Results The autopsy revealed the presence of herniated visceral organs including part of the liver, small bowel and colon in the right thoracic cavity. But these organs were covered and separated from the thoracic cavity by a membraneous but intact right diaphragm. As for the situation seen in CDH, these displaced organs led to important lung hypoplasia and obstructed venous return. The liver dysfunction resulted from the venous congestion and cardiac failure in extravascular liquid accumulation.

Conclusion(s) CDE is a rare condition resulting from impaired ingrowth of muscle fibres into the diaphragm during the first trimester of gestation. The association of CDE and NIHF has not been previously described.

OP6.9

Amniotic band disruption complex: a fetopathological study of 7 cases

Yacoubi Tahar M.; Lahmar A.; Trabelsi A.; Hmissa S.; Mokni M.

Department of Pathology, F. Hached Hospital, Sousse, Tunisia

Background The amniotic band disruption complex is a rare syndrome characterized by deformations, malformations and redistribution of fetal structures due to their strangulation by fibrous bands. Our aim is to describe the features of the lesions according to the gestational age, to precise the differential diagnosis and to advice the parents for the next pregnancies.

Methods Our study is retrospective, describing 7 cases of amniotic band disruption complex concerning fetuses, diagnosed by fetopathological examination at our department of pathology during a period of 10 years.

Results The maternal age ranged from 17 to 27 years. Consanguinity was found in one case. Two groups of lesions were seen : the first one interesting abnormalities of the skull, the central nervous system and/or of the thoraco-abdominal wall in 4 cases; and the second affecting the members (amputation, syndactily, deformations, bands and strangulating furrows) in all cases. Placenta was abnormal in all cases (Inflammation, short umbilical cord and/or single umbilical artery).

Conclusion(s) The amniotic band disruption complex have an atypical variable spectrum of anomalies affecting all the systems, leading to lethal important defects and sometimes to minor lesions compatible with living neonate. Our series, even it is not very large, confirms the correlation between the age of the setting of the abnormalities and the gestational age.

OP6.10

IDH1 mutations in gliomas

Ohgaki H.; Watanabe T.; Nobusawa S.; Kleihues P.

International Agency for Research on Cancer, Lyon, France

Background IDH1 encodes isocitrate dehydrogenase 1, which participates in the citric acid cycle and was recently reported to be mutated in gliomas.

Methods We assessed mutations in the IDH1 gene in 623 gliomas from 562 patients.

Results IDH1 mutations at amino acid residue 132 (majority, G395A; Arg->His) were frequent in low-grade diffuse astrocytomas (88%) or anaplastic astrocytoma (82%). Similarly high frequencies of IDH1 mutations were found in oligodendrogliomas (79%) and oligoastrocytomas (94%). IDH1 mutations were typically co-present with TP53 mutations in 63% of low-grade diffuse astrocytomas, and with LOH 1p/19q in 64% of oligodendrogliomas. Analysis of multiple biopsies from the same patient (51 cases) showed that there was no case in which an IDH1 mutation occurred after acquisition of a TP53 mutation or loss of 1p/19q. IDH1 mutations were detected in 36/407 glioblastomas (8.8%). Glioblastoma patients with IDH1 mutations were younger (mean 47.9 years) than those with TP53 mutations (55.2 years) or EGFR amplification (60.9 years) and were associated with significantly longer survival (mean 27.1 vs. 11.3 months; $p<0.0001$). IDH1 mutations were frequent in glioblastomas diagnosed as secondary (22/30; 73%), but rare in primary (de novo) glioblastomas (14/377; 3.7%: $p < 0.0001$). IDH1 mutations as genetic marker of secondary glioblastoma corresponded to the respective clinical diagnosis in 95% of cases.

Conclusion(s) IDH1 mutations are very early events in the development of astrocytic and oligodendroglial gliomas, and may affect a common glial precursor cell population. IDH1 mutations are the most reliable molecular marker of secondary glioblastomas available and should be used to complement clinical criteria to distinguish them from primary glioblastomas.

OP6.11

Lymphotoxin-driven hepatocellular cancer

Haybaeck J.; Zeller N.; Wolf J.M.; Wagner U.; Kurrer O.M.; Bremer J.; Weber A.; Iezzi G.; Graf R.; Clavien P.; Thimme R.; Blum H.; Nedospasov S.; Zatloukal K.; Karin M.; Kopf M.; Aguzzi A.; Heikenwalder M.

Institute of Neuropathology, Department of Pathology, University Hospital of Zurich, Zürich, Switzerland

Background Worldwide more than 500 million people are chronically infected with hepatitis B (HBV) or hepatitis C virus (HCV). In about one third of these cases the persistent infection leads to the development of hepatocellular carcinoma (HCC), the most common primary human liver cancer.

Methods Here we show in biopsies from HBV or HCV infected human livers as well as in human HCC samples a drastic increase of the cytokines lymphotoxin a (LTa) and lymphotoxin b (LTb), investigated on mRNA and on protein level. To test whether these cytokines simply correlate or if they are causally linked to disease we generated a mouse model transgenically expressing LTa and LTb specifically on hepatocytes (AlbLTab mice).

Results AlbLTab mice develop chronic hepatitis, resembling chronic hepatitis in humans, in 100% at an age of 9 months. At the age of 12 to 18 months about 30% of these mice develop HCC. Intercrosses with rag1-/- (mice

lacking B and T cells) or IkkbDhep mice (defect in NF-kB signaling) completely abolished the development of chronic hepatitis and HCC development. In contrast, AlbLTab mice backcrossed to tnfr1-/- mice developed hepatitis and HCC.
Conclusion(s) Here, we show a new model of chronic hepatitis induced HCC. Transcriptome analysis at various stages of hepatitis and HCC development reveals many similarities to virus induced hepatitis and HCC in humans and enables to dissect signaling events in AlbLTab, AlbLTab x IkkbDhep and AlbLTab x tnfr1-/-mice.

OP6.12
New genes related to oncogenic senescence in human cancer

Romagosa Pérez-P C.; Lleonart M.; López L.; Artero-Castro A.; Armengol G.; Magrans P.; Castellvi J.; Ramon YCajal S.
Dpt. Pathology, Fundació Institut de Recerca, Hospital Vall d'Hebron, Barcelona, Spain

Background Control of senescence and its biochemical pathways is a crucial factor for understanding cell transformation. Otherwise, embryonic stem cells share some features with carcinogenic cells representing a good model to study senescence bypass mechanisms in cancer. The purpose of the present study was to describe the possible role of RSK4 and other new genes related to senescence in human cancer.
Methods To study the expression of embryonic stem cell genes in primary cells, genetic screening was performed by infecting mouse embryonic fibroblasts (MEFs) with a cDNA library from embryonic stem cells. CIRP and Rplp1 were identified due to their proliferative effect in primary cells. Moreover, these genes plus RSK4, a gene previously described to be related to p53-dependent arrest, were determined by qRT-PCR, immunoblot and immunohistochemestry in different human cancer types. Finally, in vitro studies with different cell lines were used to assess the molecular pathways of senescence control through CIRP, Rplp1 and RSK4.
Results RSK4 was downregulated in malignant and premalignant tumors of colon and kidney. In vitro overexpression of RSK4 induced senescence. Otherwise, CIRP and Rplp1, overexpressed in a subgroup of human cancer, induced the ability to bypass replicative senescence in the absence of p16INK4a, P19ARF and P21WAF1 through enhancing ERK1/2 phosphorilation.
Conclusion(s) These results support the concept that RSK4 may be an important tumor suppressor gene while CIRP and Rplp1 may be considered as oncogenes due to their ability in modulating senescence in opposite ways.

OP6.13
Performance characteristics of a MicroRNA based assay to distinguish mesothelioma from adenocarcinoma

Mansukhani Mohandas M.; Taher Mohammed M.; Benjamin H.; Zhong J.; Rosenwald S.
Columbia University, New York, NY, USA

Background Distinction of mesothelioma from adenocarcinomas, despite the use of multiple immunohistochemical markers can be difficult, and there is a need for better markers. MicroRNAs 18–22nt RNAs that regulate translation are highly preserved in formalin fixed paraffin embedded (FFPE) tissue and highly tissue-specific markers. We evaluated the sensitivity and specificity of a real-time PCR assay using four miRNAs in distinguishing mesothelioma from adenocarcinoma.
Methods Total RNA from FFPE tissue from 38 mesotheliomas and 72 adenocarcinomas was analyzed. Following addition of a polyA tail and reverse transcription, expression levels of four miRNAs were analyzed using gene-specific primers and hydrolysis probes with Minor Groove Binders. The relative expression of one mesothelial-specific and three adenocarcinoma-specific miRs was used to classify the samples as high confidence mesothelioma, low confidence mesothelioma, low confidence adenocarcinoma, or high confidence adenocarcinoma. U6 was used as an amplification control.
Results 35/38 mesotheliomas and 69/72 adenocarcinomas were successfully amplified. The assay correctly identified 34/35 (sensitivity for mesothelioma, 97.1%) and 68/69 adenocarcinomas (specificity for mesothelioma 98.6%). The assay was highly reproducible.
Conclusion(s) A real-time PCR assay using four miRNAs is a highly sensitive and specific marker for mesotheliial differentation, in the differential diagnosis of mesothelioma versus adenocarcinoma.

OP6.14
Preliminary data of a molecular genetic approach to receptor tyrosine kinase family gene EGFR in thymic epithelial tumors (TET)

Marino M.; Sioletic S.; Martucci R.; Gallo E.; Gerardina M.; Lauriola L.; Di Benedetto A.; Ceribelli A.; Milella M.; Petillo L.; Facciolo F.; Palmieri G.; Conti S.
Regina Elena National Cancer Institute, Rome, Italy

Background Several observations indicated sensitivity of relapsing/metastasizing Thymic Epithelial Tumors (TET) to Cetuximab and to Tyrosine Kinase Inhibitors (TKI). Genetic status /regulatory pathways involved in the Receptor Tyrosine Kinase family activity in TET are largely unknown. Recently, a novel EGFR transcriptional regula-

tory mechanism has been described in colonic, breast, head and neck carcinomas depending on the length of a CA repeat in intron 1 [CA simple sequence repeat 1 (CASSRI)] of the EGFR gene. Furthermore, the number of CA repeats was inversely correlated to pre-mRNA EGFR synthesis.
Methods We analyzed a series of TET with respect to the EGFR gene structure by direct DNA sequencing of exon 21, microsatellite analysis of CASSRI locus and to gene copy number by EGFR/CEN-7 FISH Probe mix. KIT and K-RAS mutational status have been also investigated.
Results No mutations in EGFR, KIT and K-RAS relevant exons have been found in the cases analysed so far. Several CASSRI genotypes were found with prevalent 16/16 CA repeats genotype. The presence of long alleles (≥ 18 CA repeats) was rare. Very preliminary observations suggested a correlation between cases with heterozygous genotypes and relapsing tendency.
Conclusion(s) The observed variations in the CA repeats length could result in allele-dependent overexpression of EGFR at the transcriptional level, as detectable by immunohistochemistry. Our preliminary molecular genetic data on EGFR gene structure /regulation could contribute to biologically- targeted therapeutical approaches in TET.

OP6.15
Impacts: planning a European initiative for standardized protein analysis of archival clinical tissues

Kothmaier H.; Faoro V.; Daniele L.; Zamò A.; Rossoni R.; Schott C.; Bussolati G.; Stanta G.; Popper H.H.; Becker F.K.
Medical University of Graz, Institute of Pathology, Graz, Austria

Background The lack of standardized guidelines for protein analysis of archival tissues (AT) seems to have hampered the use of such samples in molecular analyses. IMPACTS is a new European consortium aiming to establish guidelines for AT analyses. Here we focus on the evaluation of protein analysis in AT, fixed with formalin or new fixatives, for research and diagnostic use.
Methods Tissue samples were fixed with formalin (FFPE) or a new fixative (FineFix, Milestone Srl) and inspected by histology. Five sections from three matched samples of each tissue were distributed within the consortium in order to compare the efficiency of protein recovery by immunohistochemistry, Western blot, and protein lysate microarray technology.
Results By applying an optimized protocol, proteins can be successfully extracted from FFPE and FineFix tissues. Moreover, we could show a correlation between immunohistochemical, Western blot, and protein lysate microarray results for each of the tissue fixation procedures. Differences between methods, however, were observed in the total protein yield and staining intensities for antibodies detecting membrane proteins, including E-cadherin, EGFR, and HER2.
Conclusion(s) Analysing proteins from fixed tissue samples can provide critical information for clinical decision making. Although long-term studies for formalin-substitutes such as FineFix are still missing, formalin-free tissue fixation represents a reliable alternative for protein preservation, regarding quality and quantity, as compared to FFPE tissue. The IMPACTS consortium is working towards evaluating AT sample processing for protein analysis and tap into the vast treasure chest of archived samples.

Oral presentations 7

Head & neck pathology

OP7.1
DNA double stranded break repair mechanisms in squamous cell carcinomas of the oral cavity of young and older patients

Da Silva Duval V.; Bohrer Luce P.; Kamel-Reid S.
PUCRS, Porto Alegre, RS, Brazil

Background The aim of the study was to gain further insight into DNA repair mechanisms for oral squamous cell carcinoma (OSCC) in young (< 40 yr.) and older (≥ 40 yr) patients by assessing whether young and older patients differ in their ability to repair DNA double-stranded breaks (DSBs) by both Homologous Recombination (HR) and Non-homologous End-Joining (NHEJ).
Methods DSBs were assessed using UT-SCC cell lines established from young and older patients. Global DNA damage was measured using the Comet assay after cell exposure to ionizing radiation (IR). Cells were irradiated and collected at different moments. After electrophoresis, 200 cells per sample were stained with EtBr, observed under fluorescence and submitted to image analysis.
Results In order to assess global DNA DSB repair, three experiments were performed for all cell lines using the Comet assay, and no differences were found between younger and older patients when comparing irradiated vs. non-irradiated cells. It was observed that both young and old patients' cell lines were able to repair DSBs caused by ionizing radiation in 24 hrs. To test whether there is a deficiency or compensation from one DSB mechanism, the HR and NHEJ was employed using a plasmid-based repair assay to measure the ability of the UT-SCC cell lines to perform DSB repair.

Conclusion(s) Both young and old patients' UT-SCC cell lines showed deficient DBS repair with both mechanisms. However HR efficiency was largely compromised in UT-SCC cell lines from older patients.

OP7.2

Cdc20 immunohistochemical expression is associated with aggressive behavior in squamous cell carcinoma of the oral cavity

Ambrosini Spaltro A.; Farnedi A.; Cocchi R.; Pennesi G.M.; Tosi L.A.; Foschini M.P.
Section of Anatomical Pathology, Department of Oncology and Hematology, University of Bologna, Bellaria Hospital, Bologna, Italy

Background Oral Squamous Cell Carcinoma (OSCC) can show recurrences and lymph node metastases even at an early stage presentation. Therefore numerous studies are performed to found markers of aggressive behaviour. Cell division cycle 20 (Cdc 20) is a regulator of APC/C (anaphase-promoting complex/cyclosome), which regularly degrades cyclins. APC/C activation by Cdc20 is essential for metaphase to anaphase transition. The purpose of this study is to evaluate Cdc20 immunohistochemical expression in cases of OSCC presenting in stage T1-T2 and to correlate it with follow-up.
Methods Twenty-nine cases of OSCC, presenting at T1-T2 stage, were selected. Tissues were formalin fixed and paraffin embedded. From representative blocks, an immunohistochemical analysis for Cdc20 (Santa Cruz Biotechnology, dilution 1:50) was conducted. A semiquantitative evaluation was performed and compared with the clinical outcome. Mean follow up was 40.1 ± 24.4 months (range 7 to 78 months).
Results Cdc20 expression varied from 5% and 60% of the neoplastic cells (mean: 25.9 ± 16.9 %). The follow-up revealed 13 patients with an adverse prognosis: 10 lymph node metastases, 1 recurrence, 2 recurrences with lymph node metastases. Among the 13 patients with an adverse prognosis, 10 exhibited Cdc20 higher than or 30%. Among the 16 patients showing neither recurrences nor lymph node metastases, 12 presented Cdc20 less than 30%.
Conclusion(s) Cdc20 immunohistochemical expression is higher in patients with lymph node metastases and high level of recurrences, in comparison to patients with a more favourable prognosis.

OP7.3

Prognostic value of histological predictors in squamous cell carcinoma of the oral cavity

Andrejevic-Blant S.; Monnier P.; Bron L.; Sandu K.
Institute of Pathology, CHUV-Hospital & Faculty of Biology and Medecine, Lausanne, Vaud, Switzerland

Background Among oral SCC primary site, initial stage of the tumor is a well documented marker of tumor prognosis. Various histological parameters such as pattern of front invasion, tumor thickness, degree of differentiation, inflammatory host response, stromal reaction, the pattern of bone invasion, as well as lymphatic, and perineural invasion, were shown to contribute significantly to the oncological prognosis of these tumors. The aim of our study was to collect retrospectively a number of histological criteria's on a cohort of oral SCC with long term follow up in a attempt to characterize and correlate tumor biology with clinical prognosis.
Methods Between 1995 and 2005, 54 patients were primarily operated for oral SCC. Precise clinical data was fed into a computerized database obtained from patient files. For each patient, paraffin embedded tumor specimens were retrieved and various parameters were evaluated and then correlated with both, local control and patient's survival data.
Results The pattern of front invasion, host inflammatory response, lymphatic and perineural invasion and regional lymph node status were more significant prognostic factors than the T stage status and resection margins in the overall survival and local recurrence rates.
Conclusion(s) More than adequate resection margins, it is the tumor histological pattern, that actually determines local recurrence and the overall patient survival. Adjuvant therapy and outcomes can be better anticipated in low and high risk groups patients according to histological parameters.

OP7.4

A 37 year retrospective analysis of odontogenic tumours

Soluk Tekkesin M.; Olgac V.; Aksakalli N.; Alatli C.
Istanbul University, Institute of Oncology, Department of Tumour Pathology, Istanbul, Fatih, Turkey

Background Odontogenic tumours (OTs) comprise a heterogeneous group of lesions derived from cells that specialise in odontogenesis and its products (dentine, enamel, and cement).These tumours have a specific histological structure that reflects various stages of odontogenesis and diverse clinical behavior.
Methods We rewieved 776 OTs from a total 70.752 cases diagnosed in our department between the years 1971–2008. These specimens were analysed for the distribution of age, sex and site of tumours.
Results Of these 776 OTs, 768 were benign, 8 were malignant. The most common lesions were ameloblastomas (n=197), followed by odontogenic myxomas/fibromyxomas (n = 153), odontomas (n = 149). There was female predominance (n=419, 54%). The posterior mandible was

the commonest site (n=322, 41%), followed by the premolar area of the mandible (n=128, 16.5%) and the anterior maxilla (n = 103, 13%).

Conclusion(s) When we compare our results with other countries, they are same as Africa, but in contrast, in Chile, Mexico, Canada and USA odontoma was the most common tumour, but these reports were published before the third edition of WHO new histological typing of OTs in 2005 which odontogenic keratocyst is included with the OTs and termed keratocystic odontogenic tumour (KCOT). After this new classification, there is few retrospective studies. One of them was reported in China in 2008 and the KCOT was the most common tumour.In this study, we do not included odontogenic keratocyst as a tumour like many of oral pathologists who can not accept it exactly.We have immunopathologic study of the odontogenic keratocysts in progress.

OP7.5

Sclerosing polycystic adenosis of parotid gland with in situ duct carcinoma

Losito N.; Longo F.; Fulciniti F.; Manna A.; Botti G.; Asioli S.; Foschini M.P.
INT Fondazione G.Pascale Napoli, Napoli, Italy, Italy

Background Sclerosing polycystic adenosis (SPA) of the parotid gland is a rare disease that, occasionally, can present features of atypia.

Methods Two cases of SPA affecting a 57-year-old man and a 27 year old woman are presented.

Results On Histological examination both cases showed a focally encapsulated proliferation of enlarged ducts and of glandular acinar structures with lobular growth pattern, embedded in abundant sclerotic hyalinized fibrous stroma. The majority of ducts was cystically dilated and lined by apocrine-type cuboidal cells with large granular eosinophilic GCDFP-15 positive cytoplasm, merging with foam cells resembling sebaceous differentiation. In addition, a focal intraductal epithelial proliferation, sometimes with cribriform growth pattern, always lined by myoepithelial S100, Actin, p63 positive cells was observed. These areas were interpreted as atypical epithelial hyperplasia merging with low grade ductal carcinoma in situ.

Conclusion(s) Up to date, 38 cases of SPA of the salivary glands have been reported but the nature neoplastic or pseudoneoplastic is still under discussion. The presence of foci of in situ duct carcinoma (Skalova et al. Virchows Archiv 2002;440:29–35) together with the demonstration of the clonal nature of the disease (Skalova et al. Am J Surg Pathol 2006;30(8): 939–944) support the hypothesis of a neoplastic proliferation. On the other side, even if recurrences are possible, presently none of the reported cases developed metastases, therefore excluding a malignant nature of the lesion.

OP7.6

EGFR- and downstream mutations in salivary gland carcinomas

Kosmehl H.; Dahse R.
Institute of Pathology, HELIOS Hospital Erfurt, Erfurt, Germany

Background Salivary gland carcinomas (SGC) have limited response to chemotherapy. In new molecular therapy strategies, EGFR overexpression, the absence of drug-resistance EGFR mutations and a wildtype status of KRAS and BRAF are prerequisites for a successful anti-EGFR therapy and may help to better estimate the response of tumor patients to molecular targeted therapy.

Methods We analyzed 65 SGC of the main histopathological types for the expression and the mutation status of EGFR and of its downstream effectors KRAS and BRAF.

Results EGFR over expression has been identified by immunohistochemistry in 75,4% of SGC. The mutation status of EGFR is known to be a molecular marker to identify patients most likely to benefit from EGFR tyrosine kinase inhibitors (TKI). Whereas approximately 10–30% of lung carcinoma contains EGFR mutations, only two TKI sensitivity-predicting mutations were detected in our cohort. Ras is one of the important molecules in the downstream of EGFR signaling pathway. The KRAS gene was mutated in only one sample (1.5%), 64 SGC in this cohort (98.5%) presented the KRAS wildtype. In the absence of KRAS mutations, resistance to anti-EGFR-therapies could be caused by alterations of other members of the RAS-RAF-MAPK pathway. We performed a mutational analysis of BRAF and demonstrate that codon 600 mutations are rare.

Conclusion(s) EGFR- and downstream mutations in salivary gland carcinomas should be taken in to considerations for the selection of targeted therapy strategies using EGFR-blocking antibodies or TKI.

OP7.7

Acinic cell carcinoma with high-grade transformation. a report of 13 cases with immunohistochemical study and analysis of TP53 and HER-2/neu genes

Skalova A.; Sima R.; Vanecek T.; Elmberger G.; Muller S.; Leivo I.; Passador-Santos F.; Geierova M.; Michal M.
Charles University, Faculty of Medicine in Pilsen, Pilsen, Czech Republic

Background High grade transformation (HG) of acinic cell carcinoma (AciCC) is a rare phenomenon characterized by histologic progression to HG adenocarcinoma or undifferentiated carcinoma. We report 13 new cases with examination of HER-2/neu and p53 genes.
Methods HG component was composed of glandular and solid areas with comedonecrosis. HG component of AciCC was characterized by strong membrane staining for CK18 and beta-catenin, nuclear staining for cyclin-D1, and high MIB1 index. HER-2/neu, androgen receptor, C-kit, and EGFR were absent from both LG and HG components. In contrast, S-100 protein, alpha-1-antitrypsin and lysozyme were lost only in HG foci of transformed AciCC.
Results The median age was 61 years (with range from 43 to 76). Lymph node (LN) metastases were found in 10/13 cases (77%). Distant metastases to the lungs (6), pleura (4) brain (3) and peritoneum (1), and paraaortic, paratracheal, and mediastinal LNs (4) were observed. Nine of 13 patients (70%) died from tumor dissemination, all with a median overall survival of 4.3 years (range 1–9).
Conclusion(s) HG transformed AciCC is an aggressive variant of AciCC that often follows an accelerated clinical course resulting in cancer dissemination and death of patients. Any foci of HG morphology qualify the tumor as HG transformed acinic cell carcinoma. HG transformed AciCC seems to have a high propensity for cervical lymph node metastases suggesting the need for neck dissection in management of patients.

OP7.8
Chromosome stability in tonsillar squamous cell carcinoma is associated with HPV and a favorable prognosis

Speel M.E.; Mooren J.J.; Hopman H.A.; Ramaekers C.F.; Claessen M.S.; Klussmann P.J.; Kremer B.
Maastricht University Medical Center, Maastricht, Netherlands

Background Tonsillar squamous cell carcinoma (TSCC) is frequently associated with oncogenic human papillomavirus (HPV). Because data on chromosomal alterations in TSCCs in relation to HPV are scarce, we examined chromosome 1 and 7 copy number changes in relation to the presence of HPV as well as the prognosis of TSCCs.
Methods Seventy TSCCs (36% with HPV-16 integration) with known clinical outcome and cell cycle protein expression profiles were analyzed by fluorescence in situ hybridization (FISH) using chromosome 1- and 7-specific centromere probes. Furthermore 6 HPV-positive, tumor-adjacent dysplasias were analyzed.
Results Chromosome 1 and 7 disomy was present in 26/70 TSCCs (37%) and strongly associated with HPV (16/26; $p=0.001$). Aneusomies for both chromosomes were observed in the remaining TSCCs, of which 24 tumors showed balanced and 20 unbalanced copy numbers (19 cases with higher chromosome 7 copy numbers). Aneusomies correlated significantly with tobacco- and alcohol consumption ($p=0.001$ and $p=0.007$, respectively) and a higher T-stage ($p=0.03$). Both HPV-positivity and chromosome disomy were significantly associated with favorable prognosis ($p=0.003$ and $p=0.011$, respectively). 5/6 HPV-positive, tumor-adjacent dysplasias also showed disomy for chromosomes 1 and 7.
Conclusion(s) HPV-positive TSCCs and their precursor lesions are genetically more stable than HPV-negative lesions, suggesting that HPV integration preferentially occurs in (near) diploid lesions. The high chromosome 7 copy numbers in HPV-negative tumors may point to oncogene involvement such as EGFR, which is inversely related to HPV presence. Furthermore, HPV-positivity and chromosome disomy are favorable prognosticators in TSCC.

OP7.9
Inter-observer reliability for laryngeal preneoplastic lesions

Sarioglu S.; Cakalagaoglu F.; Elagoz S.; Etit D.; Hucumenoglu S.; Koybasioglu F.; Saraydaroglu O.; Seckin S.; Uguz A.; Veral A.; Yilmazbayhan D.; Karaman I.; Ellidokuz H.
Dokuz Eylul University, Inciralti, Izmir, Turkey

Background In order to compare the interobserver reliability (IR) of World Health Organization (WHOC) and Ljubljana Classification (LC) for laryngeal preneoplastic lesions, Turkish Head and Neck Pathology Working Group members started a research project including 43 laryngeal biopsies from 11 centers from 8 cities.
Methods Seven participants evaluated the slides and gave scores according to WHOC as normal, simple hyperplasia, mild, moderate, severe dysplasia, in situ and invasive carcinoma and according to LC as normal, simple hyperplasia, basal-parabasal cell hyperplasia, and atypical hyperplasia, in situ and invasive carcinoma. The results were analyzed statistically.
Results There was positive correlation between all observers for both classifications, but it was mild for 5 comparisons with WHOC and for 4 comparisons with LC, while the rest showed moderate correlation. There was significant difference between participants both with WHOC and LC (Friedman, $p=0{,}000$; $p = 0{,}000$ respectively). Two participants gave lower scores and one participant higher scores than others by both classifications (Wilcoxon Signed Ranks Test with bonferonni correction, $p<0{,}0024$).The mean kappa values for WHOC for 21 comparisons was 0,19+ 0,078 (range 0,03–0,34) and for LC (only 6 participants could be compared with 15 comparisons) 0,25+0,059 (range 0,13–0,32) and kappa values for LC were higher (Wilcoxon Signed Rank Test, $p=0{,}025$).

Conclusion(s) This series with participants from different centers demonstrates that the IR with WHOC and LC are not satisfactory and some observers score the lesions lower or higher compared to the others. LC gives better results. Such activities may facilitate better IR results.

OP7.10
Synchronization of epithelial and stromal cell proliferation in early glottic cancer

Krstulja M.; Petkovic M.; Dragicevic S.; Ljubacev A.; Budisavljevic I.; Blaskan A.
Department Pathology, School of Medicine, University of Rijeka, Rijeka, Croatia

Background Multiparameter investigation of pathological molecular organization is a method of choice in biology. The AgNORs (interphase argirophylic nucleolar organizers), Ki67 S phase specific protein, EGFR (epidermal growth factor receptor) proliferation driver and SPARC (secreted protein acidic rich in cystein) remodelling promotor are widely used proliferation related molecules.
Methods We investigated 16 keratinizing squamous cell carcinomas with the aim to confront pT1a and pT2 glottic tumors. The epithelial cell proliferation and the accompanying stromal cell proliferation were registered with four molecular markers as mentioned above and the results expressed as proliferation index or means. To obtain cell specific results we used double staining immunohistochemistry for the stromal compartment of the tumors.
Results Positive correlation was found between proliferation of neoplastic and stromal cells in glottic pT1a squamous cell carcinoma with Ki67 and SPARC. EGFR score of the neoplastic compartment differentiated between pT1a and pT2 tumors. No positive correlation was found between the AgNOR histochemical parameters (m-AgNOR, p-AgNOR index) and Ki67 immunohistochemical index in the keratinizing pearls.
Conclusion(s) Mutiparameter molecular analysis of keratinized glottic squamous cell carcinoma revealed stage specific proliferation phenomena and differences between the molecular markers of proliferation. We briefly treatise upon the biological implications of these preliminary results.

OP7.11
Aneuploidy detection by DNA image cytometry and FISH recognizes progressive premalignant head and neck lesions

Speel M.E.; Slootweg J.P.; Van Der Laak A.J.; Otte-Höller I.; Bergshoeff E.V.; Haesevoets A.; Takes P.R.; Fleskens J.A.
Maastricht University Medical Center, Maastricht, Netherlands

Background DNA aneuploidy is a potential marker for predicting progression of premalignancies. Because tissue material (biopsies) is often limited, approaches are required to identify aneuploidy in tissue sections. Our aim was to compare DNA ploidy assessment in tissue sections by means of DNA image cytometry and FISH, and to compare their value with that of histopathological diagnosis to recognize precursor lesions at risk for progression.
Methods 7 μm-thick paraffin-embedded tissue sections of 17 oral premalignancies with known DNA ploidy status were stained for MIB-1 expression and DNA content (Feulgen-Schiff procedure), followed by ploidy analysis using QPath software. This approach enabled distinction between truncated tetraploid nuclei and aneuploid nuclei. Subsequent 4 μm-thick sections were analyzed by FISH using chromosome 1 and 7-specific centromere probes. Aneuploidy was indicated by the presence of chromosome imbalances and/or polyploidization. In addition, these approaches were applied to 50 histopathologically classified, primary laryngeal precursor lesions and results were correlated with clinical follow-up data.
Results Both in situ approaches were able to correctly classify the 17 specimens as diploid, tetraploid or aneuploid. Data of the analysis of 50 histopathologically classified, primary laryngeal precursor lesions for ploidy and their significant ($p<0.05$) correlation with clinical outcome will be presented.
Conclusion(s) Tumorigenesis of the head and neck mucosa is associated with the development of aneuploidy, and both DNA image cytometry and FISH can reliably detect aneuploid cells in tissue sections and therefore identify lesions at risk for progression.

OP7.12
Documentation of the sarcomatoid carcinomas of the upper aerodigestive tract (5 cases)

Etit D.; Altinel D.; Bayol U.; Cukurova I.
Izmir Tepecik Training and Research Hospital, Izmir, Turkey

Background Sarcomatoid carcinoma (SC) of the upper aerodigestive tract is one of the difficult diagnostic challenges for surgical pathologists. Histogenesis has been settled in favor of a divergent (mesenchymal) differentiation of a carcinoma, most often a squamous cell carcinoma. Finding the carcinoma and/or its immunohistochemical marker in the metaplastic cells supports the correct diagnosis
Methods SC cases of upper aerodigestive tract were retrieved from the Pathology Department of Tepecik Training and Research Hospital for a two-year period, from 2007 to 2009. The hematoxyline and eosine stained slides

were reviewed. The patients' age and gender and localizations of the lesions and the morphologic/immunohistochemical findings were noted.

Results There were five SCs, four males and one female, with a mean age of 65.2. Four were located on larynx, one was at the base of the tongue. All of the cases had a solid exophytic growth pattern with surface epithelial ulceration accompanying pleomorphic spindle cell component. Premalignant changes in the squamous epithelium has been observed in 3 cases. Range of 7–37 mitosis were detected per 10 high-power field. In 2 cases, atypical mitosis have been identified.

Conclusion(s) Different aspects of clinicopathological implications of 5 cases of sarcomatoid carcinoma of the upper aerodigestive tracts of the head and neck are presented. The results were compatible with the literature.

OP7.13
CTLA-4, IL17A/B/C/D/E/F, PLZF, CD27, FOXP3, RORgammaT and CD70 expression in mucosal melanoma of head and neck

Wang Yiyao B.; Shibata R.; Zhu H.; Delacure M.; Levis W.; Martiniuk F.
New York University School of Medicine, New York, NY, USA

Background Primary mucosal melanoma rarely occurs in head and neck. Cytotoxic T-lymphocyte antigen-4 (CTLA-4) has been shown highly induced in Wnt/β-catenin pathway. CD70 is a co-stimulator in T-cell activation. Recently, a report described IL17 genes observed in a skin melanoma with better prognosis. We examined expression of CTLA-4, IL17A/B/C/D/E/F, PLZF, CD27, FoxP3, RORgammaT and CD70 in 8 mucosal melanomas.

Methods 8 paraffin embedded mucosal melanomas were obtained from 2 major medical centers. All cases arose from sinonasal cavities and nasopharyngeal mucosa (3 male and 5 female, average age 71). RNA was extracted with TRIzol after deparaffinizing with xylene, first strand cDNA synthesis performed, and PCR for HGAPDH as internal control. 2 rounds of nested PCR for IL17A/B/C/D/E/F, RORgammaT, FoxP3, CD27, PLZF, CD70 and CTLA-4 were performed.

Results All mucosal melanomas were diagnosed with confirmatory immunostains. Expression of CTLA-4, IL17A/B/C/D/E/F, PLZF, CD27, FoxP3, RORgammaT and CD70 was detected by PCRs. We found 2/8 positive for CTLA4; 2/8 positive for IL17D; 2/8 positive for IL17E; 2/8 positive for RORgamma T; 2/8 positive for FoxP3; 4/8 positive for CD27; 3/8 positive for IL17A; and 6/8 positive for IL17B. PLZF; IL17C; IL17F; and CD70 were all negative.

Conclusion(s) Although 2 of 8 (20%) samples were detected for CTLA-4 and IL17 genes, results may suggest that CTLA-4 and IL17 expression in mucosal melanomas potentially associated with less aggressive behavior, while majority of mucosal melanomas have worse prognosis.

OP7.14
FAK and C-SRC expression in human benign and malignant thyroid lesions

Michailidi C.; Giaginis C.; Stolakis V.; Alexandrou P.; Klijanienko J.; Delladetsima I.; Chatzizacharias N.; Theocharis S.
University of Athens, Medical School, Athens, Greece

Background Focal Adhesion Kinase (FAK) and c-Src have been reported to regulate tumor growth, invasion, metastasis and angiogenesis. The present study aimed to evaluate the clinical significance of FAK and c-Src expression in human benign and malignant thyroid lesions.

Methods FAK and c-Src protein expression was assessed immunohistochemically in formalin-fixed, paraffin-embedded thyroid tissues obtained from 108 patients with benign (hyperplastic nodules and Hashimoto thyroiditis, $n=48$) and malignant (papillary, medullary, follicular and anaplastic thyroid carcinomas, $n=60$) lesions. The FAK and c-Src positivity, overexpression (expression in more than the mean percentage value), and intensity of staining were assessed in order to compare their expression between malignant and benign thyroid lesions, as well as between Hashimoto thyroiditis and hyperplastic lesions. FAK and c-Src protein expression was statistically analyzed in relation to TNM stage for the subgroup of malignant thyroid tumors and tumor proliferative capacity assessed by Ki67 labeling index.

Results FAK expression provided a distinct discrimination between malignant and benign thyroid lesions ($p=0.00001$), being also associated with follicular cells' proliferative capacity ($p=0.0003$). In malignant thyroid lesions, FAK expression was associated with tumor size ($p=0.0455$), capsular ($p=0.0102$), lymphatic ($p=0.0173$) and vascular ($p=0.0801$) invasion. c-Src expression was only associated with tumor size ($p=0.0169$).

Conclusion(s) The current data revealed that FAK and, to a lesser extent, c-Src expression could be considered of diagnostic utility in thyroid neoplasia. Further studies conducted on distinct malignant thyroid lesions are warranted to delineate their clinical significance and potential use as therapeutic targets.

OP7.15

Helicobacter pylori colonization in patients with and without chronic sinusitis

Emami S.; Dabiri H.; Molaei M.; Noohi S.; Fattahi A.; Safavi Naeini S.; Zojaji H.; Zali M.
Research Center for Gastroenterology and Liver Disease, Tehran, Islamic Republic of Iran

Background It has been suggested that direct reflux of gastric juice into the nasopharynx may cause mucosal edema and inflammation, leading to secondary obstruction of sinus ostia, but the exact mechanism remains unclear. In the present study, we used the PCR to investigate and compare the Helicobacter pylori status of sinonasal mucosa specimens in patients with and without chronic sinusitis.
Methods The study was performed in 97 patients, 32 with and 65 without chronic sinusitis, who were admitted to the department of Otolaryngology of Taleghani, and Erfan Hospitals from 2007 to 2008. Patients that unresponsiveness to full medical treatment were enrolled in sinusitis group. Control group selected from patients without any suspected symptoms or signs of sinusitis.
Results The mean age of the patients was 32.16±9.42 years in S-group and 28.34±8.35 years in C-group. Using multivariate logistic regression model, probable risk factors in sinusitis were evaluate: Sex had no significant role. With positive H.P., risk of sinusitis multiply by 18.24 fold (p-value<0.0001). With positive GER symptoms, risk of sinusitis was 9.83 fold (p-value=0.002). Results of PCR was positive in 23 patients,16 in S- group and 7 in C- group (p-value<0.0001).
Conclusion(s) Helicobacter pylori colonization was investigated in nasal and sinus tissues obtained from 16 patients with chronic sinusitis (in comparison with 6 patients without chronic sinusitis). These results may have interesting implications for a possible role of HP in chronic sinusitis.

Oral presentations 8

Digestive pathology

OP8.1

Optical biopsy with confocal endoscopy diagnosed by pathologist

Ferrer-Roca O.; Da Silva V.; Marcano F.; Santos-Palacios X.
University of La Laguna, La Laguna, Tenerife, Canary Islands, Spain

Background One of the main problems for the endoscopist to use confocal endoscopy is that the images obtained are morphological images closer to pathologist training and far from endoscopist background. For that reason the on line pathology diagnosis (telepathology) is of paramount importance or in case this is not possible an image data mining to extract the most-likely diagnosis to help endoscopists.
Methods We have developed the metadata structure and the ontology capable to be use by the query multimedia standard ISO/IEC 15938–12 y ISO/IEC 24800–3 in order to find out the possible image and diagnosis using the technique of the "query by example".
Results The results are that an endoscopist can get the diagnosis of a confocal images using to query the data base the confocal image.
Conclusion(s) In the present paper we showed how it works and the importance to be use in this and other field of morphological diagnosis in pathology. Particularly when morphological images are used for diagnosis by specialist not trained in histological morphology.

OP8.2

Granular cell tumor of pancreas: a rare entity with a misleading presentation

Cataldo I.; Piazzola E.; Schiavo N.; Pedica F.; Gallotti A.; Butturini G.; Segala D.; Vergine M.; Zamboni G.; Menestrina F.; Capelli P.
Anatomia Patologica, Università di Verona, Verona, Italy

Background Granular Cell Tumors (GCTs) are rare neoplasm arising from Schwann cells with an overall incidence of 0.03%. GCTs develop primarily in dermis of cervicofacial district however any site is possible. Malignant GCTs (MGCT) performs cellular atypia, or metastasize to regional lymph nodes and distant sites and are exceedingly rare. Nowadays, only 5 cases of pancreatic GCT have been reported. We describe a new case of pancreatic GCT.
Methods A 41 year-old woman was admitted to our Hospital for acute abdominal pain. Blood test, computerized tomography (CT), magnetic resonance (MRI) and contrast enhanced ultrasonography (CEU), distal splenopancreasectomy followed by pathological examination were performed.
Results Abdominal-CT showed a cystic enlargement of the main pancreatic duct (MPD) and its secondary branches, whereas Colangio-Wirsung-MRI displayed a stricture of MPD in pancreatic body, associated with a swelling in the tail. At CEU a diagnosis of mucinous neoplasm was assumed. Gross pathological examination revealed a nodular area (diameter: 8 mm) inducing mild constriction of Wirsung duct and cystic dilatation upstream. Microscopically a light partially fringed nodule

composed of clusters of eosinophilic cells with small nuclei and abundant cytoplasm was found. Neoplastic cells revealed positivity to NSE, S100 and CD68, while were negative for CK8/18. The diagnosis of GCT of the pancreas was performed.
Conclusion(s) GCTs are rare lesions. Due to their clinical presentation as nodule bearing constriction in MPD, GCTs are often mistaken for malignant pancreatic neoplasm in pre-operative diagnosis.

OP8.3
Granular complement C3 positive immune complexes are overexpressed in autoimmune pancreatitis and located at the pancreatic ductal epithelium

Detlefsen S.; Bräsen Hinrich J.; Zamboni G.; Klöppel G.
Dept. of Pathology, University Hospital Schleswig-Holstein, Campus Kiel, Kiel, Germany

Background Autoimmune pancreatitis (AIP) is a special type of chronic pancreatitis. Its pathogenesis is largely unknown. Recently, electron dense deposits have been demonstrated at the basement membrane in AIP. Aims of this study were: 1) to characterize the biochemical composition and 2) to evaluate the localization of basement membrane deposits in AIP.
Methods On snap frozen tissue blocks from five AIP patients, five alcoholic chronic pancreatitis (ACP) patients and one normal pancreas, immunofluorescence histochemistry for C1q, C3c, IgA, IgG, IgG4 and IgM and immunofluorescence double staining for C3c, IgG and IgG4 together with CK7, collagen IV and trypsin were performed. The immunofluorescence intensity was graded from 1 (focal, weak) to 4 (diffuse, strong).
Result Granular immune complexes were detected at the basement membrane of the ductal epithelium in 5/5 AIP specimens. They were strongly C3c positive (grade 4) and weakly IgG positive (grade 1) in 5/5 AIP specimens. Besides, they were focally strongly IgG4 positive (grade 2) in 2/5 AIP specimens. In 3/5 ACP specimens, there were few, sparsely distributed immune complexes, which were weakly C3c positive (grade 1). The remaining 2/5 ACP specimens were C3c negative, and 5/5 ACP specimens were IgG and IgG4 negative. In the normal pancreas, no immune complexes were found.
Conclusion(s) C3 positive granular immune complexes are strongly overexpressed at the pancreatic ductal epithelium in AIP. This may explain why the lymphoplasmacytic inflammation in AIP is centered around the pancreatic ducts.

Oral presentations 9

Breast pathology

OP9.1
Analysis of molecular markers in basal-like breast cancers predict poor response to anti-EGFR targeted therapies

Martin V.; Botta F.; Zanellato E.; Molinari F.; Bordoni A.; Crippa S.; Mazzucchelli L.; Frattini M.
Institute of Pathology, Locarno, Switzerland

Background Basal-like breast cancer (BLBC) is one of the most clinical aggressive and poor prognosis form of breast cancer. Generally BLBC patients do not benefit from hormone therapies or anti-Her2 treatments because of their triple-negative phenotype (ER-/PR-/Her2-). With the availability of additional targeted drugs, new pharmaceutical approaches are emerging for BLBCs. In particular, clinical trials with anti-EGFR drugs are currently ongoing. The predictive role of molecular markers in this setting, however, has been poorly investigated.
Methods We analyzed 38 BLBCs patients with a proficient histological profile, a triple negative phenotype and CK5/6 positive expression. PTEN and EGFR protein levels were evaluated by immunohistochemistry (IHC), EGFR gene status was investigated by FISH and EGFR, PIK3CA, K-Ras, N-Ras, H-Ras and BRAF gene mutations were assessed through direct sequencing of DNA extracted from formalin-fixed paraffin-embedded tissue sections.
Results IHC revealed EGFR protein overexpression in 29/38 (77%) and PTEN loss of expression in 28/38 (74%) patients. FISH identified EGFR gene copy number gain in 17/33 (51%) patients (FISH+). Sequencing analyses identified PIK3CA mutations in 3/38(8%) patients, whereas no mutation has been found for the other investigated genes. Overall, among FISH+ BLBCs, 12/17(70%) showed PTEN loss of expression and/or PIK3CA mutation. FISH+ profile was statistically related to patients' older age (> 50 years) ($p<0.02$).
Conclusion(s) Our results suggest that: 1) the efficacy of anti-EGFR drugs in BLBCs patients could be impaired by PTEN alterations; 2) targets other than EGFR should be identified to treat BLBC patients younger than 50.

OP9.2

Columnar cell lesions are the early precursors of some forms of invasive breast carcinoma: a new genetic map for the evolutionary pathway of low nuclear grade breast neoplasia (LNGBN) family

Abdel-Fatah Mohamed Ahmed T.; Powe G.D.; Lambros M.; De Biase D.; Savage K.; Mackay A.; Reis-Filho J.S.; Ellis I.O.

Division of Pathology, School of Molecular Medical Sciences and Nottingham University Hospitals Trust, University of Nottingham, Nottingham, Nottinghamshire, United Kingdom

Background There is evidence to suggest that a number of low nuclear grade invasive breast cancers (LNGBC) and putative precursor lesions may consist in a family of interrelated lesions.

Methods To identify the molecular genotypic profile of lesions belonging to the LNGBN family, 15 LNGBCs and matched coexisting columnar cell lesions (CLLS), ductal carcinoma in situ (DCIS) and lobular neoplasia (LN) were microdissected and subjected to high-resolution array-comparative genomic hybridization (aCGH), single nucleotide polymorphisms (SNPs) analysis, and loss of heterozygosis analysis. Results were validated using fluorescence and chromogenic in situ hybridisation and immunohistochemistry.

Results We observed that at the genetic level, lesions from the same patient displayed remarkably similar patterns of genetic aberrations (Spearman's correlations 0.55–0.89; $p<0.00001$). All CLLs, low grade DCIS, LN and their matching invasive carcinoma harboured gain/amplification of 1q31–32 and loss of 16q12, 16q21 and 16q23. In addition to the aberrations found in CCLs, in situ and matching invasive components displayed additional genetic aberrations. Amplification of cyclin D1 was detected by CISH in lobular carcinoma and their matching LN and flat epithelial atypia.

Conclusion(s) Our results provide strong circumstantial evidence to suggest that CCLs are the earliest morphologically identifiable non-obligate precursors of more advanced lesions in the LNGBN family and that loss of 16q and gain 1q are the earliest genetic changes in this family of lesions that activate luminal pathway.

OP9.3

Genetic similarities and differences in duct carcinoma in situ of the breast

Flamminio F.; Morandi L.; Foschini M.P.; Eusebi V.

Section of Anatomical Pathology, Department of Oncology and Hematology, University of Bologna, Bellaria Hospital, Bologna, Italy

Background It has been suggested that ductal carcinoma in situ (DCIS) develops within a single lobe. This view has been challenged by a study of DCIS using large sections. It was found that well differentiated (G1) DCIS/DIN1 is a multicentric condition in 76.9% of the cases. Aim of the study is to find out genetic similarities (clonality) or differences among multiple foci of DCIS.

Methods Ten randomly selected cases of multiple DCIS foci on large sections were laser-microdissected and studied for mtDNA analysis and for Comparative Genomic Hybridization analysis (CGH).

Results Five cases DCIS were G1 DCIS/DIN1, five cases were G2 DCIS/DIN2. The mtDNA analysis indicated that four cases of G1 DCIS/DIN1, distant more than 30 mm, showed mtDNA differences. The fifth case displayed foci with mtDNA differences, even if located more closely (12 mm). Three cases of G2 DCIS/DIN2, distant 11, 35, 72 mm respectively, showed similar mtDNA features. Two cases, distant 26 and 40 mm respectively, showed mtDNA differences. The CGH analysis indicated that three cases of G1 DCIS/DIN 1, distant more than 48 mm, showed genomic differences. Two cases, distant 12 and 30 mm respectively, showed same changes. Two cases of G2 DCIS/DIN2, distant 35 and 72 mm respectively, showed same alterations in common; three cases, distant 11, 26 and 40 mm respectively, showed different genomic profile.

Conclusion(s) Distance is not the only discriminant to establish the origin of multiple foci of DCIS from the same lobe.

OP9.4

High resolution array comparative genomic hybridization (ACGH) identifies mouse double minutes 4 (MDM4) as one of the early genetic changes in breast cancer development: mdm4 is a new independent prognostic and predictive marker

Abdel-Fatah Mohamed Ahmed T.; Powe G.D.; Lambros M.; Reis-Filho J.S.; Ellis I.O.

Division of Pathology, School of Molecular Medical Sciences and Nottingham University Hospitals Trust, University of Nottingham, Nottingham, Nottingham, Nottinghamshire, United Kingdom

Background Genome-wide aCGH identified recurrent amplification/gain of chromosome 1:202,752,134–202,862,753 in 86% and 7% of low (LGBC) and high grade breast cancers, respectively. MDM4 gene maps to this locus. We hypothesised that it may be a candidate oncogene and tested this hypothesis by determining its

association with clinical outcome and biological features in BC.

Methods MDM4-mRNA expression levels were assessed in 2 independent sets of gene expression arrays. Protein expression levels were assessed using immunohistochemistry in series of 1081 BCs with long term follow up and series of 140 cases of LGBCs with matched normal breast tissue and precursor lesions.

Results MDM4 mRNA expression levels significantly correlated with copy number (Pearson's correlation$n$=0.55, p= 0.0001) and this gene is overexpressed when amplified (Mann-Whitney U test p = 0.0018). Mdm4 was overexpressed in 17% of BC and was associated with low grade, ER+ and normal expressions of p53, ATM and BRCA1. In cases showing coexistent precursors with invasive component, MDM4 expression was identical in both lesions. On multivariate analysis that included NPI, MDM4-overexpression was an independent prognostic marker for patients survival outcomes [HR, 0.4; p<0.0001]. In high risk patients who had received systemic adjuvant therapy, MDM4-overexpression predicted better response to both hormone- [HR, 2.7; p< 0.0001] and chemo-therapies [HR, 6.7; p=0.008].

Conclusion(s) Mdm4 is an independent prognostic and predictor of BC providing new avenues for therapeutic intervention.

OP9.5

A curious association between breast lobular neoplasia and proliferation of myoepithelial/ basal cells

Shousha S.; Peston D.
Charing Cross Hospital, London, United Kingdom

Background Staining for E-Cadherin differentiates between in situ lobular neoplasia (negative) and ductal carcinoma in situ (positive). Cases where positive and negative cells are seen in the same foci have been described in the literature and interpreted as mixed in situ ductal and lobular neoplasia. We here present 3 cases of in situ neoplasia where E-Cadherin positive and negative proliferating cells were present in the same foci, but the positive cells proved to be of myoepithelial/basal type rather than 'ductal' type

Methods The three patients presented with breast lumps consisting mostly of multiple solid foci of in situ neoplasia. One case was also associated with small foci of invasive lobular carcinoma. Sections were stained for E-Cadherin, CD10, smooth muscle actin (SMA) and cytokeratins (CK) 5/6, 14 and 8/18.

Results The in situ lesions consisted of well defined solid structures composed of two separate populations one being neoplastic lobular (negative for E-cadherin, CD10, CK 5/6 and 14 and SMA; and positive for CK 8/18 and ER), and the other is myoepithelial/ basal (positive for E-cadherin, CD10, CK 5/ 6, 14 and 8/18 and negative for SMA and ER).

Conclusion(s) We suspect that these combined lobular myoepithelial/ basal cell lesions are more common than is thought, and may include at least some of the cases reported as mixed ductal/ lobular in situ carcinoma. The cases emphasize a close relationship between proliferation of lobular and myoepithelial/ basal cells, in certain circumstances, that deserves further investigation.

OP9.6

A new method of complete shaved margin assessment to identify a subgroup of breast cancer patients who might not require radiation therapy; A cohort study in japan

Ichihara S.; Sato Y.; Hayashi T.; Hasegawa M.; Moritani S.
Nagoya Medical Center, Nagoya, Aichi, Japan

Background Radiation reduces local recurrence in the breast following breast conservation surgery. There is, however, controversy as to the necessity of radiation of breast in all patients. We have developed a new method of complete shaved margin assessment in wide local excision (Histopathology 2001,39,85–92, Rinsho Byori 2003,51,905–909.) to identify a subgroup who might not require radiation therapy.

Methods Using an adjustable mould to prevent the three-dimensional specimen from distorting during fixation, the new method requires fewer blocks than sequential slicing to guarantee the negative margin. We prospectively studied consecutive 103 wide local excisions (Stage 0=15, Stage I= 53, Stage IIA=26, Stage IIB=8, Stage IIIA=1) examined by this method during a two year period between June 2003 and May 2005.

Results To date, of ninety cases with margin negative, only two patients (2.2%) developed local recurrence and four, distant metastasis. One patient with local recurrence was considered due to lymphatic spread. The other case was considered as a true multicentric basal-like carcinoma.

Conclusion(s) In conclusion, our cohort study suggests that the negative margin assured by complete shaved margin evaluation showed very much lower recurrence rates after breast conservation surgery for breast cancer even if radiation therapy is omitted.

OP9.7

Anti COL11, a new marker of infiltrating breast cancer

Garcia Pravia C.; Fuentes Martinez N.; Garcia Ocaña M.; Del Amo Iribarren J.; De Los Toyos J.; Fresno Forcelledo Florentino M.; Simon Buela L.; Barneo Serra L.
Hospital Universitario Central de Asturias, Oviedo, Asturias, Spain

Background Early and accurate diagnosis of breast cancer can be achieved by core biopsy. Pitfalls and problems in differential diagnosis with benign lesions (e.g. sclerosing adenosis) can occur when dealing with a limited sample of tissue. We have validated the new antibody anti-proCOL11A1 in this setting.
Methods 52 benign and 51 malignant samples of breast tissue were evaluated. Gene expression on a subset of the above samples was evaluated by Q-RTPCR. A new polyclonal antibody anti-proCOL11A1 against the less homologous region between proCOL11A1 and other procollagens was generated. Immunostaining was double blind scored by two pathologists and by means of the image analysis software Qwin. Sensitivity and specificity were depicted as a receiver operator characteristics (ROC) analysis.
Results Q-RT-PCR showed overexpression of COL11A1 gene in malignant samples. Anti-proCOL11A1 stained fibroblasts in 98% of malignant samples, and in 13% of benign samples. Specificity and sensitivity were 92% and 96% respectively. When we compared sclerosing adenosis (SA) and infiltrating ductal breast cancer (IDC), 11% of SA and100% of IDC were positive for anti-proCOL11A1. Specificity and sensitivity were 96 and 98%, respectively.
Conclusion(s) The new antibody anti-proCOL11A1 recognizes desmoplastic fibroblasts of IDC and can be useful for differential diagnosis with benign lesions, particularly sclerosis adenosis.

OP9.8

Are Src kinase family members (SKFMS) expressed in human breast cancer?

Elsberger B.; Zino S.; Jordan F.; Shiels P.; Edwards J.
Glasgow Royal Infirmary/ University of Glasgow, Glasgow, Scotland, United Kingdom

Background The aim of this study was to assess the levels of Src kinase and SKFM expression in breast carcinomas.
Methods m-RNA expression of eight SKFMs was assessed by quantitative real time PCR in 52 patients with invasive breast cancer.
Results Median age of the patients was 60 yrs. Median size of breast cancer was 25 mm, 42% were pathologically graded G2 and 50% G3. ER status was known in all patients (18 ER neg/34 ER pos). 60% of breast cancer patients were LN positive. Every SKFM expression was quantified in all tissue samples. Src and Lyn were most and Blk was the least expressed SKFM. No association was observed between SKFM and tumour grade, size and LN positivity. c-Src (p=0.01) and Fyn (p=0.03) were expressed at higher levels in lobular compared to ductal carcinomas, whereas Yes (p=0.006) was only expressed in ductal carcinomas. Lck and Lyn were expressed at higher levels in ER negative tumours compared to ER positive tumours (p=0.03, p=0.01). All SKFMs correlated with c-Src expression; strongest correlation observed was with Lyn (p<0.001, CC=0.805) and least with Yes (p=0.003, CC= 0.489). High Fgr expression was significantly associated with decreased disease specific survival in ER positive patients (mean: 39 months versus 123 months, p=0.014).
Conclusion(s) Src and Lyn are expressed in higher levels in invasive breast cancer tissue. Only Fgr was associated with decreased disease specific survival, especially in ER positive patients. c-Src, Lck, Lyn, Fyn and Yes warrant further investigations in a larger cohort.

OP9.9

Characterization of oncocytic breast carcinoma

Ragazzi M.[1]; Reis-Filho J.S.[2]; De Biase D.[1]; Ramadan Sezgin S.[3]; Lambros B.M.[2]; Farnedi A.[1]; Tallini G.[1]; Eusebi V.[1]
[1]Department of Haematology and Oncological Sciences "L. &A. Seragnoli", Section of Anatomical Pathology, Ospedale Bellaria, University of Bologna, Bologna, Italy, [2]The Breakthrough Breast Cancer Research Centre, Institute of Cancer Research, London, United Kingdom, [3]Department of Pathology, Anadolu Medical Center, Kocaeli, Turkey

Background Bona fide oncocytic breast carcinomas (OC BCs) are composed of mitochondria-rich (mt-rich) cells and there are only few cases described in literature. Our aim is to characterize the morphological and immunohistochemical features of mt-rich and OC BCs.
Methods The morphological and immunohistochemical characteristics of 14 selected OC BCs were compared with those of 84 consecutive BCs. Immunohistochemistry was performed in both cohorts with antibodies for Ab anti-mitochondria, GCDFP-15, chromogranin, estrogen receptors, progesteron receptors, androgen receptors, c-erbB2, CK7, CK14, EMA, CD68. Positivity for the anti-mictochondria antigen was estimated by immunohistochemistry (Lab Vision, Ab-2, Clone MTC02) and scored based on staining intensity and percentage of positive cells (≥ 70% 3+: OC BCs; < 70% 3+/2+: mt-rich BCs).
Results 19 out of 84 BCs were reclassified as "OC" with overall immunohistochemical pattern not different from bona fide OC cases. 10 out of 84 BCs were reclassified as "mt-rich".
Conclusion(s) Till now, the incidence of mt-rich/OC BCs has been underestimated. OC BCs have distinct morphological and immunohistochemical features. Our results and previous molecular genetic data support the contention that mt-rich/OC BCs are a distinct entity.

Oral presentations 10

IT in pathology - Miscellaneous

OP10.1

Radiologic-pathologic correlation: novel developments in the way pathologists incorporate multimodal imaging findings into pathology

Furuya K.; Maeda T.; Kikuchi T.; Ishimaru Y.; Nakamura S.; Miyagawa M.
Ehime Prefectural Central Hospital, Matsuyama City, Ehime Prefecture, Japan

Background The remarkable progress has achieved in information technology related to medicine and the consequent incorporation of radiologic findings into pathology has improved the understanding of the radiologic-pathologic correlation and has encouraged research.
Methods Conferences - based on multimodal radiologic imaging including PET-CT and pathological imaging, wherein gross and microscopic images are obtained through virtual microscopy - have brought to light studies such as (1) Relationships between the hepatocellular carcinoma (HCC) gross types, dedifferentiation (DD) score and DD gradient (DD-G) and FDG uptake. (2) Pulmonary cryptococcosis and FDG-PET, and (3) Two-step autopsy: Dissecting some organs along the axial plane and then assembling all the fragments of each organ.
Results 1. The 179 cases of surgical resection of HCC comprised 4 gross types. Nodular HCCs were further classified into the macro-subnodular and micro-subnodular types. The gross types were strongly correlated with DD scores, DD-G and FGD uptake and efficacy of TAE and RFA. These novel indices and division of nodular HCCs into 2 subtypes have useful clinical applications. 2. Of 4 patients with pulmonary cryptococcosis, 2 patients had a remarkably high FDG uptake, and their microscopic findings suggested FDG uptake by the fungi. 3. With the two-step autopsy, most clinicians were more inclined to use the radiologic-pathologic correlation on near position to pathomorphology.
Conclusion(s) Radiologic-pathologic conferences bring to light ongoing developments in research and encourage original research.

OP10.2

Texture classifiers for breast cancer outcome prediction

Konsti J.; Ahonen T.; Lundin M.; Joensuu H.; Pietikäinen M.; Lundin J.
University of Helsinki, Helsinki, Finland

Background Development of virtual microscopy and more efficient texture classification algorithms facilitates automated classification of whole-slide tumor samples.
Methods Tissue microarray breast cancer samples (n= 1928) from the FinProg series were digitized using whole slide scanning. A teaching set of 30 samples were annotated by an experienced breast pathologist. Local binary pattern (LBP) texture features were extracted from sub-samples, using a Matlab algorithm. LBPs from teaching set were clustered into 50 clusters with K-means clustering. LBP cluster frequencies in the histological images for the remaining cases (n = 1898) were extracted. A logistic regression model was fitted with a split sample method, using randomly 50% of the data as a training dataset. Clusters were compared to histological grading, by using 10-year distant disease free survival (DDFS) as an endpoint.
Results The AUC-values in the train set for the LBP texture classifier was 0.61, as compared to 0.63 for histological grade alone. By adding histological grade to the texture classifier model, AUC-value increased significantly to 0.69 (p=0.0009). In the test set the texture classifier was a significant predictor of 10-year DDFS with an AUC of 0.58 (CI95% 0.54–0.63), but did not improve the accuracy when added to a model which included histological grade (AUC 0.64; p = 0.61).
Conclusion(s) Automated classification of tumor samples is feasible. We were able to construct a texture classifier that significantly predicted 10-year DDFS in a large series of patients with breast cancer. Further studies are needed to select appropriate training image datasets to improve the classification accuracy.

OP10.3

A cognitive approach to microscopy analysis applied to automatic breast cancer grading

Roux L.; Tutac A.; Veillard A.; Dalle J.; Racoceanu D.; Loménie N.; Klossa J.
Université Joseph Fourier, Singapore, Singapore

Background Analysis of medical images in histopathology is a tedious manual work sometimes inconsistent and subjective. Our project aims at developing a cognition-driven visual explorer for pathology; the first proof of concept focuses on the domain of breast cancer grading.
Methods We propose a radical change in medical practice by introducing a cognition-driven medical imaging environment facilitating decision-making for histopathology based on modelisation. The cognitive microscope will be effectively using dynamic knowledge bases, rules and medical ontologies in order to setup the bases of a cognition-driven medical imaging. Semantic approaches

for indexing, retrieval and visual positioning, based on medical ontologies, will enable the use of multi-scale interactive image analysis, semantic annotation and browsing of different modalities. Pervasive adaptation and a continuous learning of implicit medical knowledge will maintain the quality level of the analysis performed by the system.

Results A first prototype has been developed. It can perform breast cancer grading, semantic indexing, image analysis using medical knowledge, and validation through CBIR (content-based image retrieval).

Conclusion(s) With the cognitive microscope, the pathology diagnosis accuracy will be enhanced by integrating earlier stage diagnostic modalities including mammography, breast echo, and clinical information (such as history and physical examination) as well as the use of stored expert knowledge in similar virtual slides, such as indicators, reasoning and decision-making, enabling safer decision-making for histopathology.

OP10.4
Arrangement of large scale web slide seminars. Experiences from the ECP 2007 and ECP 2009

Lundin M.; Konsti J.; Lundin J.
Department of Oncology, Institute of Clinical Medicine, University of Helsinki, Helsinki, Finland and Folkhälsan Research Center, Helsinki, Finland

Background In 2007 the WebMicroscope team arranged the web slide seminars of the ECP, with more than more than 100 speakers and 800 registered participants. Based on experiences from this event, an improved administration system was introduced for the ECP 2009.

Methods In 2007 text and image material was collected by the chairs and organizers of the congress, and indexed by the webmicroscope team. In 2009 this task was distributed on the 126 speakers, who could edit their own cases, inspect the result in real-time, and function as a discussion moderator.

Results In ECP 2007 all 154 seminar slides were digitized by the WebMicroscope team, but 2 years later a substantial proportion was expected to be scanned by the speakers. After upload, all files were automatically converted to a wavelet file format. To enable fast viewing over the internet, a network of mirror servers was setup. A connection speed measurement tool automatically guided the user's browser to use the optimal server. In ECP 2007 the average viewing speed with the network was 3.1 Mbit/s, as compared to 1.9 Mbit/s using single servers. A good viewing speed (>2Mbit/s) was observed in 32 of 37 countries (86%), compared to 25 of 37 (68%) using single servers. An improved monitoring system was implemented for the ECP 2009.

Conclusion(s) Arrangement of large scale web based slide seminars requires careful planning and a networked design.

OP10.5
Computer-aided image analysis: expanding the boundaries of digital pathology

Dobson L.; Conway C.; Colgan O.; Costello S.; O'Shea D.
SlidePath, Dublin, Ireland

Background The introduction of personalized medicine regimes has led to a growing incidence of the use of biomarkers for diagnostic purposes. Nonetheless, many recent reports have documented the variability and subjectivity of manual interpretation of biomarker expression in immunohistochemically (IHC) stained slides, highlighting the lack of tools for objective and standardized assessment.

Methods With digital microscopy gaining momentum in today's laboratory environment, the potential for Image Analysis to play a role in diagnostic pathology is greatly anticipated. SlidePath have created a number of algorithms for quantification of nuclear, membrane, and intracellular biomarker expression in full face sections, annotated regions of interest or Tissue Microarray (TMA) cores. In addition, SlidePath have developed a bespoke algorithm which specifically quantifies HER-2 protein expression, taking into consideration both the intensity and continuity of membrane bound staining.

Results With particular focus on breast pathology and HER-2, research findings will be presented demonstrating how Image Analysis can prove to be an indispensable support tool for pathologists in order to diagnose and monitor disease progression. In addition, the potential of combining TMA technology with Image Analysis to substantially accelerate biomarker validation studies will also be discussed.

Conclusion(s) Computer-aided Image Analysis has great potential to offer objective and quantitative measurement of IHC staining in digital slides, whilst concomitantly introducing a high degree of automation. This seminar details the promises and pitfalls of Image Analysis technology and describes how software solutions for virtual microscopy have progressed far beyond the development of digital slide viewers.

OP10.6
Development of an online image analysis platform for digital whole slide specimen

Lundin J.; Konsti J.; Lundin M.
Institute of Clinical Medicine and Folkhälsan Research Center, University of Helsinki, Helsinki, Finland

Background Virtual slides consist of massive amounts of data and are therefore commonly kept on image servers. Application of image analysis on whole slide specimens opens up entirely new possibilities for probing large specimen areas. However, downloading the image data to the user's computer for the analysis is not an efficient solution. Here we introduce an approach were the image analysis is performed server-side and discuss the advantages.
Methods A web application was programmed that combines the functionality of an image web server (IWS) and image processing software (ImageJ and Matlab). Whole slide images of tissue microarray slides stained with immunohistochemical (IHC) methods were digitized with a virtual slide scanner (Zeiss Mirax Scan) at a 0.23 micrometer/pixel resolution and uploaded to the image web server (www.webmicroscope.net).
Results Image analysis algorithms developed with two commonly used image processing software were successfully implemented to be run server-side. Algorithms for IHC and fluorescence in-situ hybridization quantization were applied on the whole slide specimens. Results of the analyses were stored in a database which contains other clinico-pathological data related to the examined samples.
Conclusion(s) It is feasible to run computer vision algorithms server-side and to apply them on digitized wholes slide specimen. The server based "cloud computing" approach has many advantages, which include speed, standardization of image analysis procedures, immediate implementation of updates and no need to install software other than a web browser.

OP10.7
Knowledge modeling of breast cancer grading using OWL-DL formalism

Tutac Eunice A.; Racoceanu D.; Loménie N.; Leow Kheng W.; Roux L.; Cretu I.V.; Putti T.
Politehnica University of Timisoara, Timisoara, Timis, Romania

Background Histopathological grading of breast carcinoma has become a highly relevant assessment tool for prognosis in modern pathology practice. Sharing this domain knowledge among concerned people (pathology community/academia) or software agents is useful for alleviating inter-observer agreement inconsistencies, therefore terminology consensus modeling is required. With the ontologies' advent in the semantic web world, using this formalism in medical domain captured a lot of interest in the recent years.
Methods We propose a novel ontology-based modeling of breast cancer grading (BCG) in an interactive approach. We use Ontology Web Language-Description Logics (OWL-DL) combined with Semantic Web Rules Language (SWRL), which provides high level of expressivity and reasoning. Nottingham Grading System's concepts such as tubule formation, nuclear pleomorphism, mitotic figures are encoded as classes in Protégé OWL-DL. Medical rules assigned to each criterion, complemented with slide analysis visual information are represented as properties.
Results Based on expert guidance from Pathology Department of Singapore National University Hospital which provided us breast cancer biopsy slides, we collected the domain knowledge information and translated into a BCG ontology model. Validation in terms of consistency checking and class hierarchy automated classification was achieved under Pellet reasoner.
Conclusion(s) Hybrid modeling (structural and rule component) is a non-trivial task from complexity standpoint. However, we gained expressivity and concept satisfiability via OWL-DL reasoning service. We envision an accurate BCG knowledge modeling represents a solution for improving the inter-observer k-coefficient. Currently, integration in a virtual microscope platform to assist in breast cancer diagnosis is ongoing.

OP10.8
The correlation between nuclear size and protein expression level of prognostic and predictive biomarkers in breast carcinoma by computer assisted technology

Kolatt T.; Lifschitz-Mercer B.; Solar I.
Applied Spectral Imaging, Migdal Haemek, Israel

Background Nuclear size and pleomorphysm is a morphologic feature for histologic grading of breast cancer, considered as an important prognostic factor. The immunohistochemical assessment of the hormonal receptors ER and PR, the proliferation marker KI67 and mutations of the tumor suppressor gene P53, serve as additional prognostic biomarkers. New image analysis tools allow, for the first time, to explore the nuclear size versus protein expression level relationship in breast carcinomas.
Methods Formalin fixed araffin embedded sections of breast carcinoma are subjected to H&E and immunohistochemical staining. An automatic scoring analysis through computer assisted technology provides for each detected nucleus its physical size and its expression level as deduced by its color and optical density (scores 1+, 2+, 3+). Population of such nuclei forms the bi-variant distribution function.

Results There is a tight positive correlation between the nuclear size and the expression level. Size Probability Distribution Functions (PDFs) of nuclei that express proteins that reside within normal breast tissue (ER, PR), are made out of "normal population" and "tumor population". Size PDFs for nuclei that over-express markers which are specific for tumor progression (KI67, P53) do not show the "normal population" component.
Conclusion(s) The size over-expression relation provides a new viewpoint of tumorogenesis and etiology as it may be referred to as an evolution track sampler and not as a snapshot of the tumor state alone. Moreover, it may serve as a new quantitative index for prognosic evaluation.

OP10.9
How much of diagnostic pathology research is not formally funded?

Khong Y.
SA Pathology, North Adelaide, South Australia, Australia

Background Workload increase, workforce shortage, a dollar-value corporatisation culture and a global financial crisis are likely factors to affect the research output of diagnostic pathologists by increasing the need to have all research formally funded.
Methods The proportion of research that is funded that was published in three clinical pathology journals (Pathology [Australia and New Zealand], Journal of Clinical Pathology [United Kingdom] and American Journal of Clinical Pathology [United States of America]) in 2008 was measured against type of publication (original, case reports, reviews, other) and subspecialty.
Results Of the 591 papers, 181 (30.6%) were funded and 410 (69.4%) were unfunded. Papers classified as original research (240 of 395; 60.8%) were more likely to be funded than case reports (90/104; 86.5%) or reviews (73/84; 86.8%) (chi-squared test $p<0.0001$). 269 of 383 (70.2%) anatomical pathology/cytology, 49 of 78 (62.8%) haematology/transfusion medicine, 31/40 (77.5%) microbiology/virology, and 40/59 (67.8%) chemical pathology and 16/18 immunology publications were unfunded (chi-squared test NS). 491 papers were identified as emanating from pathology laboratories: 249 of 307 papers from hospital pathology laboratories and 92/173 papers from university departments of pathology were unfunded (chi-squared test $p < 0.0001$); the affiliation of 11 laboratories was unclear.
Conclusion(s) A sizeable proportion of diagnostic pathology research, including original research, which tended to be funded, would not be realised if pathologists were to rely solely on formal funding for their research.

Oral presentations 11

Breast pathology

OP11.1
Does chromosome 17 centromere copy number predict polysomy in breast cancer? A fluorescence in situ hybridisation and microarray-based cgh analysis

Marchiò C.; Lambros M.; Gugliotta P.; Verdun Di Cantogno L.; Botta C.; Pasini B.; Tan D.; Mackay A.; Bussolati G.; Ashworth A.; Reis-Filho J.S.; Sapino A.
Dept of Biomedical Sciences and Human Onncology, Turin, Italy

Background Approximately 8% of breast cancers show increased copy numbers of chromosome 17 centromere (CEP17) by fluorescence in situ hybridisation (FISH) (i.e. average CEP17 signals > 3.0 per nucleus). Currently, this pattern is believed to represent polysomy of chromosome 17. HER2 amplified cancers harbour complex patterns of genetic aberrations of chromosome 17, in particular involving its long arm. We hypothesised that aberrant copy numbers of CEP17 in FISH assays may not necessarily represent true chromosome 17 polysomy.
Methods Eighteen CEP17 polysomic cases and 10 CEP17 disomic cases, as defined by dual-colour FISH, were studied by microarray-based comparative genomic hybridisation (aCGH), which was performed on microdissected samples using a 32K tiling-path bacterial artificial chromosome microarray platform. Additional FISH probes for SMS (17p11.2) and RARA (17q21.2) were employed as references for chromosome 17 copy number.
Results Eleven out of the 18 polysomic cases harboured gains of 17q encompassing the centromere, one displayed 17q gain sparing the centromeric region and only one could be defined as polysomic. The remaining five cases displayed amplification of the centromeric region. Among these, one case, showing score 2+ by IHC and 8.5 HER2 mean copy number, was classified as not-amplified by HER2/CEP17 ratio and as amplified by HER2/SMS ratio.
Conclusion(s) True polysomy of chromosome 17 is a rare event in breast cancer and CEP17 copy number > 3.0 in FISH analysis is frequently related to gain or amplification of the centromeric region.

OP11.2
Effects of mammographic screening in trieste (Italy) at the end of first round

Zanconati F.; Haxhiymeri O.; Martellani F.; Romano A.; Bonifacio D.; Leonardo E.; De Pellegrin A.; Zacchi A.; Bandiera V.; Giudici F.; Franzo A.; Tonutti M.; Di Bonito L.
UCO Citodiagnostica e Istopatologia, Trieste, Italy

Background Trieste is one of the italian areas with the highest incidence of breast carcinoma (Age Standardazied Ratio European Incidence 133,6). Mammographical screening has been active since 2006 involving women (50–69 years old).
Methods 33000 women were invited to undergo screening mammography (1/1/ 2006–12/31/2007) with compliance equal to 50%. We wanted to evaluate screening's impact in breast cancer diagnosis comparing data from first round (2006–2007) with the ones from 2004–2005. Cytohistological samples were analyzed by the Cytodiagnostic and Histopathology Department where all breast surgical specimens from entire province are submitted.
Results In the two years before screening activation (2004–2005) 486 women had been investigated, 246 had carcinoma. pTis represented 5% of cases (12); Subclinical lesions (pT1a+pT1b) were 19% (46 cases); pT1c lesions were 34% (84 cases); Lesions with diameter larger than 2 cm were 42% (104 cases). In the following two years (2006–2007) 697 women were investigated, 363 had breast carcinoma. Tis were 10% (37 cases; 73% of them screening detected); Subclinical lesions (T1a+T1b) were 27% (98 cases; 59% of them screening detected); T1c lesions were 33% (119 cases; 55% screening detected). Lesions with maximum diameter larger than 2 cm were 30% (109 cases; 24% of them screening detected).
Conclusion(s) Breast screening introduction has led to an increase both of Tis cases (+208%) and of invasive carcinoma (+39%). The observed growth is due to increase of subclinical lesions (T1a+T1b), while lesions larger than 2 cm maintained steady.

OP11.3
Evaluation of chromatin modifying enzymes and modified histones in breast cancer

Makretsov N.; Howat W.; Dawson S.; Morris L.; Lequesne J.; Blows F.; Driver C.; Provenzano E.; Pharoah P.; Caldas C.
Memorial University, St John's, NL, Canada

Background Chromatin modifications represent a level of epigenetic transcriptional regulation. They alter the structure of chromatin, occluding certain DNA regions and exposing others for the transcription machinery, leading to gene silencing or expression and play a significant role in breast cancerogenesis. This study focuses on initial evaluation of antibodies against several chromatin modifying enzymes and modified histones in invasive breast cancer.
Methods Clinically annotated tissue microarrays (700 invasive breast cancers) was used. Automated image analysis using the standard biomarkers (Estrogene Receptor, Progesterone Receptor, Ki67, TP53) and ARIOL slide scanner was validated in Receiver-Operator Curve (ROC) analysis. Pathologist scoring was used as standard. We optimized the antibodies against chromatin modifying enzymes- HDAC1, HDAC2, HDAC5, CBP, EZH2, MTA2, MTA1, SIRT1 and LSD1, and antibodies against modified histones: H2B-acetyl-K12, H3-acetyl K14, H3-dimethyl-K4, and H4-acetyl-K5. Kaplan-Meier method, log-rank test and Cox regression models were used.
Results ER, PR, Ki67 and TP53 were of significance by automated image analysis, and proved the validity of our approach. CBP, SIRT1 and H3-acetyl-K14 were associated with improved survival, while LSD1, MTA1, EZH2, H4-acetyl-K5 and H3-dimethyl-K4 were associated with poor survival. The other antibodies were of no significance in our analysis. Three markers- H3-dimethyl-K4, H4-acetyl-K5 and H3-acetyl-K14 were of significance in multivariate analysis.
Conclusion(s) Chromatin modifying enzymes and histone modifications are of potential clinical significance in breast cancer according to our pilot evaluation. Further rigorous validation is required as these markers may serve potential therapeutic targets. Supported by ACSBI-UICC fellowship.

OP11.4
Expression pattern of CD24 and CD44 isoforms in micropapillary carcinoma of the breast

Simonetti S.; Zlobec I.; Kilic E.; Stasio L.; Pettinato G.; Terracciano L.; Insabato L.
Università di Napoli Federico II, Naples, Italy

Background Micropapillary carcinoma (MPC) of the breast is a very aggressive tumor with early lymph node metastases and poor prognosis. Expression of some isoform variants of CD44 and CD24 is associated to lymph node metastasis and poor prognosis in several tumors. A specific pattern of expression of CD44 and CD24 is considered a index of stem cell capability of breast cells: CD44+/CD24−/low belonging to the basal cell group associated to worst prognosis and CD44−/CD24+ corresponding to luminal cell types, which correlate with a better clinical behavior.
Methods We studied immunohistochemically protein markers CD24, CD44v5 and CD44v9 on 31 MPCs and compared their expression to 22 high-grade invasive ductal carcinomas of the breast (DCs).

Results CD24 expression was observed in 18/22 (81%) DCs of which 12 (66%) showing a strong cytoplasmic staining and 6 (44%) with apical positivity. In 27/31 (87%) MPCs CD24 immunoreactivity was identified with a characteristic apical localization. In MPCs we observed an inverted apical staining of CD24. In normal breast tissue CD24 expression was not found. We found a CD44−/CD24+ combination in 6 (27%) DCs and 7 (22%) MPs and a CD44+/CD24− association in 2 (9%) DCs and in 3 (9.6%) MPs, without a significant difference between both type of tumors.
Conclusion(s) In conclusion, this study demonstrated that MPC represent a distinct entity of breast carcinoma and that the inverted apical membrane pattern of CD24 expression is useful for distinguishing MPC from other forms of breast cancer.

OP11.5
Gene expression profiling in under-vacuum stored breast carcinomas: a pilot study

Sapino A.; D'Armento G.; Molinaro L.; Macrì L.; Cavicchini A.; Bussolati G.
Department of Biomedical Sciences and Human Oncology University of Turin, Turin, Italy

Background MammaPrint is a FDA-approved molecular test for breast carcinomas which determines whether the patient is at low or high risk of disease recurrence. Being the test based on gene expression profiling technology, the sample collection and storage are crucial. According to manufacturer's instructions breast carcinoma specimens should be sampled fresh within 1 h from excision and stored in specific solution. Alternatively, the reliability of the test has been estimated to be far from high. To circumvent the problems connected with conditions and timing of specimens collection/ sampling, and specifically the practical feasibility of sampling immediately after tissue removal, we have adopted for the study purposes a formalin-free sample collection method based on under-vacuum preservation.
Methods Thirty-one consecutive breast carcinomas were collected under-vacuum conditions at surgical theatres and kept at 4°C up to sampling. Prior to gross sampling for diagnostic purposes a core of fresh tissue was obtained and immediately stored in RNA Retain solution. The specimens were sent by courier to Agendia laboratories to perform MammaPrint.
Results The time elapsed between surgical excision and sampling varied from 1 h to 72 h. All cases proved to be analysable, regardless of magnitude of the time-gap between surgical excision and sampling.
Conclusion(s) These results provide evidence on the reliability of the under-vacuum tissue collection in preserving RNA integrity and suggest a way to circumvent feasibility issues related to collection of fresh samples to be analysed by molecular tests.

OP11.6
Genotypic intratumoral heterogeneity in breast carcinoma with Her-2/neu amplification: evaluation according to ASCO/CAP criteria

Brunello E.; Brunelli M.; Manfrin E.; Miller K.; Remo A.; Reghellin D.; Bersani S.; Gobbo S.; Eccher A.; Martignoni G.; Bonetti F.
Anatomia Patologica, Università di Verona, Verona, Italy

Background There is concern that heterogeneity of Her-2/neu gene amplification within a tumor may affect treatment response due to the selection of resistant subclones lacking this alteration. We sought to evaluate the intratumoral heterogeneity in breast carcinoma with Her-2/neu amplification.
Methods We selected thirty ductal breast carcinomas with strong 3+ Her-2/neu immunoexpression and Her-2/neu gene amplification on whole tissue sections by FISH and built two microarray blocks. Amplification was scored sec. ASCO/CAP criteria. Moreover, high grade (ratio > 4.0) versus low grade amplification (ratio 2.2>×<4.0) and polysomy of chromosome 17 were evaluated.
Results On whole tissue sections, 20/30 (66.7%) showed a high grade Her-2/neu gene amplification whereas 10/30 (33.3%) showed a low grade amplification. Fourteen out of twenty (70%) with high grade Her-2/neu gene amplification did not show intratumoral genotypic heterogeneity. The remaining 30% showed at least one core with a low grade gene amplification. Among the 10 cases with low grade Her-2/neu gene amplification 60% did not show intratumoral heterogeneity. In four cases 2/3 cores showed polysomy of chromosome 17 without gene amplification.
Conclusion(s) Overall, 4/30 (13.3%) ductal breast cancer with Her-2/neu gene amplification on whole tissue sections may show a "not amplified pattern" in other part of the tumour. Genotypic heterogeneity is more restricted to breast carcinomas that show low grade Her-2/neu gene amplification.

OP11.7
Lower incidence of triple negative breast cancers within a screening program

Cannizzaro C.; Manfrin E.; Nottegar A.; Falsirollo F.; Brunello E.; Gobbato M.; Reghellin D.; Schiavo N.; Remo A.; Menestrina F.; Bonetti F.
Anatomia Patologica, Università di Verona, Verona, Italy

Background Triple negative breast cancers (TNc) (ER-, PR-, Her2/neu-) are about 10–17% of diagnosed carcino-

mas and are associated with poor prognosis. Screen detected breast cancers (SDBc) have a better prognosis than symptomatic ones but little is known about TNc in a screening context. In the current study, we analyze the role of TNc in a breast cancer screening series.

Methods We investigated TNc in a series of 253 SDBc diagnosed between July 1999–2006 in the Breast Cancer Screening Program in Verona. The cancer series were stratified according to the histological type, size (T), lymph node status (N) and proliferative index.

Results In our series, invasive TNc assess on 3,1 % (8/253) and in situ TNc on 1,58% (4/253). In invasive TNc series the detection rate was higher in the first screening round (87,7% of cases). The prevalent histopathological aspects were ductal type (87,7%), pT1 (62,5%), pN0 (75 %), G2-G3 (100%) and Ki-67≤20% (62,5%). In "in situ" TNc series, the detection rate was higher in the subsequent screening rounds (75% of cases). 75% of in situ TNc were ≤ 2 cm, 50% were G, 100% were ductal and 75% showed Ki-67 index ≤ 20%.

Conclusion(s) In our experience TNc represent a lower percentage of SDBc (3,1%) when compared to symptomatic ones in the literature (10–17%). The positive prognostic variables of screen detected cancers such as small size, high percentage of negative lymph nodes and low proliferative index, are also present in TNc subset.

OP11.8

Margin width and size as predictors of residual tumour in breast conserving therapy of ductal carcinoma in situ

Decker T.; Ruhnke M.; Obenaus R.; Kettritz U.; Roterberg K.; Tio J.; Hungermann D.; Korsching E.; Böcker W.
Breast Unit, Institute of Pathology, University Hospital Muenster, Muenster, Germany

Background Residual tumour is the main risk factor for local recurrence of ductal carcinoma in situ (DCIS). Aim of the study was to identify pathologic factors useful in defining the risk of residual tumour after breast conserving therapy (BCT).

Methods From 1992 – 2003 at the Berlin-Buch Breast Unit in 247 of 371 DCIS patients of primary BCT was performed. All patients with margins< 10 mm had a re-operation. Residual tumour risk was evaluated with respect to whole size of DCIS, margin status, nuclear grade, and comedo necroses after standardized pathological investigation. Margin width was recorded as < 1 mm, 1–10 mm, and >10 mm). Lesions were grouped by size: ≤15 mm, >15–40 mm, or >40 mm.

Results All DCIS ≤ 15 mm had margins >10 mm. Residual DCIS was found in 90% (101/112) of margins < 1 mm, and 79% (61/77) of margins 1–10 mm. The rate of residual DCIS by size was 27% (36/132) for >15–40 mm, and 98% for >40 mm, respectively. On univariate and multivariate analysis margin width and lesion size significantly predicted for residual DCIS ($p<0.0001$) whereas grade and necrosis did not.

Conclusion(s) Margin status of BCT specimens in DCIS is statistically the most important predictive factor for residual disease but its predictive power is essentially influenced by the size of DCIS, which should be considered in therapeutic decision making.

OP11.9

Mixed micropapillary-ductal carcinomas of the breast: a genomic and immunohistochemical analysis of morphologically distinct components

Marchiò C.; Iravani M.; Natrajan R.; Geyer F.; Lambros M.; Savage K.; Mackay A.; Schmitt F.; Bussolati G.; Ellis I.O.; Ashworth A.; Sapino A.; Reis-Filho J.S.
Department of Biomedical Sciences and Human Onncology, Turin, Italy

Background Micropapillary carcinoma (MPC) is a rare histological special type of breast cancer frequently admixed with invasive ductal carcinomas of no special type (IDC-NSTs). We demonstrated that pure MPCs constitute a distinct entity at the morphological and genetic levels. In this study we aimed to define whether mixed MPCs have genomic aberrations similar to pure MPCs and to investigate whether the distinct morphological components of MPCs harbour different genetic aberrations.

Methods 10 mixed MPCs and 20 IDC-NSTs matched for grade and oestrogen receptor (ER) status were profiled using high-resolution microarray comparative genomic hybridisation (aCGH). We also generated tissue microarrays containing 24 pure and 40 mixed MPCs and performed immunohistochemistry for ER, PR, Ki-67, HER2, cytokeratin (CK) 5/6, CK14, CK17, EGFR, topoisomerase-IIα, cyclin D1, caveolin-1 and E-cadherin. HER2, TOP2A, EGFR, CCND1, MYC and FGFR1 gene status was assessed by in situ hybridisation.

Results Mixed MPCs harbour patterns of genomic aberrations and phenotype (82.5% luminal, 17.5% HER2) similar to those of pure MPCs. We observed that the papillary and non-papillary components of mixed MPCs harbour strikingly similar genomic profiles. When compared to grade and ER matched IDC-NSTs, mixed MPCs more frequently harboured amplification of multiple regions on 8q ($p<0.05$) and displayed significantly higher proliferative rates ($p < 0.0001$).

Conclusion(s) Mixed-MPCs are more closely related to pure MPCs than to IDC-NSTs and micropapillary differentiation, even focally, is associated with the presence of

genetic aberrations usually found in a subgroup of aggressive luminal cancers.

Oral presentations 12

Endocrine pathology

OP12.1
An FGFR4 polymorphism is implicated in the progression of neuroendocrine tumors

Serra S.; Zheng L.; Chetty R.; Ezzat S.; Asa S.L.
Department of Pathology, UHN, Toronto, Ontario, Canada

Background A polymorphism of FGFR4Gly/Arg388 is associated with poor outcome in several cancers. We examined the effects of FGFR4Gly/Arg388 in pancreatic endocrine tumor cells in vitro and in vivo and its correlation with clinicopathologic parameters of neuroendocrine carcinomas.
Methods 83 PETs and BON1 cells were genotyped. BON1 cells were stably transfected with FGFR4/Gly388 or FGFR4/Arg388, injected into SCID mice intraperitoneally (orthotopic) or subcutaneously, tumor growth and spread was monitored and complete autopsy was performed.
Results There was a positive but not significant trend between FGFR4/Arg388 and tumor size, lymph node and liver metastasis, MIB1 > 2%, mitoses > 2/HPF, and VIP production. Benign tumors and insulinomas were more frequently WT; tumors of uncertain behavior and well-differentiated carcinomas were more often associated withFGFR4/Arg388. Non-transfected BON1 cells are homozygous FGFR4/Gly388. In subcutaneous xenografts, FGFR4/Arg388-transfected cells formed significantly larger tumors (mean volume: 1955 mm3) than FGFR4/Gly388 (916 mm3) and controls (828 mm3) (p=0.43). FGFR4/Arg388 tumors weighed 1.25 g (0.97–1.40 g); FGFR4/Gly388 tumors weighed 0.68 g (0.43–1.00 g) (p=0.05) and controls weighed 0.73 g (0.43–1.18 g) (p=0.05). In the orthotopic model, FGFR4/Arg388 total weight was higher, 2.07 g (1.37–2.87 g) than FGFR4/Gly388, 1.23 g (0.57–1.78 g) (p>0.01) and control 0.97 g (0–1.8 g) (p=0.05). FGFR4/Arg388 nodules were larger than the other groups and exhibited greater spread throughout the peritoneum and liver.
Conclusion(s) We developed an orthotopic model of neuroendocrine carcinoma that develop intraperitoneal growth resembling human pancreatic neuroendocrine carcinomas. Our data support the hypothesis that FGFR4/Arg388 plays a key role in the progression of neuroendocrine tumors.

OP12.2
Endocrine tumors of appendix. Presentation of 8 cases

Malinowska M.; Ptaszynski K.
Oncology Center-Institute, Warszawa, Poland

Background Appendiceal endocrine tumors (AETs) are the second most common gastrointestinal endocrine tumors with a relative frequency of 30–25%. Malignant neoplasms constitute 17% of all AET cases. The malignant potential of these tumors is difficult to predict.
Methods A group comprised of 5 females and 1 male (mean age 25 years; range 16–45; this range excludes a 74-year old male with goblet cell carcinoid). All patients underwent simple appendectomy and have been referred to the Department of Pathology of Oncology Center–Institute in Warsaw. Immunohistochemical and histochemical staining of synaptophysin, chromogranin A, Ki-67 and mucicarmin were performed. A proliferative index, tumor grade, tumor size and pTNM stage were investigated to evaluate prognostic parameters.
Results Four cases showed an appearance of well-differentiated endocrine tumor with uncertain malignant behavior, 3 cases were well-differentiated endocrine carcinomas and 1 case appeared as a goblet cell carcinoid. One patient had 2 tumors. The Ki-67 labeling index was low (1%-2%). 3 tumors invaded submucosa and muscularis propria, 3 invaded subserosa/mesoappendix and 2 invaded serosa. No significant correlation was found between tumor grade and Ki-67 index as well as between tumor size and Ki-67 index.
Conclusion(s) The findings suggest that tumor size, tumor grade and Ki-67 index do not accurately predict malignant behavior of AETs. The best predictor of the outcome appeared to be a current TNM staging system.

OP12.3
Genomic identification of biomarkers of behavior of pancreatic endocrine tumors

Bauersfeld J.; Thomas G.D.; Kuick R.; Vinco M.; Sanders D.; Giordano J.T.
Department of Pathology, University Hospital of Zurich, Zurich, Switzerland

Background Endocrine tumors of the pancreas are difficult to classify into benign and malignant categories, and as such are often diagnosed as pancreatic endocrine tumors (PETs). The recent WHO classification has improved the situation, but there is still a need for additional molecular biomarkers to provide independent assessment of the risk of malignant behaviour.
Methods To identify potential biomarkers of malignant behaviour, genome-wide transcriptional profiles were gen-

erated for a cohort of 46 PETs from 29 patients using commercially available DNA microarrays. PETs analyzed represented sporadic and syndromic (MEN1) forms, primary metastasizing and non-metastasizing tumors. For validation of the potential biomarkers we performed AQUA and immunohistochemistry on 3 tissue arrays with 110 PET samples.

Results Using F-tests and selection criteria of $p<.01$ and fold change > 1.5 in either direction, comparison of 8 PETs with proven metastases (PET-M) to 6 PETs without metastases (PET-N) yielded 255 unique genes whose expression was increased in the PET-M group. Differentially expressed genes included genes related to tumor invasion and metastases as well as other biological processes. Preliminary results from immunhistochemical and AQUA based validation for several of these biomarkers using tissue arrays containing an independent set of PETs are promising and ongoing.

Conclusion(s) Genomic investigations of pancreatic endocrine tumors will yield novel biomarkers that will permit a more refined assessment of their risk of malignant behaviour. Applications of these biomarkers to pathology practice will improve management of patients with PETs.

OP12.4

Serotonin-producing pancreatic endocrine tumors (5HT-PETS): appropriate nomenclature and different biopathology with intestinal ec-cell tumors

La Rosa S.; Franzi F.; Albarello L.; Capella C.
Ospedale di Circolo, Varese, Italy

Background 5HT-PETs are rare neoplasms composed of EC-cells that have been traditionally named carcinoids likewise gut EC-cell tumors. However, the use of term carcinoid is now discouraged because it has failed to convey adequately the great pathologic variety of such tumors. The majority of published 5HT-PETs have been described as case reports and studies analyzing the morphological similarities or differences with intestinal EC-cell neoplasms have never been reported.

Methods We studied nine pancreatic and twenty intestinal serotonin-producing neoplasms using the diazonium reaction and antibodies directed against pancreatic hormones, gastrin, serotonin, substance P, S100, VMAT1, VMAT2, CDX2, alpha-hCG, prostatic acid phosphatase (PAP) and aFGF.

Results All 5HT-PETs were nonfunctioning and, according to the WHO classification, one case was classified as benign, 5 as uncertain behavior and 3 as well differentiated carcinomas. Intestinal tumors were malignant, while the appendiceal ones were benign. The lack of stromal and peritumoral fibrosis, of S100-positive sustentacular cells, of substance P and aFGF immunoreactivity, the low immunohistochemical expression of CDX2 and PAP, the low positivity at the diazonium reaction, and the strong expression of VMAT2 in 5HT-PETs were the main morphological features differentiating 5HT-PETs from the intestinal 5HT tumors.

Conclusion(s) 5HT-PETs show a different immunophenotype from intestinal EC-cell tumors and we suggest using the term "serotonin-producing tumor" instead the term "carcinoid" to diagnose a PET composed of serotonin-immunoreactive cells. The term carcinoid may be retained only in the case of tumors associated with the typical carcinoid syndrome.

OP12.5

VHL and hypoxia signalling in sporadic pancreatic endocrine tumors

Schmitt M.A.; Schmid S.; Rudolph T.; Anlauf M.; Moch H.; Heitz P.; Komminoth P.; Perren A.
Institute of Surgical Pathology, University Hospital Zurich, Zurich, Switzerland

Background Sporadic PET rarely harbour somatic VHL mutations, but the chromosomal location of the VHL gene is frequently deleted in sporadic PET and a subset of sporadic PET shows active hypoxia signals on mRNA and protein level. The aim of this study was to correlate epigenetic and genetic VHL alterations to hypoxia signalling in order to identify the frequency of functional VHL inactivation in sporadic PET.

Methods VHL gene mutation, VHL deletion and promoter methylation analyses were performed. Quantitative RNA expression levels of VHL and CA-9 were studied. HIF-1α as well as the HIF target proteins CA-9 and GLUT-1 were investigated by semiquantitative immunohistochemistry.

Results VHL mutations were absent in all 37 PET examined. VHL deletion was found in 14 of 79 tumors (18%) by FISH and methylation of the VHL promoter was detected in 2 of 35 tumors (6%). HIF-1α was expressed in 19% of PET, CA-9 and GLUT-1 protein was expressed in 27% and 30% of PET, respectively. Protein expression of the HIF-1α downstream target CA-9 correlated significantly with the expression of CA-9 mRNA ($p<0.001$) and VHL loss ($p < 0.05$) as well as with HIF-1α ($p<0.005$) and GLUT-1 immunohistochemistry ($p < 0.001$).

Conclusion(s) We conclude that VHL gene inactivation by promoter methylation or VHL hemizygous deletion in nearly 25% of PET leads to an activation of the HIF-pathway. Our data suggest that VHL inactivation is an important mechanism for the development of a subset of sporadic PET.

OP12.6

Analysis of thyroid tumors by a microscopic score combined with immunohistochemistry on tissue microarray (CK19, HBME1, Galectin 3 and TPO)

Renaud F.; Devos P.; Saussez S.; Aubert S.; Verhulst P.; Pigny P.; Bouchind'Homme B.; Do Cao C.; Pattou F.; Carnaille B.; Wemeau J.; Leteurtre E.
CHR-U, Lille, France

Background Distinction between follicular adenoma and encapsulated follicular variant of papillary thyroid carcinoma remains one of the most difficult area in thyroid surgical pathology. We previously proposed a score based on five morphological criteria (ovoid nuclei, lack of polarization, nuclear grooves, enlarged nuclei, dark staining colloid) illustrating the variety of morphologic presentations in the histopathological categories of adenoma and PTC. Our objective was now to evaluate immunohistochemical markers on the same series.
Methods We performed a detailed immunohistochemical analysis on a tissue microarray constructed from paraffin-embedded blocks of 66 papillary thyroid carcinoma and 66 adenoma previously evaluated with the score.
Results Immunostaining for HBME1, CK19, Galectin 3 and TPO showed a significant statistical association between stained cells percentage (cut off 20% positive cells) and diagnosis of malignancy and also between stained cells percentage and presence of microscopic criteria ($p<0{,}0001$). The microarray data showed that CK19 had a sensitivity and specificity of 95% and 89% respectively, HBME1 (70%, 97%), Galectin 3 (91%, 83%) and TPO (81%, 91%) for the diagnosis of malignancy. Linear discriminant analysis between criteria of the morphological score and immunohistochemical markers revealed that in our series CK19 is useful to discriminate carcinoma versus adenoma and gives informations complementary to morphological examination.
Conclusion(s) This original study compared immunohistochemistry performance to a microscopic score. In our series CK19 immunohistochemistry can indeed complete morphological examination.

OP12.7

Evaluation of DNA repair related molecules expression in human benign and malignant thyroid lesions

Michailidi C.; Stolakis V.; Zarros A.; Zira A.; Tsourouflis G.; Delladetsima I.; Klijanienko J.; Theocharis S.
University of Athens, Medical School, Athens, Greece

Background Dysfunction of DNA repair related mechanisms is considered as a crucial cause for malignant transformation. In the present study, the clinical significance of important proteins' expression involved in DNA repair, namely MLH1, MSH2 and MGMT, was examined in thyroid lesions.
Methods MLH1, MSH2 and MGMT expression was assessed immunohistochemically in formalin-fixed, paraffin-embedded thyroid tissues obtained from 79 patients with benign (hyperplastic nodules and Hashimoto thyroiditis, $n=36$) and malignant (papillary, medullary, follicular and anaplastic carcinomas $n=43$) lesions. The MLH1, MSH2 and MGMT positivity, overexpression, and intensity of immunostaining were assessed in order to compare their expression between malignant and benign lesions, and within benign subgroup between Hashimoto thyroiditis and hyperplastic lesions. Additionally, in the subgroup of malignant thyroid tumors, protein expression was statistically analyzed in relation to TNM stage and tumor proliferative capacity assessed by Ki67 labeling index.
Results MGMT positivity as well as MLH1 and MSH2 overexpression provided a distinct discrimination between malignant and benign thyroid lesions ($p=0.004$, $p=0.042$, and $p=0.021$, respectively). In malignant lesions, MSH2 intensity of immunostaining was associated with tumor size ($p=0.003$). Additionally, in benign lesions MLH1 overexpression was differently contributed between hyperplastic nodules and Hashimoto thyroiditis ($p=0.005$).
Conclusion(s) The current data revealed that DNA repair related molecules could be considered of diagnostic utility in thyroid neoplasia. Further studies are warranted to delineate their implication in pathogenesis and their potential use as therapeutic targets in thyroid neoplasia.

OP12.8

Increased FOXP3 positive lymphocytic infiltrates are associated to aggressive behaviour in papillary thyroid carcinoma

Volante M.; Tavaglione V.; Rapa I.; Righi L.; Papotti M.
University of Turin, Department of Clinical and Biological Sciences, Orbassano, Turin, Italy

Background FOXP3 is a transcription factor specifically expressed by regulatory T lymphocytes (Tregs) that act as negative modulators of immune response in several pathological conditions, including cancer. The aim of this study was to investigate the correlation between the density of Treg population and clinical pathological parameters in papillary thyroid carcinoma.
Methods A series of 111 consecutive papillary thyroid carcinomas was investigated. The phenotype of lymphocytic infiltrates was immunohistochemically assessed with CD3 and FOXP3 antibodies and evaluated counting the number of intra-epithelial positive cells in 10 randomly

selected HPF of normal peri-tumoral and intra-tumoral areas. The FOXP3/CD3 ratio and the presence of morphologically evident thyroiditis were also recorded.
Results Mean FOXP3+ cells were significantly correlated with those CD3+ and presence of thyroiditis. Mean FOXP3+ cells and FOXP3/CD3 ratio were significantly higher in tumor than in peri-tumoral normal tissues. No association was found between the density of FOXP3 population in normal peri-tumoral tissue and clinical pathological variables. By contrast, higher intra-tumoral FOXP3+ density and FOXP3/CD3 ratios were significantly associated to sclerosing histotype, absence of tumor capsule, extrathyroidal extension, pT stage > 3 and vascular invasion (all $p<$ 0.0001, except for FOXP3/CD3 ratio vs vascular invasion, $p=0.007$). Higher FOXP3+ cell count was also associated to positive nodal status ($p=0.02$).
Conclusion(s) Our findings suggest that impaired T-cell specific immune response supported by enhanced intra-tumoral Treg activity might favour local and vascular dissemination in papillary thyroid carcinoma.

OP12.9

Oncocytic and mitochondrion-rich follicular thyroid tumours: one spectrum of lesions or different pathways?

Tsybrovskyy O.; Roessmann-Tsybrovskyy M.
Institute of Pathology, Graz, Austria

Background Oncocytes are currently defined as mitochondrion-rich cells, but the cut-off for separating them from non-oncocytes is poorly defined. The role of other cell organelles during oncocytic change is also unclear.
Methods Immunohistochemical markers of mitochondria and endoplasmic reticulum (ER) were applied to 470 follicular tumours (276 adenomas and 194 carcinomas), 162 normal thyroids and 296 non-neoplastic lesions (tissue microarrays). Immunohistochemistry was validated by ultrastructural examination and organelle density measurements in 15 cases.
Results Oncocytes were characterized by densely packed mitochondria resulting in homogeneous immunostaining pattern. Moreover, in most cases oncocytes displayed peculiar organelle polarity, namely predominantly basal location of mitochondria, whereas ER and the nuclei were displaced to the apical position. Non-oncocytes showed coarsely granular mitochondrial immunoreaction, uniform ER distribution throughout the cytoplasm and basally located nuclei. 14.6% of tumours contained high amounts of mitochondria comparable with those seen in typical oncocytes, but showed no oncocytic features on H&E stain and no aberrant organelle polarity ("mitochondrion-rich non-oncocytic" tumours). Clinically, this tumour group was characterized by significantly increased risk of malignancy and higher cancer recurrence rates. By contrast, oncocytic change had no impact on tumour behaviour.
Conclusion(s) True oncocytic change implies not only accumulation of mitochondria, but also aberrant spatial distribution of all major cell organelles. Defined this way, oncocytic transformation does not seem to correlate with tumour behaviour. By contrast, mitochondrion-rich non-oncocytic tumours are morphologically and clinically distinct entities, which suggests a different pathogenetic mechanism of mitochondrial accumulation.

Oral presentations 13

Digestive pathology

OP13.1

CD8+ lymphocytes/tumour budding ratio. A "defender-attacker" approach as a an example of tumour-host interaction

Lugli A.; Karamitopoulou E.; Panayiotides I.; Karakitsos P.; Rallis G.; Peros G.; Iezzi G.; Spagnoli G.; Bihl M.; Terracciano L.; Zlobec I.
Institute for Pathology, University Hospital Basel, Basel, Switzerland

Background The tumour-host interaction is an important area of investigation in terms of prognosis in colorectal cancer. Established tumour and host related factors are the epithelial-mesenchymal transition including its hallmark "tumour budding" and the adaptive immunologic microenvironment including CD8+lymphocytes. The aim of this study was to test and validate the prognostic impact of an "attacker-defender" approach defined by an established "attacker" (tumour budding) and "defender" (CD8+ lymphocytes).
Methods 300 colorectal cancer resection specimens from different Pathology centres in Basel, Switzerland, with complete clinico-pathological data were used as test set. 221 colorectal cancer samples from the Second Department of Pathology (Athens, Greece) represented the validation set. The number of buds and the presence of CD8+ T-cell per high power field were counted to obtain the CD8+ T-lymphocytes/tumour buds ratio.
Results Test set: In univariate analysis a low CD8+/buds ratio was associated with presence of lymph node metastasis ($p<0.001$), vascular invasion ($p=0.009$), infiltrating tumour border ($p=0.005$), absence of peritumoral lymphocytic infiltration ($p=0.007$) and worse survival ($p<0.001$), confirmed in multivariable analysis. Validation set: The

CD8+/buds ratio was associated with higher T stage ($p<0.001$), N stage ($p=0.041$), higher tumour grade ($p<0.001$), vascular invasion ($p=0.005$) and survival ($p<0.001$). The CD8+/buds ratio showed an increased discriminatory ability for identifying survivors and non-survivors at 5-year follow-up ($p<0.001$).

Conclusion(s) The ratio including tumour budding and CD8+ lymphocytes is an independent prognostic factor in colorectal cancer and a promising approach for a future prognostic score in colorectal cancer.

OP13.2

Analysis of EGFR gene deregulation and PIK3CA mutations in patients with squamous cell anal cancer (SCAC) treated with concurrent chemoradiation

Crippa S.; Franzetti Pellanda A.; Zanellato E.; Molinari F.; Martin V.; Saletti P.; Mazzucchelli L.; Frattini M.
Institute of Pathology, Locarno, Switzerland

Background Chemoradiation is the standard treatment for locally advanced SCAC, with complete response in 75–85% of patients. Do molecular markers predict the response to chemoradiation? Preclinical and clinical studies in several cancers have demonstrated that EGFR and PIK3CA mutations may impair the efficacy of radiotherapy or, limited to PIK3CA, fluoropyrimidines. We analyzed EGFR gene deregulation and PIK3CA mutations in patients with locally advanced SCAC who underwent concurrent chemoradiation. The results were then correlated to clinical outcome.

Methods We considered patients with concurrent chemoradiation. EGFR gene status was assessed by FISH, PI3KCA mutations by direct sequencing. Objective tumor response was evaluated by radiological and endoscopic methods; if indicated confirmatory biopsy was performed.

Results Twenty patients were investigated. Seventeen patients (85%) achieved a complete remission after chemoradiation. EGFR gene copy number gain was detected in 2/19=10% evaluable cases, and did not correlate with response. A PIK3CA point mutation was detected in 7/20=35% patients: six patients were responders, while one patient was non-responder.

Conclusion(s) • PIK3CA mutations may play a key role in the development of a subset of SCAC. • EGFR and PIK3CA alterations do not seem predict the efficacy of chemoradiation in SCAC patients, suggesting that other molecular markers should be investigated. • The presence of both EGFR gene deregulation and high frequency of PI3KCA mutation might suggests that patients with SCAC could benefit from tailored treatments against these two targets.

OP13.3

Impact of microsatellite instability, braf and specific kras mutations G12D and G13D on prognosis in lynch syndrome-associated and sporadic colorectal cancer

Lugli A.; Kovac M.; Frattini M.; Bihl M.; Rufle A.; Förster A.; Iezzi G.; Spagnoli G.; Terracciano L.; Heinimann K.; Zlobec I.
Institute of Pathology, Basel, Basel, Switzerland

Background Promising prognostic and predictive molecular features such as KRAS and BRAF gene status are now considered in the management of colorectal cancer patients. The aim of this study was to determine the combined effect of MSI, BRAF and KRAS gene status including specific mutations, on prognosis in sporadic and Lynch syndrome-associated colorectal cancer.

Methods KRAS, BRAF and MSI status were analyzed by PCR and direct sequencing of 202 sporadic and 94 Lynch syndrome-associated colorectal cancers from patients with full clinico-pathological data. Survival analysis included Kaplan-Meier and log-rank testing.

Results In sporadic cases, 3 prognostic subgroups were identified: patients with (1) BRAF mutation, (2) BRAF/KRAS wild-type tumours and (3) KRAS mutation and MSI-high (MSI-H). Stratification by specific KRAS mutation revealed a detrimental effect of codon 12 Gly->Asp (G12D) mutation on outcome. Patients with codon 13 Gly->Asp (G13D) mutations, particularly with MSI-H benefited from prolonged survival ($p=0.02$), a result also observed in Lynch syndrome patients. In both sporadic and Lynch syndrome, a trend toward increased CD8+ lymphocyte count was noted in G13D compared to G12D mutated tumours.

Conclusion(s) Our results highlight differential prognostic effects of specific KRAS mutations G12D and G13D in sporadic and Lynch syndrome-associated colorectal cancer. The favourable outcome of patients with G13D may be related to increased tumour immunogenicity, a hypothesis, which if validated, may provide a new avenue of investigation into the pathogenesis of colorectal cancer.

OP13.4

More sensitive methods to identify K-Ras mutations increase the detection of non-responder in metastatic colorectal cancer (mCRC) patients treated with anti-egfr monoclonal antibodies (MoAbS)

Molinari F.; De Dosso S.; Saletti P.; Crippa S.; Mazzucchelli L.; Marchetti A.; Bardelli A.; Frattini M.
Institute of Pathology, Locarno, Switzerland

Background Anti-EGFR MoAbs (cetuximab and panitumumab) are effective in 10–20% of mCRC patients.

Deregulations of EGFR downstream proteins (K-Ras, BRAF, PI3K, PTEN) predict MoAbs resistance. Direct sequencing, the main technique currently used to analyze K-Ras mutations, may skip the detection of mutated minor clones. Several methods have been proposed to investigate K-Ras mutations. We focused our attention on mutant-enriched PCR (ME-PCR), able to identify 0.1% of mutant alleles.

Methods We retrospectively evaluated objective tumor response, the mutational status of K-Ras, BRAF and PIK3CA by direct sequencing, and PTEN protein expression by immunohistochemistry in mCRC patients treated with cetuximab or panitumumab; mutational status of K-Ras by ME-PCR was also analyzed in K-Ras-BRAF wild-type patients. All tissue samples contained at least 70% of neoplastic cells.

Results Fifty-seven patients were considered for analysis. K-Ras mutations were detected in 17/57 (30%), BRAF mutations in 4/57 (7%), and PIK3CA mutations in 5/57 (9%) patients. PTEN loss was identified in 17/55 (31%) cases. These alterations were restricted to non-responders. Thirty-six patients exhibited K-Ras and BRAF wild-type status. The ME-PCR identified K-Ras mutations in 7/36 (19%) cases. K-Ras mutations by ME-PCR, together with PTEN loss in 4 cases or isolated in 3 cases, were identified only in non-responder.

Conclusion(s) The analyses of EGFR downstream pathways alterations are able to select mCRC patients resistant to anti-EGFR MoAbs. More sensitive methods for the detection of K-Ras mutations could be useful for this purpose.

OP13.5

Comprehensive analysis of egfr and its downstream pathways deregulation identifies the vast majority of metastatic colorectal cancer (mCRC) patients resistant to anti-egfr monoclonal antibodies (MoAbs)

Frattini M.; Molinari F.; De Dosso S.; Martin V.; Crippa S.; Saletti P.; Mazzucchelli L.
Institute of Pathology, Locarno, Switzerland

Background The anti-EGFR MoAbs cetuximab and panitumumab are active in 10–20% of mCRC patients. The absence of EGFR deregulation by gene copy number gain (CNG), the presence of mutations in K-Ras, BRAF and PIK3CA, and loss of PTEN expression have been individually linked to resistance to MoAbs. A comprehensive analysis of these markers is still lacking.

Methods We retrospectively evaluated the objective response in mCRC patients treated with cetuximab or panitumumab. EGFR gene status was assessed by FISH, K-Ras, BRAF and PIK3CA gene mutations by direct sequencing, and PTEN protein expression by immunohistochemistry.

Results Fifty-seven patients were considered for analysis. K-Ras mutations were present in 17/57=30%, and were associated with resistance to MoAbs (p=0.011). We observed BRAF mutations in 4/57=7%, PIK3CA mutations in 5/57=9% and PTEN loss of expression in 17/55=31% of patients. Absence of EGFR gene status deregulation was documented in 14/43=33% of evaluable cases. The absence of EGFR CNG and the presence of alterations in EGFR downstream members were limited to non-responders. Overall, 35/45=78% of non-responders exhibited at least one alteration in the EGFR pathway (versus 0/12 of responders, p=0.0000009).

Conclusion(s) Our data confirm that alterations in EGFR pathways members play a crucial predictive role of response to anti-EGFR MoAbs in patients with mCRC. The combined analysis of EGFR, K-Ras, BRAF, PIK3CA and PTEN led to the identification of up to 80% of non-responding patients.

OP13.6

High grade tumour budding in colorectal cancer is associated with up-regulation of βIII-tubulin expression at the invasive margin

Portyanko A.; Gorgun J.; Kovalev P.; Nerovnya A.; Bich T.; Tur G.; Letkovskaya T.; Cherstvoy E.
Belarusian State Medical University, Minsk, Belarus

Background Cell locomotion, including cancer invasion, is closely associated with the dynamics of cytoskeletal structures. Tubulin is a constitutive molecule of cytoskeleton. It was shown previously that tubulin isotype affects dynamics of microtubules. Notably, the polymerization properties of the αIII isotype are significantly different from the others. Tumor budding (TB) is known as an independent factor of poor prognosis in colorectal cancer (CRC). Hence, we investigated the possible association of TB and βIII-tubulin expression in CRC.

Methods Surgical specimens of 32 tumours were retrieved. Immunohistochemistry was performed with anti-βIII-tubulin antibody and anti-cytokeratin antibody AE1/AE3 to confirm the presence of TB. The Pixel Count Algorithm (ImageScope) was used for quantitative evaluation of immunohistochemistry.

Results The intensity of staining with anti-βIII-tubulin antibody was significantly higher at the invasive front than in the central area in 29/32 tumours (p<0.05). TB was

detected in 29 cases. Malignant cells in the region of TB expressed βIII-tubulin in 28/29 cases. Staining for βIII-tubulin was evident in cancer cells apparently budding from adjacent malignant cells which exhibited a higher degree of differentiation and negative staining for βIII-tubulin. Tumours with higher grade of TB had significantly more intensive staining of the invasive margin with anti-βIII-tubulin antibodies ($p < 0.05$).
Conclusion(s) βIII-tubulin expression is up-regulated at the invasive margin of CRC and is associated with higher grade of TB. Further investigations are needed to determine clinical implications of this finding.

OP13.7
Diffuse TOPK expression is an adverse prognostic factor in KRAS and BRAF mutated colorectal cancer

Zlobec I.; Bihli M.; Terracciano L.; Lugli A.
Institute for Pathology, University Hospital Basel, Basel, Switzerland

Background T-cell originated protein kinase (TOPK) was described in colorectal cancer as an oncogenic form of MEK, yet its prognostic effect remains to be elucidated. The aim of this study was first, to characterize the prognostic effect of TOPK in colorectal cancer in the context of KRAS, BRAF and microsatellite instability (MSI) status and second to analyze its relationship with ERK/MAPK proteins Epidermal Growth Factor Receptor (EGFR), Raf-1 kinase inhibitor protein (RKIP) and pERK.
Methods Immunohistochemistry for TOPK, EGFR, RKIP and pERK was performed on two subgroups of patients (n=391; n= 854, respectively) with full clinico-pathological data. MSI, KRAS and BRAF gene status were analyzed by polymerase chain reaction (PCR) and direct sequencing on 222 cases.
Results In both subgroups, diffuse expression of TOPK was associated with right-sided location ($p \leq 0.01$), mucinous subtype ($p \leq 0.05$), higher tumour grade ($p \leq 0.01$), EGFR over-expression ($p \leq 0.001$), KRAS and BRAF mutation ($p < 0.001$). Survival time in patients with either KRAS or BRAF mutated tumours was strongly and negatively affected by diffuse TOPK expression ($p = 0.009$).
Conclusion(s) The individualized treatment options for patients with KRAS or BRAF mutation, representing 30–40% of all cases continue to be explored. Our results demonstrate adverse outcome in KRAS or BRAF mutated colorectal cancer patients with diffuse TOPK expression suggesting that TOPK may represent a target for novel anti-cancer therapies directed toward ERK/MAPK signalling inhibition.

OP13.8
Hyperplastic polyposis syndrome in asymptomatic patients: the results from the colorectal-cancer screening program

Orlowska J.; Kiedrowski M.; Kaminski F.M.; Regula J.; Butruk E.
Histopathology Laboratory of the Dept. of Gastroenterology, Medical Center for Postgraduate Education, Warsaw, Poland

Background Patients with Hyperplastic Polyposis Syndrome (HPS) are reported to be at increased risk of colorectal cancer (CRC) with its occurrence greater than 50%. However, detailed analysis have shown that there were different frequencies of CRC in HPS, e.g. in 1/15 (6.6%), 26/57 (45.6%) and 14/17 (82.3%) in asymptomatic screening group, symptomatic patients, and retrospective material of colectomy undertaken because of CRC, respectively.
Methods In order to assess the prevalence of CRC in HPS we have analyzed data from a large colonoscopy-based screening program including 50,148 asymptomatic participants aged 40–66 years (Regula J, et al.: N Engl J Med 2006;355:1863–1872).
Results Twenty eight participants (0.056%) who fulfilled the WHO (2000) criteria for HPS were identified: 13M: 15F; mean age: 56.6y (range 48–66y). In all patients at least 20 to multiple HP were found, mostly < 5 mm, maximum up to >10–15 mm in diameter. Localization of HP proximally to the rectosigmoid was identified in 17 pts (60.7%) and was only left-sided in 11 (39.3%). In none of HPS pts neither "high risk" adenomatous lesions (more than 1 cm, villous component, HGD) nor CRC were found. There were only two pts with accompanying 1 or 2 small tubular adenomas with LGD. Five pts (17.9%) had family history of cancer of the gastrointestinal tract.
Conclusion(s) 1. High CRC prevalence in HPS is probably much exaggerated. 2. It is of great importance to judge with great caution results of previous studies on CRC prevalence in HPS.

OP13.9
Inflammation as a co-factor in colorectal neoplasia

Marszalek A.; Zebrowska M.; Banaszkiewicz Z.; Meder A.; Korenkiewicz L.; Jarmocik P.; Korenkiewicz J.
Department of Clinical Pathomorphology, Collegium Medicum Nicolaus Copernicus University, Bydgoszcz, Poland

Background Colonic polyps are heterogenous group. Recently there were described two ways of neoplasia, e.g.

well-known based on "classic" adenoma" and the "alternative" one through serrated adenoma. There is still an open question of inflammation could play a role in both ways of cancerogenesis.
Methods Between 2004–2008, from over 4500 patients examined in gastroentorologic disease out-patients clinic, in 1885 cases colonoscopy was performed with removal of 694 polyps. From removed material, 144 polyps were selected and classified into four following groups: adenoma (A), hyperplastic polyps (HP), serrated polyps (SP), and serrated adenoma (SA).
Results Biopsies were taken from patients aged from 25 to 82 years, however the average age in all group was as follows: A – 63 yrs, HP – 58 yrs, SP – 60.5 yrs, and SA – 58 yrs. In A and SA groups 65% of patients were males, while in HP and SP number of males and females was equal. Although there were some differences in number of mononuclear cells in polyps, we found a statistically significant difference only according to semi-quantitative estimation of number of eosinophils in A and SA (medium 63 and 58 cells/HPF, respectively) comparing with HP and SP (5 and 11 cells/HPF respectively). Such tendency was confirmed by expression of IL-10 which was higher in A and SA then in control tissue.
Conclusion(s) Our results proof that inflammation (reflected but intensity) in colon polyps is correlated with such lesions as adenomas and serrated adenomas.

Oral presentations 14

Urological pathology – Cardiovascular pathology

OP14.1
Immunohistochemical stain for cytokeratin 7, S100A1, and claudin 8 is valuable in differential diagnosis of chromophobe renal cell carcinoma from renal oncocytoma

Choi C.; Kim S.; Choi Y.; Jin X.; Cho Y.; Jang J.; Juhng S.
Chonnam National University Medical School, Hwasun, Chonnam, Republic of Korea

Background It is sometimes very dificult to distinguish the chromophobe renal cell carcinoma (ChRC) and renal oncocytoma (RO) either by light microscopic examination or by immunohistochemical staining. We studied the difference of cytokeratin (CK) 7, S100A1, and claudin 8 immunoreactivity between classical chromophobe renal cell carcinoma (ChRC), renal oncocytoma (RO), and tumor of overlapping histology (TOH).
Methods We performed immunohistochemical stain of CK7, S100A1, and claudin 8 in archived specimens of 24 classical ChRCs, 25 ROs, and 11 TOHs.
Results CK7 was positive in 21 out of 24 classical ChRCs, and negative in 23 of 25 ROs. S100A1 was negative in all classical ChRCs, and positive in 23 of 25 ROs. Claudin 8 was positive with membranous pattern in 14, and with cytoplasmic pattern in one of 24 classical ChRCs, respectively. However, it was positive with cytoplasmic pattern in 24 of 25 ROs. When the results of three immunomarkers were combined as a panel, classical ChRCs and ROs revealed different immunophenotypes. Accordingly, 11 TOH could be designated as six ChRCs and five ROs. We examined four TOHs by electron microscopy, and found that ultrastructural findings were concordant with the diagnoses based on immunophenotypes.
Conclusion(s) We demonstrate that classical ChRC and RO reveal very significant difference in CK7, S100A1, and claudin 8 immunoreactivity. And we suggest that a panel of three immunomarkers could be used to classify TOH as either ChRC or RO.

OP14.2
Ki-Ras 4A is an aldosterone sensitive gene in renal carcinoma

Fleming S.; King S.; Christie L.
University of Dundee, Dundee, Scotland, United Kingdom

Background Renal carcinoma is amongst the ten most common malignancies in Europe. It is a tumour which is resistant to conventional chemotherapy and radiotherapy. Recent data suggests that agents targeting growth factor receptor kinases and their downstream signalling pathways including Ras and Raf may be effective in slowing growth and possibly inducing remission. Ras mutations are however uncommon in renal cell carcinoma. Data from our previous work suggested that Ras may be upregulated by aldosterone in the nephron and may drive proliferation in response to activation of the renin angiotensin aldosterone pathway.
Methods We investigated the role of mineralocorticoid induction of K-Ras expression, the downstream signalling pathway and tumour cell growth in an in vitro model of renal cell carcinoma. Using the RCC4 cell line and a control line with the mutant VHL gene replaced by a wild type copy we treated cells with aldosterone, spironolactone or siRNA experiments to suppress KiRas4a.
Results We have shown that Ki-Ras, especially the 4a splice isoform, is induced by aldosterone and suppressed following block of the mineralocorticoid receptor by spironolactone. Suppression of Ki-Ras 4a by siRNA led to reduced kinase activity of the Akt and Raf pathways. This treatment and aldosterone blockade both suppressed tumour cell growth and increased apoptosis.
Conclusion(s) These data suggest that K-Ras is aldosterone inducible and when induced supports the proliferation of

renal carcinoma cells. This may be of importance in understanding the response to newer treatments for renal cell carcinoma.

OP14.3

Human aspartic protein napsin-A: immunoistochemical detection among renal cell neoplasms

Segala D.; Gobbo S.; Brunelli M.; Eccher A.; Chilosi M.; Bonetti F.; Menestrina F.; Martignoni G.
Anatomia Patologica, Università di Verona, Verona, Italy

Background Napsin-A is an aspartic protease expressed in the normal kidney and localized in the lysosomes of the cells lining the proximal tubules. Considering the importance of lysosomal aspartic proteases during renal cell carcinogenesis and the role of napsin-A during kidney differentiation, we sought to evaluate its immunoexpression among a wide serie of renal cell neoplasms that exhibit differentiation toward the proximal and distal tubule phenotype.
Methods We examined the expression of napsin-A in 80 consecutive renal cell neoplasms, including 30 clear cell, 20 papillary, 15 chromophobe renal carcinomas (RCCs) and 15 renal oncocytomas. Positive scoring was considered when a neoplasm expressed more than 50% of the cells with a cytoplasmic/membranous staining.
Results Napsin-A was immunoexpressed in two out of 30 (7%) clear cell RCCs, in 12/20 (60%) papillary RCCs, in 1/15 (7%) chromophobe RCCs and in 1/15 (7%) oncocytomas. One oncocytoma showed napsin-A expression focally (< 10%) in the neoplastic cells embedded in the central scar of the tumours.
Conclusion(s) The aspartic protease napsin-A is variably expressed among renal cell neoplasms and, althought is not a specific marker, napsin-A is prevalently expressed in the papillary subtype of RCCs whereas clear cell RCCs, chromophobe RCCs and oncocytomas usually do not stain for this marker.

OP14.4

Immunohistochemical profile of common epithelial neoplasms arising in the kidney

Gobbo S.; Brunelli M.; Segala D.; Chilosi M.; Cossu-Rocca P.; Bonetti F.; Menestrina F.; Martignoni G.
Anatomia Patologica, Università di Verona, Verona, Italy

Background Immunohistochemistry is the foremost ancillary technique in diagnostic surgical practice. The purpose of this study was to determine the diagnostic utility of an immunohistochemical panel we propose as valid tool in distinguishing different subtypes in a wide serie of adult renal cell neoplasms.
Methods One hundred and fifty-one consecutive renal neoplasms, including 79 clear cell, 32 papillary, 20 chromophobe renal carcinomas (RCCs) and 20 oncocytomas were analyzed with an immunohistochemical panel including CD10, parvalbumin, Cytokeratin7, AMACR-racemase, S100A1 and CD13. Positive scoring was considered when the markers were expressed in more than 10% of neoplastic cells.
Results Clear cell RCCs immunoexpressed CD10, parvalbumin, Cytokeratin7, AMACR-racemase, S100A1 and CD13 respectively in 96%, 3%, 26%, 45%, 75% and 91% of cases. Papillary RCCs showed positivity in 77%, 3%, 88%, 100%, 69% and 91% of cases. Chromophobe RCCs in 60%, 95%, 90%, 30%, 5% and 0% of cases and oncocytomas in 35%, 100%, 55%, 15%, 100% and 0% of cases.
Conclusion(s) Although there are some overlaps, subtypes of renal cell neoplasms usually show distinctive immunoexpression profiles using this panel that may be efficient in several differential diagnostic settings. Clear cell RCCs usually express CD10 and CD13 and are negative for parvalbumin and Cytokeratin7; papillary RCCs typically show CD13, AMACR-racemase and Cytokeratin7 immunoexpression; both chromophobe RCCs and oncocytomas constantly express parvalbumin and are negative for CD13 whereas S100A1 is immunoexpressed in oncocytomas but not in chromophobe RCCs.

OP14.5

Critical role of central pathology review in translational research

Aydin H.; Sercia L.; Simmerman K.; Lane B.; Elson P.; Baehner R.; Rini B.; Zhou M.
Cleveland Clinic, Cleveland, OH, USA

Background The classification and staging of renal cell carcinoma have undergone major changes recently. Therefore, archival data collection may be misleading. We evaluated 1281 renal cell carcinomas to establish the role of central expert pathology re-review in providing current information for research and clinical applications utilizing archived materials.
Methods 1281 nephrectomies performed between 1985 and 2004 for stage < 3 clear cell RCC (CCRCC) or RCC not otherwise specified (RCCNOS) were collected. The diagnosis was based on 2004 WHO classification. Fuhrman nuclear grade (FNG), perinephric fat invasion (PNI), renal sinus invasion (RSI), and gross vascular invasion (GVI) were also evaluated. Re-review results were compared to archival database.
Results 104 (5.7%) cases were originally diagnosed as RCCNOS and were not further histologically subtyped. 144

(11.2%) were misdiagnosed as CCRCC. The correct diagnoses for misdiagnosed cases were papillary RCC (52, 36.1%), chromophobe RCC (36, 25%), oncocytoma (13, 9%), unclassified RCC (23, 15.9 %) and other tumors (20, 13.8%). In evaluable cases, FNG was changed in 303/775 (39.1%) cases, with significant change (from grade 1/2 to 3/4 and vice versa) in 180 (23.2%) cases. Also, discrepancy in PNI, RSI and GVI was present in 107/831 (12.9%), 112/841 (13.3%) and 36/829 (4.3%) cases respectively. Overall pathological stage was changed in 134/827 (16.2%) cases.

Conclusion(s) A significant number of cases were found to be originally incorrectly classified, and/or graded or staged. Centralized expert review provides more accurate and up-to-date information for translational research and potential clinical applications.

OP14.6

Inflammatory cardiomyopathy: a link between myocarditis and dilated cardiomyopathy?

Chiu K.B.; Sergi C.
University of Alberta, Edmonton, Alberta, Canada

Background Inflammatory cardiomyopathy (IFCM), a distinct entity in the most recent WHO/WHF definition, is a common cause of heart failure on a basis of cardiac inflammation, with autoimmune, infectious and idiopathic forms recognized.

Methods We reviewed the etiologic and morphologic features of hearts from 22 autopsies of patients with dilated cardiomyopathy (DCM) or autoimmune diseases and 100 explanted hearts with DCM. Inflammatory foci were graded as zero, mild and moderate-marked.

Results 42 hearts (mean wt. 498 g, patients mean age 47) with DCM contained inflammatory foci graded from mild (n=17 (40%)) to moderate-marked (n=25 (60%), including 10 with granulomatous inflammation). 12 (29%) had a history of viral infection or autoimmune diseases. Immunostaining showed mixed B- and T-cell infiltrates. No etiology was found in the remaining 30 (71%) cases. In 80 hearts (mean wt. 377 g, patients mean age 51), 68 (85%) showed DCM, fibrosis without inflammation, and only 4 were associated with etiologic factors. In the remaining 12 hearts from patients with autoimmune diseases, there were no morphologic features of DCM or IFCM.

Conclusion(s) A possible connection between myocarditis and DCM has long been postulated, but the underlying mechanisms linking these two conditions are poorly understood. This study confirms previous reports that IFCM shows both morphologic features of DCM and inflammation, and is associated with viral infection or autoimmune diseases. IFCM may represent the missing link between myocarditis and DCM.

OP14.7

"Dry" preparation of aortic aneurisms at the University of Turin

Bussolati G.; Micalizio S.
Univerisity of Turin, Turin, Italy

Background The origin of the Museum of Pathological Anatomy at the University of Turin can be traced at the first half of the 19th Century.

Methods In year 1860, the then Curator of the Museum, Dr. Giovanni Gallo, handled a list of 704 specimens (426 preserved dry, 278 in alcohol) to his successor, Prof. Germano Malinverni, who had just been nominated as the first Professor of Anatomic Pathology of the University of Turin. The list was inclusive of 37 "dry" preparations of vascular lesions (the clinical and autopsy data of two cases of "true" aortic aneurisms of luetic origin were reported by Dr. G. Gallo in 1821 (Repertorio Medico-Chirugica 1, 241–247, 1821).

Results Of all preparations, only 12 "dry" preparations of aortic aneurisms are still preserved. They vividly illustrate the spatial relationships of vascular lesion with bones (vertebrae, ribs, sternum, pelvis) often deformed and escavated by the growing and pulsating mass as well as (often) the breach responsible of the fatal haemorrhage. We have evidence (both, chemical and historical) that the preparations were fixed in mercuric chloride (corrosive sublimate) with perhaps the addition of other chemical reagents (antimonium; chrome) The restoration of these historical preparation was planned following historical records and successfully conducted by cleaning with lye water and with a decoction of Saponaria Officialis. Finally, shellac was applied over the surface.

Conclusion(s) The quite unique "dry" preparations are now visible at the local Museum and at site www.oncologiaumana.unito.it/aneurisms.

OP14.8

Histopathological correlation and feasibility of atherosclerotic carotid lesion classification using T2* weighted imaging at 9.4t MRI

Goebel H.; Spehl T.; Paul D.; Markl M.; Mader I.; Harloff A.
Institute for Pathology, University of Cologne, Germany, Cologne, Nordrhein-Westfalen, Germany

Background Intraplaque hemorrhage (IH) is a major risk factor for atherosclerotic plaque progression and ischemic stroke in case of thromboembolism. Intracerebral hemorrhage can be reliably detected by T2* weighted MR imaging (T2* WI). Thus, we evaluated the feasibility of a multicontrast-MRI protocol including T2* WI to assess the specific identification of IH in carotid artery lesions (CAL) ex-vivo.

Methods Surgically removed, formalin fixed CAL of 27 patients with ≥ 70% internal carotid artery stenosis were firstly analyzed using a 3D multi-contrast MRI protocol at 9.4 Tesla consisting of T1, T2, and T2* weighted sequences with a spatial resolution ~100 μm3. Histology as the gold standard was used to establish plaque composition and to classify CAL according to modified AHA criteria. Then, corresponding 2D MRI slices were independently assessed for the presence of plaque components and AHA lesion type by two readers.
Results Mean sensitivity and specificity of both readers for IH were 87–90% and 65–79% respectively. Mean accuracy of plaque classification based on MR images and using modified AHA criteria was 87.5%.
Conclusion(s) Incorporation of T2* WI into multi-contrast MRI was feasible and allowed for a reliable identification of IH in CAL and combination of T2* weigthed imaging with standard multicontrast protocols could be beneficial to further increase accuracy of plaque assessment.

OP14.9

Malignant neoplasms in the heart. A study of four cases

Bakula Zalewska E.; Domanski H.A.
Department of Pathology, Maria Skłodowska-Curie Memorial Cancer Center and Institute of Oncology, Warsaw, Poland

Background Malignant neoplasms in the heart are uncommon; metastases are the most frequently found and sarcomas are the most common primary heart malignancies. Other malignant lesions in the heart include hematologic tumours and mesotheliomas.
Methods Four patients having malignant neoplasms of the heart were identified in the records of the Department of Pathology & Cytology, Lund University Hospital during 1998–2008. In three patients diagnoses were rendered from histological examination of heart biopsies and one tumour was found at autopsy. Biopsy from Ewing sarcoma was also evaluated cytogenetically.
Results The lesions included one angiosarcoma and one Ewing sarcoma, both of each presented with pericardial effusions. There was one diffuse large, B-cell lymphoma and one squamous cell carcinoma metastatic from the lung. There were two women and two men ranging from 28 to 81 years of age. The sarcomas were treated with chemo- and radiotherapy while the patient with lymphoma received chemotherapy alone. The patients with angiosarcoma, lymphoma and metastasis from lung carcinoma died of their disease within 3 to 10 months from presentation while the patient with Ewing sarcoma doing well after 3 years follow-up.
Conclusion(s) Malignant neoplasms of the heart are rare and display a heterogeneous spectrum of lesions. Early detection and correct diagnosis, in particular distinguishing primary heart sarcomas and hematological malignancies from metastases, is very important because of different treatment options and prognosis.

Oral presentations 15

Dermatopathology - Endocrine pathology

OP15.1

Structural, molecular and biochemical changes of collagen V is associated with cutaneous thickness in scleroderma

Teodoro Rosolia W.; Martin P.; Braga Fontes F.; Morais J.; Velosa Pereira A.; Carrasco S.; Souza Beatriz R.; Capelozzi V.L.; Yoshinari Hajime N.
Universidade de São Paulo, São Pauo, São Paulo, Brazil

Background Systemic sclerosis (SSc) is a fibrotic disease characterized by an increased extracellular matrix deposition, vasculopathy and an autoimmune dysfunction. We have found an excessive and distorted collagen type V (COLV) deposition in the skin of SSc patients that could be associated to cutaneous thickness. Our purpose was to analyze the structural, molecular and biochemical profile of COLV in skin through of patients with SSc.
Methods Six skin female SSc patients (ACR criteria: 3 diffuse and 3 limited subtype; mean age 26+13.4 year) biopsies were obtained from thorax region during pulmonary surgery and six healthy control were also obtained from thorax region during plastic surgery procedure. COLV analysis was done in fibroblasts culture, through tridimentional reconstruction (3D), Real-time RT-PCR, and immunoblotting.
Results Under 3D reconstruction collagen V, displayed as thickened and forming heterotypical fibers with collagen I in SSc, in contrasting with thin and linear pattern as the native form in the healthy controls. Molecular analysis demonstrated an increased COLV mRNA expression in SSc (1,375±0,373) patients when compared to control (0,0047±0,0013, $p < 0.05$) group. These findings were validated by immunoblotting assay.
Conclusion(s) These unusual structural, biochemical and molecular COL V profile can justify the morphological pattern viewed in skin of SSc patients. These results indicate that this remodeling is different from others fibrotic processes and bringing new insights in the treatment of this severe disease.

OP15.2
Evaluation of bcl-2 expression in aggressive and non-aggressive basal cell carcinomas

Amini E.; Salehian P.
Tehran, Islamic Republic of Iran

Background bcl-2, the well known anti-apoptotic gene, promotes cell viability without cell proliferation. Expression of the bcl-2 oncogene is reported in certain low grade neoplasms including basal cell carcinomas (BCCs). Bcl-2 expression in BCCs is contradictory, with 67–100% immunopositivity being reported. The purpose of this study was to evaluate bcl-2 expression in the indolent variants of BCC, namely superficial and circumscribed subtypes and their aggressive counterparts, infiltrative and morphea-like subtypes.
Methods Anti-human bcl-2 monoclonal antibody is used to identify its protein product in formalin-fixed tissue from 33 BCCs. 22 histopathologically non-aggressive and 11 aggressive subtypes were investigated. Quantity of decoration of tumor cells for bcl-2 was graded in the following fashion: 0 to 25%, 26% to 50%, 51 to 75% and 76% to 100%. Intensity of decoration was evaluated as slight, moderate and intense.
Results bcl-2 expression was observed in all of the BCCs, but high bcl-2 expression was statistically a significant feature of non-aggressive BCCs (p=0.001). 40% and 60% of superficial subtypes reveal 51% to 75% and 76% to 100% of tumoral cells decoration for bcl-2 respectively, and 47% and 41% for circumscribed subtypes, which also reveal 26% to 50% of decoration in 11.2% of cases. All morphea-like subtypes reveal 0% to 25% of tumoral cells decoration. In infiltrative subtypes quantitative bcl-2 expression equals 0% to 25% in 55.6% of cases, 26% to 50% in 22.2% of cases and 51% to 75% in 22.2% of cases (p = 0.004). Ultimately, of the non-aggressive subtypes bcl-2 expression equals 26% to 50%, 51% to 75% and 76% to 100% in 9%, 45.6% and 45.6% of the cases respectively. Of the aggressive subtypes bcl-2 expression equals 0% to 25%, 26% to 50% and 51% to 75% in 63.6%, 18.2% and 18.2% of the cases (p = 0.001).
Conclusion(s) Different bcl-2 expression in various non-aggressive and aggressive histopathological subtypes of BCCs suggests that despite the common derivation of these tumors from a primitive basaloid stem cell and a limited potential for metastasis, they form a heterogenous group of tumors. While the superficial and circumscribed BCCs are indolent slow- growing tumors with high bcl-2 labeling, the aggressive BCCs are infiltrative and morphea-like tumors with low bcl-2 labeling. High expression of bcl-2 may indicate a more favorable prognosis in BCCs.

OP15.3
Expression of lactadherin in melanoma and melanocytic lesions

Begon J.; Andrejevic Blant S.; Aldairi R.; Carrascosa C.; Mariotti A.
Institute of Pathology, CHUV-Hospital & Faculty of Biology and Medecine, Lausanne, Switzerland

Background Lactadherin is a secreted glycoprotein that promotes cell adhesion and cell-cell interactions, and can act in both an autocrine and paracrine manner. We have recently shown that lactadherin is associated with cholesterol/sphingolipids rich membrane microdomains of Vertical Growth Phase (VGP) and metastasis-derived, but not Radial Growth Phase (RGP) derived melanoma cells, indicating that the function of this protein is differentially regulated during melanoma progression.
Methods Reviewing melanocytic lesions cases between 2004 and 2008, we have selected 47 lesions from 33 patients, including 4 benign naevocellular naevi, 9 dysplasic naevi, 5 in situ melanoma and 19 melanomas (including lesions with nodal, dermal or distant metastases), some cases presenting more than one lesion. Tissue microarray including selected lesions and healthy skin, were prepared and slides were examined for lactadherin immunoreactivity.
Results We have found that lactadherin is not expressed in normal melanocytes nor in naevi, while it is expressed in some primary melanomas (independently from the histological type), and in their derived lymph node metastases. Interestingly we have also observed that lactadherin is expressed in in-transit metastases.
Conclusion(s) Our observations indicate that lactadherin expression increases during melanoma development and in particular in early stages of melanoma progression at the onset of metastatic activity and suggest that lactadherin may be a marker of metastatic melanoma in its early phases.

OP15.4
Non-linear laser imaging of human skin tissue

Cicchi R.[1]; Sestini S.[2]; De Giorgi V.[2]; Maio V. [3]; Lotti T.[2]; Massi D.[3]; Pavone F.S.[1]
[1]L.E.N.S. & Department of Physics, [2]Department of Dermatological Sciences, [3]Department of Human Pathology and Oncology, University of Florence, Florence, Italy

Background Non-linear microscopy is a non-invasive laser scanning imaging technique able to image up to 150 micron depth inside a biological tissue without any exogenously added probe.
Methods In this work we have combined different non-linear techniques, including two photon intrinsic fluorescence (TPE), second harmonic generation microscopy (SHG), fluorescence lifetime imaging microscopy (FLIM), and multispectral two photon emission detection (MTPE) to investigate different kinds of human cutaneous lesions on fresh biopsies.
Results Morphological and spectroscopic analyses have allowed to characterize both healthy and pathological skin samples, including tumors, as well as to discriminate between healthy and diseased dermis, in a good agreement with common routine histology. In particular, we have examined tissue samples from normal and pathological scar tissues (keloid), and skin tumors, including basal cell carcinoma (BCC) and malignant melanoma (MM). Finally, the use of 5-aminolevulinic acid as a contrast agent has been demonstrated to increase the contrast in the tumor margins detection.
Conclusion(s) The obtained results represent further support for in-vivo non-invasive non-linear imaging of diseased skin. A possible in-vivo use of this imaging technique could be helpful in skin cancer research, whereas it could be a powerful tool in the assessment of photo-ageing, laser therapy effects, effects of cosmetics, and in general in applications where a biopsy can be avoided.

OP15.5

Primary cutaneous Ewing sarcoma/primitive neuroectodermal tumor: are immunohistochemically negative for Merkel cell polyoma virus

Pulitzer M.; Scolyer R.; Jungbluth A.; Busam K.
Department of Pathology, Memorial Sloan Kettering Cancer Center, New York, New York, USA

Background Primary cutaneous Ewing sarcomas/primitive neuroectodermal tumors (ES/PNET) are rare skin tumors, which may be confused with other cutaneous small blue cell tumors, in particular Merkel cell carcinoma (MCC). Recently, a novel reagent has become available for the diagnosis of MCC: the monoclonal antibody CM2B4, which recognizes an epitope on the large T antigen associated with the Merkel cell polyoma virus (MCV). Preliminary studies have indicated high sensitivity and specificity of this antibody for MCC.
Methods Immunohistochemistry was performed on sections of formalin-fixed and paraffin-embedded tissue of seven cases of primary cutaneous ES/PNET (small cell tumors of the skin, positive for CD99 with EWS rearrangement) and 10 cases of MCC, using the antibody CM2B4.
Results Eight of 10 MCCs were positive for CM2B4. All ES/PNET tumors were completely negative for CM2B4.
Conclusion(s) Given some morphologic and immunohistochemical overlap between MCC and cutaneous ES/PNET, the antibody CM2B4 represents an additional useful diagnostic reagent. It failed to stain any cutaneous ES/PNET, suggesting that positive labeling of a cutaneous small cell tumor for CM2B4 practically excludes ES/PNET.

OP15.6

RCAS1 expression in thyroid malignant and benign lesions

Stolakis V.; Demetriou N.; Alexandrou P.; Zarros A.; Griniatsos I.; Giaginis K.; Klijanienko J.; Theocharis S.
University of Athens, Medical School, Athens, Greece

Background The tumor associated antigen "receptor-binding cancer antigen expressed on SiSo cells" (RCAS1) inhibits the growth of cells that express its receptor, inducing apoptosis. The aim of the present study was to evaluate the clinical significance of RCAS1 expression in benign and malignant thyroid lesions.
Methods RCAS1 protein expression was assessed immunohistochemically in formalin-fixed, paraffin-embedded thyroid tissues from 124 patients with benign (hyperplastic nodules and Hashimoto thyroiditis, $n=64$) and malignant lesions (papillary, medullary, follicular and anaplastic thyroid carcinomas $n=56$). The RCAS1 positivity, overexpression, and intensity of staining were assessed in order to compare the expression of RCAS1 protein between malignant and benign thyroid lesions, as well as between Hashimoto thyroiditis and hyperplastic lesions. RCAS1 protein expression was statistically correlated with TNM stage and tumor proliferative capacity (Ki67 labeling index).
Results RCAS1 positivity was noted in 71 out of 124 (57%) thyroid lesions examined. Statistically significant difference in RCAS1 positivity and overexpression was noted between thyroid malignant and benign lesions ($p=0.000103$ and $p=0.0000103$, respectively), and between Hashimoto thyroiditis and hyperplastic nodules ($p=0.02215$ and $p=0.0000779$, respectively). Statistically significant difference in RCAS1 intensity of immunostaining was noted between thyroid malignant and benign lesions ($p=$

0.000989), and between Hashimoto thyroiditis and hyperplastic nodules (p=0.003846). RCAS1 positivity, overexpression and intensity of immunostaining were not statistically significantly correlated with TNM stage and Ki67 labeling index.
Conclusion(s) Our data support evidence for implication of RCAS1 in thyroid neoplasia, based on different correlations manifested in benign and malignant lesions.

OP15.7
A routine immunohistochemical procedure for the detection of paraganglioma and pheochromocytoma patients with germline SDHB, -C, or -D gene mutations

Gaal J.; Van Nederveen F.; Favier J.; Korpershoek E.; Komminoth P.; Mannelli M.; De Bruïne A.; Badoual C.; Tissier F.; Perren A.; Gimenez-Roqueplo A.; De Krijger R.; Dinjens W.
Erasmus MC, Rotterdam, Netherlands

Background Pheochromocytomas (PCCs) and paragangliomas (PGLs) are neuro-endocrine tumors that occur sporadically and in several hereditary tumor syndromes, including the pheochromocytoma-paraganglioma (PCC-PGL) syndrome. This syndrome is caused by germline mutations in succinate dehydrogenase B (SDHB), C (SDHC), or D (SDHD) genes. Clinically, the PCC-PGL syndrome is often unrecognized although 10 to 30% of apparently sporadic PCCs and PGLs harbor germline SDH-gene mutations. Despite these figures, screening of all PCCs and PGLs for mutations in the SDH-genes to detect the PCC-PGL syndrome is rarely performed due to the workload and financial constraints.
Methods Immunohistochemistry for SDHB was performed on 220 tumors. Two retrospective series of 175 PCCs and PGLs with known germline mutation status for PCC/PGL susceptibility genes were investigated. In addition, a prospective series of 45 PCCs and PGLs was investigated for SDHB immunostaining followed by SDHB, -C, and -D mutation testing.
Results SDHB protein expression was absent in all PCCs and PGLs with a SDHB, -C, or -D mutation and present in all MEN2-, VHL-, and NF1-related paraganglionic tumors. In addition, 47 of 53 (89%) PCCs and PGLs, in which no syndromic germline mutation was identified, showed SDHB expression.
Conclusion(s) Our results demonstrate that the PCC-PGL syndrome can be diagnosed reliably by an easy-to-perform and low-cost immunohistochemical procedure. Only in patients with SDHB-negative tumors SDHB, -C, and -D germline mutation testing is indicated. SDHB immunohistochemistry on PCCs and PGLs will improve the diagnosis of PCC-PGL syndrome, which is important for surveillance of PCC and PGL patients and their family members.

OP15.8
Light chains expression of lymphoid infiltrate in fine-needle cytology of Hashimoto's thyroiditis

Zeppa P.; Cozzolino I.; Peluso A.; Troncone G.; Malapelle U.; Russo M.; Varone V.; Vetrani A.; Palombini L.
Dipartimento di Scienze Biomorfologiche e Funzionali, Università di Napoli "Federico", Napoli, Italy

Background The thyroidal lymphoid infiltrate (TLI) in Hashimoto's thyroiditis (HT) represents the substrate from which thyroid lymphoma (TL) may arise. The aim of the study was to assess the TLI in HT with flow cytometry (FC) evaluating the κ/λ light chains ratio and its molecular assessment.
Methods FNA was performed in 34 HT patients to prepare traditional smears, FC immunophenotyping and RNAlaterTM suspensions for molecular assessment. FC used antibodies were: CD3, CD5, CD10, CD19, κ and λ light chains. In four cases, high molecular weight DNA was extracted and used for polymerase chain reaction (PCR) to amplify the variable diversity joining (VDJ) region of the heavy chain Ig genes (IgH). A statistical analysis was performed to evaluate possible association between the percentage of the expressing cells (≤ 20%, >20%) and κ/λ ratio.
Results FC showed T-cells (CD3+,CD5+) in all the cases, T-cells and B-cells (CD19+,CD10+/-) in 22 cases. Light chains were expressed in 30 cases; in 13 cases in less than 20% of the cells and in 17 cases in more than 20%. Five cases showed small κ/λ ratio imbalances and PCR analysis showed diffuse bands in the gel and Gaussian curves at the heteroduplex. Statistical analysis showed a significant association between light chain restriction and low light chain expression (p<0.005).
Conclusion(s) Small light chain imbalances in HT are not sustained by heavy chain Ig gene (IgH) rearrangements. FNA coupled with FC may contribute to the discrimination of florid TLI from non-Hodgkin's lymphoma.

OP15.9
The expression of cell cycle markers in autoimmune thyroiditis

Babal P.; Kvetova M.; Urbanova A.; Janega P.
Department of Pathology, Faculty of Medicine, Comenius University Bratislava, Bratislava, Slovakia

Background Autoimmune thyroid diseases (AITD), Hashimoto thyroiditis (HT) and Grave's disease (GD), represent the most frequent thyroid gland disorders, especially in the

young population. They are accompanied by the increased risk of thyroid gland tumors. Alterations of the cell cycle regulation may be the key step in malignant transformation of affected cells.

Methods Archival FFPE tissue samples from patients with AITD and control parenchymatous goiters were used. The expression of the p53, caspase 3, NO synthase 1, 2 and 3, Bcl-2, survinin, Bax, Apaf and PCNA was analyzed by immunohistochemistry.

Results The increased expression of proapoptotic markers (caspase 3, Bax, Apaf), as well as antiapoptotic markers (bcl-2, survivin), tumor supressor protein p53, marker of the cellular proliferation PCNA and all isoforms of NO syntases were detected in HT. In GD only increased expression of antiapoptotic protein survivin and proapoptotic protein Bax was detected. The expression of other markers was less prominent, although it was slightly increased when compared to the controls.

Conclusion(s) We demonstrated increased expression of proteins involved in the regulation of apoptosis in AITD, especially in HT, which correlates with the higher incidence of malignancies in these patients in comparison with GD. Positivity of proliferative and antiapoptotic markers in HT was found predominantly in oncocytes. The change of normal thyreocytes into oncocytes could thus indicate an increased risk of malignant transformation. Autoimmune thyroid disease seems to be an interesting model for studying of precancerosis. This work was supported by Ministry of Health Slovak Republic No.2006/23-UK-02.

Oral presentations 16

Soft tissue tumors

OP16.1

Potential role of egfr signaling in giant cell tumor of bone (GCTB)

Moskovszky L.; Balla P.; Sapi Z.; Knowles H.; Athanasou N.; Jones F.; Szendroi M.; Kopper L.; Benassi M.; Picci P.; Krenacs T.

1st Department of Pathology and Experimental Cancer Research, Semmelweis University, Budapest, Hungary

Background The benign but locally aggressive and incidentally metastatic giant cell tumour of bone (GCTB) consists of osteoclatic giant cells and a mononuclear cell population including reactive monocytic and neoplastic stromal elements. Here we demonstrate a positive correlation of EGFR expression with biological aggressiveness and a proliferative response upon EGF treatment in the neoplastic cell population of GCTB.

Methods EGFR (clone:3C6) expression was studied in 450 archived TMA (tissue microarray) samples of 260 cases including 96 recurrences, 21 metastatic tumors and 6 cases of secondary osteosarcoma. Peripheral blood mononuclear cells (PBMC) were treated with combinations of MCSF, RANKL and EGF. Also, cultured CD14-negative neoplastic cells of 4 GCTB cases treated with EGF were analysed for proliferation and differentiation.

Results Half of the GCTB cases expressed EGFR showing positive correlation with tumor grade/aggressiveness and metastatic growth without major aberration in the EGFR gene. Neoplastic stromal cells were responsible for EGFR expression with elevated levels of phospho-EGFR, p-Raf1 and p-ERK1-2 suggesting an active MAPK pathway. EGF facilitated osteoclastogenesis from PBMC but without supporting osteolytic activity. CD14-negative neoplastic cells showed proliferative response to EGF, though this treatment did not increase alkaline phosphatase activity to indicate differentiation.

Conclusion(s) EGFR signaling seems active in neoplastic stromal cells of GCTB and may contribute to the pathogenesis and aggressiveness of this osteolytic tumor.

OP16.2

Activity of Topoisomerase IIα in leiomyosarcoma uteri

Avdalyan Merudzanovith A.; Lazarev Fedorovitch A.; Bobrov Petrovitch I.; Klimatchev Vasilievitch V.

Altays office of ROSC by N.N. Blochin, Barnaul, Altai, Russian Federation

Background Topoisomerase IIα participates in various transformation of DNA, for example it clears topological difficulties at its replication and transcription, thus affecting to intensity of the processes, connected first of all with proliferative activity. At mean time, there is no data in bibliographies on containing of enzymes in leiomyosarcoma uteri.

Methods Retrospective materials of 62 cases of spindle-cell leiomyosarcoma. Topoisomerase IIα expression was detected by immunohistochemical method. 10-year survival rate was detected by Caplan-Meyer method.

Results Activity of Topoisomerase IIα of neoplastic cells was indicated in 87%±5,6 of LMS, at that ex-ponential increase of enzyme was accompanied by decrease of differentiation degree of tumor: so activity increase from 5,5±1,6% up to 23,7±8,7% of cells was marked in series from high to low differentiation degree. Medium level of activity of enzyme was 17,5%. Analysis of prognostic value of expression affected logically to 10-year survival rate: in the group of Topoisomerase IIα activity up to the medium grade at medium activity index of 17,5%, 10- year recurrence-free viability came to 61,4%±7,4. At enzyme

activity more than medium grade no one being investigated survived to 10 year, and 4-year vitality came to 11,9%±4,6. At multifactorial analysis of prognostic value of number of molecular and biological characteristics activity of enzyme appeared to be independent criteria (χ^2=4,9; p=0,05).
Conclusion(s) In such a way, hyperexpressia of Top-oisomerase IIα was detected in ULMS cellules. Level of expression of enzyme affected statically authentic to differentiation degree of neoplastics cell and decade-long survival rate.

OP16.3
Alterations of the G1-S checkpoint in leiomyosarcoma of the peripheral soft tissue and its prognostic significance. A tissue microarray analysis of 70 cases treated at the same institution

Panelos I.; Beltrami G.; Scoccianti G.; Capanna R.; Mela M.; Paglierani M.; Pepi M.; Massi D.; Franchi A.
Department of Pathology, University of Ioannina Medical School, Ioannina, Greece

Background The aim of this study was to investigate the expression of cell cycle regulators p53, p16, cyclin-D1, and retinoblastoma (RB) gene protein in leiomyosarcomas in order to identify expression profiles potentially useful for clinical prognostic purposes.
Methods A tissue microarray representing 70 localized leiomyosarcomas of the limbs and limb girdles was created and immunohistochemical staining for p53, p16, cyclin-D1, and RB was performed. Staining was scored as either absent-low (< 20% of neoplastic cells) or moderate-diffuse (≥ 20%). Outcome analysis was performed for local recurrence-free survival (LFS), metastatic disease free survival (MDFS), and disease-specific survival (DSS).
Results Kaplan Meyer analysis revealed that no single alteration of the factors examined was associated with outcome, but tumors showing concomitant alteration of p16 and p53 were characterized by reduced MDFS and DSS (p=0.01 and p<0.001, respectively). In addition, patients who received adjuvant therapy consisting of radiotherapy alone or radiotherapy and chemotherapy had a better DSS than those receiving surgery alone or surgery and chemotherapy (p=0.05). In multivariate analysis, altered p16/p53 remained the only predictive parameter of MDFS and DSS (p = 0.048, HR=2.488, 95% CI 1.006–5.116; p=0.043, HR=2.488, 95% CI 1.029–5.909).
Conclusion(s) Accumulation of cell cycle alterations represent a prognostic indicator in localized soft tissue leiomyosarcoma, and in particular altered p16/p53 expression is associated with an unfavorable prognosis. This may help the clinical management of patients with leiomyosarcomas.

OP16.4
Extraskeletal mesenchymal chondrosarcoma (EMC): a clinicopathological study

Safaya R.; Jain A.
All India Institute of Medical Sciences, New Delhi, Delhi, India

Background Mesenchymal chondrosarcoma (MC), an uncommon aggressive variant of chondrosarcoma. About one thrid of MC occur in extraskeletal sites. The findings of this study emphasize the importance of adequate sampling, early diagnosis, correct & appropriate treatment to improve the life span.
Methods Between 2005 and 2008 nine cases of MC were diagnosed in the department of pathology at AIIMS. P53 & Ki67 expression was studied in all nine cases to see if there is any prognostic value of these markers.
Results Of nine cases five were found to be EMC. The extraskeletal sites involved were pleura, meninges, chest wall, nasal cavity and shoulder. The duration of symptoms varied from as low as 15 days to as long as 20 years. Of 5 cases of EMC full tumour specimens were received in three cases and biopsies were performed in 2 other cases. Patient having EMC of pleura succumed to compression due to huge pleural mass & biopsy being non-representative. Final diagnosis of MC was made on autopsy. On the biopsy material final diagnosis was hampered on account of inadequate tissue, however, MC was the first possibility. Results of P53 & Ki67 staining did not show any correlation with the clinical behaviour.
Conclusion(s) MC forms a diagnostic dilemma unless supported by adequacy of biopsy sample, clinical and radiological data, and immunohistochemistry. Although MC is a highly malignant neoplasm but early diagnosis, appropriate and adequate treatment can remarkably influence the outcome.

OP16.5
CD56, calretinin and CD34 a useful marker for differentiating schwannomas from neurofibromas

Lee S.; Park J.; Park N.; Park J.
Keimyung University School of Medicine, Daegu, Republic of Korea

Background Schwannomas (SC) and neurofibromas (NF) are two most common benign neoplasms derived from peripheral nerve. It is difficult to distinguish these two tumors by light microscopy alone in a small number of cases. The importance in separating these 2 entities lies in the selection of surgical approaches in these patients. Until now, S-100 protein, calretinin, CD34, CD56, claudin, Glut-1 have been studied for their

potential value in the differential diagnosis of these tumors.

Methods We immunohistochemically studied 50 cases of SC and 56 NF using antibodies to S-100 protein, calretinin, CD34 and CD56 to explore the usefulness in differentiating SC from NF. The archival paraffin blocks were prepared for tissue micro-array. Immunohistochemistry was performed using HRP polymer methods.

Results CD56 was positive in 39 SC (78%) and 2 NF (3.6%) (p=0.0000). Calretinin was positive in 11 SC (22%) and none of NF (p=0.0002). CD34 showed positivity in 17 SC (34%) and 39 NF (54.6%) (p=0.0002). All SC and most NF cases were positive for S-100 protein.

Conclusion(s) These results indicated that CD 56 is detected in 78% of SC and only 3.4% of NF, suggesting it is a superior marker for differentiating SC from NF. Calretinin and CD34 can be another useful markers for distinguishing these two lesions.

OP16.6

Claudin expression in gastrointestinal stromal and mesenchymal tumours

Gyorffy H.; Tokes A.; Jackel M.; Udvarhelyi N.; Kiss A.; Schaff Z.
Semmelweis University, 2nd Dept. of Pathology, Budapest, Hungary

Background Gastrointestinal stromal tumours (GIST) are rare. Their prevalence in Hungary is 129/1 million inhabitants. These tumours prove to be malignant in 20–30% of cases. Recent studies confirmed that epithelium revealing tight junction proteins, claudins (CLDN) are demonstrable in non-epithelial tumours. CLDN5 was found to be expressed by endothelial cells. Our aim was to confirm the claudin expression in GISTs, leiomyosarcomas and angiosarcomas by immunohistochemical and molecular biological methods.

Methods Formaline-fixed, paraffin-embedded tissue samples of 13 GISTs, 12 leiomyosarcomas, 10 angiosarcomas, 3 hemangiomas and 3 leiomyomas were used. Immunohistochemical examinations were performed with anti-CLDN1, -2, -3, -4, -5 and -7 antibodies. CLDN2 and -5 expressions were confirmed at protein and mRNA levels.

Results CLDN1 expressed only in leiomyosarcomas. GIST and leiomyosarcoma expressed CLDN2, -3, -4, -5 and -7 proteins. Leiomyomas expressed CLDN2 exclusively. CLDN2 and -5 expressions were features for benign and malignant vessel tumours.

Conclusion(s) Claudin expression profiles were typical in each studied tumour. Similarities of claudin expression in GISTs and leiomysarcomas suggest histogenetic connection between these tumours.

OP16.7

Mutation profile of Turkish gastrointestinal stromal tumor cases: a multicenter study

Kaygusuz G.; Suner S.; Karatayli E.; Dogusoy Bulbul G.; Ozoran Y.; Akbulut H.; Mandel Molinas N.; Kuzu I.
Ankara University, School of Medicine, Dept of Pathology, Ankara, Turkey

Background Gastrointestinal stromal tumor (GIST) is the most common mesenchymal neoplasm in the gastrointestinal tract and is associated with mutations of the KIT or PDGFRA genes. Mutation screening is becoming an important method in GIST for determination of prognostic molecular parameters and guiding targeted therapy. The purpose of this study was to analyse the clinicopathologic and mutational status of Turkish GIST cases.

Methods Parafin blocks of 43 GIST cases were analyzed by their clinical, morphological and immunophenotypic characteristics. Mutation analysis was performed on DNA extracted from parafin embedded tissues. Exons 9, 11, 13, 17 of KIT gene and exons 12, 14, 18 of PDGFRA gene were examined by direct sequencing (Applied Biosystems, Foster City, CA).

Results Patients median age was 61 years, and Male: Female was 1:0,6. Tumors were located most commonly in the stomach (46%), small intestine (21%), colorectum (11%), omentum-peritoneum (18%) or liver (4%). Two of the cases were recurrent tumors. Thirty one cases were classified in high, 8 were intermediate and 4 were low risk groups. Except two, all cases were CD117 positive. Not only point mutations but also different types of deletions with or without insertions were detected most commonly in KIT gene exon 11.

Conclusion(s) We confirmed that, paralel with the previous reports, the spindle cell morphology was mostly accompanied by mutations in KIT gene exon 11.

OP16.8

Primary synovial sarcoma of the liver

Ferlan-Marolt K.; Luzar B.; Bracko M.
Institute of Pathology, Medical Faculty Ljubljana, Slovenia

Background Concerning only two recently published cases of synovial sarcoma proceeding from the liver this origin of soft tissue neoplasia is extremely rare. We investigated the particular liver tumor and upgraded the conventional diagnosis with cytogenetic analysis.

Methods A 45-year-old man presented with fatigue and abdominal pain due to a large, highly vascular tumor mass in the left liver lobe. Hepatic lobectomy revealed a well demarcated, grayish tumor with 10 cm in diameter, comprising hemorrhagic areas. Since the neoplasm did not

extend to other organs it was defined as liver primary. Follow–up evaluation detected no widespread disease 5 months after surgery.

Results The pathologic findings corresponded with a malignant soft tissue tumor compressing adjacent liver parenchyma. It was composed of spindle cells with oval to elongate nuclei arranged in a whorled and hemangiopericytoma-like pattern. Positive immunohistochemical stains were for CD99, CD56, bcl-2, vimentin, and EMA, negative for cytokeratins, CD34, CD117, muscle actin, S100, HMB-45, chromogranin, calponin, caldesmon. With FISH cytogenetic study the specific translocation t (x;18) (p11,2; q11,2) involving the fusion of SYT gene was detected.

Conclusion(s) Synovial sarcoma with suggestive basic morphology expresses distinctive immunophenotype and cytogenetic abnormality related to X-chromosomal genes SSX1, SSX2. In distinguishing the growth from other morphologically similar sarcomas molecular tissue examination has become an obligatory diagnostic technique. Since synovial sarcomas may arise in unusual anatomic sites, the liver may also be the organ of its origin, as in our represented case.

OP16.9

The role of artificial intelligence for predicting the biological behavior of bone tumors

Sopta Petar J.; Marinkovic J.; Mijucic V.; Vucicnic Z.; Minic D.

Institute for Pathology, Belgrade, Serbia, Serbia and Montenegro

Background Score for predicting the clinical and biological tumors behavior is usually determinate using classic statistical methods such multivariate logistic regression (MVLR), but new computer tehniks, and models of artificial intelligence: classifications tree analysis (CTA) and artificial neural network (ANN) take a place in modern scoring systems.

Aim This study compared the levels of accuracy of MVLR, CTA and ANN model for the prediction of bone tumor's biological behavior

Methods Data (166 variables) from 2807 patient with bone tumors were used for analysis. We compared three models across theirs overall percentages. The best model was one with highest overall percentage.

Results Malignant bone tumors (prime and metastatic) were 1339 (47,7%) and benign 1468 (52,3%). From 166 characteristics 11 were selected and included into scoring system. Three performed scoring models showed wary high overall percentages in prediction biological behavior of bone tumors: MVLR 93, 77%, CTA 88, 2% and ANN 91, 5%.

Conclusion(s) All scoring models are very useful in prediction, most of them each ones had priority versus others. The most successive is MVLR. ANN have high sensitivity and gave ranges of variables included in score. CTA is very simple and easy for interpretation.

Oral presentations 17

Digestive pathology

OP17.1

CD34 in cirrhotic liver - reliance to dedifferentiation

Gligorijevic Velja J.; Djordjevic B.; Gligorijevic R.N.

Department for Pathology, Nis, Serbia and Montenegro

Background Dysplastic nodules are distinct nodular lesions that differ from surrounding hepatic parenchyma in terms of size, color, texture or degree of bulging at the cut surface. We investigated the angiogenic profile of regenerative, dysplastic and nodules of hepatocellular carcinoma to asses wether vascular profile is in reliance to proces of dedifferentiation of hepatocytes during the course of cirrhosis.

Methods Thirty two liver nodules from surgical biopsies of 12 patients previously undiagnosed to have cirrhosis:8 large regenerative nodules, 11 low grade dysplastic nodules, 12 high grade dysplastic nodules and 3 early HCCs. Serial sections of the nodules and surrounding cirrhotic liver tissue were stained against CD34. The assesmant of capillary units was performed according to the method proposed for vascular counting.The results were statisticaly analysed.

Results Sinusoidal capillarisation and CD34 positive forms were at the periffery of the LRNs and LGDNs and were more centraly located in HGDNs, while random in HCC. The number of capillaries was not singnificantly different in specific nodular type, but single was greatest in HGDNs. There is important statistical difference in vascular unites number among the tested groups ($p<0,001$) with greatest number of CD34 positive unites in HCC and smallest in LRN.

Conclusion(s) There is strong correlation of sinusoidal capillarysation to dedifferentiation of the liver tissue during the course of cirrhosis. The appearnce of dysplastic nodules in non selected surgical biopsies is frequent enough to challenge caution during the follow up of cirrhotic patients.

OP17.2

Chemical imaging of liver steatosis using synchrotron infrared microspectroscopy

Le Naour F.; Bralet M.; Sandt C.; Guettier C.; Dumas P.
INSERM 602, Villejuif, France

Background Liver steatosis is a frequent lesion that may progress to cirrhosis and hepatocellular carcinoma. The mechanisms of lipid accretion in liver are still l unknown.
Methods We addressed the in situ composition and distribution of biochemical compounds in steatotic liver using synchrotron FTIR (Fourier transform infrared) microspectroscopy. Infrared spectroscopy is based on the determination of absorption of infrared light due to resonance with vibrational motions of functional molecular groups. Synchrotron is a high brightness source of infrared giving high and used for histological staining or FTIR microspectroscopy. spatial resolution. This technique allows determining the chemical composition at the subcellular level and chemical imaging by visualizing the distribution of a selected band along a tissue section. The study was performed on 3 livers exhibiting macrovacuolar and microvesicular steatosis and 3 normal livers. Frozen sections were cut at 5 μm.
Results Imaging steatosis visualized anti-correlation between proteins and lipids which were highly enriched in steatotic vesicles. Unsaturated molecules followed lipid distribution suggesting an enrichment of unsaturated lipids into such steatotic vesicles. Interestingly, IR spectra performed on the non steatotic part of the fatty livers demonstrated increased lipid content despite histological aspects similar to that observed on normal liver.
Conclusion(s) Synchrotron FTIR microspectroscopy appears to be a powerful technique to study the early metabolic disturbances and the local lipid composition in steatosis. In addition, as deported IR sources are currently available, this technique could provide accurate evaluation of hepatic steatosis before liver surgery or transplantation.

OP17.3

Gamma smooth muscle actin: a marker of epithelial-mesenchymal transition for hepatocellular carcinoma?

Ghigna M.; Dos Santos A.; Benzoubir N.; Battaglia S.; Thiers V.; Demaugre F.; Bourgeade F.; Guettier C.
Centre Hospitalier-Universitaire de Bicetre, Le Kremlin Bicetre, France

Background Epithelial to mesenchymal transition (EMT) refers to a complex programme by which epithelial tumor cells shed their differentiation characteristics and acquire mesenchymal features. EMT is thought to play a role in cancer progression and has been associated with a poorer prognosis. The aim of the study is to investigate EMT in primary liver epithelial tumors.
Methods TGF-β induced EMT in HuH7 cell line resulted in strongly decreased expression of epithelial markers such as E-cadherin and in the enhanced expression of mesenchymal markers such as, vimentin and smooth muscle actin (SMA). In HuH7, TGF-β-induced EMT resulted in expression of γSMA whereas αSMA was barely detected. Immunohistochemical study for E-cadherin, vimentin, αSMA and γSMA was performed on surgical specimens of 15 HCV–related hepatocellular carcinoma (HCC).
Results E-cadherin was expressed with a membrane staining in all HCC except 2 with a mosaic pattern associating up-, down- or steady-state expression when compared to adjacent cirrhotic hepatocytes. αSMA was totally negative whereas the presence of γSMA was observed in all HCC except 2. γSMA was expressed focally with a membranous and/or canalicular staining. In some cases, a balance between the decreased expression of E-cadherin and the enhanced expression of γSMA were observed in the same tumor cells.
Conclusion(s) These results strongly suggest that γSMA could be a marker of the EMT process for liver cells. The possible correlation between γSMA expression and tumor invasiveness is currently investigated.

OP17.4

GOLPH2 expression in liver tumours and its value as a serum marker for hepatocellular carcinomas

Riener M.; Stenner F.; Liewen H.; Soll C.; Pestalozzi B.; Jochum W.; Clavien P.; Wild P.; Fritzsche F.; Moch H.; Kristiansen G.
University Hospital Zürich, Zürich, Switzerland

Background GOLPH2 has been proposed as a new serum marker for hepatocellular carcinomas (HCC), but an analysis of the tissue. expression of GOLPH2 in liver lesions has not been conducted yet.
Methods GOLPH2 protein expression was investigated in normal liver tissue (n=105), HCC (n = 170) and bile duct carcinomas (BDC; n = 114). Additionally, a newly designed sandwich ELISA was used to analyse GOLPH2 levels in the sera of patients with HCC (n = 18), HCV (n = 10), BDC (n=5) and healthy controls (n=12).
Results GOLPH2 expression in non-tumourous liver tissue correlated significantly with the presence of HCV infection

($p<0.01$). 121/170 (71%) HCC showed strong GOLPH2 expression. 97/114 (85%) BDCs showed a strong GOLPH2 expression which proved to be an independent prognostic factor for overall-survival ($p < 0.05$). GOLPH2 serum levels were significantly higher in HCC patients than in sera of healthy controls ($p < 0.05$). Furthermore, patients with HCV induced HCC displayed significantly elevated GOLPH2 levels ($p < 0.05$).

Conclusion(s) GOLPH2 protein is highly expressed in tissues of HCC and BDC patients. Serial GOLPH2 ELISA measurements appear to be a promising complementary serum marker in the surveillance of HCV induced HCC.

OP17.5

Localization of schistosoma mansoni antigen confirms the frequent coexistence of hepatic schistosomiasis with chronic viral hepatitis C. An immunohistochemical study

Akl Mahmoud M.; Hammam Ali O.; Mohamed Mahmoud S.; El Baz Gamal H.; Demerdash Ahmed Z.; Atta Ibrahim R.; Shaker Ahmed Z.
Theodor Bilharz Research Institute, Giza, Egypt

Background Aimed at confirmation of schistosomal aetiology in liver biopsies when pathomorphological features of schistosomal hepatic affection coexist with chronic viral hepatitis features inspite of the absence of Schistosoma ova or granuloma. And immunohistochemical localization (IHC) and assessment of collagen III and IV in relation to the disease severity.

Methods Fifty-two individuals with chronic liver disease were diagnosed, classified as 36 chronic hepatitis C (HCV) and 16 pure hepatic schistosomiasis. Twinty one cases out of total 36 HCV cases were proved histopathologically to have mixed viral & schistosomal hepatic lesions with no detectable schistosome ova or granuloma, the rest (15/36) were pure hepatitis C. Eight individuals used as normal controls. Liver needle biopsy specimens were obtained from all patients. Unstained sections were stained immunohistochemically with monoclonal antibodies for Schistosoma mansoni antigen (SmA) as well as collagen III and interstitial collagen IV.

Results Expression of SmA was strongly positive in all cases diagnosed as pure hepatic schistosomiasis and was significantly positive in 17/21 of the examined HCV mixed cases confirming the coexistence of hepatic schistosomiasis.

Conclusion(s) Localization of SmA by SEA monoclonal antibody, proved significantly effective in the co-diagnosis of hepatic schistosomiasis in hepatic tissue sections of chronic viral hepatitis subjects who had mixed pathology in absence of schistosome egg or granuloma.

OP17.6

Human herpesvirus type 8 in patients with cirrhosis independent of thrombocytopenia

Su C.; Chou A.; Huang W.; Lin M.
Buddhist Dalin Tzu Chi General Hospital, Chiayi County, Taiwan

Background High seropositive rate of human herpesvirus type 8 (HHV-8) antibody in cirrhotics was reported associated with severity of cirrhosis and thrombocytopenia. Severe cirrhotics always have ascites as a complication. HHV-8 DNA levels in effusion from primary effusion lymphoma patients were reported to be significantly greater than in blood. The statuses of HHV-8 antibody and DNA in cirrhotic ascites are unclear.

Methods Plasma and ascites samples were collected from 85 cirrhotics. HHV-8 antibody and DNA were detected by immunofluorescence assay and polymerase chain reaction, respectively.

Results The male patients seropositive for HHV-8 antibody were significantly younger than the seropositive female patients ($p=0.0039$). The positive rate in plasma was independent of thrombocytopenia and over six-fold greater than in ascites ($p<0.0001$). All patients positive for ascites were seropositive. More male than female seropositive patients were positive for ascites (19% vs. 9%). A higher proportion of seropositive Child-Pugh class C cirrhotics (17%) were positive for ascites than class B cirrhotics (13%). No hepatitis C virus-related ascites samples were positive for HHV-8 antibody. Neither plasma nor ascites samples from any subject were positive for HHV-8 DNA.

Conclusion(s) In cirrhotics, the positive rate and titers of HHV-8 antibody in plasma were much greater than in ascites. The positive rate in ascites seems to be associated with sex, disease severity, and disease etiology.

OP17.7

Kupffer cells in non alcoholic steatohepatitis (NASH), hepatosteatosis (HS) and normal liver

Gurbuz Y.; Besnili B.; Celebi A.
Pathology Department, Medical Faculty, Kocaeli University, Kocaeli, Turkey

Background Nonalcoholic fatty liver disease (NAFLD) is an actual health problem whose prevalence has recently risen in line with metabolic syndrome. NAFLD contain two entities: non alcoholic steatohepatitis (NASH) goes progressively with steatose, inflammation in liver and high serum transaminases and ordinary hepatosteatosis (HS). The etiology of NASH is not clear but cytokines may be one of the responsible factors. Kupffer cells which secrete cytokines may play an important role in developing inflammation in NASH.

Methods The aim of this work is to study the distribution patterns and intensity of Kupffer cells and to determine the difference in normal tissue and NAFLD in liver needle biopsies in order to find new diagnostic and prognostic histopathological parameters. With this aim, we searched histopatologigally 63 NASH, 13 HS, and 17 normal liver biopsies in detail. Then we stained the cases with CD68 with immunohistochemical method.

Results Spotty necrosis was common in most of the HS patients (61.5%) and could not be accepted diagnostic for NASH. The lipogranuloma structures were only detected in NASH group ($p<0.0001$). The prevalence of lipogranuloma and aggregate structures are directly proportionally with the Brunt grade (aggregate grade 0:25%, grade 1:51%, grade 2:80.8%, grade 3:100% $p<0.007$), (lipogranuloma grade 0:0%, grade 1:48.7%, grade 2:61.5%, grade 3:100% $p<0.006$).

Conclusion(s) Lipogranuloma formation which is clearly identified with CD68 immunohistochemical staining seems to be a patognomonic finding for NASH. We recommend performing the CD68 immunhistochemical staining to confirm the diagnosis and detect the degree of cellular injury in liver biopsy materials with NASH.

OP17.8
Mcl-1 is important for integrity and survival of hepatocytes

Weber A.; Vick B.; Boger R.; Urbanik T.; Galle P.; Schulze-Bergkamen H.
Department of Patholgoy, University Hospital Zurich, Zurich, Switzerland

Background Mcl-1 is an anti-apoptotic member of the Bcl-2 family of proteins. It inhibits apoptosis induction by interacting with pro-apoptotic family members. We recently have shown that Mcl-1 expression is induced in primary human hepatocytes after treatment with growth factors such as HGF, thereby protecting these cells against CD95-mediated apoptosis. The aim of this study was to further analyse the role of Mcl-1 for liver cell homeostasis and CD95-induced liver failure.

Methods A liver-specific Mcl-1 knock-out mouse was generated by mating Mcl-1flox/flox-mice with mice expressing the Cre-recombinase under the control of an albumin-promoter. Mcl-1flox/flox/AlbCre-mice were compared to their Mcl-1flox/wt/AlbCre littermates with respect to immunohistochemical findings and apoptosis induction.

Results At the age of 8 weeks, Mcl-1flox/flox/AlbCre-mice show a reduced body weight and a drastically reduced liver mass. Furthermore, basal serum transaminases were highly increased in these mice, indicating a basal liver damage. Mcl-1 expression was completely abrogated in hepatocytes of Mcl-1flox/flox/AlbCre-mice. This loss of Mcl-1 expression was not compensated by an increase of Bcl-xL expression. Liver damage was further increased in Mcl-1flox/flox/AlbCre-mice compared to control animals, both after induction of fulminant hepatic failure by injecting CD95-antibody and after LPS/D-Galactosamin treatment, as could be detected by enhanced hepatocyte apoptosis, liver tissue damage, and caspase-activation. Furthermore, compensatory hyper-proliferation and hepatic pericellular fibrosis occurs in Mcl 1 negative livers in response to chronic liver damage.

Conclusion(s) Our results suggest that Mcl-1 is an important anti-apoptotic factor and crucial for integrity and survival of hepatocytes.

OP17.9
Oxidative stress in hepatitis C virus infection and associated liver cirrhosis

Nosseir Mostafa Fahmy M.; Bekheet William I.; Madkour Ezzat M.; Moussa Abdel Hameid M.; Ibraheim Atta R.; Ateya M.; Abdel Ghaffar N.
Theodor Bilharz Research Institute, Giza, Imbaba, Egypt

Background Myeloperoxidase (MPO) is an important enzyme that found in neutrophils and involved in reactive oxygen species (ROS) production. The aim of the current study was to clarify the potential role of MPO in oxidative stress and liver fibrosis associated with hepatitis C virus (HCV) infection.

Methods This study was conducted on 90 subjects, 10 normal controls and 80 patients having HCV infection classified into chronic hepatitis C without cirrhosis (CHC) (50 cases) and CHC with cirrhosis (LC) (30 cases). Myeloperoxidase was assessed in plasma by ELISA technique and in liver tissue by immunohistochemistry. Malondialdehye (MDA), as a marker of lipid peroxidation and oxidative stress was also measured in plasma by spectrophotometric assay.

Results Results revealed significant increase of both plasma and hepatic tissue MPO in cirrhotic patients compared to either controls or CHC patients ($p<0.05$). Plasma and tissue MPO showed significant direct correlation with liver aminotransferases (ALT and AST), MDA and stage of hepatic fibrosis. Regression analysis revealed that both plasma and tissue MPO are independent determinant for MDA and stage of hepatic fibrosis.

Conclusion(s) The results incriminate MPO in oxidative stress that causes tissue damage in chronic HCV patients and the subsequent development of hepatic cirrhosis.

OP17.10

Anti COL11 is a useful marker of infiltrating pancreatic cancer

Fresno Forcelledo Florentino M.; Garcia Pravia C.; De Los Toyos J.; Del Amo Iribarren J.; Garcia Garcia J.; Garcia Ocana M.; Perez Basterrechea M.; Ochoa Garay G.; Martinez A.; Simon Buela L.; Barneo Serra L.

Hospital Universitario Central de Asturias, Universidad De Oviedo, Oviedo, Asturias, Spain

Background Chronic pancreatitis and pancreatic cancer are characterized by inflammatory events, and their clinical differentiation and pathological distinction can be difficult, particularly in core biopsy specimens. Our previous work (ESSR2006) identified changes in gene expression associated to pancreatic cancer, and found genes that could differentiate pancreatic cancer from chronic pancreatitis, in particular COL11A1. Aims: to confirm COL11A1 as an efficient marker that distinguishes pancreatic cancer from chronic pancreatitis.

Methods 24 cases of moderately differentiated PDAC and 16 chronic pancreatitis were studied. A polyclonal antiserum to human proCOL11A1 was generated. Immunostaining was double blind scored by two pathologists, and also quantified by means of the image analysis QWin program. Statistical analyses were performed with SPSS 13. The sensitivity and specificity of anti-proCOL11A1 were depicted as ROC curves.

Results ProCOL11A1 immunostaining was confined to the cytoplasm of stromal fibroblasts, even in areas where tumor cells were not seen. It showed a sensitivity of 92 % and a specificity of 94 % in discriminating pancreatic ductal adenocarcinoma from chronic pancreatitis.

Conclusion(s) Anti-proCOL11A1 is an efficient immunostaining that distinguishes between chronic pancreatitis and pancreatic ductal adenocarcinoma.

OP17.11

Expression pattern of claudins 3 and 5 distinguishes intestinal from pancreaticobiliary ampulla of vater carcinoma

Cataldo I.; Comper F.; Beghelli S.; Daniele E.; Chilosi M.; Scarpa A.

Anatomia Patologica, Università di Verona, Verona, Italy

Background Ampulla of Vater carcinomas (AVC) may present with "intestinal" or "pancreaticobiliary" differentiation and express distinct sets of markers consistent with the histotype they resemble. Differences in tissue morphology are connected with differences in expression of proteins involved in structural cell-cell adherens and tight junctions. The expression of the adherens junction proteins, E-cadherin and beta-catenin, has been evaluated in AVC, while no data is available for the expression of the tight junction essential proteins, claudins.

Methods To assess the expression pattern of claudin family members 1, 2, 3, 4, 5 and 7 in AVC of different histotypes and evaluate their association with previously reported markers, cytokeratin-7, cytokeratin-20, mucin-2 and caudal-type homeodomain transcription factor (CDX2), we studied 41 AVC, 24 pancreatic ductal adenocarcinomas and their matched normal duodenum and pancreatic duct epithelium by immunohistochemistry.

Results Most AVC, PDAC and normal pancreatic ducts stained for claudin-1, -4, -7 β-catenin and E-cadherin on the membrane and for claudin-2 on the cytoplasm, regardless of their histological type, while only the intestinal type AVC and normal duodenum showed staining for claudin-3 and claudin–5. Moreover, intestinal AVC showed a gain of membrane claudin-1 expression compared with duodenum epithelium.

Conclusion(s) AVC shows a peculiar claudin expression profile and the highly specific pattern of claudin-3 and claudin-5 differentiates pancreatobiliary type AVC, PDAC and pancreatic ducts from duodenum epithelium and intestinal type AVC with an higher specificity and sensitivity than previously reported markers.

OP17.12

Pathological and clinical roles of mTOR in pancreatic ductal adenocarcinomas

Handra-Luca A.; Hammel P.; Rebours V.; Sauvanet A.; Martin A.; Fagard R.; Flejou J.; Belghiti J.; Bedossa P.; Ruszniewski P.; Couvelard A.

APHP Hopital Jean Verdier Université Paris 13, Bondy, France

Background mTOR protein contributes to carcinogenesis either in the rapamycin-sensitive mTORC1 complex, interfering with cell proliferation or in the mTORC2 complex interfering with AKT and cell spreading. We aimed to analyze the expression of mTOR with respect to clinico-morphological characteristics and cell proliferation in pancreatic ductal adenocarcinoma (PDAC).

Methods The expression of phosphorylated mTOR and Ki67 was determined by immunohistochemistry in 99 primary PDAC treated by surgery. Medians of the p-mTOR score (based on intensity and percentage of stained tumour cells) and of the percentage of Ki67 stained nuclei, were used to classify tumours.Statistical analysis used the Fisher's, uni-and multivariate survival tests.

Results The median tumour size was 30 mm. Fifty-eight PDAC contained necrosis and 19 an abundant clear cell component. Fifty-two patients (out of the 80 with positive

lymph nodes) had ≥ 3 metastatic lymph nodes (median, 3). A high mTOR tumour expression was correlated to a high Ki67 index (< 0.001), an abundant clear cell component (0.01), and to lack of necrosis (0.01). A high Ki67 index (0.04), ≥ 3 lymph node metastasis (0.01), tumour necrosis (0.002), abundant clear cell component (0.03), and size ≥30 mm (0.03) correlated to a shorter overall survival on univariate analysis. On multivariate Cox model, low mTOR (0.01), high Ki67 (0.001) and ≥lymph 3node metastasis (0.002) were independent indicators of an adverse outcome.
Conclusion(s) Our results suggest that, in addition to well known prognostic indicators, an abundant clear cell component in PDAC was related to an adverse outcome. Low mTOR and high Ki67 index independently predicted a shorter survival. The correlation of high mTOR expression to a high Ki67 proliferation index suggest that PDAC could be targeted by rapamycin/rapalogs.

OP17.13
VHL expression in pancreatic adenocarcinomas

Serra S.; Chetty R.
University Health Network, Toronto, Ontario, Canada

Background VHL protein (pVHL) targets transcription factors of the hypoxia-inducible factor family for degradation and is involved in the orientation of growing microtubules. The aim of this study was to investigate pVHL expression in pancreatic ductal adenocarcinomas (PDAC).
Methods A tissue microarray composed of 44 PDAC, corresponding normal pancreas and lymph node metastases was stained for pVHL. Neoplastic glands were well-formed (P1), ill-defined and irregular (P2), and nests/cords/single cells (P3). Membrane/cytoplasm staining and intensity [0 (negative), 1+ (weak), 2+ (moderate), 3+ (strong)] were recorded.
Results 21/44 patients were females; average age 61.4 years. 90.9% of the tumors were in the head of the pancreas, 7/44 well differentiated and 31 moderately differentiated; 33/44 had lymph node involvement and 1 liver metastasis. Islets and acini were negative for pVHL, normal ducts showed weak focal positivity. pVHL was overexpressed in 41/44 cases. pVHL localization correlated with gland pattern: there was progressive loss of membranous and increase in cytoplasmic immunoreactivity from P1 to P3 (p=0.003). Moderate intensity of the staining was most frequent (p = 0.001). pVHL expression was higher in cases with cytoplasmic/membranous staining than cytoplasmic or membranous only (p = 0.037). pVHL expression was higher in smaller T1 tumors than larger T3 tumors (p>0.05). No significant difference was correlated with perineural or lymphovascular invasion.
Conclusion(s) VHL is overexpressed in PDAC with a membranous and cytoplasmic localization, although not significant, there is a loss of expression in larger tumors, while less differentiated tumors showed cytoplasmic staining.

OP17.14
Clinical significance of ephrin receptors -A2, -A4, -A5 and -A7 expression in pancreatic adenocarcinoma

Giaginis C.; Tsourouflis G.; Nikitakis N.; Zizi-Serbetzoglou A.; Kouraklis G.; Theocharis S.
University of Athens, Medical School, Athens, Greece

Background Ephrin receptors (Ephs) have been reported to be frequently overexpressed in a wide variety of malignant tumors, including breast, lung and gastrointestinal cancers, melanoma and neuroblastoma. The present study aimed to evaluate the clinical significance of Eph-A2, -A4, -A5 and -A7 in pancreatic adenocarcinoma.
Methods Eph-A2, -A4, -A5 and -A7 expression was assessed immunohistochemically on paraffin-embedded pancreatic adenocarcinoma specimens obtained from 68 patients. Ephs positivity, overexpression and staining intensity were statistically associated with patients' age and gender, TNM stage, tumor histopathological grade, and proliferative capacity (Ki-67 expression) and patients' survival.
Results Eph-A2, -A4, -A5 and -A7 positivity was noted in 66%, 87%, 98% and 87% of the examined cases, respectively. Eph-A2 positivity and overexpression was significantly associated with patients' age (p=0.003 and p = 0.0004, respectively). Eph-A4 positivity and staining intensity were significantly associated with nodal status (p = 0.046) and tumor proliferative capacity (p = 0.040), respectively. Eph-A5 and -A7 staining intensity were borderline associated with nodal status (p = 0.077) and tumor size (p = 0.054), respectively. Moderate and intense staining intensity for Eph-A5 and -A7 was significantly associated with shorter survival times (p = 0.016 and p = 0.031, respectively), being also identified as independent prognostic factors in multivariate analysis (p = 0.034 and p = 0.048).
Conclusion(s) The present study revealed that Ephs were abundantly expressed in pancreatic adenocarcinoma being correlated with clinicopathological parameters and patients survival. Further molecular and clinical studies are required to define the significance of Ephs and their ligands (ephrins) in prognosis and management of pancreatic carcinoma.

OP17.15
Morphological and immunohistochemical study of 165 gallbladders and review of literature

Mameri S.; Ould-Slimane S.; El Haiba A.
Beni-Messous, Hydra, Alger, Algeria

Background We report a study of 165 gallbladders in order to evaluate the different lesions that may occur in this organ and which may constitute precursors of gallbladder cancer realizing different carcinogenetic pathways. These lesions are already suspected in other organs.
Methods This study concerns 165 patients (80% of women and 20% of men) between 20 and 84 years old who underwent cholecystectomy for cholelithiasis diagnosed by ultrasound examination. Among these 165 cases, 03 cancers are incidentally found. The morphologic study reveals that some lesions incriminated in cancer pathogenesis of other sites are present alone or together in gallbladders: chronic inflammation, intestinal metaplasia, hyperplasia with atypia, adenoma. An immunohistochemical study using Protein 53 (P53) and Bcl 2 is performed.
Results Chronic inflammation is found in 100% of our cases and 80% are associated with gallstones. Intestinal metaplasia is present in the 3 cancer cases and in one inflammatory cholelithiasis specimen. Hyperplasia and atypical hyperplasia foci are found in the 3 neoplastic gallbladders and in 2 inflammatory ones. P53 and Bcl2 are expressed very strongly by the tumorous cells and also by the metaplastic cells and hyperplastic areas situated close to the cancer. There was no expression by the adenomatous cells.
Conclusion(s) In a recent review of literature a study reports established associations between chronic infections and some cancers and another one relates the presence of estrogen receptors in cholelithiasis gallbladder.

Oral presentations 18

Urological pathology

OP18.1

Impact of sub-stage on the clinical outcome of pT1 bladder cancer

Van Der Kwast H.T.; Van Der Aa M.; Bangma C.; Jewett M.; Van Rhijn B.
University Health Network, Toronto, Ontario, Canada

Background Management of pT1 bladder cancer is controversial. We compared the impact of two sub-staging systems on the clinical outcome of a large series of primary pT1 bladder cancer patients treated with BCG.
Methods The slides of 134 primary (first diagnosis) bladder tumors from two university hospitals (Rotterdam, the Netherlands $n=60$ and Toronto, Canada $n=74$) were reviewed and the pT1 diagnosis was confirmed. Sub-staging was done in two separate rounds, using pT1micro-invasive (pT1m) and pT1extensive-invasive (pT1e) and according to invasion of the muscularis mucosae (pT1a/pT1b/pT1c). A grade review (WHO 1973 and 2004) was also done.
Results Substage distribution was as follows: 40 pT1m and 94 pT1e; 81 pT1a, 18 pT1b and 35 pT1c. Grade review resulted in 56 G2 and 78 G3 lesions (WHO1973 system) and 26 low-grade and 108 high-grade lesions according to the WHO2004 system. In multivariate analyses, sub-staging using pT1m and pT1e was significant for progression ($p=0.001$) and disease specific survival ($p=0.021$), whereas sub-stage according to pT1a/b/c was not significant. Female gender ($p=0.006$) and CIS ($p=0.035$) were also significant predictors for progression in multivariate analysis.
Conclusion(s) Sub-stage (pT1m and pT1e) was possible in all the cases and very predictive of pT1 bladder cancer behaviour. Future studies may lead to the incorporation of sub-stage in the TNM classification system for urinary bladder cancer.

OP18.2

Altered ezrin expression in urothelial bladder tumors

Bravou V.; Athanasopoulou A.; Aroukatos P.; Nakas D.; Vandoros Panagiotis G.; Repanti M.
"Agios Andreas" General Hospital of Patras, Patras, Greece

Background Ezrin, a member of the ERM protein family, links the cell membrane to the actin cytoskeleton and has been shown to regulate survival, adhesion and migration. Altered ezrin expression has been correlated with tumor invasion and metastasis. The current study aimed to evaluate the expression profile of ezrin in urothelial bladder tumors.
Methods The protein expression of ezrin and p53 was assessed by immunohistochemistry in 91 bladder biopsies including 3 cases of cystitis and 88 urothelial bladder tumors (primary tumors or recurrences): 14 urothelial neoplasms of low malignant potential, 34 low grade and 40 high grade urothelial carcinomas. Correlations between ezrin expression and clinicopathological variables of the disease such as grade, invasion and recurrence, as well as p53 expression were evaluated.
Results In non neoplastic urothelium, ezrin showed a strong membranous and a moderate cytoplasmic localization. Cytoplasmic localization of ezrin was found in 74/88 (84.1%) urothelial tumors, while membranous ezrin immunostaining was observed in 87/88 (98.6%) cases. Low levels of membranous ezrin expression significantly correlated with high grade urothelial carcinomas ($p=0.03$) and recurrence ($p<0.001$). Membranous ezrin expression was also lower in invasive tumors ($p=0.066$) and decreased with advancing stage ($p = 0.06$). Notably there was a significant downregulation of ezrin

expression (cytoplasmic and membranous) in invasive tumor areas. There was also a negative correlation between membranous ezrin expression and p53 (p=0.05, r=-0.335) in invasive tumors.
Conclusion(s) Altered ezrin expression is probably implicated in urothelial cancer progression and correlates with aggressive features of urothelial bladder tumors.

OP18.3
D-type cyclins in superficial and muscle-invasive bladder urothelial carcinoma: correlation with clinicopathological data and prognostic significance

Levidou G.; Saetta A.A.; Karlou M.; Thymara I.; Pavlopoulos P.; Diamantopoulou K.; Patsouris E.; Korkolopoulou P.
Athens, Greece

Background The main regulatory events leading to proliferation in mammalian cells take place in G1 phase. Therefore the deranged expression of D-type cyclins may be a vital step towards oncogenesis. This study tries to elucidate the role of D-type cyclins in the tumourigenesis of both superficial (Ta-T1) and muscle-invasive (T2-T4) urothelial carcinomas (UCs), looking into their potential prognostic usefulness.
Methods Paraffin-embedded archival tissue from 157 patients with bladder UC was immunostained for cyclins D1, D2 and D3.
Results Cyclin D1 expression positively correlated with D2 and negatively with D3 and decreased with increasing grade (p=0.0001) and advancing T-category in the entire cohort (p=0.0001) and in muscle-invasive carcinomas (p=0.0033). Cyclin D2 correlated with grade (p=0.0005) and T-category (p=0.0078), a relationship which remained significant in muscle-invasive (p=0.0135). Cyclin D3 immunoreactivity increased with histological grade and T-category in the entire cohort (p=0.0001 in both relationships), in superficial (p=0.0034) and in muscle-invasive carcinomas (p=0.0036). Although both higher cyclin D1 (p=0.0001) and higher cyclin D3 levels (p=0.0032) implied a lesser probability of survival in univariate analysis only cyclin D3 remained significant in multivariate analysis. In muscle-invasive tumours lower cyclin D1 (p=0.0234), and D2 (p=0.0424) and higher cyclin D3 (p=0.0322) correlated with shortened survival in univariate analysis, with cyclin D3 remaining significant in multivariate analysis.
Conclusion(s) Cyclin D3 overexpression emerges as an independent adverse prognosticator in superficial and muscle-invasive tumours. Cyclin D1 independently indicates shortened survival only in muscle-invasive tumours.

OP18.4
Expression of GATA-3 among renal cell and urothelial neoplasms

Segala D.; Gobbo S.; Brunelli M.; Eccher A.; Gobbato M.; Vergine M.; Chilosi M.; Bonetti F.; Menestrina F.; Martignoni G.
Anatomia Patologica, Università di Verona, Verona, Italy

Background GATA-3 is a member of a transcription factor family (GATA 1–6) that binds selected GATA sites to regulate specific gene expression. Among renal cell and urothelial tumours, GATA-3 has been shown to immunolabel most of urothelial carcinomas and none of renal cell carcinomas. However, few data are available in regard to the immunoexpression of GATA-3 among different common subtypes of renal cell neoplasms.
Methods We evaluated the immunoexpression of GATA-3 in 54 renal cell neoplasms, including 25 clear cell, 10 papillary, 8 chromophobe renal carcinomas, 8 renal oncocytomas, 1 mucinous-tubular spindle cell carcinoma and 2 translocation renal carcinomas. Seven urothelial carcinomas were evaluated. We also analyzed the adjacent non-neoplastic renal parenchyma. The appropriate nuclear immunoexpression was considered as a positive result.
Results All renal cell neoplasms did not immunoexpress GATA-3 whereas 6/7 (86%) of the urothelial carcinoma stained for GATA-3 in most of the neoplastic cells (> 80%). In the non-neoplastic adjacent renal parenchyma GATA-3 showed a nuclear expression in the podocytes and in the cells lining the distal nephron.
Conclusion(s) GATA-3 protein expression represents a valid marker to distinguish urothelial carcinomas from common renal cell neoplasms and seems not to play a crucial role in the cancerogenesis of major epithelial renal neoplastic subtypes.

OP18.5
Loss of heterozygosity on chromosome 18 as a prognostic indicator of urothelial bladder cancer

Nesi G.; Cai T.; Dal Canto M.; Mondaini N.; Piazzini M.; Bartoletti R.
University of Florence, Florence, Italy

Background Somatic alterations on chromosome (Chr) 18q have been indicated as a critical step in bladder carcinogenesis. The aim of the current study was to evaluate the prognostic role of loss of heterozygosity (LOH) on Chr 18q21–23 in patients affected by low-grade, non-muscle invasive bladder cancer (NMIBC).
Methods A group of 108 consecutive patients (65 affected by low-risk NMIBC and 43 controls) were selected for this prospective study. LOH on Chr 18 was assessed on the

blood/urine pair and the primers used were D18S51, MBP LW and MBP H. The data obtained were compared with follow-up information. Results were also analysed by means of artificial neural networks (ANN).

Results Of the 65 patients with NMIBC, 38 (58.4%) showed at least one alteration on Chr 18, while 27 (41.6%) showed no alteration. In the control group, only 2 out of the 43 subjects (4.6%) showed LOH on Chr 18. At the end of follow-up, 29 patients were alive without recurrence, while 36 had experienced at least one recurrence. The Kaplan-Meier curves demonstrated a significant association between recurrence-free status and LOH on Chr 18 (p= 0.0003). At multivariate analysis, LOH on Chr 18 (p = 0.002) and the number of lesions (p = 0.03) were identified as independent predictors of recurrence-free probability. ANN confirmed the results from multivariate analysis.

Conclusion(s) This study highlights the role of LOH analysis on Chr 18 in improving recurrence prediction in patients with low-grade NMIBC.

OP18.6

The role of TGF-beta-1 protein and TGF-beta-R-1 receptor in immune escape mechanism in bladder cancer

Hammam Ali O.; Helmy Mohamed A.; El Leithy Ramzy T.; Wishahi Mohi M.
Theodor Bilharz Research Institute, Giza, Egypt

Background This study tried to clarify one of immune surveillance escape mechanisms used by tumor cells in bladder cancer hoping be able to develop targeted therapy that will sensitize the tumor cells to immune mediated apoptosis.

Methods Expression of TGF-beta-1protein and TGF-beta-R-1 receptor using immunocytochemical and immuno electron microscopic techniques in urine and peripheral blood mononuclear cells (PBMNCs).

Results Urine samples are 5 healthy controls and 60 patients classified as; 15 chronic cystitis, 45 bladder cancer associated with bilharzial infection or not. Urine examination revealed a significant decrease in the percentage of positive cases expressing TGF-beta-R1 receptor in bladder cancer compared to chronic cystitis or controls (p<.01), while TGF-beta-1 protein was increased (p<.01). Examination of PBMNCs showed a increase in the percentage of positive cases expressing both TGF-beta-1 protein and TGF-beta-R-1 receptors in bladder cancer in comparison to the control (p<.01 and p<.05) and to chronic cystitis cases (p<.05). 42 out of 45 bladder cancer revealed remarkable apoptotic changes represented by cell shrinkage, surface blebs, nuclear chromatin condensation, and vacuolated cytoplasm.

Conclusion(s) This work helps researchers and clinicians to better understand one of the escape mechanisms in bladder cancer that may facilitate the reverse of tumor escape from the immune system. TGF-beta-1 protein can be used as attractive target for anticancer therapy, and the absence of TGF-beta-R1 can be considered a marker for malignant transformation of urothelial cells in bladder cancer.

OP18.7

Role of telomerase and sFas in pathogenesis of various bladder lesions associated with schistosomiasis

Hammam Ali O.; Shaker Gamil O.; Saleh Foad A.; El Leithy Ramzy T.; Wishahi Mohdin M.
Theodor Bilharz Research Institute, Giza, Egypt

Background aim is to find the role of telomerase and sFas in pathogenesis of various bladder lesions associated with schistosomiasis and to correlate the results with clinico-pathological parameters.

Methods One hundred bladder samples, including 65 cases with bladder cancer and 25 cases with chronic cystitis and 10 as control. Telomerase activity was measured by TRAP and IHC techniques and sFas was detected by ELISA in serum.

Results TRAP activity was detected in 51/ 65 bladder cancer, with increase in number of positive cases with schistosomal urothelial carcinoma (sch. uroth.carc) and SCC compared to control and non-schistosomal urothelial carcinoma (non sch. uro.carc) (p<0.01), positive in 100 % of high grade compared to low grade uroth carc (p<0.01) and 92% positive in invasive compared to non invasive tumors (p<0.01). hTERT-protein was detected in 49/65 of bladder cancer ; with increase in number of positive cases with sch. uroth carc. and SCC compared to control and non sch. uroth carc(p<0.01), positive in 100% of high grade and invasive compared to low grade and non invasive uroth carc (p<0.01). sFas was detected in 42/65 in bladder cancer, increase in number of positive cases in SCC compared to control and non-schistosomal uroth carc (p<0.01).

Conclusion(s) Both TRAP and hTERT proteins may be of significance in development of schistosoma associated bladder cancer. they are useful marker to identify bladder carcinoma that would be amenable to therapies involve interference of tumor proliferation through telomerase inhibition.

OP18.8

Schistosoma haematobium total antigen induces dysplasia and inflammation on the urothelium of CD-1 mice

Botelho C.M.; Oliveira A.P.; Lopes C.; Correia Da Costa M.J.; Machado C.J.
CIBP - Centre for Parasite Immunology and Biology, National Institute of Health, Porto, Portugal

Background Squamous cell carcinoma of the urinary bladder has been associated with Schistosoma haematobium infection in many parts of Africa. The epidemiological association is based both on case control studies and on the close correlation of bladder cancer incidence with prevalence of S. haematobium infection within different geographic areas. A parasite tumor linkage is further suggested by the predominance of squamous cell (as opposed to transitional cell) morphology of bladder carcinomas seen in S. haematobium-endemic areas. Tumor development proceeds via a process in which a succession of genetic alterations, each conferring growth advantage, leads to the progressive conversion of normal cells into cancer cells. The cellular mechanisms linking S. haematobium infection with cancer formation are not yet defined.
Methods In the present study, we hypothesized that the parasite antigens might induce alterations in the bladder epithelial cells. For this we investigated the effects of S. haematobium total antigen in CD-1 mice normal bladders after intravesical administration of the parasite antigen. The mice were sacrificed 4 and 8 months after treatment and their bladders were analyzed histopathologically.
Results We will show alterations in the urothelium of these animals consistent with reactive atypia, dysplasia and inflammation induced by S. haematobium total antigen.
Conclusion(s) In our work we demonstrate for the first time that S. haematobium antigens are the direct cause of alterations leading to pre-neoplastic lesions in normal bladder epithelial cells.

OP18.9
Prostatectomy and preoperative findings in patients with prostate cancer (PCA) involving ≤ 1% of gland volume

Trpkov K.; Zhang J.; Yilmaz A.
University of Calgary and Calgary Laboratory Services, Calgary, Alberta, Canada

Background Minimal pCa involving ≤1% of gland volume has become increasingly common in the era of pCa diagnosed during prostatic specific antigen (PSA) screening and extended core biopsies. This study explores the prostatectomy and the preoperative findings in these patients with very limited cancers.
Methods We retrieved from our institutional database (07/2000 to 06/2007) all prostatectomies with pCa involving ≤ 1% of the gland volume and we reviewed the preoperative parameters and the prostatectomy findings. Preoperative biopsies were performed using a standard 10-core sampling. All prostatectomies were completely sampled and were reported using synoptic format.
Results During the study period, 114 (6.5%) prostatectomies of a total of 1754 prostatectomies contained tumors involving ≤ 1% of the gland volume, which corresponded to organ-confined disease with <0.5 cc pCa. On prostatectomy, 106 (93%) patients had Gleason score 6 (3+3) and 8 (7%) had Gleason score 7 (3+4). All patients had organ-confined disease (stage pT2), and none had either positive seminal vesicles or lymph nodes. Positive margins were reported in 5 (4%) patients. Median patient age was 59.1 years, interquartile range (IQR) 54.8–62.6. Abnormal digital rectal exam (DRE) was found in 23% of patients and 17% had abnormal ultrasound. Median gland volume was 52.2 cc (IQR 36.3–70.8). Median serum PSA was 5.4 ng/mL (IQR 4.1–8); 81.3% patients had PSA ≤ 10 ng/mL. Median PSA density was 0.11 (IQR 0.06–0.16); 29% had PSA density >0.15. On biopsy, 89 (78%) patients had only one positive core, while 25 (22%) had pCa in more than one core: 21 (18.4%) had pCa in 2 cores and 4 (3.6%) had 3 or more positive cores. In patients with 2 or more positive cores, 7 (28%) patients had bilateral biopsy pCa, while 18 (72%) patients had unilateral pCa: 11 (44%) in the same site, 7 (28%) in a different site. Median tumor involvement on biopsy was 1.4% (IQR 0.8–2.3%). Biopsy Gleason score 6 (3+3) was found in 107 (94%) patients; remaining 7 (6%) had Gleason score 7 (3+4).
Conclusion(s) Great majority of patients with minimal pCa involving ≤1% of the gland volume presented with favourable clinical, biopsy and prostatectomy findings. However, predicting these cases, based on the currently available preoperative parameters before a definitive treatment, remains an ongoing challenge.

OP18.10
The lack of IL-7 and BAFF/BLyS gene expression in prostate cancer as a mechanism of tumor escape from immuno-surveillance

Sorrentino C.; Magnasco S.; D'Antuono T.; Musiani P.; Di Carlo E.
"G. d'Annunzio" University, Department of Oncology and Neurosciences, Anatomic Pathology Section, Chieti, Italy

Background We previously showed that the human prostate is endowed with intraepithelial (IEL) and stromal lymphocytes which may develop lymphoid follicles (LFs) and allow a local immune response. Here, we aimed to determine whether IL-7 and BAFF/BLyS, fundamental survival factors for T- and B-cells, are expressed in the normal and neoplastic prostate and affect intra-prostatic lymphocyte homeostasis.
Methods We performed Real-Time RT-PCR of micro-dissected prostatic glands and confocal microscopy to identify cytokine sources and immunohistochemistry to characterize intraprostatic lymphocytes.

Results Prostatic epithelia constitutively produce IL-7 and, to a lesser extent, BAFF/BLyS. Indeed, we show that IL7Ralpha is expressed by intraepithelial and parafollicular T-lymphocytes, while BAFF-R is found on periglandular and mantle zone B-cells of LFs. Prostate homing B- and T-lymphocytes are scarcely proliferating, while most of them express the anti-apoptotic protein Bcl-2 and reveal a low apoptotic index in the TUNEL assay. The transition from normal to neoplastic glands is marked by a dramatic decline of IL-7 and BAFF/BLyS production. Accordingly, prostate cancer is characterized by a significant reduction of IEL and loss of LFs. B- and T-cell expression of Bcl-2 decrease, whereas the apoptotic events increase. The remaining tumor infiltrating lymphocytes are mostly CD8+ T that lack terminal differentiation and barely penetrate neoplastic glands.

Conclusion(s) The loss of epithelial IL-7 and BAFF/BLyS production in prostate cancer is associated with a severe depletion of prostate-associated lymphocytes and points to a novel tumor escape mechanism.

OP18.11

Elevated expression of adiponectin receptor 2 is associated with adverse outcome in prostate cancer

Walsh T.; Finn S.; Sinnott J.; Stark J.; Ma J.; Giovannucci E.; An Thai T.; Hung N.; Eisenstein A.; Stampfer M.; Loda M.; Mucci L.

Mid Western Regional Hospital Limerick, Limerick, Ireland

Background Adiponectin is a metabolic hormone produced by adipose tissue and is inversely related to obesity. We previously showed low circulating levels are associated with increased PCa aggressiveness. Adiponectin signals through 2 receptors, AdipoR1/R2. Here, we examine the relationship between AdipoR2 tumor expression and clinicopathological variables including PCa specific death.

Methods The study cohort includes men diagnosed with prostate cancer (1982–2006) in the prospective Physicians' Health Study and the Health Professionals Follow-up Study. Data on survival (median follow-up 10.8 years), Gleason Grade, diagnostic PSA, clinical stage, baseline obesity measures were available for 865 members of the cohorts. Immunohistochemistry for AdipoR2 and ki67 was performed on TMAs and scored with modified Allred measures.

Results AdipoR2 protein expression was upregulated in tumor compared to normal tissue, and correlated positively with Gleason grade (p=0.0141), tumor stage (p = 0.0802) and tumor ki67 proliferation (p<0.0001). In Kaplan-Meier analyses, the highest 2 quartiles of AdipoR2 tissue expression were significantly associated with the incidence of metastases and death. In Cox Models, controlling for age at diagnosis, BMI and Gleason grade, men with highest AdipoR2 tumor expression had a 3.1 fold increased risk of lethal PCa (95% CI, 1.5, 6.3 p-trend=0.0006).

Conclusion(s) AdipoR2 is overexpressed in a subset of PCa and is associated with higher stage, proliferation and higher Gleason scores. In addition, overexpression is associated with poorer prognosis over and beyond clinical measures. These data provide further links between obesity and PCa.

OP18.12

Identification and validation of differentially expressed miRNAs of prostate cancer

Kristiansen G.; Jung M.; Mollenkopf H.; Wagner I.; Miller K.; Lein M.; Stephan C.; Jung K.; Schäfer A.

University of Zurich, Zurich, Switzerland

Background We aimed to identify differentially expressed microRNAs in prostate cancer by comparing miRNA expression in tumor and normal adjacent tissue.

Methods 24 pairs of fresh frozen matched tumor and normal adjacent tissue were analysed using human miRNA-microarrays encoding probes for 470 human and 64 human viral microRNAs from the Sanger database v9.1. Regulated miRNAs were further validated in qRT-PCR using TaqMan Probes in 76 pairs of matched normal and tumor tissue. Data were normalized to hsa-miR-130b.

Results Fourteen miRNAs with expression changes greater 1.5 fold in prostate cancer were found. Unsupervised cluster analysis displayed good discrimination between normal and tumor samples. These differentially expressed miRNAs were further validated by qRT-PCR. Ten miRNAs showed a significantly decreased expression in tumor tissue with expression changes ranging from 1.33 to 3.74 fold. Five miRNAs were significantly increased with a 1.23 to 1.61 fold higher expression in tumor tissue. Importantly, a good overall classification of normal and malignant prostate tissue is possible with the combination of only two miRNAs (hsa-miR-205, hsa-miR-183). Furthermore, high rates of hsa-miR-96 are associated with a shortened recurrence-free interval after radical prostatectomy.

Conclusion(s) These findings endorse the general notion, that microRNAs posess a diagnostic and also a prognostic value, which can be clinically utilized. Prostate cancer is characterized by significant miRNA expression changes that clearly discriminate between tumor and normal tissue and that might bear prognostic significance. Further studies validating these findings in larger, clinically characterized tumor cohorts are underway.

OP18.13

Influence of hormonal deprivation therapy on relevant chemotherapy targets in prostate cancer

Kozakowski N.; Hartmann C.; Mazal Roland P.; Susani M.; Kenner L.; Marberger M.; Haitel A.
Clinical Institute of Pathology, Vienna, Austria

Background In prostate cancer neoadjuvant hormonal therapy with radiotherapy but not in combination with radical surgery has been proved to increase disease-free survival. Many patients - even after prostatectomy - experience progression of the disease and develop hormone refractory cancer after months or years. They are then candidates to other therapy regimens, but the further therapeutic options (i.e. targeted therapy) could be influenced by the preceding hormonal therapy. We therefore evaluated the effects of hormonal therapy on different relevant chemotherapy targets.
Methods Evaluation of EGFR, PDGFR, VEGFC, mTOR, p70S6-kinase, carboanhydrase IX and CerB2 expression as well as Gleason scoring were carried out in pre-treatment biopsy specimens and radical prostatectomies after hormonal deprivation from 22 patients. Duration of hormonal deprivation ranged from 17 to 592 days (mean 119 days).
Results Expression of PDGFR, VEGFC, mTOR and p70S6-kinase were significantly lowered after hormonal therapy (p=0,002, p=0,004, p=0,025 and p=0,033, respectively). Expression of EGFR and carboanhydrase IX did not show statistical significant difference between pre- and post-treatment specimens. CerB2 was never expressed in both groups. Gleason score appeared to be higher in most of the patients after therapy (p=0,001).
Conclusion(s) These results suggest that PDGFR, VEGFC, mTOR and p70S6-kinase are decreased after hormonal deprivation, whereas EGFR and carboanhydrase IX are not influenced. CerB2 seems to play no significant role in our study group. These findings could be relevant for further therapeutic schemes of prostate carcinoma.

OP18.14

Stromal-parenchymal interactions of MMP2, MMP13 and TIMP1 in prostate intraepithelial neoplasia and prostate cancer

Kogan E.; Markova A.; Shestiperov P.; Kovalenko A.; Tuong V.
Scientific Centre of Obtetrics and Gynecology, Moscow, Russian Federation

Background Matrix metalloproteinases (MMPs) play an important role in the modeling and remodeling of the extracellular matrix in both physiologic and pathologic states and thus play an important role in tumor progression. The present study was designed to investigate the expression of MMP2, MMP13 and TIMP1 on the different stages of prostate cancer (PCa) progression and in prostate intraepithelial neoplasia (PIN).
Methods Prostate biopsies and operating material from 35 patients and 3 control patients (normal prostate tissue) were used. Immunohistochemistry on paraffin sections with microwave pretreatment had been done with antibodies to MMP2, MMP13 and TIMP1 (Lab Vision). Positive and negative control reactions were done. Results were evaluated via semiquantative method and statistics analysis (the nonparametric Mann-Whitney test).
Results Accumulation of MMPs 2,13 and TIMP1 was found in parenchymal and stromal cells. TIMP1 expression was mainly detected in the endothelium of blood vessels and appeared to be more marked in PIN and localized PCa than in invasive PCa forms. MMPs are predominantly expressed in parenchyma rather in stroma.
Conclusion(s) These results suggest that TIMP1 prohibits the tumor cell invasion. The high expression of MMP2 and MMP13 in malignantly transformed epithelial cells can be associated with tumor biological aggressiveness and used to aid in predicting patient's poor prognosis.

OP18.15

Analysis of penile condylomas and dysplasia

Baydar Ertoy D.; Kulac I.; Tezel Guler G.; Gokoz O.; Gunay A.; Ozagari A.
Hacettepe, Ankara, Turkey

Background Penile condylomas (PC) constitute a group of sexually transmitted HPV related diseases. They are commonly treated with fulguration. We analyzed histomorphological features of all PC diagnosed from 2000 up-to-day in two different institutions. The prevalence of dysplastic changes was specifically investigated.
Methods Slides of 58 consecutive PC were retrieved from pathology archives and were reviewed for histological features. Clinical characteristics of patients (age, location, multifocality, size) were obtained from computer-based patient data system. Presence of dysplasia was investigated and when found graded as: low, moderate and high. Dysplastic lesions were screened for specific HPV types using commercial PCR-array hybridization assay (HPV Genoarray, HybriBio Inc.) after DNA extraction from the tissues in paraffin blocks.
Results Patients' age ranged from 20 to 62 (mean 38.4). None were HIV-infected. Histological examination revealed that 13 of 58 PC had moderate to severe dysplasia. Ten of

them could be studied for HPV genotype and five of those had high-risk types, HPV 16 or 18.
Conclusion(s) Significant dysplasia is not a rare occurance in PC, seen in 22% of cases and associated with high risk HPV 50%. We suggest at least one of the condylomatous lesions submitted to pathology for recognition. Since HPV is the major etiology in pathogenesis of penile squamous carcinomas, these patients may have to be followed-up. Finding of dysplasia or high-risk HPV may be important in counseling of female partner.

Oral presentations 19

Pulmonary pathology – Miscellaneous

OP19.1
Cytopathological cross validation of preoperative circulating tumor cell detection in patients with non small cell lung carcinoma

Hofman V.; Bonnetaud C.; Vielh P.; Molina T.; Vignaud J.; Fléjou J.; Lantuejoul S.; Piaton E.; Mourad N.; Butori C.; Mouroux J.; Paterlini-Brechot P.; Hofman P.
Laboratory of Clinical and Experimental Pathology, Nice, France

Background No current tissue biomarkers are predictive of non-small cell lung cancer (NSCLC) recurrence and metastasis onset. The preoperative detection of circulating tumor cells (CTC) could be useful for tailored therapeutic strategies. The aim of this study was to assess the presence and the frequency of CTC in NSCLC patients undergoing surgery by using cytopathological analysis after their isolation by size (ISET method).
Methods 151 patients with different pTNM stages of NSCLC have been included in this study. The presence of circulating non haematological cells (CNHC) has been assessed before surgery, blindly and independently by 10 cytopathologists on May Grunwald Giemsa stained filters. Cells have been classified in three groups according to classical cytopathological criteria of malignancy: CNHC with malignant features (CNHC-MF) or circulating tumoral cells (CTC), CNHC with uncertain malignant features (CNHC-UMF), and CNHC with benign features (CNHC-BF). We assessed interobserver agreement using Kappa (κ) as the measure of agreement.
Results 52% patients showed CNHC corresponding to CNHC-MF in 37% cases, to CNHC-UMF in 13% cases and to CNHC-BF in 2% cases. Interobserver agreement was almost perfect for CNHC-MF (κ=0.63), and moderate for CNHC-UMF (κ=0.32) diagnosis. Presence and number of CNHC was not correlated with pTNM staging.
Conclusion(s) A high percentage of NSCLC undergoing surgery show preoperative detection of CNHC. Further studies are needed to analyze the invasive potential of these CNHC and to correlate results with the risk of developing recurrence after complete surgery.

OP19.2
Molecular events at early and late stages of idiopathic pulmonary fibrosis (IPF)

Tuong Phi V.; Demoura S.; Kogan E.
Sechenov Moscow Medical Academy, Moscow, Russian Federation

Background The goal of our study was to investigate the molecular and cellular mechanisms of tissue remodeling in patients with IPF at early and late disease stages.
Methods Specimens of open lung biopsies from 30 IPF patients and 10 control patients (normal lung tissue) were used. Immunohistochemistry on paraffin sections had been done with antibodies to Apo-cas, TGFβ, PCNA, PDGF, EGFR, MMP 1, 2, 7, and TIMP 4, CD34, SMA. The nonparametric statistic Mann-Whitney test was used.
Result We found that the expressions of MMP 1, 2, 7, and TIMP-4 by epithelial cells, macrophages, fibroblasts and myofibroblast were higher in early stage of IPF than in the late one. Late stage of IPF was characterized by higher expression of PDGF, PCNA, Apo-cas by all types of cells and SMA by myofibroblasts than in early stage of disease. In addition, adenomatous structures, myofibroblast foci, and foci of angiogenesis were presented predominantly nearby the area of bronchoalveolar duct junction (BADJ) in IPF with statistically significant different expression of studied molecular markers.
Conclusion(s) We propose that IPF is chronic disease with pathological tissue repair in the early stage, following excessive accumulation of ECM components and cell proliferation in late stage, which lead to the formation of lung fibrosis and honeycombing lung. Remodeling of the regions of BADJ is the most important event that contributes to the onset and progression of adenomatosis and fibrosis in IPF.

OP19.3
Pathologic variants of COPD

Cherniaev A.; Samsonova M.
Pulmonology Research Institute, Moscow, Russia, Russian Federation

Background COPD is a disease characterized with the mixture of lesions within the lung. Discontinuity of lesions and clinical manifestation differing one patient from

another necessitate the differentiation of pathologic processes within the nosology.
Methods We analyzed the lung tissue of 15 patients underwent lung volume reduction surgery and 150 autopsies of patients died from COPD.
Results According to histological examination we propose three types of lung involvement within COPD group. First is – obstructive type due to pathology of cartilage bronchi accompanied with the lesion of bronchioles and alveoli, leading to pulmonary emphysema – bronchial-interstitial type. Second is the disease with the predominance of emphysema as a result of obstruction caused by degradation of extracellular matrix and consequent bronchiolar collapse – emphysematous type. In this type only scanty inflammatory infiltration with lymphocytes or leucocytes could be seen in alveolar wall. Third is the disease with predominance of constrictive bronchiolitis or bronchiolitis obliterans with obstructive emphysema but absence of interstitial fibrosis – true-obstructive type.
Conclusion(s) The distinguishing of different types of COPD is the first attempt to appreciate the clinical discrepancies within this disease.

OP19.4

Refractory remodelling of the microenvironment by abnormal type V collagen, apoptosis and immune response in non small cell lung cancer

Souza Da Costa P.; Ab'Saber Muxfeldt A.; Rizzardi F.; Noleto G.; Atanazio M.; Takagaki T.; Antonangelo L.; Bianchi O.; Parra Rogers E.; Teodoro W.; Capelozzi V.L.
Faculdade de Medicina da Universidade de São Paulo, São Paulo, SP, Brazil

Background Type V collagen emerging promise as inductor of death response via caspase. We examined remodeling of the microenvironment by type V collagen, tumoral/vascular apoptosis, angiogenesis, immune response and their impact on prognosis of patients with non-small cell lung carcinomas (NSCLC).
Methods Collagen, apoptosis, angiogenesis and immune cells were examined in tumor tissues from 65 patients with surgically excised NSCLC. We used immunofluoresce, immunohistochemistry, morphometry and 3D reconstruction to evaluate the amount and structure of type V collagen, endothelium apoptosis caspase 9+, tumoral cells apoptosis and microvessel density
Results Impact of these markers was tested on follow-up until death from recurrent lung cancer. It was found that a decreased and abnormal synthesis of collagen type V leads to increased angiogenesis by low endothelial death rate, and low immune response. Cox model analysis demonstrated that just four variables were significantly associated with survival time: N stage, histological subtype, type V collagen and caspase 9. Once these two variables were accounted for, none of the others related to survival. A cutpoint at the median for type V collagen and caspase 9 divided patients into two groups with distinctive prognosis.
Conclusion(s) This findings may suggesting that strategies aimed at preventing the low type V collagen synthesis, or local responses to low cell apoptosis, may have a greater impact in lung cancer.

OP19.5

Somatostatin receptor type 2 in bronchopulmonary carcinoids: new clinical and diagnostic implications

Fassan M.; Rea F.; Pennelli G.; Clemente R.; Rizzardi G.; Pizzi M.; Lazzarin V.; Lanza C.; Giacomelli L.; Rugge M.
Department of Medical Diagnostic Sciences & Special Therapies, University of Padova, Padova, Italy

Background The expression of Somatostatin receptor type 2 (sst2) by different neuroendocrine tumors represents the biological rationale of both diagnostic (scintigraphy) and therapeutic (stable somatostatin analogs) approaches. Bronchopulmonary carcinoids (BC) are uncommon neuroendocrine tumors. Their histological distinction in low-grade typical (LG-TC) and intermediate-grade atypical (IG-AC), inconsistently correlates with tumor behavior. Only anecdotic information is available on BC's sst2 expression and its possible correlation with more validated histological parameters.
Methods Sst2 immunohistochemical expression was studied in a large single-institution series of 79 radically-treated BC. The results were then compared and related to tumor grade and to other clinicopathological parameters.
Results Among the 79 considered BC, 69 (87.3%) were assessed as LG-TC and 10 (12.7%) as IG-AC. sst2 was consistently expressed in 76/79 (96.2%) cases. Although in the majority of positively stained tumors sst2 immunoreactivity was obtained in most tumor cells, a considerable part of the tumors showed an inhomogeneous pattern of staining. At the cellular level, immunohistochemical staining was observed both in the cytoplasm and at the cell membrane. A significant decreased expression pattern has been observed in IG-AC versus LG-TC (p=.048).
Conclusion(s) Sst2 is highly expressed in BC and may provide information on the diagnostic or therapeutic usefulness of somatostatin analogues in individual BC patients.

OP19.6

Systemic amyloidosis: a case report

Samsonova M.; Cherniaev A.
Pulmonoloqy Research Institute, Moscow, Russia, Russian Federation

Background It's well known that we generally see general diseases and rarely see rare diseases. But one should be ready to recognize a rare pathology even in case of unsuspected localization.
Methods A clinical case.
Results Patient (female, 60 yrs old) has the diagnosis of tuberculosis in anamnesis morbi from 2005. In September 2009, the surgery was done because of peritonitis. Laparotomy and omentectomy was perfomed. Histological analysis of biopsy of greater omentum revealed the amorphous mass accumulation with giant cell reaction and ossification. Some pathologists considered the changes to be the aseptic necrosis with calcification, the other – tuberculosis in phase of regression. As for us the diagnosis of tuberculous granulomatosis looked doubtful. Clinical examination of the patient revealed the bilateral dissemination within the lung, surgical biopsy was performed. The same amorphous masses were seen in visceral and parietal pleura, alveolar wall, around arterioles. Giant cell reaction, moderate lymphoid infiltrates could also be seen. These masses showed the diffuse glow under polarized light. Congo rot staining was also positive.
Conclusion(s) The diagnosis was formulated as diffuse variant of systemic amyloidosis with affection to the lung and omentum. The diagnostic difficulties in such cases were due to the rarity of pathology. It was quite difficult to suspect amyloidosis while examining omentum.

OP19.7

Immunophenotyping study in patients with pulmonary and extra-pulmonary sarcoidosis

Capelozzi V.L.; Da Silva Quintino P.; Narde I.; Zocolaro W.; Parra Roger E.
Faculdade de Medicina da Universidade de São Paulo, São Paulo, São Paulo, Brazil

Background Sarcoidosis is a multisystemic granulomatous disease of unknown etiology that may involve lungs, liver, lymphonodes and skin. Parenchymal involvement may improve spontaneously in most of patients, but progression to fibrosis, leading to permanent functional impairment, occurs in 20–25% and death in 5–10%. The pathological hallmark of sarcoidosis is a noncaseating epithelioid cell granuloma. The disease activity is marked by the balance of epithelioid cells, immune cells and fibrosis deposition.
Methods We reviewed our medical records over a 10-yr period to investigate the significance of the immune response in histological specimens of patients with pulmonary and extrapulmonary sarcoidosis. Inflammatory cells (macrophages, neutrophils elastase (+), CD1a and S100) and CD20, CD3, CD4, CD8 were quantified in lung (N=8), liver (N=4), lymphonodes (N=8) and skin (N=3) surgical biopsies.
Results The total density of inflammatory cells was more significantly increased in extra-pulmonary than pulmonary sites. Lymphocytes CD3+, CD4+, CD8+ and CD20+, as well as macrophages CD68+ were significantly increased in liver when compared to lung and lymphonodes. For CD20+, CD1a and S100 a significabtly increase was present in skin compared to liver, lung and lymphonode. Different proportions of neutrophils elastase+ were found among the four organs studied but this difference didn´t achieve statistical significance.
Conclusion(s) Total density of immune cells and lymphocytes present a different distribution within the pulmonary and extrapulmonary sarcoidosis. We concluded that in extrapulmonary sarcoidosis the immune response is more prominent than pulmonary, mainly in liver and skin, because the immunological mechanisms of lungs and lymphonodes has a more effective antigen clearance.
Financial Support: FAPESP, CNPq.

OP19.8

Collagen and elastic fibers evaluation in granulomatosis lung diseases

Capelozzi V.L.; Narde I.; Da Silva Quintino P.; Zocolaro Sanches W.; Parra Roger E.
Faculdade de Medicina da Universidade de São Paulo, São Paulo, São Paulo, Brazil

Background Granulomatous lung diseases, as tuberculosis and histoplasmosis, from infectious origin, and as sarcoidosis and chronic hypersensitivity pneumonitis, from non-infectious origin, are strongly associated with high morbidity and mortality. The pathogenesis of the granulomatous inflammation is often associated to the intense inflammatory response. However, the pathogenic mechanisms of theses diseases remain still unknown. In this study, we evaluated lung extracellular matrix alterations (collagen system and elastic) in granulomatous lung diseases, specially sarcoidosis, hypersensitivity pneumonitis, tuberculosis and histoplasmosis.
Methods We examined extracellular matrix (collagen and elastic fibers system) in sarcoidosis (N=21), hypersensitivity pneumonia (N=11), tuberculosis (N=11) and histoplasmosis (N=3) cases. We used the Picrosirius-polarization method, Weigert's resorcin-fuchsin histochemistry and morphometric analysis to evaluate the amount of normal parenchymal and granulomas collagen/elastic fibers.
Results The granuloma and normal parenchymal areas measurements of collagen fibers were higher in hypersensitivity pneumonitis (21,57%±8,37% and 22,07%±9,40%, respectively) compared to sarcoidosis (15,65%±2,11% and 11,33%±1,75%), tuberculosis (15,48%±6,80% and 10,97%±5,15%) and histoplasmosis (15,85%±8,93% and

9,76%±1,77%). Equally higher was the granuloma measurement of elastic fibers in hypersensitivity pneumonitis (2,99% ± 1,27%) compared to sarcoidosis (1,18%±0,37%), tuberculosis (0,15% ± 0,00%) and histoplasmosis (0,42% ± 0,18%). The comparison between infectious and non-infectious diseases showed a significant (p=0,005) higher quantity of elastic fibers in granuloma areas of non-infectious diseases (1,53±2,02) compared to infectious diseases (0,29%±0,21%).

Conclusion(s) We concluded that granulomas of HP are more fibroesclerotic than sarcoidosis and infectious, indicating a more intense reparative process due immune response activation after chronic and repeated inhalatory injury. Financial Support: FAPESP, CNPq.

OP19.9

Microarray comparative genomic hybridization analysis in malignant peritoneal mesothelioma

Serio G.; Scattone A.; Pennella A.; Buonadonna A.; Marzullo A.; Pollice L.; Musti M.; Gentile M.
Dept. of Pathology, Medical School, University of Bari, Bari, Italy

Background Malignant mesothelioma (MM) develops as a result of multiple genetic alterations. Past asbestos exposure represents the major risk factor for MM. A large number of cytogenetic studies have shown the complex nature of these changes. The most frequent events observed in MM are deletions in 1p21–22, 3p21, 4, 6q14–25, 9p21, 13q, 14q, 15q15, 17p13 and 22. Currently, high throughput methods such as a-CGH are available to study genome-wide alterations.

Methods Employing a-CGH, we studied the biopsies of eighteen patients affected by peritoneal mesothelioma. The goal of our study was to detected recurrent genomic gains and losses associated with MM survival. None patient underwent cyto-reduction but they received palliative chemotherapy. All patients had a history of occupational or domestic exposure to asbestos. Survival was taken as the duration between histological diagnosis and the date of death. No patients was alive at the time of the study.

Results A high number of genetic aberrations were detected in sixteen cases. Losses were prevalent. Each tumour harboured 0–18 aberrations of the chromosomal region and the mean numbers of chromosomal aberrations per tumour were 3.7 losses and 2.0 gains (ratio 1.85). Deletions in chromosomes 9p12-q12→q21.3-q33.3 (61%), 1q21(56%), 17p11.2→p12 (28%), 2q11.1→q13 (22%), 12p13.32 (22%) appeared to be the most frequent events. Moreover, deletion in 9q33 (39%) was associated to poor outcome

Conclusion(s) Deletion in 9q33 is a novel finding that allow us to hypothize that in this area there could be genes possibly associated with adverse prognosis.

Oral presentations 20

Breast pathology

OP20.1

Oestrogen receptor-positive breast cancer: identification of significant prognostic patho-biological subgroups

Habashy Onsy H.; Powe C.D.; Ball G.; Ellis I.O.
University of Nottingham, Nottingham, United Kingdom

Background Gene expression studies have been able to classify breast cancer (BC) into a number of different distinct biological classes which have relationships with clinical outcome. One class, the luminal group, while characterised by high oestrogen receptor expression is complicated by tumour biological heterogeneity implying the presence of subclasses. Identification and biological characterisation of ER-positive luminal-like subtypes could have important implications in clinical decision-making and patient treatment.

Methods In this detailed and novel study, we examined the protein expression of 15 biomarkers of known relevance to ER-positive BC including FOXA1, TFF1, CD71, CARM1, PELP1, RERG, TK1, TFF3, XBP1, BCL2, Cyclin B1, FoxO3a, P27, C-MYC, and BEX1 in a large (n=1902) and well characterized consecutive patient series of invasive BC using immunohistochemistry based on high throughput tissue microarray technology (TMA) with particular emphasis on ER-positive cohort of patients. The biomarkers were assessed to determine their importance or role in identifying subclasses of ER positive breast cancer and their biological and clinical relevance.

Results The results of this study demonstrate the existence of luminal subclasses that differ with respect to patient outcome. Biomarkers of good prognosis include FOXA1, Bcl2, RERG, P27 and BEX1, and markers of poor prognosis include CD71, PELP1, CARM1, TK1 and C-MYC.

Conclusion(s) Our results emphasise the biological and behavioural heterogeneity of ER-positive luminal BC and identify ER related biomarker specific associations. Subsequent bioinformatic analysis is expected to identify those biomarkers that characterise and have prognostic importance in ER positive breast cancer.

OP20.2

Pathological features of nodal micrometastases predict distant failure in patients affected by breast cancer

Di Tommaso L.; Masci G.; Del Prato I.; Orefice S.; Rubino A.; Gullo G.; Incarbone M.; Sacco R.; Alloisio M.; Eboli M.; Giordano L.; Roncalli M.; Santoro A.
Istituto Clinico Humanitas, Rozzano, Milan, Italy

Background Micrometastases (i.e. < 2-mm metastatic deposits) are frequently found during extensive pathological examination of lymph nodes in women affected by breast cancer. Despite this, their clinical relevance is still under debate. Aim of this study is to investigate if pathological features of nodal micrometastases can affect the prognosis in patients with breast cancer.
Methods We retrospectively investigated the outcome of 119 patients with nodal micrometastases from breast cancer. Median follow-up was 52 months.
Results Multifocality (p=0.008), tumor size >1 cm (p= 0.032), grade (p = 0.018), absence of estrogen (p = 0.002) and progesterone (p<0.001) receptors, and HER-2 overexpression (p=0.034) were related to worse disease free survival (DFS) on univariate analysis. In the multivariate model only tumor size (p=0.049) and receptor status (p< 0.001) were maintained. Worse DFS was also associated with sinusal localization of micrometastasis, as highlighted on both univariate (p=0.029) and multivariate analysis (p= 0.032). Overall survival (OS) was influenced by multifocality (p<0.001) and receptor status (p=0.005), the latter being significant also in a multivariate model (p=0.009).
Conclusion(s) Our results suggest that in patients affected by breast cancer, in addition to well known pathological features of primary tumor, pathological features of nodal of micrometastasis significantly correlates with worse prognosis.

OP20.3

"Piking" the right isoform for breast cancer progression

Carvalho S.; Milanezi F.; Costa Luis J.; Schmitt F.
IPATIMUP, Porto, Portugal

Background Class IA phosphoinositide3'–kinases (PI3Ks) regulate many cellular processes. Despite a clear implication of PI3K in cancer, the involvement of each of its catalytic isoforms (p110) in the development of cancer remains elusive. Until recently the spotlight had been given to p110alpha subunit due to the occurrence of activating mutations in human cancers, namely breast. However the p110beta isoform has now emerged as an interesting target, since, in an experimental model of HER2-driven tumours, mice expressing an inactive form of p110beta were protected from cancer development. In order to determine the importance of these subunits in breast cancer progression we studied the expression of p110alpha/beta in a series of invasive breast carcinomas.
Methods 21 TMAs were constructed using a series of 362 invasive breast carcinomas, and classified according to their molecular profile, using recognized markers, as: Luminal-A and -B, HER2-overexpressing and Basal-like. Then, Immunohistochemistry for p110alpha and beta was performed.
Results Strong membrane expression was observed for p110alpha in 7.95% of Luminal-A, 8.1% in Luminal-B, 20% in HER2-overexpressing and 10% of Basal-like tumours. Regarding the p110beta, we observed strong membrane expression in 83% of HER2-overexpressing tumours and a strong granular citoplasmic expression mainly restricted to Basal-like (17.1%) and Luminal-B (11.5%) tumours.
Conclusion(s) Our results show a putative role for the beta subunit in the progression of HER2-overexpressing tumours. Although the value of the granular pattern is still unclear, the immunostaining specificity justifies further studies in order to determine its significance in Basal-like and Luminal-B subgroups.

OP20.4

Pure intracystic papillary carcinoma of the breast with spread to the ipsilateral intrammary lymph node five years after needling procedure

Ichihara S.; Shimoyama Y.; Nakamura S.; Aoki M.; Oda K.; Hasegawa M.; Moritani S.
Nagoya Medical Center, Nagoya, Aichi, Japan

Background Iatrogenic epithelial cell displacement in the breast and the mechanical transport of epithelial cells into lymph nodes are recently described complications of the needle manipulations. The fate of epithelial deposits in the lymph node remains unknown.
Methods Here we describe a 67-year-old Japanese woman who developed an intracystic papillary carcinoma in the intramammary lymph node probably due to the mechanical transport of papillary carcinoma cells.
Results Over a half of an intramammary lymph node was replaced by intracystic papillary carcinoma measuring 17 mm, closely resembling the original intracystic papillary carcinoma of the ipsilateral breast with regard to immunoprofiles and morphology. Five years earlier, she had undergone a needle manipulation and surgical excision of pure intracystic papillary carcinoma of the breast. The excisional biopsy specimen of the original intracystic papillary carcinoma exhibited displaced fragments of epithelial cells within granulation tissue at the needle manipulatioin site.
Conclusion(s) This particular case exemplifies that the pure intracystic carcinoma can metastasize to the lymph node

due to mechanical transport by the needling procedures and that the cystic space containing the papillary carcinoma may be generated by a proliferating papillary carcinoma itself, through the mechanism similar to 'duct neogenesis' proposed by Tibor Tot et al.

OP20.5

Survival analysis of most expressed src kinase family members (SKFMs) in human breast carcinoma

Elsberger B.; Fullerton R.; Tan A.B.; Edwards J.
Glasgow Royal Infirmary, University of Glasgow, Glasgow, Scotland, United Kingdom

Background Pilot results, investigating mRNA expression levels of SKFMs, have shown that Src and Lyn were highest expressed in invasive breast cancer tissue, and that Lck and Lyn were higher expressed in ER negative compared to ER positive tumours.
Methods In this study, immunohistochemistry was performed on specimens from a cohort of 320 breast cancer patients for Src, activated Src, Lck, Lyn and proliferation marker Ki67 to investigate if this observation translated to protein expression and examine its association with clinical outcome measures.
Results Within the cohort, median follow-up was 6.3 years, median age was 58 years (IQR 24–90) and median tumour size of 20 mm (IQR 15–30 mm). Majority of specimens were pathologically graded as grade 2 and 3. 49% of the patients were axillary lymph node positive. High cytoplasmic c-Src and membrane Y419Src kinase expression levels were significantly associated with decreased disease specific survival (p=0.03, p=0.02). Lyn was not associated with survival at any cellular location. No correlation was observed between Lyn and Src expression. High membrane Lck expression was significantly associated with improved survival (p=0.03). No patients expressing high membrane Lck died of breast cancer. Ki67 correlated positively with tumour grade (p=0.004), nuclear c-Src (p=0.002) and activated Y419Src (p=0.003), but was not associated with survival.
Conclusion(s) High proliferation of breast tumours correlates with high expression of Src kinase and activated Src kinase leading to worse clinical outcome of breast cancer patients. Membrane Lck expression influences disease specific survival positively.

OP20.6

The UK NEQAS online auditing system for breast cancer predictive markers

Miller K.; Ibrahim M.; Herriot K.
University College London, London, United Kingdom

Background Approximately 44,000 new breast cancers emerge each year in the UK and the HER-2 testing data for almost 38,000 of these cases has been collected by UK NEQAS for both 2007 and 2008 using an excel spread sheet. The overall positivity for each of the years was around 15%. The data collection has been helpful as it provides, when coupled to external quality assessment, an early warning should any testing fall below the expected standards. With this in mind, the data collection has now been extended to hormonal receptor status for every new breast cancer.
Methods Collecting ER & PR data, as well as HER-2 test information, has meant that an on-line system becomes necessary in order to handle the amount of information efficiently. Within this system there is an automatic analysis tool that will quickly provide posivity rates for those inputting testing data.
Results The results give useful information such as, the percentage of cases that are HER-2 positive and hormonal receptor negative, cases that are HER-2 negative, ER positive, PR negative etc.
Conclusion(s) By collecting so much testing data on huge numbers of cases, it will enable the UK to establish ranges of positivity for each predictive target. Once these are in place, centres whose testing is not within the ranges will be expected to investigate. The on-line audit tool is not restricted to the UK though, all overseas subscribers can also use the system.

OP20.7

Intra-operative assessment of sentinel node biopsy for breast carcinoma using osna technique. The Charing Cross experience

Peston D.; Shousha S.; Sinnett D.
Charing Cross Hospital, London, United Kingdom

Background Sentinel lymph node biopsy (SLN) is a major surgical advance in the management of breast cancer. Intra-operative assessment of SLN, using frozen sections or imprint cytology, has a high false negative rate. One Step Nucleic Acid Amplification (OSNA) is a newly introduced automated molecular diagnostic system for SLN analysis. Charing Cross Hospital was recently involved in a multi-centeric prospective study to evaluate this technique.
Methods One hundred SLNs from breast cancer patients, detected by combined radio-isotope and blue dye, were studied. Each freshly removed node was cut into four slices. Two were immediately analysed by OSNA for cytokeratin 19 mRNA, and 2 were routinely processed for later examination of step levels using haematoxylin and eosin, and immunocytochemistry for CK19 and AE1/AE3. The results were then tabulated and compared.

Results After exclusion of samples affected by tissue allocation bias, overall concordance per lymph node of OSNA versus routine histopathology was 96% with a sensitivity of 92% and specificity of 97%. The OSNA results were achieved, on average, within 30 min for two sentinel nodes.
Conclusion(s) OSNA enables accurate intra-operative assessment of sentinel lymph nodes which can be used successfully in a typical UK hospital setting. If the node is positive the patient can undergo an immediate axillary clearance under the same anaesthetic instead of a delayed second procedure. This saves unnecessary stress for the patient and theatre time for the hospital.

OP20.8
The need for a biological grading system and its relationship to the current nottingham histological grading system (NGS)

Abdel-Fatah Mohamed Ahmed T.; Powe G.D.; Ball G.; Reis-Filho J.S.; Ellis I.O.
University of Nottingham, Nottingham, Nottinghamshire, United Kingdom

Background In this study, we hypothesised the interaction between mitotic index; MI and Bcl2, could accurately discriminate between low and high-grade breast cancer (BC) and provide a more objective and clinically valuable measure of tumor grade with prognostic significance for patients with moderately differentiated cancer.
Methods A series of 1585 invasive BC with long term follow-up were immunohistochemically profiled for apoptosis regulators and others. Mitotic index was assessed according to NGS: M1; < 10 mitoses, M2; 10 to 18 mitoses and M3; >18 mitoses. Subsequently, BC were classified according to combined MI/Bcl2 profile and compared to NGS.
Results In multivariate Cox regression models including validated prognostic factors, the MI/Bcl2 profile not only remained significantly associated with patients' outcomes but performed better than lymph node status and tumour size. Incorporation of the MI/Bcl2 profile into NPI, accurately reclassified twice as many patients into excellent (EPG) or poor prognostic groups (PPG), improving decision-making for which patients should be given systemic adjuvant therapy. Patients with M1/Bcl2±and M2/Bcl2+ (NGS G1 like) produced a better response to hormone therapy than those with M2-3/Bcl2- and M3/Bcl2+ (NGS G3 like) (HR 3.4; $p<0.0001$).
Conclusion(s) In conclusion biological grading achieved through mitosis and Bcl2 expression reclassified 70% of patients with equivocal NGS G2 into NGS G1-like with low risk versus NGS G3-like with high risk of recurrence, improving prognosis and therapeutic planning and supporting the genetic pathway model of tumour grade origin.

OP20.9
Recurrent phyllodes tumours

Busmanis I.; Tan E.; Yong W.; Tan P.
Singapore General Hospital, Singapore, Singapore

Background Phyllodes tumours (PT) of the breast are uncommon, usually benign, fibro-epithelial neoplasms, The overall local recurrence rate is approximately 21%. Controversial areas with regard to prognostication for this tumour remain the predictive factors for recurrence. There is recognition that recurrences may be of differing histologic grade compared with the original tumour. Few studies have contributed immunohistochemical (IHC) data; this would be the first retrospective IHC analysis of both recurrent as well as original tumours.
Methods Medical records of 49 patients diagnosed with recurrent PT were reviewed retrospectively over a 15 year period, and clinical and pathologic data analysed. PT were classified into 3 grades, benign, borderline (BL) and malignant, based on the degree of mitotic activity, stromal hypercellularity and atypia, overgrowth, and nature of tumour borders. Immunohistochemistry utilising antibodies to Ki-67, c-kit and p53 is performed on paraffin sections of the original and recurrent tumours.
Results Ethnicities; 44 Chinese, 4 Malay and 1 Filipina. Mean age at diagnosis 39.9 years. Mean original tumour size; 5.8 cm. Of 46 assessable cases, 59% had tumour at, or within 1 mm of the margin. 63.3% were benign, 22.4% BL, and 14.3% malignant. Local recurrence occurred after a median period of 23.7 months. 16 patients (32.6%) showed transformation: 7 benign upgraded to BL; 2 BL downgraded to benign; 4 benign, and 3 BL cases upgraded to malignant. Comparative IHC analysis is presented.
Conclusion(s) A large database of 49 Asian cases of recurrent PT is presented. In comparison with Caucasian data, patients presented at a slightly earlier age, and with a higher percentage of BL or malignant tumours. 59% of recurrent cases were originally at, or very close, to margins. A lower rate of transformation (32.6%) was seen in comparison with previous reports. IHC data is analysed retrospectively in the recurrent tumours to determine prognostic significance of immunoreactivity.

Oral presentations 21

Nephropathology

OP21.1

Columbia classification of histological variants of focal and segmental glomerulosclerosis (FSGS) and risk of recurrence after transplantation

Canaud G.; Dion D.; Zuber J.; Gubler M.; Thervet E.; Salomon R.; Legendre C.; Noel L.; Niaudet P.
Hôpital Necker, Paris, France

Background Recurrence of nephrotic range proteinuria in patients with idiopathic nephrotic syndrome (INS) and FSGS on native kidneys is associated with poor graft survival. Identification of risk factors for recurrence is therefore an important issue. In 2004, the Columbia University introduced a histological classification of FSGS that identifies five mutually exclusive variants. In non-transplant patients, the Columbia classification appears to predict the outcome and the response to treatment better than clinical characteristics alone. However, the predictive value of this classification to assess the risk of recurrence after transplantation has not been addressed.
Methods We retrospectively studied 77 patients with INS and FSGS on native kidneys who underwent renal transplantation. Of these, 42 recipients experienced recurrence of nephrotic range proteinuria.
Results At time of recurrence, minimal change disease (MCD) was the main histological feature. On serial biopsies, the incidence of MCD decreased over time, while the incidence of FSGS variants increased. The variant type observed on native kidneys was not predictive of either recurrence or type of FSGS seen on the allograft. Patients with complete and sustained remission did not developed FSGS.
Conclusion(s) In conclusion, the Columbia classification is of no help in predicting recurrence after renal transplantation or histological lesions in case of recurrence.

OP21.2

High salt intake and oxidative stress in the kidney. The role of fetal programming

Koleganova N.; Piecha G.; Ritz E.; Schirmacher P.; Gross M.
Department of Pathology, University of Heidelberg, Heidelberg, Germany

Background High salt intake causes hypertension and adverse cardiovascular and renal outcomes, but some forms of salt-mediated target organ damage are blood pressure-independent. It has been suggested that high salt intake during pregnancy influences blood pressure in the offspring. It was the purpose of the present study to clarify whether high salt intake in pregnancy and after weaning alters blood pressure and kidney morphology in the offspring
Methods Sprague-Dawley rats were fed normal (0.15%), medium (1.3%), or high (8.0%) salt diet during pregnancy and weaning. The offspring were weaned at 4 weeks of age and subsequently maintained on the same diet or switched to normal or high salt diet respectively. Kidney morphology and markers of oxidative stress were assessed at 7 and 12 weeks postnatally
Results The number of glomeruli in the offspring of the mothers on high salt was significantly lower compared to the other groups in normal and in medium salt. Compared to other offspring urinary 8-isoprostane was significantly higher in offspring of mothers on high salt irrespective of their post-weaning salt intake. Albumin excretion was higher and creatinine clearance was lower in offspring of mothers on high salt which were maintained on high salt compared with other offspring. No significant differences in telemetrically measured blood pressure were observed between the groups of offspring.
Conclusion(s) High salt intake in mothers restricts nephron number in offspring and predisposes the offspring to increased oxidative stress and disturbed kidney function.

OP21.3

High salt intake in pregnancy alters maturation of glomeruli in the rat offspring

Koleganova N.; Piecha G.; Ritz E.; Schirmacher P.; Gross M.
Department of Pathology, University of Heidelberg, Heidelberg, Germany

Background Faulty fetal programming leads to alterations in kidney morphology in the offspring. A low number of glomeruli is known to cause high blood pressure later in life. It was the purpose of the present study to clarify whether high salt intake in pregnancy alters kidney development in the offspring.
Methods Sprague-Dawley rats were fed normal, medium or high salt diet during pregnancy and weaning. The number of glomeruli (mature, immature, and S-shape bodies) was assessed at 1 week postnatally. The expression of proteins of interest was assessed at 1 week postnatally and at term.
Results There was no difference between the groups with respect to litter size, birth weight, and placenta size. At age 1 week the number of S-shaped bodies was significantly lower and the number of mature glomeruli and layers of developing glomeruli was higher in the offspring of

mothers on high-salt compared to the other groups. As a net result total number of glomeruli was significantly lower in the offspring of mothers on high-salt compared to the other groups. At 1 week of age in the offspring of mothers on high salt the glomeruli were bigger compared to lower salt intake. The expression of Pax-2 and FGF-2 was significantly lower in the offspring of mothers on high-salt consistent with their causative role.
Conclusion(s) We conclude that high maternal salt intake during pregnancy accelerates maturation of glomeruli in the offspring, but reduces the final number of glomeruli.

OP21.4

Intensity, mean and total optical density of immune deposits in renal diseases

Sarioglu S.; Unlu M.; Sakar M.; Camsari T.; Turkmen Mehmet A.; Ellidokuz H.
Dokuz Eylul University, Inciralti, Izmir, Turkey

Background In this series of renal diseases, semiquantitative scores (SS) for staining of direct immunfluorescein (DIF) examination were compared with mean intensity, mean optical density (MOD), total optical density (TOD) measurements by image analysis. The properties and methods of quantification are described in different diseases.
Methods Twenty-seven (54%) IgA nephropathy, 8(16%) membranous nephropathy, 8(16%) membranoproliferative glomerulonephritis, 7(14%) systemic lupus erithematosus nephritis (SLE-N) cases were diagnosed by clinical, light, DIF and electron microscopic features. Each case was evaluated by SS for IgG, IgA, IgM, C3, C1q, lambda and kappa previously. Intensity, MOD and TOD were determined by image analysis software.
Results There was positive correlation between SS; and intensity and TOD for 199 positive stained images (Spearman's Test, r=0,433, p=0,000 and; r=0,440 p=0,000 respectively) but not with MOD. TOD was important for determining SS by linear regression (p: 0.000). For 2 SLE-N cases, SS and intensity for IgG, IgA were same, but TOD measurements could demonstrate that actually IgG was predominant. When all the cases were considered, creatinine at the time of biopsy was only mildly correlated with intensity and TOD of IgM (r=0,44, p=0,004; and r=0,42, p=0,07; respectively).
Conclusion(s) It seems SS given by the pathologists are determined related to TOD. SS present similar results with intensity and TOD, but for some SLE-N cases only TOD allowed discrimination of the predominantly deposited antibody. The relation of intensity and TOD with clinical features might be evaluated for further information.

OP21.5

Non-heart beating donors are associated with a major and early increase in renal graft fibrosis quantified by an automatized image software analysis

Ferlicot S.; Frangie C.; Jacquet A.; Beaudreuil S.; Durrbach A.; Charpentier B.; Guettier C.; Francois H.
Bicetre Hospital, Le Kremlin Bicêtre, France

Background Non-heart beating donors (NHBD) represent a potential source of kidney donors in an era of organ shortage although resulting in delayed graft function (DGF) and poorer outcome due to interstitial fibrosis.
Methods We used image analysis on Sirius red stained sections to precisely measure the percentage of area of cortical fibrosis. Twelve patients received a first kidney transplant from 9 NHBD.
Results The mean age of NHBD was 42±10 years. Warm ischemia was less than 2 h, cold ischemia less than 18 h. Seven patients had DGF necessitating dialysis; 2 patients experienced acute rejection episode, one patient returned to dialysis and was detransplanted 2 months after transplantation. The starting of graft function occurred around 25± 17 days after transplantation. Seven patients had a pre-implantation graft biopsy. All but 2 patients (one death, one immediate functioning kidney graft) had a kidney biopsy between day 7 and 15 post-transplantation. We found an increase in interstitial graft fibrosis from 4.2±0.6% at the time of transplantation to 24.7±11% (p<0.05) between 7 to 15 days after transplantation. After 306±119 days of follow-up, 10 patients still have a functioning kidney transplant (83.3%) with an average of serum creatinine of 183±82 μmol/l.
Conclusion(s) Although the quality of grafts was good and a rare occurrence of acute rejection episodes, we found an early significant increase in renal graft fibrosis with a poor outcome possibly due to warm ischemia.

OP21.6

The significance of peritubular capillary basement membrane laminations in native and transplant kidneys

Liapis G.; Singh H.; Gasim Mohamed A.; Hogan S.; Nickeleit V.
Chapel Hill, North Carolina, USA

Background Peritubular capillary basement membrane laminations (PTCL) in renal transplants have attracted

increasing interest as potential markers of chronic, possibly antibody mediated, rejection. The aim of our study is to determine the diagnostic significance of PTCL in transplant biopsies.

Methods 548 renal biopsies were analyzed (360 native kidney and 187 transplant specimens). PTCL was evaluated by electron microscopy in 3 representative capillaries per case. Cases were grouped into: A) minor PTCL abnormalities (up to 4 circumferential layers), and B) significant PTCL abnormalities (> 5 circumferential layers). Groups A and B were correlated with more than 20 histologic findings/diagnoses in transplant and native kidneys.

Results PTCL group B was found in 23/360 (6.4%) of native kidneys and significantly correlated only with the presence of thrombotic microangiopathies (9/23), and the degree of chronic injury, i.e. interstitial fibrosis/tubular atrophy, global glomerulosclerosis, arteriosclerosis and arteriolosclerosis ($p<0.05$). In contrast, 35.8% (67/187) of transplant biopsies demonstrated group B PTCL ($p<0.05$ compared to native biopsies). In addition to chronic injury group B PTCL was significantly associated with severe peritubular capillaritis (31/50), transplant glomerulopathy (34/52), C4d positivity (29/49), transplant endarteritis and sclerosing arteriopathy (35/56; all $p<0.05$).

Conclusion(s) Marked multilamination of peritubular capillary basement membranes is most common in transplant biopsies and associated with acute or chronic rejection induced endothelial/capillary injury. Our observations justify the use of PTCL as adjunct markers to diagnose "chronic cellular or antibody mediated" rejection.

OP21.7

Unusual evolution of type II membranoproliferative glomerulonephritis associated with factor I mutation

Servais A.; Frémeaux-Bacchi V.; Bollée G.; Grünfeld J.; Lesavre P.; Noël L.
Necker Hospital, Paris, France

Background The role of uncontrolled activation of alternative pathway due to C3 nephritic factor (C3NeF) is suggested in the pathophysiology of type II membranoproliferative glomerulonephritis (MPGN II). Furthermore three patients with MPGN II associated with homozygous Factor H (FH) mutation have been published. Clinical evolution is usually severe.

Methods We report a patient with heterozygous Factor I (FI) mutation and atypical evolution.

Results A six-year old girl presented with lipodystrophy, proteinuria, and normal renal function. First renal biopsy showed MPGN II with ribbon-like aspect of glomerular basement membranes, mild mesangial proliferation, and few mesangial deposits stained by C3 antiserum. Electron microscopy study confirmed the presence of dense deposits in the lamina densa. A second and a third biopsies were performed 8 and 34 years later respectively showing a progressive extension of the deposits with moderate glomerular proliferation. During follow-up, proteinuria increased but renal function remained normal. Initial complement analysis showed consumption of alternative pathway with decreased C3 and C3NeF detection. Then C3 level and C3NeF detection were fluctuant with transient C3 normalization and absence of C3NeF. Antigenic FH and FI levels were normal. Genetic screening found an heterozygous mutation localized in FI gene.

Conclusion(s) This 34-year follow-up of a MPGN II is characterized by persistent normal renal function despite of increasing C3 deposits on iterative renal biopsies. Uncontrolled activation of the alternative pathway with transient C3NeF is implicated in the pathophysiology of the disease. Evolution may be modulated by the FI mutation.

OP21.8

Deceased donor kidney evaluation. The turning point

Goldberg C.J.; Amante M.; Re L.; Petroni J.; Rial C.M.; Galdo T.M.; Casadei H.D.
Facultad de Ciencias Medicas, Buenos Aires, Caba, Argentina

Background Clinical and histopathological scoring systems were developed to allow a better identification of kidneys associated with standard versus increased risk of graft failure. The aim of our study was to evaluate if post-transplant outcome showed a correlation with either histopathological and/or clinical scores in a cohort of deceased donor (DD) kidney recipients

Methods For the histological analysis, we used the Histological Score (HS), developed by Remuzzi et al. For our clinical analysis, we chose the deceased donor score (DDS). 95 primary DD transplants recipients performed between 01/01/04 and 12/31/06 were analysed.

Results No significant association was found between both scoring systems ($p=0.734$) DGF incidence and 12 month acute rejection rate did not correlate with neither scoring system. 2-year-patient survival showed a trend toward a relationship with DDS (grade A 96%, grade B: 90%, grade C 86%) but no correlation with the HS (mild 88%, moderate: 96%) 2-year graft survival was strongly influenced by the different DDS categories ($p=0.01$), however

no such correlation was found with the HS categories (p= 0.925) 2-year creatinine levels also demonstrated a significant correlation with DDS, but not with the HS.
Conclusion(s) In conclusion, the allocation of kidneys based on a clinical scoring system (DDS) constitutes a useful tool at the moment of accept or discard an offered kidney, showing strong association with relevant post-transplant events. The histological information alone does not correlate with outcomes,but is very usefull at the turning point.

OP21.9
Immunohistochemical study of the inflammatory infiltrate and the proliferative index in the tubulointerstitium in human glomerulonephritis

Petrusevska K.G.; Kostadinova-Kunovska P.S.; Grcevska P. L.; Banev G.S.; Jovanovik R.; Polenakovik Haralampie M.
Institute of pathology, Medical faculty, Skopje, Yugoslav Former Republic of Macedonia

Background The aim of the study was to define the role of inflammatory cells and proliferative index in the renal biopsies of glomerulonephritic lesion in developing of the interstitial fibrosis.
Methods We used archival biopsies from 50 patients, previously diagnosed as primary glomerulopathies (PG) with light microscopy, immunofluorescence and electron microscopy. Urine and blood samples were collected at the time of biopsy for creatinine in the serum and 24-hour total protein excretion. LSAB immunoperoxidase staining on paraffin sections was performed for CD20cy, CD43, CD68, HLA-DRa, LCA, and Ki67. Morphometric analysis of the interstitial fibrous tissue (IF) was done by the Image Analyzing System Lucia M-Nikon on trichrome Mason`s stained tissue samples. The data were statistically analyzed with StatSoft, 2001.
Results The results showed mostly focal inflammatory reaction in the interstitium of all types of PG. It was composed of T lymphocytes (58.26%), macrophages (22.92%), B lymphocytes (18.62%). The IC-s were found in the interstitium, among the tubular epithelial cells (TEC), between the TEC and tubular basement membrane or within the TBM (tubulitis). There was enhanced proliferation of TEC-s with positive correlation with IC-s. The extent of IF was 18.75% ± 5.04. There was positive correlation between the presence of T lymphocytes and IF as well as between the analyzed subpopulations of ICs and the concentration of creatinine in the serum of the patients.
Conclusion(s) There is association of the interstitial IC-s and processes in the tubulointerstitial compartment in glomerular disease.

Oral presentations 22

Cardiovascular pathology – Pulmonary pathology

OP22.1
Ventricular unloading increases 20s proteasome protein expression and restores proteasomal function in a subset of patients

Wohlschlaeger J.; Sixt Urs S.; Tatjana Stoeppler T.; Vahlhaus C.; Schmid C.; Peters J.; Schmid Werner K.; Baba A.H.
Institute of Pathology and Neuropathology, University Hospital of Essen, Germany

Background The Ubiquitin/Proteasome (UPS) system breaks down misfolded and normal proteins including cell cycle regulatory proteins involved in cardiac hypertrophy. Chronic heart failure (CHF) is associated with increased cardiomyocyte cellular mass, indicative of increased synthesis and/or impaired breakdown of proteins by the UPS. Ventricular unloading is associated with decreased cardiac hypertrophy and reversible regulation of numerous molecular systems ("reverse cardiac remodelling").
Methods In 23 paired myocardial specimens (before and after unloading) Ubiquitin and 20S Proteasome were immunohistochemically investigated and morphometrically quantified with regard to cardiomyocyte hypertrophy, DNA content and Cyclins, PCNA and the pRb/E2F-1 pathway. The plasma 20S Proteasome concentrations were measured by ELISA. In a subset of patients, proteasomal activity was determined in tissue lysates.
Results In CHF, the 20S Proteasome protein expression is significantly decreased compared to controls and significantly increases after unloading. Cardiomyocyte 20S Proteasome expression correlates negatively with cell size, mean DNA content and with Cyclins D1 and A, PCNA and the pRb/E2F-1 pathway. 20S Proteasome plasma concentrations are significantly increased after unloading. In a subset of patients there is increased proteasomal enzymatic activity after unloading.

Conclusion(s) 20S Proteasome protein expression is increased after ventricular unloading and associated with decreased cardiomyocyte hypertrophy, mean DNA content and cell cycle regulatory proteins, which are mediators of cardiac hypertrophy. This is in accordance with the proteasomal function of breakdown of misfolded and functional proteins involved in the pathogenesis of cardiac hypertrophy.

OP22.2

C4d immunostaining in the follow-up of cardiac transplantation

Fedrigo M.; Tona F.; Gambino A.; Frigo A.; Poli F.; Benazzi E.; Caforio A.; Feltrin G.; Toscano G.; Gerosa G.; Valente M.; Thiene G.; Annalisa A.
Departement of Medical-Diagnostic Science and Special Therapies, Padova, Italy

Background Aim of present study was to assess the role of C4d positive staining on endomyocardial biopsies (EMB) in the development of micro-vasculopathy and in the outcome of patients.
Methods 822 endomyocardial biopsies (EMB) were obtained from 120 patients who had undergone heart transplantation at our centre since 2004. Immunostaining for C4d was performed in all biopsies with affinity-purified anti human C4d polyclonal antibody (AbdBiomedica). Coronary blood flow velocity in the left anterior descending coronary artery was detected by contrast-enhanced transthoracic echocardiography (CE-TTE) at rest and during intravenous infusion of adenosine (0.14 mg/kg/min) in all the patients. CFR was obtain as the ratio of hyperaemic diastolic peak of velocity (DPV) to resting DPV.
Results 40 patients showed C4d capillary positive staining, 9 of them fulfilled three major criteria for humoral rejection (7,5%). Ten patients showed C4d capillary positive staining on more than one subsequent EMB. Patients with C4d positivity showed the worst survival (p log rank 0,002), followed by patients with Antibody Mediated Rejection (p log rank 0,0162) and by patients with C4d positivity without graft dysfunction (p log rank 0,0189). Mean CFR was 3.4±0.99 in patients with C4d negative EMB and was 2.4 ± 0.97 in patients with C4d positive EMB ($p<0,05$).
Conclusion(s) C4d positive staining significantly correlates with a worse outcome, in particular with C4d positive staining with circulating antidonor antibodies. It can be regarded as a marker of early graft dysfunction and microvascular damage and can influence the outcome of the patients.

OP22.3

Computerized texture analysis of histologic sections: comparison of aortas of normotensive and hypertensive patients

Metze K.[1, 4]; Vieira G.[1, 4]; Adam R.L.[2, 4]; Ferro D.P.[1, 4]; de Thomaz A.A.[3, 4]; Cesar C.L.[3, 4]
[1]Faculty of Medical Sciences, [2]Institute of Computing, [3]CePOF, Institute of Physics, [4]National Institute of Photonics Applied to Cell Biology, University of Campinas, Brazil

Background Elastic fibers can be demonstrated in eosin-stained histologic sections by fluorescence microscopy. The aim of our study was to create an automatic computerized texture analysis system for elastic fibers, and to compare histologic slides of aortas of normotensive (NTs) and hypertensive (HTs) patients.
Methods The system composed of an inverted microscope, scan head and Argon laser was able to collect confocal backscattered fluorescence of eosin-stained slides of aortas (21 normotensive and 26 hypertensive patients from our autopsy files). Images comprising the full thickness of the vessel wall were composed by integration of several frames. For texture analysis a gliding box was running in 1-pixel steps along a predefined axis from intima to adventitia. For each step several texture features were simultaneously calculated and plotted in diagrams according to their topographic position in the vessel wall.
Results In NTs discrete architectural changes reveled by changes of the entropy values can be found more frequently at the transition between the inner and the medial third of the vessel wall. Variation of the number of elastic layers is increasing with advanced age in both NTs and HTS. In HT there is a greater distance between the elastic layers, when compared with NTs, and their number of the layers is increasing in older patients.
Conclusion The presented method provides a new tool for an objective and reproducible automatic analysis of the architecture of the aorta with the possibility of topographic quantification of the disease process. In both normotensive and hypertensive patients, discrete local alterations of the architecture appear more frequently in older patients. Aortas of HTs reveal signs

of adaptative processes. Supported by FAPESP 2007/52015-0 and CNPq 479074/2008-9

OP22.4

Stem cells homing, ventricular remodelling and cytokines profile in an animal model of heart failure

Castellani C.; Ravara B.; Gobbo V.; Franzin C.; Pozzobon M.; De Coppi P.; Vettor R.; Thiene G.; Dalla Libera L.; Vescovo G.; Angelini A.
Department of Medico-Diagnostic Sciences and Special Therapies, Padua, Italy

Background Aim of our study was to investigate the homing and differentiation of human amniotic stem cell (hAFC, like embryonic stem cells) and rat vascular stromal adipocite GFP positive cells (rGFP, vascular progenitor cells) in a rat model of heart failure.
Methods 28 male Sprague-Dowley rats were injected with monocrotaline to develop right heart failure. Four millions hAFC or rGFP cells were injected via tail vein three weeks after MCT injection. Stem cells differentiation was studied by double immunofluorescence technique. Ventricular remodelling was analized by RVM/Vol at histology and by BNP serum level and Multiplex cytokines array on serum.
Results hAFC cells were detected in the lung, heart and skeletal muscle with a homing percentage of 2.26±0.23, 0.5±0.42 and 0.36±0.41 respectively. rGFP cells were detected in the lung, heart and skeletal muscle with a homing percentage of 2.01±0.31, 0.6±0.3 and 0.8±0.4 respectively. Stem cells showed a differentiation towards smooth muscle and endothelial markers. Protein suspension array of rat serum showed that cytokines profile in rats injected with stem cells was similar to that of the controls and in particular we found high levels of anti-inflammatory IL10 and low level of pro-inflammatory TNF alfa cytokine.
Conclusion(s) These results suggest that hAFC and rGFP cells are both engrafted in the lung, heart and skeletal muscle and reduce heart failure remodelling through the IL10 pathway activation which lead to reduction of pro-inflammatory cytokines profile.

OP22.5

Cardiac variant of Fabry's disease associated to ichtyosis

Mercado M.; Tuñon T.; Amat I.; Beloqui R.; Martinez-Peñuela A.; Martinez-Peñuela J.
Hospital de Navarra, Pamplona, Navarra, Spain

Background Fabry's disease is an X -linked recessive disorder caused by deficiency of alphagalactosidase A and typically causes multi-organ dysfunction.
Methods We present a case of a 35 year old man without past medical records who came to the coronary unit after a cardiac arrest; CPR was performed with total recuperation. Echocardiography showed thickness of left ventricular wall. With the diagnosis of restrictive miocardiopathy endomyocardial biopsy was performed. He didn't show any angiokeratomas but dermatologist performed a diagnosis of vulgar ichtyosis.
Results Histology study of the biopsy revealed mild hypertrophy of cardiomyocytes containing perinuclear vacuoles. At electronmicroscopy the vacuoles contained electron dense inclusions of different configuration, the most frequent being the so-called "zebra body", which consists of lamellar parallel or concentric inclusions with alternating electron-dense and clear bands suggesting a Fabry's disease. The diagnosis was confirmed by detection of a very low level of alphagalactosidase A activity in serum. Similar findings were found on skin biopsy.
Conclusion(s) This case was classified as a cardiac variant of Fabry's disease, when deposition in myocardium causes cardiac hypertrophy and the infiltration of the conduction is severe occult ventricular arrhythmias could cause sudden death. An early recognition and treatment of this entity with enzyme replacement therapy may avoid fatal outcomes. Electron microscopy is a reliable method to study and to diagnose Fabry's disease. We'll report the clinical and morphological response after five months of recombinant human alphagalactosidase A replacement.

OP22.6

Hemodynamic support by left ventricular assist devices reduces cardiomyocyte DNA content and increases myocardial stem cells in the failing human heart

Wohlschlaeger J.; Levkau B.; Brockhoff G.; Stypmann J.; Schmid C.; Pomjanski N.; Böcking A.; Baba A.H.
Institute of Pathology and Neuropathology, University Hospital of Essen, Germany, Essen, Germany

Background Whether adult cardiomyocytes have the capacity to regenerate in response to injury is an issue of debate. In human heart failure, cardiomyocytes harbour a polyploid genome. A unique opportunity to study the mechanism of such polyploidisation is provided through the setting of hemodynamic support by left ventricular assist devices (LVAD). Hence we assessed cardiomyocyte ploidy status, number of nuclei per cell and myocardial stems cells in paired samples prior to and after LVAD support.
Methods In 23 paired myocardial samples, cardiomyocyte ploidy was investigated by DNA cytometry and the number of binucleated cardiomyocytes was counted. Myocardial stem cells were investigated by immunofluorescence.

Results The mean cardiomyocyte DNA content and the number of polyploid cardiomyocytes declined significantly after LVAD. The decrease in polyploidy correlated with an increase in cardiomyocytes with diploid DNA. After unloading, a significant increase of CD117+/MEF-2+ stem cells suggestive of commitment to cardiomyocytes was noted.
Conclusion(s) The clear correlation between a decrease in polyploidy and increase of diploidy after LVAD suggests a numerical increase of diploid cardiomyocytes either through cell cycle progression with completion of mitosis or by stem cell commitment to cardiomyocyte lineage.

OP22.7

Diverse prognostic roles of akt isoforms, PTEN and PI3K in tumor epithelial cells and stromal compartment in non-small cell lung cancer

Al-Saad S.; Donnem T.; Al-Shibli K.; Persson M.; Bremnes R.; Busund L.
University hospital of Northern Norway Tromso, Tromso, Norway

Background By tissue microarray methodology we evaluated the expression of altered Akt isoforms, PTEN and PI3K and their prognostic significance in 335 non-small cell lung cancer (NSCLC) tumors.
Methods Tumor tissue was sampled and immunohistochemicaly quantified in 335 tumors from stage I to IIIA non-small cell lung cancer patients both from tumor epithelial cells and surrounding stromal tissue in resected specimens. Correlations were made with clinicopathologic variables. In addition, the expression of these markers was compared to 20 lung tissue cores from patients without any history of malignancy.
Results A significantly higher PTEN expression was observed in control tissue compared with tumor (p= 0.001). In univariate analyses, high tumor epithelial cell expression of non-phosphorylated Akt2 (p=0.014) was a positive prognisticator for disease-specific survival (DSS), while high tumor epithelial cell expression of p-Akt Thr308 (p=0.045) was a negative prognosticator. High stromal expression of total Akt3 (p=0.0008) and total PI3K (p= 0.0003) correlated with a good prognosis. In the multivariate analysis, tumor epithelial cell expression of p-Akt Thr308 (p=0.0009) and Akt2 (p=0.004) and the stromal cell expression of Akt3 (p=0.0008) and PI3K (p=0.012) were independent prognostic factors for DSS.
Conclusion(s) High expression of non-phosphorylated Akt2 and low expression of p-Akt Thr308 in tumor epithelial cells are independent predictors of improved survival in primary NSCLC. In stromal cells, high expression of total Akt3 and total PI3K are both favourable independent prognostic indicators.

OP22.8

High level of carbonic anhydrase IX (CAIX) in tumour tissue and plasma is associated with non-small cell lung carcinoma (NSCLC) progression and poor survival of patients

Ilie M.; Hofman V.; Mazure N.; Butori C.; Lassalle S.; Bonnetaud C.; Mouroux J.; Vénissac N.; Pouysségur J.; Hofman P.
Laboratory of Clinical and Experimental Pathology, Nice, France

Background Hypoxia is a consequence of the rapid growth of many tumours, including lung cancer. CAIX is a hypoxia-inducible member of the CA family and a protein maintaining intracellular and extracellular pH-reportedly also influences regulation of cell proliferation, oncogenesis, and tumour progression. The objective of this study was to evaluate the potential role of CAIX as a prognosis biomarker in NSCLC.
Methods TMA-immunohistochemistry analysis was used to study CAIX expression in NSCLC from 560 patients who underwent surgery between 2001 and 2008. ELISA assay was performed to measure CAIX serum level in 170 of these patients and in 55 healthy individuals. A follow-up (median 35 months) was performed to track recurrence after surgery.
Results All normal lung tissue samples were negative for CAIX expression, whereas 80% of lung cancers expressed CAIX. High tissue expression of CAIX was correlated with poor prognosis for NSCLC patients. The mean serum CAIX level in NSCLC patients was higher (45.40+4.81 pg/ml) than in healthy individuals (2.47+ 0.63 pg/ml). A high serum CAIX level and a high CAIX immunostaining were significantly related with shorter overall and disease-free survival, but independently of pTNM stage
Conclusion(s) The current results indicated that CAIX is a strong predictor of recurrence, progression and overall survival of patients with NSCLC. CAIX could be in the future a diagnostic, prognostic and therapeutic molecular biomarker in lung cancers.

OP22.9

Lymphatic fluctuation in parenchymal remodelling stage of organizing pneumonia, nonspecific interstitial pneumonia and idiopathic pulmonary fibrosis

Ab'Saber Muxfeldt A.; De Araujo Lima C.; Parra Roger E.; De Carvalho Ribeiro C.; Kairalla Adib R.; Capelozzi V.L.
Faculdade de Medicina da Universidade de São Paulo, São Paulo, SP, Brazil

Background Because the superficial lymphatics in the lungs are distributed in the subpleural, interlobular and peribroncovascular interstitium, lymphatic impairment

would occur in the lungs of idiopathic interstitial pneumonias (IIPs) and increase its severity. We investigated lymphatic distribution in different remodelling stage of IIPs by immunohistochemistry using D2-40 antibody.
Methods Pulmonary tissue was obtained from 45 patients with criptogenic organizing pneumonia/organizing pneumonia (COP/OP, $N=6$), nonspecific interstitial pneumonia (NSIP/NSIP, $N=20$) and idiopathic interstitial fibrosis/usual interstitial pneumonia (IPF/UIP, $N=19$). D2-40+ lymphatic dilatation (LDI) and density (LDE) in the lesions were quantitatively determined and associated to remodelling stage score.
Results LDE decreased with the advance from OP up to NSIP. However, LDE abruptly increased from NSIP up to UIP with the advanced process of remodelling stage of the lesions. Cox regression model showed statistical significance low risk of death for patients with high FVC, but high risk for male, median age >66 yrs and lymphatic density < than 14,04%.
Conclusion(s) Lymphatic impairment occurs in the lungs of IIPS and increase its severity according to remodelling stage. The results suggest that disruption of the superficial lymphatics would impair alveolar clearance, delay organ repair and cause severe disease progress mainly in patients with IPF/UIP. Therefore, lymphatic distribution may serve as a surrogate marker for the identification of patients at greatest risk for death in IIPS.

OP22.10

Protective effects of iloprost in cellular and animal models of ventilator-induced lung injury

Birukov G.K.; Cokic I.; Fu P.; Junjie X.; Birukova A.A.
University of Chicago, Chicago, IL, USA

Background Mechanical ventilation at high tidal volume may cause pulmonary capillary leakage and acute lung inflammation resulting in ventilator-induced lung injury. To test the hypothesis that iloprost, synthetic analogue of prostaglandin I2, may attenuate lung inflammation and barrier disruption caused by pathologic lung distension, we used in vivo two-hit model of ventilator-induced lung injury and in vitro model of pulmonary endothelial cells exposed to pathologic cyclic stretch and agonist stimulation.
Methods Mice received triple intraperitoneal injections of iloprost (i/v, 2 μg/kg) at 0, 40 and 80 min after onset of high tidal volume (30 ml/kg) ventilation (HTV) combined with administration of thrombin receptor activating peptide 6 (TRAP6, i/t, 12 mg/kg). After 4 h, bronchoalveolar lavage (BAL), histological analysis, and measurements of Evans blue accumulation in the lung tissue were performed. In vitro, effects of iloprost on endothelial barrier dysfunction were assessed in EC exposed to thrombin and pathologic (18%) cyclic stretch.
Results Combination of HTV and TRAP6 enhanced accumulation of neutrophils in BAL fluid and lung parenchyma, increased BAL protein content and endothelial permeability monitored by Evans blue measurements. These effects were markedly attenuated by iloprost. In vitro, high magnitude cyclic stretch enhanced thrombin-induced EC paracellular gap formation and phosphorylation of myosin light chain and myosin phosphatase, which were inhibited by pretreatment with iloprost.
Conclusion(s) Iloprost exhibits potent protective effects against lung endothelial barrier dysfunction and vascular leak in the in vivo and in vitro two-hit models of ventilator-induced lung injury.

OP22.11

Serpin B3 transgenic mice are more susceptible to lung fibrosis and epithelial proliferation

Lunardi F.; Pontisso P.; Rea F.; Villano G.; Gnoato M.; Agostini C.; Valente M.; Calabrese F.
University of Padua, Padua, Italy

Background Idiopathic pulmonary fibrosis (IPF) is a devastating fibrotic lung disease where an abnormal re-epithelization is frequently observed. Serpin B3/B4 is a serin protease inhibitor, recently correlated to fibrotic process and lung function impairment in human IPF. To confirm the role of serpin B3 in fibrosis and epithelial dysfunction, serpin B3 transgenic mice (TM) challenged with bleomycin (BLM) were studied.
Methods The study was performed in 40 C57BL/6 mice: 20 TM and 20 wild-type (WT). Intratracheal instillation of BLM was performed in 13 TM and 13 WT, the remained animals were treated with placebo. Mice were sacrificed 48 h (Group 1) and 30 days (Group 2) after treatment. AR and fibrosis extension were quantified by morphometry. Apoptosis and proliferation indexes (AI and PI), the presence of bronchiolisation, dysplasia and neoplasia were also evaluated.
Results In the Group 1 no significant differences were observed, while in the Group 2 TM/BLM presented a more extended fibrosis than WT/BLM mice ($p=0.04$). PI was significantly higher in TM mice than in WT, when treated either with BLM ($p = 0.006$) or with placebo ($p = 0.04$). Although no statistically significant, neoplastic transformation was more evident in TM than in WT (43 vs 14%).
Conclusion(s) Serpin B3 plays an important role in the fibrogenesis of BLM-induced lung damage and it seems to influence epithelial proliferation and neoplastic transformation.

OP22.12

The prognostic value of intraepithelial and stromal innate immune system cells in non-small cell lung carcinoma

Al-Shibli Ibrahim K.; Al-Saad S.; Donnem T.; Persson M.; Bremnes R.; Busund L.
Nordland Central Hospital, Bodo, Norway

Background The major value of prognostic markers in potentially curable non-small cell lung carcinoma (NSCLC) should be to guide therapy after surgical resection. The prognostic significance of tumor infiltrating macrophages, their growth factor, M-CSF, and its receptor, CSF-1R, as well as natural killer cells and dendritic cells, is controversial and not fully understood, especially in the tumor stroma. The aim of this study is to elucidate the prognostic significance of these cells/markers in the epithelial and stromal compartments of NSCLC.
Methods Tissue microarrays from 335 resected NSCLC, stage I-IIIA were constructed from duplicate cores of viable and representative neoplastic epithelial and stromal areas. Immunohistochemistry was used to evaluate cells in epithelial and stromal areas with respect to CD68 (macrophage marker), M-CSF, CSF-1R, CD56 (NK cell marker) and CD1a (dendritic cell marker).
Results In univariate analysis, increasing numbers of stromal CD1a+ (p=0.011) and CD56+ cells (p=0.014) correlated significantly with an improved disease-specific survival. No such relation was noted for epithelial CD1a+ and CD56+ cells, or for CD68+ cells, M-CSF and CSF-1R neither in stromal or epithelial areas. In multivariate analysis, stromal CD56+ cells was an independent prognostic factor for DSS.
Conclusion(s) High density of stromal CD56+ cells is an independent factor associated with an improved prognosis in resected NSCLC, suggesting that these cells might mediate an antitumor immune response in the tumor stroma.

OP22.13

The prognostic value of intraepithelial and stromal T cells, mast cells and plasma cells in non-small cell lung carcinoma

Al-Shibli Ibrahim K.; Donnem T.; Al-Saad S.; Andersen S.; Bremnes R.; Busund L.
Nordland Central Hospital, Dept of Pathology, Bodo, Norway

Background The major value of prognostic markers in potentially curable non-small cell lung carcinoma (NSCLC) should be to guide therapy after surgical treatment. Although tumor infiltrating T lymphocytes and plasma cells have been documented in NSCLC, a clear association with clinical outcome, especially for the stromal component, has not been well established. The aim of this study is to elucidate the prognostic significance of these cells/markers in the epithelial and stromal compartments of NSCLC.
Methods Tissue microarrays from 335 resected NSCLC, stage I-IIIA were constructed from duplicate cores of viable neoplastic epithelial and stromal areas. Immunohistochemistry was used to evaluate the infiltration of T cells (CD3), mast cells (CD117) and plasma cells (CD138) in epithelial and stromal areas.
Results In univariate analysis, increasing numbers of stromal CD3+ (p=0.001) and epithelial CD3+ cells (p=0.004) correlated significantly with an improved disease-specific survival. No such relation was noted with plasma cells or mast cells. In multivariate analysis, stromal CD3+ cells was an independent prognostic factor for DSS (HR 1.925, CI 1.216–3.048, p=0.005).
Conclusion(s) The presence of T cells (detected by CD3 positivity) is an independant factor which correlates with improved clinical outcome in NSCLC. This significance is clearer in the tumor stroma. Neither plasma cells nor mast cells are prognostic indicators in our cohort.

OP22.14

Type V collagen nasal tolerance decrease pulmonary collagen mRNA and TGF-beta expression in experimental model of systemic sclerosis

Velosa Pereira A.; Teodoro Rosolia W.; Konno R.; Parra Roger E.; Oliveira C.C.; Katayama L.M.; Capelozzi V.L.; Yoshinari Hajime N.
Faculdade de Medicina da Universidade de São Paulo, São Paulo, Brazil

Background To evaluate the inflammatory process, collagen deposition, mRNA collagen synthesis, TGF-beta expression in the lung tissue in an experimental model of scleroderma (SSc) after type V collagen (COL V)-induced nasal tolerance.
Methods Female New Zealand rabbits (N=12) were immunized with 1 mg/ml of COL V in Freund's adjuvant (IM). After 150 days, six immunized animals were tolerated by nasal administration of COL V (25 microgramas/day) (IM-TOL), daily during 60 days. The inflammatory cells were evaluated by point counting. The collagen content was determined by morphometry and types I, III and V collagen mRNA expression by Real-time PCR. The morphological aspects were evaluated by immunostaining.
Results IM-TOL, when compared to IM, presented decreased lymphocytes (4.33±1.71 vs. 11.45±2.52), macrophages (5.7433±2.27 vs. 7.66±1.568) and monocytes

(1.9158±0.7332 vs. 27.67±3.72) as well as significant reduction in collagen content around the small vessels (0.371±0.118 vs. 0.874±0.282, $p<0.001$) and bronchioles (0.294±0.139 vs. 0.646±0.172, $p<0.001$). The lung tissue of IM-TOL, when compared to IM, showed decreased immunostaining of types I, III and V collagen, reduced mRNA expression to types I (0.10±0.07 vs. 1.0± 0.528, p=0,002) and V (1.12±0.42 vs. 4.74±2.25, p= 0,009) collagen, in addition to decreased TGF-beta expression.

Conclusion(s) COL V-induced nasal tolerance in the experimental model of SSc decreased the inflammatory process and regulated the pulmonary remodeling process, inhibiting collagen deposition and collagen I and V mRNA synthesis. Additionally, it decreased TGF-β expression, indicating a promising therapeutic option for human scleroderma treatment.

OP22.15

UbcH10 may be a useful tool in the prognosis of lung carcinomas

Bellevicine C.; Berlingieri M.; Sanchez-Cespedes M.; Pallante P.; Natella V.; Varone V.; Iaccarino A.; Guerriero E.; Iannario E.; Fusco A.; Troncone G.

Dipartimento di Scienze Biomorfologiche e Funzionali, Università degli studi Federico II, Naples, Italy

Background The UbcH10 gene codes for a cell cycle-related protein that is involved in mitosis completion. Previous studies of our group suggest its expression as a valid indicator of the aggressive status of epithelial and lymphoid neoplasms. Here we investigated its role in lung non-small cell carcinomas (NSCC).

Methods A NSCC tissue microarray with complete clinical-pathological and molecular data, was analysed and compared to those derived from non-neoplastic lung tissues. The labelling of the mitotic figures ensured the validity of immunoreactivity. UbcH10 expression data were also evaluated by RT-PCR. Prospectively collected NSCC cases were analyzed by flow cytometry evaluating UbcH10 protein levels during the different phases of the cell cycle.

Results UbcH10 expression was strongly related to malignancy at both trascritional and translational levels. Flow cytometry of prospectively collected NSCC cases showed that UbcH10 expression is cell-cycle dependent, steadily increasing in S phase, peaking in G2/M phase and dramatically decreasing in G0/G1 phases. Clinical-pathological correlations showed that UbcH10 is significantly associated with the large cell and squamous NSCC histotypes and with a lesser degree of differentiation. Pearson's correlation test analysis showed that UbcH10 expression was closely associated with intense Ki-67 staining (,427) and with mutational status of both p53 (,466) and EGFR (,340). A significant relationship between UbcH10 expression and overall survival was also observed (,505).

Conclusion(s) UbcH10 overexpression is a novel prognostic marker associated with the most aggressive lung carcinomas.

Oral presentations 23

Digestive pathology

OP23.1

Expression of p-Smad2 and SnoN in GISTs

Bravou V.; Damaskou V.; Kotsikogianni I.; Verras D.; Repanti M.

"Agios Andreas" General Hospital of Patras, Patras, Greece

Background Gastointestinal stromal tumours (GISTs) are the most common mesenchymal tumors of the gastrointestinal tract originating from interstitial cells of Cajal (ICCs). The TGFβ/Smad signaling pathway plays a pivotal role in organogenesis, oncogenesis, inflammation and repair and it was recently shown that it may affect the development and differentiation of ICCs. However, the role of TGFβ/Smad signaling in GISTs is currently unknown.

Methods The expression profile of p-Smad2 and SnoN, a modulator of TGF/Smad responses was assessed by immunohistochemistry in 29 primary KIT positive GISTs (8 low risk, 7 intermediate risk and 14 high risk). Correlations with cell proliferation assessed by Ki67, cell cycle regulators p21, p27 and prognostic factors of GISTs (risk grading system by Fletcher et al and location) were evaluated.

Results Nuclear pSmad2 expression was found in 29/29 (100%) of the cases. Expression of SnoN was cytoplasmic or cytoplasmic and nuclear. Cytoplasmic and nuclear SnoN expression was found in 28/28 (100%) and 18/28 (64.3%) cases respectively. There was no correlation of pSmad2 or SnoN with risk grade, number of mitoses, tumor size, Ki67, p21 or p27. However expression of p-Smad2 and cytoplasmic SnoN was higher in tumors of the small intestine compared to gastric GISTs (p=0.05 and p=0.014 respectively).

Conclusion(s) Expression of the TGFβ signaling components pSmad2 and SnoN is a frequent finding that may contribute to GIST pathogenesis. However the prognostic significance of this finding remains to be determined.

OP23.2

Systematic analysis of proteins from different signalling pathways in the tumour centre and the invasive front of colorectal cancer

Karamitopoulou E.; Zlobec I.; Panayiotides I.; Karakitsos P.; Peros G.; Rallis G.; Lugli A.
University of Athens, 2nd Dept of Pathology, Halandri-Athens, Attiki, Greece

Background In colorectal cancer, the functional impact of proteins from different signalling pathways varies between tumour centre and tumour front. The epithelial-mesenchymal transition at the invasive front is recognized as a crucial step in colorectal cancer carcinogenesis. Aim of this study was to identify potential differences in protein expression between tumour centre and tumour front of colorectal cancer.
Methods Twenty proteins from different signalling pathways (EGFR, pERK, RHAMM, RKIP, b-Catenin, E-Cadherin, pAKT, p16, p21, Ki67, bcl2, VEGF, APAF-1, MUC1, EphB2, MMP7, pSMAD2, CDX2, Laminin5g2, MST1) involved in colorectal cancer progression were studied on 221 well characterized colorectal cancer samples using receiver operating characteristic curve (ROC) analysis for defining appropriate protein cut-off scores.
Results Mean protein expression between tumour front and tumour centre varied statistically significantly for pSMAD2 ($p=0.002$), pERK, RKIP, E-Cadherin, pAKT, bcl2, VEGF, EphB2, MMP7, CDX2, Laminin5g2, MST1, APAF-1 ($p<0.001$ each). pAKT, bcl2, VEGF, APAF-1, pERK, EphB2, RKIP, CDX2 ($p<0.001$ each), E-Cadherin ($p=0.028$), pSMAD2 ($p=0.047$) and MST1 ($p=0.004$) were more frequently expressed in tumour centre, whereas MMP7 ($p=0.002$) and Laminin5g2 ($p<0.001$) over-expression was associated with the invasive tumour front. In multivariable analysis, only VEGF ($p<0.001$), RKIP ($p=0.009$) and Laminin5g2 ($p<0.001$) were the most relevant protein markers discriminating between tumour centre and tumour border.
Conclusion(s) In colorectal cancer progression, VEGF over-expression seems to play a major role in tumour centre whereas Laminin5g2 positivity combined with loss of RKIP promote tumour invasion at the front.

OP23.3

The multi-marker phenotype EphB2/Bcl2/ Laminin5g2 differentiates between low grade and high grade tumour budding in colorectal cancer

Karamitopoulou E.; Lugli A.; Panayiotides I.; Karakitsos P.; Peros G.; Rallis G.; Zlobec I.
University of Athens, 2nd Dept of Pathology, Halandri-Athens, Attiki, Greece

Background Tumour budding is, according to 3rd edition of "Prognostic Factors in Cancer" published by UICC (2006), an additional prognostic factor in colorectal cancer. A tumour bud is defined as a single tumour cell or tumour cell cluster up to five cells at the invasive tumour front. Indeed, a significant difference in survival has been detected in colorectal cancer patients with low- compared to high-grade budding. Therefore, the aim of this study was to identify which potential protein markers differ in expression between low- and high-grade budding.
Methods Established and promising prognostic proteins such as EGFR, pERK, RHAMM, RKIP, b-Catenin, E-Cadherin, pAKT, p16, p21, Ki67, bcl2, VEGF, APAF-1, MUC1, EphB2, MMP7, pSMAD2, CDX2, Laminin5g2 and MST1 were analyzed on 221 colorectal cancer samples with complete clinico-pathological data. Receiver operating characteristic curve (ROC) analysis was used to determine appropriate protein cut-offs.
Results Low- and high-grade budding were defined as ≤ 6 and >6 tumour buds, respectively. Between low- and high-grade budding, mean protein expression was statistically different for RKIP, E-Cadherin, bcl2, EphB2 and Laminin5g2 ($p<0.001$, each). Over-expression of Laminin5g2 ($p=0.003$) and loss of E-Cadherin, RKIP, EphB2 and bcl2 ($p<0.001$ each) was associated with high-grade budding. In multivariable analysis, only bcl2 ($p=0.001$), EphB2 ($p<0.001$) and Laminin5g2 ($p=0.009$) were the most relevant protein markers discriminating between low- and high-grade budding.
Conclusion(s) The multi-marker phenotype Laminin5g2+/ EphB2-/bcl2- is associated with high-grade budding and implies an increased aggressive behaviour in colorectal cancer.

OP23.4

Screening for lynch syndrome in a series of 869 colorectal carcinomas

Musulen E.; Sanz C.; Benito L.; Ariza A.
Hospital Universitari Germans Trias i Pujol, Badalona, Barcelona, Spain

Background To present a colorectal carcinoma (CRC) before the age of 50 years as well as to have a mucinous or medullary (M/M) CRC before the age of 60 years are both accepted criteria to suspect Lynch syndrome (Bethesda guidelines). The aim of the present study is to evaluate the efficiency of these criteria.
Methods A series of 869 primaries CRC prospectively resected were included. In all cases the followed scheme analysis were performed: immunohistochemical (IHC) expression of mismatch repair protein genes (MLH1, MSH2, and MSH6); microsatellite instability (MSI) analy-

sis amplifying 5 different microsatellites (NR21, NR24, NR27, bat25, and bat26) when the 3 IHC were positive in patients aged <50 years and in M/M CRC in patients aged <60 years. In those cases with LMH1(-) the V600E B-raf gene mutation was analyzed by sequentiation. A CRC was considered pathologic if presented one of the followed conditions: 1) MSH2 and MSH6(-); 2) MSH6(-); 3) MLH1 (-) with wild type B-raf gene; 4) MSI-H (≥ 2 mutated microsatellites).

Results Eighty one patients aged ≤50 years, 77 CRC were M/M, 93 patients metl suspicious criteria, and 45 patients had CRC considered pathologic according to above conditions. Young age (< 50 years) and M/M CRC appeared as strong risk factors with statistical significance (p=0,029 and p=0,000). Of those 45 patients identified as possible Lynch syndrome only 10 met Bethesda criteria.

Decades	Nº of cases	Nº HPV positive
1920–29	112	35 (31.2%)
1930–39	685	344 (50.2%)
1940–49	86	40 (46.5%)
1950–59	88	82 (93.1%)
1060–69	65	58 (87.6%)
1070–79	50	46 (92.0%)
1980–89	56	47 (83.9%)
1990–99	31	24 (77.4%)
2000–05	41	39 (95.1%)
Total	1214	714 (86.6%)

Conclusion(s) We strongly recommend including all patients with CRC in the screening for Lynch syndrome.

OP23.5

Diagnosis of colonic adenomas with confocal endoscopy by inexperienced pathologist and endoscopyst

Jimeno M.; Lopez-Ceron M.; Zabalza M.; Rodriguez De Miguel C.; Castells A.; Llach J.; Pellise M.
Hospital Clinic, Barcelona, Spain

Background Endomicroscopy is a newly developed diagnostic tool which enables in vivo microscopy with subcellular resolution during ongoing endoscopy. It uses stimulated light emission based on the application of fluorescent agents (intravenous fluorescein), whose distribution throughout the entire tissue results in a bright contrast over a laser light stimulation. The aim of this study is to evaluate its value to asses the grade of dysplasia in colonic adenomas by both a pathologist and an endoscospist without experience in this technique.

Methods 23 programmed pacients to perform polipectomy were included. Almost 30 images of each polyp were taken with confocal endoscopy (Pentax EPK-1000). Based on architectural and cytologic changes both specialists made an individual diagnosis of dysplasia. The anatomopathologic diagnosis was taken as the gold standard. Polyps were classified as HGD (high grade dysplasia) or LGD (low grade dysplasia).

Results 27 adenomas were studied (main size 18,9± 7,7 mm). Final diagnosis was HGD in 20 (74%) and LGD in 7 (26%). Sensibility (Se) to detect HGD for both specialists was 42,9%. Specificity (Sp), predictive positive and negative values (PPV, PNV) showed higher statistical power, particularly for the diagnosis of the pathologist.

Conclusion(s) Confocal endoscopy can be a useful tool to classify dysplasia in colonic polyps by a pathologist, and probably also effective for an instructed endoscopist.

OP23.6

Expression and methylation profile of DNA repair genes in Greek colon adenocarcinoma patients

Michailidi C.; Theocharis S.; Stolakis V.; Kouraklis G.; Katsaronis P.; Troungos C.
University of Athens, Medical School, Athens, Greece

Background This study aimed to analyze DNA promoter methylation in the following repair genes: hMLH1, MGMT, APC, CDH1, as also hMLH1 and MGMT expression.

Methods Genomic DNA was isolated from surgical tissue samples (malignant, normal) obtained from 45 colon cancer patients. DNA was subjected to chemical modification followed by Methylation Specific PCR (MSP). Results were associated with patients' gender and age, tumours' histological grade and stage. Additionally, MGMT and hMLH1 expression was examined immunohistochemically.

Results Promoter methylation for hMLH1, MGMT, APC and CDH1 genes was observed in (11%, 60%, 24% and 87%, respectively). In 65% of the cases, methylation in two or more of the examined genes was noted. An association between methylation of CDH1 gene and Dukes' stage was found (stages A, B, C, D; p=0.004; stages A, B, C vs D; p=0.0001). Moreover an association between methylation in two or more genes in contrast with well and moderately versus poorly differentiated tumors, was found (p=0.008). Alterations in methylation status were also noted between normal and malignant tissues. Immunohistochemical hMLH1 and MGMT expression was noted in 44% and 51% of the malignant samples, respectively.

Conclusion(s) The promoter of CDH1 gene found to be very frequently methylated, being related with Dukes' stage. Furthermore hypermethylation in two or more genes seems to be related with tumor characteristics. This work and CM were supported by Stavros Niarchos Foundation.

OP23.7

Long-term prognostic impact of isolated tumour cells in pN0 colorectal cancer

Mescoli C.; Albertoni L.; Pucciarelli S.; Giacomelli L.; Fassan M.; Clemente R.; Lanza C.; Nitti D.; Rugge M.
Department of Medical Diagnostic Sciences & Special Therapies, University of Padova, Padova, Italy

Background The prevalence of Isolated Tumour Cells (ITC) in regional lymph-nodes (LNs) from pN0 colorectal cancer (CRC) is controversial and has never been assessed in large series of consecutive, prospectively collected patients.
Methods ITCs were assessed (MNF116-immunohistochemistry) in 5,016 LNs harvested from 308 surgically treated (R0) CRC-patients (LNs mean number/patient: 16.2; range: 1–107). All the considered cases were consecutive, and were prospectively collected. No LNs metastasis were assessed at routine histology assessment (pN0). From each LN, two histology sections (5 micron-thick; 70–100 micron apart) were considered. Cancer outcome was clinically assessed as disease-free survival (mean follow-up = 58.4 months, range = 6–77).
Results ITC were documented in 156/308 (50.5%) patients (ITC+ve LNs: 496/5016 [9.9%]). The mean number of harvested LNs significantly differed in ITC+ve versus ITC-ve group (18 versus 13). ITC-status significantly correlated with both p-Stage and vascular tumour invasion. CRC relapsed in 16/308 (5.2%) cases. Twelve out the 16 relapses (75%) were documented among 156 ITC+ve patients (7.6%). Four out of the 16 CRC relapse (25%) were documented among 152 ITC-ve patients (2.6%). CRC relapse significantly correlated with the ITC+ve status (OR=3.36; 95%CI=1.0–14.4; p=0.020). The disease-free survival time for ITC-ve versus ITC+ve cases was 38.8 versus 28.8 months, respectively (p=0.043).
Conclusion(s) In CRC-pN0 patients, ITCs in regional LNs identifies patients at higher risk of cancer recurrence. ITCs are reliable marker of early relapsing disease and ITC+ve status could imply adjuvant therapy in that pN0-subgroup of patients who are currently excluded from any post-surgical treatment.

OP23.8

Mucins in neoplastic spectrum of colorectal polyps: can they provide predictions?

Molaei M.; Mansoori B.; Mashayekhi R.; Fatemi S.; Vahedi M.; Zali M.
Research Center for Gastroenterology and Liver Disease, Tehran, Islamic Republic of Iran

Background The significance of expression of different mucins in succession of malignant transformation of colorectal polyps is not determined yet. The aim of the present study was to determine the pattern of expression of MUC1, MUC2, MUC5AC and MUC6 in colorectal polyps and to evaluate the applicability of using mucin expression in predicting the extent of malignanttransformation in colorectal polyps.
Methods A total of 453 polyp specimens comprising 36 hyperplastic polyps, 15 serrated adenomas, 258 tubular adenomas, 114 tubulovillous adenomas, and 31 villous adenomas were included in this study, and were immunostained for MUC1, MUC2, MUC5AC and MUC6 by using mucin specific antibodies.
Results MUC1 and MUC6 were absent in all hyperplastic polyps and their expression was higher in serrated and traditional adenomas. Only 5 cases including 2 serrated adenomas, 1 tubulovillous adenoma, and 2 villous adenomas stained negative for MUC2. The highest expression of MUC5AC was observed in serrated adenomas followed by tubular adenomas. Binary logistic regression analysis indicated that absence of staining for MUC1, MUC5AC, and MUC6, and negative staining for MUC2 would increase the risk of invasion in colorectal polyps. Ordinal regression analysis demonstrated a positive association between the level of staining for MUC1 and risk of being of high configuration/grade in colorectal polyps.
Conclusion(s) MUC1, MUC2, MUC5AC, and MUC6 have the potential to be used as predictors of malignant transformation or invasion in colorectal polyps. The most reliable predictions can be achieved by determining the level of expression of MUC1. Keywords: colorectal polyps, MUC1, MUC2, MUC5AC, MUC6.

OP23.9

Expression of barrier genes in the colonic mucosa of IBD patients

De Hertogh G.; Arijs I.; Van Assche G.; Vermeire S.; Geboes K.; Schuit F.; Rutgeerts P.
Pathology, UZ KULeuven, Leuven, Belgium

Background The intestinal epithelium acts as a barrier to nocious luminal compounds. This depends on normal expression of barrier genes. This expression is disturbed in ulcerative colitis (UC) and Crohn's disease (CD). It is unclear whether this is primary or a consequence of inflammation. Our aims were 1) to investigate barrier gene expression in UC and CD before and after infliximab (IFX) therapy; 2) to compare gene expression profiles in responders and controls.
Methods Colonic mucosal biopsies were obtained from 24 active UC and 19 CD patients before and after IFX, and from 6 controls. Patients were classified as responder (8 UC, 12 CD) or not based on combined endoscopic and histological

scores. RNA was isolated, labelled and hybridized to the Affymetrix HG-U133 Plus 2.0 array. Differential gene expression was analyzed with R/Bioconductor software.

Results Various barrier genes were abnormally expressed in active disease. Expression normalized in most UC responders. However, 4 genes remained abnormally expressed in CD responders: 1) MUC1 and MUC4 showed persistent upregulation (x 2.32 for MUC1 and x 2.80 for MUC4); 2) the AJC protein CXADR remained significantly underexpressed (x 0.47); 3) the xenobiotic transporter protein OCTN2 also remained downregulated (x 0.43). These findings were confirmed by RT-PCR and immunohistochemistry.

Conclusion(s) A primary intestinal mucosal barrier defect may contribute to the development of clinical CD. This defect may persist even with endoscopic and histological mucosal healing after successful therapy. In contrast, no such defect could be demonstrated in UC.

OP23.10
Programmed cell death 4 (PDCD4) protein in esophageal cancer

Fassan M.; Parente P.; Ruol A.; Pennelli G.; Rizzetto C.; Giacomelli L.; Lanza C.; Battaglia G.; Pizzi M.; Zaninotto G.; Ancona E.; Rugge M.
Department of Medical Diagnostic Sciences & Special Therapies, University of Padova Padova, Italy

Background Programmed cell death 4 (PDCD4) is a new putative tumour suppressor gene implied in transformation, tumorigenesis, and cell invasiveness. Recent studies demonstrated PDCD4 down-regulated in different human cancers as well as in cancer cell lines. Moreover, loss of Pdcd4 expression has been associated to unfavourable cancer outcome.

Methods A screening for genes down-regulated in esophageal cancers (Oncomine database) disclosed PDCD4 as one of the most consistently involved. Based on such biological rationale, the immunohistochemical expression of Pdcd4 protein has been assessed in 111 consecutive esophageal cancers (63 adenocarcinomas and 48 squamous cell carcinomas) and paired non-cancer samples.

Results Pdcd4 immunostain was significantly reduced in cancer versus non-cancer samples ($p<0.001$). In all cases, normal esophageal mucosa consistently expressed nuclear Pdcd4, which was significantly less expressed (37/111 cases; 33.3%) or completely lost (31/111 cases; 27.9%) in cancer samples. An inverse correlation was disclosed between nuclear Pdcd4 expression and tumour p-stage ($p=0.002$), pT ($p<0.001$), nodal metastasis ($p=0.038$), and with both vascular ($p=0.005$) and perineural invasion ($p=0.004$). Nuclear Pdcd4 expression was associated with longer disease free- ($p=0.011$) and overall-survival ($p=0.021$).

Conclusion(s) These findings support the tumour suppressor function of PDCD4 and suggest a prognostic impact of nuclear Pdcd4 expression. Additional functional studies should inquire on both the PDCD4 role in the multistep esophageal oncogenesis and its clinical usefulness in prognosticating esophageal precancerous lesions with divergent cancer risk.

OP23.11
Prognostic impact of isolated tumour cells in pN0 esophageal cancer

Mescoli C.; Fassan M.; Zaninotto G.; Giacomelli L.; Ruol A.; Parente P.; Lazzarin V.; Pennelli G.; Ancona E.; Rugge M.
University of Padova - Department of Medical Diagnostic Sciences & Special Therapies, Padova, PD, Italy

Background Esophageal cancer (EC) early recurs even after radical surgery. In pN0 EC, the prevalence of isolated tumour cells (ITC) in regional lymph-nodes (LN) ranges between 8% and 62%. The prognostic impact of ITC in EC is controversial.

Methods ITC prevalence in 2,253 LNs regional from 115 surgically treated (R0) pN0-ECs (Squamous: 66; Adenocarcinoma: 29; non-otherwise specified EC [TGR1]: 20) has been assessed (MNF116-immunohistochemistry). From each collected LN, two histology sections (70–100 micron apart) were considered. Cancer outcome was assessed as both disease-free and overall survival (mean follow-up= 29.5 months, range=0.7–60.6).

Results ITCs were documented in 30/115 (26%) pN0-ECs (62/2253 LNs [2.8%]). Mean number of harvested LNs (19.4) did not differ between ITC+ve versus ITC-ve group. No difference in ITC prevalence was noted according to tumour location, p-Stage, cancer's histotype/grade, neo-adjuvant/adjuvant therapy. The disease-free survival time was 30 versus 23 months for ITC-ve versus ITC+ve cases ($p=0.7$). The actuarial median overall-survival was 30 versus 28 months for ITC-ve versus ITC+ve cases ($p=0.4$). When ITC+ve cases were stratified according to number of ITC+ve LNs (< 5 versus ≥ 5), significantly longer disease-free survival was associated to the subgroup of cases < 5 ITC+ve LNs (30 versus 20 months; Cox-Hazards model: HR=4.85; 95% CI=1.02–22.93; $p=0.004$).

Conclusion(s) High prevalence of ITC is documented in LNs regional to EC. The crude prevalence of ITC+ve nodes does not affect the long-term cancer outcome. The number of ITC+ve LNs significantly correlates with cancer relapse.

OP23.12

Intercountry (Italy-Japan) agreement and residual discrepancies in the diagnosis of superficial gastric lesions after Paris and Vienna classifications

Tosi P.; Vindigni C.; Ambrosio M.; Onorati M.; Marini M.; Frosini G.; Cevenini G.; Gotoda T.; Taniguchi H.
University of Siena, Siena, Italy

Background The Paris endoscopic classification and the Vienna histopathological classification aimed to reduce the interobserver discrepancies and in particular those between Western and Japanese endoscopists and pathologists in the diagnosis of superficial gastric lesions.
Methods Forty-eight consecutive superficial gastric lesions were collected and endoscopically and histopathologically diagnosed at Siena University Hospital. Endoscopic photographs as well as histopathological slides, without any diagnostic indications, were then sent to Japanese endoscopists and pathologists working at the National Cancer Center in Tokyo. The Japanese endoscopists and pathologists sent their diagnoses back to the endoscopists and pathologists in Siena.
Results The correlations between Paris endoscopic types and Vienna histopathological categories is high in both the independent Italian and Japanese evaluations. However, the agreement between Italian and Japanese endoscopists is moderate due to the difficult evaluation of the height of the lesions, in particular when they are mixed. The agreement on the size of the lesions is fairly good. The probability of the same allocation to the Vienna categories of a single case is 87%, disagreements remaining in dysplasia grading, between dysplasia and in situ carcinoma, and on cancer invasion of the lamina propria.
Conclusion(s) The results indicate that use of the Paris and Vienna classifications has reduced but not eliminated the discrepancies between Western and Japanese endoscopists and pathologists in the diagnosis of these lesions.

OP23.13

Gastric atrophy diagnostic accuracy: comparison of OLGA and baylor with serum biomarkers

El-Zimaity Mt.H.; Riddell H.R.; Opekun R.A.; Abudayyeh S.; Graham Y.D.
McMaster, Hamilton, Ontario, Canada

Background The extent of gastric atrophy decides the risk for gastric cancer. This study compares two histopathology staging systems (OLGA, and Baylor) that provide an index of gastric atrophy. OLGA incorporates the updated Sydney recommendations but combines antrum and corpus atrophy scores for a final atrophy score associated with cancer risk. Baylor scores the antrum and corpus independently. In Baylor, corpus atrophy stage (and thus cancer risk) is dependent on location. As corpus atrophy starts at the incisura and extends in continuity proximally and towards the greater curve, atrophy in a distal biopsy is early and atrophy in the most proximal location is advanced.
Methods We examined biopsies from 127 patients. We compared corpus atrophy grade (Sydney and Baylor) and stage (OLGA and Baylor) with serum biomarker for corpus atrophy (pepsinogen I:II ratios - sPGI:PGII).
Results Baylor's corpus atrophy score is superior to Sydney's average score from all biopsies ($p<0.0001$), and to OLGA's stage ($p=0.0003$). Also, patients with autoimmune gastritis were easily missed using OLGA while readily identified using Baylor (low antral score, high corpus score).
Conclusion(s) By following Sydney's biopsy site and scoring recommendations, OLGA systematically underestimated the presence of corpus atrophy and thus cancer risk. In addition, diagnostic information was lost in lumping comparative measures (antral versus corpus atrophy). Baylor's recommendations for biopsy sites and atrophy stage best define the extent of atrophy, and therefore cancer risk.

OP23.14

Expression of genotypes CagA and VacA and their correlation with hystophathological changes in Hp chronic gastritis

Baruti A.; Manxhuka-Kerliu S.; Petrusevska G.; Kamberaj X.; Ahmetaj H.; Jovanovich R.
Institute of Pathology, Prishtina, Kosova, Serbia and Montenegro

Background The presence of CagA and VacA genes are considered the two major virulent markers of H. pylori gastritis. The aim of this study was to detect dominant CagA and VacA genotypes in patients with chronic H. pylori gastritis, correlation among CagA and VacA genotypes and morphological changes in gastric mucosa infected with H.pylori as well as coinfection frequency of H. pylori in patients with CagA genotypes and VacA subtypes.
Methods Biopsy specimens of 100 Hp-infected patients, obtained from the antrum and corpus of the stomach, by gastroscopy have been analyzed histologicaly. Formalin-fixed paraffin-embedded tissue blocks were sliced 4 mm thick and placed in sterilized 1.5 ml centrifuge tubes. The genotyping of VacA and CagA was done by PCR.

Results The CagA and VacA genotypes have been detected in 79% of H. pylori-positive gastric biopsy specimens. The CagA genotype was detected in 19%, VacA s1 in 29%, VacA s2 in 23%, VacA m1 in 12% and VacA m2 in 17% of cases. The VacA s1/s2 allele and VacA m2 subtype were detected in 2.53% of cases. Statistical analysis showed no difference in detection of the CagA and VacA of gastric biopsy specimens ($p<0,0001$).

Conclusion(s) The early detection of CagA and VacA genotypes as well as their sybtypess has the significant importance in prevention the complications of Hp gastritis such as gastric cancer.

OP23.15
Pleomorphic phenotypes of gastrointestinal stromal tumors (GISTS) at metastatic sites. 145 lesions in 30 autopsy cases without imatinib treatment

Sakamoto K.; Sakurai S.
Gunma University Graduate School of Medicine, Maebashi, Gunma, Japan

Background A molecular targeting drug, imatinib mesylate, has been reported as effective against advanced and/or metastatic GISTs. However, secondary resistance to the drug has been reported and the mechanism of resistance is not fully clarified. Therefore understanding the characteristics of advanced and/or metastatic GISTs is necessary for an appropriate treatment strategy. In this study we analyzed the histological and immunohistochemical phenotypes of metastatic GISTs without imatinib treatment and clarified the pleomorphism of metastatic GISTs.

Methods We examined 30 autopsy cases in which the patient died of multiple metastases of GISTs without imatinib treatment. In those cases, total 145 metastatic sites were examined by histological and immunohistochemical expression of KIT and CD34. As to KIT-negative tumor sites, we analyzed the expression of other receptor tyrosine kinase, HER2, EGFR, MET, PDGFRa and b.

Results 10 of 145 metastatic sites lacked KIT expressions, and 6 of those tumors expressed PDGFRb whereas expression of HER2, EGFR, MET and PDGFRa was not observed in any of these metastatic sites.

Conclusion(s) The histological morphology and immunohistochemical phenotypes of metastatic GISTs vary among lesion even in the cases without imatinib treatment. KIT-independent mechanism might participate in the proliferation of GISTs in the late stage and that might be a cause of secondary imatinib resistance. Now, we are analyzing PDGFRb gene mutations and amplification in KIT-negative and PDGFRb-positive GISTs.

Poster session 1

Breast pathology

P1.1
MGMT expression in breast neoplasia: correlations with clinicopathological variables

Michailidi C.; Tsourouflis G.; Stolakis V.; Sampani A.; Vgenopoulou S.; Klijanienko J.; Troungos C.; Theocharis S.
University of Athens, Medical School, Athens, Greece

Background O6-Methylguanine-DNA-methyltransferase (MGMT) is an enzyme involved in the repair of damages induced by endogenous and environmental alkylating agents. Abnormal MGMT expression has been correlated with solid tumor patients' prognosis. The aim of this study was to examine the clinical significance of MGMT expression in human breast clinical material.

Methods MGMT expression was examined immunohistochemically on paraffin-embedded tissue sections obtained from 102 breast benign and malignant lesions. MGMT positivity, overexpression and intensity of immunostaining were correlated with patients' age and TNM stage, tumor histological type and grade, as well as with mitotic activity.

Results MGMT positivity was noted in 29% of malignant, 25% of benign and 70% of in situ breast tumors. MGMT overexpression was noted in 70% of malignant, 33% of benign and 36% of in situ MGMT positive cases. MGMT positivity, overexpression and intensity of immunostaining provided a distinct discrimination between malignant, benign and in situ breast tumors ($p=0.0001$, $p=0.043$ and $p=0.008$, respectively). MGMT positivity was correlated with tumor size (T, $p=0.001$), while a trend with nodular metastasis (N, $p=0.060$) was also noted.

Conclusion(s) Our study reported alterations in MGMT expression in the progression of breast neoplasia, and correlations with clinicopathological variables important for patients' management. Further molecular and clinical studies are required in order to delineate the participation of MGMT in breast cancer development, progression, prognosis and treatment.

P1.2
Paxillin expression and EMT markers in breast ductal carcinoma in situ (DCIS)

Logullo F.A.; Pasini S.F.; Nonogaki S.; Osorio C.; Soares A.F.; Brentani MM.
UNIFESP, São PAulo, São Paulo, Brazil

Background Detection and treatment of DCIS has increased considerably but it is not yet possible to predict its biological behavior. EMT, epithelial mesenchymal transition, is a cellular transdifferentiation program that enables epithelial transformed cells to acquire mesenchymal properties, including traits of motility and invasiveness. Paxillin, a focal adhesion-associated protein involved in cell motility Is one of the factors associated to EMT. In an attempt to evaluate EMT markers in initial breast cancer we assessed the pattern and distribution of paxillin expression in 94 DCIS lesions (49 cases comprised pure DCIS and 45 cases of infiltrative carcinomas with a DCIS component) and its correlation to other EMT proteins, ER, PR and HER-2 expression and to clinical outcome.
Methods Samples were assembled in Tissue micro array. ER, PR, HER-2, Paxillin, e-cadherin, cathenin, TGFbeta1 were assessed by immunohistochemistry. Statistical analysis used a chi-square test.
Results From 94 cases studied, paxillin immunoreactivity was positive in 81%. Of the biomarkers analyzed only TGFbeta1 and beta catenin expression were correlated to paxillin expression (p=0.003 and p=0.009). In the DCIS subset with invasive component, paxillin and HER-2 expression were correlated (p=0.026). Paxillin expression did not correlate with morphological variables. None of the biomarkers analyzed were associated to survival.
Conclusion(s) We found high positive percentage of paxillin expression in DCIS without prognostic significance. HER-2 correlation only in DCIS associated to invasive lesions suggests the possibility that paxillin may be part of HER-2 pathway in this subset.

P1.3
VEGFR and HIF-1a evaluation in triple negative breast cancer

Fakhruddin N.; Farhat F.
AUBMC and HHUMC, Beirut, Lebanon

Background Tumoral angiogenesis is a therapeutic target for many solid tumors, including breast carcinoma. Vascular endothelial growth factor (VEGF) and its associated gene transcriptional activator under hypoxic conditions, known as the hypoxia inducible factor -1 alpha (HIF-1α) are two of several factors implicated in pathogenesis. These factors were correlated with high metastatic potentials and poor clinical prognostic outcomes evident in the low response to hormonal therapy, radiotherapy, or chemotherapy. Breast cancer is known to respond to hormonal or monoclonal antibody (Trastuzumab) treatment; however, triple negative breast cancer (TNBC, immunohistochemically showing no expression of estrogen receptors, progesterone receptors, or c-erbB2) is an aggressive category that does not show such a response. These tumors exhibit morphological signs of hypoxia, including central fibrosis or necrosis, thus hypoxia-induced angiogenesis can be implicated in the aggressive characteristics of TNBC and consequently, the possibility of employing antiangiogenesis therapy as a target and an adjuvant therapy to the already established protocols.
Methods Immunohistochemical evaluation of VEGFR, HIF-1α, and CD31 for microvessel density counting was performed on sections obtained from paraffin reserved archival TNBC tissues. VEGFR and HIF-1α are evaluated using a two tier score, while microvessel density counting is performed manually. In addition, quantitative real-time polymerase chain reaction (qRT-PCR) for pre-translational evaluation (mRNA evaluation) using tissues from the same paraffin reserved blocks is performed. A statistical analysis is conducted correlating the findings to the histological and the clinical data.
Results Expected date: July 2009.
Conclusion(s) Expected date: July 2009.

P1.4
A benign mesothelial inclusion in axillary sentinel lymph node resection for breast cancer. About a series of 1850 sentinel lymph node procedures

Croce S.; Marin C.; Casnedi S.; Wittersheim A.; Loussert L.; Mathelin C.
University Hospital, Strasbourg, France

Background Benign lymph node inclusions are uncommon and represent a potential source of false positive diagnosis of malignancy. Their rate is growing up with sentinel lymph node (SLN) procedure because of the exhaustive analysis of the nodes by multi-level sectioning and systematic immunostaining. We describe here an observation of benign mesothelial inclusion. To our knowledge, such a situation was never described in axillary sentinel lymph nodes.
Methods We analyzed 1850 axillary sentinel node procedures in patients affected by breast carcinoma who underwent surgery between 2000 and 2008. The SLNs were analyzed by H&E and AE1-AE3 immunostaining at 500 μm intervals until tissue exhaustion.
Results 6 epithelial (annexial/mammary gland tissue) inclusions and 1 mesothelial benign inclusion were detected, which represents a frequency of 0.2% and 0.03% respectively in our series. These cases did not induce a false positive diagnosis of malignancy. As usual, the epithelial inclusions were identified focally in subcapsular location but the mesothelial inclusion was localized in an extensive circumferential subcapsular and

paracortical fashion making the differential diagnosis with metastatic deposits difficult. The mesothelial nature was suggested by H&E cellular morphology (large cells in a monolayer distribution) and confirmed by IHC (calretinin positivity and BERP4 negativity). In this case the SLN was excised in a context of a large DCIS without microinvasion.
Conclusion(s) We reported the first observation of a benign mesothelial inclusion in an axillary SLN.

P1.5
AKT and trail status in young women with breast cancer. Implications in therapy resistance

Georgescu A.; Stoicea M.; Enache S.; Andrei F.; Vasilescu F.; Dobrea C.; Ceausu M.; Cionca F.; Comanescu M.; Butur G.; Ardeleanu C.
Victor Babes National Institute of Pathology, Bucharest, Romania

Background Breast cancer in young women is more aggressive, has worse prognosis and reduced survival compared to older women. AKT is a key mediator in cell proliferation, migration and survival. High AKT expression is associated with suppressed apoptosis, tumor genomic instability and therapy resistance. Also, AKT and estrogen receptors (ER) are interrelated, AKT mediating tamoxifen resistance in breast cancer. TRAIL induces apoptosis and is important for cancer therapy, selectively destroying tumor cells, and sparing normal cells. Tumor cells may evade TRAIL-mediated apoptosis by means of regulators like AKT.
Methods A retrospective study was done on 19 consecutive cases of primary invasive ductal carcinomas in young women (mean age=27.84 years, range 23–31 years) on formalin-fixed paraffin-embedded tumoral tissue, using an indirect bistadial immunohistochemical technique, and antibodies for AKT, TRAIL and ER.
Results Eighteen cases showed positive reaction for AKT (94.73%), almost double as usually reported. TRAIL was positive in 11 tumors. ER was positive in 13 cases. Statistical correlations were noticed between ER and AKT. AKT and TRAIL expressions were encountered in high histological grade tumors; there was a single tumor (G3) both AKT and TRAIL negative.
Conclusion(s) The ER-AKT correlation may explain the poor prognosis and aggressiveness in breast cancer in young women. As a theoretical possibility, we suggest that, when co-expressed, AKT's potential as negative prognostic factor could diminish TRAIL's positive prognostic potential. AKT inhibitors could represent a novel therapeutic strategy in breast cancers resistant to classical therapies.

P1.6
Axillary lymph node dissection in breast cancer patients with sentinel lymph node micrometastases

Gomez Dorronsoro L.M.; Aizcorbe Garralda M.; Sanz De Pablo Angel M.; Dominguez F.; Trujillo R.; De Miguel Medina C.; Ruiz De Azua Y.; Gonzalez Alvarez G.
Hospital de Navarra, Pamplona, Navarra, Spain

Background Immunohistochemical (IHC) analysis in determining micrometastases in the SLN has increased the number of patients with positive SLN. To prevent unnecessary ALND, there are studies, that try to identify histological parameters that might predict additional axillary metastasis
Methods 524 patients underwent SLN biopsy for breast cancer, 41 patients were found to have micrometastases and 37 underwent ALND. Tumoral and micrometastases size, histological grade, presence of lymphovascular invasion, and IHC or hematoxylin-eosin detection of the micrometastases were analyzed in order to determine their value in predicting additional positive nodes
Results The median micrometastases size in those without additional positive nodes was 1 mm and 1.25 mm in those with additional axillary metastasis. Non-significant Mann-Whitney test. The diagnosis with IHC or HE did not show significant differences with Fishers' test. No significant differences were observed in tumoral size with the Mann-Whitney test. - No significant differences were also observed in histological grade and lymphovascular invasion.
Conclusion(s) Even though the size of the sample is insufficient to establish a firm statistical analysis, no significant differences were found in the histological parameters analyzed in order to predict which patients with micrometastases would not be expected to benefit from completion ALND. ALND would most probably be unnecessary in patients with SLN micrometastases, since in these cases the axillary lymph node invasion rate is similar to the failure rate of the technique (SLN determination and biopsy) admitted in the medical literature.

P1.7
Basal-like breast carcinoma in needle core biopsies

Chmielik E.; Lange B.; Goraj-Zajac A.; Budryk M.; Lange D.
Maria Sklodowska-Curie Memorial Cancer Center and Institute of Oncology, Gliwice, Silesia, Poland

Background The study analysed morphological, immunohistochemical and clinical features in breast invasive carcinomas which were diagnosed as basal-like type of invasive ductal carcinoma (BLIDC) on the basis of needle core biopsies (NCB).
Methods We reviewed slides including 21(11.7%) breast carcinomas: 20 primary ones and one after a 7-year

recurrence; immunohistochemical slides for ER, PR, HER-2, CK 5/6, CK17, CK 18, p53, the results of BRCA1 testing and clinical information. Morphological features, intensity of lymphocytic infiltration, necrosis, fibrous and/or hyalinised stroma, nuclear pleomorphism and mitoses were studied. Semiquantitative evaluation of basal cytokeratin- and CK 18-positive cancer cells was performed.

Results BRCA1 cases of BLIDC (3/21) were triple negative and just in one case p53 was overexpressed. All sporadic BLIDC (18/21) were ER- and PR-negative but three cases were scored 3+ and four cases scored 2+ for HER-2. Overexpression of p53 was noted in 11/18 carcinomas. At least one cytokeratin (CK 5/6 or CK17) was positive in all cases.5–30% cancer cells expressed CK 5/6 in 53% BLIDC and there were more than 30% positive cells in 29% BLIDC. CK 17 was expressed in 10–30% neoplastic cells in 36% BLIDC, and more than 30% positive cancer cells were noted in 56% of cases. CK 18 was positive in all BRCA1 cases and in 75% sporadic cases.

Conclusion(s) CK 17 is recommended as the first basal marker when seeking immunohistochemical confirmation of basal-like type of breast cancer in NCB when number of cancer cells is small.

P1.8

Benign glandular inclusions in an axillary sentinel lymph node of a patient with ipsilateral breast invasive carcinoma

Tengher-Barna I.; Rodrigues A.; Uzan M.; Ziol M.
Hôpital Jean Verdier AP-HP, Bondy, France

Background Biopsy of axillary sentinel lymph nodes (SLN) is a standard of care in the management of breast cancer. Although the finding of benign glandular inclusions is well recognized, it has been very rarely reported in axillary lymph node.

Methods Designated individual lymph node specimens were identified, grossly examined and blocked at interval of approximately 3 mm. After formalin fixation and paraffin inclusion, 4 levels at a separation of 300 micrometers were examined on hematoxylin and eosin stained sections and on Cytokeratin (AE1/AE3) immunostained sections.

Results A 50-year-old women underwent a breast lumpectomy with biopsy of sentinel lymph nodes for a nodule diagnosed as an invasive carcinoma, 11 mm of greatest size, grade SBR I. Four individual lymph nodes were identified. On one single level of one of the SLN, we observed on AE1-AE3 immunostained section several small positive glands and cysts. Other lymph nodes were negative for metastasis. We concluded to the diagnosis of benign glandular inclusions. The benign nature of this lesion was supported by the following criteria: proximity of the subcapsular sinus, lack of cytological atypia or stromal reaction, presence of a basement membrane, myoepithelial lining assessed with p63 immunostaining, association with squamous inclusion cysts.

Conclusion(s) The systematic practice of cytokeratin immunostaining on SLN for breast carcinoma leads to disclose rare benign glandular inclusions. To describe histological features for distinguishing benign glandular inclusions from metastasis is important to avoid false-positive diagnosis.

P1.9

Can Ki67 proliferation index in breast core biopsies of invasive cancer predict neoadjuvant therapy response?

Kanbour-Shakir A.; Kanbour Ibrahim A.; Trucco G.
Pittsburgh, PA, USA

Background Studies showed significant correlation between high Ki67 Proliferation Index (Ki-PI) and survival. There are inconsistent data regarding the value of Ki67 in predicting response of breast cancer to neoadjuvant therapy, some with higher Ki67 had better response, others showed no association. We evaluates Ki-PI role in core biopsy of breast cancer in predicting response to neoadjuvant therapy.

Methods All patients with core biopsy diagnosis of breast cancer at Magee-Womens Hospital during 6 months period had Ki67 immunostaining routinely. Only those with post neoadjuvant therapy excisional biopsy were included. Response assessed as % tumor reduction (TR) and correlated with Ki-PI and tumor type.

Results 31 patients had breast cancer on core biopsy followed by neoadjuvant therapy.25 infiltrating ductal carcinoma (IDC, NOS), 2 infiltrating lobular carcinoma (ILC), 3 IDC–Basal type and 1 IDC-Secretory type. Linear correlation is present between Ki-PI7 and TR in all IDC, NOS/ILC cases, the higher Ki-PI the more TR. An inverse correlation between the Ki-PI and TR in others, 3 IDC–Basal with high Ki-PI (95%, 90% & 75%) and low/no TR; one IDC-Secretory with low (5%) Ki-PI and 90% TR.

Conclusion(s) Ki-PI can predict neoadjuvant therapy response in all breast cancers and correlates with tumor types: All IDC-NOS/ ILC with high Ki-PI had better TR; IDC-Basal with high Ki-PI had low/no TR and IDC-Secretory with low Ki-PI had high TR. We recommend the use of immunostaining Ki67-PI in breast cancer to predict neoadjuvant therapy response.

P1.10

CD10. An important marker in the profiling of triple negative breast cancer

Phan S.; Shousha S.; Gojis O.
Charing Cross Hospital, Hammersmith, London, United Kingdom

Background Patients who are negative for ER, PR and HER-2, so called triple negative breast cancer (TNBC) accounts for 10–15% of all breast cancers. Within TNBC, there exists a subgroup that expresses CD10. CD10 is a myoepithelial cell marker in normal breast tissues. CD10 expression has been found to correlate with poor prognosis, metastasis and hormonal receptors negativity. However, the significance of CD10 expression by cancer cells has not yet been explored. This study investigates the relationship between CD10 expression by breast cancer cells and the clinicopathological parameters, the recurrence-free/survival intervals within the TNBC population. The relationship between CD10 expression and the basal markers CK5/6, CK14 and EGFR is also examined.
Methods Immunohistochemical staining for CD10, CK5/6, CK14, and EGFR were performed on 71 TNBC patients. The relationship between CD10 expression and clinicopathological parameters was investigated statistically. The correlation between CD10 and CK5/6, CK14, EGFR expression was also examined.
Results 26% of TNBC patients expresses CD10. In the younger patients (< 50 yrs), CD10 expression increases the risk of lymph node metastasis. There is also a slightly higher risk of recurrence amongst CD10 positive patients. There is a significant correlation between CD10 expression and the basal markers Ck5/6 and EGFR, but not CK14.
Conclusion(s) CD10 is a potential predictor for lymph node metastasis in the younger TNBC patients. CD10, CK5/6 and EGFR should be used together as a diagnostic marker for identifying the basal phenotype in TNBC patients.

P1.11
CGH analysis of basal-like type of breast cancer. Comparison with chromosomal imbalance pattern in HER2+ type

Sanfeliu E.; Andreu F.; Carrera R.; Bueno A.; Rigola M.; Vazquez J.; Rey M.
UDIAT - Corporacio Sanitaria Parc Tauli, Sabadell, Barcelona, Spain

Background The most consistent immunophenotype of basal-like breast tumours, by gene-expression profile, is negativity for hormone receptors and HER2 (triple-negative type), positivity for vimentin, EGFR, cytokeratin 8/18, and cytokeratin 5/6, variable for myoepithelial (SMA, p63, CD10). We investigated if these cancers have distinguishing genetic alterations, by CGH.
Methods CGH performed on frozen material from 12 cases of triple-negative. Immunophenotypic profile evaluation with cytokeratin 5/6, cytokeratin 17, EGFR and p63. Comparison results with chromosomal imbalance pattern observed in 10 cases of HER2 positive breast cancer.
Results Of 12 cases, 10 (80%) positivity for EGFR, cytokeratin 5/6 and/or cytokeratin 17. Gain at 1q (91.6%), 8q (75%), 3q, 7q (66.6%) and 1p, 6q, 11q, 12p, 2q (50%); and loss in 17p (75%), 19p (66.6%), 1p (58.3%) and 8p, 16p, 17q (41.6%). Opposite, HER2 gains in 17q (90%), 1q, 8q (80%), 16p, 19q, 20q (60%) and 7q (50%); and losses in 3p, 5q, 11q, 14q (50%), 4q, 9p, 13q (40%) and 6q, 8p, Xq (30%).
Conclusion(s) Chromosomal imbalance pattern of basal-like showed increased prevalence for losses at 16p, 17q (correlation with pure myoepithelial carcinomas) and 19p, opposite HER2 group, gains in these regions and at 20q and 7q. Gains at 6q and 11q present in up to 50% of basal-like group, but losses in HER2. Gains at 1q and 8q indicate shorter disease-free and overall survival times, common to both groups. Different CGH profiles demonstrate inherent differences in molecular evolution of these groups.

P1.12
Comparison between silver and flourescence in situ hybridization for detecting HER2 gene status in breast cancer

De La Cruz Mera A.; De La Cruz Dávila A.
Centro Oncologico de Galicia, La Coruna, Spain

Background For the validation of HER2 gene status, in breast cancer, fluorescence in situ hybridization (FISH) and immunohistochemistry (IH) are the most commonly used techniques. The purpose of this study is to compare and validate the efficacy of a newly silver enhanced in situ hybridization (SISH) technique in determination of the HER2 status, because the essential thing is to ensure that HER2 testing results are accurate and reliable.
Methods Routinely processed paraffin sections of 120 invasive breast carcinomas were selected. We performed IH with rabbit monoclonal antibody 4B5; FISH with the direct labelled manual PathVysion Kit; and SISH with the Ventana´s Benchmark automated slide stainer using two sections, one for assessment of HER2 gene amplification and the other for chromosome 17.
Results The new ASCO/CAP guidelines were used to interpret HER2 status. The immunohistochemical study was positive in 21 cases (17, 5%), equivocal in 17 cases (14, 1%) and negative in 82 cases (68, 4%). FISH and SISH reached identical results and identified gene amplification in 26 cases (21, 6%); in all out of the positives (17, 5%), in 4 out of the equivocal (3, 3%) and 1 out of the negatives (0,8%).
Conclusion(s) In conclusion SISH is an accurate and practical approach to screen HER2 status in breast cancer. The results are comparable to those obtained with FISH, but

SISH has the advantage of being a complete automated technique (more suitable for standardization) and can be visualized by an ordinary light microscope.

P1.13

Diagnosing papillary lesions using vacuum-assisted breast biopsy: should conservative or surgical management follow?

Nonni A.; Zagouri F.; Sergentanis N.T.; Lazaris A.; Patsouris E.; Zografos C.G.
Athens, Greece

Background This study evaluates the underestimation rate of papilloma lesions diagnosed with vacuum-assisted breast biopsy (VABB), taking into consideration the greater volume excised.
Methods 56 women with a diagnosis of a papilloma lesion after VABB (Mammotest; Fischer Imaging, Denver, CO, USA) were evaluated. At least 24 cores were excised in all cases (mean 74, range 24–96 cores) and a preoperative diagnosis was established. Subsequently, open surgery using hook-wire localization followed. A second, postoperative diagnosis was independently and blindly made. The association between the pathological types and Breast Imaging Report and Data System (BI-RADS) classification, as well as the discrepancy between preoperative and postoperative diagnoses, was evaluated.
Results The underestimation rate of papillary lesions was 3.6%. When the papillary lesions did not coexist preoperatively with any other precursor breast lesions, the underestimation rate was 0%. The underestimation rate did not differ with age, BI-RADS category or type of lesion.
Conclusion(s) Conservative management of patients with a papillary lesion diagnosis may follow when the extended VABB protocol is adopted and a great tissue volume is excised. However, when diagnosing a coexisting papillary lesion with a precursor breast lesion, open surgery should follow, given the high probability of a postoperative cancer diagnosis.

P1.14

Epithelial CD10 expression in invasive breast carcinoma and secondary deposits

Trihia H.; Gavressea T.; Lekka J.; Tzaida O.; Iakovidou J.; Arapantoni-Dadioti P.
Metaxa, Pireaus, Athens, Greece

Background CD10 is a zinc-dependent peptidase (metalloproteinase), commonly expressed in lymphoid stem cells, various lymphoma subtypes, renal cell carcinoma and endometrial stromal sarcoma cells. CD10-positive cells have been reported in the stroma of breast carcinomas. A few studies have suggested that expression of CD10 in the stroma of invasive breast carcinomas is associated with aggressive behaviour. CD10 expression has also been identified in breast epithelial cells.
Methods The aim of our study was to evaluate epithelial CD10 expression in 96 breast carcinomas and their secondary deposits and to examine associations with clinicopathological variables.
Results In 14 out of 82 cases (17%) there was focal or diffuse epithelial positive expression of CD10. In 14 out of 79 cases (17, 7%) there was CD10-positive epithelial expression in the secondary deposits, of which 3 cases had also positive expression in the primary tumor. In 4 of the 14-positive primary cases (3%) there was also positive stromal expression of CD10.
Conclusion(s) In our study is confirmed the positive epithelial expression of CD10 in breast carcinomas. The positive cases were of high grade carcinomas with positive lymph nodes. Although the significance of the positive expression of CD10 in breast epithelial carcinoma cells needs further investigation, CD10 positivity in epithelial cells should not rule out the possibility of primary breast cancer during the work-up of a metastatic adenocarcinoma.

P1.15

Epstein-Barr virus and breast cancer: lack of evidence for an association in iranian women

Kadivar M.; Joulaee A.; Monabati A.
Iran University of Medical Science, Tehran, Islamic Republic of Iran

Background Epstien-Barr virus, an oncogenic ubiquitous herpesvirus, infects more than 90% of the population worldwide. EBV is associated with certain malignancies such as Burkitt's lymphoma and nasopharyngeal carcinoma. Recent interest has focused on the possibility that EBV may also be involved in the pathogenesis of breast cancer. If substantiated, this finding not only broadens understanding of breast cancer etiology but also has implications for prevention and treatment.
Methods To asess the EBV presence in breast carcinoma in an Iranian series, breast biopsy specimens from 100 women with breast carcinoma were collected. The following control biopsy specimens were obtained from 42 women: 13 fibroadenoma, 9 benign epithelial proliferation (adenosis and sclerosing adenosis), 9 usual ductal hyperplasia, 4 atypical ductal hyperplasia, 4 non-proliferative fibrocystic changes, and 3 normal breast tissue. The EBV-infected cells were identified by means of immunohistochemical analysis,

using monoclonal antibody against Epstein-Barr virus-encoded nuclear antigen 2 (EBNA-2) and late membrane protein 1 (LMP-1). Polymerase chain reaction (PCR) was used to amplify EBV DNA, with primers that cover the EBV encoded RNA (EBER) and BamHIW regions.
Results EBV encoded nuclear antigen 2 and late membrane protein 1 immunohistochemistry were negative in all breast cancer and control specimens. Using PCR, none of the 100 breast cancer samples or the control specimens showed detectable EBV DNA.
Conclusion(s) Our findings suggest that EBV may not play a significant role in the pathogenesis of breast cancer in Iranian patients.

P1.16
Evaluation of HER2 IHC and FISH in breast cancer with digital pathology platform

Micsik T.; Krenács T.; Ficsor L.; Molnár B.
Ist Department of Patology and Experimental Cancer Research, Semmelweis University, Budapest, Hungary

Background The evaluation of HER2 immunohistochemistry is crucial in determining the therapy of breast cancer. Immunohistochemically 3+ positive Her2 protein expression alone make patients eligible for Herceptin therapy, while – or + cases couldn't benefit from anti-HER2 therapy. 2+ cases are the most problematic ones since these require further FISH or CISH validation to determine the HER2 copy number. As FISH and CISH evaluation needs special equipments it would be helpful to substitute or facilitate the evaluation with an automated IHC evaluation.
Methods 3DHistech provides comprehensive platform including instrumentation and software for digital microscopic scanning and evaluation of the electronic slides. We performed HER2 IHC and FISH on TMAs created from hundred breast cancer cases and then analyzed the scanned reactions with digital pathology software tools (Histoquant, MembraneQuant, FISHQuant) capable of automated and standardized IHC and FISH measurements.
Results Digital pathology provided effective and powerful tools for automated evaluation of HER2 status and we found good correlation between the results of the digital and manual evaluations.
Conclusion(s) Automated evaluation performed with the Mirax-platform could be used in matching the IHC- and FISH-positivity with each other and might be helpful in determining HER2-positivity and thus anti-HER2 therapy in a quick and easy way. More digital experience will be collected to test if it is possible to substitute the difficulties of FISH evaluation with a new standardized digital IHC evaluation protocol.

P1.17
Expression HGF/SF and C-MET in invasive ductal carcinomas

Bilgin G.; Pestereli E.H.; Colak T.; Erdogan G.; Karaveli S.F.
Akdeniz University, Antalya, Turkey

Background Hepatocyte growth factor/scatter factor (HGF/SF) and C-MET induce mitogenic, motogenic, morphogenic behaviour, angiogenesis, tubul/lumen formation in normal breast tissue and in breast carcinoma. Especially co-expression of C-MET and HGF in breast carcinoma provides tumor cell proliferation, distruption of intercellular junctions, migration through the extracellular matrix, protection from apoptosis and leads to expression of differentiated phenotypes. The aim of this study is to investigate HGF/SF and C-MET in invasive ductal carcinomas.
Methods We used parafin-embedded blocks from excisional biopsy, lumpectomy, mastectomy of 103 patients that diagnosed as invasive ductal carcinoma from 1998 to 2002 in Akdeniz University Medical Faculty Pathology Department to analyze expression of HGF/SF and C-MET by immunohistochemistry. The results compared with other histopathological parameters (size, nuclear and histologic grade, stage, lymph node status, hormon receptor status, cerbB2 expression) and prognosis.
Results We found that strong HGF/SF, C-met expression were associated with high nuclear grade (p=0,027). Also strong C-met expression correlated with invasive tumour size (p = 0,073). No relationship was found with histologic grade, stage, lymph node positivity and cerbB2 expression. Although strong HGF/SF and C-MET expression was revealed in metastatic carcinomas no significant difference was found in disease free survival.
Conclusion(s) HGF/SF, C-MET could be useful prognostic factors in breast carcinomas. To evaluate the prognostic significance of HGF/SF, C-MET further studies in large series with long follow up period should be done.

P1.18
Expression of STAT1 in breast cancer: relation with hormonal status and its prognostic significance

Magkou C.; Fytou A.; Giannopoulou I.; Nomikos A.; Theohari I.; Papadimitriou C.; Dimopoulos M.A.; Nakopoulou L.
University of Athens, Papagou, Greece

Background STAT-1 is the first member of signal transducers and activators of transcription (STATs). Recent studies have demonstrated its apoptotic and anti-proliferative effect in breast cancer, therefore suggesting a

tumor suppressor role. However, its prognostic significance in breast cancer remains unclear. The aim of the present study was to gain further insight into the role of pSTAT-1 in invasive breast carcinoma and its prognostic significance during premenopause and postmenopause.

Methods A three-step immunohistochemical method (ABC/HPR) was applied on paraffin-embedded sections from 173 patients with invasive breast carcinoma to detect the expression of the proteins pSTAT-1, ER, PR, topoIIa, caspase-3 and pAKT. The results were statistically processed using chi-square test and Kaplan-Meier test.

Results PSTAT-1 protein was immunodetected in the cytoplasm and nuclei of the malignant cells (11.6% and 8.6% respectively). In premenopausal patients, cytoplasmic pSTAT-1 expression was positively correlated with stage (p= 0.018), ER (p=0.017), caspase-3 (p=0.029) and pAKT (p= 0.003). Univariate analysis showed that cytoplasmic pSTAT-1 was associated with poor overall survival (p=0.042) and STAT1/ERorPR co-expression was associated with shorter disease-free survival during premenopause (p=0.012). On the contrary, during postmenopause, pSTAT-1/ERorPR co-expression was associated with longer disease-free survival (p=0.034).

Conclusion(s) It seems that patients' hormone profile significantly influences pSTAT-1 expression. pSTAT-1 was associated with an aggressive phenotype in premenopausal women and a possible favorable phenotype in postmenopausal patients. Further investigation of pSTAT-1 hormone-dependent signaling pathways need to be performed in order to determine their role in breast cancer.

P1.19

HER-2 status determination prevalence and techniques: a Portuguese observational study

Tortosa F.; Correia L.; Alves C.; Camacho J.; Henriques I.; Goncalves M.
Hospital Santa Maria, Lisbon, Portugal

Background The importance of HER status in breast cancer treatment justifies this study aims of estimating HER-2 positive prevalence in Portuguese Hospitals.

Methods Cross-sectional study to evaluate HER2 status in adult women with diagnosis of breast cancer. Data were characterized with descriptive measures. HER-2 prevalence was estimated with 95% confidence interval (CIs). A concordance analysis between the 3 techniques, sensitivity and specificity analysis on the CISH and FISH determinations' results were conducted. Preliminary results are presented.

Results 613 women with breast cancer, mean age 58.7 years (29–94 years), 98.7% Caucasian. Tumour characteristics: moderately differentiated - 43.6%, well differentiated - 21.6%, little differentiated - 27.8%, not assessable - 7%; 38.5%, 41.3%, 15.7% and 3.8% were in stages I, II, III and IV respectively. HER-2 positive prevalence was 21% (IC95% 17.4%-24.0%). In the group with IHC 2+, 82.4% had negative results by FISH. The sensitivity and specificity of CISH versus FISH in IHC 2+ patients were 73% and 93%, respectively.

Conclusion(s) Prevalence of HER 2 positive, determined by IHC, was in accordance with international data. In our study CISH presents a good specificity and may be considered in HER2 positive patients. These results suggested that patients with negative CISH can be considered as HER2 negative and FISH may only be performed in positive CISH.

P1.20

Heterogeneous cell distribution of cell signalling factors in breast tumors correlates with hypoxia and lymph node metastasis

Ramon YCajal S.; Pons B.; Vázquez Angeles M.; Martínez Antima E.; Lirola Luis J.; Peg V.
H. U. Vall d'Hebron, Barcelona, Spain

Background Cell signalling is a crucial cellular pathway in breast carcinomas. The cell signals converge through a few pathways where downstream mTOR factors control final cap-dependent protein traslation. We studied whether the pattern of expression throughout the tumors could reflect a constitutive activation of the pathway or indicate concomitant epigenetic and microenviromental signals.

Methods We studied 36 primary tumors and 34 lymph node metastasis. By immunohistochemistry, Western-blot and/or RT- PCR we evaluated the expression of 4E-BP1, p4E-BP1, peIF4E and eIF4G. Immunohistochemistry alone was performed for pMAPK and pS6. The expression of these factors was evaluated according to a semi-quantitative score and to their tumoral distribution. Hypoxia markers included GLUT-1.

Results 4E-BP1, p4E-BP1, eIF4E and peIF4G protein showed a diffuse pattern while pMAPK and pS6 displayed a peripheral or patchy distribution. pS6 was stronger in the invasive border, the periphery of the nests and emboli. pS6 and pMAPK correlated inversely with GLUT-1 positivity. Tumors that showed a diffuse expression of pS6 and lack of GLUT1 had less lymph node involvement.

Conclusion(s) 4E-BP1 and eIF4E protein expression levels associate with high grade and lymph node involvement and show a diffuse expression while pMAPK and pS6 show a great heterogeneity and correlated with hypoxia. These results support that 4E-BP1 can reflect oncogenic activation of other cellular pathways in addition to mTOR while pS6 could be indicative of mTOR activity and should be modulated by factors related to hypoxia.

P1.21

HuR expression in breast benign and malignant lesions

Sampani A.; Tsourouflis G.; Vgenopoulou S.; Stolakis V.; Kouraklis G.; Klijanienko J.; Theocharis S.
University of Athens, Medical School, Athens, Greece

Background Dysregulation of mRNA stability is important for tumor biology, leading to abnormal expression of several proteins in malignant states. HuR, an ubiquitously expressed protein of the embryonic lethal abnormal vision (ELAV) family, stabilizes certain mRNAs, allowing increased mRNA stability and protein expression. Since HuR immunoreactivity was found to be elevated in a variety of human tumors, HuR expression on breast benign and malignant lesions was examined in this study.
Methods HuR expression was examined immunohistochemically on paraffin-embedded tissue sections of 7 fibroadenoma, 10 in situ and 32 invasive carcinoma. HuR positivity, overexpression (over the mean percentage value) and intensity of immunostaining were correlated with patients' age and TNM stage, tumor histological type and grade.
Results HuR positivity was noted in 46 out of 49 (93,8%) examined cases and overexpression in 19 out of 46 (41,3%) positive ones. The intensity of immunostaining was characterized as mild, moderate and intense in 43%, 39%, and 18%, of the HuR positive cases. HuR positivity was statistically significantly correlated with tumor histological type (p=0.05), presence of lymph nodes (N, p=0.0001) and distal (M, p=0.003) metastasis. Neither HuR overexpression or staining intensity were correlated with any of the clinicopathological variables examined.
Conclusion(s) Our study confirms the expression of HuR on breast benign and malignant lesions. Additionally, correlations between HuR expression and clinicopathological variables important for patients' management were found. Further molecular and clinical studies are required in order to delineate the participation of HuR in breast carcinogenesis.

P1.22

Image analysis as an adjunct tool to manual HER-2 IHC review

Dobson L.; Conway C.; Hanley A.; Johnson A.; Costello S.; O'Grady A.; Connolly Y.; Magee H.; O'Shea D.; Jeffers M.; Kay E.
SlidePath, Dublin, Ireland

Background Accurate determination of HER-2 status is critical to identify patients for whom trastuzumab treatment is of benefit. Although the recommended primary method of evaluation is IHC, numerous reports of variability in interpretation have raised uncertainty in the reliability of results.
Methods Recent HER-2 guidelines have suggested that image analysis could prove to be an effective tool for achieving consistent interpretation and this study aimed to assess whether SlidePath's Tissue Image Analysis system has potential as a diagnostic support tool.
Results This study revealed that image analysis could accurately classify HER-2 status, with 91% agreement (κ= 0.81) achieved between computer aided classification and the pathology review across 275 cases from two reference laboratories stained with a number of commercial antibodies targeted against the c-erbB-2 protein. Assessment of the continuity of membrane staining in addition to staining intensity was critical to distinguish between negative and equivocal cases and enabled image analysis to report a lower referral rate of cases for confirmatory FISH testing. An excellent concordance rate of 95% was also observed between gene amplification status and the automated review.
Conclusion(s) The data from this study has validated that image analysis can robustly and accurately evaluate HER-2 status in IHC stained tissue. Based on these findings, image analysis has promise as a diagnostic support tool for pathologists and biomedical scientists, and may significantly improve the standardisation of HER-2 testing by providing a quantitative reference method for interpretation of IHC staining.

P1.23

Immunoprofiling of primary breast carcinomas and consecutive distant metastases

Szasz Marcell A.; Lukacs L.; Tokes M.A.; Arato G.; Szendroi M.; Hanzely Z.; Balint K.; Fillinger J.; Soltesz I.; Kulka J.
2nd Dept. of Pathology, Semmelweis University, Budapest, Hungary

Background Most common metastatic sites of breast cancer are the bones, lung and central nervous system. The most recent classification of breast carcinomas is based on the genetic profile. Still, there are dozens of unanswered questions.
Methods 43 primary breast carcinomas and consequtive metastases to bone, lung and CNS were evaluated by immunohistochemical profiling. Genotypes were assessed indirectly based on ER, PgR, Ki67, and Her2 expression.
Results Among the primaries, which developed bone metastases there were 47% in luminalA, 15% luminal B, 31% triple-negative and 6% HER2+-ve, while in the bone metastases 61% were triple-negative. The primaries which metastatized to lung, 86% were triple-negative and 14% luminal B.68% of lung replapses were triple-negative. The primary tumors spreading to the CNS were luminal A

(50%), HER2+-ve (20%) and triple-negative (30%). CNS metastases, in 28% showed Her2-positivity, while 43% was luminal, and the remaining were triple-negative. The time to the development of bone and CNS metastases was on average 4 years, while that to the lung required 7 years.
Conclusion(s) The phenotype of breast carcinomas and their metastases frequently changes during progression. Often, the hormon receptor positive tumors loose their ERs and PgRs, while the triple-negative tumors do not change with time. There are no luminalA patients with CNS metastases, and the HER2+-ve tumors progress to the brain. While the most aggressive triple-negative carcinomas spread to the lung, the time to relapse seems longer in this subgroup.

P1.24
Increased expression of toll-like receptor 9 (CD289) in human invasive breast carcinoma

Meseure D.; Le Ray C.; Vacher S.; Lerebours F.; Trassard M.; Boudjemaa S.; Andre C.; Lidereau R.; Guinebretiere J.; Bieche I.
Centre Rene Huguenin, Saint Cloud, France

Background Toll-like receptor 9 (TLR-9) is a Pattern Recognition Receptor (PRR) expressed by immune cells that identify DNA and RNA released by necrotic and apoptotic cells. TLR-9 activation seems to play a major role in the development of an inflammatory, antiapoptotic and progrowth microenvironment. Recent studies suggest that TLR-9 could also be detected in cancer cells and implicated in cell survival, immune tolerance and Epithelio-Mesenchymal Transition (EMT).
Methods 40 invasive ductal carcinomas including 13 Triple Negative Carcinomas (TNC) were reviewed to analyse expression and functionality of TLR-9 pathway and their relationship to EMT, using RT-PCR (TLR9/CD289, MyD88, TRAF6, IRAK4, IKKE, IRF3, ZEB1, FOXC2, CDH1, VIM, ACTA2/SMA and MMP13) and immunohistochemistry(TLR9/CD289, ZEB1, FOXC2, E-cadherin, vimentin, ACTA2/SMA and MMP13).
Results TLR-9 protein expression was increased in 23/40 cases (57%) and inversely correlated with Estrogen Receptor status. High positive correlation was observed between TLR-9 mRNA and TLR-9 protein levels ($P<0.05$). Interestingly, 9 cases (69%) of TNC had a strong diffuse cytoplasmic positivity with subapical reinforcement in 4 cases. Among TNC, 3 cases presented a complete EMT phenotype (E-cadherin-, ZEB1+, FOXC2+, MMP13+ and vimentin+). Moreover, TLR-9 signalling pathway was further explored by RT-PCR.
Conclusion(s) TLR-9 pathway is activated in breast cancer epithelial cells, particularly in TNC and is associated with EMT.

P1.25
Molecular phenotype of ductal carcinoma in situ of the breast in hereditary predisposed women

Van Der Groep P.; Van Diest P.J.; Menko F.; Bart J.; De Vries E.; Van Der Wall E.
UMCUtrecht, Utrecht, Netherlands

Background Invasive breast cancers in germline BRCA1 mutation carriers have a distinct "basal" immunophenotype characterized by high expression of stem cell cytokeratins (CK) 5/6 and 14 and epidermal growth factor receptor (EGFR) and low expression of the estrogen (ER), progesterone (PR) and HER-2/neu receptors. The immunophenotype of BRCA2 related breast cancers resembles a "luminal" immunophenotype with a frequent expression of ER, PR and only "luminal" cytokeratins CK8/18. Precursor lesions for these hereditary breast cancers have hardly been studied and the immunophenotype has not yet been established. The aim of this study was therefore to evaluate the immunophenotype of DCIS and their available invasive counterparts of BRCA1 and BRCA2 mutation carriers and to compare them.
Methods DCIS lesions of 25 proven BRCA1 and 9 BRCA2 germline mutation carriers and their 22 respectively 6 accompanying invasive lesions were stained by immunohistochemistry for ER, PR, HER-2/neu, Ck5/6, Ck14, EGFR and Ki67.
Results DCIS lesions in BRCA1 mutation carriers were mostly of basal type. DCIS lesions in BRCA2 mutation carriers were mostly of luminal type. In both BRCA1 and BRCA2 mutation carriers, a high concordance between DCIS lesions and their concomitant invasive counterpart with regard to expression of individual markers as well as molecular subtype.
Conclusion(s) Similar immunophenotypes suggest that DCIS is a direct precursor lesion in hereditary breast cancer and crucial carcinogenetic events occur at an early stage in hereditary predisposed patients, possibly even before the stage of DCIS.

P1.26
NF-Kappa B expression in metastatic breast carcinomas

Pestereli E.H.; Bilgin G.; Kargi A.; Colak T.; Erdogan G.; Ozdogan M.; Karaveli S.F.
Akdeniz University, Antalya, Turkey

Background Nuclear factor-kappaB (NF-κB) is a transcription factor that plays an important role in carcinogenesis via cell proliferation and apoptosis. Its expression is relevant to tumor progression, angiogenesis, metastasis and finally induction of resistance to chemotherapy in breast

cancer. The aim of this study is to investigate the NF-κB p50 subunit expression in metastatic breast carcinomas.
Methods Primary tumor sections of 58 invasive ductal carcinomas with distant metastasis and 77 invasive ductal carcinomas without distant metastasis were retrieved from the archives of Pathology Department, Akdeniz University. NF-κB p50 expression was analysed by immunohistochemical method. Clinico pathologic variables (grade, hormon status, c-erbB2 expression, lymph node status) were retrieved from the files of patients.
Results There was no statistically significant difference between the NF-κB p50 expression and grade, hormon status, lymph node metastasis of the tumors. Among 78 c-erbB2 negative carcinomas 60 (77 %) revealed strong nuclear NF-κB p50 positivity (p=0.024). Thirtytwo of 58 (55.2%) metastatic breast carcinomas expressed strong NF-κB p50 where it was 63 of 77 (82%) in carcinomas without organ metastasis. The difference was statistically significant (p=0.001).
Conclusion(s) Our results showed inverse correlation between NF-κB p50 expression and distant metastasis in breast carcinomas (p=0.001). This result was conflicted with the previous studies that used cell lines and molecular methods. Our results should be confirmed by further molecular studies using tumor sections.

P1.27
Oncotype DX® in invasive lobular carcinoma: scores are higher in the pleomorphic variant versus the classical variant

Estrella Santiano J.; Salvatore P. S.; Chiu Y.; Hoda A. S.
Weill Cornell Medical Center, New York, USA

Background Recent data indicate that invasive lobular carcinoma of the pleomorphic variant (ILC-PV) has significantly worse recurrence-free survival than the classical variant (ILC-CV), although both variants are E-cadherin-negative and share a common molecular genetic pathway. However, the biological potential of ILC-PV at the molecular genetics level remains largely unexplored.
Methods Stage I and II, ER-positive breast carcinoma cases with concurrent Oncotype DX® testing [a 21-gene commercially available molecular test (Genomic Health, Inc, Redwood City, CA)] were categorized for morphological type (ductal versus lobular, confirmed with E-cadherin immunostain) and conventional Nottingham grade. OncotypeDx results from patients with ILC-PV were compared to those with classical invasive lobular carcinoma (ILC-PV) and invasive duct carcinoma (IDC) of all 3 grades.
Results Of the 150 stage I and II, ER-positive cases with concurrent Oncotype DX® results, 9 cases were ILC-PV, 23 were ILC-CV, 29 were IDC-well differentiated (IDC-WD), 54 were IDC-moderately differentiated (IDC-MD) and 35 were IDC-poorly differentiated (IDC-PD). ILC-PV had a significantly higher Oncotype DX® score (23.6) and corresponding 10-year projected recurrence rate (RR) (15%) compared to ILC-CV (14.8, 10y RR=9.9%, p=0.008), IDC-WD (15.5, 10y RR=10.1%, p=0.007) and IDC-MD (16.4, 10y RR=10.8%, p=0.018). There was no statistical difference between ILC-PV and IDC-PD (25.6, 10y RR=16.7%, p=0.62).
Conclusion(s) Oncotype DX® results in ILC-PV are significantly higher than in ILC-CV, IDC-WD and IDC-MD. ILC-PV scores were similar to those of IDC-PD suggesting similar biologic potential and recurrence rate for these two carcinomas.

P1.28
Possible involvement of breast cancer stem cells in tumour dissemination

Hernández Sánchez L.; Rodríguez Pinilla S.; Martínez Montero J.; Maroto Pérez A.; Idrovo Mora F.; Rodríguez Gil Y.; Garzón Martín A.; Pajares Martínez R.; Granados Alamillo M.; Sánchez Verde L.
Hospital Universitario 12 de Octubre, Madrid, Spain

Background The most cancerous clones are initiated, driven and sustained by a population of cancer stem cells (CSCs). Al Hajj (2003), found cancer stem cells in breast cancer, the first evidence in a solid tumour. They have identified and isolated the tumorigenic cells as CD44 + CD24-/low Lineage-. These cells were able to initiate tumours in mice and resemble normal stem cells in their ability of self renew, proliferate and differentiate into diverse cell types.
Methods Our aim has been to characterize CSCs, in 17 skin breast biopsies of inflammatory breast carcinomas diagnosed between 2000- 2008. Single and double immunohistochemical (IHC) staining for CD44 and CD24 was performed on paraffine sections. We choose the inflammatory cancer, because the cells in the vascular spaces, are the cells that seed the tumour a distance, and their small number eliminate the noise from the mixture of cells CD44+ CD24+ in the bulky tumour.
Results CD44+/CD24- or weakly + neoplastic cells were observed in variable proportions in the vascular spaces in 12 of the 17 cases (70%). In some cases, CD24 + cells constitute a network around cells CD44 + / CD24-, as a protective cover in a three-dimensional structure.
Conclusion(s) In spite of heterogeneity of inflammatory breast carcinoma we have shown, CSCs circulating along vascular spaces, in the majority of the cases. This argues for a possible role of CSCs to invade, home, and proliferate at sites of metastasis.

P1.29

Significance of IL-6 and PAI-1 expression in nucleic-acid based therapy of breast cancer

Cakalagaoglu F.; Salva E.; Ozkan N.; Kaya H.; Kabasakal L.; Akbuga J.
Marmara University, Istanbul, Turkey

Background Nucleic acid-based therapy for cancer is based on the delivery of nucleic acids which inducing or suppressing a specific genetic function. RNA interference (RNAi) is a relatively new discovery for inhibiting gene expression and well-used research tool in the analysis of molecular mechanisms for many diseases including cancer. IL-6 (Interleukin-6) is a pleiotropic cytokine with obviously tumor-promoting and tumor-inhibitory effects. The strong expression of PAI-1 (Plasminogen activator inhibitor type-1) was associated with high tumor grade. The aim of this study is to investigate whether or not play a role in the development of tumor of IL-6 and PAI-1 expression and also promote in the nucleic-acid based therapy of experimental breast cancer model.
Methods Experimental model induced mammary tumors in Female Spraque-Dawley rats aged 30–45 days. The administration of two i. p dose of 50 mg/kg to rats induced 75–95% incidence of tumors 70 days postcarcinogen treatment. In the rat model of breast cancer, chitosan/siRNA complexes were administered intratumorally after tumor development. Immunohistochemical examination was carried out to detect the expression of PAI-1 and IL-6 in tumor tissues.
Results We found that the expression of PAI-1 and IL-6 were higher in the tumour group compared with the siRNA therapy group and this difference was statistically significant ($p<0,05$).
Conclusion(s) This preliminary study implicate IL-6 and PAI-1 expression as a possible prognostic indicator in breast tumor.

P1.30

Silver-enhanced in situ hybridisation (SISH) detection assay for HER2 gene status determination in breast carcinoma

Patakiouta F.; Koumpanaki M.; Anestakis D.; Zafeiriou G.; Paraskevopoulos P.; Papakotoulas P.; Papazisis T.K.; Bousoulegas A.
Theagenion Cancer Hospital of Thessaloniki, Thessaloniki, Greece

Background Her2 is an important tumour marker in breast cancer. However, there is a debate over the reliability of different methods measuring the Her2 gene status. We present the results of the SISH technique used in our laboratory in the last year.
Methods 115 cases of invasive breast carcinoma were analyzed for Her2 gene status, including 5 core biopsy specimens, by bright field silver-enhanced in situ hybridization (SISH) using the automated Ventana Benchmark XT machine. All cases were previously characterized immunohistochemically (CB11) as equivocal on a protein level (Her2 2+). Evaluation was independently performed by two pathologists (FP, MK) based upon the algorithms of the manufacturers and ASCO/CAP guidelines.
Results In 12 out of all 115 cases (10.4%) the Her2 gene was amplified, whereas in 99 cases (86.1%) there was no gene amplification. Four of the cases (3.5%) were characterized as equivocal. The concordance between the two pathologists was quite high (97.4%). These results were similar to those found in most studies.
Conclusion(s) SISH is a new, rapid, fully automated technique for determining the Her2 gene status in breast carcinoma. This method also has the advantage of having a permanent end result that can be visualized by an ordinary bright field light microscope, therefore making it particularly suitable for routine application in surgical pathology.

P1.31

Topoisomerase 2A status as a prognostic and predictive factor in breast carcinoma

Olszewski T.W.; Olszewski P.W.; Mrozkowiak A.; Pienkowski T.; Bauer Kosinska B.; Piascik A.; Suszylo K.; Wojnowska A.
Institute of Oncology, Warsaw, Poland

Background Aim of the study was a correlation TOPA2a status with other well established prognostic and predictive factors (steroid receptors, HER2 status, tumour grade) of breast carcinoma as well as therapy response.
Methods Material constituted of 100 cases of invasive breast carcinoma. All cases undergone neoadjuvant chemotherapy with antracyclins. During therapy ER, PGR and HER2 status were known to oncologist. Evaluation of TOPA2a was performed retrospectively. Methods: Slides for the study were prepared from routinely made paraffin blocs for diagnostic purposes. In all cases TOPA2a status was evaluated both by immunohistochemistry and by FISH method. We implemented four-tier system for immunopathologic evaluation of TOPA2a.
Results In our material it was found that there is positive correlation among TOPA2a status, HER2 status and histologic grade and there is negative correlation between TOPA2a status and steroid receptors status. It was also found that cases with positive TOPA2a status presented better response to therapy included antracycline as one of chemotherapeutics. There were differences between TOPA2a status results evaluated by immunohistochemistry and FISH method.
Conclusion(s) Our preliminary results suggest that TOPA 2a status may be utilize as a predictive factor for patients

selection for protocols which included antracycline as one of chemotherapeutics.

P1.32

Tumour angiogenesis and hypoxia in breast carcinomas: correlation with node metastasis and prognosis

Stamos C.; Koutsopoulos Vasilios A.; Pitsiava D.; Fiska A.; Nikolettos N.; Sivridis E.; Manolas K.; Koukourakis M.; Giatromanolaki A.
Democritus University of Thrace, Alexandroupolis, Thrace, Greece

Background Hypoxia and angiogenesis are early events in tumor growth. In this study we investigated the expression of hypoxic and angiogenetic features in breast carcinomas.
Methods One hundred and twenty-seven (127) breast carcinomas of ≤2 cm in size, clinically negative axilla and distant metastases (pT1-cN0-M0) were included in this study. Using a standard immunohistochemical technique, the expression of estrogen (ER), and progesterone receptors (PgR), c-erbB-2, hypoxia inducible factor 1α (HIF1α) and vascular endothelial growth factor (VEGF) was investigated. In addition, the vascular density (VD) was examined. The median follow-up for patients alive at the time of analysis was 130 months (62–245 months).
Results Linear regression analysis revealed a significant association of c-erbB-2 expression with VEGF (p=0.05, r= 0.19) and HIF1α (p=0.03, r=0.20). HIF1α was significantly linked to VEGF (< 0.0001) expression. VEGF expression was linked high VD (p=0.04). Tumor size, number of involved lymph nodes, PgR, VEGF and VD were significant prognostic variables at univariate analysis. In multivariate analysis of these parameters, nodal involvement was the strongest independent prognostic variable (p<0.0001, t-ratio 4.90).
Conclusion(s) C-erbB-2, hypoxia and angiogenesis pathways are linked to each other and have important prognostic relevance in early breast cancer.

P1.33

Analysis of immunohistochemical expression of CD40 in breast cancer and its relation to prognosis

Slobodova Z.; Ehrmann J.; Krejci V.
Faculty of Medicine and Dentistry Palacky University and University Hospital, Olomouc, Czech Republic

Background Breast cancer is most common cancer in women worldwide and new biomarkers that could predict better prognosis are searched. CD40 was described to be expressed in haematological and epithelial tumours and its relation with inhibition of apoptosis promises to have role as a prognostic marker.
Methods Formalin fixed and paraffin embedded samples from 181 breast carcinomas were used and immunohistochemical staining with CD40 antibody was performed. Samples were divided into groups according hormonal (oestrogen receptor /ER/, progesterone receptor /PR/) and her2/neu status: 1. luminal A (ER+PR+her2-), 2. luminal B (ER+PR+her2+), 3. triple-negative (ER-PR-her2-), 4. Her2/neu (ER-PR-her2+). Results of CD40 staining were correlated with clinicopathological data in these groups.
Results Normal ducts showed cytoplasmic CD40 expression in 30% of cases, in breast tumours in 53% cases. CD40 was evaluated as an independent marker and significant positive correlation was found with Bcl-2 (p≤0,002), low stage (p≤0,016) and preoperative chemotherapy (p≤0,043). Differences in expression of CD40 between groups were statistically significant (p≤0,00003). Groups with different hormonal status showed positive correlation of CD40 in luminal A group with stage (p≤0,006) and relapse (p≤ 0,024). Correlation wasn't found with age, diseases onset, familiar history of cancer, hormonal substitutive treatment, menopausal status and adjuvant chemotherapy.
Conclusion(s) We found significant positive difference between groups with good and worse prognosis. Expression of CD40 was related with factors connected with better prognosis and these could indicate CD40 as a new predictive factor in breast cancer. Acknowledgments: Supported by MSM6198959216, 80110091.

P1.34

Assessment of multiple biological prognostic and predictive markers on breast carcinoma: a comparison between their expression in primary tumor and in metachronous recurrences or metastases

Arapantoni-Dadioti P.; Gavressea T.; Tzaida O.; Trihia H.; Valavanis C.; Lekka J.
Metaxa, Pireaus, Greece

Background To investigate the expression of molecular markers in primary breast cancer in their metachronous recurrences or metastases, estimate the percentage of discordant cases and evaluate if the detected differences could have an impact on clinical patients management.
Methods One hundred and ten cases of breast cancer in primary site and in paired metachronous distant metastases were assessed by immunohistochemistry for the ER, PgR, C-erbB2 and AR expressions. Two cases with locoregional recurrences were also included. A statistical analysis using exact MC Nemar test was performed.
Results In the primary tumor ER, PgR, C-erbB2 and AR were positively expressed in 64,5%, 58,2%, 30,9% and 56,4% respectively. In the corresponding metastatic sites, the ER, PgR C-erbB2 and AR investigation demonstrated a

total discordance up to 27, 3% (p-value: 0.136), 26, 34, %. (p-value <0.0001), 29, 1% (p-value: 0.503) and 37, 1% (p-value: 0.405), respectively, with a loss of expression of these markers to 18, 2%, 21, 8%, 18, 2%, 22, 3%, respectively.

Conclusion(s) The expression of ER, PgR, C-erbB2 and AR in the metastases can be discordant from that observed in primary tumor for some patients. From the clinical point of view, the possibility of these changes during the disease progression, make mandatory the evaluation of molecular markers in the metastatic sites whenever possible.

P1.35

Basal-like immunophenotype in triple negative breast carcinomas

Ivkovic Kapicl T.; Knezevic Usaj S.; Panjkovic M.; Nikin Z.; Plzak A.
Institute of Oncology of Vojvodina, Sremska Kamenica, Vojvodina, Serbia and Montenegro

Background Basal-like breast carcinomas, as defined by gene expression microarray analysis, express genes usually found in normal basal/myoepithelial cells. The majority lack expression of hormone receptors and HER2, hence, some trialists have adopted the convenient "triple negative" definition for basal-like cancers. Furthermore, basal-like breast cancer appears to be eligible for EGFR-targeted therapeutic modalities due to its reported EGFR immunoreactivity.

Methods A total of 117 consecutive cases of invasive ductal breast carcinomas diagnosed in our institution were screened for the triple-negative phenotype, and were subsequently evaluated for cytokeratins (CK): 5/6 and 17, and EGFR immunoexpression.

Results Triple-negative breast carcinoma was 13.68% (16/117) in our series. Expression of CK5/6 showed 26 tumours (22.22%) and 35 (29.91%) were CK17-positive. EGFR positive expression was detected in 9 tumours (7.69%), and among this group triple-negative phenotype was noted in 4 (44.4%) cases ($p=0.006$). Triple-negative phenotype showed 11 (42.3%) cases from the group of CK5/6-positive tumours and 14 (40.0%) cases from the group of CK17-positive tumours ($p=0.000$).

Conclusion(s) The majority, but not all, of the triple-negative breast carcinomas exhibit a basal-like phenotype. Thus, triple-negative should not be used as a surrogate marker for basal-like cancers. EGFR expression is more often present in the triple-negative group then in hormone receptor positive and/or HER2 positive cases. This data suggests that EGFR expression might be important as a potential target for molecular therapy in triple-negative breast cancer.

P1.36

Bilateral breast involvement in multiple myeloma: a case report with clinical and cytological findings

Akbulut M.; Kelten C.; Ege B.; Kabukcu S.; Sari I.; Düzcan E.
Medical School of Pamukkale University, Denizli, Turkey

Background Plasma cell tumors of the breast, in association with multiple myeloma are rare and even less frequently reported as a plasmacytoma.1–3 In both conditions, lesions may present as single or multiple, well-defined nodules with or without axillary lymphadenopathies. 3–5 This may clinically mimic primary breast carcinoma or reactive conditions of the breast.

Methods A 42-year-old woman presented a complaint of back pain. Radiological examination showed compression fracture in the level of T11, and the biopsy from this region was reported as "plasma cell tumor". The patient was evaluated as IgA κ myeloma with biochemical test results and bone marrow biopsy and then VAD (vincristine, adriamycine, dexamethazone) chemotherapy was started. During the chemotherapy treatment, metastatic multiple lesions in the sacrum, different levels of the vertebrae, the lungs and both breasts were revealed by radiologic examination.

Results Fine needle aspiration cytology (FNAC) from the lesions in both breasts showed numerous plasma cells and plasmablasts. Cohesive groups of malignant epithelial cells were not identified. The radiologic and the FNAC findings of multiple myeloma involvement of the breast were presented with its differential diagnoses.

Conclusion(s) In conclusion, we add a new case of bilateral breast involvement of multiple myeloma to the literature. Although multiple myeloma is rare and diagnosis based solely on cytology is difficult, it is worthwhile to consider multiple myeloma in the differential diagnosis when cytological examination reveals many discohesive cells with plasmacytoid morphology.

P1.37

Biomarkers of apoptotic pathways in triple negative breast cancer

Comanescu M.; Ardeleanu C.
Emergency Clinic Hospital Bucharest, Craiova, Romania

Background Triple negative (TN) breast cancer (negative for expression of estrogen and progesterone receptors (ER, PR) and HER2/neu protein) represent a subbtype of breast cancer associated with poor prognosis and highly aggresive behaviour. The aim of our study was to establish a correlation between imunostaining patterns of biomarkers of apoptotic pathways, in an attempt of a better understanding of the biology of this special group of highly aggresive tumors.

Methods In our study, we selected a list of 27 female patients with triple negative breast cancer, out of 232 consecutive breast tumors. We investigated the morphological parameters of all cases on hematoxylin-eosin-stained sections and expression of p53, bcl2, Bax and TRAIL immunostaining.
Results The patients were aged between 19 and 39 years old (mean 29.2). All cases in our study were ductal carcinomas. Antibodies against P53, bcl-2, Bax and TRAIL were overexpressed in 11 (40.7%), 9 (33.3), 3 (11.1) and 2 (7.4%). The expression of the immunohistochemical reactions and histological grading were studied in univariate and multivariate analysis.
Conclusion(s) The identifying of additional immunohistochemical markers to refine prognostic in TN breast cancers is very much needed.

P1.38

Breast cancer in young women: morphologic features and immunohistochemical status

Aicha B.; Ahlem L.; Alia K.; Saadia B.; Carole B.; Olfa E.; Sabah M.
Mongi Slim, Tunis, Tunisia

Background Carcinoma of the breast is the most common malignancy of women in Tunisia with an incidence of 24/100 000 women per year. The frequency of this cancer in young women (≤ 40 years) varies from 2 to 24% over the world and it's about 8, 5% in Tunisia. The purpose of this study was to analyze the morphologic and hormonal status particularities of breast cancer in a Tunisian series.
Methods A retrospective study was done in one single institution (La Marsa Hospital. Tunisia) over13 years (1997–2009).
Results 104 breast cancers were diagnosis during this period.30 (29%) of these patients were under 40 years, the mean age was 34 years ranged from 20 to 40 years. Among this population, the left breast was more commonly involved (63%). Tumor size ranged from 0.7 to 7.0 cm; 70% were >2.0 and 13% were >5.0 cm in diameter. The predominant morphology was infiltrating ductal carcinoma (93%). The majority of the cases presented as grade II (53%), lesions with intraductal carcinoma (56%) and lymph node involvement (46%). ER and PR were positive in 23% and 23% cases respectively. HER-2/neu was positive (3+) in 6%.
Conclusion(s) Breast cancer in young women is relatively frequent in the current study. It presents more aggressive histological features than in older women. ER and PR expression in breast cancers was found to be comparable to published international data, but the frequency of HER-2/neu expression was lower.

P1.39

Breast carcinoma with osteoclast-like giant cells: case report

Gecer M.; Kayahan S.; Geyyas R.; Sakirahmed D.; Karadayi N.
Pathology Department, Dr. Lutfi Kırdar Kartal Educational and Research Hospital, Istanbul, Turkey

Background Breast carcinoma with osteoclast-like giant cells is an extremely rare tumor and occurring 45- 50-year-old women, characterised by osteoclast-like giant cells, hypervascular stroma, and signs of older and recent haemorrhages on the background of the conventional type of breast carcinoma.
Methods A patient 32 years old women who presented with a long-standing benign breast nodule that was negative on fine needle aspiration biopsy but sonographically appeared suspicious for carcinoma. The patient underwent lumpectomy.
Results Macroscopic features were typical of invasive carcinoma, but with unusual brown staining. Histologically, cribriform patterns, marked stromal angiogenesis and giant cells, nest of tumors predominated in our cases. Immunohistochemical studies indicated that the multinucleated giant cells were of histocytic origin
Conclusion(s) Clinical and morphological features of this rare type of breast carcinoma indicate that it should be regarded as an unique clinical- histomorphological entity with probably better prognosis when compared to ductal invasive carcinoma.

P1.40

Breast "papillary" lesions diagnosed on fine needle aspiration cytology: correlation with histology

Gimeno J.; Pijuan L.; Gimenez A.; Soler I.; Rodriguez A.; Corominas J.; Alameda F.; Lloveras B.; Serrano S.
Hospital del Mar, Barcelona, Spain

Background Papillary lesions of the breast include papillary ductal hyperplasia as a component of fibrocystic change, solitary or multiple papillomas (papillomatosis), in situ carcinoma, and invasive ductal carcinomas. The cytologic accuracy in assessing malignancy in papillary breast neoplasms is controversial and difficult.
Methods We reviewed 20 fine-needle aspirates (FNAs) diagnosed as "papillary lesions" in our institution from 2006 to 2008. The objectives was to determine: a) the correlation of the cytologic findings with the final diagnoses at excision, b) the accuracy of FNAs diagnosis of a papillary lesion in distinguishing true papillary from non-papillary proliferations and papillomas from true papillary malignancies c) the final percentage of malignant lesions.

Results The histology showed 13 (65%) benign cases (3 solitary papillomas, 7 papillomatosis, 1 adenomioepithelioma, 2 fibrocystic change with papillary hyperplasia) and 7 (35%) malignant tumors (3 intracystic papillary carcinomas, 1 papillary invasive carcinoma, 1 tubular carcinoma, 1 ductal invasive carcinoma with cribiform pattern, and 1 ductal in-situ carcinoma with papillomatosis). Four (57,2%) out of the 7 carcinomas were classified as benign papillary lesion on FNAs and 3 (42,8%) as suspicious. Four cases were true papillary carcinomas and 3 nonpapillary.
Conclusion(s) There was an overlap in cytomorphologic features between papillary and nonpapillary benign lesions as well as between benign and malignant papillary neoplasms. Cases reported as papillary on cytology should be excised urgently for histological evaluation. In our study 35% of lesions showing papillary features on cytology proved to be malignant.

P1.41
C-erbB-2 amplification in Turkish patients with invasive ductal carcinomas of the breast

Tuzuner B.; Bas E.; Erbarut I.; Cakalagaoglu F.; Kaya H.
Marmara University, Istanbul, Turkey

Background The aims were two-fold: 1) To determine the frequency of the immunoexpression and amplification of c-erbB-2 in Turkish patients with invasive ductal carcinoma of the breast, and 2) to search the correlation of the estrogen receptor (ER), progesterone receptor (PR), tumor histologic grade, stage and amplification of the c-erbB-2 in these cases.
Methods One hundred thirty three invasive ductal carcinomas of the breast has been studied for c-erbB-2, by streptavidin- biotin horseradish peroxidase method and FISH technique. The correlations with the histopathological prognostic parameters as tumor stage, grade, lymph node status, hormonal status, and c-erbB-2 amplification have been investigated.
Results Of the 133 tumours 14% (19/133) were 3+, 9% (12/133) 2+ for c-erbB-2 by immunohistochemistry. Eight of 12 c-erbB-2 equivocal (2+) cases demonstrated amplification by FISH. Overall c-erbB-2 amplification found to be 20,3% of the cases. 33% (9/27) of the c-erb-B2 amplified cases were grade 3,67 % (18/27) were grade 2. While 67% (18/27) of the cases were stage II, 26% (7/27) of the cases were stage I.7, 4 % (2/27) of the cases were stage III. ER / PR negativity was found 63% (17/27) of the c-erbB-2 amplified cases.
Conclusion(s) In the recent study the occurence of amplification frequency has found to be 20,3% for c-erbB-2 in Turkish patients with invasive ductal carcinomas of the breast. C-erbB-2 amplification apppears to be correlated with ER / PR negativity.

P1.42
C-erbB-2 and EGFR gene expression profile in breast carcinomas

Erbarut I.; Bas E.; Cakalagaoglu F.; Kaya H.
Hakkari Devlet Hastanesi, Hakkari, Turkey

Background Breast cancers comprise very heterogeneous diseases with a wide a variety pathological entities that are reported to have distinct clinical behaviours. Overexpression of transmembrane peptide growth factor receptors such as EGFR or HER2 has been associated with poor prognosis and resistance to hormonal therapy. The main purpose of this study was to determine the immunoexpression and gene expression profile of c-erbB-2 and EGFR in invasive ductal carcinomas of the breast, not otherwise specified (IDC-NOS).
Methods Fifty nine invasive ductal carcinomas of the breast has been studied for c-erbB-2, and EGFR by immunohistochemistry and FISH technique. The majority of the cases (91.5%) were stage I or II.
Results Among the 59 IDC-NOS cases studied, EGFR protein expression occurred in 7% (4/59). EGFR amplification by FISH technique could only be demonstrated in one case. c-erbB-2 protein overexpression was found in 12% (7/59) of the cases. All of the 3+ cases by immunohistochemistry demonstrated c-erbB-2 gene amplification by FISH technique. We demonstrated a statistically significant negative correlation between the presence of ER and EGFR overexpression ($p<0.05$). There was also a tendency for positive correlation with EGFR and c-erbB-2 ($p=0.064$). The other finding of the recent study was a statistically significant correlation between c-erbB-2 overexpression and tumour high grade, PR negativity and gene amplification.
Conclusion(s) The results of the recent study supports that EGFR or HER2 overexpressions are most commonly associated with poor prognosis.

P1.43
Comparing basal and HER-2 breast carcinomas by IHQ and hypermethylation of suppressor gene RASSF1-A

Cordoba A.; Guerrero D.; Vicente F.; Ederra M.; Gómez M.; María S.; Martinez Peñuela M.J.
Hospital of Navarra, Pamplona, Navarra, Spain

Background Molecular taxonomy introduced by the Stanford Group classified breast cancer into five molecular subgroups of tumours. It is necessary to incorporate the markers used routinely in practice and molecular features in order to characterise better these subgroups. The ER-negative branch encompassed two principal subgroups of tumours: One overexpressing Her-2 and the other expressing basal/myoepithelial genes. We analysed classic varia-

bles as grade, IHQ profiles and hypermethylation of RASSF1-A in basal and Her-2 subgroups.
Methods We analysed histological grade, tumour size, lymph node involvement, basal markers (CK5/6, CK14, EGFR), p53, Bcl-2 and Ki-67 antigens in 42 basal (ER-, Her-2-) and 30 Her-2 carcinomas (ER-, Her-2-). The RASSF1-A hypermethylation was assessed by Methylation-Specific PCR (MS-PCR).
Results High histological grade, CK5/6 and EGFR expression were associated with basal subgroup ($p<0.05$). A percent of 13.3%, 40% and 23.3% of the Her-2 tumours were positive for CK5/6, CK14 and EGFR, respectively. RASSF1-A hypermethylation was more frequent in Her-2 tumours compared to basal tumours ($p<0.05$).
Conclusion(s) We should remark that the high expression of basal markers and the absence of RASSF1-A hypermethylation are useful for the better differentiation between basal and Her-2 subgroups, although these parameters are not exclusive of each subgroup. We conclude that immunohistochemistry and gene hypermethylation may characterize better those molecular subgroups that share features, as ER-negative tumours (basal and Her-2). These findings could help for a better diagnosis and treatment of breast cancer patients in the future.

P1.44
Correlation between HER2/neu and hormonal receptor status in invasive breast carcinoma in Oltenia region

Georgescu V. C.; Plesea E. I.; Georgescu C. C.; Patrana N.
Emergency County Hospital, Craiova, Dolj, Romania

Background The aim of the study was to establish the correlation between HER2/neu expression and hormonal receptors (HR) status in invasive breast carcinoma (I-BC) in Oltenia region in 2008.
Methods The studied material consisted of tumoral tissue samples from 140 cases diagnosed with I-BC. Tissue samples were processed by the classical histological technique and immunomarked both for HER2/neu following DAKO HercepTest procedure and oestrogen (ER) and progesterone (PR) receptors. HR status was assessed using Allred score.
Results HER2/neu was negative in 85% of tested cases and positive in only 15% of cases, 2/3 of the latter being 2+ and the other 1/3, 3+. Half of cases had ER+/PR+phenotype, 1/3 had ER-/PR- phenotype and the rest were either PR+(6,43%) or ER+(4,29%). Most of main phenotypes were HER2neu negative (ie 90% of the ER+/PR+cases and 80% of ER-/PR-cases). Cases with heterogenous phenotype were also predominantly HER2 negative but less than the main ones (ie 77,8% of PR+ cases and 66,7% of ER+ cases).
Conclusion(s) Our preliminary data showed that only a small part of studied cases expressed HER2/neu and HER2neu positivity was most frequently associated with ER+/ PR- phenotype, the one usually associated with a poor prognostic.

P1.45
Expression of C-kit protein in breast tissues and its correlation with malignancy

Mavropoulou S.; Papanikolaou A.; Tatsiou Z.; Anagnostou E.; Spandos V.
Xanthi General Hospital, Xanthi, Greece

Background The c-kit gene which codes transmembrane tyrosine kinase receptor protein plays an important role in several types of normal and/or neoplastic human tissues. The purpose of this study is to investigate the expression of c-kit protein in benign and malignant breast tissue.
Methods Immunohistochemical expression of c-kit in 15 primary breast cancer tissues (8 axillary lymph nodes negative, 7 lymph nodes positive) were studied, in comparison with 5 normal breast tissues and 5 benign breast lesions (fibroadenomas and fibrocystic change).
Results In primary breast cancer tissues, the expression of the c-kit was significantly reduced or negative, with no remarkable difference between the breast cancer groups (concerning histologic type, grade and axillary lymph node status). On the opposite, it was highly expressed in all cases of normal breast epithelium and in benign breast lesions it was detected with heterogeneous positivity.
Conclusion(s) The results of our study suggests that the loss of c-kit expression might correlate with malignant transformation, most likely at the early stages of breast cancer development. These data suggest that c-kit may play a role in breast tumor progression and may therefore have diagnostic, prognostic, and therapeutic implications.

P1.46
Expression of MCM-2 protein and Ki-67 antigen in breast cancer

Dziegiel P.; Wojnar A.; Kobierzycki C.; Zabel M.; Podhorska-Okolow M.
Department of Histology and Embryology Medical University of Wroclaw and Poznan, Wroclaw, Poland

Background Breast cancer is diagnosed in over one million women worldwide and is the cause of death in over 400,000 women. In breast cancer the analysis of proliferation index is very important. Ki-67 is well accepted cell nuclear protein of proliferation process. Minichromosome Maintenance Proteins (MCM) due to their involvement in DNA replication may also provide a sensitive markers of cell proliferation. The use of Ki-67 as prognostic marker in various types of tumor is

common. Studies on MCM proteins are still in the preliminary phase. The aim of the study was to analyze the expression of Ki-67 and MCM-2 and the correlation between the expressions of both proteins in breast cancer.
Methods The study material included 119 paraffin-embedded breast ductal carcinoma. Tissue sections were prepared for H&E staining and immunohistochemistry (IHC). IHC reactions were performed using mouse monoclonal antibodies: anti-Ki-67 (Clone MIB-1; DakoCytomation) and anti-MCM-2 (Clone CRCT2.1; Novocastra). Analysis of intensity of Ki-67 and MCM-2 expression was assessed with microscope (Olympus BX42) and AnalySIS 3.2 software. Percentage of positive cells in 3 areas ("Hot Spots") on each section was counted. Statistical analysis was performed with Statistica 5.1 PL software (StatSoft) using Spearman's correlation. The differences were considered significant at $p<0.05$.
Results MCM-2 was expressed more frequently than the Ki-67. Statistical analysis demonstrated strong positive correlation ($r=0.52$; $p<0.05$) between Ki-67 and MCM-2.
Conclusion(s) The obtained results demonstrate that MCM-2 protein may provide a sensitive and useful marker of proliferative potential in ductal breast cancer.

Digestive pathology

P1.47

Immunoreactivity of stellate cells for alpha-smooth muscle actin in non-alcoholic steatohepatitis

Mashayekhi R.; Molaei M.; Shateri K.; Derakhshan F.; Zali M.
Research Center for Gastroenterology and Liver Disease, Tehran, Islamic Republic of Iran

Background Mechanisms that are responsible for development of fibrosis in nonalcoholic steatohepatitis (NASH) are largely unknown. Hepatic stellate cells are the principal collagen-producing cells in many liver disease and when activated express α-smooth muscle actin (α-SMA). In this study immunoreactivity of stellate cells for α-SMA was correlated with disease activity and stage of fibrosis in cases with NASH.
Methods Biopsy specimen of 45 cases of non-alcoholic steatohepatitis were evaluated and NAFLD activity score (NAS) and stage were determined according to Kleiner system. Immunohistochemistry for α-SMA was done and the number of α-SMA positive stellate cells per mm2 of liver tissue was determined by computerized image analysis.
Results Totally 45 patients with median age of 36 (22 to 57) were evaluated.34 patients were male and 11 were female. NAS was between 1 to 7, and stages between 1a to 3. Mean number of α-SMA positive stellate cells per mm2 of liver tissue was 33.7 in stage = 0 disease and 53.5, 64.3 and 85.5 in stages 1, 2 and 3 respectively. Mean number of α-SMA positive stellate cells per mm2 of liver tissue was 33.7 in stage = 0 disease and 53.5, 64.3 and 85.5 in stages 1, 2 and 3 respectively.
Conclusion(s) Stellate cell activity determined by α-SMA immunoreactivity was significantly associated with stage of fibrosis and ballooning of hepatocytes but not with overall disease acticity (NAS), severity of steatosis or lobular inflammation.

P1.48

Is Rooibos tea treatment beneficial in liver pathology? The dual effect of strong antioxidants

Janega P.; Cerna A.; Ulicna O.; Vancova O.; Greksak M.; Babal P.
Department of Pathology, Faculty of Medicine, Comenius University Bratislava and Institute of Normal and Pathological Physiology, Slovak Academy of Sciences, Bratislava, Slovakia

Background Rooibos tea has shown potent antioxidant activity. It is especially popular because of the belief in its beneficial health effects. The presented study evaluated the effect of Rooibos tea on liver damage induced by experimental free radical injury caused by carbon tetrachloride (CCl4) administration.
Methods Experimental rats that received 10 weeks CCl4 intraperitoneally with the following 6 weeks recovery period were divided into 2 groups: with and without parallel Rooibos tea administration. The animals without CCl4 administration were analyzed as controls.
Results CCl4 administration led to an increase of liver fibrosis and steatosis as well as the increase of liver damage markers (AST, ALT). Rooibos tea administration significantly reduced the fibrosis, decreased the liver damage markers to the physiological level, reduced the level of malondialdehyde as the marker of free radical tissue injury. It led to the decrease of the TNF mediated pathway markers expression, including the proapoptotic marker apaf, but also the NFkB and inducible NO-synthase which are important in the liver regeneration. The Rooibos administration prolonged the recovery period characterized by increased liver steatosis when compared to the group without Rooibos tea treatment.
Conclusion(s) It is likely that Rooibos tea compounds with the strong antioxidant capacity can participate on reduction of liver damage when administered during the injury. On the other side the free radicals play a not negligible role in the organism especially during the tissue recovery. This can explain the extended healing period when the Rooibos tea was administered. Supported by VEGA project No.1/0524/08.

P1.49

MUC5AC expression and its biological value in cholangiocarcinoma

Pedica F.; Bortesi L.; Montagna L.; Pachera S.; Ruzzenente A.; Guglielmi A.; Chilosi M.; Menestrina F.; Capelli P.
University of Verona, Verona, Italy

Background Cholangiocarcinomas (CC) are distinguished in intrahepatic, perihilar and extrahepatic CC and 3 morphological types, as mass-forming (MF), periductal infiltrating (PI) and intraductal growth (IG). Our aim was to investigate the immunophenotype of different forms of CC to find new markers for their classification. We focused on MUC5AC antibody expression, which is detected in >50% sera of CC cases.
Methods 35 IHCC, 39 PHCC and 5 EHCC were collected. Morphologically they were subdivided as follows: IHCC were 30 MF and 5 of the MF plus PI; PHCC were classified as PI in 27 cases, 8 cases were MF plus PI and 4 were MF alone; EHCC were PI in all cases. All cases were immunohistochemically analysed for MUC5AC expression (clone CLH2, NovoCastra, 1:100). The antibody was estimated semiquantitatively: negative (-) if <5% positive cells, grade 1 (+) between 5 and 20%, grade 2 (++) between 20 and 50% and 3 (+++) >50%.
Results 30/35 (85.7%) IHCC were MUC5AC negative.26 of the 39 PHCC were MUC5AC positive (66.6%), while 13 cases were negative. Of these 13 cases, 8 cases have some positive cells, but <5%. EHCC were strongly positive in 3 cases (60%), but 2 cases have <5% positive cells.
Conclusion(s) MUC5AC demonstrated to distinguish IHCC from PHCC and correlates with morphology. These differences in MUC5AC expression support the hypothesis of a different origin of IHCC and PHCC. For these reasons MUC5AC may have some value in choosing the therapeutic options.

P1.50

S100P expression in cholangiocarcinoma

Pedica F.; Bortesi L.; Capelli P.; Cataldo I.; Montagna L.; Pedron S.; Parolini C.; Pachera S.; Campagnaro T.; Guglielmi A.; Chilosi M.; Menestrina F.; Martignoni G.
University of Verona, Verona, Italy

Background S100P is involved in the regulation of cell cycle and differentiation. Its overexpression in pancreatic ductal adenocarcinoma has been reported. Cholangiocarcinoma (CC) have histologic similarities to pancreatic adenocarcinoma and one report investigated S100P expression in CC. CC are classified into 3 groups according to their anatomic location, as intrahepatic (IHCC), perihilar (PHCC), extrahepatic (EHCC) and 3 morphological types, as mass-forming (MF), periductal infiltrating (PI) and intraductal growth (IG) type. Our aim was to analyze if S100P expression in CC is related to their anatomic classification and morphology.
Methods We collected 28 CC subdivided into 14 IHCC, 11 perihilar CC PHCC and 3 EHCC. The IHCC were all MF type but one which was MF plus IG, the PHCC were 10 PI and one case MF plus PI, while EHCC were all PI type. Immunohistochemical staining was performed applying S100P antibody (PharMinger, clone 16, 1:1000).
Results All 11 PHCC expressed S100P protein except the MF plus PI type which was negative (91%). All the EHCC expressed S100P while none of the 14 IHCC expressed S100P (0%), but MF plus IG type case expressed the antibody only in the IG component.
Conclusion(s) S100P has different expression in IHCC and PHCC, while in EHCC and PHCC it has a similar expression. These results suggest that IHCC and PHCC may have different immunophenotype and different biology. Anatomic location, morphology and ancillary studies will help in understanding the biology and etiopathogenesis of CC.

P1.51

Solid-pseudopapillary tumors of pancreas

Shchegolev A.I.; Dubova E.A.; Mishnev O.D.; Podgornova M.N.
A. V. Vishnevsky Institute of Surgery, Moscow, Russian Federation

Introduction Solid-pseudopapillary tumor (SPT) is a rare neoplasm of the pancreas that usually occurs in young females.
Method Complex morphological investigation of surgical material of 10 patients (all woman, aged 15–67), treated in 2002–2008 in the Institute, was performed.
Results In 5 cases neoplasm affected the head of pancreas, in 2 – the body and in 3 – the tail. The size of tumors varied from 2, 5x2, 5x2 to 13x9x8 cm. In 3 cases neoplasms were solid, in the other – solid-cystic. In 3 cases tumors were malignant: in 2 cases we've observed the hepatic metastasis and in 1 case – the renal metastasis. In 1 case local recurrences of the tumor (4, 6, 8 years after primary tumor removing) were observed. The liver metastases were cystic and their size was up to 25x23x14 cm. Microscopically tumors showed a variable admixture of solid monomorphous growth pattern and the pseudopapillary areas with focuses of necrosis and hemorrhage. Cytologycaly we found a single cells and aggregates of uniform malignant cells, forming branching, papillary clusters with delicate fibrovascular cores. Immunohistochemically all the tumors were vimentin, NSE, alpha-1-antitrypsin and alpha-1-antichymotrypsin diffusely positive. In 8 cases nuclei of tumor cells expressed the receptors of progesterone. We've found abnormal expression

of E-cadherin in tumor cells: it was localized in the nucleus of tumor cells, but not on membrane of cells.
Conclusion The SPTs are the tumors which are generally benign or premalignant neoplasias. Nevertheless they can behave like carcinomas. The final diagnose can made only after complete morphologic investigation.

P1.52
HSP90 is an independent predictor of recurrence in gastrointestinal stromal tumors

Kang G.; Kim K.; Park C.; Park H.; Kim J.; Kim T.
Samsung Medical Center, Seoul, Republic of Korea

Background Despite the therapeutic success of imatinib in gastrointestinal stromal tumors (GISTs), patients often develop resistances to the kinase inhibition therapy. Therefore, it is important to identify alternative targets for therapy and relevant prognostic factors.
Methods To evaluate HSP90 as a prognostic marker and therapeutic target in GISTs, 92 GISTs (35 low, 23 intermediate and 34 high-risk) were studied. In addition, clinopathologic features were compared with clinical outcome in patients with GIST after complete surgical resection.
Results HSP90 overexpression was found in 33.7% of GISTs and was correlated with non-gastric location (p=0.007), mixed histologic subtype (p=0.006), high mitotic counts (p=0.002), high risk grade (p=0.002) and specific genotypes (p=0.026). Among 25 GISTs with recurrence, 19 cases (76.0%) showed HSP90 overexpression. Cytoplasmic expression levels of HSP90 were confirmed by western blotting and matched perfectly with the results of immunohistochemistry. On univariate analysis, recurrence was predicted by histologic subtype (p=0.000), tumor size (p=0.003), mitosis (p=0.000), NIH risk grade (p=0.003) and HSP90 expression (p=0.000). On multivariate analysis, tumor size (p=0.010), mitosis (p=0.049) and HSP90 expression (p=0.001) were independent prognostic factors for recurrence-free survival in GISTs.
Conclusion(s) We found that HSP90 is an independent prognostic marker for recurrence in completely resected GISTs and may provide a therapeutic solution to the patients with imatinib-resistant GIST.

P1.53
Implication of LOH/MSI pathways in the filiation adenomas-colorectal carcinomas

El Hadj El Amine O.; Arfaoui Toumi A.; Ben Mahmoud L.; Chaar I.; Khiari M.; Lahmar A.; Khalfallah T.; Mzabi Regaya S.; Bouraoui S.
Mongi Slim, Tunis, Tunisia

Background Colorectal (CRC) neoplasms and/or preneoplasms can be prevented by interfering with the various steps of oncogenesis, which begins with uncontrolled epithelial cell replication, continues with the formation of adenomas and eventually evolves into malignancy. CRC tumors usually originate from preexisting adenomatous polyp (AP). These can be defined as well-demarcated masses of epithelial dysplasia, with uncontrolled crypt cell proliferation. Adenomatous colorectal polyps are mainly represented by tubulovillous adenomas (TVA), villous adenomas and serrated adenomas (SA). We aim to study the implication of the two main pathways of CRC carcinogenesis (MSI and LOH) in the filiation CRC adenomas-CRC carcinomas. We correlate each subtype of CRC carcinoma with the different AP it originate from.
Methods Three hundred twenty five patients with CCR were collected. Immunohistochemical analysis including antip53, antip21 ras, anti-MLH1 and anti MSH2 were performed.
Results CRC tumours consisted of 270 adenocarcinomas (AC); 70 cases among them are adenocarcinomas with mucinous component less than 50% (ACM) and 55 mucinous carcinomas (MC). We identified 260 TVA; 230 among them leads to AC and 30 to MC.19 MC originate from SA, 3 cases from polyps of peutz Jehgers PPJ.3MC with signet ring cell differentiation but without AP were also identified.40 AC originate from SA.95% of AC were characterised by LOH; 80% of MC were MSI-H.40 ACM were characterised by LOH, 20 cases were MSI-H and 10 MSI-L.
Conclusion(s) SA and PPJ are the main preneoplasms leading to MC whereas AC originates essentially from TVA.

P1.54
Loss of the CBX7 protein expression correlates with more aggressive phenotype in pancreatic cancer

Karamitopoulou E.; Pallante P.; Zlobec I.; Tornillo L.; Carafa V.; Schaffner T.; Borner M.; Esposito F.; Panayiotides I.; Brunner T.; Zimmermann A.; Terracciano L.; Fusco A.
University of Athens, 2nd Dept of Pathology, Halandri-Athens, Attiki, Greece

Background Polycomb group proteins (PcG) function as multiprotein complexes and are part of a gene regulatory mechanism that determines cell fate during normal and pathogenic development. Several studies have implicated the deregulation of different PcG proteins in tumorigenesis. Pancreatic ductal adenocarcinoma is an aggressive neoplasm with a dismal prognosis that follows a multistep model of progression through non-invasive precursor lesions called pancreatic intraepithelial neoplasia (PanIN).

Aim of this study was to investigate the role of the PcG protein CBX7 in pancreatic carcinogenesis as well as to evaluate its diagnostic and prognostic significance.
Methods We analysed immunohistochemically by using CBX7, 210 ductal adenocarcinomas of the pancreas from resection specimens, combined on a tissue microarray (TMA) including 40 PanIN cases and 40 normal controls. The results were evaluated by using receiver operating characteristic (ROC) curve analysis for the selection of cut-off scores and correlated to the clinicopathological parameters of the tumors and the survival of the patients.
Results A significantly differential, and progressively decreasing, CBX7 protein expression was found between normal pancreatic tissue, PanINs and invasive ductal adenocarcinoma. Moreover, loss of CBX7 expression was associated with increasing malignancy grade in pancreatic adenocarcinoma, whereas maintenance of CBX7 expression seemed to be associated with a longer survival.
Conclusion(s) These results suggest the detection of the CBX7 protein as a valid prognostic marker for pancreatic carcinomas.

P1.55
Sporadic colorectal carcinomas with low level microsatellite instability: a distinct subgroup with specific clinicopathological and molecular features

Azzoni C.; Bottarelli L.; Cecchini S.; D'Adda T.; Pizzi S.; Tamburini E.; Sarli L.; Bordi C.
University of Parma, Parma, Italy

Background Colorectal cancers (CRCs) with high-level microsatellite instability (MSI-H) have distinctive clinicopathological and molecular features. The biologic significance of low microsatellite instability (MSI-L) is not clearly defined. In particular, the relationship of MSI-L to microsatellite stable (MSS) and MSI-H cancers is currently under debate and the clinical usefulness of these alterations as genetic markers for the prognosis remains unclear. The objective of this study was to further clarify the characteristics of MSI-L CRCs by comparing MSI-L CRCs with MSI-H and MSS cancers, particularly with respect to disease recurrence and survival.
Methods A series of 184 primary sporadic CRCs were subdivided into three groups according to the level of MSI (94 MSS, 22 MSI-L and 68 MSI-H) and analyzed the clinicopathological features, the genetic changes at APC gene and 18q chromosome and the immunohistochemical expression of hMlh1, hMsh2, Fhit, Cox-2, p53, p21, p27 and MGMT proteins.
Results When compared with MSS, MSI-L CRCs frequently showed poorly differentiated histology. In addition, MSI-L CRCs were associated with altered MGMT and COX-2 expression ($p<0.001$) and lower levels of p53 and p21 than MSS CRCs. Three-year overall and disease-free survival rates of MSS, MSI-L and MSI-H CRCs were significant different with better survival of MSI-low CRCs than MSS CRCs.
Conclusion(s) These results indicated that sporadic MSI-L CRCs displayed distinguished clinicopathological features and significantly better survival than MSS CRCs and might form a distinct subgroup from MSS CRCs.

P1.56
A comparative study of hepatic stellate cells in alcoholic and virus induced chronic hepatitis

Egyed-Zsigmond I.; Jung J.; Lorincz-Marton G.; Georgescu D.; Gurzu S.; Mezei T.
University of Medicine and Pharmacy Targu-Mures, Romania

Background Liver injury activates quiescent hepatic stellate cells to proliferative myofibroblasts.
Methods In our retrospective study based on review of percutaneous liver biopsies to determine the reliability of the subjective semiquantitative assessment of fibrosis against objective digital image measurement by image analysis, we evaluated the evidence of fibrosis and GFAP positive quiescent hepatic stellate cells, and SMA and Desmine positive, activated myofibroblastic hepatic stellate cells in portal tracts, in perisinosoidal and in the interface zones of lobular structures.
Results The median value of fibrosis was higher in cases with B-virus hepatitis, than in C-virus and alcoholic hepatitis, there was different percentage of hepatic stellate cells infiltration between the three zones studied, but the evidence of these cells was oftener in HCV induced chronic hepatitis.
Conclusion(s) If fibrosis was strongly evident in cases with chronic B-virus hepatitis, the proportion of quiescent and myofibroblastic hepatic stellate cells increased from alcoholic-, through B-virus-, and culminate to C-virus induced chronic hepatitis.

P1.57
Adiponectin receptors expression is associated with an intestinal histotype and a longer survival in gastric cancer

Barresi V.; Grosso M.; Vitarelli E.; Giuffrè G.; Tuccari G.; Barresi G.
Department of Human Pathology, University of Messina, Messina, Italy

Background Adiponectin (ApN) is a 30 KDa adipocytokine which mediates an anti-neoplastic effect following its binding to the receptors Adipo-R1 and Adipo-R2. The expression of these receptors has been documented in gastric cancer (GC) cell lines, but only a few data exist on

their expression in GC neoplastic tissue. In addition, the expression of ApN has never been investigated in human gastric cancer up to now. Accordingly our aim was to investigate the expression of ApN, Adipo-R1 and Adipo-R2 in a series of surgically resected GC and to assess its association with the various clinico-pathological characteristics of the tumours as well as with the patients' survival.
Methods Forty-nine surgically resected GC were submitted to the immunohistochemical assays for Adipo-R1, Adipo-R2 and ApN.
Results Adipo-R1 and Adipo-R2 immuno-expression was found in 22/49 GC and in the intestinal metaplasia areas nearby the tumours, whereas only a slight immunoreactivity for these proteins was encountered in normal adjacent gastric epithelium. No ApN expression was found in any of the analysed cases. Adipo-R1/Adipo-R2 expression was significantly associated with an intestinal histotype of the tumours and with a longer overall survival of the patients.
Conclusion(s) Intestinal-type GC frequently express Adipo-R1/R2 in association with a better prognosis. Patients with an Adipo-R1-R2 positive GC may benefit of novel anti-cancer therapies based on ApN addition.

P1.58
An accurate diagnosis of hepatocellular carcinoma and cholangiocarcinoma with immunohistochemistry?

Herlea V.; Pechianu C.; Stoica-Mustafa E.; Stroescu C.; Hortopan M.; Paslaru L.; Iorgescu A.; Sobaru I.; Balan O.; Moldovan D.; Poteca A.; Vasilescu C.; Ionescu M.; Tomulescu V.; Hrehoret D.; Dima S.; Brasoveanu V.; Alexandrescu S.; Ungureanu C.; Mitulescu G.; Ciurea S.; Croitoru A.; Gheorghe C.; Popescu I.
Fundeni Clinical Institute, Bucharest, Romania

Background An accurate diagnosis, mostly for poorly differentiated carcinomas, call for differentiation between hepatocellular carcinoma (HCC), cholangiocarcinoma (CC), metastatic carcinoma (MC), and other malignant tumors, and is important in apropriate clinical management, and their proper histopathological diagnosis can be problematic.
Methods Were examined microscopically multiple sections from 98 primary liver tumors to confirm the tumor type and the degree of differentiation. In order to do the differential diagnosis, we used immunohistochemical stains, realised by ABC method, using the following primary antibodies: CEA, CK 7, 8/18, 19, 20, CD 34, Bcl-2, VEGF, Ki-67, PCNA, and p53.
Results From the 98 primary liver tumors, 67 were HCC and 31 were CC. We noticed, that the positivity for CK 7 and CK 19 was higher in CC, than in HCC, CEA was positive more frequently in CC, than in HCC, and the PCNA index was higher in CC, than in HCC.
Conclusion(s) Immunohistochemical markers are available to assist in this differential diagnosis, each with its limitations, making their use imperative.

P1.59
CD138: a new immunohistochemical marker for hepatocellular carcinoma (HCC)?

Tiniakos D.G.; Palaiologou M.; Tsioli P.; Fatourou V.; Felekouras E.; Antoniou E.; Delladetsima I.
Lab. of Histology-Embryology, Medical School, University of Athens, Athens, Greece

Background CD138 is a syndecan (transmembrane heparan sulphate proteoglycan) acting as a tuner of transmembrane signalling by regulation of cell-cell and cell-matrix interactions. CD138 is predominantly expressed in epithelial cells and plasmacytes. CD138 is upregulated promoting tumorigenesis in breast, prostate, head and neck carcinomas, while is downregulated and growth inhibitory in lung, gastric, pancreatic, colon and uterine carcinomas. Limited data is available regarding HCC. The aim of the present study was to assess the expression and sensitivity of CD138 in HCC in comparison to the established hepatocellular marker Hepatocyte (HepPar-1).
Methods Immunohistochemistry was employed on routinely-processed tissue sections of 48 surgically resected HCCs (grade I $n=8$, II $n=24$, III $n=10$, IV $n=5$), using Novolynk Polymer Detection System (Novocastra) and monoclonal antibodies to CD138 (MI30, Dako) and Hepatocyte (OCH1E5, Dako).
Results CD138 was detected in all cases of HCC in the membrane and/or cytoplasm of neoplastic cells. CD138-specific immunostaining did not correlate with tumor grade ($p>0.05$). Non-neoplastic hepatocytes showed mainly membranous immunostaining. No significant differences in CD138 expression were detected between HCC and surrounding non-neoplastic parenchyma ($p=0.216$). Hepatocyte was positive in 100% of grade I, 90.9% of grade II, 75% of grade III and 40% of grade IV HCC. The negative correlation of Hepatocyte immunoexpression with tumor grade was statistically significant ($p<0.01$).
Conclusion(s) CD138 is a highly sensitive immunohistochemical marker detected in all cases of HCC regardless of tumor grade, in contrast to Hepatocyte which shows limited sensitivity in high grade HCC.

P1.60
Clinical and morphological characteristic of mucinous cystic tumors of pancreas

Dubova E.; Podgornova M.; Shchegolev A.
A. V. Vishnevsky Institute of Surgery, Moscow, Russian Federation

Background Mucinous cystic tumors (MCT) are rare pancreatic lesions which amount 2–5% of all exocrine pancreatic tumors. They're divided into cystic adenomas, borderline tumors and cystic adenocarcinomas.
Methods We investigated 24 surgical specimens from patients with MCT, treated in the Institute in 2004–2008. All the patients were females at the age from 27 to 81 years (median – 49 years). In 16 cases (62,5%) tumor was located in the tail of pancreas, in 7 (29,2%) cases – in the body and in 2 (8,3%) cases – in the head of pancreas.
Results Histologically in 13 (54,2%) cases mucinous cystic adenoma (MCA) was diagnosed, in 3 (12,5%) cases – borderline MCT and in 8 (33,3%) cases – invasive mucinous cystic adenocarcinoma (MCAC).
Conclusion(s) We stated that MCAC frequently affects elder females (median age – 54,8 years), they're larger then MCA and always multiloculated while most of MCA's are monoloculated. Areas of hemorrhage and suppuration are often seen in MCAC's. In all types of MCT ovarium-like stroma can be seen. Stromal cells are positive for progesterone and estrogen receptors. Ovarium-like stroma more prominent in the MCA's. MCAC characterized by a high proliferative level (more then 30%), while in MCA's it minimal (not more then 2%). Borderline MCT's are characterized by the signs of both MCA's and MCAC's.

P1.61
Detection of lymph nodes in colorectal resection specimens with carcinoma. Is resampling OF pN0 cases indicated?

Olsen T.; Ingeholm P.; Bols B.; Jensen H.; Engel Hoejholt U.; Mogensen Mellon A.; Holck S.
Hilleroed Hospital, Holte, Denmark

Background Determination of the correct node status of colorectal cancer (CRC) is an important prognosticator and a key marker for the postoperative treatment implication. According to International guidelines the identification of a minimum of 12 nodes is the goal. Several authorities stress, however, the importance of collecting as many nodes as possible and recently evidence was presented by Greco et al. (Virchows Arch 2006; 449: 647–51) that resampling proved rewarding in pT3pN0 rectal cases. Thus, their pN0 status was converted to pN1 in close to 20% of cases. The aim of this study was to analyze whether resampling in our hands could reproduce these encouraging results.
Methods The study population comprised 51 consecutive CRC resection specimens that on initial examination were staged pN0, collected June-December 2007, at two Danish institutions.
Results The mean number of lymph nodes from the first routine sampling was 20, 2 (range 12–45). The resampling yielded 0 to 11 additional nodes per case. None of these nodes harboured metastatic deposits. The mean time spend on the resampling procedure was 12, 7 min producing an additional mean of 4, 3 blocks for further processing.
Conclusion(s) Given our inability to convert any node-negative cases to node-positivity combined with the significant extra workload on the part of the pathologist and the lab technician as well as the delay in issuing the pathology report, we do not recommend an additional gross examination upon an initial thorough analysis with detection of at least 12 nodes.

P1.62
Differential expression of cell cycle regulatory molecules in hepatitis C-related hepatocellular carcinoma

El Bassiouny A.; Nosseir Mostafa Fahmy M.; Zoheiry Mohamed Kamel M.; Amen Abdel Aal N.; Abdel-Hadi Mahmoud A.; Ibraheim Mostafa I.; El-Bassiouni N.; Zada S.; Saad El-Din A.
Theodor Bilharz Research Institute, Giza, Imbaba, Egypt

Background An increased risk of hepatitis C virus-related cirrhosis and/or hepatocellular carcinoma (HCC) can be explained by mechanisms other than cell proliferation.
Methods The study included 50 cases of chronic hepatitis C, 30 cases of CHC with cirrhosis, 30 cases of HCV-related HCC and 15 normal wedge liver biopsies, taken during laparoscopic cholecystectomy. Laboratory investigations & ultrasonography were done for all cases together with immunohistochemistry using primary antibodies against cyclin D1, cyclin E, p21, p27 and Rb/p105.
Results Cyclin D1 expressed nuclear staining that was sequentially increased from CHC to LC ($p<0.01$) to HCC ($p<0.001$) cases; meanwhile, cyclin E revealed nuclear positivity only in HCCs that was directly correlated to Rb/p105. Expression of p21 and p27 was significantly increased in CHC and LC compared to normal controls and HCCs with no significant difference between well- and poorly-differentiated tumors. Correlation analysis revealed direct relation between cyclin D1 and cyclin E in HCCs; however, inverse relationship was detected between cyclin D1 and p21 or p27 and between p21 and Rb/p105.
Conclusion(s) Up-regulation of cyclin D1 in CHC plays a vital role in the development and differentiation of HCC; while, cyclin E is a useful marker for monitoring tumor behavior. p21 and p27 can be used as predictive markers for HCC. Expression of Rb/p105 in CHC and LC may help to protect from malignant transformation. Its higher presentation and inverse relation with p21

and histologic grades suggest its importance in hepatic carcinogenesis.

P1.63

Dysplasia is frequent around small intestinal adenocarcinomas complicating Crohn's disease (CD)

Svrcek M.; Cosnes J.; Parc Y.; Fléjou J.
Hôpital Saint-Antoine, AP-HP, Paris, France

Background CD is associated with an increased risk of small intestinal adenocarcinoma (SIA). Unlike colorectal cancer complicating ulcerative colitis and CD, less is known about a dysplasia-adenocarcinoma sequence in CD-related SIA.
Methods All histological slides from surgical specimens with CD-related SIA examined in our hospital between 1990 and 2008 were reviewed. We focused on the characteristics of dysplasia associated with SIA (type, grade and distribution). Dysplasia was categorized into flat or elevated.
Results We identified 10 SIA. Of the 10 patients, five were male and 5 were female. The median ages at diagnosis of CD and SIA were 14 and 49.2 years, respectively. Eight SIA occurred in the ileum and one in the jejunum; one was developed in an entero-cutaneous fistula. Dysplasia was present in 6 of 10 surgical specimens. Dysplasia was found adjacent to SIA in 1 case and consisted of flat low grade dysplasia (fLGD), and distal to the carcinoma in 1 case (fLGD). Dysplasia was both adjacent and distal in 4 cases. Three cases had both low and high-grade dysplasia in adjacent and distant mucosa. Dysplasia was flat in 4 cases, elevated in 1 case and both flat and elevated in 1 case. All neoplastic lesions occurred in areas affected by active inflammation.
Conclusion(s) Our results suggest the existence of a dysplasia-adenocarcinoma sequence in SIA complicating CD. Both elevated and flat dysplasia are observed in small intestinal carcinogenesis complicating CD. Inflammation might promote carcinogenesis in SIA.

P1.64

EGFR expression and amplification are not associated with prognosis in esophageal squamous cell carcinoma

Sato-Kuwabara Y.; Neves Ivanildo J.; Soares A.F.
Depth Anatomic Pathology, Hospital A.C. Camargo, São Paulo, Brazil

Background EGFR family has four members and much attention has been focused on the expression of EGFR with therapeutic implications. There are few studies involving EGFR amplification and protein expression in cases of esophageal squamous cell carcinoma (ESCC). We aimed to verify the presence of EGFR amplification and to correlate with immunoexpression analysis and clinicopathological findings.
Methods Immunohistochemistry of 239 ESCC cases were carried out using Tissue Microarray (TMA) technique. Analyses were performed by the Automated Cellular Imaging System (DAKO), according to membrane staining pattern and were classified in Negative, Weak and Strong Positive. FISH were performed using the EGFR gene/chromosome 7 centromer probes (Vysis). Cases showing ratio gene/CEP7 ≥ 2 or a tight gene cluster were considered positive for EGFR amplification.
Results In this study, 33.9% cases were considered Negative for EGFR expression, while 32.6% were Weak and 33.5% Strong Positive. No significant association between EGFR overexpression and clinicopathological features was found. EGFR expression did not influence overall survival. FISH analysis of 53 cases, we found EGFR amplification in 35.9%, Dissomy in 11.3%, Trissomy in 34% and Polissomy in 18.9% cases. No association between EGFR amplification and clinicopathological findings and overall survival (p=0.959) were found.
Conclusion(s) Our findings indicate that EGFR expression and amplification does not influence ESCC prognosis. Further studies are necessary to better understand the role of EGFR in ESCC development.

P1.65

Endosialin as a new marker in hepatocellular carcinomas

Mogler C.; Wieland M.; Lasitschka F.; Becker R.; Augustin H.; Schirmacher P.; Longerich T.
Institute of Pathology Heidelberg, Germany

Background Hepatocellular carcinoma (HCC) is one of the most common cancers worldwide. Our aim was to identify new angiogenic markers that can possibly differ liver lesions. Endosialin, is a myofibroblastic marker, that has been associated with tumor angiogenesis.
Methods Samples of fetal, normal adult and cirrhotic liver tissues as well as dysplastic nodules and HCCs were analyzed for Endosialin expression using immunohistochemistry. Upregulation of mRNA level was measured using quantative PCR. HCC cell lines (HuH7, Hep3B, HepG2, PLC) were tested for expression by Western Immunoblotting.
Results Endosialin was detected in atypical tumor vessels and diffusely along the sinusoids in all HCCs. In contrast, sinusoidal Endosialin staining was restricted to periportal/periseptal areas in cirrhotic nodules. Focal sinusoidal expression was observed in dysplastic Nodules. Normal adult liver did not stain for Endosialin, whereas a distinct expression in the sinusoids was seen in fetal liver tissues. Endosialin mRNA was upregulated (>2fold) in 61, 5% (8/13) HCC and 40% (4/10) cirrhotic liver tissues. Corresponding peritumorous liver tissue did not show upregulation. Western Immunoblot analyses confirmed that Endosialin is not expressed by neoplastic hepatocytes.

Conclusion(s) Endosialin is highly expressed in tumor capillaries and sinusoidal cells of HCC, but not neoplastic hepatocytes. It may thus serve as diagnostic marker for the differential diagnosis of early well-differentiated HCC in needle biopsies. Since Endosialin expression was also seen in the periphery of cirrhotic nodules and dysplastic nodules, its upregulation may occur during progressive capillarization and may indicate a functional remodeling of the specialized liver sinusoids.

P1.66
Expression of cytokeratins 7 and 20, and Ki-67 in serrated adenoma of the colorectum

Zivkovic V.; Gligorijevic J.; Djordjevic B.; Ilic I.; Petrovic A.; Krstic M.
Institute of Pathology, Medical School, University of Nis, Serbia and Montenegro

Background Serrated adenoma of the colorectum is characterized by a saw-toothed structure of hyperplastic polyp and cytologic atypia of tubular adenoma. Its histogenesis and natural history still remain unclear. The presence of foci of dysplasia in the surface epithelium supports the hypothesis that these lesions have a malignant potential. The purpose of this study was to examine the expression pattern of differentiate and proliferative markers, and to evaluate the prognostic significance of serrated adenomas.
Methods We studied colonoscopic polypectomy specimens including 25 serrated adenomas, 20 hyperplastic polyps and 20 traditional tubular adenomas. The paraffin embedded tissues were immunostained for cytokeratin 7, cytokeratin 20, and Ki-67 antigen by employing labeled streptavidin-biotin (LSAB) method.
Results Immunoreaction for cytokeratin 20 was demonstrated and strongly expressed in all "polyps". Cytokeratin 7 show a strong staining in majority of hyperplastic polyps and serrated adenomas, whereas most tubular adenomas are negative. Labeling index for Ki-67 in hyperplastic polyps, serrated adenomas and tubular adenomas was as follows: 29,4%, 34,8%, 42,4%, respectively.
Conclusion(s) Distinct cytokeratin 7, and Ki-67 staining patterns are seen in serrated adenoma and tubular adenoma possibly suggest different patways of colorectal carcinogenesis, and can be diagnostically and prognostically useful.

P1.67
Expression of MDM2/p53 and its implication in the genesis and the progression of colorectal adenocarcinoma

Chaar I.; Khiari M.; Arfaoui Toumi A.; El Hadj El Amine O.; Lahmar Boufarawa A.; Khalfallah T.; Mezabi Regaya S.; Bouraoui Masmoudi S.
Mongi Slim, Tunis, Tunisia

Background Mutation in protein p53 represents an important step in colorectal CRC carcinogenesis. Its concentration, degradation and activity are controlled by an ubiquitine ligase: MDM2. We aim to study its implication in the progression and the genesis of CCR.
Methods Analyses of p53 and MDM2 were performed for 79 cases of CCR. We compared the expression of p53 and MDM2 comparatively between normal mucosa, dysplasia and adenocarcinoma.
Results Analyses of p53 and MDM2 were performed for 79 cases of CCR. we compared the expression of p53 and MDM2 comparatively between normal mucosa, dysplasia and adenocarcinoma.
Conclusion(s) In the absence of all stress in normal mucosa, the weak rate of p53 could be explained by the fact that it is not indispensable for the normal cell function. It would be due to the fixation of MDM2 on p53 misleading its degradation so it's no detection by immunochemistry. For dysplasia or tumor, where the rate of p53 increased, the cells don't received any more signal for arrest the division or apoptose and accumulation of mutations that doesn't recognize MDM2 anymore, it promote and contribute at the neoplasic transformation and progression of this cancer.

P1.68
Expression of NF-kB1 (P105) in Helicobacter-pylori positive gastric lesions

Badawy Abdel Ghany A.; El-Hindawy Ahmed A.; Mosaad M.; Omran Omar Z.; Mohamed Magdy M.
Theodor Bilharz Research Institute, Cairo, Egypt

Background H-pylori is a causative agent of peptic ulcer disease, gastric adenocarcinoma, and MALT lymphoma. It accelerates apoptosis and cell proliferation. Nuclear factor (NF-kB1) is a transcription factor required for cellular DNA replication, and has a role in apoptosis and in tumor promotion. The study aimed at assessing the proliferative activity of gastric epithelium in H-pylori gastritis through immune-histochemical tissue localization of NF-kB1 (P105).
Methods Fourty eight endoscopic biopsies from cases with chronic gastritis and fourteen gastrectomy specimens of gastric carcinoma were included. H-pylori intensity, gastritis activity and chronicity, intestinal metaplasia, and glandular atrophy were graded and correlated with P105 expression.
Results Intact control mucosa and gastric epithelial cells of non H-pylori gastritis cases expressed P105 as cytoplasmic staining in heterogenous pattern, while its nuclear expression was found in 83.3% of H-pylori gastritis, in 71.4% of areas adjacent to cancer lesions, and in 100% of cancer lesions with

labeling index of 46.8, 82.0, and 95.0 respectively. In H-pylori gastritis P105 nuclear labeling index strongly correlated positively with neutrophil influx, polypoid formation, intestinal metaplasia, and dysplasia, without definite correlation to mucosal atrophy or H-pylori colonization intensity.
Conclusion(s) H-pylori infection provokes high proliferation in gastric mucosa that can be followed up through activated NF-kB1(P105) nuclear expression as its increasing values can be used to detect consecutive line of events leading to gastric cancer (chronic active gastritis-chronic atrophic gastritis-intestinal metaplasia-dysplasia-carcinoma in situ).

P1.69
Expression of p-STAT3 in human colorectal adenocarcinoma and adenoma: correlation with clinicopathologic features

Zizi-Serbetzoglou Evangellos A.; Petrakopoulou N.; Tepelenis N.; Savvaidou V.
Tzaneion General Hospital of Piraeus, Piraeus, Attiki, Greece

Background STATs are tyrosine phosphorylated transcription factors activated by Jak family kinases. Various ligands, including interferons and growth factors induce the activation of the STATs. STATs are a key signaling in malignant transformation and tumor progression. Constitutive activation of the STAT-3 has been observed in a wide variety of human malignancies. The aim of this study was to evaluate the clinical significance of p-STAT3 expression in cases of human colorectal adenocarcinomas and adenomas.
Methods We studied immunohistochemistry 34 human colorectal adenomas and 125 primary human colorectal adenocarcinomas from which 23 were intramucosal carcinomas and 102 invasive carcinomas. p-STAT3 expression was classified into two categories, depending on the percentage of the cells stained: Negative 0–15% and positive, when more than 15% of the tumor cells are stained. The pattern of p-STAT3 immunostaining was cytoplasmic and membraneous.
Results In the adenomas only 5 of 34 (14,7%) showed immunoreactivity for p-STAT3. In contrast immunoreactivity was noted in 10 of the 23 intramucosal carcinomas, whereas strong immunoreactivity was found in 62 of the 102 invasive carcinomas. p-STAT3 immunoreactivity correlated significantly with the depth of the tumor invasion, the venous invasion ($p<0,05$) and the increasing stages of Dukes classification ($p<0,001$). There was no significant correlation between p-STAT3 immunoreactivity and the differentiation of colorectal adenocarcinomas.
Conclusion(s) The expression of p-STAT3 is an important factor, related to tumor invasion and poor prognosis of human colorectal adenocarcinomas.

P1.70
Expression of VEGF-A, VEGFR-1, VEGFR-2 and microvessel density in colorectral cancer with liver metastasis

Jeong Hui E.; Choi Duk Y.; Min Woo B.; Lee Hyuk J.
Chonnam National University Medical School, Gwangju, Republic of Korea

Background Colorectral cancer (CRC) has been increased. Liver metastasis is often developed in CRC patients. Neovascularization is a basic event for metastasis. It is associated with many angiogenic factors. VEGF has been known to an important angiogenetic factor. We tried to investigate a staus of neovascularization and the expression of VEGF-A, VEGFR-1, VEGFR-2 in CRC patients with liver metastasis.
Methods We examined the immunohistochemical expression patterns of VEGF-A, VEGFR-1, and VEGFR-2 in serial colon cancer tissue sections from 45 patients, but also in metastatic liver tissues in same patients. We also examined the extent of microvessel density of CRC and liver metastasis by immunohistochemistry using CD34, and evaluated a relation between the degree of neovascularization and the expression of VEGF.
Results There is no difference in the expression of VEGF-A, VEFGR-1 between CRC tissue and metastatic liver tissue ($p=0.46$, $p=0.20$). While the expression of VEGFR-2 and microvessel density were increased in CRC tissue ($p=0.04$, $p=0.001$) compared to metastatic liver tissue.
Conclusion(s) There was no significant difference of VEGF expression between primary CRC tissue and metastatic tissue.

P1.71
Frantz's tumour: analysis of 13 cases

Carvalho Castelo Branco T.; Maranhão Sheyla Rodrigues K.; Oliveira Kaysa Cunha E.; Amorim Soares I.; Almeida-Filho S.B.; Santos Gomes L.; Ibiapina Oliveira J.; Patrocinio R.; Cunha Carsten A.; Ribeiro Brito T.; Silva Saraiva J.
Hospital Sao Marcos, Teresina, Piauí, Brazil

Background Solid pseudopapillary tumor of the pancreas, known as Frantz's Tumor, is a rare cancer considered to have low malignant potential and that accounts for 1–2% of the exocrine pancreatic tumours. Predominantly it occurs in young females and the tumor surgical excision leads to cure in most of the cases. We report 13 cases evaluating their epidemiological, clinical, radiological, morphological and surgical parameters.
Methods It is a retrospective study of patients with the tumor which were treated in an oncology reference hospital of Piaui - Brazil, between January 1999 and January 2009.

The evaluated parameters were: sex, age, radiological features, size, localization, metastasis, surgical therapy, surgical margin and evolution.

Results Solid pseudopapillary tumors are usually seen in women – 92, 3 %. The average age of patients was 21, 1 years varying from 10 to 33. CT-scan was the main diagnostic method used – 83, 3 %. The sizes varied from 3, 1 to 18 cm, the most frequent localization was the pancreatic head (60% of 10 cases). The partial pancreatic resection was the most used therapy (66 % of 12 cases). One patient died (7, 69 %) of a surgical complication in the 44º post-operatory day.

Conclusion(s) Frantz's tumor has a favorable prognosis, the treatment is essentially surgical and is prevalent in young females, corroborating with the literature. The epidemiological, clinical and radiological information has a large diagnostic importance, and the histopathological aspect is essential for confirmation of this tumour.

P1.72

Gastroduodenal morphology in patients with inflammatory bowel disease

Bas E.; Alehah Eden A.; Hamzaoglu H.; Ertem D.; Celikel Ataizi C.
Marmara University, Istanbul, Turkey

Background It is well known that upper gastrointestinal endoscopic biopsies often show histologic abnormalities inCrohn's Disease(CD). However, recent studies suggested that similar abnormalities may occur in ulcerative colitis UC). The aim of this study was to analyze the histological appearence of gastroduodenal mucosa in adult-onset IBD and to compare biopsy findings of adult- and pediatric-onsetCD.

Methods In this retrospective study, we analyzed 216 gastroduodenal biopsy samples from patients with adult-onset UC (n=10), adult-onset CD (n=21), and pediatric-onset CD (n=11). In the evaluation of biopsies from antrum, gastric body, bulbus, and duodenum; focally enhanced gastritis (FEG), presence of H. pylori, micro-aggregates of macrophages (MM), epithelioid cell granulomas (EG), crypt distortion and diffuse duodenitis were recorded.

Results H. Pylori associated gastritis was found in 4 patients with UC (40%), 4 patients with adult-onset CD (19%), and 2 patient with pediatric-onset CD (18, 2 %). In H. pylori negative patients the diagnosis was FEG in 41, 2 % and 33, 3 % in adult- and pediatric-onset CD, respectively, but 10% in UC. MM was found in adult- and pediatric-onset CD in38, 1% and 63, 6%, respectively. EG was present in 4 patients with CD (2 adult- and 2 pediatric-onset). In patients with UC, no granuloma and MM could be detected. Duodenal biopsies revealed diffuse duodenitis in30% and low grade dysplasia in10% of the UC patients, but focal duodenitis in 19% in adult-onset CD.

Conclusion(s) FEG is common in both adult- and pediatric-onset CD, but not spesific for CD. Detecting a MM in a biopsy specimen taken from gastroduodenal mucosa seems to be a useful method for differetiating CD from UC, especially in pediatric-onset IBD.

P1.73

Hepatotrophics factors: a tool for the treatment of chronic liver diseases and before partial hepatectomy

Aloia Pinheiro Arrais T.; Cogliati B.; Araújo Maria Monteiro C.; Hernandez-Blazquez Javier F.
University of São Paulo, São Paulo, Brazil

Background Hepatotrophics factors (HF) have the ability to enhance the cell proliferation in hepatectomized rats and decrease fibrosis in cirrhotic rats. The HF can be important before in hepatic resection surgery in which the liver needs to enlarge a considerable mass volume before large hepatectomy. Thus, this study evaluated the main morphological and physiological effects of HF solution in the livers of healthy animals.

Methods We used 70 female Wistar rats divided into 7 groups of 10 animals each. The rats were treated with HF solution (dose 40 ml/kg/day) and euthanized 2, 4, 6, 8, 10 and 12 days after starting treatment (groups A to F). A control group (CT) received only saline. The biometric parameters of liver weight, proliferation of hepatocytes (PCNA), morphometry of collagen, liver biochemical function and gene expression of collagen type I were evaluated.

Results There was an increase of liver mass during the treatment. The PCNA proliferation index was 1.9, 9.7, 5.7, 4.2, 4.7, 5.2, 2.7% in CT and A to F groups respectively. Collagen morphometric analysis and gene expression decreased during the treatment. The liver function remained normal.

Conclusion(s) The results showed that the HF promotes hepatocyte hyperplasia and hypertrophy, with no change in liver function and with a decrease of volume of liver collagen content and mRNA expression. Therefore, the HF solution represents an important option for treatment of chronic liver diseases and to increase in liver mass before large hepatectomy.

P1.74

Immunohistochemical and morphometrical analysis in ductal pancreatic carcinoma

Herlea V.; Stoica-Mustafa E.; Pechianu C.; Vasilescu C.; Paslaru L.; Sajin M.; Hortopan M.; Iorgescu A.; Sobaru I.; Ionescu M.; Stroescu C.; Tomulescu V.; Dima S.; Brasoveanu V.; Ungureanu C.; Mitulescu G.; Ciurea S.; Gheorghe L.; Gheorghe C.; Croitoru A.; Cretoiu D.; Popescu I.

Fundeni Clinical Institute, Bucharest, Romania – Umf "C. Davila", Bucharest, Romania

Background Ductal pancreatic carcinoma is the most aggressive neoplasm of the pancreas, representing 80–90% of all pancreatic tumors.

Methods Our study included 230 cases of ductal pancreatic carcinoma, admited in our institute during a period of ten years. The analyzed histopathological parameters were: tumoral grade, lymph node metastases, perineural and intravascular invasion and intraglandular necrosis; the used immunohistochemical markers are: MUC 1, MUC 2, Ki 67, CD-34, CD 68, MMP-7, CEA, p21, p27, p53, F VIII, CK-7; 53 of 230 cases were morphometricaly analyzed.

Results MUC-1 and MMP-7 were positive in about 75% cases, most of them well differentiated in initial stages; CEA was positive in 83% cases; p53 was positive in 41% cases, most of them std II-III, and negative in adenosquamos and mucinos types; p21 was positive in 36% cases, and Ki-67 was positive in 40 – 45% of high grade tumors (over 20%).

Conclusion(s) Majority of ductal carcinomas were localized in cephalic region, in patients with 50–70 years, more frequent in males; the morphometrical preoperative analysis is necessary and useful; the immunohistochemical analysis is necessary for an accurate diagnosis, grading, staging, and differential diagnosis.

P1.75

Immunohistochemical detection of the somatostatin receptors in gastroenteropancreatic neuroendocrine tumors

Delektorskaya V.V.; Ponomareva M.V.

N. N. Blokhin Russian Cancer Research Centre RAMS, Moscow, Russian Federation

Background The expression of somatostatin receptor subtypes (SSTR 1–5) in neuroendocrine tumors (NETs) is the basis for somatostatin analogues treatment. The aim of this study was to determine SSTRs 1- 5 presence, cellular localization and distribution in gastroenteropancreatic NETs.

Methods We have analyzed the SSTRs subtype 1–5 expression using immunohistochemistry in a retrospective series of primary gastroenteropancreatic NETs (n 21) and their hepatic metastases (n 7) and compared the results with clinical and pathological features.

Results Gastroenteropancreatic NETs and their metastases expressed the SSTR 1–5 with different frequency and intensity. Both SSTR-2 and SSTR-5 were expressed in 75% of NETs. More than 50% of the specimens expressed SSTR 1. SSTR 3 and 4 positive were detected in 32% and 25% of the tumors, respectively. SSTRs were localized in tumor cells and surrounding structures, especially blood vessels. The immunoreactivity of SSTRs was strong on the cell membrane and less intense in the cytoplasm of the tumor cells. Analysis of primary tumors and their metastases revealed a similar pattern in receptor-subtype immunoreactivity. Among 7 hepatic metastases from small intestinal and pancreatic NETs 4 were positive for SSTR1; 6 - for SSTR2; 5 - for SSTR3 and SSTR-5; 2 - for SSTR4. There was no correlation between SSTR 1–5 expression and main clinical-pathological characteristics.

Conclusion(s) Immunohistochemical SSTR status typing can be used in the routine surgical pathologic analysis for optimizing receptor targeted diagnosis and therapy of primary and metastatic gastroenteropancreatic NETs with subtype specific somatostatin analogues.

P1.76

Immunohistochemical evaluation of nectin 3 expression in pancreatic tumours

Hirabayashi K.; Nakamura N.; Kajiwara H.; Matsui N.; Oyamada H.; Osamura R.Y.

Department of Pathikigy, Tokai University School of Medicine, Isehara, Kanagawa, Japan

Background Nectin is an adhesion molecule belonging to the immunoglobulin-like superfamily. It is an epithelial junctional complex, a receptor for virion entry, and a tumour suppressor and is involved in immune reactions. This study is aimed at to immunohistochemically elucidate nectin 3 expression in the membrane of normal and cancerous pancreatic cells.

Methods Total 83 pancreatic tumours were examined, including invasive ductal carcinoma (IDC; $n=15$), intraductal papillary mucinous adenoma (IPMA; $n = 12$), intraductal papillary mucinous carcinoma (IPMC; $n = 12$), mucinous cystadenoma (MCA;: $n=9$), endocrine tumour (n=17; well-differentiated endocrine tumours, $n = 12$; endocrine carcinoma, $n=5$), serous cystadenoma (SCA; $n=7$), acinar cell carcinoma (ACC; $n=4$), and solid pseudopapillary neoplasm (SPN; $n=7$).

Results In normal pancreatic tissues, nectin 3 was detected in the intercalated, intralobular, and interlobular ducts and in the islets of Langerhans but not in the acinar cells. Reactivity of

nectin 3 was as follows: IPMA (12/12), IPMC (12/12), IDC (15/15), SCA (7/7), MCA (9/9), SPN (7/7), ACC (1/4), well-differentiated endocrine tumour (10/12), and endocrine carcinoma (1/5). The distribution of nectin 3 expression was more focal and the intensity of expression weaker in IDC, ACC, and endocrine carcinoma than in other tumours.

Conclusion(s) Nectin 3 expression was absent or weak and focally distributed in ACC, IDC, and endocrine carcinoma. Nectin 3 may be related to invasion and malignancy of pancreatic tumours.

P1.77

Inhibition of human esophageal adenocarcinoma growth by both high and low-dose aspirin in nude mice

Ortego J.; Esquivias P.; Cebrián C.; Santander S.; Conde B.; Emperador S.; Sopeña F.; García-Gonzalez M.; Jimenez P.; Lanas A.; Piazuelo E.
Hospital Clínico Universitario, Zaragoza, Spain

Background Regular use of aspirin (ASA) has been shown to be associated associated with a reduced risk of esophageal adenocarcinoma (EAC). We examined whether treatment with ASA affects the growth of human EAC in a nude mice xenograft model.

Methods The effect of ASA was evaluated in vitro: human EAC OE33 cells line were treated with ASA (0–5 mM) to evaluate proliferation, apoptosis and migration, and in vivo: OE33 cells inoculated into athymic nude mice. OE33-derived tumours were excised and cut up. Xenografts from primary tumours were subcutaneously re-implanted into new mice which were randomized to different treatments: low-dose ASA (5 mg/kg/day) or high-dose ASA (50 mg/kg/day). For each treatment a control group was included. Tumour growth and volume were estimated. After 2 months mice were sacrificed. ASA and salicylic acid (SA) plasma levels were assessed by HPLC. Data analysis was carried out using variance analysis and anova test.

Results Cell proliferation and migration was significantly inhibited, while apoptosis was significantly increased by ASA. All tumours were poorly differentiated adenocarcinomas. Tumour progression was significantly lower in ASA-treated mice when compared to non-treated animals and proliferation index was significant decreased in tumours. Tumoral inhibition was 85% and 78.3% in ASA-5 and ASA-50 groups respectively.

Conclusion(s) Both low and high-dose ASA inhibits the growth of human EAC xenografts in nude mice, which suggests a potential role for ASA in the treatment of this type of tumours.

P1.78

Laboratory evaluation of capecitabine administration impact on the healing process of colonic anastomoses. experimental study in rats

Sioga A.; Pissanidou T.; Papamitsou T.; Ekonomou L.
Laboratory of Histology and Embryology, Aristotle University of Thessaloniki, Greece

Background Capecitabine is a fluoropyrimidine carbamate with antineoplasmatic activity, indicated for the therapy of colorectal cancer. The aim of this study was concluded to determine the impact of Capecitabine administration during perioperative period of colectomy.

Methods We studied the effect of Capecitabine in rats which underwent colectomy and hand sutured colonic anastomosis. Sixty Wistar rats where randomized in two groups of 30 rats each. In the study group capecitabine was given p. o.1 week prior the operation and through out the study. In the control group placebo medication was administrated. Both groups where further subdivided into 3 groups, each consisting of 10 animals. Rats were sacrificed in groups of 10 animals on the 3 rd, 7th and 14th postoperative day, in both study and control group.

Results All animals of study group gained weight postoperatively, in addition to controls. We found no negative impact on the healing of colonic anastomosis. Histological findings showed less necrotic effects for study animals sacrificed at 3 rd postoperative day. Routine biochemical measurements did not reveal any significant differences between control, study and specifier groups. No significant increase in IL-2, IL-6, and TNF-a serum levels was found in capecitabine-treated animals during the early and more vulnerable days of intestinal healing.

Conclusion(s) Administration of Capecitabine doesn't have negative impact on the healing of colonic anastomosis in rats, neither to the recuperation of preoperatively treated animals.

P1.79

Methylene blue assisted lymph node dissection in combination with ex vivo India ink sentinel lymph node mapping in colorectal cancer

Märkl B.; Oruzio D.; Jähnig H.; Wünsch K.; Kerwel T.; Anthuber M.; Arnholdt Martin H.; Spatz H.
Klinikum Augsburg, Augsburg, Germany

Background We recently introduced intra arterial methylene blue injection as a simple method to improve the lymph node (LN) harvest in gastrointestinal cancer. We now combined it with a novel ex vivo sentinel lymph node (SLN) mapping technique which allows histological SLN detection.

Methods Up to now 16 colorectal specimens were enrolled. In unfixed state a subserosal injection of about 2 ml India ink and an intraarterial methylene blue were performed. Lymph node dissection was carried out after formalin fixing over night. Slides were screened for lymph node metastases and SLN were identified by detecting carbon particles. In primary N0 cases all lymph nodes were step sectioned and immunohistochemically stained for pan cytoceratin.
Results India ink as well as methylene blue injection was easy to perform in all cases. The mean harvest was 37±14 LNs and the SLN detection rate was 81%. The mean SLN number was 3±1. LN metastases were found in 6 out of 15 malignant cases (40%). Skip metastases occurred in 2 cases. Both cases showed involvement of at least one entire LN. True upstaging (N0 - >N1mi) was found in one case (7%) were a SLN showed a micrometastasis after cutting additional step sections.
Conclusion(s) Combination of methylene blue technique and ex vivo sentinel mapping is feasible and has the potential for improving sensitivity of histopathological LN investigation without increasing the time of operation.

P1.80

New histological features of hepatic necrosis after imatinib treatment

De Coataudon L.; Michalak S.; Rousselet M.; Pavageau A.; Nedelcu C.; Singeorzan C.; Zidane Marinnes M.; Saint Andre J.
University Center of Pathology, Angers, France

Background Imatinib is a drug used in treatment of gastrointestinal stromal tumor. Imatinib given in doses of 400 mg daily is generally well tolerated. The adverse effects known are edema, nausea, rash, abdominal pain. Severe hepatotoxicity is rare.
Methods We report a 71 years old woman known with gastric stromal tumor and liver metastasis. She started a treatment with Imatinib at a 400 mg/day after the gastrectomy. She developed a leucopenia after 2 month of treatment, deciding to decrease the dose at 300 mg/day. The CT-scan showed a good evolution of the hepatic metastasis and the clinicians returned to the first dose. Virus serology was negative. After ten days, appeared an elevation of transaminasis, so the decision was to performe a percutaneous liver biopsy.
Results The liver biopsy showed centrolobular spotty necrosis. This area was filled by sandy macrophages infiltration. The lobule had respected architecture. In the portal spaces, there was a little lymphocytic inflammatory infiltration. These aspects are highly suggestive for resolution phase of an acute centrolobular necrotizing hepatitis. The toxic etiology was evocated and confirmed by returning to normal of hepatic function after stopping the Imatinib administration.
Conclusion(s) Seven cases with hepatic cytolysis and necrosis around the portal tracts were described. Here the necrosis was centrolobular. This rare case during the Imatinib treatment proved that a regular monitoring liver's function is to be considered and it can be resolved by discontinuing of drug.

P1.81

New preneoplasic lesion of colorectal carcinoma: "globlet cell dysplasia" leading to signet ring cell colorectal carcinoma

Ben Mahmoud L.; El Hadj El Amine O.; Arfaoui Toumi A.; Khiari M.; Gharbi L.; Regaya Mzabi S.; Bouraoui S.
Mongi Slim, Tunisia

Background Approximately 10% of all colorectal carcinomas (CRC) are mucinous, characterized by extracellular mucin. Occasionally, mucin accumulates intracellularly in these tumours, causing signet ring cell (SRC) differentiation that believed to originate from a de novo pathway. In this study, we hypothesise that SRCs arise from a preneoplasic lesion occurring in globlet cells.
Methods Two cases of mucinous CRC with SRCs differentiation and one case of signet ring cell carcinoma (SRCC) were collected among two hundred four cases of CRC. By histological examination in light of further immunohistochemical analysis of adhesion molecules and characteristics of mucin, we tried to prove that SRC in CRC may be the result of dysplasia occurring in globlet cells.
Results These cases are believed to be primary lesions of CRC. Indeed, by a combination of clinical, radiological investigations we didn't find any other primary tumors. CK18 and CK20 analysis showed positive immunostaining in the three cases which better confirm the primary colorectal nature. Morphological examination showed interesting changes in globlet cells that become progressively vacuolated; than the mucin pushes the nuclei in one side leading to a SRC phenotype. The transformed cells are characterized by MUC2 production, which are secretory mucins specific of globlet cells, and showed a progressive disruption of the E-cadherin/ β-catenin complex.
Conclusion(s) All these findings suggest that SRC in CRC may rather be the result of neoplasic transformation affecting the globlet cells than the result of a de novo pathway.

P1.82

Osteoclastic-like giant cell tumor of the pancreas associated with mucinous cystadenocarcinoma. Case report

Spasevska L.; Janevska V.; Petrusevska G.; Kostadinova-Kunovska S.; Banev S.; Dukova B.; Karadzov Z.; Orovcanec D.; Hadzimancev M.
Institute of Pathology, Faculty of Medicine, Skopje, the Former Yugoslav Republic of Macedonia

Background We report the case of 59-year-old woman with an osteoclast-like giant cell tumor (OLGT) of the pancreas associated with a mucinous cystadenocarcinoma (MCC). Conflicting opinions exist regarding the OLGT origin, whether it is mesenchymal or epithelial, neoplastic or reactive, paraneoplasic product.
Methods Ultrasonography et CT showed two adjacent large tumors involving the tail of the pancreas. Distal pancreatectomy with splenectomy, adhered segment of colon and paraaortic lymph nodes dyssection were performed.
Results The surgical specimen revealed that the first node is uniloculated cystic tumor, 14x12x12 cm, filled with mucin-haemorrhagic-necrotic material, without communication with the pancreatic duct system. The second node, 7x10x7 cm, was solid, with fibrous pseudocapsule. Microscopically the cysic tumor was composed of mucinous carcinoma cells (MCCs) and ovarian-type stroma. Focal areas of invasive carcinoma were observed in the cyst wall, not affecting the surrounding pancreas. The solid tumor was composed of pleomorphic stromal cells (PSGs) and osteoclastic-like giant cells (OGCs). There were no areas of transition between the MCC and OLGT. Immunohistochemically, MCCs stained for cytokeratin 7, 18 and 19 and stroma for inhibin, progesteron and vimentin. PSCs were strongly positive for vimentin, while OGCs for CD68 and CD45. The overexpression of p53, about 40%, was detected in a MCCs and in the PSCs.
Conclusion(s) Such results support the idea that the stroma of the OLGT is a tumor and origins from totipotential ovarian-type stroma. The OGCs are not epithelial and their histiocyte-macrofage phenotype is a possible paraneoplastic product.

P1.83
Progesterone and estrogen receptor expression in slow transit constipation

Madden E. M.; Masley M. P.; Mills E. S.; Evans F. M.; Trainer D. T.; Mawe M. G.
Fletcher Allen Health Care/University of Vermont, Burlington, VT, USA

Background Progesterone may play a role in slow transit constipation (STC), as STC occurs primarily in women and progesterone decreases colonic contractility in experimental animals.
Methods Immunohistochemistry was performed for progesterone (PR) and estrogen receptors (ER) on specimens removed for STC (n=27) and age-matched controls (n=27). Results were evaluated blindly with a computer-based stereology system.
Results Compared with controls, STC specimens had a significantly lower proportion of PR-positive smooth muscle cells in the muscularis propria of their ileum (circular layer, 18.3±2.9% vs.28.5±3.1%, p=0.02; longitudinal layer, 27.3±5.3% vs. 45.8±4.6%, p= 0.01) and distal colon (circular layer, 12.3±2.7% vs. 32.9±3.0%, p=0.0001; longitudinal layer, 18.2±3.8% vs. 37.9±6.0%, p=0.006). No significant differences in PR immunoreactivity were detected in the proximal colon (circular layer, 31.8±4.8% vs. 30.9±5.3%, p=0.90; longitudinal layer, 33.2±4.8% vs. 28.2±3.7%, p=0.47). No immunoreactivity for ER was present in cases or controls.
Conclusion(s) These data suggest that STC is associated with a decrease in PR expression in the ileum and distal colon. Our findings contradict previous theories that an overexpression of PRs may contribute to decreased colonic motility in these patients. A recent study suggested that overexpression of progesterone receptor B increases sensitivity of human muscle cells to progesterone. However, ours is the first study to look specifically at levels of PR expression in STC. Although the implication of decreased PR expression is unclear, it may represent a compensatory down-regulation of progesterone receptors due to increased sensitivity of PRs to progesterone in these individuals.

P1.84
Prognostic value of the peritumoural versus intratumoural microvessels density and invasion in colorectal carcinoma

Spasevska L.; Janevska V.; Jovanovic R.; Dukovska B.; Kostadinova-Kunovska S.; Janevski V.; Jankulovski N.; Karadza Z.; Karagjozov A.; Panovski M.; Josifovski T.
Institute of Pathology, Faculty of Medicine, Skopje, the Former Yugoslav Republic of Macedonia

Background There are controversial data on the prognostic value of the peritumoural versus intratumoural microvessels density (MVD) and invasion (MVI) in colorectal carcinoma (CRC). The aim of this paper is evaluate whether peritumoural versus intratumoural microvessels density and invasion correlate with the clinical-pathological parameters of known prognostic importance.
Methods Surgically resected specimens from 62 CRC were analyzed. Assessment of the MVD and MVI was performed by immunohistochemical detection of microvessels using CD34, CD31 and factor VIII-related antigen. The number of vessels was quantified at x200 magnification. The median of microvessels counted in ten hot-spot fields was defined as MVD. Additionally a cut-point of the 6 MVI (median value in the same areas) was used for comparation with pathological parameters.
Results The median value of the intratumoural MVD was higher than at the peritumoural margine and correlated

with the tumor type, tumor size, extramural spread and the infiltrative growth pattern ($p<0,5$), but not with the nodal and distant metastasis. Peritumoural MVD was correlated with the nodal and distant metastasis ($p<0,01$). MVI was significantly associated with the tumour budding and nodal metastasis ($p<0,01$). Invasion in more than 6 microvessels has shown high-significance correlation with the number of involved nodal (> 4) and distant metastasis ($p<0,001$).

Conclusion(s) Peritumoural MVD and MVI are related to pathological parameters indicative of poor outcome such as lymph-node status. MVI in more than 6 vessels may be used to identify patients more prone to developing distant metastasis.

P1.85

Prognostic-molecular-markers (PMM) in colon-cancer (CC) ultra-staged by sentinel-lymph-node (SLN)-mapping

Donisi M.P.; Riccardi M.; Vianello R.; Sommariva A.; Zaninotto G.; Stracca-Pansa V.

S. Giovanni e Paolo Hospital, Department of Clinical Pathology, Venezia, Italy

Background The SLN-mapping-tecnique allows to up-stage 5–20% of patients with micro-metastases that may benefit from adjuvant-chemotherapy. Several molecular-markers have negative-predictive significance in CC: microsatellite-stability (MSS), 18q-loss-of-heterozigosity (18qLOH) and k-ras-mutations (mut-kras). The aim of this study is to evaluate the prognostic significance of these markers in a group of CC-patients ultra-staged by SLN-mapping.

Methods 62 CC-patients were included in a SLN-mapping study.14 patients were pT1/T2, 44pT3 and 4pT4. DNA was extracted from macrodissected-tumor-tissue and PCR-amplified. Exon1–2 mut-kras were detected by direct-sequencing.

Results 1) To search a relationship between PMM and lymph-node-status, we focused on pT3-patients.13/44 pT3-patients (29%) were in MSS-18qLOH-mut-kras-status (9-N0 and 4-N+). 2) We searched a relationship between PMM and clinical-outcome (average follow-up-time 31-months). 29/44 patients (66%) were N0, 15 (34%) N+. 20/29 N0 patients had no relapse while 6 relapsed or died.4 of these belonged to MSS-18qLOH-mut-kras-group and 2 had at least 1 negative PMM. 10/15 N+patients had no relapse while 3 relapsed or died. 2 of these belonged to MSS-18qLOH-mut-kras-group. In 5 patients we had no clinical data (3-N0 and 2-N+).3). In 6 patients, that relapsed and belonged to the negative-prognostic-group, we found 2 mut-k-ras in codon-61, 3 glycine-to-aspartate-mutations in codons-12–13, and 1 non-aspartate-mutation in codon-13.

Conclusion(s) 1) We found no relationship between MSS-18qLOH-mut-kras and lymph-node-status. 2) Regarding to prognosis, it's advisable to associate lymph-node-status with PMM analysis. Infact, in pT3N0 patients is possible to identify a MSS-18qLOH-mut-kras-subgroup who may benefit from adjuvant-chemotherapy. 3) In this study k-ras-mutations in codon-61 and glycine-to-aspartate-mutations in codons-12–13 are associated with increased risk of relapse and death.

P1.86

Reduction of hepatocyte intercellular communication promotes an increase of liver fibrosis

Cogliati B.; Silva C.T.; Aloia Pinheiro Arrais T.; Chaible Martins L.; Real-Lima Aline M.; Hernandez-Blazquez Javier F.; Dagli Lúcia Zaidan M.

School of Veterinary Medicine and Animal Sciences, University of Sao Paulo, Sao Paulo, Brazil

Background Intercellular gap junctions, formed by connexins (Cx), are involved in control of tissue homeostasis, cellular growth and proliferation. Hepatocytes mostly express Cx32 and play an important role in liver fibrogenesis. Thus, we investigated the development of liver cirrhosis in Cx32-deficient mice (Cx32-/-).

Methods Mice were genotyped and received 3 weekly doses of 10% CCl4, for 2 months. After euthanasia, tissue and blood samples were collected for histopathological and serum biochemical analysis. Inflammatory activity index, number of apoptotic bodies and collagen content were analyzed in the hepatic tissue. Hepatocyte cellular proliferation was quantified by PCNA immunohistochemistry. Gene expression of collagen type I and matrix metalloproteinase II (MMP-2) was performed by real time RT-PCR. t-Student test was employed for statistical analysis ($p<0.05$).

Results Cx32-/- mice presented higher collagen content (23.7%), decrease of hepatocyte proliferation (47.5%) and increase in the number of apoptotic bodies (40.3%). Also, Cx32-/- mice had a higher index of inflammatory activity (20.4%) and, consequently, an increase of AST (33.2%) and ALT (19.2%) enzymes. There was an increase in collagen I mRNA in Cx32-/-, but there was no difference in MMP-2 in both genotypes.

Conclusion(s) Cx32-deficient mice presented an increase of collagen deposition in cirrhotic livers because of an imbalance between cell proliferation and apoptosis, besides the presence of more inflammatory activity. Therefore, this data showed an important role of connexin 32 in the maintenance of tissue homeostasis,

preventing fast progression of liver fibrosis by reduction of hepatocyte injury.

P1.87

Relationship between the polymorphism of p73 gene and colorectal cancer risk and survival

Arfaoui Toumi A.; Ben Mahmoud L.; El Amine El Hadj O.; Khiari M.; Chaar I.; Ben Hmida A.; Khalfallah T.; Mzabi Regaya S.; Bouraoui S.
Mongi Slim, Soukra, Tunis, Tunisia

Background Polymorphism at loci controlling cellular processes such as cell cycle, DNA repair, and apoptosis may modulate the risk of cancer. We examined the association of one linked polymorphism (G4C14-A4T14) at p73 with the risk of colorectal cancer. In the present study, we investigated whether this polymorphism was related to the risk of colorectal cancer, and whether there were relationships between the polymorphism and LOH, protein expression or clinicopathological variables.
Methods The p73 genotypes were determined by PCR-restriction fragment length polymorphism in 150 Tunisians patients with colorectal cancer and in 204 healthy control subjects. Immunohistochemistry was performed on normal mucosa, primary tumour and metastasis.
Results The frequencies of the genotypes were 53% for wild-type (GC/GC), 30% for heterozygotes (GC/AT) and 17% for variants (AT/AT) in patients, and 54, 35 and 11% in controls, respectively. The frequencies of the genotypes in the patients and controls were significantly different ($p<$ 0.05). We did not find any relationship of the genotypes with clinicopathological features ($p>$0,05). The genotype was not related to the protein. The samples that were heterozygous in normal colorectal tissue were lost in four cases of matched primary tumours. However, LOH of the p73 gene was rarely event in colorectal cancer. The patients carrying the AT allele had a better prognosis than those with the GC/GC genotype.
Conclusion(s) The AT/AT homozygotes may have a greater risk of developing colorectal cancer, while the patients who carried the AT allele had a better prognosis.

P1.88

Role of colonoscopic biopsies in distinguishing between Crohn's disease and tuberculosis

Bulbul Dogusoy G.; Celik Ferhat A.; Goksel S.; Aygun G.
Istanbul University Cerrahpasa Medical Faculty, Department of Pathology, Istanbul, Turkey

Background As the histological differential diagnosis of Tuberculosis (TB) enterocolitiscolitis and Crohn's disease (CD) can be very challenging, the aim of this study is to evaluate clinical and histologic parameters in colonic biopsy specimens to discriminate between two disorders.
Methods Gastroenterology archieves of the last seven years were reviewed and 12 cases with TB colitis and 25 cases with CD registered in the same period, were selected for this study on the basis of clinical, radiologic, microbiologic and histopathologic criteria. Clinical and histopathologic features were reviewed retrospectively.
Results A total of 14 biopsies of intestinal TB cases and 38 biopsies of 25 cases with CD were evaluated and compared. In the histopathologic features in colonoscopic biopsies, granulomas were observed in colonic mucosa or submucosa of all, with suppuration of granulomas in 11, caseous necrosis in 5, and ulceration in 9 cases with TB. However, granulomas were observed in 6 of 25 CD cases with no suppuration and caseous necrosis. Other features were also compared. EZN stain revealed presence of acid fast bacilli in 5 TB and no CD cases, however PCR studies for mycobacterium were found positive in all of TB and none of CD cases.
Conclusion(s) The results of this study demonstrated that with clinical features, histopathologic parameters in colonoscopic biopsies especially due to characteristics of granulomas are helpful to distinguish TB colitis from CD.

P1.89

Role of transforming growth factor-beta pathway in progressiveness of colorectal cancer

Gulubova Vladova M.; Manolova I.; Julianov Emilov A.; Yovtchev Petkov Y.; Peeva Teneva K.
Medical Faculty, Trakia University, Stara Zagora, Bulgaria

Background Most of all epithelial-derived tumors become resistant to the growth inhibitory effect of TGF-beta.The aim of the present study was to evaluate TGF-beta1, TGF-betaRII, Smad4 and Smad7 expression in tumor tissue of colorectal cancer (CRC) patients and to determine their relationship survival. TGF-beta expression in tumor cell cytoplasm was correlated with HLA-DR expression, with macrophages and dendritic cells.
Methods The expression of TGF-beta1, TGF-betaRII, Smad4 and Smad7 and of HLA-DR antigen, CD1a, CD83 and CD68 was evaluated immunohistochemically in 142 CRC patients (50 females and 92 males), followed-up for 6–8 years period.
Results The TGF-beta1 expression in tumor cytoplasm was observed in 127 patients (89, 4%) and of Smad4 expression - in 83, 8% patients. Smad4 expression in tumor nuclei correlated with TGF- beta1 expression in tumor cytoplasm (chi2=38.88; $p=$0,000) whereas cytoplasmic Smad4 expression correlated with TGF- betaRII on the

tumor cell membrane (chi2=23.52; p=0,000). Low HLA-DR expression and low CD83 infiltration was observed in tumor stroma in 62, 5 % of tumors (chi2=5.65; p=0,017). Increased TGF-beta expression in tumor cytoplasm correlated also with low CD68-positive cell infiltration in tumor nests (chi2=4.03; p=0,045). On univariate survival analysis, TGF-beta1 and Smad4 overexpression had a negative impact on CRC patients' survival.

Conclusion(s) Our results suggest that TGF-beta1 production by tumor cells affects the tumor environment via suppression of tumor-infiltrating immune cells and directly contributes to tumor cells aggressiveness through autocrine activation of Smad signaling.

P1.90

Strong cytoplasmic expression of COX2 and high p21-labeling index at invasive fronts of gallbladder cancer are associated with a poor prognosis

Song J.; Kim H.; Yoon Y.; Cho J.; Lee H.; Seol H.; Park S.; Chung J.; Choe G.
Seoul National University Bundang Hospital, Seongnam, Gyeonggi, Republic of Korea

Background The significance of cell cycle proteins, p21 and p53, and cyclooxygenase-2 (COX2) is still controversial in gallbladder adenocarcinoma (GC) – conflicting results exist with regards to the prognostic significance of p21 and p53 expression, and the strong association of GC with chronic inflammation makes it only natural that COX2-negativity is rarely encountered, even in non-neoplastic biliary epithelia.

Methods We explored whether the p21 and p53-labeling indices (LI) and strong cytoplasmic COX2 expression differs in the central parts (TC) and invasive fronts (IF) of GC. Paraffin-embedded whole tissue sections of 45 GCs were immunohistochemically analyzed for p21, p53 and COX2-LI at the IF and TC separately.

Results p21, p53 and COX2-LI were higher in IF compared to TC in 100% (p<0.001), 86.1% (p=0.017) and 100% (p<0.001) GCs, respectively. p21-vs-COX-LI were significantly correlated at TC and IF (p<0.05). COX2-LI-IF was correlated with perineural invasion (p= 0.008) and recurrence (p=0.067). GCs with COX2-LI-IF >30% showed decreased disease-free survival (p=0.028). GCs with high COX2 and p21-LI-IF showed decreased overall survival (p=0.051). However, COX2 and p21-LI-TC showed no clinicopathological significance.

Conclusion(s) The IF of GC is characterized by significantly increased expression of p21, p53 and strong COX2 expression, and p21 and COX2 expression at IF are associated with a poorer prognosis. Heterogeneity between TC and IF should be considered in in situ molecular studies, especially during interpretation of immunohistochemical stain results and tissue microarray construction.

P1.91

Survivin in colorectal carcinoma: its role as a prognostic marker

Ozturk Akif M.; Dane F.; Bas E.; Ozkan N.; Turhal S.; Celikel Ataizi C.
Marmara University, Istanbul, Turkey

Background In the pathogenesis of colorectal carcinoma (CRC), defects in the regulation of apoptosis has been implicated. In our study, we aimed to investigate the role of survivin, an inhibitor of apoptosis protein, in CRC patients in terms patient/tumor characteristics and survival.

Methods In tissue sections prepared from parafin-embedded tissue blocks of 143 patients, anti-survivin (clone 4F7, Neomarkers) primary antibody was applied.89 patients who received adjuvant chemotherapy and had a follow-up of at least 2 years were included for statistical analysis. The immunoexpression of survivin was scored according both to the intensity (0–4) and the percentage of stained neoplastic cells (1–4). By multiplying two scores we determined the survivin value (SV) for each case. Patients were classified as high SV (≥ 12) and low SV (≤ 12) for statistical analysis.

Results In patients with nonmetastatic disease, low SV was observed in advanced T stages (p=0.033). When patients with inadequate lymph node (LN) dissection (< 10) were excluded low SV was related to LN positivity (p=0,037). Perineural invasion, grade, presence of mucinous component, and high SV were related to survival. In Cox regression negative LN status was related to survival. No effect of SV on disease free survival was observed, but low SV caused higher cancer related deaths in the adjuvant settings (p = 0.019).

Conclusion(s) Immunoexpression of survivin predicts a better cancer spesific survival in patients who receives adjuvant therapy. Contradictory results in the literature can be explained by the fact that different antibodies detects different splice variants of survivin gene that have different regulatory functions in apoptosis machinery.

P1.92

The evaluation of VEGF and endostatin expressions and serum levels in ulcerative colitis

Savas B.; Kahramanoglu E.; Ustun Y.; Cetinkaya H.; Toruner M.; Ozden A.; Ensari A.
Ankara University, Medical Faculty, Department of Pathology, Ankara, Turkey

Background Increased serum levels and tissue expressions of VEGF, in active ulcerative colitis (UC) were shown in recent studies. However it is not clear why the healing of UC related mucosal injury is impaired despite the increased levels of angiogenic factors. We aimed to evaluate the serum levels and tissue expressions of VEGF and endostatin in UC patients.
Methods A total of 67 cases (39 UC, 28 Irritable Bowel Syndrome (IBS) cases) were studied. UC cases were grouped clinically for disease activity. Mean serum VEGF and endostatin levels were measured. VEGF and endostatin expressions were assessed with immunhistochemistry in histologicaly proved active and inactive mucosa biopsies of UC cases and IBS cases as control group.
Results Mean serum VEGF and endostatin levels in UC and IBS groups were significantly different ($p<0.05$). VEGF expression was higher in UC when compared to IBS cases ($p=0.004$), besides significant difference was found between active UC and IBS group ($p<0.05$). When active and inactive UC groups were compared with IBS cases in terms of endostatin expression difference was found between active UC and IBS ($p=0.005$). Additionally inactive mucosa showed higher endostatin expression when compared to IBS cases ($p = 0.002$).
Conclusion(s) In this study it was shown that serum levels and tissue expression of endostatin and VEGF were increased in UC patients. This result may account why the healing of mucosal injury were detained although the increased serum and tissue VEGF levels.

P1.93

The impact of the pathologist on lymph node retrieval and survival for colorectal cancer

Erdamar S.; Karakas N.; Yamac P.; Baser A.; Kutahyalioglu M.; Atac E.; Aydin A.; Mandel Molinas N.; Dirican A.; Dogusoy G.; Goksel S.
Pathology Department, Medical Faculty, Istanbul University Cerrahpasa, Istanbul, Turkey

Background The aim of this study is to identify how many lymph nodes should be examined to establish the presence or absence of lymph node metastasis, a staging factor, based on cumulative survival rate in colorectal cancer.
Methods Patients ($n=525$) who underwent radical resection for colorectal carcinoma were retrospectively analyzed in Cerrahpasa Medical College, Turkey. The clinical and pathological parameters considered in statistical analysis were age, gender, tumor location, invasion level (IL), grade, the number of examined LN, LN met, LVI, BVI, PNI and tumor size. Patients were divided in 3 groups; I:patients had < 9 ($n=195$); II: had 10–14 ($n=131$) and III:had 15 ($n=199$) LN reported.
Results Mean follow-up time was 78 10.6 months. The mean LN was 13, 8 (1–57) and 225 (43 %) of the patients had LN metastases. BVI had most significant prognostic affect in DFS ($p=0{,}001$); LN met ($p=0{,}007$) and IL ($p=0{,}028$) had highest prognostic affect in OS, in Cox analysis. In Kaplan-Meier analysis, mean ST was lower in group I (45, 44 2, 9) than in both group II (59, 6 5, 8) and III (75 4, 79), ($p=0{,}018$). The patients with 4 or more LN metastasis (36, 1 3, 7) had poor prognosis than for those with 3 LN metastases (40, 6 3, 1) and with no metastases (66, 20 3, 79), ($p<0{,}001$).
Conclusion(s) In CRC, staging accuracy and survival can be improved with increasing nodal examination by pathologists. A standardation of harvesting and reporting in lymph nodes is exteremely necessary.

P1.94

Tissue transglutaminase over-expression in celiac duodenal mucosa is remarkable but not specific for celiac disease

Gorgun J.; Portyanko A.; Kuralenia S.
BelMAPE, Minsk, Belarus

Background Tissue transglutaminase (tTG) constitutes a main autoantigen in celiac disease (CD). The aim of the study was to clarify weather celiac disease is associated with changes in tissue transglutaminase (tTG) expression in duodenal mucosa.
Methods tTG was assessed immunohistohemically (clone CUB 7402) in duodenal biopsy specimens from 22 untreated CD patients (CD), 10 normal controls (NC) with unremarkable duodenal mucosa and 9 pathological nonceliac controls (PC) (acid-related duodenitis, Waldenstrom macroglobulinemia, Crohn's duodenitis, infectious enteritis). In 17 CD patients duodenal biopsy specimens were repeatedly assessed while keeping to gluten-free diet. The Positive Pixel Count Algorithm of ImageScope was used for quantitative evaluation of immunohistochemistry.
Results tTG expression in superficial epithelium differed significantly between three groups ($p=0{,}000$). It was increased in PC in relation to NC ($p<0{,}000$) and in CD – in relation to NC ($p<0{,}000$) and PC ($p=0{,}0025$). In CD and PC, cryptal epithelium stained more intensively than in NC ($p<0{,}000$ and $p=0{,}00$ respectively), but there was no difference between CD and PC ($p = 0{,}506$). The same pattern was seen in lamina propria. Histological improvement after gluten free diet was associated with decreasing of tTG expression.
Conclusion(s) Untreated CD is associated with tTG over-expression in lamina propria and intestinal epithelium, which is reversible. tTG up-regulation does not seem to

be specific for CD and can appear in other pathological conditions. Further investigations are needed to clear up how far an altered expression and distribution of tTG contributes to CD pathogenesis.

P1.95

Undifferentiated carcinoma with osteoclast-like giant cell of the pancreas: histopathological, immunohistochemical, ultrastuctural and molecular biological studies

Murillo R.; Iglesias M.; López L.; Gimeno J.; Torner A.; Blanco P.; Martinez L.; Juanpere N.; Serrano S.
Hospital del Mar, Barcelona, Spain

Background The undifferenciated carcinoma with osteoclast-like cells is a rare neoplasm (less than 1% of the non-endocrine pancreatic tumours). Is composed of multinucleated pleomorphic to mononucleated spindle cells and variable amount of non-tumoral osteoclast-like giant cells. This tumour has a controvert histogenesis.
Methods Describe the entity from the point of view of histopathologic, immunohistochemical, ultrastructural and molecular biological studies. Women of 79 years old with painless jaundice and pruritus. The TC shows a solid lesion in the pancreatic head, without signs of invasion of the duodenum neither the inferior vein cava. A cephalic duodenopancreatectomy is performed.
Results Macroscopically the lesion was bilobulated, of tan surface without cystic component. Histologically showed a population of mononuclear spindle cell, with pleomorphism, nuclear atypia and numerous mitosis figures. Also existed a pleomorphic multinucleated component. We identified a second population of osteoclast-like giant cells, close to hemorragic areas, areas of ischemic necrosis, and osteoid matrix, without nuclear pleomorphism neither mitosis.
Conclusion(s) Immunohistochemically the spindle component express vimentin and p53 and the giant cell CD45 and CD68. We did not find ductal adenocarcinoma. Ultrastructural studies showed presence of scattered desmosomes in the pleomorphic components, a characteristic of epithelial origin. Biological molecular studies found a mutation in KRAS in the tumour component.

P1.96

Value of alpha-smooth muscle actin and glial fibrillary acidic protein in predicting early hepatic fibrosis in chronic hepatitis c virus-infection

Moussa Mohamed M.; Zakaria S.; Yossef M.; Akl M.; El-Ahwany E.; El-Raziky M.; Mostafa O.; Helmy A.; Salama R.; El-Hindawi A.
Theodor Bilharz Research Institute, Cairo, Egypt

Background Alpha-smooth muscle actin (α-SMA)-positive hepatic stellate cells (HSC's) are pericytes responsible for fibrosis in chronic liver injury. The reports concerning glial fibrillary acidic protein (GFAP) expression in human liver are still conflicting. Aim: To investigate the utility of GFAP compared to α-SMA as, an indicator of early activated HSC's, in predicting fibrosis in chronic hepatitis C (CHC) patients.
Methods With immunohistochemistry and a semi-quantitative scoring system, the expressions of α-SMA and GFAP on HSC's in liver biopsies from patients with pure CHC (n=34), hepatitis C virus-induced cirrhosis (n=24), mixed CHC/schistosomiasis (n=11) and normal controls (n= 10) were analyzed.
Results The immuno-reactivity of α-SMA and GFAP in peri-sinusoidal, peri-portal and peri-central areas was assessed. α-SMA and GFAP-positive HSC's were significantly increased in all diseased groups compared with normal controls. In pure CHC with or without cirrhosis, peri-sinusoidal α-SMA-positive HSC's were predominant in relation to GFAP-positive cells. On the other hand, GFAP-positive cells were predominant in the group of schistosomiasis as compared with the other diseased groups. It was noticed that expression of GFAP on peri-sinusoidal HSC's in CHC patients sequentially decreased with the progression of fibrosis.
Conclusion(s) GFAP could represent a useful marker, than α-SMA, of early activation of HSC's in CHC patients and seems to be an early indicator of hepatic fibrogenesis.

P1.97

A case of gastritis cystica profunda associated with an adenocarcinoma developed after partial gastrectomy

Kiroglu K.; Balik E.; Gulluoglu M.; Kapran Y.
Istanbul University Istanbul Medical Faculty Pathology Department, Istanbul, Turkey

Background Gastritis cystica profunda is a relatively rare disorder characterised by hyperplastic and cystic dilatation of gastric glands within the submucosa or muscularis mucosa. Macroscopically it may present as a submucosal tumor or as a polyp. These lesions typically occur in patients with chronic gastritis as local ischemia or mucosal prolapse is critical to the development of cysts.
Methods We report a case of a 63-year-old man who has a subtotal gastrectomy for peptic ulcer disease 40 years ago. Upper gastrointestinal endoscopic biopsy revealed an adenocarcinoma arising on the site of gastrojejunal anastomozis. The patient underwent a total gastrectomy with a Roux-en-Y esophagojejunostomy. Along with the adenocarcinoma which was 0,6 cm in diamater and located at gastrointestinal anastomozis site, there were cystic glands in the submucosa by herniation of surface epitelium, closely resembling the changes seen in colitis cystica profunda.

Results Gastritis cystica profunda may occur several years after previous gastric surgery. It may be associated with a carcinoma.
Conclusion(s) It should be included in the differential diagnosis of submucosal lesions consisted of mostly cystically dilated glands.

P1.98

A giant leiomyoma of oesophagus. A case report

Koumpanaki M.; Nikolaidou A.; Balis Christos G.; Moysidis I.; Anestakis D.; Barbetakis N.; Patakiouta F.
"Theageneion" Cancer Hospital of Thessaloniki, Thessaloniki, Greece

Background Leiomyoma is the most common mesenchymal tumour of the oesophagus. It occurs more frequently in males between the age of 30 and 35. Leiomyomas are usually located in the lower oesophagus as intramural lesions.
Methods We report a case of giant leiomyoma at the proximal oesophagus. A 46 year-old male was complaining of cervical spine and right shoulder pain. The MRI revealed a large soft tissue mass at the upper third of oesophagus, which was surrounding in a horse-shoe manner its external wall. The endoscopic assessment revealed a mass that was pressing the oesophageal wall from the outside leaving the mucosa unaffected. Surprisingly, despite its enormous size, the tumour presented no gastrointestinal symptoms.
Results The mass was surgically removed and we received an ovoid, well-circumscribed tumour, 12, 5 cm in maximal diameter, with a whitish, fascicular cut. Microscopically the tumour composed of bland spindle cells and showed low to moderate cellularity. Mitotic figures were rare. Immunohistochemically, the neoplastic cells were strongly stained for SMA, Desmin, Caldesmon and were negative for S-100, CD34 and CD117/c-kit.
Conclusion(s) Leiomyomas vary in size from a few millimeters up to 10 cm in diameter (average 2–3 cm). The majority of these neoplasms are detected incidentally during investigation of dysphagia. Tumours smaller than 5 cm are usually asymptomatic. Large tumours can also cause retrosternal discomfort, chest pain, oesophageal obstruction or regurgitation and have a slight potential for malignant tranformation.

P1.99

A rare etiology of adult intussusception: multilple granular cell tumor of gastro intestinal tract

Hicham A.; Hamdaoui R.; Hakkou M.; Benhami B.; Idrissi Dafali A.; Krati K.; Louzi A.; Belkhayat R.
Marrakech, Morocco

Background Granular cell tumors (GCT) are infrequently found in the gastrointestinal tract (GIT), and rare cases report lesions occurring simultaneously in different sites. We report a morrocan case of simultaneous ileal and coecal GCT revealed by ileocolic intussusception.
Methods A 31-year-old man was admitted to the emergency department for severe colicky pain that began 24 h prior to admission and gradually extended to the abdomen, followed by bilious vomiting and subsequent hematemesis. He had no surgical history. Abdominal CT demonstrated intestinal loops extending into the colic lumen, with thickened valvulae conniventes, and presence of minimal contrast material and air at the intestinal loops. The patient was operated and a loop appeared congested and ischemic when disclosed. An ileocolic resection was made. A the macroscopic exam, two tumors were found. The first tumor in the colonic segment and the second in the ileal part. All GCT appeared histologically benign and there was no sign of malignancy. all tumor diffusely expressed the protein S-100.
Results A the macroscopic exam, two tumors were found. The first tumor in the colonic segment and the second in the ileal part. All GCT appeared histologically benign and there was no sign of malignancy. All tumor diffusely expressed the protein S-100.
Conclusion(s) Multiple granular cell tumor is a rare cause of adult intussusception.

P1.100

An immunohistochemical study of different histological types of colon adenomas

Pap Z.; Pávai Z.; Dénes L.; Mezei T.; Kovalszky I.; Jung J.
University of Medicine and Pharmacy Targu Mures, Mures, Romania

Background Most colorectal cancers arise from adenomas through different carcinogenetic pathways. The aim of this study was to compare the immunoexpression of several proteins coded by oncogenes and tumor suppressor genes to E-cadherin, syndecan-1, Ets-1, and MMP7 immunoexpression (determined in our previous studies), to investigate their possible role in the adenoma-carcinoma sequence.
Methods We studied formalin- fixed paraffin- embedded tissue sections from 34 cases of colon adenomas: 3 hyperplastic polyps (HP), 5 serrated (SA), 8 tubular (TA), 18 tubulovillous adenomas (TVA) and from 4 cases of adenomas with intramucosal carcinomas (AC). Immunohistochemistry was performed using antibodies to p53, Bcl-2, Ki-67, APC, MSH2. Distribution of positivity was assessed using percentage expression, and the obtained values were used in establishment of an immunohistochemical grading system (scores 0–2).

Results The number of cases with p53, Bcl-2, Ki-67 overexpression increased from HPP, SA, TA to TVA. We observed decreased MSH2 expression in all cases of HPP and SA, and decreased APC expression in a third of SA and TVA cases. We found a significant association between the grade of dysplasia and p53, and APC expression respectively, and also between histological type and p53, Bcl-2, KI-67, MSH2 expression respectively. p53, Ki67 expression correlated positively with Ets1, MMP7 expression and negatively with E-cadherin, syndecan-1 expression.
Conclusion(s) Compared to classic adenomas HPP and SA represent a different immunophenotype.

P1.101
Analysis of ezrin and Moesin expression using automated cellular imaging system (ACIS) in esophageal squamous cell carcinoma

Sato-Kuwabara Y.; Kagohara Tsukamoto L.; Silva M.E.; Ayala Rocha Roja F.; Soares A.F.
Hospital AC Camargo - Dept Anatomic Pathology, São Paulo, Brazil

Background Esophageal squamous cell carcinoma (ESCC) is the sixth most frequent neoplasia in Brazil and it is associated to poor prognosis. The Ezrin-Radixin-Moesin family of actin-binding proteins is membrane-cytoskeleton linkers involved in signaling pathway acting as signal transducers. We aimed to verify the Ezrin and Moesin expression and to correlate with clinicopathological findings.
Methods Immunohistochemistry of 199 ESCC cases were carried out using Tissue Microarray technique. Analyses were performed using the Automated Cellular Imaging System - ACIS (DAKO), considering the cytoplasmic staining pattern. Cases were classified in four categories based on the percentiles of the intensity score (IS) values from ACIS analysis: Negative (IS < 25th), Weak (25th ≤ IS < 50th), Intermediate (50th ≤ IS < 75th) and Strong Positive (IS ≥ 75th).
Results This study showed no expression of Ezrin in 24.6% cases. Positive cases were divided in 25.1% Weak, 24.6% Intermediate and 25.7% Strong Positive. A significant association was found between Ezrin expression and venous invasion (p=0.011). Ezrin expression did not influence overall survival (p=0.405). Moesin expression was considered Weak Positive in 24.1%, Intermediate Positive in 25.1%, Strong Positive in 25.1% and Negative in 24.1% cases. Significant association was found between Moesin expression and histological grade (p=0.040). Moesin expression absence was significantly associated to poor survival rates (p=0.028).
Conclusion(s) Further studies are necessary to understand the role of Ezrin expression in ESCC prognosis. Our findings strongly suggest that absence of Moesin expression may be an indicator of ESCC prognosis.

P1.102
CD5 expression in benign and malignant pancreaticobiliary epithelia

Rowsell H.C.; Wong Wang-Ngai J.
University of Toronto, Toronto, ON, Canada

Background CD5 is a commonly used marker of normal T cells and certain B cell lymphomas. In our practice, we have noted strong cytoplasmic staining of biliary type epithelia. The purpose of our study is to investigate the amount and intensity of CD5 expression in benign and malignant pancreaticobiliary epithelia.
Methods We retrieved the following cases from the archives at Sunnybrook Health Sciences Centre: 16 cases of non-neoplastic gallbladder, 13 cases of carcinoma of the gallbladder or extrahepatic bile ducts, and 15 cases of pancreatic ductal adenocarcinoma. Sections of formalin-fixed, paraffin-embedded tissue were stained with an anti-CD5 antibody (4C7) and the percentage of cells staining and intensity were assessed by two pathologists.
Results All of the slides of benign gallbladder mucosa as well as benign pancreatic ductal epithelium showed strong, diffuse cytoplasmic staining for CD5 (Allred score 5, intensity 3+). Of the pancreatic adenocarcinomas, 11 out of 15 showed loss of intensity of staining and/or decreased percentage of positive cells compared to normal controls.5 out of 13 extrahepatic bile duct/gallbladder carcinomas showed diminished staining.
Conclusion(s) CD5 expression is seen in both benign and malignant pancreaticobiliary epithelia. Future studies are needed to determine if the loss of staining seen in malignant tumors can be exploited to help differentiate well-differentiated adenocarcinomas from reactive lesions such as pancreatitis or bile duct proliferations related to obstruction/stenting.

P1.103
Characterization of CD10-positive colorectal cancer in relation to P53 and P21 expression

Seada Salah L.
Benha University, Cairo, Egypt

Background Recent studies have shown that CD10-positive colorectal carcinomas have a high risk of giving rise to liver metastases. The aim of the present study is to examine CD10 expression in a group of colorectal patients in Egypt, in relation to expression of p21, p53 and clinicopathological parameters.

Methods We examined 40 cases of colorectal cancer and immunostained for CD10, p53 and p21 using the standard Streptavidin Biotin Peroxidase Method, and DAB chromogen. All clinicopathological parameters were recorded correlated statistically.
Results In the present study male to female ratio was 1:1. Site of lesion was colonic in 26 cases and rectal in 14 cases. Mean age for males and females was 42.3 and 50.2 respectively. Lymph node metastases were found in 35% and liver metastases in 5% of cases. CD10-positive tumors comprised 50% of our series. In 10 cases LN metastases were present and 2 cases had liver metastases. CD10 expression positively correlated with positive safety margin (p=0.004), and negatively with 53 expression (p = 0.008) but not with grade or stage. P21 was expressed in 65% of cases and positively correlated with female gender and with p53 expression (p = 0.05 and p = 0.047, respectively).
Conclusion(s) CD10 expression defines a subset of colorectal cancer with an apparent aggressive behavior, which suggests that early cancerous growth of colon expressing CD10 should not be overlooked which might detect aggressive cancers at an earlier stage.

P1.104
CK20 positive large cell neuroendocrine carcinoma of transverse colon: a case report and review of the literature

Anagnostou E.; Venizelos I.; Nikolaidou C.; Spandos V.; Papathomas T.
Hippokration, Thessaloniki, Greece

Background Large cell neuroendocrine carcinomas (LCNECs) are rare, poorly differentiated neoplasms, characterized by unfavourable prognosis. Immunohistochemistry plays a crucial role in the establishment of diagnosis, since these carcinomas display positivity in neuroendocrine markers and CK7, whereas they are negative for CK20.
Methods We report a case of a 70-year-old man, who was admitted with anorexia, weight loss and abdominal discomfort. The patient underwent colonoscopy, which revealed the presence of an exophytic mass, measuring 4.7 cm in greatest diameter.
Results Histopathologic analysis showed that the neoplastic cells were large and exhibited a significant degree of atypia. Immunohistochemical examination showed positivity for AE1/AE3 and chromogranin and negativity for synaptophysin and EMA. The morphological and immunohistochemical data were consistent with a LCNEC. Later on, the patient underwent a right hemicolectomy. The histological characteristics of the neoplasm were identical with those of the biopsy. An additional immunohistochemical examination showed that the neoplastic cells were positive for cytokeratin 20 and negative for cytokeratin 7. Postoperative combination chemotherapy was introduced and the patient is well 7 months after the diagnosis was made.
Conclusion(s) To the best of our knowledge there is a single reported case of a CK20-positive, CK7- negative colorectal LCNEC. We present an additional case of this unusual immunophenotype of a LCNEC located in the transverse colon.

P1.105
Clinicopathological characteristics and pattern of hMLH1, hMSH2 and hmsh6 expressions in 299 colorectal carcinomas in a cohort of multiethnic patients in Malaysia

Khoo J.; Gunn A.; Peh S.
Monash University, Johor Baru, Johor, Malaysia

Background To evaluate the prevalence of microsatellite instability in a cohort of multiethnic patients in Malaysia and to correlate to their clinicopathological characteristics.
Methods We reviewed the pathology of 299 consecutive colorectal carcinoma (CRC) specimens for their histological grade, mucinous production, lymphocytic response, presence of necrosis and growth pattern. The analysis of microsatellite status was determined by immunohistochemical staining patterns of hMLH1, hMSH2 and hMSH6.
Results In this study, there was a preponderance of male to female patients (1.3:1) with a multiethnic spectrum of Malays, Chinese and Indians. The age of patients ranged from 27 to 91 years with the mean of 59.9 years. There was an overall predominant left sided lesion (205/299, 68.6%). Microsatellite instability (MSI) was found in 42 of 299 patients (14.0%). Single hMLH1 loss was seen in majority of cases (59.5%) followed by hMSH6 (14.3%) and hMSH2 (4.8%). Nine cases (21.4%) had a combination of protein loss. MSI sporadic CRC were significantly localised to the right side (p=0.001) associated with poor differentiation (p<0.001); have presence of marked necrosis (p=0.005) and patients gave history of previous or synchronous malignancy (p = 0.026). There was no significant correlation with sex, age, stage, growth pattern or host response.
Conclusion(s) 14.0% of patients with sporadic colorectal carcinomas in the multiethnic cohort in Malaysia were found to have microsatellite instability. These tumours had distinct clinical, pathologic and biological features.

P1.106
Collagenase participation in collagen degradation during the recovery from experimental hepatic fibrosis

Rivneac V.; Rivneac E.; Pretula R.
State Medical and Pharmaceutical University "Nicolae Testemitanu", Chisinau, Republic of Moldova

Background Collagenase is the most important metalloproteinase, indispensable for collagen degradation.
Methods Collagenase activity was determined biochemically in normal, CCl4-induced fibrotic rat liver and at 7, 14, 21, 30, 45, 60 days after discontinuation of treatment. The activity of collagenase in normal and fibrotic rat liver at the 7th and 30th days after CCl4 abolition was investigated electron-histochemically. Z-Pro-Ala-Gly-Pro-4MBNA ("BACHEM") served as the substratum.
Results In liver cirrhosis a decrease of collagenase activity with 21% in comparison with normal liver was revealed. Activity remained reduced during the whole period after CCl4-treatment cessation with maximums at the 7th and 30th days, when the level of collagenase activity was close to control. Electron-histochemically was determined that in normal rat liver active collagenase is localized in Kuppfer cell and endoteliocyte lysosomes, and also extracellularly in very little quantity on hepatocytes microvillus. In fibrotic rat liver at the 7th and 30th days after CCl4 abolition reaction product was revealed mainly extracellularly on hepatocyte, macrophage and fibroblast cytolemma and on adjacent collagen fibrils.
Conclusion(s) The results suggest that during the recovery from hepatic fibrosis the active collagenase is located mainly extracellularly. There are two periods of augmentation of collagenolytical activity in liver – at the 7th and 30th days after discontinuation of CCl4-treatment. It means that the initiation of collagen degradation in liver takes place at least twice – probably, in dependence on the quantity and activity of different liver cell types.

P1.107
Collision tumor of the stomach - adenocarcinoma and neuroendocrine carcinoma. Case report and review of the literature

Mroz A.; Kiedrowski M.; Malinowska M.; Sopylo R.
Medical Center for Postgraduate Education, Maria Sklodowska-Curie Memorial Cancer Center and Institute of Oncology, Warsaw, Poland

Background Adenocarcinoma is the most common malignant neoplasm of the stomach. It is not unusual to find neuroendocrine differentiation within typical glandular histology. In the cases when 2 types of tissue is intermingled within the same tumor, the term "composite" is used, while when 2 elements are adjacent to one another without intermixing the term "collision" is generally accepted. Recently Fujiyoshi et al. reclassified the mixed endocrine and nonendocrine epithelial tumors into six categories, concerning histological patterns.
Methods We report a rare case of gastric collision tumor composed of poorly differentiated adenocarcinoma and neuroendocrine carcinoma in a 56 year old Caucasian male. The tumor was located in the gastric body and, to our knowledge, it is the tenth case described in the literature and the first in Poland.
Results Adenocarcinoma component constituted 20% of the lesion and was in more advanced stage than the neuroendocrine. Additionally adenocarcinoma was the only to metastasize to regional lymph nodes and the liver.
Conclusion(s) Detailed classifications of composite/collision tumors including their subtypes seems to be too complicated and do not point out the dualistic nature of such tumors. That's why we suggest simplifying the issue by turning back to the previously advocated binomial classification. Every case with any degree of intermixing adenocarcinoma and neuroendocrine carcinoma pattern should be designated "mixed" or "composite" tumor as synonyms while two separate sharply delineated compounds regarded as "collision" tumor.

P1.108
Collision tumor of the stomach: a case report

Unal B.; Elpek Ozlem G.; Gelen T.; Gurkan A.; Yildirim B.
Departments of Pathology, General Surgery and Internal Medicine, Akdeniz University, Antalya, Turkey

Background Collision tumor is characterized by the presence of two localized tissue types adjacently together. Gastric collision tumor composed of epithelial and non-epithelial malignant neoplasm has been rarely reported in the literature. However coexistence of adenocarcinoma and carcinoid tumor is extremely rare. Herein is described a case with features of adenocarcinoma colliding with a typical carcinoid component.
Methods Case report.
Results The patient was a 51 year-old women, suffering from epigastric pain. On endoscopic examination, an ulcerated polypoid mass was noted at the cardia of the stomach. Subsequently patient underwent a total gastrectomy. The specimen showed an ulcerated mass measuring 2, 5 x 1, 5 x 2 cm. The cut surface showed a yellowish white tumor surrounding area of the ulcer. On microscopy the tumor showed 2 different types of tissue. One was well differentiated adenocarcinoma. The other component was composed of smaller tumor cells, that express synaptophysin, chromogranin A and NSE. There was no intermixing or transition area between the 2 components. The tumor was diagnosed as a collision tumor composed of adenocarcinoma and carcinoid tumor of the stomach.
Conclusion(s) Although the presence of adenocarcinoma or carcinoid tumor individually is not notable, this collision tumor is only the eighth such case in the literature. We suggest that as more as cases are reported, the clinicopath-

ological properties, the pathogenesis of this entity will be shown in more details.

P1.109

Colonic collision tumour: an unusual presentation

Menezes Soares N.; Andrade Vianna C.; Carvalho Cristina Gouvêa A.; Gaglionone Cavalcante N.; Pires Rodrigues Cordovil A.; Lopes Gloria Silami V.; Dias Pedra E.
Hospital Universitario Antonio Pedro, Niterói, Brazil

Background Colorectal cancer is one of the most common gastrointestinal malignancies. Lymphoma is relatively uncommon. Adenocarcinoma and lymphoma together in intestinal tract are more unusual. We report a unique case to our knowledge of a collision tumour of the colon.
Methods A 73 years old man, asymptomatic, was submitted to a CT scan revealing colonic tumour without lymphadenomegaly. Colonoscopy and biopsy were performed and the analysis of H&E routine sections and immunohistochemistry led the patient to a partial colectomy and a follow up in Hematology Division and bone marrow biopsy. One month later he presented ileal obstruction. Part of his small bowel was resected and analyzed.
Results The biopsy diagnosed Adenocarcinoma. Grossly, the tumour was ulcerative/infiltrating, located in the splenic flexure and microscopically had two patterns of tissue proliferation (malignant glandular structures with moderate pleomorphism and diffusely infiltrative large cells). The second resembled Lymphoma or Undifferentiated Tumour. Immunohistochemistry was performed. The diffuse component was negative for keratin, positive for CD 45 and CD20. The final diagnosis was Moderately Differentiated Adenocarcinoma and Diffuse Large B-Cell Lymphoma. The diagnosis of the ileum was Diffuse Large B-Cell Lymphoma. The bone marrow biopsy was not infiltrated.
Conclusion(s) The careful examination of routine sections and appropriate immunohistochemistry provided precise diagnosis. The awareness of the existence of collision tumours led us to suspect of it. Further information and complementary methods were important to confirm such rare clinical entity. Thus, it must be emphasized because proper therapeutical approach is only possible with precise diagnosis.

P1.110

Colorectal signetring cell carcinoma with focus on phenotypic diversity of "signetring cells"

Gjerdrum L.; Jensen H.; Engel U.; Mogensen Mellon A.; Holck S.
Department of Pathology, Hvidovre Hospital, Hvidovre, Denmark

Background The term SRCC generally refers to carcinoma predominated by signetring cells (SRC), overruling any amount of extracellular mucin, the cut-off level being defined as 50%. Here we test the reproducibility of the existing definition of SRCC arising in colorectal cancers (CRC).
Methods 27 cases of CRC coded as SRCC from 1982 through 2007, were drawn from the files of the Department of Pathology, Hvidovre Hospital. Slides were circulated among four observers, who semiquantitatively graded the proportion of SRC (none-50 % vs. >50 %). Kappa statistic was applied.
Results The percentage of the study cases considered SRCC, ranged from 33.3–85.2% among observers, kappa value=0.217. Unanimous agreement was achieved in 9 of the cases; majority agreement was obtained in 18 cases.
Conclusion(s) A diagnosis of SRCC can easily be established when cytological features are classic and diffusely distributed. However, borderline cases do exist. In our study, the perception of the cytology of SRC varied, some using a strict, others a more relaxed definition, referring to the description of classical SRC as well as SRC with a deviating morphology. Such variants have been described as anaplastic, but are generally not commented on in relation to the formulation of the definition of SRCC. This widely different threshold for issuing a diagnosis of SRCC has no known impact on prognosis/ patient management. Nevertheless, detailed guidelines as to minimal cytologic criteria required, specifically addressing whether variants of SRC be included, seems, from an academic viewpoint, warranted.

P1.111

Common variable immunodeficiency syndrome mimicking familial adenomatous polyposis in gastrointestinal endoscopy (case report)

Molaei S.; Molaei M.; Mashayekhi R.; Pejhan S.; Zali M.
Research Center for Gastroenterology and Liver Disease, Tehran, Islamic Republic of Iran

Background Common variable immunodeficiency syndrome (CVID) includes a heterogeneous disorder characterized by reduced levels of IgG, IgA or IgM, recurrent bacterial infections with normal T-cell immunity (in 60% patients). It is the second most prevalent primary immunodeficiency disorder but the most common form of severe antibody deficiency (selective IgA deficiency is more common). It causes a wide spectrum of symptoms and signs affecting many systems of the body. The gastrointestinal tract is the largest immune organ in the body, and it is therefore expected that this immunodeficiency will affect it in some way.

Methods We present a case of nodular lymphoid hyperplasia (NLH) of the small intestine in a 31 year old man admitted for evaluation of chronic diarrhea. Endoscopy and colonoscopy revealed multiple polyps in duodenum, ileum and large intestine in favor of FAP (familial adenomatous polyposis).
Results Microscopic findings were compatible with lymphoid follicular hyperplasia and although he had no history of recurrent infection, except for frequent episodes of diarrhea from childhood, immunological profiles were in favor of CVID.
Conclusion(s) CVID should be considered in any patient with gastrointestinal manifestations especially chronic diarrhea even if not in association with recurrent bacterial infections of other organs. Diagnostic delay results in more morbidity and complications in untreated patients.

P1.112

Does sentinel lymph node in colon carcinoma improve staging accuracy? A comparative immunohistochemical and pathological RT-PCR analysis of nodal upstaging in patients with stage I-II colorectal cancer?

Cuatrecasas M.; Landolfi S.; Espin E.; Tabernero J.
Hospital Clinic, Barcelona, Spain

Background Lymph node metastasis is the most important prognostic factor and a predictor of reccurence and survival in colon cancer (CC). Lymph node analysis on hematoxylin-eosin (HE) stains is the standard method for nodal status (pN) in CC, however its sesitivity can be improved. Objectives: To identify the differences in lymph node staging between standard HE and cytokeratin immunohistochemistry (IHC) stains, using sentinel lymph node analysis in stage I-II CC patients.
Methods A prospective study was done in 70 cases, and a retrospective study of 72 cases of CC in stages I-II (pT1/pT2 N0). Identification of sentinel and other regional lymph nodes was performed in the prospective cases during surgery with blue ink. In the retrospective group all lymph nodes were evalutated. HE and cytokeratin AE1/AE3 were performed. Rectal carcinomas were excluded.
Results Most cases were negative and the pathological stage was not modified. In 8/70 (12%) cases with sentinel lymph node, and in 7/72 (8%) cases from the retrospective group with no sentinel lymph node, CK AE1/AE3 resulted positive in isolated or small grouped tumoral cells (micrometastases), not detected with HE. These patients should be re-staged as pN1 (micrometastases, IHC).
Conclusion(s) The lymph node methodology for micrometastases detection is capable of re-staging from pN0 to pN1 up to 12% of CC patients. These patients could get benefit from chemotherapy and improved survival rates.

P1.113

DOG-1 AND D2–40 in GISTs diagnosis

Enache S.; Stoicea M.; Georgescu A.; Terzea D.; Arsene D.; Mihai M.; Iosif C.; Andrei F.; Enache V.; Cionca F.; Ardeleanu C.
I. N. C. D. "V. Babes" Bucharest, Bucharest, Romania

Background Gastrointestinal stromal tumors (GISTs) are the most common mesenchymal tumors of the gastrointestinal tract, originating in the interstitial cells of Cajal or their precursors, typically expressing c-kit (CD117). In c-kit negative GISTs, additional markers are required for diagnostic accuracy. DOG-1 is a relatively new biomarker for GISTs. D2–40 is a selective marker for lymphatic endothelium and a possible biomarker for GISTs. Our study assessed the contribution of DOG-1 and D2–40 in GISTs diagnosis.
Methods A retrospective study was performed on formalin fixed, paraffin embedded samples from 20 cases of confirmed GISTs. Immunohistochemical expression of CD117, CD34, DOG-1 and D2–40 was evaluated using the EnVision system.
Results Spindle cell GISTs were encountered in 60% of cases, epithelioid cell GISTs in 30% and mixed pattern in 10%. CD117 was positive in 80% of GISTs, CD34 in 85% of tumors. DOG-1 was positive in 80% of GISTs, while D2–40 was positive in 75 % of tumors, more frequently in the spindle cell type (60%); D2–40 was also observed on intra and peritumoral microvessels, with an average of 21 microvessels/HPF, in 60% of GISTs. Within 4 CD117 negative GISTs, DOG-1 was positive in 3 cases and D2–40 in 2 cases, while both DOG-1 and D2–40 were expressed in 2 c-kit negative GISTs. A direct correlation between CD34 and D2–40 was noted ($p=0.04$).
Conclusion(s) Our study confirms DOG-1 and D2–40 as sensitive markers in the diagnosis of GISTs; they could constitute an immunohistochemical alternative in the diagnosis of c-kit negative GISTs.

P1.114

A treatment-resistans intestinal spiroketosis case for a chield

Arslan Hacer E.; Erdamar S.; Dervisoglu S.; Ozden S.; Tekand G.; Goksel S.
Cerrahpaşa University, Istanbul, Turkey

Seven year old boy admitted Cerrahpasa Medical College with rectal bleeding two years ago. In his colonoscopy there were mucosal ulserations and pseudopolyps in rectum. Histopathological examination revealed that there were spirochets at luminal surface of colonic epithelium. After diagnosis of spirochetosis which was confirmed with

Warthin-Starry and PAS staining, the patient was searched for any possible associated clinical entity. In clinical history, it's found that he had arthritis but he did not take steroid therapy. It's found also hepatosplenomegaly and mild anemia. Serological markers related with rheumatology were normal. After treatment with metronidasole for 2 months he went back to his home and he did not have any problem with bleeding during two years. Two months ago, he applied same institute with rectal bleeding again. Although his colonoscopy was normal, several biopsy were taken from different level of colon. This second histopathological examination showed that marked spirochetosis in colonic mucosa, more than the previous time. The reason we present this cases that pathologist have to aware of spirochetosis can be seen in even normal looking colonic mucosa and should inform and collaborate clinician in terms of etiology and treatment.

P1.115

EGFR and ERCC1 expression by immunohistochemistry and fluorescence in situ hybridization in resected colorectal adenocarcinoma

Kim J.; Bae B.; Shin E.; Kim H.; Park K.
Inje University Sanggye Paik Hospital, Seoul, Republic of Korea

Background Mutations of epidermal growth factor receptor (EGFR) and expression of excision repair cross-complementation group 1 (ERCC1) are related to the responsiveness to tyrosine kinase inhibitors and platinum agents. This study was performed to determine whether EGFR and ERCC1 expression are related to the prognosis of colorectal adenocarcinoma and whether EGFR and ERCC1 expressions are inter-related.
Methods We used immunohistochemistry (IHC) and fluorescence in situ hybridization (FISH) to evaluate EGFR and ERCC1 protein expression and EGFR amplification in tissue microarray of colorectal adenocarinoma from 235 patients.
Results EGFR and ERCC1 expressions are detected in tumors from 12 patients (5.1%) and 19 patients (8.1%), respectively. EGFR expressions are associated with angioinvasion ($p<0.05$) and lymph node metastasis ($p<0.05$). Patients with EGFR expression showed a tendency of shorter survival than EGFR non-expression group. EGFR amplification was noted in 25 tumors (25/183, 13.7%), but it was not related with EGFR protein expression. ERCC1 expression was not associated with EGFR protein expression or amplification.
Conclusion(s) Although EGFR amplification is not required for EGFR protein expression and the latter may have prognostic significance in resected colorectal adenocarcinoma. ERCC1 may have a minor role in colorectal adenocarinoma.

P1.116

Evaluating relationships of beta-catenin with TGF-beta1, HIF-1alpha, Ki-67 and patients' survival in human colorectal cancer

Wincewicz A.; Sulkowska M.; Koda M.; Sulkowski S.; Kanczuga Koda L.
Medical University of Bialystok, Bialystok, Poland

Background Beta catenin is well known because of its stimulatory impact on proliferation of colon epithelium. Beta-catenin accumulation is blocked by TGF-beta1 (transforming growth factor beta1) in intestinal mucosa. Moreover, beta-catenin co-operates with HIF-1alpha (hypoxia-inducible factor-1alpha) at the promoter region of HIF-1 target genes. The purpose of our work was to compare beta-catenin with expressions of HIF-1alpha, TGF-beta1, Ki67 and survival of colorectal cancer patients.
Methods 72 human, primary colorectal cancers were investigated with a complete panel of immunohistochemistry for beta-catenin, TGF-beta1, HIF-1alpha and Ki67.
Results Beta-catenin, TGF-beta1 and HIF-1alpha were accumulated in colorectal cancer cells. Expression of beta-catenin significantly associated with HIF-1alpha and TGF-beta1 as well in all colorectal cancers ($p<0.009$, $r=0.307$ and $p=0.003$, $r=0.342$, respectively). There were similar positive correlations among studied factors in selected subgroups of different clinical features and pathological characteristics. Beta-catenin failed to link with Ki67 in studied colorectal cancers. Patients' survival was not significantly associated with expression of beta-catenin, too.
Conclusion(s) Beta-catenin expression can not still be recognized as a prognostic factor in colorectal cancers due to lack of a statistically significant linkage between beta-catenin and patients' survival. Positive correlations between beta-catenin and TGF-beta1 may reflect ineffective influences of TGF-beta1 to decrease intracellular level of beta-catenin in colorectal cancer. Associations between beta-catenin and HIF-1alpha confirm previously detected interactions between HIF-1alpha with beta-catenin in cancer cell lines and our results support an idea for presence of such relationships in human colorectal cancer primary tumors.

P1.117

Evaluation of microsatellite instability and mismatch repair proteins analysis in patients with suspect of lynch syndrome in a Brazilian population

Oliveira Petrolini L.; Santos Maria Monteiro E.; Martins Oyama Mascarenhas Fonseca M.; Rossi Mauro B.; Coudry Almeida R.
Hospital AC Camargo, Sao Paulo, Brazil

Background The Lynch syndrome represents about 4% of colorectal cancer, thus, is very important to identify clinic and molecularly these families. The techniques are expensive and laborious; therefore, it is important to have screening methods with better cost-benefit relation.
Methods We aimed to identify patients with defect in DNA mismatch repair (MMR) system, using microsatellite instability evaluation (MSI-panel of 10 markers) and immunohistochemistry for the proteins MLH1, MSH2, MSH6 and PMS2. The individuals were selected according to the clinical criteria (Amsterdam I/II or Bethesda).
Results Immunohistochemistry were carried out in 95 non-related individuals. Analysis showed 7.4% loss of expression of MLH1/PMS2, 15.8% of MSH2/MSH6 and 8.5% of one isolated protein. For MSI analysis, 26/95 frozen samples were selected: 53.85% were classified as MSS, 38.46% as MSI-H and 7.69% as MSI-L. The results were correlated with clinical-pathological data and family history. Right-side tumors and mucinous component presented correlation with loss of MMR expression. All cases that demonstrated MSI-H also showed alteration in the protein expression and MSI-L and MSS samples had none.
Conclusion(s) Immunohistochemistry technique in primary colorectal tumor is an appropriate method to identify individuals with defect in MMR system and may be used as a screening methodology to identify patients with Lynch syndrome in developing countries. The identification of mutation in MMR genes using direct sequencing is essential for the care and surveillance of patients and enables predictive testing of the family members.

P1.118

Expression and clinicopathological significance of MMP-2 and its specific inhibitor TIMP-2 in gastric cancer

Halon A.; Halon L.; Donizy P.; Rudno Rudzinska J.; Kielan W.; Zolnierek A.; Matkowski R.; Rabczynski J.
Department of Patomorphology, Wroclaw Medical University, Wroclaw, Poland

Background Matrix metalloproteinase 2 (MMP-2) can degrade type IV collagen of extracellular matrices and basal membranes. Tissue inhibitors of metalloproteinases (TIMPs) maintain connective tissue integrity by modulating MMP activity. MMPs and TIMPs are strongly implicated in tumour invasion and metastasis.
Methods Formalin-fixed paraffin-embedded tissue sections from 82 gastric adenocarcinomas were immunostained using monoclonal antibodies against MMP2 and TIMP2. Immunoreactivity of two compartments (neoplastic/epithelial tissue and tumour stroma) was semiquantitatively scored based on stain intensity and percentage of reactive tissue according to Remmele Immunoreactive Score. Results were correlated with tumour grade, Lauren classification, microscopical features (ulceration and lymphocytic infiltration), pathologic stage, lymph nodes status, distant metastases and overall cancer specific survival (OS).
Results 78 of 82 (95.1%) and 40/82 (48.8%) gastric cancers expressed MMP-2 and TIMP-2, respectively. Expression of both markers in tumor stroma correlated significantly with tumor type based on Lauren classifications: higher expression was associated with intestinal tumour type. High epithelial MMP-2 immunoreactivity was significantly associated with better survival. TIMP-2 showed no association with survival in gastric cancer, but higher intensity of TIMP-2 staining in tumor cells correlated significantly with presence of distant metastases.
Conclusion(s) Our results show that high epithelial MMP-2 expression in gastric cancer is associated with better survival and high epithelial expression of TIMP-2 with metastatic disease. Aggressive diffuse histological forms of gastric cancer are associated with low MMP-2 and TIMP-2 expression in tumour stroma.

P1.119

Expression of beta catenin and E cadherin in colorectal adenocarcinomas

Khiari M.; Chaar I.; Ben Mahmoud L.; Khalfallah T.; Mzabi S.; Bouraoui S.
Mongi Slim, Tunis, Tunisia

Background The E-cadherin-catenin complex plays a crucial role in epithelial cell-cell adhesion and in the maintenance of tissue architecture. Perturbation in the expression or function of this complex results in loss of intercellular adhesion, with possible consequent cell transformation and tumour progression, particulary in colorectal adenocarcinomas.
Methods We studied the expression of beta catenin and E-cadherin in a set of 107 colorectal adenocarcinomas by using immunohistochemistry (IHC).
Results Normal colorectal mucosa showed basolateral and apical membrane staining for the E-cadherin and membrane and cytoplasmic staining for beta catenin. Most colorectal adenocarcinomas showed heterogeneous staining with variable degrees of both membrane and cytoplasmic staining for both protein. In fact, we observed strong membranous satining in most cells in a well differentiated tumours for E-cadherin. For beta catenin, it's the same besides the cytoplasmic immunostaining. We noted an important decrease of expression of both beta catenin and E-cadherin with less differentiated tumours. Moreover, our results showed that 23, 65% of colorectal carcinomas were positive for nuclear staining of beta catenin, especially

when we have metastasis. Absent beta catenin expression was found in 14 (13, 08 %) of 107 colorectal cancers. It's almost the same for the E-cadherin that is absent in 18 cases (16, 82%). The loss of the integrity of this complex is also observed in mucinous carcinomas, especially at the apical membrane.

Conclusion(s) Our results suggests that the loss of the E-cadherin-catenin complex may be involved in tumour progression.

P1.120

Expression of epithelial markers in gastrointestinal stromal tumours (GIST). A potentially serious diagnostic pitfall

Sing Y.; Ramdial K.P.; Meyiwa S.P.; Pillay N.
Nelson R Mandela School of Medicine, Durban, KwaZulu Natal, South Africa

Background GISTs are the commonest mesenchymal neoplasms of the digestive tract. Use of Gleevec has magnified the importance of accurate histopathological diagnosis. Although most GISTs are identified with ease, diagnostic problems may arise in cases presenting at metastatic sites when limited material is available and in cases exhibiting atypical morphological features. We undertook this study to establish the frequency of cytokeratin (CK) expression in GISTs and to correlate this finding with various parameters.

Methods 43 GISTs were stained for AE1-AE3, MNF116 and CAM 5.2. Cases were scored as "negative", "rare" (< 5%), "1+" (6 - 25%), "2+" (26 – 50%), "3+" (> 50%). Cases were re-appraised for a variety of histopathological and clinical parameters including site and overall risk.

Results Male predominance (M=25 and F=18), mean age of 55.4 (range 10–90 years). Sites: oesophagus=1, stomach=18, small bowel=9, rectum=2, extragastrointestinal=6 and metastatic=7.6 of 43 cases (13.95%) demonstrated CK immunopositivity. All 6 were high risk for malignancy. 3 were gastric, the remaining 3 were metastatic.

Conclusion(s) Although rare (13.95%), GISTs may express CK immunomarkers. Dot-like perinuclear accentuaton, coupled with epithelioid morphology, may lead to an erroneous diagnosis of a neuroendocrine carcinoma. Conversely, CD117 positivity has been documented in carcinosarcomas. In this setting, genetic analysis may have a key diagnostic role in preventing misdiagnosis. Caution is advised in the interpretation of CK positive tumours of the gut or their secondaries particularly when faced with limited material.

P1.121

Expression of estrogen and progesterone receptors in well-differentiated neuroendocrine tumors of the gastrointestinal tract

Rowsell H. C.; Kahn J. H.
University of Toronto, Toronto, ON, Canada

Background Expression of estrogen and progesterone receptors has been previously described in pancreatic endocrine tumors and rare neuroendocrine tumors of the breast. The purpose of our study is to investigate the expression of estrogen and progesterone receptors in well-differentiated neuroendocrine tumors (WDNET, carcinoid) of the gastrointestinal tract.

Methods Thirty-one cases of WDNETs of the gastrointestinal tract were retrieved from the archives at Sunnybrook Health Sciences Centre from 2003–2008. The primary sites were as follows: Small intestine – 16; Colon/rectum – 6; Stomach – 4; Appendix – 4; Ampulla of Vater – 1. Immunostaining was performed on formalin-fixed, paraffin-embedded tissue sections with antibodies to estrogen receptor (SP1) and progesterone receptor (1E2).

Results Normal gastrointestinal neuroendocrine cells were negative for estrogen and progesterone receptors in all cases.28 out of 31 WDNETs were negative for estrogen and progesterone receptors. One case of appendiceal WDNET was positive for estrogen receptors, a second appendiceal tumor was positive for progesterone receptors, and the ampullary tumor was positive for progesterone receptors. No cases showed co-expression of estrogen and progesterone receptors.

Conclusion(s) The majority of gastrointestinal WDNETs do not express estrogen or progesterone receptors, similar to normal endocrine cells of the gastrointestinal tract. Rare positivity was noted in two of the appendiceal tumors and one ampullary tumor in our study, which could be a potential pitfall if hormone receptors are used to differentiate between primary sites in the setting of a metastatic endocrine neoplasm.

P1.122

Expression of P27 and agnor in hepatocellular carcinoma

Seada Salah L.; Badawy Al Nasser A.; Youssef Ahmed S.
Benha University, Cairo, Egypt

Background The burden of HCC in Egypt has been increasing with a doubling in the incidence rate in the past 10 years. Therefore, identification of useful molecular prognostic markers is required. P27, a negative regulator of the G1-S phase is frequently inactivated in HCC and is

considered to be potent tumor suppressor and is now considered to be an adverse prognostic factor in HCC.
Methods Forty HCC cases have been studied, together with 26 adjacent areas, and 6 normal liver tissue. Paraffin blocks were available for all cases, where immunostaining for the anti-p27 antibody was done using the standard peroxidase method. Proliferative activity was measured by the AgNOR silver staining technique.
Results Loss of nuclear p27 was found in 22.9% and low expression (LI<50) in 37.5% of cases. Out of 29/40 (72.5%) cases with cancer on top of cirrhosis, 8 (27.5%) had loss of expression and 11 (38%), low expression. Loss of p27 correlated with advanced stage (p=0.001) and vascular invasion (p = 0.002), but not with tumor size, multiplicity, or presence of cirrhosis. AgNOR count/nucleus was 5.95 in cases with high p27 expression (LI > 50), while in the remaining loss or low expression, the mean count was 7.31, and the difference was non significant.
Conclusion(s) Investigation of both p27 and AgNOR counts in individuals with HCC, maybe useful as a prognostic indicator. However, in some cases of increased proliferation, p27 is also overexpressed, which might indicates a deregulated pathway of an aberrant clone.

P1.123
Expression of the epidermal growth factor receptors (EGFR and HER-2) in esophageal squamous cell cancer

Delektorskaya V.V.; Chemeris Jurievna G.; Kononec V.P.; Grigorchuk Ju.A.
N. N. Blokhin Russian Cancer Research Centre RAMS, Moscow, Russian Federation

Background The present study was aimed to assess EGFR and HER-2 expression in esophageal squamous cell carcinoma (ESCC) and to correlate the results with clinic-pathological findings and prognosis.
Methods The immunohistochemical staining of EGFR and HER-2 receptors were retrospectively investigated in biopsy specimens from 28 patients with T (2–3), N-any, and M-0 ESCC. The results were classified according to the Herceptest criteria (Dako): negative (0/1+), potential positive (2+) and positive (3+).
Results The EGFR expression was negative in 4/28 cases (14.3%) and positive in 24 (85.7%), of which 11 (39.3%) were 2+ and 13 (46.4%) were 3+. EGFR diffuse strong positivity was significantly related to vascular invasion (p= 0.023) in a subgroup of ESCC patients. Statistical trend towards poor outcome was observed in ESCC patients overexpressing EGFR (3+) (p=0.059). The HER-2 expression was negative in 11/28 cases (39.3%) and positive in 17 (36.8%), of which 12 (42.9%) were 2+ and 5 (17.9%) were 3+. No significant associations were found among protein expression and clinic-pathological data. Our results revealed a high rate of HER-2 overexpression in the group of ESCC patient with poor disease outcome (p=0.043).
Conclusion(s) Our data demonstrate the great potential prognostic interest of evaluation EGFR and HER-2 overexpression in ESCC. Protein overexpression of HER-2 (3+) is an indicator of poor prognosis in ESCC patients, although the results should be confirmed in a larger series.

Urological pathology

P1.124
Morphology and immunohistochemistry of primary and secondary adrenal gland neoplasms

Hortopan M.G.; Herlea V.; Stoica Mustafa E.; Pechianu C.; Iorgescu A.C.; Sobaru I.; Balan O.M.; Moldovan D.D.; Marzan L.; Voinea S.; Manu M.; Constantinescu I.; Sinescu I.
Fundeni Clinic Institute, Bucharest, Romania

Objectives 1 To describe the morphology and immunohistochemistry aspects of primary and secondary adrenal gland neoplasms.2. To identify possible correlations between various histopathology aspects (macro and microscopic) and immunohistochemistry expression of proliferation and invasive biomarkers.3. To identify (for malign tumors) through a unique or multifactor analysis, the prognostic role of morphologic and immunohistochemistry markers in predicting the survival rate or the risk of metastasis.
Material and method In this study we included 45 patients admitted and surgically treated in the Center for Urologic Surgery and Renal Transplant and diagnosed in the Pathology Department, between January 1995 and December 2005, 25 with carcinoma of cortical adrenal gland, and 20 with secondary adrenal gland neoplasm. The patients were choosing randomized, the number of cases being proportional with the number of cases diagnosed in the Pathology Department in the above mentioned period. Each case was examined and described from macroscopically, microscopically (classical H&E staining) and immunohistochemical point of view. The immunohistochemistry markers followed on these cases were: Antibody Ki-67, Proteins: Bcl-2, p21 and p27, MDM-2, Receptors: CD-44 and EGFR, Sinaptophisine.
Conclusion The immunohistochemistry biomarkers (expressing the proliferation activity, grade of invasion and cellular cohesively) as well as the classical pathologic characteristics (weight, architecture, tumoural necrosis, capsular invasion, Weiss index) are defining in the prognostic of primary and secondary adrenal gland neoplasms.

P1.125

How we are dealing with bladder biopsies (tubr specimens)? Survey among Spanish uropathologists

Gomez Dorronsoro L.M.; Algaba F.; Blanco M.; Condom E.; Congregado J.; Gallel P.; Gonzalez-Peramato P.; Guarch R.; Luque R.; Mallofre C.; Ortiz Antonio J.; Picazo Luz M.; Rodriguez-Barbero J.
Hospital de Navarra, Pamplona, Navarra, Spain

Background The uropathologists group of the Spanish Society of Pathology did some surveys to know how the pathologists really work with the urological specimens. The first inquire was about the diagnosis of prostate carcinoma and the second one was about handling and reporting transurethral resection specimens of the bladder which results are referred below.
Methods 25 questions with macroscopic and microscopic issues from bladder biopsies were sent to all memberships of the club.
Results We have collected sixteen replies, (64%). Results were summarized as follows: Most of the biopsies were received formalin fixed (75%), and tumor and resection base in 87.5% were sent in separated containers.56.25% of specimens were embedded in its totality in TURB specimens. 62% of the uropathologists gradated bladder tumor with the WHO 1973 and WHO 2004, both together, and 100% reported the pTNM for staging. PUNLMP is only rarely diagnosed by 81.25% of the uropathologists. Substaging of T1 is only scored when it was very clear in 43.75% and always in 12% respectively. Vascular-lymphatic invasion were reported with H-E stain, without ancillary techniques in 87.5%. Immunohistochemical techniques were rarely used (12%) and p53 and ki67 were only applied for early lesions.
Conclusion(s) Spanish uropathologists used similar criteria to do reports, especially related to those factors which are known to have prognostic implications. Bladder cancer grading need to become more standardized and ancillary techniques should be recommended for early diagnosis and prognosis.

P1.126

Prognostic significance of several biomolecular markers in prostate cancer

Liatkouskaya A. T.; Zakharava A. V.; Cherstvoy D. E.; Pashkevich A. L.; Sukonko G. O.; Rolevich I. A.; Masanskiy L. I.; Sagalchik M. L.; Ivanovskaya I. M.; Portyanko S. A.
Belarusian State Medical University, Department of Pathology, Minsk, Belarus

Background Prognostic significance of the proliferation index (PI) by Ki-67, of neuroendocrinal differentiation (NED) by chromogranin A, of androgen receptors (AR), p-53 and bax status, of the adhesion molecules (E-cadherin, b-catenin, CD44) and oncoprotein P504S expression has been assessed on the material obtained from 104 prostate cancers (PCa) pa-tients having undergone retropubic radical prostatectomy. The overall five-year, five-year-without-biochemical-relapse and five-year-without-clinical-progression survival rate was 94%, 45%, 84% respectively.
Methods We studied the expression of the Ki-67, chromogranin A, AR, p-53, bax, E-cadherin, b-catenin, CD44 and P504S with the use of immunostaining.
Results Kaplan-Meyer analysis revealed that unfavorable prognostic factors for PCa were presurgical PSA level (≥ 10 ng/ml), pathologic stage (pT) including the prostate capsule and the seminal vesicles invasion, Gleason score ≥7, involvement of regional lymph nodes. Among the biomolecular markers the most significant were increased PI≥5% of tumor cells, appearance of NED and the mutant p-53, also reduces of bax and reduced intensity of staining with antibodies to P504S. Regression analysis by Cox revealed independent prognostic significance for Gleason score≥7 and involvement of pelvic lymph nodes. Among the biomolecular markers independent influence upon relapse-free survival rate of PCa patients was confirmed for the mutant p53 and reduced AR and bax expression.
Conclusion(s) Patients with PI by Ki-67≥5%, availability of NED and the gene-suppressor p-53, reduced bax and with reduced intensity of staining with antibodies to P504S may be regarded as groups of high risk of tumor progression.

P1.127

Single-nodule prostatic carcinoma: pathologic features

Falzarano Moscovita S.; Zhou M.; Magi Galluzzi C.
Cleveland Clinic, Cleveland, Ohio, USA

Background Prostate cancer (PCA) is frequently a multifocal process. Few studies report on incidence and characteristic features of single-nodule PCA (snPCA).
Methods 1100 radical prostatectomies (RP) for PCA were reviewed. Tumor outline and number of PCA were determined. For each snPCA, histologic type, tumor volume (TV), location, zone of origin, Gleason score (GS), extraprostatic extension (EPE), seminal vesicles invasion (SVI), surgical margin status (SM), lymphovascular invasion (LVI), pathologic stage, and presence of palpable disease by digital rectal examination (DRE) were recorded.
Results 107 snPCA were identified. Mean age, PSA, and prostate weight were 59 years, 5.8 ng/ml and 57.4 g. snPCA involved both lobes (19.6%), left lobe (35.5%) and

right lobe (44.9%) .98.1% of snPCA originated from peripheral zone. All tumors except one were acinar PCA. GS was 6 (37.4%), 7 (39.2%) and≥8 (23.4%). Mean TV was 153 mm2. EPE, SVI and LVI were detected in 30.8%, 1.9% and 10.3% of cases, respectively. SM was positive in 14.9% of cases. Pathologic stage was T2 in 69%, T3 in 31%. In 29/76 men a nodule was detected on DRE. EPE was more likely to occur in positive DRE patients (p= 0.041). No statistical difference in prostate weight, PSA, age, SVI, SM, LVI and GS was found between patients with and without a nodule on DRE.

Conclusion(s) snPCA represents 10% of PCA. Most snPCA involve one lobe of the prostate and originate from PZ. DRE detected a nodule in more than 1/3 of cases, 44.5% of which were non-organ confined tumors.

P1.128

Variation among urogenital pathologists in diagnostic opinion of single small atypical foci in prostate biopsies

Van Der Kwast H.T.; Evans A.; Tkachuk D.; Lockwood G.; Bostwick D.; Epstein I.J.; Humphrey P.; Montironi R.; Srigley J.; Members of The Pathology Committee E.
University Health Network, Toronto, Ontario, Canada

Background We investigated the level of diagnostic agreement (kappa) for small foci of atypical glands on prostate biopsy among experts specialized in urogenital pathology and all-round pathologists with extensive experience in reading prostate biopsies.

Methods We retrieved 20 prostate biopsies with small atypical foci. HE stained slides and – if available - matched immunostained slides (n=10) were digitalized. Five experts in urogenital pathology (UGE) and seven members of the pathology committee of the European Randomized Study of Screening for Prostate Cancer (ERSPC) examined the virtual slides. Multirater kappa statistics were applied to determine agreement.

Results The kappa of UGE (0.39 (95%CI: 0.29–0.49)) was significantly higher than that of the ERSPC pathologists (0.21 (95%CI: 0.14–0.27)). UGE and ERSPC pathologists rendered in 5 and 9 biopsies respectively a diagnosis ranging from benign to carcinoma. The UGE diagnosed cancer (49%) significantly (p<0.001) more often than the ERSPC pathologists (32%), at the expense of the number of benign diagnoses, while the number of suspicious cases was about the same. If the agreement was calculated for originally diagnosed cancers and benign diagnoses the kappa's of GUE increased to 0.42 and 0.55, respectively and those of ERSPC pathologists to 0.26 and 0.27 respectively.

Conclusion(s) Although UGE demonstrate a better agreement in their diagnostic opinion of small atypical foci in prostate biopsies than their non-specialized ERSPC colleagues their level of agreement remains poor. UGE rendered more often a diagnosis of carcinoma than the ERSPC pathologists.

P1.129

Absence of gains in chromosomes 7 and 17 in renal papillary adenomas associated with adult polycystic kidney disease

Juanpere N.; Galván Belen A.; Salido M.; Espinet B.; Rodríguez M.; López L.; Murillo R.; Bielsa O.; Serrano S.; Solé F.; Lloreta J.
Hospital del Mar, Barcelona, Spain

Background Autosomal dominant polycystic kidney disease (AD-PKD) is the most common non-acquired cystic renal disease. It usually leads to end-stage renal failure and frequently associates renal papillary neoplasms. The genetic alterations shared by papillary renal adenoma (PA) and papillary renal cell carcinoma are gains in chromosomes 7 and 17, and loss of chromosome Y. The aim of this study was to analyze the genetic features of PA in the setting of AD-PKD using Fluorescent in situ Hybridization (FISH).

Methods 15 PAs from 9 AD-polycystic kidneys were analyzed with FISH (CEP3, CEP7 and CEP17). The study was performed separately in the areas of PA and in the flat epithelium of cyst walls far from the tumor.

Results In one case, two different lesions were identified: a tubulopapillary adenoma with glomeruloid cell aggregates that showed gains in chromosomes 7 and 17, and a PA that lacked genetic alterations. In seven cases, genetic abnormalities were not detected. One case could not be assessed because of the small number of tumor cells available.

Conclusion(s) In this preliminary study, the absence in most of the cases of the genetic alterations typically found in PAs suggests that PAs associated with AD-PKD have a different pathogenesis from that of sporadic PAs. Our results raise the need to perform a comparative study between sporadic PA and PA associated with renal polycystic disease in a larger series of cases.

P1.130

AMACR expression in particular subtypes of prostate carcinoma

Dema A.; Taban S.; Lazar E.; Anderco D.; Lazureanu C.; Cornianu M.; Muresan A.; Costi S.; Bucuras V.; Botoca M.; Bardan R.
University of Medicine and Pharmacy "V. Babes", Timisoara, Romania

Background Alpha-methylacyl-CoA-racemase (AMACR) is a reference immunohistochemical marker in urological pathology, extremely useful to the diagnosis of difficult prostate lesions. The aim of this study was to investigate AMACR expression in some particular subtypes of prostate carcinoma.
Methods Particular prostate carcinoma forms were selected: ductal (7 cases), carcinoma with foamy cell (9 cases), mucinous (2 cases) or pseudohyperplastic (5 cases) areas, atrophic carcinomas (3 cases), urothelial carcinomas (3 cases) together with 20 cases of conventional prostate carcinomas. IHC study was performed using following antibodies: P504S (monoclonal), p63, HMWCK, CK5/6, PSA, prostein, CK7 and CK20.
Results 5 of particular prostate carcinoma cases were devoid of immunoreactivity for AMACR: 2 ductal carcinomas, 2 urothelial carcinomas and an atrophic carcinoma. Carcinomas/areas of mucinous, foamy and pseudohyperplastic type have shown a marked heterogeneous expression of AMACR, with negative areas and portions of positive staining with variable intensity. Ninety percent of conventional prostate carcinomas cases were positive for AMACR, with diffuse reactivity in 45% of cases and heterogeneous in 55% of cases.
Conclusion(s) This study confirms the heterogeneity of AMACR expression in prostate carcinomas and the fact that for some cases of prostate conventional or particular carcinomas the marker expression is absent. For those cases the diagnosis of cancer is often very difficult in small tissue fragments and is based on data correlation provided by the usual stains with the methods for basal cell highlighting.

P1.131
CD24 and Ki-67 expression in urothelial carcinoma of urinary bladder correlates with tumor progression

Daglar E.; Kulacoglu S.
Ankara Numune Training and Research Hospital, Ankara, Turkey

Background CD24 is a glycosylated cell surface protein which has gained considerable attention in tumor research. CD24 expression have been found in several types of carcinomas that are significantly associated with a more agressive course. A cell proliferation marker, Ki-67 is a nuclear protein complex, expressed in the G1, S, G2 and M phases of the cell cycle that associated with tumor progression. The aim of our study was to determinate the expression of CD24 and Ki-67 in urothelial carcinomas of the urinary bladder and relationship of them with tumor grade and stage.
Methods 68 urothelial carcinomas, including 34 noninvasive (17 cases with low grade, 17 cases with high grade), 34 high grade, invasive (17 cases with lamina propria invasion, 17 cases with muscularis propria invasion). All cases were examinated immunohistochemically. Percentage of positive cells was evaluated for CD24 and Ki-67. Each section was also recorded for the intensity and the location of the staining (membranous and/or cytoplasmic) for CD24.
Results CD24 expression in urothelial carcinoma is associated with advanced tumor stage. Percentage of positive cells for Ki-67 staining correlates with tumor grade and stage.
Conclusion(s) Our data confirmed that Ki-67 is a prognostic marker associated with tumor progression. CD24 expression as detected by immunohistochemistry may be a new marker for predicting aggressive behaviour in urothelial carcinoma and serve as a useful target for the therapeutic approach of this tumor.

P1.132
CK 903 and p63 are useful markers in the differential diagnosis of atypical large glandular proliferations of the prostate

Gan J.; Huang H.; Delasmorenas A.
Boston Medical Center, Boston, MA, USA

Background While in prostatectomy specimens, high-grade prostatic intraepithelial neoplasia (PIN) is commonly seen within or adjacent to tumor nodules. In needle biopsies, these distinctions may be even more challenging, especially in the absence of obvious invasive cancer.
Methods 51 prostatectomy specimens from Boston Medical Center (2006–2007) were retrospectively reviewed. Immunohistochemical studies using basal cell-associated markers, CK 903 and p63, were performed on selected sections. The results were analyzed in the following morphologic groups: normal as positive control, invasive adenocarcinoma as negative control and glands with high grade PIN changes, which were further subclassify as atypical large glands with branching and with (groups A) or without nuclear stratification (group B), elongated glands with (groups C) or without branching (group D), and cribriform glands (group E).
Results The results showed that 20% of the cases in group A, 43% of the cases in group B, 41% of the cases in group C, 43% of the cases in group D and 60% of the cases in group E were negative for p63 and CK 903.
Conclusion(s) All five groups of high-grade PIN variants had overlapped morphologic features with Gleason 3 and 4 prostatic adenocarcinoma. Our results indicated that a significant percentage of cases with morphologic changes of high grade PIN may represent prostatic adenocarcinoma. P63 and CK903 should be used in small biopsies when only large glands with histological features of high-grade PIN are present in needle biopsies.

P1.133

Collagen micronodules: frequency and significance in prostate needle biopsies

Billis A.; Quintal Momesso M.; Meirelles L.; Freitas Luiz Lopes L.; Duarte Gabriela Esteves A.; Silva Augusto Moreira C.; Bisson Augusto Matioli M.; Magna Alberto L.
Dep. of Pathology, School of Medicine, University of Campinas (Unicamp), Brazil, Campinas, SP, Brazil

Background Collagen micronodules are considered histological features specific for prostate cancer. They have not to date been identified in benign glands. At the ISUP consensus conference on Gleason grading it was recommended to subtract away the collagen micronodules and grade the tumor based on the underlying glandular architecture. We studied the frequency and clinicopathological features of this lesion when present in needle biopsies.

Methods The study was based on 266 prostate needle biopsies and the correspondent radical prostatectomies. Several clinicopathological variables were studied. The data were analyzed using the Mann-Whitney test for comparison of independent samples and Fisher s exact test for comparing proportions. Time to progression-free outcome was studied using the Kaplan-Meier product-limit analysis; the comparison between the groups was done using the log-rank test.

Results The frequency of needle biopsies showing collagen micronodules was 32/266 (12.03%). Comparing patients without and with collagen micronodules in the needle biopsy for several clinicopathological variables, the findings were not statistically significant for age, clinical stage, preoperative PSA, prostate weight, Gleason grading in biopsy and radical prostatectomy, positive surgical margins, extraprostatic extension, seminal vesicle invasion, tumor extent, and PSA progression-free survival.

Conclusion(s) The frequency of collagen micronodules in needle biopsies was 12%. The presence of this feature was not associated to any adverse clinicopathologic finding. The result of this study favors the recommendation of the ISUP to subtract the collagen micronodules and grade the tumor based solely on the underlying glandular architecture.

P1.134

Contemporary grading and staging impact on grade and stage migration in prostate cancer

Falzarano Moscovita S.; Zhou M.; Klein E.; Magi Galluzzi C.
Cleveland Clinic, Cleveland, Ohio, USA

Background Tumor grade and stage are established prognostic factors in prostate cancer (PCA). PCA grading has recently undergone major revisions. We investigated the impact of current grading and staging in a subset of radical prostatectomies (RP) for PCA performed between 1988 and 2004.

Methods A genitourinary (GU) pathologist reviewed 302 RP for Gleason score (GS), extraprostatic extension (EPE), seminal vesicle invasion (SVI), stage, and surgical margin involvement (SMI). Review data were compared with those of general pathologists. Relationship between prostate-specific antigen (PSA) and pathologic characteristics was examined in early (1988–1998) and late (1999–2004) PSA-eras.

Results Patients mean age was 61.7 years. Mean PSA was 12.8 (early-PSA-era) and 7.0 ng/ml (late-PSA-era) ($p<0.0001$). Review GS was 5 (0.3%), 6 (18.5%), 7 (54.3%) and≥8 (26.8%). GS was upgraded by review in 14.6% and downgraded in 4.6% of cases. Upgrading was more likely in early-PSA-era; downgrading in late-PSA-era ($p<0.0001$). GU pathologist agreed with cases previously scored with EPE and SMI, however, more frequently judged a case positive for EPE (51%), SVI (15%) and SMI (32.8%) than general pathologists (46%, 14% and 25.5%, respectively). Review stage was T2 (48.3%) and T3 (51.7%) with an upstage in 5.6% of cases. No statistical difference was found in EPE, SVI, SMI and upstaging between early-PSA and late-PSA-era.

Conclusion(s) Our study suggests that changes in pathology practice are a significant factor in GS migration. Overall, high concordance existed for EPE (95%, k= 0.90), SVI (99%, k = 0.96), and SMI (93%, k = 0.83).

P1.135

Diagnostic value of fatty acid synthase in comparison to alpha-methylacyl-CoA racemase as prostate cancer tissue marker

Tischler V.; Fritzsche R.F.; Gerhardt J.; Jäger C.; Stephan C.; Jung K.; Dietel M.; Moch H.; Kristiansen G.
Department of Surgical Pathology, University Hospital Zurich, Zurich, Switzerland

Background Fatty acid synthase (FASN) is overexpressed in prostate carcinoma on mRNA and protein level. Its clinical significance and the potential value for tissue diagnosis is unknown. We studied the relationship between FASN and clinicopathological parameters in prostate cancer patients.

Methods FASN protein expression was analysed immunohistochemically in 622 clinically characterized prostate cancer cases and compared to adjacent normal prostate tissue. In parallel, the expression of the prostate cancer marker alpha-methylacyl-CoA racemase (AMACR), the basal cell marker p63 and the proliferation marker Ki-67 was determined.

Results FASN expression was found at low to medium intensities in normal prostate epithelium and also high grade prostatic intraepithelial neoplasia (PIN). The

strongest FASN expression was found in prostate cancer: 92.6% of cases showed a significant upregulation in comparison to adjacent normal tissue. FASN expression was significantly correlated to higher Ki-67 and AMACR levels, but not to Gleason score, pre-operative PSA levels, pT stage or margin status. Importantly, FASN was upregulated in 91 % of AMACR negative cases.

Conclusion(s) This is the first report to compare the diagnostic efficacy of FASN in comparison to AMACR. FASN is overexpressed in 92.6% of prostate cancer cases. As a single marker, it is slightly inferior to AMACR which is overexpressed in 95% of cases. However, since 90.1% of cases not labelled by AMACR were detected by FASN, it might be of use as an additional positive marker in critical lesions.

P1.136

Do multifocal tumors consist a separate entity of histological prostate cancer?

Stamatiou K.; Lardas M.; Labrakopoulos A.; Petrakopoulou N.; Zizi-Serbetzoglou A.
Tzaneion General Hospital of Piraeus, Piraeus, Greece

Background The aim of this study is to examine the occurrence of multifocal tumors among impalpable histologic carcinomas of the prostate and compare their histologic features to that of single histologic carcinomas.

Methods The study was done in 212 consecutive autopsies of men above 40 and less 98 years of age who died, of diseases other than carcinoma of the prostate diagnosed clinically. The whole prostate and seminal vesicles are sectioned and underwent pathologic examination. Diagrams were constructed by tracing the outline of each whole-mount section, and tumor maps were generated subsequently. The largest focus was considered as the index tumor. A primary and a secondary Gleason grade was assigned at each tumor and the same procedure has been followed for each of the tumor foci.

Results 39 cases of latent prostate cancer were found: 24 of them (61.53%) were multifocal tumours which contained two or more foci. Invasiveness was more frequent in multifocal tumors and related equally to the tumour volume and the histological differentiation. No statistical significance was found for capsular penetration, perineural or perivascular invasion of multifocal in comparison to single carcinomas.

Conclusion(s) According to the findings of this autopsy study the histologic features of multifocal tumours are similar to that of single histologic carcinomas. Invasiveness is related to the tumour volume (and the number of foci) and to the histological differentiation.

P1.137

Does tumor extent in needle prostatic biopsies (NPB) influence the value of perineural invasion (PNI) to predict extraprostatic extension in radical prostatectomies (RP)?

Billis A.; Quintal Momesso M.; Meirelles L.; Freitas Luiz Lopes L.; Rogerio F.; Oliveira Vismari R.; Schultz L.; Fazuoli Galvao M.; Bronner Nicolau M.; Magna Alberto L.; Ferreira U.
Dep. of Pathology, School of Medicine, University of Campinas (Unicamp), Brazil, Campinas, SP, Brazil

Background The significance of PNI by carcinoma in NPB is still controversial. The aim of our study was to find whether tumor extent in NPB influence the value of PNI to predict stage > pT2 in RP.

Methods The study was based on 266 patients with NPB matched with completely embedded RP specimens. A logistic regression model was used to relate the outcomes of prostatectomy stage > pT2 to several variables.

Results PNI was present in 48/266 (18%) biopsies. The median percentage of linear extent of adenocarcinoma in millimeters for each biopsy was 13.5%. In RP, 74/266 (27.8%) specimens showed stage > pT2. Considering all cases, in univariable analysis preoperative PSA, Gleason grade, tumor extent, and PNI significantly predicted stage > pT2; in multivariable analysis only preoperative PSA, tumor extent, and Gleason grade were significant. Analyzing only biopsies with percentage of linear extent < 13.5%, Gleason grade and tumor extent significantly predicted stage > pT2 in univariable as well as multivariable analyses but not PNI in both analyses.

Conclusion(s) In our study, PNI in NPB significantly predicted prostatectomy stage > pT2 in univariable but not in multivariable analysis. In cancers with percentage of linear extent < 13.5% there was no significant prediction in both analyses. It seems that PNI does not have predictive value in small cancers. This is important considering that a higher number of small cancers in stage T1c are currently most commonly detected.

P1.138

EGFR protein and gene level in clear cell renal cell carcinoma

Dordevic G.; Babarovic E.; Matusan Ilijas K.; Jonjic N.
Rijeka University School of Medicine, Rijeka, Croatia

Background The role of epidermal growth factor receptor (EGFR) in the pathogenesis of clear cell renal cell carcinoma (CCRCC) is still not well recognized. The aim of study was to analyze the expression of EGFR on tumor cells in CCRCC, to correlate its value with EGFR gene

copy number and to compare analyzed parameters with clinicopathological characteristics including the patients' survival.

Methods Tissue microarrays (TMA) from the cohort of 91 archive formalin fixed and paraffin embedded CCRCC were immunohistochemically stained for EGFR expression and evaluated as percentage and intensity of membranous staining (histoscore, HS). EGFR gene copy number was investigated by means of fluorescence in situ hybridization (FISH). Clinicopathologic data included tumor size, stage and nuclear grade (NG).

Results Membranous EGFR expression was detected in 84 of 91 cases (92.3%), with moderate to strong staining (HS 2 and 3) in 52 cases (57.14%), and only week cytoplasmic EGFR in 29 cases (31.86%). Overexpression of EGFR was related to bigger tumors (p=0.018), higher NG (p = 0.0002), pT stage (p = 0.036) and lower overall survival (p = 0.046). FISH method revealed polisomy 7 associated with protein EGFR overexpression in CCRCC tumor cells ($p \leq 0.001$) but not with clinicopathological parameters. No amplification was found.

Conclusion(s) Survey of CCRCC with TMA technique highlights more aggressive subtype of CCRCC with overexpression EGFR in tumors cells that might have some clinical implication. FISH analysis showed that EGFR gene dosage can influence on protein expression through polisomy rather than amplification.

P1.139

Expression of Jun activation domain-binding protein 1 in urothelial carcinoma of the upper urinary tract

Sung M.; Huang H.
Kaohsiung, Taiwan

Background Jun activation domain-binding protein 1 (Jab 1), a coactivator of transcription factor, promoted cell proliferation through the ubiquitin/proteasome pathway and its overexpression was reported in some neoplasia. To elucidate the significance of Jab 1 in urothelial carcinoma of the upper urinary tract, the expression of Jab 1 and its relationship between tumor progression were investigated.

Methods We undertook the analysis of m-RNA expression of Jab 1 in paired tumor and normal tissue by semiquantitative reverse transcription polymerase chain reaction (RT-PCR) in 33 patients of urothelial carcinoma of the upper urinary tract, including both renal and ureteral tumors, and explored the correlation between Jab 1 expression and tumor aggressiveness.

Results Urothelial carcinomas were shown overexpression of Jab 1 in 52% (17/33) cases. The incidence of Jab 1 overexpression in patients harboring invasive cancers is 68% (13/19), higher than those with non-invasive tumors (28%, 4/14). A significant correlation between high Jab1 expression and both advanced tumor stage and high tumor grade was found.

Conclusion(s) Our data suggest Jab 1 may play a significant role in tumor progression in urothelial carcinoma of the upper urinary tract.

P1.140

Expression of Pax2 and S100A1 in nephrogenic adenoma: utility in distinction of nephrogenic adenoma from its malignant mimics

Nese N.; Gupta R.; Osunkoya O.A.; Paner G.; Parakh R.; Chung F.; Alsabeh R.; Amin B.M.
Manisa, Turkey

Background Nephrogenic adenoma, an unusual benign lesion is often incidentally detected and involves the urinary tract. Seeding, implantation and growth of distal renal tubules in traumatized/inflamed urothelial mucosa may be the cause of nephrogenic adenoma. Another thought considers nephrogenic adenoma as metaplastic changes. The importance of these innocuous lesions lays in the fact that they may histomorphologically mimic malignant entities such as clear cell carcinoma of the bladder (CCC), urothelial carcinoma with glandular differentiation (UCa) and prostatic adenocarcinoma (PCa). Pax2 and S100A1 are two novel renal tubule associated markers.

Methods The utility of Pax2, S100A1 and MIB-1 in differentiating nephrogenic adenoma from its malignant mimics was analyzed in 42 conventional sections from nephrogenic adenoma (n=17), CCC (n=5), UCa (n=7) and PCa (n=13).

Results 94.1% of nephrogenic adenoma were immunoreactive with Pax2 and S100A1, while all the malignant mimics were largely non immunoreactive. The mean MIB-1 proliferation index in nephrogenic adenoma was 2% (range 0–5); 30% (range 10- 60) in CCC; 25% (range 10–40) in UCa; and 6% (range 2–30) in PCa.

Conclusion(s) The high incidence of renal tubular marker expression provides further support for tubular histogenesis of nephrogenic adenoma. The immunoprofile (Pax2+, S100A1+ and low MIB-1) typifies nephrogenic adenoma in contradistinction to the malignant lesions (Pax2 -, S100A1- and high MIB-1). An immunopanel of Pax2, S100A1 and MIB1 in the appropriate histologic context has strong diagnostic utility in the differential diagnosis of nephrogenic adenoma.

P1.141

Galectin-3 is a useful immunomarker in diagnosis of chromophobe renal cell carcinoma

Kim M.; Sung W.; Bae Y.
Yeungnam University Hospital, Daegu, Republic of Korea

Background Chromophobe renal cell carcinoma accounts for about 5% of renal epithelial tumors. Diffuse

cytoplasmic staining reaction with Hale's colloidal iron stain has been known for diagnostic hallmark of this tumor. However, distinguishing chromophobe renal cell carcinoma from other renal epithelial tumors, including clear cell renal cell carcinoma and oncocytoma is still challenging. In this study, we tried to do immunohistochemistry for galectin-3, CK20, CK7 and e-cadherin to evaluate its diagnostic usefulness of chromophobe renal cell carcinoma.

Methods 10 chromophobe renal cell carcinomas, 25 clear cell renal cell carcinomas and 4 oncocytomas were obtained at Yeungnam University Hospital from Jan.2005 to July 2009. Immunohistochemistry using galectin-3, CK7, CK20, and e-cadherin was done on tissue microarray slide. Hale's colloidal iron staining was also performed.

Results All of chromophobe renal cell carcinoma was positive in galectin-3 and e-cadherin was positive in 90% of chromophobe renal cell carcinoma (< 0.001). CK 7 was positive in 70% of chromophobe renal cell carcinoma and all cases of chromophobe renal cell carcinoma were negative in CK20. Hale's colloidal iron stain was also noted in all chromophobe renal cell carcinoma.

Conclusion(s) Expression of galectin-3 and Hale's colloidal iron stain was very useful in diagnosis of chromophobe renal cell carcinoma. This study demonstrates that a panel of galectin-3+/CK7+/e-cadherin+immunostains could be used to distinguish between chromophobe renal cell carcinoma and conventiona renal cell carcinoma, and a panel of Hale's coloidal iron+/CK20- is helpful in excluding oncocytoma.

P1.142

Heterogeneity of Gleason grade in impalpable multifocal adenocarcinomas of the prostate

Stamatiou K.; Lepidas D.; Labrakopoulos A.; Savvaidou V.; Zizi-Serbetzoglou A.

Tzaneion General Hospital of Piraeus, Piraeus, Greece

Background The current study was undertaken to compare the Gleason grades of individual adenocarcinoma foci in a given specimen with the overall Gleason grades (primary and secondary) of that specimen.

Methods Data were obtained from 40 cadaveric prostate specimens via whole-mount processing and complete sectioning. Diagrams were constructed by tracing the outline of each whole-mount section, and tumor maps subsequently were generated. The largest focus was considered the index tumor. Each specimen was assigned primary and secondary Gleason grades, and each tumor focus was assigned its own primary and secondary Gleason grades.

Results Multi-focality was frequent in impalpable PC: 24 (60%) out of 40 impalpable carcinomas, consisted of two or more small tumor foci (< 0.5 cc). Specimens containing a single tumor were excluded from further analysis Multi-focal carcinomas showed a relative homogeneity: primary Gleason grade of the index tumor corresponded to the primary Gleason grade of the remaining smaller foci in 65% of the specimens. Among multi-focal carcinomas, the larger ones presented a minor grade of homogeneity: Differences in histologic heterogeneity between multifocal prostate carcinomas of overall volume greater than 2 cc and the smaller malignancies are statistical significant. An absolute equivalence (of primary and secondary Gleason grades) has been observed in only seven cases.

Conclusion(s) The findings of the current study demonstrated that homogeneity of multi-focal PC, depends on overall tumor volume and the number of foci.

P1.143

High and heterogeneous expression of epidermal growth factor receptor (EGFR) in penile carcinoma

Silva Muglia Thomaz A.; Rocha Malagoli R.; Cubilla A.L.; Guimarães Cardoso G.; Cunha Werneck I.; Lopes A.; Soares A.F.

A. C. Camargo, São Paulo, Brazil

Background Penile squamous cells carcinoma (PSCC) is commonly notified in undeveloped countries. EGFR is a well characterized growth factor receptor that shows increased expression levels in diverse tumors. EGFR has been shown to facilitate tumor development and it is also target for therapy. We aimed to evaluate EGFR profile and frequency of expression in penile carcinomas.

Methods Sections were evaluated following the ASCO/CAP guidelines for HER2: 0, no membrane staining; 1+, barely partial membrane staining in more than 10%; 2+, weak to moderate complete membrane staining in more than 10%; 3+, strong complete membrane staining in more than 30% of the cells. Either 0 or 1+ were considered negative, 2+ were borderline and 3+ were positive. IHC hot spots were reached for evaluation. ™Immunohistochemistry (IHC) against EGFR was performed in 91 penile carcinomas selected from the files of AC Camargo Hospital, Brazil, using the monoclonal antibody EGFR 25 (Leica).

Results We found 53 cases (58, 24%) positive, 17 cases (18, 68%) borderline, 14 cases (15, 38%) negative (1+), and 4 cases (4, 4%) negative (0). Three tumors were uninterpretable due to pre-analytical artifacts. EGFR showed an important heterogeneous expression pattern along the tumor tissue showing variable IHC staining intensity.

Conclusion(s) The frequency of EGFR overexpression in PSCC is relevant, as it is in other squamous cells carcinomas. These patients might benefit from target therapy since gene mutations is also assessed. However, further studies concerning clinical data and gene analysis must be done.

P1.144

High expression of gastrin-releasing peptide receptors in the vascular bed of urinary tract cancers

Fleischmann A.; Waser B.; Reubi J.
Division of Cell Biology and Experimental Cancer Research, Institute of Pathology, University of Bern, Bern, Switzerland

Background Since there is evidence for a role of Gastrin-releasing peptide (GRP) in tumoral vessels this study aimed to test a large number of different cancers for GRP-receptor expression in tumor vascular bed.
Methods Human cancers (n=368) from different organs were analyzed using in vitro GRP-receptor autoradiography on tissue sections with the 125I-[Tyr4]-bombesin radioligand and/or the universal radioligand 125I-[D-Tyr6, ß-Ala11, Phe13, Nle14]-bombesin(6–14). GRP-receptor expressing vessels were evaluated in each tumor group for prevalence, quantity (vascular score) and GRP-receptor density.
Results The prevalence of vascular GRP-receptors was variable, ranging from 13% in prostate cancers to 92% in urinary tract cancers. Different tumor types within a given site may have highly divergent prevalence of vascular GRP-receptors (e. g. lung: small cell cancers: 0%; adenocarcinomas: 59%; squamous carcinomas: 83%). Also the vascular score ranged widely, with the highest score in urinary tract cancer (1.69), moderate scores in lung (0.91), colon (0.88), kidney (0.84) and biliary tract (0.69) cancers and low scores in breast (0.39) and prostate (0.14) cancers. Tumoral vascular GRP-receptors were expressed in the muscular vessel wall.
Conclusion(s) The tumoral vessels in all evaluated sites overexpressed GRP-receptors, suggesting a major biological function of GRP-receptors in neovasculature. The differential distribution of vascular GRP-receptors between the tumor types may point to tumor-specific mechanisms in their regulation. Urinary tract cancers express vascular GRP-receptors so abundantly, that they are promising candidates for vascular targeting in diagnosis and therapy.

P1.145

Interobserver reproducibility in the diagnosis of the prostate cancer

Zakharava V.; Liatkouskaya T.; Cherstvoy E.; Portyanko A.; Nitkin D.; Pashkevich L.; Sukonko O.; Rolevich A.; Masanskiy I.; Sagalchik L.; Ivanovskaya M.
Belarusian State Medical University, Department of Pathology, Minsk, Belarus

Background Considerable difficulties persist among pathologists in agreeing on the presence and severity of prostate cancer (PCa) when atypical small acinar proliferation (ASAP) is found in the material of prostate needle biopsy.
Methods Four oncopathologists participated in a study of 17 ASAP cases (using immunostaining cocktail of antibodies HWC (clone 34βE12), p63, AMACR) and were instructed to categorize each as either 'PCa' or 'not PCa'.
Results Overall agreement among pathologists using standard staining was 66.1%, and the multi-rater kappa value was 0.14, which is within the 'poor agreement' range. This is the evidence of the lack of distinct morphological criteria for PCa verification and of poor reliability of morphological examination as a single method. With the use of HWC-p63 cocktail, the overall agreement and the kappa coefficient increased to 85.3% and 0.53 respectively, which is within the 'moderate agreement' range and supports the expedience of their use in ASAP cases. The addition of the HWC-p63-AMACR cocktail permitted to achieve agreement among pathologists in 94.1% cases and the multi-rater kappa value was 0.78, which is within the 'excellent agreement' range. The sensitivity, the specificity and the positive predictive values of immunostaining using the triple cocktail was 94.4%, 90.9% and 96.8% respectively.
Conclusion(s) We conclude that PCa diagnosis is highly reproducible with the use of the available diagnostic criteria and HWC-p63-AMACR cocktail, which make it possible to verify the diagnosis of PCa in 97% cases of ASAP.

P1.146

Latent prostate cancer in Israel: an autopsy study comparing ethnic groups

Sandbank J.; Herbert M.; Mendlovic S.; Hermann G.; Segal M.; Zehavi S.
Assaf Harofeh Medical Center, Zerifin, Zerifin, Israel

Background In this autopsy study, we examined prostate glands from individuals immigrating to Israel from Europe, America, Asia and Africa and native-born Israelis.
Methods The study population consisted of a random autopsy population of 210 prostates of individuals between the ages of 4 and 78. Cases of carcinoma were assigned a Gleason score according to established guidelines. Results were tabulated and analyzed for three different groups: European/American-born Jews, Asian/African-born Jews and native-born Israeli Jews.
Results Ninety-two were of European/American birth, 53 of Asian/African birth and 65 were native-born Israelis. There was no difference in prostate size between the three groups. There were no cases of carcinoma found in the individuals under the age of 50. For individuals over the age of 50, the overall rate of carcinoma was 26.5% with a similar prevalence in each of the three groups.

Conclusion(s) Our results conform to other autopsy series and lend further support to the understanding that, in contrast to clinically detected prostatic adenocarcinoma, latent carcinoma of the prostate appears to show little variation among the races.

P1.147

Mechanisms of prostate cancer development: correlation of EGF, HGF and VEGF levels with the hormone refractory indicators

Popova O.; Shegai P.; Danilova T.; Bogomazova S.; Alekseev B.; Andreeva Y.; Ivanov A.; Frank G.; Paltsev M.
Moscow Medical Academy, Moscow, Russian Federation

Background The contribution of androgens to hormone refractory of prostate cancer (PC) remains unproved, but it is possible to suggest the role of non-hormonal regulators including polypeptide growth factors.
Methods The content of epidermal growth factor (EGF), hepatocyte growth factor (HGF) and vascular endothelial growth factor (VEGF) in PC culture supernatants from 91 patients in dependence on the use of neoadjuvant hormone therapy (NHT) was examined by ELISA. Parallely the association of growth factors concentration with basic indices of PC progressing and sensitivity to hormone therapy - the PSA level and PSA density was been estimated.
Results The obtained results testify to a differently directed change in regulation of HGF and EGF levels on the back of NHT and lack of the effect in relation to VEGF. Antiandrogen therapy was the best in promoting the HGF production. The quantitative increase of the HGF level appeared to be closely and positively associated with the most significant indicator in hormone refractory - the PSA rise on the back of NHT. The association of EGF production with NHT was unlike HGF been directed conversely as correlation with preoperational PSA level.
Conclusion(s) Our results allow to suggest that NHT functionally inhibiting androgen signalling leads to an enhancement in the production of factors in normal conditions negatively regulated by androgen receptor and to the contrary gets down the factors positively regulated under the influence of androgens.

P1.148

Nuclear morphometry in differential diagnosis of chromophobe renal cell carcinoma and renal oncocytoma

Choi C.; Kim S.; Kim J.; Park R.; Choi Y.; Cho Y.; Jang J.; Juhng S.
Chonnam National University Medical School, Hwasun, Chonnam, Republic of Korea

Background Chromophobe renal cell carcinoma (ChRC) is a malignant tumour and its benign counterpart is renal oncocytoma (RO). It is difficult to differentiate eosinophilic variant of ChRC (E-ChRC) from RO with overlapping histology (RO-TOH) histopathologically. In order to get objective informations of the nuclear feature, we compared the morphometric characteristics of classical ChRC (C-ChRC), E-ChRC, RO-TOH, and classical RO (C-RO).
Methods The hematoxylin-stained slides of 24 C-ChRCs, 6 E-ChRCs, 5 RO-TOHs, and 25 C-ROs were studied. The obtained parameters were longest diameter (LD), shortest diameter (SD), nearest nuclear distance (NND), diameter ratio (DR), and area (AR).
Results NND, LD, and DR were largest in C-ChRC and were smallest in C-RO, respectively. NND, SD, and DR were significantly different, however both LD and AR were not significantly different among the four disease groups. Post-hoc analysis (Mann-Whitney U test) found that these effects were mainly contributed by the differences between C-ChRC and C-RO. The C-ChRCs were more likely to have the NND > 9.5 μm (odds ratio=66.7; 95% confidence interval 6.9–645.5), and DR > 1.5 (odds ratio=17.9; 95% confidence interval 1.8–179.2) than C-ROs.
Conclusion(s) The morphometric features of NND, SD, and DR were significantly different among the four groups, especially between C-ChRC and C-RO. NND > 9.5 μm was the most important, and DR > 1.5 was the second important characteristic of C-ChRC compared with C-RO. However, E-ChRC and RO-TOH were similar in nuclear morphometric features.

P1.149

Osteopontin expression correlates with nuclear factor-κB activation and apoptosis downregulation in clear cell renal cell carcinoma

Lucin K.; Matusan-Ilijas K.; Damante G.; Fabbro D.; Dordevic G.; Hadzisejdic I.; Grahovac M.; Maric I.; Spanjol J.; Grahovac B.; Jonjic N.
Dpt of Pathology, Rijeka University School of Medicine, Rijeka, Croatia

Background Osteopontin (OPN) is a phosphoglycoprotein implicated in tumourigenicity and tumour cell metastasis. Apoptosis inhibition is one of mechanisms that contribute to development and progression of cancer and might be initiated by OPN interaction with tumour cell. The aim of this study was to establish the relation between OPN and nuclear factor- kappa B (NF-κB) expression at protein and mRNA level in specimens of clear cell renal cell carcinoma (CCRCC), and their relation to apoptosis.
Methods Expression of OPN protein and p50/65 NF-κB subunits was analyzed immunohistochemically in 94

CCRCC samples and compared mutually and to apoptotic index. Expression of OPN mRNA was analyzed using quantitative real-time PCR and compared to OPN and NF-κB protein expression in 22 CCRCC samples.
Results Statistical analysis showed the correlation of OPN expression at protein ($p<0.001$) and mRNA levels ($p=0.019$) with NF-κB activation, as well as the inverse association with apoptotic rate ($p = 0.024$). Also, activation of both NF-κB subunits showed inverse correlation with apoptotic index ($p = 0.003$).
Conclusion(s) Our data indicate that activation of NF-kB signaling pathway contributes to OPN-mediated CCRCC progression, partly by mediating prosurvival effect on tumour cells. Therefore, both molecules can constitute potential targets for therapeutic intervention in CCRCC.

P1.150

p16 expression in bladder biopsies in a small community hospital: could be helpful for differential diagnosis ?

Menendez C.; Fuente E.; Corrales B.; Palacio J.; Beridze N.; Murias C.; Argüelles M.
Hospital de Cabueñes, Gijón, Asturias, Spain

Background Bladder urothelial carcinoma (UC) is a multifactorial disease where cell cycle dysregulation has an important role with various proteins related to altered genes, like p16 ink4. The objective of this study is to assess immunohistochemical expression of p16 in different bladder lesions and see if it is useful for diagnosis of carcinoma versus reactive changes.
Methods 30 consecutive new transurethral vesical samples (TUR) divided into three groups: inflammatory/reactive/atypical lesions, non invasive low grade UC (Ta) and high grade UC (Ta, 1, 2)/CIS. p16 stains were performed in an automated device with positive controls. p16 was evaluated semiquantitatively. Nuclear staining was separately scored according to its sharp edge plus intensity. An ANOVA analysis was performed.
Results Weak positive p16 expression was observed in normal and reactive lesions. Isolated CIS and CIS adjacent to high grade UC showed strong positivity, mainly nuclear (with sharp edge); superficial UC (Ta) and invasive UC (T1-T2) had variable expression, frequently intense. Differences among those groups were statistically significative (p: 0,04), more yet between inflammatory/reactive/atypical lesions vs CIS, when nuclear p16 expression alone was considered (p: 0.001).
Conclusion(s) In spite of the variability of p16 expression and subjectivity of interpretation, there are significant differences of p16 immunoreactivity among those groups, mainly between neoplastic (especially CIS) versus reactive atypical lesions. This could be useful when diagnosing some small or partially denudated biopsies (altogether with other markers like p53 and CK20) and would also help to characterize them biologically.

P1.151

Pax8, hypoxia-inducible protein 2 (hig2), KSP-cadherin and carbonic anhydrase IX (CAIX) expression in collecting duct renal cell carcinoma (CDRCC) and papillary renal cell carcinoma (PRCC)

Abdullazade S.; Schultz L.; Netto G.; Illei P.; Sharma R.; Albadine R.; Baydar Ertoy D.
Hacettepe University, Ankara, Turkey

Background Distinguishing PRCC from CDRCC can be challenging at times on routine H&E sections. We studied immunohistochemical expression of Pax8, HIG2, KSP-Cadherin and Carbonic Anhydrase IX (CAIX) in papillary RCC (PRCC) and in collecting duct RCC (CDRCC) to evaluate their diagnostic value in distinguishing these two subtypes.
Methods Six collecting duct renal carcinomas and 45 PRCC were retrieved from surgical pathology archives of two different institutions. Representative paraffin block from each case was selected for immunohistochemistry. Immunohistochemical studies were performed using antibodies for Pax8, HIG2, KSP-Cadherin and CAIX. Stainings were scored semiquantitatively as: Negative: 0%, 1+: 1–25%, 2+: 26–50%, 3+: 51–100% of cells staining.
Results All CDRCC stained for HIG2 and Pax8. Staining was diffuse in 100% of cases for HIG2 while 67% (4/6) for Pax8. On the other hand, CAIX and KSP-Cadherin were expressed only focally (< 10% of cells) in 5 and 3 tumors respectively. Similarly, most (78% and 96% of) PRCC were HIG2 and Pax8 positive. CAIX and KSP-Cadherin expressing PRCC were rare (16% and 15%).
Conclusion(s) HIG2 and Pax8 have high sensitivity (87–100%) for both PRCC and CDRCC. CAIX and KSP-Cadherin is more frequent in CDRCC and can favor this tumor type. However their expression is very focal involving only few cells. We believe none of four markers can differentiate between two above renal carcinoma variants reliably.

P1.152

Pax8, hypoxia-inducible protein 2, KSP-cadherin and carbonic anhydrase-ix expression in mucinous tubular & spindle cell carcinoma (MTSC) and papillary renal cell carcinoma (PRCC)

Abdullazade S.; Schultz L.; Yildiz K.; Illei P.; Akkaya B.; Netto G.; Sharma R.; Albadine R.; Baydar Ertoy D.
Hacettepe University, Ankara, Turkey

Background Mucinous tubular&spindle cell carcinoma is a rare newly described type of renal cell carcinoma. Its histogenetic origin or line of differentiation is unclear. They are composed of variable proportions of tubular and spindle cell areas with focal to prominent mucinous/myxoid stroma. Although claimed to be genetically distinctive, MTSC and PRCC have significant overlaps morphologically. Here, we evaluated novel kidney markers and their differential value in distinguishing these tumors pathologically.
Methods We have performed immunohistochemistry for Pax8 (Protein Tech Group, Inc., USA), HIG2 (Novocastra, UK), CAIX (Novocastra, UK) and KSP-Cadherin (Cell Marque, USA) on 8 MSTC and 45 PRCC. Staining was evaluated semiquantitatively using a scoring system of 0–3+ for intensity and 0, 1+, 2+ and 3+ for extent (0, <25%, 25–50%, >50%).
Results All MTSC were positive for HIG2.7/8 expressed Pax8 which were diffuse (> 50%) in 5. KSP was negative in most (5/8) and only focally present in remaining 3. CAIX was positive in 7/8, but expression was focal (< 25%) in all. The immunoprofiles of PRCC were similar to MTSC for Pax8 and HIG2, positive in 96% and 78% of cases respectively. KSP and CAIX were less frequent in PRCC (15% and 16%).
Conclusion(s) MTSC and PRCC have similar IHC features. Both express HIG2 and Pax8 extensively while KSP is absent or focal. CAIX is the only molecule that is more frequently observed in MTSC in comparison with PRCC although its expression is always focal.

P1.153
Periacinar retraction clefts and D2–40 expression in prostatic cancer

Ulamec M.; Tomas D.; Cupic H.; Lenicek T.; Balicevic D.; Kruslin B.
Sestre Milosrdnice University Hospital and School of Medicine, Zagreb, Croatia

Background Diagnosis of prostatic adenocarcinoma can be complex, particularly in needle core biopsies. Periacinar retraction clefting is an useful additional criterion in setting patohistological diagnosis. Some authors suggest that clefts around tumorous tissue actually represent lymph vessel compartments.
Methods Neoplastic glands were analysed in 25 paraffin sections from radical prostatectomy specimens with prostatic adenocarcinoma diagnosis. Specimens were taken from the archive at the Ljudevit Jurak Department of Pathology, Sestre milosrdnice University Hospital, Zagreb. Each sample contained at least 30% of tumorous tissue and normal prostatic tissue that was used as an internal control. Lymph vessels were demonstrated with D2–40 antibody. Each slide was examined at 40x and 100x magnification field. Lymph vessels were counted inside tumorous tissue and compared with presence of periacinar retraction clefting in haematoxylin-eosin slides, in the same area.
Results Number of lymph vessels inside tumours tissue ranged between 2 and 75 on the one cross section (average number was 17.4). Lymph vessels that mimicked clefts inside tumours tissue ranged between 0 and 10 on the one cross section (average number was 1.33). In 30 tumorous glands with most extended clefts on each cross section number of lymph vessels ranged between 0 and 3 (average number was 0.6).
Conclusion(s) Lymph vessels can mimic periacinar clefts inside tumor, but most periacinar retraction clefts do not represent lymphatic spaces. These results suggest that clefts are probably due to stromal changes around tumorous acini.

P1.154
Prognostic factors of clear renal cell carcinoma in pT1a cases

Tsuzuki T.; Nishikimi T.; Fujita T.; Sassa N.; Fukatsu A.; Araki M.; Yoshino Y.; Hattori R.; Gotoh M.
Nagoya Daini Red Cross Hospital, Nagoya, Japan

Background The proportion of clear renal cell carcinoma (CRCC) cases diagnosed at pT1a is known to be increasing significantly. Although their prognosis is excellent in general, some cases show distant metastasis. Most of proposed prognostic factors are based on relatively large sized CRCC data. The prognostic factors for small sized CRCC, pT1a cases aren't well described.
Methods Three hundred three pT1a CRCC cases were retrieved from authors' institution files. For each case, the following pathological parameters were recorded: patient age, tumor location (upper, middle, low), Furhman grade, presence of capsule, presence of lympho-vascular invasion, growth pattern (expansive or infiltrating), presence of scar, presence of hemorrhage, and presence of necrosis.
Results Male to female ratio was 4.4. Patient's age ranged from 21 to 85 years (median 59 years, mean 58.1 years). Follow up duration ranged from one to 265 months (median 62 months). Seventeen cases showed distant metastasis. Furhman grade (grade 1+2+3 vs. 4), presence of lympho-vascular invasion, infiltrating growth pattern, and presence of necrosis were statistical significant ($p<0.0001$).
Conclusion(s) Furhman grade (less than 3 vs. 4), presence of lympho-vascular invasion, growth pattern, and presence of necrosis can be prognostic factors in CRCC in pTa cases. Growth pattern may be a new prognostic factor in CRCC.

P1.155
Spatial identification of the proteins from renal cell carcinomas by imaging mass spectrometry

Lim S.; Na C.; Lee S.; Kim W.; Chae C.; Kim K.
Seoul, Republic of Korea

Background Renal cell carcinoma (RCC) is the most common malignant renal epithelial neoplasm and has histologically diverse subtypes with variable clinical behavior. Gene or protein expression profiling has been a promising technique for refining the diagnosis and staging of RCCs. Recently imaging mass spectrometry (IMS) is emerging as new tool for the study of spatial distribution in the tissue as well as identification either protein or small molecules.
Methods In this study, we analyzed 7 RCCs by IMS including three clear cell RCCs, three chromophobe RCCs, and one papillary RCC with IMS. IMS is matrix assisted laser desorption ionization (MALDI) mass spectrometry (MS) based technology. Matrix is applied on cryosectioned-tissue and very small area of the matrix applied tissue is analyzed with MALDI-MS. The differences between each analyzed area are displayed by the imaging program. Based on the spatial distribution, region specific proteins can be identified by digesting the tissue with trypsin and analyzing it with MALDI-TOF/TOF.
Results Some proteins that are increased or decreased in RCCs were identified. The degree of expression of protein species or members to each class was used to stain the tissue section. S100A11 and ferritin were identified from papillary RCC tissue.
Conclusion(s) We successfully show the feasibility of MALDI imaging as a possible tool for the analysis of renal cell carcinomas. Identification of cancer specific proteins based on imaging mass spectrometry is considered to be new useful tool for cancer research.

P1.156
The fibrous capsule (pseudocapsule) in renal clear cell carcinoma (RCCC)

Pasechnik D.
Rostov Medical University, Rostov on Don, Russian Federation

Background The formation of fibrous capsule (FC) around the cancer is frequently observed with the development of renal clear cell carcinoma (RCCC).
Methods We studied 220 cases (94 males and 126 females, aged 37–79 years), who received nephrectomy of RCCC. A part of the tumor tissue was routinely fixed in 10% neutral formalin and was embedded in paraffin. Sections (4 μm) were stained with hematoxylin and eosin for histological diagnosis.20 cases RCCC were stained with monoclonal antibodies (DAKO) against vimentin, α smooth muscle actin (SMA), collagen I, IV, fibronectin, tenascin-C.
Results The development of FC is observed at early stages of RCCC growth. FC thickness was 1 to 3 mm, uneven. The interstitial nephritis around FC was presented in 72% of cases. FC was composed of collagen I, IV fibers, myofibroblast-like SMA- and vimentin-positive cells. Cancer cells did not express SMA. Tenascin C, fibronectin were located at the periphery of a tumor occasionally adjoined FC.
Conclusion(s) The FC was formed by host mesenchymal cells, not by RCCC cells. The fibrogenesis in the capsule of the RCCC could be regulated by many factors, including various growth factors and cytokines. The FC formation may result from interaction between tumor and host kidney and prevent the growth and invasion of RCCC.

P1.157
The impact of cancer volume and site of origin on the biologic behavior of impalpable adenocarcinoma of the prostate

Stamatiou K.; Kostakos E.; Labrakopoulos A.; Tepelenis N.; Zizi-Serbetzoglou A.
Tzaneion General Hospital of Piraeus, Piraeus, Greece

Background The present study investigates the relationship of cancer volume and site of origin of impalpable carcinoma of the prostate to local spread.
Methods Data were obtained from 212 autopsy specimens of the prostate gland, of men who died of causes other than carcinoma of the prostate, via whole-mount processing and complete sectioning. The largest focus was considered as the index tumor. A primary and a secondary Gleason grade was assigned at each tumor, and the same procedure has been followed for each of the tumor foci. Tumor volume was measured using the grid method.
Results Peripheral zone (PZ) carcinomas were much more common accounting for 85% of the cases while only 5 cases were found to originate from the transitional zone. Biologic behavior of impalpable tumors, was equally related to overall tumor volume and histological differentiation: local spread was found only in cancers that had both volume greater than 1 cc and areas of poor differentiation (Gleason grade 4). There was a clear correlation between tumor volume and local invasiveness: [$p<0.001$].
Conclusion(s) Transition zone impalpable cancers showed much less local spread than PZ cancers of comparable volume because the TZ boundary provided a barrier to cancer spread through the PZ.

P1.158
A rare kidney tumor

Sassi S.; Dhouib R.; Mrad K.; Driss M.; Abbes I.; Ben Romdhnae K.
Salah Azaeiz Institute, Tunis, Tunisia

Background Mucinous tubular and spindle cell renal carcinoma (MTSC) of the kidney is an uncommon recently recognized renal cell carcinoma with a favourable prognosis. differentiating it from other primary malignancies of the kidney is important. We report a case of MTSC in a 76- year- old woman.
Methods Hematoxylin and eosin stain and immunohistochemical studies were done. The primary antibodies used are pancytokeratin, cytokeratin 7, epithelial membrane antigen, cytokeratin 19, vimentin, cytokeratin 5/6, cytokeratins 20 and CD10.
Results The specimen received consists of a right kidney with a 35x30x25 cm tumour arising in the medial back region. The tumour was well limited of tan glistening colour. The tumor is histologically characterized by the proliferation of cuboidal and spindle cells of eosinophilic cytoplasm, an elongated and anastomosing tubules, a mucinous extracellular matrix and a low-grade nuclear cytology. Immunohistochemical study showed that the tumor cells were positive for pancytokeratin, cytokeratin 7, epithelial membrane antigen, cytokeratin 19 and vimentin. They were negative for cytokeratin 5/6, cytokeratins 20 and CD10.
Conclusion(s) MTSC is a rare low-grade tumour with a favourable prognosis which is easily identifiable morphologically. Further investigations are required to determine the frequency and true prognosis of these tumor.

P1.159
Alterations of ubiquitylation and sumoylation in conventional renal-cell carcinomas after the Chernobyl accident: a comparison with Spanish cases

Romanenko M.A.; Vozianov F.A.; Llombart-Bosch A.
Institute of Urology AMS of Ukraine, Kiev, Ukraine

Background We determined whether ubiquitylation and sumoylation processes, are involved in conventional renal-cell carcinogenesis associated with chronic, persistent low doses of ionizing radiation in patients living more that 20 years in contaminated areas after the Chernobyl accident in Ukraine.
Methods We assessed the immunohistochemical expression, on tissue microarray sections, of Ubiquitin (Ub), SUMO1, SUMO E2 conjugating enzyme Ubc9 and the cell cycle regulators p53, mdm2 and p14 ARF in 36 conventional renal-cell carcinomas and peritumoral tissue from Ukrainian patients with different degrees of radiation exposure. As control cases, eighteen cRCCs and peritumoral tissue from a Spanish cohort were analyzed.
Results Significant differences between the Ukrainian and Spanish groups were found regarding Ub overexpression, being higher in the Ukrainian cases. Furthermore, this expression was inversely associated with SUMO1 and Ubc9, with no correlation with tumor nuclear grade. Upregulation of nuclear p14ARF showed direct correlation with high levels of Ub in the same Ukrainian tumors and peritumoral tissue ($p<0.001$). There was also a trend towards a direct relation between Ub and mdm2 overexpression.
Conclusion(s) These findings suggest that ubiquitylation and sumoylation processes could be direct targets for long-term low-dose IR exposure leading to unscheduled protein degradation. Our present study can therefore provide a basis for future individual tailoring of cRCCs therapy and prophylactic measures in individuals inhabiting radio-contaminated areas.

P1.160
AMACR (Alpha-Methyl-Acyl-CoA Racemase) expression in urothelial cell carcinoma variants

Hatzianastassiou Kyriakos D.; Allamani M.; Kyrodimou E.; Papakonstantinou N.; Marinou H.; Papadimas G.; Koutselini H.
Department of Pathology, "Henry Dunant" Hospital of Athens, Athens, Attica, Greece

Background Despite its limitations and pitfalls, AMACR (alpha-Methyl-Acyl-CoA Racemase, or P504S) has been of value as an adjunct diagnostic tool for prostatic adenocarcinoma (PAC). It is known for being expressed in renal epithelial structures, a subset of renal tumors, as well as, in both normal and neoplastic urothelium - and more recently, in urothelial adenocarcinomas. Therefore, we addressed the same issue in a small series of urothelial cell carcinoma (UCC) variants.
Methods Four UCC variants were retrieved from our recent routine files and stained for AMACR (clone 13H4), while supportive immunostains were available accordingly.
Results Cases included: UCC signet-ring cell type involving the prostate on FNCB, UCC plasmacytoid/lymphoma-like variant extending to the cysteo-uterine space, mixed bladder carcinoma – predominantly small cell type, and a moderately differentiated squamous cell carcinoma of the renal pelvis. Three cases exhibited moderate to intense cytoplasmic staining that ranged from focal to extensive, while the squamous cell carcinoma was negative. Moderate focal positivity was noticed in the small cell component. Normal urothelium was less intensly positive.
Conclusion(s) Our findings, although limited to small series, if seen in conjunction with the pertinent literature, suggest that AMACR/P504S expression may represent a non-specific common denominator spanning the entire spectrum from normal urothelium to primary urothelial neoplasms and their variants. Since its expression in the upper urinary tract has already been associated with tumor

progression, it remains to be validated if squamous trans-differentiation could be hold responsible for the lack of expression in our case.

P1.161

Carcinosarcoma of the renal pelvis: a case report

Cakir C.; Hallac Keser S.; Kayahan S.; Ege Gul A.; Ergen C.; Barisik N.; Eryildirim B.; Karadayi N.
Lutfi Kirdar Kartal Educational and Research Hospital, Pathology Department, Istanbul, Turkey

Background Carcinosarcomas of the renal pelvis is very rare neoplasm. These tumors are composed of both malignant mesenchymal and epithelial elements. Histologically, it exhibits morphologic and/or immunohistochemical evidence of epithelial and mesenchymal differentiation with the presence or absence of heterologous elements. Carcinosarcomas of the renal pelvis are known to be rapid in progression and associated with a poor prognosis.
Methods We present the case of a 72-year-old man with gross hematuria and flank pain. Radiologic studies revealed a large left kidney mass. Radikal nephrectomy was performed.
Results In the renal pelvis irregular shaped 10x9x8 cm mass was seen. The cut section of the mass was gray-white, focally necrotic and hemorrhagic. The tumor had invaded the renal parenchyma was also noted. Extrarenal extension of the tumor was observed. Microscopically, on the sections infiltrating urothelial carcinoma and sarcomatous component including numerous osteoclast-like multinucleated giant cells was seen. There were also foci of squamous differentiation. Two lymph nodes locating at the hilum of the kidney showed metastasis. Immunohistochemically, epithelial component showed a diffuse reactivity for cytokeratin, whereas sarcomatous components react with vimentin, CD68 and focally SMA. There was no staining of the sarcomatous component with cytokeratin.
Conclusion(s) In the case report, the clinical presentation, histopathologic and immunohistochemical features of the case are reported and discussed in the light of literature.

P1.162

Clusterin expression in non-invasive urothelial carcinoma

Dogan Ekici A.I.; Eroglu A.; Turkeri L.; Ekici S.
Yeditepe University, Istanbul, Turkey

Background Clusterin is a circulating multifunctional glycoprotein that up-regulated during various physiological and pathological states, such as senescence, type-II diabetes mellitus, Alzheimer disease and in many neoplasms such as colonic and pituitary adenomas, colonic, hepatocellular, ovarian, urothelial and laryngeal carcinomas.
Methods We investigated the immunohistochemical Clusterin expression (Clu) in paraffin embedded archival transurethral resection specimens of non-invasive urothelial carcinoma cases [n=46; 35 (76%) male, 11 (24%) female] with mean 45 months of follow-up. We analysed the association of percent Clu (% Clu) with clinicopathological factors. SPSS for Windows V.14 was used for statistical analyses.
Results Of the 46 cases, 28 (60.9%) were <65 years and 18 (39.1%) were≥65 years. During follow-up 11 (23.9 %) of them were died of non-tumoral reasons, 1 (2.2%) bladder cancer. %Clu in cases≥65 years (50.5%) was significantly higher than %Clu in cases <65 years (32.9%) (p<0,05). %Clu in males (48.3%) was significantly higher than in females (28.8%) (p=0,04). %Clu in cases with progression (53.2%) was significantly higher than the %Clu in cases without progression (32.24%) (p = 0,04).
Conclusion(s) In conclusion; up-regulation in clusterin expression was showed in males, its association with age and progression was detected in non-invasive bladder cancer. Further studies are required to clarify the mechanism of clusterin accumulation and its probable age association in non-invasive urothelial carcinomas. It is important to know the increase in %Clu with age, therefore further studies related to clusterin expression in certain neoplasms may be designed on subjects in the same age group.

P1.163

Cyclooxygenase-2 expression on urothelial and inflammatory cells of cystoscopic biopsies and urine cytology

Moussa Mohamed M.; Omran Z.; Nossier M.; Lotfy A.; Swellam T.
Theodor Bilharz Research Institute, Cairo, Egypt

Background Cyclooxygenase-2 (COX-2) is a key inducible enzyme involved in the production of prostaglandins. It contributes to human carcinogenesis by various mechanisms. The aim of the current study was to elucidate the possible involvement of COX-2 in human bladder carcinoma by examining its expression on both urothelial and inflammatory cells in tissue biopsies and urine cytology samples of different urinary bladder lesions.
Methods A total of 65 patients were included in the study, they represented seven control cases with almost normal-looking bladder tissue; pure chronic cystitis (n= 12); premalignant lesions (18) in the form of squamous metaplasia (n=8) or urothelial dysplasia (n=10) as well as transitional cell carcinoma (TCC) (n= 18), and squamous cell carcinoma (SqCC) (n= 10). Immunohistochemistry of formalin-fixed, paraffin-embedded bllader sections and urine cytology samples was performed for all cases.

Results The score of urothelial COX-2 expression was sequentially upregulated from normal to chronic cystitis (either pure or associated with premalignant changes) (po 0.05) to malignant changes (po 0.05). However, the inflammatory cellular expression was downregulated with malignant transformation compared with chronic cystitis (po 0.05). In TCC, COX-2 was over-expressed on both urothelial and inflammatory cells in advanced tumors. Urine cytology samples were positive for COX-2 in a comparable manner to that observed in cystoscopic biopsies.
Conclusion(s) The possibility of using the differential COX-2 expression on both inflammatory and urothelial cells as markers for premalignant or malignant transformation; second, besides cystoscopy, urine cytology was found to have a high sensitivity for COX-2 expression and hence proved to be valuable in malignancy as a non-invasive substitute for cystoscopy.

P1.164
Diagnostic performance of cytokeratin-19 in cancer bladder

Nosseir Mostafa Fahmy M.; Aboul-Magd Ahmed D.; Hassanien Sayed A.; Wahdan Samir M.; Zahran Mohamed N.; Swellam Abdalla T.
Theodor Bilharz Research Institute, Giza, Imbaba, Egypt

Background Detection of urinary bladder cancer using non-invasive markers appears to be significantly accurate to hopefully reduce the use of cystoscopies among these patients.
Methods The study was conducted on 30 cases of primary bladder carcinoma (18 TCC and 12 SqCC), 8 patients of benign prostatic hyperplasia and 7 healthy volunteers. Serum and voided urine samples from all cases were subjected to Cyfra 21-1 immunoassay. Immunohistochemistry was performed on their tissue biopsies.
Results For detection of primary bladder carcinoma, the optimal cut-off concentration of serum Cyfra 21-1 that resulted in a sensitivity of 33% and 100% specificity was at 2.8 ng/ml. While, for urine Cyfra 21-1, the best receiver operating characteristic curve analysis revealed a sensitivity of 92% and 100% specificity at a threshold value of 5.8 ng/ml. Immunohistochemical tissue expression of cytokeratin-19 revealed a strong positivity in BPH. No statistical significant difference could be detected in tissue staining regarding tumor grades and stages.
Conclusion(s) Urine Cyfra 21-1 assay had promising sensitivity and specificity results that appeared to be superior to both urine cytology and FDPs assays for screening primary bladder carcinoma. While, serum Cyfra 21-1 does not show enough sensitivity to justify its application routinely, but increased level with advancing tumor grade or stage may be useful for monitoring the clinical course of the disease thus can be used as a complementary parameter. Cytokeratin-19 immunohistochemical expression, besides being an invasive maneuver, had a relatively lower reliability as a useful tumor marker.

P1.165
Ductal prostatic carcinoma exhibiting as an urethral polypoid tumour

Boila Corina A.; Loghin A.; Moldovan C.; Decaussin Petrucci M.; Ragage F.; Berger N.; Borda A.
Department of Pathology, University of Medicine and Pharmacy Târgu-Mureş, Târgu-Mures, Romania

Background Ductal Prostatic Carcinoma (PDC) is a rare variant of prostatic carcinoma accounting for less than 3% of all cases, arising from proximal prostatic ducts, rarely observed in prostatic biopsies, more often in transurethral prostatic resection (TURP) specimens. The clinical and pathological features of this variant can be mislaid with urothelial carcinoma.
Methods A 78 years old patient with obstructive syndrome and hematuria, underwent a TURP for a polypoid papillary mass situated on the anterior part of the bladder neck near the veru montanum. The PSA serum level was 7.5 ng/ml and the prostate was nodular. On microscopic examination, the exophytic mass exhibited a complex, branching architecture with papillae covered by a single layer of pseudostratified columnar epithelium. The prostatic subsequent resection cores showed an infiltration with cribriform or solid masses without central necrosis. Immunohistochemical studies showed the following pattern: PSA+(focal), P504S+, 34BE12 –, CK7-, CEA-.
Results The prostatic origin of the polypoid intra-urethral tumor is confirmed by immunohistochemistry and the tumor is classified as ductal variant of prostatic adenocarcinoma, Gleason score 8 (4+4). Despite the rather low level of the patient's serum PSA, a bone metastasis was also present.
Conclusion(s) Ductal Carcinoma is a rare and severe variant of prostatic carcinoma. Its clinical feature (low PSA level and urethral obstruction) and microscopic appearance (papillary architecture) can be mistaken for an urothelial carcinoma. Immunohistochemical studies are mandatory for the diagnosis.

P1.166
Evaluation of expression of chromatin assembly factor-1 (CAF-1) p60 in prostatic preneoplastic lesions

Staibano S.; Siano M.; Mascolo M.; Ilardi G.; Insabato L.; Altieri V.; Prezioso D.; De Rosa G.
Department of Biomorphological and Functional Sciences, Pathology Section, Federico II University, Naples, Italy

Background Prostatic adenocarcinoma is the second cause of cancer-related death for men in Western countries. High-

grade prostatic intraepithelial neoplasia (HG-PIN) and atypical small acinar proliferation (ASAP) are precancerous lesions of the prostate. In the last years, a great interest was focused on the relationship between epigenetic mechanism alterations and cancer development and progression. Chromatin assembly factor-1(CAF-1) regulates epigenetically the orderly progression of eukaryotic cells toward mitosis and has been proposed as sensible proliferation and prognostic marker in experimental and human tumors. We previously demonstrated the relationship between overexpression of p60 subunit/CAF-1 and adverse behavior of prostatic cancer. The aim of the present study was to evaluate the role of CAF-1/p60 as a new marker of tumor progression and as a predictor of biological behavior.

Methods The p60/CAF-1 expression was detected by immunohistochemistry on a selected series of prostatic preneoplastic lesions (formalin-fixed paraffin-embedded biopsies: 11 ASAP, 7 HG-PIN and 3 HG-PIN/ASAP). Results were compared with clinicopathological data and follow-up of patients.

Results We found overexpression of CAF-1/p60 in most HG-PIN and high grade adenocarcinoma, with a linear progression from low to high-grade tumors. Furthermore, the protein was strongly expressed in up to 50% of ASAP.

Conclusion(s) We hypothesize that CAF-1/p60 plays a role as marker of evolution from preneoplastic lesions to prostatic adenocarcinoma. In addition, analysis of follow-up data showed an association between highest values of CAF1/p60 and metastatic cancer, suggesting for this protein a role as prognostic marker for prostate cancer.

P1.167

Expression of E-cadherin in upper urothelial carcinoma

Jankovic-Velickovic Goluba L.; Dolicanin Z.; Djordjevic B.; Tasic D.; Marjanovic Tomislava G.
Institute of Pathology, Clinical Centre, Nis, Serbia and Montenegro

Background The aim of this study was to compare E-cadherin (E-CD) expression (normal or aberrant) among different types of invasion (nodular, trabecular, infiltrative) of the upper urothelial carcinoma (UUC).

Methods Samples from 45 patients with UUC were analyzed with monoclonal anti-human E-CD antibody. E-CD expression was consider normal if staining was present in > 90% of the tumor cells. Aberrant expression were defined as those giving negative (complete absence of immunoreactivity), focally positive (<10% of the cells are dyed) or heterogeneous reactivity (10–90% of the cells are dyed).

Results Nodular type of invasion was detected in 30 (67%) UUC, trabecular in 6 (13%), infiltrative in 6 (13%) cases, while pTa stage was present in 3 (7%) of UUC. Aberrant expression of E-CD was found in 17/45 (38%) and normal membranous in 28/45 (62%) of UUC. The prevailing aberrant pattern was heterogeneous (15 specimens, 33%). Aberrant expression of E-CD was found in nodular, trabecular and infiltrative type of invasion in 9 (20%), 4 (9%), 4 (9%) respectively. There was no difference in expression of E-CD depending of type of invasion ($x2=2.91$, $p=0.087$).

Conclusion(s) The results of our study did not confirm difference in expression of E-cadherin in different types of invasion in UUC while prevailing pattern of aberrant E-CD expression was the heterogeneous type.

P1.168

Expression of maspin in normal prostate and prostatic carcinomas

Lovric E.; Gatalica Z.; Eyzaguirre E.; Kruslin B.
Department of Pathology and Cytology, County Hospital "Čakovec", Čakovec, Croatia

Background Maspin is a serine protease with tumor suppressor activity. It plays an important role in preventing basement membrane invasion, suppression of tumor growth, vascularization and metastasis. Overexpression of maspin may enhance hypoxia induced apoptosis. We analyzed the expression of maspin in various cell types in normal prostate and prostatic adenocarcinomas.

Methods Formalin fixed, paraffin embedded prostatic biopsies from 42 patients (34 carcinomas, and 8 normal) were evaluated with anti-maspin antibody (G167-70, Pharmingen), and anti-cytokeratins antibody (34ß E12, DAKO). Automated immunohistochemical procedures were used (LSAB2, DAKO).

Results Maspin was strongly expressed in basal cells in every case of normal glands, and also weakly expressed in luminal cells in a number of cases. Normal stromal cells (fibroblasts and smooth muscle) were weakly positive. Epithelium of prostatic carcinoma in 27 of 34 cases showed cytoplasmic and nuclear expression of maspin, predominantly in prostatic carcinomas Gleason score 6 and 7. Stromal cells surrounding carcinomas expressed maspin similarly to the normal tissue. In controls, basal cells were identified by strong staining with 34ß E12, while prostatic carcinomas were consistently negative.

Conclusion(s) Maspin is expressed strongly in cytoplasm of the basal cells of normal prostatic glands. This is consistent with its proposed role as tumor suppressor in malignant transformation in prostate. However, some low grade prostatic carcinomas, showed abnormal nuclear maspin expression. Follow up studies are needed to address prognostic significance of maspin aberrant expression in prostatic carcinomas.

P1.169

Expression of PDGFR-β in renal cell carcinoma

Mallofre C.; Petit A.; Gaspa A.; Nadal A.; Mellado B.
Dpt. Pathology, Hospital Clínic, Universitat de Barcelona, Barcelona, Spain

Background Recent studies about molecular biology of Clear Cell Renal Cell Carcinoma (CRCC) has established VEGF and PDGF mediated tumor angiogenesis as relevant therapeutic targets. Inhibitors targeting PDGFR-β receptor have been proved effective controlling tumoral growth and are undergoing clinical testing in metastatic CRCC patients. Neverheless, little is known about the tissular expression of PDGFR-β in this tumor type.
Methods Three TMA from 97 CRCC specimens were constructed. Immunohistochemical study was performed using polyclonal antibody PDGFR-β. Expression of PDGFR-β on tumor cells and vessels were assessed. Both the extent and intensity of staining were taken into account in a three grade score.
Results 83,5% (81) CRCC showed no expression of PDGFR-β in tumor cells; low staining was seen in 12,4% (12) of cases and high in 4,1% (4) of them. In contrast, vascular expression of PDGFR-β was detected in 51,6% (50) cases.29 of them exhibiting diffuse and 21,6 focal expression.
Conclusion(s) Our results highlight low expression of PDGFR-β in tumor cells and document for the first time, vascular expression of this receptor in CRCC tissue samples. This data supports PDGFR-β as a mediator of angiogenesis in this tumor type. The consideration of vascular expression of PDGFR-β as a therapeutic marker deserves further investigation.

Pediatric and fetal pathology

P1.170

Correlation between prenatal ultrasound and postmortem findings in fetuses with central nervous system anomalies terminated in the second trimester

Akgun H.; Ozgun T.; Aydin A.; Ozturk F.; Okten T.; Basbug M.
Erciyes University Medical Faculty, Department of Pathology, Kayseri-Turkey, Kayseri, Turkey

Background The aim of the study was to compare the consistency of Central nervous system (CNS) anomalies detected by second trimester prenatal ultrasound examination with the findings in fetal autopsies following the termination of pregnancy (TOP) in the second trimester.
Methods In a 4-year long prospective study, 107 second-trimester TOP was performed due to fetal malformation diagnosed by second trimester-ultrasound examination at a tertiary referral center. Ultrasound findings were compared with fetal autopsy findings.
Results There were 107 prenatally diagnosed malformed fetuses that were analyzed following the TOP. There were 53 (49%) CNS anomalies (isolated $n=24$, multiple anomaly $n=19$) out of the 107 cases. Hydrocephaly ($n=34$, 40%) and neural tube defects ($n=18$, 18%) were the two most common CNS anomalies. Fourteen cases had anencephaly (26.4%), there were 13 cases with encephalocele (25.5%), 5 cases with Dandy-Walker syndrome (9.4%), one cases with agenesis of corpus callosum (1.8%) and one case with holoprosencephaly (1.8%). Only neural tube defects were not diagnosed in two cases with multiple anomalies in prenatal ultrasound. Other anomalies were diagnosed in prenatal sonography and were confirmed by fetal autopsy.
Conclusion(s) Evaluation of fetal autopsies following TOP enables diagnosis of pathologies undetected by prenatal ultrasound alone, leading to better preconceptional counseling for subsequent pregnancies. This study confirms that developmental anomalies in the central nervous system are frequent and that ultrasound diagnoses are in good concordance with the autopsy diagnoses.

P1.171

Expression of EGFR and HER2 in pediatric enbryonal brain tumours

Stefanaki K.; Patereli A.; Doussis Anagnostopoulou I.; Moschovi M.; Van Vliet Constantinidou C.; Karamolegou K.; Sfakianos G.; Prodromou F.; Karentzou O.
Dept of Pathology Agia Sofia Children's Hospital, Athens, Greece

Background Medulloblastoma[MB], Atypical Teratoid rhabdoid tumour [ART]and CNS PNET show overlapping histological features and different genetic pathways. The role of EGFR and HER2 in their pathogenesis has not been elucidated. The aim of this study was to investigate EGFR and HER2 expression in 36 embryonal brain tumours in correlation with histology, Ki-67, and p-53 oncoprotein.
Methods Our material comprised 27 MB, 7 ART and 2PNET. The Bond Polymer kit was used for the detection of Ki-67/MIB-1, p-53 [DO-7], EGFR [EGFR 25] and HER2 [CB 11].
Results High Ki67 expression [> 25%] was observed in all MB being increased [> 50%] in 8 cases, while p-53 was detected in 25 MB showing a high expression [> 10%] in 16 cases. EGFR and HER2 were observed in 10 /27 [37%] and 17/27 [63%] MB showing a heterogenous expression. Although there was no correlation of EGFR or HER2 expression with MB subtype, HER-2 expression increased in undifferentiated areas. A high EGFR and HER2 expres-

sion was observed in 5 MB with a high Ki-67 [> 50%]. In 3 A high p-53/HER2 expression was observed in 7 MB. High Ki67 and p-53 expression was revealed in all ART and PNET, while EGFR and HER2 were detected in 3 and 6/7 ART respectively with high expression.
Conclusion(s) EGFR and HER2 expression is variable in pediatric embryonal brain tumours. HER2 expression in a considerable number of MB [63%] and ART [85%] suggests that it may be implicated in their pathogenesis representing a potential target for novel therapies.

P1.172
Lung morphology in systemic diseases in children

Toran N.; Ferreres Carles J.; Garrido M.; Garcia-Peña P.; Lindo E.; Semidey Eugenia M.; Ramón YCajal S.
Hosptal Vall d'Henron, Barcelona, Spain

Background Systemic diseases in children could involve the pulmonary parenchyma as the first manifestation. Lung biopsy contributes to the diagnosis and the therapeutic management of the patient. This work presents the correlation between radiological and histological findings.
Methods During the last six years we reviewed 3000 patients with systemic disease. The most frequent radiological examination techniques were Chest X-ray/ High Resolution Computed Tomography (HRCT), following by MRI in some cases. In 34 cases (1.2% of patients) lung biopsy was performed.
Results Connective tissue disorders showed with HRCT ground glass pattern, subpleural nodules or linear dense areas, displayed histological interstitial pneumonitis, fibrosis or cholesterol granulomas. Systemic lupus erythematous presenting massive pulmonary hemorrhage had a radiological pattern of consolidation. In acquired immunodeficiencies with unusual pattern of lung disease we found angioinvasive Aspergillosis and mycetomas. In immunodeficiency syndromes with alveolar or ground-glass pattern, morphologically predominated lymphoid interstitial pneumonia, lymphohistiocytic infiltrates or organizing pneumonia. In chronic granulomatous disease with focal destruction on HRCT, lung abscess were present. The radiological finding of cysts and densities in Langerhan's disease showed morphological septal infiltration of CD1a+histiocytes. In vasculitis, confluent alveolar opacities in HRCT corresponded to perivascular granuloma. Cystic fibrosis presented bronchiectasis in HRCT and in the biopsy.
Conclusion(s) In 66% of children with systemic disorders the correlation between radiological findings and the morphological lesions was good. In a 20% of the patients morphological diagnosis was mandatory for classifying the disease and to begin a prompt treatment to prevent its progression.

P1.173
Pediatric brain tumor in 2005–2008 in Uludağ University

Elezoglu B.; Tolunay S.
Bursa, Turkey

Background In turkey, pediatric brain tumor comes after the leukemia and lymphoma.5 year survival rate is %50–60. Survi depends on histologic types.
Methods We have evaluated pathology report of 80 patient 15 and under 15 years old in 2005–2008. Their diagnoses were meningioma, pilocytic astrocytoma, gioblastoma multiforme, craniopharngioma, choroid plexus papilloma, medulloblastoma, dermoid tumor, ependimoma, oligodendroglioma.
Results We have evaluated tumor location, tumor type, age, sex, clinical information.
Conclusion(s) We represented pediatric brain tumor with pathologic and clinical sign.

P1.174
Significance of meconium-stained amniotic fluid in preterm deliveries

Staribratova Ivanova D.
Medical University-Plovdiv, Plovdiv, Bulgaria

Background Meconium staining of the amniotic fluid has been considered to be a sign of fetal hypoxia. However, it has been demonstrated that hypoxia is not usually present. The causes underlying meconium staining of amniotic fluid are not well-known, but infection may be involved in some cases.
Methods To better understand this, placental membrane and umbilical cord were sectioned from cases with preterm delivery. Antepartum death was excluded from the study. Cases were classified according to the color of amniotic fluid into two groups: meconium stained and clear amniotic fluid. Perinatal complications were defined in our study as: (1) intrapartum death (IPD) or postpartum death (PPD); (2) one or more of the following: 1-min Apgar score <3,5-min Apgar score <7 or small for gestational age. 75 women in premature labor were evaluated.
Results Amniotic fluid was stained with meconium in 30 cases. Infection was significantly more prevalent among women with meconium in the amniotic fluid; 25 of 30 women with meconium staining, and 15 of 75 women with clear fluid had infections. The most common bacteria found in women with meconium staining were Ureaplasma urealyticum and mixed bacterial strains.
Conclusion(s) The study indicates that meconium staining of amniotic fluid is associated with an increased risk for infection and premature delivery but not significantly with fetal hypoxia.

P1.175

Aberrations of ALK gene in neuroblastoma: a potential therapeutic target

Noguera R.; Subramaniam Mani M.; Piqueras M.; Tadeo I.; Berbegall A.; Villamón E.; Navarro S.
University of Valencia, Valencia, Spain

Background Anaplastic Lymphoma Kinase (ALK) is a transmembrane tyrosine kinase receptor implicated in neuronal autocrine differentiation and physiology. Recent evidence indicates ALK to be a major predisposition gene as well as a potential therapeutic target for neuroblastoma.
Methods In this study, we used a break-apart ALK DNA probe to analyze the copy number aberrations of ALK gene in a tissue microarray (TMA) of 50 well characterized primary neuroblastomas. Out of these tumors, 28 were classified as poorly differentiated, 10 as NOS and 12 as undifferentiated neuroblastomas.
Results ALK aberrations (amplification, 1/45; gain 15/45 and loss/imbalance 11/45) were detected in 27 of 45 (60%) of neuroblastomas. No significant correlation was observed between ALK gene aberrations and aberrations of MYCN, 17q, 11q and 1p36. The median OS time was 84, 51 months (95% IC 71, 26–97, 76), whereas the median EFS time was 70, 82 months (95% IC 56, 02–85, 62). Interestingly, we found ALK aberrations in metastatic neuroblastomas (stage 4: 14/22) and also in localized neuroblastomas (stages 1, 2, 3 and 4 s:12/21).
Conclusion(s) This is the first TMA-based-interphase-fluorescence in situ hybridization (FISH) study to assess the frequency of copy number aberrations of ALK gene and its possible association with MYCN, 17q, 11q and 1p36 status in formalin fixed paraffin embedded (FFPE) clinical samples of neuroblastomas. Our data suggest that ALK copy number aberrations are frequent genetic alterations in the development of neuroblastomas and it represents a novel potential therapeutic target. Grants: ISCIII (606/2007; PI06/1576; RD06/0020/0102) and Fundación Inocente, Inocente (PI4/07-36).

P1.176

Activation of the PI3K/AKT pathway and its regulation by thioredoxin in neuroblastoma

Sartelet H.; Rougemont A.; Fabre M.; Bosq J.; Oligny L.; Vassal G.
CHU Sainte Justine, Montreal, Quebec, Canada

Background Neuroblastoma is a malignant pediatric tumor with poor survival. The PI3K/AKT pathway contributes to tumor aggressiveness. Thioredoxin (Trx) a PTEN inhibitor is overexpressed in many tumors. The objective of this study was to explore the PI3K/AKT pathway activation and its regulation by Trx-1 in neuroblastoma.
Methods TRKB, p-p70S6K, 4EBP1 and p-mTOR. A semi-quantitative score based on the percentage of positive cells was used. Using neuroblasts cell lines, we investigated the variation of cell viability and AKT activity induce by several AKT inhibitors and Trx-1 used as single agents or in combination. „ IGF1Rβ, PDGFRαTissue microarrays were constructed from 101 primary tumors. Immunohistochemical study was performed using antibodies against: PI3K, AKT, pAKT, PTEN, pPTEN, Trx-1, EGFR, HER2, VEGFR1, VEGFR2, VEGF, PDGFR.
Results AKT was activated in nearly all neuroblastomas despite a high expression of PTEN but in correlation with pPTEN and Trx-1 ($p<0.01$) two PTEN inhibitors. Among membrane receptors studied, only IGF1R, TRKB and VEGFR1 were correlated with the presence of pAKT, as well as the downstream protein p70S6K (all $p<0.01$). In neuroblasts, LY294002 and RAD001 but not Deguelin significantly decreased cells viability and AKT activity. Trx-1 up-regulated AKT activation and decreased the cytotoxicity of AKT inhibitors and of doxorubicin a chemotherapeutic agent commonly used in the treatment of neuroblastoma.
Conclusion(s) The PI3K/AKT pathway is activated in neuroblastoma, and VEGFR1, TRKB, IGF1R and Trx-1 are preferentially committed to this activation. Trx-1 is a potential target for specific treatment in neuroblastoma.

P1.177

Alveolar rhabdomyosarcoma with positive neuroendocrine markers: report of 3 cases

Bellefqih S.; Gaillard D.; Lorenzato M.; Luquet I.; Ploton D.; Delattre O.; Birembaut P.
CHU Reims Hopital Maison Blanche, Reims, France

Background Alveolar rhabdomyosarcoma (ARMS) may be extremely difficult to distinguish from primitive blue round cell tumors without immunohistochemistry and/or genetic study. We report 3 cases of ARMS with neuroendocrine phenotype.
Methods 3 cases of ARMS were analysed using histological, immunohistochemical, ploidy, ultrastructural, and molecular genetic techniques.
Results The three patients were boys aged 11 (case 1), 15 (case 2) and 4 years (case 3). The tumours were located respectively in the nasal ala groove, the retroperitoneum and the hand. Cases 1 and 3 had lymph node metastases at time of presentation. Microscopically, cases 1 and 2 had morphologic features of small blue round cell tumors; case 3 was composed of compact sheets of medium to large tumor cells. Alveolar architecture was present in all cases. Tumor cells were desmin+(3/3), myogenin+(3/3), synaptophysin+(3/3), CD56+ (3/3), NSE (2/3), AE1/3+ (2/3).

Chromogranin-A, CD99, S100 protein, EMA and CD45 were negative. Ki67 index was > 70% (3/3). DNA content was tetraploid (3/3). Ultrastructurally, sarcomeric filaments were seen in all cases, while neuroendocrine granules were absent. PAX3/FKHR fusion transcript was identified in cases 2 and 3 and t(2;13)(q35;q14) translocation in case 3. FISH analysis is pending for the cases 1 and 2.

Conclusion(s) Aberrant expression of neuroendocrine markers in ARMS may be a potentially serious diagnostic pitfall. These findings emphasize the need to use a panel of markers and genetic studies to improve primitive blue round cell tumors diagnosis regardless of the patient's age and the tumour location.

P1.178

An immunohistochemical study of tenascin-C expression in the developing human lung

Lambropoulou M.; Chatzaki E.; Simopoulou M.; Koutlaki N.; Kiziridou A.; Jivannakis T.; Limberis V.; Grammatikopoulou I.; Deftereou T.; Papadopoulos N.
Department of Histology-Embryology, Democritus University of Thrace, Alexandroupolis, Greece

Background Aim of this study was to investigate the role of tenascin-C in the developing human lung, during the pseudoglandular, canalicular and saccular stage of lung maturation.

Methods Formalin-fixed, paraffin-embedded lung tissue from thirty embryos at the pseudoglandular (10–16w, no= 10) the canalicular (17–23w, no = 10) and the saccular stage (24–27w, no = 10), were investigated for the expression of tenascin-C by immunohistology.

Results The tenascin-C distribution patterns observed differed significantly between the stages of embryogenesis. During the pseudoglandular stage, the density of immunoreactive cells was higher in the condensing mesenchyme surrounding the epithelial glands than in the epithelial cells, whereas the opposite was observed in the canalicular stage. During the saccular stage, the pattern of immunoreactivity was lower than those of the pseudoglandular and canalicular stage, in both epithelial and mesenchymal cells, but it was highly expressed in the basement membranes.

Conclusion(s) This restricted spatiotemporal distribution suggests that tenascin-C has a key role 1) in mesenchymal tissue remodeling during the pseudoglandular stage, a period that describes the development of the complete bronchial tree and 2) on the epithelial cell shape and function during the canalicular stage, a period that describes the formation of pneumocytes type I and pneumocytes type II. The later, will produce the surfactant, a phospholipid-rich fluid capable of lowering surface tension at the air-alveolar interface. During the saccular stage, tenascin-C was present mainly in the basement membranes surrounding the acinar and vascular structures, indicating a supporting and mechanical role.

P1.179

Analysis of the PI3K signaling pathway in neuroblastic tumours. preliminary study

Izycka-Swieszewska E.; Drozynska E.; Grajkowska W.; Klepacka T.; Perek D.; Kobierska-Gulida G.; Koltan S.; Jaskiewicz K.; Stefanowicz J.; Szurowska E.; Dembowska B.; Wozniak A.
Medical University of Gdansk, Gdansk, Poland

Background The PI3 kinase plays a complex role in cell biology and metabolism. Signaling pathway through PI3K is activated in many malignant tumors. The role of this signal transduction stream is not well known in neuroblastic tumors.

Methods In this study multiple components of PI3K signaling pathway were evaluated by immunohistochemistry in tissue arrays containing 110 neuroblastic tumors. The phosphospecific antibodies against PI3K 110, PI3K 85, pAKT, pmTOR, PTEN, p70S6K, 4EBP1 were used. The expression was assessed semiquantitatively as negative, weak, moderate or strong, depending of the number of positive cells and labeling intensity.

Results PTEN expression was found in all tumors, however in 30% of cases the expression was weak. Cytoplasmic PI3K 100 was observed in 92%, PI3K 85- in 95% of tumors. pAKT (Ser-473) cytoplasmic staining was detected in 82% with variation of intensity. Weak to moderate expression of pmTOR (Ser-2481) characterized 78% of cases. Nuclear and cytoplasmic p70S6K labeling was found in 90% cases and cytoplasmic 4EBP1 in 85% neuroblastic tumors. The most intense expression of components of PI3K/AKT/mTOR pathway were observed in poorly differentiated and chemotherapy pretreated tumors.

Conclusion(s) Activation of PI3K signaling pathway is a common event in neuroblastic tumors. This fact creates the possibility of patients treatment with selective inhibitors of this pathway. Granted by Polish MNE project N40117631/3867.

P1.180

Changes of weight indexes at symmetrical and asymmetrical types of intrauterine growth retardation

Myroshnychenko Sergeevich M.; Yakovtsova A.; Gargin V.; Tveretinov A.; Nazaryan R.
Kharkov National Medical University, Izum, Kharkiv region, Ukraine

Background The weight of the child is an extent integrative parameter of intrauterine growth and dynamics of weight curve - reflectance of his adaptive capabilities. The purpose of the our research was the detection of dynamics of weight indexes at symmetrical and asymmetrical types of IUGR.
Methods For achievement of the purpose, the analysis of archive materials of autopsies of fetuses and newborns with IUGR in term of gestation 21–42 weeks.
Results During the analysis of 2329 archive materials of autopsies is detected 350 cases with IUGR (15, 03%). The fetuses among perished have compounded 79, 14% (277 cases), neonatal - 20, 86% (73 cases). It was fixed at estimation of the types of IUGR, that the symmetrical type was detected for 28% (98 cases) and asymmetrical - for 72% (252 cases). The body weight has compounded 0,915 kg at symmetrical type of IUGR and 0,892 kg at asymmetrical type in gestational term of 28 weeks, that is lower than average weight parameters on 0,209 kg and 0,232 kg accordingly. The body weight has compounded 2,192 kg at symmetrical type and 1,875 kg at asymmetrical type in gestational term of 37 weeks, that is lower than average weight parameters on 0,579 kg and 0,896 kg accordingly.
Conclusion(s) Thus, for children with asymmetrical type of intrauterine growth retardation the deficit of the body weight is expressed in the greater degree as contrasted by the children with symmetrical types of intrauterine growth retardation.

P1.181

Detection of Epstein Barr virus by chromogenic in situ hybridization in cases of extra-hepatic biliary atresia

Mahjoub Elham F.; Shahsiah R.; Azmoudeh Ardalan F.; Iravanloo G.; Najafi Sani M.; Zarei A.; Monajemzadeh M.; Farahmand F.; Mamishi S.
Tehran University of Medical Sciences, Tehran, Islamic Republic of Iran

Background Extra-hepatic biliary atresia (EHBA) is an important cause of neonatal cholestasis. Several infectious agents have been proposed as etiologic factors such as Rotavirus and Reovirus. There is limited data on the role of Epstein Barr virus (EBV) infection in EHBA, so we decided to study the presence of EBV virus in a series of 16 proven EHBA cases by Chromogenic in situ hybridization (CISH) technique.
Methods In the current study a total of 16 liver wedge biopsies of proven cases of EHBA were selected in a period of 4 years. CISH staining for EBV-encoded RNA (EBER) transcript was performed.
Results The review of H&E-stained slides of liver biopsies revealed fibrosis and marked ductular proliferation. In CISH-stained slides, EBV trace was observed in hepatocytes in two cases and in biliary epithelium in one case of EHBA.
Conclusion(s) Considering the association of hepatitis with the Epstein-Barr virus in later life, it is likely that EBV hepatitis and its complications occur in the neonatal/perinatal period. Since EHBA is a relatively rare disease, a similar study on wedge biopsies of this number of proven cases of EHBA has not been performed to date. Current observation proposes the need for a study of larger series and employing other methods for confirming the etiologic role of EBV in EHBA cases.

P1.182

Gingival granular cell tumor in new born (congenital epulis): immunohistochemical study of 7 cases

Yacoubi Tahar M.; Lahmar A.; Trabelsi A.; Hmissa S.
Department of Pathology, F. Hached Hospital, Sousse, Tunisia

Background Congenital epulis is a benign tumor of the new born arising in the gingiva, mimiking morphologically granular cell tumor. Our aim is to contribute to the determine its histogenesis using an immunohistochemistrical study: mesenchymal markers, neuro-endocrine markers, neuronal markers, vascular markers, muscular markers, epithelial markers, oestrogen and progesterone markers, proliferating and apoptotic markers, Carcino-Embryonal-Antigen, glial markers and histiocytic markers.
Methods Our study is retrospective, concerning 7 cases of congenital epulis diagnosed in our department during a period of 14 years, occurring in new borns in whom the pregnancy was unremarkable. We used a large panel of antibodies that the choice was based on hypothesis found in the literature.
Results The age of the new borns ranged from 2 to 16 days. Lesions were located in the upper maxilla in 6 cases and in the lower in the remaining case. The expression of the vimentine and the neuron specific enolase (NSE) was diffuse and strong in all cases. Positivity was also found in all cases using the Proliferating Cell Nuclear Antigen (PCNA) antibody. Tumoral cells didn't express apoptotic markers (bcl2) and were negative for p53.
Conclusion(s) Our results agree with those found in the literature and let us to consider congenital epulis as a mesenchymal lesion with a neuro-ectodermal differentiation, having a prouved proliferating tendancy.

P1.183

HER receptor family in neuroblastic tumors. Immunohistochemical and FISH analysis

Izycka-Swieszewska E.; Wozniak A.; Drozynska E.; Grajkowska W.; Kobierska-Gulida G.; Perek D.; Klepacka T.; Jaskiewicz K.; Limon J.
Dpt of Pathology, Medical University of Gdansk, Gdansk, Poland

Background HER receptor family takes part in the cancerogenesis and different tumors progression. It is also involved in the development of the autonomic nervous system. Neuroblastic tumors are common pediatric embryonal neoplasms of the adrenal medulla and autonomic ganglia. The aim of study was to examine the expression of EGFR, HER2, HER3 and HER4 in 117 neuroblastic tumors.
Methods The clinical data included patients' age, location of tumor, stage of disease, event free survival. Pathological data: histological type, MKI, proliferation index, NMYC status. The tissue microarrays were constructed. The expression of HERRs was assessed semiquantitatively on immunolabeled TMAs based on the number of positive cells and staining intensity. FISH analysis with molecular probes for EGFR and HER2 was performed with examination of at least 100 neoplastic nuclei.
Results The presence of EGFR was detected in 95% of cases, HER2- 80%, HER3- 85% and HER4 in 88%. EGFR expression was the strongest among HERRs. HER2 was related to the differentiation of the tumor and proliferative index. The expression level of HERRs wasn't correlated with tumor stage, neither tumor location. FISH analysis of EGFR showed no changes in gene copy number. FISH analysis of HER2 showed no amplification, but relative increase in gene copy number in 15 cases.
Conclusion(s) Expression of HERRs is frequent in neuroblastic tumors and takes part in tumor evolution. High expression of EGFR and HER2 in neuroblastoma isn't caused by gene amplification. Granted by Polish Government- project N40117631/3867.

P1.184
Histopathological study of 17 placentas of women with clinical and serological diagnosis of dengue

Lopes Silami V.; Alvarenga C.; Menezes Soares N.; Coelho J.; Boechat Elizabeth M.; Brasil P.; Nogueira R.; Dias Pedra E.; Silva Cássia Lauria Goncalves R.; Gaglionone Cavalcante N.; Carvalho Cristina Gouvêa A.; Gouvêa Luísa Figueira A.; Andrade Vianna C.
Universidade Federal Fluminense, Niterói, Rio de Janeiro, Brazil

Background Brazil has had several epidemics of dengue for the last three decades. Virus DENV 1, DENV 2 and DENV 3 have been identified in our population. The severe evolution in pregnant women and the absence of a clinicopathological study led us to investigate vertical transmission of the disease and morphologic changes in placentas.
Methods We analysed 17 placentas from the Services of Anatomic Pathology of Hospital Universitário Antonio Pedro and Hospital Azevedo Lima. Serological tests, virus isolation and immunohistochemistry were performed at Instituto Oswaldo Cruz.
Results The maternal and gestational ages ranged from 16 to 38 years and from 10 to 42 weeks, respectively. We had dengue fever in 6 cases, hemorrhagic fever in 4 cases, shock syndrome in 1 case and dengue with complications in 6 cases. The serological tests evidenced IgM in all cases. There were 2 maternal deaths, 4 abortions, 1 still-born death and 1 newborn death. The placentas weight was appropriate to gestational ages. The microscopic study showed umbilical vasculitis (1 case), funisitis (2 cases), coriodeciduitis (8 cases), intervillositis (3 cases), villitis (7 cases), villous edema (4 cases), villous immaturity (4 cases) and basalis deciduitis (3 cases). Eight placentas exhibited alterations related to ischemic injury.
Conclusion(s) Face to the importance of this disease in our country and the lack of studies of infection during pregnancy we believe it may be an important trigger for future studies for the understanding of the vertical transmission of dengue.

P1.185
Inflammatory myofibroblastc tumor of small bowel in a child

Casco F.; Moreno-Rodríguez M. M.; González-Menchén A.; Sánchez Frías M.; Rangel Mendoza Y.
Pathology Department, H.U. Reina Sofia, Cordoba, Spain

Background Inflammatory myofibroblastic tumor (IMFT) is a rare clinicopathological entity characterized by a dense inflammatory cell component amid myofibroblastic proliferation with characteristic histopathology and immunohistochemical findings. Although the lung is the site commonly associated, it may occur in the gastrointestinal tract too.
Methods Female 8-years-old child with acute abdominal pain. Abdominal ultrasound showed small bowel invagination, and 5 cm. of small bowel were resected.
Results On gross examination serous surface had an umbilicted as "glove finger" lesion. At inner surface, a 2, 5 cm. polipoid lesion with fibrin deposits was seen. The cut surface was white-tan, solid and fleshy. Microscopically, it consisted of fusiform cells proliferation with many intermixed inflammatory cells. Immunohistochemical profile was Desmin, CD 34and ALK positives.
Conclusion(s) IMFT is a very rare lesion that affects predominantly children and young adults. Originally considered to represent an aberrant inflammatory response to tissue injury with the myofibroblast as the primary cell type and an associated mixed inflammatory cell infiltrate, is now classified as a neoplasm on the basis of its potential for local recurrence, infiltrative growth, vascular invasion and malignant transformation.

P1.186
Intrauterine growth restriction (IUGR): visfatin and vaspin expression in decidual tissue

Geronatsiou K.; Papachristou D.; Kourea H.; Papadaki H.
Medical School of Patras, Patras, Greece

Background Intrauterine growth restriction (IUGR) is fetal failure to achieve the intrinsic growth potential. Adipokines profoundly influence insulin sensitivity and energy metabolism. Visfatin, is a visceral fat-specific adipokine, exerting insulin-mimetic effects in various tissues. Visceral adipose tissue-derived serine protease inhibitor (vaspin) is a novel adipokine with insulin-sensitizing effects. The aim of this study was to investigate the expression pattern of visfatin and vaspin in human decidua at different stages of gestation in IUGR.
Methods Paraffin embedded placental sections, from 45 fetuses with IUGR and endometrial demise were examined by immunohistochemistry for vaspin and visfatin expression. The cases were divided in two groups according to gestational age (GA) (group A: 0–28w, $n=20$, group B: 29–40w, $n=25$). Percentage and intensity of staining were recorded and the cut-off for high expression was set at 30%. Statistical analysis was performed by Kendall's tau and Mann-Whitney tests.
Results Visfatin expression was high in 84% of group A and low in 72% of group B. Vaspin expression was high in 85% of group A and low in 76% of group B. Visfatin and vaspin expression-levels was significantly higher in early GA and negatively correlated with fetal weight, foot length and liver weight ($p<0.05$).
Conclusion(s) Our findings indicate a gestational age-dependent expression of visfatin and vaspin in human decidua in the background of IUGR. Both adipokines might contribute to the development of pregnancy disorders. Further studies are needed to elucidate the pathophysiological significance of visfatin and vaspin in pregnancy-related complications.

P1.187
Kidneys structural elements formation in cases of intrauterine growth restriction at 20–22 weeks of gestation

Reshetnikova Sergeyevna O.; Sysoyenko Pavlovich A.
Lugansk State Medical University, Lugansk, Ukraine

Background Epidemiological and experimental studies support the idea that intrauterine alterations of the placental-fetal environment may cause the changes in the development of fetal tissues, followed by diseases in adults. The aim of present study was to confirm the relation between kidneys morphology changes and fetal intrauterine growth restriction (IUGR).
Methods 20 pairs of fetal kidneys (including 10 pairs of kidneys in cases of IUGR) from the late medical abortions because of psychotherapeutic reasons at 20–22 weeks of gestation were weighted, studied macroscopically and microscopically. Volume fractions of the major renal components were determined from 5mmk paraffin sections.
Results have shown reduction of fetal weight and length in IUGR group; renal weight and volume were also smaller than at controls. There were also increase of immature glomeruli and cortex stroma VFs, as well as VFs of stroma and vessels at renal medulla. Mature glomeruli and tubules VF were below the control parameters. Statistics showed the increased number of correlations between organometric and stereometric indices of fetal weight, length and kidneys parameters in cases with IUGR.
Conclusion(s) Morphological alterations in kidneys in cases of the fetal growth restriction might represent an important structural background in the pathogenesis of adult renal pathologies.

P1.188
Malignant gliomas as second malignant neoplasms in pediatric oncological patients. One center experience

Kobierska-Gulida G.; Izycka-Swieszewska E.; Stefanowicz J.; Drozynska E.; Niedzwiecki M.; Maciejka-Kapuscinska L.; Bien E.; Stachowicz-Stencel T.; Zaucha R.; Szurowska E.; Balcerska A.
Medical University of Gdansk, Dpt. of Pathology, Gdansk, Poland

Background Malignant high-grade gliomas are the most common secondary neoplasms in children cured of acute lymphoblastic leucaemia (ALL). They can also develop in different pediatric cancer survivors, since the main predisposing factor is cranio-spinal irradiation.
Methods We present clinical, histological and immunohistochemical analysis of five cases of secondary gliomas developing in four ALL and one orbital RMS survivors aged 9–15 years, treated in our Center (period 1992–2008).
Results The tumors developed 3- 6.5 years after completion of oncological treatment. All tumors were supratentorial and contrast-enhancing. Two were well demarcated, two-infiltrating, one presented as intracerebral hematoma. Two patients underwent stereotactic biopsy, three patients were operated after the initial biopsy. Overall survival was: 5, 10 and 19 months. Two alive patients receive chemotherapy-one with glioma relapse after 8 years and one- three months since the recognition. Histologically all tumors were cellular- rich, made of small neoplastic astrocytes. Two anaplastic astrocytomas and three glioblastomas were recognized. All tumors expressed vimentin and GFAP, however GFAP in two cases had low intensity. Nestin was detected in three cases. Proliferative index (Ki-67) was up to 60%. The late relapse of glioblastoma showed poorly differentiated neoplasm with focal coexpression of glial and neuronal markers.

Conclusion(s) Presented secondary gliomas were composed of primitive astrocytes in part nestin-positive which can suggest their origin from glial stem cells injured by aggressive treatment of primary neoplasm. Undifferentiated morphology and not always typical immunophenotype can cause diagnostic problems.

P1.189

Neuroblastoma of adrenal medulla with spinal metastases and long survival. A case report

Gorbacheva Y.; Bublievsky D.; Novikov V.; Evzikov G.; Paltseva E.
Moscow Medical Academy, Moscow, Russian Federation

Background Neuroblastoma is usually seen in young children. The typical sites of localization are adrenal medulla and sympathetic ganglia. The overall 3-year survival rate for patients with neuroblastoma is around 30%.
Methods Morphological and immunohistochemical study with antibodies to synaptophysin and chromogranin A were performed.
Results We present a case of adrenal neuroblastoma with unusual long survival. A 21-year-old man had a history of radical adrenalectomy for neuroblastoma when he was 2-year-old. Patient was treated by chemotherapy several times because he had recurrent metastases. The results of therapy were good and the remissions period was long. Extradural metastases at C7-Th2 spine level were revealed two years ago. Patient was operated successfully with good recovering. He had recently presented with numbness and paresthesia of lower half trunk and extremities, deep lower paraparesis, impossibility of autonomous walking. MRI showed extradural lesions at Th5–6 and Th11–12 spine levels with spinal cord compression. Patient was operated again. Histological examination showed aggregation of small tumor cells with round hyperchromatic nuclei and scant cytoplasm, foci of necrosis and haemorrhages, mitotic figures. Synaptophysin and chromogranin A immunoreactivity was detected in tumor cells. Having regard to medical history and immunomorphological findings metastasis of adrenal medulla neuroblastoma was diagnosed. After surgery the patient shows decreasing of perceptibility disturbance, increasing strength of extremities; he walks with support.
Conclusion(s) Thus, the presented case is extraordinary with regard to age, clinical presentation and rapid patient's rehabilitation.

P1.190

Pediatric papillary-cystic acinic cell carcinoma shows strong expression of MiT tumor family protein TFE3

Ngan B.; Zielenska M.; Ho M.; Forte V.
Div. of Pathology, Hospital for Sick Children, University of Toronto, Toronto, Ontario, Canada

Background Over-expression of TFE3 protein as a consequence of Xp11 translocation is present in papillary pediatric renal cell carcinoma (PPRC) and alveolar soft part sarcoma. We report a papillary-cystic acinic cell carcinoma (PCACC) that presented in the right accessory parotid gland of a 13 year old girl. The diagnostic investigations of a papillary neoplasm led to this immunohistochemistry and molecular study of TFE3 expression in PCACC.
Methods A review of pediatric salivary gland pathology records revealed 12 cases of pleomorphic adenoma (PA), 4 cases of acinic cell carcinoma (ACC) and 2 cases of mucoepidermoid carcinoma (MC). Immunohistochemistry was performed on PCACC & ACC with antibodies to TFE3, MiTF, HMB45, MART-1, S-100, cytokeratin, TTF-1, CD10, CD15 and BCL10. TFE3 and MITF immunostains were also performed on 3 randomly chosen PA and 1 MC. PCR was used to detect ASPL-TFE3. PPRC tissues were used as positve control. Electron microscopy was also performed.
Results PCACC had stong nuclear TFE-3 expression.3 ACC had background TFE3. None of them express MiTF.2 ACC expressed weak cytoplasmic BCL10. ASPL-TFE3 fusion was negative.
Conclusion(s) Only PCACC of the salivary gland strongly expressed TFE3 protein. Expression was not due ASPL-TFE3 fusion. MiTF was not expressed. Others had reported TFE3+ PEComa, Melanotic Xp11 translocation renal cancers, adrenal cortical carcinoma, granular cell tumors, bile duct carcinoma and myxofibrosarcoma. We found that PCACC of the salivary gland shares similar aberrant TFE3 expression with these members of the MiT tumor family.

P1.191

Plexogenic pulmonary arteriopathy in a 2 year-old boy

Boudjemaa S.; Pages P.; Coulomb A.; Capron F.
Armand Trousseau, Paris, France

Background The plexiform lesion is the hallmark of plexogenic pulmonary arteriopathy (PPA) that accompanies severe idiopathic pulmonary arterial hypertension (PAH). Actually, idiopathic PAH is distinguished from PAH secondary to specific pathologic conditions. Pathomechanisms explaining the morphologic changes of pulmonary vasculature include endothelial and thrombocytic dysfunction, deregulated vasoconstriction, coagulation abnormalities and cancer like growth.
Methods A 2 year-old boy, followed-up for repeated episodes of bronchiolitis, was admitted to the reanimation department of our institution for respiratory distress, abdominal pain, fever and loss of consciousness, with anemia and thrombopenia. His condition deteriorated rapidly and he presented a pulmonary failure, with a

respiratory rate at 60/min, sub-costal and sub-sternal recession and a grade 3/6 systolic murmur, leading to diagnose a PAH. Despite medical manoeuvres, he remained in a low cardiac output and died two days later.
Results At autopsy, the lungs were heavy, dense, purplish and not lobulated. There was not cardiac malformation as suspected by clinicians. A polysplenia was present. Histologically, there was a widespread pulmonary arteriopathy with intimal fibrosis, marked medial hyperplasia and glomeruloid proliferative lesions. Distal to the plexiform lesion, dilated vessels were present, with microthrombosis. This pattern was consistent with plexiform (complex) arteriopathy. Familial and genetic investigations are undertaken to identify mutation of BMPR2.
Conclusion(s) The role and the impact of pathomechanisms of this poor prognosis disease have to be better defined. Recent identification of responsible gene mutations in subgroups of patients has shed light into the modus of inheritance.

P1.192
Pulmonary hypertension in cases with congenital heart malformations

Duganovska S.; Tolovska M.; Petrusevska G.; Bogoeva B.; Janevska V.; Kostadinova S.; Dukova B.
Insitute of Pathology, Skopje, the Former Yugoslav Republic of Macedonia

Background We analysed the morphology of congenital heart malformations (CHM) and changes in lung blood vessels in cases of developed left-right shunt.
Methods We used standard tissue staining: HE, Van Gieson-Elastica, trichrom Masson and Reticulin. We performed histomorphometrical analysis using the LUCIA M - NIKON Image analysing system. The thickness of the media of the lung muscle arteries has been measured and then compared to the complete total diameter of the blood vessel. Thickness coefficient obtained was compared to the graduation results acording to the Heath-Edwards classification (I, II, III, IV) and to the control group.
Results The changes in lung blood vessels in a group of 38 cases of CHM were classified according to the above mentioned classification system. Most of the cases were classified in group I (63, 1%), group II (18, 4%) regarding the cases with VSD, AV-canal, PDA, ASD/VSD; group III (7, 8%) regarding the cases with VSD, CoA, TGA+VSD; group IV (10,5%) regarding the cases with VSD, AV-canal, Single ventricle. Microscopically, there were aneurismal, plexiform and dilatation lesions of the blood vessels.
Conclusion(s) Results obtained from this study emphasize the necessity of lung biopsy while evaluating reversible and irreversible phases of the disease, which is very important for further surgical treatment of children with CHM.

P1.193
Role of preoperative infra-red laser therapy in hypertrophic skin scar treatment

Severgina Olegovna L.; Severgina Serafimovna E.; Lopatin Vyacheslavovich A.; Batyunin Vladimirovich V.
Medical Sechenov Academy, Moscow, Russian Federation

Background Hypertrophic skin scar formation is an important aesthetical problem. The aim of this study was a search of optimal surgical treatment in combination with preoperative laser therapy (LT).
Methods We studied skin incision biopsies of the hypertrophic scar adjacent areas, obtained during the operation of scar removal from 16 patients.10 patients underwent 10th day preoperative course of infra-red 690ηm-wave LT.6 patients were included into control group – without preoperative LT. We investigated all specimens under light microscopy; immunhistochemical reactions with monoclonal antibodies to VEGF, CD34 and CD68 were done. We also averaged vascular density level in dermal papillary layer.
Results The number of dermal papillary layer vessels was increased in patients with LT; we also found local proliferation of epidermal basal layer cells on apical parts of dermal papillae and perivascular CD68+ lymphoid infiltrates. Vascular density level was 4, 82 mm² in patients with LT vs 3, 32 mm² in patients without LT. Overexpression of VEGF was found on endothelium, all epidermal layers and dermal cells; in same areas VEGF+dermal cells form chain-like structures. CD34 expression was found only on endothelial cells, it was significantly higher after LT.
Conclusion(s) Preoperative LT stimulated local microcirculation and cell proliferation in scar adjacent areas. Presence of VEGF+and CD34+ cell populations confirmed high grade of angiogenesis activity after LT treatment, which intensified wound healing.

P1.194
Two cases of neurocytoma with atypical features in children

Jou C.; Suñol M.; Rovira C.; Puy R.; Cusi V.
Hospital Sant Joan de Deu, Esplugues de Llobregat, Barcelona, Spain

Background Neurocytomas are very uncommon central nervous system tumours in childhood. They are well circumscribed, low grade supratentorial intraventricular neoplasms. Some tumours with neurocytic features have been reported in extraventricular locations. Atypical neurocytomas show proliferation index > 2–3% or atypical histological features. They can be more aggressive and associated with recurrences.
Methods Case1: A 2-year-old boy was referred to our hospital after some episodes of loss of conscience and vomits. MIR

showed a well-defined neoformation arising from the left temporal lobe. A wide surgical resection was performed. Case 2: A 13-year-old girl was admitted presenting headache during fourth months. MIR showed an intraventricular tumour arising from frontal ventricular horn. A surgical resection was performed.

Results Both cases showed similar histology: a monotonous proliferation of uniform neurocytes with perinuclear halos and moderately pleomorphic nuclei, disposed in sheet-like growth pattern with neuropil-like areas. The cells were inmunoreactive for synaptophisin. MIB1 labelling index was 22% in the first case and 10% in the second. The diagnostic was atypical neurocytoma, one of them in extraventricular location.

Conclusion(s) Neurocytomas in childhood are exceedingly rare. Differential diagnosis includes oligodendroglioma, clear cell ependymoma, clear cell meningioma, medulloblastoma, cerebral neuroblastoma, subependymal giant cell astrocytoma, and dysembryoplastic neuroepithelial tumour. Subtotal resection, atypical histological features, and high cell proliferation rates correlate with recurrences. MIB-1 proliferation index is commonly used in an attempt to predict biologic behaviour.

P1.195

A case of propionic acidemia (clinical and autopsy report)

Tolovska-Stojanovic M.; Sofijanova A.; Tasic V.
Institute of Pathology, Skopje, the Former Yugoslav Republic of Macedonia

Background Propionic acidemia is rare autosomal recessive disorder due to deffective enzyme propionyl-coenzyme A carboxilase, which results in accumulation of propionic acid. The clinical picture varies from mild psychomotor retardation to severe metabolic decompensation with vomiting, dehydration, encephalopathy and, rarely, fatal outcome.

Methods A 13-month-old male infant was admitted to the Children's Hospital with severe acidosis and dehydration. His vomiting intensified and his general state worsened and presented with weakness, hypotonia, sopor, tachypnea and dyspnea. The laboratory investigations revealed severe metabolic acidosis, urine pH = 5, mild hypokaliemia, hypophosphatemia and hypouricemia, suggesting tubular disfunction. He developed severe anaemia, low platelets, humoral immunodefficiency, high concentration of creatinine and the assay of the urinary organic acids revealed increased concentration of 3OH-propionic acid.

Results Autopsy and histology findings were non-specific. The liver was enlarged with severe steatosis. The brain showed severe spongiosis-like degenerative changes with homogenisation and loss of the neuron`s nuclei. The cerebellar tissue showed decreased external granular cell layer with focal Purkinye-cell loss. Myocardium was degenerated with interstital fibrosis and consecutive pulmonary edema.

Conclusion(s) Propionic acidemia is the most common organic acidemia with prevalence between 1:35000–75000 population, but the real prevalence is not known because in the neonatal period is misdiagnosed as sepsis. In our case the diagnosis was established clinically and on the basis of elevated urinary concentrations of 3OH propionic acid. Mutational analysis of the both genes responsible for propionic acidemia is in progress. The autopsy findings supported the clinical diagnosis.

P1.196

Bilateral frontal polymicrogyria. An autopsy case report

Chun Y.; Choi J.; Chi J.
Cheil General Hospital, Kwandong University College of Medicine, Seoul, Republic of Korea

Background Polymicrogyria may result from both genetic and environmental factors and occurs as an isolated finding or as part of a syndrome with multisystem involvement. Bilateral frontal polymicrogyria is a recently recognized syndrome characterized by symmetric polymicrogyria of both frontal lobes that presents as delayed motor and language development, spastic quadriparesis, and variable mental retardation. However, its postmortem findings are not fully elaborated.

Methods We describe an autopsy case of bilateral frontal polymicrogyria from a male fetus delivered at 22 weeks of gestation due to extensive chorioamnionitis.

Results The brain showed bilateral symmetric distribution of polymicrogyria in the frontal lobes, sparing the prefrontal area and the base of frontal lobe. Microscopically, the cortical plate of polymicrogyria was thinner than that of a normal cortex of the same gestational age, but there was no difference in cellullarity and maturation of cortical neurons. The white matter and ventricular surface and leptomeninges showed no inflammatory change. The placenta showed chorioamnionitis, but no funnisitis or villitis. Chromosomal study of the fetal tissue revealed 46, XY.

Conclusion(s) Although this case is associated with severe chorioamnionitis, we did not see the evidence of inflammatory change or hypoxic-ischemic damage in either the polymicrogyria or normal cortex. It is quite unlikely that chorioamnionitis per se could have lead to bilateral symmetric polymicrogyria of the frontal lobes in this case. Genetic study is necessary because it might be associated with genetic factors.

P1.197

Chronic placental intervillositis and villitis: relationship to pregnancy outcome

Downey P.; Kelehan P.; Mooney E.E.
National Maternity Hospital, Dublin, Ireland

Background Chronic intervillositis is characterised by histiocytic inflammation in the intervillous space. It is associated with recurrent miscarriage and a poor pregnancy outcome. Whilst early descriptions of intervillositis included cases with concurrent villous inflammation, recent literature has excluded cases with villitis and secondary inflammation. As villitis may also be associated with pregnancy complications, we examined cases of intervillositis and evaluated the role of co-existent villitis.
Methods Sixty-two placentas with intervillous inflammation were identified. Intervillositis was graded as mild, moderate, or severe. Co-existent villitis was classified as present or absent. Results were compared to clinical outcome data and available demographic details. Cases with malaria were excluded.
Results Concurrent villitis was seen in 34% of cases (n=21). Intervillositis alone was associated with fetal loss in 57% of cases (n= 24), but when concurrent villitis was present, the mortality rate was 14% (n=3). Intervillositis alone was significantly associated with earlier pregnancy loss – mean of 25.6 weeks compared with 35.7 weeks for pregnancies with concurrent villitis (p=0.0073). After 37 weeks (n=23), rates of fetal loss were similar: intervillositis alone 18% (n= 2) and with villitis 17% (n= 2). Although severe intervillositis tended to be associated with earlier fetal loss, this finding was not significant (p=0.1736).
Conclusion(s) Co-existence of villitis with intervillositis does not increase the rate of stillbirth.

P1.198
Congenital generalized myofibromatosis (CGM) as a cause of sudden death

Toran N.; Garcia-Fontgivell Francesc J.; Landeyro J.; Elguezabal A.; Gené M.; Pujol J.; Sirvent Josep J.
Hosptal Vall d'Henron, Barcelona, Spain

Background Infantile myofibromatosis is a distinctive mesenchymal disorder with different clinical forms, including solitary, multicentric, and generalized with visceral involvement. The generalized form has been documented in 25–37% of patients, being the most clinically ominous form, most cases are progressive and cause death by compromising the heart, lungs, or gastrointestinal tract as the case we report.
Methods Newborn female with congenital subcutaneous multicentric tumors. Normal echocardio.5 days later, she suddenly died. The autopsy was performed.
Results Morphological findings: multiple nodules (0'5 - 3 cm) grayish white, firm cut surface, in subcutaneous tissue, striated muscle, diaphragm and intestine. Serous pericardial effusion and pulmonary condensation. The microscopic study showed tumoral nodes in lung, thymus, trachea and heart. The nodules displayed a spindle cell population with oval nuclei and eosinophilic cytoplasm but in the central part the cells were more primitive, with low mitotic rate, forming isolated whorls and intravascular projections. Immunohistochemical staining revealed positivity for SMA, calponin, CD34 and vimentin. Cytokeratines, CD117, desmin and S-100 protein were negative. The diagnosis was CGM, attributing the cause of sudden death to massive pericardia effusion.
Conclusion(s) CGM is an unusual disorder of unknown etiology in infants. These tumors are present at birth or might develop during the first weeks of life. Prognosis is worse if visceral involvement exists. In a newborn with multicentric infantile myofibromatosis complete evaluation of the patient is crucial. Differential diagnosis: a) neurofibromatosis, skin spots (S-100 protein +), b) Langerhans' cell histiocytosis, involving bone and skin (CD1+).

P1.199
Congenital toxoplasmosis: an important cause of morbidity and mortality in children of anti-toxoplasma IgG+ and IgM- and HIV seropositive women

Lopes Silami V.; Azevedo Martins Lopes K.; Setúbal S.; Menezes Soares N.; Ferraz P.; Castro Carolina Monteiro A.; Oliveira Artimos S.; Dias Pedra E.; Pires Rodrigues Cordovil A.; Andrade Vianna C.; Gaglionone Cavalcante N.; Carvalho Cristina Gouvêa A.; Gouvêa Luísa Figueira A.
Universidade Federal Fluminense, Niterói, Rio de Janeiro, Brazil

Background Congenital transmission of toxoplasmosis occurs in acute phase in pregnancy. We have observed transmission in immunosuppressed women with latent infection. Our aim was to emphasize the importance of the examination of the placenta and the necropsy in these cases.
Methods We analysed two cases at the Service of Anatomic Pathology of Hospital Universitario Antonio Pedro. Both pregnant were HIV+ and anti-toxoplasma IgG+ without IgM. In the first case the woman had urinary tract infection, was treated, the ultrasound revealed fetal death and the delivery was induced. In the second case the pregnancy was interrupted in the 39th week and the placenta was examined.
Results The necropsy of the still-born (first case) showed hydrops fetalis, hepatosplenomegaly, pericarditis and miocarditis with many forms of T. gondii. We also observed diffuse necrotizing vilitis with parasites. The immunohistochemistry study was positive in sections of

placenta and heart. The gross examination of the placenta (second case) showed enlargement of the placenta with greenish and opalescent membranes. The histologic examination revealed funisitis, umbilical vasculitis, coriodeciduitis, villitis and intervillositis (hematogenous infection). The newborn was followed-up and presented corioretinitis, nystagmus, hepatosplenomegaly, anti-toxoplasma IgM and intracranial calcifications in the CT (congenital toxoplasmosis).
Conclusion(s) Although the risk of vertical transmission is low in women with latent toxoplasmosis this diagnosis should always be considered in the children in our country because of the high prevalence of this disease specially in HIV seropositive mothers.

P1.200
Features of immunochemical analysis of chorionic gonadothropin in the women's placenta at smoking family
Gubina-Vakulik G.; Belyayev S.; Mylovydova G.
Kharkiv National Medical University, Kharkiv, Ukraine

Background Morphological researches of placenta at mother's smoking reveal reduction of actively functioning placenta tissue. The purpose of research is to study features of immunochemical analysis of chorionic gonadothropin in placenta in the situations: 1)mother smoked before and during pregnancy - gr. M, 2)father smokes – gr. F, 3)both parents smoke – gr. MF, 4)both smoked, but a pregnant woman gave up smoking – grM1F.
Methods In each of the groups there were 10 cases, the control group also comprised 10 cases. The content of tiocyonate (nicotine metabolite) was determined in urine of pregnant women. Besides the common histological analysis, there has been carried out the immunochemical detection of chorionic gonadothropin with luminescent visualization and an estimation of luminescence intensity in standard units.
Results Chorionic gonadothropin production in gr. C occurs in sycitium of quantity of villi. In basic groups the sites of specific luminescence are found out less often and displaced in the region of syncytial nodules. Cytofotometric study of this hormone production activity testifies to its increase in the basic groups: MF > M > M1F > F >C. There is a positive correlation (r = +0,61) between the content of tiocyonate in urine and intensity of luminescence in syncitium.
Conclusion(s) Chorionic gonadothropin production areas in a woman's placenta at smoking family are observed less often, but hormone production in them is increased. There is a compensatory mechanism supporting a level of placenta function.

P1.201
Ganglioglioma in a pediatric case: a unique and rare tumor
Gurer E.; Ozbudak I.; Eren Karanis M.
Akdeniz University School of Medicine Department of Pathology, Antalya, Turkey

Background Gangliogliomas are slowly growing neuroepithelial tumors composed of in combination neoplastic ganglion cells and glial cells. Their incidence is range between 0.4–1.3% in all brain tumors.
Methods We presented a 5 year-old girl with a history of seizures ranging in duration from first year of life to one month before. The tumor was 4.5x3 cm in dimension which was localized in temporal region and gross total resection was performed.
Results Tumor was pink-white colored and calcified appearance. Microscopically, tumor was composed of multipolar, dysmorphic neurons and neoplastic glial cells. Ki 67 labelling index was found approximately 2%. P53 labelling also was seen. The patient was diagnosed as Ganglioglioma grade II according to WHO classification.
Conclusion(s) Since gangliogliomas are rare and have difficulties for differential diagnosis for pathologist. Therefore, presented case was discussed and evaluated in the light of the literature.

P1.202
Mesenchimal hamartoma of the liver: a case report
Ristovski Tale M.; Filipovski V.; Jovanovic R.; Janevska V.; Cadikovski V.
Institute of Pathology, Faculty of Medicine, University "Ss Kiril and Metodij", Skopje, the Former Yugoslav Republic of Macedonia

Background Mesenchymal hamartoma of the liver (MHL) is a rare lesion occurring mainly in infants and children. This report describes a case of MHL of the liver in a 9 month - old girl.
Methods We used clinical data, gross examination, microscopic and immunohistochemical analysis.
Results The patient presented with progressive abdominal distension and elevated serum alpha fetoprotein level. Preoperative radiological examination revealed well defined, large cystic and partially solid mass in the right lobe of the liver. On gross examination, the tumor is well circumscribed, solitary mass wit dimenssion of 18 cm. The tumor mass measured 1200 gr. Deep dissection of the mass showed multilocular cystic compartments separated from fibromixomatous tissue. The cysts were variable in size and filled wit mucoid, pink fluid. On microscopic examinations of the lesion,

multilocular cysts were observed, lined by flattened epithelium and surrounded by a mesenchymal component. The branching bile ducts without atypia, dilated vessels and lymphatics also were present. An immunohistochemical panel consisting of desmin, smooth-muscle actin, S-100, vimentin, CD-34, carcinoembryonic antigen, cytokeratin-7, cytokeratin-8, cytokeratin-17, cytokeratin-18, cytokeratin-19, and cytokeratin-20 was applied to paraffin sections. Immunoreactivity for cytokeratin-7 and cytokeratin-19 was observed in cystic epithelium and ductal structures.

Conclusion(s) In conclusion MHL in infants seems to be related to neoplastic origin or developmental anomaly in bile duct plate formation. This case is the first case in practice of our institution.

P1.203

Morphological analysis of fetuses and placentas of pregnant hypertensive rats (SHRs) subjected to physical training

Abate Tavares Resende ESilva D.; Olegário Pacheco J.; Rossi ESilva Calciolari R.; Faleiros Guimaraes A.; Barbosa Neto O.; Miranda Correa R.; Castro Costa Da Cunha E.; Dias Da Silva José V.; Reis Antônia M.
UFTM, Uberaba, Minas Gerais, Brazil

Background Evaluate the effects of exercise training over arterial pressure (AP), heart rate (HR) and morphological alterations in placentas and fetuses in hypertensive pregnant rats.

Methods Spontaneously hypertensive rats (SHRs), and normotensive rats (WKY), distributed into four groups: a) hypertensive gestation sedentary (HSE) and hypertensive gestation trained (HCE), normotensive gestation sedentary (NSE) and normotensive gestation trained (NCE). On day 20 of pregnancy animals were euthanized, fetuses and placentas were weighted and measured. To analyze placental vessels, was done imunohistochemistry technique to factor VIII.

Results Trained rats presented smaller values of MAP compared to sedentary rats (T=89, 000; p=0,028). The number of placental vessels of SHRs was significant higher when compared to WKY (F=19, 077; p<0,001). In relation to fetal length, trained pregnant rats presented higher values (T= 2637, 500; p=0,003). SHRs presented smaller fetal weight compared to WKY (t=-2, 761; p=0,007), however, fetuses from trained rats presented higher weights compared to fetuses from sedentary rats (T=2696, 000; p=0,007). Placental volume of normotensive pregnant rats, those who practice exercise presented higher values compared to sedentary rats, although the same didn't happened with hypertensive pregnant rats (F=9, 503; p=0,003).

Conclusion(s) Exercise training causes a lowering of AP in pregnant SHRs could contribute to an increase in number of placental vessels. Besides that, SHRs trained presented higher fetal length, although fetal weight was smaller compared to SHRs sedentary. In placentas, there was no positive repercussion.

P1.204

Parasitic conjoined twins: internal and detached

Ege Cigdem B.; Yalcin N.; Koltuksuz U.; Savran B.; Gurckaya E.
Pamukkale, Denizli, Turkey

Background Conjoined twinning (CT) is a rare occurence. Although the exact cause is unknown, CT has been regarded as an error in blastogenesis of zygotes.

Methods In these two case reports, two types of parasitic conjoined twins, internal and detached, were presented. Both deliveries were by cesarean section at 38th and 39th gestation week. Both female co-twins were without congenital anomalies, and survived.

Results The internal one was located in its co-twin's subcutaneus sacrococcygeal area. It weighed 750 g measuring 22x12x10 cm. The head had no facial structures but some scalp hair. The detached one was of a 1085 g fetus measuring 21x12x5 cm and without a head and two upper extremities.

Conclusion(s) The teratology of these malformations is discussed, and attention is drawn to the degeneration of some parts of the embryo and/or fusion to the other embryo as possible causes.

P1.205

Pathomorphology of the thymus in fetuses from mothers with type 1 diabetes mellitus

Sorokina Victorovna I.; Kupriyanova Sergeevna L.
Kharkiv Medical, Kharkiv, Ukraine

Background The influence of type 1 diabetes mellitus (DM) in the mother on the morphofunctional peculiarities of the fetal thymus with respect to the stage of the mother's disease and fetus anthropometry findings was investigated.

Methods The autopsy material included 99 cases of intranatal fetal death. Methods: organometry, histology, histochemistry, immunohistochemistry, morphometry and statistical analysis.

Results The revealed pathomorphological peculiarities of the fetal thymus result from metabolic and vascular disorders in the mother's organism and vary depending on the mother's disease severity. Irrespective of the mother's disease severity, specific changes in the fetal thymus from the mothers with type 1 DM are collagen formation disturbance in the vascular and stromal components of the

thymus; disorders of maturation, proliferation, and T-lymphocyte differentiation; immaturity of lymphoid component in the fetal thymus from mothers with type 1 DM; reduction of thymalin-producing activity; disturbance of interleukin-producing activity of the fetal thymus from mothers with type 1 DM; increase of endothelin producing function of both arteries and veins; increase of apoptosis as a sign of antigenic stimulation characteristic for type 1 DM.

Conclusion(s) The obtained findings prove the necessity of prevention, timely and adequate treatment as well as close attention to risk groups among the children from mothers with type 1 DM and working out the methods of prevention of vascular and metabolic manifestations in fetuses from mother with type 1 DM.

P1.206

Pelvic cyst in a 32 week old fetus. An unusual presentation of "persistent cloaca"

Guimarães S.; Baptista P.; Ramalho C.; Cunha M.; Jesus J.; Silva G.; Brandão O.; Matias A.
Hospital S. João, Porto, Portugal

Background A 35 year-old pregnant women was referred to our centre at 32 weeks due to a fetal ovarian cyst. A cystic mass was confirmed with 99x83x67mm, probably arising from the left adnexa. A bilateral pyelic dilatation was identified. Ultrasound-guided puncture was performed (280 mL). Hormonal levels were below those expected for an ovarian cyst. Fetal karyotype was 46, XX. Cytologic examination revealed squamous cells without atypia. The cyst refilled the next day and the hypothesis of a rectal dilatation arose. MRI showed: pelvic cyst in which both ureters ended; bladder was slightly distended; uterus and rectum were not identified. A HELLP syndrome developed at 33 weeks and a caesarean-section was performed. The newborn had an Apgar score of 2/4/4 and 2000 g, and besides the pelvic mass, presented with: ambiguous genitalia, anal atresia and small anterior fistula. The newborn died 2 h after birth.

Methods A complete necropsy examination of a female newborn was performed.

Results The most important features were: very dilated uterus and vagina, filled with a serous fluid (hydrometrocolpos) and dilated bladder, both ending in a elongated urethra-like cloaca; rectal atresia with a small non-functioning fistula to the vagina and a hypoplastic anus. There was also a "borderline" pulmonary hypoplasia.

Conclusion(s) We present a case of a hydrometrocolpos with a prenatal diagnosis of a pelvic cyst. MRI can be very helpful, but in some cases, like this one, the diagnosis is only made by an autopsy examination.

P1.207

Perinatal stress organs evaluated through immunohistochemical and morphometrical techniques

Corrêa Rosa Miranda R.; Reis Antônia M.; Teixeira De Paula Antunes V.; Castro Costa Da Cunha E.; Olegário Pacheco J.
Triângulo Mineiro Federal University, Uberaba, Minas Gerais, Brazil

Background The aim of this study was to evaluate through immunohistochemical and morphometrical techniques the morphology of the organs that had been previously described in the literature as stress organs.

Methods We analysed 146 cases, with Perinatal Hipoxia/Anoxia PHA, Ascending Infection (AI) and Congenital Malformations. The hematoxilina-eosina stain was used to the analysis of the adrenal gland vacuolization; hepatic steatosis and extramedular eritropoiesis quantification in the liver (LI). For the LI fibrosis the Picro-sírius method was used. For the immunohistochemical analyses we used the antibodies CD68 (DAKO®) in the thymus.

Results The degree of vacuolization was higher in the cases with AI. In the thymus the number of macrophages was significantly higher in the cases with PAH. There was no difference regarding the frequency of steatosis between the groups of cause of death. There was a positive and significant correlation between the degree of steatosis and the gestational age. In the liver the cases with PAH and AI presented the bigger percentage of hepatic fibrosis. The focuses of eritropoiesis varied in accordance with the gestational age.

Conclusion(s) With the improvement of the perinatal care and the survival of the premature which had been exposed to intrauterine stimulus like PAH and AI, the description of the morphological injuries of the stress organs will help in future autopsy studies, and in the prevention of the diseases in the childhood. Grants: CAPES, CNPq, FAPEMIG, FUNEPU, UFTM.

P1.208

Primary intracranial malignant fibrous histiocytoma in a 2 month-old boy

Taeeun K.; Suh Y.
Dpt. of Pathology, Samsung Medical Center, Sungkyunkwan University School of Medicine, Seoul, Republic of Korea

Background Malignant fibrous histiocytoma (MFH) in the pediatric age group is extremely rare and 3 cases of intracerebral MFH aged 2 and 5 years been reported in literature.

Methods Authors report a case of primary intracranial MFH occurring a 2-month-old boy.
Results He had presented with left facial palsy. Magnetic resonance imaging demonstrated a 3.5 cm-sized, well-defined enhancing mass in the left middle cranial fossa. The tumor affected left temporal base with dural adhesion and bone destruction, and a gross total removal of the mass was performed. Histologically, there was a highly cellular tumor composed of a mixture of fibroblast-like spindle-shaped cells forming storiform patterns, round to oval cells, osteoclast-like giant cells, and intermingled with inflammatory cells. Atypical mitotic figures and occasional necrosis were seen in the tumor. Immunohistochemically, tumor cells were strong positive for CD68 and focal positive for S-100, but negative for GFAP and EMA, smooth muscle actin, desmin, pancytokeratin and anaplastic lymphoma kinase. Ultrastructurally, tumor cells had lysosomes and abundant, usually undilated rough endoplasmic reticulum, which were consistent with histiocytes. Histopathological and ultrastructural findings of the tumor were consistent with malignant fibrous histiocytoma. During chemotherapy, he suffered from bloody stool and underwent endoscopic biopsy from the sigmoid colon. Metastatic lesion was incidentally found on the sigmoid colon. However, there was no evidence of metastasis in other organs including the bone.
Conclusion(s) MFH should be included in differential diagnosis of pediatric intracranial tumors, even though intracranial MFH is very rare.

P1.209

Retroperitoneal neuroblastoma in 30 year old woman. Case report

Dukova B.; Duganovska S.; Petrusevska G.; Filipovski V.; Bogdanovska M.
Institute of Pathology, Skopje, the Former Yugoslav Republic of Macedonia

Background Neuroblastomas arise from neural crest-derived cells in the sympathetic ganglia and adrenal medulla. We present a retroperitoneal neuroblastoma in 30 year old woman with lymph node metastases and involving the left obturatory canal. There were 13 tumor masses with 1000gr weight and largest diameter of 10 cm.; some lined by a pseudocapsule.
Methods The tissue samples were formalin fixed, paraffin embedded and standard HE stained. Additional immunohistochemical analyses were performed with NSE, Chromogranin, Vimentin, S-100, MIC2, Synaptophysin.
Results Histologically we found dense cellular tumor composed of small cells with round dark nuclei and scant cytoplasm – "lymphocyte like". Homer-Wright rosettes with central neuropil were also present. There were large areas of necrosis and hemorrhage. The tumor invades the pseudocapsule and spreads in paravertebral and presacral lymph nodes. We assessed some better differentiated areas in tumor mass found in obturatory canal resembling mature ganglion cells, chromaffine cells and focuses of calcification. Tumor cells showed high positive signal on immunohistochemical staining for NSE, Chromogranin, Vimentin, S-100, moderate signal on MIC2 and no signal on Synaptophysin.
Conclusion(s) Although neuroblastoma is most common malignant tumor in childhood we emphasize the possibility that it can be found in adults also. Screening tests for metabolites of catecholamines should be performed.

P1.210

Type 2 infantile hemangioendothelioma / infantile angiosarcoma: an autopsy case report

Afonso M.; Vizcaíno J.; Eisele R.; Encinas A.; Lopes C.
Instituto Português de Oncologia do Porto Francisco Gentil, Porto, Portugal

Background Hepatic tumours in the perinatal period are rare, representing less than 5% of the total. Infantile Hemangioendothelioma (IHE) is the second most common in this age group and can be divided into two histologic types: type 1 and type 2. Type 2 is extremely rare and is sometimes referred as Infantile Angiosarcoma.
Methods Sections of 10% neutral-buffered formalin fixed paraffin embedded material were stained with standard H&E technique. Immunostains were performed with avidin-biotin-peroxidase method.
Results We report an autopsy case of a female neonate who died 14 days after birth due to acute abdominal haemorrhage and hepatic laceration, followed by renal failure. Macroscopically, there was a voluminous liver, with solid and haemorrhagic multinodular areas. Microscopically there was a diffuse involvement by a vascular proliferation of poorly formed anastomosing channels with papillae and a complex branching pattern lined by atypical endothelial cells. The mitotic index was low (1 mitosis/10 HPF), so as the proliferative index (Ki67 <1%). These changes were consistent with Congenital Type 2 IHE/Infantile Angiosarcoma.
Conclusion(s) Although the significance of type 2 changes in IHE remains controversial, our case had a fulminant outcome. Despite extensive prenatal screening, clinical and imagiologic investigation, there was no suspicion of hepatic or vascular neoplasm and the final diagnosis was only made on autopsy.

P1.211

Werdnig Hoffmann disease

Eugenia M.
Emergency Hospital County Targu mures, Mures, Romania

Background Spinal muscular infantile dystrophy (werdnig Hoffmann Diasease) is the most Well-known autosomal-recesive familial neuromuscular disease seen in child. The debut is at birth or during childhood. The preccity of the debut is an unfavorabile sign.
Methods We present three cases of spinal muscular infantile dystrophy, studied in the last year, with a clinical suspicion of the disease and myogen EMG. Muscular biopsies were done and the biopsies were sampling on ice and paraffin stains. Usual coloration was done, and also special colorations: PAS hematoxilin, Gomori argentic stain, tricrome and van Gieson coloration.
Results Unfortunately, two of the children died at two months. The necropsy was done and diagnostic was formulated using multiple biopsies from different places, including cardiac muscle. For one the cases, an ADN examination was done. For third case, a nine year old boy, the diagnostic was a mild dystrophy. For all the cases the muscular biopsy presented the caracteristic features or fetal muscle:round fibers, often small, some angulated, containg little glycogen, PAS positive with central nuclei. Toghether there are bigger fibers, showing degenerative aspects end erased or lost transversal striations.
Conclusion(s) A diagnostic of spinal muscular infantile dystrophy (werdnig Hoffmann disease) was formulated. Spinal muscular infantile dystrophy is a genetic disease, with a serious outcome. The diagnostic of the muscular biopsies is extremely important. The genetic examination is very important for the prevention of multiple familial transmissions.

P1.212

Absence of the septum pellucidum associated with a midline fornical nodule and ventriculomegaly - a report of two autopsy cases

Chun Y.; Kim H.; Hong S.; Chi J.
Cheil General Hospital, Kwandong University College of Medicine, Seoul, Republic of Korea

Background Absence of the septum pellucidum is a congenital defect in the development of the midline telencephalic structures. It rarely occurs in isolation, but is usually associated with additional malformations of the brain. Septo-optic dysplasia should be differentiated from isolated absence of the septum pellucidum.
Methods We report two fetal autopsy cases at 36 and 25 weeks of gestation that revealed the partial absence of the septum pellucidum with ventriculomegaly.
Results In each case, the brain showed mild dilatation of both frontal horns of the lateral ventricles, normal third and fourth ventricles and no aqueductal stenosis. The posterior portion of the septum pellucidum was absent and the fornices were fused in a single midline nodule, abnormally displaced to a caudal position and lodged in the foramina of Monro. The brain base showed well developed optic nerves. Maternal estriol and fetal pituitary hormones were not checked.
Conclusion(s) We think that the caudally displaced fornix in the absence of the septum pellucidum may have intermittently obstructed the foramina of Monro and induced mild ventriculomegaly. We can not exclude septo-optic dysplasia with certainty, even though normal appearance of the optic nerves.

P1.213

Congenital disorder of true cyclopia: a rare case report

Lambropoulou M.; Alexiadis G.; Chatzaki E.; Simopoulou M.; Giannoudi T.; Jivannakis T.; Grapsas X.; Deftereou T.; Grammatikopoulou I.; Papadopoulos N.
Department of Histology-Embryology, Democritus University of Thrace, Alexandroupolis, Greece

Background Cyclopia is a rare type of holoprosencephaly and a congenital disorder characterized by the failure of the embryonic forebrain to properly divide the orbits of the eye into two cavities. As a result a birth defect in which only one eye is developed. Generally, cyclopia occurs in the second week of gestation and can be caused by chromosome abnormalities, as well as, gene mutations.
Methods We present a rare case of true cyclopia in a female fetus (32 weeks of gestation). There were orbital malformations- true cyclopia - single median eye in single median orbit and a non-functioning nose in the form of proboscis measuring 15 mm in length and 10 mm in diameter with a single orifice above the central eye.
Results The radiographic findings included fusion of the thalami with resultant absence of the third ventricle. The cerebrum was presented as a “pancakelike” mass of tissue located anteriorly in the skull. A single large ventricle was posteriorly. There was absence of the interhemispheric fissure, falx cerebri and corpus callosus. The outer appearance of the rest of the body was normal, except of the existence of an extra finger in both the above limbs (polydactylia).
Conclusion(s) Cyclopia is the most severe malformation of holoprosencephaly with a single median orbit that may be anophthalmic, monophthalmic, or synophthalmic. Approximately 1.05 in 100,000 births are identified as cyclopian, including stillbirths and the sex distribution shows a female predominance.

P1.214

The etiology of hydrops fetalis: series of stillborn autopsy in the central region of Thailand

Taweevisit M.
Chulalongkorn University, Pathumwan, Bangkok, Thailand

Background Hydrops fetalis (HF) is a life-threatening problem in fetuses and newborns. The purpose of this study is to analyze the etiology of HF among fetal death in a central region of Thailand.
Methods The author retrieved the autopsy reports mentioned HF between 2000 and 2008 at King Chulalongkorn Memorial Hospital together with reviewing the clinical information, fetal ultrasounds, and laboratory data.
Results There were 74 autopsies (36 male and 38 female) with a mean gestational age of 29 weeks. The causes were identified in 87.7% and no immune hydrops was detected. Anemic cause was dominant (38.4%), followed by cardiovascular anomaly (21.9%), thoracic space-occupying lesion (8.2%); fetal infection (6.8%); and tumor or tumor-like lesion (4.2%). Chromosomal/genetic abnormalities were suspicious in 2.7%. The following diagnoses were grouped as miscellaneous (5.6%) and made in one instance each: placental vascular thrombosis, maternal diabetic mellitus, intestinal lymphagiectasia, and Beckwith-Wiedemann syndrome. No identifiable etiology was 12.3%. In anemic cause, it consisted of Hb Bart (20.5%), twin-twin transfusion syndrome (8.2%), HbH (4.1%), lung hemorrhage (1.4%) and unspecified (4.1%). Four out of 14 cases in the group of cardiac defect (19%) whose mothers had previous abortions, 1 or 2 times (p=0.028).
Conclusion(s) Hb Bart HF showed the highest incidence in central region of Thailand. Interestingly, even small numbers of cases, we speculate that congenital cardiac anomaly may link with a history of abortion in their mothers by some genetic and/or environmental factors.

P1.215
Omental-mesenteric myxoid hamartoma mimicking malignancy in a 14-month-old child (a case report)

Zabolinejad N.; Bazrafshan A.; Dehghanian P.
Mashhad University of Medical Sciences, Mashhad, Khorasan, Islamic Republic of Iran

Background The omental-mesenteric myxoid hamartoma (OMMH) is a very rare lesion, mainly seen in children and characterized by multiple omental and mesenteric nodules, which may be confused with malignant neoplasm. Microscopically, these lesions consist of a richly vascularized myxoid stroma with plump mesenchymal cells. This lesion has a benign clinical course without recurrence during follow up.
Methods We present a 14-month-old boy that was referred with history of abdominal distension, fever and vomiting for 3 months. Enhanced computed tomography (CT) revealed a huge well-demarcated hypodense and spherical mass which displaced bowel loops without obvious penetration to the intestinal walls.
Results Histological and immunohistochemical examinations confirmed the diagnosis of OMMH. No evidence of recurrence was noted during 3 years follow up.
Conclusion(s) OMMH is a very rare lesion and because of its aggressive appearance, differential diagnosis with malignancy is warranted. The clinical picture of our case also led to high suspicion of malignancy. However by consideration of histological and immunohistochemical findings we could achieve the correct diagnosis.

Cytopathology

P1.216
Solid pancreatic lesions diagnosed by endoscopic ultrasound guided fine needle aspiration

Cabezas A.; Alcaraz E.; Aparicio Ramón J.; Martínez-Sempere J.; Perez-Mateo M.; Aranda Ignacio F.
Hospital General Universitario de Alicante, Alicante, Spain

Background The incorporation of Endoscopic Ultrasound Guided Fine Needle Aspiration (EUS-FNA) has become in the field of pancreatic lesions. Following study is based on the experience of 2 years since the incoming of the procedure in our hospital.
Methods There have been realized 68 EUS-FNA of solid pancreatic lesions in a period of 2 years. Some material is set aside to the cell block and liquid-based processing (Thin prep). The needle used is 22–25 G and the number of passes considered optimum is 3.
Results The number of solid pancreatic lesions punctured was 68, 43 males (63%) and 25 females (37%). The average size of the lesions was 24 mm (range 5–60 mm), being the most frecuent location, the head (71%), followed by the body (22%) and the tail (7%). Only in 2 of the cases, the sampling was unsatisfactory. In 18 cases there were subsequent correlation (surgical specimen or core biopsy), confirming the diagnosis in 14 cases. The sensibility and specificity of the procedure was 71% y 100%, respectively.
Conclusion(s) In our way, EUS-FNA is probably the simplest method for the classification of solid pancreatic lesions. It has a high specificity and sensibility (70 %), depending the latter on the quality of the sampling. We think is necessary the presence in situ of a cytopathologist since it allows the communication with the endoscopist during the procedure, the valuation of the material as well as the classification of the lesion.

P1.217

Study of the mediastinum using real-time endobronchial ultrasound (EBUS)-guided transbronchial needle aspiration (TBNA) compared to conventional and EBUS-guided TBNA

Pijuan L.; Sánchez-Font A.; Curull V.; Albert S.; Santos J.; Vollmer I.; Gayete A.; Trampal C.; Lloveras B.; Rodriguez A.; Alameda F.; Serrano S.
Hospital del Mar, Barcelona, Spain

Background Conventional transbronchial needle aspiration (C-TBNA) and EBUS-guided TBNA are minimally invasive methods for mediastinal study. A new endoscope with a built-in linear probe ultrasonography on the tip enables real-time EBUS-guided TBNA. We report our initial experience using real-time EBUS-guided TBNA with rapid on site cytologic evaluation (ROSE) compared to C-TBNA ("blind" procedure) and EBUS-guided TBNA previously undertaken in our institution.
Methods A total of 182 TBNA samples (150 patients) were obtained from mediastinal lymph nodes detected by CT and/or PET scan. We performed 73 C-TBNA, 70 EBUS-guided TBNA, and 39 real-time EBUS-guided TBNA. Cytology specimens were categorized as positive, negative or inconclusive, using the ROSE method in the real-time EBUS-guided TBNA. Final diagnosis was based on mediastinal biopsy results, surgery and/or clinical follow-up.
Results The efficiency of the TBNA using C-TBNA was 43.8% and 54.3% using EBUS-guided TBNA; with inconclusive TBNA rates of 56.2% and 45.7% respectively. Using the real-time EBUS-guided TBNA in combination with ROSE, improved the efficiency to 89.7% with only 10.3% inconclusive TBNA. No complications with TBNA were reported.
Conclusion(s) EBUS-guided TBNA is a safe and useful method for mediastinal lymph node study. A positive diagnosis avoids more invasive diagnostic procedures. Real-time EBUS with ROSE improves the diagnostic yield of TBNA compared to C-TBNA and EBUS-guided TBNA. ROSE when positive is very useful to reduce the duration of a procedure.

P1.218

Negative cervico-vaginal samples, HPV positive: must be re-screened?

Alameda F.; Lloveras B.; Pijuan L.; Gimferrer E.; Albert S.; Bosch M.; Romero E.; Soler I.; Musset M.; Bellosillo B.; Muñoz R.; Carreras R.; Serrano S.
Hospital del Mar, Barcelona, Spain

Background To assess the results of CV-liquid based negative – HC-II positive re-screened cases.
Methods 1379 Liquid based (ThinPrep) automated screened (Imager, Cytyc Hologic) CV negative samples. Hybrid Capture II in all cases. Re-screening of 228 CV-HPV+ samples.
Results 965 (70%) from primary screening centers (PSC) and 414 (30%) from the Obstetrics and Gynecology Department (OGD), corresponding to LSIL or post surgical controls.228 cases were HC-II+ (16.5%). Fourteen cases (1.01% of total cases) were re-informed as ASCUS (9 cases), or LSIL (5 cases), eigth of them from PSC, L 7 ASCUS 1 LSIL) and six from the OGD (2 ASCUS and 4 LSIL). None of them was reclassified as ASC-H or HSIL. The mean viral load (MVL) of all cases, 228 HCI+ cases and the re-classified ones, was 133.5, 163 and 616.5. If we use the MVL to dfferentiate between those cases that must be re-screened, using 133.5 the NPV is 97%, the specificity is 86.9%, the sensitivity is 57% and the PPV is 22%. Using a VL of 163 as a cutt-off, the results are similar. Consequently if we would re-screen only the cases with a VL greather than 133.5 or 163 we woud miss 2 LSIL and 4 ASCUS cases, or 2 LSIL and 3 ASCUS respecfully, but we wouldn't had to re-screen 193 or 191 negative cases (84.6% or 83.7%).
Conclusion(s) HPV positivity and viral load could help us to select the cases must be re-screened.

P1.219

The significance of fine needle aspiration biopsy in the differential diagnosis of the cystic lesions

Bayol U.; Vardar E.; Deniz A.; Isin E.
Izmir Tepecik, Izmir, Turkey

Background To evaluate the role of fine needle aspiration cytology in the diagnosis of hydatid cysts and to emphasize in the differential diagnosis in cystic lesions.
Methods In the Department of Pathology in Izmir, FNAB were performed in many patients with cystic occupying lesions. Twenty-six cases of hydatid cyst were diagnosed primarily by fine needle aspiration cytology.
Results In all cases, large fragments of acellular acidophilic stained material, finely lamellated, were found. In early post-procedural period there were no complications related to FNAB puncture. Serological and/or histologic studies confirmed the diagnosis of hydatid cyst. The location and number of the patients of the cyst hydatic were given in below. Liver 14 Lung 4 Gallbladder 2 Kidney 1 Adrenal 1 Gluteal soft tissue 1 Breast 1 Serebrum 1 Omentum 1.

Conclusion(s) When acellular, laminated fragments suggestive of a laminated layer are identified on slides, hydatid cyst should be considered in the differential diagnosis of cystic lesions, even in atypical locations and in the absence of hooklets, protoscolices or both.

P1.220

Rapid intraoperative cytology in the evaluation of breast cancer-comparative study of two staining methods

Kyurkchiev P.G.; Tzvetkov G.I.; Shopov B.K.; Jurukov N.I.; Birdanov G.J.; Pavlova R.Z.
Sofia, Bulgaria

Background To evaluate the contribution of two staining methods on touch imprints from breast carcinoma and lymph node metastases.
Methods Thirty-nine patients with primary breast tumors underwent imprint cytology performed on primary tumor and lymph node samples during primary surgical treatment. Cytological specimens were stained with the Haemacolor and hematoxylin-eosin (HE) techniques. Histologic sections from the lesions were studied and compared with the cytologic findings.
Results Touch imprints from the primary breast tumor stained with Haemacolor were positive for tumor cells in 92% of the patients, these stained with HE were positive in 92% of the patients. Touch imprints from the lymph nodes stained with Haemacolor were positive for tumor cells in 94% of the patients, these stained with HE were positive in 89% of the patients.
Conclusion(s) Haemacolor and HE stainings presented clear cellular details in detecting malignant cells in imprints from the primary lesion, while Haemacolor staining gave more accurate results in lymph node touch imprints. Both staining methods could be useful in intraoperative detection of breast tumor cells.

P1.221

A simple and efficient procedure that enables miRNA array analyses from single thyroid in vivo FNA

Kiss K.; Rossing M.; Glud M.; Nielsen Cilius F.; Bennedbaek Noe F.; Friis-Hansen L.
Department of Pathology, Copenhagen University Hospital, Herlev Section Gentofte, Hellerup, Denmark

Background MicroRNA (miRNA) expression profiling and classification of tissue obtained from fine-needle aspirates (FNA) could be a major improvement of the preoperative diagnosis of thyroid nodules. Before this can be implemented in the clinical setting, a robust and non-toxic method for obtaining sufficient quantity and quality of RNA from single in vivo FNA has to be established. RNA later is a non-toxic stabilization agent that preserves RNA. However, due to the high density of RNAlater, pelleting of the tissue samples is difficult, and causes a low recovery of RNA insufficient for subsequent miRNA array expression analyses. We therefore developed a simple centrifugation method for capturing tissue stored in RNAlater on a 0.45-μm filter.
Methods FNA from 24 patients with a solitary cold thyroid nodule was stored in Trizol, liquid nitrogen, or RNAlater. The tissue stored in RNAlater was either pelleted by centrifugation or captured on the 0.45-μm filters. RNA was extracted using the Trizol method.
Results Capturing FNA tissue samples on the filters increased the RNA yield 10 fold, maintained RNA pureness, thus permitting miRNA array expression profiling and allowing comparable levels of known microRNAs of thyroid nodules regardless of preservation technique.
Conclusion(s) The modified RNAlater protocol is well suited for isolating RNA from single thyroid in vivo FNA in the clinical setting.

P1.222

Anal human papillomavirus genotype distribution and cytologic abnormalities among HIV-infected homosexual men

Costes V.; Damay A.; Fabre J.; Didelot J.; Boule N.; Segondy M.
Department of Pathology, CHRU Montpellier, France

Background The aim of this study was to determine the prevalence of human papillomavirus infection, the HPV genotype distribution and the prevalence of cytologic abnormalities in anal canal specimens collected from HIV-infected homosexual men.
Methods Anal samples were collected into a PreservCyt solution for liquid-based cytology and HPV-testing. We used the MagNA Pure compact DNA isolation kit I and the MagNA Pure compact extractor.
Results 64 anal samples from 58 patients were tested. HPV-DNA was detected in 46 (71.9%) samples.44 (68.8%) patients were infected with at least one HR HPV, 27 (42.2%) patients were infected with at least one LR HPV, 2 (3.1%) patients were infected with LR HPV only, and 37 (57.8%) patients had a multiple HPV infection with 2 to 9 different types. A total of 139 HPV isolates (101 HR HPV and 38 LR HPV) were identified, the most prevalent HPV-types being: HPV 16 (26.1%), HPV 53 (26.1%) and HPV 39 (23.9%). Anal squamous intraepithelial lesions (SIL) were detected in 22 cases (34.9%), 19 (30.2%) being classified as low-grade SIL and 3 (4.8%) as high-grade SIL. Six samples (9.5%) were classified as atypical squamous cells of undetermined significance (ASCUS).

Conclusion(s) We observed a high prevalence of HPV and HR HPV infection, and of cytological abnormalities including high-grade lesions. Anal cytological and HPV screening of the homosexual HIV-infected patients should be considered in order to prevent progression to anal cancer.

P1.223

Biliary brush cytology combined with immunocytochemical staining for IMP3 provides superior diagnostic sensitivity for detection of pancreaticobiliary malignancies

Parab Sanjay M.; Daniza M.; Cartun W.R.; Ligato S.
Hartford Hospital, Hartford, CT, USA

Background Biliary brush cytology is an important diagnostic tool in the evaluation of patients with bile duct strictures. In this study, we evaluated the immunocytochemical expression of insulin-like growth factor (IGF) mRNA-binding protein 3 (IMP3), also known as KOC/L523S, to assess the performance of this marker for the detection of malignant cells in bile duct brushing specimens.
Methods Sixty-four patients who underwent ERCP and bile duct brushing for bile duct stricture were studied. Diagnoses were: 37 cases negative for malignancy, 14 cases atypical, not diagnostic for malignancy, and 13 cases suspicious/positive for malignancy. Alcohol-fixed, PAP-stained slides were immunostained with mAb to IMP3 (Dako). Results were recorded as negative (< 5% cells positive) or positive (> 5% cells positive). The atypical, not diagnostic cytology cases were considered negative for statistical analysis.
Results 39 of the 64 patients were diagnosed with malignancy based on biopsy, FNA or clinical progression of disease. The sensitivity of routine cytology for the detection of malignancy was 33.3% (13/39), immunocytochemical -IMP3 expression was 64.1% (25/39), and the combined sensitivity was 71.8% (28/39) with a $p<0.0001$. The specificity of both tests was 100%.
Conclusion(s) Our study shows that IMP3 improves significantly the sensitivity of routine cytology for the detection of malignancy in bile duct specimens. The combined use of biliary brushing cytology and IMP3 provides the highest yield for diagnosing malignancy in the pancreatico-biliary system.

P1.224

Hodgkin/Reed-Sternberg cells in a lymph node diffusely infiltrated with mantle cell lymphoma - a case report

Klopcic U.; Jancar J.
Institute of Oncology, Department of Cytopathology, Ljubljana, Slovenia

Background Association of Hodgkin lymphoma (HL) and mantle cell lymphoma (MCL) is very rare with only four cases described in the literature so far. We present a case where Hodgkin/Reed-Sternberg (HRS) cells were detected in a lymph node othervise diffusely infiltrated by MCL.
Methods The patient has been treated for MCL for five years and recently noted enlarged left supraclavicular lymph node. Fine needle aspiration biopsy showed a dominant population of small to medium sized lymphoid cells with some scattered large HRS-like cells. Immunocytochemistry for cyclin D1 was positive in small to medium sized lymphoid cells, while HRS-like cells were CD15 and CD30 positive. Flow cytometric analysis confirmed the infiltration of lymph node by MCL.
Results Lymph node was excised and histology closely resembeld cytology: a monotonous diffuse proliferation of small-medium sized B cells with scatered HRS cells. There was no reactive background, typical for HL around HRS cells. HRS and MCL cells were EBV negative. Translocation t(11;14) was demonstrated by FISH in MCL component.
Conclusion(s) Scattered HRS cells within MCL are an exceptional finding with unknown prognostic significance. Although our case cannot be classified as a composite lymphoma, we can hypothesize that 1) the reactive background of HL might not have developed yet due to the early stage of HL, or 2) that the reactive background of HL was overgrown by MCL component.

P1.225

Mediastinal mass diagnosed as malignant melanoma. Case presentation and literature review

Abuomar A.; Cabezas A.; Muñoz C.; Sanchez M.; Herrero J.
Hospital de Torrevieja, Torrevieja, Alicante, Spain

Background Although skin is the most common site for primary malignant melanoma, it also appears wherever melanocytes are present. Mediastinum is a rare location of primary malignant melanoma.
Methods We report a case of a 75 years old woman with asymptomatic mediastinal mass. Chest computered tomography (CT) scan reported: leyomioma of the esophagus as a first diagnostic possibility. Representative material obtained by ecoendoscopy with Fine Needle Aspiration (FNA) showed atypical polygonal cells with hyperchromatic oval nucleus with prominent nucleoli and abundant eosinophilic cytoplasm with brown granules. Frequent mitotic figures were seen. Neoplastic cells stained for HMB45 and S100 protein. Esophageal mucosa was normal. Extensive examination of the patient was done, but no other lesion suggesting a primary origin was found.
Results In contrast to metastatic mediastinal involvement, there have been only a twelve case reports in literature of

melanoma presenting primarily in the mediastinum. Range of age: 11–75 with a slight male preponderance (M:F= 1.3:1). Most were asymptomatic or presented nonspecific chest discomfort. One case presented laryngeal nerve palsy, other with severe dysfagia.
Conclusion(s) The primary mediastinal origin of melanoma is difficult to prove. In our opinion a definitive diagnosis should base on the morphology of the melanoma as well as on the absence of other patent or formerly resected primary lesions in melanocyte-rich localizations like skin, mucosa and eye.

P1.226
Papillary thyroid microcarcinoma. Fine needle biopsy diagnosis and accuracy

Ivanova S.R.; Kovacheva R.; Ivanova B.R.; Shinkov A.; Kanev N.; Sechanov T.
Lab of Pathomorphology and Cytopathology University Hospital of Endocrinology, Sofia, Bulgaria

Background Papillary thyroid microcarcinoma (a thyroid nodule < 1 cm) is the most common subtype thyroid carcinoma. With the widespread use of the thyroid ultrasound and fine needle biopsy (FNB) it become possible to diagnose cytologically very small thyroid carcinomas. The aim of this study was to evaluate the diagnostic accuracy of the FNB suspicious for papillary thyroid microcarcinoma (PTMC) by cytohistological correlation.
Methods Forty FNB classified as positive for PTMC (n= 24) and suspicious for PTMC (n=16) were included. In all patients (5 - male, 35 - female, mean age 40.8 y) high frequency ultrasonography of the thyroid gland was performed and thyroid nodules with size up to 1 cm and echographic signs suspicious for malignancy were selected for FNB under echographic control (using free-hand technique, without aspiration). The cytologic smears were stained with MGG and the presence of different cytologic parameters (hypercellularity, papillary clusters, intranuclear inclusions and grooves) was evaluated.
Results In 22 (91.7 %) patients with positive cytology PTMC was proved at surgery. In the remaining 2 cases the histology was negative for cancer (false-positive). In 12 (75 %) cases with suspicious cytology the histology showed papillary carcinoma and in the rest 4 cases - benign nodule. Lymph node metastases were found in 4 (11.8%) cases.
Conclusion(s) The diagnostic algorithm, including thyroid ultrasonography, FNB under echographic control and cytology of suspicious thyroid nodules is very sensitive for preoperative diagnosis of papillary thyroid microcarcinoma.

P1.227
Recognition of follicular variant of papillary thyroid carcinoma in fine needle aspiration

Jeong J.; Shon Y.; Park J.
Kyungpook National University Hospital, Daegu, Republic of Korea

Background The diagnosis of follicular variant of papillary thyroid carcinoma (FVPTC) in fine needle aspiration (FNA) is difficult, because FVPTC often shows nuclear features of papillary thyroid carcinoma (PTC) focally, and it can even be similar to follicular neoplasm. The purpose of this study was to identify the sensitive or specific cytologic features of FVPTC.
Methods A total of 51 cases of FNA specimens diagnosed as FVPTC on histology were examined retrospectively. The original cytologic diagnoses were variable, including 20 cases of atypical follicular lesion, 13 cases of PTC, 8 cases of follicular neoplasm, 6 cases of benign follicular lesion, and 4 cases of insufficient specimen. We evaluated several commonly-mentioned cytologic features.
Results Nuclear grooves, fine chromatin or nuclear clearing, micronucleoli, colloid, intranuclear inclusions, and papillae were present in 96%, 92%, 67%, 59%, 47%, 2% respectively. Fine chromatin and nuclear grooves were the most sensitive cytologic features. We could find fine chromatin, nuclear grooves, and/or intranuclear inclusions rarely, even in the 6 false negative cases, although they were mostly limited to form the diagnosis by observing low cellularity, so those features were thought to be specific.
Conclusion(s) There is no definite criteria for the diagnosis of FVPTC. But we could suggest FVPTC and reduce false negative in FNA by carefully searching for some helpful cytologic features, like fine chromatin, nuclear grooves, and intranuclear inclusions, in cases without definite papillary structure.

P1.228
The comparison between monolayer and conventional cytology in the diagnostic of cervical cancer

Weyerstahl T.; Trauner A.
Laboratory for Cytology and Molecular Biology Dr. T. Weyerstahl, Munich, Germany

Background To observe the cytological-histological approach of 196 cervical biopsy cases and evaluate the difference between conventional and monolayer cytology.
Methods The significance of difference was evaluated with the Fisher exact test.
Results 182 biopsy cases were histological diagnosed as positive.152 of these cases were cytological diagnosed

(conventional smear) as: 4 cases without any cytological anomaly (PAPI-II), 51 cases of mild and/or moderate dysplasia (PAP IIID), 70 carcinoma in situ cases (PAP IV) and 4 cases of invasive carcinoma (PAP V).23 cases were with cytological report as questionable. The remaining 30 cases of positive biopsy were cytological diagnosed with the monolayer method. The distribution of the PAP results was: 12 IIID cases, 13 PAP IV cases and 5 cases of PAP III. There were not cases of invasive carcinoma and PAPI-II cases. The value of negative histological reports (n=14) was the same by conventional (n=7) and by monolayer methods (n= 7) and showed the same distribution of PAP: one case of PAP I-II, 4 cases of PAP IIID, one CIS and one case with cytological report as questionable. There were not cases of invasive carcinoma.

Conclusion(s) 18, 9% cases of monolayer method to 4, 4% conventional cytology cases were with negative histology.81, 1% monolayer cases to 95, 6% conventional cytology cases were with positive histology. There is a statistical significant difference (p=0,0120) between conventional and monolayer cytology in relation to negative histology and no significant difference (p = 0,5909) in relation to positive histology.

P1.229
The difference between the conventional and the monolayer cytology in the cervical cancer diagnostic

Trauner A.; Weyerstahl T.
Praxis Doctor Weyerstahl, Munich, Germany

Background To observe the cytological-histological approach of 174 cervical biopsy cases and evaluate the difference between conventional and monolayer cytology.

Methods The significance of difference between the PAP-test result of Thinprep (PAP TC) and the PAP-test results of conventional cytology (PAP CC) in relation to the histological reports was evaluated by Chi Square (Yates) test.

Results 8 of all cervical biopsy cases showed benign histological changes. The percentage relation between PAP TC to the PAP CC was: 0,0% TC to 33,3% CC by cases without any cytological abnormality (NILM), 80,0% TC to 33,3% CC by cases of mild and/or moderate dysplasia (PAP IIID), 20,0% TC to 33,3% CC by cases of severe dysplasia/ CIS (PAP IV). There were not cases with cytological report as questionable (PAP III) and cases of invasive carcinoma (PAP V).166 biopsy cases showed cervical intraepithelial neoplsia, carcinoma in situ or invasive carcinoma. The percentage relation between PAP TC and PAP CC was: 0%TC to 3,0% CC by NILM; 32,3% TC to 35,6% CC by IIID cases, 51,6% TC to 44,4% CC by PAP IV, 0,0%TC to 3,0% CC by cases of PAP V and 16,1% TC to 14,1% CC by PAP III.

Conclusion(s) 13,9% cases of the monolayer method were with benign lesions and 86,1% monolayer cases with positive histology. With conventional cytology were 2, 2% of the cases with benign lesions and 97, 8% of the cases with positive histology. There is a statistical significant difference (p=0,025) between conventional and monolayer cytology in relation to the histology.

P1.230
The role of bronchial brushing for diagnosis bronchoscopically "no visible" lung carcinoma

Stojanovic V.I.
Center for Pathology, Nis, Serbia and Montenegro

Background Fiberoptic bronchosopy is the most common modality used to diagnose endobronchial carcinoma. Endobronchial abnormalities underwent fiberoptic bronchial biopsy and bronchial brushing. A combination of both techniques to increase the diagnostic yield for endobronchial malignant tumours.

Methods We had taken in analysis 30 patients hospitalized in clinik for pulmonary disease. They had endoscopically signs of chronical inflammation, without visible tumors. Specimen for cytological procedures was dyed by May-Grunwald-Gimsa method. Specimen for patohistologic analysis was taken from eventually suspected places and were routinely processed and dyed by the HE method.

Results Bronchial brushing were positive for maligant cells in all cases. The diagnosis of lung carcinoma was confirmed with bronchial biopsy in 20 cases - 10 squamos cell, 7 adeno and 3 small cell type lung carcinomas. In 10 cases bronchial biopsy were with signs of chronical inflammmation. In those cases cell typing were made on bronchial brushing, becose the typing of lung carcinoma was important for therapeutic decisions.

Conclusion(s) Bronchial biopsy provides the definitive histological diagnosis in most cases, but accompanig cytological procedures can increase diagnostic yield. The results from brushing were related to the quality of the techique and the experience of the pathologist. There is a good corelation between biopsy and brushing in cases where the biopsy was not uninterpretable. In our study, in those cases brushings confirmed a cancer and type of cancer in all cases.

P1.231
Utility of D2–40, desmin, calretinin, CK5/6 and MOC-31 in differentiating mesothelioma from adenocarcinoma in pleural effusions

Barnes M.; Tabatabai L.Z.
University of California San Francisco, San Francisco, CA, USA

Background Differentiation between mesothelioma and adenocarcinoma remains one of the most problematic areas in effusion cytology. Recent studies have suggested that the novel lymphatic endothelial marker D2–40 may be useful in the diagnostic workup of effusions. We tested D2–40 along with Desmin, Calretinin, CK5/6 and MOC-31 to help establish the utility of these antibodies in cytologic specimens.
Methods Forty-five archival, formalin-fixed, paraffin embedded cell blocks of pleural effusions representing 13 reactive effusions, 11 mesotheliomas, and 21 metastatic adenocarcinomas were retrieved. All cases were immunostained with anti-D2–40, Desmin, Calretinin, CK5/6, and MOC-31 and the immunoreactions were evaluated in a blinded fashion by two pathologists.
Results D2–40 showed membranous staining in 82% of mesotheliomas and 77% of benign effusions. Desmin was negative in all malignant cases and positive in 85% of benign effusions. Calretinin and CK5/6 were positive in 100% and 64% of mesotheliomas, and 92% and 64% of benign effusions, respectively. All metastatic adenocarcinomas were positive for MOC-31 and negative for D2–40, Desmin, Calretinin and CK5/6.
Conclusion(s) D2–40 was not as sensitive as Calretinin, and due to its sometimes focal and weak positivity, it should be interpreted cautiously in limited cellularity samples. Desmin was useful in differentiating benign from malignant effusions, but not in distinguishing between malignancies. CK5/6 was the least sensitive mesothelial marker. Calretinin and MOC-31 were the most sensitive in detecting mesothelial and epithelial differentiation, respectively, and are recommended in staining panels used to evaluate effusion specimens.

P1.232
Value of thyroid transcription factor-1 and cytokeratin 7 and cytokeratin 20 immunostaining in differentiating metastatic pulmonary from extrapulmonary adenocarcinoma in pleural effusion samples

Almeida Mendes M.; Pestana I.; Lopez D.
Santa Maria, Lisboa, Portugal

Background The aim of our study is to assess the utility of thyroid transcription factor-1(TTF-1) and the combined cytokeratin (ck7 and ck20) immunoprofile as a marker for identifying the primary site of metastatic adenocarcinoma in pleural effusions.
Methods Cytologic pleural samples of 140 patients with adenocarcinomas were reviewed. A panel of monoclonal antibodies (CK7, CK20 and TTF-1) was applied to Papanicolaou stained smears. The results were correlated with the primary origin of the metastatic adenocarcinoma. The primary sites were: lung (n=63), breast (n=42), ovary (n=12), stomach (n= 10), colon (n=4), pancreas (n=3), kidney, bladder and uterus (two of each).
Results Among the 63 cases of metastatic pulmonary adenocarcinoma, 46 cases showed nuclear staining for TTF-1 in most of the tumor cells (sensitivity, 73.2%). None of the 77 cases of metastatic extrapulmonary adenocarcinoma expressed TTF-1 (specificity, 100%). All TTF-1 positive adenocarcinomas were also ck7 positive, thus being conclusive of pulmonary origin. The CK7-/CK20+ immunophenotype was seen in 6/10 gastric and 4/4 colonic adenocarcinoma and not seen in lung, ovary, breast or pancreas adenocarcinomas. The CK7+/CK20- immunophenotype was seen in 100%, 80 % and 100% of cases that originated in the lung, breast and ovary respectively.
Conclusion(s) TTF-1 proofed to be a sensitive and highly specific immunomarker for distinguishing between metastatic pulmonary and extrapulmonary adenocarcinoma in effusion cytology specimens. CK20 positivity with CK7 negativity was conclusive of metastatic gastrointestinal adenocarcinoma.

P1.233
What have we done, as a cancer screening center, in 2008?

Bagci P.; Coskunoglu Zeynep E.; Yazar Gokdemir O.; Saracoglu N.
Rize Research and Training Hospital, Rize, Turkey

Background Cancer screening centers are the most important development of Turkish health care system. The goal of these centers are to screen the most common cancers. Here in this study we share the cervical and anal smear results of our center.
Methods We reviewed archives of our center, obtained positive smears and follow ups of the patients, to see what we have done in 2008.
Results We have screened 4941 cervical smears, and reported 120 of them as positive. Fifty percent of them were ASCUS / AGUS-reactive, 26.6 % were ASCUS / AGUS, 13.3 % were LGSIL, 5 % were HGSIL, 3 % were ASC-H and 3 % of them were reported as carcinoma. The median age was 41, 8 (17–74). We have screened 562 anal smears, only from women. Only 4 of them (0.7 %) were reported as positive. Three of them were ASCUS and 1 of them was AGUS, found out to be endometrial carcinoma with an invasion to the rectum.
Conclusion(s) Our results were correlated with the literature. The management of the SILs, ASC-Hs and carcinomas were good enough, but we decided to improve our follow up criterias for ASCUS-AGUS cases by shortening the interval. We decided to go on with our routine procedure for anal smears and try to add males to the screening. As a result, we can say that the Cancer Screening Centers attained their goal for the moment.

P1.234

CD Differentiation clusters and γ-interferon content of patients, infected with different C-hepatitis virus genotypes after introduction of hemopoietic human cord blood precursor cells

Volobuyeva O.; Klimova O.; Maliy V.
Government Institution Institute of General and Urgent Surgery Academy of Medical Sciences of Ukraine, Kharkiv, Ukraine

Background Determination of CD differentiation clusters expression intensity and γ-interferon content in blood serum of hepatocirrhosis patients, infected with different C-hepatitis virus genotypes, before and after introduction of hemopoietic cord blood precursor cells.
Methods 24 patients had diagnosis, confirmed by HCV RNA and virus genotype detection (15 patients had 1a-genotype, 9 patients -3a-genotype). γ-interferon content was determined by IFA method, expression level of immunocompetent cell CD receptors -by immunofluorescence method.
Results We detected: CD3+, CD4+, CD8+, CD34+ expression decrease by 30–54%; CD11+, CD16+, CD162+ level rise by 10–18% against control points, γ-interferon concentration decrease by 70% against reference values. After introduction of hemopoietic cord blood precursor cells, CD34+ increased by 15% for 1a-genotype and by 25% for 3a-genotype; CD16+ expression remained unchanged, CD4+, CD8+, CD162+ expression reached control values. γ-interferon content increased by 5 times for 1a-genotype, and by 11 times against control points for 3a-genotype.
Conclusion(s) Immunologic parameters changes, we verified, correlated with significant amelioration of clinical disease indications (abatement of asthenovegetative and pain syndromes and edemas). Hepatocirrhosis patients, infected with different C-hepatitis virus genotypes, showed different intensity of differential CD markers expression and γ-interferon concentration, which may be used for patients' state severity evaluation and therapeutic efficacy monitoring. Single transfusion of hemopoietic cord blood precursor cells caused patients' state improvement.

P1.235

Preneoplasic lesions of uterine cervix on conventional pap smears: eosinophilic dysplasia

Gramada E.; Micu V.G.; Slavnea Mariana A.; Tudorica Catalina L.; Andrei Theodor R.; Staniceanu F.; Maniu A.
Colentina University Hospital, Bucharest, Romania

Background For more complete results of cervical cytological aspects, the pathologists from the Colentina University Hospital studied the qualitative changes of the exfoliative cells using also the new data of morphologically findings presented in their article by Ma et al. (Am J Surg Pathol 2004; 28: 1474–1484). After koilocytic changes, these findings (including lack of normal maturation, relative eosinophilia of the cytoplasm and distinct cell bordes compared with conventional HSIL, mild to moderate increased nuclear to cytoplasmic ratio), were the most important criteria we analyzed.
Methods Our study involved 143 cases, women between 25–45 years old, with clinical suspicion (of the gynecologist) for dysplastic lesions. We purposed to correlate the cytologic findings on conventional Paps with histopathological aspects. We used Papanicolaou stain of the smears, Bethesda classification was used to interpret the cytologic findings.
Results We found 91 cases (63.63%) with mild dysplasia, 43 cases (30.16%) with ASC-H and 9 cases (6.21%) with HSIL; all the cases of the latter group were positive for oncogenic HPV types (after HPV tests). After three months, we repeted the investigation for the women with ASC-H and we observed that only in 23% of the cases the cytological abnormalities persisted, as well as eosinophilic dysplasia.
Conclusion(s) We observed a concordance of 93, 22% between the cytological findings (including koilocitic atypia, eosinophilic dysplasia, atypical mitosis) and the histopathological aspects.

P1.236

The alterations of figures of non-specific resistance and expression of clusters differentiation of cd t-lymphocytes in experimental model in animals with burn stricture of esophagus and after introduction of fetal hemopoietic cell-predecessors

Boyko V.; Klimova O.; Bozhkov A.; Savvi S.; Kordon T.; Volobueva O.
Government Institution "Institute of General and Urgent Surgery of Academy of Medical Sciences of Ukraine", Kharkiv, Ukraine

Background The process of healing includes accumulation of organic acids in the zone of tissue necrosis, leukoproteases activation, change of function of non-specific factors of resistance and T-system immunity, local inflammatory reactions.
Methods The study used the following methods: microscopic for phagocytic activity of neutrophilic granulocytes, immunofluorescent for receptor's density CD3+, CD4+, CD8+, CD50+, CD54+, HLA-DR II class, spectrophometric and radioisotopic for RNA and DNA synthesis speed. The object of research was serum and forming blood elements of intact and experimental rats with chemical burn of esophagus.

Results The investigation revealed the increase of phagocytic activity of neutrophils in animals with post burn stricture of esophagus. These animals had reliable decrease of expression of clusters of CD4+ T-lymphocytes differentiation and increase of CD8+-lymphocytes. Combined fermental preparations and xenogenic transplantation of prenatal hemopoietic progenerator cells contributed to stimulation of phagocytic function of neutrophils and normalization of expression of CD4+ and CD8+-markers of differentiation of immunocompetent cells. There was also found the positive decrease of density of receptors of adhesion molecules CD50+, CD54+ and antigens HLA-DR II class. After introduction of cellular xenotransplantats of phetal origin we noted the increase of RNA and DNA synthesis speed in parenchymatous organs.
Conclusion(s) The use of stem hemopoietic cells contributes to induction of myocytes of tissue-specific regeneration without conjunctive cicatrix formation.

P1.237

Preliminary study regarding value of endobronhoscopic ultrasound-guided transbronhic fine needle aspiration (EBUS-TBNA) in positive and differential Diagnosis of the mediastinal tumors

Popescu C. F.; Plesea E.I.; Saftoiu A.; Ioncica; A.-M.; Comanescu V.; Gheone D.; Cazacu S.
Emergency County Hospital, University of Medicine and Pharmacy, Craiova, Romania

Background The aim of this preliminary study is to assess the value of *EBUS-TBNA* in pulmonary cancer diagnosis and staging, because mediastinal adenopathies biopsy is very difficult.
Methods 18 cases with pulmonary tumor (PT) diagnosed on computed tomography were selected. EBUS-TBNA involved PT in all cases and both PT and paratraheal and subcarinal lymph node (LN) groups in 5 cases. Smears stained with Giemsa and Papanicolaou techniques were made in all cases and cellular blocks in only 12 cases. Cellular tumoral fenotype was assessed by immunostaining with TTF-1; cytokeratines AE1/AE3 and 7; EMA; CEA; cromogranine (Cromo), synaptophysine (Syn), CA19-9, cytokeratine 20 and MUC 1 mucine antibodies.
Results 10 of 13 cases with PT smears only were malignant.3 of 5 cases with both PT and LN smears were malignant on PT smear, 2 of them being malignant also on contralateral LN smear. 7 cases presented scuamous carcinoma phenotype with AE1/AE3, CEA, EMA and TTF-1 (focally) positivty. Other 5 cases presented pulmonary adenocarcinoma phenotype with diffuse positivity for CK7, TTF-1 and CEA. In one case, 2 simultaneous tumors, pulmonary and pancreatic were present. Intense positivity for TTF-1 of pancreatic tumor suggested its pulmonary origin.
Conclusion(s) Our preliminary data suggested that EBUS-FNA is a reliable adjuvant method in establishing the nature of a PT, staging pulmonary malignancies and assessment of uncertain mediastinal lymphadenopathy allowing a better selection of patients for adjuvant chimiotherapy.

Poster session 2

Breast pathology

P2.1

Extranodal B-cell lymphoma of a breast, malt type. Case report

Babic M.; Gajanin R.; Pavlovic-Tomasevic S.; Kukic B.
General Hospital Gradiska, Gradiska, Republic of Serpska, Bosnia and Herzegovina

Background Lymphomas make from 0.12 to 0.53% of all malignant breast tumors. There are 40- 70% B- lymphomas from which MALT lymphoma participate with 44%. Of all lymphomas with high-grade of malignity, the most common one is Burkitt´s lymphoma, while the MALT lymphoma is the most common one among lymphomas with low grade of malignity.
Methods Case report: A female, 64 years, came in because of a palpatory lesion in right breast.. The removed tumor, dimensions 30x30x20 mm was brown and hemorrhagic, not clearly limited ad it took hold on the breast's tissue.
Results Looking HE slides, we´ve seen small cell infiltration in the fat tissue and ducts –lymphoepithelial lesion, which is focally nodular. Imunohystochemistry report: EMA -, Pan CK -, NSE-, CD3-, CD4-, CD5-, CD8-, LCA +, CD20+, CD79a+, bcl-2+ CD43+, Ki 67 is 30%. Our diagnosis is: Low grade extranodal marginal zone B-cell lymphoma, MALT type.
Conclusion(s) Back in 1972, Wisemen and Liao gave several criterias for diagnosis of the primary malignant lymphoma of a breast, and they are: 1.regular pathological evaluation; 2.close relation of breast tissue and lymphoid infiltrations; 3.exclusions of any other lymphomas as non-existence of breast lymphoma earlier. Fiveyears survival with an operative treatment, chemotherapy and radiation is about 85%.

P2.2

Fine-needle aspiration biopsy of breast carcinoma presented with abscess formation

Kelten C.; Sen Turk N.; Kesen Z.; Akbulut M.
Pamukkale, Denizli, Turkey

Background FNAC of breast carcinomas may include a rich lymphoplasmocytic infiltration. Acute inflammatory infiltrate however, is an uncommon finding in breast carcinomas.
Methods A 38-year-old woman presented with a mass in the upper outer quadrant of right breast for two weeks. In her physical examination, a palpable, tender breast mass was found within the upper external quadrant of the right breast without axillary lymphadenopathies. Mammography showed a suspicious microcalcified mass with irregular margin (3 cm in diameter). This mass showed both solid and cytic components on ultrasound evaluation.
Results Fine needle aspiration biopsies (FNAC) from solid and cystic areas of the mass were performed. The smears showed small groups of atypical cells (nuclear pleomorphism, hyperchromasia, prominent nucleoli) in a background predominantly composed of polymorphonuclear leukocyte. No other inflammatory cells were observed. The patient then had undergone breast conservative surgery with sentinel lymph node dissection in a different hospital.
Conclusion(s) The clinical and the cytological findings of some breast carcinomas, such as invasive ductal carcinoma-not otherwise specified or medullary carcinoma, may mimic abscess formation. Ultrasound-directed FNAC from both solid and cystic components of breast masses may reveal groups of carcinoma cells better.

P2.3
HER2 assessment in breast cancer. Further progress 1: computer-assisted image analysis by VIAS™

Di Palma S.; Ping B.; Faulkes C.; Lavender L.
RSCH University of Surrey, Guildford, Surrey, United Kingdom

Background Determination of HER2 status by Silver In Situ Hybridization (SISH) in breast carcinoma is an accurate method to assess patient eligibility for trastuzumab therapy. However, histological assessment is time consuming and quantification may be challenging for some laboratories. The aim of this study is to test if the use of the Ventana Image Analysis System (VIAS™) helps the pathologist to assess HER2 status with a standardised method. Our work includes the use of an interactive light microscope, a digital camera and algorithm for SISH software.
Methods We examined the feasibility of real time capture and quantification of HER2 and chromosome 17 (Chr17) signals and HER2/Chr17 ratio by the VIAS™, using 50 cases of breast carcinoma previously evaluated by SISH. The series included highly amplified, equivocal and not amplified cases. In selected areas of the tumour, we used VIAS™ to quantify the absolute HER2 and Chr17 gene copy number and the HER2/Chr17 ratio. Results were compared against manual counts.
Results Assessment of HER2 status using the VIAS™ correlated well with manual results, both in terms of absolute HER2 and Chr17 gene copy number and HER2/Chr17 ratio.
Conclusion(s) Our experience showed that VIAS™ is an easy to use system combining traditional microscopy with computer-assisted image analysis. It is a useful tool for the quantification of HER2 SISH signals and it may have special application in counting HER2 signals in equivocal cases.

P2.4
HER2 assessment in breast cancer. Further progress 2: single- slide-light microscopy-automated-dual colour silver in situ hybridisation (DC-SISH)

Di Palma S.; Ping B.; Faulkes C.; Lavender L.
RSCH University of Surrey, Guildford, Surrey, United Kingdom

Background Bright field ISH has been successfully used to assess HER2 status with accepted limitation that chromosome 17(Chr17) is not in the same slide. The most recent development is fully automated DC-SISH which uses a DNP- labelled HER2 DNA probe detected via SISH, and a DNP- labelled Chr17 oligoprobe detected via chromogenic ISH (CISH) with fast red and naphthol phosphate, allows the detection of HER2 genes and Chr17 on the same slide. Our aim is to compare single colour SISH with DC-SISH to determine if DC-SISH is a viable alternative.
Methods 50 breast carcinomas previously evaluated using two separate SISH-HER2 and Chr17, slides and selected HER2 highly amplified and not amplified cases were re-tested using DC-SISH, and concordance analysed. UK NEQAS cell lines SK-BR-3, MDA-MB-453, MDA-MB-175 and MDA-MB-231 were used as controls.
Results Non-amplified and highly-amplified cases were identified by DC-ISH. Interpretation of equivocal/very low amplified cases was also facilitated. Our results indicate a high consensus between HER2 single probe and CHR17-corrected SISH and DC-ISH.
Conclusion(s) DC-SISH is an alternative to FISH by using a HER2 and Chr17 ISH probe on the same slide. In light microscopy, black HER2 genes dots and red Chr17 centromere dots in the same cell fits in the pathologist's workflow. Our data suggests that, for equivocal cases, using DC-ISH to evaluate HER2 and CHR17 on the same slide makes histological assessment easier and quicker.

P2.5

HER-2 protein overexpressed breast cancer without gene amplification shows higher hormone receptor expression than her-2 protein overexpressed breast cancer with gene amplification

Koo J.; Shin E.; Jung W.; Yang W.
Yonsei University, Seoul, Republic of Korea

Background Cases of breast cancer showing human epidermal growth factor receptor-2 (HER-2) protein overexpression without corresponding gene amplification have been found in immunohistochemistry (IHC) and fluorescent in situ hybridization (FISH) results. In this study, we investigated the clinicopathologic characteristics of cases showing HER-2 protein overexpression breast cancer without gene amplification (IHC3+/FISH-) and compared them to cases showing HER-2 protein overexpression breast cancer with gene amplification (IHC3+/FISH+).
Methods This study was conducted on 84 patients with HER-2 IHC3+ breast cancer. The clinicopathologic factors analyzed included tumor size, histologic grade, nuclear grade, nodal involvement, and hormone receptor status.
Results HER-2 IHC3+/FISH- breast cancer was found in 14 out of 84 tumors (16.7%) and showed a statistically significant lower histologic and nuclear grade (p=0.000) and higher expression of estrogen receptor (ERs) (p = 0.011) and progesterone receptors (PRs) (p = 0.015) than HER-2 IHC3+/FISH+ breast cancer.
Conclusion(s) HER-2 IHC3+/FISH- breast cancer could be a subgroup showing lower histologic/nuclear grade and higher expression of ERs/PRs.

P2.6

Histologic detection of additional nodal metastases in breast carcinoma with positive sentinel node

Mustac E.; Matusan Ilijas K.; Marijic B.; Smokvina A.; Jonjic N.
School of Medicine University of Rijeka, Rijeka, County of Rijeka, Croatia

Background Axillary lymph node dissection (ALND) is an important procedure in the staging of breast cancer patients. A lymph node defined as sentinel lymph node (SLN) would be the first to receive tumoral drainage. The aim of this study was to estimate the likelihood of additional disease in the axilla after SLN mapping.
Methods A total of 259 breast carcinomas and SLN biopsies followed by ALND were examined. The patient median age was 59 years, approximately 75% of them postmenopausal. Tumor size was 1.4±0.8 cm (almost 80% in pT1).
Results SLNs were positive in 59 of 259 (22.8%) carcinomas, 30 (11.6%) with micrometastases (< 2.0 mm) and 29 (11.2%) with metastases. Tumor size (p=0.004) and presence of lymphovascular invasion (LVI) (p = 0.034) were found to be significant predictors of pathologically positive SLN. Positive non-SLNs were present mostly in patients with metastasis > 2 mm in SLN (p=0.003), in carcinoma with higher nuclear grade (p = 0.044), decreased ER (p = 0.042), and PR (p = 0.042). Finally, lymph node status (pN) following SLN and ALND was found to be significantly associated with tumor size (p = 0.006), LVI (p = 0.037), PR (p = 0.023) and Her-2 status (p<0.001).
Conclusion(s) These results point to detailed analysis of primary tumor and SLN that may increase the precision of patient selection for further axillary surgery or radiotherapy.

P2.7

Immunohistochemical phenotype of breast cancer before and after neoadjuvant chemotherapy

Burkadze G.; Tsikhiseli G.; Khardzeishvili O.; Gudadze M.; Khomasuridze T.; Gachechiladze M.; Turashvili G.
N. Kipshidze Central University Hospital, Tbilisi, Georgia

Background In Georgia most breast cancer patients are diagnosed at advanced stages, and neoadjuvant chemotherapy (NAC) is often used. It is unknown but important how NAC changes the immunohistochemical (IHC) phenotype of tumor.
Methods We retrospectively analyzed data from 78 patients with invasive ductal carcinoma (IDC) diagnosed on both core needle biopsies (CNB) and surgical specimens. IHC data (ER/PR, HER2, Ki67, p53) were available before and after NAC. In surgical specimens pathological response to NAC was assessed using Miller-Payne's grading system.
Results Analysis of pre-chemotherapy IHC data revealed 40 ER+ (51%), 42 PR+ (54%), 13+ HER2+ (17%), 55 Ki67+ (71%), and 21 p53+ (27%) cases. In surgical specimens, Grade 4–5 response was seen in 12 (15%), Grade 2–3 in 57 (73%) and Grade 1 in 9 (12%) patients. Comparison of pre- and post-surgical IHC data showed ER/PR loss in 5 (6%) and 14 (18%) patients, respectively, while initially ER- 7 (9%) and PR- 2 tumors (3%) were ER+ and PR+ after NAC. HER2 could not be evaluated in 4 (5%) patients due to pathological response. Ki67 and p53 expression was decreased in 31 (40%) and 5 (6%) patients, respectively.
Conclusion(s) IHC phenotype of IDC differs between CNB and surgical specimens, suggesting that histological and IHC examination after NAC is important not only for the assessment of chemotherapeutical efficacy but also for the accurate selection of adjuvant treatment. This study was funded in part by the Georgian National Science Foundation (GNSF/STO7/6-223).

P2.8

Metastastic small cell lung carcinoma of the breast diagnosed in fna material

Fytili P.; Hatzis O.; Valeri R.; Boglou K.; Kokkori I.; Angel J.; Destouni C.
Theagenio Cancer Hospital of Thessaloniki, Greece

Background Small cell lung carcinoma is a very aggressive tumor, which disseminates widely and has a poor overall prognosis. The most usual sites of metastasis are regional lymph nodes, liver, adrenal, bone, kidney and brain. We report a case of a woman with breast metastasis of small cell lung carcinoma diagnosed in FNA material.A 63-year-old woman with a known history of small cell lung carcinoma presented with a 2x2 cm solid lump in her left breast. The patient's disease was first diagnosed 1.5 years ago with lymphnode and adrenal metastasis, treated with chemotherapy. She was in follow-up and free of disease till her recent presentation.
Methods An FNA using a 21 G syringe was performed and the material was processed using conventional and liquid based cytology (Thin Prep technique).Immunocytochemistry using the appropriate monoclonal antibodies followed.
Results The smears revealed a large number of small round or ovoid neoplastic cells with scant cytoplasm, in aggregates producing a "crash artefact", with moulding of the nuclei and "salt and pepper" like chromatin. These findings were consistent with a small cell carcinoma. Immunocytochemistry using monoclonal antibodies against EMA, Vimentin, S-100, Synaptophysin, Chromogranin, NSE and CD 56 followed, confirming the initial diagnosis.
Conclusion(s) We present this case because of its rareness and also to point out the usefulness of FNA for the correct diagnosis in order to achive the optimal therapeutic management of these patients.

P2.9

Molecular classification of breast cancer cell lines using four immunohistochemical markers

Tang P.; Subik K.; Lee J.; Baxter L.; Strzepek T.; Costello D.; Crowley P.; Hung M.; Bonfiglio T.; Hicks Grant A.
University of Rochester, NY, USA

Background Molecular classification for breast carcinomas has been increasedly used in clinical studies with simple surrogate panel of immunohistochemistry (IHC) markers. The objective of current project was to study the molecular classification on commonly used breast cancer cell lines by IHC analysis.
Methods Sixteen breast cancer cell lines were harvested by cell scraper, washed in saline, and frozen as cell pellets. They were then fixed in formalin and made into cell blocks. IHC analyses were performed on each cell block. ER and PR were recorded as Allred scores. HER2 was scored as positive if > 30% of tumor cells showed 3+ membrane staining. EGFR was designated as positive if any tumor cells showed 1+ positive stain. Any strong cytoplasmic stain was considered as positive for CK5/6. The definitions for each molecular subtype were based on the expression of ER, HER2, EGFR and CK5/6.
Results Among 16 cell lines, MCF-7 and ZR-75-1 fell within the luminal A subtype. None belonged to luminal B subtype. SKBR,-3, MDA-MD-435 and AU 565 fell within the HER2 over-expression subtype. MDA-MB-231, MCF-12A, HBL 100, Hs 598 T, MCF-10A, MCF-10F, BT-20, MDA-MB-468 and ER-483 belonged to basal-like subtype. MDA-MB-453 belonged to unclassified subtype. BT-474 could not be classified based on current IHC-based definition.
Conclusion(s) The clinical and biologic heterogeneity in breast carcinomas revealed by gene expression profiling is present among different breast cancer cell lines. Attention should be paid when choosing a cell line for any study.

P2.10

Mucinous cystadenocarcinoma and columnar cell mucinous carcinoma of the breast

Erdogan G.; Bilgin G.; Ozbey C.; Pestereli E.H.; Karaveli S.F.
Akdeniz University, Antalya, Turkey

Background Mucin producing carcinomas are characterized by production of abundant extracellular and intracellular mucins in breast carcinomas. Both mucinous cystadenocarcinomas and columnar cell mucinous carcinomas are generally composed of columnar cells with basally located bland nuclei and abundant intracytoplasmic mucin.
Methods We present two unusual cases of primary mammary mucin producing carcinomas. The patients had no history of concurrent or subsequent ovarian or pancreatic malignancy. A 76-year-old female presented with a large breast lump and underwent mastectomy. Gross inspection revealed a well-demarcated multilocular cystic tumour with fibrous septa, containing abundant bloody and mucinous material. Cysts of various sizes consisting of dilated ducts were lined by atypical tall columnar cells exhibiting a focal protruding papillary structure with a delicate fibrovascular core. The diagnosis was mucinous cystadenocarcinoma Other case was 50 year old woman with breast tumor which was composed of compact to loose aggregation of round and convulated glands lined by a single layer of tall, columnar epithelium with basal nuclei. Columnar cell mucinous carcinoma was diagnosed.
Results Immunohistochemistry showed strong positivity for cytokeratin (CK) 7, overexpression of p53, and high proliferation index and was negative for CK20, eostrogen and progesterone receptors and c-erbB2.

Conclusion(s) Mucinous cystadenocarcinoma and columnar cell mucinous carcinoma are rare variants of breast carcinomas. Total removal of the tumor with detailed histolopathologic and immunohistochemical examination can make a correct diagnosis and a distinction from other mucin-producing breast tumors. In addition diagnosis of a metastatic tumor should be excluded.

P2.11

Neoadjuvant therapy in breast cancer: scoring system with predictive value of pathologic response obtained in core needle biopsy

Aranda Ignacio F.; Peiró G.; Niveiro M.; Alcaraz E.; Adrover E.; Muci T.; Seguí J.; Alenda C.
Hospital General Universitario de Alicante, Alicante, Spain

Background To validate a scoring system with predictive value of pathologic response to neoadjuvant therapy (NAT) in breast carcinoma (BC).
Methods Tumour tissue was obtained by 12–14 G CNB in 208 patients with BC, and surgical specimens after NAT (anthracycline ± taxanes). Pathological/immunohistochemical variables: histological type and grade/HG (Nottingham), nuclear grade, estrogen and progesterone receptors (cutoff 10%), bcl-2 protein (50%), Ki-67 (30%), p53 (40%) and Her-2 (Positive: 3+ and 2+ with FISH amplified). The scoring system with only variables with statistical significance (negative=1 pt and positive=2 pts). Assessment of response: a) pathologic complete response (pCR) if not evidence of tumor cells in the breast or axillary lymph nodes; b) near-pathologic complete response (near-pCR) if microscopical residual cells only in the breast. Statistical analysis: chi square and Fisher´s exact test.
Results pCR was obtained in 11.5% and near-pCR in 22%. Association between pCR and Her-2 positivity, high Ki-67, p53 positive, and high HG was found (all <0.02). Regarding the near-pCR: high Ki-67, Her-2 positive, high HG and bcl-2 (all $p<0.02$). Cases with low score (5–6): pCR in 2% and near-pCR in 9%; those with intermediate score (7) pCR in13% and for near-pCR in 24%; and those with high score (8–10) pCR in 21% and near-pCR in 35% (all $p<0.0001$).
Conclusion(s) The scoring system based in pathological variables obtained in CNB can se useful to predict the pathological response in patients with NAT.

P2.12

Pathological and biological (Ki-67 and $p27^{KIP1}$ expression) effects of neoadjuvant aromatase inhibitor therapy for breast cancer patients

Oba H.; Kurosumi M.; Ninomiya J.; Yoshida T.; Takei H.; Inoue K.; Tabei T.
Saitama Cancer Center, Kitaadachi-Gun, Saitama-Ken, Japan

Background Neoadjuvant therapy (NAT) using aromatase inhibitor is expected to have benefits for postmenopausal hormone receptor-positive breast cancer patients. The aim of this study is to clarify the pathological effects of exemestane and significance of Ki-67 and p27 < sup > kip1 </sup > expression.
Methods Postmenopausal 48 women with hormone receptor-positive 49 breast cancers were treated with exemestane (25 mg/day) for 4 months before surgery. Pathological response was categorized into 5 degrees, e.g., Grade 0 (no response), Grade 1a (slight effect), Grade 1b (moderate effect; marked degeneration and/or disappearance of tumor cells in 1/3 to 2/3 area), Grade 2 (same effect over 2/3 area) and Grade 3 (complete response), respectively. Ki-67 labeling index (Ki-67LI) and p27 < sup > kip1 </sup > immunohistochemical expression of needle biopsied specimens were compared with those of remaining tumors.
Results Pathological partial response (pPR; Grade 1b and 2) was recognized 38.8% (19/49) of patients. The pPR rate was 40.6% (13/32) in ER(+)PgR(+) group and 35.3% (6/17) in ER(+)PgR(-) group. Furthermore, low Allred score (score 0, 2) of PgR group also revealed high response rate (40.0%, 4/10). Ki-67LIs decreased after NAT in 39 tumors (79.6%). Expression rate of nuclear p27 < sup > kip1 </sup > decreased in 21 tumors (70.0%) in non-responding (grade 0–1a) group and in 9 tumors (47.4%) in responding (grade 1b-2) group.
Conclusion(s) It is demonstrated that preoperative treatment of exemestane might be effective for breast cancer patients and reduce not only tumor size but also cell cycle activity according to Ki-67LIs and p27 < sup > kip1 </sup > expression.

P2.13

Periductal stromal sarcoma-phylloedes tumor. Are they part of the same spectrum? A case report

Trihia H.; Gavressea T.; Perakis N.; Arapantoni-Dadioti P.
Metaxa, Pireaus, Greece

Background Phylloedes tumors are uncommon fibroepithelial neoplasms, described in young women. They were originally described in 1838 and they are thought to arise from periductal connective tissue/stroma. They have been historically given a large number of names, including periductal stromal sarcoma. In the following years, the designation ‘periductal stromal tumor/sarcoma’ (PDSS) was used specifically by Burga & Tavassoli to designate a specific group of biphasic tumors that lack the phylloedes or leaf-like growth pattern and rather exhibit cuffs of circumscribed periductal spindle cell proliferations that infiltrate the surrounding adipose tissue.
Methods A 33 year old Asian/Syrian woman presented with a six month history of a palpable peri-areolar breast nodule of her right breast. In mammography and ultrasound

examination there were multiple nodules, in close proximity of each other, up to 15 mm.
Results Microscopically, there were two well-defined nodules with focal phylloedes pattern, a fibroadenoma and areas with coalesced sarcomatous cuffs with vague nodularity in areas. The findings were of combined features of both phylloedes tumor/sarcoma and PDSS, indicating an intimate relationship between the two entities.
Conclusion(s) Our findings are more in agreement with Lee, who suggested that the stromal cellularity of periductal stromal tumors is like phylloedes tumors'. And so it may be better to regard PDSS as a variant of phylloedes tumor rather than as a distinct entity.

P2.14
Sarcoma and pregnancy

Moleiro W.; Kneubil Cassilha M.; Waitzberg Flávia Logullo A.; Alves De Seixas M.
UNIFESP, São Paulo, São Paulo, Brazil

Background Fifteen years old patient, 34 weeks pregnant, presents at the physical exam a fast growing, well delimited, mobile, fibroelastic nodule measuring 8 cm, located at the retroareolar region of the right breast. The breast ultrasound, showed a hiperecogenic nodule with hipoecoic areas, heterogeneous, with umprecise limits, measuring 6,4 x 6,8 x 2,6 cm. The core biopsy revealed atipical fusocelular proliferation of low mitotic rate, considering malignant phyllodes tumor, sarcoma or metaplastic carcinoma. The patient was submitted to tumorectomy with margins during pregnancy. Anatomopathologic report revealed high grade lipossarcoma.
Methods Case report.
Results The patient was submitted to cesarean section at 39 weeks of pregnancy. Currently the patient is submitted to clinical control every 2 months.
Conclusion(s) The primary sarcoma of the breast rare, accounting for less than 1% of all malignant breast neoplasm. Clinically, they present themselves as fast growing mobile masses. The average size is 4 to 6 cm, and the average age at the time of diagnosis is the sixth decade. Histologically, before considering a breast neoplasm as a sarcoma, it is fundamental to rule out the possibility of a metaplastic carcinoma showing other mesenquimal elements, because these lesions present different biological behavior. Sarcomas usually have poor prognosis due to preference to haemathogenic matastasis. Surgical ressection is the standard treatment. As lymphonodal metastasis are rare, the treatment does not include axilar lymphadenectomy. The quimotherapy and radiotherapy role aren´t clear. While other site located sarcoma are responsive to radiotherapy, the ideal breast sarcoma treatment isn´t established, due to the rarity of these lesions.

P2.15
Significance of the topographic distribution of axin protein in invasive breast carcinomas: relation with invasion and angiogenesis

Theohari I.; Giannopoulou I.; Alexandrou P.; Papadimitriou C.; Dimopoulos A.; Nakopoulou L.
National and Kapodistrian University of Athens, Athens, Attiki, Greece

Background AXIN plays central role in Wnt signaling pathway and serves as a scaffold protein that coordinates the action of several molecules through the formation of a multiprotein complex that degradates β-catenin. When this complex is dysfunctional, β-catenin translocates into the nucleus where it functions as a transcription factor of various genes, such as MMPs and VEGFs. Our aim was to investigate the expression pattern of AXIN and correlate it with β-catenin gene copy numbers and protein expression, clinicopathologic parameters and markers of invasion and angiogenesis.
Methods Immunohistochemistry was used for the detection of AXIN in 232 invasive breast carcinomas. β-catenin gene copy number were evaluated with Real Time PCR in 80 specimens.
Results AXIN was detected in 68,5% and in 68,5% of cancer and stromal cells, respectively. The expression in cancer cells was inversely correlated with β-catenin gene copy numbers (p=0.035), but no associations were observed with any of β-catenin protein forms. Cancerous expression was positively related to tumor stage (p = 0.028), VEGFR-1 (p = 0.001) and MMP-9 (p = 0.011) expression. Stromal expression was positively associated with lymph nodes (p = 0.048), c-erbB-2 (p<0.001), VEGF-A (p=0.021) and VEGF-C (p = 0.035) expression.
Conclusion(s) The above results seem to verify the functional interaction between AXIN and β-catenin. AXIN expression is related to breast carcinomas with an aggressive phenotype, through its correlations with markers of invasion and angiogenesis. Moreover, AXIN negatively influences patients' prognosis, as reflected by its associations with positive lymph nodes and advanced stage.

P2.16
Similarity in genetic alterations in multiple synchronous or metachronous breast cancer

Kovács A.; Danielsson A.; Parris T.; Karlsson P.; Helou K.
Sahlgrenska University Hospital, Göteborg, Sweden

Background Breast cancer patients are more prone to develop multiple breast tumors in one or both breasts. Classical histological parameters are insufficient, no specific biochemical marker is available to discern multiple

primary tumors from local or metastatic spread. It is uncertain to classify the newly detected tumors as primaries, local or metastatic spread.
Methods High resolution array CGH on 80 synchronous and metachronous tumors from 40 patients with bi- or unilateral invasive breast tumors. The purpose was to place genetic concordance between tumors in these four clinical categories. Similarity scores and concordance within tumor pairs were estimated by breakpoint and segmentation analysis with consideration of outliers due to copy number polymorphisms.
Results The overall genomic instability based on segment basepairs and the pattern of genomic imbalances differed among the four clinical diagnostic groups. The bilateral pairs diagnosed synchronous were characterized by lower frequency of both copy number gain and losses compared to the other groups. In several tumors with high level DNA amplifications and high genomic instability in the primary tumor, few additional alterations were seen in the corresponding tumor after several years.
Conclusion(s) Both genetic preposition and exogenous influence might explain those tumors which exhibit few identical breakpoints and discordant alteration patterns. Our genetic data supports both different entities, predominant in those pairs with different histological types, and metastatic spreading from the primary tumor. Genetic profiling may allow distinction between multiple tumors with different loco-regional and systemic therapeutic needs.

P2.17
Synchronous axillary lymph nodes involvement by breast cancer and nodal marginal zone lymphoma: report of a case

Kelten C.; Sen Turk N.; Akbulut M.; Kabukcu S.; Yaren A.; Erdem E.; Düzcan E.
Medical School of Pamukkale University, Denizli, Turkey

Background In cases without previous history of radiotherapy and/or chemotherapy, it is rare to find the involvement of ipsilateral axillary lymph nodes in conjunction with breast carcinoma metastasis and lymphomatous proliferasyon synchronously (tumor in tumor).
Methods We report an unusual condition in a 66-year-old woman who presented swelling in her left axillary region for a period of one month. Radiologic evaluations revealed a suspicious mass with microcalcifications in the upper external quadrant of her left breast and also bilateral enlarged axillary lymph nodes.
Results The excisional biopsy of the breast mass showed invasive ductal carcinoma with a predominant intraductal carcinoma component. The patient then underwent modified radical mastectomy with left axillary dissection. All 22 axillary lymph nodes were completely involved with the lymphomatous proliferation, consisting with nodal marginal zone B-cell lymphoma by immunohistochemistry. Two out of 22 also included invasive ductal carcinoma metastasis in the background of lymphoma.
Conclusion(s) It is important to identify coincident tumors for proper treatment. The possibility to encounter breast carcinoma and lymphomatous involvement simultaneously should take into consideration in the presence of exaggerated axillary lymph nodes (unilateral or bilateral) and/or cervical/supraclavicular lymphadenopathies with a relatively small size breast mass by clinic/radiologic examinations. Carefull histologic examination as well as immunohistochemical staining are important to correct diagnosis.

P2.18
The significance of EGFR protein expression and copy numbers in invasive breast carcinomas

Alexiadis E.; Papanikolaou E.; Theohari I.; Giannopoulou I.; Papadimitriou C.; Dimopoulos A.; Nakopoulou L.
National and Kapodistrian University of Athens, Athens, Attiki, Greece

Background HER family receptors are critically involved in the development and progression of breast cancer. EGFR overexpression occurs in approximately 16–36% of breast cancers, but a higher percentage (70%) is observed in triple-negative breast carcinomas (ER-, PR-, HER2-). Moreover, this subtype is usually accompanied by an aberrant BRCA1 pathway. Our aim was to evaluate the amplification status of EGFR and correlate it with the expression of steady state and phosphorylated EGFR proteins, clinicopathologic and biologic parameters.
Methods Real Time PCR and immunohistochemistry were performed in 116 tissue paraffin sections to determine EGFR copy number and the expression pattern of EGFR, phospho-EGFR, ER, PR, HER2 and BRCA1.
Results Steady state and phospho-EGFR were detected in 8,6% and 27,6% of cases, respectively. Increased copy numbers of EGFR were detected in 7,8% of the cases, 56% of which showed phospho-EGFR and 44% EGFR overexpression. The patients harboring amplified EGFR were found to have negative ER (p=0,023) and HER2 status (p = 0,009) and decreased BRCA1 expression (p = 0,043). Furthermore, the tumors with EGFR amplification tended to be of higher nuclear grade and positive lymph nodes.
Conclusion(s) EGFR amplification seems to occur more frequently in patients with an immunoprofile similar to that observed in patients with triple-negative breast cancer and is related to a more aggressive phenotype, compared to the expression of EGFR proteins. The above results might be useful for the development of new targeted therapy in

breast cancer, based mainly on the presence of amplified EGFR.

P2.19

Topoisomerase II-alpha (Topo II-a) and HER2/neu expression in primary breast cancer and metastatic axillary nodes

Anestakis D.; Nikolaidou A.; Dimitriadis I.; Moysidis I.; Baliaka A.; Patakiouta F.
Theagenio Cancer Hospital, Thessaloniki, Greece

Background Evaluation of biological markers(BM) is mainly done at the primary site. In the adjuvant therapy of breast cancer, the target is control of micrometastases. Heterogeneity in the expression of biological markers between the primary and metastatic site exists.
Methods To evaluate the expression of (TopoII-a) and Her2/neu from the primary and metastatic site with potential predictive value. Formalin-fixed, paraffin-embedded specimens from 60 women were stained for (TopoII-a) [clone Ki-S1, Dako] and Her-2/neu [polyclonal rabbit, Dako]. Only nuclear staining was considered for (TopoII-a) and membrane staining for Her-2/neu.
Results In twenty-eight (46,6%) patients were TopoII-a (+) in the primary tumour, and 20(33,3%) in the metastatic nodes. The subgroup of patients with TopoII-a(+) primary tumours, 6 patient (21,4%) were negative in the nodes. The percentage of Her2/neu(+) primary tumours 83,3% and 80% in the metastatic nodes. Within the subgroup of patients with Her2/neu(+) primary tumours, one patient (1,6%) was negative in the node. Eight patients (13,3%) had discordant results for Her2/neu intensity. The percentage of discordant overall marker status in the primary tumour and its metastatic nodes was 3,4% for Her2/neu and 22 % for (TopoII-alpha). For the subgroup of patients with positive BM in the primary tumour, the percentage of discordance was 3,3% for Her2/neu and 13,3% for TopoII-a.
Conclusion(s) No biological marker had 100% concordant results. Future studies aiming to evaluate the predictive value of BM in the adjuvant therapy of breast cancer should take into account a possible difference between the primary and the metastatic sites.

P2.20

Two cases of myoid hamartoma of the breast: case report and review of the literature

Arakawa A.; Kato C.; Hayashi T.; Kasumi F.; Yao T.
Juntendo School of Medicine, Bunkyouku, Tokyo, Japan

Background Mammary myoid hamartomas are relatively rare benign neoplasms and considered as a variant of mammary hamartoma. The origin of this tumor is still uncertain. Hamartoma of the breast is subclassified adenolipoma, chondrolipoma and myoid hamartoma. We reported two cases of myoid hamartomas of the breast with ultrasonographical, histological, clinical findings and some review of literature.
Methods We have reviewed surgical pathology report between 2005 and 2008, and found two cases of myoid hamartoma of the breast.
Results Two patients with myoid hamartomas aged 43 and 38 years old. The size of those tumors measured 1.7 cm and 1.2 cm in diameter at the first time of detected tumor. Both tumor in patients increased in size two times during six months and in other one, four times during 29 months. Histologically, those two tumors showed that normal mammary ducts and lobules surrounded by spindle stroma with interlacing bundles. Those spindle stroma shows strongly positive for smooth muscle actin, immunohistochemically. And those spindle stromal cells show negative for S-100.
Conclusion(s) We reported two cases of myoid hamartoma of the breast. Increase of the size of tumors might be considered as malignancy or other fibroepithelial neoplasms, however, myoid hamartoma should be one of differentials.

P2.21

Unusual presentation of sarcoidosis as a breast lump

Ventura L.; Pizzorno L.; Ciccozzi A.; Mercurio C.; Bafile A.
Department of Pathology, San Salvatore Hospital, L'Aquila, Italy

Background Sarcoidosis is a granulomatous disease of unknown etiology that may affect multiple organs. Breast involvement is rare (1% of the cases) and usually occurs in patients with known systemic disease. We report an extremely rare case of primary breast sarcoidosis presenting as a lump.
Methods A 59-year-old woman without significant clinical history underwent bilateral screening mammography, showing an ill-defined mass in the upper inner quadrant of the left breast. Multiple, bilateral, smaller nodules were also identified. Ultrasonography of the main nodule revealed an irregular hypoechoic mass measuring 19x12x10 mm. Multiple stereotactic core biopsies were then performed. Histologic slides were stained with H&E, PAS, Ziehl-Neelsen and Grocott methods and immunostained for AE1/AE3 cytokeratins, CD68, S100 and CD1a.
Results Microscopic examination showed noncaseating granulomas with epithelioid histiocytes and Langhans-type multinucleated giant cells, among lobules and ducts. Occasional asteroid and Schaumann bodies were evident. Giant cells were CD68+, histiocytes were CD68+, S100- and CD1a-. Theere was no evidence of microorganisms or foreign bodies. A subsequent CT scanning of the thorax showed multiple dense

masses in both lungs and the presence of enlarged mediastinal lymph nodes.
Conclusion(s) Mammary sarcoidosis may present as a clinically suspect nodule that needs to be differentiated from malignancy. Sarcoidosis should always be considered in the differential diagnosis of granulomatous breast lesions. The diagnosis relies on the exclusion of other causes of granulomatous mastitis, such as infectious or foreign bodies.

P2.22
Can D2-40 and CD-31 immunohistochemistry in core biopsy for invasive breast carcinoma predict lymph node status?

Trucco G.; Jones M.; Kanbour-Shakir A.
MWH/UPMC/University of Pittsburgh, Pittsburgh, PA, USA

Background Since the status of the axillary lymph nodes is one of most important prognostic factor in breast carcinoma, we try to correlate the presence of lymphovascular space involvement (LVSI) in core biopsies with the presence of metastasis.
Methods 315 cases of invasive breast carcinoma were diagnosed at Magee Women Hospital by core biopsy, followed by a final surgical procedure over seven months. Five H&E levels and ICH stains (D2-40 and CD31, DAKO) were routinely used in the core biopsies for the detection of LVSI.
Results IHC highlight the presence of LVSI in 41 (13%) of core biopsies.109 (34.6%) final excisions have positive and 206 negative lymph nodes. 23 (7.3%) cases show positive LVSI in the core biopsies and positive LN and concordance of negative LVSI and negative LN occurs in 188 (60%) cases. The positive (PPV) and negative (NPV) predictive values are 56% and 69%. Six of the 18 false positive cases are patients who received neoadjuvant chemotherapy with partial to complete clinical response. The false negative cases are 86.
Conclusion(s) The small size of breast core biopsies maybe the reason of the limited predictive value of IHC for the detection of LVSI. While LVSI outside the tumor worsens the prognosis, this may not be true for the LVSI within the tumor. To be cost effective IHC should be used only to confirm possible LVSI detected on H&E sections.

P2.23
C-erbB-2 and the "triple-state" in early breast carcinomas

Sivridis E.; Stamos C.; Fiska A.; Nikolettos N.; Koutsopoulos Vasilios A.; Koukourakis M.; Giatromanolaki A.
Democritus University of Thrace, Alexandroupolis, Thrace, Greece

Background Although c-erbB-2 expression is an ominous prognostic indicator in breast carcinomas, there are suggestions that lack of this oncogene, when combined with analogous lack of estrogen and progesterone receptors – "triple-negative phenotype", is linked with an equally poor prognosis. We investigated this hypothesis in a series of early ductal breast carcinomas.
Methods A total of 116 specimens with early breast cancer, defined as tumors of ≤ 2 cm in size and clinically negative axilla, were studied immunohistochemically for ER, PgR and c-erbB-2 expression. The median follow-up was 131 months (range 62–245 months).
Results ER positive tumors had a favorable clinical course, compared to ER negative neoplasms, but only for the first 10 years of follow-up (p=0.04). Prognosis was poorer for the PgR negative cases, relative to PgR positive tumors (p = 0.005), but this stood true for the entire investigation period. Triple-negative breast carcinomas had a poor prognosis, while triple-positive tumors had a favorable outcome. However, if triple-positive and -negative cases were excluded from the original sample, the remaining c-erbB-2 positive cases were connected with poor prognosis, relative to the remaining c-erbB-2 negative tumors.
Conclusion(s) C-erbB-2 oncogene has a complex biological role in early breast carcinomas for its expression characterizes subgroups of patients with both favorable (triple-positive phenotype) and unfavorable prognosis (c-erb-B2 positive cases after excluding triple-positive and triple-negative tumors) – a phenomenon presumably due to activation of different biological pathways. Elucidation of these pathways may determine subgroups of patients with tumors requiring different targeted agents.

P2.24
Computer assisted morphometric analysis of breast and colonic carcinoma cells

Aschie M.; Craciun A.; Papuc A.; Dobre A.; Poinareanu I.; Iliesiu A.; Deacu M.; Bosoteanu M.; Aschie I.; Sarbu V.
"Ovidius" University, Constanta, Romania

Background Computer assisted morphometric analysis is a step forward in evaluation of morphology based on multiparametric single cell analysis.
Methods Our study consists on analysis of morphometric parameters such as: mean nuclear area, mean cytoplasmatic area and mean N/C ratio on 36 cases of breast carcinoma and 40 cases of colonic carcinoma. Morphometry analysis was accomplished with Lucia Net Laboratory Imaging-Eclipse Net Software. For every carcinoma case was calculated the mean value for every parameter on 10–20 cells and analyzed with SPSS system.

Results The mean nuclear area for breast carcinoma was 42,5±1,36 μm² for well differentianted, 52,54±9,22 μm² for moderate differentiated and 61,22±13,40 μm² for poore differentiated carcinoma. Mean cytoplasmatic area was 74,72±2,64 μm² for G1 carcinoma, 65,27±11,49 μm2 for G2 carcinoma and 72,83±19,09 μm² for G3 carcinoma and N/C ratio was 0,56±0,01 for G1 cases, 0,81±0,12 for G2 cases and 0,85±0,15 for G3 cases. On colonic carcinoma cases the mean nucleare are was 194,34±5,06 μm² for G1 cases, 164,425±3,01 μm² for G2 cases and 125,175 ± 3,17 μm2 for G3 casea. The mean cytoplasmatic area was 199,84±18,54 μm² for G1 cases, 124,5±7,11 μm² for G2 cases and 86,86±8,17 μm² for G3 cases. The mean N/C ratio was 0,98±0,10 for G1 cases, 1,32±0,09 for G2 cases and 1,45±0,14 for G3 cases.

Conclusion(s) Morphometric analysis revealed the increase of nuclear area and N/C ratio concordant with differentiation grade on breast carcinoma and the increase of N/C ratio, decrease of nuclear and cytoplasmatic area according with differentiation of colonic carcinoma.

P2.25

Correlation of BRCA1 expression with immunohistochemicals markers in sporadic breast carcinomas

Papuc A.; Aschie M.; Dobre A.; Iliesiu A.; Poinareanu I.; Craciun A.; Stanisici J.; Iacub G.; Baltatescu G.; Lacurezeanu V.; Badiu D.; Cretu A.; Enciu M.
Clinical Emergency County Hospital of Constanta, Constanta, Romania

Background Breast carcinomas still represent an important cause of death in women, despite the important discoveries in the genetics and etiology of this malignancy. BRCA1 is an important tumor suppressor gene involved in the etiology of familial and sporadic breast carcinoma and participates together with BRCA2 in DNA double-strand break repair.

Methods Our study investigates the immunohistochemical detection of BRCA1 protein expression in sporadic breast carcinomas and its relations with other molecular markers including ER, PR and HER2 status. For this purpose a total of 80 cases of formalin-fixed paraffin – embedded tissues of breast carcinoma were selected and immunostained using monoclonal antibody to BRCA1, ER, PR, HER2, p53 and Ki67.

Results We found high-level expression of BRCA1 protein in normal mammary epithelium and various degrees of reduced expression in breast carcinoma. 52% of breast carcinoma showed reduced BRCA1 protein expression. This reduced expression correlates with ER and PR negative status, HER2 over expression, moderate expression of p53 and Ki 67. Also we observed an association between reduction of BRCA1 expression and poor carcinoma differentiation and poorly differentiated nuclear grade.

Conclusion(s) Our results suggest that BRCA1 may play an important role in breast carcinogenesis and emphasizes the potential value as prognostic marker in sporadic breast carcinoma.

P2.26

Experience of CISH technique in routine diagnostics of HER2-positive breast cancer

Petrov Venedictovich S.; Mazitova Marsovna F.; Khasanov Shamilyevich R.; Raskin Alexandrovich G.
Kazan Cancer Center, Dept. Pathology, Kazan, Russian Federation

Background Chromogenic hybridization in situ (CISH) was created as a cheaper and simpler alternative of FISH but isn't used yet in routine practice.

Methods We studied 337 samples of breast cancer with known positive immunohistochemical (IHC) reaction of HER2 "++" using CISH. 3 cases of Paget's disease (2 HER2-positive and negative) were also analyzed by CISH. The moderate amount of HER2 marks was calculated in 60 nuclei of each case. Amplification was concluded if moderate amount of HER2 marks is > 6,2; over-expression of HER2 without amplification was concluded if moderate amount of HER2 marks is <5,0. 5 < marks <6,2 – such condition was concluded as ambiguous.

Results Gene amplification was revealed in 180 cases (53,4%), amplification wasn't revealed in 139 samples (41,2%), and ambiguous cases consist of 18 samples (5,4%). Moderate amount of HER2 marks was 8,05, ranged from 6,33 to 12,4 in cases with gene amplification; 3,1 - ranged from 1,6 to 4,95 in samples without gene amplification. IHC HER2-positive Paget's disease was accompanied by gene amplification; in IHC HER2-negative case amplification wasn't revealed.

Conclusion(s) 53,4% of HER2 2+ IHC patients presented gene amplification by CISH. Chromogenic hybridization in situ allows establishing HER2 gene status in 94,6% of cases and may be used in routine diagnostic practice.

P2.27

GATA-3 expression in breast cancer

Cantaloni C.; Bragantini E.; Ferro A.; Cazzolli D.; Gasperetti F.; Doglioni C.; Eccher C.; Dalla Palma P.; Barbareschi M.
S. Chiara, Trento, Italy

Background GATA-3 is a transcription factor involved in human growth and differentiation. According to gene

expression data GATA-3 is highly expressed in the luminal A subtype of breast cancer and may be related with favourable pathologic features, including negative lymph node and positive oestrogen receptor (ER) status. GATA-3 levels were also found to be a prognostic marker, with low expression predicting for breast cancer recurrence and shorted overall survival.
Methods Our case series consists of 197 consecutive cases of invasive breast cancer in which GATA-3 expression was assessed by immunohistochemistry on tissue microarrays. GATA-3 immunoreactivity was scored as low to absent (score 0–1) and strong (score 2–3) on a semiquantitative basis. Follow-up data were collected for 45 cases.
Results GATA-3 expression was nuclear and was assessed as percentage of positive cells and intensity of staining. 225 of 248 (90%) cases were GATA-3 positive. GATA-3 expression is statistically related with ER+ (p: 0.00001) and PgR+ tumours (p: 0.0001), with lower tumour grade (p: 0.0150). No association was observed with tumour size and nodal status. Survival analysis showed a trend for prolonged overall survival and GATA-3 high expression.
Conclusion(s) Our preliminary study is in keeping with literature data suggesting that GATA-3 expression is related to ER pathway and may be of pathogenetic relevance. However, given its strict relation to ER expression, additional studies with multivariate analysis are needed to verify if its possible clinical role as prognostic/predictive marker.

P2.28
Heat shock protein90 in lobular neoplasia of the breast

Nonni A.; Zagouri F.; Sergentanis N.T.; Lazaris A.; Patsouris E.; Zografos C.G.
Athens, Greece

Background To evaluate the immunohistochemical expression of Hsp90 and to examine whether Hsp90 expression is associated with estrogen receptor alpha (ER-alpha) and beta (ER-beta) immunostaining in lobular neoplasia (LN) of the breast.
Methods Tissue specimens were taken from 44 patients with LN. Immunohistochemical assessment of Hsp90, ER-alpha and ER-beta was performed both in the lesion and the adjacent normal breast ducts and lobules; the latter serving as control. As far as Hsp90 evaluation is concerned: i) the percentage of positive cells, and ii) the intensity was separately analyzed. Additionally, the Allred score was adopted and calculated. Accordingly, Allred score was separately evaluated for ER-alpha and ER-beta.
Results Hsp90 immunoreactivity was mainly cytoplasmic in both the epithelial cells of normal breast (ducts and lobules) and LN. Some epithelial cells of LN also showed nuclear staining, but all the LN foci mainly disclosed a positive cytoplasmic immunoreaction for Hsp90. In addition, rare intralobular inflammatory cells showed a slight immunoreaction. The intensity score of Hsp90 staining was statistically significant ($p=0.029$, Wilcoxon matched-pairs signed-ranks test). The Hsp90 Allred score in LN was significantly lower than in the normal adjacent tissue. Within the LN foci, the Hsp90 Allred score was neither associated with ER-alpha, nor with ER-beta percentage.
Conclusion(s) Hsp90 was lower in LN foci both at the level of intensity and Allred score, a finding contrary to what might have been expected, given that high Hsp90 expression is detected in invasive breast carcinomas.

P2.29
Immunohistochemical study of lobular carcinoma of the breast

Böör V.A.; Jurkovic P.I.; Dudrikova K.; Babjakova L.; Kocan P.
University P.J.Šafárik, Kosice, Slovakia

Background Expanding role in mammary pathology is played by immunohistochemistry, which is widely used for subtyping of breast carcinomas. A growing evidence has been accumulated to support the idea of a heterogenous character of non-classic forms of the invasive lobular carcinoma, the second most common histological type of breast cancer.
Methods Expressions of PCNA, Ki-67, p53, bcl-2, ER and PR with controls, E-cadherin, 34betaE12, c-erbB2 and Herceptest in 42 consecutive biopsy cases of invasive lobular carcinoma of the breast have been analyzed in our Institute through the years 2003–2008.
Results The lobular nature of the classic variant of invasive lobular carcinoma was confirmed by negative expression of E-cadherin and positive staining with 34betaE12. Three cases were reclassified as carcinomas with mixed or hybrid ductal and lobular character and additional two cases as tubulolobular carcinoma with lobular morphology and characteristic E-cadherin positivity. Almost all cases revealed ER and PR positivity. Results of the immunoreactivity of p53 and bcl-2 were variable and inconsistent for adequate evaluation. Relatively important differencies have been found in the c-erbB2 and Herceptest immunoreactivity.
Conclusion(s) Characteristic loss of E-cadherin expression in the invasive lobular carcinoma and its usefullness for differential diagnosis between invasive lobular and invasive ductal carcinomas of the breast was also confirmed by our study. Precaution is recommended in unequivocal cases, while abberant positive expression may cause misinterpretations. Immunohistochemical characteristics of tubulolobular carcinoma support its ductal differentiation despite the dominant lobular growth pattern of this tumor subtype.

P2.30

Immunoprofile of four cases of primary neuroendocrine tumor of the breast

Anestakis D.; Tsobanidou C.; Andreadis C.; Konstantinidis I.; Kleontas A.; Patakiouta F.
Theagenio Cancer Hospital, Thessaloniki, Greece

Background Primary neuroendocrine cancers encompass a heterogeneous group of tumors showing morphological features similar to those of neuroendocrine neoplasms of both the gastrointestinal tract and the lung. They are very rare tumors that express neuroendocrine markers in more than 50% of the cell population. The histogenesis and behavior of these neoplasms is still unclear. Herein we describe the immunoprofile of four cases of primary breast neuroendocrine tumors.

Methods Four patients with primary neuroendocrine cancers treated surgically were examined retrospectively. The age of the patients ranged from 52 to 79 years (mean 65,5 years). Two of the neoplasms were in the right and two in the left breast. The tumor ranged in greatest diameter from 2,2 to 3,5 cm. Representative sections of the tumor specimens were immunostained for CK7, CK20, CEA, NSE, Chromogranin, Synaptophysin, CD57, E-cadherin, TTF1, S-100, ER, PR, C-erb2.

Results The neoplasms were solid neuroendocrine carcinomas. All the tumor were positive for the NSE, CEA, E-cadherin, ER, PR and were negative for the Chromogranin, CD57, TTF1, Cerb2, CK20. Three of four cases were positive for the S-100, Synaptophysin, CK7.

Conclusion(s) The results suggest that primary neuroendocrine carcinoma would be originated from ductal cell. Applification of this panel of antibodies might expected to increase the occurancy of the diagnosis especially in difficult cases.

P2.31

Interconnection of immunoreactivity type at patients with myastenia with character of tumoral damage of thymus

Klimova O.; Boyko V.; Bozhkov A.; Drosdova L.; Kudrevich A.; Mylovydova G.
Government Institution "Institute of General and Urgent Surgery of Academy of Medical Sciences of Ukraine", Kharkiv, Ukraine

Background The study covered correlation between immunophysiological reactions, thymom types and clinical current of illness.

Methods The clusters of differentiation CD (2, 3, 4, 6, 8, 19), phenotype antigens HLA-DR II class, content of serumal cytotoxical factors, cytokins (IL-2, IL 4, IL-6, IL-8) concentration were determined by immunocytochemical and immunofluorescent methods.

Results The examined patients with thymus tumors had: lymphoepithelial thymom (LET) – 59%, epithelial (ET) – 24%, lymphoid (LT) – 9% and granulomatous (GT) – 8%. Patients with LT frequently had HLA-DR1, HLA-DR5 phenotypes, LET – HLA-DR3, HLA-DR7, ET – HLA-DR1, HLA-DR3. HLA-DR5, HLA-DR52 phenotypes were associated with GT. There was revealed a CD2+ reliable increase in 1,5 times at LT and GT. The patients with LT had increased CD4+ T-helpers levels; CD16+, CD8+ level was decreased. CD4+ subpopulation was significantly decreased at LET and ET. Patients with LET showed the double increase of CD19+ and CD16+ in comparison with referent quantities. The frequentative increase of IL-4 to 623,0±37,3 pkg/ml was also revealed at LET group. After thymusectomia IL-4 decreased to 5,6±0,99 pkg/ml at patients with favorable clinical course. The decrease of IL-2, IL-4, IL-6 was defined at GT.

Conclusion(s) The study found the interconnection of immunoreactivity type at patients with myasthenia with the character of tumoral damage of thymus. It defined HLA-DR3, DR5, DR7 at malignant local-spreaded thymoms at 100% of patients. The significant increase of IL-4 and CD19+ was revealed at LET.

P2.32

Invasive apocrine carcinoma of the breast: a clinico-pathological and immunohistochemical study of nine cases

Villena N.; Soler M.; Climent F.; Petit A.; Taco R.; Blazquez A.; Gumà A.; Pla M.; Sirvent J.; Gil M.; Condom E.
Hospital Universitari de Bellvitge, Barcelona, Spain

Background Apocrine carcinoma (AC) is a rare variant of breast carcinoma with an estimated incidence of 0.3–4%. The objective of our study was to determine the clinico-pathological and immunohistochemical features of AC, focussing on its possible relationship with basal-type tumors.

Methods Nine cases of AC (8 women, one man) diagnosed during 2007–2008 were evaluated for the immunohistochemical expression of estrogen/progesterone receptor (HR), EGFR, HER-2neu, androgen receptor(AR), GCDFP-15, cytokeratin5/6, vimentin and p63.

Results The incidence of AC was 1.2%. Age ranged from 30 to 86 years (median 64.8). In mammography, 6 tumors (66.6%) had spiculated edges. Tumor size was between 9 and 25 mm (median16.6 mm). Histologic grade was I in 1 patient, II in 5 and III in 3; 4 cases showed associated apocrine intraductal carcinoma and 5 had apocrine adenosis and/or metaplasia with atypia. One case was HER-2 neu+ and 2 were HR+. Six cases (66.6%) had a triple negative

pattern, three of which displayed a basal phenotype with cytokeratin5/6 and/or EGFR positivity. Vimentin and p63 were negative in all cases. All 9 tumors were AR+ and 8 (88.8%) were GCDFP-15+.
Conclusion(s) The clinico-pathological characteristics in this study are similar to those in the literature. Radiologically, AC was similar to conventional ductal breast carcinoma. More than 50% of the patients showed associated apocrine metaplasia with atypia. Two thirds of cases were triple negative and half of them had basal phenotype. In comparison with published data, we found a higher percentage of AR+ (100%) and GCDFP-15+ (88.8%) cases.

P2.33
MMP9 expression in relation with SDF1/CXCR4 axis in invasive breast carcinomas and their microenvironment

Papatheodorou G.H.; Kalofonos P.H.; Scopa D.C.; Dimopoulos P.; Leotsinidis M.; Varakis N.J.; Papadaki H.
School of Medicine, University of Patras, Patras, Achaia, Greece

Background SDF-1 / CXCR4 axis and MMP9 are involved in various steps of tumorogenesis such as tumor growth, angiogenesis and metastasis. The goal of present study is to demonstrate immunohistochemical distribution of the aforementioned molecules in invasive breast carcinomas and possible correlation of their expression patterns with tumor pathological parameters.
Methods We investigated paraffin embedded tissue samples from 96 invasive breast tumors using immunohistochemistry for the understudy molecules. Statistical analyses were performed to evaluate potential differences in immunohistochemical expression and correlations with tumor parameters.
Results In the majority of the cases, adjacent normal breast tissue showed no immunopositivity for CXCR4 and MMP9 while almost half of them were highly positive for SDF1. A significant statistical correlation between SDF1 expression in fibroblasts of adjacent normal breast tissue and tumor grade was noticed (r=0.20, p<0.05), while tumor size was greater in cases with CXCR4 expression in intratumoral fibroblasts (p<0.05). In cancerous epithelial cells, cytoplasmic MMP9 expression was correlated with cytoplasmic CXCR4 immunolocalization (r=0.191, p<0.05). MMP9 expression was also correlated with the expression of CXCR4 in intratumoral fibroblasts (r=0.250, p<0.05) while a statistically significant correlation between MMP9 expression in intratumoral fibroblasts with expression of CXCR4 and SDF1 in intratumoral vessels (r=0.219, p< 0.05 and r=0.257, p<0.05, respectively) was also noticed.
Conclusion(s) Our result suggests possible interaction between SDF-1/CXCR4 axis and MMP9 and point out the involvement of tumor microenvironment in tumorigenesis.

P2.34
Primary leiomyosarcoma of the breast: a case report

Pané M.; Paúles M.; Soler T.; Alarcón I.; Climent F.; Petit A.; Prieto L.; Pla M.; Condom E.
Ciutat Sanitària i Universitària de Bellvitge, Barcelona, Spain

Background Leiomyosarcoma of the breast is a rare neoplasm accounting for less than 1% of breast malignancies. It usually presents in women in the sixth decade as enlarging palpable masses. A proper diagnosis is important since its management and prognosis are different from those of epithelial and other mesenchymal breast neoplasms.
Methods The patient was a 50 year-old asymptomatic woman. A screening mammography detected a lump on the upper external quadrant of her right breast. Ultrasonography showed a hypoechoic nodule. A core biopsy displayed a spindle cell proliferation with marked atypia and mitotic figures devoid of epithelial elements.
Results Immunohistochemistry showed the tumor cells to be positive for actin, desmin and vimentin, and negative for CK7, CK5.6 and CK903. A diagnosis of leiomyosarcoma was rendered.The patient underwent tumour excision with wide margins. The specimen contained a well delimited tumour measuring 9 mm. Histologically it was made of interlacing fascicles of spindle-shaped atypical cells with 7 mitosis per 10 high-power fields. There were no epithelial elements. The immunohistochemical study was repeated and confirmed the diagnosis.
Conclusion(s) Primary sarcomas of the breast are uncommon. Among these, leiomyosarcomas are exceptional. For breast leiomyosarcoma a complete excision with wide margins is the safest treatment strategy and lymphadenectomy is not necessary. They have a better prognosis than other breast malignancies. Differential diagnosis includes Phyllodes tumour and metaplastic carcinoma. Both have epithelial components detectable by extensive sampling and immunohistochemistry. Angiosarcoma and melanoma should also be kept in mind.

P2.35
The histological and biological markers to predict early distant metastasis after neoadjuvant chemotherapy in breast cancer

Tokuda E.; Arakawa A.; Yao T.; Takahashi Y.; Horimoto Y.; Shimizu H.; Kosaka T.; Abe I.; Senuma K.; Nakai K.; Miura H.; Saito M.; Kasumi F.
Dept. of Breast Surgery, Juntendo University, Tokyo, Japan

Background Recently neoadjuvant chemotherapy (NAC) has become the standard treatment for locally advanced breast cancer, however, there are some cases with worse prognosis because of early metastasis after operation. We investigated the factor of early distant metastasis (DM) within one year after operation, such as patient's clinical background, effectiveness of chemotherapy, pathological and biological factors. So, we examined immunohistological stains of these markers and analyzed these factors as predictors of the early metastasis.
Methods We investigated 100 patients underwent NAC, operated between July 2006 and January 2008 at the breast centre in Juntendo University breast centre, Tokyo. Those patients included 17 patients with DM within one year after operation (the early). All patients received NAC as 3 weekly FEC plus Taxans. The adjuvant therapy was done after operation considering hormone receptor status. We have done immunohistochemical study such as hormone receptors, HER2 status, Ki67, EGFR, CK5/6, VEGF and CD24/44.
Results The mean age of patients with the early was 46 years old younger than that of all cases (54.6 years old). There was no case of pathological CR with the early, and all the early had lymph node metastasis. Estrogen-receptor-negative and HER2/neu -negative are significant features as the early, and we analyzed the immunostains of Ki67, EGFR, CK5/6,CK14 for basal cell type breast cancer, and CD44/CD24 which indicates cancer stem cell.
Conclusion(s) We hereby report that the factors as pathological and histological markers are useful to predict early DM after NAC.

P2.36
The role of estrogen receptor (ER) β1 and ERβ2 in ERα-negative breast carcinoma

Chantzi Ioannis N.; Filippidis T.; Goutas N.; Vassilaros S.; Kittas C.; Alexis N.M.; Tiniakos D.G.
Medical School, Athens, Greece

Background Estrogen receptor (ERα) is of primary importance in breast cancer prognosis and treatment. The recently discovered ERβ1 and its isoforms may also be important in this respect and their role could vary depending on ERα expression. To assess the role of ERβ1 and ERβ2 in ERα-negative breast carcinoma, we correlated their level of expression with clinicopathological parameters, patient prognosis and response to treatment.
Methods Routinely-processed sections of 97 ERα-negative breast carcinomas from 97 women (27–77 years, mean=54) followed-up for 7–152 (mean=60) months, were subjected to immunohistochemistry using ERβ1- and ERβ2-specific antibodies. Immunostaining was semi-quantitatively evaluated using Histoscore (range 0–7).
Results ERβ1- and ERβ2-positivity (Histoscore≥5; 5= median value) was detected in 66 of 97 (68%) and 65 of 96 (68%) cases, respectively. ERβ1 and ERβ2 were co-expressed in 51(53%) cases. ERβ1- and ERβ2-expression were correlated (Spearman r=0.393, p=0.01). ERβ1-positivity was negatively correlated with tumour grade (p = 0.039). ERβ2-positivity was positively related to lymph node metastasis ($p<$ 0.001). Tumour grade (p=0.013) and size (p=0.052), lymph node metastasis (p=0.01) and ERβ2-expression (p=0.007) were significantly higher in patients who relapsed. In multivariate analysis, grade and ERβ2-status were the most important variables to predict relapse (p=0.004 and 0.014, respectively). ERβ1- and ERβ2-status were not related to overall survival. In patients receiving chemotherapy (± radiotherapy), ERβ2-positivity was correlated with lower relapse-free survival (p=0.023).
Conclusion(s) In ERα-negative breast carcinoma: a) ERβ1 and ERβ2 are frequently and concurrently expressed, b) ERβ1-positivity is not related to patient survival, c) ERβ2-positivity indicates poor prognosis and response to therapy.
Support: grant 04ED644 jointly funded by GSRT-Greece and EU.

P2.37
Unusual breast tumors in Isfahan (Iran)

Rajabi P.; Rajabi M.; Afshar Moghaddam N.; Heidarpour M.; Neshat A.; Rajabi F.
Pathology Department, Faculty of Medicine, Isfahan, Islamic Republic of Iran

Background The majority of breast cancers are carcinomas (mostly of ductal type) and very few are non-epithelial tumours.
Methods The reports of the patients with the diagnoses of unusual breast malignancies between 2002 and 2007 were reviewed. Age, gender, clinical details, type of specimen and diagnoses were recorded.
Results One patient presented with mammary skin lesions which was a recurrent angiosarcoma in a mastectomy scar. The most common diagnosis was lymphoma (6/14). Two diffuse large B-cell lymphomas, 3 marginal zone lymphomas and one bilateral Burkitt lymphoma in a 24 year pregnant woman. Two cases were metastatic embryonal rhabdomyosarcoma, one in a 21 year-old girl with origin of orbital rhabdomyosarcoma and the other in an 11 year-old girl which had been originated from retroperitoneal rhabdomyosarcoma. One of the cases was a metastatic Merkel cell carcinoma in a 42 year old woman. The

original lesion was skin of axillary region, followed by axillary lymph node metastasis and finally the substance of the breast was almost entirely replaced by multiple large nodules, macroscopically simulating primary breast cancer. Other cases were a malignant fibrous histiocytoma in a 28 year-old woman, one liposarcoma arising in phyllodes tumor, one metastatic gestational choriocarcinoma in a 22 year-old woman and one pure SCC in a 74 year old woman which of course was a malignant epithelial tumor.

Conclusion(s) Malignant non-epithelial tumors were rare and most of them were lymphomas. Only three metastases were found; two of them were in children and their type was rhabdomyosarcoma.

P2.38

A comparative study of immunohistochemical and chromogenic in situ hybridization (CISH) evaluation of HER2 status in breast cancer

Hristova Lubomirova S.; Vlahova I.A.; Dikov Iliichev T.
Medical University of Sofia, Sofia, Bulgaria

Background The aim of the study was to comparate IHC and CISH results in parallel evaluation of HER2 oncoproteine expression and HER2 gene amplification. The study has been sponsored by ROCHE-Bulgaria EOOD.

Methods Examination was made of a total of 605 biopsies with preliminarily established HER2 status by immunohistochemistry, in 16 local laboratories in Bulgaria. The determining of the amplification of the HER2 gene was carried out using SPOT-Light® HER2 CISH™ Kit, ZYMED® Laboratories Inc. CISH examination was made in Central laboratory of Clinical Pathology, University Aleksandrovska Hospital, Medical University of Sofia.

Results The examined cases were divided into 3 groups according to the results from IHH evaluation: HER2 0-1+ - 68 cases; HER2 2+ - 432 cases and HER2 3+ - 105 cases. In 8 out of 68 HER2 immunohistochemistry negative tumors there was proven a gene amplification (11.76%). In surprise, a high level of discordance was registered in HER2 3+ positive cases. Only 59 out of 105 carcinomas were CISH positive (56.20%). The main group of the study was HER2 2+ immunohistochemistry low positive tumors, 32.87% of which were CISH positive. Totally, HER2 gene amplification was observed in 34.54% of the examined biopsy materials.

Conclusion(s) The study shows that chromogenic in situ hybridization is recommendable as control of the results of IHC testing in local laboratories, predominantly in HER2 3+ positive cases.

P2.39

Equivocal (2+) HER-2/neu results by immunohistochemistry in breast carcinoma: "normalizing" reduces need for FISH testing

Estrella Santiano J.; Salvatore P. S.; Hoda A.S.
Weill Cornell Medical Center, New York, USA

Background Mounting evidence indicates that HER-2/neu status is therapeutically crucial in early and late stage breast carcinoma. ASCO-CAP 2007 guidelines require reflex flourescent in situ hybridization (FISH) testing to determine gene amplification in cases with equivocal (2+) HER-2/neu expression by immunohistochemistry (IHC). However, background staining of benign and malignant glandular epithelium artifactually increases degree of IHC positivity. We studied "normalization" to improve efficiency of reflex FISH testing by optimizing IHC scoring (Gown, AM et al: Mod Pathol 2008;21:1271-7).

Methods Stage 1, ER-positive, lymph node-negative breast carcinomas which were originally reported as equivocal (2+) for Her-2/neu by IHC, and had available confirmatory FISH results, were evaluated. Degree of staining of benign breast epithelium was subtracted from degree of staining in invasive carcinoma cells and a "Normalized" IHC Score (NIS) was obtained. NIS was then compared to FISH results.

Results NIS was obtained by consensus review in 37 cases. Per NIS, 3/37 (8%) were positive (3+), 12/37 (32%) were equivocal (2+) and 22/37 (59%) were negative (0–1+). NIS decreased the number of cases with equivocal (2+) HER-2/neu score by 68% (25/37). Discordance was observed in 3/37 cases (8%). One NIS-positive (3+) case was negative (ratio <1.8) by FISH, another NIS-positive (3+) case was borderline-positive (ratio=1.8–2.2) by FISH. One NIS-negative case (0) had low-degree positivity by FISH (ratio=2.3).

Conclusion(s) NIS increases efficiency of reflex testing by decreasing equivocal HER-2/neu results (68% of cases in our study).

P2.40

Evaluation of prognostic markers in negative estrogen - progesterone receptor breast cancers

Frangou-Plemenou M.; Kairi-Vassilatou E.; Karandrea D.; Apostolidi M.; Vouza E.; Tsantopoulos M.; Kondi-Pafiti A.
Aretieon University Hospital, Athens, Greece

Background In primary breast cancer estrogen (ER) and progesterone (PR) receptor status is very useful in predicting response to endocrine therapy and prognosis. Negative ER, PR cases have poor prognosis and limited therapeutical options.

Methods 101 out of 623 tissue samples from operable primary breast adenocarcinomas were ER, PR negative. In all these cases tumor grade, cerbB-2, p53 expression and the amplification of HER-2 gene by CISH were known.
Results 66,3% of negative ER/PR cases were Gr. III, 13,6% were Gr. II, 4,8% were Gr. I, 10,8% were in situ and 3,8% were lobular. CerbB-2 (++/+++) was found in 52,3% versus 37,3% in the total. P53 expression was 59,5% versus 26,6% of the total samples. HER-2 was amplified in 36,6% of the cerbB-2 (++/+++) cases versus 16,8% of the total. CerbB-2 (-/+) cases expressed amplified HER-2 in the 47,6% versus 2,4% of the total. Cases with co-expression of cerbB-2 (+)/p53 (+) had HER-2 amplified in 94,7% versus 62,5% of cerbB-2(+)/p53(-) cases.
Conclusion(s) The majority of ER/PR negative breast tumors were poorly differentiated. The positivity of cerbB-2, p53 is higher than the total group. CerbB-2 (+)/p53 (+) cases had almost all amplified HER-2. CerbB-2 negative cases showed a percentage of amplified HER-2 that may be due to post translational events in these low differentiated tumor cells. It is useful though to test CISH in all ER/PR (-) patients in order to find those that may benefit from targeting therapy.

P2.41
HER2 immunoexpression in invasive breast cancer: morpho-clinic and prognostic correlations

Muresan Anca Maria M.; Lazar E.; Raica M.; Dema A.; Campean A.; Suciu C.; Costi S.; Cornea R.; Faur A.; Sargan I.
University of Medicine and Pharmacy, Timisoara, Timis, Romania

Background The breast cancer is the most frequent malignant tumor of women with high capacity of metastasing. The HER2 status evaluation is important in the management of patients with breast cancer, in determining the possible application of trastuzumab therapy.
Methods We included 60 patients with primary breast cancer in this study. The tumors samples were fixed in 10% formalin and paraffin embedded, colored with Hematoxilin-Eosin (HE); for HER2 determination we used the avidin-biotin complex immunohistochemical method.
Results The positive reaction was noted as 3+ (a strong complete membrane immunostaining in > 10% of tumor cells). From 60 carcinomas, 16 were HER2 positive.We have interpreted the score of 0–1 as negative.
Conclusion(s) The HER2 positivity was correlated with the size of the tumor; our data show no correlation between the HER2 status and the invasion of axillary lymph nodes; the carcinomas which are not infiltrative ductal, known as having a better prognostic, were HER2 negative.

P2.42
Histologic diagnosis of one hundred painful breast masses

Fakhrjou A.; Montazeri V.; Mirzazadeh S.
Tabriz University of Medical Sciences, Faculty of Medicine, Tabriz, East Azarbijan, Islamic Republic of Iran

Background The presence of a mass in the breast could be a serious source of stress an anxiety, primarily due to the assumption of a malignant underlying pathology. This study aimed at evaluating the histologic diagnosis of one hundred painful breast masses.
Methods In a cross-sectional setting, 100 hundred patients with a breast painful lump referred to Tabriz Imam Hospital and private pathology laboratories were evaluated. Fine needle aspiration and excisional biopsy was carried on for all patients and the definite histological diagnosis was made accordingly. The effect of age on the final diagnosis was also assessed.
Results One hundred patients, 98 females and 2 males with the mean age of 37.86±8.79 (18–52) years were enrolled. The pain of the lump was constant in 59 cases and fluctuating in 41 patients. Four patients suffered from severe pain. Eighty four patients revealed to have a benign histologic finding whereas malignant pathology in 16 patients. The benign pathologies consisted of the fibrocystic disease (50 cases), fibroadenoma (30 cases), abscess (2 cases) and gynecomastia (2 males). The malignant pathology was ductal carcinoma. The sensitivity and specificity of a painful lump for a malignant disease was 31% and 69% in patients older than 40 years.
Conclusion(s) The current study showed that majority of the patients with a painful breast mass would ultimately have a benign diagnosis, especially in younger ages; however they should be thoroughly evaluated.

P2.43
Paget`s disease of the nipple with invasion

Nielsen Banely B.
Regionshospital Randers, Randers No, Denmark

Background Paget`s disease of the nipple is considered an extension of tumor cells from an underlying breast carcinoma to the nipple epidermis. A case is presented of a 53-years old women with Paget`s disease of the nipple, where unexpectedly, the Paget cells demonstrated invasion of the nipple stroma, representing invasive carcinoma.
Methods The examined tissue were a sentinel node biopsi, a lumpectomi and a subsequent mastectomi specimen. In total 65 tissue bloks were taken for histologic examination including immune staining.
Results Microscopy showed a 7 mm well differentiated invasive ductal carcinoma (IDC) in the nipple stoma and

Paget´s disease. The Paget cells in the epidermis were in direct continuity with the invasive carcinoma and showed the same positive reaction to estrogen and Her-2 receptor. Whereas CEA was negative. In the breast tissue DCIS was found, but without invasion after extensive tissue sampling. Further, there was no direct relation between the IDC in the nipple and the DCIS in the breast. The sentinel node was found negative.
Conclusion(s) The breast tissue was without invasive carcinoma and no continuity between the DCIS in the breast and the IDC located in the nipple was demonstrated. Contrary, the Paget cells were continously with the invasive carcinoma and also showed the same immune profile. It is therefore concluded, that the IDC orginated from the the Paget cells and represent what one could call invasive Paget`s disease of the nipple.

P2.44
Preliminary results with the 3DHISTEC essential breast immunostaining kit

Cserni G.
Bács-Kiskun County Teaching Hospital, Department of Pathology, Kecskemét, Hungary

Background The estrogen receptor (ER), progesterone receptor (PR) and HER-2 status of breast cancers are routinely evaluated as they drive therapeutic decisions. The histological grade of breast cancers is also routinely evaluated and influences the prognosis and treatment of the disease.
Methods SP1 (anti-ER), SP2 (anti-PR) and SP3 (anti-HER-2) rabbit monoclonal antibodies along with the B56 (Ki-67 specific) mouse monoclonal antibody all supplied as part of an essential breast kit by 3DHISTECH, Hungary were evaluated against the external QA validated gold standard of antibodies used in our laboratory or the mitotic score component of the combined histological grade.
Results 62 specimens were analyzed. The ER and PR statuses were 100% and 98% concordant, respectively, with the two antibodies compared when any staining was considered positive. The overall kappa values for ER and PR categories based on the Allred quick scores were 0.64 and 0.76 reflecting substantial agreement between the two tests compared. For the HER-2 status there was only one relevant mismatch, the remaining 10 positive and 51 negative cases had concordant results. Tumors having a score of 1, 2 and 3 as part of the histological grading scheme had an increasing estimated proportion of Ki-67 nuclear staining: 11%, 23% and 44%, respectively.
Conclusion(s) The antibodies tested are reliable, and could probably be used with similarly good results in an automated system aiming at a standardized quantitative assessment of ER, PR, and HER-2 statuses and proliferation rate currently developed by 3DHISTECH.

P2.45
The study of an immunohistochemical aggressivity marker in mammary carcinomas

Muresan Anca Maria M.; Lazar E.; Raica M.; Dema A.; Campean A.; Suciu C.; Cioroboreanu R.; Sargan I.
University of Medicine and Pharmacy, Timisoara, Timis, Romania

Background The mammary cancer is the most frequent malign tumor encountered in females, characterized by a high distant metastasis tendency. Among the potential prognosis factors, we mention the biomarkers that measure or are associated with biologic processes involved in the tumorous progression.
Methods Using the immunohistochemical method of ABC Elite staining and the p53 human anti-protein mouse monoclonal antibody, the DO 7 clone (1:500 dilution) on tissue sections fixed in 10% formaldehyde and included in paraffin, we have obtained a red staining of the tumorous cells' nuclei.
Results Out of 40 mammary carcinomas where we have immunohistochemically determined the p53 protein, we have assessed that 29 of them proved to be negative, 6 had a moderate staining and 5 had an intense staining. The p53 immunoreactivity was more frequently encountered in pre-menopausal women and in invaded axillary lymph nodes tumors. We remarked a strong connection between the p53 overexpression and the studied tumors' grading.
Conclusion(s) The results of the p53 staining present some variations (between 21.5% and 52% with different antibodies and on a different number of cases). In the studied cases, the percentage of p53 positive cells was of 27.5%. The p53 protein overexpression can be useful in establishing the mammary carcinomas prognosis, only if it is analyzed in connection with other factors, thus improving the information provided by them: therefore it contributes to the identification of the patients with an increased risk of disease progression.

P2.46
Two cases of malignant phyllodes tumor of the breast treated with ifosfamide

Takahashi Y.; Saito M.; Kasumi F.; Yao T.; Arakawa A.; Miura H.; Nakai K.; Senuma K.; Abe I.; Kosaka T.; Shimizu H.; Tokuda E.; Mouri K.
Department of Breast Surgery, Juntendo, Tokyo, Japan

Background Malignant phyllodes tumor of the breast are rare. Primary standard treatment is surgical resection, but optimal treatment for metastatic disease of malignant

phyllodes tumor has not been established yet. Metastatic phyllodes tumor is not responsive to chemotherapy and radiotherapy, generally.
Methods Two patients of malignant phyllodes tumor with distant metastasis, who were treated with combination of ifosfamide and doxorubicin are reported. We examined the predictive factors of chemotherapeutic effect and prognosis, histopathologically and immunohistochemically.
Results Case 1: 50 years old woman was performed total mastectomy on January 2004, for rapidly enlarged malignant phyllodes tumor. On February 2005, metastatic adrenal tumor was found, which was not operable. After six curse of combined chemotherapy of ifosfamide and doxorubicin, a partial response was obtained. Additionally, the patient was treated with ifosfamide alone and long stable status of this disease have lasted 42 months since metastasis was found. Case 2: 55 years old woman was performed tumorectomy on October 2006, pathology report showed malignant phyllodes tumor. Six months later, local recurrence and lung metastasis appeared. Mastectomy was done on August 2007, and lung metastasis was not operable. Combination chemotherapy of ifosfamide and doxorubicin has started. A stable status of disease have lasted 11 months, however, the patient died of rapidly progressive disease.
Conclusion(s) Among metastatic malignant phyllodes tumor, some has chemosensitivity for ifosfamide and doxorubicin. We examined the relations of the predictive factor of chemotherapeutic effect and prognosis factor with histopathological and immunohistochemical finding.

P2.47
Two cases of mucinous breast carcinoma in patients younger than 60 years old

Gramada E.; Zurac S.A.; Nichita L.; Cohal M.; Gafton M.; Popp C.G.; Simeanu I.D.; Staniceanu F.; Andreescu B.; Rebosapca A.
Colentina University Hospital, Bucharest, Romania

Background Mucinous carcinoma (MC) is an uncommon breast neoplasm generally associated with a good prognosis. More common in older women (median age over 60), MC accounts for 2% of all breast cancers, its frequency dramatically increasing with the patients' age. Two forms are described: pure MC (consisting in clusters of small epithelial cells floating in abundant extracellular mucin), and mixed variants (associating areas of others types of mammary carcinomas, most frequently invasive ductal carcinoma NOS).
Methods We report 2 cases of MCs of the breast in women younger than 60 years old (36 and respectively 58 years).
Results Our first case revealed pure MC, well differentiated grade I, stage pT2; the second one was mixed MC carcinoma with small areas of invasive ductal carcinoma NOS and invasive lobular carcinoma, also well differentiated grade I. Estrogen and progesterone indexxes were similar (50–55%). Also, both of the tumors had PCNA index of 50–60%. In the second case the diagnosis of malignancy was obvious but the first case consisted in pools of mucin with small groups or isolated cells floating within it; large parts of the tumor were paucicellular, imposing a differential diagnosis with a mucocele-like lesion.
Conclusion(s) Distinguishing between cases with pure type of MC, mixed type of MC and other types of breast invasive carcinoma and/or benign lesions has outmost importance in respect of their different clinical behavior and expected outcome.

Digestive pathology

P2.48
Gastric cancer: correlation between muc1 immunohistochemical expression and clinicopathological factors

Lazar D.; Taban S.; Dema A.; Cornianu M.; Lazar E.; Goldis A.; Sporea I.
University of Medicine and Pharmacy "V. Babes", Timisoara, Romania

Background The aim of our study was to correlate the immunohistochemical MUC1 expression with the clinicopathological factors.
Methods We have evaluated the immunohistochemical expression of MUC1 on a batch of 61 patients operated for gastric cancer in County Hospital Timisoara, Romania.
Results We identified 41 cases with positive MUC1 immunoreactions (67,2%). We found a significantly higher immunostaining in patients over 61 years (55,2%) (p= 0.046513).We noticed positive MUC1 immunoreactions in 64,5% of antral, 73,3% of corporeal, 70% of pangastric, 66,7% of gastric stump and in 50% of cardial carcinomas. We observed an increased frequency of the MUC1 positive immunoreactions in carcinomas with glandular differentiation (73,7%), in comparison with the diffuse type (53%). Tubular and papillary adenocarcinomas showed positive immunostaining in a significantly higher number of cases (78,6%; 80%), in comparison to signet-ring cell and anaplastic carcinomas (53%; 3,3%) (p = 0.000635). MUC 1 immunohistochemical expression does not correlate with lymphovascular invasion. G1 carcinomas became positive for MUC1 in 100% of cases.Our results do not reveal any correlation between MUC1 and pT, pM and pTMN stage. We have remarked a significantly higher number of positive

immunoreactions in patients presenting lymphonodular metastasis (72,1%) in comparison to those without lymphonodular metastasis (55,6%) (p = 0.047969).Patients with MUC1 positive carcinomas presented a five years survival rate significantly lower in comparison those with MUC1 negative carcinomas (12,2% vs.25%, p = 0.0368).
Conclusion(s) MUC1 immunohistochemical expression correlates with the histological type of gastric cancer, with the degree of differentiation and the presence of lymphonodular metastasis. MUC1 immunohistochemical expression represents an important prognostic factor in patients with gastric cancer.

P2.49
Gastric metastasis of the uterine cervix. A rare entity
Chaabouni N.; Sassi S.; Abbes I.; Mrad K.; Dhouib R.; Driss M.; Ben Romdhane K.
Salah Azaeiz Institute, Tunis, Tunisia

Background We report a rare complication of an advanced cervical squamous cell carcinoma metastatic to the stomach presenting with acute peritoneal syndrome caused by a gastric perforation.
Methods Five- micrometer-thik sections were cut on formalin-fixed paraffin-embedded tissue s and stained with hematoxylin and eosin
Results Grossly, the specimen received consists of a partial gastrectomy measured 14 cm at the level of the large curvature and 7 cm at the level of the small one. In the opening and at 1 cm of the fundic margin, there was an irregular perforated ulceration measuring 2 cm of major axis near the small gastric curvature.The diagnosis of gastric metastases was confirmed by clinical history and by the finding of numerous vascular space involvements by squamous cell carcinoma in the gastric mucosa at microscopic examination
Conclusion(s) Gastric metastasis in cervical carcinoma is a late manifestation of advanced malignancy and heralds a poor prognosis. It may present with features of upper gastro intestinal bleeding and the diagnosis requires a multidisciplinary approach to its management.

P2.50
Gastrointestinal stromal tumor (GIST) arising in a Meckel's diverticulum: a case report
Kopaka M.; Kara P.; Tsigka A.; Lianou A.M.; Diamanti E.; Argyriou P.; Lariou K.
"Evaggelismos" General Hospital, Athens, Greece

Background Tumors within Meckel's diverticulum (MD) are rare with a reported frequency of 0,5 to 3,2% and only few cases of gastrointestinal stromal tumor (GIST) developed in MD have been published in the literature. We report a case of a GIST arising in a MD and causing small bowel obstruction. A 80-year old male presented to the emergency department with symptoms and signs of small bowel obstruction. Surgery was performed and an ischemic MD was identified as the cause of the obstruction.
Methods Macroscopically the diverticulum measured 4x2x1 cm and on the longitudinal section of the tip an ill-defined grey-tan mass of 3 cm was revealed. After tissue processing, Hematoxylin-Eosin staining was performed as well as immunohistochemical staining for CD117, CD34, S-100, desmin, b-Catenin, SMA, bcl-2 and Ki-67.
Results Microscopic examination revealed a tumor with spindle cell proliferation arranged in a fascicular pattern, with extensive areas of hemorrhage. No necrosis was found and mitotic activity was low, estimated to be <5/50 HPF. Immunohistochemically the tumor cells show strong positive reaction to CD117 and moderate positivity to SMA and bcl-2.Staining with CD34, S100, desmin and b-catenin were negative. Immunoreactivity for Ki-67 showed a low mitotic rate of≈2%. The diagnosis of a low grade GIST in a MD was confirmed.
Conclusion(s) Although that tumors arising in MD are very rare, the surgeon should always keep in mind this possibility in his differential diagnosis of unexplained abdominal symptoms.

P2.51
Glomangiomatosis of the stomach: a case presentation
Cosic Micev Luka M.; Micev Tomislav M.; Todorovic V.; Drndarevic N.; Alempijevic T.; Knezevic S.
Clinical Centre of Serbia, Belgrade, Serbia and Montenegro

Background Glomangiomatosis is a rare condition and refers to multiple angiomatous type of glomus tumors that has been described in a variety of anatomical sites, usually in the peripheral soft tissues, but extremely rare in the stomach.
Methods We present a case of multiple glomangiomas occupying large distal gastric segment in a 18 yrs old male patient who suffered right upper quandrant abdominal pain, abdominal discomfort and short interval intermittent nausea. Unlike other six solitary gastric glomus tumours we examined in last fifteen years, the endoscopy described „etat mammelonné".
Results Gross examination revealed large and ill defined area of diffuse thickening of the antral and distal corporal gastric segment, measuring 130x65 mm in greatest diameters and covered with intact mucosal nodular folds. Histologically, sessile masses and micronodular thin-walled vascular structures were surrounded by small masses or scattered cells and agreggates of uniform glomus cells, often forming organoid architecture in conjunction with

vascular channels. These cells with round nuclei rarely showed clear perinuclear zone and scanty cytoplasm, focal atypia and low mitotic activity (1/50 HPF). We have not observed necrosis or vascular invasion. Immunostaining showed alpha-smooth muscle actin and variable but significant CD34 and pericellular net-like collagen IV positivity, but a lack of CD117, desmin and S-100 protein immunoexpression. In 30 months follow-up there was no relapse or any signs of the disease.

Conclusion(s) Glomangiomatosis is rare cause of abdominal pain and might broaden differential diagnosis of painful diffuse infiltrative gastric lesions, which is crucial for appropriate treatment.

P2.52

Helicobacter spp DNA in mucosa of Swedish patients with cholecystitis

Stenram U.; Karagin P.; Nilsson H.; Wadstrom T.; Ljungh A.
Department of Pathology, Lund, Sweden

Background Helicobacter DNA in cholecystitis mucosa has been reported with prevalences from 2% to 83% in different countries. Several authors claim that Helicobacter is especially found in areas of gastric metaplasia. We examined a series of patients from Southern Sweden.

Methods Paraffin embedded samples (5–10 mg tissue) from the mucosa of 54 consequtive patients with acute or chronic cholecystitis were studied by Helicobacter DNA specific PCR-assay and sequence analysis.

Results Helicobacter DNA was found in 9 out of the 54 patients in acute as well as in chronic cholecystits, in total 17%. Sequence analysis displayed similarity to H pullorum in all cases, and lower similarity to H canadensis. There was very little gastric metaplasia.

Conclusion(s) The prevalence was higher than in a recent German study but lower than in a few examinations from non-Western countries. H pullorum has been found by one previous author, H canadensis by none. More cases will be examined. The paraffin embedded specimens are composed of epithelial as well as stromal elements, and Helicobacter may be present only in the epithelium. The sampling strategy may have great influence on the results. The presence of non-pylori species may not be dependent on gastric metaplasia.

P2.53

Hepatic lesions induced by olive leaf extract in mice

Arantes-Rodrigues R.; Henriques A.; Vasconcelos-Nóbrega L.C.; Ginja Dinis M.; Colaco A.A.; Palomino F.L.; Fernandes Horácio T.; Lopes Silva C.; Oliveira A.P.
University of Trás-os-Montes and Alto Douro, Vila Real, Portugal

Background Olive leaf extract-d-lenolate (OLE) is pointed as a very effective dietary supplement that is used to prevent and treat various tumours, hypertension and many other diseases. The aim of this work was to investigate the effect of OLE in mice liver histology.

Methods Female ICR mice were distributed into groups of ten animals, I, II, and III, and treated with 0.25%, 0.50% and 0.75% of OLE in their food during fourteen weeks, respectively. One group of ten animals was used as negative control. After completing the period of exposure animals were euthanized and collected samples were collected from liver, spleen, urinary bladder, kidneys, and lungs. Conventional histological techniques, reticulin and Masson's Trichrome stains were performed.

Results In the course of the study animals from groups II and III showed icterius, lost weight ($p<0.05$), and 2 and 5 animals died, respectively. Liver macroscopic observation showed a green coloration and dilated bile ducts in animals exposed to OLE. Histological study of organs collected from animals treated with OLE revealed no changes, with the exception of liver. Control animals did not show macroscopic neither microscopic changes. The livers collected from group I showed bile ductal hyperplasia and from groups II and III revealed changes in architecture, fibrosis, cholestasis, bile ductal hyperplasia, areas of necrosis, liver inflammatory infiltrate and several mitosis.

Conclusion(s) The results obtained in this research revealed that OLE might contain dangerous liver substances that could be responsible by liver damages.

P2.54

High-grade neuroendocrine carcinoma of the ascending colon, diagnosed synchronously with two colonic adenocarcinomas.

Anagnostou E.; Katsiki E.; Marakis G.
Hippokration, Thessaloniki, Greece

Background High-grade neuroendocrine carcinomas are aggressive neoplasms, characterized by poor prognosis. These tumors are frequently associated with synchronous or metachronous primary malignancies. However, the coexistence of a neuroendocrine tumor and adenocarcinoma has been rarely reported.

Methods We report a case of a 71-year-old man, who was admitted with anorexia, weight loss and anaemia. The patient underwent a colonoscopy, which revealed the presence of two colonic masses, located in the right colic flexure and the in the middle of the ascending colon. Consequently, a right hemicolectomy was performed. On gross examination, during the opening of the bowel, an

exophytic and an ulcerative tumor were observed, with greatest diameters of 5.5 and 4.5 cm, respectively.
Results Histopathologic analysis of multiple sections from the exophytic mass showed the presence of an intramucosal adenocarcinoma, while tunica muscularis and serosa were infiltrated by a high-grade neuroendocrine carcinoma. The neoplastic cells of the latter tumor exhibited positivity to synaptophysin and chromogranin and high expression of the proliferation index Ki-67. Sections from the ulcerative tumor showed features of conventional colonic adenocarcinoma, moderately differentiated. The neoplasm infiltrated the entire colonic wall, with extension to the pericolic fatty tissue. The patient has no signs of recurrence or metastasis, 3 months after surgical treatment.
Conclusion(s) Coexistence of adenocarcinoma and neuroendocrine tumors has been reported by a few case studies. We report this case due to its rarity, emphasizing on the pathogenesis and possible relationship of such combined tumors.

P2.55
H-ras oncogene expression and angiogenesis in experimental liver cirrhosis

Unal B.; Bozova S.; Elpek Ozlem G.
Serik State Hospital, Akdeniz University, Department of Pathology, Antalya, Arapsuyu, Turkey

Background H-ras oncogene may not only affect cell proliferation but also contributes to angiogenesis by influencing both proangiogenic and anti-angiogenic mediators. Although, H-ras oncogene expression in liver diseases has been investigated, the association of H-ras oncogene expression with angiogenesis during liver fibrogenesis has not been evaluated. The aim of this study was to investigate the relationship between H-ras expression and angiogenesis during experimental liver fibrogenesis.
Methods Cirrhosis was induced by male Wistar rats (n: 30) by intraperitoneal administration of diethyl nitrosamine (DEN) (100 mg/kg, once a week). The serial sections from liver tissues were stained with anti-CD34 and anti-H-ras antibodies before being quantitated by light microscopy.
Results H-ras expression was lower in the control group (0.66%)compared to the DEN-treated rat groups (19.5%) ($p<0.01$). Its expression gradually increased according to the severity of fibrosis. Moreover H-ras expression was found to be correlated with angiogenesis ($p<0.01$).
Conclusion(s) Our results revealed that similar to tumor related angiogenesis. H-ras might contribute to the wound healing response to liver injury as a promotor of angiogenesis. Although our data needs to be clarified with further molecular studies in experimental models, the relationship between angiogenesis and H-ras expression suggests that H-ras could be a potential target in the manipulation of angiogenesis in chronic inflammatory liver diseases ending with cirrhosis.

P2.56
Immunohistochemical assessment of neuroendocrine differentiation in colorectal carcinomas and its relation with age, sex, grade and stage

Shahzadi Zohourian S.; Shayanfar N.
Iran University of Medical Sciences, Tehran, Islamic Republic of Iran

Background Neuroendocrine differentiation has not been proved to have effects in behavior of colorectal carcinomas. The aim of this study was Immunohistochemical evaluation of neuroendocrine differentiation in colorectal cancer.
Methods In this cross-sectional study, 83 paraffin blocks from patients admitted in Rasoul-e-akram hospital, Tehran, Iran during 2003 to 2008 evaluated in pathology department in December 2008. All sections stained with immunohistochemistry method for neuron specific enolase (NSE) and Chromogranin A(CgA). All histologic and epidemiologic data analyzed, accordingly.
Results Median age of patients was 56 yrs. 44 cases (53%) were female and 39 cases (47%) were male. According to TNM staging system, 11% of cases were in stage I, 29% in IIa, 7% in IIb, 2% in IIIa, 23% in IIIb, 24% IIIc and 2% were in stage IV. 13 cases (16%) were NSE positive.15 cases (18.1%) were CgA positive.In grades II and III, NSE and CgA were significantly higher than grade I ($p<0.001$). CgA incidence was higher significantly in mucinous carcinomas ($p<0.05$).
Conclusion(s) Less than 20% of colorectal cancers showed neuroendocrine differentiation. There's no significant relationship between NSE and CgA incidence with stage or tumor site. There is a relationship between histologic grade and above mentioned markers; this finding may help us in our knowledge about tumor behavior.

P2.57
Immunohistochemical expression of EGFR and VEGF in colorectal carcinoma and their correlation with clinicopathological features

Vasilakaki T.; Skafida E.; Glava C.; Katsamagkou E.; Grammatoglou X.; Zissis D.; Delliou E.
Tzaneion General Hospital of Piraeus, Athens, Greece

Background Colorectal carcinomas account for about 10% of deaths in the world, especially in developed countries. The aim of this study was to investigate the expression of EGFR and VEGF in colorectal carcinoma and to correlate them with clinicopathological parameters.

Methods Immunohistochemical staining for EGFR and VEGF was carried out on paraffin embedded tissue sections 4 μm of thickness from specimens of 90 patients who underwent surgery for colorectal cancer. Data about sex, age, size and location of the tumour, grade, necrosis, depth of invasion, inflammatory response, vascular invasion and status of lymph-nodes were obtained from all patients. The staining degree was evaluated as weak, moderate and strong. VEGF and EGFR expression were classified in two groups corresponding to the percentage of positive carcinoma cells: low (< 25%) and high (> 25%).
Results Tumor cells showed positive staining for EGFR in 42 cases (47%) and for VEGF in 81 (90%). The degree of staining with EGFR was moderate to strong in the cell's membrane. The degree of staining with VEGF was moderate to strong mainly in the cytoplasm. All cases of the VEGF-positive group had high expression (> 25%), while the EGFR-positive group had high expression (> 25%) in 9 cases and low expression (< 25%) in 33 cases. There was no relationship between the expression of EGFR and VEGF and all of the parameters ($p>0.05$).
Conclusion(s) This study suggests that EGFR and VEGF appear not to be reliable prognostic factors in colorectal carcinomas.

P2.58

Immunohistochemical expression of transforming growth factor beta-1 in chronic liver diseases

Goussia A.; Nesseris I.; Mouladaki A.; Baltayiannis G.; Siozopoulou V.; Ntoulia A.; Zois C.; Tsianos E.; Malamou-Mitsi V.
Department of Pathology, Medical School, University of Ioannina, Ioannina, Greece

Background Transforming growth factor beta-1 (TGB-β1) has many biological properties involving regulation of cell growth, apoptosis and repair processes, including fibrosis. The aim of the present study was to investigate the role of TGB-β1 in different phases of chronic liver diseases.
Methods Liver biopsies from 70 patients with chronic liver diseases treated at the Department of Hepato-Gastroenterology, Medical School, University of Ioannina, Greece, were studied. The diagnoses were: chronic hepatitis B (35 patients), chronic hepatitis C (26 patients), alcohol chronic liver disease (9 patients). Histological activity of inflammation and staging of fibrosis were performed according to the Scheuer scoring system. Sections from formalin-fixed, paraffin embedded tissues were stained immunohistochemically with the TGB-β1 primary antibody (Menarini). The evaluation of TGB-β1 was done semiquantitatively as follows: 0, absence of immunoreaction; 1, 1–10% positive cells; 2, 11–50% positive cells1; 3, > 50% positive cells.
Results Cytoplasmic staining of TGB-β1 was detected in hepatocytes, mesenchymal and inflammatory cells. Expression of TGB-β1 in hepatocytes was observed in 18 patients (51.43%) with chronic hepatitis B, 14 patients (53.85 %) with chronic hepatitis C and in 2 patients (22.22%) with alcoholic disease. A statistically significant correlation was observed between TGB-β1 expression and the stage of fibrosis but not with the activity of inflammation.
Conclusion(s) TGB-β1 expression in hepatocytes correlates with the degree of fibrosis in chronic liver diseases. TGB-β1 seems to play a role in liver fibrogenesis by activating both mesenchymal and parenchymal hepatic cells.

P2.59

Inflammatory myofibroblastic tumor of the ileum causing intestinal invagination

Adouni O.; Chelly I.; Tangour M.; Nfoussi H.; Mekni A.; Azouz H.; Boujelbène N.; Haouet S.; Kchir N.; Sebai F.; Zitouna M.
Tunis, Tunisia

Background Inflammatory myofibroblastic tumor (IMT) is a rare spindle cell lesion of indeterminate malignant potential occurring in various organs and of unknown aetiology. Entero-enteric invagination is a very rare event in adults, in which a single (often malignant) cause is identified as triggering the invagination. We report a case of an ileal IMT causing intestinal invagination.
Methods A 61-year-old woman presented with a 2-week history of worsening abdominal pain. The diagnosis of ileo-ileal invagination was made.
Results Laparotomy and segmental small bowel resection were performed revealed gross intussusception and a palpable intraluminal pedunculated mass measuring 5 cm, from which a histological diagnosis of IMT was made.
Conclusion(s) IMT has been described as a neoplasm composed of spindle cells admixed with numerous inflammatory cells, including plasma cells and lymphocytes. IMT occurs most commonly in the lungs. Extrapulmonary sites have also been reported and include the genitourinary tract, gastrointestinal tract, pelvis, head and neck, and extremities. Although these tumors are typically benign, IMTs have an uncertain malignant potential and may show local recurrence, infiltrative growth, vascular invasion, and malignant sarcomatous transformation. The differential diagnosis for spindle cell tumors includes IMT, leiomyoma, leiomyosarcoma, rhabdomyosarcoma, malignant fibrous histiocytoma, inflammatory fibrosarcoma, intra-abdominal fibromatosis, and gastrointestinal stromal tumor. The etiologic factors responsible for the development of IMT are not clearly understood. IMT is a rare spindle cell tumor with an uncertain malignant potential. Thus, early recognition and complete surgical resection are

necessary to avoid recurrences and prevent spread of locally aggressive tumors.

P2.60

Intraductal papillary mucinous neoplasms of pancreas

Dubova E.; Shchegolev A.; Mishnev O.D.; Pavlov K.
A.V. Vishnevsky Institute of Surgery, Moscow, Russian Federation

Background Intraductal papillary mucinous neoplasms (IPMN) are pancreatic exocrine lesions composed of dilated main or branch ducts lined by mucin producing atypical epithelium, which usually proliferates in a papillary fashion.
Methods In 2004–2008 we observed 11 IPMNs. 10 patients were men and 1 was woman at age from 36 to 71.
Results 9 patients had main duct IPMNs (mdIPMNs) and 2 patients had branch duct IPMNs (bdIPMNs). Diameter of main pancreatic duct in mdIPMNs varied from 1 to 7 cm. In 4 cases of mdIPMNs we've found a dilated accessory duct. All of the bdIPMNs were multiloculated adenomas and their cystic-dilated ducts ranged from 3 to 15 mm. The mdIPMNs in 2 cases were histologically graded as IPMB and in 7 cases - as IPMC. In 4 cases of the mdIPMNs we've detected the intestinal-type IPMN. The neoplastic cells consistently expressed MUC2, MUC5AC, CDX2 and CK20, but were negative for MUC1. In all cases of the bdIPMN and in 5 cases of mdIPMNs we've detected the pancreatobiliary type of IPMN. The lesions were positive for MUC1 and consistently expressed MUC5AC but not MUC2. The tumor cells also expressed CK7, CK8, CK19, but not CDX2 and CK20. The tumors demonstrated a progressive increase in cell proliferation from adenomas, to borderline tumors, to carcinomas, detected by expression Ki-67. The tumor cells of malignant IPMN showed high level of expression of p53.
Conclusion(s) To detect the type and pattern of IPMN immunohistochemical investigation need to be performed.

P2.61

Ito cells in liver lesions and liver cirrhosis

Dmitrovic B.; Kurbel S.; Horvat D.
Osijek Clinical Hospital, Osijek, Croatia

Background The aim of the study was to determine the association between the number of activated Ito cells with the activity and the stage of the chronic liver disease.
Methods The study included 31 patients with liver lesion and 32 patients with liver cirrhosis after completion of diagnostic procedures with liver biopsy. Liver lesion patients were diagnosed as: hepatitis C (17) and B (8) and ethylism (6). Liver cirrhosis causes were ethylism (10), hepatitis C (8) and B (6), PBC (5), hemochromatosis (2) and Wilson's disease (1). Ito cells were identified with smooth muscle actin.
Results The subgroups of the patients according to the etiology of the disease differed significantly in the disease activity (p=0.0462; Kruskal-Wallis test). Those subgroups of the patients did not differ in the stage of the disease (p = 0.54). The number of the activated Ito cells did not differ between those subgroups (p = 0.06737; Kruskal-Wallis test). A significant difference was found between the subgroups of the patients formed according to the Child-Plough classification (p = 0.0013), dominantly between stages C and A. Furthermore, the liver lesion and liver cirrhosis subgroups differed significantly in the cell number (p = 0.0002).
Conclusion(s) The study showed that the disease activity 7 and the disease stage 3 were the cut-off scores by which one could expect the disease progression toward liver cirrhosis. The disease activity by different etiology was accompanied by the different number of activated cells in the initial stages, while the difference disappeared with the later development of cirrhosis.

P2.62

Lymph node micrometastases in patients with gastric carcinoma: immunohistochemical evaluation

Vélez D.; Ramos P.; Olmedilla G.; Busteros J.; Marcos R.; Gutiérrez A.
"Príncipe de Asturias" University Hospital, Alcalá de Henares, Madrid, Spain

Background Lymph node status is a major determinant of disease recurrence after curative resection for gastric carcinoma. In this study, we evaluate the clinicopathologic significance of micrometastases to lymph nodes, confirmed by immunostaining with cytokeratins.
Methods A total of 738 lymph nodes from 44 patients with gastric carcinoma, pTXN0M0, who underwent gastric resection between 1996 and 2003 at the Principe de Asturias Hospital were studied. Tissue preparations were stained with hematoxylin and eosin (H&E), and six consecutive sections were newly prepared from each lymph node for immunohistochemical staining (antibodies against cytokeratin AE1/3).
Results Micrometastases were confirmed in 23 lymph nodes (3.11%) by immunostaining for citokeratin, and in 11 patients (25%), who were then up-staged. Between the two histologic types of gastric carcinoma, the diffuse type had more micrometastases than the intestinal type.
Conclusion(s) Immunohistochemical staining can be an useful method to detect micrometastatic lymph nodes, and have also an impact on staging and survival in patients with gastric carcinoma.

P2.63

Mallory-Denk-Body-like cytoplasmic inclusions in the cholangiocarcinoma component of a case of combined hepatocellular and cholangiocarcinoma

Aigelsreiter A.; Pixner T.; Denk H.; Lackner C.
Institute of Pathology, Medical University of Graz, Graz, Styria, Austria

Background Mallory-Denk-bodies (MDBs) are cytoplasmic protein inclusions found in hepatocellular carcinoma (HCC). MDBs mainly consist of the oxidative stress-induced misfolded keratins (K) 8 and 18, sequestosome 1/p62 (p62) and ubiquitin. MDBs in HCCs are often associated with steatohepatitic features, i.e. steatosis, neutrophilic granulocyte inflammation and cellular ballooning. However, data concerning cytoplasmic inclusion bodies in cholangiocarcinoma are limited.
Methods We report a case of combined hepatocellular and cholangiocarcinoma (HCC/CCC) with steatohepatitic features in the HCC component and intracellular inclusions resembling MDBs in both tumor components. Tumor components and inclusions were characterized by immunohistochemistry using antibodies against hepatocellular antigen (Hepar1), K7, K8/18, p62 and ubiquitin.
Results The HCC component displayed trabecular and pseudoglandular growth pattern with steatohepatitic features. Its tumor cells were decorated by Hepar1 antibodies. In the areas with steatohepatitic features the tumor cells lost cytoplasmic K8/18-expression, whereas MDBs were labelled with K8/18, p62 and ubiquitin antibodies. The CCC component presented as tubular adenocarcinoma with variable fibrous stroma. Most tumor cells contained irregularly formed cytoplasmic inclusions which were labelled by K7, K8/18, p62 and ubiquitin antibodies. Tumor cells were negative with Hepar1-antibodies and showed loss of cytoplasmic K7 and K8/18 expression.
Conclusion(s) MDB-like cytoplasmic inclusions consisting of K7, K8/18, p62 and ubiquitin can occur in the CCC component of CCC/HCC. The aetiology of the MDB-like inclusions and the loss of cytoplasmic K expression are unknown; like in HCC with steatohepatitic features oxidative stress may play an important pathogenetic role.

P2.64

Markers of neuroendocrine cell differentiation and gastric cancer progression

Ananiev Rumenov J.; Gulubova Vladova M.
Medical Faculty, Trakia University, Stara Zagora, Bulgaria

Background It was found that mainly chromogranin A (CHA) and less other endocrine cell (EC) markers such as gastrin (GAS), somatostatin (SOM) and serotonin (SER) immunostained the ECs in gastric cancers. The expression of isoenzymes glutation-S-transferase (GST-pi) and Cu/Zn superoxide dismutase 1 (SOD1) in gastrointestinal ECs is not studied. The aim of our study was to determine the EC presence in gastric cancers and its prognostic value for patients, and whether GST-pi-positive and SOD1-positive ECs could be useful as EC markers.
Methods The study included 53 gastric cancers, resected in University Hospital in Stara Zagora. The patients' population consisted in 21 females and 32 males with median age of 67 years. ECs were displayed using immunohistochemistry with antibodies against CHA, SER, GAS, SOM, GST-pi and SOD1.
Results In the overlying mucosa ECs were most in number immunostained for CHA, followed by GST-pi, GAS, SER, SOM, and SOD1. In tumors CHA-positive ECs were the prevailing cell type followed by SOM, GST-pi GAS, SER, and SOD1. The lower GST-pi –positive ECs in tumor tissue correlated with more advanced tumor stage (chi2=4.56, p= 0.033). On serial sections it was shown that some CHA, GAS, SER, and SOM-positive ECs in the tumor and in overlying mucosa were also GST-pi- and SOD1-positive.
Conclusion(s) In conclusion we may state that the presence of high EC numbers in gastric cancer is related to early tumor stage; and that GST-pi is a good marker for gastric ECs.

P2.65

Mdm2 in colon carcinoma: an immunohistochemical and fluorescence in situ hybridization study

Hav M.; Libbrecht L.; Pattyn P.; Peeters M.; Praet M.; Pauwels P.
Department of Pathology, Ghent University Hospital, Ghent, Belgium

Background New pharmacological agents targeting mdm2-p53 axis are available. By blocking p53 degradation mediated by mdm2, wild-type p53 could restore its function and induce tumour cell apoptosis, especially when these cells express high p53 levels as a result of chemo and/or radiation therapy. These molecules could be effective in the subset of patients whose mdm2 protein levels are particularly high. Published studies on mdm2 status showed conflicting results. In this study, we checked mdm2 status by immunohistochemistry (IHC) and Fluorescence In Situ Hybridization (FISH). FISH is less susceptible to interobsever variation. We correlated mdm2 gene amplification status with mdm2 protein expression.
Methods We examined 38 cases of invasive colon carcinoma. Mdm2 IHC and FISH were performed on paraffin-embedded sections. Mdm2 protein expression was recorded based on staining pattern (cytoplasmic or nuclear), staining intensity (weak, moderate, or strong), and proportion of tumour cells stained. We then correlated mdm2 protein expression with the FISH result.

Results Of the 38 cases, 11 (26%) showed mdm2 amplification. Mdm2 nuclear positivity was seen in 13 cases (34%). There was no correlation between mdm2 amplification and mdm2 nuclear positivity. Cytoplasmic positivity was seen more frequently in amplified cases (10 cases, 91%) than in non-amplified cases (18 cases, 67%).
Conclusion(s) Contrary to the published results, we showed the presence of mdm2 amplification in 26% of cases. We also observed that there was a positive correlation between mdm2 amplification and cytoplasmic staining regardless of the staining intensity.

P2.66
Microsatellite status, lymph node status and loco-regional inflammatory response: prognostic factors for right-sided colorectal cancer?

Beuvon F.; Canard G.; Leconte M.; Dousset B.; Terris B.
GH Cochin Saint Vincent-de-Paul, Paris, France

Background To study the prognostic value of histopathological local anticancer immune response and microsatellite status in a homogenous series of right side tumor colorectomies.
Methods A rectrospective unicenter study of a cohort of 164 patients who underwent ride side colectomy for cancer. All histology slides were analyzed by 2 pathologists for tumor invasion (VELIPI), microsatellite status and loco-regional inflammatory reaction: lymph node number, size and functional status. A loco-regional inflammatory score (LRI) was established which included 4 parameters: presence of Crohn-like infiltrate, intra-epithelial lymphocytes, node size and germinal center hyperplasia. Patient survival was evaluated using uni- and multi-variate analysis.
Results 135 patients were included in this study. Excluded were 4 deaths and 23 lost to follow-up. 33 patients (24.4%) were microsatellite instable (MSI) and 102 (75.5%) were microsatellite stable (MSS). Using univariate analysis, histopathological prognostic factors associated with increased survival included MSI (p= 0.019) and high LRI score (p = 0,003). Factors associated with poor prognosis were VELIPI postitivity (p = 0.009), lymph node involvement (p = 0.001) and synchronous metastases (p = 0.025). In multivariate analysis, independent factors for poor prognosis were lymph node involvement (p = 0.001) and synchronous metastases (p = 0.025). Excluding these confounding factors, MSI status was an independent prognostic factor associated with increased survival (p = 0,031) and linked to high LRI score.
Conclusion(s) • MSI status is a good prognostic factor linked to high LRI score. • Increased lymph node size correlated with increased remission and survival. • Local immune response is implicated in the control of tumor progression.

P2.67
Midkine expression and angiogenesis in colorectal carcinoma

Ay N.; Erdogan G.; Elpek Ozlem G.; Erdogan O.; Gürer S.
Akdeniz University, Antalya, Turkey

Background Midkine (MK) is a heparin-binding growth factor that is expressed in various human cancers and plays important roles in cell transformation and angiogenesis. Recent studies indicated that MK was involved in genesis and development of colorectal carcinomas (CRC). However in these tumors the relationship among MK expression, angiogenesis and prognosis has not been documented. The purpose of this study was to investigate whether MK expression was associated with angiogenesis and survival in patients with CRC.
Methods Tumour specimens from 61 patients diagnosed as CRC were included in this study. Serial sections from paraffin embedded tissues stained anti-midkine and anti-CD34 antibodies. Angiogenesis assessed as microvessel densitiy (MVD). Chi-square test, Kaplan-Meier method and Cox regression analysis were used for statistical analysis.
Results MK expression was observed in 36 of the cases (59%). Non-neoplastic mucosa was consistently negative. Any relationship was not observed between MK expression and clinicopathologic parameters, so MK expression failed to predict tumor behaviour. Moreover MK expression was not associated with MVD. On the other hand the prognosis was significantly worse in patients with high MVD (> 5.8). Survival analysis revealed that although MK expression had no impact on prognosis, MVD was an independent prognostic variable.
Conclusion(s) Our results revealed that MK expression has no prognostic relevance in CRC. However MVD could be reliable indicator of prognosis. Although our data needs to be clarified with further molecular studies, the lack of correlation between MK expression and MVD suggests that MK has no impact on CRC related angiogenesis.

P2.68
Nuclear ploidy and proliferative level of tumor cells of the hepatocellular cancer

Shchegolev A.; Dubova E.; Pavlov K.
A.V. Vishnevsky Institute of Surgery, Moscow, Russian Federation

Background The purpose of the study was to investigate nuclear ploidy and proliferative level of different grade hepatocellular carcinoma cells.
Methods We investigated surgical specimens from 17 patients with hepatocellular carcinoma (HCC) treated in the Institute in the 2007–2008. There were 10 males and 7 females at the age from 18 to 66 years.

Results Median nuclear ploidy level of normal hepatic cells at the densitometric investigation of Felgen-staned specimens was 2,6 (little higher then diploid chromotype). Nuclear ploidy level of HCC cells was much higher then in normal hepatic cells. Nuclear ploidy level of HCC cells is invert correlate with tumor differentiation: medial nuclear ploidy levels of well differentiated HCC cells similar to those in tetraploid cells and medial nuclear ploidy levels of poorly differentiated HCC cells was 5,5. Proliferative level of normal hepatic cells was 0,5%. Proliferative level of well differentiated HAC cells was 5.2 times higher then in normal hepatic cells. Highest level of Ki-67-positive cells was in poorly differentiated HCC, though in undifferentiated HCC proliferative level was lower then in moderate and poorly differentiated HCC. This feature associated with prevalence of cell injury and apoptosis in undifferentiated HCC cells.
Conclusion(s) Thus in HCC we observed tumor cells enlargement, increasing of nuclear ploidy levels and the number of proliferative cells. This features reflects phasic pattern of tumor growth. Investigation of cell proliferation level in comparison to nuclear ploidy level is accurate and specific criteria of tumor differentiation level.

P2.69
Overexpression of P150, a part of the large subunit of the eukaryotic translation initiation factor 3, in colon cancer

Haybaeck J.; Spizzo G.; Mikuz G.; Brunhuber T.; Salvenmoser W.; Bänziger R.; Bachmann F.; Schäfer G.; Burger M.M.; Obrist P.
Department of Pathology, University Hospital Zürich, Zürich, Switzerland

Background P150 – a 150 kD protein- was isolated from virally and oncogene transformed mouse cell lines, partially purified and cloned. P150 is part of the large subunit of the eukaryotic initiation factor 3 with sequence homologies to centrosomin A. A significant correlation between p150 expression and malignancy in breast, cervical and esophageal cancer have been recently demonstrated.
Methods 110 colorectal carcinomas of different grades and stages including lymph node and liver metastases were compared to adjacent normal mucosa by immunohistochemistry. Western blot analysis of selected cases reconfirmed the expression levels determined by immunohistochemistry. Additionally immune electron- and laser scanning microscopy was performed.
Results All investigated carcinomas revealed high levels of p150 protein compared to normal adjacent mucosa. The staining intensity was slightly heterogeneous, and positivity was correlated to the tumor grade with statistically significant differences of p150 expression between normal and neoplastic mucosa ($p<0,0001$, Kruskal-Wallis test). Western blots confirmed these results with higher expression levels of p150 in the tumor. Immunogold labelling and laser scanning microscopy investigation presented high expression levels of p150 on the rough endoplasmic reticulum and polyribosomes, which attest p150 to be associated with the protein synthesis.
Conclusion(s) Thus, we suggest that p150 plays an important role in development and growth of colorectal carcinomas. Furthermore, it might provide us with reliable information on the biological behaviour of the tumor and the possible clinical course of the disease.

P2.70
Prognosis criterions of insolvency of anastomosis of large intestine

Klimova O.; Boyko V.; Kryvorotko I.; Sushkov S.
Government Institution "Institute of General and Urgent Surgery of Academy of Medical Sciences of Ukraine", Kharkiv, Ukraine

Background The insolvency of anastomosis of large intestine is the complication at quarter of patients operated regarding colorectal cancer. The process of collagen formation with further induced metabolization is completed by proline and oxyproline formation. The redundant increase of oxyproline concentration causes disturbance of rheological properties of blood. The principle of functioning of biological systems is based on phenomenon of substrate inhibition or activation. Amino acid methionine can be metabolized by consistent methylation in alternative way with sufficient amount of vitamins B11, B12 and folic acid into creatinine and adrenaline.
Methods In study have been used photocolorimetrical and immunohistochemical methods at patients with suppuration of large intestine. The study investigated the expression of main markers of cytotoxicity CD175S, CD40 in biopsy material, figures of interchange process of conjunctive tissue – metabolites of collagen proline and oxyproline in urine.
Results The research has shown that the patients with insolvency of large intestine anastomosis had significant increase of oxyproline presence in urine to 214,0+12,3 ml/d at norm 27,2+5,7 ml/d and increase of cytotoxicity markers CD175S, CD40 expression in 1,2 times as compared to control.
Conclusion(s) The alteration of collagen metabolites concentration, reliable increase of expression of cytotoxicity markers of hemopoietic cell-predecessors and receptors of FNO family could be used as prognosis criterions of insolvency of anastomosis for complications prophylaxis.

P2.71

Serous oligocystic adenoma of the pancreas

Tangour M.; Chelly I.; Azzouz H.; Daghfous A.; Mekni A.; Nfoussi H.; Adouni O.; Boujelbene N.; Juini M.; Haouet S.; Kchir N.; Zitouna M.
Rabta, Dar Chaabane el Fehri, Nabeul, Tunisia

Background Serous oligocystic adenoma of the pancreas is a rare, newly recognized neoplasm made of few, relatively large cysts, lined by uniform glycogen-rich cuboidal epithelial cells. It accounts for less than 1% for all exocrine pancreatic tumours. It occurs at the 6th decade with no sex predilection, commonly in the pancreatic head and body.
Methods We report a case of 56 year-old woman presented with 6 months history of right-sided abdominal pain.
Results Physical examination was unremarkable. Magnetic resonance imaging (MRI) revealed an oligocystic mass located in the pancreatic tail, adherent to the spleen and measuring about 7 cm in greatest dimension. The patient underwent a spleno-pancreatectomy. Grossly, the tumour was well defined, and disclosed macrocystic appearance, without central stellate scare. Microscopic examination showed that cystic cavities were lined by uniform, serous, cuboidal cells.
Conclusion(s) Diagnosis of the macrocystic variant of pancreatic serous cystadenoma is challenging for the clinician because it can be confused preoperatively with the mucinous counterpart which is characterized by a malignant potential and requires surgical excision. Extensive sampling of the surgical specimen is needed in order to distinguish this neoplasm from pseudocystic lesions.

P2.72

Spindle and giant cell type undifferentiated carcinoma of the common bile duct: report of two cases and review of the literature

Tsai C.
Dept. of Anatomical Pathology, Far Eastern Memorial Hospital, Pan-Chiao, Taipei, Taiwan

Background Undifferentiated carcinoma of spindle and giant cell type arising from extrahepatic bile duct is very rare. We report two cases of this type of carcinoma in the common bile duct.
Methods From the archive of the Department of Anatomical Pathology in Far Eastern Memorial Hospital between 1998 and 2008, 27 primary carcinomas of extrahepatic bile duct underwent surgical resection were retrieved. Reviewing the histopathological features, two cases fulfilled the diagnosis of undifferentiated carcinoma of spindle and giant cell type.
Results Both cases (57 and 43 years old respectively) were males presenting obstructive jaundice due to fungating masses over common bile duct. Both tumors were composed mainly of anaplastic spindle cells arranged in fascicles or solid sheets with frequent giant cells, mixed with small foci of ordinary carcinoma. Immunohistochemically, the sarcomatoid tumor cells of both cases were positive for cytokeratin, but negative for actin, S-100, CD34, and CD117. Case 1 had lymph node metastasis at the time of presentation and passed away 7 months later due to disseminated tumors. Case 2 was live and well 10 months after operation.
Conclusion(s) Searching the English literature, only 9 cases of spindle cell carcinoma of extrahepatic bile duct have been reported. All these cases, plus our additional two, were people of the Far East. Genetic or ethnic factor may play some role in the tumorigenesis of this peculiar type of tumor.

P2.73

Study of Wnt pathway and colorectal cancer using protein analysis

Martins Oyama Mascarenhas Fonsêca M.; Oliveira Petrolini L.; Kuwabara Sato Y.; Silva Maria E.; Elias Pessoa I.; Santos Maria Monteiro E.; Rossi Mauro B.; Coudry Almeida R.
Hospital AC Camargo, Sao Paulo, Brazil

Background Wnt signaling is integrally associated with colorectal carcinogenesis and is considered an early event. However the role of this pathway in tumor recurrence and patient outcome is poorly understood. The increased in Wnt ligands or mutation in APC or CTNNB1 genes has been shown to alter the expression of several downstream molecules. Aim: This study was designed to test the hypothesis that early alteration can dictate the fate of colorectal tumors. We performed a systematic evaluation of several proteins, such as, Wnt 2, 3 and 5, frizzled, dishevelled, beta-catenin, APC, Gsk3-B, Axin, Tcf 4, Lef 1, MITF, Cyclin D1, c-Myc, MMP7, COX-2, p120 and Kaiso.
Methods Tumours from 30 patients with colorectal cancer in stage II and III was analyzed using a semiquantitative immunohistochemistry and the results were compared with recurrence and patient outcome.
Results Patients expressing Tcf4 had a reduced overall survival when compared with other patients (p=0,019). No correlation with Wnt proteins and recurrence was observed in this study. MITF protein was negative in all colorectal tumours.
Conclusion(s) These results indicate that Tcf4 may constitute a marker of poor prognosis and could be used in the development of drugs that target specific types of Wnt induced tumors.

P2.74

The colorectal carcinomas and their immunophenotypes

Gurzu S.; Jung I.
University of Medicine and Pharmacy of Targu Mures, Targu Mures, Romania

Background Colorectal carcinomas (CRC) are intensly studied in the literature but the exact role of immunohistochemically (IHC) markers are not established yet. In many papers the expression of new markers was analysed but it is very difficult to know which of them have a prognostic value. In our paper we tried to clasify the CRC depending of their immunophenotype.
Methods We analysed the clinico-pathological features (age and sex of patients, histological grade, the pTNM staging) of 200 surgical specimens with colorectal carcinomas and we performed IHC reactions with the following antibodies, provided by LabVision: p53, bcl-2, c-erbB-2. We tried to establish the prognostic importance of these parameters depending by the following immunophenotypes: p53/bcl-2, p53/c-erbB-2 and bcl-2/c-erbB-2.
Results We observed that the cases with the immunophenotype p53+/bcl-2- presented lymph node metastases in 50% of cases and angiolymphatic invasion in more than 65% of cases. The CRC with the immunophenotype p53-/bcl-2+ were better differentiated and more than 60% were diagnosed without lymph node metastases or angiolymphatic invasion. We also proved that the c-erbB-2 was an independent prognostic factor in CRC and was not correlated with p53 or bcl-2 expression.
Conclusion(s) The CRC with the immunophenotype p53+/bcl-2- were correlated with that parameters which showed a worse prognosis. This immunophenotype, in correlation with the number of lymph node metastases, pTNM stage, the aspects of microsatellite instability and also the BRAF and k-RAS mutation remain the main prognostic and predictive factors in CRC.

P2.75

The microsatellite instability and its correlations in colorectal carcinomas

Jung I.; Gurzu S.; Szentirmay Z.; Mezei T.; Cimpean Maria A.; Raica M.
University of Medicine and Pharmacy of Targu-Mures, Romania, Targu-Mures, Romania

Background Many studies revealed that the colorectal carcinomas (CRC) with microsatellite instability (MSI) had a better prognosis compared with the MSS (microsatellite stable) cases. In our paper we tried to analyse the correlations of this parameter with other classical and modern prognostic factors.
Methods We analysed the clinico-pathological features (age and sex of patients, histological grade, the pTNM staging) of 200 surgical specimens with colorectal carcinomas and we performed IHC reactions with the following antibodies, provided by LabVision: p53, bcl-2, VEGF-A, VEGF-C. Using the Real Time PCR, we determined the MSS and MSI colorectal carcinomas.
Results We observed that, compared with the MSS colorectal carcinomas, the MSI cases were poorlier differentiated, presented lymph node metastases and positivity for p53 in a few number of cases. The angio- and lymphangio-immunophenotypes, determined with VEGF-A and VEGF-C, the angiolymphatic invasion and also the bcl-2 expression did not presented differences between MSS and MSI cases.
Conclusion(s) The MSI colorectal carcinomas seems to have a better prognosis than MSS cases but this parameter should be appreciate only in correlation with other classical and modern prognostic factors.

P2.76

A calcifying fibrous tumor of the liver

Wittersheim A.; Croce S.; Renard C.; Weingertner N.; Rosso E.; Casnedi S.
University Hospital of Strasbourg, Strasbourg, France

Background Calcifying fibrous tumor is a rare lesion. It occurs predominantly in subcutaneous and deep soft tissues but has also been described in the pleura and the peritoneum. Visceral localization is extremely uncommon. To date, only few cases were reported in the lung, stomach, gallbladder and adrenal gland.
Methods A 26-year-old woman presented with abdominal discomfort. US and RMN imaging showed a large solid mass with scattered calcifications involving the right liver, mimicking a fibrolamellar hepatocellular carcinoma.
Results The wedge resection of the liver weighed 300 g and was subtotally replaced by a well-circumscribed, homogeneous, firm, pale mass measuring 8.5 cm. The tumor was composed of a poorly cellular collagenous tissue with bland spindle cells, a mild lymphoplasmacytic inflammatory infiltrate and scattered dystrophic calcifications. The diagnosis was supported by the lack of IHC reactivity for keratin, SMA, ALK, S100, CD34, CD117. The Ki67 proliferative index was at 1%. Due to overlapping morphologic features, the differential diagnosis are solitary fibrous tumor, schwannoma and inflammatory myofibroblastic tumor suggesting for some authors that calcifying fibrous tumor may reflect a late sclerotic phase in the evolution of an inflammatory myofibroblastic tumor. Calcifying fibrous tumor is considered as a benign lesion. Although recurrence has been demonstrated, complete local excision appears to be adequate management.

Conclusion(s) To our knowledge, this is the first case report of calcifying fibrous tumor of the liver. It appeared as a solitary mass and simple wedge resection is the treatment of choice.

P2.77

A case of primary squamous cell carcinoma of the liver, producing G-CSF

Watanabe J.; Nakashima O.; Yano H.
Yame General Hospital, Yame, Fukuoka, Japan

Background Primary squamous cell carcinoma of the liver is extremely rare. We examined a case of primary liver squamous cell carcinoma producing granulocyte-colony stimulating factor (G-CSF).
Methods Case Report: The patient was 54-year-old female. Symptoms were persisting high fever, abdominal pain and anorexia. A mass was detected in the left lobe of the liver, which was low-echoic, low-density with slight contrast on enhanced CT, low-intensity in T1-weighted and high-intensity in T2-weighted MRI. WBC count was 14,000 and G-CSF level was 74 pg/ml. The patient underwent extended left hepatectomy.
Results The resected tumor was 8 X 6 X 4 cm, whitish, solid, and contained a small cavity. The tumor was moderate~poorly differentiated squamous cell carcinoma associated with partial keratinization, and contained small ductular elements without mucin secretion. Moderate infiltration of neutrophils was found in and around the tumor. Immunohistochemically, the tumor cells were Involucrin (+), AE1/AE3 (+), CK19 (+), CA19-9 (+), CEA (+), CK7 (–), CK8 (–), CD20 (–), hepatocyte-A (–), PIVKA-II (–), AFP (–), and positive for anti-G-CSF staining. Based on these findings, the tumor was diagnosed as squamous cell carcinoma originating from the liver. After surgery, high fever had gone and WBC count and serum G-CSF level returned to normal.
Conclusion(s) This tumor was most probably producing G-CSF. Our current case was thought to be the squamous cell carcinoma originating from liver stem cells.

P2.78

Clinical, pathological and molecular features of early onset

Pilozzi E.; Duranti E.; Ferri M.; Zardo G.; Ruco L.
II Facoltà di Medicina e Chirurgia, Università La Sapienza, Rome, Italy

Background Early onset colorectal carcinomas are suggestive of hereditary predisposition. They often occur in the context of Lynch syndrome, show microsatellite instability (MSI) and right colon localization. Series of early onset colorectal carcinoma MSI-, mainly localized on the left colon, have been reported. We selected 22 cases of early onset left-sited carcinoma and investigated clinical, pathological and molecular features.
Methods Fifteen sigmoid and 7 rectal carcinomas (≤ 50 years, age range: 27–50) were collected. Pathological (grading, stage, vascular invasion, intraepithelial tumor-infiltrating lymphocytes) and molecular (MSI and K-RAS mutation) features were evaluated. Cancer family history was available in 11/22 patients.
Results 18/22 (81%) carcinoma were well/moderately differentiated; 3 (13%) showed mucinous differentiation; 65% showed vascular invasion; 3/22 (13%) showed intraepithelial tumor-infiltrating lymphocytes; 20/22 (90%) were T3 or T4 at the diagnosis and 60% had lymph nodes metastasis. None of the 22 cases showed MSI; 8/19 (42%) showed K-RAS point mutation at codon 12, 6 of them (75%) were > 45 years old. 7/11 had a relative (> 50 years) with a malignant epithelial neoplasm. In 5/7 it was a first relative (2 colon, 1 stomach, 1 lung, 1 breast).
Conclusion(s) Our results suggest that early onset sigmoid and rectal carcinomas lack molecular evidence of DNA repair abnormalities. Most are high stage at the diagnosis. They do not show the typical histological features (mucinous differentiation and intraepithelial tumor-infiltrating lymphocytes) of Lynch syndrome carcinoma. K-RAS mutations turned out to be prevalent in patients >45.

P2.79

Colorectal adenosquamous and squamous cell carcinoma. Case reports

Staniceanu F.; Tebeica T.; Tudorica Catalina L.; Zurac S.A.; Micu V.G.; Tudose I.; Slavnea Mariana A.; Croitoru A.
Colentina University Hospital, Bucharest, Romania

Background Squamous cell carcinoma (SCC) and adenosquamous carcinoma (ASC) are rare aggressive subtypes of colorectal carcinoma with interesting issues concerning histogenesis, prognosis and appropriate management, the clinicopathologic behavior being mostly unknown.
Methods We analyzed all primary cases of colorectal SCC and ASC diagnosed in our department over the last 4 years. Histological features were reviewed and histochemical and immunohistochemical studies were performed in order to highlight specific characteristics of the tumours.
Results From a pathological database of 331 colorectal cancers, ten pacients were identified (2 males and 8 females), with a mean age of 62.5 (range, 32–82) years. We counted 1 case of pure squamous cell carcinoma and 9 cases of mixed adenosquamous carcinoma. The gross appearance of carcino-

mas varied within large limits but all of them showed the same rectosigmoidian location. Moreover, 3 patients presented with advanced stage disease – either regional lymph node or liver metastasis. Most of the cases had high grade of anaplasia, the cytonuclear pleomorphism and the proliferation indexes being higher in the squamous component than in pure adenocarcinomatous counterpart.

Conclusion(s) We report our experience with an increased incidence and exclusive rectosigmoidian location of ASC and SCC. Moreover, the overall histopathological appearance and the immunohistochemical phenotype of the analyzed cases sustain the hypothesis of squamous metaplasia of the glandular adenomatous epithelium with subsequent malignant transformation as possible mechanism of ASC and SCC histogenesis. High biological aggressiveness should draw attention over the importance of correct diagnosis of these rare colonic neoplasms.

P2.80

Combination of multiple primary carcinomas: breast adenocarcinoma, intestinal adenocarcinoma, urinary bladder transitional cell carcinoma and endometrial endometrioid adenocarcinoma

Kapranou A.; Kordelas A.; Sotiropoulou G.; Koutlis G.; Terzi M.; Petala M.; Sfiniadakis I.
Naval Hospital of Athens, Athens, Greece

Background We report a case of a woman with a history of breast carcinoma in whom intestinal adenocarcinoma, urinary bladder transitional cell carcinoma and endometrial endometrioid adenocarcinoma were diagnosed within one month period.

Methods A 58 years old woman with a history of breast cancer diagnosed and treated five years ago, underwent colonoskopy in order to investigate haematochezia. The histology of resected specimen taken from a large bowel mass was intestinal adenocarcinoma. A mass in the urinary bladder was revealed and specimen with cystoscopy was taken with the suspicion of metastasis from the intestinal adenocarcinoma. The histology showed urinary bladder transitional cell grade II carcinoma without muscle invasion. The patient underwent sigmoid recection and hysterectomy.

Results The histologic examination of sigmoid revealed a TNM Stage IIB intestinal adenorcinoma. The histologic examination of the uterus revealed a TNM Stage II endometrial endometrioid adenocarcinoma.

Conclusion(s) The incidence of multiple primary malignant neoplasms in the same patient increases with age and they are encountered more frequently nowadays than in the past, the phenomenon is still considered to be rare. The combination of the four different neoplasms (breast, sigmoid colon, bladder and endometrium) in one patient described above, to the best of our knowledge, has never been reported before.

P2.81

Composite endocrine tumor-adenocarcinoma of the stomach: a case report

Tzaida O.; Vogiatzis P.; Stanc-Giannakopoulos G.; Valavanis C.; Arapantoni-Dadioti P.
Metaxa, Piraeus, Greece

Background Composite tumors of the gastrointestinal tract are uncommon neoplasms characterized by an intimate admixture of glandular and endocrine components with a wide range of histological appearances.

Methods A 69 year old male presented with dyspepsia and epigastric pain. Gastric endoscopy revealed a protuberant, umbelicated lesion with central ulcer at the greater curvature of the gastric body. Laboratory investigation revealed significantly elevated serum chromogranin levels. The biopsy showed gastritis and a few aggregates of cells suggestive of endocrine differentiation. A partial gastrectomy was performed.

Results Grossly, the lesion measured 18x9 mm. Microscopically, a composite tumor localized at the mucosa and submucosa was revealed. The prevalent endocrine component was composed of uniform round to oval cells with slight nuclear atypia and low mitotic count (0–1 mitosis/10 hpf) arranged in organoid/solid nests. A strong and diffuse immunoreactivity with keratins, endocrine markers and gastrin was detected. The minor glandular component had the appearance of a well differentiated tubular adenocarcinoma with focal mucinous differentiation.

Conclusion(s) Based on the tumor dimensions and histology, the diagnosis was: composite, well differentiated endocrine tumor of uncertain malignant potential admixed with an early adenocarcinoma. The patient is free of disease at 23 months after surgery. Whether the long term prognosis of this tumor is different from that of conventional gastric adenocarcinoma remains to be determined, making mandatory the long term follow up of these patients.

P2.82

Composite malignant tumor of colon (adenocarcinoma + neuroendocrine carcinoma): a case report

Lazar E.; Lazureanu Codruta D.; Lazar D.; Baderca F.; Cojocaru S.
University of Medicine and Pharmacy "V. Babes", Timisoara, Timis, Romania

Background Even if they are rare, tumors with a conventional carcinoid and a glandular (adenoma or carcinoma) component, in both, "collision" or "composite"

patterns, can occur at any level of the gastro-intestinal tract.

Methods Tissue fragments from 58-year-old male with an ascending colon tumor were fixed in 4% buffered formalin, paraffin embedded and HE stain. Further immunohistochemical investigations were made with DAKO antibodies (CK, Chr A, Sy, CD20, CD30, CD45RO, S-100, Vim and HMB45), LSAB system and DAB visualization.

Results Histopathological appearance revealed a tumor composed of intermingled pseudoglands, some with mucinous secretion, with nests of cell with "salt and pepper" nuclei. 2 out of 15 examined regional lymph nodes, presented metastases. Immunohistochemistry showed reactions positive for CK adenocarcinoma - intense, carcinoid - weak, the latter being positive also for Sy, Chr and S-100; CD20 and CD45RO were positive in the reactive lymphocytes.

Conclusion(s) Considering the rarity of this lesion - a composite tumor (neuroendocrine carcinoma + adenocarcinoma) with metastases in the regional lymph nodes we think that the dual mechanisms involved in the oncogenesis (epithelial line and neuroendocrine) and the presence of regional metastases are factors of a poor prognosis.

P2.83

Correlations between the immunohistochemical expression of the cellular proliferation index (Ki-67) and the clinicopathological factors in gastric cancer

Lazar D.; Taban S.; Dema A.; Cornianu M.; Lazar E.; Goldis A.; Sporea I.
University of Medicine and Pharmacy "V. Babes", Timisoara, Romania

Background We assessed the immunohistochemical expression of the Ki-67 antigen in 61 patients with gastric cancer, the correlation with clinicopathological factors and the prognosis of the patients.

Methods We used the primary MIB1 antibody pre-diluted, using the LSAB technique, DAB visualisation. The quantification of the reaction was performed by appreciating the marking index Ki-67 (MI Ki-67). The tumor cells were considered Ki-67 positive in the presence of brown nuclear staining of granular or diffuse type. The tumor invasion front has shown the most numerous Ki-67 positive cells.

Results In the gastric carcinomas we remarked various Ki-67 scores. For a proper grouping of the results we classified gastric carcinomas into two categories: carcinomas with high MI Ki-67 (≥ 45%) and carcinomas with low MI Ki-67 (≤ 45%). We noticed an increased frequency of high MI Ki-67 carcinomas in males and also in the tumors developed at cardia level and those extended in the entire stomach in the moment of diagnosis ($p<0.001$). The results of our study do not reveal any correlation between the Lauren Classification of gastric carcinomas,the lymphovascular invasion,the depth of tumor invasion,the TNM stage and the Ki-67 score ($p>0.05$).

Conclusion(s) In our study,immunohistochemical assessment of the tumor proliferation does not represent a prognostic factor, but seems to be useful in identifying of a group of patients with aggressive tumors, needing adjuvant postoperatory chemotherapy.

P2.84

Enterobius vermicularis, an uncommon cause of acute appendicitis, a report of three cases

Coskunoglu E.; Bagci P.; Dokumcu Zafer U.; Erbarut I.
Rize Research and Training Hospital, Rize, Turkey

Background Enterobius vermicularis (EV) has a broad geographic range and is a common human parasite infecting about 10% of population in developed countries, located predominantly in the caecum and appendix. It is suggested that, EV infestation can present with symptoms resembling acute appendicitis, although it does not necessarily cause acute appendicitis.

Methods We present three cases of enterobiasis of appendix presented with clinical features of acute appendicitis, two of which are pathologically confirmed as acute appendicites and one diagnosed as reactive lymphoid hyperplasia.

Results First case is a 26 year-old male who is clinically diagnosed as acute appendicites. Pathological evaluation of the specimen revealed parasites with features compatible with EV in the lumen of the appendix, without evidence of acute neutrophilic inflammation. The second and the third cases are 12 and 11 year-old females who also are clinically diagnosed as acute appendicites. In both cases, the appendix lumen contained EV. Pathological analysis revealed acute neutrophilic inflammation in both specimens.

Conclusion(s) EV infestation may present with symptoms resembling acute appendicitis, although it does not necessarily cause acute inflammation. It is also not clear yet, whether the invading parasites actually cause the inflammation or are the parasites incidental findings where inflammation is already present.

P2.85

Expression of TLR4 and MUC5AC in H. pylori infected gastric epithelium

Kang M.; Hyun J.; Hwang M.; Sagong S.; Kim J.; Park J.; Lee S.; Lee S.
Inje University, College of Medicine, Busan, Republic of Korea

Background Helicobacter pylori (H. pylori) infection plays major role in development of gastritis, ulcer, and gastric malignancy. It alters mucin expression of gastric surface epithelial cells. Toll-like receptor 4 (TLR4) is a receptor for lipopolysaccharide (LPS) of gram negative gacteria and plays major role in immune and inflammatory response. The aim of this study is to investigate the correlation between the expression of TLR4, MUC5AC and H. pylori infection, histologic findings in chronic gastritis. And also we analyzed the correlation between TLR4 and MUC5AC expressions in H. Pylori-associated chronic gastritis.
Methods Immunohistochemical stains for TLR4 and MUC5AC were done in a total of 112 gastric fiberscopic biopsy samples which were taken from body or antrum of stomach. HE stained slides were reviewed for histologic grading of chronic inflammation, activity, intestinal metaplasia and H. pylori in gastritis based on Sydney system. H. pylori status was determined by immunohistochemistry.
Results TLR4 expression was positively correlated with severity of H. pylori infection ($p<0.01$) and activity ($p<0.01$) in chronic gastritis. MUC5AC expression was also positively correlated with severity of H. pylori infection ($p<0.05$). But there was no correlation between expressions of TLR4 and MUC5AC in gastritis.
Conclusion(s) H. pylori infection affects the expression of TLR4 and MUC5AC in gastric surface epithelium and TLR4 is considered a key regulator of H. pylori infection and active inflammation but not in MUC5AC expression of gastric epithelium.

P2.86

Extra–gastrointestinal stromal tumor of the pancreas: case report

Benyacoub-Abid L.; Trabelsi A.; Mtimet A.; Ben Mabrouk M.; Hammedi F.; Rammeh S.; Sriha B.
Farhat Hached, Sousse, Tunisia

Background Gastrointestinal (GI) stromal tumors are the most common kind of mesenchymal tumors that arise from the GI tract. These tumors tend to present with higher frequency in the stomach and small bowel. Furthermore, the extra-gastrointestinal stromal tumors (EGIST) tend to be more common in patients greater than 50 years of age.
Methods We report the case of a 52-year-old woman which presented with abdominal pain and epigastric mass. Preoperatively, computed tomography (CT) revealed a hypervascular mass, 11.0 cm in diameter, in the pancreatic head. The surgery confirmed large tumor of the head of the pancreas. A duodenopancreatectomy was performed and the tumor was radically removed.
Results Histologically, the tumor was composed of spindle and epithelioid components, and only a few mitotic features were seen. Immunohistochemically, most of the tumor cells were positive for c-kit (CD 117) and alpha-smooth muscle actin, but negative for CD34. This neoplasm was finally diagnosed as a malignant gastrointestinal stromal tumor (GIST) of the head of the pancreas.
Conclusion(s) Stromal tumors of an extra-gastrointestinal origin are rare. They are immunohistochemically similar to their GI tract counterparts. Primary pancreatic GI stromal tumors are very rare, with only 4 previous cases reported.

P2.87

Gastric ulcer disease

Zubritsky N.A.
Municipal Institution "Taldom Central Regional Hospital", Taldom, Moscow Region, Russian Federation

Background The purpose of the present study was to determine the prevalence of gastric ulcer disease (GUD) on the post-mortem material obtained at the Municipal Institution "Taldom Central Regional Hospital" over a 15-year period from 1993 to 2007.
Methods Comprehensive analysis of 830 post-mortem examinations.
Results We revealed 21 cases (15 men and 6 women, mean age 56 years) of GUD that had been the primary cause of death. All ulcers were chronic, and in an exacerbation phase, which fact had been confirmed histologically, with the most common localization being the lesser curvature of the stomach (15 cases) and the largest size of the ulcer encountered amounting to 11x8.5 cm. In three cases, GUD had taken course on the background of chronic alcohol intoxication, and in one case - on the backgroundof diabetes mellitus. The immediate causes of death appeared to have been as follows: posthaemorrhagic anaemia (17 cases), peritonitis (3 cases), and pulmonary thromboembolism accompanied by peritonitis (1 case).
Conclusion(s) GUD as a primary cause of death amounted to 2.53% amongst 830 post-mortem examinations of adults at our general somatic hospital over 15 years. The most frequently encountered localization of ulcers was the lesser curvature of the stomach (71%). Acute posthaemorrhagic anaemia secondary to profuse haemorrhage from an arrosion-stricken blood vessel in the ulcer's bottom was the most frequent immediate cause of death (81%).

P2.88

Granular cell tumor of the cecum with extensive hyalinization and calcification

Lim S.; Hong R.
Chosun University, Gwangju, Republic of Korea

Background Granular cell tumor (GCT) is a benign tumor, which is rare in the gastrointestinal tract. Initially attributed to neural origin through immunohistochemistry, there has been controversy with increasing reports of GCTs of non-neural origin. Furthermore, GCTs could be regarded as lesions that reflect a local metabolic or reactive change rather than a true neoplasm.
Methods We experienced a case of GCT arising in the cecum of 55-year-old man, which was removed by laparoscopic resection. He had a 2-month history of abdominal pain and diarrhea. Other than this tumor, endoscopic examination revealed a 5 mm-sized polyp in the descending colon and multiple tiny polyps in the sigmoid colon and rectum.
Results Gross examination revealed that the cecal tumor was 1.5x1.0x0.7 cm-sized, feeled as hard consistency, and on cut sections are mixed with yellowish and whitish-colored portions. The tumor was located at the mucosa to the subserosa, and composed of plump histiocyte-like tumor cells with abundant granular eosinophilic cytoplasm which were immunoreactive for S-100 protein, and characteristically, accompanied by extensive hyalinization and focal dystrophic calcification.
Conclusion(s) Accompanying extensive hyalinization with focal dystrophic calcification suggests that GCT might be a non-neoplastic reactive lesion.

P2.89
Histological and phenotypic heterogeneities of a choriocarcinoma of the sigmoid colon

Bamba M.; Takemura S.; Nagata H.; Fukuda K.; Masuyama M.; Shigematsu T.; Kobayashi T.; Kushima R.; Sugihara H.
Department of Pathology, Saiseikai Shiga Hospital, Imperial Gift Foundation Inc., Ritto, Shiga Prefecture, Japan

Background In the gastrointestinal tract, choriocarcinomas have been reported to be characterized by a biphasic tumor growth with choriocarcinomatous and adenocarcinomatous components (CC and AC). However, there are only a few reports that analyze the relationship between the CC and AC. We analyze this point in a case of choriocarcinoma of the sigmoid colon with histological and phenotypic heterogeneities.
Methods A 63-year-old female was diagnosed as having a sigmoid colon cancer with multiple hepatic and pulmonary metastases. She underwent sigmoidectomy. There was no tumor in the pelvic organs. The patient died 1 month after diagnosis and a necropsy of hepatic metastases was undergone. Sections of colonic tumor, which consisted largely of CC and partly of AC, and hepatic metastases, which included only CC, were immunostained for hCG, CK7, CK20, MUC2, CD10, CDX2 and p53. Moreover, CC was analyzed for TP53 mutations.
Results CC was hCG(+), CK7(+), CK20(-), MUC2(-), CD10(+), CDX2(-/+) and p53-overexpression (diffusely+). In contrast, AC was hCG(-), CK7(-), CK20(+), MUC2(+), CD10(-), CDX2(+) and p53-overexpression (regionally+). The density of positive cells was similar between CC and a region of AC. In CC, a deletion in exon 5 of TP53 was found.
Conclusion(s) Because p53-overexpression, probably due to a deletion of TP53 in CC, was commonly found in CC and a region of AC, both components of the tumor may possibly be of a common origin despite distinct phenotypic differences. Therefore, CC could derive through transdifferentiation from a subclone of AC.

P2.90
Idiopathic hepatic fibrosis in the newborn

Gurzu S.; Jung I.; Szentirmay Z.; Lorinczi G.; Shaff Z.
University of Medicine and Pharmacy of Targu Mures, Targu-Mures, Romania

Background It is very difficult to establish the hepatic fibrosis etiology in the newborn because the criteria of differentiating among the known etiology, the genetic modifications and the idiopathic disease are not clearly established.
Methods Our paper is a case presentation.
Results Case report: We present the case of a twelve days old girl, born in due time, by caesarian section because of pelvin presentation. The 28 years old mother, health. The pregnancy evolution was normal. Birth weight: 2900 g. Apgar score: 6 after 1 min, 7 after 5 min. She presented a respiratory distress syndrome, cutaneous spots, hepatosplenomegaly and jaundice. The hemogram revealed: leucocitosis, anemia, thrombocitopenia, hyperbilirubinemia. Her general condition became worse and death was installed. Necropsy revealed: hepatic fibrosis with cholestasis and jaundice, bilateral confluent bronchopneumonia with Aspergillus granuloma in lungs. The immunohistochemistry (IHC) revealed biliary pseudocanaliculi in liver, positive for Cytokeratin 7. We also observe the positive immunostain for α-1-antitrypsin in liver and lung. Based on the data of the literature, on the clinical, macroscopycal, microscopycal and IHC features, we excluded the following diagnosis: materno-fetal infection (TORCH syndrome), billiary atresia with cholestatic jaundice, congenital hepatitis, primary sclerosing cholangitis, cystic fibrosis, progressive familial intrahepatic cholestasis, α-1-antitrypsin deficiency and Wilson syndrome.
Conclusion(s) The idiopathic hepatic fibrosis in the new born is very rare and it is necessary to exclude all the other possibility for establish this diagnose.

P2.91

Inflammatory fibroid polyp of the ileum complicated with intussusception: a case report

Kostov Sima M.; Dragovic Bosko S.; Petkovic Sekula A.; Mijovic Zarko Z.; Mihailovic Slavoljub D.; Stojanovic Petko M.

Military Hospital of Nis, Department of Pathology, Nis, Serbia and Montenegro

Background Inflammatory fibroid polyps (IFP) are an extremely rare benign, non-neoplastic lesions of uncertain origin, that may occur in many different locations in the gastrointestinal tract, especially the stomach and small bowel. These lesions can cause abdominal pain, gastrointestinal bleeding, intestinal obstruction or intussusception. We present a case of an adult male patient with ileal intussusception due to an inflammatory fibroid polyp. Diagnosis was made preoperatively with abdominal ultrasound and computerized tomography.

Methods From formalin-fixed, paraffin-embedded tissues were sectioned at 5μm thick sections and were stained with haematoxylin and eosin (HE), Alcian Blue - Periodic Acid Schiff (AB-PAS) and Masson Trichrome.

Results Macroscopically, resected ileal segment was 27x5x4,5 cm in diameter. While opening, a solid, a sessile a polypoid lesion 4,5x4,0x3.5 cm in diameter projecting into the lumen was found. Its surface was covered with ulcerated mucosa. Microscopically, the surface of the polypoid lesion was covered by ulcerated mucosa characterized by inflammatory exudate and granulation tissue. It is composed of a fibrous and edematous stroma containing many variable-sized blood vessels and a diffuse inflammatory infiltrate, including eosinophils, plasma cells, lymphocytes, macrophages and mast cells. Bundles of smooth muscle cells separated by connective tissue stroma were also noted. Trichrome stain highlighted the collagenous fibrous tissue background.

Conclusion(s) In case of an intestinal inflammatory fibroid polyp causing ileal intussusception, the treatment is surgical. Since they can mimic malignant stromal lesions, the differential diagnosis must be done very carefully.

P2.92

KRAS mutation as a new target in colorectal carcinoma. A pilot study

Hristova Lubomirova S.; Bichev Naydenov S.; Mitkova Velichkova A.; Vlahova I.A.; Dikov Iliichev T.; Kaneva Petrova R.; Kremensky Marinov I.

Medical University of Sofia, Sofia, Bulgaria

Background Several years ago immunohistochemical identification of EGFR membrane oncoproteine was a brief hope for target therapy of colorectal carcinoma (CRC). Nowadays mutations in the KRAS gene predict a negative response of anti-EGFR target therapies. The aim of this study was to introduce KRAS molecular genetic testing on paraffin embedded surgical biopsies of CRC patients and compare the results with pathomorphological data.

Methods Sixteen patients with CRC were examined: 12 man and 4 women. All of the cases were staged according to their histological differentiation and pTNM system. Examined tissue areas were tested by pathologist, assessed adequate for tumor density and optimal carcinomas' invasive regions. DNA was extracted by NucleoSpin kit. KRAS mutation screening was performed by TheraScreen Kit, allowing detection of 7 common somatic mutations in codons 12 and 13 of the gene. The test is based on ARMS allele specific PCR technology which triggers a real time PCR reaction leading to a fluorescent output via Scorpions technology.

Results Histological grading of the examined cases ranged G2 – G3, with pT status mainly: pT2 – pT3. In 5 cases a hepar metastases were histologicaly verified. We have detected KRAS mutations in five (31%) Bulgarian CRC patients. Three of the patients carried mutations 12 Ala, 12 Ser and 12 Val, respectively, whereas 12 Asp was found in two patients.

Conclusion(s) Our results were in agreement with previous studies demonstrating that KRAS was mutated in 30 -50% of the CRC cases.

P2.93

Liver histology after preoperative chemotherapy and radiofrequency-assisted liver resection of hepatic colorectal metastases

Micev Tomislav M.; Cosic Micev Luka M.; Bulajic P.; Milicevic M.

Clinical Centre of Serbia, Belgrade, Serbia and Montenegro

Background Neoadjuvant systemic chemotherapy is frequently used prior to hepatic resection of colorectal cancer liver metastases (CRCLM) and provokes histologic alterations of liver tissue not involved by tumor (NTLT). The aim of this study was to assess histologic alterations in the non-tumor bearing liver in the resected specimens after liver resection using the novel technique of radiofrequency-assisted liver resection (RALR), which is thought to be transfusion-free, easy and safe.

Methods Detailed histological examination of NTLT from 59 specimens of transfusion-free RALR made for CRCLM in last three years was compared to histological changes in NTLT from 38 specimens of standard liver resections made

for CRCLM which all needed blood transfusion after signficant blood loss (> 1 unit of PRBC transfusion).
Results The main histologic alterations in both examined groups of NTLT include portal and/or porto-portal fibrosis and moderate macrovacuolar steatosis (30–60% of hepatocytes) with similar distribution between groups. However, there were significant differencies in vascular abnormalities, particularly in the presence of hemorrhagic centrilobular necrosis (10,2% in RALR vs 31,5% in non-RALR group) and peliosis (15,2% in RALR vs 36,8% in non-RALR group), but were not significant in the presence of sinusoidal dilataton and congestion as well as surgical necrosis.
Conclusion(s) Severe vascular abnormalities such as hemorrhagic centrilobular necrosis and peliosis are less frequent in cases of RALR of CRCLM and they might be associated with better clinical outcome in these patients.

P2.94
Mucinous adenocarcinoma versus signet ring cell carcinoma of the stomach and largebowel

Kepil N.; Goksel S.; Yagci T.; Dirican A.; Cetin Erdamar S.; Dogusoy G.
Istanbul University Cerrahpasa Medical Faculty, Istanbul, Turkey

Background The stomach and largebowel reside in same system and their carcinoma classification is very similar. However, they have significant differences in embryogenetic and functional characteristics. These two regions also show differences in carcinogenesis.Besides studies investigating differences between mucinous carcinoma and signet ringcell carcinoma in these locations in terms of morphological, behavioural, molecular, genetic features are limited.
Methods 57 colorectal, 21 gastric MAC and 3 colorectal, 54 gastric SRCC cases were included in the study.TMA blocks were formed with tumor tissues of all cases.MLH-1, MSH-2 and p53 protein expressions were investigated immunohistochemically.BRAF mutation was detected by PCR.The associations among clinicopathological, immunohistochemical parameters and presence of BRAF mutation were evaluated.
Results Colorectal SRCCs were extremely rare(0.37%) in all of colorectal carcinoma in same period. Gastric SRCCs (70%) were significantly frequent than gastric MAC ($p<$ 0.001) and colorectal MACs (95%) were significantly frequent than gastric MACs ($p<0.001$). Gastric MACs were more aggressive compared to gastric SRCCs and colorectal MACs regarding invasion depth, lymph node metastasis, lymphovascular invasion frequency.BRAF mutation was detected in 42.9% of gastric MACs, 35.1% of gastric SRCCs, and 38.6% of colorectal MACs.Co-missing of MLH-1 and MSH-2 was 14.2% at gastric MACs, 3.8% at gastric SRCCs and 5.5% at colorectal MACs.p53 expression was 28,5% at gastric MACs and 38.8% at gastric SRCCs.p53 expression was significantly more frequent at colorectal MACs compared to gastric MACs ($p=0.017$).
Conclusion(s) We observed a lot of similar findings for gastric and colorectal MACs were exhibiting opposite frequency.Colorectal MACs were rather exhibiting similar characteristics with gastric SRCCs.

P2.95
Mucoepidermoid carcinoma of duodenum: an extremely rare neoplasm

Sakonlaya D.; Chonprasertsook S.; Tomtitchong P.
Division of Pathology, Faculty of Medicine, Thammasat University (Rangsit Campus), Amphur Khlongluang, Pathumthani, Thailand

Background Primary small-bowel malignancies are rare, accounting for 2.1% of all gastrointestinal cancers. Most common histological types are carcinoid, adenocarcinoma, lymphoma, and sarcoma. Mucoepidermoid carcinoma (MEC) is a malignancy composed of epidermoid, intermediate, glandular, and mucus cells in varying proportions. Although it is the most common salivary gland cancer, MEC rarely occurs in other organs. We herein reported a case of MEC on unusual site, duodenum.
Methods Case report of duodenal MEC with endoscopic, radiographic, and histological studies.
Results A 43 year-old Thai female with history of alcohol abuse had suffered from progressive postprandial abdominal discomfort, nausea and vomiting for one year with significant weight loss. Physical examination revealed mildly tender epigastrium without palpable mass. Initially diagnosed as dyspepsia and treated as outpatient for a month with no improvement, patient was finally admitted to hospital due to severe electrolyte imbalance and oliguria associated with severe vomiting. Clinically stable after fluid resuscitation, esophagogastroduodenoscopy was performed and revealed whitish plaques at duodenum. Biopsy showed intermediate-grade MEC. Subsequent CT scan revealed diffusely thickened wall of 2nd-3 rd part of duodenum causing partial gastric outlet obstruction. Exploratory laparotomy demonstrated advanced tumor involving 2nd-4th part of duodenum, proximal jejunum with extension to small-bowel mesentery and transverse mesocolon and carcinomatosis peritonei. By gastrojejunostomy, symptoms of obstruction were relieved. At time of this report, patient was waiting for chemotherapy and long-term follow-up data are still required.

Conclusion(s) A case of duodenal MEC presenting with small-bowel obstruction was reported.

P2.96

Neoplastic cells containing paneth granule-like granules in early gastric cancer. a distinct morphological variant of gastric-type well-differentiated adenocarcinoma of the stomach

Haraoka S.; Iwashita A.; Iwashita I.
Department of Pathology, Chikushi Hospital, Fukuoka University, Chikushino-Shi, Japan

Background The pyloric cells having intracytoplasmic eosinophilic granules are sometimes observed in the gastric antral glands. These granules contain lysozyme. We report three cases of early gastric cancer that are histologically characterized by well-differentiated adenocarcinoma composed predominantly of neoplastic cells containing Paneth granule-like eosinophilic granules.
Methods Case reports: Three patients are 66-, 73-, and 69-year-old men. Endoscopic examination revealed a shallow depressed lesion (2 cm in diameter) in one case and a superficial elevated lesion (1 cm in diameter) in two cases. Distal gastrectomy or endoscopic submucosal dissection was performed.
Results Histological examination showed a well-differentiated tubular adenocarcinoma invading into the submucosal layer in all cases. The majority of tumor cells had distinct coarse eosinophilic granules in the plump cytoplasm. Immunohistochemically, tumor cells with the eosinophilic granules were positive for lysozyme and MUC-6, and tumor cells in the superficial portion were positive for MUC-5 AC.
Conclusion(s) The characteristic histological features of these tumors were as follows: a) well-differentiated adenocarcinoma of gastric mucinous phenotype showing a double layered-structure comprising a upper portion of foveolar cell differentiation and a lower portion of pyloric cell differentiation, and b) tumor cells containing Paneth granule-like eosinophilic granules. To our knowledge, there are only a few case reports of advanced gastric cancer with neoplastic Paneth cells. These cases are extremely rare and regarded as a distinct morphological variant of gastric (pyloric gland)-type well-differentiated adenocarcinoma of the stomach.

P2.97

Oesophageal cancer

Zubritsky N.A.
Municipal Institution "Taldom Central Regional Hospital", Taldom, Moscow Region, Russian Federation

Background The present study was undertaken to identify the incidence rate of oesophageal cancer (OC) on the post-mortem material obtained at the "Taldom Central Regional Hospital" over the period from 1993 to 2007.
Methods Comprehensive analysis of 830 post-mortem examinations.
Results We revealed four cases (all being men averagely aged 60 years) of advanced and then considered inoperable ulcerated OC (with the tumours localizing in the middle third of the oesophagus) which turned out to have been the primary cause of death. Histology revealed a keratinizing type of squamous cell carcinoma with invasion of all oesophageal membranes in all the cases; with invasion of the pericardium and that of the wall of the left main bronchus - 1 case each. The immediate causes of death were as follows: bilateral abscessing pneumonia in 2 cases, sepsis and cachexia - 1 case each. Mention must be made that in two cases discrepancies were revealed between the clinical and pathologic diagnoses, pertaining to group III, i.e., by a complication of the prior disease (clinically unrecognized pneumonia and sepsis, referred to herein above).
Conclusion(s) OC as a primary cause of death appeared to have accounted for 0.48% amongst a total of 830 post-mortem examinations od adults at our general somatic hospital over 15 years. Making an early diagnosis of OC requires systematic and regular oncological screening of the population living in the Taldom Region of the Moscow District with appropriately engaging an endoscopic method of examination.

P2.98

Primary adenocarcinoma of gallbladder with components of invasive micropapillary morphology: report of two cases

Endo M.; Chiba R.; Iwama N.
Sendai Kousei Hospital, Sendai, Miyagi, Japan

Background Carcinoma with invasive micropapillary (IMP) morphology has been known as a distinctive variant in several organs, because of not only its unique histological character but its highly malignant potential. Here two cases of primary adenocarcinoma of gallbladder with IMP morphology were reported.
Methods Case one: 73 y.o. female. Cholecystectomy and lymphadenectomy was performed for a gallbladder tumor. A nodular tumor was seen in fundus of the gallbladder, 18 mm in diameter. Histopathologically, it was adenocarcinoma invaded perimuscular connective tissue (pT2) with a metastasis to regional lymph node (pN1). Case two: 71 y.o. male. Extended right lobectomy of liver and lymphadenectomy was performed for a tumor of gallbladder. Histopathologically, the tumor was adenocarcinoma

originated from the gallbladder and invaded into the liver(pT4) with metastases to regional lymph node (pN1). Immunohistostains for EMR, MUC1, D2-40 and podplanin were performed for examining the IMP characters.

Results Both tumor had large components of IMP morphology. The lesions had small tight clusters of carcinoma cells floating in clear spaces. Apical membrane expression of EMA and MUC1 immunostains confirmed the clusters had reversed polarization (so-called "inside-out" pattern). The reversed polarization indicated IMP pattern. D2-40 and podplanin immunostains also proved the spaces weren't small lymphatic channels.

Conclusion(s) Both of the tumors had lymph node metastases. Although case one in particular was pT2, it already had lymph node metastasis. Thus, carcinoma with IMP morphology had aggressive behavior, and it should be recognized the rare but important variant could also arise from gallbladder.

P2.99

Primary liver cancer

Zubritsky N.A.
Municipal Institution "Taldom Central Regional Hospital", Taldom, Moscow Region, Russian Federation

Background The work was aimed at determining the incidence of primary liver cancer (PLC) based on post-mortem material obtained at the "Taldom Central Regional Hospital" between 1988 and 2007.

Methods Comprehensive analysis of 1,235 post-mortem examinations.

Results We revealed 9 advanced and inoperable cases (6 men and 3 women, averagely aged 71) of PLC that proved to have been the primary cause of death. In all the nine cases, tumours had grown multicentrically; in 3 cases, PLC had developed on the background of progressing small-nodular hepatocirrhosis. Amongst the immediate causes of death were the following: more frequently encountered was acute posthaemorrhagic anaemia, having developed secondary to breakthrough haemorrhage into the abdominal cavity from the disintegrating hepatic tumorous nodes (5 cases), followed by hepatic and renal insufficiency (2 cases), pneumonia in the presence of hepatargy, and pulmonary thromboembolism – 1 case each. In five cases, discrepancies were revealed between the clinical and pathological diagnosis, pertaining to group II, i.e., by the underlying disease, belonging to category 2 (i.e., proper diagnosis would not necessarily have influenced the outcome of disease).

Conclusion(s) PLC as a primary cause of death amounted to 0.73% of the 1,235 post-mortem examinations of adults at our general somatic hospital over a 20-year period. To detect PLC at an early stage requires systematic and regular oncological screening amongst the population of the Taldom Region of the Moscow District to be carried out involving present-day methods of examination.

P2.100

Primary squamous cell carcinoma of the stomach: a case report

Choi K.; Shin D.; Sol M.; Lee J.
Pusan National University Yangsan Hospital, Yangsan-Si, Gyeongnam, Republic of Korea

Background Pure squamous cell carcinomas (SCC) develop rarely in the stomach. Pathogenesis remains obscure and controversial. To date, fewer than 100 cases of primary SCC of the stomach have been reported. A generally poor prognosis has been reported in the literature.

Methods We report a case of SCC of the stomach in a 61-year-old male with complaint of weight loss for several months. Total gastrectomy was performed.

Results There was a 7.0x6.7x4.5 cm tumor in the cardia with an ulcer on its top. On histological examination, a moderately differentiated squamous cell carcinoma was seen. In all sections, there was neither adenocarcinoma nor squamous dysplasia. Tumor cells extended to serosa and perigastric regional lymph node was also involved. To clarify the role of human papillomvarus (HPV) and Epstein-Barr virus (EBV) infection in the carcinogenesis of SCC arising in the stomach, we used DNA chip microarray for HPV infection and in situ hybridization for EBV infection. We found no evidence of HPV and EBV infection in our case. Postoperative CT scan one month later showed tumor recurrence and dissemination of the tumor to jejunum and pancreas. He is in the course of low dose FP chemotherapy.

Conclusion(s) Primary SCC is extremely rare in the stomach. They resemble squamous cell carcinomas arising elsewhere in the body. There was no evidence of relationship between HPV or EBV infection and carcinogenesis in our case.

P2.101

Prognostic significance of p53 expression in gastric carcinomas

Lazar E.; Lazar D.; Dema A.; Taban S.; Cornianu M.; Lazureanu Codruta D.; Muresan A.; Costi S.; Faur A.
University of Medicine and Pharmacy "V. Babes", Timisoara, Timis, Romania

Background In the case of gastric cancer, the role of p53 protein accumulation as prognostic factor is controversy. Various results are due to the different methods of study

regarding patients` selection, immunohistochemical techniques used and the quantifying systems for immunoreactions.
Methods We studied the p53 expression in 61 patients with gastric carcinomas and the correlation with clinicopathological factors (gender, age, location, macroscopic and histological type, degree of tumor differentiation and TNM stage) and patients` survival. We used the monoclonal antibody DO7 with EnVision technique and DAB visualization.
Results p53 was positive in 25 gastric cancers (41%) - 41,9% cases in men and 38,9% women. We found positive p53 in all the carcinomas developed in the upper third of the stomach (100%), in 53,3% of the corporeal tumors, 50% of the pangastric tumors; we noticed a significantly increased immunoreaction of p53 for the intestinal type carcinomas. p53 positive stainings were more frequently encountered in moderate/poor differentiated carcinomas and those associated with lymphovascular invasion; according to pT and pN stage, we remarked a significantly increase of the number of p53 positive cases (p=0.02291 and p = 0.038264). Five years survival rate for patients with p53 positive carcinomas was significantly lower in comparison to the patients p53 negative (8% vs. 22,2%, p = 0.0326).
Conclusion(s) Immunohistochemical evaluation of p53 protein represents an important prognostic factor, allowing the selection of a group of patients with an aggressive therapeutic indication, such as extensive lymphadenectomy and adjuvant chemotherapy.

P2.102

Successful treatment of poorly-differentiated endocrine rectal carcinoma. A case report

Gajanin Bosko R.; Kecman G.; Gojkovic Z.; Babic M.; Amidzic L.
Pathology Department, Clinical Center of Banja Luka, Banja Luka, Republika Srpska, Bosnia and Herzegovina

Background Poorly-differentiated endocrine carcinoma (PDEC) is very rare. Colorectal PDEC is a highly malignant tumor and is like neuroendocrine lung carcinoma in behavior, morphological, histochemical and immunochemical characteristics.
Methods Case report: A 47-year old man had PDEC (small cell variant) in rectal ampulla in June 2004. His first symptom was blood in the stool. On CT scan, an irregular tumor mass has been verified. During colonoscopy, the mass was biopted, and histologically confirmed as poorly-diferentiated large intestine carcinoma. Resection of sigmoid colon and rectum followed the diagnostics. In histological report, tissue of the tumor located in rectum was verified.
Results Morphologically, tissue of the tumor was composed of solid aggregation of small cells. Positive immunoreactivity of tumor cells has been noticed for the following antibodies: chromogranin A, Synaptophysin, CK (AE1/AE3), EMA, CEA and Ki 67 (30 %). Negative for NSE and TTF1 antibodies. In definitive histological report, diagnosis of PDEC was established in pT3N2M0 stage. Patient received adjuvant i.v. chemotherapy (Cisplatin 100 mg/m2/per day x 3 days, and etoposid 100 mg/ m2/ per day on days 2 and 3). After the treatment, the patient has been regularly monitored. At the moment (April 2009), he is in a good general condition, without recidivation of the disease and deposits in other organs.
Conclusion(s) It is necessary to differentiate PDEC from other types of neoplasms. Our case report shows the efficiancy of combination of surgical treatment and chemotherapy in treatment of PDEC of the large intestine without distant metastases.

P2.103

Synchronous adenocarcinoma and mucosa-associated lymphoid tissue (MALT) lymphoma in a single stomach

Hammedi F.; Rammeh S.; Beizig N.; Trabelsi A.; Abid Ben-Yacoub L.; Jomaa W.; Ben Abdelkader A.; Mokni M.; Sriha B.
Sousse, Tunisia

Background Gastric adenocarcinoma is one of the most common malignancies, whereas primary gastric lymphoma is relatively uncommon, occurring in only 1–7% of all malignant neoplasms of the stomach. The occurrence of both malignant gastric lymphoma and adenocarcinoma in the same patient is very rare. Since the first case reported by Rabinovitch et al. about 60 cases of synchronous occurrence of gastric adenocarcinoma and lymphoma have been published in English literature. Here, we report a single case of a gastric adenocarcinoma with a synchronously gastric low-grade MALT lymphoma.
Methods We report a 50-year-old man who was initially diagnosed to have gastric MALT lymphoma by a gastric biopsy. Imaging studies revealed diffuse thickening of the stomach extending to the pancreas and the spleen. There was also multiple regional lymph nodes enlargement. A total gastrectomy with caudal pancreatectomy and splenectomy were performed.
Results Pathological findings revealed a gastric low-grade MALT lymphoma collided with gastric adenocarcinoma. The regional lymph nodes were infiltrated by the MALT lymphoma. The pancreas and the spleen were infiltrated by the adenocarcinoma. Synchronous gastric adenocarcinoma with primary gastric low-grade MALT lymphoma was made.
Conclusion(s) Gastric MALT lymphoma patients should be carefully examined by endoscopy, and any suspicious area must be biopsied considering the possibility of coexisting adenocarcinoma. The prognosis of patients with double primary gastric lymphoma and adenocarcinoma has yet to

be clarified due to the lack of any long term follow-up observations.

P2.104

Tactile-like corpuscles in gastric mucosa. A case report

Moysidis I.; Xirou P.; Koumbanaki M.; Vladika N.; Traiannidis D.; Patakiouta F.
"Theageneion" Cancer Hospital of Thessaloniki, Thessaloniki, Neoi Epivates, Greece

Background Tactile corpuscle-like structures, also known as tactoid bodies or Wagner-Meissner-like corpuscles, are neurogenic lamellated formations composed predominantly of Schwann cells, perineural cells or both. They are usually encountered in certain types of nerve sheath tumours and intradermal nevi.
Methods A 41 year-old male, complaining of dysphagia, was endoscopically investigated in our hospital. Two biopsies from the gastro-oesophageal junction were taken and sent for histopathologic evaluation.
Results Light microscopic examination of routine H-E sections revealed the presence of round to oval tactile corpuscle-like structures in the lamina propria of the gastric mucosa. These corpuscles were consisted of elongated slender cells with eosinophilic cytoplasm and pale nucleus, which were immunohistochemically strongly positive for S-100 protein.
Conclusion(s) Only two cases of this rare phenomenon have been described in the literature. In the first case, these structures were found in the normal gastric mucosa of an oesophagogastrectomy performed for gastroesophageal adenocarcinoma, while in the other they were found in the benign intestinal mucosa of a colectomy done for colonic adenocarcinoma. The morphological and immunohistochemical characteristics of these structures suggest that they are similar to tactile corpuscle-like structures described in peripheral nerve sheath tumours or dermal nevi and are of schwannian origin. Whether these structures represent embryonic remnants of sensory nerve system in the viscera or could be the potential source of neurogenic tumours in the lamina propria of gastric mucosa need to be further investigated. In any case, they should not be misinterpreted as neurogenic lesions in small biopsies.

P2.105

The presence of Helicobacter pylori infection in children with giardiasis

Monajemzadeh M.; Haghi Ashtiani M.; Sahams S.; Mahjar Ali A.; Najafi Sani M.
Tehran University of Medical Sciences, Tehran, Islamic Republic of Iran

Background Helicobacter pylori is one of the most important factors in the pathogenesis of upper gastroduodenal diseases. H. pylori is thought to be transmitted by several mechanisms involving the fecal-oral pathway and the isolation of H. pylori from feces and the consumption of uncooked vegetables contaminated by raw sewage in the water supply have been suggested to be key factors in the this transmission. Giardiasis is also a common cause of recurrent abdominal pain. Few reports are present that mentioned the predisposition effects of giardiasis and H. pylori infections to each other especially in children, thus, as an attempt to investigate the association of Helicobacter pylori infection in children infected with Giardia lamblia was done.
Methods We performed a case-control study in children with and without giardiasis in Tehran, Iran. Helicobacter pylori and giardia infection were identified by antigen detection test and parasitological evaluation of stool samples, respectively.
Results The frequency of Helicobacter pylori infection in case group (subjects with giardiasis) was greater than that in control group (subjects without giardiasis). The only variable remaining independently associated with Helicabacter pylori infection was the presence of Giardia lamblia in feces (OR=4.5, CI=1.4–13.7).
Conclusion(s) We conclude that H. pylori infection was significantly associated with giardiasis in children. The relationship observed between G. lamblia and H. pylori infection may have several reasons. Further studies to investigate this relationship are needed.

P2.106

The significance of tumor paranchym types in the gastric and colorectal mucinous and signet ring cell carcinoma

Goksel S.; Kepil N.; Yagci T.; Dirican A.; Erdamar Cetin S.; Dogusoy G.
Istanbul University, Pathology Department of Cerrahpasa Medical Scool, Istanbul, Turkey

Background Signet ring cell carcinoma(SRCC) and mucinous adenocarcinoma(MAC) are distinct subtypes of gastric and colorectal adenocarcinoma. However, MAC may contain signet ring cells(SRC) and vice-versa SRCC may contain extracellular mucin pool(ECMP). The aim of this study is to investigate the meaning of the percentages of the ECMP and SRC in these tumor.
Methods The study groups consisted of 54 gastric SRCC, 21 gastric MAC, 57 colorectal MAC and 3 colorectal SRCC cases. We visually estimated the amounts of ECMP, SRC, and prismatic cell(PC) components in the tumors. The cases were subgrouped with respect to the percentages of the ECMP, and according to the SRC /PC ratios. In all cases, p53, MLH-1, MLH-2 expressions and BRAF mutation were investigated.

Results All of the colorectal and gastric SRCCs had ECMP. SRC were present as 95% at gastric MAC and 38,5% at colorectal MAC. While the occurrence of pure PC pattern in colorectal MAC was 61,4%, it was 9,5% in gastric MAC ($p<0.001$). Conversely, pure SRC pattern was more frequent in gastric MAC than in colorectal MAC(38% and 8,8% respectively) ($p<0.001$). Mixed pattern was seen in two localizations. There were no significant correlation among the amount of ECMP, tumor paranchym cell pattern, MLH1, MLH2, p53 expression, and BRAF mutation.
Conclusion(s) Gastric MAC and colorectal MAC have different morphological features in terms of ECMP and tumor cell type. Contrary to gastric MAC, colorectal MAC mostly presented itself by pure patterns.

P2.107
Adenosquamous carcinoma of the pancreas: case report and immunohistochemical study

Skafida E.; Grammatoglou X.; Glava C.; Zissis D.; Pasxalidis N.; Katsamagkou E.; Vasilakaki T.
Tzaneion General Hospital of Piraeus, Athens, Greece

Background Adenosquamous carcinoma of the pancreas is a rare variant of pancreatic exocrine carcinoma with less favorable prognosis than common ductal cell carcinoma of the pancreas. Preoperative diagnosis of this tumour is difficult.
Methods We report the case of a 70-year-old man who came to our hospital with abdominal pain, anorexia and jaundice. Imaging of the abdomen showed a mass in the head of the pancreas. Curative pancreaticoduodenectomy was performed.
Results Histological examination of the pancreatic tumor showed an adenosquamous carcinoma, extensively infiltrative, with perineural invasion, involvement of peripancreatic lymph nodes and all the thickness of the duodenum wall. The tumor exhibited a biphasic malignant growth composed of a well-to-moderate differentiated adenocarcinoma and well-to-poorly differentiated squamous cell carcinoma. On immunohistochemical examination the tumor cells were positive for CKAE1 and CKAE3. Cam5.2 and Ker7 were reactive predominantly in the adenocarcinoma component and in few of the squamous cells. Immunoreactivity for CK5/6 was restricted to the squamous component, while the glandular component was negative. A few of the tumor cells were immunoreactive with CEA and Ca19-9. All tumor cells were negative for Ker20, chromogranin and synaptophysin. The patient received postoperative adjuvant chemotherapy and survived for 6 months after surgery since prognosis of adenosquamous carcinoma is poor with only a few patients surviving more than 1 year.
Conclusion(s) Pancreatic adenosquamous carcinoma is a rare aggressive subtype of ductal adenocarcinoma. Squamous metaplasia of the pancreatic ductal epithelium occurs most commonly in the setting of chronic pancreatitis.

P2.108
An uncommon tumor of exocrine pancreas: pleomorphic carcinoma with osteoclast-like giant cells and ductal adenocarcinoma

Bagci P.; Kucuk O.; Kepil N.; Goksel S.; Kalafat H.
Rize Training and Research Hospital, Department of Pathology, Rize, Turkey

Background Poorly and undifferentiated carcinomas of the pancreas are infrequent. Osteoclast-like giant cell tumors associated with ductal and pleomorphic carcinomas only in a few articles in the English literature.
Methods A 51 year-old male presented with a history of jaundice, nausea and vomiting during a month. Endosonography showed a tumor of 4 cm in diameter, invased head of pancreas and central veins, and protruted to the lumen of duodenum.
Results Macroscopic examination of the Whipple resection specimen revealed a 2 cm polypoid tumor in the common bile duct with a 4 cm invasion to the head. At microscopic examination, intraductal papillary mucinous neoplasm through Wirsung duct and usual ductal adenocarcinoma was seen in the head. But only the polypoid part of the tumor showed pleomorphic carcinoma features and osteoclast-like giant cell differantiation. Giant cells did not express any cytokeratin subtypes, while pleomorphic cells did.
Conclusion(s) It was like two different tumors were together; one with invasive and usual carcinoma morphology and one with a polypoid and pleomorphic morphology with osteoclast-like giant cells. Differantial diagnose with primary and metastatic mesenchymal tumors is important, as the prognosis is so different.

P2.109
Angiodysplasia of ileum

Kimula Y.
Nozaki Tokusyukai Hospital, Osaka, Japan

Background Angiodysplasia of intestine is a rare disease in Asian countries. 6 papers from Japan were reported, so far. Two cases were reported in this paper.
Methods 74-year-old man had abdominal pain and was admitted for the operation to the ileus. The ileum lump sized 3 cm in diameter was removed because of the passage disturbance. Histopathological examination revealed the

angiodysplasia and the fibromuscular hyperplasia of ileum causing the thickened wall. 60-year-old woman visited our hospital for the anemia and occasional syncope. During the therapy for the anemia, for the syncope and hemotemesis she had been undertaken the resection of ileum to cecum. Histopathology examination revealed the angiodysplasia of ileum.

Results After resection of intestinal angiodysplasia, both 2 persons are fine without any symptom.

Conclusion(s) Before operation, it is difficult to diagnose the intestinal angiodysplasia showing various symptom.

P2.110

Coexistence of colonic adenocarcinoma with uterine endometrioid adenocarcinoma (case report)

Cumurcu S.; Bayol U.; Sonmez G.; Gunay Yardim B.; Turelik O.
Tepecik Research and Training Hospital, Izmir, Turkey

Background Synchronous gynecologic tumors associated with endometrial neoplasms have been published several times. Endometrial adenocarcinoma associated with non-polyposis coli is also detailed by pathological and cinical features. Coexistence of colon carcinoma and endometrial adenocarcinoma is very unusual.

Methods Case: 76 years old woman applied surgery clinic with complaint of abdominal distension. She had ascite, large pelvic and colonic mass on physical examination and radiologic images. Kolonoscopic examination and microscopic evaluation of the adenomas excised revealed tubular adenomas. She had been undertaken to surgery for excision of adherent large pelvic and colonic masses.

Results Microscopic and immunohistochemical evaluation of the tumor masses revealed adenocarcinomas of descenden colon and endometrial cavity and metastasis of both tumors on omentum.

Conclusion(s) This unusual coexistence of colonic and endometrial adenocarcinomas are presented for details of differential diagnosis.

P2.111

Diagnostic methods of gastrointestinal stromal tumors of stomach

Lapidus N.; Shamarin A.
The North Estonian Regional Hospital, Tallinn, Harjumaa, Estonia

Background GIST is the most frequent non-epithelial tumor of the alimentary tract. The interstitial cells of Cajal or primitive progenitor cells are thought to be the cells of origin. Incidence: 0,1–1,0%. Age: 14–93 years, also in children and neonatals. Gender: no preference. Symptoms: abdominal pain, bleeding, rarely obstraction. Size: 0,5–30 cm. Radiological differential diagnosis: mesenchymal, neuroendocrine neoplasms, adenocarcinoma, lymphoma. Morphology: tumors are spindle or epithelioid type. They may show differentiation toward muscle or neural elements, the both structures simultaneously or showno differentiation. Mutations: may be mutation of CD117(c-kit) or PDGRa. It correlates with different clinical behavior. Oncologists use the mutational status as a predictive parameter for therapy planning. Immunohistochemically: C-kit(CD117), CD34, SMA, VIM, NSE markers may be positive. Tumor grade: low and high. Metastasis: most often liver,peritoneum, lungs. Treatment: surgical excision with following treatment with imatinib mesylate. Prognosis: 5-year survival rate is 56%. The standard criteria for prognosis are tumor size and mitotic activity. Evaluation of malignancy (according to Miettinen et al.): probably benign, probably malignant, uncertain or low malignant potential.

Methods A 67 years old patient has been diagnosed with GIST of the stomach in our hospital.

Results The surgery has been performed.

Conclusion(s) The diagnosis should be confirmed morphologically and immunohistochemically. The molecular changes are very important for prognosis and treatment.

P2.112

Diagnostic use of AMACR in hepatocellular carcinoma

Willemoe Linno G.; Vainer B.
Pathology Department, Hvidovre Hospital and Rigshospitalet, Copenhagen, Denmark

Background α-methylacyl coenzym A racemace (AMACR or P504S) is a mitochondrial and peroxisomal protein present in a variety of human cells. Demonstration of increased expression is used diagnostically in prostatic adenocarcinoma. AMACR is also produced by normal hepatocytes and it has been postulated that demonstration of AMACR expression or its pattern of distribution is useful in the diagnosis of hepatocellular carcinoma (Jiang. Hum Pathol 2003;34, uzman. Appl Immunohistochem Mol 2006;14. Li. J Exp Clin Canc Re 2008;27). The aim of the present study was to evaluate whether immunohistochemical staining for AMACR can be used in a routine histopathologic setting.

Methods Immunohistochemical staining for AMACR was performed on paraffin embedded tissue from livers resected for HCC during 1980–2006 at Rigshospitalet, Copenhagen, Denmark (n=44). Tumour sections as well as surrounding non-neoplastic tissue was studied. In both tumour and non-tumour tissue intracellular localisation and staining pattern

was assessed and the staining intensity of AMACR was graded.
Results The fraction of stained tumour cells was not significantly different from the fraction of stained non-tumour cells in the same patients (p=0.97). A significantly lower staining intensity was observed in clear cell areas (p = 0.005), but the AMACR expression did not correlate with the HCC type and could not distinguish neoplastic from non-neoplastic liver cells.
Conclusion(s) AMACR is not applicable as a tool in the histopathologic diagnosis of hepatocellular carcinoma.

P2.113
Hepatoid gastric adenocarcinoma. A case report

Zizi-Serbetzoglou Evangellos A.; Savvaidou V.; Tepelenis N.; Petrakopoulou N.; Farmakis N.; Manoloudaki K.
Tzaneion General Hospital of Piraeus, Piraeus, Attiki, Greece

Background Hepatoid adenocarcinoma (HAC) is a peculiar type of extrahepatic adenocarcinoma generally characterized by adenocarcinomatous and hepatocellular carcinoma (HCC)- like foci. HAC has been found in different organs, such as the stomach, lung, pancreas, esophagus, papilla of Vater, colon, bladder, kidney, uterus and peritoneal organ.
Methods A 72 year-old male presented to the gastrointestinal clinic with dyspeptic symptoms of four months duration. There was no documented weight loss and the clinical examination revealed no abnormality. Upper G1 endoscopy showed an ulcerative, central excavated tumor mass with a mean diameter of 15 cm. Biopsy was reported as" poorly differentiated, adenocarcinoma". Total gastrectomy was performed and the resected specimen was sent for further histological examination.
Results The microscopic examination showed an adenocarcinoma which consisted of two patterns. The first was an adenocarcinoma which had a tubular pattern with prominent glandular differentiation. The second morphological pattern consisted of sheets and islands of neoplastic cells with hepatoid differentiation. In the immunohistochemical examination the cells with the hepatoid differentiation were positive for HepPar1 and negative for high- and low molecular weight keratins. After all the diagnosis of hepatoid gastric adenocarcinoma was established.
Conclusion(s) The hepatoid gastric adenocarcinomas have generally an unfavorable prognosis. The majority have already metastasized by the time of diagnosis, mostly to the liver and lymph nodes. Our patient is free of disease 6 months after the initial diagnosis.

P2.114
Immunohistochemical study of the apoptotic and proliferative mechanisms of the colorectal sessile serrated adenoma

Ziak D.; Dvorackova J.; Cegan M.; Nieslanik J.
CGB laboratory S.A., Ostrava, Czech Republic

Background In the large series of colorectal carcinomas 5.8% were associated with an adjacent serrated adenoma. Studies examining molecular alterations in serrated adenomas demonstrated different genetic alterations than those traditionally seen in the adenoma-carcinoma sequence.
Methods In our study we examined mechanisms of the apoptosis and proliferation of the sessile serrated adenoma of colorectum with help of the immunohistochemical methods. We used this antibodies: Survivin, P53, P63, P27, P21, BAX, Bcl 2, FAS(CD95), Glutation transferase(GST), Caspase 3, Caspase 8, COX 2, Matrix metalopreteinase, Ki67, PCNA and Topoisomerase 2- alpha. We analysed expression of this antibodies in morphological defined patterns of this lesion.
Results Analysis and results of our examinations will be matter of the poster presentation.
Conclusion(s) We expect that our study will prove that serrated adenoma is a tumor with low proliferative aktivity and its growth would be maintained by a low extent of cell loss by apoptosis that the neoplastic process in serrated adenoma is characterised by the disorder of cell maturation, migration and exfoliation.

P2.115
Malakoplakia of the cecum. A case report

Gianna K.; Xirou P.; Nikolaidou A.; Anestakis D.; Paikos D.; Patakiouta F.
Theagenio Cancer Hospital, Thessaloniki, Greece

Background Malakoplakia is a distinctive rare granulomatous disorder and has been described in numerous anatomic locations, most commonly the genitourinary tract. The pathogenesis of malakoplakia remains poorly understood and is presently regarded as an acquired defect in the host macrophage response to a bacterial infection.
Methods A 73-year-old man was investigated in our hospital for liver and pulmonary metastases. Colonoscopy revealed two small polypoid lesions in the cecum, which were biopsied.
Results Histological and histochemical features of the lesions were consistent with malakoplakia of the cecum.

Conclusion(s) Malakoplakia is a peculiar host reaction to chronic infection that is stimulated by an inability to completely metabolise certain bacteria. It usually involves the bladder, while the colon is the commonest site of extraurogenital involvement. An association between malakoplakia and various diseases, including carcinomas, adenomas and immune deficiency, has been documented. Macroscopically colonic malakoplakia most frequently presents as one or more polypoid lesions, 3 mm to 4 cm in maximum diameter, usually in the rectosigmoid and cecum. Histologically collections of histiocytes with granular eosinophilic cytoplasm, known as von Hansemann's cells, accumulate in the lamina propria of the mucosa. The diagnosis rests upon the identification of intracellular and extracellular Michaelis-Gutmann bodies, which appear as target or ring-like structures and are highlighted with the Von Kossa stain for calcium or with iron stains. Differential diagnosis includes storage diseases, Whipple's disease, MAI and fungal infections. Our patient died 4 months after diagnosis due to widespread metastatic disease of unknown primary.

P2.116

Malignant hemangioendothelioma of the mesentery. Report of a case

Abou M.; Bouabdellah K.; Fatiha B.; Fatima B.
Oran, Algeria

Background We report a case of malignant hemangioendothelioma of the mesentery in a 22 old years male who was hospitalised for an abdominal tumor with pain and hemorragic syndrome.
Methods Macroscopic study showed a voluminous tumor of 18 cm length with necrosis and hemorragy.
Results Microscopic study showed a malignant vascular proliferation eh cells of the mesenteric vessels with many nuclear atypies and a high mitotic level. An immunohistochemistry study with monoclonal antibody CD34 (Dako) on parafine showed a strong membranar staining of the tumoral cells which proved the vascular origin of the neoplasm.
Conclusion(s) Malignant hemangioendothelioma of the mesentery is a rare tumor and the pronostic is poor because early metastasis and hemorragic syndrom.

P2.117

MALT lymphoma of the stomach. Case report

Filipovski Aleksandar V.; Janevska Boris V.; Banev Gjorgji S.; Dukova B.
Institute of Pathology, Skopje, Macedonia, the Former Republic of Yugoslav

Background A 74 year old male was clinically diagnosed with a gastrtic carcinoma on the grounds of endoscopy combined with imiging techniques. However the biopsy specimen from the tumor mass in the stomach did not confirm the diagnosis of gastric cancer. Gastrectomy and omentectomy was performed with additional biopsis from the pancreas and lymph nodes.
Methods The specimens were routinly formalin fixed and embedded in paraffin blocks. A routin Hematoxyllin-Eosin stain was performed, and additional immunohistochemistry was performed on the tumor specimens.
Results The gross gastric speciment showed a homegenous grey-white infiltration of the cardia, fundus, and antrum of the stomach. There were areas of ulceration and the gastric wall reached thickness of 2 sm, a picture resembling linitis plastica. However microscopy was confusing, and the lesion showed dense inflamatory substrate that masked the tumor cells and the case posed a diagnostic challenge. Immunohistochemistry was performed, and the results pointed toward MALT lymphoma of the stomach.
Conclusion(s) MALT lymphomas of the stomach are not rare. However sometimes they may pose a diagnostic challenge as in our case when the lesion is accompanied by massive inflamation.

P2.118

Mature cystic teratoma of the pancreas diagnosed by endoscopic ultrasound-guided fine needle aspiration. Report of a case

Alcaraz E.; Cabezas A.; Aparicio J.; Paya A.; Perez-Mateo M.; Aranda I.
University Hospital of Alicante, Murcia, Spain

Background Mature cystic teratoma of the pancreas is a extremely rare neoplasm. Endoscopic Ultrasound (EUS) - guided fine needle aspiration (FNA) has become a usefull method in the diagnosis of pancreatic cystic lesions. We report a case of mature cystic teratoma in the body of the pancreas preoperatively diagnosed and successfully treated with distal pancreatectomy with splenectomy. Characteristics, preoperative detection and differencial diagnosis of this rare pathology are also discussed.
Methods This report documents the findings of a 49-year-old-woman presenting epigastric tenderness and Computerized Tomography (CT) images of a 8.5 cm pancreatic multicystic mass. The cytological smears from the EUS-FNA showed different types of epithelium (mucinous, ciliated and squamous) and gave the preoperative diagnosis of mature cystic teratoma.
Results Conclusion(s) EUS-FNA is a helpful method in the preoperative diagnosis of pancreatic lesions. A on-site cytopathologist evaluation is necessary to check the smears

in aim to obtain a good sampling. The whole smears must be examined, even several sections from the cell blocks in order to detect the different types of epithelium.

P2.119

Primary colorectal non-Hodgkin lymphoma

Hammedi F.; Rammeh S.; Abid Ben-Yacoub L.; Trabelsi A.; Beizig N.; Jomaa W.; Ben Abdelkader A.; Sriha B.
Sousse, Tunisia

Background Primary colorectal non-Hodgkin's lymphomas (NHL) are rare tumors that comprise 0.5 to 2% of large bowel malignancies and 10 to 20% of gastrointestinal lymphomas. Therefore, it has received little attention in the literature. We present the clinical and pathological features of 6 cases primary colorectal lymphomas diagnosed in our institution in over a 16-year period.
Methods This study included six primaries colorectal NHL collected over 16 years (from 1990 to 2006). The data of every patient included: Age, sex, presenting symptoms and signs, extent of the disease at diagnosis and the type of resection performed and histopathological examination.
Results Over the 16 years of the study 169 gastrointestinal NHL were diagnosed in our institution, 6 (3.5%) of these lymphomas were located in the large bowel. There were 4 males and 2 females. Ages varied from 14 to 77 years. Weight loss, right iliac palpable mass and bowel habit alterations were the most common symptoms. Definitive diagnostic was set with histological evaluation of the surgical specimen in all colon tumors. The tumors were located in caecum (1 case), right colon (3 cases), left colon (1 case) and rectum (1 case). Three cases corresponded to B large cell lymphomas, 2 were T cell lymphomas and one was a low grade MALT lymphoma.
Conclusion(s) Primary colorectal lymphoma is a rare condition. We present our experience of primary colorectal lymphomas over a 16-year period to characterize his natural history and identify prognostic factors.

P2.120

Primary signet ring cell carcinoma of the sigmoid

Tepelenis N.; Kontostolis S.; Sfikakis G.P.; Petrakopoulou N.; Zizi-Serbetzoglou A.
Tzaneion General Hospital of Piraeus, Athens, Greece

Background Primary Signet ring cell carcinoma of the colorectum is rare in comparison with other forms of adenocarcinoma of the large intestine. It constitutes between 0,1 % and 2,4% of all colorectal carcinomas. Ninety-nine percent occurs in the stomach, with the rest arising in other organs, including the breast, gallbladder, pancreas, urinary bladder and colon. Despite its rarity, this neoplasm merits recognition and differentiation from ordinary adenocarcinomas because of certain clinical, pathological and biological differences.
Methods Case Report: We report a case of a 70 year old man who presented to our hospital with a sharp abdominal pain. He reported a 3 months history of loss of weight, altered bowel habits, tenesmus, bleeding and presence of mucus per rectum. CT scan was performed and showed a rectosigmoid mass measuring approximately 5x4 cm. The patient was submitted for surgical resection.
Results Microscopic examination of the tumor showed an adenocarcinoma. The majority of neoplastic cells had morphological features of "signet-ring cells"(neoplastic cells with abundant intracytoplasmic mucin and peripherally placed nuclei), which constituted more than 80% of the tumor. According to the criteria of WHO classification the tumor was classified as signet-ring carcinoma.
Conclusion(s) Signet ring carcinoma have been associated with poor prognosis, with poor response to chemotherapy and associated with microsatellite instability. The majority of signet-ring adenocarcinomas presented at TNM stages II and III or (Duke's stage B and C).

P2.121

Undifferentiated carcinoma with osteoclast-like giant cells of the pancreas: a case report

Benyacoub-Abid L.; Rammeh S.; Trabelsi A.; Ben Abdelkader A.; Jomaa W.; Hammedi F.; Beizig N.; Mokni M.; Sriha B.
Farhat Hached, Sousse, Tunisia

Background Pancreatic undifferentiated carcinoma with osteoclast-like giant cells is rare. It resembles giant cell tumor of bone. An epithelial origin is now established and this tumor has been recently considered as a variant of ductal adenocarcinoma of the pancreas in the last WHO histological classification.
Methods We report a 70-year-old woman who presented with pain in the left hypochondrium and weight loss. Imaging studies revealed a 3 cm inhomogeneous mass in the tail of the pancreas with multiple metastatic liver masses. A biopsy of a liver nodule was performed.
Results Pathological findings revealed a cellular neoplasm composed of pleomorphic mononuclear cells and osteoclast-like multinucleated giant cells. A diagnosis of

undifferentiated carcinoma with osteoclast-like giant cells of the pancreas was made.
Conclusion(s) Pancreatic undifferentiated carcinoma with osteoclast-like giant cells may have a more favourable prognosis than the usual ductal adenocarcinoma. More recently a mean survival of 12 months has been reported. We report this case with a review of literature.

P2.122
Analysis of MLH1 promoter methylation in colorectal carcinomas with microsatellite instability

Gafà R.; Ulazzi L.; Maestri I.; Negrini M.; Lanza G.
Department of Experimental and Diagnostic Medicine, University of Ferrara, Italy

Background Microsatellite analysis and immunohistochemistry for DNA mismatch repair proteins (MMRPs) demonstrated great utility in the identification of Lynch syndrome. However, the majority of MMR-deficient colorectal carcinomas are sporadic and produced by hypermethylation of the MLH1 promoter. The aim of our study was to evaluate the role of MLH1 promoter methylation analysis in the distinction between MLH1-negative sporadic and hereditary carcinomas. Methods The study included 370 colorectal adenocarcinomas. Microsatellite analysis was performed using the five markers of Bethesda plus BAT40 and a fluorescence based PCR method. MMRPs expression (MLH1, MSH2, MSH6, PMS2) was evaluated by immunohistochemistry. MLH1 promoter methylation (C-region, proximal relative to the transcription start of the MLH1 gene) was determined by methylation-specific PCR.
Results MLH1 promoter methylation was detected in 198 of 272 (72.8%) MSI-H carcinomas, whereas all the 98 MSS/MSI-L tumors analyzed were unmethylated. Among MSI-H tumors, MLH1 methylation was found in 196/222 (88.3%) MLH1-negative carcinomas and in 2 of 50 (4%) MLH1-positive carcinomas ($p<0.001$). MLH1-negative tumors of patients aging <56 years were less frequently methylated (8/14, 57.1%) than tumors of patients aging 56–70 years (46/55, 83.6%) and of patients older than 70 years (142/153, 92.8%) ($p<0.001$).
Conclusions Our data confirm that MLH1 promoter methylation is the major mechanism leading to MSI-H in colorectal cancer. Analysis of MLH1 methylation in conjunction with clinical data and MMRPs expression pattern may be relevant in the selection of patients with suspected Lynch syndrome for genetic testing.

P2.123
Current trends in the epidemiologic and pathological characteristics of gist in Korea, 2003–2004

Cho M.-Y.; Sohn J.H.; Kim J.M.; Kang D.Y.; Kim K.-M.; Kim W.H.; Park Y.S.; Park H.S.; Park J.B.; Jung E.S.; Sook C.J.; S.-Y. Jin
Department of Pathology Wonju College of Medicine Yonsei University, Sungkyungkwan University, Inha University, Chungnam National University, Seoul National University, Ulsan University, Chonbuk National University, Daegu Catholic University, Catholic University, Soonchunhyang University, Dong-A University, The Gastrointestinal Pathology Study Group of Korean Society of Pathologists

Background and objectives Despite remarkable progress in understanding and treating gastrointestinal stromal tumor (GIST) during last two decades, the pathologic characteristics of GIST is not yet clear. Furthermore, the concrete diagnostic criteria of malignant GIST is still uncertain.
Materials and methods We search the data of GISTs nationwide collected from 38 hospitals in Korea from 2003 to 2004. The tumors were subclassified by the diagnostic criteria from NIH consensus meeting.
Results We collected the pathology reports of 1208 GIST. The tumor is most common in 7th decade (31.2%) and sex ratio was 1:1.1(F:M). The tumors were 1.2% in esophagus, 60.1% in stomach, 23.2% in small intestine, 5.6% in large intestine, 8.1% in extraintestinal tract. The metastatic and recurrent tumors were found in 3%. The most common extraintestinal site of GIST was omentum and mesentery (45.9%). In immunohistochemical stains, c-kit immunoexpression was found in 96.2%, and CD34 in 81.1%, actin in 35.8%, s-100 in 16.2%. The high risk group was more common in intestine (46.2%) and extraintestinal site (54.9%) than other site.
Conclusion The GISTs with high risk of aggressive behavior were more prevalent than very low risk and intermediate risk group. The extraintestinal GISTs are more common in Korea than western country. Intestinal

GISTs are more malignant than gastric one at the time of diagnosis.

Urological pathology

P2.124
Expression of VEGF-A, VEGFR-3, CD105 and CD34 in prostatic adenocarcinomas

Diamantopoulou K.; Chranioti S.; Kariotis I.; Delakas D.; Tsangli-Thoma E.
District General Hospital Attikis, "K.A.T", Athens, Kifissia, Greece

Background Angiogenesis is a fundamental stage in tumor progression and metastatic pathway. Vascular endothelial growth factor (VEGF) and its receptor (VEGFR-3/Flt4) seem to be key regulators of angiogenesis associated with prostate cancer. We have studied the expression of VEGF-A, VEGFR-3, CD105 and CD34 in prostatic adenocarcinomas and their potential value as diagnostic and prognostic markers.
Methods An immunohistochemical study was performed using VEGF-A, VEGFR-3, CD105 and CD34 in both cancer and peripheral benign areas of 64 radical prostatectomy specimens, diagnosed at "Asklepieio Voulas" hospital during 2004 to 2008, further categorized with Gleason score: 6, 26 cases; 7 (4+3), 28 cases; 8, 7 cases and 9 (4+5), 3 cases. 2/64 displayed both acinar, ductal and neuroendocrine differentiation. 21/64 had a greatest diameter per block of PCa 0,2–0,7 cm and 43/64 0,9–2 m. 10/64 showed invasion of the prostatic pseudocapsule, with another 6 cases extending to periprostatic tissue. One case with Gleason score 7 showed invasion of seminal vesicles.
Results VEGF-A expression was low in 48 cases (75%) and moderately high in 16 cases (25%). VEGFR-3 showed cytoplasmic and nuclear staining in both benign and malignant prostatic glands. A high endoglin microvessel count was demonstrated in 10 cases (15,62%) with high Gleason score. Biochemical recurrence with high PSA levels (> 4 ng/mm^3) was noted in one case. All patients are alive, free of metastatic disease.
Conclusion(s) VEGF-A seems to be important for inducing prostate cancer intratumoral lymphangiogenesis. Both VEGF-A and VEGFR-3 remain to be investigated as possible targets of anti-angiogenic therapeutic strategies.

P2.125
Giant polypoid leiomyosarcoma of the bladder: report of a case

Tan A.; Gokcol Erdogan I.; Bayol U.; Sen Korkmaz N.
Izmir Tepecik Training and Research Hospital, Izmir, Turkey

Background Non-urothelial neoplasms of the bladder account for fewer than 5% of all bladder tumors. Sarcoma appears to be the most usual mesenchymal malignancy of the bladder, with leiomyosarcomas being the most common type in adults.
Methods Case: A 75-year-old-male with gross hematuria for 1.5–2 months was presented.
Results Cystoscopic examination revealed a large pedunculated polipoid mass originating from the posterior wall of the bladder and filling the cavity, 12 cm in diameter. With mesencymal tumor diagnosis of transuretral resection, radical cystoprostatectomy was performed. On the immunohistochemical evaluation, according to the smooth muscle actine (SMA) positivity and CD 34, S-100, epithelial membran antigen (EMA), CK-7, CK-20, desmin, myoglobulin, CD 68, CD 117 negativity, the neoplasm was diagnosed as leiomyosarcoma. The MIB-I proliferation index was 40%.
Conclusion(s) We present the case to point out the giant size and the polypoid appearence of the neoplasm.

P2.126
Giant seminoma with signet ring cells in a retroperitoneal undescended testis

Condom-Mundo E.; Taco R.; Villena N.; Alarcon I.; Pane M.; Vidal A.; Serrano T.
Hospital de Bellvitge-IDIBELL, Hospitalet de Llobregat, Barcelona, Spain

Background Several morphologic variants of classical seminoma have been reported. Among these, the presence of prominent signet ring cells is exceedingly rare.
Methods Histological and immunohistochemical study of a huge retroperitoneal mass in a 46 year old man.

Results The resected tumor measured 24 cm and invaded the muscular wall of the sigmoid colon, which was resected en-bloc. On pathologic examination, the tumor turned to be a classical seminoma arising from an undescended retroperitoneal testis. In many areas with scant stromal component, the discohesive tumor cells showed a prominent signet ring cell appearance. The cytoplasmic vacuoles did not stain for any of the histochemical stains for mucin. The immunohistochemical study showed the tumor cells, including the signet ring ones, to be positive for PLAP and CD117, and negative for AFP, HCG and epithelial markers.
Conclusion(s) The histologic diagnosis of classical seminoma is usually straightforward. On occasion, however, architectural and/or cytologic deviations from the typical histologic appearance are seen. In the last years, variant patterns including intertubular, tubular, and microcystic have been well characterized. More recently, two cases have been published of testicular seminoma with large numbers of tumor cells displaying a prominent cytoplasmic vacuolization resulting in a signet ring cell appearance. To be aware of this morphologic variant is important in order to avoid confusion with the many conditions having signet ring cells, especially when limited biopsy material is available and/or when the seminoma presents in unusual locations.

P2.127
Malignant fibrous histiocytoma of kidney: report of a case

Sen Turk N.; Kelten C.; Ozkalay Ozdemir N.; Düzcan E.
Medical School of Pamukkale University, Denizli, Turkey

Background Primary renal malignant fibrous histiocytoma is extremely rare. It is indistinguishable from more frequent renal cell carcinomas, clinically and radiologically. Although radical surgery, MFH shows a strong predilection for local recurrence and the prognosis is generally poor.
Methods We report a case of primary renal MFH in a 43-year-old woman presented with left-flank pain. Ultrasonography and computerized tomography of the abdomen revealed a 10x9x7 cm sized, well-defined renal mass with a lobulated contour. The contralateral kidney and renal functions were normal. Metastatic work-up was negative. The patient underwent left radical nephrectomy.
Results Gross examination of the specimen revealed a huge, yellowish white, partly necrotic neoplasm in renal parenchyma, perirenal fat and adrenal tissue. Microscopically, the tumor was extensively necrotic and composed of pleomorphic spindle to polygonal cells arranged in fascicles and storiform structures. Frequent mitotic figures were seen. Immunohistochemical staining for vimentin and CD68 were positive while pan-cytokeratin, smooth muscle actin, S-100, HMB-45 and desmin were negative. The microscopic and immunohistochemical findings thus indicated a storiform-pleomorphic type of MFH. Two years after nephrectomy the patient presented with multipl bilateral lung metastasis.
Conclusion(s) Primary renal MFH is a tumor of the middle-aged and elderly, with equal sex distrubition, and a prediliction for the left kidney. It can not be differentiated clinically and radiologically from other common renal mass lesions so that histopathology is essential. The overall prognosis is unfavourable with a recurrence rate of more than 50% and a 5-year-survival rate only 14%.

P2.128
Morphological changes of peritubular tissue in ageing testis

Plesea E.I.; Enache Danut S.; Georgescu V.C.; Pop T.O.
Craiova University of Medicine and Pharmacy, Craiova, Dolj, Romania

Background Morphologic changes in Peritubular Tissue (PT) sheets, basement membrane (BM) and lamina propria (LP), of human ageing testis were assessed.
Methods The studied material consisted of testicular tissue samples from 28 cases with orchiectomy for prostate adenocarcinoma. Tissue samples were processed by the classical histological technique and stained, on serial slides, with Hematoxilin-Eosin, Goldner trichrome and immunomarked for smooth muscle actin and collagen IV. Images were acquired and measured with an image analysis software. The assessed parameters were: thicknesses of BM (BM-Th), LP (LP-Th), Hyalin "Collar" (HyC-Th) and PT (PT-Th). 30 seminferous tubules (ST) were randomly selected for each case with X40 objective and 5 random determinations for each ST and parameter were performed. Mean thickness (M-x-Th) for each ST, case and age group were calculated (x=assessed parameter). Regression line (RL), Slope (m) and Slope Significance Test ("p") were calculated to assess correlation between each parameter and ageing.
Results M-PT-Th was 6,6 µm, with discretely decreasing RL (m=-0,041) and “p”=0,82. M-BM-Th was 0,6 µm, representing around 9% of PT, with discretely decreasing RL (m=-0,012) and “p”=0,309). The internal LP layer, revealed, not rarely, areas of collagen focal denseness, with frequent foci of hyaline degeneration which, sometimes had circumferential, "collar"-like disposal around the ST. M-Hyc-Th was 2 µm with discretely decreasing RL (m=-0,05) and “p”=0,73.
Conclusion(s) PT undergoes, with ageing, degenerative changes especially in its internal layer, with "mosaic",

focal distribution and no tendency to advance with ageing as showed "p" values determined for assessed parameters.

P2.129
Neuroendocrine carcinoma with minor malignant stromal component of the root of the penis: a case report

Vecchini G.; Vogiatzis P.; Ntoula E.; Lekka I.; Arapantoni-Dadioti P.
Metaxa, Piraeus, Greece

Background Neuroendocrine carcinomas of the genitourinary tract are uncommon neoplasms, most often of the small cell type and usually located in the urinary bladder. We present a case of neuroendocrine carcinoma (non-small cell type) with minor malignant stromal component, located in the root of the penis.
Methods A 59 y.o. man with clinical history of hypospadias presented a reddish zone in the ventral-proximal portion of the penis and small palpable left inguinal nodes. The biopsy showed a "high grade carcinoma". No distant metastases were identified. A radical penectomy with perineal urethrostomy was performed.
Results Grossly, the tumor extensively infiltrated the root of the penis, destroying the urethra and cavernous bodies. Histologically, the prevalent component consisted of intermediate to large cells with amphophilic cytoplasm, large nuclei with prominent nucleoli and many mitoses. The architecture was highly variable with insular, trabecular, pseudoglandular, rosette-like and diffuse patterns. Focal peripheral palisading was present as well as extensive areas of necrosis. Strong and diffuse immunoreactivity with keratins, chromogranin, synaptophysin and CD56 was identified. A minor stromal component was intimately admixed with variable morphology and cellularity, ranging from highly cellular epithelioid to low grade myxoid spindle cell-like sarcoma.
Conclusion(s) Two months later, pulmonary metastases were identified and the resected inguinal nodes showed extensive infiltration by the neuroendocrine component. The clinical follow-up confirms the aggressive nature of these tumors, dictating prompt diagnostic and therapeutic procedures.

P2.130
Pathological changes of contractile wall of the epididymis in men with obstructive azoospermia

Ibrayeva A.; Alchibayev M.; Ismoldayev Y.; Fedotovskikh G.; Enin E.
Scientific Center of Urology, Almaty, Kazakhstan

Background The time taken for spermatozoa to appear in the ejaculate is very high (6–12 months) after the microsurgical repair of obstructive azoospermia (Matthews et al., 1995). The cause of this fact is structural changes in the contractile wall with alteration of transport and storage function of spermatozoa (Pelliccione et al., 2004). The objective is study of histological and ultrastructural changes of contractile wall of the caput epididymis in men with obstructive azoospermia.
Methods The contractile wall in the tubules of the caput epididymis was analyzed by light microscopy and transmission electron microscopy in 8 patients with a bilateral postinflammatory congestive obstruction of the epididymis. Six specimens from the caput epididymis, obtained from fertile men who had undergone an orchidectomy because of testicular cancer, served as control.
Results The contractile wall was strongly thickened when compared with controls (74,5±6,2 μ vs 18,23±3,2 μ), the flat myoid cells were partially replaced by large smooth muscle cells with features of contractile activity (a large number of myofilaments coalescing into dense bodies) coexisting with secretory activity (a developed Goldgi complex and endoplasmic reticulum, scattered lipid inclusions and a thickened continuous basement membrane-like material).
Conclusion(s) The increased mechanical forces on the epididymal wall, proximal to the obstruction, can activate the differentiation of myoid cells into smooth muscle cells. After the microsurgical repair of the obstruction for restore an altered transport and storage of spermatozoa require some time to realign phenotype of smooth muscle cells.

P2.131
Prevalence of latent prostatic carcinoma in Russia: the autopsy study

Kovylina Vladimirovna M.; Pushkar Urievich D.; Govorov Victorovich A.
Moscow State University of Medicine and Dentistry, Moscow, Russian Federation

Background The incidence of prostate cancer has increased substantially all over the world since it became common practice to screen asymptomatic men for the disease. The aim of this study was to investigate the true prevalence and features of latent prostate cancer in Russia in a detailed pathological study.
Methods One hundred autopsied cases (are ranged from 32 to 80) with no history of urological diseases were examined for prostate cancer and high grade prostatic intraepithelial neoplasia. All the prostates were completely embedded.
Results The prevalence of prostate cancer in this study was 36.4%. The most common Gleason scores were 2+2, 2+3 and 3+3 (61%) followed by 3+4 and 4+4 (39%) patterns. High grade prostatic intraepithelial neoplasia was present in

28 (28%) cases, of which 19 cases were associated with the presence of cancer and 9 were free of cancer. Eight prostate glands contained multifocal tumors with a total of 45 tumors in 36 specimens. Of 45 cancerous foci 86.7% were localized in the peripheral zone. Seventeen prostates out of 36 contained tumors with a volume greater than 0.5 cc and 7 - greater than 1.5 cc.

Conclusion(s) Tumors in elderly men were more likely to be larger and poorly differentiated. The probability to find a tumor with a volume larger than 1.5 cc in our study is higher than in other autopsy studies. This may be partially explained by the fact of insufficient use of screening programs in Russian Federation.

P2.132

Proliferative inflammatory atrophy and prostatic intraepithelial neoplasia in benign prostatic hyperplasia after the Chernobyl accident in Ukraine

Iemelianova A.A.; Romanenko M. A.; Harkonen P.; Vozianov F.A.
Institute of Urology AMS of Ukraine, Kiev, Ukraine

Background During the 23-year period subsequent to the Cherbobyl accident the morbidity of prostate cancer in Ukraine has increased from 12.0 to 28.2 per 100000 of male population. The prevalence of chronic prostatitis, proliferative inflammatory atrophy (PIA) and prostatic intraepithelial neoplasia (PIN) in men who underwent surgery for benign prostatic hyperplasia (BPH) was studied.

Methods BPH samples were obtained by adenomectomy from 116 Ukrainian patients operated between 2006 and 2008 consisting of 86 patients living in Cesium 137 (137Cs) contaminated areas (group 1) and 30 patients from non-contaminated areas (control group 2). Ki-67, p53, p27Kip-1 proteins were immunohistochemically investigated in BPH from all patients.

Results The incidences of chronic prostatitis, PIA, PIN and incidentally detected prostate carcinoma were 60.4, 28.1, 31.3 and 12% in group 1; 43.3, 18.3, and 10% in group 2, respectively. Greatly elevated levels of Ki-67, p53 associated with decreased levels of p27Kip-1 in BPH, especially in areas of PIA and less PIN among the patients living in the radio-contaminated areas of Ukraine to compare with group 2 patients were obtained with statistically significant differences.

Conclusion(s) Our study suggests that chronic long-term low-dose radiation exposure might result in the increase of chronic inflammation and it is now found to be associated with increased incidences of PIA and PIN in BPH accompanied by p53, p27KIP-1 alteration which in turn could lead to prostate carcinogenesis

P2.133

Purely sarcomatoid renal cell carcinoma or endometrial stromal sarcoma? A case with atypical presentation

Moreno-Rodríguez M.M., Casco F.G., Merchán-García, González-Menchen A., Sánchez-Frías M.E., Rangel-Mendoza Y.
Servicio de Anatomía Patológica, H.U. Reina Sofía, Unidad de Urología, H. Valle de Los Pedroches, Pozoblanco, Córdoba, Spain

Background A sarcomatoid component can occur in all histologic subtypes of renal cell carcinoma (RCC) and indicates an aggresive tumor. Flank pain and hematuria are the most common symptoms. We report a patient with acute abdominal pain at presentation.

Methods 75-years-old woman with acute abdominal pain. Massive hemoperitoneum and left renal mass were confirmed by images techniques. Left radical nephrectomy was performed and patient died later.

Results Pathologic examination confirmed a 5-cm renal tumor with invasion of the perinephric fat. Histologic examination revealed poorly differentiated sarcomatoid tumor, containing enlarged pleomorphic or malignant spindle cells. Immunohistochemical study was positive to CD10, RE, RP and negative to Cytokeratins, EMA, S-100, CD34, Actina, Desmina and HMB-45.

Conclusion(s) Sarcomatoid RCC is not a distinct histologic entity and represents high-grade transformation in different subtypes of RCC. To the best of our knowledge, acute abdominal pain at presentation and torpid evolution as in this case has not been reported yet. She died many hours later by massive hemoperitoneum and hypovolemic shock. The diagnosis of purely sarcomatoid RCC, like endometrial stromal sarcoma, needs an adequate sampling, diligent searching for epithelial elements, and an appropriate immunohistochemical panel. The presence of sarcomatoid histology should be reported in cases of RCC because it portends an adverse prognosis (less than one year).

P2.134

Sarcomatoid carcinoma of the ureter. A case report

Mrcela M.; Blazicevic V.; Galic J.; Simunovic D.; Koprolcec D.
University Hospital Osijek, Osijek, Croatia

Background Sarcomatoid carcinoma or sarcomatoid variant of urothelial carcinoma is the term that should be used

for all biphasic malignant neoplasm's exhibiting morphologic and/or immunochistochemical evidence of epithelial and mesenchymal differentiation with or without heterologous elements.

Methods We described a case of biphasic malignant neoplasm of the ureter. The patient was 68-years-old woman admitted to the clinic because of painless hematuria, cystoscopically visible tumor protruding from right ureteral orifice, hydronephrosis and affunction of the right kidney. She underwent right nephroureteroctomy. The tumor consisted of four polypoid intraluminal masses that fulfill distal part of the ureter and infiltrate ureteral wall.

Results The majority of the tumor was composed of epithelial elements that show squamous or glandular differentiation and only focal urothelial differentiation. Stroma was abundant fibromixoid or highly cellular composed of atypical mesenchymal spindle cells with high mitotic rate evidence. Epithelial elements react with cytokeratin 10/13 and focally with cytokeratins 7, 8, 18 and 20. The epithelial elements were strongly NSE positive while Synaptophyisn and Chromogranin A showed only focal positivity. Atypical mesenchymal spindle cells showed immunoreactivity for Vimentin while Desmin and Actin were negative. The tumor infiltrated ureter wall and spread into periureteral fat tissue as well as into vascular spaces.

Conclusion(s) Sarcomatoid carcinoma of the ureter is a rare aggressive neoplasm with unknown biology. Molecular studies suggest a monoclonal origin for both tumor components. In our case, epithelial component consisted of various epithelial cell types while stroma consisted of undifferentiated mesenchyma.

P2.135

SNAI1 expression is related to clinical recurrence and associated with cadherin switching and vascular proliferation in localized prostate cancer

Halvorsen J.O.; Gravdal K.; Haukaas S.; Akslen L.
Haukeland University Hospital, Bergen, Norway

Background SNAI1 is a zinc-finger transcriptional factor inducing epithelial to mesenchymal transition (EMT) through repression of E-cadherin. We have recently shown that the presence of an E- to N-cadherin switch as well as proliferation of immature tumour vessels are related to disease progression in prostate cancer. The aim of this study was to examine SNAI1 expression and the relation to these novel markers in localized prostate cancer.

Methods Tissue microarray sections from 104 patients treated with radical prostatectomy, and with long follow-up, were immunostained for SNAI1 and studied in relation to an E- to N-cadherin switch and vascular proliferation by Nestin/Ki-67 co-expression.

Results Increased SNAI1 expression at the tumour-stromal interphase was found in 54 of 104 prostatic carcinomas. This expression pattern was significantly associated with high Gleason score (p=0.019) and large tumour diameter (p = 0.010). Increased expression of SNAI1 was also associated with the cadherin switch demonstrated by reduced E-cadherin and increased N-cadherin expression (p = 0.039), and with high vascular proliferation (p = 0.03). Further, SNAI1 expression was associated with both time to biochemical failure (p = 0.003) and clinical recurrence (p = 0.030).

Conclusion(s) Increased expression of SNAI1 was significantly associated with disease progression in prostate cancer, and linked to both EMT by cadherin switching and vascular proliferation, suggesting that these processes may be co-regulated. These novel data might be important for patient selection and targeted therapy in prostate cancer.

P2.136

Synchronous bilateral leiomyomas of epididymis: a case report

Mavropoulou S.; Tatsiou Z.; Kalogeris K.; Milioudis N.; Nasos P.
Xanthi General Hospital, Xanthi, Greece

Background Leiomyomas are benign neoplasms that may arise from any organ containing smooth muscle. The majority of genitoourinary leimyomas are found in the renal capsule, but this tumor has also been reported in the ureter, bladder, urethra, prostate, seminal vesicles, penis, epididymis, spermatic cord, tunica dartos and tunica albuginea. Synchronous bilateral leiomyomas of the epididymis is extremely rare and only 7 cases have been reported thus far.

Methods We report the case of a 50-year-old patient who presented with a 2-year history of painless intra-scrotal masses which were enlarged gradually. CT-scanning and ultrasonography revealed paratesticular masses. On surgical exploration, two solid encapsulated masses at the tail of the epididymis were found, so conservative excision of the tumors was performed.

Results Gross pathologic examination showed firm, grayish to white masses, 3 cm and 7 cm in maximum diameter, the cut surface of which showed a whorled pattern. Microscopic examination showed interlacing elongated fascicles of spindle cells with abundant eosinophilic cytoplasm. The nuclei were regular, long, blunt, and did not exhibit atypia or mitotic figures. Immunohistochemical studies demonstrated positive smooth muscle actin stain and desmin and negative β-hCG stain, confirming the diagnosis of epididymal leiomyomas. The patient 7 months later has no evidence of recurrent or metastatic disease.

Conclusion(s) We report an extremely rare case of bilateral epididymal leiomyomas. Although no long-term follow-up study has been reported, it is presumed that they are benign in nature and do not recur. Nevertheless, regular outpatient follow-up is still recommended.

P2.137

The role of the cyclin D1 and TGFB expression in the development of the atypia in probable precancerous lesions of the prostate

Zakharava V.; Liatkouskaya T.; Cherstvoy E.; Pashkevich L.
Belarusian State Medical University, Department of Pathology, Minsk, Belarus

Background Postatrophic hyperplasia (PAH) and proliferative inflammatory atrophy (PIA) of the prostate demonstrate both overlapping histological features and biological properties common with prostate cancer (PCa).
Methods We studied the expression of the cyclin D1, TGFb and a cocktail of basal cells (BC) markers (HWC (clone 34bE12) and p63) with the use of immunostaining.
Results The cyclin D1 was expressed in all cases, its expression was the highest in the cases PCa and decreased in the direction of benign prostatic hyperplasia (BPH), PAH and PIA, atypical adenomatous hyperplasia (AAH). In the groups PAH, PIA and AAH, reliable differences of the cyclin D1 expression was absent, that is the evidence of the likeness of their biological potential. The expression of TGFb was focally in all the cases with prevalent expression in the cytoplasm of epithelial, endothelial and smooth muscle cells. The TGFb expression was highest in the cases BPH, decreased in the direction of AAH and PAH and was lowest in the PIA and PCa. According to the regression model, the increase of the cyclin D1 expression and the decrease of the TGFb expression contribute to the increase of the degree of BC layer fragmentation.
Conclusion(s) The present study demonstrated that based on the pattern of the cyclin D1 and TGFb expression PAH and PIA occupy the intermediate position between BPH and PCa, closer based to PCa.

P2.138

The value of some immunohistochemical methods in optimizing the diagnosis of prostate cancer

Dema A.; Lazar E.; Taban S.; Anderco D.; Lazureanu C.; Cornianu M.; Bucuras V.; Botoca M.; Bardan R.; Cornea R.; Faur A.
University of Medicine and Pharmacy "V.Babes", Timisoara, Romania

Background Information provided by usual stains is sometimes insufficient to certify or exclude prostate carcinoma, cases which require further IHC investigation. The aim of this study was to investigate, using AMACR and basal cell markers, a number of prostate lesions difficult to classify on usual stains.
Methods We selected 30 cases of prostate lesions, identified on TURP (6 cases) and PB (24 cases) specimens, which were diagnosed as atypical acinar proliferations or suspicious for adenocarcinoma on usual stain grounds. For IHC study, conducted on additional consecutive sections from paraffin blocks, markers for basal cells (CK5/6 / HMWCK / p63) and AMACR were used.
Results In 9 of the 30 cases (30%) the suspect focus on PB material wasn't found anymore on the IHC stained sections. Of the 21 remaining cases, 16 (76.19%) were classified on the basis of IHC stains as benign lesions (6 cases), PIN foci (2 cases) and prostate carcinomas (8 cases).
Conclusion(s) The combined detection of basal cells markers and AMACR reduces the number of equivocal or false diagnoses. Proving the malignancy by IHC investigation avoid repeatead biopsy in patients with initial uncertain diagnosis on usual stain. To clarify the difficult prostate lesions in the PB material is preferable to use antibodies cocktails (p63/AMACR, HMWCK/AMACR) and standardized protocol for paraffin blocks section.

P2.139

Tissue microarray of prostate cancer: successful survival stratification based on the heterogeneously distributed tumour markers Bcl-2 and Ki67

Fleischmann A.; Schlomm T.; Huland H.; Mirlacher M.; Simon R.; Sauter G.; Erbersdobler A.
Institute of Pathology, Bern, Switzerland

Background The utility of tissue microarrays (TMA) for survival analysis in case of heterogeneously distributed tumour markers has been questioned. Bcl-2 and mitotic activity (Ki67) are heterogeneously distributed markers in prostate cancer. We determined their prognostic relevance in a large scale TMA of more than 2300 hormone naïve prostate cancer patients undergoing radical prostatectomy and having complete follow-up information.
Methods One cancer tissue core (diameter 0.6 mm) per prostatectomy specimen was transferred to the TMA. Bcl-2 expression (negative, weak, strong) was correlated with histopathological and immunohistochemical (Ki67) tumor features and biochemical failure. Cancers with strong Bcl-2 overexpression were investigated for Bcl-2 gene translocation, amplification and polysomy by fluorescence in situ hybridization (FISH).

Results Bcl-2 expression was significantly up-regulated in tumours with aggressive phenotype as indicated by high Gleason score ($p<0.0001$), advanced stage ($p<0.0001$) and high mitotic activity ($p=0.0114$). The different Bcl-2 expression levels translated into significantly different survival curves showing better outcome for patients with lower Bcl-2 levels. The prognostic information obtained from the anti-apoptotic Bcl-2 was independent from the mitotic activity (Ki67) of the cancer. FISH analysis detected no genetic aberration of the Bcl-2 gene.
Conclusion(s) TMA technology has also the potential to link the expression of heterogeneously distributed tumour markers to specific clinical courses. In addition, the large scale of tumours allowed supplementary survival stratification of the Bcl-2 positive subgroup according to the BCL-2 expression level and the mitotic activity.

P2.140
Two very rare and distinct variants of renal angiomyolipomas in a patient with tuberous sclerosis: epithelioid angiomyolipoma sclerosing variant and angiomyolipoma with epithelial cysts (AMLEC)

Vizcaíno Ramón J.; Encinas A.; Beirão I.; Silva P.; Branco F.; Lopes C.
Centro Hospitalar do Porto-Hospital Geral Stº António, Oporto, Portugal

Background Angiomyolipomas are well-characterized triphasic tumors composed of varying amounts of vascular, smooth muscle and mature adipous elements. Angiomyolipomas usually occurs in the kidney, but can occasionally involve the liver and the retroperitoneum. Angiomyolipoma with epithelial cysts is a recently described distinct cystic variant of angiomyolipoma.
Methods Samples fixed in 10% neutral-buffered formalin and embedded in paraffin. Paraffin sections were stained with standard routine stains (H&E and Masson trichrome). Immunostains were performed with avidin-biotin-peroxidase method.
Results We describe a 55 years-old-woman with tuberous sclerosis complex, associated to TSC2 gene mutation, with bilateral renal cysts and a 9.6 cm "renal/peri-renal mass". The microscopic analysis of a needle core biopsy sample displayed an epithelioid sclerosing neoplasia. No renal parenchyma or adipous tissue were observed. Immunostains showed diffuse positivity of the neoplastic cells for desmin, α-actin and HMB-45 and negativity for CAM5.2, S100 and CD45. These features were consistent with a renal or extra-renal sclerosing neoplasm of pericytic cells. The subsequent study of the nephrectomy specimen revealed a sclerosing variant of epithelioid angiomyolipoma and additionally displayed an adjacent lesion with morphological and immunohistochemical features of an AMLEC.
Conclusion(s) The specimen presented two rare lesions combined together, to our knowledge, neither described nor associated with a tuberous sclerosis patient before. The differential diagnosis between sclerosing PEComa of the retroperitoneum and sclerosing variant of epithelioid angiomyolipoma may be impracticable in needle core biopsy sample.

P2.141
ZK 191 784 inhibits invasion of prostate cancer cell lines by modulating matrix metalloproteinase and ICAM-1 levels

Stio M.; Martinesi M.; Ambrosini S.; Treves C.; Zuegel U.; Steinmeyer A.; Simoni A.; Nesi G.
University of Florence, Florence, Italy

Background Low serum levels of 1,25(OH)2D3 have been associated with increased risk and a more aggressive behaviour of prostate cancer. In this research, we examined the effects of 1,25(OH)2D3 (1,25D) and its analogue ZK 191 784 (ZK) on secreted matrix metalloproteinases (MMPs), as well as on ICAM-1 protein levels in human prostate cancer cell lines LNCaP and DU-145. In order to study the mechanisms of action of vitamin D derivatives, the expression of vitamin D receptor (VDR) was assessed.
Methods The cells were incubated with vehicle (control), 1,25D or ZK under serum-free conditions for 48 h. MMP-2 and MMP-9 activity was determined by gelatin zymography, while ICAM-1 and VDR levels were estimated by Western Blot analysis.
Results A marked decrease in the gelatinolytic activity of both MMP-9 and MMP-2 is caused by 1,25D and ZK in DU-145 and LNCaP cell lines. When compared to the control, densitometric analysis showed a distinct dose-dependent decrease in MMP activity with the maximum reduction after incubation with ZK. VDR expression in cells treated with vitamin D derivatives was up-regulated in comparison to the control. Contrariwise, the adhesion molecule ICAM-1 was down-regulated in the cells incubated with 1,25D or ZK.
Conclusion(s) These findings support the hypothesis that vitamin D-based therapies may be of use in preventing and managing advanced prostate cancer.

P2.142
Adenocarcinoma of the renal pelvis. An unusual metastatic tumor from a primary colonic neoplasm

Taban S.; Dema A.; Lazar E.; Cornianu M.; Lazar D.
University of Medicine and Pharmacy V. Babes, Timisoara, Romania

Background Metastasis to the renal pelvis are a rare clinical entity. To our knowledge, there are only a few case reports described in the literature.
Methods We present the case of a 68-year old male with a synchronous colonic and renal pelvis tumors.
Results The patient was admitted to the hospital with left flank pain. Magnetic resonance imaging and colonoscopy demonstrated stenosis of the ureter and a polipoid tumor of the sigmoid. Left nephroureterectomy and sigmoidectomy were performed. Histopathological examination showed a moderate differentiated adenocarcinoma of the colon. In the renal pelvis, just proximal to the ureter was identified a nodular irregular neoplasm without invading adjacent renal parenchyma. The renal tumor had similar histopathological aspects to the sigmoid tumor. Immunohistochemical assessment of the renal pelvis adenocarcinoma revealed positive expressions for cytokeratin 20 and carcinoembryonal antigen, but not cytokeratin 7.
Conclusion(s) The histopathological diagnosis of a renal pelvis adenocarcinoma being a metastasis from a primary colonic neoplasm represents a challenge for pathologists.

P2.143
Asymptomatic phaeochromocytoma of the bladder co-existing with carcinoma

Boujelbene N.; Chelly I.; Adouni O.; Tangour M.; Benfadhel S.; Nfoussi H.; Azzouz H.; Mekni A.; Kchir N.; Haouet S.; Zitouna M.
Rabta, Tunis, Tunisia

Background Phaeochromocytoma of the urinary bladder is a rare neoplasm that accounts for less than 0.06% of all bladder tumours and less than 1% of all phaeochromocytomas.
Methods We present a case of phaeochromocytoma of the urinary bladder in co-existence with a transitional cell carcinoma in 60-years old woman with a good past health and with no history of hypertension admitted for left pyelonephritis.
Results Radiologic investigations revealed a trigonal submucosal tumour associated with a tumour of the upper urinary tract. Cystoscopy with biopsy specimens was performed. The histological diagnosis was pheochromocytoma of the bladder. Endocrinologic examination disclosed normal levels of serum and urinary noradrenalin. A partial cystectomy with left nephroureterectomy was undertaken. The histopathological diagnosis indicated pheochromocytoma in coexistence with transitional cell carcinoma of the upper urinary tract.
Conclusion(s) Since paragangliomas of the urinary bladder are rare and not easily recognised, histological examination is often the only leading key to diagnosis. We report one further case of phaeochromocytoma of the urinary bladder, with the exceptional features of absence of symptoms connected with phaeochromocytoma and association with bladder carcinoma and we discuss the difficulties in diagnosis and treatment.

P2.144
Cellular congenital mesoblastic nephroma: case report

Carvalho Castelo Branco T.; Carvalho Sousa Ribeiro J.; Reis Aguiar M.; Santos Gomes L.; Ibiapina Oliveira J.; Sobral Andrea Santos K.; Miranda Goncalves E.
Hospital Sao Marcos, Teresina, Piauí, Brazil

Background Congenital mesoblastic nephroma is a rare pediatric renal tumor (about 3–10% of all cases). It comprises two histologic subtypes, namely classic and cellular, with the second accounting for 42–63% of all cases and more associated with poor prognosis. It is a diagnostic challenge to the pathologists due to its close differentials with other commoner pediatric renal tumors.
Methods Case report: A 2-years-old girl with an abdominal mass of renal origin was diagnosed with cellular mesoblastic nephroma after left nephrectomy confirmed by histopathological examination. On gross examination, there was an extensive, granular and whitish tumoral lesion occupying almost the entire kidney, invading renal sinus and capsule and perirrenal fat, with areas of hemorrhage and necrosis. The surgical margins were negative. Histologically, it showed ovoid spindle cells, mitoses and no cellular atypia. The immunohistochemical study was positive for vimentin. Adjuvant chemotherapy was realized, but even though there was reccurence in the first year, presenting itself as unresectable tumor, with no response to neoadjuvant chemotherapy. The patient progressed to death.
Results Study of a cellular congenital mesoblastic nephroma case and its recurrence.
Conclusion(s) Mesoblastic nephroma is presumed to originate from proliferating nephrogenic mesenchyme. The cellular variant demonstrates hemorrhage, necrosis, and solid sheets of packed ovoid spindle cells, with low cellular density, mitoses and apoptotic cells. It can invade adjacent structures and tends to be more aggressive, with a relapse-free survival of 85% versus 100% for classic variant.

P2.145
Coexistence of non-invasive papillary urothelial carcinoma with extranodal marginal zone lymphoma (mucosa-associated lymphoid tissue - malt lymphoma)

Zorzos Savas C.; Anagnostakis D.; Hatzianastassiou D.; Kouvidou C.; Tsagkatakis M.; Karanastasis D.; Androulaki A.
'Elpis' General Hospital, Athens, Attika, Greece

Background We present a case of extranodal marginal zone lymphoma (MALT lymphoma) of the bladder mucosa in a 88-year-old man.
Methods TUR-B(T) tissue material was submitted for histology, and based on the findings, the diagnosis was supported by immunohistochemistry and PCR.
Results Sections showed non-invasive papillary urothelial carcinoma, low grade (WHO 2004) that coexisted with a diffuse lymphocytic infiltration of the lamina propria and muscularis propria, having morphological and immunohistochemical features compatible with extranodal marginal zone lymphoma of mucosa-associated lymphoid tissue (MALT lymphoma).
Conclusion(s) Primary urinary bladder lymphomas are rare, and although MALT lymphoma is more frequent than any other type, the coexistence with urothelial carcinoma is exceedingly rare and may be overlooked due to the rather frequent, reactive lymphocytic infiltration in the latter.

P2.146
Condyloma acuminatum of urinary bladder

Delliou E.; Papamichail V.; Grammatoglou X.; Skafida E.; Glava C.; Vasilakaki T.
Tzaneion General Hospital of Piraeus, Piraeus, Athens, Greece

Background Condyloma acuminatum typically effect the external genitalia or perianal region. Extension to the urinary tract is infrequent and especially the bladder involvement is rare. This almost always occurs in patients with cutaneous condyloma
Methods We report a case of a 63-year-old female presented with history of dysuria lasting 3 months. Physical examination revealed hypogastric pain. Cystoscopy revealed an exophytic cauliflower like lesion in the trigone of the urinary bladder measuring 1,8x1, cm. Biopsy was performed.
Results The histologic examination of the biopsy sample showed papillary growth of squamous epithelium and the presence of koilocytosis. The diagnosis was condyloma acuminatum.
Conclusion(s) Condyloma acuminatum represents a benigh proliferation of squamous epithelium.It is caused by human parillomavirus (HPV) which is sexually transmitted. Condyloma of the urinary tract is a rare finding and is usually associated with coexistent condylomata of external genitalia. Histologically they are composed of nodular or papillary growths of squamous epithelium displaying koilocytosis. The stroma is well-vascularized with mild lymphocytic infiltration. They are characterized by increased p53 protein expression and aneuploid DNA content. Local therapy represents the first line of treatment, which might be effective for isolated superficial condylomas. When the disease is extensive cystectomy is often required.

P2.147
Expression of p53 protein in prostate cancer

Dumitriu S.; Roznovan S.; Ungureanu C.; Morosanu E.; Butcovan D.; Radulescu D.
UMF Iasi, Romania

Background The aim of this study is to investigate the prevalence of abnormalities of p53 gene in a group of prostate carcinoma and to determine whether acinar and non-acinarcarcinomas can be related to different genotypes. Methods.We examined paraffin sections of 60 prostate carcinomas for the expression of p53 protein using a panel of antibodies.
Methods We examined paraffin sections of 60 prostate carcinomas for the expression of p53 protein using a panel of antibodies.
Results No p53 expression was observed in any acinar carcinomas independently of the Gleason score. Between non acinar carcinomas only the small cell and the transitional cell carcinomas presented detectable abounts of p53 protein in tumor cell nuclei.
Conclusion(s) The prevalence of p53 overexpression in prostate carcinoma is relatively low compared with mayn other tumors. In our study, the overexpression of p53 only in a small-cell carcinoma and in a transitional cell carcinoma suggests the loss of the suppressing role of p53 gene.

P2.148
Intratesticular angiomyoma

Milias S.; Papathanasiou M.; Melitas C.
Department of Pathology, 424 General Military Hospital, Thessaloniki, Greece

Background To present an unusual tumor of the testis masquerading malignancy.
Methods The patient was male 24 years old with a painless nodule in the left testis. The U/S revealed a multicystic lesion with the differential diagnosis of teratoma. During the intraoperative consultation we received a solid-microcystic, elastic, whitish, nodule measured 1 cm on greatest diameter.
Results The consultation was negative for malignancy, so only the tumor was excised in healthy margins. Microscopic examination revealed a well circumscribed tumor with elongated smooth muscle cells with incomplete fascicular arrangement, surrounding thick- walled veins, sometimes dilated. No atypia, necrosis or mitoses were observed. Immunohistochemical expression showed positivity of the tumor cells for vimentin, desmin, SMA and a-sma, and negativity for CEA, EMA, AE1/AE3. CD31 and CD34 revealed the vascularity of the tumor.

Conclusion(s) Angiomyoma is a benign tumor of the soft tissue of the extremities, trunk, head and neck. Intratesticular angiomyoma (angioleiomyoma) is an unusual benign tumor, which may cause diagnostic problems, simulating a malignancy in U/S examination and therefore may lead to unnecessary orchiectomies

P2.149

Localized malignant mesothelioma of spermatic cord

Iravanloo G.; Eftekhari H.; Ghaderi-Sohi S.
Tehran University of Medical Sciences, Tehran, Islamic Republic of Iran

Background Malignant mesothelioma is an uncommon neoplasm derived from the surface cells of the serous membrane and approximately one third of cases involve the peritoneum.
Methods A 79 year old diabetic man with history of asbestosis was referred to our center because of right spermatic cord swelling and pain. Histologically the tumor was characterized by proliferation of epithelioid cells with papillary and tubular arrangement, the cells were positive for Calretinine, Cytokeratin, EMA & MIC2, which indicating a mesothelial cell origin.
Results The adjuvant chemotherapy was started for the patient but liver metastasis occurred and the tumor spread to abdominal cavity. Consequently the patient died after 6 months without any response to chemotherapy.
Conclusion(s) The spermatic cord in an unusual primary site for malignant mesothelioma and this case highlights the need to consider the diagnosis of well-described pathologies at unusual site.

P2.150

Malignant mesothelioma of the tunica vaginalis

Moreno-Rodríguez M.M.; Casco F.G.; Carrasco Aznar J.C.; González-Menchén A.; Ruiz García J.; Robles Casilda R.
Servicio de Anatomía Patológica y Unidad de Gestión Clínica de Urología, H.U. Reina Sofía, Córdoba, Spain

Background Malignant mesothelioma (MM) is a tumor that occurs most frequently in the pleura, peritoneum and pericardium. It is extremely rare in the tunica vaginalis. We report a case of MM of the tunica vaginalis (MMTV).
Methods 43-years-old man presented left hydrocele since he was 14-years-old. Ultrasonography found a hydrocele with hyperechoic fluid. The procedure was hydrocelectomy. The tunica vaginalis of hydrocelectomy showed granulated surface and two nodular tumors. Five weeks later a radical orchiectomy was performed. It showed a peritesticular diffuse tumor of 8,5 cm in high dimension.
Results Microscopically, it was of the epithelial type and showed both tubulopapillary and diffuse growth patterns. The cells population consisted of cuboidal epithelial-like cells with abundant and eosinophilic or vacuolated cytoplasm. Immunohistochemical profile was: calretinin, cytokeratins 5/6, EMA and WT1 positives; CEA negative. We therefore diagnosed the tumor as a MMTV. We did not undertake further treatment, because there were no other effective therapies for MM.
Conclusion(s) MMTV is a very rare malignancy, it accounts just 0,3–5% of all cases of MM. The etiology of MM is unknown, but asbestos exposure has been suggested as a risk factor. Our patient was no apparent history of asbestos exposure. Many patients present signs of hydrocele, but we did not find other case with long term evolution as our patient.

P2.151

Metachronous bilateral multifocal nonfamilial renal cell carcinoma: a case report

Nikolaidou C.; Katsiki E.; Thanos P.; Patsiaoura K.
Pathology and Urology Departments, Hippokration General Hospital, Thessaloniki, Greece

Background Bilateral renal cell carcinoma (RCC) is a rare tumor with a reported incidence of about 3% to 5% of all patients with RCC. Patients with metachronous bilateral RCC pose a significant challenge considering their high mortality and the poor quality of life in cases dialysis becomes necessary.
Methods We present the case of a 63-year-old man who was admitted to our hospital to have a left radical nephrectomy due to the presence of multifocal nonfamilial RCC. Sixteen months later an other tumor was revealed in the contralateral kidney and an open partial nephrectomy followed in order to maintain renal function.
Results Sections from the left kidney revealed two foci of maximum diameter 3,5 cm and 1 cm corresponding to papillary RCC types 1 and 2. Sections from the excised segment of the right kidney revealed two foci of maximum diameter 1,5 cm and 0,3 cm corresponding to clear cell RCC. The patient is disease free.
Conclusion(s) I. The main issue in patients with metachronous bilateral nonfamilial RCC is the safe and adequate excision of these tumors with maintainance of renal function. II. Long-term survival rates of these patients are moderate but patients with a longer primary-free interval have a more favorable prognosis. III. More meticulous studies are required in order to understand better the histopathologic and genetic profile of these tumors.

P2.152

Molecular markers and histopathological characteristics of germinative testicular tumors

Poinareanu I.; Aschie M.; Papuc F.A.; Iliesiu A.; Craciun A.A.; Dobre A.; Iacub G.; Stanisici J.; Badiu L.D.; Cretu A.; Deacu M.; Bosoteanu M.; Tode V.
Ovidius University Constanta, Constanta, Romania

Background Germinative testicular tumoral pathology affects especially active sexual men who have capacity of reproduction. The paper is justified by trying to improve management in their complex pathology group with majore risks, having the purpose of a fast psycho-social integration for the orchidectomised patient, after post surgical treatment, taking into consideration the histopathological and immunohistochemical type.
Methods We chose to study patients with malignant testicular tumors from 2000 to 2008, hospitalized in surgery departments of Emergency County Clinical Hospital Constanta, 68 cases with malignant testicular tumors.
Results The frequency is arising from 2007 to 2008, with a pick in 2005 and the tumoral type was germinal tumors (52 cases). To all patients from our study, the chorionic gonadotropin (beta-hCG) and alfafetoprotein serological level was high, without specificity. Immunohistochemical expression of PLAP and AFP was classified as follows: absent/weak (cytoplasmic staining less intense than in adjacent normal germ cell) and strong (staining of similar intensity to that of normal germ cells).
Conclusion(s) Testicular cancer is the most frequent cancer for a young man (15–30 years old). Its incidence still rising and it doubled in the last 20 years. The tumor development is not associated with changed serological markers: the differential diagnosis is very hard. Immunohistochemistry confirm the diagnosis.

P2.153

Monocarboxylate transporters 2 and 4 are upregulated in prostate carcinoma

Gomes Pértega N.; Vizcaino Ramon J.; Pinheiro C.; Baltazar F.
Hospital Geral de Santo António, Porto, Portugal

Background Highly proliferative cancer cells maintain high rates of glycolysis, producing large amounts of acids, mainly lactic acid. Monocarboxylate transporters (MCTs) are transmembrane proteins that, by promoting the efflux of the accumulating acids, play a key role in the maintenance of tumour intracellular pH. As a result, they constitute attractive targets for cancer therapy. There are evidences for the upregulation of MCTs in some solid tumours, however, there are no data on prostate cancer.
Methods This study aims to characterize the immunoexpression of MCT1, 2, 4 and CD147 (MCT1 and MCT4 chaperone), in a series of 114 of prostate carcinomas (paraffin-embedded samples) organized into tissue microarrays and evaluate their clinico-pathological value.
Results MCT2 and MCT4 were more frequently expressed in tumour cells than in the adjacent normal epithelium, while MCT1 was significantly decreased in tumour cells. There were no significant differences in CD147 expression between the normal epithelium and tumour cells. Staining for MCT4 and MCT2 was mainly observed in the cytoplasm of tumour cells, suggesting that they could have important functions in the membrane of some cellular organelles. There was a positive association between MCT4 and low PSA levels, affected surgical margin and presence of biochemical recurrence. However, there were no significant correlations between CD147, MCT1 and MCT2 expressions and the clinico-pathological data.
Conclusion(s) These results support a metabolic pathway different from glycolysis in prostate cancer, where the participation of MCTs is poorly understood.

P2.154

Perirenal undifferentiated sarcoma. A new case report

Petrescu N.A.; Berdan G.; Damian D.; Jinga V.; Ambert V.; Constantin I.; Vasilescu F.; Ardeleanu C.
"Prof. Dr. Th. Burghele" Hospital, Bucharest, Romania

Background Retroperitoneal sarcomas account a very small procent of all malignant tumors. Liposarcoma is the most common type of retroperitoneal sarcoma. We report the case of a 59-years old woman hospitalized for intermittent pain in the left lombar side. CT revealed a tumoral mass in perinephric tissue of the upper pole of the left kidney. The kidney and tumoral mass were removed. Grossly, the tumor size was 8/7/4 cm with nodular areas, grey-white colour and firm.
Methods Tumoral fragments were fixed in formaldehyde 10%, paraffine embedded and processed as standard technique; the sections were stained with HE,VG and immunohistochemically with VIM, HMB-45, ACT, CD34, CK19, MNF116, S100, Ki67, cd117.
Results Microscopically examination showed a proliferation composed by round, polygonal and spindle cells with hyperchromatic atypical nuclei some of them having bizarrely aspects, prominent nucleoli, clear or pale eosinophilic cytoplasm. We observed some areas with different pattern: mixoid, hyaline and osseous. Immunohistochemically analyses emphasized: VIMENTINE diffusely positive in tumoral cells, HMB 45, Calretinine and CK19 negative, ACT and CD34 negative but positive in vessels, MNF116 and S100 positive in rare tumoral cells, Ki67 positive in 25% tumoral cells, Cd117 positive in mastocytes.

Conclusion(s) Histopathological and immunohistochemical data established diagnosis of undifferentiated sarcoma, because of lacking of characteristic clinical presentations.

P2.155

Primary choriocarcinoma of the renal pelvis: a rare case

Lianou A.M.; Argyrakos T.; Kyriakou F.; Diamanti E.; Kopaka M.; Savvani A.; Vourlakou C.; Koutsoukou A.
Evaggelismos, Athens, Attiki, Greece

Background We present the case of a 35-year old female who was admitted to the emergency department of our hospital in a comatose state due to, as it was later established, an extensive intracerebral hematoma situated at the left parieto-occipital lobe for which she underwent decompressive craniotomy. Her personal history involved two gestations, the last one 10 months before admission. The patient had breastfed until one month before the incident. Computed tomography revealed the presence of a soft density mass in the right paratracheal area, a solitary nodule in the liver and a space occupying lesion at the inferior pole of the right kidney. β-HCG was repeatedly measured >200000 mIU/ml. Fine needle aspiration of the liver was performed that was followed by radiofrequency ablation of the liver mass and right nephrectomy.
Methods Macroscopical examination of the kidney revealed a gray-red tan mass of the inferior pole. Immunohistochemical stains were also performed.
Results Microscopic examination of the renal tumor and the liver mass revealed the presence of a malignant neoplasm composed of syncytiotrophoblastic and cytotrophoblastic cells in an extensively hemorrhagic and necrotic background. Immunophenotypically the tumor cells showed intense expression of β-HCG, CK7, Ker34βE12, PLAP and p63, a weak positivity for Uroplakin while CK20 was negative.
Conclusion(s) The morphological, immunophenotypical and serological findings were diagnostic of primary choriocarcinoma of the renal pelvis. The patient died approximately 45 days after admission. Choriocarcinoma of the kidney, primary or metastatic, is rarely reported in the literature.

P2.156

Primary osteosarcoma of bladder treated with cystectomy

Galic J.; Mrcela M.; Simunovic D.
University Hospital Osijek, Osijek, Croatia

Background Bladder osteosarcoma is extremely rare tumor. There are about 30 cases described in the literature. Poor prognosis with lethal outcome within one year could be expected, although successful treatments were reported. We present a case of primary bladder osteosarcoma successfully treated with cystectomy, free of the disease for two years.
Methods A 63 years old man was admitted with history of blood in urine during the last month. CT showed 5 cm bladder mass and suspected infiltration of rectum. Transurethral resection was performed and after histology revealed osteosarcomma a cystectomy was done.
Results Histology found a mesenhimal malignant tumor made from spindle like cells, areas of osteoid surrounded with malignant osteoblast type cells showing trabeculae resembling structures, cartilage with atypical forms of hondrocytes and osteoclasts. Areas of urothelium were of normal structure and without atypical or malignant cells. Immunochemistry staining was positive for vimentin, S-100, CD31, CD99, CD68 and Ki67, but negative for cytokeratin, epithelial membrane antigen (EMA) and desmin.
Conclusion(s) Bone forming bladder tumors can be divided into the three groups: carcinosarcoma, transitiocellular carcinoma with osseous metaplasia and osteosarcoma. Historically four origin theories were proposed: mesenchymal remains of Wolfian body, blood transfer of cells, metaplasia and theory of alkaline-phosphatase rich mucosa triggering osteogenic differentiation into neoplastic mesenchymal cells has been held for true. Our case showed that with good coordination of pathologist and urologist combined with prompt and aggressive therapy even a locally advanced disease can be treated.

P2.157

Prostatic blue naevus

Mercado Gutierrez, M.; Gomez Dorronsoro M.; Cordoba Iturriagagoitia A.; Amat Villegas I.; Martinez-Peñuela M.A.; Beloqui Perez De Obanos R.; Martinez-Peñuela V.J.
Hospital de Navarra, Pamplona, Navarra, Spain

Background Prostatic blue nevus or melanosis is very uncommon. The incidence is unknown but it could be around 4%.
Methods We present two cases: First one is an 83 year old man with a 3 year history of prostatism, on physical examination a grade IV prostatic hypertrophy was found, Trans urethral resection was performed; the other one is an 84 year old man with a year history of urinary incontinence and hematury cistoscopy revealed multiple bladder stones a cystolitholapaxy and prostatic adenectomy was performed.
Results Microscopic examination revealed in the first case a brow yellow pigment in the spindle cells located between the muscle bundles of the prostate and the stroma close to

or away from the glands. In the second an intraprostatic adenocarcinoma Gleason 3+3 was found and the pigmented lesion was between the tumoral glands, the prostatic stroma and in other sections it was incorporated into the cytoplasm of the tumoral cells. The melanic origin of the pigment was proven by the negative for Perls staining and the inmunoreactivity for S 100.

Conclusion(s) Extracutaneous nevus is very uncommon the finding in the prostatic tissue is incidental in the context of a prostatectomy or TUR. About its origin is speculated that the melanin is produced in the stromal melanocytes that migrated from the neural crest and later transfer into the glandular hyperplasic or neoplasic epithelium. Blue nevus in the prostate is a benign lesion that could be confused with other pigmented lesions.

P2.158

Prostatic foamy gland carcinoma. A clinical-morphologic study of 3 cases

De Anda González J.; Quintero Becerra J.; Alvarado Cabrero I.
Centro Médico Nacional Siglo XXI, Hospital de Oncologìa, IMSS, Distrito Federal, México

Background The prostatic foamy gland carcinoma is a recently histologic variant of prostatic adenocarcinoma, and is characterized by abundant foamy cytoplasm and minimal cytologic atypia. Many years ago, people believed that variant prostatic adenocarcinoma should be classified as an intermediated-grade carcinoma, but, this variant of prostatic adenocarcinoma is often associated with an aggressive behavior. However, there is limited information in the literature about the biologic nature of this histologic variant.

Methods We examined 120 needle biopsy, to the Oncology´s Hospital, CMN, during a 18 months period (July 2007 to December 2008) and we collected 3 cases with foamy gland prostate carcinoma.

Results Patients ranged in age from 61 to 74 years (mean 69.3 years). The serum PSA level at the time of the biopsy from 10.2 ng/dl to >150 ng/dl. Positive cores involved by foamy gland carcinoma, from 17%, to 75%. The Gleason scores was 4 +3, 4+4 and 4+5. Nuclear enlargement was observed in 1 of 2 cases, in 2 cases intrauminal dense pink secretion were identified. All the cases were associated with typical adenocarcinoma. One patient had extraprostatic extension, the 3 patients received radiotherapy adyuvant.

Conclusion(s) We concluded that the prostatic foamy gland carcinoma often have an aggressive behavior, and need to recognized from other benignant and malignant conditions. In our hospital, the prostatic foamy gland carcinoma always had aggressive behavior.

P2.159

Pure choriocarcinoma of the testis revealed by multiple lung metastases

Preda O.; Fülop E.; Moldovan C.; Borda A.
Emergency County Hospital, Tîrgu Mureş, Romania

Background Choriocarcinoma usually occurs as a component of mixed germ cell tumors. Pure choriocarcinoma is extremely rare, representing 0.1 – 0.3% of all testicular germ cell tumors. Due to its highly malignant potential it is often discovered at an advanced stage, most commonly involving the lung, the liver and the brain.

Methods We present the case of 16 years-old patient with no previous medical record, admitted to the hospital with dyspnea and fatigability. Radiologic examination revealed multiple bilateral opacities of the lung, very suggestive for a metastatic disease. Detailed physical examination suggests a right testicular mass and ultrasound examination confirmed the presence of a tumor. Serum hCG concentration was very elevated. Consecutively a right orchidectomy was performed.

Results Macroscopically, the testicular parenchyma was partially replaced by a hemorrhagic and necrotic tumor. The tumor was entirely composed of an admixture of cytotrophoblasts, syncytiotrophoblasts and intermediate trophoblastic cells, reminiscent of immature placental villi, circling and invading blood vessels. Unspecified intratubular germ cell neoplasia was present in the surrounding testicular parenchyma. Immunohistochemistry showed intense positivity for both hCG and cytokeratin antibodies. After 1 year and 3 chemotherapy cycles the patient is alive and symptom free.

Conclusion(s) Pure choriocarcinoma, an exceptionally rare testicular tumor, is very often discovered by distant metastases as the first sign of disease. Symptoms like dyspnea and fatigability, associated with high hCG serum levels, in a young patient, may suggest the presence of a lung metastases of a testicular choriocarcinoma.

P2.160

Sarcomatoid carcinoma of the penis: the rare case

Carvalho Castelo Branco T.; Santos Gomes L.; Ibiapina Oliveira J.; Cunha Carsten A.; Patrocinio R.; Barros Wobber Cardoso W.; Siqueira Aparecida S.; Araujo Klerton Luz J.; Almino Luisa Brito Ferreira M.
Hospital Sao Marcos, Teresina, Piauí, Brazil

Background The cancer of penis is a rare tumor with a higher incidence in individuals from 50 years and related to low socio-economic conditions and education. In most developed nations including the United States, its incidence is less than 1 per 100.000 men/year, while in Brazil this

tumor accounts for 2% of all cases of cancer in males. Squamous cell carcinoma represents 95–97% of malignant tumors of the penis. The sarcomatoid tumors are a rare variant, accounting for only 1–2% of cancers that usually affect younger patients and has reserved prognosis because of its invasive nature and high histological grade. The authors report an unusual case of sarcomatoid carcinoma of the penis.
Methods Case report: Patient of 55-years-old with a penis lesion with rapid growth for 3 months. Urological examination demonstrate the vegetans lesion in the ventral glans. The surgical procedure was a penectomia and grossly evaluation showed a 5.1 x 5.0 cm irregular white grey mixed exophytic masses. On cut surface, corpus spongiosum and cavernosum are not involved. Histologically, it is composed predominantly of atypical spindle cells with focal squamous differentiation, accentuated nuclear pleomorphism and numerous mitotic figures. The spindle cells was positive to p63 and high molecular weight keratin by immunohistochemistry.
Results The histomorphological findings correlated with immunohistochemical panel showed it was sarcomatoid carcinoma of the penis.
Conclusion(s) This is an unusual variant of squamous cell carcinoma of the penis with reserved prognosis and lack of data in the literature.

P2.161
Squamous cell carcinoma of the urinary bladder: a case report and immunohistochemical study

Glava C.; Grammatoglou X.; Skafida E.; Moustou E.; Katsamagkou E.; Vasilakaki T.
Tzaneion General Hospital of Piraeus, Piraeus, Athens, Greece

Background Primary squamous cell carcinoma of the urinary bladder is a rare tumour. The prevalence of squamous cell carcinoma depending on geographic location and usually associated with chronic inflammation due to chronic urinary tract infections, urinary calculi, long-term indwelling catheters or bladder diverticula.
Methods A 72 year-old-woman came to the emergency department of our hospital with gross hematuria. Her past medical history included episodes of cystitis caused by vescical stones. Bimanual examination and endoscopic evaluation revealed a fungating mass in the bladder neck. Cystoscopic biopsies were taken.
Results Histological examination of the mass showed a well-to-moderate differentiated squamous carcinoma. Squamous differentiation was characterized by irregular and infiltrative nests or sheets of polygonal cells with distinct cellular borders, eosinophilic cytoplasm and varying degrees of keratinization. The tumour elicited areas of necrosis and demonstrated muscle wall invasion. The non neoplastic tissue showed extensive squamous metaplasia. The immunohistochemical study showed that the tumor cells were positive for CK5/6 and COX-2 and negative for CK19 and CK20. Some of the tumour cells were immunoreactive with P63. COX-2 was expressed homogeneously and intensely in the cytoplasm of neoplastic cells. Squamous metaplastic epithelium also expressed COX-2.
Conclusion(s) Squamous cell carcinoma occur in a younger age group in association with schistosomiasis in 83% of the cases. Radical cystectomy with urinary diversion appear to be the treatment of choice but five-year survival rates are still unsatisfactory, ranging from 27% to 33%.

P2.162
The effect of RAD001 on urothelial lesions induced by N-butyl-N-(4-Hydroxybutyl) nitrosamine in ICR male mice

Vasconcelos-Nóbrega L.C.; Colaco A.A.; Santos L.L.; Vala H.; Palomino F.L.; Lopes Silva C.; Oliveira A.P.
Instituto Superior Politécnico de Viseu, Viseu, Portugal

Background Rapamycin and its analogues have shown an important anticancer activity in preclinical and clinical studies. RAD001, a rapamycin analog, is a antibiotic with potent antiproliferative effect against a variability of mammalian cell types. The chemopreventive efficacy of RAD001 was evaluated in an experimental model of invasive urinary bladder cancer.
Methods 52 ICR mice were randomized into four groups, I, II, III, and IV. Groups I, III, and IV received N-butyl-N-(4-hydroxybutyl) nitrosamine (BBN) in drinking water during twelve weeks. Group II was used as negative control. Groups I and II were euthanized one week after ending BBN exposition. Group III was treated with RAD001, 2 days a week, during six weeks. Animals from groups III and IV were sacrificed one week after ending treatment and were collected samples from urinary bladder.
Results In group I were found 67% of simple hyperplasia, 100% of dysplasia, 33,3% of carcinoma in situ (CIS) and 33% of invasive carcinoma. Urinary bladders from control group revealed no changes. No evidence of host toxicity was found among animals treated with RAD001. The incidence of urothelial lesions in animals treated with RAD001 was simple hyperplasia 64%, dysplasia 85%, CIS 7% and invasive carcinoma 43%. On the other hand, group IV showed simple hyperplasia 77%, dysplasia 100%, CIS 15% and invasive carcinoma 54%.
Conclusion(s) Our study showed that animals treated with RAD001 presented a lower preneoplastic and tumour incidence than animals not treated.

P2.163

Thyroid metastasis as primary manifestation of clear cell renal cell carcinoma

Preda O.; Bejan L.; Fülop E.; Moldovan C.; Imre A.; Borda A.
Emergency County Hospital, Tîrgu Mureş, Romania

Background Metastases in the thyroid are uncommon. The most common sites of primary tumors are breast, kidney and lung. There are few reported cases of thyroid metastasis as the primary manifestation of a renal cell carcinoma.
Methods A 64-years-old man was admitted with an initial diagnosis of bilateral goiter. The patient underwent a left thyroid lobectomy and a diagnosis of malignancy was established on frozen sections. Consequently, a total thyroidectomy was performed.
Results On gross examination, both thyroid lobes were enlarged: the right lobe was almost totally replaced by a white grayish, ill circumscribed, solid tumor and in the left lobe multiple colloidal nodules were present. Tumor architecture was solid with focal areas of acinar pattern. The cells were polygonal, with abundant clear or eosinophylic cytoplasm, distinct cell borders and moderately enlarged eccentric nuclei with conspicuous nucleoli. Since architectural and cytological features were not characteristic for any primary thyroid tumor, an immunohistochemical study was carried out. Tumor cells were negative for thyroglobulin and calcitonin, while citokeratin 7 and CD10 showed a diffuse membranous positivity.
Conclusion(s) The differential diagnosis of a clear cell thyroid neoplasm must include metastatic clear cell renal cell carcinoma. When no previous history of renal cell carcinoma is available to the pathologist, immunohistochemical studies are mandatory for the diagnosis. In our case the immunohistochemical profile allowed us to establish the diagnosis of clear cell renal cell carcinoma metastasis in the thyroid.

P2.164

Unusual metastasis of a testicular germ cell tumor

Borda A.; Preda O.; Loghin A.; Decaussin-Petrucci M.; Ragage F.; Berger N.
University of Medicine and Pharmacy, Tîrgu Mures, Romania

Background Metastases in the thyroid, especially from testicular tumor are extremely rare. Fine needle aspiration (FNA) can exclude a primary thyroid tumor, but can not always establish the primary origin of the lesion.
Methods We present the case of a 26 years old man, with a history of a growing mass in the left lobe of the thyroid, associated with a bilateral lymph node enlargement. At FNA both thyroid nodule and lymph nodes were cystic, containing a troublous mucinous material. The samples were very cellular, exhibited a hemorrhagic, necrotic and dirty background. The cellular clusters consisted of rather uniform cells, with abundant eosinophilic cytoplasm. The nuclei were hypercromatic with coarse chromatin, round or fusiform in shape.
Results The morphologic features of these samples were uncharacteristic for any primary thyroid tumor. A complete examination of the patient was recommended and revealed a left testicular tumor with elevated alpha-fetoprotein serum level. The 3,5 cm grayish, mucinous testicular tumor displayed the features of a non-seminomatous germ cell tumor with two components: a majority of yolk sac tumor and a minor component of embryonal carcinoma with some vascular invasions. Following orchidectomy the patient received several chemotherapeutic cures. Two years after the treatment he is alive with no recurrences.
Conclusion(s) In the presence of an unusual cytological aspect at FNA, a metastasis in the thyroid should be evocated. The origin of this metastasis can be often assessed only by complete clinical examination of the patient.

P2.165

Ureteritis cystica presenting with atrophic kidney: report of a case

Emil Sayhan S.; Tan A.; Unluoglu S.; Bayol U.
Izmir Tepecik Training and Research Hospital, Izmir, Turkey

Background Ureteritis cystica is a rare proliferative condition which is found predominantly in the bladder, renal pelvis and upper ureter. It may occlude the ureteral lumen and should be considered in the reasons of atrophic kidney.
Methods Case: A 65-year-old-female with a two-year-history of right flank pain which increased in the last two months was presented.
Results Abdominal ultrasonography revealed right-sided atrophic kidney. Nephroureterectomy was performed. On the gross examination, along the ureter wall, there were numerous polyps, 0.5 cm in maximum diameter, protruding into the lumen. On the histopathological evaluation, ureteritis cystica and chronic pyelonephritis was detected.
Conclusion(s) In conclusion, ureteritis cystica is a benign and indolent lesion which needs to be kept in mind among the causes of the renal atrophy

P2.166

Wilms tumor in an adult patient: a case report

Nikolaidou C.; Thanos P.; Katsiki E.; Patsiaoura K.
Pathology and Urology Departments, Hippokration General Hospital, Thessaloniki, Greece

Background Wilms tumor is the most frequent renal tumor in children but very rare in adults. It represents a malignant embryonal neoplasm derived from nephrogenic blastemal cells that often shows divergent patterns of differentiation.
Methods We present the case of a 35-year-old man who was admitted to our hospital in order to perform radical nephrectomy due to the presence of a rounded mass of maximum diameter 10 cm in the right kidney.
Results Multiple sections from the tumor revealed a malignant neoplasm mainly composed of undifferentiated blastemal cells and few cells differentiating toward epithelial and stromal lineages. The blastemal cells were small, closely packed, mitotically active with rounded overlapping nuclei, small nucleoli and scant cytoplasm. The main architectural pattern was the diffuse blastemal pattern but there were areas with nodular and serpentine patterns. Immunohistochemically there was expression for Vimentin and local expression for the low molecular weight cytokeratin AE1. The diagnosis of Wilms tumor was made, the patient received 3 circles of chemotherapy and is disease-free.
Conclusion(s) Wilms tumor in adults is a rare entity. The different histopathologic types influence both type of treatment and prognosis which is inferior to that of children. Nearly 90% of the syndromic cases and 33% of the sporadic cases of Wilms tumor have a deletion of chromosome 11p13 in their somatic cells involving the WT 1 gene.

P2.167

Xanthogranulomatous cystitis: a challenging imitator of bladder cancer

Ekici S.; Dogan Ekici A.I.; Midi A.; Eroglu A.; Ruacan S.
Maltepe University, Istanbul, Turkey

Background Xanthogranulomatous cystitis (XC) is a rare benign chronic inflammatory disease mimicking malignancy.
Methods 57-year-old maLE presented with pollakuria, nocturia, disuria, left flank pain and a mass on the right lower abdomen. Abdominopelvic Computerized tomography (CT) demonstrated grade-2 hydroureteronephrosis with an obstructing 10 mm stone in the lower third of the left ureter, and a 60x55mm urinary bladder solid mass lesion at the anterolateral wall of the bladder with a central cavity of necrosis. The mass presented local perivesical invasion at the anterolateral side. Cystouretroscopy revealed a mass protruding into the bladder cavity with edematous but smooth surface. The rest of the bladder mucosa was normal. CT-guided bladder needle biopsy revealed fibrosis and necrotic material. Surgical exploration and partial cystectomy was performed. Frozen section analysis could not rule out malignancy because of necrosis and presence of epitheliod and clear cells. Therefore, nerve sparing radical cystoprostatectomy, orthotopic neobladder and ureterolithotomy were performed.
Results Gross examination of bladder revealed a yellow mass with areas of necrosis. Histologically, fibrosis, numerous plasma cells, eosinophyls and immunohistochemically CD68 positive epithelioid and foamy macrophages were detected. Prostatic adenocarcinoma [Gleason score 6 (3+3)] within the prostate was found.
Conclusion(s) The diagnosis was XC and prostatic adenocarcinoma. The patient was free of disease and continent 6 months postoperatively. To our knowledge, the presented case of XC is the 21st to be reported in the English literature and the first case associated with prostatic adenocarcinoma.

P2.168

Disangiogenesis role in varicocele formation

Severgina Olegovna L.; Severgina Serafimovna E.; Leonova Vassilyevna L.; Menovschikova Borisovna L.; Derunova Ivanovna T.
Medical Sechenov Academy, Moscow, Russian Federation

Background The mechanisms of varicocele formation are still unclear.
Methods The aim of this research was the morphological analysis of vessel biopsies obtained during the operative treatment of left sided varicocele of sixteen 11–15-year old boys. These specimens were studied under the light microscopy; immunohistochemical reactions with monoclonal antibodies to VEGF, CD34 and alfa-SMA were also done.
Results The morphological analysis of the biopsies revealed a scattered type of v.spermatica sinistra branching. In all biopsies we found three different types of veins according to their diameter, wall thickness and grade of wall sclerosis. Multiple round formations with identical diameter were also detected in majority of biopsies. These formations were composed of longitudinally, tangentially and circularly oriented bundles of smooth muscle cells surrounded with thin connective tissue capsules; they had narrow lumens lining with flattened epithelium and containing single erythrocytes. During the immunohistochemical reaction the overexpression of VEGF and CD34 on flattened epithelium lining round formation lumens were detected; alfa-SMA

mild expression was revealed on single smooth muscle cells. That proved the belonging of these formations to the vascular system; they can be considered as malformed vessels with anomalous cell differentiation – incomplete angiogenesis structures.

Conclusion(s) We suppose that the main reason for varicocele formation is a scattered type of v.spermatica sinistra branching leading to congestive effect. Presence of incomplete angiogenesis structures confirms direct connection between disangiogenesis and varicocele formation.

P2.169

Microbial causes of hospital urinary-tract infections in elderly female patients after catheterization of the urinary bladder

Patiakas S.; Tziamalis M.; Hoursalas I.; Rousos K.; Akritopoulou K.
General Hospital of Kastoria, Greece

Background Study of microbial causes of urinary tract infections in female patients after catheterization of the urinary bladder

Methods 63 female patients were studied, admitted to our Hospitals and subjected to catheterization of the urinary bladder during admission. All have a negative urine culture during the first 24 h of hospitalization, while urine samples were taken on a daily basis for microscopic examination and culture.

Results In 36 patients (57,1%) all urine cultures during their hospitalization were negative. But after catheterization microbiuria (bacteria in urine) was detected in 27 patients (42,9%). In 15 patients (55,6%) out of these 27, microbiuria was not accompanied by pyuria, while in the other 12 patients (44,4%) microbiuria represented cystitis. In order of frequency, the following microbial strains were isolated: E.coli was identified in 15 patients (55,6%), Candida sp in 4 (14,8%), Pseudomonas aeruginosa in 3 (11,1%), Acinetobacter sp in 2 (7,4%), Proteus sp in 2 (7,4%) and Enterococcus in 1 patient (3,7%).The resistance of enterobacterial microbes to antibiotics was as following: Ampicillin 62,9%, Amoxycillin / Clavulanic acid 11,1%, Cefuroxime 22,2%, Piperacillin 33,4%, Piperacillin/Tazobactam 3,7%, Cotrimoxazole 37% and Fluoroquinolones 11,1%.

Conclusion(s) The percentage of hospitalized elderly female patients with urinary bladder catheter who present microbiuria is relatively high (43%). In the vast majority of these cases E.coli is the cause, while it is not uncommon to detect Candida sp. and Pseudomonas aeruginosa.

Cardiovascular pathology

P2.170

Highly organized lymphoid infiltrates develop in the aortic adventitia of aortic aneurysms due to either chronic aortitis or longstanding atherosclerosis

Dingemans W.; Van Der Loos C.; Ploegmakers H.; Bruneval P.; Sheppard M.; Van Der Wal A.
Academic Medical Centre, Amsterdam, Netherlands

Background Atherosclerosis, presently considered a chronic inflammatory disease, is associated with the development of adventitial infiltrates. These infiltrates increase dramatically with the severity of intimal plaque formation, and ultimately may show a distinct follicular organization, with close resemblance to Mucosa associated lymphoid tissue (MALT). Whether this response is specific for atherosclerosis or occurs also in autoimmune chronic aortitis is unknown.

Methods Retrospective analysis of paraffin blocks of transmural aortic wall segments with histologically proven (autoimmune) chronic aortitis (n=39) and 11 tissue blocks from atherosclerotic aneurysms. Microanatomy and immunophenotype of adventitial infiltrates was studied with monoclonal antibodies reactive with lymphocyte subsets (CD45RO, CD45RA, CD20), plasmacells (CD138), microvessels (CD31), high endothelial venules (HECA 452), BCL6 and CD21 (follicular organization).

Results 97% of cases of aortitis and 91% of atherosclerotic aortas showed distinct adventitial lymphoplasmocellular (CD138, CD20, CD45RA positive) inflammation. Inflammatory activity was severest in (non atherosclerotic) chronic aortitis. Follicular organization with active germinal centers (BCL-6, CD21 positive) within these infiltrates was found in 59% of aortitis and 55 % atherosclerosis cases. Endothelium of microvessels within the infiltrated areas showed HECA 452 expression (71% in aortitis and 40% in atherosclerosis) indicating differentiation into high endothelial venules. In non-inflamed aortic segments, adventitial infiltrates were scarce or absent.

Conclusion(s) Adventitial lymphofollicular inflammation resembling MALT occurs in autoimmune chronic inflammatory aortic diseases and in atherosclerosis. We propose the term VALT (vascular associated lymphoid tissue).

P2.171

Synovial sarcoma in the heart

Henriques De Gouveia Mota R.; Andrade João M.; Neves Manuel J.; Silva J.A.; Melo Queirós J.; Luísa Crespo C.
Instituto Nacional de Medicina Legal, I.P., Lisboa, Portugal

Background Heart "masses" may correspond to tumoriform lesions – like thrombus, mice – or to tumors, either begnin or malignant; and among the last, both primary and metastatic. The authors present the case of a rare cardiac secondary neoplasm.
Methods A 60-year-old male was transferred to our hospital due to a cardiac mass that induced cardiorespiratory distress and severe thrombocytopenia. A transthoracic echocardiography showed that it occluded the right ventricle and moved backwards to the right atrium and forwards to the pulmonary artery during systole. An endomyocardial biopsy revealed a monomorphic proliferation of fusiform cells, highly mitotic and positive for vimentin, CD99 and Bcl2.
Results The histological pattern and the immunohistochemical profile were consistent with the diagnosis of Monophasic Sarcomatoid Synovial Sarcoma, which was confirmed by the knowledge of a previous surgery to a synovial sarcoma of the spermatic cord.
Conclusion(s) Synovial sarcoma is a rare cardiac tumor, primary or metastatic. It may be biphasic with epithelioid and spindle areas or monophasic. The monomorphic type may be underestimated, requiring immunohistochemistry for differential diagnosis and genetic study for final diagnosis. Intra-cardiac location is variable. Symptoms range from minimal to lifethreatning, as in the present case. The prognosis is usually dim and therapeutic options depend on the clinical status.

P2.172

Vascularization of the cusps in calcific aortic stenosis

Steiner I.; Krbal L.
The Fingerland Department of Pathology, Hradec Kralove, Czech Republic

Background In developed countries, calcific aortic stenosis (CAS) has become the most common acquired valvular disease. It is considered a form of atherosclerosis and, like the latter, of inflammatory origin. Majority of cases of CAS are classified etiologically as senile ("degenerative") – of a previously normal aortic valve with three cusps, or based on congenitally malformed – bicuspid aortic valve. The aim of our work was to study patterns of both blood and lymphatic vessels in CAS.
Methods Histology and immunohistochemistry (CD31 for blood vessels; D2-40 for lymphatic vessels) in 28 surgical cases of CAS.
Results The 28 cases comprised 18 of the senile type and 7 of the bicuspid valve type; in 3 cases the type was indeterminate. CD31-positive blood vessels were present in all 28 cases. In 14, there were D2-40-positive lymphatics in addition. Vascularization was associated with lymphocytic infiltrates in 24 cases. Five valves contained metaplastic bone tissue. Between both types of CAS there was no difference in the incidence of vascularization, lymphocytic infiltration, or bone formation.
Conclusion(s) There is a paucity of data on vascularization of heart valves and virtually nothing is known about valvular lymphatics. Normal aortic valves are avascular. In CAS, our finding of both blood and lymphatic vessels together with lymphocytic infiltrates supports the inflammatory theory on its pathogenesis. The term "degenerative" thus seems inappropriate.

P2.173

Anatomo-clinical researches on pericardium

Parascan Misu-Mihai L.; Candea Vasile V.; Laky Dezideriu D.
Dept. of Pathology Urgency, Cardiovascular Disease Institute "Prof. Dr. C.C. Iliescu", Bucharest, Romania

Background Aim: Anatomoclinical study was effectuated in our Clinic for offer a synthesis about all the cases with pericardial disease cytologically and / or histopathologically examinated.
Methods Were effectuated cytological exams from pericardial fluid MGG stained and classic histologically stained (HE, VG) from pericardial biopsies harvested by surgeons (Iliescu V, Vasile R, Moldovan H, Iosifescu A, Cosa F, Baila S, Radulescu B, Cornea A, Rotareasa B, Vasilescu A, Stiru O, Somacescu T, Mihalcescu D) in perioada 1999 – 2008.
Results From total of 140 cases histological exams of pericardium were been: fibrinous and serofibrinous pericarditis: 63 cases (39 male, 24 female); caseous pericarditis: 4 cases (3 male, 1 female); purulent or supurative pericarditis: 19 cases (4 male, 15 female); chylous effusions containing malignant mediastinal neoplasms: 29 cases (9 male; 20 female); constrictive pericarditis: 22 cases (11 male, 11 female); hemorrhagic pericarditis: 14 (9 male, 5 female); serous pericarditis: 5 (2 male, 3 female). About sex variability, I was founded male predominance in the fibrinous and serofibrinous pericarditis and female predominance in malignant mediastinal neoplasms with metastasis in pericardium.
Conclusion(s) The majority of pericardium cases from total are fibrinous and serofibrinous pericarditis; the next (by numuber) is the serosanguineous effusions in the frame of malignant mediastinal neoplasms: after them are hemorrhagic and purulent or suppurative pericarditis; the serous and caseous pericarditis are rare.

P2.174
Cell characteristics of small arteries of chronic thromboembolic pulmonary hypertension

Ishibashi-Ueda H.; Hao H.; Hirano K.; Ikegami C.; Matsuyama T.; Ikeda Y.; Nakanishi N.; Ogino H.
National Cardiovascular Center, Suita, Osaka, Japan

Background Chronic thromboembolic pulmonary hypertension (CTPAH) is one of the major diseases among pulmonary arterial hypertension (PAH). Small vessel pulmonary arteriopathy of CTPAH has been considered as the mechanistic similarity to idiopathic PAH and would contribute to prognosis of CTPAH. To clarify the cell characteristics of small vessels of CTPAH, we compared pulmonary artery smooth muscle cells (PASMC) of neointima from CTPAH to those of idiopathic PAH by histopathology, immunohistochemistry, and ex-vivo cell biology.
Methods Fifty pulmonary endarterectomy specimens from CTPAH cases were reviewed histopathologically. Neointimal cells obtained from recent 6 cases and normal PASMCs were examined by cell culture system and the cell characteristics and Rho-kinase activity were analyzed by immunofluorescence.
Results Mean minimum vessel diameter of 50 surgical specimens was 3.5 mm and consistent with small vessels. Neointimal obstructive proliferation showing recanalization (colander lesion) with rich extra-cellular matrix were recognized in 34 cases (68 %). Micro-thrombi in distal site of pulmonary arteries were very rare. The cultured cells from neointima obtained by endarterectomy of CTPAH cases showed slow-growing with bizarre blebbing and the characteristics of smooth muscle cells (SMC), positive to alpha-SMC actin, and myosin heavy chain but exhibited no character of endothelial cells, and very low activity of Rho-kinase.
Conclusion(s) In our data, neointima of small pulmonary arteries in CTEPH showed different characteristics from normal PASMC. This may be related to small-vessel vasculopathy of CTPAH.

P2.175
Cardiomyopathy in adult Sanfilippo A syndrome: right-sided more than left!

Ballantyne Cirino M.; Silva J.; Sergi C.; Chiu B.
University of Alberta, Edmonton, AB, Canada

Background Sanfilippo A syndrome (SAS), mucopolysaccharidosis (MPS) type IIIA, is an inborn lysosomal storage disorder with autosomal recessive inheritance caused by a deficiency of heparan sulphamidase activity. SAS usually presents in childhood with neurodegeneration leading to death in teenage years.
Methods We report two cases occurring in sisters both with onset in childhood and underwent bilateral hip arthroplasty in their early 30's, but without neurological, ophthalmic, hepatic symptoms or coarsening of features as classically described. The older sister had an orthotopic heart transplant for dilated cardiomyopathy (DCM) at the age of 45. She is alive and well. The younger sister died due to heart failure awaiting transplantation. Both hearts were extensively studied by light and electron microscopy.
Results Morphologically both hearts showed DCM with predominantly right ventricular involvement. Light microscopy showed ballooned cardiomyocytes and fibromyxoid changes and extensive replacement of the myocardium by adipose tissue in the right ventricle. Ultrastructural studies revealed an impressive accumulation of typical zebra bodies, membranous cytoplasmic bodies and membrano-granulo-vacuolar inclusions in cardiomyocytes.
Conclusion(s) The clinical presentations in these siblings are atypical, without neurological or hepatic symptoms. The interesting association with a predominantly dilated right ventricular pathology observed in both cases increases the spectrum of MPS III. Physicians evaluating adults must remain aware of the inherited metabolic disorders-related dilated cardiomyopathy.

P2.176
Genetic analysis of sudden cardiac death victims in forensic practice

Michaud K.; Elger B.; Mangin P.
University Center of Legal Medicine, Geneva - Lausanne, Switzerland

Background Current recommendations for post-mortem examination in cases of sudden cardiac death include genetic analysis (molecular autopsy). However, molecular autopsy seems to be taking place only in a few academic centres.
Methods In order to assess the current practice of different forensic institutions, we contacted the members of forensic medicine associations (International Academy of Legal Medicine, German, Swiss, French Societies of Legal Medicine and Mediterranean Academy of Forensic Sciences) and asked them to fill in an on-line questionnaire. The questions concerned the routine procedures applied in cases of sudden cardiac death (forensic autopsy including macroscopical and microscopical heart examination, conduction tissue examination, immunohistochemistry and electron microscopy, biochemical markers, sampling and storing appropriate material for genetic and toxicological analyses) and some aspects concerning legal and ethical questions raised by genetic analyses in post-mortem and multidisciplinary collaborations.

Results We received 97 answers mostly from European countries. The responses to the questionnaire show that routine practice varies widely and that genetic testing is practice only by minority of respondents. The link between post-mortem investigation and clinical assessment of the families of a sudden cardiac death victim is still very rare. The more detailed results of our survey will be presented and discussed.
Conclusion(s) Genetic analysis of sudden cardiac death victims takes place only in a few academic centres in Europe. Therefore, the reason of that should be analysed and role of all implicated medical practitioners should be revised.

P2.177
Lyme disease myocardiopathy. Light and transmission electron microscopic study

Lalosevic D.; Vuckovic D.; Stojsic-Milosavljevic A.; Momcilov-Popin T.; Lalosevic V.; Stojsic D.
Faculty of Medicine, Clinical Center of Vojvodina, Novi Sad, Serbia and Montenegro

Background At the Cardiology Clinic in Sremska Kamenica, Serbia, a myocardial biopsy was introduced as routine procedure on the start of 1990-s. In series of 304 patients, a six were diagnosed as Lyme disease myocarditis or myocardiopathy. Light and transmission electron microscopic (TEM) study of these cases were performed.
Methods Bioptic samples from the hearth right ventricle were taken through the right femoral vein using the myocardial biotome No. VII after hearth catheterization.The myocardial tissue samples were fixed in 10% formalin for light, and in 2,5% glutar-aldehide/cacodylate buffer, postfixed in 1% osmium tetroxide/cacodylate buffer for TEM and appropriate processed.
Results Both light and TEM findings were classified in circumstance of the myocardiocyte damages, interstitial inflammatory infiltrate and vascular lesions. Mitochondrial damage and necrosis of some myocardiocytes, lymphocytes and macrophages in the interstice, and swelling of the endothelial cells were found. In one case on TEM photographs, we recognized the fragments of Borrelia burgdorferi located in the lumen of capillaries. These fragments represented convoluted and transversal sections of some borrelia, constantly 0.2 micrometers in thickness. The capillary lumen with borrelia fragments was filled with a debris and fibrin. In the interstice, activated macrophages were seen. In the neighbouring cardiocytes, contractile departments were focally destroyed.
Conclusion(s) The Borrelia-induced damage of heart microcirculation with fibrin deposits, constitutes the morfologic picture of the activation of inflammatory mediators and coagulation factors as the first step in the Lyme myocardiopathy.

P2.178
Pathomorphology of the cardiac nervous system in ischemia

Gargin V.; Markovsky V.; Nazaryan R.; Shkolnik V.
Kharkov National Medical University, Kharkiv, Ukraine

Background The link between atherosclerosis progression, cardiac ischemia and changes in autonomic nervous system is elusive. We hypothesized that depression of cardiac innervation relates to increased risk of cardiac ischemia. The performed investigation demonstrated morphofunctional changes in the intracardiac nervous system in acute form of coronary artery disease.
Methods We studied 573 autopsy cases (aged 39–87 years) between 3 h and 17 days after an acute coronary event. The histological, histochemical, immunomorphological, morphometric methods were used.
Results Dystrophic and reactive changes in intracardiac innervation develop in acute form of ischemic heart disease. Dystrophic and destructive changes of the nerve elements consist in swelling of neurons with perinuclear edema, focal pyknosis of the neurons, granular disintegration of the nerve fibers, lumpy disintegration of the neuron bodies, fragmentation and vacuolization of the nerve fibers, disturbance of ribonucleoprotein accumulation, reduction of activity of histochemical reactions of cholinergic and adrenergic structures, increase in the amount of atrophic neurons and reduction in the number of active ones, appearance of mosaic nervous network with areas of low and high density. The reactive changes in the nervous fibers can be characterized by varicose dilation of the nerve fibers, uneven argyrophilia, deformation of axial cylinders, changes in the size of the nucleus and its ectopy.
Conclusion(s) The changes in the morphofunctional state of the intracardiac nervous system cause myocardial tissue hypoxia, increased endothelial dysfunction, changes in the sensitivity of the cardiomyocytes to catecholamines, their damage and sclerotic processes.

P2.179
Cadmium cardiomyopathy

Jancic Arandjel S.; Najman Joza S.; Jancic Slavisa N.; Goronja Dragoljub A.; Radivojcevic Milos U.; Bojanic Zoran N.
Institute of Pathology, Faculty of Medicine, Kragujevac, Serbia and Montenegro

Background Carcinogens effects of cadmium on lungs, testicles and prostate are well known, but there are not many published articles about effects of cadmium on myocardium. The aim of our research is micromorpholog-

ical examination of rat's myocardium when they were chronically treated with cadmium.

Methods The study was carried out on 30 male albino Wistar rats (weighing 120 g (+/- 10 g), 35–37 days old. The animals were raised in controlled laboratory conditions. Ten animals from the control group did not undergo the treatment. The 20 experimental rats were exposed to 15 mg of CdCl2 /L drinking water. After 90 days, all animals were victimized and after the macroscopic inspection of the heart, the myocardial tissue was taken, routinely processed and embedded in paraffin. On sections 5 micrometers thin classical HE method, histochemical PAS-AB (pH 2, 5), van Gieson and Gommori method was applied and for showing mastocytes we used cytochemical Toluidine blue technique.

Results Noticeable atrophy and hydropic degeneration of subendocardial localized muscles fibers, with focal presence of myocytolysis. Endothelial cell hyperplasia and edema of the intima is present on arteriolar type blood vessels. These changes, focally, cause an occlusion of the arterioles. Fibrocytes, histiocytes and mastocytes are multiplied perivascularly. Mastocytes are polymorphic and hypergranulated. In myocardium, multifocally, there are capillary bleedings. In all layers of myocardium, perivascularly, fibrosis is prominent.

Conclusion(s) Cadmium causes morphological changes on myocardium and small blood vessels and it has strong vasculotrophic effects.

P2.180

Cardiac light chain deposition disease. Report of one case

Tangour M.; Chelly I.; Azzouz H.; Boujelbene N.; Adouni O.; Nfoussi H.; Mekni A.; Haouet S.; Kchir N.; Zitouna M.; Houman H.
Rabta, Tunis, Tunisia

Background Nonamyloidotic deposition is a rare multisystemic disorder associated with plasma cell dyscrasias. It's due to the deposition of Congo Red negative, amorphous and granular material by electron microscopy. These deposits are positive for light or heavy chains on immunohistochemical study. Cardiac involvement is uncommon and usually described in the advanced stages of the disease.

Methods We report a case of 42 year-old woman with no past medical history, presented with dyspnea, and lypothymia of tow months duration.

Results Echocardiography showed features suggestive of restrictive cardiomyopathy. Electrophoresis of the patient's serum revealed a monoclonal spike in the gamma globuline region which was of Ig K nature on immunofixation. Laboratory data, myelogramme, and skeletal survey were unremarkable. Bone marrow biopsy showed marrow plasmocyte component occupying nearly 10% of the specimen. Salivary glands and abdominal fat were normal. Histological examination of a biopsy specimen taken from the cardiac septum revealed an important deposition of smooth and eosinophilic material. This deposits was Congo Red negative and showed positivity for kappa light chains on immunohistochemical study. The diagnosis of light chain deposition disease was made.

Conclusion(s) Although uncommon, light chain deposition disease must be considered in the differential diagnosis of cardiac dysfunction. Physicians have to be aware from multisystemic involvement.

P2.181

Changes of endothelial cells preceding the formation of erosions in coronary arteries and aorta in atherosclerosis

Solovjeva N.; Lysenko A.
Moscow Medical Academy, Department of Pathology, Moscow, Russian Federation

Background To determine the changes of endothelial cells (EC) and frequency of the micro-focuses of destruction (MFD) over atherosclerotic lesions in coronary arteries (CA) and an aorta (AO).

Methods Autopsy material was collected from 16 men and 23 women aged 35–92. It was received the imprints of fatty streaks, plaques and unaffected surfaces of 39 AO subjects and 19 right CA subjects. The samples were stained on Romanovsky-Gimsa

Results Multiple MFD of EC (diameter – 0,2–1,3 mm) were found over atherosclerotic lesions of AO and CA. All focuses were dividing on three types: destructive lesions with accumulation of surrounding EC and hematogenous cells; dystrophic alterations with conservation of endothelial layer integrity; erosions at full destruction of EC. AO intimae showed EC MFD in 79,5 % of patients. In total 107 focuses of various types were revealed: over fatty streaks - 15, over plaques - 85 and on unaffected fields - 7. Frequency of EC MFD at acute myocardial infarction (AMI) (53 focuses) in comparison with a cardiosclerosis (42 focuses) was higher in 1,3 times. CA intimae exhibited EC MFD in 63,2 % of patients. Totally 53 focuses were revealed. Frequency of EC MFD at AMI (34 focuses) of CA was 2 times higher in comparison with cardiosclerosis (17 focuses).

Conclusion(s) Described EC MFD of three types over atherosclerotic lesions of AO and CA demonstrate a transition from a stable endothelialized plaque to a plaque erosion.

P2.182
Immunohistochemical investigation of collagen I and collagen III in myocardium with systolic and diastolic CHF

Popova O.; Solomahina N.
Moscow Medical Academy, Moscow, Russian Federation

Background The investigation designed to compare the intensity of immunohistochemical staining to collagen I and collagen III in the myocardium of patients having the systolic and diastolic heart insufficiency (S-CHF and D-CHF).
Methods The autopsies material of 11 patients aged 75–93 years (80. 0±1.2), (5 males and 6 females) with the ischemic disease of heart, dead of progressive S-CHF (EF <40%) (n=6) and D-CHF (EF >40%) (n=5) was stained against collagen-I and collagen-III on paraffin sections. The results of immunohistochemical reactions were evaluated semiquantitatively according to the 5-scale-number. The data obtained was carried out through the sum of ranks using the criterion Mann-Whitney. Differences were considered reliable with p(U) <0,05.
Results It was revealed the reliably large intensity of immunohistochemical staining of collagen- III in D-CHF group than in S-CHF with the endomysial localization (mean score 1.4 and 0.6, p(U)=0.05), perimysial localization (mean score 1.6 and 0.5, p(U) = 0.04), perivascular localization (mean score 1.6 and 1.0, p(U) = 0.03). It was not any statistical significance in intensity of immunohistochemical reaction to the collagen I between D-CHF and S-CHF: with the endomysial localization (mean score 0.6 and 0.5, p(U)=1.00), perimysial localization (mean score 1.4 and 1.3, r(U)=0.82), perivascular localization (mean score 1.4 and 1.6, p(U) = 0.39).
Conclusion(s) In the myocardium of patients dead in the result of the progressive D-CHF a reliable increase of the endomysial, perimysial and perivascular collagen III was revealed in comparison with the persons dead from the progressive S-CHF.

P2.183
Investigation of HbA1c as precocious indicator of cardiovascular aggravation in not diabetic individuals

Hoursalas I.; Patiakas S.; Mitsikaris D.; Charalampous C.
"Onasio" Heartsurgery Center of Athens, Kastoria, Greece

Background To investigate the likely cross-correlation between HbA1c and the degree of cardiovascular tax.
Methods We have studied 117 not diabetic individuals, age 32 until 62 years, with positive familial background of diabetes, however without cardiovascular diseases. In all the levels of HbA1c the lypidemic profile and the arterial pressure were measured, while the dimensions and the mass of left ventricle as well as distention of the ascenda aorta were calculated.
Results 34 individuals presented high prices HbA1c (medium price 6,01), 48 intermediate prices HbA1c (5,11), and 35 low prices HbA1c (4,09). The individuals that belong in the team of high HbA1c had considerably bigger pressure of pulse, mass of left ventricle, higher arterial pressure and lower distention of the ascenda aorta, comparatively with the individuals of team with low prices HbA1c. The statistical analysis showed powerful cross-correlation of HbA1c with the blood pressure (r=0,29, p=0,01), the mass of left ventricle (r=0,31, p=0,008), and ascenda aorta (r=0,30, p=0,03).
Conclusion(s) It is proved, consequently, that the HbA1c constitutes an independent factor that is related so much with the decreased elasticity of aorta, what with the increased mass of left ventricle and in particular, even in her low levels, under even from those of diabetic limen.

P2.184
Morphological analysis of autopsied cases of transposition of the great arteries

Glumac D.S.; Levicanin Z.M.; Stevanovic M.R.; Lekic V.B.; Djuricic M.S.; Sopta P.J.; Radojevic-Skodric M.S.; Vasiljevic D.J.
Institute of Pathology, Medical School, University of Belgrade, Belgrade, Serbia and Montenegro

Background The transposition of the great arteries (TGA) can be defined as situs inversus of conus (or infundubulum), with atrio-ventricular concordance and ventriculo-arterial discordance.
Methods All data are obtained from the register of congenital heart diseases from 1947. to 2008. year. In this study, we found 400 autopsied cases of TGA. The aim of this study is to describe and classify our autopsied cases of TGA, using segmental analysis, and modified Rokitansky autopsy technique, as our methodology.
Results The major frequency has a TGA with intact atrial and ventricular septum (55%), then TGA with ventricular septal defect (22.25%), TGA with ventricular septal defect and pulmonary stenosis (5.25%), TGA with isolated pulmonary stenosis (1.5%), and finally, the fifth group was TGA with complex associated cardiac anomalies (13%).
Conclusion(s) Some authors do not accept such a classification of TGA, saying that associated anomalies exclude the TGA as morphological substrate, but in our opinion, TGA could be associated with other complex cardiac anomalies. This morphological analysis and our classification of TGA are very important for the choice of adequate therapy, depending on the morphology of TGA, and we found that over 60% of the cases (the first 3 groups) could undergo the Switch procedure for correction of TGA.

P2.185

Peroxisome proliferator-activated receptor-gamma and Retinoid X receptor-alpha expression in the high-risk carotid atherosclerotic plaque

Giaginis C.; Klonaris C.; Katsargyris A.; Papadopouli K.; Kouraklis G.; Theocharis S.
University of Athens, Medical School, Athens, Greece

Background Peroxisome proliferator-activated receptor-gamma (PPAR-gamma), a ligand-activated transcription factor, which forms heterodimers with the Retinoid X Receptors (RXRs) has been recognized as a crucial player in several cardiovascular diseases, including atherosclerosis. The present study aimed to evaluate the clinical significance of PPAR-gamma and RXR-alpha expression in patients with high-risk atherosclerotic lesions.
Methods PPAR-gamma and RXR-alpha expression was assessed immunohistochemically in paraffin-embedded carotid plaque specimens from 126 patients. Immunohistochemical scoring was based on both staining intensity and the amount of positive stained cells within carotid plaques and was statistically analyzed with patients' clinicopathological parameters.
Results PPAR-gamma expression in macrophages was significantly reduced in patients presenting coronary artery disease (p=0.048) and coronary artery bypass grafting/percutaneous transluminal coronary angioplasty (CABG/PTCA) (p=0.028), and borderline in those treated with statins (p=0.097). PPAR-gamma expression in fibroblasts was borderline reduced in hyperlipidemic patients (p=0.098) and in those treated with antiplatelets (p=0.061). RXR-alpha expression in macrophages was borderline reduced in patients treated with statins (p=0.051) and in those presenting advanced stenosis grade (p=0.072). RXR-alpha expression in fibroblasts was significantly reduced in patients treated with statins (p=0.045), and borderline in patients presenting hyperlipidemia (p=0.071), coronary artery disease (p=0.072) and peripheral angiopathy (p=0.057).
Conclusion(s) The present study revealed down-regulation of PPAR-gamma and RXR-alpha expression in patients with high-risk atherosclerotic lesions. Further molecular and clinical studies are required to delineate and confirm the significance of PPAR-gamma and RXR-alpha in the management of high-risk atherosclerotic patients.

P2.186

Sudden death due to an unrecognized cardiac hydatid cyst: a case report

Benkhedda G.; Boudeffeur N.; Lamouti A.
Blida, Algeria

Background Echinococcosis is an endemic disease,most common in scheep-raising communities,usually caused by the tapeworn echincoccus granulosis. The most common sites of infection are the liver and the lungs.cardiac hydatid cysts are very rare.It has been reported that cardiac involvement is seen in about 0,5–3% of human echinococcosis cases.
Methods We reported a case of an 40-year-old-femal, who died suddently.
Results The post-mortem examination revealed an isolated cyst in the left ventricule of heart.The cyst measuring 10 cm long axis,contained white-colored fragments of a membrane, associated to small vesicles. Microcopic examination ascertained the diagnosis of echinococcosis.
Conclusion(s) Cardiac echinococcosis is rare,but due to its insidious presentation and affinity to cause sudden death, it is important that it be identified in the histopathological examination.

P2.187

Two cases of calcific embolism

Arena V.; Pennacchia I.; Bonadia N.; Arena E.; De Giorgio F.; Capelli A.
Università Cattolica del Sacro Cuore, Roma, Italy

Background We describe two unusual cases of embolization.
Methods Case1: 74 year-old man transported unconscious to ICU with a severe coronary syndrome associated with acute renal failure (ARF). Case 2: 68 year-old man, diabetic, with an ulcer of the toe. Amputation was suggested to prevent ostemielitis.
Results Case 1: At necropsy acute myocardic ischemia (MI) was identified as the cause of death. Other findings were a mild ventricular hypertrophy and a calcified bicuspid aortic valve. At histology, calcific emboli, likely originated from the calcified valve, were noted both in the coronary microcirculation and in the renal arterioles and were considered the cause of the MI and the ARF. Case 2: The day after, the patient was found in cardiac arrest. The clinical suspicion was of a MI. At necropsy, the heart did not show sign of ischemic damage but on histological examination, pulmonary vessels showed a diffuse microembolization of calcified particles was noted. Microscopically the CNS examination displayed a thrombosis of the internal carotid artery with a fragment of bone inside. The cause of the emboli was presumed to be the bone erosion caused by diabetic ulcer. The pulmonary embolization was explained with the venous return, while the cerebral embolization was due to a persistent patent foramen ovale.
Conclusion(s) These cases highlight firstly, the importance of an accurate histopatological sampling to clarify cases in which the macroscopic examination is not

decisive; secondly, other unusual sources of emboli should be kept in mind by both clinicians and pathologists.

P2.188

A tuberculous myocarditis associated with right heart failure

Grigoriu C.; Arsenescu Georgescu C.; Butcovan D.
UMF "Gr. T. Popa", Iasi, Romania

Background Tuberculous myocarditis associated with right heart failure is rare. Tuberculosis is an important public health problem considering to spare four organs: heart, skeletal muscle, thyroid and pancreas.
Methods We present a case of tuberculous myocarditis diagnosed on a post-mortem cardiac biopsy.
Results The patient, a girl of fifteen years old, presented with history suggestive of congestive heart failure. We describe the clinical presentation, investigations and outcome of this case.
Conclusion(s) In conclusion, the involvement of myocardium in tuberculosis is rare. Increasing recognition of the entity and the use of endomyocardial biopsy may help us for detecting of more cases of this "curable" form of cardiopathy.

P2.189

Arrhythmogenic right ventricular cardiomyopathy. Case report

Sramek Zatler S.; Iternicka Z.
Department for Pathology and Cytology, General Hospital, Celje, Slovenia

Background The arrhythmogenic right ventricular cardiomyopathy (ARCV) is a primary heart muscle disease characterized by the progressive myocardial atrophy of the right ventricle, with a massive fibro-fatty replacement.
Methods Case report
Results A 21-year-old woman was found at home without any vital signs. At the hospital the ventricular arrhythmia was confirmed. Sudden death occurred in the General Hospital Celje at the Intensive Care Unit (ICU) within 10 h. Toxicological analyses were negative. At the autopsy the heart weight was 445 g and the heart consisted of diffuse transmural myocardium atrophy (3 mm) in the right ventricular free wall, with the replacement by fatty tissue. The myocardial loss accounted for a parchment like a translucent look of the right ventricular free wall. There was also an aneurysm of the free wall. At external examination, the right side of the heart appears yellowish. Sections of the free wall of the right ventricle clearly showed the disappearance of the myocardium with the transmural fatty replacement. At a higher magnification there was evidence of patchy myocarditis with myocyte death and round cell inflammatory infiltrates.
Conclusion(s) In investigations of out-of-hospital deaths in young people (youth) the question whether toxic substances are involved is always raised. In our case the 21-year-old woman was on a diet under medical control and the toxicological analysis was negative. The autopsy showed massive fatty infiltration of the right ventricle, in the absence of coronary artery and valve disease.

P2.190

Expressing of some angiogenic mediators at peripheric arteriovenous and venous malformations

Pavlov K.; Shchegolev A.; Dubova E.; Mishnev O.D.
A.V. Vishnevsky Institute of Surgery, Moscow, Russian Federation

Background The problem of peripheric vascular malformations morphological diagnostic is still of current importance.
Methods Complex morphological investigation of surgical specimens from patients with vascular malformations, treated in the Institute in 2004 - 2007 was performed. Light microscopy of specimens from 5 patients with peripheric arteriovenous malformation (AVM) and 5 patients with peripheric venous malformation (VM) with immunohistochemistry (using monoclonal antibodies against VEGF, TGFβ1, TGF β1R) was performed.
Results In all cases of AVM we've found abnormal arteries and abnormal dilated veins with vascular wall thickening, intimal hyperplasia and direct arteriovenous shunts. In cases of VM we've found dilated vascular caverns and abnormal veins with local thinning of their wall. We've detected a focal moderate expression of VEGF and TGFβ1 in endothelial cells of little and medium caliber veins of VM. Expression of VEGF and TGFβ1 in endothelial cells of large caliber veins was low. We've detected a focal moderate expression of TGFβ1 receptor in endothelial cells of little and medium caliber veins of VM. We've detected focal moderate expression of VEGF in endothelial cell of AVM. Expression of TGFβ1 and TGFβ1 receptor in endothelial cells of arteries, veins and arteriovenous shunts of AVM.
Conclusion(s) Moderate and high expression of some mediators of angiogenesis (such as VEGF, TGFβ1 and its receptor) in endothelial cells of peripheric vascular malformations suppose to be one of the factors, leading to the recurrence of this lesions after surgical treatment.

P2.191

Fluorescence of "intact" human myocardium by infarction

Anestiadis V.; Tsiple I.; Anestiadi V.V.; Ciobanu V.
Centre for Pathobiology and Pathology, Chisinau, Republic of Moldova

Background The study aimed towards finding new criteria for the determination of the duration in time of myocardial infarction (MI).
Methods Fifty-two hearts from persons (PRS) deceased from MI, in which MI beginning was documented clinically and by ECG, were selected. Thirty hearts of PRS deceased almost instantaneously from traumas served as controls. In each case we did 1000 measurements of myocardial primary fluorescence (MPF) at the wavelength of 360 nm, both in the necrotic (ischaemic) zone (NZ) and in extrainfarctic zones (EZ).
Results During 8–12 h from MI beginning, the MPF decreased concordantly in both zones, being 89.6–2.3% of controls. At 24 h after MI onset MPF in NZ was 78.8–4.3%, in EZ 84.4–3.1% of controls. Minimal NZ MPF was on Days 4–5 and 9–10 (66.3–2.5% and 62.6–2.1% of controls, $p<0.001$). EZ MPF on Days 4–5 was 77.4–3.5%, on Days 9–10 82.3–2.2% and on Days 14–15, 85.7–2.8%, remaining even up to Days 30–35 of MI 7.3–0.8% below controls. MPF variations in time were approximated by splines.
Conclusion(s) By solving a system of equations, which included formulae for EZ and NZ MPFs, it was possible to determine the time elapsed from the MI onset, with an accuracy of 9.6 h.

P2.192

Isolated coronary amyloidosis with giant cell reaction

Arena V.; Pennacchia I.; De Giorgio F.; Bonadia N.; Capelli A.
Università Cattolica del Sacro Cuore, Roma, Italy

Background Cardiac amyloid involvement may simulate cardiomyopathy, congestive heart failure, coronary heart disease, valvular heart disease or arrhytmia.
Methods We report a case of a 74 year-old man, admitted to our ICU because of progressive dyspnoea and chest pain. An ECG showed transient non-specific changes with ST elevation without reciprocal ST depression. On the basis of the clinical presentation and the result of ECG, a clinical suspicion of myocarditis was raised. Although a corticosteroid treatment was immediately started, the patient died from progressive heart failure a few hours after the admission. Autopsy was performed.
Results The heart (450gr) was enlarged and dilated. The myocardium was waxy and pale with few areas of fibrosis. At histology, deposits of amyloid with giant cells reaction were found in the walls of intramyocardial vessels of both ventricles. Histological examination of specimens from other organs did not reveal amyloid deposits. Bone marrow examination showed infiltration by well differentiated plasma cells (70%). Although only 10% of patients with multiple myeloma develop amyloid disease, their prognosis is very poor, especially in the presence of cardiac amyloidosis. In our case, the cardiac involvement was the primary cause of death on the basis of the extensive coronary localization, and the presence of giant cells was presumed to be a foreign body reaction to amyloid.
Conclusion(s) Because cardiac involvement in amyloidosis is associated with a rapidly progressive course and high mortality, a rapid and accurate diagnosis is essential to aid in the selection of therapy.

P2.193

Myocardial infarction and cardiac insufficiency in rheumatoid arthritis

Bély M.; Apáthy A.
Department of Pathology, Policlinic of the Order of the Brothers of Saint John of God in Budapest, Hungary, Budapest, Hungary

Background Myocardial infarction (MI) and cardiac, or cardiorespiratoric insufficiency (CI), may be the consequence of complications of RA, or consequence of various associated diseases accompanying RA. The aim of this study was to determine: the prevalence and spectrum of MI and CI caused by complications of RA or caused by associated atherosclerosis (Ath) accompanying RA.
Methods A randomized (non-selected) autopsy population of 161 in-patients with RA was studied.
Results (1) MI and/or CI – related to complications of RA - led to death in 41 (25.5%) of 161 RA patients. MI was caused by coronary arteritis and/or arteriolitis in 12 of 161 RA patients (coronary arteritis and thrombosis of the main coronary artery with a large myocardial infarct in 1, coronary arteriolitis and myocardiocytolysis in 11 cases). CI was the direct cause of death in 29 of 161 patients as consequence of complications of RA. RA related complications leading to CI were carditis (endo-, myo-, epi- or pancarditis) in 10, systemic vasculitis in 6 (without myocardial infarcts), amyloidosis A in 7, and polyserositis (with, or without interstitial pneumonitis) in

6 of 29 cases. (2) Ath accompanied RA in 74 (45.96%) of 161 patients and led to death as MI and/or CI in 37 (22.98%) of 74 cases.
Conclusion(s) MI and/or CI were the leading cause of death of RA patients and led to death in 78 (48.4 %). i.e. nearly in half of 161 RA patients.

P2.194
Study of the glycosylated hemoglobin as a prognostic indicator of coronary disease in diabetic patients
Patiakas S.; Hoursalas I.; Tziamalis M.; Mitsikaris D.
General Hospital of Kastoria, Greece

Background To investigate the possibility of using HbA1c as a prognostic indicator for the outcome of the coronary control in diabetic patients, considering that it represents a recognized indicator of retrospective regulation of blood glucose level, while, it is known that there is a positive correlation between the diabetes and the coronary disease.
Methods The study involved 57 diabetic patients (41 men and 16 women), who were under anti-diabetic medication (21 with insulin and 36 with tablets), and underwent a coronary angiography. For all of them, before the coronary angiography, the level of HbA1c was measured by the chromatographic method.
Results Patients who received anti-diabetic tablets presented a statistically significant increase of the HbA1c level, in comparison to those under insulin treatment: 6,64± 2,4 νs. 6,12±1,6 mg/dl respectively, $p<0{,}001$. Moreover, statistically significant increase of the HbA1c level was found in men in relation to the women. According to the results of the coronary angiography control, there was no such difference noticed between the two sexes, as far as the condition of the affected coronary arteries is concerned: men 1,62±1,3, women 1,60±1,2, $p=0{,}974$. However, in total, there was a statistically significant positive correlation between the HbA1c level and the number of affected coronary arteries.
Conclusion(s) It is, therefore, proved that the HbA1c level represents a useful prognostic indicator for the severity of the coronary disease.

P2.195
Sudden cardiac death from unrecognized cardiac sarcoidosis
Grigoriu Anda C.; Butcovan D.; Florea I.
University of Medicine and Pharmacy, Iasi, Romania

Background In sarcoidosis, cardiac involvement can become apparent at any stage of the disease, and may precede or follow extra-cardiac manifestations by several years. At diagnosis, a clinically apparent cardiac sarcoidosis is rare but in 17% of these cases sudden death may be the initial presentation of the disease.
Methods Case report: A healthy 20 years old man died suddenly in a public place with no history of trauma or drug abuse including alcohol consumption or smoking.
Results At autopsy, the only abnormality was a heart weighting 1162 g, with a marked concentric thickening of the left ventricular wall and some fibrotic scarring in the myocardium. The coronary arteries and the cardiac valves were grossly normal. Microscopically, the myocardium had a diffuse and extensive interstitial fibrosis with focal lymphocytic inflammation and scattered giant cells without characteristic granulomas. However, in the hilar lymph nodes and the pulmonary broncho-vascular bundles there were multiple non-caseating granulomas.
Conclusion(s) A significant number of cases of myocardial sarcoidosis are discovered at autopsy and are never suspected antemortem. Cardiac involvement is of critical importance, due to its poor prognosis if left untreated.

P2.196
Viable chlamydia pneumonia in aorta and coronary arteries endothelial cells in atherosclerosis
Lysenko A.; Solovjeva N.
Moscow Medical Academy, Department of Pathology, Moscow, Russian Federation

Background To detect Chlamydia pneumonia (Ch.p.) and change endothelial cells (EC) of aorta (AO) and coronary artery (CA) in atherosclerosis
Methods Autopsy material was collected from 16 men and 30 women aged 35–92. It was received the imprints of fatty streaks, plaques and unaffected surfaces of 46 AO subjects and 12 CA subjects. The samples were stained on Romanovsky-Gimsa. In 5 cases the monoclonal antibodies against Ch.p. were used.
Results At cytological investigation viable Ch.p. was found in 26 (56,5%) from 46 AO EC subjects and in 7 (58,3%) from 12 CA EC. Immunocytochemisry confirmed the presence of Ch.p. in 3 AO cases of 5 performed. In infected EC Ch.p. was revealed in three morphological forms: inclusions, spots and aggregates. The early stage of bacterium reproduction was presented by inclusions with individual bodies - diameter of inclusion - 7 μm. As a result of replication the diameter of inclusion could enlarge to 31 μm. EC containing the inclusions had intact nuclei and cytoplasm. The dead EC never contain inclusions and show damage intracytoplasmic membranes, chromatin condensation but no nuclear fragmentation. Such form of cells death is known as aponecrosis. Aponecrotic cells may provoke the inflammatory response

Conclusion(s) In human EC Ch.p. is detected in three morphological forms: inclusions, spots and aggregates. Ch.p. leads to an extensive infected and aponecrotic death EC over fatty streaks and plaques of AO and CA. Destroyed EC cause an inflammatory response.

P2.197

Clinico-pathological features of a cardiac sarcoma originating from the right ventricle

Butcovan D.; Tinica G.; Radulescu D.
UMF "Gr. T. Popa", Iasi, Romania

Background Cardiac tumors are rare tumors representing 0,3% from all cardiac surgeries. Malignant tumors, almost all of which are sarcomas, account for 25% of primary cardiac tumors.
Methods We describe a primary right ventricular sarcoma, presenting with tricuspid outflow tract obstruction, developed early after a severe lung infection, diagnosed by using histological and immunohistochemical methods.
Results The patient underwent open-heart surgery with minimal invasive right thoracotomy and a partial surgical excision of the cardiac tumor, as a palliative procedure. After histological processing, the microscopic examination revealed a high grade pleomorphic, undifferentiated sarcoma, confirmed immunohistochemically.
Conclusion(s) The malignant cardiac tumors continues to have a poor prognosis despite of the individualization of the approach. Whatever applied treatment is, the improving of patient's quality life is an important objective, and as a rule the early diagnosis is imperative.

P2.198

Correlation of the platelet parameters, B12 and folic acid in patients with coronary heart disease

Hoursalas I.; Patiakas S.; Palaiologou M.; Tziamalis M.; Alexidis I.; Charalampous C.
"Onasio" Heartsurgery Center of Athens, Kastoria, Greece

Background To compare the parameters of the full blood count, the B12 and the folic acid, between patients with known coronary heart disease and the general population.
Methods 144 patients (102 men and 42 women, with an average age of 63,4±7,5 years) with known coronary heart disease (previous myocardial infarction and unstable angina), and 140 healthy people (102 men and 38 women, with an average age of 64,2±7,8 years) who formed the control group, were included in the study. For all of them the absolute number of eosinophils, the platelet number (PLT), and the mean platelet volume (MPV) were measured by an hematology analyzer, while, when considered necessary, a blood slide was also examined. Moreover, the levels of B12 and folic acid were measured by a biochemical analyzer.
Results Although the absolute platelet number as well as the levels of B12 and folic acid, didn't differ significantly between the two groups, the MPV was found >11 fl in 126 out of 144 patients with known coronary heart disease (percentage 87,5%), while in 106 (percentage 73,6%) an eosinophil level <1% was noted.
Conclusion(s) It is, therefore, proved that in the coronary patients a statistically significant increase of MPV as well as a decrease of the percentage of eosinophils is found. This can be a useful indicator in patients under an acute phase of an ischemic episode and also as a criterion of differential diagnosis in patients with coronary disease.

P2.199

Cystic medial necrosis in Marfan and non-Marfan aortic dissection

Amalinei C.; Manoilescu I.; Hurduc C.
University of Medicine and Pharmacy, Iasi, Romania

Background Aortic dissection has an increasing incidence, with a higher prevalence in men, being associated with atherosclerosis, hypertension, hereditary connective tissue disorders, such as Marfan and Ehlers-Danlos Syndromes, congenital cardiac anomalies, such as aortic coarctation or bicuspid aortic valve, trauma, vascular inflammation, and pregnancy. Cystic medial necrosis represents a histologic marker for Marfan Syndrome and for a subgroup of non-Marfan patients.
Methods We present two cases from the files of the Legal Medicine Institute, with sudden death and post-mortem diagnosis. They were both men, aged 45 and 50 years old respectively. We used routine paraffin-embedding tehnique, followed by several stainings that revealed the modifications in the components of the extracellular matrix of the aortic wall (HE, Elastic van Gieson, Masson's trichrome, Alcian blue).
Results In both cases, degenerative changes in the aortic media, including fragmentation and loss of elastic laminae, loss of smooth muscle cells, and deposition of mucopolysaccharides and/or collagen were noted, associated with aneurysm and chronic adventitial inflammation in the last case. Our diagnoses were of Marfan acute aortic dissection, type A Stanford, in one case, and of an acute onset of a non-Marfan chronic aortic dissection, type A Stanford, associated with an aneurysm, in the other case.
Conclusion(s) Although a severe condition, due to improved clinical diagnostic tools, aortic dissection is a

relatively uncommon necropsy diagnosis; its variable aspects are based on different morhological substrates and etiopathogenical mechanisms, sharing a relatively frequent histologic hallmark: the cystic medial necrosis.

P2.200

Ischemic and atheromatous lesions in cardiac sudden death

Enache A.; Chatzinikolaou F.; Njau S.; Vladika N.; Koumpanaki M.
Medicine and Pharmacy Victor Babes, Timisoara, Romania

Background We performed an analysis of 917 cases of sudden death which were autopsied at Timisoara Institute of Legal Medicine.
Methods We observed the correlation between macroscopic autopsy diagnostic and histopathologic microscopic diagnostic, the age, the sex and the presence of preexistent pathological lesions with a role in thanatogenesis.
Results We observed the correspondence between the macroscopic autoptic diagnostic and the microscopic diagnostic which showed, in 34% of the cases, the presence of preexistent cardiac affections. These were represented by myocardial lipomatosis, different degrees of intramyocardic sclerosis, direct and indirect signs of cardiac anoxia associated with atherosclerotic and fibrosclerogenic lesions. Acute myocardic infarct and myocardic sclerosis were the most frequent cause of death met in these cases. Ischemic phenomena were associated with complete thrombotic manifestations (68%) at the myocardic vessels and partial thrombosis (32%) which proofs the thanatogenerator syndrome. On the study lot, there were ruptures of atherom plaques or intraluminal thrombosis in 12% of the cases of death with coronary causes at an old age and they were associated with fibrilar proliferations and focuses of lipidic charge set mainly perivascularly.
Conclusion(s) In ischemic or coronary thrombotic cases of sudden death the autopsy shows acute modifications. If the recent thrombotic phenomena are small and do not totally occlude the coronary lumenum it is possible that they are not directly observed. In these cases the autopsy will show different states of evolution of the infarct scar.

P2.201

Natural history of disease and cause of death in transposition of the great arteries

Stevanovic M.R.; Lekic V.B.; Glumac D.S.; Levicanin Z.M.; Sopta P.J.; Djuricic M.S.; Radojevic-Skodric M.S.; Vasiljevic D.J.
Institute of Pathology, Medical School, University of Belgrade, Belgrade, Serbia and Montenegro

Background Total transposition of the great arteries (TGA) is a heart disease which occurs in 2 - 4% of all congenital malformations, and if not treated causes 20% of cardiac death. It is defined as situs infundibuli in which aorta goes out of the right ventricle, and pulmonal truncus goes out of the left ventricle. Hemodynamic factors are essential in pathogenesis of the disease on which depends life of the patient with heart failure.
Methods Data taken from the Register of congenital heart failure and Museum of congenital heart failure, in period 1947 - 2007. This study analyzed 400 autopsied cases of TGA. This research gives description and classification of pathological morphology of TGA relaying on segmental approach. Analysis is conduced by Rokitansky method.
Results The most common cause of death (43.75%) were pulmonary complications, such as pneumonia, asphyxia, respiratory distress syndrome of newborns. The second causes were cardial (39.5%), such as heart failure and cardiac shock. Sepsis was confirmed in 5.75% of all cases. Mostly extracardial malformations were found in spleen (49%), lungs (30%), thymus (8%), situs inversus (8%) and other.
Conclusion(s) Three most common causes of death are shown to be pneumonia, heart failure and sepsis, which correspond to data from literature. The most frequent extracardial malformation is asplenia.

P2.202

Sclerosing angiomatoid transformation of the spleen a rare vascular lesion

Mahzouni P.; Amjadi E.; Taheri D.; Mesbah A.
Isfahan Faculty of Medicine, Isfahan, Islamic Republic of Iran

Background Abstract: Sclerosing angiomatoid nodular transformation (SANT) is a vascular lesion of spleen that only a few cases have been reported to date. We report a case of sclerosing angiomatoid nodular transformation (SANT) of spleen in a 20 years old man who refered with gastroenteritis, abdominal pain and leukopenia. By sonography a large hypoehoic mass was seen in spleen and computed tomography showed a hypodense mass lesion in spleen. The mass was enlarged after 5 months so he underwent splenectomy. On microscopic examination, the tumor showed granuloma like multinodules that were composed of slilt like vascular spaces. These vascular nodules are surrounded by hyalinized/sclerotic stroma, fibroblasts, lymphoplasma cells, macrophages and hemosidrin-laden macrophages. Immunohistochemical staining of nodules showed a mixture of CD31+, CD34+, and CD8- in endothelial cells surrounded by a variable

numbers of actin positive pericytes. The main differential diagnosis of SANT includes littoral cell angioma, splenic hemangioendothelioma, inflammatory myofibroblastic tumor and hamartoma But their morphologic and immuhistochemical staining are different from SANT.
Methods this is the case report
Results this is the case report
Conclusion(s) this is the case report.

P2.203
Tears and dissections of the aorta: anatomo-clinical correlations

Parascan Misu-Mihai L.; Candea Vasile V.; Laky Dezideriu D.
Dept. of Pathology, Urgency Cardiovascular Disease Institute "Prof. Dr. C. C. Iliescu", Bucharest, Romania

Background Aim: Presenting our personal experience concerning the morphopathological substratum and the physiopathological factors involved in the pathogenesis of tears and dissections of the aorta.
Methods We presented 146 cases: 76 necropsical and 70 resections of the aorta, out of which four were frust Marfan Syndromes, 102 in male and 44 in female patients. According to age groups, most of the patients were aged between 51 and 60 and between 61 and 70, 27 were over 70 year-old and 20 were under 40. Histological slades col. HE, VG, elastic stain, PAS-Alcian, Gomori were made and the morphological data were correlated with clinical and paraclinical ones.
Results Eight cases alone appeared in the abdominal and thoracic aorta, followed by B-type dissections. The most frequent complication were: hemopericard (24 cases), hemothorax, mediastinal and retroperitoneal hematomas. The autopsies also revealed left ventricular hypertrophy (32 cases), evolutive atherosclerosis (58 cases), strokes (10 cases), renal, splenic and mesenteric infarcts (27 cases), aortic failure (14 cases), abdominal aneurisms (42 cases) and acute pericarditis (5 cases).
Conclusion(s) The various lesions of the aortic media structures are caused by a worsening of the nocuous action of the hemodynamic, enzymatic and genetic factors, mostly idiopatic, generating tears and dissections of the aorta with hemorrhagic complications that can only be remedied through rapid resections and surgical prosthesis.

P2.204
The uric acid as factor of cardiovascular danger and kidney damage in hypertension patients

Rousos K.; Patiakas S.; Tziamalis M.; Tsigaridaki M.; Charalampous C.
Health Center "Alexandria", General Hospital of Veria, Greece

Background The correlation of uric acid with the presence of damage in organ-target hypertension patients was investigated. The role of uric acid as independent factor of cardiovascular danger and kidney's damage was appreciated.
Methods 247 patients (109 men and 138 women) with average age 62,5 years that they were suffered from hypertension, were studied in the Hypertentionist Exterior Surgery of Pathological Clinic in collaboration with the Microbiological Laboratory. The known factors of cardiovascular danger were thoroughly recording with special questionnaire and the patients whose was receiving diuretic, allopourinoli and the alcoholics were excluded. Finally, the Left Ventricle Mass Index (LVMI) was calculated with ECHO-Doppler and was determined the uric acid levels.
Results Considerably, higher uric acid levels were found in hypertension patients with at least a damage in tissue-target (hypertrophy of left abdomen, ischemic cardiopathy, vasclar cerebral episode etc), comparatively with patients without damage. (Corresponding medium uric acid values: 6,2+/-1,31 and 4,9+/-1,46 mg/dl). Certainly, the patients with uric acid >5,5 mg/dl were found to have caused damage in more than one tissue-target. In relative analysis it was found correlation between the value of uric acid and the LVMI. The cholesterol and triglyceride levels, the catharsis of creatinine, the age and the hypertension play important role, but the uric acid definitely remains as important factor of left ventricle hypertrophy.
Conclusion(s) We conclude that uric acid constitutes important independent factor of cardiovascular danger.

P2.205
Ultra structural and histopathological lesions study of coronary arteries of Alloxan induced diabetes mellitus in dog

Valilou M.; Sohrabi I.; Soleimani J.; Mohammadnejhad D.
Department of Pathology, Faculty of Veterinary Medicine, Islamic Azad University, Shabestar Branch, Shabestar, East-Azerbaijan, Islamic Republic of Iran

Background Diabetes mellitus is one of the most common disease of endocrine glands in body that is diagnosed by malfunction in natural metabolism of carbohydrate, fat and protein. This disease involves most tissues of the body and the consequent deficiencies reduce their efficiency, cause infections and disease in body. Alloxan is a chemical which is used in creating experimental diabetes in animals.
Methods In this research, 9 German shepherd's dog were provided, 5 of which was considered as our experimental group and the remainig 4 was considered as our control group. The necessary examinations were conducted to

guarantee their health and we approved the absence of diabetes with Intravenous Tolerance Test (IVGTT). We injected intravenously Alloxan monohydrate with 100 mg/kg in experimental group. In experimental group, if the symptoms were indicating the death and in control group (after end of experimental group) we took samples tissue of coronary arteries. We scrutinized microscopic and ultral structural deficiencies.
Results In the endothelial cells of coronary arteries, we could see vacuolization of cytoplasm, transitional vesicles decrease and basal membrane was thicken.
Conclusion(s) Diabetes mellitus is a potent risk factor for the development of coronary atherosclerosis.

P2.206
Mitral valve prolapse and sudden cardiac death in the young

Rizzo S.; Peralta A.; Abudurheman A.; Thiene G.; Basso C.
Dept Medico-diagnostic Sciences, University of Padua Medical School, Padua, Italy

Background Mitral valve prolapse (MVP) occurs in up to 5% of the general population. Aim of the study was to evaluate the prevalence of MVP in young sudden death (SD) victims and the pathological substrate of electrical instability.
Methods Hearts from young SD victims with MVP and 15 age-matched controls whith extracardiac causes of death (mean age 28 years) were investigated according to the European protocol with sampling of the valve leaflets and myocardium. Primary antibodies against the phosphorilated form of Smad 2 were used in selected cases.
Results MVP was the cause of SD in 27 (10 M, 17 F, mean age 29,7 years) out of 481 cardiovascular SDs (6%). MVP leaflets had a four-fold increase in thickness compared to the normal valves (2,09±0,23, $p<0,0001$) with fragmented elastin and collagen and accumulation of proteoglycans. Significant replacement-type fibrosis was observed in MVP, particularly at the base of papillary muscle (100%). By histomorphometry, fibrosis was 26,9±10,9% vs 7,2±4,7% in controls ($p<0,0001$) and cardiomyocyte diameter was 17,6±4,9 vs 13,2±0,8 ($p=0,0006$). Increased nuclear staining for p-Smad-2 in valve leaflets and cardiac interstitium was found in MVP ($p=0.02$).
Conclusions MVP is a no-so rare cause (6%) of arrhythmic SD in the young. Replacement-type fibrosis of the ventricular myocardium, even in the setting of still competent mitral valves, may explain the electrical instability. These findings suggest a potential role for risk stratification of late-enhancement cardiac magnetic resonance in MVP patients.

Haematopathology

P2.207
Phospho-tyrosine profiling of mantle cell lymphoma cells suggests the BCR signalling pathway as a potential therapeutic target

Zamò A.; Pighi C.; Gu T.; Mancini F.; Parolini C.; Pedron S.; Bertolaso A.; Parisi A.; Barbi S.; Polackiewitz R.; Cecconi D.; Chilosi M.; Menestrina F.
Dept. of Pathology, University of Verona, Verona, Italy

Background Very few studies have attempted the investigation of mantle cell lymphoma (MCL) by proteomic tools. We studied MCL cell lines using the PhosphoScan approach. We then investigated the importance of the identified pathways for the survival of MCL cell lines using a functional validation approach.
Methods We analysed MCL cell lines MAVER-1, Jeko-1, Rec-1 and Granta-519. Following phospho-peptide identification, we determined the most represented pathways. For SYK inhibition, we used Piceatannol, determining the LD50 for each cell line. Apoptosis was tested by Annexin V. The modifications of P-SYK and downstream molecules were analysed by flow cytometry, immunofluorescence and western blotting.
Results 421 peptides were identified, corresponding to 341 proteins. The most represented pathways suggest the tonic activation of the B-cell receptor signalling. Inhibition of the upstream molecule SYK by Piceatannol, followed by the reduction of downstream target phosphorylation, caused apoptosis of MCL cells. Immunofluorescence studies showed a compartment transition of P-SYK after inhibition.
Conclusion(s) The BCR signalling pathway is therapeutically promising, and recent data indicate that it might be important in the pathogenesis of B-CLL and DLBCL. Its importance in MCL was suggested by gene expression studies. We show that tonic BCR signalling might be one of the mechanisms driving cell survival and proliferation in MCL, and that the inhibition of SYK might be a viable therapeutic approach. More studies are needed to verify the importance in vivo of this pathway.

P2.208
UbcH10 is a novel lymphoid proliferation marker associated with the G2/M cell cycle phase

Guerriero E.; Berlingieri M.; Pallante P.; Ferraro A.; Iaccarino A.; Malapelle U.; Bellevicine C.; Desiderio D.; Natella V.; Fusco A.; Troncone G.
Università degli studi Federico II, Naples, Italy

Background The UbcH10 ubiquitin-conjugating enzyme plays a key role in regulating mitosis completion. We have previously reported that UbcH10 overexpression is associated with aggressive thyroid, ovarian and breast carcinomas. The aim of this study was to investigate UbcH10 expression in human lymphomas.
Methods Cell lines and tissue samples of Hodgkin's lymphoma (HL) and of non-Hodgkin's lymphoma (NHL) were screened for UbcH10 expression at transcriptional and translational levels.
Results UbcH10 expression was related to the grade of malignancy. In fact, it was low in indolent tumours and high in a variety of HL and NHL cell lines and in aggressive lymphomas. It was highest in Burkitt's lymphoma, as shown by quantitative real-time polymerase chain reaction and by tissue microarray immunohistochemistry. Flow cytometry of cell lines confirmed that UbcH10 expression is cell-cycle dependent, steadily increasing in S phase, peaking in G2/M phase and dramatically decreasing in G0/G1 phases. We also showed that UbcH10 plays a relevant role in lymphoid cell proliferation, since blocking of its synthesis by RNA interference inhibited cell growth.
Conclusion(s) Taken together, these results indicate that UbcH10 is a novel lymphoid proliferation marker encompassing the cell cycle window associated with exit from mitosis. Its overexpression in aggressive lymphomas suggests that UbcH10 could be a therapeutic target in this setting.

P2.209

Immunotopography of cells expressing markers of histiocytic and dendritic cells in thymus

Bai M.; Papoudou-Bai A.; Karatzias G.; Doukas M.; Stefanaki K.; Kanavaros P.
Department of Pathology, Medical School, University of Ioannina, Ioannina, Greece

Background Since histiocytic and dendritic cells play key roles in the thymic function and pathology we analyzed the immunotopography of cells expressing markers of histiocytic and dendritic cells in normal thymus.
Methods Twenty normal thymuses from newborns, children, adolescents and adults were studied by paraffin-section immunohistochemistry using antibodies against pan-cytokeratin, S100 protein, CD1a, CD207, CD123, CD11c, CD68 and CD163.
Results In thymuses from newborns and children S100 protein, CD1a, CD207, CD123 and CD11c positive cells were found in the medullary region and in Hassall corpuscles [HC]. CD123 was not detected in HC. In thymuses from adolescents and adults reduced number of S100 protein, CD1a, CD207, CD123 and CD11c positive cells were found in the medullary region but not into HC. In all thymuses CD11c positive cells were also found in the cortical region and CD68 and CD163 positive cells were found in both cortical and medullary region. By double immunostaining the neural/neuroendocrine markers neurofilaments, chromogranin, synaptophysin and tyrosine hydroxylase were detected only in cells expressing pan-cytokeratin.
Conclusion(s) The detection of S100 protein, CD1a, CD207 and CD11c positive dendritic cells in the medullary region and into HC in newborns and children, may reflect an important role of HC in the cooperation of epithelial and dendritic cells in the process of T-cell differentiation. The absence of S100 protein, CD1a, CD207 and CD11c positive dendritic cells into HC in adolescents and adults may reflect the age-related thymic involution.

P2.210

Metachronous follicular lymphoma in a patient with prostatic adenocarcinoma: a case report and review of the literature

Venizelos I.; Anagnostou E.; Papathomas T.; Spandos V.; Massa E.
Hippokration, Thessaloniki, Greece

Background Prostate cancer is associated with several secondary malignant neoplasms. Synchronous hematolymphoid malignancies, mainly coincidental non-Hodgkin's lymphoma discovered during pelvic lymphadenectomy for prostatic adenocarcinoma, albeit rare, have been reported. We present a case of a metachronous presentation of follicular lymphoma in a patient with a previously diagnosed prostatic acinar adenocarcinoma.
Methods We report a case of a 65-year-old man, who underwent a prostate biopsy due to relatively elevated PSA levels (PSA=7.5 ng/ml). Histopathologic examination of showed the presence of acinar adenocarcinoma, Gleason score 7 (4+3). A year later, he presented with fatigue, weight loss and palpable lymph nodes in the right inguinal region., which were surgically removed.
Results On histology, the architecture of the lymph nodes was effaced by the presence of multiple lymphoid follicles of variable size, which consisted of centroblasts (>60%) and centrocytes. The lymphoma cells showed positivity for CD20, CD79a and bcl-2, while they were negative to CD3, CD5, CD10, CD23 and cyclin D1. So, the diagnosis of follicular non-Hodgkin lymphoma, grade IIIA was made. The patient received chemotherapy with rituximab-CHOP and is well 8 months after the establishment of the diagnosis.
Conclusion(s) We present a rare case of follicular non-Hodgkin lymphoma in the background of a previously

diagnosed prostatic adenocarcinoma. We recommend that any lymph node enlargement in patients with prostate cancer should be investigated.

P2.211

Promoter hypermethylation of multiple genes in ocular adenxal malt lymphoma

Kim Y.; Kim W.; Jeon Y.; Choung H.; Kim C.
Boramae Hospital, Seoul, Republic of Korea

Background Aberrant methylation of CpG islands in promoter regions is one of the major mechanisms for silencing of tumor suppressor genes in various types of human cancers including non-Hodgkin's lymphomas. Ocular adnexal MALT lymphoma (ocular MALToma) is the most common lymphoma arising in the ocular adnexa. But little is known about the pathogenesis of this tumor. In this study, we investigated the aberrant promoter methylation status of known or suspected tumor suppressor genes in ocular MALToma and correlated them with the clinical parameters.
Methods 24 cases of ocular MALToma were examined for the methylation status of nine genes (p16, p14, DAPK, RASSF1A, CDH1, MGMT, MT1G, THBS1 and RARβ) using methylation specific PCR. Clinical information was obtained from reviewing medical records.
Results CpG islands methylation was variously found in nine genes as follows; DAPK (95.8%), CDH1 (75%), THBS1 (33.3%), RARβ (33.3%), MT1G (29.2%), p16 (16.7%) and MGMT (8.3%). RASSF1A and p14 methylation was not detected in any of 24 ocular MALTomas. All cases showed more than one gene methylated, and overall methylation index was 0.32. Of nine genes tested, MT1G methylation status was significantly correlated with the progression free survival (p= 0.001). There was no correlation between methylation status and other clinical parameters such as age, sex and primary site of tumor.
Conclusion(s) In ocular MALTomas, DAPK and CDH1 were highly methylated and p16 methylation was rare. MT1G methylation status might be used to predict the treatment response in ocular MALToma.

P2.212

A comparative study between clinical behavior and real time quantitative reverse transcriptase polymerase chain reaction results in chronic myelogenous leukemia cases

Pávai Z.; Pap Z.; Bödör C.; Benedek I.; Köpeczi B.; Horváth E.; Muresan C.; Vasile K.; Dénes L.
University of Medicine and Pharmacy Targu Mures, Targu Mures, Romania

Background During the past year we managed to introduce the RQPCR method for CML follow-up. This study correlates our results with clinical data, and therapeutic response of the patients.
Methods We performed the follow-up of 11 patients from the Hematology and Transplantation Clinic. We studied the BCR/ABL fusion gene using an ABI 7500 Real-Time PCR System, and the primers and protocols recommended by the Europe Against Cancer Program.
Results Our lot comprised 7 male and 4 female patients, mean age 49 years. The diagnosis was established by cytogenetic exam, and the mean follow-up period was 3 years. Three new patients received Hydrea, while 8 patients received Imatinib following Hydrea treatment, and 2 of them had allogenous transplantation. During the follow-up period the fusion gene remained under the detection threshold in 4 cases. Its expression displayed not significant decrease in one case, and significant decrease in another case. Two male patients around the age of 49 had poor, respectively no therapeutic response to Imatinib therapy, so dasatinib had been introduced, but the results didn't improve. We lost one of them.
Conclusion(s) Our results suggest the successful implementation of the method, and the results reflect the condition of the patients. At the same time, we emphasize the importance of determination of the specific mutations in order to establish a correct and timely diagnosis of refractory cases.

P2.213

A monoclonal antibody anti-BDCA2 (CD303) highly specific for plasmacytoid dendritic cell neoplasms on paraffin sections

Lonardi S.; Rossini C.; Ungari M.; Marocolo D.; Petrella T.; Vergier B.; Balme B.; Facchetti F.
Spedali Civili, Brescia, Solferino, Italy

Background Tumoral proliferations of Plasmacytoid dendritic cells (PDC) may occur as "differentiated" PDC associated with other myeloid leukemias or as blastic PDC neoplasms (BPDCN)(WHO-2008). Immunohistochemistry is required for PDC identification, but none of the most commonly used markers (e.g.: CD123, CD2AP, TCL1, BCL11a) is totally PDC-restricted. We report a novel monoclonal antibody recognizing on paraffin sections BDCA2 (CD303), the most specific marker for these cells.
Methods Anti-BDCA2 antibody (clone 124B3.13) was applied on 10 cases of reactive lymph nodes, normal thymi (2), 4 cases of PDC tumoral proliferation associated with chronic myelomonocytic leukemia (CMML), 15

cases of BPDCN, 55 cases of acute myeloid leukemia (AML; all FAB subtypes), and 14 acute lymphoblastic leukemias (ALL; 10 B, 4 T). Specimens (including skin and bone marrow) were fixed in buffered formalin; bone marrow biopsies were decalcified with EDTA.

Results PDC were strongly stained by anti-BDCA2 in all reactive tissues, in the cases of PDC tumor associated with CMML and in 13 (86,7%) cases of BPDCN. In contrast, none of the AML and LBL reacted with anti-BDCA2; interestingly, in many of these cases scattered BDCA2+ PDC were identified. No other cells were found to be labeled by anti-BDCA2.

Conclusion(s) This anti-BDCA2 antibody is a very sensitive and specific marker for PDC on paraffin sections. It should be used as a first-choice immunohistochemical reagent for this cell population, particularly in neoplastic conditions where distinction from other blastic leukemias can be challenging.

P2.214

Autoimmune lymphoproliferative syndrome. A rare cause of splenomegaly

Ferreira C.; Tortosa F.; Lopes C.; Loidi L.; Albuquerque A.; Silva S.; Sousa A.; Santos C.; Piris M.; Fernandes A.
Department of Pathology, Hospital de Santa Maria, Lisbon, Portugal

Background Autoimmune Lymphoproliferative Syndrome (ALPS) is a rare inherited disorder with a childhood onset, caused by defects in apoptotic genes and characterized by organomegalies, autoimmune phenomena and an expansion of DNαβ,T-cells. We describe a family with an unusual form of presentation of ALPS.

Methods Members of three generations of a family in which splenomegaly and cytopenias were relevant findings were analyzed. Routine procedures for histology, immunohistochemistry and molecular studies were applied to the spleen specimens of two members. Sequencing of the FAS gene was performed in three members; immunological characterization and apoptosis of peripheral T-cells were studied in two members.

Results Splenomegaly and lymphadenopathies were discovered in a 29 years-old man during the staging of a seminoma. Ten years latter he was splenectomised. The spleen weighted 3550 g and had a perifolicular proliferation of CD57+, DN T-cells. A diagnosis of ALPS was purposed. A heterozygous mutation in the FAS gene of the patient and his daughters was found. The peripheral T-cells of the patient and his symptomatic daughter revealed a DNαβ,T-cells expansion and defective lymphocyte apoptosis in vitro. His father had a splenic small B-cell lymphoma; latter he developed a Hodgkin lymphoma and died during chemotherapy.

Conclusion(s) This family case emphasizes the importance of recognizing this entity in the differential diagnosis of splenomegaly and cytopenias. These patients have an increased risk for developing lymphomas. The patient's father had had a history of splenomegaly for years, probably due to ALPS, that was complicated by lymphoma.

P2.215

Comparative proteomic analysis of DLBCL from HIV+ and HIV- individuals by two-dimensional differential gel electrophoresis (2D-DIGE)

Canzonieri V.; De Re V.; Spina M.; Simula M.; Pavan A.; Toffoli G.; Perin T.; Massi D.; Tirelli U.
Aviano Cancer Center, National Cancer Institute, Aviano, Pordenone, Italy

Background Diffuse large B-cell lymphomas (DLBCL) are associated with different morpho-phenotypes and clinical outcome. Despite treatments (CHOP for GC subtype and R-CHOP for both GC and ABC-like subtypes), several patients remain unresponsive and/or experience relapse(s). The aim was to investigate whether an integrated proteomic and immunoistochemical approach may discriminate proteins expression profile between HIV+ and HIV- DLBCLs with good clinical response upon R-CHOP.

Methods Two dimensional fluorescence difference gel electrophoresis (2D-DIGE) was used to identify proteins that are differentially expressed in affected lymph nodes from 8 patients (5 HIV- and 3 HIV+) with DLBCL and good clinical response upon R-CHOP at 5 years follow-up. Immunohistochemistry identifies selected proteins in tumor tissues.

Results Data analysis by 2D-DIGE showed a limited number (23/250 analyzed, <10%) of differentially expressed proteins ($p \leq 0.05$) in HIV+ vs. HIV- DLBCLs. Difference spans ranged from a maximum of 3.53 times (anti-trypsin) to a minimum of -2.91 times (serpin). Proteins were clustered as cytoskeletric, extracellular matrix proteins, metabolic enzymes and proteins involved in the unfolding endoplasmatic process. Immunohistochemistry confirmed the high expression of proteins of histiocytes/macrophagic lineage.

Conclusion(s) We found a similar protein expression profile in HIV+ vs. HIV- DLBCLs. For several proteins there was good agreement between proteomic and immunohistochemical findings, providing insights into the biomolecular mechanisms involved in these malignancies and their possible use as biomarkers for good clinical response.

P2.216

EBV infection and deregulation of apoptotic pathways in PTLDS

Ghigna M.; Reineke T.; Rincé P.; Fabre M.; Durbach A.; Samuel D.; Joab I.; Guettier C.; Tingely M.; Lucioni M.; Paulli M.; Besson C.; Raphael M.
Centre Hospitalier-Universitaire de Bicetre, Le Kremlin Bicetre, France

Background PTLDs include a wide spectrum of lymphoproliferative disorders, possibly complicating the clinical course of solid organ or bone marrow recipients. We studied the expression pattern of apoptotic molecules in PTLD and we compared their expression with the presence of EBV expression of latent and replicative viral proteins. This would allow new insights in EBV linked lymphomagenesis.
Methods The analysed apoptotic molecules included: bcl-2, the antiapoptotic molecules Bax, Bim and PUMA, PARP and p53. Their expression has been tested by immunohistochemistry; the detection of EBV was also performed by ISH using EBER probes. A series of 53 PTLD was collected from 3 institutions (Bicêtre, Zurich and Pavia University Hospitals). Thirty-four out of 53 PTLD have EBV positive status and 19 are EBV negative. They are mainly adult onset PTLD and show DLBCL histology.
Results Bim, PUMA and PARP expression, showed a significant correlation with EBV status (EBV+ PTLD group: Bim+: 5/28, PUMA+: 4/34, PARP+: 3/34 vs EBV- PTLD group: Bim+: 10/17, PUMA+: 10/15, PARP+: 9/19 $p<0{,}005$). Any correlation between Bcl-2, Bax and p53 expression and EBV status was evidenced.
Conclusion(s) PUMA and Bim are BH-3 only pro-apoptotic proteins having an important role in lymphocyte cellular homeostasis. Their loss of expression is significantly correlated wth EBV status. These results suggest a significant impact of EBV infection on apoptosis pathways deregulation in PTLD and underline biological specificities in EBV linked lymphomagenesis.

P2.217

Epidemiological study of hemoglobinopathies in North Greece

Mitsikaris D.; Patiakas S.; Xiropoulou E.; Alexidis I.; Rousos K.
Diagnostic Center of Thessaloniki "Hemotest", Thessaloniki, Greece

Background To study cases of hemoglobinopathies in areas of North Greece and islands of the Aegean.
Methods A total of 3248 samples of patients were studied for anemia control, prenatal control, as well as pediatric cases. Blood tests were performed, hemoglobin electrophoresis, quantitative determination of HbA2 and HbS on columns, as well as HbF determination using immunodiffusion.
Results Homozygous b-thalassemia was revealed in 4 cases (0,12%). It concerns children aged <10 months with increased fractions of HbA2 and HbF in electrophoresis, in the families of which no prenatal control was performed.Heterozygous b-thalassemia (increased HbA2 fraction, hypochromia, anisocytosis, microcytosis, target cells and basophilic stain) was found in 342 cases (10,53%), while microsickle-cell anemia (positive sickle-cell test and increased HbA2 and HbS fractions in electrophoresis) was found in 2 cases (0,06%). Finally, homozygous sickle-cell anemia was found in 2 cases (0,06%) and heterozygous sickle-cell anemia in 3 cases (0,09%).
Conclusion(s) Therefore, it is proven that thalassemic syndromes are widely common in Mediterranean people like in Greece, where approximately 3.500 people suffer from thalassemia and 7,5% of Greek people are carriers of the disease, especially in some parts of Greece like the islands of the Aegean. As a result, the systematic effort to inform the public about the importance of the test is crucial, in order to avoid the births of children with the disease.

P2.218

Expression profiles of P27Kip1 and its phosphorylated form on Threonine-187 in B-cell lymphomas

Sirinian C.; Symeonidis A.; Giannakoulas N.; Vlotinou E.; Melachrinou M.
Dept. Pathology, Medical School University of Patras, Egio, Greece

Background Deregulated phosphorylation of p27 is implicated in tumorigenesis. P27-phosphorylation on Threonine-187 (pThr187p27) is involved in the poly-ubiquitination and degradation of the protein. We studied the p27 and pThr187p27 expression in B-cell lymphomas and their association with the proliferation index (PI).
Methods Paraffin-sections from 113 B-cell lymphomas [84 aggressive (66 DLBCLs, 13 MCLs, 5 FLs Gr 3) and 29 indolent (9 FLs {3 Gr 1, 6 Gr 2}, 10 MZLs, 10 SLLs)] were immunostained for p27, pThr187p27 and Ki-67. The expression of pThr187p27 was analyzed in relation to α-tubulin by immunofluorescence in HeLa cells.
Results Aggressive lymphomas showed a significant higher expression ($p<0.001$) of pThr187p27 [29.53%], while p27 expression predominated in indolent [69.39%] ($p<0.001$). The majority of DLBCLs showed a weak expression of p27. A positive and significant correlation between pThr187p27 immunoexpression and PI was detected in both groups. Moreover, a positive immunostaining for

pThr187p27 was observed in most of the mitotic lymphoma cells. The co-expression of pThr187p27 and α-tubulin in HeLa cells showed that pThr187p27 was accumulated in the nucleus during prophase, on centromeres and chromosomes during metaphase, on chromosomes at anaphase and relocated to the midbody at telophase.
Conclusion(s) The increased expression of pThr187p27 in aggressive lymphomas and its association with PI suggest that protein overexpression may be related with tumor aggressiveness. The expression pattern of pThr187p27 during mitosis in HeLa cells resembles the profile of mitotic kinases, indicating its possible involvement in mitosis.

P2.219
mTOR pathway activation in bone marrow biopsies of multiple myeloma

Cappia S.; Merlini R.; Bacillo E.; Tavaglione V.; Saglio G.; Papotti M.; Guglielmelli T.
AOU San Luigi Gonzaga, Orbassano, Turin, Italy

Background The mammalian target of rapamycin (mTOR) is a serine/threonine-specific protein kinase, downstream of the P13-K/AKT pathway. Previous in vitro studies on multiple myeloma (MM) demonstrated the therapeutic potential of rapamycin in combination with chemotherapy.
Methods Phosphorylated forms of AKT(Ser 473), mTOR (Ser2448), P70S6K(Thr389) and 4EBP1(Thr37,Trh46) were immunohistochemically analysed in bone marrow biopsy sections of 90 MM patients. The results were scored by a semiquantitative method, the HSCORE obtained multiplying staining intensity (0=negative, 1=weak, 2= moderate, 3=strong) by percentage of positive cells. Specimens with an HSCORE of ≥30 were classified as positive. Wilcoxon test was used to compare mTOR expression with clinical and laboratory data (sex, age, bone lesion location, isotype, Beta2-microglobulin, haemoglobin, creatinine and albumin serum levels).
Results Cytoplasmic p-AKT and p-mTOR expression was found in 54/90 (60.0 %) and 56/90 (62.2%) cases, respectively. Predominantly nuclear p-P70S6K and p-4E-BP1 were detected in 64 (71.1%) and 48 (53.3%) cases, respectively. In the 56 p-mTOR positive MM, significant correlation were observed with the expression of p-AKT (42/56, $p=0.003$), p-4E-BP1 (39/56, $p<0.001$) and (49/56, $p<0.001$). A statistically significant ($p=0.03$) correlation was also found between p-mTOR expression and serum levels≥3 g/dl of Beta2-microglobulin, a known marker of poor prognosis for MM.
Conclusion(s) A subgroup of MM patients with AKT/mTOR/P70S6K/4E-BP1 pathway activation was identified and found associated to poor prognosis. mTOR pathway phosphoprotein immunoprofiling could be useful to select patients for mTOR inhibitor therapies in combination with chemotherapy.

P2.220
Pathohistological and immunohistochemical analysis of bone marrow and blood telomerase activity in chronic myeloid leukemia

Jovanovic R.; Janevska V.; Spasevska L.; Chevreska L.; Stojanovski Z.; Petrusevska G.
Institute of Pathology, Skopje, the Former Yugoslav Republic of Macedonia

Background Chronic myeloid leukemia (CML) is a myeloproliferative disorder affecting all age groups, with peak incidence between 50–60 years.
Methods We analyzed 38 CML bone marrow (BM) biopsies. In 15 of the patients we also analyzed blood samples for relative telomerase activity (RTA). As a control for the RTA we used the results from our previous study (47 healthy, age matched persons). In all biopsy samples, we evaluated the degree of myelofibrosis and elevation in blast, megakaryocyte and eosinophil counts. The results were expressed in a semi-quantitative manner as low-grade, moderate and high-grade increase. We also performed immunostainings (IS) for Bcl-2, p53, and Ki-67. IS were expressed in a semi-quantitative manner as (1+), (2+) and (3+) signal.
Results The degrees of increase in blast, megakaryocyte and eosinophil counts were neither inter-correlated, nor correlated to the peripheral blood RTA. We found (2+) signal for Ki-67 (52,6% cases) and Bcl-2 (18,4% cases) with no (3+) cases, while p53 showed (2+) signal in 45% and (3+) signal in 8% of the cases, with significant correlation bertween the blast count increase and the IS expression of p53 ($p<0,01$) and Ki-67 ($p<0,01$). The mean RTA was significantly higher (15,9), compared to the controls (9,28) ($p<0,01$).
Conclusion(s) There is a significant correlation between the degree of blast count increase and the IS expression of p53 ($p<0,01$) and Ki-67 ($p<0,01$). Patients with increased p53 expression in BM show significantly higher blood RTA ($p<0,05$).

P2.221
Assessment of bone marrow plasma cell infiltrates in multiple myeloma

Stifter S.; Babarovic E.; Seili Bekafigo I.; Valkovic T.; Marijic B.; Lucin K.; Duletic Nacinovic A.; Jonjic N.
Department of Pathology, Rijeka University School of Medicine, Rijeka, Croatia

Background Assessment of bone marrow aspirates (BMA) as well as bone marrow biopsy (BMB) is an integral and important part of the standard algorithm used in multiple myeloma (MM) diagnosing and monitoring, so the methods should be accurate. The aim of this study was to compare plasma cell infiltrates evaluated in BMA and BMB with patients' clinical parameters.
Methods In a retrospective study, 79 patients with MM were classified according to cytological grading of the neoplastic cells as those expressing plasmacytic (mature) and plasmablastic (immature) differentiation (WHO criteria), degree of myeloma cells infiltration (%), and the pattern of neoplastic infiltration (diffuse, nodular, interstitial). The presence of marrow fibrosis and the normal haematopoesis were also studied. Plasma cells number and distribution in BMB was determined by independent pathologist count and image analysis software on CD138 stained sections.
Results Plasmablast morphology was more often present in BMB with up to 50% of plasma cell infiltrates (t-test=2.93; p=0.005). The agreement in results of assessment plasma cells infiltrates using the computer-assisted image analysis system and BMA, and BMB was r=0.4; p<0.05, r=0.80; p <0.05, respectively. The significantly higher percentage of tumor cells was observed in clinical stage II and III (p= 0.05), while overall survival was longer in patients with mature plasma cell morphology (p<0.05).
Conclusion(s) Obtained preliminary results suggest that usefulness of combined analyses when ever possible in order to achieve more accurate and predictive information.

P2.222

B-cell lymphoma unclassifiable, with features intermediate between DLBCL and Burkitt lymphoma showing unusual genetic features

Zorzos Savas C.; Ioannou M.; Hatzianastassiou D.; Anagnostakis D.; Kouvaras E.; Koukoulis K.G.; Androulaki A.
'Elpis' General Hospital, Athens, Attika, Greece

Background To present a case of B-cell lymphoma, unclassified with features intermediate between diffuse large B-cell lymphoma (DLBCL) and Burkitt lymphoma (BL) with paradoxical genotype, regarding a 45-year-old man presenting with generalized peripheral lymphadenopathy, fever and cahexia.
Methods A cervical lymph node was biopsied and the submitted material was evaluated by means of immunohistochemistry and FISH.
Results The morphology was compatible with a Burkitt-like lymphoma exhibiting diffuse proliferation of medium to large-sized transformed cells and typical "starry sky" macrophages. Immunohistochemically, the neoplastic cells expressed B-cell markers with intense co-expression of bcl-2. Using a split probe for BCL2, the majority of the lymphoid cells showed triple fused signals, suggestive of trisomy 18. MYC rearrangement was not seen.
Conclusion(s) This type of unclassifiable B-cell lymphoma is heterogenous and is not considered a distinct disease entity but it is useful in allowing the classification of cases not meeting the criteria of BL or DLBCL. Genotype features similar to those of our case are exceedingly rare.

P2.223

B-cell lymphoma unclassifiable, with features intermediate between DLBCL and classical Hodgkin lymphoma

Zorzos Savas C.; Hatzianastassiou D.; Anagnostakis D.; Papadaki T.; Androulaki A.
'Elpis' General Hospital, Athens, Attika, Greece

Background To present a case of B-cell lymphoma, unclassified with features intermediate between diffuse large B-cell lymphoma (DLBCL) and classical Hodgkin lymphoma (CHL) in a peripheral lymph node associated with mediastinal disease and lung infiltration.
Methods A cervical lymph node was biopsied and the submitted material was evaluated by means of immunohistochemistry and PCR for IG rearrangement.
Results The morphology was compatible with a classical Hodgkin lymphoma, nodular sclerosis with an area of diffuse neoplastic cell proliferation. Immunohistochemically the neoplastic cells showed a preserved B-cell programe demonstrated by strong expression of CD20, CD79a, bcl6, PAX5, CD30, and CD15, favoring the diagnosis of grey zone lymphoma. PCR analysis showed oligoclonality.
Conclusion(s) This type of unclassifiable lymphoma has overlapping morphologic and immunohistochemical features between classic Hodgkin lymphoma and DLBCL, pursuing a more aggressive clinical course and unfortunately there is no consensus on the preferred treatment.

P2.224

Bone marrow involvement by B-lineage non-Hodgkin lymphomas. Clonal detection using the biomed-2 protocl on marrow aspirates

Vermi W.; Medicina D.; Marocolo D.; Rossi G.; Borlenghi E.; Ferrari S.; Ungari M.; Facchetti F.
University of Brescia, Brescia, Italy

Background The evaluation of bone marrow involvement in B-NHL patients is critical with respect to staging and assessment of treatment response. Flow

cytometry of bone marrow aspirates together with the histopathological evaluation of trephine biopsy represent a standardized approach for such analysis. The present study was aimed to evaluate the usefulness clonality analysis using the BIOMED-2 protocol on marrow aspirates of B-NHL patients.

Methods Bone marrow biopsies and aspirates were obtained from 65 consecutive patients with suspicious or known B-cell lymphoma and from eight cases from patients with non-B-cell hematological malignancies (CTR). Marrow aspirates were obtained immediately after the trephine biopsy. DNA was purified using QIAamp DNA Blood Mini Kit. BIOMED-2 primers set and GeneScanning analysis were used for detection of complete IGH rearrangements (VH-JH).

Results Amplifiable DNA was obtained from 71 samples (97.2%). The clonal detection rate in patients with documented marrow involvement was 90.7% (39/43); negative cases were represented by post-germinal centre lymphomas (2 follicular, 1 splenic marginal-zone and 1 diffuse large cell lymphomas). Notably, clonality was detected in 3/20 (15%) of morphologically negative cases; in two of them the clone was identical to that detected in the original B-cell tumor. No clonal rearrangements were found in the CTR group.

Conclusion(s) Detection of marrow involvement by B-NHL is obtained with a high sensitivity by the BIOMED-2 protocol on marrow aspirates. This procedure might be considered complementary to bone marrow biopsies in follow-up studies.

P2.225

Congenital aggressive variant of langerhans cells histiocytosis with CD56 +/ E-cadherin- phenotype

Lucioni M.; Beluffi G.; Fiandrino G.; Zecca M.; Inzani F.; Viglio A.; Nicola M.; Stronati M.; Necchi V.; Riboni R.; Locatelli F.; Paulli M.

Foundation IRCCS Policlinico San Matteo, Pavia, Italy

Background In children less than 2 years cutaneous involvement is the most frequent presentation of Langerhans cell histiocytosis (LCH). Cutaneous LCH can be localized or associated with dissemination and organ dysfunction. The clinical course is variable from spontaneous regression to fatal outcome. Herein we describe a case of congenital LCH presenting in the skin and pursuing an aggressive clinical course.

Methods A female newborn presenting with congenital cutaneous lesions (rashes, petechiae and small papules) who rapidly developed pulmonary infiltrates and osteolytic lesions. On the fourth day of life the patient underwent skin biopsy.

Results Histologic examination of skin biopsy showed a dermal infiltrate of medium to large cells, some of them with grooved to lobulated nuclei, others with more pleomorphic nuclei and prominent nucleoli. The phenotype of the cellular infiltrate (CD1a+, S-100+, Langerin+/-) was in keeping with LC origin. Numerous mitoses (15 per 10 HPF) and high Ki-67 proliferation index (20%) were found. Lesional LCs lacked E-Cadherin but deeply stained for CD56. On such findings a histopathological diagnosis of LCH was made; the presence of cytologic atypia, the high mitotic index and Ki-67 rate suggested an aggressive variant. The clinical course was rapidly fatal despite chemotherapy and the patient dead on 16th day.

Conclusion(s) So far, no strict correlation between morphology and prognosis has been documented in LCH, but, in our case, peculiar morphological and immunohistochemical features (CD56 expression and E-Cadherin negativity) seem to predict an aggressive clinical course.

P2.226

Determination of apoptosis and proliferation status in different immunophenotypic profiles of diffuse large B-cell lymphoma

Sen Turk N.; Ozsan N.; Caner V.; Karagenc N.; Düzcan F.; Düzcan E.; Hekimgil M.

Medical School of Pamukkale University, Denizli, Turkey

Background The aim of this study was to investigate the expression profiles of apoptosis-associated proteins, apoptotic index, and proliferetion index in different immunophenotypic profiles of diffuse large B-cell lymphoma.

Methods Immunophenotypic profiles were determined according to bcl6/CD10/MUM1 expresion patterns and classified as germinal center B-cell like phenotype (GCB) and activated B-cell like phenotype (ABC) in total of 101 samples of diffuse large B-cell lymphomas. The expression profiles of apoptosis-associated proteins including bcl2, bcl-xl, bax, bak and bid were determined by IHC while TUNEL method was used to determine apoptotic index. Proliferation index was measured by Ki67.

Results Twenty nine samples were classified as GCB phenotype (28.7%) and 72 samples (71.3%) as ABC phenotype. The proliferation index was significantly higher in GCB profile than in the ABC profile. The expression of bcl6 was positively correlated with the expression of bcl2 (r=0.226, p=0.023), the apoptotic index (r=0.272, p=0.006) and the proliferation index (r=0.515, p≤0.001), and significant negative correlation was observed with the expression of bax (r=-0.221, p=0.027). The expression of MUM1 showed significant positive correlation with the expression of bcl-xl (r=0.295,

$p=0.003$), bid ($r=0.313$, $p=0.002$), apoptotic index ($r=0.341$, $p\leq0.001$) and proliferation index ($r=0.330$, $p=0.001$).

Conclusion(s) Our results suggested that bcl6 may be reponsible for significantly high proliferation index observed in germinal center B-cell like phenotype.

P2.227

Focal follicular lymphoma in the lymph node of the gallbladder neck. The significance of diagnosis in clinical management

Parasi A.; Karacosta A.; Karayannis M.; Fameli M.; Dogan A.
Department of Pathology, General Hospital Nikaia-Piraeus, Piraeus, Greece

Background Partial involvement of lymph nodes (LN) by follicular lymphoma (FL) and "in situ" FL/intrafollicular neoplasia are terms which need further clarification. The "in situ" FL has recently been recognized by the revised WHO classification. Some of the cases already have FL elsewhere, other develop FL later or remain without evidence of FL.

Methods We present a case of focal involvement of the gallbladder neck LN by an FL, grade 1, in a 64-year old woman, who underwent operation for chronic cholecystitis. The LN was found macroscopically.

Results Microscopic examination showed a focal, subtle architectural disturbance, with some follicles containing a population of small B- cells with centrocytic cytology and CD20, CD10, bcl-2 protein expression. Further investigation of the patient did not reveal either nodal or gastrointestinal lymphoma or bone marrow infiltration, except for slight splenomegaly. Six months after diagnosis, no splenectomy has been performed and the patient is under surveillance. We presume that the lesion represents a focal infiltration by FL (which possibly originated from the spleen), rather than an early in situ FL of the LN of the gallbladder neck. Our case is interesting because a focal or "in situ" FL of gallbladder LN has not been described in the literature until now.

Conclusion(s) The careful microscopic examination of an LN, excised for other reasons, and proper immunohistochemistry can lead to the diagnosis of a subclinical FL.

P2.228

Histiocytic sarcoma arising from low grade B-cell lymphomas: molecular/genetic evidence of clonal relationship between two morphologically and immunophenotypically distinctive neoplasms

Wang E.; Hutchinson B.
Duke University Medical Center, Durham, NC, USA

Background Rare cases of histiocytic sarcoma (HS) have been reported in association with indolent B-cell neoplasms. The clonal relationship between these neoplasms remains unclear, although recent data suggest a transdifferentiation from follicular lymphoma (FL) to HS. We investigate this clonal relationship in two cases of B-cell lymphoma with subsequent HS.

Methods Diagnosis was based on morphology and immunohistochemical analysis according to WHO criteria. PCR-based immunoglobulin gene rearrangement and FISH for IgH/bcl-2 were performed on paraffin imbedded sections.

Results A 62 year old female with splenic marginal zone lymphoma (SMZL), treated with chemotherapy, developed groin lymphadenopathy one year after diagnosis. Lymph node biopsy showed HS. PCR for IgH gene rearrangement detected identical clonal rearrangements in both the spleen and the lymph node, each of 114 base pairs. A 61-old female with a remote history of FL (17 years) developed supraclavicular lymphadenopathy and multiple other infiltrating foci. Lymph node biopsy demonstrated HS. Bone marrow biopsy showed low level involvement by FL. PCR analysis of the lymph node detected a clonal rearrangement of the IgH gene and FISH analysis revealed IgH/bcl-2 fusion, a genetic hallmark for FL.

Conclusion(s) HS secondary to indolent B-cell lymphoma harbors a clonally rearranged immunoglobulin gene. IgH/bcl-2 fusion in HS secondary to FL suggests a clonal relationship between HS and FL, and thus a possible transdifferentiation. This concept could be extended to clonal evolution of other indolent B-cell lymphomas, such as SMZL, into HS.

P2.229

Immunohistochemical demonstration of NPMc+ acute myeloid leukemia: biological and clinical features related to cytoplasmic nucleophosmin expression

Mehes G.; Bedekovics J.; Rejtö L.; Hevessy Z.; Kappelmayer J.; Ujfalusi A.; Kajtár B.; Udvardy M.
Department of Pathology, University of Debrecen, Debrecen, Hungary

Background The mutation of the nucleophosmin gene (NPM1) is the most frequently occurring genetic aberration in acute myeloid leukemia (AML). Due to the obvious impact on disease outcome the current WHO classification also defines the new (provisory) entity of "AML with NPM mutation". NPM1 exon 12 mutations affect both the nuclear complexing as well as the nuclear export signaling (NES) domain resulting in accumulation of the NPM protein in the cytoplasm of leukaemic cells. The effect of the gene mutation can be directly demonstrated by immunohistochemistry (NPMc+).

Methods The study focussed on the critical evaluation of NPM positivity in archival material diagnosed in our center between 2005 and 2008. Biological and clinical characterization of NPMc+ AML was done using embedded bone marrow samples and smears.
Results 6 out of the 41 adult AML cases presented with cytoplasmic NPM immunostaining (14,6%). All but one were female patients, and all filled the criteria of de novo AML with no recurrent cytogenetic aberrations (6/23, 26,1%). The NPMc+ group displayed M2 or M4 morphology, low CD34, c-kit and HLA-DR expression making a clear phenotypic distinction from the unaffected cases possible. These results are in good agreement with previous studies. IHC staining demonstrated arteficial cytoplasmic staining in 4 cases possibly due to mechanical effects on the cells.
Conclusion(s) In conclusion, with critical interpretation immunohistochemistry is well applicable for the identification of NPM mutated AML in the daily hematopathology practice.

P2.230

Luetic lymphadenitis with macro-lymphoid nodules and B-cell pseudoclonality, potentially mimicking lymphoma

Fisogni S.; Medicina D.; Vermi W.; Bossini P.; Fappani L.; Rossini C.; Giardini R.; Facchetti F.
Spedali Civili di Brescia, Brescia, Italy

Background Lymphadenitis secondary to Treponema pallidum (Tp) infection typically shows follicular hyperplasia and capsular fibrosis, that may be associated with inflammatory pseudotumor-like changes. Here we report a case of Tp lymphadenitis showing a very unusual and hitherto undescribed reactive pattern consisting in multiple large lymphoid nodules simulating lymphoma.
Methods A 36 years old male in good general conditions presented with 5x2.5 cm cervical lymphadenopathy. In addition to routine histology, immunohistochemistry was performed using different anti-leucocyte antibodies and the anti-Tp polyclonal antibody (Biocare Medical); molecular analysis for B-cell clonality was performed using the BIOMED-2 protocol for heavy and light chains on DNA extracted form multiple paraffin blocks.
Results The node showed, in addition to pronounced follicular hyperplasia and capsule fibrosis, multiple large nodules containing numerous CD20+TCL1+IgD+ mantle B-cells, admixed with CD3+PD1 intrafollicular T-cells, endothelial cells, sparse histiocytes, plasma cells and neutrophils. Immunohistochemistry for Tp showed innumerable spirochetes within these nodules. PCR analysis revealed a clonal population for FR2-FR3 frameworks of IgH gene in a single tissue block, but a polyclonal pattern in another.
Conclusion(s) A recent outbreak of syphilis has been observed in Western Europe and pathologist should be aware of the multiple forms of histological presentation of the infection. The macronodular reactive pattern here reported is particularly worrisome, since it may simulate follicular lymphoma or Lymphocyte predominance Hodgkin lymphoma. B-cell molecular pseudoclonality was also observed in this case, pointing to the importance to correlate molecular results with histology.

P2.231

Modulation of lymph node sinus endothelial expression of LSECTin, DC-SIGN, DC-SIGNR, Lyve-1 and CD31 with local environment

Soilleux E.; Wheeldon S.; Cotterill A.; Gramberg T.; Poehlmann S.
Oxford University, Oxford, Oxfordshire, United Kingdom

Background LSECtin is a recently identified C-type lectin encoded in a gene cluster with DC-SIGN, DC-SIGNR and CD23 on chromosome 19p13.3. Antibody or ligand-mediated engagement triggers rapid LSECtin internalisation, suggesting it acts as an antigen uptake receptor that may recognize host or pathogen-derived proteins. We demonstrated that LSECtin expression is restricted to liver, lymph node and bone marrow sinus endothelial cells.
Methods We used standard immunohistochemical techniques to investigate whether LSECtin, DC-SIGN and DC-SIGNR, the functionally related protein Lyve-1, and PECAM-1 (CD31) demonstrated modulation of their expression levels on lymph node sinus endothelium in relation to local microenvironment.
Results In granulomatous conditions, there was some loss of LSECtin, DC-SIGN and DC-SIGNR and little change in Lyve-1 or CD31 expression. In conditions with necrosis (Kikuchi's lymphadenitis and caseating granulomatous inflammation), there was marked LSECtin, and more moderate DC-SIGN and DC-SIGNR downregulation, with Lyve-1 and CD31 upregulation. When metastatic melanoma or squamous cell carcinoma was present in the lymph node strong expression of LSECtin, DC-SIGN and DC-SIGNR was seen, but Lyve-1 and CD31 expression was less prominent. In Castleman's disease, only CD31 expression was seen on any foci of hyaline vascular proliferation.
Conclusion(s) LSECtin, DC-SIGN, DC-SIGNR, Lyve-1 and CD31 show modulation of expression by lymph node sinus endothelial cells in response to the environment within the lymph node. Further studies are needed to determine whether this modulation of expression may be used as a diagnostic or prognostic feature.

P2.232

Morphopathological praticularities of non-Hodgkin lymphoma in Romanian black sea area. A 5 years study

Dobre A.; Aschie M.; Papuc F.A.; Craciun A.A.; Poinareanu I.; Iliesiu A.; Iacub G.
Clinical County Hospital Constanta, Constanta, Romania

Background Lymphoma is a type of cancer that originates in lymphocytes of the immune system. Non-Hodgkin lymphoma are malignant proliferation of lymphocytes originated in lymph nodes. There are 40.000 new cases in every year for non-Hodgkin lymphoma. In Romania, non-Hodgkin lymphoma incidence is 5,1/100.000.
Methods We chose to study patients with malignant non-hodgkin lymphoma from 2004–2008, hospitalized in County Hospital Constanta. The diagnosis was established on the basis of paraclinical investigations, histopathological exams.
Results There were 65 non-Hodgkin lymphoma patients that distinguish a median diagnostic age of 61–70 years. Microscopical study of the specimens showed that the predominant tumoral type was Diffuse Small Cell Lymphocytic Lymphoma, followed by Lymphoblastic Lymphoma and Diffuse mixed lymphoma. Sex distribution for each lymphoma form showed no sex preference in Diffuse small cell lymphocytic lymphoma, Mixt follicular lymphoma, Histiocitic lymphoma. In case of Large cell anaplastic lymphoma Hodgkin-like, Mixt follicular and difuse lymphoma, Burkitt lymphoma, Diffuse mixed lymphoma, Lymphoblastic lymphoma there was evidentiated some degree of sex determinism. Burkitt lymphoma was diagnosed in younger ages and other lymphomas were diagnosed in older ages.
Conclusion(s) Median diagnosis age in Constanta, Romania is 60–70 years old, showing a belay diagnosis age than in USA, Australia or developed European countries. Sex ratio on studied cases was M/F=3/2. Microscopical study of the specimens showed that the predominant tumoral type was Diffuse Small Cell Lymphocytic Lymphoma.

P2.233

Peroxiredoxin IV is overexpressed in multiple myeloma

Demasi Paula A.; Ortega M.; Lima Silvia C.; Araújo Soares N.; Araújo Cavalcanti V.
São Leopoldo Mandic Institute and Research Center, Campinas, São Paulo, Brazil

Background Multiple myeloma (MM), the second most prevalent hematological cancer, is a multi-focal plasma cell proliferation in bone marrow, usually presenting highly malignant behavior. Thanks to the overload of immunoglobulin production, MM cells are constantly exposed to endoplasmic reticulum stress and increased levels of hydrogen peroxide, the main byproduct of oxidative protein folding. Cells respond to such stress by activating the unfolded protein response (UPR), which is crucial for MM cell survival. Peroxiredoxin (Prx) IV is the endoplasmic reticulum-located member of the Prx family, which comprises ubiquitous proteins with the ability to catalyse peroxide detoxification.
Methods To investigate the participation of Prx IV in the UPR, we studied its expression in tissue samples from MM patients by immunohistochemistry and we also performed quantitative PCR utilizing plasma cells isolated from bone marrow mononuclear cells from healthy and MM donors.
Results All MM samples were positive for Prx IV, with cell staining proportion higher than 85 percent. In addition, results from qPCR demonstrated that Prx IV expression levels in plasma cells from MM patients were significantly increased, corresponding to at least ten fold those observed in plasma cells from healthy donors.
Conclusion(s) In conclusion, we demonstrated that Prx IV is overexpressed in multiple myeloma cells, suggesting that this protein could participate in the UPR, functioning in the elimination of the potentially damaging by-products of disulfide bond formation, thus providing protection against oxidative stress-induced apoptosis to MM cells.

P2.234

Primary intracranial meningeal marginal zone B-cell lymphoma of malt type with an extensive plasmacytic differentiation. A case report

Campr V.; Hrabal P.; Koren J.; Mohapl M.; Mrhalova M.
Teaching Hospital Motol, Prague, Czech Republic

Background Primary intracranial low grade lymphoma of dura is a rare neoplasm. The preoperative diagnosis is usually meningioma or subdural hematoma. The most common type is marginal zone B-cell lymphoma of MALT type. The plasmacytic differentiation of tumour is common, but only rarely plasma cells are prevailing.
Methods We are reporting a case of 59 year old woman. She underwent control MRI examination two years after evacuation of arachnoid cyst and a bioptical diagnosis of chronic pachymeningitis. MRI findings were consistent with a diagnosis of meningioma.
Results Histologically there was predominantly plasmacytic infiltration of thickened fibrotic dura. The infiltrate was centered on several small lymphoid aggregates. Immunohistologically the plasma cells expressed CD138,

MUM1 and kappa light chains; lambda chains and CD56 were negative. Small B-lymphocytes were CD20 and BCL2 positive; CD10, BCL6, cyclin D1 and CD5 were negative. There were CD23 positive networks of follicular dendritic cells and a disperse admixture of CD5 positive small T-lymphocytes. The nuclear positivity of Ki67 was found in approximately 10 % of tumour cells. The complete staging work-up including bone marrow trephine biopsy ruled out any systemic lymphomatous involvement. The only pathological finding was triclonal gammopathy IgA/kappa (13 g/l).

Conclusion(s) The patient was treated with systemic chemotherapy plus rituximab and intrathecal Methotrexate, followed by a local radiotherapy (40 Gy in total). The 1-year follow-up confirms a complete remission, the patient is alive and well. (Supported by VZ MZ CR 00064203/6704.)

P2.235

Rare morphologic variants of multiple myeloma: study of 208 cases at first diagnosis

Fameli M.; Iordanidis F.; Marinos L.; Georgiadou D.; Xilouri I.; Kokkini G.; Papadaki H.; Papadaki T.
Hematopathology Dpt, Evangelismos, Athens, Greece

Background The purpose of this study is to alert the pathologists and hematologists in peculiar morphologic variants of myelomatous cells, in multiple myeloma (MM), with certain diagnostic difficulties, mainly on bone marrow trephines (BMT).

Methods Materials-Methods: 208 patients with BMT (EDTA decalcification), with MM (infiltration~20%-90%). Immunohistochemistry: CD3, CD20, CD30, CD34, CD56, CD117, CD138, cyclin D1, MUM-1, PAX-5, MIB-1, CIg, MPO, LAT-1, Glycophorine C, Cytokeratines. Five patients had follow up biopsies (1- 4, total 15).

Results 34/208 (16.3%) cases showed a peculiar morphology of the myelomatous cells. Four groups, were divided, mimicking A: foamy histiocytes: 19/34 (55.9%), B: anaplastic cells 12/34 (35.3%), C: AML 2/34 (6%), D: megakaryoblasts 1/34. Immunophenotype: CD138+, MUM-1+, CD20-, CD56 + (66.6% group A, 10% group B), cyclin D1+ (50% group A, 25% group B). In group A, α-heavy chain restriction was demonstrated in 9/14 (~ 64.3%) cases, while λ-light chain restriction was observed in 11/19 (58%) cases. In group B, κ-light chain predominated: 9/12 (~ 75%) cases showed κ-light chain restriction, 5/12 (41.6%) with only κ-light chain presentation. No morphological differentiation was noted in follow up BMTs.

Conclusion(s) 1) MM cases with peculiar morphology represented approximately 16% of our material and caused severe problems in the differential diagnosis on H&E sections, which requires additional studies with a broad panel of immunohistochemical markers. 2) CIgA (λ) and Cig (κ) restriction were predominated in groups A and B respectively. Future steps: study of the potential correlation between morphological diversity and prediction.

P2.236

Rare form of splenic vascular lesions: sclerosing angiomatoid nodular transformation

Zurac S.A.; Micu V.G.; Nichita L.; Andrei T.R.; Simeanu I.D.; Ene E.A.; Tebeica T.; Staniceanu F.
University of Medicine and Pharmacy Carol Davila, Colentina University Hospital, Bucharest, Romania

Background Primary splenic tumors are uncommon, usually consisting in vascular proliferations. One of the most recently described lesions is sclerosing angiomatoid nodular transformation (SANT). It was first mentioned in October 2004 by Martel et al in a series of 25 cases. Few other cases have been reported since.

Methods We report one case of SANT in a 54-years-old man. An abdominal CT scan performed eighteen months after the symptoms onset (mild pain in upper left quadrant of the abdomen worsened by effort) revealed in the medium third of the spleen a hypoecogenic solitary nodular 34 mm mass, apparently well-delineated and a 7 mm cyst in the fifth hepatic segment. Splenectomy was performed for clinical assumption of a splenic lymphoma.

Results Gross examination revealed a slightly enlarged spleen (13/7.5/3 cm, 190 g); within the spleen, adjacent to the hillum, a firm brown-yellowish 4,5/3,5/3 cm mass was present without sharply peripheral demarcation. Microscopically, the tumor had vague polycyclic appearance; numerous concentric rings of collagen fibers septate masses of interconnected sinusoidal vascular spaces lined by plump endothelial cells interspersed with spindle/ stellate cells. Vessels of the angiomatoid nodules were positive for CD31, CD34 and weak positive for CD8.

Conclusion(s) SANT is a vascular benign tumor of the spleen, included in a large spectrum of similar lesions such as: splenic hamartoma, isolated diffuse hemangiomatosis, littoral cell angioma, hemangioendothelioma, angiosarcoma. We discuss the differential diagnosis and the correlations between clinical and pathological aspects of this new entity.

P2.237

Recording of changes in hemoglobin, hematocrit, Fe and TIBC in patients with malignacy at the duration of chemotherapy

Xiropoulou E.; Patiakas S.; Barbantonakis N.; Tsigaridaki M.; Rousos K.
General Hospital Of Goumenissa, Kastoria, Greece

Background The changes in hematocrit, haemoglobin and iron values as well as iron-binding ability were investigated in the neoplasmatic patients during chemotherapy.
Methods 67 patients were examined (9 men and 13 women): 7 were suffered from breast cancer, 5 from lung cancer, 4 from thick intestine cancer, 3 from prostate cancer and 3 with various other type of cancers. 1st sample of blood was received before the administration of chemotherapeutic schedule. 2nd and 3 rd blood sample were received 3 rd and 7th day after the administration, respectively.
Results The percentage increase of iron values average between 1st and 2nd sample was 215%, while in another case this increase was sixfold higher. On the contrary, the higher reduction between second and third sample was 98%, while the average value reduced at 51%. The fluctuation in TIBC was lower, (changes <20%), while almost stable remained the values of hematocrit and hemoglobulin values in the various measurements.
Conclusion(s) 1)The iron values and the total iron-binding ability are very high the 3 rd day during chemotherapy, while the measurements return in their normal range afterwards the 7th day. 2)Reversely, the hematocrit and hemoglobulin values were not significantly influenced. 3) The simultaneous examination of bone marrow during the chemotherapy would potentially help in the explanation of our observations. Moreover, our findings should be confirmed with further studies.

P2.238
Reticulin fiber density and microvessel density in pediatric all cases

Tezcan G.; Akkaya B.; Kupesiz G.; Yesilipek A.; Hazar V.
Akdeniz University School of Medicine, Antalya, Turkey

Background The prognosis of ALL has improved mainly because of risk stratified approach for treatment according to prognostic factors. The aim of this study was evaluation of BMstroma in respect to MVD and RFD and investigation of these factors in relation to other proposed prognostic factors.
Methods We retrospectively evaluated MVD and RFD in sections from diagnostic BM biopsies from children with ALL.
Results A hundred nineteen specimens were available. RFD was found higher in B-lineage-ALL compared to T-lineage-ALL ($p<0.05$). MVD was not found different in B-and-T-lineage leukemias. MVD and RFD did not differ in respect to sex and being at the age of below or above 6 years. Although anemia (hemoglobin <10gr/dL) was not associated with MVD or RFD, there was a correlation between MVD and WBC count being above 20.000/mm^3. RFD was inversely correlated with WBC. In patients presenting with hepatomegaly MVD was found higher ($p=0.008$).All patients were treated according to ALL-BFM-chemotherapy protocol. Responses were evaluated on 8th, 15th and 33th days. In respect to MVD and RFD, there was no any statistical difference between responders and nonresponders. Median DFS and OS were 33 and 102 months, respectively.
Conclusion(s) The principal finding was association between the expression of B-lineage-markers and presence of BM-fibrosis. Despite small size of this group, ability of distinct immunphenotypes of ALL to stimulate a fibrotic reaction in BM seems different. MVD was found higher in patients presenting with higher WBC and with hepatomegaly but not found to have affect on survival.

P2.239
Rosai-Dorfman disease of the bone: a rare case of extranodal manifestation

Pokieser W.; Hackl M.; Wantke F.; Weigl G.; Chott A.
Institute of Pathology and Microbiology; Wilhelminenspital, Vienna, Austria

Background Rosai-Dorfman disease (RDD) is a rare, non-neoplastic disorder usually characterized by sinus histiocytosis and massive lymphadenopathy. Extranodal disease is frequent, but localized bone involvement is very rare.
Methods We present two consecutive patients with RDD in order to illustrate a diagnostically challenging case of extranodal disease as compared to the prototypical node-based manifestation. Case 1: A 43-year-old male reported on a more than one year history of bone pain localized to the left knee. Radiological examination showed multiple lesions involving proximal tibia and patella without cortical erosion or remodelling, suggestive of a lymphomatous process. All other tests were normal. Case 2: A 62-year-old female presented with massive cervical lymphadenopathy and dyspnoea due to bilateral pleural effusion. Fine needle aspiration cytology of an enlarged cervical lymph node contained large cells with uniformly round to oval shaped nuclei.. Subsequently, a lymph node biopsy was performed. CT-scans demonstrated abdominal lymphadenopathy.
Results Histology in both cases revealed characteristic features of RDD. Immunhistochemically the histiocytes were S100+, CD14+, and CD68R+, but negative for CD1a and CD30. The abundant plasma cells present in the bone biopsy were polytypic.
Conclusion(s) Outside the well preserved nodal microenvironment the diagnosis of RDD may require a high level of suspicion. The characteristic S-100+ histiocytes represent the sole clue suggestive of the disease after ruling out subtle involvement of large cell lymphoma.

P2.240

Frequency of gastrointestinal system hemorrhage cases in the population and correlation with their blood types

Rousos K.; Patiakas S.; Xiropoulou E.; Tsigaridaki M.; Charalampous C.
Health Center of "Alexandria", General Hospital of Veria, Veria, Greece

Background To document all the cases of patients admitted in the our General Hospitals, with gastrointestinal system hemorrhage.
Methods A total of 6758 patients were studied, 71 out of which (1,05%) had a history of melena stools or hemoptysis and were hospitalized for gastrointestinal bleeding. In all these patients anemia was discovered by the blood tests, which were followed by determination of the blood type and cross-referenced with gel card system.The hemodynamic state of the patients was studied on a daily basis and any blood transfusions were documented.
Results Out of 71 patients, 28 (39%) were in a good hemodynamic state and there was no need for a transfusion, while the remaining 43 (61%) were transfused with more than two (2) blood units. It concerned 12 patients (28%) with blood type O(+), 24 (55,8%) A(+), 2 (4,7%) O(-), 3 (7%) A(-), 1 (2,7%) AB(+) and 1 (2,7%) B(+).
Conclusion(s) Therefore, it is proven that gastrointestinal system hemorrhage is not so rare and in many cases a blood transfusion is needed in order to treat the hemorrhage. As far as blood types are concerned, the frequency of gastrointestinal hemorrhage cases coincides with the frequency of the blood groups in the general population, however in blood group A, an increased number of cases was documented in our study.

P2.241

Investigation of the frequency and the causes of thrombocytopenia

Xiropoulou E.; Patiakas S.; Charalampous C.
General Hospital of Goumenissa, Kastoria, Greece

Background To search for the causes, and also the frequency of thrombocytopenia.
Methods 145 cases of patients with thrombocytopenia (95 men, 47 women and 3 children) were registered. The count was made by an automatic analyzer, and afterwards followed the control of the blood smears in the common microscope.
Results 126 cases of real thrombocytopenia were confirmed by the study, while in the rest 19 cases (percentage 13,1%) pseudothrombocytopenia was found, since clumps of platelets were found in the blood smear examination. The 83 cases appeared in men, the 41 in women and 2 in children. Severe thrombocytopenia (PLT <50×103/mm3) appeared in 8 patients (6,35%), moderate thrombocytopenia (PLT 50-100×103/mm3) in 49 patients (38,9%), and mild thrombocytopenia (PLT 100-140×103/mm^3) in 69 patients (54,75%). In relation to the etiology, the following were found: CAUSES DISEASES Infections 25 (19,8%) Cancer 22 (17,5%) Hepatopathy 17 (13,5%) Blood diseases15 (11,9%) Drugs 13 (10,3%) Idiopathic thrombocytopenia 1 (0,8%) DIC 2 (1,6%) Others 31 (24,6%).
Conclusion(s) 1) The microscopic examination of the blood is absolutely necessary, particularly in patients with severe thrombocytopenia, considering that the percentage of psudothrombocytopenia (13,1%), is not negligible at all. 2) The men appear to have thrombocytopenia much more often than the women. 3) The majority of these cases (93,65%) refers to mild or moderate thrombocytopenia. 4) The most common causes of secondary thrombocytopenia are the infections, the cancer, the several blood diseases and drugs.

P2.242

Nodular lymphocyte predominant Hodgkin lymphoma with unusual morphology, mimicking granulomatous lymphadenitis

Hatzianastassiou Kyriakos D.; Mavrantonis C.; Papadaki T.; Androulaki A.
Department of Pathology, "Henry Dunant" Hospital of Athens, Athens, Attica, Greece

Background A 79-year old woman with long-standing history of myasthenia gravis presented with abdominal lymphadenopathy and fever.
Methods Laparoscopic surgical biopsy of a mesenterial lymph node was performed and the submitted material was evaluated by means of histochemisty for mycobacteria sp., immunohistochemistry and PCR for IG rearrengement.
Results The overall morphology was deceptively similar to that of a granulomatous lymphadenitis. However, very rare L&H cells were seen in association with the epitheliod aggregates. Their immunophenotypic profile was typical of NLPHL: CD45+, CD79a+, CD20+, PAX5+, BOB1+, EMA+, CD30-, CD15-.
Conclusion(s) This morphological variation is very unusual in the setting of NLPHL.

P2.243

Persistent polyclonal b lymphocytosis (PPBL). Report of three cases

Kanellis G.; Georgiadou D.; Foudoulaki A.; Kokkini G.; Stefanoudaki A.; Papadaki T.
Evangelismos, Athens, Greece

Background PPBL is a rare lymphoproliferative disorder of unknown etiology and mild biologic behavior affecting younger women, predominantly smokers.
Methods Three female patients, ages 35, 33 and 40, all with splenomegaly, leukocytosis and increased serum polyclonal IgM, were evaluated. Bone marrow biopsies (BMB, $n=3$), peripheral blood smears (PB, $n = 3$) and spleen samples ($n=1$) were studied by (i) flow cytometry (PB); (ii) morphology (Giemsa stains of PB smears and H&E sections of biopsy material); (iii) immunohistochemistry, (IHC) (paraffin); (iv) molecular analysis (PCR) for IgH gene rearrangements and bcl-2/IGH rearrangements.
Results (1)PB: lymphocytosis with "typical" PPBL morphology; polyclonal expansion of IgM + IgD + CD27+ B cells. (2) BMB Moderate small lymphocytic infiltration mainly intrasinusoidal and or interstitial. IHC: CD20 + CD79α + CD27/ + SIgMDκ+ = SIgMDλ + CD5-CD23-bcl2 + bcl6-CD10-DBA44-CD3-. Limited number of T cells (CD3 + CD20-) and polyclonal plasma cells (PCs). (3) Spleen. Prominent expansion of the marginal zone with a "biphasic like" lymphocytic cytology and a moderate lymphocytic infiltration of the red pulp (cords and sinuses), mimicking splenic marginal zone lymphoma (SMZL). Immunophenotypically the expanded lymphocytes were identified as marginal zone cells (CD20 + CD79a + bcl2 + CD21 + CD35 + SigMDκ+ =SigMDλ + CD10-bcl6-CD27 -/+ DBA44-CD5-CD23-CyclinD1). Additionally, polyclonal IgM + PCs in both the germinal centers and the red pulp. PCR analysis of the BMB and spleen samples revealed a polyclonal pattern of IgH gene rearrangements; one case tested bcl-2/IGH +.
Conclusion(s) Our findings (i) alert pathologists to the similarity between PPBL and SMZL both in the BMB and/or the spleen; (ii) support the recent hypothesis that B cells of PPBL are an abnormal expansion of memory (IgM + IgD + CD27+) B cells of the splenic marginal zone.

P2.244

Plasmatocytic neoplasm presenting as a paravertebral mass with an unusual amyloid deposition pattern

Gavriil A.
Athens, Greece

Background 25% of plasmacytomas and 10% of multiple myelomas show amyloid deposition among the neoplastic cells. These depositions are usually in the form of bands or in a fibrillary fashion. We present a case of an unusual pattern of amyloid deposition, reminiscent of thyroid follicles.
Methods A 60 year old male patient was admitted to hospital complaining of localised pain in the lumbar region. Physical examination revealed a paravertebral mass approx. 1,5 cm in diameter.
Results The specimen consisted of multiple brown tissue fragments. Microscopy revealed neoplastic tissue consisting solely of mature plasma cells. The main finding was the deposition of an amorphous eosinophilic substance, surrounded by histiocytes and multinucleated giant cells. These depositions were mainly forming round masses, giving the impression of thyroid follicles. The neoplastic process showed evidence of bone invasion. Imunohistochemical phenotyping showed positivity for κ-light chain, CD79a, CD 138 and CD 56. The amorphous eosinophilic substance reacted positively to Congo-Red and was also birefrigent under polarised light. A trephine bone marrow biopsy performed a week later showed limited interstitial infiltration (10%) by mature plasma cells of the same immunophenotype.
Conclusion(s) Multiple myeloma is known to present in the majority of cases as a bone lesion, sometimes with soft tissue extension. The presence of a paravertebral lession invading bone is a rather unusual presentation. Another uncommon finding is the formation of round amyloid depositions in such a fashion as colloid in the thyroid follicles.

P2.245

Primary anaplastic large cell lymphoma of the stomach: case report

Barisik Ozdemir N.; Keser Hallac S.; Gecer Ozgun M.; Gul Ege A.; Ablan E.; Cakir C.; Karadayi N.; Bildik N.
Dr. Lutfi Kirdar Kartal Educational and Research Hospital, Department of Pathology, Istanbul, Turkey

Background Anaplastic large cell lymphoma (ALCL) is a subgroup of non-Hodgkin's lymphoma first described by Stein et al in1985. The most common involvement sites of ALCL are lymph nodes, followed by skin, bone, soft tissue, lung and liver. Involvement of the stomach is very rare in literature.
Methods Retrospective evaluation of a patient with ALCL of the stomach.
Results A 43 year old female patient admitted to our hospital with complaints of abdominal pain, nausea, difficulty in swallowing and weight loss for the last three month. Ulcerovegetating mass, 3–4 cm in diameter was found in the cardia of the stomach at upper GI endoscopy. Pathologic examination of the endoscopic biopsy revealed, malignant cells determined on the ulcer ground. During surgery vegetating mass, 12x9x2cm in sizes was determined in cardia and total gastrectomy was performed. On microscopic examination of the mass; there were malignant cells on stroma that show diffuse infiltration.These were

abundant cytoplasm with irregular nucleus and prominent nucleolus. Immunohistochemical examination was performed and positive staining with CD 30, EMA, ALK-1, and vimentin were found while no staining was found with LCA, CD3, CD20, CD4, CD79 alpha, S-100, melan-A, Desmin, CD38, kappa, lambda, EBV, CK, CD117, CD34, synaptophysn. The pathological diagnosis was primary gastric anaplastic large cell lymphoma, common variant null cell type.
Conclusion(s) ALCL of the stomach is rare and Immunohistochemical evaluation is necessary in the pathologic diagnosis.

P2.246
Primary ovarian follicular lymphoma: a case report and review of the literature

Venizelos I.; Anagnostou E.; Papathomas T.; Spandos V.
Hippokration, Thessaloniki, Greece

Background The gynecologic tract has been well described as a site of involvement for non-Hodgkin's lymphoma (NHL). Primary (localized) NHL of the ovary is extremely rare, comprising less than 10% of NHLs with ovarian involvement.
Methods We report a case of a 51-year-old woman, who was presented with abnormal genital bleeding. After physical and ultrasound examination, the patient underwent an abdominal hysterectomy and bilateral salpingo-oophorectomy due to the presence of multiple leiomyomas. Gross examination revealed the presence of a solid tumor of the left ovary, measuring 2.5 cm in greatest diameter. The mass was solid, with elastic consistency and whitish colour.
Results Histopathologic analysis of sections from the ovarian tumor showed nodular and partially diffuse growth of small lymphoid cells. The lesional cells were characterized by round or irregular nucleus and inconspicuous cytoplasm. Mitoses were scant. Centroblasts were less than 5/HPF. Immunohistochemical examination showed positivity of the lymphoid cells to CD20, CD79a, CD10, and bcl-2. The abovementioned findings were consistent to primary ovarian follicular lymphoma, grade 1. Complete screening of the patient excluded other possible tumor sites. Chemotherapy was introduced and the patient is free of detectable disease 4 months after initiation of treatment.
Conclusion(s) After extensive review of the English literature, we detected 21 documented cases of primary ovarian NHL, 3 of them of follicular type. We report a case of a primary follicular lymphoma of the ovary, additional to this short list.

P2.247
Study of the level of B12 and folic acid in elderly patients with neuropsychic disorders

Charalampous C.; Patiakas S.; Palaiologou M.
Internal Medicine Clinic of Psychiatric Hospital of Thessaloniki, Kastoria, Greece

Background To study the incidence of memory and depression disorders in elderly patients with megaloblastic anemia.
Methods 87 elderly patients were included in the study, and 44 of them suffered from megaloblastic anemia.The levels of B12 and folic acid were measured. Out of the 44 patients: a) 21 -group I- aged 62–76 years old, presented light to severe memory disorders, and b) 23 patients -group II-aged 65–78 years old, presented light to severe depression. The rest 33, were all healthy-group III- aged 64–77 years old.
Results Between group I and II, a statistically significant difference (p=0,04) in relation to B12 level was found, without any positive correlation between the B12 level and the severity of the memory disorders. Moreover, in group II, an important deficiency of B12 was found in 13 patients out of 18-percentage 83,3%- while there was no positive correlation between low levels of folic acid and depression.
Conclusion(s) 1)The measurement of B12 in the serum of patients with memory disorders is very useful and it should not be omitted, since it can often reveal their causal factor, and 2) in contradiction to the levels of folic acid that don't seem to relate to depression symptoms, the reduction of the B12 level is an important risk factor for the appearance of depression, and consequently, its measurement should never be omitted in these cases.

P2.248
Systemic mastocytosis associated with hematological disorders

Fameli M.; Parasi A.; Papanikolaou A.; Vallianatou K.; Michailidou A.; Markidou F.; Filiotou A.; Kokkini G.; Laoutaris N.; Papadaki T.
Hematopathology Dpt, Evangelismos, Athens, Greece

Background The association of Systemic Mastocytosis (SM) with clonal, non-mast cell hematological disorders (NMHD), accounts for about 20%-30% of SM cases and represents a unique subcategory in the WHO classification (2008).
Methods During a ten year period, we revealed eleven cases [bone marrow trephines (BMT)] with NMHD associated with SM. The patients were three females and eight males, with mean age 66 years (43–86). BMT were examined with a broad immunohistochemical panel including CD2, CD25, CD68, CD117, mast cell tryptase.

Results All patients underwent BMT for hematological reasons, other than mastocytosis: CML=4, CMML=2, ET=1, AML=2, MDS=2, ET=1, while no one had clinical signs of SM. Histological evaluation of the neoplastic mast cells revealed two patterns: 1)variable sized clusters of mast cells with minimal or moderate cellular atypia, paratrabecular or perivascular distribution (6/11), 2) paratrabecular, hardly recognized small number of elongated mast cells trapped in fibrous tissue. Immunophenotype: mast cell tryptase +, CD25+, CD117+ (11/11) CD2+ 7/11. One case showed activating point mutation D816V for KIT. Follow up BMT in three patients showed that while the NMHD became minimal or absent, the neoplastic mast cell component was almost unchanged.

Conclusion(s) Our results 1) Confirm the value of BMT, since there are no clinical symptoms indicating the coexistence of SM and pathologists are the first ones who identify and confirm the neoplastic mast cell population. 2) Recognition of simultaneous presence of SM with NMHD, is critical for treatment planning, due to mast cell resistance to most cytoreductive agents.

P2.249

Three cases of indolent systemic mastocytosis in R. of Macedonia

Bogdanovska M.; Petrusevka G.; Kostadinova S.; Necovski P.; Stojanovic A.; Pavkovic M.; Janevska V.; Spasevska L.; Duganovksa S.; Dukova B.
Institute of Pathology, Skopje, the Former Yugoslav Republic of Macedonia

Background To present three cases with indolent systemic mastocytosis and follow up of the disease for at least 5 years.

Methods We used clinical histories and skin and bone marrow biopsies procedured by standard histological techniques (HE, Giemsa, Reticulin) and immunohistochemical analyses for LCA, CD117, CD3, CD20, CD33, CD68, CD15 and tryptase. Two patients were 34- and 35-years old males, and one 39 years old female. The patient had constitutional symptoms and classical Darier`s sign. Physical examination revealed numerous typical macular and maculopapular pigmented lesions. Other laboratory investigations were negative.

Results In the bone marrow biopsies we found partially disturbed architecture with paratrabecular and perivascullar patchy accumulations of spindled mast cells, consisting about 50% from the bone marrow cellularity. The focal lesions were comprised of varying proportions of mast cells, central core of lymphocytes, more rarely increased number of eosinophils. Focally, marked reticulin fibrosis could be found. Immunophenotype of the cells was as follows: LCA ++ - lymphoid cells and mast cells, CD117+ and tryptase + mast cells, CD3+ few lymphoid cells, CD20+ lymphoid aggregates, CD33+ myeloid cell lineage, CD68++ myelomonocytic cell lineage, CD15+ granulocytic cells. Histological examination of the skin biopsies revealed substantially lesser number of perivascular mastocytes besides obvious changes of the skin. We were not able to do cytogenetic and molecular analyses.

Conclusion(s) Follow up of the patients showed good condition for almost 5 years in two patients and for almost 7 years in third female patient, without therapy.

P2.250

Papillary adenocarcinoma of the thymus. A case report

Baliaka A.; Xirou P.; Christoforidou B.; Balis Christos G.; Barbetakis N.; Patakiouta F.
"Theagenio" Cancer Hospital, Thessaloniki, Greece

Background Papillary adenocarcinoma of the thymus is a rare type of primary thymic carcinoma and only a few cases have been reported in the literature.

Methods A 73-year-old man presented with a tumour in the upper lobe of the right lung. The tumour was surgically resected and proved to be a squamous cell lung carcinoma. During the operation, an anterior mediastinal tumour was found and, after a month, a second operation was performed in order to excise it.

Results Macroscopically the mediastinal tumour, measuring 3,7 cm in maximum diameter, was encapsulated with lobulated, white and firm cut surface. Histological and immunohistochemical features of the tumour were consistent with papillary adenocarcinoma of the thymus.

Conclusion(s) Papillary adenocarcinoma of the thymus occurs equally in males and females in their sixth to seventh decades of life. It usually presents as an enlarging anterior mediastinal mass, is more or less encapsulated and on cut sections appears lobulated, white and firm. Histologically it shows a tubulopapillary proliferation of cuboidal to columnar cells, with scattered psammoma bodies, highly reminiscent of papillary carcinoma of the thyroid. Immunohistochemically tumour cells are positive for CEA, CD5, Leu-M1 and BerEP4, whereas they are negative for CD20, thyroglobulin, pulmonary surfactant apoprotein and calretinin. Differential diagnosis includes mediastinal thyroid neoplasms, germ cell tumours, malignant mesothelioma, metastatic adenocarcinomas and adenocarcinomas of

foregut cyst origin. Prognosis is obscure, since the number of reported cases is limited. Our patient received no further treatment and remains alive 3 months after initial diagnosis.

P2.251
Diffuse large B cell primary bone and nodal lymphomas. Apoptosis related proteins, cell cycle and adhesion molecules studied by immunohistochemistry and FISH in 122 cases

Lima F.P.; Amstalden E.M.I.; Vassallo J.; Oliveira C.R.G.C.; Soares F.A.; Brousset P.
Department of Pathology, State University of Campinas, Campinas, São Paulo, Brazil; Institute of Orthopedic and Trauma of São Paulo University, São Paulo, Brazil; Department of Pathology, Hospital Antônio Cândido Camargo, São Paulo, Brazil; Center of Physiopathology of Toulouse-Purpan and Department of Pathology, Paul-Sabatier University, Toulouse, France

Objectives To evaluate the immunoexpression of proteins related to apoptosis and cell cycle (Bcl-2; Bcl-6; Bax; p53; pRB); adhesion molecules (CD29; CD62L; CD51); stages of B-cell differentiation and *BCL2*; *MYC; PAX5, BCL6, BCL-1/Cyclin D1* and *ALK* genes of diffuse large B-cell (DLBCL) primary bone (PBL) and nodal lymphomas.
Material/methods DLBCL (n=122) PBL (n=76) and nodal (n=46) were collected by TMA. Clinical, morphological, immunophenotypic and molecular features were compared. Detection of proliferation cell markers, proteins related to apoptosis; stages of B-cell differentiation germinal center(GC) and non germinal center(non-GC) and adhesion molecules were evaluated by IH method. The cytogenetic study was analyzed by FISH.
Results Both groups of DLBCL exhibited strong immunoexpression of proteins related to apoptosis and cellular cycle proteins, while the immunoexpression of adhesion molecules was weak/ absent. 63 PBL cases: 59% was GC and 41% was non-GC. Better outcome was associated with absence of adhesion molecules: CD29, CD62L and CD51 in both groups. Apoptosis molecules (Bax and p53) were related to worst behavior and pRB to favorable one in PBL. Bcl-2 and Bcl-6 were expressed in both lymphoma groups. Rearrangement of BCL2 (n=9/32) and MYC (n=3/32) were found, whereas PAX5, BCL6, BCL-1/Cyclin D1 and ALK genes were in germ line configuration. The majority of cases with rearrangements were of GC phenotype.
Conclusions These results suggest that bone DLBCL represents a specific particular extranodal B-cell lymphoma group.

Poster session 3

Dermatopathology

P3.1
Regulatory T (TREG) cells in cutaneous Leishmania major infection of young adults

Fischer M., Tenner-Racz K., Racz P.
Hamburg, Germany

Background Treg cells are involved in the regulation of immune responses against Leishmania (L) infection. To date, limited information on the role of intralesional Treg cells in human cutaneous leishmaniasis is available. We analyzed skin biopsies obtained from German military personnel with acute cutaneous leishmaniasis (ACL) who acquired the infection in Northern-Afghanistan where L. major is prevailing.
Methods Paraffin sections of the skin from 22 persons were analysed. Beside haematoxylin/eosin and Giemsa stains immunohistochemistry (CD4, CD8, FOXP3, CD25, CD68, lysozyme, CD1a, DC-LAMP, DEC-205, CD83, S-100 protein) was performed. Double labelling (CD4+FOXP3 and FOXP3+CD25) was done using the APAAPand the biotin-avidin-peroxidase methods. Quantitative image analysies was performed with a Zeiss AxioImager M1 microscope.
Results In ACL the FOXP3+CD25+ Treg cells are elevated. The parasitic burden and the elevation of intralesional Treg cells seem to correlate with each other. L was not detected in bone marrow derived dendritic cells. The host cells were CD68+ or lysozyme+ macrophages. The intralesional Treg cells were not associated with unresponsiveness to treatment.
Conclusion(s) Our observation is consistent with the experimental data suggesting that Treg cells play an important role in the persistence of L. major. It is possible that Treg cells exert a suppressive effect on the immunologic activation of macrophages thereby rendering them unable to eliminate the parasites. The numbers of Treg cells had no effect on therapy as reported in L. guyanensis infection (Bourreau et al. JID 2009).

P3.2
Interstitial granulomatous dermatitis: a distinctive histological pattern with variable clinical expression. Description of five cases

Colato C.; Peruzzi L.; Menestrina F.; Girolomoni G.
Department of Pathology, University of Verona, Verona, Italy

Background Interstitial granulomatous dermatitis (IGD) is a peculiar inflammatory reaction pattern with protean clinical presentation. Usually it is associated with autoimmune or connective tissue diseases, but correlation to lymphoproliferative disorders, solid neoplasms, drugs and infections has been also reported. The histologic differential diagnosis for this entity is broad and clinicopathologic correlation is essential to identify the underlying cause.
Methods We describe the clinical, serologic, and histologic features in five patients with IGD. Skin biopsy specimens were examined and correlated with the clinical and laboratory findings.
Results The study included 1 man and 4 women with erythematosus plaques (2 cases), patches (1 case), papules (1 case) and urticaria-like lesions (1 case). Lesions were asymptomatic or moderately itchy, bilateral and symmetrically distributed on the trunk and extremities. In three patients the cutaneous lesions were associated with the clinical and serologic findings of an autoimmune disease (rheumatoid arthritis, spondyloarthropathy and autoimmune thrombocytopenia). The histological examination disclosed a moderate to dense, diffuse dermal inflammatory infiltrate composed mostly of histiocytes distributed interstitially and focally in palisaded array around small sclerotic collagen bundles. In one case mucin deposition was observed and in 2 cases vacuolar interface dermatitis was also noticed. Immunohistochemical staining for CD68 confirm the histiocytic predominance of the infiltrate.
Conclusion(s) IGD identify a rather uniform histological pattern associated with variable clinical presentation. Classification of IGD remains controversial. Recognition of IGD is important as patients may have an underlying systemic autoimmune condition.

P3.3

Equine/animal-type melanoma (pigment synthesizing melanoma): a very rare variant of melanoma with indolent clinical course. A case report

Palumbieri G.
Hospital "Mons. R. "Dimiccoli", Barletta, Italy

Background Animal-type melanoma is an extremely rare low-grade variant of melanoma with prominent pigment synthesis and with indolent clinical behaviour. In 1832 W. Dick first reported a variant of melanoma in horses and termed it equine melanotic disease. By 1925 Darier described a similar lesion in humans and termed it melanosarcoma. It is reported a case of animal-type melanoma of the back, in a 33 year old men who presented an black nodule of the skin, near shoulder-blade, for over three years.
Methods The neoformation was tamponate formalin fixed, embedded in paraffin, and stained with ematoxylin-eosin. Immunohistochemical stains were performed using the avidin-biotin immunoperoxidase method.
Results At gross examination the cutaneous nodule, having a diameter of 1,3 cm, appeared exophytic, oval and black, with well defined edges. Histopathological and immunoistochemical features: the skin biopsy specimen revealed an exophityc heavily pigmented neoplasm occupyng the whole dermis and focally extended into the subcutaneous tissue. The atypical melanocytes showed short spindle-shaped and epithelioid morphology; they were arranged in perifollicular-perieccrine confluent sheet, fascicles and nodules, with evidence of junctional and intra-epidermal components, with focally pagetoid pattern; there was epidermal hyperplasia with focus of erosion. Mitoses were sparse. TILs were non-brisk. The Breslow thickness was 5.0 mm.
Conclusion(s) Animal-type melanoma is a distinct variant of melanoma with less aggressive clinical behaviour, but the lesion has metastatic potential, therefore full excision with sentinel node biopsy and long term follow up are indicated.

P3.4

Primary cutaneous spindle cell B-cell lymphoma. A case report

Incardona P.; Fisogni S.; Galletti A.; Gulotta T.; Fontana L.; Tironi A.
Spedali Civili, Brescia, Lombardia, Italy

Background Primary cutaneous spindle cell B-cell lymphoma represents an unusual morphological variant of diffuse large B-cell lymphoma (DLBCL), categorised in the WHO/EORTC classification, firstly described by Cerroni. We report a case of cutaneous lymphoma in who the spindle cell morphology may represent a diagnostic pitfall for the pathologist among dermal spindle cells proliferations (e.g. mesenchimal and epithelial).
Methods We examine a skin biopsy of a solitary lesion located on the scalp of a 40-year-old man. After the evaluation of hematoxilin&eosin slides (2–3 microns thick-sections), a wide immunohistochemical panel was performed, including mesenchimal, epithelial and lymphoid markers.
Results The histological examination revealed a dermo-hypodermic proliferation with a diffuse pattern of growth and a focal storiform arrangement, showing a grenz-zone against epidermis. The prevalent medium-sized spindle cell component merged with aggregates of large rounded nucleolated cells, preferentially deeply located. The immunophenotype revealed a positivity for LCA/CD45RB, evidencing the "lymphoid" nature of the neoplasm, and conversely a negativity for CK AE1/AE3, Vimentin, CD34,

CD68, S100, CD21+35. Further analysis showed the following phenotype: CD20+, CD79a+, CD10+, Bcl6+, Bcl2-, CD30-, ALK1; mitotic index (Mib1/Ki67) 80%. A complete staging, including bone marrow biopsy, performed after our diagnosis, was negative, confirming the cutaneous origin.

Conclusion(s) Primary cutaneous spindle cell B-cell lymphoma represents a morphological variant of DLBCL that may cause relevant diagnostic problems, as showed in our case. Mandatory remains a careful morphological examination, searching a large cell component that may represents a useful diagnostic clue, before any other stain.

P3.5

Acral lentiginous melanoma: a case series

Zarra I.; Driss M.; El Euch D.; Dhouib R.; Sassi S.; Mrad K.; Abbes I.; Ben Osmane A.; Ben Romdhane K.
Dermatolgy Department, La Rabta Hospital, Tunis, Tunisia

Background The epidemiology of melanoma varies widely in different ethnic groups. In Tunisia, a highly sunny country inhabited by mostly white people, the acral lentiginous melanoma (ALM) was the most common one. It is characterized by a lentiginous pattern of proliferation of the intraepidermal component of the tumour. The aim of this work is to study the characteristics of this type of melanoma and compare the prognostic histologic factors with the other types.

Methods We conducted a retrospective study in the department of dermatology and pathology in Tunis from 1981 to 2007 (27 years). For each patient we collected the epidemiological, histological and clinical features.

Results Forty six cases of melanoma were enrolled. Forty of them were ALM. The sex ratio M/F was about 1, with a mean age of 61 years. The anatomical localization was the sole in 12 cases. The mean Breslow thickness was 6 mm [1–12.5 mm]. The Clarck level was IV in 8 cases. There was regional nodal metastasis in 6 of cases, with no visceral metastasis.

Conclusion(s) Our study shows some particularities of melanoma in Tunisia: (i) its incidence was low; (ii) the sole was the most common site among both sexes, (iii) The ALM was the most common subtype of melanoma. This form showed particular histological features comparatively other type concerning Breslow index, Clarck level, and mitotic rate.

P3.6

Basal cell carcinoma with myoepithelial differentiation

Bodo K.; Ott A.; Stacher E.; Liegl-Atzwanger B.
Institute of Pathology, Graz, Austria

Background Basal cell carcinoma (BCC) is the most common malignant skin tumor. They are thought to arise from pluripotential cells in the epidermis or the hair follicle. Various lines of differentiation within BCCs have been reported. Herein we report two rare case of a BCCs with myoepithelial differentiation occurring in the face female patients 70 and 80 years old.

Methods Formalin fixed, routinely processed, and paraffin embedded, four-micron thick, H&E stained sections were evaluated. Immunohistochemical studies were performed with antibodies against Pan-CK, EMA, CK14, p-63, SMA, SM-Myosin, S-100, GFAP.

Results Morphologically the tumors were composed of well demarked tumor nodules located in the dermis and connected with the epidermis. The tumor cells showed hyaline/ granular cytoplasmic inclusions with an eccentrically placed nucleus (mimicking signet ring cells/ plasmacytoid morphology). Mitotic activity was spare (1/10 HPF) apoptotic bodies were present. Pleomorphism or tumor necrosis was absent. Immunohistochemical evaluation demonstrated tumor cells with a myoepithelial phenotype. The tumor cells strongly expressed Pan- CK, p-63, SMA and focally S-100.

Conclusion(s) BCC with myoepithelial differentiation are rare BCC subtypes with predilection to the face. They seem to have the same clinical and prognostic characteristics as regular BCCs. The awareness and, to some extent, the knowledge of this rare subtype of BCCs expands the differential diagnoses of skin tumors with myoepithelial differentiation and may help to collect additional examples for further investigation.

P3.7

CDKN2A but not TP53 mutations nor HPV presence predict poor outcome in metastatic squamous cell carcinoma of the skin

Küsters-Vandevelde V.H.; Van Leeuwen A.; Verdijk A.M.; Koning N.M.; Quint G.W.; Melchers J.W.; Ligtenberg J.M.; Blokx A.W.
Canisius Wilhelmina Hospital, Nijmegen, Netherlands

Background Genetic alterations in metastatic cutaneous squamous cell carcinoma (CSCC) which might serve as prognostic biomarkers are not well investigated. We aimed to investigate the mutation status and protein expression of the CDKN2A (INK4a-ARF) and TP53 genes in metastatic CSCCs and correlated this with clinicopathological variables, HPV presence and survival data.

Methods Sequence analysis of the CDKN2A and TP53 genes was performed on formalin fixed and paraffin embedded tissue of 35 metastases and their primary tumors, and was correlated with immunohistochemical stainings for

p53, p16 and p14. Beta-PV and mucosal HPV DNA was detected using PCR based assays.
Results CDKN2A was mutated in 31% of the metastases and their primary tumors, while the TP53 gene was mutated in 51% of the metastases. P53 protein expression proved to be significantly associated with missense type of TP53 mutations (p=0.002), while there was no significant effect of CDKN2A mutations on p16 and p14 expression. No persistent HPV types were detected. CDKN2A mutations were significantly associated with disease-specific death (p = 0.001). At univariate Cox´s regression analysis tumor size (p = 0.010), invasion depth (p = 0.030) and CDKN2A mutations (p = 0.040) were significantly related to shorter disease-specific survival. At multivariate Cox's regression analysis only tumor size had an adverse effect on survival (p = 0.002).
Conclusion(s) This study reveals an novel association between the presence of CDKN2A mutations and CSCC-related death in metastatic CSCCs. Our data do not support a role for oncogenic HPV in metastatic CSCC.

P3.8
Clinicopathological and immunohistochemical differences of squamous cell carcinoma arising in burn scars and nonburn scars

Sakiz D.; Yener S.; Kabukcuoglu F.
Pathology Department, Şişli Etfal Education and Research Hospital, Istanbul, Turkey

Background Burned skin tissue is the major problem not only for cosmetic and reconstructive reasons but also for neoplastic transformation. Poor vascularization, repeated damage, inflammation and toxin production may be responsible for malignancy. Squamous cell carcinoma (SCC) is the most common type of tumor arising in burn scar. We aimed to investigate clinicopathological and immunohistochemical differences of cutaneous SCC arising burn scar and nonburn scar areas.
Methods 15 cases of burn scar carcinoma and 23 cases of nonburn scar carcinoma were included in this study. Expression of p53, E-cadherin and β-catenin was evaluated by immunohistochemistry.
Results The mean age for diagnosis of burnscar SCC was 59,6 and nonburn scar SCC was 69 years. In burn scar SCC, the extremities were most frequently affected, while nonburn scar SCC's were seen most frequently in the face and neck area. Two of bum scar SCC and one of nonburn scar SCC had metastasis. There were no ıstatistical differences with staining distribution, staining intensity, staining pattern and staining index by p53, E-cadherin and β-catenin among burn scar SCC and nonburn scar SCC.
Conclusion(s) Mutation of p53 gene is a well-known entity in SCC of the skin. In this study we found the same staining properties in burn scar SCC and nonburn scar SCC with p53. Our findings suggest that mutation of p53 may play role in carcinomatous transformation of the burn scar tissue.

P3.9
Cutaneo myoepithelial carcinoma (malignant myoepithelial tumor of skin)

Garcia-Sanchez S.; Elices M.; Nieto S.
Hospital del Henares, Madrid, Spain

Background Benign and malignant neoplasms of myoepithelial cells are a rare but well characterized group of tumors, among which salivary gland is the more fracuently and best known. Reported studies suggests a continous spectrum of cutaneous mioepitelial neoplasms ranging from benign mixed tumor of the skin to cutaneous myoepithelioma and myoepithelial carcinoma.
Methods Specimen was submitted from surgical area, and processing in paraffin blocks. Sections was stained with hematoxiline-eosine. Sections were studied inmunohistochemically with automated inmunostainig Ventana (Vitro, Master Diagnostics).
Results At scanning magnification the lesion is dermal located, showed a well-circumscribed shaped, and compossed of fascicled of spindle ceels with eosinophilic cytoplasm and ovoid nuceli, with, focally, agregated of more epithelioid neoplasitc cells. Ductal differentiation was nor seen. Nuclear pleomorfism in epitheliod and spindle-cell areas was moderate, with abundant mitotic figures, some of them atypical, and necrotic areas very frecuent. The neoplastics cells was positive for cytoqueratin AE1 AE3, specific muscle actin, p63, and focally for S-100. EMA, CEA and Melan A was negative. Ki-67 index was positive in 50% of tumor cells.
Conclusion(s) The present study shows a case of myoepithelial carcinoma and the histologic an inmunohistochemical caracteristics of this type of tumors.

P3.10
Cutaneous marginal zone B-cell lymphoma (MALT-type) occurring in a skin tattoo

Nikolaidis A.; Antoniadis G.; Kouvidou C.; Tsinga A.; Kara P.; Argyrakos T.; Rontogianni D.
Evangelismos General Hospital, Athens, Greece

Background Tattoo reactions are histologically diverse. In general, dermal changes predominate, although epidermal changes as acanthosis or spongiosis can also be seen. The

chronic inflammatory infiltrate can be nodular, lichenoid or granulomatous. Occasionally, the infiltrate may be so dense as to suggest a diagnosis of cutaneous lymphoma.
Methods A case of Cutaneous marginal zone B-cell lymphoma (MALT-type) in a tattoo is presented. A 35 year old patient developed swelling in the red colored areas of her tattoo, which was administered 10 years ago.
Results Histological examination of a biopsy specimen revealed reactive lymphoid follicles surrounded by small lymphocytes which colonize germinal centers.The interfollicular infiltrate was composed of small to medium-sized, centrocyte- like or monocytoid cells and plasmacytes. The immunohistochemical results (CD20+, CD23-, CD5-, bcl-6-, CD10-, Cyclin D1-, bcl-2+, monoclonal λ light chain) were consistent with the diagnosis of cutaneous marginal zone B-cell lymphoma (MALT-type).
Conclusion(s) Cases with pseudolymphomatous hypersensitivity reaction to tattoo pigment have also been described. Awareness of this type of reaction to tattoo pigment and immunohistochemistry can help prevent the erroneous diagnosis of lymphoma. The development of marginal zone B-cell lymphoma MALT-type in this patient may be related to the persistent abnormal immune response to the chronic stimulus of the dye of the tattoo.

P3.11
Different protein expressions between Spitz nevus and melanoma

García-Martín R.; Garrido M.; Ortiz P.; Ballestin C.; Rodriguez-Peralto J.
12 de Octubre, Madrid, Spain

Background Spitz nevus is an infrequent, usually acquired melanocytic nevus, composed of spindle and/or epithelioid melanocytes than can be confused with melanoma. Although some immunohistochemical markers can aid in the differential diagnosis, there are no molecular or immunohistochemical techniques that can be used to establish an entirely safe diagnosis. In order to clarify this problem we design this study to compare the different protein expression between Spitz nevus and melanomas.
Methods We selected from our files 90 patients: 51 females (56.6%) and 39 males (43.4%). We performed 3 tissue arrays with 62 vertical growth phase malignant melanomas and 28 Spitz nevus. We studied all the cases with 23 proteins related with cell cycle, apoptosis, DNA instability, membrane and epithelial-mesenchymal receptors and other typical melanocytic molecules.
Results Nine of these 23 proteins presented significant statistical differences between Spitz nevus and malignant melanomas, but the most important ones were Cyclin D1, p21, Survivin, Topoisomerase IIa and Ki 67, especially Suirvivin that was observed in 69% of malignant melanomas and 0% in Spitz nevus, Topoisomerase IIa 15% in Spitz nevus and 79% in melanomas and p21 positive in 91% Spitz nevus and 27% malignant melanomas.
Conclusion(s) The present study demonstrates that malignant melanomas and Spitz nevus show different protein expressions that may be useful to perform the differential diagnosis of both conditions. However, more studies are necessaries to confirm our findings, especially in difficult diagnostic cases.

P3.12
Diffuse cutaneous amyloidosis expressing strong signals for Apo AI and transthyretin, both of wild type, and for Apo E. A report of an exceptional case

Elleder M.; Feit J.; Kovacevicova M.; Vlaskova H.
Institute of Inherited Metabolic Disorders, 1st Medical Faculty and University Hospital, Charles University in Prague, Prague, Czech Republic

Background In contrast to localized cutaneous amyloidosis, generalized cutaneous amyloidosis is a rare condition. We describe an elderly woman with an unremarkable personal and family history who developed a diffuse orange skin discoloration. The skin biopsy revealed amyloidosis which was then subjected to multiple analyses.
Methods Standard histology, electron microscopy, immunohistochemistry, DNA analysis of WBC gDNA (Apo AI and TTR genes).
Results Amyloid with a typical Congo red induced dichroism, a strong signal for the amyloid P component, and a typical ultrastructure, had uniformly infiltrated the subepidermal region, obliterating the papillary layer. Amyloid deposition was also seen periadnexally, around vessels and nerves and deep in the dermis around elastic fibers. Immunohistochemistry showed uniform strong staining for transthyretin (TTR), apoproteins AI and E. Serum Amyloid A protein, and Ig light chains were not detected. Sequencing of Apo AI and TTR genes failed to show any pathogenic mutations. Both serum Apo AI and TTR levels were within normal range.
Conclusion(s) The case was classified as acquired amyloidosis with a predominant cutaneous localization. The immunohistochemical amyloid profile points to participation of three proteins. Two of them, Apo AI and TTR, are known to belong to the list of amyloid building proteins. The standard analytic procedures are unable to distinguish which of them was responsible for the amyloid fibril formation.

P3.13

Erythema elevatum diutinum: two cases in patients with aids

Vazquez Navarrete S.; Espinel Vazquez M.; Jimenez Peña R.; Martin Jaramillo J.; Diaz Lagama A.
Hospital del SAS de la Linea, La Linea, Cadiz, Spain

Background Erythema elevatum diutinum ("EED") is an extremely rare form of cutaneous vasculitis characterized by plaques and nodules that are distributed symmetrically over the superficial surfaces of the extremities and joints. The pathogenesis is believed to be immune complex mediated and is associated with hematological, autoimmune and infectious diseases.
Methods We describe two cases of EED in patients with AIDS that were intravenous drug abusers and where the CD4+ lymphocyte cell count was below 200/mm3. In one we could study clinically and histologically the early and late lesions demonstrating once again that the histopathologic features of EED can vary according to the evolutionary stage of the lesions.
Results We have reviewed the clinical presentation, histopathology, etiology and treatment options and believe that HIV should be considered as a possible causative agent in EED.
Conclusion(s) HIV infections should be investigated, especially in atypical and exacerbated clinical manifestations in EED.

P3.14

Fluorescence in situ hybridization (FISH) in pigmented neoplasm diagnostics

Frank G.; Ryazantseva A.; Zavalishina L.; Andreeva Y.
Herzen's Oncological Institute, Moscow, Russian Federation

Background Early identification of cutaneous melanoma is a very important proposition for timely treatment. However, sometimes there are some difficulties for pathologists in recognition of starting of transformation by morphologic criteria only. Aim: studying material obtained from patients with different pigmented neoplasms to compare morphological diagnosis and cytogenetic data for detection starting of malignant transformation.
Methods Specimens of 22 patients were divided into 3 groups: dysplastic nevi – 10 cases, malignant melanoma – 11 cases and 1case – indeterminate diagnosis, presumably nevus. FISH performed on 5 μm paraffin sections using multi coloured probe LSI RREB1/LSI MYB/LSI CCND1/CEP 6 (Abbott).
Results In 7 samples from first group genetic alterations have not been identified. However, 3 cases showed multiple genetic alterations: amplification of CEP6 (polysomy of chromosome 6) was observed in all three cases, in two cases we observed gene RREB1 amplification, gene CCND1 amplification was observed in one case, and the loss of MYB and CCND1 genes was also detected in one case. Perhaps it may be indicative of early malignant transformation. In group 2 all patients revealed multiple genetic abberations. Amplification of RREB1 gene was observed in 10 cases, CCND1 – in 5 cases, MYB – in 6 cases, and polysomy of chromosome 6 was observed in 5 cases. We also confirmed the presumptive diagnosis of 1 patient.
Conclusion(s) Detection of genetic aberration using FISH may be an additional diagnostic tool in the diagnosis of complex cases of pigmented skin neoplasms.

P3.15

Intralymphatic atypical T-cell proliferation arising in a cutaneous hemangioma

Ardighieri L.; Lonardi S.; Vermi W.; Medicina D.; Cerroni L.; Facchetti F.
Spedali Civili, Brescia, BS, Italy

Background Intravascular lymphoma (IVL), is a rare and aggressive variant of non-Hodgkin lymphoma, mostly of B-cell origin, characterized by the proliferation of atypical large lymphocytes filling small blood vessels. Skin involvement by IVL is frequent and it may present as an hemangioma-like eruption or it can colonize a preexisting angioma. We report a unique case of atypical T-cell proliferation involving the lymphatic vessels within a cutaneous hemangioma and showing a benign clinical evolution.
Methods A 69 year-old woman presented with a pyogenic granuloma-like solitary cutaneous lesion on the arm, which was evaluated with histopathological, immunohistochemical, in-situ hybridization and PCR-clonality studies.
Results Histology revealed an hemangioma containing some vessels filled by large atypical lymphocytes showing mitoses, very high proliferation index (MIB1 ca. 100%) and pronounced apoptosis. Phenotypically, the atypical lymphoid cells were of T origin (CD2+CD3+CD4+CD5+CD7-CD8-ZAP70+LAT+CD20- CD30+/-CD56-Granzyme B-TIA1-), with an effector-memory-like regulatory T-cell phenotype (CD45RO+CD25+FOXp3+); some expressed CCR7, a lymph-node homing molecule. EBV was negative (LMP1 and EBER); the TCR analysis by polymerase chain reaction revealed a polyclonal T-cell population. Interestingly, the atypical cells were exclusively located within lymph vessels (CD31-/+ podoplanin+). Clinical examination was unremarkable and the evolution uneventful after 9 months of follow-up.

Conclusion(s) The blastic morphology, the CD4-restricted phenotype and the high proliferation suggested an IVL, but the lack of clonality and the benign clinical evolution favoured a reactive nature of the process. This uncommon intralymphatic T-cell proliferation might reflect an immune response driven by memory-like regulatory T-cells migrating to draining lymph nodes.

P3.16

Keratin expression patterns in human epidermal tumors mirror developmental stages of fetal histogenesis

Karelina Vasiljevna T.
NSLIJH, New York, USA and N.N. Blokhin Cancer Research Centre of Russian Academy of Medical Sciences, Moscow, Russia

Background Cell origin and differentiation status of human skin epithelial tumors are controversial issues.
Methods Immunostaining with monoclonal antibodies on fetal and tumor frozen sections.
Results Keratins (Ks) expression patterns of superficial clinically benign basal cell carcinomas (BCCs) (K8-positive-K17-positive), exhibit resemblance to earliest embryonic epithelium still un-committed to appendageal versus inter-appendageal fate and to early appendageal placodes, but not to any adult epidermal structures including outer root sheath of hair follicle. Both recurrent and morpheaform BCCs with more aggressive clinical features were predominantly K8-positive-K17-negative, imitating pattern of inter-appendageal keratinocytes, and again did not fit to any adult epidermal pattern. In general, BCCs consist of tumor cells expressing K17 that do or do not co-express K5, K8, and K14. Such patterns of tumor expression can be considered as mosaic embryonic basal cell phenotypes at different stages of fetal epidermal maturation. Squamous cell carcinomas (SCCs) were uniformly negative for K8 and only focally reactive for K6 and K17 in hyperkeratotic zones. This pattern was characteristic of the inter-appendageal compartment of embryonic epidermis at the stage of hair follicle maturation. Metatypical BCCs being of an intermediate typology between BCCs and SCCs exhibit distinct patterns of K8 and K17 expression, which corresponds to phenotypes both of inter-appendageal (K8-negative-K17-negative) and appendageal (K8-positive-K17-positive) keratinocytes at intermediate stages of fetal life.
Conclusion(s) The study of embryonic patterns of specific markers expression greatly improves interpretation of data on differentiation status of human skin epithelial tumors.

P3.17

p16 is consistently expressed in ocular sebaceous carcinoma

Singh K.
Brown University, Providence, RI, USA

Background The assessment of mapping biopsies for involvement by sebaceous carcinoma frequently poses diagnostic problems for the pathologist. Identifying single lying tumor cells and differentiating them from goblet cells can be difficult. The co-existent inflammation makes this task more unachievable. The immunohistochemical markers like epithelial membrane antigen and carcino-embryonic antigen, used to identify sebaceous carcinoma have low sensitivity. We investigated p16 and EMA expression in ocular sebaceous carcinoma.
Methods P16 and EMA immunohistochemical staining was performed on sebaceous cell carcinoma (n=9), squamous cell carcinoma (n=5) and benign squamous epithelium (n=7) on paraffin embedded tissue. The p16 expression was assessed as: 0, <5%; 1+, 5–10%; 2+, 10–50% & 3+ >50%.
Results All sebaceous carcinoma cases (9/9) showed 3+, nuclear and cytoplasmic staining for p16. The pagetoid tumor cells were strongly positive. p16 stained benign sebaceous & apocrine glands, reactive fibroblasts, foreign body giant cells and metaplastic squamous epithelium. Only one squamous cell carcinoma showed 2+ nuclear expression. EMA was 0 – 2+ positive in sebaceous carcinoma cases. The pagetoid tumor cells were EMA negative. EMA also stained normal squamous epithelium.
Conclusion(s) P16 consistently stains the solid and pagetoid cells of sebaceous carcinoma. In small conjunctival and eyelid mapping biopsies, p16 would be more reliable than EMA in identifying pagetoid tumor cells. In presence of inflammation, EMA is positive in plasma cells with faint expression in tumor cells and normal squamous epithelium while p16 selectively highlights the tumor cells.

P3.18

Role of flow cytometry in cutaneous lympho-proliferative lesions: trento hospital experience

Boi S.; Leonardi E.; Bauer P.; Micciolo R.; Bragantini E.; Morelli L.; Licci S.
S.Chiara, Trento, Italy

Background The diagnosis of cutaneous lymphomas (CL) is a very complex area of dermatopathology. To achieve a correct diagnosis morphologic observation is usually integrated with specific immunohistochemical techniques and molecular biology analysis. Flow cytometry (FC) is a technique of cellular analysis very useful and accurate in hematological diagnosis.

Methods In the suspect of cutaneous lymphoma (CL), the dermatologists perform two punch biopsies: one is sent immediately without any fixative solution for FC analysis, the other is sent with formalin for morphological and molecular biology examinations. We examined 53 cutaneous biopsies. The results of FC were evaluated together with standard histology, immuno-histochemistry and PCR results and compared with clinical information.
Results FC evidenced monoclonality in 90% of the cases diagnosed histologically as CL and in 2 cases histologically diagnosed as atypical dermatitis. 22 cases showed B Cell phenotype and 26 T Cell one. In 5 cases both phenotypes were expressed. Cell size: medium-small in 75% of T CL, medium-large in 53% of BCL. We evidenced BCL both with light and heavy chain rearrangement and TCL with alfa/beta and gamma/delta TCR alterations. In TCL the CD4/CD8 ratio ranged from 2 to 9.
Conclusion(s) FC helps to distingue between benign and neoplastic condition, to diagnose and characterize lymphoma and determine minimal residual disease in patients with acute leukemia or chronic lymphoproliferative disorders. FC has some important features: rapidity and the statistical reliability of the measurements with the possibility of multiparametric analysis.

P3.19
Skin biopsies in patients with connective tissue diseases

Bogoeva Gligor B.
Institute of Pathology, Skopje, Macedonia, the Former Yugoslav Republic of Macedonia

Background The aim of the study was to find the correlation between the clinical and morphological and immunofluorescence findings of skin biopsy specimens obtained from these patients.
Methods A total analysed 110 skin biopsy specimens obtained from patients with connective tissue disease: 42 patients with systemic sclerosis, 22 patinets with dermatomyositis, 25 patients with Raunoyd's phenomenon, 6 patients with vasculitis, 4 patients with SLE and 1 patient with polyarteritis nodosa were analysed. 80 females and 30 males, 3–78 years old were included in the study. Skin biopsies were routinely stained with HeEo. For hystochemistry, PAS, Weighert resorcine fuchsine, and Van Gieson staining were used.
Results Skin biopsies revealed characteristic findings: epidermal atrophy, degenerative changes and swelling of collagen tissue. Capillaries showed thickening of the basal membrane, hypertrophy of endothelial cells, perivascular edema and lymphocytic infiltration. 70% of the affected blood vessels were PAS positive. Skin biopsy were stained for direct immunofluorescence with antihuman fluorescent antiserum: IgG, IgM, IgA, IgE and C3. Granular or linear deposits of immunoglobulines at dermal-epidermal junction was demonstrated in 20 patients with systemic sclerosis, 5 patients with dermatomyositis, 2 patients with systemic lupus erythematosus and 3 patients with vasculitis. 70% of patients' sera exhibit antinuclear antibodies detected with idnirect immunofluorescence.
Conclusion(s) We registered correlation between clinical and morphological and immunofluorescence findings of skin biopsies obtained from patients with connective tissue diseases. These results confirm autoimmune etiology of connective tissue diseases and emphases the need of immunofluorescence investigations in these patients.

P3.20
Stromal immunophenotype in nevi and melanomas with regression

Zioga A.; Panelos I.; Batistatou A.; Balassi E.; Simou N.; Malamou-Mitsi V.
Department of Pathology, University Hospital of Ioannina, Greece

Background Stromal remodeling, characterized by loss of CD34-positive fibrocytes and appearance of α-smooth muscle actin (SMA)-positive myofibroblasts, has been observed in many invasive carcinomas. Regarding melanocytic lesions there are only rare reports, suggesting differences with epithelial neoplasms. Furthermore, the stroma has not been examined in regressed nevi and melanomas. The aim of the present study was to investigate the immunophenotype/nature of fibrocytic cells in the stroma of regressed skin melanocytic tumours.
Methods The immunohistochemical expression of CD34 and α-SMA was examined in paraffin-embedded tissue sections from 10 melanomas (M/F: 5/5, median age: 49 yrs) and 5 nevi (M/F: 2/3, median age: 28 yrs) with regression.
Results The stroma of both nevi and melanomas was devoid of SMA-positive myofibroblasts, in the regressed as well as in the non-regressed areas. Stromal CD34+ fibrocytes were rare within the dermal component of all tumours, whereas they were abundant in the adjacent tumour-free stroma. In both nevi and melanomas, CD34+ cells were also rare in the areas with early regression, which were characterized by intense inflammation. In later stages of regression, the presence of fibrosis was accompanied by the appearance of CD34+ fibrocytes, in both benign and malignant tumors.
Conclusion(s) The stromal immunophenotype in benign and malignant melanocytic tumours without or with early regression is similar and thus can not aid in the differential diagnosis.Late regression is accompanied by re-appearance of few CD34+ fibrocytes in both nevi and melanomas.

P3.21

The determination of the biological behaviour at benign, diagnostically difficult and malignant melanocytic laesions by using FISH and its comparision in the imunohistochemistry

Buzrla P.; Dvorackova J.; Uvirova M.
Faculty Hospital Ostrava, Ostrava - Poruba, Czech Republic

Background The determination of the biological behaviour at benign, diagnostically difficult and malignant melanocytic laesions is the problematic clinical process for surgical pathologists, dermatologists and oncologists. The major aim of our investigation were the genes named RREB1, MYB, CCND and the detection of their chromosomal abnormalities by FISH, followed by immunohistochemistry.
Methods For this investigation were selected 42 melanocytic laesions – 10 malignant melanomas, 4 superficial spreading melanoma, 2 lentigo maligna, 1 lentigo maligna melanoma, 3 nodular melanomas, 12 common naevi, 5 Spitz naevi, 2 atypical Spitz naevi, 9 dysplastic naevii and 4 blue naevii - which genes were examined by Four Colour FISH VysisR LSIR RREB1/LSIR MYB/LSIR CCND1/CEPR 6 probes and then by immunohistochemical antibodies (Ki-67, p21, p27, p53, cyclin D1).
Results There was detected the amplification of one gene in one of diagnostically difficult laesions. Malignant laesions were accompanied with the numerical or structural aberrations of chromosomes in 100%.
Conclusion(s) The results of our investigation are in harmony with other results in the medical literature. The FISH investigation by Four Colour FISH VysisR LSIR RREB1/LSIR MYB/LSIR CCND1/CEPR 6 probes are considered the effective detection of numerical and structural aberrations of chromosomes. On its basis, the prediction of the biological behaviour is very important for the treatment of the melanocytic laesions.

P3.22

The importance of consumption of epidermis (COE) in malignant melanoma (MM) and the relationship with clinicopathologic prognostic parameters

Seckin S.; Ozgun E.
Ankara Numune Research and Training Hospital, Ankara, Turkey

Background COE defines the thinning of epidermis due to the attenuation of the basal and suprabasal layers and the loss of rete ridges adjacent to melanocytes. The purpose of this study is to reveal the value of COE for MM as additional diagnostic criteria and to evaluate the relation with clinicopathologic findings.
Methods Clinically age, sex and localization, histopathologically type of tumor, Breslow Index, ulceration, Clark Level, mitosis/mm², growth phase type, lymphocytic infiltration were assessed in 34 MM cases. Presence of COE was noted and the relation with clinical and histopathological parameters was searched. Statistical analysis was performed.
Results COE was observed in 61,8 % of cases (21/34). There has been a positive correlation between COE and male sex, head-neck localization, superficial spreading MM, increase in Breslow Index and presence of ulceration. However, it wasn't significant statistically. Furthermore, the decrease in mitosis has supported the increase in COE, yet it wasn't significant statistically. This is thought to be emanating from the restricted number of cases. No association could be established between the other evaluated parameters and COE.
Conclusion(s) As COE has been observed in most of the cases, we are urged to consider that COE could be a histopathological criteria for the MM diagnosis. Moreover, the existence of a correlation between the COE and the increase in Breslow Index and the presence of ulceration highlights the remarkable importance of COE as a probable bad prognostic indicator.

P3.23

Ultrastructural proof of polyomavirus in Merkel cell carcinoma tumour cells and its absence in small cell carcinoma of the lung

Wetzels C.; Hoefnagel J.; Bakkers J.; Dijkman H.; Blokx W.; Melchers W.
Radboud University Nijmegen Medical Centre, Nijmegen, Netherlands

Background A new virus called the Merkel Cell Polyomavirus (MCPyV) has recently been found in Merkel Cell Carcinoma (MCC). MCC is a rare aggressive small cell neuroendocrine carcinoma primarily derived from the skin, morphologically indistinguishable from small cell lung carcinoma (SCLC). So far the actual presence of the virus in MCC tumour cells on a morphological level has not been demonstrated, and the presence of MCPyV in other small cell neuroendocrine carcinomas has not been studied yet.
Methods We investigated MCC tissue samples from five patients and SCLCs from ten patients for the presence of MCPyV-DNA by PCR and sequencing. Electron microscopy was used to search ultrastructurally for morphological presence of the virus in MCPyV-DNA positive samples.
Results MCPyV was detected in two out of five primary MCCs. In one MCC patient MCPyV-DNA was detected in the primary tumour as well as in the metastasis, strongly suggesting integration of MCPyV in the cellular DNA of

the tumour in this patient. In the primary MCC of another patient viral particles in tumour cell nuclei and cytoplasm were identified by electron microscopy, indicating active viral replication in the tumour cells. In none of the SCLCs MCPyV-DNA was detected.
Conclusion(s) Our results strongly suggest that MCPyV is an oncogenic polyomavirus in humans, and is potentially causally related to the development of MCC but not to the morphological similar SCLC.

P3.24
Acral calcanean malignant melanoma case report

Stanculescu V.M.; Sajin M.; Simion G.; Milosescu A.; Bruma G.; Nistor A.; Guran R.; Oproiu A.
University Emergency Hospital Bucharest, Bucharest, Romania

Background The malignant melanoma is the most aggressive cutaneous neoplasm, associated with sunlight exposure. It begins with a radical growth phase, but then over time starts a vertical growth phase, invading down into the dermis and developing the potential for metastases to distant sites. The aim of this comunication is to report a clinical case of a 71 years old man. He was hospitalized in the surgery department on the 23 of March 2009 for a red-brown, flat, round-oval macule, 4 cm diameter, with ulcerated center and irregular borders, localizated on the right calcaneum. It appeared 4 months ago.
Methods Materials and Methods: the tumoral fragments were fixed in 10% formaldehyde solution, paraffin-embedded, cut and stained with Hematoxiylin–Eosin and Van Gieson.
Results Macroscopically: 3 tumoral fragments with firm consistency 2/2/2 cm each. Microscopically: the tumoral cells are large polygonal, spindle shaped and bizarre with eosinophilic cytoplasm, very pleomorphic nuclei, proeminent nucleoli and scanty melanin pigment, grouped in nests or single cells. The tumoral cells fill the papillary dermis. Histopathology Diagnosis: acral malignant melanoma, Clark III; Differential Diagnosis: leiomyosarcoma; IHC: HMB 45 (+), Melan A (+/-), p100 (+), Vimentin (+), KI 67 (+), CK (-); SMA (-)
Conclusion(s) The prognosis is correlates best with the microscopic depth of invasion. There is a progressive potential for metastasis.

P3.25
Basal cell carcinomas of the eyelids

Radulescu D.; Costea C.; Ungureanu C.; Stolnicu S.; Dumitriu S.; Niculescu G.; Butcovan D.
University of Medicine and Pharmacy "Gr. T. Popa" Iasi, Iasi, Romania

Background Basal cell carcinoma is the most common skin malignancy. Eyelids represent a special location of the basal cell carcinoma due to proximity of the eyeball. The aim of this study is to evaluate the incidence of basal cell carcinoma located on the eyelids and to examine the histological types of this neoplasm.
Methods We included in this study 80 patients with basal cell carcinoma of the eyelids. We made a comparison between clinical and histological features of basal cell carcinoma located on eyelids and in other locations.
Results About 18% of all tumours were located on the eyelids and most of them were situated on the lower eyelid. We observed nodularulcerative clinical type in 94.5% of the tumours.
Conclusion(s) The histological nodular type was the most common one found on eyelids. It was more common on eyelids than on trunk and extremities. Superficial type was less frequently found on the eyelids. Infiltrative type was significantly more observed on the eyelids compared with other locations of head and neck region.

P3.26
Cutaneous blastomycosis in an immunosuppressed patient

Efstratiou I.; Fotiadou A.; Pervana S.; Pazarli E.; Matzarakis I.
Papageorgiou Hospital, Thessaloniki, Greece

Background Primary cutaneous blastomycosis is rare in Europe. We report a case of a 49-years-old man with a history of kidney transplantation 2 years ago. Small papules appeared on the skin of right knee. The clinical picture favoured a diagnosis of Kaposi s sarcoma.
Methods After surgical excision the specimen measuring 5,5*2,5*0,5 cm was histologically examined.
Results Sections stained with HE and PAS revealed the typical features of blastomycosis. No signs of recurrence have been reported 3 years after excision.
Conclusion(s) Despite the known geographical prevalence, deep fungal infections are not so rare especially among immunosuppressed patients in our region.

P3.27
Dermoscopic, histopathological and cytodiagnostic correlations in cutaneous melanomas

Costache M.; Simionescu O.; Sajin M.; Georgescu M.; Bura M.; Ene A.
"Victor Babes" National Institute of Pathology, Bucharest, Romania

Background Cutaneous melanoma is a tumor resulting from the malign proliferation of melanocytes. Digital

dermoscopy is a non-invasive, clinical method of diagnosis in melanoma, by means of which the tumour is studied with the dermoscope. The cytodiagnostic is a simple method and a fast one too, which contributes at cancer localization, and it provides a cellular study.

Methods A comparative dermoscopic, cytologic and histopathologic study has been made on 173 cases of cutaneous melanic tumors. Skin biopsy enables histopathological confirmation of diagnosis in standard hematoxylin-eosin staining.

Results Elementary lesions in melanoma visible with the dermoscope are: the irregular pigmentary network, spots and globules distributed at the periphery, pseudopodes, "radial flow", white-bluish veil, irregular vascular pattern, depigmentation and multitude of colors. There are dermoscopic diagnosis algorithms, some of them entirely handled by computers, used in screening procedures meant to detect melanoma in the early stage. The results of the cytodiagnostic in 137 cases were exacts and confirmed by the histopathological exam. However in 36 cases, the cytodiagnostic was false negative, in which the pacients had acrals melanomas with massive descuamations of epithelial cells or the tumour were melanomas arised from nevic tumours.

Conclusion(s) The cytodiagnosis in melanoma is a simple and rapid method of orientation which can be checked by a histopathologic examination. The diagnosis is facilitated by the abundant tumoral cells that appear on the imprints and smears obtained even by the simplest apposition in situ, due to the loss of intercellular cohesion.

P3.28

Expression of CD99 in normal and pathologic skins

Choi G.; Park S.; Kee S.; Park C.
Mizmedi, Seoul, Republic of Korea

Background CD99 is a 32 kD type I glycoprotein, encoded in MIC2 gene. It has been known to play an important role in apoptosis, cell adhesion, migration and transportation of protein to the cell surface. Function and expression pattern of CD99 in the skin are not well established except in malignant melanoma, spitz nevi, atypical fibroxanthoma and actinic keratosis. We herein evaluated CD99 expression in the normal skins and various adnexal tumors.

Methods The immunohistochemical expression of CD99 was investigated in the normal adult and fetal skins and in various adnexal tumors. Additionally, expression of CD99 was confirmed in differentiating keratinocytes using normal human epidermal keratinocytes (NHEK) culture model.

Results In the adult skin, CD99 was strongly expressed in the membrane of basal keratinocytes, outer root sheath (ORS), follicular papilla and bulge, which harbor harbor stem cells. CD99 immunoreactivity was gradually decreased upward from basal layer and it was not identified in the granular layer. Down regulation of CD99 on differentiated keratinocytes was also demonstrated by in vitro NHEK culture model. In the fetal skin, CD99 was not expressed on the priderm but the pattern of expression became similar to that of the adult skin as gestational age was later. In various skin adnexal tumors, CD99 was strongly immunopositive for tumor cells in basal cell carcinoma, and pilomatrixoma.

Conclusion(s) The differential expression of CD99 may provide useful information for specific diagnosis of skin tumors and, possibly, cutaneous stem cell research.

P3.29

Granuloma faciale: report of a case and review of the literature

Avraam K.; Kouvidou C.; Anastasiadis G.; Nikolaidis A.; Theofanous E.; Frangia K.; Noutsis K.
Evangelismos General Hospital, Athens, Greece

Background GF is a rare condition of unknown pathogenesis that is often clinically misdiagnosed and can easily be confused with often skin diseases. Sarcoidosis, lymphoma, lupus erythematosus and basal cell carcinoma are the main differential diagnoses.To avoid the incorrect treatment the correct diagnosis is of a primary importance.

Methods We report of a 50 year old man which consulted to the dermatological department with a facial lesion of 4 years duration. A dermatological examination revealed a single red-brown soft, elevated, well circumscribed plaque of 1x1,5 cm over the nasal dorsum extending to the left malar region.

Results In the histological examination of the biopsy material the epidermis was intact; grenz zone was observed in the papillary dermis and a dense predominantly perivascular infiltrate of the reticular dermis consisting of abundant neutrophils, lymphocytes, plasmacytes, histiocytes and a varying number of eosinophils. Leukocytoclasia and fibrin in some vessel walls were also observed.Differential histological diagnosis were erythema elevatum diutinum, angiolymphoid hyperplasia with eosinophilia and histiocytosis X.

Conclusion(s) GF almost exclusively envolves the face, although it has been reported in extrafacial locations. It is considered as a variant of leukocytoclastic vasculitis confined to the skin. Although this condition is benign the treatment is often unsatisfactory.

P3.30

Histological criteria in cutaneous melanoma

Dumitriu S.; Radulescu D.; Stolnicu S.; Costea C.; Ungureanu C.; Morosan E.; Butcovan D.
University of Medicine and Pharmacy "Gr. T. Popa", Iasi, Romania

Background The efficacy of the histological criteria currently used in the diagnosis of cutaneous melanoma is still to be defined.
Methods We made a quantitative analysis for 10 histological diagnostic parameters (dimension >6 mm, asymmetry, poor circumscription, suprabasal melanocytes, absence of maturation, cytological atypia, melanin in deep cells, mitoses, necrosis and dermal lymphocytic infiltrate) of 85 melanomas.
Results Most of the parameters were significantly associated with melanoma. Dimension > 6 mm, cytological atypia, asymmetry, cytological atypia, dermal lymphocitic infiltrate and absence of maturation presented a high sensitivity (> 85%). On the other hand absence of maturation, necrosis, mitoses, suprabasal melanocytes and melanin in deep cells presented a high specificity (> 90%).
Conclusion(s) Not all the parameters showed to have the same diagnostic value. Absence of maturation and suprabasal melanocytes were the most sensitive and specific histological features. Dimension >6 mm, cytological atypia, mitoses, suprabasal melanocytes were additional reliable diagnostic features, that showed a high sensitivity and a high specificity.

P3.31

Immunohistochemical and molecular study of multiple skin tumours in a renal transplant patient

Kamina S.; Doukas M.; Zioga A.; Batistatou A.; Grepi K.; Lykissas M.; Fotika C.; Bassukas D.I.; Malamou-Mitsi V.
University Hospital of Ioannina, Ioannina, Greece

Background The development of skin cancers is a known problem in renal transplant patients. However, the molecular mechanisms for this phenomenon have not been elucidated yet. The aim of the present study was to examine the expression of proteins involved in differentiation, adhesion and cell-cycle regulation, as well as the possible role of HPV infection, in multiple skin tumours from a 39-year-old male, who received a renal transplant 15 years ago.
Methods Over the last six years 4 squamous cell carcinomas (SCC), and 2 keratoacanthomas (KA) have been excised. In these tumours the immunohistochemical expression of p63, p53, syndecan, β-catenin, p16, cyclin A and cyclin D1 were examined. Furthermore, in situ hybridization for HPV/DNA detection was performed.
Results All tumours showed variable p63 immunostaining, with a basal layer-like distribution in KA, all layer distribution in in situ SCC, and diffuse expression in invasive SCC. p53 expression was comparable to that of p63. Expression of cyclins A and D1, was similar in all neoplasms, with mostly peripheral distribution. Reduced/aberrant β-catenin and syndecan expression was noted mainly in the invasive SCC, where mostly cytoplasmic p16 expression was also present. HPV was not detected by in situ hybridization in any of the neoplasms.
Conclusion(s) Our results indicate that SCC and KA, which have developed in the presented transplanted patient, have similar molecular profile with those developing in the general population.

P3.32

Immunohistochemical evaluation of four prognostic markers in malignant melanoma

Radulescu D.; Costea C.; Stolnicu S.; Ungureanu C.; Dumitriu S.; Morosan E.; Niculescu G.; Butcovan D.
University of Medicine and Pharmacy "Gr. T. Popa" Iasi, Iasi, Romania

Background In the last few years the incidence of cutaneous malignant melanoma increases all over the world and that is why a proper standardization for estimating the evolution of malignant melanoma would be of great importance.
Methods We examined the expression of four markers (Ki-67, bcl2, p16, p53) in 50 cases of primary malignant melanoma clasified as Clark II, Clark III and Clark IV.
Results bcl2 was negative in all cases. The Ki-67 labeling index was between 10% to 60%. The p16 was positive in seven cases diagnosed as Clark III. P53 presented positivity in 18 cases and weak reactivity in five cases.
Conclusion(s) Our cases presented a high Ki-67 labeling index mostly in those of Clark IV. The p16 functions as a tumour suppresor gene and its loss plays a role in dysregulation of cell proliferation. Mutated p53 accumulates in the affected cell nuclei and p53 overexpression corelates with a worse prognostic The loss of bcl2 expression is associated with tumour progression and have a prognostic value in pacients with malignant melanoma.

P3.33

Increased density of dermal nerve fibers in the affected dermatomes after herpes zoster therapy

Zografakis C.; Tiniakos D.G.; Kouloukoussa M.; Kittas C.; Stavrianeas N.
Medical School, University of Athens, Athens, Greece

Background Herpes zoster (HZ) is a neurocutaneous disease sometimes followed by irreversible skin damage, sensory abnormalities and, in many patients, persistent pain (postherpetic neuralgia-PHN). We assessed cutaneous nerve fiber density in the affected dermatomes at the time of acute HZ infection and after 3 months and correlated the results with type of treatment and appearance of PHN.
Methods Punch skin biopsies were taken from 35 patients (22 males,mean age 62.4±12.5 years) with acute HZ not affecting cranial nerves and antiviral therapy was started (Brivudin $n=13$, Valacyclovir $n=11$, Famciclovir $n=11$). PHN appeared in 10 patients (35%). Repeat biopsies from the same area were performed 3 months later. Immunohistochemistry for PGP9.5 (pan-neural marker) was applied on paraffin sections from pre- and post-treatment biopsies. Number of free nerve endings or nerve fibers per mm of epidermis´ length was recorded.
Results Epidermal free nerve endings' density was 2.18± 2.49/mm in the acute stage and 2.69±2.96/mm after 3 months ($p=0.09$). Nerve fiber density in the papillary dermis was 12.05±4.78/mm and 14.17±5.71/mm, respectively ($p=0.004$). There was no significant difference in dermal nerve fiber density between patients who developed PHN (12±4.4/mm) and those without (14.7±6.1/mm) ($p=0.37$). No significant differences were found in relation to type of antiviral therapy.
Conclusion(s) Three months after acute HZ infection, nerve fiber density is increased only in the dermis, probably reflecting nerve regeneration. Presence of PHN or type of antiviral treatment does not affect nerve fiber density in the skin of HZ patients.

P3.34
Merkel cell carcinoma: problems of differential diagnosis

Bastian A.E.; Tudose I.; Andrei T.R.; Socoliuc G.C.; Lazaroiu C.; Zurac S.A.; Staniceanu F.; Rebosapca A.; Andreescu B.
Colentina University Hospital, Bucharest, Romania

Background Merkel cell carcinoma (MCC) is a highly aggressive primary cutaneous small cell neuroendocrine carcinoma. It has similar histopathologic appearance with small cell pulmonary carcinoma (SCPC) but has less aggressive behaviour (overall 5 years survival rate 40–60%).
Methods We report 11 cases of MCC. We analyzed both tumor morphologic characteristics and immunohistochemical (IHC) expression of CK20, NF, BerEP4, MNF116, chromogranin, S100 and TTF1).
Results Our group showed a slight feminine predominance (63.63%) with 62 years old average. Most lesions were painless firm subcutaneous nodules (median diameter 1.9 cm), dark-reddish, located in the head&neck (5 cases), forearm, thigh and calf (4 cases). Microscopic examination revealed dermal/subcutaneous infiltration by monotonous round-to-ovoid cell proliferation with solid/nest-like arrangement. The tumoral cells present scanty amphophilic cytoplasm, fine granular round-to-ovoid nuclei and numerous mitotic figures. One tumor associated squamous cell carcinoma areas; another patient associated non-Hodgkin malignant lymphoma. All the cases showed intense staining for NF and chromogranin; all but one cases were positive for CK20 (all in 'dot-like' pattern). The differential diagnosis included metastatic SCPC, malignant lymphoma, amelanotic malignant melanoma, poorly differentiated carcinoma.
Conclusion(s) The differentiation between MCC, SCPC and malignant lymphoma may sometimes be difficult. We report two unusual cases of MCC, one CK20 negative, the other in a patient concomitantly diagnosed with malignant lymphoma. Based on IHC phenotype (MNF116, chromogranin and 'dot-like' NF positivity, TTF1 and lymphoid markers negativity), along with the absence of any pulmonary primary tumor, definite diagnoses of MCCs were established.

P3.35
Mismatch repair proteins expression in sebaceous gland tumors

Company Margarita M.; Terrasa F.; Ibarra J.; Taberner R.
Hospital Son Llatzer, Palma de Mallorca, Spain

Background Muir-Torre syndrome (MTS) is characterized by the coexistence of sebaceous gland tumors of the skin and visceral malignancies. The majority of the MTS-associated tumors reveal mutations in DNA mismatch repair (MMR) genes and microsatellite instability. Here we investigate the MMR gene expression in a variety of sebaceous gland tumors, with or without associated visceral malignancy and its association with tumor location and histology.
Methods We studied the expression of MSH2, MSH6 and MLH1 in 15 consecutive sebaceous hyperplasias, 12 sebaceous adenomas, 4 sebaceous carcinomas and 3 colorectal carcinoma and using immunohistochemistry and paraffin-embedded sections obtained from 32 patients.
Results The normal sebaceous glands and sebaceous hyperplasias were positive for MSH2, MSH6 and MLH1. Concurrent loss of MSH2 and MSH6 was found in 3/12 (25%) sebaceous adenomas and in 1/4 (25%) sebaceous carcinoma. No loss of MLH1 was found in any case. High concordance was showed between MMR expression in

sebaceous lesions and extracutaneous neoplasm in the same patient.
Conclusion(s) This study confirms the value of immnohistochemistry to identify tumors with abnormalities of mismatch repair genes. Cutaneous sebaceous neoplasias with MMR deficiency are associated with anatomic location (outside of head and neck) and histology (cystic and keratoacanthomalike). Solitary sebaceous hyperplasias do not associate with MTS. All cases with MMR deficiency was due to loss MSH2 and MSH6 and this probably represents a germline defect. The sebaceous glands lesions are often the presenting sign of MTS.

P3.36
Notch1 in cutaneous malignant melanoma
Ene A.; Mihalcea Chitu A.; Florescu A.; Costache M.; Ionica E.
University of Bucharest, Bucharest, Romania

Background Melanoma is a malignant tumor of the neural-crest derived cells named melanocytes. Physiologically, these cells reside in the basal epidermal layer and provide pigmentation to skin or other tissues. Melanoma is characterized by an increased aggressivity due to its high ability of proliferation and invasion. Because of a high increase of melanoma incidence, cutaneous melanoma has become a public health problem and an important subject for research. The aim was to evaluate Notch1 protein expression in cutaneous malignant melanoma by comparison with normal skin.
Methods Five cases of cutaneous melanoma and normal skin samples were assessed for Notch1 expression. Immunofluorescent staining was performed on 5 micron thickness criosections. Primary antibodies were applied and incubated over night at 4°C. FITC-labeled goat anti mouse secondary antibodies were used to detect the primary immune reaction for Notch1. The samples were examined using light and UV microscopy. For the Western blot technique the WesternBreeze kit was used.
Results Notch1 expression in normal skin was detected in the epidermis and also in hair follicles, sweat glands, sebaceous glands and blood vessels. Melanoma cells showed moderate to high levels of expression of Notch1. In cytoplasmatic and nuclear lysates, Notch1 expression was also detected using the Western blot technique.
Conclusion(s) A possible explanation for the results is that Notch1 expression is correlated with increased aggressivity and also the activation of the Notch pathway, but further studies are needed. Notch signaling pathway can be used as a diagnostic and prognostic tool in melanoma therapy.

P3.37
Pilomatrical carcinosarcoma of the head: report of a very rare case
Alexopoulou E.; Zourou I.; Manailoglou G.; Kalodimos G.; Fericean Monika A.
Achillopouleion Hospital Volos Hellas, Volos, Magnesia, Greece

Background Pilomatrical carcinoma is the rare malignant counterpart of pilomatricoma, with most cases occurring in the head and neck of adults. When a sarcomatous component is also present we refer to the extremely rare pilomatrical carcinosarcoma.
Methods Our case was a 85-years-old woman who presented with a dermal tumor, measuring 5.5 cm at greatest dimension, at the iniac region of the scalp. A broad surgical excision took place and histology showed a malignant neoplasm with a biphenotypic morphology. One part of the tumor was the epithelial element of pilomatrical carcinoma with necrosis and calcification. The other part was a sarcomatoid stroma with spindle cells showing a whorled configuration and a remarkable mitotic activity.
Results Immunohistochemistry confirmed the carcinomatous nature (pancytokeratin +) of the first and the sarcomatoid nature (vimentin+) of the second element. Subsequently the cells of the latter showed positivity for CD68 and smooth muscle actin (focally), while the results for desmin and CD34 were negative / suggestive of fibrohistiocytic origin.
Conclusion(s) The patient refused any therapeutical approach. The tumor recurred shortly after and she died 12 months later.

P3.38
Primary cutaneous adenoid cystic carcinoma: a case report and immunohistochemical study
Glava C.; Grammatoglou X.; Skafida E.; Katsamagkou E.; Moustou E.; Vasilakaki T.
Tzaneion General Hospital of Piraeus, Piraeus, Athens, Greece

Background Primary cutaneous adenoid cystic carcinoma (ACC) is a rare slow-growing malignancy with only few cases (65) reported in the literature. It has characteristics of indolent and progressive course and high incidence of perineural and local recurrence.
Methods An 80-year-old woman came to our hospital with a mass measuring 2,5x1,5 cm in the occipital region of the scalp, which underwent surgical removal with clean margins.

Results Histological examination of the mass showed a cutaneous adenoid cystic carcinoma. The tumor characteristically consisted of basophilic cells with a distinct adenoid or cribriform pattern in the dermis. On immunohistochemical examination the tumor cells were positive for EMA, CKAE1, CKAE3, and Vimentin and negative for CEA. A considerable number of tumor cells were immunoreactive with S100p. CT scan did not reveal any masses, lymphadenopathy or distant metastases. No postoperative radiotherapy or adjuvant chemotherapy was given and within three-year follow-up no recurrence was reported.

Conclusion(s) Adenoid cystic carcinoma is an uncommon type of cancer that most commonly develops in the salivary glands. In some cases ACC may arise in other primary sites such as skin, breast, lung, trachea, cervix, prostate gland, paranasal sinuses or other areas. ACC seldom metastasizes to the regional lymph nodes or distant organs. Primary treatment for this cancer regardless of body site is surgical removal with clean margin. Adjuvant radiotherapy is commonly given following surgery to help limit local failure.

P3.39

Primary Hodgkin lymphoma of the skin. A case report

Petrakopoulou N.; Savvaidou V.; Tepelenis N.; Zizi-Serbetzoglou A.
Tzaneion General Hospital of Piraeus, Piraeus, Greece

Background Primary cutaneous Hodgkin disease (PCHD) is exceedingly rare. Most older reports purporting to describe cutaneous HL were really depictions of lymphomatoid papulosis (LyP) or CD30+ anaplastic large cell lymphoma (ALCL).

Methods We present a case of a 59-year-old-man who presented to our hospital because of a slow growing skin mass. A surgical excision of the skin followed.

Results The microscopic examination, revealed variable nodules in the dermis and the subcutis. They were composed of an admixture of inflammatory cells and few cells morphologically identical to HRS cells. Immunohistochemically these cells were positive for CD30 and CD15 and negative for other markers such as CD45RO and CD3. In the differential diagnosis CD30 positive disorders such as ALCL, MF, HL and LyP were taken into considerarion. ALCL was excluded by the polymorphous background of inflammatory cells. Moreover nodules of MF can contain cells that resemble RS cells but the infiltrate usually contains a range of large lymphocytes with hyperchromatic irregularly shaped nuclei, whereas the reactive T cells in the infiltrate of HL are smaller and are all of fairly uniform size. The diagnosis of cutaneous Hodgkin lymphoma was established. After further diagnostic procedures there was no evidence of disease in any other organ or lymph node tissue.

Conclusion(s) PCHD is extremely rare. According to the literature some patients can have a benign course without systemic disease whereas others can develop mixed cellularity Hodgkin disease in lymph nodes.

P3.40

Profound sarcoid-like skin reaction to exogenous pigment deposits mimicking blue nevus with a worrisome change in its clinical features

Hatzianastassiou Kyriakos D.; Tsiougou M.; Nikita E.
Pathology Department "Henry Dunant" Hospital of Athens, Athens, Attica, Greece

Background A 32-year-old Caucasian female sought medical advice for a flat to slightly papular pigmented lesion on the mid-extensor surface of her right forearm. The lesion had remained unremarkable for at least 10 years; however, she reported that it had slowly grown palpable within the last year, following her pregnancy.

Methods Surgical excision biopsy was performed and the lesion was submitted for histology.

Results Sections showed a profound non-necrotic epithelioid granulomatous (sarcoid-like) reaction spanning throughout the dermis and extending to the subcutis. It appeared to be elicited by finely dispersed black pigment granules within, or in association to the histiocytic population and surrounded a nidus of "foreign body" type giant cell reaction to coarser black pigment granules. Masson-Fontana for melanin was negative, and immunohistochemistry failed to reveal elements of blue nevus, either classic or epithelioid. The pigment distribution had a linear, bottom-heavy pattern. Additionally, knife chattering and scratching artifacts were noted, as well as, occasional birefringent particles colocating with the pigment granules.

Conclusion(s) The lesion was diagnosed as mixed granulomatous, predominantly sarcoid and focally "foreign body" type reaction to exogenous pigment deposits. We present this case not only because it mimicked a blue nevus with worrisome change in its clinical features, but also because traumatic pigment deposits, just like normal tattoos are a favored site for the development for sarcoid-like reaction in prone individuals. After 20 months, she has not shown clinical evidence of sarcoidosis.

P3.41

Sjögren syndrome: histopathologic criteria. What means an aggregate of more than 50 mononuclear cells

Rotter A.
Institute of Pathology, Ljubljana, Slovenia

Background Sjöegren syndrome is an autoimmune disease with the antibodies directed against the salivary glands. The "gold standard" for diagnosis is histological evaluations of the glands. According to the American-European Consensus Group positive focus score, i.e. one or more aggregates of >50 mononuclear cells on 4 mm2 fulfill the criteria. However, there is no clear-cut instruction on how large the cells-counting field or aggregate should be. It thus depends on the pathologist to decide.
Methods Specimens of glands were treated with CD79a and CD3 to mark lymphocytes B and T. We took into account all cells distributed in a fashion close to aggregation with >50 in number, dividing aggregates into closely packed (overlapping) and dispersed (mostly without overlapping).
Results The comparison between overlapping aggregates with > 50 cells/4 mm^2 (positive score) and dispersed aggregates with > 50 cells/4 mm^2 (considered negative score) will be presented in relation to possible error in deciding to sign out a negative biopsy score.
Conclusion(s) We want to stress the fact that counting cells only in very close packages is probably not the only histological pattern and that larger aggregates of > 50 cells should also be taken in account. If infiltrates of > 50 mononuclear cells are so important for a diagnosis of Sjögren syndrome, they should be counted on definite unit of area (e.g. 0,25 mm^2) regardless of aggregation forms.

P3.42

Evaluation of differential diagnostic criteria for dysplastic nevus and malignant melanoma

Craciun A.A.; Aschie M.; Poinareanu I.; Dobre A.; Papuc F. A.; Iliesiu A.; Deacu M.; Bosoteanu M.; Iacub G.; Stanisici J.; Baltatescu I.G.; Enciu M.; Lacurezeanu I.V.
Clinical County Emergency Hospital Constanta, Constanta, Romania

Background Dysplastic nevus and malignant melanoma represent a very important pathology of our times because of their difficult differential diagnosis, the increased incidence in young individuals and high mortality of the latter. This paper tries to point out aspects of differential diagnosis between these two entities.
Methods We chose to study patients diagnosed in the Pathology Department of Emergency County Clinical Hospital Constanta with benign and malignant melanocytic tumors from 2007 to 2008 (244 cases).
Results The microscopic aspects of dysplastic nevus encountered consisted of junctional or compound nevi with mild/moderate cyto-architectural atypia, atypical melanocytes mainly in the basal layer, accompanied by an dermal or junctional inflammatory infiltrate. The microscopic features of malignant melanoma group includes epithelioid cell form, spidle cell form, pigmanetated forms, non-pigmentated forms and acral lentiginous melanoma, mostly associated, accompanied by epidermal ulceration and inflammatory infiltrate.
Conclusion(s) The incidence of melanocytic tumors is higher in females, regardless the type of tumour (common nevus, dysplastic nevus or malignant melanoma) and prefer younger people. The clinical diagnostic criteria between dysplastic nevus and malignant melanoma are not concluded because these lesions can have similar macroscopic aspects (irregular borders, uneven pigmentation and variate sizes). The thorough examination of microscopic slides is the best method for establishing the diagnosis of dysplastic nevus or malignant melanoma.

P3.43

Seladin-1/DHCR24 is implicated in melanoma progression through lipid rafts-dependent cross-talk with notch signaling

Sturli N.[1], Rosati F.[1], Morello M.[1], Di Serio C.[2], Gokoz O.[3], Paglierani M.[4], Tarantini F.[2], Massi D.[4], Danza G.[1]
[1]Department of Clinical Physiopathology, Unit of Endocrinology, [2]Department of Critical Care Medicine and Surgery, [4]Department of Human Pathology and Oncology, University of Florence, [3]Department of Pathology, Hacettepe University, University of Florence, Italy

Background Malignant melanoma aggressive growth and cell resistance to apoptosis derive from aberrant activation of cell signals dependent from lipid rafts, cholesterol-rich membrane microdomains able to activate molecules involved in signal transduction. The identification of deranged gene expression is crucial to understand the melanoma pathogenesis. Seladin-1/DHCR24, an antiapoptotic protein which catalyses the last step of cholesterol biosynthesis, is more expressed in melanoma metastases vs. primary lesions, protecting cells against apoptosis. Melanoma tumorigenesis is also associated with up-regulation of Notch receptors and ligands. The aim of the study was to characterize Seladin-1 expression in normal skin, melanocytic nevi and melanoma and identify molecular mechanisms that link Seladin-1 with tumour progression.
Methods Immunohistochemistry with anti-Seladin-1 Ab was performed on the different tissue specimens. Primary (A375) and metastatic (WM266-4) melanoma cell lines were used. Gene expression was determined by quantitative

real time PCR and cell cholesterol by GC/MS. Lipid rafts distribution was visualised by confocal microscopy.
Results and conclusions Seladin-1 was more expressed and differently localized in primary and metastatic tumours vs. normal skin and benign lesions. Higher Seladin-1 gene expression and cell cholesterol were found in WM266-4 vs. A375. Increase of lipid rafts after transient transfection of Seladin-1 in A375 suggests a raft-dependent activation of pro-oncogenic signals. Different gene expression of Notch receptors, ligands and target genes (HES1, HEY1) indicate a stronger activation of Notch signalling in metastatic vs. primary melanoma cell lines suggesting a raft-dependent crosstalk between this pathway and Seladin-1.

P3.44
CD4+, CD56+ haematodermic (plasmacytoid dendritic cell) neoplasm: a "two-faced" entity

Mariotti G.[1]; Massi D.[2]; Alterini R.[3]; Delfino C.[1]; Santucci M.[2]; Rigacci L.[3]; Pimpinelli N. [1]
Depts. of [1]Dermatological Sciences, [2]Human Pathology and Oncology, and [3]Haematology, University of Florence Medical School, Florence, Italy

Background CD4+, CD56+ hematodermic (plasmacytoid dendritic cell) neoplasm (HDN) usually presents in the skin with or without concurrent extracutaneous involvement, and. show non-epidermotropic infiltrates of medium-sized cells with a CD4+, CD56+, CD8-, CD7 +/-, CD2-/+, CD45RA+, C68+/-, CD123+, TCL1+ phenotype and a EBV- and TCR germline configuration genotype. HDN is more frequently characterized by "eruptive" cutaneous presentation lesions, and less frequently by a single/regional presentation. The course is generally aggressive, with a poor prognosis (median survival, 14 months) and no significant difference in survival between patients presenting with or without concurrent extracutaneous disease. The end stage of the disease is characterized by leukaemic dissemination and withering course thereafter.
Methods A series of 9 patients (7 males and 2 females; age range 34–81 years) with HDN were studied. Four of 9 patients presented with a solitary tumour on the trunk, as opposed to the other 5 with more classic, "eruptive" presentation. In all cases, the aforementioned histological, immunophenotypic, and genotypic features were seen.
Results We found significantly different figures in terms of progression-free survival between the localized and the widespread skin involvement group at presentation (median 23 months vs. 9 months, with a long survivor – 34 months – in the first group), notwithstanding the patients with localized lesions had been initially treated with radiotherapy (taking into consideration the poor prognosis in spite of aggressive treatment) different from the eruptive lesions' group.
Conclusions To date, no single prognostic marker is predictive of a globally different course in HDN. Yet, these results suggest the possible indication to treat HDN patients with localized lesions with a non-aggressive approach (radiotherapy), thus preserving a relatively efficient immune status and maintaining a reasonably good quality of life.

Gynecopathology

P3.45
Molecular interactions of adenomyosis and endometrial adenocarcinoma (EA)

Kogan E.; Niziaeva N.; Ezova S.; Demura T.; Grechukhina O.
Scientific centre of obtetrics and gynecology, Moscow, Russian Federation

Background The combination of adenomyosis and EA is a rare condition.The aim of our study was to investigate molecular interactions of adenomyosis and EA.
Methods The study was performed on serial sections of uteri taken from 11 patients aged 48–68 with combination of adenomyosis and highly and moderately differentiated EA of I and II grade. The majority of patients were found to have transformation of endometrial hyperplasia into EA. Morphological and immunohistochemical analysis was performed on paraffin sections of tissues. We used MMP-1,2,7,9, TIMP-1,4, COX-2, PCNA, Apo-CAS, EGFR, VEGF as monoclonal antibodies. Results were evaluated with the help of quantitative and semi quantitative methods and statistic analysis.
Results Based on immunohistochemical analysis adenomyosis and EA have different pathogenesis. Epithelial cells in EA had significantly higher expression of PCNA, Apo-CAS, VEGF, p53, EGFR, COX and lower expression of E-cadherin compared to adenomyosis. High level of MMP-7 was detected in both parenchyma and stroma of adenomyosis and was almost absent in EA. The MMP-9 expression was significantly higher in epithelial cells in EA in comparison with adenomyosis. MMP-2 was significantly higher in stroma of adenomyosis compared to that in EA.
Conclusion(s) Obtained morphological and immunohistochemical results indicate that adenomyosis and EA may both originate from the basal layer of endometrium. However, further development of these lesions is based on different molecular mechanisms.

P3.46
Morphological and molecular characteristic of uterine sarcomas in patients with adenomyosis

Ezova L.; Kogan E.; Niziaeva N.; Demura T.; Unanjan A.
Scientific centre of obtetrics and gynecology, Moscow, Russian Federation

Background The aim of our study was to identify morphological and molecular features of uterine sarcomas in patients with adenomyosis.
Methods The study was made on surgical materials (excised uteri) from 5 patients with uterine sarcoma aged 48–71. Morphological and immunohistochemical analysis was performed on paraffin sections. We used monoclonal antibodies for MMP-1, MMP-2, MMP-9, TIMP-1, PDGF, GT, FGF VEGF, SMA, Desmin, Vimentin, Cytokeratin 7 and 20. Results were evaluated with the help of quantitative and semi quantitative methods and statistic analysis.
Results Morphological examination revealed combination of adenomyosis and endometrial stromal sarcoma with low malignant potential, adenomyosis and leiomyosarcoma, adenomyosis and carcinosarcoma, adenomyosis and endometrial adenocarcinoma and adenosarcoma simultaneously. We observed active foci of adenomyosis with stromal predominance and high expression of MMPs, PDGF in all cases. In one case of endometrioid stromal sarcoma neoplastic tissue spread from foci of adenomyosis. Hyperplasia of leiomyocytes was found in myometrium adjacent to adenomyosis with transition into leiomyosarcoma in one case. Four patients were diagnosed to have atrophic endometrium or endometrium with complex hyperplasia without atypia.
Conclusion(s) Obtained results show possible association of stromal sarcoma with active foci of adenomyosis and development of leiomyosarcoma from leiomyocytes hyperplasia in adenomyosis.

P3.47

Activation of signalling pathways in cervical squamous cell carcinoma (CSQCC): new prognostic markers

Alameda, F.; Menendez S.; Rovira A.; Albanell J.; Muñoz R.; Carreras R.; Serrano S.; Rojo F.
Hospital Del Mar, Barcelona, Spain

Background Membrane receptor dysregulation is a frequent event in cancer that leads to proliferation, migration, invasiveness and survival. Membrane signals are mainly transduced by the MAPK (ERK, p38 and JNK), PI3K/AKT and NF-kB pathways. The analysis of the activation of these pathways could identify tumors with an aggressive behaviour.
Methods A TMA was built from 38 CSQCC. Total and activated (phosphorylated, –p-) EGFR, JNK, p38, ERK1/2, AKT, NF-kB subunits and the MAPK phosphatase 1 (MKP-1) were studied.
Results EGFR was detected in 50% of cases and p-EGFR, in 10%. The activated signalling proteins were observed in 31% (ERK), 54% (AKT), 55% (p38), 30% (JNK) and 24–64% (NF-kB subunits) of tumors. Only p-ERK correlated with stage and disease relapse (p= 0.001). MKP-1 was expressed in 40% of cases, mainly in patients with poor response to adjuvant therapy (p = 0.001). P-ERK correlated with MPK-1 (p<0.001), suggesting a regulatory mechanism, and conversely, MKP-1 was associated with a low activation of JNK (p=0.036) and p38 (p=0.011).
Conclusion(s) Signalling mediated by ERK1/2 might be associated with an aggressive behaviour in CSQCC. ERK signalling could drive to a compensatory upregulation of MKP-1, which induce a downregulation of the pro-apoptotic pathways JNK and p38 and, consequently, resistance to the therapy. In conclusion, MKP-1 could be used as a prognostic factor in CSQCC and postulates as a target to sensitize tumors to systemic therapies.

P3.48

Association of ERCC1 protein expression to platinum resistance in epithelial ovarian cancer

Waldstrom M.; Steffensen Dahl K.; Jacobsen A.
Department of Pathology, Vejle Hospital, Vejle, Denmark

Background Platinum-based chemotherapy is the cornerstone for treatment of ovarian cancer, but some patients are resistant to the treatment. Data have suggested a potential use of ERCC1 (Excision repair cross-complementation group 1 enzyme) as a predictor of clinical resistance to platinum-based chemotherapy. The aim of the study was to investigate if immunohistochemical expression of ERCC1 protein was associated with resistance to standard combination carboplatin and paclitaxel chemotherapy.
Methods Formalin-fixed, paraffin-embedded tissue sections from 101 patients were used for immunohistochemical staining for the ERCC1 protein. The percentage of positive tumor cells in each slide were scored as 0 if 0 % of the tumor cells were positive, 0.1 if 1 %-9 %, 0.5 if 10 %-49 % and 1.0 if 50 % or more were positive. A semi quantitative H-score was calculated by multiplying the staining intensity (0–3) with the percentage score. The tumor was considered positive when the H-score was > 1.0.
Results ERCC1 protein overexpression was found in 13.9 % of the tumors. Platinum resistance were found in 75 % of the tumors with positive ERCC1 protein expression compared to 27 % among the patients with negative tumor staining for ERCC1 (p=0.0013). These findings translated into a significant difference in progression free survival in both univariate (p = 0.0012) and in multivariate analysis (p = 0.006).
Conclusion(s) The data presented suggests a positive association between positive ERCC1 protein expression and clinical resistance to platinum-based chemotherapy.

P3.49

Chromatin assembly and biological behavior of cervical cancer

Staibano S.; Nugnes L.; Mascolo M.; Lo Muzio L.; Giovannelli L.; Vecchione M.; De Rosa G.
Department of Biomorphological and Functional Sciences, Federico II University, Pathology Section, Faculty of Medicine and Surgery, Napoli, Italy

Background Squamous cell carcinoma (SCC) of the uterine cervix, pathogenetically related to high risk papilloma virus infection, is the second most common tumor in women. It has been shown that genetic alterations and epigenetic events influence the clinical behavior of this tumor. Chromatin assembly factor -1(CAF-1) p60 protein is a new putative prognostic marker for malignant tumors. It belongs to a molecular complex (formed by p48, p60 and p150) with a pivotal role in regulation of proliferation-related chromatin assembly and DNA damage processing in eukaryotic cells. The aim of this study was to evaluate the role of CAF-1/p60 as prognostic marker for cervical epithelial lesions.
Methods The p60 expression was investigated and scored semiquantitatively on a selected series of 26 cases of SCC and 46 cases of preneoplastic cervical lesions (formalin fixed and paraffin embedded tissues retrieved from the archives of the Department of Biomorphological and Functional Sciences, Pathology Section, University of Naples "Federico II"). All the samples were analysed for HPV by RT-PCR.The results were compared to the clinicopathological data and follow up of patients.
Results CAF-1/p60 expression showed a linear increase from L-SIL to H-SIL and invasive SCC. In particular, the cases of metastatic SCC presented the highest expression of the protein.
Conclusion(s) These preliminary results allow us to hypothesize a prognostic role for CAF-1/p60 in cervical cancer.

P3.50

Neurotrophin expression in the eutopic endometrium of women with and without endometriosis

Foster G.W.; Boutross-Tadross O.; Maharaj-Briceño S.
McMaster University, Hamilton, Ontario, Canada

Background The neurotrophins receptor Tyrosine receptor kinase B (Trk B) is over expressed in several cancers and we have recently demonstrated that Trk B and its ligand Brain Derived Neurotrophic Factor (BDNF) are expressed in endometriosis associated ovarian cancer with greater staining in more aggressive tumors. Trk B is thought to be important in cancer cell resistance to apoptosis. We therefore hypothesized that Trk B expression would be increased in the endometrium of women with endometriosis compared to healthy women.
Methods Endometrial samples were collected from women with endometriosis or healthy controls undergoing benign gynecologic surgery at McMaster University Medical Centre. All procedures were approved by the McMaster University Research Ethics Board. Samples were processed for routine histology, immunohistochemistry, and Western blot analysis. Data were compared by t-test and a p value <0.05 was considered significant.
Results BDNF and Trk B were localized to the epithelial cells of endometrial glands and stroma. BDNF and Trk B were localized in the proliferative and secretory phases of the cycle with diminished staining late in the secretory phase. Western blot analysis demonstrated expression of both the full-length and truncated isoforms of Trk B, with elevated levels observed in the endometrium from women with endometriosis vs. healthy controls.
Conclusion(s) BDNF and TrkB are expressed in the human endometrium and may play a role in the pathobiology of endometriosis.

P3.51

Relevance of proteins involved in resistance to apoptosis and hypoxia in post-radiation recurrences of endometrioid carcinomas of the endometrium

Pallarés Quixal J.; Santacana M.; Matias-Guiu X.; Lopez S.; Yeramian A.; Llobet D.; Dolcet X.; Oliva E.
Hospital Universtitari Arnau de Vilanova, Almacelles, Lleida, Spain

Background Endometrial carcinoma (EC) is treated with surgery and radiotherapy. A significant number of patients present with advanced disease. Post-radiation recurrences of EC are usually associated with increased risk of metastases. Alterations of genes of the extrinsic and intrinsic apoptosis pathways have been involved in resistance to radiotherapy in other types of tumors and may be involved in post-radiation recurrences of EC.
Methods Ten post-radiation recurrences of EC were evaluated by immunohistochemistry (IHC) compared to a group of 95 primary EC. The IHC panel included estrogen (ER) and progesterone receptors (PR), p53, Ki 67, E-cadherin, beta-catenin, PTEN, HIF-alpha, CK2, FLIP, BAX, Bcl-xL, CD.44, MLH-1, MSH-2, MSH-6, and members of the NF-kb family of genes.
Results Overall, post-radiation recurrences showed decreased expression of ER and PR, and increased expression of p53 in comparison with primary EC. Interestingly, the vast majority of the recurrences exhibited beta-catenin nuclear expression (66.7 %). Flip immunoexpression was

also significantly higher in the recurrences than the primary EC ($p=0.00$). Moreover, postradiation recurrences showed frequent nuclear expression for members of the NF-kb family of genes (p65, p50, p52, C-REL, Rel-B and IKK).
Conclusion(s) Alterations of genes involved in the control of apoptosis and hypoxia may play a role in resistance to radiation in EC. Moreover, nuclear expression of beta-catenin is also frequent in post-radiation recurrences of EC and may play a role in resistance to radiation.

P3.52

Aggressive angiomyxoma of the cervix mimicking a cervical polyp. Report of an unusual case and review of the literature

Hadjileontis C.; Paplomata E.; Balaxis D.; Kafanas A.
Serres General Hospital, Serres, Northern Greece, Greece

Background Aggressive angiomyxoma is a rare mesenchymal tumor predominantly affecting the vulva, pelvis and perineum of reproductive-age females. The tumor may locally recur after surgery and in rare cases it has been reported to metastasis.
Methods We present the case of an aggressive angiomyxoma of the uterine cervix in a 29–year-old asymptomatic woman. The tumor was preoperatively diagnosed as a uterine cervical polyp and it was removed with an electrocautery blade electrode under general anesthesia. It originated from the external cervical os as a polypoid mass, and its base of about 1,5 cm in diameter was fulgurated. The surgical specimen measured 5X4X1,5 cm, it was glistening white, soft, solid and was send for histological examination.
Results Microscopic examination revealed a densely vascular, poorly circumscribed neoplasm, composed of spindle-shaped cells widely spaced from each other in myxoid stroma. Immunohistochemical examination showed positive reaction of the spindle cells to desmin and smooth muscle actin, while they were negative to S-100 protein and CD34 antigen. The latest revealed the rich vascular network of the neoplasm. Proliferation index antigen Ki67 was practically negative. These findings were consistent with aggressive angiomyxoma.
Conclusion(s) Aggressive angiomyxoma primarily affecting the cervix in the form of a polypoid mass, has not until now been reported in literature, it seems however to share the same morphologic and behavioural characteristics with the ones reported for its usual locations. Several aspects of the entity are discussed.

P3.53

Anaplastic-type extra-axial ependymomas of the ovary. Report of 2 cases mimicking juvenile granulosa cell tumour and malignant struma ovarii

Stolnicu S.; Macedo Pinto I.; Ariza A.; Hincu M.; Puscasiu L.; Nogales F.F.
University of Medicine, Targu Mures, Romania

Background Extra-axial locations of ependymomas such as ovary and broad ligament are rare with only 18 cases reported to date, the majority occurring in young and mature women, often with a malignant behaviour and not teratoma-associated.
Methods Patients aged 32 and 35, respectively with 15 cm right-sided stage-III and stage-I tumours. The latter had bilateral mature teratomata, left one overgrown by a 7 cm ependymoma. Case 1 had omental metastases and recurred after chemotherapy. Case 2 had chemotherapy and a follow-up of 13 years without recurrences. Initial diagnoses before consultation were juvenile granulosa cell tumour – JGCT- and malignant struma ovarii-MSO-.
Results Microscopically both had minor mixopapillary areas, with predominance of cellular anaplastic areas with clear oligodendroglial-like cells with numerous rossettes and pseudorossetttes and pseudofollicular, colloid containing spaces, present in case 1 metastases. Fibrillary cytoplasms and characteristic perivascular arrangement favoured diagnosis of ependymoma, findings supported by a characteristic immunophenotype of GFAP-CD56-ER-PR and Vim+++. Clear, oligodendroglia-like cells were negative for GFAP but positive for NSE-CD57. Additional positivity for ER-PR-CK18 and 34βE12 was present in both cases. Case 2 had areas of HMB45+ pigmentation, a fact very rarely described in cerebral ependymoma.
Conclusion(s) Patient's age and histology with pseudofollicular, colloid spaces, vacuolated, clear cells were suggestive of JGCT. However the presence of perivascular pseudorosettes, fibrillary cytoplasm and papillary areas together with a typical immunophenotype led to correct diagnosis. ER-PR-CK18-34βE12+ immunophenotype was characteristic of extra-axial ependymoma and different from axial CNS neoplasms.

P3.54

Bilateral ovarian malignant mixed mullerian tumor with associated choriocarcinomatous areas. Case report

Staniceanu F.; Zurac S.A.; Gramada E.; Tebeica T.; Tudose I.; Stoica A.; Bacaliuc S.
University of Medicine and Pharmacy Carol Davila, Colentina University Hospital, Bucharest, Romania

Background Malignant mixed Müllerian tumor (MMMT) is a rare neoplasm of the female genital tract. Very few

cases of MMMT associate areas of choriocarcinoma. Two such cases were reported in Medline indexed medical literature, both originating within uterus.
Methods We report a case of bilateral ovarian MMMT in a 49-year-old postmenopausal woman, admitted with abdominal pain and significant weight loss (20 kg during 3 moths). The patient underwent total hysterectomy with bilateral adnexectomy and omentectomy.
Results Both ovaries had tumorous appearance with solid areas and cystic cavities covered by papillary surface. Multiple nodular omental lesions were identified. Histologically, both ovarian tumors presented intermingled carcinomatous and sarcomatous components. The carcinomatous component consisted in a high-grade serous type carcinoma, with immunohistochemical expression for AE1/AE3, CK7, CK20, CA125, estrogen receptors (ER) and progesteron receptors (PR); limited areas of choriocarcinoma were identified in the right ovarian tumor, with focal positivity for beta-HCG. The sarcomatous component mostly consisted in homologous malignant undifferentiated spindle-cell sarcoma, limited areas of heterologous rhabdomyosarcoma being present. The sarcomatous cells were positive for SMA, focal positive for desmin (the heterologous component), and negative for ER, PR and CA125. The omental metastases had purely carcinomatous appearance (serous type). Based on histopathological and immunohistochemical findings, the diagnosis of bilateral MMMT of the ovary stage IIIC was established.
Conclusion(s) Our case is, at least in our knowledge, the first case of MMMT of the ovary with choriocarcinomatous component ever reported in the medical literature.

P3.55

Breast carcinoma metastatic to a tamoxifen related endometrial polyp

Tille J.; Ambrosetti A.; Nobahar M.; Vlastos G.; Pelte M.
Department of Clinical Pathology, University Hospital of Geneva, Geneva, Switzerland

Background Secondary tumors involving the uterus are rare and most of them come by contiguous spread. Metastasis to a Tamoxifen-related polyp is even rarer, with only twelve cases reported.
Methods Case report.
Results Case report: A 50-year-old woman presented with metrorrhagia 11 months after a lumpectomy and sentinel lymph node biopsy for breast ductal carcinoma. Ductal carcinoma measured 1,5 cm and one of the four sentinel lymph node contained isolated tumor cells. Medical complementary treatment consisted of chemotherapy and radiotherapy followed by Tamoxifen. Hysteroscopy showed polyps and polypectomies was performed. Microscopically, the polyps consisted of dilated glands lined by a stratified columnar epithelium with regular outlines in a fibrous stroma containing thick-wall dilated vessels. Within the stroma, there were multiple foci of cohesive tubular structure composed of large cells with nuclei enlargement, a coarse chromatin clumping and a prominent nucleoli. Similar cells were also seen within lymphatic vessels. Immunohistochemically, ductal carcinoma and metastasis were positive for cytokeratin-19 and ER but negative for GCDFP-15 and PR. A hysterectomy was performed with no residual tumor.
Conclusion(s) We report the thirteen case of ductal breast carcinoma metastasis in a Tamoxifen endometrial polyp. In previous reports 9 cases were related to Tamoxifen therapy, 6 were ductal, 6 lobular and one apocrine carcinoma. Pathologists should be aware of this possibility in women of previous breast carcinoma.

P3.56

Embryonal (botryoides) rhabdomyosarcoma associated with a primitive neuroectodermal tumour (PNET)

Stolnicu S.; Nicolae A.; Goez E.; Hincu M.; Nicolau R.; Nogales F.F.
University of Medicine, Targu Mures, Romania

Background Embryonal rhabdomyosarcoma botryoides (ERB) is a rare tumor that occurs in young women in cervical location. Unusual elements such as cartilage and focal pleomorhic areas can be found. Association with PNET has not been previously reported.
Methods 12 year old presented with massive bleeding after the spontaneous elimination of a large (12 cm) polypoid tumor. Inspection of the cervix revealed no remaining tumour. Patient had only chemotherapy and is alive and well 8 months later.
Results The fleshy and congestive polypoid formation were lined by an endocervical-type epithelium which was also present in glands embedded in an extensive mesenchymal loose matrix surrounded by a characteristic periglandular cambium layer. Numerous fascicles of mature striated muscle fibres were present. Multiple foci of small cells arranged in a trabecular, adamantiform pattern of PNET were found, that were positive for CD99, NSE, CD56 and synaptophysin but negative for FLI-1 protein, cytokeratins and muscle markers. FISH for EWSR1 was also negative. Rhabdomyosarcomatous areas were positive for myosin and myogenin; Ki67 index over 60%.
Conclusion(s) Heterologous components of ERB may include, as in this case, metaplastic cartilage. This case is unique as it shows a concomitant PNET pattern with its distinctive small basophilic cells, adamantiform arrangement and a characteristic immunophenotype. The absence

of FLI-1 and negative EWSR1 FISH is a known phenomenon in many uterine neuroectodermal tumors, which seem to have a central type of PNET, rather than a peripheral one.

P3.57

European guidelines for quality assurance in cervical cancer screening: impact of sectioning of cervical cone biopsies for the histopathological detection of cervical cancer

Strojan Flezar M.; Gutnik H.; Pizem J.; Ellis K.; Don O.; Perunovic B.
Institute of Pathology, Faculty of Medicine University of Ljubljana, Ljubljana, Slovenia

Background European guidelines for quality assurance in cervical cancer screening (2008) acknowledge different techniques of sectioning cervical excision cone biopsies (LLETZ). This study aims to compare sensitivity of cervical carcinoma detection of two methods that produce a substantially different workload.
Methods We compared two year workload comprising 820 cases from Royal Hallamshire Hospital, Sheffield and 94 from Institute of Pathology, Ljubljana University, all of which had a previous diagnostic biopsy of high-grade intraepithelial neoplasia. The assessment of LLETZ in the UK laboratory comprised sectioning in 3 mm intervals, examining 3 levels per block whilst in the Slovenian laboratory, cones were cut in 3 mm thick tissue blocks and with 10 100 μm spaced levels per block approximating sectioning of a cone in total, generating on average 24 and 65 sections per case respectively. Relevant histopathological variables were compared using Fisher exact test.
Results Although the Slovenian laboratory examined significantly larger number of levels per cone biopsy this method did not offer higher sensitivity in detection of invasive carcinoma either cumulatively or for pT1a1 (35/820 vs 6/94, $p>0.05$, 30/820 vs. 5/94, $p>0.05$). The detection rates for high-grade intraepithelial neoplasia (CIN2+3) were similar (584/820 vs 71/94, $p>0.05$).
Conclusion(s) A method with large number of levels per cervical cone biopsy does not increase sensitivity, but substantially affects pathologist's workload, and has an impact on the costs and laboratory resources so may need to be reconsidered.

P3.58

Genotype distribution of cervical human papillomavirus DNA in women with cervical lesions: Malabo, Equatorial Guinea

Moro Rodríguez E.; García Espinosa B.; Nieto Bona M.; Silva L.; Piernas C.; Carro P.; Cortés Lambrea L.
Universidad Rey Juan Carlos, Alcorcón, Madrid, Spain

Background HVP vaccine is a useful tool in preventing cervical cancer.
Methods As a result of a campaign against cervical cancer in Equatorial Guinea following cytological screening in which a total of 1680 women were included, finally 26 women were treated surgically with a loop diathermy conization (LEEP). These cases were studied histologically and paraffin samples for each case were genotyped applying a commercial kit that recognized 35 different types of HPV – Clinical Arrays (R) Genomica.
Results Cytological diagnoses included 17 high grade SIL, 1 indeterminate SIL, 5 ASC-H and 3 AGUS. Histological diagnosis results in 3 cases of stage IA cancer of FIGO, 9 CIN-3, 8 CIN-2, 2 CIN-1, 3 flat condylomas and mild dysplasia of the endocervical epithelium. The histopathological results showed a high correlation (84.6%) between cytological diagnoses and the final surgical pathology. The genotyping was performed in 25 cases of which 15 cases were positive for HPV (60%). In 4 cases were identified the HPV-16, 4 HPV-33, 2 HPV-58, 1 HPV-18, 1 HPV-31, 1 HPV-52, 1 HPV-82, and a co-infection of HPV-16 and 58.
Conclusion(s) The prevalence HPV types in the African area vary in comparison to other regions, particularly in Europe and USA. Thus, vaccination against HPV 16, 33 and 58 should be considered in the geographic region of West Africa and specifically in Equatorial Guinea.

P3.59

HPV types distribution in invasive carcinoma of the uterine cervix from 1920 to 2005 in Portugal

Felix A.; Alemany L.; Bosch X.F.
Instituto Portugues de Oncologia de Lisboa, Faculdade de Ciencias Medicas Lisboa, Lisboa, Portugal

Background HPV infection is causally linked to invasive cervical cancer. Our aim was to describe the distribution of HPV genotypes in cervical carcinomas in Portuguese women.
Methods We retrieved 1214 cases diagnosed and treated in the IPOLFG-Lisboa (1920–2005). The DNA HPV types were evaluated from Bouin (1920–44) or formalin fixed, paraffin-embedded tumor samples. HPV detection was done using SPF-10 PCR, followed by DEIA and LiPA25 (version1). Samples were tested at ICO (Barcelona-Spain).
Results Patient's mean age at diagnosis was 53.3 years. SCC was the most common histological type (91.6%). The presence of DNA HPV in cervical carcinomas was detected in 714 cases. Table 1 shows some results. Single, multiple and unknown types were identified in 93.4%; 2.3% and 4.34%. The most prevalent DNA viruses were HPV 16 and 18 with an overall prevalence of 66.3%, followed by HPV 33, 45, 31, 35, 52. Table 1: Decades Nº Nº HPV(+ve);

1920–29 112 35(31.2%); 1930–39 685; 344(50.2%); 1940–49 86 40(46,5%); 1950–59 88 82(93,1%); 1060–69 65 58 (87.6%); 1070–79 50 46(92.0%); 1980–89 56 47(83.9%); 1990–99 31 24(77,4%); 2000–05 41 39(95.1%); Total 1214 714(86.6%).

Conclusion(s)1 - HPV DNA was found in 58.8% of all cases, with low rates of detection in material diagnosed in the first 3 decades (1920–1940). 2 - The lower rate of HPV detection was related with poor quality of DNA, probably due to the fixative used. 3 - The most common viruses in invasive cervical carcinomas from Portuguese women were HPV 16, 18, 33, 45, 31, 35, 52, 4 - Patient's mean age at diagnosis of invasive carcinoma was slightly lower in the beginning of the 20th century compared to last decades.

P3.60
Identification of NLRP7 mutation in a Tunisian family with recurrent hydatidiform mole

Landolsi H.; Rittore C.; Gribaa M.; Yacoubi M.; Touitou I.
Laboratoire d'anatomie et de cytologie pathologiques, CHU Farhat Hached, Sousse, Tunisie

Background Familial recurrent hydatidiform moles (FRHM) are a rare recessive condition in which molar tissues have biparental contribution to their genome. One maternal locus responsible for this condition has been mapped to 19q13.4 and the causative gene, NLRP7, identified. Several affected families have been described. Our objective was to look for the presence of NLRP7 mutation in a Tunisian family with RHM in two sisters.

Methods Molecular analyses were conducted on genomic DNA extracted from the peripheral white blood cells of the two patients, their two sisters (with no RHM), and the parents. All exons of the NLRP7 gene were sequenced in both directions for the two patients. A high resolution melting (HRM) analysis was also performed for quick screening and confirming mutation in the two patients, their sisters and the parents.

Results Sequencing and HRM curves demonstrated an homozygous stop codon, p.E570X (c.1708G>T), mutation in exon 4 in the two sisters with RHM and a third sister who presented with non-molar abortion. The fourth asymptomatic sister and the parents were heterozygous for this mutation.

Conclusion(s) These findings confirm and extend previous studies on NLRP7 mutations, as a cause of recurrent reproductive wastage. This mutation was recently reported for the first time in an Asian patient with 3 complete hydatidiform moles. Here we show that p.E570X is involved in gestational pathology other than RHM. Moreover, this is the first case of FRHM reported in Tunisia and the second case with North-African origin.

P3.61
Ovarian serous tumor with mural nodule of sarcomatoid carcinoma and reactive changes

Basheska Trajce N.; Veljanoska S.; Zografski G.
Department of Histopathology and Clinical Cytology, University Clinic of Radiotherapy and Oncology, Medical Faculty, Skopje, the Former Yugoslav Republic of Macedonia

Background Serous ovarian tumors with mural nodules are very infrequent, with only a dozen of cases described, including four cases of sarcomatoid carcinoma. We report a first case of a mural nodule with features of both sarcomatoid carcinoma and prominent sarcoma-like reactive changes associated with ovarian serous cystic tumor.

Methods A 52-year-old woman underwent left salpingo-oophorectomy and partial omentectomy because of a cyst. Forty-five months previously a total abdominal hysterectomy with right salpingo-oophorectomy and left ovarian resection had been performed. Postoperatively the patient received full-dose chemotherapy and is clinically free of disease at 76 months' follow-up.

Results Within the wall of the largest locule of the left ovarian multilocular cyst, 12.5 cm in diameter that had ruptured at operation, there was a 4x4x1.5 cm nodule. The smaller locules were lined with benign serous epithelium, while the largest locule had morphology of a serous borderline tumor with small foci of superficial invasion. The mural nodule was composed of carcinomatous nests intermingled with pleomorphic mononuclear cells, multinucleated giant cells, histiocytes and other inflammatory cells. The luminal epithelium and underlying pleomorphic cells were diffusely positive for cytokeratin and epithelial membrane antigen, and focally positive for vimentin. Benign spindle cells and multinucleated giant cells were vimentin positive. The ovarian capsule was not invaded.

Conclusion(s) This study confirms the usefulness of immunohistochemistry in distinguishing variant forms of mural nodules in cystic ovarian tumors. It further suggests that malignant nodules in serous tumors do not necessarily carry a poor prognosis.

P3.62
P57KIP2 immunohistochemical expression: a useful diagnostic tool in discrimination of complete hydatidiform mole from its mimics

Sarmadi S.; Izadi-Mood N.; Abbasi A.; Tavangar S.
Mirza Koochak Khan Hospital, Tehran University of Medical Sciences, Tehran, Islamic Republic of Iran

Background Classification of molar pregnancies are typically defined by histologic and genetic criteria,but histological findings still form the main diagnostic tool in the differential diagnosis of the molar gestations. Also, the histologic criteria are subjective and demonstrate considerable interobserver variability between pathologists. Recently, several studies have showed the usefulness of p57KIP2 immunohistochemistry as an ancillary diagnostic tool for molar gestations. The p57KIP2 gene is strongly paternally imprinted and maternally expressed and because complete hydatidiform mole (CHM) lacks a maternal genome, p57KIP2 immunostaining is absent, whereas partial hydatidiform mole (PHM) & hydropic abortuses reveal positive staining.
Methods We evaluated p57KIP2 immunohistochemical expression in 89 cases with histological diagnosis including: 22 CHM, 32 PHM, 20 hydatidiform mole (HM), when the histological features were lacking to differentiate exactly between CHM and PHM & 15 suggestive for PHM.
Results P57 expression in villous cytotrophpblast was absent in 22 of 22 CHM, and 7 of 32 PHM, 15 of 20 HM and 1 of 15 suggestive for PHM. In all cases, maternal deciduas showed diffuse and strong P57 expression, whereas syncytiotrophoblast was negative, which served as internal positive and negative controls respectively for P57 immunostaining.
Conclusion(s) This study confirms that P57 immunostaining can reliably identify CHM irrespective of gestational age and can be used in association with the histological finding for distinguish CHM from its mimics in challenging cases.

P3.63

Phosphorylated-4E-BP1 expression correlates with aggressive tumours and prognosis in endometrial carcinomas

Castellvi J.; Garcia A.; Ruiz Marcellan C.; Peg V.; Salcedo M.; Gil Moreno A.; Hernandez Losa J.; Ramon YCajal S.
Hospital Vall d'Hebron, Barcelona, Spain

Background Cell growth and their signalling pathways are known to be altered in endometrial cancer, mostly in type I carcinomas, and they play a crucial role in the carcinogenic process. Two main pathways transmit the proliferative signal from the membrane receptors to the nucleus: PI3K-AKT-mTOR and RAS-RAF-ERK. The aim of our work was to study the relative importance of the factors involved in these pathways, and evaluate their correlation with the clinico-pathological features of the tumors and their prognosis.
Methods We studied by immunohistochemistry 120 endometrial carcinomas, including 93 type I and 27 type II carcinomas, and 18 control cases, on tissue microarrays. The factors included were HER2, p53 and the phosphorylated forms of AKT, ERK and 4E-BP1.
Results HER2 was overexpressed in 11%, and 30% of carcinomas showed activation of AKT and ERK. The phosphorylated form of 4E-BP1 was expressed in the cytoplasm (31%) and nucleus (63%), and the latter was only found in carcinomas. The nuclear expression of phospho-4E-BP1, and HER2 overexpression were the only factors with prognostic significance.
Conclusion(s) The expression of the activated form of 4E-BP1 correlates with aggressive phenotypes and prognosis, and can reflect the activation status of PI3K-AKT-mTOR and RAS-RAF-ERK pathways, regardless of the upstream oncogenic alterations, and therefore, can be considered as a "funnel factor".

P3.64

Potential epigenetic changes in endometrial hyperplasia

Carvalho L.; Alarcão A.; Gomes A.; Teixeira P.; Silva Reis M.; Simões Da Silva T.; Sousa V.; Couceiro P.
Instituto de Anatomia Patológica, Coimbra, Portugal

Background The endometrial carcinoma is the second most common malignancy of the female genital tract in Portugal. The aim of this study focused on simple hyperplasia of the endometrium in two age groups: women younger than 50 years and over (transition between pre-and post-menopause).
Methods The endometrial carcinoma is the second most common malignancy of the female genital tract in Portugal. The aim of this study focused on simple hyperplasia of the endometrium in two age groups: women younger than 50 years and over (transition between pre-and post-menopause).
Results The protein expression in the samples of the younger group was increased when compared with women over 50 years. Of the 20 cases studied by MS-PCR, 17 were unmethylated and 3 were hypermethylated. Of the 17 cases negative for MLH1 hypermethylation, 12 had positive expression for the respective protein. Two cases of the 3 hypermethylated had no detectable MLH1 protein expression in IHC.
Conclusion(s) The actual detection of changes in preneoplastic lesions of the endometrium seemed to be important since in these 2 groups of patients a different potential risk of developing endometrial carcinoma was traced. Silenced and hypermethylated genes can be reexpressed after administration of drugs that promote deme-

thylation and MLH1 seems to be important in endometrial carcinogenesis.

P3.65
Sertoli cell tumors of the ovary: a clinicopathologic and immunohistochemical study

Dimitriadis I.; Anestakis D.; Tsompanidou C.; Nikolaidou A.; Kartsiounis H.; Patakiouta F.
Theageneion Cancer Hospital, Thessaloniki, Greece

Background Ovarian Sertoli cell tumors are rare and their morphologic spectrum, behavior and factors influencing the latter are not clearly established. They may be mimicked by many different tumors and immunohistochemistry may aid in this differential.
Methods We studied the clinicopathologic features of 4 Sertoli cell tumors, including the immunohistochemical profile of them. The patients, ranged from 25 to 45 years (a.m. 32,25 years). The tumors ranged from 3.5 to 7 cm. They were all unilateral, solid and yellow. The predominant microscopic pattern was tubular, other patterns were cords or trabeculae. The cells (2 tumors) had pale to densely eosinophilic cytoplasm, but (2 tumors) were composed of cells with clear cytoplasm. Two of the tumors had mild τo moderate cytologic atypia and mitotic activity (≤ 5 mitoses/10 [HPFs]).
Results Immunohistochemical stains showed positivity for AE1/AE3 in 3 of 4 tumors. EMA, Keratin7, Keratin 20 were negative in all the tumors. Inhibin and Chromogranin were positive in all tumors. Calretinin in 3 of 4. Vimentin in 3 of 4. SMA in 1 of 4.
Conclusion(s) EMA, Inhibin, and Chromogranin are the most helpful immunomarkers serving to exclude two common mimics of Sertoli cell tumors (endometrioid carcinoma [Inhibin-, EMA+; Chromogranin-] and carcinoid tumor [Inhibin-, EMA+; Chromogranin+]). Most Sertoli cell tumors are stage I, unilateral, cytologically bland, and clinically benign, but occasional examples are high stage, and about 11% of stage I tumors have worrisome histologic features that may portend an adverse outcome.

P3.66
Uterine tumor with neuroectodermal differentiation (malignant ectomesenchymoma)

McCubbin K.; Cooper K.
Fletcher Allen Health Care/Univeristy of Vermont, Burlington, Vermont, USA

Background Malignant ectomesenchymomas (MEM) are rare tumors featuring mesenchymal and neuroectodermal elements which are most commonly found in the pediatric population. Histologically they are characterized by a mixture of rhabdomyosarcoma with either ganglioneuroma, neuroblastoma, or malignant peripheral nerve sheath tumor. The presented case features a uterine MEM in a 59 year-old female.
Methods A 59 year-old female underwent hysterectomy for a pelvic mass detected on ultrasound examination. Gross and histologic examination were performed, as well as a panel of immunohistochemical stains.
Results Gross examination revealed a 10 cm exophytic mass arising from the posterior endometrium and extending to the serosa. Histopathologic examination revealed predominantly small round blue cell morphology with high mitotic activity and foci of necrosis. Other areas exhibited rhabdomyosarcomatous differentiation, with larger cells containing amphophillic cytoplasm and nucleoli. A single focus of epithelial carcinoma was identified. Immunohistochemical stains supported the diagnosis.
Conclusion(s) MEMs are rare tumors featuring mesenchymal and neuroectodermal tissues, arising primarily in soft tissue in infants. Our unique case presents a uterine tumor in an adult arising in association with an endometrial adenocarcinoma or carcinosarcoma. Several theories have been proposed regarding the origin of uterine neuroectodermal tissues. One theory is that of ectopic migration of neural crest cells, however a recent theory suggests that uterine neuroectodermal tissues may represent a "neometaplastic" process of cells of Mullerian origin. This theory is supported by our case, in which neuroectodermal tumor is admixed with epithelial carcinoma.

P3.67
A giant angioleiomyoma of the broad ligament. A case report

Koumpanaki M.; Nikolaidou A.; Moisidis I.; Anestakis D.; Zafeiriou G.; Patakiouta F.
Theagenion Cancer Hospital of Thessaloniki, Thessaloniki, Greece

Background Angioleiomyoma (synonyms: vascular leiomyoma, angiomyoma) is a benign mesenchymal neoplasm composed of smooth muscle cells and thick-walled vessels. It is usually a small, solitary, pain-producing lesion that occurs in the subcutis of the lower extremities. The patients are usually females between the forth and sixth decade.
Methods We report a case of giant angioleiomyoma of the broad ligament of a 62 year-old female. The tumour was discovered in a routine check-up with CT scan. The patient, who had no prior symptoms, had underwent total hysterectomy 18 years ago for uterine leiomyomas. MRI revealed a tumour with a soft-tissue mass consistency and increased vascularization located in the area of the excised left ovary.

Results The mass was surgically removed and we received a well-demarcated tumour, sized 13X9X3 cm, with a tanned-brownish, solid, glistening cut-surface. Microscopically the tumour composed of smooth muscle cells punctuated with numerous thick-walled blood vessels. Myxoid change and pseudoverocay bodies were also observed. Immunohistochemically, the neoplastic cells were positive for SMA, Vimentin and Caldesmon and were negative for S-100, CD34, HMB45, CD57 and calretinin.
Conclusion(s) In early literature, angioleiomyomas were considered as cutaneous leiomyomas, from which they were later distinguished because of their different clinical and histological features. Since then, they have been also found in other areas, such as the oral cavity, uterus and rarely in the broad ligament in variable sizes (up to 12 cm). Differential diagnosis should also include a swannoma and an angiomyolipoma.

P3.68
Aberrant nuclear Cdx2 expression in morule-forming tumors in different organs, accompanied by the cytoplasmic reactivity

Wani Y.; Notohara K.; Nakatani Y.; Matsuzaki A.
Kurashiki Central Hospital, Kurashiki, Okayama, Japan

Background The aim of this study is to examine Cdx2 expression in various morule-forming lesions in different organs, including the evaluation of cytoplasmic immunoreactivity.
Methods We selected morular cases as follows; thyroid papillary carcinoma, (n=3), well differentiated fetal adenocarcinoma (WDFA) (n=4), gastric adenoma, intestinal type (n= 1), gastric adenocarcinoma, pyloric gland type (PGT) (n= 1), Pyloric gland adenoma(duodenum; n = 1, gallbladder; n= 6), colonic adenoma(n=1), endometrial polyp (n=4), endometrial hyperplasia(n=13), uterine endometrioid carcinoma (n= 13), ovarian endometrioid borderline tumor/adenocarcinoma (n= 5). Immunostaining of Cdx2 was basically followed by the method in our previous study. Briefly, morular and glandular LI (%) were also calculated separately by counting positive cells in foci of SM and in the surrounding glandular cells. Regarding cytoplasmic reactivity, fine granular staining was only considered significant and scored as follows; >1–30% positive cells; focal, >30%; diffuse.
Results All but five cases (1; thyroid, 2; lung, 2; endometrium) (90.4%) showed nuclear reactivity of Cdx2, whose morular LIs were higher than glandular LIs, in contrast to equally high LIs in both areas in each case of gastric and colonic adenoma, intestinal type. 15 cases (28.8%) showing nuclear Cdx2 expression were accompanied by cytoplasmic reactivity (diffuse; 11, focal; 4) both in morular and glandular areas. Of interest, all five cases lacking nuclear expression presented cytoplasmic reactivity (diffuse; 2, focal; 3) in morules as well as in adjacent glands.
Conclusion(s) Both nuclear and cytoplasmic staining patterns suggested a close link between Cdx2 expression and morular forming.

P3.69
Adenoid cystic carcinoma of the Bartholin's gland, a case report

Mohammed H.; Soloy-Nilsen H.; Al-Shibli K.
Nordland Central Hospital, Department of Obstetrics and Gynecology, Bodo, Norway

Background Carcinoma of the vulva is the fourth frequent malignancy in the female genital system. Bartholine gland carcinoma represents 0.1% to 5% of vulvar carcinomas, and adenoid cystic carcinoma is a rare subtype.
Methods We report a case of vulvar adenoid cystic carcinoma in a 42 years old female with Adenomatous Polyposis Coli (APC). Because of pelvic pain and dyspareunia was she reffered for gynecological examination and a mass in the introitus was found and thought to represent an infected bartholine cyste. Intraoperative findings were suspicious (an infiltrative vulvar mass).
Results Biopsy from the vulvar lesion showed a neoplasm composed of cuboidal-columnar cells in solid nests mixed with duct-like structures, reticular and cribriform patterns. Perineural infiltration was identified with S100 immunohistochemistry. The tumor showed rich hyaline (PAS +) material. The ductal luminal cells were positive for keratin 7, while the basal cells were positive for cytokeratin 5/6 and actin. Both CD117 and Bcl2 were positive. The diagnosis was adenoid cystic carcinoma, grade I. The patient was treated by vulvectomy followed by radiotherapy. The ingunal lymph nodes were negative for metastases, bilaterally.
Conclusion(s) Adenoid cystic carcinoma of the Bartholine gland is a rare malignancy with a morphologic and phenotypical picture similar to the salivary gland counterpart. There is a known association with APC which may suggest that the abnormal products of the mutated genes result in the inappropriate activation of the Wnt signalling pathway and the growth of adenoid cystic carcinoma.

P3.70
Borderline Brenner tumors of the ovary-report of two cases

Arnogiannaki N.; Martzoukou I.; Biteli M.; Negris V.; Gakidis P.; Michelis V.; Aslanidis O.; Sofopoulos M.
St. Savvas, Athens, Attiki, Greece

Background Borderline Brenner tumor (BBT) is a rare entity accounting for 1:1000 ovarian tumors. Our study presents two cases of BBT and approaches the problem of differential diagnosis.
Methods 1. A 50-year-old patient was admitted for abnormal vaginal bleeding and abdominal pain. U/S and CT exhibited a 20x19x15cm mass of the right ovary. 2. A 70-year-old patient was admitted for urinary difficulties. U/S and CT revealed a 14x11.5x10cm mass of the left ovary. Neither case had evidence of metastatic disease. Both patients underwent a total hysterectomy and epiploectomy. Tumors appeared circumscribed, multilobulated and firm. The gross section revealed a large, multicystic component containing a polypoid mass and foci of white-yellowish solid areas.
Results Histologically, in both cases the diagnosis confirmed BBT. Cysts were lined by broad papillae with fibrovascular cores covered by transitional cells, resembling a low grade papillary transitional cell carcinoma of the urinary tract. In the first case tumor cells showed mild atypia, nuclear grooves and sparse mitoses while in the second one severe atypia as well as squamous and mucinous metaplasia. No invasion was demonstrated in both cases. Tumors' immunoprofile was positive for CK7, Pankeratin, EMA, EGFR, CEA, P63 and negative for CK20, S100, Vimentin, SMA, Estrogen, Progesterone, Ca125, P53.
Conclusion(s) BBTs are rare ovarian tumors displaying benign, borderline and malignant variants. The borderline condition, together with the atypical or malignant features, requires also the presence of benign elements and by definition the absence of obvious stromal invasion. The correct diagnosis is important since their prognosis is excellent unlike its malignant counterparts.

P3.71
Carcinosarcoma of uterus and ovary: a comparative histological and clinical analysis

Jamali M.; Rasty G.; Rouzbahman M.; Clarke B.
University Health Network, Toronto, Ontario, Canada

Background Carcinosarcomas of uterus and ovary are high-grade malignancies of the female genital tract. The objective of this study is to compare these two groups in terms of their different components, clinical stage and correlation of pathological parameters with patient outcome.
Methods The database at University Health Network was searched and 42 and 6 cases of uterine carcinosarcoma (UC) and ovarian carcinosarcoma (OC), respectively, were retrieved in the period of 2001–2009. Types and percentages of different components as well as pathologic and clinical stage and patient outcome were documented.
Results The epithelial component in UC made 53.3% of the tumour, which was serous, endometrioid and mixed cell types in 16, 11 and 15 cases, respectively. The mesenchymal element was mainly homologous (28, 66.7%). In OC, the epithelial component was 70% of the tumour with which was serous, endometrioid and mixed cell types in 3, 1 and 2 cases respectively. The mesenchymal element was homologous in 50% of cases. In UC, 20 were FIGO stage I, 3 stage II, 15 stage III and 4 patients stage IV. In OC, one was FIGO stage I, one stage II, 3 stage III and one stage IV.
Conclusion(s) Serous carcinoma appeared to be the most common epithelial component in this series for both UC and OC. The sarcomatous component is mainly homologous in UC and heterologous in OC. Thus, OC shows a less favourable outcome in comparison to its uterine counterpart in higher stages of disease.

P3.72
Clinical significance and molecular analysis of endometrial adenocarcinoma type 1 with minute type 2 component

Kanbour-Shakir A.; Kanbour A.; Trucco G.; Elishaev E.
Pittsburgh, PA, USA

Background Endometrial adenocarcinoma (EA) are common tumors with type 1 being 80–85%, estrogen related, predominantly endometrioid with low/moderate differentiation and type II, 10–15 %, non-estrogen dependant, high grade carcinoma, predominantly serous or clear cell type. Mixed type I and II, have at least 10% of minor component. Mixed carcinomas with 25% or more high grade component have poor prognosis. The significance of minute <5% of type II within type 1 endometrial cancer is analyzed.
Methods Three cases of minimally invasive type I EA containing microscopic foci <5% of type II clear cell component are presented.
Results All three patients had superficially invasive endometrioid adenocarcinoma with microscopic foci of clear cell component and no cervical or lymphovascular invasion. First patient had had clear cell adenocarcinoma involving both ovaries. Molecular analysis (identity test) of both ovarian cancer were of the same clonal origin to endometrial clear cell component but different from the type 1 cancer. Second patient had negative staging and positive clear cell carcinoma in the pelvis wash. Third patient had negative staging and pelvic wash, but fourteen months later she developed positive ascites with clear cell adenocarcinoma.
Conclusion(s) This limited study suggests that even a small focus of clear cell <5 % of tumor within type I endometrial adenocarcinoma may lead to higher clinical stage, tumor

recurrence and have prognostic impact. We recommend extensive sampling of type I endometrial adenocarcinoma for the presence of a clear cell component.

P3.73

Expression and clinical significance of FAK and SRC proteins in human endometrial adenocarcinoma

Chatzizacharias N.; Giaginis C.; Gatzidou E.; Sfiniadakis I.; Theocharis S.
University of Athens, Medical School, Athens, Greece

Background Focal Adhesion Kinase (FAK) is a protein tyrosine kinase, localized in the focal adhesions, which, when activated, has been shown to interact with Src, another kinase of tyrosine, regulating several cellular signaling pathways. Both enzymes have been implicated in malignant transformation and disease progression. The aim of the present study was to evaluate the clinical significance of FAK and Src expression in endometrial adenocarcinoma.
Methods FAK and Src protein expression were assessed immunohistochemically in tumoral specimens obtained from 43 endometrial adenocarcinoma patients and were statistically analyzed in relation to various clinicopathological parameters and tumor proliferative capacity, reflected by Ki-67 labeling index.
Results FAK positive staining was significantly associated with FIGO disease stage (p=0.046), while FAK overexpression was significantly associated with patients' age (p = 0.009). FAK staining intensity was not associated with the clinicopathological parameters examined and tumor proliferative capacity. No statistically significant associations were noted between Src positivity, overexpression or staining intensity and the clinicopathological parameters examined, except for a borderline association between Src positivity and patients' age (p = 0.094). FAK expression was positively correlated with Src expression; however, without reaching statistical significance.
Conclusion(s) The current study supports evidence that FAK but not Src protein expression was associated with clinicopathological parameters important for endometrial adenocarcinoma patients' management. However, further research effort is warranted to delineate whether FAK protein may represent a potential marker of malignant transformation and could serve as a potential target for therapeutic disruption of endometrial adenocarcinoma progression.

P3.74

Female adnexal tumor of probable wolffian origin that recurred 13 years later: a case report

Mori I.; Ozaki T.; Taniguchi E.; Shintaku M.; Kakudo K.
Wakayama Medical University, Wakayama, Japan

Background Female adnexal tumor of probable wolffian origin (FATPWO) is a rare tumor. In the literature of 2009, 72 cases were counted. Although most cases follow benign clinical course, about 10% cases resulted recurrence or metastasis. We report a case that recurred after 13 years.
Methods The patient was 53 years old female. She underwent simple hysterectomy under a diagnosis of uterine leiomyoma. During operation, multi-nodular tumors up to 6 cm were found between uterine cervix and urinary bladder. No direct connection to the uterus was identified. Tumors were also found on the peritoneal surface of the intestine.
Results The cut-surface was light brown without hemorrhage or necrosis. Microscopically, tumor cells show large, oval, relatively uniform nuclei with few mitotic figures. Cytoplasm was wide and faintly eosinophilic. Tumor cells were chiefly arranged in trabecular structures divided by thin stroma with foci of glandular structures. Apparent invasive growth was found. Tumor cells revealed positive reaction for keratin and vimentin while negative for inhibin, CA19-9, and CEA. MIB-1 labeling index was lower than 5%. The patient had a history of pelvic tumorectomy 13 years ago that arose from parametrium of left Fallopian tube. Because of severe degenerative change, no histological diagnosis was made at that time. We retrieved the old slides, and the microscopic features were similar.
Conclusion(s) Finally, we diagnosed this tumor as FATPWO. Recurrence after 13 years was the longest period as far as we could find.

P3.75

Giant uterine leiomyoma. Case report

Guran R.; Bruma G.; Stanculescu M.; Nistor A.; Simion G.; Sajin M.; Moldovan D.
Emergency University Hospital Bucharest, Bucharest, Romania

Background Leiomyomas are the commonest benign pelvic tumors in women. Despite the high incidence, it is uncommon to encounter a giant fibroid as in this case: a 59-year old female presented with a 10-year history of gradually increasing abdominal distension, accentuated in the last year along with difficulty in walking and symptoms of urinary obstruction. She went a full clinical and radiological investigation showing a large abdomino-pelvic mass of uncertain origin and the angiography revealed a highly vascularized tumor.
Methods Total abdominal histerectomy and bilateral salpingo-oopherectomy, including the mass and a fragment of omentum, were performed. All anatomical pieces were fixed in 10% formaldehyde solution, paraffin-embedded, cut and stained (HE and VG).

Results I. Freeze-down histopathology. Macroscopically: a 32 kg, boselated, encapsulated tumor measuring 44/41/22 cm, with a whitish, whorled cut surface without any necrotic areas. Microscopically: fibroma. II. Paraffin-embedded histopathology: Macroscopically: Uterine corpus 10/6/8 cm; hemoragic endometrium; the myometrium shows one leiomyoma measuring 1 cm and another subserous leiomyoma only a few mm in size. Right adnexa - ovary 3/2/1 cm; salpinx 8/0,7 cm. Left adnexa - ovary 2/1/1 cm; salpinx 3/0,3 cm. A 30/10/1 cm omentum fragment without any lymphatic nodules grossly identified. Microscopically: Giant uterine leiomyoma showing whorled bundles of well-differentiated, regular, spindle-shaped smooth muscle cells; proliferative endometrium; bilateral ovarian and salpingian atrophy; mature adipose tissue with mesothelial inflamatory reactivity.
Conclusion(s) The presence of giant abdomino-pelvic tumors is uncommon and may reach incredible size without producing appreciable symptoms.

P3.76
Malignant mixed Müllerian tumor evolving on endometrial polyp in a patient with sertoli-leyding cell tumor. An extremly rare coexistence of tumors with no recorded relevance

Hadjileontis C.; Agelidou E.; Taravanis T.; Kafanas A.
Serres General Hospital, Serres, Northern Greece, Greece

Background The overall risk of malignancy in endometrial polyps is less than 2%, while degeneration of endometrial polyps in to malignant mixed Müllerian tumor (carcinosarcoma) is estimated to accound about 0,36% of the cases. Sertoli-Leyding cell tumors on the other hand comprise less than 1% of ovarian neoplasms and are more comonly seen in young patients. Until now, no correlation has been reported between the coexistence of these three entities.
Methods We present the case of a 67 year-old patient with no history, who presented with postmenopausal uterine bleeding. Allthough no histological examination was performed, the patient underwent total hysterectomy and bilateral salpingo-oophorectomy, due to radiologic findings compatible with endometrial carcinoma.
Results The endometrial cavity was filled by a polypoid mass measuring 4,5 cm in diameter, arisiging from the fundic region of the uterine corpus. The mass was found to be a hyperplastic polyp. Confined within the projecting part of the polyp, a malignant neoplasm was noted, consisting of both stromal and glandular malignant elements, the immunohistochemical profile of which confirmed the histological diagnosis of carcinosarcoma. Furthermore, a circumscriped yellow nodule was found in the right ovary, presenting with histological and immunohistochemical features of Sertoli-Leyding cell tumor.
Conclusion(s) We discuss the coexistence of these three different tumors, differential diagnosis and the patients' clinical course.

P3.77
Malignant myxoid solitary fibrous tumor of the uterus: a rare case

Vizcaíno J.; Peixoto C.; Encinas A.; Afonso M.; Silva P.; Lopes C.
Centro Hospitalar do Porto-Hospital Geral Stº António, Oporto, Portugal

Background Malignant myxoid neoplasms of the uterus are extremely rare. Indeed, only few entities of primary uterine pure mesenchymal tumors bearing myxoid changes and malignant features have been described, including myxoid malignant leiomyosarcoma, myxoid endometrial stromal sarcoma, and myxoid liposarcoma.
Methods Sections of 10% neutral-buffered formalin fixed paraffin embedded material were stained with standard technique (H&E). Immunostains were performed with avidin-biotin-peroxidase method.
Results We describe the case of a 31 year-old woman submitted to resection of a 391 g mass received in multiple gelatinous greyish fragments. Microscopically it was a myxoid neoplasia consisting of fascicles of atypical spindle cells, haemangioperycitoma-like vascular pattern admixed with collagen bundles. The mitotic index was 4 mitosis/10HPF. Immunostains showed diffuse positivity of the neoplastic cells for CD34, CD99, BCL-2 and progesterone receptor, and negativity for CAM5.2, α-actin, HHF-35, caldesmon, desmin, CD10, α-inhibin, estrogen receptor and S100. Myxoid malignant solitary fibrous tumor (SFT) was diagnosed. The hysterectomy specimen revealed residual tumor.
Conclusion(s) SFT of the uterus is very rare. Our search results revealed only two cases of benign uterin SFT reported so far. To the best of our knowledge, no malignant case was described to date. Although rare, myxoid malignant SFT should be considered in the differential diagnosis of uterine primary malignant myxoid tumors.

P3.78
Mature cystic ovarian teratoma with well developed cerebellum. A case report

Fericean A.; Kalodimos G.; Zourou I.; Karamouti M.; Koutsogiannis G.; Georgadakis G.; Alexopoulou E.
Achillopouleion Volos Hellas, Volos, Magnesia, Greece

Background Mature ovarian teratomas usually consist of an epithelial cyst lining of epidermal type and of a wall

harbouring mature mesodermal, endodermal and ectodermal derivatives. Neural tissue is frequently encountered, with glial tissue to predominate, while organized brain tissue (including cerebrum and cerebellum) is a rare finding.

Methods We present the case of a 19 year old Caucasian female patient who was admitted to our hospital for acute lower abdominal pain and abnormal uterine bleeding. Ultrasound revealed the presence of bilateral cystic ovarian tumours. A laparotomy was performed and the tumours were removed.

Results Histology showed bilateral mature cystic teratomas. The tumour of the left ovary contained only well-differentiated skin and adnexa, while the right ovarian tumour revealed the presence of skin and adnexa, adipose tissue with blood vessels and peripheral nerves, cartilage, respiratory epithelium, intestinal tissue, smooth muscle and fibrous tissue as well as an area composed of mature neurons intermingled with the processes of astrocytes. The same tumour also included a well formed cerebellum measuring 30 mm in greatest diameter and having a structure similar to that found in normal mature cerebellum, with a single row of Purkinje cells and absence of Obersteiner external granular layer, indicating an advanced stage of development.

Conclusion(s) According to the literature, our patient is the second youngest female of reproductive age with a well-differentiated cerebellum of approximately normal size in an ovarian teratoma.

P3.79

Nose skin metastasis of uterine endometrial adenocarcinoma: case report

Keser Hallac S.; Yavuzer D.; Ergen C.; Gul Ege A.; Barisik Ozdemir N.; Cakir C.; Karadayi N.; Gumus M.; Bilici A.
Dr. Lutfi Kirdar Kartal Educational and Research Hospital, Department of Pathology, Istanbul, Turkey

Background Endometrial adenocarcinoma is one of the most common gynecological tumors. Distant metastasis may involved the lungs, heart, skin, and bones. Metastases to the nose skin is an unusual distant metastasis localization.

Methods Case:3 months ago, 67-year-old female patient's; who was adenosquamous subtyped endometrioid adenocarcinoma diagnosed; sample mass which was located on right side of the nose wall was sent to our clinic. The biopsy was off-white color and in 0.5x 0.4x0.3 cm sizes. Adenocarcinoma was detected showing focally squamous differentiation in microscopic examination. The tumor was showing similar features with the endometrium adenocarcinoma in the patient's story. Tumor cells with estrogen and progesterone receptors showed positive staining.

Results With immunohistochemical and morphological findings the case assessed as it is compatible with the endometrium adenocarcinoma nose skin metastasis. Chemotherapy is applied to the patient. The patient is still under control who shows partial response to chemotherapy.

Conclusion(s) The rare that shows unusually located skin metastasis is presented in the ligth of literature information.

P3.80

P16 protein doesn't correlate with high risk HPV, neither with HER receptors expression

Koumoundourou S.D.; Mpota N.V.; Gerbesi M.; Ravazoula K.P.
University Hospital of Patras Rio, Patras, Achaia, Greece

Background P16 is a member of the family of Cyclin-Dependent- Kinase-Inhibitors while HER proteins interact with Cyclins and CDKs. The aim of this study was the evaluation of p16, HPV and HER/2, HER/3 and HER/4 proteins in cervical lesions and the correlation of their expression with each other, with the type of carcinoma (invasive vs in situ) and with coilocytic atypia.

Methods 75 specimens of cervical carcinomas were used (42 infiltrative and 33 in situ). The expression of all molecules was studied by immunohistochemistry. The staining cut-off was the staining of at least 5% of the tumor cells. The statistical analysis was implemented using SPSS13.

Results All specimens were p16 positive. 11 invasive (26,2%) and 12 in situ (36,3%) carcinomas immuoreacted with HPV antibody. 24 infiltrative (57,1%) and 9 (27,3%) in situ carcinomas were HER3 positive, while 22 (52,4%) and 15 (45,4%) respectively showed HER/4 immunopositivity. 8 cases of invasive carcinomas (19%) revealed HER/2 positivity. HER proteins were strongly associated with one another while HER/4 expression was strongly correlated with HPV (p=0,007). HER/3,4 had a significant association with coilocytic atypia. p16 was nuclear in coilocytes and cytoplasmic in carcinomas cells.

Conclusion(s) HER receptors are overexpressed in cervical carcinomas correlating with high risk HPV. Expression of P16 was independent from HPV. This leads to the conclusion that p16 is always present in high grade cervical lesions and helps in the differential diagnosis rather than the prognosis of squamous cervical lesions.

P3.81

P16(INK4A) immunostaining in cytological and histological specimens from the uterine cervix: a comparative study

Kampas I.L.; Milias S.; Giomisi A.; Papachatzopoulos S.; Melitas K.
Cytopathology Department, 424 Military Hospital of Thessaloniki, Thessaloniki, Greece

Background The gene p16INK4a is a protein that in case of dysplastic intraepithelial lesions, this protein is overexpressed due to the transforming activity of the E7 of all high risk-HPV types. Thus, the detection of p16 INK4a in cervical intraepithelial lesions seems to be an unfavorable prognostic factor. The aim of this study was to investigate the expression of p16 INK4a in cytologic and corresponding histologic with dysplastic lesions.
Methods Thirty five cervical ThinPrep specimens, diagnosed as ASCUS, LGSIL, HGSIL, were included in our study. The women with these abnormal Pap test underwent biopsy. Both of cytology and tissue specimens were processed for p16 INK4a (clone E6H4, DakoCytomation) immunostaining. The findings were evaluated in relation to cyto-histo-morphology.
Results The diagnostic findings in both of cytologic and histologic samples were concordant in the majority of them. The protein was overexpressed in all of HGSIL specimens. In a small percentage of LGSIL samples p16 INK4a was detected. In cytologic smears positivity of p16 was observed in isolated cells. On the other hand in tissue samples the positive reaction was characterized by diffuse strong nuclear and cytoplasmic staining.
Conclusion(s) The results of our study showed concordance of p16 INK4a expression in cytologic and corresponding histologic specimens. p16 INK4a seems to be a specific and easily performed biomarker, which offers prognostic information about early dysplastic lesions, contributing to the management and monitoring of HPV affected women.

P3.82

p53 in ovarian mucinous borderline tumours

Mora M.; Gaggero G.; Pigozzi S.; Fulcheri E.
Department of Pathology, National Institute for Cancer Research, Genoa, Liguria, Italy

Background A new carcinogenetic model of ovarian epithelial tumours have recently been proposed paying attention to clinic, prognostic and genetic features: it divides Type I carcinomas -with indolent growth, genetic stability and mutation in KRAS, BRAF, PTEN- from Type II ones -with rapid growth, high rate of p53 mutation and genetic instability-. Since few data have been reported in literature about p53 mutation in mucinous borderline tumours of ovary (MBT), we evaluated the p53 mutation rate in MBT and correlated it with histotype (endocervical -EMBT- versus intestinal -IMBT-), detected by morphology and by immunohistochemical markers of intestinal differentiation.
Methods 21 MBT (age range 24–80, 1 monolateral and 20 bilateral) were reviewed and tissue sections were immunoassayed for p53 (DO-7), cdx2 (Cdx2–88) and CK20 (K320.8).
Results Considering both morphological and immunohistochemical data, we obtained 18 (86%) IMBT (6 cdx2+ and 14 CK20+) and 3 (14%) EMBT (0 cdx2+ and 0 CK20+). 5 cases (24%, all IMBT) showed diffuse p53 expression (> 75% of neoplastic cells); 4 cases (19%, 3 EMBT, 1 IMBT) showed focal p53 expression (< 25% of neoplastic cells) and 12 cases (57%) showed no p53 expression (< 5% of neoplastic cells). Correlation between p53 expression and histotype was statistically not significant (Fischer-test).
Conclusion(s) We found unexpected high rate of p53 mutation in 5 IMBT, contrasting to previous literature reporting low p53 mutation rate in MBT. In literature however IMBT are supposed to have higher malignant potential than EMBT that are more frequently bilateral and endometriosis-associated.

P3.83

Pathogical findings and immunophenotype evaluation in lipoma of the uterus: report on 7 cases

El Hadj El Amine O.; Bouraoui S.; Kassar A.; Goutalier C.; Lahmar A.; Mzabi S.
Mongi Slim, Tunis, Tunisia

Background Lipoleiomyoma of the uterus is an extremely rare, benign, uterine tumour. Only 200 cases were reported in the literature. This rare disease was unknown for a long time. Their histogenesis remains controversial. We aim to describe the clinical and pathological aspects of uterine lipoleiomyoma and to try to specify, by an immunohistochemical study, its degenerative or tumoral nature.
Methods We underwent a retrospective study collecting uterine lipoleiomyomatous lesions over 20 years among 3500 uterine leiomyomas. We performed an immunohistochemical study including anti-vimentin, anti-smooth muscle actin, anti PS-100, anti-desmin, anti-factor VIII and anti-HMB-45. The results were correlated with the pathogenesis of this lesion.

Results 7 cases were identified represented by 2 pure Lipoma. Which exceptional lesions and 5 Lipoleiomyoma. Two cases were located to the endocervical cavity. All the others were lesions of the uterine body. Immunohistochemical analysis showed an expression of PS 100 only in lipocytes whereas leiomyomatous cells express only smooth muscle actin.
Conclusion(s) Our study supports the benign tumoral nature of the fatty uterine lesions. Lipoleiomyomatous cells may originate from the transformation of a totipotent mesenchymal cell and not from a degenerative process.

P3.84
Primary ovarian hydatidiform mole: a case report

Mavropoulou S.; Tatsiou Z.; Proskinitopoulou A.; Vlahos G.; Kefalas P.; Chouchos N.
Xanthi General Hospital, Xanthi, Greece

Background Primary ovarian ectopic pregnancy comprises up to 3% of all ectopic gestations. Primary ovarian gestational trophoblastic disease is an extremely rare condition with only a few cases been reported in the English literature.
Methods We report the case of a 31-year-old woman, who was admitted to the hospital for suspected ectopic pregnancy, with acute pelvic pain at 5 weeks after her last menstrual period. Laboratory examination showed positive pregnancy test and elevated serum beta-human chorionic gonadotropin (beta-hCG). Pelvic ultrasonography revealed a heterogeneous cystic mass of the right adnexa. Accordingly, a diagnostic laparoscopy for suspected extrauterine pregnancy was performed. A ruptured hemorrhagic mass of the right ovary with maximum diameter 3,5 cm was found, accompanied with hemoperitoneum and a partial wedge resection of the right ovary followed. The uterus, both fallopian tubes, and the left ovary were normal.
Results Histological examination revealed an ovarian partial hydatidiform molar pregnancy, with small vascularized chorionic villi with nucleated red cells admixted with enlarged oedematous villi with central cisterns, proliferative trophoblast with no evidence of atypia and with scalloped villous surface forming trophoblastic inclusions. A compressed ovarian tissue was observed at the periphery, with decidual reaction of the ovarian stroma adjacent to a corpus luteum. Serial beta-hCG measurements showed a decline without need for adjuvant chemotherapy.
Conclusion(s) Although primary ovarian pregnancy is a very rare event, attention should be paid to the uncommon possibility of gestational trophoblastic disease. Careful follow-up with serial serum beta-hCG levels is required to detect persistent disease.

P3.85
Primary peritoneal and ovarian carcinosarcomas

Gualco M.; Mora M.; Bruzzone M.; Truini M.; Fulcheri E.
Department of Pathology, National Institute for Cancer Research, Genoa, Liguria, Italy

Background Extragenital Mullerian carcinosarcomas (MMMT) are rare. They may arise in the peritoneum as a part of the Secondary Mullerian System (SMS). However some cases are associated with peritoneal endometriosis that may arise from the SMS thus confirming a unique etiologic way. Ovarian carcinosarcomas are more frequent but rare (< 1% of ovarian neoplasms) and may arise from mullerian inclusion or endometriosis similarly to extragenital peritoneal counterparts.
Methods We reviewed all primary mullerian peritoneal neoplasms from 1999 to 2008.
Results 7 primary extrauterine carcinosarcomas were observed (age: 62–72 years), 6 ovarian (O-MMMT, 4 monolateral and 2 bilateral) and 1 peritoneal (P-MMMT). O-MMMT had heterologous sarcomatous component in 4 cases and omologous in 2 cases. The carcinomatous component was endometrioid in 3 cases, serous in 2 cases and mixed (serous/clear cells) in 1 case. The P-MMMT had heterologous sarcomatous component and endometrioid epithelial component with foci of clear cell differentiation. A primary peritoneal endometrioid adenocarcinoma (PEA) was observed (58 y.o. patient) showing endometrioid component with foci of transitional differentiation. The endometrioid malignant component of all cases exhibited p53 overexpression. No foci of endometriosis were demonstrated in all cases.
Conclusion(s) The so-called mullerian adenosarcoma (with overgrown and malignant stromal component) frequently arise from well documented peritoneal endometriosis. Rare PEAs (with overgrown and malignant epithelial component) are reported. The many similarities between epithelial components of all these neoplasms, including MMMT, seem to confirm the unique pathogenesis and the absence of endometriosis seems to stress the mullerian origin of these tumours.

P3.86
Pseudo-Meigs syndrom or not?

Mameri S.; Khaili R.; Ould-Slimane S.; Ayyach A.
Beni-Messous, Hydra, Alger, Algeria

Background We report the case of a 57 year old postmenopausal woman admitted in Obstetric-Gynecology Unit because of ascite and pelvic tumor. Clinical examination revealed a moderate ascite and a palpable mass of lower abdomen. Ultrasound scan confirmed the presence of

intraperitoneal fluid with a solid ovarian tumor and a large Fallopian tube mass. The fluid was free of malignant cells at the cytologic examination.The patient underwent surgical therapy, a total hysterectomy with annexectomy. The ascite was resolutive immediately after surgery.
Methods Macroscopically, there was a right tumoral ovary of 2 cms and a homolateral big Fallopian tube of 7 cms occupied by a well-circumscribed white nodular tissue. Uterus, uterine cervix and left annexectomy presented no abnormalities. Several samples of the ovarian and Fallopian tube lesions are realized, stained with hematoxyline-eosine.
Results Microscopic study shows that the ovarian tumor was a benign fibroma and the Fallopian tube one a granulosa tumor with few cytologic atypia, rare mitosis and a preserved capsula.
Conclusion(s) Pseudo-Meigs syndrom is characterized by the co-existence of peritoneal and/or pleural fluid and ovarian or pelvic tumors. This fluid accumulation which regresses after excision tumor seems to be related to lymphatic obstruction caused by rare pathologic conditions (benign or malignant) described in the literature. Can we consider this case associating an ascite with ovarian and Fallopian tube tumors as one other unique entity?

P3.87

Resection margin status in conization specimens as prognostic marker for recurrences in high-grade squamous intraepithelial lesions (HSIL) of the uterine cervix

Jasar Nijazi D.; Kostadinov J.; Panchevski N.; Matevska-Anastasovska E.; Badzakov N.; Timcheva S.; Lazarevski S.; Sardzovski B.; Kubelka-Sabit K.
Mala Bogorodica-Sistina, Skopje, the Former Yugoslav Republic of Macedonia

Background The aim of this study was to evaluate the prognostic significance of the resection margins in association with the recurrence risk in conization specimens from patients with HSIL.
Methods In this retrospective study, 277 women with HSIL were included. Eighty-eight of them were diagnosed with CIN-II (32%), 127 with CIN-III (46%) and 62 with CIS (22%). Ultrascision knife conization technique was performed in all patients, in a period 2003–2007. Mean age of the patients was 32.3 years (range, 17–55 years). During the follow-up period (12 to 60 months, mean 35), the results of control biopsies/PAP-smears were accessible for 87 patients only.
Results From a total of 87 patients, 35 (40%) had clear margins, while in 52 margins were unclear (60%). There were 7/28 recurrences in the CIN-II group (26%), 9/39 (24%) in the CIN-III group and 5/20 (25%) in the CIS group. When chi-square test was performed to investigate the statistical relation between the resection margins and recurrences of CIN in each of the three groups, there was no significant correlation ($p>0.05$).
Conclusion(s) In our material, the relation between resection margins and recurrence of CIN, was not statistically significant. According to the literature, clear resection margins in a conization specimen is not an optimal predictive factor for recurrence. Other prognostic markers should be investigated in order to define the risk of recurrence in patients with HSIL.

P3.88

Sarcomatoid squamous cell carcinoma of the vulva: a case report

Lazureanu Codruta D.; Lazar E.; Dema A.; Cornianu M.; Costi S.; Faur A.; Cornea R.
University of Medicine and Pharmacy Timisoara, Timis, Romania

Background Sarcomatoid features of squamous cell carcinoma type of vulvar cancer appears to be associated with a poorer clinical outcome.
Methods A 70-year-old woman with a 3 months history of tenacious pruritus and burning vulvar sensation underwent partial vulvectomy for a 1.5 cm ulcerative-infiltrative mass, with 2 cm free of lesion margins and left inguinal lymph node dissection. Tissue samples were fixed in buffered 4% formalin solution, paraffin embedded and stain with HE, then, vulvar biopsies were investigated with Dako antibodies pan-cytokeratin, vimentin and Ki-67 antigen, using LSAB system and DAB visualization.
Results The pathologic findings were consistent for an intermediate-differentiated squamous cell carcinoma with superficial tendency to keratin pearl formation and deepness spindling morphology. The tumor was ulcerated and it's depth of invasion was 2 mm (pT1b). On immunohistochemistry stain, both squamous and spindle cell components were positive for pan-cytokeratin, the sarcoma-like area being also immunoreactive for vimentin. The mitotic index of Ki-67 antigen was higher in deep portion (12% vs. 5% superficially). No metastases were found in the regional lymph node (T1bN0Mx - FIGO stage Ib).
Conclusion(s) Due to the rarity of cases reported in the literature and the biological aggressiveness, is important to actively search for the sarcomatoid variant of vulvar squamous cell carcinoma. A complex strategy must integrate clinical examination with classic histopathology and immunohistochemistry to point out a possible poorer prognosis.

P3.89

Sertoli-Leydig cell tumor with heterologus element

Benkhedda G.; Lamouti A.
Blida, Algeria

Background Sertoli-Leydig cell Tumor (SLCT) is a rare ovarian tumor that belongs to the group of sex-cord stromal tumors.These constitute less than 0,5% of ovarian tumors. Most tumors are unilateral,confined to the ovaries,and seen during the second and third decades of life. 50% of these tumors are characterized by the presence of testicular structures that procduce androgens in 50% of cases.
Methods We report the case of a young woman aged 24 years with an SLCT. The heterologus element was in the form of mucinous epithelium of the gastro-intestinal type.
Results *Macrocopy: ovarian mass measuring 13 cm long axis.the external surface was smooth.A cut section of the specimen revealed solid as well as cyst areas filled with clear fluid.Solid areas are fleshy and pale yellow or grey. *Microscopy: tumor composed of poorly formed cords, nests,and tubules of tumors cells.Leydig cells are found in clusters at the periphery of the cellular lobules or adixed with other elements. Large areas showed dilated glands lined by mucinous epithelium of gastro-intestinal type. *Immunohistochemical: sertoli cell tumors are positive for keratins, vimentin, calretinin, alpha-inhibin and negative for EMA.
Conclusion(s) Heterologus elements are observed in approximately 20% of SLCT.They occur in those of intermediate or poor differentiation or in retiform tumors.A gastro intestinal struture is rarely reported in thes tumors. The prognostic factors in these tumors are their stage, degree of differentiation and capsular rupture.

P3.90

Squamous metaplasia (AIM), from high-grade cervical intraepithelial neoplasia (CIN III). The role of CK17, p16 and p63 expression, in distinguish atypical immature

Papaspyrou I.; Mitropoulou G.; Sotiropoulou M.; Pateli A.; Pavlou V.; Markaki S.
Alexandra, Athens, Greece

Background The diagnosis of AIM has poor intra-and interobserver reproducibility on hematoxylin and eosin (H&E) stained sections, because of its resemblance to CIN III. The aim was to determine whether AIM can be reclassified into metaplasia and CIN III, based on p16 and CK17 immunohistochemistry.
Methods Seventy-two formalin-fixed paraffin-embedded cervical punch biopsy specimens and cone excisions containing varying proportions of dysplasia and metaplasia were analyzed immunohistochemically with antibodies to CK17, p16 and p63.P16 was classified positive when intense diffuse cytoplasmic and nuclear immunoreactivity of the entire cervical squamous epithelium was observed. CK17 immunoreactivity was cytoplasmic and was scored positive with a single cell stain.
Results From the 72 cases, 32 were regarded as AIM. Dysplastic cells of CIN III, demonstrated uniform immunoreactivity for p16 and p63, but were CK17 negative. In AIM all proliferating cells were immunoreactive with antibodies to CK17 and p63, but p16 was negative. Based on the reciprocal immunoreactivity of CK17 and p16 30/32 cases of AIM were reclassified as atypical immature metaplasia, and 2/32 cases who stained both for CK17 and p16, were classified as CIN III.
Conclusion(s) The biological and clinical significance of the diagnosis of AIM is unclear. AIM should not be used as a diagnostic term in histopathology, it should rather serve as a helpful histological descriptor of a worrisome lesion which needs further work-up.

P3.91

Struma ovarii: a report of five cases

Moysidis I.; Nikolaidou A.; Xirou P.; Vladika N.; Voutsas M.; Patakiouta F.
"Theageneion" Cancer Hospital of Thessaloniki, Thessaloniki, Neoi Epivates, Greece

Background Struma ovarii is a rare and highly specialized form of mature ovarian teratoma, characterized by the presence, entirely or predominantly, of mature thyroid tissue in the ovary. The peak incidence occurs during the fifth decade of life. Malignant transformation and thyrotoxicosis are rare, but important complications of this entity.
Methods We report 5 cases of struma ovarii. In our study, clinical features, laboratory findings and histologic characteristics are reviewed.
Results The patients' age ranged between 47–77 years. The most common symptom was pelvic pain. Radiographic exams (US, CT), revealed a unilateral location in all cases. All patients were operated, one of them had salpingo-oophorectomy, and the other four had hysterectomy. The tumours had a solid and/or cystic appearance, a greyish-white colour, and soft to firm consistency. The size ranged between 1,8–13 cm. Histologically they were composed of benign follicular thyroid structures, which were immunohistochemically positive for thyroglobulin.
Conclusion(s) Struma ovarii is a benign germ cell tumour of the ovary. It is presented during reproductive life and rarely before puberty. Approximately 5% of all cases show malignant transformation. The tumour is usually nonfunctional and only 8% of patients present symptoms and signs of hyperthyroidism. Histologically it is composed of typical rounded thyroid follicles filled with eosinophilic, homogenous, gelatinous colloid, lined with a single-layered cuboidal or columnar epithelium. Immunohistochemically the neoplastic cells are positive for T3, T4 and Thyroglobulin. Due to its rarity, there are no precise therapeutic protocols.

P3.92

Ten-year evaluation of pathological findings in cases of hysterectomy in javaheri hospital, Tehran, 1998–2008

Mozaffari Kermani R.; Tabatabaee S.
Tehran, Islamic Republic of Iran

Background This study was conducted to determine the relationship of pathological findings with clinical findings in patients undergoing hysterectomy and to consider the surgical indications leading to hysterectomy in Javaheri Hospital, Tehran, 1998–2008.
Methods In this descriptive-analytical study, clinical data of 450 in-patients who suffered from gynecologic complaints and underwent hysterectomy in Javaheri Hospital from 1998 to 2008 in Tehran were analyzed, with respect to their pathological microscopic findings.
Results The mean age of the patients is 47.1±7.3 years. The most frequent types of endometrial pathologic findings are endometrial polyp (27.3%), and disordered proliferative endometrium (21.3%). The most frequent type of myometrial pathologic findings are leiomyomas (42.3%) (intramural type in 73%) and adenomyosis in 31.2%of cases. The most frequent clinical findings leading to hysterectomy are dysfunctional uterine bleeding (dysmenorrhea) (57.2%) and abdominal pain (38.5%). Abdominal pain is the most frequent symptom in patients with leiomyoma (75% of cases). There is a significant statistical association between clinical symptoms and pathological findings of endometrium and myometrium ($p<0.01$).
Conclusion(s) Dysmenorrhea is the most frequent patients' complaint leading to hysterectomy.

P3.93

Uterine leiomyosarcoma metastatic to the cerebellum: a case report

Benizelos J.; Anagnostou E.; Papathomas T.; Spandos V.; Kampas L.; Rasala V.; Sioutopoulou D.; Destouni C.; Tatsiou Z.; Tsantila I.
Hippokration, Thessaloniki, Greece

Background Leiomyosarcoma is a malignant neoplasm of the uterine corpus, with a highly aggressive course due to its tendency to recur and metastasize after initial resection. The most frequent sites of metastases are the lung, intraperitoneal, pelvic and paraaortic lymph nodes as well as the liver.
Methods We present a case of a 51-old-year woman, which underwent a hysterectomy and bilateral salpingo-oophorectomy due to a uterine tumor. Histologically, the diagnosis of leiomyosarcoma was made. Adjacent lymph nodes were free of metastases. Six months later, she presented equilibrium disorders and nystagmus. A cranial MRI scan was performed and confirmed the presence of a 1.5 cm mass, located in the cerebellum.
Results Histopathologic analysis of the excised tissue fragments showed infiltration of cerebellar tissue from spindle-shaped neoplastic cells, with prominent nuclear atypia. Mitoses were numerous and coagulative necrosis was additionally noted. Immunohistochemical examination showed positivity of the neoplastic cells for desmin and SMA, while they were negative for GFAP, AE1/AE3, LCA and EMA. A whole-brain radiation and adjuvant chemotherapy was introduced. The patient died 3 months after the diagnosis of metastasis was made.
Conclusion(s) Cerebral metastasis of uterine leiomyosarcoma is extremely rare with 15 documented cases. Review of the literature, we failed to demonstrate metastasis of this neoplasm to the cerebellum.

P3.94

Vascular endothelial growth factor (VEGF) and Cox-2 expression in mucinous ovarian adenocarcinoma: relationship with pathologic features

Sotiropoulou M.; Papaspirou I.; Mitropoulou G.; Pateli A.; Politou C.; Pavlou V.; Markaki S.
Alexandra, Athens, Greece

Background Cycloxygenase (Cox-2) and Vascular Endothelial Growth Factor (VEGF) have been reported to be significant related to carcinogenesis and progression of various cancers. Aim of this study was the determination of the Cox-2 and VEGF's expression in mucinous carcinomas, the correlation with the type of invasion and other pathologic parameters.
Methods Forty (40) primary mucinous carcinomas were subclassified according to the criteria of Lee and Scully into 19 expansile and 21 infiltrative subtypes. Nuclear grade was histologically evaluated in all cases as mild, moderate and severe.Mitotic count was done in at least 10 HPF and measured as few (≤ 4), moderate (5–9) and many(≥ 10) /10 HPF. VEGF and Cox-2 expression were studied by immunohistochemistry.
Results Positive VEGF reactivity was in 39 (97,5%) and in 27(67,5%) of tumors. There was not any difference in expression between infiltrative and expansile types and nuclear grade. Many mitoses there are in 70% of VEGF (+) and 60% Cox-2 (+) of cases, while moderate are in 50% and 12,5% and few in 21% and 0%. There are many mitoses in 16% of expansile and 38% of infiltrative tumors.
Conclusion(s) VEGF and Cox-2 were expressed in most of primary mucinous ovarian carcinomas. The expression was positively correlated with mitotic count but not with mode of invasion nor with nuclear grade. Further studies using molecular models are required to explain why a mucinous tumor has an expansile or infiltrative pattern of invasion.

P3.95

A rare case of carcinoma in situ of the cervix with extension into endometrium

Bruma G.; Simion G.; Sajin M.; Badea I.; Guran R.; Nistor A.; Stanculescu V.M.
Emergency University Hospital, Bucharest, Romania

Background Endocervical carcinoma in situ originates at the squamocolumnar junction and from there may grow to replace large areas of the ecto- and endocervical surface. It usually spreads to uterus as invasive carcinoma; very rarely it can spread along the endometrium as carcinoma in situ. Clinical: Enlarged uterus, pelvic pain, purulent discharge. Ecography-distended uterine cavity with hyperechogenic content. Purpose: We present the case of a 62 year old patient addmited in the gyneacology section for severe dysplasia of the cervix and endometrium found in a curreting biopsy for a purulent discharge. Total histerectomy with bilateral salpingo-oophorectomy was performed.
Methods All anatomical pieces - uterus and cervix, right and left adnexa - were fixed in 10% formaldehyde solution, paraffin-embedded, cut and stained (Hematoxilyn-Eosin and Van-Gieson).
Results Macroscopically:cervix-thickened reddish anterior lip; uterus-increased in size with a thickened and irregular endometrium; fallopian tubes-purulent content. Microscopically: Sections from cervix and endometrium showed uniform thickened epithelium with carcinoma in situ changes that were limited to the epithelium, without infiltration into the stroma, covering the entire endometrial surface. Histopathology diagnosis: carcinoma in situ of the cervix with extension into endometrium; purulent salpingitis. Immunohistochemistry: p53, p16, Ki67 – positive
Conclusion(s) Very rarely carcinoma in situ of the cervix spreads along the endometrium as carcinoma in situ.

P3.96

Cervical high grade squamous intraepithelial lesions, from cytology to immunohistochemistry

Pop M.D.; Pop F.
University of Medicine Carol Davila, Bucharest, Romania

Background The aim of this presentation is to look for consensus data in cervical citology concerning LSIL and HSIL lesions and correlations with immunohistochemical findings on biopsy or excisional material. Using the immunohistochemical panel markers CD34, Ki-67, CEA, laminin and CK34BE12 we estimate that the boundery between CINIII, CIS and carcinoma with microinvasion is reliable.
Methods The study material was obtained from 20 patients presenting for screening cytology. The lesions were found to be in the spectrum of HSIL some of which possibly invasive. The subsequent cervical biopsies that raised controversies on histology were elucidated using the immunohistochemical panel: CK34BE12, CD34, CEA, Ki-67, laminin. The monoclonal antibodies were from Novocastra for paraffin embedded material. An ABC technique with DAB detection system was subsequently used.
Results Nine out of 20 patients had a suspicion of invasion on cytologic examiantion. In 4 out of 9 cases the microinvasion was demonstrated using immunohistochemistry. CD34 labels the fibroblastic subepithelial stroma of the cervix and in doing so isolates the epithelial small islands of microinvasion that are further highlighted by the cytokeratin immunostain with CK34BE12. CEA is also positive in most of the cases showing criteria for CIS and microinvasive carcinoma. Laminin confirms the disruption of basal membrane in microinvasive carcinoma.
Conclusion(s) Separating CIS from microinvasive carcinoma is significant for therapy. The proposed immunohistochemical panel sharpens the limit between the two.

P3.97

Differential diagnostic value of immunohistochemical markers Cytokeratin 7, Cytokeratin 20, CDX2 and beta catenin in metastatic adenocarcinomas of the peritoneum

Poriazova G.E.; Zaprianov N.Z.; Markova M.D.; Milchev P.N.
Medical, Plovdiv, Plovdiv, Bulgaria

Background Immunohistochemistry is a useful diagnostic tool in pathology. The knowledge in this area is constantly growing. In cases with low differentiated adenocarcinomas of the peritoneum colorectal and ovarian carcinomas have to be excluded first.
Methods Three groups of metastases from adenocarcinomas in the peritoneum were studied retrospectively and prospectively: metastases from colorectal carcinoma, ovarian adenocarcinoma and from adenocarcinomas with an unknown primary site of origin. Immunohistochemical examination was performed with DAKO antibodies using streptavidin-biotin immunoperoxidase analysis. Sixty patients, of which 30 with CRC metastases in the peritoneum, 30 with ovarian adenocarcinoma metastases in the peritoneum and 15 with peritoneal metastases of unknown primary site of origin were studied retrospectively and prospectively.
Results The immunohistochemical expression was evaluated using a semi-quantitative method. The ovarian adenocarcinomas are mostly positive for Cytokeratin 7 (in 86,66%), while colorectal carcinomas are mostly positive

for Cytokeratin 20 (in 83,33%). Regarding Beta catenin, in colorectal carcinomas the expression is mostly nuclear (in 76,66 %) and in ovarian carcinomas mostly membrane (in 70 %). In cases of uncertain expression of the markers mentioned above, CDX2 was used. Positive nuclear expression was observed only in intestinal tumours (in 93,33%).
Conclusion(s) For differential diagnosis between ovarian and colorectal adenocarcinomas, the use of antibodies, determining the intestinal differentiation of the tumours like Cytokeratin 20, Beta catenin and CDX2 is recommended.

P3.98

Elevated expression of RNA-binding protein IGF2BP3 correlates with poor prognosis in ovarian carcinoma

Gradhand E.; Mrotzek M.; Thomssen C.; Hüttelmaier S.; Hauptmann S.
Institut für Pathologie, Halle, Germany

Background Correlation of IGF2BP3 (IMP3) expression with survival of patients with ovarian cancer.
Methods Immunhistochemical expression analyses using a monoclonal IGF2BP3 (IMP3) directed antibody. Paraffin embedded samples used comprised: 103 ovarian carcinomas, 5 Bordeline Tumors, 4 regular ovarian surface epitheliums, 2 regular fallopian tubes. For statistical analyses, Chi-square-Test and log-rank test by Kaplan-Meier were performed.
Results IGF2BP3 was not expressed in normal ovarian surface epithelium and 4 of 5 Borderline Tumors. In Ovarian Cancer 32 cases (31%) were completely negative, 12 (12%) were scattered in less than 5% tumour cells. In 59 cases more than 5% of the tumor cells were positive up to a range of 90%. Mean expression was 23% marked tumor cells. Patients with more than 23% IGF2BP3 (IMP3)-expressing tumor cells showed a considerable reduced overall survival.
Conclusion(s) Recent studies indicated that IGF2BP1 expression was negatively correlated with survival of patients with ovarian cancer. Here, we demonstrate that similar to IGF2BP1, IGF2BP3 expression is correlated with reduced overall survival in patients with ovarian carcinomas.

P3.99

Glassy cell carcinoma of the uterine cervix. Report of one case with a review of the literature

Ryme D.; Driss M.; Abbes I.; Sassi S.; Mrad K.; Ben Slama S.; Ben Romdhane K.
Tunis, Tunisia

Background Glassy cell carcinoma of the uterine cervix is described as a poorly differentiated adenosquamous cancer. It is a rare tumor, accounting for only 1.6% of all cervical cancers; however, the prognosis is said to be extremely poor due to rapid progression and high resistance to radiation therapy. We report a patient with glassy cell carcinoma of the uterine cervix and we discuss this case with reference to reports in the literature.
Methods A 72-year old patient was admitted to Salah Azaiez Institute for irregular post-coital vaginal bleeding of short duration. Gynaecological examination revealed an ulcerated polyploidy lesion of the anterior exocervix. The diagnosis of poor differentiated carcinoma was made on biopsy. Radical hysterectomy with bilateral salphingo-oophorectomy and pelvic lymph node dissection specimens were received.
Results Tumour of 3.5/2.5 cm in diameter was exophytic and ulcerated with distortion of the cervix and invasion into the adjacent myometrium. Pathological findings showed nests and sheets of large cells with abundant granular cytoplasm and large nuclei with macronucleoli. Stromal eosinophilic, lymphocytic, and plasmacytic infiltrations were seen. Polymerase chain reaction did not reveal human papilloma virus. The patient was staged as having FIGO stage I. It has been 2 years, to date, since the initial treatment, and our patient is alive and disease/recurrence free.
Conclusion(s) Although glassy cell carcinoma runs an aggressive clinical course, an early diagnosis may help in a more effective management and offer a better prognosis.

P3.100

HPV types in female anogenital invasive squamous cell carcinoma (SCC)

Felix A.; Martins L.; Lourenco H.; Alemany L.; Bosch X.F.
Instituto Portugues de Oncologia de Lisboa Faculdade de Ciencias Medicas, Lisboa, Portugal

Background SCC of the female anogenital region is associated with HPV infection. Our aim was to describe the distribution of HPV types in SCC of the cervix; vagina; vulva and anus in Portuguese women.
Methods We retrieved 214 cases diagnosed and treated from 1989–2007 in the IPOLFG. DNA HPV types were evaluated from formalin fixed and paraffin embedded tumor samples. HPV detection was done using SPF-10 broad-spectrum primers PCR, subsequently followed by DEIA and genotyping by LiPA25(version1 and 2). Samples were tested at ICO (Barcelona-Spain) and at IPOLFG (Lisbon-Portugal).
Results HPV DNA was found in 161 cases of invasive SCC from cervix (n=113); vagina (n=21); vulva (n=48); anus (n=32). HPV DNA positivity and HPV16 were detected in 97.3%/66.6%; 81.0%/42,1%; 18.7%/77,7%;

and 78.1%/87,5% of cervix; vagina; vulva, anus, respectively. Multiple HPV types were seen in 9.7% of cervical; in 19% of vaginal and in 4% of anal cancers. Unknown HPV types were only detected in cervical carcinomas (2.7%). The five more common HPV types found in each locations were almost the same.

Conclusion(s) 1-HPV DNA is very frequent in female anogenital invasive SCC being present in 161 of the 214 cases (75%). 2-The distribution of HPV genotypes in Portuguese cases is similar to the reported in other populations being HPV16 virus the most frequent type (71.4%). 3-In the Portuguese population, SCC from vulva is also less frequently associated with HPV infection compared to other SCC arising in the female anogenital region. 4-Multiple HPV were more frequent in vaginal SCC cases.

P3.101

Immunoreactivity of CD99 and Melan-A in ovarian fibromas/fibrothecomas

Miliaras D.; Meditskou S.
Medical School of University of Thessaloniki, Thessaloniki, Greece

Background Sex cod-stromal tumors comprise a group of ovarian neoplasms with different as well as overlapping histological, immunohistochemical and clinical characteristics. Various antibodies have been recently used in order to define the immunoprofile of each category, including CD99 and Melan-A. The reason we have undertaken this investigation is because fibromas/fibrothecomas is the least studied category within this group.

Methods Paraffin sections from 26 ovarian fibromas/fibrothecomas were immunostained for CD99 and Melan-A. Immunohistochemical reaction was evaluated in a 0 to 3 scale.

Results Nine tumors (34,6%) were positive to CD99: 6 with +2 reaction, and 3 with +1 reaction. All tumors were negative to Melan-A.

Conclusion(s) In contrast to what is already known from the limited literature regarding the immunoprofile of ovarian fibromas/fibrothecomas, some of these tumors may present a weak to moderate reaction to CD99, as other tumors within this group.

P3.102

KIT/PDGFRA expression and mutation in testicular seminoma and ovarian dysgerminoma

Suh K.; Choi S.; Kim E.
Chungnam National University School of Medicine, Daejeon, Republic of Korea

Background KIT and PDGFRA (platelet-derived growth factor receptor alpha) genes encode KIT and PDGFRA, which belong to the type III transmembrane tyrosine kinase receptor family. Stem cell factor (SCF)/KIT-mediated signaling is known to play a role in normal spermatogenesis, and the alteration of KIT plays a central role in the pathogenesis of seminomas/dysgerminomas (SD).

Methods To determine the role of immunoreactivity and mutation of the KIT and PDGFRA genes, we analyzed 20 seminoma cases and 9 dysgerminoma cases for c-kit and PDGFRA expression and for mutation of the KIT (exon 11, 13, and 17) and PDGFRA (exon 12 and 18) genes using PCR-SSCP methods.

Results Immunohistochemically, c-kit was positive in 25 (100%) of 25 SD cases, and 1 (25%) of 4 spermatic seminomas (SS). PDGFRA results were positive in 16 (64%) of 25 SD cases, and 2 (50%) of 4 SS cases. The correlation between seminoma histologic type and c-kit expression was demonstrated (p=0.0035). PDGFRA expression was not statistically correlated with the histologic type or expression of KIT. Two seminoma cases and one dysgerminoma case showed mutation in exon 17 of KIT. One seminoma case and one dysgerminoma case showed mutation in exon 12 of PDGFRA.

Conclusion(s) These results indicate that the expression of c-kit is observed in a majority of SD cases. C-kit expression is negative in most SS cases. However, the significance of a histopathologic correlation between KIT/PDGFRA expression and mutation was not demonstrated.

P3.103

Massive ovarian oedema metachronous to a mature cystic teratoma

Patsiaoura K.; Anagnostou E.; Spandos V.; Agelidou S.
Hippokration, Thessaloniki, Greece

Background Massive ovarian oedema is an unusual cause of ovarian enlargement in young women. There are a few case reports of lesions associated with massive oedema in the same ovary. The metachronous appearance of a massive oedema accompanied with a contralateral mature cystic teratoma has been reported only once.

Methods We report a case of a 28-year-old woman, who underwent a left salpingo-oophorectomy prior to 15 years due to a mature cystic teratoma. The patient was referred to the emergency room after recurrent episodes of lower abdominal pain. An ultrasound examination confirmed a solid enlargement of the right ovary, with hypoechogenic areas. The patient underwent a laparoscopy and a solid mass with dimensions of 9.5x7.5x5 cm was excised, which arose from the right ovary.

Results Histopathological analysis showed severe interstitial oedema throughout the ovary. Ovarian stromal cells

were scattered within abundant oedematous fluid, which separated several ovarian structures. Superficial cortex was preserved, containing dilated follicles. Immunohistochemical examination was positive for vimentin, whereas negative for S100 protein. CD34 positivity confirmed the presence of many vessels within the mass. The above-mentioned data, were consistent with a massive ovarian oedema. The patient had an uneventful recovery and she is free of recurrence a year after the oophorectomy.

Conclusion(s) Massive ovarian oedema is a lesion frequently misdiagnosed as a neoplasm due to its manifestation as a large pelvic mass. We report this case due to its rarity, emphasizing on the pathogenesis and the differential diagnosis of this entity.

P3.104
mTOR is activated in ovarian carcinomas and correlates with eIF-4E and prognosis

Noske A.; Lindenberg J.; Darb-Esfahani S.; Weichert W.; Buckendahl A.; Lehmann A.; Sehouli J.; Dietel M.; Denkert C.
Charité, Berlin, Germany

Background Due to the unfavourable prognosis of ovarian cancer patients and chemo-resistance, novel anticancer therapies are urgently needed. The mTOR-pathway, which may be targeted by agents like Rapamycin or RAD001 is a promising target for such approaches.

Methods We investigated the expression of molecules of the p-mTOR pathway in primary ovarian carcinomas by immunohistochemistry and compared expression data with clinicopathological characteristics and patient outcome. We further determined the effect of mTOR inhibition by Rapamycin on protein expression as well as cell proliferation in ovarian cancer cell lines.

Results We observed an expression of p-mTOR, p-4EBP1 and p-eIF-4E in a subpopulation of ovarian carcinomas and improved overall survival for patients with p-mTOR and p-eIF-4E positive carcinomas. In ovarian cancer cell lines, a different expression pattern and activation state was observed as well as an up-regulation of p-AKT and inhibition of the cell proliferation by Rapamycin.

Conclusion(s) The data indicate the importance of the mTOR pathway in ovarian carcinomas and suggest that mTOR inhibition may be effective in a subset of these tumors.

P3.105
Ovarian serous borderline tumors in women in reproductive age

Musizzano Y.; Pacella E.; Marchiolé P.; Toletone A.; Fulcheri E.
Department of Pathology, University of Genoa, Italy

Background Recent studies tend to classify serous ovarian tumors (SOTs) into two subtypes depending on different genetic mutations; particularly, predictive value has been suggested for p53 immunoreactivity (p53-index). We evaluated histopathological and clinical features of borderline serous tumors (SBTs) affecting fertile women.

Methods We reviewed all SBTs diagnosed between 2000 and 2008. Clinical and histological data, including p53-index, were compared; all patients were strictly followed up.

Results 18 of 30 SBTs occurred in women in reproductive age (23–42 y.o.), treated by radical (10 patients) or conservative (8 patients) surgery based on preoperative stage and on the woman's wish to preserve fertility. Pathological examination showed superficial (4 cases), endocystic (1 case) and mixed growth pattern; nodal metastases were detected in 3 patients, and peritoneal implants in 8 cases, 4 of them being invasive. p53-index resulted <25% in 12 cases. At follow-up, two patients relapsed despite radical surgery. Conversely, two conservatively treated women (p53-index ≤20%) underwent term pregnancy and delivery. No significant correlation was found between p53-index, nodal or peritoneal involvement and relapses; anyway, mean and median p53-index were higher in cases with microinvasion.

Conclusion(s) Our findings seem to confirm that SBTs belong to a prognostically more favorable SOTs subtype, and the majority of them show low p53-index. This increases our confidence in proposing conservative surgery to women yearning for preservation of their fertility; anyway, strict follow-up is mandatory, as well as for high-risk women.

P3.106
Ovarian steroid cell tumour: case report and review of the literature

Vasilakaki T.; Grammatoglou X.; Savvaidou V.; Glava C.; Skafida E.; Delliou E.
Tzaneion General Hospital of Piraeus, Athens, Greece

Background Ovarian steroid tumours are rare sex-cord stromal tumours with malignant potential. The majority of these tumours produce several steroids, particularly testosterone. Various virilizing symptoms are common. These tumours are divided in three subtypes: stromal luteoma, Leydig cell tumour and steroid cell tumour, the latter being the most common of these three subtypes accounting for approximately 60% of cases.

Methods We report the case of a 40-year-old woman with mental disorder who presented with 3 years of amenorrhea

and progressive virilizaton (temporal balding and hirsutism). Her plasma testosterone level was elevated. A transvaginal pelvic ultrasound showed a 6,8x5,5x3,5 cm left ovarian mass. Hysterectomy with bilateral salpingo-oophorectomy was performed.

Results Histological examination showed a steroid cell tumour. The tumour was composed of two cell types. The predominant cell type was polygonal with abundant spongy cytoplasm. Interspersed within these cells were aggregates of polygonal cells with a glandular eosinophilic cytoplasm. Mitotic figures were rare. There was no evidence of necrosis, hemorrhage or invasion. On immunohistochemical examination the tumour cells were positive for inhibin, CD99, MelanA and Vimentin and negative to actin, CKAE1, CKAE3, progesterone and estrogen receptors. No postoperative radiotherapy or adjuvant chemotherapy was given.

Conclusion(s) Ovarian steroid tumours account for less than 0,1% of all ovarian tumours and are usually benign and unilateral. The primary treatment is surgical excision of the primary lesion and there are no reports of effective radiation or chemotherapy.

P3.107

p53, p63, p21, Rb, mdm2 and Ki-67 expression in normal placenta, partial and complete hydatidiform mole

Landolsi H.; Yacoubi M.; Gribaa M.; Lahmar Boufaroua A.; Trabelsi A.; Hidar S.; Hmissa S.
Laboratoire d'anatomie et de cytologie pathologiques, CHU Farhat Hached, Sousse, Tunisia

Background Gestational trophoblastic diseases are characterized by an abnormal proliferating trophoblastic tissues and are classified as partial hydatidiform moles (PHM), complete hydatidiform moles (CHM), invasive moles, choriocarcinomas and placental site trophoblastic tumors. Malignant transformation in gestational trophoblastic tumours is likely a multistep process and involves multiple genetic alterations including activation of oncogenes and inactivation of tumour suppressor genes. In this study we investigate the potential expression of p53, p63, p21, Rb and mdm2 oncoproteins and a proliferation marker Ki-67 (MIB-1), in non-molar hydropic abortions (HA), PHM and CHM.

Methods Expression of the above oncoproteins was determined immunohistochemically by specific antibodies for these proteins on formalin-fixed paraffin sections of 17 HA, 13 PHM and 26 CHM.

Results Positive staining for p53 was significantly stronger in CHM than in PHM (p=0.03) and HA (p<10-4) and in PHM than HA (p=0.03). The expression of p21 and mdm-2 was significantly higher in CHM and PHM than HA (p< 10-8 and p<10-4 respectively). CHM expressed significantly stronger staining of Rb and Ki-67 than HA (p= 0.0025 and p = 0.02 respectively), but there was no significant difference between CHM and PHM and between PHM and HA. There was no significant difference in distribution of p63 positive cells between HA, PHM, and CHM.

Conclusion(s) Altered expression of p53, p21, mdm2, Rb and Ki-67 may be important in the pathogenesis of hydatidiform mole. Over-expression of p53 in CHM may be predictive with more aggressive behaviour.

P3.108

Prevalence and genotype identification of HPV infection with cytological diagnosis in a population of Turkish women

Eren F.; Erenus M.; Bas E.; Ahiskali R.; Yoldemir T.
Marmara University School of Medicine Department of Pathology, Istanbul, Turkey

Background Type specific distribution of HPV differs between regions around the world. The aim of this study was to evaluate the prevalence of HPV genotypes in Turkish women and correlate the data with cytology and certain sociodemographic data to provide information for future management and prevention policies.

Methods 492 women (age: 19–85) who referred to gynecology outpatient clinics were recruited from May -August 2008. All women answered a standard questionnaire. Split sampling was used for obtaining specimens for cytological examination. HPV typing were identified by PCR DNA microarray method which enables identification of 35 types. HPV typing and cytological examination were blinded.

Results Prevalence of HPV was found to be 16,5 % with 75% being in the high risk group. Type 16 was the most frequent HPV type (34%) followed by types 6 (12%) and 53 (11%). 79% of HPV positive women had normal cytology. The highest prevalence was observed in women aged <30 years (36%) and aged 31–40 (35%). The prevalence was significantly higher in women younger than 40 when compared with older woman. 65.2% of HPV (+) women had higher education levels and 34% were single. HPV positivity was significantly associated with marital status and higher education levels.

Conclusion(s) This study showed that HPV infections in our population involve numerous types even in patients with normal cytology and associated with higher education and income levels.

P3.109

Primary mesonephric adenocarcinoma of the cervix: a case report and review of the literature

Ramadan Sezgin S.; Yapicier O.; Gucer F.; Onat H.
Anadolu Medical Center, Kocaeli, Turkey

Background Mesonephric adenocarcinoma is a rare tumor of the cervix. The course of most of the reported mesonephric adenocarcinomas in the literature is usually indolent but here we present a case with widespread peritoneal implants.
Methods Case: A 58 year-old woman with vaginal bleeding admitted to our institution. Pelvic magnetic resonance imaging(MRI) revealed cervico-vaginal 7,5x5,4x4 cm mass with regular contours. Abdominal computed tomography(CT) showed ascites. Cervical punch biopsy was performed.
Results Microscopically, the tumor was composed of predominantly atypical round to polygonal cells arranged in tubular, retiform and solid patterns. Spindle cell component was observed in solid areas. Atypical cells were positive with cytokeratin 7 and epithelial membrane antigen (EMA). Multifocal immunoreactivity was observed with vimentin and CD10. No immunoreactivity was detected with estrogene and progesterone receptors, chromogranine, synaptophysin, carcinoembryonic antigen (CEA) or calretinin. Histomorphologic and immunohistochemical findings were consistent with mesonephric adenocarcinoma.
Conclusion(s) At present there is no concensus on a standardised treatment protocol for malignant mesonephric tumors of the cervix. In contrast to the most of the stage I cases presented in the literature, our case is assessed as a stage IV, inoperable carcinoma due to peritoneal involvement. Our patient is having chemotherapy at the moment. The prognosis of mesonephric adenocarcinoma is uncertain because of the small number of cases reported.

P3.110

Primary vaginal mucinous adenocarcinoma of endocervical type arising from vaginal adenosis in a patient with uterus didelphys

Kelten C.; Ozkalay Ozdemir N.; Yildirim B.; Akbulut M.
Medical School of Pamukkale University, Denizli, Turkey

Background Primary vaginal adenocarcinomas are rare neoplasms. Primary mucinous adenocarcinomas of the vagina (intestinal or endometrial type) have been reported only in a few cases. Due to its rarity, little is known about its aetiology and clinical behavior.
Methods A 42-year-old woman, gravida: 4, para: 2, with a history of uterus didelphys, presented with the complaint of irregular vaginal bleeding and left inguinal pain. The patient has been followed because of leiomyoma uteri. She had no history of in utero diethylstilboestrol (DES) exposure. On physical examination and radiologic evaluation (ultrasound), no abnormality was found except leiomyoma uteri. The patient had undergone vaginal total hysterectomy with bilateral oophorectomy.
Results Macroscopic examination showed only intramural leiomyoma. However, microscopic examination of the vaginal samples revealed vaginal adenosis and carcinoma composed of irregular infiltrative glands, unexpectedly. Malign glands were lined by both endocervical and endometrial type columnar epithelium. The lesion was diagnosed as primary vaginal mucinous adenocarcinoma of endocervical type. Immunohistochemical staining and mucin histochemistry supported the diagnosis. Other pathologic findings were chronic cervicitis, proliferative endometrium, adenomyosis and leiomyoma uteri.
Conclusion(s) We report a primary vaginal mucinous adenocarcinoma probably arising from vaginal adenosis in a patient with uterus didelphys without in utero DES exposure. It is important to distinguish this rare lesion from the other metastatic adenocarcinomas (cervix, endometrium, ovary or gastrointestinal tract) to the vagina.

P3.111

Reproducibility determination of WHO classification of endometrial hyperplasia / well differentiated adenocarcinoma and comparison with computerized morphometric data

Izadi-Mood N.; Yarmohammadi M.; Ahmadi S.; Iravanloo G., Haeri H., Meysamie A., Khaniki M.
Department of Pathology of Mirza Koochak Khan Hospital, Tehran, Islamic Republic of Iran

Background Endometrial hyperplasia constitutes a wide range of histomorphologic features associated with high intra and interobserver diagnostic variability. Although traditional microscopic diagnosis is by far the most applicable method and the gold standard for histomorphologic diagnosis, digitized image analysis has been used as a powerful adjunct to maximized the histologic data retrieval and to add some detailed objective criteria for correct diagnosis in difficult cases.
Methods A series of 100 endometrial curettage specimens with diagnosis of endometrial hyperplasia or well differentiated adenocarcinoma were blindly reviewed by 5 pathologists; their intra and interobserver reproducibility determined and further compared to the objective morphometric data.
Results The results were assessed using the weighted kappa statistics. Mean intraobserver kappa value was 0.8690. Mean interobserver kappa values by diagnostic category

were: simple hyperplasia without atypia: 0.7441; complex hyperplasia without atypia: 0.3379; atypical hyperplasia: 0.3473, and well-differentiated endometrioid carcinoma: 0.6428; with a kappa value of 0.5372 for all cases combined. Interobserver agreement was in substantial rate for simple hyperplasia and well differentiated adenocarcinoma but was in fair limit for complex hyperplasia and atypical hyperplasia. Intraobserver agreement was almost perfect. Morphometric findings were closely compatible with routine WHO classification made by one expert pathologist; however, diagnosis of complex hyperplasia and atypical hyperplasia made by other pathologists were not concordant with morphometric data.
Conclusion(s) It may be necessary to make some revisions in WHO classification for endometrial hyperplasia.

P3.112
Serous carcinoma of the endometrium arising in an endometrial polyp with choriocarcinomatous differentiation: a case report and review of the literature

Akbulut M.; Gundogan M.; Soysal E.M.
Pamukkale University, Denizli, Turkey

Background Endometrial serous carcinoma with choriocarcinomatous differentiation is an extremely rare occurrence with poor prognosis.
Methods We report the pathologic findings, and immunohistochemical profile in a case of a 55 years old woman, who was presented with a history of postmenopausal bleeding.
Results Endometrial curettage revealed serous carcinoma arising in an endometrial polyp with highly pleomorphic tumor cells and multinucleated syncytiotrophoblastic giant cells. Hysterectomy specimen showed endometrial intraepithelial carcinoma without myometrial invasion.
Conclusion(s) Choriocarcinomatous differentiation is extremely rare in endometrial serous carcinomas.

P3.113
The clinicopathological study of epithelial ovarian carcinoma and borderline ovarian tumor complicated with endometriosis

Suzuki C.; Arakawa A.; Miyakuni Y.; Yao T.; Mitsuhashi N.; Takeda S.
Juntendo School of Medicine, Bunkyouku, Tokyo, Japan

Background There are some patients with ovarian malignancy (carcinoma and low potential malignancy (LPM)) who are associated with endometrtiosis and it is also well-known about the ovarian malignancy arising from endometriosis.
Methods Two hundred forty patients with ovarian carcinoma and borderline ovarian tumor were treated at Juntendo University Hospital between 2000 and 2006. Thirty seven out of 240 patients had association with endometriosis. We investigated association ovarian carcinoma or borderline ovarian tumor with endometriosis, clinicopathologically.
Results Clinically, chief complaints of those patients at first time visit were abnormal bleeding (23%) and lower abdominal pain (23%) The percentage of detecting by screening test was 29%. Thrity seven patients with ovarian malignancy had 26 ovarian carcinomas and 11 LPMs. In 37 patients with ovarian malignancy combined with endometriosis, 11 cases were clear cell carcinoma (including one LPM), 11 cases were endometrioid adenocarcinoma (including one LPM), 6 cases were serous carcinoma (including 4 LPM), 4 cases were mucinous LPM, 4 cases were mixed epithelial tumor (including 2 LPM) and one was adenosquamous carcinoma. Among 26 ovarian carcinoma patients, 19 cases were stage I, 2 cases were stage II, 2 cases were stage III and 3 cases were stage IV.
Conclusion(s) The patients with ovarian endometriosis should be also considered as combination with ovarian malignancy.

P3.314
The role of pathologic results and clinical presentations in predictive value of transvaginal ultrasonographic findings: differentiating benign from malignant ovarian neoplasms

Mozaffari-Kermani R.; Montaser-Kouhsari L.
Tehran, Islamic Republic of Iran

Background The correlation between pathologic ovarian microscopic findings with clinical presentations and ultrasonographic findings has been determined. There was various accuracy of ultrasonography for differentiating benign from malignant ovarian lesions.
Methods Total of 208 patients were candidate for ovarian lesions biopsy at the Javaheri hospital at Tehran, Iran, between June 1997 and Dec 2009. We designed a model in which age, pathologic results, clinical presentations as well as sonographic parameters were considered for the pathologic assessments.
Results Mean age for patients was 40.9±10.8 (range 14–75) years. 201/208 (96.6%) had benign lesion and 7/208 (3.4%) had malignant tumor. The majority of benign specimens were follicular cyst (25%, $n=52$) and luteal cyst (19.7%, $n=41$) and among malignant specimens, Serous cystadenocarcinoma was the most common (2.9%, $n=7$). Abdominal pain (65.9%) and AUB (32.7%) were the most common clinical symptoms. The sensitivity and specificity of transvaginal ultrasonography were 99% and 57.1%,

respectively. In our designed model, age (OR 1.13 [1.03 – 1.27]; p=0.01) and the presence of echoic or multilocular cyst (OR 18.8 [1.3–250]; p = 0.031) in sonographic study greatly influenced the diagnosis of malignant from benign ovarian lesions.

Conclusion(s) Our macroscopic pathological findings revealed that ultrasonography effectively results in earlier diagnosis and decreases unnecessary surgical staging procedures. This study showed that advanced age and the presence of echogenicity and multilocularity in sonographic study are two independent predictors for malignant ovarian lesions.

P3.115

Tubal (tubo-endometrial) metaplasia of the endometrium (TEM). A frequent source of misdiagnosis of malignancy. A study of 64 cases

Nogales F.F.; Goez E.; Nicolae A.; Aneiros-Fernandez J.; Stolnicu S.
University of Granada, Spain

Background TEM is a condition of uncertain significance that is not frequently recognized or reported and consists of glands with eosinophilic, ciliated and intercalary cells. Its real incidence and associations are not known. Formerly, many such lesions were considered as "CIS". Its architecture may be complex and can be confused with atypical hyperplasia or well differentiated adenocarcinoma. Recently, p16 has proven to be a reliable marker of TEM that may be useful in identifying TEM in cases with a diagnostic difficulty.

Methods Routine and consultation material comprising 64 endometrial biopsies and hysterectomies. Immunohistochemistry performed for p16-Bcl-2-p53-ER-PR-Ki67.

Results TEM in endometrial biopsy material associated to: 13 cyclic, 12 polyps, 2 adenomyomas and 6 adenocarcinomas and 19 simple, 4 complex without atypia and 8 atypical hyperplasias. Histologically TEM was reduced to isolated simple glands 53, 9 had a complex papillary or cribriform pattern. Atypia present in 2. Coexistent mucinous metaplasia in 3 from these cases. Misdiagnosis of atypical hyperplasia or carcinoma occurred in 6 cases. All of the cases positive for p16.

Conclusion(s) TEM to be recognized as a differential element in the diagnosis of atypical hyperplasia and adenocarcinoma in lesions with eosinophilic cells and a cribriform- papillary architecture, including cases with additional mucinous papillary metaplasia. TEM is frequently present in various types of hyperplasia and in the vicinity of adenocarcinoma and thus, its significance is to be assessed. P16 positivity helps in establishing a differential diagnosis.

P3.116

Umbilical endometriosis in pregnancy without previous surgery: a case report

Nfoussi Hamza H.; Chelly I.; Adouni O.; Boujelbene N.; Azzouz H.; Tangour M.; Mekni A.; Haoeut S.; Kchir N.; Zitouna M.
La Rabta, Ariana, Tunis, Tunisia

Background The presence of extrapelvic endometriosis has been reported in many organs. Up to 40% of patients present with umbilical lesions. In 75% of the women, umbilical endometriosis develops spontaneously, as it did in the present case. Objective: To illustrate the influence of pregnancy on primary umbilical endometriosis.

Methods Case report: We report a case of umbilical endometriosis in a pregnant woman at 20 weeks of gestation. The patient revealed rapid enlargement of a reddish-brown polypoid nodule within the umbilical depression with the typical history of monthly bleeding from the umbilicus. She reported now permanent umbilical bleeding as well as continuous umbilical pain. A total excision of the umbilic and a transabdominal ultrasound examination were performed. The excised tissue measured 1,5 cm in diameter.

Results Histologically, it showed endometrial glands surrounded by endometrial stroma with strong decidual reaction. The diagnosis of endometriosis was confirmed. The pelvic ultrasound examination did not identify ovarian cysts of a possible endometriotic nature. No therapy was given. At 2-month follow-up evaluation, there were no signs of recurrence of the disease.

Conclusion(s) Spontaneous umbilicus endometriosis is a rare disease that can worsen during pregnancy.

P3.117

Use of immunohistochemistry criteria in definition of the prognosis of superficial cancers of ovaries

Petrov S.; Antoneeva A.
Kazan Medical University, Kazan, Russian Federation

Background Taking into account high morbidity of cancer of ovaries, including young women, and as importance of elaboration of morphological criteria of the prognosis of morbidity of cancer.

Methods 112 cases of the superficial cancers of ovaries removed by surgical way (endometrial, serous and mucinosis) have been investigated. Research was carried out with the traditional morphological methods, the full stereometric analysis of a tissue, research of proliferous activity (PCNA, Ki67) and factors of a progression (Bcl2 and p53).

Results Carried out research has shown, that cancer tumours of ovaries, has medullary structure and possess mainly sinus type of a blood channel. Thus appeared, that the level of blood supply is high enough at small volume of necrosis. At the same time a level lymphoid infiltration as a whole low with the tendency to lowering at progressing. During progressing of cancer of ovaries in primary tumoral knot the increase in mutations with increase of quantity of neoplastic cells expressioning a gene p53 is revealed. It is known, that a product of this gene is nuclear a protein though to be involved in the control of the cell cycle, apoptosis, and the maintenance of genetic stability.
Conclusion(s) In these conditions there is an increase of proliferous activity, that authentically proves to be true of expression PCNA and Ki67, finding out high activity, and as infringements of apoptosis with hiperexpression of oncoprotein Bcl-2.

P3.118

Uterine malignant mixed mullerian tumors in two women, having been treated with tamoxifen and aromatase inhibitor for breast carcinoma

Koumoundourou Sp.D.; Aletra C.; Nikolaou M.; Tsoukas A.; Papadopoulou M.; Ravazoula P.
University Hospital of Patras Rio, Patras, Achaia, Greece

Background Two female patients aged 74 and 64 years presented with endometrial bleeding during the last 3 and 2 weeks respectively, with accompanying U/S findings of endometrial hyperplasia.
Methods Both sustained a dilatation curettage and the diagnosis was that of MMMT.
Results In the first patient, an heterologous element of chondrosarcoma was also recognized. Both patients, had a history of invasive ductal breast carcinoma eight and seven years ago (Grade III, stage T1cNo, and Grade II and Stage II respectively) for which they had received radiotherapy, chemotherapy (CMF) and tamoxifen (1 mg/d for 5 years followed by aromatase inhibitor till the day of the current diagnosis).
Conclusion(s) Uterine MMMTs are rare malignant neoplasms of mesodermal derivation usually arising de novo. However, recently, a few cases have been reported developed after tamoxifen therapy for breast cancer. Tamoxifen acts like an agonist in the endometrial epithelium and is often correlated with endometrial carcinoma development. The fact that tamoxifen is also related with the development of MMMTs, makes necessary to study the way that this molecule stimulates both endometrial glands and stroma and induces their malignant transformation.

P3.119

Benign fibroepithelial polyp of the vagina. A case report

Savvaidou V.; Petrakopoulou N.; Moustou E.; Tepelenis N.; Manoloudaki K.; Zizi-Serbetzoglou A.
Tzaneion General Hospital of Piraeus, Piraeus, Attiki, Greece

Background Fibroepithelial polyps of the vagina are quite rare lesions. Although benign they can be confused with botryoides sarcoma, rhabdomyosarcoma and mixed mesodermal tumor because of their bizarre histology. The stellate and multinucleated stromal cells which characterize these lesions ultrastructurally resemble fibroblasts and myofibroblasts and sometimes, there is a collection of functional fibroblasts that may be capable of differentiation along two or more cell lines.
Methods We report a case of a 69-year old woman who presented to the gynecological clinic of our Hospital complaining of vaginal bleeding. A gynecological examination followed which revealed a stulky, well circumscribed, pedunculated vaginal polyp of smooth consistence, with a mean diameter of 10 cm. A surgical excision of the polyp followed and the specimen was sent to our Laboratory for further histological examination.
Results Microscopically, the lesion was lined by a non-keratinizing, glycogen producing squamous epithelium. The subepithelial stroma was oedematous and contained spindle and asteroid cells. Some of these cells showed nuclear hyperchromasia. Mitoses were scant. Immunohistochemically, the cells stained strongly for desmin and CD34. The stains for actin, vimentin, oestrogens, progesterone and S100p were negative. After all the diagnosis of benign fibroepithelial polyp of the vagina was established.
Conclusion(s) Benign fibroepithelial polyps of the vagina are generally treated by local excision. Recurrence is extremely uncommon.

P3.120

Breast-like carcinoma of the vulva of colloid type

Sassi S.; Dhouib R.; Driss M.; Mrad K.; Abbes I.; Ben Romdhane K.
Salah Azaeiz Institute, Tunis, Tunisia

Background Breast-like carcinoma of the vulva is extremely rare. It derived from so called mammary- like glands which share features of eccrine, apocrine, and mammary glands. We report a case of MTSC in a 72-year- old woman without a clinical history of a breast carcinoma.
Methods Hematoxylin and eosin stain (H&E). Immunohistochemical studies were done. The primary antibodies used

are estrogen receptors, progesterone receptors, cytokeratin 7 and cytokeratin 20.
Results Grossly, the specimen received consists of a vulvar excisional biopsy specimen revealing a 3.5/3/1.5 cm, multinodulated lesion with a glistening appearance and soft consistency. Microscopic examination of formalin-fixed tissue sections showed a carcinoma infiltrating the dermis within an abundant mucoïd material. Immunohistochemical stains revealed that the tumor cells were positive for estrogen receptors, progesterone receptors, and focally positive for the cytokeratin 7. They were negative for the cytokeratin 20.
Conclusion(s) Primary breast carcinoma of the vulva is very rare. The diagnosis of this tumor is based on a morphologic pattern consistent with breast carcinoma, presence of estrogen and/or progesterone receptors, absence of primary adenocarcinoma elsewhere metastasing to the vulva and/or the positivity for common breast.

P3.121
Complete hydatiform mole case report

Stanculescu V.M.; Sajin M.; Bruma G.; Guran R.; Nistor A.; Simion G.; Cirstoiu M.; Secara D.
Emergency University Hospital, Bucharest, Romania

Background Complete hydatiform mole is a gestational trophoblastic disease caused by abnormal gametogenesis and fertilization. The aim of this comunication is to report a clinical case of a 24 years old pregnant woman, who had got 15 weeks gestational age. She was urgently hospitalized in the obstetrics-gynaecology department on the 5 th of March 2009 for vaginal bleeding. The serum hCG: > 20000 mIU/mL.
Methods Materials and Methods: the placental fragments were fixed in 10% formaldehyde solution, paraffin-embedded, cut and stained with Hematoxiylin–Eosin and Van Gieson.
Results Macroscopically: evident transparent villous vesicles as a "bunch of grapes", 1–30 mm in diameter. Microscopically: the molar villi are avascular, with cisterns, irregular in shape and sizes with secondary club-like extensions. The hyperplastic trophoblast is circumferential with nuclear pleomorphism.The intermediate trophoblast in the intervillous space and the implantation site is also hyperplastic with marked nuclear atypia and hypercromasia. Differential Diagnosis: -partial hydatiform mole - hydropic abortus IHC: CD34 (-), p57 (-), hCG (+), inhibina (+), p53 (+).
Conclusion(s) the evacuation of CM has not reduced the frequency of persistent disease but has reduced the frequency of molar metastases and choriocarcinoma.

P3.122
Ovarian endometrioid adenocarcinoma coexistent with benign and borderline endometrioid cystadenofibroma: a case report

Rammeh S.; Ferchichi L.; Abid Ben-Yacoub L.; Hammedi F.; Trabelsi A.; Jomaa W.; Beizig N.; Sriha B.
Sousse, Tunisia

Background Malignant endometrioid adenofibroma / cystadenofibroma is recognized as a distinct category of epithelial ovarian cancer and yet is rarely reported with confusing terms: malignant ovarian adenofibromas, ovarian endometrioid carcinoma with adenofibromatous pattern, endometrioid adenocarcinoma coexistent with adenofibroma...The relationship between this tumor and its benign counterparty (adenofibroma / cystadenofibroma) and the frequency and features of carcinomas developed on these benign tumours are little known.
Methods We report a case of a 36-year-old woman.
Results She's a 36-year-old woman with a FIGO stade Ia, 12 cm solid and cystic ovarian tumor. The cystic component showed features of cystadenofibroma. The solid area (3 cm surface) was composed of irregularly shaped endometriotic glands with malignant cytologic features, squamous metaplasia and a confluent growth pattern with invasion of the stroma.
Conclusion(s) We describe this unusual tumor and review the literature.

P3.123
Proliferation markers (Ki-67 and PCNA) and the tumor suppressor gene designated pten as evaluating elements for the malignancy potential in atipical endometrial hyperplasia

Sajin M.; Chefani A.; Lazaroiu A.; Simion G.; Costache M.; Caruntu I.; Georgescu M.; Secara D.; Carstoiu M.
Universitary Emergency Hospital Bucharest, Bucharest, Romania

Background Atipical Endometrial Hyperplasia (increase in gland/stroma ratio, disorder number and shape of the glands like modifications of the glandular epithelium: exhibits loss of nuclear polarity, stratification, etc) is a lesion associated with the uterine leiomyomas. The Study was realized at the Universitary Emergency Hospital Bucharest, Romania on 579 endometrium biopsies taken in the period 2004–2008 from women with ages between 45 and 55.
Methods Material and methods: Hematoxylin –eosin stained slides of endometrial formalin fixed, paraffin embedded tissue has emphasized in 150 cases the simple

hyperplasia (SH), in 211 cases the complex hyperplasia (CH), in 53 cases the simple atypical hyperplasia (SAH) and in 165 cases the complex atypical hyperplasia (CAH). We performed the indirect tristadial ABC method of IHC for 3 antibodies: PTEN, Ki-67 and PCNA on formalin fixed embedded tissue taken by biopsies from 80 cases (14 SH, 12 CH, 54 SAH and CAH).
Results PTEN was focal positive for SAH, diffuse for CAH and for some cases of SH and CH. Ki-67 and PCNA were also very frequent in group SAH and CAH.
Conclusion(s) PTEN, Ki-67 and PCNA take part in the process of endometrial carcinogenesis following probably molecular pathways and determine the malignity potential of atypical hyperplasia of endometrium.

P3.124
Sertoliform endometrioid carcinoma of the ovary

Boujelbene N.; Driss M.; Dhouib R.; Sassi S.; Karima M.; Abbes I.; Ben Slama S.; Khecherem N.; Ben Romdhane K.
Tunis, Tunisia

Background Sertoliform endometrioid carcinoma of the ovary (SEC) is an uncommon variant that bears histologic similarity to Sertoli and Sertoli-Leydig cell tumors (SLTs). We discuss the elements of the differential diagnosis and insist upon the value of epithelial membrane antigen in identifying SEC.
Methods A 59-year-old postmenopausal woman presented with a one year history of progressive enlargement of an abdominal mass. Pelvic sonography and abdominal computed tomography showed a pelvic mass measuring 12 X 10 X 10 cm. A staging operation with total abdominal hysterectomy, bilateral salpingo-oophorectomy, infracolic omentectomy and pelvic lymph node dissection was performed. Microscopically, the right ovarian tumor consisted of small hollow tubules, anastomosing cords and trabeculae, and tightly packed nests. Component of typical endometrioid carcinoma was noted only focally. The tumor cells were diffusely immunoreactive for epithelial membrane antigen and negative for inhibin and calretinin.
Results Discussion: Clinically, SEC affects an older population, while patients with Sertoli-Leydig cell tumors have an average age of 25 years and may exhibit endocrine manifestations. The most important histologic features used to distinguish the 2 entities is the presence of areas with the usual pattern of endometrioid carcinoma. The cells in the sertoliform component are immunoreactive for cytokertin, epithelial membrane antigen, while inhibin and calretinin stain negatively.
Conclusion(s) Adequate sampling, a careful search for areas of conventional endometrioid carcinoma, and immunohistochemical studies are helpful in the evaluation of ovarian tumors with sex cord-stromal features.

P3.125
The expression of p16, p53 and Ki-67, in uterine smooth muscle tumors: an immunohistochemical analysis

Papaspyrou I.; Mitropoulou G.; Pateli A.; Sotiropoulou M.; Peitsidis P.; Pavlou V.; Markaki S.
Alexandra, Athens, Greece

Background Recent studies reported the overexpression of P16 protein in uterine leiomyosarcomas. However the potential role of immunohistochemistry of P16, P53 and Ki-67 in differential diagnosis of leiomyosarcomas and leiomyoma variants has not been well assessed.
Methods In this study we have compared the expression of three biomarkers p16, p53 and Ki-67 in 38 cases of uterine smooth muscle tumors, including 15 usual LM, 8 BLM and 15 LMS. All specimens had been routinely fixed in formalin and processed in paraffin wax. Each case was scored on the extent of staining: negative (< 5%), focal (5–25%), mediate (26–75%) and diffuse (> 75%).
Results Negative immunoreactivity for p16 was seen in100% of usual LM, 50% of BLM and 40% of LMS. Among p16 positive neoplasms 50% of BLM and 13,3% of LMS shows focal expression. 46% of LMS shows mediate to diffuse expression of p16. P53 positive expression was observed in 6% of usual LM, 12% of BLM and 53% of LMS. Negative immunoreactivity for p53 was seen in 93,3% of usual LM, 87% of BLM and 46% of LMS. Ki-67 positivity was seen in approximately 47% of LMS, while showed negative expression in 100% of usual LM, 100% of BLM and 53% of LMS.
Conclusion(s) P16 in combination with p53 and Ki-67 may be of value in the assessment of problematic uterine smooth muscle tumors, although further studies with follow-up are necessary to confirm this.

P3.126
Tubal (tubo-endometrial) metaplasia of the cervix (TEM): a possible source of error with endocervical adenocarcinoma

Nicolae A.; Goez E.; Aneiros-fernandez J.; Stolnicu S.; Nogales F.F.
University of Granada, Granada, Spain

Background TEM is a p16+ condition of uncertain significance. In the cervix it is not often recognized and may have cellular and architectural features similar to endocervical adenocarcinoma such as multistratification, loss of polarity and papillary formations. Its diagnosis may

be difficult in cervical biopsies involving squamo-columnar junction and surgical specimens with deep parietal involvement.
Methods 2 cervical biopsies, 2 polyps and 9 hysterectomy specimens containing TEM were analysed. All patients were perimenopausal. Immunohistochemistry for p16-CEA-Bcl-2-Ki67-ER-PR-CD10 was performed.
Results Foci of TEM were localised preferentially in squamo-columnar junction. 4 cases had papillary "florid" architectural complexity and were localised deeply into the cervical muscular wall. 1 case was continuous with mesonephric hyperplasia and other occurred in a post-irradiation cervix. Glands were not surrounded by endometrial stromal cuffs. All cases were p16 positive, CEA negative and exhibited a low Ki67 index.
Conclusion(s) Squamo-columnar junction TEM can mimic in situ adenocarcinoma, as it is found in similar location. When TEM occurs in an architecturally complex "florid" fashion with multiple deep intramuscular foci in the cervical wall, it may be confused with minimal deviation adenocarcinoma, mesonephric rests and tunnel clusters. Diagnosis should be strictly done by demonstration of ciliated and intercalary "peg" cells in complex glandular structures. P16 positivity does not mean necessarily that this is a HPV related lesion, as it is a constant marker of endometrial TEM. In such cases, CEA negativity and low ki67 would support a diagnosis of TEM.

Head & neck pathology

P3.127
An unusual case of meningioma with osseous metaplasia (review of metaplastic meningiomas)

Gunay Yardim B.; Cumurcu S.; Bayol U.; Bardakci S.
Tepecik Research and Training Hospital, Izmir, Turkey

Background Meningiomas comprising scattered or sheets of cells with lipomatous, chondroid, osseous or xanthomatous like matur mesenchimal differentiations called metaplastic meningiomas. While lipomatous change is common, osseous metaplasia is very exceptional. Among meningiomas in the archive of our institute, only 6 (3 lipomatous, 2 xanthomatous, 1 osseous) of 280 cases were metaplastic. This very unusual osseous metaplastic meningioma is presented with clinical, radiological and pathological features.
Methods Case: 60 years old woman with complaint of back and leg ache for nearly 3 years applied neurosurgery clinic. By examining weakness of right knee flexion-pollex dorsiflexion and hipoesthesia under thoracal 7 dermatome the patient had lomber MRI and cranial CT. On MRI 12x14 mm. hipointense, nodular lesion bulging back at thoracal 11 level existed. Cranial CT revealed nodular lesion on the right frontal region which consequent for parasagittal meningioma. The patient didn't permit the excision of the parasagittal lesion, so only the spinal nodule was excised.
Results Microscopic evaluation of the spinal nodule revealed osseous metaplastic focus among the classical meningomatous areas. The lesion was diagnosed as meningioma with osseous metaplasia.
Conclusion(s) This very unusual osseous metaplastic meningioma is presented with clinical, radiological and pathological features.

P3.128
Diagnosis of myotonic and myofascial syndroms of acute and chronic neck pain

Filipovich Nicolaevich A.; Filipovich Semenovna N.
Research Institute of Medical Assessment and Rehabilitation, Minsk, Belarus, Minsk, Belarus

Background The prevailing myotonic syndromes were identified which were the musculus obliquus capitis inferior syndrome (39.4%); superscapular area syndrome (33% of patients); musculus scalenus anterior and musculus scalenus medius syndromes (18.9%); musculus pectoralis minor syndrome (9.7%). Hypodynamia caused system disorders were noted in 78.3% patients including excessive body mass and fat content; reduced blood circulation rate and heartbeat volume and the pronounced decrease of PWC170. The most informative spondylographic findings were reduced thickness of posterior areas of intervertebral disks from CI to CVII (77.9%), cervical lordosis impression (76.4%) and uncovertebral arthroses (58.2%).
Methods The dynamic monitoring of 195 patients. An extended neurological examination was carried out which included roentgenometry of cervical and vertebrocranial areas of spinal column, electromyography of 7 to 9 relevant muscles, finding of the "key" muscle and the overall computer aided assessment of osteomuscular, cardiorespiratory and oxygen transport system disorders.
Results Clinical and electromyographic criteria for diagnosis of myotonic and myofascial syndromes of neck pain were identified based on the occurrence rates. The role of major system disorders in pathogenesis of neurological manifests of neck pain was studied. New therapeutic approaches to stopping pain and myotonic syndromes were developed; the effectiveness of early rehabilitation measures was demonstrated.
Conclusion(s) The most seriously affected ("key") muscles in neck pain patients were found. Diagnosis and treatment strategies for neck pain patients were developed.

P3.129

Distant metastases to the head and neck. Don't forget about them!

Gene Heym A.; Terrasa Sagristá F.; Gómez Bellvert C.; Ibarra De La Rosa J.; Hamdan Ah'mad H.
Hospital Comarcal de Inca, INCA, Balearic Islands, Spain

Background Metastatic tumors to the head and neck region are very rare. The most common sites of metastatic tumors to this area are the lung, kidney, breast and colon. Most cases affect the maxillary sinus and jawbones and rarely the oral soft tissues. Cutaneous metastases may also be the first indication of a visceral cancer. Symptoms are frequently indistinguishable from those of a primary tumor, and in 20% of the cases, the metastatic lesion may be the first indication of a tumor at a distant site. Histological evaluation and immunohistochemical techniques are essential to separate metastatic versus primary carcinoma.
Methods We reviewed clinical histories of 6 cases of distant tumors metastazing to the H&N that presented at 3 hospitals in Mallorca between the years 2002 and 2008. Hematoxylin & Eosin slides were examined and a battery of stains where performed to characterize these neoplasms (CK7, CK20, CK AE1/AE3, CK5/6, CK8, HepPar1, CEA, TTF1, Vimentin and CD10). Symptoms, location, histology, distant origin site and clinical outcome are discussed.
Results Most frequent origin sites where the lung and kidney, followed by colon and liver. They were found in the sinus, gingiva, lip and skin. In 1 case, the metastases was the first symptom of a kidney tumor.
Conclusion(s) We emphasize the importance of including metastatic tumors in the differential diagnosis of H&N masses, being sometimes the first indication of an undiscovered malignancy at a distant site.

P3.130

Histochemical character of amyloid plaques and cerebral amyloid angiopathy in Alzheimer disease

Apáthy A.; Bély M.; Majtényi K.; Sebestyén T.; Szentjóbi Szabó T.
Department of Rheumatology, National Institute of Rheumatology and Physiotherapy Budapest, Hungary, Budapest, Hungary

Background Amyloid plaques (AP) and cerebral amyloid angiopathy (CAA) are associated diseases. The pathogenesis of AP and CAA is different. The aim of this study was to determine the histochemical characteristics of amyloid beta deposits (Ab) of APs and CAA in Alzheimer's disease (AD).
Methods Isolated cerebral Ab were studied in a selected autopsy population of 12 in-patients with clinically diagnosed AD.
Results AP and CAA were observed in all of 12 patients with AD. In CAA the Ab were localized to the walls of small arteries and arterioles of the leptomeninges (mainly within the sulci) and less frequently in the cortical and subcortical region of the brain. No amyloid deposits were detected in the wall of venules and veins neither in leptomeninges, nor in the brain tissue. The Ab of AP were stable and resistant after performate pretreatment for 20 sec. The Ab of CAA were very sensitive: after one second of performate pretreatment; the birefringence of Ab disappeared.
Conclusion(s) We found histochemical differences between Ab deposits of AP and CAA. Our results imply that AP and CAA may occur together but are independent phenomena of AD. Amyloidosis is a progressive, cumulative process, involving in its early stage only a few structures in some organs, and increasingly more in the later stages of the disease. Amyloid deposition begins in organs and tissue structures that are frequently involved and later show marked deposition of amyloid.

P3.131

Analysis of metastatic signature in glottic squamous-cell carcinoma through oligonucleotide microarrays

Alós L.; Conde L.; Moyano S.; Vilaseca I.; Moragas M.; Jares P.; Cardesa A.; Nadal A.
Hospital Clínic, Universitat de Barcelon, Barcelona, Catalunya, Spain

Background The low prevalence of nodal metastases in glottic squamous-cell carcinoma (GSCC) is attributed to anatomic characteristics. However, some patients develop nodal metastases while others do not, in spite of similar local growth, suggesting that metastatic ability is restricted to some, but not all, glottic carcinomas. We suggest that metastatic ability could be reflected in different mRNA expression profile in primary tumors. To avoid the biass generated by small tumors, cases with nodal metastases were compared to locally advanced tumors, T3 or T4 according to UICC/AJC TNM classification.
Methods Total RNA from 22 GSCCs with fresh frozen tissue available from patients with advanced stages (3 and 4, M0), eleven with nodal metastases and eleven without them, was extracted, purified and labeled for hybridization using the One Cycle Target Labeling kit (Affymetrix, Santa Clara, CA), starting with 2 μg. Labeled cRNA was hybridized to Human Genome U133 Plus 2.0 gene Arrays (Affymetrix) and scanned on an Affymetrix Scanner 3000. Raw data were normalized using the Robust Multichip Average expression summary consisting of background adjustment, quantile normalization, and summarization. Prophet is a web-based tool for microarray data (www.gepas.org) that pre-selects the genes with the best predic-

tion accuracy. Algorithm support vector machine was used.
Results A preliminary set of ten predictor genes with a cross-validation error of 0.1818 and a cluster of 55 differentially expressed genes were obtained.
Conclusion(s) Mathematic algorithms allow the definition of a metastatic signature in a disease with a low metastatic potential.

P3.132
Survey of oral cavity biopsies in the school of dentistry - University Camilo Castelo Branco, Brazil - during the period of 1997–2009

Costa E.; Innocencio Fernando L.; Varoli Paes F.; Costa C.; Rodrigues Fabiano M.
University Camilo Castelo Branco, Sao Paulo, Brazil

Background The prevalence of oral lesions recorded, the anatomic location and the specimens distribution about the type, sex and age were evaluated. Each case was classified in eleven distinct groups, presented number and that lesions which obtained the higher percentage of occurrences.
Methods The aim of this research was to realize a survey of oral lesions in the School of Dentistry (Unicastelo), during the period of 1997–2009, 197 clinical files were analyzed with their retrospectives histopathological diagnosis certificates.
Results The results demonstrated predominance of proliferative non neoplasic lesions, with sixty cases, fibrous inflammatory hyperplasia represented the most common entity (38%).
Conclusion(s) The female sex predominated and the higher percentage of these cases occurred in the first life decade.

P3.133
Altered expression of cell adhesion molecules E-cadherin, desmoglein-2, B4 integrin, CD44s (HCAM) and ICAM-1 in acinic cell and salivary ductal adenocarcinomas

Andreadis D.; Poulopoulos A.; Nomikos A.; Epivatianos A.; Christidis K.; Barbatis C.; Antoniades D.
Dental School, Aristotle University of Thessaloniki, Thessaloniki, Greece

Background This descriptive, immunohistochemical study investigates the expression of E-cadherin a member of adherence junctions, the hemidesmosomal receptor b4-integrin, the most common desmosomal cadherin desmoglein-2 (Dsg-2), the hyaluronan-receptor CD44s and the ICAM-1 in two salivary gland tumors; acinic cell and salivary ductal adenocarcinomas.
Methods Formalin – fixed, paraffin – embedded tissue specimens of 7 acinic cell and 3 salivary ductal adenocarcinomas were studied using an automated Envision/HRP immunohistochemical technique.
Results In acinic cell adenocarcinomas, E-cadherin, b4-integrin and CD44s were mainly strongly expressed along the membrane of intercellular contacts, whereas Dsg-2 was moderately presented only in cytoplasm. ICAM-1 staining was heterogeneous based on staining intense and percentage of positive cells. Regarding salivary ductal adenocarcinomas E-cadherin was moderately to strongly expressed on cell membrane in 2/3 cases, whereas Dsg-2 was located in the cytoplasm of the 3 cases. B4-integrin and ICAM-1 showed a membrane or membrane/cytoplasmic respectively, heterogeneous, case-related, pattern of expression, regarding the intense of staining and the percentage of positive neoplastic cells, whereas CD44s was expressed moderately along the membrane of cells located upon the basal membrane of neoplastic structures.
Conclusion(s) For both of the tumors, Dsg-2 showed a standard pattern of cytoplasmic expression, in contrast to its normal membrane presence, whereas a reduction of E-cadherin and CD44s membrane staining was observed. B4-integrin, on the other hand, revealed a specific profile depending on tumor subtype.

P3.134
Correlation of E-cadherin, β-catenin, p63 and claudin-4 with tumor grade and survival in laryngeal carcinomas

Koumoundourou D.; Sirinian C.; Ravazoula P.; Mastronikolis N.; Papadas T.
University Hospital of Patras, Rio, Patra, Greece

Background E-Cadherin and β-catenin are p63 related proteins, playing an important role in both cell adhesion and signaling. P63 is implicated in the formation of ectodermally derived tissues and all three proteins are involved in the tumorigenesis of squamous carcinoma of head and neck region. On the other hand, Claudin4 is a component of tight junctions, implicated in tumor progression. The purpose of the present study was the assessment of the above proteins in laryngeal carcinomas and their correlation with tumor Grade and patients' survival.
Methods 54 paraffin embedded specimens of laryngeal carcinomas (with a mean follow-up time of 76 months during which 22 patients died of their disease) were immunohistochemically stained for all proteins' expression, trying to assess any potential association with each other and with tumor Grade, Stage and patients' outcome. Statistical analysis was assessed using SPSS 13.
Results P63 overexpression was strongly correlated with E-Cadherin (p=0,01) and β-catenin (p = 0,023) and inversely was correlated with Claudin4 (p = 0,018). A statistically significant reverse association was found between E-

Cadherin overexpression and tumor Grade (p = 0,045), while E-Cadherin and Claudin4 were poor prognostic factors for patients' survival (Kaplan-Meier plots, p = 0,022 and 0,016 respectively).
Conclusion(s) P63 related proteins and Claudin4 are involved in the development of laryngeal squamous carcinomas and are crucial molecules in tumor progression. They are also strong prognostic factors for patients' outcome, since their abnormal overexpression gives the tumor cells an increased malignant potential.

P3.135
Epithelial cell adhesion alterations in salivary gland neoplasms. the paradigm of E-cadherin, desmoglein-2 and b4 integrin
Andreadis D.; Poulopoulos A.; Nomikos A.; Epivatianos A.; Christidis K.; Barbatis C.; Antoniades D.
Dental School, Aristotle University of Thessaloniki, Greece

Background This immunohistochemical study investigates the expression of E-cadherin a member of adherence junctions, the hemidesmosomal receptor b4-integrin, and the most common desmosomal cadherin desmoglein-2 in benign and malignant salivary gland neoplasms.
Methods Formalin – fixed, paraffin – embedded tissue specimens of different subtypes of 54 benign and 31 malignant tumors were studied using an automated Envision/HRP immunohistochemical technique.
Results Normally, E-cadherin and desmoglein-2 were strongly expressed along the membrane of intercellular contacts, whereas beta4-integrin in cell-basal membrane interface in both acinar and ductal salivary epithelium. Although, E-cadherin was strongly expressed in Warthin's tumor, myoepitheliomas and oncocytomas, a reduction and/or absence of E-cadherin was already observed in pleomorphic adenoma at the peripheral cells of the duct-like or island structures, and those exhibiting plasmacytoid / stromal differentiation,. In malignant tumours this marker showed a weak to moderate loss of expression or cytoplasmic expression related to tumour subtype and grade of malignancy. Dsg-2 showed a switch from exclusive membrane to membrane/cytoplasmic presence in benign neoplasms, followed by a reduced, grade- related, cytoplasmic and rarely membranous expression. In contrast, beta-4 integrin revealed an unpolarised heterogenous membrane and/or cytoplasmic staining in the majority of both benign and malignant cases.
Conclusion(s) The pattern of E-cadherin and Dsg-2 expression indicates a strong relation with the grade of neoplastic transformation, whereas the unpolarized staining of beta4-integrin may play a more general role in tumor formation and expansion.

P3.136
Expression of NFk-B and pten proteins in salivary gland tumors cell lines
Marques Maria Freire Soares Y.; Mantesso A.; Araújo Cavalcanti V.; Pinto Jr Santos D.; Sousa Cantanhede Orsini Machado S.
University of São Paulo, São José dos Campos, São Paulo, Brazil

Background The salivary gland tumors comprise a group of tumors with a complex process of tumorigenesis. The balance of regulatory oncogenes or tumor suppressors and respective proteins are unclear, but our previous studies have shown overexpression of akt expression in pleomorphic adenoma (PA) and adenoid cystic carcinoma (ACC). The NFk-B and PTEN expression may play an important role on activation of Akt pathway. None previous studies have shown the response of cell lines from these tumors. The aim of this study was to analyse the NFk-B and PTEN expression in PA and ACC cell lines.
Methods Two cell lines of salivary gland tumors, previously diagnosed as ACC and PA in accordance with the latest WHO classification were retrieved from School of Dentistry of the University of São Paulo. Samples of both lesions were cultured for analysis. The anti-PTEN and anti-NF-kB antibodies were used to western blotting and immunoflorescence analysis.
Results Western blotting analysis revealed overexpression of NFk-B and PTEN in both cell lines. Immunofluorescence evaluation showed nuclei and cytoplasmatic NFk-B and PTEN staining in the ACC cell line. The PA cell revealed only cytoplasmatic staining of both proteins.
Conclusion(s) The overexpression of NFk-B and PTEN protein in PA and ACC may represent important activators of akt pathway and, the nuclear expression of PTEN and NFk-B in ACC may predict a possible response to adjuvant therapies. In conclusion, NFk-B and PTEN expression showed an important participation by AKT pathway in salivary gland neoplasms.

P3.137
Glucose transporter-1 expression in squamous cell carcinoma of larynx
Ozbudak I.; Turhan M.; Erdogan G.; Guney K.; Ozbilim G.
Akdeniz University School of Medicine, Department of Pathology, Antalya, Turkey

Background Development of malignant tumor is an energy-dependent process supported by increased glucose metabolism. Glucose transporter-1 (GLUT-1) mediates the glucose uptake and facilitates anaerobic glycolysis. Elevated levels of GLUT-1 expression have been shown to be

associated with malignancy. The aim of this study was to investigate its expression in squamous cell carcinoma (SCC) of larynx.

Methods Eighty-four tumor samples from patients with laryngeal SCC were studied immunohistochemically for GLUT-1 expression. The intensity and the percentage of the stained tumor cells with distinct cytoplasmic staining were evaluated. The available data of clinical information including age, gender, clinical stage and pathological information including histologic grade were collected.

Results The cohort included 80 men and 4 women with a mean age of 59.54±10.36 years (range, 33 – 84). All the samples except one of laryngeal SCCs were immunoreactive with GLUT-1. Expression of GLUT-1 was observed in neoplastic cells, preferentially along the luminal border of tumor islands. Normal pseudostratified epithelium was negative. There was no significant correlation with the gender, age or stage. However, a significant difference was found between the tumor grades in GLUT-1 expression (p= 0.016). Well-differentiated laryngeal SCCs had higher GLUT-1 expression compared to moderate and poor differentiated laryngeal SCCs (p = 0.013).

Conclusion(s) In conclusion, GLUT-1 is commonly expressed in laryngeal SCCs. It shows characteristic membranous expression with predilection for the luminal surface of tumor islands. GLUT-1 expression strongly correlates with tumor differentiation in laryngeal SCCs.

P3.138

Homeobox genes expression in oral squamous cell carcinomas according to clinical parameters of aggressiveness

Nunes Daumas F.; Rodini De Oliveira C.; Okamoto Keith O.; Xavier Calo F.; Michaluart Jr.P.; Carvalho Brasilino M.; Alvares Madeira A.; Tajara Helena E.; Gencapo H.
Universidade de São Pulo, São Paulo, São Paulo, Brazil

Background The search for molecular markers to improve diagnosis, to individualize treatment and to predict behavior of oral squamous cell carcinomas has been the focus of several studies. The present study investigates if homeobox genes may be relevant molecular markers of prognosis and/or tumor aggressiveness in squamous cell carcinoma of the tongue and/or floor of the mouth.

Methods Tumor samples were classified as more or less aggressive based on TNM staging system, and after microarray analysis of tumors and their non tumoral margins, HOXC13, HOXD10, HOXD11, IRX4, PROX1 and ZHX1 were selected, validated by qRT-PCR, and correlated to clinico-pathological parameters.

Results Increased expression of HOXD10 and HOXD11 in less aggressive tumors in comparison to their margins was observed. A decreased expression of PROX1 and ZHX1 was observed in margins compared to their respective tumors. These results suggest that the altered expression of HOXD10 and HOXD11 may participate in the development of squamous cell carcinoma of the tongue and/or floor of the mouth, while PROX1 and ZHX1 probably present loss of function or are silenced in these tumors. There was a weak statistical correlation between expression of homeobox genes and some clinical and histopathological parameters. IRX4 was associated with a decreased overall survival.

Conclusion(s) Additional studies are necessary to understand the participation of homeobox genes in oral squamous cell carcinoma; however, our results suggest they are related to aggressiveness.

P3.139

Medulloblastoma: Tunisian experience of 55 cases

Chelly I.; Nfoussi H.; Azzouz H.; Adouni O.; Mekni A.; Tangour M.; Boujelbene N.; Haouet S.; Kchir N.; Zitouna M.
La Rabta, Ariana, Tunis, Tunisia

Background Medulloblastoma is a rapidly-growing tumor of the cerebellumMedulloblastoma is relatively rare, accounting for less than 2% of all primary brain tumors and 18% of all pediatric brain tumors. Objective: To describe epidemiological characteristics of medulloblastoma in a Tunisian population.

Methods A retrospective study of 55 medulloblastoma operated during 15 years was undertaken. We investigated the age-related location, gender distribution and the histology of this tumor.

Results Of the 55 medulloblastoma, 32 (58%) occurred in children and 23 (42%) in adults. The median age at diagnosis in pediatric group was 7,32 years, with a male: female ratio of 1,3. In adults, the median age was 34,8 with a male:female ratio of 1,4. In children, medulloblastoma arose most often near the vermis (46%). In adults this tumor tends to occur in the body of the cerebellum, (40%). Microscopic examination revealed that desmoplastic nodular medullobastoma was found in the majority of both pediatric and adult tumors (63%). Classic pattern was found in 35% of cases. Only one case has a large-cell pattern. The MIB-1 proliferating index was higher in children (19,02%) than in adults (10,06%). Immunohistochemistry for bcl-2 and p-53 showed a high expression of these proteins in pediatric group that revealed the agressivity of this tumor.

Conclusion(s) The incidence and distribution of medulloblastoma in this Tunisian study show a high frequency of desmoplastic type in both pediatric and adults patients. There is a correlation between MIB-1 proliferating index, bcl-2, p53 and the aggressive behaviour of this tumor.

P3.140

Oral hairy leukoplakia: study of histopathological and citopathological features, using immunochemistry, in situ hybridization and PCR

Dias Pedra, E.; Silva-Junior A.; Milagres A.; Rocha Lage M.; Israel Simões M.; Maciel Abreu V.; Macedo Pessanha J.; Menezes Soares N.; Fontana Christina T.; Ferreira Soares S.; Lopes Silami V.

Universidade Federal Fluminense, Niterói, Rio de Janeiro, Brazil

Background Oral Hairy Leukoplakia (OHL) is a unique possibility to study EBV replication in vivo. As it can be the first manifestation of immunocompromised, the accurate diagnosis is crucial. Morphological aspects, although characteristic, are still not established as the preferential diagnostic tool. The aim of study was to describe histo/cytopathological aspects and demonstrate that the cytopathic effects of EBV on keratinocytes are sufficient to define diagnosis of OHL.

Methods Oral biopsy (n=25) and scrapes of the tongue (n= 25) were selected from the archives of oral pathology, all confirmed as OHL. Were investigated histo/cytopathological features; EBV proteins (LMP-1 and BZLF1) by immunohistochemistry (IHC); EBER-PNA and DNA-EBV in situ hybridization (ISH) and DNA-EBV polymerase chain reaction (PCR).

Results EBV cytopathic effects were identified in all biopsy and smears. DNA-EBV and EBER were identified by ISH in all seven tissue selected and, by PCR, in all 25 scrapes. Nuclear and/or cytoplasmic LMP1 and nuclear BZLF1 immunopositivity were observed in all biopsies as well as in six scrapes tested. The comparative analysis demonstrated that either ISH or IHC stained cells nuclei with specific changes (nuclear inclusions, ground glass and nuclear beading). In none of the cases it was observed positivity in sites where cytopathic effects were not present.

Conclusion(s) a) Immunohistochemical for BZLF1 can be used as an EBV replicative infection markers; b) EBV cytopathic effects are pathognomonic for histopathological diagnosis of OHL; c) Cytopathology is the recommended technique for OHL diagnosis.

P3.141

Pathology of the myoepithelial cells as one of the reasons of the disorder of the secretion liberation from nasal glands in chronic rhinitis

Ivanova Nikolaevna O.

Institute for Sorption and Endoecology Problems (National Academy of Sciences of Ukraine), Kiev, Ukraine

Background It is known that the discoordination between the secretion synthesis and liberation in the nasal glands is significant manifestation of chronic rhinitis. However, the potential role of myoepithelial cell pathology in the disorder of liberation of the nasal gland secretion has not yet been sufficiently explored.

Methods Ninety-three biopsies taken for diagnostic reasons from nasal mucosa of patients with chronic rhinitis – average residents of Kiev (group I, n=40) and liquidators of the Chernobyl accident consequences (group II, n=53) – were examined by light-microscopic histochemistry and transmission electron-microscopy.

Results Various pathological changes were observed in the myoepithelial cells in both groups, being more expressed in group II: the cytoplasm edema and vacuolization; destruction of the actin-myosin complex (disappearance of the dense bodies and disarrangement of the contractile filaments), nucleus pyknosis, and mitochondrial edema and destruction. These changes demonstrate the contractile disfunction of myoepithelial cells. In addition, the decrease in number of the mitochondria-rich cells in the collector ducts of the glands in the group II patients (11%, as opposed to 23% in group I) might cause changes in the nasal secrete rheological properties and its thickening. Hence, the increased density of secretion obstructed its liberation from the nasal glands.

Conclusion(s) Pathology of the myoepithelial cells and the decrease in number of the mitochondria-rich cells are among the reasons of the disorder of the secretion liberation from nasal glands.

P3.142

Pleomorphic adenoma in salivary glands: an epidemiologic study of 406 cases in a Brazilian population

Oliveira Aparecida F.; Duarte Carla Barroso E.; Costa Teles A.; Taveira Teixeira C.; Máximo Abreu A.; Alencar Cássia R.; Vencio Franco E.

Department of Pathology, Tropical Pathology and Public Health Institute of the Universidade Federal de Goiás (UFG), Goiânia, Goiás, Brazil

Background Pleomorphic adenoma is the most frequent salivary tumor, representing 45 to 74% of all salivary gland neoplasms. The aim of this study was to describe the epidemiological data of pleomorphic adenoma in a Brazilian population.

Methods The cases were selected over a period of 10 years (1996 to 2005) from the Pathology Department, Cancer Hospital Araújo Jorge in Goiânia-Goiás, Brazil.

Results From the 599 salivary gland tumors diagnosed, 67.8% were pleomorphic adenoma. The women were more frequently affected 63.3%, although no statistical difference was found relating to the other types of tumors (55.9% $p>0.05$). The mean age of patients with pleomorphic adenoma was significantly lower than other salivary gland tumors (42.6±16.1 vs. 53.8±16.9 years $p<0.05$). The ages ranged from 5 to 86 years, and the most frequent group was 35 to 49 with 34%, while in the other types of salivary gland tumors the ages ranged from 50 to 64 with 37.8% ($p<0.05$). In pleomorphic adenoma, the median age for women was significantly higher than for men with 42 vs. 39 years, respectively. Pleomorphic adenoma significantly affected the parotid gland with 73.9% (298 cases), followed by the submandibular gland with 18.1%. In both genders, the parotid gland was more affected by pleomorphic adenoma, with no statistical difference ($p>0.05$).
Conclusion(s) Therefore, pleomorphic adenoma was more frequent in the parotid gland and in women, affecting mainly young people compared to the other salivary gland tumors.

P3.143
Study of growth factors and receptors in carcinoma ex pleomorphic adenoma

Furuse C.; Miguita L.; Soares Borges A.; Rosa Garcia A.; Altemani A.; Araújo Soares N.; Araújo Cavalcanti V.
São Leopoldo Mandic Institute and Research Center, Campinas, SP, Brazil

Background Carcinoma ex-pleomorphic adenoma (CXPA) is a rare malignant salivary gland tumor derived from a pre-existed pleomorphic adenoma. It is a good model to study the evolution of carcinogenesis, starting with in situ areas to frankly invasive carcinoma. Growth factors are associated with several biological and neoplastic processes by transmembrane receptors.
Methods To investigate by immunohistochemistry the expression of some growth factors and its receptors (EGFR, FGF, FGFR-1, FGFR-2, HGF, c-Met, TGF-β1, TGFβR-II and IGF) in the progression of CXPA, we used ten cases of CXPA in several degrees of invasion- intracapsular, minimally and frankly invasive carcinoma with only epithelial component. Slides were evaluated qualitatively and semi-quantitatively according to the percentage of stained tumor cells from 0 to 3 (0=less than 10% of cells; 1=10–25% of cells; 2=25–50% of cells; 3=more than 50% of cells).
Results Malignant epithelial cells showed stronger expression than luminal cells of benign residual pleomorphic adenoma for all antibodies since in situ CXPA. Most of the intracapsular, minimally and frankly invasive CXPA presented score 3. However, score 2 was more evident in the frankly invasive one. In small nests of invasive carcinoma, negative cells were observed (except for EGFR) probably indicating that the proliferative process is replaced by the invasive mechanism.
Conclusion(s) Taking together all these data infers that these factors may contribute to cell proliferation during initial phases of the tumor.

P3.144
The immunohistochemical and viral profile of oral plasmablastic lymphomas in a South African population sample

Boy C.S.; Van Heerden B.M.; Van Heerden F.W.
University of Pretoria, Pretoria, South Africa

Background Oral plasmablastic lymphoma (OPBL) was originally described in 1997 as an AIDS-associated tumour and less than 200 cases have since been reported in the literature. The tumour is classified by the WHO (2001) as a rare subtype of diffuse large B cell lymphoma with distinctive immunophenotypic features. There is contradiction in the literature with regard to the true nature of these neoplasms and their immunophenotype expression.
Methods Immunohistochemical investigations were performed on 37 cases of OPBL using CD45, CD3, CD20, CD79a, CD38, CD138, MUM1, and Ki-67. Positivity was recorded based on the percentage of positive staining cells: single <5%; focal <20%; intermediate 20–70%; diffuse >70% of cells. In-situ hybridisation was performed using EBV encoded small nuclear RNA's (EBER1/2) probes and was recorded as positive or negative.
Results All cases were negative for CD20 with only focal reactive T-cells detected with CD3. Diffuse and strong positive staining was found with Ki-67 and MUM1 antibodies. Variable immunoreactivity was found with CD79a, CD38 and CD138. EBV was detected in 35 (95%) cases.
Conclusion(s) OPBL are mostly seen on the gingiva and should only be diagnosed with a panel of immunohistochemical markers and clinical features. The true nature of these neoplasms as an entity should be further investigated with molecular and genetic studies.

P3.145
Biphasic meningeal tumor that includes solitary fibrous tumor and meningioma, case report

Demir H.; Oz B.; Ozturk A.; Dagistan Y.; Ethemoglu B.; Taskin Murat M.
Istanbul Univercity Cerrahpasa Medical Faculty, Istanbul, Turkey

Background Intracranial solitary fibrous tumors are typically presents as a dural based lesion. Radiologically and morphologically, they can be confused with fibrous meningioma. In contrast to meningiomas, solitary fibrous tumors express CD34 and they are negative for EMA. We report a case of solitary fibrous tumor that associated with meningioma.
Methods 59 year old woman presented with headache for one year. Cranial MR showed an extra-axial lesion that was considered as a meningioma. Right frontal craniotomy was performed and the tumor removed totally. On microscopic examination two different tumors were observed. The first one included irregular fascicules made of spindle cells with long, oval nucleus and elongated cytoplasm. Thin hyalinizing and collagenous septa were accompanied to these cells. The second one included the meningothelial cells showed whorl pattern. Necrosis was not observed. The first described areas, solitary fibrous tumor, showed cytoplasmic positivity with CD34. The second one, meningioma, showed membranous positivity with EMA. The proliferative index was 1–2 percent with Ki 67 and mitotic figures were 0–1 in ten hpf in both tumors.
Results We report the case as solitary fibrous tumor that includes focally meningioma areas.
Conclusion(s) Synergy of solitary fibrous tumor and meningioma is reported very rare on the literature. Meningeal solitary fibrous tumors are benign tumors and totally resection is a prognostic factor. Our case was considered as a Grade I tumor, because of low proliferative index, low mitotic activity and absence of necrosis.

P3.146
CD117 expression with molecular analysis of muations in ISH-EBV positive undifferentiated nasopharyngeal carcinomas

Iosif Ileana C.; Georgescu A.; Ceausu M.; Vasilescu F.; Arsene D.; Mihai M.; Terzea D.; Dobrea C.; Enache S.; Visan A.; Butur G.; Ardeleanu C.
Victor Babes National Institute of Pathology, Bucharest, Romania

Background EBV-encoded non-polyadenylated RNAs (EBERs) is often used as a marker to detect EBV-infected undifferentiated nasopharyngeal carcinoma (UNPC) cells. Aim of our study was to detect the presence and significance of CD117 in UNPC tumor cells with positive ISH (in situ hybridization) reaction for EBV.
Methods 13 formalin fixed paraffin embedded tissue samples from patients (mean=38,84 years, M:F=8:5) diagnosed with primary UNPC were analyzed using standard HE stain and Dako EnVision IHC detection system for CD117. ISH has been done using a detection kit from Novocastra for EBER transcripts of EBV. PCR for c-kit mutations of exons 9 and 11 was performed on all CD117 positive cases.
Results In the study group 10 of 13 cases (77%) were UNPC of Regaud type, with a high mitotic index (about 5–6 mitoses/HPF); 7 of 10 cases of Regaud type (70%) have expressed CD117. All cases were positive for EBER. None mutations were detected by PCR on 9 and 11 exons of c-kit gene. The potential of CD117 as a target for therapy should be considered, even in the absence of c-kit gene mutations and other mechanisms of this protein overexpression should be take into account.
Conclusion(s) Even if there is a high sensibility of CD117 in EBV positive Regaud type UNPC, this marker is independent for biological tumor behavior, therefore requires further studies on larger cohorts and needs to be compared with other prognostic markers with already demonstrated value.

P3.147
Dentin matrix protein 1 (DMP1) in developing human salivary gland

Dias Santos Souza R.; Araújo Cavalcanti V.; Araújo Soares N.; Furuse C.
São Leopoldo Mandic School of Dentistry, Campinas, São Paulo, Brazil

Background Dentin Matrix Protein 1 (DMP1) is an acidic phosphoprotein expressed mainly in the extracellular matrix of dentin and bones and it is associated to the mineralization of these tissues. DMP1 was also found in non-mineralized tissues such as brain, liver, kidney, muscles and pancreas.
Methods The aim of this research was to investigate the presence and distribution of DMP1 in developing human salivary glands by immunohistochemistry. Major and minor salivary glands from different sites of 10 human fetuses in different gestational ages (14 a 24 weeks), fixed in formol 10% and embedded in paraffin, were analyzed.
Results DMP1 was expressed in the nucleus and cytoplasm, and no differences were observed between major and minor glands. At the beginning of the development, in the early phase of branching and canalization, positivity was observed in all inner and outer cells, but some negative cells were noted in completely fulfilled lobules. In the early acinic cells differentiation, no staining was observed. In this stage, outer cells of ductal structures were also negative to DMP1, especially the ones with more flattened morphology.
Conclusion(s) Based on the fact that the DMP1 was not observed in the cells in differentiation, we can conclude that DMP1 may have a role in the proliferation process but not in the differentiation mechanism of the salivary gland.

P3.148

Epidermal growth factor receptor (EGFR), cyclin D1 and P16 gene expressions in nasopharyngeal carcinoma

Gonzalez Serrano Teresa M.; Vargas Teresa M.; Ruiz Molina I.; Galera Ruiz H.; Casco F.G.; Gonzalez Campora R.
Hospital Infanta Margarita, Cabra, Córdoba, Spain

Background Nasopharyngeal carcinoma is an sporadic and unusual neoplasia in western countries while it is endemic in certain geographical areas such as South East Asia and Mediterranean countries. Recent studies have focused on the identification of genetic changes implicated in the biopathologic behaviour of nasopharyngeal carcinoma. Besides environmental factors, genetic susceptibility, Epstein-Barr virus infection and alterations in the cell cycle due to disregulation of factors such as Epidermal Growth Factor Receptor (EGFR), p16 and cyclin D1 have been involved in the tumorigenesis.
Methods Material and methods: Gene expression has been studied on paraffin embedded tissue sections from 30 cases by FISH methodology with probes; LSI EGFR (7q12)/ CEP7,LSI p16 (9q21)/CEP 9 and LSI cyclin D1 (11q23)/ CEP 11. The centromeric probes of chromosomes 7, 9 and 11 were used as control probes.
Results Amplification of cyclin D1 in 36,6% of the cases, amplification of gene EGFR in 10% and deletion of the gene p16 in 36,6% were observed.
Conclusion(s) First, the FISH method on paraffin embedded tissue has been improved by introducing some technical modifications. Second, we try to contribute to increase the knowledge about biomolecular mechanisms of the genesis of nasopharyngeal carcinoma.

P3.149

FGF-2 is overexpressed in myoepithelial cells of in situ areas of carcinoma ex-pleomorphic adenoma

Martinez Ferreira E.; Demasi Dias A.; Miguita L.; Altemani A.; Araújo Soares N.; Araújo Cavalcanti V.
São Leopoldo Mandic Institute and Research Center, São Paulo, Brazil

Background Increasing emphasis has been placed on the role of myoepithelial cells in the in situ to carcinoma transition. These cells are placed at the interface between luminal epithelial cells and the stromal compartment, which favors their cross-talk with all other cell types comprising the tumor microenvironment.
Methods We have investigated FGF-2 expression in CXPA in situ areas as well as in cells cultured under conditions attempting to simulate the cellular interactions of this tumor stage by immunofluorescence and immunohistochemistry. We also have performed a quantitative real time and Western blotting to validate the results.
Results We have observed by immunohistochemistry that myoepithelial cells of CXPA in situ areas overexpress FGF-2. In addition, our immunofluorescence results, supported by qPCR and Western blotting, demonstrated that the expression of FGF-2 in the myoepithelial cells was in fact increased by stimulation with the conditioned medium from malignant cells. Low molecular weight FGF-2, known to be primarily released from the cells to exert its biological activity through receptors, was the predominant FGF-2 form detected in the myoepithelial cells. Specific FGF-2 receptors were found in the malignant epithelial but not in the myoepithelial cells of CXPA, indicating a paracrine role for myoepithelial cell-derived FGF-2.
Conclusion(s) Abnormal paracrine myoepithelial/epithelial cell interactions and also myoepithelial/stromal cell interactions could favor tumor growth, invasion and metastasis. Based on this, FGF-2 signaling cascade could be viewed as a candidate intervention target aiming the blockage of CXPA progression.

P3.150

Human developing salivary glands: expression of mucins according to the morphogenesis stages

Ianez Fraga R.; Teshima Harumi T.; Coutinho-Camillo Malheiros C.; Buim Cavicchioli M.; Soares A.F.; Lourenco Vanessa S.
Hospital A C Camargo, São Paulo, SP, Brazil

Background Formation of salivary glands starts with proliferation of epithelial cells from stomatodeum into the underlying ectomesenchyme, culminating in complex structures formed by a ductal network and acinar bulbs. Mucins participation during salivary gland morphogenesis process is still obscure, but they may contribute to luminal space formation.
Methods Using immunohistochemistry we investigated the participation of mucins MUC1, 2, 3, 4, 5 and 6 in developing human salivary glands obtained from foetuses ranging from weeks 4 to 24 of gestation and in fully developed salivary glands.
Results Mucins 1, 3 and 4 were detected in during salivary gland development, being stronger in all ductal segments by the final phases of branching morphogenesis, and in mature glands. Acinar cells were negative for all mucins, except for MUC1 in mature salivary glands. Mucins 2, 5 and 6 were negative.
Conclusion(s) Mucins appear to be important to maturation and maintenance of ductal network in human salivary glands.

P3.151

Immunohistochemical analysis in primary and recurrent pleomorphic adenoma of salivary gland tumors

Oliveira Aparecida F.; Duarte Carla Barroso E.; Alencar Cássia R.; Vencio Franco E.
Department of Pathology, Tropical Pathology and Public Health Institute of the Universidade Federal de Goiás (UFG), Goiânia, Goiás, Brazil

Background Pleomorphic adenoma is the most common lesion of salivary gland tumors. Although, it represents a benign tumor, pleomorphic adenoma may exhibit recurrence and locally aggressive behavior. The aim of this study is to identify protein expression in the primary and recurrent tumors of pleomorphic adenoma.
Methods Immunohistochemical expression of estrogen receptor, progesteron receptor, E-cadherin, Bcl-2, p53, Ki-67, EGFR and c-erbB-2 were investigated in 8 cases of recurrent pleomorphic adenoma, and 9 cases of primary tumors without recurrence. Normal salivary glands were used as controls.
Results Thirty percent of recurrent tumors showed overexpression for p53, Ki67, Bcl2, estrogen receptor and c-erbB2. Membrane associated E-cadherin was overexpressed in 75% of the primary tumors and in 70% of the respective recurrent tumors, mainly in focal areas beside the fibrous capsule.
Conclusion(s) In conclusion, the overexpression of the estrogen receptor, Bcl-2 and c-erbB2 might be useful proteins as predictors of recurrence in pleomorphic adenoma. It is possible that the E-cadherin is an important biomarker if detected in the primary tumor.

P3.152

Immunohistochemistry analysis of WNT pathway in oral squamous cell carcinoma

Buim Eliza Cavicchioli M.; Lourenco Vanessa S.; Carvalho Candido K.; Soares A.F.
Hospital A.C. Camargo, São Paulo, Brazil

Background β-catenin is key downstream effector of the WNT signaling pathway to regulate cell growth/survival. This pathway is activated by stabilized the β-catenin protein, which accumulates in the cytoplasm, and then translocates to the nucleus. It then binds to the T-cell factor/lymphoid-enhancer factor to activate genes, such as cyclin D1, c-myc, MMP7, and contributes to the oncogenesis of various humans cancers. This study analyzed the profiles of Wnt-1, β-catenin, cyclin D-1, MMP-7 expression in oral squamous cell carcinoma (OSCC).
Methods We performed immunohistochemistry for WNT-1, β-catenin, cyclin D1, MMP-7 in 129 OSCC included in one Tissue Microarray. The results were evaluated quantitatively by the Automated Cellular Imaging Systems (ACIS III, DAKO). Mann-Whitney and Spearman tests were used for statistical analysis.
Results Wnt-1 and MMP-7 protein had high expression in OSCC. The β-catenin accumulation in the cytoplasm and particularly in the nuclei was observed in almost all tumors. However, no correlation was observed among β-catenin, WNT-1, MMP-7 expression and morphological parameters (histological grade, vascular and perineural invasion, recorrence, and clinical stage). Higher cyclin D1 immunoreactivity was observed incases with lymph node metastasis than in those without (p=0,006). Expression of WNT-1 protein showed strong correlation with MMP7 (r=0,64; p<0,001) and regular correlation with β-catenin (r=0,30; p=0,004) and cyclin D1 (r=0,30; p=0,005).
Conclusion(s) Our results suggested activation of WNT/β-catenin pathway in OSCC tumorigenesis. Importantly, it was suggested that β-catenin expression might be associated with lymph node metastasis.

P3.153

Losses of chromosomal material are a common feature in acinic cell carcinomas of salivary glands

Passador-Santos, F.; Scheinin I.; Jee Jaa K.; Hagström J.; Mäkitie A.; Knuutila S.; Stenman G.; Skalová A.; Elmberger G.; Leivo I.
Department of Pathology, Haartman Institute, University of Helsinki, Helsinki, Finland

Background Acinic Cell Carcinomas (AciCCs) are salivary gland tumors characterized by a proliferation of cells containing various amounts of serous acinar cell differentiation. Additionally, cases with dedifferentiated tumor growth in addition to conventional AciCC occur rarely. Array-Comparative Genomic Hybridization (a-CGH) is an important tool for assessing gains and losses of chromosomal material at the genomic level. This study was designed to find possible prognostic markers using a-CGH technique.
Methods Eight Formalin Fixed Paraffin Embedded (FFPE) and seven Fresh-Frozen cases of AciCCs were selected. Twelve cases exhibited conventional acinic cell pattern and three cases had areas of dedifferentiation. Genomic DNA from the tumors was extracted according to standard procedures after macrodissection. The a-CGH technique was applied using 4x44k and 244 K oligonucleotide-based CGH arrays (Agilent® Technologies). Digestion, labeling and hybridization were done according to manufacturer's protocol. The array slides were scanned using Agilent's confocal scanner. The data was processed using Feature

Extraction software v9.5 and analyzed using DNA Analytics software v4.0.76 (Agilent® Technologies).
Results We identified chromosomal aberrations in 11 cases. Losses were more common than gains. The most prevalent losses were observed at 1p21.1-p31.1, 1p35.1-p36.13, 11q22.1-qter, and 15q11.2-q21.2. Gains at 1p31.3-p34.3 and 1q21.1-qter can occur but were not prevalent.
Conclusion(s) Chromosomal aberrations were identified in 73,3% of cases studied. Losses were more common than gains. Identification of relevant genes localized at aberrant regions could reveal biological mechanisms involved in the pathogenesis of AciCCs.

P3.154
Meningeal hemangiopericytoma. What is about predictive factors?

Chelly I.; Nfoussi H.; Azzouz H.; Boujelbene N.; Mekni A.; Tangour M.; Adouni O.; Khaldi M.; Haouet S.; Kchir N.; Zitouna M.
La Rabta, Ariana, Tunis, Tunisia

Background background and objective: Meningeal hemangiopericytoma is a rare tumor that has a relentless tendency for local recurrence and metastases outside the CNS. Histological criteria for grading are not yet firmly established.This study was designed to investigate the clinicopathological and biology behavior of primary meningeal hemangiopericytoma in order to deduce predictive factors of recurrence and / or metatasis.
Methods Clinical data, combined with histopathology and immunohistochemistry of 14 cases of meningeal hemangiopericytoma were reviewed.
Results The average age of patients with primary meningeal hemangiopericytoma was 43.35 year-old (21–72 years). The ratio of male to female was 0,75. The tumors were supratentorial in nine cases, infratentorial in three cases, tentorial in one case and located in the spinal cord in the last one. Histologically, CNS-HPCs were similar to their soft tissue counterparts. Four cases had focal necrosis and three case displayed frank anaplasia. Mitotic figures were present in most of the tumors with variation from zero to ten mitoses per 10 high-power fields. Immunohistochemistry for Ki-67 (MIB-1) antibody ranged from zero to more than 20%. All patients underwent surgery with gross-total resection in all cases. Only three patients received postoperative radiation therapy. One of them recurred after 1 year. Four of the 11 non irradiated tumours recurred locally after six, seven and eight months, and five years. No distant metastases were noted.
Conclusion(s) As in literature, there were almost no correlation between patient prognosis, clinical and histopatholgic features and therapeutic modalities.

P3.155
Metallothionein expression is associated to metastatic behavior of adenoid cystic carcinoma of the salivary glands

Cardoso Vitorino S.; Brazão-Silva M.; Faria P.; Dias F.; Eisenberg Amaral A.; Loyola Mota A.
Federal University of Uberlandia, School of Dentistry, Uberlandia, MG, Brazil

Background Metallothionein (MT) is a scavenger protein that has been enrolled in aggressive tumoral behavior. It has been suggested as a marker of myoepithelial cells and is more frequently detected in adenoid cystic carcinomas with worse histological pattern.
Methods In order to evaluate MT as a predictive marker for metastasis development in adenoid cystic carcinoma of the salivary glands (ACC), we detected this protein by streptavidin-biotin-peroxidase immunohistochemistry in 40 primary non-metastasizing (PNM) and 8 primary metastasizing (PM) tumors. Semiquantitative analysis assessed pattern (nuclear or cytoplasmic) of expression, intensity of staining, proportion of positive cells, and proportion of nuclear positivity.
Results MT staining was observed in all of the samples. Nuclear positivity was a prominent feature in many lesions, while cells with ductal differentiation were usually negative. All of the obtained values for MT staining were constantly higher in PM than PNM cases. Mean intensity of staining was significantly higher in PM rather than PNM tumors. Distinct cut-off values could be traced to segregate only PNM cases.
Conclusion(s) Results of the present study substantiate the hypothesis of association between MT expression and biological behavior of ACC. In fact, it was possible to identify non-metastatic lesions according to specific semiquantitative patterns of staining. Therefore, this protein should be subject of further investigation to elucidate its participation in the development of this neoplasm.Financial support: FAPEMIG, CNPq.

P3.156
p53 and bcl2 in lip squamous cell carcinoma

Fontes A.; Martins Trierveiler M.
University of Sao Paulo, Sao Paulo, Brazil

Background The p53 tumor suppressor gene has an important role in carcinogenesis, particularly in the photocarcinogenesis, as it shows to be very susceptible to mutation by ultraviolet radiation (UV). The UV radiation is the most important factor that causes lip squamous cell carcinoma. Other mechanism altered by the damaging effect of photocarcinogenesis is apoptosis, that is responsi-

ble for the cell death. Many proteins are involved in the apoptosis mechanism, and one of these proteins is bcl2, that promotes the prevention of cell death by increasing the rate of cell division. This study had the aim of analyzing the presence and distribution of p53 and bcl2 proteins in lip squamous cell carcinoma.
Methods Sections of 14 cases diagnosed as lip squamous cell carcinoma were submitted to the anti-p53 and anti-bcl2 antibodies in imunohistochemistry reactions.
Results The results showed that all cases had peripheral staining for both proteins. The basal layer of epithelium and the invasive front island were stained for both markers. The p53 showed nuclei staining while the bcl2 staining was mostly cytoplasmic.
Conclusion(s) The results suggest that the expression of p53 and bcl2 in the peripheral areas means that the staining is only at the invasive front areas. This pattern of staining confirms the less aggressive behavior of lip squamous cell carcinoma if compared of the another kinds of oral carcinoma.

P3.157
Somatic mutations in mitochondrial DNA of oncocytic cells in warthin tumours

Guimarães S.; Leal N.; Máximo V.
Hospital S. João, Porto, Portugal

Background Oncocytic cells have a cytoplasm filled with large number of abnormal mitochondria. This accumulation may be the result of an alteration in mitochondrial DNA (mtDNA), or a consequence of mutations in nuclear DNA that encodes mitochondrial proteins. There is only one study describing alterations in mtDNA in Warthin tumours. In oncocytic thyroid tumours, there is an association between this tumours and the existence of polymorphisms in mitochondrial genes encoding complex V of the mitochondrial respiratory chain and a higher frequency of alterations in displacement-loop (D-loop).
Methods Nineteen Warthin tumours and the non neoplastic parenchyma in 13 cases, were studied regarding the CD, mutations in D-loop and in subunits 6 and 8 of the complex V (ATPase) of the mitochondrial respiratory chain. DNA extraction was performed from samples obtained using microdissection.
Results Instability in the D-loop region was detected in 63.2% of the Warthin tumours and in one case in the adjacent normal tissue; somatic mutations in ATPase 6 were detected in 5.3% of the cases. Mutations in the 8 subunit were not found. Mutations in ATPase 6 showed some preference by oncocytic phenotype. The authors did not obtain evidence favouring the existence of a determinant role for the instability of the D-loop region in the process of oncocytic transformation of Warthin tumours.
Conclusion(s) Alterations in mtDNA of Warthin tumours do not differ substantially from those obtained in Hürthle cells tumours, both with respect to the type of alterations and to their frequency.

P3.158
Spindle epithelial tumor with thymus-like differentiation (SETTLE) of the thyroid. A case report

De Anda González J.; Llamas-Gutiérrez F.; Albores-Saavedra J.; Ángeles Ángeles A.
Instituto Nacional De Ciencias Médicas y Nutrición Salvador Zubiran, Distrito Federal, Mexico

Background Spindle epithelial tumors with thymus–like differentiation (SETTLE) is a rare tumor, and it is considered to develop from ectopic thymic tissue or remnants of branchial pouches. Occurs most frequently in children and adolescents, and his differential diagnosis is important. The treatment of these tumor consist of surgical excision with or without adyuvant therapy. The prognosis and the clinical course are uncertain, someone showing delayed metastases.
Methods A 56 years old women with symptoms of primary hyperparathyroidism, and a neck mass that was present for 2 years. During the operation the surgeon found that the tumor was in continuity with the thyroid gland. On the gross examination, there was a 1.1x0.9x0.9 cm unencapsulated mass. Microscopically there were predominant spindle cells, with tubulopapillary epithelial elements. Nuclear atypia was mild to moderate and mitotic figures were there. There wasn´t necrosis.
Results The immunohistochemical stains were vimentin, smooth muscle actin and cytokeratin AE1/AE3 positive. Epithelial elements were positive for epithelial membrane antigen (EMA), and there weren´t reactivity for thyroglobulin, calcitonin and CD34. The final diagnosis was SETTLE.
Conclusion(s) We considerer that this tumor should be differentiated from other thyroid tumors and in particular from malignant neoplasm for example: CASTLE, malignant teratomas and synovial sarcoma.

P3.159
Angio-architectonics and prognosis of laryngeal squamous cell carcinoma

Lushnikov E.; Gorban N.
Medical Radiological Research Center, Obninsk, Kaluga, Russian Federation

Background Clinical course and prognosis of laryngeal carcinoma are dependent on various factors including tumor angiogenesis. Objective. To investigate a correlation be-

tween angio-architectonics of laryngeal carcinoma and clinical course, character of pathomorphims after treatment, and prognosis.

Methods As a material we used biopsies from laryngeal invasive squamous carcinoma in 61 patients (aged from 34 to 77 years old) treated at the Medical Radiological Research Center RAMS. Microvessel density, total vascular perimeter, and cut square of vessels were assessed based on the Factor FVIII immunoexpression of endothelial cells. Comparative analysis of angio-architectonics was made in tumors of different stage, level of differentiation, metastasizing properties, character of pathomorphism, and tumor relapse after treatment. Survival analysis was made by Kaplan-Meier Test, significance of differences were confirmed by Cox''F Test.

Results Level of vascularization and peculiarities of blood vessels morphology influenced on a possibility of tumor relapse after treatment, on overall and disease-free survival. High level of vascularization of tumor and dendritic type of blood vessels morphology were favourable prognostic factors. Microvessel density (less than 17) and perimeter of vascular wall were associated with high risk of tumor relapse, and low overall and disease-free survival. Vascular cut square did not influence clinical and biological behavior of tumors. Level of post-treatment pathomorphism was not dependent on peculiarities of angio-archirectonics of laryngeal squamous cell carcinoma.

Conclusion(s) Angio-architectonics could be used as a factor of clinical course and prognosis of laryngeal squamous cell carcinoma.

P3.160

Clinicopathological features and immunohistochemical markers in neurofibroma of the oral cavity

Fontes A.; Campos Sampaio M.; Marocchio Sassa L.; Nunes Daumas F.; Sousa Cantanhede Orsini Machado S.
University of Sao Paulo, Sao Paulo, Brazil

Background To review clinical, histopathological and immunohistochemical features of 16 isolated Neurofibromas (NFs) of the oral cavity, and also provides insights to help in its differential diagnoses.

Methods Clinical and histopatological features of 22 oral NFs were obtained and reviewed. Immunohistochemical reactions included S-100, CD-34, GLUT-1, EMA, Ki-67, p53 and Colagen IV. Histochemical reactions for Alcian blue were also performed.

Results Clinically, the preferential location was the maxillary bones, tongue and buccal mucosa, affecting more women. Microscopically, uniformly distributed spindle-shaped cells with elongated, ovoid and thin nuclei and scant cytoplasm were seen. Immunostaining revealed that the tumor cells weakly expressed GLUT-1, ColIagen IV, Ki-67 and p53. They were variably positive for CD-34, S-100 protein, membrane epithelial antigen (EMA). Positive histochemical reaction for Alcian blue was observed.

Conclusion(s) The different types of nerve sheath cells observed reinforce the hypothesis of the heterogeneous cell population in NFs. The strong positivity for S-100 suggests that the lesions were most composed by S-100-positive Schwann cells than other cells. The low immunostaining for p53 and Ki-67 can indicate that NFs massively composed by S-100-positive Schwann cells present low potential of aggressiveness and malignant transformation.

P3.161

Correlation between dysplasia and ploidy status in oral potentially malignant disorders

Van Zyl W.A.; Langenegger E.E.; Van Heerden B.M.; Boy C.S.; Van Heerden F.W.
University of Pretoria, Pretoria, South Africa

Background Potentially malignant disorders (PMD) is a group of oral disorders of which some are associated with squamous cell carcinoma development (SCC). Histological grading of dysplastic lesions is currently the method of choice to predict the risk of SCC development in PMD. The purpose of this study was to correlate epithelial dysplasia of PMD with the ploidy status.

Methods All cases of PMD were retrieved from the archives of the Department of Oral Pathology and Oral Biology, University of Pretoria, and graded as mild, moderate or severe dysplasia according to the WHO criteria. Thirty cases of each group were selected for flow cytometry analyses. Flow cytometry was performed on four 50 μm sections of the formalin-fixed paraffin-embedded tumour blocks using a DAPI solution to stain the nuclei. A Partec PAS II flow cytometer equipped with a 100 W mercury lamp was used for ploidy analysis. A minimum of ten thousand cells were counted in each case.

Results Aneuploidy was found in 13% of mild, 40% of moderate and 50% of severe epithelial dysplasia cases.

Conclusion(s) Aneuploidy determination by high resolution flow cytometry may be a marker to predict biological behaviour in PMD and can be an additional tool in determining the prognosis of oral dysplastic lesions.

P3.162

Evaluation of lymphangiogenesis in premalignant conditions of the head and neck mucosa

Palomba A.; Gallo O.; Brahimi A.; Franchi A.
Azienda Ospedaliera Universitaria Careggi, Firenze, Italy

Background The purpose of this study was to determine whether lymphangiogenesis occurs in the early steps of cancerogenesis of the upper aerodigestive tract mucosa, in the transition from normal mucosa to dysplasia to invasive carcinoma.
Methods We immunostained 18 specimens of normal mucosa, 38 precancerous lesions, and 3 microinvasive carcinomas with the lymphatic marker D2-40. In each sample we determined the number of lymphatics per unit area (lymphatic vessel density, LVD) and the percent area occupied by the lymphatic vessels (lymphatic vascular area, LVA) by computer-assisted morphometric analysis. The results were compared with those obtained in 60 samples of invasive squamous cell carcinoma.
Results No significant difference was observed between normal mucosa,hyperplasia/ mild dysplasia (n=28), moderate/severe dysplasia (n=10), and microinvasive carcinoma in terms of LVD (p=0.9) and of LVA (p = 0.3). Similarly, no significant difference was observed for both LVD and LVA according to the site of biopsy (larynx vs. pharynx vs. oral cavity, p = 0.7 and p = 0.3, respectively). Considering risk factors, there was no significant association with smoking history (p = 0.1 for LVD and p = 0.7 for LVA), whereas LVA was directly associated with alcohol consumption (p = 0.005). Finally, invasive carcinomas presented a significantly higher LVD than normal mucosa, precancerous lesions and microinvasive carcinoma (p<0.001), while no difference was observed for LVA (p=0.9).
Conclusion(s) Lymphangiogenesis does not occur in premalignant lesions of the upper aero-digestive tract. At variance with the process of angiogenesis, lymphangiogenesis is a late event associated with the development of an invasive phenotype.

P3.163
Extraosseous aneurysmal giant cell lesion of the neck

Bayol U.; Vardar E.; Arikan Etit D.; Cumurcu S.
Izmir Tepecik Training and Research Hospital, Izmir, Turkey

Background Aneurysmal bone cyst (ABC) is a benign tumor of bone. Histologically, it is composed of blood-filled cystic spaces separated by fibrous septa that contain an admixture of fibroblasts, variable numbers of osteoclast-type giant cells, and reactive woven bone. ABC may arise de novo or areas resembling ABC can be found in other benign and malignant bone tumors that have undergone secondary cystic change. ABC developing in soft tissue is extremely rare. Giant cell tumors (GCT) of soft tissue resembling osseous GCTs are uncommon but distinct entities. Both ABC and GCT may overlap and ABC may hide GCT radiologically and histologically. They both can recur locally malignant transformation is extremely rare. Here we present an extraosseous aneurysmal giant cell lesion of the neck.
Methods A 78 year-old-male patient presented with a recurrent mass in the left submandibular region.
Results Light microscopy showed a lesion neighbouring the salivary gland continues with skeletal muscle and adipous tissue composed of a bony structure surrounding a multicystic central area made up of anastomosing cavernous blood channels separated by fibrous septa that contained osteoid like material and osteoclastic giant cells that strongly reminiscing aneurysmal bone cyst.
Conclusion(s) This unique case is presented with clinical and histologic findings that could be either an ABC or a GCT of soft tissues as the first case in the literature to our knowledge.

P3.164
Extremely rare lesion “a tongue cyst containing granules of saprophytic actinomycetes”. A case report

Kubota N.; Hori M.; Tsukinoki K.; Dohi M.; Kubota E.
Kanagawa Dental College Hospital, Yokosuka, Kanagawa, Japan

Background Actinomyces israelii, which causes actinomycosis, is known to grow saprophytically in oral cavity. We report a case of tongue cyst containing granule of saprophytic actinomycetes in the lumen.
Methods A 64-year-old woman visited our hospital with a chief complaint of a mass of the tongue. Under the diagnosis of benign tumour, the mass was resected. Sectioning of the resected specimen revealed an 4 mm cystic lumen filled with some spherical structures. Histopathological examination showed a cyst wall composed of fibrous connective tissue and lined with stratified squamous epithelium. The spherical structures were deeply stained with hematoxylin, and showed hypha-like structures, which were stained black with Grocott’s stain and were Gram-positive. There were no peripheral club-shaped structures seen, nor inflammatory cells observed. Immunohistochemical staining suggested that the lining epithelium was not derived from salivary duct epithelium.
Results These findings led to the diagnosis of a tongue cyst containing granules of saprophytic actinomycetes in the lumen.
Conclusion(s) It is well known that actinomycetes are saprophytes in the oral cavity, and cause actinomycosis. They sometimes inhabit palatine tonsillar crypts and other sites in a saprophytic manner, proliferate, and form sulfer granule. Some views hold that lesions involving these granules of saprophytic actinomycetes represent saprophytic actinomycosis. The present lesion is consistent with this concept. We speculate that actinomycetes proliferated saprophytically in the lumen of a pre-existing cyst, forming sulfer granule. The absence of previous reports of similar cases makes this an extremely rare condition.

P3.165

High risk human papillomavirus infection and p16INK4a protein expression in oral and oropharyngeal cancer in non-smoking and non-alcoholic patients

Laco J.; Vosmikova H.; Novakova V.; Celakovsky P.; Dolezalova H.; Tucek L.; Ryska A.
Charles University Faculty of Medicine, The Fingerland Department of Pathology, Hradec Kralove, Czech Republic

Background To investigate high-risk human papillomavirus (HR-HPV) infection in non-smoking and non-alcoholic patients with oral (O-SCC) and oropharyngeal (OP-SCC) squamous cell carcinoma.
Methods A total of 24 O-SCC and 22 OP-SCC were analyzed by immunohistochemistry for p16INK4a protein (p16) expression and by chromogene in situ hybridization (CISH) and polymerase chain reaction (PCR) for HR-HPV DNA presence.
Results The p16 expression was detected in 7/24 (29%) O-SCC and in 22/22 (100%) OP-SCC. Using CISH, HR-HPV DNA was observed in 6/24 (25%) O-SCC and in 21/22 (95%) OP-SCC. HR-HPV DNA was found in 2/24 (8%) O-SCC and in 18/22 (82%) OP-SCC by PCR. OP-SCC showed significantly higher tumor grade (p=0.0005), more frequent lymph node involvement (p = 0.0063), higher p16 expression (p< 0.0001) and more frequent HR-HPV DNA presence using both CISH and PCR (p<0.0001), when compared to O-SCC. The sensitivity and specificity of p16 expression for HR-HPV DNA presence were 0.96 and 0.84 when compared to CISH and 1.00 and 0.65, when compared to PCR. The sensitivity and specificity of CISH for HR-HPV DNA presence compared to PCR were 1.00 and 0.82.
Conclusion(s) Our results confirm a definite ethiologic role of HR-HPV in pathogenesis of OP-SCC, which are characterized by higher tumor grade and tendency for lymph node dissemination. Supported by Research project of the Ministry of Health of the Czech Republic No. 00179906.

P3.166

Juvenile psammomatoid ossifying fibroma of the mandible. A case report

Balis Christos G.; Vladika N.; Xirou P.; Vahtsevanos K.; Ntomouchtsis A.; Patakiouta F.
"Theagenion" Cancer Hospital, Thessaloniki, Greece

Background Juvenile ossifying fibroma is a rare, benign, but potentially aggressive fibro-osseous tumour of the craniofacial bones.
Methods A 33-year-old male patient, presented with a 3 year slowly expansile lesion of the left side of the mandible. Facial asymmentry was clinically evident. The CT scan revealed a cystic lesion of the mandible, measuring 7,5x6,5 cm, containing bony septums. Incisional biopsy was followed by surgical resection of the mass via hemimandibulectomy. Reconstruction was performed with titanium plate 2,7 and costochondral graft from the 6th rib.
Results Grossly a well circumscribed tumor, measuring 9x6,5x6 cm, of white-tan colour and bony consistency, containing multiple cystic spaces, with hemorrhagic content, divided by fibrous or bony septums. Histological features of the tumour were consistent with Juvenile Psammomatoid Ossifying Fibroma. The surgical excision was complete.
Conclusion(s) Juvenile Psammomatoid Ossifying Fibroma is a benign neoplasm, commonly affecting the maxilla but also other bones including the mandible. Microscopically is characterized by a fibroblastic stroma containing small ossicles resembling psammoma bodies. The stroma varies from being loose and fibroblastic to intensly cellular with minimal intervening collagen. Treatment consists of complete surgical removal. Incomplete excision has been associated with a high local recurrence rate. Our patient remains alive and well 9 months after surgical treatment, without evidence of residual disease.

P3.167

Oncocytic lipoadenoma of the right parotid gland

Yaegashi H.; Sakuma T.; Endo Y.; Ono S.; Takayama K.; Tomichi N.
Iwate Prefectural Central Hospital, Morioka, Iwate Prefecture, Japan

Background Oncocytic lipoadenoma of salivary glands is an extremely rare benign neoplasm. So far only 3 cases have been reported in English literature.
Methods We report a case of oncocytic lipoadenoma in the right parotid gland occurring in a 50-year-old man who was admitted to the hospital with a 2-year history of slowly growing soft mass. CT and MRI showed a 4-cm mass in a superficial lobe with a relatively clear margin and heterogenous signals. A right partial parotidectomy was performed.
Results Macroscopically, the mass was well circumscribed, measuring 5 x 3.5 x 3 cm. Histologically, it was surrounded by a thin fibrous capsule, and was composed of an admixture of mature adipose tissue and oncocytic glandular elements with focal sebaceous change. The mature adipocytes accounted for approximately half of the tumour area. The oncocytes were diffusely positive for CAM5.2, cytokeratin (CK)5/6, CK14, CK18 and 34βE12, and coarsely positive for CK7 and AE1/AE3. In addition, a small number of cells of the basal layer showed strong reactivity with CK5/6, CK14 and 34βE12, indicating basal differentiation. EMA highlighted the luminal surface of the oncocytes, whereas their cytoplasm was negative. Alpha-SMA, CD10 and p63 were negative, indicating a lack of myoepithelial differentiation. Only the adipocytes in the mature adipose tissue were positive for S-100 protein.

Conclusion(s) Our case is the fourth reported case of oncocytic lipoadenoma of the salivary glands. Immunohistochemistry suggested that oncocytes had luminal and basal differentiation, and that neoplastic glandular elements were homologous with striated ducts.

P3.168
Post-transplant lymphoproliferative disordes of oral cavity: a case report

Saracibar Nieves M.; Caton Blanca M.; Etxegaray Leire M.; De Diego Julia M.
Santiago Apostol, Vitoria-Gasteiz, Alava, Spain

Background Post-transplant lymphoproliferative disorders (ptld) are abnormal proliferation of lymphocytes in the inmunocompromised host following transplantation. Ptld is most often seen in the gastro-intestinal tract and very rarely in the oral cavity. Most of them are of b-cell origin, related with Epstein-Barr virus infection, and behaved as malignant lesions if left untreated.
Methods Clinical case: a 59 year-old woman was referred to the department of oral and maxillofacial surgery for evaluation and treatment of a mass on the tongue. She had undergone a kindney transplant 15 years before. She was treated with azathioprima for 20 years.
Results Microscopic examination revealed a large ulcerated and hyperplastic neoplastic proliferation of lymphoreticular origin, composed of a dense and tightly packed hyperchromatic pleomorphic cells including large lymphocytic plamacytoid and inmunoblastic cells. Immunohistochemical stains revealed positivity with cd20, cd79a, pax 5, cd3, cd30, lmp-1, and eber.
Conclusion(s) Ptld was first reporter by starzl in 1968 in renal transplant recipients. The frecuency range from 1%-10% depending on the organ transplanted. Lesions in the oral cavity may present sinply as swellings with or without symptoms. A reduction in inmunosupression is the most common management strategy. Dental specialist must always maintain a high level of suspicion to rule out ptld as intraoral masses in a setting of chronic inmunosupression to treat them properly.

P3.169
Primary malignant melanoma of the parotid gland: a case report and review of the literature

Malta F.; Tsinga A.; Theofanous E.; Takou A.; Argyriou P.; Savvani A.; Prigouris P.; Kouvidou C.
Evangelismos General Hospital, Athens, Greece

Background Malignant melanomas of the parotid gland are relatively uncommon. They occur almost invariably as metastases from a primary tumour located in the region of scalp, or mucous membranes of the nose, paranasal sinuses or throat. Primary malignant melanomas are extremely rare.
Methods We report a 80-year old woman which presented to the Otolaryngology Department for a persistence, progressively enlarging, firm and fixed mass in the parotid gland. B-scan ultrasonography showed a parotid neoplasm diagnosed as carcinoma by fine-needle aspiration. The patient treated by total parotidectomy with excision of the skin.
Results The histology revealed a low differentiation neoplasm with morphological features compatible with malignant melanoma. The immunohistochemical expression of S100, Melan A, HMB45 and Micropthalmia trancriptor factor confirmed the diagnosis. A reprospective search for a primary melanocytic lesion was negative and the melanoma was considered as primary in the parotid gland. Despite radiotherapy for brain metastases and adjuvant chemotherapy for lung and lymph nodes metastases, she died 16 months after the initial operation.
Conclusion(s) The majority of previously reported cases appear to represent metastatic lesions, often from cutaneous head and neck primaries. Primary malignant melanomas is assumed that they originate in the glandular tissue or in the intraglandular lymph node. The existence of melanocytes in the interlobular duct of the parotid gland has also been reported. The effectiveness of adjuvant treatment such as radiotherapy, chemotherapy or immunotherapy remains controversial.

P3.170
Primary sinonasal choriocarcinoma

Bell D.; Luna Armando M.
MD Anderson Cancer Center, Houston, Texas, USA

Background Choriocarcinoma usually arises in the uterus and gonads. However, it can also occur in extragonadal locations such as mediastinum,sacroccocygeal region and pineal gland. Primary sinonasal chroriocarcinoma, to the best of our knowledge, has not been previously described.
Methods We report two cases of primary sinonasal choriocarcinoma.
Results Two male patients of 45 and 49 years of age complained of epixtasis and nasal obstruction of several months duration. CAT scan of the sinuses revealed opacity of the left nasal cavity and ethmoid sinus in one patient and a destructive lesion of the maxillary sinus in the other. Histologically the lesions exhibited cytotrophoblastic and syncytiotrophoblastic cells in a hemorrhagic background. The tumor cells expressed panCK and beta-chorionic gonadotrophin (HCG). They were negative for OCT4, AFP, S-100 protein and pan melanin. CAT scan of the

abdomen and thorax were negative. Testicular ultrasounds were negative. The serum levels of HCG were 20,000 and 13,000 mIU/ml respectively. One patient, treated with maxillectomy, neck dissection and postoperative radiotherapy followed by 5 course of VIP chemotherapy (cisplatinum, etoposide, ifosfomide), died with brain metastases 13 months after diagnosis. The other patient received only VIP chemotherapy, and he is alive, with tumor, 7 months after diagnosis.

Conclusion(s) These cases demonstrated the widespread distribution of germ cell tumors in the human body and lead to further support of the existence of primary choriocarcinomas in the sinonasal tract. Correct identification of this neoplasm is therefore important for institution of specific therapy.

P3.171

Proliferative verrucous leukoplakia: lack of association with human papillomavirus (HPV) and Epstein-Barr virus (EBV) infection

Hakim S.; Moyano S.; Caballero M.; Diaz A.; Bailon E.; Ordi J.; Nadal A.; Cardesa A.; Alos L.
Department of Pathology, Hospital Clinic, IDIBAPS, University of Barcelona, Spain

Background Proliferative verrucous leukoplakia (PVL) is a rare form of oral leukoplakia with a high risk to malignant transformation. Its aetiology is still unknown. We have studied a series of PVL to evaluate the possible relationship with oncogenic viruses including human papillomavirus (HPV) and Epstein-Barr virus (EBV).

Methods Nine patients diagnosed of PVL were retrospectively evaluated. The clinicopathological features were analyzed. Tissues were tested by PCR using the SPF10 primer to detect HPV DNA, and by in situ hybridization for mRNA of EBER1/2 gene of the Epstein-Barr virus (EBER). Immunohistochemical studies for p16 INK4a and p53 were also performed.

Results The patients (six female, three male) presented a mean age of 62 years (range 37–74). The gingiva was the most common site of PVL, followed by floor of mouth and palatal mucosa. Eight of nine cases (89%) progressed to carcinoma. The neoplasms developed more frequently in the jaws and tongue. Six patients (75%) presented conventional squamous cell carcinomas and two (25%) developed both conventional and verrucous carcinomas. All the lesions were negative for HPV and EBV. Immunohistochemistry for p16INK4a was negative in all cases, whereas p53 was positive in 2 of 9 cases (22%).

Conclusion(s) PVL is a distinct form of leukoplakia that usually presents in women older than 50. It is an aggressive oral lesion that tends to progress to multifocal squamous cell carcinoma, and lacks association with HPV and EBV infection.

P3.172

Solitary intramedulary plasmacytoma of the skull temporal bone mimicking aggressive meningioma: a case report

Adouni O.; Chelly I.; Boujelbène N.; Ben Hamouda K.; Mekni A.; Azouz H.; Nfoussi H.; Tangour M.; Khaldi Mohamed M.; Haouet S.; Zitouna M.; Kchir N.
Departement of Pathology La Rabta Hospital, Tunis, Tunisia

Background Intracranial plasmacytomas are rare and infrequently diagnosed by imaging due to their resemblance to the more common meningioma. We present a patient presenting with an intracerebral mass mimicking a meningioma on MRI.

Methods A 70-year-old woman consulted for a frontotemporal tumefaction becoming painful with speech disturbance and crural monoparesis. MRI revealed a left temporal extra-axial mass with a dural tail mimicking meningioma. The patient underwent craniotomy and partial resection of the mass.

Results Histology revealed sheets of plasma cells with mild atypia and occasional mitotic figures. Immunohistochemistry demonstrated the plasma cells to be positive for CD 138 and CD 79a with kappa light chain restriction. Search for multiple myeloma was negative.

Conclusion(s) Solitary intracranial plasmocytomas are rare tumors which can involve the skull, meninges or brain. According to the origin of neoplastic cells, the solitary plasmacytomas are subdivided into solitary bone and extramedullary plasmacytoma. The solitary bone plasmacytoma derives from bone marrow and is characterized by bone erosion. The differential diagnosis of an intramedullary plasmacytoma includes meningioma, which has a similar MRI appearance. The final diagnosis is based on the histopathologic and immunohistochemical examination. Intracranial plasmocytomas require a differential approach and a meticulous examination since the presence or absence of multiple myeloma radically affects prognosis. The gold standard of treatment for plasmocytoma is its total removal and adjuvant radiation therapy. A large extra-axial mass with an important lytic lesion should have led to the diagnosis of plasmocytoma.

P3.173

Undifferentiated stratified epithelium of nasal mucosa as a universal transitional form of nasal epithelium in its reparative and pathological regenerations

Ivanova Nikolaevna O.
Institute for Sorption and Endoecology Problems (National Academy of Sciences of Ukraine), Kiev, Ukraine

Background The role of undifferentiated stratified epithelium (USE) in regeneration of nasal mucosa is not

sufficiently investigated. This research is focused on nasal epithelial regeneration in chronic rhinitis patients, liquidators of consequences of the Chernobyl Disaster.

Methods Ninety-three biopsies taken for diagnostic reasons from nasal mucosa of patients with chronic rhinitis – average residents of Kiev (group I, $n=40$) and liquidators of the Chernobyl accident consequences (group II, $n=53$) – were examined by light-microscopic histochemistry and transmission electron-microscopy.

Results In both groups, the successive nidal degeneration, alteration, necrosis and desquamation of pseudostratified ciliated epithelium and uncovering the basal membrane were observed. Reparative regeneration of epithelial defect commenced with formation of flattened cell monolayer later replaced with 3–4-layer cuboidal transitional USE. The latter was replaced with pseudostratified ciliated epithelium if the pathogenic factor had been eliminated (a similar process is observed after mechanical injury of nasal mucosa and in nasal epithelial differentiation in embryogenesis). In the case of pathological regeneration (chronic inflammation or strong damaging factor), the USE was replaced with stratified squamous metaplasia (I - 7%; II - 62%), stratified cuboidal metaplasia (I - 33%; II - 73%), with fibrovascular papillae (I - 20%; II - 70%), or the joint presence of these characters (I - 7%; II - 49%).

Conclusion(s) USE is universal transitional form in both reparative and pathological regenerations of nasal epithelium. Reparative regeneration of nasal epithelium recapitulates its prenatal development.

P3.174

Analysis of aurora-A and aurora-B expression in human glioblastomas. Clinicopathological correlations

Samaras V.; Stamatelli A.; Samaras E.; Arnaoutoglou C.; Arnaoutoglou M.; Stergiou I.; Konstantopoulou P.; Varsos V.; Karameris A.; Barbatis C.

Department of Histology and Embryology, National and Kapodistrian University of Athens, Medical School, Athens, Greece

Background In the present study, we targeted at a comparative immunohistochemical analysis of aurora-A and aurora-B expression in forty patients with glioblastomas, attempting to identify any association with Ki-67 index and patients' clinical features. The impact of various treatment modalities and proliferative activity in patients' outcome was also assessed.

Methods Immunohistochemistry in formalin-fixed and paraffin-embedded tissue sections was utilized.

Results Aurora-A expression was higher in tumors demonstrating high Ki-67 expression ($p=0.01$) and was positively, though marginally, related to aurora-B expression ($p = 0.085$). Aurora-B expression was not linked to Ki-67 expression ($p = 0.182$). Lower aurora-A immunohistochemical expression, chemotherapy administration and tumors localization in one lobe of the brain implied a greater probability of patients' survival, in univariate analysis ($p = 0.044$, $p = 0.008$, $p = 0.041$, respectively). Ki-67 and aurora-B immunoreactivity were not associated with patients' survival ($p = 0.918$ and $p = 0.539$, respectively).

Conclusion(s) To our knowledge, for the first time the association between aurora-A and aurora-B expression, the correlation of aurora-A with Ki-67 index and the prognostic impact of aurora-A expression were assessed in glioblastomas. Though we addressed a prognostic connotation of aurora-A, we suggested a complicated role of aurora-A and aurora-B within glioblastomas, mandating further examination in larger series so as definite conclusions to be drawn.

P3.175

Angiogenic and lymphangiogenic microvessel density in recurrent pleomorphic adenoma

Soares Borges A.; Altemani A.; Araújo Cavalcanti V.

São Leopoldo Mandic Research Center, Campinas, São Paulo, Brazil

Background Recurrent pleomorphic adenoma (RAP) is an uncommon and challenging disease. The aim of this study was to determine if there is a difference between RAP and the pleomorphic adenoma (PA) without recurrence related to tumor blood and lymphatic vascularization. Moreover, we compared the microvessel density (MVD) between cell-rich areas (predominance of epithelial cells) and cell-poor areas (predominance of myxoid and chondroid areas) of the stroma of PA and RPA. In addition, immunohistochemical staining for the Ki-67 antigen was conducted simultaneously to evaluate cell proliferation in PA and RPA.

Methods 19 cases of PA and 24 cases of RPA, blood and lymphatic vessels were analyzed by immunohistochemical technique using the antibodies CD34, CD105, D2-40 and Ki-67.

Results Comparing no-recurrent with recurrent tumor, no significant difference was found in terms of lymphatic vascular density, microvessel density and proliferation index. When MDV and proliferation index were compared to different areas in cellular composition (cell-rich and cell-poor areas) there was a significant difference in the PA, as well as, in RPA.

Conclusion(s) This study shows that although RPA presents more aggressive clinical behavior than PA, there is no difference between tumor blood and lymphatic vascularization, suggesting that there is no correlation between vascularity and risk of recurrence. Furthermore,

vascularized stroma in PA as well as RPA, depends on the proportion of the cellular composition.

P3.176

Apoptotic signaling in oral squamous cell carcinoma and association with clinicopathological characteristics

Coutinho-Camillo Malheiros C.; Lourenco Vanessa S.; Kowalski Paulo L.; Soares A.F.
AC Camargo, Sao Paulo, Brazil

Background Oral cancer holds the eighth position in the cancer incidence ranking worldwide and oral squamous cell carcinoma (OSCC) implies quite significant mortality and morbidity rates. Apoptosis is a genetically programmed form of cell death and aberrations of the apoptotic mechanisms that cause excessive or deficient programmed cell death have been linked to a wide array of pathologic conditions.
Methods In this study, using a Tissue Microarray (TMA) comprising 229 cases of OSCC, we have analyzed the immuno-expression of Apaf1, cytochrome c, caspase 9, Smac/DIABLO, survivin and p53. The results were quantitatively analyzed using an automated imaging system (ACIS III) and statistical analyses were performed by the Mann-Whitney test.
Results Downregulation of Apaf1, caspase 9 and survivin was associated with the presence of vascular invasion (p= 0.0019, p = 0.0560, p = 0.0368, respectively). Expression of caspase 9 was also associated with tumor occurring in the floor of mouth (p = 0.0078). Survivin expression was also associated with moderately/well differentiated tumors (p = 0.0096) and with tumor occurring in the floor of mouth (p = 0.0097). Smac/DIABLO, cytochrome c and p53 proteins were not significantly associated to any of the clinicopathological characteristics analyzed. Overall survival probabilities were not statistically different between the cases presenting low or high expression of the proteins studied.
Conclusion(s) Our results showed the involvement of apoptotic proteins in OSCC tumorigenesis and suggest that the expression of apoptotic molecules might be used as a prognostic indicator in oral squamous cell carcinoma.

P3.177

Chondromyxoid fibroma of the head with unusual calcifications. Report of two cases

Wang B.; Morris L.; Rihani J.; Lebowitz R.; Yuan S.; Steiner G.
New York University School of Medicine, New York, NY, USA

Background Chondromyxoid fibroma (CMF), a rare benign tumor, usually affects metaphyses of long bone in childhood. Rarely, CMF occurs in skull base, parasinuses, and mandible, which may be difficult to distinguish from chondrosarcoma or chordoma. We report 1 case of CMF involving sphenoid sinus mimicking a chondrosarcoma and 2nd case involving a recurrent lesion in mandible. Both cases were calcified on images and histology.
Methods Medical records, clinical manifestations, radiographic imaging, and pathologic slides of 2 CMF cases were reviewed. The extent literature was systematically reviewed. Case 1: 52 year-old female complained vertigo. CT scan showed a 2 cm heterogeneous calcified mass within the left sphenoid sinus, protruding into the left nasal cavity. Differential included a chondrosarcoma. Case 2: 50 year-old male presented a 3 cm right mandibular mass with dense paresthesia, at the site of previous excision for a cementifying fibroma 23 years ago.
Results Both Case 1 and 2 were diagnosed as Chondromyxoid Fibroma. Immunostains for 2 cases reveal that tumor cells were positive for Vimentin and SMA, but negative for S-100, CD34, Cytokeratin AE1/AE3 and EMA. Follow up: Case 1 patient is doing well (lost F/U on case 2).
Conclusion(s) Although CMF rarely affects in head region, it can mimic a chondrosarcoma or chordoma on both imaging and morphology. It can be calcified. One should always be aware of this entity to avoid unnecessary over diagnosis and treatment.

P3.178

Correlation of microvessel density and proliferation index in undifferentiated nasopharyngeal carcinoma

Taweevisit M.; Thorner S.P.
Chulalongkorn University, Pathumwan, Bangkok, Thailand

Background Undifferentiated nasopharyngeal carcinoma (UNC) is a highly malignant tumor with an endemic distribution. Both proliferation index (PI) and microvessel density (MD) are commonly determined on such tumors; however, the relationship between these two parameters has not been well studied.
Methods To determine the association between MD and cellular proliferation in UNC, the authors studied a series of 60 cases in patients of Southeast Asian origin. Cellular proliferation was determined by Ki67 immunostaining and vessel proliferation by CD31 immunostaining based on areas of increased staining (‘hot spots’). Ki67 results were scored on a scale of 0-4+ and CD31 results as a microvessel density/mm2.
Results The mean of the MD in the Ki67-negative group (25 cases) was 22/mm2, whereas in the Ki67-positive group

(35 cases) the mean was 35/mm2, a difference that was statistically significant ($p<0.001$). Moreover, MD significantly increased as the Ki67 score increased ($p<0.001$). However, the 'hot spots' for MD did not correspond in tissue sections to areas of increased cellular proliferation.
Conclusion(s) Because of the significant association between PI and MD, it may be practical for pathologists in routine practice to determine only one of these two prognostic factors when dealing with UNC. We suggest the PI, since this measurement is easier to perform and can be done on small biopsies that may not contain enough surface area for MD determination.

P3.179
D2-40 expression in salivary gland tumors

Giorgadze T.; Saqi A.; Pang C.; Eleazar J.; Miller E.L.; Rentz W.M.
Wayne State University, Detroit, Michigan, USA

Background D2-40 is a novel monoclonal antibody, well-established as a specific marker for lymphatic endothelium. D2-40 also highlights myoepithelial cells in the breast and is strongly expressed in skin adnexal tumors. We evaluated diagnostic utility of D2-40 immunostaining pattern in salivary gland tumors.
Methods Immunoreactivity of 60 neoplasms including 7 pleomorphic adenomas (PA), 2 monomorphic adenomas, 6 Warthin's tumors, 2 oncocytomas, 1lipoma, 5 mucoepidermoid carcinomas (MEC), 12 adenoid cystic carcinomas (AdCC), 6 polymorphous low-grade adenocarcinomas, 3 salivary duct carcinomas (SDC), 3 squamous cell carcinomas (SCC), 3 epithelial-myoepithelial carcinomas, 2 carcinomas ex pleomorphic adenoma, 3 acinic cell carcinomas, 1 poorly differentiated carcinoma, 1 diffuse large B-cell lymphoma, 1 metastatic melanoma, and that of adjacent non-neoplastic salivary gland (NNSG) was assessed. Immunostaining was evaluated as negative (< 1%), focally positive (1–10%), diffusely positive (> 10%).
Results D2-40 showed intense cytoplasmic immunoreactivity both in myoepithelial and cuboidal epithelial cells in 11/12 AdCC of different morphologic forms, and intense cytoplasmic staining of stellate cells in 3/7 PA. MEC (2/5) and SCC (1/3) showed a focal membranous pattern of immunoreactivity that was observed neither in AdCC nor in PA. SDC (1/3) demonstrated focal positivity only in myoepithelial cells surrounding the neoplastic ducts. All other tumors were consistently negative for D2-40 expression. Focal positivity in 7/37 NNSG was found in myoepithelial cells surrounding ducts and acini adjacent to the advancing tumor edge.
Conclusion(s) D2-40 is strongly expressed in AdCC and can be used in distinguishing AdCC from other salivary gland neoplasms with overlapping morphologic features.

P3.180
Demyelinisation process rate in adolescents

Filipovich Nicolaevich A.; Chapko Jakovlevich I.; Zagorskaya Vladimirovna T.
Research Institute of Medical Assessment and Rehabilitation, Minsk, Belarus

Background 4 groups of patients were distinguished: (1) latent phase (16.6%), (2) slow progradient phase (33.1%), (3) acute phase (35.4%) and (4) fast progradient phase (14.9%). Characteristic of group 1 were slight increase in MTA of blood serum, decreased CD4+ (33.9% compared to 40.1% in control) and increased CIC levels (94.65 optical units compared to 69.32 in control). In group 2 with MTA level as high as 22.1, clear decrease of T-lymphocyte, CD22+, CD4+ and CIC levels was noted, along increase in CD8+ level and weak induction of TNF-α. In group 3 MTA level was 40.2 units coupled with increased CD8+, IL-2P+, Ig G, A, M, TNF-α, IL-8 and CIC and decreased T-lymphocyte and CD22+ levels. In group 4 MTA level was as high as 79.3; high level of CD4+, CD8+, IL-2P+, IgG, I and CIC and low level of T-lymphocytes and CD22+ were noted.
Methods 127 multiple sclerosis patients 15 to 19 years old were examined. CT and MRI of cerebrum and spinal cord, conventional clinical methods, immunoassays and a patented radioimmunobiological assay for measuring the myelinotoxic activity (MTA) of blood serum and spinal fluid were used.
Results The MRI findings (decreasing T-1 W signal and increasing T-2 W signal) were diagnostically important in 91.4% of cases and the CT findings were important in 42.6% cases.
Conclusion(s) Measurement of blood serum MTA in combination with immunoassay and MRI findings helps to correctly estimate the rate of demyelinization in multiple sclerosis patients.

P3.181
Gum tissue remodelling in cases of chronic periodontitis and calcium hydroxide application

Morozov Anatoliyovich S.; Mudra Nikolayevna V.
Lugansk State Medical University, Lugansk, Ukraine

Background Acute and chronic inflammation in a pulp and a periodontium may result in inflammatory processes of maxillofacial area and a neck, complicate patient's diseases of internal organs and systems. Present investigation was designed to examine the effect of the calcium hydroxide treatment on the periapical healing in cases of chronic periodontitis.
Methods 50 volunteers were enrolled while receiving dental care. The main group included 40 patients. Their scheme of

the treatment included usage of calcium hydroxide treatment by Pro-root for the sealing of their cavities. 10 patients were treated by routine scheme without Pro-root treatment (group of comparison).
Results The results have shown favorable result of the filling of root canals with calcium hydroxide drugs. There were stimulation of periapical healing, osteogenesis and cementogenesis up to the full healing of the bone at most cases of Pro-root applications in cases of chronic periodontitis. These data support the idea that in teeth with chronic periodontitis, dressing of the root canal with calcium hydroxide is highly effective in arresting external inflammatory processes and root resorptions.
Conclusion(s) Calcium hydroxide considerably decreases the permeability of exposed dentin for the penetration of bacterial components towards the pulp. Calcium hydroxide stimulate the underlying pulp to form secondary dentin, which may seal off the tubules on the pulpal site of dentin. That is why a dressing of the root canal with calcium hydroxide suggestive to be performed in teeth with chronic periodontitis.

P3.182
Immunohistochemical study of myoepithelial cells during human salivary gland morphogenesis

Ianez Fraga R.; Lourenco Vanessa S.; Buim Cavicchioli M.; Soares A.F.
Hospital A C Camargo, São Paulo, SP, Brazil

Background Salivary gland morphogenesis is a process divided in initial bud, pseudoglandular, canalicular and terminal bud phases. During these phases differentiation of glandular components, including myoepithelial cells occurs. The presence of specific markers of these cells during glandular morphogenesis is not fully understood.
Methods Using immunohistochemistry, we evaluated the expression of smooth muscle actin (SMA), calponin, caldesmon, CD10, CD29, S-100 protein, glial fibrillary acidic protein (GFAP) and p63 in myoepithelial cells during salivary gland morphogenesis in order to understand the maturation process of myoepithelial cells and explore their possible use in the diagnosis of salivary gland lesions. For that, specimens of salivary glands dissected from human fetuses from 8 to 26th weeks of gestation (from natural miscarriages) were used. Adult salivary glands were considered as controls.
Results From canalicular stage of salivary gland morphogenesis, the protein p63 was colocalized with SMA, calponin, CD29 and S-100 protein in myoepithelial cells around the terminal sacs, immature acinar lobules and intercalated ducts. In adult normal salivary glands expression of these proteins was observed in myoepithelial cells. GFAP, CD10 and caldesmon were not detected neither during morphogenesis nor in adult salivary glands. The protein p63 was also detected in basal cells of the entire ductal system.
Conclusion(s) Myoepithelial cells could be identified from canalicular phase of gland morphogenesis. Smooth muscle actin, calponin, CD29, p63 and S-100 protein are good markers for myoepithelial cells, although not specific to this cell type.

P3.183
Lymphomas of salivary glands-case report and review of literature

Faur A.; Lazar E.; Cornianu M.; Dema A.; Lazureanu C.; Muresan A.
University of Medicine and Pharmacy "V. Babes", Timisoara, Timis, Romania

Background Lymphomas primary located in the salivary gland tissue are very rare and constitute about 2–5% of all salivary gland neoplasm.
Methods A study has been carried out for seven years on 204 cases of salivary gland tumors and only 2 cases (females, 71 and 49-years-old) of salivary gland lymphomas were diagnosed. The 4 μ-thick formalin-fixed paraffin-embedded tissue samples were stained with hematoxilin and eosin (HE). For the immunohistochemical analysis we used the antibodies: LCA (2B11, Dako), CD20 (L26, Dako), cytokeratin (MNF 116, Dako), p53 (DQ-7, Dako) and PCNA (PC-10, Dako).
Results Both tumors were composed of a diffuse proliferation of lymphoid cells with lymphoepithelial lesions. In the first case the lymphoid cells within and around the ducts are typically larger than the rest. Other lymphoid cells are small, medium-sized to large cells with a scant cytoplasm and atypical nuclei containing distinct nucleoli. In the second case we notice a great variability of number and morphology of the lymphocytes: large lymphoid cells with pleomorphic nuclei and prominent nucleoli, lymphoplasmacytic cells and multinucleated malignant lymphoid cells.
Conclusion(s) In the cases that we evaluated we demonstrated the lymphoid origin of the cells using LCA and the B-cell lineage with CD20. For the proliferation rate we used PCNA and p53. The histopathology and immunohistochemistry suggested in the first case a low-grade diffuse large B-cell mucosa associated lymphoid tissue lymphoma and in the second case a high-grade extranodal marginal zone B-cell lymphoma.

P3.184
Mesenchymal chondrosarcoma of the nasopharinx and acinic cell carcinoma of the parotid gland synchronous in a child

Amat Villegas I.; Lobo Moran C.; Zozaya Alvarez E.; Martinez Penuela M.A.; Beloqui Perez De Obanos R.; Mercado Gutierrez R.
Hospital de Navarra, Pamplona, Navarra, Spain

Background Up to our knowledge, this is the first case report of the coexistence of a nasopharyngeal mesenchymal chondrosarcoma (MC) and a parotid acinic cell carcinoma (AAC) affecting in our case an 11 year old girl.
Methods MC is a high grade sarcoma with an aggressive clinical behaviour and strong tendency toward late recurrences and distant metastases. Morphologically, it is a biphasic tumor constituted of undifferentiated small round cell areas intermixed with islands of hyaline cartilage. It typically occurs in young adults and the treatment usually requires excision with wide margins but frequently this is not feasible because of the specific anatomic location of the lesion.
Results AAC is an unusual malignant salivary gland neoplasm that mainly occurs in the parotid gland. The presence of cytoplasmic zymogen granules (PAS positive) is highly specific of this entity. Affected patients range from young children to adults. According to recent studies, pediatric malignant salivary gland neoplasms have a good prognosis.
Conclusion(s) We present the first case report of a MC associated to an ACC. The patient was an 11-year-old girl without previous medical records and was seen in our hospital because of a parotid mass, with the additional clinical finding of an asymptomatic pharyngeal lesion.

P3.185

Myoepithelial carcinoma ex pleomorphic adenoma showing an exophytic growth at the uvula of palate. Report of a case

Kaku T.; Ohuchi T.; Wada T.; Tateno M.; Uemura T.; Kobayashi H.
Helath Sciences University of Hokkaido, Ishikari-Tobetsu, Hokkaido, Japan

Background Carcinoma ex pleomorphic adenoma (Ca-ex - PA) is a malignant tumor that shows histological evidence arising in or from a benign pleomorphic adenoma. Myoepithelial carcinoma(MEC) is a rare tumor accounting for less than 1% of salivary gland neoplasms and is uncommon in carcinoma ex pleomorphic adenma and only a few cases are reported in the literature. In this report, we present a case of a myoepithelial ca-ex-PA of the uvula.
Methods Case report: A 63-year-old male was referred to a clinic of otorhinolaryngology for examination of a pedunculated mass hanging down from the uvla. The patient complained of mild disturbance when swallowing. MRI of the oral cavity and neck found a solid lesion arising from the uvula, 55x30x35mm in size with extension to the soft palate.
Results Carcinomatous tissue was made up of malignant myoepithelial cells, appearing as a mixture of atypical spindle and plasmacytoid cells, arranged in sheets, cords or nests of different sizes. The myoepithelial growth showed the features of local malignancy, infiltrating into the remainig adenomatous tissue. The mitotic figures were found but only a few. Immunohistochemical investigation showed that the carcinoma cells were positive for pancytokeratin, S-100 protein and p63 and so on. These data confirmed that the carcinoma cells were myoepithelial.
Conclusion(s) We present a case of MEC ex pleomorphic adenoma. The rarity of this case is related to both histogenesis from a pre-existing pleomorphic adenoma and location in the uvula.

P3.186

p53 decrease after drug exposure in squamous cell carcinoma from larynx and oral cavity

Fanni D.; Nemolato S.; Coni P.P.; Senes G.; Fanari M.; Massidda B.; Faa G.; Proto E.
Anatomia Patologica AOU Cagliari, Cagliari, Italy

Background Cancer treatment is currently empirical. Many evidences suggest that the same tumour in different patients may shows different chemosensitivity indeed. It would be useful to test selected anticancer drugs individually and predict the effect of chemotherapy, in order to achieve a higher response rate. Multiple in vitro tests have been developed over the past five decades. However, none of these tests has been applied clinically and no standard method has been established yet.
Methods Fresh specimens from larynx and oral cavity squamous cell carcinoma were incubated in an oxigenated medium for 30 min with cisplatin (at 75 µg/ml), docetaxel (at 35 and 100 µg/ml) and 5-fluroluacile (at 800 and 1000 µg/ml). Cases interpretation was performed by histological examination of H-E stained sections and by immunohistochemical analysis for p53.
Results Oedema, apoptosis and necrosis were the morphological modifications in drug-treated specimens from malignant tumor. In squamous cell carcinoma from larynx and oral cavity, immunoreactivity for p53 changed in vitro after cisplatin exposure and after docetaxel exposure; less relevant results were observed with 5-flurouracil exposure. Reactivity for p53 changed differently with different chemotherapeutic agents.
Conclusion(s) The significance of modification in p53 reactivity in tumor cells after drug exposure for a very short time could be in correlation with p53 status, which is considered a relevant factor in determining the efficacy of anticancer treatments.

P3.187

p63, E-cadherin/β-catenin complex and low molecular weight cytokeratins in basaloid squamous cell carcinoma of the larynx

Drougou A.; Tsopanomichalou M.; Lefantzis D.; Kefala M.; Vafiadis A.; Tsamouri M.; Papazoglou G.; Barbatis C.
Department of Pathology, Hellenic Red Cross Hospital 'Korgialenion-Benakion', Athens, Attiki, Greece

Background Basaloid squamous cell carcinoma (BSCC) is a rare aggressive variant of squamous cell carcinoma with male predominance. The diagnosis is based on morphological features and confirmed by the expression of low molecular weigh cytokeratins (LWCK) as detected by 34βE12. The purpose of this study is to investigate the connection of p63, a member of p53 family, predominantly localized in the basal layer of stratified epithelia, to the E-Cadherin/β-catenin complex and cytokeratins 14 and 19, as these molecules interact in other tumors.
Methods The immunohistochemical expression of the aforementioned molecules was studied in 12 laryngectomy specimens from 10 male and 2 female patients treated for BSCC in our hospital.
Results Strong p63 nuclear positivity of all tumor cells was present in 9/12 cases with concomitant expression of 34βE12, CK14, CK19 and reduced or lost membranous E-Cadherin/β-catenin complex. p63 negativity in 2/3 cases was correlated with cytoplasmic-nuclear translocation of β-catenin with marked reduction of E-Cadherin and minimal, focal CK14 positivity compared to diffuse expression in all other cases. CK19 expression was maintained in all cases.
Conclusion(s) This is the first study of β-catenin in BSCC and we observed similar reduction or loss of the complex to the reported data on poorly differentiated SCC. Despite the morphological basaloid features of all tumors we observed an aberrant p63 negative phenotype associated with loss of certain LWCKs and in some cases β-catenin abnormal overexpression. These findings need further investigation.

P3.188

Pleomorphic adenoma of the nasal septum: a case report

Cornianu M.; Lazar E.; Lazureanu C.; Faur A.; Costi S.; Cornea R.
Universitatea de Medicina si Farmacie Timisoara, Timisoara, Timis, Romania

Background Pleomorphic adenoma is the most frequent benign salivary glands tumors but unusual in the sinonasal region. Most of them arise in the nasal septum and the rest on the lateral nasal wall or turbinates. They may also occur in the minor salivary glands of the hard and soft palate.
Methods We present the case of a 53-year-old female who presented with right nasal obstruction, occasional epistaxis and facial pain. The radiological examination showed a polypoid tissue mass in the right nasal cavity. The 4 μ-thick formalin-fixed paraffin-embedded tissue samples were stained with hematoxilin and eosin (HE). For the immunohistochemical analysis we used the antibodies: cytokeratin, and S100 protein.
Results Histologically the tumor was characterized by an architectural rather than cellular pleomorphism, with a greater myoepithelial cellularity and a poor mixoid stroma. The myoepithelial cells were arranged in sheets, islands and trabeculae and were positive for S-100 protein.
Conclusion(s) The intranasal mixed tumor differs from its counterparts in the major salivary glands by a greater cellularity and less myxoid stroma. The rarity of mixoid stroma in intranasal mixed tumors has been cited as a pathologic reason for the low recurrence rate. Because of their unusual presentation, these tumors have been often misdiagnosed and treated in a more aggressive way that is necessary. Furthermore, if unilateral nasal obstruction is the main symptom for a patient, we suggest pleomorphic adenoma as a possible diagnosis.

P3.189

Post-traumatic inflammation in the lower jaw fractures and trombocytes gel application

Morozov Anatoliyovich S.; Gavrilov Alekseyevich V.
Lugansk State Medical University, Lugansk, Ukraine

Background Lower jaw fractures are one of the most frequently diagnosed pathology in the oral surgery practice. They are commonly complicated with inflammation of oral and facial soft tissues. In severe cases it may result in osteomyelitis. The aim of present study was to find out the effect of the thrombocytes membrane application in reduction of the inflammatory reaction in patients with the lower jaw fractions.
Methods Twenty-three patients with uncomplicated jaw fractures got the application of the thrombocytes gel as an additional method of treatment (main group). Thirty patients had the reposition and fixing of jaws fragments by the teeth fixating devices without application of the thrombocytes gel (group of comparison).
Results The findings presented the positive effect of the application of thrombocytes membrane developed from thrombocytes gel at the area of the lawyer jaw fracture under the mucosal and periosteum layers. Plasma rich with platelets filled the alveolus of the tooth (or teeth) extracted from the line of the fracture. The naked eye examination of the zone of trauma, clinical data, and radiological control of the patient's treatment results confirmed the acceleration of the bone repair.

Conclusion(s) The formation and maturation of a bone callous at the zone of the lower bone fracture may be related to the stimulation of the repair process by platelets growth factors.

P3.190

Primary diffuse large B-cell lymphoma of the oral cavity

Nfoussi Hamza H.; Chelly Ennaifer I.; Tangour M.; Azzouz H.; Turki A.; Adouni O.; Mekni A.; Boujelbene N.; Haouet S.; Kchir N.; Zitona M.
La Rabta, Ariana, Tunis, Tunisia

Background Lymphomas arising within the oral cavity account for only 3.5% of all oral malignancies. Diffuse large B-cell lymphoma is a non-Hodgkin lymphoma subtype characterized by diffuse proliferation of large neoplastic B lymphoid cells.
Methods Case report: A 67-year-old man was seen complaining of a painless lesion in his mouththat had been increasing in size for the past nine months. Extra oral examination revealed asymmetry and swelling of the left side of the face. Intra-oral exam showed a soft mass on the right side of the palate, containing some eroded areas. Computed tomography revealed destruction of the maxilla and zygomatic bone and invasion of soft tissue on the left side. There were no signs of the disease elsewhere in the body.An incisional biopsy was performed.
Results Histological exam revealed neoplastic sheets of lymphoid cells with a solid growth pattern. Individually, cells showed scarce cytoplasm and large nucleus. The malignant cells were immunopositive for CD20 and vimentine. CK, CD3 and S-100 were immunonegative.
Conclusion(s) Clinician should be aware of the diagnostic problems since a correct diagnosis is required to plan adequate treatment.

P3.191

Primary malignant melanoma of the conjuctiva. A case report

Skafida E.; Petrakopoulou N.; Glava C.; Grammatoglou X.; Tepelenis N.; Vasilakaki T.
Tzaneion General Hospital of Piraeus, Piraeus, Athens, Greece

Background Conjuctival melanoma is a rare condition with an incidence of 0,2 to 0,8 per million in white populations. It may arise without an apparent precursor lesion or it may be a sequela of a nevus or of so called “aquired melanosis”. Metastatic spread is very uncommon.
Methods A 60 year-old-female, otherwise healthy presented to our Hospital with a fifteen month history of a slow growing protruding massive pigmented tumor on the right eye. An excisional biopsy with wide margins followed.
Results Histological examination showed a prominent nesting of atypical melanocytes in the junctional region with invasion of the underlying substantia propria. Pagetoid extension into the overlying epithelium was noted. The tumor cells were epithelioid, showing pleomorphic nuclei, prominent nucleoli, atypical mitoses and abundant cytoplasm. There was loss of maturation of the deeply situated cells. The thickness of the tumor was 1.8 mm. Very near to the one surgical margin a region of primary acquired melanosis with atypia was seen. The immunohistochemical examination showed marked positivity of the tumor cells for HMB45 and S100p. No lymph nodes of the head and neck were palpable in our patient.
Conclusion(s) Malignant melanoma of the conjuctiva is a very rare lesion. It occurs in three clinical settings (in junction with a nevus, de novo and on the basis of PAM with atypia). Histopathologic findings associated with a poor prognosis include a tumor thickness of greater than 0,8 mm and involvement of the surgical margin.

P3.192

Primary malignant melanoma of the submandibular gland

Patsiaoura K.; Anagnostou E.; Tsantila I.; Karasmanis I.; Gougousis S.
Hippokration, Thessaloniki, Greece

Background Malignant melanomas are unusual tumors in the salivary glands, and most frequently represent metastatic lesions. Primary salivary gland melanomas are rare but well-described tumors, which exclusively refer to the parotid. Submandibular gland as a primary site of melanoma has not yet been reported.
Methods We report a case of a 70 year-old woman, which presented a rapidly-growing enlargement of the right submandibular area. Surgical excision of a mass, which merged from the submandibular gland was performed. This lesion had dimensions of 6.5x9x1.5 cm, it was solid and yellowish-tan.
Results Histopathologic analysis of sections from the lesion showed features of salivary gland. The presence of a neoplasm, in a peripheral position of the gland was noted, characterised by high cellularity. The neoplastic cells were relatively uniform. Their nuclei were round, pale-stained or clear with prominent nucleoli, while the cytoplasm was scant and eosinophilic. Immunohistochemical examination was positive to melan-A, HMB-45 and vimentin, while the lesional cells were negative to LCA, CD20, CD57, chromogranin, EMA, synaptophysin and cytokeratins AE1/AE3. These findings were consistent with malignant melanoma of the submandibular gland. Complete screening

excluded other possible primary tumor sites. The patient has no signs of recurrence 6 months after the tumor resection.
Conclusion(s) After extensive review of the literature, we demonstrated a single case of metastatic malignant melanoma in the submandibular gland but no case reports documenting primary melanoma in this specific site. This case further supports that this neoplasm can occur in virtually any anatomic location.

P3.193
Prognostic value of MAGE-3 and NY-ESO-1 expression in pharyngeal cancer

Sarcevic B.; Pastorcic-Grgic M.; Dosen D.; Knezevic F.
University Hospital for Tumours, Zagreb, Croatia

Background Studies on cancer-testis antigens (CTA) in head and neck squmous cell cancer are limited. Detection of CTA gene products by immunohistochemistry was only attempted in one study.
Methods This restrospective study included 90 patients with pharyngeal squamous cell cancer treated at the Department of Head and Neck Surgery of the University Hospital for Tumours between 1996 and 1999. TNM stage at the time of diagnosis, treatment, follow up and survival data were collected. Follow up for disease free patients was 5 years. Immunohistochemistry was done under standard conditions on tumour tissue of each patient embedded in paraffin blocks using monoclonal antibody 57B for the detection of multiple MAGE-A gene products and monoclonal antibody B9.8.1.1 for NY-ESO-1 detection.
Results MAGE-A gene products were detectable in 70.0% and NY-ESO-1 in 33.3% out of 90 patients with pharyngeal squamous cell cancer. No correlation was established between MAGE-A and NY-ESO-1 expression with TNM staging at presentation. Survival analysis showed a trend towards a shorter 5-year disease free survival in the group of patients bearing MAGE-A positive tumours. In contrast, a trend towards a prolonged five year disease free survival was observed in the group pf patients bearing NY-ESO-1 positive tumours.
Conclusion(s) According to the results, detection of MAGE-A gene products appears to be associated with poor prognosis, but NY-ESO-1 protein detection appears to represent a relatively favorable prognostic marker in the patients with pharyngeal squamous cell cancer.

P3.194
Rare tumour of the mandible: report of 3 cases

Soluk Tekkesin M.; Barut O.; Aksakalli N.; Olgac V.
Istanbul University, Institute of Oncology, Department of Tumour Pathology, Istanbul, Fatih, Turkey

Background Intraosseous lipoma is a rare benign bone tumour which originates from mature lipocytes.It accounts for approximately 0.1% of primary bone tumours.The most frequent localisation are calcaneus and the femur. 60% of it arises from long bones,skull and jaws 10%, pelvis %10 and rest from ribs,sacrum and spine.
Methods Case 1: A 33 year-old female patient was referred to oral surgery clinic for swelling in the right side of the mandible.A computed tomographic examination showed a well-circumscribed radiolucency with areas of calcification. Case 2: A 37 year-old female patient presented with a well-defined round radiolucency, 25–30 mm in diameter with a sclerotic border in the midline mandible.The lesion was asymptomatic, there was no expansion of the jaw. Case 3: The last patient was a 47 year-old female who had an osteolytic lesion in the anterior mandible was detected incidentally.
Results All of the lesions were treated with tumour resections under local anesthesia. Microscopically, the lesions were composed of primarily of mature adipocytes among thin trabeculae of lamellar bone. No evidence of hematopoietic tissue was detected,only normal-appearing bone marrow elements were present at the periphery of the lesion in case 1.Thin fibrous septa and capillary-like vessels occasionally were seen.
Conclusion(s) Only 15 cases of intramandibular lipoma have been reported since 1948. Clinically and radiographically, this rare and distinct entity is discriminated from central giant cell granuloma,simple bone cyst,some odontogenic cysts and focal osteoporotic bone marrow defect, whereas histologically, intraosseous well differantiated liposarcoma should be kept in mind.

P3.195
Renal cell carcinoma: a rare metastasis to the tongue. A case report

Altinel D.; Etit D.; Bayol U.; Beyhan R.
Izmir Tepecik Training and Research Hospital, Izmir, Turkey

Background Metastasis of renal cell carcinoma (RCC) to the head and neck is an uncommon phenomenon and tongue metastasis is extremely rare which has been reported in only a handful of cases in the literature.
Methods A 67-year-old-male with a two-cm-mass on his tongue.
Results Punch biopsy of the tongue revealed a malignant neoplasm with clear cell features. During the diagnostic work-up, a renal mass was found radiologically and immunohistochemical positivity of EMA and Vimentine with the histopathological evaluation supported the metastatic origin from the kidney. The excision of the tongue

mass and the radical nephrectomy material confirmed the diagnosis.
Conclusion(s) RCC metastases to the tongue are infrequent which can cause difficulties in diagnosis and proper management. Among the clear cell neoplasms, the metastasis of RCC should always be considered in the differential diagnosis.

P3.196
Sclerosing rhabdomyosarcoma of the parotid gland
Volavsek M.; Lamovec J.
Institute of Pathology, Faculty of Medicine, University of Ljubljana, Ljubljana, Slovenia

Background Salivary gland sarcomas are extremely rare, with poor prognosis. A case of slowly progressing parotid gland sclerosing rhabdomyosarcoma is reported.
Methods Surgical specimens were routinely processed using HE and immunohistochemistry.
Results 60 year old male with right parotid swelling had total parotidectomy (subsequent irradiation, total dose 66 Gy). Modified right sided neck dissection was negative (0/17). Five recurrences were excised in five years. Postoperative chemotherapy (6 cycles doxorubicin, ifosphamid) resulted in partial regression of last residuum. No distant metastases were found at any time. Patient is alive with disease. Firm, grey and macroscopically well circumscribed primary tumour measured 25x22mm. Irregularly distributed cells infiltrated gland and surrounding connective/fatty tissue, with prominent perineural invasion. They grew in focally abundant hyalinized/chondroid/myxiod matrix with numerous irregular thick, keloid-like collagen fibers. Cell margins were unclear, cytoplasm scanty, amphophilic/slightly eosinophilic, nuclei irregular, mitoses numerous (25 mitoses/10 hpf). Histologically, primary/recurrent/residual tumours varied only slightly, except for myoid strap tumour cells with abundant eosinophilic cytoplasm appearing in recurrences, being most prominent in first (intermixed with more primitive looking cells, no terminally differentiated rhabdomyoblasts). Immunophenotype was diagnostic of sclerosing rhabdomyosarcoma: all tumour cells of primary/recurrent tumours (MyoD1+, vimentin+, CD56+), numerous cells (MSA+, SMA+, calponin+); rare cells (desmin+); variable cell number (CD34+, myoglobin+), negative reaction (cytokeratins, EMA, S-100, melanA, HMB-45).
Conclusion(s) Sclerosing rhabdomyosarcoma, a newly described subtype of rhabdomyosarcoma, is rare, mostly described in adults and often located in head and neck. To our knowledge this is the first reported case of primary sclerosing rhabdomyosarcoma of parotid gland.

P3.197
Sialoblastoma: case report
Kayahan S.; Gecer M.; Yavuzer D.; Karadayi N.
Dr.Lutfi Kırdar Kartal Educational and Research Hospital Pathology Department, Istanbul, Turkey

Background Sialoblastoma is a rare, aggresive and potentially malignant congenital, epithelial tumor of the salivary gland.
Methods A patient 3 years old girl who presented with right parotid swelling. The tumor grew in a period of 6 months. Ultrasonography revealed a tumor mass 2,5 cm in diameter. Parotidectomy was performed.The resection margins were negative. But tumors was recurred 3 months later.
Results Histologically tumor was characterized by solid nests of epithelial cells intermingled with proliferating ductal structures lined by a double layer of cells.The ductal companent showed membranous expression of cytokeratins.Actin was pronounced at the periphery of the neoplastic islands. The differantial diagnoses include pleomorphic adenoma, basal cell adenoma, adenoid cystic carcinoma and teratoma.
Conclusion(s) Sialoblastoma is a uncommon congenital/perinatal salivary tumor that varies in histologic features and biologic potential.Distant metastases are rare. The patient's prognosis is likely to be determined by the tumor grade as well as tumor stage at presentation and the extent of resection.

P3.198
The comparison of D2-40 immunoreactivity with clinicopathologic parameters in laryngeal carcinoma
Kibar Y.; Bakir K.; Güldür Emin M.
Gaziantep Hospital Department of Pathology, Gaziantep, Turkey

Background Laringeal SCC is the most common malignant neoplasm of head and neck area. Lymphangiogenesis is an early indication of the lymph node metastases. In this study, some clinicopathologic parameters were compared with lymphatics and D2-40-stained tumor cells.
Methods This study included 114 cases of larynx SCC diagnosed at Gaziantep University, Medical Faculty, Pathology Department (1997–2008). D2-40-stained lymphatic vessels in

intratumoral and peritumoral areas were counted. Additionaly, D2-40 immunoreactivity was examined in tumor cells.
Results On D2-40 immunohistochemical examination, the number of peritumoral lymphatics ranged from 0–41. Within the tumor, the number of lymphatics was between 0–30. Lymph vessel numbers (LVN) in cases without lymph node metastases was found to be lower. When the lymphatic numbers in peritumoral area were compared with stage, the increase in the number of lymphatics in stage 4 cases, was observed to be significant. When D2-40 staining in tumor cells was compared with grade, well-differentiated tumors had higher staining ratios than moderate/poorly differentiated tumors. This finding is statistically significant (p=0.011). No significant correlation was found between LVN in peritumoral and intratumoral areas, tumor grade, tumor site and lymph node metastases.
Conclusion(s) D2-40 immunoreactivity was not observed as a prognostic parameter in larynx SCC in our study. No other study on the correlation between grade and D2-40 immunoreactivity has been found in the literature. This is why we are inclined to think that the results we obtained will contrubute to the literature.

P3.199

The expression of SOCS1 and TLR4-NFKB pathway molecules in neoplastic cells as potential biomarker for the aggressive tumor phenotype in laryngeal carcinoma

Starska K.; Forma E.; Lewy-Trenda I.; Stasikowska O.; Brys M.; Krajewska W.; Lukomski M.
Medical University of Lodz, Poland, Department of Laryngological Oncology, Lodz, Poland

Background Suppressor of cytokine signaling 1 (SOCS1) is the key regulator of cytokine-mediated innate and adaptive immunity. One of the molecular mechanisms of SOCS1 is connected with inhibition of TLR4-NFκB pathway.
Methods To investigate NFκB (p65 subunit) nuclear and cytoplasmic expression in 45 tumor samples of advanced laryngeal carcinoma IHC staining was performed. To determine the mRNA expression levels of TLR4, IRAK1, TRAF6 and SOCS1 in isolated neoplasm cells and non-cancerous adjacent mucosa epithelial cells RT-PCR was used. The relationships between certain clinicopathological characteristics and the mRNA expression of the molecules mentioned earlier were investigated.
Results Significant differences of TLR4-NFκB pathway molecules and SOCS1 mRNA expression in laryngeal tumor cells and normal adjacent mucosa. Positive relationships of TRAF6 in tumor margin cells with the histological grade and the mode of tumor invasion as well as the TFG total score were highlighted. Significant positive correlations were found between the TLR4 in tumor central cells and the TFG total score. Negative relationships of SOCS1 in tumor central cells with the histological grade were also noted. Significant positive correlations were found between the cytoplasmic NFκB(p65) and the mode of invasion as well as TFG total score.
Conclusion(s) Our findings confirmed the importance of SOCS1 and TLR4-NFκB pathway molecules as potential biomarkers for assessment of the aggressive tumor phenotype in laryngeal carcinoma.

P3.200

Update of thyroid lesions in Enugu, Nigeria (January 1st 2000 - December 31st 2004)

Nzegwu A.M.; Ezume E.R.; Njeze G.E.; Njeze N.R.; Olusina D.B.; Ugochukwu A.I.
University of Nigeria Medical School, Enugu, Nigeria

Background The thyroid is affected by a variety of lesions, with few Nigerian reports. Abstract updates literature and highlights thyroid lesions, age and sex variations, necessary for adequate planning and resource allocation for diagnoses and treatment, leading to early detection especially of the malignant subtypes.
Methods Study analyzes data from thyroidectomies from Morbid Anatomy department of UNTH. Slides from paraffin blocks of all thyroidectomies were independently reviewed by two pathologists to identify the lesions.
Results 163 thyroidectomies were received, from 141 females and 22 males. Most common is multinodular goiter 72 (44.2%); mean 39.5 yrs (SD) 12.9. Simple colloid goiter 31 (19%), mean 38.7 years SD12.7. Diffuse toxic goiter 5 (3.1%). Thyroid adenomas (follicular), 17 (10.4%), mean 21–54 years. 9 cases (5.5%) of follicular thyroid carcinoma. Papillary carcinoma 13 (8%). Hashimoto's thyroiditis presents in females with 3 (1.8%). Tuberculosis of the thyroid and medullary carcinoma each 1 (0.6%). Anaplastic carcinoma and secondary carcinoma each has 1 (0.6%). Lymphangioma 1(0.6%), Rosai Dorfmanns disease 3 (1.8%). Thyroglossal cyst 3 (1.8%). Neurofibromatosis 1 (0.6%). Simple colloid goiter has the greatest female preponderance, with a ratio of 30 females; 1 male.
Conclusion(s) Goiter, adenoma and carcinoma remain the most common thyroid pathologies. There are significant decreases in non-malignant lesions over the past years, largely as a result of increases in compliance to use of iodized salts and flour. This has reduced especially female suffers. But malignant lesions have increased making it likely to have a different etiology unrelated to iodine deficiency.

Pulmonary pathology

P3.201

Differential gene expression profiles of radioresistant lung cancer cell lines established by fractionated irradiation

Choi Duk Y.; Jeong Hui E.; Min Woo B.; Kim Y.; Nam Woo S.; Ahn Ja S.; Kim Chul Y.; Choi C.
Chonnam National University Medical School, Gwangju, Republic of Korea

Background The response of tumor cells to radiotherapy may be accompanied by complex mechanism. Although it is not known what proportion of the treatment failure is associated with gene related radio-resistance, it will be possible to use these informations to sensitize radioresistant tumor cells and improve radiocurability. We tried to identify differentially expressed genes between parent and radio-resistant cell lines established by fractionated irradiation.
Methods Two lung cancer cell lines (A549, NCI-H1650) were irradiated at sequential doses ranging from 2 Gy to 6 Gy at two-week intervals for 8 times. To determine whether radioresistant cancer cell line was successfully established, clonogenic assay was performed. We compared the expression profiles of each parent and radioresistant cell lines on a cDNA microarray consisting of 48,804 genes (Illumina beadarray).
Results Four radioresistant cell lines (A549-2 Gy, A549-5 Gy, H1650-2 Gy, and H1650-5 Gy) were established. Unsupervised hierarchial cluster analysis showed significant difference in gene expression profile between parent and radioresistant cell lines, respectively. We identified 72 genes in A549 radioresistant cells and 657 genes in H1650 radioresistant cells, which revealed more than two-fold difference. They were genes of Wnt pathway, inflammation, angiogenesis, and apoptosis. Some of the genes of WNT pathway, such as AXIN2, MMP7, NKD2, PCDH9, WNT5A, and WNT5B were verified by subsequent quantitative real time-PCR.
Conclusion(s) Global gene analysis of radioresistant cell lines may provide new insights into the mechanism underlying radioresistance and therapeutic strategies can be introduced to sensitize the radioresistant lung cancer cells.

P3.202

Introducing new perspectives in lung cancer prognosis; lymphangiogenesis excels angiogenesis and successfully defines subsets of patients with poor prognosis at the time of diagnosis

Arkoumani E.; Hardavella G.; Galanis P.; Constantopoulos S.; Stefanou D.
Department of Pathology, Medical School, University of Ioannnina, Dourouti Ioannina, Greece

Background Introducing new prognostic crossroads in lung carcinomas would be of vital importance. While angiogenesis' prognostic potential starts trembling, lymphangiogenesis, a promising successor, hasn't been thoroughly studied. The present study aims to crash test angiogenesis' with lymphangiogenesis' expression in non small cell (NSCLC) and small cell lung carcinomas (SCLC) and determine their prognostic impact.
Methods 96 NSCLC and 50 SCLC specimens were retrospectively studied and immunohistochemically stained for Vascular Endothelial Growth Factor-VEGF, VEGF-R1-Flt1, VEGF-R2-Flk1 and lymphangiogenetic factor CD105 (DBS California-Menarini Hellas). Evaluation of expression, assessment of lymphatic invasion (L.I) and correlation with clinical data and 5-year survival followed.
Results VEGF was more expressed in NSCLC while CD105 in SCLC (NSCLC, p=0.002, SCLC, p = 0.04). VEGF didn't associate with epidemiological/clinical data. Its two receptors associated with stage in NSCLC (Flt1, p = 0.026, Flk1, p = 0.005). CD105 expression associated with metastasis (NSCLC, p = 0.003, SCLC, p = 0.05) and stage (NSCLC, p = 0.003, SCLC, p = 0.004). SCLC patients with high VEGF and CD105 expression had low 5-year survival although not statistically significant. L.I associated with stage and metastasis in NSCLC (p<0.005). Specification of target organ metastasis wasn't associated with any factor.
Conclusion(s) VEGF and CD105 expressed differently in NSCLC and SCLC. CD105 presented as a potentially independent prognostic factor unlike VEGF which was devoid of prognostic significance. Assessment of lymphangiogenesis at the time of diagnosis could be capable of defining subsets of patients with poor outcome thus highlighting exciting possibilities in lung cancer prognosis.

P3.203

The stem cell marker CD133 (prominin-1) selectively identify mesenchimal stroma of pulmonary blastoma tumors

Liguori G.; Cantile M.; Franco R.; Anniciello A.; Cerrone M.; Manna A.; Pinto A.; Camerlingo R.; Scognamiglio G.; Pirozzi G.; Rocco G.; Botti G.
INT Fondazione Pascale, Napoli, Campania, Italy

Background Adult Pulmonary Blastomas (PB) is classified as pulmonary sarcomatoid carcinoma, in which the activation of an epithelial-mesenchimal transition program is fundamental in their development and progression. PB is a biphasic tumor, composed of primitive epithelial component, resembling well-differentiated low-grade fetal adenocarcinoma and primitive mesenchymal stroma, with blastematous cells and occasional foci of true sarcomatous differentiation. Recent data have demonstrated that tumors

generally contain a variable amount of cancer stem-like cells, with self-renewing capacity and responsible for tumor maintenance and metastasis.

Methods Lobectomy in a case of PB has been performed in a male smoking patient 82 yrs old. Fresh neoplastic tissue was selectively obtained in order to have a stabilized cell line and characterize stem cell component by the stem cell marker CD133 (prominin-1). Moreover, immunohistochemistry characterization was performed including CD 133 expression on paraffin embedded tissue.

Results CD133-positive cells isolated from primary culture obtained of a PB tissue sample are located prevalently in mesenchimal component of tumoral tissue, supporting the idea that the epithelial-mesenchimal transition in biphasic development of PB is probably related to oncogenic mutations modulating the expansion of stem/progenitor cells in this cancer tissue.

Conclusion(s) In other pulmonary sarcomatoid carcinomas the composition of the metastases reveal an predominat ephitelial composition suggesting that epithelial cells could contribute more effectively than sarcomatous component to metastasis formation. Thus, it's priority understand the role of primitive mesenchimal stroma in PB tumor progression and metastasis.

P3.204

Treatment with collagen v increases caspase-9 expression in experimental model of lung cancer

Parra Roger E.; Vargas Mutai C.; Bielecki Cavallari L.; Ribeiro Mauro J.; Balsalobre De Andrade F.; Teodoro Rosoglia W.; De Souza W.; Capelozzi V.L.
Faculdade de Medicina da Universidade de São Paulo, São Paulo, Brazil

Background Recently, collagen V (COL V) has shown efficient as tumoral and endothelial apoptotic-promoter emerging promise as inductor of death response via caspase 9. In this study, we sought to examine the interface of COL V and endothelial apoptosis in experimental lung cancer.

Methods Four groups of mice Balb/c males were studied: a) control (n=10), b) animals that received two doses of 3 g/kg intraperitoneal of Uretane (n= 10), c) animals that received two doses of 3 g/kg intraperitoneal of Uretane and treatment with COL V intranasal administration of 20 mug for 2 months after 2 months of uretane administration (n= 10). The mice were sacrificed after 6 months. Lung histological sections underwent hematoxylin-eosin, immunofluoresce for COL V and immunohistochemistry for Caspase 9 methods for morphometric analysis.

Results Collagen V (7.19±2.81) and caspase 9 (5.99 ± 2.55) densities in tumoral area were lower when compared with normal surrounding parenchyma (12.31±0.79) and control (9.67±3.20) groups. The intranasal COL V administration in animals with lung cancer increased the caspase 9 expression rate by tumoral endothelial cells (16.06±4.36) when compared with other groups (p<0.01).

Conclusion(s) Collagen V intranasal treatment induces increased endothelial immune expression of caspase 9 in tumoral areas of experimental lung cancer, thus leading to decreased angiogenesis by high endothelial death rate. Further studies will be required in randomized and prospective trials to validate the therapeutic efficacy of type V collagen. Financial supported: FAPESP.

P3.205

A study of immunohistochemical differential expression in lung and breast cancers

Nonaka D.; Chiriboga L.; Yang M.
New York University School of Medicine, New York, USA

Background The risk of developing a second primary cancer is increased in patients with breast cancer, and the lung is one of the major sites involved. Furthermore, the lung is the major metastatic site for breast cancers. A distinction between metastatic breast cancer and primary lung cancer is often histologically difficult, and both generally show CK7+/CK20-.

Methods 201 pulmonary carcinomas (162 adenocarcinomas, 39 squamous) and 115 invasive mammary carcinomas (89 ductal, 24 lobular, 2 mixed type) were studied. PE-10, TTF-1, ER, GATA-3, mammaglobin, and GCDFP-15 immunostains were performed. The extent of staining was graded to focal (< 50%) and diffuse reaction (>50%).

Results In mammary carcinomas, ER, GATA-3, mammaglobin, and GCDFP-15 were expressed in 74, 72, 62, and 54%, respectively, while TTF-1 and PE10 were negative. The expression was diffuse in ER and GATA-3, and variable in mammaglobin and GCDFP-15. 17% were negative for ER, GATA-3, and mammaglobin. All lung squamous cell carcinomas were negative for all markers studied. TTF-1 and PE10 were positive in 81 and 61% of pulmonary adenocarcinomas. None of TTF-1(-) tumors expressed PE-10. GCDFP-15 was variably expressed in 7% of adenocarcinomas, and ER was focally expressed in 1.2% of adenocarcinomas.

Conclusion(s) 83% of mammary carcinomas were positive for mammaglobin, GATA-3, and/or ER. Thus, when a metastasis from breast cancer is suspected in the lung, a panel of the three markers is recommended. GCDFP-15 is unreliable due to its occasional expression in pulmonary adenocarcinomas.

P3.206

Analysis of the prognostic impact of nestin expression in nonsmall cell lung cancer

Skarda J.; Kolar Z.; Janikova M.; Chmelova J.; Krejci V.; Zapletalova J.; Langova K.; Klein J.; Grygarkova I.; Kolek V.; Fridman E.; Kopolovic J.
Department of Pathology Medical Faculty Palacky University, Olomouc, Czech Republic

Background The expression of nestin in tumour cells can be associated with the degree of tumour differentiation, biological potential of tumour and degree of neoangiogenesis.
Methods Immunohistochemical detection of nestin was performed by indirect immunohistochemistry using available anti-bodies on tissue microarrays were constructed from 115 formalin-fixed paraffin-embedded non-small cell lung cancer samples and 35 brain metastasis. The H-score and degree of nestin positive vascularisation evaluated semi-quantitatively in areas of the most prominent vascularisation were determined. The parameters were correlated with each other and with disease-free and overall survival.
Results Significantly higher expression of nestin was found in brain metastases of squamous cell carcinomas compared to brain metastases of adenocarcinomas (p=0.003). In sqamous cell carcinomas and adenocarcinomas a significantly higher expression of nestin was found in brain metastases compared to primary tumours (p<0.0001, p=0.034). There was significantly higher occurrence of nestin positive vascularisation in brain metastases of adenocarcinomas than primary adenocarcinomas (p = 0.044). In brain metastasis, there was significantly higher occurrence of nestin positive vascularisation in poorly differentiated adenocarcinomas than in well-differentiated adenocarcinomas (p = 0.927) or poorly differentiated primary adenocarcinomas (p = 0.008). Kaplan-Meier curves of disease-free and overall survival showed no significant correlation with nestin expression except for better overall survival of patients with brain metastasis and high nestin expression than patients with brain metastasis and low nestin expression (p = 0,043).
Conclusion(s) Our results suggest that the immunohistochemical expression of nestin may be an important diagnostic marker.

P3.207

Cathepsin-k expression in benign clear cell "sugar" tumor of the lung

Gobbo S.; Pea M.; Martignoni G.; Zamboni G.; Brunelli M.; Chilosi M.; Bonetti F.
Anatomia Patologica - Università di Verona, Verona, Italy

Background Cathepsin-k is a papain-like cysteine protease that recently has been shown to be constantly, strongly and diffusely immunoexpressed in lymphangioleiomyomatosis. Lymphangioleiomyomatosis can be considered as part of the spectrum of proliferative lesions that have been previously defined under the name of "perivascular epithelioid cell tumours" (PEComas), including angiomyolipoma, clear-cell "sugar" tumour of the lung and extrapulmonary sites. The aim of this study is to evaluate cathepsin-k immunoexpression in clear-cell "sugar" tumour of the lung.
Methods We collected 3 clear-cell "sugar" tumours of the lung analysing the immunoexpression of cathepsin-k. We tested also cathepsin-k expression in 20 pulmonary adenocarcinomas, 20 squamous cell carcinomas of the lung and in 20 clear cell renal cell carcinomas.
Results All the clear-cell "sugar" tumours were diffusely and strongly immunoreactive for cathepsin-k whereas none pulmonary adenocarcinoma, squamous cell carcinoma of the lung and clear cell renal cell carcinoma showed immunoreaction for this marker.
Conclusion(s) We demonstrated that: 1) Cathepsin-k is constantly and strongly expressed in benign clear cell "sugar" tumor of the lung and can be useful in their differential diagnosis with other primary and metastatic epithelial neoplasms of the lung. 2) The expression of cathepsin-k is an additional proof of the close relationship between benign clear cell "sugar" tumor and lymphangioleiomyomatosis of the lung.

P3.208

Decreased sirtuin expression in COPD

Isajevs S.; Svirina D.; Taivans I.; Strazda G.; Kopeika U.
University of Latvia, Faculty of Medicine and Pathology Centre of East Clinical University Hospital of Riga, Riga, Latvia

Background COPD is characterized by persistent and modified inflammatory responses in lung tissue. Human sirtuin (SIRT1), an antiaging and antiinflammatory protein, is a metabolic NAD (+) -dependent protein/histone deacetylase that regulates proinflammatory mediators by deacetylating histone and nonhistone proteins. The aim of our study was to compare the expression of sirtuin in large, small airways and lung parenchyma in nonsmokers, asymptomatic smokers and smokers with COPD.
Methods 13 nonsmokers, 11 current smokers and 10 smokers with moderate COPD undergoing lung resection for a solitary peripheral non-small cell carcinoma were enrolled in the study. Immunohistochemical methods were used to analyze sirtuin expression in the airways and lung parenchyma.
Results Obtained results showed the non-uniform sirtuin expression throughout the bronchial tree. COPD patients had decreased sirtuin expression both in large airways and

alveolar walls compared to nonsmokers and asymptomatic smokers. In lung parenchyma sirtuin was mainly expressed in macrophages, but in large airways in lymphocytes. A positive correlation between airflow limitation (FEV1%) and sirtuin positive cells in large airways and lung parenchyma was revealed (Rho = +0.50, p=0.003 and Rho = +0.64; p<0.0004). In addition, a negative correlation was observed between the pack-years smoking history and the number of SIRT1 positive cells (Rho=-0.34; p=0.01). No differences were found between groups in sirtuin expression in small airways.
Conclusion(s) COPD is characterized by decreased sirtuin expression in alveolar macrophages and lymphocytes in large airways. Sirtuin expression throughout the bronchial tree is non-uniform.

P3.209
Detection of K-RAS mutations in tumour samples of patients with non-small-cell lung cancer using pyrosequencing

Hwang T.; Oh Young S.; Kim Seop W.
Konkuk University Medical Center, Seoul, Republic of Korea

Background Somatic mutations of the K-RAS oncogene have been assessed as a mechanism of de-novo resistance to epidermal growth factor receptor (EGFR) tyrosine-kinase inhibition in patients with non-small-cell lung cancer (NSCLC), and to anti-EGFR monoclonal antibodies in patients with metastatic colorectal cancer (mCRC). Most of the clinical samples obtained from benign or malignant neoplasm represent heterogenous tissue containing tumor cells and a considerable proportion of non-neoplastic stromal and inflammatory cells. To detect a minority of mutant alleles among abundant wild-type alleles, a careful dissection and a sensitive technique is required.
Methods Various mixtures of DNA from K-RAS mutant cell line and wild-type cell line were analysed by pyrosequencing and chain termination sequencing. A total of 117 NSCLC samples including 84 adenocarcinomas, 20 squamous cell carcinomas, 4 adenosquamous cell carcinomas, 6 large cell carcinomas, 1 mucoepidermoid carcinoma, 1 sarcomatoid carcinoma, and 1 carcinoma, type undetermined were analysed for K-RAS mutations at codon 12,13, and 61 by pyrosequencing. Either cytology specimens or paraffin embedded tissue sections were used.
Results K-RAS mutation was detected in 13(11.1%) of total 117 NSCLCs;12(14.3%) of 84 adenocarcinomas and one(5.0%) of 20 squamous cell carcinomas. Rest of the tumors did not reveal K-RAS mutation.
Conclusion(s) We found that pyrosequencing was superior to the chain termination sequencing and K-RAS mutation was more frequently detected in cytology specimens than in paraffin embedded tissue sections.

P3.210
Double organic lesions due to tuberculosis

Enache A.; Chatzinikolaou F.; Njau S.; Vladika N.; Theoharis S.
Medicine and Pharmacy Victor Babes, Timisoara, Romania

Background The TB related sudden death is rarely reported as cause of death in the literature and when is so the thanatogenerating syndrome is due to bronchopneumonia and/or hemoptysis, isolated or associated. During 2007 and 2008 we investigated the sudden death cases caused by tuberculosis with double localisations.
Methods From the forensic necropsies performed at IML Timisoara we found 28 cases of death by tuberculosis.
Results The majority of the cases 95% were males. In 14 of the cases (50%) we found a fibrocavitary form, 8 of the cases had a fibronodular form, 3 cases had an ulcerative form and 2 cases were of miliar form. Some cases presented unassociated pulmonary tuberculosis, some presented pulmonary tuberculosis associated with broncho-pneumonia, 1 case presented tuberculosis associated with pulmonary carcinoma, and some presented pulmonary tuberculosis associated with pericardial tuberculosis or hepatic granular tuberculosis and an association of pulmonary tuberculosis and hepatic tuberculosis granulia. Cardiac complications of tuberculosis causing sudden death can take many forms and are rare, but lethal.
Conclusion(s) The study shows that sudden death caused by pulmonary tuberculosis mainly affects male and social cases. The microscopic observations show bioorganic lesions of tuberculous nature in 80% of the cases which mainly affect the lungs and the kidneys. Other associations were observed between the lungs and the hepatic granulia.

P3.211
Estrogen receptors and aromatase in Japanese female patients with pulmonary adenocarcinoma: a comparison between BAC and non-BAC

Abe K.; Miki Y.; Ono K.; Kikuchi N.; Suzuki S.; Takahashi T.; Sasano H.
Tohoku University School of Medicine, Sendai, Miyagi, Japan

Background We attempted to examine the correlation between histological subtypes of pulmonary adenocarcinoma (bronchioalveolar carcinoma (BAC) vs non-BAC) and the status of estrogen receptors and aromatase, one of the estrogen-producing enzymes in order to explore an involvement of estrogens in these cancers.

Methods Fifty-six female cases with pulmonary adenocarcinoma (15 BAC cases and 41 non-BAC cases) were retrieved for imuunohistochemical study of ERα, ERβ, progesterone receptor (PR) aromatase and Ki67. Nuclear immunoreactivity for ERα, ERβ and PR was counted among 1000 cells, and defined "positive" with over 10% positivity. Cytoplasmic stain for armoatase over 10% of cancer lesion was defined as "positive". Ki67 labeling index was also obtained by counting 1000 cells.
Results ERα was negative for all cases, and PR was detected only in 10 cases. ERβ was positive among 33 cases (58.9%). Aromatase was detected among 45 cases (80.4%). Only among non-BAC cases, ERβ and aromatase expression demonstrated highly concordance (Fisher's exact test, p=0.019) but no significant correlation was detected in BAC cases. The ratio of ERβ immunoreactivity in non-BAC cases was higher than that in BAC cases especially among aromatase-positive cases, but difference did not reach statistical significance. Ki67 LI and ERβ expression also tended to be correlated.
Conclusion(s) Cell proliferation of non-BAC is considered to be partially regulated by ERβ, especially among aromatase-positive cases in female lung adenocarcinomas.

P3.212

Fluorescence in situ hybridization (FISH) in fresh pleural fluid improves cytological diagnosis

Rosolen Cristina Batista D.; Kulikowski Domenici L.; Capelozzi V.L.; Acencio Marques Pagliarelli M.; Bottura G.; Melaragno I.; Smith Arruda Cardoso M.; Vargas Suso F.; Antonangelo L.
Pulmonaru Division - Heart Institute and Investigate Laboratory (LIM03) of University Sao Paulo Medical School, Sao Paulo, Brazil

Background A diagnosis of malignant effusions is based on the finding of malignant cells in pleural fluid. Small number of malignant cells, tumor histological subtypes and presence of reactive mesothelial cells are some of the difficulties faced by cytologists. Ancillary methods are frequently associated with pleural cytology and improve diagnosis sensitivity. The search for chromosomal aneuploidies in pleural fluid cells may improve the cytological diagnosis.
Methods Interphasic cells from ten fresh malignant (n=7) or paramalignant (n=3) pleural effusion samples were analyzed by fluorescence in situ hybridization (FISH) using centromere specific Alpha satellite DNA probes labeled with Spetrum red and Spectrum green for chromosomes 11 and 17, respectively. FISH was performed according to direct modified labeling protocols. FISH images were captured on an Axioplan 2 imaging fluorescence microscope (Zeiss®, Göttingen, Germany) and analyzed with ISIS software. At least 200 metaphases for each probe were analyzed. Malignant cells were characterized by the presence of extra FISH signals.
Results All pleural samples showed trisomic or tetrasomic clones. This finding suggests that chromosones11 and 17 are frequently involved with malignant pleural effusions.
Conclusion(s) The combination of cytological examination with cell DNA testing may increase the accuracy of pleural fluid diagnosis, mainly in those cases with suspicious malignant cells.

P3.213

Immunohistochemical analysis of peripheral benzodiazepine receptors (PBR), p53 and antiapoptotic proteins bcl-2 and bcl-xl in Lung adenocarcinoma

Naroditsky I.; Eidel J.; Ben-Izhak O.; Cohen E.; Kremer R.
Rambam Medical Center, Haifa, Israel

Background Lung cancer is the leading cause of cancer death in the world. Despite early cancer detection and surgery and adjuvant therapy the long-term survival rate has only slightly improved. Peripheral benzodiazepine receptors (PBR) are expressed at high levels in different cancers and correlates with aggressive behavior. The aim of this study was to investigate the prognostic significance of PBR in lung cancer (previously unstudied) along with expression of p53, bcl-2 and bcl-xl.
Methods We investigated 74 tumor tissue samples from patients with different stages and grades of lung adenocarcinoma. All samples were stained immunohistochemically for bcl 2, bcl-xl, p53 and PBR and their expression levels were analyzed by semi quantitative method.
Results Survival analysis revealed a significant association between bcl-2, bcl-xl and patient prognosis. The PBR expression levels inversely correlated with bcl-2 levels but not with the prognosis.
Conclusion(s) The inverse correlation of PBR with bcl-2 suggests its relation to apoptosis. As opposite to the previous studies of PBR expression in different tumors, in our studies no correlation with prognosis was found. Additional studies should be undertaken to investigate the role of PBR in lung tumors development and the possibility of its role as a therapeutic target.

P3.214

Lung cancer as a second primary malignancy in women with a history of previous radiotherapy

Pillay N.; Baithun I.S.; Sheaff M.; Merve A.
Royal London Hospital, London, United Kingdom

Background Women who have had previous radiotherapy as part of their treatment for breast carcinoma develop lung cancer. Studies investigating this association use data extracted from cancer registries whose criteria for assigning the determination of a second primary tumour are largely clinically based. To our knowledge, there has not been a pathology based study in which the criterion for diagnosis of a second primary malignancy in the lung has been based on TTF-1 immunohistochemistry. The objectives were therefore to document the incidence of a "true" second primary malignancy and to evaluate its histopathological spectrum.
Methods Ninety six women with a diagnosis of lung cancer were identified from pathology records between 03/2004–02/2009. The following parameters were examined: previous malignancy, history of radiotherapy and tobacco use. In addition the histology and TTF-1 expression were re-confirmed.
Results Fifteen women developed TTF-1 positive lung cancer following treatment for breast (n=13) and laryngeal carcinoma (n=2). Ten had a history of radiotherapy and six of these patients were also smokers. The histopathological spectrum included adenocarcinoma (n=10), small cell neuroendocrine carcinoma (n= 1), squamous cell carcinoma (n=3), and undifferentiated pleomorphic sarcoma (n=1).
Conclusion(s) Smoking and radiotherapy are independent risk factors for the development of lung cancer. Their combined use is multiplicative and is responsible for the increasing incidence of lung cancer as a second primary malignancy in women. This is the first pathology based study to document this using TTF-1 immunohistochemistry as a more objective tool of determining primary malignancy.

P3.215

Maspin, VEGF and p53 expressions in primary lung cancer and relationship with clinicopathologic parameters

Bircan A.; Bircan S.; Kapucuoglu N.; Songur N.; Ozturk O.; Akkaya A.
Dept. of Pulmonary Medicine, Suleyman Demirel University School of Medicine, Isparta, Turkey

Background Maspin, a member of the serine protease inhibitors, has been shown to inhibit tumor progression and metastasis. We aimed to investigate maspin, p53 and VEGF expressions by immunohistochemistry in non-small cell lung cancer (NSCLC) and small cell lung cancer (SCLC).
Methods Twenty-eight squamous cell carcinoma (SCC), 18 adenocarcinoma (AC) and 17 SCLC tissue biopsies showing squamous and glandular differentiation or small cell morphology were selected. Medical records of these patients were reviewed from archival files.
Results The incidence of maspin positivity was significantly higher in NSCLC (84.8%) and SCC (89.3%) than SCLC (52.9%) (p=0.013, p = 0.021, respectively). Its mean percentages were significantly different between NSCLC and SCLC, and also SCLC and SCC or AC (p = 0.0001, p = 0.0001, p = 0.038, respectively). In ACs, maspin expression was tend to be positive correlated with the p53 expression (p = 0.053, r=0.464), and maspin positive cases had significantly higher T status in contrast to negatives (p=0.036). In SCC, the stage of disease was positively correlated with p53 (p = 0.007, r=0.536) and negatively correlated with VEGF expressions (p=0.013, r=-0.498). Multivariate analysis demonstrated the stage of disease was a significant and independent prognostic parameter in NSCLC (p=0.031).
Conclusion(s) Although maspin expression is higher in SCC and AC, our data did not indicate its prognostic significance. However, the findings in AC may suggest that maspin expression is regulated by p53 and might be a poor prognostic factor due to the relationship with the higher T status.

P3.216

MUC1 and bcl-2 expression in pre-invasive lesions and adenosquamous carcinoma of the lung

Demirag F.; Cakir E.; Bayiz H.; Yazici Eren U.
Ataturk Chest Diseases and Chest Surgery Education and Research Hospital, Department of Pathology, Ankara, Turkey

Background Adenosquamous carcinoma of the lung is composed of adenocarcinoma and squamous cell carcinoma with each comprising at least 10% of the tumor. Atypical adenomatous hiperplasia (ADH), bronchiolar columnar cell dysplasia (BCCD), basal cell dysplasia (BCD), columnar cell dysplasia (CCD), bronchial epithelial dysplasia with transitional differentiation (BEDT) and squamous dysplasia (SD) were preinvasive lesions. The aim of this study was to define preinvasive lesions in adenosquamous carcinomas and to investigate the role of MUC1 and bcl-2 in the pre-invasive and invasive parts of adenosquamous carcinoma.
Methods 31 patients with adenosquamous carcinoma were selected. All slides were reviewed. The ratio of squamous to glandular differentiation, preinvasive lesions, features of tissues around the tumor, stroma of the tumor, necrosis, perineural and vascular invasion were detected. Blocks contained squamous cell carcinoma, adenocarcinoma and preinvasive lesions were selected for immunohistochemistry. MUC1 and bcl-2 was done by immunoperoxidase method using the avidine-biotin complex (ABC). It was evaluated semiquantitatively according to the percentage of cells staining cytoplasmic or membranous.

Results SD, BCCD, BEDT, AAH and CCD were found in 23, 6, 3, 1 and 2 patients respectively. MUC-1 was positive in 30 squamous component, in 28 adenocarcinoma component and in 23 preinvasive lesions. Bcl-2 was positive in 18 squamous component, in 14 adenocarcinoma component and in 11 preinvasive lesions.
Conclusion(s) Squamous dysplasia is the most preinvasive lesion for adenosquamous carcinoma. MUC1 ve bcl-2 expression were strongly associated with preinvasive lesions in adenosquamous carcinomas.

P3.217

Pathology of pulmonary arterioles in COPD and idiopathic lung fibrosis (IPF). Do the similarity and difference give the key to pathogenesis?

Mikhaleva L.; Nekludova G.; Bykanova A.; Cherniaev A.; Samsonova M.
Research Institute of Human Morphology, Moscow, Russia, Russian Federation

Background Secondary pulmonary hypertension (PH) determines the prognosis of survival in COPD and IPF. The aim of the investigation was to analyze the structural changes of pulmonary arterioles in order to recognize the pathogenetic peculiarities of PH in these conditions.
Methods We examined patients with COPD (n=19) and IPF (n= 18). Systolic pulmonary pressure (PAPs) was measured by means of echocardiography. Vasoreactivity test with vasodilators (NO and iloprost) were used to assess the reversibility of PH. Lung tissue specimens for histological examination (H&E, Van-Gison, immunostaining with antibodies to SMA, vimentin, desmin) were obtained during lung volume reduction surgery (COPD) or open lung biopsy (IPF).
Results Morphometric examination depicts similar changes of pulmonary arterioles: intimal thickening (5,4 times more in COPD and 4,3 – in IPF as compared to control), medial hypertrophy (%med=2,8 times more in COPD and 2,2 in IPF) resulted in arteriolar wall thickening and luminal narrowing. Moderate increase of PAPs was revealed in COPD (42,8±11,1) and IPF (41,8 ± 12,6 mmHg). PAPs correlated with %med in COPD (r=0,77) and IPF (r=-0,76). Vasoreactivity test proved the more PAPs the better response in COPD but not in IPF. Careful histological examination showed that medial thickening was accompanied with myoelastofibrosis in IPF but not COPD, proved by immunohistochemistry.
Conclusion(s) Smooth muscle hypertrophy in arterioles comes together with fibroblast and myofibroblast proliferation in IPF but not COPD, which explain poor prognosis of pulmonary hypertension.

P3.218

Pleural osteochondromatosis

Slavova Georgieva Y.; Mihova A.; Plochev M.; Petrov Borisov D.; Djambazov V.; Marinova D.
Univercity Hospital of Lung Diseases, Sofia, Bulgaria

Background We present the case of a 58-year-old female patient with complaints of prolonged cough for 7 months, followed by 3-month pain in the left chest half. The surgical interventions discover multiple coral-shaped formations in both parietal and visceral pleura, all connected with the pleura with soft tissue „foot". 8 of the formations with yellowish-gray color and glistening surface were removed. The size of the largest formation is 9.5/7.8/5 cm, with focal formation of foliar, overlapping structures (16 in number), the largest foliar structure has a size of 5.5/2.5/0.2 cm.
Methods Hematoxylin-eosin, Masson, immunohistochemically - CK5 / 6, Calretinin.
Results Microscopically we observed sections with characteristics of mature, colagenized, fibrous tissue, and areas with structure of hyaline cartilage in the form of nodules and foliar formations, with foci characterized with bone tissue with morphology of spongy bone with eburneus. The bone tissue is connected to the cartilage described by means of endochondral ossification. Matrix prevails in the cartilagenous tissue, where chondrocytes are located individually or in groups. The cells are scattered, without a specific order or structure, resembling hondrome. The surface of these formations consists of a layer of connective tissue, covered with a row of flattened cells with immuunophenotype of mesotel (+ CK5 / 6 and Calretinin).
Conclusion(s) So far, no description has been made of similar formations of the pleura. The lesion is most likely metaplastic and is similar to synovial osteochondromatosis. By analogy with the latter, we offer the term pleural osteochondromatosis for a similar type of lesions.

P3.219

Primary synovial sarcoma of the lung: a case report and review of the literature

Fytili P.; Mygdakos N.; Valeri R.; Barbetakis N.; Gkogkou C.; Tsilikas C.; Destouni C.
Theagenio Cancer Hospital of Thessaloniki, Greece

Background A male, 49 years of age,was admitted to our hospital for a surgical resection of a known synovial sarcoma (SS),diagnosed one year ago.At that time, a nodular mass was discovered in the upper lobe of the right lung by CT, measuring approximately 75 mm at its maximum diameter. The histopathological examination of the lung biopsy revealed a malignant neoplasm, of high grade malignancy consistent with a SS. The patient

received systematic chemotherapy and radiotherapy with no improvement of his condition. Therefore surgical excision of the mass was decided. During surgery, n unresectable, necrotic mass 100 mm in diameter was revealed and an FNA was performed.
Methods The material,was processed by Liquid Based Cytology (ThinPrepTechnique) and immunocytochemistry by the corresponding monoclonal antibodies followed.
Results The smears showed necrotic and degenerated material with many inflammatory cells. Among them many malignant tumor cells single or in clusters were present. The cells appeared fusiform shaped with oval nuclei and granular chromatin. Nucleoli were inconspicuous. Immunocytochemistry was positive for Vim(3+), CK7(2+), Bcl2(2+), CD99(2+), S100(2+) and negative for EMA and CK19. Our diagnosis was consistent with the initial diagnosed SS.
Conclusion(s) PSS is a rare mesenchymal spindle cell tumor, which occurs in young to middle aged adults. The lung is the second most common location after the extremities. Cough with haemoptisis are the most often clinical manifestations, followed by chest pain. There are only rare reports of PSS diagnosed by cytology in the literature. Therefore we present this case describing the cytomorphologic findings and we review the relevant literature.

P3.220

Pulmonary collision cancer of metastasic colonic carcinoma and primary lung adenocarcinoma. Report of a case

González-Piñeiro A.; Fiaño-Valverde C.; Fernández-Vázquez P.; Pérez-Rodríguez A.
Xeral-Cíes, Vigo, Pontevedra, Spain

Background Collision tumors is defined as two independent neoplasm invading each other or in close proximity and they have been reported in various organs. Collision tumors of the lung are rare. We report the first case, to our knowledge in the English literature, of a collision tumor composed of a metastatic colonic adenocarcinoma coexisting with a primary lung adenocarcinoma.
Methods Case presentation: A 65-year old man with a history of colonic carcinoma pT3 pN0 two years before, who develop a radiological mass on the right lower lobe. It was diagnosed by transthoracic FNAC as metastatic colonic carcinoma and a lobectomy with hiliar lymph node dissection was performed.
Results Pathological examination revealed a 5,5 cm tumor with the coexistence of two different components, each element was clearly distinguished and touched each other, even in inmunohistochemical studies, with clearly different expression of CK7, ck20, TTF-1 and CDX-2. The pulmonary adenocarcinoma shows pleural invasion and metastatic disease at hiliar lymph node.
Conclusion(s) Collision tumors of the lung are rare. This is the firs case reported of this combination of pulmonary adenocarcinoma and metastatic colonic carcinomas in the lung. It is difficult to diagnose collision tumor before surgical resection, because there are no characteristic clinical features.The recognition of this rare tumor is important as they will dictate appropriate treatment strategies depending on each of the tumor components.

P3.221

Pulmonary metastasis from malignant phyllodes tumor of the breast

Dimitriadis I.; Tsompanidou C.; Stergiou E.; Boukovinas I.; Angel I.; Kiziridou A.
Theageneion Cancer Hospital, Thessaloniki, Greece

Background Phyllodes tumors are rare fibroepithelial tumors that make up less than 1% of all breast neoplasms. Based on histological growth pattern, number of mitoses, pleomorfism and stroma characteristics tumors are classified as malignant, borderline or benign. Malignant phyllodes tumors are associated with a 25% incidence of distant metastasis which is invariably fatal within 24 months. The most frequent sites of metastases are the lung, soft tissue, bone and pleura.
Methods We present a case of a 54-year old postmenopausal woman who had history of mastectomy and radiotherapy because of malignant phyllodes tumor of the breast. The patient had no symptoms. One year after mastectomy chest x-ray and computer tomography (CT) scan demonstraded bilateral pulmonary tumors. The left mass in the lower lobe measured 5,5 cm and the right mass in the lower lobe was 1,3 cm. Brain and abdominal CT were unremarkable. At one stage operation for resection of bilateral lung tumors was performed.
Results Macroscopically the left and the right lung neoplasms were firm, grey tumours measured 5,5X3X2 cm and 1,3X1X0,8 cm respectively. Microscopically both lung tumours showed histological features of metastatic lesion of malignant phyllodes tumor similar to those of the primary tumor of the breast.
Conclusion(s) Careful follow up of the patients with malignant phyllodes tumors of the breast is necessary to confirm the early diagnosis of metastasis from this tumor.

P3.222

Pulmonary sclerosing hemangioma with lymph node metastasis and multiple lung involvement

Ozbilim G.; Ozbudak I.; Ozbey C.; Erdogan G.; Erdogan A.; Ozbudak O.
Akdeniz University School of Medicine Department of Pathology, Antalya, Turkey

Background Pulmonary sclerosing hemangioma has been considered benign based on the slow-growing, it has uncertain histogenesis and biologic behavior To date, no case has been reported with poor prognosis due to sclerosing hemangioma, however its clinical characteristics of multiple spread and lymph node metastasis have not yet been elucidated.
Methods We presented a 32 year-old woman with a history of chest pain. The radiological studies revealed multiple central and peripheral masses originating in the left lung. The patient underwent elective thoracotomy.
Results Tumor was diagnosed as pulmonary sclerosing hemangioma with multiple lung involvement. Immunohistochemical staining was positive for EMA, TTF-1 and Vimentin in both round stromal cells and cuboidal surface cells. However, Pancytokeratin positivity was detected in only cuboidal surface cells. A metastatic focus in mediastinal lymph node of 5 was also determined. During the follow-up, there was no recurrence or metastasis.
Conclusion(s) We would like to emphasize that the awareness of the sclerosing hemangioma with lymph node metastasis and multiple lung involvement is important for clinicians and pathologists. Although the tumor is considered to be benign, possible nodal metastases should be kept in mind, particularly during the work-up of enlarged regional lymph nodes in pulmonary sclerosing hemangioma.

P3.223

Pulmonary sclerosing hemangioma with tuberculosis lymphadenitis

Ozbudak I.; Ozbudak O.; Oz N.; Eren Karanis M.; Okudan H.; Ozbilim G.
Akdeniz University School of Medicine Department of Pathology, Antalya, Turkey

Background Pulmonary sclerosing hemangioma is a relatively rare benign tumor of uncertain histogenesis. It is composed of round stromal cells and cuboidal surface cells. Architecturally, pulmonary sclerosing hemangioma comprises a mixture of four histological patterns named as papillary, solid, sclerotic and hemorrhagic.
Methods We presented a 54 year-old woman with a history of cough and chest pain. The radiological studies revealed a nodule, approximately 3 cm in diameter originating in the inferior lobe of left lung and multiple mediastinal pathologic lymphadenopathies. The patient underwent elective thoracotomy.
Results The lesion from lung was diagnosed as pulmonary sclerosing hemangioma with characteristics microscopic features. Immunohistochemical staining was confirmatory as round stromal cells and cuboidal surface cells are positive for EMA and TTF-1 but Pancytokeratin positivity was detected in only cuboidal surface cells. During the work-up of mediastinal lymphadenopathies, tuberculosis lymphadenitis was detected and the acid-fast basils were confirmed by Ziehl-Nielsen staining.
Conclusion(s) We would like to emphasize that the awareness of the sclerosing hemangioma with tuberculosis lymphadenitis in mediastinal lymph nodes is important for clinicians and pathologists during the work-up of cases. Because when a patient presented with a mass in the lung and pathologic mediastinal lymphadenopathy, the physicians usually regarded as malignant neoplasm with lymph node metastasis. Therefore, intraoperative frozen section should be done on the cases which don't have preoperative diagnosis to avoid the over-treatment.

P3.224

Squamous cell of the lung. One methylation signature

Carvalho L.; Silva Reis M.; Gomes Isabel A.; Silva L.; Alarcão A.; Couceiro P.; Sousa V.
Instituto de Anatomia Patológica, Coimbra, Portugal

Background Lung cancer is one of the main causes of death in the World. Lung carcinogenesis has to be understood either in bronchial epithelium and normal lung parenchyma to know the sequence of genetic and epigenetic abnormalities in pre-neoplastic lesions and after determine adequate therapies to prevent neoplastic evolution. In the accumulation of genetic and epigenetic abnormalities, methylation is a normal biochemical reaction to control cell cycle, may become aberrant and unmethylated CpG-rich areas in or near the promoter region of genes have been associated with transcriptional inactivation of tumour suppressor related genes and also of genes that inhibit metastasis, apoptosis, angiogenesis, and DNA repair in the evolution of human cancer. Promoter hypermethylation has been proposed as a prognostic biomarker.
Methods The aim of this retrospective study was the determination of a methylation profile of 40 squamous cell carcinomas, evaluating the methylation status of DNA repair genes hMLH1 and hMSH2 using Methylation-Specific PCR and respective protein expression by Immunohistochemistry (IHC) collected from surgical specimens in different TNM stages.

Results The MLH1 and MSH2 IHC expression was reduced in the carcinomas when compared with respective normal tissue. In only two cases hypermethylation of the promoter of these DNA repair genes was present.
Conclusion(s) These findings open a potential clinical application of methylation status both in pre-neoplastic lesions and in small biopsies of non-surgical lung cancer. The implications of this preliminary study will be useful in accessing individual risk.

P3.225
Analysis of micropapillary pattern in 145 lung adenocarcinomas

Cakir E.; Demirag F.; Yilmaz A.; Sahin S.; Yazici Eren U.; Aydin M.
Ataturk Chest Diseases and Chest Surgery Education and Research Hospital, Department of Pathology, Ankara, Turkey

Background Micropapillary pattern is defined as papillary tufts without fibrovascular core. Lung adenocarcinoma with micropapillary pattern have been reported to have a worse biological behaviour. We analysed the pathological and clinical features of micropapillary pattern positive cases.
Methods A series of 145 consecutively resected pulmonary adenocarcinomas were reviewed. Clinical features and presence of micropapillary, acinar, papillary, bronchioloalveolar and solid patterns, necrosis, differentiation, lymphovascular and perineural invasion, status of visceral pleura were examined.
Results Of the 145 adenocarcinoma cases 130 (89%) were mixed histological pattern, 12 were solid and 3 were acinar pattern. The most common combination of the four patterns were acinar and solid accounting for 37% of the cases. Micropapillary pattern observed in 49 cases (35 male, 14 female, age range 37 to 71 years, mean 56.6 years). Numbers of micropapillary pattern positive cases with clinical stage I, II, III and IV diseases were 18 (36%), 9 (18%), 16 (32%) and 6(8%), respectively. Of the 49 micropapillary pattern positive cases 26 showed tumour necrosis, 20 lymphovascular and 11 perineural invasion. 77% of micropapillary pattern positive tumors were well differentiated, 5% were poorly differentiated. Visceral pleural invasion observed in 73% of micropapillary pattern positive cases.
Conclusion(s) Micropapillary pattern in lung adenocarcinoma is regarded as a distinct prognostic marker. A micropapillary component occuring in lung adenocarcinoma should be noted in the pathology report. The presence of this component should alert the clinician to search more carefully for metastases and have a closer follow-up on these patients.

P3.226
Diagnostic utility of p63 expression in differential diagnosis of lung carcinoma

Bir F.; Aksoy Altinboga A.; Satiroglu Tufan L.
Pamukkale University, Denizli, Turkey

Background The aim of this study was to investigate the relation between p63 expression and pathological differential diagnosis of lung carcinoma.
Methods Expression of p63 in 62 lung carcinomas were investigated immunohistochemically. In six selected cases mRNA analysis were performed by using RT-PCR.
Results When p63 staining of the cases were evaluated, 24 of 25 (%96) squamous cell carcinomas were strongly positive. Six of 20 adenocarcinomas and one (%100) large cell carcinoma (except neuroendocrine carcinoma) were mildly positive. p63 staining was statistically significantly positive in squamous cell carcinoma compared to other tumors ($p<0.002$). There was a significant statistical differrence among squamous cell carcinoma and adenocarcinoma ($p<0.002$). In three of 6 cases, DNp63 was strongly positive (3/3) squamous cell carcinoma, mildly positive in one (1/1) adenocarcinoma and negative in carcinoid tumor. TAp63 was strongly positive in non-tumoral lung, but was negative in all tumors, except one squamous cell carcinoma.
Conclusion(s) Our data suggested that when poorly differentiated squamous cell carcinoma had strong and widespread staining for p63 immunohistochemically, p63 can be a useful marker in differentiating squamous cell carcinoma from adenocarcinoma and squamous cell carcinoma from large cell neuroendocrine carcinoma. Our RT-PCR results also reveal that, along with immunohistochemical staining, when diagnosis is difficult in poorly differentiated adenocarcinoma and large cell neuroendocrine carcinoma evaluation of p63 mRNA can be useful.

P3.227
Hard metal disease in two patients with interstitial diffuse lung disease

Montero Angeles M.; Morell F.
Hospital Universitario Vall d'Hebron, Barcelona, Spain

Background Hard metal lung disease is an unusual form of occupational lung disease which can occur in individuals exposed to hard metals. Clinically, the condition resembles to hypersensitivity pneumonitis, which eventually evolves to pulmonary fibrosis, depending mainly on individual susceptibility. Histologically, the lesion shows different patterns: descamative interstitial pneumonia, hypersensitivity pneumonitis, giant cell interstitial pneumonia and usual interstitial pneumonia.

Methods We present two cases that correspond to different types of workers: a 37 year-old woman, who worked as a jewellery polisher for two years. On histology, she showed a fibrotic Non-Specific Interstitial Pneumonia with abundant multinucleated giant cells some of them with emperipolesis. The second case, a 56 year-old woman who worked at a wheel factory for years. She presented Usual Interstitial Pneumonia pattern with centrilobular fibrosis and abundant intraalveolar macrophages.
Results Both cases were studied under Scanning Electron Microscopy, and both of them showed different types of metals.
Conclusion(s) - Hard metal lung disease depends on individual susceptibility, and there is no correlation between intensity and the accumulation of dust. - As the functional and radiological findings are non-specific, and there are no laboratory tests available to establish the diagnosis, it is important to study the broncoalveolar lavage or the lung tissue to look for direct or indirect signs of the disease, as giant cell with emperipolesis or different types of hard metals.

P3.228

Histological features of metastatic adenocarcinoma (adenocarcinosis) of the pleura

Kosjerina Z.; Kern I.; Kayser K.; Kosjerina Ostric V.; Bozanic S.; Goldman T.; Kayser G.
Institute of Lung Diseases, Sremska Kamenica, Serbia and Montenegro

Background Metastatic adenocarcinoma (MA) involved pleura, may sometimes take the histological features very similar to epithelial malignant mesothelioma.
Methods The material of the study included 13 biopsy samples of the pleura. The quantity of cellular elements, as well as the intensity and distribution of IHH staining were determined by the semiquantitative method.
Results Of the total of 13 MAs, malignant cells were arranged as solid collections in 7/13 samples, papillary, tubular or acinar formations in 2/13 cases respectively. Malignant cells varied in size, being most commonly of the medium (9/13), small, or large size (2/13) respectively. The cells were diversely shaped as well: polygonal in 6, oval and cylindric in 2 samples respectively. The cytoplasm of the malignant cells was moderately abundant in quantity 4 times, poor 9 times. The nucleus was most commonly large (9/13), oval in shape (8/13), with fine chromatin (4/13). The nucleolus was most frequently tiny (6/13), unprominent (9/13). The papillas were coated with a row of moderately large polygonal or cuboid cells. All 13 biopsy samples were positive to BerEp4 (8 and 5 intensive or moderately stained samples respectively). Immunopositivity to MOC31 was registered in 12/13 biopsies (with intensive or moderately staining malignant cells in 5 and 7 biopsies respectively). Carletinin was negative in all biopsy samples, but CK 5/6 was poor positive in 2 biopsies.
Conclusion(s) MA is most commonly solid, then papillary, tubular and acinar. BerEp4 and MOC31 are nearly always positive, unlike Carletinin and CK 5/6.

P3.229

Morphometric image analysis of squamous dysplasia and squamous cell bronchial carcinoma

Mijovic Zarko Z.; Mihailovic Slavoljub D.; Kostov Sima M.
Institute of Pathology, Medical Faculty of Nis, Nis, Serbia and Montenegro

Background Lung cancers are preceded by a series of preneoplastic lesions. Squamous dysplasia may be precursor to squamous cell bronchial carcinoma. The aim of this study was morphometric image analysis of squamous dysplasia and squamous cell bronchial carcinoma.
Methods At Institute of Pathology, Medical faculty University of Nis, formalin-fixed, paraffin-embedded bronchoscopic mucosal samples from 10 patients with moderate squamous dysplasia and 10 patients with squamous cell bronchial carcinoma were retrieved from pulmonary pathology archives. Serial histologic sections of 4 μm thickness were prepared for staining with hematoxilin and eosin and analyzed using a computer-assisted interactive image analysis system LUCIA M 3.51 ab (Nikon) at objective 40x. The binary images were manually edited. Four nuclear variables were estimated. In each case a hundred nuclei were measured. A statistical analysis was performed using Student's t-test.
Results All measured four nuclear variables: equivalent diameter, nuclear area, volume of equivalent sphere and circularity were found to be significantly different between squamous dysplasia and squamous cell bronchial carcinoma ($p<0.001$). The values of nuclear variables of squamous cell carcinoma were significantly larger than in squamous dysplasia.
Conclusion(s) Morphometric image analysis may be helpful ancillary tool in distinguishing squamous dysplasia from squamous cell bronchial carcinoma in bronchoscopic biopsy specimens.

P3.230

Neuroectodermal tumour of the lung with divergent differentiation towards malignant melanoma and atypical carcinoid

Pilozzi E.; Cacchi C.; D'Andrilli A.; Pini B.; Scarpino S.; Ruco L.
II Facoltà di Medicina e Chirurgia, Università La Sapienza, Rome, Italy

Background The possibility that lung cells of neuroectodermal origin may undergo melanocytic differentiation is sustained by description of rare cases of lung carcinoids with cells containing melanin and expressing melanocytic antigens. Moreover rare cases of primary lung melanoma have been reported. Since normal melanocytic cells are not present in bronchial mucosa, it has been suggested that melanoma cells may derive from disperse neuroendocrine cells or from a pluripotent stem cells. In the present report we describe a case of lung neoplasm with unambiguous divergent differentiation toward atypical carcinoid and malignant melanoma.
Methods A 62 years old woman presented with a well circumscribed 5 cm lung tumour that was extensively characterized by immunohistochemistry. To assess the frequency of melanocytic differentiation in carcinoid tumours, 37 cases of lung carcinoid (31 typical and 6 atypical) were immunostained for S100, MART-1 and HMB45.
Results The tumour was made of melanomatous areas (melanin-positive, HMB45+, MART-1+) intermingled with atypical carcinoid areas (CD56+, cromogranin A+, synaptophisin+, TTF1+). The patient had no history of excised cutaneous pigmented lesion, nor any evidence of primary malignant melanoma elsewhere. A very tiny group of HMB45+ cells was observed in only one of the 37 immunostained carcinoids, suggesting that focal melanocytic differentiation is rare.
Conclusion(s) Our results indicate that melanocytic differentiation is a rare event in carcinoids, and provide additional evidence that a common stem cell may be responsible for the development of the few cases of primary melanoma of the lung.

P3.231

Prognosic value of immunohistochemical expression of hMLH1, hMSH2, PTEN and AKT in non-small cell lung carcinoma (NSCLC)

Vasilescu F.; Georgescu A.; Iosif C.; Dobrea C.; Andrei F.; Mihai M.; Dumitrescu M.; Dinu B.; Ardeleanu C.
Victor Babes National Institute of Pathology, Bucharest, Romania

Background Lung cancer continues to be the leading cause of cancer death in many industrialized countries. Despite advances in therapy, surgery methods, and protein markers, there are not well established the prognostic factors of NSCLC. The only criterion with prognostic value remains the tumor stage.
Methods We investigated the immunohistochemical expression of hMLH1, hMSH2, PTEN and AKT in 47 paraffin-embedded tissue specimens of NSCLC in different tumor stages. Eighteen of them were diagnosed with squamous cell carcinoma, 20 with adenocarcinoma, 5 with adenosquamous carcinoma and 4 with large cell carcinoma. None of them received treatment before surgery.
Results PTEN was positive in 70,21% of cases (range 10% to 95%). AKT was positive in 95,74% of cases in isolated cells, focal or diffuse areas. MLH was positive in 44 cases (93,61%) and MSH in 43 cases (91.48%) both of range in between 3% and 90%. We didn't find any correlations between protein expressions of these markers with invasion, lymph node metastasis and survival.
Conclusion(s) As a result of our study, the absence of any correlation between the expression of hMLH1, hMSH2, PTEN and AKT, and clinical prognostic factors with already accepted value, don't recommend them as prognostic biomarkers.

P2.232

Prognostic value of EGFR protein expression and gene amplification in patients with lung adenocarcinoma

Panjkovic Dusanko M.; Eri Z.; Knezevic Usaj S.; Tadic Latinovic L.; Ivkovic Kapicl T.; Karapandzic A.
Institute of pulmonary diseases of Vojvodina, Sremska Kamenica, Vojvodina, Serbia and Montenegro

Background The epidermal growth factor receptor (EGFR) is associated with the genesis of many human tumors including lung carcinoma. One of the elevation mechanisms of the EGFR expression is the gene amplification.
Methods This investigation was analysis of the protein expression by immunohistochemistry (IHC) and EGFR gene amplification by chromogen in situ hybridization (CISH) in lung adenocarcinoma tissue obtained from 90 patients. The parameters were analysed in regard to the disease free period and patients' overall survival over a 60-month follow-up period.
Results Protein EGFR overexpression was found in 37,78%, while gene amplification was presented in 11,11% cases. A difference in the disease-free period and the overall survival has been established for diverse stages of the disease. No differences regarding the final outcome of the disease were established between the groups according to the EGFR protein expression. Considering the EGFR gene amplification in the tumor, a statistically significant difference in the length of the disease-free period and survival was registered between the examined groups, registering a better final outcome in the groups with an increased gene copy number and the presence of EGFR gene amplification compared to the group with normal gene copy number for EGFR in the tumor. Disease stage was the only independent prognostic factor according to the multivariant analysis.

Conclusion(s) Further investigations are needed for the evaluation of the prognostic and predictive value of EGFR in lung adenocarcinoma.

P2.233
Prognostic value of vascular endothelial growth factor expression in lung adenocarcinoma

Tadic Latinovic L.; Eri Z.; Knezevic Usaj S.; Panjkovic M.
Banja Luka, Bosnia and Herzegovina

Background Lung adenocarcinoma is most common cell type in fimales (smokers and non smokers) and in non smoking males. Vascular endothelial growth factor (VEGF) plays a pivotal role in the development of physiological and pathological neovascularisation. High expression of vEGF in tumors has been found to be associated with poor prognosis in some studies, but not in others. The aims of this study were to determine the prognostic value of VEGF in operable lung adenocarcinomas.
Methods Tumor tissue were obtained for 107 patients with operable lung adenocarcinomas and complete follow up informations for five years included. No adjuvant therapy was given prior surgery. Specimens were stained with anti- VEGF antibody. VEGF expression in tumor cells was assessed by: percentage of stained area, intensity staining and final score (product of area and intensity).
Results Expression of VEGFwhere almost same in a patients with mediastinal nodal metastasis when compared with non metastsizing cases without statistical significance (p=0,269). VEGF expression was more intense in a patients with IIIA stage disease when compared with the other lower stages. Ther was statistical significance (p = 0,044). Furthermore, log rank analysis showed significant association with poor survival by higher disease stages (p = 0,022). VEGF expression in tumor cells was not prognostic factor for survival time (p = 0,114).
Conclusion(s) The most important prognostic factor for lung carcinomas is pathological stage.

P3.234
Sialadenoma papilliferum of the bronchus

Honda Y.; Ishihara S.; Iyama K.
Department of Surgical Pathology, Kumamoto University Hospital, Kumamoto, Kumamoto, Japan

Background Sialadenoma papilliferum is a rare salivary gland tumor, mostly occur on the intraoral mucosa. There are sporadic cases of sialadenoma papilliferum of the esophagus, nasopharynx, nasal cavity. Only one case of sialadenoma papilliferum of the bronchus has been reported previously.
Methods A small poplypoid tumor, 5 mm in size, in the luminal wall of the right superior lobe bronchus was resected from a 75-year-old man. The resected tumor was examined histologically and immunohistochemically.
Results Histologically, exophytic papillary lesion of the tumor were lined by columnar or metaplastic non-keratinizing stratified squamous epithelium. Glandular component of cysts and duct-like structures in the submucosa were lined by a double layer epithelium composed of luminal cuboidal or columnar cells and basal cuboidal or flattened cells. There were no features indicating malignancy. The luminal cells were immunohistochemically positive for cytokeratin (CK) 7, CK 8/18, CK 19, CEA and epithelial membrane antigen (EMA), and negative for CK 20, CK 5/6, CK 14, vimentin, p63, S-100 protein, smooth muscle actin (SMA), calponin or glial fibrillary acidic protein (GFAP). On the other hand, basal cells were positive for CK 5/6, CK 14, vimentin, p63 and S-100 protein, and negative for CK 7, CK 8/18, CK 19, CK 20, CEA, EMA, SMA, calponin or GFAP.
Conclusion(s) We report the second case of sialadenoma papilliferum of the bronchus. Awareness of such rare lesions is important for both pathologist and clinician.

P3.235
VEGF-A and bcl-2 expression in different tissues after cardiac surgical interventions

Jung I.; Gurzu S.; Kovacs J.; Azamfirei L.
University of Medicine and Pharmacy of Targu-Mures, Romania

Background The VEGF (Vascular Endothelial Growth Factor) and apoptosis seem to play an important role in the Multiple Organ Failure Syndrome (MOFS). In this paper we analysed the expression of VEGF and bcl-2 in different tissues, trying to understand the pathogenesis of MOSF.
Methods We used the antibodies VEGF-A, clones VG1 and bcl-2, clone 100/D5 (LabVision). With VEGF-A, we analysed the angiogenic phenotype of different tissues (lung, myocardium, pancreas, kidney, liver) from 40 necroptic cases. All the patients died after cardiac surgical interventions. We also analysed the aspects of apoptosis with bcl-2.
Results In myocardium, VEGF-A marked normal muscle cells but the areas with degeneration were negative. Bcl-2 expression was diffuse or focal in these fibers, with overexpreesion in subendocardial areas. In liver, VEGF marked only normal hepatocytes but bcl-2 marked the degenerated hepatocytes. In kidney, VEGF marked the normal tubes but bcl-2 expression was observed in necrotic tubes. VEGF also marked the pancreatic tissue, bronchial epithelium and the endothelium in lung. The bcl-2 expression was also observed in alveolocites, macrophages and bronchial epithelium.

Conclusion(s) VEGF expression increases in hypoxic condition but the overexpression of bcl-2 in myocardium, degenerated hepatocytes and renal tubes with necrosis prove an intense anti-apoptotic activity. This means that, after a major trauma like cardiac surgery the defending mechanisms consists in pro-angiogenic and anti-apoptotic activities. The latest seems to play an important role in epithelial regeneration.

P3.236
Effect of cholesterol rich diet, recurrent infection and possible treatment modalities on pulmonary vascular system: an experimental study

Ozbudak O.; Ozbudak I.; Turkay C.; Sahin N.; Ozdem S.; Turkay M.; Ozbilim G.
Akdeniz University School of Medicine Department of Pulmonary Medicine, Antalya, Turkey

Background Infectious agents may lead to inflammation, atherosclerosis and thrombotic vascular events. The atherosclerotic effect of hypercholesterolemia on vascular system is well-known. However, limited studies were done on the therapeutic and preventing agents. The aim of this study was to investigate the effects of infection and/or cholesterol rich diet combined with antibiotic, anti-inflammatory agent and red wine on pulmonary arteries.
Methods Fifty-nine rats were able to be evaluated. Six groups were done as follows: Control rats (Group I), infected rats (Group II), infected rats fed by cholesterol rich diet (Group III), infected rats fed by cholesterol rich diet and treated by antibiotics (Group IV), infected rats fed by cholesterol rich diet and treated by anti- inflammatory agent (Group V), infected rats fed by cholesterol rich diet and red wine (Group VI). The sections of central pulmonary arteries were examined for thickness of intima and medial wall by computerized image analysis.
Results A significant difference was found between the groups in thickness of intima (p=0.000). Rest of the groups had more intimal thickening than the Group I (p = 0.000). Group III had thicker intima than Group IV and V (p = 0.009, p = 0.011 respectively). There was no significant difference between the groups in thickness of media (p = 0.432).
Conclusion(s) Infection and a cholesterol rich diet have a synergistic effect on atherosclerosis in pulmonary arteries. However, antibiotics and anti-inflammatory agents could be useful in prevention.

P3.237
EGFR expression in lung squamous cell carcinoma and correlation with prognosis

Vuckovic L.; Tadic Latinovic L.; Eri Z.; Savjak D.; Nenezic T.; Vukmirovic F.; Golubovic M.
Clinical Center, Podgorica, Serbia and Montenegro

Background Lung carcinoma is a frequent malignant disease with a poor percent 5-year survival. One of the most frequent histology type is squamous cell carcinoma. Expression of Epidermal Growth Factor Receptor is increased in many malignant diseases. The purpose of this study is to verify the grade of expression EGFR in squamous cell carcinoma of the lung and its correlation with prognosis.
Methods In this study 120 patients were examined who in the moment of an operative treatment were in I, II and IIIA stage of disease (40 patients in each stage). Observation interval lasted five years. Imunohistochemical analyses was done. Following score system was used: 0 – there is no colouring or less then 10% cells are coloured, score 1 – scanty membranous positivity is observed in more than 10% of cells, score 2 – weak or middle complete membranous positivity is observed in more than 30% of cells and score 3- strong, complete membranous positivity is observed in more than 30% of cells.
Results In the examined group of patients there were 105 men and 15 women. Most of them had an age range 50 to 69. The great number of patients expressed score 1 and score 2. Important statistic connection of EGFR grade expression with survival interval in all 3 examined stages of spreading disease wasnt improved.
Conclusion(s) Expression grade of EGFR doesnt correlate with prognosis of patients with lung squamous cell carcinoma treated in stage I, II and IIIA.

P3.238
Oncocytoma of the lung. Case report

Nenezic T.; Savjak D.; Vuckovic L.; Vukmirovic F.; Golubovic M.
Clinical Center, Podgorica, Serbia and Montenegro

Background Oncocytoma is a rare tumour which occurs among elders. It has its orrgin in oncocites large cells with granular acidophilics cytoplasma replaced with large mitochondria.Tumour is charasteristically well demarked uniformly expanse.
Methods Patient 73 years old had symptoms, like: pain in the thoraces, preath obstruction, suffocating, coughing up and hemophtisia. Lingula was in whale obstructed with neoplasma. After surgical removment, specement of tumor was examined at Department of Pathology. Hematoxillin and eosin coloration was used.
Results The sectioned surface of tumour was characteristically mahagony brown, homogeneous and centrally scarred. Histologically: tumor was composed of a uniform population of plump cells orranged in alveolar type nests, trabeculae or even tubules. The cytoplasm was granular and acidophilic. The chromatin was finely granular and evenly

dispersed. Nucleoli were inconspicuous and mitoses were rare. Haemorrhage and necrosis were absent even in the largest examples. Diagnosis was oncocytoma.
Conclusion(s) Oncocytoma is a benign tumour which occurs among elders with well prognosis.

P3.239
Pathological perspective of lung cancer histological type changings trends

Stojsic M.J.; Adzic T.; Markovic J.; Milovanovic I.; Maric D.; Branislava M.
Institute for Pulmonary Diseases and Tuberculosis, Clinical Centre Serbia, Belgrade, Serbia and Montenegro

Background The lung cancer is most frequently diagnosed malignant disease all over the world. In men, it is the first cause of mortality and in women, it is on the third place, just after breasts and intestinal but before cervical cancer.
Methods Retrospective analysis of the most frequent histological types of lung cancer on tissue spacemans obtained on bronchoscopy and percutaneous needle biopsy. The changing of histological type were analysed from 1985 to 2005 according to patients' age and geneder, in total number and noth genders separately. Analysis was based on histologically confirmed primary lung cancer in 6289 patients, 16.6% females and 83.1% males. Statistical significance was established by Chi-Square Test ($\chi 2$) test at the level of significance $p<0.05$ with software package SPSS for Windows, version 10.0.
Results The highest frequency of squamous cell carcinoma (SCC) was noted in total number of patients in all investigated years (58.0%), and separately in male (60.4%) and female (45.7%) patients. This histological type was predominant in all age groups in both genders: 180 (38.1%) females i and 1318 (41.6%) in group 5.00 and 1318 (41.6%).
Conclusion(s) SCC has the highest frequency in undeveloped countries in contrary to AC with the highest frequency in developed ones. Continuous prevention against smoking and its cessation, improving working conditions and socioeconomic conditions is a strategy for decreasing of all histological types of lung cancer patients.

P3.240
Pulmonary carcinoid tumorlets in association with aspergilloma (fungus ball)

Abensur Athanazio D.; Medeiros F.; Costa A.L.; Athanazio P.R.
Federal University of Bahia, Salvador, Bahia, Brazil

Background Pulmonary carcinoid tumorlets are otherwise typical carcinoid tumors that measure ≤5 mm in greatest dimension. Their neoplastic behavior or even metastatic potential is still matter of debate. They are usually found in association with chronic fibrosing lung disease such as tuberculosis and bronchiectasis. The occurrence of carcinoid tumorlets next to aspergilloma (fungus ball) has not been previously reported.
Methods Case report.
Results A 63 year old female patient, with previous history of long-term rheumatoid arthritis treated with diverse immunosuppressive drugs, underwent surgical resection of two segments of the left lung due to extensive honeycomb appearance. Both specimens exhibited an extensive bronchiectasis pattern with multiple cavities containing purulent material. The larger cavity (5 cm in diameter) proved to be an aspergilloma at microscopy. Two small foci of neuroendocrine proliferation in the periphery of this lesion were observed.
Conclusion(s) This case highlights the importance of future studies, such as case series of with careful examination of peripheric areas of aspergillomas, to evaluate in which extent the disease is related to carcinoid tumorlets or even typical carcinoid tumors. Such information would be valuable for the follow-up recommendations of patients after treatment of aspergilloma (fungus ball).

P3.241
Would patients with primary pulmonary carcinomas 40 years and younger profit from small molecule tyrosine kinase inhibitors?

Gruber-Moesenbacher U.[1]; Eiter H.[2]; Cerkl P.[3]; Popper H.[4]
[1]Institute of Pathology, [2]Department of Radiooncology, [3]Department of Pulmonology Universitary Teaching Hospital Feldkirch, Austria; [4]Institute of Pathology, Medical University Graz, Austria

Introduction Approximately 50 new pulmonary carcinomas are diagnosed in our institution yearly. Patients below the age of 40 years are rare. Between 2003–2005 we diagnosed.9 patients, 5 females and 4 males.
Materials and methods Tumors were diagnosed on biopsies (5) or resection specimen (4) according to WHO classification of lung tumors 2003. Specimen of 8 patients could be analysed for mutations of the EGFR-gene (TheraScreen: EGFR29 MutationKit DXSdiagnostics).
Results Most patients presented with high stage. Metastasis were found in pericardium, liver, brain, lung and bone. Overall survival was between 6 months and 3 years 7 of 9 tumours were low grade adenocarcinomas, mixed types, 1 mucoepidermoid carcinoma 1 large cell carcinoma. 2 resected tumors had large central scars, 1 showed invasion of pulmonary arteries. Chemotherapy was based on a combination of Gemcitabine, Cisplatin, and Vinorelbine, first- and second line.

Discussion and conclusion Pulmonary carcinomas in young smoking patients usually behave more aggressively as we could find in our cases. These patients might have had a benefit from therapy with small molecule tyrosine kinase inhibitors (Gefitinib or Erlotinib), even as first-line therapy. We retrospectively analysed mutations in exons 18–21 of the EGFR gene, which is required for prediction of success of treatment.

Electron microscopy

P3.242

Endotheliocytes desquamation in hemomicrovessels of bronchial mucosa of liquidators of Chernobyl disaster

Segeda Prokofievna T.
Institute for Sorption and Endoecology Problems, National Academy of Sciences of Ukraine, Kiev, Ukraine

Background Long-term own studies of peculiar structural features of microvasculature elements in bronchial mucosa of individuals exposed to low intensity radiation action, gives evidence to considerable damages caused to endothelium.
Methods Please consider results of electron microscopy studies of broncho-bioptic specimens of individuals suffering with chronic bronchitis: 142 liquidators of Chernobyl Disaster Y1986, and 26 patients of nosological control group.
Results It was established, that frequency of endotheliocytes desquamation of liquidators was higher vs. those of the reference group, and has been registered within the whole study period (1989 - 2001). In the process of endothelial cells desquamation under the influence of radiation, their considerable quantity was registered in vessels lumens, sometimes even resulting in obturation of the latter. Obvious alteration features were not registered in predominant amount of desquamated cells of the liquidators. Monitoring surveys inside the vessels have shown prevailing amounts of individual endotheliocytes with distinct signs of necrobiosis. Stimulation of endotheliocytes death of the liquidators resulted in: a) decrease of hemomicrovessels walls thickness; b) registration of fenestrated endothelium; c) vessels walls integrity damages; d) multiplication of vascular basal membrane.
Conclusion(s) Endotheliocytes desquamation activation in hemomicrovessels of patients-liquidators has pathogenetic significance for violation of microcirculation.

P3.243

Electron-microscopic examination of the liver biopsy in injection drug users with the chronic hepatitis C

Reshetnikova Sergeyevna O.; Ovcharenko Alekseyevich N.; Zinchenko Vladiimirovna O.; Pinsky Leonidovich L.
Lugansk State Medical University, Lugansk, Ukraine

Background It is widely accepted that injection drug users (IDUs) are at risk for contracting a chronic hepatitis C (CHC), which can cause liver cirrhosis and carcinoma. Morphological investigation of a liver biopsy could be helpful for assigning the severity of the hepatic damage.
Methods Fifteen liver biopsies (12 men and 3 women, 22 - 34 years old) were taken for histological and electron-microscopic examinations from the IDUs with CHC. Diagnosis of CHC supported by the presence of anti-HCV, biochemical indicators and confirmed by the positive test for HCV RNA.
Results The results have shown the hepatocellular damage including lipid degeneration and hepatocytes necrotic foci accompanied with lympho- macrophages infiltration in the portal tracts. Thin strands of collagen fibers extended from the portal tracts. Steatosis was an important pathological implication. The centrilobular hepatocytes were more affected. The fat droplets varied from minute ones scattered in the cytoplasm to coalesced droplets filled entire cytoplasm of cells. They had the appearance of the cypolasmic bodies changeable in sizes and electron density. Cytoplasm in most of cells was presented by distended clear globules, while the nucleus flattened and displaced to the periphery of the cell. The mitochondria were enlarged, sometimes with a giant forms formation. The smooth endoplasmic reticulum was hyperplastic.
Conclusion(s) These data suggests the performance of the liver biopsy to detect the severity of changes in CHC and any success in the treatment of hepatic pathology.

P3.244

Ethanol and carbon tetrachloride hepatotoxicity in rats. Ultramicroscopically comparative evaluation

Dima-Cozma C.; Pandele G.; Stolnicu S.; Dobrescu G.; Radulescu D.
Gr. T. Popa University of Medecine and Pharmacy, Iasi, Romania

Background Most drugs and other foreign substances could induce liver injury. At least 5 mechanisms that primarily involve the hepatocyte produce liver injury, some of them being identified by ultramicroscopic evaluation. The objective of this study was to assess the differences in morphological evolution of hepatotoxicity obtained with ethanol or carbon tetrachloride (CCl4) in rats.
Methods Chronic liver injury was induced in 40 rats who received CCl4 (N=14), ethanol (N = 14) or saline solution (N = 12, control rats) and the morphology was evaluated at 4, 8 and 12 weeks by optically and electronically microscopic examination. For histological assessment, liver samples were fixed in 4% formalin and stained with hematoxylin and eosin. Ultramicroscopically, the samples were evaluated at Philips CM 100.

Results The evolution of alterations (blood congestion, steatosis, fibrosis and cirrhosis) was more rapidly in tetrachloride hepatotoxicity. The precocious lesions were also demonstrated in electronic microscopy (disruption of actin filaments and mitochondrial DNA, blebbing of the cell membrane, rupture and cell lysis). The most important mechanisms implicated in liver injury was intracellular dysfunction, loss of ionic gradients, decline in ATP levels, actin disruption, cell swelling and cell rupture, cholestasis and inhibition of mitochondrial function. Cirrhosis was induced after a mean period of 8 weeks in tetrachloride group and 12 weeks in ethanol group.
Conclusion(s) The study compare 2 experimental models of hepatic cirrhosis, realised with ethanol or carbon tetrachloride and identify optically and ultramicroscopically evolution.

P3.245
Pitfalls in tumour pathology solved by EM: the "multiform" patterns of adenoid cystic carcinoma of salivary gland

Resta L.; Rossi R.; Fiore G.M.; Palumbo M.; Piscitelli D.
University of Bari, Dept. of Pathology, Bari, Italy

Background The routine collection of a sample for ultramicroscopy in each case of salivary gland neoplasia led us to assemble a series of more than 40 patients.
Methods Ultrastructural study was useful to confirm the diagnostic hypothesis based on morphological and immunoistochemical findings and of primary importance in 5 cases. In particular, two cases diagnosed as acinic cell carcinoma (of follicular pattern) and clear cell carcinoma NOS were re-evaluated after the ultrastructural microscopy and diagnosed as adenoid cystic carcinoma.
Results The usual cyto-architectural pattern of adenoid cystic carcinoma may become confuse when the cells are larger then normal, with evident and anphophil and/or clear cytoplasm. The accumulation of the PAS-positive basal membrane-like protein among neoplastic cells may mimic the protein accumulation observed in the follicular structure of acinic cell carcinoma or the hyaline stroma of other carcinomatous proliferation. The ultrastructural aspect of adenoid cystic carcinoma is characterized by luminal ductal cells and abluminal basal and myoepithelial cells. The cytoplasm is poor of subcellular orgenelles, shows many process and desmosomes. The nuclei are irregular in shape, with clear matrix and evident nucleoli. Beyond the basal lamina, the granular interstitial space is composed by glycosaminoglycans and proteins of the basal membrane.
Conclusion(s) In some instance, the ultrastructural findings result to be more important than the confusing immunophenotype in the diagnosis of adenoid cystic carcinoma of the salivary glands.

P3.246
Placentas of well controlled diabetic mothers and healthy newborns show ultrastructural damages. A mechanism of compensation?

Resta L.; Rossi R.; Fiore G.M.; Palumbo M.; Piscitelli D.
University of Bari, Dep. of Pathology, Bari, Italy

Background Diabetes in pregnancy can lead to severe consequences both for mother and fetus. Many studies therefore aim to identify the histological characteristics of the placenta during diabetes, as chorioangiosis and "dysmaturity. Few ultrastructural studies has been reported in well controlled diabetes.
Methods The study was carried out on 5 diabetic placentae and 4 of normal placentae. The women with diabetes (3 of type 1 and 2 gestational diabetes) were aged between 24 and 39. All of the patients were receiving insulin treatment, so their glucose profile was fairly low. A full-thickness chorionic biopsy was performed immediately at birth, and 1–2 mm fragments processed for electron microscopy.
Results In diabetic placentae, the capillaries were more numerous but with a reduced diameter. Many of them were some distance from the villus basement membrane. The endothelium often appeared swollen, due to the presence of several endothelial cells with thicker, electrondense cytoplasm with varying degrees of vacuolisation. The trophoblast showed excess intracytoplasmic vacuoles. Various focal points were observed where electron-dense protein bodies accumulated in a finely structured intra- or sub-membranous location, sometimes with minute calcifications.
Conclusion(s) Our study shows that also in well treated and non complicated diabetic women, alteration in ultrastructure of terminal villi vessels are present. Degenerative and proliferative changes in endothelium as well as in trophoblast may interfere with maternal-fetal exchanges. Accumulation of electrondense material in basal membrane may be a sign of immunodeposits.

P3.247
Ultrastructural alterations of hepatocytes at design and treatment of intrahepatic portal hypertension by means of applications of laser intrahepatic portocaval shunt in the experiment

Boyko V.; Mylovydova G.; Avdosyev Y.; Grigorov Y.; Nalcha I.
Government Institution "Institute of General and Urgent Surgery of Academy of Medical Sciences of Ukraine", Kharkiv, Ukraine

Background The aim of this study was to investigate at ultrastructural level the effectiveness of laser intrahepatic

portocaval shunt for decreasing pressure in portal vein and prophylaxis of hemorrhages from esophagus and stomach veins.

Methods There was carried out the electron microscopic research of small parts of liver from zone at the large distance from the place of shunts formation at mechanical and laser methods in the experiment.

Results The electron microscopic research of state of liver cells after setting of intrahepatic stent revealed predomination of synthetic and reparative processes over catabolic process. Essential normalization of ultrastructural architectonics of hepatocytes was marked. The mitochondria swelling degree increased, the vacuolization of cisterns of granular and agranular endoplasmatic networks decreased. Hepatocytes with large number of glycogen granules, ribosomes and polysomes in cytoplasm represented the structural equivalent of compensate-adapted and reparative processes on submicroscopic level. The main group had the full recovery of submicroscopic architectonics of all cellular and intracellular components of liver parenchyma.

Conclusion(s) Morphofunctional comparative characteristic of formation of shunt by mechanical method and using laser radiation shows the advantage of the last. Visual characteristic revealed less traumatic effect of laser shunt in the first days after its formation caused by less damaging influence on hepatocytes; the fast formation of epithelial cover on the surface of created canal; the minimal damage of hepatocytes by laser radiation.

P3.248

Amyloid deposits polarizations optical characteristics of systemic and localized AL-lambda

Apáthy A.; Bély M.
Department of Rheumatology - National Institute of Rheumatology and Physiotherapy Budapest, Hungary, Budapest, Hungary

Background The aim of this study was to define the polarizing microscopic characteristics of systemic AL-lambda and localized AL-lambda deposits.

Methods amyloidosis was studied in a selected autopsy population of 5 in-patients with B-cell lymphoma and compared with 5 biopsies of extranodal plasmacytoma of epipharynx (nasopharynx) or vocal cord with localized AL deposits. Systemic immunoglobulin light-chain AL.

Results Microscopically all types of amyloid deposits were eosinophilic, congophilic and with polarized light appeared birefringent, showing a specific apple green color.There was a basic difference between systemic and localized AL amyloid deposits in relation to the blood vessels when viewed under polarized light. The systemic AL deposits were always present within the vessel walls (with, or without extravascular deposition between the collagen fibrils). The localized AL amyloid deposits (with, or without proliferation of undifferentiated immunoblasts and plasmablasts) were never observed within the vessel walls; the amyloid deposits were exclusively localized to extravascular tissues. Under polarized light the localized AL deposits exhibited in some areas extremely intensive "crystalloid-like" accumulations and birefringence of amyloid filaments.

Conclusion(s) The production of amyloid precursors related to the cardiovascular system becomes generalized via the bloodstream, producing systemic forms of amyloidosis. The local production of immunoglobulin light chains is not directly related to the systemic circulation and remains a localized process of organ- or tissue-limited isolated amyloidosis. According to our interpretation the "crystalloid-like" birefringence represent the stage dependent maturation (or fragmentation) of deposited amyloid protein filaments, indicative of an advanced stage of deposition.

Poster session 4

Soft tissue tumors

P4.1

Morphologic and functional characteristic of smooth muscles' new growth of uterus under amplification of nucleolar organizers

Avdalyan Merudzanovich A.; Bobrov Petrovich I.; Lazarev Fedorovitch A.
Altay's office of ROSC by N.N.Blochin, Barnaul, Altai, Russian Federation

Background It was recently discovered participation of argyrophilic proteins of nucleolar organizer areas (Ag-NOR - proteins) in regulation of mitotic cycle. According to data, the level of Ag-NOR expression correlates with that of transcript activity of ribosome genes and also with indexes of proliferate cells activity. Objective of the work is investigation of the activity of Ag-NOR of invariable myometrium, leiomyomas and leiomyosarcoma corpus uteri myocytes.

Methods Materials of investigation are 41 uterus, removed on account of myoma. 36 cases were cellu-lar leiomyomas, fibromyoma, bizzare leiomyomas; 6 - high-grade and 5 are low-grade differ-entiated leiomyosarcomas. Histological sections of tumours were AgNO3 imbued by two-stage method of Y. Daskal et al., 1980.

Results Results of the investigation made demonstrated that despite phase of the menstrual cycle the average number of

silver granules per 1 myocyte nucleus in invariable myometrium totaled 3,42±0,11. In cellular leiomyoma, high-differentiated and low-differentiated leiomyosarcoma number of silver granules per 1 myocyte nucleus in invariable myometrium totaled 6,01±0,22, 12,11 ± 0,46 and 18,8±1,06 respectively ($p<0,05$). In bizzare leiomyoma number of silver granules totaled 6,6±0,33. The minimal number of silver granules was recorded in fibroma with marked sclerosis and hyalinosis i.e. 2,1±0,19.

Conclusion(s) Thus, calculation of the number of silver granules per 1 myocyte nucleus can be assume as a basis to differential diagnostics between cellular leiomyoma and high-differentiated leiomyo-sarcoma and can be a sign of retrogression of their differentiation.

P4.2
Retroperitoneal mesenchymal chondrosarcoma (case report)

Amini E.; Shayanfar N.; Mirzamani N.
Tehran, Islamic Republic of Iran

Background Mesenchymal chondrosarcoma (MC) was first described in 1959. MC is a rare tumor arising in bone or soft tissue which is composed of well differentiated cartilage within a proliferation of primitive mesenchymal cells. MC occurs most often in the second and third decades of life. The prognosis is poor and local recurrence and metastases are frequent.

Methods A 32 year old, white female consulted a physician for abdominal pain, nausea and vomiting. Computed tomographic (CT) scan of the abdomen disclosed a huge retroperitoneal mass with large area of necrosis located at the left side with probable diagnosis of kidney tumor. Left nephrectomy and splenectomy was performed for the patient. During surgery a retroperitoneal mass occupying the left side with adhesion to the adjacent viscera was detected and removed.

Results Histopathological examination revealed mesenchymal chondrosarcoma.

Conclusion(s) Case report.

P4.3
Basal carcinoma: high local malignancy in face localization

Tamas C.; Shaukat S.; Popa L.; Stolnicu S.; Radulescu D.
Plastic and Reconstructive Surgery Department, University of Medicine and Pharmacy "Gr. T. Popa", Iasi, Romania

Background Basal cell carcinoma (BCC) known as a skin tumor with low general malignancy, has high risk of recurrence in face localization; the special morphological features of the face and the latency of the patients in first presentation to the physician, are reasons for bad functional and esthetic post-operatory results.

Methods We are reporting 130 cases operated during last 5 years, histologically confirmed as facial BCC. We performed correct oncollogical excision in ~95%; 6 patients needed re-excision. Local flaps were used in 120 cases and pedicled (9) or free flaps (omentum 1 case).

Results Our study confirmed the predominance of the facial BCC on male over 55 (90%), and the localization mainly in the eyelids, orbital regions and central face, (38%). We operated facial BCC also in young people (4 cases) with low sun exposure. High local aggresivity is particular for the inferior eyelid localization (~52% from the orbital BCC) and medial epicanthus (30% from the orbital BCC). On three situations we had to eliminate the eyeball because of cancer invasion and we covered the defect with local (1 frontal flap), pedicle (1 temporal flap) or free transferred (free omentum) flap.

Conclusion(s) BCC, known as a skin cancer with very low general aggresivity, often affecting old people, with good evolution in time, can be fatal in face localization due to particular anatomy of the region.

P4.4
Chordoma. A retrospective clinico-pathological study of 42 cases surgically treated

Sopta Petar J.; Skender Gazibara M.; Mijucic V.; Manojlovic E.; Poleksic Z.; Milinkovic Z.
Institute for Pathology, Belgrade, Serbia and Montenegro

Background Chordoma is a malignant neoplasm believed to arise from notochord remnants. It accounts 3 to 4 % of primary bone tumors and is localized along the axial skeleton. Aim: The aim of this study was to analyze the clinico-pathological findings, oncological and functional outcome of the patients with surgically treated chordoma.

Methods From 1995 to 2008, 42 patients with chordoma were diagnosed and surgically treated. All biopsies were stained by: HE, Vimentin, CK AE1/AE3, S-100 protein, EMA, Ki 67.

Results The extent of the lesion was defined according to Weinstein-Boriani-Biagini system. Frankel classification was used to define the level of neurological lesion. The biopsy material was analyzed for cell type, cell pleomorphism, presence of necrosis, bleeding, mixoid transformations, and hyaline cartilage. The results of treatment have been divided into chordomas of the spine above the sacrum, sacral and cranial localization. The follow-up of the patients lasted up to 65 months; the presence of rest/relapse of the tumor was being determined as well as the origins of metastasis.

Conclusion(s) The localization of the lesion and the type of surgical resection are the most important parameters influencing the clinical course of the disease. Tumors with prominent cell pleomorphism and higher Ki67 expression have fast relapse. En bloc resection, even the marginal one, is the therapeutic method of choice.

P4.5
Chordomas: evaluation of EGFR and c-METgenes expression

Walter-Rodriguez B.; Begnami M.; Quezado M.
National Cancer Institute/NIH, Bethesda, USA

Background Chordomas are rare primary malignant bone tumors of grim prognosis. Most patients are dead of disease within 10 years given high local recurrences rates or metastasis. Surgery with clean margins is the best treatment. High degree of resistance to radiation and chemotherapy is encountered. Development of targeted molecular therapy, as demonstrated by encouraging preliminary results with Gleevec, would be helpful in treating chordomas. We evaluate the expression of EGFR and c-MET genes in a group of 27 sacral chordomas to determine their potential use in chorodmas therapy.
Methods Twenty seven primary, sacral chordomas were reviewed. H&E slides were evaluated to confirm diagnosis. Immunohistochemistry for EGFR and c-MET was performed.
Results All chordomas were of conventional type. Nuclear pleomorphism, mitosis and/or necrosis were seen in 7 tumors. EGFR expression was focal and strong in 7/26 cases. c-MET expression was difuse and strong in 20/27 cases. All cases that expressed EGFR also expressed c-MET staining.
Conclusion(s) c-MET expression is common in chordomas; EGFR expression is less commonly observed and usually focal. Both EGFR and c-METoverexpression may be a marker of potential response to targeted molecular therapy in the treatment of chordomas.

P4.6
Description of two cases of pigmented villonodular synovitis with atypical features

Arena V.; Pennacchia I.; Bonadia N.; Capelli A.
Università Cattolica del Sacro Cuore, Roma, Italy

Background Pigmented villonodular synovitis (PVNS) is a proliferative disorder that affects synovial lined joints, bursae, and tendon sheaths. PVNS is capable of local recurrence and considerable destruction of the joint, but not of distant metastasis.
Methods We describe two cases of PVSN with features of questionable malignant transformation. Case 1: 28 year-old man with a 20x11x8cm mass involving the popliteal fossa. Case 2: 49-year-old woman with a recurrent PVSN of the wrist.
Results Histologically the cases were very similar: they were composed of an histiocitic proliferation with interposed giant cells and hemosiderin. Zones of pink hyaline material surrounded and entrapped groups of mononuclear and multinuclear histiocytes. No maturational zoning nor necrosis were observed. A mild inflammatory component was present. In some areas the pattern of growth was solid and the histiocytes appeared larger, mainly round to oval, with hypercromatic nuclei sometimes showing prominent nucleoli with higher nucleo-cytoplasmatic ratio and atypical mitotic figures.
Conclusion(s) In agreement with Bertoni we believe that malignant PVNS is a true entity that can arise in a previous PVNS or can be primary too. These cases contain only few areas with some worrisome histological features; however not all the criteria to make a full diagnosis of malignancy were satisfied. In such cases, a definite diagnosis is not possible given the paucity of atypical areas. We think that similar lesions should be described in the pathology report as PVNS with foci of atypical proliferation. A close follow up should be strongly recommended.

P4.7
Differential expression of HEY2 between desmoid-type fibromatosis and fibrosarcomas

Carvalho Candido K.; Buim E.M.; Reis L.L.; Soares A.F.; Cunha Werneck I.
Hospital A C Camargo, São Paulo, Brazil

Background Fibroblastic tumors represent a group of tumors that include since benign tumors to high grade sarcomas.. Between these two extremes, desmoid-type fibromatosis (DTF), are clonal tumors, with fibroblastic proliferation and local aggressiveness but without metastatic potential. The aim of this study was to determine differential gene expression profile and define molecules able of discriminating among Desmoid-type fibromatosis (DTF) and fibrosarcoma (FS).
Methods Using a cDNA platform representing 4608 genes, we seeked for gene that could discriminate desmoid-type fibromatosis (19 samples) from fibrosarcomas (04 samples). Validation was done in 124 samples (112 DTF and 12 FS) by immunohistochemistry and 25 samples by Quantitative RT-PCR.
Results cDNA microarray results pointed a set of genes that discriminate DTF from fibrosarcomas. Among differential expressed genes selected for validation, HEY2 (hairy/enhancer of split related - YRPW - motif 2) was able to separate precisely DTF from fibrosarcomas. QRT-PCR and Immunohistochemi-

cal results corroborate with cDNA data with DTF showing higher expression levels of Hey2 than fibrosarcomas. Mathematical analysis showed significative statistical values of differential expression between these two groups.
Conclusion(s) Our results pointed Hey2 protein and transcript as a potential discriminator of biological behaviour between fibroblastic tumors.

P4.8
Epithelioid perineurioma

Le U.; Mech J.J.; Cooper K.
University of Vermont Fletcher Allen Health Care, Burlington, VT, USA

Background Perineuriomas represent a subset of benign peripheral nerve sheath tumors composed of perineurial cells. They are classified by location as either intraneural or extraneural and can be diagnostically challenging due to histologic overlap with other tumors. Recently, an unusual epithelioid perineurioma was described which was reminiscent of a meningioma with a proliferation of epithelioid cells and focal intranuclear pseudoinclusions.
Methods We describe the clinicopathologic and immunohistochemical features of the second case of an unusual epithelioid variant of perineurioma.
Results The patient is a 15 year old male with a 1 cm mass on his right index finger. Histologic examination demonstrated a variably cellular component admixed with collagen which focally exhibited whorling. The cellular areas consisted of trabeculae of loosely aggregated epithelioid cells which stained positive for epithelial membrane (EMA) and factor XIIIa and negative for S100, desmin, smooth muscle actin (SMA), CD34, CD68, and keratin, thus confirming the diagnosis of an epithelioid variant of perineurioma. There was no necrosis or mitoses.
Conclusion(s) Perineuriomas are benign peripheral nerve sheath tumors which can exhibit many morphologies. Variants that have been described include the extraneural soft tissue, sclerosing, reticular (retiform), intraneural, and now the epithelioid subtype. It is important to correctly differentiate this benign tumor from other malignant mesenchymal neoplasms, such as epithelioid sarcoma (cytokeratin+, CD34+), dermatofibrosarcoma protuberans (CD34+, factor XIIIa-), and smooth muscle tumors (SMA+).

P4.9
Extrapulmonary inflammatory myofibroblastic tumor: a study of 17 cases

Chaabouni S.; Sellami Dhouib R.; Driss M.; Sassi S.; Mrad K.; Abbes I.; Chaabouni N.; Kilani H.; Ben Romdhane K.
Tunis, Tunisia

Background Inflammatory myofibroblastic tumor (IMT) is a spindle cell proliferation of uncertain pathogenesis, with a distinctive fibroinflammatory and even pseudosarcomatous appearance. Although the lung is the best known and most common site, IMT occurs in diverse extrapulmonary locations.
Methods A retrospective review of 17 cases of extrapulmonary IMT was performed at our institution from 2003 to 2007.
Results Our study concerned 10 female and 7 male patients between the ages of 4 and 70 years. Tumor location included eye/orbit (4 cases), mesentery (2 cases), retroperitoneum (2 cases), spleen (2 cases), soft tissue (2 cases), skin (1 case), pancreas (1 case), liver (1 case), adrenal gland (1 case) and vagina (1 case).The lesions ranged in size from 1,5 to 18 cm. All tumors were firm and white or tan with variable myxoid change. Three basic histologic patterns were recognized: myxoid, vascular and inflammatory areas resembling nodular fasciitis; compact spindle cells with intermingled inflammatory cells resembling fibrous histiocytoma; and dense plate-like collagen resembling a desmoid tumor or a scar.
Conclusion(s) IMT is a benign non metastasizing proliferation of myofibroblats with a potential for recurrence and persistent local growth. Differential diagnosis is influenced by the site of presentation and the dominant histologic pattern. Immunohistochemistry does not play a major role in confirming the diagnosis, due to the variable expression and lack of specificity of myofibroblastic markers. Anaplastic lymphoma kinase (ALK) positivity is helpful if present, but its absence does not exclude the diagnosis.

P4.10
Immunohistochemical expression of E-cadherin, β-catenin and topoisomerase IIα in leiomyosarcomas

Batistatou A.; Panelos J.; Gogou P.; Pakos E.; Tsekeris P.; Apostolikas N.; Stefanou D.; Malamou-Mitsi V.
University Hospital of Ioannina, Ioannina, Greece

Background β-catenin is a key-molecule in several signaling pathways, involved in cell adhesion (mainly via E-cadherin binding), differentiation and proliferation. Topoisomerase IIα is mainly expressed in proliferating cells and has been shown to be component of the nuclear β-catenin/TCF-4 complex. The expression of E-cadherin, β-catenin and topoisomerase IIα has been associated with clinical outcome of several neoplasms, including sarcomas. The aim of the present study was to examine the expression of these proteins in leiomyosarcomas.
Methods The immunohistochemical expression of E-cadherin (CM170B, Biocare Medical), β-catenin (DBS, Menarini, Hellas) and topoisomerase IIα (clone Ki-S1,

DAKO) was examined in paraffin-embedded tissue sections from 38 leiomyosarcomas (17 retroperitoneal, 14 of extremities, 7 of other sites). All surgical margins were negative and the mean patient follow-up was 36 months.
Results Expression of E-cadherin was negative in all tumours. Membranous and/or cytoplasmic immunostaining for β-catenin was noted in the majority of tumours (23/38, 60%), while nuclear staining was not observed. Topoisomerase IIα was expressed in 33/38 tumours (87%). There was no correlation between β-catenin, topoisomerase IIα and survival. The size of tumours was significantly correlated with survival.
Conclusion(s) Nuclear expression of β-catenin is not observed in smooth muscle tumours, even in deep locations, a feature that can aid in the differential diagnosis with fibromatosis. Traditional parameters, such as size, are more useful in predicting outcome of leiomyosarcomas than expression of E-cadherin, β-catenin and topoisomerase IIα, which have been proved prognostically useful in other tumours.

P4.11
Molecular classifiers that separate desmoid-type fibromatosis from other mesenchymal tumor types

Carvalho Candido K.; Cunha Werneck I.; Simões C.A.; Reis L.L.; Soares A.F.
Hospital A C Camargo, São Paulo, Brazil

Background Desmoid-type fibromatosis (DTF) are clonal tumors with fibroblastic proliferation and local aggressiveness but without metastatic potential. We defined gene signatures capable of discriminating DTF from other soft tissue tumors (STT).
Methods Using a cDNA platform representing 4608 genes, we seeked for genes that discriminate DTF (16 samples) from other histological types of STT (51 samples including: synovial sarcoma, fibrosarcoma, leiomyosarcoma, MPNST, and others). Validation of differential expression was done in 65 samples by quantitative PCR (Q-PCR), with TaqMan detection system.
Results cDNA microarray results pointed a set of genes that discriminate DTF from the other histological types of STT analyzed. Among differential expressed genes identified in our analysis, the genes NUP98 (Nucleoporin 98 kDa), GGA3 (Golgi associated gamma adaptin 3), FUCA1 (Fucosidase alpha - L1), SMYD2 (SET and MYND domain containing 2), ENTPD7 (Ectonucleoside triphosphate diphosphohidrolase), and SETD7 (SET domain containing -lysine transferase-7) precisely discriminated DTF from the remaining samples. Additionally, ENTPD7 gene could also discriminate DTF from fibrosarcomas. QRT-PCR confirmed that DTF have higher SMYD2 (p=0,0170), ENTPD7 (p<0,0001) and SETD (p=0,0306) transcript levels than all other STT histological types. On the other side, NUP98 (p = 0,0113), GGA3 (p = 0,0034) and FUCA1 (p = 0,0102) showed lower expression levels in fibromatosis group.
Conclusion(s) Our results indicated that NUP98, GGA3, FUCA1, SMYD2, ENTPD7, and SETD7, together or individually, could precisely discriminate DTF from other mesenchymal tumors. Moreover, ENTPD7 was able to discriminated DTF from fibrosarcomas.

P4.12
Oooppss is it an alveolar soft part sarcoma of bone?

Dervisoglu S.; Aydin O.; Demirkesen C.; Calay Z.; Folpe A.
Istanbul University Cerrahpasa Medical Faculty Pathology Department, Istanbul, Turkey

Background Alveolar soft part sarcoma (ASPS) is a rare soft tissue tumor affecting principally adolescents and young adults, representing mainly in the lower extremities and head-neck. Primary bone involvement is an exceedingly unusual presentation for ASPS. The radiologic examination usually reveales a lytic expansile appearance with ill-defined margins and cortical destruction.
Methods We report a case of ASPS with an unusual clinical and radiologic presentation, discuss the differential diagnosis and review literature.
Results Our case was a 19 year old woman having an expansile mass with a thin calcified rim in her 11th rib, sent for consultation. The case was previously diagnosed as metastatic adenocarcinoma and osteosarcoma by two different laboratories respectively. The microscopic examination revealed a mesenchymal tumor composed of round polygonal cells showing a partially spindled pattern of growth and focal areas of chondroosteoid like material. Osteosarcoma diagnosis was unlikely due to low mitotic activity, presence of sclerotic rim and absence of permeative infiltration pattern. The atypical histologic features with focal S-100 positivity and the reticulin pattern were reminiscent of a chondroblastoma. The tumor cells were positive for TFE3 which was the key point of our final diagnosis; ASPS.
Conclusion(s) Primary involvement of bone in ASPS is very rare and there are only 19 cases in literature. Our case is unique with its localization, radiologic findings and the unusual focal spindled growth pattern causing diagnostic difficulties. ASPS should be taken in differential diagnosis of bone tumors with unusual radiologic and microscopic features.

P4.13
Perineurial cells in granular cell tumor

Izquierdo-García Miguel, F.; Suárez-Vilela D.; Honrado-Franco E.
Hospital de León, León, Spain

Background Granular cell tumor is a neoplasm of the nerve sheath composed of cells s-100 positive, of probably origin in schwann cells. Perineurium is made up by perineurial cells. These cells are also found in some nerve sheath tumors as neurofibroma or schwannoma. However they have not been well studied in granular cell tumors.
Methods We study 30 cases of granular cell tumor with EMA, claudin-1 and GLUT-1 antibodies, immunohistochemical markers for perineurial cells.
Results 14 cases (47%) did not show perineurial cell proliferation. The resting 16 showed different degrees of perineurial cell proliferation: 5 light proliferation; 5 light or moderate proliferation, depending of the areas; 6 moderate proliferation. In two cases the proliferation was extensive. In the other 14 cases it was limited around the nerve fascicles included inside the tumor, in continuity with the perineurium, being most of the tumor free of perineurial cells.
Conclusion(s) Perineurial cells are involved in 53% of the granular cell tumors not as a component of the neoplasm but as hyperplasia or proliferation of the perineurium. As epithelial hyperplasia is commonly associated to granular cell tumor, likewise we think this proliferation of the cells of the perineurium could be induced by the tumor instead of being neoplastic. In our hands claudin-1 more sensitive marker for perineurial cells than EMA and GLUT-1.

P4.14

Phosphaturic mesenchymal tumors: what about them?

Quezado M.; Collins T.M.; Merino M.J.
LP/National Cancer Institute/NIH, Bethesda, USA

Background Phosphaturic Mesenchymal tumors (PMT) are rare tumors associated with oncogenic osteomalacia (OO) due to renal phosphate wasting. They can be mistaken for other bone or soft tissue tumors including hemangiopericytoma, osteosarcoma, and chondrosarcoma. Association with OO and expression of fibroblastic growth factor-23 (FGF23) helps in rendering the correct diagnosis. Upon removal of the neoplasms, most patients are cured. We will describe the H&E morphology and immunohistochemistry (IHC) of 11 cases of PMT.
Methods Twelve patients with a clinical diagnosis of oncogenic osteomalacia and localization of tumors biochemically and by imaging studies were included. H&E and IHC slides were reviewed.
Results The patients included 7 males and 4 females, from 19 to 63 yo (1 patient did not show a lesion in the specimen). Eight tumors occurred in bone and 3 involved soft tissues. H&E revealed a spectrum of "mesenchymal" tumors. They were composed of spindle to epithelioid cells, occasionally with cytoplasmic clearing. Giant cells were frequent, many around cystic spaces. Adipose tissue, lamellar bone, and chrondroid or osteoid matrix were observed. Ten tumors were benign with no cell atypia, mitotic activity or necrosis. One tumor was malignant, diagnosed upon development of metastatic lung disease; original tumor showed increased cellularity, cell pleomorphism and increased mitotic activity. By IHC, consistent staining was of vimentin and FGF23.
Conclusion(s) Phosphaturic mesenchymal tumors are morphologically diverse. Awareness of their morphology can allow their recognition and avoid confusion with other tumors which could lead to unnecessary aggressive treatment.

P4.15

Small cell osteosarcoma of bone. A morphological, immunohistochemical and genetic study of 10 cases

Llombart Bosch A.; Machado I.; Alberghini M.; Bacchini P.; O'Sullivan M.; Bertoni F.
Pathology Department, Valencia University, Valencia, Spain

Background Differential diagnosis of Small Cell Osteosarcoma (SCO) is difficult, especially in cases in which osteoid deposition is absent or minimal.
Methods Ten SCO were studied to assess whether the morphological, immunohistochemical (IHC) and genetic features can differentiate them from other srct (Ewing's sarcoma (Es), lymphoma, rhabdoid tumor, synovial sarcoma and mesenchymal chondrosarcoma). The cases were selected from 865 srct of bone (Prothets EU Project Nº 503036). Two cases were transferred into xenograft for several passages. IHC: osteonectin, osteocalcin, ezrin, fibronectin, PLAP, CD99, bcl-2, CAV1, vimentin, Ki-67, p16, p53, p21, LCA, CK, EMA, E-cadherin, EGFR, CD31, CD34, ckit, Her-2, β-catenin, epithelial-mesenchymal transition markers, mTor, INI1 and TP52. PAS, Masson's tricomic, FISH EWS,TLS/FUS and SYT break apart and RT-PCR were done.
Results All SCO cases possessed an srct morphology with osteoid formation (focal/minimal or extensive) and positivity for osteonectin, osteocalcin, CD99, ezrin, CAV1, Bcl2, vimentin, c-kit, p53, p21 and epithelial mesenchymal transition markers. PLAP, CK, p16, mTor and EMA showed heterogeneous staining, while Ki-67(MIB1) had a high proliferation index (over 50% of tumor cells). INI was negative in one case. The xenograft tumors presented similar findings. FISH analysis and RT-PCR found no evidence of EWS, TLS/FUS or SYT rearrangement in any case.

Conclusion(s) SCO is an unusual type of bone sarcoma in which IHC, FISH and molecular biology techniques provide distinction from other srct with overlapping morphology. Support: EuroBoNeT Consortium (018814), European Commission.

P4.16

TFE3 in tumors of pecoma family: immunohistochemical and molecular study

Panizo A.; Sola I.; Aisa G.; Labiano T.; Pardo J.
Clinica Universidad de Navarra, Pamplona, Navarra, Spain

Background Immunoreactivity for TFE3 is a sensitive marker of tumors with known translocations involving the TFE3 gene. Several cases of PEComas have been reported to be TFE3 positive. We performed a study of TFE3 immunoreactivity and ASPL/TFE3 translocation in PEComa family tumors.
Methods 51 renal AML, 2 hepatic AML, 6 PEComas, 2 lymph node (lymphangioleiomyomatosis) LAM, 1 lung LAM, and 1 sugar tumor of the lung, were studied. We performed IHC using the polyclonal antibody to TFE3 (Santa Cruz). TFE3 nuclear immunoreactivity was semiquantified based on Allread score: intensity (0–3) and % of positive tumor cells (0–5). Cases showing a combined score of >3 were defined as positive. RT-PCR with primers designed in detecting both ASPL/TFE3 fusion transcripts, was performed.
Results Nuclear immunoreactivity for TFE3 was observed in 43 cases (68,3%): 36 renal AML (average score 5,08), 5 PEComas (average score 6,67), 1 hepatic AML, and 1 lymph node LAM. Of the 43 positive cases, 26 (60,6%) showed strong, 15 (34,9%) moderate, and 2 (4,7%) weak nuclear labeling. TFE3 immunoreactivity was observed in all ASPS control cases. All 4 ASPS contained a fusion transcript, whereas none of the AML or PEComas showed ASPL/TFE3 transcripts.
Conclusion(s) PEC neoplasms are frequently immunoreactive for TFE3. The nuclear TFE3 immunoreactivity precludes its use in discriminating epithelioid renal AML or PEComas from TFE3 renal carcinomas or ASPS. TFE3 immunoreactivity in these tumors is not related with ASPL/TFE3 translocation, so the mechanism of TFE3 overexpression is not known.

P4.17

Angiomyofibroblastoma-like tumor (cellular angiofibroma) of male genital tract with comparison to female angiomyofibroblastoma

Orellana R.; Soler M.; Saez A.; Bagué S.; Sanfeliu E.; Rey M.
Corporació Parc Tauli. UDIAT-CD, Sabadell, Barcelona, Spain

Background Cellular angiofibroma is a histological distinctive benign mesenchymal neoplasm composed of spindle cells and prominent stromal blood vessels, that usually arises in vulvovaginal region. Cases in males have been called "angiomyofibroblastoma-like tumor" because they share clinicopathologic features and immunoprofile of vulvovaginal angiomyofibroblastoma.
Methods We describe two cases: para-scrotal mass in 63-year-old male, and tumor in vulvovaginal region in 53-year-old female.
Results Both lesions were superficially located, and appeared as well-circumscribed nodules measuring 6,5 cm. and 3 cm, respectively. Microscopically, they were composed of spindle cells proliferating between numerous medium to large-sized, thick-walled hyalinized vessels with perivascular fibrinoid deposition and scarce mature adipocytes. Mitotic activity was absent. Occasional pleomorphic atypical cells were identified. Tumor cells of vulvovaginal lesion were vimentin and CD34 positive. The tumor cells of para-scrotal lesion were positive for vimentin, CD34 and oestrogen receptor, but not for S-100 protein, CD99, actin and desmin.
Conclusion(s) The differential diagnosis of this distinctive tumor includes aggressive angiomyxoma, angiomyofibroblastoma, spindle cell lipoma, pleomorphic hyalinizing angiectatic tumor, schwannoma and solitary fibrous tumor. Distinguishing the various entities is clinically important but may be difficult because of the overlapping morphologic features. Immunohistochemistry is of limited value, and histologic features are the mainstay in the diagnosis of these entities. In our cases, desmin was absent although this finding has been described in postmenopausal cases. Pleomorphic cells were interpreted as degenerative changes ("ancient") in both cases. Care must be taken in misdiagnosing this rare tumor as sarcoma.

P4.18

Benign lipomatous tumors: how difficult can it be?

Popp C.G.; Zurac S.A.; Bastian A.E.; Socoliuc C.G.; Stoican D.; Croitoru A.; Andreescu B.; Rebosapca A.
Colentina University Hospital, Bucharest, Romania

Background Benign lipomatous tumors (BLT) are the most common soft tissue tumors with solitary lipoma as leader in respect of frequency. Several rarer variants of BLT have been described (angiolipoma AL, myolipoma, chondroid lipoma, spindle cell lipoma SCL/pleomorphic lipoma PL).
Methods We report 13 cases of lipoma variants (10 ALs, 1 SCL and 2 PL) out of 157 BLT diagnosed between 2002–2005. We analyzed histological pattern, stroma, vasculature, nuclear aspects, presence of giant cells, regularity in size of adipocytes, presence of atypical cells and lipoblasts, edge of tumor and the adequacy of excision.
Results Our group presented male predominance (males: females=12:1 – one woman with AL) in young adulthood (median age 36.4 years). All the lesions were small (median

diameter 1.96 cm) yellow-reddish, located in the extremities (7 ALs) and ear (2ALs, 1 SCL). 3 ALs presented highly vascular areas with prominent cellularity and bland morphology; one case had occasionally giant cells; one other case had occasional areas of hemorrhage and necrosis. PLs and SCL revealed dense CD34+ spindle/stellate cell population with bland nuclei in a variable myxoid matrix; no mitoses or necrosis were present; many giant cells with prominent nuclear pleomorphism were identified in the PLs; the overall histopathological appearance in each case of PL and/or SCL prone to misdiagnose these lesions as malignant.

Conclusion(s) Recognizing different variants of BTL is important because diagnostic pitfalls might include a large number of malignant soft tissue tumors with severe subsequent consequences on the outcome of the patient.

P4.19

Desmoplastic fibroblastoma in adolescence

Riga D.; Chatzis O.; Goupou E.; Tziakou P.; Machaira E.
District General Hospital Attikis "K.A.T", Athens, Kifissia, Greece

Background DF is a very rare, benign, soft tissue tumor that arises in the subcutaneous tissue or skeletal muscle of adults. It presents as a well-circumscribed, firm, white to grey-tan, painless nodule on the neck, upper arm, forearm, shoulder, hand, lateral thigh, abdomen, ankle and foot. The male/female incidence ratio is 4/1. Although most patients are in their 5th or 6th decade of life, few cases have been reported in children. Lesions range from 1 to 20 cm (median 4 cm).

Methods A 13-year-old boy noticed a painless, immobile nodule on the right side of the neck (supraclavicular region) 3 months earlier. The patient had neither relevant medical history, nor clinical symptoms. The tumor was totally excised. Our Department received a well-circumscribed specimen measuring 3,8x3,5x2,8 cm, with grey-tan cut surface and firm consistency.

Results Microscopically, the lesion was hypocellular with spindle and stellate-shaped cells, with elongated nuclei, embedded in a hypovascular, fibrotic stroma. No calcifications, tumor necrosis, or mitotic figures were detected. Immunohistochemically the tumor cells were positive for Vimentin, a1ACT and negative for S-100, Desmin and CD34.

Conclusion(s) The clinical, macro-microscopic and immunohistochemical data led us to the diagnosis of DF, despite its low incidence rate in children, Our differential diagnosis included desmoid fibromatosis, fibroma of tenton sheath, low-grade fibromyxoid sarcoma, nodular fasciitis, elastofibroma and juvenile hyaline fibromatosis. No recurrence after total excision has been reported after a period of 3 years.

P4.20

Differential diagnosis of small round cell tumors (SRCT), fluorescence in situ hybridization (FISH) and immunohistochemical (IHC) study

Ptaszynski K.; Szumera Cieckiewicz A.; Pekul M.; Nowecki Z.
MSC Memorial Cancer Centre and Institute of Oncology, Warsaw, Poland

Background Small round cell tumors of bone and soft tissue constitute a frequent diagnostic problem when only histopathology and immunohistochemistry is used. A molecular testing is necessary in many cases.

Methods We analysed 125 cases with the initial diagnosis of small round cell tumor (SRCT). Histopathology, IHC and FISH testing with commercially available probes were performed.

Results In several cases IHC and/or FISH analysis contributed significantly in final diagnosis of a classic or non-classic SRCT. We found also cases with difficult to interpret FISH results. Signals in some cases showed no genetic aberration. Some cases showed negative results due to technical problems.

Conclusion(s) Molecular testing is necessary in many cases of SCRT for final diagnosis.Interpretation of molecular testing in some cases is a difficult task.

P4.21

Heterotopic mesenteric ossification presenting as an isolated pelvic mass

Athanazio Abensur D.; De Carvalho A.L.; Silva N.; Azevedo Filho VO..; Athanazio P.R.
Federal University of Bahia, Salvador, Bahia, Brazil

Background There are 28 unequivocal reports of heterotopic mesenteric ossification ("intraabdominal myositis ossificans'') (HMO/IMO) in English literature. Most cases present as poorly defined lesions in intraabdominal structures causing intestinal obstruction. Small well-delineated solid mass was reported only once in a case with no previous history of trauma.

Methods Case report.

Results A 67 year old female patient sought the Surgery service because of an incidental finding of calcified mass in the left adnexal region. Her surgical history includes two cesarean operations (last one 35 years ago) and uterine leiomyoma removal ten years ago. The tumor was located in the retro-rectal adipose tissue and broad ligament. At

macroscopy, it was a 9.0 x 4.5 cm well delineated tumor. The cut surface had a soft grayish glistering center while the periphery appeared grayish-white and densely calcified. Microscopically, the tumor exhibited a hypercellular population of immature stromal cells lacking cytologic atypia. The classic zonation phenomenon described in myositis ossificans was easily observed with orderly progression of osteoid formation to mature bone from the center to tumor periphery.

Conclusion(s) Awareness on HMO/IMO may avoid an erroneous diagnosis of extraskeletal osteosarcoma. This case differs from most cases of HMO/IMO since is the third reported in females and lacks a diffuse involvement leading to obstructive symptoms. Past surgical events are too old to be obviously implicated in tumor emergence. Alternatively, such insidious evolution may explain the organization of a reactive process into a silent isolated mass.

P4.22

Meningothelial-like whorls in a retroperitoneal cellular schwannoma: a potential diagnostic pitfall

Santi R.; Franchi A.; Valeri A.; Veltri M.; Nesi G.
University of Florence, Florence, Italy

Background Whorl-like, concentric, discrete nodules typically occur in meningiomas and perineurial cell neoplasms, but occasionally they are observed in neoplasms of different histogenesis. In particular, meningothelial-like whorls are a peculiar finding of a specific variant of dedifferentiated liposarcoma. A retroperitoneal cellular schwannoma with meningothelial-like whorls as a characteristic histological feature is herein reported.

Methods We describe the clinico-pathological findings of an asymptomatic 40-year-old female patient with an 8.5 cm retroperitoneal mass incidentally detected.

Results At microscopic examination the tumour was composed of spindle-shaped cells arranged in elongated fascicles and meningothelial-like whorls were frequently identified. The cells were diffusely and strongly positive for S100-protein, whereas they were negative for MDM-2 staining. The diagnosis of cellular schwannoma was established.

Conclusion(s) In the presence of a retroperitoneal mass in an adult patient, dedifferentiated liposarcoma is one of the most likely clinical diagnoses. Histologically, meningothelial-like whorls may be a potential diagnostic pitfall. Pathologists should be aware of the occurrence of meningothelial-like whorls in cellular schwannomas. Immunohistochemical findings support the diagnosis.

P4.23

Metabolic profiling of atypical and benign meningioma by NMR

Morales J.; Monleon D.; Gonzalez-Darder J.; Talamantes F.; López-Ginés C.; Celda B.; Cerdá-Nicolás M.
Universitat de València, Valencia, Spain

Background Meningiomas add up to 30% of CNS tumours. Atypical meningiomas show a high index of recurrence 5 years after complete resection. Sometimes, meningiomas with histological diagnosis of benign meningioma show clinical characteristics of atypical meningioma. Additional criteria for better classification of meningiomas will improve clinical decisions. We show differences in molecular profiles of benign and atypical meningiomas based on NMR spectra.

Methods HRMAS spectra were obtained for 30 samples of human meningioma tissue (23 benign and 7 atypical). The whole study was performed at 4ºC. All samples were analyzed by post-HRMAS histopathology to assess tissue integrity and double validate histological diagnosis. Multivariate statistical analysis was performed. Robust Principal Component Analysis (RPCA) was applied to the set of spectral vectors. Principal components chosen explained at least 90% of the variance.

Results NMR spectra showed adequate signal-to-noise ratios with well resolved spin-spin multiplicities. Resonances were assigned by methods described elsewhere. The comparison among spectra shows clear differences between benign and atypical meningiomas. The phospholipids pattern and other well known signals like Alanine and Lactate seem to have some correlation with the meningioma grade.

Conclusion(s) HRMAS allows discriminating between molecular profiles of benign and atypical meningiomas. Metabolic discrimination between benign and atypical meningioma according to the PCA, include the metabolites which can be seen by MRS 'in vivo'. These metabolites may be the basis for a non-invasive classification of benign and atypical meningioma.

P4.24

Microcystic/reticular schwannoma of the pancreas: a potential diagnostic pitfall

Bodo K.; Malliga Eugenia D.; Lackner C.; Tsybrovskyy O.; Liegl-atzwanger B.
Institute of Pathology, Graz, Austria

Background Schwannomas occurring in the pancreas head are rare. Herein we report a case of a microcystic/ reticular schwannoma of the pancreas head with encasement of the portal vein and the truncus coeliacus.

Methods Cytology smears as well as formalin fixed, routinely processed, and paraffin embedded, four-micron thick, H&E stained sections were evaluated. Immunohistochemical studies were performed with antibodies against CKs, EMA, p-63, S-100, GFAP, NFP, KIT, SMA and desmin.
Results Cytology revealed malignant tumor cells consistent with an adenocarcinoma (G2). Histological evaluation showed a multi-nodular unencapsulated tumor with focal infiltration into pancreas parenchyma and striking microcystic and reticular lesional growth pattern. Anastomosing and intersecting strands of spindle cells with eosinophilic cytoplasm set in a myxoid partly collagenous stroma, small clusters of epithelioid tumor cells as well as a small tumor focus resembling a conventional schwannoma were observed. The tumor cell nuclei were round oval and tapered and showed inconspicuous small nucleoli. Degenerative nuclear atypia was seen. Mitotic activity was spares (1/50 HPF). Pleomorphism or necrosis was absent. The tumor showed strong nuclear and cytoplasmic positivity for S-100 and focal positivity for GFAP, whereas all other markers were negative.
Conclusion(s) Microcystic/reticular schwannoma is a distinctive morphologic variant of schwannoma with predilection for visceral locations. The awareness and, to some extent, the knowledge of this rare tumor in the pancreas is needed to achieve the correct diagnosis and to avoid confusion especially with pancreatic adenocarcinomas.

P4.25

Molecular detection of SS18-SSX fusion transcripts in synovial sarcoma: analysis of conventional RT-PCR, real time PCR and dual color FISH

Mohammadtaheri Z.; Nassiri M.; Olczyk J.; Mohammadi F.
National Research Institute of Tuberculosis and Lung Disease, Tehran, Islamic Republic of Iran

Background The diagnosis of synovial sarcoma was based on the morphological feature and immunohistochemistry. However, sometimes immunohistochemistry can not resolve the diagnostic problem and in these, genetic analysis for the detection of SS18 gene rearrangement has been found to be a powerful diagnostic tool for making the diagnosis of synovial sarcoma.
Methods Tissue microarray of 14 cases including 12 cases of synovial sarcoma (including 10 monophasic and 2 biphasic) diagnosed based on morphology and immunohistochemical staining and two other types of sarcoma as negative control was prepared and FISH was performed. Amplifiable cDNA was obtained from all cases and presence of SS18-SSX1, SS18-SSX2 and SS18-SSX4 were tested using RT-PCR.
Results SS18-SSX fusion products were found in 9 (75%) cases of synovial sarcoma using Real Time PCR. Of these, 4 cases including one biphasic type harbor SS18-SSX1 and 3 cases, all monophasic type revealing SS18-SSX2 by conventional RT-PCR. Fourteen cases in a tissue microarray, analysed by fluorescence in situe hybridization (FISH), revealed that 8 (66%) showed SS18 rearrengement: one RT-PCR positive case reported as negative by FISH. Used in combination, FISH and quantitative RT-PCR, 11 from 12 (91%) cases showing gene rearrangement.
Conclusion(s) Combination of FISH and Real Time PCR are the most sensitive tools for detecting translocation in synovial sarcoma.

P4.26

Molecular events in the angiogenesis initiation of human sarcomas

Llombart Bosch A.; López Guerrero J.; Machado I.; Mayordomo E.; Zambelli D.; Carda C.; Giner F.; Calabuig Fariñas S.; García Casado Z.; Pellín A.; Scotlandi K.; Picci P.; Peydró Olaya A.
Pathology Department, Valencia University, Valencia, Spain

Background Angiogenesis is crucial for the growth and spread of tumors. We have used a nude mice model to study the initiation of angiogenesis in xenotransplanted human sarcomas.
Methods Tumors, 0.3–0.4 cm in size, from fifteen human sarcomas [Ewing's sarcoma (ES), osteosarcoma (OS), chondrosarcoma (Chs), synovial sarcoma (SS), gastrointestinal stromal tumor (GIST) and fibrosarcoma (FS)] were implanted into the backs of athymic Balb-c nude mice. The mice were sacrificed at 24, 48, 72 h, 7, 14, 21 and 28 days from implantation. The expression of 96 angiogenesis related genes was studied. Serum levels of both human and mice VEGF were evaluated by ELISA. TC, LAP and SK ES cell lines were tested for two tyrosine-kinase inhibitors (TKI) (NVP-AEW541 and BEZ-235) as potential angiogenesis-inhibitors.
Results After 24–48 h from implantation all tumors expressed high levels of angiogenic factors. Co-option together with vascular mimicry is observed. Cluster analysis showed that the expression profiles at 48 h and 1 week had similar behavior, mainly in ES and OS. ELISA experiments showed that the levels of mouse VEGF did not change during the experiment, indicating that the induction of angiogenesis is locally produced. In vitro studies revealed that NVP-AEW541 TKI is more effective at inhibiting angiogenesis than BEZ-235.
Conclusion(s) The model herein presented offers an excellent way to study the initiation of tumor angiogenesis

and provides new ways of assessing the activity of potential inhibitory agents associated with tumor growth. EC Euro-BoNeT (018814) 6THFP.

P4.27
Neurofibroma with multifocal schwannoma-like nodules: a unique entity

Ozbudak I.; Gurer E.; Gokhan G.; Akkaya B.
Akdeniz University School of Medicine, Department of Pathology, Antaalya, Turkey

Background Neurofibroma is a benign nerve sheath tumor composed of a variable mixture of Schwann, perineurial-like and fibroblastic cells. The distinction of Schwannoma and neurofibroma is clinically important, not only for diagnosing neurofibromatosis but, on occasion for excluding a diagnosis of malignant peripheral nerve sheath tumor.
Methods We presented a 17 year-old boy with a history of palpable mass on the right supraclavicular region. The radiological studies revealed a soft tissue tumor extending from right supraclavicular neurovascular bundle to the second costa of right hemithorax. The patient underwent elective thoracotomy and surgical excision of mass.
Results The tumor composed of Schwann cells with ovoid to thin, elongated nuclei and scant cytoplasm and fibroblasts which embedded in a myxoid and edematous stroma. Architecturally, tumor showed nodular configuration composed entirely of Schwann cells, some featuring Verocay bodies. Immunohistochemical staining for S-100 was confirmatory for Schwann cells. Neurofilament and EMA were positive sparsely within the tumor. The patient was diagnosed as neurofibroma with multifocal schwannoma-like nodules.
Conclusion(s) We would like to point out a unique entity, neurofibroma with multifocal schwannoma-like nodules, for clinicians during the work-up of nerve sheath tumors and for pathologists in the differential diagnosis of these tumors.

P4.28
Nuclear localization of phosphorylated ezrina in osteosarcoma

Di Cristofano C.; Miraglia A.; Leopizzi M.; Ferrara A.; Sardella B.; Moretti V.; Petrozza V.; Della Rocca C.
Sapienza University of Rome, Rome, Italy

Background Ezrin is a membrane-cytoskeleton linker protein involved in regulating growth and metastatic behaviour of cancer cells. Ezrin is present in the cytoplasm in an inactive form, after phosphorylation ezrin assumes an active conformations and moves to the cell membrane. Recently, ezrin was found to be related to metastatic potentiality in osteosarcoma and its high expression was associated with poor outcomes. The specific mechanism or mechanisms by which ezrin mediates the metastatic process remains to be elucidated. This study evaluated expression and subcellular localization of phosphorylated (p-ezrin) and not phosphorylated ezrin (ezrin) in osteosarcomas.
Methods We studied 54 osteosarcomas (9 yr mean follow-up) and 6 benign bone lesions. Expression and localization p-ezrin and ezrin were assessed using immunohistochemistry (IHC) and immunofluorescence (IF) analysis on TMA paraffin sections and cultured cells (143B) of osteosarcoma. For the analysis were used anti-ezrin AB (3C12; Tyr 354 and Thr567).
Results 58%of osteosarcoma showed ezrin cytoplasmic localization, in the largest part (81%) of this cases a nuclear p-ezrin (Tyr354) localization was also present. The IF analysis confirmed the p-ezrin nuclear localization. P-ezrin nuclear localization was associated to ezrin expression (p= 0.001). Cytoplasmic and nuclear p-ezrin localization was associated to malignant neoplasm (p = 0,01 and p = 0,02 respectively). Ezrin expression was associated with high grade osteosarcomas (p = 0,04).
Conclusion(s) Ezrin had a prevalent cytoplasmic localization in osteosarcoma confirming its role of membrane-cytoskeleton linker protein. The nuclear localization of p-ezrin active forms in osteosarcomas suggests a possible role of transcription factor in cancer.

P4.29
Pacinian neuroma of the foot, an exceedingly rare painful lesion: a case report

Palumbieri G.
Hospital "Mons. R. Dimiccoli", Barletta, Italy

Background Pacinian neuroma is a rare benign hyperplasia or hypertrofy of the pacinian corpuscles. Pacinian corpuscles are mechanoreceptors: they are oval to round and they consist of a central core of packed lamellae, which enclose a nerve terminal and are surrounded by a cellular layer, within a laminated capsule. It is reported a case of Pacinian neuroma of the ball of the foot, in a 50 year old women who presented with a very painful small lump at the bifurcation of the 1° plantar common digital nerve; it produce metatarsalgia for over a year during both normal and tip-toe deambulation. Morton's neuroma was clinical diagnosis.
Methods Lump of fibro-fatty tissue (mm 15x8x6), once removed, was tamponate formaline fixed and routinely processed for inclusion in paraffin. Sections were stained with haematoxilin-eosin and immunohistochemical investigations were performed.

Results Histologically, the lesion was characterized by grape like cluster of normal-enlarged size pacinian corpuscles intermixed with few small nerve fibers and surrounded by fibrosis. At immunoistochemistry, the central core of pacinian corpuscles were positive for S-100 protein, while outer lamellae were positive for EMA.
Conclusion(s) Pacinian neuroma is a rare lesion of unknown aetiolology (local trauma often is reported), usually observed in the hand, with about 70 cases reported in literature, but it is extremely rare in the foot (only a few cases have been published). This diagnosis should be considered in the differential diagnosis of painful lesions of hand and foot.

P4.30

Post-traumatic and postcombustional malignant tumors of the scalp with high agressivity

Tamas C.; Turliuc D.; Stanescu C.; Stolnicu S.; Radulescu D.
Plastic and Reconstructive Surgery Department, University of Medicine and Pharmacy "Gr. T. Popa", Iasi, Romania

Background The etiology of skin cancers is not known but a long list of possible causes exists. Neglected posttraumatic and postcombustional injuries may be trigger for malignant tumors of the scalp.
Methods We report 9 cases operated between 2003–2009. The excisions were performed by the neurosurgeon, including dura-mater when necessary, and we reconstructed with various local flaps combined with skin grafts, trapezius or free omentum.
Results Most of the patients were males (7) aged over 65, and the scalp tumors were squamous-cell carcinoma (SCC) in 6, basal-cell carcinoma (BCC) in 2 and sarcoma in 1. All the patients reported scalp neglected injuries some years before tumoral development like: burns (5 SCC), crushed wounds (3) or radiotherapy (female, 70 years, SCC). A patient with postcombustional scar declared a very long history (20 years) with periods of local instability (inflamated ulcers of the scalp) followed by 2–3 month of new thin layer of skin. He developed a wide tumor covering the fronto-temporal left scalp and zygomatic fossa, interesting dura-mater. We reconstructed dura with fascia lata and the defect of scalp with free omentum flap.
Conclusion(s) Neglected posttraumatic and postcombustional wounds on the scalp can be a cause for the development of malignant tumors. Correct oncological excision can not be performed after long local evolution and reconstruction needs complex techniques.

P4.31

Primary leiomyosarcoma of the heart. A case report

Lund H.
Institute of Pathology, Aalborg Hospital, Aalborg, Denmark

Background Primary tumors of the heart are rare and usually benign, most being myxomas. Twenty-five percent are malignant and dominated by sarcomas. Among these, leiomyosarcomas are exceptionally rare. Secondary tumors are far more common than primary tumors.
Methods A 54-year old male presented with dyspnea and symptoms of right heart failure. Chest computed tomography and transesophageal echocardiography showed a large tumor in the right atrium attached to the atrial wall by a stalk. A cardiac myxoma was expected and surgery performed.
Results A large greyish lobulated tumor of firm consistency measuring 8x6x5 cm was seen. Microscopically, the tumor consisted of spindle cells with blunt-ended nuclei, forming fascicles at right angels. Pleomorphism, high mitotic activity and frequent foci of necrosis were identified. The tumor involved the surgical margins (stalk). Immunohistochemical stains for vimentin, desmin and the smooth muscle markers ASMA and SMMS1 were positive. The tumor was classified as a leiomyosarcoma, malignancy grade 3.
Conclusion(s) In general, surgical resection is the treatment of choice for primary cardiac tumors. Complete resection is often impossible for malignant tumors and adjuvant chemotherapy and irradiation may be given. Heart transplantation is another option. This patient had right atrial recurrence after 19 months, and a heart transplantation was successfully performed; at this point the tumor was almost the same size as initially. Due to backache MRI was performed 17 months after transplantation revealing metastatic disease in the lumbar spine and pelvis.

P4.32

Primary soft tissue giant cell tumor of the neck

Rys J.; Kruczak A.; Marczyk E.; Skotnicki P.; Wasilewska A.; Vogelgesang M.; Moskal J.; Ambicka A.; Dyczek S.
Center of Oncology, Cracow, Poland

Background The giant cell tumor of low malignant potential (GST-ST) is a very rare neoplasm of soft parts. The majority of tumors are localized superficially (in subcutaneous tissue) and occur in the proximal parts of the extremities. Arm, thigh, knee, and leg are the most common locations. The GST-STs situated in the muscle of the neck are extremely rare.
Methods The authors report a case of primary giant cell tumor of soft part localized in the trapezius muscle of a 19-year-old woman. The cytological and histological picture of the tumor is presented.
Results The smears obtained by fine needle aspiration biopsy revealed the typical picture of the tumor. It consisted of the mixture of multinucleated osteoclast-like cells and

the mononuclear bland looking spindle cells. They grouped together or they were dispersed as single cells. The cytologic findings of the tumor were so suggestive that a diagnosis of giant cell lesion was made. The diagnosis was confirmed histologically after the surgical removal of the whole tumor. Histologically, the tumor was characterized by a multinodular growth pattern with osteoclast–like giant cells admixed with spindle cell. They were stained for vimentin and CD68; the CD68 immunoreactivity was characteristically strong and diffuse in the osteoclast-like giant cells and focal in the mononuclear stromal cells.
Conclusion(s) GST-ST is a rare soft tissue counterpart of giant cell tumor of bone. It presents a distinctive cytological and histological picture.

P4.33
Rare case of a bilateral elastofibroma

Tziakou P.; Riga D.; Goupou E.; Diamantopoulou K.; Machaira E.; Pikoulas K.
District General Hospital Attikis "K.A.T", Athens, Kifissia, Greece

Background Elastofibroma is a fibroelastic tumour-like lesion that occurs primarily in the soft tissue between the lower portion of the scapula and the chest wall and lies deep within latissimus dorsi and rhomboid muscles, often with attachment to the periosteum of the ribs. It may be a response to repeated trauma occurring in individuals over the age of 55 with a striking predominance in women.
Methods A 57 year old female patient presented with a slowly growing painless mass at the lower portion of her left scapula. MRI revealed the presence of this mass outside the thoracic cavity, lying deep within the latissimus dorsi together with a second smaller mass, being undetected with palpation, at the lower portion of the right scapula. The diagnosis of possible bilateral elastofibromas was given followed by simple excision. Our Department received two white-brownish tissue specimen measuring 10X8,5X4,5 cm and 4X3x2 cm with grey-white cut surface and elastic consistence.
Results Microscopically, both lesions were composed of a mixture of paucicellular collagenous stroma and large, coarse, deeply eosinophilic elastic fibers scattered throughout which were reactive to Masson-Trichrome and Vimentin.
Conclusion(s) Radiologically detected subclinical bilateral involvement comprises up to 10% of all reported cases. Although the clinical and histologic features are characteristic, the most important differential diagnostic consideration is desmoid fibromatosis, which differs by its higher cellularity. Simple excision remains the treatment of choice due to the benign nature of the lesion, the lack of any report of malignant transformation and the rareness of recurrence.

P4.34
Retroperitoneal lymphangioleiomyomatosis arising from cystic endometriosis

Fukunaga M.
Jikei University Daisan Hospital, Tokyo, Japan

Background Lymphangioleiomyomatosis (LAM) is included in a family of perivascular epithelioid cell tumors (PEComa). Its histogenesis is controversial.
Methods A case of retroperitoneal LAM arising from cystic endometriosis is described and the histogenesis is discussed.
Results A 25-year-old woman with no history of tuberous sclerosis or hormonal therapy presented with a painless, palpable abdominal mass. Computed tomographic and magnetic resonance imaging studies of the abdomen demonstrated a 4 cm cystic mass in the retroperitoneum. Macroscopically, the excised retroperitoneal cyst was multilocular and measured 4.0 X 3.5 X 3.5 cm. Histologically, the lesion demonstrated three components. The first were multiple cysts or glands lined by columnar epithelial cells with cilia. The second component was a condensation of endometrial-type small stromal cells immediately subjacent to the cystic epithelium or glands. The third component was a thick exterior wall composed of plump spindle cells with clear to palely eosinophilic cytoplasm in a fascicular pattern, and slit-like vascular spaces, resembling LAM. Immunohistochemically, the epithelium and glands were positive for cytokeratin 7. The endometrial-type stroma cells were positive for vimentin and CD10. The cells of the LMA-like component showed positive staining for HMB45, alpha-smooth muscle actin, muscle actin and h-caldesmon.
Conclusion(s) The lesion, LAM arising from endometriosis, represents a distinctive pathologic entity that should be recognized and studied further. This type of lesion should be included in the differential diagnosis of retroperitoneal cystic lesions.

P4.35
Sclerosing epithelioid fibrosarcoma

Goupou E.; Tziakou P.; Riga D.; Machaira E.; Staikidou I.; Giannikouris G.
District General Hospital Attikis "K. A. T.", Athens, Kifissia, Greece

Background SEF is a very rare fibrosarcoma variant which occurs in young and middled-aged adults. It is localized mainly in soft tissues, but it can also be primary in bone.It is a clinically aggressive but histologically low-grade sarcoma with unsatisfactory treatment results.
Methods A 20-year old Polish male presented with frequent urination and a swelling in the right limb present

for 2 weeks. CT scan revealed a 15x8x7,5 cm poorly demarcated mass, in the right iliac fossa, with destruction of the adjacent sacrum. The tumor was not totally excised. Our Department received a poorly circumscribed, multinodular specimen measuring 8x5x3,5 cm, with a firm, whitish cut surface and foci of necroses.

Results Microscopically, the largest portion of the tumor was of low cellularity in a dense hyalinized stroma, but some areas were more cellular. The neoplastic cells were predominantly epithelioid in appearance with nests, cords, strands and Indian file patterns of growth. Mitotic figures were inconspicuous. Extensive necrosis were seen. Immunohistochemically, the tumor cells were positive for Vimentin, CD99, MDM2, Ki-67 and negative for EMA, cytokeratins, neural markers, Desmin, SMA, CD68, LCA, CD34 and HMB45.

Conclusion(s) The clinical, macro-microscopical and immunohistochemical data led us to the diagnosis of SEF. The differential diagnosis includes a wide range of both benign and malignant lesions composed of epithelioid cells including desmoid tumour, nodular fasciitis, low-grade fibromyxoid sarcoma, synovial sarcoma, MFH, MPNST, infiltrating signet-ring adenocarcinoma, sclerosing lymphoma and clear-cell sarcoma.

P4.36

Senescence markers in Schwannomas

Romagosa Pérez-P C.; Simonetti S.; Serrano C.; López L.; Esquinas M.; Moliné T.; Somoza R.; Huguet P.; Ramon YCajal S.

Dpt. Pathology, Hospital Vall d'Hebron. Fundació Institut de Recerca, Barcelona, Spain

Background Senescence is the irreversible growth arrest of cell cycle caused by aging or different stresses. Schwannomas are benign mesenchymal tumors that frequently present pleomorphic cells. The objective of this study was to assess p16, Ki67 and B-galactosidase expression in this group of tumors to demonstrate the possible role of senescence in the development of Schwannomas.

Methods Retrospective study of 27 cases of Schwannoma, diagnosed during the period from 2003 to 2006 in the Pathology Department of the "Hospital Vall d'Hebron" in Barcelona, Spain. Immunohistochemical staining for P16 and Ki67 was done in all the cases, evaluating positivity in pleomorphic and non-pleomorphic cells separately. Moreover, B-galactosidase histochemistry staining was done in those cases where frozen tissue was available ($n=3$).

Results A 59.3% (16/27) of cases showed p16 positivity > or = 60% of cells. There were no cases with p16=0. Ninety percent of cases with p16 < 60% (10/11) showed higher positivity for p16 in pleomorphic cells than in the non-pleomorphic ones. All cases showed Ki67 positivity in <5% of total cells, being totally negative in the pleomorphic ones. B-galactosidase staining was highly positive in all three cases.

Conclusion(s) This study has shown a high expression of p16 in Schwannomas, specially in pleomorphic cells. This results together with the high B-galactosidase activity and the low rates of ki67 positivity, suggest that Schwannomas could be part of the group of benign senescent tumors like nevus.

P4.37

Skull-base metastases from a malignant solitary fibrous tumor of the liver. Case report and review of the literature

Singeorzan C.; Michalak Provost S.; De Coataudon Tramanoir L.; Nedelcu C.; Rousselet Chapeau M.

CHU Angers, Angers, France

Background Initially thought to be limited to the pleura, solitary fibrous tumor (SFT) has now been reported in numerous extrathoracic sites. Among the benign and malignant forms of the tumor, the benign course is three to four times more common than the malignant one. Metastatic malignant SFT has been rarely described.

Methods We report a case of a liver's SFT occurring in a white man, initially resected when the patient was 54 years old and recurring 7 years later. Nine years after the resection of the first liver tumor the patient presented powerful cervical pain. MR Imaging showed a large skull-base tumor.

Results Histopathological examination showed malignant oval and round-cell proliferation with high cellularity, areas of necrosis and high mitotic activity. Some cells were bigger with cytoplasmic hyaline grains or more atypical with hyperchromatic, multilobed nuclei. Immunohistochemically, the tumor cells were positive for CD34, HBA71, bcl-2 and negative for all the other tested antibodies. On the other hand, the clinical evaluation showed the presence of no other tumor. The skull – base tumor was compared to the liver's SFT (diagnose confirmed by experts), the final conclusion being that it was the metastases of the liver's SFT.

Conclusion(s) There have been only 38 cases of SFTs of the liver reported in the literature. To the best of our knowledge, this is the first reported case of malignant SFT of the liver metastatic to the skull-base.

P4.38

Solitary fibrous tumour: a presentation of two cases

Nikolaidou A.; Moysidis I.; Koumpanaki M.; Christoforidou B.; Vasileiadis K.; Patakiouta F.

"Theageneion" Cancer Hospital of Thessaloniki, Thessaloniki, Greece

Background Solitary fibrous tumour is an uncommon spindle cell neoplasm, which is believed to be of mesenchymal origin. Extrapleural SFTs are very rare and can occur occasionally in extraserosal soft tissues or parenchymatous organs.
Methods We present two cases of SFT. Case1: A 61 year-old woman presented to the hospital complaining of a slowly enlarging mass in her left supraclavicular fossa. Clinical examination revealed the presence of a firm, nontender, 5X3,6X2 cm sized nodule. Case2: A 53 year-old woman was complaining of a mass at the right side of the lower anterior abdominal wall. Clinical examination revealed the presence of an ovoid, firm, nontender, 6,5x6x4 cm sized tumour.
Results In both cases, surgical excision was performed. Grossly, the tumours had a grey-white, solid cut surface. Microscopically, the tumours were composed of uniform spindle cells with separating bands of collagen. Marked variations of cellularity were observed. The cells had indistinct cellular borders, eosinophilic cytoplasm and ovoid to elongated nuclei. Mitotic figures were rare. Immunohistochemically, the neoplastic cells were positive for CD34 and bcl-2, but were negative for S-100, desmin, CK AE1/AE3 and CD117/c-kit.
Conclusion(s) Initially, SFTs were thought to be of mesothelial origin because they had been noted to arise only from mesothelium-lined surfaces. Since then, however, these tumours have also been observed in extrapleural and extraserosal areas, which suggests a mesenchymal cell origin. The differential diagnosis should always include a haemangiopericytoma, which has a similar morphologic and immunohistochemical profile.

P4.39
Synovial sarcoma. Clinical and morphological characteristics

Janevska V.; Spasevska L.; Kostadinova-Kunovska S.; Zafiroski G.; Samardziski M.; Vasilevska V.; Jovanovic R.; Filipovski V.
Institute of Pathology, Faculty of Medicine, Skopje, the Former Yugoslav Republic of Macedonia

Background Synovial sarcomas (SS) are frequent soft-tissue tumors with specific imaging and histologic appearance.
Methods 30 cases of SS were analyzed using clinical symptoms, imaging and histopathological parameters, including immunostainings for vimentin, EMA, CK7, CK19 and MIC2. Patients were treated with surgical excision, chemotherapy in 8 and adjuvant radiation in 12 cases. The follow-up period was 3–10 years.
Results Most of the patients had slow growing solitary soft-tissue mass, with pain in more than 50% of the cases. The plain radiography appearance was nonspecific. At ultrasound (US) the predominant finding was nodular, solid, hypoechogenic, well defined soft-tissue mass. MR imaging showed heterogenous multilobulated soft-tissue mass with high signal intensity, especially at T2-weighted images in 21 patients, and triple sign in 15. Limbs were the most involved localization. Wide local excision was made in 11 pacients, radical in 6, marginal in 9 and intralesional in 4. Six surgical specimens were smaller than 5 cm. There were 9 monophasic, 20 biphasic and 1 poorly differentiated SS. Nine cases were high grade. Five cases were completely negative, 25 cases were positive for vimentin and EMA, 19 of them for MIC2, 8 for CK19, 17 for CK7. Twelve patients died during the follow-up period and 17 had recurrence of the disease.
Conclusion(s) Clinical symptoms and the radiographic features were not specific. MRI in combination with US was diagnostic in most of the cases. Positive stainings for vimentin and epithelial markers in correlation with the histologic features were diagnostic for SS.

P4.40
A challenging case of epithelioid angiosarcoma of the thoracic wall

Lazureanu Codruta D.; Baderca F.; Lazar E.; Burlacu O.; Nicodin A.
University of Medicine and Pharmacy, Timisoara, Timis, Romania

Background A correct diagnosis of the epithelioid variant of an angiosarcoma of the thoracic wall is very difficult due to it's rarity, multiple possible origins (pleura, bone, striated muscle as primary or it can be a metastatic tumor) and to it's epithelial features on routine stain, which are readily misjudged.
Methods A 48-year-old male was admitted to the Thoracic Surgery Department with a 9 months history of right inferior thoracic (T10-T12) paravertebral mass, which became painful after a back trauma; dyspnea and hemoptysis were associated. Fragments of 10 cm large tumorectomy specimen (striated muscle, dense connective tissue, adipose tissue, lymph nodes and intercostal nerves) were routinely processed, with further immunohistochemical investigations for 1 block, using Dako antibodies CKAE1/AE3, CK7, CK20, CEA, vimentin, S-100 protein, CD34, CD31, von Willebrand factor, D2-40/podoplanin, Ki-67 antigen, in En Vision system, DAB visualization.
Results The histological and immunohistochemical aspects were indicative for soft tissue epithelioid angiosarcoma, which was misdiagnosed on frozen and HE sections as a carcinoma, because of the cohesiveness and nesting proper-

ties of the malignant cells, together with the presence of lymph node metastases. The Ki-67 index was high (20%). The patient was discharged with adjuvant therapy indication: radiotherapy and chemotherapy. The tumor locally recurred 12 months afterwards.
Conclusion(s) The poor outcome (local recurrence) correlates with the tumor large size and a high Ki-67 antigen value.

P4.41
Adamantinoma bifocal with tubular diffrentiation. A case report
Ouahioune W.; Baiche D.; Benchenouf M.; Cherifi H.; Asselah F.; Saighi Bouaouina A.
Department of Patholgy. Ehs Douera - Alger, Algiers, Algeria

Background Adamantinoma is a rare low grade malignant tumor of long bones. It's often clinically, radiologicaly and histologicaly mistaken for metastatic carcinoma, Ewing's sarcoma and numerous other lesions. The histogenesis of this tumor is not clear.
Methods We report the case of male patient aged 20 years, who was treated for bifocal tumor of tibia.
Results The first biopsy conclued to Ewing's sarcoma. The second biopsy confirmed diagnosis of bifocal adamantinoma with tubular differentiation. After 3 years, patient developped pulmonary metastasis.
Conclusion(s) Adamantinoma is a rare bone tumor, but we must remember this diagnosis because the recurrence and metastasis are not rare.

P4.42
Elastofibroma
Nistor A.; Simion G.; Sajin M.; Bruma G.; Guran R.; Stanculescu M.; Tudor A.; Barbulescu C.
Emergency University Hospital, Bucharest, Romania

Background Elastofibroma is an ill defined fibroelastic tumor-like lesion that occurs primarly in the soft tissue between the lower portion of the scapula and the chest wall. It is caracterised by a large number of coarse, enlarged, elastic fibers. We report the case of a 58 year-old caucasian woman who presented with a round,13/5/4 cm tumor located in the right subscapular region, deep under the latissimus dorsi muscle, with fibrous tissue areas admixed with fat areas on CT scan. The diagnosis of elastofibroma was suspected.
Methods After fixation in 10% formaldehyde, the tumor was oriented, paraffine-embedded and stained with hematoxylin-eosin and van Gieson. Histological examination was performed.
Results Macroscopically: tumoral mass of 13/5/4 cm, grey-white with small yellow areas, ill defined, firm. Microscopically:The lesion was composed of a collagenous matrix with altered elastic fibers and mature adipose cells. The elastic fibers were fragmented, arranged like small(petaloid) globules, disks or cords with serrated margins. Histopatology diagnosis: elastofibroma.
Conclusion(s) Elastofibroma is an unusual benign lesion, cured by simple excision, with very rare local recurrence. A 2 years-follow up in this case has shown no tumoral recidive.

P4.43
Expression and significance of EGFR in malignant peripheral nerve sheath tumor
Issakov J.; Keizman D.; Meller I.; Meimon N.; Ish-Shalom M.; Sher O.; Merimsky O.
Sourasky Medical Center, Tel Aviv, Israel

Background Malignant peripheral nerve sheath tumor (MPNST) is an aggressive sarcoma. Epidermal growth factor receptor (EGFR) has been implicated in the pathogenesis of several cancers, and is a treatment target. There is little information regarding its role in MPNST.
Methods Malignant peripheral nerve sheath tumor (MPNST) is an aggressive sarcoma. Epidermal growth factor receptor (EGFR) has been implicated in the pathogenesis of several cancers, and is a treatment target. There is little information regarding its role in MPNST.
Results Included 46 patients (mean age 41±19 SD; 30 male, 65%). 43% (n=20) of them overexpressed EGFR in the primary tumor, and had a higher prevalence of advanced stage tumors (≥ IIc, 46% versus 80%, p=0.011). Patients without overexpression had a higher prevalence of tumors with a low mitotic rate (31% versus 0%, p = 0.049). Neurofibromatosis was more prevalent in patients with EGFR overexpression (75% versus 42%, p = 0.007). 5 years disease free survival (mean 30.1 versus 17.4 months, p = 0.048), time to progression (mean 9.2 versus 5.2 months, p = 0.005) and 5 years survival (52% versus 25%, p = 0.041, mean 54 versus 43 months) were significantly higher among patients without overexpression.
Conclusion(s) EGFR appeared to play a role in MPNST progression, and its overexpression is correlated with worse prognostic variables and course. Studies evaluating it as a target for therapy in these tumors appear warranted.

P4.44
How to avoid overdiagnosis of GISTs from other neoplasms?
Michej W.; Ptaszynski K.
Cancer Centre Institute, Warsaw, Poland

Background Gastrointestinal stromal tumors (GISTs) are the most common neoplasms of mesenchymal origin of

stomach and small bowel. They derive from precursors of Cajal's cells and express positive reaction with CD117 antibody. There are a few neoplasms, which clinically and microscopically are similar to GISTs, but treatment of them is not the same.

Methods Between 2002 and 2009 in our Department there were about 500 cases, which were suspected as GISTs. Specimens were sent from other pathologic departments from whole of Poland to consult and make immunohistochemical examination. More of them were GISTs, but 48 were diagnosed as another neoplasms. 10 cases were leyomyosarcomas, 5 leyomomas, 13 neural tumors,, 1 melanoma, 9 fibromatosis, 4 SFT, 1 was liposarcoma.

Results Microscopically: the spindle cells were seen mostly mixed with epitheliod ones. Neoplasms did not express a positive reaction with CD 117 antibody apart from melanoma, CD 34 reaction was postitve in SFT.SMA was positive in neoplasms derived from muscle tissue.S-100 were positive in tumors originated from neural tissue and in liposarcoma. Melan A, HMB 45 and MIT F reactions were expressed in melanoma. Immunohistochemical examinations were negative in firomatosis.

Conclusion(s) It is very important to make good recognition of GISTs and carefully diversify from other neoplasms.. The implication is very simple – treatment will be incorrect.

P4.45

Intramuscular myxoma of psoas muscle: a case report

Nikolaidou A.; Moysidis I.; Anestakis D.; Koumpanaki M.; Balis Christos G.; Patakiouta F.
"Theageneion" Cancer Hospital of Thessaloniki, Thessaloniki, Greece

Background Intramuscular myxoma is a rare, benign mesenchymal tumour, affecting skeletal muscles. Clinically is a painless, mobile, slow growing mass. It usually arises in large muscles of the thigh, and shoulder. The growing rate varies and large lesions maybe painful and cause numbness and muscle weakness.

Methods We report a case of an IMM in the right psoas muscle. A 74 year-old man presented to the Surgical clinic of our hospital with a history of worsening pain in the right iliac fossa. Physical examination revealed a tender, firm mass in the RIF. CT scan showed a hypodense, well defined lesion.

Results Surgical excision was performed, and intraoperatively a 9,5 cm mass was found confined to the right psoas muscle. We received a well-circumscribed tumour, weighing 195grams and measuring 9,5x8,5x6,5 cm. On gross examination, the tumour presented a greyish-white colour, a gelatinous aspect and an elastic consistency. Microscopically the tumour was composed of small, uniform, cytologically bland spindle and stellate shaped cells, with tapering eosinophilic cytoplasm and small nuclei. The cells were separated by abundant myxoid extracellular stroma containing very sparse capillary sized blood vessels. There were no necrotic areas or features of malignancy. Findings consistent with an intramuscular myxoma.

Conclusion(s) Conventional intramuscular myxoma is usually a non-recurrent tumour. Differential diagnosis is between a group of neoplasms in which myxoid change can be a prominent feature (liposarcoma, myxofibrosarcoma,), and a variety of non-neoplastic disorders resulting in focal mucinous degeneration of the soft tissue (nodular fasciitis, localized myxoedema).

P4.46

Pelvic malignant fibrous histiocytoma behind prostate with incidental discovery of adenocarcinoma of the prostate

Apostolaki A.; Negris V.; Theodoropoulou G.; Xekotea A.; Biteli M.; Righa M.; Koufopoulos N.
St. Savvas, Athens, Attika, Greece

Background Malignant fibrous histiocytoma (MFH) is the most common sarcoma of soft tissue in late adult life, between 50 and 70 years, located mainly in the lower extremity (49%) and less frequently in the abdominal cavity or retroperitoneum (16%).We report a case of pelvic pleomorphic MHF,located within the periprostatic tissue of a patient with a concurrent prostatic adenocarcinoma.

Methods A 54-year old man presented urine retention.US and CT showed a 11 cm maximum diameter mass located behind the prostate.Firstly,a rectal needle biopsy revealed a prostatic adenocarcinoma.A second biopsy through the mass confirmed the malignancy.Radical prostatectomy and tumor excision were performed.Tumor cut surface was whitish to yellow with haemorrhagic foci.Solid configuration,cystic degeneration and an elastic,partially gelatinous consistency were observed.

Results Histologically the presence of spindle-shaped fibroblast-like cells in storiform and fascicular patterns of growth was demonstrated. Pleomorphic giant cells with bizarre nuclei were observed.Tumor cells were immunoreactive for CD68 and CD57,slightly positive for Vimentin,SMA and negative for CD117,CD34 and Caldesmon.

Conclusion(s) MFHs are painful solitary multilobulated masses located mainly on the lower extremity.Tumor size varies between 5 and 10 cm of diameter.Cut surface is generally gray to white. The storiform-pleomophic type, the most common, is characterized by sheets of bizarre eosinophilic cells. Differential diagnosis should exclude pleomorphic liposarcoma,pleomorphic rhabdomyosarcoma,pleomorphic carcinoma and Hodgkin's disease.Metastases usually occur

within 2 years of diagnosis,mainly to the lung,lymph nodes, liver and bone.Prognosis of pelvic tumors is poorer than those of extremities.Treatment of choice is surgical therapy.

P4.47
Testicular rhabdomyosarcoma. Case report

Arnogiannaki N.; Theodoropoulou G.; Xecotea A.; Michelis V.; Gakidis P.; Aslanidis O.; Papathanasaki A.
St. Savvas, Athens, Attiki, Greece

Background Rhabdomyosarcoma is the most common paratesticular malignant tumor in infants and young adults.The middle age of appearance is 19 years.It is located usually within the scrotum.Testicular parenchyma is rarely involved. We describe here a case of an alveolar and pleomorphic type rhabdomyosarcoma.
Methods A 19-year-old boy with a long standing palpable right testicular mass was submitted.AFP and b-HCG were negative. MRI revealed enlarged epididymis. FNA was not diagnostic.Radical right orhiectomy was performed. We received separately the testis with spermatic cord and a large circumscribed, uncapsulated mass, measured 5x4,5x4 cm from the inferior pole of the testis. The tumor was firm, with gray-white cut surface, fibrous consistency. The testis was parenchymal.
Results The histologic pattern was an alveolar type of rhabdomyosarcoma with pleomorphic areas. Immunochistochemically cells were positive for Myoglobulin, MyoD1, SMA, Desmin, negative for S-100, HCG, AFP, Vimentin, CD117, CD30, PLAP, Ker CAM5-2, Panker.
Conclusion(s) Testicular tumors represent 0.58–2.09% of all male tumors.1–2% of these tumors are sarcomatous.A small percentage are rhabdomaysarcomas, usually presented as a large intrascrotal painful masses of 1–20 cm diameter. They are circumscribed,never encapsulated, generally gray-white cut surface with fibrous consistency. Microscopically, alveolar type is composed of ill-defined aggregates of poorly differentiated, round or oval pleomorphic cells, showing central loss of cellular cohesion and formation of irregular alveolar spaces. The pleomorphic type is characterized by loosely arranged, haphazardly oriented, small and large, round cells, some with deep eosinophilic cytoplasm. Diferential diagnosis should exclude liposarcoma and other polymorphic sarcomas. Metastases occured through the blood stream and lymphatics (pelvic lymph nodes metastases). Treatment of choice is radical orhiectomy and retroperitoneal lymphadenectomy.

P4.48
Vaginal cellular angiofibroma. A case report

Pitino A.; Squillaci S.; Spairani C.; Barbero M.
Anatomical Pathology, Asti, Piemonte, Italy

Background Cellular angiofibroma (CA) is an uncommon neoplasm that was originally described. in 1997. Since then, this tumor, predominantly involving vulvar soft tissues in women and inguinoscrotal region in men, has subsequently received great attention, with about 60 cases reported to date.
Methods A 19-year-old woman presented with a 2,5 cm. painless vaginal mass which was locally excised. The specimens were routinely stained with H&E. Immunohistochemical studies were performed for vimentin, desmin, smooth muscle actin (ASMA), h-caldesmon, S-100, CD31, CD34, estrogen (ER) and progesterone (PR) receptors.
Results Grossly, the tumor was rubbery, with a greyish homogeneous cut surface. Microscopically, it was a well-demarcated lesion, composed of monotonous, spindle to ovoid cells, with bland oval to fusiform nuclei and lightly eosinophilic ill defined cytoplasm. The cells were arranged in sheets, sometimes loosely dispersed in a myxoid matrix, often around a delicate net of branching thick vessels with occasional perivascular fibrosis. The tumor contained hypercellular areas and an average of 1–2 mitoses per 10 HPF but lacked significant nuclear atypia. Immunoreactivity for vimentin, ASMA, CD34, ER and PR was present. None for other markers was observed.
Conclusion(s) CA is a rare neoplasm which follows a benign course. The differential diagnosis includes: other vulvovaginal mesenchymal lesions such as aggressive angiomyxoma, a paucicellular, usually desmin positive tumor, with locally infiltrative growth, benign tumors with very low risk of local recurrence (postoperative spindle cell nodule, nodular fascitis, neurofibroma) and malignant tumors (synovial sarcoma and liposarcoma).

Endocrine pathology

P4.49
Sialyltransferases expression. New perspective markers of thyroid gland pathology

Janega P.; Urbanova A.; Celec P.; Babal P.
Department of Pathology, Faculty of Medicine, Comenius University Bratislava and Institute of Normal and Pathological Physiology, Slovak Academy Of Sciences, Bratislava, Slovakia

Background Thyroid cancer belongs to the most frequent endocrine diseases. The difficult differential diagnosis between benign and malignant lesions often complicates its histopathological evaluation.
Methods The cases of well differentiated thyroid gland tumors (malignant papillary and follicular carcinomas and benign follicular adenomas) and parenchymatous goiters were analyzed by real-time-PCR for the expression of sialyltransferases 1,4A,4B and 4C and neuraminidases 1

and 2. The results were correlated with the evaluation of protein sialylation by lectin histochemistry.
Results The follicular cell in benign goiter and adenomas shows weak expression of sialic acid (10,6±1,6% and 5,7± 1,3% respectively). The significant increase of sialic acid positivity is documented during malignant transformation in follicular and papillary carcinoma (22,34±2,6%, 22,41± 0,9% respectively) and correlates with the significant increase of sialyltransferase 4C and 4B expression found in these tumors, which are specific for alpha-2,3-linkage of sialic acid. A parallel decrease of neuraminidase 1 transcription in the papillary (by 77,1%) and neuraminidase 2 (by 58,5%) in the follicular carcinoma was documented.
Conclusion(s) The changes of protein sialylation represent new perspective markers of thyroid gland pathology and may become a diagnostic aid, especially in respect to the differential diagnostics of the follicular thyroid gland lesions. This work was supported partially by Ministry of Health of the Slovak Republic under the project 2006/23-UK-02.

P4.50
Claudins-1,3,4,5 and -7 expression during human thyroid development: an immunohistochemical analysis

Colato C.; Ambrosetti M.; Dardano A.; Monzani F.; Filetti S.; Chilosi M.; Menestrina F.; Ferdeghini M.
Depatment of Pathology, University of Verona, Verona, Italy

Background Thyroid follicles develop from aggregates of unpolarized precursor cells. Tight junctions (TJs) are dynamic structure, that at different stages of epithelial tissue development play an essential role in maintaining integrity and physiological function of thyroid follicles. Claudins (CLDNs) are the major components of TJs. Tissues are characterized by distinctive CLDNs patterns changing during differentiation and tumor formation. CLDNs expression during thyroid ontogenesis is unknown.
Methods To examine CDLNs-1,3,4,5, and 7 immunohistochemical distribution and staining pattern in human foetal thyroid glands. Eighteen thyroid glands were obtained from human fetuses (gestational age range: 15–22 weeks). Immunostaining was performed using polyclonal (CLDNs-1 and 3) and monoclonal (CLDNs-4, 5 and 7) antibodies.
Results CDLN-7 was constantly expressed showing strong, diffuse and linear basolateral positivity. CDLN-4 and 5 immunostaining was similar to CDLN-7 but weaker. CDLN-1 exhibited a weak, focal membranous staining at gland periphery. CLDN-3 immunoreactivity was negative.
Conclusion(s) CDLN-7 and 4 are constitutively expressed in thyroid epithelium during ontogenesis at a similar level from foetal up to adult thyroid tissue, thus suggesting an essential role in architectural stability of follicular cells. CLDN-1 was expressed at the border of the foetal gland where the first follicles, containing colloid, are localized. Conversely, CLDN-1 was absent in adult normal tissue while up-regulated in thyroid cancer, thus emerging as an oncofetal antigen and a potential marker of thyroid cancer. Our study demonstrates CLDN-5 expression in thyroid gland, suggesting its possible role in normal and neoplastic adult thyroid tissue.

P4.51
Epstein-Barr virus infection in the development of autoimmune thyroid diseases

Urbanova A.; Babal P.; Janega P.
Department of Pathology, Faculty of Medicine, Comenius University Bratislava, Bratislava, Slovakia

Background Autoimmune thyroid diseases (AITD) afflicts up to 10% of the worldwide population.The etiology of the AITDs remains unclear but it is believed that both genetic and environmental factors are important in their development.Serological and epidemiological data suggest that viral infection could play a possible role in their pathogenesis.The presented study focused on the direct detection of Epstein-Barr virus(EBV) in thyroid gland biopsies from patients with Hashimoto's thyroiditis (HT) and Grave's disease (GD).
Methods Detection of EBV infected cells was achieved through immunohistochemistry and in situ hybridisation (ISH). For immunohistochemistry antibodies against viral latent membrane protein (LMP) were used. ISH technique demonstrated EBV presence through the expression of EBV-encoded small nuclear RNA (EBERs) transcripts.
Results Immunopositivity of LMP was found only in HT. The specimens of GD were negative for this marker. EBER nuclear positivity was found in 84,7% cases of HT and in 62% cases of GD.In Hashimoto's thyroiditis EBER was also prominent in lymphocytes. Grave's disease demonstrated EBER positivity predominantly in follicular epithelial cells.
Conclusion(s) The presented high prevalence of EBV strongly indicates a causal role of this infectious agent in AITD. An interesting finding was the intensive nuclear positivity of both LMP and EBER mainly in follicular epithelial cells in some cases of HT with few infiltrating lymphocytes. This strong epithelial positivity in the early phase of the disease could imply the role of EBV in the initiation of the autoimmune process. This work was supported by Ministry of Health Slovak Republic, project No.2006/23-UK-02.

P4.52

Diagnostic value of galectin-3, HBME-1 and cytokeratin-19 immunoexpression in thyroid tumors of different malignant potential

Abrosimov Yur'evitch A.; Dvinskikh Yur'evna N.; Lushnikov Fedorovitch E.
Endocrinological Research Center, Moscow, Russian Federation

Background Differential diagnosis between benign and malignant thyroid tumors originated from follicular epithelium is sometimes difficult even after full pathologic review.The group of tumors of uncertain malignancy concerns either atypical adenomas or the recently called "tumors of uncertain malignant potential". Hyalinizing trabecular tumor that is regarded by many pathologists as benign or tumor of uncertain malignancy could also be a source of diagnostic difficulties.
Methods We studied the diagnostic value of galectin-3, HBME-1 and cytokeratin-19 immunoexpression in four groups of benign (follicular adenoma, 17 cases), malignant (follicular carcinoma and follicular variant of papillary carcinoma, 23 cases), follicular and well differentiated tumors of uncertain malignant potential (12 cases) and hyalinizing trabecular tumor (7 cases). Immunohistochemistry was performed on 4 um thick sections with the appropriate Dako and Novocastra Laboratories monoclonal antibodies. Preliminary heat-induced antigen retrieval was carried out.
Results Most of follicular adenoma and hyalinizing trabecular tumor cases demonstrated negative immunostaining for all of three markers. Immunoexpression of galectin-3 and its combination with HBME-1 was useful diagnostic test for malignant tumors with high levels of sensitivity (96%), specificity (88%) and accuracy (93%). The group of tumors of uncertain malignant potential was heterogeneous in terms of galectin-3 and HBME-1 immunoexpression.
Conclusion(s) Negative immunostaining in most of cases of follicular adenoma and hyalinizing trabecular tumor confirmed benign character of these tumors. The co-expression of galectin-3 and HBME-1 in tumors of uncertain malignancy may suggest malignant potential in some of these tumors.

P4.53

The use of HBME-1 and CK19 in the differential diagnosis of benign from malignant thyroid lesions

Tanoglidi A.; Mourtzoukou E.; Tsopanomichalou M.; Pantzartzi D.; Tsikou Papafragou A.; Berger N.; Barbatis C.
Hellenic Red Cross Hospital, Department of Pathology, Athens, Greece

Background The distinction between malignant from benign thyroid lesions albeit easy for the majority can be very difficult at times, as there are cases with subtle differences, and the current terminology relevant to prognosis is still under scrutiny. HBME-1 and CK19 have shown high sensitivity but variable specificity for malignancy and the aim of this study is to evaluate the immunohistochemical expression of both molecules in the differential diagnosis of benign from atypical/malignant thyroid nodules.
Methods From 114 total thyroidectomies the following sites were studied: normal thyroid (49), nodular/diffuse hyperplasia (40/5), adenoma (20), atypical adenoma (10), adenomatoid nodule (3), thyroiditis Hashimoto/de Quervain/lymphocytic (13/2/4), focal nuclear clearing in hyperplastic nodules (4), adenomas (6), and atypical adenomas (1) and papillary carcinoma (PTC) (71). The topography, distribution and the % of positive cells were assessed.
Results All normal thyroid follicles were HBME-1 negative in contrast to positive PTCs (68/71),hyperplastic micro follicles at sites of inflammation (14/15), areas with nuclear clearing (9/12) and atypical adenomas (9/10). Infrequent and focal positivity was observed in hyperplastic (7/40), adenomatoid nodules (0/3) and adenomas (6/20). CK19 was frequently expressed in all lesions but in malignant and suspicious areas there was concomitant expression of both molecules.
Conclusion(s) HBME-1 antigen is an important marker for distinguishing malignant/atypical lesions from benign epithelium. In our lesions simultaneous positivity for the two molecules increased the specificity and improved our diagnostic ability.

P4.54

DLK is a novel immunohistochemical marker for adrenal gland tumors

Turanyi E.; Dezso K.; Paku S.; Nagy P.
Semmelweis, Budapest, Hungary

Background Delta-like protein (DLK) has a quite restricted distribution in the human body, but it is present in fetal and adult adrenal gland. We have investigated if this expression is maintained in adrenal gland derived tumors.
Methods Thirty six adrenocortical tumors, including four carcinomas, 13 phaeochromocytomas and several differentialdiagnostically related tumor blocks has been collected from our archives. The sections has been stained for DLK by standard ABC based immunohistochemistry using DAB as chromogen.
Results All the studied cortical tumors stained positively as well as the examined phaeochromocytomas. Thus, DLK is a very sensitive marker for adrenal tumors of cortical and

medullary origin. Renal cell carcinomas (13), presenting the major differential diagnostic problem for cortical tumors were all negative, as well as melanomas (11), which similar to high portion of adrenocortical tumors react with melan A. However, all paragangliomas (4), some carcinoids (3/22) and thyroid medullary carcinomas (5/11) were also positive for DLK.

Conclusion(s) This novel immunohistochemical marker seems usefull for the identification of adrenocortical tumors while it has limited value for the distinction of pheochromocytomas from diagnostically related neuroendocrine tumors.

P4.55

Evaluation of cannabinoid receptor (CB)-1 and -2 expression in human benign and malignant thyroid lesions

Giaginis C.; Stolakis V.; Zira A.; Zarros A.; Klijanienko J.; Delladetsima I.; Tsourouflis G.; Theocharis S.
University of Athens, Medical School, Athens, Greece

Background Endocannabinoids are suppressors of key cell-signalling pathways involved in cancer cell growth, invasion, and metastasis. Two types of cannabinoid receptors (CBs) have been identified so far: the central (CB-1) and peripheral (CB-2). Endocannabinoids present variable selectivity for these receptors, while their pharmacological manipulation could be of great importance for novel targeted anti-tumor approaches. The present study aimed to evaluate the clinical significance of CB-1 and CB-2 expression in benign and malignant thyroid lesions.

Methods CB-1 and CB-2 protein expression was assessed immunohistochemically in formalin-fixed, paraffin-embedded thyroid tissues from 98 patients with benign (hyperplastic nodules and Hashimoto thyroiditis, $n=46$) and malignant lesions (papillary, medullary, follicular and anaplastic thyroid carcinomas $n=55$). CB-1 and CB-2 positivity was compared between malignant and benign thyroid lesions, as well as between Hashimoto thyroiditis and hyperplastic lesions. Additionally, CB-1 and CB-2 expression was statistically analyzed in relation to TNM stage for the subgroup of malignant tumors and tumor proliferative capacity assessed by Ki67 labeling index.

Results Only CB-1 positivity provided a distinct discrimination between malignant and benign thyroid lesions ($p=0.007$). On the other hand, in malignant thyroid lesions, CB-2 expression was associated with tumor size ($p = 0.002$).

Conclusion(s) The current data revealed that CB-1 and CB-2 expression could be considered of diagnostic utility in thyroid neoplasia. Further studies conducted on distinct malignant thyroid lesions are warranted to delineate the clinical significance of CBs expression and their potential use as therapeutic targets in thyroid neoplasia.

P4.56

Haemopoietic malignancies of the sella and pituitary gland

Bravi I.; Mauri F.; Horncastle D.; Mehta A.; Hyam J.; Mendoza N.; Ascani S.; Naresh K.; Roncaroli F.
Imperial College, London, United Kingdom

Background Sellar involvement from haemopoietic malignancies is usually secondary to a systemic disease and accounts for about 1% of pituitary metastases; primary sellar lymphomas are exceedingly uncommon.

Methods We present one surgical index case of chronic lymphocytic leukaemia (CLL) and 11 post-mortem cases of acute myeloid leukaemia (AML) and non-Hodgkin's lymphoma (NHLs) retrieved between 1970 and 2008. We have also reviewed 123 published papers between 1980 and 2009. Langherans cell histiocytosis was not included in this study.

Results Although AML and CLL are the most common leukaemias affecting the sellar region, almost all subtypes of NHL have been documented, with about 50% of them being diffuse large B-cell lymphoma. Plasma cell neoplasms (PCNs) and Hodgkin's lymphoma (HL) are the least common. AML characteristically present with diabetes insipidus whereas CLL, NHL, PCNs and HL usually present with signs and symptoms of mass effect and hypopituitarism. Neuroimaging features are indistinguishable from adenomas but, unlike adenohypophyseal cell tumours, leukaemias and lymphomas often involve neurohypophysis and cranial nerves. Adenohypophysis is usually infiltrated from the stalk or the surrounding tissue; in only a minority of cases is the gland primarily involved. PCNs invariably invade the sellar bones and only secondarily extend to the pituitary. Interestingly, all our cases of AML but not CLL and NHLs expressed prolactin receptors in neoplastic cells.

Conclusion(s) Haemopoietic malignancies involving the pituitary gland may represent a challenging diagnostic problem and should be considered in the differential diagnosis of non-functioning lesions of the sella.

P4.57

Microvessel and lymphatic vessel density and VEGFR-3 expression of papillary carcinoma of thyroid gland

Koo H.; Cheong H.
Department of Pathology, Ewha Womans University School of Medicine, Seoul, Republic of Korea

Background In papillary carcinoma of thyroid gland, the tumor size and lymph node metastasis are important

prognostic factors and their relationship with angiogenesis is controversial. This study was performed to see the correlation between CD34-positive microvessel density (MVD), D2-40-positive lymphatic vessel density (LVD), and VEGFR-3 expression and various clinical parameters of papillary thyroid carcinomas of size larger than 1.0 cm (PTCs) and smaller than 1.0 cm (papillary thyroid microcarcinomas, PTMCs).

Methods 197 samples including 113 cases of PTC and 84 cases of PTMC were analyzed. Thirty pairs of patients from PTMC and PTC matched for clinical characteristics were selected for immunohistochemical staining.

Results The MVD in combined PTMC and PTC groups showed an increasing tendency in tumors with lymph node metastasis. Because the PTMCs and PTCs did not show difference in MVD, LVD, and VEGFR-3 expression, the differences in nodal metastasis between these two groups must be related to other factors. The LVD was higher in patients of age over 45, which was more apparent in PTC group. In addition, LVD was significantly higher in PTMCs of larger size than smaller ones. There was no difference of VEGFR-3 expression in PTMC according to tumor size.

Conclusion(s) Because the correlation between clinical parameters and papillary carcinoma of thyroid gland showed variable results according to analyzing factors, the treatment of the patients should be individually planned based on their clinical presentations and other tumor risk profiles.

P4.58

The value of BRAFV600E mutation analysis for the therapeutic decision making in patients with thyroid nodule

Hwang T.; Kim Kyeong S.; Han Seung H.; Lim Dug S.; Kim Seop W.

Konkuk University Medical Center, Seoul, Republic of Korea

Background BRAFV600E mutation analysis has been proposed as a valuable adjunctive tool for refining the cytological diagnosis of thyroid nodules. To define a clinical value of BRAFV600E mutation analysis in the routine patient care, fine needle aspiration biopsy and BRAFV600E mutation analysis were performed.

Methods DNA was extracted after follicular cells were scraped from cytology slide and BRAFV600E mutation was analysed by pyrosequencing method.

Results Among 410 cases, 5 (1.2%), 230 (56.1%), 54 (13.2%), 27 (6.6%), 88 (21.5%), and 6 (1.5%)cases were cytologically dignosed as an inadequate specimen, benign nodule, indeterminate cytologic feature, suspicious for papillary carcinoma(PC), PC, and follicular neoplasm(FN) or suspicious for FN, respectively. None of the 230 benign nodules showed BRAFV600E mutation. Twenty one 38.9%) of 54 indeterminate cases, 23 (85.2%) of 27 cases suspicious for PC, 81 (92.1%) of 88 PC cases showed BRAFV600E mutation. All 6 cases diagnosed as FN or suspicious for FN did not reveal BRAFV600E mutation. All patients diagnosed as suspicious for PC or PC were recommended to have an operation and all of these patients turned out to have PC regardless of their BRAFV600E status. All 21 patients with positive BRAFV600E mutation and indeterminate cytologic feature were recommended to have an operation. Among them 10 patients underwent surgery and 9 patients had a PC and one patient had a nodular goiter.

Conclusion(s) We found that BRAF analysis provide a great help to make a therapeutic decision when the FNAB results are equivocal.

P4.59

Adrenal oncocytic tumor. Report of 2 cases and prognostic value of three different histopathological scoring systems

Decaussin-Petrucci M.; Ragage F.; Loghin A.; Borda A.; Berger N.

Centre Hospitalier Lyon Sud, Hospices Civils de Lyon, Université Lyon 1, Pierre Benite, France

Background Oncocytic adrenocortical neoplasms are rare. Clinical outcome and biologic behavior of these tumors are difficult to predict. The Weiss system is considered to be predictive of the biologic behavior of adrenocortical neoplasms. Nevertheless, a modified Weiss scoring was proposed in 2004 for oncocytic tumors. The Weiss Revisited Index (WRI) presented by Aubert is another way to evaluate agressivity of these tumors. We tested these systems on adrenocortical oncocytic tumors to determine whether they can predict clinical outcome.

Methods Two cases of adrenal oncocytic tumors were examined. The classical and the modified Weiss systems and WRI were evaluated.

Results The size was 5.5 cm and 9 cm respectively and the weight 82 g and 95 g. The two cases were exclusively composed of oncocytic cells, arranged in diffuse or solid patterns. Immunohistochemical profil was the same for the two cases: AE1-AE3 +/-, chromogranin A -, synaptophysin +, PS 100-, EMA -, Melan A+, inhibin +. The classical Weiss score for the both cases was 3 (diffuse architecture, less than 25% clear cells, high nuclear grade), the modified Weiss was 0 as the WRI. Follow up was obtained for each patient (mean: 5 years): no recurrence or metastases were noticed.

Conclusion(s) If the classical Weiss score is inadequate for oncocytic adrenocortical tumors, the modified Weiss score or

the WRI seems an interesting alternative. Larger series are necessary to confirm these results.

P4.60
Expression of E-cadherin in papillary thyroid carcinoma

Bich T.; Nerovnya A.; Cherstvoy E.
Belarussian State Medical University, Minsk, Belarus

Background The E-cadherin plays a crucial role in epithelial cell-cell adhesion, in the maintenance of tissue architecture and differentiation. Changes in the expression or function of E-cadherin results in loss of intercellular adhesion, with possible consequent cell transformation and tumour progression.
Methods The expression of E-cadherin were immunohistochemically studied in 37 papillary thyroid carcinomas (PTC), in 11 regional metastatic PTC and in 3 PTC with cataplasia to anaplastic carcinoma.
Results E-cadherin expression levels decrease has been detected in solid structures of PTC in comparison with papillary (p=0,01) and folliculary (p<0,01) structures. Such regularity for E-cadherin expression in different variants of PTC was not found. Papillary thyroid carcinomas with cataplasia to anaplastic carcinoma demonstrated significantly lower level of E-cadherin expression in comparison with main group of PTC (p=0,03). The increased expression of E-cadherin has been detected in regional metastatic cells of PTC cases compared to the primary thyroid tumor of the same patients (p = 0,03).
Conclusion(s) The significant downregulation of E-cadherin expression was revealed alongside with the reducing level of PTC cell differentiation. Cancer cells in the regional metastasis of PTC had higher level of E-cadherin expression in comparison to the primary tumor. These results suggest that the epithelial cell-cell adhesion increases in metastatic cells of PTC.

P4.61
Immunohistochemical analysis of IgG4 In Hashimoto's autoimmune thyroiditis

Li Y.; Nishihara E.; Mori I.; Miyauchi A.; Kakudo K.
Wakayama Medical University, Wakayama, Japan

Background IgG4-related sclerosing disease is a recently recognized systemic inflammatory entity involving pancreas, liver, lung, kidney, retroperitoneum and so on. All these lesions shared histologic features such as: diffuse lymphocytic infiltration by many IgG4-positive plasma cells, progress fibrosis, occasional eosinophilic infiltration and obliterative phlebitis.
Methods 70 cases of surgical samples from clinicopathologically confirmed Hashimoto's autoimmune thyroiditis were analyzed. Immunostaining of IgG4 and IgG were performed on paraffin sections and the histopathological characterisitics of these cases were also evaluated.
Results Based on immunohistochemical staining of IgG4 and IgG, Hashimoto's autoimmune thyroiditis could be classified into two groups. 17 cases showed diffuse or nodular dense infiltration of abundant IgG4-positive plasma cells (IgG4-positive plasma cell-rich group), whereas the remaining 53 cases had only a few IgG4-positive plasma cells (IgG4-positive plasma cell-poor group). Histopathologically, IgG4-positive plasma cell-rich group presents with severe lymphoplasmacytic infiltration, dense fibrosis, marked follicular cell degeneration, lymphoid follicle formation and oxyphilic change, while IgG4-positive plasma cell-poor group presents with relatively mild or absent in the above histological characteristics. In addition, serum IgG4 concentrations were significantly higher in IgG4-positive plasma cell-rich group than poor group.
Conclusion(s) Hashimoto's autoimmune thyroiditis can be subclassified into two groups, in regard of IgG4-positive plasma cell population: IgG4 thyroiditis (IgG4-positive plasma cell-rich group) and non-IgG4 thyroiditis (IgG4-positive plasma cell-poor group).

P4.62
Investigation of the magnesium level in patients with type II diabetes

Tziamalis M.; Patiakas S.; Akrtopoulou K.; Charalampous C.; Koufos L.; Lytra E.
Dialysis Unit of General Hospital of Kastoria, Kastoria, Greece

Background To register the magnesium level (Mg) in blood samples of diabetic patients, to compare them with those of healthy people, and to investigate their possible correlation with the levels of the glycated hemoglobin (Hba1c).
Methods The level of Mg as well as that of Hba1c were measured in the blood samples of 92 patients with type II diabetes and of 50 healthy people.
Results table A: patients with diabetes Mg < 1,8 mg/dl: Hba1c < 7: Men/Women: 1/1, Hba1c 7–10: Men/Women: 4/5, Hba1c > 10: Men/Women: 2/1, Mg: 1,8–2,4 mg/dl: Hba1c < 7 :Men/Women: 12/15, Hba1c 7–10: Men/Women: 17/27, Hba1c > 10: Men/Women: 4/3, table B: control group Mg<1,8 mg/dl: Men/Women: 1/2 Mg: 1,8–2,4 mg/dl: Men/Women: 23/24.
Conclusion(s) It is, therefore, proved that a great percentage of 15,2% of the diabetic patients suffers from hypomagnesaemia, - fact that undoubtedly underlines the necessity of a therapeutic intervention -. It should be mentioned that the corresponding percentage in the healthy-general

population of the similar age, barely reaches the level of 6%. Moreover, it is shown that the Mg level measured remains to the lowest normal values (1,8–2 mg/dl) at a great percentage of the rest diabetic people (14,1%).

P4.63

Morphological aspects of the high-frequency electrochemical destruction of thyroid nodules

Kanibolotskiy Alekseevich A.; Galkin Nikolaevich V.; Pimonova Sergeevna I.
Moscow Clinical Hospital, Moscow, Russian Federation

Background In recent years steadfast growth of thyroid nodulose pathology is noted. Thyroid nodules are re-vealed in 30% of adults. The aim of this investigation was to prove the efficacy and safety of a new miniinvasive method of thyroid nodulose pathology treatment – high-frequency electrochemical destruction (HFED).
Methods The electrothermic influence was carried out by monopolar electrocoagulation with 1760 kGz fre-quency and impulse period in 15 microseconds with the help of apparatus« ECHF-300»after pre-liminary injection into the thyroid paren-chyma of 2% NaCl solution. Power of the HFED oscillated from 40 to 70 Wt, and duration – from 2 to 10 seconds. The investigation included the research on operatively removed thyroid glands (n=40) and on adult corpses (n=20).
Results The destruction in thyroid parenchyma had spherical form and consisted of precisely distinguished zones of coalification, coagulative necrosis, parabiotic alteration, mor-phologically invariable paren-chyma. Zone of necrotic injury was achieved from 0.2 to 5 mm in diameter. The destruction zone was limited by capsule of the nodule and afterwards it was replaced by connective tissue. Trachea, recurrence laryngeal nerves, parathyroid glands were intact.
Conclusion(s) The HFED causes firm coagulative necrosis of thyroid parenchyma inside the capsule of the nodule. Zone of necrosis has precisely limited boundaries, its size enlarges with increasing of power and duration of the HFED. Absence of alteration in trachea, recurrence laryngeal nerves, parathy-roid glands and other surrounding tissues, proves safety of the HFED and permits using of this method in clinic.

P4.64

Prognostic factors in evaluation of adrenal pheochromocytoma (PHE)

Janicka-Jedynska M.; Wozniak A.; Biczysko M.; Zurawski J.; Bulak-Joniec J.; Kaczmarek E.
Poznan University of Medical Sciences, Poznan, Poland

Background PHEs are not common neoplasms, however they are of great clinical importance because of the catecholamines secretion and arterial hypertension. Histo-logical diagnosis of typical case of PHE is relatively easy. Most of PHEs are benign neoplasms. Malignant PHEs constitute about 10% (2,4 -26%). According to WHO recommendations, metastasis is the only one single criteri-on of PHE malignancy because conventional histological features may be also present in benign PHE. There are multiple systems of scoring of various PHE histological features, which however are not compatible and do not give confirmation of PHE malignancy. Therefore other prognos-tic factors are searched for. The aim of the study was examination of Ki 67, p53, bcl-2 and VEGF expression with reference to microscopic picture and clinical course.
Methods All archival cases of PHEs (50) from last 12 years were found (including 6 malignant). The following histo-logical features were evaluated: presence of necrosis, invasion of capsule and vessels, cellularity, atypical mitoses and type of growth. Immunoreactivity for Ki 67, p53, bcl-2 and VEGF was studied.
Results Proliferative activity was significantly higher in malignant PHEs (at least 5%) than in benign ones. P53 expression has been reported in only 1 malignant PHE (in all benign PHEs it was negative). There were no differences in bcl-2 expression between both studied groups. Most benign PHEs showed only focal positive VEGF expression. Significantly more intense immunoreactivity was observed in malignant PHEs.
Conclusion(s) Ki 67,p53 and VEGF are usefull prognostic factors in evaluation of adrenal PHE.

P4.65

Prognostic significance of cytokeratin19 in pancreatic endocrine tumours

Bragantini E.; Barbi S.; Beghelli S.; Capelli P.; Falconi M.; Scarpa A.
Università degli Studi di Verona, Verona, Italy

Background Pancreatic endocrine tumours are rare neo-plasm, whose behaviour is difficult to predict. Recent 2004 WHO classification gives clear criteria to define prognosis of PET, but despite these criteria some tumours show a more aggressive course. Recent studies highlighted the role of immunohistochemical markers such as CK19, CD99, P27 as prognostic markers for pancreatic endocrine tumors. The aim of this study was to evaluate the prognostic value of CK19 expression in PETs.
Methods Immunohistochemical expression of CK19 was searched in 149 PETs using tissue microarrays.
Results CK19 was detected in 100/149 primary tumours (67.1%). At univariate analysis, CK19 expression showed a significant correlation with tumour dimension, presence of nodal or distant metastasis and 5 years survival. The

significance of CK19 disappeared when WHO 2004 classification was entered into the multivariate Cox analysis.
Conclusion(s) CK19 is an index and marker of malignancy but it is not an independent prognostic marker.

P4.66
Quantitative fine needle aspiration cytology of nodular goiter

Mihailovic Slavoljub D.; Kostov Sima M.; Mijovic Zarko Z.
Institute of Pathology, Nis, Serbia and Montenegro

Background Thyroid nodules are common clinical findings, and the vast majority of them are benign lesions. Several diagnostic tests, especially fine needle thyroid aspirate cytology, have been used to differentiate benign from malignant thyroid nodules pre operatively. A cytological diagnosis of malignancy allows the patient to be informed that an operation for cancer is likely and preoperative staging procedures to be carried out. The aim of this study was to estimate nuclear morphometric variables in fine needle thyroid aspirate cytology (FNAC).
Methods At Institute of Pathology, University of Nis, from January 2003 to December 2006 a total of 205 FNACs were done on 198 patients. In 44 patient comparisons with histopathology was done. Six nuclear variables were estimated by ImageJ analytical software: area, mean optical density, Feret's diameter, perimeter, circularity, and integrated optical density (IOD).
Results Nuclear area, Feret's diameter, and perimeter were significantly larger in cancer patient compared to benign and suspect cases. On the other hand, optical density of epithelial cell nuclei was significantly smaller in cancer patients. Differences between benign and suspect lesions were not statistically significant.
Conclusion(s) Our results suggest that quantitative analysis of fine needle thyroid aspirates can be useful in routine cytopathological practice.

P4.67
Serum cytokines and growth factors levels in pituitary adenomas behaviour using xMAP technology

Tanase C.; Raducan E.; Mihai S.; Georgescu M.; Ionita A.; Poroschianu M.; Cruceru L.; Codorean E.; Ogrezeanu I.
"Victor Babes" National Institute of Pathology, Bucharest, Romania

Background Serum cytokines/growth factors levels have been investigated in relationship with invasiveness in pituitary adenomas in order to evaluate the involvement of this potential biomarkers in pituitary tumor cell proliferation.
Methods We have investigated 22 serum samples of subjects with pituitary adenomas (15 non-invasive and 7 invasive adenomas) and 7 samples as control group. Cytokines and growth factors levels were determined using xMAP technology (Luminex 200).
Results Increased levels of IL-1beta, IL-6 and TNFalpha were found in 27%, 32% respectively 41%. Cytokines expression was significantly higher in invasive pituitary adenomas 86% versus non-invasive ones 7%. TNFalpha level was up to 1,8 fold higher than control, while IL-6 and IL-1beta were 4 respectively 4,7 fold higher. We have noticed a positive correlation between the cytokines level and the tumoral invasiveness. Growth factors values obtained by xMAP array were comparable with the outline obtained by ELISA tests. Mean value for soluble VEGF in patients versus control was 1.6 fold in Luminex and 2 fold in ELISA analysis. Soluble bFGF mean value was 1.2 fold higher when Luminex technology was used and 1.6 fold in ELISA quantification.
Conclusion(s) Our findings demonstrate that cytokines and angiogenic factors levels are closely linked to the tumoral pituitary behaviour. Expression of cytokines/angiogenic factors are strongly related to tumor invasion and in this way may act as factors supporting pituitary tumour expansion. This project was supported by Grant PNII 62-087.

P4.68
Usefulness of CK19, HBME-1 and galectin-3 immunohistochemistry in differential diagnosis of follicular thyroid tumors

Cornianu M.; Golu I.; Dema A.; Taban S.; Costi S.; Faur A.; Lazar E.; Zosin I.
Universitatea de Medicina si Farmacie Timisoara, Timisoara, Timis, Romania

Background Well-differentiated encapsulated thyroid tumors with follicular architecture may cause diagnostic difficulties.The aim of the present study was to evaluate the expression and diagnostic value of cytokeratin 19 (CK19), HBME-1 and galectin-3 (Gal-3) in distinguishing between well-differentiated follicular neoplasm and tumors with uncertain malignant potential (TUMP).
Methods The study group consisted in 41 cases of thyroid tumors (14 benign, 27 malignant: 18PTC, 5FTC, 4TUMP), immunostained with CK19 (RCK108, 1:150, Dako, USA), HBME (HMBE-1, 1:100Dako, USA) and Gal-3 (5170, 1:50 Sigma –Aldrich, USA). Staining was scored as positive when >10–50% of the lesion cells showed positive immunostaining.
Results CK19 was expressed in 94.44% PTC, 60% FTC, 50% TUMP and 41.66 FA (p=0.006). HBME-1 was positive in 83.3% PTC, 80% FTC, 50% TUMP and 25% FA (p = 0.006). Gal-3 showed positive reactivity in 94%

PTC, 60% FTC and 16.6 % of benign lesions ($p = 0.001$). Regarding TUMP, the positive immunoreaction for CK19 (moderate and diffuse), along with HBME-1 immunoexpression allowed the inclusion in the FVPTC category for 2 out of 4 cases. The expression of all markers was significantly associated with differentiated thyroid carcinoma (DTC). The sensitivity for the diagnosis of DTC was 81.5% with CK19, 77.8% with HBME-1, and 81.5% with Gal-3. The specificities of these markers were 64.3%, 71.4% and 85.71%, respectively.

Conclusion(s) An immunohistochemical panel consisting of CK19, HBME-1 and galectin-3 can make a correct distinction between malignant and benign thyroid lessions.

P4.69

Von Hippel-Lindau disease and parasympathetic paragangliomas

Gaal J.; Van Nederveen F.; Korpershoek E.; Erlic Z.; Robledo M.; Oldenburg R.; Neumann H.; Dinjens W.; De Krijger R.
Erasmus MC, Rotterdam, Netherlands

Background Von Hippel-Lindau (VHL) disease is a hereditary tumor syndrome manifested by haemangioblastomas, clear cell renal cell carcinomas and phaeochromocytomas. Although these aforementioned tumors are the hallmarks of VHL, a multitude of other rare tumors can occur and even be the sole manifestation of the disease. One of these rare tumors is parasympathetic paraganglioma (pPGL). The occurrence of pPGL has been described in the literature in several cases, but the involvement of the VHL tumor suppressor gene has never been proven in tumor tissue.

Methods The pPGL from 2 patients with VHL disease, were available for analysis. From the two formalin fixed paraffin embedded tumors, DNA was isolated and mutation analysis was performed by direct sequencing of the VHL gene. To rule out other underlying genetic causes of the pPGL, mutation analysis by direct sequencing of the SDHB, SDHC and SDHD genes, was also performed. LOH analysis was performed for 3 microsatellite loci near the VHL gene.

Results Mutation analysis revealed no mutations in the SDHB, SDHC and SDHD gene, but direct sequencing of the VHL gene revealed the p.Arg64Pro and the p.Tyr98His mutation. Analysis of the tumor tissues revealed loss of the VHL wild type allele indicating that these tumors occurred in the context of VHL disease.

Conclusion(s) These findings suggest that pPGL do occur in the context of VHL disease and so clinicians should be aware of the potential presence of pPGL in VHL disease.

P4.70

Diffuse sclerosing variant of papillary carcinoma of the thyroid (case report)

Keser Hallac S.; Gul Ege A.; Cakir C.; Barisik Ozdemir N.; Geyyas R.; Karadayi N.; Kandemir Onak N.
Dr. Lutfi Kirdar Research and Education Hospital, Istanbul, Turkey

Background Diffuse sclerosing variant of papillary thyroid carcinoma (PTC) is an uncommon variant of PTC that shows diffuse involvement of the thyroid, dense sclerosis, extensive squamous metaplasia, patchy to dense lymphocytic infiltrate, numerous psammoma bodies, and marked lymphatic permeation during histological examination. The cinical behavior of this variant of PTC remains uncertain.

Methods Case: A year ago, papillary carcinoma was detected in the piece of right thyroidectomy of a 33-year-old female patient and complementary left thyroidectomy was performed. The thyroid gland was hard and gritty. Grey-white colored areas were observed. Histologically, there is diffuse involvement of thyroid lobe with dense fibrosis, extensive squamous metaplasia with morphologically benign nuclei, patchy lymphoid infiltration with germinal centres, psammoma bodies. One of the perithyroidal lymph node contained metastatic carcinoma.

Results The case was considered as the diffuse sclerosing variant of papillar carcinoma.

Conclusion(s) The case is presented since diffuse sclerosing variant of papillary carcinoma of the thyroid is rare.

P4.71

Expression and diagnostic availability of p63 and CD56 in papillary thyroid carcinoma

Park J.; Jeong J.; Jang E.; Shon Y.; Jung J.
Kyungpook National University Hospital, Daegu, Republic of Korea

Background Differential diagnoses of well differentiated thyroid tumors are often difficult. Especially, distinguishing papillary thyroid carcinoma (PTC) including follicular variant (FVPTC) from follicular tumor is problematic. Only few studies have evaluated about p63 and CD56 in thyroid tumors. The purpose of this study is to evaluate the diagnostic availability of p63 and CD 56, as well as Galectin-3 and HBME-1.

Methods A total of 267 cases were studied. The well differentiated thyroid tumors included 129 cases of PTC, 80 cases of follicular tumor (FT). 40 cases of nodular hyperplasia (NH), and 18 cases of undifferentiated carcinoma (UC) were also included. We made the tissue microarray (TMA), and assessed expression of p63, CD56, Galectin-3 and HBME-1.

Results P63 revealed positive in order of UC (22%), PTC (15%), FT (1%), NH (0%). P63 was not sensitive (sensitivity: 16%), but specific (specificity: 91%) and revealed very high positive predictive value (95%) for PTC. CD56 revealed no specific tendency, and was neither sensitive (sensitivity: 39%) nor specific (specificity: 59%) for PTC. Galectin-3 and HBME-1 were relatively sensitive (sensitivity: 88%, 80%) and specific (specificity: 83%, 58%) for PTC.

Conclusion(s) P63 is a useful marker for PTC in distinguishing from other thyroid lesions, and cocktail with other markers including Galectin-3 and HBME-1 can improve the diagnostic accuracy. And p63 is specific for PTC and UC, so it could be associated with the progression of thyroid carcinoma or poor prognosis. CD56 is not thought to be considerably useful.

P4.72

Gastrin and adhesive molecules in neuroendocrine cancer of GI tract. Preliminary study

Nasierowska-Guttmejer A.; Lipinski M.; Cwikla J.
Central Clinical Hospital, Ministry of Intern Affairs, Warszawa, Mazowieckie, Poland

Background The goal of the study was the evaluation of IHC markers in metastasing neuroendocrine cancers. Our material comprised 10 patients with tumors located in: stomach (1), duodenum (1), small bowel(6) and appendix (1) and one metastasis of undetermined origin. There were 6 females and 4 males. In 5 cases patients developed carcinoid syndrome. The patients went through surgery, PRRT, SST. Two of the cases were poorly differentiated neuroendocrine cancers, the others were well differentiated.

Methods IHC staining for gastrin, somatostatin, CD57, E-cadherin and beta-catenin was made using DAKO antibodies. All the cases were confirmed neuroendocrine using standard set of antibodies (synaptophysin, chromogranin, MIB1).

Results In 2 poorly differentiated cancers there was no secretion. Somatostatin was negative, gastrin and CD57 were diffuse positive, beta-catenin and E-cadherin were negative or lowered. In eight well differentiated cancers somatostatin expression was weak to moderate, CD57 was moderate to high, gastrin was weak to moderate. Beta-catenin and E-cadherin expression were lowered and localized in membranes and cytoplasm.

Conclusion(s) There was no expression of somatostatin and lower expression of adhesive markers in poorly differentiated cancers than in well differentiated cancers. There's necessity of further continuation of this study on larger groups of patients.

P4.73

Giant myelolipoma presenting as acute abdomen due to haemorrhage

Gakiopoulou H.; Antoniou E.; Delladetsima I.; Agrogiannis G.; Givalos N.; Stofas A.; Tseleni S.; Kostakis A.; Patsouris E.
A' Department of Pathology, Medical School, National and Kapodistrian University of Athens, Greece

Background Adrenal myelolipomas are relatively rare nonfunctioning, usually asymptomatic benign tumors of unclear pathogenesis, incidentally found at radiological examination or autopsy. Giant myelolipomas are rare tumors which may give symptoms related to mass effect, haemorrhage or rupture. We report on a case of a giant myelolipoma measuring 31 cm and presenting as an acute abdomen due to haemorrhage.

Methods Clinical, laboratory, and pathologic findings are presented.

Results A male patient aged 52 was admitted from the emergency department with a chief complaint of abdominal pain. Physical examination revealed an acute abdomen. Laboratory data showed hematocrit 20. US revealed a huge mass with extensive haemorrhagic areas and no definite conlusion about the site of origin, not excluding a possible liver mass. Surgical resection was performed showing tumor's origin from the right adrenal gland. Gross inspection revealed a rather well circumscribed tumor of 5200gr and~31 cm in greatest diameter. On sections, tumor showed fatty consistency with extensive areas of hemorrhage. Microscopic examination demonstrated an admixture of mature adipose tissue with trilineage mature haematopoietic elements, hemorrhagic areas and compressed normal adrenal cortex at the periphery of the tumor. A diagnosis of a giant adrenal gland myelolipoma was reported.

Conclusion(s) To our knowledge, our current case represents one of the largest lesions in the literature. Although most myelolipomas are clinically silent tumors, they may rarely achieve huge dimensions being at risk of spontaneous rupture with hemorrhage and life-threatening shock.

P4.74

Immnunoexpression of several papillary carcinoma markers in solid cell nests (SCNS) of the human thyroid gland

Cameselle Teijeiro J.; Caramés N.; Alberte Lista L.; Abdulkader I.; Alfonsín Barreiro N.; Reyes Santías R.; Sobrinho Simões M.
Clinical University Hospital of Santiago, Santiago de Compostela, Spain

Background Solid cell nests (SCNs) of the thyroid are single or multiple clusters of 2 cell types referred to as main cells and C cells. SCNs harbor the minimal properties of a stem cell phenotype and may thus represent a pool of stem cells of the adult thyroid. According to the cancer stem cell hypothesis, a histogenetic relationship between SCNs and some thyroid carcinomas has been widely debated in the literature. We investigated this relationship in the SCNs of 7 thyroid glands.
Methods The study was performed using antibodies against: alpha-fetoprotein (AFP), alkaline phosphatase (ALPP), and Oct-4 (stem cells markers); p63, CEA, and galectin-3 (SCN markers); and thyroglobulin (TG), CK19, and Hector Battifora mesothelial cell (HBME-1) (papillary thyroid carcinoma markers). In situ hybridization for TG was also performed using a commercial single stranded DNA probe (Cenbimo, Spain).
Results The main cells of SCNs were positive for p63, galectin-3, CEA, CK19 and HBME-1, and negative for AFP, ALPP and Oct-4. Except for the mixed follicles, negativity for TG in SCNs was confirmed both at protein and mRNA levels.
Conclusion(s) The immnunoreactivity for galectin-3, CK19, and HBME-1 and the negativity for AFL, ALPP and Oct-4 support a histogenetic link between the main cells of SCNs and papillary thyroid carcinoma rather than a classic stem cell nature of these cells. Supported by grant PI060209 from the Instituto de Salud Carlos III (Ministry of Health and Consumer Affairs), Spain.

P4.75
Merkel cell carcinoma. Immunohistochemical study in a group of 11 patients

Jirásek T.; Matej R.; Pock L.; Mandys V.
Third Faculty of Medicine, Prague, Czech Republic, Czech Republic

Background The aim of our work was to confirm an immunohistochemical profile of routine markers of epithelial and neuroendocrine differentiation in eleven cases of Merkel cell carcinoma, as well as to study the expression of two markers of early phases of neuronal differentiation, namely reelin and class III β-tubulin, markers which have not yet been studied in Merkel cell carcinomas.
Methods Immunostaining for cytokeratin 20, cytokeratin 7, thyroid transcription factor 1 (TTF-1), NSE, chromogranin-A and cytokeratin MNF-116, as well as immunodetection of class III β-tubulin with monoclonal antibodies TU-20 and TuJ-1 and immunodetection of reelin using clone 142 antibody was performed.
Results In all the investigated tumours the characteristic "dot-like" pattern of cytokeratin 20 immunoexpression, as well as negative immunostaining for cytokeratin 7 and TTF-1 were disclosed; all the tumours showed neuroendocrine differentiation, expressing either neuron specific enolase (NSE) or chromogranin A (CgA), or both. The characteristic "dot-like" pattern was detected using MNF-116 in high proportion of tumours, including two samples of local recurrence of one of the carcinomas, where neoplastic cells have lost the expression of cytokeratin 20. The majority (91%) of Merkel cell carcinomas showed positive immunodetection of class III β-tubulin when TU-20 antibody was used, while TuJ-1 immunostaining was surprisingly negative in all the investigated tumours. Detection of reelin was negative in almost all the studied Merkel cell carcinomas.
Conclusion(s) Class III β-tubulin could be a potentially useful marker of Merkel cell carcinoma while reelin immunodetection is almost negative.

P4.76
Parathyroid-like thyroid follicular lesions: a review of 5 cases and associated diagnostic pitfalls

Sirintrapun J.; Cimic A.; Logani S.
Emory University, Decatur, Georgia, USA

Background We have encountered cases where circumscribed intrathyroidal tissue morphologically mimicking parathyroid proved to be thyroid tissue leading to erroneous interpretation at time of frozen section examination. In this report we describe the histologic spectrum of these parathyroid-like thyroid follicular lesions.
Methods We reviewed the histologic features of 5 thyroid follicular lesions which mimicked parathyroid tissue. Size and location of these lesions and clinical indication for surgery were recorded from the clinical and pathology reports. Immunohistochemistry was performed using thyroid transcription factor (TTF1) staining and a panel including thyroglobulin(TG), parathyroid hormone(PH), chromogranin(CG), synaptophysin(SY) and calcitonin (CA). Seven control intra and extra-thyroidal parathyroid glands were stained with TTF1.
Results The 5 intra-thyroidal lesions ranged from 0.3 to 2.7 cm, all occurring in females 35 to 70 yrs in age. Clinical hyperparathyroidism was seen in 2 patients. The frozen section was ambiguous in 1 case and was designated as parathyroid tissue in another. Histologic features mimicking parathyroid included round nuclei with salt and pepper chromatin and moderate amount of eosinophilic cytoplasm. One case showed focal aggregates of cells with clear and oxyphilic cytoplasm.
Conclusion(s) The morphologic resemblance of these thyroid lesions to parathyroid tissue was striking and lead to error on at least one frozen section examination. This

error was more likely to occur with small (< 1 cm) lesions since an intra-thyroidal parathyroid is unlikely to present as a clinically discernable nodule. Pathologists should be aware of these histologic variations in thyroid follicular lesions.

P4.77

Quantitative investigation of the neuroendocrine cells in superficial and deep gastric mucosa inflammation

Kozlowski Waclaw W.; Jochymski C.; Markiewicz T.
Lodz, Poland

Background To the present moment there is lack of commonly accepted proofs on the participation of neuroendocrine gastric mucosal cells in the stomach inflammation pathomechanism. One of the possible reasons of this state of knowledge are various examination methods used by different authors.
Methods Paraffin blocks from gastric oligobiopsies were the material which was collected from 35 women and 34 men. Chronic inflammations were graded according to modified Whitehead's classification. Helicobacter pylori was evaluated according to the system from Sydney. Neuroendocrine cells of gastric pylori were counted in circular, oblique short, oblique long and oblong gastric glands sections. The Pearson linear correlation factor and linear regression factor were calculated.
Results Gastric mucosa inflammation type did not have a significant influence on cells localization in gastric mucosa. The number of CgA cells diminished in gchs gastric antrum among patients, who were over 50 years old. The increase of CgA cells number was found in gchs gastric antrum with Hp colonization. In these cases D cells number diminished.
Conclusion(s) 1. The most representative measurement for individual types of cells in the case of CgA cells this is long oblique cross-section gland, in the cases of D cells short oblique and in the cases EC short oblique cross-section of gastric mucosal glands. 2. In gchs gastric antrum with Hp pylori colonization CgA cells number significantly increases while D cells number decreases.

P4.78

Study of the iron and ferritin level in the blood samples of patients with goiter during their treatment with thyroxin

Palaiologou M.; Patiakas S.; Hoursalas I.; Alexidis I.; Xiropoulou E.
University of Athens, Kastoria, Greece

Background To study the levels of iron and ferritin in the serum of euthyroid patients with goiter and to investigate any possible changes during their treatment with thyroxin.
Methods For 63 euthyroid women, (average age of 46,8 years), we measured the levels of iron and ferritin, as well as the levels of total and free thyroid hormones, and the level of TSH, before and after three months of the beginning of the thyroxin treatment, and the results were compared with those of 65 healthy women of similar age.
Results In the patients under thyroxin treatment, the mean value of ferritin increased from the level of 54,1 ± 42,8 ng/ml before the treatment to 73,5 ± 61,2 ng/ml in the first trimester. On the contrary, the serum iron level didn't show any significant change (it decreased from 87,2 μg/dl to 80,7 μg/dl), while the levels of T3 and T4 increased significantly (p=0,022 and p = 0,005 respectively), and the TSH, as expected, was reduced (p<0,001). Finally, it should be mentioned that there was no significant difference noted in the control group as far as the serum ferritin level is concerned (p=0,5 approximately), while no statistically significant correlation was found to any of the thyroid function's parameters.
Conclusion(s) It is, therefore, proved that the thyroxin treatment with inhibition doses in euthyroid women with goiter results to the increase of the serum ferritin level.

P4.79

Study on C-cell hyperplasia of the thyroid gland

Krstic M.; Katic K.; Katic V.; Gligorijevic J.; Mitic I.; Petrovic A.
School of Medicine, Nis, Serbia and Montenegro

Background C-cell hyperplasia (CCH) is an uncommon proliferation of C cells within the follicles of the thyroid gland and refers to two different pathologic conditions with neoplastic and reactive potential. Reactive (physiological) CCH is considered to be caused by a stimulus from outside the cells. Having in the mind that there are both contradictory data on the reactive CCH and its microscopy criteria, the object of our study was both histological and immunohistochemical examinations of CCH, induced by the following pathophysiologic conditions: Lymphocytic and Hashimoto's thyroiditis, goitrous hypothyroidism, follicular tumors, Hurtle cell adenoma, papillary carcinoma, anaplastic carcinoma and parathyroid adenoma, from 44 operated patients.
Methods Paraffine sections were stained with: HE, Van Gieson, AB-PAS (AB=2.5) and LSAB2 immunohistochemical method, by using antibodies to chromogranin A, NSE, calcitonin, somatostatin and synaptophysin. Student's T test was used, for statistical analysis.
Results An increase in the size and numbers of C-cells (more than 7 cells per visual field at the magnification of 200) has been discovered, multifocal and nodular, inside

the thyroid tissue.Their localization is often in groups and intrafollicular, often encircling and completely obliterating the follicular space. In one autopsy case with hyperparathyroidism that has been associated with MEN I, we have found microscopic medullary thyroid carcinoma.
Conclusion(s) The authors have concluded that secondary CCH is not so rare, but possible pathogenetic relationship between CCH and some thyroid lesions is not always known.

P4.80
The contribution of the pathologist to hyperparathyroidism diagnosis. Our experience (163 cases)

Puras Gil A.; Tejada X.; De Miguel C.; Echegoyen A.; Rezola M.; Anda E.; Salvador P.; Solozabal C.
Hospital Virgen del Camino, Pamplona, Navarra, Spain

Background Hyperparathyroidism diagnosis is the task of Parathyroid Working Group. The pathologist confirms the especifity of tissue in intraoperative biopsy and makes a presumptive diagnosis. The definitive diagnosis is the work of the team, but the pathologist is still an important member of the group and acquires a more relevant role if there are clinical- pathologic discrepancies.
Methods A retrospective study (163 cases, 1994–2008). Age, MIBI, weight, chronic renal failure (CRF), morphologic findings : "Adenoma criteria" and cytoplasmic lipid droplets; PTH intraoperatively and gamma-cámara. The CDPs have been carefully checked.
Results 109 women, 54 men, predominant localization in lowers; weight: 254–2950 mg in Adenomas and 4660–6183 in Carcinomas; 125 Adenomas (76.7%, 5 athypical), 3 Carcinomas (1.8%) and 35 Hyperplasia (21.5%) : 14 secondaries.« Adenoma criteria»were present in the mayority of Adenomas but«pseudo-rim»in some Hyperplasias. In 4 cases clinically« double Adenomas», secondary Hyperplasia was diagnosed. The MIBI and gamma-camara were useful in Adenomas, excepting«Hürthle transformation»of the neighbouring thyroid; intraoperative PTH was only useful in the Adenomas.
Conclusion(s) 1) The pathologist´s report is essential in WGP diagnosis. 2) We recommend preoperative study by the team if there are DCP. 3) The adenoma criteria will are a help in IB. 4) All«double adenomas»were hyperplasia. 5)Detection of intraoperative PTH has a very limited value.

P4.81
Unusual presentation of poorly differentiated thyroid carcinoma: intranasal metastasis in the form of a well differentiated thyroid malignancy

Börcek P.; Kulacoglu S.; Ergoz Seren E.
Ankara Numune Research and Training Hospital, Ankara, Turkey

Background Poorly differentiated thyroid carcinomas are follicle cell derived cancers of the thyroid which stand in between well differentiated and anaplastic thyroid carcinomas. It is regarded conventional for this group of tumors to metastasize via lymphatic or hematogenous routes, the most favorable sites being lungs, liver, bones and brain. However, sinonasal spaces are very exceptionally affected by the metastases of thyroid carcinomas and a very limited number of cases have been presented in the literature.
Methods A 48 year-old male patient admitted with epistaxis was operated for a left intranasal mass which was clinically thought to be an inflammatory nasal polyp or angiofibroma.
Results The histopathological examination revealed metastasis from a well differentiated thyroid tumor which consisted of follicular structures lined by ground glass nuclei, filled with colloidal material and showed strong and diffuse immunohistochemical positivity with thyroglobulin. The patient was then detected to have a thyroid mass and underwent total thyroidectomy, which demonstrated a surprising histomorphology: a poorly differentiated thyroid carcinoma with better differentiated areas.
Conclusion(s) Intranasal metastases of thyroid origin are exceedingly rare and if it ever occurs, it is most probably from a well differentiated thyroid malignancy. Metastasis from a poorly differentiated thyroid carcinoma into nasal cavity has never been reported before. To make things more interesting in this particular case, the metastasis was from the minor well differentiated component of a more aggressive tumor.

P4.82
Well differentiated thyroid carcinoma with distant metastasis

Zelaya M.; Tejada X.; Rezola M.; Echegoyen A.; Puras A.; De Miguel C.; Anda E.
Hospital Virgen del Camino, Pamplona, Navarra, Spain

Background Even though Well Differentiated Thyroid Carcinoma (WDTC) rarely produced distant metastasis, we did a research into our records with WDTC in stage M1 diagnosed and treated by our Thyroid Working Group (TWG) in order to determine factors that can influence the prognosis and survival of these patients.
Methods We studied the medical records in our Institute from 1988–2008. 520 WDTC diagnosed and treated by our TWG, making a retrospective study of 31 patients (6%) with WDTC and distant metastasis M1. All of them were treated with total thyroidectomy followed by the administration of radioactive iodine (except 2 cases that died), 33.3% needed a second cervical intervention; 61.2% had more than one dose of Radioiodine; 9.7% required bone metastases surgery and 6.5 % local radiotherapy. Follow up was 9.9 years.

Results Mean patient age, 52 years (18–78); 77.4% females. 26 (80.6%) were diagnosed at the beginning of the disease. Being predominantly papillary carcinomas (67%). Only one metastasis, in 27 (87 %): lungs (74.2%), and bone (9.7%) most frequent. Four of them with multiple metastasis lungs, bone, skin and brain, 11(35.5%) died during the process (mean time 10 years), 35.5% are in complete remission, 13 % are stable with metastasis and 16% in progression.
Conclusion(s) 1) Most of the metastases are diagnosed at the beginning of the disease the lungs being the only metastasis. 2) Worse prognosis factors are >45 years old and extrapulmonar metastasis.

P4.83

Carcinoma rates in the east coast of the Black Sea Region of Turkey

Bagci P.; Coskunoglu Zeynep E.; Saracoglu N.; Eryigit H.
Rize Research and Training Hospital, Rize, Turkey

Background As one of the biggest cities in the east coast of Black Sea Region, Rize had said to be affected by the Chernobyl disaster in 1986. We wanted to study the rate of all types of carcinomas in our region in the 23 rd year of the disaster.
Methods We made an epidemiological study and reviewed the archieves of our pathology department between the years 2004- 2008; found out the number of the carcinomas and the rates among total biopsies.
Results The patients were between 11–99 years; and the median age was 59,6. Most carcinomas were seen between 60–79 years of age (43%). There was male predominance (53%). Skin carcinomas were the most common type in all years (40%) and in every year. Female genital tract carcinomas were the most common cancer type in females, while lung carcinomas were the most common in males. Thyroid carcinomas were the second common carcinoma in both sex.
Conclusion(s) The most common carcinomas in both sex (female genital tract and lung) had poor correlation with radiation. Thyroid carcinoma rates were significant, associated directly with radiation. But we still need larger epidemiological studies and long term analysis to correlate Chernobyl disaster and carcinoma rates in our region.

P4.84

Expression of immunohistochemical markers in thyroid carcinoma and adenoma

Iliesiu A.; Aschie M.; Papuc A.; Poinareanu I.; Craciun A.; Dobre A.; Iacub G.; Stanisici J.; Enciu M.; Deacu M.; Bosoteanu M.; Cretu A.
Clinical Emergency County Hospital, Constanta, Romania

Background Thyroid cancers account for 2% of all the cancers in Romania.Papillary thyroid carcinoma (PTC) is the most common histological type of thyroid cancer (75–80%) It derives from the follicular cells of the endoderm. The management of differentiated (papillary and follicular) thyroid cancer is a challenge because there have been no prospective randomized trials of treatment and none are likely to be done, given the typically prolonged course and relative infrequency of these tumors.
Methods We examined 94 thyroid tumors removed the Clinics of Endocrinological Surgery of C.I.Parhon Institute and Departments of Surgery of Clinical Emergengy County Hospital Constanta diagnosed in the Department of Pathology with diagnoses confirmed according to the criteria provided by the WHO classification. All of the patients had been operated between 2002 and 2008.
Results Galectin-3 was expressed in 19 of the 27 cases (70.4%) of papilary carcinoma.CK19 was expressed in 22 of the 27 cases (81.5%) of papilary carcinoma.p53 was expressed in 6 of the 27 cases (22.2%) of papilary carcinoma.Ki-67 was expressed in 1 of 27 cases (3.7%) of papilary carcinoma.
Conclusion(s) In our study macroscopic features were not relevant. Galectin-3 is a candidate marker for the differential diagnosis between malignant and benign thyroid lesions, and especially between follicular carcinoma and follicular adenoma in the patients over 20 years old.In our opinion, CK19 is also useful for differentiating between the follicular variant of papillary carcinoma and follicular carcinoma, and between papillary carcinoma and the papillary area of nodular hyperplasia.

P4.85

Metastatic small cell carcinoma to the thyroid gland: case report

Gul Ege A.; Keser Hallac S.; Ergen C.; Barisik Ozdemir N.; Cakir C.; Kandemir Onak N.; Karadayi N.; Tuncay E.
Dr. Lutfi Kirdar Kartal Educational and Research Hospital, Department of Pathology, Istanbul, Turkey

Background Secondary involvement of the thyroid gland by malignant metastases is uncommon. The primary cancers in these cases are commonly renal cell carcinoma, lung cancer, and breast cancer. Usually metastatic thyroid disease is identified upon autopsy, and only sporadic cases are encountered in clinical material.
Methods Case: The patient was 55-year-old male with fatigue and weight loss complainings in the last one year; bilateral multiple nodules were detected in patient's thyroid ultrasonography. Hypoactive and hyperactive nodules were detected in thyroid scintigraphy. The patient underwent bilateral total thyroidecthomy. In macroscopic examination,

a large number of thyroid nodule were detected on both lobes. Microscopically, tumoral lesions seen as multifocal small groups on both lobes. Neoplastic cells showed small hyperchromatic nuclei and undistinguishable nucleoli and frequent mitosis. Tumor cells as immunohistochemically showed positive staining with chromogranin, synaptophysin, NSE, cytokeratin and TTF-1. Histology and immunohistochemistry were charecteristic of small cell carcinoma.
Results Depending on our report the patient was clinically investigated. A mass was determined on the patient's lungs. It is determined that the tumor on thyroid is metastasis. As a result chemotherapy was applied to patient.
Conclusion(s) In cases of small cell carcinoma metastases to the thyroid gland is presented in the light of literature information.

P4.86
Rare case of a primary metastatic carcinoid tumour arising in a tailgut cyst

Wöhlke M.; Sauer J.; Dommisch K.; Görling S.; Hinze R.
Schwerin, Germany

Background Tailgut cysts are unusal benign multiloculated cystic malformations between the rectum and the sacrum arising from persistent remnants of the postanal gut. Only a few cases of carcinoid tumours within a tailgut cyst have been reported to date. On rare occasions there is malignant transformation. Metastasis is only known in one of these cases reported in the literature.
Methods Case report.
Results We report the rare occurrence of a carcinoid tumour arising in a tailgut cyst with primary liver and lymph node metastases in a 55-year-old woman presented with sacral pain since 6 weeks. MRI of the pelvis showed a soft tissue tumour in the presacral space. The resected specimen demonstrated histologically a cystic lesion lined by a benign both squamous and focally mucinous cuboidal epithelium with bundles of smooth muscle in the wall. Additionally, a solid tumour measured 28 mm in greatest dimension was indentified within the wall. Positivity for Synaptophysin and Chromogranin on immunostains indicates a carcinoid tumour. In the subsequently performed OctreoScan metastases in liver and presacral soft tissue were identified. After a peptide receptor radionuclide therapy a nearly complete tumour regression was achieved. After a follow-up of 17 months stable serum levels of Chromogranin A and Serotonin were slightly beyond the norm.
Conclusion(s) To our knowledge this is the second report about a metastatic carcinoid tumour within a tailgut cyst. The neuroendocrine nature of the tumour determines the therapeutical approach and the prognosis.

P4.87
Thyroid hemiagenesis. Benign developmental variant or something more?

Zabel M.; Ruchala M.; Szaflarski W.; Szczepanek E.; Czarnywojtek A.; Moczko J.; Pietz L.; Nowicki M.; Niedziela M.; Sowinski J.
Department of Histology and Embryology, University of Medical Sciences in Poznan, Poznan, Poland

Background Thyroid hemiagenesis (TH) is an anomaly resulting from the developmental failure of one thyroid lobe. Ethiopathogenesis, clinical significance and management of patients in whom TH was diagnosed, are still a matter of debate. The aim of the study is to provide the first systematic analysis of a large cohort of subjects with TH.
Methods 40 patients with TH are described in comparison to a control group of 80 subjects. Serum concentrations of TSH, freeT4, freeT3 and autoantibodies were measured. Ultrasonography and Tc-99 m thyroid scintiscan were performed, followed by aspiration biopsy. The SHH gene were amplified and subjected for bidirectional sequencing.
Results Although patients with TH were usually clinically euthyroid, among those subjects the observed TSH and freeT3 levels were significantly higher. Furthermore, higher incidence of associated functional, morphological and autoimmunological thyroid disorders in patients presenting TH was noted. The results of the SHH analysis in 5 out of 40 patients did not reveal any abnormalities in coding sequence.
Conclusion(s) The obtained results suggest, that people with TH are more likely to develop thyroid pathology, in ethiopathogenesis of which sustained TSH overstimulation of the undersized gland might play major role. So far, genetic analysis has been shown no abnormalities in SHH. However, further studies will encompass other genes being involved in the organism development such as PAX8 and TTF-1.

P4.88
Unusual distribution of psammoma bodies related to thyroid papillary carcinoma. Presentation of three cases

Bella M.; Combalia N.; Orellana R.; Marques G.; Barcons S.; Sanfeliu E.; Bueno A.; Casalots A.; Rey M.
UDIAT-CD - Corporació Parc Taulí, Sabadell, Barcelona, Spain

Background Psammoma bodies (PB) are usually found in papillary carcinomas (PC), associated with neoplastic cells or structures. We present three cases with unusual distribution of PB in surgical specimens of thyroidectomy and cervical lymph node dissection. Under these circumstances, the clinical management can be controversial.

Methods From 180 surgical specimens of thyroidectomy ± lymph node dissection with diagnosis of PC, identification of cases with unusual distribution of PB; review of all histologic material; new histologic and immunohistochemical techniques on lymph nodes with isolated PB sentinel lymph node technique (SLNT) with cytokeratins CAM5.2 and 19).
Results We identified 3 unusual cases. 1: PC of 2,5 cm. in right lobe, with many PB along this lobe, non-related to PC cells, and moderate lymphocytic thyroiditis in all non-neoplastic thyroid. 2: PC of 0,9 cm. in left lobe, with many tumor associated PB, and some PB in one ipsilateral cervical lymph node, without epithelial cells (SLNT). 3: PC of 0,4 cm. in left lobe, many PB in the same lobe, Hashimoto's thyroiditis in all non-neoplastic thyroid, and many PB in some ipsilateral cervical lymph nodes, without epithelial cells (SLNT).
Conclusion(s) 1. Psammoma bodies in the same thyroid lobe where papillary carcinoma exits and in ipsilateral cervical lymph nodes can represent lymphatic migration of these structures, or spontaneous regression in locations where papillary carcinoma previously existed. 2. Considering psammoma bodies in lymph node as evidence of metastatic disease can be discussed.

Molecular pathology

P4.89
Detection of human papilloma virus integration and chromosomal aberrations in cervical epithelial cells using fluorescence in situ hybridization (FISH)

Sokolova A.I.; Song M.; Policht F.; Sitailo S.; O'Hare A.; Morrison L.
Abbott Molecular Inc, Des Plaines, Illinois, USA

Background FISH technique can visualize individual HPV infected cells and determine whether HPV is integrated into the host genome. It also allows for the detection of chromosomal aberrations indicative of genomic instability and associated with malignant transformation.
Methods 35 different genomic loci were tested on a set of histological specimens. Following evaluation, chromosomal loci 3q26 (TERC) and 8q24 (MYC) were selected as the best performers. These two probes were formulated into final probe set along with a biotin-labeled HPV DNA probe cocktail targeting high risk types, and applied to cervical histological and cytological specimens for testing by FISH.
Results Cells with episomal and integrated states of HPV were easily distinguished. The episomal state of the virus was observed as diffuse nuclear staining, whereas integrated HPV appeared as a punctate staining pattern. The percent of specimens with HPV integration correlated with disease severity ranging from 1 infected cell per 1250 uninfected cells in ASCUS, to 1 infected cell per 200 uninfected cells in LSIL group, to 1 HPV infected cell per 50 uninfected epithelial cells in HSIL group. Frequency and degree of chromosome aberrations strongly correlated with disease progression ($p<0.05$).
Conclusion(s) Detection of HPV in individual cells combined with the detection of chromosomal aberrations identifies genetically unstable HPV infected cells. This may prove to be a useful tool for clinicians in stratifying patients with atypical and mild lesions into low risk and high risk progression categories.

P4.90
HOX D13 expression across 79 tumor tissue types and its prognostic role in pancreatic cancer

Cantile M.; Franco R.; Forte I.; Cerrone M.; Anniciello A.; Liguori G.; Manna A.; Corrado A.; Aquino G.; Terracciano L.; Cillo C.; Botti G.
INT Fondazione Pascale, Naples, Italy

Background HOX genes control normal development and primary cellular processes. Locus D HOX genes play an important role in limb generation and mesenchymal condensation. During normal morphogenesis, HOXD13 is involved in the determination of the terminal digestive and urogenital tracts and deregulation has been detected in different tumor types such as breast, cervical, melanoma, atrocytomas and in the neuro-endocrine differentiation of human advanced prostate cancers.
Methods We have investigated the epidemiology of HOXD13 expression in human tissues and its potential deregulation in the carcinogenesis of specific tumors by immunohistochemistry. HOXD13 homeoprotein expression has been detected using microarray technology comprising more than 4000 normal and neoplastic tissue samples including 79 tumor categories. Validation of HOXD13 expression has been performed, at mRNA level, by qReal Time PCR, for selected tumor types.
Results Significant differences are detectable between specific normal tissues and corresponding tumor types with the majority of cancers showing an increase in HOXD13 expression. In contrast, pancreas and stomach tumor subtypes display the opposite trend. Interestingly, detection of the HOXD13 homeoprotein in pancreas-TMA shows that its negative expression has a significant and adverse effect on the prognosis of patients with pancreatic cancer independent of the T or N stage at the time of diagnosis.
Conclusion(s) Our study identify pancreatic cancer as one of the most affected by the HOXD13 homeoprotein and underlines the way homeoproteins can be associated to human cancerogenesis.

P4.91

Inhibitors of histone deacetylases potentiate the formation of AR/SMRT complex and suppress ar transcriptional activity in prostate cancer cell lines

Trtkova K.; Paskova L.; Matijescukova N.; Kolar Z.
Laboratory of Molecular Pathology and Department of Pathology, Faculty of Medicine, Palacky University, Olomouc, Czech Republic

Background Signaling through androgen receptor (AR) plays a critical role in prostate cancer progression. The transcription activity of the AR can be regulated by coactivators or corepressors. Corepressors SMRT (silencing mediator for retionid and thyroid hormone receptors) and N-CoR (nuclear receptor corepressor) that form complex together with histone deacetylase 3 (HDAC3) exhibit histone deacetylase activity (HDAC). Inhibitors HDACs: sodium butyrate (NaB) and trichostatin (TSA) have shown antiproliferative and proapoptotic effects on prostate cancer cells and they could be used as the potential therapeutic agents.
Methods Androgen-dependent prostate cancer cell line (LNCaP) and androgen-independent prostate cancer cell lines (C4-2, DU145 and PC3) were treated with NaB and TSA. The effects of NaB and TSA on AR, HDAC2 and HDAC3 protein expressions were assessed by Western blot analyses. The ChIP method together with qPCR and co-immunoprecipitation assay were used to investigate the potential role of SMRT in the suppression of AR activity by NaB.
Results NaB declines AR transcription activity and activates SMRT in LNCaP and C4-2 cells, and on the other hand in these cell lines the NaB reduces AR protein expression and increases AR-SMRT complex formation.
Conclusion(s) The inhibitory effect of NaB on AR gene transcription and expression seems to be specific and unique for prostate cancer cell lines containing AR. This study was supported in part by IGA NR9475-3/2007 and MSM 6198959216.

P4.92

KRAS mutations correlates with P53 status in colorectal carcinomas

Rodon N.; Roman R.; Verdu M.; Calvo M.; Garcia-Pelaez B.; Gonzalez M.; Pubill C.; Puig X.
BIOPAT, Barcelona, Spain

Background KRAS mutations, present in approximately 30–50% of colorectal carcinomas (CRC) has been recently associated with lack of response to anti-EGFR therapy, poor prognosis and high mitotic activity. Nevertheless, its relation to other histopathological and molecular parameters has not been well established. Our first approach was to determine correlations between KRAS status and histopathologic and molecular findings in an univariate analysis using a retrospective series of 337 CRC cases.
Methods 25 histopathological features were evaluated, including Ki67 and p53 immunoexpression. Mutational analysis of P53 and BRAF was carried out by direct sequencing. Statistical analysis was performed by Kruskal-Wallis and Fisher's exact tests.
Results KRAS mutations were identified in 144 out of 337 cases (42.7%). BRAF V600E was found in 32 cases out of 318 (10.1%), 31 of them in KRAS wild-type group ($p<0.001$). 72 cases out of 144 with KRAS mutated contained P53 mutations (50%). In the KRAS wild-type group, 133 cases (70%) harbour P53 mutations ($p<0.001$). The p53 immunoexpression was also significantly higher in the KRAS wild-type group ($p=0.009$). Significant differences were also observed between KRAS mutations and mucinous ($p = 0.001$) and solid tumoral patterns ($p = 0.010$).
Conclusion(s) KRAS (42.7%) and BRAF V600E (10.1%) mutations were found to be mutually exclusive in agreement with published data. The P53 mutated status is significantly associated with KRAS wild-type ($p<0.001$) but is also frequent in the KRAS mutated group, suggesting P53 inactivation arises through independent pathways. A multivariate analysis would be required to further analyse these correlations.

P4.93

PCR-based testing for drug-sensitising EGFR mutations in lung cancer patients

Dahse R.; Berndt A.; Kosmehl H.
Helios Klinikum Erfurt, Erfurt, Germany

Background Epidermal growth factor receptor (EGFR) signal blocking is an important goal for targeted therapy strategies in two ways: competitive inhibition of EGF binding by an antibody or of the receptor tyrosine kinase by small molecules. Recently, ligand-independent EGFR activating mutations were identified in non-small cell lung cancer (NSCLC). Two hotspot mutations located in exon 19 and exon 21 account for about 90% of all EGFR mutations.
Methods We designed a Bi-PASA (bidirectional PCR amplification of specific alleles) assay to detect the most common exon 19 deletion (codons 746–750) and an allele-specific PCR for the L858R mutation in exon 21. To validate the assays for use in clinical diagnostics, 35 lung adenocarcinoma samples were analyzed.
Results Both assays provided the predicted amplification pattern for normal and mutant genotypes with high specificity and sensitivity. In serial dilution experiments, the mutant alleles were detectable in mixed samples with an at least 6-fold excess of normal DNA. Three exon 19 deletions were identified in the tumor samples.

Conclusion(s) Both assays are fast and easy to perform in any routine PCR laboratory with no special equipment other than thermocyclers. The costeffective test identifying ligand-independent EGFR activation, selected 3 out of 35 NSCLC patients who had maximal benefit from receptor tyrosine kinase inhibition and were prevented from side effects of an antibody-based therapy.

P4.94

Protein expression profile in different nerve sheath tumor entities focused on tumor stem cell markers

Hauser-Kronberger C.; Rösch S.; Alinger B.; Santner F.; Kiesslich T.
University Hospital Salzburg, Salzburg, Austria

Background Malignant peripheral nerve sheath tumor (MPNST) is a tumor originating mainly from schwann cells. Besides spontaneous occurrence, MPSNT in some cases arises from benign schwannoma but usually from benign neurofibroma. The assumption for the establishment of a specific non-invasive therapy is the appreciation of pathogenesis and involved cellular mechanisms as well as the knowledge of tumor behavior. The aim of the present study was the detection of a specific protein expression profile in different nerve sheath tumor entities focused on tumor stem cell markers.
Methods Immunohistochemical analysis of MPNST cells, derived from a purchased cell line, was performed. Additional real-time PCR was done in order to verify the protein expression on mRNA level. In a second step different entities such as MPNST (n=5), benign neurofibroma (n= 5) and benign schwannoma (n= 5) were analysed on paraffin sections for expression of Notch1, Nestin, b-Catenin, S100, CD44 and CD133.
Results In case of MPNST cell line we found positive results for Notch1, Nestin, ß-Catenin, participants of Hedgehog pathway, CD44 and CD133. Staining for S100 showed negative results. Between and within the three entities we found differentiating expression-profiles concerning Nestin, S100, CD44 and CD133 with a tendency towards separation between benign and malign origin.
Conclusion(s) Benign neurofibroma, schwannoma and MPNST showed different geneexpression profile for stem cell markers indicating different prognosis and biological behavior.

P4.95

Sensitive detection of KRAS mutations using mutant-enriched PCR and reverse-hybridization teststrips

Kriegshaeuser G.; Holzer B.; Rauscher B.; Schuster E.; Kury F.; Zeillinger R.; Oberkanins C.
ViennaLab Diagnostics GmbH, Vienna, Austria

Background The KRAS gene encodes a GTPase, which plays a vital role in cellular signaling processes. Mutated forms are potent oncogenes and found in many human cancers. KRAS mutations are also predictive for the response to cancer therapy with certain anti-EGFR monoclonal antibodies.
Methods We have developed a reverse-hybridization StripAssay targeting 10 mutations in codon 12 and 13 of the KRAS gene. The test is based on PCR in the presence of a wild-type KRAS suppressor, followed by hybridization of PCR products to teststrips presenting a parallel array of allele-specific oligonucleotide probes. The performance of the StripAssay was evaluated on DNA obtained from cultured cell lines, from formalin-fixed paraffin-embedded tissue and from stool.
Results Using serial dilutions of DNA from various KRAS-mutated tumor cell lines into normal DNA, each of the 10 mutations was shown to be detectable at levels as low as 1%. DNA samples containing various proportions of mutated KRAS were analyzed by the StripAssay in direct comparison to real-time PCR, dideoxy sequencing and pyrosequencing. While all methods correctly identified samples containing 25% mutated DNA, dideoxy sequencing and pyrosequencing failed to detect levels of 12.5% or lower. Both the StripAssay, as well as real-time PCR, unambiguously identified 10%, 5% and 1% of KRAS-mutated DNA in the presence of excess wild-type DNA.
Conclusion(s) The simultaneous detectability of 10 different mutations with excellent sensitivity will make the StripAssay a very useful tool for the assessment of the KRAS mutation status in cancer patients.

P4.96

A prognostic implication of epithelial mesenchymal transition markers in non-small cell lung cancer

Al-Saad S.; Al-Shibli K.; Donnem T.; Persson M.; Bremnes R.; Busund L.
University Hospital of Northern Norway Tromso, Tromso, Norway

Background Vimentin, NFκB p105, fascin, E-cadherin, TGF-β, Par6 and atypical PKC are molecular markers which play an important role in cell differentiation. Herein we investigate their prognostic impact in primary non-small cell carcinoma (NSCLC).
Methods Tumor tissue samples from 335 resected patients with stage I to IIIA were used. Tissue microarrays (TMAs) were constructed from duplicate cores of both neoplastic cells and stromal cells and were immunohistochemically evaluated.
Results In univariate analyses, high tumor epithelial cell expression of NFκB p105 (p=.02) and E-cadherin (p=.03)

were positive prognostic indicators for disease-specific survival (DSS), while high tumor epithelial cell expression of vimentin (p=.001) was a negative prognostic indicator. High expression of NFκB p105 (p=.001) and Par6 (p=.0001) in the stromal compartment correlated with a good prognosis. In multivariate analyses, the tumor epithelial cell expression of NFκB p105 (p=.0001) and vimentin (p=.005) and the stromal cell expression of NFκB p105 (p=.007) and Par6 (p=.0001) were independent prognostic factors for DSS.

Conclusion(s) High expression of NFκB p105 and low expression of vimentin in tumor epithelial cells are independent predictors of better survival in primary NSCLC. In stromal cells, high expression of NFκB p105 and Par6 are both favourable independent prognostic indicators.

P4.97
Aurora B kinase in malignant mesothelioma: immunohistochemical detection and potential drug target

Orecchia S.; Libener R.; Salvio M.; Arnolfo E.; Bensi T.; Betta P.
Azienda Ospedaliera Nazionale, Alessandria, Italy

Background Aurora kinases represent a family of highly related serine/threonine kinases overexpressed in a variety of human cancers, including malignant mesothelioma, suggesting their implication in oncogenesis and tumour progression and indicating their targeting as an attractive and novel anticancer therapy approach. In the present study we evaluated the expression of Aurora B kinase in malignant mesothelioma cell lines and the antiproliferative effects of AZD1152 (gift of Astra Zeneca), a dihydrogen phosphate prodrug of a specific pyrazoloquinazoline Aurora B kinase inhibitor.

Methods Three malignant pleural mesothelioma cell lines and an anti-Aurora B kinase monoclonal antibody (BD Transduction Laboratories; 1:200 dilution) were used. The IC50 of AZD1152 and the effects of AZD1152 on mesothelioma cell growth were analyzed using the MTT assay. AZD1152 prodrug was preliminarily activated by in vitro incubation with human plasma at 37°C for 24 h and subsequently the cell lines were exposed to the active drug at 50 nmol/ L for 24 h. All the experiments were carried out in triplicate.

Results All the cell lines showed positive nuclear staining for Aurora B kinase in a varying proportion of cells. AZD1152 inhibited cell proliferation of cell lines with an average IC50 value of 20 μM.

Conclusion(s) All 3 mesothelioma cell lines showed moderate sensitivity to Aurora B kinase inhibition by AZD1152. A further investigation using the active moiety AZD1152-HQPA is in progress in order to fully explore the therapeutic potential of Aurora B kinase inhibition in malignant mesothelioma cells.

P4.98
Chromosomal abnormalities of brain tumors: cytogenetic analyses of 54 patients, twelve-month experience

Dvorackova J.; Urbanovska I.; Uvirova M.; Buzrla P.
Faculty Hospital Ostrava, Ostrava - Poruba, Czech Republic

Background The molecular genetic alterations associated with the initiation and progression of central nervous system tumors are complex and poorly understood at present. This thesis aims at the further elucidation of the molecular genetics of important central nervous tumors. Specific gene mutations, loss of heterozygosity, deletions and/or amplifications of entire chromosomes and genes were described in brain tumors.

Methods For the detection of most frequent chromosomal changes in brain tumors we used I-FISH with locus specific and/or α-satellite probes (Abbott-Vysis).

Results 54 patients have been investigated to detect the specific deletion of p53, RB1, PTEN, p16 genes, and the deletion of locus 1p,1p36, 19q13, 22q11.2 amplifications of EGFR gene, polysomy of chromosome 7 and monozomy of chromosome 10 and 14. In the study molecular cytogenetic analysis were succesfull in 50 patients (92,6%) and were uninformative in 4 (7,4%).

Conclusion(s) The cytogenetic analyses were correlated with the morfological date (19 astrocytic tumors, 12 glioblastoma multiformae, 2 oligodendrogliomas, 19 meningeomas 1 meduloblastoma, 1 neurinoma) and clinical outcome. A systematic molecular cytogenetic analysis may advance diagnosis, discovery, classification and in some case also a treatment of brain tumors.

P4.99
Dlk1 inhibits migration but not proliferation of activated hepatic stellate cells isolated from rat liver

Huang C.; Tsai P.; Tai M.; Wu C.; Chou M.; Huang Y.; Huang Lynn L.; Chuang J.
Chang Gung Memorial Hospital-Kaohsiung Medical Center, Kaohsiung County, Taiwan

Background Activation of hepatic stellate cells has been known to play a crucial role in liver fibrosis. We previously found that Dlk1, a cytokine associated with cell differentiation, was significantly over-expressed in the early stage

of liver fibrosis during the progression of biliary atresia. To further explore the role of Dlk1 in liver fibrosis, we performed functional study for Dlk1 on the primary cell culture of hepatic stellate cells.
Methods Recombinant soluble protein of Dlk1 extracellular domain (0, 10, 100 and 1000 ng/ml, respectively) was added in the culture medium of hepatic stellate cells isolated from rat liver after in-vitro activation for 7 days on the culture plates. To evaluate cell proliferation, WST-1 assay was performed after Dlk1 treatment for 72 h. Transwell migration assay was also performed to study the effect with Dlk1 treatment. Furthermore, mRNA expressions of alpha-smooth muscle actin, desmin and procollagen alpha 1 (I) were also analyzed by quantitative RT-PCR.
Results Cell migration of activated hepatic stellate cells was significantly inhibited by Dlk1 treatment with a dose-dependent manner, whereas cell proliferation was not significantly influenced by Dlk1 treatment. In addition, mRNA expressions of alpha-smooth muscle actin, desmin and procollagen alpha 1 (I) showed a trend to be down regulated with increased concentration of Dlk1 treatment.
Conclusion(s) Dlk1 may inhibit cell migration of activated hepatic stellate cells and could have some roles for the regulation of liver fibrosis.

P4.100
Evaluation of BIOMED-2 PCR primers for detection of clonality in follicular lymphoma on formalin-fixed, paraffin-embedded samples

Berget E.; Helgeland L.; Molven A.; Vintermyr Karsten O.
Haukeland University Hospital, Bergen, Norway

Background The use of BIOMED-2 PCR primers has been introduced as a standard procedure for assessing B-cell clonality (Leukemia 2003, 17: 2257–2317). Due to high prevalence of spontaneous somatic mutations in follicular lymphomas, this entity poses a special challenge in PCR-based clonality analysis. The aim of our study was to evaluate the performance of the BIOMED-2 primers in detecting B-cell clonality in archival material of follicular lymphomas.
Methods Formalin-fixed paraffin-embedded (FFPE) samples from one hundred patients diagnosed with follicular lymphoma were obtained from the archives of the Department of Pathology, Haukeland University Hospital, Bergen, Norway. All cases were reevaluated and diagnosed according to the World Health Organization classification of lymphoid neoplasms (WHO 2008). DNA was extracted by standard methods.
Results BIOMED-2 primers showed an improved rate of clonality detection as compared to previously used consensus PCR primers (J. Clin. Path. 1990, 43: 888–890; J. Clin. Mol. Path. 2002, 55: 98–101). Detection of clonality in follicular lymphoma was significantly improved by a combination of different sets of heavy and light immunoglobulin gene analyses. The fraction of positive clonal PCR assays was less than reported for fresh or frozen samples (Leukemia 2003, 17: 2257–2317).
Conclusion(s) Our study underscores that the assessment of clonality in follicular lymphoma is challenging, at least in FFPE tissue, and that the use of a combination of BIOMED-2 PCR primer sets may improve the sensitivity of clonality detection in B-cell follicular neoplasias.

P4.101
Integrin-linked kinase (ILK) expression correlates with progression of astrocytomas to higher malignancy grades with involvement of wnt pathway components

Grande Mendes R.; Teixeira Paulo Castro V.; Franco Fabiano M.; Engelman Fátima Brasil M.
Universidade Federal de São Paulo - UNIFESP, Pouso Alegre, Minas Gerais, Brazil

Background The glial neoplasms are responsable for 60% of the CNS tumors and glioblastoma is by far the commonest and most malignant of the astrocytic tumors. Composed of a heterogenous mixture of poorly differentiated neoplastic astrocytes, glioblastomas primarily affect adults and are located preferentially in the cerebral hemispheres. These tumors may originate from lower-grade astrocytomas (WHO grade II) or anaplastic astrocytomas (WHO grade III), but more frequently, they appear de novo, with no evidence of a precursor lesion. The treatment of glioblastomas is palliative, with a median survival of approximately 12 months. Therefore, it is mandatory to make efforts to understand molecular mechanisms of the genesis and biological behavior of these tumors. Integrin-linked kinase (ILK) has been implicated in the development and progression of several human malignancies. However, the role of ILK in astrocytomas progression is not established in vivo nor its downstream effectors in the disease have been identified.
Methods We studied the immunoexpression of ILK, β-catenin and phosphorylated glicogen synthase kinase 3β (pGSK-3β) in 30 low grade and 30 high grade astrocytomas.
Results The levels of ILK expression correlated strongly with tumor progression to a higher grade of malignancy. Up-regulation of pGSK-3β associated with nuclear translocation of β-catenin correlated significantly with both ILK expression and tumor progression.
Conclusion(s) Our results suggest that ILK may play an important role in progression of human astrocytomas in vivo through possibly modulation of Wnt signaling pathway components.

P4.102

KRAS and BRAF mutations in colorectal cancer and matched distant metastasis

Colarossi C.; Scarpulla S.; Costanzo R.; Ferlito G.; Aiello E.; Memeo L.

Mediterranean Institute of Oncology, Viagrande, Catania, Italy

Background KRAS or BRAF mutations in metastatic colorectal cancer are associated with clinical resistance to treatment with EGFR–targeted monoclonal antibodies. Only few reports have evaluated whether BRAF and KRAS status matches in primary tumor and metastatic sites.
Methods We evaluated KRAS (exon 2) and BRAF (exon 15) by DNA sequencing in a cohort of 16 colorectal adenocarcinoma patients (median age 67 years; range 42 to 92 years; 9 men and 7 women) in primary tumor (11 colon; 5 rectum) and matched metastases (14 liver; 2 omentum).
Results KRAS mutations were found in 3 of 16 primary tumors (18%; always G12D), while BRAF mutations only in 1 of 16 cases (6%; V600E). The percentage of KRAS mutations in metastatic sites was slightly higher then primary tumors (4 of 16; 25%; 3 G12D and 1 G12S). None of the patients carried both mutations (in primary tumor or metastasis); the occurrence of the mutations was a mutually exclusive phenomenon, as expected by literature. All 3 patients with mutated KRAS showed the same mutation in the metastatic sites while one patient with a G12S mutation in the liver metastasis had a wild type KRAS in the primary tumor.
Conclusion(s) The patient with BRAF mutation presented the same mutation also in the liver metastasis. We observed overall concordance between primary tumor and metastasis in the vast majority of patients. The evaluation of the KRAS and BRAF mutations can be performed in either primary tumor or metastatic sites.

P4.103

K-ras mutation in colorectal cancer treated with cetuximab

Barbareschi M.; Girlando S.; Soini B.; Cuorvo L.; Fasanella S.; Cantaloni C.; Piccolo A.; Prosdocimi F.; Galligioni E.; Dalla Palma P.

S. Chiara, Trento, Italy

Background K-ras is mutated in a high percentage of colorectal cancer (CRC) and is related to sensitivity to anti-EGFR monoclonal antibodies.
Methods We retrospectively analyzed the mutational status of k-ras in 28 metastatic CRC patients treated with irinotecan + cetuximab after treatment failure with irinotecan based chemotherapy. The main characteristics were: 17 men, 11 women; median age: 57 years. The metastatic sites were the liver in 12 patients, lung in 2 patients and both in 14 patients. Genomic DNA was extracted from paraffin-embedded tissue blocks of the primary tumors, amplified and sequenced for k-ras and b-raf genes using the ABIPrism 310 analyzer.
Results Three cases were excluded because DNA was poorly preserved. Of the remaining 25 cases 12 had wild type k-ras and 13 had mutated k-ras. The response rate was 27% (3/12) in the k-ras wild type patients and 7% (1/13) in the mutated k-ras patients. Thirteen cases were analyzed for b-raf gene mutation: twelve cases were wild type and one was mutated. The b-raf mutated case was not mutated for k-ras; 9 out of 12 wild type b-raf were k-ras mutated and 3 were wild type for both genes.
Conclusion(s) Our results are in keeping with studies showing that in CRC there is a correlation between the k-ras status and response to cetuximab, but suggest that additional markers are needed for better patient selection. b-raf mutation could be an adjunctive criterium but analysis of other genes could provide additional information.

P4.104

Loss of DNA repair O6-methylguanine-DNA methyltrans-ferase (MGMT) expression, occurs in oligodendroglial tumors early and does not correlate with radiotherapy response

Martinez Carlos J.; Sepulveda Manuel J.; Cabello A.; Ricoy Ramon J.; Troncone G.

Instituto Oftalmico Hospital G Marañon, Madrid, Spain

Background To analize O6-methylguanine-DNA-methyl-transferase (MGMT) protein expression in oligodendroglial tumors and assess the possible association with radiotherapy response.
Methods MGMT and Ki-67 expression was evaluated in seventy-three patients (32 low- grade oligodendrogliomas, 21 anaplastic oligodendrogliomas, 9 low-grade oligoastrocytoma and 11 anaplastic oligoastrocytomas). Survival univariate analysis was made constructing survival curves using Kaplan-Meier method and comparing subgroups by log-rank probability test. The association between MGMT loss of expression and survival was also evaluated in the group treated with radiation therapy using the log rank test.
Results Most cases showed negative or weak MGMT expression, from 0 to 23.2%, (median labelling index 1.2%). There were no differences in MGMT expression between high and low-grade tumors nor between oligodendrogliomas and oligoastrocytomas. Ki-67 overexpression had strong prognostic influence on survival ($p<0.0001$, Hazard Ratio 4.51). MGMT downregulation was not predictive of survival. Also, the absence of MGMT

immunostaining was not an independent prognostic factor of treatment response in the group treated with radiotherapy.
Conclusion(s) Down-regulation of MGMT expression occurs in oligodendroglial tumors since early phases. Low or negative MGMT protein expression at similar proportions in low and high grade tumors strongly suggest that this alteration could play a pathogenetic role in the initiation of oligodendroglial neoplastic development. - MGMT protein downregulation prevents DNA repair, allowing the accumulation of mutations that could lead to neoplastic transformation as a result of the impairement of a fundamental genomic protective pathway.

P4.105
mRNA expression of collagen V gene increased in pulmonary fibrosis of systemic sclerosis

Parra Roger E.; Teodoro Rosolia W.; De Morais J.; Katayama L.M.; De Souza R.; Yoshinari Hajime N.; Capelozzi V.L.
Faculdade de Medicina da Universidade de São Paulo, São Paulo, São Paulo, Brazil

Background Our previous studies done with animal model of systemic sclerosis (SSc) had proven that fibrosis was due to increased amount of abnormal collagen type V (Col V). We propose to analysis Col V in lung tissue of SSc patients.
Methods We examined the amount of collagen V and mRNA chains expression using immunofluorescence, Real-time PCR and computer morphometric analysis in 15 open lung biopsies of patients with SSc. The pulmonary function tests were analyzed and correlated with collagen amount and PCR chains expression. Normal lung tissue was obtained from 8 individuals who had died from traumatic injuries.
Results Immunofluorescense showed abnormal dense thick Col V bundles in the interstitium and histomorphometry revealed higher amount of distorted Col V fibers, when compared with control group. In SSc patients there were increased [α1(V)] and [α2(V)] mRNA chains expression when compared with control, but [α2(V)] was proportionally raised compared to control group. High levels of collagen V were inversely associated to VC (r=-0.72; p= 0.002), FCV (r=-0.76; p<0.001) and FEV1 (r=-0.89; p< 0.001) pulmonary function tests.
Conclusion(s) We conclude that abnormal Col V fibers are overproduced in SSc patients and it could plays an important role in the pathogenesis of SSc, since this molecule regulates tissue collagen assembly. This aberrant histoarchitecture observed in SSc can be related to over-expression of [α2(V)] gene of unknown origin. Financial supported: FAPESP, CNPq.

P4.106
Ursodeoxycholic acid induces apoptotic death through activation of ERK1/2 and A-SMase in gastric cancer cells

Lim S.; Han S.
Chosun University, Gwangju, Republic of Korea

Background Ursodeoxycholic acid (UDCA) is well recognized as its cyto-protective and anti-apoptotic role, and suppressor of cholestatic liver diseases and colorectal cancer development. Presently, we demonstrate that UDCA induces cell death in human gastric cancer cells.
Methods We investigated the effect of UDCA on SNU601 and SNU638 cells through the evaluation of molecular mechanism of cell death as well as morphologic changes.
Results UDCA triggered cell death mainly through apoptosis with low level of autophagic death in both cells. Upon UDCA exposure, the number of clone formation was linearly decreased with increasing UDCA concentration. UDCA-induced apoptosis was completely blocked by z-IETD, z-LEHD, and z-VEID, and partially suppressed by z-DEVD. In accordance with this, UDCA activated caspases (3, 6, 8, and 9), indicating that UDCA induces extrinsic and intrinsic apoptotic pathways. In SNU601, UDCA increased ERK1/2 phosphorylation, not affecting p38MAPK or JNK activity. Unexpectedly, suppression of ERK pathway by PD98059, or U0126 significantly decreased UDCA-triggered apoptosis. We examined whether some membrane events are involved in the UDCA-induced cell death. Imipramine, A-SMase inhibitor strongly suppressed UDCA-induced apoptosis, indicating that UDCA-induced apoptosis is mediated through A-SMase activation. Prevention of ERK decreased UDCA-induced SMase activation, but inhibition of A-SMase activity did not affect ERK activation. These results suggest that ERK activation is an upstream event of SMase activation.
Conclusion(s) UDCA induces apoptosis by activating ERK1/2 – A-SMase pathway in SNU601 gastric cancer cells.

P4.107
Expression of human MxA protein in liver cirrhosis and in primary & secondary liver cancers

Vassilev M.; Kyoseva D.; Mihailov I.; Vlasov V.; Spassov L.
Hospital Lozenets, Sofia, Bulgaria

Background Human MxA protein is under the transcriptional control of type I interferons and it was shown to be up-regulated in hepatitis C virus related hepatocellular carcinoma (HCC) (Chaerkady, JProteome Res 2008) as compared to surrounding tissue. We compared the expression of MxA protein by immunohistochemistry in liver

cirrhosis (Ci), hepatocellular and chloangiocellular carcinoma (CCC) and in metastatic colon cancer (MCC).
Methods A total of 67 retrospective paraffin embedded surgical sections were stutied. MxA protein was visualized by monoclonal antibody (Hochkeppel, NovartisPharma, Basel) or rabbit antiserum (Julkunen, NPHI, Helsinki) and visualized using DAKO DAB+ Envison kit. Omission of the first antibody or irrelevant antibody was used as negative control. Each entire slide was evaluated and assigned a score for frequency & intensity; total score was then calculated by multiplication.
Results The majority of the hepatocytes expressed diffuse cytoplasmic staining of high intensity. The neoplastic cells showed less frequent and intense staining. There was significantly lower total score for MxA expression in HCC than in surrounding cells (paired t-test, p=0,0005). Mean score±SD for hepatocytes for Ci(22), HCC(25), CCC(8), MCC(12) were: 10.7±3.2; 12.4±1.6; 12.4±2.8; 11.0±3.4 respectively. Mean score± SD for neoplastic cells for HCC(25), CCC(8), MCC(12) were: 7.6±3.9; 8.3±3.8; 6.5±4.01 respectively. Unpaired comparisons showed significant differences between normal and neoplastic cells in HCC (p=0.001) and MCC (p = 0.003), but not in CCC.
Conclusion(s) The discrepancy between the proteomics and our IHC study can be explained, either by derangement of translation of MxA protein in HCC, or by patient selection bias.

P4.108

"Forgotten organs" for metastases

Katic V.; Gligorijevic J.; Katic K.; Krstic M.; Snezana J.; Zivkovic V.
School of Medicine, Nis, Serbia and Montenegro

Background The ability to migrate and invade into surrounding tissues, blood, and lymphatic vessels is one of the halmarks of cancer and a prerequisite for local tumor progression and metastatic spread. However, the underlying mechanisms controlling cell invasiveness remain poorly understood.
Methods We analyzed the histological parameters and immunohistochemical expression in 6 metastatic tumors of the unusual localizations.
Results (1) autopsy case: Sudden cardiac death, 40 days after removal of the original hyroid carcinoma. Intramyocardial tumour nodules of the right atrium and ventricular septum were macroscopically seen. Abdominal granullar cell ovarian metastasis found after 23 years from its diagnosis and surgical therapy. (3) Splenic subcapsular metastasis of the ovarian cystadenocarcinoma, was ressected after four years from its cytologic diagnosis in the massive ascites. (4) An 17 year- old boy, had sigmoid colon metastasis of choriocarcinoma of the testis. (5) Gastroduodenal mucosa and submucosa were infiltrated with epitheloid melanoma of the eye. (6) A 46-year -old woman, had signet ring cell breast tumor metastatic from the stomach.
Conclusion(s) We point out the four pathways of invasion : retrograde lymphatic extension, hematogenous spread, direct contiguous extension and transvenous extension. But, the pathway of invasion, as well as the time of invasion, often are not predictable.

P4.109

Genetic and epigenetic alterations in sporadic basal cell carcinomas

Stamatelli A.; Saetta A.; Vlachou C.; Michalopoulos N.; Gigelou F.; Aroni K.; Patsouris E.
1st Department of Pathology, Medical School, National and Kapodistrian University of Athens, Athens, Greece

Background Recently it has become evident that along with genetic mutations epigenetic alterations, a mechanism for tumor suppressor gene inactivation, seem to play a key role in the pathogenesis of human cancer. We searched for epigenetic alterations of hMLH1, RASSF1A, DAPK, APC, DCR1 and DCR2 genes and B-Raf mutations in Basal Cell Carcinomas (BCC) in association to the clinicopathological parameters and the histological subtypes of the tumours.
Methods Fifty BCCs were analysed by methylation-specific PCR (MSP) in order to assess the methylation status of hMLH1, RASSF1A, DAPK, APC, DCR1 and DCR2 genes after sodium bisulfite treatment of the tumour DNA. hMLH1 and DCR1 gene expression was investigated by immunohistochemistry. B-Raf mutations were studied by High-Resolution Melting analysis (HRM).
Results High frequency of promoter methylation occurred in DCR1 (32%), DCR2 (44%), RASSF1 (32%) and APC (32%) genes whereas methylation of DAPK was moderate (15%) and methylation of hMLH1 was absent. No B-Raf V600E mutation was detected. There was no correlation between the frequency of the promoter methylation of the above mentioned genes and the clinicopathological features or the histological subtypes of the tumours.
Conclusion(s) The high frequency of RASSF1A, DCR1, DCR2 and APC genes methylation may suggest that methylation may be an important pathway in the tumorigenesis of BCC given that there is a potential relationship between methylation and exposure to solar UV-radiation which is the main cause of BCC development. Nevertheless, further studies are mandatory to elucidate the above mentioned conclusion.

P4.110

Optimization of DNA extracted from formalin fixed-paraffin embedded tissue (FFPET), stored for seven years, tested by PCR to M. tuberculosis

Iwamura Sadayo Miazato E.; Barcelos D.; Silva Souza M.; Funabashi Silva K.; Franco Fabiano M.
Paulista Medical School, Federal University of São Paulo-EPM/UNIFESP (Department of Pathology), São Paulo, Brazil

Background New diagnostic approaches have emerged with the advent of PCR technique and DNA extraction and purification methods have been routinely performed in clinical laboratories. The ability to study DNA extracted from archival formalin fixed-paraffin embedded tissue (FFPET) enables valuable retrospective testing. However, it is difficult to obtain good quality genomic DNA. This represents a factor for false negative results in the procedure.
Methods An analytical approach to the DNA quality and PCR performance in paraffin embedded specimens (spleen and lung necropsy samples, previously tested by PCR, in 2002) with the diagnosis of miliary tuberculosis were used to evaluate the influence of the seven years of storage. The DNA were extracted from 10μm slices of FFPET using phenol/chloroform and centricon or using commercial kits (QIAamp DNA mini and GFX). Specimens were submitted to PCR for amplification of the human beta-actin gene and separately for the insertion sequence IS6110, specific from the M. tuberculosis complex. The DNA extracted was analyzed in NanoDrop spectrophotometer and the concentration adjusted for PCR.
Results This study will present the optimization and the best performance protocol, even in non buffered formalin fixed specimens after seven years of storage.
Conclusion(s) Probably, molecules derived from the fixation procedure, and imbalance in the quantity of starting material in the DNA extraction and PCR, interfered with the detection of M. tuberculosis in stored FFPET. The QIAamp DNA mini Kit presented best results.

P4.111

Real-time quantitative allele-suppression (clamped) PCR assay for the determination of K-ras mutational status from paraffin embedded tumor samples

Fazakas F.; Kajtár B.; Török M.; Pór A.; Kovács I.; Méhes G.
Department of Pathology, University of Debrecen, Debrecen, Hungary

Background Response to anti-EGFR therapy is depending on the wild-type KRAS gene in colorectal carcinoma. Most of the function gaining mutations are located in the codons 12 and 13 of the KRAS gene. Genotyping of the critical region is challenging due to lack of standardization in tissue processing, difficulties in DNA integrity and unpredictable mutant/wild type allele ratio. A commercially available KRAS genotyping kit performed generally well, however, the lack of wild type controls and exact genotyping, as well as abnormal melting profiles proved to be serious limitations.
Methods A clamped PCR assay with a TaqMan probe as a reporter was developed enabling the absolute and relative (clamped versus non-clamped) quantification and direct sequencing of the mutant allele.
Results Altogether 136 colorectal adenocarcinomas were analyzed so far. We identified unambiguously 10 different mutations in 47 samples (35%), six were located in codon 12 and four in codon 13. The mutant alleles had at least 1% relative abundance compared to the wild type alleles. 12 out of the remaining 89 wild type samples showed late amplification suspicious of minimal quantities of mutant alleles. However, multiple G>A transitions could be demonstrated by sequencing of the clamped area in all of them. The transitions were considered as artefacts as microdissection did not reveal true genetic heterogenity in these tumors.
Conclusion(s) The method presented is sensitive, fast and reliable, also minimizing the chance of false positivities.

P4.112

The significance of the HPV determination for the agreement between cytology and histology in the cervical cancer diagnostic

Weyerstahl T.; Trauner A.
Laboratory for Cytology and Molecular Biology Dr. T. Weyerstahl, Munich, Germany

Background 196 reports of cervical biopsy were registered in our laboratory in 2008. 14 of these were diagnosed as cases with benign histological changes. The distribution of the corresponding 14 PAP results was: 2 cases without any cytological anomaly (PAP I-II), 8 cases of mild and/or moderate dysplasia (PAP IIID), 2 cases of severe dysplasia/CIS (PAP IV) and 2 cases with cytological report as questionable (PAP III). There were no cases of invasive carcinoma (PAP V). The distribution of the remaining 182 biopsy diagnoses was: 51 cervical intraepithelial neoplsia, 111 carcinoma in situ and 20 invasive carcinoma with corresponding 182 PAP results of: 4 PAP I-II cases, 63 IIID cases, 83PAP IV cases, 28 PAP III cases and 4 PAP V. 103 of all 196 PAP test results were accompanying with a result of HPV detection (HCII test, QIAGEN).
Methods PAP results versus histology reports showed the sensitivity and specificity of PAP test. The significance of difference was evaluated by Fisher exact test.
Results The PAP test combined with HPV determination showed 99,0% sensitivity (96 of 97 cases were true positive) and 16,7% specificity (1 of 6 cases were true negative). The

PAP test without HPV determination showed 96,5% sensitivity (82/85) and 12,5% specificity (1/8).
Conclusion(s) There is no statistical significant difference (p=0,9162) between cases of PAP test with HPV results and PAP test without HPV results in relation to histology reports.

P4.113
Patterns of 1p/19q chromosomal abnormalities among glial neoplasms

Schiavo N.; Brunelli M.; Martignoni G.; Menestrina F.; Gobbo S.; Eccher A.; Ghimenton C.
Anatomia Patologica, Università di Verona, Verona, Italy

Background Loss of 1p/19q is considered an important diagnostic and favourable prognostic parameter in glial neoplasms, particularly in oligodendrogliomas. Fluorescent in situ hybridization (FISH) is one of the most used technique for investigation of 1p/19q status in paraffin-embedded tissues. We evaluated different pattern of 1p and 19q status among glial neoplasms.
Methods To test 1p/9q region the FISH Vysis-kit was used in a series of 49 glial neoplasms (26 oligodendrogliomas, 16 astrocytomas, 7 oligoastrocytomas) and 5 gliotic brain tissue as controls. For each case were evaluated 1p/19q signals of at least 200 nuclei and combinations of cut-off were calculated to distinguish different patterns.
Results 69,2% of cases of oligodendrogliomas showed chromosome 1p/19q deletions, 11,5% were not deleted, 11,5% presented gains of 1p signals, 7,8% presented a polysomy pattern. Among cases with 1p/19q deletions, 12 cases (46,2%) presented also clones of neoplastic cells with gains and loss at 1p associated with deletion of 19q. Astrocytomas showed chromosome 1p/19q deletions in 6,2% of cases, polysomy in 81,2% whereas 7% were not deleted. Three cases of oligoastrocytomas showed deletions, 3 polysomy and one with gains of 1p.
Conclusion(s) 1p/19q loss is more frequent in oligodendroglioma than in astrocytoma, the latter characterized by a polysomy pattern. Interestingly, oligodendrogliomas present molecular different subgroups such as isolated clones with gains or heterogeneity clones with gains and loss of 1p associated to loss of 19q. These pattern of chromosomal abnormalities need to be set differently to evaluate potential clinical outcomes.

P4.114
Immunohistochemical expression of WT1 in gliomas

Schiavo N.; Dell'Agnola C.; Frizziero M.; Sava T.; Lupidi F.; Ghimenton C.
Anatomia Patologca, Università di Verona, Verona, Italy

Background WT1 was described in 1990 as a tumour suppressor gene associated with nephroblastoma. Interaction with p53, Bcl-2, IGF1R, CMYC genes have been described with oncogenic-oncosuppressor effects. WT1 target therapy have been proposed in various type of neoplasms and its inhibition on glioblastoma culture cells determines regression of proliferation. WT1 express positively in neoplastic astrocytes and correlates with grade of gliomas. Only few cases of oligodendroglial neoplasms have been studied.
Methods 70 glial neoplasms (30 oligodendrogliomas, 8 oligoastrocytomas, 32 glioblastomas) fixed in FineFIX-paraffine embedded, have been tested with Monoclonal WT1, Clone 6F-H2. Glioblastomas included also 7 GBMO, 2 Gliosarcomas, 3 small cell glioblastomas and 6 giant cell glioblastomas. A score system was established (1+ =0–30%; 2+ =31–60%; 3+ =61–100%).
Results WT1 staines cytoplasmatically. Gemistiocytes, mini-gemistiocytes, perivascular and subpial neoplastic astrocytes stain particularly strongly. 88% of GBM presented score 3+ without histological differences. Gliosarcomas presented a lower expression in the sarcomatous component. Score of astroytomas cases: 61,5% 3+; 23,5% 2+; 15% 1+. 70% of high grade astrocytomas were 3+. Score of oligodendrogliomas cases: 70% 1+; 20% 2+; 10% 3+. 100% grade II oligodendroglioma scored 1+. Score of grade III oligodendroglioma: 64% 1+; 24% 2+; 12% 3+. Score of oligoastrocytomas: 87,5% 1+; 12,5% 3+.
Conclusion(s) WT1 could be a useful diagnostic marker to distinguish astrocytic and oligodendroglial tumor. In astrocytic neoplasms (astrocytomas and glioblastoma) WT1 correlates with neoplastic grade. WT1 expression in oligoastrocytomas is probably the mirror of astrocytic/oligodendroglial component. We are investigating about an eventual prognostic correlation.

IT in pathology

P4.115
Automated image analysis of nuclear immunomarkers in breast cancer: data on 2064 cases tissue microarrays

Makretsov N.; Dawson S.; Mercer J.; Provenzano E.; Howat W.; Morris L.; Blows F.; Driver K.; Pharoah P.; Caldas C.
Memorial University, St John's, NL, Canada

Background The aim of this study was to evaluate the clinical utility of automated analysis of routine nuclear immunomarkers in breast cancer as a highthroughput validating platform for new biomarkers.
Methods Tissue microarrays containing 2064 breast carcinomas and immunohistochemical stainings for estrogen receptor (ER), progesterone receptor (PR), Ki67 and p53

were performed and slides digitalized by ARIOL (Applied Imaging Inc, USA) system. The images were scored semi-quantitatively (Allred method) by the pathologists in order to obtain the standard for training of automated algorithms. The images were scored automatically by ARIOL, ImageJ (NIH, USA) and MATLAB v7.4 (Natick, USA) software using the customized algorithms; ROC and Kaplan-Meier analyses were performed.

Results Overall, the automated ER scoring reached 94 % sensitivity and 95 % specificity (comparable between all three different software and algorithms used), PR -88 and 90%, P53- 88 and 93%, Ki67- 83 and 77%, and p53, respectively. The automated scores for all biomarkers were of prognostic significance comparable to the manual scores. There was consistently high agreement between manual pathologist and automated scores for ER, PR and P53 with kappa 0.7–0.8, and substantial agreement for Ki67 scoring with kappa 0.5.

Conclusion(s) Automated digital image analysis of nuclear immunomarkers in breast cancer is a sensitive and specific screening tool; it can be applied to novel candidate antibodies with a nuclear staining pattern in translational research settings. Supported by ACSBI-UISS fellowship.

P4.116

Nanopathology: nano-sized particles in human tonsil tissues

Dvorackova J.; Kukutschova J.; Kratosova G.; Zelenik K.; Kominek P.; Bielnikova H.
Faculty Hospital Ostrava, Ostrava - Poruba, Czech Republic

Background The 21st century opened with a revolution due to nanotechnology as special emerging technology. We have heard about nanobiotechnology, nanomedicine, nanomaterials, nanoparticles, etc. Applications of nano-technologies in the field of medicine are growing rapidly. Areas such as disease diagnosis, drug delivery and molecular imaging are being investigated intensively. The aim of the study was to identify nano-sized particles in human tonsils tissues as an entering filter of air breathed.

Methods Three main groups of tonsil samples were chosen for evaluation of the fine-particles presence. First group of samples were randomly selected tonsils of children undergoing “cold” tonsillectomy, second group tonsil samples of dead born children, and third group were tonsils with histologically proved spinocellular carcinoma. Dehydrated tissue samples were analyzed using scanning electron microscope with X-ray microanalysis (SEM-EDX), which enabled analysis of particles morphology and elemental composition.

Results Presence of various nanostructured metallic agglomerates in all groups assessed was confirmed. Dominant metals found almost in all tissues analyzed were iron and zinc. Differences were found between groups of various age, lifestyle, living environment affected by industrial processes and last but not least diagnose.

Conclusion(s) The study allowed to ascertain that environmental pollution may strongly affect human health. Through SEM-EDX analysis it was possible to verify character and composition of particles, unintentionally released into the environment by industrial processes and road traffic, which were present in pathological tissues.

P4.117

Quality control, diagnosis and delegation aid for the gross pathology field

Buono J.; Xavier C.
L’Anapath, Aix-en-Provence, BdR, France

Background In the ame of quality control improvements in samples management, the gross preparation is polar importance. It’s delegation on a larger number of acts needs the establishment of a specific controlled and assisted training.

Methods To address these issues, we developed a new kind of samples labeling and numbering for reducing biopsy cassettes and slides identification errors. This process uses a laser source and a separate laboratory software module, MacroDigit™ system that works without additives. The cassettes previously engraved with numbers, different from the cases numbers usually employed are immediately available even though the cassette number is unknown. For each sample or lesion observed, the system requires inputs: descriptions and pre-set data, some of them obligatory, through a tactile interface integrated to the gross table.

Results The technician uses interactive and adaptable forms to all practices. He makes pictures, audio comments, all indexed at each stage of the gross act, allowing a posteriori control. He can refer at cutting guides and database of previous same acts. Alert messages are automatically generated depending on the context met, thus facilitating a secured delegation. Simultaneously, requests forms are digitized, fees automatically integrated, technical colorations proposed and corresponding slides automatically generated.

Conclusion(s) This approach has quickly found its place in the team, reducing the stress caused by supplies labeling and identification, thus avoiding a potential error source. It led to establish a training program for technical team, leading the laboratory to productivity and quality enhancement.

P4.118

Recognition of tumor cell by image analysis in oligodendroglioma at Ki-67 staining

Markiewicz T.; Grala B.; Warowny M.; Osowski S.; Kozlowski W.
Military Institute of the Health Services, Warsaw University of Technology, Warsaw, Poland

Background Many studies have reported that Ki-67 index in oligodendroglioma is significant in discrimination of patients into groups of good and worse prognosis. The referred cut-off value varies from 3% (Heegaard) to 5% (Coons) MIB-1 positive cells. For exact evaluation of Ki-67 index, recognition between tumor and non-neoplastic cells in Ki-67 staining is necessary. We proposed method based on textural image analysis in automatic evaluation of digital images.
Methods Digital images of Ki-67 stained tissue of the brain tumor is acquired using Olympus microscope and camera. Selected areas are processed automatically by developed system in order to count and recognize immunonegative and immunopositive cells. The recognition between neoplasm and non-neoplastic cells, such as lymphocytes, microglia or stroma cells, was done on the basis of Unser texture features (i.e. mean, contrast, homogeneity and energy), generated for any nuclei of immunonegative cell independently.
Results The developed system with texture based neoplasm cell recognition was applied for counting Ki-67 index in 25 specimens of oligodendroglioma. Using texture analysis, we increased the accuracy of Ki-67 index evaluation, correcting absolute values from 0.1% to 1.8% (depending on homogeneity of tumor). The average discrepancy of index value between system and expert's results were reduced from 0.4% to 0.1% in absolute values.
Conclusion(s) The texture analysis is potentially a very useful tool in automatic quantitative image analysis for neoplasm cell recognition at Ki-67 staining and can support well the medical diagnosis of selected brain tumors.

P4.119

A quantitative study of the comparative features of liver's regulatory mechanisms at the norm and delta hepatitis

Kamilov Haydarovich F.; Hidirov B.; Saidalieva M.; Aliev B.; Hidirova M.; Turgunov A.
Tashkent Institute of Postgraduate Medical Education, Tashkent, Uzbekistan

Background Molecular-genetic and cellular aspects of viral hepatitis pathogenesis are definitively not established. It can be reached by applying modern technology for the quantitative analyzing functioning regulatory mechanisms (regulatorika) of living systems at molecular-genetic and cellular levels with using methods for biological, mathematical modeling and computing experiment. In the given work the biological, mathematical and computer modeling liver regulatorika at the norm and viral hepatitis type D (HDV) on molecular-genetic level are considered.
Methods For mathematical modeling the methods of the quantitative studying functioning regulatory mechanisms (regulatorika) of living systems at molecular-genetic and cellular levels have been used.
Results In quantitative research the following modes of considered process have been received: clarification, symbiosis, auto-oscillations and irregular fluctuations (chaos), sharp destructive changes ("black hole" effect) which define various clinical forms of the HDV infection.
Conclusion(s) Developed mathematical model and computer program CM-HDV can be used for quantitative researching infectious process regularities in hepatocyte under viral hepatitis type D and carry out diagnostics and predict characteristic stages of disease including beginning of liver cirrhosis in delta hepatitis. (The research is supported by RUz grant A-17-Ф009).

P4.120

Internet web conferencing strategies for broadcasting pathology meetings

Alfaro L.; Gómez L.; Angulo A.; Catalá P.; Berzosa J.; Zaragozá F.
Fundacion Oftalmologica del Mediterraneo, Valencia, Spain

Background Two meetings were held in our institution in early 2009. A regional pathology meeting of eastern Spanish (Valencian) Society, and a meeting on Telepathology and Informatics for pathologists. We offered the chance to attend those meetings through a Internet video broadcasting.
Methods Our hospital is connected to an intranet covering 25 hospitals. This is a broadband connection with 2 Megabits/s. There is besides an open Internet connection with 512 Kbits/s. We broadcasted simultaneously sound and images for both nets with different approaches. A video camera was recording images from the speakers, sent to a computer with a USB video capture device (Hauppage WINTV-HVR900H), and broadcasted through a video streaming generated with VLC player software. Simultaneously PowerPoints presentations were transformed from its VGA signal into video (RGB) with an AverMedia AVerKey330Convertor. For saving maximum bandwidth, this second signal was sent every 10 seconds through FTP in the form of.jpg files to a external server hosting the web page were observers followed the transmission. This webpage was built with two parallel screens: one receiving video from the

room, and a second refreshing every 10 seconds to actualize PowerPoint images.
Results Video and sound transmission was fluid and efficient in the 2 Megabit Intranet. Slower Internet line was easily saturated, so video was replace with sequences of fixes images.
Conclusion(s) Technology for broadcasting Pathology meetings is available with a minimum cost. Adaptation to bandwidth conditions is necessary, but lines are continuously increasing speed and facilitating these activities.

Nephropathology

P4.121
Transgelin in renal fibrosis

Karagianni F.; Kypreou K.; Politis P.; Kavvadas P.; Sountoulidis A.; Agapaki A.; Vlachakos D.; Goumenos D.; Charonis A.
Biomedical Research Foundation of the Academy of Athens, Athens, Greece

Background Renal fibrosis is common in several renal diseases; however, several aspects of its pathophysiology are not yet known at the molecular level.
Methods We have applied proteomic analysis of renal cortex samples in the well established rat model of Unilateral Ureteric Obstruction (UUO). Proteomic analysis indicated that among other macromolecules, transgelin expression may be differentially regulated in this fibrotic model. In order to further confirm our results, we have studied the expression of transgelin at three levels: using the HK2 cell culture system, using the animal model of UUO where renal tissue samples from four categories of animals (sham operated or ligated and sacrificed after 2 or 8 days) were analyzed and compared and finally using biopsy material from patients.
Results Transgelin expression was found increased after ligation at the protein level, using Western Bloting and immunocytochemistry. In double immunofluorescence experiments only partial co-localization of transgelin and αSMA was observed. Transgelin expression was also found increased at the mRNA level.. Transgelin showed a preferential distribution in the tubulointerstitial compartment surrounding Bowman's capsule. These findings suggest that a subgroup of fibroblasts may exist around Bowman's capsule, phenotypically different from the rest of renal interstitial fibroblasts. Using renal biopsy material from patients suffering from several renal diseases, we have observed that depending on the disease, either the glomerular or the tubulointerstitial compartment or both exhibited increased expression of transgelin.
Conclusion(s) These results provide strong evidence that transgelin is a macromolecule involved and up-regulated in specific cells during renal fibrosis.

P4.122
C4d staining in peritubular capillaries and morphological analysis of renal allograft biopsies

Faleiros G.A.; Aguiar F.C.; Breda C. L.; Abate T.R.D.; Rodrigues P.M.; Llaguno M.M.; Reis A.M.
University of Triangulo Mineiro, Uberaba, Minas Gerais, Brazil

Background C4d deposition in peritubular capillaries has been described as a marker of humoral renal graft rejection. Aims:characterize the epidemiological and clinical features of kidney transplant patients of the Nephropathology-Department of the University of Triangulo Mineiro, and to analyze morphologically and by immunohistochemistry their biopsies.
Methods To analyze the fibrosis were calculate the percentage per area of the examined field(%F). For C4d detection was used the immunohistochemistry and for IgA, IgG,IgM,C3,C1q was used direct immunofluorescence. Diagnoses were made according to the presence of C4d (C4d0,C4d1,C4d2,C4d3) and classified according to Banff 07.
Results The mean age was 41.1 years and had positive correlation with %F. The median of %F was 1% in C4d0, 1% in C4d1, 2% in C4d2, 3% in C4d3. The correlation between %F and C4d was positive. Rejection mediated by antibodies(RMA) represented 36.7%, rejection mediated by cells(RMC) 16.7%, borderline lesions(BL) 25% and interstitial fibrosis/tubular atrophy(TF/TA) 18,3%. Mean %F for acude RMA was 2%, acude RMC 1%, chronic RMA 5%, BL 2.5%, TF/TA 4%. There was positivitity for IgM and C3 in all groups. C4d3 showed a higher %F, with elevated serum creatinine levels.
Conclusion(s) C4d is an important marker of humoral renal graft rejection and essential to determine the diagnosis. The co-expression of C4d with IgG and C3 could indicate the activation of the classical complement pathway. The relation between C4d, fibrosis and creatinine levels may be indicative of renal function decline and worse prognosis.

P4.123
Chronic transplant glomerulopathy. Clinical and histological characteristics

Perkowska-Ptasinska A.; Ciszek M.; Urbanowicz A.; Kwiatkowski A.; Galazka Z.; Paczek L.; Glyda M.; Debska-Slizien A.; Dziewanowski K.; Rydzewski A.; Durlik M.
Department of Transplantology and Nephrology, Warsaw Medical University, Warsaw, Poland

Background Chronic transplant glomerulopathy (TG) is one of chronic lesions developing secondary to persistent,

or repetitive injury to glomerular endothelium. There is limited data about histological and clinical characteristics of that lesion including its impact on graft survival.
Methods We retrospectively analyzed all 152 cases of chronic transplant glomerulopathy recognized in Transplantation Institute, and compared it with 86 non-TG cases matched for the stage of advancement of chronic interstitial, tubular and vascular lesions.
Results In comparison to control TG was associated with lower survival rate (83% vs 49%, $p<0.0001$) higher incidence of proteinuria (34% vs 88%, $p<0.0001$), and higher incidence of HCV infection (45% vs. 33%, p= 0.0033). Morphological analysis (Banff 07 classification) revealed higher incidence of C4d deposition in PTC (77% vs 1%, $p<0.0001$), and glomeruli (66% vs 0%, $p<$ 0.0001), as well as an acute transplant glomeurlopathy (14% vs 0%, $p<0.0001$) and endarteritis ("v", 9% vs 0%, p=0.005). Banff scores for inflammatory infiltrates ("i" and "ti" score), and PTC-itis were also higher in TG biopsies.
Conclusion(s) Chronic transplant glomerulopathy is associated with poorer graft survival and higher proteinuria than other chronic kidney transplant lesions. In substantial percentage of cases TG is associated with C4d deposition in both PTC and glomerular capillaries, and co-occurrence of inflammatory interstitial and vascular infiltrates which is in contrast to other common chronic lesions in kidney graft.

P4.124
Fibronectin glomerulopathy in a 34-year old male: case report

Coric M.; Brcic I.; Brcic L.; Dotlic S.; Kuzmanic D.
Zagreb, Croatia

Background Fibronectin glomerulopathy is a rare autosomal dominant familial kidney disease. It presents with proteinuria, microscopic hematuria, and hypertension that lead to end-stage renal failure in the second to sixth decade of life.
Methods The patient is a male who developed low-grade proteinuria at 25 years of age. At 34 years of age he presented with nephrotic-range proteinuria (6 g per day), low serum albumin, and severe hypertension (220/ 130 mmHg). His father had a renal disease and died of myocardial infarction at the age of 33. Renal biopsy showed enlarged glomeruli with massive deposits of fibronectin in the mesangium and subendothelial spaces. These deposits also showed scant immunoreactivity for immunoglobulins and complement proteins. Fibronectin deposits showed focal fuchsinophilia with the SFOG trichrome stain. Fibronectin deposits were detected in the peripheral loop and mesangium by immunohistochemistry. By electron microscopy the deposits in the mesangium and the subendothelial spaces appeared to be arranged in a fine granular pattern.
Results He received a multidrug treatment titrated against urinary protein excretion and after 20 months, urinary protein excretion is about 2 g per day; blood pressure is 160/90 mm Hg; and his renal function is now stable.
Conclusion(s) Immunohistochemistry and electron microscopy is essential for diagnosing fibronectin glomerulopathy in patients with positive family history and distinctive clinical findings. If the disease is properly diagnosed the patient's condition can be improved, at least temporarily, with multidrug treatment.

P4.125
Immunoexpression of adhesion molecules and inflammatory cell profile in vascular lesions of type III acute rejection of the renal allograft

Soares F.M.; Franco Fabiano M.; Medina-Pestana Osmar J.
Federal University of Sao Paulo, Sao Paulo, Brazil

Background Acute severe vascular rejection of the renal allograft (Banff type III) is characterized by transmural arteritis and/or fibrinoid necrosis of the vessel wall, but it is object of debate if these lesions are pathogenetically distinct entities.
Methods Seventy explanted renal allografts with type III rejection were analyzed. Vascular lesions were classified as i) "FN"- fibrinoid necrosis; ii) "TA"- transmural arteritis and iii) "M"- mixed fibrinoid necrosis and transmural arteritis. Tissue underwent immunoperoxidase testing for: i) CD4, CD8, CD20 and CD68 in vessel wall and interstitial inflammatory cells; ii) C4d in peritubular capillaries; iii) ICAM-1 and VCAM-1 in vessel walls. Groups were compared by Fisher Exact Test, corrected by Bonferroni in multiple comparisons (p=0,018).
Results Statistically significant differences were observed in: I) The finding of CD4 and CD8-lymphocytes and CD68-hystiocytes in vessel walls was higher in TA and M lesions than in FN lesions; II) Endothelial and arterial tunica media immunoexpression of ICAM-1 and VCAM-1 was more consistently observed in TA and M lesions than in FN lesions. No statistically significant differences were registered regarding C4d positivity in peritubular capillaries and the immunoprofile of interstitial inflammatory cells.
Conclusion(s) Active vascular inflammation and T-cell interactions may be involved in the increased positivity of ICAM-1 and VCAM-1 in type III renal allograft rejection. Peritubular capillary C4d positivity in all patterns of

lesions suggests that both TA and FN lesions may be antibody-mediated.

P4.126

Immunohistochemical characteristic of tubulointerstitial changes in patients with primary glomerulopathies

Savosh V.V.; Letkouskaya A.T.; Cherstvoy D.E.; Sukalo V.A.; Tur I.N.
Belarussian State Medical University, Minsk, Belarus

Background The purpose of our study was to ascertain the possible relationships between number of interstitial myofibroblasts, TGF-b and interstitial deposition of matrix proteins in the renal tissue of patients with primary glomerulopathies.
Methods We studied the expression of the a-SMA, TGF-b, collagen types IV and fibronectin with the use of immunostaining in 96 needle renal biopsy specimens from children with minimal change disease, immunoglobulin A nephropathy, membranoproliferative glomerulonephritis, and focal segmental glomerulosclerosis.
Results Interstitial myofibroblasts were detected in the interstitial tissue as well as in the periglomerular areas. TGF-b immunostaining was found in the renal cortex within epithelial cells of the proximal tubule and in surrounding interstitial cells. Greater immunostaining for type IV collagen was present in the peritubular basement membrane. There was a significant correlation between level of proteinuria and interstitial a-SMA expression, and tubular expression of TGF-b ($p<0,05$). Interstitial a-SMA expression was significantly higher in patients with nephrotic proteinuria level compared with patients with urinary protein excretion less then 1 g/l. A highly significant correlation was also evident between the number of interstitial myofibroblasts and interstitial deposition of collagen types IV and fibronectin ($p<0,05$).
Conclusion(s) We found that tubulointerstitial changes in the renal tissue of patients with proteinuric glomerulopathies were accompanied by increases number of interstitial myofibroflasts and expression of collagen type IV and fibronectin. The TGF-b overexpression within tubular epithelial cells in patients with nephrotic syndrome, suggest the activation of these cells by filtered protein.

P4.127

Macrophage infiltration in kidney tissue in children with primary glomerulopathies

Krylova-Alefirenko Viktorovna A.; Letkovskaya A.T.; Tur I.N.; Cherstviy Davydovich E.; Sukalo V.A.
Belarusian State Medical University, Minsk, Belarus

Background Macrophages contribute to the initial damage and progression of various glomerulopathies. We have conducted the study to assess predictive value of CD68 expression in renal tissue.
Methods 87 children (2 to 17 years, median 13), with primary glomerulopathies were enrolled (25 with IgA-nephropathy, 30 with non-IgA MesPGN, 11 with FSGS, 15 with MCNS, 6 with MPGN). 36 children were followed for at least 12 months (13 to 60, median 19). According to clinical data at the most recent follow-up patients were divided in progressive (n=(n=11) and stable (n=25) groups. Monoclonal mouse anti-human CD68 (DAKO) were used to identify macrophages in kidney biopsy samples.
Results Number of glomerular macrophages was correlated with renal function impairment at onset (p=0,281, r=0,009), degree of proteinuria (p=0,332, r=0,002) at biopsy, mesangial proliferation (p=0,588, $r<0,001$) and glomerulosclerosis (p=0,262, r=0,015), glomerular deposits of IgG (p=0,335, r=0,024) and C3c (p=0,278, r=0,014). Interstitial macrophage accumulation was correlated with renal function impairment at onset (p=0,273, r=0,010), acute phase reactants (p=0,286, r=0,007), degree of proteinuria (p=0,316, r=0,003), serum creatinine (p=0,331, r=0,020), GFR (p=-0,288, r=0,007) at biopsy, mesangial proliferation (p=0,312, r=0,003) and glomerulosclerosis (p=0,393, $r<0,001$), interstitial fibrosis (p=0,375, $r<0,001$), tubular atrophy (p=0,264, r=0,021), glomerular deposits of IgG (p=0,375, r=0,011). Patients with progressive course had significantly higher scores of glomerular (p=0,004) and interstitial macrophages (p=0,023).
Conclusion(s) Glomerular and interstitial macrophages are related with some predictors of poor renal outcome and might be considered to be predictors of progressive course of primary glomerulopathies in children.

P4.128

Membranoproliferative glomerulonephritis in the setting of multicentric angiofollicular lymph node hyperplasia (Castleman's disease) complicated by Evan's syndrome

Gakiopoulou H.; Paraskevakou H.; Marinaki S.; Voulgarelis M.; Korkolopoulou P.; Lazaris A.; Tzirakis M.; Agrogiannis G.; Stofas A.; Boletis J.; Patsouris E.
A' Department of Pathology, Medical School, National and Kapodistrian University of Athens, Greece

Background Systemic Castleman's disease is a lymphoproliferative disorder which has been associated with autoimmune phenomena. We report a rare case of the plasma cell variant of Castleman's disease associated with autoimmune hemolytic anemia and autoimmune thrombo-

cytopenia (Evan's syndrome) and complicated by mixed nephrotic-nephritic syndrome and acute renal failure due to glomerulopathy with microscopic and immunofluorescence findings compatible with a membranoproliferative glomerulonephritis (MPGN) type I. To the best of our knowledge constellation of all these disorders is reported for the first time.

Methods Clinical, laboratory and pathologic findings are presented.

Results A 17 year old boy with a history of plasma cell type Castleman's disease complicated by Evan's syndrome, presented with mixed nephrotic-nephritic syndrome followed by rapid deterioration of his renal function. Serologic examination demonstrated hypocomplementemia. Renal biopsy showed diffuse mesangial hyperplasia, basement membrane thickening and double contours on PAS and silver stains. Immunofluorescence microscopy demonstrated immunodeposits of IgG (+++), IgM(++), C3 (+++), C1q (++) and κ light chain (++) with a peripheral subendothelial localization. A diagnosis of membranoprolipherative glomerulonephritis was supported.

Conclusion(s) Although proteinuria is a common manifestation in patients with Castleman's disease, glomerulonephritis has been infrequently reported. To our knowledge, there are only five previous reports describing the occurrence of MPGN/MPGN-like glomerulopathy in Castleman's disease. Moreover, coexistence of Castleman's disease, Evan's syndrome and membranoproliferative glomerulonephritis is reported for the first time.

P4.129

Modulation of inflammation by mesenchymal stem cell is determinant for better outcome after acute kidney injury

Semedo P.; Palasio C.; Oliveira C.; Cenedeze Antonio M.; Teixeira Paula Antunes V.; Reis Antonia M.; Pacheco-Silva A.; Câmara Olsen Saraiva N.
Federal University of São Paulo, São Paulo, Brazil

Background Therapy with stem cells has showed to be promising for acute kidney injury (AKI), although how it works is still controversial. Modulation of the inflammatory response is one possible and interesting mechanism behind it. Most of published data relies on early time and whether the protection is still maintained after that is not known. We analyzed whether immunemodulation pattern continues after 24/48hours of reperfusion.

Methods Mesenchymal stem cell (MSC) - from bone of Wistar-EPM, after 3–5 passages, cells were submitted to FACS (Bencton Dickson) for phenotypic analyses (CD73, CD90 and CD 31). In addition, MSC were submitted to differentiation in adipocyte/osteocyte. AKI - bilaterally clamping renal pedicles (60 min). Six hours after injury, MSC (2x105 cells)-administered intravenously.

Results MSC-treated animals presented the lowest serum creatinine compared to controls, and lower expression of IL-1b, IL-6 and TNFa and higher expression of IL-4 and IL-10. However, 48 h after reperfusion - decrease in Th1 cytokines was less evident and IL-6 was markedly up regulated. PCNA analysis showed that regeneration occurs faster in kidney(MSC-treated) than in control 24hours. And also ratio of Bcl2/Bax was higher at treated animals after 24/48 h. ATN also is reduced (H&E analysis) on MSC-treated-kidney. Moreover, repair/regeneration in H&E analysis is highly increased in 24 h and it is sustained in 48 h.

Conclusion(s) Our data demonstrated that indeed MSC act early after injury, changing the inflammation profile toward Th2 profile that ultimately determines the organ outcome.

Grant: CNPq, Fapemig, Fapesp, Funepu, UFTM, UFSP

P4.130

Renal disease in HIV+ childrens

Serrano Griselda A.; Balbarrey Z.; Monteverde M.; Rodriguez Rilo L.; Goldberg C.J.
Hospital de Pediatria Juan P. Garrahan, Ciudad Jardin del Palomar, Buenos Aires, Argentina

Background HIV patients may develop several renal manifestation which vary depending on age, races and socioeconomic factors. HIV-associated nephropathy (HIVAN) may present with nephrotic syndrome and progressive renal disease. Collapsing focal and segmental glomerulosclerosis, microcystic tubular dilatation and mononuclear interstitial inflammation are frequent pathological findings. Thrombotic microangiopathy (TM) is not uncommonly reported among adults. In our institution, TM in pediatric patients is quite common, though rarely biopsied. The progression to end-stage renal disease and dyalisis may be rapid. Less than 50% develop HIVAN and diffuse mesangial hypercellularity (DMH) is the most usuall finding.

Methods 612 HIV-infected children were followed between 1989 and 2006 in 2 central hospitals in Buenos Aires. Ages ranged from 13 to 168 months. 11 had renal disease. 7 had clinical and haemathological evidence of TM. We report 3 HIV childrens biopsied with renal disease.Biopsies were performed under ultrasonography guide and routinely processed as kidney samples, with immunofluorescence in 2/3.

Results 2/3 patients with nephrotic syndrome showed diffuse mesangial hipercellularity, focal segmental glomerulosclerosis, atrophic tubules,and scanty interstitial lymphocytes. Immunofluorescence was negative and DMH was diagnosed. 1/3 showed TM. 7/8 of the non-biopsied cases

has HUS. As the frecuency of HUS in our country is high, only severe complicated cases get a kidney biopsy. The final non-biopsed case (1/8) had tubular proteinuria. The three patients biopsied died.
Conclusion(s) HIVAN in children has low incidence. In our experience there is a predominance of DMH and a high frequency of HIV-associated HUS. Non collapsing glomerulopathy was detected.

P4.131
Renal pathology associated with renin signal sequence mutation
Hulkova H.; Zivna M.; Ivanek R.; Sikora J.; Claes K.; Kapp K.; Elleder M.; Kmoch S.
Institute of Inherited Metabolic Disorders, First Medical Faculty and University Hospital, Charles University Prague, Prague, Czech Republic

Background A primary function of renin is the conversion of angiotensinogen to angiotensin, with the subsequent production of aldosterone. The renin angiotensin system (RAS) has also other widespread and diverse roles, including modulating erythropoiesis, cardiac hypertrophy and functioning through local RAS systems in many organs. Recessive mutations causing complete loss of renin synthesis resulted in renal tubular dysgenesis. With the exception of premature stop codon leading to benign hyperproreninemia, no other non-lethal mutations of the renin gene have been reported to date. We identified, using positional cloning, a family with the autosomal dominant inheritance of early onset hyperuricemia, anemia, chronic progressive kidney failure and a deletion of a leucine residue in the signal peptide of renin.
Methods Histology and immunohistochemistry performed in kidney biopsies of three patients. In-vitro functional studies and ultrastructural analysis.
Results In-vitro analysis showed that the mutation affected renin translocation and endoplasmic reticulum (ER) processing, resulting in reduced renin biosynthesis. Cultivated cells expressing the mutant protein showed activated ER stress, unfolded protein response, and reduced growth rate. Renal biopsies revealed progressive tubulointerstitial nephropaty, secondary focal and segmental glomerular sclerosis, and nephron loss. Expression of renin and other renal RAS components were decreased in kidney biopsy specimens.
Conclusion(s) The signal sequence mutation decreased renin biosynthesis and gradually reduced the viability of renin expressing cells due to chronic ER stress, affecting intrarenal RAS and leading to nephron loss and progressive kidney damage.

P4.132
A unclassifying renal cell carcinoma in a 36 year old man
Arslan Hacer E.; Uygun N.
Cerrahpaşa University, Istanbul, Turkey

Background A 36 year old man presented with shortness of breath,coughing and back pain.Clinical and radiologic examination of the lung showed multıple mass,medistinal lympadenomegali and heterogenous mass in the right kidney.
Methods Tru-cut biopsy ”unclassifying type in renal cell carcinoma” were reported. Right radical nephrectomy was performed.Hematoxylin-eosin staining revealed tubules and papillary architecture,clear cytoplasm and large nucleus, prominent nucleoli.Tumor extended renal capsule,perinephric fatty tissue,pelvis renalis,surrenal and all lymph nodes.
Results On these basis of these findings,the case was reported as “Translocation Renal Cell Carcinoma”.
Conclusion(s) Cytogenetic studies are ongoing.

P4.133
Changes in the tubular basement membrane in primary glomerulopathies
Kostadinova-Kunovska S.; Petrusevska G.; Jovanovic R.; Grcevska L.; Bogdanovska M.; Janevska V.; Kocmanovska-Petreska S.; Polenakovic M.
Institute of Pathology, Faculty of Medicine, Skopje, the Former Yugoslav Republic of Macedonia

Background Changes in the renal tubulointerstitial compartment have been found in almost all glomerular diseases. The damaged tubular epithelial cells (TECs) participate in the process of interstitial fibrosis through the mechanism of epithelial-mesenchymal transition (EMT) during which mature epithelial cells become myofibroblasts and deposit excessive amounts of extra-cellular matrix.
Methods We analyzed 50 renal biopsies from primary glomerulopathies stained with HE, PAS, Trichrom Masson and immunostained with Collagen IV, Cytokeratin, E-cadherin, Vimentin and aSMA. Semi-thin sections were stained with PASM.
Results The tubular basement membranes (TBM) in the fields of interstitial fibrosis and tubular atrophy were thickened on PAS and Collagen IV stainings, and delaminated on the PASM staining, with solitary inflammatory cells inside the TBM and between the TBM and TECs. Atrophic tubules were lined with flattened cuboidal TECs which showed weaker signal for Cytokeratin and E-cadherin (in comparison to non-atrophic tubules), as well as positivity for Vimentin, but not for aSMA.

Conclusion(s) In order to preserve their integrity, the damaged TECs initially express vimentin and produce larger amounts of collagen IV, which stabilizes their epithelial phenotype. We hypothesize that in due time, the damaged TECs start producing other types of collagen (I, III, VI), thus altering the composition of TBM, decreasing its stabilizing role and making way for their transformation into myofibroblasts positive for aSMA, ready to migrate into the interstitium and contribute to the interstitial fibrosis.

P4.134

Collagenofibrotic glomerulonephropathy

Reis Antonia M.; Custodio Bichuette F.; Ferreira Diniz Rabelo R.; Rodrigues Laura Pinto M.; Faleiros Carolina A.; Oliveira Aparecida F.; Correa Rosa R.
Federal University of Triângulo Mineiro, Uberaba, Minas Gerais, Brazil

Background Collagenofibrotic glomerulopathy (CG) - recently defined entity characterized by deposition in the mesangial glomerulus and in the subendothelial space of type III collagen fibers - spiraled and frayed collagen fibrils. Clinically it presents with nephrotic syndrome. The reported cases are still rare, principally in the West counties, as it is the knowledge in the diagnosis of this disease.
Methods Case reports.
Results Case 1: female patient, 21 years old, white; patient was previously healthy. No familiar history of renal diseases. She had proteinuria (1,6 g/24 h) and microscopic haematuria with one year of evolution. Case 2: female patient, 15 years old, white, with edema and hypertension for two months; urine analyses showed proteinuria of 2,49 g/24 h and dyslipidemia (total colestherol: 426 mg/dl and triglycerides: 264 mg/dl), without other alterations; she presented partial answer to the use of corticosteroids. Renal biopsy: in both cases, at light microscopy, the only alteration was discrete mesangial hipercelularity; the immunofluorescence was negative. The electronic microscopy found massive accumulation of spiraled and frayed collagen fibrils in mesangial and subendothelial areas compatible with collagen type III. At picrosírius method under polarized light, the fibers displayed birefringence and greenish staining, highly suggestive of type III collagen.
Conclusion(s) These cases of CG are probably the first ones to be reported in Brazil and in South America. Even being rare the CG deserves distinction as a differential diagnosis in the cases of nephrotic syndrome, mainly in adolescents/young adults. The CG illustrates the importance of electronic microscopy for diagnosis and best understanding of glomerulopathies. Grant: CNPq, Fapemig, Funepu, UFTM

P4.135

Development of tubular atrophy in old spontaneously hypertensive rats

Leh S.; Hultström M.; Iversen B.
Renal Research Group, Institute of Medicine, University of Bergen, Bergen, Norway

Background The pathogenesis of tubular atrophy in hypertensive renal disease is unknown. Here we investigate the relationship between arteriolar wall hypertrophy, glomerular changes and tubular atrophy using serial sections and morphometry.
Methods Old spontaneously hypertensive rats (SHR, 60 weeks, $n=7$) and normotensive Wistar Kyoto (WKY) rats (60 weeks, $n=3$) were used. Serial sections from glomeruli and corresponding proximal tubules and afferent arterioles from WKY (5 glomeruli) and SHR (5 normal glomeruli, 10 glomeruli with segmental sclerosis, 13 glomeruli with ischemic changes) were investigated. Afferent arteriolar media thickness, glomerular capillary volume fraction (indicating blood flow) and diameter of proximal tubular cross sections (indicating atrophy) were measured.
Results There was a significant correlation between glomerular capillary volume fraction and tubular diameter ($r=0.58$, $p=0.004$). Glomerular capillary volume fraction was also correlated with afferent arteriolar media thickness ($r=0.44$, $p=0.001$). Glomerular capillary volume fraction from glomeruli with segmental sclerosis was slightly reduced compared with normal SHR glomeruli ($p=0.03$), but was not different from WKY glomeruli. Glomerular capillary volume fraction from glomeruli with ischemic changes was reduced compared with all other groups ($p<0.001$ vs. WKY and SHR normal, $p=0.04$ vs. SHR segmental sclerosis). Only glomeruli with ischemic changes showed significant reduced proximal tubular diameter ($p<0.002$ vs. all other groups).
Conclusion(s) In conclusion, a relationship between segmental glomerulosclerosis and tubular atrophy could not be verified in old spontaneously hypertensive rats. We propose, that tubular atrophy is a functional consequence of glomerular ischemic capillary collapse probably secondary to arteriolar wall hypertrophy.

P4.136

Diagnostic findings in 3349 consecutive renal transplant biopsies, over a 8-year period, from the kidney and hypertension hospital

Franco Fabiano M.; Marujo Iglesias F.; Godofredo R.A.; Galante N.; Pestana Osmar Medina De Abreu J.
Paulista Medical School, Federal University of São Paulo, São Paulo, Brazil

Background The Kidney and Hypertension Hospital, from UNIFESP, is the largest renal transplantation center in the world, with around 549 renal transplantations per year. The Nephropathology Unit of our Medical Center consequently sees around 604 graft biopsies annualy. We aimed to analyze the frequency of the histopathological diagnoses in 3349 consecutive graft biopsies, over an 8-year period.
Methods The data were obtained from two database programs from the UNIFESP-EPM, Pathology Dept.
Results The most frequent findings were: Acute rejection (24.2%), Acute Tubular Necrosis (22.5%) and Chronic Transplant Nephropathy (21.4%). Other frequent diagnoses were: Chronic rejection (5.0%), Infarction (3.1%), Acute pyelonephritis (3.7%) and other infections (1.5%). Other histopathological findings amounted to 9.3% of the cases and, in 480 biopsies (5.9%), the sample was insufficient for diagnosis. Frequently, a single biopsy presented more than one histopathological feature.
Conclusion(s) There are very few similar studies for comparison in the literature. In the present series, acute rejection was seen in 24.2% of the cases, compared to a frequency between 12% and 30%, reported in other studies. Chronic rejection represented 5.0%, similarly to the value in other studies. Acute pyelonephritis was more frequent in our series (3.7%) when compared to the literature (1.6%).

P4.137
Histologic predictors of renal outcome in lupus nephritis

Cakalagaoglu F.; Tosuner Z.; Ari E.; Tuglular S.; Kaya H.
Marmara University, Istanbul, Turkey

Background Systemic lupus erythematosus (SLE) an autoimmune disorder which predominantly affects young women is frequently complicated by renal involvement. The first lupus nephritis (LN) classification was formulated by Pirani and Pollak in 1974. The new classification was modified by ISN (International Society of Nephrology) /RPS(Renal Pathology Society) in 2003. In the present study we reclassified LN patients by using the ISN/RPS classification and investigated the relationship between renal outcome variables and clinicopathologic features.
Methods We studied 34 patients with LN (26 female, 8 male, mean age of 34 years old) and were followed from 12 to 312 months, with a mean of 72 months. Clinical data of patients were collected from hospital files.Patients with biopsy diagnosed lupus nephritis were retrospectively classified according to the ISN/RPS.
Results The prevalance of each category was follows: Class III 32%, Class IV-S 38%, Class IV-G 17%, Class V 3%, class VI 6%.One patient was combined class III and class V.There was no class I and Class II in our series. Patients with class VI had massive proteinuria levels than other cases.Patients with class VI showed higher rate end stage renal disease. Both class IV-S and class IV-G showed higher scores of activitiy and chronicity indices. Subendothelial hyaline deposits were positive correlated with renal prognosis in our class IV and class III patients.
Conclusion(s) The ISN/RPS classification provided beneficial pathologic information. Data suggest that subendothelial hyaline deposits may be predictor in LN patients.

P4.138
Post-transplant membranous glomerulonephritis as a manifestation of chronic antibody mediated rejection

Jeong H.; Lim B.; Kim M.; Kim Y.; Kim S.
Yonsei University College of Medicine, Seoul, Republic of Korea

Background Autoimmune or alloimmune responses to unspecified glomerular antigens are considered as a pathogenetic mechanism in membranous glomerulonephritis (MGN) developing after transplantation.
Methods We tested C4d positivity using polyclonal antibody in renal allograft biopsy samples diagnosed as post-transplant MGN. A total of 18 cases (16 M and 2 F), including 2 recurrent and 7 de novo forms were the subject of the study.
Results Mean age of recipients at transplant were 38.2 yrs. Nine recipients (5 de novo, 1 recurrent and 3 unknown forms) received grafts from the opposite gender and 33% from the living related donors. Number of HLA-DR mismatch was one or more in 50% of unrelated donors. The biopsy indication was proteinuria in 67% with nephrotic range in 39%. On light microscopy, stage II was the most common ($n=9$). In addition to glomerular capillay IgG deposits, all but 2 cases having only sclerotic glomeruli were C4d-positive in glomerular capillary walls. Nine cases (3 de novo, 2 recurrent and 4 unknown forms) were also positive in cortical peritubular capillaries (PTCs): diffuse in 8 cases and focal in 1 case. Two of 3 cases associated with acute rejection and 3 of 4 cases associated with chronic rejection were PTC C4d-positive. The PTC C4d positivity increased with stages of MGN, but was not consistent in the follow-up biopsies/graft nephrectomy.
Conclusion(s) A higher frequency of PTC C4d positivity suggests an involvement of chronic antibody mediated injury in the evolution of post-transplant MGN.

P4.139

Role of HIF1a in renal cell carcinoma and consecutive bone metastases

Szendroi A.; Kardos M.; Tokes A.; Idan R.; Timar J.; Szendroi M.; Kulka J.; Szasz Marcell A.
Semmelweis University, Budapest, Hungary

Background Hypoxia may contribute to local and/or systemic tumor progression. HIF1a, targeting the transcription of over 50 genes involved in many aspects of cancer biology including cell survival, invasion and angiogenesis, is an essential component in changing the transcriptional response of tumors under hypoxia.
Methods 65 patients, who developed bone metastases after being treated for renal cell carcinoma, and 20 patients with no recurrence on long-term follow-up were evaluated for clinical and pathological parameters. Formalin-fixed, paraffin-embedded tissue was used to extract RNA and construct tissue microarray (TMA) from the samples. The expression levels of the HIF2a gene and those regulated by HIF1a: GLUT1, LDH5, GAPDH, CAIX, VEGFR, EGFR and EPOR were evaluated by qPCR analysis. Reference gene was B2M. The results of the PCR were confirmed with immunohistochemistry performed on the TMAs (HIF1a, EGFR, phosphoEGFR).
Results HIF1a (p=0,001), HIF2a (p=0,001), VEGFR (p=0,002) and EPOR (p=0,001) showed significant fold change in the metastatizing renal cancer patients as compared to non-metastatizing patients. Upon comparing the primary tumors with diatant metastases, HIF2a expression was elevated (p=0,034). The expression of LDH5 (p=0,061) was decreased and CAIX (p=0,059) was higher as well. The immunohistochemial data was in concordance with the PCR analysis.
Conclusion(s) The pharmacological manipulation of HIF1a in vivo has showed marked effects on tumor growth, and it could be the next personalized target for drug therapy. We also plan to evaluate the role of vHL and it's relation to the disease in this set of patients.

P4.140

Spectrum of biopsy-proven renal diseases in adults: a 6 year review of five regional renal biopsy databases in Poland

Perkowska-Ptasinska A.; Danilewicz M.; Halon A.; Klinger M.; Durlik M.; Okon K.; Andrzejewska A.; Szynaka B.; Mroz A.; Wagrowska-Danilewicz M.
Department of Transplantology and Nephrology, Warsaw Medical University, Warsaw, Poland

Background This is a first report on epidemiology of kidney diseases in Poland based on kidney biopsy databases from 5 nephropathological centers.
Methods All adult native kidney biopsies recognitions collected in years 2002–2007 in Warsaw, Lodz, Cracow, Wroclaw and Bialystok were retrospectively analyzed for histological type of renal disease and demographic data. Biopsies were processed for light and immunofluorescence microscopy, and electron microscopy in some cases.
Results The total number of analyzed diagnostic biopsies was 3259. Male to female ratio was 1782:1477, the mean age was 40.4 years (range 17–89). The most common recognition was glomerulopathy with the most prevalent type being IgA nephropathy (15.5%), followed by focal segmental glomerulosclerosis (FSGS) (14.8%), membranous nephropathy (10.37%), mesangial proliferative glomerulonephritis (9.02%), membrano-proliferative glomerulonephitis (8.35%), extracapillary glomerulonephritis (7.5%), and minimal change disease (4.3%). Among secondary nephropathies the most prevalent were lupus nephritis, and renal amyloidosis (9.6% and 4.8% of all diagnostic biopsies, respectively). Tubulointerstitial nephritis was reported in 2.36 % of all renal biopsies.
Conclusion(s) In Poland the most common disease recognition upon kidney biopsy in adults is chronic glomerulonephritis with a domination of IgA nephropathy. The most common type of glomerular injury is FSGS. Lupus nephritis predominates among secondary types of glomerulonephritis. This report constitutes the basis for the future Polish Registry of Renal Biopsies.

P4.141

A case of lupus nephritis presenting as Guillian-Barré syndrome: a case study and review of the literature

Caldas Lucia Ribeiro M.; Castro A.; Carvalho Filho A.; Tulius M.; Lozoya C.
Universidade Federal Fluminense, Niteroi, Rio de Janeiro, Brazil

Background To describe a case of systemic lupus erythematous (SLE) associated with severe diffuse lupus nephritis, class IV-G (A) diagnosed seven years after the appearance of an acute motor inflammatory polyneuropathy (Guillain-Barré-like syndrome - GBS).
Methods Diagnosis of a case of SLE and GBS by peripheral nerve biopsy and kidney biopsy.
Results This is an atypical clinical presentation of SLE revealed at the beginning with polineuropathy similar to GBS whose diagnosis was revealed after the development of nephritis.
Conclusion(s) SLE is a multisystemic chronic inflammatory disease with unknown etiology and autoimmune pathogenesis represented by autoantibody formation. The clinical manifestations are polymorphic and the clinical course is characterized by exacerbations and relapses of symptoms.

Nephritis is a classic and frequent form of SLE manifestation with prognostic implications after its diagnosis. Several neurological disorders are described in association with SLE, with frequent occurrence in lupus nephritis patients. Neurolupus, similar to lupus nephritis has a worse prognosis in the clinical evolution of the disease. Acute motor inflammatory polyneuropathy is one of the neurological manifestations of neurolupus similar to GBS. In this case report the neurological manifestation preceded the SLE diagnosis as an isolated clinical finding for a long period of time.

P4.142

Atypical renal angiomyolipoma

Vazquez Navarrete S.; Jimenez Peña R.; Diaz Lagama A.; Pinzon Bohorquez J.
Hospital del SAS de la Linea, La Linea, Cadiz, Spain

Background Renal Angiomyolipomas (AML) are unsual benign mesenchymal tumors composed of variable proportion of three distinct elements: adipocytes, smooth muscle and abnormal blood vessels. Although most of these tumors are easy to recognize some may differ greatly in the predominant component and show unsual histologic features.
Methods We describe a case of atypical AML of the kidney in a 43 years old women and we studied the clinicopathologic and the inmunohyistochemical features.
Results Microscopic examination reveled a neoplasm composed of pleomorphic epithelioid cells with numerous multinucleated cells, spindle cells, adipocytes and thick walled blood vessels. The epithelioid cells had a clear o pale eosinophilic cytoplasm which were sometimes located mainly in perivascular areas. The tumour was inmunoreactive for HMB-45, Vimentin and Smooth Muscle Actin while CKAE1-CKAE3, EMA, CEA, CD68, CD31, CD34, Factor VIII and S100 protein were negative.
Conclusion(s) In conclusion this AML variant can give rise to diagnostic confusion with RCC, renal sarcomas or metastases involving the kidney. Recognition of the characteristic pleomorphic epithelioid cells and their distribution with respect to blood vessels in the tumour, along with an inmunohistochemical panel, should allow the correct diagnosis to be made.

P4.143

BK virus nephropathy. Review of five cases

Mosquera Reboredo Manuel J.; Vázquez Martul E.; Pombo Otero J.; Alvarez Rodríguez R.; Vázquez Bartolomé P.; Hermida Romero T.; Fernández Rivera C.; Alonso Hernández A.; Valdés Cañedo F.
Complexo Hospitalario de A Coruña, Galicia, Spain

Background BK virus is member of the poliomavirus family and is related to JC and SV40 viruses.In human primoinfecction occurs in childhood with high seroprevalence rates(60–80%) in adults. BK virus cause a tubulointertitial nephritis due reactivation of latent infection in a immunocompromised host.In last years BK virus nephropathy has emerged as a significant cause of allograft loss linked to use of newer potent immunosuppressive drugs. Urine cytology is the screening technique looking for cells with viral inclusions(decoy cells).In positive cases renal biopsy is requires and usually show a tubulointertitial nephritis with focal tubulitis, that can mimic acute cellular rejection, and viral inclusions in tubular epithelium.Immunohistochemical staining(SV40 antigen),electron microscopic and DNA virus detection by PCR are useful for differential diagnosis between both entities.
Methods Review of BK virus nephropathy in our center.
Results Five BK virus nephropathy had been diagnosed in last 5 years in our center.Urine cytology,renal biopsy, electron microscopic and immunohistochemical study was made in all cases.All biopsies showed tubuloinerstitial infiltrate,viral inclusions in tubular epithelium and different grade of fibrosis and tubular atrophy.Inmunohistochemistry was positive in all cases and electron microscopic showed viral particles in two cases.DNA detection by PCR in paraffin-embedded tissue was positive in two cases.All patients lost graft function One patient developed a bladder adenocarcinoma three year after BK nephropathy diagnosis. All malignant cells were positive for SV40 antigen in inmunohistochemistry.
Conclusion(s) BK virus nephropathy is an important cause of graft loss. We propose that BK virus are involve in development of bladder adenocarcinoma

P4.144

Glomus tumour. Report of an unusual localization

Tortosa F.; Correia L.; Fernandes A.
Hospital de Santa Maria, Lisbon, Portugal

Background Glomus tumour is a rare benign, well-circumscribed, solitary mesenchymal neoplasm, usually located in the subungueal region of the fingers or affecting the deep dermis or subcutaneous tissues of the upper or lower extremities; it is generally associated with paroxysmal pain. It only rarely has been found involving visceral organs. Primary renal glomus tumours are extremely rare. Six previous cases of renal glomus tumours have been reported in the english literature, one of which was seen in the renal capsule. We report an additional case.
Methods A 65-year-old woman presented with a renal tumour detected by computed tomographic scan. A total nephrectomy was performed and revealed a 4,5 cm encap-

sulated tumour with a hemorrhagic cut surface, located in the inferior pole of the kidney.
Results Histologically, it had the usual morphology of a glomus tumour. The immunohistochemistry study showed positivity of tumour cells for vimentin, smooth muscle actin and collagen IV; they were negative for cytokeratin (AE1/AE3), desmin, HMB-45, CD31, CD34 and CD117. A diagnosis of glomus tumour was established.
Conclusion(s) Glomus tumour arising in visceral organs is rare, and those arising in kidney are extremely rare. To date, this case has followed a benign course without evidence of local recurrence or metastasis.

P4.145

Investigation of calcium channel competitors' effect in the kidney's operation in hypertensive of patients

Tziamalis M.; Patiakas S.; Palaiologou M.; Lytra E.; Koufos L.; Akrtopoulou K.
Dialysis Unit of General Hospital of Kastoria, Kastoria, Greece

Background The changes in kidney's operation were studied at the duration of treatment with calcium channels' competitors in patients with newly arterial hypertension diagnosed.
Methods 86 not diabetic patients (31 men and 55 women) means age 58,4 years, with recently (< 6 months) arterial hypertension diagnosed were studied. Calcium inhibitors (nifedipine, aminlodipine, lasidipine, felodipine etc) were administrated in these patients. The laboratorial - biochemical factors of the kidney's operation (urea, creatinine, electrolytes and urine acid) were determinated in all patients, at the treatment's beginning and after three months. The examinations were accomplished after 12 h fast with the chemoluminescence method. The statistically analysis was performed using $\chi 2$ test.
Results There were not ascertain statistically significant difference ($p<0{,}001$) in the indicators of kidney's operation in the patients before the treatment's beginning and afterwards three months. There was observed a lightly bending tendency of urea's values.
Conclusion(s) In the present study, it is obvious that the treatment with calcium competitors does not influence the kidney's operation in the hypertension patients.

Infectious disease pathology

P4.146

Application of the scientific method to create and implement sustainable pathology and general laboratory services programs in resource limited countries for PLWHA

Stevens Isis M.; Constantine N.; Croxton T.; Kelley W.
University of Maryland School of Medicine, Baltimore, Maryland, USA

Background There is a sincere need for quality laboratory systems for PLWHA and other HIV-associated pathologies. The Scientific Method was employed to create sustainable solutions for improving pathology and general laboratory services through capacity building and strengthening of laboratory systems.
Methods Program goals were to improve site level identification of various maladies for PLWHA via appropriate laboratory diagnostics. The Scientific Method was employed by 1) identifying the need for increased confirmatory diagnosis, forming a hypothesis of "If GLP, Quality Systems, and training are introduced, then diagnostic services and knowledge sharing in laboratory services will flourish"; 2) Designing programs around the needs; 3) Making observation through continuous monitoring; 4) Interpreting; and 5) reporting data to show areas of success and room for improvement.
Results Since 2006, over 400 laboratory staff, clinicians, surgeons, and pathologists have been mentored in QA/QC, GLP in specimen collection, processing, interpretation, and results reporting in 3 PEPFAR countries. Overall, programs were successful in comprehension of material presented, confidence of the participants in employing Quality Systems practices at sites, and sustainable transitioning to National Partners, all evidence that concepts were well understood and implemented.
Conclusion(s) Using this method highlighted challenges for improvement in the need for standardization of laboratory services, more personnel, enhanced communication, and documentation at various levels. However, this trend showed significant improvement in services and will undoubtedly build capacity in laboratory services to prove the sustainability theory.

P4.147

AIDS and changes in the immune status of genital tract

Corrêa Rosa Miranda R.; Cavellane Lourencini C.; Rocha Penna L.; Da Silva Beatriz R.; Faria Aparecido H.; Teixeira De Paula Antunes V.; Reis Antônia M.
Triângulo Mineiro Federal University, Uberaba, Minas Gerais, Brazil

Background It was demonstrated that HIV infection is associated with changes in the immune status of mucosal surfaces. The aim of this study was to evaluate the thickness of the epithelium of the uterine cervix and its association with AIDS, with the nutritional status and the number of Langerhans cells.
Methods Were used fragments of the uterine cervix from 25 women autopsied between 1980 and 2008, which were divided into two groups: without AIDS ($n=14$) and with AIDS ($n=11$). The measurement of the whole cervical

epithelium was performed through the system Image J and to immunohistochemical marking of Langerhans cells was used anti-S100.

Results The cervical epithelium was significantly thinner in women with AIDS and women considered undernourished, independently of AIDS. The number of Langerhans cells observed in the epithelium of the uterine cervix was significantly lower in the group of women with AIDS, and these women presented a higher frequency of immature or morphologically changed Langerhans cells.

Conclusion(s) We conclude that probably AIDS and undernutrition cause a reduction in the thickness of cervical epithelium and in the number and functions of Langerhans cells, contributing to changes in local immunity, which favors the onset of symptoms and opportunistic infections in the uterine cervix. The local deficient immunity associated with a thinner epithelium and more severe morphological changes could promote co-infection, reinfection and spread of the virus in patients with AIDS.

Grants: CAPES, CNPq, FAPEMIG, FUNEPU, UFTM.

P4.148

Chronic hepatitis with dual B and C hepatitis viruses infection: particularities of the histopathologic appearance

Zurac S.A.; Staniceanu F.; Popp C.G.; Nichita L.; Stoica A.; Bastian A.E.; Micu V.G.; Streinu Cercel A.

University of Medicine and Pharmacy Carol Davila, Colentina University Hospital, Bucharest, Romania

Background Chronic hepatitis due to dual infection with hepatitis B virus (HBV) and hepatitis C virus (HCV) is a severe liver disease with higher risks of developing cirrhosis or hepatocellular carcinoma than monoviral counterparts. Despite the high frequency of HBV-HCV chronic hepatitis reported to date, scant information regarding histopathological features is available.

Methods We analyzed 38 cases of HBV-HCV chronic hepatitis (BC group) versus 355 cases HBV chronic hepatitis (B group) and 756 cases HCV chronic hepatitis (C group). We analyzed necroinflammatory activity and fibrosis using Ishak semiquantitative score and also ground glass cells, pigment deposition, liver cell dysplasia; statistical analysis used Chitest and Student test (level of statistic significance $p<0.05$).

Results The necroinflammatory activity was significantly higher in BC group than in B group (P-BC/B=1.7×10–5) or C group (P-BC/C=6×10–11) due to higher portal inflammation and interface hepatitis; intralobular activity was similar (P-BC/B=0.5, P-BC/C=0.49). The fibrosis was also higher in BC group (P-BC/B=0.0003, P-BC/C=0.045). High fibrosis correlates with higher necroinflammatory activity in BC group than B or C groups. Slightly heavier hemosiderin deposition and lesser ground glass cells were present in BC group versus B group. Presence of small cell liver dysplasia associates mild necroinflammatory activity (P=6×10–6) and important fibrosis (P=1×10–212) in BC group.

Conclusion(s) HBV-HCV chronic hepatitis has a more severe course than HBV or HCV single infection chronic hepatitis (both a higher grading and staging with a tendency of more severe grading for an already severe staging).

P4.149

Conjunctival rhinosporidiosis: one case report

Ríos-Mazó Marilu D.; Dehollain Paula A.; Mazo Delia A.; Bermudez C.; Vera G.; Castillo M.

IVSS Hospital Raul Leoni Otero, Ciudad Guayana, Bolívar, Venezuela

Background Rhinosporidiosis is a rare chronic infectious granulomatose entity caused by Rhinosporidium, currently considered a cyanobacterium, Microcistis aeruginosa. It is of worldwide distribution although most described cases are from India and Sri Lanka. In Venezuela it is reported with more incidence in the states of Portugesa and Barinas (Venezuelan plains). It usually affects men between 20 and 40 years and is classified as an antropozoonosis that appears as nodular or polypoid slow-growing masses, highly vascularized and friable, that primarily affect the mucous membranes of the nasal region and more rarely the conjunctiva but can also affect other organs.

Methods We report the case of a school girl, 11 years old, from the state of Bolívar, who consults for progressive tumor growth of three months of evolution in caruncle of her right eye, painless, which causes discomfort. Surgical removal is decided. Macroscopically the tumor was ovoid, 0.5 x 0.4 cm, pink and soft. Microscopic examination of the tissue sections showed cystic structures observed in the mucosa with spheres of Rhinosporidiosis in different stages of maturation.

Results Macroscopically the tumor was ovoid, 0.5 x 0.4 cm, pink and soft. Microscopic examination of the tissue sections showed cystic structures observed in the mucosa with spheres of Rhinosporidiosis in different stages of maturation.

Conclusion(s) We concluded the diagnosis as ocular Rhinosporidiosis. After the extraction, the patient progressed satisfactorily without recurrence. We expose this case with a literature review given the rare condition manifested in an unusual age group.

P4.150

Correlation between oral and cervical human papillomavirus infection in HIV+ and HIV- patients

Lima Deus Moura M.; Costa Riera C.; Pereira Maria Miranda S.; Coelho Castro A.; Hernandes Tome P.; Aguiar L.; Ortega Lopez K.; Magalhaes Gallottini M.
University of São Paulo, São Paulo, PI, Brazil

Background Human papillomavirus (HPV) is one of the most prevalent sexually transmitted viruses worldwide with both oral and genital manifestations. The high prevalence of HPV infection among HIV+ individuals provides an opportunity to elucidate the relationship between oral and cervical HPV-infection in this group of subjects. Objective: to evaluate the possible association between oral and cervical infections in HIV-positive and negative patients.
Methods Eighty-six HIV+ (group 1) and 100 HIV- (group 2) women were recruited consecutively from a gynecologic clinic between April 2008 and March 2009. All subjects were given cervical and oral examination. Cytological samples were evaluated by the Hybrid Capture II technique from oral and cervical scrapings. Statistical analysis was performed using chi-square test and p values < 0.05 were considered significant.
Results HPV-DNA was detected in cervical scrapings from 43 (50%) HIV-positive subjects and from 45 (45%) HIV-negative subjects ($p=0.4959$). In oral samples, HPV-DNA was observed in 11 subjects from group 1 and in 2 subjects from group 2 ($p=0.0096$). High-risk HPV subtypes were prevalent in both groups and no difference between the groups was detected ($p=0.6801$). No subject showed macroscopic oral HPV-related lesion, whereas 13 (15.11%) from group 1, and 17 (17.00%) from group 2, presented with macroscopic genital lesion ($p=0.2129$).
Conclusion(s) HPV-DNA was more frequent in oral mucosa of HIV+ patients than HIV-. There was no association between oral and cervical HPV infection in HIV+ and HIV- patients.

P4.151

Identification of HPV-16 and epithelial dysplasia in papillomatous orogenitais lesions

Dias Pedra E.; Oliveira Paula S.; Rodrigues Resende F.; Silva-Junior A.; Ferreira Maria Soares S.; Rocha Lage M.; Pires Rodrigues Cordovil A.; Fontana Christina T.; Ferraro Tereza Lima C.; Menezes Soares N.; Lopes Silami V.
Universidade Federal Fluminense, Niterói, Rio de Janeiro, Brazil

Background Condylomata acuminata is a common sexually transmitted disease caused by Human papillomavirus (HPV) that often leads to persistent infections and recurrence. It is associated with non-oncogenic HPV 6/11 in more than 95% of cases. However, few studies have investigated the association of oncogenic types or epithelial dysplasia these lesions. The aim of the present study was to investigate the frequency of immunoreactivity to the antibody HPV16, location of mitoses and proliferating keratinocytes in genital condylomata acuminata and oral papillomas.
Methods Genital ($n=50$) and Oral ($n= 50$) lesions from HIV- and HIV+ patients were evaluated by histopathology and immunohistochemistry for Ki-67/HPV (Dako®) and HPV16 (CAMVIR-1, Biocare®), according to the manufacturer's guidelines. The main aspects investigated were positivity to HPV and HPV16, proliferation cell rate and abnormally superficial mitoses.
Results 78% and 52% of genital and 14% and 14% of oral showed immunoreactivity to HPV16 and HPV, respectively. Proliferating keratinocytes were observed in surface layers by 86% of genital and 36% of oral lesions. Abnormally superficial mitoses occurred in 66% of genital and 34% of oral lesions. The positive keratinocytes were more numerous in HIV patients.
Conclusion(s) Histopathological features indicative of epithelial dysplasia, even as association of oncogenic HPV16 with benign papillomatous lesions is common, especially in the genitals. But, should be confirmed by ISH since the manufacturers reported occasional reactions with HPV6/11. We believe that all lesions associated with HPV should be evaluated by histopathology and type of HPV.

P4.152

Identifying HIV infection in diagnostic histopathology tissue samples

Van Der Walt D.J.; Moonim T.M.; Alarcon L.; Freeman J.; Mahadeva U.; Lucas B.S.
St Thomas' Hospital, London, United Kingdom

Background St Thomas' Hospital, London is a referral Institute which sees a large number of HIV cases and haemato-oncology referrals. This study includes cases which presented clinically as lymphoma, tumour / inflammatory masses, unknown - which eventually turned out to be HIV associated pathology.
Methods 3 year period (2005–2007). Immunohistochemistry (IHC) records for p24 use on fixed tissue samples retrieved. Diagnostic biopsies, referrals & autopsy material Dako anti HIV-1 p24 antibody (clone Kal-1, dil 1:40). Case inclusion criteria – morphologically suspicious of HIV on H&E slides. Review of all 123 cases.
Results 37/123 cases (30%) showed positive expression of p24 in lesional follicular dendritic cells (FDCs). 11/37 cases were not clinically suspected to be HIV positive and had no

prior serologic evidence of HIV infection. These cases represented lymph node biopsies, tonsillar and nasopharyngeal biopsies and a parotid. In addition to expression on FDCs, in 22/37 (60%), p24 also highlighted mononuclear cells and macrophages. p24 was also identified HIV in lymphoid tissue in non-lymphoid organs such as the lung, anus, salivary gland and brain. Negative staining occurred in occasional known HIV positive cases, probably related to treatment or tissue processing.

Conclusion(s) Histopathology is of use in identifying HIV in tissue samples from lymph nodes and non-lymphoid organs. P24 IHC identifies HIV in morphologically appropriate scenarios but could be negative following therapy. P24 can pick up cases not known to be HIV positive allowing early treatment and better outcomes. In the future, p24 should be utilised in the systematic work-up of suspicious cases.

P4.153
Old infectious entities re-appearing because the population change in some neighbourhoods in Barcelona

López L.; Iglesias M.; Garcia M.; Murillo R.; Corominas J.; Casado B.; Munné A.; Serrano S.
Hospital del Mar, Barcelona, Spain

Background Gastrointestinal infections are a major cause of morbidity and mortality worldwide. Some unusual etiologic agents have been remerge because of immunocompromising conditions as well as sexual practices and immigrant populations, such as CMV, Mycobacterium tuberculosis, spirochetal infections, Whipple's disease, viral, parasitic and helmintic infections. Histologically the differential diagnosis of those infectious processes has to be done with the more usual clinical entities because they can have a similar clinical presentation and they can resemble microscopically.

Methods We searched for gastrointestinal infections cases diagnosed during the last five years (2003–2008), and correlated the histologic findings with the etiologic agents and the differential diagnosis.

Results The incidence of gastrointestinal infections has increased significantly in the last 5 years in our hospital (13/12058 vs 33/13475, p=0.01). Of 36 identified infectious the patogenous agents were 16 CMV, 3 Treponema sp, 2 Mycobacterium tuberculosis, 3,Tropheryma whippelii, 7 protozoal infections, 1 Strongiloides stercolaris, 1 Leishmania and 3 herpetic infection. Clinically, they usually present with abdominal pain and diarrhea. Grossly, ulcers are the most common in the endoscopy. Histologically, the type of inflammation can be quite different between pathogens, although not specific.

Conclusion(s) The study of the endoscopic biopsy has to include this type of pathology in the differential diagnosis. Moreover, microscopic findings are the most useful for the diagnosis because both clinical symptoms and gross findings are not specific of any of the entities in the differential diagnosis.

P4.154
Particularity of liver steatosis in chronic hepatis c with normal ALT levels

Aliev B.; Kamilov Haydarovich F.; Musabaev E.
Institute of Virology, Tashkent, Uzbekistan

Background Chronic hepatitis C (CHC) usually runs an asymptomatic clinical course. A number of histological features have been cited for their potential diagnostic value, including small-droplet fatty change. In this investigation particularity of the hepatic steatosis in the patients with CHC and persistently normal serum alanine aminotransferase (ALT) levels was studied (PNALT).

Methods We examined sections of formalin fixed, paraffin-embedded liver biopsies from 25 patients with CHC and PNALT stained by Hematoxylin and Eosin,Van Gieson's picro-fuchsin collagen stains. Histology activity index served to asses grading and staging of CHC infection.

Results A liver biopsy showed the presence of mild hepatitis and of microvesicular steatosis affecting about 30% of hepatocytes in 13 patients with CHC and PNALT. In the liver of the patients also was estimated appearance of lymphoid follicles and/or aggregates (F/A) within portal tracts and parenchyma. Concerning hepatic parenchymal steatosis a direct cytopathic effect of the virus has been considered. We also suggest that HCV-related hepatic steatosis might be the result of increased virus-induced iron storage eliciting a free-radical-mediated peroxidation - alteration of hepatic lipid metabolism.

Conclusion(s) Steatosis and lymphoid F/A are the major diagnostic features of CHC with PNALT.

P4.155
The importance of bone marrow biopsy in diagnosing fever of unknown origin in patients with aids

Menezes Soares N.; Damião Moreira R.; Lusis Kopschitz Praxedes M.; Pires Rodrigues Cordovil A.; Gabriel Henrique Daumas A.; Orlando P.E.; Damasceno Annete J.; Goncalves Andrade M.; Martins Dias M.; Augusto Uliana R.; Almeida Passalini R.; Lopes Gloria Silami V.; Dias Pedra E.
Hospital Universitario Antonio Pedro, Niterói, Rio de Janeiro, Brazil

Background Patients with AIDS have a greater probability of having bone marrow infections. Fever of unknown origin

is one of the main indications of bone marrow biopsy. Recent studies have shown specific diagnosis by biopsy in one third of patients with advanced disease.
Methods We analyzed bone marrow biopsies from the Anatomic Pathology Service of Hospital Universitário Antônio Pedro (5 years period). There were 100 biopsies from patients with AIDS. We observed H&E routine staining, Wade, Grocott and PAS.
Results The main clinical data were cytopenias (40 cases), fever and cytopenias (28 cases) and only fever (22 cases). There were 74 men and 26 women, with ages ranging from 4 to 61 years. Biopsies were able to diagnose 21 cases of histoplasmosis, 11 of atypical mycobacteriosis, 3 of Parvovirus sp., 3 of tuberculosis and 2 of histoplasmosis and Parvovirus sp. The positivity for infectious diseases in 40% of the biopsies confirmed it has good sensibility for the etiologic diagnosis of fever of unknown origin in patients with AIDS. Patients with fever associated with cytopenias and fever as the unique symptom had the greater percentages of positivity. The presence of granulomas was the most important morphologic feature for the diagnosis and the identification of the microorganisms.
Conclusion(s) We concluded bone marrow biopsy is simple, safe and very useful in the diagnosis of unknown origin fever in patients with advanced stages of AIDS and it enables specific therapy.

P4.156

Cerebral abscess as a complication of bronchiectasiae. Case report of autopsy finding

Filipovski Aleksandar V.; Janevska Boris V.; Banev G.S.; Dukova B.
Institute of Pathology, Skopje, the Former Yugoslav Republic of Macedonia

Background A 35 year old male died of septic condition with diagnosed suppurative meningitis. Autopsy was performed in order to discover the origin of this septic condition.
Methods A standard autopsy protocol was performed. Sections from every organ were taken for histology analysis. The sections were routinly fixed in 10% formalin fixative. The paraffin blocks were routinle stained with Hematoxyllin-Eosin for histological analysis.
Results The autopsy yelded a surprising discovery of bronchiectasie, that were not previosly diagnosed, with hematogenic spread of the infection to the cerebral cortex. Multiple small abscesses formed a confluent abscess measuring 5 sm in the left frontotemporal region of the brain. The abscess protruded into the ventricular sistem and into the subarachnoid space.
Conclusion(s) Brain abscesses due to complications from bronchiectasiae is a well known fact. However this condition is seldom found in this modern antibiotic era. This case report stresses the importence of the diagnosis of this condition.

P4.157

Cerebral hydatid cyst: case report

Yavuzer D.; Ergen C.; Dalbayrak S.; Yilmaz T.; Karadayi N.
Dr. Lutfi Kirdar Kartal Educational and Research Hospital, Department of Pathology, Istanbul, Turkey

Background Hydatid disease (echinococcosis) is a worldwide zoonosis produced by the larval stage of the Echinococcus tapeworm. It is usually endemic in regions where sheep raising is common (such as Middle Orient, Mediterranean, south of America, north of Africa and Australia). The principal localization of human infection are the liver and lung. It is rarely observed in the brain (0.5–4.5%). Headache and vomiting are the most common initial signs of cerebral hydatid disease.
Methods Case: A 17-year-old female was admitted to Department of Neurosurgery after a three-month history of intense headache. Cranial computed tomography (CT) and magnetic resonance imaging (MRI) scans revealed a large heteregeneous multiloculated mass in the right occipital lobe with marginal rim enhancement. She was operated and frozen section investigation was performed during surgery. Microscopically, we observed multipl small cystic areas containing fragments of eosinophilic laminated membrane and some protoscolices that surrounded by imflammatory reaction and fibrosis.
Results The diagnosis was hydatid cyst and total surgical resection was performed.
Conclusion(s) Hydatid cyst must be considered in the differantial diagnosis of cerebral space-occupying lesions, especially in endemic areas.

P4.158

Clinico-pathologic evaluation of the canine heartworm infestation

Ranjbar-Bahadori S.; Ashrafi-Helan J.; Jamshidi K.; Kashefinejad M.
Islamic Azad University, Garmsar Branch, Garmsar, Tehran, Islamic Republic of Iran

Background Heartworm or Dirofilaria immitis is a nematode that lives in right ventricle, pulmonary artery and posterior vena cava.
Methods One hundred and twenty two stray dogs were trapped and examined for D. immitis. Then, five dogs with dirofilariasis were selected and hematological and serum biochemical values were assessed in these dogs. Necropsy

of infected dogs was also performed for histopathological examination.
Results The assessment of hematological parameters showed mild anemia in dogs with D. immitis, with a significant decrease ($p<0.05$) in the number of red blood cells. Data analysis also showed an increase in number of eosinophil. However, there was no significant difference between infected and non-infected dogs ($p>0.05$). Significant difference was detected for AST activity between groups with higher activity of AST in infected dogs ($p<0.05$). In microscopic examination of renal tissue, severe congestion in medullary and cortical juxtamedulary portions along with inflammatory cell infiltration of inflammatory cell were noticed. In cardiac tissue, there was vascular engorgement, and interfibrilar accumulation of edematous fluid in myocardial muscle fibers. In pulmonary tissue, emphysamatous foci as well as areas of interstitial pneumonia were found. In histopathological sections prepared from eye, except congestion and edema, particularly in retina of eye, no other lesion was observed. There were scattered foci of coagulative necrosis in hepatic tissue.
Conclusion(s) Assessment of blood and biochemical parameters can be used for diagnosis of D. immitis and this nematode can involve some organs of infected animals because of its circulating microfilariae.

P4.159
Estimation sepsis severity based on detection of systemic inflammation development: application of systemic inflammation scale

Zotova Vladimirovna N.; Gussev Yuryevich E.
Scientific Research Institute of Immunology and Phisiology, Ural Branch of Russian Academy of Sience, Yekaterinburg, Russian Federation

Background A theory and a methodology of Systemic Inflammation (SI) studying is the significant part of PIRO concept. We consider SI development from the position of typical pathological process, rather than the syndrome model. SI diagnostics is based on two principles: 1) a definition of level of systemic inflammatory reaction (SIR) (not SIRS), that characterizes the innate immune mechanisms of local inflammation focus; 2) a detection of different SI phenomena: systemic alteration, distress-reaction of neuroendocrine system, DIC, MOD. The SI scale created on the base allows to enter SI and pro-SI, and to define dominate phenomena and stage of SI.
Methods The patients of the following groups entered into the retrospective study: healthy persons ($n=50$); elderly persons ($n=22$); patients with sepsis on 1–3 days ($n=90$) and on 5–7 days ($n=25$) after admission at ICU. The patients with MODS including shock ($n=52$) and lethal outcomes (LO) ($n=24$) were studied separately as well.
Results We identified SI development in patients with sever sepsis, septic shock and lethal outcomes in 61.4%, 100% and 87.5% of cases respectively. AUC values predicted LO for SOFA, SI scale and more then 2 criteria SIRS achieved 0.95, 0.95 and 0.72 respectively.
Conclusion(s) SI scale intends for identification dominate pathogenic mechanisms of MOD and therefore for correction pathogenic and in some cases etiologic treatment. The scale doesn't interchange SOFA and other scale of MOD.

P4.160
Kaposi sarcoma with concomitant intralesional tuberculosis

Sing Y.; Ramdial K.P.; Subrayan S.; Sookhdeo D.; Ramburan A.; Calonje E.; Sydney C.
Nelson R Mandela School of Medicine, Durban, KwaZulu Natal, South Africa

Background Co-lesional cutaneous AIDS-KS and TB is undocumented. In documenting concomitant cutaneous AIDS-KS and TB, assiduous appraisal of KS for granulomatous inflammation and optimal investigation thereof to confirm a tuberculous etiology is stressed.
Methods Retrospective appraisal of all skin biopsies diagnosed as KS and TB
Results 9 males and 7 females, 21 to 44 years. Skin biopsy findings were the sentinel of HIV infection in 9/16 patients and of visceral TB in 8/16 patients. In 5 patients, the current skin lesions served as the basis for confirmation of non-compliance to anti-tuberculous treatment. M. tuberculosis was cultured from sputum or nodal tissue. Histological assessment confirmed nodular and plaque KS in 12 and 4 cases each, respectively. Necrotising, non-necrotising and a combination of both was present in 8, 3 and 5 biopsies each, respectively. AFB on ZN staining and corroboration of M. tuberculosis on PCR confirmed TB in 15/16 biopsies. The biopsy with histological appearance of lichen scrofulosorum in plaque KS did not demonstrate AFB or M. tuberculosis DNA, however the cutaneous clinical lesions, association with nodal TB and response to anti-tuberculous therapy, confirmed a clinicopathological diagnosis of lichen scrofulosorum in KS.
Conclusion(s) Characterised by aetiological and histomorphological diversity, granulomatous inflammation in KS requires optimal use and appraisal of histopathological and molecular techniques to confirm M. Tuberculosis aetiology, as the identification of KS and TB may serve as a clue to HIV infection, systemic TB, therapeutic non-compliance and as a poor prognostic parameter of KS.

P4.161

Rhino-orbital mucormycosis in a bone marrow transplant recipient

Diamanti E.; Argyrakos T.; Lianou A.M.; Kara P.; Kopaka M.; Manaka C.; Vourlakou C.; Karakasis D.
Evaggelismos, Athens, Attiki, Greece

Background We present the case of a 35-year old male with acute biphenotypic leukemia, diagnosed in November 2005, who received bone marrow transplant from a non-relative compatible donor. Two years after the transplantation the patient was admitted to our hospital due to fatigue and dyspepsia and 10 days later he developed periorbital edema and a necrotic lesion in the hard palate. Magnetic resonance scan revealed an inflammatory lesion of the soft tissues of the skull extending to the right ophthalmic orbit suspecting a fungal infection. A diagnostic biopsy was performed that led to the surgical excision of the right ophthalmic bulb.
Methods Examination of the biopsy and of the excised ophthalmic bulb revealed infiltration of the bulb by a fungal mould in a background of severe inflammatory response.
Results The observed fungi were characterized by irregular in diameter and in wall thickness, elongated or round hyphae with right angle formation and without septa. The surrounding tissues were ischaemic with areas of hemorrhagic necrosis, invasion by the fungi of the optical nerve, the mandible and the blood vessels with subsequent thrombosis of them.
Conclusion(s) The morphological characteristics of the fungi established the diagnosis of orbital Zygomycosis (Mucormycosis). The patient was treated with liposomal Amphotericin B and Posaconazole. Four months later the patient relapsed with a subsequent spreading of the fungus to the brain and he is currently being treated in the intensive care unit.

P4.162

Sudden death during sports activity. An unusual cause

Henriques De Gouveia Mota R.; Nikolic Gaspar D.; Eiras Maria L.; Costa Santos Matias F.; Costa Santos Matias J.
Instituto Nacional de Medicina Legal, I.P., Lisboa, Lisboa, Portugal

Background Sudden Death is a universal everlasting concern, since it occurs unexpectedly and as a consequence of a broad spectrum of causes.
Methods The authors report a case of an apparently healthy 49-year-old male that dropped dead during athletics training, immediately after complaining of chest pain. A postmortem examination was performed.
Results The autopsy revealed diffuse pulmonary œdema, œdema of the myocardial intersticium and signs of acute, "functional" heart dilation, coronary atherosclerosis, generalized organ vascular congestion, fibrous thickning of splenic and hepatic capsules, as well as multiple necrotic liver granulomas, eosinophil-rich (with degranulation), some of which contain foreign bodies whose morphology is consistent with Schistosoma mansoni's eggs. Toxicology was negative.
Conclusion(s) Schistosomiasis affects 200 million people in the world. Some are assymptomatic and other present either acute or chronic disease. Death may result from different underlying mechanisms. In the present case, the data suggests that the final, sudden and unexpected event may have supervened from anaphylatic reaction with acute lung œdema as a consequence of parasitic allergic hepatitis aggravated by the effort of sports activity.

P4.163

A study on infections of Candida species, distribution and their resistance to commonly used antifungal drugs

Charalampous C.; Patiakas S.; Mitsikaris D.; Palaiologou M.; Alexidis I.; Xiropoulou E.
Internal Medicine Clinic of Psychiatric Hospital of Thessaloniki, Kastoria, Greece

Background To study the cases of the isolation of different Candida (C.) species from cultivations of biological fluids, their distribution and thei resistance to commonly used antifungal drugs.
Methods Instrument of our study was 63 cases in which Candida was isolated.The fungus was found in urine,pus, stools, bronchial secrations and other biological fluids. All these were vaccinated in selective nutritive mediums (Saboureaud with TTC) and were incubated in 37 C for 1–4 days however their identification and antifungogramm was done with the API and ATB Fungus.
Results There were found 46 cases with C. albicans (percentage 73%), 7 with C. tropicalis(11%), 3 with C. lusitaniae (4.8%), 2 with C.parapsilosis (3.2%), furthermore three other different species.Their resistance was, for C. albicans which was isolated from the majority of the cases, 11% in Amphotericine B, 31.7% in Ketoconasole, 22.2% in Mikonazole, 1.6% in Nystatine, 9.5% in Fluocytosine and 36.5% in Econasole
Conclusion(s) 1) C. albicans dominates the case of fungal isolations with percentage of 73%. Its resistance -even though low in Amphotericine B – was concidered increased in the most antifungal drugs. 3) This fact is considered particularly concening, if we take into account a)that in 15 cases (32.6%) Candida was the cause of an infectious disease and not just a colonisation and b) that the

systematic infections from Candida are a more and more increasing problem for patients under chemotherapy, those under Cortisole therapy, immunodeficient, premature babies, transplanted, polytraumatised.

P4.164

Characteristics of fatal SIRS cases of 2006–2009 years in Riga

Kleina R.
Riga Stradins University, Riga, Latvia

Background Aim is to evaluate the most common variations of SIRS and MODS in some hospitals of Riga
Methods We have investigated 70 fatal SIRS cases from pathology records of Riga Easter Clinical University Hospital, Pathology Centre and clinical epicrises. Histological specimens were stained with H/E and some immunohistochemical methods. We took into consideration also some laboratory tests. Sepsis cases were verified bacteriologically and/or microscopically.
Results The most common reasons of SIRS were: urgent surgery cases (27,4%), bacterial endocarditis (12,9%), infectious diseases including HIV cases (30,6%). Patients were from home without treatment, isolation hospital, prisons and different departments of general hospitals. The mean age of patients with SIRS and HIV was 39 years, but in others 60,1. The amount of leucocytes was a bit increased, but in more permanent cases around 30000.Liver tests were elevated due to alcoholism. Staphyloccocus aureus was proved in 41,6%. In 14,8% of cases diagnosis of SIRS was missed.
Conclusion(s) 1. Mainly fatal cases of SIRS were from surgery due to gastrointestinal diseases with peritonitis and compromised immune status in bacterial endocarditis and lung pathologies. 2. Between concomitant diseases in young patients were HIV infection but in more aged - severe atherosclerotic complications, hepatic steatosis and diabetes mellitus type 3. There is a lack of direct correlations between laboratory tests and severity of SIRS as secondary inflammatory changes of organs were expressed in 32% but predominantly were microcirculatory, injury and coagulation disturbances.

P4.165

Characterization of the cellular phenotype of the lalt in the false vocal cords in autopsies of individuals with aids

Abate Tavares Resende ESilva D.; Olegário Pacheco J.; Rossi Esilva Calciolari R.; Salge Marques A.; Reis Antônia M.; Teixeira Antunes V.; Castro Costa Da Cunha E.; Miranda Correa R.
UFTM, Uberaba, Minas Gerais, Brazil

Background In individuals infected with aids there is a decrease in the number of cells responsible for immune response, which influences the cell population of lymphoid follicles (LF) found in the false vocal cords (FVC).
Methods We studied 71 larynges of autopsied adults in the Hospital of Triângulo Mineiro Federal University. For the morphological analysis of LF were used the hematoxylin-eosin staining and Picro-sirius. The immunohistochemistry was performed with antibodies: Anti-CD20, anti-CD3, anti-CD68 and anti-Follicular Dendritic Cells.
Results Of the patients studied 52 (73.2%) had aids. In patients with HIV, the number of T lymphocytes significantly varied ($p=0.007$), the same happened with the macrophages ($p=0.024$) when compared with the patients without aids, even when linked to respiratory infection. The amount of fibrosis was lower in patients with aids ($p=0.002$), and in these cases, the cell number observed was lower in those who presented respiratory infection. In relation to malnutrition, the aids patients had lower body mass index ($p=0.002$), when malnutrition was isolated there were no significant differences in the cells examined.
Conclusion(s) The LF in FVC represent the immune status of patients with aids, with reduction of immune cells and changes in fibrosis' distribution. The malnutrition does not appear to directly influence the amount of cells of the immune system.

P4.166

Nanoparticles and prions. "A dangerous duet"?

Tereshchenko Pavlovna V.; Bezuglaya Vladimirovna M.
Institute for Sorption and Endoecology Problems (National Academy of Sciences of Ukraine), Kiev, Ukraine

Background Nanopathologies and prion infections present two urgent medical-biological problems. Our goal was search for possible links between these concepts. Scientific data were used as material.
Methods Analytical methods were applied.
Results It is accepted nowadays that nanoparticles (NPs) are capable of altering tertiary structure of proteins with transformation of their functions, i.e. they promote the appearance of pathological invasive forms of prion-protein. Hence, NPs can act as inducers/stimulators of conformational prion-associated pathology. It is also known that pathological invasive forms of prion-protein are extremely resistant towards physicochemical impact. It is widely thought that prion is the last living organism to die. As the sizes of pathogenic prion-proteins, determined on the basis of their molecular mass (33–35 kD), do not exceed 100 nm, they can be conditionally defined as "biological nanoparticles". The fact that both

traditional NPs and invasive prions differ markedly from basic objects in usual physicochemical state says for such interpretations, i.e. in this case the size essentially determines the properties. An indirect argument confirming this fact is the following: viruses, sized both below and above 100 nm, reveal the trend to environmental resistance and unpredictability increase with decrease of their size.
Conclusion(s) 1) Rapid development of nanotechnologies poses the danger of increased morbidity of prion-associated diseases. 2) Theoretical possibility of elimination of prion-protein conformations using NPs can not be excluded.

Miscellaneous

P4.167
Medical rehabilitation for patients with myotonic syndrome of lumbar osteochondrosis

Filipovich Nicolaevich A.; Smychek Borisovich V.
Research Institute of Medical Assessment and Rehabilitation, Minsk, Belarus, Minsk, Belarus

Background 78 patients 21 to 60 years old with myotonic syndrome of lumbar osteochondrosis were examined.The examination included the assessment of neurologic condition of muscles, CT and MRI of back bone lumbar department.
Methods Clinical methods, electromyography, revasography
Results In 69.2% MT-syndrome patients the associated damage of two or more muscles was found to prevail. The most vulnerable muscles appeared to be gastrocnemius, gluteus medius, quadriceps femoris, rectus abdominis and externalis obliquus, peroneal, piriform and lumbar quadrate muscles, gluteus maximus, gluteus minimus, adductor and abductor thigh muscles. Medical rehabilitation course for malfunctioning extremity was tested on 27 MT syndrome patients. The course included oral reception of katadolon pills, 8 to 10 sessions of traction on Fintrac-471 table with applied effort of 3 to 55 kg and acupuncture of points of general action as well as those of vascular autonomic nervous system orientation (G14, MJ6, E36, RP6, TR5, V40) and locally-segmented points related to problematic muscles (AT60, VB30 with deep introduction to stimulate piriform muscle; VB 34, VB41, F3). The course consisted of 12–15 sessions.
Conclusion(s) After treatment, pain in malfunctioning extremity completely disappeared in 19 patients, or essentially decreased in 6 patients while the tolerance to physical activity increased. We have also found that katadolon not only had analgesic and neuroprotective, but also myorelaxing effect on muscles of pelvic girdle and feet in patients with acute and chronic pain syndrome.

P4.168
Original model of secondary osteoarthritis following spontaneous cranial cruciate ligament rupture in dogs

Teodoro RosoliaW.; Silva Coutinho A.; Yoshinari Hajime N.
Universidade de São Paulo, São Pauo, São Paulo, Brazil

Background We describe an original experimental model of OA which permit us to understand the pathogenesis of OA, doing laboratorial analysis of joint material collected at different time after Spontaneous Cranial Cruciate Ligament Rupture in Dogs (CCLR).
Methods Twenty male animals, younger than 5 years old (20 to 40 kg) with CCLR were submitted to arthrotomy for articulation stability and had articular fragments removed for analysis. The Group A (10 animals) was operated before 20 days of CCLR and Group B (10 animals) after 20 days of lesion. Seven animals with pre-existent OA (MI), and 7 normal animals (MII) were the control groups. The animals were submitted to clinical and radiological evaluations. For the morphological study, the cartilage fragments were stained with H&E and Picrossirus. The score for OA severity was quantified using Safranin-O stainning.
Results Radiographic data showed that narrowing of joint space, osteophytes and erosions were more prominent in Group B animals. Histological exams done in animals from Group A showed irregularities on articular surface, reduction on the number of chondrocytes and collagen fibers remodeling. Animals from Group B exhibited deep fibrillations, presence of chondrocytes clusters on the intermediate area of cartilage, osteophytes and total disorganization of the collagen fibers net.
Conclusion(s) The spontaneous model of canine OA reproduces the clinical, radiological and morphological alterations viewed in human OA. We conclude that this model is useful to test drugs and to understand OA pathogenesis.

P4.169
The immunoassay and MTA test of blood serum. Help to assess the progress of demyelinisation process in multiple sclerosis patients

Filipovich Nicolaevich A.
Research Institute of Medical Assessment and Rehabilitation, Minsk, Belarus, Minsk, Belarus

Background 4 groups of patients were distinguished: (1) latent phase with low MTA level (7.6±1.2 units against 3.9±0.82 in control group), (2) slow progradient phase (20.4±0.68), (3) acute phase (40.7±0.83) and (4) fast progradient phase (75.6±4.9).
Methods CT and MRI of cerebrum and spinal cord, immunoassay and a patented radioimmunobiological assay

for measuring the myelinotoxic activity (MTA) of blood serum were carried out.
Results In group 1 the increase of T-a lymphocyte (from 28.0±2.9 to 41.6±2.1%), CD22 (from 9.56±0.81 to 28.5± 0.15%). In group 2 the significant decrease of CD22 (16.0±0.58%; $p<0.001$), CD4 (25.7±1.29%) and CIC (84.34±3.88) levels in blood serum was observed whereas CD8 level increased (31.4±1.1%) and a small induction of inflammation cytokines was noted (TNF-α=39.7± 2.9 pg/ml; IL-8=412.0±12.4 pg/ml). In group 3 the increase of CD8 (29.6±2.41%), IL-1.2 (16.6±0.7%), IgG (15.3±1.9), IgA (2.57±0.22), IgM (2.41±0.15 pg/ml), CIC (94.65±3.1) levels were observed while CD22 level decreased (17.0±0.63%; $p<0.001$).
Conclusion(s) In group 4 the increase of CD4 (36.7± 0.20%); CD8 (18.3±1.5%), IL-2R+ (18.0±0.65%; $p<$ 0.001), IgG (14.3±0.74), IgA (2.63 ± 0.26), IgM (2.61± 0.13 g/l) and CIC (105.36±3.39) levels in blood serum was observed whereas the CD22 declined to 18.0±0.96%; $p<$ 0.001. A significant decline of CD8 antigen level (from 29.6±2.41 to 18.3±1.5%; $p<0.001$) coupled with the CIC level (from 94.65±3.1 to 105.36±3.39) compared to those in group 3 patients were noted.

P4.170
The long term results of rehabilitation of multiple sclerosis patients

Filipovich Nicolaevich A.
Research Institute of Medical Assessment and Rehabilitation, Minsk, Belarus, Minsk, Belarus

Background Long term results of treatment of multiple sclerosis were studied. The dynamic monitoring of 110 patients over the period of 1 to 1.5 years following the successful in-hospital treatment of MS was carried out.
Methods Clinical methods, CT and MRI of cerebrum and spinal cord, and a patented radioimmunobiological assay of the myelinotoxic activity (MTA) of blood serum were used.
Results Four groups of patients were distinguished: group 1 (36 patients; 32.7%) – patients with low MTA level (4.56*0.7 units) after successful hormone therapy. No rehabilitation was required out afterwards. Group 2 included 41 patients (37.3%) with low MTA level (3.76*0.81) after hormone and corrector therapy; a rehabilitation course was carried out at a later stage. Group 3 consisted of 22 patients (20.0%) that required long term immunomodulating therapy due to a higher rate of demyelinisation (MTA= 19.2*0.43). The remaining 11 patients (group 4, 10.0%) with moderate rate of demyelinisation (16.4*0.52) were prescribed general health improvement therapy and rehabilitation based on intensive motional activity and physical exercise.
Conclusion(s) Hormone therapy helps to reduce the demyelinisation rate to acceptable level within 2 to 4 month. The subsequent rehabilitation helps to achieve the extended remission period. However, long time after treatment of acute MS the hormone therapy is not justified.

P4.171
Use of fMRI and MTA assay of blood serum for diagnosis of initial phase of multiple sclerosis

Filipovich Nicolaevich A.; Filipovich Semenovna N.
Research Institute of Medical Assessment and Rehabilitation, Minsk, Belarus, Minsk, Belarus

Background Two groups of patients were distinguished on the basis of MTA measurements. Group 1 included 46 mono-symptomatic patients with slightly increased MTA of blood serum (9.8±1.3 units compared to 3.9±0.82 in control group) and spinal fluid (11.2±1.2 units compared to 5.9±1.4 in control group). Group 2 consisted of patients with polysymptomatic course of MS. Clear increase in MTA level (18.9±0.92 for blood serum and 23.4±0.7 for spinal fluid) compared to both control group and group 1 was noted.
Methods RI of cerebrum and spinal cord and a patented method for measuring the myelinotoxic activity (MTA) of blood serum and spinal fluid were used. 75 initial MS patients 16 to 35 years old were examined.
Results onosymptomatic start of MS was found in 46 (61.3%) patients, and polysymptomatic MS in 29 (38.7%) patients. MRI of cerebrum and spinal cord revealed focal points of decreasing T-1 W / increasing T-2 W signal in 50 (70.7%) of examined patients. Therefore, the diagnostic importance of MRI of cerebrum and spinal fluid at the initial phase of MS is not very high.
Conclusion(s) he diagnostic importance of MRI of cerebrum is not high at the initial stage of MS. However, MRI in combination with MTA assay of blood serum greatly helps to reveal the initial MS in vast majority of cases.

P4.172
Pathologists and the Stendhal´s syndrome (Florence syndrome)

Cortés Amparo V.
Hospital Universitario Dr. Peset, Valencia, Valencia, Spain

Background Pathologists have the privilege of facing daily the microscopic world, which presents an unlimited variety of images, some of them surprising and wonderful. This study tries to verify if there is a relationship between the beauty of the human body tissues and other forms that exist in nature and even in art. Can the pathologist suffer

Stendhal's syndrome (= overdose of beauty) or the vision of these charming shapes can be healthy for him/her?
Methods Searching for outstanding normal and pathologic microscopic images in my own archive, textbooks and the web. Reading texts that relate science and art. Searching for thoughts and sentences possibly useful in this context coming from writers, phylosophers, scientists and from other cultures.
Results There is a strong connection between some of the microscopic patterns and other structures found in nature as well as in universal symbols belonging to human knowledge.
Conclusion(s) Although the pathologist's main role is to diagnose lesions accurately, during this process it is possible to live pleasant and gratifying moments if he/she tries to look not only with the eyes, but also with a deep sensitivity for discovering and enjoying the small wonders that exist in our daily work.

P4.173
Does lactoferrin behave as an oncofetal antigen in osteocartilagineous tumours?

Ieni A.; Barresi V.; Grosso M.; Tuccari G.
Department of Human Pathology, Messina, Italy

Background Lactoferrin (Lf) is an 80 kDa basic iron-binding glycoprotein which has been extensively investigated by immunohistochemistry in many human normal and neoplastic tissues. Nonetheless, it has never been evaluated in human osteocartilagineous tissue.
Methods In the present study, Lf expression was investigated by immunohistochemistry in 25 foetal or embryonal human bone and cartilagineous tissues (8–34 weeks of gestation), in 10 adult normal bone samples as well as in 57 formalin-fixed paraffin-embedded osteocartilagineous tumours.
Results Lf expression was found in the cytoplasm, and sometimes in the nucleus, of mesenchymal periosteal cells, chondroblasts and osteoblasts, in embryonic and foetal skeleton samples. In particular, the immunoreactivity for this iron-binding glycoprotein increased from the tenth to twenty-sixth weeks of gestation, and it disappeared by the end of pregnancy and in the adult normal osteocartilagineous specimens. Pertaining to the neoplastic osteocartilagineous samples, Lf immunoexpression was encountered in 10/10 giant cell tumours, 5/7 osteoid osteomas, 3/3 chondroblastomas, 3/3 chondromyxoid fibromas as well as in a single case of adamantinoma and myeloma.
Conclusion(s) Basing on our findings we may hypothesize that Lf behaves as an oncofetal antigen, which is present at high concentrations in the embryo and fetus during early development of life, playing a role in bone growth, by the contrast, Lf was undetectable or present at low concentrations in the adult tissues; where it appears as the result of activation of the controlled genes by a yet unknown mechanism in association with cancer.

P4.174
High quality immunohistochemistry staining performance: the use of specific structures/elements in normal control tissue

Mansson Svensson S.; Nielsen M.; Them Andersen B.; Bagge Nielsen S.; Feldballe Rasmussen O.
Dako A/S Denmark, Glostrup, Denmark

Background A key prerequisite for monitoring optimal protocol performance is to use proper controls. In this study, we show the power of using easy accessible control tissue with well-defined marker-specific control structures. This approach was integrated during development of a new series of 110 high quality FLEX Ready-to-Use antibodies.
Methods Optimal reaction pattern in control and clinical tissue was described in collaboration with nine internationally acknowledged experts within immunohistochemistry. For each marker, marker-specific control structures, comprising high expression (HE) and low expression (LE) cellular elements/structures in specific control tissue, were defined. These were typically present in normal tissue.
Results Generally, easily accessible normal control tissue such as tonsil, colon/appendix and liver was used to monitor protocol performance. The staining intensity for a given marker and protocol was typically stable among different samples for the majority of normal tissue types, whereas generally it varied among different clinical tissues. Within the normal control tissue, a variety of cellular elements/structures showed variable intensity for many of the markers included. However, when evaluating marker-specific HE and LE structures, changes in protocol and performance were easily reflected.
Conclusion(s) Designated easy accessible control tissue with well-defined cellular structures/elements reflecting variations in protocol performance is a superior tool to monitor IHC protocol performance. These controls are recommended as part of Dako´s new FLEX Ready-to-Use antibody series and can be implemented by the individual laboratories as controls to increase quality and standardize immunohistochemistry performance in the daily routine.

P4.175
Immunohistochemical analysis of antigen expression in hepatoblastomas

Patsiaoura K.;Katsiki E.; Nikolaidou C.; Tatsiou Z.
Pathology Department, Hippokration General Hospital, Thessaloniki, Greece

Background Hepatoblastoma, although rare, is the most common malignant neoplasm of the liver in children and 90% are seen in the first 5 years of life. The histological diagnosis of hepatoblastoma relies on the identification of typical morphologic features but in many cases especially in needle core biopsies, it must be distinguished from other pediatric small round blue cell tumors involving the liver.
Methods Cases selected for our study were those where an initial diagnosis of hepatoblastoma was made, five on needle biopsy, four on liver segmectomy and one on liver lobectomy speciements. We reviewed ten cases of hepatoblastomas admitted to our department from 1991 to 2009. The patients were 3 males and 7 females from 5 months to 12 years old. All cases were stained with a panel of antiodies including CD99, Hep Par 1, bcl2, CD56, Desmin, Vimentin, AFP, AE1/AE3, NSE, LCA and S-100.
Results Our results showed variable immunophenotype of the hepatoblastoma cells but no marker was exclusively diagnostic. They revealed immunoreactivity for antigens which are most commonly associated with other malignancies. This suggest that hepatoblastomas can express many different antigens showing potential for differentiation toward epithelial, neural and mesenchymal lineages.
Conclusion(s) Clinical, imaging and histological findings is a useful triad for the diagnosis. Pathologists should know that hepatoblastomas may express a wide range of antigens. Further studies are needed for understanding better the complexity of these tumors.

P4.176
Immunohistochemical expression of SPARC is correlated with recurrence, survival and malignant potential in meningioma

Bozkurt Uyar S.; Ayan E.; Bolukbasi F.; Elmaci I.; Sav A.
Marmara University, Institute for Neurological Sciences, Department of Pathology, Istanbul, Turkey

Background SPARC (secreted protein, acidic and rich in cysteine) (Osteonectin) is matricellular glycoprotein that regulates cell function by interacting with different extracellular matrix proteins. The aim of this study was to evaluate expression of SPARC with proliferation index, p53 reactivity in WHO grade I, grade II and grade III meningiomas and correlate with clinical features of the patients.
Methods We studied 111 meningiomas, 69 were benign, 34 were atypical and 8 were anaplastic meningiomas of various histological types. We evaluated the immunohistochemical expression of SPARC, Ki-67 (MIB-1) and p53 in meningiomas.
Results A high immunohistochemical score (4–6) for SPARC was more frequent in atypical and anaplastic meningiomas than in benign meningiomas ($p<0.01$). MIB-1 proliferation index showed significant association between tumor grades in meningiomas ($p<0.01$). At the end of a mean follow-up period of 47.53±25.04 months, 30 tumors recurred. A high SPARC expression was significantly associated with tumor recurrence ($p=0.02$). The immunoreactivity of p53 protein and MIB-1 score were significantly higher in recurrent meningiomas than in non-recurrent meningiomas. The cumulative survival of patients with high SPARC expression was significantly lower than patients with low SPARC expression. The high SPARC expression scores were mostly identified in meningothelial, fibrous and chordoid meningiomas, low SPARC expression scores were mostly spotted in secretory and psammomatous meningiomas.
Conclusion(s) To evaluate SPARC expression might help assessing recurrence risk and survival estimation in meningiomas.

P4.177
Primary glioblastomas: correlation of EGFR amplification (FISH, qPCR, SNPs) with mRNA level and protein expression status

Cerdá-Nicolás M.; Gil-Benso R.; Ferrer-Luna R.; Benito R.; Serna E.; Quilis V.; Monleon D.; Morales J.; Celda B.; Gonzalez-Darder J.; Lopez-Gines C.
Department of Pathology, Valencia, Spain

Background Glioblastoma multiforme continues to be the most common primary brain tumour in adults with a rapidly progressive and fatal course despite current therapies. EGFR is frequently overexpressed, amplified and most rarely mutated in primary glioblastoma. The aim of this study was to investigate of EGFR amplification status in primary glioblastomas.
Methods We have studied 40 cases of glioblastomas by FISH analysis in metaphases and in paraffin sections. The analysis of copy number alterations of EGFR was validated by quantitative PCR and SNPs microarrays. Gene expression profiles were obtained using Affymetrix microarrays; and inmmunohistochemical EGFR expression was analyzed with a monoclonal mouse anti-human EGFR clone H11, that recognizes the wild-type EGFR and the EGFRvIII.
Results We have observed that in 42% of the cases the type of amplification of EGFR was doubles minutes and a strong immunohistochemical expression. We have detected another type of amplification, with extra copies of EGFR inserted in different locus of chromosome 7, present in 28% of cases. Using SNP arrays, we inferred the presence of copy number gains in the region of the EGFR locus. Gene copy numbers at 7p12.1 were validated by quantitative PCR, the values varied between 1.9 and 227.8 copies. The expression of EGFR mRNA varied between 119 to 3200 a.u.

Conclusion(s) The amplification of EGFR in glioblastomas is characterized for an important heterogeneity. This event has been correlated with mRNA level and protein expression status.

P4.178

Cav-1 expression in diffuse gliomas: a reliable diagnostic marker?

Barresi V.; Buttarelli F.; Vitarelli E.; Arcella A.; Antonelli M.; Giangaspero F.
University of Messina, Messina, Italy

Background Caveolin-1 (cav-1) has been proposed as an immunohistochemical marker able to distinguish astroglial from oligodendroglial tumors. In addition, it has been suggested that the reduction of cav-1 expression in glioblastoma cells increases their proliferative and invasive potential, suggesting a higher biological aggressiveness of cav-1 negative glioblastoma cells.
Methods In the present study we investigated cav-1 immuno-expression in a series of 73 diffuse gliomas in an attempt to verify the usefulness of cav-1 immunostaining in the differential diagnosis of astrocytoma versus genetically proven oligodendroglioma and mixed oligoastrocytoma. Moreover, to seek a correlation, if any, between the biologic features and cav-1 expression, the latter was correlated with histological grade, proliferation index, Epidermal Growth Factor Receptor (EGFR) and p53 expression.
Results No significant differences in terms of cav-1 expression were observed between astrocytomas, oligodendrogliomas and oligoastrocytomas. In addition, cav-1 expression was not correlated with 1p/19q status in oligodendrogliomas and mixed oligoastrocytomas. Low cav-1 expression correlated with a higher Ki-67 labelling index (LI) and the absence of p53 over-expression in glioblastomas and it was significantly associated with EGFR over-expression in anaplastic astrocytomas.
Conclusion(s) In conclusion, the present study indicates that cav-1 is not useful as a diagnostic marker to differentiate grade II astrocytomas from oligodendrogliomas. In addition, our data suggest that cav-1 expression is correlated with the absence of EGFR over-expression in anaplastic astrocytomas. Further verification will have to be undertaken to demonstrate if cav-1 expression is an independent predictor of biological aggressiveness in high grade gliomas.

P4.179

Comparative immunohistochemical and quantitative morphological study of convexital and basal meningiomas

Vlodavsky E.; Sabo E.; Soustiel J.
Rambam Medical Center, Haifa, Israel

Background There are very few references in the literature concerning the relationship between anatomic location of meningioma and its biological behavior. Clinical experience and few published studies suggest, that basal meningomas have lower risk of recurrence, than convexital ones. The goal of this study was to compare wide spectrum of morphological characteristics of these two groups in attempt to explain their biological differences.
Methods Detailed pathological examination of 30 basal and 60 convexital meningiomas (Simpson grade I, WHO grade I) was performed with immunohistochemical staining for progesterone receptors, p53, MDM-2 bcl-2, Ki67 (Mib1), TUNEL for evaluation of apoptosis and CD-31 to reveal blood vessels. Proliferation and apoptotic indeces, blood vessel density, nuclear area, nuclear area/box ratio, perimeter and roundness of nuclei were counted. Statistical analysis was performed by ANOVA test.
Results Recurrence rate in 5 years in our study was 2% for basal and 9% for convexital meningiomas. Most tumors in both groups were of meningotheliomatous, fibrous or transitional type. Significant statistical difference was revealed in proliferation index (2±0.4% in basal vs 4± 1.5% in convexital), mean nuclear area (30.42±8.0 vs 41.25±16.0) and density of blood vessels/square μ. MDM-2 immunostaining was more intense in convexital meningiomas, but this difference was not significant.
Conclusion(s) We revealed that convexital meningiomas have higher proliferation rate, their cells have larger nuclei and they have densier blood supply network. These characteristics may be important for explanation of higher rate of recurrences of convexital meningiomas.

P4.180

Diffuse leptomeningeal glioneuronal tumors: a new entity?

Gardiman P.M.; Fassan M.; Orvieto E.; Calderone M.; Denaro L.; D'Avella D.; Perilongo G.
Department of Pathology, University Hospital of Padova, Padova, Italy

Background Glioneuronal tumors are a group of primary brain neoplasms recently acquired in the WHO Classification of Central Nervous System (CNS) characterized by mixed immunohistochemical profile combining neuronal/glial markers.
Methods We report four paediatric cases of diffuse leptomeningeal tumors admitted to our Institution between 1990–2007 with unusual and similar clinical, radiological and neuropathologic features.
Results In these cases MRI revealed a tetraventricular hydrocephalus with thickened enhancing subarachnoid spaces without intraparenchymal mass coexisting with

small cystic lesions widespread in the brain. In all cases a dural biopsy was performed. The thickened desmoplastic leptomeninges appared diffusely infiltrated by a monotonous population of oligo-like cells without cytologic atypia, mitosis, necrosis or endothelial proliferation. In one case, from a secondary lesion developed after two years from the initial presentation, the tumour showed oligodendrocyte-like cells intermingled with "ganglioid" cells occasionally arranged in perivascular pseudorosettes or pseudopapillary structures. The immunohistochemical features strongly suggest a glioneuronal commitment of the neoplasm (synaptophysin and Neu-N positive, GFAP patchly positive). All cases presented an indolent follow-up.

Conclusion(s) We are proposing to descriptively designate this case series as "diffuse leptomeningeal glioneuronal tumors". Further studies and larger validation are needed to test our hypothesis and to consider "leptomeningeal glioneuronal tumors" as a separate nosological entity in the CNS tumors classification.

P4.181

Immunohistochemical study of angiogenesis after local administration of platelet-rich plasma in a patellar tendon defect

Agrogiannis G.; Lyras D.; Kazakos K.; Verettas D.; Botaitis S.; Kisiridis G.; Kokka A.; Trigka E.; Fragkou P.; Kallitsis E.; Kavantzas N.; Patsouris E.

1st Department of Pathology, School of Medicine, National and Kapodistrian University of Athens, Greece

Background Platelet-rich plasma (PRP) is an autologous concentration of platelets in a small volume of plasma, which contains several growth factors.Considering that the low-healing capacity of tendon is associated with a reduced blood supply compared with other tissues and that tendon healing and remodelling require angiogenesis, a process that is tightly controlled by growth factors [16], we postulated that an application of PRP might significantly enhance angiogenesis in the patellar tendon after resecting its central third.

Methods A full thickness defect was made in the central portion of the patellar tendon of 48 New Zealand white rabbits. Platelet-rich plasma (PRP) gel was then applied and filled the tendon defect. The same procedure was performed in the control group, without the application of PRP. Animals were sacrificed after one, two, three, and four weeks. Histological and immunohistochemical analyses using a monoclonal antibody against CD31 were performed, while computer aided image analysis was carried out for vessel density.

Results The histological examination showed a superior healing process in the PRP group compared with the control group. Especially in the third week, the tissue formed in the PRP group was more mature and dense with less elastic fibres remaining. Neovascularisation was significantly higher in the PRP group during the first two weeks and significantly lower in the third and fourth weeks ($p<0.0001$).

Conclusion(s) Histological examination and study of angiogenesis showed that the application of PRP enhances and accelerates the tendon healing process.

P4.182

Infantile hepatic hemangioendothelioma (IHHE). Case report and literature review

Patsiaoura K.; Katsiki E.; Nikolaidou C.

Pathology Department, Hippokration General Hospital, Thessaloniki, Greece

Background IHHE is a primary vascular tumor of the liver and the commonest mesenchymal tumor in infancy. The tumor is seldom solitary and it is classified into two types, which frequently coexist. About 10%-15% of cases present with features of congestive heart failure and a variety of anomalies are associated with IHHE.

Methods We present a case of an one month old infant showing fever and a palpable abdominal mass. The patient had no cutaneous manifastations or other anomalies. On CT-scanning an intrahepatic mass was revealed and liver segmectomy was performed. Macrospopically, the tumor was solitary, with a maximum diameter of 7,5 cm, red-brown with fibrotic areas.

Results The tumor was composed by numerous vascular channels admixed with areas of hemorrhage and necrosis, supported by fibrous stroma containing many entrapped bile ducts. The channels were lined by plump or flattened endothelial cells. Focally, the tumor cells had a solid pattern of growth. Immunohistochemically the cells were positive for CD34 and Factor VIII. The morphological and immunohistochemical findings were consistent with IHHE.

Conclusion(s) The natural history of IHHE is variable and has a histologically benign nature but few tumors (IHHE type II) have and aggressive course with metastasis and death from disseminated disease. It is crucial to make the differential diagnosis mainly from angiosarcoma. Our patient had an uneventful recovery and is free of symptoms 6 months after surgery.

P4.183

Liver transplantation for primary angiosarcomas presented with unusual clinical manifestations

Patsiaoura K.; Katsiki E.; Nikolaidou C.; Imvrios G.; Papanikolaou V.

Pathology Department, Transplantation Unit, Hippokration General Hospital, Thessaloniki, Greece

Background Hepatic angiosarcoma is a primary non-epithelial malignant tumor of the liver accounting for less than 2% of all primary hepatic malignancies. Most of them have unknown etiology and their prognosis is very poor.
Methods Among 300 patients who underwent liver transplantation between 1990 and 2009 two patients were incidentally transplanted due to a misleading clinical diagnosis. We report these two cases of a 35 and a 66-year old men with initial clinical diagnosis of cirrhosis of unknown etiology. Both patients presented with jaundice, weight loss and splenomegaly. Liver function tests were slightly abnormal.
Results Sections from both hepatectomy speciments revealed the presence of multifocal malignant neoplasm composed of many large vascular spaces lined by malignant highly atypical cells sometimes with polypoid projections. The neoplastic cells had different shape, hyperchromatic nuclei and eosinophilic cytoplasm. Immunohistochemical staining was strongly and diffusely positive for vascular endothelial markers CD34, Factor VIII and Ulex europeous lectin and negative for cytokeratins. The non-neoplastic parenchyma showed atrophy of hepatocytes and cholestasis but without features of cirrhosis.
Conclusion(s) Hepatic angiosarcoma is a rare primary sarcoma of the liver. Clinical diagnosis is usually difficult due to unspecific symptoms and signs. Angiosarcomas have an aggressive behavior, progress rapidly and therefore have no indication for liver transplantation. Our patients died 2 and 4 months after transplantation.

P4.184
Myeloid metaplasia in a lymph node of a patient with chronic idiopathic myelofibrosis

Petrakopoulou N.; Tepelenis N.; Savvaidou V.; Zizi-Serbetzoglou A.
Tzaneion General Hospital of Piraeus, Piraeus, Greece

Background: Development and growth of hematopoetic tissue outside of the bone marrow is termed extamedullary hematopoesis (EMH). The occurrence of EMH after birth is usually considered abnormal. Non hepatosplenic EMH is often associated with myelofibrosis. Specific treatment may not be required unless NHS-EMH is accompanied by symptoms. 15% of EMH involves the lymph nodes.
Methods We present a case of a 60-year-old man with a long time history of idiopathic myelofibrosis, who came to our Hospital complaining of lymph nodes enlargement in the right axilla, fatique and weakness. The lymph nodes were painless after palpation. A surgical excision of the enlarged lymph nodes followed. The specimen was sent to our Laboratory for further histopathological examination.
Results The microscopic examination revealed in the lymph nodes extramedullary hematopoesis with extension in the paracortical area consisting of primary immature granulocytes (myeloperoxidase positive), several megakaryocytes and a small number of erythrocytes. The patient remained in the Hematology clinic of our Hospital for further treatment.
Conclusion(s) The occurrence of NHS-EMH is rare. Most cases of NHS-EMH occur in the setting of hematologic disease with myelofibrosis being the most frequent diagnosis. The most frequent site of NHS-EMH is the spinal column followed by lymph nodes and retroperitoneum.

P4.185
Proteomics technologies in pancreatic cancer early diagnosis

Tanase C.; Popescu D.; Albulescu L.; Dima S.; Albulescu R.; Popa A.; Neagu M.; Hinescu M.; Bulman A.
"Victor Babes" National Institute of Pathology, Bucharest, Romania

Background Multiple technologies that measure expression levels of proteins in human samples offer a potential for detection and understanding tumor formation. Pancreatic cancer is one of the most devastating human malignancies. Thus, there is a great need of new biomarkers for early diagnosis in this pathology.
Methods Our data were obtained using two cutting-edge proteomic profiling technologies: Luminex xMAP multiplexed biomarkers (pancreatic cancer associated cytokines, chemokines, signal transduction proteins, angiogenic and growth factors) and SELDI-TOF-MS. Both technologies provided robust discrimination between pancreatic cancer patients and normal-matched controls.
Results We investigated the individual and combined utility of the two approaches for protein expression analysis in 17 cases. Cytokines expression (IL-6, IL-10, VEGF, IL-1 beta, IL-8, bFGF, IL-12, TNF alpha) was strongly correlated with tumor stage, proliferation markers and clinical aggressiveness in pancreatic carcinoma. Overexpression of multiple signaling molecules (c-KIT, EGFR, p38, ERK/MAPK, JNK, IRS1, HSP27) found in tumoral samples sustained the high amplification of growth signals levels in pancreatic cancer. The possible biomarkers discovered by SELDI-TOF-MS may be applied in early pancreatic cancer detection.
Conclusion(s) Combining serum protein profiling using multiplexed assays and mass spectrometry can prove to be an effective strategy for the discovery of new proteins in pancreatic cancer. In addition to using less-invasive techniques, these proteins may become molecular biomarkers useful for diagnosis, prognosis and could be

involved in this pathology as therapy targets. The project was supported by Grant PN II 41-020.

P4.186

Reliability of morphological studies from evidence-based medicine perspective

Tanasijchuk Sergeevna I.
Institute for Sorption and Endoecology Problems (National Academy of Sciences of Ukraine), Kiev, Ukraine

Background One of the central issues of morphological diagnostics is selection of informative group of features, as well as the efficient algorithm of their using.
Methods Analysis of the large-scale array of morphology papers, done within the last 5 years, demonstrated absence of any reliable efficiency appraisal of proposed diagnostic criteria. On the one hand, low reliability of such investigations is related to overestimation of diagnostic significance of such criteria, on the other hand – to incorrect extrapolation of results received at one sample group for estimation of another. Thus, the efficiency of diagnostic criteria will be appraised inclusive of their utility for a certain application.
Results Analysis scheme may be presented as follows: 1) to define operating characteristics of proposed parameters – sensitivity (Se) and specificity (Sp); 2) to appraise the correlation of wastage (w) from the false-positive and the false-negative results (with the aim of morphologic diagnosis, it makes sense to assimilate amount of such mistakes, and thus consider w=1); 3) to calculate prevalence (Pr) of a disease for the medical facility, where the new diagnostic approach is planned for implementation; 3) the criteria will be considered efficient if the following is correct: for cases with $2Pr \leq 1$ $Sp \geq 1 - Pr(1 + Se)/1 - Pr$; for cases with $2Pr \geq 1$ $Se \geq -(1 - Pr)Sp/Pr$ 4) to define convergence and reproducibility of the proposed criteria or diagnostic schemes at the additional blind selection of samples.
Conclusion(s) Substantiality of the defined analysis algorithm was proved on a wide range of cytological, histological, immunohistochemical studies.

P4.187

Alterations in phospholipid fractions in MS patients

Filipovich Nicolaevich A.
Research Institute of Medical Assessment and Rehabilitation, Minsk, Belarus

Background Four groups of patients were distinguished: (1) latent phase with low MTA level (19 patients; 18.1% of all; MTA = 7.6±1.2 units against 3.9±0.82 in control group; $p<0.05$), (2) slow progradient phase (36 patients; 34.3%; MTA = 20.4±0.77; $p<0.001$), (3) acute phase (33 patients; 31.4%; MTA = 40.9±0.83; $p<0.001$) and (4) fast progradient phase (17 patients; 16.2%; MTA = 75.7±4.9; $p<0.001$).
Methods 105 multiple sclerosis patients 15 to 19 years old were examined against the control group of 20 healthy people. CT and MRI of cerebrum and spinal cord, phospholipid assay and a patented radioimmunobiological assay for measuring the myelinotoxic activity (MTA) of blood serum were used.
Results In all four groups of MS patients clear decline in phosphatidic acids level (0.044±0.009 mmol/l to 0.029±0.007 against 0.085±0.003 in control, $p<0.001$), lysolecithine (0.19±0.002 to 0.15±0.024; 0.044±0.009 in control, $p<0.001$), sphingomyeline (0.34±0.04 to 0.23±0.04; 0.31±0.023 in control, $p<0.01$ or 0.001) and prephosphatidylethanolamine (0.043±0.007 to 0.027±0.003; 0.054±0.006 in control, $p<0.05$ and 0.001) was observed. In groups 1, 2 and 3 low levels of phosphatidylcholine 2 (0.048±0.002 to 0.091±0.002 mmol/l; 0.20±0.03 in control, $p<0.01$ and 0.001) and phosphatidylserine (0.14±0.017 to 0.17±0.04; $p<0.05$ and 0.001) were noted. Group 4 with the highest MTA level differed from the other groups by an increased phosphatidylinositol level (0.21±0.003 mmol/l; $p<0.001$).
Conclusion(s) The increased MTA of blood serum clearly correlates MS progress and decreased level of major phospholipid fractions; it may indicate a need for phospholipid metabolism correction.

P4.188

Angiogenesis in gastric cancer. Prognostic importance

Vukmirovic F.
Clinical Center of Montenegro, Podgorica, Serbia and Montenegro

Background The new blod vessels which generation tumor inducer is a important in process of growth, prognosis and metastasis of tumors. We investigate the relationship between the angiogenesis and clinicopathologic features to related with prognosis in gastric cancer patients.
Methods To asses tumor angiogenesis, microvascular density (MVD) were analyzed immunohistochemically in 83 primary gastric cancers. Any single brown-stained cell with Factor VIII, that indicates an endothelial cell, was counted as a single vessel. Branching structures were counted as a single vessel unless there was a discontinuity in the structure. Vessels were counted in 4 regions, with the highest vascular density, at 200-magnification, and the average number of microvessels was recorded.
Results The microvascular density for 83 tumor speciment ranged from 17,5–51,5 with a mean MVD of 33,17±7,95.

Mean microvascular density was chosen as the cut-off point, 38 patients were categorized as a low MVD and 45 patients as a high MVD. There was no significant relationship between angiogenesis and age, sex, and histological type of gastric cancer. A significant correlation was found between the angiogenesis in early and advanced gastric cancer, and between gastric cancer with and without regional lymph node metastasis. Angiogenesis was significantly associated with poor survival. Multivariate survival analysis showed that stage of dissease and angiogenesis were independent prognostic factors.

Conclusion(s) Angiogenesis is one of the most important prognostic factors for gastric cancer patients, and therapeutic inhibition of angiogenesis may advance poor prognosis of gastric cancer patients.

P4.189

Angiogenesis in pterygium and normal conjunctiva

Herbert M.; Sandbank J.; Mendlovic S.; Hermann G.; Segal M.; Zehavi S.
Assaf Harofeh Medical Center, Zerifin, Israel

Background Chronic exposure to ultraviolet radiation has been found to correlate with the development of a pterygium. It has been suggested that inflammation and angiogenesis also contribute to the formation of pterygia. Our aim was to investigate angiogenesis in pterygia compared to superior bulbar conjunctival tissue, an area not exposed to ultraviolet radiation, as a control.

Methods Twenty-eight primary pterygium specimens were obtained from the eyes of 28 patients who underwent pterygium excision with conjunctival autograft. A fragment of temporal conjunctiva was taken from the same eyes for immunohistochemical staining that was performed using rabbit anti-human von Willebrand Factor (Factor VIII). Microvascular density was compared between the pterygium specimens and the normal conjunctiva tissue by morphometric examination. Statistical analysis was performed using the paired t-test.

Results Microvascular counts were significantly higher in the pterygium specimens.

Conclusion(s) The statistically significant differences in vascularity values between the pterygium and the normal conjunctiva in the same eye suggest that angiogenesis play a role in pterygium formation.

P4.190

Association of EBV virus and thymic epithelial tumor

Mohammadi F.; Mohammadtaheri Z.; Dorudinia A.; Nadji A.
National Research Institute of Tuberculosis and Lung Disease, Tehran, Islamic Republic of Iran

Background The thymus is a lymphoepithelial organ composed of epithelial cells and lymphocytes. Primary tumor of thymus are uncommon and no definite risk factor is introduced for development of this tumor. This study was conducted to evaluate the presence of EBV genome in thymic epithelial tumor.

Methods EBV genome (EBNA1 and EBNA2) were determined via nested PCR on DNA extract of 41 paraffin embedded specimen including 16 thymic epithelial tumor as subject cases and 25 mediastinal lymph node as controls.

Results A total of 41 individuals, including 16 thymus tumor patients (7 females and 9 males) and 25 controls (9 females and 16 males), were recruited into this study, with mean ages of 37±19.81 (S.D.) and 47.64±19.21 (S.D.) years, respectively. Nested PCR assay reveal that 31.25% of cases with positive EBNA1. We had no EBNA2 in our cases.

Conclusion(s) Our findings support the association of EBV with thymic epithelial tumor and we may suggest that this association is due to endemic nature of EBV infection, or ethnicity.

P4.191

Beneficial effect over T-cell responses in rheumatoid arthritis of human adipose-derived mesenchymal stem cells

O'Valle F.; Gonzalez-Rey E.; Gonzalez M.; Varela N.; Hernadez-Cortes P.; Rico L.; Büscher D.; Gomez Morales M.; Garcia Del Moral R.; Delgado M.
University of Granada, Granada, Spain

Background Adult mesenchymal stem cells were recently found to suppress effector T-cell and inflammatory responses and have emerged as attractive therapeutic candidates for immune disorders. In rheumatoid arthritis (RA), a loss in the immunological self-tolerance causes the activation of autorreactive T cells against joint components and subsequent chronic inflammation. The aim of this study is to characterize the immunosuppresive activity of human adipose-derived mesenchymal stem cells (hASCs) on collagen-reactive T cells from RA patients.

Methods We investigated the effects of hASCs on collagen-reactive RA human T-cell proliferation and cytokine production, as well as on the production of inflammatory mediators by monocytes and fibroblast-like synoviocytes from RA patients.

Results hASCs suppressed antigen-specific response of T cells from RA patients. hASCs inhibited the proliferative response and the production of inflammatory cytokines by collagen-activated CD4 and CD8 T cells. In contrast, the number of IL-10-producing T cells and monocytes significantly augmented upon hASC-treatment. The suppressive activity of hASCs was both cell-to-cell contact-dependent

and -independent. hASCs also stimulated the generation of FoxP3-expressing CD4+CD25+ regulatory T cells with capacity to suppress collagen-specific T-cell responses. Finally, hASCs donwregulated the inflammatory response and the production of matrix-degrading enzymes by synovial cells isolated from RA patients.
Conclusion(s) Our work identifies to hASCs as key regulators of immune tolerance with capacity to suppress T-cell and inflammatory responses to induce the generation/activation of antigen-specific regulatory T cells.

P4.192
Cardio-pulmonary involvement in liver cirrhosis. Morphopathologic features
Dima-Cozma C.; Stolnicu S.; Pandele G.; Dumitriu S.; Radulescu D.
Gr. T. Popa University of Medecine and Pharmacy, Iasi, Romania

Background Cirrhosis of the liver and consecutive portal hypertension are characterised by cardiovascular and pulmonary abnormalities, defined as cirrhotic cardiomyopathy, hepato-pulmonary syndrome or porto-pulmonary hypertension. Alcoholic and non-alcoholic causes of cirrhosis was associated with an equal degree of ventricular dysfunction, with no specific morphological changes between the causality of liver cirrhosis.
Methods The objective of this study was to describe and discuss, the morphologic changes observed in cardiac tissue and pulmonary vasculature in patients with demonstrated liver cirrhosis. We studied 55 necroptic cases with alcoholic or viral liver cirrhosis and we assessed the alterations of cardiac and pulmonary structures. The samples were fixed in 4% formalin and stained with hematoxylin-eosin and elastic-van Gieson for pulmonary samples.
Results Histologic examination of the liver demonstrated changes consistent with alcoholic liver disease in 20 cases and with postviral cirrhosis in 35 cases. In patients with alcoholic cirrhosis the cardiac lesions were more severe, but no specific comparatively with those seen in viral cirrhosis: widespread focal interstitial myocardial fibrosis, acute and chronic inflammation. Pulmonary hypertension associated with portal hypertension was present in 8,8 % of cases, in some patients with coexistent thromboembolic lesions, which may also contribute to vascular obstruction. Medial hypertrophy of muscular arteries and plexiform lesions were the predominant features in most of the cases with pulmonary hypertension.
Conclusion(s) The current morphopathologic study assessed the most important lesions observed in cirrhotic cardiomyopathy and suggests that pulmonary hypertension secondary to cirrhosis commonly has plexogenic lesions on histologic examination.

P4.193
Comparison study of automated quantification between JPEG and JPEG2000 in immunohistochemical stained nuclei
López C.; Jaen J.; Lejeune M.; Escriva P.; Salvado T.M.; Pons E.L.; Alvaro T.; Baucells J.; Garcia-Rojo M.; Cugat X.; Bosch R.
Hospital de Tortosa Verge de la Cinta, Tortosa, Tarragona, Spain

Background High quality images in pathology generate a great amount of information that requires considerable storage capacity. Image compression allows files size reduction. Computer-assisted quantification of immunohistochemically stained nuclear markers could be affected by standard JPEG compressed format. JPEG2000 compression could provide improvements in picture quality. The aim of this study is compare the computer-assisted count variability in immunohistochemical nuclear markers, using JPEG and JPEG2000 compressed formats as compared to the original TIFF images.
Methods Quantification was performed with two distinct immunohistochemical nuclear markers in a total of 329 DI: 47 DIs captured from original uncompressed TIFF format, 141 DIs converted to different JPEG compressed formats (47 with 1:3(minimum), 47 with 1:23(medium) and 47 with 1:46(maximum) compression ratio) and 141 DIs converted to JPEG2000 compressed formats with the same compression ratios. The differences between TIFF versus JPEG formats were compared to those obtained between TIFF versus JPEG2000 formats at the different levels of compression.
Results JPEG2000 compression have lower automated count differences in around 80% of cases than JPEG compression at minimum and medium compression ratio. Otherwise, in images with low complexity, JPEG and JPEG2000 have similar count efficiency that TIFF original images in around 90% of cases in all compression levels.
Conclusion(s) This work presents a new approach for the automatic quantification in which JPEG2000 compression could be an effective method to reduce files size and storage capacity without compromise the detection rate of nuclear immunohistochemical markers.

P4.194
Does PRP gel promote the expression of IGF-I in the early phase of tendon healing? An experimental study in rabbit's patellar tendon defect model
Agrogiannis G.; Lyras D.; Kazakos K.; Verettas D.; Botaitis S.; Kisiridis G.; Kokka A.; Trigka E.; Fragkou P.; Kallitsis E.; Kavantzas N.; Patsouris E.
Athens, Greece

Background Platelet-rich plasma (PRP) is an autologous concentration of platelets in a small volume of plasma, which contains several growth factors. This stydy aims to test the hypothesis that a single application of PRP gel in a patellar tendon defect influences the spatial and temporal expression of IGF-I during tendon healing.
Methods 24 animals received PRP (PRP group) which apllied as gel and 24 served as untreated controls (Control group). Six animals (12 limbs) from each treatment-group were sacrificed after one, two, three and four weeks following treatment. Histological and immunohistochemical staining along with image analysis were performed in order to evaluate our results.
Results Histology revealed faster healing process in the tendons of PRP group compared to control group. A superior expression of IGF-I was found in PRP group in comparison with the controls ($p<0.0001$). At 4th week of healing, a superior expression of the growth factor was showed in the endotenon of control group, in comparison with the endotenon of the PRP group ($p<0.0001$).
Conclusion(s) The superior healing process and the over-expression of IGF-I in PRP group suggest that PRP may become medically quite useful for the enhancement and acceleration of tendon healing.

P4.195
Early defects in human t-cell development severely affect distribution and maturation of thymic stromal cells: relevance to the pathophysiology of omenn syndrome

Poliani L.P.; Ravanini M.; Gennery R.A.; Villa A.; Roifman C.; Facchetti F.; Notarangelo D.L.
Department of Pathology, University of Brescia, Brescia, Italy

Background Null mutations in genes involved in early T-cell development cause severe combined immunodeficiency (SCID). However, hypomorphic mutations in these genes result in a complex phenotype with residual T-cell development and immune-dysreactivity. Omenn Syndrome (OS), prototype of such conditions, is due to hypomorphic mutations in different genes, suggesting a common pathophysiological mechanism. Thymocytes and thymic epithelial cells (TECs) cross-talk is essential to preserve thymic architecture and maturation of TECs, dendritic cells (DCs) and Foxp3+ T-cells (nTreg). We hypothesize that genetic defects that abrogate or severely affect early stages of T-cell development result in profound abnormalities in TECs and DCs maturation, and affect central tolerance (CT) induction, thus providing a basis for OS genetic heterogeneity.
Methods We performed detailed immunophenotypical analysis of thymic architecture and DC/nTreg distribution, in nine patients representative of six different genetic defects leading to complete or partial block in T-cell development.
Results Profound abnormalities of TECs differentiation (with lack of Claudin-4 and AIRE expression) and severe reduction of thymic DCs were identified in SCID, reticular dysgenesis and OS. OS also showed profund nTreg depletion. In contrast, IL2RG-R222C hypomorphic mutation permissive for T-cell development allowed for TEC and nTreg maturation and Claudin-4 and AIRE expression.
Conclusion(s) Data provide a unified mechanism by which severe defects of thymopoiesis may impinge on TECs homeostasis and on deletional and non-deletional mechanisms of CT, favouring immune-dysreactive manifestations, as in OS.

P4.196
Evaluation of cytotoxicity and tissue reaction to titanium oxide nanofibres

Mandys V.; Jirasek T.; Rubacek L.; Kocka V.
Depatrment of Pathology, Third Faculty of Medicine, Charles University in Prague, Prague, Czech Republic

Background The aim of our work was to evaluate cell and tissue reactions to titanium oxide nanofibres in in vitro and in vivo experiments.
Methods Cellular reactions were studied in permanent cell lines, T47D and HT1197, maintained with a standard culture medium, exposed for a short-time (3–4 days) to sterile titanium oxide nanofibres. Tissue reaction was evaluated in subcutaneous tissue of laboratory rats, where samples of titanium oxide nanofibres were implanted under sterile conditions for 7, 22 and 91 days. Excided tissue samples containing implanted nanofibres were processed by a routine histological technique and the slides were evaluated under an optical microscope.
Results In vitro experiments showed that titanium oxide nanofibres did not cause visible cytotoxic effect in both cell lines. Cell morphology, adhesion and growth properties were not affected by the presence of titanium oxide. Titanium oxide nanofibres implanted into the subcutaneous tissue induced prominent inflammatory and granulomatous reaction evident already 7 days after implantation and persistent to day 91, where tissue fibrotisation was also detectable.
Conclusion(s) The results point at the importance of adequate evaluation of interactions of new nanomaterials with biological systems to characterise potential risks for human and animal health.

P4.197
Expression of double cortin and nestin in malignant brain tumors

Pal L.; Behari S.; Kumar R.; Mahapatra Kumar A.
Sanjay Gandhi PostGraduate Institute of Medical Sciences, Lucknow, Uttar Pradesh, India

Background Biology of brain tumors is enigmatic. Nestin an intermediate filament is expressed in undifferentiated cells during development also expressed in cancer stem cells. Double Cortin (DCX) a microtubule associated protein is involved in neuronal migration. Re-expression of these antigenically primitive proteins in brain tumors not clear. Hence this study has been conceptualised.
Methods Formalin fixed sections from 28 glial tumors, 10 medulloblastomas and 5 mixed glioneuronal tumors were immunostained with nestin and DCX antibodies. GFAP and NeuN immunohistochemistry was performed to confirm glial and neuronal components. Subventricular region of foetal brain was taken as positive control.
Results Nestin positivity noted in all glioblastomas (n=10) and gemistocytic astrocytomas (n=4). In oligodendrogliomas (n=8) nestin immunoreactivity was strong at invasive margin. Medulloblastomas were negative. Two papillary glioneuronal tumors expressed nestin in glial component. DCX and nestin was negative in dysembryoplastic neuroepithelial tumors (n=3). All gliomas expressed DCX with accentuation in infiltrative zone in oligodendrogliomas. Low grade astrocytomas (n=5) were negative.
Conclusion(s) Nestin a marker for stem cells/progenitor cells is expressed during development and in certain malignant tumors. DCX is expressed in migrating neuroblasts. Aberrant expression of these primitive proteins in high grade tumors probably suggest remodelling of cell cycle and migration during tumor progression. The microenvironment at the margin of invasive tumor may be different from that of circumscribed tumor and may induce DCX expression. Low grade tumors did not express these markers and histologically were more circumscribed. More studies are needed to elucidate the concept.

P4.198

Expression of TGF- β1 during the tendon healing, after application of platelet rich plasma

Agrogiannis G.; Lyras D.; Kazakos K.; Verettas D.; Botaitis S.; Kisiridis G.; Kokka A.; Trigka E.; Fragkou P.; Kallitsis E.; Kavantzas N.; Patsouris E.
1st Department of Pathology, School of Medicine, National and Kapodistrian University of Athens, Greece

Background The aim of this study is to find out the spatial and temporal expression of TGF-b1 during the tendon healing, after application of Platelet Rich Plasma (PRP) in a patellar tendon defect model in rabbits.
Methods 48 mature New Zealand rabbits,were used. Equal numbers of animals from PRP and Control group were sacrificed at 4 time points (1st, 2nd, 3rd, and 4th week). A full thickness patellar tendon substance was excised from its central portion and PRP filled the tendon defect. No PRP was applied in the tendon defect of controls. Histological and immunohistochemical sections with an anti-TGF-β primary antibody were made for the evaluation.
Results An acceleration of the healing process was observed in the PRP group in comparison with the control group. TGF-β1 expression was detected in inflammatory cells, endothelial cells, macrophages, and tenocytes.Stronger immunoexpression was detected in epitenon and in the repair site. PRP group showed stronger and more extensive staining at 1st and 2nd week (p<0.0001), whereas control group showed more extensive staining at the 3 rd and 4th week (p<0.0001).
Conclusion(s) Our study demonstrates that locally application of PRP result in overexpression of TGF-b1 into epitenon and the repair site of the healed tendon defect

P4.199

Focal cortical dysplasias of the brain. Size and geometry of the tissue extracellular space

Zamecnik J.; Vargova L.; Homola A.; Marusic P.; Krsek P.; Sykova E.
Department of Pathology and Molecular Medicine, Charles University Prague, 2nd Medical Faculty and Faculty Hospital Motol, Prague, Czech Republic

Background Focal cortical dysplasia (FCD) of the brain represents a prominent cause of pharmacoresistant epilepsy. The epileptogenesis in FCD is supposed to result from the alteration of the synaptic transmission; however, neurons themselves also communicate by extrasynaptic transmission mediated by the diffusion of neuroactive substances in the extracellular space (ECS). Therefore, changes in ECS size and geometry might contribute to the epileptogenicity of FCD.
Methods The size and geometry of the ECS were studied in resected brain cortex of 19 non-malformed samples and in samples of FCD type I in 4 patients and FCD type II in 6 patients by the real-time iontophoretic method. The diffusion measurements revealed the ECS volume fraction (ECS volume/total tissue volume) and the geometrical factor "tortuosity", reflecting various ECS diffusion barriers. The results were correlated with the histopathology.
Results In control cortex - ECS volume fraction = 0.23± 0.01, tortuosity = 1.46±0.01 (mean±SEM). In both FCD type I and FCD type II, tortuosity was significantly increased (1.61±0.01 and 1.69±0.02, respectively). ECS volume fraction was not significantly changed in FCD.
Conclusion(s) Despite the unchanged size, the ECS of FCD has increased tortuosity reflecting the increase of diffusion barriers in the ECS. We propose that disturbed extrasynaptic transmission through the ECS of such cortex, along with altered diffusion parameters, represents another

factor contributing to the epileptogenicity of FCD. Supported by IGA NS9915-4 and VZ MZO 00064203.

P4.200

Hepatocellular carcinoma with syncytial giant cell in an adult with alcoholic cirrhosis after consumption of hypericum perforatum/ St John's mort

Ioachim E.; Lampri E.; Harissis H.; Simou N.; Malamou-Mitsi V.
Ioannina, Greece

Background Hepatocellular carcinoma (HCC) often develops in patients with underlying liver disease. Its type with syncytial giant cell is extremely rare in adults.
Methods We report the clinicopathologic features of an unusual HCC occurring in an adult with alcoholic cirrhosis who had consumed unknown quantity of hypericum perforatum/ St John's mort (SJW).
Results The tumor was characterized by multinuclear epithelial cells of the syncytial type similar to that seen in infantile giant cell hepatitis. Moreover, these giant cells displayed the same nuclear atypia and immunohistochemical profile as the other HCC cells and were therefore part of the tumor itself and not entrapped nonneoplastic cells.
Conclusion(s) Hepatocellular giant cell carcinoma in adults has been previously reported, but the cells were osteoclast-like and not epithelial type as it was in the presenting patient. Futhermore, the HCC seems to have been arisen in the field of cirrhosis. Its etiology is probably the alcoholism. However, the possible etiopathogenic role of chronic consumption of the herb SJW, which is a known hepatotoxic one, in combination with the presence of syncytial giant cells cannot be excluded.

P4.201

Localised corneal amyloidosis secondary to keratoconus

Singh K.
Brown University, Providence, RI, USA

Background Secondary amyloidosis of cornea has multiple etiologies like phlyctenular disease, trauma, trachoma, trichiasis, syphilis, and hereditary endothelial dystrophy. Amyloidosis is rarely described with keratoconus. Primary corneal dystrophy with amyloid deposition is histopathologically similar to secondary corneal amyloidosis.
Methods Three corneas from two cases with clinical diagnosis of keratoconus were studied. One patient underwent bilateral keratoplasty. Congo red stain was done to confirm amyloid.
Results Histopathological examination confirmed keratoconus. All the three corneas showed central thinning with normal thickness peripheral corneal button. Bowmans membrane showed multiple breaks. Amyloid was deposited between the Bowmans membrane and corneal stroma. The amyloid deposits were sub-epithelial, nodular & gelatinous and showed apple green birefringence. The endothelium was intact. In one of the corneal button, due to extensive cautery artifacts, amyloid was identified retrospectively on repeat examination.
Conclusion(s) Corneal amyloidosis should be considered in keratoconus patients with unusual forms of central corneal opacification. The lesions of secondary, local corneal amyloidosis are all subepithelial in location. With the exception of gelatinous droplike dystrophy where the amyloid is deposited in the subepithelial space, primary amyloidoses of the cornea all have amyloid deposits situated deep in the stroma. It is hypothesised that the corneal epithelium produces amyloidogenic protein secondary to chronic surface irritation, which is deposited in subepithelium. Primary corneal dystrophy with amyloid deposition is diagnosed by identifying the associated genetic abnormality.

P4.202

Mediastinal cystic changes

Vukmirovic F.
Clinical Center of Montenegro, Podgorica, Serbia and Montenegro

Background Mediastinal cysts are rare pathological entity and they consist 10 to 15 percent of radiological detected masses of this region.
Methods In our study we include 163 patients which were operated due to radiologicaly detected mediastinal tumor mass in ten year period of time (1992–2003).
Results From 163 diagnosed mediastinal masses we found 29 cystic formations (17,8%). We documented 14 (48,3%) mesothelial and 15 (51,7%) non-mesothelial cysts. Bronchogenic (5 cases or 33,3%) and dermoid (4 cases or 26,7%) cysts were the most frequent of non-mesothelial cysts, thymic cysts we found in 3 (20%) patients while parathyroid cysts had only 1 (6,7%) patient. Cystic tumors were diagnosed in 3 (20%) cases, from which 2 (13,3%) cavernose lymphangiomas and 1 (6,7%) cystic schwannoma.
Conclusion(s) Though, rare changes, mediastinal cysts are very diverse group of pathological changes. We have to emphasize that some mediastinal tumors can have cystic apperance.

P4.203

New automated technique for evaluation of HER2 amplification by FISH in breast cancer

López C.; Bosch R.; Lejeuene M.; Salvado T.M.; Muñoz E.; Subirats N.; Pons E.L.; Alvaro T.; Jaen J.
Hospital de Tortosa Verge de la Cinta, Tortosa, Tarragona, Spain

Background The HER2 gene, amplified in 10 to 35% of invasive human breast carcinomas, has prognostic and therapeutic implications. Overexpression of HER2 protein can be detected by immunohistochemistry(IHC) and it is the routine diagnostic technique. Fluorescent in situ hybridisation(FISH) technique is used to detect HER2 gene amplification in the unclear diagnostics with IHC. The detection of HER2 gene amplification involves the subjectivity of manual signal quantification. This study shows a preliminary study where an alternative automated methodology of FISH evaluation is used for diagnostic.
Methods Twenty paraffin embedded breast sections were stained using HercepTest(IHC) and scored by a pathologist. FISH was performed using the HER2 FISH-pharmDx™ fluorescent probe and scored by a biologist and an automated quantitative image analysis using Image-Pro® Plus 5.0 program with the appropriate algorithms developed in our laboratory. Three diagnostics results were compared between them.
Results 14 cases were scored by IHC as negative(0 or 1+), 4 as intermediate (2+) and 2 as positive (3+). FISH automated and manual evaluations obtain the same diagnostic result: 17 not amplified(score <2) and 3 cases amplified (score≥2). The FISH scoring technique was consistent with all negative and the positive IHC scores(0, 1+ versus not amplified and 3+ versus amplified). One of four unclear IHC diagnosed cases (2+) was amplified by FISH.
Conclusion(s) These preliminary data suggest that our new automated method may provide a consistent alternative to visual IHC and FISH scoring especially for IHC 2+.

P4.204

RUNX3, S100A4 and COX2 immunohistochemical expression in colorectal adenocarcinomas

Milias S.; Eleftheriadis E.; Constantaras C.; Zaramboukas T.
Department of Pathology, 424 General Military Hospital Thessaloniki, Greece

Background RUNX3 is tumor suppressor in several cancers and especially for gastrointestinal ones. COX2 is overexpressed and correlated with gastric cancer. S100A4 is believed to be a marker for metastatic disease. We would like to examine the combination of immunohistochemical expression of these three antibodies in colorectal adenocarcinomas.
Methods We examined 45 archival colectomies for adenocarcinomas and 10 colectomies for non neoplastic purposes. 32 cases were medial differentiated adenocarcinomas stage B2 (n=13) and C2 (n= 19), 10 cases were low differentiated adenocarcinomas Stage B2 (n=3) and C2 (n=7) while the rest cases (n=3) were high differentiated ones stage A (n=1) and B2 (n=2). Polyclonal antibodies for RUNX3, S100A4 and COX2 were used.
Results The analysis of the immunohistochemical results revealed dense focal cytoplasmic expression for S100A4 and/or COX2 in 12/17 stage C2 adenocarcinomas and 5/16 stage B2 adenocarcinomas. On the contrary RUNX3 was expressed in 1 case stage C2 adenocarcinoma, 2 cases of stage B2, the unique case of stage A and 6/10 cases of the non-neoplastic colectomies.
Conclusion(s) Our data suggest that a panel of antibodies including RUNX3, S100A4 and COX2, among others, could be used, as prognostic markers for colorectal adenocarcinomas.

P4.205

Solid pseudopapillary tumor of the pancreas (SPT). An incidental finding, case report and literature review

Dehollain Paula A.; Ríos Marilu D.; Mazó Delia A.; Bermudez C.; Martínez A.; Hernández L.
Centro Médico Integra, Caracas, Distrito Federal, Venezuela

Background Solid pseudopapillary tumor (SPT) of the pancreas is a rare neoplasm of uncertain histogenesis and neuroendocrine epithelial growth pattern that shows cystic and solid, pseudopapillary formations. It can be classified as a tumor of low malignant potential and treatment requires complete excision. It is known by many different names, but in 1996 was appointed as the TSP by the World Health Organization. It represents between 1–3% of pancreatic tumors, appearing as a painful abdominal mass in most patients.
Methods We describe a case of a 23 year old female patient, who after a car accident presented Grade II Spleen Injury and Grade III Hepatic Injury. She undergoes surgery finding hemoperitoneum and a retroperitoneal tumor that occupied head, body and tail of the pancreas, with multiple adhesions of intestinal loops and omentum. A corpo-caudal pancreatectomy with complete resection of the tumor is done.
Results We received an encapsulated tumor of 14x9 cm, solid and cystic, with hemorrhagic foci. Microscopically it showed a solid growth pattern with papillary and cystic areas. The tumor cells are uniform with scant cytoplasm, regular nucleus with occasional indentations and granular chromatin. They are arranged around axes of fibrous connective vascularized tissue.
Conclusion(s) Immunohistochemical studies were performed with vimentin, α1-antitrypsin and enolase, concluding diagnose as Solid pseudopapillary tumor of pancreas. The patient progressed satisfactorily. We emphasize the importance of the case because of the clinical

presentation and incidental surgical findings of an unusual neoplasm.

P4.206
Subependymoma: the rare neoplasm of central nervous system

Carvalho Castelo Branco T.; Ibiapina Oliveira J.; Santos Gomes L.; Araujo Klerton Luz J.; Tavares Carolina Brito A.; Almino Luisa Brito Ferreira M.; Oliveira Marcos C.; Vale Pessoa B.; Alencar Jose F.; Carvalho Sousa Ribeiro J.; Reis Aguiar M.; Morais Pereira L.
Hospital Sao Marcos, Teresina, Piauí, Brazil

Background The subependymoma is a rare benign neoplasm of the central nervous system that is characterized by slow-growing and often affects the ventricular wall. The true incidence of subependymoma is difficult to determine because these tumours frequently remains asymptomatic and are often found incidentally at autopsy. In two studies, they accounted for approximately 8% of ependymal tumours. They occur in all age groups and both sexes, but most commonly in middle-age and elderly males. The fourth ventricule is involved most often (30–40%), followed by lateral ventricules (30–40%). The authors report a case with typical presentation of subependymoma.
Methods Case report: Male patient, 56-years-old, healthy, suddenly presenting important headache. Neurological evaluation and imaging examinations was done. MRI showed well-defined nodular mass located in the lateral wall of the fourth ventricle, with hypointense at T1 and T2 in hyperintense, measuring 3.5 cm and associated ventricular dilatation. Craniotomy made with excision of the tumor. Mycroscopically, a neoplasm characterized by cluster of isomorphic nuclei embedded in a dense fibrillary matrix with frequent focus of calcifications and lobular architecture; mitoses are absent. The patient progressed well in the postoperative period, without neurological complaints.
Results The neurosurgical findings were nodular and firm lesion located in the IV ventricule wall confirmed by classic histopathologic findings.
Conclusion(s) Subependymomas are rare neoplasm of central nervous system carry a good prognosis and surgical removal is usually curative.

P4.207
The histopathology diagnosis of the gastric lesions in obese patients with sleeve gastrectomy. Before of after?

Vrabie Doina C.; Petrescu A.; Waller M.; Munteanu R.; Copaescu C.
University of Bucharest, Bucharest, Romania

Background In developed western culture, a lean body is considered to reflect good self-control. The prevalence of obesity has been increasing in recent decades.Our study emphasizes the frequent histopathological gastric lesions detected postsurgery, on surgical specimens.
Methods We investigated 87 surgical interventions, performed between 2007–2008, June, which have been registered for bariatric therapy (sleeve gastrectomy). The specimens have been fixed in buffered formalin and then, stained with hematoxilin eosin.
Results In our study, the females are especially affected (66.66%), comparative with males (34%). The analysis of the age range shows that the most affected are the young patients, between 31–40 years old (39.08%). The frequent histopathological lesions encountered on microscopy were: oxintic cells hyperplasia (63.21%), ulcerations (34.48%), the lymph nodes hyperplasia in lamina propria (33.33%), active gastritis (22.98%) and other lesions (10.34%). The oxintic cells hyperplasia was noted in fundic and corpus mucosa and it was the most constant lesion encountered in obese patients.
Conclusion(s) Our study outlines that the most important area of the gastric mucosa, from histopathological point of view and for patients with morbid obesity, is the fundus and the most affected cells are the oxintic ones. We concluded that the histolopathology, on surgical specimens is very important because of the general picture of the gastric mucosa shown, but it can not be excluded the endoscopy, which can interrupt the surgical mechanism because of the lesions found.

P4.208
Audit of retained organs at autopsy

Bakhiet Mohamed S.; Crotty B.T.
St. Vincents University Hospital, Dublin, Ireland

Background Retention of organs is sometimes required in order to accurately establish the cause of death (COD) at autopsy. The aim of this study was to determine the number of postmortem where organs were retained in a 1-year period and the indications for organ retention. We aimed also to determine the contribution of findings in the retained organs to the COD and to Study variation of rates of organ retention between individual consultants.
Methods Approx. 170 autopsies are performed annually in SVUH. Of them, an organ was retained in 28.3% of PMs in the year 2006. Autopsy reports from 49 PMs where organs were retained were reviewed extracted were: Consultant supervising PM, indication for organ retention, COD and estimation as to whether organ retention confirmed the COD and/or resulted in a new diagnosis.
Results The brain represented 80% of the retained organs. Consultant A, B, C and D retained 22.4%, 10.5%, 31.4% &

60.9% of their PMs performed respectively. The cause of death confirmed in 1/3 of the cases and a new diagnosis added in approximately 2/3 of the cases (1/3 show major findings).
Conclusion(s) • Brain represents most of the retained organs • Consultants differ in frequency in which they retain organs • The indication for organ retention is usually not stated. In only one of 49 autopsies was the indication clearly stated. • It is a good practice to retain the brain when there is no apparent COD.

P4.209
Bacillar osteoarthritis. Considerations on three cases with hip arthroplasty
Sîrbu P.; Cretu A.; Radulescu D.; Petreus T.; Stolnicu S.; Asaftei R.; Botez P.
"Gr.T. Popa" University of Medicine and Pharmacy, Iasi, Romania

Background Regarding the increased number of tuberculosis cases reported in Romania in the past 5 years, we have observed the involvement of the bacillary impregnation in osteoarticular pathology.
Methods The authors present the cases of three patients with hip arthroplasty and diagnosed with bacillary osteoarthritis. First case, male, 72 years, with a acetabular fracture, secondary coxarthrosis was operated with hip replacement using a total hip prosthesis. It was clinically examined postoperative, with a favorable evolution and he returned after 1,5 years with pain and decementation. During revision he was diagnosed a bacillary osteoarthritis demanding a large drainage intervention and Austin-Moore spacer implantation, continued with tuberculostatic treatment. 2nd case, female, 68 years with left side coxarthrosis was operated with an uncemented total hip prosthesis. 7 months from surgery she was diagnosed with bacillary osteoarthritis of the left knee (knee arthrodesis continued by tuberculostatic treatment). 3 rd case, female, 73 years, operated for a femoral neck fracture; intraoperative - tuberculous trochanteritis but we have performed hemiartrhoplasty continued by tuberculostatic treatment.
Results A tuberculostatic treatment managed for 12 months, led to stabilization and cure of the bacillary process in all three cases.
Conclusion(s) The presented cases raised three questions: for the first case, was the tuberculosis inoculated on the hip prosthesis or was preexistent and was exacerbated after surgery? For the second case, was there a bacillary osteoarthritis of the hip and the knee tuberculosis was secondary? For the third case, was the hip arthroplasty a risky one?

P4.210
Cerebral metastasis from urinary bladder cancer: α case report
Nesseris I.; Lambri E.; Zigouris A.; Pahatouridis D.; Mihos E.; Alexiou G.; Zikou A.; Voulgaris S.; Goussia A.
Department of Pathology, University of Ioannina, Ioannina, Greece

Background Cerebral metastasis from urinary bladder carcinoma is exceedingly rare and accounts for less than 1% of all brain metastases. Herein we report a case of cerebral metastasis from a transitional cell bladder carcinoma (TCC) occurring 7 months after a total cystectomy and radical prostatectomy followed by chemotherapy and radiotherapy.
Methods A 71-year-old man was admitted to the Neuropathology Department after an episode of loss of consciousness. Imaging studies revealed a space-occupying lesion in the right frontal lobe. The patient was operated and a solid and partially cystic tumor was excised.
Results The surgical material measured 1X1X0.3 cm in total dimensions. Histologic examination revealed a malignant neoplasm invading the brain cortex. The neoplastic cells were arranged in solid clusters or in papillary structures with central fibrovascular cores. The cells were large, with abundant pale or clear cytoplasm and ovoid pleomorphic nuclei. Immunohistochemically, tumor cells were positive for keratin 7, keratin 20 and CD10 antigen. The histological diagnosis was consistent with a metastatic carcinoma, with histopathological features suggesting urothelial origin. The patient received radiotherapy but died 18 months later due to systemic disease.
Conclusion(s) In patients with known TCC, brain metastasis, although rare, should not be excluded and in follow-up examination any alterations in neurological status should be thoroughly evaluated. In the published cases, brain metastases were detected in a time period between 7 and 40 months after surgery. Total excision of the mass followed by radiotherapy was the treatment of choice.

P4.211
Clinicopathological analysis of histologically confirmed intracranial germ cell tumors in Korea
Suh Y.; Lee D.
Dpt. of Pathology, Samsung Medical Cener, Sungkyunkwan University, School of Medicine, Seoul, Korea, Republic of Korea

Background Intracranial germ cell tumors (GCT) are a heterogeneous group of lesions, and it is difficult to determine the relative prognosis of a specific type of tumors.

Methods To investigate the clinical presentations including survival and prognostic factors of intracranial germ cell tumor (GCT), 62 patients diagnosed with histologically confirmed GCT in Samsung Medical Center were retrospectively analyzed. There were 45 male and 17 female patients. The median follow-up period on the 51 patients was 28 months.
Results Histologically, intracranial GCTs consisted of germinoma (48.4%), mixed GCT (27.4%), teratoma (19.4%), and pure nongerminomatous GCTs (4.8%). The pediatric patients under 18 years comprised 60% of cases with incidence peaking in 16 to 20 years of age. The most frequent site was the pineal glands followed by the suprasellar region, basal ganglia, cerebral hemisphere, cerebellum, and lateral ventricle. The 5-year overall survival (OS) and event free survival (EFS) for patients with germinoma compared to NGGCTs was 100% versus 84.9% (p=0.059) and 91.7% and 64.5% (p=0.022). The EFS for patients with normal tumor markers compared to those with elevated markers was 82.6% and 70.2%. Two out of 4 patients with either α-FP > 10,000 mg/ml or β-HCG > 10,000 mIU/ml died of disease.
Conclusion(s) Even though aggressive chemo- and radiotherapy have improved treatment outcomes, NGGCT still harbored a poorer prognosis. Elevated tumor markers alone may not be the direct adverse prognostic factor except when they are extremely high.

P4.212
Collision metastasis of breast and rectal carcinoma

Gasparinho G.; Silva J.; Fonseca R.; Claro I.; Nobre-Leitão C.; Chaves P.
Instituto Português de Oncologia de Lisboa Francisco Gentil, Lisboa, Portugal

Background Collision tumours are rare entities, defined by the simultaneous occurrence of histologically different neoplasms in the same organ. Various chemokine receptors, namely CCR6 and CCR7, have a role in determining the metastatic destination of tumour cells. In this case of a patient with collision metastasis, we analyzed the expression of the chemokine receptors CCR6 and CCR7 in order to elucidate a possible common metastatic pathway.
Methods Female, 55-year-old, with a history of invasive breast carcinoma with hepatic metastases and a rectal neuroendocrine carcinoma. During a course of chemotherapy, the patient died and an autopsy was performed.
Results A pulmonary thromboembolism of the right pulmonary artery was the cause of death. Other findings included multiple hepatic nodules; pulmonary hilar adenopathies and a local recurrence of neuroendocrine carcinoma. Histological analysis showed two distinct patterns both in the liver and in the hilar lymph nodes. Immunohistochemistry with anti-GCDFP15 and neuroendocrine markers confirmed collision metastases of both primaries. Chemokine receptors expression was positive for CCR6 and CCR7 in both tumours.
Conclusion(s) As far as we know, this is the first reported case of collision metastases concerning breast carcinoma and rectal neuroendocrine carcinoma. Hepatocytes constitutively express CCL20, which attracts and selects CCR6+ cancer cells and therefore chemotaxis via CCR6 might be the common mechanism by which different malignant tumours metastasize to the same organs, even within the same patient, as we report. Inhibition of chemokine signalling might be useful in patients with multiple malignant tumours, sharing a metastatic "molecular facilitator" profile.

P4.213
Correlations between histological type, clinical behaviour, and prognosis in type A thymoma

Butcovan D.; Grigoriu C.; Radulescu D.
UMF "Gr. T. Popa", Iasi, Romania

Background Medullary thymoma is a rare benign epithelial tumor, arising late in life with no mortality after surgery alone.
Methods We present the case of a 70 years old man, admitted at Cardiovascular Institute, for a compressive mediastinal tumor, treated by tumorectomy and morphologically diagnosed.
Results By applying histological and immunohistochemical techniques we evidentiated the characteristic and particular tumoral features. The tumor crossed by broad fibrous bands was composed from predominantly keratin positive spindle epithelial cells and scant immature lymphoid cells. Reticulin fibers individually surround most cells. We discuss the relation between the thymoma clinicopathological and prognostic features, resulting a clear correlation between histological type and clinical study. We also compared the Muller-Hermelink classification with WHO classification, pointing the importance of establishing an accurate tumor grading and staging and of appreciation of thymoma clinical behavior, as well.
Conclusion(s) Medullary thymoma remain the best prognosis thymic tumor.

P4.214
Cranial computer assisted tomographic features in hydrocephalus: implications for the involved aetiopathogenic mechanisms/management options

Onyekwelu E.U.
Royal Victoria Teaching Hospital, Banjul, Greater Banjul, Gambia

Background Hydrocephalus could be isolated (congenital/acquired) or related to neural tube defects. It is usually suggested by its clinical features, diagnosed at transfontanelle ultrasound and confirmed and evaluated further at CT, MRS, MRA, and SPECT. Their effective management/outcome are contingent on elucidation/localizations of the basic structural defects and its aetiopathogenic mechanisms.Ventriculo-peritoneal shunt surgery or lumbar peritoneal,ventriculocisternostomy,endoscopic third ventriculostomy,and ventriculo-ureteral shunts are occasionally indicated in more difficult cases.
Methods This review concerned the features demonstrated at cranial CT scan, evaluated, validated, interpreted and reported in a standardized manner in anticipation of definitive intervention.
Results 45 cases were related to genetic hydrocephalus and compatible TORCHES complex congenital hydrocephalus, 35 cases were prematurity, meningoencephalitic and tumour related acquired hydrocephalus, 37 cases were related to neural tube defects. Warburg Walker syndrome/Type II Lissenencephaly 2. Associated clinical features were hemiplegia, poor nuchal regulation, regressional milestones, micropthalmia, impaired executive functions, and consanguinity/endogamy. The features demonstrated at CT were a panhydrocephalus, agenesis/absence of the corpus callosum, alobar poroencephaly and poroencephalic cysts were most commonly associated with congenital hydrocephalus in addition to lissenencephaly in Walker-Warburg syndrome whereas in the TORCHES Complex infection group Schinzenencephaly, microgyria, pachygyria and cortical dysplasias were the principally featured CT findings. Amongst the tumour related group medulloblastomas were determined with most certainty because of exact localization.
Conclusion(s) Neuro-imaging a valuable tool in aetiopathologic classification of hydrocephalus indicates area of neuropathological interest and directs neuroprotective options.

P4.215
Determination of functional MDR-activity of rheumatoid arthritis patients

Micsik T.; János G.; Lorincz A.; Borgulya G.; Jakab K.; Peták I.; Schwab R.
Ist Department of Patology and Experimental Cancer Research, Semmelweis University, Budapest, Hungary

Background Rheumatoid arthritis is a chronic inflammatory disease of small articulations ending up often in invalidism. In contrast with the many therapeutic efforts the effectiveness of the therapy cannot be foretold. Recent research showed that MDR1(MultiDrug Resistance protein 1) and MRP1(Multidrug resistance Related Protein 1) transporters causing chemoresistency in tumor cells may have pathophysiological role in different chronic diseases. MRP1 transporter is pumping out methotrexate (MTX) from the cells and research data of elevated MDR1/MRP1 expression of RA-patients show the potential prognostic role of these proteins.
Methods Functional MDR Activity Factor (MAF) was determined in six peripheral blood leukocyte populations (granulocyte, monocyte, lymphocyte, CD4+, CD8+, CD19+ cells) with MDQAssayTM in 58 RA patients responding well or not or intolerant to MTX-therapy and in 50 healthy individuals ans subsequently statistically analyzed.
Results We didn't find significant differences in the MAF-values of the RA-patients according to their responder-rate to MTX-therapy, but the MAF-values were significantly lower in RA-patients than in healthy individuals. An interesting and clinically relevant finding was the difference found in the MAF-values of the CD19+ cells of RA-patients intolerant to MTX-therapy.
Conclusion(s) We couldn't demonstrate any significant difference in the functional MDR-activity of MTX-responder and MTX-nonresponder RA patients. Althought functional MDR-determination cannot foretell the success rate of MTX-treatment, it might be useful in predicting and avoiding the harmfull side effects of MTX-treatment. Another interesting finding was that MTX has decreased the functional MDR-activity of RA-patients as a sign of their immunsupression.

P4.216
Dysmorphic nuclei of renal cells in progeria: an ultrastructural study

Onorati M.; Falzarano Moscovita S.; Rossi B.; Rollo F.; Del Vecchio Teresa M.
University of Siena, Siena, Italy

Background Progeria is a rare, genetic disorder that causes premature aging in children, shortly after birth. There are several forms of progeria, related to different genetic alterations. The classic type is Hutchinson-Gilford Progeria Syndrome (HGPS), typically caused by a point mutation in the human nuclear lamin A (LMNA) gene. Other progeroid syndromes have been associated with nuclear lamin A abnormalities, which lead to a characteristic abnormal nuclear morphology, often described as "blebbing", "herniation" or "denting". We report the ultrastructural findings of renal cells in a patient with progeria.
Methods A 25 year-old woman with progeria underwent a kidney needle biopsy due to persistent proteinuria.
Results Focal Segmental Glomerulosclerosis was observed by light microscopy. Immunofluorescence microscopy showed mesangial IgM deposits. Ultrastructural analysis highlighted nuclear dysmorphism of glomerular and cortical collecting tubule cells and endothelial cells of cortical

vessels; conversely, proximal and distal tubular cell nuclei were found almost unaltered.
Conclusion(s) Nuclear dysmorphism has been reported in fibroblast and lymphocyte cultures from patients with progeroid syndromes and other diseases, collectively known as laminopathies. It has been observed that lamina structural defects worsen with cell aging and stress. We describe nuclear alterations in renal cells of a 25 year-old woman with progeria. We found that nuclei are normal or slightly altered in proximal and distal tubular epithelium, compared to glomerular and vascular cells. The disruption of the normal nuclear architecture may impair important nuclear functions leading to organ dysfunction and premature aging in patients with progeria.

P4.217
Evaluation of CyclinD1, CyclinE, p21RAF and P27Kip-1 in retinal membranes

Aletra C.; Papadopoulou M.; Koumoundourou D.; Ravazoula P.; Batistatou A.
Department of Pathology, University General Hospital of Patras, Patras, Greece

Background Introduction: Membranes developing in retina during diabetic retinopathy, hyperplastic vitreoretinopathy, trauma, and membranes of macula lutea cause shrinkage of the retina and loss of its function. Several pathophysiologic mechanisms lead to these membranes' development. In diabetic retinopathy the major event is neovascularisation while in the other cases there is proliferation of fibroblasts from metaplastic melachromatic epithelium. It is also known that Cyclin-D1 regulates the activity of CDKs and the entry into the S-Phase while CyclinE regulates G1/S transition. Moreover, p21WAF-1 protein inhibits CDKs and p27Kip-1 is implicated in G1 arrest. Perspectives: The purpose of the present study was to evaluate the role of Cyclin D1, CyclinE, p21WAF-1 and p27Kip-1 in the development of retinal membranes.
Methods 20 paraffin embedded specimen of retinal membranes (12 of hyperplastic vitreoretinopathy, 3 of diabetic retinopathy, 4 of macula lutea and 1 following trauma) were used. The proteins' expression was studied by immunohistochemistry.
Results Cyclin D1, Cyclin E and p21RAF were not detected in any of the cases studied. P27Kip-1 protein was positive in 5 cases of hyperplastic vitreoretinopathy. The immunoreaction was strong and was detected in the nucleus of membrane fibroblasts.
Conclusion(s) Different mechanisms are responsible for membrane development.In cases of hyperplastic vitreoretinopathy P27Kip-1 protein seems to play an important role in the development and maintenance of retinal membranes. Other molecular pathways should be investigated in order to comprehend retina pathology.

P4.218
General character of methodic approaches in study of biological effects of low dose radiation and nanopathology

Tereshchenko Pavlovna V.; Degtyaryova Victorovna L.; Kartel Timofeevich N.
Institute for Sorption and Endoecology Problems (National Academy of Sciences of Ukraine), Kiev, Ukraine

Background We possess the results of long-term complex clinical-morphological studies of the impact of Chernobyl disaster factors of human organism. It has been established that small doses of low intensity ionizing radiation and other anthropogenic pollutants usually act differently from high ones, i.e. predominantly without "dose-effect" dependence. Other methodic approaches were developed for estimation of their realization.
Methods We are also currently interested in nanopathology. Nanoparticles and nanomaterials differ from substances in integral phase form or macroscopic dispersions by their chemical, physical or biological effect, which is determined by corresponding laws of quantum physics. The goal of analytical studies was justification of possibility of using methodic approaches we have developed for small doses in investigation of effect of nano-sized particles on human organism.
Results Small doses of low intensity ionizing radiation and nanoparticles possess several common features, i.e. high reactivity, cumulative effects, high ability to penetrate cellular and subcellular membranes, induction of free radicals and active oxygen forms formation, ability for additive and synergic interactions with other contaminants, and migration along foodchains.
Conclusion(s) It is expedient to use methodic approaches, concerning realization of small doses, in study of nanoparticles' biological effects, with the following representative characteristics: 1) disease pathomorphism; 2) accelerated organism ageing; 3) components of a scale we have developed, with emphasis on cambial tissue elements, immunocompetent cells, and connective tissue system.

P4.219
Hystological characteristics of periprosthetic tissue around metal-on-metal hip prostheses

Cör A.; Milosev I.; Pisot V.
College of Health Care, Izola, Slovenia

Background The most noteworthy advantage of a metal-on-metal (M-M) total hip prostheses is low were rate and

avoidance of polyethylene (PE) particles. The goal of the present study was to evaluate the histological characteristics of the tissue around M-M THR.

Methods Between 2003 and 2009 a consecutive series of tissue samples from 29 revised THRs with M-M articulation and samples from two control groups (control group I: THRs made of CoCrMo alloy and control group II: THRs made of Ti-based ally stem and Al2O3 femoral head and polyethylen cup) were analysed. Histopathological and immunohistochemical analyses of periprosthetic tissue samples were performed in order to determine general cellular features.

Results The retrieved periprosthetic tissue showed granulomtous tissue with varying numbers of macrophages with different cytoplasmatic amount of metal particles. The characteristic histological features in periprosthetic tissue from M-M THRs were diffuse lymphocytes in 16 (62%) of cases and perivascular lymphocytic cuffs in 15 (58%) cases. However, there was no correlation between the degree of metalosis and the intensity of lymphocytic infiltration. In comparison with tissue from control groups the lymphocytic infiltration was much more intense and the presence of foreign body type giant cells was much less marked.

Conclusion(s) The M-M bearing may be considered a viable alternative to either polyethylene or ceramic implants, however, outstanding and unresolved issues continue to exist. One of them is extensive lymphocytic infiltration which might be a sign of type IV or cell-mediated hypersensitivity reaction.

P4.220

Immunohistochemical peculiarities and immune cells infiltrate of the tumors in patients treated with implanted titanium scaffolds embedded by modified autologous white blood cells

Zagrebin Valentinovich L.; Kuzmin Anatolyevich K.; Raspopina Evgenyevna A.; Samoylov Vladimirovich M.; Mishnev D.O.

Central Clinical Hospital of the Russian Academy of Sciences, Moscow, Russian Federation

Background Immunotherapy in the patients with inoperable tumors rapidly develops last years. We have obtained earlier positive experimental results on our original patent method on the implantation of the titanium scaffolds embedded by autologous white peripheral blood cells exposed to electrophoresis with zinc ions. Here we present first clinical data in this direction.

Methods Scaffolds were implanted to 30 patients with various inoperable tumors (adenocarcinomas, squamous cell carcinomas, melanomas). Biopsies of tumors and their metastasis obtained repeatedly in period 3–12 months after implantation were investigated with routine histological and immunohistochemical (Ki67, P53, cyclin E, P27, Bcl-2, Bax, caspase 3, E-cadherin, CD44, CD4, CD8, CD56, CD68) methods.

Results Significant inflammation and fibroplastic reaction were observed in all cases but with different intensiveness. In many metastatic biopsy objects fibrous inflammatory tissue prevailed upon tumor tissue many times. Considerable decrease Ki67 and P53 expression was shown. However other apoptotic, adhesive and cell cycle parameters were contradictious. There are prevalence of CD8+ and CD68+ cells among immune cells infiltrating tumors tissue. Quantity of CD8+, CD68+ and NK-cells increased eventually in part of patients. All immunohistochemical parameters varied notably in different tumor types and in different patients.

Conclusion(s) So, considerable influence of this original scaffold method upon tumors is obvious. However this influence and it mechanisms in neoplasias of the different nature require further investigations.

P4.221

Management of hepatocarcinoma metastasized to proximal humerus: case report

Sîrbu P.; Friedl W.; Radulescu D.; Petreus T.; Stolnicu S.; Asaftei R.; Botez P.

"Gr.T. Popa" University of Medicine and Pharmacy, Iasi, Romania

Background Metastatic involvement of the musculoskeletal system is one of the most significant clinical issues facing orthopedic oncologists.

Methods The authors report the case of a 48 years old male who was diagnosed by x-ray examination with fracture of the upper diaphysis of the left humerus on a lytic lesion. The MRI showed a tumor with slight expansive and lytic effect on the humeral bone. Bone biopsy showed a metastasis of a clear-cell carcinoma with unknown origin. Following complete imagistic examination, the ultrasonographic exam and the liver CT discovered a nodule in the VIIIth segment. Hepatic biopsy puncture confirmed a mid differentiated G2 hepatocarcinoma, with small and medium tumor cells, with eosinophilic or amphophilic cytoplasm, with atypical nuclei, disposed as clusters and trabeculas. Percutaneous nodule ablation by ethanol was performed, under ultrasonographic control SonoVue. The MRI of the left shoulder after 2,5 months showed a significant extension of the tumor with partial involvement of the axillary nerves and vessels. The patient was operated with oncologic resection of the proximal humerus and reconstruction with a proximal humeral modular replacement prosthesis type Mutars.

Results The reconstruction procedure was a success and the secondary complete imaging exam showed no new metastasis.
Conclusion(s) Even if the hepatocarcinoma metastasizes less commonly to bone, the authors experience with minimally invasive treatment of the liver nodule, as well as the oncological reconstruction of the humerus, completed with an adequate chemotherapic treatment, represent the premises of short and medium term promising results.

P4.222
Mediastinal neuroblastoma: case report
Bermudez C.; López J.; Ríos Marilú D.; Dehollain Paula A.; Mazó Delia A.; Penso M.
Instituto Oncologico Dr. Luis Razetti, Caracas, Distrito Capital, Venezuela

Background The neuroblastomas are malignant tumors originated from the sympathetic nervous system, that usually affect children under five years old and sporadically adults.
Methods We report a case of a female patient, 34 years old, with no history of pathological significance, which refers thoracic pain for 10 months, without response to medical treatment. CT chest scans report a nodular lesion in posterior mediastinum that displaces without infiltrating adjacent structures. Lateral right posterior thoracotomy was performed, removing a soft, grayish-white lobulated tumor, with round margins, and foci of hemorrhage and necrosis.
Results Microscopic examination of the tissue sections revealed small round cells, some with differentiation toward ganglion cells and intermediate mitotic / karyorrhexis index, scattered in abundant fibrillary background alternating with areas of hemorrhage and necrosis.
Conclusion(s) Immunohistochemical studies were performed revealing positivity for S-100 protein, CD56, Neuron-specific enolase and Chromogranins, concluding diagnose as Nodular differentiating Neuroblastoma according to the modified Shimada classification. The patient is currently in good general conditions, with monitoring by medical oncology. We consider this as an exceptional case because of the patient's age and the tumor's combination with an immature histological type.

P4.223
Morphological ground for experimental tissue sealing method of front abdominal wall wound
Mylovydova G.; Boyko V.; Sushkov S.; Lelytsia A.; Pasternak O.
Government Institution "Institute of General and Urgent Surgery of Academy of Medical Sciences of Ukraine", Kharkiv, Ukraine

Background Prevention of visceral-parietal adhesions of laparotomic wound.
Methods Rats, used for this study, were divided into main and control groups. First group had front abdominal wall wound sealed with silk sutures, tissue sealing method IK-300 M1(analogue LigaSure, USA) has been used on second (main) group. Wound sealing of front abdominal wall was assessed in 14 days by second surgery; pictures of sutured wound, histological materials were taken for evaluation of tissue inflammation and grade of adhesions.
Results In main group adhesions have occurred only in one rat suffered from eventration, others had no signs of adhesions. Evaluation of front abdominal laparotomic wound of control group has discovered the following: two rats had omentum adhesions, the rest of group suffered from even more severe adhesions connected to sutures. Histological assessment of main group (treated with tissue sealing method) has discovered minimal tissue inflammation, granular tissue growth and macrophageal reaction. Histological assessment of control group appeared to have extended tissue reaction with acute inflammation. Granular tissue had many foreign body giant cells and macrophages. Muscle fibers were in condition of bionecrosis. Blood vessels wall appeared to be thickened and had hyalinization signs.
Conclusion(s) Thermal tissue sealing method appeared to cause less tissue inflammation and more reparative changes according to histological and macroscopic evaluation. Thermal tissue sealing method leads to reduction of post surgery adhesions and tissue inflammation, which can lead to reduction of intestinal obstruction caused by post surgical adhesions.

P4.224
Paleohistologic findings in the left eye of Maria d'Aragona (1503–1568)
Ventura L.; Urbani V.; Di Franco M.; Mercurio C.; Fornaciari G.
Department of Pathology, San Salvatore Hospital, L'Aquila, Italy

Background The artificial mummy of the Renaissance noblewoman Maria d'Aragona showed obesity, osteoarthritis, periodontitis, a left arm syphilitic ulcer, and a paravulvar condyloma. The presence of naturally preserved left orbital content prompted us to examine it to identify ocular structures and traces of luetic alterations.
Methods The specimen measured 36x50x24 mm, consisting of brown, cardboard-like structures. Eyelids, medial canthus, muscles and optic nerve were recognized. CT scanning helped to locate the globe, prior to sectioning. Rehydration in Sandison solution for 48 and formalin post-

fixation for 24 h were followed by routine processing and embedding. Sections were stained with H&E, PAS, Masson, van Gieson, Gomori and Grocott methods.
Results Microscopy showed eyelid's connective tissue with glandular empty spaces. Orbital muscles were surrounded by collagen and fat. The sclera was composed of thick collagen bundles and covered by Bruch's membrane, a line of large brownish granules (retinal pigment epithelium), choroid, and a layer of smaller granules, abundant in ciliary body and iris. The anterior segment was identified by cornea, iris and ciliary body. Neither cellular material nor pathological changes were detected. Fungal spores and hyphae were distributed throughout the tissues.
Conclusion(s) No attempt was made by the embalmers to preserve the eye, that underwent spontaneous mummification. The main ocular components were recognized, with post-mortem colonization by fungi. The absence of corneal-uveal alterations, and the failure to identify retina and vessels hindered the demonstration of syphilitic involvement. Molecular and ultrastructural investigations are planned to obtain additional information.

P4.225

Primary CNS meningiomas treated with neurosurgery in the Military Institute of Health Services in Warsaw

Grala B.; Kozlowski W.; Markiewicz T.
Military Institute of Health Services, Warszawa, Poland

Background Meningiomas are common central nervous system (CNS) tumours. In adults they account for about 25% of CNS tumours. Despite their relative frequency, so far no attempts were made to describe large group of primary meningiomas treated with neurosurgery in the Military Institute of Health Services in Warsaw, Poland.
Methods We evaluated postoperative specimens of 615 cases of primary meningiomas treated with neurosurgery from April 1997 to April 2009. Two pathologists evaluated meningioma type and grade, according to recent WHO Classification of Tumours of the CNS issued in 2007. Analysed cases were grouped by gender, age and tumour localisation.
Results Of 615 cases 574 were WHO grade I (93.3%), 30 - grade II (4.9%) and 11 – grade III (1.8%). Of grade I the most common type was meningothelial meningioma (216 cases). Of grade II, 27 were atypical meningiomas. Of grade III, 7 were anaplastic and 4 papillary. Overall male to female ratio was: 1:2.9. Depending on grade it was 1:3.2, 1:2 and 2.7:1 for grade I to III respectively. Peak incidence of meningiomas was in sixth decade for both sexes. The most common site of tumour development was supratentorial (76.3%), followed by infratentorial (12%), intraspinal (10.2%) and intraventricular (1.5%). Among psammomatous meningiomas 35.1% (13 of 37) arose intraspinally.
Conclusion(s) In our material we observed significantly greater imbalance in occurrence of meningiomas between females and males. WHO assumed this ratio to be 1.7:1; in our study it was 2.9:1.

P4.226

Review and new studies of sleep disorders in Brazilian patients at Sao Paulo city

Costa E.; Rodrigues Fabiano M.; Costa C.; Varoli Paes F.; Ranieri A.
University Camilo Castelo Branco, Sao Paulo, Brazil

Background Sleep disorders encompass pathology of very diverse origin with clinical expressions as varied as insomnia, hypersomnia, breathing disorders, complex motor disorders, etc. Some of these processes can be diagnosed clinically, while for the evaluation, diagnosis and treatment of others a battery of tests are required that are carried out in a sleep laboratory.
Methods We review the different diagnostic tests available in the sleep units: polysomnography, respiratory poligraphy, multiple sleep latency test, maintenance of wakefulness test, Osler test, video- EEG for sleep and actigraphy in 56 patients of University Camilo Castelo Branco Clinical Center, during 2008.
Results Besides establishing the pertinence of the indication of the study, such evaluation must establish the type of test to be carried out. Each case was classified in ten distinct groups, presented number and that disorders which obtained the higher percentage of occurrences origin deficit of melatonine.
Conclusion(s) In this brazilian studies we can affirm that the complexity and the cost of these tests, their indication must be based on a suitable evaluation and clinical exploration of the subject.

P4.227

Systemic disorders in patients with neck pain

Filipovich Nicolaevich A.; Filipovich Semenovna N.
Research Institute of Medical Assessment and Rehabilitation, Minsk, Belarus

Background 267 patients 30 to 69 years old with MT-syndromes of cervical osteochondrosis were examined including 140 males and 127 females. The selected patients neglected their problem for 2 to 3 month or longer and resultingly suffered from pain syndrome (moderate in

70,8% and serious in 29,2%), long period of low motional activity, excessive body weight, posture abnormalities (47,8%), cervical lordosis flattening with limited mobility of cervical backbone department, the reflective tension of shoulder girdle and hypotrophy of various muscles (scalene, deltoid, supraspinatus, infraspinatus, biceps, triceps, tener and hypotener).

Methods Clinical methods, radiographic.

Results Regarding the condition of major body systems, the patients were divided in two groups: Group 1 – 157 (58,8%) patients radiographic and clinical evidence of moderate cervical osteochondrosis, and Group 2 – 110 (41,2 %) patients with pronounced radiographic and clinical evidence of cervical osteochondrosis. In group 2 serious alterations in cardiovascular system were found including the decreased heart stroke, and reduced blood circulation rate. Even the increased heart contraction frequency coundnot provide enough oxygen per body mass. As a result considerable decrease in working capacity (PWC 170) in such patients took place.

Conclusion(s) In comparison with control group, all patients in the Group 1 were characterized by decreased muscle and increased fat component of total body weight which was an evidence of permanent alterations in skeletomuscular system. The decreased thorax excursion and relevant muscle hypotrophy stimulated the hypoxia development.

P4.228

Transmission of metastasizing high-grade hepatocellular carcinoma from a donor with liver cirrhosis

Aigelsreiter A.; Stiegler P.; Pichler M.; Stöger H.; Roob J.; Horn S.; Ratschek M.; Höfler G.; Lackner C.
Institute of Pathology, Medical University of Graz, Graz, Styria, Austria

Background Donor malignancy transmission is a rare complication in organ transplantation. Donors are evaluated for malignancy including review of medical data and macroscopic organ assessment by procuring surgeons. Since ischemia time is crucial, transplantation is often performed without organ evaluation by a pathologist. Allograft removal and discontinuation of immunosuppression is beneficial after transplantation of organs from donors with prior undetected malignancy.

Methods We present a 54-year-old male patient with lung metastases 16 months after transplantation of a grossly normal kidney from a 58-year-old male donor with liver cirrhosis without history or macroscopic evidence of malignancy.

Results A few hours after kidney transplantation the cirrhotic liver was evaluated by a pathologist and haemorrhagic tumors were found at the cut surface. Nine hours later, after it was learned that the donor had malignant disease, the kidney transplant was removed and immunosuppression discontinued. Pathological assessment revealed hemorrhagic kidney tumors of up to 7 mm. Histology of the donors' liver-, kidney- and the recipients' lung-tumors showed solid high-grade carcinoma. Immunohistochemistry of the donors' liver tumors was suggestive of high-grade hepatocellular carcinoma. Short-tandem-repeat-(STR)-PCR-analysis of donor- and recipient tumors revealed an allelic profile indicative of donor origin.

Conclusion(s) Our patient developed donor derived metastatic hepatocellular carcinoma after only 9 h of kidney reperfusion and despite withdrawal of immunosupression. Since liver cirrhosis represents a precancerous condition, we suggest organ donations from individuals with cirrhosis should be considered only after examination by a pathologist to prevent transmission of occult liver cancer.

P4.229

Traumatic injuries of human sympathetic ganglia

Dabuzinskiene A.; Ratkevicius A.
Kaunas University of Medicine, Kaunas, Lithuania

Background Studies of human sympathetic ganglia more actual have became of their influences relationship on pathology of target organs. Experimental studies of decentralization and axotomy have given evidence for variety of morphological changes. Our aim was to investigate possible respondent changes of neurochemical features of human neurons after strangulation and mechanical trauma.

Methods We were examined 12 sympathetic ganglions of 8 cadavers, from 42 to 71 years old, 6 men, and 2 women. Reason of death: strangulation (5), mechanical trauma (3). Delay time 12- 18 h. 5μm thick paraffin sections were prepared for immunolabeling to synaptophysin. We were used monoclonal mouse antisynaptophysin (DAKO), clone SY 38, dilution 1:20. Synaptophysin positive areas were counted and data statistical analysis was performed.

Results In ganglia after strangulation we found synaptophysin positive terminals and clusters of vesicles-dot like, different size structures, mainly located nearby neurons. Several single vesicles were disseminated in bundles of nerve fibers. Synaptophysin positive structures were placing completely and incompletely layered circumference of neurons. In some regions of ganglions we detected strongly immunopositive various shape structures as possible markers of damaged enlarged neuritis and sprout baskets. Only single dot like structures were located closely to blood vessels related to neuron. We didn't find any specific differences in morphology of ganglions after trauma in comparison with control group.

Conclusion(s) Morphology of sympathetic ganglia imunohistochemistry of synaptophysin was similar after strangulation and trauma. These results suggest that time after influence on ganglion was to short for coming observable changes.

P4.230

Again on the European Centre of Pathology

Zubritsky N.A.
Municipal Institution "Taldom Central Regional Hospital", Taldom, Moscow Region, Russian Federation

Background The structural organization of the European pathoanatomical service (EPAS) has currently achieved such a level of development that there seems to have arisen a need for creation in Europe of a united, up-to-date, organizational, methodical, consultative and statistical centre on studying human pathology at a qualitatively new level – the European Centre of Pathology (ECP). Otherwise, the EPAS, being a system of measures aimed at improving diagnosis, treatment and research, will sooner or later be drowned in the already available and currently increasing flood of information. The aim of creating the ECP is to unite all national pathologists on the grounds of their membership in the European Society of Pathology, to establish on the European scale common standards and requirements imposed upon pathological anatomy (standardization), as well as to unify the knowledge on pathology (unification). In other words, pathologists must think and express themselves in one professional language. In what country the ECP must be organized? In my opinion, the centre should be set up a country situated in the heart of Europe, such as Austria (in Innsbruck). The problems of financing the ECP should be settled with due regard in relation to the interests of all the countries concerned.
Methods None.
Results None.
Conclusion(s) Hence, the creation of such an ECP having no counterpart in the world pathoanatomical practice will undoubtedly be a powerful breakthrough in European Pathology.

P4.231

Clear cell chondrosarcoma of bone

Trabelsi A., Hammedi F., Rammeh S., Hmissa S., Beizig N., Bedoui A., Sriha B.
Department of Pathology, Farhat Hached Hospital, Sousse, Tunisia

Background Clear cell chondrosarcoma is a rare, low-grade variant of chondrosarcoma that comprises approximately 2% of all chondrosarcomas. It was initially described by Unni et al. in 1976 and was called "Clear-cell Variant of Chondrosarcoma". Because of it's rarity this lesion is still being confused with benign or more malignant bone tumors, both radiologically and histologically. This malignant tumor has been described in a number of anatomic sites and has shown a particular tendency to involve the epiphyseal ends of long bones.
Method In this report, we describe another case of clear cell chondrosarcoma that arises from the chondro-costal region.
Results There is a 49-year-old man patient presented with cervico-thoracic masse measuring 10 cm. On admission, computed tomography (CT) revealed a lobulated enhancing mass that measured approximately 10.0 cm in diameter. Because the biopsy results reported a malign clear cell tumor, the lesion was completely excised. Microscopically, the neoplasm consisted of small and indistinct lobular groups of cells that had round, large, centrally located nuclei with clear cytoplasm and distinct cytoplasmic boundaries. Immunohistochemically confirmed the diagnosis.
Conclusion Clear cell chondrosarcoma is a low-grade and slow-growing tumor. Cure can be achieved by wide local excision in the majority of cases.

P4.232

Galectin-3 expression in pituitary adenomas as marker of aggressive behaviour

Marucci G.; Righi A.; Menetti F.; Farnedi A.; Mazzatenta D.; Frank G.; Faustini-Faustini M.; Agati R.; Morandi L.; Foschini M.P.
Section of Pathology, Department of Haematology and Oncology of the University of Bologna, Bellaria Hospital, Bologna, Emilia Romagna, Italy

Background Galectin-3 (Gal-3) belongs to the family of carbohydrate-binding proteins with high affinity for beta-galactoside. It's expressed in a variety of endocrine tumors, including pituitary adenomas and carcinomas, specifically those producing prolactin (PRL) and adrenocorticotropic (ACTH) hormone. Recent studies indicate that Gal-3 has an important role in pituitary cell proliferation and tumour progression, with a higher expression in ACTH and PRL carcinoma compared with adenomas. The present study has been conducted in order to speculate if Gal-3 could be a negative predictive factor of clinical behaviour in pituitary adenomas.
Methods 61 cases of PRL (31) and ACTH (30) adenomas were selected. All cases were stained with a monoclonal antibody directed against Gal-3. Semiquantitative scoring of positivity was performed on a 3-tiered scale (1 = < 10%, 2 = >10% and<50%, 3 = ≥ 50% of cells).

Results The immunoreactivity for Gal-3 was:1+ in 41%, 2+ in 36% and 3+ in 21,4% of the cases. One ACTH adenoma (1,6%) resulted negative. The mean duration of follow-up was 82.7 months: 34 (55,7%) patients were cured, 13 (21,3%) patients had controlled tumour, 13 (21,3%) had not controlled tumour, while the negative case evolved in pituitary carcinoma. All cases showing 1+ staining were cured or controlled; nine out of 13 (69,2%) not controlled cases showed 3+ staining and 4 showed 2+ staining; this difference showed a trend toward statistical significance.
Conclusion(s) Gal-3 expression in PRL and ACTH pituitary tumours seems to be correlated with a tendency to disease progression.

P4.233

Geographic variation and environmental conditions as cofactors in *chlamydia psittaci* association with ocular adnexal lymphomas: a comparison between Italian and African samples

Carugi A.[1]; Onnis A.[1]; Antonicelli G.[1]; Rossi B.[1]; Mannucci S.[1]; Luzzi A.[1]; Lazzi S.[1]; Bellan C.[1]; Tosi G.M.[2]; De Falco G.[1]; Leoncini L.[1]
[1]Dept. Human Pathology and Oncology, [2]Dept. of Ophthalmology and Neurosurgery, University of Siena, Italy

Non-Hodgkin's lymphomas develop from nodal and extra-nodal tissue. A particular extra-nodal lymphoma type arises from B cells of the marginal zone (MZ) of mucosa-associated lymphoid tissue (MALT). The aetiology of MZ lymphomas suggests that they are associated with chronic antigenic stimulation by microbial pathogens, among which *Helicobacter pylori*-associated gastric MALT lymphoma is the best studied. Recently, MALT lymphomas have been described in the context of chronic conjunctivitis, which can be associated with *Chlamydia* spp. infection. Studies from Italy showed the presence of *Chlamydia psittaci* in 87% of ocular adnexal lymphomas (OAL) and the complete or partial regression of the lymphoma after *C. psittaci* eradication by antibiotic treatment, in four out of nine cases. However, this finding was not confirmed by other studies, suggesting that the association with *C. psittaci* is not a constant parameter in OAL, and that this variability may depend on geographic heterogeneity. Interestingly, none of the studies up to now has been carried out in the African population, where a strong association between infectious agents and the occurrence of human neoplasms has been reported. This study was designed to investigate the possible association of *Chlamydia psittaci* in cases retrieved from Africa, compared to cases from Italy. Our results showed that there was a marked variation between the two geographical areas in terms of association with *C. psittaci*, as 17% (5/30) of the samples from Italy were positive for *C. psittaci*, whereas no association with this pathogen was observed in any of the African samples, suggesting that other cofactors may determine the OAL occurrence in those areas. OAL cases are often characterized by down-regulation of p16/INK4a expression and promoter hypermethylation of the *p16/INK4a* gene has been described in *H. pylori*-associated gastric MALT lymphoma. Therefore, we investigated whether *C. psittaci* may determine such an epigenetic alteration in OAL. Our results showed a partial methylation of *p16/INK4a* promoter in *C. psittaci*-negative cases, whereas no hypermethylation of this gene was found in *C. psittaci*-positive cases, suggesting that mechanisms other than promoter hypermethylation lead to *p16/INK4a* silencing in *C. psittaci*-positive cases. In addition, FISH analysis revealed chromosomal translocations only in a few cases, independently of *C. psittaci* association. From our findings, we may conclude that the role of epidemiologic, environmental, and genetic factors, as well as the involvement of other infectious agents, must be considered in the aetiology of this disease.

P4.234

Myc disregulation relies on miRNA altered expression

Onnis A.; Antonicelli G.; Lazzi S.; De Falco G.; Leoncini L.
Dept of Human Pathology and Oncology, University of Siena, Italy

A key player in cell growth regulation is represented by *MYC*, which is able to induce both cell proliferation and cell death. Interestingly, its expression is often dysregulated in most human tumors (approximately 70%), because of alterations in signal transduction pathways or due to genomic aberrations. The *MYC* oncogene is commonly mutated/amplified in tumors, or over-expressed as a consequence of a reciprocal translocation, as in the case of Burkitt lymphoma. Recent findings link *MYC* to altered expression of small non-coding RNAs, the microRNAs (miRNAs), which have been documented altered in most human tumors. It is well-known that *MYC* can regulate up to 10–15% of all genes, but increasing evidence suggests that *MYC* is also able to modulate miRNA expression. Changes in miRNA expression are highly informative for the classification and the prognosis of cancer, and altered expression of specific miRNAs has been shown to be relevant for malignant transformation. miRNAs have been implicated in various cancers, acting either as oncogenes or tumor suppressors. It has been recently demonstrated that *MYC* activates the expression of a cluster of six miRNAs on human chromosome 13, the miR-17–92 cluster, by directly binding to this *locus*. The miR-17–92 cluster is directly regulated by *MYC*, depending on growth stimuli. This cluster is known to be over-expressed in a variety of B-cell lymphomas, including diffuse large B-cell lymphomas

(DLCBL), follicular lymphomas (FL), and mantle cell lymphomas (MCL), either at the RNA or at the DNA levels, suggesting amplification events. Dysregulation of the miR-17–92 cluster may contribute to lymphomagenesis by repressing tumor suppressor genes and/or via anti-apoptotic activity. Two members of the miR-17–92 cluster, miR-17-5p and miR-20a, in turn control the expression of an important transcription factor, E2F1 which is essential for the G1-S phase passage. Expression of E2F1 is known to be induced by c-*MYC*, and in turn controls c-*MYC* expression, with a positive feedback loop. Intriguingly, a strong *MYC*-induced up-regulation of this gene is observed only at the transcriptional level, whereas a modest increase is observed at the protein level, suggesting a greatly reduced translational yield. These findings support a model in which the miR-17-92 cluster limits c-*MYC*-mediated induction of E2F1 expression, preventing uncontrolled reciprocal activation of these gene products. This reveals a mechanism through which c-*MYC* simultaneously activates E2F1 transcription and limits its translation, allowing a tightly controlled proliferative signal, and highlights the active role of c-*MYC* in regulating miRNA expression. We have previously investigated miRNA expression in Burkitt lymphoma, observing that the expression of hsa-miR-34b is altered in Burkitt lymphoma cases lacking c-*MYC* translocation, which suggests a different pathogenetic mechanisms in these cases. With this in mind, we decided to analyze the expression of specific miRNAs, possibly regulated by c-*MYC,* whose expression could be altered upon *MYC* dysregulation in primary tumors of aggressive B-cell lymphomas. In particular, we focused on miRNAs supposed to be targets of c-*MYC*. Collectively, our results support the hypothesis that additional factors involved in *MYC* deregulation also exist, as *MYC* transcription levels may vary immensely from one tumor to another, independent of translocation. microRNA dysregulation upon *MYC* overexpression may significantly contribute to lymphomagenesis. All of the primary tumors of aggressive B-cell lymphomas we analyzed showed a common trend of miRNA expression, with the exception of hsa-miR-9*. Its down-regulation, in fact, seems to specifically identify a particular subset of BL, cases lacking *MYC* translocation. This finding suggests that it may be relevant for malignant transformation in these cases and identifies it as a promising novel candidate for clinical tumor cell marker.

P4.235

MicroRNA deregulation in HIV-related lymphoid malignancies

De Falco G.; Luzzi A.; Morettini F.; Onnis A.; Bellan C.; Leoncini L.

Dpt. Human Pathology and Oncology, University of Siena, Italy

The incidence of non-Hodgkin's lymphoma (NHL) is greatly increased in HIV-infected individuals. Interestingly, HIV-related tumours may arise even in the presence of high CD4-positive cell counts, suggesting that tumours may not arise as a consequence of the immunodeficiency, but rather the HIV itself may have an oncogenic role. Although the molecular mechanisms underlying HIV-mediated transformation are not clearly understood, the Tat protein of HIV is a likely candidate to contribute to tumour pathogenesis in HIV-infected patients. Extensive evidence indicates that Tat is a cofactor in the development of AIDS-related neoplasms, and the protein has also been found to have an oncogenic role *in vitro* and *in vivo*. The molecular mechanism underlying Tat's pleotropic activity may include the generation of functional heterodimers of Tat with cell cycle proteins, but this may not be sufficient for neoplastic transformation *in vivo*. Recent findings indicate a complex interplay between viral proteins and host transcription regulatory machineries. In particular, evidences indicate that virus may interfere with cellular regulation of several physiological processes exerted by a recently described class of small non-coding RNAs, the microRNAs. In addition, many reports in the last several years have linked Tat transactivation to chromatin remodelling *in vitro* and *in vivo*. We aimed to investigate whether Tat may dysregulate the expression of chromatin remodelers, and whether this may contribute to HIV-associated transformation. Our results show that Tat is able to modulate the expression of some chromatin remodelers, as DNA-methyltransferases and acetyltransferases. In particular, ectopic expression of Tat leads to a marked up-regulation of the acetyltransferase p300, and a dramatic down-regulation of DNMT1, which regulates DNA hypermethylation. This modulation seems to occur at the post-transcriptional level, as mRNA expression for both genes remains unaffected by the ectopic expression of Tat. We then investigated whether this modulation may rely on Tat-mediated dysregulation of specific microRNAs, which have these genes as targets. Their expression was therefore tested both in HIV-positive vs. HIV-negative lymphoma primary tumors, and in human cell lines transfected with Tat. Our results demonstrated that microRNA expression is strongly down-regulated in HIV-positive primary tumors, as compared to normal reactive lymph nodes and HIV-negative tumors. This result was further confirmed *in vitro*, in human cell lines transfected with Tat. Whether such down-regulation may depend on promoter hypermethylation or on mutations of the microRNA sequences is currently under investigation. Collectively, our results suggest a role for the HIV Tat protein in microRNA dysregulation, which may eventually contribute to malignant transformation.

P4.236

Hepatic response to transplantation of human umbilical cord blood stem cells in CCL4-injured liver in mice

Greish S.[1]; El Barbary M.[1]; Eldin M. [2]; Yousef A.[1]; Abd El All H.[3]

[1]Department of Physiology, [2]Department of Internal Medicine, [3]Department of Pathology, Suez Canal University, Ismailia, Egypt

Background Human umbilical cord blood (HUCB) contains stem / progenitor cells, which can differentiate into a variety of cell types. They can differentiate into hepatocytes in vitro and in vivo and can ameliorate fibrosis. **Objectives** The aim of this study was to investigate the hepatic response to transplantation of HUCB stem cells in carbon tetrachloride (CCl_4) injured liver in mice, as regard liver function, histopathology (HP) and immunohistochemistry (IHC).

Design Experimental study.

Material and methods Hepatic fibrosis was induced by CCl_4. HUCB stem cells were infused systemically through the tail vein immediately in group 1 (G1) and after one week of receiving CCl_4 in G2. The control groups were mice receiving only CCl_4 (G3) or were only perfused with saline (G4). Administration of CCl_4 for G1, G2 and G3 and saline for G4 was continued for 10 weeks. After that, blood from all groups was collected for assessment of liver function. All mice were sacrificed under anesthesia, and the hepatic tissue was processed through paraffin embedding to study the extent of liver damage by HP and IHC. The transdifferentiation of HUCB was evaluated by monoclonal mouse anti-human hepatocytes.

Results The level of alanine aminotransferase (ALT) in mice treated with stem cells after CCl_4 administration was significantly lower while serum albumin was significantly higher compared to group 3 ($p=0.001$), whereas serum total and direct bilirubin levels were similar among all groups. On HE basis, stem cells treated mice (G1 and G2) showed improvement compared to the non treated group as regards liver cell ballooning degeneration, portal tract inflammation, piecemeal necrosis, portal tract fibrosis and bridging fibrosis ($p>0.001$). However, liver inflammation and fibrosis were more pronounced in G2 mice compared to G1 ($p>0.001$). Human hepatocytes were identified in all injured mice liver in both G1 and G2 groups. The percentage ranged from 5% to 25%. They were identified allover the lobules with a perivascular concentration (non significant).

Conclusion HUCB stem cells can transdifferentiate into hepatocytes when infused in mice with injured liver causing improvement in both liver function test and histology. Key words: carbon tetrachloride (CCl_4), human umbilical cord blood stem cells, liver fibrosis and monoclonal mouse anti-human hepatocytes.

P4.237

Stem cell factor immunohistochemical expression in vitiligo vulgaris

Abd El All H.S.[1]; Abd El Kareem G.F.[2]; El Maged R.A.[2]; Ayada M.M.[2]

[1]Departments of Pathology and [2]Dermatology, Faculty of Medicine, Suez Canal University, Ismailia, Egypt

Background disturbed cytokines had been implicated in melanocytes destruction in vitiligo. **Aim** to clarify one of the mechanisms involved in melanocytes by evaluating the immunohistochemical (IHC) expression of stem cell factor (SCF) in vitiligo.

Materials and methods this case control study involved 68 skin specimens from lesional ($n=34$) and non lesional ($n=34$) biopsies, assessed by hematoxylin and eosin (H&E) and Masson Fontana (MF). SCF was evaluated by IHC and was tested for association with histopathological changes and disease progression.

Results In the lesional biopsies, the central zone showed nearly absence of melanocytes while in the peripheral one decreased number was noted compared to the non lesional biopsies ($p<0.05$). Dermal lymphocytic infiltrate were observed and was more pronounced in generalized vitiligo ($p=0.04$). In non lesional biopsies, epidermal SCF expression was strong in 70.6% and moderate in 29.4%, while strong staining for dermal endothelial cells and fibroblasts was encountered in 97%. In the lesional biopsies, epidermal SCF was mild, moderate and strong representing 79.4%, 14.7% and 5.9% respectively, while mild (97%) and moderate (3%) staining was seen in dermal endothelial cells and fibroblasts. The over all immunoreactivity was significantly lower in lesional biopsies compared to non lesional ones ($p<0.001$). Strong association has been found between decreased SCF expression and extent of depleted melanocytes ($p<0.05$), and was more pronounced in generalized vitiligo ($p<0.01$). Furthermore, significant association has been identified between decreased SCF immunoreactivity and progressive disease course ($p<0.05$).

Conclusion The study showed decreased expression of SCF in lesional biopsies of vitiligo. Therapy directed to restore SCF might be helpful to patients. Key words: vitiligo, stem cell factor, IHC.

P4.238

Lack of CCR7 expression is rate limiting for lymphatic spread of pancreatic ductal adenocarcinoma

Sperveslage J.[1; 8]; Frank S.[1]; Heneweer C.[2]; Emme D.[3]; Egberts J.[3]; Schniewind B.[3]; Bergmann F.[4]; Giese N.[5]; Friedl P.[6; 7]; Alexander S.[7]; Häsler R.[8]; Kalthoff H.[3]; Klöppel G.[1] ; Sipos B.[1; 9]

[1]Department of Pathology, [2] Department of Diagnostic Radiology, [3]Molecular Oncology Section, Department of General Surgery, University of Kiel, Germany; [4] Department of Pathology and [5] Department of Surgery, University of Heidelberg, Germany; [6] Department of Cell Biology, NCMLS, Radboud University Nijmegen Medical Centre, Nijmegen, Netherlands; [7] Rudolf Virchow Center, DFG Research Center for Experimental Biomedicine, Würzburg, Germany; [8] Institute for Clinical Molecular Biology, University Hospital Schleswig-Holstein, Kiel, Germany; [9] Department of Pathology, University of Tübingen, Germany

Background CCR7 is a major regulator of activated immune cells that are directed to lymph nodes. We studied the role of CCR7 in lymphatic spread and tumor growth in pancreatic ductal adenocarcinomas (PDACs), which are highly metastatic to lymph nodes.

Methods and results CCR7 was expressed in the majority (10/12) of PDAC cell lines at mRNA level. FACS analysis revealed low constitutive CCR7 protein expression in most cell lines; however, CCR7 was significantly elevated in 7 of 11 cell lines. Wild type CCR7 transfected Pt45P1 and Colo357 cells showed enhanced migration towards CCL21 in transwell migration assays. Orthotopically injected CCR7 transfected Pt45P1 cells gave rise to significantly larger tumors in a nude mouse model than mock transfected and CCR7 negative cells (CCL21-KDEL transfected). In addition, CCR7 transfected Pt45P1 tumors showed a higher frequency of lymph node metastases than mock transfected and CCR7 negative tumors. Likewise, of 126 human PDACs 46% exhibited moderate-to-strong CCR7 expression by immunohistochemistry, which correlated with high rates of lymph vessel invasion and the presence of lymph node metastases. Moreover, in PDAC completely lacking CCR7 expression, high rates of lymph vessel invasion and > 3 lymph node metastases were not detected. The analysis of immunofluorescence stains revealed a significant upregulation of CCL21 in peritumoral and intratumoral lymph vessels compared with lymph vessels in disease-free pancreata.

Conclusion CCR7 expression significantly promotes lymphatic spread in PDAC. Lymph vessel invasion of PDAC cells may be additionally enhanced by upregulation of CCL21 in tumor-associated lymph vessels, representing a previously unknown factor of lymphatic spread.

P4.239

Novel prognostic markers of insulinomas

Alkatout I.[1]; Sitek B.[2]; Stühler K.[2]; Bauersfeld J.[3]; Anlauf M.[4]; Perren A.[5]; Beghelli S.[6]; Scarpa A.[6]; Raffel A.[7]; Meyer H.E.[2]; Klöppel G.[1]; Sipos B.[1; 8]

[1]Department of Pathology, University of Kiel, Germany; [2]Medizinisches Proteom-Center, Ruhr-University Bochum, Germany; [3]Department of Pathology, University of Zürich, Switzerland; [4] Department of Pathology, University Düsseldorf, Germany; [5]Department of Pathology, University of Bern, Switzerland; [6]Department of Pathology, University of Verona, Italy; [7]Department of Surgery, University of Düsseldorf, Germany; [8] Department of Pathology, University of Tübingen, Germany

Background The biological behavior of pancreatic endocrine tumors (PET) is difficult to predict on the basis of classical histological criteria. Benign and malignant PET can be identified with certainty on the basis of tumor size, rate of proliferation and the presence of metastasis. However, a number of tumors must be categorized as neuroendocrine tumors with uncertain biological behavior. The discovery of novel prognostic markers would allow a better stratification of patients for post-operative diagnostic and therapeutic approaches.

Method Microdissected cells from 10 benign and 10 malignant insulinomas were subjected to a procedure combining fluorescence dye saturation labelling with high resolution two-dimensional gel electrophoresis. Differentially expressed proteins were identified using nanoLC-ESI-MS/MS and validated by immunohistochemistry on tissue microarrays containing 68 well-characterized insulinomas.

Results 18 differentially expressed spots were identified representing 9 up or downregulated proteins. The proteins were validated by means of a tissue microarray containing 68 insulinomas (benign, malignant and of uncertain malignant potential). The classical histopathological features and survival data were analysed in relation to the expression of novel candidates. Aldehyddehydrogenase-1a, Gelsolin, TPD52 binding protein and Voltage-dependent anion-selective channel protein 1 showed a significant different expression in benign and malignant insulinomas in proteomic and immunohistochemical analysis. Low TPD52 and high VDAC1 expression predicted the malignant behaviour of insulinomas with 75% specificity and 82% sensitivity.

Conclusion VDAC1 and TPD52 have been identified as novel marker which may help to estimate the prognosis of insulinomas. The overexpression of ALDH1a in malignant insulinomas is worth further investigations regarding its putative role as stem cell factor.

P4.240
The identification of the oncoprotein C-erbB-2 in normal endometrium and in endometrial carcinoma

Sisovsky V.[1;2;3]; Palkovic M.[1;2]; Repiska V.[4]; Danihel L.[1;2]
[1]Department of Pathology and [4]Institute of Medical Biology, Genetics and Clinical Genetics, Faculty of Medicine, Comenius University and Faculty Hospital with Policlinics in Bratislava, Slovak Republic; [2]Pathological-Anatomical Workplace, Health Care Surveillance Authority, Bratislava, Slovak Republic; [3]Department of Molecular Biology, Faculty of Natural Sciences, Comenius University in Bratislava, Slovak Republic

Background C-erbB-2 oncoprotein is a 185 kDa transmembrane tyrosine kinase belonging to the epidermal growth factor receptor family. Activation of C-erbB-2 by dimerization triggers intracellular signaling events, which are crucial for cell growth, differentiation and survival. **Aim** To evaluate a possible association between morphological appearance of normal endometrium and of endometrial carcinoma (ECa), and between the degree of C-erbB-2 expression and of clinical findings.
Methods A total of 90 archival formalin-fixed and paraffin-embedded biopsy (hysterectomy and curettage) tissue specimens with proliferative (PE) and secretory (SE) endometrium, endometrioid (EC) grade G1 (ECG1) and G3 (ECG3), serous (SC) and clear cell (CCC) subset of ECa were evaluated by immunohistochemistry (IHC) for the C-erbB-2 expression in cell membrane of endometrial epithelial cells. The protein expression was evaluated by light microscopy semiquantitatively.
Results The expression of C-erbB-2 was low in PE and in SE, with progressively increase with the grade of differentiation of EC to SC. The expression of C-erbB-2 was the highest in CCC that corresponded with worse clinical course of oncological illness.
Conclusions There is low expression of C-erbB-2 in PE and in SE. Malignant changes of endometrium are accompanied by a increased in C-erbB-2 expression. The quantity of C-erbB-2 is directly proportioned to the grade of differentiation of EC (type I). The highest expression of C-erbB-2 is associated with aggressive (mainly CCC, less SC) type (type II) of ECa. Evaluation of C-erbB-2 expression in ECa by IHC, could be relevant component, which may be useful in clinical practice. Supported by the grant 2007/28-UK-05 MZSR.

P4.241
The prognostic value of the tumour protein p53 in endometrial carcinoma

Sisovsky V.[1;2;3]; Palkovic M.[1;2]; Bucekova B.[1]; Porubsky J.[1]; Repiska V.[4]; Danihel L.[1;2]
[1]Department of Pathology and [4]Institute of Medical Biology, Genetics and Clinical Genetics, Faculty of Medicine, Comenius University and Faculty Hospital with Policlinics in Bratislava, Slovak Republic; [2]Pathological-Anatomical Workplace, Health Care Surveillance Authority, Bratislava, Slovak Republic; [3]Department of Molecular Biology, Faculty of Natural Sciences, Comenius University in Bratislava, Slovak Republic

Background The TP53 is a tumor suppressor gene encoding a DNA-binding phosphoprotein p53 that is involved in the regulation of the cell cycle; it has an inhibitory effect on cell proliferation and transformation and an activating effect on DNA repair and apoptosis. Mutation of the TP53 results in a mutant p53 with a longer half-life that accumulates in the cells and lack of the above presented functions.
Aim To evaluate a possible association between morphological appearance of normal endometrium and of endometrial carcinoma (ECa), and between the degree of p53 expression and of clinical findings.
Methods A total of 60 archival formalin-fixed and paraffin-embedded biopsy (hysterectomy and curettage) tissue specimens with proliferative endometrium (PE), endometrioid (EC) grade G1 (ECG1) and G3 (ECG3), serous (SC) and clear cell (CCC) subset of ECa were evaluated by immunohistochemistry (IHC) for the p53 expression in nuclei of endometrial epithelial cells. The findings were evaluated by light microscopy semiquantitatively.
Results The p53 expression was related only to aggressive (SC and ECG3, less CCC) types of ECa. In SC the expression of p53 was the highest and it correlated with the worse clinical course of oncological illness. In PE and in ECG1 was not found the p53 expression.
Conclusion The p53 expression is the important prognostic marker of ECa. Its evaluation by IHC is a relatively cheap and simple method usable for clinical practice. The p53 expression is related only to aggressive (SC and ECG3) types of ECa. Supported by the grant 2007/28-UK-05 MZSR and the Governor Ing.T.Bucek, 2006-07 LCI D-122.

Author index